PURINERGIC PHARMACOLOGY

EDITED BY: Francisco Ciruela and Kenneth A. Jacobson
PUBLISHED IN: Frontiers in Pharmacology

frontiers Research Topics

ISSN 1664-8714
ISBN 978-2-88945-947-6
DOI 10.3389/978-2-88945-947-6

About Frontiers

Frontiers is more than just an open-access publisher of scholarly articles: it is a pioneering approach to the world of academia, radically improving the way scholarly research is managed. The grand vision of Frontiers is a world where all people have an equal opportunity to seek, share and generate knowledge. Frontiers provides immediate and permanent online open access to all its publications, but this alone is not enough to realize our grand goals.

Frontiers Journal Series

The Frontiers Journal Series is a multi-tier and interdisciplinary set of open-access, online journals, promising a paradigm shift from the current review, selection and dissemination processes in academic publishing. All Frontiers journals are driven by researchers for researchers; therefore, they constitute a service to the scholarly community. At the same time, the Frontiers Journal Series operates on a revolutionary invention, the tiered publishing system, initially addressing specific communities of scholars, and gradually climbing up to broader public understanding, thus serving the interests of the lay society, too.

Dedication to Quality

Each Frontiers article is a landmark of the highest quality, thanks to genuinely collaborative interactions between authors and review editors, who include some of the world's best academicians. Research must be certified by peers before entering a stream of knowledge that may eventually reach the public - and shape society; therefore, Frontiers only applies the most rigorous and unbiased reviews.
Frontiers revolutionizes research publishing by freely delivering the most outstanding research, evaluated with no bias from both the academic and social point of view. By applying the most advanced information technologies, Frontiers is catapulting scholarly publishing into a new generation.

What are Frontiers Research Topics?

Frontiers Research Topics are very popular trademarks of the Frontiers Journals Series: they are collections of at least ten articles, all centered on a particular subject. With their unique mix of varied contributions from Original Research to Review Articles, Frontiers Research Topics unify the most influential researchers, the latest key findings and historical advances in a hot research area! Find out more on how to host your own Frontiers Research Topic or contribute to one as an author by contacting the Frontiers Editorial Office: researchtopics@frontiersin.org

PURINERGIC PHARMACOLOGY

Topic Editors:
Francisco Ciruela, Universitat de Barcelona, Spain
Kenneth A. Jacobson, National Institute of Diabetes and Digestive and Kidney Diseases, National Institutes of Health, United States

Citation: Ciruela, F., Jacobson, K. A., eds. (2019). Purinergic Pharmacology. Lausanne: Frontiers Media. doi: 10.3389/978-2-88945-947-6

Table of Contents

frontiers in Pharmacology

EDITORIAL
published: 23 January 2019
doi: 10.3389/fphar.2019.00021

Editorial: Purinergic Pharmacology

Francisco Ciruela[1,2]* *and Kenneth A. Jacobson*[3]

[1] Unitat de Farmacologia, Departament Patologia i Terapèutica Experimental, Facultat de Medicina, IDIBELL, L'Hospitalet de Llobregat, Universitat de Barcelona, Barcelona, Spain, [2] Institut de Neurociències, Universitat de Barcelona, Barcelona, Spain, [3] Molecular Recognition Section, Laboratory of Bioorganic Chemistry, National Institute of Diabetes and Digestive and Kidney Diseases, National Institutes of Health, Bethesda, MD, United States

Keywords: adenosine, G protein-coupled purinergic receptors, ATP, purinergic signalling, adenosine transport, caffeine, purinergic pathophysiology, ligand-gated purinergic ion channels

Editorial on the Research Topic

Purinergic Pharmacology

The purine nucleotides and nucleosides constitute important extracellular signaling molecules acting as neurotransmitters and neuromodulators. Indeed, extracellular adenosine 5′-triphosphate (ATP) and adenosine, tightly controlled by nucleotidases, ribokinases, deaminases, and transporters, signal through a rich array of purinergic receptors. These receptors, which emerged early in evolution, are among the most abundant in living organisms controlling many physiological actions, thus becoming promising therapeutic targets in a wide range of pathological conditions. Thus, while P1 receptors are selective for adenosine, a breakdown product of ATP, P2 receptors are activated by purine nucleotides, as well as P2Y receptors being activated by pyrimidine nucleotides. Interestingly, purinergic receptors, both G protein-coupled (i.e., P1 and P2Y) and ligand-gated ion channel (i.e., P2X) receptors, are involved in many neuronal and non-neuronal mechanisms, including pain, immune responses, exocrine and endocrine secretion, platelet aggregation, endothelial-mediated vasodilatation and inflammation, among others.

Purinergic receptors are ubiquitously expressed throughout the body, thus compromising the specificity of receptor subtype-selective drugs and increasing the possibility of side effects upon pharmacological intervention. However, the extracellular levels of purines may fluctuate enormously, thus distinct purinergic receptors responding differently to low and high concentrations of endogenous purines are called into action while cells are exposed to multiple purinergic signaling molecules. Therefore, the same cell usually concurrently expresses different subtypes of P1 and P2 receptors, which allows the integration of purinergic transmission into short- and long-term signaling events. Consequently, drug selectivity constitutes another important pharmacological goal within the purinergic field. Indeed, the development of potent and selective synthetic agonists and antagonists for purinergic receptors has been the subject of medicinal chemistry research for decades. In addition, allosteric modulators of purinergic receptors have been successfully developed. Interestingly, these compounds allow the manipulation of the endogenous purinergic system in an event-responsive and temporally specific manner, thus offering a unique therapeutic window when compared to orthosteric compounds. Finally, the functioning of the purinergic system could be also manipulated by modulating the metabolism and/or uptake of extracellular purine nucleotides and nucleosides. Overall, there is no doubt that purinergic pharmacology is growing fast and becoming an attractive field for pharmacotherapeutic development.

In this timely research topic, an overview of the purinergic pharmacology is provided through 61 articles written by 439 authors. This successful compilation contains 15 reviews, 5 mini reviews, 3 hypothesis and theory papers, 1 perspective, and 37 original research papers. The reviews summarize the currently available knowledge on the role of purinergic signaling, focusing

OPEN ACCESS

Edited and reviewed by:
Salvatore Salomone,
Università Degli Studi di Catania, Italy

***Correspondence:**
Francisco Ciruela
fciruela@ub.edu

Specialty section:
This article was submitted to Experimental Pharmacology and Drug Discovery, a section of the journal Frontiers in Pharmacology

Received: *21 December 2018*
Accepted: *09 January 2019*
Published: *23 January 2019*

Citation:
Ciruela F and Jacobson KA (2019) Editorial: Purinergic Pharmacology. Front. Pharmacol. 10:21. doi: 10.3389/fphar.2019.00021

on the pathophysiology and its therapeutic potential (Burnstock), for example, in mast cell degranulation and its most relevant disease, asthma (Gao and Jacobson), pulmonary arterial hypertension (Alencar et al.), amyotrophic lateral sclerosis (Sebastião et al.), neurodevelopmental disorders (Fumagalli et al.), epilepsy (Alves et al.), neurological diseases with motor symptoms (Oliveira-Giacomelli et al.), motivational dysfunction and depression (López-Cruz et al.), and inflammatory diseases (Savio et al.), In addition, some of the reviews provide more mechanistic opinions, for instance on purinergic transmission in psychostimulant addiction (Ballesteros-Yáñez et al.), carotid body physiology (Conde et al.), and platelet heterogeneity (Koupenova and Ravid). Also, some hints about the molecular mechanism of ligand binding and activation by adenosine (Carpenter and Lebon) and ATP (Di Virgilio et al.) receptors is provided. Finally, the impact of adenosine transport in purinergic signaling is also reviewed (Pastor-Anglada and Pérez-Torras).

Subsequently, five minireviews highlight diverse aspects of purinergic signaling. For instance, the role of adenosine and its receptors in T cell development in the thymus (Köröskényi et al.) and the regulation of the activity of immune cells and enteric nervous system (Dal Ben et al.). Thus, the most promising purine-based strategies are summarized for the treatment of inflammation-related disorders, including the recent development of nanobodies against key targets of purinergic system (Menzel et al.). Next, the current knowledge on the pathophysiological involvement of purinergic receptors in white and brown adipocytes and their potential use in metabolic disorders is reviewed (Tozzi and Novak). Also, the recent emerging data involving the ATP-gated P2X7 ion channel as a potential drug target for central nervous system disorders including neuropsychiatric conditions (Bhattacharya).

In the section "Hypothesis and Theory" the molecular determinants of small-molecule ligand (i.e., BzATP and ivermectin) binding at P2X receptors is reviewed grounded in structure-based docking studies (Pasqualetto et al.). Next, the interplay of adenosine receptors with muscarinic acetylcholine and neurotrophin receptors in the mammalian neuromuscular junction controlling synapse elimination and neurotransmission release is considered (Tomàs et al.). Also, the formation of adenosine A_{2A} and dopamine D_2 receptor heterotetramers and adenylate cyclase type 5 complexes in striatopallidal neurons are postulated as an integrative device tuning adenosine and dopamine signaling and therefore behavioral effects of adenosine/dopamine-based ligands (Ferré et al.). Finally, a perspective paper discusses the current limitations and highlights future research directions to achieve adenosine receptor-mediated cardioprotection (Lasley).

The research topic contains a series of original research papers covering important aspects of purinergic pharmacology. Thus, several papers focus on the role of adenosine receptors in cancer cells proliferation (Gessi et al.), morphologically altered hippocampal neurons (Pinheiro et al.), hippocampal slices subjected to oxygen and glucose deprivation (Fusco et al.), instrumental animal learning (Li et al.), and rodent models of movement disorders (Núñez et al.). Indeed, the interest of targeting adenosine receptors is also shown by the design of a non-imaging high throughput approach to screen drugs in native receptors (Arruda et al.) and their detection in human brain using positron emission tomography (PET) ligands (Mishina et al.). In addition, some molecular clues about adenosine receptor function are also given, for instance, the formation of transcellular trimeric complexes involving CD26, adenosine deaminase and adenosine A_{2A} receptor ($A_{2A}R$) (Moreno et al.), the $A_{2A}R$-mediated control of glutamatergic synaptic plasticity in prefrontal cortex interneurons (Kerkhofs et al.) and the adenosine A_{2B} receptor ($A_{2B}R$)-mediated control of epithelial-mesenchymal transition by tuning the cAMP/PKA and MAPK/ERK balance (Giacomelli et al.). Also, it is speculated whether $A_{2A}R$ may be useful to sustain contractility in failing human hearts and upon ischemia and reperfusion (Boknik et al.). Finally, the role of caffeine in controlling glutamatergic synaptic transmission in human cortical neurons (Kerkhofs et al.) and its adverse effects in an Alzheimer's disease animal model (Baeta-Corral et al.) are investigated.

The role of the purinergic system in microglia and astrocytic function both *in vitro* and *in vivo* is studied in glaucoma (Rodrigues-Neves et al.), prostaglandin E2 signaling (Paniagua-Herranz et al.), extracellular vesicle-based cell communication (Drago et al.), cell migration (Adzic and Nedeljkovic) and proliferation (Quintas et al.). Similarly, the impact on T cells (Shinohara and Tsukimoto; Soslow et al.) and cytokine-induced killer cell function (Horenstein et al.) is also explored. Interestingly, extracellular signaling by guanine-based purines was explored in cultured cells (Pietrangelo et al.; Zuccarini et al.) and in rodent models of movement disorders (Massari et al.).

The extracellular ATP/adenosine ratio is a key element for immune responses, including post-inflammatory ileitis, as described in this research topic (Vieira et al.). Thus, the tissue-nonspecific alkaline phosphatase enzyme and Pannexin-1 channel seem to play an important physiological role regulating the levels of extracellular ATP (Sebastián-Serrano et al.), which ultimately will activate cell surface P2XRs and P2YRs. In addition, it seem that ATP release, at least in the suprachiasmatic nucleus, is under the control of these two kinds of purinergic receptors (Svobodova et al.). Interestingly, P2XRs are allosterically modulated by trace metals (i.e., zinc) and other drugs (i.e., ivermectin) (Latapiat et al.), which also can form heterotrimeric P2X4/P2X7 receptors (Schneider et al.). Importantly, P2X7R is up-regulated and promotes a fibrogenic phenotype in systemic sclerosis (SSc) fibroblasts, thus becoming a potential therapeutic target in SSc patients (Gentile et al.). Conversely, P2YR expression seems to play a key role in eye physiology. Thus, changes in the $P2Y_2/P2Y_1$ expression ratio correlates well with an increment in the intraocular pressure in an animal model of glaucoma (Fonseca et al.). Also, $P2Y_{12}R$ blockade facilitate the clearance of lysosomal waste in retinal pigmented epithelial cells, which is relevant for age-related macular degeneration management

(Lu et al.). Furthermore, a clinical study revealed that $P2Y_{12}R$ blockade does not contribute to risk of osteoporotic fractures in stroke patients, a common adverse effect of transient ischemic attack treatment (Jørgensen et al.). In a separate context, the $P2Y_6R$ regulates chemokine (i.e., CXCL10) secretion in mouse intestinal epithelia cells, thus regulating gut homeostasis (Salem et al.).

As a neurotransmitter, ATP is stored in secretory vesicles, a process mediated by the vesicular nucleotide transporter (VNUT). In this research topic it is demonstrated that cerebellar granule cells express functional VNUT and that may be implicated in the initial stages of granule cell development (Menéndez-Méndez et al.). Finally, the issue also reports the generation and characterization of a valuable, new tool to study ectonucleotidase nucleoside triphosphate diphosphohydrolase-8 (NTPDase8) (Pelletier et al.) and the characterization of uridine adenosine tetraphosphate's (Up4A) physiological role in *in vivo* heart failure model, i.e., swine aortic banding (Zhou et al.).

Overall, this research topic provides new insights into the vast physiological roles of purinergic signaling and its structural and mechanistic basis. This field offers enormous possibilities for translation of basic science into novel treatments for chronic and acute diseases, while at the same time it presents a challenge to achieve selectivity of drug action.

AUTHOR CONTRIBUTIONS

All authors listed have made a substantial, direct, and intellectual contribution to the work, and approved it for publication.

ACKNOWLEDGMENTS

We would like to thank all authors for their highly valuable contribution. Also, we would like to acknowledge the work of reviewers whose constructive input contributed to improving the quality of the articles. Finally, we would like to acknowledge the support of MINECO-AEI/FEDER, UE (SAF2017-87349-R), the Catalan government (2017 SGR 1604), Fundació la Marató de TV3 (Grant 20152031), FWO (SBO-140028) to FC and NIDDK Intramural Research Program (ZIADK031117) to KJ.

Conflict of Interest Statement: The authors declare that the research was conducted in the absence of any commercial or financial relationships that could be construed as a potential conflict of interest.

frontiers in Pharmacology

ORIGINAL RESEARCH
published: 19 October 2018
doi: 10.3389/fphar.2018.01200

PBF509, an Adenosine A_{2A} Receptor Antagonist With Efficacy in Rodent Models of Movement Disorders

Fabiana Núñez[1,2], Jaume Taura[1,2], Juan Camacho[3], Marc López-Cano[1,2], Víctor Fernández-Dueñas[1,2], Naomi Castro[3], Julio Castro[3] and Francisco Ciruela[1,2]**

[1] Unitat de Farmacologia, Departament Patologia i Terapèutica Experimental, Facultat de Medicina, IDIBELL, Universitat de Barcelona, L'Hospitalet de Llobregat, Barcelona, Spain, [2] Institut de Neurociències, Universitat de Barcelona, Barcelona, Spain, [3] PaloBiofarma S.L., Barcelona, Spain

Adenosine A_{2A} receptor ($A_{2A}R$) antagonists have emerged as complementary non-dopaminergic drugs to alleviate Parkinson's disease (PD) symptomatology. Here, we characterize a novel non-xhantine non-furan $A_{2A}R$ antagonist, PBF509, as a potential pro-dopaminergic drug for PD management. First, PBF509 was shown to be a highly potent ligand at the human $A_{2A}R$, since it antagonized $A_{2A}R$ agonist-mediated cAMP accumulation and impedance responses with K_B values of 72.8 ± 17.4 and 8.2 ± 4.2 nM, respectively. Notably, these results validated our new $A_{2A}R$-based label-free assay as a robust and sensitive approach to characterize $A_{2A}R$ ligands. Next, we evaluated the efficacy of PBF509 reversing motor impairments in several rat models of movement disorders, including catalepsy, tremor, and hemiparkinsonism. Thus, PBF509 (orally) antagonized haloperidol-mediated catalepsy, reduced pilocarpine-induced tremulous jaw movements and potentiated the number of contralateral rotations induced by L-3,4-dihydroxyphenylalanine (L-DOPA) in unilaterally 6-OHDA-lesioned rats. Moreover, PBF509 (3 mg/kg) inhibited L-DOPA-induced dyskinesia (LID), showing not only its efficacy on reversing parkinsonian motor impairments but also acting as antidyskinetic agent. Overall, here we describe a new orally selective $A_{2A}R$ antagonist with potential utility for PD treatment, and for some of the side effects associated to the current pharmacotherapy (i.e., dyskinesia).

Keywords: PBF509, Parkinson's disease, adenosine A_{2A} receptor, catalepsy, label-free, tremor, hemiparkinsonism, antagonist

OPEN ACCESS

Edited by:
Vsevolod V. Gurevich, Vanderbilt University, United States

Reviewed by:
David Blum, INSERM U1172 Centre de Recherche Jean-Pierre Aubert, France
Rodrigo A. Cunha, Universidade de Coimbra, Portugal

****Correspondence:***
Julio Castro
jcastro@palobiofarma.es
Francisco Ciruela
fciruela@ub.edu

Specialty section:
This article was submitted to Experimental Pharmacology and Drug Discovery, a section of the journal Frontiers in Pharmacology

Received: *05 July 2018*
Accepted: *01 October 2018*
Published: *19 October 2018*

Citation:
Núñez F, Taura J, Camacho J, López-Cano M, Fernández-Dueñas V, Castro N, Castro J and Ciruela F (2018) PBF509, an Adenosine A_{2A} Receptor Antagonist With Efficacy in Rodent Models of Movement Disorders. Front. Pharmacol. 9:1200. doi: 10.3389/fphar.2018.01200

INTRODUCTION

Parkinson's disease (PD) is a neurodegenerative condition affecting around 1% of the population over the age of 65 (Meissner et al., 2011). PD is characterized by bradykinesia, tremor, and rigidity, which are secondary to the loss of dopamine neurons in the substantia nigra (Poewe and Mahlknecht, 2009). The main therapeutic approach consists of administrating L-3,4-dihydroxyphenylalanine (L-DOPA) or dopamine receptor agonists, thus recovering the functioning of dopaminergic transmission (Poewe, 2009). However, a number of adverse effects appear upon the long consumption of dopamine-like based drugs (Huot et al., 2013). From these, dyskinesia is the most reported one, since, in most cases, it critically impedes the normal life of patients. Rotation of dopamine-like based drugs is a normal strategy to diminish the appearance of these secondary effects, but it seems clear that there is a need in PD clinics for searching novel agents that may improve the management of the pathology (Schapira et al., 2006).

From the new drugs developed not only to improve the clinical features of classical drugs but also to alleviate their undesired side effects, adenosine A_{2A} receptor ($A_{2A}R$) antagonists appear to be the most promising ones. Interestingly, $A_{2A}Rs$ are expressed in GABAergic enkephalinergic neurons together with dopamine D_2 receptors (D_2R), which are the main target of PD drugs (Gerfen et al., 1990). In addition, it has been largely studied the presence of reciprocal functional interactions between both receptors, a phenomenon that has been postulated to permit a fine-tuning modulation of the basal ganglia functioning (for review see Ferre et al., 2004). Furthermore, it was recently demonstrated that both receptors form receptor complexes (i.e., oligomers), in which a direct receptor-receptor interaction may drive the functional interplay between $A_{2A}R$ and D_2R (Fernández-Dueñas et al., 2015). Nevertheless, apart from the plausible pre- and post-synaptic mechanism mediating its effects (Schiffmann et al., 2007), it has been clearly shown that $A_{2A}R$ antagonists show an antiparkinsonian efficacy, and that they may also be used to lessen undesired side effects of dopaminergic-like based drugs. In such way, the obtained pre-clinical information points to the use of $A_{2A}R$ antagonists as valuable agents for: (i) providing motor benefits by themselves, (ii) potentiating the benefit of dopamine agonists, or (iii) preventing the development of dopamine-like drugs induced dyskinesias (for review see Hauser and Schwarzschild, 2005; Jenner et al., 2009). In line with this, randomized clinical studies have been performed to assess the efficacy of these new $A_{2A}R$-based drugs (for review see Vallano et al., 2011). Indeed, an $A_{2A}R$ antagonist (i.e., istradefylline) (Jenner, 2005) has been licensed in Japan (Nouriast®) as an adjuvant to L-DOPA treatment in order to reduce off-times produced by the dopaminergic drug (Mizuno et al., 2010; Kondo and Mizuno, 2015; Müller, 2015).

The development of new $A_{2A}R$ antagonists is consequently a main objective in PD therapeutics, since they may represent alternative or complementary drugs to deal with the symptomatology associated with the pathology. Importantly, it is crucial the information gained in pre-clinical studies, which may permit to properly screen the better candidates to be tested in randomized clinical studies. However, finding the optimal animal model is not a simple task, and it is usually mandatory to demonstrate the activity of any new drug in a variety of them. Here, we describe the effectiveness of PBF509, a novel selective and potent $A_{2A}R$ antagonist, in several rat animal models of movement impairment: (i) the pilocarpine-induced tremulous jaw movement (TJM), (ii) the hemiparkinsonian animal model, and (iii) the L-DOPA induced dyskinesia (LID). Importantly, we show the activity of this new antiparkinsonian drug in comparison with other well-known $A_{2A}R$-based agents, aiming to prompt its future use in randomized clinical trials.

MATERIALS AND METHODS

Drugs

PBF509 (Mediavilla-Varela et al., 2017), synthesized by PaloBiofarma, was dissolved in 0.5% methylcellulose for oral administration. All other compounds were obtained from external sources: 6-hydroxydopamine (6-OHDA), benserazide, pilocarpine, haloperidol (Sigma-Aldrich, St. Louis, MO, United States), 3,4-Dihydroxy-L-phenylalanine (L-DOPA; Abcam Biochemicals, Cambridge, United Kingdom), CGS21680, SCH442416, (Tocris Bioscience, Ellisville, MO, United States).

Antibodies

The primary antibodies used were rabbit anti-TH polyclonal antibody (Millipore, Temecula, CA, United States), mouse anti-$A_{2A}R$ monoclonal antibody (Millipore) and rabbit anti-α-actinin polyclonal antibody (Santa Cruz Biotechnology, Santa Cruz, CA, United States). The secondary antibodies were horseradish peroxidase (HRP)-conjugated goat anti-rabbit and goat anti-mouse IgG (Pierce Biotechnology, Rockford, IL, United States), and Cy2-conjugated donkey anti-rabbit and Cy2-conjugated donkey anti-mouse antibodies (Jackson ImmunoResearch Laboratories).

cAMP Accumulation Inhibition Assay

cAMP accumulation was measured using the LANCE *Ultra* cAMP kit (PerkinElmer, Waltham, MA, United States) (Taura et al., 2016). In brief, HEK-293 cells permanently expressing the $A_{2A}R^{SNAP}$ construct (Fernández-Dueñas et al., 2015) were incubated in the absence or presence of increasing concentrations of SCH442416 or PBF509 before stimulating the cells with CGS21260 ($\sim EC_{80}$) for 30 min at 22°C with adenosine deaminase (0.5 U/ml; Roche). Eu-cAMP tracer and U*Light*™-anti-cAMP reagents were prepared and added to the sample according to the LANCE® *Ultra* cAMP Kit instruction manual. 384-wells plate was incubated 1 h at 22°C in the dark and was then read on a POLARstar microplate reader (BMG LABTECH, Durham, NC, United States). Measurement at 620 and 665 nm were used to detect the TR-FRET signal and the concomitant cAMP levels were calculated following manufacturer's instructions. Data were fitted by non-linear regression using GraphPad Prism 5 (GraphPad Software).

Concentration-response curves were carried out by assaying different ligand (i.e., PBF509 and SCH442416) concentrations ranging between 10 nM to 30 μM. Data was expressed as K_B by following the formula reported by Leff and Dougall (1993):

$$K_B = IC_{50}/[2 + ([A]/[A_{50}])^n]^{(1/n)} - 1$$

Where IC_{50} is the concentration of compound that inhibits CGS21680 effect by a 50%; [A] is the concentration of CGS21680 employed in the assay, $[A_{50}]$ is the CGS21680 EC_{50} value and n is the Hill slope of the curve.

Cellular Impedance Assay Label-Free

The xCELLigence RTCA system (Roche) was employed to measure changes in cellular impedance correlating with cell spreading and tightness, thus being widely accepted as morphological and functional biosensor of cell status (Xu et al., 2016). Accordingly, we assessed the impact of $A_{2A}R$ blockade in cellular impedance (Solly et al., 2004; Stallaert et al., 2012; Hillger et al., 2015). To this end, HEK-293 cells permanently expressing the $A_{2A}R^{SNAP}$ construct (Fernández-Dueñas et al., 2015) were growth in Dulbecco's modified Eagle's medium (DMEM) (Sigma-Aldrich) supplemented with 1 mM sodium pyruvate (Biowest,

Nuaillé, France), 2 mM L-glutamine (Biowest), 100 U/mL streptomycin (Biowest), 100 mg/mL penicillin (Biowest), and 1.5% (v/v) fetal bovine serum (Gibco) in presence of 0.5 U/ml of adenosine deaminase. The 16-wells E-plates (Roche) were used. Wells were coated with 50 µl fibronectin (10 µg/ml). Plates were placed at 37°C for 1 h. After removing coating liquid, plates were washed three times with 100 µl Milli-Q-water before use. The background index for each well was determined with supplemented DMEM (90 µl) in the absence of cells. Data from each well were normalized to the time point just before compound addition using the RTCA software providing the normalized cell index (NCI). Subsequently, cells (90 µl re-suspended in supplemented DMEM were then plated at a cell density of 10,000 cells/well and grown for 18 h in the RTCA SP device station (Roche) at 37°C and in an atmosphere of 5% CO_2 before ligand (i.e., CGS21680) addition. For the concentration-response inhibition of CGS21680-mediated effect the cells were first incubated with the corresponding antagonist (i.e., PBF509 or SCH442416) for 1 h and then CGS21680 ($\sim EC_{80}$) was added. Cell index values were obtained immediately following ligand stimulation every 15 s for a total time of at least 100 min. For data analysis, ligand (i.e., SCH442416 and PBF509) responses were transformed to ΔNCI after subtracting baseline (i.e., vehicle control) to correct for any ligand-independent effects. The ΔNCI was then taken at 30 min after the agonist addition to build the concentration-response curve. ΔNCI were expressed in % considering 1 µM of CGS21680 as the 100% and the vehicle as the 0%.

Animals

Sprague-Dawley rats (Charles River Laboratories, L'Arbresle, France) weighing 240–250 g were used. The University of Barcelona Committee on Animal Use and Care approved the protocol. Animals were housed and tested in compliance with the guidelines provided by the Guide for the Care and Use of Laboratory Animals (Clark et al., 1997) and following the European Union directives (2010/63/EU). All efforts were made to minimize animal suffering and the number of animals used. Rats were housed in groups of three in standard cages with *ad libitum* access to food and water and maintained under a 12 h dark/light cycle (starting at 7:30 AM), 22°C temperature, and 66% humidity (standard conditions). All animal model observations were made between 9:00 AM and 1:00 PM.

Haloperidol-Induced Catalepsy

Rats (n = 10) were randomly assigned to treatment groups and behavioral testing was performed blind to treatment. The dopamine D_2 receptor (D_2R) antagonist, haloperidol (1 mg/kg, s.c.) was administered to induce catalepsy. Thirty minutes after the haloperidol administration, rats experienced a full cataleptic response. At this time point, for each rat the state of catalepsy was tested by gently placing their front limbs over an 8-cm high horizontal bar. The intensity of catalepsy was assessed by measuring the time the rats remain in this position being completely immobile for a maximum of 120 s. Only rats that remained cataleptic for the entire 120 s were used for subsequent drug testing. After 30 min of the baseline measurement vehicle (0.5% methylcellulose and 2% DMSO) or PBF509 was administered orally via gavage (3, 10, or 30 mg/kg, p.o.) and the catalepsy was then determined at 15, 30, and 60 min PBF509 administration. For each time point the number of responding rats and the total cataleptic time for each animal was determined.

Pilocarpine-Induced TJM

Rats were placed in the observation chamber (30 cm diameter and 40 cm high clear glass chamber with a mesh floor and elevated 40 cm from the bench) to habituate during 5 min before being orally administered with vehicle (0.5% methylcellulose and 2% DMSO) or the indicated $A_{2A}R$ antagonist (i.e., SCH442416 and PBF509), followed (20 min) by pilocarpine (1 mg/kg; i.p.). Five minutes after pilocarpine injection TJMs were counted for 1 h (divided into six tests of 10 min each). TJMs were defined as rapid vertical deflections of the lower jaw that resembled chewing but were not directed at any particular stimulus (Salamone et al., 1998). Each individual deflection of the jaw was recorded using a mechanical hand counter by a trained observer, who was blind to the experimental condition of the rat being observed (Gandía et al., 2015).

Hemiparkinsonian Animal Model

Experimental hemiparkinsonism was induced in rats by unilateral injection of 6-OHDA in the medial forebrain bundle as previously described (Fernández-Dueñas et al., 2015). Accordingly, rats were stereotaxically injected with 6-OHDA (8 µg of 6-OHDA in 4 µl of saline solution containing 0.05% ascorbic acid) at: AP (anterior-posterior) = −2.2 mm, ML (medial-lateral) = −1.5 mm and DV (dorsal-ventral) = −7.8 mm with respect to bregma (Paxinos and Watson, 2007). To minimize damage to noradrenergic neurons, rats were pretreated with desipramine hydrochloride (10 mg/kg, i.p.) 20 min before surgery. Then, 3 weeks after the lesion the extent of dopamine deafferentation was validated by assessing the rotating behavioral response to L-DOPA administration. In brief, rats were injected with L-DOPA (50 mg/kg, i.p.) in the presence of benserazide hydrochloride (25 mg/kg, i.p.) and the number of full contralateral turns recorded during a 2 h period. Dopamine deafferentation was considered successful in those animals that made at least 200 net contralateral rotations. Thereafter, animals were housed during 3 weeks before used.

To test the effect of $A_{2A}R$ antagonists in the hemiparkinsonian animal model compounds were orally administered in vehicle (0.5% methylcellulose and 2% DMSO) 40 min before the administration of benserazide (25 mg/kg; i.p.). Subsequently, L-DOPA (4 mg/kg; i.p.) was delivered 20 min later and placed in the rotametry chambers, as previously described (Hodgson et al., 2009). The number of contralateral rotations was recorded during a 2-h period.

LIDs and Abnormal Involuntary Movements (AIMs) Rating

L-DOPA-induced dyskinesias were triggered to the hemiparkinsonian rats (see above) by twice a day administration

of L-DOPA (4 mg/kg, i.p.) plus benserazide hydrochloride (15 mg/kg, i.p.) during 22 consecutive days. Subsequently, the L-DOPA-induced AIMs were scored by a blinded experimenter following a rat dyskinesia scale previously described (Winkler et al., 2002). In brief, rats were injected with L-DOPA, placed individually in transparent plastic cages and observed every 20 min during 220 min. Thus, three subtypes of AIMs were monitored (i.e., axial, forelimb, and orolingual) and their respective severity scored from 0 to 4 as previously described (Winkler et al., 2002). Enhanced manifestations of otherwise normal behaviors, such as rearing, sniffing, grooming, and gnawing, were not included in the rating. Accurate AIM ratings were subsequently performed on treatment days 1, 7, 14, and 22 during the chronic L-DOPA administration phase. We computed integrated AIM scores for each animal and testing session using the sum of all three AIM subtypes and expressed as the area under the curve (AUC).

Gel Electrophoresis and Immunoblotting

Sodium dodecyl sulfate polyacrylamide gel electrophoresis (SDS/PAGE) was per-formed using 10% polyacrylamide gels. Proteins were transferred to PVDF membranes using a semidry transfer system and immunoblotted with the indicated antibody and then HRP-conjugated rabbit antigoat (1:30,000) or goat anti-rabbit IgG (1:30,000). The immunoreactive bands were developed using a chemiluminescent detection kit (Pierce) and the Amersham Imager 600 (GE Healthcare Europe GmbH, Barcelona, Spain).

Immunohistochemistry

Rat brains were fixed and coronal sections (50–70 μm) obtained as previously described (Taura et al., 2015). Slices were collected in Walter's Antifreezing solution (30% glycerol, 30% ethylene glycol in PBS, pH 7.2) and kept at −20°C until processing.

For immunohistochemistry, previously collected slices were washed three times in PBS, permeabilized with 0.3% Triton X-100 in PBS for 2 h and rinsed back three times more with wash solution (0.05% Triton X-100 in PBS). The slices were then incubated with blocking solution (10% NDS in wash solution; Jackson ImmunoResearch Laboratories, Inc., West Grove, PA, United States) for 2 h at R.T. and subsequently incubated with rabbit anti-TH polyclonal antibody (1 μg/ml) and mouse anti-A_{2A}R monoclonal antibody (1 μg/ml) overnight at 4°C. After two rinses (10 min each) with 1% NDS in wash solution, sections were incubated for 2 h at R.T. with either Cy2-conjugated donkey anti-rabbit (1:200) or Cy2-conjugated donkey anti-mouse (1:200) antibodies before being washed (10 min each) two times with 1% NDS in wash solution and two more times with PBS and mounted on slides. Fluorescence images of whole brain coronal sections were obtained using a SteREO Lumar.V12 fluorescence stereoscope (Carl Zeiss MicroImaging GmbH, Oberkochen, Germany).

Statistics

The number of samples (n) in each experimental condition is indicated in figure legends. When two experimental conditions were compared, statistical analysis was performed using an unpaired *t*-test. Otherwise, statistical analysis was performed by one-way analysis of variance (ANOVA) followed by Bonferroni *post hoc* test. Statistical significance was set as $P < 0.05$.

RESULTS

Functional Activity of PBF509 at Human Recombinant A_{2A}R

PBF509 is a structurally novel non-xanthine and non-furan A_{2A}R antagonist. The affinity of PBF509 for all four human adenosine receptors was recently reported by means of classical radioligand competition binding assays using membrane extracts from cells expressing A_1R, A_{2A}R, A_{2B}R, and A_3R (Mediavilla-Varela et al., 2017). Thus, PBF509 bound A_{2A}R with high affinity ($K_i = 12 \pm 0.2$ nM) and showed 416-, 208-, and 83-fold selectivity over the A_3R, A_1R, and A_{2B}R, respectively (Mediavilla-Varela et al., 2017).

In functional assays, PBF509 did not show any agonist efficacy in HEK cells permanently expressing the human $A_{2A}R^{SNAP}$ (data not shown). However, PBF509 completely antagonized the agonist-mediated cAMP accumulation in $A_{2A}R^{SNAP}$ expressing HEK cells (**Figure 1**), thus showing a K_B value of 72.8 ± 17.4 nM (**Figure 1**). Interestingly, while the PBF509 K_B value was significantly different [$F_{(1,60)} = 11.5$, $P < 0.005$] from the one found for a well characterized A_{2A}R antagonist (Todde et al., 2000), SCH442416 ($K_B = 28.8 \pm 7.2$ nM; **Figure 1**), it was within the same range as previously described (Mediavilla-Varela et al., 2017). Thus, these results suggested that PBF509 was equipotent in blocking A_{2A}R-mediated cAMP accumulation at the moderate nanomolar range.

Next, we aimed to characterize the functional activity of PBF509 using a label-free technology. To this end, the whole-cell agonist-mediated impedance responses were monitored in the presence or absence of PBF509 using a biosensor method. Once

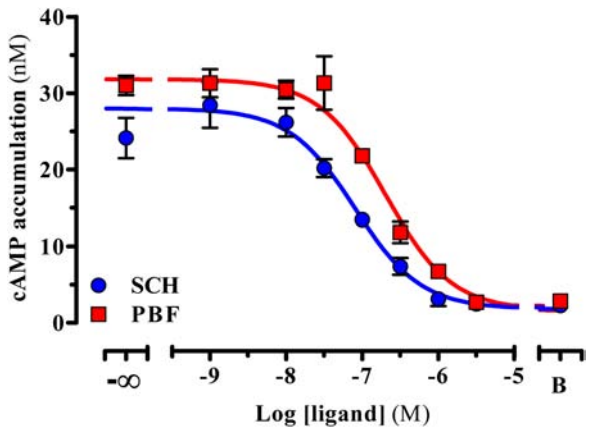

FIGURE 1 | Inhibition of A_{2A}R-mediated cAMP accumulation. Inhibition of the CGS21680-mediated cAMP accumulation. A SCH442416 and PBF509 concentration-response inhibition curve of CGS21260-mediated cAMP was assessed in HEK-293 cells permanently expressing the $A_{2A}R^{SNAP}$. Data are representative of three separate experiments performed in duplicate.

completed the optimization of the assay (see section "Materials and Methods"), we first tested the CGS21680-mediated changes in morphology (i.e., impedance) of $A_{2A}R^{SNAP}$ expressing HEK cells, which were recorded in real-time. Interestingly, addition of CGS21680 resulted in an immediate and concentration-dependent increase of impedance (**Figure 2A**). The EC_{50} found for this CGS21680-mediated impedance change was of 127 ± 74 and 61 ± 31 nM, for measurements performed at 30 and 60 min, respectively (**Figure 2B**). As the potency value did not significantly differ between the two time points measured [$F_{(1,21)}$ = 1.256, P = 0.274], we assessed the ability of PBF509 to block the CGS-induced impedance change at 30 min (**Figure 2C**). Of note, while SCH442416 showed a K_B value of 0.2 ± 0.07 nM, PBF509 displayed a K_B of 8.2 ± 4.2 nM (**Figure 2C**). Thus, the PBF509 inhibitory potency of $A_{2A}R$-mediated impedance increase was within the low nanomolar range, following the same tendency to that displayed by SCH442416. Overall, the two functional assays used confirmed a lower potency of PBF509 vs. SCH442416 in blocking the $A_{2A}R$-mediated signaling, which ranged from 2.5-fold in the cAMP assay and 40-fold in the label-free approach. Importantly, the potency values derived from the label-free assay provided a proof-of-principle that this biosensor technology can be applied to pharmacologically characterize $A_{2A}R$-based drugs.

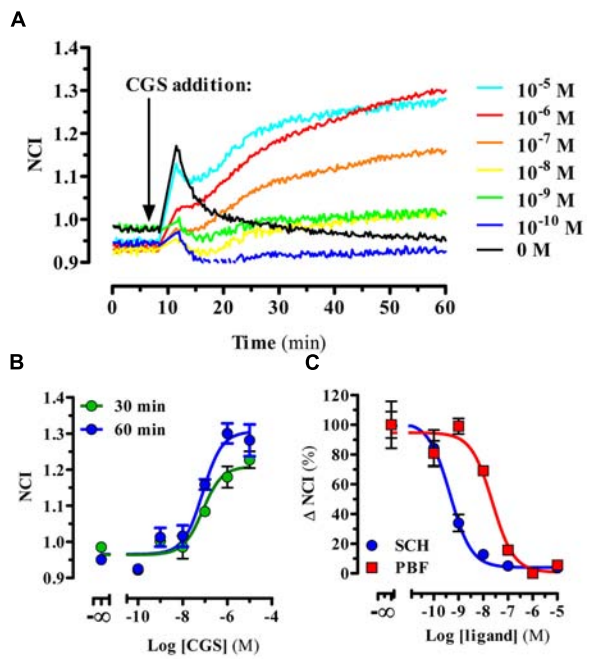

FIGURE 2 | PBF509 blocks $A_{2A}R$-mediated whole cell label-free responses. **(A)** Representative example of the $A_{2A}R^{SNAP}$ cells impedance signal in response to CGS216980 (10 μM–100 pM) over the time. Cell lines were stimulated with the $A_{2A}R$ selective agonist CGS21680 18 h after seeding (10,000 cells/well) and the impedance signal recorded over 60 min as described in materials and methods. **(B)** Concentration-response curves of CGS21680 derived from the normalized cell index (NCI) shown in **(A)** within 30 or 60 min after agonist addition. EC_{50} values of CGS21680 were 127 ± 74 and 61 ± 31 nM at 30 and 60 min, respectively. **(C)** Inhibition of the CGS21680-mediated impedance signal. Cell lines were pre-incubated for 60 min with increasing concentrations of SCH442416 and PBF509 (10 μM–100 pM) before stimulation with CGS21680 (500 nM). Concentration-response curves of SCH442416 and PBF509 were derived from ΔNCI within 30 min after agonist addition. Data are representative of three separate experiments performed in duplicate.

PBF509 Attenuates Haloperidol-Induced Catalepsy

Once determined the potency and intrinsic activity of PBF509 we aimed to determine the pro-dopaminergic nature of this compound *in vivo*. To this end, we evaluated the ability of PBF509 to block D_2R antagonist-mediated catalepsy. PBF509 dose-dependently attenuated the cataleptic effects of haloperidol when administered 1 h after haloperidol injection (**Figure 3**). Interestingly, the anticataleptic activity of PBF509 was observed after 15 min of administration at all the doses tested (3, 10, and 30 mg/kg) and lasted for at least 1 h post-administration of PBF509 (**Figure 3**). These results are in good agreement with the early description of anticataleptic activity of $A_{2A}R$ antagonists (Kanda et al., 1994).

PBF509 Attenuates Pilocarpine-Induced Tremulous Jaw Movements

The adenosinergic system has emerged as a potential target for the treatment of parkinsonian symptoms, including tremor (Schwarzschild et al., 2006). Indeed, $A_{2A}R$ antagonists have been shown to be efficacious to reduce drug-induced tremor (Simola et al., 2004). Accordingly, we aimed to test whether PBF509 was able to reduce pilocarpine-induced tremulous jaw movements (TJMs), an animal model of parkinsonian tremor previously

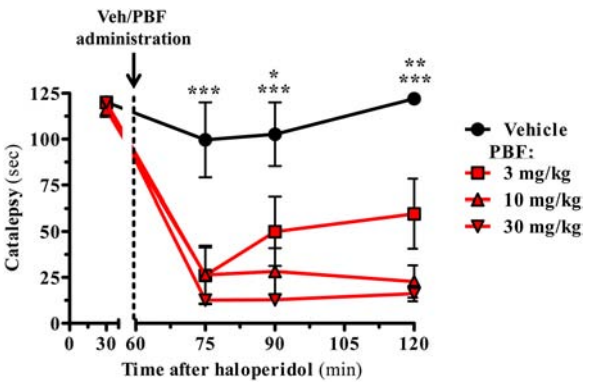

FIGURE 3 | PBF509 reverses haloperidol-induced catalepsy. Rats were pretreated with haloperidol (1.0 mg/kg, s.c.) and 1 h later the selected cataleptic animals were orally administered with either vehicle or PBF509 (3, 10, and 30 mg/kg, p.o.). The time spent in a cataleptic position was measured after 15, 30, and 60 min after PBF509 administration. The data represent the mean time spent cataleptic ± SEM over a period of 120 s measurement (n = 3–8 animals/group). The cataleptic behavior was calculated and compared within groups by a two-way ANOVA followed by Bonferroni's *post hoc* test. Group differences were calculated by a non-parametric Kruskal Wallis ANOVA followed by a Dunn's post-test as Gaussian distribution was missing. *P < 0.05, **P < 0.01, ***P < 0.001. The alpha-error level was set to 0.05.

used (Salamone et al., 2013; Gandía et al., 2015). Interestingly, PBF509 dose-dependently attenuated pilocarpine-induced TJMs, being effective at the lowest dose tested (0.3 mg/kg; **Figure 4**). It is important to mention here that PBF509 showed similar potency to SCH442416 in reducing TJMs (**Figure 4**). Thus, these results suggested that parkinsonian rest tremor, which is relatively resistant to dopamine-replacement therapy, might be potentially targeted by PBF509.

Effect of PBF509 on L-DOPA-Induced Turning Behavior

Next, we aimed to evaluate the antiparkinsonian effectiveness of PBF509 using the unilateral 6-OHDA lesioned rat, a classic and widespread toxin-based animal model of experimental parkinsonism (Schwarting and Huston, 1996). To this end, we first validated the extent of the 6-OHDA lesion in our hemiparkinsonian animal model by monitoring the striatal tyrosine hydroxylase (TH) density, a marker of dopaminergic innervation. As expected, a significant reduction (∼75%) of TH density in the lesioned striatum (L) was observed by immunoblot (**Figures 5A,B**) and immunohistochemistry (**Figure 5C**), thus corroborating the 6-OHDA-mediated loss of striatal dopaminergic innervation. Interestingly, when the $A_{2A}R$ immunoreactivity was assessed not significant differences ($P = 0.193$) between the healthy (R) and the lesioned (L) striatum were observed (**Figure 5**).

In the hemiparkinsonian animal model, an asymmetry in motor behavior is produced upon administration of dopaminergic agents (i.e., L-DOPA), a consequence of the unilateral dopamine depletion in the nigrostriatal pathway (Duty and Jenner, 2011). Accordingly, pro-dopaminergic compounds can promote contralateral rotations of lesioned animals upon submaximal L-DOPA dosing (4 mg/kg, for our hemiparkinsonian rats). The administration of $A_{2A}R$ antagonists, either SCH420814 (preladenant) or PBF509, up to 3 mg/kg, to 6-OHDA lesioned rats did not result in asymmetric turning behavior (**Figure 6**). However, both compounds dose-dependently induced a contralateral turning behavior when administrated before the

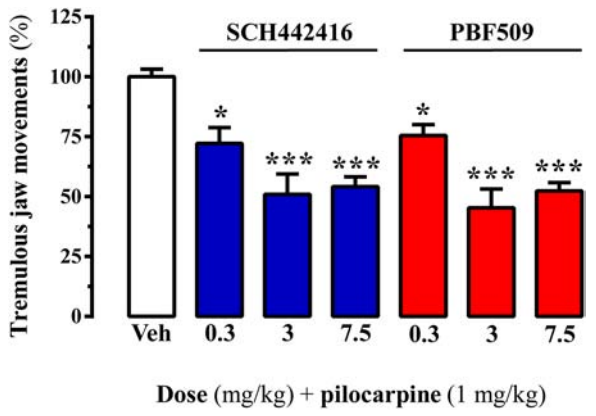

FIGURE 4 | PBF509 attenuates pilocarpine-induced tremulous jaw movements. Effect of different doses of SCH442416 and PBF509 on pilocarpine-induced tremulous jaw movements. The number of jaw movements were recorded during 1 h in rats orally administered with vehicle (Veh), SCH442416 or PBF509 (0.3–7.5 mg/kg) before (20 min) pilocarpine administration (1 mg/kg, i.p.). Values correspond to the mean ± SEM of 6–7 animals for each condition and expressed as percentage of the TJMs observed in the vehicle. TJMs were absent in animals no treated with pilocarpine. The asterisks denote data significantly different from the vehicle condition: $^{*}P < 0.05$ and $^{***}P < 0.001$, one-way ANOVA with a Bonferroni's *post hoc* test.

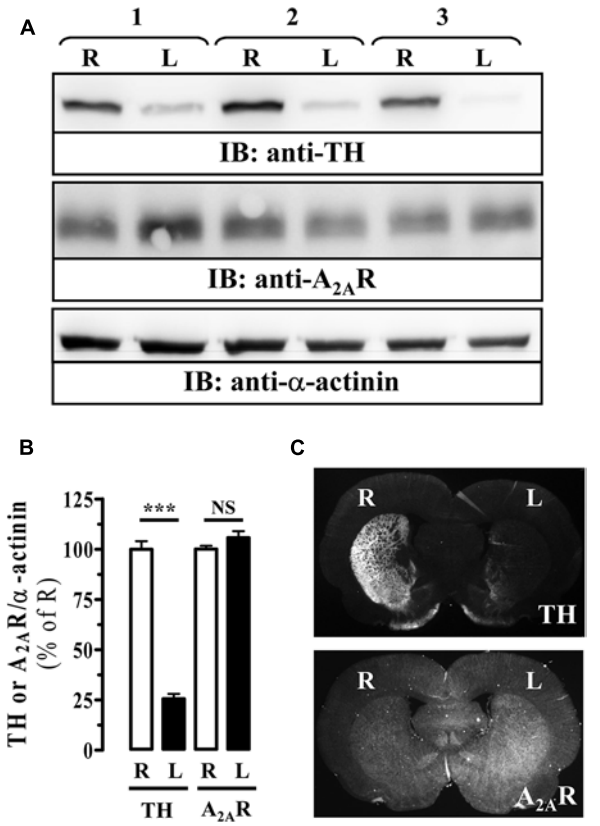

FIGURE 5 | Immunoreactivity of $A_{2A}R$ in the striatum of 6-OHDA-lesioned rats. **(A)** Immunoblot analysis of TH and $A_{2A}R$ density in striatal membranes from control (R) and 6-OHDA lesioned (L) striatal hemisphere. Striatal membranes were analyzed by SDS–PAGE and immunoblotted using a rabbit anti-TH polyclonal antibody (1 μg/ml), a mouse anti-$A_{2A}R$ monoclonal antibody (1 μg/ml) and a rabbit anti-α-actinin polyclonal antibody (1 μg/ml). A HRP-conjugated anti-rabbit or anti-mouse IgG (1/30,000) was used as a secondary antibody. The immunoreactive bands were visualized by chemiluminescence. Load control used for quantitating was α-actinin. A representative blot for three different lesioned animals is shown. **(B)** Quantification of TH and $A_{2A}R$ density in striatal membranes from control (R) and 6-OHDA lesioned (L) striatal hemisphere. The immunoreactive bands corresponding to TH and $A_{2A}R$ in each striatal hemisphere were normalized by α-actinin immunoreactivity. Data are expressed as percentage of the control (R) TH or $A_{2A}R$ density ± SEM of three independent experiments. Asterisks indicate data significantly different from the control condition: $^{***}P < 0.0001$ by Student's *t*-test. NS: not statistically significant. **(C)** Photomicrographs showing, by means of TH staining (upper panel), the loss of dopaminergic innervation in the lesioned striatum (L) compared to the non-lesioned (R) striatum, and the density of $A_{2A}R$ (lower panel) in 6-OHDA-lesioned rat brain coronal slices (see section "Materials and Methods").

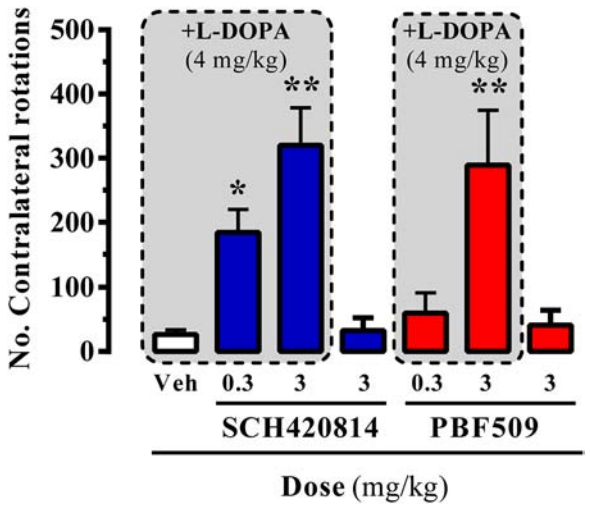

FIGURE 6 | PBF509-mediated potentiation of L-DOPA-induced contralateral rotations in 6-OHDA-lesioned rats. The number of contralateral rotations in 6-OHDA-lesioned rats orally administered with vehicle (Veh) or SCH420814 and PBF509 (0.3 and 3 mg/kg) in the absence or presence of L-DOPA (4 mg/kg) was monitored during a 2 h period. Values correspond to the mean ± SEM of 10–15 animals for each condition. The asterisks denote data significantly different from the vehicle condition: $^{*}P < 0.05$ and $^{***}P < 0.001$, one-way ANOVA with a Bonferroni's *post hoc* test.

subthreshold dose of L-DOPA (**Figure 6**). Overall, PBF509 was able to enhance the effects of L-DOPA with a minimum efficacious dose (MED) of 3 mg/kg p.o., and equal in efficacy to SCH420814 at this dose.

PBF509 Reduces L-DOPA-Induced Dyskinesia (LID)

Chronic L-DOPA use in PD is often associated with the development of LIDs. Accordingly, alleviating this adverse side effect related to PD therapy constitutes a therapeutic challenge. Interestingly, a relationship between $A_{2A}R$ and LIDs has been established, thus an increased striatal $A_{2A}R$ density has been reported in experimental animal models of LID (Zeng et al., 2000) and in PD patients with dyskinesia (Calon et al., 2004; Ramlackhansingh et al., 2011). Here, we aimed to assess the potential antidyskinetic activity of PBF509. To this end, we induced LIDs to our 6-OHDA lesioned rats by chronic L-DOPA administration and the emergence of abnormal involuntary movements (AIMs) over time was monitored. Indeed, a time L-DOPA-dependent AIMs manifestation was observed (**Figure 7A**). Thus, AIM severity increased during the first 40 min post-injection and remained significantly ($P < 0.01$) elevated for an additional 40 min in one-week L-DOPA administrated animals (**Figure 7A**, Day 7). A follow up of these animals over time showed that after 2 weeks of L-DOPA administration the AIMs remained robustly ($P < 0.001$) elevated during 80 min and after 3 weeks the animals showed a longer and sustained LIDs incidence (**Figure 7A**). Interestingly, the observed time-course in our LID animal model resembled the so called peak-dose dyskinesia in PD (Fahn, 2000). Subsequently, we next demonstrated that chronic L-DOPA treatment of hemiparkinsonian rats prompted a significant increase (15 ± 2%, $P < 0.05$) of striatal $A_{2A}R$ density in the lesioned hemisphere (**Figure 7B**), in agreement to that

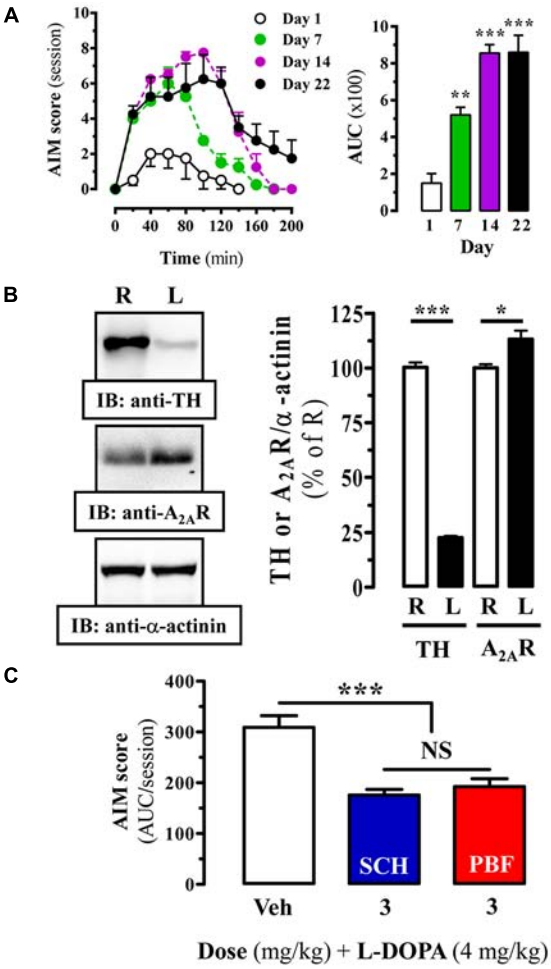

FIGURE 7 | Effect of PBF509 in LID rats. **(A)** L-DOPA induced-motor side effects (i.e., LIDs) development upon chronic (22 days) L-DOPA (4 mg/kg) administration. AIM score was measured during a 220-min on days 1, 7, 14, and 22 after the corresponding daily L-DOPA administration. The total AIMs score over 200 min was quantified and expressed as area under the curve (AUC) ± SEM ($n = 8$). $^{**}P < 0.01$ and $^{***}P < 0.001$ one-way ANOVA with Dunnett's *post hoc* test when compared to day 1. **(B)** Immunoreactivity of $A_{2A}R$ in the striatum of dyskinetic rats. TH and $A_{2A}R$ density in striatal membranes from control (R) and 6-OHDA lesioned (L) striatal hemisphere of LID animals was analyzed by immunoblot and quantified as described in **Figure 4**. Data are expressed as percentage of the control (R) TH or $A_{2A}R$ density ± SEM of three independent experiments. Asterisks indicate data significantly different from the control condition: $^{***}P < 0.001$, $^{*}P < 0.05$ by Student's *t*-test. **(C)** LID attenuation in chronic (22 days) L-DOPA (4 mg/kg) administered rats following administration of $A_{2A}R$ antagonists. The total AIM score (area under the curve, AUC) obtained over 220 min following co-administration of L-DOPA (4 mg/kg) plus vehicle (Veh), SCH420814 (3 mg/kg) and PBF509 (3 mg/kg) are presented as mean score ± SEM ($n = 6$). The asterisks denote data significantly different from the vehicle condition: $^{***}P < 0.001$, one-way ANOVA with a Bonferroni's *post hoc* test. NS: not statistically significant.

described previously. Then, under these experimental conditions, we assessed the antidyskinetic activity of PBF509. The drug was used at the antiparkinsonian MED (3 mg/kg, p.o.), and it showed an antidyskinetic efficacy similar to that observed for SCH420814 (**Figure 7C**). Overall, while PBF509 showed a robust antiparkinsonian activity it also displayed antidyskinetic efficacy.

DISCUSSION

Dopamine augmentation constitutes the first line therapy in PD. Hence, L-DOPA or direct dopamine agonists (i.e., ropinirole, pramipexole, apomorphine) are regular drugs for PD clinical management (Poewe and Mahlknecht, 2009). Interestingly, while dopamine-targeted therapies allow proper management of PD, associated motor disturbances have considerable side effects both after acute and chronic regimes (i.e., hallucinations, constipation, nausea, somnolence, on-off effects, dyskinesia) (Eggert et al., 2008). In addition, these therapies usually display an efficacy decline along the disease development and do not address other disease disturbances frequently associated to PD (i.e., mood, postural instability, or cognitive disturbances). Accordingly, alternative approaches modulating dopaminergic neurotransmission in PD have emerged as potential alternatives to manage PD therapy-associated side effects (Fox et al., 2008). Indeed, $A_{2A}R$ blockade has been demonstrated to be effective in both preclinical and clinical PD studies (Vallano et al., 2011; Pinna, 2014). Interestingly, it has been proposed that the mechanism behind the pro-dopaminergic activity of $A_{2A}R$ antagonists may rely in part to the existing functional and molecular interaction (i.e., heteromerization) of $A_{2A}R$ and D_2R within the striatum (Ferre et al., 2004; Fernández-Dueñas et al., 2015). Thus, a mutual trans-inhibition between these two receptors has been largely described (Ferre et al., 2008). In addition to this postsynaptic site of action, striatal $A_{2A}R$ show also presynaptic expression on glutamatergic terminals of the cortico-limbic-striatal and thalamo-striatal pathways forming heteromeric complexes with adenosine A1 receptors (Ciruela et al., 2006) and driving striatal circuits controlling motor function independently of dopaminergic signaling (Schiffmann et al., 2007).

The initial work identifying novel $A_{2A}R$ antagonists focused on purine and xanthine derivatives, principally built from adenosine and the naturally occurring antagonist caffeine. In parallel, further effort was set on non-xanthine furan-based derivatives, such as triazolotriazines and triazolopyrimidines (e.g., ZM241385, BIIB014 and SCH420814). However, regardless of the good affinity and selectivity shown, these $A_{2A}R$ antagonists have, in general, high molecular weight, thus they are complex and difficult to synthesize. In addition, they display poor water solubility, and their furan group precludes replacement by empirical medicinal chemistry. Here, we characterize the functional activity of PBF509, a new non-xanthine and non-furan competitive antagonist with high affinity and selectivity for the $A_{2A}R$ (Mediavilla-Varela et al., 2017), through a highly sensitive TR-FRET-based cAMP accumulation assay in $A_{2A}R$ expressing cells. Interestingly, to further characterize the its activity we implemented a label-free xCELLigence assay based on the real-time impedance recording of $A_{2A}R$ expressing cells. Thus, upon similar physiological conditions of the xCELLigence assay (i.e., regular cell culture growing), PBF509 displayed comparable potency in blocking the $A_{2A}R$-mediated signaling when compared to the cAMP assay. Noteworthy, apart from revealing PBF509 antiparkinsonian efficacy, our work led to the description of a whole-cell label-free approach for investigating $A_{2A}R$-mediated drug responses in $A_{2A}R^{SNAP}$ expressing HEK cells, which may allow cellular assays with minimal modifications and increased sensitivity over traditional label-based methodologies.

PBF509 was effective in reducing catalepsy induced by haloperidol, a D_2R antagonist. Interestingly, anticataleptic properties have been classically used to predict clinical efficacy for antiparkinsonian drugs (i.e., pramipexole) (Maj et al., 1997). Thus, our results suggested that PBF509-induced $A_{2A}R$ blockade provided a counterbalance to the loss of D_2R-mediated effects in the basal ganglia indirect pathway, as previously described for other $A_{2A}R$ antagonists (Shiozaki et al., 1999). Moreover, PBF509-mediated $A_{2A}R$ blockade reduced pilocarpine-induced tremulous jaw movements and potentiated L-DOPA-induced contralateral rotations in unilaterally 6-OHDA-lesioned rats, which is consistent with previous findings using other $A_{2A}R$ antagonists (Hodgson et al., 2009). In addition, PBF509 showed antidyskinetic efficacy in the LID animal model, which correlated well with the increased striatal $A_{2A}R$ expression. Overall, our results support the potential usefulness of PBF509 in PD management, including its ability to reduce dyskinesia when used in combination with L-DOPA in PD treatment.

A number of $A_{2A}R$ antagonists have been proposed as antiparkinsonian agents and tested in preclinical PD animal models. For instance, ST-1535 (Rose et al., 2006; Tronci et al., 2007) and related metabolites (i.e., ST3932 and ST4206) (Stasi et al., 2015), and JNJ40255293 (Atack et al., 2014), which are based on the purine adenosine. Also, the xanthine-based compounds, as KW6002 (istradefylline) (LeWitt et al., 2008) and the non-xanthine SCH58261 (Simola et al., 2004), SCH420814 (preladenant) (Hodgson et al., 2009), and BIIB014 (vipadenant) (Gillespie et al., 2009), amongst others. However, among the $A_{2A}R$ antagonists undergoing clinical trials (Vallano et al., 2011; Pinna, 2014), only the xanthine istradefylline has been approved for manufacturing and marketing (in Japan, 2013), thus becoming the world's first antiparkinsonian agent of a first-in-class $A_{2A}R$ antagonist. In clinical trials, Nouriast® (istradefylline) improved wearing-off phenomena and was well tolerated by PD patients treated with L-DOPA. On the other hand, the non-xanthine preladenant did not prove itself to be more effective than placebo during Phase-III trials, and was discontinued in 2013, as it was vipadenant. Similarly, despite the robust preclinical pharmacology and good pharmacokinetic properties of JNJ40255293, its development was halted due to preclinical toxicity. Here, we have described a selective non-xanthine and non-furan $A_{2A}R$ antagonist with efficacy in rat models of movement disorders and without preclinical toxicity. Interestingly, in a double-blind, placebo-controlled, Phase-I clinical trial (NCT01691924) of single ascending oral doses in

32 healthy male volunteers, PBF509 showed safety, tolerability and feasibility. Thus, the compound is currently in prospective Phase-II clinical trials for PD.

In summary, PBF509 demonstrated remarkable potential in experimental animal models of movement disorders, including PD and LID, thus becoming an excellent candidate for clinical A_{2A}R-based treatment of PD motor symptoms. In addition, the ability of PBF509 to alleviate non-motor symptoms associated with PD (i.e., memory and mood impairments and sleep disturbances) will deserve future clinical attention.

AUTHOR CONTRIBUTIONS

FN performed the *in vivo* experiments. JT performed the *in vitro* experiments. JaC synthesized the PBF509. ML-C performed the *in vivo* experiments and analyzed the data. VF-D designed the experiments and wrote the paper. NC conceived and supervised the project. JlC conceived and supervised the project and designed the experiments. FC conceived and supervised the project, designed the experiments, analyzed the data, and wrote the paper.

FUNDING

This work was supported by MINECO-AEI/FEDER, UE (SAF2017-87349-R), the Catalan government (2017 SGR 1604), Fundació la Marató de TV3 (Grant 20152031), FWO (SBO-140028) to FC.

ACKNOWLEDGMENTS

We thank Esther Castaño and Benjamín Torrejón, from the CCiT-Bellvitge Campus of the University of Barcelona for the technical assistance.

REFERENCES

Atack, J. R., Shook, B. C., Rassnick, S., Jackson, P. F., Rhodes, K., Drinkenburg, W. H., et al. (2014). JNJ-40255293, a novel adenosine A2A/A1 antagonist with efficacy in preclinical models of Parkinson's disease. *ACS Chem. Neurosci.* 5, 1005–1019. doi: 10.1021/cn5001606

Calon, F., Dridi, M., Hornykiewicz, O., Bédard, P. J., Rajput, A. H., and Di Paolo, T. (2004). Increased adenosine A2A receptors in the brain of Parkinson's disease patients with dyskinesias. *Brain* 127, 1075–1084. doi: 10.1093/brain/awh128

Ciruela, F., Casadó, V., Rodrigues, R. J., Luján, R., Burgueño, J., Canals, M., et al. (2006). Presynaptic control of striatal glutamatergic neurotransmission by adenosine A1-A2A receptor heteromers. *J. Neurosci.* 26, 2080–2087. doi: 10.1523/JNEUROSCI.3574-05.2006

Clark, J. D., Gebhart, G. F., Gonder, J. C., Keeling, M. E., and Kohn, D. F. (1997). Special report: the 1996 guide for the care and use of laboratory animals. *ILAR J.* 38, 41–48. doi: 10.1093/ilar.38.1.41

Duty, S., and Jenner, P. (2011). Animal models of Parkinson's disease: a source of novel treatments and clues to the cause of the disease. *Br. J. Pharmacol.* 164, 1357–1391. doi: 10.1111/j.1476-5381.2011.01426.x

Eggert, K. M., Reese, J. P., Oertel, W. H., and Dodel, R. (2008). Cost effectiveness of pharmacotherapies in early Parkinson's disease. *CNS Drugs* 22, 841–860. doi: 10.2165/00023210-200822100-00005

Fahn, S. (2000). The spectrum of levodopa-induced dyskinesias. *Ann. Neurol.* 47, S2–S9.

Fernández-Dueñas, V., Taura, J. J., Cottet, M., Gómez-Soler, M., López-Cano, M., Ledent, C., et al. (2015). Untangling dopamine-adenosine receptor-receptor assembly in experimental parkinsonism in rats. *Dis. Models Mech.* 8, 57–63. doi: 10.1242/dmm.018143

Ferre, S., Ciruela, F., Canals, M., Marcellino, D., Burgueno, J., Casado, V., et al. (2004). Adenosine A2A-dopamine D2 receptor-receptor heteromers. Targets for neuro-psychiatric disorders. *Parkinsonism Relat. Disord.* 10, 265–271. doi: 10.1016/j.parkreldis.2004.02.014

Ferre, S., Quiroz, C., Woods, A. S., Cunha, R., Popoli, P., Ciruela, F., et al. (2008). An update on adenosine A2A-dopamine D2 receptor interactions. Implications for the function of G protein-coupled receptors. *Curr. Pharm. Design* 14, 1468–1474. doi: 10.2174/138161208784480108

Fox, S. H., Brotchie, J. M., and Lang, A. E. (2008). Non-dopaminergic treatments in development for Parkinson's disease. *Lancet Neurol.* 7, 927–938. doi: 10.1016/S1474-4422(08)70214-X

Gandía, J., Morató, X., Stagljar, I., Fernández-Dueñas, V., and Ciruela, F. (2015). Adenosine A2A receptor-mediated control of pilocarpine-induced tremulous jaw movements is Parkinson's disease-associated GPR37 receptor-dependent. *Behav. Brain Res.* 288, 103–106. doi: 10.1016/j.bbr.2015.04.001

Gerfen, C. R., Engber, T. M., Mahan, L. C., Susel, Z., Chase, T. N., Monsma, F. J. Jr., et al. (1990). D1 and D2 dopamine receptor-regulated gene expression of striatonigral and striatopallidal neurons. *Science* 250, 1429–1432. doi: 10.1126/science.2147780

Gillespie, R. J., Bamford, S. J., Botting, R., Comer, M., Denny, S., Gaur, S., et al. (2009). Antagonists of the human A(2A) adenosine receptor. 4. Design, synthesis, and preclinical evaluation of 7-aryltriazolo[4,5-d]pyrimidines. *J. Med. Chem.* 52, 33–47. doi: 10.1021/jm800961g

Hauser, R. A., and Schwarzschild, M. A. (2005). Adenosine A2A receptor antagonists for Parkinson's disease: rationale, therapeutic potential and clinical experience. *Drugs Aging* 22, 471–482. doi: 10.2165/00002512-200522060-00002

Hillger, J. M., Schoop, J., Boomsma, D. I., Slagboom, P. E., IJzerman, A. P., and Heitman, L. H. (2015). Whole-cell biosensor for label-free detection of GPCR-mediated drug responses in personal cell lines. *Biosens. Bioelectron.* 74, 233–242. doi: 10.1016/j.bios.2015.06.031

Hodgson, R. A., Bertorelli, R., Varty, G. B., Lachowicz, J. E., Forlani, A., Fredduzzi, S., et al. (2009). Characterization of the potent and highly selective A2A receptor antagonists preladenant and SCH 412348 [7-[2-[4-2,4-difluorophenyl]-1-piperazinyl]ethyl]-2-(2-furanyl)-7H-pyrazolo[4,3-e][1,2,4]triazolo[1,5-c]pyrimidin-5-amine] in rodent models of movemen. *J. Pharmacol. Exp. Ther.* 330, 294–303. doi: 10.1124/jpet.108.149617

Huot, P., Johnston, T. H., Koprich, J. B., Fox, S. H., and Brotchie, J. M. (2013). The pharmacology of L-DOPA-induced dyskinesia in Parkinson's disease. *Pharmacol. Rev.* 65, 171–222. doi: 10.1124/pr.111.005678

Jenner, P. (2005). Istradefylline, a novel adenosine A2A receptor antagonist, for the treatment of Parkinson's disease. *Expert Opin. Investig. Drugs* 14, 729–738. doi: 10.1517/13543784.14.6.729

Jenner, P., Mori, A., Hauser, R., Morelli, M., Fredholm, B. B., and Chen, J. F. (2009). Adenosine, adenosine A 2A antagonists, and Parkinson's disease. *Parkinsonism Relat. Disord.* 15, 406–413. doi: 10.1016/j.parkreldis.2008.12.006

Kanda, T., Shiozaki, S., Shimada, J., Suzuki, F., and Nakamura, J. (1994). KF17837: a novel selective adenosine A2A receptor antagonist with anticataleptic activity. *Eur. J. Pharmacol.* 256, 263–268. doi: 10.1016/0014-2999(94)90551-7

Kondo, T., and Mizuno, Y. (2015). A long-term study of istradefylline safety and efficacy in patients with Parkinson disease. *Clin. Neuropharmacol.* 38, 41–46. doi: 10.1097/WNF.0000000000000073

Leff, P., and Dougall, I. G. (1993). Further concerns over Cheng-Prusoff analysis. *Trends Pharmacol. Sci.* 14, 110–112. doi: 10.1016/0165-6147(93)90080-4

LeWitt, P. A., Guttman, M., Tetrud, J. W., Tuite, P. J., Mori, A., Chaikin, P., et al. (2008). Adenosine A2A receptor antagonist istradefylline (KW-6002) reduces "off" time in Parkinson's disease: a double-blind, randomized, multicenter clinical trial (6002-US-005). *Ann. Neurol.* 63, 295–302. doi: 10.1002/ana.21315

Maj, J., Rogóz, Z., Skuza, G., and Kołodziejczyk, K. (1997). The behavioural effects of pramipexole, a novel dopamine receptor agonist. *Eur. J. Pharmacol.* 324, 31–37. doi: 10.1016/S0014-2999(97)00066-6

Mediavilla-Varela, M., Castro, J., Chiappori, A., Noyes, D., Hernandez, D. C., Allard, B., et al. (2017). a novel antagonist of the immune checkpoint protein adenosine A2a receptor restores tumor-infiltrating lymphocyte activity in the context of the tumor microenvironment. *Neoplasia* 19, 530–536. doi: 10.1016/j.neo.2017.02.004

Meissner, W. G., Frasier, M., Gasser, T., Goetz, C. G., Lozano, A., Piccini, P., et al. (2011). Priorities in Parkinson's disease research. *Nat. Rev. Drug Discov.* 10, 377–393. doi: 10.1038/nrd3430

Mizuno, Y., Hasegawa, K., Kondo, T., Kuno, S., Yamamoto, M., and Group, J. I. S. (2010). Clinical efficacy of istradefylline (KW-6002) in Parkinson's disease: a randomized, controlled study. *Mov. Disord.* 25, 1437–1443. doi: 10.1002/mds.23107

Müller, T. (2015). The safety of istradefylline for the treatment of Parkinson's disease. *Expert Opin. Drug Saf.* 14, 769–775. doi: 10.1517/14740338.2015.1014798

Paxinos, G., and Watson, C. (2007). *The Rat Brain in Stereotaxic Coordinates*, 6th Edn. Vol. 170, Cambridge, MA: Elsevier Academic Press, 547–612.

Pinna, A. (2014). Adenosine A2A receptor antagonists in Parkinson's disease: progress in clinical trials from the newly approved istradefylline to drugs in early development and those already discontinued. *CNS Drugs* 28, 455–474. doi: 10.1007/s40263-014-0161-7

Poewe, W. (2009). Treatments for Parkinson disease–past achievements and current clinical needs. *Neurology* 72, S65–S73. doi: 10.1212/WNL.0b013e31819908ce

Poewe, W., and Mahlknecht, P. (2009). The clinical progression of Parkinson's disease. *Parkinsonism Relat. Disord.* 15(Suppl. 4), S28–S32. doi: 10.1016/S1353-8020(09)70831-4

Ramlackhansingh, A. F., Bose, S. K., Ahmed, I., Turkheimer, F. E., Pavese, N., and Brooks, D. J. (2011). Adenosine 2A receptor availability in dyskinetic and nondyskinetic patients with Parkinson disease. *Neurology* 76, 1811–1816. doi: 10.1212/WNL.0b013e31821ccce4

Rose, S., Jackson, M. J., Smith, L. A., Stockwell, K., Johnson, L., Carminati, P., et al. (2006). The novel adenosine A2a receptor antagonist ST1535 potentiates the effects of a threshold dose of L-DOPA in MPTP treated common marmosets. *Eur. J. Pharmacol.* 546, 82–87. doi: 10.1016/j.ejphar.2006.07.017

Salamone, J. D., Collins-Praino, L. E., Pardo, M., Podurgiel, S. J., Baqi, Y., Müller, C. E., et al. (2013). Conditional neural knockout of the adenosine A(2A) receptor and pharmacological A(2A) antagonism reduce pilocarpine-induced tremulous jaw movements: studies with a mouse model of Parkinsonian tremor. *Eur. Neuropsychopharmacol.* 23, 972–977. doi: 10.1016/j.euroneuro.2012.08.004

Salamone, J. D., Mayorga, A. J., Trevitt, J. T., Cousins, M. S., Conlan, A., and Nawab, A. (1998). Tremulous jaw movements in rats: a model of parkinsonian tremor. *Prog. Neurobiol.* 56, 591–611. doi: 10.1016/S0301-0082(98)00053-7

Schapira, A. H., Bezard, E., Brotchie, J., Calon, F., Collingridge, G. L., Ferger, B., et al. (2006). Novel pharmacological targets for the treatment of Parkinson's disease. *Nat. Rev. Drug Discov.* 5, 845–854. doi: 10.1038/nrd2087

Schiffmann, S. N., Fisone, G., Moresco, R., Cunha, R. A., and Ferre, S. (2007). Adenosine A2A receptors and basal ganglia physiology. *Prog. Neurobiol.* 83, 277–292. doi: 10.1016/j.pneurobio.2007.05.001

Schwarting, R. K., and Huston, J. P. (1996). The unilateral 6-hydroxydopamine lesion model in behavioral brain research. Analysis of functional deficits, recovery and treatments. *Prog. Neurobiol.* 50, 275–331. doi: 10.1016/S0301-0082(96)00040-8

Schwarzschild, M. A., Agnati, L., Fuxe, K., Chen, J.-F. F., and Morelli, M. (2006). Targeting adenosine A2A receptors in Parkinson's disease. *Trends Neurosci.* 29, 647–654. doi: 10.1016/j.tins.2006.09.004

Shiozaki, S., Ichikawa, S., Nakamura, J., Kitamura, S., Yamada, K., and Kuwana, Y. (1999). Actions of adenosine A2A receptor antagonist KW-6002 on drug-induced catalepsy and hypokinesia caused by reserpine or MPTP. *Psychopharmacology* 147, 90–95. doi: 10.1007/s002130051146

Simola, N., Fenu, S., Baraldi, P. G., Tabrizi, M. A., and Morelli, M. (2004). Blockade of adenosine A2A receptors antagonizes parkinsonian tremor in the rat tacrine model by an action on specific striatal regions. *Exp. Neurol.* 189, 182–188. doi: 10.1016/j.expneurol.2004.05.027

Solly, K., Wang, X., Xu, X., Strulovici, B., and Zheng, W. (2004). Application of real-time cell electronic sensing (RT-CES) technology to cell-based assays. *Assay Drug Dev. Technol.* 2, 363–372. doi: 10.1089/adt.2004.2.363

Stallaert, W., Dorn, J. F., van der Westhuizen, E., Audet, M., and Bouvier, M. (2012). Impedance responses reveal β_2-adrenergic receptor signaling pluridimensionality and allow classification of ligands with distinct signaling profiles. *PLoS One* 7:e29420. doi: 10.1371/journal.pone.0029420

Stasi, M. A., Minetti, P., Lombardo, K., Riccioni, T., Caprioli, A., Vertechy, M., et al. (2015). Animal models of Parkinson's disease: effects of two adenosine A2A receptor antagonists ST4206 and ST3932, metabolites of 2-n-Butyl-9-methyl-8-[1,2,3]triazol-2-yl-9H-purin-6-ylamine (ST1535). *Eur. J. Pharmacol.* 761, 353–361. doi: 10.1016/j.ejphar.2015.03.070

Taura, J., Fernández-Dueñas, V., and Ciruela, F. (2015). Visualizing G protein-coupled receptor-receptor interactions in brain using proximity ligation in situ assay. *Curr. Protoc. Cell Biol.* 67, 17.17.1–17.17.16. doi: 10.1002/0471143030.cb1717s67

Taura, J., Fernández-Dueñas, V., and Ciruela, F. (2016). Determination of GPCR-mediated cAMP accumulation in rat striatal synaptosomes. *Neuromethods* 110, 455–464. doi: 10.1007/978-1-4939-3064-7_28

Todde, S., Moresco, R. M., Simonelli, P., Baraldi, P. G., Cacciari, B., Spalluto, G., et al. (2000). Design, radiosynthesis, and biodistribution of a new potent and selective ligand for in vivo imaging of the adenosine A(2A) receptor system using positron emission tomography. *J. Med. Chem.* 43, 4359–4362. doi: 10.1021/jm0009843

Tronci, E., Simola, N., Borsini, F., Schintu, N., Frau, L., Carminati, P., et al. (2007). Characterization of the antiparkinsonian effects of the new adenosine A2A receptor antagonist ST1535: acute and subchronic studies in rats. *Eur. J. Pharmacol.* 566, 94–102. doi: 10.1016/j.ejphar.2007.03.021

Vallano, A., Fernandez-Duenas, V., Pedros, C., Arnau, J. M., and Ciruela, F. (2011). An update on adenosine A2A receptors as drug target in Parkinson's disease. *CNS Neurol. Disord. Drug Targets* 10, 659–669. doi: 10.2174/187152711797247803

Winkler, C., Kirik, D., Björklund, A., and Cenci, M. A. (2002). L-DOPA-induced dyskinesia in the intrastriatal 6-hydroxydopamine model of Parkinson's disease: relation to motor and cellular parameters of nigrostriatal function. *Neurobiol. Dis.* 10, 165–186. doi: 10.1006/nbdi.2002.0499

Xu, Y., Xie, X., Duan, Y., Wang, L., Cheng, Z., and Cheng, J. (2016). A review of impedance measurements of whole cells. *Biosens. Bioelectron.* 77, 824–836. doi: 10.1016/j.bios.2015.10.027

Zeng, B. Y., Pearce, R. K., MacKenzie, G. M., and Jenner, P. (2000). Alterations in preproenkephalin and adenosine-2a receptor mRNA, but not preprotachykinin mRNA correlate with occurrence of dyskinesia in normal monkeys chronically treated with L-DOPA. *Eur. J. Neurosci.* 12, 1096–1104. doi: 10.1046/j.1460-9568.2000.00988.x

Conflict of Interest Statement: The authors declare that the research was conducted in the absence of any commercial or financial relationships that could be construed as a potential conflict of interest.

The reviewer RC declared a past co-authorship with the authors to the handling Editor.

frontiers in Pharmacology

REVIEW
published: 14 June 2018
doi: 10.3389/fphar.2018.00627

Who Is Who in Adenosine Transport

Marçal Pastor-Anglada[1,2] and Sandra Pérez-Torras[1,2]**

[1] Molecular Pharmacology and Experimental Therapeutics, Department of Biochemistry and Molecular Biomedicine, Institute of Biomedicine, University of Barcelona, Barcelona, Spain, [2] Oncology Program, National Biomedical Research Institute on Liver and Gastrointestinal Diseases – CIBER ehd, Institut de Recerca Sant Joan de Déu, Barcelona, Spain

Extracellular adenosine concentrations are regulated by a panel of membrane transporters which, in most cases, mediate its uptake into cells. Adenosine transporters belong to two gene families encoding Equilibrative and Concentrative Nucleoside Transporter proteins (ENTs and CNTs, respectively). The lack of appropriate pharmacological tools targeting every transporter subtype has introduced some bias on the current knowledge of the role of these transporters in modulating adenosine levels. In this regard, ENT1, for which pharmacology is relatively well-developed, has often been identified as a major player in purinergic signaling. Nevertheless, other transporters such as CNT2 and CNT3 can also contribute to purinergic modulation based on their high affinity for adenosine and concentrative capacity. Moreover, both transporter proteins have also been shown to be under purinergic regulation via P1 receptors in different cell types, which further supports its relevance in purinergic signaling. Thus, several transporter proteins regulate extracellular adenosine levels. Moreover, CNT and ENT proteins are differentially expressed in tissues but also in particular cell types. Accordingly, transporter-mediated fine tuning of adenosine levels is cell and tissue specific. Future developments focusing on CNT pharmacology are needed to unveil transporter subtype-specific events.

Keywords: adenosine, transporters, CNT, ENT, purinergic signaling

OPEN ACCESS

Edited by:
Kenneth A. Jacobson, National Institutes of Health (NIH), United States

Reviewed by:
Elsa Fabbretti, University of Trieste, Italy
Rennolds S. Ostrom, Chapman University, United States

****Correspondence:***
Marçal Pastor-Anglada
mpastor@ub.edu
Sandra Pérez-Torras
s.perez-torras@ub.edu

Specialty section:
This article was submitted to Experimental Pharmacology and Drug Discovery, a section of the journal Frontiers in Pharmacology

Received: *13 March 2018*
Accepted: *24 May 2018*
Published: *14 June 2018*

Citation:
Pastor-Anglada M and Pérez-Torras S (2018) Who Is Who in Adenosine Transport. Front. Pharmacol. 9:627. doi: 10.3389/fphar.2018.00627

INTRODUCTION

Oscillation of extracellular adenosine levels is physiologically relevant because this nucleoside is the agonist of four P1 receptors known to modulate many biological functions (Fredholm et al., 2011; Burnstock, 2017). Indeed, adenosine concentrations in the extracellular milieu are determined by the balance between its appearance and its removal. In most cases adenosine appearance is the result of the sequential metabolic action of various ecto-nucleotidases on nucleotide precursors, ATP being the first nucleotide in this cascade (Dos Santos-Rodrigues et al., 2014; Nguyen et al., 2015; Pastor-Anglada et al., 2018). However, in particular cell types, there is experimental evidence supporting the possibility of adenosine also being released from cells (Almeida et al., 2003). Extracellular adenosine disposal is similarly mediated by either metabolism, Adenosine Deaminase (ADA) being the enzyme responsible for its conversion into inosine, or by its uptake into cells, where it is likely to be metabolized and trapped as AMP after being phosphorylated by Adenosine Kinase (ADK). The relative contribution of each particular

mechanism to the oscillations of adenosine levels may be cell-specific and dependent upon the tissue microenvironment, but is not well-known, although some attempts to address this issue have been done (Nguyen et al., 2015). In any case, adenosine removal from the extracellular milieu is likely to play a major role in regulating adenosine concentrations.

Adenosine cannot freely permeate biological membranes and its transport across them occurs via selected adenosine transporter proteins. Accordingly, transport processes are key modulators of extracellular adenosine disposal. In this contribution, we plan to provide an updated and critical view on the particular transporter subtypes likely to mediate adenosine transport. Evidence supporting the link between transport processes and purinergic signaling will be also discussed.

ADENOSINE TRANSPORT MECHANISMS

All adenosine transporters identified so far belong to the SoLute Carrier (*SLC*) superfamily, in particular, to gene families *SLC28* and *SLC29* (Young et al., 2013; Young, 2016; Pastor-Anglada et al., 2018). *SLC28* genes encode three transporter subtypes known as human Concentrative Nucleoside Transporters 1, 2, and 3 (hCNT1, hCNT2, and hCNT3). The *SLC29* family has four members, thereby resulting in four transporter subtypes, known as human Equilibrative Nucleoside Transporters 1, 2, 3, and 4 (hENT1, hENT2, hENT3, and hENT4). Evidence for additional transporter subtypes, generated by mRNA splicing has been provided for hCNT3 and hENT2, in both cases leading to shorter proteins than their corresponding wild type transporters. Nevertheless, in all cases these small variants appear to be localized in intracellular compartments (Errasti-Murugarren et al., 2009; Grañé-Boladeras et al., 2016) and are unlikely to play any significant role in purinergic signaling. Nevertheless, it has been shown that hENT2 splice variants can regulate wild type hENT2 abundance and function at the plasma membrane (Grañé-Boladeras et al., 2016).

The type of translocation processes implicated in adenosine transport (i.e., "concentrative" versus "equilibrative") and the affinity binding of adenosine to its transporter proteins are key determinants of adenosine transport efficacy.

hCNTs are obligatory inward transporters which take advantage of the sodium gradient to accumulate nucleosides in the cells. Nucleosides and sodium are co-transported with translocation stoichiometry 1:1 (hCNT1 and hCNT2) and 1:2 (hCNT3). Indeed, those CNT proteins showing the ability to transport adenosine are excellent candidates to promote adenosine disposal from the extracellular milieu due to their concentrative capacity. hENTs are potentially bidirectional, vectorial transport being determined by the nucleoside concentration gradient across the membrane. Nevertheless, it is probable that in some circumstances, functional coupling of adenosine influx with its intracellular phosphorylation by ADK enables cells to trap this nucleoside as AMP thereby building up a transmembrane adenosine gradient which will favor unidirectional import of adenosine. It is not known whether adenosine release via these transporters can be explained by some sort of inefficient, not necessarily uncontrolled coupling between metabolism and transport.

As introduced above, affinity is also a critical parameter when discussing the adenosine transport capacity of each nucleoside transporter subtype. Reported physiological adenosine concentrations are very low, often below 1 μM (Fenton and Dobson, 1992; Espinoza et al., 2011; Rose et al., 2011; Westermeier et al., 2011), although under certain conditions, such as hypoxia or in tumor microenvironments where ATP levels can increase considerably, adenosine can also accumulate above normal physiological concentrations (Blay et al., 1997) reviewed in de Andrade Mello et al. (2017) and Di Virgilio and Adinolfi (2017). As shown in **Table 1**, apparent Km values for adenosine vary among transporter subtypes, although some intrinsic variability is observed for the same transporter subtype, probably as a result of the experimental set used to calculate this parameter.

Adenosine transport can be determined either by influx measurements of its radiolabeled form or, at least for CNT-type transporters, by electrophysiological means. In order to get accurate determinations of kinetic parameters it is important to overexpress a particular subtype on a nucleoside-transport null background, which indeed is very rare, although two mammalian non-commercial cell lines lacking CNT- and ENT-related activity had been engineered for this purpose (Mackey et al., 1998; Ward et al., 2000). On the other hand, determination of adenosine uptake kinetic constants of endogenous transporters is a big challenge. In general trends, most cell lines do not retain hCNT-related activity, because hCNT expression is highly dependent upon cell differentiation. Moreover, kinetic determinations in primary cells are not easy either because they co-express several transporter subtypes showing overlapping substrate selectivity.

Nucleoside uptake by each particular nucleoside transporter subtype cannot be determined directly. This is a limitation likely to result in experimental variability. CNT-mediated transport is Na-dependent, but uptake determinations in saturating sodium concentrations (normally 120 mM NaCl) incorporate CNT- and ENT-related transport as well a variable (often small) residual component likely to be associated with non-specific binding, to which even the support where the cells grow on can contribute to. Thus, uptake measurementsin the absence of sodium are required, being this cation often replaced by choline (120 mM Choline Cl). CNT-type activity can be calculated by subtracting uptake rates measured in the absence of Na from the total uptake activity measured in a Na-containing medium. Needless to say, uptake rates should be measured in initial velocity conditions for proper calculation of kinetic constants. This can be experimentally challenging, particularly when transporters are overexpressed. Under these conditions substrate uptake can be very fast and short uptake time points might be needed (seconds). As mentioned above, it is not correct to assume that endogenous ENT-type proteins are responsible for all apparent uptake activity measured in the absence of sodium. This means in practice that direct measurements of ENT-related activity cannot be performed either. Thus, ENTs must be pharmacologically inhibited to figure out their

TABLE 1 | Affinity constants of human adenosine transporters.

Gene name protein	Experimental model	Type of assay	Af. ct. (μM)	Reference
SLC29A1	Human Erythroleukemia K562 cells.	Adenosine influx	75	Boleti et al., 1997
ENT1	Endogenous transporters.	Adenosine influx	32	Celis et al., 2017
	Human Umbilical Vein Endothelial Cells (HUVEC).	Adenosine influx	53	Casanello et al., 2005
	Endogenous transporters.	Adenosine influx	59	Muñoz et al., 2006
	Placental microvascular endothelial cells. Endogenous transporters.		61	Salomón et al., 2012
			82	Escudero et al., 2008
	Heterologous expression in PK15NTD (Nucleoside Transporter Deficient) cells.		40	Ward et al., 2000
SLC29A2	Human Umbilical Vein Endothelial Cells (HUVEC).	Adenosine influx	49	Celis et al., 2017
ENT2	Endogenous transporters.	Adenosine influx	102	Muñoz et al., 2006
	Placental microvascular endothelial cells. Endogenous transporters.	Adenosine influx	77	Salomón et al., 2012
			98	Escudero et al., 2008
	Heterologous expression in PK15NTD (Nucleoside Transporter Deficient) cells.		140	Ward et al., 2000
SLC29A3	hENT3AA, mutated to reach the plasma membrane in	Adenosine influx pH 5.5	1860	Baldwin et al., 2005
ENT3	*Xenopus laevis* oocytes.	Adenosine influx pH 5.5	1620	Rahman et al., 2017
	Δ36hENT3, deleted to reach the plasma membrane in *Xenopus laevis* oocytes.		1800	Kang et al., 2010
SLC29A4	Expression in *Xenopus laevis* oocytes.	Adenosine influx pH 5.5	780	Barnes et al., 2006
ENT4				
SLC28A2	Expression in *Xenopus laevis* oocytes.	Adenosine influx	8	Yao et al., 1996
CNT2		Adenosine influx	6	Che et al., 1995
		Electrophysiology	18	Larráyoz et al., 2006
		Electrophysiology	23	Li et al., 2001
SLC28A3	Expression in *Xenopus laevis* oocytes	Adenosine influx	15	Ritzel et al., 2001
CNT3	Heterologous expression in yeast	Electrophysiology	18	Gorraitz et al., 2010
	Heterologous expression in HeLa cells	Adenosine influx	2.2	Damaraju et al., 2005
		Adenosine influx	2.4	Errasti-Murugarren et al., 2008

Interaction of nucleoside transporters with adenosine has been addressed either by determining the influx of radiolabeled adenosine into cells or, for hCNTs, by monitoring adenosine-induced Na^+currents in Xenopus laevis oocytes expressing a particular CNT subtype protein. Apparent affinity constants (Af. ct.) are all given in μM for a better comparison among all NT subtypes. Endogenous transporters refer to kinetic determinations performed using cell lines which express hENT1 and hENT2 endogenously, being the contribution of each subtype calculated by selectively inhibiting either hENT1 alone or both hENTs, as explained in the text. Adenosine uptake by hENT3 and hENT4 can only be measured at acidic pH. Kinetic determinations using the intracellular transporter hENT3 can only be performed if the wild type protein is modified in a way that sorting signals are blocked, thereby allowing the protein to reach the plasma membrane and determine function. Whether these relatively small structural alterations can significantly impact on adenosine affinity is not known. hCNT1 is not included in the table because, as explained in the text, even though some adenosine affinity constants have been reported, its translocation efficacy is extremely poor and we think it cannot be considered an adenosine transporter in a physiological context.

contribution to the remaining transport activity measured in sodium-free medium. Indeed, both plasma membrane ENTs (ENT1 and ENT2) can be simultaneously blocked by μM concentrations of dipyridamole and dilazep, whereas ENT1 can be selectively inhibited by nM concentrations of the nucleoside analog NBMPR (Young et al., 2013; Young, 2016; Pastor-Anglada et al., 2018). Accordingly, ENT1 activity corresponds to the NBMPR-sensitive component whereas ENT2 contribution to nucleoside uptake can be calculated by subtracting the ENT1 activity from the dipyridamole-sensitive component (ENT1 and ENT2 working simultaneously). At this moment, the reader can easily understand to what extent accurate measurements of endogenous nucleoside transport activity can be challenging in primary cells co-expressing all types of transporter proteins.

As introduced above, electrophysiology might be suitable for accurate kinetic measurements taking advantage of the fact that hCNT proteins are electrogenic when they translocate nucleosides and sodium. The two-electrode voltage clamp technique has been broadly used in transporter biology for this purpose (Lostao et al., 2000; Larráyoz et al., 2004; Smith et al., 2004; Slugoski et al., 2008; Gorraitz et al., 2010). The cRNA coding for a specific transporters is injected in *Xenopus laevis* oocytes and, in normal conditions, transporter function can be assessed after 2 days. Oocytes are clamped and inward sodium currents triggered by the addition of a particular hCNT substrate are recorded. Indeed, the intensity of the applied current to compensate for the transient depolarization associated with sodium influx, reflects transport activity. In this particular set up, initial velocity conditions can be easily achieved, endogenous activity is not interfering and currents may be a more direct way of measuring hCNT transport function than when using radiolabeled adenosine influx determinations. However, the oocyte membrane might show physicochemical properties different from mammalian plasma membranes. To what extent the membrane environment of a particular nucleoside transporter determines function and, eventually, substrate specificity is not really well-known. In this regard, when studying a novel polymorphic hCNT3 variant identified in our laboratory several years ago (Errasti-Murugarren et al., 2008), we observed that hCNT3 can indeed be found in different membrane microdomains, hCNT3 proteins located in lipid rafts being more active than the ones off rafts (Errasti-Murugarren et al., 2010).

There are many experimental issues which are likely to affect hCNT-related activity measurements and this may explain published variability in substrate specificity (adenosine affinity constants). Despite all these experimental issues, in general terms, it seems that the transporter proteins showing the highest affinity for adenosine are hCNTs, in particular, hCNT2 and hCNT3. In our hands, apparent Km values for adenosine in HEK293 cells expressing hCNT3 are the lowest reported so far among all nucleoside transporter proteins, 2.4 μM. Nevertheless, what makes hCNT3 an excellent candidate to modulate extracellular adenosine levels is the fact that it shows a huge capacity to concentrate nucleosides inside cells, because of its unique stoichiometry. Nevertheless, as will be discussed below, hCNT3 is not ubiquitously expressed, meaning that in some particular cell types hCNT2 would be the one to do the job.

The role of hCNT1 in adenosine regulation requires a more detailed explanation because there has been an argument in the past about whether or not this protein is an adenosine transporter. Apparent Km values for adenosine have been calculated for rCNT1 when it was expressed in oocytes and transport assays were performed using radiolabeled nucleosides (Yao et al., 1996). In this set up, an apparent Km of 26 μM was reported and discussed to be similar to the one calculated for uridine (37 μM) (Huang et al., 1994). Nevertheless, under these conditions the Vmax for uridine was 300 fold higher than the one calculated for adenosine (Yao et al., 1996). The same laboratory reported very low, almost negligible, substrate-induced Na-inward currents when using saturating concentrations of adenosine (100 μM) in oocytes expressing the human CNT1 ortholog (Smith et al., 2004). In our hands currents were undetectable using the same experimental approach (Larráyoz et al., 2004). In summary, we believe hCNT1 cannot be considered an adenosine transporter protein. However, we generated some evidence suggesting the possibility that adenosine can instead bind to the transporter protein without being translocated. Evidence for adenosine binding is quite consistent. Most sodium-coupled transporters, among them hCNTs, show some sodium leakage in the absence of the co-substrate (a nucleoside in our case). Leakage can be similarly measured as a current and is dependent upon membrane potential. Adenosine was shown to block what are called pre-steady state and steady state currents of the transporter protein associated with sodium-leakage (Larráyoz et al., 2004). This can be understood as the consequence of adenosine binding to the transporter protein. The physiological relevance of this event is not known.

Regarding ENT proteins, most available literature points to ENT1 and ENT2 as major players in the regulation of adenosine levels. Although apparent Km values are definitely higher (even much higher for hENT2) than the ones reported for hCNT2 and hCNT3, efficient coupling with adenosine phosphorylation would contribute to generate a huge transmembrane adenosine gradient which thermodynamically would favor influx via these transporter proteins. As discussed below, ENT1 is by far the most studied member within the *SLC29* gene family and different laboratories have provided consistent evidence supporting a role for this particular subtype in adenosine signaling. ENT3 is mostly localized in intracellular compartments (probably mitochondria and lysosomes) but, in any case, its affinity for adenosine seems to be low enough as to preclude any role for this transporter protein in adenosine regulation (Baldwin et al., 2005; Kang et al., 2010; Hsu et al., 2012; Rahman et al., 2017).

Similarly to CNT1, ENT4 also requires some detailed explanations, because its role in adenosine signaling is still on debate. ENT4 is evolutionarily distant from the other three members of the family (Young et al., 2013) and, when cloned and functionally expressed it was reported to show poor affinity for nucleosides, whereas it could translocate monoamine neurotransmitters such as dopamine and serotonin (Engel et al., 2004). In fact the laboratory that generated all this information claimed ENT4 to be renamed as PMAT, from Plasma Membrane Amine Transporter. Interestingly, ENT4/PMAT shows functional similarity with organic cation transporters (OCTs), which means that this protein can act as a polyspecific OCT as the *SLC22* gene members encoding for hOCT1, 2, and 3. Some common substrate structural determinants between nucleoside transporters and OCTs can be hypothesized. Indeed the three hOCT proteins can efficiently translocate the antiviral nucleoside analog lamivudine. Moreover, they can also interact with several other nucleoside-based antiviral drugs such as zidovudine, abacavir, and others (Minuesa et al., 2009). Nevertheless, none of the OCT proteins can transport natural nucleosides. The possibility of ENT4 playing a role in adenosine transport was raised by Barnes et al. (2006) several years ago. These authors demonstrated that serotonin transport via ENT4 was not pH-dependent, whereas adenosine transport was. Apparent Km values for adenosine at acidic pH (5.5) were in the high micromolar range but still were considered to be compatible with ENT4 being an adenosine transporter protein in physiological conditions associated with acidosis.

In summary, we have briefly dissected and discussed the basic biochemical principles and events governing adenosine transport into cells, by highlighting which are the best transporter candidates to regulate extracellular adenosine levels, and therefore, adenosine-mediated purinergic signaling.

ADENOSINE TRANSPORTERS AND PURINERGIC SIGNALING

Once the plasma membrane transporters likely to be implicated in the regulation of adenosine levels have been identified, we will discuss what is the physiological evidence supporting a functional link between a particular transporter subtype and purinergic regulation.

Several experimental approaches have been used in this regard. NT transporter pharmacology is still poorly developed and no subtype-specific inhibitors are available for CNT proteins, although this is not the case for ENTs. Indeed, high-affinity inhibition of ENT1 by NMBPR has proven very helpful. In fact, the determination of NMBPR-specific binding sites has been used by different authors to quantify ENT1 expression at the plasma membrane, even long before ENT1 was identified at the molecular level (Pickard et al., 1973; Dahlig-Harley et al., 1981;

Marangos et al., 1982). Besides the pharmacological approach, functional genomics is also available for ENT1, since Choi colleagues reported the first NT-subtype knock out mouse model (Choi et al., 2004; Oliveros et al., 2017). Probably because of these circumstances, we can say that ENT1 is the most studied transporter among the two families (*SLC28* and *SLC29*), with plenty of literature showing a link between ENT1 function and purinergic regulation. Another experimental approach suitable for the analysis of adenosine transporters as players in the purinome, comes from the evidence that selected NT subtypes (including ENT1) are under purinergic control. This means that their function is regulated by P1 (but probably also by P2) type receptors. In the classical set up of purinome function one would envisage NT proteins being stimulated by adenosine acting on P1 receptors, thereby promoting extracellular adenosine removal and ending the purinergic signaling. Moreover, changes in the expression of particular NT subtypes in physiological and pathophysiological conditions known to be associated with increased adenosine levels, further support the role particular NT proteins might play in purinergic regulation.

ENT Proteins

ENT1 expression in the rat and human brain has been mapped by different means (i.e., NBMPR binding, mRNA *in situ* hybridization and others). ENT1 shows broad cellular and regional distribution and its role in adenosine signaling is relatively well-understood (Parkinson et al., 2011). Adenosine is known to be neuroprotective in various pathological conditions such as stroke (Cunha, 2016). This is the reason why physiological mechanisms governing adenosine extracellular levels have been comprehensively studied. A probable dual role of ENT proteins either as influx or efflux transporters has been reported in the CNS. Indeed, rat cortical neurons when cultured alone are able to release adenosine after *N*-methyl-D-aspartate (NMDA) stimulation, whereas the NMDA-triggered increase in extracellular adenosine concentration appears to be related to nucleotide degradation when neurons are co-cultured with astrocytes (Zamzow et al., 2008). In rat hippocampal slices it has been shown that ATP is able to promote adenosine release via ENT-type proteins, which in turn might activate A2A receptors (Almeida et al., 2003). Subsequently, A2A activation might promote adenosine uptake, as shown in hippocampal synaptosomes (Pinto-Duarte et al., 2005). In fact, adenosine uptake via ENT-type transporters appears to reduce extracellular adenosine levels in hypoxia which suggests that ENT proteins and probably ENT1 in particular might be suitable targets for the treatment of cerebral ischemia (Zhang et al., 2011). Interestingly, adenosine in the brain has also been related to addictive behaviors, among them alcohol addiction. It has been known for a long time that ethanol increases extracellular adenosine by inhibiting in a somehow selective manner ENT1 function (Nagy et al., 1990). Nevertheless the most conclusive evidence supporting this pharmacological effect comes from functional genomics. The ENT1 knock out mouse model shows reduced acute responses to ethanol intake and increased addiction to alcohol (Choi et al., 2004). This animal model has also been useful in the understanding of ENT1-related adenosine signaling in other organs. In fact, ENT1-null mice show increased adenosine plasma levels and are cardioprotected (Rose et al., 2010, 2011). Similarly, ENT1 appears to be implicated in adenosine-related protection in the liver during ischemia and reperfusion (Zimmerman et al., 2013).

Moreover, adenosine contributes to chronic kidney disease, particularly in diabetes. Increased adenosine signaling via A2B receptors has been reported to be involved in diabetic glomerulopathy (Cárdenas et al., 2013), and increased adenosine levels in insulin-deficient states have been associated with down-regulation of ENT2 transport function in podocytes (Alarcón et al., 2017). In a complementary manner, in proximal tubule cells, decreased ENT1 function has also been related to fibrosis in diabetic nephropathy (Kretschmar et al., 2016). In fact, ENT1 null mouse shows a spontaneous tendency to develop renal fibrosis whereas ENT1 silencing in human kidney epithelial (HK) cells results in the promotion of epithelial-to-mesenchymal transition (EMT) (Guillén-Gómez et al., 2012). Promotion of EMT in HK2 cells can be mimicked by TFG-β1, whereas adenosine itself mediates TFG-β1 release from glomeruli of diabetic rats via A2B receptor activation (Roa et al., 2009).

The involvement of ENT proteins in the regulation of adenosine tone in vascular endothelium has been comprehensively studied using Human Umbilical Vein Endothelial Cells (HUVECs) and Placenta Microvascular Endothelial Cells (PMECs) as experimental models (review in Sobrevia et al., 2011; Pardo et al., 2013). As in other cell types, it has been shown that control of extracellular adenosine levels via P1 receptors also involves hENT modulation, in particular the hENT1 and hENT2 subtypes (Escudero et al., 2008; Pardo et al., 2013). In some cases, opposite effects on each transporter protein have been reported, thereby suggesting either some sort of physiological compensation or an hENT-subtype specific effect impacting on the ability of removing from the extracellular milieu not only adenosine but also some of its catabolites. hENT2 is indeed a suitable hypoxanthine transporter. Interestingly, we have recently shown that hENT1 and hENT2 can form oligomers hENT1-hENT1, hENT2-hENT2, but also hENT1-hENT2, with multiple functional consequences (Grañé-Boladeras et al., 2002).

Overall, it is within this framework that the pharmacological use of ENT inhibitors such as dipyridamole and dilazep can be understood (Figueredo et al., 1999). Nevertheless, at least for cardioprotection, it has recently been argued that ENT4 could become a better target than ENT1, because of the more restricted tissue expression pattern of the former ENT subtype (Yang and Leung, 2015). As discussed above, ENT4 was shown to be a suitable cardiac adenosine transporter at acidic pH (Barnes et al., 2006). Then, the idea these authors discuss is that most cell types may rely upon ENT1 for nucleoside salvage purposes, thereby making any ENT1-targeting drug more likely to present adverse effects than newly developed molecules targeting ENT4.

CNT Proteins

As discussed above, hCNT2 and hCNT3 should be, by far, the best candidates for efficient removal of adenosine from the extracellular milieu. This statement is based upon their apparent high affinity for adenosine and for its concentrative

capacity which is even 10 fold higher for hCNT3 than hCNT2. Nevertheless, hCNT pharmacology is very poor, even though some hCNT subtype specific inhibitors have been recently proposed (Kumar Deokar et al., 2017). In this regard the structural modeling of human CNT subtypes (Arimany-Nardi et al., 2017; Kumar Deokar et al., 2017; Latek, 2017; Mulinta et al., 2017) based upon the crystal structure of the *Vibrio cholerae* CNT ortholog (Johnson et al., 2012) might be particularly useful for future specific inhibitor design. This has been a major bottleneck to study the probable impact of acute CNT pharmacological inhibition on adenosine signaling. Nevertheless there is solid experimental evidence showing that CNT2 and CNT3 are under purinergic regulation, which suggests they contribute, as ENTs, to modulate extracellular adenosine levels and P1 signaling.

In liver parenchymal cells CNT2 is expressed at the basolateral (sinusoidal) and apical (canalicular) plasma membranes (Duflot et al., 2002; Govindarajan et al., 2008). In rat primary hepatocytes and hepatocarcinoma FAO cells the activity of this transporter protein is under purinergic regulation via A1 receptors (Duflot et al., 2004). This effect is relatively rapid (peaking between 5 and 10 min after agonist addition) and consistent with increased transport capacity (Vmax effect). Interestingly the magnitude of the effect (transport fold-induction) is dependent upon glucose concentration, being lower at high glucose (10 vs. 5 mM glucose). Indeed, CNT2 up-regulation could be blocked by inhibitors of KATP channels and mimicked by openers, which establishes a putative link between energy metabolism and purinergic regulation of CNT2. All the protein machinery likely to be implicated in this phenomenon, this is the KATP channel subunits Kir6.1, Kir6.2, SUR2A, SUR2B, as well as the transporter itself and A1 receptors were shown to co-localize in FAO cells. The physiological impact of the reduction of adenosine removal capacity triggered by high-glucose is not clear, although decreased hENT1 function and expression have been reported in HUVEC from diabetic patients and shown to be mimicked by high glucose in the culture medium (Sobrevia et al., 2011). It is interesting to keep in mind that extracellular adenosine has been reported to be able to modulate the AMP-dependent kinase AMPK, by a mechanism which depends on transporter function, also involving CNT2 in some cell types (Aymerich et al., 2006). Overall, CNT2 appears to be a suitable candidate to modulate purinergic signaling in hepatocytes, particularly considering that hCNT1 is not an adenosine transporter and hCNT3 expression in hepatocytes appears to be negligible. Interestingly, CNT2 function has recently been identified in primary rat bile duct epithelial cells where it is similarly found in both plasma membrane domains, apical and basolateral of cholangiocytes (Godoy et al., 2014). Luminal ATP, via P2Y receptors, down-regulates apical (lumen-facing) CNT2 activity by a Ca^{++}-dependent mechanism. Cholangiocytes also express CNT3 and its apical function is similarly down-regulated by nucleotides, such as ATP. However, A2A agonists (i.e., adenosine), acting from the luminal side, specifically activate apical CNT3, without modifying CNT2 function. CNT3 activation is consistent with transporter trafficking from intracellular vesicles to the plasma membrane. In practice this means that CNT2 and probably to more extent CNT3 are contributing to end up the purinergic regulation of bile flow by removing adenosine from the bile canaliculus. It makes sense that the adenosine precursor ATP reduces adenosine removal capacity by inhibiting both CNT2 and CNT3, whereas the differential regulation of both transporters by adenosine acting on A2A receptors may reflect basal (CNT2 and CNT3) and adenosine-induced (CNT3) capacity for its own removal.

CNT2, in parallel with ENT1, has also been mapped in the adult rat brain by *in situ* hybridization (Guillén-Gómez et al., 2004). Indeed, CNT2 is broadly distributed in the CNS with significant overlapping with ENT1. More recently, others have identified the CNT2 protein in plasma and vesicle membranes isolated from rat striatum (Melani et al., 2012). The possibility of CNT2 also playing a role in adenosine signaling in the brain is also supported by the evidence that its activity can be up-regulated by P1 receptor activation in differentiated neural PC12 cells (most probably A1 and A2A) (Medina-Pulido et al., 2013). CNT2 activation is relatively rapid, as in hepatocytes, peaking 15 min after P1 agonist addition. Interestingly, caffeine has been reported to inhibit CNT2 function with an apparent Ki value of 103 μM (Lang et al., 2004). Although this concentration might significantly exceed the one found in blood after coffee ingestion, it could still be relevant in heavy coffee drinkers (Nehlig and Debry, 1994). Taking together these observations suggest ENT1 may not be the only player regulating adenosine signaling in the brain, which in fact is consistent with the relatively mild phenotype of the ENT1 null mice.

Last, but not least, several physiological and pathophysiological observations also support a role for hCNT2 and hCNT3 as proteins relevant to purinergic signaling. The three hCNT genes are expressed in the nephron and accurate anatomic analysis of their distribution along it reveals a longitudinal pattern of expression consistent with nucleoside renal tubule reabsorption but also with adenosine-mediated tubulo-glomerular feedback regulation (Schnermann, 2015). Indeed, the three transporter proteins are expressed in the proximal convoluted tubule (PCT), where most nutrient reabsorption (glucose, amino acids) take place, but only the two adenosine transporters (CNT2 and CNT3), not CNT1, are also expressed in very specific distal segments of the nephron, the cortical collecting duct (CCD) (CNT3) and the outer medullary collecting duct (OMCD) (CNT2). This anatomical distribution is more consistent with adenosine signaling than with nucleoside reabsorption. Distribution of CNTs along the gastrointestinal tract (Pastor-Anglada et al., 2018) also points to this dual role of adenosine transporters. In fact, the CNT2 encoding gene (*SLC28A2*) is, by far, the one which is down-regulated the most (sevenfold) in inflamed ileon mucosa from Crohn's patients (Pérez-Torras et al., 2016). Even though the impact of inflammation is broad and down-regulates a broad cohort of genes, those associated with the purinome (transporters, receptors, and ectonucleotidases) are greatly affected.

In the rat brain, CNT2 is also down-regulated in situations known to be associated with increased adenosine concentrations. CNT2 mRNA levels are decreased in cortical samples from sleep-deprived rats, whereas ENT1 mRNA is not affected at all under the same circumstances (Guillén-Gómez et al., 2004).

CNT2-related mRNA tends to recover when animals are allowed to sleep. On the other hand, experimental ischemia *in vivo*, induced in rats by intraluminal middle cerebral arterial occlusion, also regulates nucleoside transporter encoding genes (Medina-Pulido et al., 2013). In this study, transcripts of both ENTs (ENT1 and ENT2) and the three CNT members were quantified in the ipsilateral cortex (infarcted) and compared to the contralateral cortex as its own control. Indeed, the mRNA levels of hENT1, hCNT2, but also hCNT3 (poorly studied in the brain), the three transporters more likely to modulate adenosine tone, were decreased in the infarcted tissue with no changes observed for hCNT1 and hENT2.

CONCLUDING REMARKS AND FUTURE PERSPECTIVES

Nucleoside transport by each particular nucleoside protein subtype cannot be measured directly, thereby resulting in some experimental variability likely to impact on the determination of adenosine affinity constants. Despite this limitation, we can conclude that adenosine transport mechanisms across the plasma membrane are well-understood with the only exception of ENT4, for which a clear role in the regulation of adenosine tone in some tissues (i.e., heart) still awaits clarification. Nevertheless, in general trends, who is who in adenosine transport is well-known.

Less clear is how each transporter subtype contributes to modulate adenosine levels, an issue of particular interest considering most cells show some apparent redundancy in the expression of adenosine transporters. ENT1 is by far the most studied adenosine transporter. This may be explained, as discussed above, not necessarily because of its ubiquitous expression, but because pharmacological tools and functional genomics have provided better chances to study it than for the other adenosine transporters. Nevertheless, the contribution of the other subtypes, particularly CNTs (CNT2 and CNT3) should not be ruled out and deserves further investigation.

Although CNT and ENT subtype expression appears to be polarized in (re)absorptive epithelia, thus allowing vectorial flux of substrates, in other epithelial cell types CNT and ENT proteins appear to be located in both poles (apical and basolateral), thereby anticipating other roles beyond absorption (Pastor-Anglada et al., 2018). Moreover, non-epithelial cells, such as adipocytes (Guallar et al., 2007) and immune system cells (Soler et al., 1998, 2001; Minuesa et al., 2009, 2011) also express ENT and CNT proteins. Whether particular subtypes are under purinergic regulation in these cells and tissues has not been properly addressed until now. Last, but not least, there is also the possibility of local regulation of selected adenosine transporters even at the single cell level, thereby providing some sort of compartmental regulation of biological functions. In this regard, ENT and CNT protein interactomics might help to unveil novel regulatory events likely to facilitate the fine tuning of purinergic regulation.

AUTHOR CONTRIBUTIONS

MP-A conceived the review and wrote the first draft of the manuscript. SP-T critiqued and revised the manuscript. SP-T and MP-A read the final version of the manuscript and approved it for submission.

FUNDING

This work was funded by SAF2011-23660 and SAF2014-52067-R (MINECO, Spain), Fundación Ramón Areces (Spain), and FEDER (European Union). MPET is a member of the Oncology Program of CIBER EHD. CIBER is an initiative of Instituto de Salud Carlos III (Spain).

ACKNOWLEDGMENTS

The authors would like to acknowledge past and present members of the MPET laboratory.

REFERENCES

Alarcón, S., Garrido, W., Cappelli, C., Suárez, R., Oyarzún, C., Quezada, C., et al. (2017). Deficient insulin-mediated upregulation of the equilibrative nucleoside transporter 2 contributes to chronically increased adenosine in diabetic glomerulopathy. *Sci. Rep.* 7:9439. doi: 10.1038/s41598-017-09783-0

Almeida, T., Rodrigues, R. J., de Mendonça, A., Ribeiro, J. A., and Cunha, R. A. (2003). Purinergic P2 receptors trigger adenosine release leading to adenosine A2A receptor activation and facilitation of long-term potentiation in rat hippocampal slices. *Neuroscience* 122, 111–121. doi: 10.1016/S0306-4522(03)00523-2

Arimany-Nardi, C., Claudio-Montero, A., Viel-Oliva, A., Schmidtke, P., Estarellas, C., Barril, X., et al. (2017). Identification and characterization of a secondary sodium-binding site and the main selectivity determinants in the human concentrative nucleoside transporter 3. *Mol. Pharm.* 14, 1980–1987. doi: 10.1021/acs.molpharmaceut.7b00085

Aymerich, I., Foufelle, F., Ferré, P., Casado, F. J., and Pastor-Anglada, M. (2006). Extracellular adenosine activates AMP-dependent protein kinase (AMPK). *J. Cell Sci.* 119(Pt 8), 1612–1621. doi: 10.1242/jcs.02865

Baldwin, S. A., Yao, S. Y., Hyde, R. J., Ng, A. M., Foppolo, S., Barnes, K., et al. (2005). Functional characterization of novel human and mouse equilibrative nucleoside transporters (hENT3 and mENT3) located in intracellular membranes. *J. Biol. Chem.* 280, 15880–15887. doi: 10.1074/jbc.M414337200

Barnes, K., Dobrzynski, H., Foppolo, S., Beal, P. R., Ismat, F., Scullion, E. R., et al. (2006). Distribution and functional characterization of equilibrative nucleoside transporter-4, a novel cardiac adenosine transporter activated at acidic pH. *Circ. Res.* 99, 510–519. doi: 10.1161/01.RES.0000238359.18495.42

Blay, J., White, T. D., and Hoskin, D. W. (1997). The extracellular fluid of solid carcinomas contains immunosuppressive concentrations of adenosine. *Cancer Res.* 57, 2602–2605.

Boleti, H., Coe, I. R., Baldwin, S. A., Young, J. D., and Cass, C. E. (1997). Molecular identification of the equilibrative NBMPR-sensitive (es) nucleoside transporter and demonstration of an equilibrative NBMPR-insensitive (ei) transport activity in human erythroleukemia (K562) cells. *Neuropharmacology* 36, 1167–1179. doi: 10.1016/S0028-3908(97)00136-6

Burnstock, G. (2017). Purinergic signalling: therapeutic developments. *Front. Pharmacol.* 8:661. doi: 10.3389/fphar.2017.00661

Cárdenas, A., Toledo, C., Oyarzún, C., Sepúlveda, A., Quezada, C., Guillén-Gómez, E., et al. (2013). Adenosine A(2B) receptor-mediated VEGF induction promotes diabetic glomerulopathy. *Lab. Invest.* 93, 135–144. doi: 10.1038/labinvest.2012.143

Casanello, P., Torres, A., Sanhueza, F., González, M., Farías, M., Gallardo, V., et al. (2005). Equilibrative nucleoside transporter 1 expression is downregulated by hypoxia in human umbilical vein endothelium. *Circ. Res.* 97, 16–24. doi: 10.1161/01.RES.0000172568.49367.f8

Celis, N., Araos, J., Sanhueza, C., Toledo, F., Beltrán, A. R., Pardo, F., et al. (2017). Intracellular acidification increases adenosine transport in human umbilical vein endothelial cells. *Placenta* 51, 10–17. doi: 10.1016/j.placenta.2017.01.120

Che, M., Ortiz, D. F., and Arias, I. M. (1995). Primary structure and functional expression of a cDNA encoding the bile canalicular, purine-specific Na(+)-nucleoside cotransporter. *J. Biol. Chem.* 270, 13596–13599. doi: 10.1074/jbc.270.23.13596

Choi, D. S., Cascini, M. G., Mailliard, W., Young, H., Paredes, P., and McMahon, T. (2004). The type 1 equilibrative nucleoside transporter regulates ethanol intoxication and preference. *Nat. Neurosci.* 7, 855–861. doi: 10.1038/nn1288

Cunha, R. A. (2016). How does adenosine control neuronal dysfunction and neurodegeneration? *J. Neurochem.* 139, 1019–1055. doi: 10.1111/jnc.13724

Dahlig-Harley, E., Eilam, Y., Paterson, A. R., and Cass, C. E. (1981). Binding of nitrobenzylthioinosine to high-affinity sites on the nucleoside-transport mechanism of HeLa cells. *Biochem. J.* 200, 295–305. doi: 10.1042/bj2000295

Damaraju, S., Zhang, J., Visser, F., Tackaberry, T., Dufour, J., Smith, K. M., et al. (2005). Identification and functional characterization of variants in human concentrative nucleoside transporter 3, hCNT3 (SLC28A3), arising from single nucleotide polymorphisms in coding regions of the hCNT3 gene. *Pharmacogenet. Genomics* 15, 173–182. doi: 10.1097/01213011-200503000-00006

de Andrade Mello, P., Coutinho-Silva, R., and Savio, L. E. B. (2017). Multifaceted effects of extracellular adenosine triphosphate and adenosine in the tumor-host interaction and therapeutic perspectives. *Front. Immunol.* 8:1526. doi: 10.3389/fimmu.2017.01526

Di Virgilio, F., and Adinolfi, E. (2017). Extracellular purines, purinergic receptors and tumor growth. *Oncogene* 36, 293–303. doi: 10.1038/onc.2016.206

Dos Santos-Rodrigues, A., Grane-Boladeras, N., Bicket, A., and Coe, I. R. (2014). Nucleoside transporters in the purinome. *Neurochem. Int.* 73, 229–237. doi: 10.1016/j.neuint.2014.03.014

Duflot, S., Calvo, M., Casado, F. J., Enrich, C., and Pastor-Anglada, M. (2002). Concentrative nucleoside transporter (rCNT1) is targeted to the apical membrane through the hepatic transcytotic pathway. *Exp. Cell Res.* 281, 77–85. doi: 10.1006/excr.2002.5641

Duflot, S., Riera, B., Fernández-Veledo, S., Casadó, V., Norman, R. I., Casado, F. J., et al. (2004). ATP-sensitive K(+) channels regulate the concentrative adenosine transporter CNT2 following activation by A(1) adenosine receptors. *Mol. Cell Biol.* 24, 2710–2719. doi: 10.1128/MCB.24.7.2710-2719.2004

Engel, K., Zhou, M., and Wang, J. (2004). Identification and characterization of a novel monoamine transporter in the human brain. *J. Biol. Chem.* 279, 50042–50049. doi: 10.1074/jbc.M407913200

Errasti-Murugarren, E., Cano-Soldado, P., Pastor-Anglada, M., and Casado, F. J. (2008). Functional characterization of a nucleoside-derived drug transporter variant (hCNT3C602R) showing altered sodium-binding capacity. *Mol. Pharmacol.* 73, 379–386. doi: 10.1124/mol.107.041848

Errasti-Murugarren, E., Molina-Arcas, M., Casado, F. J., and Pastor-Anglada, M. (2009). A splice variant of the SLC28A3 gene encodes a novel human concentrative nucleoside transporter-3 (hCNT3) protein localized in the endoplasmic reticulum. *FASEB J.* 23, 172–182. doi: 10.1096/fj.08-113902

Errasti-Murugarren, E., Molina-Arcas, M., Casado, F. J., and Pastor-Anglada, M. (2010). The human concentrative nucleoside transporter-3 C602R variant shows impaired sorting to lipid rafts and altered specificity for nucleoside-derived drugs. *Mol. Pharmacol.* 78, 157–165. doi: 10.1124/mol.110.063552

Escudero, C., Casanello, P., and Sobrevia, L. (2008). Human equilibrative nucleoside transporters 1 and 2 may be differentially modulated by A2B adenosine receptors in placenta microvascular endothelial cells from pre-eclampsia. *Placenta* 29, 816–825. doi: 10.1016/j.placenta.2008.06.014

Espinoza, J., Espinoza, A. F., and Power, G. G. (2011). High fetal plasma adenosine concentration: a role for the fetus in preeclampsia? *Am. J. Obstet. Gynecol.* 485, e424–e487. doi: 10.1016/j.ajog.2011.06.034

Fenton, R. A., and Dobson, J. G. Jr. (1992). Fluorometric quantitation of adenosine concentration in small samples of extracellular fluid. *Anal. Biochem.* 207, 134–141. doi: 10.1016/0003-2697(92)90514-8

Figueredo, V. M., Diamond, I., Zhou, H. Z., and Albert Camacho, S. (1999). Chronic dipyridamole therapy produces sustained protection against cardiac ischemia-reperfusion injury. *Am. J. Physiol.* 277(5 Pt 2), H2091–H2097. doi: 10.1152/ajpheart.1999.277.5.H2091

Fredholm, B. B., IJzerman, A. P., Jacobson, K. A., Linden, J., and Müller, C. E. (2011). International Union of Basic and Clinical Pharmacology. LXXXI. Nomenclature and classification of adenosine receptors–an update. *Pharmacol. Rev.* 63, 1–34. doi: 10.1124/pr.110.003285

Godoy, V., Banales, J. M., Medina, J. F., and Pastor-Anglada, M. (2014). Functional crosstalk between the adenosine transporter CNT3 and purinergic receptors in the biliary epithelia. *J. Hepatol.* 61, 1337–1343. doi: 10.1016/j.jhep.2014.06.036

Gorraitz, E., Pastor-Anglada, M., and Lostao, M. P. (2010). Effects of Na+ and H+ on steady-state and presteady-state currents of the human concentrative nucleoside transporter 3 (hCNT3). *Pflugers Arch.* 460, 617–632. doi: 10.1007/s00424-010-0846-9

Govindarajan, R., Endres, C. J., Whittington, D., LeCluyse, E., Pastor-Anglada, M., Tse, C. M., et al. (2008). Expression and hepatobiliary transport characteristics of the concentrative and equilibrative nucleoside transporters in sandwich-cultured human hepatocytes. *Am. J. Physiol. Gastrointest. Liver Physiol.* 295, G570–G580. doi: 10.1152/ajpgi.00542.2007

Grañé-Boladeras, N., Spring, C. M., Hanna, W. J., Pastor-Anglada, M., and Coe, I. R. (2016). Novel nuclear hENT2 isoforms regulate cell cycle progression via controlling nucleoside transport and nuclear reservoir. *Cell Mol. Life Sci.* 73, 4559–4575. doi: 10.1007/s00018-016-2288-9

Grañé-Boladeras, N., Williams, D., McKenzie, T., and Naydenova, Z. (2002). Oligomerisation of Equilibrative Nucleoside Transporters: a novel regulatory and functional mechanism involving PKC and PP1. *FASEB J.* 517, 201–205.

Guallar, J. P., Cano-Soldado, P., Aymerich, I., Domingo, J. C., Alegre, M., Domingo, P., et al. (2007). Altered expression of nucleoside transporter genes (SLC28 and SLC29) in adipose tissue from HIV-1-infected patients. *Antivir. Ther.* 12, 853–863.

Guillén-Gómez, E., Calbet, M., Casado, J., de Lecea, L., Soriano, E., Pastor-Anglada, M., et al. (2004). Distribution of CNT2 and ENT1 transcripts in rat brain: selective decrease of CNT2 mRNA in the cerebral cortex of sleep-deprived rats. *J. Neurochem.* 90, 883–893. doi: 10.1111/j.1471-4159.2004.02545.x

Guillén-Gómez, E., Pinilla-Macua, I., Pérez-Torras, S., Choi, D. S., Arce, Y., Ballarín, J. A., et al. (2012). New role of the human equilibrative nucleoside transporter 1 (hENT1) in epithelial-to-mesenchymal transition in renal tubular cells. *J. Cell Physiol.* 227, 1521–1528. doi: 10.1002/jcp.22869

Hsu, C. L., Lin, W., Seshasayee, D., Chen, Y. H., Ding, X., Lin, Z., et al. (2012). Equilibrative nucleoside transporter 3 deficiency perturbs lysosome function and macrophage homeostasis. *Science* 335, 89–92. doi: 10.1126/science.1213682

Huang, Q. Q., Yao, S. Y., Ritzel, M. W., Paterson, A. R., Cass, C. E., Young, J. D., et al. (1994). Cloning and functional expression of a complementary DNA encoding a mammalian nucleoside transport protein. *J. Biol. Chem.* 269, 17757–17760.

Johnson, Z. L., Cheong, C. G., and Lee, S. Y. (2012). Crystal structure of a concentrative nucleoside transporter from *Vibrio cholerae* at 2.4 A. *Nature* 483, 489–493. doi: 10.1038/nature10882

Kang, N., Jun, A. H., Bhutia, Y. D., Kannan, N., Unadkat, J. D., and Govindarajan, R. (2010). Human equilibrative nucleoside transporter-3 (hENT3) spectrum disorder mutations impair nucleoside transport, protein localization, and stability. *J. Biol. Chem.* 285, 28343–28352. doi: 10.1074/jbc.M110.109199

Kretschmar, C., Oyarzún, C., Villablanca, C., Jaramillo, C., Alarcón, S., Perez, G., et al. (2016). Reduced adenosine uptake and its contribution to signaling that mediates profibrotic activation in renal tubular epithelial cells: implication in diabetic nephropathy. *PLoS One* 11:e0147430. doi: 10.1371/journal.pone.0147430

Kumar Deokar, H., Barch, H. P., Barch, H. P., and Buolamwini, J. K. (2017). Homology modeling of human concentrative nucleoside transporters (hCNTs)

and validation by virtual screening and experimental testing to identify novel hCNT1 Inhibitors. *Drug Des.* 6:146. doi: 10.4172/2169-0138.1000146

Lang, T. T., Young, J. D., and Cass, C. E. (2004). Interactions of nucleoside analogs, caffeine, and nicotine with human concentrative nucleoside transporters 1 and 2 stably produced in a transport-defective human cell line. *Mol. Pharmacol.* 65, 925–933. doi: 10.1124/mol.65.4.925

Larráyoz, I. M., Casado, F. J., Pastor-Anglada, M., and Lostao, M. P. (2004). Electrophysiological characterization of the human Na(+)/nucleoside cotransporter 1 (hCNT1) and role of adenosine on hCNT1 function. *J. Biol. Chem.* 279, 8999–9007. doi: 10.1074/jbc.M311940200

Larráyoz, I. M., Fernández-Nistal, A., Garcés, A., Gorraitz, E., and Lostao, M. P. (2006). Characterization of the rat Na+/nucleoside cotransporter 2 and transport of nucleoside-derived drugs using electrophysiological methods. *Am. J. Physiol. Cell Physiol.* 291, C1395–C1404. doi: 10.1152/ajpcell.00110.2006

Latek, D. (2017). Rosetta Broker for membrane protein structure prediction: concentrative nucleoside transporter 3 and corticotropin-releasing factor receptor 1 test cases. *BMC Struct. Biol.* 17:8. doi: 10.1186/s12900-017-0078-8

Li, J. Y., Boado, R. J., and Pardridge, W. M. (2001). Differential kinetics of transport of 2′,3′-dideoxyinosine and adenosine via concentrative Na+ nucleoside transporter CNT2 cloned from rat blood-brain barrier. *J. Pharmacol. Exp. Ther.* 299, 735–740.

Lostao, M. P., Mata, J. F., Larrayoz, I. M., Inzillo, S. M., Casado, F. J., and Pastor-Anglada, M. (2000). Electrogenic uptake of nucleosides and nucleoside-derived drugs by the human nucleoside transporter 1 (hCNT1) expressed in Xenopus laevis oocytes. *FEBS Lett.* 481, 137–140. doi: 10.1016/S0014-5793(00)01983-9

Mackey, J. R., Mani, R. S., Selner, M., Mowles, D., Young, J. D., Belt, J. A., et al. (1998). Functional nucleoside transporters are required for gemcitabine influx and manifestation of toxicity in cancer cell lines. *Cancer Res.* 58, 4349–4357.

Marangos, P. J., Patel, J., Clark-Rosenberg, R., and Martino, A. M. (1982). [3H]nitrobenzylthioinosine binding as a probe for the study of adenosine uptake sites in brain. *J. Neurochem.* 39, 184–191. doi: 10.1111/j.1471-4159.1982.tb04717.x

Medina-Pulido, L., Molina-Arcas, M., Justicia, C., Soriano, E., Burgaya, F., Planas, A. M., et al. (2013). Hypoxia and P1 receptor activation regulate the high-affinity concentrative adenosine transporter CNT2 in differentiated neuronal PC12 cells. *Biochem. J.* 454, 437–445. doi: 10.1042/BJ20130231

Melani, A., Corti, F., Stephan, H., Müller, C. E., Donati, C., Bruni, P., et al. (2012). Ecto-ATPase inhibition: ATP and adenosine release under physiological and ischemic in vivo conditions in the rat striatum. *Exp. Neurol.* 233, 193–204. doi: 10.1016/j.expneurol.2011.09.036

Minuesa, G., Huber-Ruano, I., Pastor-Anglada, M., Koepsell, H., Clotet, B., and Martinez-Picado, J. (2011). Drug uptake transporters in antiretroviral therapy. *Pharmacol. Ther.* 132, 268–279. doi: 10.1016/j.pharmthera.2011.06.007

Minuesa, G., Volk, C., Molina-Arcas, M., Gorboulev, V., Erkizia, I., Arndt, P., et al. (2009). Transport of lamivudine [(-)-beta-L-2′,3′-dideoxy-3′-thiacytidine] and high-affinity interaction of nucleoside reverse transcriptase inhibitors with human organic cation transporters 1, 2, and 3. *J. Pharmacol. Exp. Ther.* 329, 252–261. doi: 10.1124/jpet.108.146225

Mulinta, R., Yao, S. Y. M., Ng, A. M. L., Cass, C. E., and Young, J. D. (2017). Substituted cysteine accessibility method (SCAM) analysis of the transport domain of human concentrative nucleoside transporter 3 (hCNT3) and other family members reveals features of structural and functional importance. *J. Biol. Chem.* 292, 9505–9522. doi: 10.1074/jbc.M116.743997

Muñoz, G., San Martín, R., Farías, M., Cea, L., Vecchiola, A., Casanello, P., et al. (2006). Insulin restores glucose inhibition of adenosine transport by increasing the expression and activity of the equilibrative nucleoside transporter 2 in human umbilical vein endothelium. *J. Cell Physiol.* 209, 826–835. doi: 10.1002/jcp.20769

Nagy, L. E., Diamond, I., Casso, D. J., Franklin, C., and Gordon, A. S. (1990). Ethanol increases extracellular adenosine by inhibiting adenosine uptake via the nucleoside transporter. *J. Biol. Chem.* 265, 1946–1951.

Nehlig, A., and Debry, G. (1994). Potential teratogenic and neurodevelopmental consequences of coffee and caffeine exposure: a review on human and animal data. *Neurotoxicol. Teratol.* 16, 531–543. doi: 10.1016/0892-0362(94)90032-9

Nguyen, M. D., Ross, A. E., Ryals, M., Lee, S. T., and Venton, B. J. (2015). Clearance of rapid adenosine release is regulated by nucleoside transporters and metabolism. *Pharmacol. Res. Perspect.* 3:e00189. doi: 10.1002/prp2.189

Oliveros, A., Starski, P., Lindberg, D., Choi, S., Heppelmann, C. J., Dasari, S., et al. (2017). Label-Free neuroproteomics of the hippocampal-accumbal circuit reveals deficits in neurotransmitter and neuropeptide signaling in mice lacking ethanol-sensitive adenosine transporter. *J. Proteome Res.* 16, 1445–1459. doi: 10.1021/acs.jproteome.6b00830

Pardo, F., Arroyo, P., Salomón, C., Westermeier, F., Salsoso, R., Sáez, T., et al. (2013). Role of equilibrative adenosine transporters and adenosine receptors as modulators of the human placental endothelium in gestational diabetes mellitus. *Placenta* 34, 1121–1127. doi: 10.1016/j.placenta.2013.09.007

Parkinson, F. E., Damaraju, V. L., Graham, K., Yao, S. Y., Baldwin, S. A., Cass, C. E., et al. (2011). Molecular biology of nucleoside transporters and their distributions and functions in the brain. *Curr. Top. Med. Chem.* 11, 948–972. doi: 10.2174/156802611795347582

Pastor-Anglada, M., Urtasun, N., and Pérez-Torras, S. (2018). Intestinal nucleoside transporters: function, expression and regulation. *Comp. Physiol.* (in press).

Pérez-Torras, S., Iglesias, I., Llopis, M., Lozano, J. J., Antolín, M., Guarner, F., et al. (2016). Transportome profiling identifies profound alterations in crohn's disease partially restored by commensal bacteria. *J. Crohns Colitis* 10, 850–859. doi: 10.1093/ecco-jcc/jjw042

Pickard, M. A., Brown, R. R., Paul, B., and Paterson, A. R. (1973). Binding of the nucleoside transport inhibitor 4-nitrobenzylthioinosine to erythrocyte membranes. *Can. J. Biochem.* 51, 666–672. doi: 10.1139/o73-083

Pinto-Duarte, A., Coelho, J. E., Cunha, R. A., Ribeiro, J. A., and Sebastião, A. M. (2005). Adenosine A2A receptors control the extracellular levels of adenosine through modulation of nucleoside transporters activity in the rat hippocampus. *J. Neurochem.* 93, 595–604. doi: 10.1111/j.1471-4159.2005.03071.x

Rahman, M. F., Askwith, C., and Govindarajan, R. (2017). Molecular determinants of acidic pH-dependent transport of human equilibrative nucleoside transporter 3. *J. Biol. Chem.* 292, 14775–14785. doi: 10.1074/jbc.M117.787952

Ritzel, M. W., Ng, A. M., Yao, S. Y., Graham, K., Loewen, S. K., Smith, K. M., et al. (2001). Molecular identification and characterization of novel human and mouse concentrative Na+-nucleoside cotransporter proteins (hCNT3 and mCNT3) broadly selective for purine and pyrimidine nucleosides (system cib). *J. Biol. Chem.* 276, 2914–2927. doi: 10.1074/jbc.M007746200

Roa, H., Gajardo, C., Troncoso, E., Fuentealba, V., Escudero, C., Yáñez, A., et al. (2009). Adenosine mediates transforming growth factor-beta 1 release in kidney glomeruli of diabetic rats. *FEBS Lett.* 583, 3192–3198. doi: 10.1016/j.febslet.2009.09.003

Rose, J. B., Naydenova, Z., Bang, A., Eguchi, M., Sweeney, G., Choi, D. S., et al. (2010). Equilibrative nucleoside transporter 1 plays an essential role in cardioprotection. *Am. J. Physiol. Heart Circ. Physiol.* 298, H771–H777. doi: 10.1152/ajpheart.00711.2009

Rose, J. B., Naydenova, Z., Bang, A., Ramadan, A., Klawitter, J., Schram, K., et al. (2011). Absence of equilibrative nucleoside transporter 1 in ENT1 knockout mice leads to altered nucleoside levels following hypoxic challenge. *Life Sci.* 89, 621–630. doi: 10.1016/j.lfs.2011.08.007

Salomón, C., Westermeier, F., Puebla, C., Arroyo, P., Guzmán-Gutiérrez, E., Pardo, F., et al. (2012). Gestational diabetes reduces adenosine transport in human placental microvascular endothelium, an effect reversed by insulin. *PLoS One* 7:e40578. doi: 10.1371/journal.pone.0040578

Schnermann, J. (2015). Concurrent activation of multiple vasoactive signaling pathways in vasoconstriction caused by tubuloglomerular feedback: a quantitative assessment. *Annu. Rev. Physiol.* 77, 301–322. doi: 10.1146/annurev-physiol-021014-071829

Slugoski, M. D., Smith, K. M., Mulinta, R., Ng, A. M., Yao, S. Y., Morrison, E. L., et al. (2008). A conformationally mobile cysteine residue (Cys-561) modulates Na+ and H+ activation of human CNT3. *J. Biol. Chem.* 283, 24922–24934. doi: 10.1074/jbc.M801793200

Smith, K. M., Ng, A. M., Yao, S. Y., Labedz, K. A., Knaus, E. E., Wiebe, L. I., et al. (2004). Electrophysiological characterization of a recombinant human Na+-coupled nucleoside transporter (hCNT1) produced in Xenopus oocytes. *J. Physiol.* 558(Pt 3), 807–823.

Sobrevia, L., Abarzúa, F., Nien, J. K., Salomón, C., Westermeier, F., Puebla, C., et al. (2011). Review: differential placental macrovascular and microvascular endothelial dysfunction in gestational diabetes. *Placenta* 32(Suppl. 2), S159–S164. doi: 10.1016/j.placenta.2010.12.011

Soler, C., Felipe, A., Mata, J. F., Casado, F. J., Celada, A., Pastor-Anglada, M., et al. (1998). Regulation of nucleoside transport by lipopolysaccharide, phorbol esters, and tumor necrosis factor-alpha in human B-lymphocytes. *J. Biol. Chem.* 273, 26939–26945. doi: 10.1074/jbc.273.41.26939

Soler, C., Valdés, R., Garcia-Manteiga, J., Xaus, J., Comalada, M., Casado, F. J., et al. (2001). Lipopolysaccharide-induced apoptosis of macrophages determines the up-regulation of concentrative nucleoside transporters Cnt1 and Cnt2 through tumor necrosis factor-alpha-dependent and -independent mechanisms. *J. Biol. Chem.* 276, 30043–30049. doi: 10.1074/jbc.M10180 7200

Ward, J. L., Sherali, A., Mo, Z. P., and Tse, C. M. (2000). Kinetic and pharmacological properties of cloned human equilibrative nucleoside transporters, ENT1 and ENT2, stably expressed in nucleoside transporter-deficient PK15 cells. Ent2 exhibits a low affinity for guanosine and cytidine but a high affinity for inosine. *J. Biol. Chem.* 275, 8375–8381. doi: 10.1074/jbc.275. 12.8375

Westermeier, F., Salomón, C., González, M., Puebla, C., Guzmán-Gutiérrez, E., Cifuentes, F., et al. (2011). Insulin restores gestational diabetes mellitus-reduced adenosine transport involving differential expression of insulin receptor isoforms in human umbilical vein endothelium. *Diabetes* 60, 1677–1687. doi: 10.2337/db11-0155

Yang, C., and Leung, G. P. (2015). Equilibrative nucleoside transporters 1 and 4: which one is a better target for cardioprotection against ischemia-reperfusion injury? *J. Cardiovasc. Pharmacol.* 65, 517–521. doi: 10.1097/FJC. 0000000000000194

Yao, S. Y., Ng, A. M., Ritzel, M. W., Gati, W. P., Cass, C. E., and Young, J. D. (1996). Transport of adenosine by recombinant purine- and pyrimidine-selective sodium/nucleoside cotransporters from rat jejunum expressed in Xenopus laevis oocytes. *Mol. Pharmacol.* 50, 1529–1535.

Young, J. D. (2016). The SLC28 (CNT) and SLC29 (ENT) nucleoside transporter families: a 30-year collaborative odyssey. *Biochem. Soc. Trans.* 44, 869–876. doi: 10.1042/BST20160038

Young, J. D., Yao, S. Y., Baldwin, J. M., Cass, C. E., and Baldwin, S. A. (2013). The human concentrative and equilibrative nucleoside transporter families, SLC28 and SLC29. *Mol. Aspects Med.* 34, 529–547. doi: 10.1016/j.mam.2012.05.007

Zamzow, C. R., Xiong, W., and Parkinson, F. E. (2008). Adenosine produced by neurons is metabolized to hypoxanthine by astrocytes. *J. Neurosci. Res.* 86, 3447–3455. doi: 10.1002/jnr.21789

Zhang, D., Xiong, W., Albensi, B. C., and Parkinson, F. E. (2011). Expression of human equilibrative nucleoside transporter 1 in mouse neurons regulates adenosine levels in physiological and hypoxic-ischemic conditions. *J. Neurochem.* 118, 4–11. doi: 10.1111/j.1471-4159.2011.07242.x

Zimmerman, M. A., Tak, E., Ehrentraut, S. F., Kaplan, M., Giebler, A., Weng, T., et al. (2013). Equilibrative nucleoside transporter (ENT)-1-dependent elevation of extracellular adenosine protects the liver during ischemia and reperfusion. *Hepatology* 58, 1766–1778. doi: 10.1002/hep.26505

Conflict of Interest Statement: The authors declare that the research was conducted in the absence of any commercial or financial relationships that could be construed as a potential conflict of interest.

frontiers in Pharmacology

REVIEW
published: 01 June 2018
doi: 10.3389/fphar.2018.00526

Caffeine and Selective Adenosine Receptor Antagonists as New Therapeutic Tools for the Motivational Symptoms of Depression

Laura López-Cruz[1†], John D. Salamone[2] and Mercè Correa[1,2]*

[1] *Àrea de Psicobiologia, Universitat Jaume I, Castellón de la Plana, Spain,* [2] *Behavioral Neuroscience Division, University of Connecticut, Storrs, CT, United States*

OPEN ACCESS

Edited by:
Francisco Ciruela, Universitat de Barcelona, Spain

Reviewed by:
Rodrigo A. Cunha, Universidade de Coimbra, Portugal
Olga Valverde, Universitat Pompeu Fabra, Spain

****Correspondence:***
Mercè Correa
correa@uji.es

†Present address:
Laura López-Cruz, Department of Psychology and MRC/Wellcome Trust Behavioural and Clinical Neuroscience Institute, University of Cambridge, Cambridge, United Kingdom

Specialty section:
This article was submitted to Experimental Pharmacology and Drug Discovery, a section of the journal Frontiers in Pharmacology

Received: *19 January 2018*
Accepted: *01 May 2018*
Published: *01 June 2018*

Citation:
López-Cruz L, Salamone JD and Correa M (2018) Caffeine and Selective Adenosine Receptor Antagonists as New Therapeutic Tools for the Motivational Symptoms of Depression. Front. Pharmacol. 9:526. doi: 10.3389/fphar.2018.00526

Major depressive disorder is one of the most common and debilitating psychiatric disorders. Some of the motivational symptoms of depression, such anergia (lack of self-reported energy) and fatigue are relatively resistant to traditional treatments such as serotonin uptake inhibitors. Thus, new pharmacological targets are being investigated. Epidemiological data suggest that caffeine consumption can have an impact on aspects of depressive symptomatology. Caffeine is a non-selective adenosine antagonist for A_1/A_{2A} receptors, and has been demonstrated to modulate behavior in classical animal models of depression. Moreover, selective adenosine receptor antagonists are being assessed for their antidepressant effects in animal studies. This review focuses on how caffeine and selective adenosine antagonists can improve different aspects of depression in humans, as well as in animal models. The effects on motivational symptoms of depression such as anergia, fatigue, and psychomotor slowing receive particular attention. Thus, the ability of adenosine receptor antagonists to reverse the anergia induced by dopamine antagonism or depletion is of special interest. In conclusion, although further studies are needed, it appears that caffeine and selective adenosine receptor antagonists could be therapeutic agents for the treatment of motivational dysfunction in depression.

Keywords: adenosine receptors, dopamine, caffeine, antidepressants, anergia, fatigue, anxiety

MAJOR DEPRESSION DISORDER: SYMPTOMATOLOGY AND CURRENT TREATMENT

Major depression disorder (MDD) is one of the most debilitating disorders in the world, and the most commonly diagnosed according to the World Health Organization. The Diagnostic and Statistical Manual in its last edition (DMS-5) defines this disorder as a set of symptoms including: depressed mood, decreased interest or pleasure in almost all activities nearly every day, appetite changes (changes in body weight), sleep disturbances, feelings of worthlessness or guilt, diminished ability to concentrate or indecisiveness, psychomotor agitation or retardation and fatigue or loss of energy (American Psychiatric Association, 2013).

Although depression is typically defined as an affective disorder, it also appears that some symptoms such as psychomotor retardation, fatigue, and loss of energy are related to deficits in motivation, specifically in activational aspects of motivation. Motivated behavior is directed toward or away from particular stimuli, but it also is characterized by a high degree of activity, effort, vigor, and persistence (Salamone and Correa, 2002, 2012). People with depression commonly show profound activational impairments, such as lassitude, listlessness, fatigue, and anergia (low self-reported energy) that affect their motivation (Tylee et al., 1999; Stahl, 2002). In fact, among depressed people, energy loss and fatigue are the second most commonly reported symptoms, only behind depressed mood itself (Tylee et al., 1999), and depressed patients with anergia are more common than patients with anxiety related symptoms (Tylee et al., 1999; Drysdale et al., 2017). Furthermore, in depressed patients "lack of energy" was the factor that correlated to problems with fatigability, inability to work, and psychomotor retardation, loading most strongly onto a second order general depression factor (Gullion and Rush, 1998). Many people with MDD have fundamental deficits in reward seeking, exertion of effort, and effort-related decision making that do not simply depend upon any problems that they may have with experiencing pleasure (Treadway et al., 2009). Lack of energy is the symptom most highly correlated with a lack of social function in depressed patients, and is correlated with various work-related impairments such as days in bed, days of lost work, and low work productivity (Swindle et al., 2001). In addition, this cluster of symptoms can be highly resistant to treatment (Stahl, 2002); they are the best predictors of lack of remission after antidepressant drug treatment (Stahl, 2002; Gorwood et al., 2014).

PHARMACOLOGICAL TREATMENTS FOR THE ACTIVATIONAL SYMPTOMS IN DEPRESSION

The severity of effort-related motivational symptoms in depression is related to problems with social function, employment absence, and treatment outcomes (Tylee et al., 1999; Stahl, 2002). Patients with high scores in psychomotor retardation also have longer duration of illness, an earlier age of onset, and more depressive episodes (Calugi et al., 2011; Gorwood et al., 2014). These symptoms are a predictor of delayed response to treatment with either interpersonal psychotherapy or selective serotonin (5-HT) reuptake inhibitor pharmacotherapy (Frank et al., 2011), often remaining as residual symptoms even in patients in remission (Stahl, 2002; Fava et al., 2014; Gorwood et al., 2014).

Most of the present treatment strategies for MDD focus on drugs that block the inactivation (i.e., inhibitors of enzymatic breakdown or uptake) of the monoamine neurotransmitters 5-HT and norepinephrine (NE). The classical antidepressants include monoamine oxidase inhibitors (MAOIs), which affect one of the major catabolic enzymes for monoamines (Quitkin et al., 1979), and drugs that inhibit uptake of one or more monoamines (Feighner, 1999; Yıldız et al., 2002). Although 5-HT and NE reuptake inhibitors have become the most frequently prescribed medications for MDD, they fail to complete symptom remission in 40–60% of all patients (Rush and Trivedi, 1995; Fava et al., 2014), and it is widely accepted that at least 20% of all depressed patients do not respond adequately to most antidepressant drugs (Crown et al., 2002). Many common antidepressants, including 5-HT transport inhibitors such as fluoxetine, are relatively ineffective at treating anergia and fatigue, and in fact, can induce or exacerbate these symptoms (Padala et al., 2012; Stenman and Lilja, 2013; Fava et al., 2014).

Interestingly, some clinical studies suggest that drugs that inhibit dopamine (DA) transport, such as the catecholamine uptake inhibitor bupropion, are relatively more effective than 5-HT uptake inhibitors for treating effort-related motivational symptoms (Rampello et al., 1991; Stahl, 2002; Demyttenaere et al., 2005; Pae et al., 2007). Furthermore, individual differences in behavioral traits can differentiate between depressed patients that are more responsive to bupropion (i.e., motivated, achievement-oriented, active, exercise-oriented people) vs. fluoxetine (people with mood problems, irritability, and rumination) (Bell et al., 2013). Stimulant drugs that are not considered to be antidepressants in the classical sense, such as methylphenidate and modafinil, have been shown to increase energy and motivation in depressed patients (Zisook et al., 2006). Thus, clinical studies, together with preclinical investigations (e.g., Salamone et al., 2006, 2007; Salamone and Correa, 2012; Argyropoulos and Nutt, 2013; Heath et al., 2015), have led to the suggestion that DA systems and related circuits are particularly involved in effort-related motivational symptoms.

ADENOSINE RECEPTORS CO-LOCALIZATION WITH DA RECEPTORS

In addition, another possible therapeutic target for the anergia component of depression is adenosine receptors. Adenosine is a neuromodulator in the central nervous system (CNS) that plays an important role in the regulation of synaptic transmission and neuronal excitability (Cunha, 2001; Sebastião and Ribeiro, 2009). Several subtypes of adenosine receptors are expressed in the brain, with A_1 and A_{2A} G-protein-coupled receptors being the most abundant (Jacobson and Gao, 2006; Fredholm et al., 2011). A_{2A} receptors are expressed at high levels in the striatum and olfactory bulbs and tubercle (Fredholm et al., 2011), but also in areas such as amygdala, hippocampus or prefrontal cortex (Cunha et al., 1994; Pandolfo et al., 2013; Simões et al., 2016). Adenosine A_1 receptors have a higher widespread distribution in the brain, with a somewhat higher concentration in hippocampus (Schwarzschild et al., 2006). All these regions are involved in the regulation of complex processes such as cognition, motivation, and emotion (Hauber and Sommer, 2009; Salamone and Correa, 2012) that seem to be altered in MDD.

The spatial distribution of adenosine receptors within the brain (Fredholm et al., 2011) allows a wide range of effects, including modulation of other neurotransmitter

systems (Cunha, 2001). Thus, adenosine A_{2A} receptors are highly expressed postsynaptically in DA rich areas such as neostriatum and accumbens (Acb) (Johansson and Fredholm, 1995; Johansson et al., 1997; DeMet and Chicz-DeMet, 2002; Rebola et al., 2005). In fact, it has been demonstrated that in these areas, there is a functional interaction between DA D_2 and adenosine A_{2A} receptors (see **Figure 1**), which are co-localized on enkephalin-containing medium spiny neurons and converge onto the same signal transduction pathways in an antagonistic way (Ferré et al., 1997, 2008; Fuxe et al., 2003; Ferré, 2008; Beggiato et al., 2014). Similarly, A_1 and D_1 receptors antagonistically interact on substance P-containing medium spiny neurons (Ferré et al., 1997, 2008).

The behavioral significance of this interaction has frequently been studied in the context of neostriatal motor functions and pathologies (Ferré et al., 1997; Correa et al., 2004; Collins et al., 2010). Thus, selective A_{2A} receptor antagonists are being tested in clinical trials for pathologies involving DAergic dysfunctions such as Parkinson disease, and positive results indicate that they can be used as adjuvant therapies (Hung and Schwarzschild, 2014). Caffeine actions on A_1 and A_{2A} adenosine receptors (Ferré, 2008), has promoted its study as an alternative preventive or therapeutic tool for parkinsonian symptoms (Prediger, 2010). Moreover, within the last years, the motivational significance of DA-adenosine receptor interactions has become apparent with regard to processes such as behavioral activation, and effort-related decision-making impaired in depression or other pathologies (Salamone et al., 2006; Salamone and Correa, 2009).

In the present review, we focus on studies that assessed the effect of adenosine antagonists on different aspects of depression in humans, as well as in animal models. Special emphasis will be placed on motivational/psychomotor symptoms induced by DA depletions and studies related to DA-adenosine interactions in pathological symptoms related to effort-related decision-making.

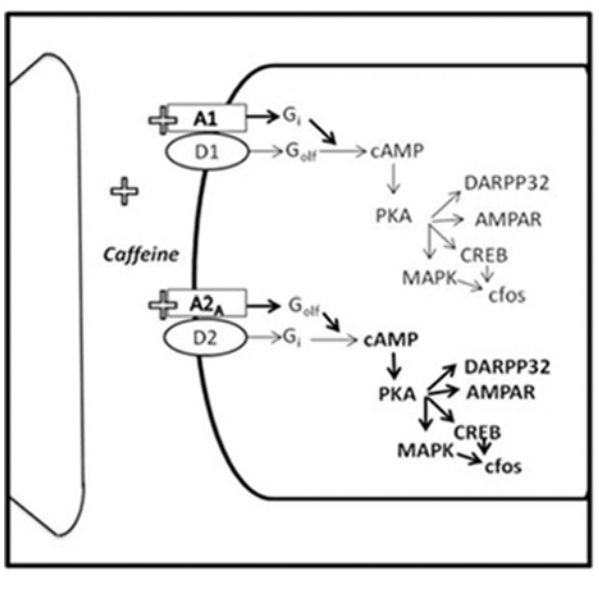

FIGURE 1 | Impact of caffeine on the functional interaction between adenosine and DA receptors. A_1R and $A_{2A}R$, adenosine A_1 and A_{2A} receptors; D_1, DA type 1 receptor; D_2, DA type 2 receptor (adapted from Ferré, 2008).

CAFFEINE CONSUMPTION AND DEPRESSION

Caffeine is a naturally occurring methylxanthine that acts mainly as a non-selective A_1 and A_{2A} adenosine receptor antagonist (Fredholm et al., 1999). This methylxanthine is found in common beverages including coffee, tea, soft drinks, and products containing cocoa, as well as a variety of medications and dietary sources (Barone and Roberts, 1996; Wikoff et al., 2017), ranking as one of the most commonly consumed dietary ingredients throughout the world (Heckman et al., 2010). Daily intake of caffeine among consumers in United States is about 280 mg, and higher intakes are estimated in some European countries (Barone and Roberts, 1996). Caffeine is typically consumed in order to increase alertness, arousal and energy (Malinauskas et al., 2007). Its consumption has been related to changes in cognitive performance and mood in normal population (Smith, 2013; Pasman et al., 2017). However, it enhances performance more in fatigued than well-rested subjects (Lorist et al., 1994; Childs and de Wit, 2008).

There are very few studies on the relation between caffeine consumption and depression-related symptoms, and in many cases, its use is related to self-medication patterns. Some of these studies focus on the role of caffeine as a drug that prevents depression, while others discuss caffeine as a possible treatment for existing depression. Thus, secondary analyses of large epidemiological databases with similar number of men and women indicate that in non-clinical samples that do not work, consumption of caffeine (around 150 mg/day as average) was associated with a reduced risk of depression (Smith, 2009). Also, in a longitudinal study in women free from depressive symptoms at baseline, high levels of caffeine consumption (>550 mg/day) was negatively correlated with the appearance of depressive symptoms (Lucas et al., 2011). In fact, the relative risk for depression was highest for those women with lower caffeine consumption (<100 mg/day) (Lucas et al., 2011). However, in women with multiple sclerosis high doses of caffeine (>400 mg/day) increased the prevalence of MDD (Patten et al., 2000). Moreover, in non-clinical samples, although caffeine consumption at moderate doses was related with decreases in suicide risk (Kawachi et al., 1996; Tanskanen et al., 2000; Lucas et al., 2014), excessive consumption (750 mg/day) was correlated with a higher risk of suicide (Kawachi et al., 1996; Tanskanen, 1997; Lucas et al., 2014). Thus, from the present studies, it seems that intermediate levels of caffeine consumption (300–550 mg/day) produce beneficial effects in non-clinical populations, but not in people with some neurological pathologies. Higher doses will have negative effects, even in non-clinical populations.

Multiple reports have lent support to the idea that depressed people could use caffeine as self-medication. It has been reported that psychiatric patients show a relatively high degree of caffeine consumption compared to the normal population (Greden et al., 1978; Leibenluft et al., 1993; Rihs et al., 1996). This appears to be particularly true in patients that have experienced depressive symptoms (Leibenluft et al., 1993). Different profiles of patients (i.e., with alcohol dependence, seasonal affective disorder, and people with MDD) have been shown to have higher levels of caffeine consumption after experiencing depressive symptoms (as shown by the Hamilton Rating Scale for depression) (Hamilton, 1967; Leibenluft et al., 1993). Specially, among youth with depression, there generally is higher caffeine consumption that in the general population (Whalen et al., 2008). Moreover, the degree of caffeine consumption seems to be a predictor of improvement of somatic symptoms (fatigue among them), and hostility in depressed patients medicated with fluoxetine (Worthington et al., 1996), suggesting that caffeine could be an effective co-treatment for some of the symptoms of depression. However, it is important to note that, at high doses or in people with susceptibility, caffeine is also known to increase anxiety and insomnia (for a review Temple et al., 2017), two side effects that can contribute to worsen MDD. At high doses, however, it has been demonstrated that caffeine may not act as an adenosine receptor antagonist, and other underlying mechanisms seem responsible of its negative effects (for a recent review Fredholm et al., 2017).

IMPACT OF CAFFEINE ON ENERGY/FATIGABILITY AND BEHAVIORAL ACTIVATION IN HUMANS

A wide range of studies demonstrate that caffeine can increase alertness and subjective energy, and also reduce fatigue (Johnson et al., 1990b, 1991; Yu et al., 1991; Smith et al., 1992, 1997; Lieberman, 2001), thus acting as an ergogenic substance. Caffeine has been demonstrated to increase feelings of efficiency, self-confidence, motivation to work (Fredholm et al., 1999), and to improve psychomotor performance (Rees et al., 1999). The behavioral effects of caffeine can be influenced by the baseline arousal levels and also by the nature of the task requirements. It has been argued that the most evident effects of caffeine on fatigue would be expected in situations of low arousal or high fatigue, or in tasks placing high demands on controlled processing (Bachrach, 1966; Lieberman et al., 1987). In fact, beneficial effects of caffeine have been observed in people in low states of alertness, such as after benzodiazepines administration (Johnson et al., 1990b), sleep loss (Childs and de Wit, 2008; Paech et al., 2016), when the person has a cold (Smith et al., 1997), or when the experiment is done in the early morning (Smith et al., 1992). In addition, a broad range of studies have reported effects of caffeine withdrawal on different markers of motivation using descriptors such as fatigue, decreased energy or vigor, lethargy, amotivation for work, etc. (for a review see Juliano and Griffiths, 2004). For example, in controlled studies, after 10 days of high levels of caffeine consumption (1,250 mg/day), withdrawal results in increased subjective ratings of headache, sleepiness, laziness, and fatigue, as well as decreased alertness, activation and vigor (Juliano et al., 2012). Abstinence from intermediate doses in daily coffee and cola consumers (579 mg/day), increased ratings of drowsy/sleepy, fatigue/tired, lazy/sluggy/slow-moving, decreased ratings of active/energetic/excited and motivation to work, and impaired performance on psychomotor tasks (Liguori and Hughes, 1997). Even at low quantities (100 mg/day, in a controlled study), caffeine withdrawal increased ratings of lethargy, fatigue, tiredness, and sluggishness, and decreased ratings of energy, motivation and urge to work (Griffiths et al., 1990).

EFFECT OF CAFFEINE AND ADENOSINE ANTAGONISTS ON CLASSIC ANIMAL MODELS OF DEPRESSION

Preclinical studies have been trying to elucidate the effect of caffeine and selective adenosine antagonists on classical animal models of depression (El Yacoubi et al., 2001). Two of the classic tests for the assessment of antidepressant properties of different substances in rodents are the forced swim test (FST) and the tail suspension test (TST). In the FST animals develop an immobile posture in an inescapable cylinder filled with water (Porsolt et al., 1977; Petit-Demouliere et al., 2005). The TST is based on the observation that a mouse suspended by the tail shows alternating periods of agitation and immobility (Steru et al., 1985). Classical antidepressants reduce immobility time in these paradigms, which have become the gold standard to evaluate antidepressant effects of multiple drugs or to show depressive symptoms induced by behavioral manipulations (Armario and Nadal, 2013). In this regard, learned helplessness has been considered as one of the causes for developing depression in vulnerable individuals that suffer stressful life events. This phenomenon is reproducible in animal models in which the depressive-like state is induced either by chronic uncontrollable and unpredictable stressors (CUS), typically electrical foot-shock (Overmier and Seligman, 1967), but also by chronic mild stress (CMS) induced by irregular exposure to a combination of different types of stressors over a period of weeks (Willner, 2005). In addition, animals that develop learned helplessness show a disruption in escape performance as well as decreases in weight gain, increased immobility in the FST or TST, and reduced locomotion, all symptoms associated to some degree with depression (Seligman, 1972). After the administration of substances with antidepressant properties, animals exposed to CUS or CMS display escape-directed behaviors, reducing time of immobility (Porsolt et al., 1977; Steru et al., 1985).

All these tests and manipulations have been used to study the therapeutic properties of caffeine and selective adenosine antagonists or genetic deletion of adenosine receptors in rodents. In one of the seminal papers, Porsolt et al. (1977) demonstrated that an acute dose of caffeine reduced immobility time in the FST in Sprague-Dawley rats. In later studies, this effect has been confirmed using other strains of rats and mice, after

acute or repeated administration of a broad range of doses (3.0–30.0 mg/kg) and using diverse animal tests (FST, TST) (Kulkarni and Mehta, 1985; Kaster et al., 2004, 2015; Robles-Molina et al., 2012; Kale and Addepalli, 2014; Minor and Hanff, 2015; Szopa et al., 2016). In accordance with the effects of caffeine, adenosine A_{2A} receptor antagonists have also been effective in these tests. Thus, SCH58261 and istradefylline (KW6002) reduced total immobility time in both the TST and the FST in mice (El Yacoubi et al., 2001). SCH58261 also reduced immobility time in a selectively bred 'helpless' mice strain in the TST (El Yacoubi et al., 2001). Moreover, A_{2A} receptor knockout (A_{2A}KO) mice showed reductions in immobility time compared to wild type (WT) animals in both tests (El Yacoubi et al., 2001).

Using the learned helplessness model for inducing depressive symptoms, it has been demonstrated that acute doses as well as chronic administration of caffeine can reduce the impact of CUS (Woodson et al., 1998; Hunter et al., 2003; Minor et al., 2008; Pechlivanova et al., 2012; Kaster et al., 2015). Thus, pharmacological or genetic blockade of A_{2A} receptors not only prevented but also reversed CUS-induced behavioral and physiological signs of depression such as decreased weight gain, increased corticosterone levels, escape behavior impairments in a shuttle box, increased immobility time in the FST and TST, increased anxiety, and decreased locomotion and spatial reference memory (Kaster et al., 2015). However, caffeine only reverted the deficits of reference memory but did not reverse mood-related alterations (Machado et al., 2017) in mice genetically selected to display 'depressive'-like symptoms (El Yacoubi et al., 2003). Consistent with these findings, mice that received the selective A_{2A} receptor antagonist istradefylline, as well as the constitutive A_{2A}KO mice, were protected from the CUS-induced behavioral impairments in the FST, TST, and memory tests (Kaster et al., 2004), suggesting a key role for A_{2A} receptors in acute and chronic stress-induced depressive effects.

Based on these results some researchers have focused on adenosine receptor antagonists, including caffeine, as tools to reverse behavioral impairments induced by pharmacological manipulations of the adenosine system (Kulkarni and Mehta, 1985; Minor et al., 1994a, 2008; Woodson et al., 1998; Hunter et al., 2003; Pechlivanova et al., 2012). Thus, high doses of acutely administered adenosine (50.0–100.0 mg/kg, intraperitoneally IP) (Kulkarni and Mehta, 1985), or its analoge 1-chloroadenosine (2.0 mg/kg, IP) induce immobility in the FST in mice, and caffeine as well as theophylline (8.0 mg/kg, IP), reversed this effect (Kulkarni and Mehta, 1985). Theophylline, is a psychoactive methylxanthine found in tea and other substances, and is also a metabolite of caffeine that acts as a non-selective adenosine antagonist for A_1/A_{2A} receptors as well (Gu et al., 1992). Increases of adenosine in the central nervous system have been also associated with escape deficits in the inescapable shock paradigm (Kulkarni and Mehta, 1985; Minor et al., 1994b; Woodson et al., 1998; Minor and Hanff, 2015). Thus, it has been demonstrated that intraventricular (ICV) administration of NBTI [S-(4-nitrobenzyl)-6-theoinosine], an equilibrative nucleoside transporter (ENT) blocker that increases extracellular adenosine levels blocking its reuptake (see **Figure 2**), impaired escape latency in rats (Jacobson et al., 1992; Noji et al., 2004) at the same level that rats preexposed to 100 inescapable tail shocks, and potentiates escape impairments produced by 50 inescapable tail shocks (Minor et al., 2008). Moreover, ICV administration of erytrho-9(2-hydroxy/3/nonyl adenine (ENHA), a selective adenosine deaminase (ADA) inhibitor which blocks adenosine metabolism, mimicked the effect of inescapable shock (Woodson et al., 1998). This manipulation increases the concentration of extracellular adenosine by blocking the major degradation pathway. Low doses of caffeine reversed escape deficits induced by EHNA (Woodson et al., 1998). The reversal effects of caffeine appear to be specific to actions on adenosine receptors, and not as a general stimulant psychomotor effect, since amphetamine exacerbated the behavioral impairments induced by inescapable shocks (Minor et al., 1994a). In addition, caffeine reversed the escape deficit produced by a bilateral injection of glutamate into the prefrontal cortex of rats (Hunter et al., 2003). This escape deficit induced by glutamate in the prefrontal cortex has been also associated with enhanced adenosine (Petty et al., 1985), since increases in glutamate are counterbalanced by an increase in adenosine production and release (Deckert and Gleiter, 1994; Kerkhofs et al., 2018).

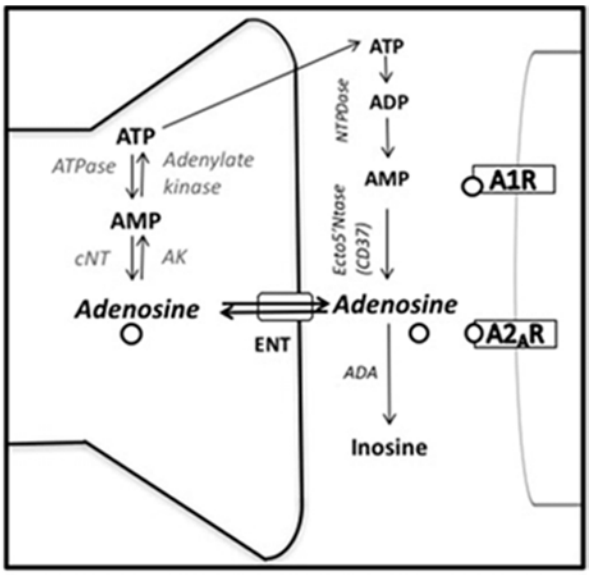

FIGURE 2 | Adenosine synthesis and metabolism. ADA, adenosine deaminase; AK, adenosine kinase; A_1R and A_{2A}R, adenosine A_1 and A_{2A} receptors; cNT, cytosolic endo-nucleotidase; ENT, equilibrative nucleoside transporter; Ecto5′Ntase (CD73), 5′-ectonucleotidase; NTPDase, nucleoside triphosphate dephosphorylase (adapted from Ruby et al., 2011).

Caffeine has also been used to enhance the effect of monoaminergic antidepressants (especially 5-HT/NE uptake inhibitors) that are being used in clinical practice, and have been demonstrated to reduce immobility in classical animal tests of depression. Thus, caffeine at low doses that do not have an effect on their own can potentiate the effects of desipramine, imipramine, duloxetine, fluoxetine and paroxetine, in animals tested on the FST (Robles-Molina et al., 2012; Kale and Addepalli, 2014; Szopa et al., 2016). In addition, a low dose of caffeine

can also improve the effect of bupropion (a DA/NE uptake inhibitor), potentiating extracellular levels of DA and NE (Kale and Addepalli, 2014).

IMPACT OF ADENOSINE ANTAGONISTS ON BEHAVIORAL ACTIVATION: PRECLINICAL STUDIES

Tasks measuring behavioral activation and effort-based functions have been suggested as potential animal models for the motivational symptoms of depression (Salamone, 2007; Markou et al., 2013; Salamone et al., 2016). Thus in the animal literature, as in the human data, there are studies showing how caffeine and selective adenosine antagonists affect the willingness to work depending on the demands of the task. In operant tasks with different work demands, caffeine and theophylline produced rate-dependent effects on lever pressing to obtain palatable food in rats (Randall et al., 2011). Moderate doses of caffeine and theophylline (5.0–20.0 mg/kg) increased responding on the low task with low response demands; a fixed interval 240 s (FI-240 s) schedule. However, higher doses (10–40 mg/kg) decreased responding on a fixed ratio 20 (FR20), schedule that typically generates high rates of responding (Randall et al., 2011). A_{2A} receptor antagonists increased lever pressing in the low effort-demanding task (FI-240 s) but did not suppress the high effort task (FR20) in the dose range tested. In fact, there was a tendency for istradefylline to increase FR20 responding at a moderate dose. A_1 antagonists failed to increase lever-pressing rate, but decreased FR20 responding at higher doses. These results suggest that the work potentiating effects of methylxanthines are mediated by their actions on adenosine A_{2A} receptors, while their A_1 receptor antagonistic action could be mediating the suppressant effects.

Progressive ratio (PR) schedules, which require gradually increasing work output, have been also employed to explore the effect of caffeine on motivation to work for sucrose or food in rats and monkeys (Buffalo et al., 1993; Brianna Sheppard et al., 2012; Retzbach et al., 2014). Acutely and chronically moderate doses of caffeine (5–25 mg/kg) elevated PR lever pressing for sucrose (Brianna Sheppard et al., 2012; Retzbach et al., 2014). Caffeine had no effect on inactive lever presses suggesting that this increase was not due to an increase in general motor activity (Retzbach et al., 2014). Recently, our laboratory has demonstrated that caffeine has differential effects on PR performance depending on baseline individual differences (SanMiguel et al., 2018). Caffeine (5.0–10.0 mg/kg) increased responding for a solution containing sucrose in low baseline responders, but decreased lever pressing (10.0–20.0 mg/kg) in high responders (SanMiguel et al., 2018). However, in rhesus monkeys intravenous (IV) caffeine (10.0 mg/kg) decreased percent of task completed, and breakpoint in a PR for palatable food (Buffalo et al., 1993), possibly because this dose directly administered in the blood stream resulted in higher levels in the brain.

Thus, from studies in rats and monkeys it seems that high doses of caffeine have an impairing effect on performance in tasks that evaluate willingness to work for a reinforcer if performance is already high. Methylxanthines can help to increase work output when the requirement of the task is low. However, selective A_{2A} receptor antagonists seem to be beneficial independently of the baseline performance, as demonstrated also in goals directed tasks (Li et al., 2016).

EFFORT BASED DECISION-MAKING DEFICITS INDUCED BY INTERFERENCE WITH DA FUNCTION: POTENTIAL THERAPEUTIC ROLE OF ADENOSINE ANTAGONISTS

Activational aspects of motivation (i.e., vigor, persistence, work output) are highly adaptative because they enable organisms to overcome obstacles or work-related response costs that separate them from significant stimuli (Salamone and Correa, 2002, 2012; van den Bos et al., 2006). An important feature of adaptive behavior, in the face of work-related challenges, is effort-related decision making. Regularly, organisms must make cost/benefit analyses in which they weigh the value of a stimulus relative to the cost of obtaining it (Salamone et al., 2007, 2016). People with MDD show impairments in estimation, anticipation, and recall of reinforcing stimuli (Pizzagalli, 2014), and also show a reduced likelihood of selecting high effort activities in human tasks of effort-related decision making (Treadway et al., 2012; Yang et al., 2014).

Extensive animal data have demonstrated that Acb DA is a key mediator of effort-based decision-making processes (for a review see Salamone et al., 2016). Interference with DA transmission biases behavior toward less valued rewards that involve less effort and less activity. In these preclinical studies addressing the effort-related decision-making process, animals are given a choice between a more valued reinforcer that can only be obtained by engaging in a more demanding (higher effort) activity vs. a low effort/low value option. One such procedure is a T-maze task that provides an effort-related challenge by having a vertical barrier in the arm with the higher reward density (HD) vs. an arm that contains a lower density of reward (LD) and has no barrier (Salamone et al., 1994; Cousins and Salamone, 1996; Cousins et al., 1996; Mott et al., 2009; Pardo et al., 2012). In this procedure, rodents choose to climb the barrier to get more reward in 90% of the trials, once they have been trained (Cousins and Salamone, 1996; Pardo et al., 2012). In operant tasks animals are given a choice between lever pressing for the more preferred reward (in FR5 or PR schedules) vs. approaching and consuming a less preferred reinforcer that is concurrently freely available in the chamber (Salamone et al., 1991; Randall et al., 2012; Pardo et al., 2015). When tested on the concurrent FR5/free reward choice task, rats typically spend most time pressing the lever for the preferred reward and less consuming freely available food or fluids (Salamone et al., 1991; Pardo et al., 2015). In contrast, rats tested on the PR/chow choice task show more individual variability, and tend to disengage more readily from the PR lever pressing component because of the increasing work requirement (Randall et al., 2012, 2014). Research with these concurrent

choice tasks has shown that interference with DA transmission via DA depletions or DA receptor antagonism typically biases rodents toward the low effort-low reward option (Salamone et al., 1991; Salamone and Correa, 2009; Worden et al., 2009; Pardo et al., 2012; Randall et al., 2012, 2014; Yohn et al., 2015).

Using these effort related choice procedures, it has been demonstrated that the catecholamine depleting agent and vesicular transport inhibitor (VMAT-2) tetrabenazine (TBZ), reduces selection of high effort alternatives, but animals compensate by increasing the amount of free less preferred reinforcer consumed (Nunes et al., 2013; Randall et al., 2014; Pardo et al., 2015; Yohn et al., 2015, 2017). TBZ depletes monoamines, with its greatest impact being upon striatal DA (Pettibone et al., 1984; Tanra et al., 1995; Nunes et al., 2013). TBZ is used as a therapeutic drug to treat Huntington's disease patients, and it induces symptoms of depression in humans, including fatigue (Frank, 2010; Guay, 2010; Rodrigues et al., 2017). TBZ has also been used in the FST and TST rodent models of depression (Kent et al., 1986; Wang et al., 2010). Although the effort-related effects of TBZ are attenuated by the DA uptake blocker bupropion (Nunes et al., 2013; Randall et al., 2014; Yohn et al., 2015) which is been used as an antidepressant, other classical drugs for the treatment of depression such as the 5-HT uptake inhibitors fluoxetine and citalopram, and the NE uptake inhibitor desipramine, failed to reverse the effects of TBZ, and higher doses even led to further behavioral impairments (Yohn et al., 2015, 2016b,c).

In addition to DA, adenosine also is involved in these effort related decision-making processes (Farrar et al., 2007, 2010; Hauber and Sommer, 2009; Mott et al., 2009; Salamone and Correa, 2009). Microinjections of adenosine A_{2A} receptor agonists into the Acb produced effects on instrumental behavior and effort-related choice that resembled those produced by Acb DA receptor antagonism or depletion (Font et al., 2008; Mingote et al., 2008). In addition, considerable evidence indicates that DA D_2 and adenosine A_{2A} receptors interact to regulate effort-related functions (Salamone and Correa, 2009, 2012). Thus, adenosine A_{2A} receptor antagonists were able to reverse the shift in choice toward a low effort alternative induced by administration of the D_2 antagonists haloperidol and eticlopride (Farrar et al., 2007, 2010; Mott et al., 2009; Salamone et al., 2009; Worden et al., 2009; Pardo et al., 2012, 2013). Moreover, A_{2A} KO mice were resistant to the effects of haloperidol on performance of the T-maze barrier task (Pardo et al., 2012). Recently, it has been demonstrated that A_{2A} KO mice are also resistant to the anergia inducing effects of D_2 antagonism in a paradigm in which animals can choose between exercising on a much preferred running wheel or sedentary consuming sweet food (Correa et al., 2016). In contrast, adenosine A_1 antagonists were ineffective at reversing the effort-related effects of either the D_1 receptor antagonist ecopipam or the D_2 receptor antagonist eticlopride (Salamone and Correa, 2009; Nunes et al., 2010; Pardo et al., 2012).

The therapeutic effect of caffeine and theophylline on effort-related choice behavior after the administration of D_2 antagonists has also been reported in rats tested on the concurrent FR5/chow feeding choice task. Caffeine partially attenuated the effects of haloperidol, increasing the lever pressing and decreasing the free chow intake in haloperidol-treated rats (Salamone et al., 2009) and the same pattern of results were observed in a more recent study in which caffeine reversed the anergia-like effect induced by TBZ in an adapted version of the T-maze task with RW (Correa et al., 2016) increasing the time running (effortful option) and decreasing the time spent eating free available sweet pellets (sedentary option) (López-Cruz et al., 2018). This behavioral effect was supported by changes in an intracellular marker of DA neurotransmission [phosphorylated form of DARPP-32; pDARPP-32(Thr34)] in the striatum (López-Cruz et al., 2018). Similarly, theophylline reversed the effects induced by this D_2 antagonist in mice tested in the T-maze barrier task (Pardo et al., 2012). Furthermore, several papers have reported that the adenosine A_{2A} receptor antagonist MSX-3 can reverse the effort-related effects of TBZ across multiple tasks (Nunes et al., 2013; Randall et al., 2014; Yohn et al., 2015). All these findings suggest that the reversal effects induced by methylxanthines on anergia induced by DA D_1 and D_2 receptor antagonism could be mediated mainly by A_{2A} receptors.

Mental fatigue associated with high attentional demands can also be overcome by the use of psychostimulants such as amphetamine or caffeine (Silber et al., 2006; Peeling and Dawson, 2007). For instance, caffeine restores memory performance in sleep-deprived or aged humans, a finding replicated in rodent animal models (Cunha and Agostinho, 2010). In cost/benefit decision-making tasks involving the evaluation of the costs related to high attention-demands, rats can choose between engaging in hard trials (difficult visuospatial discrimination) leading to more reward versus easy trials leading to less reward (Cocker et al., 2012). Under basal conditions, animals chose high effort/high reward trials more than low-effort/low reward trials. However, there are substantial baseline differences. Amphetamine increases the selection of high effort/high reward trials in animals that usually do not choose this option, but it decreases the selection of the high cognitive demand trials in animals that usually choose them. A high dose of caffeine decreased choice of high effort/high reward trials in animals that usually choose them as did amphetamine, but it did not increase the selection in the ones that usually did not choose them (Cocker et al., 2012).

A_{2A} RECEPTOR ANTAGONISTS HAVE THERAPEUTIC ACTIONS ON CYTOKINE-INDUCED FATIGUE

Cytokines are signaling molecules for the immune system mediating physiological responses to infection (Dantzer, 2001). These molecules also mediate a set of behavioral signs that include depressed activity and loss of interest or motivation (Kent et al., 1992). Compared to the general population, depressed patients have elevated levels of proinflammatory cytokines such as tumor necrosis factor alpha (TN-alpha) interleukin-1β (IL-1β), and IL-6 (Dowlati et al., 2010; Hiles et al., 2012). Fatigue, loss of energy and psychomotor slowing are reported to occurred in patients receiving treatment with IFN-α or with high levels of IL-6 (Miller et al., 2009; Goldsmith et al., 2016b). Moreover,

many inflammatory stimuli have been found to target reductions in ventral striatal neural function, and decreased synthesis of striatal DA, which is possibly related to symptoms of reduced motivation and motor retardation (Felger and Treadway, 2017). Studies with IL-6 indicate that this cytokine is responsive to stress, and is implicated in the production of depression-like effects in mice, including actions on traditional tests such as the FST, TST, and social interaction tests (Sukoff Rizzo et al., 2012). In anergia related studies, IL-6 and IL-1β reduced the tendency to work for food when an alternative food source (concurrently available chow) could be obtained through minimal effort (Nunes et al., 2014; Yohn et al., 2016a).

Brain cytokine signaling involves adenosine signaling at adenosine A_{2A} receptors (Hanff et al., 2010). These receptors regulate IL-1β and LPS linked to pathological behavioral and physiological responses such as anxiety (Chiu et al., 2014) or neuroinflammation (Brothers et al., 2010; Simões et al., 2012). Adenosine A_{2A} receptor signaling provides inhibitory feedback on proinflammatory cytokine signaling in peripheral immune cells (Sitkovsky and Ohta, 2005). Thus, the effects of IL-6 and IL-1β were attenuated through co-administration of the adenosine A_{2A} receptor antagonist MSX-3, as well as the major stimulant methylphenidate, which blocks catecholamine uptake (Nunes et al., 2014; Yohn et al., 2016c). Though previous work has shown that MSX-3 had no effect of FR5/chow-feeding choice performance when administered on its own (Farrar et al., 2007), MSX-3 produced a very robust reversal of the behavioral effects of IL-6 and IL-1β, restoring the baseline behavioral pattern of responding (i.e., increasing lever pressing and decreasing chow consumption) to a normal level (Nunes et al., 2014; Yohn et al., 2016c). These results highlight the therapeutic potential of adenosine A_{2A} receptor antagonism for pathologies related to neuroinflammation (Simões et al., 2012; Cunha, 2016).

ANERGIA AND FATIGUE INFLUENCE DECISION-MAKING IN HUMANS WITH DEPRESSION

Translational studies in humans have implemented tasks that evaluate the decision-making process in normal as well as psychiatric patients. The effort expenditure for rewards task (EEfRT; Treadway et al., 2009), is based on the operant lever pressing choice tasks described above (Salamone et al., 1991). In the human version of this task, subjects choose on each trial between a high cost/high reward option (HC/HR) and low cost/low reward option (LC/LR) to obtain different monetary rewards. The HC/HR trials required 100 button presses with the non-dominant pinky finger within 21 s, and subjects were eligible to win higher amounts that varied per trial between $1.24–4.30. In contrast, the LC/LR option only required 30 button presses with the dominant index finger during 7 s, and subjects could win $1.00 for each successfully completed trial.

Patients with MDD were significantly less likely to make HC/HR choices relative to controls, and this result was not related with depression-related differences in psychomotor speed (Treadway et al., 2012). The effect of caffeine on this task in depressed patients has not been explored, but it was assessed in normal subjects. Thus, in the normal population, caffeine (200 mg), significantly increased the speed of responses compared to placebo (Wardle et al., 2012). However, caffeine did not have an effect on percentage of HC/HR choices (Wardle et al., 2012). In fact, it decreased effortful choices in high cardiovascular responders (subjects with high arterial pressure in response to caffeine) (Wardle et al., 2012). These results contrast with studies showing that, during exercise, caffeine decreases the perception of effort in humans (Doherty and Smith, 2005), improving performance particularly for endurance testing (Doherty and Smith, 2004). Thus, caffeine may only improve performance in highly demanding situations.

CONCLUSION AND FURTHER DIRECTIONS

Although many available treatments for MDD provide relief for individuals with depressed mood, no single therapeutic modality provides a full and permanent recovery across all the symptoms of MDD in the majority of patients (McClintock et al., 2011). Clinicians have come to emphasize the importance of taking into account effort-related motivational symptoms in depression (Tylee et al., 1999; Stahl, 2002; Demyttenaere et al., 2005; Salamone et al., 2016). Decreased psychomotor speed, referred to clinically as psychomotor retardation, fatigue and anergia are cardinal symptoms of MDD that have been associated with poor antidepressant treatment response (Goldsmith et al., 2016a). Even among patients in remission, anergia and psychomotor retardation are pervasive symptoms (Gorwood et al., 2014). Thus, novel pharmacological targets are being investigated in clinical and preclinical studies.

There are promising results shown in epidemiological studies as well as in animal models, about the impact of caffeine and selective adenosine receptor antagonists on these symptoms. Is worth noting that the epidemiological studies have revealed a relation between caffeine consumption and decreased risk for developing depression (Lucas et al., 2011), and some reports demonstrate the use of caffeine as a self-medication among depressed patients (Leibenluft et al., 1993). However, it seems clear that more controlled studies are needed to explore the effect of caffeine across a wide variety of depressive symptoms, and it seems necessary to test more selective drugs for A_{2A} receptors.

Systematic studies of the effects of methylxanthines on animal models of depression and anergia have shown efficacy at improving parameters related with initiation and maintenance of behavior in order to escape an aversive situation, but also in order to pursue valued reinforcers and achieve goals (Kulkarni and Mehta, 1985; Woodson et al., 1998; Hunter et al., 2003; Minor et al., 2008; Randall et al., 2011; Pechlivanova et al., 2012). As with the human data, these therapeutic actions depend upon the dose administered, since high doses of caffeine and theophylline not only do not improve depressive symptoms, but can in fact promote anxiety (Correa and Font, 2008; López-Cruz et al., 2014). Moreover, it is important to take into consideration that the use of high doses of caffeine and other methylxanthiness,

specially, among the elder, could also have severe side effects such as tachycardia, gastric discomfort, or insomnia (Frozi et al., 2018). All these side effects could in fact worse the symptoms of MDD. Both in humans and in animal studies, the therapeutic actions of methylxanthines also seem to be dependent on the basal estate; for instance they seem to be effective when subjects are in a state or fatigue, tiredness or sleepiness (Johnson et al., 1990a; Smith et al., 1992; Childs and de Wit, 2008), or when the DArgic system is compromised. Such effects are less evident when humans and rodents are under "normal" conditions.

Several A_{2A} selective receptor antagonists have also shown to reverse motivational impairments induced by DA antagonism or depletion in animal models of anergia (Farrar et al., 2007; Mott et al., 2009; Salamone et al., 2009; Pardo et al., 2012; Correa et al., 2016). Furthermore, a recent report indicates that istradefylline can improve fatigue-related symptoms in Parkinson's disease patients (Abe et al., 2016; Sako et al., 2017). Adenosine A_{2A} receptors might be involved in these processes through their interaction with DA D_2 receptors in the Acb, region highly involved in the activational component of motivation (for a review see Salamone and Correa, 2012).

Consistent with these findings, it has been demonstrated that the rank order of clinical effectiveness in depressed patients with psychomotor retardation, paralleled the specificity of antidepressants as DA-mimetic agents (Rampello et al., 1991). Antidepressants such as bupropion have demonstrated to have therapeutical effects on motivational symptoms in humans (Pae et al., 2007) and in animal models or anergia (Nunes et al., 2013; Randall et al., 2014; Yohn et al., 2015). In animal studies, caffeine was shown to improve the effects of antidepressants such as bupropion, duloxetine, and desipramine (Robles-Molina et al., 2012; Kale and Addepalli, 2014; Kale and Addepalli, 2015; Szopa et al., 2016). These studies have led to the suggestion that caffeine could be used as an enhancer of antidepressant pharmacotherapy (for a review see Kale et al., 2010), a suggestion that is consistent with the clinical trials for antiparkinsonian effects showing that A_{2A} receptor antagonists can be a good adjuvant in the treatment of motor symptoms (Hung and Schwarzschild, 2014).

However, determination of the predominant symptomatology is key to therapeutic success. Recent neuroimage data from patients with depression indicate that they can be clustered based on four different connectivity profiles ('biotypes') that are associated with differences in clinical symptoms (Drysdale et al., 2017). Thus, reduced connectivity in anterior cingulate and orbitofrontal areas supporting motivation was most severe in biotypes 1 and 2, which were characterized partly by increased anergia and fatigue (Drysdale et al., 2017). This type of objective diagnostic can help to identify different type of patients that could benefit from different type of antidepressant therapies. For instance, in patients affected by anxious depression a selective inhibitor of 5-HT reuptake appears to be more effective than a selective inhibitor of DA reuptake (Rampello et al., 1995), and caffeine in those type of depressed patients may worsen the anxiety symptomatology. However, adenosine A_{2A} receptor antagonism may offer an alternative therapeutic strategy for treating effort-related motivational dysfunctions in humans, probably with lower abuse liability and fewer major stimulant motor effects compared to DA uptake inhibitors.

AUTHOR CONTRIBUTIONS

All authors listed have made a substantial, direct and intellectual contribution to the work, and approved it for publication.

FUNDING

This research was supported by a grant from MEC (PSI2015-68497-R), ME- FPU (AP2010-3793) Spain, and from NIH/NIMH (R03MH094966-01A1), United States.

REFERENCES

Abe, K., Fujita, M., and Yoshikawa, H. (2016). Effectiveness of istradefylline for fatigue and quality of life in Parkinson's disease patients' and of their caregivers. *APD* 5, 24–28. doi: 10.4236/apd.2016.52004

American Psychiatric Association (2013). *Diagnostic and Statistical Manual of Mental Disorders*, 5th Edn. Washington, DC: American Psychiatric Association. doi: 10.1176/appi.books.9780890425596

Argyropoulos, S. V., and Nutt, D. J. (2013). Anhedonia revisited: is there a role for dopamine-targeting drugs for depression? *J. Psychopharmacol.* 27, 869–877. doi: 10.1177/0269881113494104

Armario, A., and Nadal, R. (2013). Individual differences and the characterization of animal models of psychopathology: a strong challenge and a good opportunity. *Front. Pharmacol.* 4:137. doi: 10.3389/fphar.2013.00137

Bachrach, H. (1966). Note on the psychological effects of caffeine. *Psychol. Rep.* 18:86. doi: 10.2466/pr0.1966.18.1.86

Barone, J. J., and Roberts, H. R. (1996). Caffeine consumption. *Food Chem. Toxicol.* 34, 119–129. doi: 10.1016/0278-6915(95)00093-3

Beggiato, S., Antonelli, T., Tomasini, M. C., Borelli, A. C., Agnati, L. F., Tanganelli, S., et al. (2014). Adenosine A2A-D2 receptor-receptor interactions in putative heteromers in the regulation of the striato-pallidal gaba pathway: possible relevance for Parkinson's disease and its treatment. *Curr. Protein Pept. Sci.* 15, 673–680. doi: 10.2174/1389203715666140901103205

Bell, D. S., Shipman, W. M., Cleves, M. A., and Siegelman, J. (2013). Which drug for which patient? Is there a fluoxetine responding versus a bupropion responding personality profile? *Clin. Pract. Epidemiol. Ment. Health* 9, 142–147. doi: 10.2174/1745017901309010142

Brianna Sheppard, A., Gross, S. C., Pavelka, S. A., Hall, M. J., and Palmatier, M. I. (2012). Caffeine increases the motivation to obtain non-drug reinforcers in rats. *Drug Alcohol Depend.* 124, 216–222. doi: 10.1016/j.drugalcdep.2012.01.008

Brothers, H. M., Marchalant, Y., and Wenk, G. L. (2010). Caffeine attenuates lipopolysaccharide-induced neuroinflammation. *Neurosci. Lett.* 480, 97–100. doi: 10.1016/j.neulet.2010.06.013

Buffalo, E. A., Gillam, M. P., Allen, R. R., and Paule, M. G. (1993). Acute effects of caffeine on several operant behaviors in rhesus monkeys. *Pharmacol. Biochem. Behav.* 46, 733–737. doi: 10.1016/0091-3057(93)90570-J

Calugi, S., Cassano, G. B., Litta, A., Rucci, P., Benvenuti, A., Miniati, M., et al. (2011). Does psychomotor retardation define a clinically relevant phenotype of unipolar depression? *J. Affect. Disord.* 129, 296–300. doi: 10.1016/j.jad.2010.08.004

Childs, E., and de Wit, H. (2008). Enhanced mood and psychomotor performance by a caffeine-containing energy capsule in fatigued individuals. *Exp. Clin. Psychopharmacol.* 16, 13–21. doi: 10.1037/1064-1297.16.1.13

Chiu, G. S., Darmody, P. T., Walsh, J. P., Moon, M. L., Kwakwa, K. A., Bray, J. K., et al. (2014). Adenosine through the A_{2A} adenosine receptor increases

IL-1β in the brain contributing to anxiety. *Brain Behav. Immun.* 41, 218–231. doi: 10.1016/j.bbi.2014.05.018

Cocker, P. J., Hosking, J. G., Benoit, J., and Winstanley, C. A. (2012). Sensitivity to cognitive effort mediates psychostimulant effects on a novel rodent cost/benefit decision-making task. *Neuropsychopharmacology* 37, 1825–1837. doi: 10.1038/npp.2012.30

Collins, L. E., Galtieri, D. J., Collins, P., Jones, S. K., Port, R. G., Paul, N. E., et al. (2010). Interactions between adenosine and dopamine receptor antagonists with different selectivity profiles: effects on locomotor activity. *Behav. Brain Res.* 211, 148–155. doi: 10.1016/j.bbr.2010.03.003

Correa, M., and Font, L. (2008). Is there a major role for adenosine A_{2A} receptors in anxiety? *Front. Biosci.* 13, 4058–4070.

Correa, M., Pardo, M., Bayarri, P., López-Cruz, L., San Miguel, N., Valverde, O., et al. (2016). Choosing voluntary exercise over sucrose consumption depends upon dopamine transmission: effects of haloperidol in wild type and adenosine A2AKO mice. *Psychopharmacology* 233, 393–404. doi: 10.1007/s00213-015-4127-3

Correa, M., Wisniecki, A., Betz, A., Dobson, D. R., O'Neill, M. F., O'Neill, M. J., et al. (2004). The adenosine A_{2A} antagonist KF17837 reverses the locomotor suppression and tremulous jaw movements induced by haloperidol in rats: possible relevance to parkinsonism. *Behav. Brain Res.* 148, 47–54. doi: 10.1016/S0166-4328(03)00178-5

Cousins, M. S., Atherton, A., Turner, L., and Salamone, J. D. (1996). Nucleus accumbens dopamine depletions alter relative response allocation in a T-maze cost/benefit task. *Behav. Brain Res.* 74, 189–197. doi: 10.1016/0166-4328(95)00151-4

Cousins, M. S., and Salamone, J. D. (1996). Skilled motor deficits in rats induced by ventrolateral striatal dopamine depletions: behavioral and pharmacological characterization. *Brain Res.* 732, 186–194. doi: 10.1016/0006-8993(96)00519-7

Crown, W. H., Finkelstein, S., Berndt, E. R., Ling, D., Poret, A. W., Rush, A. J., et al. (2002). The impact of treatment-resistant depression on health care utilization and costs. *J. Clin. Psychiatry* 63, 963–971. doi: 10.4088/JCP.v63n1102

Cunha, R. A. (2001). Adenosine as a neuromodulator and as a homeostatic regulator in the nervous system: different roles, different sources and different receptors. *Neurochem. Int.* 38, 107–125. doi: 10.1016/S0197-0186(00)00034-6

Cunha, R. A. (2016). How does adenosine control neuronal dysfunction and neurodegeneration? *J. Neurochem.* 139, 1019–1055. doi: 10.1111/jnc.13724

Cunha, R. A., and Agostinho, P. M. (2010). Chronic caffeine consumption prevents memory disturbance in different animal models of memory decline. *J. Alzheimers Dis.* 20(Suppl. 1), S95–S116. doi: 10.3233/JAD-2010-1408

Cunha, R. A., Johansson, B., van der Ploeg, I., Sebastião, A. M., Ribeiro, J. A., and Fredholm, B. B. (1994). Evidence for functionally important adenosine A_{2a} receptors in the rat hippocampus. *Brain Res.* 649, 208–216. doi: 10.1016/0006-8993(94)91066-9

Dantzer, R. (2001). Cytokine-induced sickness behavior: mechanisms and implications. *Ann. N. Y. Acad. Sci.* 933, 222–234. doi: 10.1111/j.1749-6632.2001.tb05827.x

Deckert, J., and Gleiter, C. H. (1994). Adenosine–an endogenous neuroprotective metabolite and neuromodulator. *J. Neural Transm. Suppl.* 43, 23–31.

DeMet, E. M., and Chicz-DeMet, A. (2002). Localization of adenosine A_{2A}-receptors in rat brain with [3H]ZM-241385. *Naunyn Schmiedebergs Arch. Pharmacol.* 366, 478–481. doi: 10.1007/s00210-002-0613-3

Demyttenaere, K., De Fruyt, J., and Stahl, S. M. (2005). The many faces of fatigue in major depressive disorder. *Int. J. Neuropsychopharmacol.* 8, 93–105. doi: 10.1017/S1461145704004729

Doherty, M., and Smith, P. M. (2004). Effects of caffeine ingestion on exercise testing: a meta-analysis. *Int. J. Sport Nutr. Exerc. Metab.* 14, 626–646. doi: 10.1123/ijsnem.14.6.626

Doherty, M., and Smith, P. M. (2005). Effects of caffeine ingestion on rating of perceived exertion during and after exercise: a meta-analysis. *Scand. J. Med. Sci. Sports* 15, 69–78. doi: 10.1111/j.1600-0838.2005.00445.x

Dowlati, Y., Herrmann, N., Swardfager, W., Liu, H., Sham, L., Reim, E. K., et al. (2010). A meta-analysis of cytokines in major depression. *Biol. Psychiatry* 67, 446–457. doi: 10.1016/j.biopsych.2009.09.033

Drysdale, A. T., Grosenick, L., Downar, J., Dunlop, K., Mansouri, F., Meng, Y., et al. (2017). Resting-state connectivity biomarkers define neurophysiological subtypes of depression. *Nat. Med.* 23, 28–38. doi: 10.1038/nm.4246

El Yacoubi, M., Bouali, S., Popa, D., Naudon, L., Leroux-Nicollet, I., Hamon, M., et al. (2003). Behavioral, neurochemical, and electrophysiological characterization of a genetic mouse model of depression. *Proc. Natl. Acad. Sci. U.S.A.* 100, 6227–6232. doi: 10.1073/pnas.1034823100

El Yacoubi, M., Ledent, C., Parmentier, M., Bertorelli, R., Ongini, E., Costentin, J., et al. (2001). Adenosine A_{2A} receptor antagonists are potential antidepressants: evidence based on pharmacology and A_{2A} receptor knockout mice. *Br. J. Pharmacol.* 134, 68–77. doi: 10.1038/sj.bjp.0704240

Farrar, A. M., Pereira, M., Velasco, F., Hockemeyer, J., Müller, C. E., and Salamone, J. D. (2007). Adenosine A_{2A} receptor antagonism reverses the effects of dopamine receptor antagonism on instrumental output and effort-related choice in the rat: implications for studies of psychomotor slowing. *Psychopharmacology* 191, 579–586. doi: 10.1007/s00213-006-0554-5

Farrar, A. M., Segovia, K. N., Randall, P. A., Nunes, E. J., Collins, L. E., Stopper, C. M., et al. (2010). Nucleus accumbens and effort-related functions: behavioral and neural markers of the interactions between adenosine A_{2A} and dopamine D_2 receptors. *Neuroscience* 166, 1056–1067. doi: 10.1016/j.neuroscience.2009.12.056

Fava, M., Ball, S., Nelson, J. C., Sparks, J., Konechnik, T., Classi, P., et al. (2014). Clinical relevance of fatigue as a residual symptom in major depressive disorder. *Depress. Anxiety* 31, 250–257. doi: 10.1002/da.22199

Feighner, J. P. (1999). Mechanism of action of antidepressant medications. *J. Clin. Psychiatry* 60(Suppl. 4), 4–11; discussion 12.

Felger, J. C., and Treadway, M. T. (2017). Inflammation effects on motivation and motor activity: role of dopamine. *Neuropsychopharmacology* 42, 216–241. doi: 10.1038/npp.2016.143

Ferré, S. (2008). An update on the mechanisms of the psychostimulant effects of caffeine. *J. Neurochem.* 105, 1067–1079. doi: 10.1111/j.1471-4159.2007.05196.x

Ferré, S., Fredholm, B. B., Morelli, M., Popoli, P., and Fuxe, K. (1997). Adenosine-dopamine receptor-receptor interactions as an integrative mechanism in the basal ganglia. *Trends Neurosci.* 20, 482–487. doi: 10.1016/S0166-2236(97)01096-5

Ferré, S., Quiroz, C., Woods, A. S., Cunha, R., Popoli, P., Ciruela, F., et al. (2008). An update on adenosine A_{2A}-dopamine D_2 receptor interactions: implications for the function of G protein-coupled receptors. *Curr. Pharm. Des.* 14, 1468–1474. doi: 10.2174/138161208784480108

Font, L., Mingote, S., Farrar, A. M., Pereira, M., Worden, L., Stopper, C., et al. (2008). Intra-accumbens injections of the adenosine A_{2A} agonist CGS 21680 affect effort-related choice behavior in rats. *Psychopharmacology* 199, 515–526. doi: 10.1007/s00213-008-1174-z

Frank, E., Cassano, G. B., Rucci, P., Thompson, W. K., Kraemer, H. C., Fagiolini, A., et al. (2011). Predictors and moderators of time to remission of major depression with interpersonal psychotherapy and SSRI pharmacotherapy. *Psychol. Med.* 41, 151–162. doi: 10.1017/S0033291710000553

Frank, S. (2010). Tetrabenazine: the first approved drug for the treatment of chorea in US patients with Huntington disease. *Neuropsychiatr. Dis. Treat.* 6, 657–665. doi: 10.2147/NDT.S6430

Fredholm, B. B., Bättig, K., Holmén, J., Nehlig, A., and Zvartau, E. E. (1999). Actions of caffeine in the brain with special reference to factors that contribute to its widespread use. *Pharmacol. Rev.* 51, 83–133.

Fredholm, B. B., Jzerman, A. P., Jacobson, K. A., Linden, J., and Müller, C. E. (2011). International union of basic and clinical pharmacology. LXXXI. Nomenclature and classification of adenosine receptors–an update. *Pharmacol. Rev.* 63, 1–34. doi: 10.1124/pr.110.003285

Fredholm, B. B., Yang, J., and Wang, Y. (2017). Low, but not high, dose caffeine is a readily available probe for adenosine actions. *Mol. Aspects Med.* 55, 20–25. doi: 10.1016/j.mam.2016.11.011

Frozi, J., de Carvalho, H. W., Ottoni, G. L., Cunha, R. A., and Lara, D. R. (2018). Distinct sensitivity to caffeine-induced insomnia related to age. *J. Psychopharmacol.* 32, 89–95. doi: 10.1177/0269881117722997

Fuxe, K., Agnati, L. F., Jacobsen, K., Hillion, J., Canals, M., Torvinen, M., et al. (2003). Receptor heteromerization in adenosine A_{2A} receptor signaling: relevance for striatal function and Parkinson's disease. *Neurology* 61, S19–S23. doi: 10.1212/01.WNL.0000095206.44418.5C

Goldsmith, D. R., Haroon, E., Woolwine, B. J., Jung, M. Y., Wommack, E. C., Harvey, P. D., et al. (2016a). Inflammatory markers are associated with decreased psychomotor speed in patients with major depressive disorder. *Brain Behav. Immun.* 56, 281–288. doi: 10.1016/j.bbi.2016.03.025

Goldsmith, D. R., Rapaport, M. H., and Miller, B. J. (2016b). A meta-analysis of blood cytokine network alterations in psychiatric patients: comparisons between schizophrenia, bipolar disorder and depression. *Mol. Psychiatry* 21, 1696–1709. doi: 10.1038/mp.2016.3

Gorwood, P., Richard-Devantoy, S., Baylé, F., and Cléry-Melin, M. L. (2014). Psychomotor retardation is a scar of past depressive episodes, revealed by simple cognitive tests. *Eur. Neuropsychopharmacol.* 24, 1630–1640. doi: 10.1016/j.euroneuro.2014.07.013

Greden, J. F., Fontaine, P., Lubetsky, M., and Chamberlin, K. (1978). Anxiety and depression associated with caffeinism among psychiatric inpatients. *Am. J. Psychiatry* 135, 963–966. doi: 10.1176/ajp.135.8.963

Griffiths, R. R., Evans, S. M., Heishman, S. J., Preston, K. L., Sannerud, C. A., Wolf, B., et al. (1990). Low-dose caffeine physical dependence in humans. *J. Pharmacol. Exp. Ther.* 255, 1123–1132.

Gu, L., Gonzalez, F. J., Kalow, W., and Tang, B. K. (1992). Biotransformation of caffeine, paraxanthine, theobromine and theophylline by cDNA-expressed human CYP1A2 and CYP2E1. *Pharmacogenetics* 2, 73–77. doi: 10.1097/00008571-199204000-00004

Guay, D. R. (2010). Tetrabenazine, a monoamine-depleting drug used in the treatment of hyperkinetic movement disorders. *Am. J. Geriatr. Pharmacother.* 8, 331–373. doi: 10.1016/j.amjopharm.2010.08.006

Gullion, C. M., and Rush, A. J. (1998). Toward a generalizable model of symptoms in major depressive disorder. *Biol. Psychiatry* 44, 959–972. doi: 10.1016/S0006-3223(98)00235-2

Hamilton, M. (1967). Development of a rating scale for primary depressive illness. *Br. J. Soc. Clin. Psychol.* 6, 278–296. doi: 10.1111/j.2044-8260.1967.tb00530.x

Hanff, T. C., Furst, S. J., and Minor, T. R. (2010). Biochemical and anatomical substrates of depression and sickness behavior. *Isr. J. Psychiatry Relat. Sci.* 47, 64–71.

Hauber, W., and Sommer, S. (2009). Prefrontostriatal circuitry regulates effort-related decision making. *Cereb. Cortex* 19, 2240–2247. doi: 10.1093/cercor/bhn241

Heath, C. J., Bussey, T. J., and Saksida, L. M. (2015). Motivational assessment of mice using the touchscreen operant testing system: effects of dopaminergic drugs. *Psychopharmacology* 232, 4043–4057. doi: 10.1007/s00213-015-4009-8

Heckman, M. A., Weil, J., and Gonzalez de Mejia, E. (2010). Caffeine (1, 3, 7-trimethylxanthine) in foods: a comprehensive review on consumption, functionality, safety, and regulatory matters. *J. Food Sci.* 75, R77–R87. doi: 10.1111/j.1750-3841.2010.01561.x

Hiles, S. A., Baker, A. L., de Malmanche, T., and Attia, J. (2012). A meta-analysis of differences in IL-6 and IL-10 between people with and without depression: exploring the causes of heterogeneity. *Brain Behav. Immun.* 26, 1180–1188. doi: 10.1016/j.bbi.2012.06.001

Hung, A. Y., and Schwarzschild, M. A. (2014). Treatment of Parkinson's disease: what's in the non-dopaminergic pipeline? *Neurotherapeutics* 11, 34–46. doi: 10.1007/s13311-013-0239-9

Hunter, A. M., Balleine, B. W., and Minor, T. R. (2003). Helplessness and escape performance: glutamate-adenosine interactions in the frontal cortex. *Behav. Neurosci.* 117, 123–135. doi: 10.1037/0735-7044.117.1.123

Jacobson, K. A., and Gao, Z.-G. (2006). Adenosine receptors as therapeutic targets. *Nat. Rev. Drug Discov.* 5, 247–264. doi: 10.1038/nrd1983

Jacobson, K. A., van Galen, P. J., and Williams, M. (1992). Adenosine receptors: pharmacology, structure-activity relationships, and therapeutic potential. *J. Med. Chem.* 35, 407–422. doi: 10.1021/jm00081a001

Johansson, B., and Fredholm, B. B. (1995). Further characterization of the binding of the adenosine receptor agonist [3H]CGS 21680 to rat brain using autoradiography. *Neuropharmacology* 34, 393–403. doi: 10.1016/0028-3908(95)00009-U

Johansson, B., Georgiev, V., and Fredholm, B. B. (1997). Distribution and postnatal ontogeny of adenosine A_{2A} receptors in rat brain: comparison with dopamine receptors. *Neuroscience* 80, 1187–1207. doi: 10.1016/S0306-4522(97)00143-7

Johnson, L. C., Freeman, C. R., Spinweber, C. L., and Gomez, S. A. (1991). Subjective and objective measures of sleepiness: effect of benzodiazepine and caffeine on their relationship. *Psychophysiology* 28, 65–71. doi: 10.1111/j.1469-8986.1991.tb03388.x

Johnson, L. C., Spinweber, C. L., and Gomez, S. A. (1990a). Benzodiazepines and caffeine: effect on daytime sleepiness, performance, and mood. *Psychopharmacology* 101, 160–167.

Johnson, L. C., Spinweber, C. L., Gomez, S. A., and Matteson, L. T. (1990b). Daytime sleepiness, performance, mood, nocturnal sleep: the effect of benzodiazepine and caffeine on their relationship. *Sleep* 13, 121–135.

Juliano, L. M., and Griffiths, R. R. (2004). A critical review of caffeine withdrawal: empirical validation of symptoms and signs, incidence, severity, and associated features. *Psychopharmacology* 176, 1–29. doi: 10.1007/s00213-004-2000-x

Juliano, L. M., Huntley, E. D., Harrell, P. T., and Westerman, A. T. (2012). Development of the caffeine withdrawal symptom questionnaire: caffeine withdrawal symptoms cluster into 7 factors. *Drug Alcohol Depend.* 124, 229–234. doi: 10.1016/j.drugalcdep.2012.01.009

Kale, P. P., and Addepalli, V. (2014). Augmentation of antidepressant effects of duloxetine and bupropion by caffeine in mice. *Pharmacol. Biochem. Behav.* 124, 238–244. doi: 10.1016/j.pbb.2014.06.005

Kale, P. P., and Addepalli, V. (2015). Enhancement of nootropic effect of duloxetine and bupropion by caffeine in mice. *Indian J. Pharmacol.* 47, 199–201. doi: 10.4103/0253-7613.153430

Kale, P. P., Addepalli, V., Bafna, P. A., and Prabhavalkar, K. S. (2010). Caffeine-induced augmentation of antidepressant therapy. *J. Exp. Clin. Med.* 2, 282–286. doi: 10.1016/j.jecm.2010.09.001

Kaster, M. P., Machado, N. J., Silva, H. B., Nunes, A., Ardais, A. P., Santana, M., et al. (2015). Caffeine acts through neuronal adenosine A_{2A} receptors to prevent mood and memory dysfunction triggered by chronic stress. *Proc. Natl. Acad. Sci. U.S.A.* 112, 7833–7838. doi: 10.1073/pnas.1423088112

Kaster, M. P., Rosa, A. O., Rosso, M. M., Goulart, E. C., Santos, A. R., and Rodrigues, A. L. (2004). Adenosine administration produces an antidepressant-like effect in mice: evidence for the involvement of A_1 and A_{2A} receptors. *Neurosci. Lett.* 355, 21–24. doi: 10.1016/j.neulet.2003.10.040

Kawachi, I., Willett, W. C., Colditz, G. A., Stampfer, M. J., and Speizer, F. E. (1996). A prospective study of coffee drinking and suicide in women. *Arch. Intern. Med.* 156, 521–525. doi: 10.1001/archinte.1996.00440050067008

Kent, S., Bluthe, R. M., Dantzer, R., Hardwick, A. J., Kelley, K. W., Rothwell, N. J., et al. (1992). Different receptor mechanisms mediate the pyrogenic and behavioral effects of interleukin 1. *Proc. Natl. Acad. Sci. U.S.A.* 89, 9117–9120. doi: 10.1073/pnas.89.19.9117

Kent, T. A., Preskorn, S. H., Glotzbach, R. K., and Irwin, G. H. (1986). Amitriptyline normalizes tetrabenazine-induced changes in cerebral microcirculation. *Biol. Psychiatry* 21, 483–491. doi: 10.1016/0006-3223(86)90190-3

Kerkhofs, A., Xavier, A. C., da Silva, B. S., Canas, P. M., Idema, S., Baayen, J. C., et al. (2018). Caffeine controls glutamatergic synaptic transmission and pyramidal neuron excitability in human neocortex. *Front. Pharmacol.* 8:899. doi: 10.3389/fphar.2017.00899

Kulkarni, S. K., and Mehta, A. K. (1985). Purine nucleoside–mediated immobility in mice: reversal by antidepressants. *Psychopharmacology* 85, 460–463. doi: 10.1007/BF00429665

Leibenluft, E., Fiero, P. L., Bartko, J. J., Moul, D. E., and Rosenthal, N. E. (1993). Depressive symptoms and the self-reported use of alcohol, caffeine, and carbohydrates in normal volunteers and four groups of psychiatric outpatients. *Am. J. Psychiatry* 150, 294–301. doi: 10.1176/ajp.150.2.294

Li, Y., He, Y., Chen, M., Pu, Z., Chen, L., Li, P., et al. (2016). Optogenetic activation of adenosine A_{2A} receptor signaling in the dorsomedial striatopallidal neurons suppresses goal-directed behavior. *Neuropsychopharmacology* 41, 1003–1013. doi: 10.1038/npp.2015.227

Lieberman, H. R. (2001). The effects of ginseng, ephedrine, and caffeine on cognitive performance, mood and energy. *Nutr. Rev.* 59, 91–102. doi: 10.1111/j.1753-4887.2001.tb06995.x

Lieberman, H. R., Wurtman, R. J., Emde, G. G., and Coviella, I. L. (1987). The effects of caffeine and aspirin on mood and performance. *J. Clin. Psychopharmacol.* 7, 315–320. doi: 10.1097/00004714-198710000-00004

Liguori, A., and Hughes, J. R. (1997). Caffeine self-administration in humans: 2. A within-subjects comparison of coffee and cola vehicles. *Exp. Clin. Psychopharmacol.* 5, 295–303. doi: 10.1037/1064-1297.5.3.295

López-Cruz, L., Pardo, M., Salamone, J. D., and Correa, M. (2014). Differences between the nonselective adenosine receptor antagonists caffeine and theophylline in motor and mood effects: studies using medium to high doses in animal models. *Behav. Brain Res.* 270, 213–222. doi: 10.1016/j.bbr.2014.05.020

López-Cruz, L., SanMiguel, N., Carratalá-Ros, C., Monferrer, L., Salamone, J. D., and Correa, M. (2018). Dopamine depletion shifts behavior from activity based

reinforcers to more sedentary ones and adenosine receptor antagonism reverses that shift: relation to ventral striatum DARPP32 phosphorylation patterns. *Neuropharmacology* doi: 10.1016/j.neuropharm.2018.01.034 [Epub ahead of print].

Lorist, M. M., Snel, J., Kok, A., and Mulder, G. (1994). Influence of caffeine on selective attention in well-rested and fatigued subjects. *Psychophysiology* 31, 525–534. doi: 10.1111/j.1469-8986.1994.tb02345.x

Lucas, M., Mirzaei, F., Pan, A., Okereke, O. I., Willett, W. C., O'Reilly, É. J., et al. (2011). Coffee, caffeine, and risk of depression among women. *Arch. Intern. Med.* 171, 1571–1578. doi: 10.1001/archinternmed.2011.393

Lucas, M., O'Reilly, E. J., Pan, A., Mirzaei, F., Willett, W. C., Okereke, O. I., et al. (2014). Coffee, caffeine, and risk of completed suicide: results from three prospective cohorts of American adults. *World J. Biol. Psychiatry* 15, 377–386. doi: 10.3109/15622975.2013.795243

Machado, N. J., Simões, A. P., Silva, H. B., Ardais, A. P., Kaster, M. P., Garção, P., et al. (2017). Caffeine reverts memory but not mood impairment in a depression-prone mouse strain with up-regulated adenosine A_{2A} receptor in hippocampal glutamate synapses. *Mol. Neurobiol.* 54, 1552–1563. doi: 10.1007/s12035-016-9774-9

Malinauskas, B. M., Aeby, V. G., Overton, R. F., Carpenter-Aeby, T., and Barber-Heidal, K. (2007). A survey of energy drink consumption patterns among college students. *Nutr. J.* 6:35. doi: 10.1186/1475-2891-6-35

Markou, A., Salamone, J. D., Bussey, T. J., Mar, A. C., Brunner, D., Gilmour, G., et al. (2013). Measuring reinforcement learning and motivation constructs in experimental animals: relevance to the negative symptoms of schizophrenia. *Neurosci. Biobehav. Rev.* 37, 2149–2165. doi: 10.1016/j.neubiorev.2013.08.007

McClintock, S. M., Husain, M. M., Wisniewski, S. R., Nierenberg, A. A., Stewart, J. W., Trivedi, M. H., et al. (2011). Residual symptoms in depressed outpatients who respond by 50% but do not remit to antidepressant medication. *J. Clin. Psychopharmacol.* 31, 180–186. doi: 10.1097/JCP.0b013e31820ebd2c

Miller, A. H., Maletic, V., and Raison, C. L. (2009). Inflammation and its discontents: the role of cytokines in the pathophysiology of major depression. *Biol. Psychiatry* 65, 732–741. doi: 10.1016/j.biopsych.2008.11.029

Mingote, S., Font, L., Farrar, A. M., Vontell, R., Worden, L. T., Stopper, C. M., et al. (2008). Nucleus accumbens adenosine A_{2A} receptors regulate exertion of effort by acting on the ventral striatopallidal pathway. *J. Neurosci.* 28, 9037–9046. doi: 10.1523/JNEUROSCI.1525-08.2008

Minor, T. R., Chang, W. C., and Winslow, J. L. (1994a). Stress and adenosine: I. Effect of methylxanthine and amphetamine stimulants on learned helplessness in rats. *Behav. Neurosci.* 108, 254–264.

Minor, T. R., and Hanff, T. C. (2015). Adenosine signaling in reserpine-induced depression in rats. *Behav. Brain Res.* 286, 184–191. doi: 10.1016/j.bbr.2015.02.032

Minor, T. R., Rowe, M., Cullen, P. K., and Furst, S. (2008). Enhancing brain adenosine signaling with the nucleoside transport blocker NBTI (S-(4-nitrobenzyl)-6-theoinosine) mimics the effects of inescapable shock on later shuttle-escape performance in rats. *Behav. Neurosci.* 122, 1236–1247. doi: 10.1037/a0013143

Minor, T. R., Winslow, J. L., and Chang, W. C. (1994b). Stress and adenosine: II. Adenosine analogs mimic the effect of inescapable shock on shuttle-escape performance in rats. *Behav. Neurosci.* 108, 265–276.

Mott, A. M., Nunes, E. J., Collins, L. E., Port, R. G., Sink, K. S., Hockemeyer, J., et al. (2009). The adenosine A_{2A} antagonist MSX-3 reverses the effects of the dopamine antagonist haloperidol on effort-related decision making in a T-maze cost/benefit procedure. *Psychopharmacology* 204, 103–112. doi: 10.1007/s00213-008-1441-z

Noji, T., Karasawa, A., and Kusaka, H. (2004). Adenosine uptake inhibitors. *Eur. J. Pharmacol.* 495, 1–16. doi: 10.1016/j.ejphar.2004.05.003

Nunes, E. J., Randall, P. A., Estrada, A., Epling, B., Hart, E. E., Lee, C. A., et al. (2014). Effort-related motivational effects of the pro-inflammatory cytokine interleukin 1-beta: studies with the concurrent fixed ratio 5/ chow feeding choice task. *Psychopharmacology* 231, 727–736. doi: 10.1007/s00213-013-3285-4

Nunes, E. J., Randall, P. A., Hart, E. E., Freeland, C., Yohn, S. E., Baqi, Y., et al. (2013). Effort-related motivational effects of the VMAT-2 inhibitor tetrabenazine: implications for animal models of the motivational symptoms of depression. *J. Neurosci.* 33, 19120–19130. doi: 10.1523/JNEUROSCI.2730-13.2013

Nunes, E. J., Randall, P. A., Santerre, J. L., Given, A. B., Sager, T. N., Correa, M., et al. (2010). Differential effects of selective adenosine antagonists on the effort-related impairments induced by dopamine D1 and D2 antagonism. *Neuroscience* 170, 268–280. doi: 10.1016/j.neuroscience.2010.05.068

Overmier, J. B., and Seligman, M. E. (1967). Effects of inescapable shock upon subsequent escape and avoidance responding. *J. Comp. Physiol. Psychol.* 63, 28–33. doi: 10.1037/h0024166

Padala, P. R., Padala, K. P., Monga, V., Ramirez, D. A., and Sullivan, D. H. (2012). Reversal of SSRI-associated apathy syndrome by discontinuation of therapy. *Ann. Pharmacother.* 46:e8. doi: 10.1345/aph.1Q656

Pae, C. U., Lim, H.-K., Han, C., Patkar, A. A., Steffens, D. C., Masand, P. S., et al. (2007). Fatigue as a core symptom in major depressive disorder: overview and the role of bupropion. *Expert Rev. Neurother.* 7, 1251–1263. doi: 10.1586/14737175.7.10.1251

Paech, G. M., Banks, S., Pajcin, M., Grant, C., Johnson, K., Kamimori, G. H., et al. (2016). Caffeine administration at night during extended wakefulness effectively mitigates performance impairment but not subjective assessments of fatigue and sleepiness. *Pharmacol. Biochem. Behav.* 145, 27–32. doi: 10.1016/j.pbb.2016.03.011

Pandolfo, P., Machado, N. J., Köfalvi, A., Takahashi, R. N., and Cunha, R. A. (2013). Caffeine regulates frontocorticostriatal dopamine transporter density and improves attention and cognitive deficits in an animal model of attention deficit hyperactivity disorder. *Eur. Neuropsychopharmacol.* 23, 317–328. doi: 10.1016/j.euroneuro.2012.04.011

Pardo, M., López-Cruz, L., San Miguel, N., Salamone, J. D., and Correa, M. (2015). Selection of sucrose concentration depends on the effort required to obtain it: studies using tetrabenazine, D1, D2, and D3 receptor antagonists. *Psychopharmacology* 232, 2377–2391. doi: 10.1007/s00213-015-3872-7

Pardo, M., Lopez-Cruz, L., Valverde, O., Ledent, C., Baqi, Y., Müller, C. E., et al. (2012). Adenosine A_{2A} receptor antagonism and genetic deletion attenuate the effects of dopamine D_2 antagonism on effort-based decision making in mice. *Neuropharmacology* 62, 2068–2077. doi: 10.1016/j.neuropharm.2011.12.033

Pardo, M., López-Cruz, L., Valverde, O., Ledent, C., Baqi, Y., Müller, C. E., et al. (2013). Effect of subtype-selective adenosine receptor antagonists on basal or haloperidol-regulated striatal function: studies of exploratory locomotion and c-Fos immunoreactivity in outbred and A_{2A}R KO mice. *Behav. Brain Res.* 247, 217–226. doi: 10.1016/j.bbr.2013.03.035

Pasman, W. J., Boessen, R., Donner, Y., Clabbers, N., and Boorsma, A. (2017). Effect of caffeine on attention and alertness measured in a home-setting, using web-based cognition tests. *JMIR Res. Protoc.* 6:e169. doi: 10.2196/resprot.6727

Patten, S. B., Metz, L. M., and Reimer, M. A. (2000). Biopsychosocial correlates of lifetime major depression in a multiple sclerosis population. *Mult. Scler.* 6, 115–120. doi: 10.1177/135245850000600210

Pechlivanova, D. M., Tchekalarova, J. D., Alova, L. H., Petkov, V. V., Nikolov, R. P., and Yakimova, K. S. (2012). Effect of long-term caffeine administration on depressive-like behavior in rats exposed to chronic unpredictable stress. *Behav. Pharmacol.* 23, 339–347. doi: 10.1097/FBP.0b013e3283564dd9

Peeling, P., and Dawson, B. (2007). Influence of caffeine ingestion on perceived mood states, concentration, and arousal levels during a 75-min university lecture. *Adv. Physiol. Educ.* 31, 332–335. doi: 10.1152/advan.00003.2007

Petit-Demouliere, B., Chenu, F., and Bourin, M. (2005). Forced swimming test in mice: a review of antidepressant activity. *Psychopharmacology* 177, 245–255. doi: 10.1007/s00213-004-2048-7

Pettibone, D. J., Totaro, J. A., and Pflueger, A. B. (1984). Tetrabenazine-induced depletion of brain monoamines: characterization and interaction with selected antidepressants. *Eur. J. Pharmacol.* 102, 425–430. doi: 10.1016/0014-2999(84)90562-4

Petty, F., McChesney, C., and Kramer, G. (1985). Intracortical glutamate injection produces helpless-like behavior in the rat. *Pharmacol. Biochem. Behav.* 22, 531–533. doi: 10.1016/0091-3057(85)90270-9

Pizzagalli, D. A. (2014). Depression, stress, and anhedonia: toward a synthesis and integrated model. *Annu. Rev. Clin. Psychol.* 10, 393–423. doi: 10.1146/annurev-clinpsy-050212-185606

Porsolt, R. D., Le Pichon, M., and Jalfre, M. (1977). Depression: a new animal model sensitive to antidepressant treatments. *Nature* 266, 730–732. doi: 10.1038/266730a0

Prediger, R. D. (2010). Effects of caffeine in Parkinson's disease: from neuroprotection to the management of motor and non-motor symptoms. *J. Alzheimers Dis.* 20(Suppl. 1), S205–S220. doi: 10.3233/JAD-2010-091459

Quitkin, F., Rifkin, A., and Klein, D. F. (1979). Monoamine oxidase inhibitors. A review of antidepressant effectiveness. *Arch. Gen. Psychiatry* 36, 749–760. doi: 10.1001/archpsyc.1979.01780070027003

Rampello, L., Nicoletti, G., and Raffaele, R. (1991). Dopaminergic hypothesis for retarded depression: a symptom profile for predicting therapeutical responses. *Acta Psychiatr. Scand.* 84, 552–554. doi: 10.1111/j.1600-0447.1991.tb03193.x

Rampello, L., Nicoletti, G., Raffaele, R., and Drago, F. (1995). Comparative effects of amitriptyline and amineptine in patients affected by anxious depression. *Neuropsychobiology* 31, 130–134. doi: 10.1159/000119183

Randall, P. A., Lee, C. A., Podurgiel, S. J., Hart, E., Yohn, S. E., Jones, M., et al. (2014). Bupropion increases selection of high effort activity in rats tested on a progressive ratio/chow feeding choice procedure: implications for treatment of effort-related motivational symptoms. *Int. J. Neuropsychopharmacol.* 18:yu017. doi: 10.1093/ijnp/pyu017

Randall, P. A., Nunes, E. J., Janniere, S. L., Stopper, C. M., Farrar, A. M., Sager, T. N., et al. (2011). Stimulant effects of adenosine antagonists on operant behavior: differential actions of selective A_{2A} and A_1 antagonists. *Psychopharmacology* 216, 173–186. doi: 10.1007/s00213-011-2198-3

Randall, P. A., Pardo, M., Nunes, E. J., López Cruz, L., Vemuri, V. K., Makriyannis, A., et al. (2012). Dopaminergic modulation of effort-related choice behavior as assessed by a progressive ratio chow feeding choice task: pharmacological studies and the role of individual differences. *PLoS One* 7:e47934. doi: 10.1371/journal.pone.0047934

Rebola, N., Canas, P. M., Oliveira, C. R., and Cunha, R. A. (2005). Different synaptic and subsynaptic localization of adenosine A_{2A} receptors in the hippocampus and striatum of the rat. *Neuroscience* 132, 893–903. doi: 10.1016/j.neuroscience.2005.01.014

Rees, K., Allen, D., and Lader, M. (1999). The influences of age and caffeine on psychomotor and cognitive function. *Psychopharmacology* 145, 181–188. doi: 10.1007/s002130051047

Retzbach, E. P., Dholakia, P. H., and Duncan-Vaidya, E. A. (2014). The effect of daily caffeine exposure on lever-pressing for sucrose and c-Fos expression in the nucleus accumbens in the rat. *Physiol. Behav.* 135, 1–6. doi: 10.1016/j.physbeh.2014.05.038

Rihs, M., Muller, C., and Baumann, P. (1996). Caffeine consumption in hospitalized psychiatric patients. *Eur. Arch. Psychiatry Clin. Neurosci.* 246, 83–92. doi: 10.1007/BF02274898

Robles-Molina, E., Millán, D., Hong, E., Huang, F., and Villafaña, S. (2012). Increased antidepressant-like effect of desipramine combined with central stimulants (caffeine and amphetamine) in mice. *Open Life Sci.* 7, 391–396. doi: 10.2478/s11535-012-0028-1

Rodrigues, F. B., Duarte, G. S., Costa, J., Ferreira, J. J., and Wild, E. J. (2017). Tetrabenazine versus deutetrabenazine for Huntington's disease: twins or distant cousins? *Mov. Disord. Clin. Pract.* 4, 582–585. doi: 10.1002/mdc3.12483

Ruby, L., Adams, C. A., Mrazeck, A. D., and Choi, D. S. (2011). "Adenosine signaling in anxiety," in *Anxiety Disorders*, ed. V. Kalinin (Rijeka: InTech). doi: 10.5772/19423

Rush, A. J., and Trivedi, M. H. (1995). Treating depression to remission. *Psychiatr. Ann.* 64(Suppl. 15), 7–12. doi: 10.3928/0048-5713-19951201-03

Sako, W., Murakami, N., Motohama, K., Izumi, Y., and Kaji, R. (2017). The effect of istradefylline for Parkinson's disease: a meta-analysis. *Sci. Rep.* 7:18018. doi: 10.1038/s41598-017-18339-1

Salamone, J., Correa, M., Mingote, S., Weber, S., and Farrar, A. (2006). Nucleus accumbens dopamine and the forebrain circuitry involved in behavioral activation and effort-related decision making: implications for understanding anergia and psychomotor slowing in depression. *Curr. Psychiatry Rev.* 2, 267–280. doi: 10.2174/157340006776875914

Salamone, J. D. (2007). Functions of mesolimbic dopamine: changing concepts and shifting paradigms. *Psychopharmacology* 191:389. doi: 10.1007/s00213-006-0623-9

Salamone, J. D., and Correa, M. (2002). Motivational views of reinforcement: implications for understanding the behavioral functions of nucleus accumbens dopamine. *Behav. Brain Res.* 137, 3–25. doi: 10.1016/S0166-4328(02)00282-6

Salamone, J. D., and Correa, M. (2009). Dopamine/adenosine interactions involved in effort-related aspects of food motivation. *Appetite* 53, 422–425. doi: 10.1016/j.appet.2009.07.018

Salamone, J. D., and Correa, M. (2012). The mysterious motivational functions of mesolimbic dopamine. *Neuron* 76, 470–485. doi: 10.1016/j.neuron.2012.10.021

Salamone, J. D., Correa, M., Farrar, A., and Mingote, S. M. (2007). Effort-related functions of nucleus accumbens dopamine and associated forebrain circuits. *Psychopharmacology* 191, 461–482. doi: 10.1007/s00213-006-0668-9

Salamone, J. D., Correa, M., Yohn, S., Lopez Cruz, L., San Miguel, N., and Alatorre, L. (2016). The pharmacology of effort-related choice behavior: dopamine, depression, and individual differences. *Behav. Process.* 127, 3–17. doi: 10.1016/j.beproc.2016.02.008

Salamone, J. D., Cousins, M. S., and Bucher, S. (1994). Anhedonia or anergia? Effects of haloperidol and nucleus accumbens dopamine depletion on instrumental response selection in a T-maze cost/benefit procedure. *Behav. Brain Res.* 65, 221–229. doi: 10.1016/0166-4328(94)90108-2

Salamone, J. D., Farrar, A. M., Font, L., Patel, V., Schlar, D. E., Nunes, E. J., et al. (2009). Differential actions of adenosine A_1 and A_{2A} antagonists on the effort-related effects of dopamine D_2 antagonism. *Behav. Brain Res.* 201, 216–222. doi: 10.1016/j.bbr.2009.02.021

Salamone, J. D., Steinpreis, R. E., McCullough, L. D., Smith, P., Grebel, D., and Mahan, K. (1991). Haloperidol and nucleus accumbens dopamine depletion suppress lever pressing for food but increase free food consumption in a novel food choice procedure. *Psychopharmacology* 104, 515–521. doi: 10.1007/BF02245659

SanMiguel, N., Pardo, M., Carratalá-Ros, C., López-Cruz, L., Salamone, J. D., and Correa, M. (2018). Individual differences in the energizing effects of caffeine on effort-based decision-making tests in rats. *Pharmacol. Biochem. Behav.* 169, 27–34. doi: 10.1016/j.pbb.2018.04.004

Schwarzschild, M. A., Agnati, L., Fuxe, K., Chen, J. F., and Morelli, M. (2006). Targeting adenosine A_{2A} receptors in Parkinson's disease. *Trends Neurosci.* 29, 647–654. doi: 10.1016/j.tins.2006.09.004

Sebastião, A. M., and Ribeiro, J. A. (2009). Tuning and fine-tuning of synapses with adenosine. *Curr. Neuropharmacol.* 7, 180–194. doi: 10.2174/157015909789152128

Seligman, M. E. (1972). Learned helplessness. *Annu. Rev. Med.* 23, 407–412. doi: 10.1146/annurev.me.23.020172.002203

Silber, B. Y., Croft, R. J., Papafotiou, K., and Stough, C. (2006). The acute effects of d-amphetamine and methamphetamine on attention and psychomotor performance. *Psychopharmacology* 187, 154–169. doi: 10.1007/s00213-006-0410-7

Simões, A. P., Duarte, J. A., Agasse, F., Canas, P. M., Tomé, A. R., Agostinho, P., et al. (2012). Blockade of adenosine A_{2A} receptors prevents interleukin-1β-induced exacerbation of neuronal toxicity through a p38 mitogen-activated protein kinase pathway. *J. Neuroinflammation* 9:204. doi: 10.1186/1742-2094-9-204

Simões, A. P., Machado, N. J., Gonçalves, N., Kaster, M. P., Simões, A. T., Nunes, A., et al. (2016). Adenosine A_{2A} receptors in the amygdala control synaptic plasticity and contextual fear memory. *Neuropsychopharmacology* 41, 2862–2871. doi: 10.1038/npp.2016.98

Sitkovsky, M. V., and Ohta, A. (2005). The "danger" sensors that STOP the immune response: the A2 adenosine receptors? *Trends Immunol.* 26, 299–304. doi: 10.1016/j.it.2005.04.004

Smith, A., Thomas, M., Perry, K., and Whitney, H. (1997). Caffeine and the common cold. *J. Psychopharmacol.* 11, 319–324. doi: 10.1177/026988119701100406

Smith, A. P. (2009). Caffeine, cognitive failures and health in a non-working community sample. *Hum. Psychopharmacol.* 24, 29–34. doi: 10.1002/hup.991

Smith, A. P. (2013). Caffeine, extraversion and working memory. *J. Psychopharmacol.* 27, 71–76. doi: 10.1177/0269881112460111

Smith, A. P., Kendrick, A. M., and Maben, A. L. (1992). Effects of breakfast and caffeine on performance and mood in the late morning and after lunch. *Neuropsychobiology* 26, 198–204. doi: 10.1159/000118920

Stahl, S. M. (2002). The psychopharmacology of energy and fatigue. *J. Clin. Psychiatry* 63, 7–8. doi: 10.4088/JCP.v63n0102

Stenman, E., and Lilja, A. (2013). Increased monoaminergic neurotransmission improves compliance with physical activity recommendations in depressed

patients with fatigue. *Med. Hypotheses* 80, 47–49. doi: 10.1016/j.mehy.2012.10.007

Steru, L., Chermat, R., Thierry, B., and Simon, P. (1985). The tail suspension test: a new method for screening antidepressants in mice. *Psychopharmacology* 85, 367–370. doi: 10.1007/BF00428203

Sukoff Rizzo, S. J., Neal, S. J., Hughes, Z. A., Beyna, M., Rosenzweig-Lipson, S., Moss, S. J., et al. (2012). Evidence for sustained elevation of IL-6 in the CNS as a key contributor of depressive-like phenotypes. *Transl. Psychiatry* 2:e199. doi: 10.1038/tp.2012.120

Swindle, R., Kroenke, K., and Braun, L. A. (2001). "Energy and improved workplace productivity in depression," in *Investing in Health: The Social and Economic Benefits of Health Care Innovation: Research in Human Capital and Development*, Vol. 14, eds I. Farquhar, K. Summers, and A. Sorkin (Bingley: Emerald Group Publishing Limited), 323–341.

Szopa, A., Poleszak, E., Wyska, E., Serefko, A., Wośko, S., Wlaź, A., et al. (2016). Caffeine enhances the antidepressant-like activity of common antidepressant drugs in the forced swim test in mice. *Naunyn Schmiedebergs Arch. Pharmacol.* 389, 211–221. doi: 10.1007/s00210-015-1189-z

Tanra, A. J., Kagaya, A., Okamoto, Y., Muraoka, M., Motohashi, N., and Yamawaki, S. (1995). TJS-010, a new prescription of oriental medicine, antagonizes tetrabenazine-induced suppression of spontaneous locomotor activity in rats. *Prog. Neuropsychopharmacol. Biol. Psychiatry* 19, 963–971.

Tanskanen, A. (1997). Coffee, caffeine and mental health. *Duodecim* 113, 191–196.

Tanskanen, A., Tuomilehto, J., Viinamäki, H., Vartiainen, E., Lehtonen, J., and Puska, P. (2000). Heavy coffee drinking and the risk of suicide. *Eur. J. Epidemiol.* 16, 789–791. doi: 10.1023/A:1007614714579

Temple, J. L., Bernard, C., Lipshultz, S. E., Czachor, J. D., Westphal, J. A., and Mestre, M. A. (2017). The safety of ingested caffeine: a comprehensive review. *Front. Psychiatry* 8:80. doi: 10.3389/fpsyt.2017.00080

Treadway, M. T., Buckholtz, J. W., Cowan, R. L., Woodward, N. D., Li, R., Ansari, M. S., et al. (2012). Dopaminergic mechanisms of individual differences in human effort-based decision-making. *J. Neurosci.* 32, 6170–6176. doi: 10.1523/JNEUROSCI.6459-11.2012

Treadway, M. T., Buckholtz, J. W., Schwartzman, A. N., Lambert, W. E., and Zald, D. H. (2009). Worth the "EEfRT"? The effort expenditure for rewards task as an objective measure of motivation and anhedonia. *PLoS One* 4:e6598. doi: 10.1371/journal.pone.0006598

Tylee, A., Gastpar, M., Lépine, J. P., and Mendlewicz, J. (1999). DEPRES II (Depression research in European society II): a patient survey of the symptoms, disability and current management of depression in the community. DEPRES steering committee. *Int. Clin. Psychopharmacol.* 14, 139–151. doi: 10.1097/00004850-199905030-00001

van den Bos, R., van der Harst, J., Jonkman, S., Schilders, M., and Spruijt, B. (2006). Rats assess costs and benefits according to an internal standard. *Behav. Brain Res.* 171, 350–354. doi: 10.1016/j.bbr.2006.03.035

Wang, H., Chen, X., Li, Y., Tang, T.-S., and Bezprozvanny, I. (2010). Tetrabenazine is neuroprotective in Huntington's disease mice. *Mol. Neurodegener.* 5:18. doi: 10.1186/1750-1326-5-18

Wardle, M. C., Treadway, M. T., and de Wit, H. (2012). Caffeine increases psychomotor performance on the effort expenditure for rewards task. *Pharmacol. Biochem. Behav.* 102, 526–531. doi: 10.1016/j.pbb.2012.06.016

Whalen, D. J., Silk, J. S., Semel, M., Forbes, E. E., Ryan, N. D., Axelson, D. A., et al. (2008). Caffeine consumption, sleep, and affect in the natural environments of depressed youth and healthy controls. *J. Pediatr. Psychol.* 33, 358–367. doi: 10.1093/jpepsy/jsm086

Wikoff, D., Welsh, B. T., Henderson, R., Brorby, G. P., Britt, J., Myers, E., et al. (2017). Systematic review of the potential adverse effects of caffeine consumption in healthy adults, pregnant women, adolescents, and children. *Food Chem. Toxicol.* 109(Pt 1), 585–648. doi: 10.1016/j.fct.2017.04.002

Willner, P. (2005). Chronic mild stress (CMS) revisited: consistency and behavioural-neurobiological concordance in the effects of CMS. *Neuropsychobiology* 52, 90–110. doi: 10.1159/000087097

Woodson, J. C., Minor, T. R., and Job, R. F. (1998). Inhibition of adenosine deaminase by erythro-9-(2-hydroxy-3-nonyl)adenine (EHNA) mimics the effect of inescapable shock on escape learning in rats. *Behav. Neurosci.* 112, 399–409. doi: 10.1037/0735-7044.112.2.399

Worden, L. T., Shahriari, M., Farrar, A. M., Sink, K. S., Hockemeyer, J., Müller, C. E., et al. (2009). The adenosine A_{2A} antagonist MSX-3 reverses the effort-related effects of dopamine blockade: differential interaction with D_1 and D_2 family antagonists. *Psychopharmacology* 203, 489–499. doi: 10.1007/s00213-008-1396-0

Worthington, J., Fava, M., Agustin, C., Alpert, J., Nierenberg, A. A., Pava, J. A., et al. (1996). Consumption of alcohol, nicotine, and caffeine among depressed outpatients. Relationship with response to treatment. *Psychosomatics* 37, 518–522. doi: 10.1016/S0033-3182(96)71515-3

Yang, X.-H., Huang, J., Zhu, C.-Y., Wang, Y.-F., Cheung, E. F. C., Chan, R. C., et al. (2014). Motivational deficits in effort-based decision making in individuals with subsyndromal depression, first-episode and remitted depression patients. *Psychiatry Res.* 220, 874–882. doi: 10.1016/j.psychres.2014.08.056

Yıldız, A., Gönül, A. S., and Tamam, L. (2002). Mechanism of actions of antidepressants: beyond the receptors. *Bull. Clin. Psychopharmacol.* 12, 194–200.

Yohn, S. E., Arif, Y., Haley, A., Tripodi, G., Baqi, Y., Müller, C. E., et al. (2016a). Effort-related motivational effects of the pro-inflammatory cytokine interleukin-6: pharmacological and neurochemical characterization. *Psychopharmacology* 233, 3575–3586. doi: 10.1007/s00213-016-4392-9

Yohn, S. E., Errante, E. E., Rosenbloom-Snow, A., Somerville, M., Rowland, M., Tokarski, K., et al. (2016b). Blockade of uptake for dopamine, but not norepinephrine or 5-HT, increases selection of high effort instrumental activity: implications for treatment of effort-related motivational symptoms in psychopathology. *Neuropharmacology* 109, 270–280. doi: 10.1016/j.neuropharm.2016.06.018

Yohn, S. E., Lopez-Cruz, L., Hutson, P. H., Correa, M., and Salamone, J. D. (2016c). Effects of lisdexamfetamine and s-citalopram, alone and in combination, on effort-related choice behavior in the rat. *Psychopharmacology* 233, 949–960. doi: 10.1007/s00213-015-4176-7

Yohn, S. E., Gorka, D., Mistry, A., Collins, S., Qian, E., Correa, M., et al. (2017). Oral ingestion and intraventricular injection of curcumin attenuates the effort-related effects of the VMAT-2 inhibitor tetrabenazine: implications for motivational symptoms of depression. *J. Nat. Prod.* 80, 2839–2844. doi: 10.1021/acs.jnatprod.7b00425

Yohn, S. E., Thompson, C., Randall, P. A., Lee, C. A., Müller, C. E., Baqi, Y., et al. (2015). The VMAT-2 inhibitor tetrabenazine alters effort-related decision making as measured by the T-maze barrier choice task: reversal with the adenosine A_{2A} antagonist MSX-3 and the catecholamine uptake blocker bupropion. *Psychopharmacology* 232, 1313–1323. doi: 10.1007/s00213-014-3766-0

Yu, G., Maskray, V., Jackson, S. H., Swift, C. G., and Tiplady, B. (1991). A comparison of the central nervous system effects of caffeine and theophylline in elderly subjects. *Br. J. Clin. Pharmacol.* 32, 341–345. doi: 10.1111/j.1365-2125.1991.tb03909.x

Zisook, S., Rush, A. J., Haight, B. R., Clines, D. C., and Rockett, C. B. (2006). Use of bupropion in combination with serotonin reuptake inhibitors. *Biol. Psychiatry* 59, 203–210. doi: 10.1016/j.biopsych.2005.06.027

Conflict of Interest Statement: JS has received grants from Merck-Serrono, Pfizer, Roche, Shire, and Prexa. MC has received a grant from Servier.

The other author declares that the research was conducted in the absence of any commercial or financial relationships that could be construed as a potential conflict of interest.

frontiers in Pharmacology

ORIGINAL RESEARCH
published: 03 May 2018
doi: 10.3389/fphar.2018.00418

Microglia $P2Y_{13}$ Receptors Prevent Astrocyte Proliferation Mediated by $P2Y_1$ Receptors

*Clara Quintas[1,2], Nuno Vale[1,3], Jorge Gonçalves[1,4] and Glória Queiroz[1,4]**

[1] Laboratory of Pharmacology, Department of Drug Sciences, Faculty of Pharmacy, University of Porto, Porto, Portugal, [2] REQUIMTE/LAQV, University of Porto, Porto, Portugal, [3] REQUIMTE/UCIBIO, University of Porto, Porto, Portugal, [4] MedInUP, University of Porto, Porto, Portugal

Cerebral inflammation is a common feature of several neurodegenerative diseases that requires a fine interplay between astrocytes and microglia to acquire appropriate phenotypes for an efficient response to neuronal damage. During brain inflammation, ATP is massively released into the extracellular medium and converted into ADP. Both nucleotides acting on P2 receptors, modulate astrogliosis through mechanisms involving microglia-astrocytes communication. In previous studies, primary cultures of astrocytes and co-cultures of astrocytes and microglia were used to investigate the influence of microglia on astroglial proliferation induced by ADPβS, a stable ADP analog. In astrocyte cultures, ADPβS increased cell proliferation through activation of $P2Y_1$ and $P2Y_{12}$ receptors, an effect abolished in co-cultures (of astrocytes with ∼12.5% microglia). The possibility that the loss of the ADPβS-mediated effect could have been caused by a microglia-induced degradation of ADPβS or by a preferential microglial localization of $P2Y_1$ or $P2Y_{12}$ receptors was excluded. Since ADPβS also activates $P2Y_{13}$ receptors, the contribution of microglial $P2Y_{13}$ receptors to prevent the proliferative effect of ADPβS in co-cultures was investigated. The results obtained indicate that $P2Y_{13}$ receptors are low expressed in astrocytes and mainly expressed in microglia. Furthermore, in co-cultures, ADPβS induced astroglial proliferation in the presence of the selective $P2Y_{13}$ antagonist MRS 2211 (3 μM) and of the selective $P2Y_{12}$ antagonist AR-C66096 (0.1 μM), suggesting that activation of microglial $P2Y_{12}$ and $P2Y_{13}$ receptors may induce the release of messengers that inhibit astroglial proliferation mediated by $P2Y_{1,12}$ receptors. In this microglia-astrocyte paracrine communication, $P2Y_{12}$ receptors exert opposite effects in astroglial proliferation as a result of its cellular localization: cooperating in astrocytes with $P2Y_1$ receptors to directly stimulate proliferation and in microglia with $P2Y_{13}$ receptors to prevent proliferation. IL-1β also attenuated the proliferative effect of ADPβS in astrocyte cultures. However, in co-cultures, the anti-IL-1β antibody was unable to recover the ADPβS-proliferative effect, an effect that was achieved by the anti-IL-1α and anti-TNF-α antibodies. It is concluded that microglia control the $P2Y_{1,12}$ receptor-mediated astroglial proliferation through a $P2Y_{12,13}$ receptor-mediated mechanism alternative to the IL-1β suppressive pathway that may involve the contribution of the cytokines IL-1α and TNF-α.

Keywords: $P2Y_{13}$ receptors, $P2Y_1$ receptors, microglia, cell proliferation, astrocyte-microglia communication, IL-1β, anti-IL-1α, anti-TNF-α

OPEN ACCESS

Edited by:
Francisco Ciruela, Universitat de Barcelona, Spain

Reviewed by:
Alexander A. Mongin, Albany Medical College, United States
Dmitry Lim, Università degli Studi del Piemonte Orientale, Italy

***Correspondence:**
Glória Queiroz
gloria@ff.up.pt

Specialty section:
This article was submitted to Experimental Pharmacology and Drug Discovery, a section of the journal Frontiers in Pharmacology

Received: *17 November 2017*
Accepted: *10 April 2018*
Published: *03 May 2018*

Citation:
Quintas C, Vale N, Gonçalves J and Queiroz G (2018) Microglia $P2Y_{13}$ Receptors Prevent Astrocyte Proliferation Mediated by $P2Y_1$ Receptors. Front. Pharmacol. 9:418. doi: 10.3389/fphar.2018.00418

INTRODUCTION

Astrocytes and microglia respond to all types of central nervous system (CNS) insults, undergoing through several morphological and functional changes to adapt to the requirements of the surrounding inflammatory response. Microglia initiate a response that starts with their activation and with a rapid mobilization to the site of injury, to phagocyte death cells and to remove cell debris (Hanisch and Kettenmann, 2007). Astrocytes also become reactive, coursing with glial fibrillary acidic protein up-regulation, hypertrophy and, in some cases, proliferation, to form a glial scar that limits the damaged area and prevents widespread inflammation (Sofroniew, 2014).

Pro-inflammatory cytokines attain high extracellular concentrations at the early stages of the inflammatory response and trigger, or modulate, the course of astrogliosis (Buffo et al., 2010). Since microglia are the main source of inflammatory mediators, these cells are regarded as active players in orchestrating the progression of astrogliosis. Microglia activation, and an increase in microglia-derived mediators, are primary events that occur in the inflammatory response, even before the astrocytes response (Zhang et al., 2010), supporting the relevance of a continuous communication between microglia and astrocytes during inflammatory insults, to control astrogliosis.

Purinergic signaling plays a central role in the microglia-astrocyte communication during the CNS inflammatory response. Nucleotides, leaked from dying or damaged cells, act as damage-associated molecular patterns, signaling the damage and triggering different actions through activation of ionotropic P2X or metabotropic P2Y receptors, expressed in astrocytes and microglia (Di Virgilio et al., 2009). For example, ATP and its metabolite ADP, activate microglia $P2Y_1$, $P2Y_{12}$ and $P2X_4$ receptors (Ohsawa et al., 2007; De Simone et al., 2010) that act as sensors to guide microglia to the site where the inflammatory response is occurring (Davalos et al., 2005). In astrocytes, activation of $P2Y_1$ and $P2Y_{12}$ receptors causes hypertrophy and stimulates proliferation, to create the glial scar that confines the lesion site, restraining the secondary neuronal damage (Franke et al., 2004; Quintas et al., 2011a).

It is also known that inflammatory mediators, released by microglia, modulate the expression and function of G protein-coupled receptors that induce an increase in $[Ca^{2+}]_i$ in astrocytes (Hamby et al., 2012). $P2Y_1$ receptors are metabotropic receptors which, in astrocytes, mediate an increase in $[Ca^{2+}]_i$ (Fischer et al., 2009) and trigger astroglial proliferation, an hallmark of astrogliosis (Franke et al., 2004). Therefore, it is expectable that microglia inflammatory mediators may modulate $P2Y_1$ receptors activity and consequently, influence astrogliosis progression.

We have previously confirmed that astroglial proliferation may be induced not only by activation of astrocyte $P2Y_1$ receptors, but also by $P2Y_{12}$ receptors (Quintas et al., 2011a). It was further demonstrated that $P2Y_{1,12}$ receptor-mediated astroglial proliferation is inhibited in co-cultures of astrocytes and microglia, when microglia P2Y receptors are also activated (Quintas et al., 2011b). In those studies, it was excluded the possibility that the loss of the ADPβS-mediated effect could have been caused by a microglia-induced metabolisation of the compound or by a preferential microglial localization of $P2Y_1$ or $P2Y_{12}$ receptors, but it was evident that microglial P2Y receptors induced the release of diffusible paracrine mediator(s) to prevent ADPβS-mediated astroglial proliferation. Since ADPβS also activates $P2Y_{13}$ receptors, this subtype arise as a promising candidate to mediate this microglia-astrocytes communication.

Expression of $P2Y_{13}$ receptors was previously detected in microglia from the whole brain of mice (Crain et al., 2009), but also in astrocytes of several brain regions (Fumagalli et al., 2004; Carrasquero et al., 2005; Fischer et al., 2009), and functional studies support the relevance of these receptor subtypes in both types of cells. $P2Y_{13}$ receptors activation was shown to elicit $[Ca^{2+}]_i$ increase in microglia (Zeng et al., 2014) and astrocytes (Carrasquero et al., 2009; Fischer et al., 2009) and to mediate the release of several pro-inflammatory cytokines by microglia, such as IL-1β, IL-6 and TNF-α (Liu et al., 2017).

In the previous studies, P2Y receptor-mediated astrocyte proliferation was induced by ADPβS, a stable ADP analog selective for $P2Y_1$, $P2Y_{12}$ and $P2Y_{13}$ receptors (Quintas et al., 2011a). However, the mechanisms behind this P2Y receptor-mediated communication between microglia and astrocytes are still largely unknown, namely the subtype of receptors involved and the identity of such mediator(s). Therefore, the aim of the present study was to clarify the role of each of these P2Y receptor subtypes in the microglia modulation of astroglial proliferation.

It is concluded that microglial $P2Y_{12}$ and $P2Y_{13}$ are the receptor subtypes involved in preventing astroglial proliferation mediated by ADPβS in co-cultures of astrocytes and microglia. As far as putative mediator(s) are concerned, the present study further shows that, in spite of all indications that microglia-derived IL-1β could be a strong candidate to prevent ADPβS-induced astroglial proliferation, the microglial P2Y receptor inhibition of astrocyte proliferation occurs through a IL-1β independent mechanism, which involves the release of IL-1α and TNF-α.

MATERIALS AND METHODS

Drugs and Antibodies

The following antibodies and drugs were used: goat anti-mouse IgG conjugated to Alexa Fluor 488 from Invitrogen (Barcelona, Spain); rabbit polyclonal anti-$P2Y_{13}$ from Alomone Laboratories (Jerusalem, Israel); mouse monoclonal anti-CD11b, and goat anti-rabbit IgG conjugated to horseradish peroxidase from Santa Cruz Biotechnology (Santa Cruz, CA, United States); 5-bromo-20-deoxyuridine (BrdU), rabbit polyclonal anti-BrdU, rabbit polyclonal anti-α tubulin, goat anti-rabbit IgG conjugated to Alexa Fluor 594 from Abcam (Cambridge, United Kingdom); rabbit and mouse anti-glial fibrillary acidic protein (anti-GFAP), recombinant rat interleukin-1β, rabbit polyclonal anti-interleukin-1β antibody, adenosine 5'-*O*-(3-thio)-diphosphate tetralithium (ADPβS), 2′-(4-hydroxyphenyl)-5-(4-methyl-1-piperazinyl)-2,5′-bi-1H-benzimidazole trihydrochloride hydrate (Hoechst 33258), penicillin and streptomycin from Sigma-Aldrich (Sintra, Portugal); 2-(propylthio)adenosine-5′-*O*-(β,γ-difluoromethylene)triphosphate tetrasodium (AR-C66096),

2-[(2-chloro-5-nitrophenyl) azo]-5-hydroxy-6-methyl-3-[(phosphonooxy)methyl]-4-pyridinecarboxaldehyde disodium (MRS 2211) and (1R*,2S*)-4-[2-Iodo-6-(methylamino)-9H-purin-9-yl]-2-(phosphonooxy)bicyclo[3.1.0]hexane-1-methanol dihydrogen phosphate ester tetraammonium (MRS 2500) from Tocris (Bristol, United Kingdom); *methyl*-[^{3}H]-thymidine (specific activity 80–86 Ci.mmol^{-1}) and enhanced chemiluminescence (ECL) Western blotting system from Amersham Biosciences (Lisbon, Portugal); goat polyclonal IL-1α antibody, mouse polyclonal TNF-α antibody from ThermoFisher Scientific (Lisbon, Portugal). Stock solutions of drugs were prepared with distilled water and kept at −20°C. Solutions of drugs were prepared from stock solutions diluted in culture medium immediately before use.

Cell Cultures

Animal handling and experiments were conducted according to the guidelines of the Directive 2010/63/EU of the European Parliament and the Council of the European Union and the Organismo Responsável pelo Bem-Estar Animal (ORBEA) from ICBAS-UP. Primary cortical astroglial cultures were prepared from offspring of Wistar rats (Charles River, Barcelona, Spain) as previously described (McCarthy and de Vellis, 1980). Briefly, the brains were placed in ice-cold Dulbecco's phosphate buffered calcium-free saline solution (DPBS) containing 0.2% glucose. The meninges and blood vessels were removed from hemispheres and after washing twice with ice-cold DPBS, they were cut into small pieces in culture medium, i.e., Dulbecco's modified Eagle medium containing 3.7 g/L $NaHCO_3$, 1.0 g/L D-glucose and stable glutamine, supplemented with 50 U/ml penicillin, 50 μg/ml streptomycin. Tissue from two hemispheres was dissociated by triturating in 10 ml culture medium. The cell suspension obtained was passed through a 40-μm pore nylon mesh and then centrifuged at 200 × *g* for 5 min and the supernatant discharged. Centrifugation followed by cell suspension was repeated twice and the pellet obtained was suspended in culture medium supplemented with 10% foetal bovine serum (FBS), and seeded at a density of 2×10^5 cells/ml. Cultures were incubated at 37°C in a humidified atmosphere of 95% air, 5% CO_2 and the medium was replaced 1 day after preparation and subsequently twice a week. Confluent co-cultures of astrocytes and microglia were obtained at DIV14-18.

To prepare highly enriched astroglial cultures, that were named astrocytes cultures, confluent co-cultures were shaken overnight at 200 rpm to detach microglia sitting on the top of the astroglial monolayer and then trypsinized and subcultured to remove microglia trapped within the astroglial monolayer (Saura, 2007).

The suppernant obtained from confluent co-cultures after shaken overnight, which was enriched in microglia, was not discharged being used to prepared microglia cultures as previously described (Ni and Aschner, 2010; Deierborg, 2013). Briefly, the suppernant of shaken co-cultures was collect in 50 ml tubes previously cooled to 4°C and centrifuged at 1000 rpm for 10 min at 4°C. The supernant was discarded, the pellet obtained was resuspended in complete medium and cells were seeded at a density of 10^6 cells/ml. The surface of the supports used for culturing micoglia were previously coated with poly-L-lysine for better cell adhesion. To promote selective adhesion of microglia, culture medium was changed 1 h after seeding and replaced by complete medium containing 5 ng/ml M-CSF to promote microglial growth.

Co-cultures were used in experiments at DIV23. Highly enriched astrocyte cultures and microglia cultures were used at DIV6 after purification. All types of cultures were synchronized to a quiescent phase of the cell cycle, by shifting serum concentration to 0.1% FBS for 48 h before performing the experiments.

DNA Synthesis

At DIV23, cultures grown in 24-well plates, were incubated with ADPβS, IL-1β, or solvent for 48 h and methyl-[^{3}H]-thymidine was added to the medium in the last 24 h, at a concentration of 1 μCi/ml. When present, antagonists were added to the medium 1 h before ADPβS. IL-1β and the anti-ILs antibodies tested were added at the same time as ADPβS. At the end of the 48 h period of incubation, cells were rinsed with PBS, fixed with 10% of trichloroacetic acid for 30 min at 4°C, washed with ice-cold 5% trichloroacetic acid and rinsed again with PBS. Protein content and methyl-[^{3}H]-thymidine incorporation were evaluated after cell lysis with 0.2 M NaOH. The effect of drugs in cell proliferation was determined by *methyl*-[^{3}H]-thymidine incorporation, quantified by liquid scintillation spectrometry (Beckman LS 6500, Beckman Instruments, Fullerton, CA, United States) and normalized by the protein content determined by the Bradford method.

Immunocytochemistry

Cell cultures grown on 13 mm round coverslips were fixed in 4% paraformaldehyde and 4% sucrose in phosphate buffered saline (PBS; 100 mM NaH_2PO_4, 50 mM NaCl, pH adjusted to 7.3) and then incubated with 10% FBS, 1% bovine serum albumin, 0.1% Triton X, 0.05% NaN3 in PBS for 1 h. For double labeling astrocytes and microglia, and for $P2Y_{13}$ receptors localization, cultures were incubated overnight at 4°C with the following primary antibodies, diluted in 5% FBS, 1% bovine serum albumin, 0.1% Triton X, 0.05% NaN3 in PBS: rabbit or mouse anti-glial fibrillary acidic protein (anti-GFAP, 1:600), mouse anti-CD11b (1:50) and rabbit anti-$P2Y_{13}$ (1:200). Visualization of GFAP, CD11b and $P2Y_{13}$ receptors positive cells was accomplished upon 1 h incubation, at room temperature, with the secondary antibodies anti-rabbit IgG conjugated to Alexa Fluor 594 and anti-mouse IgG conjugated to Alexa Fluor 488 (both at 1:400). In negative controls, the primary antibody was omitted. Cell nuclei were labeled with Hoechst 33258 (5 μg/ml) for 1 min at room temperature. To evaluate the percentage of microglia, the two types of cultures were processed in parallel and about 200 cells were counted in each culture. The number of CD11b positive cells was expressed as percentage of the total number of cells counted. Images were captured with Lionheart^{TM} FX Automated Microscope (Biotek, United Kingdom).

BrdU Staining

In astrocyte cultures, proliferation of astrocytes or contaminating microglia was identified through double labeling of GFAP or CD11b and 5-bromo-20-deoxyuridine (BrdU) positive cells. Astrocytes cultures grown on 13 mm round coverslips were incubated with ADPβS 300 μM for 48 h. BrdU (100 μM) was added to the medium for the last 24 h, after which time the cells were incubated with mouse anti-CD11b (1:50) for 30 min at 37°C and then fixed with in 4% paraformaldehyde and 4% sucrose in PBS for 15 min at room temperature. Coverslips were washed with PBS and then incubated for 20 min with methanol to permeabilize the membranes. The BrdU epitope was exposed by incubating the cells in 2 M hydrochloric acid for 1 h at 37°C followed by neutralization with 0.1 M sodium borate, pH 8.5 for 20 min. Cell cultures were blocked with 3% FBS and then incubated with mouse anti-GFAP (1:600) and rabbit anti-BrdU (1:300) for 1 h, at room temperature. Visualization of GFAP or CD11b and BrdU positive cells was accomplished upon 1 h incubation, at room temperature, with the secondary antibodies anti-rabbit IgG conjugated to Alexa Fluor 594 and anti-mouse IgG conjugated to Alexa Fluor 488 (both at 1:400). In negative controls, the primary antibody was omitted. Images were captured with Lionheart^{TM} FX Automated Microscope (Biotek, United Kingdom).

Real Time RT-qPCR Analysis

RNA was extracted from astrocyte and microglia cultures with the RNeasy Mini Kit (QIAGEN), according to manufacturer's instructions. RNA purity and concentration was confirmed using a Synergy HT spectrophotometer (Biotek, United Kingdom). Nine hundred ng of RNA (astrocytes) or 70 ng of RNA (microglia) were used as a template for reverse-transcriptase reactions using the NZY First-Strand cDNA Synthesis kit (NZYTech). The primer sequences, listed in **Table 1**, were designed and evaluated with Beacon Designer^{TM} Software 7 (PREMIER Biosoft). Primer specificity was assessed through NCBI BLAST analysis prior to use and, for each sample following PCR, it was verified that the dissociation curve had a single peak with an observed Tm consistent with the amplicon length. Standard dilutions of the cDNA were used to check the relative efficiency and quality of primers. Negative controls (no template cDNA) were included in all qPCR.

qPCR amplifications were performed in duplicate, using 0.125 μM of each primer,10 μl of 2X iTaqTM Universal SYBR Green Supermix (Bio-Rad) and 1 μl of template cDNA. qPCRs were carried out on a CFX96 Touch^{TM} Real-Time PCR Detection System (Bio-Rad) and conditions were as follows: 95°C for 3 min followed by 40 cycles of denaturation at 95°C for 10 s, 60°C annealing temperature for 30 s. Melting curves of the PCR amplicons were then generated with temperatures ranging from 55°C to 95°C, with increments of 0.5°C at a rate of 10 s/step. The melting curve data were analyzed with the CFX Manager^{TM} (ver. 2.0, Bio-Rad). The data obtained were analyzed using the method described by Pfaffl (2001). Ct values from duplicate measurements were averaged, and relative expression levels were determined by the $2^{-\Delta C_T}$ method. While PCRs were run to 40 cycles, all detected genes had Ct values below 31 in all of the samples examined. For each analysis GAPDH and β-actin were used for normalization.

Western Blot Analysis

Cell cultures were rinsed with ice-cold PBS and total cell protein extracted in lysis buffer with protease inhibitors (1 mM Na_3VO_4, 1 mM NaF, 1 mM PMSF, 2 μg/ml aprotinin and 2 μg/ml leupeptin). Ceramic beads with 1.4 mm were added to the samples, which were disrupted with two cycles of 15 s at 5800 rpm in the Precellys Evolution homogenizer (Bertin Instruments, France). The lysate was incubated on ice for 1 h and then centrifuged at 20,000 × *g* for 45 min at 4°C. The protein concentration was determined in the supernatant and equal amounts of protein (50 μg) were boiled at 70°C for 10 min in 6x sample buffer (0.35 M Tris–HCl at pH 6.8, 10% SDS, 30% glycerol, 9.3% dithiothreitol, 0.01% bromphenol blue, 5% mercaptoethanol) and subjected to 12% SDS-PAGE (SDS-polyacrylamide gel electrophoresis). Proteins were electrotransferred onto nitrocellulose membranes overnight at 40 V in transfer buffer. Membranes were blocked at room temperature for 2 h with 5% of bovine serum albumin in PBS, and then probed for 2 h at room temperature with primary polyclonal antibody rabbit anti-$P2Y_{13}$ (1:200) followed by the secondary antibody goat anti-rabbit IgG conjugated to horseradish peroxidase (1:10,000). Immunoblots were then stripped by incubation in stripping buffer (62.5 mM Tris-HCl, 100 mM 2-mercaptoethanol and 2% SDS, pH adjusted to 6.8) for 15 min at 50°C and blocked overnight with 5% of bovine serum albumin in PBS. Subsequently, membranes were re-probed with the primary polyclonal antibody rabbit anti-atubulin (1:1000) for 1 h at room temperature, followed by the secondary antibody. Immunocomplexes were detected using Novex ECL Chemiluminescent kit (Life Technologies) and ChemiDoc MP Imaging System (Bio-Rad, Portugal).

TABLE 1 | Primer sequence table.

Gene	Forward primer	Reverse primer
$P2Y_1$	5′-CTGATCTTGGGCTGTTATGG-3′	5′-GCTGTTGAGACTTGCTAGAC-3′
$P2Y_{12}$	5′-TGTTCCTGCTGTCACTGCCTAA-3′	5′-CTCGTGCCAGACCAGACCAA-3′
$P2Y_{13}$	5′-TGCACTTTCTCATCCGTGGT-3′	5′-GGCAGGGAGATGAGGAACAT-3′
β-actin	5′-CTGTGCTATGTTGCCCTA-3′	5′-CCGATAGTGATGACCTGAC-3′
GAPDH	5′-TTCAACGGCACAGTCAAG-3′	5′-TACTCAGCACCAGCATCA-3′

Statistical Analysis

Data are expressed as means ± standard errors of the mean (S.E.M.) from n independent cell cultures tested in triplicated, or duplicated in qRT-PCR experiments. Statistical analysis was carried out using the unpaired Student's *t*-test or one-way analysis of variance (ANOVA) followed by Dunnett's multiple comparison test. Statistical analysis performed on $2^{-\Delta C_T}$ data was carried out using one-way ANOVA followed by Bonferroni's *post hoc* comparisons tests. *P*-values lower than 0.05 were considered to indicate significant differences.

RESULTS

Characterization of Glial Cultures

Two types of cell cultures were prepared, astrocytes being the predominant cell type. When no treatment was applied, cultures could be described as a monolayer of astrocytes containing a significant percentage of microglia 12.5 ± 0.2% ($n = 4$). Cultures obtained under these conditions were named astrocyte-microglia co-cultures or, more briefly, co-cultures. Confluent astrocyte-microglia co-cultures were treated to eliminate microglia (see section "Materials and Methods"), resulting in cell cultures of astrocytes with much less microglia (1.6 ± 0.1%; $n = 4$). Cultures obtained under these conditions were named astrocyte cultures. Both types of cultures, co-cultures and astrocyte cultures, were used in the experiments to identify microglia P2Y receptor subtype(s) and to explore potential paracrine mechanisms involved in the control of the ADPβS-induced astroglial proliferation.

Glial P2Y Receptor Subtype(s) Involved in the Modulation of ADPβS-Induced Astroglial Proliferation

The proliferative effect of ADPβS was compared in astrocyte cultures and in co-cultures to clarify the influence of microglia in the astrocyte proliferation elicited by this more stable ADP analog, selective for $P2Y_1$, $P2Y_{12}$ and $P2Y_{13}$ receptors.

In astrocyte cultures, ADPβS (1–300 μM), increased astroglial proliferation in a concentration-dependent manner, up to 201 ± 10% ($n = 4$; **Figure 1**). Although astroglial cultures had about 2% of contaminating microglia (see above), proliferation of astrocytes and microglia was differentiated through a double labeling of GFAP or CD11b with 5-bromo-20-deoxyuridine (BrdU), to identify the type of BrdU positive cells. The results indicate that the main proliferating cells, the BrdU positive cells, were astrocytes (**Figure 2**).

The proliferative effect caused by ADPβS (300 μM) was antagonized by MRS 2500 (1 μM), a selective antagonist of $P2Y_1$ receptor, by AR-C66096 (0.1 μM), a selective antagonist of $P2Y_{12}$ receptor, but not by MRS 2211 (3 μM), a selective antagonist of $P2Y_{13}$ receptor (**Figure 2A**). No additive antagonism was observed when both MRS 2500 (1 μM) and AR-C66096 (0.1 μM) were tested simultaneously (**Figure 3A**).

In co-cultures, ADPβS failed to cause astroglial proliferation. However, the ADPβS-induced astroglial proliferation was almost restored in the presence of MRS 2211 (3 μM), reaching proliferation levels similar to those observed in astrocyte cultures, and only partially restored by AR-C66096 (0.1 μM). When $P2Y_{12}$ and $P2Y_{13}$ receptors were blocked simultaneously, ADPβS proliferative effect was similar to that observed in the presence of the $P2Y_{13}$ antagonist alone (**Figure 3B**).

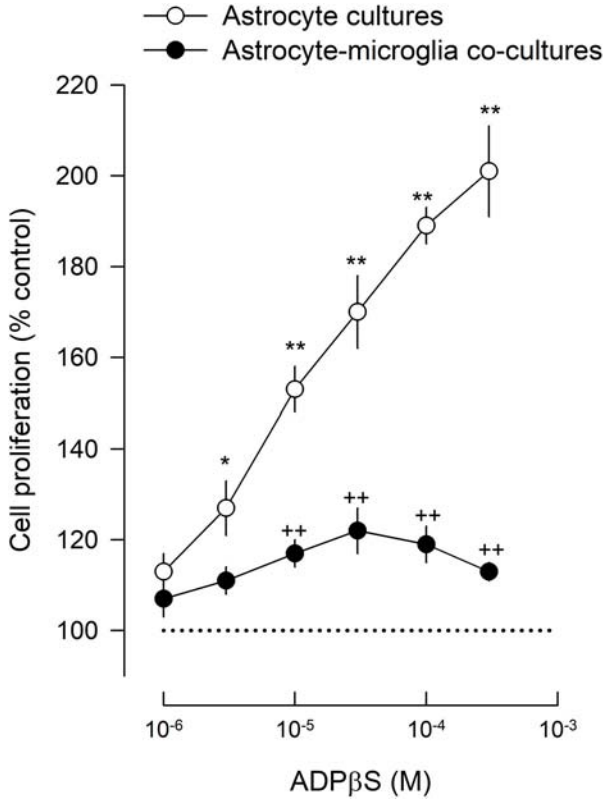

FIGURE 1 | Astroglial proliferation in astrocyte cultures and astrocyte-microglia co-cultures induced by ADPβS. Cultures were incubated with ADPβS or solvent for 48 h and *methyl*-[^{3}H]-thymidine (1 μCi/ml) was added in the last 24 h. Cell proliferation was estimated by *methyl*-[^{3}H]-thymidine incorporation and expressed in percentage of control. Values are means ± SEM from 4 different cultures. $^*P < 0.05$ and $^{**}P < 0.01$, significant differences from control (solvent). $^{++}P < 0.01$, significant differences from the ADPβS in astrocyte cultures.

Expression and Cellular Localization of $P2Y_{13}$ in Glial Cultures

$P2Y_1$ and $P2Y_{12}$ receptor subtypes are known to be expressed both in astrocytes (Fumagalli et al., 2003; Franke et al., 2004; Amadio et al., 2010) and microglia (Bianco et al., 2005; Ohsawa et al., 2007; De Simone et al., 2010) and expression levels of these receptor subtypes was found to be similar in both types of cultures, without any predominant cell-type localization (Quintas et al., 2011b). Therefore, considering these observations, and the results from the pharmacological approach, it remains to be explored a putative role for $P2Y_{13}$ receptor as candidate to mediate the loss of ADPβS-induced astroglial proliferation in co-cultures. Therefore, the expression of $P2Y_{13}$ receptors was

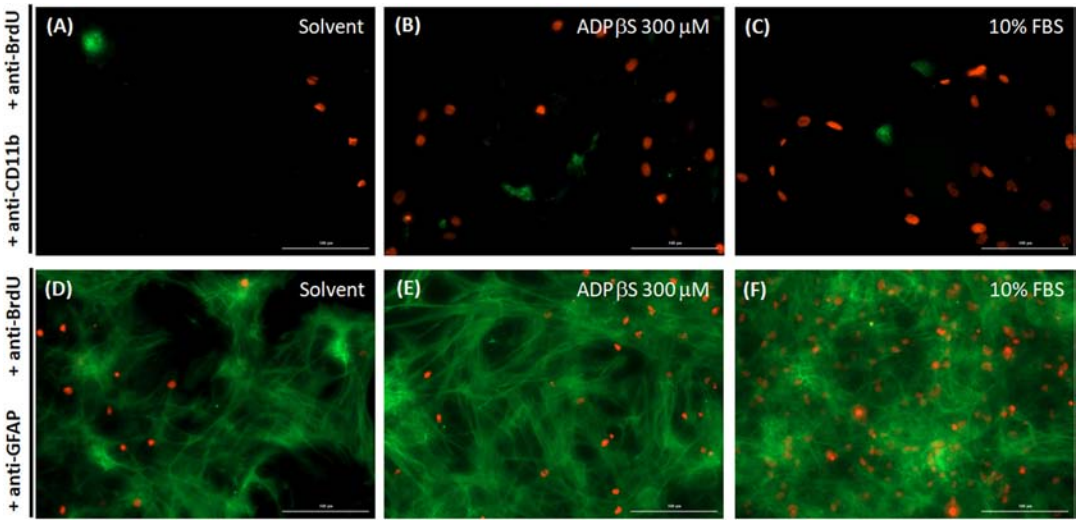

FIGURE 2 | BrdU staining and its cellular localization in astrocyte cultures. Astrocyte cultures were incubated with solvent **(A,D)**, ADPβS **(B,E)** or 10% FBS, a positive control for cell proliferation **(C,F)**, for 48 h. BrdU (100 μM) was added to the medium for the last 24 h and then stained with rabbit anti-BrdU (Alexa Fluor 594, red) to visualize BrdU incorporation. Microglia were then co-labeled with mouse anti-Cd11b (**A–C**; Alexa Fluor 488, green) and astrocytes, with mouse anti-GFAP (**D–F**; Alexa Fluor 488, green). BrdU positive nuclei co-localize mainly with astrocytes, showing they are the main proliferating cells within the astrocyte cultures. Representative images from 3 different cultures. Scale bar: 100 μm.

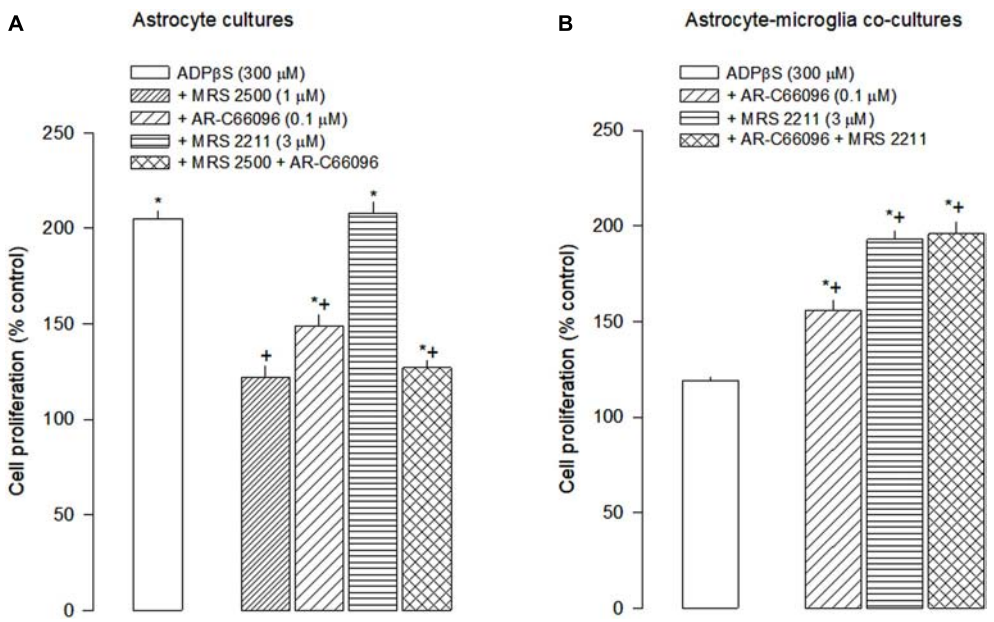

FIGURE 3 | Pharmacological characterization of P2Y receptors involved in the modulation of ADPβS-mediated astroglial proliferation. **(A)** Astrocyte cultures and **(B)** astrocyte-microglia co-cultures were incubated with ADPβS or solvent for 48 h and *methyl*-[^{3}H]-thymidine (1 μCi/mL) was added in the last 24 h. The P2Y antagonists: MRS 2500 (anti-$P2Y_1R$), AR-C66096 (anti-$P2Y_{12}R$) and MRS 2211 (anti-$P2Y_{13}R$) were added to the medium 1 h before ADPβS. Cell proliferation was estimated by *methyl*-[^{3}H]-thymidine incorporation and expressed in percentage of control. Values are means ± SEM from 6 to 10 different cultures. $^*P < 0.05$, significant differences from control (solvent).$^+P < 0.05$, significant differences from ADPβS alone.

further analyzed in both types of cultures and their cellular localization was characterized in co-cultures.

In western blot assays, $P2Y_{13}$ receptors expression was evidenced by two immunoreactive bands of 32 and 52 kDa that reacted with the anti-$P2Y_{13}$ antibody. These bands were absent in the presence of the $P2Y_{13}$ neutralizing peptide, indicating they represent specific epitopes for the anti-$P2Y_{13}$ receptor antibody (**Figure 4A**, see also Supplementary Material). qRT-PCR experiments confirm the expression of the three receptor subtypes in astrocyte cultures, despite the significant lower

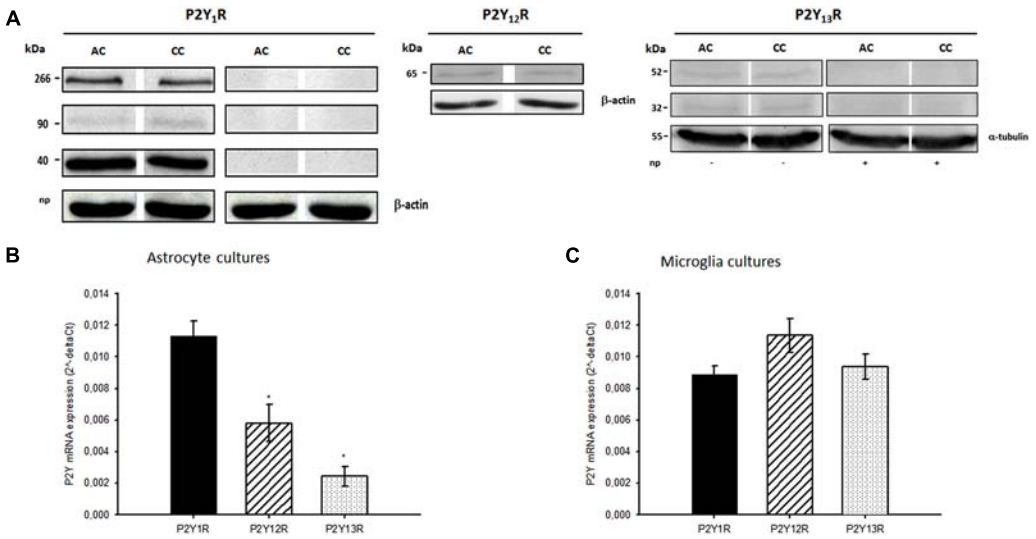

FIGURE 4 | Expression of $P2Y_1$, $P2Y_{12}$ and $P2Y_{13}$ receptors. **(A)** Representative Western blots of $P2Y_1$, $P2Y_{12}$ and $P2Y_{13}$ receptors ($P2Y_1R$, $P2Y_{12}R$ and $P2Y_{13}R$) expression in astrocyte-microglia co-cultures (CC) and astrocyte cultures (AC). $P2Y_1R$, $P2Y_{12}R$ and β-actin (43 kDa) expression data previously published by Quintas et al. (2011a,b). $P2Y_{13}$ receptors ($P2Y_{13}R$) and α-tubulin (55 kDa) expression were obtained from whole cell lysates. Two immunoreactive bands of 32 and 52 kDa specifically reacted with rabbit anti-$P2Y_{13}$ antibody. These bands were absent in the presence of the respective neutralising peptide (np). mRNA expression of P2YR in **(B)** astrocyte cultures and **(C)** microglia cultures. mRNA P2YR expression were determined using qRT-PCR and normalized to GAPDH (astrocytes cultures) or β-actin (microglial). Values are means ± SEM from 3 different cultures. $^*P < 0.05$, significant differences from $P2Y_1R$ expression.

expression of $P2Y_{12}$ and $P2Y_{13}$ receptors, when compared to that of $P2Y_1$ receptors (**Figure 4B**). In contrast, the expression of these receptor subtypes was similar in microglia cultures (**Figure 4C**). The results obtained indicate that, even though at low expression levels, $P2Y_{13}$ receptors are present in co-cultures and astrocyte cultures and that both cell types, astrocytes and microglia, express the receptor.

Immunocytochemistry analysis of co-cultures, revealed low immunoreactivity for $P2Y_{13}$ receptors in astrocytes (**Figures 5A–C**), and a preferentially localization in microglial cells ($P2Y_{13}$ receptor subtype in red and the CD11b integrin in green; **Figures 5D–F**). Although astrocytes express $P2Y_{13}$ receptors, it is clear that $P2Y_{13}$ receptors are mostly localized in microglia, and thus, may have a more relevant role in controlling the ADPβS-induced astroglial proliferation through $P2Y_{1,12}$ receptors.

On the Microglia Paracrine Mediator That Prevents the ADPβS-Induced Astroglial Proliferation

Previous studies have shown that, in co-cultures, ADPβS activates microglia P2Y receptors, inducing release of non-identified diffusible messenger(s) that attenuated its proliferative effect in astrocytes (Quintas et al., 2011b). Interleukins are potential candidates, since recently it was demonstrated that activation of microglia $P2Y_{12,13}$ receptors induces the release of IL-1β, TNF-α and IL-6 (Liu et al., 2017). Furthermore, IL-1β has been shown to decrease the activity of $P2Y_1$ receptors (Scemes, 2008). In preliminary experiments, the presence of IL-1β was detected by ELISA in the supernatant of co-cultures treated with ADPβS (not shown). Therefore, it was hypothesized that activation of microglial $P2Y_{12,13}$ receptors by ADPβS may induce release of IL-1β from microglia, which in turn interacts with $P2Y_1$ receptors expressed in astrocytes, to prevent the ADPβS-induced astroglial proliferation.

In agreement with this hypothesis, in astrocyte cultures, IL-1β attenuated ADPβS-induced astroglial proliferation, and this effect was prevented by the anti-IL-1β antibody (**Figure 6A**), supporting the view that IL-1β has conditions to exert such role. Additionally, when tested alone, the anti-IL-1β antibody had no effect, suggesting that there is no significant tonic release of IL-1β by astrocytes or by the small percentage of contaminating microglia.

Considering the hypothesis that IL-1β could be the soluble messenger produced by microglia, responsible for preventing ADPβS-induced astroglial proliferation, the anti-IL-1β antibody was tested in co-cultures to investigate whether, after IL-1β neutralization, ADPβS was able to induce astroglial proliferation. In co-cultures, when tested alone, the anti-IL-1β antibody induced cell proliferation up to 142 ± 4 ($n = 5$; $P < 0.05$), suggesting the occurrence of a basal release of IL-1β by microglia exerting a tonic inhibition of astroglial proliferation. However, the anti-IL-1β antibody was unable to restore the ADPβS proliferative effect (**Figure 6B**), indicating that there is no additional significant release of IL-1β, when ADPβS activates microglial P2Y receptors (not shown).

Following the same hypothesis, and considering the contribution of activated microglia to the release of other interleukins, such as IL-1α and TNF-α (Liu et al., 2017; Liddelow et al., 2017), that have been shown to change de reactivity of astrocytes (Liddelow et al., 2017), the interaction between

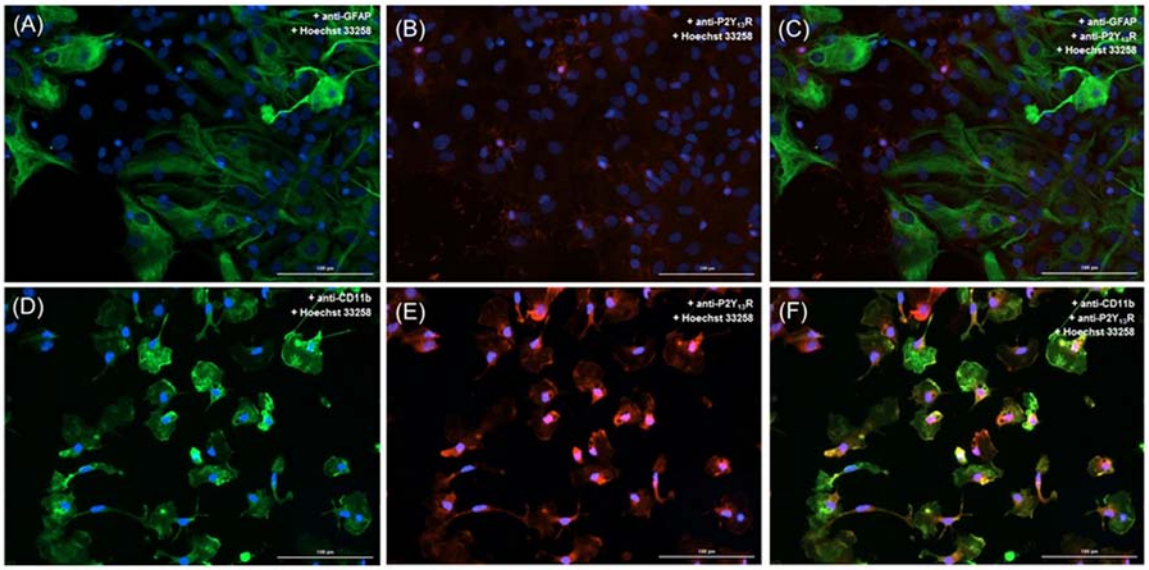

FIGURE 5 | Cellular distribution and localization of P2Y$_{13}$ receptors in astrocyte-microglia co-cultures. Astrocytes were double labeled with **(A)** mouse anti-GFAP (Alexa Fluor 488, green) and with **(B)** rabbit anti-P2Y$_{13}$ receptor (Alexa Fluor 594, red). Microglia were double labeled with **(D)** mouse anti-CD11b (Alexa Fluor 488, green) and with **(E)** rabbit anti-P2Y$_{13}$ receptor (Alexa Fluor 594, red). Nuclei were labeled with Hoechst 33258 (blue). P2Y$_{13}$ receptors (red) co-localize with astrocytes **(C)** but mainly with microglia **(F)**. Scale bar: 100 μm.

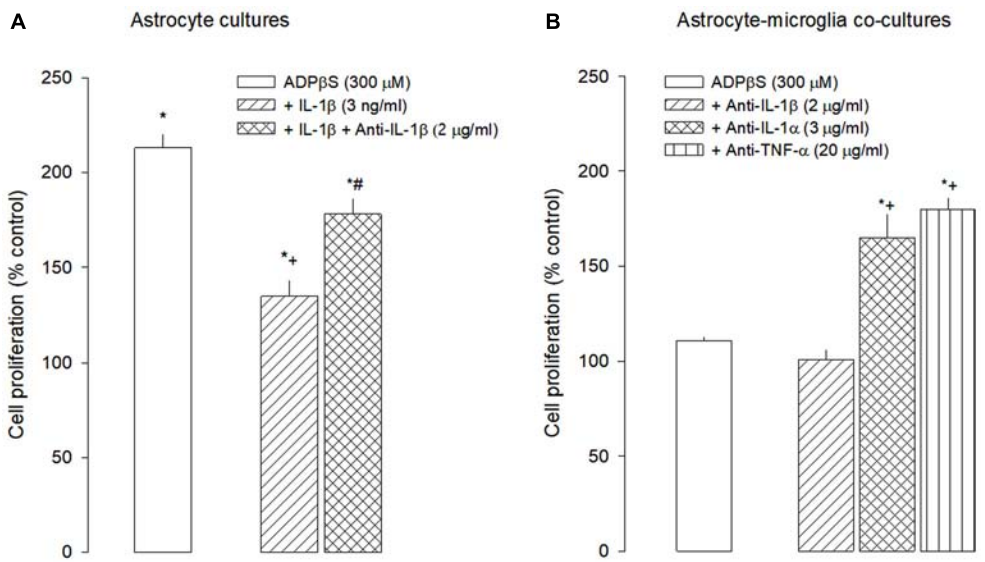

FIGURE 6 | Effect of IL-1β and anti-IL-1β antibody on proliferation induced by ADPβS in astrocyte cultures **(A)** and effect of antibodies anti-IL-1β, anti-IL-1α, and anti-TNF-α in proliferation induced by ADPβS on astrocyte-microglia co-cultures **(B)**. **(A)** Astrocyte cultures were incubated with ADPβS alone or in combination with IL-1β or IL-1β plus anti-IL-1β antibody for 48 h. **(B)** Astrocyte-microglia co-cultures were incubated with ADPβS or with anti-ILs antibodies alone or with ADPβS plus anti-ILs antibodies for 48 h. Anti-ILs antibodies, when present were added at the same time as ADPβS or solvent. *Methyl*-[^{3}H]-thymidine (1 μCi/mL) was added in the last 24 h and cell proliferation was estimated by *methyl*-[^{3}H]-thymidine incorporation and expressed in percentage of control. Values are means ± SEM from 4 to 5 different cultures. $^*P < 0.05$, significant differences from the respective control; $^+P < 0.05$, significant differences from ADPβS alone and $^\#P < 0.05$, significant differences from ADPβS plus the anti-IL-I1β antibody.

ADPβS and the antibodies anti-IL-1α and anti-TNF-α was tested in co-cultures. Unlike the anti-IL-1β antibody, both the anti-IL-1α and the anti-TNF-α antibodies had no effect when tested alone, but restored the ADPβS-proliferative effect to levels close to those observed in astrocyte cultures (**Figure 6B**). These results suggest that activation of microglia P2Y$_{12,13}$ receptors by ADPβS may induce the release of IL-1α and TNF-α that control astroglial proliferation.

DISCUSSION

Nucleotides, such as ATP and ADP are massively present in the extracellular medium during brain lesion, and were shown to activate P2Y receptors, modulating astroglial proliferation through mechanisms that involve communication between microglia and astrocytes (Quintas et al., 2011b). ADPβS is a stable ADP analog, selective for $P2Y_1$, $P2Y_{12}$, and $P2Y_{13}$ receptor subtypes, and was shown to cause cell proliferation in astrocyte cultures, an effect mediated by $P2Y_1$ and $P2Y_{12}$ receptors (Quintas et al., 2011a). The ADPβS-induced astroglial proliferation was abolished when the percentage of microglia cells increased to about 10–13% microglia (Quintas et al., 2011b). In these previous studies, it was excluded the possibility that a lower expression of $P2Y_1$ and/or $P2Y_{12}$ receptors, or a preferential microglial localization of these P2Y receptor subtypes could explain the absence of ADPβS-induced proliferative effect observed in co-cultures. It was also demonstrated that the presence of microglia did not influence metabolic degradation of ADPβS. Therefore, an activation of microglia P2Y receptors by ADPβS, was seen as the more solid explanation for the lack of ADPβS proliferative effect observed in co-cultures. However, the microglial P2Y receptor subtype(s) involved in the modulation of astroglial proliferation remained to be identified.

In the present study, it was confirmed that, in astrocyte cultures, ADPβS induces cell proliferation. Despite the minor contamination of astrocyte cultures with microglia, we have demonstrated, by BrdU incorporation, that astrocytes are the main proliferating cells. ADPβS proliferative effect in these cultures is triggered through activation of $P2Y_1$ and $P2Y_{12}$ receptor subtypes. The ADPβS proliferative effect was attenuated by the selective $P2Y_1$ receptor antagonist, MRS 2500 (1 μM; Houston et al., 2006) and by the selective $P2Y_{12}$ receptor antagonist, AR-C66096 (0.1 μM; Humphries et al., 1994). Interestingly, no additive effect was observed when both antagonists were tested simultaneously. A possible explanation is that, although they are coupled to different transduction mechanisms, they may convey in a common pathway. In fact, $P2Y_1$ receptors, are coupled to G(q) proteins and mediate astroglial proliferation through activation of phospholipase (PLC)-protein kinase C (PKC)-extracellular signal-regulated kinase 1/2 (ERK1/2) pathway (Neary et al., 2003; Quintas et al., 2011a), whereas $P2Y_{12}$ receptor activation may lead to G(i) βγ-dependent PLC-PKC-ERK1/2 pathway, as seen in 1321N1 human astrocytoma cells (Mamedova et al., 2006) or to a PLC-independent activation of PKC, as seems to occur in glioma C6 cells (Grobben et al., 2001; Van Kolen and Slegers, 2006). Therefore, $P2Y_1$ and $P2Y_{12}$ receptors subtypes, despite being coupled to different G proteins, may activate converging pathways, leading to ERK1/2 activation and cell proliferation. The results obtained in astrocyte cultures further demonstrate that $P2Y_{13}$ receptors are not involved in astroglial proliferation, because the antagonist of $P2Y_{13}$ receptor MRS 2211 (3 μM; Kim et al., 2005) did not change the ADPβS-induced astroglial proliferation.

In co-cultures, the results obtained with ADPβS on proliferation contrast with those observed in astrocyte cultures. In co-cultures, ADPβS failed to induce astroglial proliferation. However, the proliferative effect of ADPβS was restored, to levels similar to those observed in astrocyte cultures, when $P2Y_{13}$ receptors were blocked with MRS 2211, and partially recovered when $P2Y_{12}$ receptors were blocked with AR-C66096.

$P2Y_{12}$ receptors have been shown to be expressed either by microglia (Haynes et al., 2006; Ohsawa et al., 2007; De Simone et al., 2010) or by astrocytes (Fumagalli et al., 2003, 2004; Carrasquero et al., 2005; Amadio et al., 2010). Additionally, our previous studies demonstrated, by western blot and by immunocytochemical assays, that $P2Y_{12}$ receptors are expressed in both astrocytes cultures and co-cultures, by astrocytes and by microglial cells, with no preferential cellular localization (Quintas et al., 2011b). In this study, $P2Y_{12}$ receptors expression in astrocytes and microglia was further supported by quantification of $P2Y_{12}$ transcripts.

Concerning to the $P2Y_{13}$ receptors, they were expressed at low levels either in astrocyte cultures or co-cultures, which is in agreement with its lower mRNA expression in astrocytes. $P2Y_{13}$ receptors have been shown to be expressed in astrocytes of several brain regions, inducing $[Ca^{2+}]_i$ increase (Fumagalli et al., 2004; Carrasquero et al., 2009; Fischer et al., 2009), which suggest a possible role for this receptor subtype in the modulation of astrogliosis. In the present work, $P2Y_{13}$ receptors were shown to be residually expressed by astrocytes, but do not directly modulate of astroglial proliferation. Results obtained by immunocytochemistry showed that they were preferentially expressed by microglia, an observation in line with previous studies that demonstrated the expression of $P2Y_{13}$ receptors in microglia from the whole brain (Crain et al., 2009) and spinal cord, where they elicit $[Ca^{2+}]_i$ increase (Zeng et al., 2014) and the release of several pro-inflammatory cytokines, such as IL-1β, IL-6 and TNF-α (Liu et al., 2017).

From the pharmacological and molecular biology results, it may be concluded that astrocyte $P2Y_{13}$ receptors do not directly mediate astroglial proliferation, but rather act indirectly, through microglia, to regulate P2Y-mediated astroglial proliferation. The $P2Y_{12}$ receptors seem to cooperate with $P2Y_{13}$ receptors to restrain astroglial proliferation in co-cultures.

In co-cultures, $P2Y_{12}$ and $P2Y_{13}$ receptors also do not cause additive effects in preventing the ADPβS-induced astroglial proliferation. Likely, because $P2Y_{12}$ and $P2Y_{13}$ share the same transduction pathways. Both receptor subtypes are coupled to G(i) proteins (Marteau et al., 2003) and/or to an increase in $[Ca^{2+}]_i$, as described in microglial cells (Bianco et al., 2005).

We have previously shown that conditioned medium of microglia treated with ADPβS prevented the proliferative effect mediated by $P2Y_{1,12}$ receptors in astrocyte cultures, supporting the view that, in co-cultures, activation of microglia P2Y receptors induced the release of diffusible paracrine mediator(s) responsible for the inhibitory influence in the ADPβS-induced astroglial proliferation (Quintas et al., 2011b).

A recent report has shown that microglial cytokines, such as IL-1β, TNF-α and IL-6, transform astrocytes into a neuroprotective phenotype, involving downregulation of $P2Y_1$ receptors (Shinozaki et al., 2017). We have also shown that, the presence of microglia was associated with a loss of $P2Y_1$ receptor function, but without changing the expression levels (Quintas et al., 2011b). In line with our observations, it was seen a correlation between the presence of the pro-inflammatory IL-1β and the loss of $P2Y_1$ receptors function in astrocytes, without modifying its expression levels, possibly due to protein-protein interactions (Scemes, 2008). Thus, it was considered the hypothesis that microglial $P2Y_{12,13}$ receptors could induce the release of IL-1β which, acting on astrocytes, would prevent the $P2Y_{1,12}$-mediated proliferation. According to this hypothesis, IL-1β inhibited ADPβS-induced proliferation in astrocytes cultures, an effect prevented by the anti-IL-1β antibody. In co-cultures, but not in astrocyte cultures, the anti-IL-1β antibody, induced astroglial proliferation, suggesting that there is a microglial basal release of IL-1β that tonically inhibits astroglial proliferation. However, ADPβS was still unable to induce astroglial proliferation in the presence of anti-IL-1β antibody, excluding any significant contribution of IL-1β to the microglial $P2Y_{12,13}$ receptor-mediated inhibition of astroglial proliferation.

Another recent study, indicated that activated microglia release IL-1α, TNF-α and the complement factor Cq1, which are involved in phenotypical changes in astrocytes that may lead to a less proliferative and more aggressive profile to neurons (Liddelow et al., 2017). In line with this study it was hypothesized that in co-cultures, ADPβS-activated microglia could release IL-1α, TNF-α, and that these interleukins could be paracrine mediators involved in the inhibition of ADPβS-mediated astroglial proliferation. In co-cultures, both anti-IL-1α and anti-TNF-α antibodies restored, almost completely, the ADPβS proliferative effect, without causing significant effects on basal proliferation, supporting the conclusion that activation of microglia $P2Y_{12,13}$ receptors by ADPβS may induce the release of IL-1α and TNF-α that control $P2Y_{1,12}$ astroglial proliferation.

Taken together, the present results evidence the existence of two distinct pair of receptors controlling astroglial proliferation induced by extracellular purine nucleotides: $P2Y_1$ and $P2Y_{12}$ receptors, present in astrocytes and causing proliferation, and $P2Y_{12}$ and $P2Y_{13}$ receptors, present in microglia, causing a suppression of astroglial proliferation due to the release of soluble messenger(s), on a paracrine mode of communication that is independent of IL-1β, but seems to involve the release of IL-1α and TNF-α.

This purinergic interaction between microglia and astrocytes may be relevant under physiopathological conditions, during the initial phase of the inflammatory response, when there is cell death and inflammation, recruitment of microglia and other inflammatory and immune cells to remove cell debris (Burda and Sofroniew, 2014). Nucleotides are released to the lesion core at these early stages of CNS insult and may coordinate multicellular responses, activating purinergic receptors in astrocytes, microglia and surrounding cells (Buffo et al., 2010). Adenine nucleotides have been shown to induce astroglial proliferation mediated by $P2Y_{1,12}$ receptors (Franke et al., 2004; Quintas et al., 2011a) and would also act as chemotactic signals through activation of $P2Y_{12}$ receptors, causing microglia mobilization to reach the damaged site and to modulate the inflammatory response (Davalos et al., 2005). Here, we demonstrate that activation of microglial $P2Y_{12,13}$ receptors control $P2Y_{1,12}$ receptor-mediated astroglial proliferation. With the arrival of microglia to the lesion core, microglial $P2Y_{12,13}$ receptors would silence $P2Y_{1,12}$ receptor-mediated astroglial proliferation, by the release of paracrine mediators, delaying the formation of the astrocytic scar and, therefore, keeping open the path for more immune cells infiltration. As inflammation is resolved, microglia will change their phenotype, releasing astrocytes from the $P2Y_{12,13}$ proliferative brake, and pave the way for a full remodeling and repair.

ETHICS STATEMENT

Animal handling and experiments were conducted according to the guidelines of the Directive 2010/63/EU of the European Parliament and the Council of the European Union. Ethical commission of the animal house, called Organismo Responsável pelo Bem-Estar Animal (ORBEA), which in English corresponds to "Commission responsible for Animal Welfare," approved this study. Additionally, a qualified veterinary supervised the most critical part, which consisted in the euthanasia of newborn rats.

AUTHOR CONTRIBUTIONS

GQ supervised the entire work, prepared the cell cultures, and performed the experiments of DNA synthesis. CQ prepared the cell cultures and performed the experiments of immunofluorescence and molecular biology. GQ and CQ conceived and designed the experiments and analyzed the data. JG and NV analyzed the data and critically revised the manuscript. All authors discussed the results and contributed to manuscript writing.

ACKNOWLEDGMENTS

We would like to thank Maria do Céu Pereira, Mónica Caldas (Faculty of Pharmacy, University of Porto), and Paula Magalhães (i3S, University of Porto) for their technical assistance. We also thank the University of Porto, Faculty of Pharmacy for the financial support.

SUPPLEMENTARY MATERIAL

The Supplementary Material for this article can be found online at: https://www.frontiersin.org/articles/10.3389/fphar.2018.00418/full#supplementary-material

REFERENCES

Amadio, S., Montilli, C., Magliozzi, R., Bernardi, G., Reynolds, R., and Volonté, C. (2010). P2Y12 receptor protein in cortical gray matter lesions in multiple sclerosis. *Cereb. Cortex* 20, 1263–1273. doi: 10.1093/cercor/bhp193

Bianco, F., Fumagalli, M., Pravettoni, E., D'Ambrosi, N., Volonte, C., and Matteoli, M. (2005). Pathophysiological roles of extracellular nucleotides in glial cells: differential expression of purinergic receptors in resting and activated microglia. *Brain Res. Brain Res. Rev.* 48, 144–156. doi: 10.1016/j.brainresrev.2004.12.004

Buffo, A., Rolando, C., and Ceruti, S. (2010). Astrocytes in the damaged brain: molecular and cellular insights into their reactive response and healing potential. *Biochem. Pharmacol.* 79, 77–89. doi: 10.1016/j.bcp.2009.09.014

Burda, J. E., and Sofroniew, M. V. (2014). Reactive gliosis and the multicellular response to CNS damage and disease. *Neuron* 81, 229–248. doi: 10.1016/j.neuron.2013.12.034

Carrasquero, L. M., Delicado, E. G., Bustillo, D., Gutiérrez-Martín, Y., Artalejo, A. R., and Miras-Portugal, M. T. (2009). P2X7 and P2Y13 purinergic receptors mediate intracellular calcium responses to BzATP in rat cerebellar astrocytes. *J. Neurochem.* 110, 879–889. doi: 10.1111/j.1471-4159.2009.06179.x

Carrasquero, L. M., Delicado, E. G., Jiménez, A. I., Pérez-Sem, R., and Miras-Portugal, M. T. (2005). Cerebellar astrocytes co-express several ADP receptors. Presence of functional P2Y(13)-like receptors. *Purinergic Signal.* 1, 153–159. doi: 10.1007/s11302-005-6211-3

Crain, J. M., Nikodemova, M., and Watters, J. J. (2009). Expression of P2 nucleotide receptors varies with age and sex in murine brain microglia. *J. Neuroinflammation* 6:24. doi: 10.1186/1742-2094-6-24

Davalos, D., Grutzendler, J., Yang, G., Kim, J. V., Zuo, Y., and Jung, S. (2005). ATP mediates rapid microglial response to local brain injury *in vivo*. *Nat. Neurosci.* 8, 752–758. doi: 10.1038/nn1472

De Simone, R., Niturad, C. E., De Nuccio, C., Ajmone-Cat, M. A., Visentin, S., and Minghetti, L. (2010). TGF-β and LPS modulate ADP-induced migration of microglial cells through P2Y1 and P2Y12 receptor expression. *J. Neurochem.* 115, 450–459. doi: 10.1111/j.1471-4159.2010.06937.x

Deierborg, T. (2013). Preparation of primary microglia cultures from postnatal mouse and rat brains. *Methods Mol. Biol.* 1041, 25–31. doi: 10.1007/978-1-62703-520-0_4

Di Virgilio, F., Ceruti, S., Bramanti, P., and Abbracchio, M. P. (2009). Purinergic signalling in inflammation of the central nervous system. *Trends Neurosci.* 32, 79–87. doi: 10.1016/j.tins.2008.11.003

Fischer, W., Appelt, K., Grohmann, M., Franke, H., Norenberg, W., and Illes, P. (2009). Increase of intracellular Ca2+ by P2X and P2Y receptor-subtypes in cultured cortical astroglia of the rat. *Neuroscience* 160, 767–783. doi: 10.1016/j.neuroscience.2009.02.026

Franke, H., Krugel, U., Grosche, J., Heine, C., Hartig, W., and Allgaier, C. (2004). P2Y receptor expression on astrocytes in the nucleus accumbens of rats. *Neuroscience* 127, 431–441. doi: 10.1016/j.neuroscience.2004.05.003

Fumagalli, M., Brambilla, R., D'Ambrosi, N., Volonté, C., Matteoli, M., and Verderio, C. (2003). Nucleotide-mediated calcium signaling in rat cortical astrocytes: role of P2X and P2Y receptors. *Glia* 43, 218–303. doi: 10.1002/glia.10248

Fumagalli, M., Trincavelli, L., Lecca, D., Martini, C., Ciana, P., and Abbracchio, M. P. (2004). Cloning, pharmacological characterisation and distribution of the rat G-protein-coupled P2Y(13) receptor. *Biochem. Pharmacol.* 68, 113–124. doi: 10.1016/j.bcp.2004.02.038

Grobben, B., Claes, P., Van Kolen, K., Roymans, D., Fransen, P., and Sys, S. U. (2001). Agonists of the P2Y(AC)-receptor activate MAP kinase by a ras-independent pathway in rat C6 glioma. *J. Neurochem.* 78, 1325–1338. doi: 10.1046/j.1471-4159.2001.00524.x

Hamby, M. E., Coppola, G., Ao, Y., Geschwind, D. H., Khakh, B. S., and Sofroniew, M. V. (2012). Inflammatory mediators alter the astrocyte transcriptome and calcium signaling elicited by multiple G-protein-coupled receptors. *J. Neurosci.* 32, 14489–14510. doi: 10.1523/JNEUROSCI.1256-12.2012

Hanisch, U. K., and Kettenmann, H. (2007). Microglia: active sensor and versatile effector cells in the normal and pathologic brain. *Nat. Neurosci.* 10, 1387–1394. doi: 10.1038/nn1997

Haynes, S. E., Hollopeter, G., Yang, G., Kurpius, D., Dailey, M. E., and Gan, W. B. (2006). The P2Y12 receptor regulates microglial activation by extracellular nucleotides. *Nat. Neurosci.* 9, 1512–1519. doi: 10.1038/nn1805

Houston, D., Ohno, M., Nicholas, R. A., Jacobson, K. A., and Harden, T. K. (2006). [^{32}P]2-iodo-N^6-methyl-(N)-methanocarba-2′-deoxyadenosine-3′,5′-bisphosphate ([^{32}P]MRS2500), a novel radioligand for quantification of native $P2Y_1$ receptors. *Br. J. Pharmacol.* 147, 459–467. doi: 10.1038/sj.bjp.0706453

Humphries, R. G., Tomlinson, W., Ingall, A. H., Cage, P. A., and Leff, P. (1994). FPL 66096: a novel, highly potent and selective antagonist at human platelet P_{2T}-purinoceptors. *Br. J. Pharmacol.* 113, 1057–1063. doi: 10.1111/j.1476-5381.1994.tb17100.x

Kim, Y.-C., Lee, J.-S., Sak, K., Marteau, F., Mamedova, L., Boeynaems, J. M., et al. (2005). Synthesis of pyridoxal phosphate derivatives with antagonist activity at the $P2Y_{13}$ receptor. *Biochem. Pharmacol.* 70, 266–274. doi: 10.1016/j.bcp.2005.04.021

Liddelow, S. A., Guttenplan, K. A., Clarke, L. E., Bennett, F. C., Bohlen, C. J., Schirmer, L., et al. (2017). Neurotoxic reactive astrocytes are induced by activated microglia. *Nature* 541, 481–487. doi: 10.1038/nature21029

Liu, P. W., Yue, M. X., Zhou, R., Niu, J., Huang, D. J., and Xu, T. (2017). $P2Y_{12}$ and $P2Y_{13}$ receptors involved in ADPβs induced the release of IL-1β, IL-6 and TNF-α from cultured dorsal horn microglia. *J. Pain Res.* 10, 1755–1767. doi: 10.2147/JPR.S137131

Mamedova, L. K., Gao, Z. G., and Jacobson, K. A. (2006). Regulation of death and survival in astrocytes by ADP activating P2Y1 and P2Y12 receptors. *Biochem. Pharmacol.* 72, 1031–1041. doi: 10.1016/j.bcp.2006.07.017

Marteau, F., Le Poul, E., Communi, D., Communi, D., Labouret, C., and Savi, P. (2003). Pharmacological characterization of the human P2Y13 receptor. *Mol. Pharmacol.* 64, 104–112. doi: 10.1124/mol.64.1.104

McCarthy, K. D., and de Vellis, J. (1980). Preparation of separate astroglial and oligodendroglial cell cultures from rat cerebral tissue. *J. Cell Biol.* 85, 890–902. doi: 10.1083/jcb.85.3.890

Neary, J. T., Kang, Y., Willoughby, K. A., and Ellis, E. F. (2003). Activation of extracellular signal-regulated kinase by stretch-induced injury in astrocytes involves extracellular ATP and P2 purinergic receptors. *J. Neurosci.* 23, 2348–2356. doi: 10.1523/JNEUROSCI.23-06-02348.2003

Ni, M., and Aschner, M. (2010). Neonatal rat primary microglia: isolation, culturing, and selected applications. *Curr. Protoc. Toxicol.* 43, 12.17.1–12.17.16. doi: 10.1002/0471140856.tx1217s43

Ohsawa, K., Irino, Y., Nakamura, Y., Akazawa, C., Inoue, K., and Kohsaka, S. (2007). Involvement of P2X4 and P2Y12 receptors in ATP-induced microglial chemotaxis. *Glia* 55, 604–616. doi: 10.1002/glia.20489

Pfaffl, M. W. (2001). A new mathematical model for relative quantification in real-time RT-PCR. *Nucleic Acids Res.* 29:e45. doi: 10.1093/nar/29.9.e45

Quintas, C., Fraga, S., Goncalves, J., and Queiroz, G. (2011a). Opposite modulation of astroglial proliferation by adenosine 5′-O-(2-thio)-diphosphate and 2-methylthioadenosine-5′-diphosphate: mechanisms involved. *Neuroscience* 182, 32–42. doi: 10.1016/j.neuroscience.2011.03.009

Quintas, C., Fraga, S., Goncalves, J., and Queiroz, G. (2011b). P2Y receptors on astrocytes and microglia mediate opposite effects in astroglial proliferation. *Purinergic Signal.* 7, 251–263. doi: 10.1007/s11302-011-9235-x

Saura, J. (2007). Microglial cells in astroglial cultures: a cautionary note. *J. Neuroinflammation* 4:26. doi: 10.1186/1742-2094-4-26

Scemes, E. (2008). Modulation of astrocyte P2Y1 receptors by the carboxyl terminal domain of the gap junction protein Cx43. *Glia* 56, 145–153. doi: 10.1002/glia.20598

Shinozaki, Y., Shibata, K., Yoshida, K., Shigetomi, E., Gachet, C., and Ikenaka, K. (2017). Transformation of astrocytes to a neuroprotective phenotype by microglia via P2Y1 receptor downregulation. *Cell Rep.* 19, 1151–1164. doi: 10.1016/j.celrep.2017.04.047

Sofroniew, M. V. (2014). Astrogliosis. *Cold Spring Harb. Perspect. Biol.* 7:a020420. doi: 10.1101/cshperspect.a020420

Van Kolen, K., and Slegers, H. (2006). Atypical PKCzeta is involved in RhoA-dependent mitogenic signaling by the P2Y(12) receptor in C6 cells. *FEBS J.* 273, 1843–1854. doi: 10.1111/j.1742-4658.2006.05205.x

Zeng, J., Wang, G., Liu, X., Wang, C., Tian, H., and Liu, A. (2014). P2Y13 receptor-mediated rapid increase in intracellular calcium induced by ADP in cultured dorsal spinal cord microglia. *Neurochem. Res.* 39, 2240–2250. doi: 10.1007/s11064-014-1426-8

Zhang, D., Hu, X., Qian, L., O'Callaghan, J. P., and Hong, J. S. (2010). Astrogliosis in CNS pathologies: is there a role for microglia? *Mol. Neurobiol.* 41, 232–241. doi: 10.1007/s12035-010-8098-4

Conflict of Interest Statement: The authors declare that the research was conducted in the absence of any commercial or financial relationships that could be construed as a potential conflict of interest.

frontiers in Pharmacology

ORIGINAL RESEARCH
published: 24 April 2018
doi: 10.3389/fphar.2018.00393

Pharmacological Blockade of Adenosine A_{2A} but Not A_1 Receptors Enhances Goal-Directed Valuation in Satiety-Based Instrumental Behavior

Yan Li[1†], Xinran Pan[2†], Yan He[2†], Yang Ruan[2], Linshan Huang[2], Yuling Zhou[2], Zhidong Hou[2], Chaoxiang He[2], Zhe Wang[1], Xiong Zhang[1] and Jiang-Fan Chen[2,3*]*

[1] Department of Neurology, The Second Affiliated Hospital and Yuying Children's Hospital of Wenzhou Medical University, Wenzhou, China, [2] School of Optometry and Ophthalmology and Eye Hospital, The Institute of Molecular Medicine, Wenzhou Medical University, Wenzhou, China, [3] Department of Neurology, School of Medicine, Boston University, Boston, MA, United States

OPEN ACCESS

Edited by:
Francisco Ciruela,
Universitat de Barcelona, Spain

Reviewed by:
Elena Martín-García,
Universitat Pompeu Fabra, Spain
Sebastiano Alfio Torrisi,
Università degli Studi di Catania, Italy

***Correspondence:**
Xiong Zhang
zhangxiong98@gmail.com
Jiang-Fan Chen
chenjf@bu.edu

[†] These authors have contributed equally to this work.

Specialty section:
This article was submitted to Experimental Pharmacology and Drug Discovery, a section of the journal Frontiers in Pharmacology

Received: 06 December 2017
Accepted: 05 April 2018
Published: 24 April 2018

Citation:
Li Y, Pan X, He Y, Ruan Y, Huang L, Zhou Y, Hou Z, He C, Wang Z, Zhang X and Chen J-F (2018) Pharmacological Blockade of Adenosine A_{2A} but Not A_1 Receptors Enhances Goal-Directed Valuation in Satiety-Based Instrumental Behavior. Front. Pharmacol. 9:393. doi: 10.3389/fphar.2018.00393

The balance and smooth shift between flexible, goal-directed behaviors and repetitive, habitual actions are critical to optimal performance of behavioral tasks. The striatum plays an essential role in control of goal-directed versus habitual behaviors through a rich interplay of the numerous neurotransmitters and neuromodulators to modify the input, processing and output functions of the striatum. The adenosine receptors (namely A_{2A}R and A_1R), with their high expression pattern in the striatum and abilities to interact and integrate dopamine, glutamate and cannabinoid signals in the striatum, may represent novel therapeutic targets for modulating instrumental behavior. In this study, we examined the effects of pharmacological blockade of the A_{2A}Rs and A_1Rs on goal-directed versus habitual behaviors in different information processing phases of instrumental learning using a satiety-based instrumental behavior procedure. We found that A_{2A}R antagonist acts at the coding, consolidation and expression phases of instrumental learning to modulate animals' sensitivity to goal-directed valuation without modifying action-outcome contingency. However, pharmacological blockade and genetic knockout of A_1Rs did not affect acquisition or sensitivity to goal-valuation of instrumental behavior. These findings provide pharmacological evidence for a potential therapeutic strategy to control abnormal instrumental behaviors associated with drug addiction and obsessive-compulsive disorder by targeting the A_{2A}R.

Keywords: adenosine A_{2A} receptor, adenosine A_1 receptor, goal-directed behavior, habit, instrumental behavior

INTRODUCTION

Goal-directed and habitual behaviors are crucial adaptive behaviors for our daily life. Goal-directed behavior evaluates actions prospectively and can flexibly adjust action depending on environmental changes, but this comes at the cost of more cognitive resource. By contrast, habitual behavior is usually developed after repeated overtraining for days and represents automatic responses elicited by external or internal triggers during the performance of routine procedures with less cognitive loads (Dolan and Dayan, 2013). These two behavioral processes can develop in parallel or sequentially and can also reciprocally compete with each other for behavioral control

(Yin and Knowlton, 2006; Balleine and O'Doherty, 2010; Kim and Hikosaka, 2015). The balance between flexible goal-directed actions and repetitive habitual behaviors has an essential role in achieving optimal performance of behavioral task. Dysregulation of goal-directed versus habitual behaviors is considered to be a potential mechanism underlying the relapse of drug addiction (Ostlund and Balleine, 2008), obsessive compulsive disorder (Gillan et al., 2011; Robbins et al., 2012; Burguiere et al., 2015), and may contribute to the executive dysfunction in Parkinson's (Redgrave et al., 2010; de Wit et al., 2011) and Huntington's disease patients (Lawrence et al., 1998).

The striatum plays an essential role in control of goal-directed versus habitual behaviors (Yin and Knowlton, 2006; Graybiel and Grafton, 2015; Kim and Hikosaka, 2015). The dorsal medial striatum (DMS)-connecting orbitofrontal cortex (OFC) is critical for goal-directed valuation (Gremel and Costa, 2013), while the dorsal lateral striatum (DLS) and its connecting infralimbic cortex act as dual operators for habitual behavioral control (Smith and Graybiel, 2013a,b). Additionally, the accumbens nucleus (NAc)-ventral Pallidum (VP) pathway is necessary for goal-directed valuation as inactivation of NAc-VP pathway impairs the predictive learning (Leung and Balleine, 2013). Furthermore, the nigro-striatal dopamine signaling acts as a prediction error and motivational signal to drive instrumental learning (Glimcher, 2011; Rossi et al., 2013; Steinberg et al., 2013). Thus, the striatum acts as a key locus in integrating the cortico-striatal glutamate and the substantia nigra-striatal dopamine signals to control goal-directed and habitual behaviors.

The striatal control of instrumental behaviors is accomplished through a rich interplay of the numerous neurotransmitters and neuromodulators to modify the input, processing and output functions of the striatum (Lovinger, 2010). Several studies have documented the involvement of the D_2 receptor (Kwak et al., 2014), cannabinoid receptor type 1 (CB_1R) (Hilario et al., 2007) and 5-hydroxytryptamine 6 ($5\text{-}HT_6$) receptor (Eskenazi et al., 2015) in control of instrumental behavior. However, pharmacological control of instrumental behaviors is under-explored and the effective pharmacological strategies for the control of goal-directed versus habitual behaviors are lacking. Adenosine A_1 and A_{2A} receptors are highly expressed in the striatum and are increasingly recognized as important pharmacological targets for controlling cognition under normal and disease conditions (Chen et al., 2013; Chen, 2014). The Gs-coupled facilitating A_{2A} receptor ($A_{2A}R$) and Gi-coupled inhibitory A_1 receptor (A_1R) both integrate dopamine (Shen W. et al., 2008), glutamate (Kreitzer and Malenka, 2007), and BNDF (Tebano et al., 2008; Wei et al., 2014) signaling to modulate synaptic plasticity and control cognition. For example, using our newly developed chimeric rhodopsin-$A_{2A}R$ proteins (opto$A_{2A}R$), we recently demonstrated that transient activation of $A_{2A}R$ by light in a time-locked manner with reward delivery is sufficient to impair goal-directed behavior whereas focal knockdown of $A_{2A}R$ in the striatum enhances goal-directed behaviors (Yu et al., 2009; Li et al., 2016). Similarly, pharmacological blockade of $A_{2A}R$ promoted goal-directed seeking for ethanol in ENT1 knockout mice (Nam et al., 2013b) and restored goal-directed sensitivity to negative feedback in the methamphetamine (METH)-paired context (Furlong et al., 2017). These pharmacological, genetic, and optogenetic demonstrations of the cognitive "brake" mechanism of $A_{2A}R$ activation led us to propose that pharmacological blockade of the $A_{2A}R$ represents a promising therapeutic target for controlling goal-directed behaviors.

As the first step in developing an adenosine receptor-based pharmacological approach to control the goal-directed versus habitual behaviors, we coupled the $A_{2A}R$ antagonist (KW6002) and A_1R antagonist (DPCPX) with the satiety-based instrumental learning paradigm to address the effect of pharmacological blockade of the $A_{2A}R$ and A_1R on three aspects of instrumental learning processes: (i) behavioral elements of instrumental behaviors (i.e., acquisition of action-outcome contingency versus goal-evaluation) by acquisition of instrumental behavior, the devaluation test and the omission test; (ii) the instrumental learning processes by administering the $A_{2A}R$ antagonist either prior to the training (learning/encoding) or post-training (consolidation) during the random interval (RI) schedule, or immediately before the devaluation and omission tests (expression/retrieval of instrumental behaviors); (iii) the potential role of the A_1 receptor in control of instrumental learning.

MATERIALS AND METHODS

Animals

Animals were handled in accordance with the protocols approved by the Institutional Ethics Committee for Animal Use in Research and Education at Wenzhou Medical University, China. C57BL/6 male mice at least 8 weeks old (23–27 g each) were used in the experiments. The A_1R knockout mice ($A_1R^{-/-}$=$^{+/+}$) and wild-type littermate controls (A_1RC=C) have been well characterized previously (Johansson et al., 2001) and confirmed by PCR analysis of gene identification before the experiment. Mice were housed in an ambient temperature of 22 $\pm$ 0.5°C and a relative humidity of 60 $\pm$ 2% with a 12 h light/dark cycle. Mice were single-housed and underwent experiments in the light cycle.

Satiety-Based Instrumental Training and Testing

All instrumental learning experiments were performed in standard operant chambers (Med Associates). Each chamber was equipped with a retractable lever on either side of a pump with a syringe that delivered liquid reward (20% sucrose solution, 20 μl/reinforce which can be suspended from the syringe) and a house light (3 W, 24 V) mounted on the opposite side of the chamber. Training and testing procedures were performed following Rossi et al (Rossi and Yin, 2012) and illustrated in **Figure 1A**. In brief, mice were first given one 30-min magazine training session during which the sucrose solution was delivered on a random time 60 s schedule with the lever removed. Three days of continuous reinforcement (CRF) training sessions were followed to sufficiently establish the initial association between lever press and reward. At the start of the session, the house light was illuminated, and one lever was inserted into

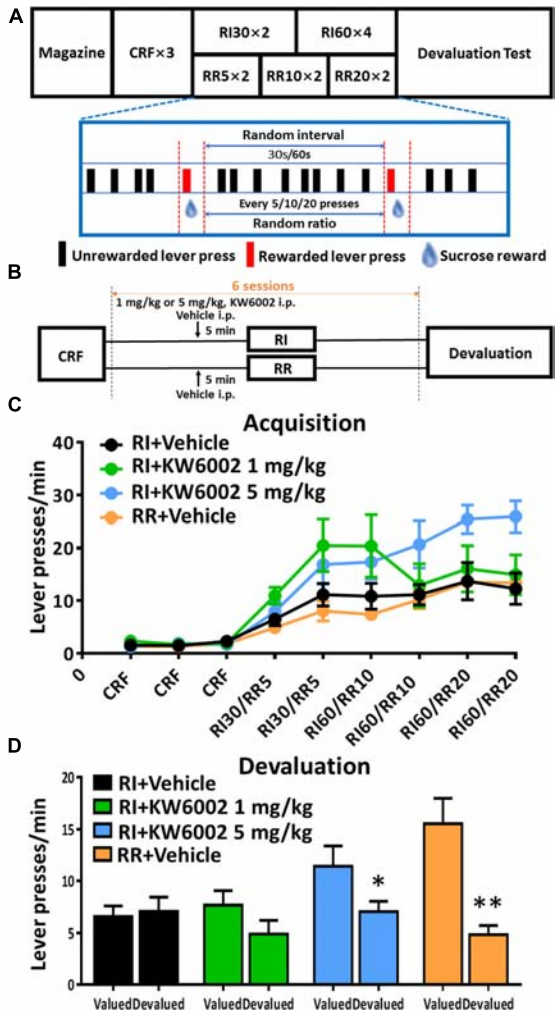

FIGURE 1 | Pharmacological blockade of A_{2A}Rs promoted goal-directed valuation. **(A)** Satiety-based instrumental behavior design schematic. Mice underwent Magazine-CRF-RI/RR-Devaluation procedure sequentially. CRF, continuous reinforcement; RI, random interval; RR, random ratio. **(B)** KW6002 and vehicle were injected intraperitoneally 5 min before daily RI training session at different doses (1 and 5 mg/kg), meanwhile vehicle was administrated 5 min before daily RR training session as another control group to form goal-directed behavior **(C)**. All mice gradually increased their lever presses in the RI/RR training sessions (training main effect: $p < 0.001$). There was the interaction effect of training sessions X drug administration groups ($p = 0.006$) and between subject effect of different drug administration groups ($p = 0.022$). The statistical significance was only observed between RI+KW6002 5 mg/kg and RR + Vehicle groups (*post hoc* by Bonferroni test, $p = 0.035$). **(D)** In the devaluation test, mice trained with RI and RR procedures performed habitual ($p = 0.755$) and goal-directed ($p = 0.002$, $^{**}p < 0.01$) behaviors, respectively, as designed. Mice received 1 mg/kg KW6002 tended to decrease their lever presses in the devalued condition but with no statistical significance ($p = 0.141$), while mice of 5 mg/kg group displayed markedly goal-directed performance in the devaluation test ($p = 0.030$, $^{*}p < 0.05$). All data was analyzed by two-way ANOVA for repeated measurement, followed by *post hoc* comparison with Bonferroni test [RI group, $n = 8$; RI+KW6002 (1 mg/kg) group, $n = 7$; RI+KW6002 (5 mg/kg) group, $n = 8$; RR group, $n = 9$].

the chamber. The house light remained illuminated and the lever remained inserted and active during the entire session. During CRF session, each lever press resulted in the delivery of one drop of 20 μl 20% sucrose solution. Sessions ended after 60 min or when 50 rewards had been earned, whichever came first. After CRF, mice underwent RI schedule which was critical for habitual learning. They were trained 2 days on RI 30 s, with a 0.1 probability of reward availability every 3 s contingent upon lever pressing, followed by 4 days on the 60 s interval schedules (0.1 probability of reward availability every 6 s contingent upon lever pressing). Just as CRF training, RI sessions ended after 60 min or when 50 rewards had been earned, whichever came first. To further confirm goal-directed behavioral pattern, we also employed random ratio (RR) training paradigm as control which contributed to goal-directed behavior. Progressively leaner schedules of reinforcement were used: CRF for 3 days, then RR 5 for 2 days (RR5; each response was rewarded at a probability of 0.2 on average), RR10 for 2 days and finally RR20 for 2 days. In the training sessions, home chows were given 1.5–2g daily to maintain 80–85% of their free-feeding weight.

Following the RI/RR training sessions, a 2-day devaluation test was conducted. A specific satiety procedure was applied to alter the current value of a specific reward. On each day the mice were allowed to have free access to home chows, which were used for maintaining their weights in the training sessions or sucrose solution which was earned by their lever pressing for at least an hour to achieve sensory-specific satiety. Immediately after the unlimited pre-feeding session, mice were given a 5-min extinction test during which the lever was inserted and pressing times were recorded without reward delivery. The order of the valued and devalued condition tests (day 1 or day 2) was counterbalanced across animals. Mice sensitive to manipulation of outcome value would significantly reduce their lever presses on the devalued condition compared with the valued condition. Then after two supplementary RI60 training sessions, mice were further evaluated by a 30-min omission test in which action-outcome contingency was altered. In the omission test, mice had to control their lever-press impulsion formed by previous training sessions for 20 s to obtain the reward. Any lever press would reset the time counter and mice would hold another 20 s not to press the lever for reward delivery.

Drug Administration

The following drugs were used in the present study: KW-6002 ((E)-1,3-diethyl-8-(3,4-dimethoxystyryl)-7-methyl-3,7-dihydro-1H-purine-2,6-dione, a selective adenosine $A_{2A}R$ antagonist) and DPCPX (8-cyclopentyl-1,3-dipropylxanthine, a selective adenosine A_1R antagonist). KW-6002 (1 mg/kg, 5 mg/kg, Sundia, United States) was suspended in dimethyl sulfoxide (DMSO, sigma), ethoxylated castor oil (Sigma) and water with a proportion of 15%:15%:70%. DPCPX (6 mg/kg, Abcam) was dissolved in 0.9% NaCl with 5% DMSO. The control mice were treated with corresponding vehicles. All the solutions were prepared immediately before administration. The administered doses of KW-6002 and DPCPX referred to previous researches (Chen et al., 2001; Prediger et al., 2004; Nguyen et al., 2014). Drugs were injected intraperitoneally (i.p.) routinely in a volume

of 0.1 ml/10 g of body weight. The specific drug administration time course depended on experimental designs: prior to (30 min before) and post (10 min after) everyday RI training for learning and consolidation periods of instrumental learning, respectively (**Figure 2A**), while treated 30 min before devaluation test/omission test, but not available in the RI training sessions for expression of instrumental behavior (**Figure 3A**).

DPCPX Concentration Detection

Considering the critical role of the striatum in control of instrumental behavior, we measured the concentration of DPCPX in the striatum of mice after intraperitoneal injection to verify the effective concentration of DPCPX. 30 min after DPCPX (6 mg/kg, i.p.) administration, the striata of mice were collected and homogenized. 0.1 ml of collected homogenate was added to a 1.5 ml centrifuge tube and followed by the addition of 0.01 ml methanol and 0.3ml of acetonitrile. The tubes were vortex mixed for 0.5 min. After centrifugation at 13,000 rpm for 10 min, 100 μl of supernatant was transferred to an auto-sampler vial. Next, 2 μl of the mixture was injected into the LC-MS/MS system for analysis. DCPCX concentrations were determined by ultrahigh performance liquid chromatography with mass spectrometry method (UHPLC-MS/MS). UHPLC-MS/MS analyses were performed by an Agilent UHPLC unit (Agilent Corporation, MA, United States) with a ZORBAX Eclipse Plus C18 column (1.8 μm, 2.1 × 50 mm, I.D. Agilent

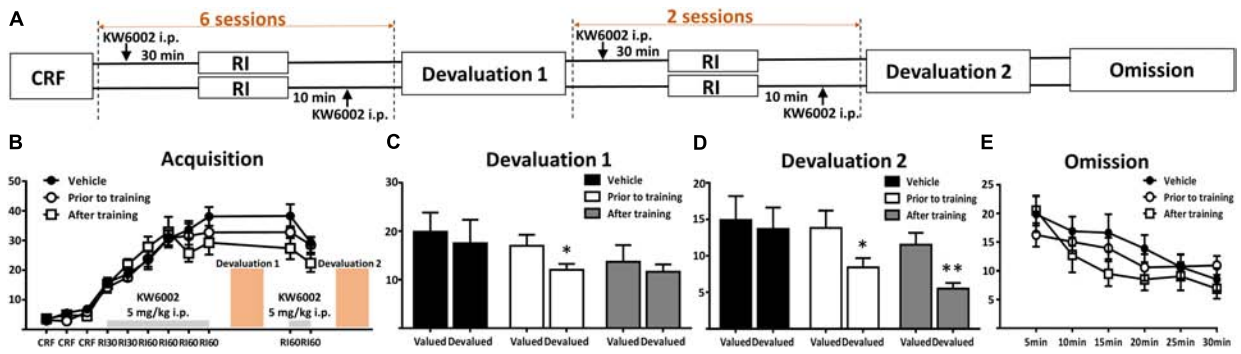

FIGURE 2 | Pharmacological blockade of A_{2A}Rs prior to and post daily training session promoted goal-directed seeking but not acquisition of instrumental conditioning. **(A)** Experimental design schematic with KW6002 injected intraperitoneally prior to and post-training. **(B)** There was no significant difference in acquisition of instrumental learning among these groups for lack of between groups effect ($p = 0.593$) and training X drug administration groups interaction effect ($p = 0.108$). **(C)** In the first devaluation test, mice with KW6002 injected prior to training showed sensitive to outcome devaluation ($p = 0.021$, $^*p < 0.05$), compared to vehicle ($p = 0.223$) and that with KW6002 treated post-training ($p = 0.539$). **(D)** Then after two additional days of RI60 training, whatever KW6002 administered prior to ($p = 0.034$, $^*p < 0.05$) or post ($p = 0.008$, $^{**}p < 0.01$) training, mice displayed sensitive to outcome devaluation in the second devaluation test compared to the vehicle group ($p = 0.482$). **(E)** All mice decreased their lever presses indistinctively in the omission test in which the action-outcome contingency was reversed, showing neither testing time X drug administration groups interaction effect ($p = 0.359$) nor between-subject effect of drug administered groups ($p = 0.836$). All data was analyzed by two-way ANOVA for repeated measurement, followed by *post hoc* comparison with Bonferroni test ($n = 8$/group).

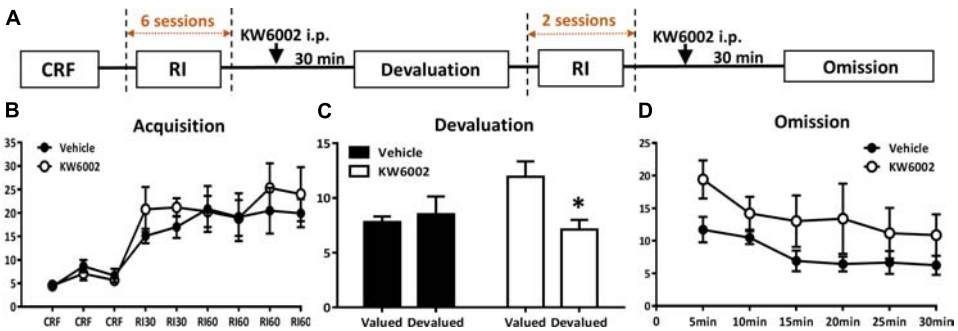

FIGURE 3 | Pharmacological blockade of A_{2A}Rs specifically in the expression phase of instrumental conditioning selectively promote goal-directed valuation but not action-outcome contingency. **(A)** Experimental design schematic with KW6002 injected intraperitoneally in the expression phase (i.e., devaluation and omission test) of instrumental behavior but not available in the training sessions. **(B)** Mice established instrumental conditioning indistinctively in the acquisition phase without between pre-manipulation groups effect ($p = 0.541$) and interaction effect of training sessions X pre-manipulation groups ($p = 0.608$). **(C)** KW6002 5 mg/kg or vehicle was administered 30 min before reward/home chow condition (i.e., devalued/valued condition). After 1-h exposure to devalued/valued condition at liberty, the devaluation test was proceeded in which reward delivery was absent and lever presses was recorded. Mice with KW6002 injected performed more goal-directed ($p = 0.017$, $^*p < 0.05$), compared to that injected with vehicle ($p = 0.710$). **(D)** After 2-day extended RI60 training sessions, KW6002 5 mg/kg or vehicle was injected 30 min before omission test. Mice of both groups significant decreased their lever presses (time main effect, $p = 0.020$). But there was neither between-subject effect of drug treatments ($p = 0.089$) nor drug treatments X testing time interaction effect ($p = 0.728$). All data was analyzed by two-way ANOVA for repeated measurement, followed by *post hoc* comparison with Bonferroni test (vehicle group, $n = 8$; KW6002 group, $n = 7$).

Corporation, MA, United States) thermostated at 25°C. The mobile phase was composed of 0.1% formic acid (A) and acetonitrile (B) with gradient as follows: 0.0 min at 50% B, 0.0–2.0 min linear increase to 98% B, and 2.0–3.5 min at 50% B and the flow rate was 0.4 ml/min. The total run time was 3.5 min. The electrospray interface was maintained at 500°C. Nitrogen nebulization was performed with a nitrogen flow of 800 l/h. Argon was used as the collision gas. DPCPX was detected in multiple reaction monitoring (MRM) scan mode with positive ion detection. The precursor-product ion pairs used for the MRM detection were m/z 305.4 → 178.1 for DCPCX.

Quantitative PCR of A_1R mRNA

Striatal tissues from A_1R KO mice and their WT littermates were analyzed by the quantitative real-time polymerase chain reaction (qPCR) procedure as we have described previously (Zhang et al., 2015) using the following forward and reverse primers for A_1R mRNA: primers: forward, 5′-CATCCTGGCTC TGCTTGCTATT-3′; reverse and 5′-TTGGCTATCCAGGCTTGTTCC-3′.

Statistical Analysis

All data presented as mean ± SEM and were processed with SPSS 17.0. Two-way ANOVA for repeated measurements was used with training/testing sessions as within-subject effect and different drug administrations/genotypes as between-subject effect, followed by *post hoc* comparison by Bonferroni test, and with $p < 0.05$ as statistical significance.

RESULTS

Pharmacological Blockade of A_{2A}Rs Promoted Goal-Directed Valuation

To perform flexible, goal-directed actions, animals must acquire the ability to encode both the *contingency* between a specific action and its outcome, and the current *value* of the outcome during instrumental conditioning (Balleine and Dickinson, 1998). We administered KW6002 (i.p. at 1 mg/kg or 5 mg/kg or vehicle) 5 min prior to everyday RI training session which was critical for establishment of habitual action (**Figure 1B**) to investigate the modulatory effect of A_{2A}R blockade on the acquisition of instrumental behaviors. To better identify goal-directed behavioral pattern, we have also included another group of mice that were trained in parallel with RR paradigm which led to goal-directed behavior as control (**Figure 1B**). All mice gradually increased their lever presses and reached a platform eventually, indicating the successful training paradigm (**Figure 1C**). Mice treated with KW6002 at 5 mg/kg significantly elevated lever presses rate (interaction effect of training sessions X drug administration groups: $F_{5,140} = 2.659$, $p = 0.006$; between-subject effect of drug administration groups: $F_{3,28} = 3.740$, $p = 0.022$): the statistical significance was observed between the RI + KW6002 5 mg/kg and the RR + Vehicle groups (Bonferroni *post hoc* test, $p = 0.035$) but absent in any other comparison pairs including RI+KW6002 5 mg/kg versus RI + Vehicle groups (*post hoc* by Bonferroni test, $p = 0.116$).

The outcome devaluation procedure was used to demonstrate the importance of the evaluative components of goal-directed actions by A_{2A}R blockade. In the devaluation test, lever presses rates between the valued and devalued conditions were compared (**Figure 1D**). Mice in the RI + Vehicle training group did not decrease lever presses in the devalued condition, showing no devaluation effect and indicating a habitual behavior ($F_{1,7} = 0.105$, $p = 0.755$), while the RR + Vehicle training group significantly decreased their lever presses ($F_{1,8} = 20.865$, $p = 0.002$), demonstrating goal-directed behavior. Notably, KW6002 at 1 mg/kg tended to decrease lever pressing rate in devalued condition compared to valued condition ($F_{1,6} = 2.867$, $p = 0.141$), whereas KW6002 at 5 mg/kg group showed markedly sensitive to outcome devaluation with decreased level pressing rate ($F_{1,7} = 7.418$, $p = 0.030$). Thus, pharmacological blockade of A_{2A}R promoted goal-directed valuation. Whether the A_{2A}R antagonist influence the acquisition of the instrumental learning need further clarification since the increased lever presses rate by KW6002 in the acquisition phase might be attributed to the improvement in instrumental learning or enhanced general motor activity effect of the A_{2A}R antagonist given the drug administration immediately (∼5 min) prior to behavioral training. Additional studies with the A_{2A}R antagonist administration 30 min prior to or post training might better dissociate the learning from motor effect of A_{2A}R antagonist.

Pharmacological Blockade of A_{2A}R at the Coding, Consolidation and Expression Phases of Instrumental Behavior Exerted Its Enhanced Effect on Goal-Directed Valuation but Not on Action-Outcome Contingency

To further determine the modulatory effect of A_{2A}R on the distinct processes of instrumental behavior (i.e., learning/coding, consolidation and expression phases), we administered KW6002 at specific time course of instrumental learning processes. Based on our previous study showing the effective biological (i.e., motor) effect of KW6002 5 mg/kg maintained for 150–170 min (Shen H.Y. et al., 2008; Yu et al., 2008), we selected the specific three time points for KW6002/vehicle administration (**Figures 2A**, **3A**): (a) prior to training (30 min before RI training) or (b) post training (10 min after RI training) or (c) prior to behavioral testing (30 min before devaluation/omission test but not available in the RI training sessions) to determine the modulatory effects of KW6002 on coding and consolidation phases as well as the expression of instrumental behavior, respectively.

Figure 2B shows that KW6002 treatment either at the prior to-training phase or post-training phase did not affect the performance of mice during the RI sessions (main effect between drug administration groups, $F_{2,21} = 0.536$, $p = 0.593$ and training sessions X drug administration groups interaction

effect, $F_{14,147} = 2.480$, $p = 0.108$). In the first devaluation test (**Figure 2C**), mice with vehicle injection formed a stable habitual behavior ($F_{1,7} = 1.787$, $p = 0.223$) as expected. Importantly, mice injected with KW6002 prior to everyday RI training session, which is the coding period, decreased their lever presses rate remarkably in the devalued condition ($F_{1,7} = 8.779$, $p = 0.021$), indicating blockade of $A_{2A}R$ enhanced goal-directed coding. However, since KW6002 post-training group did show some trend in decreasing lever pressing rate in the devaluation test, albeit not reaching statistical significance ($F_{1,7} = 0.417$, $p = 0.539$), we further explore the goal-directness promoting effect by KW6002 in the consolidation phase, by proceeding a 2-day complementary RI60 training sessions after the first devaluation test. Then we performed second devaluation test as illustrated in **Figure 2A**. After 2 additional days of RI training, both prior to-training and post-training groups significantly reduced lever presses in the devalued condition (prior to-training group, $F_{1,7} = 6.931$, $p = 0.034$; post-training group, $F_{1,7} = 13.413$, $p = 0.008$), i.e., goal-directed behavior, while control group (i.e., injected with vehicle) showed the characteristics of habitual behavior ($F_{1,7} = 0.552$, $p = 0.482$) (**Figure 2D**). Thus, KW6002 treatment in the consolidation phase of instrumental behavior promoted goal-directed behavior as well. Lastly, we performed the omission test during which the established lever press-reward association was reversed, so reward delivery depended on withholding the lever press action. As illustrated in **Figure 2E**, all mice decreased lever presses rate indistinctively in the omission test. Neither interaction effect of testing time X drug administration groups ($F_{10,105} = 1.124$, $p = 0.359$) nor main effect between drug administration groups ($F_{2,21} = 0.997$, $p = 0.836$) were detected. Thus, blockade of $A_{2A}Rs$ at the coding or consolidation phases of instrumental behavior enhanced goal-directed valuation but did not affect action-outcome association.

We then sought to investigate whether $A_{2A}R$ exerted its effect by acting on expression phase of instrumental behavior. In this experiment, KW6002 was administered 30 min before behavioral tests (devaluation and omission tests), but unavailable in all of the RI training sessions (**Figure 3A**). As expected, both pre-manipulation groups gradually increased lever presses rate and reached the platform and didn't show any difference between each other (between groups effect, $F_{1,13} = 0.395$, $p = 0.541$; interaction effect of training sessions X pre-manipulation groups, $F_{5,65} = 0.554$, $p = 0.608$) (**Figure 3B**). As **Figure 3C** shows, mice with KW6002 treatment at the expression phase displayed markedly sensitivity to outcome devaluation ($F_{1,6} = 10.857$, $p = 0.017$) compared with the controls ($F_{1,7} = 0.150$, $p = 0.710$) in the devaluation test. Thus, blockade of $A_{2A}R$ facilitated expression of goal-directed behavior. In the omission test (**Figure 3D**), both groups decreased their lever presses gradually over testing time (testing time main effect: $F_{5,65} = 4.226$, $p = 0.020$), indicating the timing effectiveness of the omission test. But the tendencies of lever-press decrease rate for the two groups were parallel as indicated by the absent of the drug treatments X testing time interaction effect ($F_{5,65} = 0.365$, $p = 0.728$), though mice injected with KW6002 apparently pressed more than that of the vehicle-treated mice (between-subject effect of drug treatments, $F_{1,13} = 3.369$, $p = 0.089$). The increased lever presses rate by KW6002 in the omission test might attribute to general motor but not learning effect of $A_{2A}R$ antagonist, for drug administration was 30 min before the test. Therefore, the action-outcome contingency may not be affected by $A_{2A}R$ antagonist.

Pharmacological Blockade and Genetic Knockout of A_1Rs Did Not Affect Acquisition or Goal-Evaluation of Instrumental Behavior

Adenosine acts on facilitating $A_{2A}R$ and inhibitory A_1R to integrate dopamine, glutamate, and BNDF signaling to modulate synaptic plasticity. We next investigated the possible involvement of A_1Rs in the modulation of instrumental behavior. To ensure the effective DPCPX drug concentration in the striatum after our A_1R pharmacological treatment paradigm, we determined the pharmacokinetic characteristic of DPCPX (**Figure 4A**) and showed the effective concentration of DPCPX in accordance with its biological effect as described previously (Baumgold et al., 1992). The A_1R antagonist DPCPX (6 mg/kg) did not affect lever pressing performance during instrumental training sessions (**Figure 4B**, main effect between drug administration groups, $F_{1,14} = 0.293$, $p = 0.597$; interaction effect of drug administration groups X training sessions, $F_{5,70} = 0.371$, $p = 0.867$). The devaluation test proceeded in drug-free condition (**Figure 4C**) revealed that mice with or without DPCPX treatment responded insensitively to satiety devaluation (DPCPX group, $F_{1,7} = 2.922$, $p = 0.131$; vehicle group, $F_{1,7} = 0.916$, $p = 0.370$). In addition, both groups of mice reduced lever presses indistinguishably in the omission test (**Figure 4D**, main effect between drug administration groups, $F_{1,14} = 0.129$, $p = 0.724$; interaction effect of drug administration groups X testing time, $F_{5,70} = 0.610$, $p = 0.580$).

To further confirm this finding by pharmacological blockade of A_1Rs, we determined the effect of genetic knockout of the A_1R on acquisition and goal-evaluation using A_1R knockout mice and their wild-type littermates. The nearly complete deletion of A_1Rs was verified by qPCR (**Figure 4E**). All mice, regardless of genotypes, increased their rate of lever pressing during the training sessions (**Figure 4F**) with no significant difference between genotypes ($F_{1,13} = 1.669$, $p = 0.219$) or interaction between training sessions and genotypes ($F_{5,65} = 1.105$, $p = 0.355$). During the devaluation test (**Figure 4G**), both A_1R KO and WT mice similarly showed insensitive to outcome devaluation (A_1R KO group, $F_{1,6} = 1.802$, $p = 0.228$; WT group, $F_{1,7} = 1.483$, $p = 0.263$), indicating that their responding was habitual. The omission test (**Figure 4H**) further confirmed the results of pharmacological blockade of A_1R by genetic knockout approach: there was neither main (genotypes) effect ($F_{1,13} = 1.521$, $p = 0.239$) nor the interaction of genotypes X testing time ($F_{5,65} = 0.260$, $p = 0.817$). This finding suggested that A_1R exerted limited effect on the control of instrumental behavior.

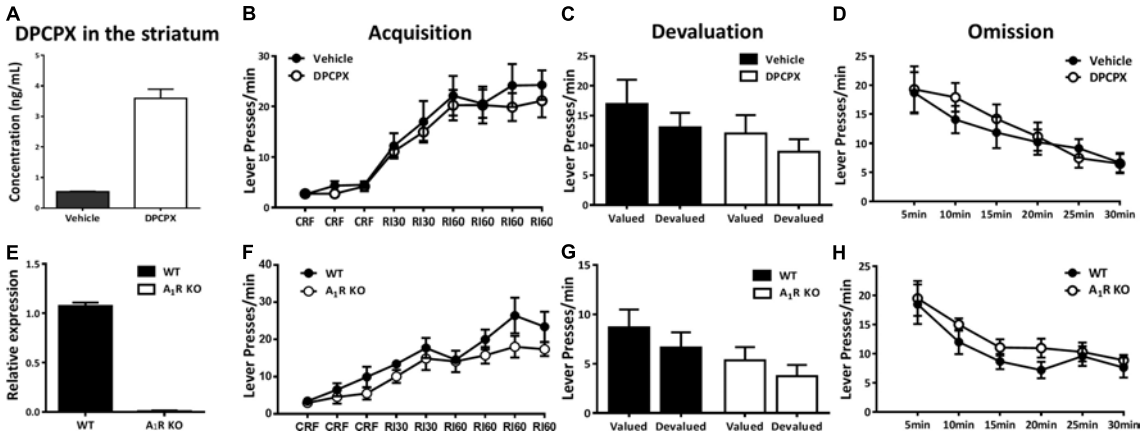

FIGURE 4 | Pharmacological blockade and genetic knockout of A_1Rs did not affect action-outcome association or goal-evaluation of instrumental behavior. **(A)** The concentration of DPCPX was detected in the striatum of mice 30 min after drug administration (n = 3/group), demonstrating the effectiveness of drug level we used. **(B)** Mice with and without DPCPX manipulation performed analogical learning curves in the acquisition of instrumental conditioning (between-subject effect, p = 0.597; drug administration X training interaction effect, p = 0.867). **(C)** Both DPCPX (p = 0.131) and vehicle (p = 0.370) groups displayed insensitive to outcome devaluation. **(D)** There didn't show any difference between DPCPX and vehicle groups in the omission test (between-subject effect, p = 0.724; drug administration X testing time interaction effect, p = 0.580). **(E)** The knockout efficiency of A_1R KO mice was confirmed by qPCR. **(F)** A_1R knockout did not affect acquisition of instrumental behavior since there lack of main effect of genotypes (p = 0.219) and training sessions X genotypes interaction effect (p = 0.355). **(G)** A_1R knockout mice and their littermates did not significantly decrease lever presses rate in the devalued condition (A_1R KO group, p = 0.228; WT group, p = 0.263). **(H)** Both groups decreased their lever presses indistinctively in the omission test (genotypes main effect, p = 0.239; genotypes X testing time interaction effect, p = 0.817). All data was analyzed by two-way ANOVA for repeated measurement.

DISCUSSION

$A_{2A}R$ Antagonist Modulate Animals' Sensitivity to Goal-Directed Valuation Without Modifying Action-Outcome Contingency

Action-outcome contingency and goal-directed valuation are two cognitive components involved in instrumental conditioning (Balleine and Dickinson, 1998). Action-outcome contingency is determined by the causal relationship between the particular actions and outcomes, while goal-directed valuation depends on the anticipation or desire for the outcome (Yin and Knowlton, 2006). Both components were acquired in the training sessions of instrumental behavior. Thus, outcome devaluation procedure was specialized to probe the importance of the evaluative component of goal-directed actions. We found that pharmacological blockade of $A_{2A}Rs$ critically promoted animals' sensitivity to outcome value (by the devaluation test) but did not affect action-outcome relationship (as manifested by similar performance in the training sessions and in the omission test). When administering 5 min prior to the training, KW6002 at 5 mg/kg apparently elevated the acquisition of learning curve. This enhancement is, however, potentially confounded by the enhanced general motor activity effect of the $A_{2A}R$ antagonist. Additional studies with the $A_{2A}R$ antagonist administering 30 min prior to or post-training can better dissociate the learning process from motor effect and clarify this issue. The selective modulation of animals' sensitivity to outcome devaluation by $A_{2A}R$ antagonist is in agreement with our recent finding that optogenetic activation of striatopallidal $A_{2A}R$ signaling in DMS alters goal-valuation as evident by the devaluation test (Li et al., 2016). On the other hand, the lack of the effect of $A_{2A}R$ antagonist on the acquisition of instrumental behaviors collaborates with similar findings by genetic inactivation of striatal $A_{2A}Rs$ (Yu et al., 2009) and optogenetic activation of striatopallidal $A_{2A}R$ signaling (Li et al., 2016).

The mechanism underlying the selective modulation of goal-valuation by the $A_{2A}R$ is not clear. The previous study that overexpression of the D_2R in the striatopallidal pathway is associated with a shift in behavioral control from habitual action to goal-directed responding but did not affect acquisition phase of instrumental learning (Kwak et al., 2014). Also, loss of striatal endocannabinoid-mediated long-term depression selectively in DLS striatopallidal neurons prevent the transition from goal-directed seeking to habitual responding behavior but did not interfere lever-press performance in the acquisition phase (Gremel et al., 2016). Given the documented antagonistic interaction of the $A_{2A}R$-D_2R and the $A_{2A}R$-CB_1R in the striatum by possibly the $A_{2A}R$-D_2R heterodimers (He et al., 2016) and $A_{2A}R$-CB_1R heterodimers (Moreno et al., 2017), these findings suggest that $A_{2A}R$ may selectively influence coding of the current value of the outcome (but not the contingency association) by the $A_{2A}R$ interaction with the D_2R and CB_1R functions in the striatum.

Moreover, this selective control of animals' sensitivity to reward valuation by $A_{2A}Rs$ might be related to a motivation factor, as $A_{2A}R$ (Mingote et al., 2008; Nam et al., 2013a) and D_2R (Trifilieff et al., 2013) activities in the striatum contribute to motivational control of behaviors. Lastly, since the $A_{2A}R$ are predominantly expressed in the striatopallidal neurons, the $A_{2A}R$ control of goal-directed valuation is further

supported by the finding from the striatal circuit studies showing that as pharmacogenetic inactivation of the striatopallidal pathway enhanced motivation by energizing the initiation of goal-directed behavior (Carvalho Poyraz et al., 2016), while optogenetic stimulation of the striatopallidal pathway suppressed motivational behavior (O'Hare et al., 2016; Vicente et al., 2016).

$A_{2A}R$ Antagonist Acts at the Coding, Consolidation and Expression Phases of Instrumental Learning to Promote Goal-Directed Behavior

Defining the specific information processing phases (i.e., learning/coding, consolidation and expression of instrumental behaviors) for $A_{2A}R$ antagonist control of goal-directed versus habitual behaviors is critical for our understanding of the neurotransmitter modulatory mechanisms and for the development of effective pharmacological strategy to control aberrant habit formation and drug addiction. Our demonstration of the enhanced goal-directed behavior by administration of KW6002 at the pre-training or post-training or expression phases suggests that $A_{2A}R$ acts at the coding, consolidation and expression phases of instrumental learning to promote animals' sensitivity to goal-directed valuation. It should be noted that the influence of the pre-training treatment paradigm on the goal-directed behavior might be partly attributed to its effect on the consolidation phase due to the relatively long-lasting effect (>2 h) of the $A_{2A}R$ antagonist KW6002. The similar control of instrumental behaviors by multiple treatment paradigms of KW6002 indicate that $A_{2A}R$ control of instrumental behaviors is largely independent of the confounding motor activity.

Various neurotransmitter systems have been implicated in control of the distinct phases of instrumental conditioning. For example, NMDA receptor signaling preferentially affected the coding (by administering NMDA antagonist at the pre-training phase) but not the expression (by administering NMDA antagonist at the post-training phase) of the instrumental conditioning (Yin et al., 2005). Furthermore, virus-induced overexpression of D_2R (Trifilieff et al., 2013) and 5-HT_6 receptor (Eskenazi and Neumaier, 2011; Eskenazi et al., 2015) preferentially affect the coding course of operant conditioning. Additionally, optogenetic activation of endocannabinoid signaling in the training session and pharmacogenetic suppression of endocannabinoid signaling in the devaluation test gated habit formation (Gremel et al., 2016), indicating that endocannabinoid modulated instrumental learning in both coding and expression sessions, consistent with the CB_1R knockout study (Hilario et al., 2007). Thus, the $A_{2A}R$ may interact with multiple neurotransmitter systems in the cortico-striatal projection pathways to integrate/modulate glutamate, dopamine and endocannabinoid signaling for instrumental behavioral control at multiple phases of information processing. Furthermore, cognitive control and working memory processes are important for the efficient control of goal-directed behavior (Buschman and Miller, 2014). We and others have documented that the $A_{2A}R$ antagonists or focal $A_{2A}R$ knockdown in the DMS significantly enhance working memory (Wei et al., 2014; Kaster et al., 2015; Li et al., 2018). Thus, it is possible that when KW6002 is administered prior to the training phase, the $A_{2A}R$ antagonist may enhance goal-directed behavior by improving working memory. On the other hand, other mechanisms (such as "off-line" processing during sleep) may contribute to the $A_{2A}R$ antagonist-mediated enhancement of goal-directed behavior when $A_{2A}R$ antagonists are administered after the training or during the expression/retrieval phase.

Pharmacological Blockade and Genetic Knockout of A_1Rs Did Not Affect Acquisition or Goal-Evaluation of Instrumental Behavior

Adenosine signaling acts at the facilitating $A_{2A}R$ and inhibitory A_1R to exert its homeostatic control of brain function. However, very limited information is available regarding the A_1R control of cognition, particularly instrumental behaviors. With its relatively high expression in the cerebral cortex, hippocampus and striatum (Reppert et al., 1991; Dixon et al., 1996), A_1R activation has a profound inhibitory control of excitatory transmission by presynaptic and post-synaptic mechanisms (Dunwiddie and Masino, 2001; Ribeiro et al., 2002). Striatal A_1Rs can preferentially interact with the striatal D_1Rs via possible A_1R-D_1R heterodimers in the striatonigral neurons to control striatal signaling and behavior (Gines et al., 2000). Accordingly, A_1Rs modulate striatal synaptic plasticity, and prevent scopolamine- and morphine-induced impairment in working memory (Hooper et al., 1996; Lu et al., 2010). However, in the fix-interval and fix-ratio operant training paradigms, A_1R antagonist failed to increase lever pressing rate, but decreased fix ratio 20 (FR20, every 20 lever presses resulted in one reward) responding at higher doses (Randall et al., 2011). Operant performance alone was insufficient to define instrumental learning modes as goal-directed or habitual actions without devaluation and omission test (Yin and Knowlton, 2006). Thus, the role of the A_1R in goal-directed versus habitual behaviors is still unknown. Our study demonstrated that pharmacological blockade or global knockout of A_1R did not affect the acquisition of instrumental learning or sensitivity to reward value or reversal of action-outcome relationship. This finding is in agreement with a recent study that DPCPX failed to reverse the effect of D_2R antagonist on effort-relevant tasks but KW6002 and caffeine (a non-selective adenosine antagonist) can (Salamone et al., 2009). These findings suggest that A_1R plays limited modulatory role in control of instrumental behavior and adenosine predominantly acts on $A_{2A}Rs$ but not A_1Rs to modulate instrumental learning.

In summary, our study demonstrated that pharmacological blockade of $A_{2A}R$ but not A_1R promote goal-directed behaviors by enhancing goal-directed valuation without affecting the action-outcome contingency and by acting at the coding, consolidation, and expression phases of goal-directed learning processes. These findings collaborates with our previous genetic and optogenetic studies, and with recent pharmacological studies of $A_{2A}R$ antagonists to control abnormal instrumental behavior in drug addiction paradigms (Nam et al., 2013a;

Pintsuk et al., 2016), providing pharmacological evidence for a therapeutic strategy to enhance goal-directed behaviors in neuropsychiatric disorders. The translational potential of $A_{2A}R$ antagonists is further enhanced by the recent demonstration of the safety profiles of the $A_{2A}R$ antagonist KW6002 in clinical phase III trials for motor benefit in >3500 Parkinson's disease patients (Chen et al., 2013) and by regular consumption of caffeine (a non-specific adenosine $A_{2A}R$ and A_1R antagonist) by 50% world population.

AUTHOR CONTRIBUTIONS

YL, YH, XZ, and J-FC designed the experiments. YL, XP, YH, YR, LH, ZW, and CH collected the data. YL, XP, YH, YZ, and ZH analyzed the data. YL, XZ, and J-FC wrote the manuscript.

FUNDING

This study was sponsored by the National Natural Science Foundation of China (Grant Nos. 81600983, 31771178, and 81600991), by the Start-up Fund from Wenzhou Medical University (Grant Nos. 89211010 and 89212012), the Zhejiang Provincial Special Funds (Grant No. 604161241), the Natural Science Foundation of Zhejiang Province of China (Grant Nos. LY15H090020, LQ16H090006, and LQ17H090005), and the Wenzhou Science and Technology Program (Grant Nos. 2016Y0725 and 2016Y0613).

REFERENCES

Balleine, B. W., and Dickinson, A. (1998). Goal-directed instrumental action: contingency and incentive learning and their cortical substrates. *Neuropharmacology* 37, 407–419. doi: 10.1016/S0028-3908(98)00033-1

Balleine, B. W., and O'Doherty, J. P. (2010). Human and rodent homologies in action control: corticostriatal determinants of goal-directed and habitual action. *Neuropsychopharmacology* 35, 48–69. doi: 10.1038/npp.2009.131

Baumgold, J., Nikodijevic, O., and Jacobson, K. A. (1992). Penetration of adenosine antagonists into mouse brain as determined by ex vivo binding. *Biochem. Pharmacol.* 43, 889–894. doi: 10.1016/0006-2952(92)90257-J

Burguiere, E., Monteiro, P., Mallet, L., Feng, G., and Graybiel, A. M. (2015). Striatal circuits, habits, and implications for obsessive-compulsive disorder. *Curr. Opin. Neurobiol.* 30, 59–65. doi: 10.1016/j.conb.2014.08.008

Buschman, T. J., and Miller, E. K. (2014). Goal-direction and top-down control. *Philos. Trans. R. Soc. Lond. B Biol. Sci.* 369:20130471. doi: 10.1098/rstb.2013.0471

Carvalho Poyraz, F., Holzner, E., Bailey, M. R., Meszaros, J., Kenney, L., Kheirbek, M. A., et al. (2016). Decreasing striatopallidal pathway function enhances motivation by energizing the initiation of goal-directed action. *J. Neurosci.* 36, 5988–6001. doi: 10.1523/JNEUROSCI.0444-16.2016

Chen, J. F. (2014). Adenosine receptor control of cognition in normal and disease. *Int. Rev. Neurobiol.* 119, 257–307. doi: 10.1016/B978-0-12-801022-8.00012-X

Chen, J. F., Eltzschig, H. K., and Fredholm, B. B. (2013). Adenosine receptors as drug targets–what are the challenges? *Nat. Rev. Drug Discov.* 12, 265–286. doi: 10.1038/nrd3955

Chen, J.-F., Xu, K., Petzer, J. P., Staal, R., Xu, Y. H., Beilstein, M., et al. (2001). Neuroprotection by caffeine and A2A adenosine receptor inactivation in a model of Parkinson's disease. *J. Neurosci.* 21:RC143.

de Wit, S., Barker, R. A., Dickinson, A. D., and Cools, R. (2011). Habitual versus goal-directed action control in Parkinson disease. *J. Cogn. Neurosci.* 23, 1218–1229. doi: 10.1162/jocn.2010.21514

Dixon, A. K., Gubitz, A. K., Sirinathsinghji, D. J., Richardson, P. J., and Freeman, T. C. (1996). Tissue distribution of adenosine receptor mRNAs in the rat. *Br. J. Pharmacol.* 118, 1461–1468. doi: 10.1111/j.1476-5381.1996.tb15561.x

Dolan, R. J., and Dayan, P. (2013). Goals and habits in the brain. *Neuron* 80, 312–325. doi: 10.1016/j.neuron.2013.09.007

Dunwiddie, T. V., and Masino, S. A. (2001). The role and regulation of adenosine in the central nervous system. *Annu. Rev. Neurosci.* 24, 31–55. doi: 10.1146/annurev.neuro.24.1.31

Eskenazi, D., Brodsky, M., and Neumaier, J. F. (2015). Deconstructing 5-HT6 receptor effects on striatal circuit function. *Neuroscience* 299, 97–106. doi: 10.1016/j.neuroscience.2015.04.046

Eskenazi, D., and Neumaier, J. F. (2011). Increased expression of the 5-HT6 receptor by viral mediated gene transfer into posterior but not anterior dorsomedial striatum interferes with acquisition of a discrete action-outcome task. *J. Psychopharmacol.* 25, 944–951. doi: 10.1177/0269881110388330

Furlong, T. M., Supit, A. S., Corbit, L. H., Killcross, S., and Balleine, B. W. (2017). Pulling habits out of rats: adenosine 2A receptor antagonism in dorsomedial striatum rescues meth-amphetamine-induced deficits in goal-directed action. *Addict. Biol.* 22, 172–183. doi: 10.1111/adb.12316

Gillan, C. M., Papmeyer, M., Morein-Zamir, S., Sahakian, B. J., Fineberg, N. A., Robbins, T. W., et al. (2011). Disruption in the balance between goal-directed behavior and habit learning in obsessive-compulsive disorder. *Am. J. Psychiatry* 168, 718–726. doi: 10.1176/appi.ajp.2011.10071062

Gines, S., Hillion, J., Torvinen, M., Le Crom, S., Casado, V., Canela, E. I., et al. (2000). Dopamine D1 and adenosine A1 receptors form functionally interacting heteromeric complexes. *Proc. Natl. Acad. Sci. U.S.A.* 97, 8606–8611. doi: 10.1073/pnas.150241097

Glimcher, P. W. (2011). Understanding dopamine and reinforcement learning: the dopamine reward prediction error hypothesis. *Proc. Natl. Acad. Sci. U.S.A.* 108(Suppl. 3), 15647–15654. doi: 10.1073/pnas.1014269108

Graybiel, A. M., and Grafton, S. T. (2015). The striatum: where skills and habits meet. *Cold Spring Harb. Perspect. Biol.* 7:a021691. doi: 10.1101/cshperspect.a021691

Gremel, C. M., Chancey, J. H., Atwood, B. K., Luo, G., Neve, R., Ramakrishnan, C., et al. (2016). Endocannabinoid modulation of orbitostriatal circuits gates habit formation. *Neuron* 90, 1312–1324. doi: 10.1016/j.neuron.2016.04.043

Gremel, C. M., and Costa, R. M. (2013). Orbitofrontal and striatal circuits dynamically encode the shift between goal-directed and habitual actions. *Nat. Commun.* 4:2264. doi: 10.1038/ncomms3264

He, Y., Li, Y., Chen, M., Pu, Z., Zhang, F., Chen, L., et al. (2016). Habit formation after random interval training is associated with increased adenosine A2A receptor and dopamine D2 receptor heterodimers in the striatum. *Front. Mol. Neurosci.* 9:151. doi: 10.3389/fnmol.2016.00151

Hilario, M. R., Clouse, E., Yin, H. H., and Costa, R. M. (2007). Endocannabinoid signaling is critical for habit formation. *Front. Integr. Neurosci.* 1:6. doi: 10.3389/neuro.07.006.2007

Hooper, N., Fraser, C., and Stone, T. W. (1996). Effects of purine analogues on spontaneous alternation in mice. *Psychopharmacology (Berl)* 123, 250–257. doi: 10.1007/BF02246579

Johansson, B., Halldner, L., Dunwiddie, T. V., Masino, S. A., Poelchen, W., Gimenez-Llort, L., et al. (2001). Hyperalgesia, anxiety, and decreased hypoxic neuroprotection in mice lacking the adenosine A1 receptor. *Proc. Natl. Acad. Sci. U.S.A.* 98, 9407–9412. doi: 10.1073/pnas.161292398

Kaster, M. P., Machado, N. J., Silva, H. B., Nunes, A., Ardais, A. P., Santana, M., et al. (2015). Caffeine acts through neuronal adenosine A2A receptors to prevent mood and memory dysfunction triggered by chronic stress. *Proc. Natl. Acad. Sci. U.S.A.* 112, 7833–7838. doi: 10.1073/pnas.1423088112

Kim, H. F., and Hikosaka, O. (2015). Parallel basal ganglia circuits for voluntary and automatic behaviour to reach rewards. *Brain* 138, 1776–1800. doi: 10.1093/brain/awv134

Kreitzer, A. C., and Malenka, R. C. (2007). Endocannabinoid-mediated rescue of striatal LTD and motor deficits in Parkinson's disease models. *Nature* 445, 643–647. doi: 10.1038/nature05506

Kwak, S., Huh, N., Seo, J. S., Lee, J. E., Han, P. L., and Jung, M. W. (2014). Role of dopamine D2 receptors in optimizing choice strategy in a dynamic and uncertain environment. *Front. Behav. Neurosci.* 8:368. doi: 10.3389/fnbeh.2014.00368

Lawrence, A. D., Sahakian, B. J., and Robbins, T. W. (1998). Cognitive functions and corticostriatal circuits: insights from Huntington's disease. *Trends Cogn. Sci.* 2, 379–388. doi: 10.1016/S1364-6613(98)01231-5

Leung, B. K., and Balleine, B. W. (2013). The ventral striato-pallidal pathway mediates the effect of predictive learning on choice between goal-directed actions. *J. Neurosci.* 33, 13848–13860. doi: 10.1523/JNEUROSCI.1697-13.2013

Li, Y., He, Y., Chen, M., Pu, Z., Chen, L., Li, P., et al. (2016). Optogenetic activation of adenosine A2A receptor signaling in the dorsomedial striatopallidal neurons suppresses goal-directed behavior. *Neuropsychopharmacology* 41, 1003–1013. doi: 10.1038/npp.2015.227

Li, Z., Chen, X., Wang, T., Gao, Y., Li, F., Chen, L., et al. (2018). The corticostriatal adenosine A2A receptor controls maintenance and retrieval of spatial working memory. *Biol. Psychiatry* 83, 530–541. doi: 10.1016/j.biopsych.2017.07.017

Lovinger, D. M. (2010). Neurotransmitter roles in synaptic modulation, plasticity and learning in the dorsal striatum. *Neuropharmacology* 58, 951–961. doi: 10.1016/j.neuropharm.2010.01.008

Lu, G., Zhou, Q. X., Kang, S., Li, Q. L., Zhao, L. C., Chen, J. D., et al. (2010). Chronic morphine treatment impaired hippocampal long-term potentiation and spatial memory via accumulation of extracellular adenosine acting on adenosine A1 receptors. *J. Neurosci.* 30, 5058–5070. doi: 10.1523/JNEUROSCI.0148-10.2010

Mingote, S., Font, L., Farrar, A. M., Vontell, R., Worden, L. T., Stopper, C. M., et al. (2008). Nucleus accumbens adenosine A2A receptors regulate exertion of effort by acting on the ventral striatopallidal pathway. *J. Neurosci.* 28, 9037–9046. doi: 10.1523/JNEUROSCI.1525-08.2008

Moreno, E., Chiarlone, A., Medrano, M., Puigdellivol, M., Bibic, L., Howell, L. A., et al. (2017). Singular location and signaling profile of adenosine A2A-cannabinoid CB1 receptor heteromers in the dorsal striatum. *Neuropsychopharmacology* 43, 964–977. doi: 10.1038/npp.2017.12

Nam, H. W., Bruner, R. C., and Choi, D. S. (2013a). Adenosine signaling in striatal circuits and alcohol use disorders. *Mol. Cells* 36, 195–202. doi: 10.1007/s10059-013-0192-9

Nam, H. W., Hinton, D. J., Kang, N. Y., Kim, T., Lee, M. R., Oliveros, A., et al. (2013b). Adenosine transporter ENT1 regulates the acquisition of goal-directed behavior and ethanol drinking through A2A receptor in the dorsomedial striatum. *J. Neurosci.* 33, 4329–4338. doi: 10.1523/JNEUROSCI.3094-12.2013

Nguyen, M. D., Lee, S. T., Ross, A. E., Ryals, M., Choudhry, V. I., and Venton, B. J. (2014). Characterization of spontaneous, transient adenosine release in the caudate-putamen and prefrontal cortex. *PLoS One* 9:e87165. doi: 10.1371/journal.pone.0087165

O'Hare, J. K., Ade, K. K., Sukharnikova, T., Van Hooser, S. D., Palmeri, M. L., Yin, H. H., et al. (2016). Pathway-specific striatal substrates for habitual behavior. *Neuron* 89, 472–479. doi: 10.1016/j.neuron.2015.12.032

Ostlund, S. B., and Balleine, B. W. (2008). On habits and addiction: an associative analysis of compulsive drug seeking. *Drug. Discov. Today Dis. Models* 5, 235–245. doi: 10.1016/j.ddmod.2009.07.004

Pintsuk, J., Borroto-Escuela, D. O., Pomierny, B., Wydra, K., Zaniewska, M., Filip, M., et al. (2016). Cocaine self-administration differentially affects allosteric A2A-D2 receptor-receptor interactions in the striatum. Relevance for cocaine use disorder. *Pharmacol. Biochem. Behav.* 144, 85–91. doi: 10.1016/j.pbb.2016.03.004

Prediger, R. D., Batista, L. C., and Takahashi, R. N. (2004). Adenosine A1 receptors modulate the anxiolytic-like effect of ethanol in the elevated plus-maze in mice. *Eur. J. Pharmacol.* 499, 147–154. doi: 10.1016/j.ejphar.2004.07.106

Randall, P. A., Nunes, E. J., Janniere, S. L., Stopper, C. M., Farrar, A. M., Sager, T. N., et al. (2011). Stimulant effects of adenosine antagonists on operant behavior: differential actions of selective A2A and A1 antagonists. *Psychopharmacology (Berl)* 216, 173–186. doi: 10.1007/s00213-011-2198-3

Redgrave, P., Rodriguez, M., Smith, Y., Rodriguez-Oroz, M. C., Lehericy, S., Bergman, H., et al. (2010). Goal-directed and habitual control in the basal ganglia: implications for Parkinson's disease. *Nat. Rev. Neurosci.* 11, 760–772. doi: 10.1038/nrn2915

Reppert, S. M., Weaver, D. R., Stehle, J. H., and Rivkees, S. A. (1991). Molecular cloning and characterization of a rat A1-adenosine receptor that is widely expressed in brain and spinal cord. *Mol. Endocrinol.* 5, 1037–1048. doi: 10.1210/mend-5-8-1037

Ribeiro, J. A., Sebastiao, A. M., and De Mendonca, A. (2002). Adenosine receptors in the nervous system: pathophysiological implications. *Prog. Neurobiol.* 68, 377–392. doi: 10.1016/S0301-0082(02)00155-7

Robbins, T. W., Gillan, C. M., Smith, D. G., De Wit, S., and Ersche, K. D. (2012). Neurocognitive endophenotypes of impulsivity and compulsivity: towards dimensional psychiatry. *Trends Cogn. Sci.* 16, 81–91. doi: 10.1016/j.tics.2011.11.009

Rossi, M. A., Sukharnikova, T., Hayrapetyan, V. Y., Yang, L., and Yin, H. H. (2013). Operant self-stimulation of dopamine neurons in the substantia nigra. *PLoS One* 8:e65799. doi: 10.1371/journal.pone.0065799

Rossi, M. A., and Yin, H. H. (2012). Methods for studying habitual behavior in mice. *Curr. Protoc. Neurosci.* 60, 8.29.1–8.29.9. doi: 10.1002/0471142301.ns0829s60

Salamone, J. D., Farrar, A. M., Font, L., Patel, V., Schlar, D. E., Nunes, E. J., et al. (2009). Differential actions of adenosine A1 and A2A antagonists on the effort-related effects of dopamine D2 antagonism. *Behav. Brain Res.* 201, 216–222. doi: 10.1016/j.bbr.2009.02.021

Shen, H. Y., Coelho, J. E., Ohtsuka, N., Canas, P. M., Day, Y. J., Huang, Q. Y., et al. (2008). A critical role of the adenosine A2A receptor in extrastriatal neurons in modulating psychomotor activity as revealed by opposite phenotypes of striatum and forebrain A2A receptor knock-outs. *J. Neurosci.* 28, 2970–2975. doi: 10.1523/JNEUROSCI.5255-07.2008

Shen, W., Flajolet, M., Greengard, P., and Surmeier, D. J. (2008). Dichotomous dopaminergic control of striatal synaptic plasticity. *Science* 321, 848–851. doi: 10.1126/science.1160575

Smith, K. S., and Graybiel, A. M. (2013a). A dual operator view of habitual behavior reflecting cortical and striatal dynamics. *Neuron* 79, 361–374. doi: 10.1016/j.neuron.2013.05.038

Smith, K. S., and Graybiel, A. M. (2013b). Using optogenetics to study habits. *Brain Res.* 1511, 102–114. doi: 10.1016/j.brainres.2013.01.008

Steinberg, E. E., Keiflin, R., Boivin, J. R., Witten, I. B., Deisseroth, K., and Janak, P. H. (2013). A causal link between prediction errors, dopamine neurons and learning. *Nat. Neurosci.* 16, 966–973. doi: 10.1038/nn.3413

Tebano, M. T., Martire, A., Potenza, R. L., Gro, C., Pepponi, R., Armida, M., et al. (2008). Adenosine A(2A) receptors are required for normal BDNF levels and BDNF-induced potentiation of synaptic transmission in the mouse hippocampus. *J. Neurochem.* 104, 279–286.

Trifilieff, P., Feng, B., Urizar, E., Winiger, V., Ward, R. D., Taylor, K. M., et al. (2013). Increasing dopamine D2 receptor expression in the adult nucleus accumbens enhances motivation. *Mol. Psychiatry* 18, 1025–1033. doi: 10.1038/mp.2013.57

Vicente, A. M., Galvao-Ferreira, P., Tecuapetla, F., and Costa, R. M. (2016). Direct and indirect dorsolateral striatum pathways reinforce different action strategies. *Curr. Biol.* 26, R267–R269. doi: 10.1016/j.cub.2016.02.036

Wei, C. J., Augusto, E., Gomes, C. A., Singer, P., Wang, Y., Boison, D., et al. (2014). Regulation of fear responses by striatal and extrastriatal adenosine A2A receptors in forebrain. *Biol. Psychiatry* 75, 855–863. doi: 10.1016/j.biopsych.2013.05.003

Yin, H. H., and Knowlton, B. J. (2006). The role of the basal ganglia in habit formation. *Nat. Rev. Neurosci.* 7, 464–476. doi: 10.1038/nrn1919

Yin, H. H., Knowlton, B. J., and Balleine, B. W. (2005). Blockade of NMDA receptors in the dorsomedial striatum prevents action-outcome learning in instrumental conditioning. *Eur. J. Neurosci.* 22, 505–512. doi: 10.1111/j.1460-9568.2005.04219.x

Yu, C., Gupta, J., Chen, J. F., and Yin, H. H. (2009). Genetic deletion of A2A adenosine receptors in the striatum selectively impairs habit formation. *J. Neurosci.* 29, 15100–15103. doi: 10.1523/JNEUROSCI.4215-09.2009

Yu, L., Shen, H. Y., Coelho, J. E., Araujo, I. M., Huang, Q. Y., Day, Y. J., et al. (2008). Adenosine A2A receptor antagonists exert motor and neuroprotective effects by distinct cellular mechanisms. *Ann. Neurol.* 63, 338–346. doi: 10.1002/ana.21313

Zhang, S., Li, H., Li, B., Zhong, D., Gu, X., Tang, L., et al. (2015). Adenosine A1 receptors selectively modulate oxygen-induced retinopathy at the hyperoxic and hypoxic phases by distinct cellular mechanisms. *Invest. Ophthalmol. Vis. Sci.* 56, 8108–8119. doi: 10.1167/iovs.15-17202

Conflict of Interest Statement: The authors declare that the research was conducted in the absence of any commercial or financial relationships that could be construed as a potential conflict of interest.

frontiers in Pharmacology

ORIGINAL RESEARCH
published: 24 April 2018
doi: 10.3389/fphar.2018.00399

The Selective Antagonism of Adenosine A_{2B} Receptors Reduces the Synaptic Failure and Neuronal Death Induced by Oxygen and Glucose Deprivation in Rat CA1 Hippocampus *in Vitro*

*Irene Fusco[1†], Filippo Ugolini[2†], Daniele Lana[2], Elisabetta Coppi[1], Ilaria Dettori[1], Lisa Gaviano[1], Daniele Nosi[3], Federica Cherchi[1], Felicita Pedata[1], Maria G. Giovannini[2] and Anna M. Pugliese[1]**

[1] Department of Neuroscience, Psychology, Drug Research and Child Health, NEUROFARBA, Section of Pharmacology and Toxicology, University of Florence, Florence, Italy, [2] Department of Health Sciences, Section of Clinical Pharmacology and Oncology, University of Florence, Florence, Italy, [3] Department of Experimental and Clinical Medicine, University of Florence, Florence, Italy

OPEN ACCESS

Edited by:
Francisco Ciruela,
Universitat de Barcelona, Spain

Reviewed by:
Rodrigo A. Cunha,
Universidade de Coimbra, Portugal
Oscar Herreras,
Consejo Superior de Investigaciones Científicas (CSIC), Spain

***Correspondence:**
Anna M. Pugliese
annamaria.pugliese@unifi.it

[†] These authors have contributed equally to this work.

Specialty section:
This article was submitted to Experimental Pharmacology and Drug Discovery, a section of the journal Frontiers in Pharmacology

Received: 09 November 2017
Accepted: 06 April 2018
Published: 24 April 2018

Citation:
Fusco I, Ugolini F, Lana D, Coppi E, Dettori I, Gaviano L, Nosi D, Cherchi F, Pedata F, Giovannini MG and Pugliese AM (2018) The Selective Antagonism of Adenosine A_{2B} Receptors Reduces the Synaptic Failure and Neuronal Death Induced by Oxygen and Glucose Deprivation in Rat CA1 Hippocampus in Vitro. Front. Pharmacol. 9:399. doi: 10.3389/fphar.2018.00399

Ischemia is a multifactorial pathology characterized by different events evolving in time. Immediately after the ischemic insult, primary brain damage is due to the massive increase of extracellular glutamate. Adenosine in the brain increases dramatically during ischemia in concentrations able to stimulate all its receptors, A_1, A_{2A}, A_{2B}, and A_3. Although adenosine exerts clear neuroprotective effects through A_1 receptors during ischemia, the use of selective A_1 receptor agonists is hampered by their undesirable peripheral side effects. So far, no evidence is available on the involvement of adenosine A_{2B} receptors in cerebral ischemia. This study explored the role of adenosine A_{2B} receptors on synaptic and cellular responses during oxygen and glucose deprivation (OGD) in the CA1 region of rat hippocampus *in vitro*. We conducted extracellular recordings of CA1 field excitatory post-synaptic potentials (fEPSPs); the extent of damage on neurons and glia was assessed by immunohistochemistry. Seven min OGD induced anoxic depolarization (AD) in all hippocampal slices tested and completely abolished fEPSPs that did not recover after return to normoxic condition. Seven minutes OGD was applied in the presence of the selective adenosine A_{2B} receptor antagonists MRS1754 (500 nM) or PSB603 (50 nM), separately administered 15 min before, during and 5 min after OGD. Both antagonists were able to prevent or delay the appearance of AD and to modify synaptic responses after OGD, allowing significant recovery of neurotransmission. Adenosine A_{2B} receptor antagonism also counteracted the reduction of neuronal density in CA1 stratum pyramidale, decreased apoptosis at least up to 3 h after the end of OGD, and maintained activated mTOR levels similar to those of controls, thus sparing neurons from the degenerative effects caused by the simil-ischemic conditions. Astrocytes significantly proliferated in CA1 stratum radiatum already 3 h after the end of OGD, possibly due to increased glutamate release.

A_{2B}receptor antagonism significantly prevented astrocyte modifications. Both A_{2B} receptor antagonists did not protect CA1 neurons from the neurodegeneration induced by glutamate application, indicating that the antagonistic effect is upstream of glutamate release. The selective antagonists of the adenosine A_{2B} receptor subtype may thus represent a new class of neuroprotective drugs in ischemia.

Keywords: apoptosis, MRS1754, PSB603, OGD, anoxic depolarization, mTOR, confocal microscopy, neurodegeneration

INTRODUCTION

Cerebral ischemic stroke represents a life threatening neurological disorder that leads to mortality and long-term disability in surviving patients. Ischemic stroke remains one of the main causes of death and disability in the western countries with only very limited therapeutic options (Dirnagl, 2012).

Acute brain injury after stroke is caused primarily by the lack of oxygen and glucose. In such conditions, mammalian neurons rapidly depolarize, and excessive release of glutamate occurs, causing excitotoxic cell death, largely due to over-activation of glutamatergic *N*-methyl-D-aspartate (NMDA) receptors. NMDA receptors are highly permeable to Ca^{2+} and are responsible for intracellular Ca^{2+} increase that reaches neurotoxic levels which, by activating cell lipases, endonucleases, proteases, and phosphatases, ultimately bring to acute excitotoxic cell death (Choi, 1992). Also, one of the early events occurring by an ischemic episode *in vivo* and during oxygen and glucose deprivation (OGD) *in vitro*, is the release of substantial amounts of adenosine (Latini et al., 1998; Melani et al., 1999; Frenguelli et al., 2007).

Adenosine exerts its biological functions via four receptors subtypes, A_1, A_{2A}, A_{2B}, and A_3 (Latini and Pedata, 2001). Many studies indicate that A_1 receptors play a prominent inhibitory tone on synaptic transmission and that adenosine selective antagonists, acting on this receptor subtype, has a protective role under ischemia (Pedata et al., 2016). Unfortunately, the development of A_1 receptor selective agonists as possible anti-ischemic drugs has been stalled by their sedative and cardiovascular side effects, including bradycardia and hypotension. Therefore, in order to identify putative targets for therapeutic intervention, the research on possible anti-ischemic drugs has focussed on the contribution of the other adenosine receptors. The role of the adenosine A_{2A} receptor under ischemia has been largely investigated (Chen et al., 2007; Pedata et al., 2014). Among adenosine receptors, the A_{2B} receptor subtype is the least studied and still remains the most enigmatic, because of the relatively low potency of adenosine for this receptor (Fredholm et al., 2011) and the very few selective ligands that have been described so far. Most of the present knowledge on A_{2B} receptors originates from their peripheral role on the control of cardiac myocyte contractility, intestinal tone, asthma, inflammation, cancer and diabetes (Feoktistov et al., 1998; Kolachala et al., 2008; Chandrasekera et al., 2010; Merighi et al., 2015; Allard et al., 2017). A_{2B} receptors play proinflammatory roles in human asthma, in chronic obstructive pulmonary disease and murine colitis (Feoktistov et al., 1998; Csóka et al., 2007; Kolachala et al., 2008). In the central nervous system (CNS), adenosine A_{2B} receptors, although scarcely, are uniformly expressed (Dixon et al., 1996) including in the hippocampus (Perez-Buira et al., 2007), but their role or function and in particular under ischemic/hypoxic conditions is still to be clarified. Understanding the processes by which the applications of these compounds confer neuroprotection should shed light on mechanisms to delay or mitigate the pathophysiological effects of ischemic injury.

In this paper we investigated the role of adenosine A_{2B} receptors during OGD in the CA1 region of rat hippocampus, the most susceptible hippocampal area to an ischemic insult. For this purpose two selective adenosine A_{2B} receptor antagonists were used. In order to characterize the OGD-induced cell injury and putative pharmacological protection, we conducted extracellular recordings of CA1 field excitatory post-synaptic potentials (fEPSPs) after a severe (7 min or 30 min) simil-ischemic insult. The response to ischemia consists of complex, concerted actions of the CNS and the peripheral immune system, that is very difficult to reproduce in *in vitro* model. However, these OGD episodes bring about irreversible depression of neurotransmission and the appearance of anoxic depolarization (AD) (Frenguelli et al., 2007; Pugliese et al., 2007). AD is a severe neuronal depolarization, which is an early and critical event that has been demonstrated both *in vivo* (Somjen, 2001) and *in vitro* (Tanaka et al., 1997; Pugliese et al., 2006). AD triggers a variety of molecular events, contributes to cell death and represents an unequivocal sign of neuronal injury (Somjen, 2001). The amount of time spent by neurons in AD is an important determinant of neuron fate. Propagation of AD from the ischemic core is one major factor contributing to neuronal death in the area surrounding the ischemic core (the penumbra) (Koroleva and Bures, 1996). The penumbra constitutes potentially salvageable tissue and hence a pharmacological treatment that delays the onset of AD would help to protect brain tissue from ischemia (Jarvis et al., 2001; Somjen, 2001).

Cell viability, extent of neuronal damage, astrocytes immunoreactivity and activation of apoptosis markers were also assessed by immunohistochemical analysis. Preliminary data were presented at the Society for Neuroscience Meeting (Ugolini et al., 2017).

MATERIALS AND METHODS

All animal experiments were performed according to the Italian Law on Animal Welfare (DL 26/2014), approved by the

Institutional Animal Care and Use Committee of the University of Florence and by the Italian Ministry of Health. All efforts were made to minimize animal sufferings and to use only the number of animals necessary to produce reliable scientific data. Male Wistar rats (Envigo, Italy, 150–200 g body weight) were used. Experiments were carried out on acute rat hippocampal slices, prepared as previously described (Pugliese et al., 2006, 2009).

Preparation of Slices

Animals were killed with a guillotine under anesthesia with isoflurane (Baxter, Rome, Italy) and hippocampi were rapidly removed and placed in ice-cold oxygenated (95% O_2–5% CO_2) artificial cerebrospinal fluid (aCSF) of the following composition (mM): NaCl 124, KCl 3.33, KH_2PO_4 1.25, $MgSO_4$ 1.4, $CaCl_2$ 2.5, $NaHCO_3$ 25, and D-glucose 10. Slices (400 μm nominal thickness) were cut using a McIlwain Tissue Chopper (Mickle Laboratory Engineering Co. Ltd., Gomshall, United Kingdom) and kept in oxygenated aCSF for at least 1 h at room temperature. A single slice was then placed on a nylon mesh, completely submerged in a small chamber (0.8 ml) and superfused with oxygenated aCSF (31–32°C) at a constant flow rate of 1.5 ml/min. The treated solutions reached the preparation in 60 s and this delay was taken into account in our calculations.

Extracellular Recordings

Test pulses (80 μs, 0.066 Hz) were delivered through a bipolar nichrome electrode positioned in the stratum radiatum of the CA1 region of the hippocampus to stimulate the Schaffer collateral-commissural pathway (**Figure 1A**). Evoked potentials were extracellularly recorded with glass microelectrodes (2–10 MΩ, Harvard Apparatus LTD, United Kingdom) filled with 150 mM NaCl. The recording electrode was placed at the dendritic level of the CA1 region to record field excitatory postsynaptic potentials (fEPSPs) (**Figure 1A**). Responses were amplified (200×, BM 622, Mangoni, Pisa, Italy), digitized (sample rate, 33.33 kHz), and stored for later analysis with LTP (version 2.30D) program (Anderson and Collingridge, 2001). The amplitude of fEPSP was measured as the difference between the negative peak following the afferent fiber volley and the baseline value preceding the stimulus artifact. In some experiments both the amplitude and the initial slope of fEPSP were quantified, but since no appreciable difference between these two parameters was observed under control conditions, in the presence of drugs or during *in vitro* ischemia, only the measure of the amplitude was expressed in the figures. When a stable baseline of evoked responses was reached, fEPSP amplitudes were routinely measured and expressed as the percentage of the mean value recorded 5 min before the application of any treatment (in particular pre-OGD). Stimulus-response curves were obtained by gradual increase in stimulus strength at the beginning of each experiment. The test stimulus strength was then adjusted to produce a response whose amplitude was 40% of the maximum and was kept constant throughout the experiment. Simultaneously, with fEPSP amplitude, AD was recorded as negative extracellular direct current (d.c.) shifts induced by OGD. The d.c. potential is an extracellular recording considered to provide an index of the polarization of cells surrounding the tip of the glass electrode (Farkas et al., 2008). AD latency, expressed in min, was calculated from the beginning of OGD; AD amplitude, expressed in mV, was calculated at the maximal negativity peak. In the text and bar graphs, AD amplitude values were expressed as positive values. The terms "irreversible synaptic failure" or "irreversible loss of synaptic transmission" used in the present work refer to the maximal time window of cell viability in our experimental model (acutely isolated hippocampal slice preparation) which, according to our previous results is 24 h (Pugliese et al., 2009).

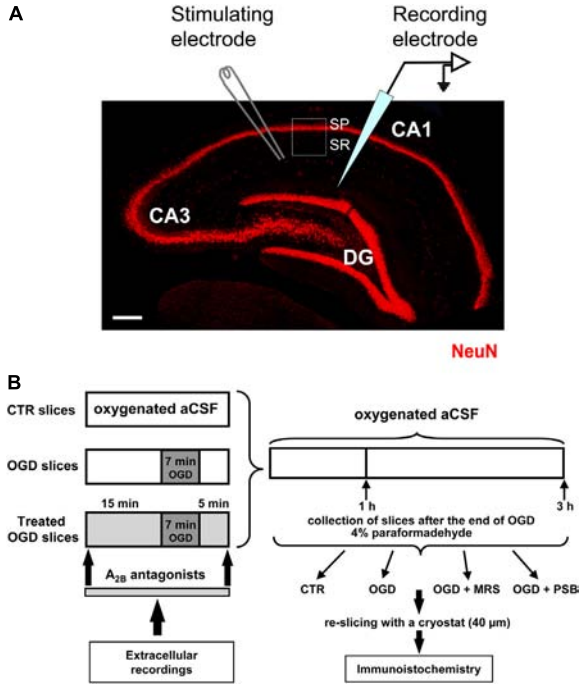

FIGURE 1 | Experimental methods. **(A)** Microphotography of an hippocampal slice showing the three subregions, the localization of the stimulating and recording electrodes and the region of interest (ROI, framed area) for the immunohistochemical analyses. SP, stratum pyramidale; SR, stratum radiatum. Scale bar: 200 μm. **(B)** Schematic representation of the experimental method.

Paired-Pulse Facilitation

To elicit paired-pulse facilitation (PPF) of fEPSP, we stimulated the Schaffer collateral-commissural fibers twice with a 40-ms interpulse interval. Double stimulation was evoked once every 15 s. The synaptic facilitation was quantified as the ratio (P2/P1) between the slope of the fEPSP elicited by the second (P2) and the first (P1) stimuli. PPF was monitored in control conditions for at least 5 min before the application of BAY606583. The effect of BAY606583 on PPF was evaluated by measuring the P2/P1 ratio during at least 5 min after 15 min of agonist application.

Drugs

Two selective adenosine A_{2B} receptors antagonists, N-(4-Cyanophenyl)-2-[4-(2,3,6,7-tetrahydro-2,6-dioxo-1,3-dip-ropyl-1H-purin-8-yl)phenoxy]-acetamide) (MRS1754) and 8-[4-[4-

(4-Chlorophenzyl) piperazide-1-sulfonyl) phenyl]]-1-propyl xanthine (PSB603) were used. D-2-amino-5-phosphonovalerate, a selective NMDA receptor antagonist was used. All these compounds were purchased from Tocris (Bristol, United Kingdom). The A_1 receptor antagonist DPCPX (8-cyclopentyl-1,3-dipropylxanthine) was purchased from SIGMA Aldrich (https://www.sigmaaldrich.com).

All drugs were dissolved in dimethyl sulphoxide (DMSO). Stock solutions, of 1000–10,000 times the desired final concentration, were stored at −20°C. The final concentration of DMSO (0.05% and 0.1% in aCSF) used in our experiments did not affect either fEPSP amplitude or the depression of synaptic potentials induced by OGD (data not shown).

Application of OGD and Adenosine A_{2B} Receptor Antagonists

The experimental method is shown in **Figure 1B**. Conditions of OGD were obtained by superfusing the slice with aCSF without glucose and gassed with nitrogen (95% N_2–5% CO_2) (Pedata et al., 1993). This causes a drop in pO_2 in the recording chamber from ∼500 mmHg (normoxia) to a range of 35–75 mmHg (after 7 min OGD) (Pugliese et al., 2003). At the end of the ischemic period, the slice was again superfused with normal, glucose-containing, oxygenated aCSF. The terms 'OGD slices' or 'treated OGD slices' refer to hippocampal slices in which OGD was applied in the absence or in the presence of A_{2B} receptor antagonists, respectively. Control slices were not subjected to OGD or treatment with A_{2B} receptor antagonists but were incubated in oxygenated aCSF for identical time intervals. All the selective adenosine A_{2B} receptors antagonists were applied 15 min before, during and 5 min after OGD. In a typical experimental day, first a control slice was subjected to 7 min of OGD. If the recovery of fEPSP amplitude after 60 min of reperfusion with glucose containing and normally oxygenated aCSF was ≤15% of the pre-OGD value, and AD developed into 7 min OGD, a second slice from the same rat was subjected to an OGD insult in the presence of the A_{2B} receptor antagonist under investigation. To confirm the result obtained in the treated group, a third slice was taken from the same rat and another 7 min OGD was performed under control conditions to verify that no difference between slices was caused by the time gap between the experiments. In some slices the OGD period was prolonged to 30 min and the A_{2B} receptor antagonists were applied 15 min before and during OGD application. After the extracellular recordings, slices were maintained in separate chambers for 1 or 3 h from the end of OGD in oxygenated aCSF at room temperature (RT). At the end, slices were harvested and fixed overnight at 4°C in 4% paraformaldehyde in PBS, cryopreserved in 18% sucrose for 48 h, and resliced as written below.

Treatment of Hippocampal Slices With Glutamate *in Vitro*

Experiments were carried out on acute hippocampal slices, prepared from male Wistar rats as described above. The A_{2B} receptor antagonists were dissolved in DMSO to obtain a stock solution suitable for a 1:2000 dilution. Slices, maintained oxygenated throughout the procedure, were incubated according to the following scheme:

- Control slices were incubated for 1 h in aCSF and then for 25 min in aCSF with DMSO (1:2000; 0.05%);
- Glutamate (GLU) treated slices were incubated 1 h in aCSF and then for 10 min with 100 μM glutamate in aCSF;
- MRS+GLU treated slices were incubated for 1 h in aCSF, then for 15 min with 500 nM MRS1754 and for further 10 min with 500 nM MRS1754 plus 100 μM glutamate, in aCSF;
- PSB+GLU treated slices were incubated for 1 h in aCSF, then for 15 min with 50 nM PSB603, and for further 15 min with 50 nM PSB603 plus 100 μM glutamate in aCSF;

After the incubation with glutamate and A_{2B} receptor antagonists, slices were further incubated for 3 h in aCSF, and then harvested and fixed overnight at 4°C in 4% paraformaldehyde in PBS, cryopreserved in 18% sucrose for 48 h, and resliced as written below.

Immunohistochemistry

One hour or 3 h after OGD, or after the incubation with glutamate and A_{2B} receptor antagonists, the 400 μm thick slices fixed in paraformaldehyde were placed on an agar support (6% agar in normal saline), included in an embedding matrix and re-sliced with a cryostat to obtain 40 μm thick slices. The more superficial sections were eliminated, while those obtained from the inner part of the slice were collected and stored in vials with 1 ml of antifreeze solution at −20°C until immunohistochemical analyses. From the 400 μm thick slices on average only a maximum of 2–3 complete 40 μm thick slices were obtained, which were then randomly allocated to the fluorescent immunohistochemical staining groups.

Antibodies Used – Primary Antibodies

Neurons were immunostained with a mouse monoclonal anti-NeuN antibody (1:200, MilliporeSigma, Carlsbad, CA, United States), astrocytes were detected by means of a polyclonal rabbit antibody anti-Glial Fibrillary Acidic Protein (GFAP, 1:500, DakoCytomation, Glostrup, Denmark), Cytochrome C with a mouse monoclonal antibody (1:200, Abcam, Cambridge, United Kingdom). Activated mTOR was detected using a polyclonal rabbit primary antibody raised against phospho-(Ser2448)-mTOR (1:100, Abcam, Cambridge, United Kingdom). Fluorescent secondary antibodies: Alexa Fluor 488 donkey anti rabbit (fluorescence in green, 1:400), Alexa Fluor 555 donkey anti mouse (fluorescence in red, 1:400), Alexa Fluor 635 goat anti-rabbit (fluorescence in far red, 1:400) (all from Life Technologies, Carlsbad, CA, United States). All primary and secondary antibodies were dissolved in Blocking Buffer (BB, 10% Normal Goat Serum, 0.05% NaN_3 in PBS-TX). All procedures were carried out with the free-floating method in wells of a 24-well plate (Cerbai et al., 2012; Lana et al., 2013).

Day 1

The sections were washed (3 times, 5 min each) in PBS-0.3% Triton X-100 (PBS-TX), blocked with 500 µl BB for 1 h, at RT under slight agitation and then incubated overnight at 4°C with the primary antibody under slight agitation.

Day 2

After washing in PBS-TX (3 times, 5 min each), sections were incubated for 2 h at room temperature in the dark with a solution containing one or two (for double immunostaining) fluorescent secondary antibodies, as appropriate. Sections were washed (3 times, 5 min each) with BB and then with 1 ml of distilled H_2O at RT in the dark, mounted on gelatinized microscopy slides, dried and coverslipped with a mounting medium containing DAPI to counterstain nuclei (Vectashield, Hard set mounting medium with DAPI, Vector Laboratories, Burlingame, CA, United States). Sections were kept refrigerated in the dark until microscopy analyses.

Day 3

Qualitative and quantitative analyses of NeuN positive neurons, CytC and phospho-mTOR positive cell bodies were performed in CA1 stratum pyramidale (SP), while astrocytes, phospho-mTOR positive dendrites and microglia were performed in CA1 stratum radiatum (SR) as shown in **Figure 1A**. Epifluorescence microscopy: sections were observed under an Olympus BX63 microscope equipped with an Olympus DP 50 digital camera (Olympus, Milan, Italy). For quantitative analysis images were acquired at 20× magnification with the digital camera.

Confocal Microscopy

Scans were taken at 0.3 µm z-step, keeping constant all the parameters (pinhole, contrast, and brightness), using a LEICA TCS SP5 confocal laser scanning microscope (Leica Microsystems CMS GmbH, Mannheim, Germany). Images were converted to green, or red using ImageJ (freeware provided by National Institute of Health[1]). The region of interest (ROI) in CA1, containing stratum pyramidalis and stratum radiatum was consistently analyzed in all slices, as shown in **Figure 1A** (Lana et al., 2014). Quantitative analyses of $NeuN^+$ neurons, HDN neurons, LDN neurons, $GFAP^+$ astrocytes, $CytC^+$ apoptotic neurons and phospho-mTOR positive cell bodies and dendrites were performed blind by two experimenters and results were averaged. Areas were expresses as mm^2. Digitized images were transformed into TIFF files and thresholded using ImageJ. Care was taken to maintain the same threshold in all sections within the same experiment. In CA1 pyramidal layer, the area labeled above the set threshold with NeuN or phospho-mTOR was calculated in pixels and expressed as $NeuN^+$ pixels/mm^2 or phospho-$mTOR^+$ pixels/mm^2. HDN neurons, LDN neurons, Cytochrome C-positive ($CytC^+$) apoptotic neurons in CA1 stratum pyramidale and $GFAP^+$ astrocytes in CA1 stratum radiatum were counted and were expressed as number of cells/mm^2. In order to evaluate mTOR activation in basal dendrites the length of phospho-$mTOR^+$ dendrites was measured at three fixed locations, equal in all slices and evenly distributed throughout the CA1 stratum radiatum ROI, and results were averaged.

[1]http://rsb.info.nih.gov/ij

Statistical Analysis

Statistical significance was evaluated by Student's paired or unpaired *t*-tests. Analysis of variance (one-way ANOVA), followed by Newman–Keuls multiple comparison *post hoc* test was used, as appropriate. *P*-values from both Student's paired and unpaired *t*-tests are two-tailed. Data were analyzed using software package GraphPad Prism (version 7.0; GraphPad Software, San Diego, CA, United States). All numerical data are expressed as the mean ± standard error of the mean (SEM). A value of $P < 0.05$ was considered significant.

RESULTS

Electrophysiological Experiments

It has been established that 7 min OGD episodes bring about irreversible depression of neurotransmission and the appearance of a severe neuronal depolarization or AD (Pugliese et al., 2006, 2007, 2009), a critical event that has been demonstrated both *in vivo* (Somjen, 2001) and *in vitro* (Fowler, 1992; Pearson et al., 2006; Pugliese et al., 2006, 2007, 2009; Frenguelli et al., 2007). Therefore, we studied the effects of two selective adenosine A_{2B} receptor antagonists, MRS1754 and PSB603, on AD development in the CA1 region of acute rat hippocampal slices under severe OGD episodes by extracellular recording of fEPSPs on 133 hippocampal slices taken from 42 rats.

The Selective Adenosine A_{2B} Receptor Antagonism Prevents or Delays AD Development and Protects From Synaptic Failure Induced by Severe OGD in CA1 Hippocampus

In agreement with our previous results (Pugliese et al., 2006, 2007, 2009), in untreated OGD slices the d.c. shift presented a mean latency of 6.04 ± 0.2 min (calculated from the beginning of OGD) and a mean peak amplitude of −6.7 ± 0.4 mV (n = 24) (**Figure 2A**). Seven min OGD exposure induced a rapid and irreversible depression of fEPSPs amplitude evoked by Schaffer-collateral stimulation, since synaptic potentials did not recover their amplitude after return to oxygenated aCSF (**Figure 2D**, n = 24, 2.5 ± 2.7% of pre-OGD level, calculated 50 min from the end of OGD). Control slices, followed for up to 3 h in oxygenated aCSF, maintained stable fEPSPs for the entire experimental time recording and never developed the d.c. shift (data not shown).

Oxygen and glucose deprivation was then applied in the presence of the selective adenosine A_{2B} receptor antagonists MRS1754 or PSB603, administered 15 min before, during and 5 min after OGD.

The two A_{2B} receptor antagonists did not modify basal synaptic transmission measured before OGD. Indeed, MRS1754 (500 nM, n = 17) did not modify fEPSPs amplitude under

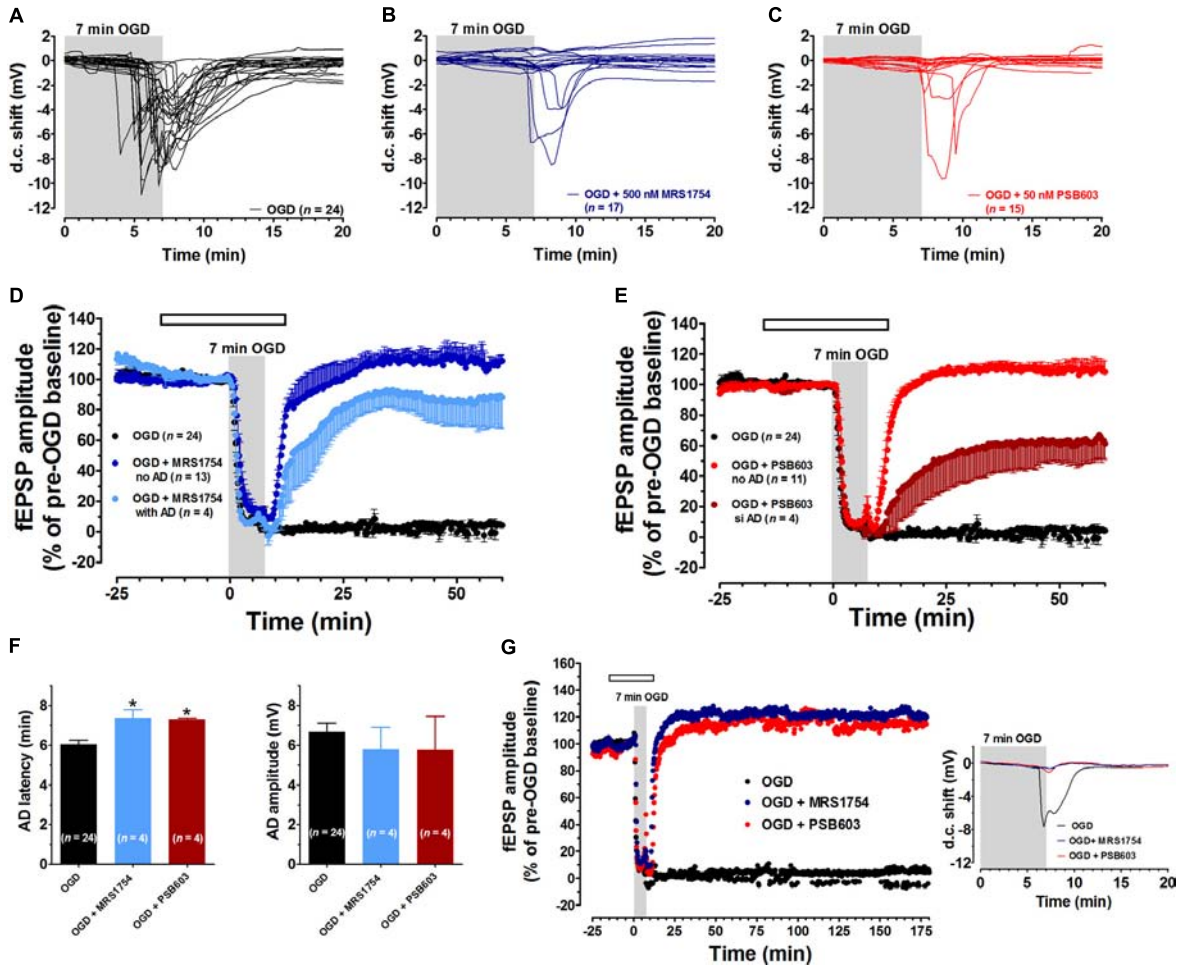

FIGURE 2 | The selective adenosine A_{2B} receptor antagonists MRS1754 or PSB603 significantly reduced the synaptic failure induced by 7 min oxygen and glucose deprivation (OGD) in the CA1 region of rat hippocampal slices. **(A–C)** anoxic depolarization (AD) was recorded as a negative direct current (d.c.) shift in response to 7 min OGD in untreated OGD slices **(A)**, in 500 nM MRS1754-treated slices **(B),** or 50 nM PSB603-treated slices **(C)**. Note that MRS1754 prevented the appearance of AD in 13 out of 17 slices, while PSB603 in 11 out of 15 slices. **(D)** The graph shows the time-course of the effect of 7 min OGD on field excitatory post-synaptic potential (fEPSP) amplitude, expressed as percentage of pre-OGD baseline in the CA1 hippocampal region in the absence (n = 24) or in the presence of 500 nM MRS1754 (n = 17). Note that, in untreated slices, the ischemic-like insult caused gradual reduction, up to disappearance, of fEPSPs amplitude that did not recover after washing in oxygenated artificial cerebrospinal fluid (aCSF). On the contrary, after reperfusion in oxygenated standard solution, a recovery of fEPSP in all MRS1754 treated OGD slices was found, even in those in which AD developed. **(E)** The graph shows the time course of the effect of 7 min OGD on fEPSP amplitude in 50 nM PSB603 treated OGD slices. Note that, after reperfusion in normal oxygenated standard solution, a recovery of fEPSP was found in all OGD-treated PSB603 slices, even those in which AD occurred. **(F, Left)** each column represents the mean ± SEM of AD latency recorded in the CA1 region during 7 min OGD in the absence or in the presence of MRS1754 (500 nM) or PSB603 (50 nM). AD latency was measured from the beginning of OGD insult. Note that when OGD was applied in the presence of MRS1754 or PSB603 the appearance of AD was significantly delayed in comparison to OGD untreated slices. *$P < 0.05$ vs. OGD, One-way ANOVA followed by Newman–Keuls Multiple comparison test. **(Right)** each column represents the mean ± SEM of AD amplitude recorded in the CA1 during 7 min OGD. The number of slices is reported in the columns. **(G)** The graph shows the time course of the effect of 7 min OGD on fEPSP amplitude in OGD-untreated slices and in 500 nM MRS1754- or 50 nM PSB603-treated slices. The selective antagonism of adenosine A_{2B} receptors counteracted the CA1 synaptic damage induced by severe OGD up to 3 h from the end of the insult. Inset: 7 min OGD induced AD was recorded untreated OGD slices, but not in the presence of 500 nM MRS1754 or 50 nM PSB603. Gray bar: OGD time duration. Open bar: time of drug application. Amplitude of fEPSPs (mean ± SEM) is expressed as percentage of pre-OGD baseline.

normoxic conditions (from 1.05 ± 0.06 mV immediately before to 1.01 ± 0.08 mV after 15 min drug application, n = 17). Also, PSB603 did not change the amplitude of synaptic potentials under normoxic conditions (from 1.32 ± 0.12 mV before to 1.35 ± 0.14 mV after 15 min drug application, n = 15). These data indicate that the blockade of A_{2B} receptors does not modify low-frequency-induced CA1 synaptic transmission under normoxic conditions, in agreement with results reported in mouse hippocampal slices (Gonçalves et al., 2015).

Nevertheless, the two A_{2B} receptor antagonists were able to prevent or delay the appearance of AD and to modify synaptic responses after OGD.

During 7 min OGD, MRS1754 prevented the appearance of AD in 13 out of 17 slices tested (**Figure 2B**). In these 13 slices

a complete recovery of fEPSPs was recorded (111.9 ± 7.4%, calculated 50 min from the end of OGD, **Figure 2D**). In the remaining 4 slices, AD developed, although at later times (**Figure 2F**, mean AD latency: 7.37 ± 0.41 min; mean peak amplitude: −5.8 ± 1.1 mV, n = 4), and, unexpectedly, was followed by a consistent fEPSP recovery (85.2 ± 15.3%, n = 4, **Figure 2D**).

During 7 min OGD, PSB603 prevented the appearance of AD in 11 out of 15 slices tested (**Figure 2C**). In these 11 slices a complete recovery of fEPSPs was found (110.4 ± 10.2%, n = 11, **Figure 2E**). In the remaining four slices in which AD appeared, a delay in AD latency was recorded (**Figure 2F**, mean AD latency: 7.33 ± 0.08 min; mean peak amplitude: −6.8 ± 1.9 mV, n = 4). Moreover, in these four PSB603-treated slices, a significant recovery of fEPSP (36.2 ± 19.7%, n = 4, **Figure 2E**) was found.

In the slices in which AD appeared in the presence of MRS1754 or PSB603, we compared the time of AD appearance in the absence and in the presence of drugs. As illustrated in **Figure 2F**, during 7 min OGD, AD appeared in OGD slices with a mean latency of 6.04 ± 0.2 min (Left panel) and a mean peak amplitude of 6.7 ± 0.4 mV (n = 24, Right panel). When 7 min OGD was applied in the presence of 500 nM MRS1754 or 50 nM PSB603 the d.c. shifts were always delayed (**Figure 2F**, Left panel), while AD amplitude values were not significantly modified in comparison to OGD slices (**Figure 2F**, Right panel).

In an experimental group of slices which never developed AD in the presence of PSB603 (50 nM) (n = 6) and MRS1754 (500 nM) (n = 6), we followed the evolution of the synaptic response for 3 h after the end of the 7 min ischemic like insult in comparison to untreated OGD slices (n = 6). As reported in the representative electrophysiological traces shown in **Figure 2G**, PSB603 (50 nM) and MRS1754 (500 nM) allowed the recovery of synaptic potentials for at least 3 h after 7 min OGD.

Furthermore, in order to confirm that both the recovery of fEPSP and the irreversible loss of neurotransmission after 7 min OGD observed in the different experimental groups were not transient, we tested slice viability 24 h after the OGD insult in control, untreated, slices and slices treated with A_{2B}-receptor antagonists. In agreement with our previously published results (Pugliese et al., 2009), we showed that untreated OGD slices, which did not recover any synaptic activity within 1 h after the insult, maintained synaptic impairment when tested 24 h later (Supplementary Figure 1A shows a representative experiment out of a total of six slices). On the contrary, MRS1754- or PSB603-treated OGD slices, which recovered initial fEPSP amplitude 1 h after OGD, preserved neurotransmission for at least 24 h after the insult (Supplementary Figure 1B shows a representative experiment out of a total of four slices, and Supplementary Figure 1C shows a representative experiment out of a total of five slices for MRS1754 and PSB603, respectively).

In order to characterize the role of adenosine A_{2B} receptors on AD development, in a next series of experiments we prolonged the OGD duration up to 30 min, in order to allow AD to unavoidably appear in all experimental groups. This longer duration of OGD is invariably associated with tissue damage (Pearson et al., 2006). We compared the latency and the magnitude of depolarizing d.c. shifts recorded in the absence or presence of PSB603 or MRS1754. As illustrated in **Figure 3A**, 30 min OGD elicited the appearance of AD in all slices, with a mean peak amplitude of −7.5 ± 0.7 mV (n = 8) and a mean latency of 5.8 ± 0.3 min, as shown in **Figures 3D,E**. When OGD was applied in the presence of 500 nM MRS1754, the d.c. shift was significantly delayed to 9.2 ± 0.7 min (**Figures 3B, D**; n = 5), although the AD amplitude (−5.7 ± 0.7 mV) was not significantly changed (**Figure 3E**). Similarly, when OGD was applied in the presence of 50 nM PSB603, the d.c. shift was significantly delayed to 7.7 ± 0.3 min (**Figures 3C,D**; n = 7) whereas AD amplitude (−7.7 ± 0.7 mV) was unchanged (**Figure 3E**).

Data in the literature demonstrate that adenosine A_{2B} receptors exert their effects through a control of A_1 receptor function in the hippocampus under simil-physiological, normoxic, conditions (Gonçalves et al., 2015). In order to test this possibility, we studied whether A_{2B} receptor antagonists were still effective in inhibiting OGD-induced alterations of synaptic transmission in the presence of the A_1 receptor antagonist DPCPX. As shown in Supplementary Figures 2A–C, we applied DPCPX before, during and after a 7 min OGD and, unexpectedly, we found that 2 out of 6 slices tested did not undergo AD and completely recovered their synaptic activity. This unexpected result was possibly due to the unselective block of A_{2A} receptors by DPCPX, as already described in hippocampal slices during OGD (Sperlágh et al., 2007). Therefore, we reduced DPCPX concentration to 100 nM and we prolonged the OGD period up to 30 min (Supplementary Figure 2D). Under these experimental conditions, DPCPX-exposed slices presented a delayed AD appearance (mean AD peak time = 8.4 ± 0.5 min) in comparison to control, untreated, OGD slices (mean AD peak time = 6.8 ± 0.2 min) thus confirming that DPCPX protects hippocampal slices from OGD insults (Supplementary Figure 2E). The time window of A_{2B} or A_1 receptor-mediated effects found in the present studies overlaps with the delay found treating the slices with glutamate receptor antagonists (Tanaka et al., 1997; Yamamoto et al., 1997), or blocking NMDA receptors that are involved both in initiation and propagation of AD (Herreras and Somjen, 1993; Somjen, 2001). In a further series of experiments, we demonstrated that D-AP5 (50 μM) significantly delayed AD appearance (from 6.8 ± 0.2 min in untreated OGD slices to 9.8 ± 1.0 min in D-AP5-treated OGD slices, Supplementary Figure 2E).

For this reason, in order to assess the involvement of A_1 receptors in A_{2B} receptor-mediated effects, we choose a different protocol. It has been shown that short-term plasticity, measured by PPF, is modified by A_{2B} receptor activation in mouse hippocampal slices in a DPCPX-sensitive manner (Gonçalves et al., 2015). We confirmed that the A_{2B} receptor agonist BAY606583, at 200 nM concentration, significantly decreased PPF in rat CA1 hippocampus (**Figure 4**), thus indicating an increase of presynaptic glutamate release upon A_{2B} receptor activation. This effect was blocked not only by the A_{2B} receptor antagonists PSB603 and MRS1754, but also by the A_1 receptor antagonist DPCPX (**Figure 4B**), thus confirming that A_{2B} receptor effects are mediated by the inhibition of the A_1 subtype, as already stated by Gonçalves et al. (2015).

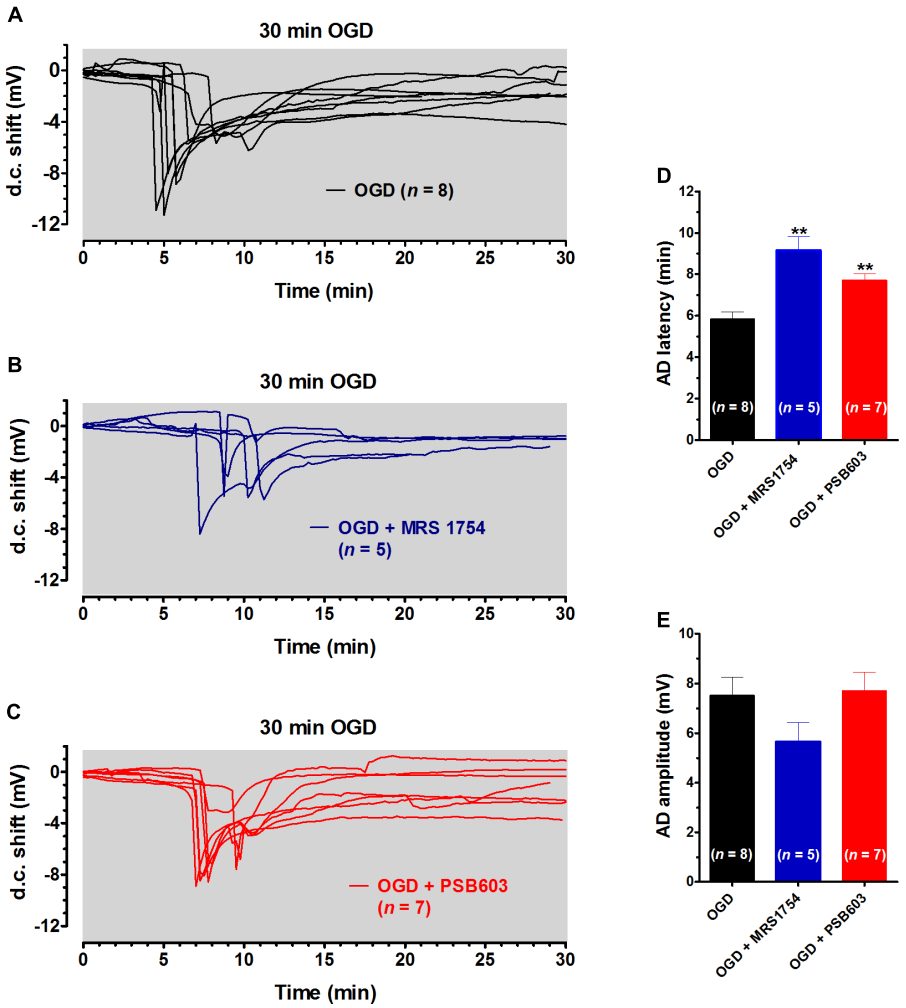

FIGURE 3 | MRS1754 and PSB603 delayed the appearance of AD induced by 30 min OGD in rat hippocampal slices. **(A–C)** The graphs show the d.c. shift traces during 30 min OGD in untreated OGD slices (**A**, $n = 8$), in the presence of 500 nM MRS1754 (**B**, $n = 5$), or 50 nM PSB603 (**C**, $n = 7$). **(D)** Each column represents the mean ± SEM of AD latency recorded in hippocampal slices during 30 min OGD in different experimental groups. AD was measured from the beginning of OGD insult. Note that both adenosine A_{2B} receptor antagonists significantly delayed AD development. $^{**}P < 0.01$ vs. OGD, One-way ANOVA followed by Newman–Keuls Multiple comparison test. **(E)** Each column represents the mean ± SEM of AD amplitude recorded in the CA1 during 30 min OGD. The number of slices is reported in the columns.

Analysis of Neuronal Damage in CA1 Stratum Pyramidale 1 and 3 h After the End of 7 min OGD

The extent of neuronal damage caused by 7 min OGD in stratum pyramidale of hippocampal CA1 was assessed by immunohistochemistry using the anti-NeuN antibody in control slices, in slices after 7 min OGD alone, and after 7 min OGD in the presence of 500 nM MRS1754 or 50 nM PSB603, both at 1 and 3 h after the end of OGD. Representative images of NeuN immunostaining in CA1 of slices collected 1 h after the end of OGD are shown in **Figures 5A–D**.

Figures 5E,F show the quantitative analyses of the area of $NeuN^+$ immunofluorescence in CA1, which represents an index of the number of pyramidal neurons, 1 and 3 h after the end of OGD, respectively. The data demonstrate that $NeuN^+$ CA1 pyramidal neurons significantly decreased both 1 h (**Figure 5E**) and 3 h (**Figure 5F**) after the end of 7 min OGD. Statistical analysis showed that 7 min OGD caused a statistically significant reduction of $NeuN^+$ area at 1 h (−29.6%, $^*P < 0.05$ vs. control slices) and at 3 h (−41%, $^*P < 0.05$ vs. control slices). The time-course of the effect, indicating that the decrease of $NeuN^+$ area was more pronounced at 3 h than at 1 h after the end of OGD, demonstrates that neuronal degeneration is an ongoing process at least at these time points.

The decrease of $NeuN^+$ area in CA1 stratum pyramidale was completely antagonized by treatment with 50 nM PSB603 (−1% at 1 h and −14% at 3 h, ns vs. control slices). This effect was statistically significant vs. 7 min OGD slices both at 1 and 3 h after the end of OGD ($^\$P < 0.05$ vs. respective OGD). Treatment with 500 nM MRS1754 completely blocked the decrease of $NeuN^+$

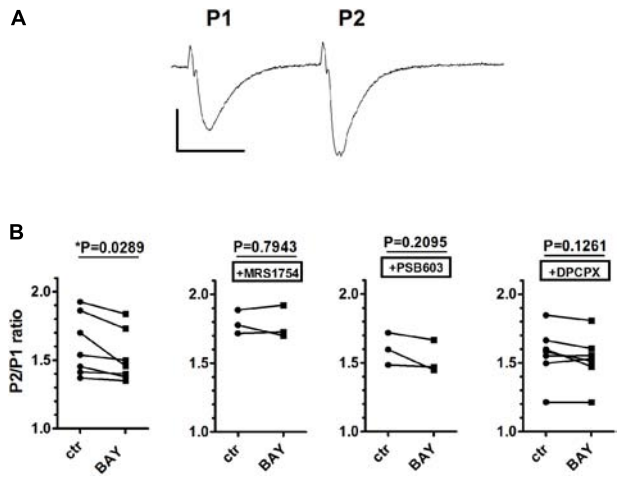

FIGURE 4 | The selective stimulation of adenosine A_{2B} receptors reduced paired-pulse facilitation (PPF) in rat hippocampal slices. **(A)** Trace of fEPSP responses to PPF protocol (40-ms interval), taken from a typical experiment. Calibration: 0.5 mV, 20 ms. **(B)** Each graph shows PPF quantified as the ratio (P2/P1) between the slope of the second fEPSP (P2) and the slope first fEPSP (P1). The effect of BAY606583 (BAY, 200 nM) on PPF was investigated in the absence (n = 7) or in the presence of MRS1754 (500 nM, n = 3), PSB603 (50 nM, n = 3), or DPCPX (100 nM, n = 7). $^{*}P < 0.05$ vs. ctr, paired Student's t-test.

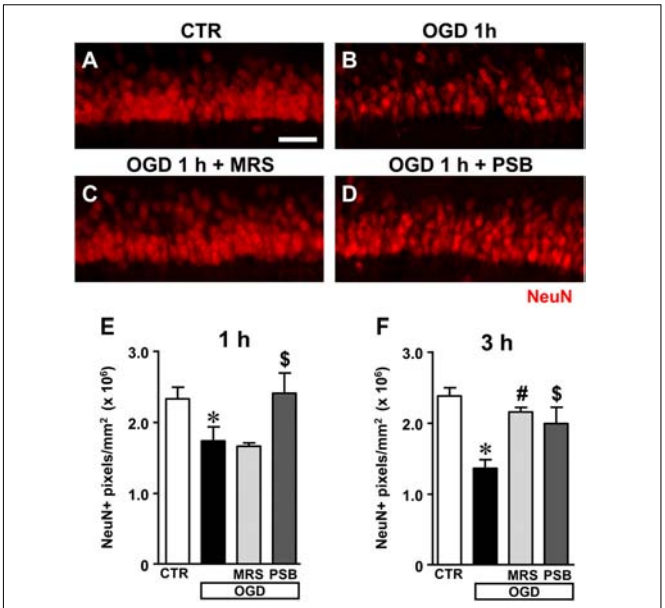

FIGURE 5 | Analysis of NeuN^{+} immunofluorescence in CA1 stratum pyramidale after the simil-ischemic insult. **(A–D)** Representative images of NeuN^{+} immunofluorescence in the ROI of CA1 of a control slice (CTR, **A**), a slice collected 1 h after 7 min OGD (OGD, **B**), a slice treated with 500 nM MRS1754 (OGD+MRS, **C**), and a slice treated with 50 nM PSB603 (OGD+PSB, **D**), all harvested 1 h after the end of 7 min OGD. Scale bar: 75 μm. **(E,F)** Quantitative analyses of NeuN^{+} immunofluorescence in the four experimental groups 1 h **(E)** and 3 h **(F)** after the end of 7 min OGD. Each column represents the area, expressed in pixels ($\times 10^6$) above a threshold, maintained constant for all slices investigated. **(E)** Statistical analysis: One-way ANOVA: $F_{(3;13)} = 6.296$, $P < 0.01$, Newman–Keuls multiple comparison test: $^{*}P < 0.05$, OGD vs. CTR; $^{\$}P < 0.05$, OGD+PSB vs. OGD. CTR, n = 6; OGD, n = 5; OGD+PSB, n = 3; OGD+MRS, n = 3. **(F)** Statistical analysis: One-way ANOVA: $F_{(3,16)} = 4.924$, $P < 0.02$; Newman–Keuls multiple comparison test: $^{*}P < 0.05$ OGD vs. CTR, $^{\#}P < 0.05$ OGD+MRS vs. OGD,$^{\$}P < 0.05$ OGD+PSB vs. OGD. CTR, n = 6; OGD, n = 3; OGD+PSB, n = 4; OGD+MRS n = 4. All data in the graphs are expressed as mean ± SEM.

area in CA1 stratum pyramidale 3 h after the end of OGD (−7% vs. control slices, ns; $^{\#}P < 0.05$ vs. OGD). MRS1754 had no effect 1 h after the end of OGD (−31.5% vs. control slices; ns vs. OGD). Therefore, antagonism of A_{2B} receptors blocked the neuronal damage induced by 7 min OGD up to 3 h after the end of the simil-ischemic insult. In the OGD slices treated either with MRS1754 or PSB603 that developed AD we found a partial reduction of neuronal damage at 1 h after the end of OGD (data not shown).

Closer examination of CA1 stratum pyramidale with confocal microscopy indicated the presence of many damaged neurons both 1 and 3 h after the end of 7 min OGD. The representative confocal z stacks in **Figures 5B**, **6B**, each obtained stacking 37 consecutive confocal z-scans (0.3 μm each, total thickness 11.1 μm) through the thickness of CA1, show that 3 h after the end of OGD the layout and morphology of CA1 pyramidal neurons was significantly different from that of the control slice (**Figure 6A**). **Figures 6A1,B1** are magnification of the framed areas in **Figures 6A,B**, and show stacks of two consecutive z-scans, 0.3 μm each, total thickness 0.6 μm, taken at 2.1 μm depth inside the neurons. It appears evident from panel **Figure 6B1** the altered morphology of pyramidal neurons after OGD, in comparison to those of the control slice shown in **Figure 6A1**. Indeed, in CA1 stratum pyramidale of OGD slices, both at 1 and 3 h after the end of OGD, we observed the presence of many neurons with nuclei that exhibit a highly condensed NeuN-positive nucleus and very faint NeuN cytoplasmic labeling (**Figures 6B,B1**, open arrows). We defined these neurons as High Density Nucleus neurons, "HDN neurons." Furthermore, we observed many NeuN^{+} neurons that have lost the NeuN^{+} nuclear immunofluorescence, an index of damaged nuclei, while NeuN^{+} immunofluorescence persists in the cytoplasm (**Figures 6B,B1**, white arrows). We defined these neurons as Low Density Nucleus neurons, "LDN neurons."

In order to better characterize this phenomenon, we performed the quantitative analysis of HDN and LDN neurons in control, 7 min OGD, 7 min OGD plus MRS1754 and 7 min OGD plus PSB603 slices at 1 and 3 h after the end of OGD. The results, presented in **Figures 6C,D**, show that HDN neurons increased significantly in 7 min OGD slices both at 1 h (+603% vs. control slices, $^{**}P < 0.01$) and 3 h (+794% vs. control slices, $^{***}P < 0.001$) after the end of OGD. The increase of damaged, HDN neurons in the CA1 area caused by the simil-ischemic insult was significantly blocked by treatment with 50 nM PSB603 at 1 and 3 h after the end of OGD (−97% at 1 h, and −77% at 3 h vs. 7 min OGD slices, both $^{\$\$\$}P < 0.001$; ns vs. controls). Conversely, treatment with 500 nM MRS1754 significantly blocked the increase of HDN neurons only 3 h after the end of OGD (−70% vs. 7 min OGD slices, $^{\#\#\#}P < 0.001$; ns vs.

control slices), but not 1 h after the end of OGD (+12% vs. OGD slices, ns; $^{\#\#}P < 0.01$ vs. control slices).

Also, as shown by the representative images in **Figures 6B,B1**, we found many LDN neurons in stratum pyramidale 1 and 3 h after the end of 7 min OGD. As demonstrated by quantitative analysis (**Figures 6E,F**) LDN neurons in stratum pyramidale were significantly increased both 1 and 3 h after OGD, in comparison to control slices. The increase of LDN neurons, in comparison to control slices, was 1489% at 1 h ($^{***}P < 0.01$ vs. control slices) and 1033% at 3 h after the end of 7 min OGD ($^{***}P < 0.01$ vs. control slices). The increase of damaged, LDN neurons brought about by the simil-ischemic insult was significantly blocked by treatment with 50 nM PSB603 both at 1 and 3 h after the end of OGD (−98% at 1 h, and −62% at 3 h vs. OGD, both $^{\$\$\$}P < 0.001$). Treatment with 500 nM MRS1754 significantly blocked the increase of LDN neurons only 3 h after the end of OGD (−52% vs. 7 min OGD,$^{\#\#\#}P < 0.001$), but not 1 h after the end of OGD (−17% vs. 7 min OGD, ns; $^{\#\#}P < 0.01$ vs. controls). These data further confirm the efficacy of the two A_{2B} receptor antagonists, and particularly of PSB603, in reducing not only the electrophysiological effects but also the morphological modifications that OGD caused on CA1 pyramidal neurons, up to 3 h after the end of the ischemic-like insult.

Analysis of Apoptotic Neurons in Stratum Pyramidale of CA1 1 and 3 h After 7 min OGD

These data demonstrate that 7 min OGD can induce neuronal damage in CA1 stratum pyramidale, as evidenced by immunohistochemical analyses that highlight conformational modifications of pyramidal neurons that may subtend cell death. Therefore, we studied whether all the above-described effects and the decrease of neurons in CA1 stratum pyramidale might be caused by apoptosis. To this end, as an apoptosis marker we used CytC, a protein which, in physiological conditions, is found in mitochondria but in the most advanced stages of apoptosis is intensely and diffusely released in the cytoplasm, where it activates caspases (Kluck et al., 1997; Yang et al., 1997; Jiang and Wang, 2004; Suen et al., 2008) and can be used as a marker of apoptosis using immunohistochemical analysis (Martínez-Fábregas et al., 2014). Using a selective antibody, CytC can be visualized in apoptotic cells as an intense and diffuse cytoplasmic immunostaining, as shown by the white arrows in the representative confocal images of an OGD slice 1 h after the end of OGD (**Figures 7A–A2**). As shown in the confocal subslice of the framed area of **Figure 7A2**, obtained stacking 17 consecutive confocal z-scans through the $CytC^+$ neuron (0.3 μm each, total thickness 5.1 μm), it is evident that the $CytC^+$ positive neuron is a LDN neuron (**Figures 7B–B2**, open arrow), thus demonstrating that LDN neurons are apoptotic.

From the quantitative analysis of $CytC^+$ neurons in CA1 stratum pyramidale, we demonstrated that both 1 and 3 h after the end of 7 min OGD many CA1 pyramidal neurons were apoptotic (**Figures 7C,D**). The increase was statistically significant in comparison to control slices both at 1 h (+277% vs. control slices, $^{***}P < 0.001$) and at 3 h (+107% vs. control slices, $^{**}P < 0.01$) after OGD. These data indicate that in CA1 area, already after 1 h from the end of OGD, neurons had clear signs of apoptotic processes. In the presence of MRS1754 or PSB603, there was a significant reduction of CytC immunostaining, both at 1 and 3 h after the end of OGD, showing that antagonism of A_{2B} receptors significantly reduced neuronal death by apoptosis at both times investigated. Indeed, treatment with MRS1754 decreased apoptotic neurons by 61% at 1 h ($^{\#\#\#}P < 0.001$ vs. 7 min OGD; ns vs. control slices) and by 33% at 3 h ($^{\#}P < 0.05$ vs. 7 min OGD; ns vs. control slices), in comparison to OGD slices. Treatment with PSB603 decreased apoptotic neurons by 63% ($^{\$\$\$}P < 0.001$ vs. 7 min OGD; ns vs. control slices) and by 46% ($^{\$\$}P < 0.001$ vs. 7 min OGD; ns vs. control slices) in comparison to OGD slices. In the OGD slices treated either with MRS1754 or PSB603 that developed AD the number of HDN and LDN neurons were partially decreased in comparison to OGD slices (data not shown).

These data indicate that in the CA1 area already 1 h after the end of OGD, when there was still no recovery of neurotransmission, neurons showed obvious signs of apoptosis. These data demonstrate that antagonism of A_{2B} receptors brought about significant protection against neuron degeneration.

Analysis of Phospho-mTOR in Area CA1 of the Hippocampus 1 and 3 h After 7 min OGD

We used a selective antibody for phospho-(Ser244)-mTOR, the activated form of mTOR, to investigate whether mTOR activation might be modified in our experimental conditions (**Figures 8A–D1**). Representative qualitative images of mTOR activation in cell bodies and dendrites of CA1 pyramidal neurons in a control slice are shown in **Figure 8A1** (green). Neurons were also immunolabelled with anti-NeuN antibody (red). The merge of the immunofluorescence (yellow-orange) in a control slice is shown in **Figure 8A**. It is evident from the images that activated mTOR is present in CA1 pyramidal neurons in basal, control conditions where it is localized both in the cell body and in neuronal apical dendritic tree spanning throughout the stratum radiatum. The simil-ischemic condition caused a significant decrease of mTOR activation 3 h after the end of OGD, as shown in the representative image of **Figures 8B,B1**. This effect is more evident in **Figures 8E,F**, that represent digital subslices obtained stacking nine consecutive confocal z-scans throughout the neuronal cell bodies (0.3 μm each, total thickness 2.7 μm) of control and OGD slices. The images clearly show that in control conditions phospho-mTOR was present both in the cell body (**Figure 8E**, open arrow) and in the dendrites (**Figure 8E**, white arrows), while 3 h after 7 min OGD activation of mTOR decreased both in cell body and dendrites (**Figure 8F**). Quantitative analysis showed that in slices harvested 1 h after the end of 7 min OGD, no significant modification of activated mTOR immunostaining was present in the neuronal cell body (**Figure 8G**) or in the apical dendrites of CA1 pyramidal neurons in any of the groups investigated (**Figure 8I**). On the contrary, in slices harvested 3 h after the

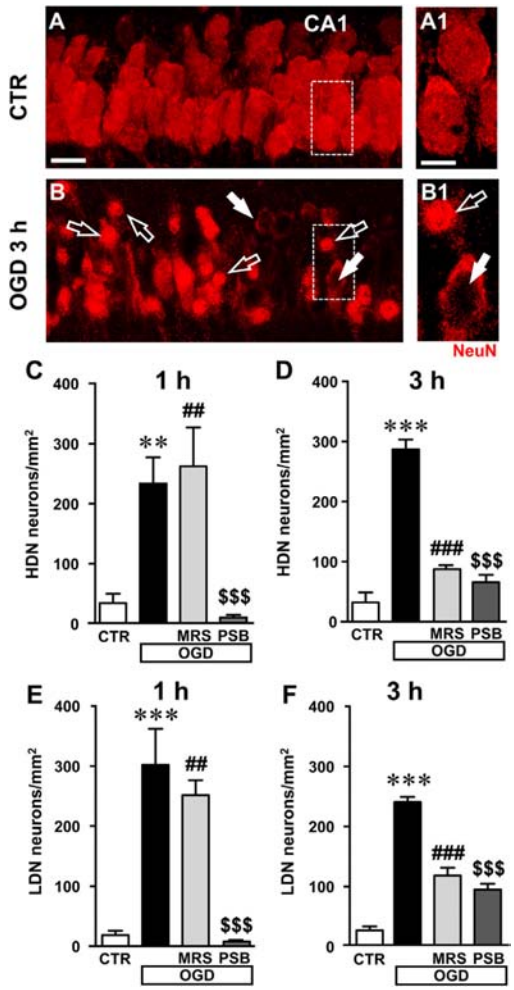

FIGURE 6 | Analysis of damaged neurons in CA1 stratum pyramidale after the simil-ischemic insult. **(A–B1)** Representative images of NeuN$^+$ immunofluorescence in the CA1 area of a control slice (CTR, **A,A1**), and of a slice harvested 3 h after the end of 7 min OGD (OGD, **B,B1**). **(A1–B1)** magnification of digital subslices of the framed areas in **A,B** (stacks of two consecutive z-scans taken at 2.1 μm depth inside the neurons, total thickness 0.6 μm). Note the presence of many HDN neurons (open arrows) and LDN neurons (white arrows) in CA1 stratum pyramidale after OGD **(B,B1)**. Scale bars: **A,B**: 25 μm; **A1,B1**: 10 μm. **(C,D)** Quantitative analyses of NeuN$^+$ HDN neurons in CA1 stratum pyramidale 1 h **(C)** and 3 h **(D)** after the end of OGD. **(C)** One-way ANOVA: $F_{(3;12)} = 11.32$, $P < 0.001$. Newman–Keuls multiple comparison test: $^{**}P < 0.01$, OGD vs. CTR; $^{\#\#}P < 0.01$, OGD+MRS vs. CTR;$^{\$\$\$}P < 0.001$ OGD+PSB vs. OGD. CTR, $n = 5$; OGD, $n = 5$; OGD+PSB, $n = 3$; OGD+MRS, $n = 3$. **(D)** One-way ANOVA: $F_{(3;12)} = 64.33$, $P < 0.001$. Newman–Keuls multiple comparison test: $^{***}P < 0.001$, OGD vs. CTR; $^{\#\#\#}P < 0.001$, OGD+MRS vs. OGD;$^{\$\$\$}P < 0.001$ OGD+PSB vs. OGD. CTR, $n = 5$; OGD, $n = 3$; OGD+PSB, $n = 4$; OGD+MRS, $n = 4$. **(E–F)**: Quantitative analysis of NeuN$^+$ LDN neurons in CA1 stratum pyramidale 1 h **(E)** and 3 h **(F)** after the end of OGD. **(E)** One-way ANOVA: $F_{(3;14)} = 13.80$, $P < 0.001$. Newman–Keuls multiple comparison test: $^{***}P < 0.01$, OGD vs. CTR; $^{\#\#}P < 0.01$, OGD+MRS vs. CTR;$^{\$\$\$}P < 0.001$ OGD+PSB vs. OGD. CTR, $n = 6$; OGD, $n = 6$; OGD+PSB, $n = 3$; OGD+MRS, $n = 3$. **(F)** One-way ANOVA: $F_{(3;12)} = 69.77$, $P < 0.001$. Newman–Keuls multiple comparison test: $^{***}P < 0.001$, OGD vs. CTR; $^{\#\#\#}P < 0.001$, OGD+MRS vs. OGD;$^{\$\$\$}P < 0.001$ OGD+PSB vs. OGD. CTR, $n = 5$; OGD, $n = 3$; OGD+PSB, $n = 4$; OGD+MRS, $n = 4$. All data in the graphs are expressed as mean ± SEM.

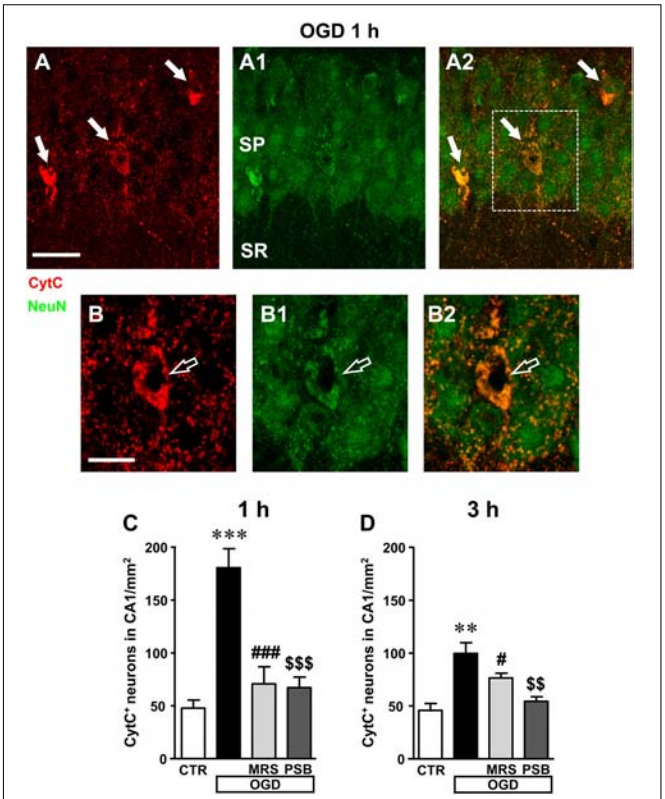

FIGURE 7 | Analysis of CytocromeC$^+$ (CytC$^+$) neurons in CA1 stratum pyramidale after the simil-ischemic insult. **(A–A2)** Representative microphotographs, taken at the laser scanning confocal microscope, of apoptotic neurons labeled with anti-CytC antibody (**A**, red), of pyramidal neurons labeled with anti-NeuN antibody (**A1**, green) and the merge of the two previous images **(A2)**. NeuN$^+$ and CytC$^+$ apoptotic neurons in CA1 stratum pyramidale are indicated by the arrows (yellow-orange color in **A2**). Scale bar: 25 μm. **(B–B2)** Subslice of the framed area in **A2**, obtained stacking 17 consecutive confocal z-scans (5.1 μm total thickness), shown at higher magnification (2×). The open arrow shows an LDN apoptotic pyramidal neuron. Scale bar: 10 μm. **(C,D)** Quantitative analysis of NeuN$^+$ and CytC$^+$ neurons in CA1 stratum pyramidale at 1 h **(C)** and 3 h **(D)** after the end of 7 min OGD. Note the significant increase of CytC$^+$ neurons both 1 and 3 h after the end of OGD. **(C)** Statistical analysis: One-way ANOVA: $F_{(3;11)} = 18.40$, $P < 0.001$, Newman–Keuls multiple comparison test: $^{***}P < 0.001$, OGD vs. CTR; $^{\#\#\#}P < 0.001$, OGD+MRS vs. OGD; $^{\$\$\$}P < 0.001$, OGD+PSB vs. OGD. CTR, $n = 4$; OGD, $n = 3$; OGD+PSB, $n = 4$; OGD+MRS, $n = 4$. **(D)** Statistical analysis: One-way ANOVA: $F_{(3;11)} = 11.41$, $P < 0.02$, Newman–Keuls multiple comparison test: $^{**}P < 0.01$, OGD vs. CTR; $^{\#}P < 0.05$, OGD+MRS vs. OGD; $^{\$\$}P < 0.01$, OGD+PSB vs. OGD. CTR, $n = 4$; OGD, $n = 3$; OGD+PSB, $n = 4$; OGD+MRS, $n = 4$. All data in the graphs are expressed as mean ± SEM.

end of 7 min OGD, we found highly significant decrease of activated mTOR immunostaining in the cytoplasm and dendrites of CA1 pyramidal neurons (**Figures 8H,J**). Indeed, statistical analysis, shown in **Figure 8H**, demonstrates that 3 h after the end of 7 min OGD there was a statistically significant reduction of activated mTOR immunostaining in the cytoplasm of CA1 pyramidal neurons (−74.8%, $^{***}P < 0.001$ vs. control slices, **Figure 8H**) in comparison to control slices. As shown in **Figure 8H**, treatment with 50 nM PSB603 blocked this effect

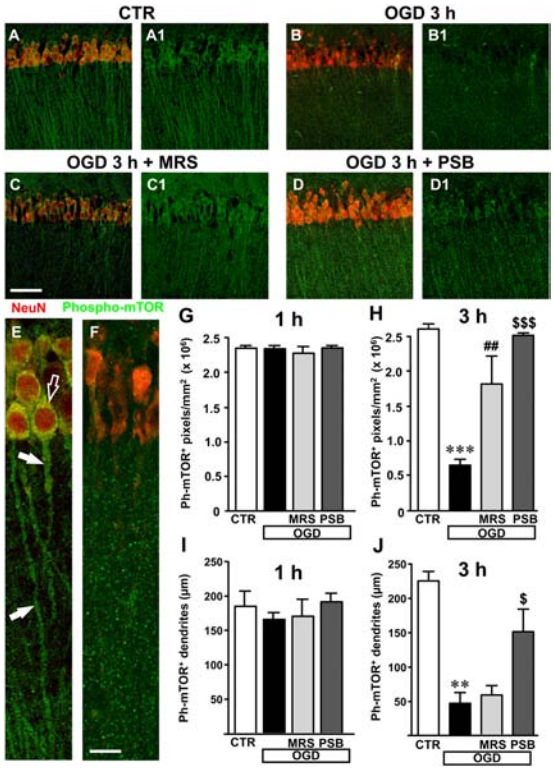

FIGURE 8 | mTOR activation in CA1 stratum pyramidale and stratum radiatum after the simil-ischemic insult. Representative microphotographs, taken at the laser scanning confocal microscope, showing immunolabelling with anti-NeuN antibody (red) and anti-phospho-mTOR antibody (green) of a control slice **(A,A1)**, a slice harvested 3 h after 7 min OGD **(B,B1)**, a slice treated with MRS1754 and harvested 3 h after 7 min OGD **(C,C1)**, and a slice treated with PSB603 and harvested 3 h after 7 min OGD **(D,D1)**. Scale bar: 75 µm. **(E,F)** Digital subslices of a control slice **(E)** and a slice collected 3 h after 7 min OGD **(F)** immunostained for phospho-mTOR (green) and NeuN (red). The open arrow shows the presence of activated mTOR in the cell body and arrows in the dendrites of pyramidal neurons in the control slice **(E)**. **(G,H)** Quantitative analysis of activated mTOR in CA1 stratum pyramidale in the different experimental conditions. Each column represents the $mTOR^+$ immunofluorescent area calculated using the ImageJ program (number of pixels above a reference, fixed threshold). **(G)** No difference among the four experimental groups, was found 1 h after the end of 7 min OGD. Statistical analysis: One-way ANOVA: $F_{(3;11)} = 0.4563$, $P > 0.05$, ns. **(H)** Slices harvested 3 h after the end of 7 min OGD. Note the significant decrease of activated mTOR in CA1 pyramidal neurons 3 h after the end of OGD. Both MRS1754 and PSB603 significantly blocked this effect. Statistical analysis: One-way ANOVA: $F_{(3;10)} = 26.99$, $P < 0.001$, Newman–Keuls multiple comparison test: $^{***}P < 0.001$, OGD vs. CTR; $^{\#\#}P < 0.01$, OGD+MRS vs. OGD; $^{\$\$\$}P < 0.001$, OGD +PSB vs. OGD. CTR, $n = 4$; OGD, $n = 3$; OGD+PSB, $n = 3$; OGD+MRS, $n = 4$. All data are expressed as mean ± SEM. **(I,J)** Quantitative analysis of phospho-$mTOR^+$ dendrites in CA1 stratum radiatum in the different experimental conditions. **(I)** Length of phospho-$mTOR^+$ dendrites in CA1 stratum radiatum 1 h after the end of 7 min OGD. No difference among the four experimental groups was observed. Statistical analysis: One-way ANOVA: $F_{(3;11)} = 0.7143$, $P > 0.05$, ns. **(J)** Length of $mTOR^+$ dendrites in CA1 stratum radiatum 3 h after the end of 7 min OGD. Note the significant decrease of activated mTOR in dendrites 3 h after the end of OGD. PSB603 significantly blocked this effect. Statistical analysis: One-way ANOVA: $F_{(3;9)} = 12.38$, $P < 0.02$, Newman–Keuls multiple comparison test: $^{**}P < 0.01$, OGD vs. CTR; $^{\$}P < 0.05$, OGD+PSB vs. OGD. CTR, $n = 3$; OGD, $n = 3$; OGD+PSB, $n = 3$; OGD+MRS, $n = 4$. All data in the graphs are expressed as mean ± SEM.

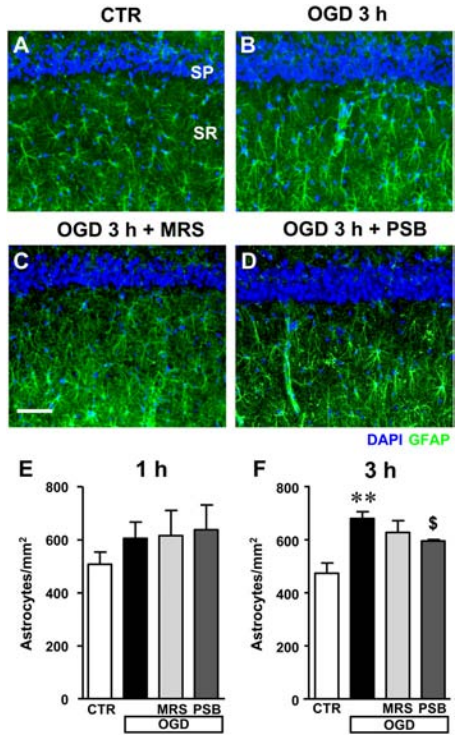

FIGURE 9 | Quantitative analysis of astrocytes in the CA1 area in the different experimental conditions after the simil-ischemic insult. **(A–D)** Representative microphotographs, taken at the epifluorescence microscope, of astrocytes immunolabelled with anti-GFAP antibodies in the stratum radiatum (green) of a control **(A)**, OGD **(B)**, OGD plus MRS1754 **(C)**, and OGD plus PSB603 **(D)** slice. Scale bar: 50 µm. **(E,F)** Quantitative analysis of astrocytes in the stratum radiatum of CA1 in control, OGD, OGD plus MRS1754, and OGD plus PSB603 slices at 1 h **(E)** and 3 h **(F)** after 7 min OGD. **(E)** No significant differences among the four experimental groups analyzed was found. Statistical analysis: One-way ANOVA: $F_{(3;18)} = 0.877$, $P > 0.05$, ns. CTR, $n = 8$; OGD, $n = 7$; OGD+PSB, $n = 3$; OGD+MRS, $n = 4$. **(F)** Statistical analysis: One-way ANOVA: $F_{(3;15)} = 6.734$, $P < 0.01$, Newman–Keuls multiple comparison test: $^{**}P < 0.01$, OGD vs. CTR; $^{\$}P < 0.05$, OGD+PSB vs. OGD. CTR, $n = 7$; OGD, $n = 4$; OGD+PSB, $n = 4$; OGD+MRS, $n = 4$. All data in the graphs are expressed as mean ± SEM.

(−4% vs. control slices, ns, $^{\$\$\$}P < 0.001$ vs. 7 min OGD), while treatment with 500 nM MRS1754 partially, but still significantly attenuated this effect (−31% vs. controls, ns, $^{\#\#}P < 0.01$ vs. 7 min OGD).

We used, as a determinant of mTOR activation in the dendrites, the analysis of the length of phospho-mTOR positive dendrites, as reported in the methods. The results shown in **Figure 8I** reveal that mTOR activation was not statistically significant among the four experimental groups 1 h after the end of 7 min OGD. However, in the slices collected 3 h after the end of 7 min OGD we found a significant decrease of mTOR positive dendrites in the stratum radiatum of the CA1 area (**Figure 8J**). From the statistical analysis we demonstrated a significant decrease of mTOR immunopositive dendrites in CA1 stratum radiatum of 7 min OGD slices 3 h after the end of OGD (−80% vs. controls, $^{**}P < 0.01$, **Figure 8J**). The

selective antagonist MRS1754, did not significantly modify this effect, while treatment with PSB603 partially, but significantly, reversed this effect (+226% vs. 7 min OGD, $^{\$}P < 0.05$). These data demonstrate that OGD significantly decreased mTOR activation and that the selective antagonism selective antagonism of A_{2B} receptors significantly reduced this impairment, a further indication of prevention of neuronal degeneration by blockade of this receptor.

Analysis of Astrocytes in CA1 Stratum Radiatum After 7 min OGD

Astrocytes were labeled with the anti-GFAP antibody and quantified in the stratum radiatum of CA1 hippocampus in the four experimental conditions: in control slices, in slices after 7 min OGD alone, and after 7 min OGD in the presence of 500 nM MRS1754 or 50 nM PSB603, both at 1 and 3 h after the end of OGD, as shown in the representative microphotographs in **Figures 9A–D**, taken at 3 h after the end of OGD.

In the stratum radiatum of slices harvested 1 h after the end of 7 min OGD we found a slight, not significant increase of astrocytes (**Figure 9E**, +19%, ns vs. controls), which became significant at 3 h after the end of 7 min OGD (**Figure 9F**, +43% vs. control slices, $^{**}P < 0.01$). Both A_{2B} receptor antagonists, partially but significantly, reduced the increase of astrocytes caused by the simil-ischemic conditions. MRS1754 decreased the number of astrocytes by 10% (ns vs. OGD), while PSB603 by 13% ($^{\$}P < 0.05$ vs. OGD).

Quantitative analysis of total microglia did not reveal statistically significant modifications in the different experimental conditions both at 1 and 3 h after the end of 7 min OGD (data not shown).

Neurodegeneration of CA1 Pyramidal Neurons Induced by Glutamate Was Not Prevented by Adenosine A_{2B} Receptor Antagonists

In order to have an insight into the mechanism of A_{2B} receptor antagonism-induced neuroprotection, we verified whether MRS1754 and PSB603 might protect CA1 pyramidal neurons from the well-known neurodegenerative effects caused by glutamate exposure. We incubated the hippocampal slices *in vitro* with 100 μM glutamate for 10 min and verified the effect of MRS1754 and PSB603 on glutamate-induced cell death (**Figures 10A–D**).

Administration of 100 μM glutamate for 10 min caused significant damage to pyramidal neurons at 3 h after the end of incubation, evidenced by the significant increase of HDN neurons in hippocampal CA1, as shown in the representative image presented in **Figure 10B**. Quantitative analysis (**Figure 10D**) demonstrated that the increase of HDN neurons was statistically significant in comparison to control slices, and that neither MRS1754 nor PSB603 protected CA1 pyramidal neurons from the excitotoxic effect of glutamate ($^{*}P < 0.05$ vs. all other groups).

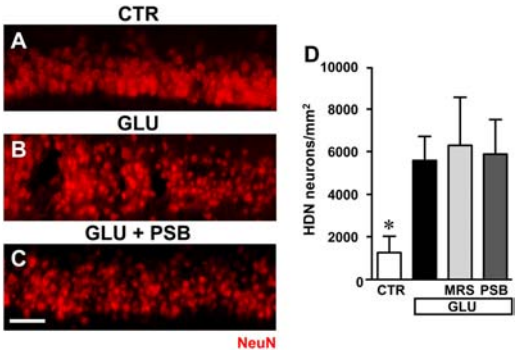

FIGURE 10 | Evaluation of glutamate induced neurotoxicity in CA1 stratum pyramidale in the different experimental conditions. **(A–C)** Representative microphotographs, taken at the epifluorescence microscope, of CA1 pyramidal neurons immunolabelled with anti-NeuN antibodies in a control slice **(A)**, a slice treated with glutamate (GLU, **B**), a slice treated with glutamate plus PSB603 (GLU+ PSB, **C**) slice. Scale bar: 50 μm. **(D)** Quantitative analyses of $NeuN^{+}$ HDN neurons in the four experimental groups 3 h after the end of drug incubation. Statistical analysis: One-way ANOVA: $F_{(3;15)} = 3.313$, $P < 0.05$, Newman–Keuls multiple comparison test: $^{*}P < 0.05$, vs. all other groups. CTR, $n = 6$; GLU, $n = 6$; GLU+PSB, $n = 3$; GLU+MRS, $n = 4$.

DISCUSSION

The putative protective role of adenosine A_{2B} receptors in cerebral ischemia was studied in the CA1 region of hippocampal slices under oxygen-glucose deprivation, an experimental condition that mimics, albeit with the limits of *in vitro* methodology, the most common causes of cerebral ischemia, such as vessel occlusion. *In vitro* slices give a partial view of the physiology of the brain because of the absence of an intact vascular system and the altered tridimensional microenvironment. These alterations involve not only neurons but also glia, and more generally the physiology of the neurovascular unit formed by astrocytes, pericytes, microglia, neurons, and the extracellular matrix (Holloway and Gavins, 2016). Nevertheless, the *in vitro* systems have many benefits such as the opportunity to obtain highly valuable information in terms of the time-course of the electrophysiological events, changes in membrane potential (AD), changes in synaptic transmission and morphological and biochemical changes in neurons and glia. Our results confirm that in the CA1 region of rat hippocampus, the application of a 7 min OGD episode induced the appearance of AD which was followed by irreversible synaptic damage and neurodegeneration of CA1 pyramidal neurons (Pugliese et al., 2003, 2006, 2009; Coppi et al., 2007; Traini et al., 2011). We now demonstrate that these events are accompanied by neurodegeneration of CA1 pyramidal neurons, with reduction of neuronal density and significant increase of apoptotic neurons. For the first time we demonstrated here that antagonism of A_{2B} receptors using the selective ligands MRS1754 or PSB603, applied before, during and after OGD, prevented or delayed the appearance of AD, and prevented the irreversible loss of neurotransmission induced by 7 min OGD. Furthermore, we demonstrated that the selective blockade of A_{2B} receptors during

a prolonged (30 min) OGD insult delays the appearance of AD indicating an extension of the time window between the start of the insult and the appearance of excitotoxic damage. Adenosine A_{2B} receptor antagonism also counteracted the reduction of neuronal density in CA1 stratum pyramidale and decreased apoptosis mechanisms at least up to 3 h after the end of the insult. Both A_{2B} receptor antagonists did not protect CA1 neurons from neurodegeneration induced by glutamate application, indicating that the antagonistic effect is upstream of glutamate release.

The hippocampus, and particularly CA1 stratum pyramidale, is one of the most vulnerable brain regions to ischemic damage. We used the acute rat hippocampal slice preparation which allows measurements of synaptic transmission with good spatial and temporal resolution. In the early phases, hypoxia/ischemia is known to induce a massive increase of extracellular glutamate levels which trigger hyperactivation of glutamate receptors, production of reactive oxygen species, pathological increase of intracellular Ca^{2+}, rapid decrease in ATP reserves and activation of various proteolytic enzymes (Káradóttir et al., 2005; Al-Majed et al., 2006; Kovacs et al., 2006). In hippocampal slices, a severe OGD insult as that applied in the present experiments (7 min) elicits the appearance of AD within the OGD period and is invariably followed by irreversible loss of neurotransmission (Frenguelli et al., 2007; Pugliese et al., 2007, 2009), an index of cell suffering, damage to neurons and to the surrounding tissue (Somjen, 2001). AD is caused by the sudden increase of extracellular K^+ and by the contemporary explosive rise in glutamate extracellular concentration (Somjen, 2001). Contemporarily to the extracellular increase of glutamate, the extracellular concentration of adenosine significantly increases, as demonstrated both in *in vivo* and *in vitro* experiments (Latini and Pedata, 2001). After 5 min OGD, adenosine reaches an extracellular concentration of 30 μM in hippocampal slices (Latini et al., 1999; Pearson et al., 2006). At such high concentration adenosine can stimulate all receptor subtypes, including the A_{2B} receptor, which exhibits affinity for adenosine with an EC_{50} in the range of 5–20 μM, lower than all other subtypes (Fredholm et al., 2011). For this reason, it is possible that activation of A_{2B} receptors occurs mainly during pathological conditions, such as inflammation, hypoxia, trauma, and ischemia (Fredholm et al., 2001).

Our data show that A_{2B} receptor antagonists, by preventing or delaying the onset of AD, prevent the irreversible loss of neurotransmission induced by 7 min OGD allowing complete recovery of synaptic potentials. We showed for the first time a partial recovery of neurotransmission was also observed in a group of hippocampal slices, treated with A_{2B} receptor antagonists, that developed AD immediately after reoxygenation. This delay of AD appearance might account for the partial recovery of neurotransmission observed in these slices. The occurrence of AD after the end of OGD period is a peculiar characteristic that we observed in our hippocampal preparation. We envisage that when the AD appears during the reoxygenation period, similarly to the phenomenon of spreading depression (Somjen, 2001), neurons are less damaged, and they can partially recover their electrical activity. Thus, even in those slices treated with the A_{2B} receptor antagonists in which AD takes place, this event is less harmful to neuronal viability. This is a substantial difference from A_{2A} receptor antagonist-mediated neuroprotection during a 7 min OGD insult. Indeed, fEPSP recovery was never observed in those few slices undergoing AD in the presence of the A_{2A} receptor blocker ZM241385, as previously published (Pugliese et al., 2009).

As to the mechanism by which A_{2B} receptor antagonists protect from hypoxia/ischemia, recent studies by Gonçalves et al. (2015) have demonstrated that in mouse hippocampus A_{2B} receptors are expressed on glutamatergic terminals anatomically comparable to those from which our recordings were performed. Their selective stimulation counteracts the predominant A_1 receptor-mediated inhibition of synaptic transmission. We confirmed this assumption by performing PPF experiments in rat hippocampal slices in which the A_{2B} receptor agonist BAY606583 was able to reduce PPF ratio, which is known to be caused by increased glutamate release at presynaptic level. This effect is counteracted not only by the A_{2B} receptor antagonists MRS1754 and PSB603 but also by the A_1 receptor antagonist DPCPX. As already hypothesized (Moriyama and Sitkovsky, 2010; Gonçalves et al., 2015), this result may be related to the existence of an A_1/A_{2B} receptor heterodimer in the CA1 hippocampal region. On these bases, our purpose was to study the possible involvement of A_1 receptors in the neuroprotective effects elicited by the two A_{2B} receptor antagonists during OGD. In accordance to data reported by Canals et al. (2008) in a model of chemical penumbra produced by a mitochondrial gliotoxin in the hippocampus *in vitro*, we would have expected conservation of synaptic transmission during the first min of OGD and acceleration of AD appearance. In our conditions, a similar response was observed only in a limited number of slices during 7 min OGD. Instead, in most of the slices we demonstrated that DPCPX induced neuroprotection during OGD, delaying AD appearance. This unexpected result may be due to a different response of A_1 receptors during OGD in our experimental conditions. Our data could also be explained considering the results obtained by Sperlágh et al. (2007) who demonstrated that DPCPX decreases glutamate release from hippocampal slices subjected to OGD and that this effect is mimicked and occluded by the A_{2A} receptor antagonist ZM241385. The same Authors hypothesize that DPCPX, even at low nanomolar concentrations, would directly bind to A_{2A} receptors during severe ischemia (in accordance with our previously published results, Pugliese et al., 2009). The rational for this assumption is that the A_{2A} receptor agonist CGS21680 displays two distinct binding sites in the hippocampus: a "typical" (striatal-like) binding site which is displayed by DPCPX only at high (submicromolar) concentrations, and an "atypical" binding site, which shows high affinity for DPCPX (Johansson and Fredholm, 1995; Cunha et al., 1996). On these bases, we can hypothesize that, in our OGD experiments, DPCPX binds to this "atypical" binding site (i.e., an A_1–A_{2A} receptor heterodimer) thus decreasing glutamate outflow and protecting hippocampal slices from OGD insults. Furthermore, when overstimulated such as during ischemia, A_1 receptors undergo desensitization (Siniscalchi et al., 1999).

This phenomenon can be further increased by A_{2B} receptors activation, triggering a vicious circle in which the beneficial effect of A_1 receptor stimulation is overcome by the noxious effect of A_{2B} receptors activation (Gonçalves et al., 2015) as already suggested for A_{2A} adenosine receptors (Pugliese et al., 2009). Further mechanistic studies suggest that the A_{2A} receptor, when stimulated, facilitates A_{2B} receptor externalization from the endoplasmic reticulum to the plasma membrane, possibly increasing the formation of the A_{2A}–A_{2B} dimer (Moriyama and Sitkovsky, 2010). All these results taken together may explain the deleterious activity of adenosine A_{2B} receptor stimulation during an ischemic insult, and the protective effect of A_{2B} receptor antagonists in this condition. Finally, observation that the A_{2B} receptor antagonists did not protect CA1 neurons from neurodegeneration induced by direct glutamate application, confirms that the mechanism underlying their protection against ischemia-induced neurodegeneration is exerted at adenosine receptors that, by the abovementioned mechanisms, regulate extracellular glutamate release. Alternatively, since OGD is above all a problem of efficient energy recovery, the demonstration that A_{2B} receptors control astrocytic and neuronal glycogen metabolism (Magistretti et al., 1986; Allaman et al., 2003) and glucose utilization by hippocampal slices (Lemos et al., 2015) may suggest an additional effect of these receptors on metabolic activity during OGD.

Severe OGD increased apoptosis and damaged CA1 pyramidal neurons at 1 and 3 h after the end of the ischemic insult. Immunohistochemistry showed that CA1 pyramidal neurons had significant morphological changes, with increased density of nuclei (HDN neurons), karyorrhexis (LDN neurons) and possibly nuclear fragmentation, as evidenced by the significantly higher number of LDN neurons and cell death after OGD. These results are in agreement with those found by Ünal-Çevik et al. (2004) in the cerebral cortex of the rat after mild ischemia. Pyknosis is typical of apoptotic cells (Elmore, 2007) and may precede karyorrhexis. We demonstrated that LDN neurons, being highly positive for CytC, were undergoing apoptosis. It has been demonstrated that CytC released into the cytosol binds to apoptotic protease activating factor-1, which leads to activation of caspase-9 which is important in neuronal cell death following ischemia (Kluck et al., 1997; Yang et al., 1997; Love, 2003; Jiang and Wang, 2004; Suen et al., 2008; Lana et al., 2014, 2016, 2017a,b; Martínez-Fábregas et al., 2014). In turn, caspase-9 is activated by high glutamate levels, as occurs during ischemia (Li et al., 2009). As reported in the literature, activation of mTOR, which has multiple roles in cells among which local protein synthesis at the dendritic and spine level (Frey and Morris, 1997; Tsokas et al., 2007; Thoreen et al., 2012), can be modified in ischemic conditions (Dennis et al., 2001; Laplante and Sabatini, 2012). As already reported (Gegelashvili et al., 2001; Maragakis and Rothstein, 2004), the decrease of mTOR activation may be secondary to the excitotoxic mechanisms evoked by massive increase of glutamate during OGD, which is known to be an important component of neuronal injury *in vitro* (Newell et al., 1995). The participation of decreased mTOR activation in OGD-induced neuronal damage is supported by our results showing decreased activation of mTOR both in the cell body and dendrites of CA1 neurons 3 h after the end of OGD.

Within the limits of the *in vitro* model and the alteration of the neurovascular unit and of neuro glia interplay, we found interesting effects on astrocytic responses. Indeed, astrocytes proliferation, possibly caused, among other stimuli, by increased release of glutamate, is one of the early events that takes place after acute focal CNS damage (Burda and Sofroniew, 2014). In accordance to our previous results (Pugliese et al., 2009), we found evidence of significant, although limited, astrocytic proliferation in CA1 stratum radiatum already 3 h after the end of OGD, possibly caused by increased glutamate release. A_{2B} receptor antagonism significantly prevented all the above neuronal and astrocytic modifications, sparing neurons from the degenerative effects caused by the simil-ischemic conditions, and reducing astrocytes proliferation. CA1 pyramidal neurons treated with the A_{2B} receptor antagonists had a similar morphology to those of control slices, had neither increased nor decreased nuclear density, did not undergo apoptosis, and had activated mTOR levels similar to those of controls.

The similar effects obtained using two different A_{2B} receptor antagonists strengthen the hypothesis that the A_{2B} receptor is involved in the mechanisms of cerebral ischemia. Nevertheless, MRS1754 seems to have lower efficiency than PSB603 on some of the parameters investigated. It is possible that the two drugs act with a different time-course or that PSB603 is more efficacious than MRS1754 in this model.

In summary, our data demonstrate that antagonists of adenosine A_{2B} receptors protect the CA1 area of the hippocampus from an acute damage induced by severe hypoxic/ischemic conditions. The mechanism likely resides in protection from the acute increase of glutamate extracellular concentrations and consequent excitotoxicity. It is worth noticing that since A_{2B} receptors have low affinity for the endogenous ligand adenosine, they are activated only at high extracellular adenosine concentrations that can be reached under pathological conditions such as ischemia, thus representing a selective target (Popoli and Pepponi, 2012).

AUTHOR CONTRIBUTIONS

MG and AP designed the research. FU, DL, DN, IF, LG, ID, and FC performed the experiments. FU, DL, EC, MG and AP analyzed the data. DL, MG, EC, AP and FP interpreted the results and the experiments. DL, MG, FU, AP and IF prepared the figures. MG and AP drafted the manuscript. DL, MG, FU, FP, AP and EC edited and revised the manuscript. All authors read and approved the final version of the manuscript.

FUNDING

DL was partly funded by Ente Cassa di Risparmio di Firenze (ECRF_2014_0663_Giovannini) and by

University of Florence Dean's Postdoctoral Fellowship. This research was funded in part by University of Florence (Fondi Ateneo Ricerca: AP, FP, and MG), and in part by MIUR-PRIN (2015E8EMCM_006, MG) and (2015E8EMCM_002, AP). The funding sources had no involvement in the conduct of the research, in preparation of the article, in study design; in the collection, analysis and interpretation of data; in the writing of the report; and in the decision to submit the article for publication.

ACKNOWLEDGMENTS

We thank Dr. F. Trombetta for the helpful technical assistance.

SUPPLEMENTARY MATERIAL

The Supplementary Material for this article can be found online at: https://www.frontiersin.org/articles/10.3389/fphar.2018.00399/full#supplementary-material

REFERENCES

Allaman, I., Lengacher, S., Magistretti, P. J., and Pellerin, L. (2003). A2B receptor activation promotes glycogen synthesis in astrocytes through modulation of gene expression. *Am. J. Physiol. Cell Physiol.* 284, C696–C704. doi: 10.1152/ajpcell.00202.2002

Allard, D., Turcotte, M., and Stagg, J. (2017). Targeting A2 adenosine receptors in cancer. *Immunol. Cell Biol.* 95, 333–339. doi: 10.1038/icb.2017.8

Al-Majed, A. A., Sayed-Ahmed, M. M., Al-Omar, F. A., Al-Yahya, A. A., Aleisa, A. M., and Al-Shabanah, O. A. (2006). Carnitine esters prevent oxidative stress damage and energy depletion following transient forebrain ischaemia in the rat hippocampus. *Clin. Exp. Pharmacol. Physiol.* 33, 725–733. doi: 10.1111/j.1440-1681.2006.04425.x

Anderson, W. W., and Collingridge, G. L. (2001). The LTP Program: a data acquisition program for on-line analysis of long-term potentiation and other synaptic events. *J. Neurosci. Methods* 108, 71–83. doi: 10.1016/S0165-0270(01)00374-0

Burda, J. E., and Sofroniew, M. V. (2014). Reactive gliosis and the multicellular response to CNS damage and disease. *Neuron* 81, 229–248. doi: 10.1016/j.neuron.2013.12.034

Canals, S., Larrosa, B., Pintor, J., Mena, M. A., and Herreras, O. (2008). Metabolic challenge to glia activates an adenosine-mediated safety mechanism that promotes neuronal survival by delaying the onset of spreading depression waves. *J. Cereb. Blood Flow Metab.* 28, 1835–1844. doi: 10.1038/jcbfm.2008.71

Cerbai, F., Lana, D., Nosi, D., Petkova-Kirova, P., Zecchi, S., Brothers, H. M., et al. (2012). The neuron-astrocyte-microglia triad in normal brain ageing and in a model of neuroinflammation in the rat hippocampus. *PLoS One* 7:e45250. doi: 10.1371/journal.pone.0045250

Chandrasekera, P. C., McIntosh, V. J., Cao, F. X., and Lasley, R. D. (2010). Differential effects of adenosine A2a and A2b receptors on cardiac contractility. *Am. J. Physiol. Heart Circ. Physiol.* 299, H2082–H2089. doi: 10.1152/ajpheart.00511.2010

Chen, J. F., Sonsalla, P., Pedata, F., Melani, A., Domenici, M. R., Popoli, P., et al. (2007). Adenosine A2A receptors and brain injury: broad spectrum of neuroprotection, multi-faced actions and "fine tuning" modulation. *Prog. Neurobiol.* 83, 310–331. doi: 10.1016/j.pneurobio.2007.09.002

Choi, D. W. (1992). Excitotoxic cell death. *J. Neurobiol.* 23, 1261–1276. doi: 10.1002/neu.480230915

Coppi, E., Pugliese, A. M., Stephan, H., Müller, C. E., and Pedata, F. (2007). Role of P2 purinergic receptors in synaptic transmission under normoxic and ischaemic conditions in the CA1 region of rat hippocampal slices. *Purinergic Signal.* 3, 203–219. doi: 10.1007/s11302-006-9049-4

Csóka, B., Németh, Z. H., Selmeczy, Z., Koscsó, B., Pacher, P., Vizi, E. S., et al. (2007). Role of A(2A) adenosine receptors in regulation of opsonized *E. coli*-induced macrophage function. *Purinergic Signal.* 3, 447–452. doi: 10.1007/s11302-007-9075-x

Cunha, R. A., Johansson, B., Constantino, M. D., Sebastião, A. M., and Fredholm, B. B. (1996). Evidence for high-affinity binding sites for the adenosine A2A receptor agonist [3H] CGS 21680 in the rat hippocampus and cerebral cortex that are different from striatal A2A receptors. *Naunyn Schmiedebergs Arch. Pharmacol.* 353, 261–271. doi: 10.1007/BF00168627

Dennis, P. B., Jaeschke, A., Saitoh, M., Fowler, B., Kozma, S. C., and Thomas, G. (2001). Mammalian TOR: a homeostatic ATP sensor. *Science* 294, 1102–1105. doi: 10.1126/science.1063518

Dirnagl, U. (2012). Pathobiology of injury after stroke: the neurovascular unit and beyond. *Ann. N. Y. Acad. Sci.* 1268, 21–25. doi: 10.1111/j.1749-6632.2012.06691.x

Dixon, A. K., Gubitz, A. K., Sirinathsinghji, D. J., Richardson, P. J., and Freeman, T. C. (1996). Tissue distribution of adenosine receptor mRNAs in the rat. *Br. J. Pharmacol.* 118, 1461–1468. doi: 10.1111/j.1476-5381.1996.tb15561.x

Elmore, S. (2007). Apoptosis: a review of programmed cell death. *Toxicol. Pathol.* 35, 495–516. doi: 10.1080/01926230701320337

Farkas, E., Pratt, R., Sengpiel, F., and Obrenovitch, T. P. (2008). Direct, live imaging of cortical spreading depression and anoxic depolarisation using a fluorescent, voltage-sensitive dye. *J. Cereb. Blood Flow Metab.* 28, 251–262. doi: 10.1038/sj.jcbfm.9600569

Feoktistov, I., Polosa, R., Holgate, S. T., and Biaggioni, I. (1998). Adenosine A2B receptors: a novel therapeutic target in asthma? *Trends Pharmacol. Sci.* 19, 148–153.

Fowler, J. C. (1992). Escape from inhibition of synaptic transmission during in vitro hypoxia and hypoglycemia in the hippocampus. *Brain Res.* 573, 169–173. doi: 10.1016/0006-8993(92)90128-V

Fredholm, B. B., IJzerman, A. P., Jacobson, K. A., Linden, J., and Müller, C. E. (2011). International union of basic and clinical pharmacology. LXXXI. Nomenclature and classification of adenosine receptors–an update. *Pharmacol. Rev.* 63, 1–34. doi: 10.1124/pr.110.003285

Fredholm, B. B., Irenius, E., Kull, B., and Schulte, G. (2001). Comparison of the potency of adenosine as an agonist at human adenosine receptors expressed in Chinese hamster ovary cells. *Biochem. Pharmacol.* 61, 443–448. doi: 10.1016/S0006-2952(00)00570-0

Frenguelli, B. G., Wigmore, G., Llaudet, E., and Dale, N. (2007). Temporal and mechanistic dissociation of ATP and adenosine release during ischaemia in the mammalian hippocampus. *J. Neurochem.* 101, 1400–1413. doi: 10.1111/j.1471-4159.2007.04425.x

Frey, U., and Morris, R. G. (1997). Synaptic tagging and long-term potentiation. *Nature* 385, 533–536. doi: 10.1038/385533a0

Gegelashvili, G., Robinson, M. B., Trotti, D., and Rauen, T. (2001). Regulation of glutamate transporters in health and disease. *Prog. Brain Res.* 132, 267–286. doi: 10.1016/S0079-6123(01)32082-4

Gonçalves, F. Q., Pires, J., Pliassova, A., Beleza, R., Lemos, C., Marques, J. M., et al. (2015). Adenosine A2b receptors control A1 receptor-mediated inhibition of synaptic transmission in the mouse hippocampus. *Eur. J. Neurosci.* 41, 878–888. doi: 10.1111/ejn.12851

Herreras, O., and Somjen, G. G. (1993). Propagation of spreading depression among dendrites and somata of the same cell population. *Brain Res.* 610, 276–282. doi: 10.1016/0006-8993(93)91411-K

Holloway, P. M., and Gavins, F. N. (2016). Modeling ischemic stroke in vitro: status quo and future perspectives. *Stroke* 47, 561–569. doi: 10.1161/STROKEAHA.115.011932

Jarvis, C. R., Anderson, T. R., and Andrew, R. D. (2001). Anoxic depolarization mediates acute damage independent of glutamate in neocortical brain slices. *Cereb. Cortex* 11, 249–259. doi: 10.1093/cercor/11.3.249

Jiang, X., and Wang, X. (2004). Cytochrome C-mediated apoptosis. *Annu. Rev. Biochem.* 73, 87–106. doi: 10.1146/annurev.biochem.73.011303.073706

Johansson, B., and Fredholm, B. B. (1995). Further characterization of the binding of the adenosine receptor agonist [3H]CGS 21680 to rat brain using autoradiography. *Neuropharmacology* 34, 393–403. doi: 10.1016/0028-3908(95)00009-U

Káradóttir, R., Cavelier, P., Bergersen, L. H., and Attwell, D. (2005). NMDA receptors are expressed in oligodendrocytes and activated in ischaemia. *Nature* 438, 1162–1166. doi: 10.1038/nature04302

Kluck, R. M., Bossy-Wetzel, E., Green, D. R., and Newmeyer, D. D. (1997). The release of cytochrome c from mitochondria: a primary site for Bcl-2 regulation of apoptosis. *Science* 275, 1132–1136. doi: 10.1126/science.275.5303.1132

Kolachala, V., Ruble, B., Vijay-Kumar, M., Wang, L., Mwangi, S., Figler, H., et al. (2008). Blockade of adenosine A2B receptors ameliorates murine colitis. *Br. J. Pharmacol.* 155, 127–137. doi: 10.1038/bjp.2008.227

Koroleva, V. I., and Bures, J. (1996). The use of spreading depression waves for acute and long-term monitoring of the penumbra zone of focal ischemic damage in rats. *Proc. Natl. Acad. Sci. U.S.A.* 93, 3710–3714. doi: 10.1073/pnas.93.8.3710

Kovacs, K., Toth, A., Deres, P., Kalai, T., Hideg, K., Gallyas, F. Jr., et al. (2006). Critical role of PI3-kinase/Akt activation in the PARP inhibitor induced heart function recovery during ischemia-reperfusion. *Biochem. Pharmacol.* 71, 441–452. doi: 10.1016/j.bcp.2005.05.036

Lana, D., Cerbai, F., Di Russo, J., Boscaro, F., Giannetti, A., Petkova-Kirova, P., et al. (2013). Hippocampal long term memory: effect of the cholinergic system on local protein synthesis. *Neurobiol. Learn. Mem.* 106, 246–257. doi: 10.1016/j.nlm.2013.09.013

Lana, D., Iovino, L., Nosi, D., Wenk, G. L., and Giovannini, M. G. (2016). The neuron-astrocyte-microglia triad involvement in neuroinflammaging mechanisms in the CA3 hippocampus of memory-impaired aged rats. *Exp. Gerontol.* 83, 71–88. doi: 10.1016/j.exger.2016.07.011

Lana, D., Melani, A., Pugliese, A. M., Cipriani, S., Nosi, D., Pedata, F., et al. (2014). The neuron-astrocyte-microglia triad in a rat model of chronic cerebral hypoperfusion: protective effect of dipyridamole. *Front. Aging Neurosci.* 6:322. doi: 10.3389/fnagi.2014.00322

Lana, D., Ugolini, F., Melani, A., Nosi, D., Pedata, F., and Giovannini, M. G. (2017a). The neuron-astrocyte-microglia triad in CA3 after chronic cerebral hypoperfusion in the rat: protective effect of dipyridamole. *Exp. Gerontol.* 96, 46–62. doi: 10.1016/j.exger.2017.06.006

Lana, D., Ugolini, F., Nosi, D., Wenk, G. L., and Giovannini, M. G. (2017b). Alterations in the interplay between neurons, astrocytes and microglia in the rat dentate gyrus in experimental models of neurodegeneration. *Front. Aging Neurosci.* 9:296. doi: 10.3389/fnagi.2017.00296

Laplante, M., and Sabatini, D. M. (2012). mTOR signaling in growth control and disease. *Cell* 149, 274–293. doi: 10.1016/j.cell.2012.03.017

Latini, S., Bordoni, F., Corradetti, R., Pepeu, G., and Pedata, F. (1998). Temporal correlation between adenosine outflow and synaptic potential inhibition in rat hippocampal slices during ischemia-like conditions. *Brain Res.* 794, 325–328. doi: 10.1016/S0006-8993(98)00304-7

Latini, S., Bordoni, F., Corradetti, R., Pepeu, G., and Pedata, F. (1999). Effect of A2A adenosine receptor stimulation and antagonism on synaptic depression induced by in vitro ischaemia in rat hippocampal slices. *Br. J. Pharmacol.* 128, 1035–1044. doi: 10.1038/sj.bjp.0702888

Latini, S., and Pedata, F. (2001). Adenosine in the central nervous system: release mechanisms and extracellular concentrations. *J. Neurochem.* 79, 463–484. doi: 10.1046/j.1471-4159.2001.00607.x

Lemos, C., Pinheiro, B. S., Beleza, R. O., Marques, J. M., Rodrigues, R. J., Cunha, R. A., et al. (2015). Adenosine A2B receptor activation stimulates glucose uptake in the mouse forebrain. *Purinergic Signal.* 1, 561–569. doi: 10.1007/s11302-015-9474-3

Li, S. Q., Zhang, Y., and Tang, D. B. (2009). Possible mechanisms of Cyclosporin A ameliorated the ischemic microenvironment and inhibited mitochondria stress in tree shrews' hippocampus. *Pathophysiology* 16, 279–284. doi: 10.1016/j.pathophys.2009.02.014

Love, S. (2003). Apoptosis and brain ischaemia. *Prog. Neuropsychopharmacol. Biol. Psychiatry* 27, 267–282.

Magistretti, P. J., Hof, P. R., and Martin, J. L. (1986). Adenosine stimulates glycogenolysis in mouse cerebral cortex: a possible coupling mechanism between neuronal activity and energy metabolism. *J. Neurosci.* 6, 2558–2562. doi: 10.1523/JNEUROSCI.06-09-02558.1986

Maragakis, N. J., and Rothstein, J. D. (2004). Glutamate transporters: animal models to neurologic diseases. *Neurobiol. Dis.* 15, 461–473. doi: 10.1016/j.nbd.2003.12.007

Martínez-Fábregas, J., Díaz-Moreno, I., González-Arzola, K., Janocha, S., Navarro, J. A., Hervás, M., et al. (2014). Structural and functional analysis of novel human cytochrome C targets in apoptosis. *Mol. Cell. Proteomics* 13, 1439–1456. doi: 10.1074/mcp.M113.034322

Melani, A., Pantoni, L., Corsi, C., Bianchi, L., Monopoli, A., Bertorelli, R., et al. (1999). Striatal outflow of adenosine, excitatory amino acids, gamma-aminobutyric acid, and taurine in awake freely moving rats after middle cerebral artery occlusion: correlations with neurological deficit and histopathological damage. *Stroke* 30, 2448–2454. doi: 10.1161/01.STR.30.11.2448

Merighi, S., Borea, P. A., and Gessi, S. (2015). Adenosine receptors and diabetes: Focus on the A(2B) adenosine receptor subtype. *Pharmacol. Res.* 99, 229–236. doi: 10.1016/j.phrs.2015.06.015

Moriyama, K., and Sitkovsky, M. V. (2010). Adenosine A2A receptor is involved in cell surface expression of A2B receptor. *J. Biol. Chem.* 285, 39271–39288. doi: 10.1074/jbc.M109.098293

Newell, D. W., Barth, A., Papermaster, V., and Malouf, A. T. (1995). Glutamate and non-glutamate receptor mediated toxicity caused by oxygen, and glucose deprivation in organotypic hippocampal cultures. *J. Neurosci.* 15, 7702–7711. doi: 10.1523/JNEUROSCI.15-11-07702.1995

Pearson, T., Damian, K., Lynas, R. E., and Frenguelli, B. G. (2006). Sustained elevation of extracellular adenosine and activation of A1 receptors underlie the post-ischaemic inhibition of neuronal function in rat hippocampus in vitro. *J. Neurochem.* 97, 1357–1368. doi: 10.1111/j.1471-4159.2006.03823.x

Pedata, F., Dettori, I., Coppi, E., Melani, A., Fusco, I., Corradetti, R., et al. (2016). Purinergic signalling in brain ischemia. *Neuropharmacology* 104, 105–130. doi: 10.1016/j.neuropharm.2015.11.007

Pedata, F., Latini, S., Pugliese, A. M., and Pepeu, G. (1993). Investigations into the adenosine outflow from hippocampal slices evoked by ischemia-like conditions. *J. Neurochem.* 61, 284–289. doi: 10.1111/j.1471-4159.1993.tb03566.x

Pedata, F., Pugliese, A. M., Coppi, E., Dettori, I., Maraula, G., Cellai, L., et al. (2014). Adenosine A2A receptors modulate acute injury and neuroinflammation in brain ischemia. *Mediators Inflamm.* 2014:805198. doi: 10.1155/2014/805198

Perez-Buira, S., Barrachina, M., Rodriguez, A., Albasanz, J. L., Martín, M., Ferrer, I., et al. (2007). Expression levels of adenosine receptors in hippocampus and frontal cortex in argyrophilic grain disease. *Neurosci. Lett.* 423, 194–199. doi: 10.1016/j.neulet.2007.06.049

Popoli, P., and Pepponi, R. (2012). Potential therapeutic relevance of adenosine A2B and A2A receptors in the central nervous system. *CNS Neurol. Disord. Drug Targets* 11, 664–674. doi: 10.2174/187152712803581100

Pugliese, A. M., Coppi, E., Spalluto, G., Corradetti, R., and Pedata, F. (2006). A3 adenosine receptor antagonists delay irreversible synaptic failure caused by oxygen and glucose deprivation in the rat CA1 hippocampus in vitro. *Br. J. Pharmacol.* 147, 524–532. doi: 10.1038/sj.bjp.0706646

Pugliese, A. M., Coppi, E., Volpini, R., Cristalli, G., Corradetti, R., Jeong, L. S., et al. (2007). Role of adenosine A3 receptors on CA1 hippocampal neurotransmission during oxygen-glucose deprivation episodes of different duration. *Biochem. Pharmacol.* 74, 768–779. doi: 10.1016/j.bcp.2007.06.003

Pugliese, A. M., Latini, S., Corradetti, R., and Pedata, F. (2003). Brief, repeated, oxygen-glucose deprivation episodes protect neurotransmission from a longer ischemic episode in the in vitro hippocampus: role of adenosine receptors. *Br. J. Pharmacol.* 140, 305–314. doi: 10.1038/sj.bjp.0705442

Pugliese, A. M., Traini, C., Cipriani, S., Gianfriddo, M., Mello, T., Giovannini, M. G., et al. (2009). The adenosine A2A receptor antagonist ZM241385 enhances neuronal survival after oxygen-glucose deprivation in rat CA1 hippocampal slices. *Br. J. Pharmacol.* 157, 818–830. doi: 10.1111/j.1476-5381.2009.00218.x

Siniscalchi, A., Rodi, D., Gessi, S., Campi, F., and Borea, P. A. (1999). Early changes in adenosine A1 receptors in cerebral cortex slices submitted to in vitro ischemia. *Neurochem. Int.* 34, 517–522. doi: 10.1016/S0197-0186(99)00028-5

Somjen, G. G. (2001). Mechanisms of spreading depression and hypoxic spreading depression-like depolarization. *Physiol. Rev.* 81, 1065–1096. doi: 10.1152/physrev.2001.81.3.1065

Sperlágh, B., Zsilla, G., Baranyi, M., Illes, P., and Vizi, E. S. (2007). Purinergic modulation of glutamate release under ischemic-like conditions in the hippocampus. *Neuroscience* 149, 99–111. doi: 10.1016/j.neuroscience.2007.07.035

Suen, D. F., Norris, K. L., and Youle, R. J. (2008). Mitochondrial dynamics and apoptosis. *Genes Dev.* 22, 1577–1590. doi: 10.1101/gad.1658508

Tanaka, E., Yamamoto, S., Kudo, Y., Mihara, S., and Higashi, H. (1997). Mechanisms underlying the rapid depolarization produced by deprivation of oxygen and glucose in rat hippocampal CA1 neurons in vitro. *J. Neurophysiol.* 78, 891–902. doi: 10.1152/jn.1997.78.2.891

Thoreen, C. C., Chantranupong, L., Keys, H. R., Wang, T., Gray, N. S., and Sabatini, D. M. (2012). A unifying model for mTORC1-mediated regulation of mRNA translation. *Nature* 485, 109–113. doi: 10.1038/nature11083

Traini, C., Pedata, F., Cipriani, S., Mello, T., Galli, A., Giovannini, M. G., et al. (2011). P2 receptor antagonists prevent synaptic failure and extracellular signal-regulated kinase 1/2 activation induced by oxygen and glucose deprivation in rat CA1 hippocampus in vitro. *Eur. J. Neurosci.* 33, 2203–2215. doi: 10.1111/j.1460-9568.2011.07667.x

Tsokas, P., Ma, T., Iyengar, R., Landau, E. M., and Blitzer, R. D. (2007). Mitogen-activated protein kinase upregulates the dendritic translation machinery in long-term potentiation by controlling the mammalian target of rapamycin pathway. *J. Neurosci.* 27, 5885–5894. doi: 10.1523/JNEUROSCI.4548-06.2007

Ugolini, F., Lana, D., Fusco, I., Coppi, E., Dettori, I., Gaviano, L., et al. (2017). "The selective antagonism of adenosine A2B receptors prevents synaptic and neuronal damage induced by oxygen and glucose deprivation in CA1 rat hippocampus," in *Proceedings of the Neuroscience 47th Annual Meeting*, Washington, DC.

Ünal-Çevik, I., Kilinç, M., Gürsoy-Ozdemir, Y., Gurer, G., and Dalkara, T. (2004). Loss of NeuN immunoreactivity after cerebral ischemia does not indicate neuronal cell loss: a cautionary note. *Brain Res.* 1015, 169–174. doi: 10.1016/j.brainres.2004.04.032

Yamamoto, S., Tanaka, E., Shoji, Y., Kudo, Y., Inokuchi, H., and Higashi, H. (1997). Factors that reverse the persistent depolarization produced by deprivation of oxygen and glucose in rat hippocampal CA1 neurons in vitro. *J. Neurophysiol.* 78, 903–911. doi: 10.1152/jn.1997.78.2.903

Yang, J., Liu, X., Bhalla, K., Kim, C. N., Ibrado, A. M., Cai, J., et al. (1997). Prevention of apoptosis by Bcl-2: release of cytochrome c from mitochondria blocked. *Science* 275, 1129–1132. doi: 10.1126/science.275.5303.1129

Conflict of Interest Statement: The authors declare that the research was conducted in the absence of any commercial or financial relationships that could be construed as a potential conflict of interest.

frontiers in Pharmacology

HYPOTHESIS AND THEORY
published: 24 April 2018
doi: 10.3389/fphar.2018.00397

Adenosine Receptors in Developing and Adult Mouse Neuromuscular Junctions and Functional Links With Other Metabotropic Receptor Pathways

Josep Tomàs†, Neus Garcia*†, Maria A. Lanuza*†, Manel M. Santafé, Marta Tomàs, Laura Nadal, Erica Hurtado, Anna Simó-Ollé, Víctor Cilleros-Mañé and Laia Just-Borràs*

Unitat d'Histologia i Neurobiologia, Facultat de Medicina i Ciències de la Salut, Universitat Rovira i Virgili, Reus, Spain

OPEN ACCESS

Edited by:
Francisco Ciruela, Universitat de Barcelona, Spain

Reviewed by:
Carles Solsona, Universitat de Barcelona, Spain
Susan B. Udin, University at Buffalo, United States

***Correspondence:**
Josep Tomàs
josepmaria.tomas@urv.cat
Neus Garcia
mariadelesneus.garcia@urv.cat
Maria A. Lanuza
mariaangel.lanuza@urv.cat

† These authors have contributed equally to this work.

Specialty section:
This article was submitted to Experimental Pharmacology and Drug Discovery, a section of the journal Frontiers in Pharmacology

Received: *06 November 2017*
Accepted: *05 April 2018*
Published: *24 April 2018*

Citation:
Tomàs J, Garcia N, Lanuza MA, Santafé MM, Tomàs M, Nadal L, Hurtado E, Simó-Ollé A, Cilleros-Mañé V and Just-Borràs L (2018) Adenosine Receptors in Developing and Adult Mouse Neuromuscular Junctions and Functional Links With Other Metabotropic Receptor Pathways. Front. Pharmacol. 9:397. doi: 10.3389/fphar.2018.00397

In the last few years, we have studied the presence and involvement in synaptogenesis and mature transmitter release of the adenosine autoreceptors (AR) in the mammalian neuromuscular junction (NMJ). Here, we review and bring together the previously published data to emphasize the relevance of these receptors for developmental axonal competition, synaptic loss and mature NMJ functional modulation. However, in addition to AR, activity-dependent mediators originating from any of the three cells that make the synapse (nerve, muscle, and glial cells) cross the extracellular cleft to generate signals in target metabotropic receptors. Thus, the integrated interpretation of the complementary function of all these receptors is needed. We previously studied, in the NMJ, the links of AR with mAChR and the neurotrophin receptor TrkB in the control of synapse elimination and transmitter release. We conclude that AR cooperate with these receptors through synergistic and antagonistic effects in the developmental synapse elimination process. In the adult NMJ, this cooperation is manifested so as that the functional integrity of a given receptor group depends on the other receptors operating normally (i.e., the functional integrity of mAChR depends on AR operating normally). These observations underlie the relevance of AR in the NMJ function.

Keywords: motor end-plate, postnatal synapse elimination, axonal competition, acetylcholine release, muscarinic acetylcholine receptors, adenosine receptors, neurotrophins, TrkB

INTRODUCTION

In addition to the main neurotransmitter-receptor signal, several signaling pathways coordinate the pre- and postsynaptic cells and associated glia in the tripartite synapses in accordance with functional demands. In the NMJ, presynaptic mAChRs directly couple ACh secretion to the regulation of the release mechanism itself (Caulfield and Birdsall, 1998; Slutsky et al., 2001; Minic et al., 2002; Santafé et al., 2003, 2004; Garcia et al., 2005). Moreover, presynaptic nicotinic ACh autoreceptors (nAChRs) are also present at the NMJ

Abbreviations: ACh, acetylcholine; AR, adenosine autoreceptors; ATP, adenosine triphosphate; EPP, evoked endplate potentials; LAL, Levator auris longus muscle; mAChR, muscarinic acetylcholine receptor; M_1, M_1-type muscarinic acetylcholine receptor; M_2, M_2-type muscarinic acetylcholine receptor; M_4, M_4-type muscarinic acetylcholine receptor; NMJ, neuromuscular junction; TrkB, tropomyosin-related kinase B receptor; TrkB-Fc, inhibitor recombinant human TrkB-Fc Chimera.

(Correia-de-Sá, 1994; Salgado et al., 2000). Also, at the NMJ, the presynaptic neurotrophin and cytokine receptors can be influenced by target-derived signals (Bibel and Barde, 2000; Roux and Barker, 2002; Pitts et al., 2006), and glutamate together with mGluR1 also mediate the signaling in this synapse (Waerhaug and Ottersen, 1993; Lück et al., 2000; Malomouzh et al., 2011; Marmiroli and Cavaletti, 2012; Walder et al., 2013).

Studies in the early 1970s Ribeiro and Walker (1973) showed that adenosine and ATP modulate the presynaptic component through purinergic receptors (adenosine P1Rs and ATP P2Rs) (Correia-de-Sá et al., 1991; Ribeiro et al., 1996). The first authors describing adenosine effects at the mammalian NMJ were (Ginsborg and Hirst, 1971, 1972; see also Singh et al., 1986). It is known that both nerve and muscle cell activity can contribute to the extracellular adenosine release (Cunha and Sebastião, 1993; Ribeiro et al., 1996).

In the last few years, we have studied the presence and involvement of AR in the synaptogenesis and transmitter release in the developing and mature mammalian NMJ (Garcia et al., 2013; Tomàs et al., 2014; Tomàs J. et al., 2017; Santafé et al., 2015; Nadal et al., 2016a,b, 2017). Here, we review and bring together previously published data to contribute to emphasizing the relevance of these receptors in this synapse. Moreover, we also discuss our previous studies in relation with the interaction between AR, mAChR and the TrkB in the control of synapse elimination during development and transmitter release in the adult NMJ.

Our results indicate that during NMJ synaptogenesis, AR (A_1R and $A_{2A}R$ subtypes) contribute to the developmental synapse elimination process, helping to define the winner of the competition between axon terminals. In the adult, AR help to modulate transmitter release by limiting spontaneous quantal leak of ACh and preserve synaptic function by reducing depression during repetitive activity. To realize these functions, several synergistic and antagonistic relations exist between AR and, at least, the mAChR subtypes (M_1, M_2, and M_4) and the TrkB receptor. These observations underlie the relevance of AR in the NMJ function.

ADENOSINE RECEPTORS LOCALIZATION IN THE NMJ

Four subtypes of AR have been cloned (A_1R, $A_{2A}R$, $A_{2B}R$, and A_3R) and despite the fact that there was some uncertainty about how they were distributed in the cells of the paradigmatic NMJ (Lynge and Hellsten, 2000; Baxter et al., 2005), some of them have been localized in the mouse synapse with confocal immunohistochemistry (Garcia et al., 2005, 2013, 2014; Wright et al., 2009). The confidence of protein localization by immunohistochemistry lies in the specificity of the antibodies used. Though the lack of signal in knockout animals was not investigated, we made an effort to characterize the commercially available antibodies by Western blotting. Our results have shown that the A_1R receptor is more abundant in adult animals, whereas the $A_{2A}R$ receptor predominates in the newborn ones (Garcia et al., 2013). Moreover, the $A_{2B}R$ and A_3R receptors are more expressed in the adult muscles than in the younger ones (Tomàs et al., 2014).

Immunofluorescence staining coupled with confocal microscopy analysis was performed to determine the localization of A_1R, $A_{2A}R$ (whose function has been further investigated) in P6 and P30 NMJ (**Figure 1**). Moreover, localization of $A_{2B}R$, and A_3R has been determined in P30 NMJ. By triple labeling of NMJ we stained each one of these protein receptors in green fluorescence together with Syntaxin or S-100 (blue fluorescence) and nAChR (red fluorescence) and we saw that

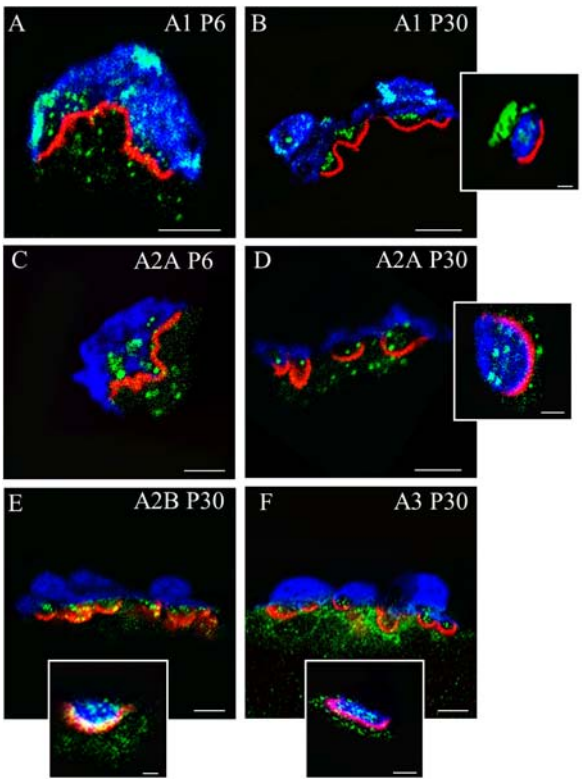

FIGURE 1 | Immunolocalization of A_1R, $A_{2A}R$, $A_{2B}R$, and A_3R receptors in the motor nerve terminals on neuromuscular synapses. Immunofluorescence staining and confocal microscopy analysis in newborn (P6) and mature (P30) mice. Triple labeling of the corresponding receptor proteins (green fluorescence) with S-100 (blue fluorescence) and rhodamine-alpha-bungarotoxin (red fluorescence). In the insets (scale bar, 1 μm), Syntaxin labeling (in blue) is showed instead of S-100. **(A–D)** Are single confocal planes from NMJs obtained using plastic embedded semithin cross-sections (0.5–0.7 μm). **(E,F)** Are single confocal planes from a projection image. In the cross-sections of the synaptic boutons, all receptors are present as a fine granular labeling in the space of the nerve terminals between the blue Schwann cell and the red postsynaptic line. In all cases, (see the insets showed as examples), the receptor proteins colocalize with Syntaxin. The bar indicates 10 μm. The images are illustrative examples of the original studies published in Garcia et al. (2014) (Garcia N., Priego M., Hurtado E., Obis T., Santafe M. M., Tomàs M., Lanuza M. A., Tomàs J. Adenosine A2B and A3 receptor location at the mouse neuromuscular junction. *J. Anat*. 225:109–117) and Garcia et al. (2013) (Garcia N., Priego M., Obis T., Santafe M. M., Tomàs M., Besalduch N., Lanuza M. A., Tomàs J. Adenosine A1 and A2A receptor-mediated modulation of acetylcholine release in the mice neuromuscular junction. *Eur. J. Neurosci*. 38:2229–2241).

the molecules were present. However, since the components of the NMJ (the nerve terminal, the Schwann cell and the muscle fiber) are juxtaposed, it is not always easy to locate the proteins with precision. Thus, in some cases, to better determine A_1R and $A_{2A}R$ localization, we used plastic embedded semithin cross-sections as a tool for high-resolution together with the triple-labeling immunofluorescence analysis. Briefly, after conventional immunohistochemistry the samples were dehydrated with increasing concentrations of ethanol and acetone, the tissue fragments were embedded in Spurr's resin in transverse orientation and sections (0.5–0.7 μm thick) were obtained (Lanuza et al., 2007; Garcia et al., 2010c; Besalduch et al., 2013). Images (A–D) correspond to a single image made in a confocal microscope from a 0,5 μm muscle semithin cross section. Images (E–F) show localization of A2BR and A3R using single confocal Z planes from a projection image of at least 10 confocal Z planes obtained every 0,5 μm. As shown in **Figure 1**, these receptors are differentially located in the three cells that configure the NMJs (Garcia et al., 2013, 2014). To the purpose of the present review, it can be noted that the four subtypes of AR are present in the motor endings, which is understood to be a requisite to modulate presynaptic function. However, some AR are localized also in the other synaptic components (for instance A_3R in the postsynaptic site) and the interpretation of the results here is not a full representation of the AR physiology.

ADENOSINE RECEPTORS ROLE DURING DEVELOPMENT

During the nervous system development there is an overwhelming production of synapses (that may promote connectiviy), followed by an activity-dependent reduction of them. Hebbian competition between axons refines connectivity and increases specificity (Purves and Lichtman, 1980; Jansen and Fladby, 1990; Sanes and Lichtman, 1999; Chen and Regehr, 2000; Nadal et al., 2016a). In newborn animals, skeletal muscle cells are innervated by various motor axons (Ribchester and Barry, 1994) but when the competition ends, the NMJs retain only one axon (Liu et al., 1994; Nguyen and Lichtman, 1996; Chang and Balice-Gordon, 1997; Sanes and Lichtman, 1999; Herrera and Zeng, 2003; Nelson et al., 2003; Wyatt and Balice-Gordon, 2003; Buffelli et al., 2004).

The postsynaptic cell and the terminal Schwann cells may be intermediary in axonal competition. A decrement in polyneuronal innervation occurs at a time when relatively little loss of the nAChR postsynaptic receptors was observed (Lanuza et al., 2002). However, in some cases, local receptor loss has been observed before the corresponding axon loss (Balice-Gordon and Lichtman, 1993). This suggest that pre- and postsynaptic changes are coordinated. Non-myelinating terminal Schwann cells at the NMJ play a role in synapse elimination (reviewed by Lee et al., 2017). A model has been proposed in which the activity of the Schwann cells promote synapse elimination by creating vacant synaptic sites that can be reoccupied by the competing axon terminals.

At the time this process occurs, several signaling mechanisms coordinate the pre- and postsynaptic cell function. First of all, presynaptic mAChR receptors allow direct competitive interaction between nerve endings because of their different activity-dependent ACh secretion (Santafé et al., 2004, 2007, 2009; Nadal et al., 2016a,b; Tomàs J. et al., 2017). Moreover, we also investigated the involvement of presynaptic AR (A_1R and $A_{2A}R$), which monitor both nerve- and muscle-derived adenosine release during the complex period of axonal elimination around P5-P9 (Garcia et al., 2013; Nadal et al., 2016a,b).

We evaluated the average number of axonal connections per NMJ from B6.Cg-Tg (Thy1-YFP) (from now YFP) and C57BL/J6 mice. To the flat and accessible mouse LAL muscle, we subcutaneously applied the unselective AR inhibitor 8-(p-sulfophenyl) theophylline (8SPT) and the agonist adenosine between P5-P15 (**Figure 2**). At P7, after the inhibition with 8SPT of the AR, we observed an acceleration of the axonal elimination on the NMJ indicating that, at this point of development, the role of AR is to delay axonal loss (Nadal et al., 2016a). In accordance, exposure to the physiological agonist adenosine resulted in a retardation of axonal elimination (i.e., a significant high number of triple innervated NMJ and a reduction in the number of dual innervated NMJ, **Figure 2Aa**). We also analyzed axonal loss after selectively blocking A_1R with 8-cyclopentyl-1,3-dipropylxanthine (DPCPX) or $A_{2A}R$ with 2-(2-furanyl)-7-(2-phenylethyl)-7H-pyrazolo[4,3-e] [1, 2, 4] triazolo[1,5-c]pyrimidin-5-amine (SCH-58261) (Nadal et al., 2016a,b). Results showed that axonal loss is accelerated by both inhibitors indicating that, in normal conditions, both receptors A_1R and $A_{2A}R$ are related with delaying axonal elimination. However, at P9 (**Figure 2Ab**), the purinergic function accelerates axonal loss to the maximum rate. Therefore, an initial delay in axonal loss at P7 (an A_1R- and $A_{2A}R$-mediated effect which can be reinforced by exogenously added adenosine) is followed by an A_1R- and $A_{2A}R$-mediated tonic acceleration of axonal loss at P9 (green arrows in **Figure 3** left, Nadal et al., 2016a). We also investigated the effect of long-term AR perturbation with 8SPT over axon number at P15. Despite the continued presence of the inhibitor, monoinnervation is achieved in about 90% of NMJ at P15 (**Figure 2Ac**) suggesting that axonal competition and loss are differentially modulated (Nadal et al., 2016a).

Axonal elimination is accompanied by changes in the structure of the nicotinic ACh receptor (nAChR) clusters in the postsynaptic site (**Figure 2B**). Based on criteria from previous studies on developing mammalian NMJ (Steinbach, 1981; Slater, 1982a,b; Bewick et al., 1996; Lanuza et al., 2002; Garcia et al., 2011), we defined several maturation stages (MS1–MS4). Changes in nAChR distribution transform the uniform nAChR oval cluster at birth (MS1) into an elongated plaque with some heterogeneities in the density of receptors (MS2). Later, they become into clusters with small zones of low receptor density (MS3) that are not innervated that lead to a mature pattern of independent primary gutters (MS4) (Nadal et al., 2016a). In relation with these changes, we found that the antagonist 8SPT, applied in the period P5–P8, had

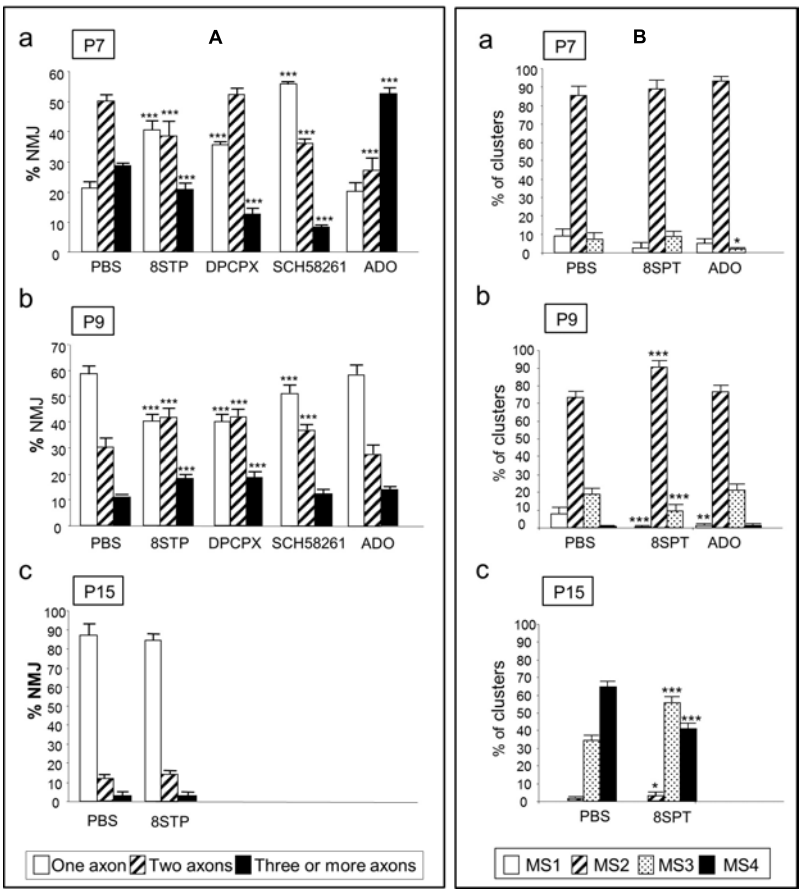

FIGURE 2 | Involvement of AR in axonal elimination and in the morphological maturation of the postsynaptic apparatus. The **(A)** shows the percentage of the singly-, dually-, and triply- (or more) innervated NMJs in the YFP control mice exposed to PBS, and after 2 (P7 in **a**), 4 (P9, in **b**) and in some cases 10 (P15, in **c**) applications (one application every day after P5) of the AR pan-inhibitor 8SPT and the AR agonist adenosine (ADO). We also studied axonal elimination after selectively blocking A_1R with the antagonist DPCPX and inhibiting A_{2A}R with SCH-58261. The **(B)** shows the percentage of the MS1–MS4 maturation stages in the NMJ of the untreated YFP control mice (exposed to PBS), and after 2 (P7 in **a**), 4 (P9, in **b**), and in some cases 10 (P15, in **c**) applications of the 8SPT and ADO. Fisher's test: $*p < 0.05$, $**p < 0.01$, $***p < 0.005$. This Figure has been adapted and redraw from the Figures 4, 8 in the original article "[Presynaptic muscarinic acetylcholine autoreceptors (M_1, M_2, and M_4 subtypes), adenosine receptors (A_1 and A_{2A}) and tropomyosin-related kinase B receptor (TrkB) modulate the developmental synapse elimination process at the neuromuscular junction]" by [Nadal, L., N. Garcia, E. Hurtado, A. Simó, M. Tomàs, M. A. Lanuza, M. Santafé, and J. Tomàs]." *Mol. Brain.* 2016, 9: 67 (doi: 10.1186/s13041-016-0248-9). The original article is an open access article distributed under the terms of the Creative Commons Attribution License (http://creativecommons.org/licenses/by/2.0), which permits unrestricted use, distribution, and reproduction in any medium, provided the original work is properly cited.

no effect on the clusters morphology when observed at P7 (**Figure 2Ba**). However, at P9 we found that MS2clusters were increased while the MS1 and MS3 ones decreased (**Figure 2Bb**), which indicates a delay in the transition from MS2 to MS3. At P15 (**Figure 2Bc**) the postsynaptic maturation is partially retained at the MS3 stage. Thus, AR are able to accelerate maturation during the P7–P15 period. Interestingly, the agonist adenosine does not unambiguously change the cluster maturation indicating that the tonic effect of the AR evidenced by using 8SPT is close to their maximum (Nadal et al., 2016a).

In summary, AR are involved in the control of the competitive interactions between nerve endings, possibly helping to determine the winner or the losers but, thereafter, axon loss seems to occur with autonomy.

ADENOSINE RECEPTORS ROLE IN THE ADULT NEUROTRANSMISSION

Once a NMJ becomes mature and monoinnervated, AR continue modulating neurotransmission. By measuring the activity-dependent efflux of radiolabelled ACh incorporated in nerve endings, Correia-de-Sá et al. (1991) showed that AR control their nerve-stimulated release. Micromolar adenosine levels reduced evoked and/or spontaneous ACh release in frog NMJs (Searl and Silinsky, 2005; Shakirzyanova et al., 2006; Adámek et al., 2010) and also in rat NMJs (Silinsky et al., 1989; De Lorenzo et al., 2006; Pousinha et al., 2010). However, in rat NMJs, submicromolar adenosine concentrations has the opposite effect (Pousinha et al., 2010). Moreover, in other studies done in mice, only very high doses of adenosine (in

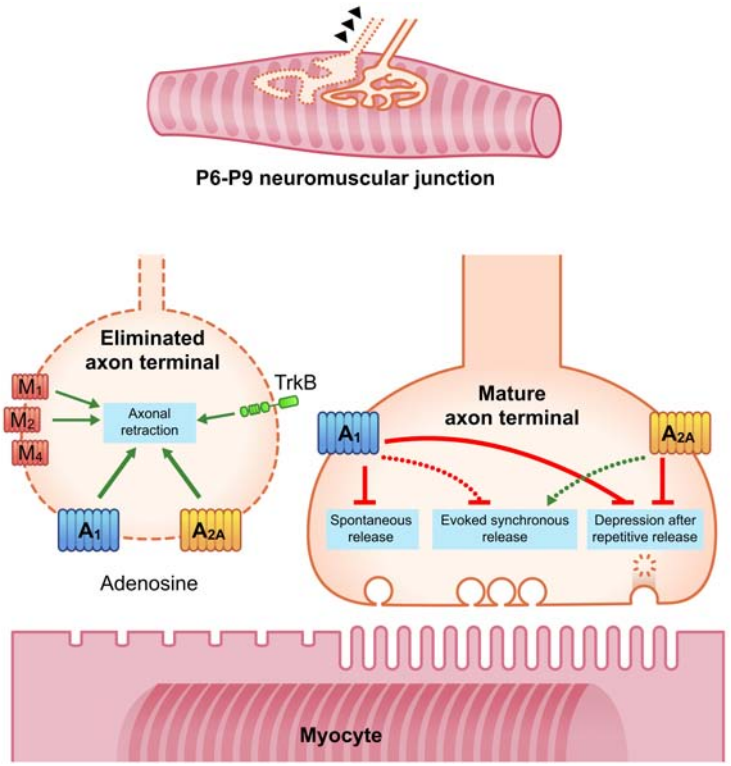

FIGURE 3 | Diagrams showing an overall representation of the data. Between P6-P9 several nerve endings are eliminated and retract whereas one nerve terminal is stabilized. Green arrows indicate stimulation or promotion; red lines indicate inhibition. During the 1st week postnatal an A_1R- and A_{2A}R-mediated tonic acceleration of axonal retraction is observed (green arrows in the eliminated axon terminal). In addition to the role of AR, at least mAChR M_1-, M_2-, and M_4-subtypes and the TrkB receptor are also involved. The downstream pathways integrate the signals related with the competitive interactions and accelerate axonal loss. In the adult NMJ, most experiments on transmitter release have been done in recording conditions that interfere with the synapse function to prevent muscle contraction. In these conditions A_1R reduces it whereas A_{2A}R increases it. Discontinuous lines in the mature axon terminal indicate these changes in conditions of safety factor reduction. In experiments with μ-CgTx-GIIIB only the voltage-dependent sodium channel of the muscle cells was shut-down, thus resulting in non-contractile muscles which have well preserved NMJ physiology and safety factor. In these conditions AR are not coupled to any immediate modulation of evoked neurotransmission. However, AR can restrict spontaneous quantal leak of ACh (A_1R) and protect synaptic function by reducing the magnitude of depression during repetitive activity (an A_1R- and A_{2A}R-mediated effect).

the range of millimolar) affected neurotransmission (Silinsky, 2004) and, in concordance, some mammalian endplates were insensitive to adenosine (Ginsborg and Hirst, 1972). Therefore, it remains unclear how and when adenosine and AR modulate neurotransmission. The majority of experiments have been done in electrophysiological recording conditions that interfere with the normal function of the NMJ to prevent muscle contraction. For example, in the ACh efflux experiments hemicholinium-3 prevents choline reuptake, high Mg^{2+} concentrations reduce ACh release and d-tubocurarine reduces postsynaptic response. In these conditions, selective agonists and antagonists of the A_1R and A_{2A}R modify ACh release. On the one hand, the A_1R agonist 2-Chloro-N^6-cyclopentyladenosine, 1 μM (CCPA) reduces it (Veggetti et al., 2008) whereas the A_{2A}R agonist 2-p-(2-Carboxyethyl)- phenethylamino-5′-N-ethylcarboxamidoadenosine hydrochloride hydrate, 1 μM (CGS-21680) increases it (Pousinha et al., 2010). However, A_1R reduces release (in high Mg^{2+} and curare blockade) when the NMJ is already weakened and because of that, the meaning of this regulation seems unclear (Garcia et al., 2013).

Because of these uncertainties, we induced muscle paralysis with μ-CgTx-GIIIB (Garcia et al., 2013; Tomàs et al., 2014; Obis et al., 2015; Santafé et al., 2015; Hurtado et al., 2017a,b), a specific inhibitor of the sodium channel of the muscle cells which preserves NMJ function (Garcia et al., 2013) and its safety factor. This experimental condition mimics the physiological conditions of this synapse in the living animals except for the absence of the contraction-dependent retrograde influence of the muscle cells (Besalduch et al., 2011; Hurtado et al., 2017a,b). We observed that 25 μM adenosine reduced (50%) the quantal content of ACh release in agreement with other authors (Ginsborg and Hirst, 1972; Ribeiro and Walker, 1975). However, in the nearly normal basal conditions (only test stimulations of 70 pulses at 0.5 Hz every 5 min in the presence of μ-CgTx-GIIIB), none of the purinergic agonists or antagonists had any effect on the evoked ACh release. In particular, we tested non-selective AR agonists and antagonists (adenosine and 8SPT, respectively), A_1R-selective agonists and antagonists (CCPA 1 μM and DPCPX 100 nM, respectively) and A_{2A}R-selective agonists and antagonists (CGS-21680 1 μM

and SCH-58261 50 nM, respectively) (Garcia et al., 2013; Tomàs et al., 2014). However, we detected that AR were still functional in reducing the spontaneous release because miniature endplate potentials (MEPP) frequency was increased by SPT8 blockade and decreased by adenosine stimulation, with A_1Rs playing the main role because only DPCPX increased MEPP frequency (Garcia et al., 2013). In addition, imposed synaptic activity (40Hz for 2 min of supramaximal stimuli) resulted in synaptic depression, an effect reduced by micromolar adenosine but potentiated by blocking AR with 8SPT. Depression in control muscles represents a ∼50% reduction of the endplate potentials (EPP) amplitude and 10 μM adenosine reduces it to a half (Garcia et al., 2013). Surprisingly, we found that depression was not affected by any selective agent, which suggested that both A_1R and A_{2A}R need to collaborate (Garcia et al., 2013; Tomàs et al., 2014). In perspective, the fact that adenosine and 8SPT modified synaptic depression, whereas A_1R and A_{2A}R ligands did not, suggested us that A_{2B}R and/or A_3R could be implicated. Thus, we investigated the A_{2B}R-selective antagonist MRS1706 (N-(4-Acetylphenyl)-2-[4-(2,3,6,7-tetrahydro-2,6-dioxo-1,3-dipropyl-1H-purin-8-yl)phenoxy]acetamide, 100 nM) and the A_3R-selective antagonist MRS1334 (1,4-Dihydro -2-methyl-6-phenyl-4-(phenylethynyl)-3,5-pyridinedicarboxylic acid 3-ethyl-5-[(3nitrophenyl)methyl] ester, 100 nM). We unexpectedly found that A_{2B}R and A_3R neither had any effect on depression (just as the A_1R and A_{2A}R selective antagonists). Thus, we concluded that two or more AR are necessary to protect against depression (Garcia et al., 2013; Tomàs et al., 2014).

In summary, these findings confirmed that in basal conditions AR are not coupled to any immediate modulation of evoked neurotransmission. However, these receptors are still crucial to preserve resources by avoiding the leak of spontaneous quantal ACh, an action which is probably implicated in their protective role against synaptic depression after repetitive activity (Tomàs et al., 2014), (the mature axonal terminal in **Figure 3**).

LINKS OF AR WITH OTHER METABOTROPIC RECEPTORS (DEVELOPMENT AND ADULTHOOD)

Activity-dependent mediators derived from the three cells of the synapse cross the extracellular cleft in all directions to generate signals in target metabotropic receptors. In the NMJ, there are other purinergic receptors apart from AR (Tsim and Barnard, 2002; Todd and Robitaille, 2006), several mAChR (Santafé et al., 2007, 2009; Wright et al., 2009; Garcia et al., 2010b), neurotrophin receptors (Gonzalez et al., 1999; Garcia et al., 2011; Santafé et al., 2015; Nadal et al., 2016a,b) cytokine receptors (Ribchester et al., 1998; Wang et al., 2002; Garcia et al., 2010a, 2012), calcitonin gene-related peptide receptors (Changeux et al., 1992; Lu and Fu, 1995; Gaydukov et al., 2016), glutamate receptors (Thomas and Sigrist, 2012; Personius et al., 2016; Tsentsevitsky et al., 2017) and neuregulin receptors (Loeb, 2003; Kummer et al., 2006; Simeone et al., 2010; Schmidt et al., 2011; Wang et al., 2017). The way a synapse operates is largely the outcome of the confluence of several signaling pathways on intracellular kinases, which phosphorylate protein targets and materialize adaptive changes to modulate transmitter release and the stability of the connection. Therefore, the appropriate knowledge of synaptic behavior needs the integrated albeit complex interpretation of the complementary function of these receptors. Thus, we studied the link and interaction of AR with mAChR and the neurotrophin receptor TrkB in the control of synapse elimination during development and transmitter release in the adult NMJ (Nadal et al., 2016a,b, 2017).

In relation with the synapse elimination process during development, in addition to the role of AR subtypes (A_1R and A_{2A}R) described above, we investigated the involvement of individual mAChR M_1-, M_2-, and M_4-subtypes and the TrkB receptor (Garcia et al., 2010b; Nadal et al., 2016a,b, 2017). Our data indicated that the three receptor sets and all subtypes considered could affect the competition between axon terminals. At P7, for instance, all these receptors taken individually (analyzed through selective inhibition) are involved in favoring initial competition and thus delaying axonal loss. The confluence of the respective downstream pathways can integrate the signals related with the competitive interactions and possibly helps to determine the nerve ending that finally wins and/or the ones that are lost. This competition concludes with the acceleration of the

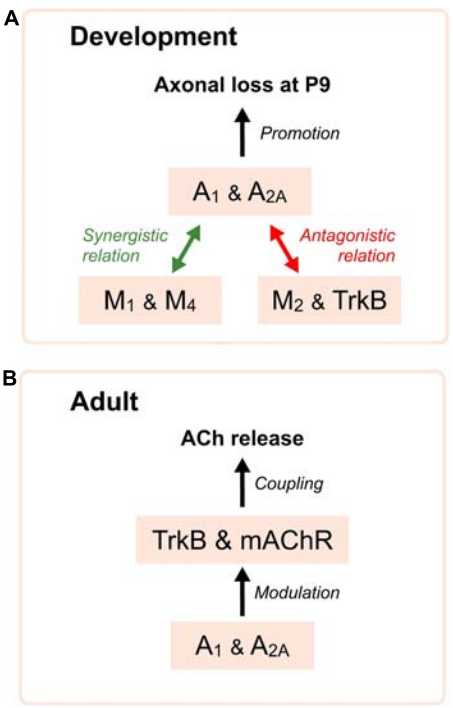

FIGURE 4 | Diagrams showing relations of AR with mAChR and TrkB receptors. In **(A)**, synergistic and antagonistic roles of the AR, mAChR and TrkB receptor during development. AR are necessary to modulate axonal loss and several synergistic (green arrows) and antagonistic (red arrows) relations are clearly observed between all receptors, which affect synapse elimination. In **(B)**, the diagram indicates that the functional integrity of the AR favors the normal operation of the mAChR and the TrkB pathways in the control of the neurotransmitter release in the adulthood.

axonal loss 2 days later (around P9; see the eliminated axonal terminal in **Figure 3**).

To study the collaboration of the AR with mAChR and TrkB, we applied two selective antagonists from two different receptors to see the additive or occlusive effects between them at P9 (Nadal et al., 2016a,b, 2017; Tomàs J. et al., 2017; Tomàs J.M. et al., 2017). These experiments showed the existence of a synergistic role between M_1 and M_4 mAChR, which potentiates the effect of both AR on axonal elimination. Contrarily, the M_2 subtype and the TrkB receptor fully occlude the effects of both A_1R and A_{2A}R. Interestingly, when both A_1R and A_{2A}R are blocked at the same time, a mutual occlusion occurs, and the result does not differ from untreated control (Tomàs J.M. et al., 2017).

Thus, both AR are necessary to modulate synapse elimination and several synergistic and antagonistic links are observed between all receptors, which regulate axonal loss (**Figure 4A**). A_1, M_1, and TrkB are coupled to stimulate PKC whereas A_{2A}, M_2, and M_4 inhibit PKA. We hypothesize that a membrane receptor-induced shifting in the protein kinases A and C activity in some nerve endings may play an important role in promoting developmental NMJ maturation.

In the adult NMJ, it is also known that A_1R and A_{2A}R as well as the M_1-, M_2-, and M_4-subtypes of mAChR and the TrkB receptor play several roles in the regulation of transmitter release (Minic et al., 2002; Santafé et al., 2003, 2004, 2007, 2009; Garcia et al., 2010b; Tomàs et al., 2011). By using selective agonists and antagonists we observed that, some receptors (i.e., A_1R as previously stated) produce minor changes in spontaneous quantal output (see **Figure 3**, right) whereas other receptors (i.e., mAChR) induce major changes in evoked release. Thus, each receptor regulates a given combination of spontaneous, evoked and activity-dependent ACh release. As it has been mentioned before, AR preserve resources by reducing spontaneous leak of neurotransmitter (an A_1R effect) and normalize the synapse function because stimulation with adenosine reduces the magnitude of depression during repetitive activity. mAChR stabilize the spontaneous quantal output of ACh and also preserve the synapse function by decreasing evoked release (mainly an M_2 action) and reducing depression. A role for the TrkB receptor is to stabilize the spontaneous quantal leak of ACh but it mainly potentiates evoked release and synaptic potentials (Tomàs et al., 2014).

We also studied the consecutive incubation with two inhibitors affecting two different receptors to see their collaboration in neurotransmission. Adenosine outflow from nerve endings may, through A_1R, reduce M_2 effect on ACh release and adenylyl cyclase may be the shared intracellular node between both pathways (Oliveira et al., 2009). We observed that non-specific AR modulation with 8SPT or adenosine abolishes the effect of a second exposure to the unselective mAChR blocker atropine, but also the effect of the M_1-selective inhibitor pirenzepine and M_2-selective blocker methoctramine. Thus, the normal operation of the AR is necessary for the normal function of the mAChRs (Tomàs et al., 2014) (**Figure 4B**). However, the same effect is observed in the other way around: a previous blockade of mAChR does not allow applied adenosine to change the above described effect on ACh release in our conditions.

Finally, it has also been reported that adenosine acting through A_{2A} receptors is able to transactivate the TrkB receptor without the need of neurotrophin binding (Lee and Chao, 2001; Lee et al., 2002; Wiese et al., 2007). Thus, AR are also implicated in the neurotrophic TrkB signaling (**Figure 4B**).

CONCLUDING REMARKS

Autoreceptors subtypes are present in the motor nerve endings in the NMJ. During development, AR modulate the competition between axon terminals, helping to define the winner and the losers (Nadal et al., 2016b). To accomplish this function, AR establish several synergistic and antagonistic relations with, at least, the mAChR subtypes and the TrkB receptor which affect synapse elimination. In the mature NMJ, AR help transmitter release by limiting the spontaneous quantal leak of ACh, which mitigates depression during repetitive activity and preserves synaptic function (Tomàs et al., 2014). In addition, the functional integrity of the AR is crucial for the normal operation of the mAChR and the TrkB pathways. These observations underlie the relevance of AR in the NMJ function.

ETHICS STATEMENT

The mice were cared for in accordance with the guidelines of the European Community's Council Directive of November 24, 1986 (86/609/EEC) for the humane treatment of laboratory animals. All experiments on animals have been reviewed and approved by the Animal Research Committee of the Universitat Rovira i Virgili (Reference number: 0233).

AUTHOR CONTRIBUTIONS

LN, EH, AS-O, VC-M, LJ-B, MS, and MT: data collection, quantitative analysis, literature search, data interpretation, and graphic design. NG and ML: statistics. JT, NG, and ML: conception and design, literature search, data interpretation, and manuscript preparation.

FUNDING

This work was supported by a grant from the Catalan Government (2014SGR344 and 2017SGR704) and a grant from MINECO (SAF2015-67143-P).

ACKNOWLEDGMENTS

We thank the reviewers for their careful reading of our manuscript and their many insightful comments.

REFERENCES

Adámek, S., Shakirzyanova, A. V., Malomouzh, A. I., Naumenko, N. V., and Vyskočil, F. (2010). Interaction of glutamate- and adenosine-induced decrease of acetylcholine quantal release at frog neuromuscular junction. *Physiol. Res.* 59, 803–810.

Balice-Gordon, R., and Lichtman, J. (1993). In vivo observations of pre- and postsynaptic changes during the transition from multiple to single innervation at developing neuromuscular junctions. - Semantic Scholar. *J. Neurosci.* 13, 834–855. doi: 10.1523/JNEUROSCI.13-02-00834.1993

Baxter, R. L., Vega-Riveroll, L. J., Deuchars, J., and Parson, S. H. (2005). A_{2A} adenosine receptors are located on presynaptic motor nerve terminals in the mouse. *Synapse* 57, 229–234. doi: 10.1002/syn.20173

Besalduch, N., Lanuza, M. A., Garcia, N., Obis, T., Santafe, M. M., Tomàs, M., et al. (2013). Cellular localization of the atypical isoforms of protein kinase C (aPKCζ/PKMζ and aPKCλ/ι) on the neuromuscular synapse. *Neurosci. Lett.* 556, 166–169. doi: 10.1016/j.neulet.2013.10.006

Besalduch, N., Santafé, M. M., Garcia, N., Gonzalez, C., Tomás, M., Tomás, J., et al. (2011). Transmitter release in the neuromuscular synapse of the protein kinase C theta-deficient adult mouse. *J. Comp. Neurol.* 519, 849–855. doi: 10.1002/cne.22551

Bewick, G. S., Young, C., and Slater, C. R. (1996). Spatial relationships of utrophin, dystrophin, beta-dystroglycan and beta-spectrin to acetylcholine receptor clusters during postnatal maturation of the rat neuromuscular junction. *J. Neurocytol.* 25, 367–379.

Bibel, M., and Barde, Y.-A. (2000). Neurotrophins: key regulators of cell fate and cell shape in the vertebrate nervous system. *Genes Dev.* 14, 2919–2937. doi: 10.1101/gad.841400

Buffelli, M., Busetto, G., Bidoia, C., Favero, M., and Cangiano, A. (2004). Activity-dependent synaptic competition at mammalian neuromuscular junctions. *Physiology* 19, 85–91. doi: 10.1152/nips.01464.2003

Caulfield, M. P., and Birdsall, N. J. (1998). International Union of Pharmacology. XVII. Classification of muscarinic acetylcholine receptors. *Pharmacol. Rev.* 50, 279–290.

Chang, Q., and Balice-Gordon, R. J. (1997). Nip and tuck at the neuromuscular junction: a role for proteases in developmental synapse elimination. *BioEssays* 19, 271–275. doi: 10.1002/bies.950190402

Changeux, J. P., Duclert, A., and Sekine, S. (1992). Calcitonin gene-related peptides and neuromuscular interactions. *Ann. N. Y. Acad. Sci.* 657, 361–378. doi: 10.1111/j.1749-6632.1992.tb22783.x

Chen, C., and Regehr, W. G. (2000). Developmental remodeling of the retinogeniculate synapse. *Neuron* 28, 955–966. doi: 10.1016/S0896-6273(00)00166-5

Correia-de-Sá, P., and Ribeiro, J. A. (1994). Potentiation by tonic A2a-adenosine receptor activation of CGRP-facilitated [3H]-ACh release from rat motor nerve endings. *Br. J. Pharmacol.* 111, 582–588. doi: 10.1111/j.1476-5381.1994.tb14777.x

Correia-de-Sá, P., Sebastião, A. M., and Ribeiro, J. A. (1991). Inhibitory and excitatory effects of adenosine receptor agonists on evoked transmitter release from phrenic nerve ending of the rat. *Br. J. Pharmacol.* 103, 1614–1620. doi: 10.1111/j.1476-5381.1991.tb09836.x

Cunha, R. A., and Sebastião, A. M. (1993). Adenosine and adenine nucleotides are independently released from both the nerve terminals and the muscle fibres upon electrical stimulation of the innervated skeletal muscle of the frog. *Pflugers Arch.* 424, 503–510. doi: 10.1007/BF00374914

De Lorenzo, S., Veggetti, M., Muchnik, S., and Losavio, A. (2006). Presynaptic inhibition of spontaneous acetylcholine release mediated by P2Y receptors at the mouse neuromuscular junction. *Neuroscience* 142, 71–85. doi: 10.1016/j.neuroscience.2006.05.062

Garcia, N., Priego, M., Hurtado, E., Obis, T., Santafe, M. M., Tomàs, M., et al. (2014). Adenosine A2B and A3 receptor location at the mouse neuromuscular junction. *J. Anat.* 225, 109–117. doi: 10.1111/joa.12188

Garcia, N., Priego, M., Obis, T., Santafe, M. M., Tomàs, M., Besalduch, N., et al. (2013). Adenosine A1 and A2A receptor-mediated modulation of acetylcholine release in the mice neuromuscular junction. *Eur. J. Neurosci.* 38, 2229–2241. doi: 10.1111/ejn.12220

Garcia, N., Santafé, M. M., Salon, I., Lanuza, M. A., and Tomàs, J. (2005). Expression of muscarinic acetylcholine receptors (M1-, M2-, M3- and M4-type) in the neuromuscular junction of the newborn and adult rat. *Histol. Histopathol.* 20, 733–743. doi: 10.14670/HH-20.733

Garcia, N., Santafé, M. M., Tomàs, M., Lanuza, M. A., Besalduch, N., Priego, M., et al. (2010a). The glial cell line-derived neurotrophic factor (GDNF) does not acutely change acetylcholine release in developing and adult neuromuscular junction. *Neurosci. Lett.* 480, 127–131. doi: 10.1016/j.neulet.2010.06.022

Garcia, N., Santafé, M. M., Tomàs, M., Priego, M., Obis, T., Lanuza, M. A., et al. (2012). Exogenous ciliary neurotrophic factor (CNTF) reduces synaptic depression during repetitive stimulation. *J. Peripher. Nerv. Syst.* 17, 312–323. doi: 10.1111/j.1529-8027.2012.00419.x

Garcia, N., Tomàs, M., Santafé, M. M., Besalduch, N., Lanuza, M. A., and Tomàs, J. (2010b). The interaction between tropomyosin-related kinase B receptors and presynaptic muscarinic receptors modulates transmitter release in adult rodent motor nerve terminals. *J. Neurosci.* 30, 16514–16522. doi: 10.1523/JNEUROSCI.2676-10.2010

Garcia, N., Tomàs, M., Santafe, M. M., Lanuza, M. A., Besalduch, N., and Tomàs, J. (2010c). Localization of brain-derived neurotrophic factor, neurotrophin-4, tropomyosin-related kinase b receptor, and p75NTR receptor by high-resolution immunohistochemistry on the adult mouse neuromuscular junction. *J. Peripher. Nerv. Syst.* 15, 40–49. doi: 10.1111/j.1529-8027.2010.00250.x

Garcia, N., Tomàs, M., Santafe, M. M., Lanuza, M. A., Besalduch, N., and Tomàs, J. (2011). Blocking p75NTR receptors alters polyinnervation of neuromuscular synapses during development. *J. Neurosci. Res.* 89, 1331–1341. doi: 10.1002/jnr.22620

Gaydukov, A. E., Bogacheva, P. O., and Balezina, O. P. (2016). Calcitonin gene-related peptide increases acetylcholine quantal size in neuromuscular junctions of mice. *Neurosci. Lett.* 628, 17–23. doi: 10.1016/j.neulet.2016.06.014

Ginsborg, B. L., and Hirst, G. (1971). Cyclic AMP, transmitter release and the effect of adenosine on neuromuscular transmission. *Nat. New Biol.* 232, 63–64. doi: 10.1038/newbio232063a0

Ginsborg, B. L., and Hirst, G. D. (1972). The effect of adenosine on the release of the transmitter from the phrenic nerve of the rat. *J. Physiol.* 224, 629–645. doi: 10.1113/jphysiol.1972.sp009916

Gonzalez, M., Ruggiero, F. P., Chang, Q., Shi, Y. J., Rich, M. M., Kraner, S., et al. (1999). Disruption of Trkb-mediated signaling induces disassembly of postsynaptic receptor clusters at neuromuscular junctions. *Neuron* 24, 567–583. doi: 10.1016/S0896-6273(00)81113-7

Herrera, A. A., and Zeng, Y. (2003). Activity-dependent switch from synapse formation to synapse elimination during development of neuromuscular junctions. *J. Neurocytol.* 32, 817–833. doi: 10.1023/B:NEUR.0000020626.29900.fb

Hurtado, E., Cilleros, V., Just, L., Simó, A., Nadal, L., Tomàs, M., et al. (2017a). Synaptic activity and muscle contraction increases PDK1 and PKCβI phosphorylation in the presynaptic membrane of the neuromuscular junction. *Front. Mol. Neurosci.* 10:270. doi: 10.3389/fnmol.2017.00270

Hurtado, E., Cilleros, V., Nadal, L., Simó, A., Obis, T., Garcia, N., et al. (2017b). Muscle contraction regulates BDNF/TrkB signaling to modulate synaptic function through presynaptic cPKCα and cPKCβI. *Front. Mol. Neurosci.* 10:147. doi: 10.3389/fnmol.2017.00147

Jansen, J. K., and Fladby, T. (1990). The perinatal reorganization of the innervation of skeletal muscle in mammals. *Prog. Neurobiol.* 34, 39–90. doi: 10.1016/0301-0082(90)90025-C

Kummer, T. T., Misgeld, T., and Sanes, J. R. (2006). Assembly of the postsynaptic membrane at the neuromuscular junction: paradigm lost. *Curr. Opin. Neurobiol.* 16, 74–82. doi: 10.1016/j.conb.2005.12.003

Lanuza, M. A., Besalduch, N., Garcia, N., Sabaté, M., Santafé, M. M., and Tomàs, J. (2007). Plastic-embedded semithin cross-sections as a tool for high-resolution immunofluorescence analysis of the neuromuscular junction molecules: specific cellular location of protease-activated receptor-1. *J. Neurosci. Res.* 85, 748–756. doi: 10.1002/jnr.21192

Lanuza, M. A., Garcia, N., Santafé, M., González, C. M., Alonso, I., Nelson, P. G., et al. (2002). Pre- and postsynaptic maturation of the neuromuscular junction during neonatal synapse elimination depends on protein kinase C. *J. Neurosci. Res.* 67, 607–617. doi: 10.1002/jnr.10122

Lee, F. S., and Chao, M. V. (2001). Activation of Trk neurotrophin receptors in the absence of neurotrophins. *Proc. Natl. Acad. Sci. U.S.A.* 98, 3555–3560. doi: 10.1073/pnas.061020198

Lee, F. S., Rajagopal, R., Kim, A. H., Chang, P. C., and Chao, M. V. (2002). Activation of trk neurotrophin receptor signaling by pituitary adenylate cyclase-activating polypeptides. *J. Biol. Chem.* 277, 9096–9102. doi: 10.1074/jbc.M107421200

Lee, Y. I., Thompson, W. J., and Harlow, M. L. (2017). Schwann cells participate in synapse elimination at the developing neuromuscular junction. *Curr. Opin. Neurobiol.* 47, 176–181. doi: 10.1016/j.conb.2017.10.010

Liu, Y., Fields, R. D., Festoff, B. W., and Nelson, P. G. (1994). Proteolytic action of thrombin is required for electrical activity-dependent synapse reduction. *Proc. Natl. Acad. Sci. U.S.A.* 91, 10300–10304. doi: 10.1073/pnas.91.22.10300

Loeb, J. A. (2003). Neuregulin: an activity-dependent synaptic modulator at the neuromuscular junction. *J. Neurocytol.* 32, 649–664. doi: 10.1023/B:NEUR.0000020640.84708.35

Lu, B., and Fu, W.-M. (1995). Regulation of postsynaptic responses by calcitonin gene related peptide and ATP at developing neuromuscular junctions. *Can. J. Physiol. Pharmacol.* 73, 1050–1056. doi: 10.1139/y95-149

Lück, G., Hoch, W., Hopf, C., and Blottner, D. (2000). Nitric oxide synthase (NOS-1) coclustered with agrin-induced AChR-specializations on cultured skeletal myotubes. *Mol. Cell. Neurosci.* 16, 269–281. doi: 10.1006/mcne.2000.0873

Lynge, J., and Hellsten, Y. (2000). Distribution of adenosine A_1, A_{2A} and A_{2B} receptors in human skeletal muscle. *Acta Physiol. Scand.* 169, 283–290. doi: 10.1046/j.1365-201x.2000.00742.x

Malomouzh, A. I., Nikolsky, E. E., and Vyskočil, F. (2011). Purine P2Y receptors in ATP-mediated regulation of non-quantal acetylcholine release from motor nerve endings of rat diaphragm. *Neurosci. Res.* 71, 219–225. doi: 10.1016/j.neures.2011.07.1829

Marmiroli, P., and Cavaletti, G. (2012). The glutamatergic neurotransmission in the central nervous system. *Curr. Med. Chem.* 19, 1269–1276. doi: 10.2174/092986712799462711

Minic, J., Molgó, J., Karlsson, E., and Krejci, E. (2002). Regulation of acetylcholine release by muscarinic receptors at the mouse neuromuscular junction depends on the activity of acetylcholinesterase. *Eur. J. Neurosci.* 15, 439–448. doi: 10.1046/j.0953-816x.2001.01875.x

Nadal, L., Garcia, N., Hurtado, E., Simó, A., Tomàs, M., Lanuza, M. A., et al. (2016a). Synergistic action of presynaptic muscarinic acetylcholine receptors and adenosine receptors in developmental axonal competition at the neuromuscular junction. *Dev. Neurosci.* 38, 407–419. doi: 10.1159/000458437

Nadal, L., Garcia, N., Hurtado, E., Simó, A., Tomàs, M., Lanuza, M. A., et al. (2016b). Presynaptic muscarinic acetylcholine autoreceptors (M1, M2 and M4 subtypes), adenosine receptors (A1 and A2A) and tropomyosin-related kinase B receptor (TrkB) modulate the developmental synapse elimination process at the neuromuscular junction. *Mol. Brain* 9, 1–19. doi: 10.1186/s13041-016-0248-9

Nadal, L., Garcia, N., Hurtado, E., Simó, A., Tomàs, M., Lanuza, M. A., et al. (2017). Presynaptic muscarinic acetylcholine receptors and TrkB receptor cooperate in the elimination of redundant motor nerve terminals during development). *Front. Aging Neurosci.* 9:24. doi: 10.3389/fnagi.2017.00024

Nelson, P. G., Lanuza, M. A., Jia, M., Li, M.-X., and Tomas, J. (2003). Phosphorylation reactions in activity-dependent synapse modification at the neuromuscular junction during development. *J. Neurocytol.* 32, 803–816. doi: 10.1023/B:NEUR.0000020625.70284.a6

Nguyen, Q. T., and Lichtman, J. W. (1996). Mechanism of synapse disassembly at the developing neuromuscular junction. *Curr. Opin. Neurobiol.* 6, 104–112. doi: 10.1016/S0959-4388(96)80015-8

Obis, T., Besalduch, N., Hurtado, E., Nadal, L., Santafe, M. M., Garcia, N., et al. (2015). The novel protein kinase C epsilon isoform at the adult neuromuscular synapse: location, regulation by synaptic activity-dependent muscle contraction through TrkB signaling and coupling to ACh release. *Mol. Brain* 8, 1–16. doi: 10.1186/s13041-015-0098-x

Oliveira, L., Timóteo, M. A., and Correia-de-Sá, P. (2009). Negative crosstalk between M1 and M2 muscarinic autoreceptors involves endogenous adenosine activating A1 receptors at the rat motor endplate. *Neurosci. Lett.* 459, 127–131. doi: 10.1016/j.neulet.2009.05.001

Personius, K. E., Slusher, B. S., and Udin, S. B. (2016). Neuromuscular NMDA receptors modulate developmental synapse elimination. *J. Neurosci.* 36, 8783–8789. doi: 10.1523/JNEUROSCI.1181-16.2016

Pitts, E. V., Potluri, S., Hess, D. M., and Balice-Gordon, R. J. (2006). Neurotrophin and Trk-mediated signaling in the neuromuscular system. *Int. Anesthesiol. Clin.* 44, 21–76. doi: 10.1097/00004311-200604420-00004

Pousinha, P. A., Correia, A. M., Sebastiao, A. M., and Ribeiro, J. A. (2010). Predominance of adenosine excitatory over inhibitory effects on transmission at the neuromuscular junction of infant rats. *J. Pharmacol. Exp. Ther.* 332, 153–163. doi: 10.1124/jpet.109.157255

Purves, D., and Lichtman, J. W. (1980). Elimination of synapses in the developing nervous system. *Science* 210, 153–157. doi: 10.1126/science.7414326

Ribchester, R. R., and Barry, J. A. (1994). Spatial versus consumptive competition at polyneuronally innervated neuromuscular junctions. *Exp. Physiol.* 79, 465–494. doi: 10.1113/expphysiol.1994.sp003781

Ribchester, R. R., Thomson, D., Haddow, L. J., and Ushkaryov, Y. A. (1998). Enhancement of spontaneous transmitter release at neonatal mouse neuromuscular junctions by the glial cell line-derived neurotrophic factor (GDNF). *J. Physiol.* 512, 635–641. doi: 10.1111/j.1469-7793.1998.635bd.x

Ribeiro, J. A., Cunha, R. A., Correia-de-Sá, P., and Sebastião, A. M. (1996). Purinergic regulation of acetylcholine release. *Prog. Brain Res.* 109, 231–241. doi: 10.1016/S0079-6123(08)62107-X

Ribeiro, J. A., and Walker, J. (1973). Action of adenosine triphosphate on endplate potentials recorded from muscle fibres of the rat-diaphragm and frog sartorius. *Br. J. Pharmacol.* 49, 724–725. doi: 10.1111/j.1476-5381.1973.tb08555.x

Ribeiro, J. A., and Walker, J. (1975). The effects of adenosine triphosphate and adenosine diphosphate on transmission at the rat and frog neuromuscular junctions. *Br. J. Pharmacol.* 54, 213–218. doi: 10.1111/j.1476-5381.1975.tb06931.x

Roux, P. P., and Barker, P. A. (2002). Neurotrophin signaling through the p75 neurotrophin receptor. *Prog. Neurobiol.* 67, 203–233. doi: 10.1016/S0301-0082(02)00016-3

Salgado, A. I., Cunha, R. A., and Ribeiro, J. (2000). Facilitation by P2 receptor activation of acetylcholine release from rat motor nerve terminals: interaction with presynaptic nicotinic receptors. *Brain Res.* 877, 245–250. doi: 10.1016/S0006-8993(00)02679-2

Sanes, J. R., and Lichtman, J. W. (1999). Developement of the vertebrate neuromuscular junction. *Annu. Rev. Neurosci.* 22, 389–442. doi: 10.1146/annurev.neuro.22.1.389

Santafé, M. M., Garcia, N., Lanuza, M. A., Tomàs, M., and Tomàs, J. (2009). Interaction between protein kinase C and protein kinase A can modulate transmitter release at the rat neuromuscular synapse. *J. Neurosci. Res.* 87, 683–690. doi: 10.1002/jnr.21885

Santafé, M. M., Lanuza, M. A., Garcia, N., Tomàs, M., and Tomàs, J. (2007). Coupling of presynaptic muscarinic autoreceptors to serine kinases in low and high release conditions on the rat motor nerve terminal. *Neuroscience* 148, 432–440. doi: 10.1016/j.neuroscience.2007.06.017

Santafé, M. M., Priego, M., Obis, T., Garcia, N., Tomàs, M., Lanuza, M. A., et al. (2015). Adenosine receptors and muscarinic receptors cooperate in acetylcholine release modulation in the neuromuscular synapse. *Eur. J. Neurosci.* 42, 1775–1787. doi: 10.1111/ejn.12922

Santafé, M. M., Salon, I., Garcia, N., Lanuza, M. A., Uchitel, O. D., and Tomàs, J. (2003). Modulation of ACh release by presynaptic muscarinic autoreceptors in the neuromuscular junction of the newborn and adult rat. *Eur. J. Neurosci.* 17, 119–127. doi: 10.1046/j.1460-9568.2003.02428.x

Santafé, M. M., Salon, I., Garcia, N., Lanuza, M. A., Uchitel, O. D., and Tomàs, J. (2004). Muscarinic autoreceptors related with calcium channels in the strong and weak inputs at polyinnervated developing rat neuromuscular junctions. *Neuroscience* 123, 61–73. doi: 10.1016/j.neuroscience.2003.09.012

Schmidt, N., Akaaboune, M., Gajendran, N., Martinez-Pena, Y., Valenzuela, I., Wakefield, S., et al. (2011). Neuregulin/ErbB regulate neuromuscular junction development by phosphorylation of α-dystrobrevin. *J. Cell Biol.* 195, 1171–1184. doi: 10.1083/jcb.201107083

Searl, T. J., and Silinsky, E. M. (2005). Modulation of Ca(2+)-dependent and Ca(2+)-independent miniature endplate potentials by phorbol ester and adenosine in frog. *Br. J. Pharmacol.* 145, 954–962. doi: 10.1038/sj.bjp.0706248

Shakirzyanova, A. V., Bukharaeva, E. A., Nikolsky, E. E., and Giniatullin, R. A. (2006). Negative cross-talk between presynaptic adenosine and acetylcholine

receptors. *Eur. J. Neurosci.* 24, 105–115. doi: 10.1111/j.1460-9568.2006.04884.x

Silinsky, E. M. (2004). Adenosine decreases both presynaptic calcium currents and neurotransmitter release at the mouse neuromuscular junction. *J. Physiol.* 558, 389–401. doi: 10.1113/jphysiol.2004.061457

Silinsky, E. M., Solsona, C., and Hirsh, J. K. (1989). Pertussis toxin prevents the inhibitory effect of adenosine and unmasks adenosine-induced excitation of mammalian motor nerve endings. *Br. J. Pharmacol.* 97, 16–18. doi: 10.1111/j.1476-5381.1989.tb11918.x

Simeone, L., Straubinger, M., Khan, M. A., Nalleweg, N., Cheusova, T., and Hashemolhosseini, S. (2010). Identification of Erbin interlinking MuSK and ErbB2 and its impact on acetylcholine receptor aggregation at the neuromuscular junction. *J. Neurosci.* 30, 6620–6634. doi: 10.1523/JNEUROSCI.5778-09.2010

Singh, Y. N., Dryden, W. F., and Chen, H. (1986). The inhibitory effects of some adenosine analogues on transmitter release at the mammalian neuromuscular junction. *Can. J. Physiol. Pharmacol.* 64, 1446–1450. doi: 10.1139/y86-245

Slater, C. R. (1982a). Neural influence on the postnatal changes in acetylcholine receptor distribution at nerve-muscle junctions in the mouse. *Dev. Biol.* 94, 23–30. doi: 10.1016/0012-1606(82)90064-1

Slater, C. R. (1982b). Postnatal maturation of nerve-muscle junctions in hindlimb muscles of the mouse. *Dev. Biol.* 94, 11–22. doi: 10.1016/0012-1606(82)90063-X

Slutsky, I., Silman, I., Parnas, I., and Parnas, H. (2001). Presynaptic M2 muscarinic receptors are involved in controlling the kinetics of ACh release at the frog neuromuscular junction. *J. Physiol.* 536, 717–725. doi: 10.1111/j.1469-7793.2001.00717.x

Steinbach, J. H. (1981). Developmental changes in acetylcholine receptor aggregates at rat skeletal neuromuscular junctions. *Dev. Biol.* 84, 267–276. doi: 10.1016/0012-1606(81)90394-8

Thomas, U., and Sigrist, S. J. (2012). Glutamate receptors in synaptic assembly and plasticity: case studies on fly NMJs. *Adv. Exp. Med. Biol.* 970, 3–28. doi: 10.1007/978-3-7091-0932-8_1

Todd, K. J., and Robitaille, R. (2006). Purinergic modulation of synaptic signalling at the neuromuscular junction. *Pflügers Arch.* 452, 608–614. doi: 10.1007/s00424-006-0068-3

Tomàs, J., Garcia, N., Lanuza, M. A., Santafé, M. M., Tomàs, M., Nadal, L., et al. (2017). Presynaptic membrane receptors modulate ACh release, axonal competition and synapse elimination during neuromuscular junction development. *Front. Mol. Neurosci.* 10:132. doi: 10.3389/fnmol.2017.00132

Tomàs, J. M., Garcia, N., Lanuza, M. A., Nadal, L., Tomàs, M., Hurtado, E., et al. (2017). Membrane receptor-induced changes of the protein kinases A and C activity may play a leading role in promoting developmental synapse elimination at the neuromuscular junction. *Front. Mol. Neurosci.* 10:255. doi: 10.3389/fnmol.2017.00255

Tomàs, J., Santafé, M. M., Garcia, N., Lanuza, M. A., Tomàs, M., Besalduch, N., et al. (2014). Presynaptic membrane receptors in acetylcholine release modulation in the neuromuscular synapse. *J. Neurosci. Res.* 92, 543–554. doi: 10.1002/jnr.23346

Tomàs, J., Santafé, M. M., Lanuza, M. A., García, N., Besalduch, N., and Tomàs, M. (2011). Silent synapses in neuromuscular junction development. *J. Neurosci. Res.* 89, 3–12. doi: 10.1002/jnr.22494

Tsentsevitsky, A., Nurullin, L., Nikolsky, E., and Malomouzh, A. (2017). Metabotropic and ionotropic glutamate receptors mediate the modulation of acetylcholine release at the frog neuromuscular junction. *J. Neurosci. Res.* 95, 1391–1401. doi: 10.1002/jnr.23977

Tsim, K. W. K., and Barnard, E. A. (2002). The signaling pathways mediated by P2Y nucleotide receptors in the formation and maintenance of the skeletal neuromuscular junction. *Neurosignals* 11, 58–64. doi: 10.1159/000057322

Veggetti, M., Muchnik, S., and Losavio, A. (2008). Effect of purines on calcium-independent acetylcholine release at the mouse neuromuscular junction. *Neuroscience* 154, 1324–1336. doi: 10.1016/j.neuroscience.2008.04.056

Waerhaug, O., and Ottersen, O. P. (1993). Demonstration of glutamate-like immunoreactivity at rat neuromuscular junctions by quantitative electron microscopic immunocytochemistry. *Anat. Embryol.* 188, 501–513. doi: 10.1007/bf00190144

Walder, K. K., Ryan, S. B., Bzdega, T., Olszewski, R. T., Neale, J. H., and Lindgren, C. A. (2013). Immunohistological and electrophysiological evidence that *N*-acetylaspartylglutamate is a co-transmitter at the vertebrate neuromuscular junction. *Eur. J. Neurosci.* 37, 118–129. doi: 10.1111/ejn.12027

Wang, C.-Y., Yang, F., He, X.-P., Je, H.-S., Zhou, J.-Z., Eckermann, K., et al. (2002). Regulation of neuromuscular synapse development by glial cell line-derived neurotrophic factor and neurturin. *J. Biol. Chem.* 277, 10614–10625. doi: 10.1074/jbc.M106116200

Wang, J., Song, F., and Loeb, J. A. (2017). Neuregulin1 fine-tunes pre-, post-, and perisynaptic neuromuscular junction development. *Dev. Dyn.* 246, 368–380. doi: 10.1002/dvdy.24494

Wiese, S., Jablonka, S., Holtmann, B., Orel, N., Rajagopal, R., Chao, M. V., et al. (2007). Adenosine receptor A2A-R contributes to motoneuron survival by transactivating the tyrosine kinase receptor TrkB. *Proc. Natl. Acad. Sci. U.S.A.* 104, 17210–17215. doi: 10.1073/pnas.0705267104

Wright, M. C., Potluri, S., Wang, X., Dentcheva, E., Gautam, D., Tessler, A., et al. (2009). Distinct muscarinic acetylcholine receptor subtypes contribute to stability and growth, but not compensatory plasticity, of neuromuscular synapses. *J. Neurosci.* 29, 14942–14955. doi: 10.1523/JNEUROSCI.2276-09.2009

Wyatt, R. M., and Balice-Gordon, R. J. (2003). Activity-dependent elimination of neuromuscular synapses. *J. Neurocytol.* 32, 777–794. doi: 10.1023/B:NEUR.0000020623.62043.33

Conflict of Interest Statement: The authors declare that the research was conducted in the absence of any commercial or financial relationships that could be construed as a potential conflict of interest.

The reviewer CS and handling Editor declared their shared affiliation.

frontiers in Pharmacology

ORIGINAL RESEARCH
published: 20 April 2018
doi: 10.3389/fphar.2018.00196

Cytokine-Induced Killer Cells Express CD39, CD38, CD203a, CD73 Ectoenzymes and P1 Adenosinergic Receptors

Alberto L. Horenstein[1], Antonella Chillemi[1], Roberta Zini[2], Valeria Quarona[1], Nicoletta Bianchi[3], Rossella Manfredini[2], Roberto Gambari[3], Fabio Malavasi[1†] and Davide Ferrari[3†]*

[1] Laboratory of Immunogenetics and CeRMS, Department of Medical Sciences, University of Torino, Torino, Italy, [2] Centre for Regenerative Medicine "Stefano Ferrari," Department of Life Sciences, University of Modena and Reggio Emilia, Modena, Italy, [3] Department of Life Science and Biotechnology, Section of Microbiology and Applied Pathology, University of Ferrara, Ferrara, Italy

OPEN ACCESS

Edited by:
Francisco Ciruela, Universitat de Barcelona, Spain

Reviewed by:
Alessandro Poggi, Dipartimento delle Terapie Oncologiche Integrate, Ospedale Policlinico San Martino, Italy
Deepak A. Deshpande, Thomas Jefferson University, United States

***Correspondence:**
Davide Ferrari
dfr@unife.it

[†] *Same authorship.*

Specialty section:
This article was submitted to Experimental Pharmacology and Drug Discovery, a section of the journal Frontiers in Pharmacology

Received: *17 November 2017*
Accepted: *21 February 2018*
Published: *20 April 2018*

Citation:
Horenstein AL, Chillemi A, Zini R, Quarona V, Bianchi N, Manfredini R, Gambari R, Malavasi F and Ferrari D (2018) Cytokine-Induced Killer Cells Express CD39, CD38, CD203a, CD73 Ectoenzymes and P1 Adenosinergic Receptors. Front. Pharmacol. 9:196. doi: 10.3389/fphar.2018.00196

Cytokine-induced killer (CIK) cells, a heterogeneous T cell population obtained by *in vitro* differentiation of peripheral blood mononuclear cells (PBMC), represent a promising immunological approach in cancer. Numerous studies have explored the role of CD38, CD39, CD203a/PC-1, and CD73 in generating extracellular adenosine (ADO) and thus in shaping the tumor niche in favor of proliferation. The findings shown here reveal that CIK cells are able to produce extracellular ADO via traditional (CD39/CD73) and/or alternative (CD38/CD203a/CD73 or CD203a/CD73) pathways. Transcriptome analysis showed the mRNA expression of these molecules and their modulation during PBMC to CIK differentiation. When PBMC from normal subjects or cancer bearing patients were differentiated into CIK cells under normoxic conditions, CD38 and CD39 were greatly up-regulated while the number of CD203a, and CD73 positive cells underwent minor changes. Since hypoxic conditions are often found in tumors, we asked whether CD39, CD38, CD203a, and CD73 expressed by CIK cells were modulated by hypoxia. PBMC isolated from cancer patients and differentiated into CIK cells in hypoxic conditions did not show relevant changes in CD38, CD39, CD73, CD203a, and CD26. CIK cells also expressed A_1, A_{2A}, and A_{2B} ADO receptors and they only underwent minor changes as a consequence of hypoxia. The present study sheds light on a previously unknown functional aspect of CIK cells, opening the possibility of pharmacologically modulated ADO-generating ectoezymes to improve CIK cells performance.

Keywords: CIK, adenosine, CD38, CD39, CD73, CD203a/PC-1, hypoxia, P1 receptors

INTRODUCTION

CIK cells are polyclonal T effector cells sharing immunological properties and receptors with NK cells. They are attracting increasing interest for their ability to perform non-MHC-restricted cytolytic activities toward susceptible autologous and allogeneic cancer cells (Schmidt-Wolf et al., 1991; Lu and Negrin, 1994). This capacity, along with their safety and easy *in vitro* generation has

opened the door to multiple applications of CIK adoptive immunotherapy against different types of cancer. Hence, CIK can be employed against solid and hematological tumors, either alone or together with chemotherapy. An experimental CIK based approach has been undertaken for the following neoplasms: chronic and acute lymphocytic leukemias, lymphomas, kidney carcinoma, renal, liver and stomach cancer, melanomas and bone sarcomas (Linn and Hui, 2010; Gammaitoni et al., 2013; Jiang et al., 2013; Sangiolo et al., 2014). CIK cells are generated by *ex vivo* cultivation of human PBMC in the presence of the cytokine interferon gamma (IFN-ɤ), the anti-CD3 monoclonal antibody OKT3, and then adding recombinant human IL-2 (rhIL-2) (Introna et al., 2007; Jiang et al., 2013; Giraudo et al., 2015). The addition of IFN-γ has the main goal of activating monocytes present in the mixed PBMC population to secrete IL-12, which favors CD58/LFA-3-mediated activation, while the binding of anti-CD3 antibody to CD3 membrane antigen expressed by T lymphocytes and the addition of IL-2 provides cells with the mitogenic stimuli they need for proliferation (Franceschetti et al., 2009). CIK cells are a heterogeneous population comprising $CD3^+CD8^+$ T cells, $CD3^+CD56^-$ T cells (from 20 to 60% of total CIK), and $CD3^+CD56^+$ double positive cells (from 40 to 80% of total CIK), as well as of a small number of $CD3^-CD56^+$ NK cells (from 1 to 10%) (Franceschetti et al., 2009; Pievani et al., 2011; Introna et al., 2013; Valgardsdottir et al., 2014).

Immune cells interact with cancer cells in the so called "tumor niche," i.e., in a localized neoplastic tissue context; therefore they are heavily influenced by the superimposed tumor conditions. Some of the most influential extracellular mediators in the niche are the nucleotides and nucleosides. Adenosine (ADO), the main nucleoside mediator generated both intracellularly and extracellularly, suppresses the anti-tumoral immune response, thus favoring metastasis to the detriment of the host organism. Once present in the extracellular *milieu*, nucleotides and nucleosides bind purinergic receptors, i.e., specific plasma membrane receptors necessary for cell-to-cell communication and named P2 (activated by ATP, UTP, ADP, UDP, UDP-glucose, and NAD^+) and P1 receptors (G protein-coupled, activated by ADO). P1 are further divided into four subtypes (A_1R, $A_{2A}R$, $A_{2B}R$, A_3R) (Burnstock, 2007; Surprenant and North, 2009; Harden et al., 2010; Plattner and Verkhratsky, 2016).

Extracellular nucleotides and nucleosides are subjected to continuous transformation. The main canonical actors of this function are four ectonucleotidases: ectonucleoside triphosphate diphosphohydrolase (NTPDase, CD39), ectonucleotide pyrophosphatase/phosphodiesterase (NPP, CD203a) or PC-1, ecto-5′nucleotidase (CD73), and alkaline phosphatases (Yegutkin, 2008; Zimmermann et al., 2012) which degrade ATP and its metabolites, eventually leading to ADO production and the subsequent activation of P1 receptors (Fredholm et al., 2001). Transformation of extracellular ATP into its metabolites requires the sequential participation of the CD39 ectoenzyme (stepwise forming extracellular AMP) subsequently metabolized by CD73 into ADO (Yegutkin, 2008; Zimmermann et al., 2012).

Another pathway generating extracellular AMP, which can then be transformed into ADO, involves participation of extracellular NAD^+ and CD38 an ADP-ribosyl cyclase/cyclic ADP-ribose (cADPR) hydrolase. Expression of CD203a (ectonucleotide pyrophosphatase/phosphodiesterase-1) accompanied by the extracellular presence of its substrate ADPR (product of the deconstruction of NAD^+ by CD38) favors the generation of additional AMP (Horenstein et al., 2013).

ADO plays multiple roles as an extracellular mediator both in physiological and pathological conditions. It is released in different tissue contexts, including neurons, kidney cells, cardiomyocytes, vascular endothelium and immune cells (Shryock and Belardinelli, 1997; Latini and Pedata, 2001; Dale and Frenguelli, 2009; Praetorius and Leipziger, 2010; Morandi et al., 2015; Silva, 2016). However, the interest in ADO and ectoenzymes involved in ADO formation (CD38, CD39, CD73 and CD203a) was prompted by growing evidence of their role in cancer biology. Indeed, ADO suppresses immune responses against tumor cells, and cancer-derived ADO is recognized as a crucial extracellular immune checkpoint target for re-establishing immune-surveillance mechanisms (Young et al., 2014; Hatfield and Sitkovsky, 2016; Allard et al., 2017).

A role in favoring cancer growth and dissemination has been described for each of the extracellular enzymes involved in nucleotide/nucleoside and NAD^+ metabolism (i.e., CD39, CD38, CD203a and CD73) and for the complexing ADO deaminase (ADA)/CD26 molecules, a controller of ADO in the extracellular space. CD39 is involved in colorectal cancer dissemination (Stagg and Smyth, 2010) as well as in the metastatic competence of non-small-cell lung cancer (NSCLC) (Schmid et al., 2015; Ferrari et al., 2017). CD73 is involved in the spread of cancer and in reducing immune-surveillance (Wang et al., 2008; Antonioli et al., 2016a,b; Ferrari et al., 2017). This is achieved by using antibodies to CD73 and CD39 (Young et al., 2014; Allard et al., 2017; Kazemi et al., 2017) to block ADO, a normal immune regulator, which is hijacked by tumors to evade immune attack. Likewise, human CD38 (Malavasi et al., 2008) is implicated in multiple myeloma, where it is main target of therapeutic treatments (Horenstein et al., 2015; Sanchez et al., 2016; Costa et al., 2017; Shallis et al., 2017). Concerning P1, $A_{2A}R$ and $A_{2B}R$ have been indicated as the main candidate receptors in cancer therapy (Beavis et al., 2013; Desmet et al., 2013; Hatfield and Sitkovsky, 2016; Allard et al., 2017; Garber, 2017; Mittal et al., 2017).

However, so far, there is no information on P1, CD39, CD38, CD203a, CD73, and CD26 expression in CIK cells. In view of the important immunosuppressive role played by ADO and the promising use of CIK cells in adoptive cancer therapy, we investigated the metabolic processes of ADO generated during the differentiation of human T cells present into the PBMC fraction into CIK cells under normoxic and hypoxic conditions.

Abbreviations: ADO, adenosine; ADA, adenosine deaminase; AR, adenosine receptor; ADPR, ADP-ribose; CD38, ADP-ribosyl cyclase/cyclic ADPR-hydrolase; CD39, ecto-nucleoside triphosphate diphosphohydrolase (NTPDase); CD73, ecto-5′-nucleotidase (5′-NT); CD203a/PC-1, ectonucleotide pyrophosphatase/phosphodiesterase-1 (NPP-1); CIK, cytokine-induced killer; EHNA, erytro-9 (2-hydroxy-3-nonyl) adenine; GIST, Gastrointestinal Stromal Tumor; PBMC, peripheral blood mononuclear cells; OS, osteosarcoma.

MATERIALS AND METHODS

CIK Cell Production and Characterization

PBMC cells from 11 donors, five healthy donors, five patients with histologic confirmed Gastrointestinal Stromal Tumors (GIST) and 1 patient with osteosarcoma (OS). Blood samples were obtained through an ongoing collaboration with Dr D. Sangiolo at the Candiolo Cancer Institute FPO-IRCCS Fondazione del Piemonte per l'Oncologia. Patients provided written informed consent for blood donation according to a protocol approved by the internal review board and ethic committee (Ethic Committee, IRCCS Candiolo Cancer Institute, Turin, Italy. Prot. CE IRCCS 244/2015).

Cryopreserved PBMC were seeded at a concentration of $2x10^6$ cells/ml according to the standard protocols (Gammaitoni et al., 2013; Sangiolo et al., 2014), including 21 days of culture in RPMI-1640 medium (Gibco BRL Life Technologies Italia, Monza, Italy) supplemented with 10% fetal bovine serum (Sigma Aldrich, MI, Italy) 100 U/ml penicillin, and 100 U/ml streptomycin (Gibco BRL Life Technologies Italia, Italy) at 37°C and 5% CO_2, with the timed addition of IFN-γ (1,000 U/ml on day 0), Ab anti-CD3 OKT3 (50 ng/ml on day 1) and IL-2 (300 U/ml on day 1 up to the end, refreshing the medium every 2-3 days) (all factors are from Miltenyi Biotec S.r.l., Calderara di Reno, BO, Italy). In parallel with the standard *ex vivo* cultures, at day 0 an aliquot (7×10^6) of PBMC was seeded (2×10^6 cells/ml) in RPMI-1640 medium with 10% fetal bovine serum, 100 U/ml penicillin and streptomycin at 37°C and 5% CO_2) but without the addition of INF-γ to perform mRNA analysis. At day 1 of culture, 3×10^6 of these cells were collected for RNA extraction. Cells were lysed in Invitrogen™ TRIzol™ (Thermo Fisher Scientific S.p.a., MI, Italy) and stored at−80°C. RNA extraction was repeated with the same procedure for each CIK cells cultures at day 14 and 21.

Phenotype of CIK cells was weekly analyzed starting from day 0 by standard flow cytometric assays. The following monoclonal antibodies (mAb) were used: CD3-FITC, CD4-PE, CD56-APC, CD8-PE, and CD314-APC (anti-NKG2D) (all mAb are from Miltenyi Biotec S.r.l., BO, Italy). Labeled cells were read on FACS Cyan (Cyan ADP, Beckman Coulter s.r.l., Cassina De' Pecchi, MI, Italy) and analyzed using Summit Software.

Evaluation of Ectoenzyme Expression on CIK Cells by Flow Cytometry

FACS analysis of $CD56^+CD3^+$ CIK cells was performed using FITC-labeled anti-CD56 (Beckman Coulter Inc., Brea CA, USA) and PE-Cy7-labeled anti-CD3 antibodies (BioLegend, Milan, Italy). Expression of ectoezymes was detected by using the following mAbs generated and purified in-house by two-step HPLC chromatography (Horenstein et al., 2003) and APC-conjugated by Aczon (BO, Italy): anti-CD38 (clone IB4), anti-CD73 (clone CB73), anti-CD203a (clone 3E8, kindly provided by J. Goding) and anti-CD26 (clone BT5.9). CD39 expression was analyzed using anti-CD39 APC mAb (clone eBioA1, eBiosciences, San Diego, CA, USA). Tests were performed on cells washed in phosphate buffered saline (PBS) containing 1% bovine serum albumin (BSA) + NaN_3 and incubated with APC-conjugated mAb for 1 h at 4°C. The samples were then washed, resuspended in PBS and acquired on a FACSort flow cytometer (Becton-Dickinson, USA) using CellQuest Software (Becton-Dickinson). Data were analyzed using FlowJo Software (TreeStar).

Expression of ADO receptors was evaluated on CIK cells gated for $CD3^+$ $CD56^+$ and assayed in PBMC and in the corresponding CIK cells using the following antibodies: purified rabbit polyclonal anti-A_1R (LifeSpan BioSciences, Inc., USA), rabbit polyclonal anti-$A_{2A}R$ and rabbit polyclonal anti-$A_{2B}R$ (Thermo Scientific, USA). PE-conjugated goat anti-rabbit Ig (Beckman Coulter, USA) was used as secondary reagent. Data were expressed as mean relative of fluorescence intensity (MRFI), obtained as follows: mean fluorescence obtained with specific mAb/mean fluorescence obtained with irrelevant isotype-matched mAb.

For FACS analysis under hypoxic culture conditions, total cryopreserved PBMC were seeded at a concentration of 2×10^6 cells/ml in a humidified CO_2 incubator (Thermo Scientific Water Jacketed 3010) and differentiated into CIK cells by using the standard procedure. Culture conditions were 21% (normoxia) or 1% (hypoxia) O_2, 5% CO_2 at 37°C. The phenotype was weekly analyzed starting from day 0 by standard flow cytometric assays.

Quantification of ADO Production by CIK Cells

CIK (1×10^6/ml) were incubated in 500 µl HBSS at 37°C and 5% CO_2 in 24 well plates (Costar Corning) and pre-treated with 50 µL of stop solution [EHNA (5 µM) + Dipyridamole (20 µM) + Levamisole (30 µM) + Deoxycoformicin (50 µM)], in the presence (or absence) of NAD^+, ADPR, ATP or AMP (100 µM). At the end of the incubation time (30 min), supernatants were collected and acetonitrile (ACN, Sigma Aldrich) was immediately added (1:2 ratio) to stabilize ADO. Samples were then centrifuged at 13,700 × g, collected and stored at −80°C until use. The presence of NAD^+, ATP, ADPR, AMP, and ADO was investigated by high-pressure liquid chromatography (HPLC, Beckman Gold 126/166NM, Beckman Coulter) equipped with a reversed-phase column (Synergi Polar C18, 5 µm; 150 × 4.5 mm, Phenomenex). The metabolites were separated using a pH 5.1 mobile-phase buffer (0.125 M citric acid and 0.025 M KH_2PO_4 containing 8% ACN) over ten min with a flow rate of 0.8 mL/min and UV detection set at 254 nm. Peak identities were confirmed by using standard compounds. The presence of ADO was also confirmed by spiking standard (50 µM ADO), followed by chromatography. The retention times (Rt, in min) of standards were: ATP, 2.00; AMP, 2.35; NAD^+, 2.8; ADPR, 3.44, and ADO; 5.56. All concentrations measured on CIK-derived supernatants were normalized to cell number and volume.

Expression Profile of Adenosinergic Ectoenzymes and P1 Purinergic Receptors in CIK Cells

The mRNA expression data of PBMC and CIK cells originate from Mesiano et al. (2017) and were deposited in the Gene Expression Omnibus repository (https://www.ncbi.nlm.nih.gov/geo/query/acc.cgi?acc=GSE97581).

Briefly, we performed the gene expression profile (GEP) of PBMC (day 1, absence of INF- γ) and CIK cells (day 14) obtained from 3 GIST patients by means of HG-U219 Array Strip (Affymetrix; Santa Clara, CA, USA) (Mesiano et al., 2017). Microarray data were analyzed by using the Partek GS 6.6 Software Package and normalized using the robust multiarray average (RMA) procedure (Irizarry et al., 2003).

Differentially expressed genes (DEGs) were then selected using a supervised approach with the ANOVA module included in Partek GS package. In particular, we considered differentially expressed genes (DEGs) all the probe sets with a fold change contrast $\geq$ 1.4 in the pairwise comparison of CIK cells with PBMCs, and a false discovery rate (FDR) (q-value) < 0.5.

Statistical Analysis

p-value was calculated using an unpaired nonparametric test, two-tailed Mann-Whitney for GraphPad Prism 6. Reported data are expressed as mean values ± SD.

RESULTS

Transcriptome Analysis on Adenosinergic Ectoenzymes

In vitro differentiation of CIK cells starts with cultivation of PBMC according to standard protocols (Gammaitoni et al., 2013; Sangiolo et al., 2014). To shed light on extracellular enzymes involved in nucleotide/nucleoside and NAD^+ metabolism we checked the expression levels of CD39, CD38, CD203a and CD73 during CIK cell differentiation. As shown in **Figure 1**, CD38 and CD39 were up-regulated in CIK cells form 3 GIST subjects (day 14) vs. PBMC (day 1, absence of INF-γ), whereas CD73 and CD203a resulted down-regulated.

Expression of Nucleotide-Hydrolyzing Ectoenzymes in PBMC and CIK Cells

Firstly, cell cultures were gated for $CD3^+CD56^+$ expression and CD38, CD39, CD203a, and CD73 were assayed both in PBMC and in the corresponding CIK cells. A representative gating of the CIK population at the third week of culture is shown in **Figure 2A**. Expression of the assayed markers is represented by white peaks (**Figure 2B**). Cytofluorometric analysis revealed that the NAD^+-consuming CD38 ectoenzyme was present in 45.7% of the PBMC while it was expressed by the vast majority (98.9 ± 1%) of CIK cells, with minor variations in mean fluorescence intensity (MFI; mean ± SD, 148 ± 25). The expression of CD39 increased during PBMC to CIK differentiation (PBMC 35.7 ± 1.89; CIK 97.9 ± 2.34). CD203a and CD73 were also monitored (**Figure 2B**). In contrast to CD38 and CD39, CD203a was barely expressed by PBMC and increased in CIK cells (PBMC 7.7 ± 0.29; CIK 14.9 ± 0.34); while expression of CD73 was almost unchanged during differentiation (28.8 ± 3.65 vs. 23.8 ± 12.1).

While day 0 corresponds to withdrawal of PBMC, day 21 is usually chosen as end of *in vitro* differentiation period to start procedures for CIK cell infusion into cancer patients. **Figure 2C** shows that $CD3^+$ $CD56^+$ CIK cells from 6 subjects 5 GIST and 1 OS) maintained the initial high levels of CD38 with a mean value of 62.5% (min 53.2%, max 75.0%) vs. 92.5% (min 81.5%, max 98.8%); CD39 had a mean value of 13.2% (min 2.3%, max 23.5%) vs. 53.3% (min 32.2%, max 75.2%) associated to a significant increase at day 21 of the expression of CD26 as compared to resting PBMC with a mean value of 20.5% (min 6.8%, max 23.1%) vs. 91.2% (min 76.5%, max 96.5%), along with minimal CD203a up-regulation with a mean value of 15.1% (min 2.5%, max 24.1%) vs. 23.5% (min. 13.6%, max 35.1%), and stable expression of CD73 with a mean value of 75.2% (min 63.5%, max 80.30%) vs. 93.6% (min 77.5%, max 97.6%). These results indicate that CIK cells are provided with a complete ectoenzymatic machinery able to produce ADO through the traditional (CD39/CD73) as well as alternative (CD38/CD203a/CD73 or CD203a/CD73) pathways.

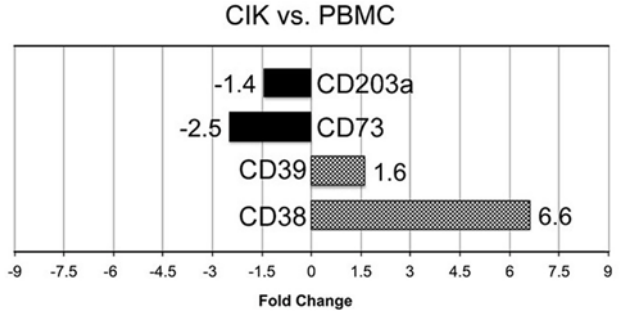

FIGURE 1 | Transcriptome analysis of CIK ectoenzymes. mRNA expression was analyzed in PBMC (day 1, absence of INF-γ) and CIK cells (day 14) obtained from 3 GIST patients. The black blocks display the transcripts that are down-regulated during CIK differentiation; whereas, the chess pattern displays the mRNAs that are up-regulated during CIK differentiation.

Extracellular ADO Production by CIK Cells

The role of ADO as potent suppressor of immune-surveillance has been well ascertained and has adopted by many cancer types as a mechanism of escape from the deleterious activity of macrophages, dendritic cells, T lymphocytes and NK (Morandi et al., 2015; Antonioli et al., 2016a,b). For adoptive immunotherapy CIK cells are usually infused as bulk into tumor bearing patients. Therefore, we checked whether the adenosinergic ectoenzymes expressed by bulk CIK cells deriving from PBMC of cancer patients were functional. To address this issue, we evaluated ADO produced by CIK cells obtained from 6 subjects (5 GIST and 1 OS). ADO release was investigated in supernatants from CIK cells incubated with NAD^+ (CD38 substrate), ADPR (CD203a substrate) and AMP (CD73 substrate) in the presence of EHNA (adenosine deaminase inhibitor).

Metabolism of Extracellular NAD^+

HPLC-assisted analysis of the supernatants of bulk CIK cells revealed the presence of non-consumed NAD^+ together with the enzymatic products ADPR and nicotinamide (NIC) ($n = 5$) (**Figure 3**). Besides the non-consumed NAD^+, which could be identified in the HPLC assay by its unique retention time (R_t) of 2.80 min, the metabolic products of CIK cells were ADPR,

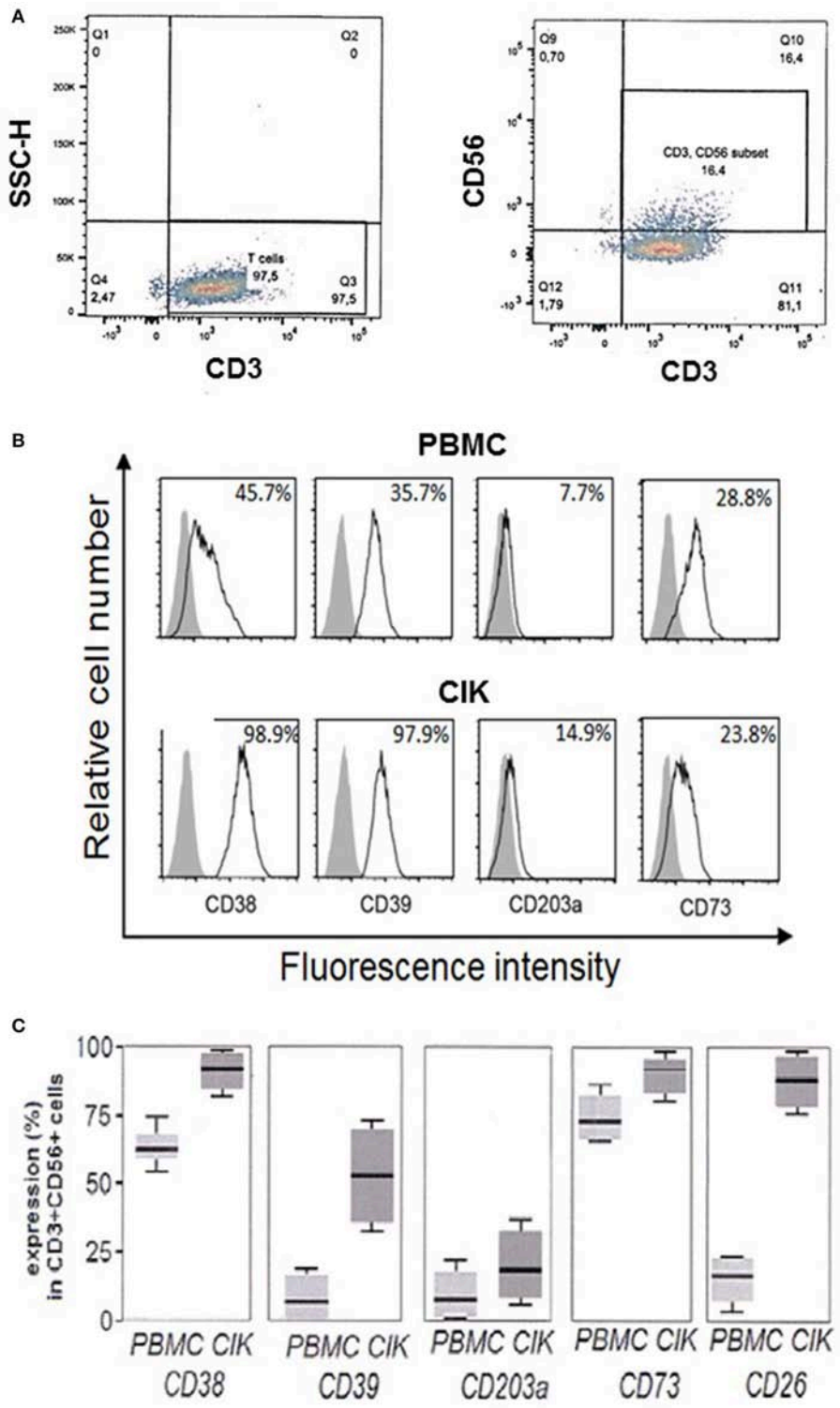

FIGURE 2 | Expression of CD38, CD39, CD203a, and CD73 in $CD3^+CD56^+$ human PBMC and in the corresponding CIK cells. **(A)** Representative gating of $CD3^+$ and $CD3^+CD56^+$ populations present in CIK cells at the third week of culture. Analysis was performed by using the fluorophores PE-Cy7 or FITC for CD3 and CD56 antigens, respectively. **(B)** Cytofluorometric expression analysis of ectoenzymes (white peaks) in PBMC at day 0 (upper panel) and CIK cells at day 21 (lower panel). CD38, CD39, CD73, and CD203a were detected by APC conjugated antibodies. Gray peaks demarcate isotype control staining. Percentage of positive cells is indicated. **(C)** Percentage of expression of the different markers in PBMC (day 0) and CIK cells (day 21). Cells were from 6 subjects (5 gastrointestinal stromal tumors and 1 osteosarcoma). In **C**, data are expressed as mean, minimum and maximum values.

NIC and AMP, exhibiting corresponding R_t of 3.44, 6.87, and 2.35 min, respectively.

The NAD^+ hydrolytic profile of CIK cells, converting extracellular NAD^+ into AMP, can be attributed to the ADP-ribosyl cyclase/cyclic ADPR-hydrolase activity of CD38 and CD203a, which exhibits nucleotide pyrophosphatase/phosphodiesterase activity. ADPR produced by CD38 upon the partial breakdown of NAD^+ can subsequently be degraded to AMP by CD203a, confirming the observations reported in other cell systems (Horenstein et al., 2015, 2016).

Since ADPR was the principal product of exogenously applied NAD^+, we wondered whether it would be source of the AMP generated by CIK cells. Thus, we tested the functional activity of CD203a by directly applying ADPR, a known substrate for this ectoenzyme (**Figure 3**). CIK cells displayed an ADPR-hydrolyzing activity leading to AMP, supporting our hypothesis that the NAD^+ converting pathway leading to AMP is operative in CIK cells concomitantly expressing CD38 and CD203a.

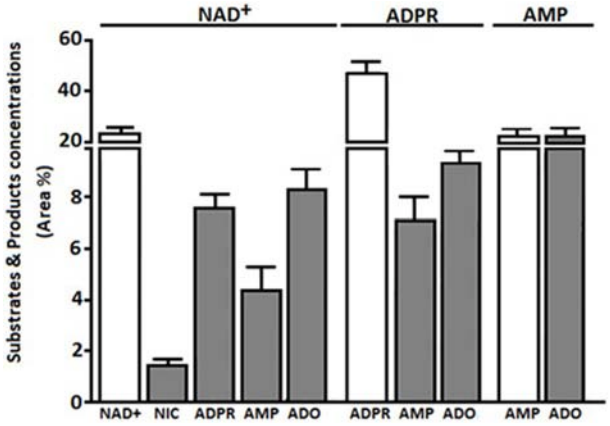

FIGURE 3 | Extracellular products of CIK enzymatic reactions using NAD^+, ADPR, and AMP as substrates. Products (NIC, ADPR, AMP, or ADO) obtained from bulk CIK cell cultures ($n = 5$) using (i) NAD^+, (ii) ADPR or (iii) AMP as substrates, were evaluated by HPLC assays in the presence of the adenosine deaminase inhibitor (EHNA) as described in Materials and Methods. Products (gray bars) are expressed as area percentage (Area %) for each enzymatic product as compared to the total components present in the ACN-treated CIK cell supernatant (100%). Substrates are represented as Area % of consumed substrate (white bars). Results indicate that bulk CIK cells efficiently hydrolyze NAD^+, ADPR and AMP to generate ADO. Of note, CIK cells produce low or undetectable amounts of ADO when incubated with NAD^+, ADPR, or AMP substrates in the absence of EHNA (not shown). The identity of peaks was confirmed by the co-migration of reference standards.

Metabolism of Extracellular ATP

The canonical adenosinergic pathway in CIK cells was investigated using ATP, a known substrate for CD39 or alternatively for CD203a (**Figures 4A,B**). Therefore, analysis ($n = 5$) of ATP consumption by CIK cells allowed a comparison of both nucleotide transformation pathways. The incubation of CIK cells with ATP led to a predominant accumulation of AMP, with low levels of ADP due to the catabolism of ATP by CD39 ectoenzyme (**Figure 4A**). However, at variance with reports pointing to the exclusive CD39-mediated ATP hydrolysis to ADP and AMP by lymphoid cells, CIK cells converted part of the ATP substrate directly to AMP, confirming the simultaneous presence of functional CD203a. This finding was confirmed by the attenuation (∼50%) of the metabolic conversion of ATP into AMP in the presence of the CD39 inhibitor POM-1 (**Figures 4A,B**). These experiments support the view that the enzymatic activity of CD203a produced AMP also by a secondary conversion of ADPR (arising from the breakdown of NAD^+ by CD38), in a CD39-independent manner.

Metabolism of Extracellular AMP

The 5′-NT CD73 is expressed on the surface of select lymphoid cells. Thus, the heterogeneous T cell population composing CIK cells, ought to display AMP-degrading activity toward ADO generation. Indeed, these cells provided the proper phenotypic background with the capacity to degrade extracellular AMP to ADO (see the complete cellular phenotype of CIK cells in **Figure 1**).

HPLC experiments confirmed that CIK cells dephosphorylate extracellular AMP (**Figure 3**). HPLC analysis showed that AMP was dephosphorylated to ADO: AMP ($R_t = 2.35$ min) was metabolized (∼80% within 30 min) by CIK cells resulting in a production of ADO ($R_t = 5.56$ min). Low level of inosine (INO, $R_t = 3.26$ min) was detected in the absence of EHNA (CD26 inhibitor) (not shown). Inhibition experiments further evinced the role of CD73 in the conversion of AMP. When CIK cells were incubated with AMP in the presence of α,β-methylene-ADP (APCP, a CD73 inhibitor), the catabolism of AMP and the formation of ADO were strongly decreased (∼80%). These results indicate that the CD73 was the predominant ectoenzyme participating in ADO generation by CIK cells.

Metabolism of Extracellular ADO

Extracellular ADO may partially accumulate in the culture medium (or tumor extracellular *milieu*) where it binds specific P1 receptors or be internalized through nucleoside transporters. Alternatively, surface adenosine deaminase (ADA), complexed to CD26, converts ADO to INO (**Figure 4B**). PBMC expressed CD26 (6.8%) and during the cytokine-dependent differentiation to CIK cells the molecule raised to 89.4%. We confirmed such feature of CIK cells by measuring the increment of ADO production upon the incubation of these cells with AMP in the presence of EHNA (an inhibitor of ADA). Consequently, ADA on the surface of CIK cells, anchored to the CD26 receptor, offer to a combination of ectoenzymes [CD38 (cyclase/hydrolase), CD203a (NPP) or CD39 (NTDase) along with CD73 (5′-NT)] a machinery for ADO generation (**Figure 4B**). Indeed, results obtained indicated that consumption of 50% of the added ATP produced AMP (20%) and ADO (23%) after 30 min of incubation (**Figure 4A**). The presence of ADO indicated that the ectoenzyme clustering on the surface of CIK cells leaded to the production of the nucleoside. The consumption of NAD^+ by CIK cell in 30 min was, however, kinetically slower. As shown in **Figure 3,** consumed NAD^+ (22%) leaded to the production of 8% of ADPR, 5% of AMP and only 8% of ADO. Taking into consideration that low metabolization of

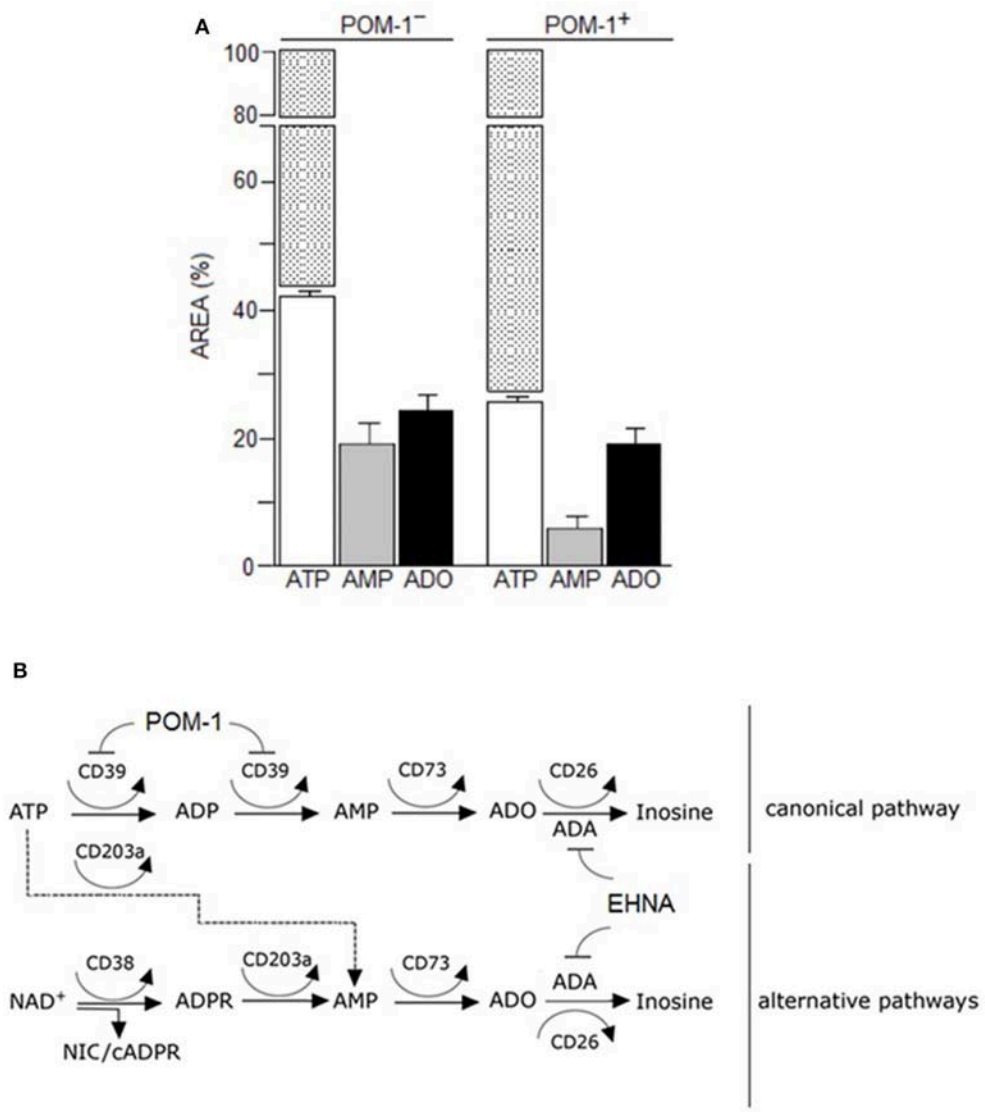

FIGURE 4 | Canonical adenosinergic pathway in CIK cells. **(A)** To prove the existence of ATP adenosinergic pathway in CIK cells, production of ADO was investigated in CIK supernatants collected 30 min after 100 μM ATP addition. White columns indicate the concentration of consumed ATP in the presence or absence of POM-1 (inhibitor of CD39). White/dotted columns indicate the total area of the substrate ATP (100%). Generated products (AMP and ADO) are indicated by grey and black columns, respectively. Data are expressed as area percentage (AREA %) of AMP and ADO. **(B)** Canonical and alternative scheme pathways of ADO production showing the enzymatic targets of POM-1 (inhibitor of CD39) and EHNA (inhibitor of adenosine deaminase, ADA).

AMP as substrate (20%) was paralleled by a high efficiency of ADO production (20%) confirmed the observation of a reduced expression of CD203a. Alternatively, a plausible explanation is a low enzymatic efficiency of CD203a to catalyze the conversion of ADPR into AMP. Accordingly, ADO production by CIK cells using NAD^+ was lower than using ATP either by CD39 or CD203a. In conclusion, CIK cells are equipped with a functional ectoenzymatic machinery leading to ADO production in the extracellular *milieu* (∼25 μmol/min/10^6 cells). However, CIK cells produced low amounts of ADO when incubated with NAD^+, ADPR, AMP, or ATP as substrates in the absence of EHNA (CD26/ADA tandem inhibitor), confirming the presence of ADA (evaluated by measuring the expression of the surrogate CD26 molecule) as shown in **Figure 3**.

Expression of P1 Receptors During CIK Cell Differentiation

Cellular responses to ADO are induced through activation of four subtypes of specific G protein-coupled receptors (A_1R, $A_{2A}R$, $A_{2B}R$, and A_3R) (Chen et al., 2013). Extracellular ADO generated by canonical (CD39/CD73) or alternative (CD38/CD203a/CD73 and CD203a/CD73) pathways, can be captured by the cells, thereby explaining its local signaling. Therefore, next step was

to detect at mRNA and protein levels, the expression of these receptors during CIK cell differentiation. As shown in **Figure 5**, mRNA expression level of $A_{2A}R$, $A_{2B}R$, and A_3R were decreased in CIK cells compared to PBMC, while A_1R expression was not changed ($n = 3$).

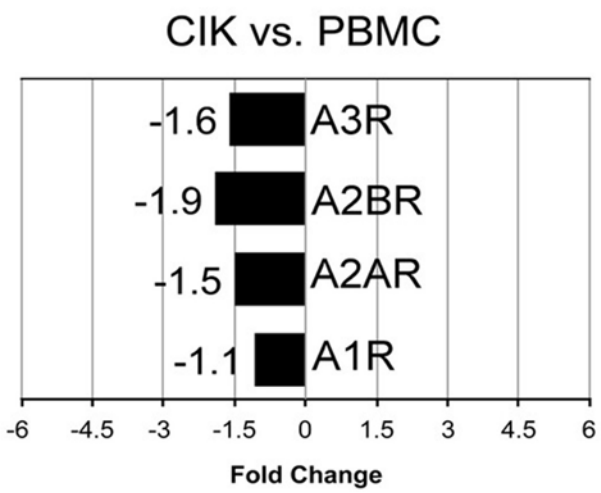

FIGURE 5 | Transcriptome analysis of P1 receptors in CIK cells. mRNA expression of A_1R, $A_{2A}R$, $A_{2B}R$, A_3R was analyzed in PBMC (day 1, absence of INF-γ) and CIK cells (day 14) obtained from 3 GIST patients as described in Materials and Methods.

To further investigate CIK immune regulation mechanisms, we analyzed the expression of ADO receptors at the protein level. Results obtained in additional patients confirmed that CIK cells of further expressed A_1R, $A_{2A}R$, and $A_{2B}R$ (see below), a feature that can be exploited by CIK cells to modulate intracellular cyclic AMP (cAMP). $A_{2A}R$ plays a role in lymphocyte deactivation by ADO and accumulation of high extracellular ADO in the absence of ADA is lymphotoxic (Huang et al., 1997; Burnstock and Boeynaems, 2014). Hence, to support cytotoxic CIK properties, the final product of the adenosinergic reaction might be devoid of an autocrine cAMP-dependent signaling. To comply with this condition, we hypothesized that a CIK active ADA/CD26 complex might scavenge pericellular ADO from the extracellular environment to facilitate their own survival and to protect its cytotoxic activities. In fact, we were unable to detect physiological levels of ADO when HPLC assays were carried in the absence of EHNA, an inhibitor of adenosine deaminase (**Figure 3**).

CIK Cell Ectoenzymes and Purinergic Receptors in Hypoxic Conditions

Hypoxic microenvironment has been shown to be one of the main drivers for the accumulation of ADO in different cancers and in some cases it increases the expression of CD39 and CD73 (Sitkovsky et al., 2014; Allard et al., 2016). CIK cells have a mixed

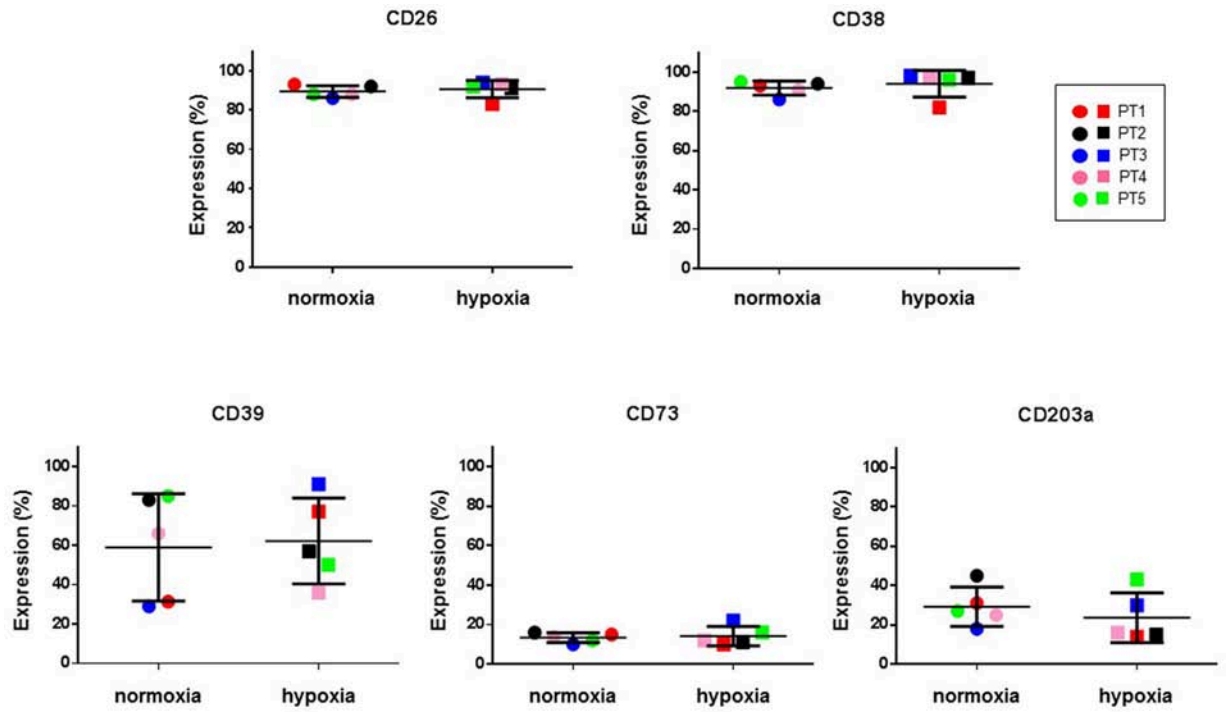

FIGURE 6 | Expression of ectoenzymes in CIK cells under normoxic and hypoxic conditions. Comparative cytofluorimetric analysis of CIK cells stained with primary antibodies to various ectonucleotidases as reported in Materials and Methods. To compare hypoxia and normoxia we used unpaired nonparametric test, two-tailed Mann-Whitney for GraphPad Prism 6. Circles, normoxia; squares, hypoxia. Patients are as following: PT1, red; PT2, black; PT3, blue; PT4, pink; PT5, green. Reported data are expressed as mean values ± SD.

T- and NK cell-like phenotype and ADO has been shown to hamper anti-tumor functions of these cells. For these reasons, the expression of CD39, CD38, CD203a and CD73 was monitored during CIK differentiation of cells from 5 patients, both in normoxic and hypoxic culture conditions. **Figure 6** shows that no significant ($p > 0.05$) differences were evidenced between values obtained in normoxia and hypoxia. ADO receptors are known to suppress immune responses against tumors. Expression analysis of A_1R, $A_{2A}R$, and $A_{2B}R$ was also performed, showing that ADO receptors only underwent minor, non-significant ($p > 0.05$) changes as a consequence of hypoxia (**Figure 7**).

DISCUSSION

Adoptive immunotherapy consists in potentiating the anticancer effects of selected immune populations. CIK cells represent a fundamental advancement in immunotherapy because of their ability to eradicate transformed cells, while sparing normal tissues (Vesely et al., 2011; Gajewski et al., 2013). However, in some cases tumors evade the killing activities of these cells. Numerous attempts are being made to enhance the potency and specificity of CIK cells (Wong et al., 2013).

Purine nucleoside adenosine (ADO) is attributed important roles in physiology and pathology. In immunity, ADO has immunosuppressive functions through activation of P1 purinergic receptors expressed by immune cells. ADO is produced from the dismantling of mono- and dinucleotides (ATP and NAD^+) and their byproducts (ADP, ADPR, AMP) by a set of ectoenzymes (CD39, CD38, CD203a, and CD73), of interest to both basic and clinical research because of their involvement in tumor biology and immune response.

The canonical pathway of ADO production originates from CD39, which metabolizes ATP. However, it was recently demonstrated that CD38 leads to an alternative pathway, whose substrate is NAD^+ (Horenstein et al., 2013). Both pathways converge into AMP, produced either from ATP/ADP (by means of CD39) or from ADPR (by means of CD203a/PC-1). AMP is then converted to ADO by CD73, the bottleneck enzyme for both adenosinergic pathways. These ectoenzymes are expressed by different normal cells (such as immune effectors) and by tumor cells. In the latter instance, these ectoenzymes grant immunosuppressive properties to the tumor cells by means of ligation of adenosine receptors (A_1R, $A_{2A}R$, $A_{2B}R$, and A_3R).

The aim of this study was to investigate expression and function of plasma membrane molecules involved in the adenosinergic pathways in PBMC and CIK cells. Here we showed that CIK cells are characterized by a combination of functional CD38, CD39, CD203a/PC-1, and CD73 ectonucleotidases. Consequently, these cells are potentially able to exploit *ex vivo* the coexistence of the canonical (CD39/CD73) and the alternative (CD38/CD203a/CD73 or CD203a/CD73) pathways. As a result they are able to generate the immunosuppressive purine nucleoside ADO, which either arises from the degradation of ATP or NAD^+ substrates. Accordingly, the substrates (ATP, NAD^+) were added to cell cultures, and their products (ADPR, NIC, AMP, ADO and INO) were quantified in the supernatants by means of a dedicated HPLC assay.

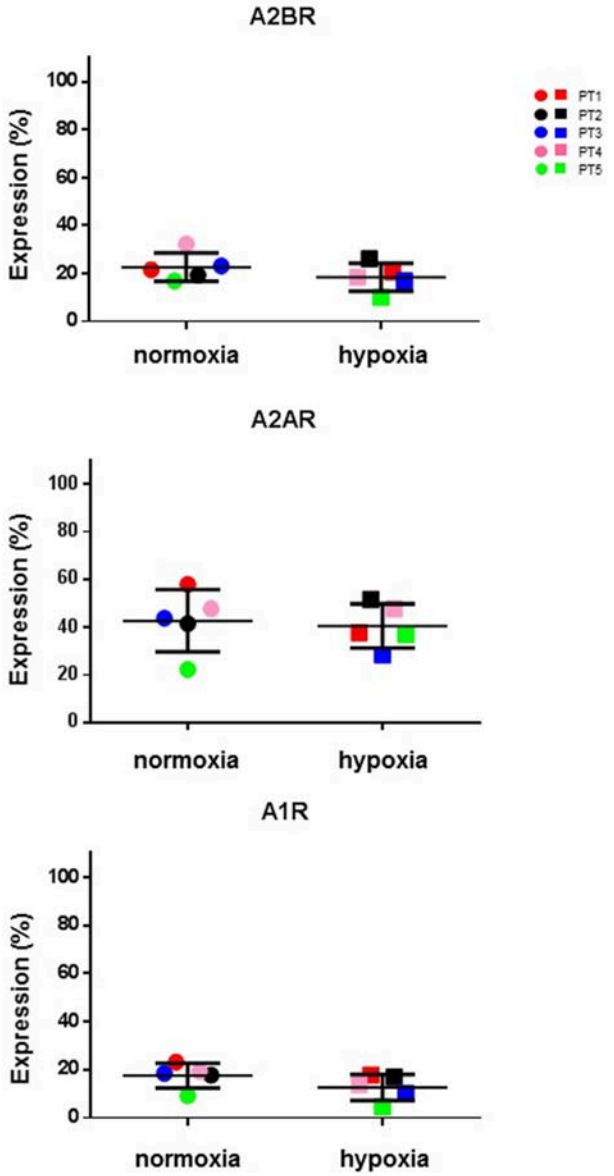

FIGURE 7 | Expression of P1 receptors in normal and hypoxic conditions. Comparative cytofluorometric analysis of A_1R, $A_{2A}R$ and $A_{2B}R$ expression in CIK cells stained with primary antibodies to various P1 receptors and detected with fluorescein (FITC)-conjugated secondary antibodies as reported in Materials and Methods. To compare data obtained in hypoxia and normoxia we used unpaired nonparametric test, two-tailed Mann-Whitney for GraphPad Prism 6. Circles, normoxia; squares, hypoxia. Patients are as following: PT1, red; PT2, black; PT3, blue; PT4, pink; PT5, green. Reported data are expressed as mean values ± SD.

At the head of the alternative network converting extracellular NAD^+ is CD38, a molecule with multiple functions. As an ectoenzyme, CD38 acts as a primary regulator of extracellular NAD^+ levels (Malavasi et al., 2008). The next component in the ectonucleotidase cascade is CD203a, an ectoenzyme initially

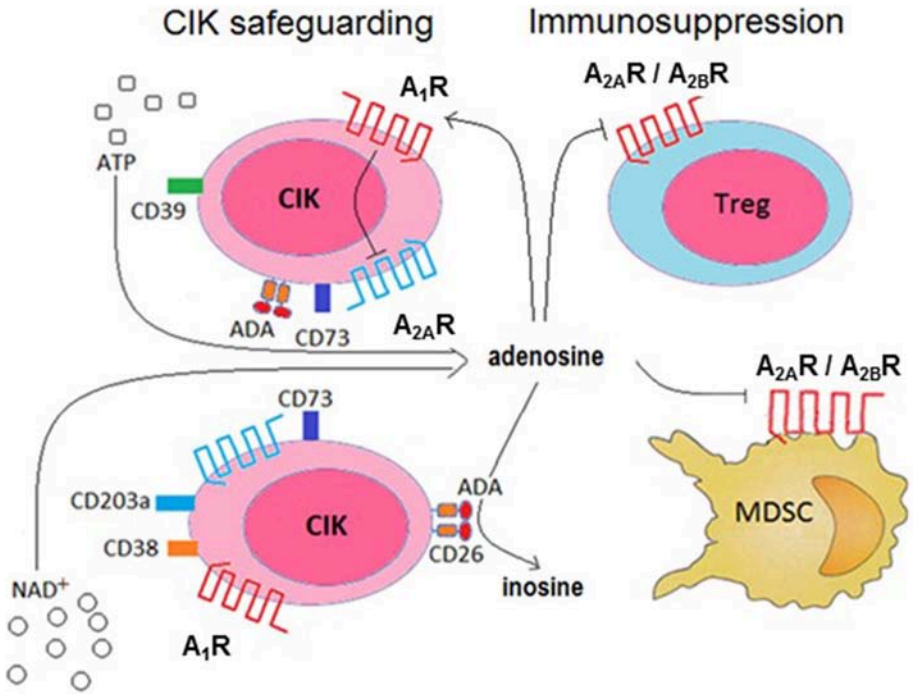

FIGURE 8 | Conceptual model of the role of ADO production, metabolism and receptor ligation in the cytotoxic activity of CIK cells. CIK cells prevent the induction of an autocrine immunosuppression by abrogating $A_{2A}R$-mediated signaling (by A_1R activation) and deamination of ADO catalyzed by the CD26/ADA complex. In turn, ADO produced by CIK cells can reduce pro-cancer immune responses through paracrine cell inhibition (e.g., Treg, MDSC functions).

known as Plasma Cell-1 (PC-1) (Goding et al., 1998). The interactions between extracellular NAD^+ and the CD38/CD203a enzymatic tandem can be exploited by CIK to generate AMP. Indeed, the addition of NAD^+ to CIK cells causes production of ADPR and NIC (products of the enzymatic activity of CD38) and AMP, in the culture supernatants. These results indicate that the outer plasma membrane of CIK cells is equipped with molecules endowed with hydrolytic activities that determine the fate of extracellular NAD^+. Lastly, we demonstrate that ADPR or AMP added exogenously to CIK cell cultures are further metabolized to produce ADO.

Extracellular ADO homeostasis is influenced by the presence of ADA, which irreversibly deaminates ADO, converting it to the related nucleoside inosine. This means that generated ADO is *in vivo* partially transformed by the cells of the surrounding environment, consequently locking the immunosuppressive effects of the nucleoside. Indeed, the low production of ADO in the absence of EHNA (a CD26/ADA inhibitor) is not ascribable to the high expression of ectonucleotidases by CIK cells. There are at least two possible explanations for this lowered production: either up-regulation of the ADA (as inferred by proxy from the increase in its surrogate, CD26) or low expression of CD203a, both of which are observed in differentiated CIK cells. Under such conditions, CIK cells would protect their ability to generate toxic effects against neoplastic cells. The remnant ADO generated by CIK cells in the extracellular medium is however available for binding to P1 purinergic receptors. Alternatively, it can be internalized by nucleoside transporters. This internalization step through the nucleoside transport was not observed in the system analyzed. Indeed, the addition of dipyridamole, an inhibitor of nucleoside transporters, was not followed by an increase in ADO. Things become even more complex considering the finding that CIK cells express high affinity A_1R and $A_{2A}R$. The presence of the two receptors would support the hypothesis that CIK cells take advantage of the P1 receptors to achieve autocrine signaling and thus self-regulation. Indeed, it is known that many cells express more than one purinergic receptor along with nucleotides degrading ectoenzymes, establishing a regulatory membrane network (Volonté et al., 2006). Therefore, trace amount of pericellular ADO may be sufficient to bind and activate (high affinity) $A_{2A}R$ on the surface of CIK cells (inducing a reduction in their immune activity). Nonetheless, $A_{2A}R$ activation is reported as being self-inhibited through the action of A_1R. This effect allow us to postulate that ADO binding to A_1R expressed by CIK cells can induce an autocrine inhibition of the nucleoside immunosuppressive effect, as depicted in **Figure 8**. Extracellular nucleoside concentrations can potentially favor (or suppress) the local immune responses, depending on its concentration as well as the relative abundance of P1 receptor subtypes expressed by CIK cells. These P1 receptor subtypes are coupled to different combinations of G-protein family members, namely A_1 receptors to G_i/G_o, A_{2a} receptors to G_s/G_{olf}, and A_{2b} receptors to G_s/G_q. Accordingly, engagement of A_{2a} and A_{2b} activates adenyl cyclase, leading to elevated levels of cellular cyclic AMP (cAMP). Instead,

A_1 stimulation inhibits adenyl cyclase, resulting in decreased cellular levels of cAMP. Accordingly, the observed biphasic effect of extracellular ADO could be explained by the peculiar functionality of A_1 and A_{2a} receptors (Cunha, 2005; Milne and Palmer, 2011).

It has been reported that hypoxia inhibit the proliferation, cytotoxicity and migration of CIK cells *in vitro* (Shi et al., 2013), hampering the effectiveness of CIK therapy. Moreover, the *ex vivo* infiltration of CIK cells in the hypoxic area is hindered, suggesting that a high expression of the complex CD26/ADA might be a condition *sine-qua-non* to warrant cytotoxicity to infused CIK cells. On this premise, we elaborate a model for CD26/ADA action at the CIK cell surface, where human ADA fine-tune ADO concentrations protecting CIK cells from an ADO mediated inhibition of proliferation. Consequently, this versatile strategy would provide a safety lock of CIK cell cytotoxic activities (**Figure 8**).

Treg cells and mesenchymal derived stromal cells (MDSC) are widely considered immune mediators of peripheral tolerance, playing a pivotal role in limiting anti-tumor immunity (Quarona et al., 2015; Chillemi et al., 2017). Therefore, pathways leading to ADO synthesis on CIK cells may contribute to the induction of paracrine suppression of the Tregs and MDSC immune activities (**Figure 8**).

A *bona fide* conclusion of the present study is that CIK cells are equipped with a surface machinery leading to ADO production. Moreover, CIK cells are characterized by the expression of ADO receptors with high affinity (A_1R and $A_{2A}R$): the activation occurs when ADO reaches 1-3 nM concentrations (Burnstock, 2007). CIK cells may produce microenvironmental ADO concentrations above the affinity constant (Ka) of adenosinergic A_1 and A_{2A} receptors present on the same cells and on immune effectors (e.g., Treg, MDSC). This sequence of events may occur *in situ* in the microenvironment or at a distance. The final outcome is an implementation by CIK cells of an autocrine/paracrine network required for optimal physiological activities. Support for this hypothesis comes from a recent study that showed T helper (Th) 17 cells ($CD26^+$) are also equipped with an adenosinergic machinery, which induces a negative regulation of the immune response of Tregs through the production of ADO (Bailey et al., 2014).

In conclusion, the results of this work consented us to highlight critical functional features of human CIK cells, not appreciated yet. Schematically, CIK cells express (i) a panel of extracellular enzymes involved in nucleotide/nucleoside and NAD^+ metabolism i.e., CD39, CD38, CD203a, and CD73. (ii) The same cells exploit the chain CD26/ADA/ADO to govern the extracellular concentration of ADO. The same effects are likely to be extended at distance, providing negative signals to T lymphocyte populations (De Meester et al., 1999). The results of this work pave the way to verify this hypothesis during the discrete steps of the induction of the CIK cells. Future studies are required to explore the functional implications of our findings within the challenging setting of solid tumors.

AUTHOR CONTRIBUTIONS

AH, FM, and DF: Conceived and designed the experiments; AH, AC, and RZ: Performed the experiments; AH, AC, FM, VQ, NB, and DF: Analyzed the data; FM, RM, and RG: Contributed reagents; AH, FM, and DF: Wrote the paper.

ACKNOWLEDGMENTS

We are thankful to Dr. Sangiolo D., Mesiano G., Grignani G., and Aglietta M for providing biological CIK samples. RZ and RM were financiated by Associazione Italiana per la Ricerca sul Cancro (AIRC), project number #10005 Special Program Molecular Clinical Oncology 5x1000 to AGIMM (AIRC-Gruppo Italiano Malattie Mieloproliferative, http://www.progettoagimm.it); AIRC project number #19818.

REFERENCES

Allard, B., Beavis, P. A., Darcy, P. K., and Stagg, J. (2016). Immunosuppressive activities of adenosine in cancer. *Curr. Opin. Pharmacol.* 29, 7–16. doi: 10.1016/j.coph.2016.04.001

Allard, D., Turcotte, M., and Stagg, J. (2017). Targeting A2 adenosine receptors in cancer. *Immunol. Cell Biol.* 95, 333–339. doi: 10.1038/icb.2017.8

Antonioli, L., Blandizzi, C., Malavasi, F., Ferrari, D., and Haskó, G. (2016a). Anti-CD73 immunotherapy: a viable way to reprogram the tumor microenvironment. *Oncoimmunology* 5:e1216292. doi: 10.1080/2162402X.2016.1216292

Antonioli, L., Yegutkin, G. G., Pacher, P., Blandizzi, C., and Haskó, G. (2016b). Anti-CD73 in cancer immunotherapy: awakening new opportunities. *Trends Cancer.* 2, 95–109. doi: 10.1016/j.trecan.2016.01.003

Bailey, S. R., Nelson, M. H., Himes, R. A., Li, Z., Mehrotra, S., and Paulos, C. M. (2014). Th17 cells in cancer: the ultimate identity crisis. *Front. Immunol.* 5:276. doi: 10.3389/fimmu.2014.00276

Beavis, P. A., Milenkovski, N., Stagg, J., Smyth, M. J., and Darcy, P. K. (2013). A2A blockade enhances anti-metastatic immune responses. *Oncoimmunology* 2:e26705. doi: 10.4161/onci.26705

Burnstock, G. (2007). Purine and pyrimidine receptors. *Cell. Mol. Life. Sci.* 64, 1471–1483. doi: 10.1007/s00018-007-6497-0

Burnstock, G., and Boeynaems, J. M. (2014). Purinergic signalling and immune cells. *Purinergic Signal.* 10, 529–564. doi: 10.1007/s11302-014-9427-2

Chen, J. F., Eltzschig, H. K., and Fredholm, B. B. (2013). Adenosine receptors as drug targets–what are the challenges? *Nat. Rev. Drug Discov.* 12, 265–286. doi: 10.1038/nrd3955

Chillemi, A., Quarona, V., Antonioli, L., Ferrari, D., Horenstein, A. L., and Malavasi, F. (2017). Roles and modalities of ectonucleotidases in remodeling the multiple myeloma niche. *Front. Immunol.* 8:305. doi: 10.3389/fimmu.2017.00305

Costa, F., Toscani, D., Chillemi, A., Quarona, V., Bolzoni, M., Marchica, V., et al. (2017). Expression of CD38 in myeloma bone niche: A rational basis for the use of anti-CD38 immunotherapy to inhibit osteoclast formation. *Oncotarget* 8, 56598–56611. doi: 10.18632/oncotarget.17896

Cunha, R. A. (2005). Neuroprotection by adenosine in the brain: From A1 receptor activation to A2A receptor blockade. *Purinergic Signal.* 1, 111–134. doi: 10.1007/s11302-005-0649-1

Dale, N., and Frenguelli, B. G. (2009). Release of adenosine and ATP during ischemia and epilepsy. *Curr. Neuropharmacol.* 7, 160–179. doi: 10.2174/157015909789152146

De Meester, I., Korom, S., Van Damme, J., and Scharpé, S. (1999). CD26, let it cut or cut it down. *Immunol Today.* 20, 367–375. doi: 10.1016/S0167-5699(99)01486-3

Desmet, C. J., Gallenne, T., Prieur, A., Reyal, F., Visser, N. L., Wittner, B. S., et al. (2013). Identification of a pharmacologically tractable Fra-1/ADORA2B axis promoting breast cancer metastasis. *Proc. Natl. Acad. Sci. U.S.A.* 110, 5139–5144. doi: 10.1073/pnas.1222085110

Ferrari, D., Malavasi, F., and Antonioli, L. (2017). A Purinergic trail for metastases. *Trends Pharmacol. Sci.* 38, 277–290. doi: 10.1016/j.tips.2016.11.010

Franceschetti, M., Pievani, A., Borleri, G., Vago, L., Fleischhauer, K., Golay, J., et al. (2009). Cytokine-induced killer cells are terminally differentiated activated CD8 cytotoxic T-EMRA lymphocytes. *Exp. Hematol.* 37, 616–628.e2. doi: 10.1016/j.exphem.2009.01.010

Fredholm, B. B., IJzerman, A. P., Jacobson, K. A., Klotz, K. N., and Linden, J. (2001). International Union of Pharmacology. XXV. Nomenclature and classification of adenosine receptors. *Pharmacol. Rev*. 53, 527–552.

Gajewski, T. F., Schreiber, H., and Fu, Y. X. (2013). Innate and adaptive immune cells in the tumor microenvironment. *Nat. Immunol.* 14, 1014–1022. doi: 10.1038/ni.2703

Gammaitoni, L., Giraudo, L., Leuci, V., Todorovic, M., Mesiano, G., Picciotto, F., et al. (2013). Effective activity of cytokine-induced killer cells against autologous metastatic melanoma including cells with stemness features. *Clin Cancer Res.* 19, 4347–4358. doi: 10.1158/1078-0432.CCR-13-0061

Garber, K. (2017). Industry 'road tests' new wave of immune checkpoints. *Nat. Biotechnol.* 35, 487–488. doi: 10.1038/nbt0617-487

Giraudo, L., Gammaitoni, L., Cangemi, M., Rotolo, R., Aglietta, M., and Sangiolo, D. (2015). Cytokine-induced killer cells as immunotherapy for solid tumors: current evidences and perspectives. *Immunotherapy* 7, 999–1010. doi: 10.2217/imt.15.61

Goding, J. W., Terkeltaub, R., Maurice, M., Deterre, P., Sali, A., and Belli, S. I. (1998). Ecto-phosphodiesterase/pyrophosphatase of lymphocytes and non-lymphoid cells: structure and function of the PC-1 family. *Immunol Rev.*161, 11–26. doi: 10.1111/j.1600-065X.1998.tb01568.x

Harden, T. K., Sesma, J. I., Fricks, I. P., and Lazarowski, E. R. (2010). Signalling and pharmacological properties of the P2Y receptor. *Acta Physiol.* 199, 149–160. doi: 10.1111/j.1748-1716.2010.02116.x

Hatfield, S. M., and Sitkovsky, M. (2016). A2A adenosine receptor antagonists to weaken the hypoxia-HIF-1α driven immunosuppression and improve immunotherapies of cancer. *Curr. Opin. Pharmacol.* 29, 90–96. doi: 10.1016/j.coph.2016.06.009

Horenstein, A. L., Chillemi, A., Quarona, V., Zito, A., Roato, I., Morandi, F., et al. (2015). NAD^+-Metabolizing ectoenzymes in remodeling tumor-host interactions: the human myeloma model. *Cells* 4, 520–537. doi: 10.3390/cells4030520

Horenstein, A. L., Chillemi, A., Zaccarello, G., Bruzzone, S., Quarona, V., Zito, A., et al. (2013). A CD38/CD203a/CD73 ectoenzymatic pathway independent of CD39 drives a novel adenosinergic loop in human T lymphocytes. *Oncoimmunology* 2:e26246. doi: 10.4161/onci.26246

Horenstein, A. L., Crivellin, F., Funaro, A., Said, M., and Malavasi, F. (2003). Design and scaleup of downstream processing of monoclonal antibodies for cancer therapy: from research to clinical proof of principle. *J. Immunol. Methods.* 275, 99–112. doi: 10.1016/S0022-1759(03)00006-1

Horenstein, A. L., Quarona, V., Toscani, D., Costa, F., Chillemi, A., Pistoia, V., et al. (2016). Adenosine generated in the bone marrow niche through a cd38-mediated pathway correlates with progression of human myeloma. *Mol. Med.* 22, 694–704. doi: 10.2119/molmed.2016.00198

Huang, S., Apasov, S., Koshiba, M., and Sitkovsky, M. (1997). Role of A2a extracellular adenosine receptor-mediated signaling in adenosine-mediated inhibition of T-cell activation and expansion. *Blood.* 90, 1600–1610.

Introna, M., Borleri, G., Conti, E., Franceschetti, M., Barbui, A. M., Broady, R., et al. (2007). Repeated infusions of donor-derived cytokine-induced killer cells in patients relapsing after allogeneic stem cell transplantation: a phase I study. *Haematologica* 92, 952–959. doi: 10.3324/haematol.11132

Introna, M., Golay, J., and Rambaldi, A. (2013). Cytokine Induced Killer (CIK) cells for the treatment of haematological neoplasms. *Immunol. Lett.* 155, 27–30. doi: 10.1016/j.imlet.2013.09.017

Irizarry, R. A., Hobbs, B., Collin, F., Beazer-Barclay, Y. D., Antonellis, K. J., Scherf, U., et al. (2003). Exploration, normalization, and summaries of high density oligonucleotide array prove level data. *Biostatistics* 4, 249–264. doi: 10.1093/biostatistics/4.2.249

Jiang, J., Wu, C., and Lu, B. (2013). Cytokine-induced killer cells promote antitumor immunity. *J. Transl. Med.* 11:83. doi: 10.1186/1479-5876-11-83

Kazemi, M. H., Raoofi Mohseni, S., Hojjat-Farsangi, M., Anvari, E., Ghalamfarsa, G., Mohammadi, H., et al. (2017). Adenosine and adenosine receptors in the immunopathogenesis and treatment of cancer. *J. Cell Physiol.* 233, 2032–2057. doi: 10.1002/jcp.25873

Latini, S., and Pedata, F. (2001). Adenosine in the central nervous system: release mechanisms and extracellular concentrations. *J. Neurochem.* 79, 463–484. doi: 10.1046/j.1471-4159.2001.00607.x

Linn, Y. C., and Hui, K. M. (2010). Cytokine-induced NK-like T cells: from bench to bedside. *J. Biomed. Biotechnol.* 2010:435745. doi: 10.1155/2010/435745

Lu, P. H., and Negrin, R. S. (1994). A novel population of expanded human CD3+CD56+ cells derived from T cells with potent in vivo antitumor activity in mice with severe combined immunodeficiency. *J. Immunol.* 153, 1687–1696.

Malavasi, F., Deaglio, S., Funaro, A., Ferrero, E., Horenstein, A. L., Ortolan, E., et al. (2008). Evolution and function of the ADP ribosyl cyclase/CD38 gene family in physiology and pathology. *Physiol. Rev.* 88, 841–886. doi: 10.1152/physrev.00035.2007

Mesiano, G., Zini, R., Montagner, G., Bianchi, N., Manfredini, R., Chillemi, A., et al. (2017). Analytic and dynamic secretory profile of patient-derived cytokine-induced killer cells. *Mol. Med.* doi: 10.2119/molmed.2017.00084. [Epub ahead of print].

Milne, G. R., and Palmer, T. M. (2011). Anti-inflammatory and immunosuppressive effects of the A2A adenosine receptor. *Sci. World J.* 11, 320–339. doi: 10.1100/tsw.2011.22

Mittal, P., Klingler-Hoffmann, M., Arentz, G., Winderbaum, L., Kaur, G., Anderson, L., et al. (2017). Annexin A2 and alpha actinin 4 expression correlates with metastatic potential of primary endometrial cancer. *Biochim. Biophys Acta.* 1865, 846–857. doi: 10.1016/j.bbapap.2016.10.010

Morandi, F., Morandi, B., Horenstein, A. L., Chillemi, A., Quarona, V., Zaccarello, G., et al. (2015). A non-canonical adenosinergic pathway led by CD38 in human melanoma cells induces suppression of T cell proliferation. *Oncotarget* 6, 25602–25618. doi: 10.18632/oncotarget.4693

Pievani, A., Borleri, G., Pende, D., Moretta, L., Rambaldi, A., Golay, J., et al. (2011). Dual-functional capability of CD3+CD56+ CIK cells, a T-cell subset that acquires NK function and retains TCR-mediated specific cytotoxicity. *Blood* 118, 3301–3310. doi: 10.1182/blood-2011-02-336321

Plattner, H., and Verkhratsky, A. (2016). Inseparable tandem: evolution chooses ATP and Ca2+ to control life, death and cellular signalling. *Philos. Trans. R Soc. Lond. B Biol. Sci.* 371:20150419. doi: 10.1098/rstb.2015.0419

Praetorius, H. A., and Leipziger, J. (2010). Intrarenal purinergic signaling in the control of renal tubular transport. *Annu. Rev. Physiol.* 72, 377–393. doi: 10.1146/annurev-physiol-021909-135825

Quarona, V., Ferri, V., Chillemi, A., Bolzoni, M., Mancini, C., Zaccarello, G., et al. (2015). Unraveling the contribution of ectoenzymes to myeloma life and survival in the bone marrow niche. *Ann. N.Y. Acad. Sci.* 1335, 10–22. doi: 10.1111/nyas.12485

Sanchez, L., Wang, Y., Siegel, D. S., and Wang, M. L. (2016). Daratumumab: a first-in-class CD38 monoclonal antibody for the treatment of multiple myeloma. *J. Hematol. Oncol.* 9:51. doi: 10.1186/s13045-016-0283-0

Sangiolo, D., Mesiano, G., Gammaitoni, L., Leuci, V., Todorovic, M., Giraudo, L., et al. (2014). Cytokine-induced killer cells eradicate bone and soft-tissue sarcomas. *Cancer Res.* 74, 119–129. doi: 10.1158/0008-5472.CAN-13-1559

Schmid, S., Kübler, M., Korcan Ayata, C., Lazar, Z., Haager, B., Hoßfeld, M., et al. (2015). Altered purinergic signaling in the tumor associated immunologic microenvironment in metastasized non-small-cell lung cancer. *Lung Cancer.* 90, 516–521. doi: 10.1016/j.lungcan.2015.10.005

Schmidt-Wolf, I. G., Negrin, R. S., Kiem, H. P., Blume, K. G., and Weissman, I. L. (1991). Use of a SCID mouse/human lymphoma model to evaluate cytokine-induced killer cells with potent antitumor cell activity. *J. Exp. Med.* 174, 139–149. doi: 10.1084/jem.174.1.139

Shallis, R. M., Terry, C. M., and Lim, S. H. (2017). The multi-faceted potential of CD38 antibody targeting in multiple myeloma. *Cancer Immunol. Immunother.* 66, 697–703. doi: 10.1007/s00262-017-1990-2

Shi, S., Wang, R., Chen, Y., Song, H., Chen, L., and Huang, G. (2013). Combining antiangiogenic therapy with adoptive cell immunotherapy exerts

better antitumor effects in non-small cell lung cancer models. *PLoS ONE* 8:e65757. doi: 10.1371/journal.pone.0065757

Shryock, J. C., and Belardinelli, L. (1997). Adenosine and adenosine receptors in the cardiovascular system: biochemistry, physiology, and pharmacology. *Am. J. Cardiol.* 79, 2–10. doi: 10.1016/S0002-9149(97)00256-7

Silva, C. L. M. (2016). Purinergic signaling in schistosomal infection. *Biomed. J.* 39, 316–325. doi: 10.1016/j.bj.2016.06.006

Sitkovsky, M. V., Hatfield, S., Abbott, R., Belikoff, B., Lukashev, D., and Ohta, A. (2014). Hostile, hypoxia-A2-adenosinergic tumor biology as the next barrier to overcome for tumor immunologists. *Cancer Immunol. Res.* 2, 598–605. doi: 10.1158/2326-6066.CIR-14-0075

Stagg, J., and Smyth, M. J. (2010). Extracellular adenosine triphosphate and adenosine in cancer. *Oncogene* 29, 5346–5358. doi: 10.1038/onc.2010.292

Surprenant, A., and North, R. A. (2009). Signaling at purinergic P2X receptors. *Annu. Rev. Physiol.* 71, 333–359. doi: 10.1146/annurev.physiol.70.113006.100630

Valgardsdottir, R., Capitanio, C., Texido, G., Pende, D., Cantoni, C., Pesenti, E., et al. (2014). Direct involvement of CD56 in cytokine-induced killer-mediated lysis of CD56(+) hematopoietic target cells. *Exp. Hematol.* 42, 1013–21.e1. doi: 10.1016/j.exphem.2014.08.005

Vesely, M. D., Kershaw, M. H., Schreiber, R. D., and Smyth, M. J. (2011). Natural innate and adaptive immunity to cancer. *Annu. Rev. Immunol.* 29, 235–271. doi: 10.1146/annurev-immunol-031210-101324

Volonté, C., Amadio, S., D'Ambrosi, N., Colpi, M., and Burnstock, G. (2006). P2 receptor web: complexity and fine-tuning. *Pharmacol. Ther.* 112, 264–280. doi: 10.1016/j.pharmthera.2005.04.012

Wang, L., Zhou, X., Zhou, T., Ma, D., Chen, S., Zhi, X., et al. (2008). Ecto-5′-nucleotidase promotes invasion, migration and adhesion of human breast cancer cells. *J. Cancer Res. Clin. Oncol.* 134, 365–372. doi: 10.1007/s00432-007-0292-z

Wong, H. C., Jeng, E. K., and Rhode, P. R. (2013). The IL-15-based superagonist ALT-803 promotes the antigen-independent conversion of memory CD8(+) T cells into innate-like effector cells with antitumor activity. *Oncoimmunology* 2:e26442. doi: 10.4161/onci.26442

Yegutkin, G. G. (2008). Nucleotide- and nucleoside-converting ectoenzymes: Important modulators of purinergic signalling cascade. *Biochim. Biophys. Acta.* 1783, 673–694. doi: 10.1016/j.bbamcr.2008.01.024

Young, A., Mittal, D., Stannard, K., Yong, M., Teng, M. W., Allard, B., et al. (2014). Co-blockade of immune checkpoints and adenosine A2A receptor suppresses metastasis. *Oncoimmunology* 3:e958952. doi: 10.4161/21624011.2014.958952

Zimmermann, H., Zebisch, M., and Sträter, N. (2012). Cellular function and molecular structure of ecto-nucleotidases. *Purinergic Signal.* 8, 437–502. doi: 10.1007/s11302-012-9309-4

Conflict of Interest Statement: The authors declare that the research was conducted in the absence of any commercial or financial relationships that could be construed as a potential conflict of interest.

frontiers in Pharmacology

ORIGINAL RESEARCH
published: 19 April 2018
doi: 10.3389/fphar.2018.00242

The $P2Y_{12}$ Receptor Antagonist Ticagrelor Reduces Lysosomal pH and Autofluorescence in Retinal Pigmented Epithelial Cells From the $ABCA4^{-/-}$ Mouse Model of Retinal Degeneration

*Wennan Lu[1], Néstor M. Gómez[1], Jason C. Lim[1], Sonia Guha[1,2], Ann O'Brien-Jenkins[1], Erin E. Coffey[1], Keith E. Campagno[1], Stuart A. McCaughey[1], Alan M. Laties[2], Leif G. Carlsson[3] and Claire H. Mitchell[1,4,5]**

[1] Department of Anatomy and Cell Biology, University of Pennsylvania, Philadelphia, PA, United States, [2] Jules Stein Eye Institute, University of California, Los Angeles, Los Angeles, CA, United States, [3] Department of Bioscience Heart Failure, Cardiovascular, Renal and Metabolic Diseases, IMED Biotech Unit, AstraZeneca, Gothenburg, Sweden, [4] Department of Ophthalmology, University of Pennsylvania, Philadelphia, PA, United States, [5] Department of Physiology, University of Pennsylvania, Philadelphia, PA, United States

OPEN ACCESS

Edited by:
Kenneth A. Jacobson,
National Institutes of Health (NIH),
United States

Reviewed by:
Alexander Oksche,
Mundipharma Research,
United Kingdom
Long-Jun Wu,
Mayo Clinic, United States

***Correspondence:**
Claire H. Mitchell
chm@upenn.edu

Specialty section:
This article was submitted to Experimental Pharmacology and Drug Discovery, a section of the journal Frontiers in Pharmacology

Received: 09 November 2017
Accepted: 05 March 2018
Published: 19 April 2018

Citation:
Lu W, Gómez NM, Lim JC, Guha S, O'Brien-Jenkins A, Coffey EE, Campagno KE, McCaughey SA, Laties AM, Carlsson LG and Mitchell CH (2018) The $P2Y_{12}$ Receptor Antagonist Ticagrelor Reduces Lysosomal pH and Autofluorescence in Retinal Pigmented Epithelial Cells From the $ABCA4^{-/-}$ Mouse Model of Retinal Degeneration. Front. Pharmacol. 9:242. doi: 10.3389/fphar.2018.00242

The accumulation of partially degraded lipid waste in lysosomal-related organelles may contribute to pathology in many aging diseases. The presence of these lipofuscin granules is particularly evident in the autofluorescent lysosome-associated organelles of the retinal pigmented epithelial (RPE) cells, and may be related to early stages of age-related macular degeneration. While lysosomal enzymes degrade material optimally at acidic pH levels, lysosomal pH is elevated in RPE cells from the $ABCA4^{-/-}$ mouse model of Stargardt's disease, an early onset retinal degeneration. Lowering lysosomal pH through cAMP-dependent pathways decreases accumulation of autofluorescent material in RPE cells *in vitro*, but identification of an appropriate receptor is crucial for manipulating this pathway *in vivo*. As the $P2Y_{12}$ receptor for ADP is coupled to the inhibitory G_i protein, we asked whether blocking the $P2Y_{12}$ receptor with ticagrelor could restore lysosomal acidity and reduce autofluorescence in compromised RPE cells from $ABCA4^{-/-}$ mice. Oral delivery of ticagrelor giving rise to clinically relevant exposure lowered lysosomal pH in these RPE cells. Ticagrelor also partially reduced autofluorescence in the RPE cells of $ABCA4^{-/-}$ mice. *In vitro* studies in ARPE-19 cells using more specific antagonists AR-C69931 and AR-C66096 confirmed the importance of the $P2Y_{12}$ receptor for lowering lysosomal pH and reducing autofluorescence. These observations identify $P2Y_{12}$ receptor blockade as a potential target to lower lysosomal pH and clear lysosomal waste in RPE cells.

Keywords: $P2Y_{12}$ receptor, ticagrelor, age-related macular degeneration, lysosomal pH, retinal pigment epithelium, lysosomal storage diseases

INTRODUCTION

In some aging diseases, the accumulation of autofluorescent lipofuscin granules can signify an impaired clearance of waste material by lysosomes. Many degradative lysosomal enzymes are pH sensitive, with optimal activity in acidic environments. Lysosomal alkalinization has been detected in models of neural degenerative diseases of accumulation, such as early-onset Alzheimer's disease (Lee et al., 2010, 2015; Coffey et al., 2014) and Stargardt's retinal dystrophy (Liu et al., 2008).

Retinal pigmented epithelial (RPE) cells are particularly sensitive to perturbations in lysosomal enzyme activity, as they are responsible for phagocytosing the lipid-rich photoreceptor outer segment (POS) tips that are shed daily. The accumulation of autofluorescent lipofuscin waste may contribute to the early pathological changes leading age-related macular degeneration (AMD); dry geographic atrophy and wet neovascularization forms of AMD are now thought to stem from the intermediate AMD stage, where RPE cells are characterized by the accumulation of intracellular lipofuscin and extracellular drusen debris (Ferris et al., 2013). The accumulation of lipofuscin in RPE cells is associated with increases in the retinoid by-product *N*-retinylidene-*N*-retinylethanolamine (A2E), and A2E levels are increased in RPE cells from the ABCA4$^{-/-}$ mouse model of recessive Stargardt's retinopathy (Charbel Issa et al., 2013). Furthermore, A2E can lead to elevation of lysosomal pH, although the delay between drug application and alkalinization suggests an indirect pathway (Holz et al., 1999; Liu et al., 2008; Toops et al., 2015). This alkalinization may reduce lysosomal activity and contribute to a secondary accumulation of oxidized lipid waste.

Restoring an acidic environment to compromised lysosomes in RPE cells is predicted to enhance activity of pH-sensitive lysosomal enzymes and improve degradation, thus reducing the pathologies associated with accumulation of waste material (Guha et al., 2014a). While several pathways capable of acidifying compromised lysosomes and improving degradative function have been identified in RPE cells, manipulation of cytoplasmic cAMP was particularly effective (Liu et al., 2008). Drugs targeting receptors coupled to stimulatory G protein (G_s) reduced lysosomal pH and enhanced the clearance of lysosomal waste and opsin turnover in RPE cells fed POSs (Liu et al., 2008; Guha et al., 2012). Importantly, this approach was also effective at lowering lysosomal pH when given to RPE cells isolated from ABCA4$^{-/-}$ mice (Liu et al., 2012; Guha et al., 2014a). While these *in vitro* experiments provided proof of concept that drugs linked to cAMP could lower lysosomal pH and enhance lysosomal degradation, the *in vivo* translation of this approach required identification of the appropriate receptor target.

Several factors make the P2Y$_{12}$ receptor antagonist ticagrelor (Brilinta) an attractive choice to target lysosomal accumulations in RPE cells. As the P2Y$_{12}$ receptor for adenosine di-phosphate (ADP) is coupled to G_i, antagonizing the P2Y$_{12}$ raises cAMP (Cattaneo, 2015). Several P2Y$_{12}$ receptor antagonists are widely used as antithrombotic agents and are approved for use in elderly patients (McFadyen et al., 2018). Ticagrelor is a reversible allosteric P2Y$_{12}$ receptor antagonist that does not require hepatic activation, removing complications associated with genetic variants of the enzyme CYP2C19 common with other P2Y$_{12}$ antagonists used clinically (Birkeland et al., 2010; Tantry et al., 2010). Ticagrelor is broadly utilized clinically to reduce the rate of thrombotic cardiovascular events in patients with acute coronary syndrome or a history of myocardial infarction (Storey et al., 2010; Bonaca et al., 2016). Finally, the P2Y$_{12}$ receptor is expressed in cultured human ARPE-19 cells (Reigada et al., 2005). In this initial study, we examined whether ticagrelor lowers lysosomal pH and reduce lysosomal autofluorescence in RPE cells from the ABCA4$^{-/-}$ mouse model of retinal degeneration.

MATERIALS AND METHODS

Animal Care and Use

All procedures were approved by the University of Pennsylvania IACUC in compliance with the Public Health Service Policy on Humane Care and Use of Laboratory Animals. C57BL/6J and ABCA4$^{-/-}$ mice were reared at 5–15 lux and sacrificed using CO_2. C57BL/6J mice were obtained from Jackson Laboratories (Bar Harbor, ME, United States). ABCA4$^{-/-}$ mice were obtained from Dr. Gabriel Travis of UCLA. All mice were negative for the RD8 mutation (Goméz et al., 2018). Mouse eyes were isolated and RPE cells processed as described previously (Liu et al., 2012).

P2Y$_{12}$ Receptor Pharmacological Agents

Ticagrelor was delivered in food or water at concentrations relevant to those used clinically in humans. The recommended maintenance dosage for ticagrelor (AZD6140) in humans of approximate mass of 90 kg is 180 mg per day; thus 2 mg/kg translated to 0.06 mg per diem for a 30 g mouse. Clinically dosed ticagrelor tablets (90 mg, Lot # YK0083 from the University of Pennsylvania pharmacy) were powdered and initially dissolved in water at 12 μg/ml to give 0.06 mg per diem, based on a mean water consumption of 5 ml per diem. (The concentration was adjusted to 10 μg/ml for later experiments to match the stated solubility more precisely, although precipitate was not detected in either concentration.) The solution was administered in tinted light-resistant bottles wrapped with black paper and refreshed every 1–2 days for 5–19 days. No clear correlation was found between exposure time or concentration, and lysosomal pH signal. Ticagrelor was delivered in food using a custom mouse diet containing 0.1% ticagrelor in Purina Lab Meal 5001 was made by MP Biomedicals (Lot #P9748, Santa Ana, CA, United States) from purified drug provided by AstraZeneca. Untreated food pellets or those containing 0.1% ticagrelor were added at 100–200 g every week and the remainder weighed to determine total food consumption. Ticagrelor has a pIC_{50} at the human P2Y$_{12}$ receptor of 8.0 (Nylander and Schulz, 2016). The pIC_{50} of ticagrelor in an ADP-induced whole blood platelet aggregation assay in humans is 6.6, similar to that in mouse. Ticagrelor is reported to be quickly absorbed from the gut, reaching a peak concentration in 1.5 h, with blood plasma levels linearly dependent on the dose (Goel, 2013).

MeS-ADP; 2-(Methylthio)adenosine 5′-diphosphate (catalogue #1624, Tocris Bio-Techne Corporation, Minneapolis, MN, United States), which has a pIC_{50} of 8.2 and 7.9 at the $P2Y_1$ and $P2Y_{12}$ receptors, respectively (Jacobson et al., 2009), was supplied pre-dissolved in water at 10 mM and diluted. AR-C66931; N^6-(2-methylthioethyl)-2-(3,3,3-trifluoropropylthio)-β,γ-dichloromethylene-ATP (a.k.a cangrelor, catalogue #5720 Tocris) with a pIC_{50} of 9.4 (Jacobson et al., 2009), was stored as a 10 mM stock solution in water. AR-C66096; 2-propylthio-betagamma-difluoromethylene ATP tetrasodium salt (catalogue #3321, Tocris) inhibits ADP-induced aggregation of washed human platelets pIC_{50} = 8.16 and was supplied pre-dissolved at a concentration of 10 mM.

Measurement of Lysosomal pH From RPE Cells

Lysosomal pH was measured as described using the dye LysoSensor Yellow/Blue DND-160 (Liu et al., 2012). In brief, RPE cells from pairs of treated and untreated mice were isolated, loaded with LysoSensor Yellow/Blue 160 DSN, washed, and loaded into wells of a plate reader; the autofluorescence in these cells was previously found to be negligible in cells loaded with LysoSensor 160 DSN (Liu et al., 2008). The limited number of cells precluded calibration to absolute pH, so data were analyzed as the ratio of light excited at 340 vs. 380 nm, an index of lysosomal pH (Guha et al., 2014a). Lysosomal pH measurements were made with UV-Star 384-well plates (Grenier Bio One) to minimize the disruption of the signal at 340 nm. As these ratios can vary from experiment to experiment, values were normalized to enable results from multiple trials to be combined. Lysosomal pH was determined from cultured ARPE-19 cells as described (Guha et al., 2013).

Polymerase Chain Reaction (PCR)

Total RNA was isolated from fresh mouse RPE/choroid cells using Trizol and the RNeasy mini kit (Qiagen, Inc.). RNA yield was determined by nanodrop 2000 spectrophotometer; 100 ng of total RNA was converted into cDNA using High Capacity RNA-to-cDNA kit (#4387406, Applied Biosystems). Primer pairs for mouse $P2Y_{12}$: Forward: CATTGCTGTACACCGTCCTG; Reverse: AACTTGGCACACCAAGGTTC; 212-bp product. PCR was performed with 2 μl first-strand DNA synthesis product, 50 mM $MgCl_2$, and10 μM of each primer with the 0.5 μl first recombinant DNA polymerase (Platinum® *Taq* DNA Polymerase; Applied Biosystems) at 95°C for 10 min, followed by 35 cycles at 95°C for 30 s, 60°C for 45 s, and 72°C for 1 min, with a final extension step at 72°C for 10 min. First-strand DNA synthesis was omitted from the negative control. Quantitative PCR (qPCR) was performed on isolated RPE/choroid from 16 month old C57BL6J or ABCA4$^{-/-}$ mice. Total RNA (100 ng) was reverse transcribed and qPCR was performed using SYBR Green and the 7300 RealTimePCR system (Applied Biosystems, Corp.) as described (Lu et al., 2017) using the following primers: A1AR- F: ATCCCTCTCCGGTACAAGACAGT, R: ACTCAGG TTGTTCCAGCCAAAC (Streitova et al., 2010); A3AR- F: AC TTCTATGCCTGCCTTTTCATGT, R: AACCGTTCTATATCTG ACTGTCAGCTT (Streitova et al., 2010); CFH- F:ACCACATGT GCCAAATGCTA; R:TGTTGAGTCTCGGCACTTTG (Radu et al., 2014); ENT1- F:CTTGGGATTCAGGGTCAGAA, R: ATC AGGTCACACGACACCAA (Eckle et al., 2013); P2Y12- F: CA TTGCTGTACACCGTCCTG, R: AACTTGGCACACCAAGG TTC (Veitinger et al., 2011). Data were analyzed using the delta-delta CT approach, with results expressed as fold change in gene expression.

Microscopy and Immunocytochemistry

Freshly isolated RPE cells from C57Bl6J mice were cultured for 1 day and fixed in 4% paraformaldehyde (PFA), rinsed with Duebcco's phosphate buffered saline (DPBS), permeabilized at room temperature in 0.1% Triton X-100 for 10 min, then blocked with 10% goat serum in SuperBlock blocking buffer (#37515, Thermo Fisher Scientific) for 60 min. Anti-mouse $P2Y_{12}$ antibody (1:50 dilution, #AS-55043A, AnaSpec, Inc., Fremont, CA, United States) was added overnight at 4°C, followed by incubation in donkey anti-rabbit Alexa-Fluor 568 (1:500 dilution; Invitrogen, Carlsbad, CA, United States). Slides were mounted in Slow Fade Gold Antifade Mountant (Thermo Fisher Scientific) and imaged using a Nikon Eclipse 600 microscope (Nikon USA, Melville, NY, United States). To quantify the autofluorescence found in RPE whole mounts from ABCA4$^{-/-}$ mice, images were obtained at 488 nm ex/>540 nm em from 16 regions using a Nikon Eclipse 600 microscope and autofluorescence was measured using the Nikon Elements software. Spectral analysis of RPE cells in ABCA4$^{-/-}$ mice was performed on 7 μm thick sections from the central 1/3rd of the retina following standard fixation (Albalawi et al., 2017) using the Nikon A1R Laser Scanning Confocal Microscope and Nikon NIS-Elements software package at the University of Pennsylvania Live Cell Imaging Core. The endogenous autofluorescent spectral profile of ABCA4$^{-/-}$ mouse RPE was collected after excitation by 406, 488, 561, and 639 lasers. The RPE layer was visualized with a 60X objective and emission was determined in 2.5 nm wide bins throughout the spectrum, grouped into 32 bins per sweep. Confocal scan settings were maintained from sample to sample, and pairs of treated and untreated sections were processed in parallel when possible to minimize day-to-day variations. ROI's were drawn along the RPE layer and corresponding emission levels were exported for analysis.

ARPE-19 Cell Culture

ARPE-19 cells (American Tissue Type Collection, Manassas, VA, United States) were grown as described previously (Reigada et al., 2005). In brief, cells were grown in 1:1 mixture of Dulbecco's modified Eagle's medium (DMEM) and Ham's F12 medium with 3 mM L-glutamine, 100 g/ml streptomycin and 10% FBS (all Thermo Fisher Scientific, Inc., Waltham, MA, United States). Cells were incubated at 37°C in 5% CO_2 and subcultured weekly with 0.05% trypsin and 0.02% ethylenediaminetetraacetic acid (EDTA).

In Vitro Autofluorescence Model

ARPE-19 cells were grown to confluence in 6-well plates, then treated with the pulse chase chloroquine/POS protocol as

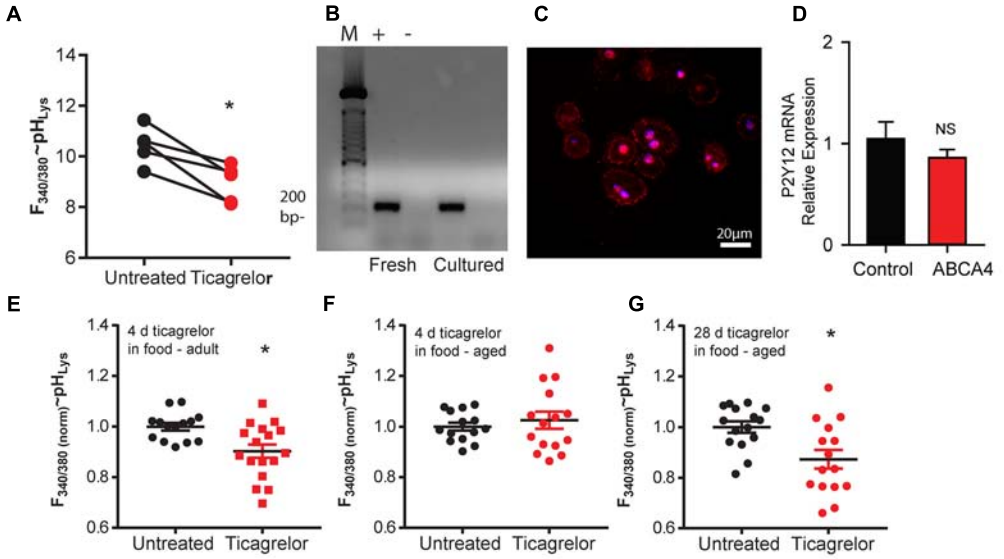

FIGURE 1 | Ticagrelor lowers lysosomal pH in ABCA4$^{-/-}$ mice. **(A)** Decline in the ratio of LysoSensor YellowBlue DNS 160 fluorescence excited at 340 vs. 380 nm in freshly isolated RPE cells from 20-month old untreated ABCA4$^{-/-}$ mice (black circles) and those treated with 10–12 μg/ml ticagrelor in water (red squares). As mice were processed in pairs in individual days, lines connect mean measurements from treated and untreated pairs processed in parallel. *p = 0.029, n = 5, each circle represents the mean of 5–6 wells. **(B)** RT-PCR (+) shows P2Y$_{12}$ receptor expression in RPE cells freshly isolated from mouse eyes (Fresh) or after 3 days in cell culture (Cultured). Bands are at the expected size of 212 bp. No product was detected when reverse transcriptase was omitted from the reaction (–). M-markers at 100 bp (see Supplementary Figure 3 for full gel). **(C)** Immunohistochemistry indicating expression of P2Y$_{12}$ near the cell membrane of freshly isolated RPE cells from 9-month-old C57BL/6J mice. **(D)** Results from quantitative PCR assessment indicating there is no significant (NS) difference between expression of P2Y$_{12}$ receptor mRNA from RPE/choroid of C57BL/6J (n = 4) and ABCA4$^{-/-}$ mice (n = 3). **(E)** Ticagrelor added to a custom diet (0.1%) for 4 days was sufficient to lower lysosomal pH in RPE cells from ABCA4$^{-/-}$ mice 7–8 months old (adult) (*p = 0.0054, n = 14–17 measurements from three mice each condition). **(F)** Exposure to ticagrelor in food for 4 days did not reduce the mean signal in RPE cells from ABCA4$^{-/-}$ mice aged 18–24 months (Old) (p = 0.514, n = 14–15 measures from three mice each condition). **(G)** Extending ticagrelor treatment to 28 days was sufficient to reduce lysosomal pH in the older mice (*p = 0.0066, n = 15 measures from three mice each condition). Throughout, data are expressed as scatter plot with mean ± SEM of the ratio of light excited at 340/380 nm; values were normalized to the mean control for each day to account for differences in LysoSensor dye loading.

described (Guha et al., 2012). Cells were incubated with 2 ml POS for 2 h; POS were isolated as previously described (Liu et al., 2012). Cells were washed thoroughly with medium to remove non-internalized POS followed by a 2 h chase in DMEM/F12. Subsequently, the medium was removed and the cells incubated for 20 h with one of the following solutions: DMEM/F12, 10 μM CHQ, CHQ + 10 μM AR-C66096. This protocol was repeated daily. After 6 days the cells were repeatedly washed, detached with trypsin, and analyzed on a flow cytometer (FACS Calibur; BD Biosciences, Heidelberg, Germany) at the Penn PDM Flow Cytometry Facility. The FITC channel (excitation laser wavelength, 488 nm; detection filter wavelength, 530 nm) was used with a gate set to exclude cell debris and cell clusters.

Magic Red Staining

Magic Red powder was reconstituted as per the manufacturer's instructions (Bio-Rad, Inc., Hercules, CA, United States). ARPE-19 cells grown on coverslips were exposed to 10 μM tamoxifen or control solution. Magic Red was diluted into PBS 1:26 and applied to the cells for 30 min, followed by a 5 min incubation of 50 nM LysoTracker Green. Magic Red was visualized at 540 nm ex and LysoTracker Green at 488 nm using the Nikon Eclipse 600, as above.

Data Analysis

All data are given as mean ± standard error of the mean. Analysis was performed using SigmaStat (Systat Software, Inc., San Jose, CA, United States) and/or GraphPad Software, Inc. (La Jolla, CA, United States). Differences between treatments were analyzed using a one-way analysis of variance (ANOVA) with indicated *post hoc* tests as appropriate, or a Student's *t*-test using unpaired or paired configuration where appropriate.

RESULTS

Systemic Delivery of P2Y$_{12}$ Antagonist Ticagrelor Lowers Lysosomal pH in RPE Cells From ABCA4$^{-/-}$ Mice

Initial experiments to determine whether ticagrelor decreased lysosomal pH in RPE cells from ABCA4$^{-/-}$ mice were carried out by adding ticagrelor to the drinking water. Mice were given free access to drinking water only or water containing 10–12 μg/ml ticagrelor for 4–19 days. Fresh solution was provided every 1–2 days. Measurements of remaining water suggested ticagrelor did not alter consumption. Age- and gender-matched ABCA4$^{-/-}$ mice used for this experiment examined

daily appeared healthy and exhibited normal behavior with no increased bleeding events noted. Previous work suggest lysosomal pH must be measured from freshly isolated RPE cells from ABCA4$^{-/-}$ mice, as the effect of lipofuscin on the lysosomal pH is altered by each cell division (Guha et al., 2014a). As such, lysosomal pH levels could only be determined accurately from only pair of one untreated and one treated mouse per day.

Ticagrelor acidified the lysosomes of RPE cells from ABCA4$^{-/-}$ mice. The lysosomal pH signal was reduced in RPE cells from treated mice as compared to untreated mice in all pairs examined, leading to a significant decline when averaged together (**Figure 1A**). The presence of the P2Y$_{12}$ receptor in mouse RPE cells was confirmed at the mRNA level (**Figure 1B**) and using immunocytochemistry; expression was concentrated near the cell membrane consistent with a membrane-associated receptor (**Figure 1C**). Quantitative PCR indicated no difference in the expression of P2Y$_{12}$ mRNA in RPE cells from C57BL/6J and ABCA4$^{-/-}$ mice (**Figure 1D**).

In a separate study, ticagrelor was added to the mouse chow to confirm the ability of oral delivery to lower lysosomal pH in the RPE cells of ABCA4$^{-/-}$ mice. Four days of exposure lowered the lysosomal pH in 7–8 month-old adult ABCA4$^{-/-}$ mice, as compared to untreated mice (**Figure 1E**). Four days of treatment did not alter the lysosomal pH of RPE cells from 18 to 24 month-old mice compared to untreated controls (**Figure 1F**), but extending treatment to 28 days significantly reduced lysosomal pH in these older mice (**Figure 1G**). Plasma levels of ticagrelor in the mice treated with ticagrelor in food were 0.89 ± 0.07 μM (n = 13) and were undetectable in untreated mice.

P2Y$_{12}$ Receptor Regulates Lysosomal pH *in Vitro*

The ability of ticagrelor to lower lysosomal pH was tested directly *in vitro* in the ARPE-19 cultured human cell line. The P2Y$_{12}$ agonist Mes-ADP raised lysosomal pH in these cells (**Figure 2A**). Addition of ticagrelor (**Figure 2B**) or P2Y$_{12}$ receptor antagonist AR-C66931 (**Figure 2C**) to the ARPE-19 cells reduced the lysosomal pH relative to MeS-ADP alone.

P2Y$_{12}$ Receptor Antagonists Reduce Autofluorescence

Lowering lysosomal pH increased clearance of autofluorescent material in prior *in vitro* work (Liu et al., 2008, 2012; Baltazar et al., 2012; Guha et al., 2012). To determine whether ticagrelor could decrease autofluorescence *in vivo*, levels were determined from 16 regions of the RPE whole mount from untreated mice and those receiving ticagrelor in food (**Figure 3A**). There was considerable variation in the autofluorescence values in untreated mice. However, comparing the pattern of autofluorescence across all regions suggested there was a greater difference in autofluorescent levels in samples from the inferior/nasal region (**Figure 3B**). Representative images show the autofluorescence in untreated (**Figure 3C**) and treated mice (**Figure 3D**). Quantification indicated that the autofluorescence

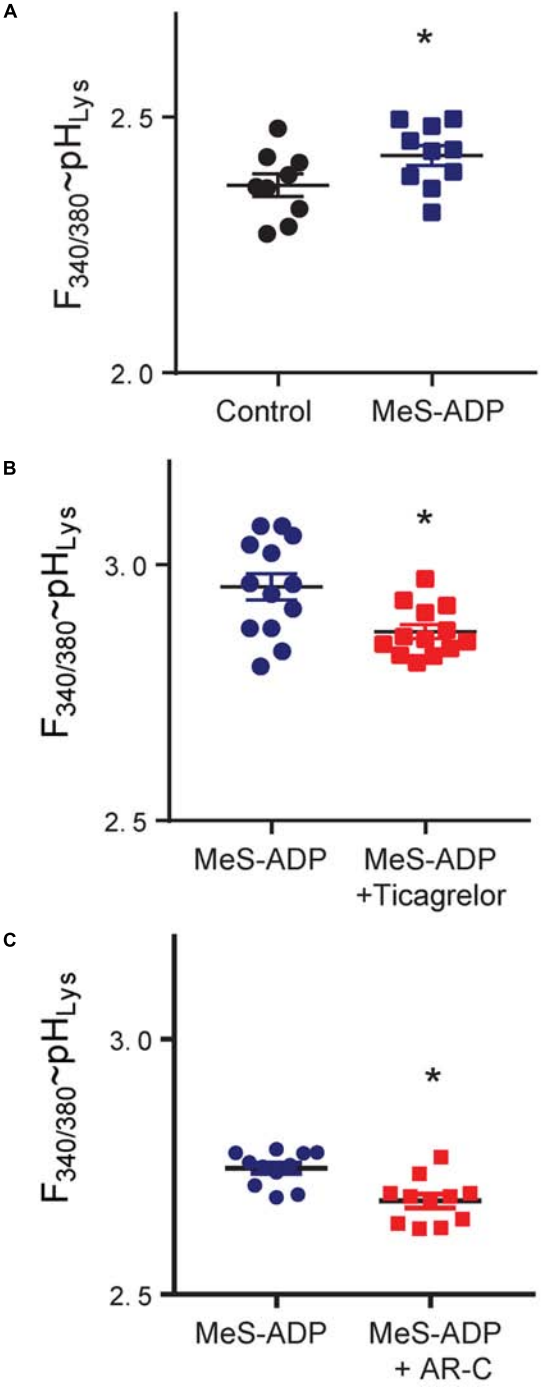

FIGURE 2 | Manipulation of the P2Y$_{12}$ receptor alters lysosomal pH in ARPE-19 cells. **(A)** The lysosomal pH of ARPE-19 cells was elevated by P2Y$_{12}$ receptor agonist methylthio ADP (MeS-ADP, 10 μM). *p = 0.002, n = 9–10. **(B)** Ticagrelor (20 μM) lowered the lysosomal pH in cells treated with MeS-ADP (*p = 0.006, n = 13). **(C)** The P2Y$_{12}$ receptor antagonist AR-C66931 (ARC, 10 μM) also reduced lysosomal pH in ARPE-19 cells treated with MeS-ADP (*p = 0.033, n = 10). Data are expressed as the ratio of fluorescence excited at 340 vs. 380 nm in cells loaded with LysoSensor Yellow/Blue DNS 160; this is indicative of lysosomal pH, although absolute ratios varied with preparation; n represents the number of wells in a single trial with figures representative of 2–4 trials.

from RPE cells in the interior/nasal regions was reduced (**Figure 3E**) in mice treated with ticagrelor. However, there was no difference in mean levels in the superior/temporal regions (**Figure 3F**).

To further characterize the effect of ticagrelor, autofluorescence in RPE cells was analyzed in retinal sections from untreated ABCA4$^{-/-}$ mice and mice treated with ticagrelor. Increased autofluorescence in the RPE cells was detected in many sections from the untreated mice, as compared to those treated with ticagrelor (**Figure 3G**). While variation in autofluorescence levels across regions and mice was considerable, quantification of the autofluorescent output for a broad range of excitation/emission pairs showed a reduction, with emission at 571, 612, and 663 nm particularly effected (**Figure 3H**).

P2Y$_{12}$ Receptor Antagonism Reduces Autofluorescence *in Vitro*

The effect of P2Y$_{12}$ antagonism on autofluorescence was determined *in vitro* using FACS analysis following application of the pulse chase protocol for loading ARPE-19 cells with POSs and alkalinizing lysosomes with chloroquine (see section "Materials and Methods"). Cellular autofluorescence was increased by chloroquine alone, but the addition of POSs increased this autofluorescence substantially (**Figure 4A**). The P2Y$_{12}$ receptor antagonist AR-C66096 reduced the autofluorescence produced by POSs in cells treated with chloroquine (**Figure 4B**). This suggests that blocking the P2Y$_{12}$ receptor reduces lipofuscin accumulation in RPE cells *in vitro*, as it does *in vivo*.

To strengthen the link between lysosomal pH and degradative enzyme activity, ARPE-19 cells were stained with Magic Red to determine cathepsin B activity. The Magic Red substrate releases fluorescent cresyl violet in organelles containing cathepsin B that is catalytically active (Creasy et al., 2007). Magic Red staining was substantial under control conditions; staining colocalized LysoTracker Green, consistent with the lysosomal localization of cathepsin B activity (**Figure 4C**). To determine whether rapid changes in lysosomal pH alter the activity of cathepsin B, cells were treated with tamoxifen, which raises lysosomal pH more rapidly and reproducibly than chloroquine in these cells (**Figure 4D**, Liu et al., 2008). Magic Red staining was absent in cells treated with tamoxifen, consistent with the pH dependence of degradative enzymes in ARPE-19 cells.

Ticagrelor and Gene Expression

The effect of ticagrelor on expression of several key genes in RPE cells was examined. Relative gene expression analysis using quantitative PCR showed a significant downregulation in the expression of the equilibrative nucleoside transporter 1 (ENT1), and complement factor H (CFH) in the RPE of mice treated with 0.1% ticagrelor in food for 14 days. There was no change in expression of mRNA for the P2Y$_{12}$ receptor, the A_1 adenosine receptor or the A_3 adenosine receptor (Supplementary Figure 1).

DISCUSSION

We found that systemic delivery of ticagrelor lowered lysosomal pH in RPE cells of ABCA4$^{-/-}$ mice. Lysosomal pH was reduced both by ticagrelor added to the drinking water, and by addition of ticagrelor to the mouse chow. Results from ticagrelor in food suggest older mice require longer treatment for lysosomal acidification. Ticagrelor, as well as the P2Y$_{12}$ antagonist AR-C66931, lowered lysosomal pH in cultured human ARPE-19 cells, showing receptor block had a direct effect on lysosomal pH in RPE cells. Ticagrelor delivered orally also reduced autofluorescence in the inferior/nasal regions of these RPE cells, while block of the P2Y$_{12}$ receptor reduced autofluorescence *in vitro* in ARPE-19 cells fed POSs. This provides the first evidence that systemic delivery of a P2Y$_{12}$ antagonist improves lysosomal dysregulation in RPE cells.

Contribution of the P2Y12 Receptor

Several observations implicate block of the P2Y$_{12}$ receptor in the lysosomal acidification by ticagrelor. Previous studies indicated that elevation of cAMP, either directly or through drugs known to target the G_s protein that stimulates adenylate cyclase, lowered lysosomal pH in RPE cells from ABCA4$^{-/-}$ mice when applied *ex vivo*, and in compromised ARPE-19 cells (Liu et al., 2008, 2012; Guha et al., 2012, 2014b). This lysosomal acidification was blocked by a protein kinase inhibitor (PKI), implicating protein kinase A in the acidification. As the P2Y$_{12}$ receptor is coupled to the inhibitory G_i protein, P2Y$_{12}$ receptor antagonists will produce similar effects (Supplementary Figure 2). Although ticagrelor can also inhibit the equilibrative nucleoside transporter 1 to raise extracellular adenosine (Nylander et al., 2013; Armstrong et al., 2014; Aungraheeta et al., 2016), it is unlikely adenosine contributes much to the response in this study as plasma levels of ticagrelor in our treated mice were 0.87 $\pm$ 0.07 μM, while plasma levels of adenosine reached half -maximal concentrations with $\sim$30 μM ticagrelor (Nylander et al., 2013). In addition, AR-C66931 does not act on ENT1 (Armstrong et al., 2014), and thus the ability of AR-C66931 to acidify lysosomes *in vitro* indicates P2Y$_{12}$ antagonism is sufficient to lower lysosomal pH in these cells. Together, this implicates the P2Y$_{12}$ receptor in mediating the effects of ticagrelor observed in this study.

Mechanisms for Reduced Autofluorescence

Ticagrelor may reduce autofluorescence from RPE cells through multiple pathways. For example, the lysosomal pH in RPE cells from ABCA4$^{-/-}$ mice is alkalinized above age-matched controls (Liu et al., 2008) and lowering lysosomal pH with ticagrelor would enhance the activity of pH sensitive degradative lysosomal enzymes. Data above using Magic Red indicate cathepsin B activity in RPE cells is decreased by moderate elevations in lysosomal pH; this parallels the rise in cathepsin D activity following lysosomal acidification in RPE cells found previously (Guha et al., 2012). Acidifying lysosomal pH in RPE cells also enhanced the turnover of opsin derived from phagocytosed

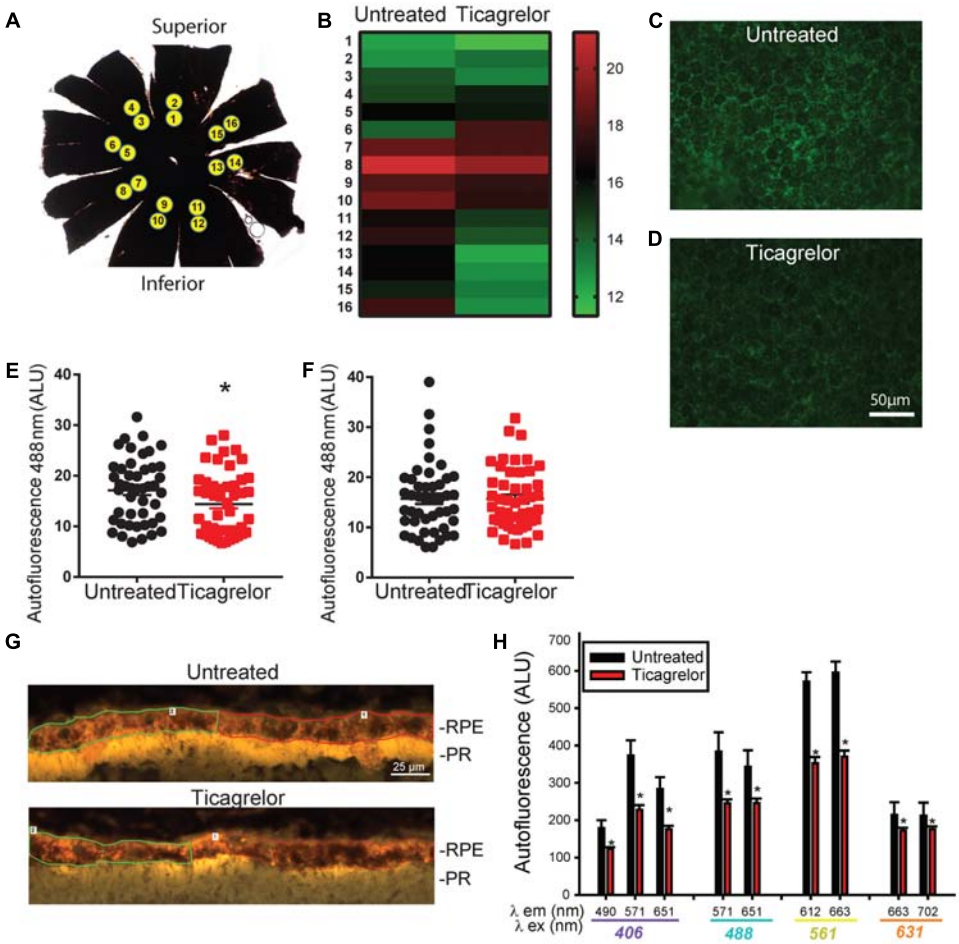

FIGURE 3 | Ticagrelor reduces autofluorescence in RPE cells from ABCA4$^{-/-}$ mice. **(A)** A RPE whole mount preparation indicating the location of images obtained for autofluorescence quantification. **(B)** Heat map illustrating variation in intensity of autofluorescence (488 nm ex/>525 nm em) in regions corresponding to those in "A." Each band is the mean of six untreated mice or mice treated with 0.1% ticagrelor in food for 28 days. Scale at right shows relative intensity. Images of autofluorescence excited at 488 nm in inferior regions of RPE wholemounts from untreated **(C)** and treated **(D)** ABCA4$^{-/-}$ mice. **(E)** Autofluorescence intensity from regions 9–16 of six mice in each condition (p = 0.039, n = 48 measurements; eight from each mouse). **(F)** Autofluorescence intensity from regions 1–8 of six mice in each condition, n = 48). Mice were 257–333 days old after ticagrelor treatment. **(G)** Images from sections of the outer retina showing the RPE and photoreceptor outer segments (POSs) in untreated 20 month old ABCA4$^{-/-}$ mice at 406 nm ex/>409 nm em. The demarcation of two regions of interest (ROI) in the RPE layer are shown. Analogous image for 20 month old ABCA4$^{-/-}$ mouse treated with 10 μg/ml ticagrelor in drinking water for 4 days. **(H)** Mean autofluorescence output for key excitation/emission pairs wavelengths (λ, as indicated; *p < 0.05, n = 16 untreated, 10 treated sections from 4 to 5 mice respectively).

POSs, suggesting pH manipulation can enhance turnover of phagocytosed waste (Baltazar et al., 2012).

In addition to modulating the activity of lysosomal enzymes, decreased autofluorescence in RPE cells may reflect an enhanced exocytosis of waste material. The *bis*-retinoid A2E is present in high levels in the RPE cells of ABCA4$^{-/-}$ mice (Mata et al., 2001). Although the endogenous breakdown of A2E is difficult (Wu et al., 2011), A2E shows a peak autofluorescence emission at 570 nm when excited at 380 nm (Sparrow et al., 1999), and the decrease in this emission in mice receiving ticagrelor suggests the A2E may be exocytosed. The TRPML1 channel contributes to the exocytosis of lysosomal waste; TRPML1 activity is pH dependent (Samie et al., 2013; Li et al., 2017), and recent studies suggest the TRPML1 channel is particularly active in RPE cells (Goméz et al., 2018). It is possible that enhanced exocytosis may contribute to the reduced autofluorescence in ABCA4$^{-/-}$ mice receiving ticagrelor, although further experiments are needed to confirm this.

Remaining Issues

Several additional issues remain unresolved in this study. For example, it is not clear why elderly ABCA4$^{-/-}$ mice required an extended treatment with ticagrelor before lysosomal pH was reduced, while there was no detectable trend between treatment length and the lysosomal acidification in mice receiving ticagrelor in their drinking water, especially as plasma concentrations of ticagrelor did not increase with prolonged dosage. Furthermore, it is unclear why the decline in RPE autofluorescence was limited to the inferior/nasal regions of the whole mounts. Regional

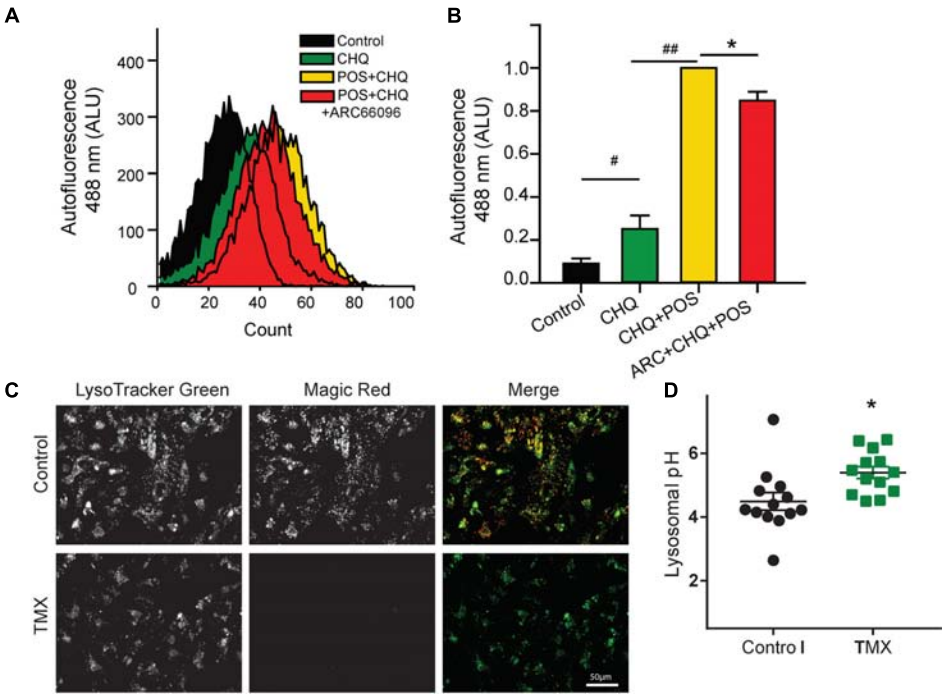

FIGURE 4 | Blocking P2Y$_{12}$ reduces RPE autofluorescence *in vitro*. **(A)** Treatment of ARPE-19 cells with POSs and 10 μM chloroquine (CHQ) using the pulse chase method led to a substantial rise in autofluorescence at 488 nm ex/>525 nm em. FACS analysis demonstrates the increased autofluorescence with the CHQ/POS treatment for >6 days. Treatment of cells with 10 μM P2Y$_{12}$ receptor antagonist AR-C66096 shifted the autofluorescence curve to the left. **(B)** Quantification of the mean autofluorescence from five independent FACS trials showing a significant reduction in POS/CHQ autofluorescence excited at 488 nm in cells treated with 10 μM AR-C66096 (#p = 0.02, ##p < 0.001, *p = 0.014, n = 5). **(C)** ARPE-19 cells displaying overlap of Magic Red and LysoTracker Green, suggesting cathepsin B activity in lysosomes under control conditions (top). Magic Red staining was eliminated by elevation of lysosomal pH with 10 μM tamoxifen (bottom). **(D)** Tamoxifen (10 μM) raises lysosomal pH in ARPE-19 cells (*p = 0.012, n = 13).

differences in photoreceptor death occur with light damage models, with degree of light and differential levels of rhodopsin implicated (Organisciak and Vaughan, 2010); both of these parameters could influence the clearance of autofluorescence by ticagrelor. The mechanisms by which ticagrelor can decrease expression of CFH and ENT1 are also unclear; neither gene is linked to the CLEAR network directly regulated by lysosomal activity suggesting a more indirect connection (Palmieri et al., 2011). As discussed above, the relative effects of ticagrelor on lysosomal degradation versus exocytosis of autofluorescent waste are also relevant. Future work is needed to address these issues.

Relevance to Human Doses

Given that ticagrelor is used in mainly elderly patients, the comparison of doses used here in mice with human dosage is relevant. Plasma levels in mice receiving 0.1% ticagrelor in food were 0.89 μM; this corresponds to 465 ng/mL and is close to levels in mice reported recently on 0.1% ticagrelor (Preusch et al., 2016). In humans receiving the standard dose of 180 mg/day, plasma concentrations of ticagrelor ranged from a maximum of 770 ng/ml 2 h after dosing to a minimum of 227 ng/mL (Storey et al., 2007, 2016). This suggests the levels of ticagrelor that lower lysosomal pH and decrease autofluorescence in mice are within the range found in patients. Whether treatments with ticagrelor can protect vision in ABCA4$^{-/-}$ mice is currently being evaluated.

Portions of this work have previously been presented in abstract form (Lu et al., 2017).

ETHICS STATEMENT

Ethics Approval and Consent to Participate: All experimental approaches on mice were approved by the Animal Care and Use Committee of the University of Pennsylvania protocol #804588.

AVAILABILITY OF DATA AND MATERIALS

All readily reproducible materials described in the manuscript, including new software, databases and all relevant raw data will be freely available to any scientist wishing to use them.

AUTHOR CONTRIBUTIONS

WL, NG, JL, SG, EC, AO, and KC performed the experiments. SM, LC, AL, and CM wrote the manuscript. CM and AL conceived of the idea.

FUNDING

This work was supported by grants from the NIH EY013434 and EY015537 and core grant EY001583 (CM), the Jody Sack Fund (WL), and AstraZeneca.

ACKNOWLEDGMENTS

We would like to thank Gabriel Baltazar for help with lysosomal pH and Magic Red measurements, Bruce Shenker and Ali Zekavat for assistance with the Flow Cytometry, Ann-Sofie Sandinge for the analysis of ticagrelor in plasma and Renato DeRita for his help coordinating with AstraZeneca.

SUPPLEMENTARY MATERIAL

The Supplementary Material for this article can be found online at: https://www.frontiersin.org/articles/10.3389/fphar.2018.00242/full#supplementary-material

REFERENCES

Albalawi, F., Lu, W., Beckel, J. M., Lim, J. C., McCaughey, S. A., and Mitchell, C. H. (2017). The P2X7 receptor primes IL-1β and the NLRP3 inflammasome in astrocytes exposed to mechanical strain. *Front. Cell. Neurosci.* 11:227. doi: 10.3389/fncel.2017.00227

Armstrong, D., Summers, C., Ewart, L., Nylander, S., Sidaway, J. E., and van Giezen, J. J. (2014). Characterization of the adenosine pharmacology of ticagrelor reveals therapeutically relevant inhibition of equilibrative nucleoside transporter 1. *J. Cardiovasc. Pharmacol. Ther.* 19, 209–219. doi: 10.1177/1074248413511693

Aungraheeta, R., Conibear, A., Butler, M., Kelly, E., Nylander, S., Mumford, A., et al. (2016). Inverse agonism at the P2Y12 receptor and ENT1 transporter blockade contribute to platelet inhibition by ticagrelor. *Blood* 128, 2717–2728. doi: 10.1182/blood-2016-03-707844

Baltazar, G. C., Guha, S., Boesze-Battaglia, K., Laties, A. M., Tyagi, P., Kompella, U. B., et al. (2012). Acidic nanoparticles restore lysosomal pH and degradative function in compromised RPE cells. *PLoS One* 7:e49635. doi: 10.1007/978-1-4614-3209-8_14

Birkeland, K., Parra, D., and Rosenstein, R. (2010). Antiplatelet therapy in acute coronary syndromes: focus on ticagrelor. *J. Blood Med.* 1, 197–219. doi: 10.2147/JBM.S9650

Bonaca, M. P., Bhatt, D. L., Storey, R. F., Steg, P. G., Cohen, M., Kuder, J., et al. (2016). Ticagrelor for prevention of ischemic events after myocardial infarction in patients with peripheral artery disease. *J. Am. Coll. Cardiol.* 67, 2719–2728. doi: 10.1016/j.jacc.2016.03.524

Cattaneo, M. (2015). P2Y12 receptors: structure and function. *J. Thromb. Haemost.* 13(Suppl. 1), S10–S16. doi: 10.1111/jth.12952

Charbel Issa, P., Barnard, A. R., Singh, M. S., Carter, E., Jiang, Z., Radu, R. A., et al. (2013). Fundus autofluorescence in the Abca4(−/−) mouse model of Stargardt disease–correlation with accumulation of A2E, retinal function, and histology. *Invest. Ophthalmol. Vis. Sci.* 54, 5602–5612. doi: 10.1167/iovs.13-11688

Coffey, E. E., Beckel, J. M., Laties, A. M., and Mitchell, C. H. (2014). Lysosomal alkalization and dysfunction in human fibroblasts with the Alzheimer's disease-linked presenilin 1 A246E mutation can be reversed with cAMP. *Neuroscience* 263, 111–124. doi: 10.1016/j.neuroscience.2014.01.001

Creasy, B. M., Hartmann, C. B., White, F. K., and McCoy, K. L. (2007). New assay using fluorogenic substrates and immunofluorescence staining to measure cysteine cathepsin activity in live cell subpopulations. *Cytometry A* 71, 114–123. doi: 10.1002/cyto.a.20365

Eckle, T., Hughes, K., Ehrentraut, H., Brodsky, K. S., Rosenberger, P., Choi, D. S., et al. (2013). Crosstalk between the equilibrative nucleoside transporter ENT2 and alveolar Adora2b adenosine receptors dampens acute lung injury. *FASEB J.* 27, 3078–3089. doi: 10.1096/fj.13-228551

Ferris, F. L. III, Wilkinson, C. P., Bird, A., Chakravarthy, U., Chew, E., Csaky, K., et al. (2013). Clinical classification of age-related macular degeneration. *Ophthalmology* 120, 844–851. doi: 10.1016/j.ophtha.2012.10.036

Goel, D. (2013). Ticagrelor: the first approved reversible oral antiplatelet agent. *Int. J. Appl. Basic Med. Res.* 3, 19–21. doi: 10.4103/2229-516X.112234

Goméz, N. M., Lu, W., Lim, J. C., Kiselyov, K., Campagno, K. E., Grishchuk, Y., et al. (2018). Robust lysosomal calcium signaling through channel TRPML1 is impaired by lipofuscin accumulation. *FASEB J.* 32, 782–794. doi: 10.1096/fj.201700220RR

Guha, S., Baltazar, G. C., Coffey, E. E., Tu, L. A., Lim, J. C., Beckel, J. M., et al. (2013). Lysosomal alkalinization, lipid oxidation, impaired autophagy and reduced phagosome clearance triggered by P2X7 receptor activation in retinal pigmented epithelial cells. *FASEB J.* 27, 4500–4509. doi: 10.1096/fj.13-236166

Guha, S., Baltazar, G. C., Tu, L. A., Liu, J., Lim, J. C., Lu, W., et al. (2012). Stimulation of the D5 dopamine receptor acidifies the lysosomal pH of retinal pigmented epithelial cells and decreases accumulation of autofluorescent photoreceptor debris. *J. Neurochem.* 122, 823–833. doi: 10.1111/j.1471-4159.2012.07804.x

Guha, S., Coffey, E. E., Lu, W., Lim, J. C., Beckel, J. M., Laties, A. M., et al. (2014a). Approaches for detecting lysosomal alkalinization and impaired degradation in fresh and cultured RPE cells: evidence for a role in retinal degenerations. *Exp. Eye Res.* 126, 68–76. doi: 10.1016/j.exer.2014.05.013

Guha, S., Liu, J., Baltazar, G. C., Laties, A. M., and Mitchell, C. H. (2014b). Rescue of compromised lysosomes enhances degradation of photoreceptor outer segments and reduce lipofuscin-like autofluorescence. *Adv. Exp. Med. Biol.* 801, 105–111. doi: 10.1007/978-1-4614-3209-8_14

Holz, F. G., Schutt, F., Kopitz, J., Eldred, G. E., Kruse, F. E., Volcker, H. E., et al. (1999). Inhibition of lysosomal degradative functions in RPE cells by a retinoid component of lipofuscin. *Invest. Ophthalmol. Vis. Sci.* 40, 737–743.

Jacobson, K. A., Ivanov, A. A., de Castro, S., Harden, T. K., and Ko, H. (2009). Development of selective agonists and antagonists of P2Y receptors. *Purinergic Signal.* 5, 75–89. doi: 10.1007/s11302-008-9106-2

Lee, J. H., McBrayer, M. K., Wolfe, D. M., Haslett, L. J., Kumar, A., Sato, Y., et al. (2015). Presenilin 1 maintains lysosomal Ca^{2+} homeostasis via TRPML1 by regulating vATPase-mediated lysosome acidification. *Cell Rep.* 12, 1430–1444. doi: 10.1016/j.celrep.2015.07.050

Lee, J. H., Yu, W. H., Kumar, A., Lee, S., Mohan, P. S., Peterhoff, C. M., et al. (2010). Lysosomal proteolysis and autophagy require presenilin 1 and are disrupted by Alzheimer-related PS1 mutations. *Cell* 141, 1146–1158. doi: 10.1016/j.cell.2010.05.008

Li, M., Zhang, W. K., Benvin, N. M., Zhou, X., Su, D., Li, H., et al. (2017). Structural basis of dual Ca^{2+}/pH regulation of the endolysosomal TRPML1 channel. *Nat. Struct. Mol. Biol.* 24, 205–213. doi: 10.1038/nsmb.3362

Liu, J., Lu, W., Guha, S., Baltazar, G. C., Coffey, E. E., Laties, A. M., et al. (2012). Cystic fibrosis transmembrane conductance regulator (CFTR) contributes to reacidification of alkalinized lysosomes in RPE cells. *Am. J. Physiol. Cell Physiol.* 303, C160–C169. doi: 10.1152/ajpcell.00278.2011

Liu, J., Lu, W., Reigada, D., Nguyen, J., Laties, A. M., and Mitchell, C. H. (2008). Restoration of lysosomal pH in RPE cells from cultured human and ABCA4(−/−) mice: pharmacologic approaches and functional recovery. *Invest. Ophthalmol. Vis. Sci.* 49, 772–780. doi: 10.1167/iovs.07-0675

Lu, W., Albalawi, F., Beckel, J. M., Lim, J. C., Laties, A. M., and Mitchell, C. H. (2017). The P2X7 receptor links mechanical strain to cytokine IL-6 up-regulation and release in neurons and astrocytes. *J. Neurochem.* 141, 436–448. doi: 10.1111/jnc.13998

Mata, N. L., Tzekov, R. T., Liu, X., Weng, J., Birch, D. G., and Travis, G. H. (2001). Delayed dark-adaptation and lipofuscin accumulation in abcr+/− mice: implications for involvement of ABCR in age-related macular degeneration. *Invest. Ophthalmol. Vis. Sci.* 42, 1685–1690.

McFadyen, J. D., Schaff, M., and Peter, K. (2018). Current and future antiplatelet therapies: emphasis on preserving haemostasis. *Nat. Rev. Cardiol.* 15, 181–191. doi: 10.1038/nrcardio.2017.206

Nylander, S., Femia, E. A., Scavone, M., Berntsson, P., Asztely, A. K., Nelander, K., et al. (2013). Ticagrelor inhibits human platelet aggregation via adenosine in addition to P2Y12 antagonism. *J. Thromb. Haemost.* 11, 1867–1876. doi: 10.1111/jth.12360

Nylander, S., and Schulz, R. (2016). Effects of P2Y12 receptor antagonists beyond platelet inhibition–comparison of ticagrelor with thienopyridines. *Br. J. Pharmacol.* 173, 1163–1178. doi: 10.1111/bph.13429

Organisciak, D. T., and Vaughan, D. K. (2010). Retinal light damage: mechanisms and protection. *Prog. Retin. Eye Res.* 29, 113–134. doi: 10.1016/j.preteyeres.2009.11.004

Palmieri, M., Impey, S., Kang, H., di Ronza, A., Pelz, C., Sardiello, M., et al. (2011). Characterization of the CLEAR network reveals an integrated control of cellular clearance pathways. *Hum. Mol. Genet.* 20, 3852–3866. doi: 10.1093/hmg/ddr306

Preusch, M. R., Rusnak, J., Staudacher, K., Mogler, C., Uhlmann, L., Sievers, P., et al. (2016). Ticagrelor promotes atherosclerotic plaque stability in a mouse model of advanced atherosclerosis. *Drug Des. Devel. Ther.* 10, 2691–2699. doi: 10.2147/DDDT.S105718

Radu, R. A., Hu, J., Jiang, Z., and Bok, D. (2014). Bisretinoid-mediated complement activation on retinal pigment epithelial cells is dependent on complement factor H haplotype. *J. Biol. Chem.* 289, 9113–9120. doi: 10.1074/jbc.M114.548669

Reigada, D., Lu, W., Zhang, X., Friedman, C., Pendrak, K., McGlinn, A., et al. (2005). Degradation of extracellular ATP by the retinal pigment epithelium. *Am. J. Physiol. Cell Physiol.* 289, C617–C624. doi: 10.1152/ajpcell.00542.2004

Samie, M., Wang, X., Zhang, X., Goschka, A., Li, X., Cheng, X., et al. (2013). A TRP channel in the lysosome regulates large particle phagocytosis via focal exocytosis. *Dev. Cell* 26, 511–524. doi: 10.1016/j.devcel.2013.08.003

Sparrow, J. R., Parish, C. A., Hashimoto, M., and Nakanishi, K. (1999). A2E, a lipofuscin fluorophore, in human retinal pigmented epithelial cells in culture. *Invest. Ophthalmol. Vis. Sci.* 40, 2988–2995.

Storey, R. F., Angiolillo, D. J., Bonaca, M. P., Thomas, M. R., Judge, H. M., Rollini, F., et al. (2016). Platelet inhibition with ticagrelor 60 mg versus 90 mg twice daily in the PEGASUS-TIMI 54 trial. *J. Am. Coll. Cardiol.* 67, 1145–1154. doi: 10.1016/j.jacc.2015.12.062

Storey, R. F., Angiolillo, D. J., Patil, S. B., Desai, B., Ecob, R., Husted, S., et al. (2010). Inhibitory effects of ticagrelor compared with clopidogrel on platelet function in patients with acute coronary syndromes: the PLATO (PLATelet inhibition and patient Outcomes) PLATELET substudy. *J. Am. Coll. Cardiol.* 56, 1456–1462. doi: 10.1016/j.jacc.2010.03.100

Storey, R. F., Husted, S., Harrington, R. A., Heptinstall, S., Wilcox, R. G., Peters, G., et al. (2007). Inhibition of platelet aggregation by AZD6140, a reversible oral P2Y12 receptor antagonist, compared with clopidogrel in patients with acute coronary syndromes. *J. Am. Coll. Cardiol.* 50, 1852–1856. doi: 10.1016/j.jacc.2007.07.058

Streitova, D., Sefc, L., Savvulidi, F., Pospisil, M., Hola, J., and Hofer, M. (2010). Adenosine A(1), A(2a), A(2b), and A(3) receptors in hematopoiesis. 1. Expression of receptor mRNA in four mouse hematopoietic precursor cells. *Physiol. Res.* 59, 133–137.

Tantry, U. S., Bliden, K. P., Wei, C., Storey, R. F., Armstrong, M., Butler, K., et al. (2010). First analysis of the relation between CYP2C19 genotype and pharmacodynamics in patients treated with ticagrelor versus clopidogrel: the ONSET/OFFSET and RESPOND genotype studies. *Circ. Cardiovasc. Genet.* 3, 556–566. doi: 10.1161/CIRCGENETICS.110.958561

Toops, K. A., Tan, L. X., Jiang, Z., Radu, R. A., and Lakkaraju, A. (2015). Cholesterol-mediated activation of acid sphingomyelinase disrupts autophagy in the retinal pigment epithelium. *Mol. Biol. Cell* 26, 1–14. doi: 10.1091/mbc.E14-05-1028

Veitinger, S., Veitinger, T., Cainarca, S., Fluegge, D., Engelhardt, C. H., Lohmer, S., et al. (2011). Purinergic signalling mobilizes mitochondrial Ca^{2+} in mouse Sertoli cells. *J. Physiol.* 589, 5033–5055. doi: 10.1113/jphysiol.2011.216309

Wu, Y., Zhou, J., Fishkin, N., Rittmann, B. E., and Sparrow, J. R. (2011). Enzymatic degradation of A2E, a retinal pigment epithelial lipofuscin bisretinoid. *J. Am. Chem. Soc.* 133, 849–857. doi: 10.1021/ja107195u

Conflict of Interest Statement: AstraZeneca partially supported this work through a granting mechanism. LC is employed by AstraZeneca, CM and AL are associated with intellectual property related to this topic.

The other authors declare that the research was conducted in the absence of any commercial or financial relationships that could be construed as a potential conflict of interest.

frontiers in Pharmacology

REVIEW
published: 16 April 2018
doi: 10.3389/fphar.2018.00267

Amyotrophic Lateral Sclerosis (ALS) and Adenosine Receptors

Ana M. Sebastião[1,2], Nádia Rei[1,2] and Joaquim A. Ribeiro[1,2]*

[1] Instituto de Farmacologia e Neurociências, Faculdade de Medicina, Universidade de Lisboa, Lisbon, Portugal, [2] Instituto de Medicina Molecular, Universidade de Lisboa, Lisbon, Portugal

In the present review we discuss the potential involvement of adenosinergic signaling, in particular the role of adenosine receptors, in amyotrophic lateral sclerosis (ALS). Though the literature on this topic is not abundant, the information so far available on adenosine receptors in animal models of ALS highlights the interest to continue to explore the role of these receptors in this neurodegenerative disease. Indeed, all motor neurons affected in ALS are responsive to adenosine receptor ligands but interestingly, there are alterations in pre-symptomatic or early symptomatic stages that mirror those in advanced disease stages. Information starts to emerge pointing toward a beneficial role of A_{2A} receptors ($A_{2A}R$), most probably at early disease states, and a detrimental role of caffeine, in clear contrast with what occurs in other neurodegenerative diseases. However, some evidence also exists on a beneficial action of $A_{2A}R$ antagonists. It may happen that there are time windows where $A_{2A}R$ prove beneficial and others where their blockade is required. Furthermore, the same changes may not occur simultaneously at the different synapses. In line with this, it is not fully understood if ALS is a dying back disease or if it propagates in a centrifugal way. It thus seems crucial to understand how motor neuron dysfunction occurs, how adenosine receptors are involved in those dysfunctions and whether the early changes in purinergic signaling are compensatory or triggers for the disease. Getting this information is crucial before starting the design of purinergic based strategies to halt or delay disease progression.

Keywords: adenosine receptors, amyotrophic lateral sclerosis (ALS), spinal cord motor neurons, neuromuscular junction, glial cells

OPEN ACCESS

Edited by:
Kenneth A. Jacobson, National Institutes of Health (NIH), United States

Reviewed by:
Rashid Giniatullin, University of Eastern Finland, Finland
Yijuang Chern, National Research Program for Biopharmaceuticals, Taiwan

****Correspondence:***
Ana M. Sebastião
anaseb@medicina.ulisboa.pt

Specialty section:
This article was submitted to Experimental Pharmacology and Drug Discovery, a section of the journal Frontiers in Pharmacology

Received: *15 December 2017*
Accepted: *09 March 2018*
Published: *16 April 2018*

Citation:
Sebastião AM, Rei N and Ribeiro JA (2018) Amyotrophic Lateral Sclerosis (ALS) and Adenosine Receptors. Front. Pharmacol. 9:267. doi: 10.3389/fphar.2018.00267

INTRODUCTION

In the present review, we will address the potential role of adenosine on amyotrophic lateral sclerosis (ALS), also known as Lou Gehrig's disease. This is one of the most devastating neurodegenerative disorders and is the most common form of Motor Neuron Diseases group. During ALS progression, both the upper motor neurons (motor neurons in the cortex) and the lower motor neurons (motor neurons in the spinal cord) degenerate or die. As a consequence of deficient input from the motor neuron, there is a progressive and terminal atrophy of skeletal muscles. All muscles under voluntary control are affected, and individuals lose their strength and the ability to move their arms, legs and body. When diaphragm and the muscles in the chest wall fail, people lose the ability to breathe without ventilation support (Nichols et al., 2013).

The incidence of this disease is 2–3/100,000 and the prevalence 4–7/100,000 (Nalini et al., 2008). The onset of symptoms is predominantly between 55 and 65 years old and the median survival of ALS patients, after the diagnosis, is 3–5 years; however, about 10% of the patients survive for 10 or more years (Wijesekera and Leigh, 2009).

The majority of cases of ALS are sporadic (sALS) (90–95%), but some cases have a positive familial history (fALS) (5–10%) (Kiernan et al., 2011). Both forms, sALS and fALS, present similar pathological and clinical features. In the case of fALS, the inheritance is autossomal dominant, but the penetrance is variable. About 20% of fALS are caused by a missense mutation in *SOD1* gene, encoding for the Cu/Zn superoxide dismutase 1 enzyme. This finding led to the first and most used rodent model for ALS, the $SOD1^{G93A}$ mouse, which in the symptomatic phase recapitulate most features of the disease, including neuromuscular dysfunction (Naumenko et al., 2011). There is still a debate whether motor neuron degeneration initially results from failure of enzymatic machinery at the level of the cell body and proximal parts of the axon that then propagates in a centrifugal way due to impaired axonal transport (Braak et al., 2013), or results from an early dysfunction at the level of the nerve terminals, with consequent synaptic dysfunction and then progressing in a 'dying back' process (Frey et al., 2000; Dadon-Nachum et al., 2011), or both (Baker, 2014). As pointed out (Dadon-Nachum et al., 2011), if cell nerve terminal degeneration precedes with axonal and cell body degeneration, early intervention focusing on motor neurons terminals could potentially delay or prevent the progressive loss of motor neurons. A functional study focusing on the activity of single end-plates demonstrated that neuromuscular transmission impairment starts long before symptomatic onset (Rocha et al., 2013). Importantly, in pre-symptomatic SOD^{G92A} mice there are functional hallmarks of dysregulated intraterminal calcium levels (Rocha et al., 2013) in consonance with the hypothesis that nerve terminal machinery designed to buffer calcium might be impaired at very early disease stages. The pathophysiological alterations at the neuromuscular junction of SOD^{G92A} mice are accompanied with alterations in the activity of adenosine receptors at the motor nerve terminals in these mice (Nascimento et al., 2014, 2015).

Mutations in the gene coding for a nuclear protein, TAR DNA-binding protein-43 are also frequent in fALS (Leblond et al., 2014). This protein has several functions in regulation of gene expression, which thus indicates a clear dysfunction at the level of the neuronal soma in some forms of ALS. ROS induce the mislocalization of TAR-DNA binding protein 43 (TDP-43) from the nucleus into the cytoplasm (Ayala et al., 2011), where it forms aggregates, an early hallmark of ALS (Neumann et al., 2006; Chou et al., 2018). Cytoplasmic mislocalization of TDP-43 is accompanied by further ROS production and overactivation AMP kinase (AMPK), an action suppressed by $A_{2A}R$ activation (Liu et al., 2015a). Importantly, $A_{2A}R$ activation in a TDP-43Tg mouse model of ALS, improved motor function (Liu et al., 2015a). Interestingly also, activation of AMPK changed the location of a mRNA stabilizer in the motor neurons of ALS patients, in mouse motor neurons, and in a motor neuron cell line, and this mislocalization was also suppressed by activation of $A_{2A}Rs$ (Liu et al., 2015b). This again reinforces the idea of a putative neuroprotective role of $A_{2A}Rs$ in ALS since impaired RNA homeostasis is a major pathway for ALS pathogenesis (Liu et al., 2017).

Mutations in *C9ORF72* are also frequently found in fALS and accounts for 10% of the sporadic cases (DeJesus-Hernandez et al., 2011; Smith et al., 2013). Motor neurons with *C9ORF72* mutations have increased expression and activity of NMDA receptors and calcium permeable AMPA receptors (Selvaraj et al., 2018; Shi et al., 2018), known to be targets for adenosine receptor-mediated modulation (Dias et al., 2012, 2013). No information so far exists on the possibility that adenosine receptor ligands may influence motor neuronal survival in this model of ALS.

Being adenosine a ubiquitous neuromodulator, affecting synaptic transmission at pre- post and non-synaptic levels, having adenosine receptors not only neuroprotective but also excitotoxic and neuroinflammatory actions, it is somehow unexpected that only relatively few studies concentrated their attention on the influence of adenosine on ALS progression. Evidence so far available highlights early dysfunctions of neuromodulation by adenosine and the ability to influence those dysfunctions through manipulation of adenosine receptors. In this review we will critically analyze data so far available.

PATHOPHYSIOLOGY OF ALS

ALS is a complex, multifactorial and multi-systemic disease, the pathophysiological mechanisms of motor neurons degeneration remaining yet incompletely known. Some of these mechanisms include RNA dysfunction, protein misfolding and aggregation, marked neuromuscular junction abnormalities, immune system deficiency, mitochondrial dysfunction, neuroinflammation, cytoskeletal derangements, desregulation of growth factors, oxidative stress, axonal disruption and apoptosis, excitotoxity (induced by glutamate), activation of nucleases and proteases and abnormal calcium metabolism (Pasinelli and Brown, 2006; Costa et al., 2010; Chou et al., 2018). It is becoming clear that ALS is a disease that involves different cell types and the communication between them, the damage that occurs in each cell population contributing to ALS pathogenicity and phenotype, thus to the progression of the disease (Taylor et al., 2016). Indeed, non-motor neuron cells, like interneurons, astrocytes, microglia, Schwann cells, skeletal muscle cells and oligodendrocytes play a crucial role in motor neuron survival, and their dysfunction impact upon motor neuron degeneration. In practical terms, a major problem that is shared with many neurodegenerative diseases is that when patients are diagnosed, the neuronal degeneration, in the case of ALS motor neuron degeneration, has already started and progressed.

Functional and structural changes at the level of the endplate are major events in ALS. It has now been realized that the functional changes may precede not only the structural ones but also the onset of symptoms. Studies conducted in our lab (Rocha et al., 2013) to investigate transmission at the diaphragm neuromuscular junction in $SOD1^{G93A}$ mice revealed that the

during the pre-symptomatic phase there is an enhanced release of ACh from nerve terminals, as determined by the mean quantal content of end-plate potentials. Also in these neuromuscular junctions the frequency of giant miniature endplate potentials (GMEPPs) was markedly increased, suggesting that the ability of the nerve terminal machinery to control cytoplasmatic [Ca^{2+}] is dysregulated. In early symptomatic (defined as moderate changes performance in the RotaRod test) $SOD1^{G93A}$ mice two groups of neuromuscular junctions were identified, both of them co-existing in the same innervated diaphragm (Rocha et al., 2013): one group, designated as group A (SOD1a group), presented significant reduction of the mean amplitude of EPP, a significant reduction of the mean amplitude of MEPPS, and a slight but not significant reduction of the quantal content of EPPs. All these changes indicate a predominant post-synaptic impairment. The frequency of GMEPPs was significantly reduced in SOD1a neuromuscular junctions, even as compared with wild type siblings, indicating that presynaptic calcium dysregulations persisted, though with opposite signal in pre-symptomatic and in symptomatic mice. The other group of neuromuscular junctions, designated as group B (SOD1b) (Rocha et al., 2013) displayed electrophysiological characteristics somehow in between those of age-matched wild type and pre-symptomatic mice, being not significantly different from any of these groups. Summarizing, data suggest (Rocha et al., 2013) an exacerbated, but already dysregulated, presynaptic activity at the mice neuromuscular junctions that do not yet display motor symptoms; once symptoms start to appear some neuromuscular junctions are already hypofunctional, some others being probably in a transition between hyper and hypofunction.

Presynaptic facilitation of neuromuscular transmission preceding motor symptoms was further confirmed in using a late onset slow progressing disease model, the $SOD1^{G37R}$ mice (Arbour et al., 2015). A recent study (Arbour et al., 2017) taking advantage of this late onset slow progressing disease model, systematically analyzed the changes in synaptic properties over the course of the disease progression and as a function of the motor unit type. Indeed, different motor units have different susceptibility to the disease, and it became clear the time course and the sequence of events associated with neuromuscular transmission dysfunction depend on the motor unit type (Arbour et al., 2017). The slow motor neurons are those that degenerate later and interestingly, they display an early and transient increase in the quantal content of endplate potentials that disappear at disease onset. In contrast, fast fatigue motor neurons, those that degenerate first, have reduced quantal content even before disease onset. Somehow in the between, fatigue resistant motor units only evidence neuromuscular transmission dysfunction after disease onset (Arbour et al., 2017). Interestingly only slow-type motor neurons display intrinsic hyperexcitability in pre-symptomatic mice (Leroy et al., 2014), pointing toward the possibility that early intrinsic hyperexcitability does not contribute to motor neuron degeneration, but rather represents an early compensatory process. It is worthwhile to note that as previously seen while using the $SOD1^{G93A}$ mice (Rocha et al., 2013), in $SOD1^{G37R}$ mice the neuromuscular transmission alterations precede the onset of motor symptoms, as well as precede motor neuron loss, axonal degeneration, and NMJ structural changes (Arbour et al., 2017).

It is nowadays clear that motor neuron degeneration in ALS also involves glial cells, namely astrocytes, oligodendrocytes, microglia, Schwann Cells and, in the case of the neuromuscular junction, perisynaptic Schwann cells (PSCs). PSCs have neuromodulatory properties close to those of astrocytes in the central nervous system, closely interacting with nerve terminals. Thus, PSCs respond to ATP and ACh released during nerve activity, which act through P2Y and muscarinic ACh receptors (mAChRs) coupled to transient increases in intracellular calcium concentration, a process that has to be kept under proper control to keep PSCs competent for their functions to modulate and to repair neuromuscular transmission (Son et al., 1996; Georgiou et al., 1999; Feng and Ko, 2008a,b). Interestingly, PSC of SOD1 mice displayed exacerbated mAChR responses and exacerbated calcium signaling, which precede functional and morphological changes at the neuromuscular junction, suggesting that the impairments of PSC functions may contribute to NMJ dysfunction and ALS pathogenesis (Arbour et al., 2015).

At the level of spinal cord and focusing in neuroinflammatory and cellular intercommunication hallmarks, it has recently been also shown a clear difference between pre-symptomatic and symptomatic stages (Cunha et al., 2017). Thus, before onset of motor symptoms, alterations in both astrocytes and microglia have been detected in the spinal cord of $SOD1^{G93A}$ mice, which comprise decreased expression of astrocytic, microglia, inflammatory and cell communication markers together with upregulation of a glutamate transporter-1 marker. In contrast, in the symptomatic stage, increased markers of inflammation became evident (Cunha et al., 2017). Microglia activation, suggestive of a switch from M1 to M2-like microglia subpopulations, have been detected in control cells exposed to exosomes derived from motor neuron-like cells transfected with mutant $SOD1^{G93A}$ (Cunha et al., 2017), thus suggesting that disease progression is promoted by cell to cell communication events. There is also a growing body of evidence showing that astrocytes expressing ALS-associated proteins impair motor neuron survival and potentiate ALS progression (Di Giorgio et al., 2007; Nagai et al., 2007; Marchetto et al., 2008; Qian et al., 2017).

Recent attention has been paid to two other ALS-related dysfunctions, TDP-43 aggregation and *C9ORF72* repeated expansion. Mutations in the gene that codes for TDP-43, *TARDBP*, may favor TDP-43 aggregation but phosphorylated TDP-43 containing aggregates also occur in sALS (Neumann et al., 2006; Chou et al., 2018). Indeed, TDP-43 aggregates are found in 97% of ALS cases of diverse etiology and constitute a major component of protein inclusions in this disease (Arai et al., 2006; Maekawa et al., 2009). TDP-43 is a nuclear protein that interacts with RNA molecules and is involved in a wide variety of relevant cellular pathways related to RNA and protein homeostasis. TDP-43 C-terminal missense mutations have been identified in ALS patients, which promote mislocalization of TDP-43 from the nucleus to the cytoplasm and lead to neurotoxicity (Gitcho et al., 2008; Nonaka et al., 2009;

Guo et al., 2011). Oxidative stress and ROS formation also favor mislocalization of TDP-43, from the nucleus to the cytoplasm (Ayala et al., 2011), being thus not surprising that SOD mutations also lead to TDP-43 pathology in mice and humans (Shan et al., 2009; Pokrishevsky et al., 2012). ROS upregulates AMP kinase (AMPK) and abnormal AMPK activity has been shown to induce TDP-43 mislocalization in a motor neuron cell line and in the spinal cord of ALS patients (Liu et al., 2015a). Interestingly, mislocalized TDP-43 in the cytoplasm triggers a positive feedback loop, leading to further ROS production and AMPK activation (Liu et al., 2015a).

The present understanding of the mechanisms that underlie motor neuron degeneration associated to expansion of a G4C2 intronic hexanucleotide of the *C9ORF72* gene, is scarce. This mutation is a common cause of fALS but also accounts for near 10% of sALS cases (DeJesus-Hernandez et al., 2011; Smith et al., 2013). A recent study has shown that the *C9ORF72* mutation is associated with an increase in GluA1 AMPA receptor subunit expression, functional expression of Ca^{2+}-permeable AMPA receptors and motor neuron vulnerability to excitotoxicity (Selvaraj et al., 2018). Interestingly, early intrinsic hyperexcitability has been detected in mixed cultures of neurons and glia derived from *C9ORF72* repeat expansion patient iPSCs (Wainger et al., 2014), but not in neuronal cultures with negligible number of glial cells (Selvaraj et al., 2018). Also, conditional medium from astrocytes expressing mutant SOD1 can induce motor neuron hyperexcitability (Fritz et al., 2013). Altogether these studies reinforce the idea that diseased astrocytes trigger excitotoxicity.

Motor neurons, astrocytes, microglia and perisynaptic Schwann cells are known to release and respond to purines, namely ATP and adenosine. Adenosine, by activating membrane receptors (A_1, A_{2A}, A_{2B}, A_3), is an endogenous and ubiquitous modulator of synaptic signaling. Released ATP is a source for extracellular adenosine, but acts on its own purinergic P2 (P2Y and P2X) receptors. So the challenging question is: How purinergic receptors affect the motor neurons and how this impacts in ALS? In this review we will only refer to adenosine receptors since the putative involvement of ATP receptors in the pathophysiology of ALS has been matter of a recent review (Volonté et al., 2016).

ADENOSINE AND ADENOSINE RECEPTORS

Adenosine is a ubiquitous endogenous neuroprotective agent, which has a central role as a neuromodulator of synaptic transmission at the central and peripheral nervous systems, protecting organs and tissues at both physiological and pathophysiological conditions. Adenosine exerts its biological effect via a class of purinergic G protein coupled receptors, which includes A_1R, $A_{2A}R$, $A_{2B}R$ and A_3R, all belonging to family of receptors named by Burnstock (1976) as P_1 purinoceptors (adenosine-sensitive) as opposed to the ATP-sensitive P2 purinoceptors. The A_1R couple to $G_{i/o}$ proteins, inhibiting the production of cyclic AMP. The A_{2A} and A_2B receptors couple to G_s, stimulating the production of cyclic AMP, whereas the A_3R may couple to $G_{i/o}$ or G_q proteins. Adenosine acts like an extracellular signaling molecule, modulating the action of several neurotransmitters (Ribeiro et al., 2003).

Adenosine A_1R are widely distributed in the brain having a widely recognized inhibitory action in synaptic transmission associated to a neuroprotective role, while $A_{2A}R$ have more restrict localizations, being predominant at the basal ganglia. However, both receptors are present in the cortex, the A_1R being the predominant in this brain area (Dunwiddie and Masino, 2001; Sebastião and Ribeiro, 2009a). $A_{2A}R$ may exacerbate excitotoxicity in several brain areas (Ribeiro et al., 2016b) as well as in motor neurons (Mojsilovic-Petrovic et al., 2006). However, $A_{2A}R$ are also able to gate the action of neuroprotective molecules as the neurotrophic factors, a mechanism known to occur in the brain (Diógenes et al., 2004) as well as in motor neurons (Wiese et al., 2007). Trophic actions of $A_{2A}R$ in cortical neurons, some of them being independent of the interplay with neurotrophic factors, have been recently identified (Ribeiro et al., 2016a). Expression of $A_{2A}R$ in spinal motor neurons is intense, being higher than that of A_1R (Kaelin-Lang et al., 1999; Ng et al., 2015).

A_1R in the spinal cord inhibit excitatory inputs (Deuchars et al., 2001) whereas $A_{2A}R$ facilitate inhibitory inputs (Brooke et al., 2004) to sympathetic preganglonic neurons, suggesting that at least in what concerns autonomic nervous system control, the opposing actions of A_1R and $A_{2A}R$ at the synaptic level may both contribute to a common outcome – a decrease in preganglionic neuron activity. The antinociceptic actions of adenosine A_1R are widely known, which involve A_1R at the dorsal horn of the spinal cord. A_3R receptors also mediate antinociception through spinal and supraspinal mechanisms (Little et al., 2015) that also involve anti-inflammation (Janes et al., 2015).

Concerning motor pattern generation, it has been for a long time described that ATP and adenosine have opposite actions in motor pattern generation, the adenosine actions being inhibitory, lowering the excitability of motor circuits (Dale and Gilday, 1996). Recent studies have shown that adenosine, via A_1R, has a general inhibitory action on ventral horn interneurons while potentially maintaining motor neuron excitability (Witts et al., 2015). Interestingly, glial cells are a predominant source of adenosine at to control motor neuron networks at the spinal cord (Witts et al., 2012; Carlsen and Perrier, 2014; Acton and Miles, 2015).

The motor nerve terminals at the neuromuscular junction have served as a model to the pioneer studies on the inhibitory action of adenosine and ATP on neurotransmitter release (Ginsborg and Hirst, 1972; Ribeiro and Walker, 1973, 1975), being now well known that endogenous adenosine inhibits neuromuscular transmission (Sebastião and Ribeiro, 1985), that ATP is a source of extracellular adenosine at the endplate (Ribeiro and Sebastião, 1987), and that adenosine can also be independently released from stimulated motor nerve endings (Cunha and Sebastião, 1993). Motor nerve terminals at the mammalian skeletal neuromuscular junction possess both inhibitory A_1R (Sebastião et al., 1990) and excitatory $A_{2A}R$ (Correia-de-Sá et al., 1991), the $A_{2A}R$ gaining particular relevance at high frequencies of nerve stimulation

(Correia-de-Sá et al., 1996). A_{2B} and A_3 receptors were also more recently detected at the mammalian neuromuscular junction (Garcia et al., 2014).

Adenosine Receptors in Health and Disease

At physiological conditions, the adenosine exerts its neuromodulation action by the activation of A_1 and A_{2A}R high affinity receptors (Sebastião and Ribeiro, 2009a), which mediate dual actions of adenosine both in health and disease (Fredholm, 2014). At pre-synaptic level, adenosine can inhibit or facilitate transmitter release through A_1R and A_{2A}R respectively; at post-synaptic level, it can modulate the actions of several neurotransmitters and it can hyperpolarize or depolarize neurons. All these receptors can be found in neurons and glia cells. While the A_1R is frequently associated to neuroprotective actions, which extend to conditions as hyperexcitability, seizures and ischemia/hypoxia, protecting neurons in response to excitotoxic injury (Boison, 2016; Cunha, 2016; Ribeiro et al., 2016b), the A_{2A}R is often associated to enhancement of excitotoxicity, since these receptors facilitate glutamate release and inhibit glutamate uptake (Popoli et al., 2003; Matos et al., 2012). However, through their ability to gate the actions of neurotrophic factors, A_{2A}R may confer a protective role under specific pathologic conditions (Sebastião and Ribeiro, 2009b; Rodrigues et al., 2014). A_1R, A_{2A}R and A_{2B}R can also influence oxygen deliver into the brain due to their influence in neurovascular coupling (Pelligrino et al., 2010).

Concerning inflammation, A_{2A}R have a duality of actions, depending on the cell type and inflammatory conditions (Haskó et al., 2008). In immune cells the global trend for A_{2A}R-mediated actions is to interrupt the proinflammatory cascade and hence limiting tissue inflammation (Sitkovsky et al., 2004; Haskó et al., 2008), contrasting with A_2B receptors that may promote overproduction of proinflammatory cytokines (Haskó et al., 2008). In the central nervous system, however, A_{2A}R mediate anti-inflammatory effects on T cells, and thus protection at early stages of inflammatory diseases; during later stages of disease, however, may contribute to sustained tissue damage within the inflamed central nervous system (Ingwersen et al., 2016). In microglia, A_{2A}R activation leads to their activation, and in such way contributing to foster neuroinflamatory cascades, thus to neurodegeneration (Dai and Zhou, 2011; Rebola et al., 2011; Santiago et al., 2014). Similarly, A_{2B}R and A_3R may mediate either anti-inflammatory or pro-inflammatory actions (Borea et al., 2017).

Adenosine Receptors in ALS

Adenosine Receptors at Spinal Cord: Implications for ALS

In accordance with the expected facilitatory influence of A_{2A}R upon excitotoxicity, A_{2A}R antagonists protect against excitotoxicity-induced motor neuron death (Mojsilovic-Petrovic et al., 2006). However, motor neuron survival after mechanical lesioning has also been shown to be increased by an A_{2A}R activation, through a mechanism that involves interplay with neurotrophines (Wiese et al., 2007). Survival of motor neurons in culture is also facilitated by A_{2A}R activation, this mechanism requiring the activity of the canonical A_{2A}R signaling pathway, cyclic AMP/protein kinase activity, as well as the activity of neurotrophin receptors, again highlighting an interplay between A_{2A}R and neurotrophins to promote motor neuron survival (Komaki et al., 2012). The apparent discrepancies between the neuroprotective actions of A_{2A}R antagonists and A_{2A}R agonists probably result from the diversity of actions that the A_{2A}R have, namely modulation of neuronal activity, neuronal survival, excitotoxicity, neuroinflammation. While facilitating the actions of neurotrophic factors A_{2A}R may promote survival and regeneration, but while enhancing excitotoxicity phenomena A_{2A}R will favor neuronal death. In addition, if neuroinflammation interferes with in the regeneration/degeneration balance A_{2A}R may again have a dual role, depending on the degree and characteristics of the inflammatory process, that it to say, if activation of the inflammatory cascade is beneficial or detrimental. Unraveling all these aspects by taking into consideration the nature of the insult and the time window for treatment is of uttermost importance to understand the role of adenosine receptors in neurodegeneration and in particular in ALS. Our poor understanding of the pathophysiology of the disease itself makes it more difficult to understand the role of adenosine receptors in this disease.

Adenosine levels are significantly elevated in the cerebrospinal fluid of ALS patients (Yoshida et al., 1999), a finding that raised the interest on the understanding the role of adenosine and adenosine receptors in ALS. The expression of A_{2A} receptors is also enhanced in lymphocytes of ALS patients (Vincenzi et al., 2013) as well as in post-mortem spinal cord of ALS patients (Ng et al., 2015). A_{2A}R expression in the spinal cord of early symptomatic $SOD1^{G93A}$ mice was also markedly increased (Ng et al., 2015), but in end-stage $SOD1^{G93A}$ mice a marked decrease was reported (Potenza et al., 2013). Mice data thus may suggest that there is an early enhancement of A_{2A}R expression in the spinal cord, followed by a decrease in latter disease states. A comparison of data obtained in the same laboratory conditions and same animal housing conditions is, however, needed to firmly conclude on biphasic changes in A_{2A}R expression during disease progression. Post-mortem human data (Ng et al., 2015), by definition related to end-stages of the disease, seems to contradict the conclusion of a late-phase decrease in A_{2A}R expression in the spinal cord. Whether the discrepancy arrives from methodological issues (post-mortem time of analysis, tissue collection procedures), species differences (mice vs. human) or from inappropriate disease model, is unknown.

Caffeine is a non-selective adenosine receptors antagonist (Pelligrino et al., 2010; Ribeiro and Sebastião, 2010; Fredholm et al., 2017) and is one of the most consumable psychoactive substances of the western diet. There is thus high interest in understanding the actions of caffeine in neurodegenerative diseases. Indeed, caffeine consumption in humans has been negatively associated with the incidence of some neurodegenerative diseases, as Alzheimer's Disease and Parkinson's Disease (de Mendonça and Cunha, 2010; Flaten et al., 2014; Laurent et al., 2014; Ascherio and Schwarzschild, 2016).

Accordingly, chronic caffeine consumption has been shown to protect several hallmarks of neurodegeneration in animal models of disease, these actions being frequently mimicked by selective $A_{2A}R$ antagonists or $A_{2A}R$ deletion (Canas et al., 2009; Kachroo and Schwarzschild, 2012; Laurent et al., 2016; Ferreira et al., 2017). Concerning ALS, however, conflicting data had recently emerged in the literature, and there are several points that are far from being understood. In clear contrast to what could be expected from previous evidence in other neurodegenerative diseases, chronic administration of caffeine significantly shortens the survival of $SOD1^{G93A}$ mice (Potenza et al., 2013). Also somehow unexpected, chronic administration of caffeine caused a marked decrease in $A_{2A}R$ levels in the spinal cord (Potenza et al., 2013) and in this aspect seems to mimic the disease itself since $SOD1^{G93A}$ mice also displayed a strong reduction in $A_{2A}R$ in the spinal cord. Both conditions (caffeine treatment and SOD^{G93A} mutation) were not additive since there were no further reduction in spinal cord $A_{2A}R$ levels in $SOD1^{G93A}$ mice treated with caffeine (Potenza et al., 2013). Caffeine can inhibit all adenosine receptors, and thus one cannot preclude that those actions of caffeine were due to antagonism of the usually neuroprotective A_1R rather than antagonism of the $A_{2A}R$. Indeed, A_1 and $A_{2A}R$ are known to strongly interact with each other (Ferre et al., 2008), including in motor neurons (Pousinha et al., 2010, 2012), and the loss of inhibitory control of A_1R upon $A_{2A}R$ may cause marked unbalance of the fine-tuning of neuronal function exerted by adenosine receptors. A selective $A_{2A}R$ antagonist, KW6002, administered daily, was recently reported to increase of motor neuron survival, delay the onset of disease and increase in the lifespan that $SOD1^{G93A}$ mice (Ng et al., 2015), which is in accordance with the usual finding that $A_{2A}R$ may exacerbate excitotoxicity.

Concerning the influence of $A_{2A}R$ agonists in ALS progression, it has been shown that treatment of $SOD1^{G93A}$ mice with CGS21680 at a very early symptomatic stage of the disease, delayed disease onset of motor symptoms and enhanced motor neuron survival (Yanpallewar et al., 2012). Interestingly, the effect of the $A_{2A}R$ agonist was similar to that resulting from genetic deletion of the truncated form of the TrkB receptor, TrkB.T1, which is overexpressed in the spinal cord of the $SOD1^{G93A}$ mice. The TrkB.T1 act as negative regulator of full-length TrkB receptor signaling, impairing the ability of its ligand, the neurotrophin Brain Derived Neurotrophic factor (BDNF), to promote neuronal survival, neuronal maturation and neuronal plasticity. Most of the actions of BDNF at synapses are triggered by $A_{2A}R$ activation (Diógenes et al., 2004; Sebastião et al., 2011; Ribeiro et al., 2016b). It is thus likely that the protective influence of $A_{2A}R$ receptor agonist in very early stages of ALS progression in SOD^{G93A} mice results from the ability of $A_{2A}R$ to facilitate full length TrkB receptor activation, thus compensating the negative influence the TrkB.T1 receptor overexpression. That $A_{2A}R$ and $A_{2A}R$ antagonists may have strict time windows to exert its beneficial influences in neurodegeneration has been already proposed (Sebastião and Ribeiro, 2009b) but data from experiments specifically addressing this point have not yet appeared.

Also particularly relevant in the context of understanding the role of $A_{2A}R$ in ALS progression was the finding that $A_{2A}R$ activation, through PKA signaling, suppresses aberrant AMPK activity as well as suppresses mislocalization of TDP-43, in the TDP-43 mouse model of ALS (Liu et al., 2015a). Taking into consideration that mislocalization of TDP-43 from the nucleus to the cytoplasm can be induced not only by mutations in the gene that codes for TDP-43 but also by ROS production, there is some overlap in the disease triggering mechanisms in the SOD mouse models and in the TDP-43 model.

Summarizing, in two models of ALS ($SOD1^{G93A}$ and TDP-43), two different $A_{2A}R$ agonists proved beneficial to improve motor neuron survival (Yanpallewar et al., 2012; Liu et al., 2015a). One study clearly showed detrimental effects of the adenosine receptor antagonist, caffeine in the survival of $SOD1^{G93A}$ mice (Potenza et al., 2013). Thus, as whole and in the specific context of ALS, $A_{2A}R$ activation seems beneficial. Importantly, $A_{2A}R$, through cAMP/PKA signaling and subsequent inhibition of AMPK may contribute to cut the positive feedback mechanism where AMPK activation by ROS leads to further mislocalization of TDP-43, which leads to further ROS production, thus to further AMPK activation. In this way, $A_{2A}R$ activation may hit a key pathophysiologic mechanism of ALS, thus reducing or even halting disease progression. Unfortunately, in the study by Liu et al. (2015a), the influence of $A_{2A}R$ activation in the time of appearance of first symptoms or in the life-span of ALS mice was not assessed. Results from such studies would indeed complement the evidence already obtained on enhancement of motor neuron survival by $A_{2A}R$ activation in two models of ALS (Yanpallewar et al., 2012; Liu et al., 2015a). Also, and taking into consideration that the agonist used by Liu et al. (2015a) already entered clinical trials for other neurodegenerative diseases, a clinical trial specifically designed for a fast devastating disease as ALS, would be of high relevance.

$A_{2A}R$ and D_2 dopamine receptors (D_2R) co-exist in motor neurons of the spinal cord of normal subjects and ALS patients (Chern et al., 2017). Activation of D_2R reverse the $A_{2A}R$-mediated prevention of ROS-induced AMPK activation and TDP-43 mislocalization in cells co-transfected with D_2R and $A_{2A}R$ (Chern et al., 2017). A_{2A}/D_2 negative interactions are well known in the basal ganglia (Fuxe et al., 2007). The evidence that they also exist at the level of the spinal cord and in a context of ALS pathophysiology (Chern et al., 2017), point toward the need of care in the use of D_2R agonists in ALS patients, as well as may suggest a beneficial role of D_2R antagonists in this disease.

From the studies mentioned above, it appears that $A_{2A}R$ agonists may prove of therapeutic value in ALS. Yet, there are several discrepancies in the literature, as the report that a selective $A_{2A}R$ antagonist may delay disease progression. To solve some discrepancies, it will be important to compare in the same colony and under the same experimental conditions, and always against age-matched control littermates, time-dependent and disease state-dependent changes in the activity and expression of adenosine receptors. The comparisons among different mouse models are also of uttermost importance to allow starting to understand the different roles of $A_{2A}R$ as a function of the etiology of the disease itself. It will be also necessary to follow

those changes in mice treated with either selective receptor ligands as well as with caffeine. Since ALS progression may not be similar at different synaptic levels, a better understanding of the time-dependent changes in $A_{2A}R$ signaling at upper and lower motor neuron levels would also allow a better understanding in the role of $A_{2A}R$ in ALS. Information of the role of A_1R in this neurodegenerative disease is scarce, which is somehow surprising on the light of the known neuroprotection exerted by these receptors. Their ability to inhibit synaptic transmission, may, however, exert a negative influence in a degenerative disease that markedly compromises information flow in the motor circuit.

Adenosine Receptors at the Neuromuscular Junction: Implications for ALS

The neuromuscular junction early served as a model to understand synaptic transmission mechanisms (Katz and Miledi, 1965), as model to understand neuromodulation by adenosine (Ginsborg and Hirst, 1972), as a model to understand the relevance of endogenous adenosine to control synaptic transmission (Ribeiro and Sebastião, 1987), and as a model to start identifying $A_{2A}R$ at synapses outside the basal ganglia (Correia-de-Sá et al., 1991; Correia-de-Sá and Ribeiro, 1994). Reasons for this are the simplicity of the model, allowing to record from a single synapse receiving input from only one nerve terminal, with a clearly identified neurotransmitter - acetylcholine. In spite of this simplicity, there are several neuromodulators released by either the pre-synaptic, the post-synaptic, the muscle itself and the perisynaptic Schwann cells, which finely tune synaptic transmission and synaptic maintenance. As widely known, ATP and adenosine are among such neuromodulators. Neurotrophic factors are also present at the neuromuscular junction and $A_{2A}R$ are also indispensable promoters of the facilitatory action BDNF, upon neuromuscular transmission (Pousinha et al., 2006), as it was firstly observed hippocampal synapses (Diógenes et al., 2004).

Having studied the action of adenosine for more than 40 years, using the neuromuscular junction as a model, and considering that this simple synaptic model could be as a sort of key (Arbour et al., 2017) to investigate novel approaches for disease therapy, and also that this particular synapse is compromised in ALS, we hypothesized (Nascimento et al., 2014, 2015) that ALS progression could be accompanied by changes in the functioning of adenosine A_1R and $A_{2A}R$, the two high affinity adenosine receptors known to be expressed at motor nerve endings (Correia-de-Sá and Ribeiro, 1994). We used a functional approach, recording endplate potentials (EPPs) and miniature endplate potentials (MEPPs), and quantifying quantal content of EPPs, from Mg^{2+}-paralyzed hemidiaphragm preparations of $SOD1^{G93A}$ mice at pre-symptomatic (absence of motor symptoms assessed by the Rota-Rod) and early symptomatic (mild but significant dysfunction at the Rota-Rod) phases of the disease. We found that at the pre-symptomatic stage the $A_{2A}R$-mediated presynaptic facilitatory action on neuromuscular transmission is exacerbated, whereas in the early symptomatic phase, this excitatory action disappears, indicating that indeed that $A_{2A}R$ function changes upon ALS progression. We then further investigated the role of A_1R in ALS using the same approach and the same disease model (Nascimento et al., 2015) and found that the $A_1R/A_{2A}R$ functional cross-talk is lost in the pre-symptomatic phase, so that the ability of A_1R to brake the action of $A_{2A}R$ is lost, which might explain the exacerbation of the $A_{2A}R$ signaling at this disease state. In addition, there was an increase of A_1R tonic activation in the symptomatic phase, suggesting that the changes adenosine modulation mediated by A_1R may be contributing to disease progression and aggravating symptoms in late disease stage. Whether the lack of A_1R-mediated inhibition of $A_{2A}R$ function, with the corresponding exacerbation of $A_{2A}R$-mediated function, corresponds to an early compensatory process that may facilitate neuromuscular transmission and confer some neuroprotection through an enhancement of the action of neurotrophic factors, remains unknown. Also unknown is if these early excitatory changes, accompanied by dysruptions of the calcium buffering at the nerve terminal (Rocha et al., 2013) and at perisynaptic Schwann Cells (Arbour et al., 2015), are a fast-track to neurodegeneration.

Summarizing, data (Nascimento et al., 2014, 2015) suggest that in ALS there is an unbalanced adenosine receptors modulation at the neuromuscular junction (**Figure 1**) that may start before first signs of motor impairment. We anticipate early compensatory alterations followed by a disruption of neuromodulatory control that may then act as an aggravating factor to exacerbate excitotoxicity, fasting neuronal death. A clear identification of the nature of these adenosine receptors changes, at different diseases states, would allow to identify new therapeutic targets based on the cause of neurodegeneration and thus to halt it.

Interestingly, adenosine A_1R at motor nerve endings, besides inhibiting the release probability, also synchronize release by removing quantal events with long latencies, an action that is sensitive to the redox potential, being abolished by oxidants (Tsentsevitsky et al., 2013). How this impacts in oxidative-stress related motor neuron diseases, as ALS, is yet unknown.

CONCLUSION AND PERSPECTIVES

A major finding in what concerns adenosinergic signaling in ALS is the existence of very early synaptic alterations, which precede motor symptoms and which are evident at the level of the neuromuscular junction as well as, most probably, at central synapses. Whether those changes are triggers for the disease or represent early compensatory modifications is yet unknown. The evidence of a positive influence of $A_{2A}R$ agonists and negative influence of caffeine, may suggest that an early enhancement of $A_{2A}R$ functioning may represent an endogenous attempt to fight the disease. The positive influence of a selective $A_{2A}R$ antagonist may, however, contradict this possibility. A better clarification of the nature of the purinergic signaling dysfunctions, their implications and their time-windows, is for sure relevant not only for a better understanding of the pathophysiology of the disease and the implications of caffeine intake, but also to guide the design of putative therapeutic strategies to halt disease progression. Specifically, it is important to know if the early exacerbation of $A_{2A}R$ signaling detected at the motor nerve endings also occurs at central synapses, in particular, at the spinal

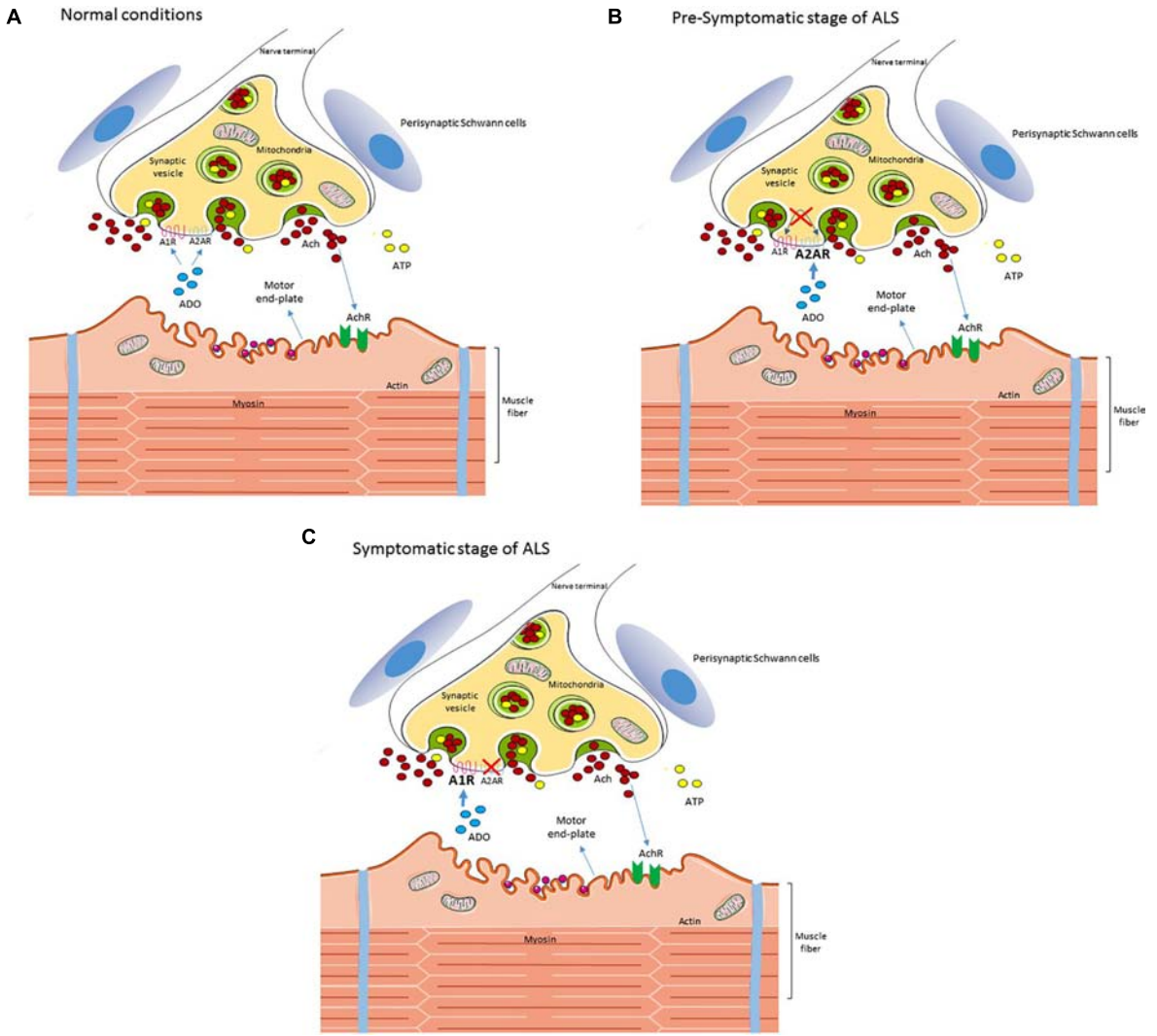

FIGURE 1 | Schematic diagram of the reported changes in adenosine signaling at the neuromuscular junction in an ALS mice model. In wild type **(A)** neuromuscular junctions, adenosine activates both inhibitory A_1R and excitatory $A_{2A}R$, modulating acetylcholine release from motor nerve terminals. In ALS mice at the pre-symptomatic stage **(B)** there is a loss of $A_1R/A_{2A}R$ functional cross-talk at the neuromuscular junction and the excitatory action of $A_{2A}R$ is exacerbated. At the symptomatic stage **(C)** there is an increase of A_1R tonic activation, which may be contributing to neurotransmission failure on late disease stages, whereas the excitatory action of $A_{2A}R$ disappears. For details see Nascimento et al. (2014, 2015). Perisynaptic Schwann cells contribute to the pool of ATP at the synaptic cleft but ATP signaling in these cells seems unchanged in ALS, in contrast with mACh signaling (Arbour et al., 2015). Interestingly, the exacerbated $A_{2A}R$ signaling at the pre-symptomatic stage correlates with an enhanced release of ACh from nerve terminals and with signs of dysregulated calcium buffering at motor nerve endings (Rocha et al., 2013; Arbour et al., 2017).

cord and motor cortex, and how selective blockade of these receptors at different disease states affects disease progression. Keeping in mind the intriguing data reported while testing the influence of caffeine in animal models, it is also of uttermost importance to understand the molecular basis of this action of caffeine, whether it has an impact in the signaling of other neuroprotective molecules, or in the signaling mediated by other adenosine receptors. This knowledge is not only important for the design of future drugs but also to guide research in patients since caffeine is present in many widely consumed beverages and is usually regarded as protective against other neurodegenerative diseases. Lastly, the putative influence of $A_{2A}R$ and A_3R in the inflammatory cascade associated to ALS has to be better understood. Indeed, recent studies have demonstrated the presence of inflammation propagating substrates in the central nervous system of patients afflicted with ALS (Khalid et al., 2017). $A_{2A}R$ receptors mediate anti-inflammatory actions and are up-regulated in lymphocytes from ALS patients(Vincenzi et al., 2013). The A_3R is a promising therapeutic target for inflammatory diseases (Jacobson et al., 2017) but these receptors have been mostly disregarded in what concerns ALS.

In conclusion, though one starts to envisage changes in the adenosinergic system at different stages of ALS progression, much more needs to be known before understanding the causal

relationship of those changes and which of them can be targeted to develop novel therapeutics toward this devastating disease.

AUTHOR CONTRIBUTIONS

All authors listed have made a substantial, direct and intellectual contribution to the work, and approved it for publication.

FUNDING

This work was supported by LISBOA-01-0145-FEDER-007391, project co-funded by FEDER through POR Lisboa 2020 (Programa Operacional Regional de Lisboa) from PORTUGAL 2020 and Fundação para a Ciência e Tecnologia (FCT) and by a Twinning action (SynaNet) from the EU H2020 program (Project Number: 692340). NR is in receipt of an FCT fellowship (PD /BD/113463/2015) and is a fellow of the M2B-Ph.D. Program.

REFERENCES

Acton, D., and Miles, G. B. (2015). Stimulation of glia reveals modulation of mammalian spinal motor networks by adenosine. *PLoS One* 10:e0134488. doi: 10.1371/journal.pone.0134488

Arai, T., Hasegawa, M., Akiyama, H., Ikeda, K., Nonaka, T., Mori, H., et al. (2006). TDP-43 is a component of ubiquitin-positive tau-negative inclusions in frontotemporal lobar degeneration and amyotrophic lateral sclerosis. *Biochem. Biophys. Res. Commun.* 351, 602–611. doi: 10.1016/j.bbrc.2006.10.093

Arbour, D., Tremblay, E., Martineau, E., Julien, J. P., and Robitaille, R. (2015). Early and persistent abnormal decoding by glial cells at the neuromuscular junction in an ALS model. *J. Neurosci.* 35, 688–706. doi: 10.1523/JNEUROSCI.1379-14.2015

Arbour, D., Vande Velde, C., and Robitaille, R. (2017). New perspectives on amyotrophic lateral sclerosis: the role of glial cells at the neuromuscular junction. *J. Physiol.* 595, 647–661. doi: 10.1113/JP270213

Ascherio, A., and Schwarzschild, M. A. (2016). The epidemiology of Parkinson's disease: risk factors and prevention. *Lancet Neurol.* 15, 1257–1272. doi: 10.1016/S1474-4422(16)30230-7

Ayala, V., Granado-Serrano, A. B., Cacabelos, D., Naudí, A., Ilieva, E. V., Boada, J., et al. (2011). Cell stress induces TDP-43 pathological changes associated with ERK1/2 dysfunction: implications in ALS. *Acta Neuropathol.* 122, 259–270. doi: 10.1007/s00401-011-0850-y

Baker, M. R. (2014). ALS—dying forward, backward or outward? *Nat. Rev. Neurol.* 10:660. doi: 10.1038/nrneurol.2013.221-c1

Boison, D. (2016). The biochemistry and epigenetics of epilepsy: focus on adenosine and glycine. *Front. Mol. Neurosci.* 9:26. doi: 10.3389/fnmol.2016.00026

Borea, P. A., Gessi, S., Merighi, S., Vincenzi, F., and Varani, K. (2017). Pathological overproduction: the bad side of adenosine. *Br. J. Pharmacol.* 174, 1945–1960. doi: 10.1111/bph.13763

Braak, H., Brettschneider, J., Ludolph, A. C., Lee, V. M., Trojanowski, J. Q., and Del Tredici, K. (2013). Amyotrophic lateral sclerosis–a model of corticofugal axonal spread. *Nat. Rev. Neurol.* 9, 708–714. doi: 10.1038/nrneurol.2013.221

Brooke, R. E., Deuchars, J., and Deuchars, S. A. (2004). Input-specific modulation of neurotransmitter release in the lateral horn of the spinal cord via adenosine receptors. *J. Neurosci.* 24, 127–137. doi: 10.1523/JNEUROSCI.4591-03.2004

Burnstock, G. (1976). Do some nerve cells release more than one transmitter? *Neuroscience* 1, 239–248.

Canas, P. M., Porciúncula, L. O., Cunha, G. M., Silva, C. G., Machado, N. J., Oliveira, J. M., et al. (2009). Adenosine A_{2A} receptor blockade prevents synaptotoxicity and memory dysfunction caused by beta-amyloid peptides via p38 mitogen-activated protein kinase pathway. *J. Neurosci.* 29, 14741–14751. doi: 10.1523/JNEUROSCI.3728-09.2009

Carlsen, E. M., and Perrier, J. F. (2014). Purines released from astrocytes inhibit excitatory synaptic transmission in the ventral horn of the spinal cord. *Front. Neural Circuits* 8:60. doi: 10.3389/fncir.2014.00060

Chern, Y., Lai, C., Liu, Y., and Lai, H. (2017). Activation of the D2 dopamine receptor hampers the protective effect of the A2A adenosine receptor on TDP-43 mislocalization. *FASEB J.* 31:LB140.

Chou, C. C., Zhang, Y., Umoh, M. E., Vaughan, S. W., Lorenzini, I., Liu, F., et al. (2018). TDP-43 pathology disrupts nuclear pore complexes and nucleocytoplasmic transport in ALS/FTD. *Nat. Neurosci.* 21, 228–239. doi: 10.1038/s41593-017-0047-3

Correia-de-Sá, P., and Ribeiro, J. A. (1994). Evidence that the presynaptic A_{2a}-adenosine receptor of the rat motor nerve endings is positively coupled to adenylate cyclase. *Naunyn Schmiedebergs Arch. Pharmacol.* 350, 514–522. doi: 10.1007/BF00173021

Correia-de-Sá, P., Sebastião, A. M., and Ribeiro, J. A. (1991). Inhibitory and excitatory effects of adenosine receptor agonists on evoked transmitter release from phrenic nerve endings of the rat. *Br. J. Pharmacol.* 103, 1614–1620. doi: 10.1111/j.1476-5381.1991.tb09836.x

Correia-de-Sá, P., Timóteo, M. A., and Ribeiro, J. A. (1996). Presynaptic A_1 inhibitory/A_{2A} facilitatory adenosine receptor activation balance depends on motor nerve stimulation paradigm at the rat hemidiaphragm. *J. Neurophysiol.* 76, 3910–3919. doi: 10.1152/jn.1996.76.6.3910

Costa, J., Gomes, C., and de Carvalho, M. (2010). Diagnosis, pathogenesis and therapeutic targets in amyotrophic lateral sclerosis, CNS and neurological disorders. *Drug Targets* 9, 764–778. doi: 10.2174/187152710793237502

Cunha, C., Santos, C., Gomes, C., Fernandes, A., Correia, A. M., Sebastião, A. M., et al. (2017). Downregulated glia interplay and increased miRNA-155 as promising markers to track ALS at an early stage. *Mol. Neurobiol.* doi: 10.1007/s12035-017-0631-2 [Epub ahead of print].

Cunha, R. A. (2016). How does adenosine control neuronal dysfunction and neurodegeneration? *J. Neurochem.* 139, 1019–1055. doi: 10.1111/jnc.13724

Cunha, R. A., and Sebastião, A. M. (1993). Adenosine and adenine nucleotides are independently released from both the nerve terminals and the muscle fibres upon electrical stimulation of the innervated skeletal muscle of the frog. *Pflugers Arch.* 424, 503–510. doi: 10.1007/BF00374914

Dadon-Nachum, M., Melamed, E., and Offen, D. (2011). The "dying-back" phenomenon of motor neurons in ALS. *J. Mol. Neurosci.* 43, 470–477. doi: 10.1007/s12031-010-9467-1

Dai, S. S., and Zhou, Y. G. (2011). Adenosine 2A receptor: a crucial neuromodulator with bidirectional effect in neuroinflammation and brain injury. *Rev. Neurosci.* 22, 231–239. doi: 10.1515/RNS.2011.020

Dale, N., and Gilday, D. (1996). Regulation of rhythmic movements by purinergic neurotransmitters in frog embryos. *Nature* 383, 259–263. doi: 10.1038/383259a0

de Mendonça, A., and Cunha, R. A. (2010). Putative neuroprotective effects of caffeine in clinical trials. Concluding remarks. *J. Alzheimers Dis.* 20(Suppl. 1), S249–S252.

DeJesus-Hernandez, M., Mackenzie, I. R., Boeve, B. F., Boxer, A. L., Baker, M., Rutherford, N. J., et al. (2011). Expanded GGGGCC hexanucleotide repeat in noncoding region of C9ORF72 causes chromosome 9p-linked FTD and ALS. *Neuron* 72, 245–256. doi: 10.1016/j.neuron.2011.09.011

Deuchars, S. A., Brooke, R. E., and Deuchars, J. (2001). Adenosine A_1 receptors reduce release from excitatory but not inhibitory synaptic inputs onto lateral horn neurons. *J. Neurosci.* 21, 6308–6320.

Di Giorgio, F. P., Carrasco, M. A., Siao, M. C., Maniatis, T., and Eggan, K. (2007). Non-cell autonomous effect of glia on motor neurons in an embryonic stem cell-based ALS model. *Nat. Neurosci.* 10, 608–614. doi: 10.1038/nn1885

Dias, R. B., Ribeiro, J. A., and Sebastião, A. M. (2012). Enhancement of AMPA currents and GluR1 membrane expression through PKA- coupled adenosine A_{2A} receptors. *Hippocampus* 22, 276–291. doi: 10.1002/hipo.20894

Dias, R. B., Rombo, D. M., Ribeiro, J. A., and Sebastião, A. M. (2013). Ischemia-induced synaptic plasticity drives sustained expression of calcium-permeable AMPA receptors in the hippocampus. *Neuropharmacology* 65, 114–122. doi: 10.1016/j.neuropharm.2012.09.016

Diógenes, M. J., Fernandes, C. C., Sebastião, A. M., and Ribeiro, J. A. (2004). Activation of adenosine A_{2A} receptor facilitates brain-derived neurotrophic factor modulation of synaptic transmission in hippocampal slices. *J. Neurosci.* 24, 2905–2913. doi: 10.1523/JNEUROSCI.4454-03.2004

Dunwiddie, T. V., and Masino, S. A. (2001). The role and regulation of adenosine in the central nervous system. *Annu. Rev. Neurosci.* 24, 31–55. doi: 10.1146/annurev.neuro.24.1.31

Feng, Z., and Ko, C. P. (2008a). Schwann cells promote synaptogenesis at the neuromuscular junction via transforming growth factor-β1. *J. Neurosci.* 28, 9599–9609. doi: 10.1523/JNEUROSCI.2589-08.2008

Feng, Z., and Ko, C. P. (2008b). The role of glial cells in the formation and maintenance of the neuromuscular junction. *Ann. N. Y. Acad. Sci.* 1132, 19–28. doi: 10.1196/annals.1405.016

Ferre, S., Ciruela, F., Borycz, J., Solinas, M., Quarta, D., Antoniou, K., et al. (2008). Adenosine A_1-A_{2A} receptor heteromers: new targets for caffeine in the brain. *Front. Biosci.* 13, 2391–2399. doi: 10.2741/2852

Ferreira, D. G., Batalha, V. L., Vicente Miranda, H., Coelho, J. E., Gomes, R., Gonçalves, F. Q., et al. (2017). Adenosine A_{2A} receptors modulate α-synuclein aggregation and toxicity. *Cereb. Cortex* 27, 718–730.

Flaten, V., Laurent, C., Coelho, J. E., Sandau, U., Batalha, V. L., Burnouf, S., et al. (2014). From epidemiology to pathophysiology: what about caffeine in Alzheimer's disease? *Biochem. Soc. Trans.* 42, 587–592. doi: 10.1042/BST20130229

Fredholm, B. B. (2014). Adenosine–a physiological or pathophysiological agent? *J. Mol. Med.* 92, 201–206. doi: 10.1007/s00109-013-1101-6

Fredholm, B. B., Yang, J., and Wang, Y. (2017). Low, but not high, dose caffeine is a readily available probe for adenosine actions. *Mol. Aspects Med.* 55, 20–25. doi: 10.1016/j.mam.2016.11.011

Frey, D., Schneider, C., Xu, L., Borg, J., Spooren, W. I., and Caroni, P. (2000). Early and selective loss of neuromuscular synapse subtypes with low sprouting competence in motoneuron diseases. *J. Neurosci.* 20, 2534–2542.

Fritz, E., Izaurieta, P., Weiss, A., Mir, F. R., Rojas, P., Gonzalez, D., et al. (2013). Mutant SOD1-expressing astrocytes release toxic factors that trigger motoneuron death by inducing hyperexcitability. *J. Neurophysiol.* 109, 2803–2814. doi: 10.1152/jn.00500.2012

Fuxe, K., Ferré, S., Genedani, S., Franco, R., and Agnati, L. F. (2007). Adenosine receptor-dopamine receptor interactions in the basal ganglia and their relevance for brain function. *Physiol. Behav.* 92, 210–217. doi: 10.1016/j.physbeh.2007.05.034

Garcia, N., Priego, M., Hurtado, E., Obis, T., Santafe, M. M., Tomàs, M., et al. (2014). Adenosine A2B and A3 receptor location at the mouse neuromuscular junction. *J. Anat.* 225, 109–117. doi: 10.1111/joa.12188

Georgiou, J., Robitaille, R., and Charlton, M. P. (1999). Muscarinic control of cytoskeleton in perisynaptic glia. *J. Neurosci.* 19, 3836–3846.

Ginsborg, B. L., and Hirst, G. D. S. (1972). The effect of adenosine on the release of the transmitter from the phrenic nerve of the rat. *J. Physiol.* 224, 629–645. doi: 10.1113/jphysiol.1972.sp009916

Gitcho, M. A., Baloh, R. H., Chakraverty, S., Mayo, K., Norton, J. B., Levitch, D., et al. (2008). TDP-43 A315T mutation in familial motor neuron disease. *Ann. Neurol.* 63, 535–538. doi: 10.1002/ana.21344

Guo, W., Chen, Y., Zhou, X., Kar, A., Ray, P., Chen, X., et al. (2011). An ALS associated mutation affecting TDP-43 enhances protein aggregation, fibril formation and neurotoxicity. *Nat. Struct. Mol. Biol.* 18, 822–830. doi: 10.1038/nsmb.2053

Haskó, G., Linden, J., Cronstein, B., and Pacher, P. (2008). Adenosine receptors: therapeutic aspects for inflammatory and immune diseases. *Nat. Rev. Drug Discov.* 7, 759–770. doi: 10.1038/nrd2638

Ingwersen, J., Wingerath, B., Graf, J., Lepka, K., Hofrichter, M., Schröter, F., et al. (2016). Dual roles of the adenosine A2a receptor in autoimmune neuroinflammation. *J. Neuroinflammation* 13:48. doi: 10.1186/s12974-016-0512-z

Jacobson, K. A., Merighi, S., Varani, K., Borea, P. A., Baraldi, S., Aghazadeh Tabrizi, M., et al. (2017). A_3 adenosine receptors as modulators of inflammation: from medicinal chemistry to therapy. *Med. Res. Rev.* doi: 10.1002/med.21456 [Epub ahead of print].

Janes, K., Wahlman, C., Little, J. W., Doyle, T., Tosh, D. K., Jacobson, K. A., et al. (2015). Spinal neuroimmune activation is independent of T-cell infiltration and attenuated by A_3 adenosine receptor agonists in a model of oxaliplatin-induced peripheral neuropathy. *Brain Behav. Immun.* 44, 91–99. doi: 10.1016/j.bbi.2014.08.010

Kachroo, A., and Schwarzschild, M. A. (2012). Adenosine A_{2A} receptor gene disruption protects in an α-synuclein model of Parkinson's disease. *Ann. Neurol.* 71, 278–282. doi: 10.1002/ana.22630

Kaelin-Lang, A., Lauterburg, T., and Burgunder, J. M. (1999). Expression of adenosine A2a receptors gene in the olfactory bulb and spinal cord of rat and mouse. *Neurosci. Lett.* 261, 189–191. doi: 10.1016/S0304-3940(99)00022-1

Katz, B., and Miledi, R. (1965). Release of acetylcholine from a nerve terminal by electric pulses of variable strength and duration. *Nature* 207, 1097–1098. doi: 10.1038/2071097a0

Khalid, S. I., Ampie, L., Kelly, R., Ladha, S. S., and Dardis, C. (2017). Immune modulation in the treatment of amyotrophic lateral sclerosis: a review of clinical trials. *Front. Neurol.* 8:486. doi: 10.3389/fneur.2017.00486

Kiernan, M. C., Vucic, S., Cheah, B. C., Turner, M. R., Eisen, A., Hardiman, O., et al. (2011). Amyotrophic lateral sclerosis. *Lancet* 377, 942–955. doi: 10.1016/S0140-6736(10)61156-7

Komaki, S., Ishikawa, K., and Arakawa, Y. (2012). Trk and cAMP-dependent survival activity of adenosine A_{2A} agonist CGS21680 on rat motoneurons in culture. *Neurosci. Lett.* 522, 21–24. doi: 10.1016/j.neulet.2012.06.003

Laurent, C., Burnouf, S., Ferry, B., Batalha, V. L., Coelho, J. E., Baqi, Y., et al. (2016). A_{2A} adenosine receptor deletion is protective in a mouse model of Tauopathy. *Mol. Psychiatry* 21, 97–107. doi: 10.1038/mp.2014.151

Laurent, C., Eddarkaoui, S., Derisbourg, M., Leboucher, A., Demeyer, D., Carrier, S., et al. (2014). Beneficial effects of caffeine in a transgenic model of Alzheimer's disease-like tau pathology. *Neurobiol. Aging* 35, 2079–2090. doi: 10.1016/j.neurobiolaging.2014.03.027

Leblond, C. S., Kaneb, H. M., Dion, P. A., and Rouleau, G. A. (2014). Dissection of genetic factors associated with amyotrophic lateral sclerosis. *Exp. Neurol.* 262, 91–101. doi: 10.1016/j.expneurol.2014.04.013

Leroy, F., Lamotte d'Incamps, B., Imhoff-Manuel, R. D., and Zytnicki, D. (2014). Early intrinsic hyperexcitability does not contribute to motoneuron degeneration in amyotrophic lateral sclerosis. *eLife* 3:e04046. doi: 10.7554/eLife.04046

Little, J. W., Ford, A., Symons-Liguori, A. M., Chen, Z., Janes, K., Doyle, T., et al. (2015). Endogenous adenosine A3 receptor activation selectively alleviates persistent pain states. *Brain* 138, 28–35. doi: 10.1093/brain/awu330

Liu, Y. J., Ju, T. C., Chen, H. M., Jang, Y. S., Lee, L. M., Lai, H. L., et al. (2015a). Activation of AMP-activated protein kinase α1 mediates mislocalization of TDP-43 in amyotrophic lateral sclerosis. *Hum. Mol. Genet.* 24, 787–801. doi: 10.1093/hmg/ddu497

Liu, Y. J., Lee, L. M., Lai, H. L., and Chern, Y. (2015b). Aberrant activation of AMP-activated protein kinase contributes to the abnormal distribution of HuR in amyotrophic lateral sclerosis. *FEBS Lett.* 589, 432–439. doi: 10.1016/j.febslet.2014.12.029

Liu, Y. J., Tsai, P. Y., and Chern, Y. (2017). Energy homeostasis and abnormal RNA metabolism in amyotrophic lateral sclerosis. *Front. Cell. Neurosci.* 11:126. doi: 10.3389/fncel.2017.00126

Maekawa, S., Leigh, P. N., King, A., Jones, E., Steele, J. C., Bodi, I., et al. (2009). TDP-43 is consistently co-localized with ubiquitinated inclusions in sporadic and Guam amyotrophic lateral sclerosis but not in familial amyotrophic lateral sclerosis with and without SOD1 mutations. *Neuropathology* 29, 672–683. doi: 10.1111/j.1440-1789.2009.01029.x

Marchetto, M. C., Muotri, A. R., Mu, Y., Smith, A. M., Cezar, G. G., and Gage, F. H. (2008). Non-cell-autonomous effect of human SOD1 G37R astrocytes on motor neurons derived from human embryonic stem cells. *Cell Stem Cell* 3, 649–657. doi: 10.1016/j.stem.2008.10.001

Matos, M., Augusto, E., Santos-Rodrigues, A. D., Schwarzschild, M. A., Chen, J. F., Cunha, R. A., et al. (2012). Adenosine A_{2A} receptors modulate glutamate uptake in cultured astrocytes and gliosomes. *Glia* 60, 702–716. doi: 10.1002/glia.22290

Mojsilovic-Petrovic, J., Jeong, G. B., Crocker, A., Arneja, A., David, S., Russell, D., et al. (2006). Protecting motor neurons from toxic insult by antagonism of adenosine A2a and Trk receptors. *J. Neurosci.* 26, 9250–9263. doi: 10.1523/JNEUROSCI.1856-06.2006

Nagai, M., Re, D. B., Nagata, T., Chalazonitis, A., Jessell, T. M., Wichterle, H., et al. (2007). Astrocytes expressing ALS-linked mutated SOD1 release factors selectively toxic to motor neurons. *Nat. Neurosci.* 10, 615–622. doi: 10.1038/nn1876

Nalini, A., Thennarasu, K., Gourie-Devi, M., Shenoy, S., and Kulshreshtha, D. (2008). Clinical characteristics and survival pattern of 1,153 patients with amyotrophic lateral sclerosis: experience over 30 years from India. *J. Neurol. Sci.* 272, 60–70. doi: 10.1016/j.jns.2008.04.034

Nascimento, F., Pousinha, P. A., Correia, A. M., Gomes, R., Sebastião, A. M., and Ribeiro, J. A. (2014). Adenosine A_{2A} receptors activation facilitates neuromuscular transmission in the pre-symptomatic phase of the SOD1(G93A) ALS mice, but not in the symptomatic phase. *PLoS One* 9:e104081. doi: 10.1371/journal.pone.0104081

Nascimento, F., Sebastiao, A. M., and Ribeiro, J. A. (2015). Presymptomatic and symptomatic ALS SOD1 (G93A) mice differ in adenosine A_1 and A_{2A} receptor-mediated tonic modulation of neuromuscular transmission. *Purinergic Signal.* 11, 471–480. doi: 10.1007/s11302-015-9465-4

Naumenko, N., Pollari, E., Kurronen, A., Giniatullina, R., Shakirzyanova, A., Magga, J., et al. (2011). Gender-specific mechanism of synaptic impairment and its prevention by GCSF in a mouse model of ALS. *Front. Cell. Neurosci.* 5:26. doi: 10.3389/fncel.2011.00026

Neumann, M., Sampathu, D. M., Kwong, L. K., Truax, A. C., Micsenyi, M. C., Chou, T. T., et al. (2006). Ubiquitinated TDP-43 in frontotemporal lobar degeneration and amyotrophic lateral sclerosis. *Science* 314, 130–133. doi: 10.1126/science.1134108

Nichols, N. L., Van Dyke, J., Nashold, L., Satriotomo, I., Suzuki, M., and Mitchell, G. S. (2013). Ventilatory control in ALS. *Respir. Physiol. Neurobiol.* 189, 429–437. doi: 10.1016/j.resp.2013.05.016

Ng, S. K., Higashimori, H., Tolman, M., and Yang, Y. (2015). Suppression of adenosine 2a receptor (A_{2A}R)-mediated adenosine signaling improves disease phenotypes in a mouse model of amyotrophic lateral sclerosis. *Exp. Neurol.* 267, 115–122. doi: 10.1016/j.expneurol.2015.03.004

Nonaka, T., Kametani, F., Arai, T., Akiyama, H., and Hasegawa, M. (2009). Truncation and pathogenic mutations facilitate the formation of intracellular aggregates of TDP-43. *Hum. Mol. Genet.* 18, 3353–3364. doi: 10.1093/hmg/ddp275

Pasinelli, P., and Brown, R. H. (2006). Molecular biology of amyotrophic lateral sclerosis: insights from genetics. *Nat. Rev. Neurosci.* 7, 710–723. doi: 10.1038/nrn1971

Pelligrino, D. A., Xu, H. L., and Vetri, F. (2010). Caffeine and the control of cerebral hemodynamics. *J. Alzheimers Dis.* 20(Suppl. 1), S51–S62. doi: 10.3233/JAD-2010-091261

Pokrishevsky, E., Grad, L. I., Yousefi, M., Wang, J., Mackenzie, I. R., and Cashman, N. R. (2012). Aberrant localization of FUS and TDP43 is associated with misfolding of SOD1 in amyotrophic lateral sclerosis. *PLoS One* 7:e35050. doi: 10.1371/journal.pone.0035050

Popoli, P., Frank, C., Tebano, M. T., Potenza, R. L., Pintor, A., Domenici, M. R., et al. (2003). Modulation of glutamate release and excitotoxicity by adenosine A_{2A} receptors. *Neurology* 61(11 Suppl. 6), S69–S71. doi: 10.1212/01.WNL.0000095216.89483.A2

Potenza, R. L., Armida, M., Ferrante, A., Pèzzola, A., Matteucci, A., Puopolo, M., et al. (2013). Effects of chronic caffeine intake in a mouse model of amyotrophic lateral sclerosis. *J. Neurosci. Res.* 91, 585–592. doi: 10.1002/jnr.23185

Pousinha, P. A., Correia, A. M., Sebastião, A. M., and Ribeiro, J. A. (2010). Predominance of adenosine excitatory over inhibitory effects on transmission at the neuromuscular junction of infant rats. *J. Pharmacol. Exp. Ther.* 332, 153–163. doi: 10.1124/jpet.109.157255

Pousinha, P. A., Correia, A. M., Sebastião, A. M., and Ribeiro, J. A. (2012). Neuromuscular transmission modulation by adenosine upon aging. *Neurobiol. Aging* 33, 2869–2880. doi: 10.1016/j.neurobiolaging.2012.01.008

Pousinha, P. A., Diogenes, M. J., Ribeiro, J. A., and Sebastião, A. M. (2006). Triggering of BDNF facilitatory action on neuromuscular transmission by adenosine A_{2A} receptors. *Neurosci. Lett.* 404, 143–147. doi: 10.1016/j.neulet.2006.05.036

Qian, K., Huang, H., Peterson, A., Hu, B., Maragakis, N. J., Ming, G. L., et al. (2017). Sporadic ALS astrocytes induce neuronal degeneration in vivo. *Stem Cell Rep.* 8, 843–855. doi: 10.1016/j.stemcr.2017.03.003

Rebola, N., Simões, A. P., Canas, P. M., Tomé, A. R., Andrade, G. M., Barry, C. E., et al. (2011). Adenosine A_{2A} receptors control neuroinflammation and consequent hippocampal neuronal dysfunction. *J. Neurochem.* 117, 100–111. doi: 10.1111/j.1471-4159.2011.07178.x

Ribeiro, F. F., Neves-Tomé, R., Assaife-Lopes, N., Santos, T. E., Silva, R. F. M., Brites, D., et al. (2016a). Axonal elongation and dendritic branching is enhanced by adenosine A_{2A} receptors activation in cerebral cortical neurons. *Brain Struct. Funct.* 221, 2777–2799. doi: 10.1007/s00429-015-1072-1

Ribeiro, F. F., Xapelli, S., Miranda-Lourenço, C., Tanqueiro, S. R., Fonseca-Gomes, J., Diógenes, M. J., et al. (2016b). Purine nucleosides in neuroregeneration and neuroprotection. *Neuropharmacology* 104, 226–242. doi: 10.1016/j.neuropharm.2015.11.006

Ribeiro, J. A., and Sebastião, A. M. (1987). On the role, inactivation and origin of endogenous adenosine at the frog neuromuscular junction. *J. Physiol.* 384, 571–585. doi: 10.1113/jphysiol.1987.sp016470

Ribeiro, J. A., and Sebastião, A. M. (2010). Caffeine and adenosine. *J. Alzheimers Dis.* 20(Suppl. 1), S3–S15. doi: 10.3233/JAD-2010-1379

Ribeiro, J. A., Sebastião, A. M., and De Mendonça, A. (2003). Adenosine receptors in the nervous system: pathophysiological implications. *Prog. Neurobiol.* 68, 377–392. doi: 10.1016/S0301-0082(02)00155-7

Ribeiro, J. A., and Walker, J. (1973). Action of adenosine triphosphate on endplate potentials recorded from muscle fibres of the rat-diaphragm and frog sartorius. *Br. J. Pharmacol.* 49, 724–725. doi: 10.1111/j.1476-5381.1973.tb08555.x

Ribeiro, J. A., and Walker, J. (1975). The effects of adenosine triphosphate and adenosine diphosphate on transmission at the rat and frog neuromuscular junctions. *Br. J. Pharmacol.* 54, 213–218. doi: 10.1111/j.1476-5381.1975.tb06931.x

Rocha, M. C., Pousinha, P. A., Correia, A. M., Sebastião, A. M., and Ribeiro, J. A. (2013). Early changes of neuromuscular transmission in the SOD1(G93A) mice model of ALS start long before motor symptoms onset. *PLoS One* 8:e73846. doi: 10.1371/journal.pone.0073846

Rodrigues, T. M., Jerónimo-Santos, A., Outeiro, T. F., Sebastião, A. M., and Diógenes, M. J. (2014). Challenges and promises in the development of neurotrophic factor-based therapies for Parkinson's disease. *Drugs Aging* 31, 239–261. doi: 10.1007/s40266-014-0160-x

Santiago, A. R., Baptista, F. I., Santos, P. F., Cristóvão, G., Ambrósio, A. F., Cunha, R. A., et al. (2014). Role of microglia adenosine A_{2A} receptors in retinal and brain neurodegenerative diseases. *Mediators Inflamm.* 2014:465694. doi: 10.1155/2014/465694

Sebastião, A. M., Assaife-Lopes, N., Diógenes, M. J., Vaz, S. H., and Ribeiro, J. A. (2011). Modulation of brain-derived neurotrophic factor (BDNF) actions in the nervous system by adenosine A_{2A} receptors and the role of lipid rafts. *Biochim. Biophys. Acta* 1808, 1340–1349. doi: 10.1016/j.bbamem.2010.06.028

Sebastião, A. M., and Ribeiro, J. A. (1985). Enhancement of transmission at the frog neuromuscular junction by adenosine deaminase: evidence for an inhibitory role of endogenous adenosine on neuromuscular transmission. *Neurosci. Lett.* 62, 267–270. doi: 10.1016/0304-3940(85)90366-0

Sebastião, A. M., and Ribeiro, J. A. (2009a). Adenosine receptors and the central nervous system. *Handb. Exp. Pharmacol.* 193, 471–534. doi: 10.1007/978-3-540-89615-9_16

Sebastião, A. M., and Ribeiro, J. A. (2009b). Triggering neurotrophic factor actions through adenosine A_{2A} receptor activation: implications for neuroprotection. *Br. J. Pharmacol.* 158, 15–22. doi: 10.1111/j.1476-5381.2009.00157.x

Sebastião, A. M., Stone, T. W., and Ribeiro, J. A. (1990). On the inhibitory adenosine receptor at the neuromuscular junction and hippocampus of the rat: antagonism by 1,3,8-substituted xanthines. *Br. J. Pharmacol.* 101, 453–459. doi: 10.1111/j.1476-5381.1990.tb12729.x

Selvaraj, B. T., Livesey, M. R., Zhao, C., Gregory, J. M., James, O. T., Cleary, E. M., et al. (2018). *C9ORF72* repeat expansion causes vulnerability of motor neurons to Ca^{2+}-permeable AMPA receptor-mediated excitotoxicity. *Nat. Commun.* 9:347. doi: 10.1038/s41467-017-02729-0

Shan, X., Vocadlo, D., and Krieger, C. (2009). Mislocalization of TDP-43 in the G93A mutant SOD1 transgenic mouse model of ALS. *Neurosci. Lett.* 458, 70–74. doi: 10.1016/j.neulet.2009.04.031

Shi, Y., Lin, S., Staats, K. A., Li, Y., Chang, W. H., Hung, S. T., et al. (2018). Haploinsufficiency leads to neurodegeneration in C9ORF72 ALS/FTD human induced motorneurons. *Nat. Med.* 24, 313–325. doi: 10.1038/nm.4490

Sitkovsky, M. V., Lukashev, D., Apasov, S., Kojima, H., Koshiba, M., Caldwell, C., et al. (2004). Physiological control of immune response and inflammatory tissue damage by hypoxia-inducible factors and adenosine A_{2A} receptors. *Annu. Rev. Immunol.* 22, 657–682. doi: 10.1146/annurev.immunol.22.012703.104731

Smith, B. N., Newhouse, S., Shatunov, A., Vance, C., Topp, S., Johnson, L., et al. (2013). The C9ORF72 expansion mutation is a common cause of ALS+/-FTD in Europe and has a single founder. *Eur. J. Hum. Genet.* 21, 102–108. doi: 10.1038/ejhg.2012.98

Son, Y. J., Trachtenberg, J. T., and Thompson, W. J. (1996). Schwann cells induce and guide sprouting and reinnervation of neuromuscular junctions. *Trends Neurosci.* 19, 280–285. doi: 10.1016/S0166-2236(96)10032-1

Taylor, J. P., Brown, R. H. Jr., and Cleveland, D. W. (2016). Decoding ALS: from genes to mechanism. *Nature* 539, 197–206. doi: 10.1038/nature20413

Tsentsevitsky, A., Kovyazina, I., Nikolsky, E., Bukharaeva, E., and Giniatullin, R. (2013). Redox-sensitive synchronizing action of adenosine on transmitter release at the neuromuscular junction. *Neuroscience* 248, 699–707. doi: 10.1016/j.neuroscience.2013.05.065

Vincenzi, F., Corciulo, C., Targa, M., Casetta, I., Gentile, M., Granieri, E., et al. (2013). A_{2A} adenosine receptors are up-regulated in lymphocytes from amyotrophic lateral sclerosis patients. *Amyotroph. Lateral Scler. Frontotemporal Degener.* 14, 406–413. doi: 10.3109/21678421.2013.793358

Volonté, C., Apolloni, S., Parisi, C., and Amadio, S. (2016). Purinergic contribution to amyotrophic lateral sclerosis. *Neuropharmacology* 104, 180–193. doi: 10.1016/j.neuropharm.2015.10.026

Wainger, B. J., Kiskinis, E., Mellin, C., Wiskow, O., Han, S. S., Sandoe, J., et al. (2014). Intrinsic membrane hyperexcitability of amyotrophic lateral sclerosis patient-derived motorneurons. *Cell Rep.* 7, 1–11. doi: 10.1016/j.celrep.2014.03.019

Wiese, S., Jablonka, S., Holtmann, B., Orel, N., Rajagopal, R., Chao, M. V., et al. (2007). Adenosine receptor A_{2A}-R contributes to motoneuron survival by transactivating the tyrosine kinase receptor TrkB. *Proc. Natl. Acad. Sci. U.S.A.* 104, 17210–17215. doi: 10.1073/pnas.0705267104

Wijesekera, L. C., and Leigh, P. N. (2009). Amyotrophic lateral sclerosis. *Orphanet J. Rare Dis.* 4:3. doi: 10.1186/1750-1172-4-3

Witts, E. C., Nascimento, F., and Miles, G. B. (2015). Adenosine-mediated modulation of ventral horn interneurons and spinal motoneurons in neonatal mice. *J. Neurophysiol.* 114, 2305–2315. doi: 10.1152/jn.00574.2014

Witts, E. C., Panetta, K. M., and Miles, G. B. (2012). Glial-derived adenosine modulates spinal motor networks in mice. *J. Neurophysiol.* 107, 1925–1934. doi: 10.1152/jn.00513.2011

Yanpallewar, S. U., Barrick, C. A., Buckley, H., Becker, J., and Tessarollo, L. (2012). Deletion of the BDNF truncated receptor TrkB.T1 delays disease onset in a mouse model of amyotrophic lateral sclerosis. *PLoS One* 7:e39946. doi: 10.1371/journal.pone.0039946

Yoshida, Y., Une, F., Utatsu, Y., Nomoto, M., Furukawa, Y., Maruyama, Y., et al. (1999). Adenosine and neopterin levels in cerebrospinal fluid of patients with neurological disorders. *Intern. Med.* 38, 133–139. doi: 10.2169/internalmedicine.38.133

Conflict of Interest Statement: The authors declare that the research was conducted in the absence of any commercial or financial relationships that could be construed as a potential conflict of interest.

frontiers in Pharmacology

REVIEW
published: 10 April 2018
doi: 10.3389/fphar.2018.00325

Purinergic Receptors in Neurological Diseases With Motor Symptoms: Targets for Therapy

*Ágatha Oliveira-Giacomelli[1], Yahaira Naaldijk[1], Laura Sardá-Arroyo[1], Maria C. B. Gonçalves[2], Juliana Corrêa-Velloso[1], Micheli M. Pillat[1], Héllio D. N. de Souza[1] and Henning Ulrich[1]**

[1] Department of Biochemistry, Institute of Chemistry, University of São Paulo, São Paulo, Brazil, [2] Department of Neurology and Neuroscience, Medical School, Federal University of São Paulo, São Paulo, Brazil

Since proving adenosine triphosphate (ATP) functions as a neurotransmitter in neuron/glia interactions, the purinergic system has been more intensely studied within the scope of the central nervous system. In neurological disorders with associated motor symptoms, including Parkinson's disease (PD), motor neuron diseases (MND), multiple sclerosis (MS), amyotrophic lateral sclerosis (ALS), Huntington's Disease (HD), restless leg syndrome (RLS), and ataxias, alterations in purinergic receptor expression and activity have been noted, indicating a potential role for this system in disease etiology and progression. In neurodegenerative conditions, neural cell death provokes extensive ATP release and alters calcium signaling through purinergic receptor modulation. Consequently, neuroinflammatory responses, excitotoxicity and apoptosis are directly or indirectly induced. This review analyzes currently available data, which suggests involvement of the purinergic system in neuro-associated motor dysfunctions and underlying mechanisms. Possible targets for pharmacological interventions are also discussed.

Keywords: Parkinson's disease, amyotrophic lateral sclerosis (ALS), multiple sclerosis, neurodegeneration, ataxia, Huntington's disease, restless leg syndrome, purinergic receptors

OPEN ACCESS

Edited by:
Francisco Ciruela, Universitat de Barcelona, Spain

Reviewed by:
Rodrigo A. Cunha, Universidade de Coimbra, Portugal
Alexandre Henriques, Neuro-Sys, France

***Correspondence:**
Henning Ulrich
henning@iq.usp.br

Specialty section:
This article was submitted to Experimental Pharmacology and Drug Discovery, a section of the journal Frontiers in Pharmacology

Received: *18 November 2017*
Accepted: *21 March 2018*
Published: *10 April 2018*

Citation:
Oliveira-Giacomelli Á, Naaldijk Y, Sardá-Arroyo L, Gonçalves MCB, Corrêa-Velloso J, Pillat MM, de Souza HDN and Ulrich H (2018) Purinergic Receptors in Neurological Diseases With Motor Symptoms: Targets for Therapy. Front. Pharmacol. 9:325. doi: 10.3389/fphar.2018.00325

INTRODUCTION

The unexpected discovery and description of non-adrenergic and non-cholinergic inhibitory nerves working through adenosine triphosphate (ATP) and its metabolites gave rise to the introduction of the purinergic system concept in the early 70's (Burnstock et al., 1970; Burnstock, 1972). Later, purines were also described as important co-transmitters in both central (CNS) and peripheral nervous systems, as they are able to modulate and be modulated by many other neurotransmission systems and signaling pathways (Burnstock, 1997, 2009; Abbracchio et al., 2009).

After proposal of purinergic neurotransmission, the following decades were dedicated to the isolation and characterization of the two families of purinergic receptors, which are distinguished by their main agonists: P1 receptors, a family of protein G-coupled metabotropic adenosine (A_1, $_{2A}A_{2A}$, A_{2B}, A_3) receptors, and P2 receptors. P2 receptors are sub-divided into P2X(1–7) channels, activated by ATP, and G protein-coupled metabotropic P2Y(1–12) receptors, which show sensitivity to ATP, adenosine diphosphate (ADP), uridine di- and triphosphate (UDP and UTP, respectively), or UDP-glucose depending on the receptor subtype. Beyond

receptors, membrane nucleotide/nucleoside transporters and channels (e.g., pannexins) as well as ectonucleotidases play important roles in purinergic signaling. These are responsible for the exchange of purines between intracellular and extracellular environments and their enzymatic extracellular conversion, respectively (Zimmermann et al., 1998; Zimmermann, 2006; Scemes et al., 2007; Abbracchio et al., 2009; Lapato and Tiwari-Woodruff, 2017).

P2X receptors are ion channels that promote a non-selective exchange of cations, mainly Ca^{2+}, Na^{+}, Mg^{2+}, and K^{+}. ATP-activation of P2X receptors is especially important for Ca^{2+}-induced intracellular signaling pathways (Surprenant and North, 2009; Puchałowicz et al., 2015). P2Y and adenosine receptors are coupled to Gq/Gi/Gs proteins, depending on the receptor subtype (Puchałowicz et al., 2015). The activation of Gq proteins triggers a signaling cascade through phospholipase C/inositol-1,4,5-triphosphate (PLC/IP3), resulting in the release of Ca^{2+} from the endoplasmic reticulum into the cytoplasm. Gs/Gi protein activation, however, will work through the stimulation/inhibition of adenylate cyclase, respectively, with subsequent up- or down-regulation of cyclic AMP (cAMP) production. Final effects of purinergic receptor-promoted signaling will depend on the cell type and other intra-/inter-cellular conditions, as i.e., in physiological embryonic and adult neurogenesis (Oliveira et al., 2016), and in various pathological scenarios, such as inflammatory (Beamer et al., 2016; Madeira et al., 2017; Przybyła et al., 2018), oncological (Allard et al., 2016; Vijayan et al., 2017; Whiteside, 2017; Kazemi et al., 2018), neurological (Burnstock et al., 2011; Stockwell et al., 2017), metabolic (Lindberg et al., 2015; Csóka et al., 2017; Parpura et al., 2017; Tozzi and Novak, 2017; Labazi et al., 2018), psychiatric (Cunha, 2008; Lindberg et al., 2015; Ortiz et al., 2015; Krügel, 2016; Cheffer et al., 2017; Oliveros et al., 2017), cognitive (Illes and Verkhratsky, 2016), and peripheral neuromuscular and/or neuromotor diseases (Robitaille, 1995; Kalmar, 2005; Burnstock et al., 2013; Jiménez et al., 2014; Bogacheva and Balezina, 2015; Puchałowicz et al., 2015; Safarzadeh et al., 2016).

In the CNS, extracellular nucleotides also participate as messengers for communication between neuronal and non-neuronal cells. As key players in neuron-glia interactions and microglial activation (Fields and Burnstock, 2006; Cunha, 2008, 2016; Färber et al., 2008; Boison et al., 2010; Lecca et al., 2012; Tsuda and Inoue, 2016; Inoue, 2017; Tsuda, 2017), both adenosine and ATP are essential modulators of neuroinflammatory responses, excitotoxicity, oxidative stress and cell death, especially via A_{2A} and P2X7 receptors activity, respectively (Cunha, 2016; Borea et al., 2017; Faas et al., 2017; Faria et al., 2017; He et al., 2017; Lu et al., 2017; Miras-Portugal et al., 2017; Vuorimaa et al., 2017). Differently from other P2X receptors, the P2X7 receptor subtype needs higher ATP concentrations for channel opening and Ca^{2+} influx and remains longer activated, recruiting pannexin pores (Volont et al., 2012; Sun et al., 2013). Through pannexin pores, large amounts of ATP are released into the extracellular environment, stimulating other purinergic receptors, and signaling cascades widely associated with pathological conditions (Bartlett et al., 2014), such as the A_{2A} receptor, which is activated by adenosine released from damaged cells or produced from ATP hydrolysis (Cunha, 2016).

Here, we explore the importance of purinergic signaling in neurological diseases with motor symptoms, including Parkinson's disease (PD), motor neuron diseases (MND), multiple sclerosis (MS), amyotrophic lateral sclerosis (ALS), Huntington's Disease (HD), restless leg syndrome (RLS), and ataxias. We discuss common mechanisms already known to be involved in these conditions (**Table 1**), revise the role of the purinergic system in demyelination processes (**Figure 1**), and discuss new insights for further neural pathologies that might have motor impairments to identify potential targets for pharmacological therapies to decelerate disease progression and improve motor activity.

MOTOR NEURON DISEASES

Motor neurons (MNs) are classified in different categories according to their soma location, electrical speed transmission, and other cellular and physiological characteristics. Regarding the location of their somas, MNs can be classified as upper or lower MNs. Lower MNs have their soma located either in the brainstem—where they control head and neck muscle contraction through cranial nerves—and in the anterior horn of the spinal cord—where their axons innervate and control skeletal muscle contraction through spinal nerves. Upper MNs have somas located in the primary motor cortex and axons that project either to the brainstem or to the spinal cord through corticobulbar and corticospinal tracts, respectively. Upper MNs axons in the brainstem interact with lower MNs, regulating their control of head and neck contraction, while upper MNs project to the spinal cord synapse with lower MNs that innervate skeletal muscles, controlling their contraction (Rezania and Roos, 2013; Verschueren, 2017).

MND are neurodegenerative conditions that affect MNs and result in motor dysfunctions without compromising sensorial neurons. MND are classified according to the damage location in relation to the spinal cord. Diseases affecting lower MNs and upper MNs are known as lower MNDs and upper MNDs, respectively. Lower MNDs include progressive muscular atrophy, spinal muscular atrophy (SMA), spinal and bulbar muscular atrophy, and monomelic amyotrophy (Hirayama disease). However, the most prevalent subtype of MND is ALS,

Abbreviations: 6-OHDA, 6-hydroxydopamine; ALS, amyotrophic lateral sclerosis; ATP, ADP, AMP, adenosine tri-, di-, monophosphate; BBG, Brilliant Blue G; BDNF, brain-derived neurotrophic factor; BzATP, 2′-3′-O-(benzoyl-benzoyl) ATP; cAMP, cyclic AMP; CNS, central nervous system; COX2, cyclooxigenase 2; EAE, encephalomyelitis; HD, Huntington Disease; Htt, huntingtin protein; IL-1β/2/6/17A/23, Interleukin 1β/2/6/17A/23; iPSC, induced pluripotent stem cells; L-DOPA, L-3,4-dihydroxyphenylalanine; LPS, lipopolysaccharide; MAPK/ERK, mitogen activated protein kinases/extracellular signal-regulated kinases signaling induction pathway; MNs, motor neurons; MND, motor neuron diseases; MPP+, 1-methyl-4-phenylpyridinium; MS, multiple sclerosis; NOX2, nicotinamide adenine dinucleotide phosphate-oxidase 2; PBMC, peripheral blood mononuclear cells; PD, Parkinson's disease; QA, quinolinic acid; ROS, Reactive oxygen species; RLS, Restless leg syndrome; SCA, Spinocerebellar ataxia; SMA, spinal muscular atrophy; SNc, substantia nigra pars compacta; SOD1 (G93A), superoxide dismutase 1 (glycin-93 to serine)-mutant mouse; TNF-α, tumor necrosis factor alpha; TrkB, tropomyosin kinase receptor b; UTP, UDP, uridine tri-, diphosphate.

TABLE 1 | Evidence of purinergic receptors involvement in neurological diseases with major motor dysfunctions.

Disease	Purinergic involvement	Model/Sample	Drug	Effects	References
ALS	P2X4 receptor positive activity modulation	MNs culture/SOD1 (G93A) mice	Preincubation with Ivermectin (10 mM); Ivermectin 12 mg per liter of water during 70 days	Neuroprotective against glutamate-induced excitotoxicity; Improves lifespan and increases ventral horn MNs numbers	Andries et al., 2007
	P2X4 receptor	SOD1 (G93A) rats	–	Strong immunoreactivity in the ventral horns	Casanovas et al., 2008
	P2X7 receptor activation	Microglial cells derived from transgenic SOD1 (G93A) mice;	BzATP (10 and 100 μM)	Increase in NOX2 activity and ROS synthesis	Apolloni et al., 2013b
			BzATP (10 μM)	Transition from microglial M2 to M1 activated phenotype, increased TNF-α production and COX2 activation	D'Ambrosi et al., 2009
		Microglia/Neuron co-culture	BzATP (10 μM)	Cell death due to ROS and NOS production	Skaper et al., 2006; D'Ambrosi et al., 2009
		Cultured rat spinal cord MNs	ATP (1–100 μM)	MNs cell death through peroxinitrite/Fas death pathway	Gandelman et al., 2013
		MNs co-cultured with SOD1G93 astrocytes	ATP (100 μM, 5 days) or BzATP (10 μM, 48 h)	Astrocytes become neurotoxic for MNs through increased oxidative stress	Gandelman et al., 2010
	P2X7 receptor deletion	$P2X7^{(-/-)}$/SOD1-G93A mice	–	Accelerates disease onset and progression, increased pro-inflammatory markers as well as astrogliosis, microgliosis, and MNs cell death	Apolloni et al., 2013a
	A_{2A} receptor antagonism	SOD1 (G93A) mice	Caffeine, 1.5 mg/day for 70 days, in drinking water	Shortened mice survival	Potenza et al., 2013
		Rat spinal cord cells culture	Chronic enprofylline treatment	Decreased MNs susceptibility to excitotoxic environment through inhibition of BDNF-promoted death pathway	Mojsilovic-Petrovic et al., 2006
	A_{2A} receptor expression or levels	SOD1 G93A mice	–	Decreased expression in spinal cord	Potenza et al., 2013
		SOD1 G93A mice and end-stage humans with ALS	–	Increased expression in spinal cord of symptomatic mice and patients	Ng et al., 2015
		ALS patient lymphocytes	–	Increased density in lymphocytes, positively related with clinical status of patients	Vincenzi et al., 2013
	A_{2A} receptor activation	SOD1 G93A mice	CGS21680, 5 mg/kg, i.p., during 4 weeks	Delays ALS onset possibly by stimulating non-truncated forms of the TrkB receptor	Yanpallewar et al., 2012
		NSC34 cells	T1–11 (30 μM)	Normalized abnormal cellular redistribution of human antigen R, found in MNs of ALS patients	Liu et al., 2015
	A_1 and A_{2A} receptors	SOD1 G93A mice presymptomatic (4–6 weeks old) symptomatic (12–14 weeks old)	N(6)-cyclopentyladenosine (50 nM); CGS 21680 (5 nM)	Impaired cross-talk between receptors in presymptomatic mice, increased A_1 receptor activation in symptomatic mice	Nascimento et al., 2015

(Continued)

TABLE 1 | Continued

Disease	Purinergic involvement	Model/Sample	Drug	Effects	References
Spinal muscular atrophy	ATP response	iPSC-derived astrocyte culture from SMA patients	ATP (10 μM)	Increased basal intracellular calcium levels accompanied by a reduced calcium response to ATP application	McGivern et al., 2013
Multiple sclerosis	P2X7 receptor expression and protein levels	Cultured PBMC from MS patients	Glatiramer acetate (50 μg/ml, 48 h) BzATP (300 μM, 30 min)	Glatiramer acetate, used to treat MS patients, reduced P2X7 receptor expression in BzATP-stimulated cells	Caragnano et al., 2012
		MS patients' spinal cords	–	Increased P2X7 receptor protein levels in microglia	Yiangou et al., 2006
		EAE rat brains	–	Increased P2X7 receptor expression related to synaptosomal fraction in the symptomatic phase and to the glial fraction in recovered rat brains	Grygorowicz et al., 2011
	P2X7 receptor polymorphisms	MS patients	–	Patients with T allele of rs17525809 polymorphism present a more prominent activity, which may contribute to MS development	Oyanguren-Desez et al., 2011
	P2X7 receptor deletion	P2X7R$^{-/-}$ EAE mice model	–	Enhanced mouse susceptibility to EAE	Chen and Brosnan, 2006
				Suppressed clinical symptoms in EAE mice	Sharp et al., 2008
	P2X7 receptor antagonism	EAE mouse model	BBG (10 mg/kg daily, delivered from pellets, during 20 days)	Antagonism improved symptoms and promoted remyelination	Matute et al., 2007
	P2Y12 receptor levels	MS patients cortical tissue	–	Reduced protein levels near demyelination areas	Amadio et al., 2010
	P2Y12 receptor deletion	P2Y12 knockout EAE mice	–	Mice developed more severe EAE related to higher release of IL-23 cytokines and imbalanced Th-cell subtype frequencies	Zhang et al., 2017
	A_{2A} receptor antagonism	MS patients	Coffee consumption exceeding 900 mL daily	Reduced MS risk in comparison to control group	Hedström et al., 2016
	A_1 receptor deletion	A1AR$^{-/-}$ EAE mice		Induced severe EAE, with more prominent demyelination, axonal injury, and microglia activation	Tsutsui et al., 2004
	A_1 receptor activation	A1AR$^{-/-}$ EAE mice	Caffeine (2 mg/kg) + adenosine amine congener (10 μg/kg), subcutaneous pump, during 25 days	Reduced EAE severity induced by A_1 receptor expression deletion	Tsutsui et al., 2004
		Cultured PBMC from MS patients	R-phenylisopropyl-adenosine (1 mM)	Inhibited IL-6 production	Mayne et al., 1999
Parkinson's disease	P2X1 receptor antagonism	H4 cells overexpressing α-synuclein	Pre-treatment with NF449 (1–5 μM) followed by 48 h treatment with ATP (3 mM, every hour)	Prevented ATP-induced α-synuclein aggregation in a dose dependent manner	Gan et al., 2015
	P2X7 receptor antagonism	6-OHDA lesioned rats	A-438079 (30 mg/kg, i.p., before lesion establishment)	Prevented depletion of dopamine in striatum without reducing dopaminergic neuron cell death	Marcellino et al., 2010

(Continued)

TABLE 1 | Continued

Disease	Purinergic involvement	Model/Sample	Drug	Effects	References
			BBG (45 mg/kg, i.p., every 48 h during 2 weeks, before lesion establishment)	Prevented loss of tyrosine-hydroxylase immunoreactivity and attenuated rotational behavior and memory deficit	Carmo et al., 2014
			BBG (50 mg/kg, i.p., daily, during 1 week, after lesion establishment)	Reverted dopaminergic neurons loss in substantia nigra and rotational behavior	Ferrazoli et al., 2017
		BV2 microglia cells	Pretreatment with BBG (1 μM)	Antagonism and/or deletion of P2X7 receptor blocked the interaction between α-synuclein and P2X7 receptors and decreased ROS production induced by α-synuclein	Jiang et al., 2015
		SH-SY5Y cells	Pretreatment with PPADS (100 μM) or AZ 11645373 (10 μM)	Prevented abnormal calcium influx induced by α-synuclein	Wilkaniec et al., 2017
	P2X7 receptor polymorphism	PBMC from PD patients	–	1513A>C (rs3751143) polymorphism increased PD risk by facilitating pore formation and cell death	Liu et al., 2013
	P2Y6 receptor antagonism	SH-SY5Y cells	Pretreatment with MRS2578 (1.0 μM)	Decreased ROS production and other inflammatory markers induced by MPP+	Qian et al., 2017
	A_{2A} receptor antagonism	6-OHDA lesioned rats	8-ethoxy-9-ethyladenine (8 mg/kg, daily, during 28 days, minipumps)	Enhanced effect of low doses of L-DOPA without increased dyskinesia	Fuzzati-Armentero et al., 2015
		MPTP treated monkeys	KW-6002 (10.0 mg/kg, orally)	Increased effect of D2 receptor agonist quinpirole, D1 receptor agonist SKF80723 and low doses of L-DOPA without increased dyskinesia	Kanda et al., 2000
		PD patients with PD gene risk variant *LRRK2* R1628P	Caffeine intake through coffee and tea consumption	Decreased PD risk in subjects with LRRK2 variant R1628P	Kumar et al., 2015
		PD patients with GRIN2A variant rs4998386-T allele	Caffeine intake through coffee consumption	Increased protective effect of GRIN2A variant rs4998386-T allele	Hamza et al., 2011; Yamada-Fowler et al., 2014
		A_{2A} receptor knockout mice, SH-SY5Y cells	SCH 58261, ZM 241385	Decreased α-synuclein aggregation, prevent neuronal death induced by extracellular α-synuclein and restrain overactivation of NMDA receptors	Ferreira et al., 2015
		Brain slices from mice treated with MPTP	Preladenant (5 μM)	Facilitated beneficial microglial responses to injury	Gyoneva et al., 2014
		Rats treated with LPS	Caffeine 10 and 20 mg/kg; KW6002 1.5 and 3 mg/kg; i.p. for 6 days	Prevented striatal dopaminergic deficit and hydroxyl radicals release	Gołembiowska et al., 2013
	A_{2A} receptor number	Mice injected with α-Syn fibrils	–	Hippocampal A_{2A} receptors number increased after injections of α-synuclein in mice	Hu et al., 2016
	A_{2A} receptor polymorphisms	PD patients	–	rs3032740 and rs5996696 polymorphisms are inversely linked to PD risk	Popat et al., 2011

(Continued)

TABLE 1 | Continued

Disease	Purinergic involvement	Model/Sample	Drug	Effects	References
Huntington's disease	P2X7 receptor antagonist	Tet/HD94 and R6/1	BBG (45.5 mg/kg, i.p., every 48 h during 28 days)	Reduce body weight loss, improve motor functions, and prevent neuronal loss	Diaz-Hernandez et al., 2009
	A_1 receptor agonist	3-NPA mouse and rat model	Pre-treatment of R-PIA (1.75 mg/kg, i.p.) 15 min prior 3-NPA application	Reduction of seizure but not prevention of neuronal loss	Zuchora and Urbańska, 2001
		3-NPA rat model	ADAC (100 μg/kg, i.p., daily for 2 days) 3 days after 3-NPA	Reduction in striatal lesion and degeneration, improvement of motor functions	Blum et al., 2002
	A_1 receptor antagonist	Intracraneal application malonate 6 μmol in Swiss-Webster mice and 3 μmol Sprague Dawley rats	Pre-treatment with CPX 1 mg/kg, i.p.	Stimulate DAergic and GABAergic neuron death	Alfinito et al., 2003
	A_{2A} receptor polymorphisms	1876 C/T		Silent mutation in A_{2A} receptor	Dhaenens et al., 2009
		1876 T/T		Accelerates HD onset by 3.5 years	
		rs2298383		Early onset of HD	Taherzadeh-Fard et al., 2010
	A_{2A} receptor antagonist	Intracranial application malonate 6 μmol in Swiss-Webster mice and 3 μmol Sprague Dawley rats	Pre-treatment with DMPX 5 mg/kg, i.p.	Provided protection to DAergic and GABAergic cells against malonate	Alfinito et al., 2003
		Human	<190 mg/day caffeine	Accelerates HD onset.	Simonin et al., 2013
		3-NPA mouse model	8-(3-chlorostyryl) caffeine (5 mg/kg and 20 mg/kg, i.p.) 2x day for 5 days prior 3-NPA application	Reduction in striatal damage	Fink et al., 2004
		R6/2 mice	SCH58261 (0.01 mg/kg, i.p.)	Reduction in striatal BDNF levels at earlier HD stage	Potenza et al., 2007
			SCH58261 (50 nM): microdialysis application in striatum)	Reduction of glutamate and adenosine level	Gianfriddo et al., 2004
			Application of SCH58261 (0.01 mg/kg, i.p.) daily for 7 days at age of 5 weeks	Reduced NMDA-induced toxicity and emotional responses	Domenici et al., 2007
		Corticostriatal slices from R6/2 mice	ZM241385 (100 nM)	Prevention of BDNF positive effect on NMDA toxicity	Martire et al., 2010
		ST14/SQ120 cells			
		Primary rat striatal culture	Pre-treatment with SCH 58261 (30 nM) prior bath application QA 900 μM	Enhanced QA-induced increase in intracellular calcium concentration	Popoli et al., 2002
		QA rat model	Pre-treatment with SCH 58261 (0.01 mg/kg, i.p.) prior to QA application	Blocked the effect of QA on striatal gliosis, EEG changes, motor activity and glutamate levels	Popoli et al., 2002
			DMPX (0.2 μg, i.p.) application 5 min after QA application	Blocked QA-induced EEG abnormalities in frontal cortex	Reggio et al., 1999

(Continued)

TABLE 1 | Continued

Disease	Purinergic involvement	Model/Sample	Drug	Effects	References
			Pre-treatment with SCH58261 (0.01 mg/kg, i.p.) 20 min before QA application	Reduction in rearing behavior and anxiety levels	Scattoni et al., 2007
			SCH58261 (0.01 and 1 mg/kg, i.p.) daily for 1 or 3 weeks	Reduction in striatal BDNF levels	Potenza et al., 2007
		Transgenic HD rat model	KW-6002 (1 and 3 mg/kg, i.p.)	No beneficial locomotor activity at 6 and 12 month age	Orrú et al., 2011
			SCH 442416 (0.3 and 1 mg/kg, i.p.)	No significant effect in reducing electromyography responses	
	A_{2A} receptor agonist	Primary rat striatal culture	Pre-treatment with CGS21680 (100 nM.) prior bath application QA 900 μM	Reduced QA-induced increase in intracellular calcium concentration	Popoli et al., 2002
		Corticostriatal slices from R6/2 mice	CGS21680 (30 nM)	Beneficial effect against NDMA-induced toxicity	Ferrante et al., 2010
		R6/2 mice	CGS21680 (5 μg/kg, i.p.) daily for 2 weeks	Delay decline in motor performance and inhibit reduction in brain weight	Chou et al., 2005
			CGS21680 (0.5 mg/kg, i.p.) daily for 3 weeks	Brain region dependent alteration in NMDA glutamate receptor subunits density	Ferrante et al., 2010
			CGS21680 (0.5 mg/kg, i.p.)	No changes in behavior compared to wild type	Martire et al., 2007
		Corticostriatal slices from R6/2 mice	CGS21680 (5 μg/kg, i.p.) daily for 2 weeks	Brain region dependent alteration in NMDA subunits	Ferrante et al., 2010
	A_{2A} receptor knockout	N171-82Q mouse model	–	Aggravate survival and motor functions and decrease in specific markers for sub-population medium spiny neurons	Mievis et al., 2011
		3-NPA mouse model	A_{2A} receptor knockout mice treated with 3-NPA	Reduction in striatal damage	Fink et al., 2004
Ataxia	A_{2A} receptor antagonism	SCA3 mice model	Caffeine (1 g/L, drinking water during 2 weeks)	Decreased synaptotoxicity and reactive gliosis	Gonçalves et al., 2013
		(TgMJD) mice	Caffeine (1 g/L, drinking water during 2 weeks)	Prevented motor symptoms and cognitive impairment	Gonçalves et al., 2013
	P2X receptors	CHO-K1 cells with mutant PKCγ	ATP (1 mM)	Increased damaging aggregation of mutant PKCγ	Seki et al., 2005
Restless leg syndrome	A_{2A} receptor	Iron deficient mice	–	Increased in striatal presynaptic neurons	Gulyani et al., 2009
	A_1 and A_{2A} receptors	Iron deficient mice	–	Decreased A_1 and D2 receptor density in animals with mild, moderate and severe deficiency; increased pre-synaptic A_{2A} receptor density in the latter	Quiroz et al., 2016

in which both upper and lower MNs are affected and where non-neuronal cells as microglia and astrocytes play a central role in its pathogenesis and progression (Rezania and Roos, 2013; Verschueren, 2017).

Amyotrophic Lateral Sclerosis

ALS is the main motor disorder in adulthood. It is characterized by a progressive loss of MNs from the motor cortex, brainstem, and spinal cord (Kiernan et al., 2011). As a result of this neuronal

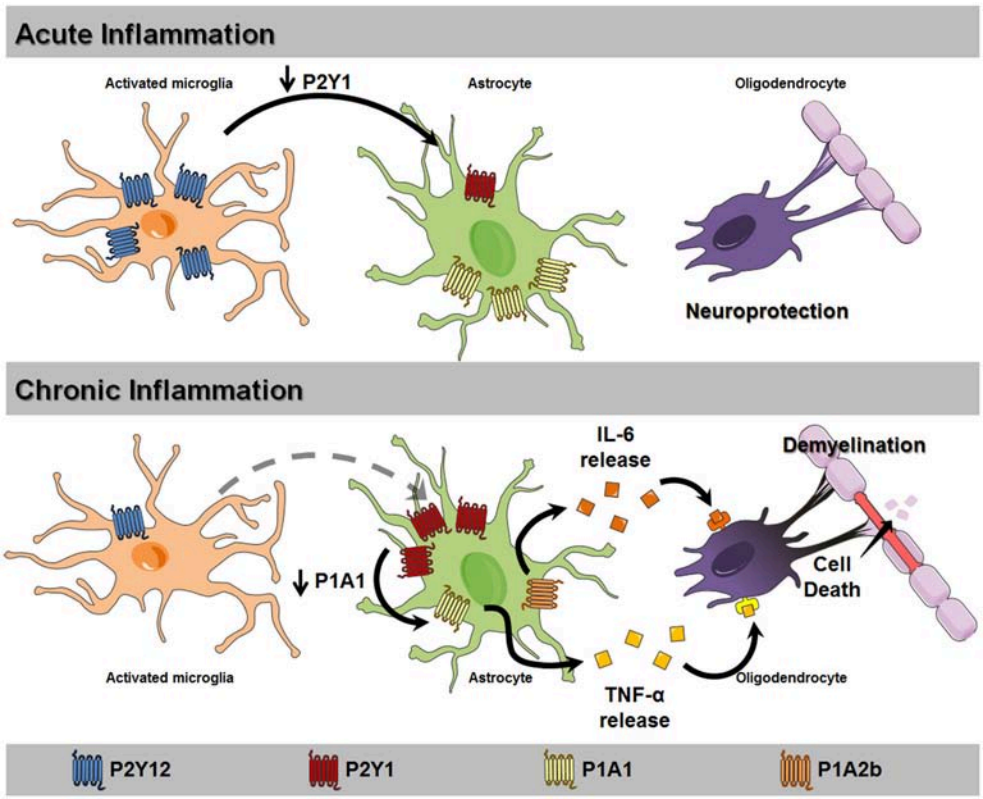

FIGURE 1 | Proposed mechanism for glial purinergic dysfunction leading to loss of myelination and cell death. In acute inflammation scenarios, microglial activation upregulates P2Y12 receptor expression and activity (blue), stimulating microglial motility to the injury site. The activation of these receptors reduces P2Y1 receptor (red) expression in astrocytes, increasing reactive astrogliosis and promoting neuroprotection. Chronic inflammation, as observed in motor neuron diseases (MND), unable of upregulating microglial P2Y12 receptor expression results in constant astrocytic P2Y1 receptor activation and reduction of A_1 receptor expression (yellow). These events result in stimulating tumor necrosis factor α (TNF-α) release, which in turn induces A_{2B} receptor activation (orange) and release of IL-6. These detrimental factors induce oligodendrocyte death and neuron demyelination, aggravating the pathological scenario.

loss, muscle weakness, spasticity, and muscle atrophy occur, inducing progressive paralysis. ALS is a very aggressive pathology that usually evolves in a fast-progressive way. Patients have a lifespan of 2–5 years after diagnosis. Death is frequently due to breathing failure. Most of ALS cases (90%) are sporadic, while a small proportion (10%) is linked to genetic mutations that usually follow an autosomal dominant transmission (Harms and Baloh, 2013; Renton et al., 2013). Cognitive impairment is also associated with ALS. In fact, 30% of ALS cases develop frontotemporal dementia (Lomen-Hoerth, 2011). The C9ORF72 mutation is responsible for the main part of ALS and frontotemporal dementia inherited cases (DeJesus-Hernandez et al., 2011).

The cause of and reasons for MNs death are still unknown. Particularly, it is still not known why this specific neuronal population is affected. However, intense research performed throughout the last two decades has uncovered several hallmarks and molecular mechanisms involved in ALS neurodegeneration. Among them, neuroinflammation, which is understood to be a maintained immune system response in the CNS, plays a central role in the pathogenesis of ALS. This response includes astrocytic and microglial activation and lymphocyte infiltration (Barbeito et al., 2010). There is strong evidence for a compromised energetic metabolism in ALS. Several genes involved in the mitochondrial electron transport chain are altered in their mRNA expression levels (Ferraiuolo et al., 2007, 2011; Lederer et al., 2007; Raman et al., 2015). Further, numerous studies reported structural and functional abnormalities in mitochondria, resulting in increased reactive oxygen species (ROS) and decreased ATP production (Jung et al., 2002; Mattiazzi et al., 2002; Menzies et al., 2002; Wiedemann et al., 2002; Browne et al., 2006), with supposed impacts on purinergic signaling. Here, we will discuss the contribution of purinergic signaling in ALS etiology.

Purinergic Involvement in ALS

P2X receptors

ATP mediates intercellular communication by acting as a messenger between neurons and glia via activation of several purinergic P2 receptors. The involvement of purinergic receptors in ALS has been documented, such as the P2X4 receptor subtype, which is implicated in neuroprotection (Andries et al., 2007) and microglial activation (Tsuda et al., 2003). Positive allosteric modulation of P2X4 receptor activity with Ivermectin

and pre-incubation with low ATP concentration has shown to induce neuroprotection against glutamate-induced excitotoxicity in MNs cultures, a phenotype observed in several ALS models. Allosteric P2X4 receptor activation also improved the lifespan of superoxide dismutase 1 (SOD1) transgenic mice harboring the G92A mutation (Gly-93 to Ala)—a conventional animal model of ALS—by 10% and increased the number of ventral horn MNs in the spinal cord (Andries et al., 2007). Ventral horns are the main neurodegenerative regions affected in ALS. These findings indicate that purinergic receptors modulate excitability, exerting neuroprotection in ALS (Miles et al., 2002). However, it has been described that the allosteric P2X4 receptor activator Ivermectin acts on AMPA receptors inhibiting glutamate excitotoxicity, which could be also responsible for these observed beneficial effects.

Interestingly, the P2X4 receptor has been suggested as a novel marker for non-typical apoptotic and degenerating MNs both in the spinal cord and in other degenerated areas, which had not been previously linked to ALS. P2X4 receptor-immunoreactivity was enhanced in the ventral horns of SOD1 (G93A) transgenic rats. These P2X4 receptor-positive cells were surrounded by microglia with a neuronophagic phenotype (Casanovas et al., 2008). Moreover, Tsuda et al. proved that the P2X4 receptor is expressed selectively in activated microglia after neural injury in the spinal cord and that this expression is required for neuropathic pain (Tsuda et al., 2003). The same study showed that pharmacological inhibition of P2X4 receptors induced a reduction in neuropathic pain, indicating a direct relationship between P2X4 receptor activation and microglial reactivity (Tsuda et al., 2003). Further studies regarding the role of P2X4 receptors in activated and resting microglia are needed for elucidating the participation of the P2X4 receptor in ALS etiology and progression.

The P2X7 receptor is expressed in microglia (Ferrari et al., 1996), spinal cord neurons (Deuchars et al., 2001; Wang et al., 2004), astrocytes (Ballerini et al., 1996), and oligodendrocytes (Matute et al., 2007). Activated microglia from the dorsolateral white matter in the spinal cord of sporadic ALS patients presented increased P2X7 receptor immunoreactivity (Yiangou et al., 2006). This receptor has been tightly linked to neuroinflammation. *In vitro* studies also showed increased densities of P2X7 and P2X4 receptors, upregulation of P2Y6 receptor expression, and decreased ectonucleotidase CD39 hydrolytic activity in transgenic mice SOD1 (G93A)-derived microglia, all indicating a potentiation of the purinergic system in ALS. In fact, SOD1 (G93A) microglia treated with ATP or 2′-3′-O-(benzoyl-benzoyl) ATP (BzATP), a potent P2X7 receptor agonist, presented a prominent transition from the microglial M2 to the M1 activated phenotype, accompanied by augmented production of tumor necrosis factor alpha (TNF-α) and cycloxygenase 2 (COX2) (D'Ambrosi et al., 2009). BzATP treatment of SOD1 (G93A) microglia also increased the presence of inflammatory markers, such as nicotinamide adenine dinucleotide phosphate-oxidase 2 (NOX2) activity and ROS production, indicating damaging effects resulting from P2X7 receptor activation (Apolloni et al., 2013b). As expected, P2X7 receptor activation in microglia-neuronal co-culture induced cell death by ROS and reactive nitrogen species generation (Skaper et al., 2006; D'Ambrosi et al., 2009). Complementary to the involvement of P2X7 receptors, Parisi et al. (2013, 2016) reported an overproduction of several microRNAs in neuroinflammation. In agreement, expression rates of these microRNAs were upregulated in ALS models upon P2X7 receptor stimulation (Parisi et al., 2016).

Astrocytes, the most abundant cell type in the CNS, show low expression of P2X7 receptor under physiological conditions. However, this potential cytotoxic receptor presents upregulated expression and increased activity following injury or under pro-inflammatory conditions (Franke et al., 2004; Narcisse et al., 2005; Lovatt et al., 2007). SOD1 (G93A) mice-derived astrocytes showed increased extracellular ATP-induced signaling as well as increased ATP hydrolysis (Gandelman et al., 2010). As previously reported for microglia, P2X7 receptor activation resulted in astrocyte cytotoxicity accompanied by production of reactive oxygen and nitrogen species that are harmful to MNs (D'Ambrosi et al., 2009).

In vitro studies presented consistent data regarding P2X7 receptor function in inflammation through microglia and astrocytes, which are detrimental for MNs survival. Low doses of ATP or BzATP induced spinal MNs death through the peroxinitrite/Fas pathway (Gandelman et al., 2013). However, *in vitro* studies fail to mimic the biological interplay between neuronal and glial cell types. Activation of the Fas pathway, or "Fas-death pathway," is required for inducing death of MNs in trophic factor deprivation environment (Raoul et al., 1999; Barthélémy et al., 2004). Fas can trigger two different signaling pathways: (1) activation of Fas-associated death domain (FADD) and caspase 8, inducing mitochondrial cytochrome c release, or (2) activation of FADD-associated protein 6 (Daxx), activating Ask1 and p38, ultimately increasing production of nitric oxide and peroxynitrite through NOS1 (Estévez et al., 1998, 2000; Raoul et al., 1999, 2002). Although the latter pathway has been described in MNs, it is not restricted to this neuronal population alone.

Though studies have linked the P2X7 receptor to neuroinflammation, surprising results have been found in ALS murine models lacking P2X7 receptor. The genetic deletion of P2X7 receptor expression ($P2X7^{-/-}$) accelerated disease onset and progression, induced neuroinflammatory responses, and produced MNs depletion at end stages of the disease in comparison with $P2X7^{+/+}$/SOD1 (G93A) animals (Apolloni et al., 2013a). The heterozygous SOD1 (G93A) P2X7 $receptor^{+/-}$ animal model did not present any significant differences in body weight, disease onset or motor performance.

While the heterozygous SOD1 (G93A) P2X7 $receptor^{+/-}$ animal model did not present any significant differences in body weight, disease onset, or motor performance, the genetic deletion of P2X7 receptor expression ($P2X7^{-/-}$), instead of improving ALS disease conditions, accelerated disease onset and progression, induced neuroinflammatory responses, and produced MNs depletion at end stages of the disease in comparison with $P2X7^{+/+}$/SOD1 (G93A) animals (Apolloni et al., 2013a). These detrimental effects on P2X7 receptor-knockout SOD1 (G93A) mice shed light on possible dual

effects of the P2X7 receptor in maintaining normal glial activation/trophic phenotypes at early stages of ALS and promoting a pronounced immunoinflammatory response in advanced stages of the disease. Moreover, P2X7 as well as P2X4 receptor expression levels were upregulated in neurons of asymptomatic SOD1 (G93A) mouse peripheral nervous system; however, more information about the mechanisms of action of these receptors in ALS is required (Volont et al., 2016).

The P2X7 receptor has been implicated in detrimental processes other than neuroinflammation. For instance, heat shock proteins that are elements involved in the unfolded protein response are also a neuroprotective mechanism against unfolded proteins that accumulate in the endoplasmic reticulum in response to stress, a phenotype associated with several ALS models. Specifically, the heat shock protein 90 (Hsp90) expression is upregulated in SOD1 (G93A) animal models as well as in ALS patients. However, it is not clear whether this upregulation is beneficial or prejudicial as *in vitro* studies reported that Hsp90 is able to induce MNs cell death through P2X7 receptor and FAS signaling (Franco et al., 2013). On the other hand, two chaperones, HSP90α and HSP70-1A, interact with A_{2A} purinergic receptors. By this interaction, they retain the receptor in the endoplasmic reticulum prior to exportation, ensuring its correct folding and acting as a protein quality control system (Bergmayr et al., 2013).

P2Y receptors

The metabotropic P2Y12 receptor has been proposed as a marker for ALS progression. It is co-expressed with CD11b in microglia and is also functional in oligodendrocytes. Its immunoreactivity is gradually lost in the dorsal and ventral horns of the spinal cord during ALS disease in the SOD1 (G93A) model, while CD68 immunoreactivity increases, indicating that P2Y12 receptor expression as marker for M2 microglia (Amadio et al., 2014). However, no specific function of this receptor has yet been described in association with either microglia or oligodendrocytes.

Adenosine receptors

Among the four adenosine receptors, the A_{2A} receptor subtype has been mostly described to be involved in ALS. *In vivo* and *in vitro* studies suggest a role of A_{2A} receptor associated with both improvement and attenuation of ALS progression, which could suggest a stage-dependent role of this receptor.

The A_{2A} receptor has been reported as the main target for caffeine, a non-selective adenosine antagonist (Fredholm et al., 1999; Karcz-Kubicha et al., 2003). The first investigation of the possible neuroprotective effect of caffeine intake and ALS development was performed in an epidemiological study, showing a reduced ALS risk in 377 European patients (Beghi et al., 2011). However, a longitudinal analysis based on over one million individuals from five cohort studies failed to demonstrate this association (Fondell et al., 2015). Similarly, an Italian case-control study found no association with caffeine intake (Pupillo et al., 2017). In the SOD1 (G93A) ALS mouse model, A_{2A} receptor blockade by chronic consumption of caffeine shortened survival and decreased motor performance (Potenza et al., 2013). An interesting finding of this study was the decrease in A_{2A} receptor protein levels only in the spinal cord from the SOD1 (G93A) control group and not in caffeine-treated animals. Whether this downregulation of receptor protein expression is due to the heterogeneity of analyzed cell types (MNs, astrocytes and microglia) or a true outcome of the disease must be determined. In fact, another study showed an increased expression of A_{2A}, but not A_1 receptors, in the spinal cords of symptomatic SOD1 (G93A) mice and in spinal cords of human end-stage ALS patients (Ng et al., 2015).

In the pathophysiology of ALS, one described mechanism that is associated with susceptibility of MNs to excitotoxic insults is activation of the receptor tropomyosin kinase receptor B (TrkB) by brain-derived neurotrophic factor (BDNF) (Fryer et al., 2001; Hu and Kalb, 2003). In this pro-death pathway, BDNF (Koh et al., 1995; Ishikawa et al., 2000; Kim, 2003) agonist stimulation of A_{2A} receptors leads to the damaging transactivation of TrkB (Lee and Chao, 2001; Rajagopal et al., 2004). This neurotoxic pathway is diminished by blockade of A_{2A} receptor in rat MNs *in vitro* injured by the levels of ALS-related mutated proteins, such as SOD1 (G85R) and p150glued (G59S) (Mojsilovic-Petrovic et al., 2006). A physical interaction between TrkB and A_{2A} receptor was demonstrated, in which their disruption by cholesterol depletion blocks the detrimental effect of BDNF to render MNs vulnerable to insult in a similar way observed by *in vitro* A_{2A} receptor blockade (Mojsilovic-Petrovic et al., 2006). In addition to pharmacological inhibition, partial genetic ablation of A_{2A} receptors in SOD1 (G93A) mice protected MNs from astrocyte-induced cell death and delayed disease progression in the mouse model (Ng et al., 2015).

During neuromuscular transmission, adenosine is an important modulator of acetylcholine release by acting on both inhibitory A_1 and excitatory A_{2A} receptors (Correia-de-Sá et al., 1991). In pre-symptomatic SOD1 (G93A) mice, a loss of functional cross-talk between A_1 and A_{2A} receptors was reported, suggesting adenosine signaling dysfunction prior to ALS onset (Nascimento et al., 2015). In the early asymptomatic ALS phase, activation of A_{2A} receptors by the agonist CGS21680 enhanced acetylcholine-evoked release, whereas this excitatory effect was no longer observed during the symptomatic phase (Nascimento et al., 2015). Intracellular Ca^{2+} homeostasis was also dysfunctional in MNs from SOD1 (G93A) mice (Fuchs et al., 2013). A_{2A} receptor activation increased the levels of cytosolic Ca^{2+} (Kobayashi et al., 1998; Palma et al., 2011), while the opposite effect was observed after A_{2A} receptor blockade (Li and Wong, 2000; Correia-de-Sá et al., 2002) and after A_1 receptor activation (De Lorenzo et al., 2004). The described loss of a functional equilibrium between A_1 and A_{2A} receptor actions in presymptomatic ALS mice could induce a hyperexcitable adenosinergic tonus in neuromuscular transmission, contributing to the Ca^{2+}-mediated excitotoxicity at initial stages of the disease (Nascimento et al., 2015). According to this hypothesis, A_{2A} receptors could act in an excitatory context during the pre-symptomatic phase, whereas A_{2A} receptor excitatory action disappears during the symptomatic phase (Nascimento et al., 2015). This stage-dependent effect of A_{2A} receptors could explain the

different effects on modulation of this receptor in ALS models. Nevertheless, further investigation of this receptor through ALS progression is needed.

Outside the neuromuscular context, only A_{2A} receptor density was up-regulated in lymphocytes from ALS patients, while A_1, A_{2B}, and A_3 receptors densities and affinities did not change compared to age-matched healthy subjects. Surprisingly, A_{2A} receptor density was positively correlated with improved clinical and functional status according to the revised ALS Functional Rating Scale (Vincenzi et al., 2013). Furthermore, cAMP production in ALS lymphocytes was increased by pharmacological stimulation of the A_{2A} receptor by its agonist CGS21680. Within the immune system, higher levels of cAMP reduce the production of pro-inflammatory mediators and increase the production of anti-inflammatory factors (Raker et al., 2016). Therefore, in addition to its described anti-inflammatory function (Sitkovsky, 2003; Haskó, 2004), these findings indicate a possible protective role for the A_{2A} receptor, specifically in the peripheral immune system.

In MNs, aberrant RNA metabolism—due to mislocalization and/or dysfunction of RNA-binding proteins—has been implicated in ALS (Strong, 2010). Human antigen R, a RNA-binding protein that translocates from nucleus to the cytoplasm, could be associated with pathogenic pathways of ALS (Liu et al., 2015). Stimulation of A_{2A} receptors with the agonist T1–11 normalized the cellular redistribution of human antigen R in the MNs cell line NSC-34, providing potential therapeutic interventions for improving the sustainability of MNs against stress and delaying ALS progression.

Conclusion

ALS is a multifactorial disease with a marked loss of MNs and an important contribution of non-neuronal cells to its pathogenesis and progression. Several works reported the involvement of diverse elements from the purinergic system in ALS, with a critical contribution to neuroinflammation through microglia and astrocyte activation. Two elements play a crucial role in ALS pathogenesis regarding the purinergic system. P2X4 and P2X7 receptors participate in microglia reactivity and astrogliosis, which both produce detrimental effects on MNs maintenance and survival. However, their involvement in ALS progression is more complex as shown *in vivo* models. There is a specific time window, at late pre-symptomatic stages of the disease, where antagonism of the purinergic P2X7 receptor may be beneficial. However, P2X7 receptor inhibition after this point produces negative effects on cell survival. During the early phase of ALS, the A_{2A} receptor mediates excitotoxicity effects on neuromuscular junction, whereas this effect is no longer observed with the progression of the disease, at the symptomatic phase. These observations indicate a possible change of function of this receptor depending on disease state. In terms of the variety of extracellular nucleotide-degrading enzymes and purinergic receptors, which assemble as homo- or heterocomplexes and vary in composition in different CNS cell types, more intense research has to be performed to clarify short- and long-term implications of purinergic signaling in ALS.

Other Motor Neuron Diseases

Spinal Muscular Atrophy (SMA) is a MND that affects MNs in the spinal cord and brainstem. Patients share manifestations similar to ALS, such as weakness, muscle atrophy/paralysis, and respiratory impairment that can lead to death (Crawford and Pardo, 1996; Lefebvre et al., 1997). The most frequent type of SMA is caused by deletions in the survival motor neuron 1 (SMN1) gene, which is involved in biosynthesis of RNA and proteins (Burghes et al., 1994; Lefebvre et al., 1995; Jablonka et al., 2000; Gabanella et al., 2007; Bebee et al., 2010; Lotti et al., 2012). High SMN1 expression in neurons and glia in a SMA transgenic mice model rescued MNs survival, indicating a non-autonomous cellular contribution in SMA (Gavrilina et al., 2008).

Currently, the only study shedding light on the involvement of the purinergic system in SMA used human induced pluripotent stem cell (iPSC)-derived astrocytes (McGivern et al., 2013). Authors reported that this population presented increased basal cytosolic Ca^{2+} concentrations and reduced responses to ATP application, suggesting a possible impairment of the purinergic system in the disease. For instance, P2Y2 receptor activation triggered intracellular Ca^{2+} mobilization in control cells, which was not observed in iPSC-derived astrocytes (Zhu and Kimelberg, 2001; Verkhratsky et al., 2012). The cause for this dysfunction, either because of altered kinetics or compromise of downstream signaling elements, still needs to be clarified. Further, this work was restricted to P2Y2 receptors, while other purinergic receptor subtypes may be involved in the same pathology. The role of the purinergic system in SMA disease should also be studied in microglia and neurons for postulating mechanisms of purinergic signaling in this MNs disorder.

Although no direct experimental evidence links the purinergic system to other previously mentioned MND, the participation of P2 and A_{2A} receptors in the physiology of peripheral nervous system is well-established. Schwann cells—peripheral glial cells responsible for myelin maintenance and injury—destroy their own myelin after peripheral nerve injury and remove myelin and cell debris (Band et al., 1986). Since demyelination is a secondary process present in MND pathophysiology, Schwann cell activity may contribute to disease progression. In fact, injured sciatic nerve induces Schwann cell proliferation via ATP activation of P2X7 receptor while A_{2A} receptors activation inhibits it, both through MAPK/ERK pathways (Stevens and Fields, 2000; Song et al., 2015).

Schwann cells located near the amphibian neuromuscular junction are activated by synaptic ATP release (Robitaille, 1998), and purinergic signaling has key roles in presynaptic modulation (Todd and Robitaille, 2006). However, as suggested by the use of suramin (a non-selective P2 receptor antagonist), activation of Schwann cells by local applications of ATP did not depend on P2 receptors, indicating a possible involvement of A_1 receptor activation by ATP metabolites (Rochon et al., 2001). An *in vitro* model of neuromuscular junction injury showed that ATP was an activating signal for Schwann cells in response to nerve function impairment, triggering purinergic signaling (Rodella et al., 2017). Xu et al. (2013) brought evidence for the involvement of purinergic signaling pathway in glia-derived neurotrophic factor (GDNF) release by Schwann cells

in nerve injure. ALS patients presented increased GDNF levels in the cerebrospinal fluid in comparison to control groups as a protective response to nerve injury (Grundström et al., 2000). Moreover, ATP and ADP released by injured nerves activated purinergic receptors that stimulate protein kinase-C and -D pathways (Xu et al., 2013). Furthermore, purinergic receptors promoted myelination processes in oligodendrocytes and inhibited them in Schwann cells. The importance of the purinergic system involvement in demyelination process in MND is clear, but a better understanding of the degenerative process is necessary for developing therapies (Xu et al., 2013).

MULTIPLE SCLEROSIS

MS is an autoimmune disease of the CNS. It is estimated to affect ∼2.5 million people worldwide and is highly incapacitating; 50% of patients will need to use a wheelchair in the years following disease onset between 25 and 45 years of age. The symptomatology of MS is heterogeneous and includes motor impairment, cognitive, visual, and sensory deficits, fatigue, and pain (Compston and Coles, 2008). The etiology of MS is unknown. However, it is speculated that environmental and genetic factors play a role in disease development (Dendrou et al., 2015).

The pathophysiology of MS is characterized by chronic inflammation, in which T cells become responsive for different myelin epitopes, triggering a cascade of events resulting in axonal demyelination and neuronal transmission impairment (Sun et al., 1991; Koehler et al., 2002). The hallmarks of MS are axonal loss, astrogliosis/microgliosis, oligodendrocytes damage, inflammatory focal lesions and T-cell activation (Goldenberg, 2012; Luo et al., 2017). There is a range of immune modulatory drugs used to alleviate MS symptoms. However, these drugs induce troubling side effects including development of other autoimmune disorders and fatal opportunistic infections (Dendrou et al., 2015). Thus, better understanding of the disease in order to develop more effective and safe treatments is needed.

Purinergic Involvement in MS

The first report of the involvement of purinergic signaling in MS came from Mayne et al. (1999), when it was found increased plasma and serum TNF-α levels in MS patients correlated with low levels of adenosine. The induced experimental autoimmune encephalomyelitis (EAE) mouse model, established by myelin oligodendrocyte glycoprotein or myelin basic protein peptide inoculation and immunization, provides some clues on the mechanical role of purinergic signaling in early-stage MS. The EAE model shows similar features as seen in the CNS of MS patients, such as infiltrating T-cells and presence of IgG antibodies as well as hind limb paralysis (Lassmann, 1983; Miller and Karpus, 1994; Eng et al., 1996; Constantinescu et al., 2011). The four purinergic receptors especially known to be involved in MS are P2X7, P2Y12, A_1, and A_{2A} receptors.

P2X receptors

The participation of P2X receptors in MS has been proposed, since they modulate astrocytes and axon-oligodendrocyte communication, which is necessary for myelination formation and repair (Butt, 2006). *Post-mortem* tissue from MS patients exhibited increased P2X7 receptor expression in microglia from spinal cord and brain white matter (Yiangou et al., 2006) in astrocytes localized in active brain lesions (Narcisse et al., 2005) and in oligodendrocytes from optic nerve samples (Matute et al., 2007). Immunohistochemistry analysis of brain sections from the frontal cortex of MS patients showed immunostaining for P2X1, P2X2, P2X3, P2X4, and P2X7 receptors, while P2X6 receptor subunits could not be detected (Amadio et al., 2010). Analysis of blood monocytes from MS patients did not show any differences in P2X7 receptor expression in comparison to healthy controls (Caragnano et al., 2012). However, monocytes from MS patients undergoing treatment with glatiramer acetate—which acts displacing myelin basic protein from the binding site on MHC-II molecules, preventing the activation of myelin-specific T cells—exhibit reduced P2X7 receptor and interleukin (IL)-1β expression, indicating that this treatment may act by decreasing P2X7 receptor pro-inflammatory effects (Caragnano et al., 2012).

Alterations in the P2X7 receptor gene have been identified in MS, leading to gain-of-function of this protein (Oyanguren-Desez et al., 2011). A polymorphism in P2X7 receptor T-allele, resulting in an Ala-76 to Val transition (A76V), induced an increase in Ca^{2+} permeability, ethidium bromide uptake, and electrophysiological responses. Also, P2X7 receptor A-allele substitution of His-155 to Tyr-382, increased Ca^{2+} influx (Oyanguren-Desez et al., 2011). Similar findings in P2X7 receptor gain-of-function due to His-155 to Tyr substitution (H155T) was previously described for leukemic lymphocytes (Cabrini et al., 2005) and suggested to be essential for ATP-dependent P2X7 receptor activation, since the residue 155 is important for P2X7 receptor protein folding (Bradley et al., 2011). On the other hand, a genetic study demonstrated that the presence of P2X7 receptor loss-of-function due to an Arg-307 to Gln (N307Q) polymorphism provided a two-fold protective effect against MS outcome (Gu et al., 2015). Thus, human P2X7 receptor variants are associated with a reduced or increased risk of MS development (Oyanguren-Desez et al., 2011; Gu et al., 2015).

In vivo studies with the EAE mouse model demonstrated that absence of P2X7 receptors resulted in a severe disease phenotype. In addition, microglia and invading brain macrophages were positive for P2X7 receptor immunostaining (Witting et al., 2006). P2X7 receptor knockout mice ($P2X7^{-/-}$), where EAE was experimentally induced, showed lower number of apoptotic lymphocytes in the CNS and increased expression of interferon γ in the spinal cord, with no alterations in TNF-α and IL-2 protein levels (Chen and Brosnan, 2006). Furthermore, P2X7 $receptor^{-/-}$ EAE mice have lower production of endocannabinoids and reduced axonal damage in comparison to wild type animals (Witting et al., 2006). The administration of a P2X7 receptor antagonist during the chronic phase of EAE in mice attenuated symptoms and tissue damage, including remyelination, by improving axonal conductivity and neurological latency (Matute et al., 2007). These results suggest that the P2X7 receptor plays a detrimental role in the development and chronic phase of MS.

A study by Sharp et al. (2008) demonstrated that the absence of P2X7 receptor results in lower frequency of EAE development, including reduced astrocyte activation with no changes in microglia, antigen responsive T-cell population, or cytokine production by splenic-T cells. These results differ from previous available data on P2X7 receptor $^{-/-}$ and EAE mice. In the former two studies, deletion of exon 5 in P2X7 receptor was used to derive the knockout mice (Chen and Brosnan, 2006; Witting et al., 2006), while in Sharp et al. (2008) exon 1 was deleted, resulting in macrophages inability to produce IL-1β. Based on these data, regulation of P2X7 receptor activation status can provide beneficial advantages for MS.

Activation of P2X7 receptors in astrocytes induces the release of purines (Ballerini et al., 1996) and limits glutamate removal from the extracellular compartment (Lo et al., 2008), eventually culminating in neuronal/oligodendrocyte excitotoxicity (Pitt et al., 2000; Matute, 2011). Upon stimulation with IL-1β, astrocytes showed P2X7 receptor expression upregulation, indicating that the P2X7 receptor expression depends on the presence of pro-inflammatory cytokines (Narcisse et al., 2005). Furthermore, a hyperactivation of P2X7 receptors in oligodendrocytes causes excitotoxicity by cytosolic Ca^{2+} overload and consequent tissue damage (Matute et al., 2007).

Yiangou et al. (2006) proposed a mechanism for the involvement of P2X7 receptor in MS: increased extracellular ATP levels caused by cell death activate P2X7 receptors in microglia and macrophages, consequently stimulate IL-1β production and release. IL-1β will induce COX2, an enzyme known to be detrimental during inflammation (Minghetti, 2004). This induction will intensify cell death and production of pro-inflammatory cytokines. In addition, in the EAE rat model, protein levels of P2X7 receptor were analyzed at symptomatic manifestation and after recovery (Grygorowicz et al., 2011). During symptom onset, P2X7 receptor was found to be overproduced in synaptosomes and in glial cells homogenates. The elevated protein level of P2X7 receptor was stable at the recovery phase mainly in the glial fraction, suggesting sustained astrogliosis. The use of P2X7 receptor antagonists, such as periodate-oxidized ATP and Brilliant Blue G (BBG), for the treatment of the neurodegenerative phase of MS has been patented (EP1655032 B1), providing novel tools for clinical and research purposes.

P2Y receptors

During inflammatory responses, P2Y receptors are up regulated in microglia to promote phagocytosis and migration, preventing oxidative stress followed by apoptosis and controlling the expression of pro-inflammatory cytokines (Förster and Reiser, 2015). In MS, the P2Y12 receptor was found in oligodendrocytes from *post-mortem* brain samples and its expression was decreased in areas corresponding to demyelination in gray and subcortical white matter (Amadio et al., 2010). Immunohistochemistry studies revealed expression of P2Y12, P2Y11, and P2Y14 receptors in the frontal cortex of MS patients (Amadio et al., 2010). However, the functions of P2Y11 and P2Y14 receptors are not known. Therefore, we will further focus on the P2Y12 receptor.

Microglia, macrophages and neuronal cells did not show any expression of P2Y12 receptors, while receptor-positive staining was found to be co-localized with myelin-binding proteins and astrocytes. In the white matter of MS patients, microglia expressing the major histocompatibility complex class II, revealed immunostaining for P2Y12 receptors, indicating that microglia possibly phagocytized myelin-bearing P2Y12 receptors (Amadio et al., 2010). Presence of P2Y12 receptors in astrocytes and oligodendrocytes suggests that signaling of this receptor is involved in remyelination.

To determine the effect of P2Y12 receptor in MS, knockout models of this receptor resulted in an enhanced EAE phenotype in mice (Zhang et al., 2017). The EAE pathology was characterized by an increase in IL-17A cytokine levels in serum, higher number of T-helper cell subset (Th17) in spleen and CNS, as well as the presence of granulocyte-macrophage colony-stimulating factor (Zhang et al., 2017). Bone marrow-derived dendritic cells from P2Y12$^{-/-}$ mice challenged to model EAE have increased release of IL-23, which is an essential factor to promote differentiation of CD4+ T cells toward the Th17 cell subtype (Zhang et al., 2017). The authors concluded that P2Y12 receptors are important for balancing Th-cell populations, and receptor function dysregulation leads to altered cytokine profiles, contributing to EAE.

Adenosine receptors

Analysis of peripheral blood mononuclear cells (PBMC) from MS patients showed that A_1 receptor protein level was significantly reduced (Mayne et al., 1999; Johnston et al., 2001), but gene expression was unaltered (Mayne et al., 1999). In healthy controls, activation of A_1 receptors in PBMCs resulted in inhibition of TNF-α while in MS patients IL-6 was inhibited and had no effect on TNF-α protein level (Mayne et al., 1999). It has been previously demonstrated that constant presence of high TNF-α levels can induce demyelination in a similar way as observed in MS patients, indicating that dysregulation of TNF-α by A_1 receptors can be an initiating factor for MS pathology (Probert et al., 1995).

Histological analyses of *post-mortem* brain tissues showed lower expression of A_1 receptor in the glial population, specifically the A_1-β receptor spliced variant (Johnston et al., 2001). Induction of the EAE model in $A_1^{-/-}$ mice caused a severe progressive-relapsing form of MS with myelin and axonal loss (Tsutsui et al., 2004). Macrophages produced IL-1β and metalloproteinase 12, as well as soluble factors that damaged oligodendrocytes. Analysis of spinal cord of $A_1^{-/-}$ EAE mice showed increased release of pro-inflammatory cytokines. In contrast, $A_1^{+/+}$ EAE mice had diminished A_1 receptor expression in microglia, corresponding to inflammation. Chronic caffeine administration upregulated A_1 receptor expression in microglia, and when treated concomitantly with A_1 receptor agonist alleviated EAE pathology in the $A_1^{+/+}$ EAE mice model (Tsutsui et al., 2004). Furthermore, coffee consumption and MS risk were recently investigated. In individuals, who reported high coffee consumption and in animal models of MS, caffeine decreased the risk of developing neuroinflammation and had neuroprotective

and anti-inflammatory properties (Hedström et al., 2016; Olsson et al., 2017).

Current therapeutic recommendations in MS include interferon-β and *glatiramer* (Wiendl et al., 2008). Worthwhile of mentioning, interferon-β treatment increases expression of CD73, responsible for the conversion of AMP into adenosine, in endothelial cells (Airas et al., 2007). Similarly, in an induced-demyelinated rat model, interferon-β treatment also enhanced CD73 activity in synaptosomes from cerebral cortex (Spanevello et al., 2006). CD73 activity is also required for lymphocyte infiltration into the CNS during EAE development (Mills et al., 2008). Thus, interference with levels of purines could be an additional factor, by which interferon-β benefits MS patients.

While the A_1 receptor subtype is an unequivocal negative modulator of MS and EAE (Tsutsui et al., 2004), the A_{2A} receptor subtype presents a complex role in this disease. Interestingly, A_{2A} receptor expression is increased in the brain of patients with secondary progressive MS, evidenced by positron emission tomography (PET) imaging of radioligand binding to the A_{2A} receptor (Rissanen et al., 2013). This receptor is both highly expressed by lymphocytes and the main mediator of anti-inflammatory effects of adenosine (Blackburn et al., 2009). In the EAE model, A_{2A} receptor-selective antagonist SCH58261 treatment protected mice from EAE induction and CNS lymphocyte infiltration (Mills et al., 2008, 2012). On the other hand, A_{2A} receptor-deficient ($A_{2A}^{-/-}$) mice developed a more severe paralysis after EAE induction, characterized by increased numbers of lymphocytes and activated macrophages/microglia in the CNS (Mills et al., 2012), severe demyelinated phenotype, axonal injury in spinal cord and cerebral cortex and pro-inflammatory cytokine profile in the CNS, blood, and spleen (Yao et al., 2012). Mechanisms of these opposite effects following genetic (knockout animal) or pharmacological (antagonists) blockade of A_{2A} receptors were revealed by assays with bone marrow chimeric mice (subjected to radiation and replacement of immune cells by bone marrow from donor animals) (Mills et al., 2012). This model also reveals the contribution of A_{2A} receptor signaling in immune and non-immune cells during EAE. In fact, $A_{2A}^{-/-}$ donor hematopoietic cells induced severe EAE, whereas the absence of A_{2A} receptor in non-immune cells protected mice from disease development. Taken together, these data demonstrate that expression of A_{2A} receptors in lymphocytes is crucial for limiting the severity of inflammation, while the A_{2A} receptor on nonimmune cells is necessary for disease development. Moreover, without A_{2A} receptor expression by blood brain barrier cells (and other non-immune cells), immune cells fail to infiltrate the CNS, protecting mice from disease development (Mills et al., 2012), similarly to the effects of pharmacological blockade of A_{2A} receptors (Mills et al., 2008, 2012).

A_3 receptor signaling is associated with degranulation of mast cells. Activation of A_3 receptor inhibits adenylate cyclase, stimulates phospholipase C and B, and induces calcium release from intracellular stores. It has been suggested that A_3 receptors may also inhibit binding of neutrophils to endothelial cells. A_3 receptor is expressed in whole brain (Safarzadeh et al., 2016). Though it is still unclear whether the A_3 receptor is involved in MS, this receptor has been demonstrated to mediate the inhibition of TNF-α production by adenosine (Lee et al., 2006; Levy et al., 2006). Therefore, this receptor may play important roles in the pathophysiology of MS and, such as for the A_{2A} receptor, A_3 receptor inhibition may be a potential therapeutic approach.

A_{2B} receptor signaling also modulates the pathogenesis of EAE phenotype. This receptor is upregulated in peripheral leukocytes of MS patients and in the mouse model. Activity inhibition of A_{2B} receptor with the selective antagonist CVT-6883 or its genetic deletion attenuated adenosine-mediated IL-6 production, infiltration of peripheral leukocytes and clinical symptoms in the EAE model (Wei et al., 2013). The presented studies suggest that adenosinergic activation of A_1 receptor regulating inflammatory cytokine TNF-α and IL-6 production is altered in MS, probably due to alterations at transcriptional levels of A_1 receptor and/or to adenosine availability (Mayne et al., 1999; Johnston et al., 2001).

Conclusion

Since current therapeutic recommendations for MS have partial efficacy on clinical outcomes and disease progression, the search for new therapeutic tools is necessary. In this context, *post-mortem* analysis of brain tissue from both MS patients and EAE mouse/rat models elicited potential therapeutic targets through: (1) blockade of P2X7 receptor and stimulation of A_1 receptor, inhibiting inflammation; (2) P2Y12 receptor stimulation, favoring remyelination; and (3) blockade of A_{2B} receptors and CD73, inhibiting the infiltration of leukocytes into the CNS.

PARKINSON'S DISEASE

Parkinson's Disease (PD) is the second most common neurodegenerative disease. Its incidence increases with age reaching over 4% of the population over 80 years old (de Lau and Breteler, 2006). PD is considered a motor disease as a reflex of its clinical symptoms, as resting tremors of extremities, muscular rigidity, postural imbalance, and bradykinesia (Braak et al., 2013). The pathology of PD is characterized by progressive loss of dopaminergic neurons in the *substantia nigra pars compacta* (SNc) and their projections to the striatum, structures associated to voluntary motor movements' control. Besides dopaminergic neuronal degeneration, the presence of protein aggregates (known as Lewy bodies) due to misfolding of α-synuclein occurs in the SNc, *locus ceruleus*, amygdala, and the CA2 area of the hippocampus (Jellinger, 2011). The mechanisms underlying these events have yet to be clarified, although a genetic predisposition associated with insults as traumatic brain injury and ischemia seems to induce α-synuclein aggregation (Shahaduzzaman et al., 2013; Kim and Vemuganti, 2017). The majority of genes linked to familial PD development, such as α-synuclein and leucine-rich repeat kinase-2 (LRRK2) apparently follow a non-Mendelian genetic inheritance pattern. Even so, people who have first-degree relatives affected by sporadic PD have increased chances of developing PD (Elbaz et al., 1999).

Mitochondrial dysfunction and purinergic receptor signaling are also involved in the mechanism of the disorder (Takenouchi et al., 2010; Hoang, 2014).

Currently, dopamine agonists as L-3,4-dihydroxyphenylalanine (L-DOPA) are the most common agents used in therapy. L-DOPA is a precursor of catecholamines such as dopamine and is able to cross the blood-brain barrier. However, long term use of L-DOPA loses efficacy and dose adjustments are needed, triggering side effects such as dyskinesias in 50% of patients after 5 years of continuous treatments (Lang, 2009; Olanow et al., 2009). Present studies on molecular aspects of PD, together with the development of new drugs and tests for improving diagnosis accuracy, will bring new therapeutics perspectives for the disease.

Purinergic Involvement in PD

P2X receptors

Although immunohistochemistry analysis did not reveal any difference between intact and lesioned striatum and SNc (Amadio et al., 2007) for P2X7 receptors, antagonism of this receptor has been shown to prevent or reverse hemiparkinsonian behavior in animals lesioned with 6-hydroxydopamine (6-OHDA), a neurotoxin that mimics PD's pathology. Acute SNc injections of the P2X7 receptor antagonist A-438059, 60 min before and 60 min after rat 6-OHDA lesion, prevented dopamine striatal deficit in comparison to the intact hemisphere, with the P2X7 receptor localized in glial cells (Marcellino et al., 2010). BBG administered in a dose of 45 mg/kg daily after 6-OHDA lesion prevented hemiparkinsonian behavior, short-term memory impairment and dopamine deficit in the striatum and SNc (Carmo et al., 2014). While these studies showed only a preventive effect of P2X7 receptor antagonism, BBG at a dose of 50 mg/kg reversed 6-OHDA lesion in striatum and SNc. In this work, BBG treatment started 1 week after 6-OHDA injection, a period of time sufficient for the lesion to settle, thus proving the reversal effect (Ferrazoli et al., 2017).

Neuronal death seems to aggravate protein aggregation observed in PD. Intense ATP release and consequent purinergic receptors activation were considered to be a key trigger. In fact, P2X1 receptor antagonism or genetic deletion reduced α-synuclein aggregation induced by ATP released by dying cells *in vitro* (Gan et al., 2015). Moreover, P2X1 receptor activation induced lysosomal dysfunction that seems to be involved in α-synuclein aggregation, since it delayed protein turnover and led to its accumulation (Gan et al., 2015). Although P2X7 receptor blockade did not result in reduction of α-synuclein aggregation in this study, ATP release triggered by α-synuclein *in vitro* activated the P2X7 receptor and mobilized the release of intracellular Ca^{2+}, showing that P2X7 receptor activation is a consequence of α-synuclein aggregation (Wilkaniec et al., 2017). Additionally, another study showed that microglial cells challenged with α-synuclein presented increased ROS production through P2X7 receptor activation, which was prevented in the presence of a receptor antagonist (Jiang et al., 2015). Thus, it seems that P2X1 receptor activation contributes to α-synuclein aggregation, which in turn modulates P2X7 receptor activity, ROS production and, finally, ATP release.

Taking into account that few studies directly link purinergic receptors with genetic predisposition to PD, the P2X7R 1513A>C polymorphism that facilitates pore formation by P2X7 receptor activation and leads to cell death (Gu et al., 2001) was shown to be a risk factor in sporadic PD in a Han Chinese population (Liu et al., 2013)

P2Y receptors

There is little data directly connecting P2Y receptors to PD. Recent studies are drawing attention to the role of P2Y6 receptors in PD development and progression. An *in vitro* study showed that P2Y6 receptor gene expression is increased in SH-SY5Y cells—a human neuroblastoma lineage that when differentiated presents markers for dopaminergic neurons—when challenged with neurotoxin 1-methyl-4-phenylpyridinium (MPP^+) (Qian et al., 2017). Thus, its antagonism or deletion decreased MPP^+ effects in cell death through reduced ROS production (Yang et al., 2017). In the CNS, UDP released by damaged cells induces expression of cytokines CCL2 and CCL3 in microglia and phagocytic activity through activation of P2Y6 receptors, indicating that this receptor subtype may be involved in inflammatory response in neurodegenerative diseases (Kim et al., 2011).

Recently, P2Y6 receptor levels were found to be increased in PBMC of PD patients younger than 80 years. To elucidate the involvement of P2Y6 receptor in these patients, the authors used an *in vitro* model of microglia challenged with lipopolysaccharide (LPS) and found increased P2Y6 receptor expression, supporting the hypothesized neuroinflammatory effect of microglia (Yang et al., 2017). Taking into account that P2Y6 receptor selective inhibition by MRS2578 is able to prevent microglial phagoptosis in a mixed neuronal/glial culture in inflammatory conditions (Neher et al., 2014), P2Y6 receptor antagonism seems to be a promising tool to attenuate neuronal death in PD by preventing lesion worsening due to phagocytosis of viable neurons.

Adenosine receptors

It is known that A_{2A} receptors are enriched in dopaminergic brain areas and that their activity modulation affects dopamine receptors (Burnstock et al., 2011). In fact, A_{2A} receptors form heterodimers with dopaminergic D2 and A_1 receptors in glutamatergic synapses, modulating the balance between excitatory and inhibitory impulses that may aggravate PD symptomatology (reviewed by Schiffmann et al., 2007). In animals, a range of A_{2A} receptor antagonists have being shown to potentiate therapeutic effect of low doses of L-DOPA in MPP^+ lesioned monkeys and marmosets and in 6-OHDA lesioned rodents (Kanda et al., 2000; Fuzzati-Armentero et al., 2015) In fact *istradefylline,* a A_{2A} receptor antagonist, was recently approved in Japan to be used concomitantly with L-DOPA treatment, once the compound enhances antiparkinsonian effect of L-DOPA and allow the usage of lower doses of L-DOPA with less long-term side effects (Zhu et al., 2014).

A_{2A} receptors are supposedly involved in synucleinopathy process. A_{2A} receptor-knock out mice presented resistance in preventing dopaminergic deficits upon α-synuclein-induced insults (Kachroo and Schwarzschild, 2012). Attempting to

clarify involved mechanisms, Ferreira et al. found that A_{2A} receptor antagonism decreased α-synuclein aggregation, prevented neuronal death induced by extracellular α-synuclein and restrained hyperactivation of NMDA-glutamate receptors (Ferreira et al., 2015). A_{2A} receptor protein expression levels are increased upon hippocampal injections of α-synuclein in mice and closely co-localized with aggregates, suggesting a pathogenic role of this receptor in synucleinopathy (Hu et al., 2016).

Moreover, A_{2A} receptor antagonism may facilitate microglial response to injury. Microglial delayed containment of debris resulted from cell death can be associated with expansion of the lesion (Gyoneva et al., 2014). Further, both caffeine and selective A_{2A} receptor antagonist KW60002 prevented rat striatal dopaminergic deficit and hydroxyl radical release in LPS-induced inflammation (Gołembiowska et al., 2013). These data suggest inflammatory modulation by A_{2A} receptor antagonism in PD models.

Two polymorphisms of A_{2A} receptor (rs71651683 or rs5996696) were inversely associated with genetic PD risk, wherein caffeine intake intensified the inverse association. Moreover, two polymorphisms in CYP1A2a (rs762551 or rs2470890), an enzyme responsible for caffeine metabolism, in homozygous caffeine consumers showed a prominent reduction in the risk of developing PD (Popat et al., 2011).

Caffeine intake interferes with other genetic risk factors for PD. Subjects with LRRK2 risk variant R1628P showed 15 times increased risk of developing PD than not caffeine consumers (Kumar et al., 2015). GRIN2A rs4998386-T allele encodes a subtype of NMDA receptor, whose activity is enhanced by A_{2A} receptor activation and leads to glutamatergic excitotoxicity. A polymorphism in the GRIN2A rs4998386-T is considered protective for PD development *per se,* but in association with caffeine consumption, it can beneficially impact PD risk in a greater magnitude (Hamza et al., 2011; Yamada-Fowler et al., 2014). However, creatine consumption that increases ATP storage accelerated PD progression in GRIN2A caffeine consumers, possibly due to ATP conversion to adenosine and later A_{2A} receptor activation (Simon et al., 2017).

Conclusion

Taken together, evidence indicates that modulation of purinergic receptor expression and activity could be useful in PD treatment in several ways: (1) reducing microglia activation by damaged cells and α-synuclein aggregation through P2X7 and P2Y6 receptors antagonism; (2) preventing α-synuclein aggregation through P2X1 and A_{2A} receptors antagonism; (3) modulating inflammatory scenario through A_{2A} receptors antagonism; or (4) preventing dyskinesia induced by L-DOPA long-term use through combined treatment with A_{2A} receptor antagonists.

OTHER NEUROLOGICAL CONDITIONS WITH MOTOR DYSFUNCTIONS

Huntington's Disease

HD is an inherited neurological disorder caused by a mutation in IT15 gene that encodes huntingtin protein (Htt) predominantly found in neurons. This mutation results in abnormal (CAG)n repeats localized in 5′ coding sequence. HD is characterized by neurodegeneration of neuronal cells located in striatum and cerebral cortex, ultimately causing neuronal dysfunction and striatal death (Vonsattel and DiFiglia, 1998; Ross and Tabrizi, 2011).

Purinergic Involvement in HD

Adenosine receptor

Adenosinergic pathway plays an essential role in HD etiology and progression, especially through the A_{2A} receptor, as observed in patients and animal models (Popoli et al., 2007). The A_{2A} receptor is highly expressed in striatum (Schiffmann et al., 1991; Fink et al., 1992) especially in GABAergic/enkephalinergic neurons (Taherzadeh-Fard et al., 2010) and in post-synaptic striatopallidal GABAergic neurons (Martinez-Mir et al., 1991; Hettinger et al., 2001), antagonizing dopamine D2 receptors (Schiffmann et al., 2007), while presynaptic A_{2A} receptor activity promotes glutamate release (Shen et al., 2013). Further, presynaptic A_{2A} receptors in glutamatergic terminals impinging into medium spiny neurons play an essential role in the initial maladaptive plasticity in animal models of HD (Li et al., 2015), suggesting its involvement in the degeneration of striatal neurons. Reduction of A_{2A} receptor expression is based on the overexpression of mutant Htt protein showing expanded poly (Q), which affects CREB binding to its promoter region in the A_{2A} receptor gene. Under stimulation, A_{2A} receptor is able to promote its own gene expression via activation of PKC/CREB signaling as well as reduce Htt aggregations (Chiang et al., 2005). Striatal cells expressing mutant Htt showed increased A_{2A} receptor density and cAMP activity due to A_{2A} receptor activation (Varani et al., 2001). As expected, transgenic HD mice showed reduced A_{2A} receptor expression (Cha et al., 1999; Glass et al., 2000; Luthi-Carter et al., 2000), while exhibiting transient increases in A_{2A} receptor density and A_{2A} receptor-dependent activation of cAMP signaling at the earlier pre-symptomatic stage (Tarditi et al., 2006).

It has been proposed that modulation of A_{2A} receptor activity either by agonists or antagonists may prove to be beneficial for HD treatment. However, available data indicate that the beneficial effect observed after stimulation or inhibition of A_{2A} receptor activity depends on the disease stage. At earlier stages of HD, the use of SCH58261 (an A_{2A} receptor antagonist) in quinolinic acid (QA)-induced HD rats and R6/2 transgenic mice reduced striatal BDNF expression, precluding BDNF control of NMDA toxicity (Potenza et al., 2007; Tebano et al., 2010). In later stages, no effect on BDNF expression was observed (Martire et al., 2010; Tebano et al., 2010). QA-induced rats reproduced neurochemical changes of NMDA receptor from HD, e.g., increased glutamate outflow, reduced adenosine levels and degeneration of A_{2A} and dopamine receptors (Beal et al., 1991; Ishiwata et al., 2002; Gianfriddo et al., 2003). Treatment with SCH58261 2-3 weeks after QA injection increased striatal glutamate release, acting as damaging factor (Gianfriddo et al., 2003).

Preventive treatment with SCH58261 before QA induction in rats minimizes the effect of QA on motor activity, striatal gliosis, electroencephalographic (EEG) changes, and glutamate levels

(Popoli et al., 2002). However, cyclooxygenase-2 (COX-2) is inhibited in microglia but increased in cortical neurons, probably as a consequence of NMDA receptors activation, leading to neurotoxicity (Minghetti, 2004). Pretreated QA-induced rats also showed less rearing behavior and no changes in baseline motor activity after 2 weeks of induction; 6 months later, rats showed reduced anxiety but no changes in learning task when compared to QA-induced rats not pre-treated with SCH58261 (Scattoni et al., 2007). These findings suggest that SCH58261 acts on damaged striatum and not on damaged hippocampus, and that different populations of striatal neurons are responsive to SCH58261 (Scattoni et al., 2007). As reviewed by Cunha (Cunha, 2016), the blockage of A_{2A} receptor improves memory and motor functions indicating hippocampal activity, contradicting the findings of Scattoni et al.

On the other hand, in primary striatal cultures treated with QA, an increase in intracellular calcium concentration was observed which enhanced in presence of SCH58261, but reduced in presence of A_{2A} receptor agonist CGS21680 (Popoli et al., 2002). Another A_{2A} receptor antagonist, 3,7-dimethyl-1-propargylxanthine (DMPX), completely blocked encephalographic changes in prefrontal cortex in QA-induced rats (Reggio et al., 1999). The beneficial effect can be due to dopamine receptor activation that provides neuroprotection as a result of abolishment of A_{2A} receptor function, since D2 dopaminergic receptors are downregulated by A_{2A} receptors in D2/A_{2A} receptor heteromers (Reggio et al., 1999).

In a transgenic rat model of HD showing 51 repeated CAG sequences, the presence of post-synaptic A_{2A} receptor antagonist KW-6002, a known stimulant of locomotion, didn't alter the locomotion pattern between 3 and 6 months old. This indicated that the animals become indifferent to A_{2A} receptor modulation during that period (Orr,ú et al., 2011). Furthermore, the presynaptic A_{2A} receptor antagonist SCH-442416 did not reduce electromyography responses (Orr,ú et al., 2011).

The function of A_{2A} receptors has been studied in HD transgenic mouse models (R6/1 with later symptoms and R6/2 with earlier symptoms), which contain the first exon of human Htt gene and 115-150 CAG repeats (Li et al., 2005). During R6/2 mouse development, A_{2A} receptor protein density and A_{2A} receptor-dependent production of cAMP slightly increased at post-natal days 7–14, before the onset of motor symptoms (Tarditi et al., 2006). On the 21st day, changes are normalized to control (Tarditi et al., 2006). A_{2A} receptor expression, but not protein density, starts decreasing, indicating that protein turnover is altered in HD (Cha et al., 1999; Tarditi et al., 2006). Reduction of A_{2A} receptor coding mRNA can be explained by regulation of A_{2A} receptor gene methylation patterns, once R6/1 mice has less hydroxymethylcytosine and higher methylcytosine levels in 5′-UTR regions of the A_{2A} receptor gene (Villar-Menéndez et al., 2013).

Since turnover of A_{2A} receptor protein is altered in HD, inhibition of this receptor function is an advisable therapeutic approach. Starting at 5 weeks, the use of the A_{2A} receptor antagonist SCH58261 in R6/2 mice ameliorated NMDA-induced toxicity and emotional/anxiety response (Domenici et al., 2007). After week 8, administration of SCH58261 leads to NMDA receptors remodeling (NR_1 and NR_{2A} receptor /NR_{2B} ratio) in striatum (Martire et al., 2010). R6/2 mice at age of 10–11 weeks old showed increased adenosine levels correlated with the presence of p38 MAPK in striatal neurons, resulting in striatal damage (Gianfriddo et al., 2004). The usage of SCH58261 greatly reduced striatal adenosine levels and glutamate outflow, suggesting that SCH58261 was acting on A_{2A} receptors located in corticostriatal glutamatergic terminals (Gianfriddo et al., 2004). When treated with SCH58261, rearing and grooming behaviors were reduced in R6/2 mice, but increased in wild type mice, suggesting that A_{2A} receptor antagonism effects on behavior depended on the presence of mutant Htt (Domenici et al., 2007). However, there are contradictory findings regarding the effect of SCH58261. While this compound has shown beneficial effect by reducing NMDA toxicity in striatum *in vivo*, it did not prevent NMDA toxicity from *in vitro* culture of corticostriatal slices obtained from R6/2 mice (Martire et al., 2010).

In order to determine whether the A_{2A} receptor is involved in HD etiology, A_{2A} receptor knockout mice were induced with mitochondrial toxin 3-nitropropionic acid (3-NPA) which blocks succinate dehydrogenase, inducing HD phenotype. Only 1 out of 8 showed striatal lesion after 3-NPA induction, indicating that the absence of A_{2A} receptor has protective effect against HD development (Fink et al., 2004). To confirm this finding, wild type mice were pre-treated with the A_{2A} receptor antagonist 8-(3-chlorostypyl)-caffeine. The animals did not show any striatal lesions after 3-NPA treatment (Fink et al., 2004). On the other hand, ablation of A_{2A} receptors in HD N171-82Q transgenic mouse model completely aggravated motor performance and survival, reducing the expression of striatal encephalin (Mievis et al., 2011). This observation suggests that early and chronic blockade of A_{2A} receptor is not favorable for HD development (Mievis et al., 2011), but memory improvement was observed in R6/2 mice with complete genetic A_{2A} receptor ablation (Li et al., 2015).

In symptomatic R6/2 mice, activation of A_{2A} receptors by CGS21680 delayed the deterioration of motor conditions, prevented reduction in brain weight, diminished the levels of choline, normalized glucose levels, and altered NMDA receptor subunit composition and basal synaptic transmission, without changing its expression (Chou et al., 2005; Martire et al., 2007; Potenza et al., 2007; Ferrante et al., 2010; Tebano et al., 2010). Cultivation of corticostriatal slices from R6/2 mice in presence of CGS21680 also showed reduced NMDA toxicity, suggesting a crosstalk between A_{2A} receptor and BDNF (Tebano et al., 2010). Treatment of striatum slices from R6/2 with CGS21680 resulted in an increase in extracellular field potential, while the opposite effect was observed in wild type slices, where the use of an A_{2A} receptor agonist potentiated toxicity via NMDA receptor activation (Martire et al., 2007).

Single nucleotide polymorphisms (SNPs) in the $ADORA_{2A}$ gene have been identified in HD patients. A C>T genotype (1876 C/T; rs5751876) SNP results in a silent mutation with unknown function and influences the age of onset of HD, while the T/T genotype increases the age of onset of HD by 3.8 years when compared to the C/C genotype (Dhaenens et al., 2009). A SNP in intron 1 (rs2298383) is linked to early onset of HD

(Taherzadeh-Fard et al., 2010). Analysis of HD patient peripheral blood cells led to increased aberrant A_{2A} receptor signaling, which correlates with the age of the patient, numbers of expanded CAG repeats and number of A_{2A} receptor ligand-binding sites (Maglione et al., 2005a,b). The linear correlation is more evident in patients suffering from chorea—an early disruption of the striatum in HD. Neutrophils from HD patients have higher A_{2A} receptor dysfunction in homozygous vs. heterozygous HD patients while no changes in A_1 or A_3 receptors are observed in peripheral blood cells (Varani et al., 2003). A_{2A}-cannabinoid CB1 receptor heterodimers exert crucial function by controlling neuronal excitability (Moreno et al., 2017), while activation of striatal A_{2A} receptors may inhibit CB1 function independent from heterodimer formation (Ferreira et al., 2015). Patients harboring high-grade HD do not possess A_{2A}-CB1 receptor heterodimers in the caudate-putamen region due to the lack of CB1 receptors (Moreno et al., 2017). Recent evidence suggests that consuming more than 190 mg/day of caffeine may accelerate HD onset (Simonin et al., 2013), contradicting findings in animal models that point toward beneficial effects of A_{2A} receptor antagonism in HD.

HD is also characterized by oxidative stress resulting from mitochondrial dysfunction, leading to GABAergic neuronal loss and proneness to DNA damage (Chiu et al., 2015). GABAergic neurons derived from HD-iPSC showed an increase in DNA damage and oxidative stress, which can be dramatically reduced by A_{2A} receptor activation (Chiu et al., 2015). Stimulation of A_{2A} receptors minimizes oxidative stress-induced apoptosis by activation of the cAMP/PKA signaling pathway (Chiu et al., 2015), which is essential for reversing the effect of reduced A_{2A} receptor activity via CREB transcription factor activation (Chiang et al., 2005). However, findings *in vivo* contradict the beneficial effect of A_{2A} receptor agonism on PKA signaling. In R6/1 mice, dopamine D1 and A_{2A} receptors are hyperactive showing greater cAMP/PKA signaling (Tyebji et al., 2015). Chronic administration of antagonists of dopamine D1 and A_{2A} receptors normalized PKA levels and improved cognitive dysfunction and synaptic plasticity. Pre-treatment of rats and mice with either 8-cyclopentyl-1,3-dipropylxanthine (CPX; A_1 receptor antagonist) or DMPX prior application of manolate (an inhibitor of mitochondria acting in striatum) showed that DMPX prevented GABAergic cell loss while CPX promotes cell death (Alfinito et al., 2003). The A_1 receptor agonist R-PIA prevented seizures but not neurodegeneration in the 3-nitropropionic acid (3-NPA) model of neurotoxicity (Zuchora and Urbańska, 2001), while the A_1 receptor agonist adenosine amine congener (ADAC) protects against excitotoxicity, delays degeneration and improves motor functions in the same model (Blum et al., 2002). In view of that, the effect of A_1 receptors depended on the respective used antagonist.

P2 receptors

The role of P2X signaling in HD has not yet been studied in detail. Evidence exists that signaling via ATP induced cell death in HD models while blockade of ATP production reduces cell loss (Varma et al., 2007). At the present, the only evidence available is the role of P2X7 receptor in HD pathogenesis. In two HD mice model, Tet/HD94 and R6/1, P2X7 receptor expression is increased, as well as P2X7 receptor-induced Ca^{2+} permeability (Diaz-Hernandez et al., 2009). Treatment with the P2X7 receptor antagonist BBG ameliorates motor coordination deficits and body weight loss while inhibiting neuronal loss. *In vitro*, neurons expressing mutant Htt are prone to cell death induction by apoptosis after P2X7 receptor stimulation (Diaz-Hernandez et al., 2009).

Conclusion

The available data on the involvement of A_{2A} receptors in HD progression is evident, suggesting that the prevention of its activation could delay disease progression. Taken together, it can be proposed that a combination of A_1 receptor agonist and A_{2A} receptor antagonist might be a good therapeutic approach for HD. It must be taken in consideration that the effect of A_{2A} receptor antagonism depends on age, doses, and length of treatment. Although antagonism of P2X7 receptor may be promising, the involvement of other P2 receptors remains unclear and needs to be investigated.

Ataxias

Ataxia, or dysfunction in motor coordination, is a major consequence of cerebellar and spinocerebellar tract dysfunction that can be induced by several factors, including genetic and sporadic forms, commonly related to immune system mechanisms (Mariotti et al., 2005). Spinocerebellar ataxia (SCA), a genetic-related form of progressive ataxia resulted by cerebellar degeneration, is classified according to mode of inheritance and gene/chromosome locus affected (Matilla-Dueñas et al., 2012). The most prevalent and severe forms of SCA are caused by an increase in CAG sequence repeats in genes that encode proteins related to disease development (Paulson et al., 2017). For example, the expansion in polyglutamine affecting ataxin-2 protein can be observed in SCA type 2, while ataxin-3 related expansion occurs in SCA type 3. Other forms of SCA can be characterized by other genetic mutations, such as the type 14, in which mutations in the protein kinase C-γ gene induce cerebellar degeneration (Seki et al., 2005).

Purinergic Involvement in Ataxias

Attempting to identify survival characteristics of some cell in SCA type 2, wild type ataxin-2 positive neurons showed resistance in cell-death induced by axotomy (Viscomi et al., 2005) and, although this lesion up-regulated P2X1 and P2X2 receptors in precerebellar nuclei (Florenzano et al., 2002) and induced P2X1 receptor in ataxin-2 positive neurons, the percentage of cells expressing P2X1 receptor was not altered (Viscomi et al., 2005). Viscomi and co-workers suggested that these purinergic receptors could influence resistance against cell death without being essential for cell survival, since there are several pathways involved in neuronal death. The elucidation of purinergic receptor involvement in SCA type 3 is focused on adenosine receptors. The blockade of A_{2A} receptors through caffeine ingestion reduced damaging morphological changes induced by mutant ataxin-3 injection. Moreover, these damaging effects were abolished in knockout mice for A_{2A} receptors (Gonçalves et al., 2013). Behavioral improvements were also observed in transgenic c57Bl6 mice expressing truncated polyglutamine

ataxin-3 with severe ataxia, reinforcing the protective effect of A_{2A} receptor antagonism in the SCA type 3 (Gonçalves et al., 2017). In the SCA type 14 *in vitro* model, stimulation of purinergic receptors with ATP transiently increased translocation of mutant protein kinase C-γ to the plasma membrane and subsequent increased damaging aggregation in the cytoplasm (Seki et al., 2005).

Restless Leg Syndrome

Restless leg syndrome (RLS) is a neurological condition characterized by an urge to move legs during rest, following a circadian cycle with worsening during night and even during sleep (named periodic limb movements of sleep). Pathophysiological mechanisms have not been fully elucidated, and conflicting results are reported in the literature. Dopaminergic transmission seems to be involved, since the use of dopaminergic-inducing drugs improved symptoms (Garcia-Borreguero and Cano-Pumarega, 2017). Due to the high affinity of the agonists with best responsiveness to RLS for D3 dopaminergic receptors, it is postulated that the D3 receptor subtype has major responsibility for RLS improvement (Ferré et al., 2018). However, the risk of symptoms worsening after long-term use of these drugs stimulated the search for alternative therapies, based on glutamatergic ligands and reversal of iron deficiency (Ferré et al., 2017). Striatal glutamatergic terminals are found to be hypersensitive in an animal model of RLS with increased glutamate and dopamine release. It is known that, besides increased dopamine release, there is a decreased synaptic D2 receptor density in this animal model (Ferré et al., 2018).

Purinergic Involvement in RLS

Recently, Ferré's group pointed at a relation between adenosine receptors and brain iron deficiency in RLS. Using an animal model for RLS, in which mice and rats adhered to an iron deficient diet, striatal presynaptic A_{2A} receptor density was upregulated (Gulyani et al., 2009). In the same animal model, A_1 receptor density was found decreased in animals with mild, moderate and severe deficiency accompanied by dopaminergic D2 receptor downregulation, and increased pre-synaptic A_{2A} receptor density in animals submitted to a more iron deficient diet (Quiroz et al., 2016). Thus, the post-synaptic A_1 receptor, which can be found as heteromers with D1 dopaminergic receptors and antagonizes their activity, as well as presynaptic A_{2A} receptors forming heteromers with D2 receptors whose activation decreases D2 receptor affinity for agonists, could be targets to improve movement impairment (Ferré et al., 1994; Ferre et al., 1996; Ferré et al., 2007, 2018). Finally, A_1/A_{2A} receptor heteromers found in the striatal glutamatergic terminals, activated by different adenosine concentrations, decreased glutamate release, a condition found in brain iron deficiency animals (Ciruela et al., 2006; Ferré, 2010).

OUTCOMES FOR HYPOTHESES ON P2 PURINERGIC SIGNALING

Although P2X7 receptor expression and levels in neurons is controversial, the involvement of this receptor in neurodegeneration is well-stated (Illes et al., 2017). Of all purinergic receptors, the P2X7 receptor has the lowest affinity for ATP, and only high concentrations of this nucleotide induce channel formation (North, 2002; Khakh and Alan North, 2006). Of the neurological diseases presented here, immune system responses and neural cell death correspond with the release of elevated levels of ATP into the extracellular space. In these scenarios, ATP in excess acts as a toxin that can directly induce oligodendrocyte death by activating P2X7 receptors, resulting in progressive neural damage (Matute et al., 2007; Domercq et al., 2009). Corroborating this idea, it is well-known that the P2X7 receptor triggers pro-inflammatory effects (Lister et al., 2007), and its antagonism can counteract chronic inflammation observed in these diseases (**Figure 2**). Thus, beneficial effects of P2X7 receptor antagonism are of interest for future therapeutic approaches.

As further investigations are necessary to better understand the real role of purinergic signaling in the diseases here presented, we also propose a novel mechanistic perspective, in which purinergic receptors from glial cells are key initiators of motor dysfunction in PD, MS, ALS and other MND. Although there is no data regarding P2Y1 receptor functions in these pathological conditions, it is known that this receptor plays a crucial role in astrocyte responses accompanied by P2Y12 and adenosine receptor activity modulation (Mamedova et al., 2006).

During an initial inflammatory response, microglial activation induces P2Y12 receptor expression level and/or activity upregulation, stimulating motility toward the injury site and resulting in reduced P2Y1 receptor expression in astrocytes. This downregulation in P2Y1 receptor expression stimulates an increase in reactive astrogliosis and a phenotypical change in order to promote neuroprotection (Haynes et al., 2006; Mamedova et al., 2006; Shinozaki et al., 2017). However, constant inflammatory responses disable microglia of stimulating P2Y12 receptor expression and activity, resulting in a permanent activation of P2Y1 receptors in astrocytes and extended ROS production (Rodrigues et al., 2015). This condition will lead to a downregulation of A_1 receptor expression, stimulating TNF-α production and release, thereby promoting IL-6 secretion through A_{2B} receptor activation. As a result, TNF-α and IL-6 accumulation damages oligodendrocytes and provoke demyelination. A scheme of this mechanism is proposed in **Figure 1**.

OVERALL CONCLUSION

The purinergic signaling system has risen in the past years as a meaningful research object for understanding and treating several pathologies, as reviewed by Burnstock (2017). Purinergic receptors and enzymes are in the spotlight for new therapeutic interventions as key regulators of neuron-glia communication, as well as modulators of many signaling pathways associated to neuroprotection, neurodegeneration, and neuroregeneration (Burnstock, 2016; Ribeiro et al., 2016). In this review, we highlighted available data linking purinergic signaling pathways to neurological diseases, such as PD, MS, ALS, and other MND, putting together published knowledge with novel hypotheses for overcoming motor dysfunctions. The evidence is summarized in **Table 1**. A common mechanism supporting P2X7 receptor

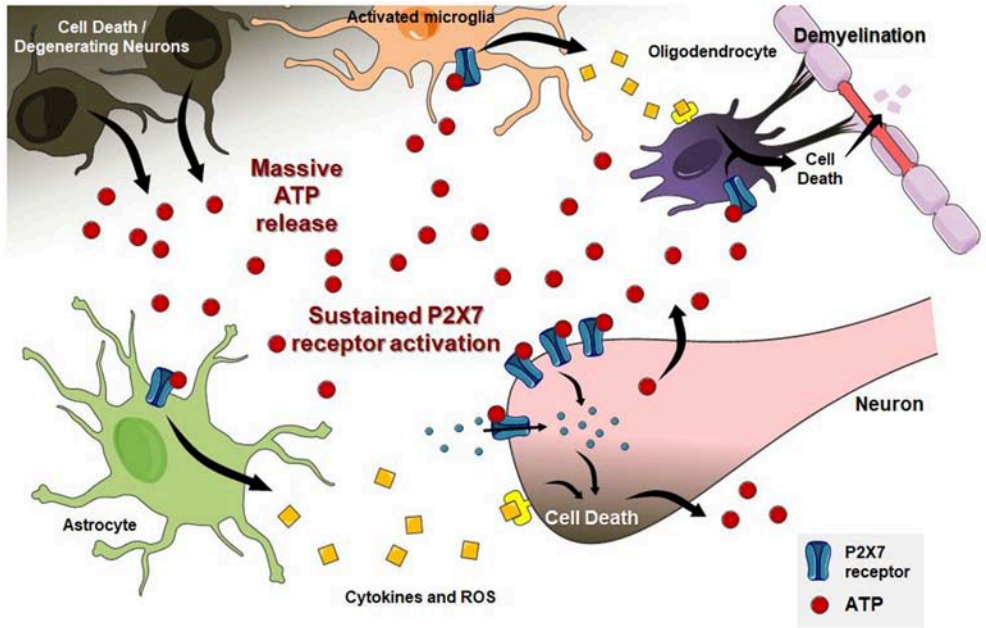

FIGURE 2 | Common mechanism involving P2X7 receptor-mediated cell death in the central nervous system under neurological diseases affecting motor functions. Degenerating neurons release large amounts of ATP, leading to sustained P2X7 receptor activation in: a. Astrocytes, inducing the release of cytokines and reactive oxygen species (ROS); b. Microglia, inducing an activated state and release of cytokines and ROS; c. Oligodendrocytes, inducing cell death and neuron demyelination; d. Neurons (in spite of the controversial discussion on expression of P2X7 receptors in this cell type), inducing pore formation, ion influx and cell death, releasing more ATP into the extracellular space. Moreover, cytokines and ROS released by astrocytes and microglia act on other neural cells, culminating in apoptotic pathway activation.

hyperactivation through high levels of ATP release during disease development is illustrated in **Figure 2**. Moreover, a novel mechanism based on purinergic modulation of glial cells is proposed in **Figure 1**. These approaches suggest novel possible research targets to understand the here presented motor dysfunctions and other factors associated to neurological impairment that have not been studied yet. Applied research will need to be conducted for the development of novel pharmacological treatments to improve patients' lifespan and quality.

AUTHOR CONTRIBUTIONS

ÁO-G: Contribution to idea proposal, organization of sections, writing PD, other MND, RLS, and Ataxia sections, figures, table. YN: Writing MS, HD, and mechanism hypothesis sections. LS-A: Writing ALS and SMA sections. MG: Writing introduction, HD, and conclusion sections. JC-V: Writing ALS section. MP: Writing MS section. HdS: Writing PD section. HU: Conceptualization of the manuscript, supervision of manuscript elaboration, editing and revision, and critical overview.

ACKNOWLEDGMENTS

HU is grateful for grant support by the São Paulo State Foundation FAPESP (Project No. 2012/50880-4) and the National Research Council CNPq (Project No. 306429/2013-6), Brazil. ÁO-G (Project No. 141979/2014-3) and MG (Project No. 870458/1997-3) are grateful for a doctorate fellowship granted by CNPq; Fellowships were granted by FAPESP to HdS (doctorate; Project No. 2012/20685-5), LS-A (doctorate, Project No. 2013/25338-4), MP (pos-doctorate, Project No. 2015/19478-3) and YN (pos-doctorate, Project No. 2015/14343-2). We thank ME Caitlyn A. Moore for English editing and comments on the manuscript.

REFERENCES

Abbracchio, M. P., Burnstock, G., Verkhratsky, A., and Zimmermann, H. (2009). Purinergic signalling in the nervous system: an overview. *Trends Neurosci.* 32, 19–29. doi: 10.1016/j.tins.2008.10.001

Airas, L., Niemela, J., Yegutkin, G., and Jalkanen, S. (2007). Mechanism of action of IFN-beta in the treatment of multiple sclerosis: a special reference to CD73 and adenosine. *Ann. N. Y. Acad. Sci.* 1110, 641–648. doi: 10.1196/annals.1423.067

Alfinito, P. D., Wang, S.-P., Manzino, L., Rijhsinghani, S., Zeevalk, G. D., and Sonsalla, P. K. (2003). Adenosinergic protection of dopaminergic and GABAergic neurons against mitochondrial inhibition through receptors located in the substantia nigra and striatum, respectively. *J. Neurosci.* 23, 10982–10987.

Allard, B., Beavis, P. A., Darcy, P. K., and Stagg, J. (2016). Immunosuppressive activities of adenosine in cancer. *Curr. Opin. Pharmacol.* 29, 7–16. doi: 10.1016/j.coph.2016.04.001

Amadio, S., Montilli, C., Magliozzi, R., Bernardi, G., Reynolds, R., and Volonté, C. (2010). P2Y12 receptor protein in cortical gray matter lesions in multiple sclerosis. *Cereb. Cortex* 20, 1263–1273. doi: 10.1093/cercor/bhp193

Amadio, S., Montilli, C., Picconi, B., Calabresi, P., and Volonté, C. (2007). Mapping P2X and P2Y receptor proteins in striatum and substantia nigra: an immunohistological study. *Purinergic Signal.* 3, 389–398. doi: 10.1007/s11302-007-9069-8

Amadio, S., Parisi, C., Montilli, C., Carrubba, A. S., Apolloni, S., and Volonté, C. (2014). P2Y 12 receptor on the verge of a neuroinflammatory breakdown. *Mediators Inflamm.* 2014:975849. doi: 10.1155/2014/975849

Andries, M., Van Damme, P., Robberecht, W., and Van Den Bosch, L. (2007). Ivermectin inhibits AMPA receptor-mediated excitotoxicity in cultured motor neurons and extends the life span of a transgenic mouse model of amyotrophic lateral sclerosis. *Neurobiol. Dis.* 25, 8–16. doi: 10.1016/j.nbd.2006.08.018

Apolloni, S., Amadio, S., Montilli, C., Volonté, C., and D'Ambrosi, N. (2013a). Ablation of P2X7 receptor exacerbates gliosis and motoneuron death in the SOD1-G93A mouse model of amyotrophic lateral sclerosis. *Hum. Mol. Genet.* 22, 4102–4116. doi: 10.1093/hmg/ddt259

Apolloni, S., Parisi, C., Pesaresi, M. G., Rossi, S., Carrì, M. T., Cozzolino, M., et al. (2013b). The NADPH oxidase pathway is dysregulated by the P2X7 receptor in the SOD1-G93A microglia model of amyotrophic lateral sclerosis. *J. Immunol.* 190, 5187–5195. doi: 10.4049/jimmunol.1203262

Ballerini, P., Rathbone, M. P., Di Iorio, P., Renzetti, A., Giuliani, P., D'Alimonte, I., et al. (1996). Rat astroglial P2Z (P2X7) receptors regulate intracellular calcium and purine release. *Neuroreport* 7, 2533–2537.

Band, H., Bhattacharya, A., and Talwar, G. P. (1986). Mechanism of phagocytosis by Schwann cells. *J. Neurol. Sci.* 75, 113–119. doi: 10.1016/0022-510X(86)90054-7

Barbeito, A. G., Mesci, P., and Boillée, S. (2010). Motor neuron–immune interactions: the vicious circle of ALS. *J. Neural Transm.* 117, 981–1000. doi: 10.1007/s00702-010-0429-0

Barthélémy, C., Henderson, C. E., and Pettmann, B. (2004). Foxo3a induces motoneuron death through the Fas pathway in cooperation with JNK. *BMC Neurosci.* 5:48. doi: 10.1186/1471-2202-5-48

Bartlett, R., Stokes, L., and Sluyter, R. (2014). The P2X7 receptor channel: recent developments and the use of P2X7 antagonists in models of disease. *Pharmacol. Rev.* 66, 638–675. doi: 10.1124/pr.113.008003

Beal, M. F., Ferrante, R. J., Swartz, K. J., and Kowall, N. W. (1991). Chronic quinolinic acid lesions in rats closely resemble Huntington's disease. *J. Neurosci.* 11, 1649–659.

Beamer, E., Gölöncsér, F., Horváth, G., Beko, K., Otrokocsi, L., Koványi, B., et al. (2016). Purinergic mechanisms in neuroinflammation: an update from molecules to behavior. *Neuropharmacology* 104, 94–104. doi: 10.1016/j.neuropharm.2015.09.019

Bebee, T. W., Gladman, J. T., and Chandler, D. S. (2010). Splicing of the survival motor neuron genes and implications for treatment of SMA. *Front. Biosci. (Landmark Ed).* 15, 1191–1204. doi: 10.2741/3670

Beghi, E., Pupillo, E., Messina, P., Giussani, G., Chiò, A., Zoccolella, S., et al. (2011). Coffee and amyotrophic lateral sclerosis: a possible preventive role. *Am. J. Epidemiol.* 174, 1002–1008. doi: 10.1093/aje/kwr229

Bergmayr, C., Thurner, P., Keuerleber, S., Kudlacek, O., Nanoff, C., Freissmuth, M., et al. (2013). Recruitment of a cytoplasmic chaperone relay by the A $_{2A}$ adenosine receptor. *J. Biol. Chem.* 288, 28831–28844. doi: 10.1074/jbc.M113.464776

Blackburn, M. R., Vance, C. O., Morschl, E., and Wilson, C. N. (2009). Adenosine receptors and inflammation. *Handb. Exp. Pharmacol.* 193, 215–269. doi: 10.1007/978-3-540-89615-9_8

Blum, D., Gall, D., Galas, M.-C., D'alcantara, P., Bantubungi, K., and Schiffmann, S. N. (2002). The adenosine A 1 receptor agonist adenosine amine congener exerts a neuroprotective effect against the development of striatal lesions and motor impairments in the 3-nitropropionic acid model of neurotoxicity. *J. Neurosci.* 22, 9122–9133.

Bogacheva, P. O., and Balezina, O. P. (2015). Postsynaptic potentiation in mouse motor synapses induced by ATP accumulation in synaptic cleft. *Bull. Exp. Biol. Med.* 159, 583–587. doi: 10.1007/s10517-015-3018-2

Boison, D., Chen, J.-F., and Fredholm, B. B. (2010). Adenosine signaling and function in glial cells. *Cell Death Differ.* 17, 1071–1082. doi: 10.1038/cdd.2009.131

Borea, P. A., Gessi, S., Merighi, S., Vincenzi, F., and Varani, K. (2017). Pathological overproduction: the bad side of adenosine. *Br. J. Pharmacol.* 174, 1945–1960. doi: 10.1111/bph.13763

Braak, H., Del Tredici, K., Rüb, U., de Vos, R. A., Jansen Steur, E. N., and Braak, E. (2013). Staging of brain pathology related to sporadic Parkinson's disease. *Neurobiol. Aging* 24, 197–211. doi: 10.1016/S0197-4580(02)00065-9

Bradley, H. J., Baldwin, J. M., Goli, G. R., Johnson, B., Zou, J., Sivaprasadarao, A., et al. (2011). Residues 155 and 348 contribute to the determination of P2X7 receptor function via distinct mechanisms revealed by single-nucleotide polymorphisms. *J. Biol. Chem.* 286, 8176–8187. doi: 10.1074/jbc.M110.211284

Browne, S. E., Yang, L., DiMauro, J.-P., Fuller, S. W., Licata, S. C., and Beal, M. F. (2006). Bioenergetic abnormalities in discrete cerebral motor pathways presage spinal cord pathology in the G93A SOD1 mouse model of ALS. *Neurobiol. Dis.* 22, 599–610. doi: 10.1016/j.nbd.2006.01.001

Burghes, A. H., Ingraham, S. E., Kóte-Jarai, Z., Rosenfeld, S., Herta, N., Nadkarni, N., et al. (1994). Linkage mapping of the spinal muscular atrophy gene. *Hum. Genet.* 93, 305–312. doi: 10.1007/BF00212028

Burnstock, G. (1972). Purinergic nerves. *Pharmacol. Rev.* 24, 509–581.

Burnstock, G. (1997). The past, present and future of purine nucleotides as signalling molecules. *Neuropharmacology* 36, 1127–1139. doi: 10.1016/S0028-3908(97)00125-1

Burnstock, G. (2009). Purinergic cotransmission. *Exp. Physiol.* 94, 20–24. doi: 10.1113/expphysiol.2008.043620

Burnstock, G. (2016). An introduction to the roles of purinergic signalling in neurodegeneration, neuroprotection and neuroregeneration. *Neuropharmacology* 104, 4–17. doi: 10.1016/j.neuropharm.2015.05.031

Burnstock, G. (2017). The therapeutic potential of purinergic signalling. *Biochem. Pharmacol.* doi: 10.1016/j.bcp.2017.07.016. [Epub ahead of print].

Burnstock, G., Arnett, T. R., and Orriss, I. R. (2013). Purinergic signalling in the musculoskeletal system. *Purinergic Signal.* 9, 541–572. doi: 10.1007/s11302-013-9381-4

Burnstock, G., Fredholm, B. B., and Verkhratsky, A. (2011). Adenosine and ATP receptors in the brain. *Curr. Top. Med. Chem.* 11, 973–1011. doi: 10.2174/156802611795347627

Burnstock, G., Campbell, G., Satchell, D., and Smythe, A. (1970). Evidence that adenosine triphosphate or a related nucleotide is the transmitter substance released by non-adrenergic inhibitory nerves in the gut. *Br. J. Pharmacol.* 40, 668–688. doi: 10.1111/j.1476-5381.1970.tb10646.x

Butt, A. M. (2006). Neurotransmitter-mediated calcium signalling in oligodendrocyte physiology and pathology. *Glia* 54, 666–675. doi: 10.1002/glia.20424

Cabrini, G., Falzoni, S., Forchap, S. L., Pellegatti, P., Balboni, A., Agostini, P., et al. (2005). A His-155 to Tyr polymorphism confers gain-of-function to the human P2X7 receptor of human leukemic lymphocytes. *J. Immunol.* 175, 82–89. doi: 10.4049/jimmunol.175.1.82

Caragnano, M., Tortorella, P., Bergami, A., Ruggieri, M., Livrea, P., Specchio, L. M., et al. (2012). Monocytes P2X7 purinergic receptor is modulated by glatiramer acetate in multiple sclerosis. *J. Neuroimmunol.* 245, 93–97. doi: 10.1016/j.jneuroim.2012.02.002

Carmo, M. R., Menezes, A. P., Nunes, A. C., Pliássova, A., Rolo, A. P., Palmeira, C. M., et al. (2014). The P2X7 receptor antagonist Brilliant Blue G attenuates contralateral rotations in a rat model of Parkinsonism through a combined control of synaptotoxicity, neurotoxicity and gliosis. *Neuropharmacology* 81, 142–152. doi: 10.1016/j.neuropharm.2014.01.045

Casanovas, A., Hernández, S., Tarabal, O., Rosselló, J., and Esquerda, J. E. (2008). Strong P2X4 purinergic receptor-like immunoreactivity is selectively associated with degenerating neurons in transgenic rodent models of amyotrophic lateral sclerosis. *J. Comp. Neurol.* 506, 75–92. doi: 10.1002/cne.21527

Cha, J. H., Frey, A. S., Alsdorf, S. A., Kerner, J. A., Kosinski, C. M., Mangiarini, L., et al. (1999). Altered neurotransmitter receptor expression in transgenic mouse models of Huntington's disease. *Philos. Trans. R. Soc. Lond. B Biol. Sci.* 354, 981–989.

Cheffer, A., Castillo, A. R., Corrêa-Velloso, J. C., Gonçalves, M. C. B., Naaldijk, Y., Nascimento, I. C., et al. (2017). Purinergic system in psychiatric diseases. *Mol. Psychiatry* 23, 94–106. doi: 10.1038/mp.2017.188

Chen, L., and Brosnan, C. F. (2006). Exacerbation of experimental autoimmune encephalomyelitis in P2X7R-/- mice: evidence for loss of apoptotic activity in lymphocytes. *J. Immunol.* 176, 3115–3126. doi: 10.4049/jimmunol.176.5.3115

Chiang, M. C., Lee, Y. C., Huang, C. L., and Chern, Y. (2005). cAMP-response element-binding protein contributes to suppression of the A2A adenosine receptor promoter by mutant huntingtin with expanded polyglutamine residues. *J. Biol. Chem.* 280, 14331–14340. doi: 10.1074/jbc.M413279200

Chiu, F. L., Lin, J. T., Chuang, C. Y., Chien, T., Chen, C. M., Chen, K. H., et al. (2015). Elucidating the role of the A2Aadenosine receptor in neurodegeneration using neurons derived from Huntington's disease iPSCs. *Hum. Mol. Genet.* 24, 6066–6079. doi: 10.1093/hmg/ddv318

Chou, S.-Y., Lee, Y.-C., Chen, H.-M., Chiang, M.-C., Lai, H.-L., Chang, H.-H., et al. (2005). CGS21680 attenuates symptoms of Huntington's disease in a transgenic mouse model. *J. Neurochem.* 93, 310–320. doi: 10.1111/j.1471-4159.2005.03029.x

Ciruela, F., Casadó, V., Rodrigues, R. J., Luján, R., Burgueño, J., Canals, M., et al. (2006). Presynaptic control of striatal glutamatergic neurotransmission by adenosine A1-A2A receptor heteromers. *J. Neurosci.* 26, 2080–2087. doi: 10.1523/JNEUROSCI.3574-05.2006

Compston, A., and Coles, A. (2008). Multiple sclerosis. *Lancet* 372, 1502–1517. doi: 10.1016/S0140-6736(08)61620-7

Constantinescu, C. S., Farooqi, N., O'Brien, K., and Gran, B. (2011). Experimental autoimmune encephalomyelitis (EAE) as a model for multiple sclerosis (MS). *Br. J. Pharmacol.* 164, 1079–1106. doi: 10.1111/j.1476-5381.2011.01302.x

Correia-de-Sá, P., Sebastião, A. M., and Ribeiro, J. A. (1991). Inhibitory and excitatory effects of adenosine receptor agonists on evoked transmitter release from phrenic nerve endings of the rat. *Br. J. Pharmacol.* 103, 1614–1620. doi: 10.1111/j.1476-5381.1991.tb09836.x

Correia-de-Sá, P., Timóteo, M. A., and Ribeiro, J. A. (2002). A2A adenosine receptor facilitation of neuromuscular transmission. *J. Neurochem.* 74, 2462–2469. doi: 10.1046/j.1471-4159.2000.0742462.x

Crawford, T. O., and Pardo, C. A. (1996). The neurobiology of childhood spinal muscular atrophy. *Neurobiol. Dis.* 3, 97–110. doi: 10.1006/nbdi.1996.0010

Csóka, B., Töro, G., Vindeirinho, J., Varga, Z. V., Koscsó, B., Németh, Z. H., et al. (2017). A2A adenosine receptors control pancreatic dysfunction in high-fat-diet-induced obesity. *FASEB J.* 31, 4985–4997. doi: 10.1096/fj.201700398R

Cunha, R. A. (2008). Different cellular sources and different roles of adenosine: A1 receptor-mediated inhibition through astrocytic-driven volume transmission and synapse-restricted A2A receptor-mediated facilitation of plasticity. *Neurochem. Int.* 52, 65–72. doi: 10.1016/j.neuint.2007.06.026

Cunha, R. A. (2016). How does adenosine control neuronal dysfunction and neurodegeneration? *J. Neurochem.* 139, 1019–1055. doi: 10.1111/jnc.13724

D'Ambrosi, N., Finocchi, P., Apolloni, S., Cozzolino, M., Ferri, A., Padovano, V., et al. (2009). The proinflammatory action of microglial P2 receptors is enhanced in SOD1 models for amyotrophic lateral sclerosis. *J. Immunol.* 183, 4648–4656. doi: 10.4049/jimmunol.0901212

DeJesus-Hernandez, M., Mackenzie, I. R., Boeve, B. F., Boxer, A. L., Baker, M., Rutherford, N. J., et al. (2011). Expanded GGGGCC hexanucleotide repeat in noncoding region of C9ORF72 causes chromosome 9p-linked FTD and ALS. *Neuron* 72, 245–256. doi: 10.1016/j.neuron.2011.09.011

de Lau, L. M., and Breteler, M. M. (2006). Epidemiology of Parkinson's disease. *Lancet Neurol.* 5, 525–535. doi: 10.1016/S1474-4422(06)70471-9

Dendrou, C. A., Fugger, L., and Friese, M. A. (2015). Immunopathology of multiple sclerosis. *Nat. Rev. Immunol.* 15, 545–558. doi: 10.1038/nri3871

De Lorenzo, S., Veggetti, M., Muchnik, S., and Losavio, A. (2004). Presynaptic inhibition of spontaneous acetylcholine release induced by adenosine at the mouse neuromuscular junction. *Br. J. Pharmacol.* 142, 113–124. doi: 10.1038/sj.bjp.0705656

Deuchars, S. A., Atkinson, L., Brooke, R. E., Musa, H., Milligan, C. J., Batten, T. F., et al. (2001). Neuronal P2X7 receptors are targeted to presynaptic terminals in the central and peripheral nervous systems. *J. Neurosci.* 21, 7143–7152.

Dhaenens, C. M., Burnouf, S., Simonin, C., Van Brussel, E., Duhamel, A., Defebvre, L., et al. (2009). A genetic variation in the ADORA2A gene modifies age at onset in Huntington's disease. *Neurobiol. Dis.* 35, 474–476. doi: 10.1016/j.nbd.2009.06.009

Díaz-Hernández, M., Díez-Zaera, M., Sánchez-Nogueiro, J., Gómez-Villafuertes, R., Canals, J. M., Alberch, J., et al. (2009). Altered P2X7-receptor level and function in mouse models of Huntington's disease and therapeutic efficacy of antagonist administration. *FASEB J.* 23, 1893–906. doi: 10.1096/fj.08-122275

Domenici, M. R., Scattoni, M. L., Martire, A., Lastoria, G., Potenza, R. L., Borioni, A., et al. (2007). Behavioral and electrophysiological effects of the adenosine A 2A receptor antagonist SCH 58261 in R6/2 Huntington's disease mice. *Neurobiol. Dis.* 28, 197–205. doi: 10.1016/j.nbd.2007.07.009

Domercq, M., Perez-Samartin, A., Aparicio, D., Alberdi, E., Pampliega, O., and Matute, C. (2009). P2X7 receptors mediate ischemic damage to oligodendrocytes. *Glia* 58, 730–740. doi: 10.1002/glia.20958

Elbaz, A., Grigoletto, F., Baldereschi, M., Breteler, M. M., Manubens-Bertran, J. M., Lopez-Pousa, S., et al. (1999). Familial aggregation of Parkinson's disease: a population-based case-control study in Europe. EUROPARKINSON study group. *Neurology* 52, 1876–1882.

Eng, L. F., Ghirnikar, R. S., and Lee, Y. L. (1996). Inflammation in EAE: role of chemokine/cytokine expression by resident and infiltrating cells. *Neurochem. Res.* 21, 511–525. doi: 10.1007/BF02527717

Estévez, A. G., Sampson, J. B., Zhuang, Y. X., Spear, N., Richardson, G. J., Crow, J. P., et al. (2000). Liposome-delivered superoxide dismutase prevents nitric oxide-dependent motor neuron death induced by trophic factor withdrawal. *Free Radic. Biol. Med.* 28, 437–446. doi: 10.1016/S0891-5849(99)00261-0

Estévez, A. G., Spear, N., Manuel, S. M., Barbeito, L., Radi, R., and Beckman, J. S. (1998). Role of endogenous nitric oxide and peroxynitrite formation in the survival and death of motor neurons in culture. *Prog. Brain Res.* 118, 269–280. doi: 10.1016/S0079-6123(08)63214-8

Faas, M. M., Sáez, T., and de Vos, P. (2017). Extracellular ATP and adenosine: the Yin and Yang in immune responses? *Mol. Aspects Med.* 55, 9–19. doi: 10.1016/j.mam.2017.01.002

Färber, K., Markworth, S., Pannasch, U., Nolte, C., Prinz, V., Kronenberg, G., et al. (2008). The ectonucleotidase *cd39* /ENTPDase1 modulates purinergic-mediated microglial migration. *Glia* 56, 331–341. doi: 10.1002/glia.20606

Faria, R. X., Freitas, H. R., and Reis, R. A. M. (2017). P2X7 receptor large pore signaling in avian Müller glial cells. *J. Bioenerg. Biomembr.* 49, 215–229. doi: 10.1007/s10863-017-9717-9

Ferré, S. (2010). Role of the central ascending neurotransmitter systems in the psychostimulant effects of caffeine. *J. Alzheimers Dis.* 20, S35–S49. doi: 10.3233/JAD-2010-1400

Ferré, S., Agnati, L. F., Ciruela, F., Lluis, C., Woods, A. S., Fuxe, K., et al. (2007). Neurotransmitter receptor heteromers and their integrative role in "local modules": the striatal spine module. *Brain Res. Rev.* 55, 55–67. doi: 10.1016/j.brainresrev.2007.01.007

Ferré, S., Earley, C., Gulyani, S., and Garcia-Borreguero, D. (2017). In search of alternatives to dopaminergic ligands for the treatment of restless legs syndrome: iron, glutamate, and adenosine. *Sleep Med.* 31, 86–92. doi: 10.1016/j.sleep.2016.08.019

Ferré, S., O'Connor, W. T., Snaprud, P., Ungerstedt, U., and Fuxe, K. (1994). Antagonistic interaction between adenosine A2A receptors and dopamine D2 receptors in the ventral striopallidal system. Implications for the treatment of schizophrenia. *Neuroscience* 63, 765–773.

Ferre, S., O'Connor, W. T., Svenningsson, P., Bjorklund, L., Lindberg, J., Tinner, B., et al. (1996). Dopamine D1 receptor-mediated facilitation of GABAergic neurotransmission in the rat strioentopenduncular pathway and its modulation by adenosine A1 receptor-mediated mechanisms. *Eur. J. Neurosci.* 8, 1545–1553.

Ferré, S., Quiroz, C., Guitart, X., Rea, W., Seyedian, A., Moreno, E., et al. (2018). Pivotal role of adenosine neurotransmission in restless legs syndrome. *Front. Neurosci.* 11:722. doi: 10.3389/fnins.2017.00722

Ferraiuolo, L., Heath, P. R., Holden, H., Kasher, P., Kirby, J., and Shaw, P. J. (2007). Microarray analysis of the cellular pathways involved in the adaptation to and progression of motor neuron injury in the SOD1 G93A mouse model of familial ALS. *J. Neurosci.* 27, 9201–9219. doi: 10.1523/JNEUROSCI.1470-07.2007

Ferraiuolo, L., Higginbottom, A., Heath, P. R., Barber, S., Greenald, D., Kirby, J., et al. (2011). Dysregulation of astrocyte-motoneuron cross-talk in mutant superoxide dismutase 1-related amyotrophic lateral sclerosis. *Brain* 134, 2627–2641. doi: 10.1093/brain/awr193

Ferrante, A., Martire, A., Armida, M., Chiodi, V., Pézzola, A., Potenza, R. L., et al. (2010). Influence of CGS 21680, a selective adenosine A 2A receptor agonist, on NMDA receptor function and expression in the brain of Huntington's disease mice. *Brain Res.* 1323, 184–191. doi: 10.1016/j.brainres.2010.01.080

Ferrari, D., Villalba, M., Chiozzi, P., Falzoni, S., Ricciardi-Castagnoli, P., and Di Virgilio, F. (1996). Mouse microglial cells express a plasma membrane pore gated by extracellular ATP. *J. Immunol.* 156, 1531–1539.

Ferrazoli, E. G., de Souza, H. D. N., Nascimento, I. C., Oliveira-Giacomelli, Á., Schwindt, T. T., Britto, L. R., et al. (2017). Brilliant blue G, but not fenofibrate, treatment reverts hemiparkinsonian behavior and restores dopamine levels in an animal model of Parkinson's disease. *Cell Transplant.* 26, 669–677. doi: 10.3727/096368917X695227

Ferreira, D. G., Batalha, V. L., Vicente Miranda, H., Coelho, J. E., Gomes, R., Gonçalves, F. Q., et al. (2015). Adenosine A $_{2A}$ receptors modulate α-synuclein aggregation and toxicity. *Cereb. Cortex* 27:bhv268. doi: 10.1093/cercor/bhv268

Fields, R. D., and Burnstock, G. (2006). Purinergic signalling in neuron-glia interactions. *Nat. Rev. Neurosci.* 7, 423–436. doi: 10.1038/nrn1928

Fink, J. S., Kalda, A., Ryu, H., Stack, E. C., Schwarzschild, M. A., Chen, J. F., et al. (2004). Genetic and pharmacological inactivation of the adenosine A2Areceptor attenuates 3-nitropropionic acid-induced striatal damage. *J. Neurochem.* 88, 538–544. doi: 10.1046/j.1471-4159.2003.02145.x

Fink, J. S., Weaver, D. R., Rivkees, S. A., Peterfreund, R. A., Pollack, A. E., Adler, E. M., et al. (1992). Molecular cloning of the rat A2 adenosine receptor: selective co-expression with D2 dopamine receptors in rat striatum. *Brain Res. Mol. Brain Res.* 14, 186–195. doi: 10.1016/0169-328X(92)90173-9

Florenzano, F., Viscomi, M. T., Cavaliere, F., Volonté, C., and Molinari, M. (2002). Cerebellar lesion up-regulates P2X1 and P2X2 purinergic receptors in precerebellar nuclei. *Neuroscience* 115, 425–434. doi: 10.1016/S0306-4522(02)00397-4

Fondell, E., O'Reilly, É. I., Fitzgerald, K. C., Falcone, G. J., Kolonel, L. N., Park, Y., et al. (2015). Intakes of caffeine, coffee and tea and risk of amyotrophic lateral sclerosis: Results from five cohort studies. *Amyotroph. Lateral Scler. Front. Degener.* 16, 366–371. doi: 10.3109/21678421.2015.1020813

Förster, D., and Reiser, G. (2015). Supportive or detrimental roles of P2Y receptors in brain pathology?–The two faces of P2Y receptors in stroke and neurodegeneration detected in neural cell and in animal model studies. *Purinergic Signal.* 11, 441–454. doi: 10.1007/s11302-015-9471-6

Franco, M. C., Ye, Y., Refakis, C. A., Feldman, J. L., Stokes, A. L., Basso, M., et al. (2013). Nitration of Hsp90 induces cell death. *Proc. Natl. Acad. Sci. U.S.A.* 110, E1102–E1111. doi: 10.1073/pnas.1215177110

Franke, H., Günther, A., Grosche, J., Schmidt, R., Rossner, S., Reinhardt, R., et al. (2004). P2X7 receptor expression after ischemia in the cerebral cortex of rats. *J. Neuropathol. Exp. Neurol.* 63, 686–699. doi: 10.1093/jnen/63.7.686

Fredholm, B. B., Bättig, K., Holmén, J., Nehlig, A., and Zvartau, E. E. (1999). Actions of caffeine in the brain with special reference to factors that contribute to its widespread use. *Pharmacol. Rev.* 51, 83–133.

Fryer, H. J., Wolf, D. H., Knox, R. J., Strittmatter, S. M., Pennica, D., O'Leary, R. M., et al. (2001). Brain-derived neurotrophic factor induces excitotoxic sensitivity in cultured embryonic rat spinal motor neurons through activation of the phosphatidylinositol 3-kinase pathway. *J. Neurochem.* 74, 582–595. doi: 10.1046/j.1471-4159.2000.740582.x

Fuchs, A., Kutterer, S., Mühling, T., Duda, J., Schütz, B., Liss, B., et al. (2013). Selective mitochondrial Ca $^{2+}$ uptake deficit in disease endstage vulnerable motoneurons of the SOD1 ^{G93A} mouse model of amyotrophic lateral sclerosis. *J. Physiol. (Lond).* 591, 2723–2745. doi: 10.1113/jphysiol.2012.247981

Fuzzati-Armentero, M.-T., Cerri, S., Levandis, G., Ambrosi, G., Montepeloso, E., Antoninetti, G., et al. (2015). Dual target strategy: combining distinct non-dopaminergic treatments reduces neuronal cell loss and synergistically modulates l -DOPA-induced rotational behavior in a rodent model of Parkinson's disease. *J. Neurochem.* 134, 740–747. doi: 10.1111/jnc.13162

Gabanella, F., Butchbach, M. E., Saieva, L., Carissimi, C., Burghes, A. H., and Pellizzoni, L. (2007). Ribonucleoprotein assembly defects correlate with spinal muscular atrophy severity and preferentially affect a subset of spliceosomal snRNPs. *PLoS ONE* 2:e921. doi: 10.1371/journal.pone.0000921

Gan, M., Moussaud, S., Jiang, P., and McLean, P. J. (2015). Extracellular ATP induces intracellular alpha-synuclein accumulation via P2X1 receptor-mediated lysosomal dysfunction. *Neurobiol. Aging* 36, 1209–1220. doi: 10.1016/j.neurobiolaging.2014.10.037

Gandelman, M., Levy, M., Cassina, P., Barbeito, L., and Beckman, J. S. (2013). P2X7 receptor-induced death of motor neurons by a peroxynitrite/FAS-dependent pathway. *J. Neurochem.* 126, 382–388. doi: 10.1111/jnc.12286

Gandelman, M., Peluffo, H., Beckman, J. S., Cassina, P., and Barbeito, L. (2010). Extracellular ATP and the P2X7 receptor in astrocyte-mediated motor neuron death: implications for amyotrophic lateral sclerosis. *J. Neuroinflammation* 7:33. doi: 10.1186/1742-2094-7-33

Garcia-Borreguero, D., and Cano-Pumarega, I. (2017). New concepts in the management of restless legs syndrome. *BMJ* 356:j104. doi: 10.1136/bmj.j104

Gavrilina, T. O., McGovern, V. L., Workman, E., Crawford, T. O., Gogliotti, R. G., DiDonato, C. J., et al. (2008). Neuronal SMN expression corrects spinal muscular atrophy in severe SMA mice while muscle-specific SMN expression has no phenotypic effect. *Hum. Mol. Genet.* 17, 1063–1075. doi: 10.1093/hmg/ddm379

Gianfriddo, M., Corsi, C., Melani, A., Pèzzola, A., Reggio, R., Popoli, P., et al. (2003). A denosine A antagonism increases striatal glutamate outflow in the 2A quinolinic acid rat model of Huntington's disease. *Brain Res.* 979, 225–229. doi: 10.1016/S0006-8993(03)02942-1

Gianfriddo, M., Melani, A., Turchi, D., Giovannini, M. G., and Pedata, F. (2004). Adenosine and glutamate extracellular concentrations and mitogen-activated protein kinases in the striatum of Huntington transgenic mice. Selective antagonism of adenosine A_{2A} receptors reduces transmitter outflow. *Neurobiol. Dis.* 17, 77–88. doi: 10.1016/j.nbd.2004.05.008

Glass, M., Dragunow, M., and Faull, R. L. (2000). The pattern of neurodegeneration in Huntington's disease: a comparative study of cannabinoid, dopamine, adenosine and GABA(A) receptor alterations in the human basal ganglia in Huntington's disease. *Neuroscience* 97, 505–519. doi: 10.1016/S0306-4522(00)00008-7

Goldenberg, M. M. (2012). Multiple sclerosis review. *P T* 37, 175–184.

Gołembiowska, K., Wardas, J., Noworyta-Sokołowska, K., Kaminska, K., and Górska, A. (2013). Effects of adenosine receptor antagonists on the *in vivo* LPS-induced inflammation model of Parkinson's disease. *Neurotox. Res.* 24, 29–40. doi: 10.1007/s12640-012-9372-1

Gonçalves, N., Simões, A. T., Cunha, R. A., and de Almeida, L. P. (2013). Caffeine and adenosine A_{2A} receptor inactivation decrease striatal neuropathology in a lentiviral-based model of Machado-Joseph disease. *Ann. Neurol.* 73, 655–666. doi: 10.1002/ana.23866

Gonçalves, N., Simões, A. T., Prediger, R. D., Hirai, H., Cunha, R. A., and Pereira de Almeida, L. (2017). Caffeine alleviates progressive motor deficits in a transgenic mouse model of spinocerebellar ataxia. *Ann. Neurol.* 81, 407–418. doi: 10.1002/ana.24867

Grundström, E., Lindholm, D., Johansson, A., Blennow, K., and Askmark, H. (2000). GDNF but not BDNF is increased in cerebrospinal fluid in amyotrophic lateral sclerosis. *Neuroreport* 11, 1781–1783. doi: 10.1097/00001756-200006050-00037

Grygorowicz, T., Sulejczak, D., and Struzynska, L. (2011). Expression of purinergic P2X7 receptor in rat brain during the symptomatic phase of experimental autoimmune encephalomyelitis and after recovery of neurological deficits. *Acta Neurobiol. Exp.* 71, 65–73.

Gu, B. J., Field, J., Dutertre, S., Ou, A., Kilpatrick, T. J., Lechner-Scott, J., et al. (2015). A rare P2X7 variant Arg307Gln with absent pore formation function protects against neuroinflammation in multiple sclerosis. *Hum. Mol. Genet.* 24, 5644–5654. doi: 10.1093/hmg/ddv278

Gu, B. J., Zhang, W., Worthington, R. A., Sluyter, R., Dao-Ung, P., Petrou, S., et al. (2001). A Glu-496 to Ala polymorphism leads to loss of function of the human P2X7 receptor. *J. Biol. Chem.* 276, 11135–11142. doi: 10.1074/jbc.M010353200

Gulyani, S., Earley, C. J., Camandola, S., Maudsley, S., Ferré, S., Mughal, M. R., et al. (2009). Diminished iron concentrations increase adenosine A_{2A} receptor levels in mouse striatum and cultured human neuroblastoma cells. *Exp. Neurol.* 215, 236–242. doi: 10.1016/j.expneurol.2008.10.007

Gyoneva, S., Shapiro, L., Lazo, C., Garnier-Amblard, E., Smith, Y., Miller, G. W., et al. (2014). Adenosine A_{2A} receptor antagonism reverses inflammation-induced impairment of microglial process extension in a model of Parkinson's disease. *Neurobiol. Dis.* 67, 191–202. doi: 10.1016/j.nbd.2014.03.004

Hamza, T. H., Chen, H., Hill-Burns, E. M., Rhodes, S. L., Montimurro, J., Kay, D. M., et al. (2011). Genome-wide gene-environment study identifies glutamate receptor gene GRIN2A as a Parkinson's disease modifier gene via interaction with coffee. *PLoS Genet.* 7:e1002237. doi: 10.1371/journal.pgen.1002237

Harms, M. B., and Baloh, R. H. (2013). Clinical neurogenetics: amyotrophic lateral sclerosis. *Neurol. Clin.* 31, 929–950. doi: 10.1016/j.ncl.2013.05.003

Haskó, G. (2004). Adenosine: an endogenous regulator of innate immunity. *Trends Immunol.* 25, 33–39. doi: 10.1016/j.it.2003.11.003

Haynes, S. E., Hollopeter, G., Yang, G., Kurpius, D., Dailey, M. E., Gan, W.-B., et al. (2006). The P2Y12 receptor regulates microglial activation

by extracellular nucleotides. *Nat. Neurosci.* 9, 1512–1519. doi: 10.1038/nn1805

He, Y., Taylor, N., Fourgeaud, L., and Bhattacharya, A. (2017). The role of microglial P2X7: modulation of cell death and cytokine release. *J. Neuroinflammation* 14:135. doi: 10.1186/s12974-017-0904-8

Hedström, A. K., Mowry, E. M., Gianfrancesco, M. A., Shao, X., Schaefer, C. A., Shen, L., et al. (2016). High consumption of coffee is associated with decreased multiple sclerosis risk; results from two independent studies. *J. Neurol. Neurosurg. Psychiatry* 87, 454–460. doi: 10.1136/jnnp-2015-312176

Hettinger, B. D., Lee, A., Linden, J., and Rosin, D. L. (2001). Ultrastructural localization of adenosine A2A receptors suggests multiple cellular sites for modulation of GABAergic neurons in rat striatum. *J. Comp. Neurol.* 431, 331–346. doi: 10.1002/1096-9861(20010312)431:3<331::AID-CNE1074>3.0.CO;2-W

Hoang, Q. Q. (2014). Pathway for Parkinson disease. *Proc. Natl. Acad. Sci. U.S.A.* 111, 2402–2403. doi: 10.1073/pnas.1324284111

Hu, P., and Kalb, R. G. (2003). BDNF heightens the sensitivity of motor neurons to excitotoxic insults through activation of TrkB. *J. Neurochem.* 84, 1421–1430. doi: 10.1046/j.1471-4159.2003.01599.x

Hu, Q., Ren, X., Liu, Y., Li, Z., Zhang, L., Chen, X., et al. (2016). Aberrant adenosine A2A receptor signaling contributes to neurodegeneration and cognitive impairments in a mouse model of synucleinopathy. *Exp. Neurol.* 283, 213–223. doi: 10.1016/j.expneurol.2016.05.040

Illes, P., Khan, T. M., and Rubini, P. (2017). Neuronal P2X7 receptors revisited: do they really exist? *J. Neurosci.* 37, 7049–7062. doi: 10.1523/JNEUROSCI.3103-16.2017

Illes, P., and Verkhratsky, A. (2016). Purinergic neurone-glia signalling in cognitive-related pathologies. *Neuropharmacology* 104, 62–75. doi: 10.1016/j.neuropharm.2015.08.005

Inoue, K. (2017). Purinergic signaling in microglia in the pathogenesis of neuropathic pain. *Proc. Japan Acad. Ser. B* 93, 174–182. doi: 10.2183/pjab.93.011

Ishikawa, Y., Ikeuchi, T., and Hatanaka, H. (2000). Brain-derived neurotrophic factor accelerates nitric oxide donor-induced apoptosis of cultured cortical neurons. *J. Neurochem.* 75, 494–502. doi: 10.1046/j.1471-4159.2000.0750494.x

Ishiwata, K., Ogi, N., Hayakawa, N., Oda, K., Nagaoka, T., Toyama, H., et al. (2002). Adenosine A_{2A} receptor imaging with [^{11}C]KF18446 PET in the rat brain after quinolinic acid lesion: comparison with the dopamine receptor imaging. *Ann. Nucl. Med.* 16, 467–475. doi: 10.1007/BF02988643

Jablonka, S., Rossoll, W., Schrank, B., and Sendtner, M. (2000). The role of SMN in spinal muscular atrophy. *J. Neurol.* 247(Suppl. 1), I37–I42. doi: 10.1007/s004150050555

Jellinger, K. A. (2011). "Parkinson's disease," in *Neurodegeneration : The Molecular Pathology of Dementia and Movement Disorders*, eds D. W. Dickson and R. O. Welle (Bassel: Wiley-Blackwell), 477.

Jiang, T., Hoekstra, J., Heng, X., Kang, W., Ding, J., Liu, J., et al. (2015). P2X7 receptor is critical in α-synuclein–mediated microglial NADPH oxidase activation. *Neurobiol. Aging* 36, 2304–2318. doi: 10.1016/j.neurobiolaging.2015.03.015

Jiménez, M., Clavé, P., Accarino, A., and Gallego, D. (2014). Purinergic neuromuscular transmission in the gastrointestinal tract; functional basis for future clinical and pharmacological studies. *Br. J. Pharmacol.* 171, 4360–4375. doi: 10.1111/bph.12802

Johnston, J. B., Silva, C., Gonzalez, G., Holden, J., Warren, K. G., Metz, L. M., et al. (2001). Diminished adenosine A1 receptor expression on macrophages in brain and blood of patients with multiple sclerosis. *Ann. Neurol.* 49, 650–658. doi: 10.1002/ana.1007

Jung, C., Higgins, C. M., and Xu, Z. (2002). Mitochondrial electron transport chain complex dysfunction in a transgenic mouse model for amyotrophic lateral sclerosis. *J. Neurochem.* 83, 535–545. doi: 10.1046/j.1471-4159.2002.01112.x

Kachroo, A., and Schwarzschild, M. A. (2012). Adenosine A_{2A} receptor gene disruption protects in an α-synuclein model of Parkinson's disease. *Ann. Neurol.* 71, 278–282. doi: 10.1002/ana.22630

Kalmar, J. M. (2005). The influence of caffeine on voluntary muscle activation. *Med. Sci. Sports Exerc.* 37, 2113–2119. doi: 10.1249/01.mss.0000178219.18086.9e

Kanda, T., Jackson, M. J., Smith, L. A., Pearce, R. K., Nakamura, J., Kase, H., et al. (2000). Combined use of the adenosine A2A antagonist KW-6002 with l-DOPA or with selective D1 or D2 dopamine agonists increases antiparkinsonian activity but not dyskinesia in MPTP-treated monkeys. *Exp. Neurol.* 162, 321–327. doi: 10.1006/exnr.2000.7350

Karcz-Kubicha, M., Antoniou, K., Terasmaa, A., Quarta, D., Solinas, M., Justinova, Z., et al. (2003). Involvement of adenosine A1 and A2A receptors in the motor effects of caffeine after its acute and chronic administration. *Neuropsychopharmacology* 28, 1281–1291. doi: 10.1038/sj.npp.1300167

Kazemi, M. H., Raoofi Mohseni, S., Hojjat-Farsangi, M., Anvari, E., Ghalamfarsa, G., Mohammadi, H., et al. (2018). Adenosine and adenosine receptors in the immunopathogenesis and treatment of cancer. *J. Cell. Physiol.* 233, 2032–2057. doi: 10.1002/jcp.25873

Khakh, B. S., and Alan North, R. (2006). P2X receptors as cell-surface ATP sensors in health and disease. *Nature* 442, 527–532. doi: 10.1038/nature04886

Kiernan, M. C., Vucic, S., Cheah, B. C., Turner, M. R., Eisen, A., Hardiman, O., et al. (2011). Amyotrophic lateral sclerosis. *Lancet* 377, 942–955. doi: 10.1016/S0140-6736(10)61156-7

Kim, B., Jeong, H. K., Kim, J. H., Lee, S. Y., Jou, I., and Joe, E. H. (2011). Uridine 5′-diphosphate induces chemokine expression in microglia and astrocytes through activation of the P2Y6 receptor. *J. Immunol.* 186, 3701–3709. doi: 10.4049/jimmunol.1000212

Kim, H. (2003). TrkB mediates BDNF-induced potentiation of neuronal necrosis in cortical culture. *Neurobiol. Dis.* 14, 110–119. doi: 10.1016/S0969-9961(03)00103-7

Kim, T., and Vemuganti, R. (2017). Mechanisms of Parkinson's disease-related proteins in mediating secondary brain damage after cerebral ischemia. *J. Cereb. Blood Flow Metab.* 37, 1910–1926. doi: 10.1177/0271678X17694186

Kobayashi, S., Conforti, L., Pun, R. Y. K., and Millhorn, D. E. (1998). Adenosine modulates hypoxia-induced responses in rat PC12 cells via the A_{2A} receptor. *J. Physiol.* 508, 95–107. doi: 10.1111/j.1469-7793.1998.095br.x

Koehler, N. K., Genain, C. P., Giesser, B., and Hauser, S. L. (2002). The human T cell response to myelin oligodendrocyte glycoprotein: a multiple sclerosis family-based study. *J. Immunol.* 168, 5920–5927. doi: 10.4049/jimmunol.168.11.5920

Koh, J., Gwag, B. J., Lobner, D., and Choi, D. W. (1995). Potentiated necrosis of cultured cortical neurons by neurotrophins. *Science* 268, 573–575. doi: 10.1126/science.7725105

Krügel, U. (2016). Purinergic receptors in psychiatric disorders. *Neuropharmacology* 104, 212–225. doi: 10.1016/j.neuropharm.2015.10.032

Kumar, P. M., Paing, S. S., Li, H., Pavanni, R., Yuen, Y., Zhao, Y., et al. (2015). Differential effect of caffeine intake in subjects with genetic susceptibility to Parkinson's Disease. *Sci. Rep.* 5:15492. doi: 10.1038/srep15492

Labazi, H., Teng, B., and Mustafa, S. J. (2018). Functional changes in vascular reactivity to adenosine receptor activation in type I diabetic mice. *Eur. J. Pharmacol.* 820, 191–197. doi: 10.1016/j.ejphar.2017.12.034

Lang, A. E. (2009). When and how should treatment be started in Parkinson disease? *Neurology* 72, S39–S43. doi: 10.1212/WNL.0b013e318198e177

Lapato, A. S., and Tiwari-Woodruff, S. K. (2017). Connexins and pannexins: At the junction of neuro-glial homeostasis & disease. *J. Neurosci. Res.* 96, 31–44. doi: 10.1002/jnr.24088

Lassmann, H. (1983). Chronic relapsing experimental allergic encephalomyelitis: its value as an experimental model for multiple sclerosis. *J. Neurol.* 229, 207–220. doi: 10.1007/BF00313549

Lecca, D., Ceruti, S., Fumagalli, M., and Abbracchio, M. P. (2012). Purinergic trophic signalling in glial cells: functional effects and modulation of cell proliferation, differentiation, and death. *Purinergic Signal.* 8, 539–557. doi: 10.1007/s11302-012-9310-y

Lederer, C. W., Torrisi, A., Pantelidou, M., Santama, N., and Cavallaro, S. (2007). Pathways and genes differentially expressed in the motor cortex of patients with sporadic amyotrophic lateral sclerosis. *BMC Genomics* 8:26. doi: 10.1186/1471-2164-8-26

Lee, F. S., and Chao, M. V. (2001). Activation of Trk neurotrophin receptors in the absence of neurotrophins. *Proc. Natl. Acad. Sci. U.S.A.* 98, 3555–3560. doi: 10.1073/pnas.061020198

Lee, J. Y., Jhun, B. S., Oh, Y. T., Lee, J. H., Choe, W., Baik, H. H., et al. (2006). Activation of adenosine A3 receptor suppresses lipopolysaccharide-induced TNF-alpha production through inhibition of PI 3-kinase/Akt and NF-kappaB activation in murine BV2 microglial cells. *Neurosci. Lett.* 396, 1–6. doi: 10.1016/j.neulet.2005.11.004

Lefebvre, S., Bürglen, L., Reboullet, S., Clermont, O., Burlet, P., Viollet, L., et al. (1995). Identification and characterization of a spinal muscular atrophy-determining gene. *Cell* 80, 155–165. doi: 10.1016/0092-8674(95)90460-3

Lefebvre, S., Burlet, P., Liu, Q., Bertrandy, S., Clermont, O., Munnich, A., et al. (1997). Correlation between severity and SMN protein level in spinal muscular atrophy. *Nat. Genet.* 16, 265–269. doi: 10.1038/ng0797-265

Levy, O., Coughlin, M., Cronstein, B. N., Roy, R. M., Desai, A., and Wessels, M. R. (2006). The adenosine system selectively inhibits TLR-mediated TNF-alpha production in the human newborn. *J. Immunol.* 177, 1956–1966. doi: 10.4049/jimmunol.177.3.1956

Li, J. Y., Popovic, N., and Brundin, P. (2005). The use of the R6 transgenic mouse models of Huntington's disease in attempts to develop novel therapeutic strategies. *NeuroRx* 2, 447–464. doi: 10.1602/neurorx.2.3.447

Li, S. N., and Wong, P. T. (2000). The adenosine receptor agonist, APNEA, increases calcium influx into rat cortical synaptosomes through N-type channels associated with A2a receptors. *Neurochem. Res.* 25, 457–459. doi: 10.1023/A:1007503907823

Li, W., Silva, H. B., Real, J., Wang, Y.-M., Rial, D., Li, P., et al. (2015). Inactivation of adenosine A2A receptors reverses working memory deficits at early stages of Huntington's disease models. *Neurobiol. Dis.* 79, 70–80. doi: 10.1016/j.nbd.2015.03.030

Lindberg, D., Shan, D., Ayers-Ringler, J., Oliveros, A., Benitez, J., Prieto, M., et al. (2015). Purinergic signaling and energy homeostasis in psychiatric disorders. *Curr. Mol. Med.* 15, 275–295. doi: 10.2174/1566524015666150330163724

Lister, M. F., Sharkey, J., Sawatzky, D. A., Hodgkiss, J. P., Davidson, D. J., Rossi, A. G., et al. (2007). The role of the purinergic P2X7 receptor in inflammation. *J. Inflamm. (Lond).* 4:5. doi: 10.1186/1476-9255-4-5

Liu, H., Han, X., Li, Y., Zou, H., and Xie, A. (2013). Association of P2X7 receptor gene polymorphisms with sporadic Parkinson's disease in a Han Chinese population. *Neurosci. Lett.* 546, 42–45. doi: 10.1016/j.neulet.2013.04.049

Liu, Y.-J., Lee, L.-M., Lai, H.-L., and Chern, Y. (2015). Aberrant activation of AMP-activated protein kinase contributes to the abnormal distribution of HuR in amyotrophic lateral sclerosis. *FEBS Lett.* 589, 432–439. doi: 10.1016/j.febslet.2014.12.029

Lo, J.-C., Huang, W.-C., Chou, Y.-C., Tseng, C.-H., Lee, W.-L., and Sun, S. H. (2008). Activation of P2X $_7$ receptors decreases glutamate uptake and glutamine synthetase activity in RBA-2 astrocytes via distinct mechanisms. *J. Neurochem.* 105, 151–164. doi: 10.1111/j.1471-4159.2007.05119.x

Lomen-Hoerth, C. (2011). Clinical phenomenology and neuroimaging correlates in ALS-FTD. *J. Mol. Neurosci.* 45, 656–662. doi: 10.1007/s12031-011-9636-x

Lotti, F., Imlach, W. L., Saieva, L., Beck, E. S., Hao, L. T., Li, D. K., et al. (2012). An SMN-dependent U12 splicing event essential for motor circuit function. *Cell* 151, 440–454. doi: 10.1016/j.cell.2012.09.012

Lovatt, D., Sonnewald, U., Waagepetersen, H. S., Schousboe, A., He, W., Lin, J. H.-C., et al. (2007). The transcriptome and metabolic gene signature of protoplasmic astrocytes in the adult murine cortex. *J. Neurosci.* 27, 12255–12266. doi: 10.1523/JNEUROSCI.3404-07.2007

Lu, W., Albalawi, F., Beckel, J. M., Lim, J. C., Laties, A. M., and Mitchell, C. H. (2017). The P2X7 receptor links mechanical strain to cytokine IL-6 up-regulation and release in neurons and astrocytes. *J. Neurochem.* 141, 436–448. doi: 10.1111/jnc.13998

Luo, C., Jian, C., Liao, Y., Huang, Q., Wu, Y., Liu, X., et al. (2017). The role of microglia in multiple sclerosis. *Neuropsychiatr. Dis. Treat.* 13, 1661–1667. doi: 10.2147/NDT.S140634

Luthi-Carter, R., Strand, A., Peters, N. L., Solano, S. M., Hollingsworth, Z. R., Menon, A. S., et al. (2000). Decreased expression of striatal signaling genes in a mouse model of Huntington's disease. *Hum. Mol. Genet.* 9, 1259–1271. doi: 10.1093/hmg/9.9.1259

Madeira, M. H., Boia, R., Ambrósio, A. F., and Santiago, A. R. (2017). Having a coffee break: the impact of caffeine consumption on microglia-mediated inflammation in neurodegenerative diseases. *Mediators Inflamm.* 2017, 1–12. doi: 10.1155/2017/4761081

Maglione, V., Cannella, M., Martino, T., De Blasi, A., Frati, L., and Squitieri, F. (2005a). The platelet maximum number of A2A-receptor binding sites (Bmax) linearly correlates with age at onset and CAG repeat expansion in Huntington's disease patients with predominant chorea. *Neurosci. Lett.* 393, 27–30. doi: 10.1016/j.neulet.2005.09.037

Maglione, V., Giallonardo, P., Cannella, M., Martino, T., Frati, L., and Squitieri, F. (2005b). Adenosine A_{2A} receptor dysfunction correlates with age at onset anticipation in blood platelets of subjects with Huntington's disease. *Am. J. Med. Genet.* 139B, 101–105. doi: 10.1002/ajmg.b.30223

Mamedova, L. K., Gao, Z.-G., and Jacobson, K. A. (2006). Regulation of death and survival in astrocytes by ADP activating P2Y1 and P2Y12 receptors. *Biochem. Pharmacol.* 72, 1031–1041. doi: 10.1016/j.bcp.2006.07.017

Marcellino, D., Suárez-Boomgaard, D., Sánchez-Reina, M. D., Aguirre, J. A., Yoshitake, T., Yoshitake, S., et al. (2010). On the role of P2X7 receptors in dopamine nerve cell degeneration in a rat model of Parkinson's disease: studies with the P2X7 receptor antagonist A-438079. *J. Neural Transm.* 117, 681–687. doi: 10.1007/s00702-010-0400-0

Mariotti, C., Fancellu, R., and Donato, S. (2005). An overview of the patient with ataxia. *J. Neurol.* 252, 511–518. doi: 10.1007/s00415-005-0814-z

Martinez-Mir, M. I., Probst, A., and Palacios, J. M. (1991). Adenosine A2 receptors: Selective localization in the human basal ganglia and alterations with disease. *Neuroscience* 42, 697–706. doi: 10.1016/0306-4522(91)90038-P

Martire, A., Calamandrei, G., Felici, F., Scattoni, M. L., Lastoria, G., Domenici, M. R., et al. (2007). Opposite effects of the A_{2A} receptor agonist CGS21680 in the striatum of Huntington's disease versus wild-type mice.*Neurosci. Lett.* 417, 78–83. doi: 10.1016/j.neulet.2007.02.034

Martire, A., Ferrante, A., Potenza, R. L., Armida, M., Ferretti, R., Pézzola, A., et al. (2010). Remodeling of striatal NMDA receptors by chronic A2A receptor blockade in Huntington's disease mice. *Neurobiol. Dis.* 37, 99–105. doi: 10.1016/j.nbd.2009.09.012

Matilla-Dueñas, A., Corral-Juan, M., Volpini, V., and Sanchez, I. (2012). *The Spinocerebellar Ataxias: Clinical Aspects And Molecular Genetics*. New York, NY: Springer.

Mattiazzi, M., D'Aurelio, M., Gajewski, C. D., Martushova, K., Kiaei, M., Beal, M. F., et al. (2002). Mutated human SOD1 causes dysfunction of oxidative phosphorylation in mitochondria of transgenic mice. *J. Biol. Chem.* 277, 29626–29633. doi: 10.1074/jbc.M203065200

Matute, C. (2011). Glutamate and ATP signalling in white matter pathology. *J. Anat.* 219, 53–64. doi: 10.1111/j.1469-7580.2010.01339.x

Matute, C., Torre, I., Perez-Cerda, F., Perez-Samartin, A., Alberdi, E., Etxebarria, E., et al. (2007). P2X7 Receptor blockade prevents ATP excitotoxicity in oligodendrocytes and ameliorates experimental autoimmune encephalomyelitis. *J. Neurosci.* 27, 9525–9533. doi: 10.1523/JNEUROSCI.0579-07.2007

Mayne, M., Shepel, P. N., Jiang, Y., Geiger, J. D., and Power, C. (1999). Dysregulation of Adenosine A 1 Receptor– Mediated Cytokine Expression in Peripheral Blood Mononuclear Cells from Multiple Sclerosis Patients. *Ann. Neurol.* 45, 633–639. doi: 10.1002/1531-8249(199905)45:5<633::AID-ANA12>3.0.CO;2-X

McGivern, J. V., Patitucci, T. N., Nord, J. A., Barabas, M. A., Stucky, C. L., and Ebert, A. D. (2013). Spinal muscular atrophy astrocytes exhibit abnormal calcium regulation and reduced growth factor production. *Glia* 61, 1418–1428. doi: 10.1002/glia.22522

Menzies, F. M., Cookson, M. R., Taylor, R. W., Turnbull, D. M., Chrzanowska-Lightowlers, Z. M., Dong, L., et al. (2002). Mitochondrial dysfunction in a cell culture model of familial amyotrophic lateral sclerosis. *Brain* 125, 1522–1533. doi: 10.1093/brain/awf167

Mievis, S., Blum, D., and Ledent, C. (2011). A_{2A} receptor knockout worsens survival and motor behaviour in a transgenic mouse model of Huntington's disease. *Neurobiol. Dis.* 41, 570–576. doi: 10.1016/j.nbd.2010.09.021

Miles, G. B., Parkis, M. A., Lipski, J., and Funk, G. D. (2002). Modulation of phrenic motoneuron excitability by ATP: consequences for respiratory-related output *in vitro*. *J. Appl. Physiol.* 92, 1899–1910. doi: 10.1152/japplphysiol.00475.2001

Miller, S. D., and Karpus, W. J. (1994). The immunopathogenesis and regulation of T-cell-mediated demyelinating diseases. *Immunol. Today* 15, 356–361. doi: 10.1016/0167-5699(94)90173-2

Mills, J. H., Kim, D.-G., Krenz, A., Chen, J.-F., and Bynoe, M. S. (2012). A2A adenosine receptor signaling in lymphocytes and the central nervous system regulates inflammation during experimental autoimmune encephalomyelitis. *J. Immunol.* 188, 5713–5722. doi: 10.4049/jimmunol.1200545

Mills, J. H., Thompson, L. F., Mueller, C., Waickman, A. T., Jalkanen, S., Niemela, J., et al. (2008). CD73 is required for efficient entry of lymphocytes into the

central nervous system during experimental autoimmune encephalomyelitis. *Proc. Natl. Acad. Sci. U.S.A.* 105, 9325–9330. doi: 10.1073/pnas.0711175105

Minghetti, L. (2004). Cyclooxygenase-2 (COX-2) in inflammatory and degenerative brain diseases. *J. Neuropathol. Exp. Neurol.* 63, 901–910. doi: 10.1093/jnen/63.9.901

Miras-Portugal, M. T., Sebastián-Serrano, Á., de Diego García, L., and Díaz-Hernández, M. (2017). Neuronal P2X7 Receptor: Involvement in Neuronal Physiology and Pathology. *J. Neurosci.* 37, 7063–7072. doi: 10.1523/JNEUROSCI.3104-16.2017

Mojsilovic-Petrovic, J., Jeong, G.-B., Crocker, A., Arneja, A., David, S., Russell, D., et al. (2006). protecting motor neurons from toxic insult by antagonism of adenosine A2a and Trk receptors. *J. Neurosci.* 26, 9250–9263. doi: 10.1523/JNEUROSCI.1856-06.2006

Moreno, E., Chiarlone, A., Medrano, M., Puigdellívol, M., Bibic, L., Howell, L. A., et al. (2017). Singular location and signaling profile of adenosine A 2A-Cannabinoid CB 1 receptor heteromers in the dorsal striatum. *Neuropsychopharmacology* 43, 964–977. doi: 10.1038/npp.2017.12

Narcisse, L., Scemes, E., Zhao, Y., Lee, S. C., and Brosnan, C. F. (2005). The cytokine IL-1beta transiently enhances P2X7 receptor expression and function in human astrocytes. *Glia* 49, 245–258. doi: 10.1002/glia.20110

Nascimento, F., Sebastião, A. M., and Ribeiro, J. A. (2015). Presymptomatic and symptomatic ALS SOD1(G93A) mice differ in adenosine A1 and A2A receptor-mediated tonic modulation of neuromuscular transmission. *Purinergic Signal.* 11, 471–480. doi: 10.1007/s11302-015-9465-4

Neher, J. J., Neniskyte, U., Hornik, T., and Brown, G. C. (2014). Inhibition of UDP/P2Y $_6$ purinergic signaling prevents phagocytosis of viable neurons by activated microglia *in vitro* and *in vivo*. *Glia* 62, 1463–1475. doi: 10.1002/glia.22693

Ng, S. K., kah, Higashimori, H., Tolman, M., and Yang, Y. (2015). Suppression of adenosine 2a receptor (A2aR)-mediated adenosine signaling improves disease phenotypes in a mouse model of amyotrophic lateral sclerosis. *Exp. Neurol.* 267, 115–122. doi: 10.1016/j.expneurol.2015.03.004

North, R. A. (2002). Molecular Physiology of P2X Receptors. *Physiol. Rev.* 82, 1013–1067. doi: 10.1152/physrev.00015.2002

Olanow, C. W., Stern, M. B., and Sethi, K. (2009). The scientific and clinical basis for the treatment of Parkinson disease (2009). *Neurology* 72, S1–S136. doi: 10.1212/WNL.0b013e3181a1d44c

Oliveira, A., Illes, P., and Ulrich, H. (2016). Purinergic receptors in embryonic and adult neurogenesis. *Neuropharmacology* 104, 272–281. doi: 10.1016/j.neuropharm.2015.10.008

Oliveros, A., Cho, C. H., Cui, A., Choi, S., Lindberg, D., Hinton, D., et al. (2017). Adenosine A2A receptor and ERK-driven impulsivity potentiates hippocampal neuroblast proliferation. *Transl. Psychiatry* 7, e1095. doi: 10.1038/tp.2017.64

Olsson, T., Barcellos, L. F., and Alfredsson, L. (2017). Interactions between genetic, lifestyle and environmental risk factors for multiple sclerosis. *Nat. Rev. Neurol.* 13, 25–36. doi: 10.1038/nrneurol.2016.187

Orr,ú, M., Zanoveli, J., Quiroz, C., Nguyen, H. P., Guitart, X., and Ferr,é, S. (2011). Functional changes in postsynaptic adenosine A 2A receptors during early stages of a rat model of Huntington disease. *Exp. Neurol.* 232, 76–80. doi: 10.1016/j.expneurol.2011.08.005

Ortiz, R., Ulrich, H., Zarate, C. A., and Machado-Vieira, R. (2015). Purinergic system dysfunction in mood disorders: a key target for developing improved therapeutics. *Prog. Neuro-Psychopharmacology Biol. Psychiatry* 57, 117–131. doi: 10.1016/j.pnpbp.2014.10.016

Oyanguren-Desez, O., Rodríguez-Antigüedad, A., Villoslada, P., Domercq, M., Alberdi, E., and Matute, C. (2011). Gain-of-function of P2X7 receptor gene variants in multiple sclerosis. *Cell Calcium* 50, 468–472. doi: 10.1016/j.ceca.2011.08.002

Palma, A. G., Muchnik, S., and Losavio, A. S. (2011). Excitatory effect of the A2A adenosine receptor agonist CGS-21680 on spontaneous and K+-evoked acetylcholine release at the mouse neuromuscular junction. *Neuroscience* 172, 164–176. doi: 10.1016/j.neuroscience.2010.10.015

Parisi, C., Arisi, I., D'Ambrosi, N., Storti, A. E., Brandi, R., D'Onofrio, M., et al. (2013). Dysregulated microRNAs in amyotrophic lateral sclerosis microglia modulate genes linked to neuroinflammation. *Cell Death Dis.* 4:e959. doi: 10.1038/cddis.2013.491

Parisi, C., Napoli, G., Amadio, S., Spalloni, A., Apolloni, S., Longone, P., et al. (2016). MicroRNA-125b regulates microglia activation and motor neuron death in ALS. *Cell Death Differ.* 23, 531–541. doi: 10.1038/cdd.2015.153

Parpura, V., Fisher, E. S., Lechleiter, J. D., Schousboe, A., Waagepetersen, H. S., Brunet, S., et al. (2017). Glutamate and ATP at the Interface Between Signaling and Metabolism in Astroglia: Examples from Pathology. *Neurochem. Res.* 42, 19–34. doi: 10.1007/s11064-016-1848-6

Paulson, H. L., Shakkottai, V. G., Clark, H. B., and Orr, H. T. (2017). Polyglutamine spinocerebellar ataxias — from genes to potential treatments. *Nat. Rev. Neurosci.* 18, 613–626. doi: 10.1038/nrn.2017.92

Pitt, D., Werner, P., and Rain, C. S. (2000). Glutamate excitotoxicity in a model of multiple sclerosis. *Nat. Med.* 6, 67–70. doi: 10.1038/71555

Popat, R. A., Van Den Eeden, S. K., Tanner, C. M., Kamel, F., Umbach, D. M., Marder, K., et al. (2011). Coffee, ADORA2A, and CYP1A2: the caffeine connection in Parkinson's disease. *Eur. J. Neurol.* 18, 756–765. doi: 10.1111/j.1468-1331.2011.03353.x

Popoli, P., Blum, D., Martire, A., Ledent, C., Ceruti, S., and Abbracchio, M. P. (2007). Functions, dysfunctions and possible therapeutic relevance of adenosine A2A receptors in Huntington's disease. *Prog. Neurobiol.* 81, 331–348. doi: 10.1016/j.pneurobio.2006.12.005

Popoli, P., Pintor, A., Domenici, M. R., Frank, C., Tebano, M. T., P.è, Zzola, A., et al. (2002). Blockade of Striatal Adenosine A 2A Receptor Reduces, through a Presynaptic Mechanism, Quinolinic Acid-Induced Excitotoxicity: Possible Relevance to Neuroprotective Interventions in Neurodegenerative Diseases of the Striatum. *J. Neurosci.* 22, 1967–1975.

Potenza, R. L., Armida, M., Ferrante, A., Pèzzola, A., Matteucci, A., Puopolo, M., et al. (2013). Effects of chronic caffeine intake in a mouse model of amyotrophic lateral sclerosis. *J. Neurosci. Res.* 91, 585–592. doi: 10.1002/jnr.23185

Potenza, R. L., Tebano, M. T., Martire, A., Domenici, M. R., Pepponi, R., Armida, M., et al. (2007). Adenosine A2A receptors modulate BDNF both in normal conditions and in experimental models of Huntington's disease. *Purinergic Signal.* 3, 333–338. doi: 10.1007/s11302-007-9066-y

Probert, L., Akassoglou, K., Pasparakis, M., Kontogeorgost, G., Kollias, G., and Levi-Montalcini, R. (1995). Spontaneous inflammatory demyelinating disease in transgenic mice showing central nervous system-specific expression of tumor necrosis factor a. *Neurobiology* 92, 11294–11298. doi: 10.1073/pnas.92.24.11294

Przybyła, T., Sakowicz-Burkiewicz, M., and Pawełczyk, T. (2018). Purinergic signaling in B cells. *Acta Biochim. Pol.* 65, 1–7. doi: 10.18388/abp.2017_1588

Puchałowicz, K., Baranowska-Bosiacka, I., Dziedziejko, V., and Chlubek, D. (2015). Purinergic signaling and the functioning of the nervous system cells. *Cell. Mol. Biol. Lett.* 20, 867–918. doi: 10.1515/cmble-2015-0050

Pupillo, E., Bianchi, E., Chi,ò, A., Casale, F., Zecca, C., Tortelli, R., et al. (2017). Amyotrophic lateral sclerosis and food intake. *Amyotroph. Lateral Scler. Front. Degener.* 19, 267–274. doi: 10.1080/21678421.2017.1418002

Qian, Y., Xu, S., Yang, X., and Xiao, Q. (2017). Purinergic receptor P2Y6 contributes to 1-methyl-4-phenylpyridinium-induced oxidative stress and cell death in neuronal SH-SY5Y cells. *J. Neurosci. Res.* 96, 253–264. doi: 10.1002/jnr.24119

Quiroz, C., Gulyani, S., Ruiqian, W., Bonaventura, J., Cutler, R., Pearson, V., et al. (2016). Adenosine receptors as markers of brain iron deficiency: Implications for Restless Legs Syndrome. *Neuropharmacology* 111, 160–168. doi: 10.1016/j.neuropharm.2016.09.002

Rajagopal, R., Chen, Z.-Y., Lee, F. S., and Chao, M. V. (2004). Transactivation of Trk neurotrophin receptors by G-protein-coupled receptor ligands occurs on intracellular membranes. *J. Neurosci.* 24, 6650–6658. doi: 10.1523/JNEUROSCI.0010-04.2004

Raker, V. K., Becker, C., and Steinbrink, K. (2016). The cAMP pathway as therapeutic target in autoimmune and inflammatory diseases. *Front. Immunol.* 7:123. doi: 10.3389/fimmu.2016.00123

Raman, R., Allen, S. P., Goodall, E. F., Kramer, S., Ponger, L.-L., Heath, P. R., et al. (2015). Gene expression signatures in motor neurone disease fibroblasts reveal dysregulation of metabolism, hypoxia-response and RNA processing functions. *Neuropathol. Appl. Neurobiol.* 41, 201–226. doi: 10.1111/nan.12147

Raoul, C., Estévez, A. G., Nishimune, H., Cleveland, D. W., deLapeyrière, O., Henderson, C. E., et al. (2002). Motoneuron death triggered by a specific pathway downstream of Fas. potentiation by ALS-linked SOD1 mutations. *Neuron* 35, 1067–1083. doi: 10.1016/S0896-6273(02)00905-4

Raoul, C., Henderson, C. E., and Pettmann, B. (1999). Programmed cell death of embryonic motoneurons triggered through the Fas death receptor. *J. Cell Biol.* 147, 1049–1062. doi: 10.1083/jcb.147.5.1049

Reggio, R., Pèzzola, A., and Popoli, P. (1999). The intrastratial injection of an adenosine A2 receptor antagonist prevents frontal cortex EEG abnormalities in a rat model of Huntington's disease. *Brain Res*. 83, 315–318. doi: 10.1016/S0006-8993(99)01489-4

Renton, A. E., Chi,ò, A., and Traynor, B. J. (2013). State of play in amyotrophic lateral sclerosis genetics. *Nat. Neurosci.* 17, 17–23. doi: 10.1038/nn.3584

Rezania, K., and Roos, R. P. (2013). Spinal Cord. *Neurol. Clin.* 31, 219–239. doi: 10.1016/j.ncl.2012.09.014

Ribeiro, F. F., Xapelli, S., Miranda-Lourenço, C., Tanqueiro, S. R., Fonseca-Gomes, J., Diógenes, M. J., et al. (2016). Purine nucleosides in neuroregeneration and neuroprotection. *Neuropharmacology* 104, 226–242. doi: 10.1016/j.neuropharm.2015.11.006

Rissanen, E., Virta, J. R., Paavilainen, T., Tuisku, J., Helin, S., Luoto, P., et al. (2013). Adenosine A2A receptors in secondary progressive multiple sclerosis: a [(11)C]TMSX brain PET study. *J. Cereb. Blood Flow Metab.* 33, 1394–1401. doi: 10.1038/jcbfm.2013.85

Robitaille, R. (1995). Purinergic receptors and their activation by endogenous purines at perisynaptic glial cells of the frog neuromuscular junction. *J. Neurosci.* 15, 7121–7131.

Robitaille, R. (1998). Modulation of synaptic efficacy and synaptic depression by glial cells at the frog neuromuscular junction. *Neuron* 21, 847–855. doi: 10.1016/S0896-6273(00)80600-5

Rochon, D., Rousse, I., and Robitaille, R. (2001). Synapse-glia interactions at the mammalian neuromuscular junction. *J. Neurosci.* 21, 3819–3829.

Rodella, U., Negro, S., Scorzeto, M., Bergamin, E., Jalink, K., Montecucco, C., et al. (2017). Schwann cells are activated by ATP released from neurons in an *in vitro* cellular model of Miller Fisher syndrome. *Dis. Model. Mech.* 10, 597–603. doi: 10.1242/dmm.027870

Rodrigues, R. J., Tomé, A. R., and Cunha, R. A. (2015). ATP as a multi-target danger signal in the brain. *Front. Neurosci.* 9:148. doi: 10.3389/fnins.2015.00148

Ross, C. A., and Tabrizi, S. J. (2011). Huntington's disease: from molecular pathogenesis to clinical treatment. *Lancet Neurol.* 10, 83–98. doi: 10.1016/S1474-4422(10)70245-3

Safarzadeh, E., Jadidi-Niaragh, F., Motallebnezhad, M., and Yousefi, M. (2016). The role of adenosine and adenosine receptors in the immunopathogenesis of multiple sclerosis. *Inflamm. Res.* 65, 511–520. doi: 10.1007/s00011-016-0936-z

Scattoni, M. L., Valanzano, A., Pezzola, A., March, Z. D., De Fusco, F. R., Popoli, P., et al. (2007). Adenosine A2A receptor blockade before striatal excitotoxic lesions prevents long term behavioural disturbances in the quinolinic rat model of Huntington's disease. *Behav. Brain Res*. 176, 216–221. doi: 10.1016/j.bbr.2006.10.004

Scemes, E., Suadicani, S. O., Dahl, G., and Spray, D. C. (2007). Connexin and pannexin mediated cell–cell communication. *Neuron Glia Biol.* 3, 199–208. doi: 10.1017/S1740925X08000069

Schiffmann, S. N., Fisone, G., Moresco, R., Cunha, R. A., and Ferré, S. (2007). Adenosine A2Areceptors and basal ganglia physiology. *Prog. Neurobiol.* 83, 277–292. doi: 10.1016/j.pneurobio.2007.05.001

Schiffmann, S. N., Jacobs, O., and Vanderhaeghen, J. J. (1991). Striatal restricted adenosine A2 receptor (RDC8) is expressed by enkephalin but not by substance P neurons: an *in situ* hybridization histochemistry study. *J. Neurochem.* 57, 1062–1067. doi: 10.1111/j.1471-4159.1991.tb08257.x

Seki, T., Adachi, N., Ono, Y., Mochizuki, H., Hiramoto, K., Amano, T., et al. (2005). Mutant protein kinase Cγ found in spinocerebellar ataxia type 14 is susceptible to aggregation and causes cell death. *J. Biol. Chem.* 280, 29096–29106. doi: 10.1074/jbc.M501716200

Shahaduzzaman, M., Acosta, S., Bickford, P. C., and Borlongan, C. V. (2013). α-Synuclein is a pathological link and therapeutic target for Parkinson's disease and traumatic brain injury. *Med. Hypotheses* 81, 675–680. doi: 10.1016/j.mehy.2013.07.025

Sharp, A. J., Polak, P. E., Simonini, V., Lin, S. X., Richardson, J. C., Bongarzone, E. R., et al. (2008). P2x7 deficiency suppresses development of experimental autoimmune encephalomyelitis. *J. Neuroinflammation* 5:33. doi: 10.1186/1742-2094-5-33

Shen, H.-Y., Canas, P. M., Garcia-Sanz, P., Lan, J.-Q., Boison, D., Moratalla, R., et al. (2013). Adenosine A2A receptors in striatal glutamatergic terminals and GABAergic neurons oppositely modulate psychostimulant action and DARPP-32 phosphorylation. *PLoS ONE* 8:e80902. doi: 10.1371/journal.pone.0080902

Shinozaki, Y., Shibata, K., Yoshida, K., Ikenaka, K., Tanaka, K. F., Correspondence, S. K., et al. (2017). Transformation of Astrocytes to a neuroprotective phenotype by microglia via P2Y 1 receptor downregulation. *Cell Rep.* 19, 1151–1164. doi: 10.1016/j.celrep.2017.04.047

Simon, D. K., Wu, C., Tilley, B. C., Lohmann, K., Klein, C., Payami, H., et al. (2017). Caffeine, creatine, GRIN2A and Parkinson's disease progression. *J. Neurol. Sci.* 375, 355–359. doi: 10.1016/j.jns.2017.02.032

Simonin, C., Duru, C., Salleron, J., Hincker, P., Charles, P., Delval, A., et al. (2013). Association between caffeine intake and age at onset in huntington's disease. *Neurobiol. Dis.* 58, 179–182. doi: 10.1016/j.nbd.2013.05.013

Sitkovsky, M., V (2003). Use of the A2A adenosine receptor as a physiological immunosuppressor and to engineer inflammation *in vivo*. *Biochem. Pharmacol.* 65, 493–501. doi: 10.1016/S0006-2952(02)01548-4

Skaper, S. D., Facci, L., Culbert, A. A., Evans, N. A., Chessell, I., Davis, J. B., et al. (2006). P2X7 receptors on microglial cells mediate injury to cortical neurons *in vitro*. *Glia* 54, 234–242. doi: 10.1002/glia.20379

Song, X. M., Xu, X. H., Zhu, J., Guo, Z., Li, J., He, C., et al. (2015). Up-regulation of P2X7 receptors mediating proliferation of Schwann cells after sciatic nerve injury. *Purinergic Signal.* 11, 203–213. doi: 10.1007/s11302-015-9445-8

Spanevello, R. M., Mazzanti, C. M., Kaizer, R., Zanin, R., Cargnelutti, D., Hannel, L., et al. (2006). Apyrase and 5'-nucleotidase activities in synaptosomes from the cerebral cortex of rats experimentally demyelinated with ethidium bromide and treated with interferon-beta. *Neurochem. Res.* 31, 455–462. doi: 10.1007/s11064-006-9039-5

Stevens, B., and Fields, R. D. (2000). Response of Schwann cells to action potentials in development. *Science* 287, 2267–2271. doi: 10.1126/science.287.5461.2267

Stockwell, J., Jakova, E., and Cayabyab, F. S. (2017). Adenosine A1 and A2A receptors in the brain: current research and their role in neurodegeneration. *Molecules* 22:676. doi: 10.3390/molecules22040676

Strong, M. J. (2010). The evidence for altered RNA metabolism in amyotrophic lateral sclerosis (ALS). *J. Neurol. Sci.* 288, 1–12. doi: 10.1016/j.jns.2009.09.029

Sun, C., Heid, M. E., Keyel, P. A., and Salter, R. D. (2013). The second transmembrane domain of P2X7 contributes to dilated pore formation. *PLoS ONE* 8:e61886. doi: 10.1371/journal.pone.0061886

Sun, J., Link, H., Olsson, T., Xiao, B. G., Andersson, G., Ekre, H. P., et al. (1991). T and B cell responses to myelin-oligodendrocyte glycoprotein in multiple sclerosis. *J. Immunol.* 146, 1490–1495.

Surprenant, A., and North, R. A. (2009). Signaling at Purinergic P2X Receptors. *Annu. Rev. Physiol.* 71, 333–359. doi: 10.1146/annurev.physiol.70.113006.100630

Taherzadeh-Fard, E., Saft, C., Wieczorek, S., Epplen, J. T., and Arning, L. (2010). Age at onset in Huntington's disease: replication study on the associations of ADORA2A, HAP1 and OGG1. *Neurogenetics* 11, 435–439. doi: 10.1007/s10048-010-0248-3

Takenouchi, T., Sekiyama, K., Sekigawa, A., Fujita, M., Waragai, M., Sugama, S., et al. (2010). P2X7 receptor signaling pathway as a therapeutic target for neurodegenerative diseases. *Arch. Immunol. Ther. Exp. (Warsz).* 58, 91–96. doi: 10.1007/s00005-010-0069-y

Tarditi, A., Camurri, A., Varani, K., Borea, P. A., Woodman, B., Bates, G., et al. (2006). Early and transient alteration of adenosine A2A receptor signaling in a mouse model of Huntington disease. *Neurobiol. Dis.* 23, 44–53. doi: 10.1016/j.nbd.2006.01.014

Tebano, M. T., Martire, A., Chiodi, V., Ferrante, A., and Popoli, P. (2010). Role of adenosine A 2A receptors in modulating synaptic functions and brain levels of BDNF: a possible key mechanism in the pathophysiology of Huntington's disease. *Rev. ScientificWorldJournal.* 10, 1768–1782. doi: 10.1100/tsw.2010.164

Todd, K. J., and Robitaille, R. (2006). Purinergic modulation of synaptic signalling at the neuromuscular junction. *Pflügers Arch. Eur. J. Physiol.* 452, 608–614. doi: 10.1007/s00424-006-0068-3

Tozzi, M., and Novak, I. (2017). Purinergic receptors in adipose tissue as potential targets in metabolic disorders. *Front. Pharmacol.* 8:878. doi: 10.3389/fphar.2017.00878

Tsuda, M. (2017). P2 receptors, microglial cytokines and chemokines, and neuropathic pain. *J. Neurosci. Res.* 95, 1319–1329. doi: 10.1002/jnr.23816

Tsuda, M., and Inoue, K. (2016). Neuron–microglia interaction by purinergic signaling in neuropathic pain following neurodegeneration. *Neuropharmacology* 104, 76–81. doi: 10.1016/j.neuropharm.2015.08.042

Tsuda, M., Shigemoto-Mogami, Y., Koizumi, S., Mizokoshi, A., Kohsaka, S., Salter, M. W., et al. (2003). P2X4 receptors induced in spinal microglia gate tactile allodynia after nerve injury. *Nature* 424, 778–783. doi: 10.1038/nature01786

Tsutsui, S., Schnermann, J., Noorbakhsh, F., Henry, S., Yong, V. W., Winston, B. W., et al. (2004). Neurobiology of disease A1 adenosine receptor upregulation and activation attenuates neuroinflammation and demyelination in a model of multiple sclerosis. *J. Neurosci.* 24, 1521–1529. doi: 10.1523/JNEUROSCI.4271-03.2004

Tyebji, S., Saavedra, A., Canas, P. M., Pliassova, A., Delgado-García, J. M., Alberch, J., et al. (2015). Hyperactivation of D1 and A 2A receptors contributes to cognitive dysfunction in Huntington's disease. *Neurobiol. Dis.* 74, 41–57. doi: 10.1016/j.nbd.2014.11.004

Varani, K., Abbracchio, M. P., Cannella, M., Cislaghi, G., Giallonardo, P., Mariotti, C., et al. (2003). Aberrant A_{2A} receptor function in peripheral blood cells in Huntington's disease. *FASEB J.* 17, 2148–2150. doi: 10.1096/fj.03-0079fje

Varani, K., Rigamonti, D., Sipione, S., Camurri, A., Borea, P. A., Cattabeni, F., et al. (2001). Aberrant amplification of A 2A receptor signaling in striatal cells expressing mutant huntingtin. *FASEB J.* 15, 1245–1247. doi: 10.1096/fj.00-0730fje

Varma, H., Cheng, R., Voisine, C., Hart, A. C., and Stockwell, B. R. (2007). Inhibitors of metabolism rescue cell death in Huntington's disease models. *Proc. Natl. Acad. Sci. U.S.A.* 104, 14525–14530. doi: 10.1073/pnas.0704482104

Verkhratsky, A., Rodríguez, J. J., and Parpura, V. (2012). Calcium signalling in astroglia. *Mol. Cell. Endocrinol.* 353, 45–56. doi: 10.1016/j.mce.2011.08.039

Verschueren, A. (2017). Motor neuropathies and lower motor neuron syndromes. *Rev. Neurol. (Paris).* 173, 320–325. doi: 10.1016/j.neurol.2017.03.018

Vijayan, D., Young, A., Teng, M. W. L., and Smyth, M. J. (2017). Targeting immunosuppressive adenosine in cancer. *Nat. Rev. Cancer* 17, 709–724. doi: 10.1038/nrc.2017.86

Villar-Menéndez, I., Blanch, M., Tyebji, S., Pereira-Veiga, T., Albasanz, J. L., Martín, M., et al. (2013). Increased 5-methylcytosine and decreased 5-hydroxymethylcytosine levels are associated with reduced striatal A2AR levels in Huntington's disease. *NeuroMolecular Med.* 15, 295–309. doi: 10.1007/s12017-013-8219-0

Vincenzi, F., Corciulo, C., Targa, M., Casetta, I., Gentile, M., Granieri, E., et al. (2013). A_{2A} adenosine receptors are up-regulated in lymphocytes from amyotrophic lateral sclerosis patients. *Amyotroph. Lateral Scler. Front. Degener.* 14, 406–413. doi: 10.3109/21678421.2013.793358

Viscomi, M. T., Florenzano, F., Amadio, S., Bernardi, G., and Molinari, M. (2005). Partial resistance of ataxin-2-containing olivary and pontine neurons to axotomy-induced degeneration. *Brain Res. Bull.* 66, 212–221. doi: 10.1016/j.brainresbull.2005.04.016

Volont,é, C., Apolloni, S., Parisi, C., and Amadio, S. (2016). Purinergic contribution to amyotrophic lateral sclerosis. *Neuropharmacology* 104, 180–193. doi: 10.1016/j.neuropharm.2015.10.026

Volont,é, C., Apolloni, S., Skaper, S. D., and Burnstock, G. (2012). P2X7 receptors: channels, pores and more. *CNS Neurol. Disord. Drug Targets* 11, 705–721. doi: 10.2174/187152712803581137

Vonsattel, J. P., and DiFiglia, M. (1998). Huntington disease. *J. Neuropathol. Exp. Neurol.* 57, 369–384. doi: 10.1097/00005072-199805000-00001

Vuorimaa, A., Rissanen, E., and Airas, L. (2017). *In vivo* PET Imaging of adenosine 2A receptors in neuroinflammatory and neurodegenerative disease. *Contrast Media Mol. Imaging* 2017:6975841. doi: 10.1155/2017/6975841

Wang, X., Arcuino, G., Takano, T., Lin, J., Peng, W. G., Wan, P., et al. (2004). P2X7 receptor inhibition improves recovery after spinal cord injury. *Nat. Med.* 10, 821–827. doi: 10.1038/nm1082

Wei, W., Du, C., Lv, J., Zhao, G., Li, Z., Wu, Z., et al. (2013). Blocking A2B adenosine receptor alleviates pathogenesis of experimental autoimmune encephalomyelitis via inhibition of IL-6 production and Th17 differentiation. *J. Immunol.* 190, 138–146. doi: 10.4049/jimmunol.1103721

Whiteside, T. L. (2017). Targeting adenosine in cancer immunotherapy: a review of recent progress. *Expert Rev. Anticancer Ther.* 17, 527–535. doi: 10.1080/14737140.2017.1316197

Wiendl, H., Toyka, K. V., Rieckmann, P., Gold, R., Hartung, H.-P., Hohlfeld, R., et al. (2008). Basic and escalating immunomodulatory treatments in multiple sclerosis: Current therapeutic recommendations. *J. Neurol.* 255, 1449–1463. doi: 10.1007/s00415-008-0061-1

Wiedemann, F. R., Manfredi, G., Mawrin, C., Beal, M. F., and Schon, E. A. (2002). Mitochondrial DNA and respiratory chain function in spinal cords of ALS patients. *J. Neurochem.* 80, 616–625. doi: 10.1046/j.0022-3042.2001.00731.x

Wilkaniec, A., Gassowska, M., Czapski, G. A., Cieślik, M., Sulkowski, G., and Adamczyk, A. (2017). P2X7 receptor-pannexin 1 interaction mediates extracellular alpha-synuclein-induced ATP release in neuroblastoma SH-SY5Y cells. *Purinergic Signal.* 13, 347–361. doi: 10.1007/s11302-017-9567-2

Witting, A., Chen, L., Cudaback, E., Straiker, A., Walter, L., Rickman, B., et al. (2006). Experimental autoimmune encephalomyelitis disrupts endocannabinoid-mediated neuroprotection. *Proc. Natl. Acad. Sci. U.S.A.* 103, 6362–6367. doi: 10.1073/pnas.0510418103

Xu, P., Rosen, K. M., Hedstrom, K., Rey, O., Guha, S., Hart, C., et al. (2013). Nerve injury induces glial cell line-derived neurotrophic factor (GDNF) expression in Schwann cells through purinergic signaling and the PKC-PKD pathway. *Glia* 61, 1029–1040. doi: 10.1002/glia.22491

Yamada-Fowler, N., Fredrikson, M., and Söderkvist, P. (2014). Caffeine interaction with glutamate receptor gene GRIN2A: Parkinson's disease in Swedish population. *PLoS ONE* 9:e99294. doi: 10.1371/journal.pone.0099294

Yang, X., Lou, Y., Liu, G., Wang, X., Qian, Y., Ding, J., et al. (2017). Microglia P2Y6 receptor is related to Parkinson's disease through neuroinflammatory process. *J. Neuroinflammation* 14:38. doi: 10.1186/s12974-017-0795-8

Yanpallewar, S. U., Barrick, C. A., Buckley, H., Becker, J., and Tessarollo, L. (2012). Deletion of the BDNF truncated receptor TrkB.T1 delays disease onset in a mouse model of amyotrophic lateral sclerosis. *PLoS ONE* 7:e39946. doi: 10.1371/journal.pone.0039946

Yao, S.-Q., Li, Z.-Z., Huang, Q.-Y., Li, F., Wang, Z.-W., Augusto, E., et al. (2012). Genetic inactivation of the adenosine A(2A) receptor exacerbates brain damage in mice with experimental autoimmune encephalomyelitis. *J. Neurochem.* 123, 100–112. doi: 10.1111/j.1471-4159.2012.07807.x

Yiangou, Y., Facer, P., Durrenberger, P., Chessell, I. P., Naylor, A., Bountra, C., et al. (2006). COX-2, CB2 and P2X7-immunoreactivities are increased in activated microglial cells/macrophages of multiple sclerosis and amyotrophic lateral sclerosis spinal cord. *BMC Neurol.* 6:12. doi: 10.1186/1471-2377-6-12

Zhang, J., Li, Z., Hu, X., Su, Q., He, C., Liu, J., et al. (2017). Knockout of P2Y 12 aggravates experimental autoimmune encephalomyelitis in mice via increasing of IL-23 production and Th17 cell differentiation by dendritic cells. *Brain Behav Immun.* 62, 245–255. doi: 10.1016/j.bbi.2016.12.001

Zhu, C., Wang, G., Li, J., Chen, L., Wang, C., Wang, Y., et al. (2014). Adenosine A2A receptor antagonist istradefylline 20 versus 40 mg/day as augmentation for Parkinson's disease: a meta-analysis. *Neurol. Res.* 36, 1028–1034. doi: 10.1179/1743132814Y.0000000375

Zhu, Y., and Kimelberg, H. K. (2001). Developmental expression of metabotropic P2Y1 and P2Y2 receptors in freshly isolated astrocytes from rat hippocampus. *J. Neurochem.* 77, 530–541. doi: 10.1046/j.1471-4159.2001.00241.x

Zimmermann, H. (2006). Ectonucleotidases in the nervous system. *Novartis Found. Symp.* 276, 113–128; discussion 128–130, 233–237, 275–281. doi: 10.1002/9780470032244.ch10

Zimmermann, H., Braun, N., Kegel, B., and Heine, P. (1998). New insights into molecular structure and function of ectonucleotidases in the nervous system. *Neurochem. Int.* 32, 421–425. doi: 10.1016/S0197-0186(97)00126-5

Zuchora, B., and Urbańska, E. M. (2001). Effect of adenosine receptor agonists on neurodegenerative and convulsive activity of mitochondrial toxin, 3-nitropropionic acid. *Polish J. Pharmacol. Pol. J. Pharmacol* 53, 69–71.

Conflict of Interest Statement: The authors declare that the research was conducted in the absence of any commercial or financial relationships that could be construed as a potential conflict of interest.

frontiers in Pharmacology

HYPOTHESIS AND THEORY
published: 09 April 2018
doi: 10.3389/fphar.2018.00243

Essential Control of the Function of the Striatopallidal Neuron by Pre-coupled Complexes of Adenosine A_{2A}-Dopamine D_2 Receptor Heterotetramers and Adenylyl Cyclase

Sergi Ferré[1], Jordi Bonaventura[1], Wendy Zhu[2], Candice Hatcher-Solis[1], Jaume Taura[3,4], César Quiroz[1], Ning-Sheng Cai[1], Estefanía Moreno[5], Verónica Casadó-Anguera[5], Alexxai V. Kravitz[6], Kimberly R. Thompson[2], Dardo G. Tomasi[7], Gemma Navarro[8], Arnau Cordomí[9], Leonardo Pardo[9], Carme Lluís[5], Carmen W. Dessauer[10], Nora D. Volkow[7], Vicent Casadó[5], Francisco Ciruela[3,4], Diomedes E. Logothetis[11] and Daniel Zwilling[2]*

[1] Integrative Neurobiology Section, National Institute on Drug Abuse, Intramural Research Program, National Institutes of Health, Baltimore, MD, United States, [2] Circuit Therapeutics, Inc., Menlo Park, CA, United States, [3] Unitat de Farmacologia, Departament de Patologia i Terapèutica Experimental, Facultat de Medicina i Ciències de la Salut, IDIBELL, Universitat de Barcelona, Barcelona, Spain, [4] Institut de Neurociències, Universitat de Barcelona, Barcelona, Spain, [5] Center for Biomedical Research in Neurodegenerative Diseases Network, Department of Biochemistry and Molecular Biomedicine, Faculty of Biology, Institute of Biomedicine of the University of Barcelona, University of Barcelona, Barcelona, Spain, [6] Eating and Addiction Section, Diabetes, Endocrinology and Obesity Branch, National Institute of Diabetes and Digestive and Kidney Diseases, Intramural Research Program, National Institutes of Health, Bethesda, MD, United States, [7] Laboratory of Neuroimaging, National Institute on Alcohol Abuse and Alcoholism, Intramural Research Program, National Institutes of Health, Rockville, MD, United States, [8] Department of Biochemistry and Physiology, Faculty of Pharmacy, University of Barcelona, Barcelona, Spain, [9] Laboratory of Computational Medicine, School of Medicine, Autonomous University of Barcelona, Bellaterra, Spain, [10] Department of Integrative Biology and Pharmacology, McGovern Medical School, University of Texas Health Science Center at Houston, Houston, TX, United States, [11] Department of Pharmaceutical Sciences, Bouvé College of Health Sciences, Northeastern University, Boston, MA, United States

OPEN ACCESS

Edited by:
Vsevolod V. Gurevich, Vanderbilt University, United States

Reviewed by:
Kevin D. G. Pfleger, Harry Perkins Institute of Medical Research, Australia
Dominique Massotte, UPR3212 Institut des Neurosciences Cellulaires et Intégratives (INCI), France

***Correspondence:**
Sergi Ferré
sferre@intra.nida.nih.gov

Specialty section:
This article was submitted to Experimental Pharmacology and Drug Discovery, a section of the journal Frontiers in Pharmacology

Received: *05 October 2017*
Accepted: *05 March 2018*
Published: *09 April 2018*

Citation:
Ferré S, Bonaventura J, Zhu W, Hatcher-Solis C, Taura J, Quiroz C, Cai N-S, Moreno E, Casadó-Anguera V, Kravitz AV, Thompson KR, Tomasi DG, Navarro G, Cordomí A, Pardo L, Lluís C, Dessauer CW, Volkow ND, Casadó V, Ciruela F, Logothetis DE and Zwilling D (2018) Essential Control of the Function of the Striatopallidal Neuron by Pre-coupled Complexes of Adenosine A_{2A}-Dopamine D_2 Receptor Heterotetramers and Adenylyl Cyclase. Front. Pharmacol. 9:243. doi: 10.3389/fphar.2018.00243

The central adenosine system and adenosine receptors play a fundamental role in the modulation of dopaminergic neurotransmission. This is mostly achieved by the strategic co-localization of different adenosine and dopamine receptor subtypes in the two populations of striatal efferent neurons, striatonigral and striatopallidal, that give rise to the direct and indirect striatal efferent pathways, respectively. With optogenetic techniques it has been possible to dissect a differential role of the direct and indirect pathways in mediating "Go" responses upon exposure to reward-related stimuli and "NoGo" responses upon exposure to non-rewarded or aversive-related stimuli, respectively, which depends on their different connecting output structures and their differential expression of dopamine and adenosine receptor subtypes. The striatopallidal neuron selectively expresses dopamine D_2 receptors (D2R) and adenosine A_{2A} receptors (A2AR), and numerous experiments using multiple genetic and pharmacological *in vitro*, *in situ* and *in vivo* approaches, demonstrate they can form A2AR-D2R heteromers. It was initially assumed that different pharmacological interactions between dopamine and adenosine receptor ligands indicated the existence of different subpopulations of A2AR and D2R in the striatopallidal neuron. However, as elaborated in the present essay, most evidence now indicates that all interactions can

be explained with a predominant population of striatal A2AR-D2R heteromers forming complexes with adenylyl cyclase subtype 5 (AC5). The A2AR-D2R heteromer has a tetrameric structure, with two homodimers, which allows not only multiple allosteric interactions between different orthosteric ligands, agonists, and antagonists, but also the canonical Gs-Gi antagonistic interaction at the level of AC5. We present a model of the function of the A2AR-D2R heterotetramer-AC5 complex, which acts as an integrative device of adenosine and dopamine signals that determine the excitability and gene expression of the striatopallidal neurons. The model can explain most behavioral effects of A2AR and D2R ligands, including the psychostimulant effects of caffeine. The model is also discussed in the context of different functional striatal compartments, mainly the dorsal and the ventral striatum. The current accumulated knowledge of the biochemical properties of the A2AR-D2R heterotetramer-AC5 complex offers new therapeutic possibilities for Parkinson's disease, schizophrenia, SUD and other neuropsychiatric disorders with dysfunction of dorsal or ventral striatopallidal neurons.

Keywords: striatopallidal neuron, adenosine A_{2A} receptor, dopamine D_2 receptor, GPCR heteromers, adenylyl cyclase, caffeine, akinesia, apathy

INTRODUCTION

One of the most noticeable functions of adenosine in the brain is the ability to impose a brake on the central dopaminergic system. This inhibitory role of adenosine is largely mediated by the activation of one subtype of adenosine receptor, the A_{2A} receptor (A2AR), particularly expressed by one type of neuron localized in the striatum, the striatopallidal neuron. The striatum is the brain area with the highest innervation of dopamine and the highest expression of dopamine receptors in the brain (Gerfen, 2004), and the striatopallidal neuron expresses the highest density of A2AR and dopamine receptors of the D_2 subtype (D2R) than any other neuron in the central nervous system (Gerfen, 2004; Schiffmann et al., 2007). It is now well accepted that adenosine controls the function of the striatopallidal neuron through intermolecular interactions between A2AR and D2R, with the formation of receptor heteromers.

Since its initial discovery, now more than 25 years ago (Ferré et al., 1991b), A2AR-D2R interactions have become a model for the study of allosteric interactions within G protein-coupled receptor (GPCR) heteromers, with the emergence of a new concept: allosteric interactions between orthosteric ligands (reviewed in Ferré et al., 2014). But recent findings indicate that the A2AR-D2R heteromer will also become a model for receptor-receptor interactions previously thought to take place downstream, on converging signaling molecules, which were often labeled as "interactions at the second messenger level." The antagonistic canonical interaction at the level of adenylyl cyclase (AC), between a Gs/olf-coupled receptor, such as the A2AR, and a Gi/o-coupled receptor, such as the D2R, represents a classical example. Thus, a recent study demonstrates that this canonical interaction is dependent on the oligomerization of A2AR and D2R and the AC subtype AC5 (Navarro et al., 2018). This discovery implies that the striatal A2AR-D2R heteromer could explain most pharmacological effects of A2AR and D2R ligands, with implications for various neuropsychiatric disorders.

The understanding of the role of striatal adenosine and A2AR-D2R heteromers in striatal function and dysfunction will be here revisited within the framework of, not only the new developments on A2AR-D2R heteromers, but also most recent developments on the function of different striatal compartments and striatal dopamine, particularly on the function of the striatopallidal neuron. First, we summarize the current knowledge of the role of dopamine in the different striatal compartments. Next, we analyze the role of adenosine-dopamine interactions in the modulation of the function of the striatopallidal neuron. We then propose a functional model for the A2AR-D2R heterotetramer-AC5 complex in the striatopallidal neuron, a complex formed by one A2AR homodimer coupled to a Golf protein, a D2R homodimer coupled to a Gi protein and its signaling molecule AC5. The model is then used to reevaluate the pharmacological effects of adenosine receptor ligands, including caffeine. Finally, it is proposed that A2AR-D2R heterotetramer-AC5 complexes localized in striatopallidal neurons can be used as targets for the treatment of neuropsychiatric symptoms, such as akinesia and apathy. We also present new results of the effect of the A2AR antagonist SCH 442416 in radioligand binding, locomotor activation and optogenetic experiments in mice, which reconcile previous studies with the same compound that were apparently incompatible with our hypothesis of a predominant population of striatal A2AR-D2R heteromers that modulate striatopallidal neuronal function.

FUNCTIONAL DISTINCTION OF STRIATAL COMPARTMENTS

The striatum is the main input structure of the basal ganglia. Although in humans and non-human primates it has been classically subdivided into nucleus accumbens (NAc), caudate and putamen, it can be functionally subdivided in three different compartments: ventral, rostral-dorsal and caudal-dorsal striata (**Figure 1A**). The ventral striatum concept has expanded from

its initial inclusion of areas innervated by the dopaminergic cells of the ventral tegmental area (VTA), mostly the NAc with its two compartments core and shell and the olfactory tubercle, to the striatal areas receiving glutamatergic inputs from the ventromedial prefrontal cortex, orbitofrontal cortex and anterior cingulate cortex (Haber and Behrens, 2014) (**Figure 1A**). In fact, the orbitofrontal cortex and the anterior cingulate cortex, respectively, receive partial and predominant dopaminergic innervation from the substantia nigra pars compacta (SNpc; Haber and Behrens, 2014). Furthermore, the ventral striatum receives afferent glutamatergic projections from the insular cortex, amygdala and hippocampus (Haber and Behrens, 2014). The rostral-dorsal striatum receives glutamatergic input from frontal and parietal association areas and the caudal-dorsal striatum from the primary motor and somatosensory cortices (**Figure 1A**). Both rostral-dorsal and caudal-dorsal striata receive their dopaminergic input from the SNpc (Haber, 2014; Haber and Behrens, 2014).

The ventral striatum forms part of decision-making brain circuits involved in reward valuation tasks, which determine and store reward values (often named as "subjective values of rewards") and constantly choose the reward to be obtained by a process of maximizing utilities associated with different options, the highest benefit/cost ratio (Kable and Glimcher, 2009). 'Delay discounting' (DD), 'effort discounting' (ED), and 'low-probability discounting' (LPD) refer to the empirical finding that both humans and animals value immediate, low-effort and high probability rewards more than delayed, high-effort and low probability rewards. A large number of behavioral and clinical studies indicate that DD, ED, and LPD are independent variables possibly involving corticostriatal circuits with different ventral striatal compartments differentially connected to different prefrontal cortical areas (Prévost et al., 2010; Stopper and Floresco, 2011). A main role of the ventral striatum, classically labeled as an interface between motivation and action (Mogenson et al., 1980), can be synthesized as determining "whether to respond" while that of the dorsal striatum is "how to respond" to reward-associated stimuli (Ferré, 2017). All reward-related, dopamine-dependent functions, including the facilitation of reward-oriented behavior and learning of stimulus-reward and reward-response associations (positive reinforcement; Wise, 2004), are simultaneously processed by the rostral-dorsal and caudal-dorsal striata. In relation to positive reinforcement, the rostral-dorsal striatum is predominantly involved in an initial, more controlled (contingent on the outcome) and less permanent learning, while the caudal-dorsal striatum is involved in a slower, less controlled (non-contingent on the outcome) but long-lasting learning (Kim and Hikosaka, 2015). The same functional dichotomy, "volitional" and "automatic" learning, but with a medial-lateral distribution, can also be demonstrated in the rodent striatum (Voorn et al., 2004; Yin and Knowlton, 2006; Balleine and O'Doherty, 2010). However, it is becoming increasingly evident that dopaminergic mesencephalic cells also process aversive-related and non-rewarded stimuli and are involved in negative reinforcement. Most dopamine cells respond by decreasing their activity upon exposure to aversive stimuli and to omission of expected rewards. Dopaminergic cells, therefore, code for positive and negative reward prediction errors, increasing their firing upon presentation of reward-related stimuli or better than expected rewards or with the termination of aversive-related stimuli and decreasing their firing upon omission of reward-related stimuli or presentation of a worse than expected reward (Steinberg et al., 2013; Chang et al., 2016).

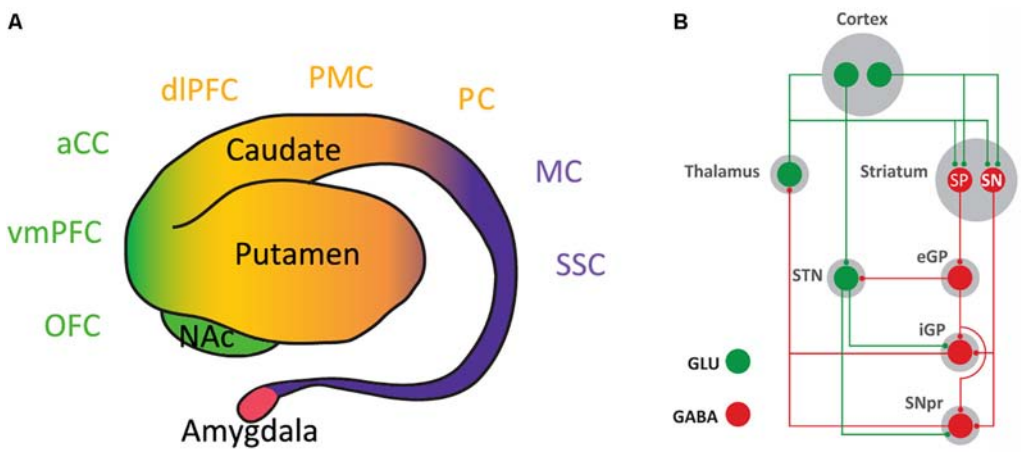

FIGURE 1 | Inputs and outputs of the striatum. **(A)** Lateral view of the striatum and amygdala (of human and non-human primates). The classical morphological subdivision of striatal compartments in nucleus accumbens (NAc), caudate and putamen nuclei can be functionally classified according to the cortical inputs in: ventral striatum (in green), which receives inputs from the ventromedial prefrontal cortex (vmPFC), orbitofrontal cortex (OFC), and anterior cingulate cortex (aCC); rostral-dorsal striatum (in orange), which receives inputs from frontal and parietal association areas, such as the dorsolateral prefrontal cortex (dlPFC), premotor cortex (PMC), and parietal cortex (PC); and caudal-rostral striatum (in purple), which receives inputs from the primary motor cortex (MC) and the somatosensory cortex (SSC). **(B)** Basal ganglia circuitry. The striatonigral neuron (SN) directly connects the striatum with the output structures of the basal ganglia: the internal segment of the globus pallidus (iGP) and the substantia nigra pars reticulata (SNpr). The striatopallidal neuron (SP) connects with the output structures by relays in the external segment of the globus pallidus (eGP) and the subthalamic nucleus (STN); GLU, glutamate.

THE A2AR-D2R-EXPRESSING STRIATOPALLIDAL NEURON

In the striatum, glutamatergic and dopaminergic inputs converge in the dendritic spines of the GABAergic medium-sized spiny neurons, which constitute more than 95% of the striatal neuronal population (Gerfen, 2004). There are two types of medium-sized spiny neurons, which define the two striatal efferent pathways that connect the striatum with the output structures of the basal ganglia, substantia nigra pars reticulata (SNpr) and internal segment of the globus pallidus (**Figure 1B**). The striatonigral neuron constitutes the *direct efferent pathway* since it connects directly with the output structures (Gerfen, 2004). The striatopallidal neuron gives rise to the *indirect efferent pathway* and connects with the pallidal complex (the external segment of the globus pallidus and the ventral pallidum), which connects with the output structures directly and through a relay in the subthalamic nucleus (Gerfen, 2004) (**Figure 1B**). While there are no apparent qualitative or quantitative differences between the glutamatergic inputs impinging on the striatonigral and striatopallidal neurons, there is a clear distinction with the receptors that process the dopaminergic signals. Thus, the striatonigral neuron expresses dopamine D_1 receptors (D1R), a prototypical Gs/olf-coupled stimulatory receptor (Golf in the striatum), while the striatopallidal neuron expresses D2R, a prototypical Gi/o-coupled inhibitory receptor (Gerfen, 2004; Bertran-Gonzalez et al., 2008). This established scheme breaks down in the most ventral striatal compartment, the shell of the NAc. The most ventral striatopallidal neurons project to the ventromedial and ventrolateral parts of the ventral pallidum, which does not connect with the output structures or relay in the subthalamic nucleus (Root et al., 2015). Instead, these regions of the ventral pallidum represent output structures of the basal ganglia themselves, since they project to the medio-dorsal thalamus, lateral hypothalamus and lateral habenula (Root et al., 2015). Furthermore, some ventral striatopallidal neurons also express D1R, with some degree of co-localization but still largely segregated from D2R (Bertran-Gonzalez et al., 2008; Frederick et al., 2015).

A mechanism by which dopamine is directly involved with positive and negative reinforcement is emerging from the study of the functional role of the direct and indirect striatal efferent pathways. Using recently developed optogenetic techniques, it has been possible to dissect a differential role of the direct and indirect pathways in mediating "Go" responses upon exposure to reward-related stimuli and "NoGo" responses upon exposure to non-rewarded or aversive-related stimuli, respectively, which depends on their different connecting output structures and their differential expression of dopamine receptor subtypes (Hikida et al., 2010, 2013; Kravitz et al., 2010, 2012; Freeze et al., 2013; Danjo et al., 2014). The differential connectivity entails that activation of striatonigral and striatopallidal neurons lead to qualitatively different behavioral responses, with the most obvious being the respective facilitation and inhibition of psychomotor activity. At this point, following Wise and Bozarth (1987), we should make the distinction between "psychomotor" and simply "motor" responses. Psychomotor responses, which include forward locomotion or withdraw, have a characteristic dependence on external stimuli; increases or decreases of dopamine enhance or diminish the responsiveness to those stimuli, respectively. The differential affinities of D1R and D2R for endogenous dopamine and their respective predominant expression in striatonigral and striatopallidal neurons provide a fine-tuning device by which bursts and pauses of dopamine neurons can differentially influence their activity (Roitman et al., 2008; Bromberg-Martin et al., 2010; Macpherson et al., 2014). Dopamine has significantly higher affinity for D2R than for D1R. Therefore, D2R are more activated than D1R by basal dopamine levels and are more sensitive to the effects of dopamine pauses, while D1R are more sensitive to dopamine bursts, to conditions of larger dopamine release. Bursts of dopamine neurons result in large dopamine release, which predominantly increases the activation of stimulatory D1R and causes the direct pathway to promote high-value reward-associated movements, whereas the lower basal dopamine levels predominantly activate D2R, which are inhibitory and remove activation of the indirect pathway, thus suppressing low-value reward-associated or high-value punishment-associated movements (Frank, 2005; Hikosaka, 2007; Dreyer et al., 2010; Hikida et al., 2010, 2013; Kravitz et al., 2012; Danjo et al., 2014). Nevertheless, we should not ignore the fact that D2R are not completely occupied by endogenous dopamine and that bursts of dopamine are also able to enhance D2R signaling, therefore participating to the psychomotor activation guided by the stimuli associated with the concomitant increase in dopaminergic cell firing. However, strong dopamine receptor activation basically promotes potentiation of corticostriatal synapses onto the direct pathway and learning from positive outcomes (positive reinforcement), while weak dopamine receptor activation promotes potentiation of corticostriatal synapses onto the indirect pathway and learning from negative outcomes (negative reinforcement) (Frank et al., 2004; Nakamura and Hikosaka, 2006; Shen et al., 2008; Voon et al., 2010).

Another important phenotypical difference between the striatopallidal and striatonigral neurons is their differential expression of adenosine receptor subtypes. The striatopallidal neurons selectively express A2AR, in fact, the highest density in the brain (Schiffmann et al., 2007). On the other hand, A2AR are absent from the striatonigral neurons, which express adenosine A_1 receptors (A1R) (Ferré et al., 1997). A2AR can then be used as a marker of the striatopallidal neuron. For instance, to identify the function of the striatopallidal neuron, studies using Bacterial Artificial Chromosome (BAC) transgenic mice have targeted the regulatory elements of either the D2R or the A2AR (Durieux et al., 2009; Valjent et al., 2009; Freeze et al., 2013). We used BAC transgenic mouse lines that express Cre recombinase under the control of regulatory elements of the D2R (D2R-Cre mice) or the A2AR (A2AR-Cre mice), allowing the selective expression of channelrhodopsin 2 (ChR2) by striatopallidal neurons (Kravitz et al., 2010; Freeze et al., 2013; Zwilling et al., 2014). This was achieved by bilateral injection of an adeno-associated virus (AAV) containing a Cre-sensitive vector with a double-floxed inverted open reading frame encoding a fusion of ChR2 and enhanced yellow fluorescence

protein into the dorsomedial striatum. Then, fiber-optic cannulas implanted immediately above the injection site allowed the local delivery of light with the concomitant selective optogenetic activation of a large fraction of dorsal striatopallidal neurons. Unilateral optogenetic stimulation led to significant ipsilateral rotational behavior, while bilateral optogenetic stimulation led to a significant decrease in locomotor activity (Kravitz et al., 2010; Freeze et al., 2013; Zwilling et al., 2014) (**Figure 2A**). These results were opposite to those obtained by the selective ablation of a large proportion of dorsal and ventral striatopallidal neurons in BAC transgenic A2AR-Cre mice by Cre-mediated expression of a diphtheria toxin receptor and diphtheria toxin injection, which led to hyperlocomotion (Durieux et al., 2009).

Altogether, these optogenetic and genetic targeting experiments agree with the increase and decrease of "NoGo" responses upon the respective activation or inactivation of striatopallidal neurons. Hypo- or hyperlocomotion represents an outcome of the respective sustained activation or deactivation of a large number of striatopallidal neurons, which more discretely should represent the respective facilitation and inhibition of withdrawal behavior from low-value reward-associated or high-value punishment-associated movements. We addressed more directly this assumption in optogenetic experiments with A2AR-Cre mice, by selectively inducing the expression of ChR2 in dorsal striatopallidal neurons and by using more discrete parameters of stimulation (Zwilling et al., 2014). **Figure 2B** shows the comparison of two different parameters of bilateral optogenetic stimulation in the dorso-medial striatum on locomotor activity. Continuous light for 1 min induced freezing and therefore an impairment of motor activity that

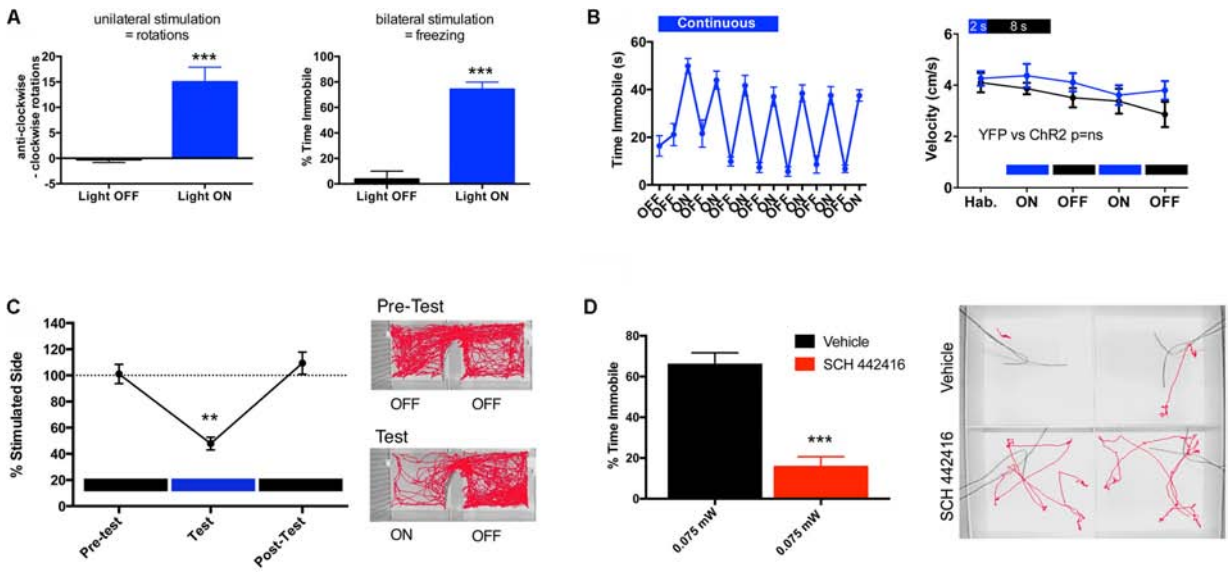

FIGURE 2 | Behavioral effects of the optogenetic stimulation of the striatopallidal neuron in mice. The adeno-associated virus (AAV) containing the Cre-sensitive pAAV5-EF1a-DIO-hChR2(H134R)-YFP virus was bilaterally injected into the dorsal-medial striatum (1 μl at coordinates M-L ± 1.5, A-P + 0.8 and D-V –3.5, relative to bregma) of a BAC transgenic A2AR-Cre mouse (C57BL/6 background). Fiber-optic cannulas were implanted 0.5 μm above the injection site and the virus was allowed to incubate for 4 weeks before the start of behavioral testing. **(A)** At high intensity of stimulation, unilateral illumination results in rotational behavior and bilateral illumination results in freezing. In **(A)** left graph, mice were unilaterally illuminated (left side) with constant light at 1 mW (measured at the fiber tip) and anti-clockwise vs. clockwise (ipsilateral vs. contralateral) rotations were recorded for a duration of 5 min; results are expressed as mean ± SEM; Student's paired *t*-test showed significant differences in the number of rotations in the illuminated condition (light ON) compared to control (light OFF) (***$p < 0.001$, $n = 4$). In **(A)** right graph, mice were illuminated bilaterally with constant light at equal intensity (1 mW per side) and time spent immobile over a period of 1 min was determined; results are expressed as mean ± SEM; Student's paired *t*-test showed significant differences between the illuminated condition (light ON) compared to control (light OFF) (***$p < 0.001$, $n = 11$). **(B)** Comparison of different light illumination paradigms; bilateral circuit activation produced different effects on motor behavior depending on the pattern of light stimulation; continuous light for 1 min induced freezing and motor impairment. In **(B)** left graph, mice were bilaterally stimulated alternating 1-min light ON/OFF blocks, while freezing (expressed as time immobile) was scored through several cycles over 15 min (results are expressed as mean ± SEM, $n = 11$). In **(B)** right graph, mice were pulse stimulated using a 2-s ON/8-s OFF illumination paradigm and did not exhibit ambulatory impairment; velocity of ambulation was monitored over 3-min bins; blue and black plots represent ambulation (in mean ± SEM) of mice injected with the virus expressing ChR-YFP ($n = 20$) or YFP (control, $n = 10$), respectively; two-way ANOVA, did not show significant differences between both groups ($p > 0.05$). **(C)** Aversive behavior driven by striatopallidal neuron activation using stimulation parameters that did not produce motor impairment; in a real-time place-preference assay pulsed light illumination (2-s ON/8 s-OFF) was triggered automatically upon entry into the predesignated 'stimulation side' of the chamber; the amount of time spent in the light-paired chamber was quantified over 20-min blocks recorded before, during and immediately after light stimulation. In **(C)** left graph, mice demonstrated a significant light-mediated aversion, a reduction in the percentage of time (in mean ± SEM) spent in the stimulated side; analyzed statistically by one-way repeated measures ANOVA and Tukey *post hoc* test (**$p < 0.01$; $n = 8$). In **(C)** right panel, example tracks show robust aversion to the left stimulation chamber during the test session. **(D)** A2AR antagonist reduces freezing phenotype. In **(D)** left graph, a 5-min pre-test injection of the A2AR antagonist SCH 442416 (3 mg/kg, i.p.) significantly reduced the percent time freezing (in mean ± SEM) at light power levels of 0.075 mW; Student's paired *t*-test showed significant difference between the groups treated with and without SCH 442416 (***$p < 0.001$; $n = 11$). In **(D)** right panel, example tracks showing SCH-mediated counteraction of optogenetically induced freezing. All behaviors were performed in custom-built arenas and activity monitored and automatically scored using a Noldus Ethovision video tracking system.

would interfere with the analysis of behavior in a real-time place-preference study. On the other hand, mice that were pulse-stimulated using a 2-s ON/8-s OFF illumination paradigm did not demonstrate ambulatory impairment (**Figure 2B**). When this pulse-stimulation was triggered when the mouse entered one of the chambers of a place-preference box, the animal showed a very significant aversion-like behavior to that side (**Figure 2C**) (Zwilling et al., 2014). These results also complement those obtained by Hikida et al. (2010, 2013) in experiments with selective bilateral inactivation of the dorsal or ventral striatopallidal neuron by means of doxycycline-dependent, pathway-specific expression of tetanus toxin (driven by the promoter of the gene coding the neuropeptide enkephalin, selectively expressed by striatopallidal neurons). A counteraction of the expression in addition to the acquisition of aversion-like behavior was also demonstrated by using an asymmetric design, with targeted unilateral inactivation of the ventral striatopallidal neurons with tetanus toxin and the contralateral infusion of a D2R agonist (but not a D2R antagonist or D1R agonists or antagonists) or an A2AR antagonist (Hikida et al., 2013). Similarly, we could demonstrate that the systemic administration of the A2AR antagonist SCH 442416 (3 mg/kg i.p.) significantly decreases the locomotor depression induced by low-intensity optogenetic stimulation of the dorsal-medial striatopallidal neurons (**Figure 2D**). These results would imply a significant role of an endogenous adenosinergic tone in the facilitation of the striatopallidal neuronal function mediated by A2AR. In fact, numerous neurochemical studies imply that A2AR signaling is especially involved in driving the activation of the striatopallidal neuron upon D2R disinhibition (see below), therefore in driving the suppression of the behavior associated with non-rewarded and punishment-associated stimuli.

THE A2AR-D2R RECEPTOR HETEROTETRAMER-AC5 COMPLEX

There is a large amount of experimental evidence indicating the existence of a predominant striatal population of A2AR and D2R that control striatopallidal neuronal function (Ferré et al., 1993, 2016; Azdad et al., 2009; Bonaventura et al., 2015). Recent studies suggested that A2AR-D2R heteromers assemble into a heterotetrameric structure, with A2AR and D2R homodimers coupled to their respective cognate Gs (more precisely the Golf isoform) and Gi proteins (Bonaventura et al., 2015). The heterotetrameric structure would provide the frame for multiple adenosine-dopamine interactions and for interactions between exogenous A2AR and D2R ligands (Navarro et al., 2014; Ferré et al., 2016). One of the most prominent interactions is the allosteric negative effect of A2AR ligands on the affinity and efficacy of D2R ligands (*allosteric interaction*) (Ferré et al., 1991b; Azdad et al., 2009; Bonaventura et al., 2015), which has been demonstrated to depend on A2AR-D2R heteromerization by the use of synthetic peptides that selectively interfere with the heteromeric interface, both in mammalian transfected cells and in striatal tissue (Azdad et al., 2009; Bonaventura et al., 2015).

In addition to the allosteric interaction, a strong reciprocal antagonistic interaction, with the ability of D2R agonists to inhibit A2AR agonist-mediated activation of AC, was first identified in mammalian transfected cells (Kull et al., 1999; Hillion et al., 2002) and more recently characterized in striatal cells in culture (Navarro et al., 2014). This represents an antagonistic Gs-Gi *canonical interaction*, the ability of an activated Gi-coupled receptor to inhibit a Gs-coupled receptor-mediated activation of AC. The A2AR-D2R canonical interaction was first observed *in situ*, in the striatum. The evidence came initially from experiments that demonstrated that the increase in the expression of the immediate-early gene *c-fos* in the striatopallidal neurons upon treatment with D2R antagonists or acute dopamine depletion could be counteracted by blocking A2AR signaling (Boegman and Vincent, 1996; Svenningsson et al., 1999). This A2AR signaling is initiated by the second messenger cyclic-AMP (cAMP), the product of AC activation. The cascade includes protein kinase A (PKA) activation, with phosphorylation of the cAMP-response element binding protein (CREB), a mechanism which is amplified by the PKA-dependent phosphorylation of 'dopamine- and cAMP-regulated phosphoprotein of molecular weight 32,000' (DARPP-32) (Svenningsson et al., 1998; Kull et al., 1999) (**Figure 3A**). A2AR-mediated activation of PKA also promotes phosphorylation of voltage dependent Ca^{2+} channels (VDCC), NMDA, and AMPA receptors (Håkansson et al., 2006; Azdad et al., 2009; Higley and Sabatini, 2010), which determines their degree of activation and, therefore, the degree of excitability of the striatopallidal neurons, which determines the degree of psychomotor depression (**Figure 3A**).

Activation of the D2R, when uninterrupted by co-activation of the A2AR (allosteric interaction), can also signal through phospholipase C (PLC) by a Gßγ subunit-dependent mechanism, which induces the release of inositol (1,4,5)-triphosphate (IP3), a second messenger that causes the release of intracellular Ca^{2+}. This, in turn results in the subsequent activation of the Ca^{2+}/calmodulin-dependent protein phosphatase calcineurin (also called protein phosphatase 2B or PP2B) (Hernandez-Lopez et al., 2000; Azdad et al., 2009) (**Figure 3A**). Phosphorylated forms of VDCC, NMDA, and AMPA receptors and DARPP-32 are main targets of PP2B. Therefore, activation of PP2B leads to a decreased neuronal excitability and represents a downstream additional mechanism of D2R-mediated inhibition of A2AR signaling (Lindskog et al., 1999) (**Figure 3A**). In addition, A2AR and D2R activation can modify gene expression through respective G protein-dependent and independent mechanisms of MAPK activation, which plays a predominant role in the mailing of signals from the synapse to the nucleus by directly activating the constitutive transcription factor Elk-1 (Besnard et al., 2011) (**Figure 3A**). Our previous work indicates that the outcome of co-activation of striatal A2AR and D2R on MAPK activation depends on the intracellular levels of Ca^{2+}, which determines the binding of two different neuronal Ca^{2+}-binding proteins, NCS-1 and calneuron-1 (Navarro et al., 2014). NCS-1 and calneuron bind to the A2AR-D2R heteromer upon low and high concentrations of Ca^{2+}, respectively. Binding of calneuron specifically alters the ability of A2AR ligands

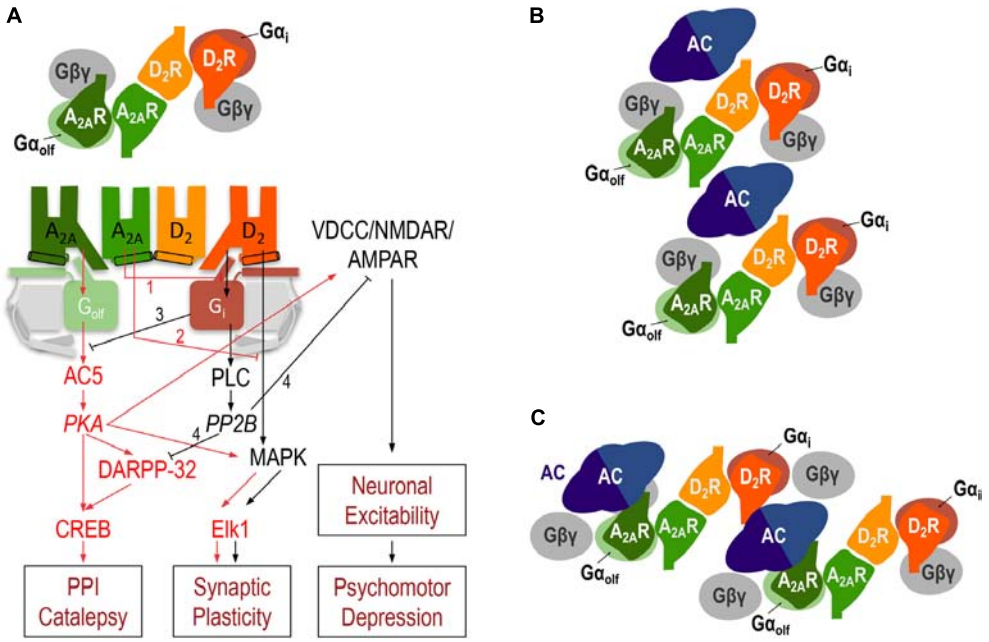

FIGURE 3 | The A2AR-D2R heterotetramer. **(A)** Model representing the striatal A2AR-D2R heteromer-dependent mechanisms that modulate different biochemical and behavioral outputs. The heterotetrameric structure of the A2AR-D2R heteromer allows multiple simultaneous and reciprocal interactions between adenosine and dopamine and exogenous A2AR and D2R ligands. Mainly, the ability of adenosine or exogenous A2AR ligands to decrease G protein-dependent (1) or G protein-independent (2) signaling by dopamine or exogenous D2R ligands (allosteric interactions) and a reciprocal antagonistic interaction, the ability of D2R agonists to inhibit the A2AR agonist-mediated activation of AC5, by means of the antagonistic Gs-Gi canonical interaction at the AC5 level (3). When uninterrupted by the canonical interaction, A2AR signals through activation of AC5 and protein kinase A (PKA) with phosphorylation of 'dopamine- and cAMP-regulated phosphoprotein of molecular weight 32,000' (DARPP-32), which facilitates PPI and catalepsy, and voltage-dependent Ca^{2+} channels (VDCC), NMDA and AMPA receptors, resulting in an increase in the excitability of the striatopallidal neuron. When uninterrupted by the allosteric interaction, D2R signals through PLC, which leads to activation of calcineurin (PP2B). PP2B dephosphorylates PKA substrates, DARPP-32, VDCC, NMDA and AMPA receptors, providing a downstream additional mechanism of D2R-mediated inhibition of A2AR signaling (4) and leading to a decrease in the excitability of the striatopallidal neuron, which facilitates psychomotor activation. A2AR and D2R activation can also modify gene expression through different mechanisms, including G protein-dependent and independent MAPK activation and activation of the transcription factor Elk-1 (see text). In **(B,C)**, schematic slice-representation viewed from the extracellular side of the minimal functional unit of the A2AR-D2R heterotetramer in complex with AC5 (see text), in the absence **(B)** and presence **(C)** of agonists, which induce a rearrangement of the heterotetramer-AC5 interfaces (modified from Navarro et al., 2018).

to allosterically modulate the GTP-independent D2R ligand-mediated MAPK activation, while binding of NCS-1 also counteracts the A2AR-mediated allosteric modulation of D2R-ligand-mediated G protein signaling (and therefore the canonical interaction). This provides a mechanism by which co-activation of A2AR and D2R in the heteromer promotes and counteracts MAPK activation upon low and high concentrations of Ca^{2+}, respectively (Navarro et al., 2014).

The question is how two apparently simultaneous reciprocal interactions between A2AR- and D2R signaling (allosteric and canonical interactions) can take place in the same cell. Based on some studies obtained with the A2AR antagonist SCH 442416, we initially hypothesized the existence of two populations of A2AR in striatopallidal neurons (Orrú et al., 2011b). One population would be forming heteromers with D2R and would mediate the allosteric interaction, while another population would not be forming heteromers with D2R and would allow the antagonistic interaction at the second messenger level, cAMP (Ferré et al., 2011; Orrú et al., 2011b). However, we recently hypothesized that the putative heterotetrameric structure of the A2AR-D2R heteromer could sustain both the allosteric and the canonical interactions (Navarro et al., 2014). In addition, based on the emergent view that considers GPCR homodimers as main functional units (Ferré et al., 2014), we postulated that heteromers are constituted by different interacting homodimers (Ferré et al., 2014; Ferré, 2015). This could be of special functional importance with heteromers formed by one homodimer coupled to a Gs/olf protein and another different homodimer coupled to a Gi/o protein. Our hypothesis was that such a GPCR *heterotetramer* would be part of a pre-coupled macromolecular complex that also includes AC5, the predominant AC subtype in the striatum (Lee et al., 2002), a necessary frame for the canonical antagonistic interaction at the AC level (Ferré, 2015). In fact, in mammalian transfected cells, using synthetic peptides with amino acid sequences of all transmembrane domains (TM) of A2AR and D2R and the putative TMs of AC5, we recently provided clear evidence for the existence of functional pre-coupled complexes of A2AR and D2R homodimers, their cognate Golf and Gi proteins and AC5 (Navarro et al., 2018). We first identified a symmetrical TM 6 interface for the A2AR and D2R homodimers and a symmetrical TM 4/TM 5 A2AR-D2R heteromeric interface. Computational analysis provided

one minimal solution, a linear arrangement with two internal interacting A2AR and D2R protomers and two external non-interacting A2AR and D2R protomers which interact with the α-subunits of the corresponding Golf and Gi proteins (**Figure 3**). Second, we found asymmetrical interfaces formed by TMs of the receptors and putative TMs of AC5 which rearrange upon agonist exposure. Computational analysis indicated the existence of a minimal functional complex formed by two A2AR-D2R heterotetramers and two AC5 molecules (**Figures 3B,C**). In fact, this quaternary structure suggests the possible formation of zig-zagged arranged high-order oligomeric structures, a higher-order linear arrangement of GPCR heteromers and effectors (Navarro et al., 2018). Finally, we could demonstrate that this macromolecular complex provides the sufficient but necessary condition for the canonical Gs-Gi interactions at the AC level (Navarro et al., 2018). The most demonstrative experiment was that destabilization of the quaternary structure of the A2AR-D2R heterotetramer, with interfering synthetic peptides with the amino acid sequence of the TMs involved in heteromeric interface, blocked the ability of a D2R agonist to counteract AC5 activation by an A2AR agonist in striatal neurons in culture (Navarro et al., 2018).

The A2AR-D2R heterotetramer therefore acts as an integrative molecular device, which allows reciprocal antagonistic interactions between adenosine and dopamine to facilitate a switch in the activation-inhibition of the striatopallidal neuron: A preferential A2AR vs. D2R activation leads to an increase in neuronal activity determined by the A2AR-mediated activation of the AC5/PKA pathway, which is potentiated by the allosteric counteraction of D2R signaling ("1" and "2" in **Figure 3A**); a preferential D2R vs. A2AR activation leads to a decrease in neuronal activity by activation of the PLC/PP2B pathway and switching off the A2A-mediated activation of AC5 through the canonical interaction ("3" in **Figure 3A**), which we have shown depends on the integrity of the A2AR-D2R heterotetramer-AC5 complex (Azdad et al., 2009; Higley and Sabatini, 2010; Navarro et al., 2014, 2018; Bonaventura et al., 2015; Ferré, 2016; Ferré et al., 2016).

The heterotetrameric structure of the A2AR-D2R heteromer provides the framework for allosteric mechanisms of A2AR ligands that could explain recent experimental findings apparently incompatible with classical pharmacology, such as the agonist-like behavior of A2AR antagonists, which includes caffeine, a non-selective adenosine receptor antagonist. The initial unexpected finding came from a human PET study. In this study, the acute administration of caffeine produced an increase in the binding of [^{11}C]raclopride, a D2R antagonist, in the putamen and ventral striatum (Volkow et al., 2015). As a significant additional finding, the caffeine-dependent increase in D2R antagonist binding in the ventral striatum correlated with an increase in alertness (Volkow et al., 2015). Considering that previous studies demonstrated antagonistic allosteric interactions between A2AR and D2R agonists, caffeine should have induced the opposite effect, a decrease in [^{11}C]raclopride binding, due to an increase in the affinity of endogenous dopamine. We therefore studied the possibility of a direct allosteric modulation of caffeine on D2R agonist binding. Both the A2AR agonist CGS 21680 and caffeine significantly decreased the binding of the D2R agonist [^{3}H]quinpirole in membrane preparations from sheep striatum and mammalian cells transfected with A2AR and D2R. We could also demonstrate that both agonist-agonist and antagonist-agonist allosteric modulations were dependent on heteromerization, since they were not observed when transfecting a mutated A2AR with impaired ability to heteromerize with D2R (Bonaventura et al., 2015). Therefore, we initially assumed that the caffeine-induced increase in [^{11}C]raclopride binding demonstrated in PET experiments could be explained by a caffeine-induced decrease in the affinity of endogenous dopamine. However, the observation that both A2AR agonists and A2AR antagonists can produce the same allosteric interaction in the A2AR-D2R heteromer, a reduction in the affinity of agonists for the D2R, contradicts the hypothesis of a key role of allosteric interactions within the A2AR-D2R heteromer as a main mechanism involved in the opposite behavioral effects of A2AR agonists and antagonists (Ferré, 2008, 2016). Nevertheless, a biphasic effect was observed when analyzing the effect of increasing concentrations of caffeine or the selective A2AR antagonists SCH 58261 and KW 6002 on the ability of a single concentration of CGS 21680 to decrease [^{3}H]quinpirole binding. Low concentrations of caffeine and the A2AR antagonists significantly counteracted the effect of CGS 21680, while high concentrations further decreased [^{3}H]quinpirole binding (Bonaventura et al., 2015). Therefore, the results implied that orthosteric A2AR agonists and antagonists produce the same allosteric modulation of D2R agonist binding within the A2AR-D2R heteromer when applied individually, but, when co-applied, they cancel out each other's effect. This could be explained by the existence of two A2AR protomers in the A2AR-D2R heteromer and allosteric interactions between orthosteric agonists and antagonists, by which simultaneous occupation of the A2AR homodimer by an agonist and an antagonist would "freeze" the ability of either ligand to allosterically modulate D2R agonist binding. The existence of allosteric interactions between orthosteric A2AR agonists and antagonists could be confirmed through binding kinetics experiments with the A2AR antagonist [^{3}H]ZM 241385. Thus, when analyzing the effect of CGS 21680, caffeine and SCH 58261, only CGS 21680 modified the dissociation rate of [^{3}H]ZM 241385 (Bonaventura et al., 2015). Considering that CGS 21680 and [^{3}H]ZM 241385 bind to the same orthosteric site (Lebon et al., 2011), the effect of CGS 21680 could be explained by co-occupation of both ligands of the two orthosteric sites in an A2AR homodimer.

The same allosteric effects on D2R agonist binding demonstrated by A2AR agonists and antagonists were also shown in functional experiments. By measuring ERK1/2 phosphorylation in transfected cells, we could demonstrate that CGS 21680 counteracts quinpirole-induced MAPK activation, that this effect of CGS 21680 can be counteracted by low concentrations of caffeine or the A2AR antagonist SCH 58261 and that high concentration of the antagonists induce the opposite effect (Bonaventura et al., 2015). We should therefore expect that in the experimental animal A2AR antagonists behave as A2AR agonists under specific conditions. In fact, in patch-clamp experiments, we could demonstrate that the A2AR

antagonist SCH 58261 counteracts the D2R antagonist-like properties of CGS 21680, but it reproduces the effect of the A2AR agonist when administered alone (Bonaventura et al., 2015). These results challenge the traditional view of competitive antagonism as the mechanism of the psychostimulant effects of caffeine (and selective A2AR antagonists). According to our model, the psychostimulant effect of caffeine can be explained by the counteraction of the allosteric interaction by co-occupation of the A2AR homodimer with caffeine and endogenous adenosine in the A2AR-D2R heterotetramer.

However, these allosteric interactions between A2AR agonists and antagonists and D2R agonists do not yet explain the increase in striatal [^{11}C]raclopride binding in human PET experiments induced by caffeine. Again, counteraction by caffeine of the inhibitory effect of endogenous adenosine on the binding of endogenous dopamine should lead to a decrease of [^{11}C]raclopride binding. It was then demonstrated that CGS 21680 and caffeine also inhibit the binding of [^{3}H]raclopride binding in membrane preparations from striatum or transfected cells (Bonaventura et al., 2015). That these results imply allosteric interactions within the A2AR-D2R heteromer was demonstrated by their disappearance upon transfection of a mutated A2AR with impaired ability to heteromerize with D2R and by using a synthetic peptide that disrupts A2AR-D2R heteromerization (Bonaventura et al., 2015). Therefore, within the A2AR-D2R heteromer, any orthosteric A2AR ligand, agonist or antagonist, exerts a negative allosteric modulation on the affinity of any orthosteric D2R ligand, agonist or antagonist. Finally, the same as with [^{3}H]quinpirole binding, we could also demonstrate a biphasic effect of caffeine on CGS 21680-mediated decrease of [^{3}H]raclopride binding (Bonaventura et al., 2015). These results would at last provide a plausible mechanism for the effect of caffeine on [^{11}C]raclopride binding in humans, by its ability to antagonize the effect of endogenous adenosine on the binding of the exogenous D2R antagonist. An alternative explanation could still be that caffeine blocks an adenosine-mediated internalization of A2AR-D2R heteromers (Hillion et al., 2002; Huang et al., 2013), thus leading to higher D2R availability along with higher [^{11}C]raclopride binding. The positive association between caffeine-induced increases in D2R availability and caffeine-induced increases in alertness (Volkow et al., 2015) would support this interpretation, since increased D2R signaling contributes to alertness (Isaac and Berridge, 2003). Irrespective of the mechanism involved, the effect of caffeine on [^{11}C]raclopride binding in human PET experiments implies its dependence on the A2AR-D2R heteromer and, therefore, that a significant proportion of striatal [^{11}C]raclopride binding visualized with PET labels A2AR-D2R heteromers. Furthermore, these results call for the need to control caffeine intake when evaluating the effect of D2R ligands in humans, not only when using them as probes for imaging studies, but also when using them as therapeutic agents in neuropsychiatric disorders.

Very different qualitative differences between several A2AR antagonists emerged when evaluating their potencies and efficacies on different *in vitro* and *in vivo* techniques. Particularly significant was the demonstration of different binding properties of the A2AR antagonist SCH 442416 depending on the presence and absence of D2R, when forming or not forming heteromers with D2R (Orrú et al., 2011a). In cells expressing A2AR and D2R, competitive-inhibition curves of the A2AR antagonist [^{3}H]ZM 241388 binding vs. increasing concentrations of SCH 442416 were clearly biphasic. On the other hand, in cells expressing only A2AR, or A1R and A2AR, the curves were monophasic. When analyzing the radioligand binding experiments with the two-state dimer model (Casadó et al., 2007; Ferré et al., 2014), the data indicated a negative cooperativity of SCH 442416 binding to the A2AR (Orrú et al., 2011b; Ferré et al., 2014), an additional demonstration of A2AR homomerization. This, in fact, was the first indication that the A2AR-D2R comprises at least two A2AR protomers, in agreement with a tetrameric structure of the A2AR-D2R heteromer. We have now been able to reproduce these findings in striatal tissue, comparing the results of competitive-inhibition experiments of [^{3}H]ZM 241388 binding vs. increasing concentrations of SCH 442416 in striatal membrane preparations of wild-type (WT) and striatal D2R knockout mice with a CRE-mediated deletion of D2R expression in A2AR-expressing neurons. The same as with mammalian transfected cells, the curves were biphasic or monophasic in the presence or absence of the D2R, respectively (**Figure 4**). The demonstration of the same binding properties of SCH 442416 in striatal tissue than in A2AR-D2R transfected cells implies that the A2AR-D2R heterotetramer represents the predominant population of A2AR and D2R in the striatum. Nevertheless, as mentioned below, striatal A2AR are also localized presynaptically, in glutamatergic terminals, where most probably do not form heteromers with D2R. These receptors, although playing a significant role in the modulation of striatal glutamate release, represent a very small fraction of the total of striatal A2AR, as compared to the postsynaptic A2AR.

REVISITING THE BEHAVIORAL EFFECTS OF ADENOSINE RECEPTOR LIGANDS IN THE FRAME OF ONE MAIN POPULATION OF STRIATAL A2AR AND D2R FORMING HETEROMERS

Considering that increases or decreases in the activity of the GABAergic striatopallidal neuron lead to the respective opposite effect on psychomotor activity and using a model that considers the A2AR-D2R heteromer as a key modulator of striatopallidal neuronal function, we could recently explain most psychomotor effects of caffeine (Ferré, 2016). This included the enigmatic caffeine-induced rotational behavior in rats with unilateral striatal dopamine denervation (Fuxe and Ungerstedt, 1974; Herrera-Marschitz et al., 1988; Casas et al., 1989; Garrett and Holtzman, 1995) and the ability of caffeine to significantly counteract the adipsic-aphagic syndrome in rodents with 6-hydroxy-dopamine-induced or genetic-induced dopamine deficiency (Casas et al., 2000; Kim and Palmiter, 2003, 2008). According to the model, under resting conditions there is a tonic activation of A2AR and D2R by the endogenous neurotransmitters which results in a predominant A2AR vs. D2R signaling and a predominant allosteric interaction (**Figure 5A**),

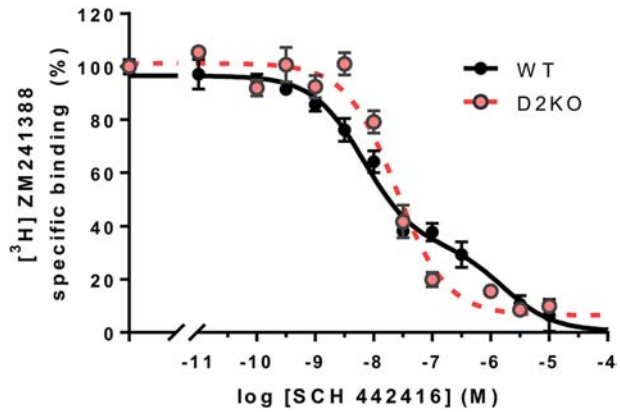

FIGURE 4 | Specific A2AR-D2R heteromer-dependent properties of SCH 442416 in mouse striatum. Transgenic conditional knockout striatopallidal neuron-Drd2-KO mice were generated by crossing mice expressing Cre driven by regulatory elements of the A2AR gene (Adora2a) [B6.FVB(Cg)-Tg(Adora2a-Cre)KG139Gsat/Mmucd; GENSAT; 036158-UCD] with mice carrying conditional D2R gene (Drd2) null alleles B6.129S4(FVB)-Drd2tm1.1Mrub/J,JAX020631 (Bello et al., 2017). Membrane preparations from the striatum of striatopallidal-Drd2-KO (red) and their CRE negative littermates (WT, black) were incubated with [^{3}H]ZM 241385 (2 nM) and increasing concentrations of SCH 442416 as described elsewhere (Bonaventura et al., 2015). Data points were fit to the two-state dimer receptor model (Casadó et al., 2007; Ferré et al., 2014), showing a biphasic curve due to negative cooperativity of SCH 442416 in WT mice (DCB = −1.8), but a monophasic curve in the conditional D2R null mice, thus reproducing the same behavior of SCH 442416 previously demonstrated in mammalian cells co-expressing A2AR and D2R and only A2AR, respectively (Orrú et al., 2011a).

which results in low psychomotor activity. Reward-related stimuli and, particularly a "better than expected" rewarding stimulus (positive reward prediction error), leads to striatal dopamine release with a predominant D2R vs. A2AR signaling, potentiated by the canonical interaction (**Figure 5B**), leading to psychomotor activation. Aversive-related stimuli or a "worse than expected" rewarding stimuli (negative reward prediction error) leads to inhibition of dopamine release, to the weakest D2R and strongest A2AR signaling, which is potentiated by the canonical interaction (**Figure 5C**), leading to psychomotor arrest.

A pathogenic hallmark of akinesia in Parkinson's disease is a pronounced hyperactivity of the striatopallidal neuron associated with the dopamine deficiency and pronounced decrease in the tonic D2R signaling. The discoveries on A2AR localization and function in striatopallidal neurons gave the rational for the recently implemented A2AR antagonists in this disease (Müller and Ferré, 2007; Morelli et al., 2009; Armentero et al., 2011). It was initially suggested that the value of A2AR antagonists as antiparkinsonian agents would depend mostly on the allosteric interaction, on the ability of A2AR antagonists to potentiate D2R signaling by concomitant administration of L-dopa or a selective D2R agonist (Ferré et al., 1991b, 1992). This was followed by behavioral studies with genetic inactivation of A2AR and D2R, which stressed the value of the canonical interaction, which was assumed to be independent of intermolecular interactions between A2AR and D2R (Chen et al., 2001). As mentioned above, the existence of the two apparently incompatible simultaneous allosteric and canonical interactions led to the hypothesis of the existence of two populations of A2AR in the striatopallidal neuron, one population forming heteromers with D2R and sustaining the allosteric interaction and another population not forming heteromers with D2R and sustaining the canonical interaction (Ferré et al., 2011; Orrú et al., 2011b). The unique pharmacological properties of SCH 442416, with its specific reduced affinity for the A2AR-D2R heteromer, due to negative cooperativity, were then exploited to attempt a pharmacological dissection of the two populations of postsynaptic A2AR. In fact, we previously used this strategy to dissect postsynaptic from presynaptic A2AR, which forms heteromers with A1R in the striatal glutamatergic terminals, where they play an important role in the modulation of glutamate release (Ciruela et al., 2006; Quiroz et al., 2009). A correlation had been shown with the higher potency of SCH 442416 to block presynaptic A1R-A2AR heteromers vs. postsynaptic A2AR-D2R heteromers and its higher potency to inhibit corticostriatal glutamate release than to produce locomotor activation (Orrú et al., 2011a). The preferential presynaptic profile of SCH 442416 was confirmed by other studies including other research groups (Hobson et al., 2013; O'Neill et al., 2014) and was suggested to provide a therapeutic approach for conditions with increased corticostriatal transmission, such as cannabinoid use disorder (Justinová et al., 2014). An apparently stronger potency of SCH 442416 to counteract locomotor depression induced by the D2R antagonist raclopride, as compared to that produced by the A2AR agonist CGS 2160, was then interpreted as the ability of SCH 442416 to also dissect the two putative postsynaptic populations of A2AR. The more sensitive population to SCH 442416 would be A2AR that do not form heteromers with D2R and that would sustain the canonical interaction (Orrú et al., 2011b). However, as mentioned before, we now know that the canonical interaction requires receptor heteromerization (Navarro et al., 2018). Therefore, we recently performed new studies on the behavioral effects of SCH 442416 upon genetic blockade of A2AR or D2R and upon administration of the A2AR agonist CGS 21680 and the D2R antagonist haloperidol, to reevaluate if they could all be explained within the framework of a predominant population of striatal postsynaptic A2AR-D2R heteromers (Taura et al., 2017).

To control strain-dependent behavioral differences and differences in drug responses, using CRISPR-Cas9 technology, we generated a D2R deficient mouse with the same genetic background as the CD-1 A2AR$^{-/-}$ mouse (Ledent et al., 1997). CD-1 D2R$^{-/-}$ mice showed a significant but relatively small reduction in spontaneous locomotor activity (Taura et al., 2017), as previously reported in D2R$^{-/-}$ C57BL/6 mice (Baik et al., 1995). This is in contrast with the pronounced akinesia and catalepsy that characterize pharmacological D2R blockade (Ferré et al., 1990; Kanda et al., 1994; Shiozaki et al., 1999). Therefore, genetic D2R blockade is associated with neuroadaptations that counteract the loss of a D2R-mediated tonic stimulatory effect of endogenous dopamine on psychomotor activity. Indeed, a recent study in inducible D2R knockout adult mice that obviated developmental compensations reported that the loss of D2R was

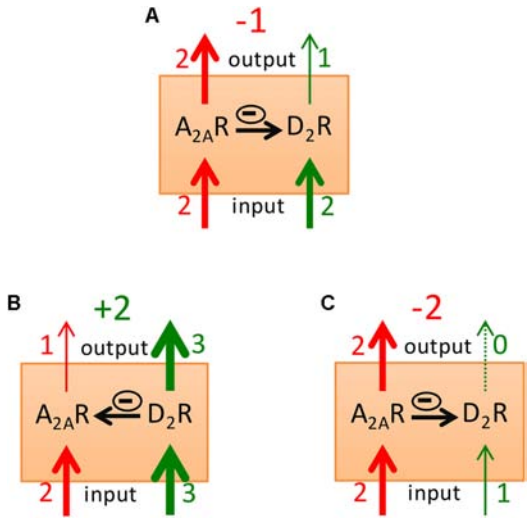

FIGURE 5 | Model of the striatal A2AR-D2R receptor heteromer as a main modulator of the excitability of the striatopallidal neuron. The relative thickness (and close number) of the red and green input arrows represents the degree of activation of the A2AR and the D2R that depends on the concentration of the corresponding neurotransmitter or exogenous ligands. The thickness (and close number) of the red and green output arrows represents the intensity of A2AR and D2R signaling, respectively, which depends on the input signal for each receptor and on the predominance of either the antagonistic or the canonical interaction (represented by horizontal arrows with a minus enclosed sign). Predominant psychomotor activation or depression will result when subtraction of the A2AR signaling from the D2R receptor signaling gives a positive or negative value (also in green or red, respectively). In **(A)**, resting condition. In **(B,C)**, processing of a positive or a negative reward prediction error, respectively.

associated with severe hypolocomotion and catalepsy (Bello et al., 2017). Likewise, the spontaneous locomotor activity of A2AR$^{-/-}$ mice was also significantly reduced, as previously reported in the A2AR C57BL/6 mouse (Yang et al., 2009). Since pharmacological blockade leads to significant locomotor activation (see below and Karcz-Kubicha et al., 2003; Orrú et al., 2011a), the reduced activity of A2AR$^{-/-}$ mice indicates the development of neuroadaptations that counteract the loss of an A2AR-mediated tonic inhibitory effect of endogenous adenosine on psychomotor activity. We also assessed sensorimotor processing of A2AR$^{-/-}$ and D2R$^{-/-}$ CD-1 mice by monitoring pre-pulse inhibitory responses (PPI) (Taura et al., 2017). As compared with WT mice, D2R$^{-/-}$ mice did not show significant differences, while A2AR$^{-/-}$ mice showed a significantly reduced PPI as previously reported (Wang et al., 2003; Moscoso-Castro et al., 2016), demonstrating a significant dependence on A2AR, but not D2R, signaling for a normal PPI. We also evaluated drug-induced catalepsy in A2AR$^{-/-}$ and D2R$^{-/-}$ mice. Our results showed that haloperidol-induced catalepsy was abolished and partially but significantly reduced in D2R$^{-/-}$ and A2AR$^{-/-}$ mice, respectively, as compared with WT mice (Taura et al., 2017), which is in agreement with previous work (Usiello et al., 2000; Chen et al., 2001; El Yacoubi et al., 2001). The results support the dependence on A2AR signaling in the catalepsy induced by pharmacological blockade of D2R, which would agree with the existence of the tonic inhibition of A2AR signaling by endogenous dopamine driven by the canonical interaction in the A2AR-D2R heteromer. Neuroadaptations occurring in the A2AR$^{-/-}$ mouse should explain the partial effect of genetic blockade of A2AR on D2R antagonist-induced catalepsy, which contrasts with the very effective blockade with A2AR antagonists (see below and Kanda et al., 1994; Shiozaki et al., 1999; Morelli and Wardas, 2001). We also assessed catalepsy induced by the A2AR agonist CGS 21680 (Ferré et al., 1991a; Kanda et al., 1994; Hauber and Münkle, 1997) in A2AR$^{-/-}$ and D2R$^{-/-}$ mice. As expected, CGS 21680 failed to induce catalepsy in A2AR$^{-/-}$ mice, but its effect was partially but significantly reduced in D2R$^{-/-}$ mice (Taura et al., 2017). Again, these results might reflect a functional antagonism related to neuroadaptations associated with genetic D2R blockade, which would tend to counteract the loss of the D2R-mediated tonic stimulatory effect of endogenous dopamine on psychomotor activity.

We then reevaluated the effect of SCH 442416 on locomotion, PPI and drug-induced catalepsy in WT, but also in A2AR$^{-/-}$ and D2R$^{-/-}$ mice. In WT CD-1 mice, SCH 442416 produced a significant and effective locomotor activation at 1 mg/kg (i.p.) (Taura et al., 2017), a dose three times lower than the minimal effective dose in Sprague-Dawley rats (Orrú et al., 2011a). As expected, SCH 44241 was unable to alter the locomotor activity in A2AR$^{-/-}$ mice and it only moderately, but significantly, increased the activity in D2R$^{-/-}$ mice (Taura et al., 2017). The decrease in the effect of the A2AR antagonist in D2R$^{-/-}$ mice would agree with a dependence on D2R signaling in the locomotor activation induced by pharmacological blockade of A2AR, due to the tonic inhibition of D2R signaling by endogenous adenosine driven by the allosteric interaction in the A2AR-D2R heteromer. In agreement with the dependence on A2AR for PPI, SCH 442416 (at the minimal dose of 3 mg/kg, i.p.) induced a blockade of PPI in WT mice (Taura et al., 2017). This is also in agreement with a previous study in rats with intracranial infusion of another A2AR antagonist (MSX-3) in the NAc (Nagel et al., 2003). SCH 442416 was obviously ineffective on the already disrupted PPI in A2AR$^{-/-}$ mice, but its disruptive effect was reduced in D2R$^{-/-}$ mice (Taura et al., 2017). This could be related to the competing effect of endogenous adenosine by the released tonic inhibition of A2AR signaling by endogenous dopamine driven by the canonical interaction in the A2AR-D2R heteromer. Finally, SCH 442416 significantly reduced haloperidol-induced catalepsy, as previously reported for other A2AR antagonists (Kanda et al., 1994; Shiozaki et al., 1999; Morelli and Wardas, 2001), but with a higher minimal dose than the one needed to produce locomotor activation (3 vs. 1 mg/kg, i.p., respectively; Taura et al., 2017). To confirm the preferential pre- vs. postsynaptic profile of SCH 442416 in mice, we also performed dose-response experiments in C57BL/6 mice on locomotor activity and counteraction of corticostriatal glutamate release using a recently introduced optogenetic-microdialysis technique (Quiroz et al., 2016; Bonaventura et al., 2017). Different to previous experiments in rats, SCH 442416 showed the same potency and efficiency as the selective A2AR antagonist KW 6002 at

eliciting locomotor activation. Both drugs produced significant activation at 1 mg/kg (i.p.) but were inefficient at 0.1 mg/kg (**Figure 6A**). At this moment, we do not have an explanation for the lower potency and efficacy of SCH 442416 in rats as compared to mice. On the other hand, SCH 442416 was able to block optogenetically induced striatal glutamate release at 0.1 mg/kg, while KW 6002 was ineffective at 1 mg/kg (**Figure 6B**). This confirmed the experimental findings in rats, demonstrating a predominant striatal presynaptic and postsynaptic A2AR blocking properties of SCH 442416 and KW 6002, respectively (Orrú et al., 2011a).

Altogether, the results with genetic and pharmacological blockade of A2AR and D2R agree with a main role of A2AR-D2R heteromers in the striatopallidal neuron in conveying locomotor activation and PPI disruption induced by A2AR antagonists and D2R agonists and catalepsy mediated by A2AR agonists and D2R antagonists. More specifically, they also agree with A2AR-D2R heteromers in striatopallidal neurons mediating all postsynaptic pharmacological effects of SCH 442416, locomotor activation, blockade of PPI and counteraction of D2R antagonist-induced catalepsy. As shown in the scheme of **Figure 3A**, the A2AR-D2R heteromer explains the qualitatively different behavioral outputs depending on direct A2AR-Golf-AC-PKA-mediated increase in excitability or indirect D2R-Gi-PLC-PP2B-mediated disinhibition of the excitability of the striatopallidal neuron, leading to catalepsy and PPI (more related to the direct activation of the PKA-DARPP-32-CREB signaling; Bateup et al., 2010; Berger et al., 2011) or just psychomotor depression, respectively. In fact, it is well known that catalepsy, with its rigidity component, is not qualitatively equivalent to a high degree of locomotor depression. Finally, and as mentioned before, depending on the intracellular concentrations of Ca^{2+}, A2AR and D2R activation and co-activation lead to differential MAPK and Elk-1 activation, with implications for gene expression and synaptic plasticity (**Figure 3A**).

A2AR-D2R HETEROMER-MEDIATED CONTROL OF THE VENTRAL VS. DORSAL STRIATOPALLIDAL FUNCTION AND IMPLICATIONS FOR NEUROPSYCHIATRIC DISORDERS. 'APATHY' VS. 'AKINESIA'

Dysfunction of the central dopamine system is involved in a variety of disorders, including Parkinson's disease, schizophrenia, and substance use disorders (SUD). The functional separation of striatal compartments in ventral, rostral-dorsal and caudal-dorsal striata allows a more syndromic sub-classification of those disorders with potentially significant new therapeutic approaches. Parkinson's disease and non-human primate models of Parkinson's disease provide the clearest illustration. The cardinal motor symptoms of Parkinson's disease, bradykinesia, rigidity and tremor (Jankovic, 2008), have been classically attributed to dysfunction of the skeletomotor system, the brain

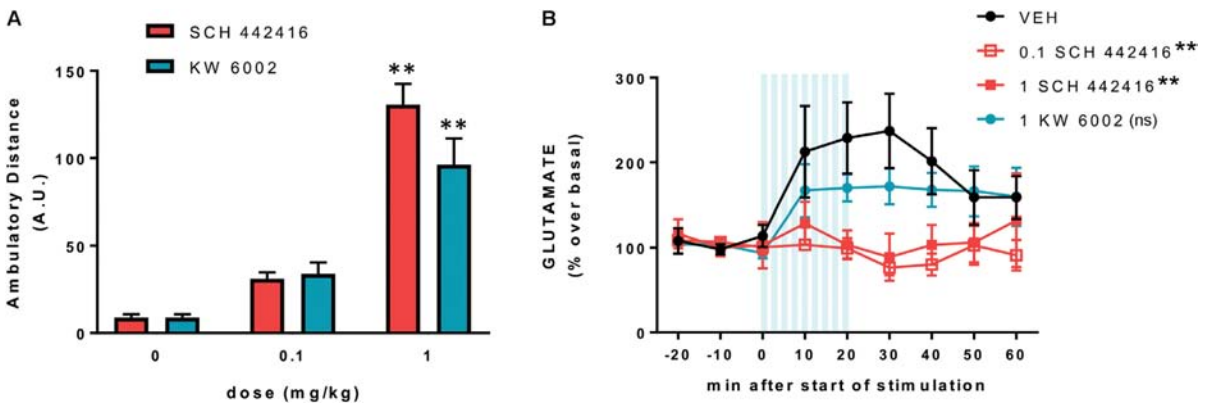

FIGURE 6 | Preferential presynaptic profile of SCH 442416 in C57BL/6 mice. **(A)** SCH 442416 shows similar potency and efficacy to KW 6002 at producing locomotor activation. Locomotor activity was measured in an open field arena as described elsewhere (Bonaventura et al., 2015); animals were injected intraperitoneally (i.p.) with vehicle (saline with 10% DMSO and 10% Tween-80) and the indicated concentrations of SCH 442416 or KW 6002 and the locomotor activity was measured for 2 h in activity chambers with 42.0 cm × 42.0 cm open fields (Coulbourn Instruments); values are mean ± SEM of the traveled distance (arbitrary units, A.U.); two-way ANOVA with Newman–Keuls *post hoc* test did not demonstrate significant differences between the two A2AR antagonists and, for both drugs, it only showed significant differences with the dose of 1 mg/kg as compared to the corresponding vehicle-treated groups (**$p < 0.01$ compared to vehicle; $n = 8$–11). **(B)** Optogenetic-microdialysis experiments were performed as described elsewhere (Bonaventura et al., 2017); briefly, C57BL/6 mice received a unilateral injection of an AAV encoding ChR2 (ChR2/H134R) fused to EYFP under control of the CaMKIIa neuronal promoter [AAV-CaMKIIa-hChR2(H134R)-EYFP] in the motor cortex. One month later, an optogenetic-microdialysis probe (Quiroz et al., 2016; Bonaventura et al., 2017) was implanted in the dorsal striatum, and glutamate in the dialysate was measured at 10-min intervals before, during, and after optogenetic stimulation of the corticostriatal terminals. Vehicle (black plot, see above) or the indicated doses of SCH 442416 (red plot) or KW 6002 (blue plot) were administered (i.p.) 10 min before the start of the stimulation. Values (in % over basal) represent mean ± SEM, normalized to the mean of the concentration of GLU present in the three samples preceding stimulation; one-way ANOVA with Newman–Keuls *post hoc* test showed a significant decrease of the transformed values (area under the curve, data from min 0 to min 60) from both groups treated with SCH 442416 (1 and 0.1 mg/kg), but not from the group treated with KW 6002, compared to the vehicle group (**$p < 0.01$ compared to vehicle; ns, non-significant; $n = 7$–8).

circuits involved in the execution and coordination of body movements. Contemporary theories embracing parallel cortical-striatal-thalamic-cortical circuits in the pathogenesis of this disorder emphasize the particular involvement of the "motor circuit," which includes motor cortical areas (DeLong and Wichmann, 2015). In fact, in Parkinson's disease, dopamine cell degeneration tends to occur initially and predominantly in the lateral part of the SNpc, which projects mainly to the caudal-dorsal striatum. Thus, there is a predominant deficit of the more "automatic" vs. "volitional" action skills and most sequential psychomotor responses need to be performed with full attention (Kim and Hikosaka, 2015). Nevertheless, with more advanced stages of Parkinson's disease the function of the more rostral striatum becomes also compromised, with deficits in "volitional" actions skills (Kim and Hikosaka, 2015). With further (or preferential) ventral degeneration of the dopamine mesencephalic nuclei (VTA) we move to the pathology of the ventral striatum, to apathy (Tremblay et al., 2015), as it has also been demonstrated experimentally in the non-human primate (Brown et al., 2012; Tian et al., 2015).

Initial studies on the psychomotor-activating effects of caffeine or selective A2AR antagonists dealt with general locomotor activity and were translationally applied to the treatment of akinesia in Parkinson's disease (see above and Müller and Ferré, 2007; Morelli et al., 2009; Armentero et al., 2011). Those initial studies implicitly considered A2AR-D2R heteromers in the dorsal striatum, but a large number of studies indicated that not only dorsal but also ventral striatopallidal neurons express A2R and A2AR-D2R heteromers (Ferré et al., 1994; Ferré, 1997; Hauber and Münkle, 1997; Pinna et al., 1997; Svenningsson et al., 1997; Ishiwari et al., 2007). More recent studies have also analyzed the effect of caffeine and A2AR antagonists on more specific reward-oriented behaviors, showing that they can increase the responsiveness to food-related stimuli, sucrose solutions, stimuli that elicit maternal behavior and self-administration (Pereira et al., 2011; Randall et al., 2011; Sheppard et al., 2012; Nunes et al., 2013; Lazenka et al., 2015). The work by Salamone's group has specifically addressed the role of adenosine and A2AR in effort-related choice behavior. Direct administration of A2AR agonists in the NAc altered effort-related choice behavior in a manner closely resembling the effects of interference with ventral striatal dopamine neurotransmission, decreasing the degree of responsiveness ("effort") to reward-associated stimuli. Furthermore, A2AR antagonists reversed the effort discounting effects of D2R antagonists (Salamone et al., 2012; Nunes et al., 2013).

Clinically, apathy has been defined as "a syndrome consisting of loss of motivation not attributable to disturbances in emotion, intellect or consciousness" (Marin, 1991). However, it is becoming obvious that apathy is a multifaceted concept that includes dissociable constructs that should correspond to dissociable neurobiological correlates (Sinha et al., 2013). We hypothesize that some if not all those dissociable correlates correspond to corticostriatal circuits involving the different functional striatal compartments and their "Go" and "NoGo" pathways. In fact, attuned with the role of dopamine in reward-associated behavior in all striatal compartments, recent studies even allow conceptualizing Parkinson's disease bradykinesia in a motivational framework (Mazzoni et al., 2007; Chong et al., 2015). Nevertheless, as defined clinically, apathy is a common non-motor symptom of Parkinson's disease (den Brok et al., 2015) that correlates negatively with dopamine innervation in the ventral striatum (Remy et al., 2005; Chaudhuri et al., 2006; Brown et al., 2012). In fact, a deficit in the dopamine modulation of the ventral striatum should translate, first, in a deficit in responsiveness, with a global inability to respond to reward- and punishment-associated stimuli (attuned with the "whether to respond" vs. "how to respond" functions of ventral vs. dorsal striatum). Second, it should lead to dysfunction of reward valuation, in alterations (increase) in DD, ED and LPD (attuned with the ventral striatum as forming part of corticostriatal circuits involved in reward valuation tasks). Indeed, non-medicated patients with Parkinson's disease have shown increases in DD and ED (Al-Khaled et al., 2015; Chong et al., 2015).

Interestingly, apathy is also a major negative symptom of schizophrenia, classically considered as a disorder associated with central hyperdopaminergic tone. Several studies have found evidence for selective dysfunction of the ventral striatum in schizophrenia, specifically hypoactivation with reward-associated stimuli (Simon et al., 2010, 2015; Strauss et al., 2015; Kirschner et al., 2016). Ventral striatal activation during reward anticipation was in fact found to be selectively and inversely correlated with apathy but not with other negative symptoms (Simon et al., 2010; Kirschner et al., 2016). Two additional findings give a clue for the mechanisms of apathy in schizophrenia, which seem to be dopamine-independent or at least not related to a decrease in the dopamine tone. First, there is a reduced functional connectivity between the orbito-frontal cortex (OFC) and the ventral striatum (Simon et al., 2015); second, there is consistent evidence that schizophrenic patients suffer from selective deficits in learning from positive outcomes, with intact learning from negative outcomes (Strauss et al., 2015). Therefore, the apathetic schizophrenic patient seems to have a selective decreased activation of the "Go" pathway, a reduction in the ratio of activation of "Go" vs. "NoGo" pathways secondary to impaired cortical-ventral striatal connectivity (Strauss et al., 2015). A similar situation would also be present in the patient with SUD, a decreased "Go"/"NoGo" pathway activation, also with reduced ventral striatal activation to reward stimuli (which can basically only be activated by the addictive drugs) (Volkow et al., 2011). Apathy is a well-known symptom in SUD, although it has been scarcely addressed experimentally (Verdejo-García et al., 2006; Verdejo-García and Pérez-García, 2008; Gjini et al., 2014). The SUD patient is motivated to procure the drug but tends to be withdrawn and apathetic when exposed to non-drug-related activities (Verdejo-García et al., 2006). In this case, however, the pathogenesis seems to follow from an initial reduction in D2R density (maybe with a concomitant relative increase of A2AR which would not be opposed by D2R forming heteromers), leading to an increased activity of the ventral striatopallidal neuronal function, of the

"NoGo" pathway. The tonic decrease in feedback activation of the ventromedial prefrontal cortex, orbitofrontal cortex and anterior cingulate cortex leads to additional dysfunction of the decision-making cortical-ventral striatal circuits (Volkow et al., 2011; Belcher et al., 2014). These changes lead to a similar situation than the non-motor symptoms in patients with Parkinson's disease, to apathy and choice impulsivity, as demonstrated by several studies indicating increase DD in patients with SUD (Belcher et al., 2014; Hamilton et al., 2015). In summary, for all types of apathy, the relative increase in the ventral striopallidal vs. striatonigral neuronal function should benefit from the treatment with A2AR antagonists, targeting A2AR-D2R heterotetramer-AC5 complexes.

CONCLUSION

A significant amount of experimental and clinical evidence demonstrates that A2AR and D2R localized in the ventral and dorsal striatopallidal neurons cannot be considered anymore as single functional units, but as forming part of complexes of the A2AR-D2R heterotetramer-AC5 complexes, which exert a fine-tuned integration of adenosine and dopamine neurotransmission. The current accumulated knowledge of the biochemical properties of the A2AR-D2R heteromer offer new therapeutic possibilities for Parkinson's disease, schizophrenia, SUD and other neuropsychiatric disorders with dysfunction of dorsal or ventral striatopallidal neurons. More generally, this knowledge implies we should modify classical views of GPCR physiology and pharmacology and include GPCR heteromers as main targets for drug development. The understanding of the biochemical properties of GPCR heteromers specifically localized in neuronal elements that form part of neuronal circuits involved in the pathophysiology of specific neuropsychiatric disorders should provide new selective pharmacological approaches with less unwanted side effects.

ETHICS STATEMENT

All animals used in the study were maintained in accordance with the guidelines of the National Institutes of Health (NIH) Animal Care, and the animal research conducted to perform this study was approved by the NIDA IRP Animal Care and Use Committee (protocols #12-BNRB-73, #15-BNRB-73, and #12-MTMD-2).

AUTHOR CONTRIBUTIONS

JB, WZ, CH-S, and KT performed the experiments and analyzed the data. SF, JB, KT, AK, VC, DL, and DZ designed the experiments. SF, JB, JT, CQ, N-SC, EM, VC-A, AK, DT, GN, AC, LP, CL, CWD, NV, VC, FC, DL, and DZ wrote the manuscript.

FUNDING

This work was supported by the intramural funds of the National Institute on Drug Abuse, "Ministerio de Economía y Competitividad", MINECO/FEDER (SAF2017-87349-R, SAF2014-54840-R, and PIE14/00034), Generalitat de Catalunya (2017 SRG 1604 and 2014-SGR-1236), and Fundació la Marató de TV3 (20140610 and 20152031).

ACKNOWLEDGMENTS

The authors apologize if they unwittingly omitted other relevant studies about the interactions between A2AR and D2R in the functional control of striatopallidal neurons.

REFERENCES

Al-Khaled, M., Heldmann, M., Bolstorff, I., Hagenah, J., and Münte, T. F. (2015). Intertemporal choice in Parkinson's disease and restless legs syndrome. *Parkinsonism Relat. Disord.* 21, 1330–1335. doi: 10.1016/j.parkreldis.2015.09.026

Armentero, M. T., Pinna, A., Ferré, S., Lanciego, J. L., Müller, C. E., and Franco, R. (2011). Past, present and future of A(2A) adenosine receptor antagonists in the therapy of Parkinson's disease. *Pharmacol. Ther.* 132, 280–299. doi: 10.1016/j.pharmthera.2011.07.004

Azdad, K., Gall, D., Woods, A. S., Ledent, C., Ferré, S., and Schiffmann, S. N. (2009). Dopamine D2 and denosine A2A receptors regulate NMDA-mediated excitation in accumbens neurons through A2A-D2 receptor heteromerization. *Neuropsychopharmacology* 34, 972–986. doi: 10.1038/npp.2008.144

Baik, J. H., Picetti, R., Saiardi, A., Thiriet, G., Dierich, A., Depaulis, A., et al. (1995). Parkinsonian-like locomotor impairment in mice lacking dopamine D2 receptors. *Nature* 377, 424–428. doi: 10.1038/377424a0

Balleine, B. W., and O'Doherty, J. P. (2010). Human and rodent homologies in action control: corticostriatal determinants of goal-directed and habitual action. *Neuropsychopharmacology* 35, 48–69. doi: 10.1038/npp.2009.131

Bateup, H. S., Santini, E., Shen, W., Birnbaum, S., Valjent, E., Surmeier, D. J., et al. (2010). Distinct subclasses of medium spiny neurons differentially regulate striatal motor behaviors. *Proc. Natl. Acad. Sci. U.S.A.* 107, 14845–14850. doi: 10.1073/pnas.1009874107

Belcher, A. M., Volkow, N. D., Moeller, F. G., and Ferré, S. (2014). Personality traits and vulnerability or resilience to substance use disorders. *Trends Cogn. Sci.* 18, 211–217. doi: 10.1016/j.tics.2014.01.010

Bello, E. P., Casas-Cordero, R., Galiñanes, G. L., Casey, E., Belluscio, M. A., Rodríguez, V., et al. (2017). Inducible ablation of dopamine D2 receptors in adult mice impairs locomotion, motor skill learning and leads to severe parkinsonism. *Mol. Psychiatry* 22, 595–604. doi: 10.1038/mp.2016.105

Berger, A. K., Green, T., Siegel, S. J., Nestler, E. J., and Hammer, R. P. Jr. (2011). cAMP response element binding protein phosphorylation in nucleus accumbens underlies sustained recovery of sensorimotor gating following repeated D_2-like receptor agonist treatment in rats. *Biol. Psychiatry* 69, 288–294. doi: 10.1016/j.biopsych.2010.08.032

Bertran-Gonzalez, J., Bosch, C., Maroteaux, M., Matamales, M., Hervé, D., Valjent, E., et al. (2008). Opposing patterns of signaling activation in dopamine D1 and D2 receptor-expressing striatal neurons in response to cocaine and haloperidol. *J. Neurosci.* 28, 5671–5685. doi: 10.1523/jneurosci.1039-08.2008

Besnard, A., Galan-Rodriguez, B., Vanhoutte, P., and Caboche, J. (2011). Elk-1 a transcription factor with multiple facets in the brain. *Front. Neurosci.* 5:35. doi: 10.3389/fnins.2011.00035

Boegman, R. J., and Vincent, S. R. (1996). Involvement of adenosine and glutamate receptors in the induction of c-fos in the striatum by haloperidol. *Synapse*

22, 70–77. doi: 10.1002/(SICI)1098-2396(199601)22:1<70::AID-SYN8>3.0.CO;2-F

Bonaventura, J., Navarro, G., Casadó-Anguera, V., Azdad, K., Rea, W., Moreno, E., et al. (2015). Allosteric interactions between agonists and antagonists within the adenosine A2A receptor-dopamine D2 receptor heterotetramer. *Proc. Natl. Acad. Sci. U.S.A.* 112, E3609–E3618. doi: 10.1073/pnas.1507704112

Bonaventura, J., Quiroz, C., Cai, N. S., Rubinstein, M., Tanda, G., and Ferré, S. (2017). Key role of the dopamine D(4) receptor in the modulation of corticostriatal glutamatergic neurotransmission. *Sci. Adv.* 3:e1601631. doi: 10.1126/sciadv.1601631

Bromberg-Martin, E. S., Matsumoto, M., and Hikosaka, O. (2010). Dopamine in motivational control: rewarding, aversive, and alerting. *Neuron* 68, 815–834. doi: 10.1016/j.neuron.2010.11.022

Brown, C. A., Campbell, M. C., Karimi, M., Tabbal, S. D., Loftin, S. K., Tian, L. L., et al. (2012). Dopamine pathway loss in nucleus accumbens and ventral tegmental area predicts apathetic behavior in MPTP-lesioned monkeys. *Exp. Neurol.* 236, 190–197. doi: 10.1016/j.expneurol.2012.04.025

Casadó, V., Cortés, A., Ciruela, F., Mallol, J., Ferré, S., Lluis, C., et al. (2007). Old and new ways to calculate the affinity of agonists and antagonists interacting with G-protein-coupled monomeric and dimeric receptors: the receptor-dimer cooperativity index. *Pharmacol. Ther.* 116, 343–354. doi: 10.1016/j.pharmthera.2007.05.010

Casas, M., Ferré, S., Cobos, A., Grau, J. M., and Jané, F. (1989). Relationship between rotational behaviour induced by apomorphine and caffeine in rats with unilateral lesion of the nigrostriatal pathway. *Neuropharmacology* 28, 407–409. doi: 10.1016/0028-3908(89)90037-3

Casas, M., Prat, G., Robledo, P., Barbanoj, M., Kulisevsky, J., and Jané, F. (2000). Methylxanthines reverse the adipsic and aphagic syndrome induced by bilateral 6-hydroxydopamine lesions of the nigrostriatal pathway in rats. *Pharmacol. Biochem. Behav.* 66, 257–263. doi: 10.1016/S0091-3057(00)00189-1

Chang, C. Y., Esber, G. R., Marrero-Garcia, Y., Yau, H. J., Bonci, A., and Schoenbaum, G. (2016). Brief optogenetic inhibition of dopamine neurons mimics endogenous negative reward prediction errors. *Nat. Neurosci.* 19, 111–116. doi: 10.1038/nn.4191

Chaudhuri, K. R., Martinez-Martin, P., Schapira, A. H., Stocchi, F., Sethi, K., Odin, P., et al. (2006). International multicenter pilot study of the first comprehensive self-completed nonmotor symptoms questionnaire for Parkinson's disease: the NMSQuest study. *Mov. Disord.* 21, 916–923. doi: 10.1002/mds.20844

Chen, J. F., Moratalla, R., Impagnatiello, F., Grandy, D. K., Cuellar, B., Rubinstein, M., et al. (2001). The role of the D(2) dopamine receptor (D(2)R) in A(2A) adenosine receptor (A(2A)R)-mediated behavioral and cellular responses as revealed by A(2A) and D(2) receptor knockout mice. *Proc. Natl. Acad. Sci. U.S.A.* 98, 1970–1975. doi: 10.1073/pnas.98.4.1970

Chong, T. T., Bonnelle, V., Manohar, S., Veromann, K. R., Muhammed, K., Tofaris, G. K., et al. (2015). Dopamine enhances willingness to exert effort for reward in Parkinson's disease. *Cortex* 69, 40–46. doi: 10.1016/j.cortex.2015.04.003

Ciruela, F., Casadó, V., Rodrigues, R. J., Luján, R., Burgueño, J., Canals, M., et al. (2006). Presynaptic control of striatal glutamatergic neurotransmission by adenosine A1-A2A receptor heteromers. *J. Neurosci.* 26, 2080–2087. doi: 10.1523/JNEUROSCI.3574-05.2006

Danjo, T., Yoshimi, K., Funabiki, K., Yawata, S., and Nakanishi, S. (2014). Aversive behavior induced by optogenetic inactivation of ventral tegmental area dopamine neurons is mediated by dopamine D2 receptors in the nucleus accumbens. *Proc. Natl. Acad. Sci. U.S.A.* 111, 6455–6460. doi: 10.1073/pnas.1404323111

DeLong, M. R., and Wichmann, T. (2015). Basal ganglia circuits as targets for neuromodulation in Parkinson disease. *JAMA Neurol.* 72, 1354–1360. doi: 10.1001/jamaneurol.2015.2397

den Brok, M. G., van Dalen, J. W., van Gool, W. A., Moll van Charante, E. P., de Bie, R. M., and Richard, E. (2015). Apathy in Parkinson's disease: a systematic review and meta-analysis. *Mov. Disord.* 30, 759–769. doi: 10.1002/mds.26208

Dreyer, J. K., Herrik, K. F., Berg, R. W., and Hounsgaard, J. D. (2010). Influence of phasic and tonic dopamine release on receptor activation. *J. Neurosci.* 30, 14273–14283. doi: 10.1523/jneurosci.1894-10.2010

Durieux, P. F., Bearzatto, B., Guiducci, S., Buch, T., Waisman, A., Zoli, M., et al. (2009). D2R striatopallidal neurons inhibit both locomotor and drug reward processes. *Nat. Neurosci.* 12, 393–395. doi: 10.1038/nn.2286

El Yacoubi, M., Ledent, C., Parmentier, M., Costentin, J., and Vaugeois, J. M. (2001). Adenosine A2A receptor knockout mice are partially protected against drug-induced catalepsy. *Neuroreport* 12, 983–986. doi: 10.1097/00001756-200104170-00024

Ferré, S. (1997). Adenosine-dopamine interactions in the ventral striatum. Implications for the treatment of schizophrenia. *Psychopharmacology* 133, 107–120. doi: 10.1007/s002130050380

Ferré, S. (2008). An update on the mechanisms of the psychostimulant effects of caffeine. *J. Neurochem.* 105, 1067–1079. doi: 10.1111/j.1471-4159.2007.05196.x

Ferré, S. (2015). The GPCR heterotetramer: challenging classical pharmacology. *Trends Pharmacol. Sci.* 36, 145–152. doi: 10.1016/j.tips.2015.01.002

Ferré, S. (2016). Mechanisms of the psychostimulant effects of caffeine: implications for substance use disorders. *Psychopharmacology* 233, 1963–1979. doi: 10.1007/s00213-016-4212-2

Ferré, S. (2017). "Adenosine control of striatal function. Implications for the treatment of apathy in basal ganglia disorders," in *Adenosine Receptors in Degenerative Diseases*, eds D. Blum and L. V. Lopes (Amsterdam: Elsevier), 231–255. doi: 10.1016/B978-0-12-803724-9.00012-0

Ferré, S., Bonaventura, J., Tomasi, D., Navarro, G., Moreno, E., Cortés, A., et al. (2016). Allosteric mechanisms within the adenosine A2A-dopamine D2 receptor heterotetramer. *Neuropharmacology* 104, 154–160. doi: 10.1016/j.neuropharm.2015.05.028

Ferré, S., Casadó, V., Devi, L. A., Filizola, M., Jockers, R., Lohse, M. J., et al. (2014). G protein-coupled receptor oligomerization revisited: functional and pharmacological perspectives. *Pharmacol. Rev.* 66, 413–434. doi: 10.1124/pr.113.008052

Ferré, S., Fredholm, B. B., Morelli, M., Popoli, P., and Fuxe, K. (1997). Adenosine-dopamine receptor-receptor interactions as an integrative mechanism in the basal ganglia. *Trends Neurosci.* 20, 482–487. doi: 10.1016/S0166-2236(97)01096-5

Ferré, S., Fuxe, K., von Euler, G., Johansson, B., and Fredholm, B. B. (1992). Adenosine-dopamine interactions in the brain. *Neuroscience* 51, 501–512. doi: 10.1016/0306-4522(92)90291-9

Ferré, S., Guix, T., Prat, G., Jane, F., and Casas, M. (1990). Is experimental catalepsy properly measured? *Pharmacol. Biochem. Behav.* 35, 753–757. doi: 10.1016/0091-3057(90)90354-K

Ferré, S., O'Connor, W. T., Fuxe, K., and Ungerstedt, U. (1993). The striopallidal neuron: a main locus for adenosine-dopamine interactions in the brain. *J. Neurosci.* 13, 5402–5406.

Ferré, S., O'Connor, W. T., Snaprud, P., Ungerstedt, U., and Fuxe, K. (1994). Antagonistic interaction between adenosine A2A receptors and dopamine D2 receptors in the ventral striopallidal system. *Implications for the treatment of schizophrenia. Neuroscience* 63, 765–773. doi: 10.1016/0306-4522(94)90521-5

Ferré, S., Quiroz, C., Orru, M., Guitart, X., Navarro, G., Cortés, A., et al. (2011). Adenosine A(2A) receptors and A(2A) receptor heteromers as key players in striatal function. *Front. Neuroanat.* 5:36. doi: 10.3389/fnana.2011.00036

Ferré, S., Rubio, A., and Fuxe, K. (1991a). Stimulation of adenosine A2 receptors induces catalepsy. *Neurosci. Lett.* 130, 162–164.

Ferré, S., von Euler, G., Johansson, B., Fredholm, B. B., and Fuxe, K. (1991b). Stimulation of high-affinity adenosine A2 receptors decreases the affinity of dopamine D2 receptors in rat striatal membranes. *Proc. Natl. Acad. Sci. U.S.A.* 88, 7238–7241.

Frank, M. J. (2005). Dynamic dopamine modulation in the basal ganglia: a neurocomputational account of cognitive deficits in medicated and nonmedicated Parkinsonism. *J. Cogn. Neurosci.* 17, 51–72. doi: 10.1162/0898929052880093

Frank, M. J., Seeberger, L. C., and O'Reilly, R. C. (2004). By carrot or by stick: cognitive reinforcement learning in parkinsonism. *Science* 306, 1940–1943.

Frederick, A. L., Yano, H., Trifilieff, P., Vishwasrao, H. D., Biezonski, D., Mészáros, J., et al. (2015). Evidence against dopamine D1/D2 receptor heteromers. *Mol. Psychiatry* 20, 1373–1385. doi: 10.1038/mp.2014.166

Freeze, B. S., Kravitz, A. V., Hammack, N., Berke, J. D., and Kreitzer, A. C. (2013). Control of basal ganglia output by direct and indirect pathway projection neurons. *J. Neurosci.* 33, 18531–18539. doi: 10.1523/JNEUROSCI.1278-13.2013

Fuxe, K., and Ungerstedt, U. (1974). Action of caffeine and theophyllamine on supersensitive dopamine receptors: considerable enhancement of receptor

response to treatment with DOPA and dopamine receptor agonists. *Med. Biol.* 52, 48–54.

Garrett, B. E., and Holtzman, S. G. (1995). Does adenosine receptor blockade mediate caffeine-induced rotational behavior? *J. Pharmacol. Exp. Ther.* 274, 207–214.

Gerfen, C. R. (2004). "Basal ganglia," in *The Rat Nervous System*, ed. G. Paxinos (Amsterdam: Elsevier), 445–508.

Gjini, K., Qazi A., Greenwald, M. K., Sandhu, R., Gooding, D. C., and Boutros, N. N. (2014). Relationships of behavioral measures of frontal lobe dysfunction with underlying electrophysiology in cocaine-dependent patients. *Am. J. Addict.* 23, 265–271. doi: 10.1111/j.1521-0391.2014.12095.x

Haber, S. N. (2014). The place of dopamine in the cortico-basal ganglia circuit. *Neuroscience* 282, 248–257. doi: 10.1016/j.neuroscience.2014.10.008

Haber, S. N., and Behrens, T. E. (2014). The neural network underlying incentive-based learning: implications for interpreting circuit disruptions in psychiatric disorders. *Neuron* 83, 1019–1039. doi: 10.1016/j.neuron.2014.08.031

Håkansson, K., Galdi, S., Hendrick, J., Snyder, G., Greengard, P., and Fisone, G. (2006). Regulation of phosphorylation of the GluR1 AMPA receptor by dopamine D2 receptors. *J. Neurochem.* 96, 482–488. doi: 10.1111/j.1471-4159.2005.03558.x

Hamilton, K. R., Mitchell, M. R., Wing, V. C., Balodis, I. M., Bickel, W. K., Fillmore, M., et al. (2015). Choice impulsivity: definitions, measurement issues, and clinical implications. *Personal. Disord.* 6, 182–198. doi: 10.1037/per0000099

Hauber, W., and Münkle, M. (1997). Motor depressant effects mediated by dopamine D2 and adenosine A2A receptors in the nucleus accumbens and the caudate-putamen. *Eur. J. Pharmacol.* 323, 127–131. doi: 10.1016/S0014-2999(97)00040-X

Hernandez-Lopez, S., Tkatch, T., Perez-Garci, E., Galarraga, E., Bargas, J., Hamm, H., et al. (2000). D2 dopamine receptors in striatal medium spiny neurons reduce L-type Ca^{2+} currents and excitability via a novel PLC[beta]1-IP3-calcineurin-signaling cascade. *J. Neurosci.* 20, 8987–8995.

Herrera-Marschitz, M., Casas, M., and Ungerstedt, U. (1988). Caffeine produces contralateral rotation in rats with unilateral dopamine denervation: comparisons with apomorphine-induced responses. *Psychopharmacology* 94, 38–45. doi: 10.1007/BF00735878

Higley, M. J., and Sabatini, B. L. (2010). Competitive regulation of synaptic Ca2+ influx by D2 dopamine and A2A adenosine receptors. *Nat. Neurosci.* 13, 958–966. doi: 10.1038/nn.2592

Hikida, T., Kimura, K., Wada, N., Funabiki, K., and Nakanishi, S. (2010). Distinct roles of synaptic transmission in direct and indirect striatal pathways to reward and aversive behavior. *Neuron* 66, 896–907. doi: 10.1016/j.neuron.2010.05.011

Hikida, T., Yawata, S., Yamaguchi, T., Danjo, T., Sasaoka, T., Wang, Y., et al. (2013). Pathway-specific modulation of nucleus accumbens in reward and aversive behavior via selective transmitter receptors. *Proc. Natl. Acad. Sci. U.S.A.* 110, 342–347. doi: 10.1073/pnas.1220358110

Hikosaka, O. (2007). Basal ganglia mechanisms of reward-oriented eye movement. *Ann. N. Y. Acad. Sci.* 1104, 229–249. doi: 10.1196/annals.1390.012

Hillion, J., Canals, M., Torvinen, M., Casado, V., Scott, R., Terasmaa, A., et al. (2002). Coaggregation, cointernalization, and codesensitization of adenosine A2A receptors and dopamine D2 receptors. *J. Biol. Chem.* 277, 18091–18097. doi: 10.1074/jbc.M107731200

Hobson, B. D., O'Neill, C. E., Levis, S. C., Monteggia, L. M., Neve, R. L., Self, D. W., et al. (2013). Adenosine A1 and dopamine d1 receptor regulation of AMPA receptor phosphorylation and cocaine-seeking behavior. *Neuropsychopharmacology* 38, 1974–1983. doi: 10.1038/npp.2013.96

Huang, L., Wu, D. D., Zhang, L., and Feng, L. Y. (2013). Modulation of A_2a receptor antagonist on D_2 receptor internalization and ERK phosphorylation. *Acta Pharmacol. Sin.* 34, 1292–1300. doi: 10.1038/aps.2013.87

Isaac, S. O., and Berridge, C. W. (2003). Wake-promoting actions of dopamine D1 and D2 receptor stimulation. *J. Pharmacol. Exp. Ther.* 307, 386–394. doi: 10.1124/jpet.103.053918

Ishiwari, K., Madson, L. J., Farrar, A. M., Mingote, S. M., Valenta, J. P., DiGianvittorio, M. D., et al. (2007). Injections of the selective adenosine A2A antagonist MSX-3 into the nucleus accumbens core attenuate the locomotor suppression induced by haloperidol in rats. *Behav. Brain Res.* 178, 190–199. doi: 10.1016/j.bbr.2006.12.020

Jankovic, J. (2008). Parkinson's disease: clinical features and diagnosis. *J. Neurol. Neurosurg. Psychiatry* 79, 368–376. doi: 10.1136/jnnp.2007.131045

Justinová, Z., Redhi, G. H., Goldberg, S. R., and Ferré, S. (2014). Differential effects of presynaptic versus postsynaptic adenosine A2A receptor blockade on Δ9-tetrahydrocannabinol (THC) self-administration in squirrel monkeys. *J. Neurosci.* 34, 6480–6484. doi: 10.1523/jneurosci.5073-13.2014

Kable, J. W., and Glimcher, P. W. (2009). The neurobiology of decision: consensus and controversy. *Neuron* 63, 733–745. doi: 10.1016/j.neuron.2009.09.003

Kanda, T., Shiozaki, S., Shimada, J., Suzuki, F., and Nakamura, J. (1994). KF17837: a novel selective adenosine A2A receptor antagonist with anticataleptic activity. *Eur. J. Pharmacol.* 256, 263–268. doi: 10.1016/0014-2999(94)90551-7

Karcz-Kubicha, M., Antoniou, K., Terasmaa, A., Quarta, D., Solinas, M., Justinova, Z., et al. (2003). Involvement of adenosine A1 and A2A receptors in the motor effects of caffeine after its acute and chronic administration. *Neuropsychopharmacology* 28, 1281–1291. doi: 10.1038/sj.npp.1300167

Kim, D. S., and Palmiter, R. D. (2003). Adenosine receptor blockade reverses hypophagia and enhances locomotor activity of dopamine-deficient mice. *Proc. Natl. Acad. Sci. U.S.A.* 100, 1346–1351. doi: 10.1073/pnas.252753799

Kim, D. S., and Palmiter, R. D. (2008). Interaction of dopamine and adenosine receptor function in behavior: studies with dopamine-deficient mice. *Front. Biosci.* 13,2311–2318.

Kim, H. F., and Hikosaka, O. (2015). Parallel basal ganglia circuits for voluntary and automatic behaviour to reach rewards. *Brain* 138, 1776–1800. doi: 10.1093/brain/awv134

Kirschner, M., Hager, O. M., Bischof, M., Hartmann, M. N., Kluge, A., Seifritz, E., et al. (2016). Ventral striatal hypoactivation is associated with apathy but not diminished expression in patients with schizophrenia. *J. Psychiatry Neurosci.* 41, 152–161. doi: 10.1503/jpn.140383

Kravitz, A. V., Freeze, B. S., Parker, P. R., Kay, K., Thwin, M. T., Deisseroth, K., et al. (2010). Regulation of parkinsonian motor behaviours by optogenetic control of basal ganglia circuitry. *Nature* 466, 622–626. doi: 10.1038/nature09159

Kravitz, A. V., Tye, L. D., and Kreitzer, A. C. (2012). Distinct roles for direct and indirect pathway striatal neurons in reinforcement. *Nat. Neurosci.* 15, 816–818. doi: 10.1038/nn.3100

Kull, B., Ferré, S., Arslan, G., Svenningsson, P., Fuxe, K., Owman, C., et al. (1999). Reciprocal interactions between adenosine A2A and dopamine D2 receptors in Chinese hamster ovary cells co-transfected with the two receptors. *Biochem. Pharmacol.* 58, 1035–1045. doi: 10.1016/S0006-2952(99)00184-7

Lazenka, M. F., Moeller, F. G., and Negus, S. S. (2015). Effects of caffeine and its metabolite paraxanthine on intracranial self-stimulation in male rats. *Exp. Clin. Psychopharmacol.* 23, 71–80. doi: 10.1037/pha0000012

Lebon, G., Warne, T., Edwards, P. C., Bennett, K., Langmead, C. J., Leslie, A. G., et al. (2011). Agonist-bound adenosine A2A receptor structures reveal common features of GPCR activation. *Nature* 474, 521–525. doi: 10.1038/nature10136

Ledent, C., Vaugeois, J. M., Schiffmann, S. N., Pedrazzini, T., El Yacoubi, M., Vanderhaeghen, J. J., et al. (1997). Aggressiveness, hypoalgesia and high blood pressure in mice lacking the adenosine A2a receptor. *Nature* 388, 674–678. doi: 10.1038/41771

Lee, K. W., Hong, J. H., Choi, I. Y., Che, Y., Lee, J. K., Yang, S. D., et al. (2002). Impaired D2 dopamine receptor function in mice lacking type 5 adenylyl cyclase. *J. Neurosci.* 22, 7931–7940.

Lindskog, M., Svenningsson, P., Fredholm, B. B., Greengard, P., and Fisone, G. (1999). Activation of dopamine D2 receptors decreases DARPP-32 phosphorylation in striatonigral and striatopallidal projection neurons via different mechanisms. *Neuroscience* 88, 1005–1008. doi: 10.1016/S0306-4522(98)00411-4

Macpherson, T., Morita, M., and Hikida, T. (2014). Striatal direct and indirect pathways control decision-making behavior. *Front. Psychol.* 5:1301. doi: 10.3389/fpsyg.2014.01301

Marin, R. S. (1991). Apathy: a neuropsychiatric syndrome. *J. Neuropsychiatry Clin. Neurosci.* 3, 243–254. doi: 10.1176/jnp.3.3.243

Mazzoni, P., Hristova, A., and Krakauer, J. W. (2007). Why don't we move faster? Parkinson's disease, movement vigor, and implicit motivation. *J. Neurosci.* 27, 7105–7116. doi: 10.1523/JNEUROSCI.0264-07.2007

Mogenson, G. J., Jones, D. L., and Yim, C. Y. (1980). From motivation to action: functional interface between the limbic system and the motor system. *Prog. Neurobiol.* 14, 69–97. doi: 10.1016/0301-0082(80)90018-0

Morelli, M., Carta, A. R., and Jenner, P. (2009). Adenosine A2A receptors and Parkinson's disease. *Handb. Exp. Pharmacol.* 193, 589–615. doi: 10.1007/978-3-540-89615-9_18

Morelli, M., and Wardas, J. (2001). Adenosine A(2a) receptor antagonists: potential therapeutic and neuroprotective effects in Parkinson's disease. *Neurotox. Res.* 3, 545–556. doi: 10.1007/BF03033210

Moscoso-Castro, M., Gracia-Rubio, I., Ciruela, F., and Valverde, O. (2016). Genetic blockade of adenosine A2A receptors induces cognitive impairments and anatomical changes related to psychotic symptoms in mice. *Eur. Neuropsychopharmacol.* 26, 1227–1240. doi: 10.1016/j.euroneuro.2016.04.003

Müller, C. E., and Ferré, S. (2007). Blocking striatal adenosine A2A receptors: a new strategy for basal ganglia disorders. *Recent Pat. CNS Drug Discov.* 2, 1–21. doi: 10.2174/157488907779561772

Nagel, J., Schladebach, H., Koch, M., Schwienbacher, I., Müller, C. E., and Hauber, W. (2003). Effects of an adenosine A2A receptor blockade in the nucleus accumbens on locomotion,feeding, and prepulse inhibition in rats. *Synapse* 49, 279–286. doi: 10.1002/syn.10240

Nakamura, K., and Hikosaka, O. (2006). Role of dopamine in the primate caudate nucleus in reward modulation of saccades. *J. Neurosci.* 26, 5360–5369. doi: 10.1523/JNEUROSCI.4853-05.2006

Navarro, G., Aguinaga, D., Moreno, E., Hradsky, J., Reddy, P. P., Cortés, A., et al. (2014). Intracellular calcium levels determine differential modulation of allosteric interactions within G protein-coupled receptor heteromers. *Chem. Biol.* 21, 1546–1556. doi: 10.1016/j.chembiol.2014.10.004

Navarro, G., Cordomí, A., Casadó-Anguera, V., Moreno, E., Cai, N.-S., Cortés, A., et al. (2018). Evidence for functional pre-coupled complexes of receptor heteromers and adenylyl cyclase. *Nat. Commun.* 9:1242. doi: 10.1038/s41467-018-03522-3

Nunes, E. J., Randall, P. A., Podurgiel, S., Correa, M., and Salamone, J. D. (2013). Nucleus accumbens neurotransmission and effort-related choice behavior in food motivation: effects of drugs acting on dopamine, adenosine, and muscarinic acetylcholine receptors. *Neurosci. Biobehav. Rev.* 37, 2015–2025. doi: 10.1016/j.neubiorev.2013.04.002

O'Neill, C. E., Hobson, B. D., Levis, S. C., and Bachtell, R. K. (2014). Persistent reduction of cocaine seeking by pharmacological manipulation of adenosine A1 and A 2A receptors during extinction training in rats. *Psychopharmacology* 231, 3179–3188. doi: 10.1007/s00213-014-3489-2

Orrú, M., Bakešová, J., Brugarolas, M., Quiroz, C., Beaumont, V., Goldberg, S. R., et al. (2011a). Striatal pre- and postsynaptic profile of adenosine A(2A) receptor antagonists. *PLoS One* 6:e16088. doi: 10.1371/journal.pone.0016088

Orrú, M., Quiroz, C., Guitart, X., and Ferré, S. (2011b). Pharmacological evidence for different populations of postsynaptic adenosine A2A receptors in the rat striatum. *Neuropharmacology* 61, 967–974. doi: 10.1016/j.neuropharm.2011.06.025

Pereira, M., Farrar, A. M., Hockemeyer, J., Müller, C. E., Salamone, J. D., and Morrell, J. I. (2011). Effect of the adenosine A2A receptor antagonist MSX-3 on motivational disruptions of maternal behavior induced by dopamine antagonism in the early postpartum rat. *Psychopharmacology* 213, 69–79. doi: 10.1007/s00213-010-2015-4

Pinna, A., Wardas, J., Cristalli, G., and Morelli, M. (1997). Adenosine A2A receptor agonists increase Fos-like immunoreactivity in mesolimbic areas. *Brain Res.* 759, 41–49. doi: 10.1016/S0006-8993(97)00214-X

Prévost, C., Pessiglione, M., Météreau, E., Cléry-Melin, M. L., and Dreher, J. C. (2010). Separate valuation subsystems for delay and effort decision costs. *J. Neurosci.* 30, 14080–14090. doi: 10.1523/jneurosci.2752-10.2010

Quiroz, C., Luján, R., Uchigashima, M., Simoes, A. P., Lerner, T. N., Borycz, J., et al. (2009). Key modulatory role of presynaptic adenosine A2A receptors in cortical neurotransmission to the striatal direct pathway. *ScientificWorldJournal* 9, 1321–1344. doi: 10.1100/tsw.2009.143

Quiroz, C., Orrú, M., Rea, W., Ciudad-Roberts, A., Yepes, G., Britt, J. P., et al. (2016). Local control of extracellular dopamine levels in the medial nucleus accumbens by a glutamatergic projection from the infralimbic cortex. *J. Neurosci.* 36, 851–859. doi: 10.1523/jneurosci.2850-15.2016

Randall, P. A., Nunes, E. J., Janniere, S. L., Stopper, C. M., Farrar, A. M., Sager, T. N., et al. (2011). Stimulant effects of adenosine antagonists on operant behavior: differential actions of selective A2A and A1 antagonists. *Psychopharmacology* 216, 173–186. doi: 10.1007/s00213-011-2198-3

Remy, P., Doder, M., Lees, A., Turjanski, N., and Brooks, D. (2005). Depression in Parkinson's disease: loss of dopamine and noradrenaline innervation in the limbic system. *Brain* 128, 1314–1322. doi: 10.1093/brain/awh445

Roitman, M. F., Wheeler, R. A., Wightman, R. M., and Carelli, R. M. (2008). Real-time chemical responses in the nucleus accumbens differentiate rewarding and aversive stimuli. *Nat. Neurosci.* 11, 1376–1377. doi: 10.1038/nn.2219

Root, D. H., Melendez, R. I., Zaborszky, L., and Napier, T. C. (2015). The ventral pallidum: subregion-specific functional anatomy and roles in motivated behaviors. *Prog. Neurobiol.* 130, 29–70. doi: 10.1016/j.pneurobio.2015.03.005

Salamone, J. D., Correa, M., Nunes, E. J., Randall, P. A., and Pardo, M. (2012). The behavioral pharmacology of effort-related choice behavior: dopamine, adenosine and beyond. *J. Exp. Anal. Behav.* 97, 125–146. doi: 10.1901/jeab.2012.97-125

Schiffmann, S. N., Fisone, G., Moresco, R., Cunha, R. A., and Ferré, S. (2007). Adenosine A2A receptors and basal ganglia physiology. *Prog. Neurobiol.* 83, 277–292. doi: 10.1016/j.pneurobio.2007.05.001

Shen, W., Flajolet, M., Greengard, P., and Surmeier, D. J. (2008). Dichotomous dopaminergic control of striatal synaptic plasticity. *Science* 321, 848–851. doi: 10.1126/science.1160575

Sheppard, A. B., Gross, S. C., Pavelka, S. A., Hall, M. J., and Palmatier, M. I. (2012). Caffeine increases the motivation to obtain non-drug reinforcers in rats. *Drug Alcohol Depend.* 124, 216–222. doi: 10.1016/j.drugalcdep.2012.01.008

Shiozaki, S., Ichikawa, S., Nakamura, J., Kitamura, S., Yamada, K., and Kuwana, Y. (1999). Actions of adenosine A2A receptor antagonist KW-6002 on drug-induced catalepsy and hypokinesia caused by reserpine or MPTP. *Psychopharmacology* 147, 90–95. doi: 10.1007/s002130051146

Simon, J. J., Biller, A., Walther, S., Roesch-Ely, D., Stippich, C., Weisbrod, M., et al. (2010). Neural correlates of reward processing in schizophrenia–relationship to apathy and depression. *Schizophr. Res.* 118, 154–161. doi: 10.1016/j.schres.2009.11.007

Simon, J. J., Cordeiro, S. A., Weber, M. A., Friederich, H. C., Wolf, R. C., Weisbrod, M., et al. (2015). Reward system dysfunction as a neural substrate of symptom expression across the general population and patients with schizophrenia. *Schizophr. Bull.* 41, 1370–1378. doi: 10.1093/schbul/sbv067

Sinha, N., Manohar, S., and Husain, M. (2013). Impulsivity and apathy in Parkinson's disease. *J. Neuropsychol.* 7, 255–283. doi: 10.1111/jnp.12013

Steinberg, E. E., Keiflin, R., Boivin, J. R., Witten, I. B., Deisseroth, K., and Janak, P. H. (2013). A causal link between prediction errors, dopamine neurons and learning. *Nat. Neurosci.* 16, 966–973. doi: 10.1038/nn.3413

Stopper, C. M., and Floresco, S. B. (2011). Contributions of the nucleus accumbens and its subregions to different aspects of risk-based decision making. *Cogn. Affect. Behav. Neurosci.* 11, 97–112. doi: 10.3758/s13415-010-0015-9

Strauss, G. P., Morra, L. F., Sullivan, S. K., and Gold, J. M. (2015). The role of low cognitive effort and negative symptoms in neuropsychological impairment in schizophrenia. *Neuropsychology* 29, 282–291. doi: 10.1037/neu0000113

Svenningsson, P., Fourreau, L., Bloch, B., Fredholm, B. B., Gonon, F., and Le Moine, C. (1999). Opposite tonic modulation of dopamine and adenosine on c-fos gene expression in striatopallidal neurons. *Neuroscience* 89, 827–837. doi: 10.1016/S0306-4522(98)00403-5

Svenningsson, P., Le Moine, C., Kull, B., Sunahara, R., Bloc, H. B., and Fredholm, B. B. (1997). Cellular expression of adenosine A2A receptor messenger RNA in the rat central nervous system with special reference to dopamine innervated areas. *Neuroscience* 80, 1171–1185. doi: 10.1016/S0306-4522(97)00180-2

Svenningsson, P., Lindskog, M., Rognoni, F., Fredholm, B. B., Greengard, P., and Fisone, G. (1998). Activation of adenosine A2A and dopamine D1 receptors stimulates cyclic AMP-dependent phosphorylation of DARPP-32 in distinct populations of striatal projection neurons. *Neuroscience* 84, 223–228. doi: 10.1016/S0306-4522(97)00510-1

Taura, J., Valle-León, M., Sahlholm, K., Watanabe, M., Van Craenenbroeck, K., Fernández-Dueñas, V., et al. (2017). Behavioral control by striatal adenosine A_{2A}-dopamine D_2 receptor heteromers. *Genes Brain Behav.* e12432. doi: 10.1111/gbb.12432 [Epub ahead of print].

Tian, L., Xia, Y., Flores, H. P., Campbell, M. C., Moerlein, S. M., and Perlmutter, J. S. (2015). Neuroimaging analysis of the dopamine basis for apathetic behaviors in an MPTP-lesioned primate model. *PLoS One* 10:e0132064. doi: 10.1371/journal.pone.0132064

Tremblay, L., Worbe, Y., Thobois, S., Sgambato-Faure, V., and Féger, J. (2015). Selective dysfunction of basal ganglia subterritories: from movement

to behavioral disorders. *Mov. Disord.* 30, 1155–1170. doi: 10.1002/mds.26199

Usiello, A., Baik, J. H., Rougé-Pont, F., Picetti, R., Dierich, A., LeMeur, M., et al. (2000). Distinct functions of the two isoforms of dopamine D2 receptors. *Nature* 408, 199–203. doi: 10.1038/35041572

Valjent, E., Bertran-Gonzalez, J., Hervé, D., Fisone, G., and Girault, J. A. (2009). Looking BAC at striatal signaling: cell-specific analysis in new transgenic mice. *Trends Neurosci.* 32, 538–547. doi: 10.1016/j.tins.2009.06.005

Verdejo-García, A., Bechara, A., Recknor, E. C., and Pérez-García, M. (2006). Executive dysfunction in substance dependent individuals during drug use and abstinence: an examination of the behavioral, cognitive and emotional correlates of addiction. *J. Int. Neuropsychol. Soc.* 12, 405–415. doi: 10.1017/S1355617706060486

Verdejo-García, A., and Pérez-García, M. (2008). Substance abusers' self-awareness of the neurobehavioral consequences of addiction. *Psychiatry Res.* 158, 172–180. doi: 10.1016/j.psychres.2006.08.001

Volkow, N. D., Wang, G. J., Fowler, J. S., Tomasi, D., and Telang, F. (2011). Addiction: beyond dopamine reward circuitry. *Proc. Natl. Acad. Sci. U.S.A.* 108, 15037–15042. doi: 10.1073/pnas.1010654108

Volkow, N. D., Wang, G. J., Logan, J., Alexoff, D., Fowler, J. S., Thanos, P. K., et al. (2015). Caffeine increases striatal dopamine D_2/D_3 receptor availability in the human brain. *Transl. Psychiatry* 5:e549. doi: 10.1038/tp.2015.46

Voon, V., Pessiglione, M., Brezing, C., Gallea, C., Fernandez, H. H., Dolan, R. J., et al. (2010). Mechanisms underlying dopamine-mediated reward bias in compulsive behaviors. *Neuron* 65, 135–142. doi: 10.1016/j.neuron.2009.12.027

Voorn, P., Vanderschuren, L. J., Groenewegen, H. J., Robbins, T. W., and Pennartz, C. M. (2004). Putting a spin on the dorsal-ventral divide of the striatum. *Trends Neurosci.* 27, 468–474. doi: 10.1016/j.tins.2004.06.006

Wang, J. H., Short, J., Ledent, C., Lawrence, A. J., and van den Buuse, M. (2003). Reduced startle habituation and prepulse inhibition in mice lacking the adenosine A2A receptor. *Behav. Brain Res.* 143, 201–207. doi: 10.1016/S0166-4328(03)00036-6

Wise, R. A. (2004). Dopamine, learning and motivation. *Nat. Rev. Neurosci.* 5, 483–494. doi: 10.1038/nrn1406

Wise, R. A., and Bozarth, M. A. (1987). A psychomotor stimulant theory of addiction. *Psychol. Rev.* 94, 469–492. doi: 10.1037/0033-295X.94.4.469

Yang, J. N., Chen, J. F., and Fredholm, B. B. (2009). Physiological roles of A1 and A2A adenosine receptors in regulating heart rate, body temperature, and locomotion as revealed using knockout mice and caffeine. *Am. J. Physiol. Heart Circ. Physiol.* 296, H1141–H1149. doi: 10.1152/ajpheart.00754.2008

Yin, H. H., and Knowlton, B. J. (2006). The role of the basal ganglia in habit formation. *Nat. Rev. Neurosci.* 7, 464–476. doi: 10.1038/nrn1919

Zwilling, D., Zhu, W., Lee, H., Gallager, I., Braithwaite, S. P., and Thompson, K. R. (2014). *An optogenetic Model to Study Motor and Psychiatric Symptoms of Parkinson's Disease. 2014 Neuroscience Meeting Planner*. Washington, DC: Society for Neuroscience.

Conflict of Interest Statement: The authors declare that the research was conducted in the absence of any commercial or financial relationships that could be construed as a potential conflict of interest.

frontiers in Pharmacology

PERSPECTIVE
published: 04 April 2018
doi: 10.3389/fphar.2018.00310

Adenosine Receptor-Mediated Cardioprotection—Current Limitations and Future Directions

*Robert D. Lasley**

Department of Physiology, Wayne State University School of Medicine, Detroit, MI, United States

Since the seminal reports of adenosine receptor-mediated cardioprotection in the early 1990s, there have been a multitude of such reports in various species and preparations. Original observations of the beneficial effects of A_1 receptor agonists have been followed up with numerous reports also implicating A_{2A}, A_3, and most recently A_{2B}, receptor agonists as cardioprotective agents. Although adenosine has been approved for clinical use in the United States for the treatment of supraventricular tachycardia and coronary artery imaging, and the selective A_{2A} agonist, regadenoson, for the latter, clinical use of adenosine receptor agonists for protecting the ischemic heart has not advanced beyond early trials. An examination of the literature indicates that existing experimental studies have several limitations in terms of clinical relevance, as well as lacking incorporation of recent new insights into adenosine receptor signaling. Such deficiencies include the lack of experimental studies in models that most closely mimic human cardiovascular disease. In addition, there have been very few studies in chronic models of myocardial ischemia, where limiting myocardial remodeling and heart failure, not reduction of infarct size, are the primary endpoints. Despite an increasing number of reports of the beneficial effects of adenosine receptor antagonists, not agonists, in chronic diseases, this idea has not been well-studied in experimental myocardial ischemia. There have also been few studies examining adenosine receptor subtype interactions as well as receptor heterodimerization. The purpose of this Perspective article is to discuss these deficiencies to highlight future directions of research in the field of adenosine receptor-mediated protection of ischemic myocardium.

Keywords: adenosine receptor subtypes, cardioprotection, chronic myocardial ischemia, co-morbidities, clinical trials

OPEN ACCESS

Edited by:
Francisco Ciruela,
Universitat de Barcelona, Spain

Reviewed by:
Francisco Westermeier,
Universidad de Chile, Chile
Vadim V. Fedorov,
The Ohio State University,
United States

***Correspondence:**
Robert D. Lasley
rlasley@med.wayne.edu

Specialty section:
This article was submitted to Experimental Pharmacology and Drug Discovery, a section of the journal Frontiers in Pharmacology

Received: *17 November 2017*
Accepted: *19 March 2018*
Published: *04 April 2018*

Citation:
Lasley RD (2018) Adenosine Receptor-Mediated Cardioprotection—Current Limitations and Future Directions. Front. Pharmacol. 9:310. doi: 10.3389/fphar.2018.00310

Although the hypothesis that adenosine could be cardioprotective first became recognized in the early to mid-1980s, it started inauspiciously. Based on observations that the post-ischemic heart was characterized by both decreased ATP content and reduced ventricular function, Reibel and Rovetto (1978) reported that a reperfusion infusion of adenosine (50 μM) in isolated perfused rat hearts did not improve ATP content, although ventricular function was not measured (Reibel and Rovetto, 1978). Several subsequent studies did yield beneficial effects of exogenous and endogenous adenosine on post-ischemic ATP content and ventricular function, but these results were based in large part on initiating treatment prior to the onset of ischemia (Humphrey and Seelye, 1982; Dhasmana et al., 1983; Ely et al., 1985). Initial reports that reperfusion infusions of adenosine could reduce infarct size (Olafsson et al., 1987; Pitarys et al., 1991), could not be replicated in subsequent

studies (Homeister et al., 1990; Goto et al., 1991; Vander Heide and Reimer, 1996). Interest in adenosine's effects in protecting the ischemic heart did not gain widespread acceptance until early 1990 when our laboratory first reported an A_1 receptor cardioprotective effect (Lasley et al., 1990). A year later Liu et al. (1991) reported a role for A_1 receptors in ischemic preconditioning to reduce myocardial infarct size. Over the next 30 years there has been an explosion in the number of adenosine receptor cardioprotection studies, primarily focusing on infarct size reduction, with all four adenosine receptor subtypes (A_1, A_{2A}, A_3, A_{2B}) being implicated (Headrick and Lasley, 2009; McIntosh and Lasley, 2012).

Despite these numerous reports in experimental models, there have been few, if any, clinical trials of adenosine receptor cardioprotection in humans. Searching the database at "ClinicalTrials.gov" with the terms "ischemic heart disease" and "adenosine" yields 192 trials; changing the disease/condition to myocardial infarction (MI) yields only 40 trials. Nearly all of these trials have related to adenosine's effects on arrhythmias, coronary blood flow, and platelets. When searching this database with "adenosine receptor" 582 trials are shown, but combining with "myocardial infarction" only 9 trials are cited, and the majority of these trials used adenosine, not a receptor analog thereof. The only adenosine receptor agonists used in cardiac related clinical trials have been the A_1 agonists Selodenoson (DTI-0009) and Capadenoson (BAY68-4986) for controlling ventricular rate in atrial fibrillation, the A_{2A} agonist regadeson and related agents for coronary imaging, and most recently the partial A_1 agonist Neladenoson bialanate (BAY1067197) for heart failure.

This limited translation of hundreds of experimental studies, in every animal species tested to date, to the clinical arena raises the question of whether the past 30 years of adenosine receptor cardioprotection investigations have been for naught. This perspective will examine limitations of our existing knowledge of adenosine-mediated protection of the ischemic heart to help guide future studies to fully understand the cardioprotective effects of adenosine therapeutics and harness its potential in humans.

LACK OF CLINICALLY RELEVANT ANIMAL MODELS

Nearly all experimental studies on adenosine receptor cardioprotection have been conducted in normal, healthy adult animals. In contrast cardioprotective interventions in humans occur in the presence of various co-morbidities, such as arterial hypertension, obesity, diabetes, hypercholesterolemia, and often advanced age. Although there are numerous reports examining the role of adenosine and its receptors in these pathologies (Long et al., 2010; Wang et al., 2010; Bot et al., 2012; Koupenova et al., 2012; Sangsiri et al., 2013; Zhang et al., 2013; Teng et al., 2014; Nayak et al., 2015; Yang et al., 2016), the only one of these areas in which adenosine cardioprotection has been examined is in healthy aged rats and mice, and results have been conflicting. Isolated heart studies in 16–18 month old mice indicate a loss in the ability of adenosine and the A_1 and A_3 adenosine receptor agonists CPA and Cl-IB-MECA to reduce ischemia-reperfusion injury (Headrick et al., 2003; Peart et al., 2014). Two studies in rat hearts have led to contradictory findings as Schulman et al. (2001) reported a loss of adenosine A_1 agonist (CCPA) preconditioning in 18–20 month-old Wistar rats, whereas Kristo et al. (2005) reported enhanced infarct size reduction in 24–26 months Fischer 344 × Brown Norway hybrid (F344 × BN) rats with the mixed (A_1 and A_{2A}) agonist AMP579. A major difference in these rat studies is that the former was conducted in an isolated perfused heart preparation, whereas the latter was conducted *in vivo*, where the effects of the circulating agonist continued into reperfusion. Interestingly in both rat and mouse studies the effects of A_1 and A_{2A} agonists on heart rate and coronary flow in aged hearts were similar to those in young adult hearts. These findings are consistent with the reports of unaltered A_{2A} agonist (regadenoson) increases in coronary flow in aged human hearts (Cerqueira et al., 2008). One of the major limitations in the field of adenosine receptor cardioprotection is the lack of studies in animal models with clinically relevant morbidities. It is likely that these co-morbidities will alter myocardial adenosine receptor subtype expression and/or signaling mechanisms, as has been reported in models of atherosclerosis and diabetes (Long et al., 2010; Cabiati et al., 2015).

TREATMENT PARADIGMS

Another deficiency in the literature, related to current experimental studies, are the experimental treatment paradigms that are typically used. The majority of experimental studies on adenosine A_1 and A_3 receptors, as well as several studies A_{2B} receptors, have involved administration of agonists prior to ischemia to reduce ischemia-reperfusion injury (Headrick and Lasley, 2009; McIntosh and Lasley, 2012). Such a treatment paradigm has relevance to open heart surgery and preservation solutions for cardiac transplantation, but there have been no clinical trials to date, even assessing safety, for the use of adenosine receptor agonists. In contrast experimental studies on adenosine A_{2A} and A_{2B} agonists have focused on reperfusion treatments for the reduction of myocardial infarct size (Headrick and Lasley, 2009; McIntosh and Lasley, 2012), which upon initial review would appear to have some clinical relevance. Initial animal studies with adenosine A_{2A} agonist reperfusion treatment, which were all successful, occurred soon after the controversial experimental results with adenosine (Olafsson et al., 1987; Homeister et al., 1990; Goto et al., 1991; Pitarys et al., 1991; Vander Heide and Reimer, 1996) and the equivocal results of the acute myocardial infarction study of adenosine (AMISTAD) trial published in 1999 (Mahaffey et al., 1999).

However, the vast majority of experimental studies have initiated treatments during late ischemia or at the onset of reperfusion. Such early reperfusion treatments in the setting of acute myocardial infarction (MI) are not feasible given the time involved from the onset of patient symptoms to the diagnosis of MI and initiation of reperfusion therapy. In fact the results of the AMISTAD-II trial indicated that patients [particularly

those receiving thrombolytic therapy, rather than percutaneous coronary intervention (PCI)] receiving intravenous adenosine within 3 h of symptom onset showed significantly reduced 1 and 6 months mortality compared with placebo (Kloner et al., 2006). Patients obtaining adenosine reperfusion treatment later than 3 h of symptom onset received no beneficial effect. These clinical observations were similar to those by (Toufektsian et al., 2006), who reported that a 1 h delay in the reperfusion administration of the highly selective A_{2A} agonist, ATL146e, failed to reduce 24 h infarct size in mice (Toufektsian et al., 2006). Interestingly, the delayed treatment did increase post-MI cardiac function and reduce inflammation. We previously reported (Lasley et al., 2001) that an intracoronary infusion of the A_{2A} agonist CGS21680, 2 h after reperfusion, increased regional preload-recruitable stroke work and stroke work area (load-insensitive parameters of cardiac contractility) in a porcine model of reversible myocardial ischemia-reperfusion injury. This effect was determined to be independent of effects on coronary blood flow, and the same infusion in normal myocardium had no effect on regional contractile function. In summary, the lack of experimental studies in clinically relevant models with appropriate treatment protocols, is likely to have contributed to the lack of clinical trials examining the efficacy of adenosine or receptor agonists for treating acute MI. The primary focus on reduction of acute injury is not only inconsistent with clinical trends of more patients living with chronic myocardial ischemia, but it also neglects some of the other recognized beneficial effects of adenosine receptors.

CHRONIC MYOCARDIAL ISCHEMIA MODELS

Another weakness in experimental models of adenosine receptor cardioprotection is the primary focus on acute cardioprotection. This is an inherent limitation of *in vitro* models, but this continues to be a significant weakness of *in vivo* models, in which the study endpoint is typically infarct size after 2–3 h of reperfusion, with only a limited number of studies extending reperfusion to 24 h. Data from the National Heart, Lung and Blood Institute (NHLBI) and other sources indicate that over the past 40 years, deaths from acute MI have decreased significantly, whereas the incidence of heart failure and deaths from heart failure have increased (Krumholz et al., 2009). Experimental studies with short durations of reperfusion exclude significant components of the post-ischemic inflammatory process, which is a primary contributor to post-MI ventricular remodeling and subsequent heart failure. Such studies also exclude the well-known modulatory effects of adenosine receptors on inflammatory processes. It is also well-recognized that adenosine receptor expression and adenosine formation are increased in chronic inflammation, similar to that seen in chronically ischemic hearts (Xaus et al., 1999; Sun et al., 2006; Hasko et al., 2008; Feoktistov and Biaggioni, 2011; Belikoff et al., 2012).

Unfortunately, there have only been a very limited number of experimental studies assessing the cardioprotective effects of adenosine and/or receptor agonists in chronic models of myocardial ischemia. In what appears to be the first such study, Villarreal et al. (2003) reported that a 2 h intravenous infusion of an adenosine kinase inhibitor, which increases endogenous adenosine levels, but not adenosine itself, in rats just prior to reperfusion (following a 2 h occlusion) increased 2 week post-MI ischemic zone wall thickness, consistent with reduced ventricular remodeling (Villarreal et al., 2003). Wakeno et al. subsequently reported that a 3 weeks treatment (twice daily intraperitoneal injections) with the non-selective agonist, 2-chloroadenosine, starting at 7-day post-MI in rats reduced cardiac remodeling and cardiac fibrosis (Wakeno et al., 2006). Based on results with multiple adenosine receptor antagonists, the authors concluded that this protective effect was due to adenosine A_{2B} receptor stimulation. More recently Sabbah et al. reported that chronic treatment with a partial A_1 receptor agonist (capadenoson), in a coronary microembolization-induced model of heart failure in canines, improved left ventricular function, decreased fibrosis, and reduced plasma n-terminal pro-brain natriuretic peptide concentrations (Sabbah et al., 2013). These beneficial effects observed in the absence of changes in heart rate, blood pressure, or renal function, but were accompanied by increased expression of left ventricular sarcoplasmic reticulum calcium ATPase activity, mitochondrial uncoupling proteins (UCP) and glucose transporters. These latter observations suggest that capadenoson's beneficial effects were due to direct effects on the heart, although the specific mechanism remains unknown.

Despite the lack of chronic experimental myocardial ischemia studies, there is evidence suggesting that adenosine may exert beneficial effects in patients with chronic myocardial ischemia. Bulluck et al. (2016) conducted a meta-analysis on the results of 13 randomized clinical trials using intracoronary or intravenous adenosine in patients with ST-segment elevation MI (STEMI). They concluded that intracoronary adenosine therapy in the presence of primary percutaneous coronary intervention (PPCI) was effective in reducing post-STEMI heart failure, but not in terms of other end-points such as death, non-fatal MI, or revascularization. They also concluded that these effects were most likely due to infarct size reduction via less reperfusion injury, although they could not exclude a role in reducing ventricular remodeling. A double blinded, placebo controlled Phase 2 clinical trial (7 days of treatment) with the A_1 partial agonist BAY1067197 (neladenoson bialanate) in patients with heart failure with reduced ejection fraction indicated that this agent was safe, although no beneficial effects on cardiac function were observed (Voors et al., 2017).

The possibility that adenosine receptors may modulate post-MI remodeling in patients highlights/emphasizes the need to conduct clinically relevant experimental chronic studies, rather than acute studies. Cardiac remodeling is due to chronic inflammation and fibrosis, mediated by immune cells and fibroblasts, both of which express at least two adenosine receptors. Adenosine A_{2A} receptors are well recognized for their anti-inflammatory effects, and there are reports that A_{2B} receptors may exert both anti- and pro-inflammatory effects (Hasko et al., 2008; Csoka et al., 2010; Feoktistov and Biaggioni, 2011; Linden, 2011; Haskó and Cronstein, 2013). Likewise, there is evidence that both A_{2A} and A_{2B} receptors regulate

fibroblast function, including cardiac fibroblasts, although there are conflicting reports on their specific effects (Zhong et al., 2005; Villarreal et al., 2009; Zhang et al., 2014; Karmouty-Quintana et al., 2015; Shaikh and Cronstein, 2016). These observations and reports of adenosine receptor involvement in various chronic diseases (Long et al., 2010; Wang et al., 2010; Bot et al., 2012; Koupenova et al., 2012; Sangsiri et al., 2013; Zhang et al., 2013; Teng et al., 2014; Nayak et al., 2015; Yang et al., 2016), clearly warrant more studies on adenosine receptor modulation of chronic myocardial ischemia.

RECEPTOR AGONISTS OR ANTAGONISTS?

One aspect related to the lack of studies on adenosine receptor modulation of chronic myocardial ischemia, which has only recently been recognized, is the issue of receptor agonism vs. antagonism. All studies examining acute myocardial ischemia models have focused on treatment with receptor agonists, and in these studies blockade or deletion of any of the four adenosine receptor subtypes has resulted in little exacerbation of ischemia-reperfusion injury. However, there are numerous reports that antagonism or deletion of adenosine receptor subtypes is protective in models of both arterial and pulmonary hypertension, pulmonary and renal fibrosis, and sepsis (Sun et al., 2006; Kolachala et al., 2008; Zhou et al., 2011; Belikoff et al., 2012; Karmouty-Quintana et al., 2012, 2013a; Zhang et al., 2013; Nayak et al., 2015). The majority of these studies have focused on the anti-inflammatory and/or anti-fibrotic effects of A_{2B} receptor blockade.

At first glance, reports that A_{2B} antagonism is beneficial in chronic disease would appear to be contradictory to the reports of beneficial effects of A_{2B} agonism in the acute phase of myocardial ischemia. However, a review of the literature indicates there is substantial evidence for adenosine receptors playing dual roles in acute vs. chronic pathologies. For example, although the anti-inflammatory role of A_{2A} receptors has been recognized for years, there are more recent reports that A_{2A} receptor stimulation prolong IL-1β release and caspase-1 activity, consistent with inflammasome activation, in murine macrophages (Ouyang et al., 2013) and brain (Chiu et al., 2014). Ingwersen et al. (2016) also reported that while A_{2A} receptor stimulation was acutely beneficial in a murine model of autoimmune neuroinflammation, chronic inflammation was reduced in A_{2A} KO mice (Ingwersen et al., 2016). The time-dependent, opposing effects of adenosine A_{2A} and A_{2B} receptors are in fact consistent with the dual role of inflammation in the post-ischemic heart. Macrophages participate in both the initial pro-inflammatory phase to remove dead and dying tissue, but the subsequent anti-inflammatory period is necessary in order for cardiac fibroblasts to differentiate into myofibroblasts, which then deposit collagen (Nahrendorf et al., 2010; Frangogiannis, 2012; Prabhu and Frangogiannis, 2016). Collagen deposition is critical for maintaining scar thickness and strength in the infarct zone, but prolonged inflammation and excess collagen deposition lead to adverse ventricular remodeling (Nahrendorf et al., 2010; Frangogiannis, 2012; Prabhu and Frangogiannis, 2016).

To date there are only a very limited number of studies assessing potential beneficial effects of adenosine receptor blockade in chronic heart disease, both in experimental models and in clinical trials. Beneficial effects of A_1 receptor antagonists in experimental models of acute heart failure have been reported going back well over a decade (Nagashima et al., 1995; Givertz et al., 2007; Greenberg et al., 2007; Slawsky and Givertz, 2009). These beneficial effects were thought to be due primarily to blockade of A_1 receptor-mediated vasoconstriction of the renal afferent artery as well as proximal tubule reabsorption of sodium. Despite these positive findings in initial small trials, a large, randomized, placebo controlled Phase 3 trial (PROTECT) with the A_1 antagonist, rolofylline, failed to significantly impact cardiac or renal primary or secondary end points (Massie et al., 2010). More recently, the beneficial effects of A_{2B} receptor antagonism in experimental models of post-MI remodeling have been reported. Toldo et al. (2012) reported that the administration of the A_{2B} antagonist, GS-6201, immediately following a permanent occlusion in mice resulted in a thicker scar, less LV hypertrophy and improved post-MI cardiac function after 4 weeks. Similar findings were reported with the same A_{2B} antagonist in a chronic occlusion-reperfusion model in rats (Zhang et al., 2014). Thus, despite numerous experimental studies reporting beneficial effects of adenosine receptor antagonists in multiple non-cardiac pathologies, there remains a paucity of similar studies in chronic heart disease.

ADDITIONAL UNRESOLVED ISSUES

In addition to the above clinical-relevance issues, there are some unresolved basic science matters related to adenosine receptor-mediated cardioprotection. Adenosine receptors are differentially expressed on multiple cells types, thus altering the tissue and organ response to even selective agonists or antagonists (Chen et al., 2013; Sheth et al., 2014). This may explain, in part, the reported time-dependent differences in acute vs. chronic effects of adenosine receptor antagonists (Karmouty-Quintana et al., 2013b). As stated earlier, all four adenosine receptors have been implicated in protection against acute myocardial ischemia-reperfusion injury, and there are multiple reports that this is mediated by all four receptor subtypes modulating the same signaling pathways, presumably in cardiomyocytes (McIntosh and Lasley, 2012). There has yet to be an explanation why cardiomyocytes would express four different adenosine receptor subtypes exerting the same effect via the same signaling pathways. As discussed previously, the lack of studies addressing adenosine receptor effects in models of chronic myocardial ischemia have hindered our knowledge of the roles of specific adenosine receptors in non-cardiomyocytes, such as endothelial cells, immune cells and cardiac fibroblasts. Species-dependent differences in the selectivity of adenosine receptor agonists and antagonists have been recognized for many years, and this topic has most recently been addressed by Alnouri et al. (2015) and Jacobson and Müller (2016). This issue has undoubtedly had effects on the interpretation of numerous

experimental studies, but its biggest impact has probably been on clinical trials, where despite reports of safety and tolerance, there remain few reports on the efficacy of adenosine receptor analogs in treating ischemic heart disease (Massie et al., 2010; Voors et al., 2017). Finally, there is increasing evidence in multiple tissues, that adenosine receptors may exert their effects, in part, via receptor dimerization (Zhan et al., 2011; McIntosh and Lasley, 2012; Chandrasekera et al., 2013; Chen et al., 2013). This aspect of adenosine receptor modulation of myocardial ischemia-reperfusion injury needs to be further explored, as this may lead to new, clinically relevant therapies.

In conclusion, nearly 30 years of experimental findings support the hypothesis that adenosine receptors modulate acute myocardial ischemia-reperfusion injury. Despite this evidence, the use of adenosine, adenosine modulators, or adenosine analogs for treatment of cardiac injury has not been accepted clinically, nor have there been many clinical trials. Clearly the next phase of research on adenosine receptor cardioprotection needs to establish the role of adenosine receptor agonists and antagonists in more clinically relevant models of myocardial ischemia.

AUTHOR CONTRIBUTIONS

The author confirms being the sole contributor of this work and approved it for publication.

REFERENCES

Alnouri, M. W., Jepards, S., Casari, A., Schiedel, A. C., Hinz, S., and Müller, C. E. (2015). Selectivity is species-dependent: characterization of standard agonists and antagonists at human, rat, and mouse adenosine receptors. *Purinergic Signal*. 11, 389–407. doi: 10.1007/s11302-015-9460-9

Belikoff, B. G., Vaickus, L. J., Sitkovsky, M., and Remick, D. G. (2012). A2B adenosine receptor expression by myeloid cells is proinflammatory in murine allergic-airway inflammation. *J. Immunol.* 189, 3707–3713. doi: 10.4049/jimmunol.1201207

Bot, I., de Vries, H., Korporaal, S. J., Foks, A. C., Bot, M., van Veldhoven, J., et al. (2012). Adenosine A2B receptor agonism inhibits neointimal lesion development after arterial injury in apolipoprotein E-deficient mice. *Arterioscler. Thromb. Vasc. Biol.* 32, 2197–2205. doi: 10.1161/ATVBAHA.112.252924

Bulluck, H., Sirker, A., Loke, Y. K., Garcia-Dorado, D., and Hausenloy, D. J. (2016). Clinical benefit of adenosine as an adjunct to reperfusion in ST-elevation myocardial infarction patients: an updated meta-analysis of randomized controlled trials. *Int. J. Cardiol.* 202, 228–237. doi: 10.1016/j.ijcard.2015.09.005

Cabiati, M., Svezia, B., Guzzardi, M. A., Mattii, L., D'Amico, A., Caselli, C., Prescimone, T., et al. (2015). Adenosine receptor transcriptomic profile in cardiac tissue of a Zucker rat model. *DNA Cell Biol.* 34, 333–341. doi: 10.1089/dna.2014.2770

Cerqueira, M. D., Nguyen, P., Staehr, P., Underwood, S. R., Iskandrian, A. E., and ADVANCE-MPI Trial Investigators (2008). Effects of age, gender, obesity, and diabetes on the efficacy and safety of the selective A2A agonist regadenoson versus adenosine in myocardial perfusion imaging integrated ADVANCE-MPI trial results. *JACC Cardiovasc. Imaging* 1, 307–316. doi: 10.1016/j.jcmg.2008.02.003

Chandrasekera, P. C., Wan, T. C., Gizewski, E. T., Auchampach, J. A., and Lasley, R. D. (2013). Adenosine A1 receptors heterodimerize with β1- and β2-adrenergic receptors creating novel receptor complexes with altered G protein coupling and signaling. *Cell. Signal.* 25, 736–742. doi: 10.1016/j.cellsig.2012.12.022

Chen, J. F., Eltzschig, H. K., and Fredholm, B. B. (2013). Adenosine receptors as drug targets–what are the challenges? *Nat. Rev. Drug Discov.* 12, 265–286. doi: 10.1038/nrd3955

Chiu, G. S., Darmody, P. T., Walsh, J. P., Moon, M. L., Kwakwa, K. A., Bray, J. K., et al. (2014). Adenosine through the A2A adenosine receptor increases IL-1β in the brain contributing to anxiety. *Brain Behav. Immun.* 41, 218–231. doi: 10.1016/j.bbi.2014.05.018

Csoka, B., Nemeth, Z. H., Rosenberger, P., Eltzschig, H. K., Spolarics, Z., Pacher, P., et al. (2010). A2B adenosine receptors protect against sepsis-induced mortality by dampening excessive inflammation. *J. Immunol.* 185, 542–550. doi: 10.4049/jimmunol.0901295

Dhasmana, J. P., Digerness, S. B., Geckle, J. M., Ng, T. C., Glickson, J. D., and Blackstone, E. H. (1983). Effect of adenosine deaminase inhibitors on the heart's functional and biochemical recovery from ischemia: a study utilizing the isolated rat heart adapted to ^{31}P nuclear magnetic resonance. *J. Cardiovasc. Pharmacol.* 5, 1040–1047. doi: 10.1097/00005344-198311000-00019

Ely, S. W., Mentzer, R. M., Lasley, R. D., Lee, B. K., and Berne, R. M. (1985). Functional and metabolic evidence of enhanced myocardial tolerance to ischemia and reperfusion with adenosine. *J. Thorac. Cardiovasc. Surg.* 90, 549–556.

Feoktistov, I., and Biaggioni, I. (2011). Role of adenosine A(2B) receptors in inflammation. *Adv Pharmacol.* 61, 115–144. doi: 10.1016/B978-0-12-385526-8.00005-9

Frangogiannis, N. G. (2012). Regulation of the inflammatory response in cardiac repair. *Circ. Res.* 110, 159–173. doi: 10.1161/CIRCRESAHA.111.243162

Givertz, M., Massie, B., Fields, T., Pearson, L., and Dittrich, H. (2007). The effects of KW-3902, an adenosine A1-receptor antagonist, on diuresis and renal function in patients with acute decompensated heart failure and renal impairment or diuretic resistance. *J. Am. Coll. Cardiol.* 50, 1551–1560. doi: 10.1016/j.jacc.2007.07.019

Goto, M., Miura, T., Iliodoromitis, E. K., O'Leary, E. L., Ishimoto, R., Yellon, D. M., et al. (1991). Adenosine infusion during early reperfusion failed to limit myocardial infarct size in a collateral deficient species. *Cardiovasc. Res.* 25, 943–949.

Greenberg, B., Thomas, I., Banish, D., et al. (2007). Effects of multiple oral doses of an A1 adenosine antagonist, BG9928, in patients with heart failure: results of a placebo-controlled, dose-escalation study. *J. Am. Coll. Cardiol.* 50, 600–606. doi: 10.1016/j.jacc.2007.03.059

Haskó, G., and Cronstein, B. (2013). Regulation of inflammation by adenosine. *Front. Immunol.* 4:85. doi: 10.3389/fimmu.2013.00085

Hasko, G., Linden, J., Cronstein, B., and Pacher, P. (2008). Adenosine receptors: therapeutic aspects for inflammatory and immune diseases. *Nature Rev. Drug Disc.* 7, 759–770. doi: 10.1038/nrd2638

Headrick, J. P., and Lasley, R. D. (2009). Adenosine receptors and reperfusion injury of the heart. *Handb. Exp. Pharmacol.* 193, 189–214. doi: 10.1007/978-3-540-89615-9_7

Headrick, J. P., Willems, L., Ashton, K. J., Holmgren, K., Peart, J., and Matherne, G. P. (2003). Ischaemic tolerance in aged mouse myocardium: the role of adenosine and effects of A1 adenosine receptor overexpression. *J. Physiol.* 549, 823–833. doi: 10.1113/jphysiol.2003.041541

Homeister, J. W., Hoff, P. T., Fletcher, D. D., and Lucchesi, B. R. (1990). Combined adenosine and lidocaine administration limits myocardial reperfusion injury. *Circulation* 82, 595–608. doi: 10.1161/01.CIR.82.2.595

Humphrey, S. M., and Seelye, R. N. (1982). Improved functional recovery of ischemic myocardium by suppression of adenosine catabolism. *J. Thorac. Cardiovasc. Surg.* 84, 16–22.

Ingwersen, J., Wingerath, B., Graf, J., Lepka, K., Hofrichter, M., Schröter, F., et al. (2016). Dual roles of the adenosine A2a receptor in autoimmune neuroinflammation. *J. Neuroinflammation*. 13:48. doi: 10.1186/s12974-016-0512-z

Jacobson, K. A., and Müller, C. E. (2016). Medicinal chemistry of adenosine, P2Y and P2X receptors. *Neuropharmacology* 104, 31–49. doi: 10.1016/j.neuropharm.2015.12.001

Karmouty-Quintana, H., Philip, K., Acero, L. F., Chen, N. Y., Weng, T., Molina, J. G., et al. (2015). Deletion of ADORA2B from myeloid cells dampens lung fibrosis and pulmonary hypertension. *FASEB J.* 29, 50–60. doi: 10.1096/fj.14-260182

Karmouty-Quintana, H., Weng, T., Garcia-Morales, L. J., Chen, N. Y., Pedroza, M., Zhong, H., et al. (2013a). Adenosine A2B receptor and hyaluronan modulate pulmonary hypertension associated with chronic obstructive pulmonary disease. *Am. J. Respir. Cell Mol. Biol.* 49, 1038–1047. doi: 10.1165/rcmb.2013-0089OC

Karmouty-Quintana, H., Xia, Y., and Blackburn, M. R. (2013b). Adenosine signaling during acute and chronic disease states. *J. Mol. Med.* 91, 173–181. doi: 10.1007/s00109-013-0997-1

Karmouty-Quintana, H., Zhong, H., Acero, L., Weng, T., Melicoff, E., West, J. D., et al. (2012). The A2B adenosine receptor modulates pulmonary hypertension associated with interstitial lung disease. *FASEB J.* 26, 2546–2557. doi: 10.1096/fj.11-200907

Kloner, R. A., Forman, M. B., Gibbons, R. J., Ross, A. M., Alexander, R. W., and Stone, G. W. (2006). Impact of time to therapy and reperfusion modality on the efficacy of adenosine in acute myocardial infarction: the AMISTAD-2 trial. *Eur. Heart J.* 27, 2400–2405. doi: 10.1093/eurheartj/ehl094

Kolachala, V., Ruble, B., Vijay-Kumar, M., Wang, L., Mwangi, S., Figler, H., et al. (2008). Blockade of adenosine A2B receptors ameliorates murine colitis. *Br. J. Pharmacol.* 155, 127–137. doi: 10.1038/bjp.2008.227

Koupenova, M., Johnston-Cox, H., Vezeridis, A., Gavras, H., Yang, D., Zannis, V., et al. (2012). A2b adenosine receptor regulates hyperlipidemia and atherosclerosis. *Circulation*. 125, 354–363. doi: 10.1161/CIRCULATIONAHA.111.057596

Kristo, G., Yoshimura, Y., Keith, B. J., Mentzer, R. M. Jr., and Lasley, R. D. (2005). Aged rat myocardium exhibits normal adenosine receptor-mediated bradycardia and coronary vasodilation but increased adenosine agonist-mediated cardioprotection. *J. Gerontol. A Biol. Sci. Med. Sci.* 60, 1399–1404. doi: 10.1093/gerona/60.11.1399

Krumholz, H. M., Wang, Y., Chen, J., Drye, E. E., Spertus, J. A., Ross, J. S., et al. (2009). Reduction in acute myocardial infarction mortality in the United States: risk-standardized mortality rates from 1995-2006. *JAMA* 302, 767–773. doi: 10.1001/jama.2009.1178

Lasley, R. D., Jahania, M. S. A., Mentzer, R. M. Jr. (2001). Beneficial effects of the adenosine A_{2a} agonist CGS 21680 in infarcted and stunned porcine myocardium. *Am. J. Physiol.* 280, H1660–H1666. doi: 10.1152/ajpheart.2001.280.4.H1660

Lasley, R. D., Rhee, J. W., Van Wylen, D. G., and Mentzer, R. M. Jr. (1990). Adenosine A_1 receptor mediated protection of the globally ischemic isolated rat heart. *J. Mol. Cell. Cardiol.* 22, 39–47. doi: 10.1016/0022-2828(90)90970-D

Linden, J. (2011). Regulation of leukocyte function by adenosine receptors. *Adv Pharmacol.* 61, 95–114. doi: 10.1016/B978-0-12-385526-8.00004-7

Liu, G. S., Thornton, J., Van Winkle, D. M., Stanley, A. W., Olsson, R. A., and Downey, J. M. (1991). Protection against infarction afforded by preconditioning is mediated by A1 adenosine receptors in rabbit heart. *Circulation* 84, 350–356. doi: 10.1161/01.CIR.84.1.350

Long, X., Mokelke, E. A., Neeb, Z. P., Alloosh, M., Edwards, J. M., and Sturek, M. (2010). Adenosine receptor regulation of coronary blood flow in Ossabaw miniature swine. *J. Pharmacol. Exp. Ther.* 335, 781–787. doi: 10.1124/jpet.110.170803

Mahaffey, K. W., Puma, J. A., Barbagelata, N. A., DiCarli, M. F., Leesar, M. A., Browne, K. F., et al. (1999). Adenosine as an adjunct to thrombolytic therapy for acute myocardial infarction: results of a multicenter, randomized, placebo-controlled trial: the Acute Myocardial Infarction STudy of ADenosine (AMISTAD) trial. *J. Am. Coll. Cardiol.* 34, 1711–1720. doi: 10.1016/S0735-1097(99)00418-0

Massie, B. M., O'Connor, C. M., Metra, M., Ponikowski, P., Teerlink, J. R., Cotter, G., et al. (2010). Rolofylline, an adenosine A1-receptor antagonist, in acute heart failure. *N. Engl. J. Med.* 363, 1419–1428. doi: 10.1056/NEJMoa0912613

McIntosh, V. J., and Lasley, R. D. (2012). Adenosine receptor-mediated cardioprotection: are all 4 subtypes required or redundant? *J. Cardiovasc. Pharmacol. Ther.* 17, 21–33. doi: 10.1177/1074248410396877

Nagashima, K., Kusaka, H., and Karasawa, A. (1995). Protective effects of KW-3902, an adenosine A1-receptor antagonist, against cisplatin-induced acute renal failure in rats. *Jpn. J. Pharmacol.* 67, 349–357. doi: 10.1254/jjp.67.349

Nahrendorf, M., Pittet, M. J., and Swirski, F. K. (2010). Monocytes: protagonists of infarct inflammation and repair after myocardial infarction. *Circulation* 121, 2437–2445. doi: 10.1161/CIRCULATIONAHA.109.916346

Nayak, S., Khan, M. A., Wan, T. C., Pei, H., Linden, J., Dwinell, M. R., et al. (2015). Characterization of Dahl salt-sensitive rats with genetic disruption of the A2B adenosine receptor gene: implications for A2B adenosine receptor signaling during hypertension. *Purinergic Signal.* 11, 519–531. doi: 10.1007/s11302-015-9470-7

Olafsson, B., Forman, M. B., Puett, D. W., Pou, A., Cates, C. U., Friesinger, G. C., et al. (1987). Reduction of reperfusion injury in the canine preparation by intracoronary adenosine: importance of the endothelium and the no-reflow phenomenon. *Circulation* 76, 1135–1145. doi: 10.1161/01.CIR.76.5.1135

Ouyang, X., Ghani, A., Malik, A., Wilder, T., Colegio, O. R., Flavell, R. A., et al. (2013). Adenosine is required for sustained inflammasome activation via the A2A receptor and the HIF-1α pathway. *Nat. Commun.* 4:2909. doi: 10.1038/ncomms3909

Peart, J. N., Pepe, S., Reichelt, M. E., Beckett, N., See Hoe, L., Ozberk, V., et al. (2014). Dysfunctional survival-signaling and stress-intolerance in aged murine and human myocardium. *Exp. Gerontol.* 50, 72–81. doi: 10.1016/j.exger.2013.11.015

Pitarys, C. J., Virmani, R., Vildibill, H. D. Jr., Jackson, E. K., and Forman, M. B. (1991). Reduction of myocardial reperfusion injury by intravenous adenosine administered during the early reperfusion period. *Circulation* 83, 237–247. doi: 10.1161/01.CIR.83.1.237

Prabhu, S. D., and Frangogiannis, N. G. (2016). The biological basis for cardiac repair after myocardial infarction: from inflammation to fibrosis. *Circ. Res.* 119, 91–112. doi: 10.1161/CIRCRESAHA.116.303577

Reibel, D. K., and Rovetto, M. J. (1978). Myocardial ATP synthesis and mechanical function following oxygen deficiency. *Am. J. Physiol.* 234, H620–H624. doi: 10.1152/ajpheart.1978.234.5.H620

Sabbah, H. N., Gupta, R. C., Kohli, S., Wang, M., Rastogi, S., Zhang, K., et al. (2013). Chronic therapy with a partial adenosine A1-receptor agonist improves left ventricular function and remodeling in dogs with advanced heart failure. *Circ. Heart Fail.* 6, 563–571. doi: 10.1161/CIRCHEARTFAILURE.112.000208

Sangsiri, S., Dong, H., Swain, G. M., Galligan, J. J., and Xu, H. (2013). Impaired function of prejunctional adenosine A1 receptors expressed by perivascular sympathetic nerves in DOCA-salt hypertensive rats. *J. Pharmacol. Exp. Ther.* 345, 32–40. doi: 10.1124/jpet.112.199612

Schulman, D., Latchman, D. S., and Yellon, D. M. (2001). Effect of aging on the ability of preconditioning to protect rat hearts from ischemia-reperfusion injury. *Am. J. Physiol. Heart Circ. Physiol.* 281, H1630–H1636. doi: 10.1152/ajpheart.2001.281.4.H1630

Shaikh, G., and Cronstein, B. (2016). Signaling pathways involving adenosine A2A and A2B receptors in wound healing and fibrosis. *Purinergic Signal.* 12, 191–197. doi: 10.1007/s11302-016-9498-3

Sheth, S., Brito, R., Mukherjea, D., Rybak, L. P., and Ramkumar, V. (2014). Adenosine receptors: expression, function and regulation. *Int. J. Mol. Sci.* 28, 2024–2052. doi: 10.3390/ijms15022024

Slawsky, M. T., and Givertz, M. M. (2009). Rolofylline: a selective adenosine 1 receptor antagonist for the treatment of heart failure. *Expert Opin. Pharmacother.* 10, 311–322. doi: 10.1517/14656560802682213

Sun, C. X., Zhong, H., Mohsenin, A., Morschl, E., Chunn, J. L., Molina, J. G., et al. (2006). Role of A2B adenosine receptor signaling in adenosine-dependent pulmonary inflammation and injury. *J. Clin. Invest.* 116, 2173–2182. doi: 10.1172/JCI27303

Teng, B., Smith, J. D., Rosenfeld, M. E., Robinet, P., Davis, M. E., Morrison, R. R., et al. (2014). A1 adenosine receptor deficiency or inhibition reduces atherosclerotic lesions in apolipoprotein E deficient mice. *Cardiovasc. Res.* 102, 157–165. doi: 10.1093/cvr/cvu033

Toldo, S., Zhong, H., Mezzaroma, E., Van Tassell, B. W., Kannan, H., Zeng, D., et al. (2012). GS-6201, a selective blocker of the A2B adenosine receptor, attenuates cardiac remodeling after acute myocardial infarction in the mouse. *J. Pharmacol. Exp. Therap.* 343, 587–595. doi: 10.1124/jpet.111.191288

Toufektsian, M. C., Yang, Z., Prasad, K. M., Overbergh, L., Ramos, S. I, Mathieu, C., et al. (2006). Stimulation of A2A-adenosine receptors after myocardial infarction suppresses inflammatory activation and attenuates contractile dysfunction in the remote left ventricle. *Am. J. Physiol.* 290, H1410–H1418. doi: 10.1152/ajpheart.00860.2005

Vander Heide, R. S., and Reimer, K. A. (1996). Effect of adenosine therapy at reperfusion on myocardial infarct size in dogs. *Cardiovasc. Res.* 31, 711–718. doi: 10.1016/S0008-6363(95)00235-9

Villarreal, F., Epperson, S. A., Ramirez-Sanchez, I., Yamazaki, K. G., and Brunton, L. L. (2009). Regulation of cardiac fibroblast collagen synthesis by adenosine: roles for Epac and PI3K. *Am. J. Physiol. Cell Physiol.* 296, C1178–C1184. doi: 10.1152/ajpcell.00291.2008

Villarreal, F., Zimmermann, S., Makhsudova, L., Montag, A. C., Erion, M. D., Bullough, D. A., et al. (2003). Modulation of cardiac remodeling by adenosine: *in vitro* and *in vivo* effects. *Mol. Cell. Biochem.* 251, 17–26. doi: 10.1023/A:1025401026441

Voors, A. A., Düngen, H. D., Senni, M., Nodari, S., Agostoni, P., Ponikowski, P., et al. (2017). Safety and tolerability of neladenoson bialanate, a novel oral partial adenosine A1 receptor agonist, in patients with chronic heart failure. *J. Clin. Pharmacol.* 57, 440–451. doi: 10.1002/jcph.828

Wakeno, M., Minamino, T., Seguchi, O., Okazaki, H., Tsukamoto, O., Okada, K., et al. (2006). Long-term stimulation of adenosine A2b receptors begun after myocardial infarction prevents cardiac remodeling in rats. *Circulation* 114, 1923–1932. doi: 10.1161/CIRCULATIONAHA.106.630087

Wang, H., Zhang, W., Tang, R., Zhu, C., Bucher, C., Blazar, B. R., et al. (2010). Adenosine receptor A2A deficiency in leukocytes increases arterial neointima formation in apolipoprotein E-deficient mice. *Arterioscler. Thromb. Vasc. Biol.* 30, 915–922. doi: 10.1161/ATVBAHA.109.202572

Xaus, J., Mirabet, M., Lloberas, J., Soler, C., Lluis, C., Franco, R., et al. (1999). IFN-gamma up-regulates the A2B adenosine receptor expression in macrophages: a mechanism of macrophage deactivation. *J. Immunol.* 162, 3607–3614.

Yang, T., Zollbrecht, C., Winerdal, M. E., Zhuge, Z., Zhang, X. M., Terrando, N., et al. (2016). Genetic abrogation of adenosine A3 receptor prevents uninephrectomy and high salt-induced hypertension. *J. Am. Heart Assoc.* 5:7. doi: 10.1161/JAHA.116.003868

Zhan, E., McIntosh, V. J., and Lasley, R. D. (2011). Adenosine A2A and A2B receptors are both required for adenosine A1 receptor-mediated cardioprotection. *Am. J. Physiol.* 301, H1183–H1189. doi: 10.1152/ajpheart.00264.2011

Zhang, H., Zhong, H., Everett, T. H., Wilson, E., Chang, R., Zeng, D., et al. (2014). Blockade of A2B adenosine receptor reduces left ventricular dysfunction and ventricular arrhythmias 1 week after myocardial infarction in the rat model. *Heart Rhythm* 11, 101–109. doi: 10.1016/j.hrthm.2013.10.023

Zhang, W., Zhang, Y., Wang, W., Dai, Y., Ning, C., Luo, R., et al. (2013). Elevated ecto-5′-nucleotidase-mediated increased renal adenosine signaling via A2B adenosine receptor contributes to chronic hypertension. *Circ. Res.* 112, 1466–1478. doi: 10.1161/CIRCRESAHA.111.300166

Zhong, H., Belardinelli, L., Maa, T., and Zeng, D. (2005). Synergy between A2B adenosine receptors and hypoxia in activating human lung fibroblasts. *Am. J. Respir. Cell. Mol. Biol.* 32, 2–8. doi: 10.1165/rcmb.2004-0103OC

Zhou, Y., Schneider, D. J, Morschl, E, Song, L, Pedroza, M., Karmouty-Quintana, H., et al. (2011). Distinct roles for the A2B adenosine receptor in acute and chronic stages of bleomycin-induced lung injury. *J. Immunol.* 186, 1097–1106. doi: 10.4049/jimmunol.1002907

Conflict of Interest Statement: The author declares that the research was conducted in the absence of any commercial or financial relationships that could be construed as a potential conflict of interest.

frontiers in Pharmacology

MINI REVIEW
published: 27 March 2018
doi: 10.3389/fphar.2018.00266

Nanobody-Based Biologics for Modulating Purinergic Signaling in Inflammation and Immunity

*Stephan Menzel, Nicole Schwarz, Friedrich Haag and Friedrich Koch-Nolte**

Institute of Immunology, University Medical Center Hamburg-Eppendorf, Hamburg, Germany

Adenosine triphosphate (ATP) and nicotinamide adenine dinucleotide (NAD^+) are released as danger signals from cells during infection and sterile inflammation. In the extracellular compartment ATP is converted by CD39, CD73, and other ecto-enzymes into metabolites that modulate the activity of T cells and macrophages. While ATP mediates pro-inflammatory signals via P2X7 and other P2 receptors, adenosine triggers anti-inflammatory signaling via the adenosine 2a receptor (Adora2a) and other P1 receptors. The latter also plays a role in maintaining an immunosuppressive tumor microenvironment. NAD^+ is converted by CD38, CD203 and other ecto-enzymes to the Ca^{2+} mobilizing messengers cyclic ADP-ribose and ADP-ribose, and to adenosine. Recent findings on the roles of CD38, CD39, CD73, CD203, P2X7, and Adora2a in inflammation and immunity underscore the potential of these proteins as drug targets. However, available small molecule inhibitors often lack specificity and mediate unwanted off-target toxicity. Nanobodies – single domain antibodies derived from heavy chain antibodies that naturally occur in camelids – display a propensity to bind functional epitopes not accessible to conventional antibodies. Like conventional antibodies, nanobodies and nanobody-based biologics are highly specific and have well-understood, tunable *in vivo* pharmacodynamics with little if any toxicity. Nanobodies thus represent attractive alternatives to small molecule inhibitors for modulating purinergic signaling in inflammation and immunity. Here we review recent progress made in developing nanobodies against key targets of purinergic signaling.

Keywords: nanobody, purinergic signaling, biologics, heavy chain antibody, antibody engineering

OPEN ACCESS

Edited by:
Kenneth A. Jacobson, National Institutes of Health (NIH), United States

Reviewed by:
Szilvia Benkö, University of Debrecen, Hungary
Gregory C. Ippolito, University of Texas at Austin, United States
Francesco Di Virgilio, University of Ferrara, Italy

***Correspondence:**
Friedrich Koch-Nolte
nolte@uke.de

Specialty section:
This article was submitted to Experimental Pharmacology and Drug Discovery, a section of the journal Frontiers in Pharmacology

Received: *03 January 2018*
Accepted: *09 March 2018*
Published: *27 March 2018*

Citation:
Menzel S, Schwarz N, Haag F and Koch-Nolte F (2018) Nanobody-Based Biologics for Modulating Purinergic Signaling in Inflammation and Immunity. Front. Pharmacol. 9:266. doi: 10.3389/fphar.2018.00266

INTRODUCTION

Purinergic signaling by extracellular ATP, NAD^+ and their metabolites is recognized as an important regulatory mechanism in inflammation and immunity (Junger, 2011; Eltzschig et al., 2012; Idzko et al., 2014; Burnstock, 2016). The intact nucleotides and their common metabolite adenosine play pro- and anti-inflammatory roles, respectively. The ecto-enzymes and receptors that mediate purinergic signaling, therefore, represent promising targets for immunomodulatory drugs (Burnstock, 2017). A number of small molecule inhibitors are available that antagonize

Abbreviations: ADCC, antibody-dependent cytotoxicity; ADP, adenosine diphosphate; ADPR, adenosine diphosphate ribose; AMP, adenosine monophosphate; ATP, adenosine triphosphate; BBB, blood brain barrier; CDC, complement-dependent cytotoxicity; GPCR, G-protein coupled receptor; HLE, half-life extended; Ig, immunoglobulin, IL-, interleukin; kD, kilodalton; NAD^+, nicotinamide adenine dinucleotide; NICD, NAD^+ induced cell death.

ionotropic (P2X) and metabotropic (P2Y) ATP-receptors, ATP- and NAD- hydrolyzing enzymes (CD38, CD39, CD73, CD203), and metabotropic (P1) adenosine receptors (Buque et al., 2016; Jacobson and Muller, 2016). Several of these show promising therapeutic benefit in animal models of inflammatory diseases and/or in animal tumor models (Buque et al., 2016; Burnstock, 2016). Recently, antibodies and nanobodies have emerged as a potent alternative class of therapeutics (Wesolowski et al., 2009; Krah et al., 2016; Steeland et al., 2016).

Nanobodies are single domain antibody fragments derived from heavy chain antibodies naturally occurring in dromedaries, llamas, and other camelids (**Figure 1A**) (Hamers-Casterman et al., 1993; Muyldermans, 2013). In these animals, the IgG2 and IgG3 isotypes lack light chains and the CH1 domain. Nanobodies correspond to the variable domain of these heavy chain antibodies (also designated VHH). VHHs carry mutations that render them highly soluble in the absence of a paired light chain. VHHs often have longer CDR3 loops than the VH domain of conventional antibodies. These long CDR3 loops can mediate binding to hidden epitopes on target proteins such as the catalytic cavity of an enzyme, the ligand binding site of an ion channel or of a GPCR (Lauwereys et al., 1998; De Genst et al., 2006; Wesolowski et al., 2009). Because of their small size (15 kD, 3 nm), nanobodies generally show excellent tissue penetration. On the other hand, these small proteins pass the renal filtration barrier, accounting for a much shorter serum half life than that of conventional antibodies. Their robust, soluble single domain format, renders nanobodies amenable for genetic fusion to other protein domains. It is much easier to link two or more nanobodies into bi- or multivalent formats than the corresponding VH+VL domains of conventional antibodies. Linkage to an albumin-specific nanobody, for example, provides a simple strategy to extend the *in vivo* half life (Tijink et al., 2008). Nanobodies, thus represent promising tools to target the key players of purinergic signaling, in particular hidden functional epitopes of these proteins (**Figure 1B**).

NUCLEOTIDE METABOLIZING ECTO-ENZYMES AS TARGET FOR NANOBODIES

Adenosine triphosphate (ATP) and nicotinamide adenine dinucleotide (NAD^+) are released as danger signals from cells during infection and sterile inflammation (Haag et al., 2007; Junger, 2011; Eltzschig et al., 2012; Idzko et al., 2014). In the extracellular compartment ATP is converted by CD39, CD73, CD203 and related enzymes into ADP, AMP, and adenosine, metabolites that modulate the activity of T cells and macrophages. NAD^+ is converted by CD38, CD73, and CD203 into nicotinamide and the Ca^{2+} mobilizing messengers cyclic ADP-ribose (cADPR) and ADP-ribose (ADPR), and finally to adenosine (**Figure 1C**). Extracellular NAD^+ is also a substrate for the CD296 family of toxin-related ecto-enzymes that modify cell surface proteins by ADP-ribosylation.

Nanobodies Targeting CD296/ARTC2.2

In response to NAD^+ released from cells during inflammation, the ARTC2.2 ecto-enzyme ADP-ribosylates the P2X7 ion channel (Adriouch et al., 2008; Laing et al., 2010) and other cell surface proteins. ADP-ribosylation of P2X7 at R125 covalently attaches the weak ligand ADP-ribose close to the ATP binding pocket.

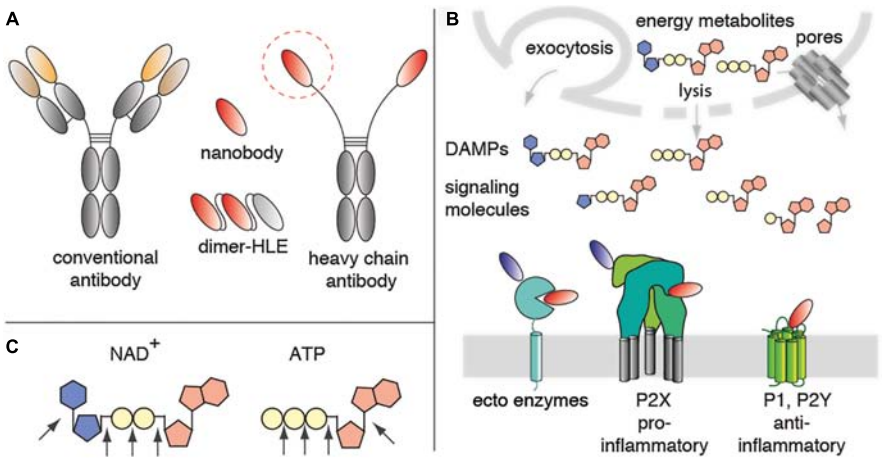

FIGURE 1 | Mediators of purinergic signaling as potential nanobody targets. **(A)** Nanobodies correspond to the variable domain of heavy chain antibodies. These single domain antibodies often contain a long CDR3 that can extend into crevices on proteins that are not accessible to conventional antibodies. Nanobodies are highly soluble and are thus easily linked into bivalent and/or bispecific formats. For example, fusion of a homodimeric nanobody to an albumin-specific nanobody yields a half-life extended dimer (Dimer-HLE). **(B)** The energy metabolites ATP and NAD^+ are released from cells during inflammation. In the extracellular space, these nucleotides function as danger associated molecular patterns (DAMPs) or signaling molecules. Immune cells express ecto-enzymes that convert pro-inflammatory ATP and NAD^+ into anti-inflammatory adenosine. Immune cells also express ionotropic ligand-gated ion channels (P2X) and metabotropic GPCRs (P1, P2Y) that respond to ATP, NAD^+ and their metabolites. These ecto-enzymes and purinergic receptors represent potential targets for immunomodulatory nanobodies. Antagonist nanobodies are illustrated schematically in red, potentiating nanobodies in blue. **(C)** Schematic diagram of NAD^+, ATP and the linkages that are targets for ecto-enzymes.

Chronic activation of P2X7 leads to cell death. This phenomenon is designated NICD (Seman et al., 2003). Regulatory T cells, NKT cells, and tissue resident memory T cells (Trm) are particularly sensitive to NICD (Hubert et al., 2010; Rissiek et al., 2014; Fernandez-Ruiz et al., 2016).

ARTC2 ecto-enzymes are not expressed by human cells because the orthologous gene in humans and other primates is inactivated by premature stop codons (Haag et al., 1994). Notwithstanding, ARTC2.2 is the first immune cell ecto-enzyme for which potent, highly specific, antagonistic nanobodies have been developed (Koch-Nolte et al., 2007). Systemic application of ARTC2.2 -blocking nanobodies in mouse models have yielded important insights that may be relevant also to nanobodies targeting other mediators of purinergic signaling. Nanobodies reach and opsonize ARTC2.2 on the surface of immune cells much faster than conventional antibodies: After intravenous or intraperitoneal injection at moderate dosage (2 mg/kg), the nanobodies completely opsonized ARTC2.2 within 10 min after injection, whereas conventional antibodies achieved this only at 2 h after injection (Koch-Nolte et al., 2007; Hubert et al., 2010; Scheuplein et al., 2010). Conversely, unbound nanobodies were rapidly eliminated via renal infiltration while conventional antibodies and nanobody-based heavy chain antibodies were shown to have a much longer half life (Bannas et al., 2014, 2015). The effective functional blockade of ARTC2.2 enzyme activity by the injected nanobodies and nanobody-based heavy chain antibodies could readily be monitored on T cells recovered from lymphatic tissues of nanobody-injected mice: both formats effectively blocked ARTC2.2-catalyzed ADP-ribosylation of cell surface proteins and ARTC2.2-mediated NICD (Koch-Nolte et al., 2007; Hubert et al., 2010; Scheuplein et al., 2010). By introducing three amino acid substitutions into the Fc domain [LSF previously shown to mediate enhanced binding of IgG to the neonatal Fc-receptor (Ghetie et al., 1997)] blockade of ARTC2.2 *in vivo* could be extended to >1 week, even after injection of only a very low dose (0.2 mg/kg) of the nanobody-based heavy chain antibody LSF mutant (Scheuplein et al., 2010). In the NOD mouse model of genetically determined type 1 diabetes, weekly injections of this ARTC2.2-blocking heavy chain antibody resulted in a significant elevation of iNKT cell numbers in lymph nodes and spleen for at least 4 weeks after injection.

During the preparation of primary lymphocytes from spleen, lymph node, blood or liver, sufficient quantities of NAD^+ are released from the mechanically stressed cells to permit ARTC2.2-catalyzed ADP-ribosylation of P2X7 and induction of NICD of Tregs, NKT, and Trm cells (Hubert et al., 2010; Rissiek et al., 2014; Fernandez-Ruiz et al., 2016). A single systemic injection of ARTC2.2-blocking nanobodies or nanobody-based heavy chain antibodies 30 min before sacrifice effectively prevents NICD of NKT cells and Tregs during cell preparation. Without such treatment ARTC2.2-expressing regulatory immune cells show poor survival during *in vitro* re-stimulation as well in adoptive transfer studies.

Nanobodies Targeting CD38

CD38, the major NAD^+-hydrolyzing ecto-enzyme, plays a decisive role in controlling the local levels of extracellular NAD^+. CD38 is expressed by various hematopoietic cells, in particular by B cells and NK cells. CD38 hydrolyzes NAD^+ to ADPR and cADPR, releasing nicotinamide. ADP-ribose is further hydrolyzed to phosphoriboside and AMP by members of the CD203 family of phosphodiesterases and eventually to adenosine by CD73. Two CD38-specific antibodies (daratumumab, isatuximab) have recently been licensed for the treatment of multiple myeloma, since these tumor cells often upregulate cell surface expression of CD38 to very high levels (van de Donk et al., 2017). The therapeutic benefit of these antibodies is thought to be mediated by their cytotoxic effects on tumor cells rather than by antagonizing the enzymatic activity of CD38. Recent evidence indicates that CD38 is also strongly upregulated by many solid tumors. It has been proposed that CD38 contributes to the immunosuppressive tumor microenvironment by hydrolyzing NAD^+ (Horenstein et al., 2015). In line with this hypothesis, blocking CD38 enzyme activity in the tumor microenvironment may be a therapeutic strategy. Isatuximab was shown to inhibit the enzymatic activity of CD38, even though its binding site is far away from the NAD^+ binding crevice, implying that this antibody acts by an allosteric mechanism (Deckert et al., 2014). Recently, 22 CD38-specific nanobodies were reported, two of which inhibited and two of which enhanced CD38 enzymatic activity (Li et al., 2016; Fumey et al., 2017). The results of epitope mapping and cocrystallization analyses indicate that these functional nanobodies, like isatuximab, act in an allosteric fashion rather than by direct binding to the active site. It is conceivable that the active site cleft of CD38 faces the plasma membrane and therefore is not easily accessible to antibodies or nanobodies. Some of the nanobodies have been shown to effectively target CD38 on human tumor cells in a mouse Xenograft model (Fumey et al., 2017) and some of these nanobodies bind independently of daratumumab and isatuximab and may, therefore, be useful for detecting cell surface CD38 in daratumumab- and isatuximab-treated patients (Oberle et al., 2017).

Other Ecto-Enzymes as Potential Targets for Inhibitory Nanobodies

Similar to ARTC2.2 and CD38, other nucleotide metabolizing ecto-enzymes including CD39, CD73, CD203, and alkaline phosphatase represent promising targets for nanobody-based antagonists and/or agonists (Yegutkin, 2008; Deaglio and Robson, 2011; Horenstein et al., 2013; al-Rashida and Iqbal, 2014) Blocking the hydrolysis of nucleotides to adenosine is predicted to promote inflammatory responses and thus may represent viable therapeutic strategies in chronic infection and oncology. Conversely, promoting the conversion of extracellular nucleotides to adenosine may be beneficial in chronic inflammation. Many of these enzymes display deep active site crevices that are difficult to block with conventional antibodies but may be accessible for nanobodies. CD73 may present an exception from this theme. The crystal structures of CD73 in closed and open conformation revealed that this enzyme undergoes a dramatic conformational rearrangement upon AMP-binding (Knapp et al., 2012). This dramatic

conformational shift may facilitate antibody mediated inhibition of CD73 by non-competitive mechanisms, e.g., by sterically blocking the shift in conformation, rather than occluding the active site (Geoghegan et al., 2016).

PURINERGIC P1 AND P2 RECEPTORS AS TARGETS FOR NANOBODIES

ATP, NAD^+ and their metabolites act as ligands for ionotropic (P2X) and metabotropic (P1, P2Y) receptors, many of which are expressed by immune cells (Burnstock and Boeynaems, 2014; Di Virgilio and Vuerich, 2015). Targeting these cell surface receptors with antagonistic and/or agonistic nanobodies thus might also provide novel therapeutic approaches in inflammation and immunity.

Nanobodies Targeting P2X7

The P2X7 ion channel is expressed by monocytes and T cells and is gated upon binding of extracellular ATP, permitting influx of calcium (Ca^{2+}) and sodium (Na^+) and efflux of potassium (K^+) (Bartlett et al., 2014; Di Virgilio et al., 2017). This triggers assembly of the inflammasome, release of the pro-inflammatory cytokine IL-1 β (IL-1β), ectodomain shedding of membrane proteins and externalization of phosphatidylserine (Ferrari et al., 2006; Giuliani et al., 2017). P2X7 is a potential therapeutic target in inflammatory diseases, such as glomerulonephritis, multiple sclerosis, and chronic pain (Bartlett et al., 2014; McInnes et al., 2014).

A set of 21 nanobodies was selected by phage display from llamas immunized with cDNA expression vectors encoding mouse and human P2X7 (Danquah et al., 2016). Six of eighteen nanobody families either blocked or enhanced activation of mouse P2X7 by both ATP and NAD^+-mediated pathways and two of three nanobody families effectively blocked ATP-mediated gating of human P2X7. Dimerization via a flexible G4S linker enhanced the potencies of both, the antagonistic 13A7 nanobody and the potentiating 14D5 nanobody to low nanomolar/high picomolar IC_{50} values. Both nanobodies modulated P2X7 function when added either before or after the ligand ATP. Intriguingly, addition of the 13A7 blocked binding of the 14D5 and vice versa, indicating that these nanobodies either bind to overlapping epitopes or to alternative conformational states of P2X7. Genetic fusion of homodimeric nanobodies to the albumin-binding nanobody Alb8 markedly increased the *in vivo* half-life from hours to days. This trimeric nanobody-format was designated HLE-dimer (half-life extended αP2X7 dimer). A similar extension of the *in vivo* half life was achieved by fusing the nanobody monomers to the hinge and Fc domains of mouse or human IgG, thereby reconstituting a bivalent heavy chain antibody format. In two different mouse models systemic administration of the P2X7-antagonistic 13A7 HLE-dimer at a moderate dosage (1 mg/kg every 3 days) significantly ameliorated inflammation scores. In the model of DNTB-induced allergic contact dermatitis, 13A7 HLE-dimer reduced local inflammation as measured by ear weight and levels of the inflammatory cytokines IL-1ß and IL-6 to a similar extent as the corticosteroid Dexamethasone. Similarly, in the model of antibody-induced glomerulonephritis, the P2X7-antagonistic 13A7 HLE-dimer significantly reduced leukocyte infiltration of glomeruli and proteinuria. In a surrogate human inflammation model with endotoxin-treated blood samples, the human P2X7 antagonistic Dano1 nanobody effectively blocked ATP-induced release of IL-1β with subnanomolar IC_{50} values, i.e., at >1.000 fold higher potency than benchmark small molecule inhibitors of P2X7. Nanobody Dano1 thus is an excellent clinical candidate.

Other Purinergic Receptors as Potential Targets for Inhibitory Nanobodies

Analogous to P2X7, P2X4, and P2X1 are expressed by immune cells and could be targets for nanobody-based antagonists and/or agonists (Burnstock, 2016). The P1 and P2Y receptors are GPCRs that respond to adenosine and purine nucleotides, respectively (Jacobson and Muller, 2016) and Adora2a and P2Y11 receptors are most relevant for inflammation and immunity (Sitkovsky et al., 2014; Young et al., 2016; Kennedy, 2017). Since these GPCRs have much smaller extracellular domains than the P2X receptors, inducing specific antibodies against GPCRs is much more challenging than in case of P2XRs. Notwithstanding, potent antagonistic nanobodies have been developed from llamas immunized with cDNA expression vectors encoding two non-purinergic lymphocyte GPCRs: CXCR4 and ChemR23, receptors for chemotactic proteins (Jahnichen et al., 2010; Claes et al., 2016; Peyrassol et al., 2016). It is thus not farfetched to propose that this strategy may also yield nanobodies targeting P1 and P2Y receptors.

ADVANTAGES AND LIMITATIONS OF NANOBODY-BASED BIOLOGICS IN PURINERGIC PHARMACOLOGY

Nanobodies directed against key players of purinergic signaling are valuable tools for research and diagnosis. Fluorochrome-conjugated nanobodies, for example, are well suited for flow cytometry, microscopy, and molecular imaging applications (Fumey et al., 2017). For example, nanobody JK36 recognizes a non-overlapping epitope on CD38 and can therefore detect cell surface CD38 by flow cytometry even in patients under treatment with daratumumab – where occupancy of CD38 by daratumumab prevents binding of most commercial diagnostic mAbs (Oberle et al., 2017). Owing to their small size, fluorochrome-conjugated nanobodies often provide much higher resolution images in fluorescence microscopy than conventional antibodies (Pleiner et al., 2015). Nanobodies have also proven useful as crystallization chaperones for 3D-structure analyses of GPCRs (Steyaert and Kobilka, 2011). On the other hand, native membrane protein-specific nanobodies usually do not work well in Western-Blot analyses, since their target epitopes are often destroyed by denaturing gel electrophoresis.

Table 1 summarizes advantages and limitations of nanobodies vs. antibodies and small molecule drugs. In contrast to most small molecule drugs, antibodies and nanobodies generally are

TABLE 1 | Advantages and limitations of nanobodies and antibodies vs. small molecule drugs in purinergic pharmacology.

	Antibodies	Nanobodies	Small molecules
Size	150 kD	15 kD	∼1 kD
Development costs	High	Moderate	Usually low
Administration	i.v., s.c.	i.v., s.c., aerosol, topical	oral, i.v.
Specificity	High	High	Variable
Off target adverse effects	None	None	P1, P2, kinases, ATPases, dehydrogenases
On target adverse effects	Depends on target	Depends on target	Depends on target
In Vivo half-life	Can be adjusted by Fc-engineering	Can be adjusted by PEGylation or fusion to albumin-specific Nb	Variable (usually short)
Metabolites	Non-toxic, biodegradable	Non-toxic, biodegradable	Potentially toxic
Tissue penetration	Slow	Excellent in periphery	Variable
Tissue specificity	Targetable (bi-specific Abs)	Targetable (bi- specific Nbs)	Variable
Albumin binding	Usually not	Via albumin-specific Nb to extend half life, usually no effect on potency	May reduce potency

not orally available, i.e., they need to be administered by infusion or subcutaneous injection. High costs of clinical development and production still are handicaps of antibodies and nanobodies (Brekke and Sandlie, 2003). On the other hand, antibodies and nanobodies show exquisite specificity to the target molecule and – in contrast to small molecules – show little if any off-target side effects (Steeland et al., 2016). Nanobodies and antibodies are biodegradable and – in contrast to small molecules – do not suffer from conversion to toxic metabolites. While antibodies display uniform pharmacodynamics and a longer *in vivo* or serum half life than small molecules and nanobodies, their large size (150 kD) limits their penetration into solid tumors and other tissues. With a small size (15 kD), excellent tissue penetration and rapid renal filtration of unbound molecules, nanobodies, however, are exceptionally well suited for *in vivo* molecular imaging applications (Chakravarty et al., 2014; Bannas et al., 2015; Rashidian et al., 2015; Beghein and Gettemans, 2017).

Antibodies and nanobodies both show little if any capacity to cross the BBB. This can be an advantage for the therapeutic targeting of purinergic enzymes and receptors in inflammation and oncology outside the nervous system, because this limits on-target side effects in the central nervous system. The BBB, however, presents a limitation for therapeutic targeting inflammation and oncology in the CNS. If desired, passage of antibodies through the BBB can be enhanced by genetic fusion or conjugation to binding modules for the transferrin receptor and other transcytosis receptors (Farrington et al., 2014). Because of their small size and modular nature, nanobodies may be suited better for this strategy than conventional antibodies. The Fc-domain of conventional antibodies can mediate unwanted complement dependent and/or cell-mediated cytotoxicity (CDC, ADCC). Here, lack of an Fc domain can be an advantage for nanobodies. If the deletion of tumor cells or certain immune cell subsets is desired for therapeutic purposes, nanobodies can readily be fused to the Fc domain of conventional antibodies to generate a nanobody-based heavy chain antibody (75 kD). Such heavy chain antibodies are amenable for the full power of Fc-engineering technologies, i.e., substitution of amino acid residues that enhance/reduce *in vivo* half life and/or cytotoxicity (Liu et al., 2017).

Most purine metabolizing ecto-enzymes and purinergic receptors are not restricted to immune cells. Many of these enzymes and receptors are also expressed by cells of the cardiovascular system and the CNS. It will thus be important to monitor potential on-target side effects of the nanobodies that modulate their target on cells of other tissues. Owing to their high solubility and modular format, nanobodies can easily be linked to other nanobodies (Els Conrath et al., 2001; Bannas et al., 2017). This opens the opportunity to generate bi-specific biologics with improved cellular specificity, e.g., by linking a purinergic receptor-specific nanobody to a nanobody directed against a tissue differentiation antigen.

CONCLUSION AND OUTLOOK

Nanobodies display a propensity to bind functional epitopes not accessible to conventional antibodies. Nanobodies that antagonize the purine-metabolizing ecto-enzymes ARTC2.2 and CD38 or the ATP-gated ion channel P2X7 have provided proof of concept for the notion that these small biologics represent attractive alternatives to small molecule inhibitors for modulating purinergic signaling in inflammation and immunity. It is thus not unlikely that caplacizumab, the first nanobody that is bound to reach the clinic next year, will pave the way for nanobody-based therapeutics also in the field of purinergic pharmacology.

AUTHOR CONTRIBUTIONS

FH and FK-N conceived the project. SM, NS, and FK-N wrote the manuscript. All authors reviewed and approved the manuscript.

FUNDING

This work was supported by Grant Nos. 310/11-1, SFB1192 B5, and Ha2369/5-1 to FK-N and FH.

REFERENCES

Adriouch, S., Bannas, P., Schwarz, N., Fliegert, R., Guse, A. H., Seman, M., et al. (2008). ADP-ribosylation at R125 gates the P2X7 ion channel by presenting a covalent ligand to its nucleotide binding site. *FASEB J.* 22, 861–869. doi: 10.1096/fj.07-9294com

al-Rashida, M., and Iqbal, J. (2014). Therapeutic potentials of ecto-nucleoside triphosphate diphosphohydrolase, ecto-nucleotide pyrophosphatase/phosphodiesterase, ecto-5'-nucleotidase, and alkaline phosphatase inhibitors. *Med. Res. Rev.* 34, 703–743. doi: 10.1002/med.21302

Bannas, P., Hambach, J., and Koch-Nolte, F. (2017). Nanobodies and nanobody-based human heavy chain antibodies as antitumor therapeutics. *Front. Immunol.* 8:1603. doi: 10.3389/fimmu.2017.01603

Bannas, P., Lenz, A., Kunick, V., Well, L., Fumey, W., Rissiek, B., et al. (2015). Molecular imaging of tumors with nanobodies and antibodies: timing and dosage are crucial factors for improved in vivo detection. *Contrast Media Mol. Imaging* 10, 367–378. doi: 10.1002/cmmi.1637

Bannas, P., Well, L., Lenz, A., Rissiek, B., Haag, F., Schmid, J., et al. (2014). In vivo near-infrared fluorescence targeting of T cells: comparison of nanobodies and conventional monoclonal antibodies. *Contrast Media Mol. Imaging* 9, 135–142. doi: 10.1002/cmmi.1548

Bartlett, R., Stokes, L., and Sluyter, R. (2014). The P2X7 receptor channel: recent developments and the use of P2X7 antagonists in models of disease. *Pharmacol. Rev.* 66, 638–675. doi: 10.1124/pr.113.008003

Beghein, E., and Gettemans, J. (2017). Nanobody technology: a versatile toolkit for microscopic imaging, protein-protein interaction analysis, and protein function exploration. *Front. Immunol.* 8:771. doi: 10.3389/fimmu.2017.00771

Brekke, O. H., and Sandlie, I. (2003). Therapeutic antibodies for human diseases at the dawn of the twenty-first century. *Nat. Rev. Drug Discov.* 2, 52–62. doi: 10.1038/nrd984

Buque, A., Bloy, N., Aranda, F., Cremer, I., Eggermont, A., Fridman, W. H., et al. (2016). Trial watch-small molecules targeting the immunological tumor microenvironment for cancer therapy. *Oncoimmunology* 5:e1149674. doi: 10.1080/2162402X.2016.1149674

Burnstock, G. (2016). P2X ion channel receptors and inflammation. *Purinergic Signal.* 12, 59–67. doi: 10.1007/s11302-015-9493-0

Burnstock, G. (2017). The therapeutic potential of purinergic signalling. *Biochem. Pharmacol.* doi: 10.1016/j.bcp.2017.07.016 [Epub ahead of print].

Burnstock, G., and Boeynaems, J. M. (2014). Purinergic signalling and immune cells. *Purinergic Signal.* 10, 529–564. doi: 10.1007/s11302-014-9427-2

Chakravarty, R., Goel, S., and Cai, W. (2014). Nanobody: the "magic bullet" for molecular imaging? *Theranostics* 4, 386–398. doi: 10.7150/thno.8006

Claes, K., Vandewalle, K., Laukens, B., Laeremans, T., Vosters, O., Langer, I., et al. (2016). Modular integrated secretory system engineering in pichia pastoris to enhance G-protein coupled receptor expression. *ACS Synth. Biol.* 5, 1070–1075. doi: 10.1021/acssynbio.6b00032

Danquah, W., Meyer-Schwesinger, C., Rissiek, B., Pinto, C., Serracant-Prat, A., Amadi, M., et al. (2016). Nanobodies that block gating of the P2X7 ion channel ameliorate inflammation. *Sci. Transl. Med.* 8:366ra162. doi: 10.1126/scitranslmed.aaf8463

De Genst, E., Silence, K., Decanniere, K., Conrath, K., Loris, R., Kinne, J., et al. (2006). Molecular basis for the preferential cleft recognition by dromedary heavy-chain antibodies. *Proc. Natl. Acad. Sci. U.S.A.* 103, 4586–4591. doi: 10.1073/pnas.0505379103

Deaglio, S., and Robson, S. C. (2011). Ectonucleotidases as regulators of purinergic signaling in thrombosis, inflammation, and immunity. *Adv. Pharmacol.* 61, 301–332. doi: 10.1016/B978-0-12-385526-8.00010-2

Deckert, J., Wetzel, M. C., Bartle, L. M., Skaletskaya, A., Goldmacher, V. S., Vallee, F., et al. (2014). SAR650984, a novel humanized CD38-targeting antibody, demonstrates potent antitumor activity in models of multiple myeloma and other CD38+ hematologic malignancies. *Clin. Cancer Res.* 20, 4574–4583. doi: 10.1158/1078-0432.CCR-14-0695

Di Virgilio, F., Dal Ben, D., Sarti, A. C., Giuliani, A. L., and Falzoni, S. (2017). The P2X7 receptor in infection and inflammation. *Immunity* 47, 15–31. doi: 10.1016/j.immuni.2017.06.020

Di Virgilio, F., and Vuerich, M. (2015). Purinergic signaling in the immune system. *Auton. Neurosci.* 191, 117–123. doi: 10.1016/j.autneu.2015.04.011

Els Conrath, K., Lauwereys, M., Wyns, L., and Muyldermans, S. (2001). Camel single-domain antibodies as modular building units in bispecific and bivalent antibody constructs. *J. Biol. Chem.* 276, 7346–7350. doi: 10.1074/jbc.M007734200

Eltzschig, H. K., Sitkovsky, M. V., and Robson, S. C. (2012). Purinergic signaling during inflammation. *N. Engl. J. Med.* 367, 2322–2333. doi: 10.1056/NEJMra1205750

Farrington, G. K., Caram-Salas, N., Haqqani, A. S., Brunette, E., Eldredge, J., Pepinsky, B., et al. (2014). A novel platform for engineering blood-brain barrier-crossing bispecific biologics. *FASEB J.* 28, 4764–4778. doi: 10.1096/fj.14-253369

Fernandez-Ruiz, D., Ng, W. Y., Holz, L. E., Ma, J. Z., Zaid, A., Wong, Y. C., et al. (2016). Liver-resident memory CD8(+) T cells form a front-line defense against malaria liver-stage infection. *Immunity* 45, 889–902. doi: 10.1016/j.immuni.2016.08.011

Ferrari, D., Pizzirani, C., Adinolfi, E., Lemoli, R. M., Curti, A., Idzko, M., et al. (2006). The P2X7 receptor: a key player in IL-1 processing and release. *J. Immunol.* 176, 3877–3883. doi: 10.4049/jimmunol.176.7.3877

Fumey, W., Koenigsdorf, J., Kunick, V., Menzel, S., Schutze, K., Unger, M., et al. (2017). Nanobodies effectively modulate the enzymatic activity of CD38 and allow specific imaging of CD38(+) tumors in mouse models in vivo. *Sci. Rep.* 7:14289. doi: 10.1038/s41598-017-14112-6

Geoghegan, J. C., Diedrich, G., Lu, X., Rosenthal, K., Sachsenmeier, K. F., Wu, H., et al. (2016). Inhibition of CD73 AMP hydrolysis by a therapeutic antibody with a dual, non-competitive mechanism of action. *mAbs* 8, 454–467. doi: 10.1080/19420862.2016.1143182

Ghetie, V., Popov, S., Borvak, J., Radu, C., Matesoi, D., Medesan, C., et al. (1997). Increasing the serum persistence of an IgG fragment by random mutagenesis. *Nat. Biotechnol.* 15, 637–640. doi: 10.1038/nbt0797-637

Giuliani, A. L., Sarti, A. C., Falzoni, S., and Di Virgilio, F. (2017). The P2X7 Receptor-Interleukin-1 Liaison. *Front. Pharmacol.* 8:123. doi: 10.3389/fphar.2017.00123

Haag, F., Adriouch, S., Brass, A., Jung, C., Moller, S., Scheuplein, F., et al. (2007). Extracellular NAD and ATP: partners in immune cell modulation. *Purinergic Signal.* 3, 71–81. doi: 10.1007/s11302-006-9038-7

Haag, F., Koch-Nolte, F., Kuhl, M., Lorenzen, S., and Thiele, H. G. (1994). Premature stop codons inactivate the RT6 genes of the human and chimpanzee species. *J. Mol. Biol.* 243, 537–546. doi: 10.1006/jmbi.1994.1680

Hamers-Casterman, C., Atarhouch, T., Muyldermans, S., Robinson, G., Hamers, C., Songa, E. B., et al. (1993). Naturally occurring antibodies devoid of light chains. *Nature* 363, 446–448. doi: 10.1038/363446a0

Horenstein, A. L., Chillemi, A., Quarona, V., Zito, A., Roato, I., Morandi, F., et al. (2015). NAD(+)-metabolizing ectoenzymes in remodeling tumor-host interactions: the human myeloma model. *Cells* 4, 520–537. doi: 10.3390/cells4030520

Horenstein, A. L., Chillemi, A., Zaccarello, G., Bruzzone, S., Quarona, V., Zito, A., et al. (2013). A CD38/CD203a/CD73 ectoenzymatic pathway independent of CD39 drives a novel adenosinergic loop in human T lymphocytes. *Oncoimmunology* 2:e26246. doi: 10.4161/onci.26246

Hubert, S., Rissiek, B., Klages, K., Huehn, J., Sparwasser, T., Haag, F., et al. (2010). Extracellular NAD+ shapes the Foxp3+ regulatory T cell compartment through the ART2-P2X7 pathway. *J. Exp. Med.* 207, 2561–2568. doi: 10.1084/jem.20091154

Idzko, M., Ferrari, D., and Eltzschig, H. K. (2014). Nucleotide signalling during inflammation. *Nature* 509, 310–317. doi: 10.1038/nature13085

Jacobson, K. A., and Muller, C. E. (2016). Medicinal chemistry of adenosine, P2Y and P2X receptors. *Neuropharmacology* 104, 31–49. doi: 10.1016/j.neuropharm.2015.12.001

Jahnichen, S., Blanchetot, C., Maussang, D., Gonzalez-Pajuelo, M., Chow, K. Y., Bosch, L., et al. (2010). CXCR4 nanobodies (VHH-based single variable domains) potently inhibit chemotaxis and HIV-1 replication and mobilize stem cells. *Proc. Natl. Acad. Sci. U.S.A.* 107, 20565–20570. doi: 10.1073/pnas.1012865107

Junger, W. G. (2011). Immune cell regulation by autocrine purinergic signalling. *Nat. Rev. Immunol.* 11, 201–212. doi: 10.1038/nri2938

Kennedy, C. (2017). P2Y11 receptors: properties. distribution and functions. *Adv. Exp. Med. Biol.* 1051, 107–122. doi: 10.1007/5584_2017_89

Knapp, K., Zebisch, M., Pippel, J., El-Tayeb, A., Muller, C. E., and Strater, N. (2012). Crystal structure of the human ecto-5'-nucleotidase (CD73): insights into the

regulation of purinergic signaling. *Structure* 20, 2161–2173. doi: 10.1016/j.str.2012.10.001

Koch-Nolte, F., Reyelt, J., Schossow, B., Schwarz, N., Scheuplein, F., Rothenburg, S., et al. (2007). Single domain antibodies from llama effectively and specifically block T cell ecto-ADP-ribosyltransferase ART2.2 in vivo. *FASEB J.* 21, 3490–3498. doi: 10.1096/fj.07-8661com

Krah, S., Schroter, C., Zielonka, S., Empting, M., Valldorf, B., and Kolmar, H. (2016). Single-domain antibodies for biomedical applications. *Immunopharmacol. Immunotoxicol.* 38, 21–28. doi: 10.3109/08923973.2015.1102934

Laing, S., Unger, M., Koch-Nolte, F., and Haag, F. (2010). ADP-ribosylation of arginine. *Amino Acids* 41, 257–269. doi: 10.1007/s00726-010-0676-2

Lauwereys, M., Arbabi Ghahroudi, M., Desmyter, A., Kinne, J., Holzer, W., De Genst, E., et al. (1998). Potent enzyme inhibitors derived from dromedary heavy-chain antibodies. *EMBO J.* 17, 3512–3520. doi: 10.1093/emboj/17.13.3512

Li, T., Qi, S., Unger, M., Hou, Y. N., Deng, Q. W., Liu, J., et al. (2016). Immuno-targeting the multifunctional CD38 using nanobody. *Sci. Rep.* 6:27055. doi: 10.1038/srep27055

Liu, H., Saxena, A., Sidhu, S. S., and Wu, D. (2017). Fc engineering for developing therapeutic bispecific antibodies and novel scaffolds. *Front. Immunol.* 8:38. doi: 10.3389/fimmu.2017.00038

McInnes, I. B., Cruwys, S., Bowers, K., and Braddock, M. (2014). Targeting the P2X7 receptor in rheumatoid arthritis: biological rationale for P2X7 antagonism. *Clin. Exp. Rheumatol.* 32, 878–882.

Muyldermans, S. (2013). Nanobodies: natural single-domain antibodies. *Annu. Rev. Biochem.* 82, 775–797. doi: 10.1146/annurev-biochem-063011-092449

Oberle, A., Brandt, A., Alawi, M., Langebrake, C., Janjetovic, S., Wolschke, C., et al. (2017). Long-term CD38 saturation by daratumumab interferes with diagnostic myeloma cell detection. *Haematologica* 102, e368–e370. doi: 10.3324/haematol.2017.169235

Peyrassol, X., Laeremans, T., Gouwy, M., Lahura, V., Debulpaep, M., Van Damme, J., et al. (2016). Development by genetic immunization of monovalent antibodies (nanobodies) behaving as antagonists of the human ChemR23 receptor. *J. Immunol.* 196, 2893–2901. doi: 10.4049/jimmunol.1500888

Pleiner, T., Bates, M., Trakhanov, S., Lee, C. T., Schliep, J. E., Chug, H., et al. (2015). Nanobodies: site-specific labeling for super-resolution imaging, rapid epitope-mapping and native protein complex isolation. *eLife* 4:e11349. doi: 10.7554/eLife.11349

Rashidian, M., Keliher, E. J., Bilate, A. M., Duarte, J. N., Wojtkiewicz, G. R., Jacobsen, J. T., et al. (2015). Noninvasive imaging of immune responses. *Proc. Natl. Acad. Sci. U.S.A.* 112, 6146–6151. doi: 10.1073/pnas.1502609112

Rissiek, B., Danquah, W., Haag, F., and Koch-Nolte, F. (2014). Technical advance: a new cell preparation strategy that greatly improves the yield of vital and functional Tregs and NKT cells. *J. Leukoc. Biol.* 95, 543–549. doi: 10.1189/jlb.0713407

Scheuplein, F., Rissiek, B., Driver, J. P., Chen, Y. G., Koch-Nolte, F., and Serreze, D. V. (2010). A recombinant heavy chain antibody approach blocks ART2 mediated deletion of an iNKT cell population that upon activation inhibits autoimmune diabetes. *J. Autoimmun.* 34, 145–154. doi: 10.1016/j.jaut.2009.08.012

Seman, M., Adriouch, S., Scheuplein, F., Krebs, C., Freese, D., Glowacki, G., et al. (2003). NAD-induced T cell death: ADP-ribosylation of cell surface proteins by ART2 activates the cytolytic P2X7 purinoceptor. *Immunity* 19, 571–582. doi: 10.1016/S1074-7613(03)00266-8

Sitkovsky, M. V., Hatfield, S., Abbott, R., Belikoff, B., Lukashev, D., and Ohta, A. (2014). Hostile, hypoxia-A2-adenosinergic tumor biology as the next barrier to overcome for tumor immunologists. *Cancer Immunol. Res.* 2, 598–605. doi: 10.1158/2326-6066.CIR-14-0075

Steeland, S., Vandenbroucke, R. E., and Libert, C. (2016). Nanobodies as therapeutics: big opportunities for small antibodies. *Drug Discov. Today* 21, 1076–1113. doi: 10.1016/j.drudis.2016.04.003

Steyaert, J., and Kobilka, B. K. (2011). Nanobody stabilization of G protein-coupled receptor conformational states. *Curr. Opin. Struct. Biol.* 21, 567–572. doi: 10.1016/j.sbi.2011.06.011

Tijink, B. M., Laeremans, T., Budde, M., Stigter-van Walsum, M., Dreier, T., de Haard, H. J., et al. (2008). Improved tumor targeting of anti-epidermal growth factor receptor nanobodies through albumin binding: taking advantage of modular Nanobody technology. *Mol. Cancer Ther.* 7, 2288–2297. doi: 10.1158/1535-7163.MCT-07-2384

van de Donk, N., Richardson, P. G., and Malavasi, F. (2017). CD38 antibodies in multiple myeloma: back to the future. *Blood* 131, 13–29. doi: 10.1182/blood-2017-06-740944

Wesolowski, J., Alzogaray, V., Reyelt, J., Unger, M., Juarez, K., Urrutia, M., et al. (2009). Single domain antibodies: promising experimental and therapeutic tools in infection and immunity. *Med. Microbiol. Immunol.* 198, 157–174. doi: 10.1007/s00430-009-0116-7

Yegutkin, G. G. (2008). Nucleotide- and nucleoside-converting ectoenzymes: important modulators of purinergic signalling cascade. *Biochim. Biophys. Acta* 1783, 673–694. doi: 10.1016/j.bbamcr.2008.01.024

Young, A., Ngiow, S. F., Barkauskas, D. S., Sult, E., Hay, C., Blake, S. J., et al. (2016). Co-inhibition of CD73 and A2AR adenosine signaling improves anti-tumor immune responses. *Cancer Cell* 30, 391–403. doi: 10.1016/j.ccell.2016.06.025

Conflict of Interest Statement: FH and FK-N receive a share of antibody sales via MediGate GmbH, a wholly owned subsidiary of the University Medical Center Hamburg-Eppendorf. SM and FK-N are co-inventors on patent applications on nanobody transgenic mice and/or CD38- or P2X7-specific nanobodies.

The other author declares that the research was conducted in the absence of any commercial or financial relationships that could be construed as a potential conflict of interest.

frontiers in Pharmacology

ORIGINAL RESEARCH
published: 26 March 2018
doi: 10.3389/fphar.2018.00255

Uridine Adenosine Tetraphosphate-Induced Coronary Relaxation Is Blunted in Swine With Pressure Overload: A Role for Vasoconstrictor Prostanoids

*Zhichao Zhou[1,2,3], Inge M. Lankhuizen[1,2], Heleen M. van Beusekom[1,2], Caroline Cheng[1,2,4], Dirk J. Duncker[1,2] and Daphne Merkus[1,2]**

[1] Division of Experimental Cardiology, Department of Cardiology, Thoraxcenter, Erasmus Medical Center, University Medical Center Rotterdam, Rotterdam, Netherlands, [2] Cardiovascular Research School Erasmus University Rotterdam, Erasmus Medical Center, University Medical Center Rotterdam, Rotterdam, Netherlands, [3] Division of Cardiology, Department of Medicine, Karolinska University Hospital, Karolinska Institutet, Solna, Sweden, [4] Department of Nephrology and Hypertension, University Medical Center Utrecht, Utrecht, Netherlands

OPEN ACCESS

Edited by:
Francisco Ciruela,
Universitat de Barcelona, Spain

Reviewed by:
Motohiro Nishida,
National Institute for Physiological Sciences (NIPS), Japan
John D. Imig,
Medical College of Wisconsin, United States

***Correspondence:**
Daphne Merkus
d.merkus@erasmusmc.nl

Specialty section:
This article was submitted to Experimental Pharmacology and Drug Discovery, a section of the journal Frontiers in Pharmacology

Received: 11 October 2017
Accepted: 07 March 2018
Published: 26 March 2018

Citation:
Zhou Z, Lankhuizen IM, van Beusekom HM, Cheng C, Duncker DJ and Merkus D (2018) Uridine Adenosine Tetraphosphate-Induced Coronary Relaxation Is Blunted in Swine With Pressure Overload: A Role for Vasoconstrictor Prostanoids. Front. Pharmacol. 9:255. doi: 10.3389/fphar.2018.00255

Plasma levels of the vasoactive substance uridine adenosine tetraphosphate (Up_4A) are elevated in hypertensive patients and Up_4A-induced vascular contraction is exacerbated in various arteries isolated from hypertensive animals, suggesting a potential role of Up_4A in development of hypertension. We previously demonstrated that Up_4A produced potent and partially endothelium-dependent relaxation in the porcine coronary microvasculature. Since pressure-overload is accompanied by structural abnormalities in the coronary microvasculature as well as by endothelial dysfunction, we hypothesized that pressure-overload blunts the coronary vasodilator response to Up_4A, and that the involvement of purinergic receptors and endothelium-derived factors is altered. The effects of Up_4A were investigated using wire-myography in isolated coronary small arteries from Sham-operated swine and swine with prolonged (8 weeks) pressure overload of the left ventricle induced by aortic banding (AoB). Expression of purinergic receptors and endothelium-derived factors was assessed in isolated coronary small arteries using real-time PCR. Up_4A (10^{-9} to 10^{-5} M) failed to produce contraction in isolated coronary small arteries from either Sham or AoB swine, but produced relaxation in preconstricted arteries, which was significantly blunted in AoB compared to Sham. Blockade of purinergic P1, and P2 receptors attenuated Up_4A-induced coronary relaxation more, while the effect of $P2X_1$-blockade was similar and the effects of A_{2A}- and $P2Y_1$-blockade were reduced in AoB as compared to Sham. mRNA expression of neither A1, A2, A3, nor $P2X_1$, $P2X_7$, $P2Y_1$, $P2Y_2$, nor $P2Y_6$-receptors was altered in AoB as compared to Sham, while $P2Y_{12}$ expression was higher in AoB. eNOS inhibition attenuated Up_4A-induced coronary relaxation in both Sham and AoB. Additional blockade of cyclooxygenase enhanced Up_4A-induced coronary relaxation in AoB but not Sham swine, suggesting the involvement of vasoconstrictor prostanoids. In endothelium-denuded coronary small arteries from normal swine, thromboxane synthase (TxS) inhibition enhanced relaxation to Up_4A compared to endothelium-intact

arteries, to a similar extent as $P2Y_{12}$ inhibition, while the combination inhibition of $P2Y_{12}$ and TxS had no additional effect. In conclusion, Up_4A-induced coronary relaxation is blunted in swine with AoB, which appears to be due to the production of a vasoconstrictor prostanoid, likely thromboxane A_2.

Keywords: Up_4A, coronary, microcirculation, purinergic receptor, hypertension, prostanoid

INTRODUCTION

Hypertension and aortic stenosis result in chronic pressure-overload of the left ventricle, producing left ventricular hypertrophy, and are considered risk factors for the development of heart failure (Khatibzadeh et al., 2013). Prolonged pressure-overload has also been shown to cause structural and functional adaptations in the coronary vasculature. Coronary flow reserve is decreased and minimal coronary resistance is increased (Duncker et al., 1993; Hamasaki et al., 2000; Galderisi et al., 2001), due to increased extravascular compression of the arterioles, decreased capillary density and vascular remodeling (Breisch et al., 1986; Tomanek et al., 1986; Bache, 1988; Hamasaki et al., 2000; van den Heuvel et al., 2001; Urbieta-Caceres et al., 2011). Functional changes in the coronary vasculature mainly result from an increase in oxidative stress and endothelial dysfunction (Rodriguez-Porcel et al., 2003; Lavi et al., 2008; Alexánderson et al., 2012) resulting in an imbalance between endothelium-derived vasodilators such as Nitric Oxide (NO) and prostacyclin and endothelium-derived vasoconstrictors like endothelin and reactive oxygen species (Vanhoutte, 1996).

Uridine adenosine tetraphosphate (Up4A) was initially identified as an endothelium-derived vasoconstrictor. A role for Up_4A in the pathogenesis of hypertension has been suggested by the observation that Up_4A-induced vascular contraction in the renal, femoral and basilar artery is potentiated in hypertension (Matsumoto et al., 2011b). In addition, the Up_4A plasma concentration in hypertensive subjects is significantly higher as compared to healthy subjects and positively correlates with blood pressure (Jankowski et al., 2007). Up_4A contains both purine and pyrimidine moieties and, like other extracellular nucleotides, exerts its vasoactive influence by binding to purinergic receptors (Matsumoto et al., 2011a; Zhou et al., 2013b), a class of receptors comprising P1 (adenosine receptors) and P2 receptors, that can be further subdivided into P2X and P2Y subtypes (Ralevic and Burnstock, 1998). Subsequent studies found that the vasoactive effect of Up_4A is not only dependent on the vascular bed but also on the species studied. Thus, Up_4A produces potent relaxation in the healthy porcine coronary vasculature (Zhou et al., 2013b) whereas vasoconstriction is observed in response to Up_4A in the murine coronary microcirculation (Teng et al., 2017). Interestingly, Up_4A-induced relaxation is attenuated in the remote coronary vasculature after myocardial infarction via downregulation of P1 receptors (Zhou et al., 2013a). Although Up_4A-induced coronary relaxation is maintained in swine with metabolic derangement, the purinergic signaling and endothelium-derived factors involved in Up_4A responses are markedly altered (Zhou et al., 2017). Altogether, these findings indicate that the effects of Up_4A in the porcine coronary vasculature change in cardiovascular disease.

Consequently, the first aim of the present study was to investigate whether prolonged pressure overload induced by AoB alters the response to Up_4A in isolated porcine coronary small arteries, and to determine the purinergic receptors and endothelium-derived factors mediating this altered vascular response to Up_4A. Interestingly, we found evidence for release of a vasoconstrictor prostanoid in response to Up_4A in AoB. As the vasoconstrictor prostanoid thromboxane A_2 (TxA_2) was recently shown to be released in response to Up_4A in renal arteries and aortas (Matsumoto et al., 2014; Zhou et al., 2015b), we further investigated whether Up_4A can induce production of TxA_2 in the porcine coronary microvasculature.

MATERIALS AND METHODS

Animals

Studies were performed in accordance with the "Guiding Principles in the Care and Use of Laboratory Animals" as approved by the Council of the American Physiological Society, and with approval of the Animal Care Committee at Erasmus Medical Center Rotterdam. Fifteen Crossbred Yorkshire X Landrace swine (2 to 3-month-old, 18.5 ± 0.3 kg at the time of surgery) of either sex entered the study. Swine were housed in the animal facility in cages with a 12/12 h light/dark cycle, *ad libitum* access to water and were fed twice per day. After 1 week of daily adaptation to laboratory conditions, animals underwent either AoB ($n = 7$) or a sham procedure (Sham; $n = 8$).

Surgery

After overnight fasting, swine were sedated with an intramuscular injection of Zoletil (Tiletamine/Zolazepam; 5 mg kg^{-1}), Xylazine (2.25 mg kg^{-1}), and Atropine (1 mg), and a small catheter was placed in an earvein for subsequent administration of fluid. Swine were intubated and ventilated with a mixture of oxygen and nitrogen (1:2 vol/vol), to which 2% (vol/vol) isoflurane was added to maintain anesthesia (Haitsma et al., 2001; Kappers et al., 2012). Under sterile conditions, the chest was opened via the fourth left intercostal space and fluid-filled polyvinylchloride

Abbreviations: AoB, aortic banding; BW, body weight; CO, cardiac output; HR, heart rate; LNAME, N^{ω}-nitro-L-arginine methyl ester HCl; LVSP, left ventricular systolic pressure measured proximal to the band; LVW, left ventricular weight at end of follow-up; MAP, mean arterial pressure measured in the descending aorta; NO, nitric oxide; PAP, pulmonary arterial pressure; PGI2, prostacyclin; PGI2S, prostacyclin synthase; PPADS, pyridoxalphosphate-6-azophenyl-2′,4′-disulfonic acid; P1-receptors, purinergic type 1 receptors; P2-receptors, purinergic type 2 receptors; SAP, systolic artery pressure measured in the descending aorta; TxS, thromboxane synthase; Up_4A, uridine adenosine tetraphosphate; U46619, 9,11-dideoxy-9α,11α-methanoepoxy Prostaglandin F2α; 8PT, 8-phenyltheophylline.

TABLE 1 | Primer information.

Receptors	Sequence		Size (bp)
A_1	5′-CCTGGCCATGCTGGCAATTGC-3′	5′-GAAGGAGAGAACCCAGCAGCC-3′	251
A_{2A}	5′-ATGTTGGGCTGGAATAGCTG-3′	5′-CACGGAGTTGGTGTGAGAGA-3′	426
A_3	5′-TACCTGCGGGTCAAGCTCACG-3′	5′-CCAGGAATGACACCAGCCAGC-3′	97
$P2X_1$	5′-TTGAACCCCATTTCTTCCTG-3′	5′-AGTGCACCACACATCTGCTC-3′	248
$P2X_4$	5′-TGTCCCCAGGCTACAATTTC-3′	5′-GGCAGCTTTTTCTCCCTTCT-3′	373
$P2X_7$	5′-CTTTTGCACCTTGAGCTTCC-3′	5′-TCCATGCTAAGGGATTCTGG-3′	152
P2Y1	5′-TTCCTGACTTGCATCAGTGC-3′	5′-CAGTGCCCGAGTAGAAGAGG-3′	157
$P2Y_2$	5′-GTGGCCTACAGCTTGGTCAT-3′	5′-GCGTGCGGAAGGAGTAGTAG-3′	235
$P2Y_4$	5′-GACTGCCGGTTTAATGAGGA-3′	5′-AGGAAAAGGACGCTGCAGTA-3′	302
$P2Y_6$	5′-CTGCTCTTGCCACCTGTGTA-3′	5′-AGGTTGGCGTAGAACAGGAA-3′	251
$P2Y_{12}$	5′-AGTGATGCCAAACTGGGAAC-3′	5′-TGAATGCCCAGATAACCACA-3′	208
COX1	5′-GGAGTTTGTCAATGCCACCT-3′	5′-GCAACTGCTTCTTCCCTTTG-3′	215
COX2	5′-GGCTGCGGGAACATAATAGA-3′	5′-GCAGCTCTGGGTCAAACTTC-3′	183
PGIS	5′-CATGCGTGCTCTGATTCACT-3′	5′-AAGCTGATGCAAAGGCAAGT-3′	233
TxS	5′-AGCAAGCAGCAGAAGAGAGG-3′	5′-TCAGAGGCTTGGACAGAGGT-3′	180
eNOS	5′-CTCTCCTGTTGGCCTGACCA-3′	5′-CCGGTTACTCAGACCCAAGG-3′	151
GAPDH	5′-TCGGAGTGAACGGATTTG-3′	5′-CCTGGAAGATGGTGATGG-3′	219

catheters were inserted into the left ventricle (LV), only in AoB swine, and in the aortic arch (Ao) of both Sham and AoB swine, for the measurement of the pressure and blood sampling for the determination of PO_2, PCO_2, pH, O_2 saturation, and hemoglobin concentration. The ascending aorta was exposed in all swine, a sterile plastic band was placed around the ascending aorta in AoB animals and gradually tightened until the systolic pressure gradient between distal aorta and proximal LV catheters reached approximately 80 mmHg. Then, the chest was closed and animals were allowed to recover, receiving analgesia (0.3 mg buprenorphine i.m.) for 2 days and antibiotic prophylaxis (25 mg kg^{-1} amoxicillin and 5 mg kg^{-1} gentamycin i.v.) for 5 days. Pressure in the proximal and distal catheters were recorded at the time of surgery, as well as 1 and 3 weeks after surgery, and the systolic pressure gradient was calculated. Due to malfunctioning of the catheters in a number of animals, pressures could not be obtained 8 weeks after the initial surgery.

Eight weeks after initial Sham and AoB surgery, animals were re-anesthetized, intubated and ventilated as described above. Pentobarbital (20 mg kg^{-1} h^{-1}) was infused to induce and maintain anesthesia. A catheter was introduced via the femoral artery into the descending aorta for measurement of mean arterial pressure. A Swan Ganz catheter was inserted via the jugular vein and advanced into the pulmonary artery for measurement of PAP and CO (via thermodilution) (van Kats et al., 2000). Following thoracotomy, hearts were arrested and immediately excised and placed in cold, oxygenated Krebs bicarbonate buffer solution.

Myograph Studies

Coronary small arteries (diameter: ∼150 μm) were dissected out from the apex of eight Sham-operated and seven AoB swine and stored overnight in cold, oxygenated Krebs bicarbonate solution of the following composition (mM): NaCl 118, KCl 4.7, $CaCl_2$ 2.5, $MgSO_4$ 1.2, KH_2PO_4 1.2, $NaHCO_3$ 25, and glucose 8.3; pH 7.4. The next day, coronary small arteries were cut into segments of ∼2 mm length and mounted in microvascular myographs (Danish Myo Technology) with separated organ baths containing 6 ml Krebs bicarbonate solution aerated with 95%O_2/5%CO_2 and maintained at 37°C (Batenburg et al., 2004; Zhou et al.,

TABLE 2 | Anatomic and hemodynamic variables.

		Sham *N* = 8	AoB *N* = 7
MAP (mmHg)	Surgery	84 ± 6	56 ± 3*
	Week 1	92 ± 2	83 ± 2*
	Week 3	88 ± 2	90 ± 3
LVSP (mmHg)	Surgery	–	155 ± 5
	Week 1	–	176 ± 8
	Week 3	–	188 ± 14
SAP (mmHg)	Surgery	99 ± 6	67 ± 4*
	Week 1	112 ± 2	100 ± 2*
	Week 3	105 ± 2	104 ± 3
Pressure gradient (mmHg)	Surgery	–	88 ± 2
	Week 1	–	82 ± 8
	Week 3	–	98 ± 6
At end of follow-up			
BW (kg)		45 ± 0.9	42 ± 1.1
LVW/BW (g kg^{-1})		2.3 ± 0.1	3.6 ± 0.1*
HR (beats min^{-1})		109 ± 3	108 ± 4
MAP (mmHg)		98 ± 5	104 ± 3
CO (L min^{-1})		4.0 ± 0.2	4.2 ± 0.1
PAP (mmHg)		19 ± 1	23 ± 1*

*AoB, aortic banding; MAP, mean arterial pressure measured in the descending aorta; LVSP, left ventricular systolic pressure measured proximal to the band; SAP, systolic artery pressure measured in the descending aorta; BW, body weight; LVW, left ventricular weight; HR, heart rate; CO, cardiac output; PAP, pulmonary arterial pressure. Those values were obtained under anesthesia at the end of follow-up. Values are mean ± SEM; *P < 0.05 vs. Sham.*

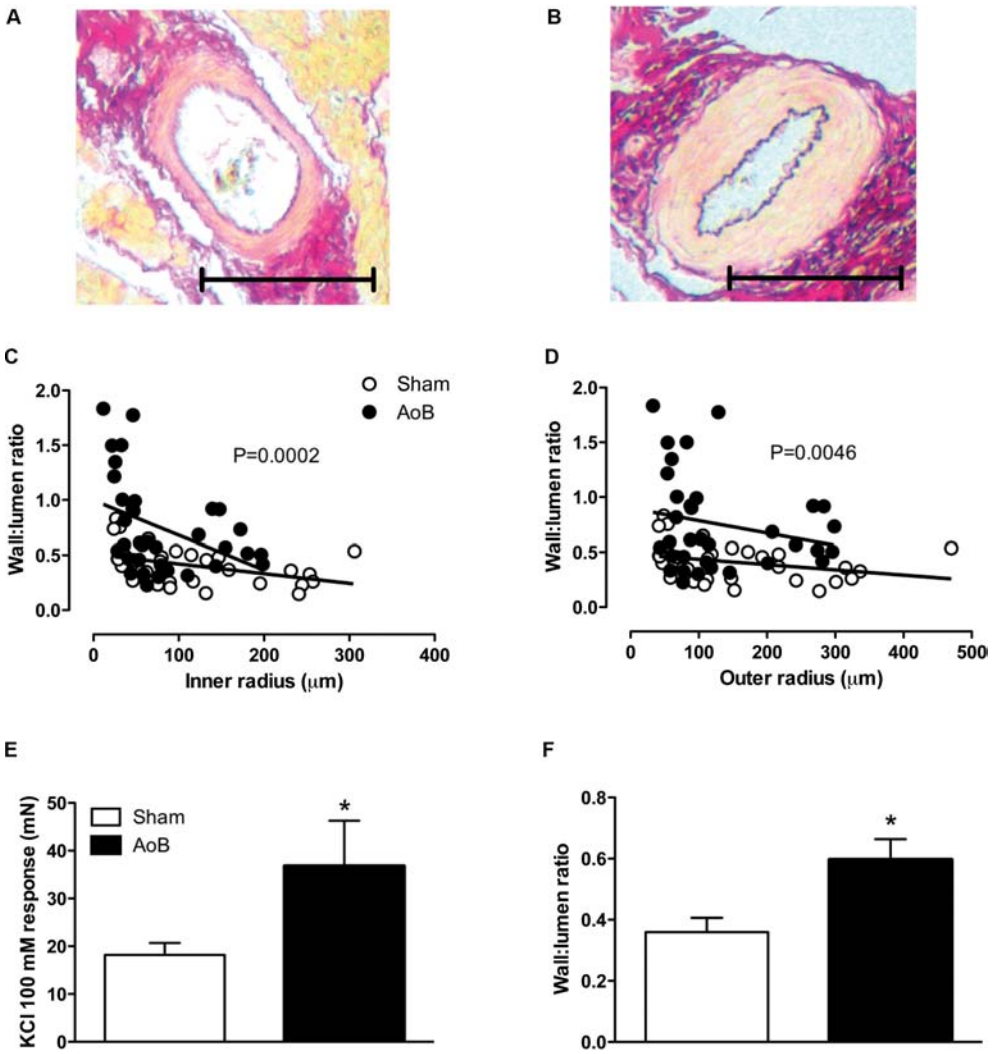

FIGURE 1 | Typical examples of coronary small arteries within the myocardium of Sham-operated swine **(A)** and swine with AoB **(B)**. The scale bar denotes 100 μm. The wall to lumen ratio both as a function of inner **(C)** and outer **(D)** was significantly increased in myocardium from swine with AoB. Shown are 34 vessels from 4 Sham-operated swine and 36 vessels from 5 AoB swine. The vasoconstrictor response to 100 mM KCl was significantly increased in vessels from AoB (n = 6) as compared to Sham (n = 8), **(E)**. The wall to lumen ratio in vessels with inner diameters ranging from 100 to 200 μm was increased in AoB as compared to Sham **(F)**. $^*P < 0.05$ AoB vs. Sham.

2013b, 2017). Changes in contractile force were recorded with a Harvard isometric transducer. Following a 30 min stabilization period, the internal diameter was set to a tension equivalent to 0.9 times the estimated diameter at 100 mmHg effective transmural pressure (Batenburg et al., 2004; Zhou et al., 2013b, 2017). At the end of the stabilization period, the vessels were exposed to 30 mM KCl twice to check the contractility. Endothelial integrity was verified by observing dilation to 10 nM substance P after preconstriction with 100 nM of the stable TxA_2 analog U46619. Then vessels were subjected to 100 mM KCl to determine maximal vascular contraction. Thereafter, vessels were allowed to equilibrate in fresh organ bath fluid for 30 min before initiating different experimental protocols (Batenburg et al., 2004; Zhou et al., 2013b). In experiments where the effect of an antagonist on the response to Up_4A was assessed, antagonists were added to the organ baths 30 min before preconstriction with U46619 and were present throughout the experiments. Only one protocol was executed per vessel and, within one protocol, all vessels were obtained from different animals.

Experimental Protocols

Coronary small arteries from both Sham and AoB swine were subjected to Up_4A in incremental concentrations ranging from 10^{-9} to 10^{-5} M in the absence and presence of preconstriction with U46619 (Zhou et al., 2013b). To assess the involvement of different purinergic receptors in the vasodilator response to Up_4A, coronary small arteries from Sham and AoB swine were pre-incubated with non-selective P1 receptor antagonist 8PT (10^{-5} M), non-selective P2 receptor antagonist PPADS (10^{-5} M), adenosine A_{2A} receptor antagonist SCH58261 (10^{-8}

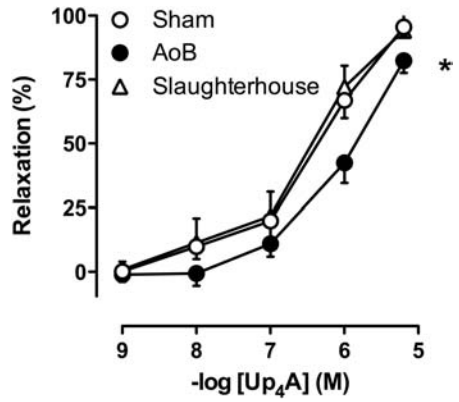

FIGURE 2 | Reduced vasodilator responses to Up_4A in coronary small arteries from swine with AoB (n = 6) as compared to Sham-operated (n = 8) or Slaughterhouse (n = 5) swine. *P < 0.05 AoB vs. Sham or Slaughterhouse.

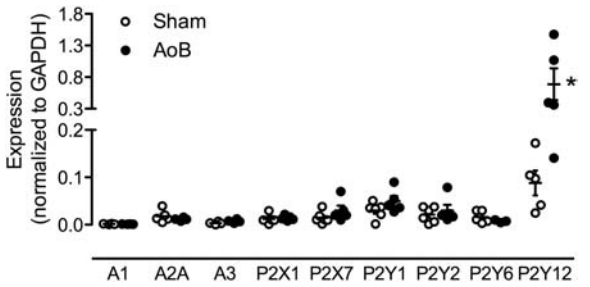

FIGURE 3 | mRNA expression of various P receptor subtypes in coronary small arteries from Sham-operated swine and swine with AoB. mRNA expression was normalized to expression of GAPDH. *P < 0.05 vs. Sham.

M), $P2X_1$ receptor antagonist MRS2159 (3×10^{-5} M), and $P2Y_1$ receptor antagonist MRS2179 (10^{-6} M) followed by preconstriction with U46619 (100 nM) (Zhou et al., 2013b) and exposed to Up_4A (10^{-9} to 10^{-5} M). To investigate if the role of endothelium-derived factors in the vasodilator response to Up_4A was altered after AoB, vessels from both Sham and AoB were exposed to Up_4A (10^{-9} to 10^{-5} M) in the absence and presence of nitric oxide synthase (NOS) inhibitor LNAME (10^{-4} M) alone or in combination with cyclooxygenase (COX) inhibitor indomethacin (10^{-5} M) (Zhou et al., 2013b). A potential role for TxA_2 in the response to Up_4A was assessed using coronary small arteries from porcine hearts (n = 5) obtained from a local slaughterhouse. The response to Up_4A of coronary small arteries of slaughterhouse pigs was similar to that of Sham-operated pigs (**Figure 2**). A subset of these vessels was de-endothelialized to mimic endothelial dysfunction of cardiovascular disease condition and exposed to the TxS inhibitor ozagrel (10^{-5} M), the $P2Y_{12}$ receptor antagonist clopidogrel (10^{-6} M), that can be converted to its active metabolites by cytochrome P450 enzymes shown to be present in the heart (Chaudhary et al., 2009; Sangkuhl et al., 2010) or a combination of ozagrel and clopidogrel prior to exposure to Up_4A.

Histology

Fresh sections of anterior wall of the left ventricle were fixed by 4% buffered formaldehyde and paraffin-embedded for histological analysis of remodeling of coronary small arteries. Sections were stained with resorcin-fuchsin as an elastin stain, photographed and inner and outer area of the coronary small arteries was assessed by planimetry (Sorop et al., 2016). Only transversely cut vessels with an inner radius below 200 μm were analyzed. Assuming circularity of the vessels, inner and outer radius were calculated as $r = \sqrt{(area/\pi)}$. Wall to lumen ratio was calculated as (outer–inner diameter)/inner diameter.

Quantitative Real-Time PCR Analysis

Following dissection, coronary small arteries (diameter: ∼150 μm) were snap-frozen in liquid nitrogen to be used for detection of purinergic receptor subtypes A_1, A_{2A}, A_3, $P2X_1$, $P2X_4$, $P2X_7$, $P2Y_1$, $P2Y_2$, $P2Y_4$, $P2Y_6$, and $P2Y_{12}$ mRNA. In addition, the expression of endothelial NOS (eNOS), cyclooxygenase (COX) 1, COX2, prostacyclin synthase (PGIS), and TxS were measured (Rondelet et al., 2003). Total RNA was extracted from 5 to 7 frozen samples per group using a Qiagen RNA kit. cDNA was synthesized from 100 ng of total RNA with iScript Reverse Transcriptase (Bio-Rad). Quantitative real-time PCR (MyIQ, Bio-Rad) was performed with SYBR Green (Bio-Rad) (Zhou et al., 2013b). Target gene mRNA levels were expressed relative to the housekeeping gene glyceraldehyde-3-phosphate dehydrogenase (GAPDH) as an endogenous control (Martino et al., 2011). The primer sequences are shown in **Table 1**.

Data Analysis and Statistics

Hemodynamic data were averaged over a time period of at least 10 s. Vascular contractions were normalized to the response to 100 mM KCl, while vascular relaxation to Up_4A was expressed as percentage of contraction to U46619 (Zhou et al., 2013b). Statistical comparison of hemodynamic data, purinergic receptor expression, vascular response to KCl and comparison of wall to lumen ratio of vessels < 200 μm between Sham and AoB swine were performed using unpaired t-tests. The effect of AoB on wall to lumen ratio was analyzed with ANCOVA, using inner or outer radius as covariant. The effects of AoB as well as drug treatment on the Up_4A response were assessed using two-way ANOVA for repeated measures. Statistical significance was accepted when $P < 0.05$ (two-tailed). Data are presented as means ± SEM.

RESULTS

Characteristics of AoB Animals

Aortic banding of the ascending aorta resulted in a systolic pressure gradient of 88 ± 2 mmHg as measured during surgery (**Table 2**). The systolic pressure gradient was stable over the time course of the experiment, as evidenced by a systolic pressure gradient of 82 ± 8 and 98 ± 6 mmHg at week 1 and week 3 after AoB (**Table 2**). Mean arterial pressure distal to the band

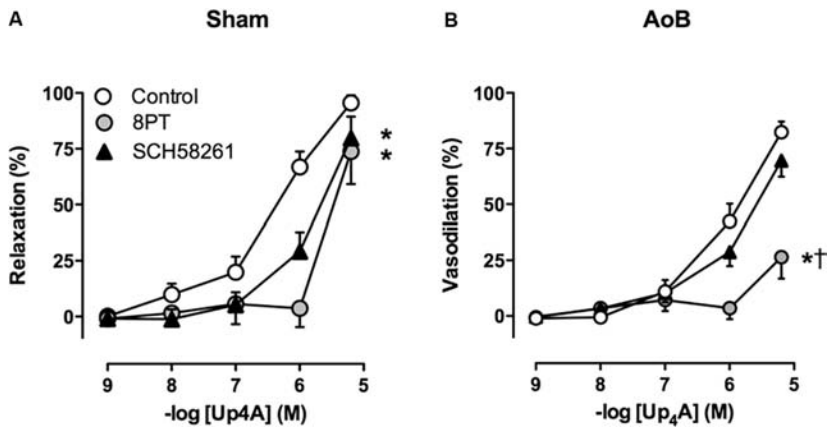

FIGURE 4 | P1 receptor blockade with 8PT attenuated relaxation to Up_4A less in coronary small arteries from Sham-operated swine (**A**, $n = 6$) as compared to coronary small arteries from swine with AoB (**B**, $n = 6$). A_{2A} receptor blockade with SCH58261 attenuated Up_4A-induced relaxation in coronary small arteries from Sham ($n = 5$), but not AoB ($n = 5$). Control data are the same as in **Figure 2** ('Sham' and 'AoB'). $^*P < 0.05$ effect of 8PT vs. corresponding control. $^\dagger P < 0.05$ effect of 8PT vs. corresponding SCH58261.

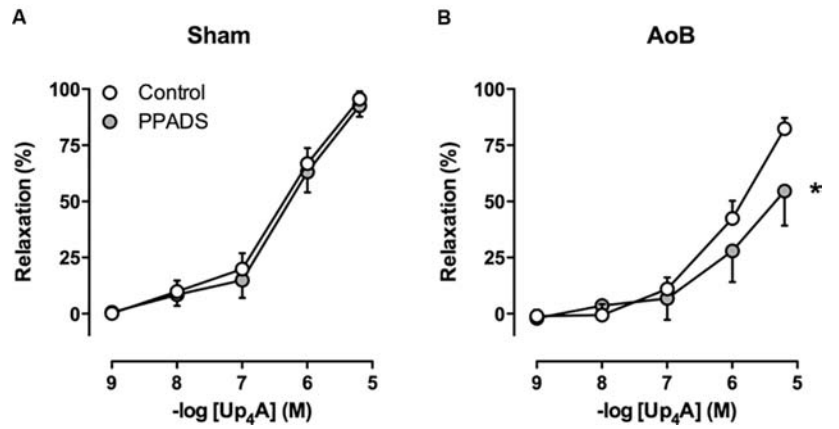

FIGURE 5 | P2 receptor blockade with PPADS had no effect on relaxation to Up_4A in coronary small arteries from Sham-operated swine (**A**, $n = 8$) but attenuated relaxation in coronary small arteries from swine with AoB (**B**, $n = 7$). Control data are the same as in **Figure 2** ('Sham' and 'AoB'). $^*P < 0.05$ effect of PPADS vs. corresponding control.

was lower in AoB as compared to Sham during surgery and 1 week after surgery, but was similar to mean arterial pressure in Sham-operated swine 3 weeks after surgery. At end of follow-up, the HR, mean arterial pressure, and CO were comparable between Sham and AoB swine, while the PAP was slightly increased in AoB (**Table 2**). Eight weeks of AoB resulted in left ventricular hypertrophy as evidenced by a 56% increase in left ventricle weight to BW ratio (**Table 2**). The wall to lumen ratio of coronary small arteries was also increased (**Figures 1A,B** for typical examples, **Figures 1C,D** for all results, **Figure 1F** for vessels with an inner diameter ranging from 100 to 200 μm) and the vascular response to 100 mM KCl in the coronary small arteries from AoB was significantly greater as compared to that from Sham (**Figure 1E**). These observations indicate that during 8 weeks of AoB, swine develop left ventricular hypertrophy as well as medial hypertrophy of the coronary microvessels.

Up_4A-Induced Coronary Relaxation Is Blunted in AoB

Cumulative concentrations of Up_4A (10^{-9} to 10^{-5} M) failed to induce vascular contraction in coronary small arteries from either Sham or AoB swine. The vasoconstrictor effect of U46619 (normalized to 100 mM KCl) was not significantly different between Sham and AoB (89 ± 15 vs. $61 \pm 9\%$, $P = 0.16$). In these preconstricted vessels, Up_4A produced concentration-dependent relaxation, but the relaxation was significantly less in vessels from AoB as compared to Sham (**Figure 2**).

Involvement of Purinergic Receptor Subtypes

Despite unaltered expression of the A_1, A_{2A}, and A_3 receptor (**Figure 3**), P1 receptor blockade with 8PT attenuated Up_4A-induced relaxation in coronary small arteries from AoB more

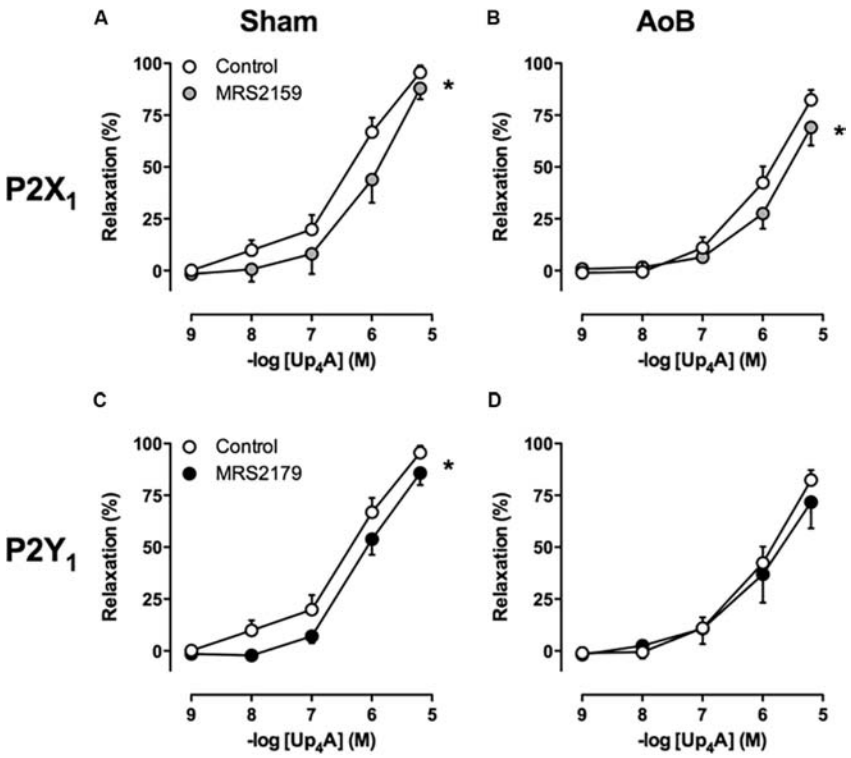

FIGURE 6 | $P2X_1$ receptor blockade with MRS2159 attenuated relaxation to Up_4A to the same extent in coronary small arteries from Sham-operated swine (**A**, $n = 8$) and from swine with AoB (**B**, $n = 6$), whereas and $P2Y_1$ receptor blockade with MRS2179 attenuated relaxation to Up_4A in coronary small arteries from Sham-operated swine (**C**, $n = 7$) but not from swine with AoB (**D**, $n = 5$). Control data are the same as in **Figure 2** ('Sham' and 'AoB').*$P < 0.05$ effect of MRS2159 or MRS2179 vs. corresponding control.

than in Sham (**Figures 4A,B**). Conversely, A_{2A} receptor blockade with SCH58261 attenuated Up_4A-induced relaxation to the same extent as 8PT in coronary small arteries from Sham, but had no effect on Up_4A-induced relaxation in AoB (**Figures 4A,B**). Non-selective P2 receptor blockade with PPADS had no effect on Up_4A-induced relaxation in coronary small arteries from Sham (**Figure 5A**), but did attenuate Up_4A-induced relaxation in vessels from AoB (**Figure 5B**). $P2X_1$ receptor blockade with MRS2159 attenuated Up_4A-induced relaxation in coronary small arteries from Sham (**Figure 6A**) and AoB swine (**Figure 6B**) to a similar extent, whereas $P2Y_1$ receptor blockade with MRS2179 attenuated Up_4A-induced relaxation in coronary small arteries from Sham (**Figure 6C**), but not AoB swine (**Figure 6D**). $P2X_1$, $P2X_7$, $P2Y_1$, $P2Y_2$ and $P2Y_6$ receptors were expressed, but no differences in expression in coronary small arteries between Sham and AoB were found (**Figure 3**). Expression of $P2Y_{12}$ receptors was higher in coronary small arteries from AoB (**Figure 3**), while expression of $P2X_4$ and $P2Y_4$ could not be detected (data not shown).

Involvement of Endothelium-Derived Factors in the Response to Up_4A

To investigate the contribution of alterations in endothelial function to the attenuated response to Up_4A after AoB, the effects of eNOS and COX inhibition on Up_4A-induced relaxation were assessed. eNOS inhibition with LNAME attenuated Up_4A-induced relaxation to the same extent in coronary small arteries from Sham and AoB swine (**Figures 7A,B**), which was corroborated by similar eNOS expression level in vessels from AoB and Sham (**Figure 8**).

In Sham-operated swine, combined inhibition of eNOS and COX (LNAME+indomethacin) attenuated Up_4A-induced relaxation to the same extent as LNAME alone (**Figure 7C**). In contrast, combined inhibition of eNOS and COX in vessels from AoB swine significantly enhanced Up_4A-induced relaxation compared to LNAME alone (**Figure 7D**), although COX1, COX2, and PGIS expression were not different in coronary small arteries between Sham and AoB (**Figure 8**). The observation that COX-inhibition enhanced the vasodilator effect of Up_4A suggests the production of a vasoconstrictor prostanoid(s). There is some evidence linking TxA_2 production to $P2Y_{12}$ receptor activation (Bhavaraju et al., 2010). Given the increased $P2Y_{12}$ receptor expression in coronary small arteries of AoB (**Figure 3**), we further investigated if TxA_2 could be the vasoconstrictor prostanoid produced in response to Up_4A, as well as the functional involvement of $P2Y_{12}$ receptor in this process. Coronary small arteries were denuded to mimic endothelial dysfunction in hypertension. Subsequently, endothelium-intact and -denuded vessels were exposed to Up_4A in the presence of the TxS inhibitor ozagrel, the $P2Y_{12}$ receptor antagonist

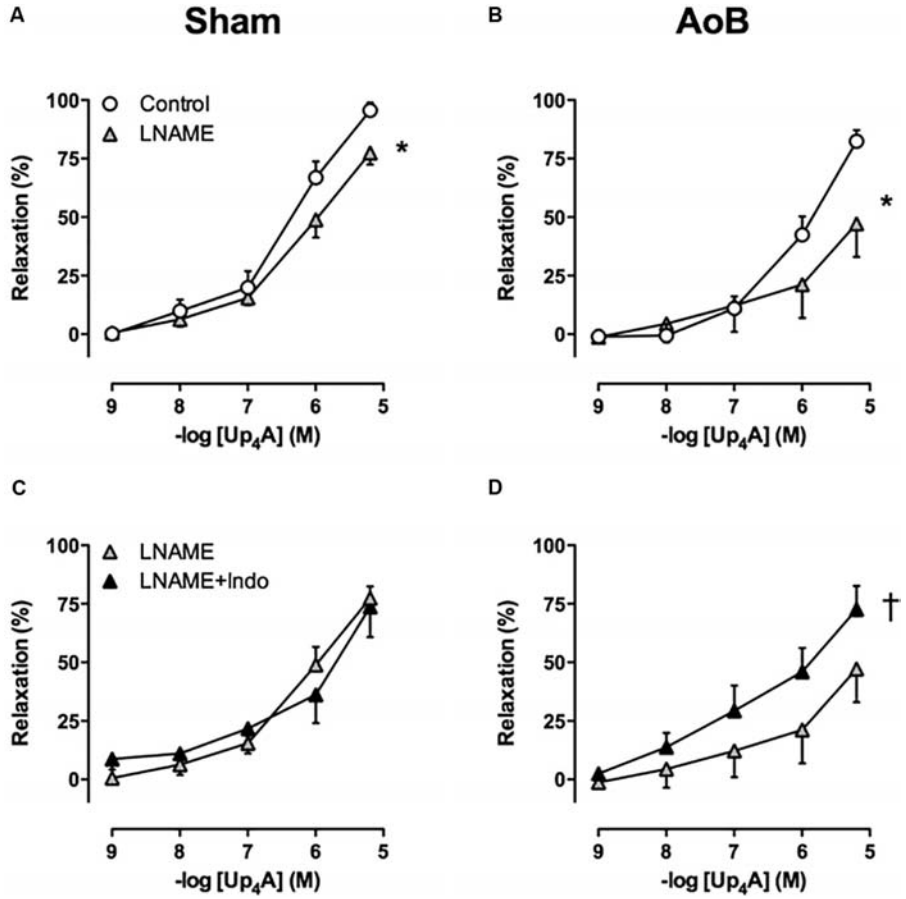

FIGURE 7 | eNOS inhibition with LNAME attenuated the response to Up_4A to a similar extent in coronary small arteries from Sham-operated swine (**A**, $n = 8$) and swine with AoB (**B**, $n = 7$). Subsequent inhibition of cyclooxygenase with indomethacin (Indo) had no effect in vessels from Sham (**C**, $n = 7$), but enhanced relaxation to Up_4A in vessels from swine with AoB (**D**, $n = 6$). Control data are the same as in **Figure 2** ('Sham' and 'AoB'). $^*P < 0.05$ effect of LNAME vs. corresponding control; $^\dagger P < 0.05$ effect of LNAME + indomethacin vs. LNAME alone.

clopidogrel or their combination. Ozagrel had no effect on the response to Up_4A in coronary small arteries with intact endothelium (**Figure 9A**), but enhanced the vasodilator response to Up_4A in denuded coronary small arteries (**Figure 9B**). Similarly, clopidogrel enhanced the vasodilator response to Up_4A in denuded coronary small arteries (**Figure 9B**), but not in coronary small arteries with intact endothelium (**Figure 9A**). As the effect of the combination of ozagrel and clopidogrel was identical to the effect of either ozagrel or clopidogrel alone (**Figure 9B**), these data are consistent with the concept that $P2Y_{12}$ receptor activation may induce TxA_2 production.

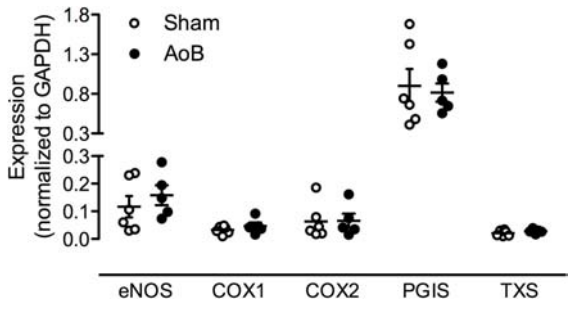

FIGURE 8 | mRNA expression of eNOS, cyclooxygenase (COX) 1 and COX2, prostacyclin synthase (PGIS) and TxS in coronary small arteries from Sham-operated swine and swine with AoB. mRNA expression was normalized to expression of GAPDH.

DISCUSSION

The main findings of the present study were that (i) AoB resulted in medial hypertrophy of coronary small arteries as evidenced by an increase in wall-to-lumen ratio and an increased KCl-induced contractile force. (ii) Up_4A-induced relaxation was reduced in coronary small arteries from AoB as compared to Sham. (iii) Blockade of P1 receptors attenuated Up_4A-induced relaxation less in coronary small arteries from Sham as compared to AoB, but the contribution of the A_{2A} receptor was reduced. (iv) P2 receptor blockade with PPADS attenuated Up_4A-induced relaxation in AoB but not Sham. (v) The response to $P2X_1$

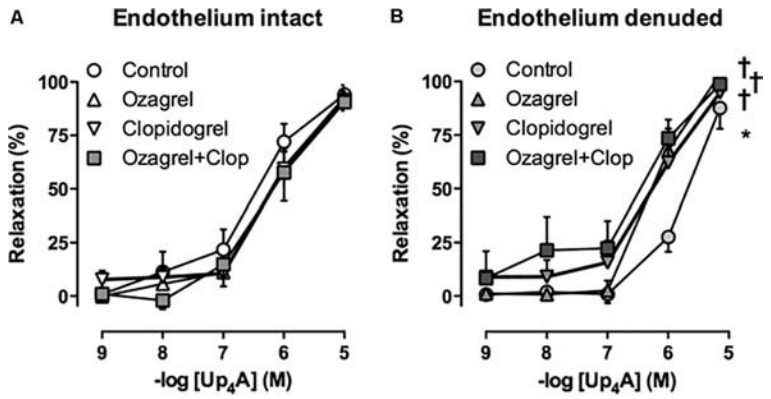

FIGURE 9 | Neither TxS inhibition with ozagrel, nor $P2Y_{12}$ receptor blockade with clopidogrel (Clop), nor the combination affected the response to Up_4A in coronary small arteries from slaughterhouse swine with intact endothelium (**A**, $n = 5$). Ozagrel and clopidogrel enhanced vasodilator response to Up_4A in denuded coronary small arteries, while the effect of the combination of ozagrel and clopidogrel was similar to the effect of either inhibitor alone (**B**, $n = 5$). Control data are the same as in **Figure 2** 'Slaughterhouse.' $^*P < 0.05$ effect of denudation; †$P < 0.05$ effect of ozagrel and/or clopidogrel vs. corresponding control.

blockade was similar in coronary small arteries from AoB and Sham. (vi) $P2Y_1$ receptor blockade attenuated Up_4A-induced relaxation in Sham, but not AoB. (vii) Expression of the $P2Y_{12}$ receptor was increased in coronary small arteries from AoB, while expression of other purinergic receptor subtypes involved in vascular tone regulation was not altered. (viii) eNOS inhibition attenuated Up_4A-induced relaxation to the same extent in Sham and AoB, whereas additional COX inhibition had no effect in Sham, but enhanced Up_4A-induced relaxation in AoB. (ix) $P2Y_{12}$ receptor blockade and/or TxS inhibition enhanced the vasodilator response to Up_4A in denuded coronary small arteries. The implications of these findings are discussed below.

Consistent with previous reports (Desjardins et al., 2005; Aubin et al., 2007), 8 weeks of AoB resulted in left ventricular hypertrophy and coronary microvascular remodeling, as evidenced by doubling of wall to lumen ratio of the coronary small arteries and doubling of the contractile response to KCl. The vasodilator response to Up_4A was blunted in coronary small arteries from swine with AoB. Up_4A exerts its vasoactive effect through interaction with purinergic receptors. In accordance with previous studies from our laboratory (Zhou et al., 2013b), coronary relaxation induced by Up_4A in swine was mediated primarily by the P1 receptors. Although the expression of the A_1, A_{2A}, and A_3 receptors was unaltered after AoB, the overall contribution of the P1 receptors to Up_4A-induced vasorelaxation was increased, while contribution of the A_{2A} receptor was reduced. These findings are different from our findings in the porcine coronary vasculature after MI (Zhou et al., 2013a) and metabolic derangement (Zhou et al., 2017), in which the reduced response to Up_4A was not due to functional loss of A_{2A} receptors. Although studies in mice (Zhou et al., 2015a) and swine (Long et al., 2010) showed that the main vasoactive effect of adenosine was mediated through A_{2A}, rather than A_{2B} receptor, we cannot exclude that altered expression of the A_{2B} receptor could explain the increased contribution of P1 receptors to the vasorelaxation to Up_4A in coronary small arteries from AoB as compared to Sham.

The assessment of the contribution of the P2 receptors to the response to Up_4A is difficult due to lack of selective antagonists of many of the P2 receptor subtypes. In general, activation of P2 receptors on endothelial cells is thought to result in vasodilation, whereas activation of P2 receptors on vascular smooth muscle cells results in vasoconstriction (Matsumoto et al., 1997; Burnstock, 2010; Zhou et al., 2013b). The non-selective P2 antagonist PPADS attenuated Up_4A-induced relaxation in coronary small arteries from swine with AoB, but not from Sham-operated swine, indicating that the contribution of P2 receptors blocked by PPADS is altered. PPADS has been shown to block $P2X_2$, $P2X_3$, $P2X_5$ (Burnstock, 2007), $P2X_7$ (Mezzaroma et al., 2011), $P2Y_1$ (Ju et al., 2003), $P2Y_2$, $P2Y_4$ (Rayment et al., 2007), and $P2Y_6$ (Schreiber and Kunzelmann, 2005) receptors. In contrast to the altered effect of PPADS, blockade of $P2X_1$ receptors attenuated the vasodilator response to Up_4A to the same extent in coronary small arteries from AoB and Sham-operated swine, which is in accordance with its unaltered expression. Conversely, despite unaltered expression of the $P2Y_1$ receptor, its vasodilator effect in response to Up_4A that was present in coronary small arteries from Sham disappeared after AoB. The observation that, in vessels from Sham-operated swine, $P2Y_1$ blockade attenuated the response to Up_4A, whereas PPADS, that has also been shown to block the $P2Y_1$ receptor, does not, suggests that PPADS also blocks a P2 vasoconstrictor receptor. The exact identity of this receptor remains to be elucidated. Interestingly, expression of the $P2Y_{12}$ receptor was increased in coronary small arteries from swine with AoB. As activation of the $P2Y_{12}$ receptor on vascular smooth muscle cells results in vasoconstriction (Wihlborg et al., 2004), increased expression of this receptor could explain the reduced vasodilator effect of Up_4A in coronary small arteries from swine with AoB. A role for the $P2Y_{12}$ receptor in the reduced vasodilator response to Up_4A is further substantiated by our observation that $P2Y_{12}$ blockade with clodipogrel enhanced the vasodilator response to Up_4A in denuded vessels, although it

had no effect on the vasodilator response in vessels with intact endothelium. Altogether, our data indicate that Up_4A-mediated activation of the $P2Y_{12}$ receptor on the vascular smooth muscle cells results in vascular contraction, while the presence of healthy endothelium prevents such response.

Since several studies have shown endothelial dysfunction in the porcine coronary vasculature following AoB (Malo et al., 2003a,b; Desjardins et al., 2005; Aubin et al., 2007), we further investigated whether the contribution of endothelial vasodilator pathways to Up_4A-induced relaxation was altered. The blunted response to Up_4A was not due to a decreased contribution of NO, as both the effect of eNOS-inhibition with LNAME and eNOS expression were similar in coronary small arteries from Sham-operated swine and swine with AoB. The unaltered expression of eNOS is consistent with another study in isolated coronary arteries from swine with AoB (Malo et al., 2003b). Also, the contribution of eNOS to bradykinin-induced relaxation was maintained (Aubin et al., 2007), despite the presence of eNOS uncoupling (Malo et al., 2003b).

Cyclooxygenase-inhibition with indomethacin potentiated the vasodilator response to Up_4A in vessels from AoB, but not Sham-operated animals, suggesting that the reduced responsiveness to Up_4A was, at least in part, due to production of a vasoconstrictor prostanoid(s). A shift in the balance from vasodilator prostanoids to vasoconstrictor prostanoids has been implicated in the pathogenesis of cardiovascular disease (Kawabe et al., 2010). A potential mechanism behind such shift may be that oxidative stress and/or endothelial dysfunction result in eNOS uncoupling, which subsequently leads to the production of peroxynitrite, that is capable of inactivating PGIS thereby causing a shift in production from prostacyclin to TxA_2 (Zou et al., 2004; Nie et al., 2006). Indeed, TxA_2 levels were increased in the myocardium of hypercholesterolemic swine with endothelial dysfunction (Chu et al., 2012). Furthermore, the presence of a healthy endothelium in the present study prevented production of TxA_2, as inhibition of TxS with ozagrel enhanced the vasodilator response to Up_4A in denuded coronary small arteries, but not in those with intact endothelium. A link between the vasoconstrictor effect of Up_4A and TxA_2 production is further supported by a recent study demonstrating that Up_4A stimulates TxA_2 production leading to vascular contraction in mouse aortas (Zhou et al., 2015b). Moreover, an enhanced contraction in response to Up_4A is mediated through activation of COX2 and production of TxA_2 in the renal vasculature of diabetic rats (Matsumoto et al., 2014). Although mRNA levels of COX1, COX2, PGIS, and TxS were unaltered in coronary small arteries from swine with AoB in the present study, it is possible that the *activity* of COX2 and/or TxS was increased following stimulation with Up_4A. Preliminary data from coronary small arteries from two swine with AoB show that inhibition of TxS with ozagrel after LNAME has a similar effect as indomethacin, suggesting that indeed, TxS activity is increased. An increased production of TxA_2 in the coronary vasculature in AoB is not unique to Up_4A, but has also been shown in response to bradykinin and serotonin (Desjardins et al., 2005). It is unlikely that the response of the coronary microvasculature to TxA_2 receptor activation was altered, as the response to the TxA_2 analog U46619 was identical in vessels from Sham and AoB swine.

There is some evidence linking TxA_2 production to activation of the $P2Y_{12}$ receptor. Thus, TxA_2 levels were reduced in human serum treated with $P2Y_{12}$ inhibitors, $P2Y_{12}$ inhibition reduced serum TxA_2 in mice, and serum TxA_2 levels were reduced in $P2Y_{12}$ knockout mice (Bhavaraju et al., 2010). Consistent with these observations, in the present study, $P2Y_{12}$ blockade enhanced the vasodilator response to Up_4A to a similar extent as TxS inhibition, and combined inhibition of $P2Y_{12}$ receptor and TxS had no additional effect as compared to each treatment alone.

A role for Up_4A in the pathogenesis of hypertension has been suggested by the observation that Up_4A-induced vascular contraction in the renal, femoral, and basilar artery is potentiated in hypertension (Matsumoto et al., 2011b), while the Up_4A plasma concentration in hypertensive subjects is significantly higher as compared to that in healthy subjects and correlates with blood pressure (Jankowski et al., 2007). The present study shows that pressure overload-induced coronary vascular remodeling results in attenuation of the vasodilator effect of Up_4A, which is accompanied by increased expression of $P2Y_{12}$ receptor. Activation of the $P2Y_{12}$ receptor on vascular smooth muscle likely results in activation of TxS and TxA_2 production in response to Up_4A, thereby blunting its vasodilator effect in the coronary microcirculation. Future experiments are required to investigate if indeed the $P2Y_{12}$ receptor is a key factor in activation of TxS in AoB animals, as well as the signal transduction pathway involved.

AUTHOR CONTRIBUTIONS

ZZ: designed and performed the experiments, interpreted the data, drafted the manuscript. IL: performed the experiments, drafted the manuscript. HvB and CC: interpreted the data, revised the manuscript. DD and DM: designed the experiments, interpreted the data, revised the manuscript.

FUNDING

This work was supported by the China Scholarship Council 2009624027 (to ZZ) and CTMM-TRIUMPH (to DD and DM) as well as by the Netherlands CardioVascular Research Initiative CVON-RECONNECT 2014-11 (to DD and DM).

REFERENCES

Alexánderson, E., Jacome, R., Jimenez-Santos, M., Ochoa, J. M., Romero, E., Cabral, M. A., et al. (2012). Evaluation of the endothelial function in hypertensive patients with 13N-ammonia PET. *J. Nucl. Cardiol.* 19, 979–986. doi: 10.1007/s12350-012-9584-z

Aubin, M. C., Gendron, M. E., Lebel, V., Thorin, E., Tardif, J. C., Carrier, M., et al. (2007). Alterations in the endothelial G-protein coupled receptor pathway in

epicardial arteries and subendocardial arterioles in compensated left ventricular hypertrophy. *Basic Res. Cardiol.* 102, 144–153. doi: 10.1007/s00395-006-0626-z

Bache, R. J. (1988). Effects of hypertrophy on the coronary circulation. *Prog. Cardiovasc. Dis.* 30, 403–440. doi: 10.1016/0033-0620(88)90005-9

Batenburg, W. W., Popp, R., Fleming, I., de Vries, R., Garrelds, I. M., Saxena, P. R., et al. (2004). Bradykinin-induced relaxation of coronary microarteries: S-nitrosothiols as EDHF? *Br. J. Pharmacol.* 142, 125–135. doi: 10.1038/sj.bjp.0705747

Bhavaraju, K., Georgakis, A., Jin, J., Gartner, T. K., Tomiyama, Y., Nurden, A., et al. (2010). Antagonism of P2Y12 reduces physiological thromboxane levels. *Platelets* 21, 604–609. doi: 10.3109/09537104.2010.511684

Breisch, E. A., White, F. C., Nimmo, L. E., and Bloor, C. M. (1986). Cardiac vasculature and flow during pressure-overload hypertrophy. *Am. J. Physiol.* 251(5 Pt 2), H1031–H1037. doi: 10.1152/ajpheart.1986.251.5.H1031

Burnstock, G. (2007). Purine and pyrimidine receptors. *Cell. Mol. Life Sci.* 64, 1471–1483. doi: 10.1007/s00018-007-6497-0

Burnstock, G. (2010). Control of vascular tone by purines and pyrimidines. *Br. J. Pharmacol.* 161, 527–529. doi: 10.1111/j.1476-5381.2010.00937.x

Chaudhary, K. R., Batchu, S. N., and Seubert, J. M. (2009). Cytochrome P450 enzymes and the heart. *IUBMB Life* 61, 954–960. doi: 10.1002/iub.241

Chu, L. M., Robich, M. P., Bianchi, C., Feng, J., Liu, Y., Xu, S. H., et al. (2012). Effects of cyclooxygenase inhibition on cardiovascular function in a hypercholesterolemic swine model of chronic ischemia. *Am. J. Physiol. Heart Circ. Physiol.* 302, H479–H488. doi: 10.1152/ajpheart.00146.2011

Desjardins, F., Aubin, M. C., Carrier, M., and Perrault, L. P. (2005). Decrease of endothelin receptor subtype ETB and release of COX-derived products contribute to endothelial dysfunction of porcine epicardial coronary arteries in left ventricular hypertrophy. *J. Cardiovasc. Pharmacol.* 45, 499–508. doi: 10.1097/01.fjc.0000159641.36900.14

Duncker, D. J., Zhang, J., and Bache, R. J. (1993). Coronary pressure-flow relation in left ventricular hypertrophy. Importance of changes in back pressure versus changes in minimum resistance. *Circ. Res.* 72, 579–587. doi: 10.1161/01.RES.72.3.579

Galderisi, M., Cicala, S., De Simone, L., Caso, P., Petrocelli, A., Pietropaolo, L., et al. (2001). Impact of myocardial diastolic dysfunction on coronary flow reserve in hypertensive patients with left ventricular hypertrophy. *Ital. Heart J.* 2, 677–684.

Haitsma, D. B., Bac, D., Raja, N., Boomsma, F., Verdouw, P. D., and Duncker, D. J. (2001). Minimal impairment of myocardial blood flow responses to exercise in the remodeled left ventricle early after myocardial infarction, despite significant hemodynamic and neurohumoral alterations. *Cardiovasc. Res.* 52, 417–428. doi: 10.1016/S0008-6363(01)00426-6

Hamasaki, S., Al Suwaidi, J., Higano, S. T., Miyauchi, K., Holmes, D. R. Jr., and Lerman, A. (2000). Attenuated coronary flow reserve and vascular remodeling in patients with hypertension and left ventricular hypertrophy. *J. Am. Coll. Cardiol.* 35, 1654–1660. doi: 10.1016/S0735-1097(00)00594-5

Jankowski, V., Meyer, A. A., Schlattmann, P., Gui, Y., Zheng, X. L., Stamcou, I., et al. (2007). Increased uridine adenosine tetraphosphate concentrations in plasma of juvenile hypertensives. *Arterioscler. Thromb. Vasc. Biol.* 27, 1776–1781. doi: 10.1161/ATVBAHA.107.143958

Ju, Y. K., Huang, W., Jiang, L., Barden, J. A., and Allen, D. G. (2003). ATP modulates intracellular Ca^{2+} and firing rate through a P2Y1 purinoceptor in cane toad pacemaker cells. *J. Physiol.* 552(Pt 3), 777–787. doi: 10.1113/jphysiol.2003.052258

Kappers, M. H., de Beer, V. J., Zhou, Z., Danser, A. H., Sleijfer, S., Duncker, D. J., et al. (2012). Sunitinib-induced systemic vasoconstriction in swine is endothelin mediated and does not involve nitric oxide or oxidative stress. *Hypertension* 59, 151–157. doi: 10.1161/HYPERTENSIONAHA.111.182220

Kawabe, J., Ushikubi, F., and Hasebe, N. (2010). Prostacyclin in vascular diseases. - Recent insights and future perspectives. *Circ. J.* 74, 836–843. doi: 10.1253/circj.CJ-10-0195

Khatibzadeh, S., Farzadfar, F., Oliver, J., Ezzati, M., and Moran, A. (2013). Worldwide risk factors for heart failure: A systematic review and pooled analysis. *Int. J. Cardiol.* 168, 1186–1194. doi: 10.1016/j.ijcard.2012.11.065

Lavi, S., Yang, E. H., Prasad, A., Mathew, V., Barsness, G. W., Rihal, C. S., et al. (2008). The interaction between coronary endothelial dysfunction, local oxidative stress, and endogenous nitric oxide in humans. *Hypertension* 51, 127–133. doi: 10.1161/HYPERTENSIONAHA.107.099986

Long, X., Mokelke, E. A., Neeb, Z. P., Alloosh, M., Edwards, J. M., and Sturek, M. (2010). Adenosine receptor regulation of coronary blood flow in Ossabaw miniature swine. *J. Pharmacol. Exp. Ther.* 335, 781–787. doi: 10.1124/jpet.110.170803

Malo, O., Carrier, M., Shi, Y. F., Tardif, J. C., Tanguay, J. F., and Perrault, L. P. (2003a). Specific alterations of endothelial signal transduction pathways of porcine epicardial coronary arteries in left ventricular hypertrophy. *J. Cardiovasc. Pharmacol.* 42, 275–286. doi: 10.1097/00005344-200308000-00018

Malo, O., Desjardins, F., Tanguay, J. F., Tardif, J. C., Carrier, M., and Perrault, L. P. (2003b). Tetrahydrobiopterin and antioxidants reverse the coronary endothelial dysfunction associated with left ventricular hypertrophy in a porcine model. *Cardiovasc. Res.* 59, 501–511. doi: 10.1016/S0008-6363(03)00390-0

Martino, A., Cabiati, M., Campan, M., Prescimone, T., Minocci, D., Caselli, C., et al. (2011). Selection of reference genes for normalization of real-time PCR data in minipig heart failure model and evaluation of TNF-alpha mRNA expression. *J. Biotechnol.* 153, 92–99. doi: 10.1016/j.jbiotec.2011.04.002

Matsumoto, T., Nakane, T., and Chiba, S. (1997). Pharmacological analysis of responses to ATP in the isolated and perfused canine coronary artery. *Eur. J. Pharmacol.* 334, 173–180.

Matsumoto, T., Tostes, R. C., and Webb, R. C. (2011a). The role of uridine adenosine tetraphosphate in the vascular system. *Adv. Pharmacol. Sci.* 2011:435132. doi: 10.1155/2011/435132

Matsumoto, T., Tostes, R. C., and Webb, R. C. (2011b). Uridine adenosine tetraphosphate-induced contraction is increased in renal but not pulmonary arteries from DOCA-salt hypertensive rats. *Am. J. Physiol. Heart Circ. Physiol.* 301, H409–H417. doi: 10.1152/ajpheart.00084.2011

Matsumoto, T., Watanabe, S., Kawamura, R., Taguchi, K., and Kobayashi, T. (2014). Enhanced uridine adenosine tetraphosphate-induced contraction in renal artery from type 2 diabetic Goto-Kakizaki rats due to activated cyclooxygenase/thromboxane receptor axis. *Pflugers Arch.* 466, 331–342. doi: 10.1007/s00424-013-1330-0

Mezzaroma, E., Toldo, S., Farkas, D., Seropian, I. M., Van Tassell, B. W., Salloum, F. N., et al. (2011). The inflammasome promotes adverse cardiac remodeling following acute myocardial infarction in the mouse. *Proc. Natl. Acad. Sci. U.S.A.* 108, 19725–19730. doi: 10.1073/pnas.1108586108

Nie, H., Wu, J. L., Zhang, M., Xu, J., and Zou, M. H. (2006). Endothelial nitric oxide synthase-dependent tyrosine nitration of prostacyclin synthase in diabetes in vivo. *Diabetes Metab. Res. Rev.* 55, 3133–3141. doi: 10.2337/db06-0505

Ralevic, V., and Burnstock, G. (1998). Receptors for purines and pyrimidines. *Pharmacol. Rev.* 50, 413–492.

Rayment, S. J., Latif, M. L., Ralevic, V., and Alexander, S. P. (2007). Evidence for the expression of multiple uracil nucleotide-stimulated P2 receptors coupled to smooth muscle contraction in porcine isolated arteries. *Br. J. Pharmacol.* 150, 604–612. doi: 10.1038/sj.bjp.0707120

Rodriguez-Porcel, M., Lerman, L. O., Herrmann, J., Sawamura, T., Napoli, C., and Lerman, A. (2003). Hypercholesterolemia and hypertension have synergistic deleterious effects on coronary endothelial function. *Arterioscler. Thromb. Vasc. Biol.* 23, 885–891. doi: 10.1161/01.ATV.0000069209.26507.BF

Rondelet, B., Kerbaul, F., Motte, S., van Beneden, R., Remmelink, M., Brimioulle, S., et al. (2003). Bosentan for the prevention of overcirculation-induced experimental pulmonary arterial hypertension. *Circulation* 107, 1329–1335. doi: 10.1161/01.CIR.0000053443.27512.33

Sangkuhl, K., Klein, T. E., and Altman, R. B. (2010). Clopidogrel pathway. *Pharmacogenet. Genomics* 20, 463–465. doi: 10.1097/FPC.0b013e3283385420

Schreiber, R., and Kunzelmann, K. (2005). Purinergic P2Y6 receptors induce Ca^{2+} and Cftr dependent Cl^{-} secretion in mouse trachea. *Cell Physiol. Biochem.* 16, 99–108. doi: 10.1159/000087736

Sorop, O., van den Heuvel, M., van Ditzhuijzen, N. S., de Beer, V. J., Heinonen, I., van Duin, R. W., et al. (2016). Coronary microvascular dysfunction after long-term diabetes and hypercholesterolemia. *Am. J. Physiol. Heart Circ. Physiol.* 311, H1339–H1351. doi: 10.1152/ajpheart.00458.2015

Teng, B., Labazi, H., Sun, C., Yang, Y., Zeng, X., Mustafa, S. J., et al. (2017). Divergent coronary flow responses to uridine adenosine tetraphosphate in atherosclerotic ApoE knockout mice. *Purinergic Signal.* 13, 591–600. doi: 10.1007/s11302-017-9586-z

Tomanek, R. J., Palmer, P. J., Peiffer, G. L., Schreiber, K. L., Eastham, C. L., and Marcus, M. L. (1986). Morphometry of canine coronary arteries, arterioles, and

capillaries during hypertension and left ventricular hypertrophy. *Circ. Res.* 58, 38–46. doi: 10.1161/01.RES.58.1.38

Urbieta-Caceres, V. H., Zhu, X. Y., Gibson, M. E., Favreau, F. D., Jordan, K., Lerman, A., et al. (2011). Reversal of experimental renovascular hypertension restores coronary microvascular function and architecture. *Am. J. Hypertens.* 24, 458–465. doi: 10.1038/ajh.2010.259

van den Heuvel, A. F., Blanksma, P. K., Siebelink, H. M., van Wijk, L. M., Boomsma, F., Vaalburg, W., et al. (2001). Impairment of myocardial blood flow reserve in patients with asymptomatic left ventricular dysfunction: effects of ACE-inhibition with perindopril. *Int. J. Cardiovasc. Imag.* 17, 353–359. doi: 10.1023/A:1011971800052

van Kats, J. P., Duncker, D. J., Haitsma, D. B., Schuijt, M. P., Niebuur, R., Stubenitsky, R., et al. (2000). Angiotensin-converting enzyme inhibition and angiotensin II type 1 receptor blockade prevent cardiac remodeling in pigs after myocardial infarction: role of tissue angiotensin II. *Circulation* 102, 1556–1563. doi: 10.1161/01.CIR.102.13.1556

Vanhoutte, P. M. (1996). Endothelium-dependent responses in congestive heart failure. *J. Mol. Cell Cardiol.* 28, 2233–2240. doi: 10.1006/jmcc.1996.0215

Wihlborg, A. K., Wang, L., Braun, O. O., Eyjolfsson, A., Gustafsson, R., Gudbjartsson, T., et al. (2004). ADP receptor P2Y12 is expressed in vascular smooth muscle cells and stimulates contraction in human blood vessels. *Arterioscler. Thromb. Vasc. Biol.* 24, 1810–1815. doi: 10.1161/01.ATV.0000142376.30582.ed

Zhou, Z., de Wijs-Meijler, D., Lankhuizen, I., Jankowski, J., Jankowski, V., Jan Danser, A. H., et al. (2013a). Blunted coronary vasodilator response to uridine adenosine tetraphosphate in post-infarct remodeled myocardium is due to reduced P1 receptor activation. *Pharmacol. Res.* 77, 22–29. doi: 10.1016/j.phrs.2013.08.007

Zhou, Z., Merkus, D., Cheng, C., Duckers, H. J., Jan Danser, A. H., and Duncker, D. J. (2013b). Uridine adenosine tetraphosphate is a novel vasodilator in the coronary microcirculation which acts through purinergic P1 but not P2 receptors. *Pharmacol. Res.* 67, 10–17. doi: 10.1016/j.phrs.2012.09.011

Zhou, Z., Rajamani, U., Labazi, H., Tilley, S. L., Ledent, C., Teng, B., et al. (2015a). Involvement of NADPH oxidase in A2A adenosine receptor-mediated increase in coronary flow in isolated mouse hearts. *Purinergic Signal.* 11, 263–273. doi: 10.1007/s11302-015-9451-x

Zhou, Z., Sorop, O., de Beer, V. J., Heinonen, I., Cheng, C., Jan Danser, A. H., et al. (2017). Altered purinergic signaling in uridine adenosine tetraphosphate-induced coronary relaxation in swine with metabolic derangement. *Purinergic Signal.* 13, 319–329. doi: 10.1007/s11302-017-9563-6

Zhou, Z., Sun, C., Tilley, S. L., and Mustafa, S. J. (2015b). Mechanisms underlying uridine adenosine tetraphosphate-induced vascular contraction in mouse aorta: Role of thromboxane and purinergic receptors. *Vascul. Pharmacol.* 73, 78–85. doi: 10.1016/j.vph.2015.04.009

Zou, M. H., Cohen, R., and Ullrich, V. (2004). Peroxynitrite and vascular endothelial dysfunction in diabetes mellitus. *Endothelium* 11, 89–97. doi: 10.1080/10623320490482619

Conflict of Interest Statement: The authors declare that the research was conducted in the absence of any commercial or financial relationships that could be construed as a potential conflict of interest.

frontiers in Pharmacology

ORIGINAL RESEARCH
published: 20 March 2018
doi: 10.3389/fphar.2018.00133

Adenosine A_{2A} Receptors Control Glutamatergic Synaptic Plasticity in Fast Spiking Interneurons of the Prefrontal Cortex

*Amber Kerkhofs[1,2], Paula M. Canas[2], A. J. Timmerman[1], Tim S. Heistek[1], Joana I. Real[2], Carolina Xavier[2], Rodrigo A. Cunha[2,3], Huibert D. Mansvelder[1] and Samira G. Ferreira[2]**

[1] Department of Integrative Neurophysiology, Center for Neurogenomics and Cognitive Research, VU University, Amsterdam, Netherlands, [2] Center for Neuroscience and Cell Biology, University of Coimbra, Coimbra, Portugal, [3] Faculty of Medicine, University of Coimbra, Coimbra, Portugal

Adenosine A_{2A} receptors ($A_{2A}R$) are activated upon increased synaptic activity to assist in the implementation of long-term plastic changes at synapses. While it is reported that $A_{2A}R$ are involved in the control of prefrontal cortex (PFC)-dependent behavior such as working memory, reversal learning and effort-based decision making, it is not known whether $A_{2A}R$ control glutamatergic synapse plasticity within the medial PFC (mPFC). To elucidate that, we tested whether $A_{2A}R$ blockade affects long-term plasticity (LTP) of excitatory post-synaptic potentials in pyramidal neurons and fast spiking (FS) interneurons in layer 5 of the mPFC and of population spikes. Our results show that $A_{2A}R$ are enriched at mPFC synapses, where their blockade reversed the direction of plasticity at excitatory synapses onto layer 5 FS interneurons from LTP to long-term depression, while their blockade had no effect on the induction of LTP at excitatory synapses onto layer 5 pyramidal neurons. At the network level, extracellularly induced LTP of population spikes was reduced by $A_{2A}R$ blockade. The interneuron-specificity of $A_{2A}R$ in controlling glutamatergic synapse LTP may ensure that during periods of high synaptic activity, a proper excitation/inhibition balance is maintained within the mPFC.

Keywords: A_{2A} receptor, prefrontal cortex (PFC), synaptic plasticity, fast-spiking interneurons, adenosine, LTP and LTD, electrophysiology

OPEN ACCESS

Edited by:
Francisco Ciruela, Universitat de Barcelona, Spain

Reviewed by:
Elena Martín-García, Pompeu Fabra University, Spain
Carl Richard Lupica, National Institute on Drug Abuse (NIH), United States

****Correspondence:***
Samira G. Ferreira
carsamira@gmail.com

Specialty section:
This article was submitted to Experimental Pharmacology and Drug Discovery, a section of the journal Frontiers in Pharmacology

Received: *02 September 2017*
Accepted: *07 February 2018*
Published: *20 March 2018*

Citation:
Kerkhofs A, Canas PM, Timmerman AJ, Heistek TS, Real JI, Xavier C, Cunha RA, Mansvelder HD and Ferreira SG (2018) Adenosine A_{2A} Receptors Control Glutamatergic Synaptic Plasticity in Fast Spiking Interneurons of the Prefrontal Cortex. Front. Pharmacol. 9:133. doi: 10.3389/fphar.2018.00133

INTRODUCTION

The prefrontal cortex (PFC) is involved in the control of cognitive and executive functions, such as decision making, working memory, inhibitory control, attention, and behavioral flexibility (Dalley et al., 2004; Euston et al., 2013). The flexible regulation of these types of behavior makes it possible to properly respond to a changing environment (Arnsten, 2009). Such flexibility is thought to require plastic changes in the strength of synaptic connections (Kandel, 1976; Mayford et al., 2012), which is heavily dependent on the action of several neuromodulators (Pawlak et al., 2010; Bloem et al., 2014; Dembrow and Johnston, 2014).

One of the neuromodulators that can impact synaptic plasticity is adenosine, which is released in an activity-dependent fashion at synapses (Cunha et al., 1996; Wall and Dale, 2013). Its actions are mediated by a balanced activation of the inhibitory A_1 receptors (A_1R) and the facilitatory A_{2A} receptors ($A_{2A}R$) (Cunha, 2008), which act predominantly on glutamatergic but also on

GABAergic signaling (Shen et al., 2008; Rombo et al., 2015; Qi et al., 2017). While A_1R control basal synaptic transmission, $A_{2A}R$ are selectively engaged in events where long-term potentiation (LTP) is induced (d'Alcantara et al., 2001; Rebola et al., 2008; Simões et al., 2016).

$A_{2A}R$ are present in the PFC (Van Dort et al., 2009; Pandolfo et al., 2013; van Aerde et al., 2013) and affect PFC-dependent behavior. Indeed, genetic elimination of $A_{2A}R$ decreases effort-based decision-making (Pardo et al., 2012), while enhancing working memory (Zhou et al., 2009; Wei et al., 2011) and reversal learning (Wei et al., 2011). Their possible pathophysiological relevance is highlighted by the ability of selective $A_{2A}R$ antagonists to attenuate working memory deficits (Horita et al., 2013; Li et al., 2015), and by the ability of caffeine, which antagonizes both adenosine receptors, to counteract cognitive behavioral deficits both in human subjects suffering from attention deficit hyperactivity disorder (ADHD; Leon, 2000) as well as in a rat model of ADHD (Pandolfo et al., 2013).

Despite the effects of $A_{2A}R$ on PFC-dependent behavior, it is not known how $A_{2A}R$ control the information flow and whether $A_{2A}R$ affect glutamatergic synaptic plasticity of information within the local PFC circuit. Therefore, we studied the impact of $A_{2A}R$ on synaptic transmission and plasticity at excitatory synapses onto pyramidal neurons and interneurons and at the network level in the medial PFC (mPFC). We found that $A_{2A}R$ are enriched at mPFC synapses, where $A_{2A}R$ blockade shifts the direction of plasticity at excitatory synapses onto layer 5 fast spiking (FS) interneurons from LTP to LTD, while it is ineffective at excitatory synapses onto layer 5 pyramidal neurons and reduces plasticity at the network level.

MATERIALS AND METHODS

Animals

All studies were conducted in accordance with the principles and procedures outlined as "3Rs" in the guidelines of EU (210/63), FELASA, and the National Centre for the 3Rs (the ARRIVE; Kilkenny et al., 2010), and were approved by the Animal Care Committee of the Center for Neuroscience and Cell Biology (ORBEA 78/2013) or by the VU University's Animal Experimentation Ethics Committee (DEC) and were in accordance with institutional and Dutch license procedures. Rats were housed in a temperature and humidity-controlled environment with 12 h light on/off cycles and *ad libitum* access to food and water.

Membrane-Binding Assay

The density of $A_{2A}R$ in total membranes or synaptosomal membranes from the PFC was estimated by a radioligand-binding assay using a supramaximal concentration of the $A_{2A}R$ antagonist ^{3}H-SCH58261 (6 nM; provided by E. Ongini, Schering-Plough, Milan, Italy), as described previously (Kaster et al., 2015; Viana da Silva et al., 2016). Specific binding was determined by the subtraction of non-specific binding measured in the presence of 3 μM XAC (Tocris).

Subsynaptic Fractionation of mPFC Synaptosomes and Western Blot Analysis

To separate the extra-synaptic (non-active) zone, presynaptic active zone and post-synaptic fractions from synaptosomes, we used a fractionation method previously described in detail (Rebola et al., 2005; Canas and Cunha, 2016). The efficiency of separation is based on the segregation of different markers in the several fractions: SNAP-25 in the presynaptic active zone, PSD-95 in the post-synaptic density (PSD) and synaptophysin outside the active zone (extra-synaptic fraction). Western blot analysis was performed with an anti-$A_{2A}R$ antibody (1:500; sc-32261 from Santa Cruz Biotechnology; Santa Cruz, CA, United States), of which selectivity was confirmed by the lack of signal in $A_{2A}R$ knockout mice (Rebola et al., 2005).

Whole-Cell-Recordings

Male Wistar rats (5–6.5 week-old) purchased from Charles River (Harlan) were decapitated, their brain was carefully removed and the mPFC was sliced in carbogen buffered (pH 7.4) ice-cold choline-based slicing solution containing (in mM): choline chloride 110, sodium ascorbate 11.6, KCl 2.5, NaH_2PO_4 1.3, $MgCl_2$ 7, $CaCl_2$ 0.5, $NaHCO_3$ 26, and glucose 10. Slices (350 μm) were kept at room temperature in aCSF oxygenated with carbogen in a holding chamber. Following recovery for at least 1 h, recordings from cells in L5 of the mPFC were made in oxygenated aCSF (flow rate of 2–3 ml/min, 32°C). Whole-cell patch-clamp recordings were made with borosilicate glass pipettes (3–6 MΩ) filled with an intracellular solution containing (in mM): K-gluconate 111, KCl 8, HEPES 10, Mg-ATP 4, K_2 phosphocreatine 10, GTP 0.4, EGTA 0.2. Biocytin (0.2–0.5%) was added to all solutions for *post hoc* cell identification, and osmolarity was adjusted to 290–295 mOsm. Pyramidal L5 cells were visualized with differential interference contrast microscopy, selected on their large and pyramidal shape and further identified by their spike profile. FS interneurons were selected based on their small, round shape and further identified by their spike profile. During recordings, neurons were kept at a holding potential close to −70 mV. Recordings were made using MultiClamp 700 A/B amplifiers (Axon Instruments, Sunnyvale, CA, United States), with sampling at 10 kHz and low-pass filtering at 3–4 kHz. Recordings were digitized with an Axon Digidata 1440A and acquired using pClamp software (Axon). After experiments were completed, slices were stored in 4% paraformaldehyde for subsequent neuronal visualization and reconstruction as previously described (Mohan et al., 2015).

Spontaneous EPSCs

Spontaneous excitatory post-synaptic currents (sEPSCs) were recorded 5–10 min before and 25–30 min after drug incubation. Acquired data were stored for off-line analysis and events were detected using MiniAnalysis software. EPSC amplitude and frequency were determined and averaged over a 5-min time-course in each condition.

Evoked EPSCs

Excitatory post-synaptic currents (EPSCs) were evoked (eEPSCs) every 3.5 s using bipolar stimulating electrodes in glass pipettes filled with aCSF positioned 100–150 μm along the cell's apical dendrite. Duration (0.5 ms) and amplitude (100–350 mA) of extracellular stimulation were controlled by Isoflex stimulators (A.M.P.I., Jerusalem, Israel) to generate a monosynaptic response. After recording a baseline for 5–10 min, drugs were added and the eEPSC response was recorded for another 20 min. In pyramidal neurons, 15 datapoints were determined and averaged in each condition (baseline, 5 min after incubation and 15 min after incubation). In FS cells, EPSC amplitude was averaged over a 5-min time-course in all conditions (baseline, 5 min after incubation and 15 min after incubation).

Long-Term Potentiation

Excitatory post-synaptic potentials (EPSPs) were evoked every 7 s (0.14 Hz) using bipolar stimulating electrodes in glass pipettes filled with aCSF positioned 100–150 μm along the cell's apical dendrite. The duration (0.5 ms) and amplitude (100–350 μA) of extracellular stimulation were controlled by Isoflex stimulators (A.M.P.I., Jerusalem, Israel) to generate a monosynaptic response. Baseline EPSP was defined with an input/output curve, stimulating at below half maximum response. After obtaining a stable baseline of 3–5 min (30–43 EPSPs), LTP was induced within 15 min of whole-cell configuration with an unpaired theta burst stimulation (TBS) protocol (10 bursts of five pulses each at 100 Hz, repeated three times). This protocol triggered an optimal potentiated response in the cells, which was more reliable than other tested protocols such as spike timing dependent potentiation (STDP), although it was still highly variable especially in pyramidal neurons. Timing of EPSPs and the induction protocol was controlled by a Master-8 stimulator (A.M.P.I.). The slope of the initial 2 ms of the EPSP was taken as a measure of EPSP strength. The change in synaptic strength was defined as the percent change in EPSP slope 20–30 min after the TBS relative to baseline. Cell input resistance was monitored by applying a hyperpolarizing pulse at the end of each sweep (−30 pA). After LTP induction, membrane potential was returned to approximate baseline value by modest current injection. Criteria for inclusion of recordings were: (1) baseline resting membrane potential < -60 mV, (2) smooth rise of EPSP and clear separation from stimulation artifact, (3) stable baseline EPSP slope, (4) less than 30% change in input resistance, (5) no AP-firing evoked by extracellular stimulation in post-pairing period. In total, five cases of extreme EPSP rundown (slope $< 20\%$ of baseline) were excluded from analysis.

Extracellular Recordings

Male Wistar rats (6–8 week-old) were purchased from Charles River Laboratories (Barcelona, Spain). Rats were anesthetized under halothane atmosphere, decapitated and the brain rapidly removed from the skull and submerged in ice-cold artificial cerebrospinal fluid (aCSF) solution of the following composition, in mM: NaCl 125, KCl 3, $MgSO_4$ 1, $CaCl_2$ 2, Na_2HPO_4 1.25 $NaHCO_3$ 25–26 and glucose 11, pH 7.4 (osmolality, ∼300 $mOsmol.kg^{-1}$), oxygenated with carbogen (95% O_2 + 5% CO_2). Coronal slices (300 μm-thick) containing the medial prefrontal cortex (mPFC) were cut with a Vibratome 1500 sectioning system (Vibratome, Germany). The slices were then transferred to a pre-chamber containing aCSF under continuous oxygenation to recover at 32°C for at least 1 h. Slices were then transferred to a submerged recording chamber where they were continuously superfused at a rate of 2–3 ml/min with oxygenated aCSF at 30–32°C. A bipolar concentric stimulation electrode SNE-100 (Kopf, Germany) was placed on the layer II/III of the mPFC delivering rectangular pulses (80–160 μA) of 0.1 ms duration applied with a Digitimer DS3 stimulator (Digitimer, Ltd., United Kingdom) once every 20 s. The evoked population spikes were recorded through an extracellular borosilicate microelectrode (filled with 4 M NaCl, 2–4 MΩ resistance) placed in the layer V of the mPFC, using an Axopatch 200B amplifier (Axon Instruments, Inc., United States), coupled to an analog/digital acquisition board (Digidata 1322A; Axon Instruments, Inc., United States). Responses were digitized at 10 kHz and continuously monitored on a personal computer via WinLTP 1.1 software (Anderson and Collingridge, 2007). Responses were quantified as the amplitude of the population spike recordings. After stabilizing the response, the input/output curve was obtained. Then the intensity of the stimulus was regulated to obtain 40–50% of the maximum response before induction of LTP. LTP was induced by delivering a train of 100 Hz (50 pulses, 0.5 s duration) for a priming effect, which was 15 min later followed by four trains of 100 Hz (50 pulses, 0.5 s duration, 1 every 10 s). Due to difficulties in inducing LTP in rat PFC slices, LTP protocols were extensively tested and this protocol, which has been used by Gemperle et al. (2003), was the most reliable one in our hands.

Experimental Design and Statistics

For membrane binding assays, PFC from five adult male Wistar rats were used, and the density of A_{2A}R in synaptosomal membranes was compared to that in total membranes using unpaired *t*-test. For Western blotting of sub-synaptic fractions, we pooled together mPFC tissue from 22 rats (30–45 days-old). This was due to the requirement of 1 g of tissue for the sub-synaptic fractionation step. For pharmacology in electrophysiology experiments, all the drugs used were dissolved in aCSF at the desired concentration and bath applied during the experiments. The drugs were diluted from stock solutions made in dimethylsulfoxide (DMSO) to their final concentrations: SCH58261 (50–100 nM from 5 mM stock solution, Tocris). All experiments were performed without application of synaptic blockers. In extracellular recordings, due to high variability in LTP magnitude, whenever SCH58261 was tested, a control slice was also done in parallel. In the end, data from 25 slices per group (from 25 different rats) were pooled together for statistical comparison using an unpaired *t*-test. For plasticity in whole-cell patch-clamp experiments,

due to cellular variability, strict exclusion criteria (see above), long duration of the experiment and high quality of slices needed, more animals were needed than are presented in our figures. When relevant and possible, we recorded one cell in control and one cell in drug condition from every animal. For the pyramidal-TBS experiment, 51 animals were used. For the FS interneuron-TBS experiment, 27 animals were used. Raw data was analyzed using Clampfit 10.4 and custom Matlab scripts. For all LTP experiments, we used the percentage of increase in EPSP slope (whole-cell recordings) or population spike amplitude (extracellular recordings) induced by the LTP protocol per cell (whole-cell recordings) or per slice (extracellular recordings) as input for statistical tests. An unpaired *t*-test was used to compare two groups consisting of multiple such experiments, comparing the percentage of LTP induction in control experiments *versus* the percentage of LTP induction in $A_{2A}R$ antagonist-treated experiments. This method for comparing differences in LTP induction in control *versus* drug treated slices is adopted from our previous research on LTP induction (Mansvelder and McGehee, 2000; Couey et al., 2007; Meredith et al., 2007; Rebola et al., 2008; Verhoog et al., 2013, 2016; Simões et al., 2016). For whole-cell spontaneous recordings, 12 slices from 10 different animals were used in sEPSC on pyramidal neurons; 2 recordings were excluded for rundown reasons (>20% change in resistance). For sEPSC on FS interneurons, 32 recordings of interneurons were made from slices of 21 different animals. Of these, 13 cells were actual FS interneurons; 1 was excluded for rundown. For eEPCS experiments on pyramidal neurons, 14 slices were used from four different animals. For eEPSC experiments on FS interneurons, eight slices from three animals were used, four animals were used in total for these experiments. All recorded sEPSCs were analyzed with MiniAnalysis software (Synaptosoft, version 6.0.7). All the statistical analysis was performed using Prism 6 (GraphPad software). Data was analyzed by using the appropriate parametric statistical test as mentioned in the text and $p < 0.05$ was taken as statistically significant.

RESULTS

$A_{2A}R$ Are Enriched in Synaptosomal Membranes and Present in All Sub-synaptic Fractions

To investigate the density and synaptic distribution of $A_{2A}R$, we compared the binding of ^{3}H-SCH58261 in total and synaptosomal membranes from the PFC. The binding density of ^{3}H-SCH58261 was higher ($n = 5$; $t_8 = 4.56$; $p = 0.0018$; unpaired *t*-test) in the synaptosomal membrane fraction (39.0 ± 3.6 fmol/mg protein) compared to the total membrane fraction (19.4 ± 2.4 fmol/mg protein; $n = 5$) from the PFC (**Figure 1A**). Given this enrichment of $A_{2A}R$ in synaptosomal membranes, we used mPFC synaptosomes (pooled from 22 rats) to separate the different subsynaptic fractions, and probed for the subsynaptic distribution of $A_{2A}R$. $A_{2A}R$ were present in all the subsynaptic fractions, inside and outside the presynaptic active zone and PSD, with a higher $A_{2A}R$ density observed outside the presynaptic active zone and PSD (**Figure 1B**). The presence of $A_{2A}R$ in all PFC sub-synaptic fractions suggests a role for $A_{2A}R$ in the control of synaptic communication in the mPFC.

$A_{2A}R$ Do Not Control Spontaneous and Evoked Excitatory Synaptic Transmission

To determine whether sEPSCs or eEPSCs are affected by $A_{2A}R$, we recorded sEPSCs and eEPSCs onto both pyramidal neurons and FS interneurons, the two largest groups of neurons in the PFC (Markram et al., 2004) and tested the effect of the selective $A_{2A}R$ antagonist SCH58261. After recording a baseline in ACSF, SCH58261 (100 nM) was incubated into the bath and cells were recorded for another 20–30 min. Spontaneous events onto pyramidal neurons were unaffected by incubation of SCH58261 (100 nM; **Figures 2A–E**) in both frequency (**Figures 2B,C**; Frequency mean control: 1.22 ± 1.2 Hz, $n = 10$; 5 min after SCH58261: 1.12 ± 0.83 Hz, $n = 10$; 25 min after SCH58261: 0.78 ± 0.46 Hz, $n = 10$; difference: $F_{2,9} = 6.05$, $p = 0.21$, ANOVA) and amplitude (**Figures 2D,E**; Amplitude

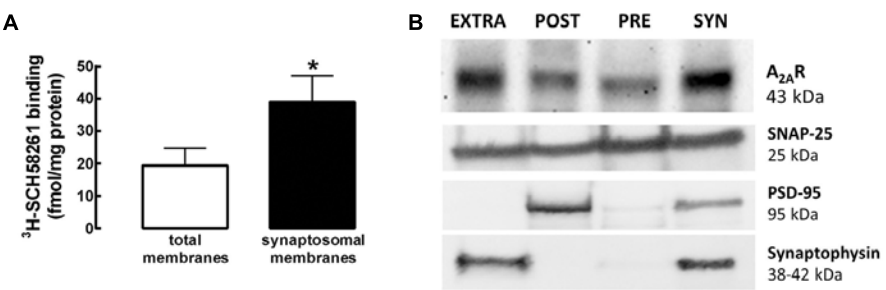

FIGURE 1 | $A_{2A}R$ are enriched in synaptosomal membranes and present in all subsynaptic fractions. **(A)** The binding density of a supra-maximal concentration of a selective $A_{2A}R$ antagonist ^{3}H-SCH58261 (6 nM) was higher in synaptosomal when compared to total membranes from Wistar rat PFC. Data are mean ± SEM of five rats; $*p < 0.05$, unpaired Student's *t*-test. **(B)** Western blots of subsynaptic fractions showing the subsynaptic distribution of $A_{2A}R$ in the mPFC (pooled from 22 rats due to the requirement of large sample size – 1 g of tissue – at the start of the subsynaptic fractionation procedure). The efficiency of separation is based on the segregation of different markers in the several fractions: SNAP-25 in the presynaptic active zone, PSD-95 in the post-synaptic density (PSD) and synaptophysin outside the active zone (extrasynaptic fraction). $A_{2A}R$ are present in all the subsynaptic fractions, inside and outside the presynaptic active zone and PSD. However, there is an enrichment outside the presynaptic active zone and PSD.

mean control: 36.38 ± 6.2 pA, $n = 10$; 5 min after SCH58261: 38.18 ± 8.9 pA, $n = 10$; 25 min after SCH58261: 37.50 ± 6.5 pA, $n = 10$; difference: $F_{2,9} = 0.95$, $p = 0.39$, ANOVA). Similarly, spontaneous events onto FS interneurons were unaffected by incubation of SCH58261 (100 nM; **Figures 2H–L**) in both frequency (**Figures 2I,J**; Frequency mean control: 3.25 ± 2.7 Hz, $n = 12$; 5 min after SCH58261: 3.50 ± 2.64 Hz, $n = 12$; 25 min after SCH58261: 3.72 ± 2.7 Hz, $n = 12$; difference: $F_{2,11} = 1.52$, $p = 0.24$, ANOVA) and amplitude (**Figures 2K,L**; Amplitude mean control: 40.34 ± 9.3 pA, $n = 12$; 5 min after SCH58261: 41.83 ± 11.5 pA, $n = 12$; 25 min after SCH58261: 41.34 ± 10.5 pA, $n = 12$; difference: $F_{2,11} = 0.32$, $p = 0.65$, ANOVA). Also, eEPSCs onto both pyramidal neurons (**Figures 2F,G**) and interneurons (**Figures 2M,N**) were unaffected by incubation of SCH58261. Specifically, the amplitude of eEPSCs onto pyramidal neurons did not differ between baseline and incubation conditions (**Figures 2F,G**; Amplitude mean control: 522.6 ± 160.4 pA, $n = 14$; 5 min after SCH58261: 574.7 ± 218.9 pA, $n = 14$; 15 min after SCH58261: 554.1 ± 239.1 pA, $n = 14$; difference: $F_{2,13} = 0.67$, $p = 0.46$, ANOVA) and likewise, the amplitude of eEPSCs onto FS interneurons did not differ between baseline and incubation conditions (**Figures 2M,N**; Amplitude mean control: 242.5 ± 107.3 pA, $n = 8$; 5 min after SCH58261: 246.5 ± 115.4 pA, $n = 8$; 15 min after SCH58261: 237.9 ± 116.1 pA, $n = 8$; difference: $F_{2,7} = 0.14$, $p = 0.79$, ANOVA). Thus, A_{2A}R do not seem necessary for excitatory synaptic transmission in the mPFC as their blockade does not affect either sEPSCs or eEPSCs in pyramidal neurons and FS interneurons.

A_{2A}R Blockade Does Not Affect Glutamatergic Synapse LTP in Layer 5 Pyramidal Neurons

Under endogenous levels of adenosine, A_{2A}R mainly act as a modulator of processes in which plasticity is engaged (d'Alcantara et al., 2001; Rebola et al., 2008; Costenla et al., 2011). Therefore, we tested whether A_{2A}R blockade affected the induction of glutamatergic synaptic plasticity in mPFC pyramidal neurons. We made whole-cell recordings from L5 pyramidal neurons (**Figures 3A,B**) and glutamatergic EPSPs were evoked by extracellular stimulation. To induce LTP, a TBS protocol was applied (Larson and Munkácsy, 2015). After recording a stable baseline of EPSPs, 10 bursts of five pulses each were given at 100 Hz (**Figure 3C**), and this was repeated three times within 30 s. Following this induction protocol, the slope of EPSPs was increased in a sustained manner, 20–30 min after the induction protocol (128.2 ± 46.6%, $n = 32$; **Figures 3D–F,H**). When slices were pre-incubated with SCH58261 (100 nM), the increase in EPSP slope (122.8 ± 59.8%, $n = 17$; **Figures 3D–F,H**) was not significantly different from control experiments without SCH58261 ($t_{47} = 0.35$, $p = 0.731$, unpaired t-test). Indeed, in the absence of SCH58261, 53% of cells showed TBS-induced LTP (17 out of 32), 28% did not show a change in EPSP slope (9 out of 32) and 19% showed a reduction in EPSP slope (6 out of 32), while in the presence of SCH58261 (100 nM), 47% of the pyramidal cells showed TBS-induced LTP (8 out of 17), 29% showed no change (5 out of 17), and 24% showed a reduction in EPSP slope (4 out of 17). These distributions were not significantly different between control and SCH58261 conditions (**Figure 3G**, chi-square test, $p = 0.52$). In both conditions – control and presence of SCH58261 – cells had on average similar resting membrane potential and input resistance (mean RMP of control: −67.6 ± 0.4 mV; mean RMP with SCH58261: −69.1 ± 0.7 mV, $t_{49} = 1.82$, $p = 0.07$, unpaired t-test; mean R input of control: 52.3 ± 4.7 mΩ; mean R input with SCH58261: 54.4 ± 7.6 mΩ, $t_{49} = 0.26$, $p = 0.80$, unpaired t-test). Thus, blockade of A_{2A}R has no significant effect on the induction of glutamatergic synaptic plasticity in L5 pyramidal neurons in mPFC slices.

A_{2A}R Blockade Shifts the Direction of Plasticity From LTP Into LTD at Excitatory Synapses Onto Layer 5 Fast Spiking (FS) Interneurons

Next, we tested the effects of A_{2A}R blockade on glutamatergic synaptic plasticity in FS interneurons. Glutamatergic synapses on FS interneurons can undergo LTP, albeit through different mechanisms than pyramidal neurons (Lamsa et al., 2007; Lu et al., 2007; Sarihi et al., 2008; Nissen et al., 2010; Sambandan et al., 2010; Huang et al., 2013). To test whether A_{2A}R are involved in this type of plasticity, we made whole-cell recordings from mPFC L5 FS interneurons (**Figure 4A**). These neurons had FS patterns, short action potential half widths, showed no inter-spike interval adaptation, and displayed fast hyperpolarization time constants and minimal hyperpolarization amplitude (**Figure 4B**). To induce LTP, we applied the same TBS protocol as in the pyramidal neuron recordings (**Figure 4C**). This induced a robust potentiation of EPSP slope in FS interneurons (159.4 ± 44.9%, $n = 10$; **Figures 4D–G,H**). When slices were pre-incubated with SCH58261 (100 nM), stimulation with the TBS protocol induced long-term depression (LTD), rather than potentiation (64.4 ± 25.2%, $n = 10$; **Figures 4D–G,H**), which was significantly different from control ($t_{18} = 5.84$, $p < 0.0001$, unpaired t-test). In the two conditions – absence or presence of SCH58261 – the resting membrane potential and input resistance were similar (mean RMP of control: −71.2 ± 0.9 mV; mean RMP with SCH58261: −69.6 ± 1.9 mV, $t_{18} = 0.75$, $p = 0.46$, unpaired t-test; mean R input of control: 164.3 ± 17.8 mΩ; mean R input with SCH58261: 160.2 ± 19.2 mΩ, $t_{18} = 0.15$, $p = 0.88$, unpaired t-test). In the absence of SCH58261, 70% of all cells displayed LTP, compared to 0% in the SCH58261 group. Conversely, 70% of all cells displayed LTD in the SCH58261 group, whereas none of the cells in the control condition displayed LTD (**Figure 4G**). This shows that A_{2A}R control the direction of plasticity at glutamatergic synapses onto FS interneurons in the mPFC.

A_{2A}R Control LTP of Population Spikes in the Layer V mPFC (mPFC)

Since population spikes represent the integrated responses of all local cells, i.e., responses from both pyramidal cells and interneurons, we next recorded population spikes to determine

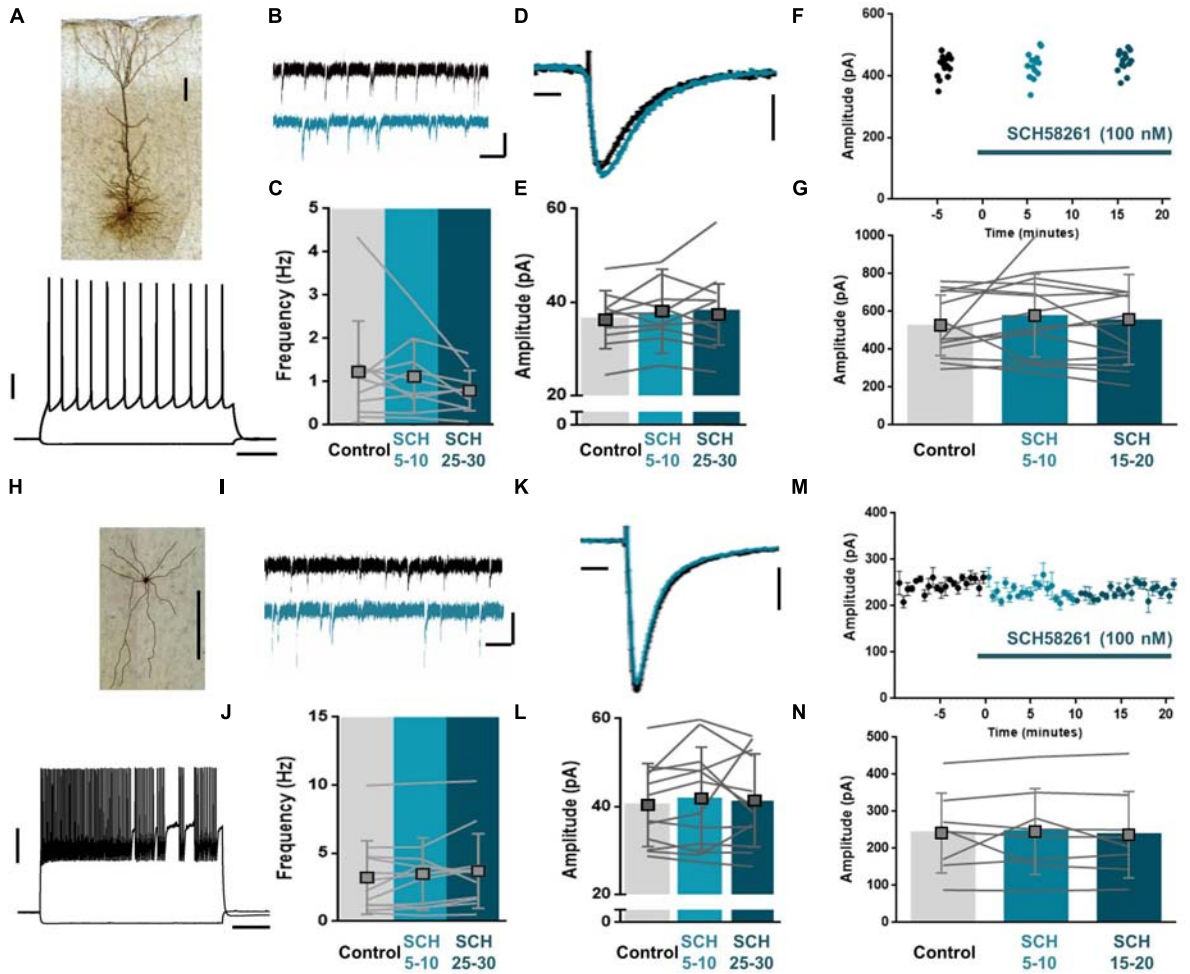

FIGURE 2 | A_{2A}R do not affect spontaneous or evoked excitatory synaptic transmission in the mPFC. Biocytin staining of layer 5 pyramidal neuron (**A**, top) and fast spiking (FS) interneuron (**H**, top) from coronal slice of rat prelimbic mPFC. Scale bars: 100 μm. Voltage responses to hyperpolarizing (–50 pA) and depolarizing (+225 pA) somatic current injections to the soma of a L5 pyramidal neuron (**A**, bottom) and to hyperpolarizing (–60 pA) and depolarizing (+400 pA) somatic current injections to the soma of a FS interneuron (**H**, bottom). Scale bars: 20 mV, 200 ms. **(B,C)** Bath application of the selective A_{2A}R antagonist, SCH58261 (100 nM, blue) did not affect the frequency of sEPSCs onto pyramidal neurons. A representative trace is depicted in control (black) and prolonged SCH58261 (100 nM, blue) wash-in condition **(B)**. The frequency over 5 min does not change after SCH58261 (100 nM, blue) wash-in; data are mean ± SD of n = 10, individual lines show the average of one cell over the course of 5 min per condition **(C)**. Scale bars: 30 pA, 50 ms. **(D,E)** Bath application of SCH58261 (100 nM, blue) did not affect the amplitude of sEPSCs onto pyramidal neurons. The average sEPSC amplitude of a representative cell is depicted in control (black) and prolonged SCH58261 (100 nM, blue) wash-in condition **(D)**. The average amplitude over 5 min does not change after SCH58261 (100 nM, blue) wash-in; data are mean ± SD of n = 10 **(E)**. Scale bars: 10 pA, 1 ms. **(F,G)** Bath application of SCH58261 (100 nM, blue) did not affect the amplitude of eEPSCs onto pyramidal neurons. The eEPSC amplitude of a representative cell is depicted during 15 sweeps in all three conditions; control (black), short- (light blue) and prolonged SCH58261 (100 nM, blue) wash-in conditions are shown **(F)**. The average amplitude does not change after SCH58261 (100 nM, blue) wash-in; data are mean ± SD of n = 14 **(G)**. **(I,J)** Bath application of SCH58261 (100 nM, blue) did not affect the frequency of sEPSCs onto interneurons. A representative trace is depicted in control (black) and prolonged SCH58261 (100 nM, blue) wash-in condition **(I)**. The frequency over 5 min does not change after SCH58261 (100 nM, blue) wash-in; data are mean ± SD of n = 12, individual lines show the average of one cell over the course of 5 min per condition **(J)**. Scale bars: 30 pA, 50 ms. **(K,L)** Bath application of SCH58261 (100 nM, blue) did not affect the amplitude of sEPSCs onto interneurons. The average sEPSC amplitude of a representative cell is depicted in control (black) and prolonged SCH58261 (100 nM, blue) wash-in condition **(K)**. The average amplitude over 5 min does not change after SCH58261 (100 nM, blue) wash-in; data are mean ± SD of n = 12 **(L)**. Scale bars: 10 pA, 1 ms. **(M,N)** Bath application of SCH58261 (100 nM, blue) did not affect the amplitude of eEPSCs onto pyramidal neurons. The average eEPSC amplitude of a representative cell is depicted over a time-course of 30 min, in which control (black), short- and prolonged SCH58261 (100 nM, blue) wash-in conditions are shown **(M)**. The average amplitude over 5 min does not change after SCH58261 (100 nM, blue) wash-in; data are mean ± SD of n = 8 **(N)**. Paired one-way ANOVA; all data are non-significant ($p > 0.05$).

whether A_{2A}R affect plasticity on the neuronal network level. To that end, we recorded extracellularly evoked AMPA receptor-mediated population spikes in mPFC layer 5 (L5) in acute brain slices, upon stimulation of L2/3 (**Figures 5A,B**). Bath application of SCH58261 (50 nM) affected the stimulus–response relationship of the network by increasing the maximum amplitude of population spikes (1.86 ± 0.03 mV in SCH58261, n = 23; 1.58 ± 0.04 mV in control, n = 26; t_{47} = 5.34,

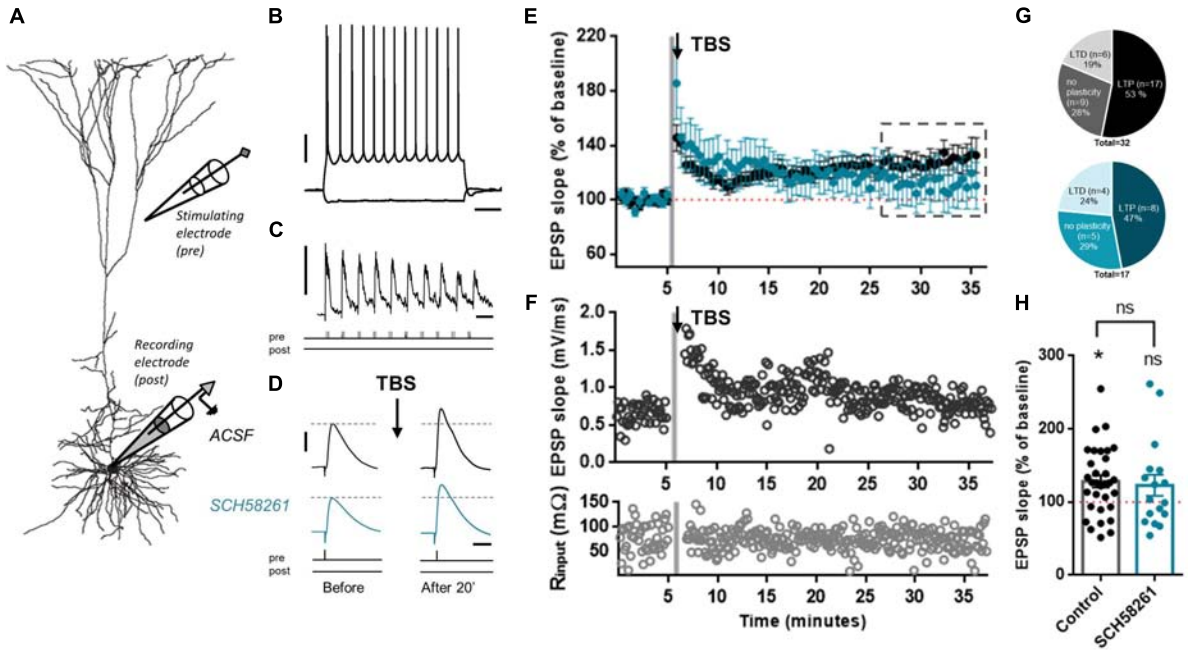

FIGURE 3 | $A_{2A}R$ blockade does not affect glutamatergic synapse LTP in layer 5 pyramidal neurons. **(A)** Biocytin reconstruction of layer 5 pyramidal neuron from coronal slice of rat prelimbic mPFC showing relative positions of recording and stimulating electrodes. **(B)** Voltage responses to hyperpolarizing (–60 pA) and depolarizing (+380 pA) somatic current injections to the soma of a L5 pyramidal neuron. Scale bars: 20 mV, 200 ms. **(C)** Plasticity induction protocol. Theta burst stimulation (TBS) was induced by stimulation of 10 bursts of five pulses each at 100 Hz, repeated three times. Scale bars: 20 mV, 200 ms. **(D)** After obtaining a baseline measure of EPSPs, TBS-LTP was induced. EPSPs were then recorded for up to 30 min to observe changes in EPSP slope. Slices were pre-incubated in either control ACSF or in ACSF with added SCH58261 (100 nM). Scale bars: 2 mV, 20 ms. **(E)** Summary time-course plot of control (black symbols) and SCH58261 (100 nM; blue symbols) experiments, showing a robust LTP in control condition, and a highly variable LTP in SCH58261 pre-incubated cells. **(F)** Example of a TBS-LTP experiment in control conditions showing slope and input resistance (top and bottom panels, respectively) *versus* time. Gray shading indicates time of TBS induction. **(G)** The fraction of cells that display LTP is slightly higher in the control condition than in the presence of SCH58261; however, fraction differences were not significant (Chi-square test, $p = 0.52$). **(H)** Summary bar chart of control and SCH58261 (100 nM) TBS-LTP experiments, showing percentage change of EPSP slope for both conditions (mean ± SEM; control: $n = 32$, SCH58261: $n = 17$). Unpaired t-test $p = 0.73$; $^*p < 0.05$ compared to baseline value of 100%, one-sample t-test.

$p < 0.0001$, unpaired t-test; **Figure 5C**). LTP of the population spike was induced by applying a single train of high-frequency stimulation (HFS), followed 15 min later by four HFS trains (50 pulses at 100 Hz, 0.5 s duration, delivered every 10 s). This induction protocol was run in the absence or presence of SCH58261, and for each experiment a naïve mPFC slice was used. Blockade of $A_{2A}R$ by SCH58261 decreased the magnitude of population spike LTP (120.7 ± 2.9% in SCH58261, $n = 25$; 130.9 ± 3.4% in control slices, $n = 25$; $t_{48} = 2.28$, $p = 0.027$, unpaired t-test; **Figures 5D–F**). These findings show that $A_{2A}R$ control plasticity at a neuronal network level in mPFC.

DISCUSSION

In the present study, we show that in the mPFC, $A_{2A}R$ control LTP at excitatory synapses onto fast-spiking interneurons rather than onto pyramidal neurons. $A_{2A}R$ did not affect spontaneous or evoked synaptic transmission in either cell type. A similar predominant role of $A_{2A}R$ on plasticity has been observed in other brain areas, including hippocampus (Rebola et al., 2008), amygdala (Simões et al., 2016), and striatum (d'Alcantara et al., 2001; Shen et al., 2008; Li et al., 2015). As in the hippocampus (Rebola et al., 2005), $A_{2A}R$ in the mPFC are enriched at synapses. However, mPFC $A_{2A}R$ are enriched outside the presynaptic active zone and PSD, whereas most of the hippocampal $A_{2A}R$ are located inside the presynaptic active zone and PSD (Rebola et al., 2005). It is conceivable that this different sub-synaptic distribution could translate into $A_{2A}R$ playing by different rules to control information flow within the mPFC. Indeed, our results show an effect of $A_{2A}R$ antagonism on the induction of LTP at excitatory synapses specifically in FS interneurons, while the antagonist was ineffective at excitatory synapses onto pyramidal neurons. At excitatory connections to FS interneurons, the blockade of $A_{2A}R$ led to LTD of their excitatory synapses, meaning that without active $A_{2A}R$, LTD would occur at these glutamatergic synapses onto FS interneurons. Thus, $A_{2A}R$ activation would be particularly important for the induction of synaptic potentiation of glutamatergic synapses in FS interneurons, while not affecting glutamatergic synapses in mPFC pyramidal neurons. At the mPFC neuronal network level, blockade of $A_{2A}R$ reduced LTP induction, suggesting a role for $A_{2A}R$ at the network level.

Target cell specificity of $A_{2A}R$ modulation has also been found in the hippocampus, although with the difference that activation

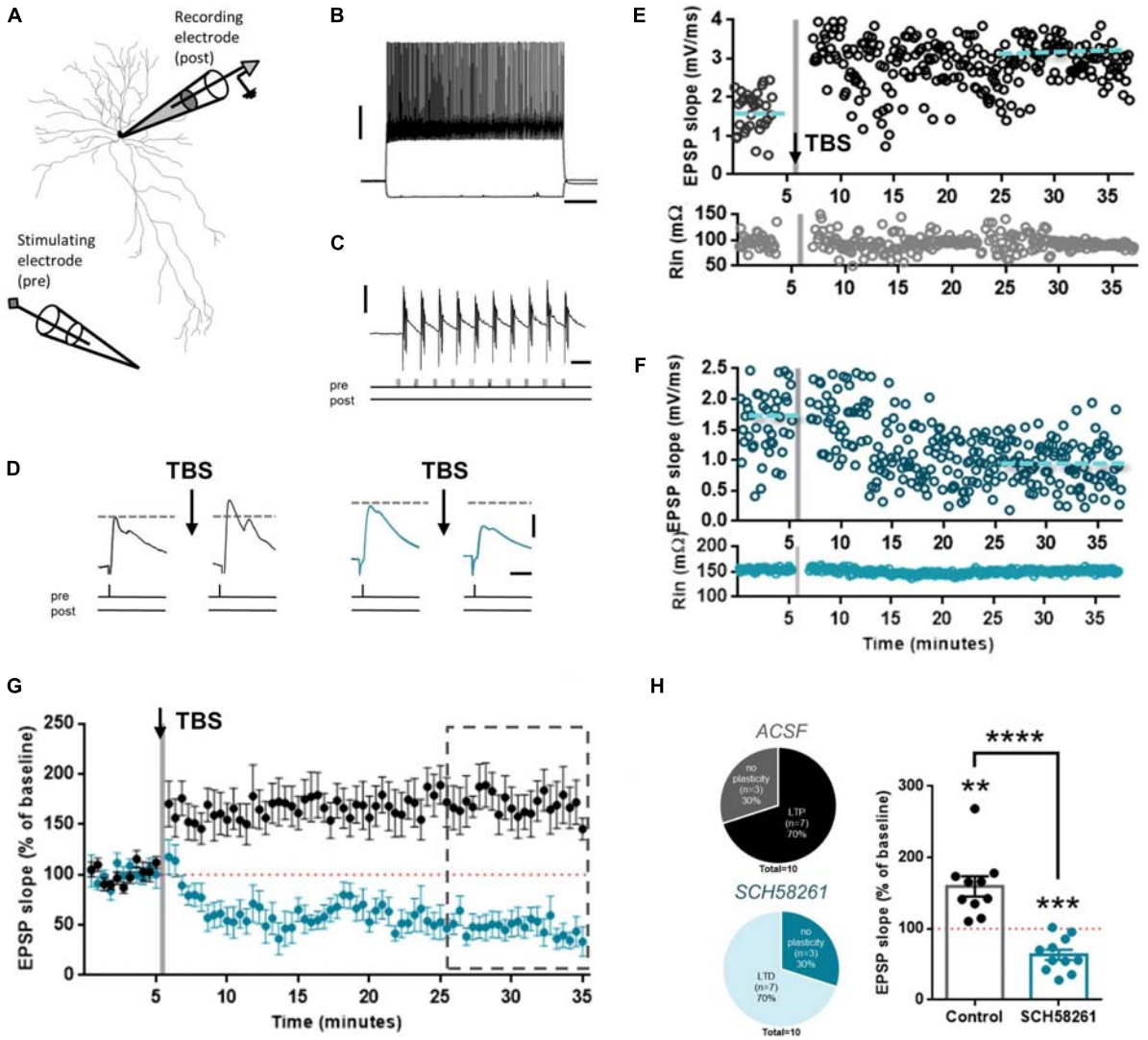

FIGURE 4 | A_{2A}R blockade shifts reverses LTP to LTD at excitatory synapses in layer 5 FS interneurons. **(A)** Biocytin reconstruction of a FS interneuron from coronal slice of rat mPFC showing relative positions of recording and stimulating electrodes. **(B)** Voltage responses to hyperpolarizing (–80 pA) and depolarizing (+360 pA) somatic current injections to the soma of a FS interneuron. Scale bars: 20 mV, 200 ms. **(C)** Plasticity induction protocol. TBS was induced by stimulation of 10 bursts of five pulses each at 100 Hz, repeated three times. Scale bars: 10 mV, 200 ms. **(D)** After obtaining a baseline measure of EPSPs, TBS-LTP was induced. EPSPs were then recorded for up to 30 min to observe changes in EPSP slope. Slices were pre-incubated in either control ACSF (black traces) or in ACSF with added SCH58261 (100 nM; blue traces). Scale bars: 2 mV, 20 ms. Representative TBS-LTP experiments in control **(E)** and 100 nM SCH58261 **(F)** conditions showing slope and input resistance (top and bottom panels, respectively) *versus* time. Gray shading indicates time of TBS induction. **(G)** Summary plot of control (black symbols) and SCH58261 (100 nM; blue symbols) experiments, showing a robust LTP in control condition, and a strong LTD in SCH58261 pre-incubated cells. (**H**, left panel) The fraction of cells that obtain plasticity is reversed in control *versus* SCH58261 conditions. In control, 70% of cells display LTP, whereas in SCH58261, 70% of cells display LTD. (**H**, right panel) Summary bar chart of control and SCH58261 (100 nM) TBS-LTP experiments, showing percentage change in EPSP slope for both conditions (mean ± SEM; control: $n = 10$; SCH58261: $n = 10$). $^{****}p < 0.0001$ compared to the respective control (*black dots*), unpaired Student's *t*-test. $^{**}p < 0.01$ compared to the hypothetical value of 100, one-sample *t*-test. $^{***}p < 0.001$ compared to the hypothetical value of 100, one-sample *t*-test.

of hippocampal A_{2A}R increased excitatory transmission to CA1 pyramidal cells but not to inhibitory interneurons (Rombo et al., 2015). The PFC is unique in the magnitude and variety of interneurons, where FS interneurons represent the largest group (Markram et al., 2004). FS interneurons are activated by feedback and feedforward excitation, and they target perisomatic regions of pyramidal neurons (Tremblay et al., 2016) to control the output of pyramidal neurons by exerting fast, powerful and uniform inhibition of their firing (Kvitsiani et al., 2013; Sparta et al., 2014). Both LTP and LTD can be generated in FS interneurons, although LTP seems to be the dominant form of plasticity expressed in this neuron subtype (Lamsa et al., 2007; Lu et al., 2007; Sarihi et al., 2008; Nissen et al., 2010; Sambandan et al., 2010). In contrast to long-term plasticity (LTP) of excitatory synapses onto pyramidal neurons, LTP at glutamatergic synapses in FS neurons is predominantly independent of NMDA receptors

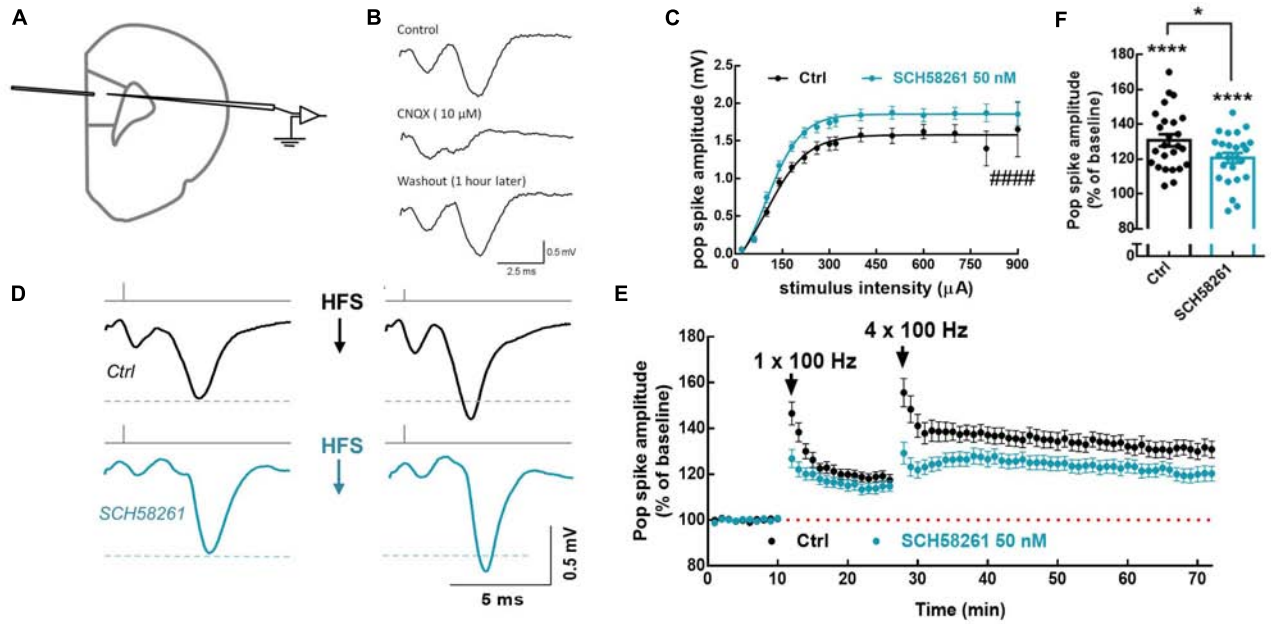

FIGURE 5 | $A_{2A}R$ facilitate LTP of population spikes in mPFC layer 5. **(A)** Positioning of the stimulating (layer 2/3 mPFC) and recording electrodes (layer 5 mPFC). **(B)** The recorded population spikes were abolished by the AMPA/kainate receptor antagonist, CNQX 10 μM. **(C)** Bath application of the selective $A_{2A}R$ antagonist, SCH58261 (50 nM; blue dots) increased the number and synchrony of cells discharging action potentials as indicated by the increase in the maximum response when the input/output response was assessed 20 min after SCH58261 superfusion. **(D)** Representative averaged traces at baseline and 30 min after the induction of LTP, in the absence and presence of SCH58261 (50 nM); SCH58261 decreased LTP magnitude. **(E)** Time course showing that SCH58261 decreased the magnitude of LTP of the population spike responses triggered by a priming train of high-frequency stimulation (HFS), followed 15 min later by four HFS trains (50 pulses at 100 Hz, 0.5 s duration, delivered every 10 s). **(F)** Summary plot displaying the variability of LTP magnitude, estimated 30 min after the induction of LTP, in the absence and presence of SCH58261 (50 nM). Data are mean ± SEM of 25 slices (from 25 rats) per group. $^{\#\#\#\#}p < 0.0001$ comparing the estimated maximum response in the presence of SCH58261 to control (*black bar/dots)*, unpaired Student's *t*-test. $^{*}p < 0.05$ comparing SCH58261 to control (*black bar/dots*), unpaired Student's *t*-test. $^{****}p < 0.0001$ compared to the hypothetical value of 100%, one-sample *t*-test.

(Lamsa et al., 2007; Sarihi et al., 2008; Nissen et al., 2010; Sambandan et al., 2010; Huang et al., 2013). In most cases, an essential role for group I metabotropic glutamate receptors (mGluRs) has been demonstrated in LTP and LTD induction in these FS interneurons (Perez et al., 2001; Lu et al., 2007; Sarihi et al., 2008; Huang et al., 2013). Whether LTP or LTD can be induced in these synapses is dependent on post-synaptic calcium fluctuations during LTP induction (Alle et al., 2001; Sambandan et al., 2010; Huang et al., 2013). $A_{2A}R$ control both NMDA receptors and voltage-sensitive calcium channels, thus potentially contributing to modulate the pattern of plasticity (Mogul et al., 1993; Gonçalves et al., 1997; Rebola et al., 2008; Azdad et al., 2009; Higley and Sabatini, 2010). Furthermore, $A_{2A}R$ heteromerize with mGluR5 (Ferré et al., 2002) and tightly interact with mGluR5 receptor function in the hippocampus, changing the efficiency of NMDA receptors (Tebano et al., 2005; Sarantis et al., 2015; Viana da Silva et al., 2016). Whether either of these mechanisms is responsible for the observed effects, should be subject to further investigation.

We here show the role of $A_{2A}R$ in normal, non-pathological, conditions by targeting the endogenous pool of adenosine acting at the $A_{2A}R$ with the $A_{2A}R$ antagonist SCH58261. In these conditions, $A_{2A}R$ act mainly as modulators of synaptic plasticity (d'Alcantara et al., 2001; Rebola et al., 2008; Simões et al., 2016). $A_{2A}R$ have an additional role in pathological conditions, where they can control microglia and astrocytes (Rebola et al., 2011; Matos et al., 2015; Orr et al., 2015; Cunha, 2016). Targeting $A_{2A}R$ with an $A_{2A}R$ agonist would mimic the situation of an additional load onto these microglia- and astrocytic located $A_{2A}R$, thereby recruiting $A_{2A}R$ that are only active in pathological conditions (Matos et al., 2012; Orr et al., 2015). As we are specifically interested in the role of the $A_{2A}R$ in non-pathological conditions, we only evaluated plastic changes under influence of the $A_{2A}R$ antagonist.

The alteration in glutamatergic synapse strength in FS interneurons by $A_{2A}R$ can have a major impact on cortical function. A decreased synaptic strength at FS interneurons has been linked to a loss of temporal fidelity of pyramidal-to-pyramidal signaling (Lamsa et al., 2005), leading to a loss of information processing (Pouille and Scanziani, 2001). Also, the selective control by $A_{2A}R$ of plasticity at glutamatergic synapses onto FS interneurons might have important implications for the excitation–inhibition balance. Indeed, if the activity of interneurons is experimentally reduced in mPFC, LTP of excitatory to pyramidal neurons is impaired (Konstantoudaki et al., 2016). Adenosine, by acting at $A_{2A}R$ at synapses of FS interneurons, could therefore provide a homeostatic

mechanism by which inhibition is ensured, thereby maintaining a proper excitation–inhibition balance (Zhang et al., 2015). FS interneurons, in particular the parvalbumin-positive FS cells, have been shown to support working memory and cognitive flexibility (Murray et al., 2015), and to be central for the control of attention (Kim et al., 2016). Therefore, abnormal A_{2A}R function might lead to impaired behavioral functioning through changes in plasticity at FS interneuron synapses. An overexpression of A_{2A}R specifically in the PFC is indeed related to cognitive and attentional deficits in a rat model of attention deficit and hyperactivity disorder (Pandolfo et al., 2013). Furthermore, genetic elimination of A_{2A}R also interferes with behaviors that involve information processing in the PFC, including working memory (Zhou et al., 2009; Wei et al., 2011) and reversal learning (Wei et al., 2011). Future research targeting selectively A_{2A}R in PFC FS interneurons will be needed to elucidate whether specifically A_{2A}R located on glutamatergic synapses in FS interneurons control PFC-related behavior.

In short, we present here a first characterization of the role of endogenous adenosine acting at A_{2A}R to affect synaptic plasticity in the mPFC, showing that A_{2A}R specifically affect plasticity of glutamatergic synapses in cortical FS interneurons. An effect of A_{2A}R manipulation on plasticity at these synapses was never shown before, therefore, further explorations into synaptic plasticity of FS interneurons in the PFC should be considered to reveal the underlying mechanism of A_{2A}R manipulation.

AUTHOR CONTRIBUTIONS

AK, HM, RC, and SF designed the research. AK, SF, AT, TH, JR, CX, PC, and RC performed the experiments. AK, SF, RC, and HM analyzed the data. AK and SF wrote the first draft of the manuscript. All authors commented on the manuscript text.

ACKNOWLEDGMENTS

Supported by Maratona da Saúde, Santa Casa da Misericórdia, GAI-FMUC and Banco Santander-Totta, NARSAD, Erasmus Mundus Joint Doctorate grant (ENC-Network) and ERDF, through Centro 2020 (project no. CENTRO-01-0145-FEDER-000008:BrainHealth 2020), and through FCT (project nos. POCI-01-0145-FEDER-007440 and PTDC/NEU-NMC/4154/2016) to RC. HM received funding for this work from the Netherlands Organization for Scientific Research (NWO; VICI grant), ERC StG "BrainSignals," EU H2020 Framework Program (agreement no. 604102 "Human Brain Project") and the EU 7th Framework Program (no. EU MSCA-ITN CognitionNet FP7-PEOPLE-2013-ITN 607508).

REFERENCES

Alle, H., Jonas, P., and Geiger, J. R. P. (2001). PTP and LTP at a hippocampal mossy fiber-interneuron synapse. *Proc. Natl. Acad. Sci. U.S.A.* 98, 14708–14713. doi: 10.1073/pnas.251610898

Anderson, W. W., and Collingridge, G. L. (2007). Capabilities of the WinLTP data acquisition program extending beyond basic LTP experimental functions. *J. Neurosci. Methods* 162, 346–356. doi: 10.1016/j.jneumeth.2006.12.018

Arnsten, A. F. T. (2009). Stress signalling pathways that impair prefrontal cortex structure and function. *Nat. Rev. Neurosci.* 10, 410–422. doi: 10.1038/nrn2648

Azdad, K., Gall, D., Woods, A. S., Ledent, C., Ferrié, S., and Schiffmann, S. N. (2009). Dopamine D_2 and adenosine A_{2A} receptors regulate NMDA-mediated excitation in accumbens neurons through A_{2A}–D_2 receptor heteromerization. *Neuropsychopharmacology* 34, 972–986. doi: 10.1038/npp.2008.144

Bloem, B., Poorthuis, R. B., and Mansvelder, H. D. (2014). Cholinergic modulation of the medial prefrontal cortex: the role of nicotinic receptors in attention and regulation of neuronal activity. *Front. Neural Circuits* 8:17. doi: 10.3389/fncir.2014.00017

Canas, P. M., and Cunha, R. A. (2016). Subsynaptic membrane fractionation. *Neuromethods* 110, 31–37. doi: 10.1007/978-1-4939-3064-7_3

Costenla, A. R., Diógenes, M. J., Canas, P. M., Rodrigues, R. J., Nogueira, C., Maroco, J., et al. (2011). Enhanced role of adenosine A_{2A} receptors in the modulation of LTP in the rat hippocampus upon ageing. *Eur. J. Neurosci.* 34, 12–21. doi: 10.1111/j.1460-9568.2011.07719.x

Couey, J. J., Meredith, R. M., Spijker, S., Poorthuis, R. B., Smit, A. B., Brussaard, A. B., et al. (2007). Distributed network actions by nicotine increase the threshold for spike-timing-dependent plasticity in prefrontal cortex. *Neuron* 54, 73–87. doi: 10.1016/j.neuron.2007.03.006

Cunha, R. A. (2008). Different cellular sources and different roles of adenosine: A1 receptor-mediated inhibition through astrocytic-driven volume transmission and synapse-restricted A_{2A} receptor-mediated facilitation of plasticity. *Neurochem. Int.* 52, 65–72. doi: 10.1016/j.neuint.2007.06.026

Cunha, R. A. (2016). How does adenosine control neuronal dysfunction and neurodegeneration? *J. Neurochem.* 139, 1019–1055. doi: 10.1111/jnc.13724

Cunha, R. A., Vizi, E. S., Ribeiro, J. A., and Sebastião, A. M. (1996). Preferential release of ATP and its extracellular catabolism as a source of adenosine upon high- but not low-frequency stimulation of rat hippocampal slices. *J. Neurochem.* 67, 2180–2187. doi: 10.1046/j.1471-4159.1996.67052180.x

d'Alcantara, P. D., Ledent, C., Swillens, S., and Schiffmann, S. N. (2001). Inactivation of adenosine A_{2A} receptor impairs long term potentiation in the accumbens nucleus without altering basal synaptic transmission. *Neuroscience* 107, 455–464. doi: 10.1016/S0306-4522(01)00372-4

Dalley, J. W., Cardinal, R. N., and Robbins, T. W. (2004). Prefrontal executive and cognitive functions in rodents: neural and neurochemical substrates. *Neurosci. Biobehav. Rev.* 28, 771–784. doi: 10.1016/j.neubiorev.2004.09.006

Dembrow, N., and Johnston, D. (2014). Subcircuit-specific neuromodulation in the prefrontal cortex. *Front. Neural Circuits* 8:54. doi: 10.3389/fncir.2014.00054

Euston, D. R., Gruber, A. J., and Mcnaughton, B. L. (2013). The role of medial prefrontal cortex in memory and decision making. *Neuron* 76, 1057–1070. doi: 10.1016/j.neuron.2012.12.002

Ferré, S., Karcz-Kubicha, M., Hope, B. T., Popoli, P., Burgueño, J., Gutiérrez, M. A., et al. (2002). Synergistic interaction between adenosine A2A and glutamate mGlu5 receptors: implications for striatal neuronal function. *Proc. Natl. Acad. Sci. U.S.A.* 99, 11940–11945. doi: 10.1073/pnas.172393799

Gemperle, A. Y., Enz, A., Pozza, M. F., Lüthi, A., and Olpe, H. R. (2003). Effects of clozapine, haloperidol and iloperidone on neurotransmission and synaptic plasticity in prefrontal cortex and their accumulation in brain tissue: an in vitro study. *Neuroscience* 117, 681–695. doi: 10.1016/S0306-4522(02)00769-8

Gonçalves, M. L., Cunha, R. A., and Ribeiro, J. A. (1997). Adenosine A_{2A} receptors facilitate $^{45}Ca^{2+}$ uptake through class A calcium channels in rat hippocampal CA3 but not CA1 synaptosomes. *Neurosci. Lett.* 238, 73–77. doi: 10.1016/S0304-3940(97)00803-3

Higley, M. J., and Sabatini, B. L. (2010). Competitive regulation of synaptic Ca^{2+} influx by D2 dopamine and A_{2A} adenosine receptors. *Nat. Neurosci.* 13, 958–966. doi: 10.1038/nn.2592

Horita, T. K., Kobayashi, M., Mori, A., Jenner, P., and Kanda, T. (2013). Effects of the adenosine A_{2A} antagonist istradefylline on cognitive performance in rats with a 6-OHDA lesion in prefrontal cortex. *Psychopharmacology* 230, 345–352. doi: 10.1007/s00213-013-3158-x

Huang, S., Huganir, R. L., and Kirkwood, A. (2013). Adrenergic gating of Hebbian spike-timing-dependent plasticity in cortical interneurons. *J. Neurosci.* 33, 13171–13178. doi: 10.1523/JNEUROSCI.5741-12.2013

Kandel, E. R. (1976). *Cellular Basis of Behavior: An Introduction to Behavioral Neurobiology*. San Francisco, CA: W.H. Freeman.

Kaster, M. P., Machado, N. J., Silva, H. B., Nunes, A., Ardais, A. P., Santana, M., et al. (2015). Caffeine acts through neuronal adenosine A_{2A} receptors to prevent mood and memory dysfunction triggered by chronic stress. *Proc. Natl. Acad. Sci. U.S.A.* 112, 7833–7838. doi: 10.1073/pnas.1423088112

Kilkenny, C., Browne, W. J., Cuthill, I. C., Emerson, M., and Altman, D. G. (2010). Improving bioscience research reporting: the ARRIVE guidelines for reporting animal research. *PLOS Biol.* 8:e1000412. doi: 10.1371/journal.pbio.1000412

Kim, H., Ährlund-Richter, S., Wang, X., Deisseroth, K., and Carlén, M. (2016). Prefrontal parvalbumin neurons in control of attention. *Cell* 164, 208–218. doi: 10.1016/j.cell.2015.11.038

Konstantoudaki, X., Chalkiadaki, K., Tivodar, S., Karagogeos, D., and Sidiropoulou, K. (2016). Impaired synaptic plasticity in the prefrontal cortex of mice with developmentally decreased number of interneurons. *Neuroscience* 322, 333–345. doi: 10.1016/j.neuroscience.2016.02.048

Kvitsiani, D., Ranade, S., Hangya, B., Taniguchi, H., Huang, J., and Kepecs, A. (2013). Distinct behavioural and network correlates of two interneuron types in prefrontal cortex. *Nature* 498, 363–366. doi: 10.1038/nature12176

Lamsa, K., Heeroma, J. H., and Kullmann, D. M. (2005). Hebbian LTP in feed-forward inhibitory interneurons and the temporal fidelity of input discrimination. *Nat. Neurosci.* 8, 916–924. doi: 10.1038/nn1486

Lamsa, K. P., Heeroma, J. H., Somogyi, P., Rusakov, D. A., and Kullmann, D. M. (2007). Anti-Hebbian long-term potentiation in the hippocampal feedback inhibitory circuit. *Science* 315, 1262–1266. doi: 10.1126/science.1137450

Larson, J., and Munkácsy, E. (2015). Theta-burst LTP. *Brain Res.* 1621, 38–50. doi: 10.1016/j.brainres.2014.10.034

Leon, M. R. (2000). Effects of caffeine on cognitive, psychomotor, and affective performance of children with Attention-Deficit/Hyperactivity Disorder. *J. Atten. Disord.* 4, 27–47. doi: 10.1177/108705470000400103

Li, W., Silva, H. B., Real, J., Wang, Y.-M., Rial, D., Li, P., et al. (2015). Inactivation of adenosine A_{2A} receptors reverses working memory deficits at early stages of Huntington's disease models. *Neurobiol. Dis.* 79, 70–80. doi: 10.1016/j.nbd.2015.03.030

Lu, J., Li, C., Zhao, J.-P., Poo, M., and Zhang, X. (2007). Spike-timing-dependent plasticity of neocortical excitatory synapses on inhibitory interneurons depends on target cell type. *J. Neurosci.* 27, 9711–9720. doi: 10.1523/JNEUROSCI.2513-07.2007

Mansvelder, H. D., and McGehee, D. S. (2000). Long-term potentiation of excitatory inputs to brain reward areas by nicotine. *Neuron* 27, 349–357. doi: 10.1016/S0896-6273(00)00042-8

Markram, H., Toledo-Rodriguez, M., Wang, Y., Gupta, A., Silberberg, G., and Wu, C. (2004). Interneurons of the neocortical inhibitory system. *Nat. Rev. Neurosci.* 5, 793–807. doi: 10.1038/nrn1519

Matos, M., Augusto, E., Machado, N. J., dos Santos-Rodrigues, A., Cunha, R. A., and Agostinho, P. (2012). Astrocytic adenosine A2A receptors control the amyloid-β peptide-induced decrease of glutamate uptake. *J. Alzheimers Dis.* 31, 555–567. doi: 10.3233/JAD-2012-120469

Matos, M., Shen, H.-Y., Augusto, E., Wang, Y., Wei, C. J., Wang, Y. T., et al. (2015). Deletion of adenosine A_{2A} receptors from astrocytes disrupts glutamate homeostasis leading to psychomotor and cognitive impairment: relevance to schizophrenia. *Biol. Psychiatry* 78, 763–774. doi: 10.1016/j.biopsych.2015.02.026

Mayford, M., Siegelbaum, S. A., Kandel, E. R., Long-term, N. R., Lüscher, C., Malenka, R. C., et al. (2012). Synapses and memory storage. *Cold Spring Harb. Perspect. Biol.* 4:a005751. doi: 10.1101/cshperspect.a005751

Meredith, R. M., Holmgren, C. D., Weidum, M., Burnashev, N., and Mansvelder, H. D. (2007). Increased threshold for spike-timing-dependent plasticity is caused by unreliable calcium signaling in mice lacking fragile X gene fmr1. *Neuron* 54, 627–638. doi: 10.1016/j.neuron.2007.04.028

Mogul, D. J., Adams, M. E., and Fox, A. P. (1993). Differential activation of adenosine receptors decreases N-type but potentiates P-type Ca^{2+} current in hippocampal CA3 neurons. *Neuron* 10, 327–334. doi: 10.1016/0896-6273(93)90322-I

Mohan, H., Verhoog, M. B., Doreswamy, K. K., Eyal, G., Aardse, R., Lodder, B. N., et al. (2015). Dendritic and axonal architecture of individual pyramidal neurons across layers of adult human neocortex. *Cereb. Cortex* 25, 4839–4853. doi: 10.1093/cercor/bhv188

Murray, A. J., Woloszynowska-Fraser, M. U., Ansel-Bollepalli, L., Cole, K. L. H., Foggetti, A., Crouch, B., et al. (2015). Parvalbumin-positive interneurons of the prefrontal cortex support working memory and cognitive flexibility. *Sci. Rep.* 5:16778. doi: 10.1038/srep16778

Nissen, W., Szabo, A., Somogyi, J., Somogyi, P., and Lamsa, K. P. (2010). Cell type-specific long-term plasticity at glutamatergic synapses onto hippocampal interneurons expressing either parvalbumin or CB1 cannabinoid receptor. *J. Neurosci.* 30, 1337–1347. doi: 10.1523/JNEUROSCI.3481-09.2010

Orr, A. G., Hsiao, E. C., Wang, M. M., Ho, K., Kim, D. H., Wang, X., et al. (2015). Astrocytic adenosine receptor A_{2A} and G_s-coupled signaling regulate memory. *Nat. Neurosci.* 18, 423–434. doi: 10.1038/nn.3930

Pandolfo, P., Machado, N. J., Köfalvi, A., Takahashia, R. N., and Cunha, R. A. (2013). Caffeine regulates frontocorticostriatal dopamine transporter density and improves attention and cognitive deficits in an animal model of attention deficit hyperactivity disorder. *Eur. Neuropsychopharmacol.* 23, 317–328. doi: 10.1016/j.euroneuro.2012.04.011

Pardo, M., Lopez-Cruz, L., Valverde, O., Ledent, C., Baqi, Y., Müller, C. E., et al. (2012). Adenosine A_{2A} receptor antagonism and genetic deletion attenuate the effects of dopamine D_2 antagonism on effort-based decision making in mice. *Neuropharmacology* 62, 2068–2077. doi: 10.1016/j.neuropharm.2011.12.033

Pawlak, V., Wickens, J. R., Kirkwood, A., and Kerr, J. N. D. (2010). Timing is not everything: neuromodulation opens the STDP gate. *Front. Synaptic Neurosci.* 2:146. doi: 10.3389/fnsyn.2010.00146

Perez, Y., Morin, F., and Lacaille, J. (2001). A Hebbian form of long-term potentiation dependent on mGluR1a in hippocampal inhibitory interneurons. *Proc. Natl. Acad. Sci. U.S.A.* 98, 9401–9406. doi: 10.1073/pnas.161493498

Pouille, F., and Scanziani, M. (2001). Enforcement of temporal fidelity in pyramidal cells by somatic feed-forward inhibition. *Science* 293, 1159–1163. doi: 10.1126/science.1060342

Qi, G., van Aerde, K., Abel, T., and Feldmeyer, D. (2017). Adenosine differentially modulates synaptic transmission of excitatory and inhibitory microcircuits in layer 4 of rat barrel cortex. *Cereb. Cortex* 27, 4411–4422. doi: 10.1093/cercor/bhw243

Rebola, N., Canas, P. M., Oliveira, C. R., and Cunha, R. A. (2005). Different synaptic and subsynaptic localization of adenosine A_{2A} receptors in the hippocampus and striatum of the rat. *Neuroscience* 132, 893–903. doi: 10.1016/j.neuroscience.2005.01.014

Rebola, N., Lujan, R., Cunha, R. A., and Mulle, C. (2008). Adenosine A_{2A} receptors are essential for long-term potentiation of NMDA-EPSCs at hippocampal mossy fiber synapses. *Neuron* 57, 121–134. doi: 10.1016/j.neuron.2007.11.023

Rebola, N., Simões, A. P., Canas, P. M., Tomé, A. R., Andrade, G. M., Barry, C. E., et al. (2011). Adenosine A_{2A} receptors control neuroinflammation and consequent hippocampal neuronal dysfunction. *J. Neurochem.* 117, 100–111. doi: 10.1111/j.1471-4159.2011.07178.x

Rombo, D. M., Newton, K., Nissen, W., Badurek, S., Horn, J. M., Minichiello, L., et al. (2015). Synaptic mechanisms of adenosine A_{2A} receptor-mediated hyperexcitability in the hippocampus. *Hippocampus* 25, 566–580. doi: 10.1002/hipo.22392

Sambandan, S., Sauer, J.-F., Vida, I., and Bartos, M. (2010). Associative plasticity at excitatory synapses facilitates recruitment of fast-spiking interneurons in the dentate gyrus. *J. Neurosci.* 30, 11826–11837. doi: 10.1523/JNEUROSCI.2012-10.2010

Sarantis, K., Tsiamaki, E., Kouvaros, S., Papatheodoropoulos, C., and Angelatou, F. (2015). Adenosine A_{2A} receptors permit mGluR5-evoked tyrosine phosphorylation of NR2B (Tyr1472) in rat hippocampus: a possible key mechanism in NMDA receptor modulation. *J. Neurochem.* 135, 714–726. doi: 10.1111/jnc.13291

Sarihi, A., Jiang, B., Komaki, A., Sohya, K., Yanagawa, Y., and Tsumoto, T. (2008). Metabotropic glutamate receptor type 5-dependent long-term potentiation of excitatory synapses on fast-spiking GABAergic neurons in mouse visual cortex. *J. Neurosci.* 28, 1224–1235. doi: 10.1523/JNEUROSCI.4928-07.2008

Shen, H. Y., Coelho, J. E., Ohtsuka, N., Canas, P. M., Day, Y. J., Huang, Q. Y., et al. (2008). A critical role of the adenosine A_{2A} receptor in extrastriatal neurons

in modulating psychomotor activity as revealed by opposite phenotypes of striatum and forebrain A_{2A} receptor knock-outs. *J. Neurosci.* 28, 2970–2975. doi: 10.1523/JNEUROSCI.5255-07.2008

Simões, A. P., Machado, N. J., Gonçalves, N., Kaster, M. P., Simões, A. T., Nunes, A., et al. (2016). Adenosine A_{2A} receptors in the amygdala control synaptic plasticity and contextual fear memory. *Neuropsychopharmacology* 41, 2862–2871. doi: 10.1038/npp.2016.98

Sparta, D. R., Hovelsø, N., Mason, A. O., Kantak, P. A., Ung, R. L., Decot, H. K., et al. (2014). Activation of prefrontal cortical parvalbumin interneurons facilitates extinction of reward-seeking behavior. *J. Neurosci.* 34, 3699–3705. doi: 10.1523/JNEUROSCI.0235-13.2014

Tebano, M. T., Martire, A., Rebola, N., Pepponi, R., Domenici, M. R., Grò, M. C., et al. (2005). Adenosine A_{2A} receptors and metabotropic glutamate 5 receptors are co-localized and functionally interact in the hippocampus: a possible key mechanism in the modulation of N-methyl-d-aspartate effects. *J. Neurochem.* 95, 1188–1200.

Tremblay, R., Lee, S., and Rudy, B. (2016). GABAergic interneurons in the neocortex: from cellular properties to circuits. *Neuron* 91, 260–292. doi: 10.1016/j.neuron.2016.06.033

van Aerde, K. I., Qi, G., and Feldmeyer, D. (2013). Cell type-specific effects of adenosine on cortical neurons. *Cereb. Cortex* 25, 772–787. doi: 10.1093/cercor/bht274

Van Dort, C. J., Baghdoyan, H. A., and Lydic, R. (2009). Adenosine A_1 and A_{2A} receptors in mouse prefrontal cortex modulate acetylcholine release and behavioral arousal. *J. Neurosci.* 29, 871–881.

Verhoog, M. B., Goriounova, N. A., Obermayer, J., Stroeder, J., Hjorth, J. J. J., Testa-Silva, G., et al. (2013). Mechanisms underlying the rules for associative plasticity at adult human neocortical synapses. *J. Neurosci.* 33, 17197–17208. doi: 10.1523/JNEUROSCI.3158-13.2013

Verhoog, M. B., Obermayer, J., Kortleven, C. A., Wilbers, R., Wester, J., Baayen, J. C., et al. (2016). Layer-specific cholinergic control of human and mouse cortical synaptic plasticity. *Nat. Commun.* 7:12826. doi: 10.1038/ncomms12826

Viana da Silva, S., Haberl, M. G., Zhang, P., Bethge, P., Lemos, C., Gonçalves, N., et al. (2016). Early synaptic deficits in the APP/PS1 mouse model of Alzheimer's disease involve neuronal adenosine A_{2A} receptors. *Nat. Commun.* 7:11915. doi: 10.1038/ncomms11915

Wall, M. J., and Dale, N. (2013). Neuronal transporter and astrocytic ATP exocytosis underlie activity-dependent adenosine release in the hippocampus. *J. Physiol.* 591, 3853–3871. doi: 10.1113/jphysiol.2013.253450

Wei, C. J., Singer, P., Coelho, J., Boison, D., Feldon, J., Yee, B. K., et al. (2011). Selective inactivation of adenosine A_{2A} receptors in striatal neurons enhances working memory and reversal learning. *Learn. Mem.* 18, 459–474.

Zhang, P., Bannon, N. M., Ilin, V., Volgushev, M., and Chistiakova, M. (2015). Adenosine effects on inhibitory synaptic transmission and excitation–inhibition balance in the rat neocortex. *J. Physiol.* 593, 825–841. doi: 10.1113/jphysiol.2014.279901

Zhou, S.-J., Zhu, M.-E., Shu, D., Du, X.-P., Song, X.-H., Wang, X.-T., et al. (2009). Preferential enhancement of working memory in mice lacking adenosine A_{2A} receptors. *Brain Res.* 1303, 74–83. doi: 10.1016/j.brainres.2009.09.082

Conflict of Interest Statement: RC is a scientific consultant for the Institute for Scientific Information on Coffee.

The other authors declare that the research was conducted in the absence of any commercial or financial relationships that could be construed as a potential conflict of interest.

frontiers in Pharmacology

ORIGINAL RESEARCH
published: 19 March 2018
doi: 10.3389/fphar.2018.00219

Adenosine A_{2A} Receptor Blockade Modulates Glucocorticoid-Induced Morphological Alterations in Axons, But Not in Dendrites, of Hippocampal Neurons

Helena Pinheiro[1,2†], Rita Gaspar[1,2†], Filipa I. Baptista[1,2], Carlos A. Fontes-Ribeiro[1,2,3], António F. Ambrósio[1,2,3] and Catarina A. Gomes[1,2,3]*

[1] Coimbra Institute for Clinical and Biomedical Research, Faculty of Medicine, University of Coimbra, Coimbra, Portugal, [2] Center for Innovation in Biomedicine and Biotechnology, University of Coimbra, Coimbra, Portugal, [3] Faculty of Medicine, University of Coimbra, Coimbra, Portugal

OPEN ACCESS

Edited by:
Francisco Ciruela,
Universitat de Barcelona, Spain

Reviewed by:
Luca Ferraro,
University of Ferrara, Italy
Maria José Diógenes,
Universidade de Lisboa, Portugal

***Correspondence:**
Catarina A. Gomes
catarina.gomes@fmed.uc.pt

[†] Co-authors

Specialty section:
This article was submitted to Experimental Pharmacology and Drug Discovery, a section of the journal Frontiers in Pharmacology

Received: 18 September 2017
Accepted: 27 February 2018
Published: 19 March 2018

Citation:
Pinheiro H, Gaspar R, Baptista FI, Fontes-Ribeiro CA, Ambrósio AF and Gomes CA (2018) Adenosine A_{2A} Receptor Blockade Modulates Glucocorticoid-Induced Morphological Alterations in Axons, But Not in Dendrites, of Hippocampal Neurons. Front. Pharmacol. 9:219. doi: 10.3389/fphar.2018.00219

The exposure to supra-physiological levels of glucocorticoids in prenatal life can lead to a long-term impact in brain cytoarchitecture, increasing the susceptibility to neuropsychiatric disorders. Dexamethasone, an exogenous glucocorticoid widely used in pregnant women in risk of preterm delivery, is associated with higher rates of neuropsychiatric conditions throughout life of the descendants. In animal models, prenatal dexamethasone exposure leads to anxious-like behavior and increased susceptibility to depressive-like behavior in adulthood, concomitant with alterations in neuronal morphology in brain regions implicated in the control of emotions and mood. The pharmacologic blockade of the purinergic adenosine A_{2A} receptor, which was previously described as anxiolytic, is also able to modulate neuronal morphology, namely in the hippocampus. Additionally, recent observations point to an interaction between glucocorticoid receptors (GRs) and adenosine A_{2A} receptors. In this work, we explored the impact of dexamethasone on neuronal morphology, and the putative implication of adenosine A_{2A} receptor in the mediation of dexamethasone effects. We report that *in vitro* hippocampal neurons exposed to dexamethasone (250 nM), in the early phases of development, exhibit a polarized morphology alteration: dendritic atrophy and axonal hypertrophy. While the effect of dexamethasone in the axon is dependent on the activation of adenosine A_{2A} receptor, the effect in the dendrites relies on the activation of GRs, regardless of the activation of adenosine A_{2A} receptor. These results support the hypothesis of the interaction between GRs and adenosine A_{2A} receptors and the potential therapeutic value of modulating adenosine A_{2A} receptors activation in order to prevent glucocorticoid-induced alterations in developing neurons.

Keywords: dexamethasone, adenosine A_{2A} receptor, development, hippocampal neurons, morphology

INTRODUCTION

The regulation of glucocorticoid (GC) levels during pregnancy is a major governing mechanism for the transition of the fetus to the extra-uterine life. During pregnancy, the levels of GC in the fetus are maintained lower than the mother's circulating levels and, toward the delivery, the intrauterine levels of GC rise, inducing fetal maturation (Thorburn et al., 1977). Once in the circulation, GC exerts a plethora of effects at the peripheral level and in the brain, by binding to mineralocorticoid (MR) and glucocorticoid receptors (GRs). Since endogenous GC have a higher affinity to MR, low levels of GC bind preferentially these receptors (Myers et al., 2014). Under stress conditions, the fetal hypothalamic-pituitary-adrenal (HPA) axis is activated in the earlier stages of development, inducing tissue differentiation, with detrimental effects later in life (Fowden and Forhead, 2015).

The administration of GC during prenatal and early life development mimics early-stress effects, being highly concerning. However, synthetic GC, such as dexamethasone (DEX), administrated in women at risk of preterm delivery to accelerate fetal lung maturation, are a crucial clinical tool to increase preterm infants survival (Brownfoot et al., 2008). Nevertheless, synthetic GC are up to 20 times more potent than endogenous GC and have higher affinity to GR (contrasting with endogenous GC), triggering different mechanisms likely implicated in their detrimental effects (Fowden and Forhead, 2015). Indeed, the antenatal exposure to synthetic GC was shown, both in humans and animal models, to have long-term effects on HPA axis regulation (Nagano et al., 2008), brain structure and behavior, neurosensory, neuroendocrine, and cardio-metabolic functions (Constantinof et al., 2016).

A brief antenatal exposure to DEX induces long-term behavioral alterations, such as decreased locomotor activity and exploratory behavior, increased susceptibility to depressive-like behavior (Oliveira et al., 2006), anxious-like behavior (Caetano et al., 2016), and altered fear-response in adulthood (Oliveira et al., 2012). The antenatal exposure to GC affects the normal development of the hippocampus, leading to a decrease in hippocampus size and an increase in the number of apoptotic cells during early life (Noorlander et al., 2014). Alterations in the hippocampal structure were reported also in models of early life stress induced by maternal separation, such as atrophy of mossy fiber density (Huot et al., 2002) and dendrites (Batalha et al., 2013). Thus, cytoarchitecture alterations in neurons due to DEX exposure may underlay the behavioral alterations.

Recent observations of A_{2A} receptor (A_{2A}R)-GR interaction in the hippocampus (Batalha et al., 2016) suggest that that A_{2A}R may be modulating DEX-induced effects in hippocampal neuronal cytoarchitecture during development. Indeed, the modulation of A_{2A}R has been regarded as a valuable therapeutic target in neuropsychiatric disorders (Cunha et al., 2008) and in the regulation of neuron morphology. The activation of A_{2A}R in neuronal differentiated PC12 cells demonstrated that A_{2A}R contributes to the increase in the number and length of neurites (Cheng et al., 2002; Charles et al., 2003). In primary cortical neurons, the activation of A_{2A}R increases axonal elongation and dendritic branching during neuronal development (Ribeiro et al., 2016). The modulation of neuronal morphology by A_{2A}R was also reported *in vivo*. Both the administration of caffeine in early life, a non-selective antagonist (Juárez-Méndez et al., 2006) and the treatment with a specific A_{2A}R antagonist in adulthood (Batalha et al., 2013) lead to alterations in neurons morphology, demonstrating that the blockade of A_{2A}R has an impact *in vivo* throughout all life span.

To test the hypothesis of A_{2A}R-GR interaction in hippocampal neuronal morphology we analyzed the effects of exposure to DEX on the morphology of hippocampal neurons during early development in the presence and absence of an A_{2A}R selective antagonist.

We report that DEX exposure induces a differential effect in the dendrites and axon of developing hippocampal neurons, characterized by dendritic atrophy and axonal hypertrophy. Whereas the effect in the increase in axonal length was dependent on the activation of A_{2A}R, the effect in the dendrites depends on the activation of GR, and not on A_{2A}R. These data suggest that the effects of DEX during development rely on distinct mechanisms in the different neuronal compartments.

MATERIALS AND METHODS

Primary Rat Hippocampal Neuronal Cultures

Primary cultures of hippocampal neurons were obtained from Wistar rats, as previously described (Baptista et al., 2013). Pregnant females (gestational day 18) were anesthetized with isoflurane, and sacrificed by cervical dislocation. Pups were delivered by cesarean operation and sacrificed by decapitation using surgical scissors. Briefly, the hippocampi from each hemisphere were macrodissected and dissociated chemically in a 0.15% trypsin solution (Sigma-Aldrich). Trypsinization reaction was blocked with 10% fetal bovine serum. Then, the hippocampi were mechanically dissociated in Neurobasal medium (Gibco) 0.025 mM glutamate (supplemented with 0.5 mM L-glutamine (Sigma), 2% B27, 0.1% gentamycin (Gibco) and plated at a low density (3000 cells/coverslip) in 16 mm coverslips previously coated with poly-D-lysine (0.1 mg/ml, Sigma). Hippocampal neurons cultures were maintained in an incubator at 37°C, 5% CO_2, until the end of the experiments. Four days after plating, at day *in vitro* (DIV) 4, half of the total medium volume was replaced by supplemented Neurobasal medium without glutamate, to avoid excitotoxicity.

All procedures involving animals were approved by the Animal Welfare Committee of the Faculty of Medicine of the University of Coimbra and were conducted in accordance with the European Community directive guidelines for the use of animals in laboratory (2010/63/EU), transposed into the Portuguese law in 2013 (Decreto-Lei 113/2013).

Pharmacological Treatment

At DIV1, hippocampal neurons were treated with DEX (250 nM, Acros Organics), a concentration that leads to GR nuclear translocation under the control of adenosine A_{2A} receptors

(unpublished data), and/or the selective A_{2A}R antagonist SCH58261 (SCH, 50 nM, Tocris) [this concentration is selective for A_{2A}R (Zocchi et al., 1996)], and/or the GR antagonist (RU486) mifepristone (MIF; 1 μM, Tocris) and the selective A_{2A}R agonist CGS21680 (CGS, 30 nM). DEX binds preferentially to GR (Kornel et al., 1982) and this concentration of MIF is able to abolish DEX effects *in vitro* (Kamradt et al., 2000; Kimura et al., 2011). When the effects of DEX were tested in the presence of the A_{2A}R antagonist, SCH was added 15 min before DEX, whereas in the case of the GR antagonist, MIF was added immediately before DEX.

Immunocytochemistry

Hippocampal neurons were fixed in 4% PFA and 4% sucrose in PBS solution (137 mM NaCl, 2.7 mM KCl, 10 mM $NaH_2PO_4.2H_2O$, 1.8 mM KH_2PO_4 in miliQ water, pH = 7.4) for 10 min, at RT. After permeabilization/blocking (PBS 5% BSA, NZYtech, 0.1% Triton X-100, Sigma), coverslips were incubated overnight with the primary antibody (1:1000, polyclonal rabbit anti-TUJ1, Covance), at 4°C, and for 2 h at RT with the secondary antibody (1:1000, polyclonal goat anti-rabbit, Thermo Fisher Scientific) after washing with PBS solution. Then, coverslips were incubated for 10 min with DAPI (1:5000 in PBS, Invitrogen) to stain nuclei, and mounted on microscope slides with glycergel mounting medium (DAKO).

Morphometric Analysis of Hippocampal Neurons

Neuronal morphology was analyzed at DIV2 and DIV5, to evaluate the influence of the pharmacological treatments upon the initial development of the axon at DIV2 and the elongation of the dendrites at DIV5 (Dotti et al., 1988, #438). For naming purposes, in this study, the major processes at DIV2 were solely considered as axons. Images of neurons were acquired in a fluorescence microscope Zeiss Axio Imager 2 linked to Zeiss AxioCam, using a 20× objective lens (Plan Apochromat 20×/0.8) and processed by Zen Blue software (Zeiss). The settings of the acquisition were maintained throughout all experiments. Two main criteria were taken into consideration for the selection of neurons: the acquisition of neurons whose neurites were clearly distinguishable and not overlaid with others, and the proximity to other neurons (in a radius of 1000 μm) to avoid morphologic alterations due to lack of trophic support derived from other neurons.

Images were imported to the Neurolucida software (MBF Bioscience) and distinguished axons and dendrites were manually reconstructed, taking into consideration their morphological differences, by a researcher blinded to the treatment conditions. The major branch in each cell with a constant caliber was regarded as the axon, whereas the smaller neurites with taper ending were considered dendrites. All ramifications were considered, regardless of their length. At DIV2, 180 cells were reconstructed for each condition, in a total of six independent experiments. At DIV5, 120 cells were reconstructed for each condition, in a total of five independent experiments.

Morphometric data (branched structure analysis) was obtained in Neurolucida Explorer software, and the number of axons/dendrites, mean length of axons/dendrites, and total numbers of ramifications of each were analyzed.

Statistical Analysis

Statistical analysis was carried out in GraphPad Prism version 5 (GraphPad Software Inc.). All graphic values are expressed as mean ± standard error of the mean (SEM). Comparison between two independent means was done by Student's *t*-test. To assess differences between three groups, a one-way analysis of variance (ANOVA) was used, followed by a Tukey's Multiple Comparison Test, to compare all groups. Differences were considered significant at $p < 0.05$.

RESULTS

Exposure to DEX Has a Differential Effect in Different Neuronal Compartments, Inducing Axon Hypertrophy and Dendrite Atrophy

To assess the effects of DEX upon neuronal morphogenesis, primary hippocampal neurons were treated with DEX (250 nM) after 24 h in culture and neuronal morphology was analyzed after 2 and 5 days in culture (**Figure 1**), by manual reconstruction, using Neurolucida software. Morphometric data were analyzed considering the number and length of dendrites and axons, and the respective ramification.

We observed that DEX treatment did not alter neuronal morphology after 2 days in culture (Supplementary Figure 1). Contrastingly, at 5 days in culture DEX exposure induced a pronounced decrease in the mean length of the dendrites: 107.6 ± 6.6 μm ($p < 0.001$), as compared with non-treated (NT; 150.7 ± 8.1 μm) (**Figure 1d**). However, no statistical effect was detected upon their number and number of ramifications. In the axon, DEX induced the opposite effect, increasing its length: 1139.2 ± 86.1 μm ($p < 0.01$), as compared with NT (811.5 ± 57.6 μm) (**Figure 1g**).

Thus, exposure of hippocampal neurons to DEX induces a contrasting modulation of neuronal morphology, characterized by axonal hypertrophy and dendritic atrophy.

DEX-Induced Increase in Axon Length Is Dependent on the Activation of Adenosine A_{2A} Receptors

To understand if the activation of A_{2A}R is implicated in the modulation of neuronal morphology induced by DEX, we analyzed the impact of DEX in hippocampal neurons under the pharmacological blockade of A_{2A}R, using a selective antagonist (SCH58261) (**Figure 2**). Hence, primary hippocampal neurons were treated with 250 nM DEX in the absence or presence of 50 nM SCH58261, and neuronal morphology was analyzed after 5 days in culture.

The blockade of A_{2A}R was not able to prevent the atrophy in the length of the dendrites induced by DEX (110.0 ± 5.4 μm),

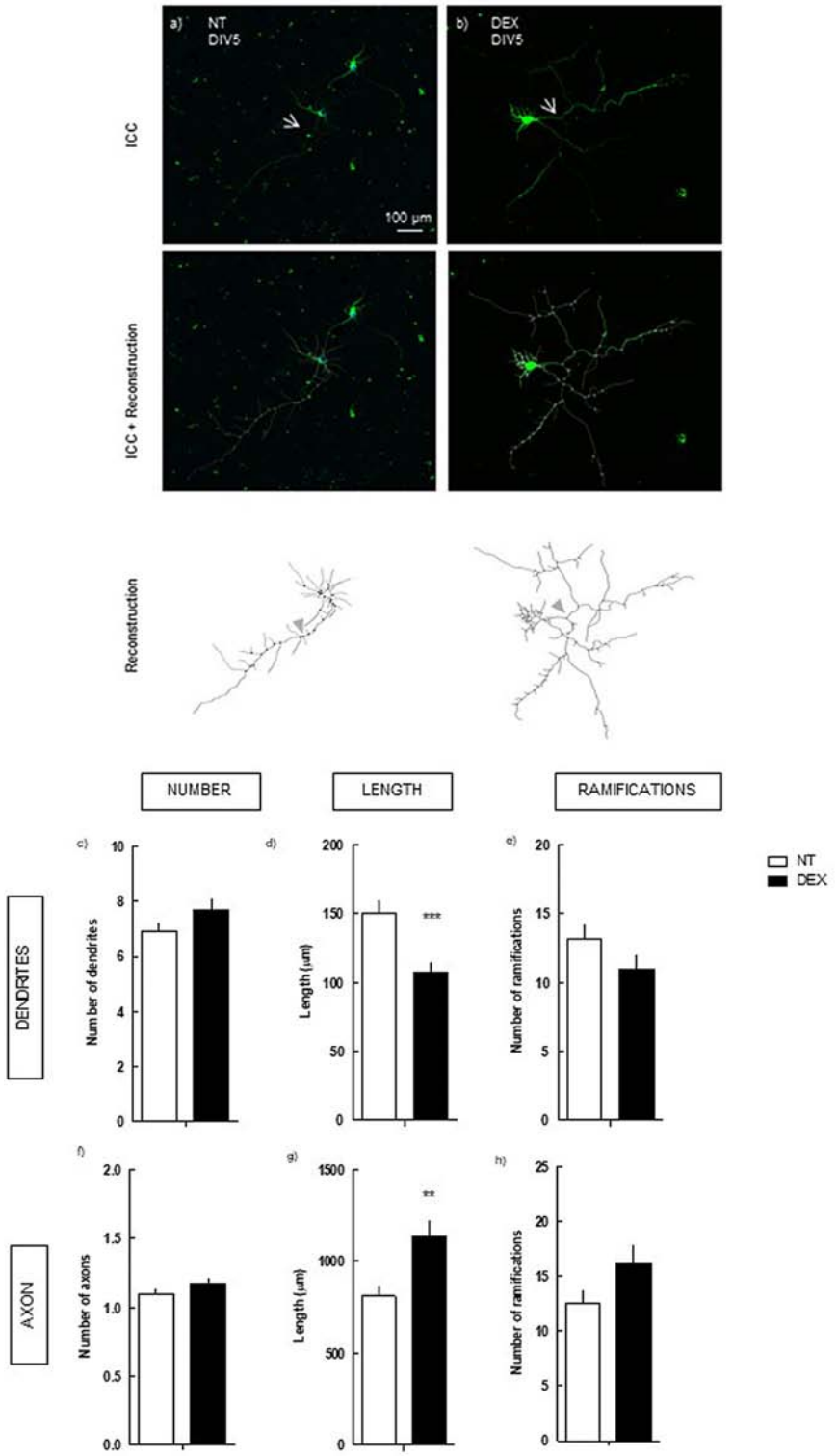

FIGURE 1 | Effect of DEX treatment (4 days treatment) on hippocampal neurons (DIV5). Hippocampal neurons from ED18 rats were cultured *in vitro* for 5 days (DIV5) and treated with DEX (250 nM) at 24 h in culture. Neuronal morphology was assessed by manual reconstruction in Neurolucida software **(a,b)** and morphometric data were acquired in Neurolucida Explorer, regarding the number **(c)**, length **(d)** and number of ramifications **(e)** of dendrites and the number **(f)**, length **(g)**, and number of ramifications **(h)** of axons (identified with an arrow in the representative images). Results are expressed as mean ± SEM of 120 cells, from five independent experiments. Statistical significance was assessed by *t*-student test: $^{**}p < 0.01$, $^{***}p < 0.001$, comparing DEX treatment with NT. ICC, immunocytochemistry; NT, non-treated; DEX, dexamethasone.

comparing with DEX alone (107.6 ± 6.6 μm). Indeed, the effect of A_{2A}R plus DEX, which induced a similar decrease as DEX alone, was significantly different ($p < 0.001$) from NT cells (150.7 ± 8.1 μm). The treatment with SCH *per se* induced a decrease in the length of the dendrites similar to the effect of DEX treatment (**Figure 2f**), indicating that both DEX and SCH induce similar alterations in dendrites' length.

Regarding the number of dendrites, although DEX treatment did not induce a significant alteration, there was a tendency to increase. Regarding the treatment with SCH, there was an increase in the number of dendrites, both in the absence (8.4 ± 0.3; $p < 0.05$) and presence of DEX (9.0 ± 0.4; $p < 0.001$), comparing with NT (6.9 ± 0.3).

Conversely, in the axon, A_{2A}R blockade prevented the increase ($p < 0.001$) in the length induced by DEX (752.4 ± 60.8 μm), comparing with DEX alone (1139.2 ± 86.1 μm; **Figure 2i**), having a similar length as in NT cells (811.5 ± 57.6 μm; n.s.).

These findings show that there is an uncouple in the mechanisms underlying the effect of DEX exposure in dendrites and axon, demonstrating the requirement of the activation of different receptors.

DEX-Mediated Increase in Axon Length Is Not Exclusively Modulated by the Activation of A_{2A}R

Given that the blockade of A_{2A}R *per se* led to alterations in neuronal morphology similar to those observed in the blockade of A_{2A}R combined with DEX, we aimed to clarify if the rescue of the axon length is not mediated solely by the blockade of A_{2A}R activation by tonic adenosine, instead of a modulation dependent on GR. Thus, we analyzed the effect of a selective A_{2A}R agonist, 30 nM CGS 21680, in neuronal morphology.

We observed that, in the absence of DEX, the activation of A_{2A}R does not lead to significant alterations in neuronal morphology, not in the dendrites or axon (**Figure 3**).

These results indicate that the DEX-induced axonal hypertrophy, although dependent on the activation of A_{2A}R requires also the activation of GR, indicating a crosstalk between A_{2A}R/GR.

Surprisingly, even though the blockade of A_{2A}R *per se* led to alterations in dendrites' morphology, these alterations were not observed by the selective activation of A_{2A}R. This indicates that the maintenance of adenosine tonic levels is crucial for neuronal morphology, although the overactivation of A_{2A}R does not alter morphology.

DEX-Induced Decrease in Dendrite Length Is Dependent on the Activation of Glucocorticoids Receptors

Considering that synthetic glucocorticoids, namely DEX, have a high affinity to GR (Kornel et al., 1982), we sought to confirm if the effects of DEX on the morphology of neurons are dependent on the activation of GR. To test this hypothesis, primary hippocampal neurons were treated with 250 nM DEX, in the absence or presence of the antagonist of GR, 1 μM MIF (**Figure 4**).

The blockade of GR prevented the alteration in the length of the dendrites induced by DEX (147.1 ± 8.6 μm; $p < 0.001$) as compared with DEX alone (107.6 ± 6.6 μm) (**Figure 4f**), to values similar to NT cells (150.7 ± 8.1 μm; n.s.). Additionally, the treatment with MIF *per se* led to an increase ($p < 0.01$) in the number of dendrites (8.6 ± 0.4) as compared with NT (6.9 ± 0.3) (**Figure 4e**), demonstrating a hypertrophic effect of the blockade of endogenous glucocorticoids.

The increase in the length of the axon induced by DEX was not prevented by the blockade of GR (1069.1 ± 88.7 μm), as compared with DEX alone (1139.2 ± 86.1 μm, n.s.) (**Figure 4i**). In contrast to the observations in dendrites, the effect of DEX in the presence of MIF in the axon is similar to the effect of DEX alone, indicative of two different mechanisms overriding DEX effects in axon and dendrites.

Indeed, we demonstrate that whereas the effect of DEX in the dendritic morphology depends on the direct activation of GR, the effects on the axon are modulated by the activation of A_{2A}R.

The observation that the blockade of GR *per se* leads to an increase ($p < 0.05$) in the number of ramifications in the axon (18.7 ± 2.0) as compared with NT (12.5 ± 1.2), is in line with the possible hypertrophic effect of blocking the action of endogenous glucocorticoids raised above. However, the hypertrophic effect of GR blockade could be also due to an increase in the activation of mineralocorticoid receptors by tonic glucocorticoids, rather than the lack of GR activation.

DISCUSSION

The development of the brain is tightly regulated by environmental factors. Thus, negative environmental stimuli, such as prenatal and early life stress, which lead to increased levels of glucocorticoids can have a long-term impact in the brain cytoarchitecture and function (Oliveira et al., 2006, 2012; Leão et al., 2007). Similarly, glucocorticoid treatments, such as DEX, also lead to detrimental effects in the brain. However, the implementation of these approaches in women in risk of preterm birth was an undoubtable advance in the increase of survival rates of premature newborns (Brownfoot et al., 2008). Therefore, it is crucial to understand the modulating effects of glucocorticoid exposure in the developing brain in order to develop new pharmacological approaches to circumvent their negative effects.

In the present work, we reported that a long-term exposure to DEX in developing hippocampal neurons leads to a differential modulation of neuronal morphology, characterized by dendrites' atrophy and axonal hypertrophy. The observation that DEX did not alter neuronal morphology after 24 h of exposure (Supplementary Figure 1) indicates that DEX-mediated effects in morphology are delayed or restricted to later stages of development.

The delay in DEX effects is in line with previous observations in PC12 cells, in which the treatment with a low dose of DEX leads to an increase in cell growth only after 72 h of exposure, as indicated by the total protein/DNA ratio (Jameson et al., 2006). As that method does not discriminate cell morphology, the results

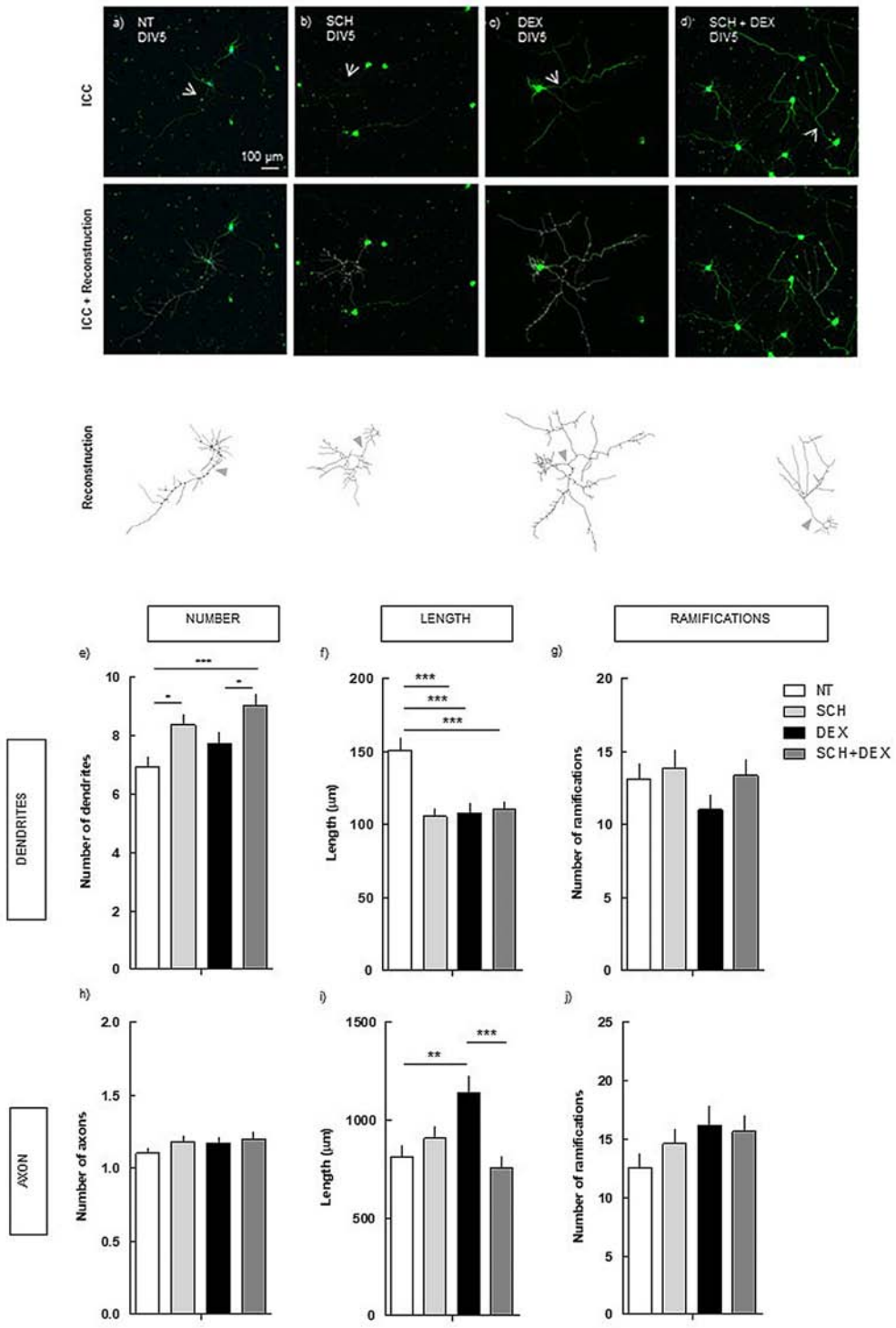

FIGURE 2 | Effect of the blockade of A_{2A}R *per se* and on DEX exposure (4 days treatment) in hippocampal neurons (DIV5). Hippocampal neurons from ED18 rats were cultured *in vitro* for 5 days (DIV5). Cultured neurons were treated with the A_{2A}R antagonist, SCH (50 nM), or with the A_{2A}R antagonist and/or DEX (250 nM; at 24 h in culture). SCH was added 15 min before DEX. Neuronal morphology was assessed by manual reconstruction in Neurolucida software **(a–d)** and morphometric data were acquired in Neurolucida Explorer, regarding the number **(e)**, length **(f)**, and number of ramifications **(g)** of dendrites and the number **(h)**, length **(i)**, and number of ramifications **(j)** of axons (identified with an arrow in the representative images). Results are expressed as mean ± SEM of 120 cells, from five independent experiments. Statistical significance was assessed by one-way ANOVA followed by Tukey's Multiple Comparison Test: $*p < 0.05$, $**p < 0.01$, $***p < 0.001$, as indicated by the horizontal lines above the columns. ICC, immunocytochemistry; NT, non-treated; SCH, SCH58261, A_{2A}R antagonist; DEX, dexamethasone; SCH+DEX, SCH58261 + Dexamethasone.

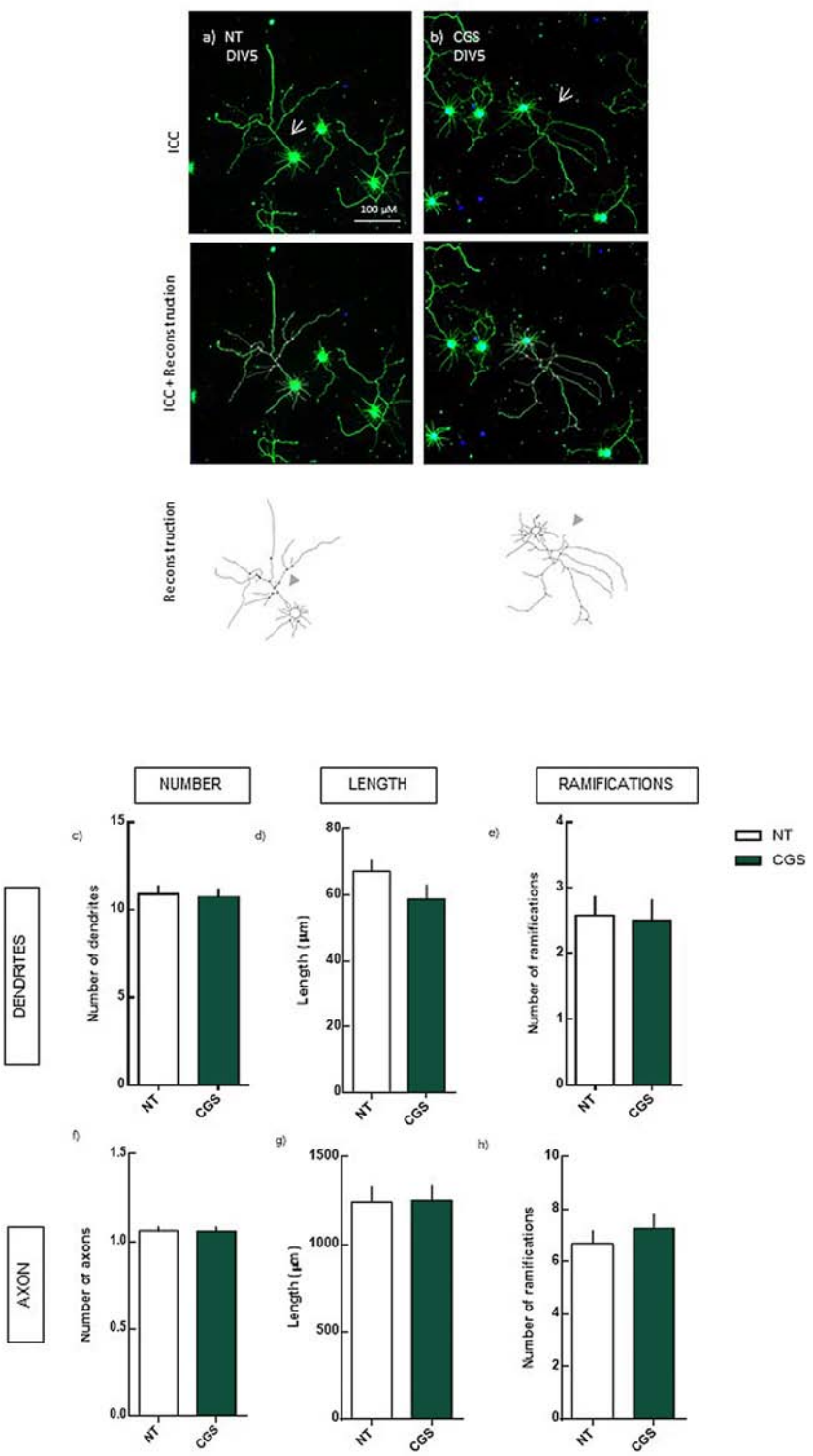

FIGURE 3 | Effect of the selective activation of A_{2A}R (4 days treatment) in hippocampal neurons (DIV5). Hippocampal neurons from ED18 rats were cultured *in vitro* for 5 days (DIV5). Cultured neurons were treated with the A_{2A}R agonist, CGS (30 nM), at 24 h in culture. Neuronal morphology was assessed by manual reconstruction in Neurolucida software **(a,b)** and morphometric data were acquired in Neurolucida Explorer, regarding the number **(c)**, length **(d)**, and number of ramifications **(e)** of dendrites and the number **(f)**, length **(g)**, and number of ramifications **(h)** of axons (identified with an arrow in the representative images). Results are expressed as mean ± SEM of 97–100 cells, from four independent experiments. No statistical significance comparing NT with CGS treatment, assessed by *t*-student test. ICC, immunocytochemistry; NT, non-treated; CGS, CGS21680, A_{2A}R agonist.

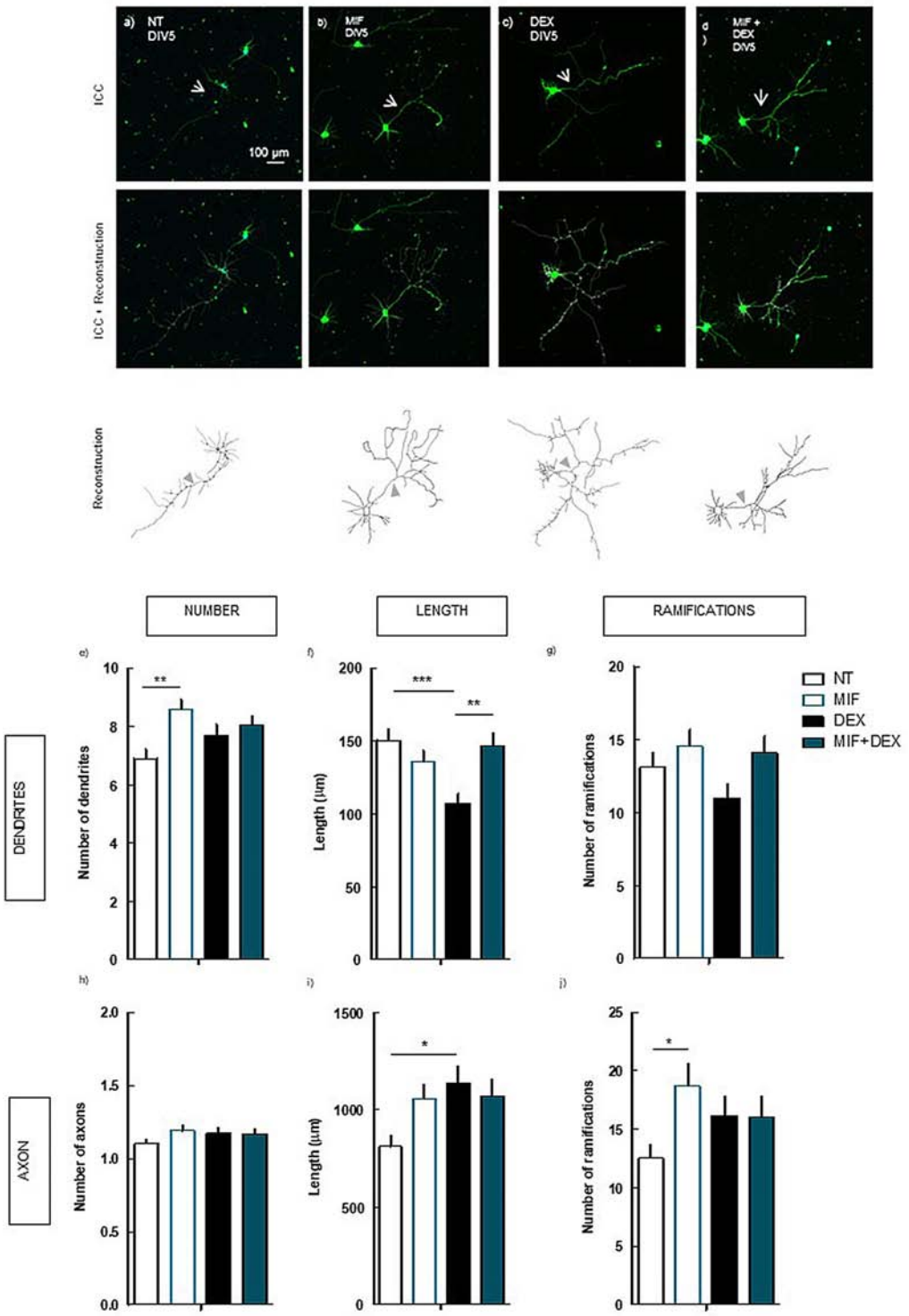

FIGURE 4 | Effect of the blockade of GR *per se* and on DEX exposure (4 days treatment) in hippocampal neurons (DIV5). Hippocampal neurons from ED18 rats were cultured *in vitro* for 5 days (DIV5). Cultured neurons were treated with the GR antagonist, MIF (1 μM), or with the GR antagonist and/or DEX (250 nM; at 24 h in culture). Neuronal morphology was assessed by manual reconstruction in Neurolucida software **(a–d)** and morphometric data were acquired in Neurolucida Explorer, regarding the number **(e)**, length **(f)**, and number of ramifications **(g)** of dendrites and the number **(h)**, length **(i)**, and number of ramifications **(j)** of axons (identified with an arrow in the representative images). Results are expressed as mean ± SEM of 120 cells, from five independent experiments. Statistical significance was assessed by one-way ANOVA followed by Tukey's Multiple Comparison Test: $^{*}p < 0.05$, $^{**}p < 0.01$, $^{***}p < 0.001$, as indicated by the horizontal lines above the columns. ICC, immunocytochemistry; NT, non-treated; MIF, mifepristone, GR antagonist.; DEX, dexamethasone; MIF+DEX, mifepristone + dexamethasone.

do not oppose our observations, once the differential effect in dendrites and axon may lead to an overall increase in cell area. However, in a different study exploring the effect of high doses of DEX (5 μM) it was observed that DEX exposure for 48 h leads to an overall inhibition of neurite development (Beaujean et al., 2003), contrasting with the present observations that DEX does not induce any effect 24 h after treatment. This discrepancy could be due to the higher concentration of DEX or differences in the susceptibility of the PC12 cell line comparing with cultured hippocampal neurons. In a different cell line, HiB5 cells, it was also observed that the exposure to DEX in a concentration in the same range of the concentration in the present study (10^{-7} M) also inhibits neurite development (Son et al., 2001), which may indicate that cell lines and hippocampal primary neurons may respond differently to DEX exposure.

Overall, there is a lack of understanding regarding the direct effect of DEX in neurons. Over the last two decades, few studies were developed to explore the effects of DEX exposure *in vitro*, which could highly contribute to the dissection of the effects observed at the organism level.

In *in vivo* models, it is interesting to notice that several reports showed dendritic atrophy, resulting from either stress or glucocorticoid exposure in brain regions such as the prefrontal cortex (Brown et al., 2005; Anderson et al., 2016) and the hippocampus (Sousa et al., 1999, 2000; Silva-Gómez et al., 2013). However, alterations in axonal morphology were not yet reported, probably due to the difficulties associated with the analysis of axonal morphology *in vivo* given the higher complexity of this cellular compartment. Nevertheless, alterations in axonal morphology can alter brain connectivity and are implicated in psychiatric disorders. In a genetic model of schizophrenia, it was observed an impair in axonal growth and branching, which leads to cognitive deficits and high incidence of emotional problems (Mukai et al., 2015).

Although the activation of A_{2A}R in the brain is well documented as a modulator of synaptic transmission and plasticity, these receptors are also implicated in neuronal morphologic development *in vivo*. The modulation of A_{2A}R activation was previously reported to impair brain connectivity trough axonal development alterations in a model of *in utero* exposure to an A_{2A}R antagonist. This impairment leads to a delay in axonal migration, which is associated to cognitive deficits in adulthood (Silva et al., 2013). Considering the report that A_{2A}R activation induces axonal elongation *in vitro* by inducing an increase in microtubule dynamics and growth speed (Ribeiro et al., 2016), we speculate that the modulation of DEX axonal effect by A_{2A}R could be due to a similar mechanism.

However, in the present study, the treatment with an A_{2A}R agonist did not alter neuronal morphology, suggesting that the effects of A_{2A}R modulation in hippocampal neurons are different from the ones in cortical neurons, or that the differences in these results are due to the analysis of neuronal morphology in a different time interval in neuronal development, once we analyzed morphology at day 5 in culture whereas in the referred study the analysis of cortical neurons was at day 3. Indeed, it is interesting that although the activation of A_{2A}R is necessary for the effects of DEX in the axon, as seen by the blockade of DEX-effect in the presence of the A_{2A}R antagonist, the activation of A_{2A}R does not alter neuronal morphology. This indicates that DEX-effect is not exclusively mediated by A_{2A}R, further supporting the hypothesis of a GR–A_{2A}R crosstalk.

Interestingly, in microglia, we previously described such a putative interaction. It is well documented that A_{2A}R are also important regulators of microglia morphology (Gyoneva et al., 2009, 2014; Orr et al., 2009; Caetano et al., 2016). We described that *in utero* exposure to DEX induces long-term alterations in microglia morphology which correlate with anxiety-like behavior, and that this alterations are recovered by A_{2A}R blockade in a gender-specific manner (Caetano et al., 2016). However, we observed only a partial recovery of microglia morphologic alterations induced by DEX accompanied by a complete recover in behavior might indicate additional targets mediating A_{2A}R blockade effects, namely neurons. This prompted us to understand the direct effects of DEX exposure in neurons, and the therapeutic potential of A_{2A}R blockade.

Although we previously observed a DEX and A_{2A}R gender-specific effect in microglia *in vivo*, in this study, we did not discriminate the sex of the fetuses, due to restrictions in the numbers of animals available to perform neuronal cultures. However, since the neurons suffer a reprogramming upon culture, and are from then on cultured in the same conditions, we do not expect such striking differences in the data obtained.

In what concerns GR–A_{2A}R crosstalk, it was recently described that the blockade of A_{2A}R activation blocks GR translocation to the nucleus, thus impairing GR activation-induced transcriptional alterations (Batalha et al., 2016). Accordingly, the effects of DEX in the axon are blocked by the simultaneous treatment with the A_{2A}R antagonist, suggesting that the axon hypertrophy is dependent on GR transcriptional activity.

However, there is a discrepancy between DEX-effects on dendrites and axons. The dendritic atrophy is independent of the blockade of A_{2A}R, which might suggest that the effects on dendrites may be due to GR effects that do not require nuclear translocation and are due to GR non-genomic effects.

On the other hand, the axonal effects were abolished by the blockade of A_{2A}R, which disrupts nuclear translocation, indicating that DEX effect on the axon depends on GR genomic action. Although, it is interesting to notice that the DEX effect was not present after 24 h of DEX exposure in either the dendrites or the axon. If the effects in the dendrites are indeed modulated by GR non-genoimc effects, the decrease in dendrites length could potentially be achieved earlier than the increase in the axon, once it would not depend on transcriptional alterations. This point could be clarified by a closer monitoring of the morphological alterations induced by DEX to pinpoint a more accurate moment of the outset of dendritic and axonal alterations.

Additionally, according to this hypothesis, the effect of DEX in the axon should be similarly blocked in the presence of GR antagonist or A_{2A}R antagonist, once both should block the receptor translocation to the nucleus. These results would be explained if the increase of GR nuclear translocation upon activation of A_{2A}R was independent on the presence of GR ligands, as DEX.

It is also possible that the distribution of A_{2A}R is differential in axon and dendrites, leading to a significant effect upon the GR signaling in the axon, but not in the dendrites. It is important to address all these hypotheses to further understand the nature of GR–A_{2A}R interaction and, consequently, the putative pharmacological modulation of A_{2A}R activation.

Furthermore, since the present results indicate that DEX effects on axonal morphology are dependent on the activation of A_{2A}R, clarifying the mechanisms underlying these receptors crosstalk can be crucial to understand DEX action on neuronal morphology. As it was previously described, the activation of A_{2A}R in cortical neurons promotes the growth speed of microtubules in the axonal growth cone, leading to axonal elongation (Ribeiro et al., 2016). In future work, it is also important to understand how glucocorticoid exposure modulates neuronal morphology, considering the possibility that the effect of DEX may be as well dependent on microtubule dynamics.

Understanding the mechanistic relation of GR and A_{2A}R and the nature of A_{2A}R morphological modulation in neurons and other cell types is crucial to the further development of A_{2A}R blockade therapies.

The genetic and pharmacological blockade of A_{2A}R was described as anxiolytic in a model of chronic stress in males, both as a preventive and therapeutic tool (Kaster et al., 2015). Additionally, the chronic blockade of A_{2A}R in adulthood is able to revert behavioral, electrophysiological and neuronal morphological alterations induced by maternal separation (Batalha et al., 2013), clearly demonstrating its pharmacological potential in psychiatric pathologies.

However, the response can differ according to gender (Caetano et al., 2016) and it can be prejudicial when administered during development. The blockade of A_{2A}R during development leads to a delay in axonal migration and consequent neuronal excitability, resulting in an increase in the susceptibility to seizures (Silva et al., 2013). Thus, understanding the different pathways induced by A_{2A}R activation in these conditions is essential to further pursue the neuropsychiatric pharmacological advantages of its blockade.

CONCLUSION

Although the use of synthetic GC in clinics is essential due to their beneficial effects in several pathologies, it is important to have a full understanding of their potential deleterious effects, namely in the CNS. The previous described effects of GC exposure in the morphology and physiology of neurons probably underlie the observed neuropsychiatric disturbances. Thus, given the therapeutic potential of A_{2A}R blockade in neuropsychiatric disorders, it is essential to fully comprehend the mechanisms of GR and A_{2A}R interaction, as well as the mechanisms responsible for the modulation of the brain cytoarchitecture by these receptors.

AUTHOR CONTRIBUTIONS

HP designed the experiments with CG, performed the experiments, and wrote the manuscript. RG performed hippocampal neurons primary cultures and immunocytochemistry for the experiment with A_{2A}R agonist treatment. FB assisted in hippocampal neurons primary cultures and revised the manuscript. AA revised the manuscript. CG supervised HP, contributed to the design of the experiments, and revised the manuscript. All authors discussed the results, contributed to and approved the final manuscript.

FUNDING

This work was supported by the Portuguese Foundation for Science and Technology (PEst UID/NEU/04539/2013), COMPETE-FEDER (POCI-01-0145-FEDER-007440), and Centro 2020 Regional Operational Program (CENTRO-01-0145-FEDER-000008: BrainHealth 2020). FB is supported by a fellowship from the Portuguese Foundation for Science and Technology (SFRH/BPD/86830/2012). FB and RG are supported by fellowships from the Portuguese Foundation for Science and Technology (SFRH/BPD/86830/2012 and PD/BD/114116/2015, respectively).

SUPPLEMENTARY MATERIAL

The Supplementary Material for this article can be found online at: https://www.frontiersin.org/articles/10.3389/fphar.2018.00219/full#supplementary-material

REFERENCES

Anderson, R. M., Glanz, R. M., Johnson, S. B., Miller, M. M., Romig-Martin, S. A., and Radley, J. J. (2016). Prolonged corticosterone exposure induces dendritic spine remodeling and attrition in the rat medial prefrontal cortex. *J. Comp. Neurol.* 524, 3729–3746. doi: 10.1002/cne.24027

Baptista, F. I., Pinto, M. J., Elvas, F., Almeida, R. D., and Ambrósio, A. F. (2013). Diabetes alters KIF1A and KIF5B motor proteins in the hippocampus. *PLoS One* 8:e65515. doi: 10.1371/journal.pone.0065515

Batalha, V. L., Ferreira, D. G., Coelho, J. E., Valadas, J. S., Gomes, R., Temido-Ferreira, M., et al. (2016). The caffeine-binding adenosine A2A receptor induces age-like HPA-axis dysfunction by targeting glucocorticoid receptor function. *Sci. Rep.* 6:31493. doi: 10.1038/srep31493

Batalha, V. L., Pego, J. M., Fontinha, B. M., Costenla, A. R., Valadas, J. S., Baqi, Y., et al. (2013). Adenosine A(2A) receptor blockade reverts hippocampal stress-induced deficits and restores corticosterone circadian oscillation. *Mol. Psychiatry* 18, 320–331. doi: 10.1038/mp.2012.8

Beaujean, D., Rosenbaum, C., Müller, H.-W., Willemsen, J. J., Lenders, J., and Bornstein, S. R. (2003). Combinatorial code of growth factors and neuropeptides define neuroendocrine differentiation in PC12 cells. *Exp. Neurol.* 184, 348–358. doi: 10.1016/j.expneurol.2003.07.007

Brown, S. M., Henning, S., and Wellman, C. L. (2005). Mild, short-term stress alters dendritic morphology in rat medial prefrontal cortex. *Cereb. Cortex* 1991, 1714–1722. doi: 10.1093/cercor/bhi048

Brownfoot, F. C., Crowther, C. A., and Middleton, P. (2008). Different corticosteroids and regimens for accelerating fetal lung maturation for women

at risk of preterm birth. *Cochrane Database Syst. Rev.* CD006764. doi: 10.1002/14651858.CD006764.pub2

Caetano, L., Pinheiro, H., Patrício, P., Mateus-Pinheiro, A., Alves, N. D., Coimbra, B., et al. (2016). Adenosine A2A receptor regulation of microglia morphological remodeling-gender bias in physiology and in a model of chronic anxiety. *Mol. Psychiatry* 22, 1035–1043. doi: 10.1038/mp.2016.173

Charles, M.-P., Adamski, D., Kholler, B., Pelletier, L., Berger, F., and Wion, D. (2003). Induction of neurite outgrowth in PC12 cells by the bacterial nucleoside N6-methyldeoxyadenosine is mediated through adenosine A2a receptors and via cAMP and MAPK signaling pathways. *Biochem. Biophys. Res. Commun.* 304, 795–800. doi: 10.1016/S0006-291X(03)00666-1

Cheng, H.-C., Shih, H.-M., and Chern, Y. (2002). Essential role of cAMP-response element-binding protein activation by A2A adenosine receptors in rescuing the nerve growth factor-induced neurite outgrowth impaired by blockage of the MAPK cascade. *J. Biol. Chem.* 277, 33930–33942. doi: 10.1074/jbc.M201206200

Constantinof, A., Moisiadis, V. G., and Matthews, S. G. (2016). Programming of stress pathways: a transgenerational perspective. *J. Steroid Biochem. Mol. Biol.* 160, 175–180. doi: 10.1016/j.jsbmb.2015.10.008

Cunha, R. A., Ferré, S., Vaugeois, J.-M., and Chen, J.-F. (2008). Potential therapeutic interest of adenosine A2A receptors in psychiatric disorders. *Curr. Pharm. Des.* 14, 1512–1524. doi: 10.2174/138161208784480090

Dotti, C. G., Sullivan, C. A., and Banker, G. A. (1988). The establishment of polarity by hippocampal neurons in culture. *J. Neurosci.* 8, 1454–1468.

Fowden, A. L., and Forhead, A. J. (2015). Glucocorticoids as regulatory signals during intrauterine development. *Exp. Physiol.* 100, 1477–1487. doi: 10.1113/EP085212

Gyoneva, S., Orr, A. G., and Traynelis, S. F. (2009). Differential regulation of microglial motility by ATP/ADP and adenosine. *Parkinsonism Relat. Disord.* 15(Suppl. 3), S195–S199. doi: 10.1016/S1353-8020(09)70813-2

Gyoneva, S., Shapiro, L., Lazo, C., Garnier-Amblard, E., Smith, Y., Miller, G. W., et al. (2014). Adenosine A_{2A} receptor antagonism reverses inflammation-induced impairment of microglial process extension in a model of Parkinson's disease. *Neurobiol. Dis.* 67, 191–202. doi: 10.1016/j.nbd.2014.03.004

Huot, R. L., Plotsky, P. M., Lenox, R. H., and McNamara, R. K. (2002). Neonatal maternal separation reduces hippocampal mossy fiber density in adult Long Evans rats. *Brain Res.* 950, 52–63. doi: 10.1016/S0006-8993(02)02985-2

Jameson, R. R., Seidler, F. J., Qiao, D., and Slotkin, T. A. (2006). Adverse neurodevelopmental effects of dexamethasone modeled in PC12 cells: identifying the critical stages and concentration thresholds for the targeting of cell acquisition, differentiation and viability. *Neuropsychopharmacology* 31, 1647–1658. doi: 10.1038/sj.npp.1300967

Juárez-Méndez, S., Carretero, R., Martínez-Tellez, R., Silva-Gómez, A. B., and Flores, G. (2006). Neonatal caffeine administration causes a permanent increase in the dendritic length of prefrontal cortical neurons of rats. *Synapse* 60, 450–455. doi: 10.1002/syn.20318

Kamradt, M. C., Mohideen, N., and Vaughan, A. T. (2000). RU486 increases radiosensitivity and restores apoptosis through modulation of HPV E6/E7 in dexamethasone-treated cervical carcinoma cells. *Gynecol. Oncol.* 77, 177–182. doi: 10.1006/gyno.1999.5724

Kaster, M. P., Machado, N. J., Silva, H. B., Nunes, A., Ardais, A. P., Santana, M., et al. (2015). Caffeine acts through neuronal adenosine A2A receptors to prevent mood and memory dysfunction triggered by chronic stress. *Proc. Natl. Acad. Sci. U.S.A.* 112, 7833–7838. doi: 10.1073/pnas.1423088112

Kimura, M., Moteki, H., and Ogihara, M. (2011). Inhibitory effects of dexamethasone on epidermal growth factor-induced DNA synthesis and proliferation in primary cultures of adult rat hepatocytes. *Biol. Pharm. Bull.* 34, 682–687. doi: 10.1248/bpb.34.682

Kornel, L., Kanamarlapudi, N., Travers, T., Taff, D. J., Patel, N., Chen, C., et al. (1982). Studies on high affinity binding of mineralo- and glucocorticoids in rabbit aorta cytosol. *J. Steroid Biochem.* 16, 245–264. doi: 10.1016/0022-4731(82)90173-X

Leão, P., Sousa, J. C., Oliveira, M., Silva, R., Almeida, O. F. X., and Sousa, N. (2007). Programming effects of antenatal dexamethasone in the developing mesolimbic pathways. *Synapse* 61, 40–49. doi: 10.1002/syn.20341

Mukai, J., Tamura, M., Fénelon, K., Rosen, A. M., Spellman, T. J., Kang, R., et al. (2015). Molecular substrates of altered axonal growth and brain connectivity in a mouse model of schizophrenia. *Neuron* 86, 680–695. doi: 10.1016/j.neuron.2015.04.003

Myers, B., McKlveen, J. M., and Herman, J. P. (2014). Glucocorticoid actions on synapses, circuits, and behavior: implications for the energetics of stress. *Front. Neuroendocrinol.* 35:180–196. doi: 10.1016/j.yfrne.2013.12.003

Nagano, M., Ozawa, H., and Suzuki, H. (2008). Prenatal dexamethasone exposure affects anxiety-like behaviour and neuroendocrine systems in an age-dependent manner. *Neurosci. Res.* 60, 364–371. doi: 10.1016/j.neures.2007.12.005

Noorlander, C. W., Tijsseling, D., Hessel, E. V. S., de Vries, W. B., Derks, J. B., Visser, G. H. A., et al. (2014). Antenatal glucocorticoid treatment affects hippocampal development in mice. *PLoS One* 9:e85671. doi: 10.1371/journal.pone.0085671

Oliveira, M., Bessa, J. M., Mesquita, A., Tavares, H., Carvalho, A., Silva, R., et al. (2006). Induction of a hyperanxious state by antenatal dexamethasone: a case for less detrimental natural corticosteroids. *Biol. Psychiatry* 59, 844–852. doi: 10.1016/j.biopsych.2005.08.020

Oliveira, M., Rodrigues, A.-J., Leão, P., Cardona, D., Pêgo, J. M., and Sousa, N. (2012). The bed nucleus of stria terminalis and the amygdala as targets of antenatal glucocorticoids: implications for fear and anxiety responses. *Psychopharmacology* 220, 443–453. doi: 10.1007/s00213-011-2494-y

Orr, A. G., Orr, A. L., Li, X.-J., Gross, R. E., and Traynelis, S. F. (2009). Adenosine A(2A) receptor mediates microglial process retraction. *Nat. Neurosci.* 12, 872–878. doi: 10.1038/nn.2341

Ribeiro, F. F., Neves-Tomé, R., Assaife-Lopes, N., Santos, T. E., Silva, R. F. M., Brites, D., et al. (2016). Axonal elongation and dendritic branching is enhanced by adenosine A2A receptors activation in cerebral cortical neurons. *Brain Struct. Funct.* 221, 2777–2799. doi: 10.1007/s00429-015-1072-1

Silva, C. G., Métin, C., Fazeli, W., Machado, N. J., Darmopil, S., Launay, P.-S., et al. (2013). Adenosine receptor antagonists including caffeine alter fetal brain development in mice. *Sci. Transl. Med.* 5:197ra104. doi: 10.1126/scitranslmed.3006258

Silva-Gómez, A. B., Aguilar-Salgado, Y., Reyes-Hernández, D. O., and Flores, G. (2013). Dexamethasone induces different morphological changes in the dorsal and ventral hippocampus of rats. *J. Chem. Neuroanat.* 47, 71–78. doi: 10.1016/j.jchemneu.2012.12.004

Son, G. H., Geum, D., Jung, H., and Kim, K. (2001). Glucocorticoid inhibits growth factor-induced differentiation of hippocampal progenitor HiB5 cells. *J. Neurochem.* 79, 1013–1021. doi: 10.1046/j.1471-4159.2001.00634.x

Sousa, N., Lukoyanov, N. V., Madeira, M. D., Almeida, O. F., and Paula-Barbosa, M. M. (2000). Reorganization of the morphology of hippocampal neurites and synapses after stress-induced damage correlates with behavioral improvement. *Neuroscience* 97, 253–266. doi: 10.1016/S0306-4522(00)00050-6

Sousa, N., Paula-Barbosa, M. M., and Almeida, O. F. (1999). Ligand and subfield specificity of corticoid-induced neuronal loss in the rat hippocampal formation. *Neuroscience* 89, 1079–1087. doi: 10.1016/S0306-4522(98)00311-X

Thorburn, G. D., Challis, J. R., and Currie, W. B. (1977). Control of parturition in domestic animals. *Biol. Reprod.* 16, 18–27. doi: 10.1095/biolreprod16.1.18

Zocchi, C., Ongini, E., Conti, A., Monopoli, A., Negretti, A., Baraldi, P. G., et al. (1996). The non-xanthine heterocyclic compound SCH 58261 is a new potent and selective A2a adenosine receptor antagonist. *J. Pharmacol. Exp. Ther.* 276, 398–404.

Conflict of Interest Statement: The authors declare that the research was conducted in the absence of any commercial or financial relationships that could be construed as a potential conflict of interest.

frontiers in Pharmacology

ORIGINAL RESEARCH
published: 16 March 2018
doi: 10.3389/fphar.2018.00152

Extracellular Guanosine 5′-Triphosphate Induces Human Muscle Satellite Cells to Release Exosomes Stuffed With Guanosine

Tiziana Pietrangelo[1†], Ester S. Di Filippo[1†], Marcello Locatelli[2], Francesco Piacenza[3], Marco Farina[4], Eleonora Pavoni[4], Andrea Di Donato[5], Denise Innosa[6], Mauro Provinciali[3] and Stefania Fulle[1]*

[1] Dipartimento Neuroscienze Imaging and Scienze Cliniche, Università degli Studi "G. d'Annunzio" Chieti-Pescara, Chieti, Italy, [2] Dipartimento di Farmacia, Università degli Studi "G. d'Annunzio" Chieti-Pescara, Chieti, Italy, [3] IRCCS-Istituto Nazionale di Riposo e Cura per Anziani, Polo Scientifico e Tecnologico, Centro di Tecnologie Avanzate nell'Invecchiamento, Ancona, Italy, [4] Dipartimento di Ingegneria dell'Informazione, Università Politecnica delle Marche, Ancona, Italy, [5] Harvard John A. Paulson School of Engineering and Applied Sciences, Harvard University, Cambridge, MA, United States, [6] Facoltà di Bioscienze e Tecnologie Agro-Alimentari e Ambientali, Università di Teramo, Teramo, Italy

OPEN ACCESS

Edited by:
Francisco Ciruela, Universitat de Barcelona, Spain

Reviewed by:
Martina Piccoli, Fondazione Città della Speranza, Italy
Wataru Aoi, Kyoto Prefectural University, Japan

***Correspondence:**
Tiziana Pietrangelo
tiziana.pietrangelo@unich.it

[†] These authors have contributed equally to this work.

Specialty section:
This article was submitted to Experimental Pharmacology and Drug Discovery, a section of the journal Frontiers in Pharmacology

Received: *14 November 2017*
Accepted: *13 February 2018*
Published: *16 March 2018*

Citation:
Pietrangelo T, Di Filippo ES, Locatelli M, Piacenza F, Farina M, Pavoni E, Di Donato A, Innosa D, Provinciali M and Fulle S (2018) Extracellular Guanosine 5′-Triphosphate Induces Human Muscle Satellite Cells to Release Exosomes Stuffed With Guanosine. Front. Pharmacol. 9:152. doi: 10.3389/fphar.2018.00152

The extracellular guanosine 5′-triphosphate, GTP, has been demonstrated to be an enhancer of myogenic cell differentiation in a murine cell line, not yet in human muscle cells. Our hypothesis was that GTP could influence also human skeletal muscle regeneration, specifically in the first phases. We tested GTP stimulus on human muscle precursor cells established in culture by human satellite cells derived from Vastus Lateralis of three young male. Our data show that extracellular GTP (a) up-regulated miRNA (specifically miR133a and miR133b) and myogenic regulator factor and (b) induces human myogenic precursor cells to release exosomes stuffed with guanosine based molecules (mainly guanosine) in the extracellular milieu. We think that probably these exosomes could be addressed to influence by means of their content (mainly guanosine) in paracrine or autocrine manner the surrounding cells and/or at distance other muscles or tissues.

Keywords: satellite cells, guanosine, guanosine 5′-triphosphate, myomiRNA, exosomes, skeletal muscle regeneration

INTRODUCTION

It has been extensively demonstrated that extracellular nucleotides are important intercellular messengers that mediate their signals through activation of P2 purinoceptors on the cell membrane (Burnstock, 2017). However, to date no indication exists about other ways of nucleotide signaling. In the last years, the communication by extracellular vesicles in muscle has received a great attention due to their importance as intercellular mediators bearing proteins, lipids, RNAs, and miRNAs through the entire body (Murphy et al., 2017). Exosomes are secreted by cells and released in the extracellular *melieu* where they could keep in contact with the surrounding cells or could be captured into the flowing blood or the lymph and addressed to the entire body. In this manner, the exosomes, and specifically their content, keep in contact different tissues influencing them as physiologycal mediators and/or pathological inductors. The adult skeletal muscle stem cells, satellite cells, provide a high degree of plasticity to muscles. During youth, the activated

satellite cells form new myofiber and make hypertrophic the existing ones; during adulthood they compensate for muscle turnover due to daily wear (Yin et al., 2013). Recently, it has been demonstrated that satellite cells are involved in the cellular turnover in response to the ingestion of protein dense foods and exercise (Burd and De Lisio, 2017). Moreover, the skeletal muscle regeneration greatly relies on the dynamic interplay between satellite cells and their cellular niche. The 3D culture model of fibers has been demonstrated to be physiologically relevant to study *in vitro* this niche and the signals present in it (Said et al., 2017; Kasper et al., 2018). The interest on studying skeletal muscle regeneration is exponentially increasing due to also its implication in nutritional aspects, exercise and healthy life. Many papers and reviews outline the role of satellite cells in muscle homeostasis during exercise stimulus or in pathological conditions, when the relative roles of intrinsic vs. extrinsic factors contribute to satellite cell dysfunction (Pietrangelo et al., 2015; Cornelison, 2018).

The pools of satellite cells are activated to proliferate under myogenic regulator factors that control both an initial boost of proliferation and differentiation. These phases influence and in turn are influenced both by myogenic regulator factors as Myogenin and by myo-microRNA, specifically miR-1, miR133a/b, and miR-206 (Drummond et al., 2011; Di Filippo et al., 2017). To date, the study of the role of nucleotide signaling in skeletal muscle regeneration is underestimated. We previously demonstrated that extracellular GTP is able to bind specific sites on plasma membrane and it participates in the early phases of myogenic differentiation process of murine C2C12 cells, modifying the plasma membrane potential toward hyperpolarized state and accelerating the proliferative boost (Pietrangelo et al., 2002, 2006a; Mancinelli et al., 2012). To date it is not known whether extracellular GTP also affects the human satellite cells in the phases of differentiation process. We therefore, hypothesize that extracellular GTP could influence the satellite stem cells via both typical signal transduction (binding on receptors) and/or by release of exosomes stuffed with guanosine based molecules.

MATERIALS AND METHODS

Cell Cultures

The Vastus Lateralis skeletal muscle biopsies were obtained by means of tiny percutaneous needle-biopsy (Pietrangelo et al., 2011).

The subjects who volunteered to have Vastus lateralis needle-biopsy to collect satellite cells provided written informed consent. The study was conducted according to the Helsinki Declaration (as amended in 2000) and approved by the Ethics Committee of the Università degli Studi "G. d'Annunzio" Chieti-Pescara, Italy (protocol no. 773 COET).

To obtain satellite sells, the skeletal muscle was processed according to the method described in Mancinelli et al. (2016). Human satellite cells were isolated from three young male volunteers (22.7 ± 2.1 years; $n = 3$), were grown as human myogenic precursor cells (MPCs) at 37°C in 5% CO_2 humidity, in Growth Medium (GM): HAM's Nutrient Mixture F10 medium (Euroclone, Milan, Italy, product #ECB7503SL) supplemented with 20% fetal bovine serum (FBS; Hyclone, Euroclone, product #SH30070.03), 100 U/ml penicillin, 100 μg/ml streptomycin, 50 μg/ml gentamycin (Euroclone, product #ECM0011B) and 1% glutamax. The MPCs were plated at a confluence of 15,000 cells/cm^2 and maintained for 2 days in Growth Medium. After 2 days in GM, the cells were cultivated with fresh GM for additional 24 h (CTR-undiff) or stimulated by addition of 500 μM GTP for the following 24 h (GTP-undiff). Differentiation was induced by replacing the GM with the Differentiation Medium (DM) on cells plated on growth condition 3 days before. The differentiating cells were regularly cultivated for 24 h (CTR-diff) or stimulated by addition of 500 μM GTP for 24 h (GTP-diff). DM is composed of DMEM high Glucose (Euroclone, product #ECB7501L) supplemented with 5% heat-inactivated Horse Serum (HS) (56°C, 30 min) (HS; Euroclone, product #ECS0091L), 50 μg/ml gentamycin (Euroclone, product #ECM0011B), 10 μg/ml insulin (Sigma–Aldrich, Milan, Italy, product #I-0516) and 100 μg/ml of apo-transferrin (Sigma–Aldrich, product #T2036).

Immunocytochemistry and Flow Cytometric Analysis

To estimate the myogenic purity of our cultures, we performed immunocytochemistry assays using Desmin as a marker. Desmin is a cytoskeletal intermediate filament protein early expressed in myogenic cell populations and not in fibroblasts. The myogenic purity of each MPC culture was estimated using Desmin antibody D33 as marker (DAKO, product #M0760). Specific antibody binding was revealed using the streptavidin biotinylated peroxidase visualization reagent (StreptABComplex DAKO). The percentage of desmin positive myoblasts was estimated as the number of positive cells vs. the total number of cells. Furthermore, human cell cultures were analyzed by flow cytometric analysis for surface myogenic markers using CD56 Mouse monoclonal antibody (Abcam, Cambridge, United Kingdom) and 5.1H11 policlonal antibody [Developmental Studies Hybridoma Bank (DSHB), Iowa City, IA, United States] (Di Filippo et al., 2016).

Gene Expression Profile

The RNA was extracted from the human MPCs in undifferentiated cells (CTR-undiff) and with GTP stimulation for 24 h (GTP-undiff), and also in differentiation medium for 24 h (CTR-diff) and with GTP stimulation 24 h (GTP-diff)

TABLE 1 | Gradient elution profile used for the four analytes.

Time (min)	Flow rate (mL/min)	%A	%B
0	1 mL/min	100	0
5		80	20
7		80	20
7.10		100	0
18		100	0

TABLE 2 | Calibration parameters for the four analytes.

Analytes	Retention times (min)	Wavelengths (nm)	LOQ (LOD) (μg/mL)	Linearity (μg/mL)	r^2
GTP	3.34 ± 0.03	256	0.1 (0.03)	0.1–5	0.9987
GDP	3.64 ± 0.05	256	0.1 (0.03)	0.1–5	0.9996
GMP	4.46 ± 0.08	256	0.1 (0.03)	0.1–5	0.9997
Guanosine	6.03 ± 0.06	259	0.1 (0.03)	0.1–5	0.9980

LOD, limit of detection; LOQ, limit of quantification.

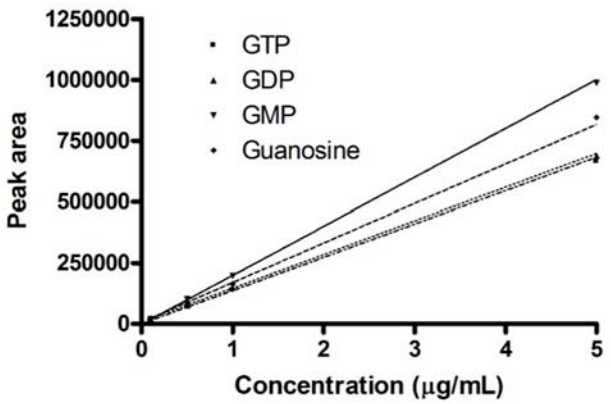

FIGURE 1 | Calibration curves. Calibration curves obtained for the four guanosine-based analytes. The graph shows the concentrations of guanosine-based molecules and the relative peak area measured on the developed HPLC procedure.

using PureLink RNA mini kit (Life Technologies). After RNA quantification using a NanoDrop^{TM} spectrophotometer, 500 ng was processed to obtain cDNA by High Capacity cDNA Reverse Transcription (#4368814; Applied Biosystems). We evaluated by quantitative real-time PCR the following genes: paired box (Pax) 7 (#4331182, Hs00242962_m1); myogenic differentiation (MyoD) 1 (#4331182, Hs00159528_m1), myogenin (#4331182, Hs 01072232GEXper-design_m1). Glyceraldehyde-3-phosphate dehydrogenase (GAPDH; #4331182, Hs99999905_m1) was used as the internal control, and the data are shown as difference in cycle threshold (ΔCt). An Applied Biosystems Prism 7900HT Sequence Detection System was used, with the Sequence Detector Software (SDS version 2.0; Applied Biosystems) (Di Filippo et al., 2017).

GTP-Dependent microRNA Expression Profile

To perform the microRNA analysis, small RNA extractions from the human MPCs in undifferentiated cells (CTR-undiff) and with GTP stimulation for 24 h (GTP-undiff), and also in differentiation medium for 24 h (CTR-diff) and with GTP stimulation 24 h (GTP-diff) was isolated using PureLink miRNA Isolation kits (Invitrogen, Life Technologies) following the manufacturer instructions and according to the procedure of Mancinelli et al. (2016). We also evaluated the following microRNA, called myomiRs: has-miR-1 (#0 02222); has-miR-206 (#00 0510); has-miR-133b (#00 2247); has-miR-16-5p (#00 0391). miR-16 was used as an internal control. The relative quantification of the miRNA targets was carried out using the ΔCt formula ($Ct_{miRNAofinterest}$ e Ct_{miR-16}), according to the Ct method.

Exosome Isolation and Purification From Cellular Media

Exosomes have been purified from both GM and DM and from media conditioned with cell culture as CTR-undiff and -diff and GTP-undiff and -diff samples following the method published by Thery et al. (2006). In detail, after a first centrifugation

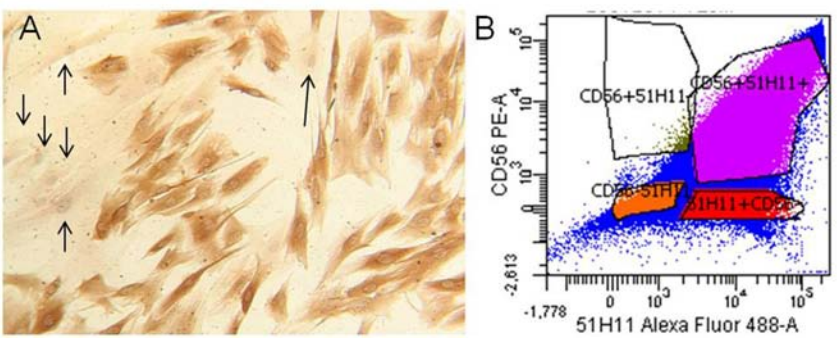

FIGURE 2 | Human myogenic precursor cells (MPCs). Human MPCs characterization. **(A)** Representative example of Desmin-positive (brown) and Desmin-negative (arrows) cells revealed by biotin-streptavidin complex method. **(B)** Representative example of flow cytometric analysis for two surface myogenic markers (CD56 and 5.1H11). In the example the percentage of CD56+/5.1H11+ cells was 75.1% and CD56–/5.1H11– cell was 11.2%.

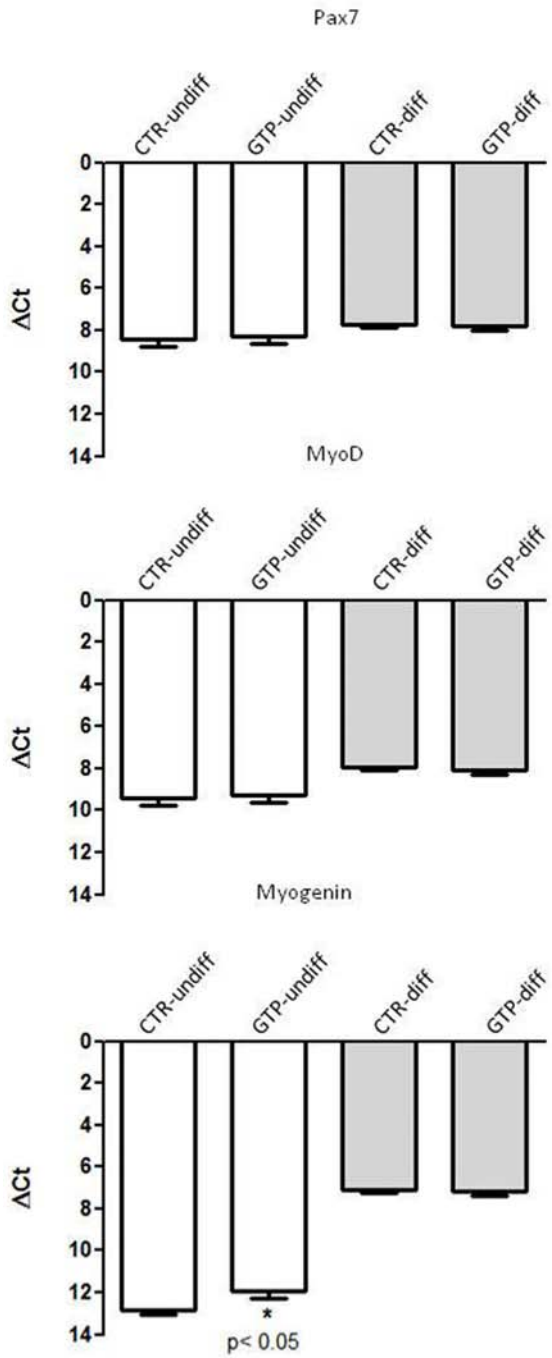

FIGURE 3 | GTP-dependent Myogenic regulator factors in human MPCs. The graphs show the relative expression of Pax7, MyoD, and Myogenin genes in undifferentiated MPCs (CTR-undiff) and with GTP stimulation (GTP-undiff) and in MPCs after 24 h of differentiation medium (CTR-diff) and with GTP stimulation (GTP-diff). The data are as mean and SD for $n = 3$ independent experiments, each performed in triplicate.

10 min at 300 *g*, 4°C to pellet cells, the conditioned-cell culture media was centrifuged 20 min at 2,000 *g*, 4°C in order to remove dead cells. The supernatant was then centrifuged 30 min at 10,000 *g*, 4°C to remove cell debris. The resulting supernatant was centrifuged 70 min at 1,00,000 *g*, 4°C to collect the pellet containing exosomes. A final step at the same speed was performed to obtain purified exosomes. The resulting pellet was resuspended in 150 μL of PBS. All the centrifugation steps were performed with the Sorvall Discovery 90SE Centrifuge.

Western Blotting for Exosome Identification

Exosomes were lysed with Exosome Resuspension Buffer (Thermo Fisher Scientific, Cat # 4478545), and denatured for 5 min at 75°C, loaded onto Bolt™ 4–12% Bis-Tris Plus Gels (invitrogen REF NW04120BOX), run at 150 V for 35 min and transferred to nitrocellulose membrane with iBlot 2 Dry Blotting System (Thermo Fisher Scientific, Cat # IB21001). Membrane was blocked 1 h at RT with 5% Skim-milk (Sigma–Aldrich) in TBS buffer supplemented with 0.1% Tween-20 (Sigma–Aldrich), the membrane was incubated overnight at 4°C with primary antibodies, as follows: CD63 (MX-49.129.5, sc-5275, Santa Cruz Biotechnology, Inc.) at 1:200, CD81 (1.3.3.22, sc-7637, Santa Cruz Biotechnology, Inc.) at 1:200. After incubation with anti-mouse IgG, HRP-linked Antibody (Cell Signaling Technology) at 1:5000 for 1 h at RT. Immunodetection was performed with the LiteAblot PLUS enhanced chemiluminiscent substrate (EuroClone). Images were taken at UVITEC machine (Cambridge).

Guanosine-Based Molecules Determination by HPLC-PDA

For the guanosine based-molecules separation was used a mobile phase composed by phosphate buffer (pH 7, concentration 40 mM) as solvent A and acetonitrile as solvent B at a flow rate of 1 mL/min. The column used for analytes resolution is the XTIMATE C18 (4.6 mm × 250 mm, 5 μm, Welch, Shanghai, China) and the system was thermostated at 25°C (±1°C). The gradient profile used to resolve the four compounds was reported in **Table 1**. The samples (20 μL) were directly injected into the HPLC-PDA system after a preliminary centrifuged at 12,000 rpm and without further pre-treatment. All the analytes were detected and quantified at their corresponding maximum wavelengths, such as 256 nm for GTP, GDP, GMP, and 259 nm for guanosine (**Table 2**).

During the method development, several parameters have been tested and optimized, such as column, mobile phase composition and temperature. The first parameter evaluated was the mobile phase composition, which was optimal when consisting of phosphate buffer (pH 7, concentration 40 mM) and acetonitrile. The column used for analytes resolution is the XTIMATE C18 (4.6 mm × 250 mm, 5 μm, Welch, Shanghai, China). Among the evaluated parameters, however, it is also necessary to remember the type of elution chosen. Firstly, was tested isocratic elution with PBS and AcN in ratio 97:3 in order to retain the more hydrophobic compounds and to reduce the total run-time. Isocratic conditions were tested in order to avoid transferability drawbacks. Unfortunately, these conditions do not

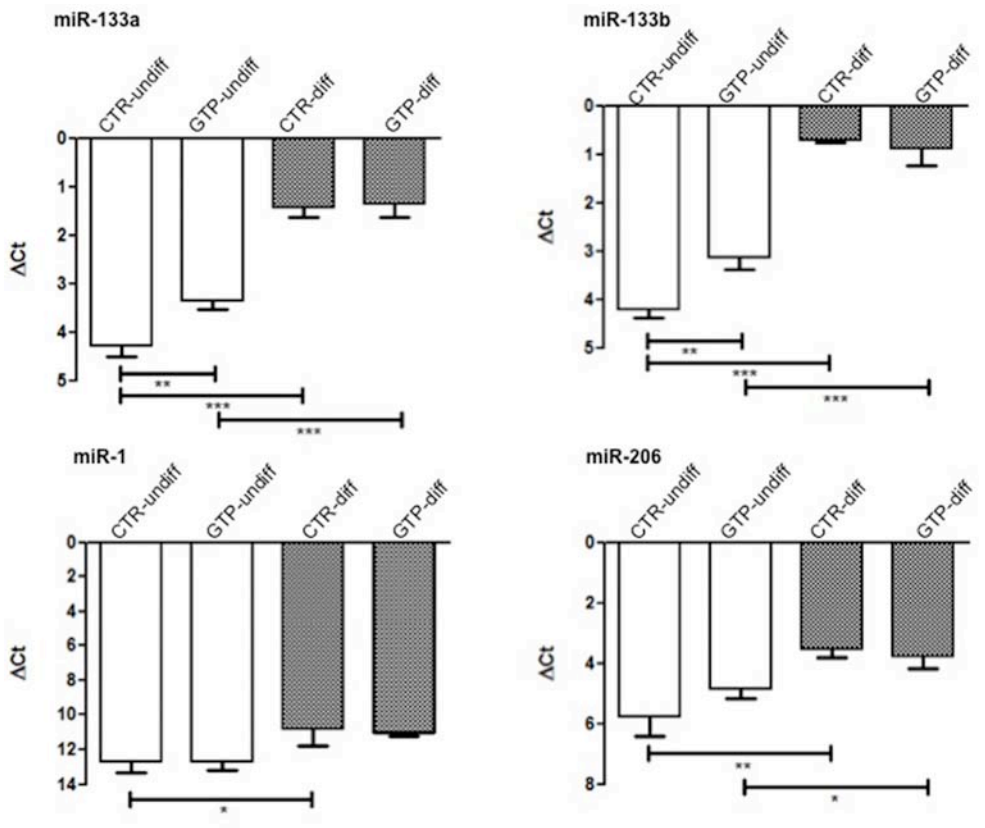

FIGURE 4 | microRNA expression profile in human MPC cells after GTP stimulation. The graphs show the relative expression of miR-133a, miR-133b, miR-1, and miR-206 both in myoblasts (CTR-undiff), in cells differentiated for 24 h in DM (CTR-diff) and in 500 μM GTP-stimulated myoblasts and differentiating cells (GTP-undiff and GTP-diff, respectively). Mean ± SD, $n = 3$ independent experiments, each performed in triplicate. *$p < 0.05$, **$p < 0.005$, ***$p < 0.0001$.

allow to fully resolving the analyte peaks and it was therefore necessary to proceed using gradient elution. Some gradient elution profiles were tested and the best conditions in terms of total run-time and peaks resolution were observed using the gradient reported in **Table 1** at 25°C.

In this range of linearity (**Figure 1**), the HPLC procedure fulfills the validation parameters as requested by International Guidelines (CDER and CVM Guidance for Industry, 2001; Taverniers et al., 2004; ICH, 2005).

Preliminary analysis of exosomes deriving from fresh media GM and DM, revealed the only presence of GDP as 0.10–0.12 ± 0.01 μg mL^{-1}.

Nanometric Scanning of Exosomes by Atomic Force Microscopy

The exosomes derived from media conditioned by MPCs in presence or not of extracellular GTP were scanned to analyze their physical properties. Experimental data were obtained using the NT-MDT Solver Pro P-47 AF. The measurements were collected in semi-contact mode by using a probe with a resonant frequency of 130 kHz and a spring constant of 4.4 N/m (HA_NC ETALON, NT-MDT). The images were obtained by plotting the error signal (mag) over 256 × 256 (x,y) positions; the mag signal is related to the oscillation amplitude of the cantilever and corresponds to the error signal of the feedback loop when working in semi-contact mode; the error signal is used for a more detailed information on the surface topography. Particle size distribution was performed with Nova Software in 1 μm × 1 μm scan area and by using a threshold of 10 nm. A statistical *t*-test has been used to evaluate the significance between the diameter distribution ($p < 0.05$).

Statistical Analysis

Data were expressed as means ± standard deviations. Statistical significance was set at $p < 0.05$ and was calculated using the unpaired Student's *t*-test. Prism5 GraphPad software (Abacus Concepts GraphPad Software, San Diego, CA, United States).

RESULTS

Human Myogenic Precursor Cells

We obtained three different human MPC culture named #1 (85.31% desmin positivity), #2 (61.6% desmin positivity), and #3 (77.8% desmin positivity). The MPC cultures were analyzed by flow cytometric analysis for surface myogenic markers using the mouse monoclonal antibody CD56 (Abcam,

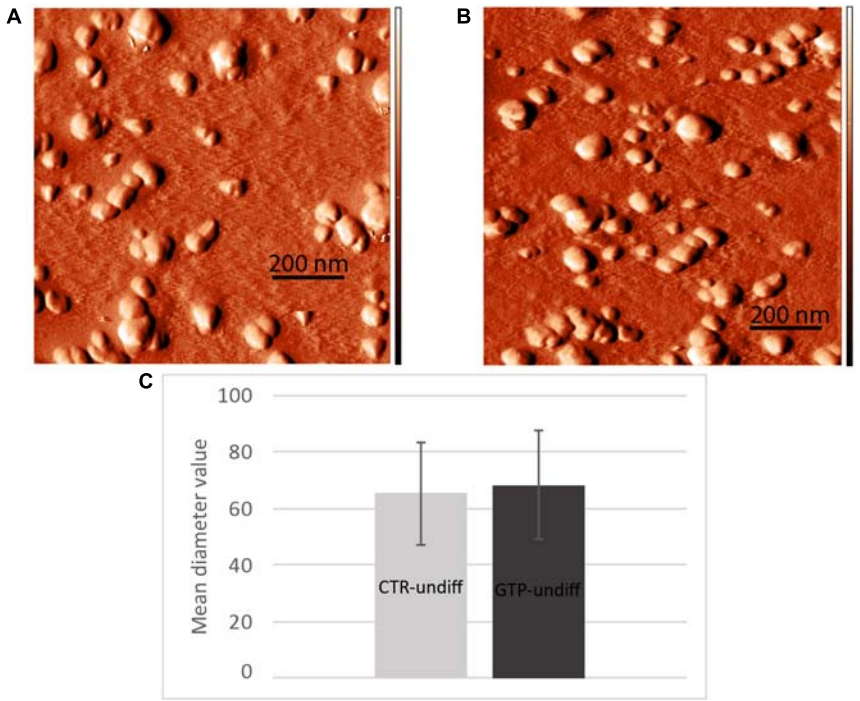

FIGURE 5 | Nanometric scanning of exosomes by atomic force microscopy. The exosomes are rounded shaped structures showing dimensions of about 60–70 nm as mean diameter. Images represent an example of exosome topography acquired in semicontact scanning. AFM error signal images obtained in semi-contact mode [scan area 1 μm × 1 μm (x,y)] of undifferentiated control (**A**, CTR-undiff) and GTP-treated (**B**, GTP-undiff) exosomes. Mean diameter particle size distribution **(C)** evaluated in 1 μm × 1 μm scan area by using a threshold of 10 nm.

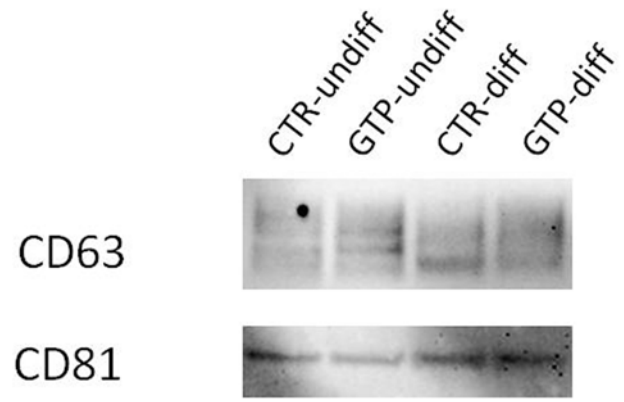

FIGURE 6 | Western blotting for exosome identification. Representative image of Western blotting analysis of CD63 and CD81 expression on exosomes obtained by cell culture media named CTR-undiff and CTR–diff and GTP-undiff and GTP-diff samples. The image showed the presence of these proteins in the exosome samples we isolated by ultracentrifugation (see section "Materials and Methods").

Cambridge, United Kingdom) and policlonal antibody 5.1H11 [Developmental Studies Hybridoma Bank (DSHB), Iowa City, IA, United States] to confirm the percentage of myogenicity. The percentage of $CD56^{+}/5.1H11^{+}$ cells was 75.1% and those $CD56^{-}/5.1H11^{-}$ was 11.2% (**Figure 2**).

Quantitative Gene Expression RT-PCR on Myogenic Regulatory Factors

The most important myogenic regulatory factors such as Pax7, MyoD, and Myogenin were assessed in our samples in order to investigate their involvement with GTP stimulation. Pax7 and MyoD1 did not change their expression in our samples, neither with respect to undifferentiated and 24-h differentiation (**Figure 3**). Myogenin was up-regulated after 24 h of differentiation stimulation both in CTR-diff and GTP-diff compared to CTR-undiff and GTP-undiff. Strikingly, we found Myogenin up-regulated after 24 h of 500 μM GTP stimulation in growth medium (GTP-undiff compared to CTR-undiff), but no differences were found in 24-h differentiated samples between CTR-diff and GTP-diff (**Figure 3**).

GTP-Induced microRNA Modulation

miR-133a and miR-133b were significantly up-regulated after 24 h of 500 μM GTP stimulation of myoblasts (GTP-undiff) compared to control (CTR-undiff). Furthermore, these microRNAs were found highly up-regulated in differentiation media both in CTR-diff and in GTP-diff. Also miR-1, that in myoblasts (CTR-undiff; GTP-undiff) does not change its expression, in differentiative condition, was slightly up-regulated both on CTR-diff and GTP-diff both at the same extent. Similarly, miR-206 was significant up-regulated after 24 h of differentiation stimulation both CTR-diff and

GTP-diff compared to CTR-undiff and GTP-undiff, but no differences were found between CTR-diff and GTP-diff (**Figure 4**).

Nanometric Scanning of Exosomes by Atomic Force Microscopy

The images obtained by AFM (**Figures 5A,B**) show the typical round-shaped structure of exosomes with diameter values ranging between 30 and 100 nm. Specifically, the diameter values were 65 ± 18 and 68 ± 19 nm for CTR-undiff and GTP-undiff exosomes, respectively (**Figure 5C**). Both samples, control and GTP-treated exosomes, were analyzed in terms of diameter distribution and as can be seen from the images, the exosomes were not found to be significantly different ($p < 0.05$).

Western Blotting for Exosome Identification

The western blot analysis using antibodies CD63 and CD81 (specifically expressed on exosomes), revealed the presence of these proteins on our isolated nanovesicles (**Figure 6**).

HPLC-PDA Guanosine-Based Molecules Determination Into Exosomes

The exosomes obtained by both simple and cell-conditioned media with and without GTP were analyzed to detect guanosine-based molecules. The herein reported HPLC-PDA method allows quantify simultaneously the four guanosine-based molecules in exosomes extracted from culture media. The gradient elution allows separate and analyze these compounds better than isocratic condition, within an overall runtime of 18 min. The quantitative data are reported in **Table 3**.

DISCUSSION AND CONCLUSION

We previously demonstrated that extracellular GTP binds its specific binding site on C2C12 myoblasts and triggers specific signal transduction that lead the myoblasts to increase the intracellular calcium and to hyperpolarize the plasma membrane (Pietrangelo et al., 2006a). However, GTP works also as intracellular signal, it triggers molecules for the G-coupled receptor signaling or its de-phosphorylation is instrumental for effector enzyme activation. In addition, GTP shows inhibitory effect at uncoupling proteins of the mitochondrial anion carrier protein family (Woyda-Ploszczyca and Jarmuszkiewicz, 2017). Low mitochondrial potential increases the inhibitory effect of GTP. In particular, GTP–GDP inhibits the proton leak mediated by these carriers across the inner mitochondrial membrane in lizard skeletal muscle mitochondria (Rey et al., 2008). In the cytoplasm GTP is present at mM level but also externally its effective concentration is in the order of 100s of micromolar (Azzu and Brand, 2010). Moreover, the cells are able to phosphorylate guanosine molecule to obtain GMP, GDP, and GTP and in turn they could be released. However, in the extracellular space, the ectonucleotidase binds and hydrolyze the GTP to GDP, GMP, and guanosine (Kovács et al., 2011). In this scenario, it is difficult to understand how guanosine-based molecules and particularly GTP could be secreted in the extracellular space and directed toward cell target, escaping the ectonucleotide degradation. The exosomes are small vesicles that protect and carry molecules to specific target. Our hypothesis that the GTP-incubated cells could produce some categories of exosomes stuffed with guanosine-based purines has been verified because we found mainly guanosine in the exosomes, but also GTP, GDP, and GMP even if in few samples. Specifically, the human MPCs that we stimulated with 500 μM extracellular GTP for 24 h, both in proliferative and differentiative conditions,

TABLE 3 | Concentration of guanosine-based molecules contained into exosome samples deriving from three different MPC culture of young subjects.

Samples	Concentration (μg mL^{-1})			
	GTP	GDP	GMP	Guanosine
#1 Exosomes from CTR-undiff	nd	nd	nd	nd
#1 Exosomes from CTR-diff	nd	nd	nd	nd
#1 Exosomes from GTP-undiff	nd	0.10 ± 0.01	nd	1.70 ± 0.18
#1 Exosomes from GTP-diff	nd	0.36 ± 0.04	nd	2.52 ± 0.25
#2 Exosomes from CTR-undiff	nd	nd	nd	nd
#2 Exosomes from CTR-diff	nd	nd	nd	nd
#2 Exosomes from GTP-undiff	nd	nd	0.15 ± 0.02	4.17 ± 0.35
#2 Exosomes from GTP-diff	0.33 ± 0.03	0.19 ± 0.01	nd	0.20 ± 0.02
#3 Exosomes from CTR-undiff	nd	nd	nd	nd
#3 Exosomes from CTR-diff	nd	nd	nd	nd
#3 Exosomes from GTP-undiff	nd	nd	nd	1.51 ± 0.12
#3 Exosomes from GTP-diff	0.16 ± 0.02	0.17 ± 0.02	nd	0.70 ± 0.05

nd, not detected. #1, #2, #3 three different young volunteers from whom we obtained myogenic precursor cells. CTR-undiff = the exosomes obtained from the medium conditioned with the human MPC cells in proliferative state for3 days in GM. CTR-diff = the exosomes obtained from the medium conditioned with the human MPC cells in differentiative state for 24 h. GTP-undiff = the exosomes obtained from the medium conditioned with the human MPC cells in proliferative state for additional 24 h after 2 days of regular cultivation in GM. GTP-diff = the exosomes obtained from the medium conditioned with the human MPC cells in differentiative state in presence of 500 μM extracellular GTP for 24 h.

secreted exosomes stuffed with guanosine in the range of 1.51–4.17 and 0.2–2.5 $\mu g\ mL^{-1}$, respectively. This result suggests that extracellular GTP influences skeletal muscle exosome release in order to direct guanosine molecules via exosomes as both paracrine and endocrine transmission in the body. We think that these exosomes containing guanosine could influence surrounding cells in the niche of regenerating skeletal muscle and in addition could spread out in all other muscles of the body and other tissue via blood and/or lymphatic fluxes. The scenario we envisioned if that the extracellular free GTP could derive from a damaged skeletal fiber after injury or after vigorous muscle contractions following specific training and/or could be released physiologically during muscle growth. The extracellular free GTP stimulus in a specific fiber, could influence the entire skeletal tissue on the same muscle (Vastus Lateralis, for instance) or other skeletal muscles in the body via exosomes stuffed with guanosine, probably in a different manner with respect to the typical binding of ligand on a receptor. In our previous paper (Pietrangelo et al., 2006a) we demonstrated a specific free GTP effect in the first stage (the proliferative phase of myogenesis) of murine skeletal muscle regeneration. Here, we confirm that free GTP stimulates human MPCs in the proliferative boost phase of differentiation. In fact, extracellular GTP up-regulated the miR-133a and miR133b expression. These myo-miRNA are specifically linked to myogenic proliferation (La Rovere et al., 2014). The enhancer toward the differentiation process mediated by free extracellular GTP is confirmed by Myogenin gene upregulation during proliferation state. These results are in concordance with the fact that the pool of satellite cells is activated to proliferate under myogenic regulator factors that control both an initial boost of proliferation and a push of differentiation (Ceafalan et al., 2014). In conclusion, we think that free extracellular GTP elicited two effects: miRNA-myogenic regulator factor modulation and exosome stuffed with guanosine and guanosine-based molecules secretion. We think that these effects are sequential, in the sense that free GTP immediately influence MPC proliferation-differentiation step and in turn after 24 h induces secretion of exosomes contained-guanosine both in proliferative and differentiative conditions.

At the current state of the study, we do not have evidence for saying that exosome contained-guanosine based molecules could influence regeneration or differentiation. What we can hypothesize for future study is that these exosome stuffed with guanosine and guanosine based molecules (GMP, GDP, GTP) could be transferred into other tissues as neuronal and glial ones where exert specific effects (Gysbers et al., 2000; Pietrangelo et al., 2006b; Guarnieri et al., 2009; Giuliani et al., 2012, 2015; Mancinelli et al., 2014).

AUTHOR CONTRIBUTIONS

All authors listed have made a substantial, direct and intellectual contribution to the work, and approved it for publication.

FUNDING

This study was funded by Università degli Studi "G. d'Annunzio" Chieti-Pescara (2012N8YJC3_003 PRIN) to TP.

ACKNOWLEDGMENTS

The authors would like to thank Dr. Elisa De Luca for her kindly collaboration during the first steps of this project. They also thank Dr. Tereza Jandova for English language revision.

REFERENCES

Azzu, V., and Brand, M. D. (2010). The on-off switches of the mitochondrial uncoupling proteins. *Trends Biochem. Sci.* 35, 298–307. doi: 10.1016/j.tibs.2009.11.001

Burd, N. A., and De Lisio, M. (2017). Skeletal muscle remodeling: interconnections between stem cells and protein turnover. *Exerc. Sport Sci. Rev.* 45, 187–191. doi: 10.1249/JES.0000000000000117

Burnstock, G. (2017). Purinergic signalling: therapeutic developments. *Front. Pharmacol.* 8:661. doi: 10.3389/fphar.2017.00661

CDER and CVM Guidance for Industry (2001). *Bioanalytical Method Validation*. Silver Spring, MD: Food and Drug Administration.

Ceafalan, C. L., Popescu, B. O., and Hinescu, M. E. (2014). Cellular players in skeletal muscle regeneration. *Biomed Res. Int.* 2014:957014. doi: 10.1155/2014/957014

Cornelison, D. (2018). "Known unknowns": current questions in muscle satellite cell biology. *Curr. Top. Dev. Biol.* 126, 205–233. doi: 10.1016/bs.ctdb.2017.08.006

Di Filippo, E. S., Mancinelli, R., Marrone, M., Doria, C., Verratti, V., Toniolo, L., et al. (2017). Neuromuscular electrical stimulation improves skeletal muscle regeneration through satellite cell fusion with myofibers in healthy elderly subjects. *J. Appl. Physiol.* 123, 501–512. doi: 10.1152/japplphysiol.00855.201

Di Filippo, E. S., Mancinelli, R., Pietrangelo, T., La Rovere, R. M., Quattrocelli, M., Sampaolesi, M., et al. (2016). Myomir dysregulation and reactive oxygen species in aged human satellite cells. *Biochem. Biophys. Res. Commun.* 473, 462–470. doi: 10.1016/j.bbrc.2016.03.030

Drummond, M. J., McCarthy, J. J., Sinha, M., Spratt, H. M., Volpi, E., Esser, K. A., et al. (2011). Aging and microRNA expression in human skeletal muscle: a microarray and bioinformatics analysis. *Physiol. Genomics* 43, 595–603. doi: 10.1152/physiolgenomics.00148.2010

Giuliani, P., Ballerini, P., Buccella, S., Ciccarelli, R., Rathbone, M. P., Romano, S., et al. (2015). Guanosine protects glial cells against 6-hydroxydopamine toxicuity. *Adv. Exp. Med. Biol.* 837, 23–33. doi: 10.1007/5584_2014_73

Giuliani, P., Romano, S., Ballerini, P., Ciccarelli, R., Petragnani, N., Cicchitti, S., et al. (2012). Protective activity of guanosine in an in vitro model of parkinson's disease. *Panminerva Med.* 54(1 Suppl. 4), 43–51.

Guarnieri, S., Pilla, R., Morabito, C., Sacchetti, S., Mancinelli, R., Fanò, G., et al. (2009). Extracellular guanosine and GTP promote expression of differentiation markers and induce S-phase cell-cycle arrest in human SH-SY5Y neuroblastoma cells. *Int. J. Dev. Neurosci.* 27, 135–147. doi: 10.1016/j.ijdevneu.2008.11.007

Gysbers, J. W., Guarnieri, S., MariggioÌ, M. A., Pietrangelo, T., FanoÌ, G., and Rathbone, M. P. (2000). Extracellular guanosine 5′-triphosphate enhances nerve-growth-factor-induced neurite outgrowth via increases in intracellular calcium. *Neuroscience* 96, 817–824. doi: 10.1016/S0306-4522(99)00588-6

ICH (2005). *International Conference on Harmonisation of Technical Requirements for Registration of Pharmaceuticals for Human Use*. Geneva: ICH.

Kasper, A. M., Turner, D. C., Martin, N. R. W., and Sharples, A. P. (2018). Mimicking exercise in three-dimensional bioengineered skeletal muscle to

investigate cellular and molecular mechanisms of physiological adaptation. *J. Cell. Physiol.* 233, 1985–1998. doi: 10.1002/jcp.25840

Kovács, Z., Juhász, G., Palkovits, M., Dobolyi, A., and Kékesi, K. A. (2011). Area, age and gender dependence of the nucleoside system in the brain: a review of current literature. *Curr. Top. Med. Chem.* 11, 1012–1033. doi: 10.2174/156802611795347636

La Rovere, R. M., Quattrocelli, M., Pietrangelo, T., Di Filippo, E. S., Maccatrozzo, L., Cassano, M., et al. (2014). Myogenic potential of canine craniofacial satellite cells. *Front. Aging Neurosci.* 6:90. doi: 10.3389/fnagi.2014.00090

Mancinelli, R., Di Filippo, E. S., Verratti, V., Fulle, S., Toniolo, L., Reggiani, C., et al. (2016). The regenerative potential of female skeletal muscle upon hypobaric hypoxic exposure. *Front. Physiol.* 7:303. doi: 10.3389/fphys.2016.00303

Mancinelli, R., La Rovere, R. M., Fulle, S., Miscia, S., Marchisio, M., Pierdomenico, L., et al. (2014). Extracellular GTP is a potent water-transport regulator via aquaporin 5 plasma-membrane insertion in M1-CCD epithelial cortical collecting duct cells. *Cell Physiol. Biochem.* 33, 731–746. doi: 10.1159/000358648

Mancinelli, R., Pietrangelo, T., Burnstock, G., Fanò, G., and Fulle, S. (2012). Transcriptional profile of GTP-mediated differentiation of C2C12 skeletal muscle cells. *Purinergic Signal.* 8, 207–221. doi: 10.1007/s11302-011-9266-3

Murphy, C., Withrow, J., Hunter, M., Liu, Y., Tang, Y. L., Fulzele, S., et al. (2017). Emerging role of extracellular vesicles in musculoskeletal diseases. *Mol. Aspects Med.* doi: 10.1016/j.mam.2017.09.006 [Epub ahead of print].

Pietrangelo, T., D'Amelio, L., Doria, C., Mancinelli, R., Fulle, S., and Fano, G. (2011). Tiny percutaneous needle biopsy: an efficient method for studying cellular and molecular aspects of skeletal muscle in humans. *Int. J. Mol. Med.* 27, 361–367. doi: 10.3892/ijmm.2010.582

Pietrangelo, T., Di Filippo, E. S., Mancinelli, R., Doria, C., Rotini, A., Fanò-Illic, G., et al. (2015). Low intensity exercise training improves skeletal muscle regeneration potential. *Front. Physiol.* 6:399. doi: 10.3389/fphys.2015.00399

Pietrangelo, T., Fioretti, B., Mancinelli, R., Catacuzzeno, L., Franciolini, F., FanoÌ, G., et al. (2006a). Extracellular guanosine 5′-triphosphate modulates myogenesis via intermediate Ca2+-activated K+ currents in C2C12 mouse cells. *J Physiol.* 572, 721–733.

Pietrangelo, T., Guarnieri, S., Fulle, S., Fanò, G., and Mariggiò, M. A. (2006b). Signal transduction events induced by extracellular guanosine 5′ triphosphate in excitable cells. *Purinergic Signal.* 2, 633–636. doi: 10.1007/s11302-006-9021-3

Pietrangelo, T., MariggioÌ, M. A., Lorenzon, P., Fulle, S., Protasi, F., Rathbone, M., et al. (2002). Characterization of specific GTP binding sites in C2C12 mouse skeletal muscle cells. *J. Muscle Res. Cell Motil.* 23, 107–118. doi: 10.1023/A:1020288117082

Rey, B., Sibille, B., Romestaing, C., Belouze, M., Letexier, D., Servais, S., et al. (2008). Reptilian uncoupling protein: functionality and expression in sub-zero temperatures. *J. Exp. Biol.* 211(Pt 9), 1456–1462. doi: 10.1242/jeb.012328

Said, S. R., Mustafa, A. G., Asfour, H. A., and Shaqoura, E. I. (2017). Myogenic satellite cells: biological milieu and possible clinical applications. *Pak. J. Biol. Sci.* 20, 1–11. doi: 10.3923/pjbs.2017.1.11

Taverniers, E., Van Bockstaele, M., and De Loose, M. (2004). Trends in quality in the analytical laboratory. II. Analytical method validation and quality assurance. *Trend Anal. Chem.* 23, 535–552. doi: 10.1016/j.trac.2004.04.001

Thery, C., Clayton, A., Amigorena, S., and Raposo, G. (2006). Isolation and characterization of exosomes from cell culture supernatants and biological fluids. *Curr. Protoc. Cell Biol.* 30, 3.22.1–3.22.29. doi: 10.1002/0471143030.cb0322s30

Woyda-Ploszczyca, A. M., and Jarmuszkiewicz, W. (2017). The conserved regulation of mitochondrial uncoupling proteins: from unicellular eukaryotes to mammals. *Biochim. Biophys. Acta* 1858, 21–33.

Yin, H., Price, F., and Rudnicki, M. A. (2013). Satellite cells and the muscle stem cell niche. *Physiol. Rev.* 93, 23–67. doi: 10.1152/physrev.00043.2011

Conflict of Interest Statement: The authors declare that the research was conducted in the absence of any commercial or financial relationships that could be construed as a potential conflict of interest.

frontiers in Pharmacology

MINI REVIEW
published: 14 March 2018
doi: 10.3389/fphar.2018.00212

Purinergic Ligands as Potential Therapeutic Tools for the Treatment of Inflammation-Related Intestinal Diseases

*Diego Dal Ben[1], Luca Antonioli[2], Catia Lambertucci[1], Matteo Fornai[2], Corrado Blandizzi[2] and Rosaria Volpini[1]**

[1] Medicinal Chemistry Unit, School of Pharmacy, University of Camerino, Camerino, Italy, [2] Department of Clinical and Experimental Medicine, University of Pisa, Pisa, Italy

Inflammation-related intestinal diseases are a set of various conditions presenting an overactive enteric immune system. A continuous overproduction of pro-inflammatory cytokines and a decreased production of anti-inflammatory modulators are generally observed, while morpho-functional alterations of the enteric nervous system lead to intestinal secretory and motor dysfunctions. The factors at the basis of these conditions are still to be totally identified and current therapeutic strategies are aimed only at achieving and maintaining remission states, by using therapeutic tools like aminosalicylates, corticosteroids, immunomodulators, biological drugs (i.e., monoclonal antibodies), and eventually surgery. Recent reports described a key role of purinergic mediators (i.e., adenosine and its nucleotides ATP and ADP) in the regulation of the activity of immune cells and enteric nervous system, showing also that alterations of the purinergic signaling are linked to pathological conditions of the intestinal tract. These data prompted to a series of investigations to test the therapeutic potential for inflammation-related intestinal conditions of compounds able to restore or modulate an altered purinergic signaling within the gut. This review provides an overview on these investigations, describing the results of preclinical and/or clinical evaluation of compounds able to stimulate or inhibit specific P2 (i.e., P2X7) or P1 (i.e., A_{2A} or A_3) receptor signaling and to modify the adenosine levels through the modulation of enzymes activity (i.e., Adenosine Deaminase) or nucleoside transporters. Recent developments in the field are also reported and the most promising purine-based therapeutic strategies for the treatment of inflammation-related gastrointestinal disorders are schematically summarized.

Keywords: inflammation, intestinal diseases, intestinal immune system, modulators, purinergic receptors, purinergic ligands, adenosine, therapeutic tools

OPEN ACCESS

Edited by:
Kenneth A. Jacobson, National Institutes of Health (NIH), United States

Reviewed by:
Rodrigo A. Cunha, University of Coimbra, Portugal
Eberhard Weihe, Philipps University of Marburg, Germany

****Correspondence:***
Rosaria Volpini
rosaria.volpini@unicam.it

Specialty section:
This article was submitted to Experimental Pharmacology and Drug Discovery, a section of the journal Frontiers in Pharmacology

Received: *16 October 2017*
Accepted: *26 February 2018*
Published: *14 March 2018*

Citation:
Dal Ben D, Antonioli L, Lambertucci C, Fornai M, Blandizzi C and Volpini R (2018) Purinergic Ligands as Potential Therapeutic Tools for the Treatment of Inflammation-Related Intestinal Diseases. Front. Pharmacol. 9:212. doi: 10.3389/fphar.2018.00212

INTRODUCTION

Inflammatory bowel diseases (IBDs) comprise Crohn's disease and ulcerative colitis and are conditions presenting an overactive intestinal immune system. The exact etiology of these diseases is still unclear but may be related to genetic predisposition or environmental factors and is characterized by an inappropriate immune response taking to morpho-functional alterations of

the host's enteric nervous system and intestinal secretory and motor dysfunctions. A loss of balance between the production of pro-inflammatory cytokines and anti-inflammatory mediators has been observed. Current therapeutic strategies are based on anti-inflammatory agents and targeted to achieve and maintain the remission state.

It is well established that during inflammation ATP is extracellularly released, a process involving pannexins or connexins and promoted by various stimuli (Eltzschig et al., 2012; Idzko et al., 2014). Extracellular ATP (eATP) is then degraded to adenosine by the ectonucleotidases CD39 and CD73 (Allard et al., 2017). While eATP generally plays a pro-inflammatory role through the activation of P2 (P2X and P2Y) purinergic receptors, the ATP degradation to adenosine usually represents a stop-signal for the inflammation process, with adenosine playing as anti-inflammatory agent through the activation of its P1 receptor targets. Adenosine is then removed from the extracellular environment by nucleoside transporters and/or metabolic enzymes.

Over the years increasing evidences pointed out a critical involvement of the purinergic system in the pathophysiology of IBDs, thus spurring the research toward the evaluation of the potential therapeutic benefits in terms of anti-inflammatory activity, arising by pharmacological targeting of purinergic pathways (Hasko and Cronstein, 2004; Hasko and Pacher, 2008; Hasko et al., 2008; Burnstock, 2011, 2014; Burnstock et al., 2017). Furthermore, the involvement of ATP in the enteric motor dysfunctions associated with bowel inflammation is a hot topic deserving further investigations.

P2 PURINERGIC RECEPTORS

P2X Purinergic Receptors

P2X receptors are ligand-gated ion channels activated by eATP and permeable to Na^+, K^+, and Ca^{2+} (North and Jarvis, 2013; North, 2016). Seven P2X subtypes are known that may assemble as homo- or heterotrimers. Upon prolonged stimulation, some subtypes like the P2X7R undergo a rearrangement with the formation of a pore permeable to large molecules.

P2XR modulators are of great interest for several potential therapeutic applications, like treatment of pain, cough, cancer, and inflammation-related diseases (Burnstock and Kennedy, 2011; Syed and Kennedy, 2012; Muller, 2015). P2XR agonists are ATP derivatives obtained by modification of the purine base (i.e., 2-meSATP), the ribose ring (i.e., BzATP), or the polyphosphate chain (like the stable analogs αβ-meATP, βγ-meATP, and ATPγS) (Coddou et al., 2011; Dal Ben et al., 2015; Lambertucci et al., 2015).

P2XR antagonists are generally negatively charged molecules like TNP-ATP (Virginio et al., 1998) and analogs (Dal Ben et al., 2017), the irreversible inhibitor oxidized ATP (o-ATP) (Murgia et al., 1993), the P2X3R antagonist A-317491, and the polyanion suramin and its derivatives. Further classes of P2XR inhibitors are uncharged molecules based on heterocyclic scaffolds and behaving as non-competitive (allosteric) antagonists (Muller, 2015). A relevant number of structural classes of compounds were developed as P2X7R inhibitors (Park and Kim, 2017) given the key role of this receptor in pain and inflammation-related conditions (Arulkumaran et al., 2011; Gulbransen et al., 2012; De Marchi et al., 2016; Burnstock and Knight, 2017; Di Virgilio et al., 2017). P2X7R-targeting compounds have been developed also as radiolabeled molecules to be used as pharmacological tools or markers (Donnelly-Roberts et al., 2009; Lord et al., 2015; Fantoni et al., 2017; Territo et al., 2017; Jin et al., 2018).

The potent, selective, and orally bioavailable P2X7R antagonist AZD9056 was studied in phase-two clinical trials for the treatment of rheumatoid arthritis (RA) and chronic obstructive pulmonary disease (COPD) showing to be well tolerated (2005-004110-32_Clinical_Trial_Results, 2005; Keystone et al., 2012). The efficacy and safety of AZD9056 was also clinically assessed in the management of patients affected by moderate/severe Crohn's disease. Although the lack in change of inflammatory parameters, this study demonstrated that AZD9056 has the potential to improve symptoms, in particular abdominal pain, in patients with IBDs (Eser et al., 2015). Other P2X7R antagonists (CE-224,535 and GSK1482160) were studied in clinical trials for RA and inflammatory pain conditions or showed (JNJ47965567) ability to enter the CNS.

In a rat model of trinitrobenzene sulfonic acid (TNBS) colitis, the administration of the P2X7R inhibitor A740003 determined a reduction of T-cell and macrophage infiltration in the lamina propria, followed by a reduction in tissue TNF and IL-1β concentrations, with a consequent amelioration of inflammation severity (Marques et al., 2014). In parallel, Neves et al. (2014) reported that mice lacking P2X7Rs and subjected to TNBS or dextran sulfate sodium (DSS) treatment failed to develop intestinal inflammation or other symptoms associated with colitis, thus indicating a protective role resulting from P2X7R blockade. In the same study, by exploring the expression of this receptor subtype in colonic mucosa of IBD patients, the authors observed high P2X7R levels in inflamed epithelium and lamina propria, where it colocalizes more with dendritic cells and macrophages, leading to hypothesize a role of P2X7R signaling in the pathogenesis of IBDs. Furthermore, Cesaro et al. (2010) pointed out the pivotal role of P2X7R in the complex cross-talk occurring between intestinal epithelial cells and immune cells. The pharmacological stimulation of P2X7R in a human colonic epithelial cell monolayer induced caspase-1 activation and IL-1β release, pro-inflammatory mediators critically involved in the recruitment of polymorphonuclear leukocytes within the intestinal mucosa in the presence of inflammation. Subsequently, several preclinical studies performed in animal models of colitis revealed a significant role of P2X7R in the pathophysiology of intestinal inflammation (Marques et al., 2014; Neves et al., 2014; Wan et al., 2016). Increasing efforts have been made to investigate the involvement of purinergic pathways in the pathophysiology of enteric motor dysfunction typically observed in the presence of intestinal inflammation, although the available data are fragmentary (Antonioli et al., 2013). Recently, Antonioli et al. (2014b) provided evidence about a marked increase in P2X7R immunostaining, and an enhanced modulating action of these receptors on colonic neuromotility in a rat model of DNBS-induced colitis.

Beside the importance of the P2X7R in the gastrointestinal diseases described in literature, recent papers suggest that even other P2X subtypes could play a relevant role the gastrointestinal pathophysiology (Paulino et al., 2011; Weng et al., 2015; Guo et al., 2016). Antagonists of the P2X3R showed promising activity in alleviating inflammatory and neuropathic pain in preclinical studies. A-317491 reduced visceral hypersensitivity in an experimental model of colitis, suggesting P2X3R as target for the treatment of inflammation-related abdominal pain syndromes (Deiteren et al., 2015).

P2Y Purinergic Receptors

P2Y receptors are G protein-coupled receptors of which eight subtypes ($P2Y_1$, $P2Y_2$, $P2Y_4$, $P2Y_6$, and $P2Y_{11-14}$) are currently known. The endogenous agonists of these receptors are ATP, ADP, UTP, UDP, and UDP-glucose, with each P2Y subtype presenting peculiar pharmacological properties and preference for di- or triphosphate nucleotides (Jacobson and Muller, 2016). P2YRs are widely expressed in the body and involved in several biological functions. Beside the well-known inhibition of platelet aggregation, for which $P2Y_{12}R$ modulators like Clopidogrel, Prasugrel, Cangrelor, and Ticagrelor are approved for human use, P2YRs play important roles in neurotransmission and modulation of immune system (Le Duc et al., 2017).

P2YR ligands were developed by modification of endogenous ligands at the base (i.e., 2-thioUTP or 2-MeSATP), the sugar (i.e., MRS2365), or the phosphate chain (i.e., PSB1114) (von Kugelgen, 2006; Jacobson et al., 2012; Conroy et al., 2016; Jacobson and Muller, 2016). Dinucleoside derivatives are also ligands of the P2YRs. Diquafosol (approved in Japan for the treatment of Dry Eye disorder) and Denufosol (clinically evaluated for bronchial indication in cystic fibrosis) are representative compounds of this category and are endowed with dual $P2Y_2/P2Y_4$ receptor agonist profile. Suramin-based compounds are also P2YR modulators. Yet, several P2YR ligands belong to other structural classes not necessarily containing negatively charged functions (Conroy et al., 2016).

Considering the role of the $P2Y_2$, $P2Y_6$, and $P2Y_{12}$ receptors in the inflammation-related conditions, compounds acting on these P2Y subtypes have been evaluated in such frames. $P2Y_{12}R$ antagonists present interesting potential to prevent a chronic inflammation promoted by this protein and to modulate the inflammatory pain (Thomas and Storey, 2015; Beko et al., 2017). Focusing on the bowel-related conditions, Grbic et al. (2008), investigating the role of ATP receptors in the pathogenesis of intestinal inflammation, reported that the pro-inflammatory cytokines TNF-α or IFN-γ determined an increased expression of $P2Y_2$ and $P2Y_6$ receptors in the colonic mucosa of mice with DSS colitis (Grbic et al., 2008; Degagne et al., 2013). Noteworthy, the pharmacological activation of $P2Y_2R$ via 2-thioUTP in a mouse model of DSS-induced colitis reduced the disease activity index and histological score values as well as a decrease in bacterial translocation to the spleen when compared with untreated mice, thus highlighting a protective role of $P2Y_2R$ in sustaining the remission phase in this experimental model of colitis (Degagne et al., 2013). By contrast, stimulation of the $P2Y_6R$ led to the activation of calcium-independent PKCδ upstream of ERK1/2, followed by the stimulation of c-fos phosphorylation and the recruitment of c-fos/c-jun dimers at level of the AP-1 motif located within the core promoter region of IL-8 gene, thus determining an increase of IL-8 release (Grbic et al., 2012). Despite these encouraging results, further investigations are needed to evaluate the putative beneficial effect of $P2Y_2$ and $P2Y_6$ receptor ligands in counteracting intestinal inflammation.

Considering the enteric motor dysfunction associated to intestinal inflammation, interesting findings were provided about the involvement of $P2Y_1R$ in the regulation of colonic neuromuscular activity in a model of TNBS-induced colitis in guinea-pig (Strong et al., 2010). Inflamed colonic specimens displayed a marked decrease in the fecal pellet output and a significant reduction of inhibitory junction potential (IJP). Of note, the pharmacological analysis of the determinant of IJP revealed that the purinergic component, mediated by $P2Y_1R$, was impaired, despite immunohistochemical assays did not display significant alterations of nerve fiber density in circular muscle strips from animals with colitis (Strong et al., 2010).

P1 ADENOSINE RECEPTORS

Adenosine Receptors (P1 receptors or ARs) are G protein-coupled receptors known as four subtypes (A_1AR, $A_{2A}AR$, $A_{2B}AR$, and A_3AR). Like the other Purinergic Receptors, ARs are widely expressed in the body and regulate many physiological functions. The endogenous ligand adenosine has a short half-life as it is internalized by nucleoside transporters and/or quickly modified to inosine by Adenosine Deaminase (ADA) or to AMP by Adenosine Kinase (ADK).

Medicinal chemistry efforts were aimed at developing compounds presenting higher metabolic stability and improved potency and selectivity compared to the endogenous ligand (Cristalli and Volpini, 2003; Jacobson and Gao, 2006; Wilson and Mustafa, 2009; Ciruela, 2011). A key modification of adenosine is the introduction of a *N*-alkyl-carboxamido function in the 4′-position to obtain NECA (*N*-ethyl) or MECA (*N*-methyl) derivatives, with an improved potency at all the ARs. Typical A_1AR and A_3AR agonists contain bulky groups in the N^6-position combined with modifications in the 2-position (Kim et al., 1994; Kiesman et al., 2009; Volpini et al., 2009). Reference A_3AR agonists are IB-MECA and Cl-IB-MECA, in clinical trials for inflammation-related conditions (RA and psoriasis) (Borea et al., 2015; Jacobson et al., 2017). $A_{2A}AR$ agonists are generally NECA derivatives presenting complex chains in the 2-position (i.e., CGS21680, ATL-146e, and ATL-313 where the 4′-carboxamido group is further modified). High $A_{2A}AR$ affinity and selectivity was obtained by inserting a bulky arylalkyl function in the N^6-position to obtain UK-432097 (de Lera Ruiz et al., 2014).

About the molecules able to block the AR function, AR antagonists are generally divided in non-xanthine- and xanthine-based derivatives. Non-xanthine AR antagonists are based on a large variety of scaffolds (generally heterocycles). Reference compounds for pharmacological studies at ARs may be found within this heterogeneous group, some of which were developed

also as water-soluble molecules, pro-drugs, and radiolabeled compounds. Xanthine-based AR antagonists contain the A_{2A}AR inhibitor Istradefylline that was approved to market in Japan as antiparkinsonian tool (Jacobson and Muller, 2016).

At present, most of available studies investigating the role of AR signaling in several experimental models of colitis showed remarkable beneficial effects upon pharmacological modulation of A_{2A}AR (Odashima et al., 2005; Cavalcante et al., 2006; Naganuma et al., 2006; Rahimian et al., 2010; Antonioli et al., 2011; Pallio et al., 2016). The A_{2A}AR agonists ATL-146e or ATL-313 significantly reduced mucosal inflammation of colon, with a marked decrease in pro-inflammatory cytokine levels and in leukocyte infiltration and an increase of levels of anti-inflammatory cytokines (Naganuma et al., 2006; Odashima et al., 2006). Recently Pallio et al. (2016) demonstrated the beneficial effects arising from A_{2A}AR stimulation with polydeoxyribonucleotide in two experimental models of colitis. In the DSS model polydeoxyribonucleotide could counteract the hemorrhagic diarrhea, improve the weight loss, and restore the anatomic integrity of damaged epithelial and mucosal layers. In the DNBS model, polydeoxyribonucleotide markedly reduced the inflammatory response as well as the granulocytic infiltration into the mucosal and submucosal layers and, therefore, decreased the pro-inflammatory cytokines TNF and IL-1β, MPO activity and lipid peroxidation in colon samples. Noteworthy, polydeoxyribonucleotide treatment also affected Bax and Bcl-2 expression, reducing apoptotic and necrotic cells in all tissue layers. By contrast, no beneficial effects have been reported upon administration of CGS21680 in mouse model of DSS-induced colitis (Selmeczy et al., 2007). Further investigations are needed to better characterize the therapeutic potential of A_{2A}AR agonists in IBDs. A number of evidences reported that aging is often associated with a chronic, low-grade systemic inflammatory condition (Laflamme et al., 2017), that could predispose to the gastrointestinal alterations typical of the elderly subject (Remond et al., 2015). Recently, it has been demonstrated that the reduction of A_{2A}AR in the digestive tract of aged mice, contributes to an increased inflammation and lower ability to

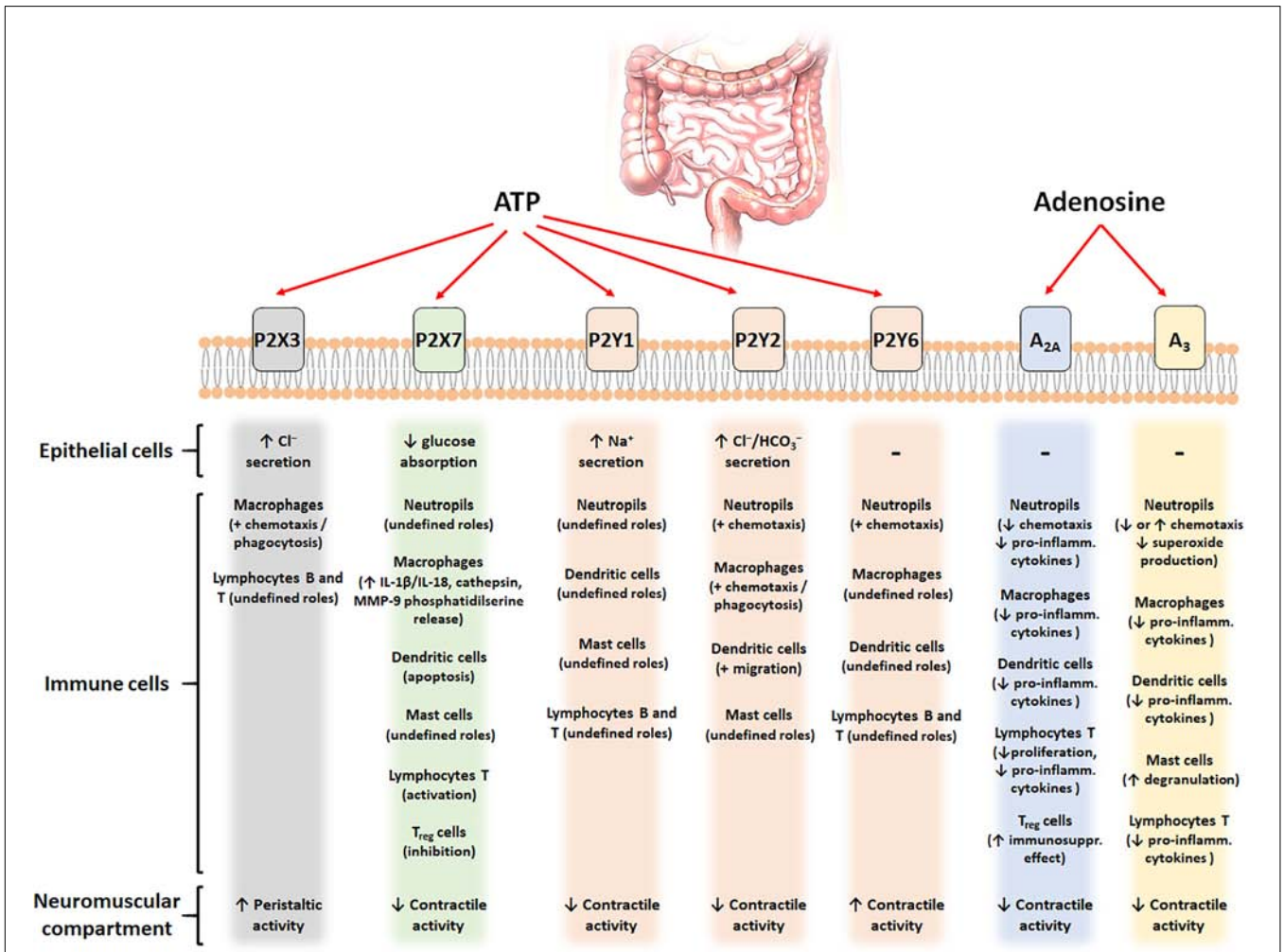

FIGURE 1 | Schematic figure with the putative contribution of the main purinergic signals (ATP and adenosine) and their different receptors (P2X3, P2X7, $P2Y_{1,2,6}$, A_{2A}, and A_3) in different cell types of the intestinal tract.

TABLE 1 | Promising pharmacological tools acting on purinergic receptors to manage intestinal disorders.

Intestinal Diseases	Pharmacological Target
Inflammatory bowel diseases (IBDs)	P2X7R antagonists
	A_{2A}AR agonists
	A_{2B}AR antagonists
	A_3AR agonists
Irritable bowel syndrome (IBS)	P2X3R antagonists
	P2X7R antagonists
	A_3AR agonists (?)
Functional motor disorders	A_1AR antagonists (post-operative ileus)
	A_{2A}AR antagonists (functional dyspepsia)
	A_{2B}AR antagonists (constipation)
	A_3AR antagonists (constipation)
Visceral pain	P2X3R antagonists
	P2X7R antagonists
	A_1AR agonists (?)
	A_{2A}AR agonists (?)
	A_3AR agonists (?)
Diarrhea	P2X3R antagonists
	$P2Y_1$R antagonists (?)
	$P2Y_2$R antagonists (?)
	$P2Y_6$R antagonists (?)
	A_{2A}AR agonists
	A_{2B}AR antagonists
	A_3AR agonists (?)

The (?) symbols indicate that the therapeutic potential arises from some literature contributions but is not yet clearly confirmed.

counteract gut infection with deleterious effects in the elderly (Rodrigues et al., 2016).

Another promising option aimed at counteracting the bowel inflammation is the pharmacological stimulation of A_3AR (Gessi et al., 2008; Antonioli et al., 2014a). The administration of IB-MECA revealed to afford a protective role in murine models of intestinal inflammation (Mabley et al., 2003; Guzman et al., 2006). In detail, the pharmacological engagement of A_3AR determined the inhibition of several cytokine/chemokine/inflammatory genes, thus promoting a marked down-regulation of several pro-inflammatory mediators (MIP-1α and MIP-2, IL-1, IL-6, IL-12) and the production of reactive species of oxygen, determining an improvement of the intestinal damage (Guzman et al., 2006). A recent preclinical study by Ren et al. (2015) showed that the pharmacological stimulation of A_3AR with Cl-IB-MECA inhibited the NF-κB pathway in the colonic epithelia of DSS colitis mice. The inhibition of both NF-κB activation and IκBa phosphorylation caused a reduction of pro-inflammatory cytokines expression in colonic epithelia of inflamed animals.

Finally, the evidence supporting an over-expression of A_{2B}AR in experimental colitis has sparked interest on the potential therapeutic implications of these intriguing receptor subtype (Kolachala et al., 2005). The same research group (Kolachala V. et al., 2008; Kolachala V.L. et al., 2008) demonstrated also a critical role of intestinal epithelial A_{2B}AR in the pro-inflammatory activity exerted by adenosine in animals with TNBS or DSS colitis. The treatment with the A_{2B}AR antagonist ATL-801 to mice with experimental colitis ameliorated several inflammatory parameters, leading to a beneficial impact on the disease progression (Kolachala V. et al., 2008). By contrast, Frick et al. (2009) reported a detrimental effect exerted by the A_{2B}AR inhibitor PSB1115 in the acute phase of DSS-induced colitis, thus questioning the beneficial effect of A_{2B}AR blockade in the management of IBDs.

REGULATION OF EXTRACELLULAR ADENOSINE LEVELS

Several authors investigated the efficacy of pharmacological treatments aimed at increasing the levels of endogenous adenosine, through the blockade of pivotal catabolic enzymes, as an alternative way to counteract intestinal inflammation. eATP is rapidly degraded to adenosine by ectonucleotidases CD73 and CD39. Genetic deletion of these enzymes prompts a higher susceptibility to inflammatory states or more severe progression of inflammation in IBD experimental models (Idzko et al., 2014; Longhi et al., 2017). Polymorphisms taking to lower ectonucleotidases expression takes to analog scenarios (Idzko et al., 2014). By contrast, blockade of nucleoside transporters leads to an increase of extracellular adenosine levels, with a consequent improvement of the inflammation course in IBD models (Ye and Rajendran, 2009). The extracellular levels of adenosine are also regulated by the activity of metabolic enzymes like ADK and ADA (Cristalli et al., 2001). The blockade of these enzymes is associated to anti-inflammatory effects and was preclinically tested as strategy to ameliorate intestinal inflammation-related conditions. Siegmund et al. (2001) reported, for the first time, an anti-inflammatory effect of the ADK inhibitor GP515 in a mouse model of colitis. Encouraging ameliorative effects were observed also following the inhibition of ADA in murine models of intestinal inflammation (Antonioli et al., 2007, 2010, 2012; La Motta et al., 2009), with reduction of the colonic inflammatory damage and decrease in tissue levels of pro-inflammatory cytokines (IL-1β, IL-6, TNF-α, IFN-γ, and chemokine C-X-C motif ligand 10), as well as a reduction of neutrophil infiltration and ROS production (Antonioli et al., 2007, 2010; Brown et al., 2008; La Motta et al., 2009). Noteworthy, it was observed that the attenuation of colonic injury, following ADA blockade, was mediated mainly by the engagement of A_{2A}AR and, to a lesser extent, A_3AR (Antonioli et al., 2010).

CONCLUSION

Several pre-clinical studies pointed out a key role for the purinergic system in the modulation of inflammatory and immune responses. Furthermore, clinical evaluation of purinergic ligands for the treatment of inflammation-related conditions (i.e., RA and psoriasis but also IBDs for a P2X7R inhibitor) showed a good tolerability of these molecules and suggests further investigations for this strategy. **Figure 1** and

Table 1 provide a schematic overview of the purinergic signal contributions in the intestinal tract and the most promising purine-based therapeutic strategies for the intestinal disorders.

Despite clinical studies demonstrated an encouraging profile in terms of tolerability for AZD9056, a novel P2X7R antagonist, it displayed a limited efficacy in the management of patients affected by moderate/severe Crohn's disease. In parallel, an increasing interest has been payed toward the A_{2A}AR (and the A_3AR) agonists as viable way to manage digestive dysfunctions. However, despite promising the available evidences are limited to the pre-clinical phase and deserve further translational and clinical insights before highlighting their therapeutic potential. In this context, Michael Sitkovsky (Fredholm et al., 2007; Ohta and Sitkovsky, 2009) undoubtedly provided several of the most eminent scientific evidences about the therapeutic potential of ligands acting on this receptor subtype, paving the way toward their next clinical employment.

Apart from animal studies, the unique window of opportunity to grasp the relevance of part of the purinergic system, operated by adenosine receptors, in intestine function, is offered by the consumption of caffeine, which only known target at non-toxic conditions is the antagonism of adenosine receptors. In this regard, there are evidences, despite conflicting, about the association between caffeine consumption and the onset and development of gastrointestinal-related disorders. In particular, several authors reported a direct association between coffee consumption and some functional digestive disorders (i.e., gastro-oesophageal reflux, dyspepsia, irritable bowel syndrome) (Boekema et al., 1999; DiBaise, 2003).

These data boost the medicinal chemistry toward the synthesis of novel pharmacological entities acting selectively on specific purinergic receptors/enzymes and endowed with improved pharmacodynamic and pharmacokinetic profiles. These molecules would definitively help to clearly depict the pathophysiological role and the therapeutic potential of these proteins and would represent a key step for the development of useful tools for the management of intestinal inflammatory disorders (Burnstock, 2017a,b; Burnstock et al., 2017).

AUTHOR CONTRIBUTIONS

DDB and LA drafted this manuscript. DDB, LA, CL, MF, CB, and RV were responsible for idea conception, critical evaluation, and manuscript review.

ACKNOWLEDGMENTS

The authors acknowledge the contributions of University of Camerino (Progetto FAR FPI000042) in supporting the works.

REFERENCES

2005-004110-32_Clinical_Trial_Results (2005). Clinical Trials for 2005-004110-32: A Randomised, Double-blind, Placebo-controlled, Parallel Group, Multicentre, Phase II Study to Assess The Efficacy of AZD9056 (single oral 400 mg dose) When Administered for 4 Weeks in Patients with Moderate to Severe COPD [Online]. Available at: https://www.clinicaltrialsregister.eu/ctr-search/search?query=2005-004110-32

Allard, B., Longhi, M. S., Robson, S. C., and Stagg, J. (2017). The ectonucleotidases CD39 and CD73: novel checkpoint inhibitor targets. *Immunol. Rev.* 276, 121–144. doi: 10.1111/imr.12528

Antonioli, L., Colucci, R., La Motta, C., Tuccori, M., Awwad, O., Da Settimo, F., et al. (2012). Adenosine deaminase in the modulation of immune system and its potential as a novel target for treatment of inflammatory disorders. *Curr. Drug Targets* 13, 842–862. doi: 10.2174/138945012800564095

Antonioli, L., Colucci, R., Pellegrini, C., Giustarini, G., Tuccori, M., Blandizzi, C., et al. (2013). The role of purinergic pathways in the pathophysiology of gut diseases: pharmacological modulation and potential therapeutic applications. *Pharmacol. Ther.* 139, 157–188. doi: 10.1016/j.pharmthera.2013.04.002

Antonioli, L., Csoka, B., Fornai, M., Colucci, R., Kokai, E., Blandizzi, C., et al. (2014a). Adenosine and inflammation: what's new on the horizon? *Drug Discov. Today* 19, 1051–1068. doi: 10.1016/j.drudis.2014.02.010

Antonioli, L., Fornai, M., Colucci, R., Awwad, O., Ghisu, N., Tuccori, M., et al. (2010). The blockade of adenosine deaminase ameliorates chronic experimental colitis through the recruitment of adenosine A2A and A3 receptors. *J. Pharmacol. Exp. Ther.* 335, 434–442. doi: 10.1124/jpet.110.171223

Antonioli, L., Fornai, M., Colucci, R., Awwad, O., Ghisu, N., Tuccori, M., et al. (2011). Differential recruitment of high affinity A1 and A2A adenosine receptors in the control of colonic neuromuscular function in experimental colitis. *Eur. J. Pharmacol.* 650, 639–649. doi: 10.1016/j.ejphar.2010.10.041

Antonioli, L., Fornai, M., Colucci, R., Ghisu, N., Da Settimo, F., Natale, G., et al. (2007). Inhibition of adenosine deaminase attenuates inflammation in experimental colitis. *J. Pharmacol. Exp. Ther.* 322, 435–442. doi: 10.1124/jpet.107.122762

Antonioli, L., Giron, M. C., Colucci, R., Pellegrini, C., Sacco, D., Caputi, V., et al. (2014b). Involvement of the P2X7 purinergic receptor in colonic motor dysfunction associated with bowel inflammation in rats. *PLoS One* 9:e116253. doi: 10.1371/journal.pone.0116253

Arulkumaran, N., Unwin, R. J., and Tam, F. W. (2011). A potential therapeutic role for P2X7 receptor (P2X7R) antagonists in the treatment of inflammatory diseases. *Expert Opin. Investig. Drugs* 20, 897–915. doi: 10.1517/13543784.2011.578068

Beko, K., Kovanyi, B., Goloncser, F., Horvath, G., Denes, A., Kornyei, Z., et al. (2017). Contribution of platelet P2Y12 receptors to chronic Complete Freund's adjuvant-induced inflammatory pain. *J. Thromb. Haemost.* 15, 1223–1235. doi: 10.1111/jth.13684

Boekema, P. J., Samsom, M., van Berge Henegouwen, G. P., and Smout, A. J. (1999). Coffee and gastrointestinal function: facts and fiction. A review. *Scand. J. Gastroenterol. Suppl.* 230, 35–39. doi: 10.1080/003655299750025525

Borea, P. A., Varani, K., Vincenzi, F., Baraldi, P. G., Tabrizi, M. A., Merighi, S., et al. (2015). The A3 adenosine receptor: history and perspectives. *Pharmacol. Rev.* 67, 74–102. doi: 10.1124/pr.113.008540

Brown, J. B., Lee, G., Grimm, G. R., and Barrett, T. A. (2008). Therapeutic benefit of pentostatin in severe IL-10-/- colitis. *Inflamm. Bowel Dis.* 14, 880–887. doi: 10.1002/ibd.20410

Burnstock, G. (2011). Purinergic signaling in the gastrointestinal tract. *World J. Gastrointest. Pathophysiol.* 2, 31–34. doi: 10.4291/wjgp.v2.i2.31

Burnstock, G. (2014). Purinergic signalling in the gastrointestinal tract and related organs in health and disease. *Purinergic Signal.* 10, 3–50. doi: 10.1007/s11302-013-9397-9

Burnstock, G. (2017a). Purinergic Signalling: therapeutic developments. *Front. Pharmacol.* 8:661. doi: 10.3389/fphar.2017.00661

Burnstock, G. (2017b). The therapeutic potential of purinergic signalling. *Biochem. Pharmacol.* doi: 10.1016/j.bcp.2017.07.016 [Epub ahead of print].

Burnstock, G., Jacobson, K. A., and Christofi, F. L. (2017). Purinergic drug targets for gastrointestinal disorders. *Curr. Opin. Pharmacol.* 37, 131–141. doi: 10.1016/j.coph.2017.10.011

Burnstock, G., and Kennedy, C. (2011). P2X receptors in health and disease. *Adv. Pharmacol.* 61, 333–372. doi: 10.1016/B978-0-12-385526-8.00011-4

Burnstock, G., and Knight, G. E. (2017). The potential of P2X7 receptors as a therapeutic target, including inflammation and tumour progression. *Purinergic Signal.* doi: 10.1007/s11302-017-9593-0 [Epub ahead of print].

Cavalcante, I. C., Castro, M. V., Barreto, A. R., Sullivan, G. W., Vale, M., Almeida, P. R., et al. (2006). Effect of novel A2A adenosine receptor agonist ATL 313 on Clostridium difficile toxin A-induced murine ileal enteritis. *Infect. Immun.* 74, 2606–2612. doi: 10.1128/IAI.74.5.2606-2612.2006

Cesaro, A., Brest, P., Hofman, V., Hebuterne, X., Wildman, S., Ferrua, B., et al. (2010). Amplification loop of the inflammatory process is induced by P2X7R activation in intestinal epithelial cells in response to neutrophil transepithelial migration. *Am. J. Physiol. Gastrointest. Liver Physiol.* 299, G32–G42. doi: 10.1152/ajpgi.00282.2009

Ciruela, F. (2011). Adenosine receptors. *Biochim. Biophys. Acta* 1808, 1231–1232. doi: 10.1016/j.bbamem.2011.03.007

Coddou, C., Yan, Z., Obsil, T., Huidobro-Toro, J. P., and Stojilkovic, S. S. (2011). Activation and regulation of purinergic P2X receptor channels. *Pharmacol. Rev.* 63, 641–683. doi: 10.1124/pr.110.003129

Conroy, S., Kindon, N., Kellam, B., and Stocks, M. J. (2016). Drug-like antagonists of P2Y receptors-from lead identification to drug development. *J. Med. Chem.* 59, 9981–10005. doi: 10.1021/acs.jmedchem.5b01972

Cristalli, G., Costanzi, S., Lambertucci, C., Lupidi, G., Vittori, S., Volpini, R., et al. (2001). Adenosine deaminase: functional implications and different classes of inhibitors. *Med. Res. Rev.* 21, 105–128. doi: 10.1002/1098-1128(200103)21:2<105::AID-MED1002>3.0.CO;2-U

Cristalli, G., and Volpini, R. (2003). Adenosine receptors: chemistry and pharmacology. *Curr. Top. Med. Chem.* 3, 355–469. doi: 10.2174/1568026033392282

Dal Ben, D., Buccioni, M., Lambertucci, C., Marucci, G., Thomas, A., and Volpini, R. (2015). Purinergic P2X receptors: structural models and analysis of ligand-target interaction. *Eur. J. Med. Chem.* 89, 561–580. doi: 10.1016/j.ejmech.2014.10.071

Dal Ben, D., Marchenkova, A., Thomas, A., Lambertucci, C., Spinaci, A., Marucci, G., et al. (2017). 2',3'-O-Substituted ATP derivatives as potent antagonists of purinergic P2X3 receptors and potential analgesic agents. *Purinergic Signal.* 13, 61–74. doi: 10.1007/s11302-016-9539-y

de Lera Ruiz, M., Lim, Y. H., and Zheng, J. (2014). Adenosine A2A receptor as a drug discovery target. *J. Med. Chem.* 57, 3623–3650. doi: 10.1021/jm4011669

De Marchi, E., Orioli, E., Dal Ben, D., and Adinolfi, E. (2016). P2X7 receptor as a therapeutic target. *Adv. Protein Chem. Struct. Biol.* 104, 39–79. doi: 10.1016/bs.apcsb.2015.11.004

Degagne, E., Degrandmaison, J., Grbic, D. M., Vinette, V., Arguin, G., and Gendron, F. P. (2013). P2Y2 receptor promotes intestinal microtubule stabilization and mucosal re-epithelization in experimental colitis. *J. Cell. Physiol.* 228, 99–109. doi: 10.1002/jcp.24109

Deiteren, A., van der Linden, L., de Wit, A., Ceuleers, H., Buckinx, R., Timmermans, J. P., et al. (2015). P2X3 receptors mediate visceral hypersensitivity during acute chemically-induced colitis and in the post-inflammatory phase via different mechanisms of sensitization. *PLoS One* 10:e0123810. doi: 10.1371/journal.pone.0123810

Di Virgilio, F., Dal Ben, D., Sarti, A. C., Giuliani, A. L., and Falzoni, S. (2017). The P2X7 receptor in infection and inflammation. *Immunity* 47, 15–31. doi: 10.1016/j.immuni.2017.06.020

DiBaise, J. K. (2003). A randomized, double-blind comparison of two different coffee-roasting processes on development of heartburn and dyspepsia in coffee-sensitive individuals. *Dig. Dis. Sci.* 48, 652–656. doi: 10.1023/A:1022860019852

Donnelly-Roberts, D. L., Namovic, M. T., Surber, B., Vaidyanathan, S. X., Perez-Medrano, A., Wang, Y., et al. (2009). [3H]A-804598 ([3H]2-cyano-1-[(1S)-1-phenylethyl]-3-quinolin-5-ylguanidine) is a novel, potent, and selective antagonist radioligand for P2X7 receptors. *Neuropharmacology* 56, 223–229. doi: 10.1016/j.neuropharm.2008.06.012

Eltzschig, H. K., Sitkovsky, M. V., and Robson, S. C. (2012). Purinergic signaling during inflammation. *N. Engl. J. Med.* 367, 2322–2333. doi: 10.1056/NEJMra1205750

Eser, A., Colombel, J. F., Rutgeerts, P., Vermeire, S., Vogelsang, H., Braddock, M., et al. (2015). Safety and efficacy of an oral inhibitor of the purinergic receptor P2X7 in adult patients with moderately to severely active Crohn's disease: a randomized placebo-controlled, double-blind, phase IIa study. *Inflamm. Bowel Dis.* 21, 2247–2253. doi: 10.1097/MIB.0000000000000514

Fantoni, E. R., Dal Ben, D., Falzoni, S., Di Virgilio, F., Lovestone, S., and Gee, A. (2017). Design, synthesis and evaluation in an LPS rodent model of neuroinflammation of a novel 18F-labelled PET tracer targeting P2X7. *EJNMMI Res.* 7:31. doi: 10.1186/s13550-017-0275-2

Fredholm, B. B., Chern, Y., Franco, R., and Sitkovsky, M. (2007). Aspects of the general biology of adenosine A2A signaling. *Prog. Neurobiol.* 83, 263–276. doi: 10.1016/j.pneurobio.2007.07.005

Frick, J. S., MacManus, C. F., Scully, M., Glover, L. E., Eltzschig, H. K., and Colgan, S. P. (2009). Contribution of adenosine A2B receptors to inflammatory parameters of experimental colitis. *J. Immunol.* 182, 4957–4964. doi: 10.4049/jimmunol.0801324

Gessi, S., Merighi, S., Varani, K., Leung, E., Mac Lennan, S., and Borea, P. A. (2008). The A3 adenosine receptor: an enigmatic player in cell biology. *Pharmacol. Ther.* 117, 123–140. doi: 10.1016/j.pharmthera.2007.09.002

Grbic, D. M., Degagne, E., Langlois, C., Dupuis, A. A., and Gendron, F. P. (2008). Intestinal inflammation increases the expression of the P2Y6 receptor on epithelial cells and the release of CXC chemokine ligand 8 by UDP. *J. Immunol.* 180, 2659–2668. doi: 10.4049/jimmunol.180.4.2659

Grbic, D. M., Degagne, E., Larrivee, J. F., Bilodeau, M. S., Vinette, V., Arguin, G., et al. (2012). P2Y6 receptor contributes to neutrophil recruitment to inflamed intestinal mucosa by increasing CXC chemokine ligand 8 expression in an AP-1-dependent manner in epithelial cells. *Inflamm. Bowel Dis.* 18, 1456–1469. doi: 10.1002/ibd.21931

Gulbransen, B. D., Bashashati, M., Hirota, S. A., Gui, X., Roberts, J. A., MacDonald, J. A., et al. (2012). Activation of neuronal P2X7 receptor-pannexin-1 mediates death of enteric neurons during colitis. *Nat. Med.* 18, 600–604. doi: 10.1038/nm.2679

Guo, W., Sui, Q. Q., Gao, X. F., Feng, J. F., Zhu, J., He, C., et al. (2016). Co-localization of Pirt protein and P2X2 receptors in the mouse enteric nervous system. *Purinergic Signal.* 12, 489–496. doi: 10.1007/s11302-016-9515-6

Guzman, J., Yu, J. G., Suntres, Z., Bozarov, A., Cooke, H., Javed, N., et al. (2006). ADOA3R as a therapeutic target in experimental colitis: proof by validated high-density oligonucleotide microarray analysis. *Inflamm. Bowel Dis.* 12, 766–789. doi: 10.1097/00054725-200608000-00014

Hasko, G., and Cronstein, B. N. (2004). Adenosine: an endogenous regulator of innate immunity. *Trends Immunol.* 25, 33–39. doi: 10.1016/j.it.2003.11.003

Hasko, G., Linden, J., Cronstein, B., and Pacher, P. (2008). Adenosine receptors: therapeutic aspects for inflammatory and immune diseases. *Nat. Rev. Drug Discov.* 7, 759–770. doi: 10.1038/nrd2638

Hasko, G., and Pacher, P. (2008). A2A receptors in inflammation and injury: lessons learned from transgenic animals. *J. Leukoc. Biol.* 83, 447–455. doi: 10.1189/jlb.0607359

Idzko, M., Ferrari, D., and Eltzschig, H. K. (2014). Nucleotide signalling during inflammation. *Nature* 509, 310–317. doi: 10.1038/nature13085

Jacobson, K. A., Balasubramanian, R., Deflorian, F., and Gao, Z. G. (2012). G protein-coupled adenosine (P1) and P2Y receptors: ligand design and receptor interactions. *Purinergic Signal.* 8, 419–436. doi: 10.1007/s11302-012-9294-7

Jacobson, K. A., and Gao, Z. G. (2006). Adenosine receptors as therapeutic targets. *Nat. Rev. Drug. Discov.* 5, 247–264. doi: 10.1038/nrd1983

Jacobson, K. A., Merighi, S., Varani, K., Borea, P. A., Baraldi, S., Aghazadeh Tabrizi, M., et al. (2017). A3 adenosine receptors as modulators of inflammation: from medicinal chemistry to therapy. *Med. Res. Rev.* doi: 10.1002/med.21456 [Epub ahead of print].

Jacobson, K. A., and Muller, C. E. (2016). Medicinal chemistry of adenosine, P2Y and P2X receptors. *Neuropharmacology* 104, 31–49. doi: 10.1016/j.neuropharm.2015.12.001

Jin, H., Han, J., Resing, D., Liu, H., Yue, X., Miller, R. L., et al. (2018). Synthesis and *in vitro* characterization of a P2X7 radioligand [^{123}I]TZ6019 and its response to neuroinflammation in a mouse model of Alzheimer disease. *Eur. J. Pharmacol.* 820, 8–17. doi: 10.1016/j.ejphar.2017.12.006

Keystone, E. C., Wang, M. M., Layton, M., Hollis, S., and McInnes, I. B. (2012). Clinical evaluation of the efficacy of the P2X7 purinergic receptor antagonist AZD9056 on the signs and symptoms of rheumatoid arthritis in patients with active disease despite treatment with methotrexate or sulphasalazine. *Ann. Rheum. Dis.* 71, 1630–1635. doi: 10.1136/annrheumdis-2011-143578

Kiesman, W. F., Elzein, E., and Zablocki, J. (2009). A1 adenosine receptor antagonists, agonists, and allosteric enhancers. *Handb. Exp. Pharmacol.* 193, 25–58. doi: 10.1007/978-3-540-89615-9_2

Kim, H. O., Ji, X. D., Siddiqi, S. M., Olah, M. E., Stiles, G. L., and Jacobson, K. A. (1994). 2-Substitution of N6-benzyladenosine-5'-uronamides enhances selectivity for A3 adenosine receptors. *J. Med. Chem.* 37, 3614–3621. doi: 10.1021/jm00047a018

Kolachala, V., Asamoah, V., Wang, L., Obertone, T. S., Ziegler, T. R., Merlin, D., et al. (2005). TNF-alpha upregulates adenosine 2b (A2b) receptor expression and signaling in intestinal epithelial cells: a basis for A2bR overexpression in colitis. *Cell. Mol. Life Sci.* 62, 2647–2657. doi: 10.1007/s00018-005-5328-4

Kolachala, V., Ruble, B., Vijay-Kumar, M., Wang, L., Mwangi, S., Figler, H., et al. (2008). Blockade of adenosine A2B receptors ameliorates murine colitis. *Br. J. Pharmacol.* 155, 127–137. doi: 10.1038/bjp.2008.227

Kolachala, V. L., Vijay-Kumar, M., Dalmasso, G., Yang, D., Linden, J., Wang, L., et al. (2008). A2B adenosine receptor gene deletion attenuates murine colitis. *Gastroenterology* 135, 861–870. doi: 10.1053/j.gastro.2008.05.049

La Motta, C., Sartini, S., Mugnaini, L., Salerno, S., Simorini, F., Taliani, S., et al. (2009). Exploiting the pyrazolo[3,4-d]pyrimidin-4-one ring system as a useful template to obtain potent adenosine deaminase inhibitors. *J. Med. Chem.* 52, 1681–1692. doi: 10.1021/jm801427r

Laflamme, C., Mailhot, G. B., and Pouliot, M. (2017). Age-related decline of the acute local inflammation response: a mitigating role for the adenosine A2A receptor. *Aging* 9, 2083–2097. doi: 10.18632/aging.101303

Lambertucci, C., Dal Ben, D., Buccioni, M., Marucci, G., Thomas, A., and Volpini, R. (2015). Medicinal chemistry of P2X receptors: agonists and orthosteric antagonists. *Curr. Med. Chem.* 22, 915–928. doi: 10.2174/0929867321666141215093513

Le Duc, D., Schulz, A., Lede, V., Schulze, A., Thor, D., Bruser, A., et al. (2017). P2Y receptors in immune response and inflammation. *Adv. Immunol.* 136, 85–121. doi: 10.1016/bs.ai.2017.05.006

Longhi, M. S., Moss, A., Jiang, Z. G., and Robson, S. C. (2017). Purinergic signaling during intestinal inflammation. *J. Mol. Med.* 95, 915–925. doi: 10.1007/s00109-017-1545-1

Lord, B., Ameriks, M. K., Wang, Q., Fourgeaud, L., Vliegen, M., Verluyten, W., et al. (2015). A novel radioligand for the ATP-gated ion channel P2X7: [3H] JNJ-54232334. *Eur. J. Pharmacol.* 765, 551–559. doi: 10.1016/j.ejphar.2015.09.026

Mabley, J., Soriano, F., Pacher, P., Hasko, G., Marton, A., Wallace, R., et al. (2003). The adenosine A3 receptor agonist, N6-(3-iodobenzyl)-adenosine-5'-N-methyluronamide, is protective in two murine models of colitis. *Eur. J. Pharmacol.* 466, 323–329. doi: 10.1016/S0014-2999(03)01570-X

Marques, C. C., Castelo-Branco, M. T., Pacheco, R. G., Buongusto, F., do Rosário, A. Jr., Schanaider, A., et al. (2014). Prophylactic systemic P2X7 receptor blockade prevents experimental colitis. *Biochim. Biophys. Acta* 1842, 65–78. doi: 10.1016/j.bbadis.2013.10.012

Muller, C. E. (2015). Medicinal chemistry of P2X receptors: allosteric modulators. *Curr. Med. Chem.* 22, 929–941. doi: 10.2174/0929867322666141210155610

Murgia, M., Hanau, S., Pizzo, P., Rippa, M., and Di Virgilio, F. (1993). Oxidized ATP. An irreversible inhibitor of the macrophage purinergic P2Z receptor. *J. Biol. Chem.* 268, 8199–8203.

Naganuma, M., Wiznerowicz, E. B., Lappas, C. M., Linden, J., Worthington, M. T., and Ernst, P. B. (2006). Cutting edge: critical role for A2A adenosine receptors in the T cell-mediated regulation of colitis. *J. Immunol.* 177, 2765–2769. doi: 10.4049/jimmunol.177.5.2765

Neves, A. R., Castelo-Branco, M. T., Figliuolo, V. R., Bernardazzi, C., Buongusto, F., Yoshimoto, A., et al. (2014). Overexpression of ATP-activated P2X7 receptors in the intestinal mucosa is implicated in the pathogenesis of Crohn's disease. *Inflamm. Bowel Dis.* 20, 444–457. doi: 10.1097/01.MIB.0000441201.10454.06

North, R. A. (2016). P2X receptors. *Philos. Trans. R. Soc. Lond. B Biol. Sci.* 371:20150427. doi: 10.1098/rstb.2015.0427

North, R. A., and Jarvis, M. F. (2013). P2X receptors as drug targets. *Mol. Pharmacol.* 83, 759–769. doi: 10.1124/mol.112.083758

Odashima, M., Bamias, G., Rivera-Nieves, J., Linden, J., Nast, C. C., Moskaluk, C. A., et al. (2005). Activation of A2A adenosine receptor attenuates intestinal inflammation in animal models of inflammatory bowel disease. *Gastroenterology* 129, 26–33. doi: 10.1053/j.gastro.2005.05.032

Odashima, M., Otaka, M., Jin, M., Horikawa, Y., Matsuhashi, T., Ohba, R., et al. (2006). A selective adenosine A2A receptor agonist, ATL-146e, prevents concanavalin A-induced acute liver injury in mice. *Biochem. Biophys. Res. Commun.* 347, 949–954. doi: 10.1016/j.bbrc.2006.06.185

Ohta, A., and Sitkovsky, M. (2009). The adenosinergic immunomodulatory drugs. *Curr. Opin. Pharmacol.* 9, 501–506. doi: 10.1016/j.coph.2009.05.005

Pallio, G., Bitto, A., Pizzino, G., Galfo, F., Irrera, N., Squadrito, F., et al. (2016). Adenosine receptor stimulation by polydeoxyribonucleotide improves tissue repair and symptomology in experimental colitis. *Front. Pharmacol.* 7:273. doi: 10.3389/fphar.2016.00273

Park, J. H., and Kim, Y. C. (2017). P2X7 receptor antagonists: a patent review (2010-2015). *Expert Opin. Ther. Pat.* 27, 257–267. doi: 10.1080/13543776.2017.1246538

Paulino, A. S., Palombit, K., Cavriani, G., Tavares-de-Lima, W., Mizuno, M. S., Marosti, A. R., et al. (2011). Effects of ischemia and reperfusion on P2X2 receptor expressing neurons of the rat ileum enteric nervous system. *Dig. Dis. Sci.* 56, 2262–2275. doi: 10.1007/s10620-011-1588-z

Rahimian, R., Fakhfouri, G., Daneshmand, A., Mohammadi, H., Bahremand, A., Rasouli, M. R., et al. (2010). Adenosine A2A receptors and uric acid mediate protective effects of inosine against TNBS-induced colitis in rats. *Eur. J. Pharmacol.* 649, 376–381. doi: 10.1016/j.ejphar.2010.09.044

Remond, D., Shahar, D. R., Gille, D., Pinto, P., Kachal, J., Peyron, M. A., et al. (2015). Understanding the gastrointestinal tract of the elderly to develop dietary solutions that prevent malnutrition. *Oncotarget* 6, 13858–13898. doi: 10.18632/oncotarget.4030

Ren, T., Tian, T., Feng, X., Ye, S., Wang, H., Wu, W., et al. (2015). An adenosine A3 receptor agonist inhibits DSS-induced colitis in mice through modulation of the NF-kappaB signaling pathway. *Sci. Rep.* 5:9047. doi: 10.1038/srep09047

Rodrigues, L., Miranda, I. M., Andrade, G. M., Mota, M., Cortes, L., Rodrigues, A. G., et al. (2016). Blunted dynamics of adenosine A2A receptors is associated with increased susceptibility to *Candida albicans* infection in the elderly. *Oncotarget* 7, 62862–62872. doi: 10.18632/oncotarget.11760

Selmeczy, Z., Csoka, B., Pacher, P., Vizi, E. S., and Hasko, G. (2007). The adenosine A2A receptor agonist CGS 21680 fails to ameliorate the course of dextran sulphate-induced colitis in mice. *Inflamm. Res.* 56, 204–209. doi: 10.1007/s00011-006-6150-7

Siegmund, B., Rieder, F., Albrich, S., Wolf, K., Bidlingmaier, C., Firestein, G. S., et al. (2001). Adenosine kinase inhibitor GP515 improves experimental colitis in mice. *J. Pharmacol. Exp. Ther.* 296, 99–105. doi: 10.1016/S0016-5085(00)84448-0

Strong, D. S., Cornbrooks, C. F., Roberts, J. A., Hoffman, J. M., Sharkey, K. A., and Mawe, G. M. (2010). Purinergic neuromuscular transmission is selectively attenuated in ulcerated regions of inflamed guinea pig distal colon. *J. Physiol.* 588, 847–859. doi: 10.1113/jphysiol.2009.185082

Syed, N. I. H., and Kennedy, C. (2012). Pharmacology of P2X receptors. *WIREs Membr. Transp. Signal.* 1, 16–30. doi: 10.1002/wmts.1

Territo, P. R., Meyer, J. A., Peters, J. S., Riley, A. A., McCarthy, B. P., Gao, M., et al. (2017). Characterization of 11C-GSK1482160 for targeting the P2X7 receptor as a biomarker for neuroinflammation. *J. Nucl. Med.* 58, 458–465. doi: 10.2967/jnumed.116.181354

Thomas, M. R., and Storey, R. F. (2015). Effect of P2Y12 inhibitors on inflammation and immunity. *Thromb. Haemost.* 114, 490–497. doi: 10.1160/TH14-12-1068

Virginio, C., Robertson, G., Surprenant, A., and North, R. A. (1998). Trinitrophenyl-substituted nucleotides are potent antagonists selective for P2X1, P2X3, and heteromeric P2X2/3 receptors. *Mol. Pharmacol.* 53, 969–973. doi: 10.1124/mol.54.6.979

Volpini, R., Buccioni, M., Dal Ben, D., Lambertucci, C., Lammi, C., Marucci, G., et al. (2009). Synthesis and biological evaluation of 2-alkynyl-N6-methyl-5′-N-methylcarboxamidoadenosine derivatives as potent and highly selective agonists for the human adenosine A3 receptor. *J. Med. Chem.* 52, 7897–7900. doi: 10.1021/jm900754g

von Kugelgen, I. (2006). Pharmacological profiles of cloned mammalian P2Y-receptor subtypes. *Pharmacol. Ther.* 110, 415–432. doi: 10.1016/j.pharmthera.2005.08.014

Wan, P., Liu, X., Xiong, Y., Ren, Y., Chen, J., Lu, N., et al. (2016). Extracellular ATP mediates inflammatory responses in colitis via P2X7 receptor signaling. *Sci. Rep.* 6:19108. doi: 10.1038/srep19108

Weng, Z. J., Wu, L. Y., Zhou, C. L., Dou, C. Z., Shi, Y., Liu, H. R., et al. (2015). Effect of electroacupuncture on P2X3 receptor regulation in the peripheral and central nervous systems of rats with visceral pain caused by irritable bowel syndrome. *Purinergic Signal.* 11, 321–329. doi: 10.1007/s11302-015-9447-6

Wilson, C. N., and Mustafa, S. J. (2009). *Adenosine Receptors in Health and Disease: Handbook of Experimental Pharmacology*, Vol. 193. Berlin: Springer. doi: 10.1007/978-3-540-89615-9

Ye, J. H., and Rajendran, V. M. (2009). Adenosine: an immune modulator of inflammatory bowel diseases. *World J. Gastroenterol.* 15, 4491–4498. doi: 10.3748/wjg.15.4491

Conflict of Interest Statement: The authors declare that the research was conducted in the absence of any commercial or financial relationships that could be construed as a potential conflict of interest.

The handling Editor declared a past co-authorship with one of the authors DDB.

frontiers in Pharmacology

REVIEW
published: 07 March 2018
doi: 10.3389/fphar.2018.00193

The Metabotropic Purinergic P2Y Receptor Family as Novel Drug Target in Epilepsy

*Mariana Alves, Edward Beamer and Tobias Engel**

Department of Physiology & Medical Physics, Royal College of Surgeons in Ireland, Dublin, Ireland

Epilepsy encompasses a heterogeneous group of neurological syndromes which are characterized by recurrent seizures affecting over 60 million people worldwide. Current anti-epileptic drugs (AEDs) are mainly designed to target ion channels and/or GABA or glutamate receptors. Despite recent advances in drug development, however, pharmacoresistance in epilepsy remains as high as 30%, suggesting the need for the development of new AEDs with a non-classical mechanism of action. Neuroinflammation is increasingly recognized as one of the key players in seizure generation and in the maintenance of the epileptic phenotype. Consequently, targeting signaling molecules involved in inflammatory processes may represent new avenues to improve treatment in epilepsy. Nucleotides such as adenosine-5′-triphosphate (ATP) and uridine-5′-triphosphate (UTP) are released in the brain into the extracellular space during pathological conditions such as increased neuronal firing or cell death. Once released, these nucleotides bind to and activate specific purinergic receptors termed P2 receptors where they mediate the release of gliotransmitters and drive neuronal hyperexcitation and neuroinflammatory processes. This includes the fast acting ionotropic P2X channels and slower-acting G-protein-coupled P2Y receptors. While the expression and function of P2X receptors has been well-established in experimental models of epilepsy, emerging evidence is now also suggesting a prominent role for the P2Y receptor subfamily in seizure generation and the maintenance of epilepsy. In this review we discuss data supporting a role for the P2Y receptor family in epilepsy and the most recent finding demonstrating their involvement during seizure-induced pathology and in epilepsy.

Keywords: epilepsy, status epilepticus, pharmacoresistance, purinergic signaling, metabotropic P2Y receptors

OPEN ACCESS

Edited by:
Francisco Ciruela,
Universitat de Barcelona, Spain

Reviewed by:
Bashkim Kadriu,
National Institute of Mental Health (NIH), United States
João O. Malva,
University of Coimbra, Portugal

****Correspondence:***
Tobias Engel
tengel@rcsi.ie

Specialty section:
This article was submitted to Experimental Pharmacology and Drug Discovery, a section of the journal Frontiers in Pharmacology

Received: *20 October 2017*
Accepted: *20 February 2018*
Published: *07 March 2018*

Citation:
Alves M, Beamer E and Engel T (2018) The Metabotropic Purinergic P2Y Receptor Family as Novel Drug Target in Epilepsy. Front. Pharmacol. 9:193. doi: 10.3389/fphar.2018.00193

INTRODUCTION

The primary treatment for epilepsy is the use of anti-epileptic drugs (AEDs). These drugs control seizures by shifting the balance of inhibitory and excitatory drive in the brain (Bialer et al., 2013). 30% of patients, however, are pharmacoresistant to all available AEDs and between 40 and 50% of patients on AEDs suffer adverse effects (Baker et al., 1997). Current major goals of epilepsy research are to develop treatment strategies that impact upon disease emergence and progression, show efficacy within the currently pharmacoresistant cohort and have a lower burden of adverse effects. To this end, the role of neuroinflammation in icto- and epileptogenesis is

receiving growing attention (Terrone et al., 2017). Purinergic signaling provides a mechanism by which hyperexcitation can lead to an inflammatory response and whereby inflammation can lead to hyperexcited networks. As such, the targeting of purinergic signaling is a promising strategy for developing new treatment options (Engel et al., 2016). Purinergic signaling is mediated via two families of purinergic receptors: ionotropic P2X receptors and metabotropic P2Y receptors (Burnstock, 2007), both receptor subtypes responding to extracellular adenine or uridine nucleotides. While much of the focus of purinergic signaling in epilepsy has focussed on the P2X receptor family, the role of P2Y receptors in epilepsy has, to date, received much less attention (Engel et al., 2016; Rassendren and Audinat, 2016; Beamer et al., 2017). In this review, we summarize data from the emerging field and suggest directions in which P2Y research in epilepsy should develop.

SEIZURES, STATUS EPILEPTICUS, AND EPILEPSY

Seizures are a transient symptom resulting from abnormally excessive or synchronous neuronal firing in the brain (Fisher et al., 2014). In general, seizures do not last longer than 1–2 min and are self-limiting (Jenssen et al., 2006). Prolonged or recurrent seizures without intervening recovery periods, however, are classified as status epilepticus, a medical emergency (Betjemann and Lowenstein, 2015). Beyond epilepsy, seizures can have many etiologies, including acute insults, such as fever, hypoxia, low blood sugar, brain tumors, lack of sleep, substance abuse, or traumatic brain injury (TBI). Seizures can be classified according to their etiology, semiology, and anatomical focus (Chang et al., 2017). The transition from seizures to status epilepticus is often due to a failure of endogenous anticonvulsant mechanisms, such as the internalization or desensitization of γ-aminobutyric acid $(GABA)_A$ receptors (Naylor and Wasterlain, 2005; Wasterlain et al., 2009; Betjemann and Lowenstein, 2015). Status epilepticus is the second most common neurological emergency behind stroke, with an annual incidence of 10–41 cases per 100,000 (Hesdorffer et al., 1998). It is associated with high mortality (up to 20%), morbidity and considerable costs to the health-care system (Betjemann and Lowenstein, 2015) and can cause severe damage to the brain, leading to serious neurological complications such as cognitive impairment (Korngut et al., 2007), and the development of chronic epilepsy (Hesdorffer et al., 1998).

Where seizures are recurrent and spontaneous, epilepsy is diagnosed. According to the International League Against Epilepsy (ILAE), epilepsy is defined by any of the following conditions: "(1) at least two unprovoked (or reflex) seizures occurring $>$ 24 h apart; (2) one unprovoked (or reflex) seizure and a probability of further seizures similar to the general recurrence risk (at least 60%) after two unprovoked seizures, occurring over the next 10 years; and (3) diagnosis of an epilepsy syndrome" (Fisher et al., 2014). Epilepsy is one of the most common neurological disorders, globally. With an incidence of $\sim$1%, epilepsy affects over 65 million people worldwide (Moshe et al., 2015). This is associated with a global disease burden of 7M disability adjusted life years (DALYs) (Leonardi and Ustun, 2002) and with an estimated annual cost of over €20 billion in Europe alone according to the World Health Organization (2010). Beside the occurrence of spontaneous seizures, epilepsy is associated with an increased mortality and co-morbidities such as anxiety and depression, which severely impact quality of life (Moshe et al., 2015). Epilepsy affects people of all ages, but is most common in the young and, particularly, the elderly (Everitt and Sander, 1998). Epilepsy can either be innate or acquired, arise due to genetic mutations or via epigenetic mechanisms (Chen et al., 2017), structural or metabolic alterations (Reid and Staba, 2014), infection and immune dysregulation (Vezzani et al., 2011), some combination thereof or, as is often the case, be of unknown etiology (idiopathic epilepsy) (Pal et al., 2016). Common mutations underlying epilepsy include those affecting the function of ion channels, such as the Na^+ channel, Voltage-Gated Sodium Channel Alpha Subunit (SCN1A) (Kasperaviciute et al., 2013), reducing the action potential threshold in neurons. Structural causes often arise as a result of changes in neuronal network connectivity following an initial insult to the brain, such as head injury, stroke, or status epilepticus (Pitkanen et al., 2015). Epileptogenesis, the process of a normal brain becoming epileptic, is usually the result of a precipitating injury and characterized by an interplay of factors including ongoing cell death, inflammation and synaptic and axonal plasticity changes (Pitkanen et al., 2015). Temporal lobe epilepsy (TLE), the most prevalent form of acquired epilepsy, is characterized by hippocampal sclerosis, including neuronal loss, mossy fiber sprouting and the formation of aberrant neuronal networks which can form a unilateral seizure focus, typically in the CA3 region of the hippocampus (Rao et al., 2006), from which seizures often generalize. Possibly because of the importance of these network changes, TLE is associated with a particularly high prevalence of pharmacoresistance (Zhao et al., 2014).

Current Treatments for Epilepsy and Status Epilepticus

Over 25 AEDs are currently used in the clinic (Bialer and White, 2010). Despite the relatively large range of options available, where the mechanisms of action are understood, they fit into three broad categories: increasing inhibitory transmission (e.g., the glutamate decarboxylase catalyst, Gabapentin), decreasing excitatory transmission [e.g., the non-competitive alpha-amino-3-hydroxy-5-methyl-4-isoxazoleproprionic acid (AMPA) receptor antagonist, Perampanel] and blockade of voltage-gated ion channels (e.g., Na^+ channel blocker, lamotrigine) (Bialer and White, 2010). In most cases, AEDs have multiple actions and are incompletely understood. For example, Topiramate exerts an inhibitory effect on Na^+ conductance, enhances GABA neurotransmission via unknown mechanisms, and antagonizes AMPA receptors (Shank et al., 2000). While there is a superficial diversity in mechanisms, all treatment options rely on the concept of redressing a balance between excitatory and inhibitory drive. This has proven largely successful in controlling seizures, but no treatments have been developed that act on the emergence or progression

of the epileptic condition. Further, approximately 30% of patients remain pharmacoresistant to all available AEDs; in most cases leaving surgery as their sole remaining option (Moshe et al., 2015). Choice of treatment strategy is based on seizure type, epilepsy syndrome, health problems, other medication used, lifestyle of the patients and considerations such as pregnancy (Moshe et al., 2015; Kinney and Morrow, 2016). AEDs are the frontline treatment for epilepsy. Although strides have been made in terms of safety, tolerability, and pharmacokinetics with the new generation of AEDs, such as felbamate, gabapentin, lamotrigine or oxcarbazepine, the number of patients resistant to all treatments has not moved from 30% for approximately 80 years (Bialer et al., 2013; Moshe et al., 2015) and the search for mechanisms which could disrupt the emergence or progression of the disease remains elusive. There is therefore an urgent need to identify new drug targets which can show efficacy in patients who are currently refractory to available treatment, and can demonstrate a disease modifying effect.

When treating status epilepticus, time is a key factor and terminating the seizure is the number one priority for preventing lasting damage. A protocol for treatment of status epilepticus has been developed whereby, a first line treatment is administered within 5–10 min of seizure onset, a second line treatment is administered within 20–40 min and a third line treatment around 60 min following seizure onset (Shorvon et al., 2008). The best first line treatment is with benzodiazepines, such as lorazepam, diazepam, or midazolam (Betjemann and Lowenstein, 2015). Evidence supporting the best treatment strategy for second and third line treatments is weaker, however current practice involves the use of AEDs such as fosphenytoin, valproic acid or levetiracetam (Glauser et al., 2016) and anesthetic drugs (Betjemann and Lowenstein, 2015). As with epilepsy, approximately 30% of status epilepticus patients are refractory to available drug treatment and these patients are particularly vulnerable to adverse clinical outcomes (Novy et al., 2010). In summary, the drug development challenges for epilepsy and status epilepticus are similar, with a need in both cases for drugs which show efficacy in currently pharmacoresistant patients, while reducing comorbidities and adverse drug effects. In the case of epilepsy, preventing the emergence or progression of the disorder is also an important goal.

New Directions in Drug Development for Epilepsy

While drugs targeting excitatory and inhibitory drive have proven widely successful in controlling seizures (Bialer et al., 2013), it seems likely that in order to modify disease progression or offer efficacious drug treatment to currently pharmacoresistant epilepsy patients, alternative targets, with a novel mechanism of action, must be sought. Several experimental and clinical findings have demonstrated an important role for neuroinflammation in both icto- and epileptogenesis (Vezzani et al., 2011, 2016). High levels of inflammatory mediators are present in the brains of both experimental rodent models of epilepsy and epilepsy patients (Aronica et al., 2017) and these processes have therefore received much attention in recent years. Selective blockade of the pro-inflammatory cytokine, Interleukin-1β (IL-1β), has been shown to reduce seizures in *in vivo* models of epilepsy (Ravizza et al., 2008; Vezzani et al., 2009), while in an epileptogenesis-resistant animal, the Amazon rodent, *Proechimys*, no acute brain inflammatory response was found following experimentally-induced status epilepticus (Scorza et al., 2017).

Following an insult, such as a seizure or period of status epilepticus, pro-inflammatory cytokines, such as IL-1β, tumor necrosis factor-α (TNF-α) and IL-6 are released in the brain, primarily from astrocytes and microglia (Terrone et al., 2017). These pro-inflammatory cytokines exert a number of effects that contribute to a reduction in the seizure threshold and emergence of chronic epilepsy. Experimental evidence demonstrates that pro-inflammatory cytokines can have an effect on the firing properties of neurons directly, through the modulation of voltage-gated Na^+, Ca^{2+}, and K^+ ion channels (Viviani et al., 2007), facilitation of excitatory neurotransmission through both pre- and post-synaptic mechanisms, and disinhibition via antagonism of $GABA_A$ receptors (Garcia-Oscos et al., 2012). The effect of inflammation on seizures and epilepsy, however, is not limited to direct modulation of the excitatory/inhibitory balance. Gliosis, gliotransmission, increased permeability of the blood–brain barrier (BBB) and subsequent influx of peripheral cells and modulatory molecules, neuronal cell death and the aberrant reorganization of neuronal networks can all be consequences of a neuroinflammatory response (Vezzani et al., 2012). The causality between hyperexcitation, excitotoxicity, and neuroinflammation is circular and, as described below, intercellular signaling through purines is an important mediator of these processes, making purinergic receptors an attractive treatment target.

PURINERGIC SIGNALING

It was not until 1972 that the role of adenosine-5′-triphosphate (ATP) as an intercellular molecule, was first described by Burnstock (1972). Today, it is well-recognized that a wide variety of nucleotides, including ATP, function as either sole or co-transmitter in both the peripheral and central nervous system (CNS). ATP can act as a fast, excitatory neurotransmitter or as a neuromodulator and is involved in a vast array of short- and long-term physiological and pathological processes including inflammation, cellular survival, proliferation, cellular differentiation, and synaptic plasticity (Burnstock et al., 2011; Khakh and North, 2012; Idzko et al., 2014). It has therefore been implicated in numerous different diseases of the CNS including epilepsy (Burnstock, 2017).

Purine Release in the Brain

Purines and pyrimidines are a well-established source of energy in all living cells. These molecules, however, also play an important role in intercellular communications within the CNS (Lecca and Ceruti, 2008; Idzko et al., 2014). Adenine and uridine nucleotides are present in almost every synaptic and secretory vesicle where they are either present alone, functioning as a fast neurotransmitter or co-stored with classical neurotransmitters

(e.g., GABA or glutamate) (Abbracchio et al., 2009). Under physiological conditions, adenine and uridine nucleotides are usually present at micromolar concentrations in the extracellular space; however, under pathological conditions (e.g., inflammation, hyperexcitability, and cell death) extracellular nucleotide levels can reach the milimolar range (Dale and Frenguelli, 2009; Idzko et al., 2014; Rodrigues et al., 2015). ATP [and most likely uridine-5′-triphosphate (UTP)] can enter the extracellular space by crossing the compromised membranes of damaged and dying cells (Rodrigues et al., 2015). In addition, purines are actively released from different cell types including neurons, astrocytes, microglia, and endothelial cells to act as neuro- and glio-transmitters (Lecca and Ceruti, 2008; Rodrigues et al., 2015). Several mechanisms have been proposed to contribute to the release of nucleotides into the extracellular medium including cell damage, exocytosis of secretory granules, vesicular transport involving the vesicular nucleotide transporter (VNUT) and membrane channels such as ABC transporters, pannexins, connexins and via purinergic receptors themselves (Lecca and Ceruti, 2008; Rodrigues et al., 2015). Once released into the extracellular space, adenine and uridine nucleotides are rapidly metabolized by ectonucleotidases (e.g., ecto-nucleoside triphosphate diphosphohydrolases, ectonucleotide pyrophosphatase, alkaline phosphatases, ecto-5′-nucleotidase, and ecto-nucleoside diphosphokinase) into different breakdown products including adenosine-5′-diphosphate (ADP), adenosine, uridine-5′-diphosphate (UDP), and uridine. These metabolites, in turn, are important neurotransmitters/neuromodulators in their own right, with specific receptors for each expressed throughout the CNS (Zimmermann, 2006; Burnstock, 2007).

Direct evidence for ATP release during seizures is mixed. Large elevations in ATP on electrical stimulation of the cortex (Wu and Phillis, 1978) provided the first direct evidence that high levels of neuronal activity could induce the release of ATP. Subsequently, stimulation of the Schaffer collateral in hippocampal slices was demonstrated to induce ATP release in a Ca^{2+}-dependent, but glutamate receptor activation-independent manner (Wieraszko et al., 1989), suggesting the release of ATP was pre-synaptic. While ATP release was not detected following high frequency stimulation or electrically-induced epileptiform seizure like events in hippocampal slices (Lopatar et al., 2015), the induction of epileptiform activity in rat hippocampal slices with the use of the mGluR5-agonist, (S)-3,5-Dihydroxyphenylglycine induced the release of ATP through pannexin hemichannels (Lopatar et al., 2015). ATP release was also elevated in hippocampal slices in a high K^+ model of seizures (Heinrich et al., 2012). Dona et al. (2016) used microdialysis and high-performance liquid chromatography in order to attempt to measure extracellular concentrations of ATP and its metabolites *in vivo* after pilocarpine-induced status epilepticus and following the onset of chronic epilepsy. They found no change in ATP concentrations for 4 h following status epilepticus, but a marked increase in ATP metabolites, including adenosine monophosphate (AMP) and ADP. Concentrations of ATP and all metabolites were reduced during chronic epilepsy, but ATP was elevated by 300% during spontaneous seizures. Because ectonucleotidases rapidly hydrolyze ATP in the extracellular space and the concentration and activity of these enzymes are increased following seizures (Nicolaidis et al., 2005), it is difficult to measure changes in ATP release directly. Less interest has been shown in investigating UTP release following seizures, however, Koizumi et al. (2007) demonstrated that following kainic acid (KA)-induced-seizure-like events in hippocampal slices, extracellular concentrations of UTP were elevated approximately threefold (Koizumi et al., 2007).

Whereas the anticonvulsive properties of the nucleoside, adenosine, are well-documented (Boison, 2016), the possible contribution of extracellular nucleotides to seizure pathology is a relatively new research area (Engel et al., 2016). The discovery of increased extracellular levels of ATP in seizure-prone rats was one of the first studies to suggest a functional contribution of extracellular nucleotides to seizures (Wieraszko and Seyfried, 1989). Demonstrating a direct impact on seizures, another early study showed that the microinjection of ATP analogs into the prepiriform cortex led to the generation of motor seizures (Knutsen, 1997). More recent evidence implicating extracellular nucleotides in seizure generation stems from studies showing that the injection of ATP into the brain of mice led to the development of high spiking on the electroencephalogram (EEG) and exacerbated seizure severity during status epilepticus (Engel et al., 2012; Sebastian-Serrano et al., 2016). In contrast, treatment with UTP decreases the rate of neuronal firing in epileptic rats (Kovacs et al., 2013) and in mice subjected to status epilepticus (Alves et al., 2017). Further, UTP metabolites such as uridine reduce epileptic seizures in patients with epileptic encephalopathy (Koch et al., 2017).

P2 Receptor Family

Once released, extracellular adenine and uridine nucleotides bind to and activate specific cell surface receptors termed P2 receptors which are ubiquitously expressed and functional on all cell types in the CNS (Burnstock, 2007). The P2 family of receptors include the ionotropic P2X channels and the metabotropic P2Y receptors. The fast acting P2X channels are a family of seven cation-permeable ionotropic receptor subunits (P2X1-7) which form both homo- and hetero-trimers, depolarizing the cell membrane upon activation (Khakh and North, 2006). All P2X receptors are activated by their main endogenous agonist, ATP, and are permeable to small cations including Na^+, K^+, and Ca^{2+}. All P2X receptor subunits share a common topology with two transmembrane domains, a large extracellular loop and an intracellular amino and carboxyl terminus (Khakh and North, 2006; Burnstock, 2007). Much attention has been paid to the study of P2X receptors over the past decades, in particular in diseases of the CNS (Burnstock et al., 2011; Saez-Orellana et al., 2015). P2X receptor activation has been implicated in numerous pathological conditions including neurodegeneration, inflammation, ischemia, brain trauma, and hyperexcitability (Engel et al., 2016; Burnstock, 2017). Among the P2X receptor subtypes, the P2X7 receptor has attracted by far the most attention as a potential therapeutic target for brain diseases (Sperlagh and Illes, 2014; Rech et al., 2016).

While the P2X receptor family is made up of fast acting ligand-gated ion channels, the metabotropic P2Y receptor family

consists of eight G-protein coupled slower-acting receptors: $P2Y_1$, $P2Y_2$, $P2Y_4$, $P2Y_6$, $P2Y_{11}$, $P2Y_{12}$, $P2Y_{13}$, and $P2Y_{14}$ (von Kugelgen, 2006; Burnstock, 2007). In contrast to P2X channels, P2Y receptors can be activated by more than one substrate including the adenine nucleotides ATP ($P2Y_2$ and $P2Y_{11}$) and ADP ($P2Y_1$, $P2Y_{12}$, and $P2Y_{13}$) and the uridine nucleotides UTP ($P2Y_2$ and $P2Y_4$), UDP ($P2Y_6$ and $P2Y_{14}$), and UDP-glucose ($P2Y_{14}$). P2Y receptors contain the typical features of G-protein-coupled receptors which includes an extracellular amino terminus, intracellular carboxyl terminus and seven transmembrane-spanning motifs (Jacobson et al., 2015). P2Y receptors can be further subdivided into groups based on their coupling to specific G proteins. $P2Y_1$, $P2Y_2$, $P2Y_4$, $P2Y_6$, and $P2Y_{11}$ receptors are coupled to Gq proteins, which stimulate phospholipase C, ultimately resulting in the subsequent release of Ca^{2+} from intracellular stores and activation of protein kinase C (PKC). Of these, $P2Y_{11}$ receptor can also couple to Gs, stimulating adenylate cyclase and increasing the production of cyclic adenosine monophosphate (cAMP) (von Kugelgen, 2006). $P2Y_{12}$, $P2Y_{13}$, and $P2Y_{14}$ are coupled to Gi proteins, inhibiting adenylate cyclase and thereby decreasing cAMP production (von Kugelgen, 2006).

Involvement of P2Y Receptor Signaling in Brain Inflammation and Excitability

P2Y receptors are involved in a myriad of different cellular functions and pathological processes pertinent to the process of epileptogenesis and epilepsy including neuroinflammation, neurodegeneration, synaptic reorganization, and changes in neurotransmitter release (von Kugelgen, 2006; Jacobson and Boeynaems, 2010; Pitkanen et al., 2015; Guzman and Gerevich, 2016) making them an attractive antiepileptic therapeutic target.

Inflammatory processes in the brain have received much attention over recent years and are thought to play a major role in seizure-induced pathology and the development of epilepsy (Vezzani et al., 2011). The principle ligands for P2Y receptors are the purine, ATP, the pyrimidine, UTP, and their metabolites, such as ADP and UDP (Burnstock, 2007). The role of each receptor in neuroinflammation is dictated by its affinity for different ligands and downstream targets. ATP is both released as a result of inflammation and promotes pro-inflammatory mechanisms. This circular causality can underpin a positive feedback loop whereby neuroinflammation becomes self-sustaining (Idzko et al., 2014). Less is known about the role of UTP in mediating neuroinflammation. The role of different P2Y receptors in mediating neuroinflammation and cell death seems to be divergent (Forster and Reiser, 2015), depending on downstream signaling pathways and mutually antagonistic actions, but is incompletely understood. The $P2Y_1$ receptor, activated by the ATP metabolite ADP, is expressed also on astrocytes and activated under conditions of oxidative stress, prompting the release of IL-6 (Fujita et al., 2009). IL-6 has been shown to play an anti-inflammatory role during 'classic signaling' involving the binding of IL-6 to the membrane-bound IL-6 receptor which induces the dimerization of the β-receptor glycoprotein 130 (gp130). In contrast however, IL-6 is also critical for pro-inflammatory signaling in a process termed 'trans-signaling,' whereby IL-6 stimulates distant cells which only express gp130 in the absence of the IL-6 receptor (Rothaug et al., 2016). A more recent study has shown that in a chronic model of epilepsy, astrocytes from kindled rats show enhanced Ca^{2+}-dependent signaling and astroglial hyperexcitability, which requires the activation of the $P2Y_1$ receptor (Alvarez-Ferradas et al., 2015). $P2Y_1$ antagonism prevented cognitive deficits and neuronal damage in a model of ischemia in mice (Carmo et al., 2014). A recent study also showed improved histological and cognitive outcomes in a model of TBI in mice provided by $P2Y_1$ receptor antagonism (Choo et al., 2013). Activation of astrocytic $P2Y_2$ receptors promotes astrocyte activation and migration via an interaction with αV-integrin (Wang et al., 2005). The $P2Y_2$ receptor has also been shown to play a protective role against chronic inflammation-induced neurodegeneration in a model of Alzheimer's disease (Kong et al., 2009). A role for the uridine-sensitive $P2Y_4$ receptor in mediating neuroinflammation has not been established (Beamer et al., 2016), with progress hamstrung by a lack of specific tools for targeting this receptor. The $P2Y_6$ receptor promotes the activation of microglia and the adoption of a phagocytic phenotype following activation by the UTP metabolite UDP (Koizumi et al., 2007). This is dependent on downstream signaling involving phospholipase C and PKC. Other studies have suggested a role for the $P2Y_{12}$ receptor in microglial activation (Ohsawa et al., 2010), showing that activation of integrin-β1 in microglia through $P2Y_{12}$ is involved in directional process extension by microglia in brain tissue. As discussed in more detail below, $P2Y_{12}$-dependent process extension has been shown to be increased following status epilepticus in mice (Eyo et al., 2014).

The effects of P2Y signaling are not limited to inflammatory processes and cellular survival alone. P2Y signaling also impacts directly on neuronal excitability, synaptic strength, and synaptic plasticity (Guzman and Gerevich, 2016). Presynaptic P2Y receptors have been shown to affect the release of different neurotransmitters including glutamate, noradrenaline and GABA, most likely by reducing presynaptic Ca^{2+} influx (Fischer et al., 2009). $P2Y_1$, $P2Y_2$, and $P2Y_4$ inhibit the release of glutamate in the hippocampus (Mendoza-Fernandez et al., 2000; Koizumi et al., 2003; Rodrigues et al., 2005), possibly through the inhibition of voltage-activated Ca^{2+} channels (VACCs) (Gerevich et al., 2004). Using the same mechanism, the release of noradrenaline in the hippocampus was also blocked via $P2Y_1$, $P2Y_{12}$, and $P2Y_{13}$ activation (Csolle et al., 2008). Similarly, activation of $P2Y_4$ with UTP blocks the release of the inhibitory neurotransmitter GABA from cerebellar basket cells (Donato et al., 2008). P2Y receptors alter the expression/function of other membrane receptors and voltage-gated ion channels. $P2Y_1$ triggers the desensitization or internalization of the metabotropic glutamate receptor 1 (mGluR1) (Mundell et al., 2004) and inhibits *N*-methyl-D-aspartate (NMDA) receptor channels (Luthardt et al., 2003). $P2Y_1$ also increases the sensitivity of the $GABA_A$ receptor (Saitow et al., 2005) and inhibits P2X receptors (Gerevich et al., 2007). P2Y receptor activation can lead to the inhibition of VACCs (Diverse-Pierluissi et al., 1991) thereby potentially influencing neuronal excitability and synaptic

plasticity. P2Y receptors also block potassium channels [e.g., voltage-gated potassium channel subunit KvLQT2,3 (Filippov et al., 2006) or G protein-coupled inward rectifying channels 1, 2, and 4 (GIRK1,2,&4)] (Filippov et al., 2004), inhibiting membrane hyperpolarisation and thereby facilitating an increased frequency of neuronal firing (Brown and Passmore, 2009; Guzman and Gerevich, 2016). On a network level, $P2Y_1$ increases the firing of GABAergic inhibitory neurons either directly or via $P2Y_1$-dependent activation of astrocytes in the hippocampus, eventually leading to an increase in inhibitory-postsynaptic currents (IPSCs) in pyramidal neurons (Bowser and Khakh, 2004). In a more recent study, Jacob et al. (2014) showed that astrocytic $P2Y_1$ activation increases extracellular concentrations of GABA by inhibiting Ca^{2+} signaling dependent GABA transport (Jacob et al., 2014). In conclusion, while P2X receptors excerpt a mainly facilitatory effect on synaptic transmission (Khakh and North, 2012), the effects of P2Y receptors seem to be context-specific, either increasing or decreasing neuronal firing by altering excitatory and inhibitory neurotransmitter release or altering receptor function (e.g., NMDA and $GABA_A$) and channel conductance (e.g., voltage-gated KCNQ2/3 potassium channel) (Guzman and Gerevich, 2016).

PURINERGIC SIGNALING AS A NOVEL DRUG TARGET IN EPILEPSY

Mounting evidence has accumulated over the past decades demonstrating a causal role for purinergic signaling in numerous pathological conditions ranging from cancer (Di Virgilio, 2012), cardiovascular disease (Ralevic, 2015), blood cell diseases (McGovern and Mazzone, 2014) to diabetes (Fotino et al., 2015) and brain diseases (Puchalowicz et al., 2014). Among brain diseases, intervention in purinergic signaling has been postulated as a new therapeutic avenue for acute insults to the brain such as stroke (Kuan et al., 2015) and TBI (Kimbler et al., 2012) and for chronic brain diseases including neurodegenerative diseases (e.g., Huntington's, Alzheimer's, and Parkinson's disease) (Miras-Portugal et al., 2016), neuropsychiatric disorders (e.g., depression and schizophrenia) (Burnstock et al., 2011) and also epilepsy (Beamer et al., 2017). Emphasizing the potential for targeting purinergic signaling as a promising new therapeutic strategy, several compounds are already used in the clinic, including the $P2Y_2$ agonist Diquafosol for the treatment of dry eye (Lau et al., 2014) or Clopidogrel, a $P2Y_{12}$ antagonist used for the treatment of thrombosis (Sarafoff et al., 2012) while others have progressed into clinical trials such as antagonists of the ionotropic P2X3 used against refractory chronic cough (Abdulqawi et al., 2015) and P2X7 receptors used against rheumatoid arthritis (Keystone et al., 2012) and other inflammatory conditions (Rech et al., 2016).

To date, most of the studies performed to elucidate the changes in expression and functional contribution of purinergic P2 receptors to seizures and epilepsy have focused on the P2X receptor subtype, in particular the P2X7 receptor (reviewed in Beamer et al., 2017), with relatively little attention paid to the P2Y receptor family. The lack of apparent interest was largely due to a lack of suitable tools (e.g., drugs to manipulate P2Y function) and the strong focus on fast synaptic effects conferred by the ionotropic P2X receptors (Engel et al., 2016). Recent studies using experimental animal models of status epilepticus and epilepsy and analysis of patient brain tissue, however, suggest a prominent role for P2Y signaling during seizures and the development of epilepsy (**Table 1**). In the last section of this review we describe in detail the evidence linking a pathological activation of the metabotropic P2Y receptors to seizure generation and seizure-induced pathology and discuss the antiepileptic potential of drugs targeting P2Y signaling.

P2Y Expression Following Status Epilepticus

One of the earliest studies analyzing P2Y expression changes following status epilepticus used the intraperitoneal KA-induced status epilepticus mouse model (Avignone et al., 2008). Here, the authors observed an increase in transcription of *P2ry*$_6$, *P2ry*$_{12}$, and *P2ry*$_{13}$ in the hippocampus. In another study using the intraperitoneal pilocarpine mouse model, Rozmer et al. (2016) show an increase in $P2Y_1$ activity in neuronal progenitor cells following status epilepticus. In a more recent study, our group published a comprehensive analysis of changes in transcription and expression across the entire P2Y family of receptors following status epilepticus using two different mouse models: the intraamygdala KA mouse model of status epilepticus (Mouri et al., 2008) and the intraperitoneal pilocarpine mouse model of status epilepticus (Alves et al., 2017). Both, intraamygdala KA and intraperitoneal pilocarpine-induced status epilepticus increased the transcription of the uridine-sensitive P2Y receptors *P2ry*$_2$, *P2ry*$_4$, and *P2ry*$_6$ in the hippocampus. At the same time, the transcription of the adenine-sensitive receptors *P2ry*$_1$, *P2ry*$_{12}$, and *P2ry*$_{13}$ was downregulated. At the protein level, hippocampal levels of $P2Y_1$, $P2Y_2$, $P2Y_4$, and $P2Y_6$ were increased and $P2Y_{12}$ was decreased following status epilepticus. No immunohistochemistry was performed to identify cell types expressing the different P2Y receptors. Thus, these results show that changes in the transcription of P2Y receptors following status epilepticus closely correlate with the known profile of agonists (i.e., adenine-sensitive receptors are downregulated and uridine-sensitive receptors are upregulated) and, at the protein level, the G-protein coupling of the receptors with P2Y receptors coupled to Gq being increased and P2Y receptors coupled to Gi being downregulated or not changed (Alves et al., 2017).

P2Y Expression During Chronic Epilepsy

Much less is known about the expression profile of P2Y receptors during epilepsy. To date, the only study carried out characterizing P2Y expression in experimental epilepsy was undertaken using the intraamygdala KA mouse model (Alves et al., 2017). In this model, mice become epileptic after a short latent period of 2–5 days (Mouri et al., 2008). Analysis of the hippocampus 14 days-post status epilepticus revealed increased *P2ry*$_1$, *P2ry*$_2$, and *P2ry*$_6$ transcription and increased $P2Y_1$, $P2Y_2$, and $P2Y_{12}$ protein levels. No changes were observed for the remaining receptors. Thus, P2Y upregulation seems to be the predominant response during experimental epilepsy, probably due to an increase in

TABLE 1 | Summary of the main findings of P2Y receptor expression and function during status epilepticus and epilepsy in experimental models of epilepsy and patient brain.

Disease process/stage	Epilepsy models/patients	Brain region	Techniques/drugs	Main results	Reference
Status epilepticus	i.p. KA-induced status epilepticus in mice	Hippocampus	GFP reporter mice; hippocampal slices; qPCR; UDP (broad-spectrum P2Y receptor agonist) and 2-MeSADP treatment ($P2Y_1$, $P2Y_{12}$, $P2Y_{13}$ agonist)	Upregulation of *P2ry*$_6$, *P2ry*$_{12}$ transcripts after status epilepticus; transient downregulation of the *P2ry*$_{13}$ transcript 3 h following status epilepticus and increased *P2ry*$_{13}$ transcript 48 h post-status epilepticus; increased microglia currents after treatment with UDP and 2-MeSADP	Avignone et al., 2008
Status epilepticus	i.p. and i.c.v. KA-induced status epilepticus in mice	Hippocampus	$P2Y_{12}$ knock-out mice	Increased seizure phenotype; reduced hippocampal microglial processes	Eyo et al., 2014
Status epilepticus	i.p. KA-induced status epilepticus in mice	Hippocampus	GFP reporter mice; hippocampal slices and two photon microscopy; 2-MeSADP treatment ($P2Y_1$, $P2Y_{12}$, $P2Y_{13}$ agonist)	Increased velocity of microglia process extension toward a pipette containing 2-MeSADP following induction of status epilepticus	Avignone et al., 2015
Status epilepticus	i.p. pilocarpine-induced status epilepticus in mice	Hippocampus	IH	$P2Y_1$ activated in neuronal progenitor cells following status epilepticus	Rozmer et al., 2016
Status epilepticus and epilepsy	i.a. KA-induced epilepsy in mice; i.p. pilocarpine-induced statusepilepticus in mice	Hippocampus (mice and patients)	WB; qPCR; i.c.v. treatment with ADP and UTP (broad-spectrum P2Y receptor agonists)	Status epilepticus: Increased *P2ry*$_2$, *P2ry*$_4$, and *P2ry*$_6$ and decreased *P2ry*$_1$, *P2ry*$_{12}$, *P2ry*$_{13}$, and *P2ry*$_{14}$ transcript levels; increased $P2Y_1$, $P2Y_2$, $P2Y_4$, and $P2Y_6$ and decreased $P2Y_{12}$ protein levels. ADP exacerbates seizure severity; UTP decreases seizure severity and neuronal death	Alves et al., 2017
	TLE patient brain			Epilepsy: Increased *P2ry*$_1$, *P2ry*$_2$, and *P2ry*$_6$ transcripts in mice; increased $P2Y_1$, $P2Y_2$, and $P2Y_{12}$ protein levels in mice. Increased $P2Y_1$ and $P2Y_2$ and decreased $P2Y_{13}$ protein levels in TLE patients	
Epilepsy	Patients with intractable epilepsy associated with focal cortical dysplasia	Cortex	WB; IH	Increased $P2Y_1$, $P2Y_2$, and $P2Y_4$ expression in astrocytes	Sukigara et al., 2014
Epilepsy	Rapid kindling protocol in rats	Hippocampus	Hippocampal slices; treatment with $P2Y_1$ antagonist MRS2179	Enhanced spontaneous Ca^{2+}-dependent signaling and astroglial hyperexcitability via $P2Y_1$ antagonism	Alvarez-Ferradas et al., 2015

GFP, green fluorescent protein; i.a., intraamygdala; i.c.v., intra-cerebro-ventricular; IH, immunohistochemistry; i.p., intraperitoneal; qPCR, quantitative polymerase chain reaction; TLE, temporal lobe epilepsy; WB, western blot.

inflammatory processes in the epileptic brain. In the same study, resected hippocampal samples from drug-refractory epilepsy patients were also analyzed. In these samples, as seen before in hippocampal samples from epileptic mice, the predominant response was an upregulation of P2Y receptors with $P2Y_1$ and $P2Y_2$ significantly upregulated. Of note, the only exception, and in contrast to findings from the mouse model of epilepsy, expression of the $P2Y_{13}$ receptor was found at lower levels in the epileptic brain compared to controls (Alves et al., 2017). In another previous study using brain tissue from patients suffering from intractable epilepsy associated with focal cortical dysplasia, Sukigara et al. (2014) showed increased levels of $P2Y_1$, $P2Y_2$, and $P2Y_4$. Interestingly, the authors reported the main increase to be in astrocytes (Sukigara et al., 2014). Thus, P2Y receptor expression is altered during epilepsy, however, in contrast to status epilepticus, the main response was an upregulation of the P2Y receptor family.

P2Y Function During Status Epilepticus

Despite the involvement of P2Y signaling in numerous pathological processes believed to play a key role during epilepsy, a possible involvement of the different P2Y receptor subtypes to seizure-induced pathology remains poorly explored and only three recent studies have suggested a functional contribution of P2Y receptors to seizures or seizure-induced pathology. The first study demonstrating a causal role for P2Y signaling during status epilepticus used mice deficient in $P2Y_{12}$ (Eyo et al., 2014). $P2Y_{12}$ is one of the most important therapeutic targets of the P2Y receptor family, with $P2Y_{12}$ agonists already routinely used in the clinic as an antithrombotic agent (Cattaneo, 2015). Eyo et al. (2014) report a $P2Y_{12}$-dependent extension of microglial process toward neurons following KA-induced status epilepticus. Neuronal NMDA receptor activation led to an influx of Ca^{2+}, stimulating ATP release, which subsequently activated microglial $P2Y_{12}$ receptors, which, in turn stimulated the extension of the processes. Interestingly, $P2Y_{12}$ knock-out mice, in which this process was inhibited, showed an increased seizure severity (Eyo et al., 2014). Thus, the authors concluded that microglial $P2Y_{12}$ receptors are necessary for microglia-neuron interaction during status epilepticus and that microglial process extension via $P2Y_{12}$ may serve an anti-ictal function. In a later study, Avignone et al. (2015) demonstrate that microglial processes extend toward a pipette containing methylthio-ADP, an agonist for $P2Y_1$, $P2Y_{12}$, and $P2Y_{13}$ (and a weak agonist for $P2Y_{11}$). The velocity of this chemotaxis was increased in activated microglia following status epilepticus. Because they also found an upregulation of $P2Y_{12}$ in activated microglia, the authors attributed this receptor as the likely mediator of this response (Avignone et al., 2015). More recently, our group has shown seizure altering properties of the broad-spectrum P2Y agonists ADP and UTP in the intraamygdala KA mouse model (Alves et al., 2017). Once status epilepticus was established, mice treated with ADP showed an increased seizure severity and mice treated with UTP showed a strong reduction in seizure severity and accompanying seizure-induced cell death (Alves et al., 2017). These results are in line with protective cellular mechanisms acting during status epilepticus regarding the P2Y receptor family with adenine-sensitive receptors being generally downregulated during status epilepticus and uridine-sensitive receptors being upregulated (**Figure 1**).

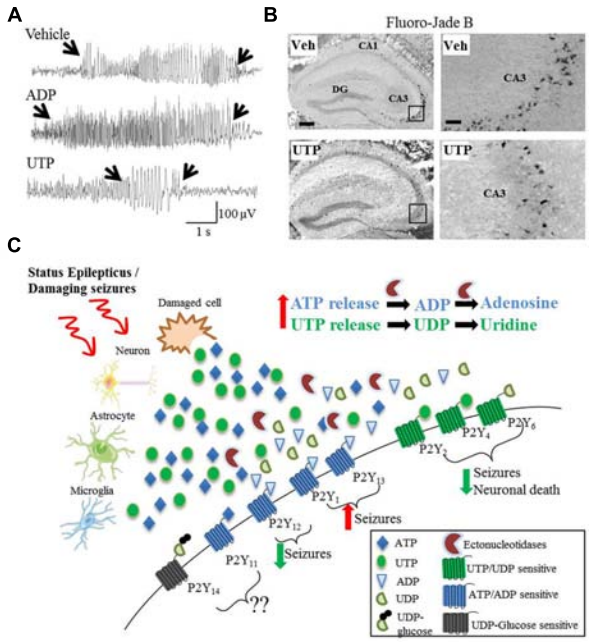

FIGURE 1 | Divergent effects on seizures and seizure-induced pathology of different P2Y agonists. **(A)** Representative EEG traces recorded during intraamygdala KA-induced status epilepticus showing pro-convulsive effects of ADP treatment, while UTP acts as potent anti-convulsive. **(B)** UTP protects against neuronal cell death following status epilepticus, visualized with the neuronal-cell death marker Fluoro-Jade B. **(C)** Hypothetical model of P2Y receptor function during and after status epilepticus or damaging seizures. During and following status epilepticus, purines (e.g., ATP and UTP) are actively released from different cell types including neurons, astrocytes and microglia or enter the extracellular space from damaged/necrotic cells. While the activation of UTP/UDP-sensitive P2Y receptors ($P2Y_2$, $P2Y_4$, and $P2Y_6$) may has anticonvulsive and neuroprotective effects, the activation of ATP/ADP-sensitive P2Y receptors ($P2Y_1$ and $P2Y_{13}$) may be pro-convulsive. The role of $P2Y_{11}$ and $P2Y_{14}$ have not been studied so far and therefore are unknown. Counterintuitively, $P2Y_{12}$ is ATP/ADP-sensitive, but seems to be anticonvulsive and neuroprotective.

In conclusion, while these results demonstrate a causal role for P2Y signaling during status epilepticus, we are still far from a clear and comprehensive picture of how individual P2Y receptors impact on seizure pathology.

P2Y Function During Chronic Epilepsy

Although results from functional studies during status epilepticus and changes in expression of P2Y receptors during epilepsy strongly suggest a role for these receptors in epilepsy, to date, no studies have been performed to determine the functional contribution of P2Y receptors to epileptogenesis or the epileptic phenotype. Possible reasons are the lack of centrally available P2Y-targeting drugs and the lack of mouse models with conditional deletion of P2Y receptors, both essential for the study of the involvement of P2Y receptors during epilepsy.

CONCLUSION AND FUTURE PERSPECTIVES

What remains to be done to establish P2Y receptors as potential drug target for epilepsy in the future? Despite the exciting emerging data revealing P2Y signaling in the brain, we are only at the beginning of understanding the potential role in seizure generation and during epileptogenesis. Recent studies have shown distinct changes in expression of the P2Y receptor family following status epilepticus and during seizures and a functional contribution has been postulated using broad-spectrum P2Y agonists (ADP and UTP) (Alves et al., 2017) and *P2Y*$_{12}$ knock-out mice (Eyo et al., 2014), there are many key issues, however, which will have to be resolved before considering P2Y receptors as valid drug target.

(i) Studies have demonstrated altered P2Y receptor expression following status epilepticus and during epilepsy (Alves et al., 2017). To get a better picture about the potential role of P2Y signaling during seizure-related pathologies, however, we must determine what cell types (e.g., neurons vs. glia; inhibitory vs. excitatory neurons) express the receptor and their sub-cellular localization (e.g., somatic vs. synaptic). (ii) Treatment of mice during status epilepticus with P2Y broad-spectrum agonists suggest a role of these receptors in seizure generation and seizure-induced pathology (Alves et al., 2017), however, we still do not know the role of individual P2Y receptors during seizures, with the only exception being the P2Y$_{12}$ receptor (Eyo et al., 2014). P2Y receptor-specific, centrally available drugs or P2Y knock-out mice, if possible cell-specific, must be used to determine the possible impact of the different P2Y receptors on seizures and epilepsy. (iii) P2Y receptors have been shown to be involved in numerous pathological processes in the brain (Beamer et al., 2016), however, signaling downstream of P2Y during seizures and epilepsy remains elusive, with the only exception being P2Y$_{12}$ functioning on microglia (Eyo et al., 2014). P2Y receptors have been shown to alter both excitatory (e.g., glutamate) and inhibitory neurotransmitter release in the brain (Garcia-Oscos et al., 2012), therefore, future studies must determine whether P2Y signaling impacts on the release of neurotransmitters and what neurotransmitters are altered during seizures. Do seizure-induced changes in P2Y function impact on the function of other cell membrane channels/receptors (e.g., potassium channels, calcium channels, NMDA receptors, GABA receptors) thereby altering neuronal excitability? (iv) Different P2Y receptors respond to different agonists (e.g., UTP, UDP, ATP, and ADP) (von Kugelgen, 2006), however, we still do not know at what concentrations these nucleotides are available during seizures/epilepsy and when, where and from which cell types these nucleotides are released or what mechanisms (e.g., ectonucleotidases) are responsible for extracellular nucleotide concentration changes. (v) To date, studies have solely used the KA and pilocarpine mouse model of status epilepticus to analyze P2Y signaling during seizures (Avignone et al., 2008, 2015; Eyo et al., 2014; Alves et al., 2017). These mouse models rely, however, on chemically-induced seizures and only recapitulate certain aspects of the disease (Reddy and Kuruba, 2013). Results must therefore be confirmed in other models of acute seizures and chronic epilepsy. (vi) To date, we do not know what drives P2Y receptor expression during seizures. The clear expression pattern according to P2Y receptor agonists during status epilepticus, however, points toward common pathways. The identification of what drives P2Y expression during and following seizures may also therefore provide much needed new target genes for seizure control. (vii) While changes in P2Y receptor expression and, to an extent, function, have been analyzed in hippocampal tissue, extrahippocampal brain areas, in particular the cortex, may also contribute to the epilepsy phenotype (Thompson and Duncan, 2005; Helmstaedter, 2007). Status epilepticus is associated with significant extrahippocampal injury, including in the cortex (Fujikawa et al., 2000) and cortical thinning has also been reported in patients with pharmacoresistant TLE (Bernhardt et al., 2010). Consequently, the P2Y expression profile must also be analyzed in non-hippocampal brain regions. (viii) Data obtained by using the broad-spectrum agonists ADP and UTP with ADP exacerbating and UTP decreasing seizure pathology (Alves et al., 2017), suggest that a mix of antagonist (e.g., adenine-specific receptors) and agonists (e.g., uridine-specific receptors) may provide better protection than single receptor targeting.

In conclusion, P2Y signaling is altered during and after status epilepticus and during epilepsy. Functional studies demonstrate an involvement of P2Y receptors in seizure pathology. Despite promising results, however, we are only at the beginning of understanding the role of P2Y signaling during seizures to ultimately establish P2Y targeting as possible therapeutic avenue in epilepsy.

AUTHOR CONTRIBUTIONS

MA wrote the manuscript and designed the Figure and Table. EB edited the manuscript. TE wrote and edited the manuscript.

FUNDING

This work was supported by grants from the Science Foundation Ireland (Project No. 13/SIRG/2098) to (TE), the Health Research Board Ireland (Project No. HRA-POR-2015-1243) to (TE), and the H2020 Marie Skłodowska-Curie Actions Individual Fellowship (Project No. 753527) to (EB).

REFERENCES

Abbracchio, M. P., Burnstock, G., Verkhratsky, A., and Zimmermann, H. (2009). Purinergic signalling in the nervous system: an overview. *Trends Neurosci* 32, 19–29. doi: 10.1016/j.tins.2008.10.001

Abdulqawi, R., Dockry, R., Holt, K., Layton, G., McCarthy, B. G., Ford, A. P., et al. (2015). P2X3 receptor antagonist (AF-219) in refractory chronic cough: a randomised, double-blind, placebo-controlled phase 2 study. *Lancet* 385, 1198–1205. doi: 10.1016/S0140-6736(14)61255-1

Alvarez-Ferradas, C., Morales, J. C., Wellmann, M., Nualart, F., Roncagliolo, M., Fuenzalida, M., et al. (2015). Enhanced astroglial Ca2+ signaling increases excitatory synaptic strength in the epileptic brain. *Glia* 63, 1507–1521. doi: 10.1002/glia.22817

Alves, M., Gomez-Villafuertes, R., Delanty, N., Farrell, M. A., O'Brien, D. F., Miras-Portugal, M. T., et al. (2017). Expression and function of the metabotropic purinergic P2Y receptor family in experimental seizure models and patients with drug-refractory epilepsy. *Epilepsia* 58, 1603–1614. doi: 10.1111/epi.13850

Aronica, E., Bauer, S., Bozzi, Y., Caleo, M., Dingledine, R., Gorter, J. A., et al. (2017). Neuroinflammatory targets and treatments for epilepsy validated in experimental models. *Epilepsia* 58(Suppl. 3), 27–38. doi: 10.1111/epi.13783

Avignone, E., Lepleux, M., Angibaud, J., and Nagerl, U. V. (2015). Altered morphological dynamics of activated microglia after induction of status epilepticus. *J. Neuroinflammat.* 12:202. doi: 10.1186/s12974-015-0421-6

Avignone, E., Ulmann, L., Levavasseur, F., Rassendren, F., and Audinat, E. (2008). Status epilepticus induces a particular microglial activation state characterized by enhanced purinergic signaling. *J. Neurosci.* 28, 9133–9144. doi: 10.1523/JNEUROSCI.1820-08.2008

Baker, G. A., Jacoby, A., Buck, D., Stalgis, C., and Monnet, D. (1997). Quality of life of people with epilepsy: a European study. *Epilepsia* 38, 353–362.

Beamer, E., Fischer, W., and Engel, T. (2017). The ATP-gated P2X7 receptor as a target for the treatment of drug-resistant epilepsy. *Front. Neurosci.* 11:21. doi: 10.3389/fnins.2017.00021

Beamer, E., Goloncser, F., Horvath, G., Beko, K., Otrokocsi, L., Kovanyi, B., et al. (2016). Purinergic mechanisms in neuroinflammation: an update from molecules to behavior. *Neuropharmacology* 104, 94–104. doi: 10.1016/j.neuropharm.2015.09.019

Bernhardt, B. C., Bernasconi, N., Concha, L., and Bernasconi, A. (2010). Cortical thickness analysis in temporal lobe epilepsy: reproducibility and relation to outcome. *Neurology* 74, 1776–1784. doi: 10.1212/WNL.0b013e3181e0f80a

Betjemann, J. P., and Lowenstein, D. H. (2015). Status epilepticus in adults. *Lancet Neurol.* 14, 615–624. doi: 10.1016/S1474-4422(15)00042-3

Bialer, M., Johannessen, S. I., Levy, R. H., Perucca, E., Tomson, T., and White, H. S. (2013). Progress report on new antiepileptic drugs: a summary of the Eleventh Eilat Conference (EILAT XI). *Epilepsy Res.* 103, 2–30. doi: 10.1016/j.eplepsyres.2012.10.001

Bialer, M., and White, H. S. (2010). Key factors in the discovery and development of new antiepileptic drugs. *Nat. Rev. Drug Discov.* 9, 68–82. doi: 10.1038/nrd2997

Boison, D. (2016). Adenosinergic signaling in epilepsy. *Neuropharmacology* 104, 131–139. doi: 10.1016/j.neuropharm.2015.08.046

Bowser, D. N., and Khakh, B. S. (2004). ATP excites interneurons and astrocytes to increase synaptic inhibition in neuronal networks. *J. Neurosci.* 24, 8606–8620. doi: 10.1523/JNEUROSCI.2660-04.2004

Brown, D. A., and Passmore, G. M. (2009). Neural KCNQ (Kv7) channels. *Br. J. Pharmacol.* 156, 1185–1195. doi: 10.1111/j.1476-5381.2009.00111.x

Burnstock, G. (1972). Purinergic nerves. *Pharmacol. Rev.* 24, 509–581.

Burnstock, G. (2007). Physiology and pathophysiology of purinergic neurotransmission. *Physiol. Rev.* 87, 659–797. doi: 10.1152/physrev.00043.2006

Burnstock, G. (2017). Purinergic signalling: therapeutic developments. *Front. Pharmacol.* 8:661. doi: 10.3389/fphar.2017.00661

Burnstock, G., Krugel, U., Abbracchio, M. P., and Illes, P. (2011). Purinergic signalling: from normal behaviour to pathological brain function. *Prog. Neurobiol.* 95, 229–274. doi: 10.1016/j.pneurobio.2011.08.006

Carmo, M. R., Simoes, A. P., Fonteles, A. A., Souza, C. M., Cunha, R. A., and Andrade, G. M. (2014). ATP P2Y1 receptors control cognitive deficits and neurotoxicity but not glial modifications induced by brain ischemia in mice. *Eur. J. Neurosci.* 39, 614–622. doi: 10.1111/ejn.12435

Cattaneo, M. (2015). P2Y12 receptors: structure and function. *J. Thromb. Haemost.* 13(Suppl. 1), S10–S16. doi: 10.1111/jth.12952

Chang, R. S., Leung, C. Y. W., Ho, C. C. A., and Yung, A. (2017). Classifications of seizures and epilepsies, where are we? - A brief historical review and update. *J. Formos. Med. Assoc.* 116, 736–741. doi: 10.1016/j.jfma.2017.06.001

Chen, T., Giri, M., Xia, Z., Subedi, Y. N., and Li, Y. (2017). Genetic and epigenetic mechanisms of epilepsy: a review. *Neuropsychiatr. Dis. Treat.* 13, 1841–1859. doi: 10.2147/NDT.S142032

Choo, A. M., Miller, W. J., Chen, Y. C., Nibley, P., Patel, T. P., Goletiani, C., et al. (2013). Antagonism of purinergic signalling improves recovery from traumatic brain injury. *Brain* 136(Pt 1), 65–80. doi: 10.1093/brain/aws286

Csolle, C., Heinrich, A., Kittel, A., and Sperlagh, B. (2008). P2Y receptor mediated inhibitory modulation of noradrenaline release in response to electrical field stimulation and ischemic conditions in superfused rat hippocampus slices. *J. Neurochem.* 106, 347–360. doi: 10.1111/j.1471-4159.2008.05391.x

Dale, N., and Frenguelli, B. G. (2009). Release of adenosine and ATP during ischemia and epilepsy. *Curr. Neuropharmacol.* 7, 160–179. doi: 10.2174/157015909789152146

Di Virgilio, F. (2012). Purines, purinergic receptors, and cancer. *Cancer Res.* 72, 5441–5447. doi: 10.1158/0008-5472.CAN-12-1600

Diverse-Pierluissi, M., Dunlap, K., and Westhead, E. W. (1991). Multiple actions of extracellular ATP on calcium currents in cultured bovine chromaffin cells. *Proc. Natl. Acad. Sci. U.S.A.* 88, 1261–1265.

Dona, F., Conceicao, I. M., Ulrich, H., Ribeiro, E. B., Freitas, T. A., Nencioni, A. L., et al. (2016). Variations of ATP and its metabolites in the hippocampus of rats subjected to pilocarpine-induced temporal lobe epilepsy. *Purinergic Signal.* 12, 295–302. doi: 10.1007/s11302-016-9504-9

Donato, R., Rodrigues, R. J., Takahashi, M., Tsai, M. C., Soto, D., Miyagi, K., et al. (2008). GABA release by basket cells onto Purkinje cells, in rat cerebellar slices, is directly controlled by presynaptic purinergic receptors, modulating Ca2+ influx. *Cell Calcium* 44, 521–532. doi: 10.1016/j.ceca.2008.03.006

Engel, T., Alves, M., Sheedy, C., and Henshall, D. C. (2016). ATPergic signalling during seizures and epilepsy. *Neuropharmacology* 104, 140–153. doi: 10.1016/j.neuropharm.2015.11.001

Engel, T., Gomez-Villafuertes, R., Tanaka, K., Mesuret, G., Sanz-Rodriguez, A., Garcia-Huerta, P., et al. (2012). Seizure suppression and neuroprotection by targeting the purinergic P2X7 receptor during status epilepticus in mice. *FASEB J.* 26, 1616–1628. doi: 10.1096/fj.11-196089

Everitt, A. D., and Sander, J. W. (1998). Incidence of epilepsy is now higher in elderly people than children. *BMJ* 316:780.

Eyo, U. B., Peng, J., Swiatkowski, P., Mukherjee, A., Bispo, A., and Wu, L. J. (2014). Neuronal hyperactivity recruits microglial processes via neuronal NMDA receptors and microglial P2Y12 receptors after status epilepticus. *J. Neurosci.* 34, 10528–10540. doi: 10.1523/JNEUROSCI.0416-14.2014

Filippov, A. K., Choi, R. C., Simon, J., Barnard, E. A., and Brown, D. A. (2006). Activation of P2Y1 nucleotide receptors induces inhibition of the M-type K+ current in rat hippocampal pyramidal neurons. *J. Neurosci.* 26, 9340–9348. doi: 10.1523/JNEUROSCI.2635-06.2006

Filippov, A. K., Fernandez-Fernandez, J. M., Marsh, S. J., Simon, J., Barnard, E. A., and Brown, D. A. (2004). Activation and inhibition of neuronal G protein-gated inwardly rectifying K(+) channels by P2Y nucleotide receptors. *Mol. Pharmacol.* 66, 468–477. doi: 10.1124/mol.66.3

Fischer, W., Norenberg, W., Franke, H., Schaefer, M., and Illes, P. (2009). Increase of intracellular Ca2+ by P2Y but not P2X receptors in cultured cortical multipolar neurons of the rat. *J. Comp. Neurol.* 516, 343–359. doi: 10.1002/cne.22079

Fisher, R. S., Acevedo, C., Arzimanoglou, A., Bogacz, A., Cross, J. H., Elger, C. E., et al. (2014). ILAE official report: a practical clinical definition of epilepsy. *Epilepsia* 55, 475–482. doi: 10.1111/epi.12550

Forster, D., and Reiser, G. (2015). Supportive or detrimental roles of P2Y receptors in brain pathology?–The two faces of P2Y receptors in stroke and neurodegeneration detected in neural cell and in animal model studies. *Purinergic Signal.* 11, 441–454. doi: 10.1007/s11302-015-9471-6

Fotino, C., Vergani, A., Fiorina, P., and Pileggi, A. (2015). P2X receptors and diabetes. *Curr. Med. Chem.* 22, 891–901.

Fujikawa, D. G., Itabashi, H. H., Wu, A., and Shinmei, S. S. (2000). Status epilepticus-induced neuronal loss in humans without systemic complications or epilepsy. *Epilepsia* 41, 981–991.

Fujita, T., Tozaki-Saitoh, H., and Inoue, K. (2009). P2Y1 receptor signaling enhances neuroprotection by astrocytes against oxidative stress via IL-6 release in hippocampal cultures. *Glia* 57, 244–257. doi: 10.1002/glia.20749

Garcia-Oscos, F., Salgado, H., Hall, S., Thomas, F., Farmer, G. E., Bermeo, J., et al. (2012). The stress-induced cytokine interleukin-6 decreases the inhibition/excitation ratio in the rat temporal cortex via trans-signaling. *Biol. Psychiatry* 71, 574–582. doi: 10.1016/j.biopsych.2011.11.018

Gerevich, Z., Borvendeg, S. J., Schroder, W., Franke, H., Wirkner, K., Norenberg, W., et al. (2004). Inhibition of N-type voltage-activated calcium channels in rat dorsal root ganglion neurons by P2Y receptors is a possible

mechanism of ADP-induced analgesia. *J. Neurosci.* 24, 797–807. doi: 10.1523/JNEUROSCI.4019-03.2004

Gerevich, Z., Zadori, Z., Muller, C., Wirkner, K., Schroder, W., Rubini, P., et al. (2007). Metabotropic P2Y receptors inhibit P2X3 receptor-channels via G protein-dependent facilitation of their desensitization. *Br. J. Pharmacol.* 151, 226–236. doi: 10.1038/sj.bjp.0707217

Glauser, T., Shinnar, S., Gloss, D., Alldredge, B., Arya, R., Bainbridge, J., et al. (2016). Evidence-based guideline: treatment of convulsive status epilepticus in children and adults: report of the guideline committee of the American epilepsy society. *Epilepsy Curr.* 16, 48–61. doi: 10.5698/1535-7597-16.1.48

Guzman, S. J., and Gerevich, Z. (2016). P2Y receptors in synaptic transmission and plasticity: therapeutic potential in cognitive dysfunction. *Neural Plast.* 2016:1207393. doi: 10.1155/2016/1207393

Heinrich, A., Ando, R. D., Turi, G., Rozsa, B., and Sperlagh, B. (2012). K+ depolarization evokes ATP, adenosine and glutamate release from glia in rat hippocampus: a microelectrode biosensor study. *Br. J. Pharmacol.* 167, 1003–1020. doi: 10.1111/j.1476-5381.2012.01932.x

Helmstaedter, C. (2007). Cognitive outcome of status epilepticus in adults. *Epilepsia* 48(Suppl. 8), 85–90.

Hesdorffer, D. C., Logroscino, G., Cascino, G., Annegers, J. F., and Hauser, W. A. (1998). Risk of unprovoked seizure after acute symptomatic seizure: effect of status epilepticus. *Ann. Neurol.* 44, 908–912. doi: 10.1002/ana.410440609

Idzko, M., Ferrari, D., and Eltzschig, H. K. (2014). Nucleotide signalling during inflammation. *Nature* 509, 310–317. doi: 10.1038/nature13085

Jacob, P. F., Vaz, S. H., Ribeiro, J. A., and Sebastiao, A. M. (2014). P2Y1 receptor inhibits GABA transport through a calcium signalling-dependent mechanism in rat cortical astrocytes. *Glia* 62, 1211–1226. doi: 10.1002/glia.22673

Jacobson, K. A., and Boeynaems, J. M. (2010). P2Y nucleotide receptors: promise of therapeutic applications. *Drug Discov. Today* 15, 570–578. doi: 10.1016/j.drudis.2010.05.011

Jacobson, K. A., Paoletta, S., Katritch, V., Wu, B., Gao, Z. G., Zhao, Q., et al. (2015). Nucleotides acting at P2Y receptors: connecting structure and function. *Mol. Pharmacol.* 88, 220–230. doi: 10.1124/mol.114.095711

Jenssen, S., Gracely, E. J., and Sperling, M. R. (2006). How long do most seizures last? A systematic comparison of seizures recorded in the epilepsy monitoring unit. *Epilepsia* 47, 1499–1503. doi: 10.1111/j.1528-1167.2006.00622.x

Kasperaviciute, D., Catarino, C. B., Matarin, M., Leu, C., Novy, J., Tostevin, A., et al. (2013). Epilepsy, hippocampal sclerosis and febrile seizures linked by common genetic variation around SCN1A. *Brain* 136(Pt 10), 3140–3150. doi: 10.1093/brain/awt233

Keystone, E. C., Wang, M. M., Layton, M., Hollis, S., McInnes, I. B., and D1520C00001 Study Team (2012). Clinical evaluation of the efficacy of the P2X7 purinergic receptor antagonist AZD9056 on the signs and symptoms of rheumatoid arthritis in patients with active disease despite treatment with methotrexate or sulphasalazine. *Ann. Rheum. Dis.* 71, 1630–1635. doi: 10.1136/annrheumdis-2011-143578

Khakh, B. S., and North, R. A. (2006). P2X receptors as cell-surface ATP sensors in health and disease. *Nature* 442, 527–532. doi: 10.1038/nature04886

Khakh, B. S., and North, R. A. (2012). Neuromodulation by extracellular ATP and P2X receptors in the CNS. *Neuron* 76, 51–69. doi: 10.1016/j.neuron.2012.09.024

Kimbler, D. E., Shields, J., Yanasak, N., Vender, J. R., and Dhandapani, K. M. (2012). Activation of P2X7 promotes cerebral edema and neurological injury after traumatic brain injury in mice. *PLoS One* 7:e41229. doi: 10.1371/journal.pone.0041229

Kinney, M. O., and Morrow, J. (2016). Epilepsy in pregnancy. *BMJ* 353:i2880. doi: 10.1136/bmj.i2880

Knutsen, T. M. (1997). "Adenosine and ATP in epilepsy," in *Purinergic Approaches in Experimental Therapeutics*, eds K. A. Jakobson and M. F. Jarvis (New York, NY: Wiley-Liss), 432–447.

Koch, J., Mayr, J. A., Alhaddad, B., Rauscher, C., Bierau, J., Kovacs-Nagy, R., et al. (2017). CAD mutations and uridine-responsive epileptic encephalopathy. *Brain* 140, 279–286. doi: 10.1093/brain/aww300

Koizumi, S., Fujishita, K., Tsuda, M., Shigemoto-Mogami, Y., and Inoue, K. (2003). Dynamic inhibition of excitatory synaptic transmission by astrocyte-derived ATP in hippocampal cultures. *Proc. Natl. Acad. Sci. U.S.A.* 100, 11023–11028. doi: 10.1073/pnas.1834448100

Koizumi, S., Shigemoto-Mogami, Y., Nasu-Tada, K., Shinozaki, Y., Ohsawa, K., Tsuda, M., et al. (2007). UDP acting at P2Y6 receptors is a mediator of microglial phagocytosis. *Nature* 446, 1091–1095. doi: 10.1038/nature05704

Kong, Q., Peterson, T. S., Baker, O., Stanley, E., Camden, J., Seye, C. I., et al. (2009). Interleukin-1beta enhances nucleotide-induced and alpha-secretase-dependent amyloid precursor protein processing in rat primary cortical neurons via up-regulation of the P2Y(2) receptor. *J. Neurochem.* 109, 1300–1310. doi: 10.1111/j.1471-4159.2009.06048.x

Korngut, L., Young, G. B., Lee, D. H., Hayman-Abello, B. A., and Mirsattari, S. M. (2007). Irreversible brain injury following status epilepticus. *Epilepsy Behav.* 11, 235–240. doi: 10.1016/j.yebeh.2007.04.016

Kovacs, Z., Slezia, A., Bali, Z. K., Kovacs, P., Dobolyi, A., Szikra, T., et al. (2013). Uridine modulates neuronal activity and inhibits spike-wave discharges of absence epileptic Long Evans and Wistar Albino Glaxo/Rijswijk rats. *Brain Res. Bull.* 97, 16–23. doi: 10.1016/j.brainresbull.2013.05.009

Kuan, Y. H., Shih, H. C., Tang, S. C., Jeng, J. S., and Shyu, B. C. (2015). Targeting P(2)X(7) receptor for the treatment of central post-stroke pain in a rodent model. *Neurobiol. Dis.* 78, 134–145. doi: 10.1016/j.nbd.2015.02.028

Lau, O. C., Samarawickrama, C., and Skalicky, S. E. (2014). P2Y2 receptor agonists for the treatment of dry eye disease: a review. *Clin. Ophthalmol.* 8, 327–334. doi: 10.2147/OPTH.S39699

Lecca, D., and Ceruti, S. (2008). Uracil nucleotides: from metabolic intermediates to neuroprotection and neuroinflammation. *Biochem. Pharmacol.* 75, 1869–1881. doi: 10.1016/j.bcp.2007.12.009

Leonardi, M., and Ustun, T. B. (2002). The global burden of epilepsy. *Epilepsia* 43(Suppl. 6), 21–25.

Lopatar, J., Dale, N., and Frenguelli, B. G. (2015). Pannexin-1-mediated ATP release from area CA3 drives mGlu5-dependent neuronal oscillations. *Neuropharmacology* 93, 219–228. doi: 10.1016/j.neuropharm.2015.01.014

Luthardt, J., Borvendeg, S. J., Sperlagh, B., Poelchen, W., Wirkner, K., and Illes, P. (2003). P2Y(1) receptor activation inhibits NMDA receptor-channels in layer V pyramidal neurons of the rat prefrontal and parietal cortex. *Neurochem. Int.* 42, 161–172.

McGovern, A. E., and Mazzone, S. B. (2014). Neural regulation of inflammation in the airways and lungs. *Auton. Neurosci.* 182, 95–101. doi: 10.1016/j.autneu.2013.12.008

Mendoza-Fernandez, V., Andrew, R. D., and Barajas-Lopez, C. (2000). ATP inhibits glutamate synaptic release by acting at P2Y receptors in pyramidal neurons of hippocampal slices. *J. Pharmacol. Exp. Ther.* 293, 172–179.

Miras-Portugal, M. T., Gomez-Villafuertes, R., Gualix, J., Diaz-Hernandez, J. I., Artalejo, A. R., Ortega, F., et al. (2016). Nucleotides in neuroregeneration and neuroprotection. *Neuropharmacology* 104, 243–254. doi: 10.1016/j.neuropharm.2015.09.002

Moshe, S. L., Perucca, E., Ryvlin, P., and Tomson, T. (2015). Epilepsy: new advances. *Lancet* 385, 884–898. doi: 10.1016/S0140-6736(14)60456-6

Mouri, G., Jimenez-Mateos, E., Engel, T., Dunleavy, M., Hatazaki, S., Paucard, A., et al. (2008). Unilateral hippocampal CA3-predominant damage and short latency epileptogenesis after intra-amygdala microinjection of kainic acid in mice. *Brain Res.* 1213, 140–151. doi: 10.1016/j.brainres.2008.03.061

Mundell, S. J., Pula, G., McIlhinney, R. A., Roberts, P. J., and Kelly, E. (2004). Desensitization and internalization of metabotropic glutamate receptor 1a following activation of heterologous Gq/11-coupled receptors. *Biochemistry* 43, 7541–7551. doi: 10.1021/bi0359022

Naylor, D. E., and Wasterlain, C. G. (2005). GABA synapses and the rapid loss of inhibition to dentate gyrus granule cells after brief perforant-path stimulation. *Epilepsia* 46(Suppl. 5), 142–147. doi: 10.1111/j.1528-1167.2005.01022.x

Nicolaidis, R., Bruno, A. N., Sarkis, J. J., and Souza, D. O. (2005). Increase of adenine nucleotide hydrolysis in rat hippocampal slices after seizures induced by quinolinic acid. *Neurochem. Res.* 30, 385–390.

Novy, J., Logroscino, G., and Rossetti, A. O. (2010). Refractory status epilepticus: a prospective observational study. *Epilepsia* 51, 251–256. doi: 10.1111/j.1528-1167.2009.02323.x

Ohsawa, K., Irino, Y., Sanagi, T., Nakamura, Y., Suzuki, E., Inoue, K., et al. (2010). P2Y12 receptor-mediated integrin-beta1 activation regulates microglial process extension induced by ATP. *Glia* 58, 790–801. doi: 10.1002/glia.20963

Pal, D. K., Ferrie, C., Addis, L., Akiyama, T., Capovilla, G., Caraballo, R., et al. (2016). Idiopathic focal epilepsies: the "lost tribe". *Epileptic Disord.* 18, 252–288. doi: 10.1684/epd.2016.0839

Pitkanen, A., Lukasiuk, K., Dudek, F. E., and Staley, K. J. (2015). Epileptogenesis. *Cold Spring Harb. Perspect. Med.* 5:a022822. doi: 10.1101/cshperspect.a022822

Puchalowicz, K., Tarnowski, M., Baranowska-Bosiacka, I., Chlubek, D., and Dziedziejko, V. (2014). P2X and P2Y receptors-role in the pathophysiology of the nervous system. *Int. J. Mol. Sci.* 15, 23672–23704. doi: 10.3390/ijms151223672

Ralevic, V. (2015). P2X receptors in the cardiovascular system and their potential as therapeutic targets in disease. *Curr. Med. Chem.* 22, 851–865.

Rao, M. S., Hattiangady, B., Reddy, D. S., and Shetty, A. K. (2006). Hippocampal neurodegeneration, spontaneous seizures, and mossy fiber sprouting in the F344 rat model of temporal lobe epilepsy. *J. Neurosci. Res.* 83, 1088–1105. doi: 10.1002/jnr.20802

Rassendren, F., and Audinat, E. (2016). Purinergic signaling in epilepsy. *J. Neurosci. Res.* 94, 781–793. doi: 10.1002/jnr.23770

Ravizza, T., Noe, F., Zardoni, D., Vaghi, V., Sifringer, M., and Vezzani, A. (2008). Interleukin converting enzyme inhibition impairs kindling epileptogenesis in rats by blocking astrocytic IL-1beta production. *Neurobiol. Dis.* 31, 327–333. doi: 10.1016/j.nbd.2008.05.007

Rech, J. C., Bhattacharya, A., Letavic, M. A., and Savall, B. M. (2016). The evolution of P2X7 antagonists with a focus on CNS indications. *Bioorg. Med. Chem. Lett.* 26, 3838–3845. doi: 10.1016/j.bmcl.2016.06.048

Reddy, D. S., and Kuruba, R. (2013). Experimental models of status epilepticus and neuronal injury for evaluation of therapeutic interventions. *Int. J. Mol. Sci.* 14, 18284–18318. doi: 10.3390/ijms140918284

Reid, A. Y., and Staba, R. J. (2014). Limbic networks: clinical perspective. *Int. Rev. Neurobiol.* 114, 89–120. doi: 10.1016/B978-0-12-418693-4.00005-4

Rodrigues, R. J., Almeida, T., Richardson, P. J., Oliveira, C. R., and Cunha, R. A. (2005). Dual presynaptic control by ATP of glutamate release via facilitatory P2X1, P2X2/3, and P2X3 and inhibitory P2Y1, P2Y2, and/or P2Y4 receptors in the rat hippocampus. *J. Neurosci.* 25, 6286–6295. doi: 10.1523/JNEUROSCI.0628-05.2005

Rodrigues, R. J., Tome, A. R., and Cunha, R. A. (2015). ATP as a multi-target danger signal in the brain. *Front Neurosci* 9:148. doi: 10.3389/fnins.2015.00148

Rothaug, M., Becker-Pauly, C., and Rose-John, S. (2016). The role of interleukin-6 signaling in nervous tissue. *Biochim. Biophys. Acta* 1863(6 Pt A), 1218–1227. doi: 10.1016/j.bbamcr.2016.03.018

Rozmer, K., Gao, P., Araujo, M. G., Khan, M. T., Liu, J., Rong, W., et al. (2016). Pilocarpine-induced status epilepticus increases the sensitivity of P2X7 and P2Y1 receptors to nucleotides at neural progenitor cells of the juvenile rodent hippocampus. *Cereb. Cortex.* 27, 3568–3585. doi: 10.1093/cercor/bhw178

Saez-Orellana, F., Godoy, P. A., Silva-Grecchi, T., Barra, K. M., and Fuentealba, J. (2015). Modulation of the neuronal network activity by P2X receptors and their involvement in neurological disorders. *Pharmacol. Res.* 101, 109–115. doi: 10.1016/j.phrs.2015.06.009

Saitow, F., Murakoshi, T., Suzuki, H., and Konishi, S. (2005). Metabotropic P2Y purinoceptor-mediated presynaptic and postsynaptic enhancement of cerebellar GABAergic transmission. *J. Neurosci.* 25, 2108–2116. doi: 10.1523/JNEUROSCI.4254-04.2005

Sarafoff, N., Byrne, R. A., and Sibbing, D. (2012). Clinical use of clopidogrel. *Curr. Pharm. Des.* 18, 5224–5239.

Scorza, C. A., Marques, M. J., Gomes da Silva, S., Naffah-Mazzacoratti, M. D., Scorza, F. A., and Cavalheiro, E. A. (2017). Status epilepticus does not induce acute brain inflammatory response in the Amazon rodent Proechimys, an animal model resistant to epileptogenesis. *Neurosci. Lett.* doi: 10.1016/j.neulet.2017.02.049 [Epub ahead of print],

Sebastian-Serrano, A., Engel, T., de Diego-Garcia, L., Olivos-Ore, L. A., Arribas-Blazquez, M., Martinez-Frailes, C., et al. (2016). Neurodevelopmental alterations and seizures developed by mouse model of infantile hypophosphatasia are associated with purinergic signalling deregulation. *Hum. Mol. Genet.* 25, 4143–4156. doi: 10.1093/hmg/ddw248

Shank, R. P., Gardocki, J. F., Streeter, A. J., and Maryanoff, B. E. (2000). An overview of the preclinical aspects of topiramate: pharmacology, pharmacokinetics, and mechanism of action. *Epilepsia* 41(Suppl. 1), S3–S9.

Shorvon, S., Baulac, M., Cross, H., Trinka, E., Walker, M., and TaskForce on Status Epilepticus of the Ilae Commission for European Affairs (2008). The drug treatment of status epilepticus in Europe: consensus document from a workshop at the first London Colloquium on Status Epilepticus. *Epilepsia* 49, 1277–1285. doi: 10.1111/j.1528-1167.2008.01706_3.x

Sperlagh, B., and Illes, P. (2014). P2X7 receptor: an emerging target in central nervous system diseases. *Trends Pharmacol. Sci.* 35, 537–547. doi: 10.1016/j.tips.2014.08.002

Sukigara, S., Dai, H., Nabatame, S., Otsuki, T., Hanai, S., Honda, R., et al. (2014). Expression of astrocyte-related receptors in cortical dysplasia with intractable epilepsy. *J. Neuropathol. Exp. Neurol.* 73, 798–806. doi: 10.1097/NEN.0000000000000099

Terrone, G., Salamone, A., and Vezzani, A. (2017). Inflammation and Epilepsy: preclinical findings and potential clinical translation. *Curr. Pharm. Des.* doi: 10.2174/1381612823666170926113754 [Epub ahead of print].

Thompson, P. J., and Duncan, J. S. (2005). Cognitive decline in severe intractable epilepsy. *Epilepsia* 46, 1780–1787. doi: 10.1111/j.1528-1167.2005.00279.x

Vezzani, A., Balosso, S., Aronica, E., and Ravizza, T. (2009). Basic mechanisms of status epilepticus due to infection and inflammation. *Epilepsia* 50(Suppl. 12), 56–57. doi: 10.1111/j.1528-1167.2009.02370.x

Vezzani, A., Balosso, S., and Ravizza, T. (2012). Inflammation and epilepsy. *Handb. Clin. Neurol.* 107, 163–175. doi: 10.1016/B978-0-444-52898-8.00010-0

Vezzani, A., French, J., Bartfai, T., and Baram, T. Z. (2011). The role of inflammation in epilepsy. *Nat. Rev. Neurol.* 7, 31–40. doi: 10.1038/nrneurol.2010.178

Vezzani, A., Fujinami, R. S., White, H. S., Preux, P. M., Blumcke, I., Sander, J. W., et al. (2016). Infections, inflammation and epilepsy. *Acta Neuropathol.* 131, 211–234. doi: 10.1007/s00401-015-1481-5

Viviani, B., Gardoni, F., and Marinovich, M. (2007). Cytokines and neuronal ion channels in health and disease. *Int. Rev. Neurobiol.* 82, 247–263. doi: 10.1016/S0074-7742(07)82013-7

von Kugelgen, I. (2006). Pharmacological profiles of cloned mammalian P2Y-receptor subtypes. *Pharmacol. Ther.* 110, 415–432. doi: 10.1016/j.pharmthera.2005.08.014

Wang, M., Kong, Q., Gonzalez, F. A., Sun, G., Erb, L., Seye, C., et al. (2005). P2Y nucleotide receptor interaction with alpha integrin mediates astrocyte migration. *J. Neurochem.* 95, 630–640. doi: 10.1111/j.1471-4159.2005.03408.x

Wasterlain, C. G., Liu, H., Naylor, D. E., Thompson, K. W., Suchomelova, L., Niquet, J., et al. (2009). Molecular basis of self-sustaining seizures and pharmacoresistance during status epilepticus: the receptor trafficking hypothesis revisited. *Epilepsia* 50(Suppl. 12), 16–18. doi: 10.1111/j.1528-1167.2009.02375.x

Wieraszko, A., Goldsmith, G., and Seyfried, T. N. (1989). Stimulation-dependent release of adenosine triphosphate from hippocampal slices. *Brain Res.* 485, 244–250.

Wieraszko, A., and Seyfried, T. N. (1989). Increased amount of extracellular ATP in stimulated hippocampal slices of seizure prone mice. *Neurosci. Lett.* 106, 287–293.

Wu, P. H., and Phillis, J. W. (1978). Distribution and release of adenosine triphosphate in rat brain. *Neurochem. Res.* 3, 563–571.

Zhao, F., Kang, H., You, L., Rastogi, P., Venkatesh, D., and Chandra, M. (2014). Neuropsychological deficits in temporal lobe epilepsy: a comprehensive review. *Ann. Indian Acad. Neurol.* 17, 374–382. doi: 10.4103/0972-2327.144003

Zimmermann, H. (2006). Ectonucleotidases in the nervous system. *Novartis Found. Symp.* 276, 113-128; discussion 128–130, 233–117, 275–181.

Conflict of Interest Statement: The authors declare that the research was conducted in the absence of any commercial or financial relationships that could be construed as a potential conflict of interest.

frontiers in Pharmacology

ORIGINAL RESEARCH
published: 06 March 2018
doi: 10.3389/fphar.2018.00192

Circadian ATP Release in Organotypic Cultures of the Rat Suprachiasmatic Nucleus Is Dependent on P2X7 and P2Y Receptors

*Irena Svobodova[1], Anirban Bhattaracharya[1], Milorad Ivetic[1], Zdenka Bendova[2] and Hana Zemkova[1]**

[1] Department of Cellular and Molecular Neuroendocrinology, Institute of Physiology of the Czech Academy of Sciences, Prague, Czechia, [2] Department of Physiology, Faculty of Science, Charles University, Prague, Czechia

OPEN ACCESS

Edited by:
Francisco Ciruela, Universitat de Barcelona, Spain

Reviewed by:
Juan C. Saez, Pontificia Universidad Católica de Chile, Chile
Susanna Amadio, Fondazione Santa Lucia (IRCCS), Italy
Lin-Hua Jiang, University of Leeds, United Kingdom

***Correspondence:**
Hana Zemkova
zemkova@biomed.cas.cz

Specialty section:
This article was submitted to Experimental Pharmacology and Drug Discovery, a section of the journal Frontiers in Pharmacology

Received: *17 November 2017*
Accepted: *20 February 2018*
Published: *06 March 2018*

Citation:
Svobodova I, Bhattaracharya A, Ivetic M, Bendova Z and Zemkova H (2018) Circadian ATP Release in Organotypic Cultures of the Rat Suprachiasmatic Nucleus Is Dependent on P2X7 and P2Y Receptors. Front. Pharmacol. 9:192. doi: 10.3389/fphar.2018.00192

The circadian rhythms in physiological and behavioral functions are driven by a pacemaker located in the suprachiasmatic nucleus (SCN). The rhythms continue in constant darkness and depend on cell-cell communication between neurons and glia. The SCN astrocytes generate also a circadian rhythm in extracellular adenosine 5′-triphosphate (ATP) accumulation, but molecular mechanisms that regulate ATP release are poorly understood. Here, we tested the hypothesis that ATP is released via the plasma membrane purinergic P2X7 receptors (P2X7Rs) and P2Y receptors (P2YRs) which have been previously shown to be expressed in the SCN tissue at transcriptional level. We have investigated this hypothesis using SCN organotypic cultures, primary cultures of SCN astrocytes, ATP bioluminescent assays, immunohistochemistry, patch-clamping, and calcium imaging. We found that extracellular ATP accumulation in organotypic cultures followed a circadian rhythm, with a peak between 24:00 and 04:00 h, and the trough at ∼12:00 h. ATP rhythm was inhibited by application of AZ10606120, A438079, and BBG, specific blockers of P2X7R, and potentiated by GW791343, a positive allosteric modulator of this receptor. Double-immunohistochemical staining revealed high expression of the P2X7R protein in astrocytes of SCN slices. PPADS, a non-specific P2 antagonist, and MRS2179, specific P2Y1R antagonist, also abolished ATP rhythm, whereas the specific P2X4R blocker 5-BDBD was not effective. The pannexin-1 hemichannel blocker carbenoxolone displayed a partial inhibitory effect. The P2Y1R agonist MRS2365, and the P2Y2R agonist MRS2768 potentiated ATP release in organotypic cultures and increase intracellular Ca^{2+} level in cultured astrocytes. Thus, SCN utilizes multiple purinergic receptor systems and pannexin-1 hemichannels to release ATP.

Keywords: suprachiasmatic nucleus, organotypic cultures, astrocytes, P2X7 receptor, P2Y1 receptor, P2Y2 receptor, pannexin-1 hemichannel, ATP release

INTRODUCTION

The suprachiasmatic nucleus (SCN) of the anterior hypothalamus is the principal circadian pacemaker in mammals (Moore and Eichler, 1972; Stephan and Zucker, 1972). In most species, including rat, the SCN has two subdivisions that differ in neuronal input and neuropeptide contents. The ventrolateral part of the SCN receives glutamatergic inputs from retinal ganglion cells and produces vasoactive intestinal polypeptide, whereas the dorsomedial part does not receive a direct visual input and produces arginine vasopressin (AVP) (Moore and Card, 1985; Jacomy et al., 1999). Circadian rhythm in AVP secretion parallels rhythm of electrical activity in SCN neurons (Inouye and Kawamura, 1979; Groos and Hendriks, 1982; Pennartz et al., 2002) and both these rhythms are mediated by the expression of clock genes (Reppert, 1998). The SCN generates also a circadian rhythm in extracellular adenosine 5′-triphosphate (ATP) accumulation, which negatively correlates with the electrical activity and AVP secretion rhythms (Yamazaki et al., 1994; Womac et al., 2009). Extracellular ATP levels fluctuate rhythmically within the rat SCN *in vivo* and SCN-derived SCN2.2 cell cultures containing 80% astrocytes (Womac et al., 2009; Burkeen et al., 2011), indicating that oscillations in ATP release are intrinsic properties of SCN astrocytes. However, the pathway by which ATP travels from the cytosol of SCN cells to the extracellular space is still unknown.

ATP release from astrocytes was originally thought to be vesicular and dependent on Ca^{2+} (Fumagalli et al., 2003; Pascual et al., 2005; Pangrsic et al., 2007). Consistent with this hypothesis, large amounts of ATP have been detected in the dense-core vesicles and lysosomes of astrocytes (Hong et al., 2016). Changes in intracellular Ca^{2+} levels in rat SCN2.2 cells, however, are inversely related to the circadian variations in extracellular ATP accumulation (Burkeen et al., 2011). Moreover, genetic disruption of the vesicular release mechanism had no effect on circadian ATP release in cultured mouse cortical astrocytes (Marpegan et al., 2011), indicating that circadian ATP release might occur via a non-vesicular pathway, possibly through conductive mechanisms involving pore-forming molecules such as pannexin-1 hemichannels (Stout et al., 2002; Schenk et al., 2008; Iglesias et al., 2009; Li S. et al., 2011) or purinergic P2X7 receptor (P2X7R) channel (Khakh and Sofroniew, 2015). P2X7R is ATP-gated ion channel (Surprenant et al., 1996) that can form a large pore itself (Khakh and Lester, 1999) or after interaction with another transmembrane molecule (Pelegrin and Surprenant, 2006; Locovei et al., 2007). The P2X7R has been detected in astrocytes (Narcisse et al., 2005; Sperlágh et al., 2006; Hamilton et al., 2008) and complexes with pannexin to promote Ca^{2+}-independent gliotransmitter release (Ballerini et al., 1996; Wang et al., 2002; Duan et al., 2003; Hamilton et al., 2008; Carrasquero et al., 2009; Nörenberg et al., 2011b). As shown in our previous RT-PCR analysis, P2X7R is the second most highly expressed P2X subunit in the SCN after the P2X2R which are localized on presynaptic nerve terminals in the SCN (Bhattacharya et al., 2013). In addition to transcripts for P2X receptors, several P2Y receptors (P2Y1 and P2Y2) have also been identified in the SCN (Bhattacharya et al., 2013). Thus, in this work, we tested the hypothesis that P2X7Rs and P2YRs are associated with circadian ATP release from SCN astrocytes. We have investigated this hypothesis using organotypic cultures of rat brain slices containing the SCN, primary cultures of SCN astrocytes, ATP bioluminescent assays, immunohistochemistry, patch-clamping, and calcium imaging.

MATERIALS AND METHODS

Animals and Brain Slices

The Animal Care and Use Committee of the Czech Academy of Sciences approved the experiments of the present study. Experiments were performed in Wistar rats of both genders, 16- to 21-days-old, which were kept under a controlled 12–12-h light-dark cycle from birth with food and water available *ad libitum*. Animals had lights on from 6 a.m. to 6 p.m. Brains were removed after decapitation and placed into ice-cold (4°C) oxygenated (95% O_2 + 5% CO_2) artificial cerebrospinal fluid (ACSF) that contained: 130 mM NaCl, 3 mM KCl, 1 mM $MgCl_2$, 2 mM $CaCl_2$, 19 mM $NaHCO_3$, 1.25 mM NaH_2PO_4 and 10 mM glucose (pH 7.3–7.4; osmolality 300–315 mOsm).

Organotypic Culture Preparation

Coronal sections of the hypothalamus (∼350 μm thick) were cut from ∼1 × 1 mm tissue blocks containing the SCN using a vibratome (DTK-1000, D.S.K. Dosaka, Japan). In some experiments, the SCN was punctured out from slices. Three slices were cut from one animal and then transferred onto one cell culture insert with a pore size of 0.001 mm (BD Falcon, Tewksbury, MA, USA). Culture inserts with 3 slices, further referred to as the organotypic cultures, were placed in 6-well plates (BD Falcon) and submerged in 1 ml of Neurobasal A medium supplemented with 2% serum-free B-27, 50 U/ml penicillin, 50 μg/ml streptomycin and 0.5 mM L-glutamine (all from Thermo Fisher Scientific, Waltham, MA) saturated with a 95% air and 5% CO_2 mixture. Plates containing inserts with slices/cultures were incubated in a humidified 5% CO_2 atmosphere at 37°C. Slices were cultured in Neurobasal medium for 7 days before starting ATP accumulation assays to allow slices to stabilize.

Acute Slices

Hypothalamic slices (200–300 μm thick) containing SCN were incubated as described previously (Kretschmannova et al., 2003; Vavra et al., 2011; Bhattacharya et al., 2013). Briefly, the slices were allowed to recover for at least 1 h in oxygenated ACSF at 32–33°C before being transferred into a recording chamber. During the experiments, slices were fixed with a platinum U-shaped wire to the bottom of the chamber and submerged in continuously flowing oxygenated ACSF at 1–2 ml min^{-1} at room temperature. Slices were viewed with an upright microscope (Olympus BX50WI, Melville, NY, USA) mounted on a Gibraltar movable X-Y platform (Burleigh) using water immersion lenses (60x and 10x) and Dodt infrared gradient contrast (Luigs & Neumann, GmbH, Germany). SCN regions were identified by their position relative to the third ventricle and the optic chiasm in a coronal hypothalamic section as described previously (Kretschmannova et al., 2003; Bhattacharya et al., 2013).

Primary Cultures of SCN Astrocytes

Postnatal day 2–5 newborn rats were euthanized by decapitation. SCN regions were dissected from ∼600 μm thick hypothalamic slices and cells were dissociated after treatment with trypsin, according to published methods (Watanabe et al., 1993; Bhattacharya et al., 2013). Next, cells were purified on a discontinuous protein gradient, and ∼100,000 cells were placed on coverslips coated with a 1% poly-L-lysine solution (Sigma) in 35 mm culture dishes (BD Falcon) and cultured in Neurobasal A medium with 2% B27 supplement and 0.5 mM L-Glutamine in a humidified CO_2-containing atmosphere at 37°C until use (14–21 days).

Measurement of ATP Production

ATP secretion by SCN cells into the medium from the above organotypic cultures was measured every 4 h over a 24–48 h incubation period. Extracellular ATP concentrations in the medium were determined using an ATP bioluminescent assay. Before assay, at 8:00 h, cultures were washed with ATP-free Dulbecco's Modified Eagle's Medium (DMEM; Thermo Fisher Scientific, Waltham, MA) supplemented with 50 U/ml penicillin and 50 μg/ml streptomycin, and then incubated with fresh ATP-free DMEM-based medium in a humidified 5% CO_2 atmosphere at 37°C for 4 h. In our experimental protocol spanning 24–48 h, media (1 ml) above the slices were collected every 4 h starting at 12:00 h. Samples were collected as a full volume of medium (1 ml) and were replaced with fresh ATP-free DMEM. Media samples were then stored at −20°C for 3 days, and the ATP concentration was then measured using an ATP Bioluminescence Assay Kit CLS II (Hoffmann-La Roche AG, Basel, Switzerland).

Treatments were performed by completely replacing the medium with fresh drug-containing culture medium every 4 h. Each tested drug was added at 8:00 h, and the cultures were exposed to these drugs over a 24–48 h incubation period. In control experiments, the protocol was identical and the medium was replaced with fresh drug-free culture medium every 4 h.

Immunohistochemistry

Adult male rats were deeply anesthetized with thiopental (50 mg/kg) and perfused through the aorta with heparinized saline followed by phosphate-buffered saline (PBS; 0.01 M sodium phosphate/0.15 M NaCl, pH 7.2) and 4% paraformaldehyde in PBS. Brains were removed, postfixed for 12 hrs at 4°C, cryoprotected in 20% sucrose in PBS overnight at 4°C, and stored at −80°C. Brains were sectioned into series of 30-μm-thick free-floating coronal slices throughout the rostral-caudal extent of the SCN. Levels of P2X7 receptor protein in astrocytes were assessed using anti-GFAP conjugated with Cy3 (ab49874, Abcam, Cambridge, United Kingdom) mouse monoclonal, 1:1,000, anti-P2X7 (APR-004, Alomone Labs, Israel) rabbit, 1:1,000. The P2X7 labeling was visualized using Alexa Fluor® 488-conjugated secondary anti-rabbit antibody (Invitrogen, Carlsbad, CA; dilution 1:500). The images were acquired with confocal microscope Leica TCS SP2.

Calcium Imaging

For intracellular Ca^{2+} fluorescence imaging, primary 14-21 days-old SCN cultures, that were enriched in astrocytes, were incubated in 2 ml ACSF containing 1 μM of membrane-permeant ester form of Fura-2 (Fura-2AM, Invitrogen, Molecular Probes) and 0.15% dispersing agent Pluronic F-127 for 30–45 min in carbogen atmosphere (95% O2 and 5% CO2). After 15 min of washing in fresh ASCF, Fura-2 fluorescence from single cells was measured using a MicroMAX CCD camera (Princenton Instruments, USA) and an Olympus BX50WI epifluorescent microscope coupled to a monochromatic illumination system (T.I.L.L., Photonics). Hardware control and image analysis were performed using MetaFluor software (Molecular Devices). Cells were examined under a water immersion objective during exposure to alternating 340- and 380-nm light beams. The emitted light images at 515 nm were acquired through a d 40 × 0.9 NA objective, and the intensity of light emission was measured. The ratio of light intensity (F_{340}/F_{380}) reflects changes in intracellular free Ca^{2+} concentration ($[Ca^{2+}]_i$) and was followed in ∼20 single cells simultaneously at the rate of one point per second.

Patch Clamp Recordings

Action potentials were recorded from SCN neurons in acutely isolated slices using standard whole-cell patch clamp techniques with an Axopatch-200B amplifier (Molecular Devices, Sunnyvale, CA, USA). Patch pipettes were pulled on the horizontal Flaming Brown P-97 model puller (Sutter Instruments, Novato, CA, USA) from borosilicate glass (World Precision Instruments, Sarasota, FL) and polished by heat to a tip resistance of 4–6 MΩ. Data were captured and stored using the pClamp 10 software package in conjunction with the Axon™ Digidata® 1550A A/D converter (Molecular Devices). Signals were filtered at 1 kHz and sampled at 2 kHz. Drugs were diluted and applied in a N-2-hydroxyethylpiperazine-N′-2-ethanesulfonic acid (HEPES)-buffered extracellular solution containing: 142 mM NaCl, 3 mM KCl, 1 mM $MgCl_2$, 2 mM$CaCl_2$, 10 mM glucose and 10 mM HEPES, pH was adjusted to 7.3 with 1 M NaOH; osmolality was 300–315 mOsm. Patch electrodes used for whole-cell recording were filled with an intracellular solution containing: 140 mM KCl, 3 mM $MgCl_2$, 0.5 mM $CaCl_2$, 10 mM HEPES, and 5 mM EGTA; pH was adjusted to 7.2 with KOH. The osmolality of the intracellular solutions was 285–295 mOsm. ATP and drugs were applied in HEPES-buffered extracellular solution delivered to the recorded cells by a gravity-driven microperfusion system containing nine glass tubes with a common outlet of ∼300 μM in diameter. The application tip was routinely positioned ∼500 μm away from the recorded cell and ∼50 μm above the surface of the slice.

Experimental Design and Statistical Analysis

Each experiment was performed on 12 independent organotypic cultures prepared from 12 animals (3 control and 3 × 3 experimental, drug-treated, cultures). Each study was repeated on cultures derived from 3 to 7 different dissections. ATP release in each experiment represents a mean of ATP release from

three cultures. Throughout the manuscript, "n" is defined as the numbers of independent experiments. Cumulated ATP secretion was calculated as a sum of all 4 h data points obtained from each of the incubated cultures at the end of incubation period. Statistical comparison of multiple groups was made by using one-way analysis of variance in SigmaStat 2000 v9.0, followed by Tukey's *post-hoc* test for comparison to a single control, or the Student's *t*-test for comparison between two groups ($^{**}p < 0.01$ and $^{*}p < 0.05$). Graphing was performed using SigmaPlot (Systat Software) and CorelDraw (Corel Corporation) software. All values are reported as the means ± SEM and sample sizes are $n = 3$–7.

Chemicals

3-[[5-(2,3-dichlorophenyl)-1*H*-tetrazol-1-yl]methyl] pyridine hydrochloride (A438079); Apyrase; D-2-Amino-5-phosphonopentanoic acid (AP5); *N*-Cyano-*N*"-[(1*S*)-1 -phenylethyl]-*N*'-5-quinolinyl-guanidine (A804598);*N*-[2-[[2-[(2–Hydroxyethyl)amino]ethyl]amino]-5-quinolinyl]-2-tricyclo[3.3.1.13,7]dec-1-ylacetamide dihydrochloride (AZ10606120); 5-(3-Bromophenyl)-1,3-dihydro-2*H*-benzofuro [3,2-*e*]-1,4-diazepin-2-one (5-BDBD); 7-Chloro-5-(2-chlorophenyl)-1,5-dihydro-4,1-benzothiazepin-2(3*H*)-one (CGP37157); 2-[(3,4-Difluorophenyl)amino]-*N*-[2-methyl-5-(1-piperazinylmethyl)phenyl]-acetamide trihydrochloride (GW791343); pyridoxalphosphate-6-azophenyl-2′, 4′-disulfonic acid (PPADS); 2-deoxy-*N*6-methyladenosine 3,5-bisphosphate tetrasodium salt (MRS2179); [[(1*R*,2*R*,3*S*,4*R*,5*S*)-4-[6-Amino-2-(methylthio)-9*H*-purin-9-yl]-2,3-dihydroxybicyclo[3.1.0]hex-1-yl]methyl] diphosphoric acid mono ester trisodium salt (MRS2365) and Uridine-5′-tetraphosphate δ-phenyl ester tetrasodium salt (MRS2768) were purchased from Tocris-Cookson (Bristol, UK). Brilliant Blue G (BBG); 2′-3′-O-(4-benzoylbenzoyl)-ATP (BzATP); carbenoxolone (CBX); nifedipine and all other drugs and chemicals were from Sigma (St. Louis, MO). The A438079, AZ10606120, 5-BDBD, CGP37157, nifedipine and PPADS were used at 1 nM−10 μM from a 10 mM working stocks in DMSO; hence, 0.00001–0.1% (v/v) DMSO vehicle controls were applied in parallel to these incubations.

RESULTS

Characterization of the Circadian ATP Release in SCN Organotypic Cultures

Organotypic SCN cultures maintain the clear organization of SCN cells along the dorsoventral axis (Figure S1) and exhibit circadian rhythm in secretion of AVP for up to 2 weeks *in vitro*, with a phase that is consistent with the light regime experienced by the donor animal (Svobodova et al., 2003). Our present study shows that ATP accumulation in the medium also followed a circadian rhythm: the peak occurred between 24:00 – 04:00 h, and the trough occurred at ∼12:00 h (**Figures 1A–D**, open circles). The time points of the peak and trough were stable in 62 of 66 independent control cultures (94%). In the remaining 6% of cultures ($n = 4$), either no rhythm was observed or the peak did not occur between 24:00 and 04:00 h; these cultures were

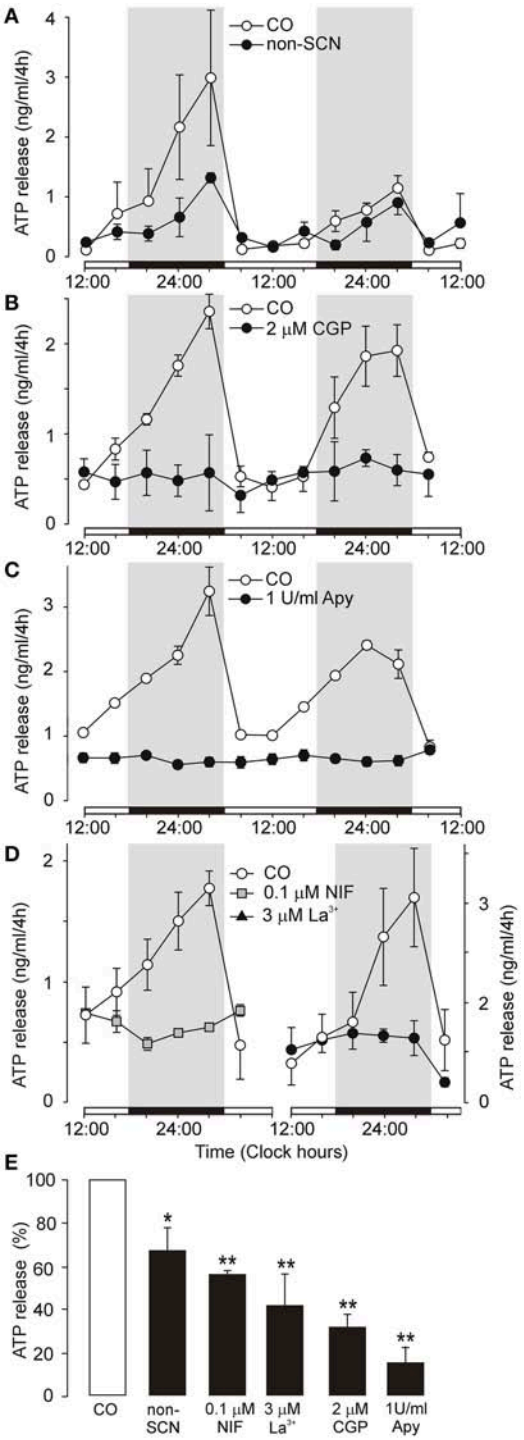

FIGURE 1 | Endogenous circadian oscillations of ATP release in organotypic cultures of the rat SCN. **(A–C)** Examples of an ATP rhythm measured during 2 days in control cultures (open symbols) and experimental cultures (closed symbols). Comparison of ATP rhythm in control organotypic cultures containing the SCN (CO) and organotypic cultures lacking the SCN (non-SCN) **(A)**. Inhibition of ATP release by a selective inhibitor of Na^{+}-Ca^{2+} exchange in mitochondria, the benzothiazepine CGP37157 (CGP) **(B)**, basal ATP release in the presence of ecto-ATPase, apyrase (Apy) **(C)** and inhibition of ATP release by the L-type Ca^{2+} channel inhibitor nifedipine (**D**, left panel) and *(Continued)*

FIGURE 1 | a non-selective voltage-gated Ca^{2+} channel blocker La^{3+} (**D**, right panel). Summary histogram showing cumulated ATP release at the end of the incubation period in control cultures (open column) and experimental cultures (black columns) **(E)**. Medium was sampled every 4 h and the ATP content was quantified (in ng/ml). ATP release was spontaneous, with a circadian rhythm that is a continuation of the endogenous rhythm in the SCN *in vivo*. Open horizontal bars on X axes thus indicate the light periods experienced by donor animals (from 12:00 to 24:00 h and from 24:00 to 12:00 h) and solid bars indicate the dark periods (12 h). Treatments were performed by completely replacing the medium with fresh drug-containing culture medium every 4 h throughout the whole incubation period. Tested drugs were applied at 08:00 h and measurements started at 12:00 h. Parallel cultures from the same experiments are shown. Data are presented as the means ± SEM, each study was repeated on cultures derived from 3 to 6 different dissections (experiments). Statistical significance of differences between control and experimental groups: $^{*}P < 0.05$ and $^{**}P < 0.01$.

discarded. These data show that circadian rhythm of ATP release peaks at an opposite phase to the previously described AVP secretory rhythm that peaked at ∼12:00 h in similar organotypic SCN cultures (Svobodova et al., 2003).

We monitored extracellular ATP accumulation in organotypic cultures from which the SCN was removed to determine the role of the SCN. In non-SCN cultures, the circadian rhythm of extracellular ATP accumulation was still present (**Figure 1A**), but exhibited lower robustness, and cumulated ATP release was significantly reduced compared to control SCN-containing cultures (66 ± 11%, $n = 3$, $P < 0.05$; **Figure 1E**). Thus, in addition to the SCN, other hypothalamic nuclei located near the SCN that also express components of the molecular clock, such as the lateral hypothalamus and supraoptic nucleus (Abe et al., 2002; Guilding et al., 2009), contribute to circadian ATP release rhythms but with a lower efficacy as compared to the SCN.

Next, we performed a bath application of selective inhibitor of the mitochondrial Na^{+}-Ca^{2+} exchange transporter CGP37157 (White and Reynolds, 1997) to examine a possible link between extracellular ATP accumulation and mitochondrial function (Burkeen et al., 2011). The effective threshold concentration of CGP37157 that inhibited ATP release was 200 nM (43 ± 8% of control, $n = 3$, $P < 0.01$; not shown), and a 2 μM treatment inhibited ATP release to 31 ± 6% of control ($n = 4$; **Figure 1B**). Incomplete inhibition of extracellular ATP accumulation after treatment with CGP37157 indicates that ATP is released as a transmitter, not as a metabolite.

We also wanted to determine basal ATP release that persists after ATP hydrolysis. *In vivo*, the ecto-nucleotide triphosphate diphosphohydrolase family of enzymes (eNTPDases) hydrolyze extracellular ATP and/or ADP to AMP and adenosine (Zimmermann, 2000). The addition of apyrase (1 U/ml), a soluble ecto-nucleotidase, completely abolished the ATP secretory rhythm (**Figure 1C**). However, apyrase did not remove all ATP, as basal ATP concentrations were observed in the bath (14 ± 8% of control, $n = 3$; **Figure 1E**), most probably reflecting ATP contained in a compartment not accessible to apyrase such as exosomes. Adenosine (100 nM) was not effective inducer of ATP release (124 ± 15% of control, $n = 3$; Figure S2), suggesting that endogenous ATP does not act at adenosine P1 receptors following extracellular metabolism.

To examine the dependence on extracellular Ca^{2+}, we tested the effect of voltage-gated Ca^{2+} channel blockers. Consistent with a hypothesis that astrocytes release ATP by Ca^{2+}-dependent mechanism (Fumagalli et al., 2003) and express voltage-gated calcium channels (Yan et al., 2013), nifedipine (0.1 μM), the L-type Ca^{2+} channel inhibitor, and La^{3+} (3 μM), a non-selective voltage-gated Ca^{2+} channel blocker, abolished ATP rhythm and significantly inhibited cumulated ATP release (nifedipine: 56 ± 3% of the control, $n = 3$, $P < 0.05$; La^{3+}: 41 ± 15% of the control, $n = 3$, $P < 0.01$, **Figures 1D,E**). Since Ca^{2+} channel blockers significantly, but not completely inhibited ATP release, these results indicate that Ca^{2+} -independent mechanism(s) might also play a role in evoking ATP release.

Dependence of Extracellular ATP Accumulation on P2X7R Activity

We examined the effects of several selective P2X7R antagonists to investigate the role of P2X7R in ATP release from SCN organotypic cultures (**Figures 2**, **3**). At low concentrations (1–10 nM), negative allosteric modulator AZ10606120 (Michel et al., 2007) reduced the amplitude of the circadian ATP rhythm (**Figures 2A,B**) and partially inhibited cumulated ATP release (10 nM: 44 ± 16% of the control, $n = 3$, $P < 0.01$; **Figure 2E**). At higher concentrations (100 nM–1 μM), AZ10606120 completely inhibited extracellular ATP rhythm (**Figures 2C,D**) to approximately basal levels (100 nM: 24 ± 7% of the control, $n = 4$, $P < 0.01$; 1 μM: 16 ± 3% of the control, $n = 3$, $P < 0.01$; **Figure 2E**), similar to levels observed in the presence of apyrase (**Figure 1C**).

Another selective P2X7R antagonist, the structurally unrelated negative allosteric modulator A438079 (Donnelly-Roberts et al., 2009), also inhibited ATP release in a concentration-dependent manner (**Figures 3A,B**). The effective threshold concentration was 10 nM (data not shown), and at concentrations of 100 nM and 1 μM, ATP release was inhibited to 44 ± 7% ($n = 4$, $P < 0.01$) and 30 ± 5% ($n = 3$, $P < 0.01$) of the control level, respectively (**Figure 3E**). Treatment with the classical P2X7R antagonist Brilliant Blue G (BBG; 200 nM) (Jiang et al., 2000) abolished the ATP rhythm (**Figure 3C**) and inhibited ATP release at the end of the incubation period to 48 ± 11% of control levels ($n = 3$, $P < 0.01$; **Figure 3E**). In contrast GW791343 (100 nM), a positive allosteric modulator of rat P2X7R (Michel et al., 2008), enhanced the amplitude of ATP release rhythm (**Figure 3D**) and extracellular ATP accumulation to 144 ± 6% of control levels ($n = 3$, $P < 0.01$; **Figure 3E**).

We also used double-label immunohistochemistry to examine the expression of P2X7R in combination with the astrocytic marker GFAP. As shown in **Figure 4**, a relatively high signal for the P2X7R protein colocalized with GFAP was observed throughout the SCN region. Experiments examining the expression of P2XRs in a mixed population of glia cells in 4 days-old culture also showed that astrocytes express P2X7R (Figure S3A), while microglia express mainly P2X4R (Figure S3B) and exhibit much lower expression of P2X7R as compared to astrocytes (Figure S3A).

Thus, P2X7R plays an important role in the circadian accumulation of extracellular ATP in SCN organotypic cultures,

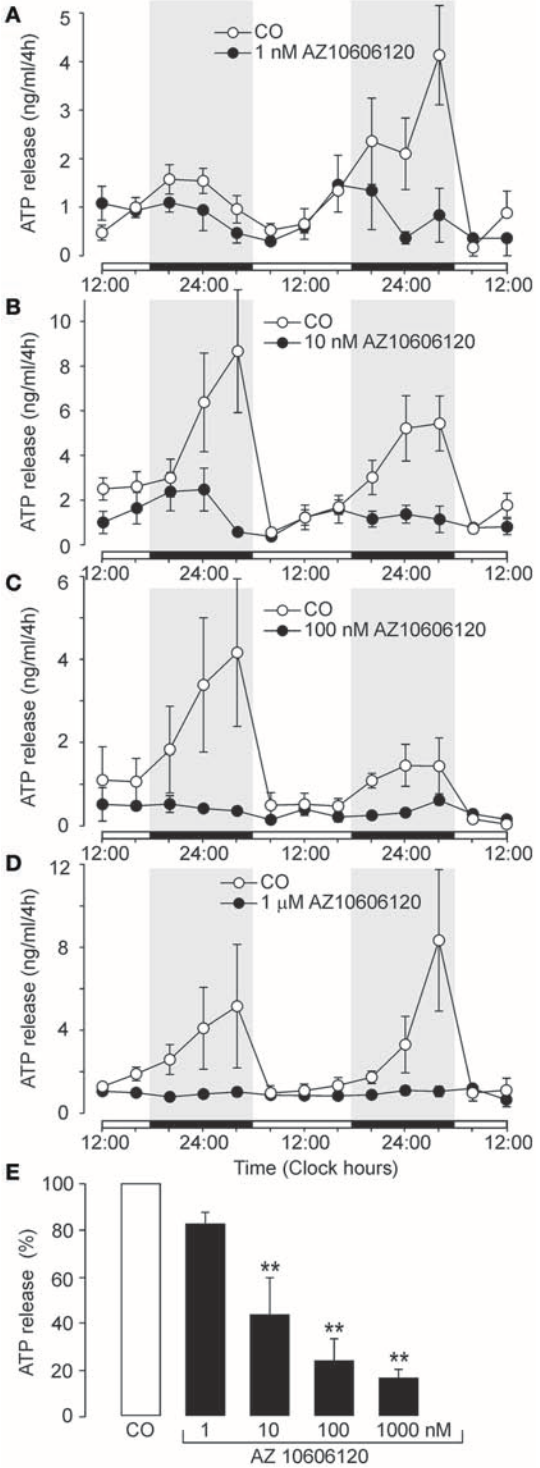

FIGURE 2 | Inhibition of circadian ATP release by the selective P2X7R blocker AZ10606120. **(A–D)** Examples of the ATP release rhythm in control cultures (open symbols) and cultures incubated with the P2X7R negative allosteric modulator AZ10606120 (closed symbols): 1 nM **(A)**, 10 nM **(B)**, 100 nM **(C)**, and 1 μM **(D)**. Summary histogram comparing the effects of various concentrations of AZ10606120 on cumulated ATP release **(E)**. Data are presented as the means ± SEM of three to six experiments. $^{**}P < 0.01$ compared to the control.

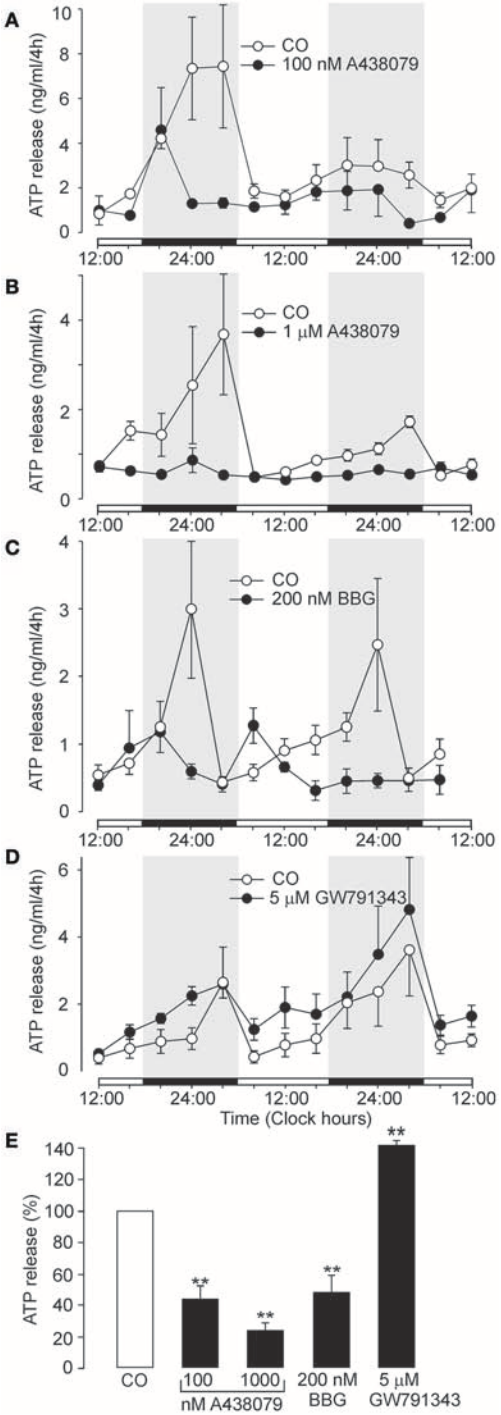

FIGURE 3 | Inhibition of circadian ATP release by the selective P2X7R inhibitors A438079 and BBG, and potentiation by positive allosteric modulator GW791343. **(A–D)** Examples of the ATP release rhythm in control cultures (open symbols) and cultures treated with selective P2X7R modulators (closed symbols). Inhibitory effects of 100 nM A438079 **(A)**, 1 μM A438079 **(B)**, and 200 nM BBG **(C)**, and potentiating effect of the positive allosteric modulator GW791343 at 5 μM concentration **(D)**. Summary graph comparing the effects of positive and negative modulators on cumulated ATP **(E)**. Data are presented as the means ± SEM of three to seven experiments. $^{**}P < 0.01$ as compared to the control.

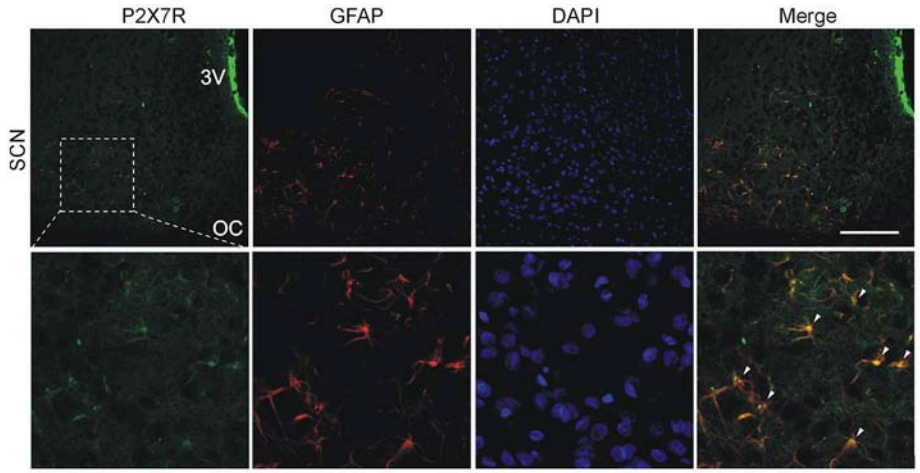

FIGURE 4 | Cellular localization of P2X7Rs in the SCN. Immunohistochemical staining of rat hypothalamic slices containing the SCN, optic chiasm (OC) and the third ventricle (3V). P2X7R immunoreactivity (green) is present on SCN cell somata. DAPI (blue) stains cell nuclei and astrocytes were identified using anti-GFAP antibodies (red). Scale bar: 100 μm **(upper row)**. Colocalization of P2X7R with the astrocyte marker. Arrowheads show representative structures that are double-labeled with anti-P2X7R and anti-GFAP antibodies **(lower row)**. Figure represents example of experiment that was performed on three animals.

and astrocytes represent the source of P2X7R-dependent circadian ATP release.

Role of Pannexin-1 Hemichannel in ATP Release

We also considered whether the pannexin-1 hemichannel might contribute to extracellular ATP accumulation. Inhibition of astrocytic panneixn-1 hemichannels by carbenoxolone (CBX, 10 μM), which might have also a minor inhibitory effect on connexin hemichannles and gap junction channels (Li M. et al., 2011), reduced the amplitude of the circadian rhythm of ATP release (**Figure 5A**) and partially inhibited cumulated ATP release (44 ± 9% of the control, $n = 4$, $P < 0.01$; **Figure 5E**). This data indicate that pannexin-1 hemichannels, alone or in complex with P2X7R, play a role in ATP release.

Dependence of Extracellular ATP Accumulation on P2Y1R and P2Y2R Activity

In addition to P2X7R, transcripts for P2X1-5 and several P2Y receptors (P2Y1R, P2Y2R and P2Y12R) have also been identified in the SCN (Bhattacharya et al., 2013). The non-selective P2 receptor antagonist PPADS (10 μM) (North, 2002) (Coddou et al., 2011) almost completely inhibited the ATP rhythm (**Figure 5B**) and extracellular ATP accumulation (28 ± 6% of the control, $n = 3$, $P < 0.01$; **Figure 5E**), whereas the P2X4R-selective negative allosteric modulator 5-BDBD (2 μM) (Balázs et al., 2013) did not exert a significant effect (79 ± 11%, $P > 0.05$; $n = 3$; **Figures 5C,E**). Treatment with the P2Y1R-selective antagonist MRS2179 (1 μM) reduced the amplitude of the ATP rhythm (**Figure 5D**, left panel) and inhibited ATP secretion to 44 ± 12% of control levels ($n = 5$, $P < 0.01$; **Figure 5E**). In contrast, the P2Y1R-selective agonist MRS2365 (1 nM) potentiated extracellular ATP accumulation (**Figure 5D**, right panel) to 186 ± 25% of control levels ($n = 3$, $P < 0.01$; **Figure 5E**). Similar effect was observed with the P2Y2R-selective agonist MRS2768 (0.5 μM; 231 ± 32%, $P > 0.05$; $n = 2$; data not shown). These results showed that, in addition to P2X7R and pannexin-1 hemichannels, metabotropic P2YRs also participate in circadian ATP release.

Ca^{2+} Signals Mediated by P2X7 and P2Y Receptors in Primary Cultured SCN Astrocytes

P2Y1R and P2Y2R are coupled to Gq/11 and may thereby contribute to extracellular ATP accumulation by stimulating phospholipase C (PLC) and mobilizing intracellular Ca^{2+} (Abbracchio and Burnstock, 1994). We examined the effects of the P2Y1R agonist MRS2365, the P2Y2R agonist MRS2768, ATP, and the prototypic P2X7R agonist 2′-3′-O-(4-benzoylbenzoyl)-ATP (BzATP) on the intracellular Ca^{2+} concentration ($[Ca^{2+}]_i$) in primary cultures of SCN astrocytes preincubated with Fura-2AM ($n = 16$ cultures, ∼20 cells per culture; **Figure 6** and Figure S4). Single cell calcium measurements showed that both ATP and BzATP induced increases in $[Ca^{2+}]_i$, and the amplitude of the BzATP-induced response was the same as or greater than the ATP-induced responses (**Figure 6A**), indicating the presence of functional P2X7R. Consistent with this finding, both ATP- and BzATP-induced increases in $[Ca^{2+}]_i$ were depressed by treatment with the P2X7R-selective blockers AZ10606120 (1 μM, 60 ± 9% inhibition, $n = 3$; **Figures 6A,G**) and A804598 (1 μM, 25 ± 6% inhibition, $n = 4$; **Figures 6B,C,H**). ATP-induced responses were also partially reduced by MRS2179 (10 μM, 57 ± 9% inhibition, $n = 3$; **Figures 6D,I**), indicating involvement of P2Y1R.

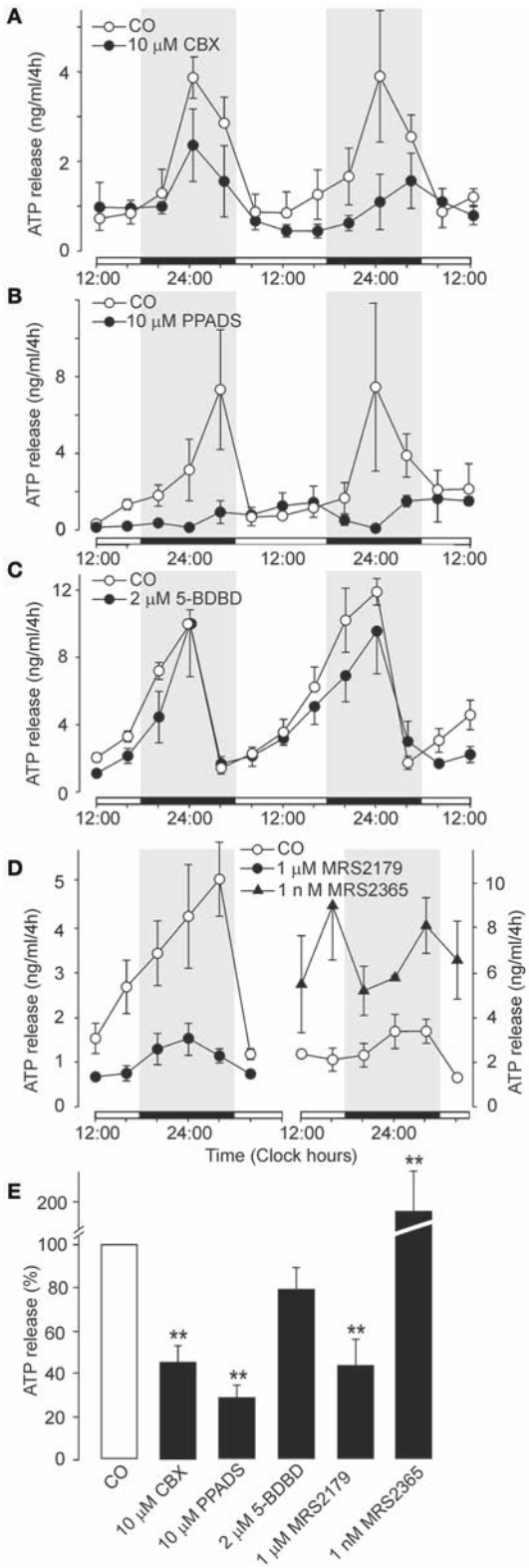

FIGURE 5 | Effects of carbenoxolone and other P2 receptor blockers on the circadian rhythmicity of ATP release. **(A)** Partial inhibitory effect of the pannexin-1 hemichannel blocker carbenoxolone (CBX). **(B)** Inhibition by *(Continued)*

FIGURE 5 | the non-specific P2 receptor blocker PPADS. **(C)** Lack of an effect of the P2X4R-selective antagonist 5-BDBD. **(D)** Circadian ATP release was significantly decreased by the P2Y1-selective inhibitor MRS2179 (left panel) and potentiated by the P2Y1R-selective agonist MRS2365 (right panel). **(E)** Summary graph showing the effects of the tested drugs on ATP release at the end of the incubation period. Data are presented as the means ± SEM of three to four experiments. $^{**}P < 0.01$ compared to the control.

Application of the P2Y1R-selective agonist MRS2365 elevated $[Ca^{2+}]_i$ in a concentration-dependent manner (**Figure 6E**), and a similar effect was observed with the P2Y2R-selective agonist MRS2768 (**Figure 6F**). Based on these results, both P2X7Rs and P2YRs may stimulate intracellular calcium signals in SCN astrocytes and thereby participate in the Ca^{2+} dependent ATP release.

Electrophysiological Evidence for the Lack of an Effect of P2X7R and Mitochondrial Blockers on SCN Neuronal Activity

We examined the effect of A438079, A 804598, AZ10606120, and CGP 37157 on firing of action potentials by SCN neurons in acutely isolated hypothalamic slices to exclude the possibility that the P2X7R antagonists and blocker of the mitochondrial Na^+/H^+ exchanger used in this study might have non-specific effects on ATP release due to their influence on the electrical activity of SCN neurons (**Figure 7**). Although 100 μM ATP induced an increase in the frequency of action potentials, the preapplication of P2X7R antagonist A438079 had no effect on ATP-induced response (**Figure 7A**). Application of P2X7R antagonists A438079 (**Figure 7B**) or AZ10606120 (not shown) was also without any effect. Application of CGP37157 slightly reduced the amplitude of action potentials without any effect on the firing frequency (**Figure 7C**). These results provide evidence that the inhibitory effects of P2X7R and mitochondrial blockers on ATP release are not associated with the inhibition of neuronal activity.

DISCUSSION

The main finding of our study is that specific P2X7R and P2Y1R antagonists inhibited circadian extracellular ATP accumulation in organotypic SCN cultures, and specific P2X7R, P2Y1R, and P2Y2R agonists elevated intracellular calcium levels in primary cultures of SCN astrocytes, suggesting that both receptors contribute to the circadian rhythmicity of ATP release that might occur via a vesicular or a non-vesicular pathway (**Figure 8**).

Non-vesicular pathways for ATP release from intact cells may include gap junction proteins like connexins (Stout et al., 2002) or pannexin-1 hemichannels (Schenk et al., 2008; Suadicani et al., 2012) and ATP-gated P2X7R channels (Pellegatti et al., 2005; Hamilton et al., 2008; Nörenberg et al., 2011a). In the brain, both neurons and astrocytes express connexins and form gap junctions, primarily with their own cell type (Contreras et al., 2004). Gap junctional networks of astrocytes are more common and generally more extensive, whereas little evidence is available

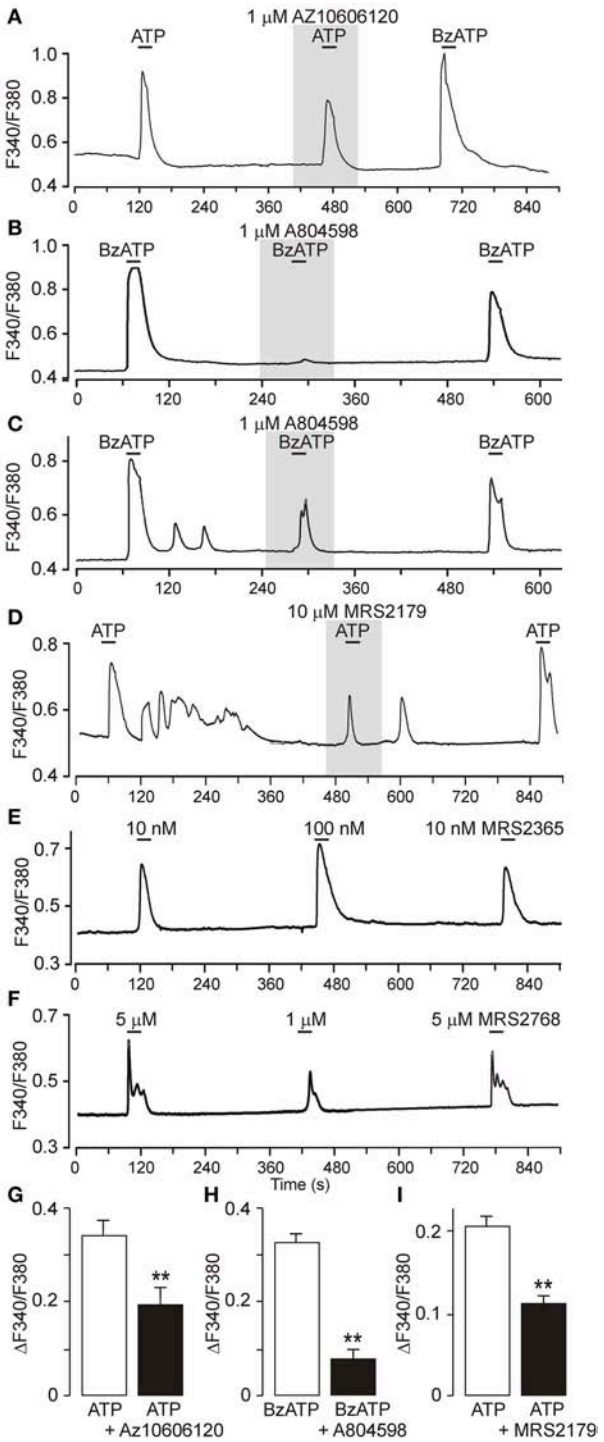

FIGURE 6 | Calcium signaling mediated by P2X7R and P2Y1R in primary cultures of SCN astrocytes. **(A)** Increases in intracellular calcium in cultured SCN astrocytes in response to ATP and BzATP (both 50 μM) and partial inhibition of the ATP-induced $[Ca^{2+}]_i$ increase by the P2X7R blocker AZ 10606120. The ratio of light intensity (F_{340}/F_{380}) reflects changes in intracellular calcium concentration ($[Ca^{2+}]_i$). **(B,C)** BzATP-induced $[Ca^{2+}]_i$ increases completely **(B)** or partially **(C)** inhibited by the P2X7R blocker A438079. **(D)** Inhibition of ATP-induced responses in the presence of

(Continued)

FIGURE 6 | the P2Y1R-selective blocker MRS2179. **(E)** Concentration-dependent elevation of astrocytic calcium levels by the P2Y1R agonist MRS2365. **(F)** Concentration-dependent effect of the P2Y2R agonist MRS2768. **(G–I)** Summary graphs showing the effects of P2 receptor agonists and antagonists on astrocytic $[Ca^{2+}]_i$. Data are presented as the means ± SEM of three to four experiments. $^{**}P < 0.01$ compared with the control.

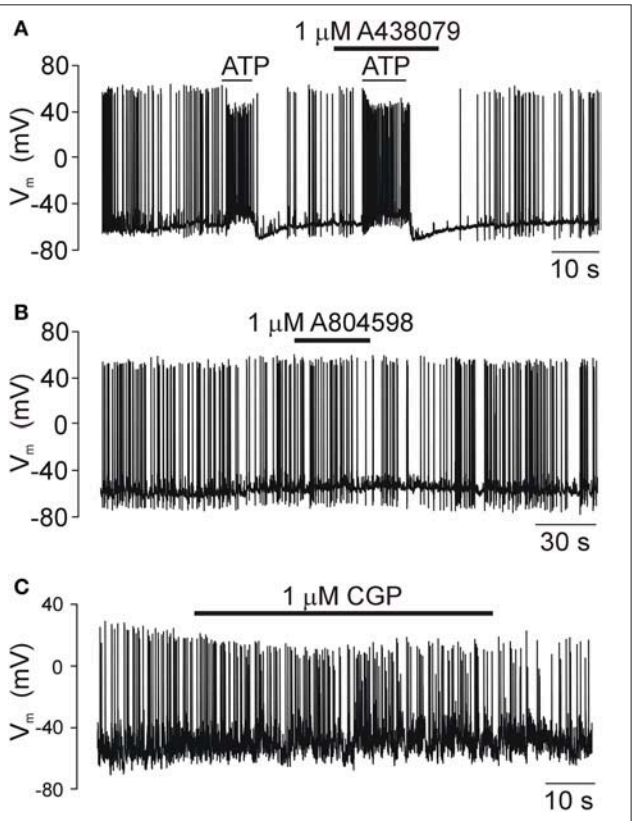

FIGURE 7 | The electrical activity of SCN neurons in acutely isolated slices is not modulated by P2X7R and mitochondria blockers. **(A)** The exogenous ATP application induced an increase in the frequency of action potentials as a result of the increased frequency of depolarizing GABAergic currents caused by the high concentration of chlorides in our intracellular solution (see the section Materials and Methods). The P2X7R-selective inhibitor A438079 had no effect on ATP-induced firing. **(B)** Prolonged application of A804598, another P2X7R blocker, also failed to change the electrical activity of SCN neurons. **(C)** A selective inhibitor of Na^+-Ca^{2+} exchanger in the mitochondria CGP37157 (CGP), gradually reduced the amplitude of action potentials with no effect on frequency. Traces shown in this figure are representative of 5–6 similar recordings.

for gap junctions among SCN neurons (Welsh and Reppert, 1996; Colwell, 2000). The P2X7R protein is also well-documented to be expressed on astrocytes (Narcisse et al., 2005; Sperlágh et al., 2006; Hamilton et al., 2008; Kamatsuka et al., 2014; Zhao et al., 2016), whereas its expression in neurons is still questionable (Illes et al., 2017). Our present study also shows the expression of the P2X7R protein in SCN astrocytes. Together with the ability of the P2X7R and pannexin-1 hemichannel blockers to reduce extracellular ATP accumulation, these data suggest that

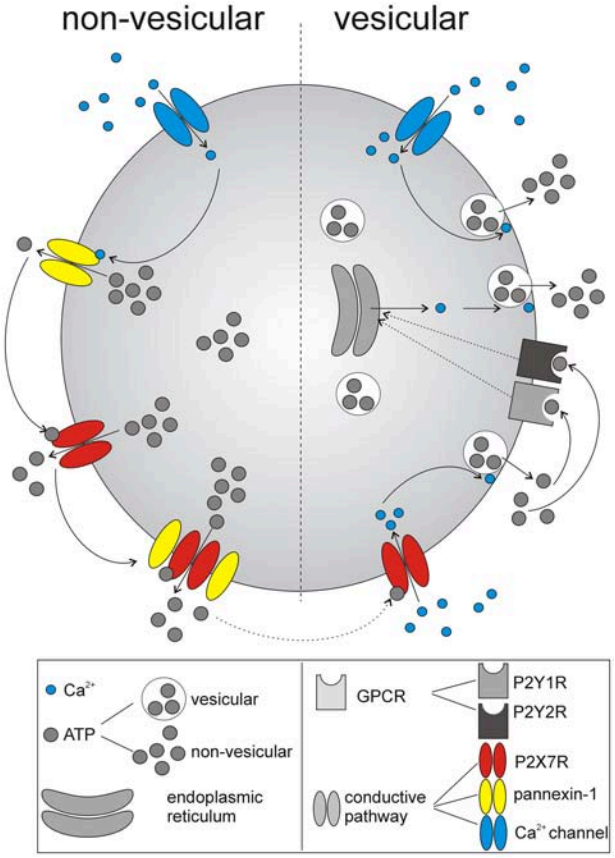

FIGURE 8 | Schematic summary of identified mechanism underlying ATP release from SCN astrocytes. The initial non-vesicular release (predominantly Ca^{2+}-independent) of ATP from astrocytes in the SCN is potentially associated with P2X7R and pannexin-1 hemichannel activation. Released ATP further stimulates P2X7R, and G-protein coupled P2YRs (GPCRs), P2Y1Rs, and P2Y2Rs, that evoke Ca^{2+}-dependent, vesicular. release of ATP. Thus, multiple purinergic P2 receptor systems, with the contribution of gap junction channels, control release of ATP from SCN astrocytes.

P2X7R alone or in complex with pannexin may function as a permeation channel for Ca^{2+}-independent astrocytic ATP release. Similar functions of P2X7Rs have been proposed for the Ca^{2+}-independent release of gliotransmitters, such as purines (Ballerini et al., 1996), GABA (Wang et al., 2002), L-glutamate and D-aspartate (Duan et al., 2003; Cervetto et al., 2013; Di Cesare Mannelli et al., 2015), D-serine (Pan et al., 2015) and ATP (Anderson et al., 2004; Suadicani et al., 2012), from cultured astrocytes. These results may also explain why circadian ATP release in SCN2.2 cells is independent of changes in intracellular Ca^{2+} concentrations (Burkeen et al., 2011) and occurs in cultured mouse cortical astrocytes even after disruption of the vesicular release mechanism (Marpegan et al., 2011).

However, astrocytic $[Ca^{2+}]_i$ is high in SCN slices during the night (Brancaccio et al., 2017), indicating that Ca^{2+}-dependent release of vesicular ATP could also contribute to circadian ATP release. P2X7R activation increases $[Ca^{2+}]_i$ in rat cerebellar astrocytes (Carrasquero et al., 2009; Nörenberg et al., 2011b; Illes et al., 2012), primary human fetal astrocytes in culture (Narcisse et al., 2005)and rat SCN astrocytes (Bhattacharya et al., 2013). This effect has been also demonstrated to be associated with the P2X7R-dependent and Ca^{2+}-dependent release of vesicular ATP (Ballerini et al., 1996; Suadicani et al., 2012) and glutamate (Cervetto et al., 2013) in astrocytes. The involvement of P2Y1R in mediating ATP-evoked Ca^{2+} signals and Ca^{2+}-dependent release of vesicular gliotransmiters is well-established in astrocytes (Fumagalli et al., 2003; Verkhratsky et al., 2009). Our finding that ATP release rhythm in SCN organotypic cultures is significantly inhibited by the voltage-gated Ca^{2+} channel blockers is consistent with the possibility that activation of P2X7R produces membrane depolarization and subsequent activation of Ca^2 entry via voltage-gated Ca^{2+} channels. Finally, increases in $[Ca^{2+}]_i$ might activate pannexin-1 hemichannels (Stout et al., 2002) which is also relevant for the ATP release through conductive mechanisms.

A P2Y1R agonist (MRS2365), and P2Y2R agonist (MRS2768) increased $[Ca^{2+}]_i$ and potentiated astrocytic ATP release in our study. However, it is noteworthy that P2Y11R is another possible target for ATP (von Kügelgen and Wetter, 2000). This receptor is also coupled to Gq/11 and has been recently identified in cultured fetal human cortical astrocytes (Muller and Taylor, 2017). However, no selective agonists or antagonists are available yet, and thus the role of P2Y11 in the SCN could not be tested. Metabotropic P2Y1Rs and ionotropic P2X7Rs have been demonstrated to be involved in autocrine stimulation of astrocytic Ca^{2+} signals in intact optic nerves (Hamilton et al., 2008) and astrocyte-to-astrocyte Ca^{2+}-mediated communication in culture (Fumagalli et al., 2003). Our data suggest that both P2X7 and P2Y receptors are involved in ATP-induced ATP release from SCN astrocytes, and that the P2X7R-stimulated ATP release is mediated by both Ca^{2+}-dependent and Ca^{2+}-independent pathway (see scheme, **Figure 8**).

Our observations raised two important questions. First, we do not know whether the rhythmic ATP secretion from astrocytes normally plays a role in controlling circadian rhythms. Genetically manipulated cortical astrocytes in culture in which IP(3) signaling is inhibited display normal circadian rhythms in clock gene expression despite the presence of arrhythmic extracellular ATP accumulation (Marpegan et al., 2011). Thus, rhythmicity in ATP release is not required for the molecular clockwork. On the other hand, extracellular ATP and its metabolites may function as paracrine modulators in the SCN. We found previously that ATP application modulates the synaptic activity of SCN neurons and via presynaptic P2X2Rs potentiates GABA release (Bhattacharya et al., 2013). Enhanced ATP release could potentially contribute to the low excitability of SCN neurons during the night. Second, further studies are needed to clarify the molecular mechanism by which P2X7 channels are rhythmically activated. Currently, no evidence has been reported suggesting day-night variability in the expression of the P2X7R mRNA or protein in the SCN. Astrocytes respond to many neurotransmitters, but ATP and glutamate are the most prominent (van den Pol et al., 1992; Bhattacharya et al., 2013) and both evoke $[Ca^{2+}]_i$ signals that

might trigger the further release of ATP or glutamate (Haydon, 2001; Illes et al., 2012). Glutamate is released from astrocytes in SCN slices during the night period (Schousboe et al., 2013; Brancaccio et al., 2017), similar to ATP (Yamazaki et al., 1994; Womac et al., 2009). Provided that the glutamate-evoked Ca^{2+}-dependent ATP release stimulates the P2X7Rs and the P2YRs, this mechanism could initiate ATP-induced ATP release. Surprisingly, the glutamate-evoked increase in astrocytic $[Ca^{2+}]_i$ in the intact optic nerve is significantly reduced in P2X7R knock-out mice (Hamilton et al., 2008). However, the control of P2X7R-dependent ATP release by glutamate in SCN astrocytes needs further investigation.

In conclusion, we provide evidence for the involvement of P2X7Rs, P2Y1Rs, and P2Y2Rs in circadian ATP release from astrocytes in SCN organotypic cultures. Purinergic signaling via P2X7Rs is well-known to play important roles in neurodegeneration, neuroprotection and neuroregeneration, and our results might improve our understanding of the roles of these receptors in the healthy central nervous system.

AUTHOR CONTRIBUTIONS

IS prepared organotypic and primary cultures, performed ATP luciferin-luciferase assays, and contributed to the conception of the work; AB did calcium imaging; MI carried out electrophysiological experiments; ZB performed immunohistochemistry; HZ designed the experiments and wrote the manuscript. All authors analyzed data, contributed to drafting the work, approved the version to be published and agree to be accountable for all aspects of the work.

FUNDING

This work was supported by grants from the Grant Agency of the Czech Republic (16-12695S and 304/12/G069), the Ministry of Education, Youth and Sports of the Czech Republic within the LQ1604 National Sustainability Program II (Project BIOCEV-FAR) and by the project BIOCEV (CZ.1.05/1.1.00/02.0109). Microscopy was performed in the Laboratory of Confocal and Fluorescence Microscopy, which is co-financed by the European Regional Development Fund and the state budget of the Czech Republic, project no. CZ.1.05/4.1.00/16.0347, CZ.2.16/3.1.00/21544 and CZ.2.16/3.1.00/21515.

SUPPLEMENTARY MATERIAL

The Supplementary Material for this article can be found online at: https://www.frontiersin.org/articles/10.3389/fphar.2018.00192/full#supplementary-material

REFERENCES

Abbracchio, M. P., and Burnstock, G. (1994). Purinoceptors: are there families of P2X and P2Y purinoceptors? *Pharmacol. Ther.* 64, 445–475. doi: 10.1016/0163-7258(94)00048-4

Abe, M., Herzog, E. D., Yamazaki, S., Straume, M., Tei, H., Sakaki, Y., et al. (2002). Circadian rhythms in isolated brain regions. *J. Neurosci.* 22, 350–356.

Anderson, C. M., Bergher, J. P., and Swanson, R. A. (2004). ATP-induced ATP release from astrocytes. *J. Neurochem.* 88, 246–256. doi: 10.1111/j.1471-4159.2004.02204.x

Balázs, B., Dankó, T., Kovács, G., Kóles, L., Hediger, M. A., and Zsembery, A. (2013). Investigation of the inhibitory effects of the benzodiazepine derivative, 5-BDBD on P2X4 purinergic receptors by two complementary methods. *Cell. Physiol. Biochem.* 32, 11–24. doi: 10.1159/000350119

Ballerini, P., Rathbone, M. P., Di Iorio, P., Renzetti, A., Giuliani, P., D'Alimonte, I., et al. (1996). Rat astroglial P2Z (P2X7) receptors regulate intracellular calcium and purine release. *Neuroreport* 7, 2533–2537. doi: 10.1097/00001756-199611040-00026

Bhattacharya, A., Vavra, V., Svobodova, I., Bendova, Z., Vereb, G., and Zemkova, H. (2013). Potentiation of inhibitory synaptic transmission by extracellular ATP in rat suprachiasmatic nuclei. *J. Neurosci.* 33, 8035–8044. doi: 10.1523/JNEUROSCI.4682-12.2013

Brancaccio, M., Patton, A. P., Chesham, J. E., Maywood, E. S., and Hastings, M. H. (2017). Astrocytes control circadian timekeeping in the suprachiasmatic nucleus via glutamatergic signaling. *Neuron* 93, 1420.e5–1435.e5. doi: 10.1016/j.neuron.2017.02.030

Burkeen, J. F., Womac, A. D., Earnest, D. J., and Zoran, M. J. (2011). Mitochondrial calcium signaling mediates rhythmic extracellular ATP accumulation in suprachiasmatic nucleus astrocytes. *J. Neurosci.* 31, 8432–8440. doi: 10.1523/JNEUROSCI.6576-10.2011

Carrasquero, L. M., Delicado, E. G., Bustillo, D., Gutiérrez-Martín, Y., Artalejo, A. R., and Miras-Portugal, M. T. (2009). P2X7 and P2Y13 purinergic receptors mediate intracellular calcium responses to BzATP in rat cerebellar astrocytes. *J. Neurochem.* 110, 879–889. doi: 10.1111/j.1471-4159.2009.06179.x

Cervetto, C., Alloisio, S., Frattaroli, D., Mazzotta, M. C., Milanese, M., Gavazzo, P., et al. (2013). The P2X7 receptor as a route for non-exocytotic glutamate release: dependence on the carboxyl tail. *J. Neurochem.* 124, 821–831. doi: 10.1111/jnc.12143

Coddou, C., Yan, Z., Obsil, T., Huidobro-Toro, J. P., and Stojilkovic, S. S. (2011). Activation and regulation of purinergic P2X receptor channels. *Pharmacol. Rev.* 63, 641–683. doi: 10.1124/pr.110.003129

Colwell, C. S. (2000). Rhythmic coupling among cells in the suprachiasmatic nucleus. *J. Neurobiol.* 43, 379–388. doi: 10.1002/1097-4695(20000615)43:4<379::AID-NEU6>3.0.CO;2-0

Contreras, J. E., Sánchez, H. A., Véliz, L. P., Bukauskas, F. F., Bennett, M. V., and Sáez, J. C. (2004). Role of connexin-based gap junction channels and hemichannels in ischemia-induced cell death in nervous tissue. *Brain Res. Brain Res. Rev.* 47, 290–303. doi: 10.1016/j.brainresrev.2004.08.002

Di Cesare Mannelli, L., Marcoli, M., Micheli, L., Zanardelli, M., Maura, G., Ghelardini, C., et al. (2015). Oxaliplatin evokes P2X7-dependent glutamate release in the cerebral cortex: a pain mechanism mediated by Pannexin 1. *Neuropharmacology* 97, 133–141. doi: 10.1016/j.neuropharm.2015.05.037

Donnelly-Roberts, D. L., Namovic, M. T., Surber, B., Vaidyanathan, S. X., Perez-Medrano, A., Wang, Y., et al. (2009). [3H]A-804598 ([3H]2-cyano-1-[(1S)-1-phenylethyl]-3-quinolin-5-ylguanidine) is a novel, potent, and selective antagonist radioligand for P2X7 receptors. *Neuropharmacology* 56, 223–229. doi: 10.1016/j.neuropharm.2008.06.012

Duan, S., Anderson, C. M., Keung, E. C., Chen, Y., Chen, Y., and Swanson, R. A. (2003). P2X7 receptor-mediated release of excitatory amino acids from astrocytes. *J. Neurosci.* 23, 1320–1328.

Fumagalli, M., Brambilla, R., D'Ambrosi, N., Volonté, C., Matteoli, M., Verderio, C., et al. (2003). Nucleotide-mediated calcium signaling in rat cortical astrocytes: Role of P2X and P2Y receptors. *Glia* 43, 218–203. doi: 10.1002/glia.10248

Groos, G., and Hendriks, J. (1982). Circadian rhythms in electrical discharge of rat suprachiasmatic neurones recorded *in vitro*. *Neurosci. Lett.* 34, 283–288. doi: 10.1016/0304-3940(82)90189-6

Guilding, C., Hughes, A. T., Brown, T. M., Namvar, S., and Piggins, H. D. (2009). A riot of rhythms: neuronal and glial circadian oscillators in the mediobasal hypothalamus. *Mol. Brain* 2:28. doi: 10.1186/1756-6606-2-28.

Hamilton, N., Vayro, S., Kirchhoff, F., Verkhratsky, A., Robbins, J., Gorecki, D. C., et al. (2008). Mechanisms of ATP- and glutamate-mediated calcium signaling in white matter astrocytes. *Glia* 56, 734–749. doi: 10.1002/glia.20649

Haydon, P. G. (2001). GLIA: listening and talking to the synapse. *Nat. Rev. Neurosci.* 2, 185–193. doi: 10.1038/35058528

Hong, Y., Zhao, T., Li, X. J., and Li, S. (2016). Mutant huntingtin impairs BDNF release from astrocytes by disrupting conversion of Rab3a-GTP into Rab3a-GDP. *J. Neurosci.* 36, 8790–8801. doi: 10.1523/JNEUROSCI.0168-16.2016

Iglesias, R., Dahl, G., Qiu, F., Spray, D. C., and Scemes, E. (2009). Pannexin 1: the molecular substrate of astrocyte "hemichannels." *J. Neurosci.* 29, 7092–7097. doi: 10.1523/JNEUROSCI.6062-08.2009

Illes, P., Khan, T. M., and Rubini, P. (2017). Neuronal P2X7 receptors revisited: do they really exist? *J. Neurosci.* 37, 7049–7062. doi: 10.1523/JNEUROSCI.3103-16.2017

Illes, P., Verkhratsky, A., Burnstock, G., and Franke, H. (2012). P2X receptors and their roles in astroglia in the central and peripheral nervous system. *Neuroscientist* 18, 422–438. doi: 10.1177/1073858411418524

Inouye, S. T., and Kawamura, H. (1979). Persistence of circadian rhythmicity in a mammalian hypothalamic island containing the suprachiasmatic nucleus. *Proc. Natl. Acad. Sci. U.S.A.* 76, 5962–5966. doi: 10.1073/pnas.76.11.5962

Jacomy, H., Burlet, A., and Bosler, O. (1999). Vasoactive intestinal peptide neurons as synaptic targets for vasopressin neurons in the suprachiasmatic nucleus. Double-label immunocytochemical demonstration in the rat. *Neuroscience* 88, 859–870. doi: 10.1016/S0306-4522(98)00259-0

Jiang, L. H., Mackenzie, A. B., North, R. A., and Surprenant, A. (2000). Brilliant blue G selectively blocks ATP-gated rat P2X(7) receptors. *Mol. Pharmacol.* 58, 82–88. doi: 10.1124/mol.58.1.82

Kamatsuka, Y., Fukagawa, M., Furuta, T., Ohishi, A., Nishida, K., and Nagasawa, K. (2014). Astrocytes, but not neurons, exhibit constitutive activation of P2X7 receptors in mouse acute cortical slices under non-stimulated resting conditions. *Biol. Pharm. Bull.* 37, 1958–1962. doi: 10.1248/bpb.b14-00000

Khakh, B. S., and Lester, H. A. (1999). Dynamic selectivity filters in ion channels. *Neuron* 23, 653–658. doi: 10.1016/S0896-6273(01)80025-8

Khakh, B. S., and Sofroniew, M. V. (2015). Diversity of astrocyte functions and phenotypes in neural circuits. *Nat. Neurosci.* 18, 942–952. doi: 10.1038/nn.4043

Kretschmannova, K., Svobodova, I., and Zemkova, H. (2003). Day-night variations in zinc sensitivity of GABAA receptor-channels in rat suprachiasmatic nucleus. *Brain Res. Mol. Brain Res.* 120, 46–51. doi: 10.1016/j.molbrainres.2003.09.017

Li, M., Kawate, T., Silberberg, S. D., and Swartz, K. J. (2011). Pore-opening mechanism in trimeric P2X receptor channels. *Nat. Commun.* 1:44. doi: 10.1038/ncomms1048

Li, S., Bjelobaba, I., Yan, Z., Kucka, M., Tomic, M., and Stojilkovic, S. S. (2011). Expression and roles of pannexins in ATP release in the pituitary gland. *Endocrinology* 152, 2342–2352. doi: 10.1210/en.2010-1216

Locovei, S., Scemes, E., Qiu, F., Spray, D. C., and Dahl, G. (2007). Pannexin1 is part of the pore forming unit of the P2X(7) receptor death complex. *FEBS Lett.* 581, 483–488. doi: 10.1016/j.febslet.2006.12.056

Marpegan, L., Swanstrom, A. E., Chung, K., Simon, T., Haydon, P. G., Khan, S. K., et al. (2011). Circadian regulation of ATP release in astrocytes. *J. Neurosci.* 31, 8342–8350. doi: 10.1523/JNEUROSCI.6537-10.2011

Michel, A. D., Chambers, L. J., Clay, W. C., Condreay, J. P., Walter, D. S., and Chessell, I. P. (2007). Direct labelling of the human P2X7 receptor and identification of positive and negative cooperativity of binding. *Br. J. Pharmacol.* 151, 103–114. doi: 10.1038/sj.bjp.0707196

Michel, A. D., Chambers, L. J., and Walter, D. S. (2008). Negative and positive allosteric modulators of the P2X(7) receptor. *Br. J. Pharmacol.* 153, 737–750. doi: 10.1038/sj.bjp.0707625

Moore, R. Y., and Card, J. P. (1985). Visual pathways and the entrainment of circadian rhythms. *Ann. N.Y. Acad. Sci.* 453, 123–133. doi: 10.1111/j.1749-6632.1985.tb11805.x

Moore, R. Y., and Eichler, V. B. (1972). Loss of a circadian adrenal corticosterone rhythm following suprachiasmatic lesions in the rat. *Brain Res.* 42, 201–206. doi: 10.1016/0006-8993(72)90054-6

Muller, M. S., and Taylor, C. W. (2017). ATP evokes Ca2+ signals in cultured foetal human cortical astrocytes entirely through G protein-coupled P2Y receptors. *J. Neurochem.* 142, 876–885. doi: 10.1111/jnc.14119

Narcisse, L., Scemes, E., Zhao, Y., Lee, S. C., and Brosnan, C. F. (2005). The cytokine IL-1beta transiently enhances P2X7 receptor expression and function in human astrocytes. *Glia* 49, 245–258. doi: 10.1002/glia.20110

Nörenberg, W., Hempel, C., Urban, N., Sobottka, H., Illes, P., and Schaefer, M. (2011a). Clemastine potentiates the human P2X7 receptor by sensitizing it to lower ATP concentrations. *J. Biol. Chem.* 286, 11067–11081. doi: 10.1074/jbc.M110.198879

Nörenberg, W., Schunk, J., Fischer, W., Sobottka, H., Riedel, T., Oliveira, J. F., et al. (2011b). Electrophysiological classification of P2X7 receptors in rat cultured neocortical astroglia. *Br. J. Pharmacol.* 160, 1941–1952. doi: 10.1111/j.1476-5381.2010.00736.x

North, R. A. (2002). Molecular physiology of P2X receptors. *Physiol. Rev.* 82, 1013–1067. doi: 10.1152/physrev.00015.2002

Pan, H. C., Chou, Y. C., and Sun, S. H. (2015). P2X7 R-mediated Ca(2+) -independent d-serine release via pannexin-1 of the P2X7 R-pannexin-1 complex in astrocytes. *Glia* 63, 877–893. doi: 10.1002/glia.22790

Pangrsic, T., Potokar, M., Stenovec, M., Kreft, M., Fabbretti, E., Nistri, A., et al. (2007). Exocytotic release of ATP from cultured astrocytes. *J. Biol. Chem.* 282, 28749–28758. doi: 10.1074/jbc.M700290200

Pascual, O., Casper, K. B., Kubera, C., Zhang, J., Revilla-Sanchez, R., Sul, J. Y., et al. (2005). Astrocytic purinergic signaling coordinates synaptic networks. *Science* 310, 113–116. doi: 10.1126/science.1116916

Pelegrin, P., and Surprenant, A. (2006). Pannexin-1 mediates large pore formation and interleukin-1beta release by the ATP-gated P2X7 receptor. *EMBO J.* 25, 5071–5082. doi: 10.1038/sj.emboj.7601378

Pellegatti, P., Falzoni, S., Pinton, P., Rizzuto, R., and Di Virgilio, F. (2005). A novel recombinant plasma membrane-targeted luciferase reveals a new pathway for ATP secretion. *Mol. Biol. Cell.* 16, 3659–3665. doi: 10.1091/mbc.E05-03-0222

Pennartz, C. M., de Jeu, M. T., Bos, N. P., Schaap, J., and Geurtsen, A. M. (2002). Diurnal modulation of pacemaker potentials and calcium current in the mammalian circadian clock. *Nature* 416, 286–290. doi: 10.1038/nature728

Reppert, S. M. (1998). A clockwork explosion! *Neuron* 21, 1–4.

Schenk, U., Westendorf, A. M., Radaelli, E., Casati, A., Ferro, M., Fumagalli, M., et al. (2008). Purinergic control of T cell activation by ATP released through pannexin-1 hemichannels. *Sci. Signal.* 1:ra6. doi: 10.1126/scisignal.1160583.

Schousboe, A., Bak, L. K., and Waagepetersen, H. S. (2013). Astrocytic control of biosynthesis and turnover of the neurotransmitters glutamate and GABA. *Front. Endocrinol.* 4:102. doi: 10.3389/fendo.2013.00102

Sperlágh, B., Vizi, E. S., Wirkner, K., and Illes, P. (2006). P2X7 receptors in the nervous system. *Prog. Neurobiol.* 78, 327–346. doi: 10.1016/j.pneurobio.2006.03.007

Stephan, F. K., and Zucker, I. (1972). Circadian rhythms in drinking behavior and locomotor activity of rats are eliminated by hypothalamic lesions. *Proc. Natl. Acad. Sci. U.S.A.* 69, 1583–1586. doi: 10.1073/pnas.69.6.1583

Stout, C. E., Costantin, J. L., Naus, C. C., and Charles, A. C. (2002). Intercellular calcium signaling in astrocytes via ATP release through connexin hemichannels. *J. Biol. Chem.* 277, 10482–10488. doi: 10.1074/jbc.M109902200

Suadicani, S. O., Iglesias, R., Wang, J., Dahl, G., Spray, D. C., and Scemes, E. (2012). ATP signaling is deficient in cultured Pannexin1-null mouse astrocytes. *Glia* 60, 1106–1116. doi: 10.1002/glia.22338

Surprenant, A., Rassendren, F., Kawashima, E., North, R. A., and Buell, G. (1996). The cytolytic P2Z receptor for extracellular ATP identified as a P2X receptor (P2X7). *Science* 272, 735–738. doi: 10.1126/science.272.5262.735

Svobodova, I., Vanecek, J., and Zemkova, H. (2003). The bidirectional phase-shifting effects of melatonin on the arginine vasopressin secretion rhythm in rat suprachiasmatic nuclei *in vitro*. *Brain Res. Mol. Brain Res.* 116, 80–85. doi: 10.1016/S0169-328X(03)00254-7

van den Pol, A. N., Finkbeiner, S. M., and Cornell-Bell, A. H. (1992). Calcium excitability and oscillations in suprachiasmatic nucleus neurons and glia *in vitro*. *J. Neurosci.* 12, 2648–2664.

Vavra, V., Bhattacharya, A., and Zemkova, H. (2011). Facilitation of glutamate and GABA release by P2X receptor activation in supraoptic neurons from freshly isolated rat brain slices. *Neuroscience* 188, 1–12. doi: 10.1016/j.neuroscience.2011.04.067

Verkhratsky, A., Krishtal, O. A., and Burnstock, G. (2009). Purinoceptors on neuroglia. *Mol. Neurobiol.* 39, 190–208. doi: 10.1007/s12035-009-8063-2

von Kügelgen, I., and Wetter, A. (2000). Molecular pharmacology of P2Y-receptors. *Naunyn Schmiedebergs Arch. Pharmacol.* 362, 310–323. doi: 10.1007/s002100000310

Wang, C. M., Chang, Y. Y., Kuo, J. S., and Sun, S. H. (2002). Activation of P2X(7) receptors induced [(3)H]GABA release from the RBA-2 type-2 astrocyte cell line through a Cl(-)/HCO(3)(-)-dependent mechanism. *Glia* 37, 8–18. doi: 10.1002/glia.10004

Watanabe, K., Koibuchi, N., Ohtake, H., and Yamaoka, S. (1993). Circadian rhythms of vasopressin release in primary cultures of rat suprachiasmatic nucleus. *Brain Res.* 624, 115–120. doi: 10.1016/0006-8993(93)90067-W

Welsh, D. K., and Reppert, S. M. (1996). Gap junctions couple astrocytes but not neurons in dissociated cultures of rat suprachiasmatic nucleus. *Brain Res.* 706, 30–36. doi: 10.1016/0006-8993(95)01172-2

White, R. J., and Reynolds, I. J. (1997). Mitochondria accumulate Ca2+ following intense glutamate stimulation of cultured rat forebrain neurones. *J. Physiol.* 498 (Pt 1), 31–47. doi: 10.1113/jphysiol.1997.sp021839

Womac, A. D., Burkeen, J. F., Neuendorff, N., Earnest, D. J., and Zoran, M. J. (2009). Circadian rhythms of extracellular ATP accumulation in suprachiasmatic nucleus cells and cultured astrocytes. *Eur. J. Neurosci.* 30, 869–876. doi: 10.1111/j.1460-9568.2009.06874.x

Yamazaki, S., Ishida, Y., and Inouye, S. (1994). Circadian rhythms of adenosine triphosphate contents in the suprachiasmatic nucleus, anterior hypothalamic area and caudate putamen of the rat–negative correlation with electrical activity. *Brain Res.* 664, 237–240. doi: 10.1016/0006-8993(94)91978-X

Yan, E., Li, B., Gu, L., Hertz, L., and Peng, L. (2013). Mechanisms for L-channel-mediated increase in [Ca(2+)]i and its reduction by anti-bipolar drugs in cultured astrocytes combined with its mRNA expression in freshly isolated cells support the importance of astrocytic L-channels. *Cell Calcium* 54, 335–342. doi: 10.1016/j.ceca.2013.08.002

Zhao, H., Zhang, X., Dai, Z., Feng, Y., Li, Q., Zhang, J. H., et al. (2016). P2X7 receptor suppression preserves blood-brain barrier through inhibiting RhoA activation after experimental intracerebral hemorrhage in rats. *Sci. Rep.* 6:23286. doi: 10.1038/srep23286

Zimmermann, H. (2000). Extracellular metabolism of ATP and other nucleotides. *Naunyn Schmiedebergs. Arch. Pharmacol.* 362, 299–309. doi: 10.1007/s002100000309

Conflict of Interest Statement: The authors declare that the research was conducted in the absence of any commercial or financial relationships that could be construed as a potential conflict of interest.

frontiers in Pharmacology

ORIGINAL RESEARCH
published: 02 March 2018
doi: 10.3389/fphar.2018.00170

Haploinsufficient TNAP Mice Display Decreased Extracellular ATP Levels and Expression of Pannexin-1 Channels

Álvaro Sebastián-Serrano[1,2†], Laura de Diego-García[1,2], David C. Henshall[3,4], Tobías Engel[3,4] and Miguel Díaz-Hernández[1,2]*

[1] Department of Biochemistry and Molecular Biology, Veterinary School, Complutense University of Madrid, Madrid, Spain, [2] Instituto de Investigación Sanitaria del Hospital Clínico San Carlos, Madrid, Spain, [3] Department of Physiology and Medical Physics, Royal College of Surgeons in Ireland, Dublin, Ireland, [4] FutureNeuro Research Centre, Dublin, Ireland

OPEN ACCESS

Edited by:
Francisco Ciruela,
Universitat de Barcelona, Spain

Reviewed by:
Nathalie Rouach,
Collège de France, France
Michael F. Jackson,
University of Manitoba, Canada

***Correspondence:**
Miguel Díaz-Hernández
migueldiaz@ucm.es

†Present address:
Álvaro Sebastián-Serrano,
Instituto de Investigaciones Biomédicas "Alberto Sols", Consejo Superior de Investigaciones Científicas, Universidad Autónoma de Madrid, Madrid, Spain; Centro de Investigación Biomédica en Red Enfermedades Neurodegenerativas, Instituto de Salud Carlos III, Madrid, Spain

Specialty section:
This article was submitted to Experimental Pharmacology and Drug Discovery, a section of the journal Frontiers in Pharmacology

Received: 15 October 2017
Accepted: 15 February 2018
Published: 02 March 2018

Citation:
Sebastián-Serrano Á, de Diego-García L, Henshall DC, Engel T and Díaz-Hernández M (2018) Haploinsufficient TNAP Mice Display Decreased Extracellular ATP Levels and Expression of Pannexin-1 Channels. Front. Pharmacol. 9:170. doi: 10.3389/fphar.2018.00170

Hypophosphatasia (HPP) is a rare heritable metabolic bone disease caused by hypomorphic mutations in the *ALPL* (in human) or *Akp2* (in mouse) gene, encoding the tissue-nonspecific alkaline phosphatase (TNAP) enzyme. In addition to skeletal and dental malformations, severe forms of HPP are also characterized by the presence of spontaneous seizures. Initially, these seizures were attributed to an impairment of GABAergic neurotransmission caused by altered vitamin B6 metabolism. However, recent work by our group using knockout mice null for TNAP (TNAP−/−), a well-described model of infantile HPP, has revealed a deregulation of purinergic signaling contributing to the seizure phenotype. In the present study, we report that adult heterozygous (TNAP+/−) transgenic mice with decreased TNAP activity in the brain are more susceptible to adenosine 5′-triphosphate (ATP)-induced seizures. Interestingly, when we analyzed the extracellular levels of ATP in the cerebrospinal fluid, we found that TNAP+/− mice present lower levels than control mice. To elucidate the underlying mechanism, we evaluated the expression levels of other ectonucleotidases, as well as different proteins involved in ATP release, such as pannexin, connexins, and vesicular nucleotide transporter. Among these, Pannexin-1 (Panx1) was the only one showing diminished levels in the brains of TNAP+/− mice. Altogether, these findings suggest that a physiological regulation of extracellular ATP levels and Panx1 changes may compensate for the reduced TNAP activity in this model of HPP.

Keywords: tissue-nonspecific alkaline phosphatase (TNAP), adenosine 5′-triphosphate (ATP), hypophosphatasia (HPP), P2X7 receptor (P2X7R), pannexin 1 (Panx1), seizure, epilepsy, connexins

Abbreviations: ATP, adenosine 5′-triphosphate; BSA, bovine serum albumin; CNS, central nervous system; CSF, cerebrospinal fluid; DAB, 3, 3′-diaminobenzidine; DAPI, 4′,6-diamidine-2′-phenylindole dihydrochloride; EEG, electroencephalogram; FBS, fetal bovine serum; GABA, γ-aminobutyric acid; HPP, hypophosphatasia; i.c.v., intracerebroventricular; M-MLV, Moloney murine leukemia virus; Panx1, pannexin-1; PBS, phosphate-buffered saline; PBS-T, PBS-buffer containing 0.1% (v/v) Tween-20; PFA, 4% paraformaldehyde in PBS; P2X7R, P2X7 receptor; qRT-PCR, quantitative real-time PCR; S.E.M., standard error of the mean; TMS, Tris-maleate sucrose buffer; TNAP, tissue-nonspecific alkaline phosphatase; TNAP−/−, *Akp2* knockout mice; TNAP+/−, heterozygous TNAP mice; VNUT, vesicular nucleotide transporter; WT, wild type.

INTRODUCTION

Intracellular ATP, best known as the main source of chemical energy along with its involvement in many crucial cellular processes, is also widely recognized to act as either sole transmitter or co-transmitter in both the peripheral and CNS (Burnstock, 2013; Rodrigues et al., 2015). In the CNS, the extracellular concentration of ATP is tightly regulated under physiological conditions via different mechanism controlling its release and degradation (Burnstock, 2016). ATP can reach the cerebral parenchyma through exocytotic and conductive release (Lazarowski et al., 2011). Exocytosis of ATP requires prior storage of ATP in secretory vesicles via VNUT (Sawada et al., 2008). Additional mechanisms of nucleotide release include ATP-binding cassette transporters, connexin or pannexin hemichannels (Dubyak, 2006; Scemes et al., 2007). During pathological conditions, however, rupture of the plasma membrane because of cell death or damage causes intracellular ATP to be directly released, thereby rapidly increasing extracellular ATP levels (Rodrigues et al., 2015).

In the extracellular space, ATP and other nucleotides undergo rapid hydrolysis by enzymes called ectonucleotidases. These enzymes are found at the plasma membrane and possess an extracellularly oriented catalytic site. This enzyme family includes ecto-nucleoside triphosphate diphosphohydrolases (E-NTPDases), ecto-nucleotide pyrophosphatase/phosphodiesterases (E-NPPs), alkaline phosphatases and ecto-5′-nucleotidase (Zimmermann, 2006). Regarding alkaline phosphatases, their mammalian isoforms share an optimum alkaline pH and are anchored to the membrane via a glycosylphosphatidylinositol anchor (Millan, 2006). TNAP is expressed in a multitude of tissues including liver, bone, kidney, and brain. In the adult mammalian CNS, TNAP represents the only isoform of alkaline phosphatases and is associated with the blood vessel endothelium and with neuropil, including synaptic contacts (Langer et al., 2008). Hypophosphatasia is a rare, inborn-error-of-metabolism characterized by defective mineralization of bone and/or teeth caused by loss-of-function mutations in the gene encoding TNAP (*ALPL* in humans and *Akp2* or *Alpl* in mice) (Whyte et al., 2015). Clinical symptoms differ with age of onset, with the perinatal form being the most severe. Neonates affected by HPP suffer from impairment of bone mineralization, respiratory distress, and spontaneous seizures which ultimately lead to death within weeks after birth (Whyte et al., 2015).

Initial studies using *Akp2* knockout (TNAP−/−) mice, a well-establish model of infantile HPP, suggested that seizures were a consequence of diminished levels of GABA in the brain, caused in turn by a defective metabolism of vitamin B6 (Waymire et al., 1995; Narisawa et al., 1997, 2001). However, our group recently identified additional phenotypes in TNAP−/− mice including increased proliferation of neural precursors, altered neuronal morphology, and augmented neuronal activity (Sebastián-Serrano et al., 2016). These morphological alterations were found to result from persistent activation of the purinergic P2X7 receptor (P2X7R), caused by the high concentrations of extracellular ATP derived from a deficient activity of TNAP. Moreover, we demonstrated that exogenous ATP or TNAP antagonists were able to trigger seizures in adult mice, with heterozygous TNAP (TNAP+/−) mice being more sensitive to ATP-induced seizures than WT mice. Accordingly, the blockage of P2X7R prevented seizure occurrence in the HPP mouse model (Sebastián-Serrano et al., 2016).

Current enzyme replacement therapy has shown skeletal, respiratory, and functional improvements as well as prevention of seizures in the most severe perinatal cases. However, several adverse side effects such as vascular calcification which has been described as comorbidity of aging, diabetes mellitus, or chronic kidney disease have been reported (Millan and Whyte, 2016). Hence, new alternative therapeutic strategies independent on ALPs targeting are currently explored. Based on our previous results, in the present study we tried to determine whether factors regulating extracellular ATP levels can be considered as potential therapeutic targets for HPP via avoiding the pathological increase of extracellular ATP concentration caused by a deficiency in TNAP activity. To address this point, we decided to use TNAP+/− mice for several reasons; although they present a decreased genetic load of alkaline phosphatase, they do not develop spontaneous seizures (Waymire et al., 1995; Narisawa et al., 1997), they are more sensitive to ATP-induced seizures than WT mice (Sebastián-Serrano et al., 2016) and they have a higher life expectancy than TNAP−/− mice, who die around postnatal day 10. Using this mouse model, we measured CSF levels of ATP, studied possible ecto-ATPase activity compensations by other ectonucleotidases and finally, focused on some of the main proteins implicated in the extracellular release of ATP.

MATERIALS AND METHODS

Animals

All animal procedures were carried out at the Complutense University of Madrid, in compliance with National and European regulations (RD1201/2005; 86/609/CEE) following the guidelines of the International Council for the Laboratory Animal Science. The protocol was approved by the Committee of Animal Experiments of the Complutense University of Madrid and the Environmental Counseling of the Comunidad de Madrid, Spain. All surgery was performed under isoflurane anesthesia, and all efforts were made to minimize suffering.

TNAP−/− mice were generated by the inactivation of the mouse *Akp2* gene, as previously described (Narisawa et al., 1997) and generously provided by Prof. Jose L. Millán (Sanford Burnham Medical Research Institute, La Jolla, CA, United States). WT, TNAP+/− and TNAP/− mice came from heterozygous TNAP+/− breeding pairs and were housed with food and water available *ad libitum* and maintained in a temperature-controlled environment on a 12/12 h light/dark cycle with light onset at 08:00 A.M.

PCR Genotyping

Genomic DNA was obtained from tail biopsies using Wizard® SV Genomic DNA Purification System (Promega, Madison, WI, United States) according to the manufacturer's protocol.

Simple PCR reactions were carried out using DNA Amplitools Master Mix (Biotools, Madrid, Spain), specific primers (400 nM each) and 5 μL of genomic DNA in a final volume of 25 μL. Animals were genotyped using specific primers for TNAP Forward 5′-TGCTGCTCCACTCACGTCGAT-3′ and Reverse 5′-AGTCCGTGGGCATTGTGACTA-3′. PCR was carried out over 40 cycles of 94°C for 30 s, 58°C for 1 min, and 72°C for 5 min.

PCR amplification products were electrophoresed on a 1.5% (w/v) agarose gel and stained with SYBR® Safe DNA Gel Stain (Life Technologies, Foster City, CA, United States). PCR bands were visualized by gel imaging system Gel Logic 200 Imaging System (Kodak, Rochester, NY, United States).

Tissue Processing for Immunohistochemistry

Adult animals were anesthetized using a mix of ketamine (80–200 mg/kg) and xylazine (7–20 mg/kg) diluted in PBS (137 mM NaCl, 2.7 mM KCl, 5 mM Na_2HPO_4 $7H_2O$, 1.4 mM KH_2PO_4; pH 7.4) and administered as a single intraperitoneal injection. Mice were perfused transcardially with PBS followed by cold PFA (pH 7.4) (Sigma-Aldrich). Perfused brains were dissected immediately and placed overnight in 4% PFA at 4°C for post-fixation. Excess PFA was removed with three PBS washes. Next, fixed brains were placed in 30% sucrose in PBS overnight at 4°C for cryoprotection. Then samples were embedded in OCT compound (Sakura) and frozen using dry ice. Finally, 30 or 50 μm floating sections were cut in parasagittal planes with a cryostat (CM1950, Leica Microsystems) and stored in a solution of 30% ethylene glycol, 30% glycerol and 0.1 M PBS at −20°C until processed.

Enzyme Histochemistry

Alkaline phosphatase activity on brain slices from adult WT and TNAP+/− mice was detected using BCIP/NBT (0.35 mM BCIP, 0.37 mM NBT, 5 mM $MgCl_2$, 100 mM Tris buffer, pH 9.5) as a dark precipitating substrate according to the manufacturer's protocol (Sigma-Aldrich, St. Louis, MO, United States). Briefly, free-floating sections were washed twice with PBS and rinsed with Tris-HCl buffer (pH 7.5) and incubated with substrate about 40 min until optimal staining intensity was obtained. After washing with Tris-HCl buffer, sections were mounted on glass slides with an anti-fading solution. To quantify the enzymatic reaction, we measured the amount of BCIP/NBT precipitate deposited on the hippocampus of WT and TNAP+/− mice. Values correspond to the mean intensity value of the pixel in eight bytes images containing the hippocampus (0–255 scale with 0 = white and 255 = black).

ATPase activity was visualized as previously described (Gampe et al., 2015). Briefly, brains sections from adult WT and TNAP+/− mice were washed in PBS and pre-treated with TMS (0.25 M sucrose, 50 mM Tris-maleate, 2 mM $MgCl_2$, pH 7.4) for 30 min at room temperature. The enzymatic reaction was carried out in TMS-buffered substrate solution stabilized with 3% dextran T 40 (Roth) [TMS-S; 2 mM $Pb(NO_3)_2$, 5 mM $MnCl_2$, 2 mM $MgCl_2$, 50 mM Tris-maleate, pH 7.4, plus 0.25 M sucrose] containing the substrate 1 mM ATP (Sigma-Aldrich) for 90 min at 37°C. The lead the dark orthophosphate precipitated, as a result of nucleotidase activity, was visualized as a brown deposit after to incubate sections for 1 min in an aqueous solution of $(NH_4)_2S$ (1% v/v) (Sigma-Aldrich). Subsequently, sections were washed twice with PBS and mounted on glass slides with an anti-fading solution. To quantify the enzymatic reaction, we measured the amount of orthophosphate precipitate deposited on the hippocampus of WT and TNAP+/− mice. Values correspond to the mean intensity value of the pixel in eight bytes images containing the hippocampus (0–255 scale with 0 = white and 255 = black).

Immunohistochemistry Techniques

Fresh-frozen parasagittal brain sections from adult WT and TNAP+/− mice were stained free-floating using the biotin–avidin–peroxidase method, with DAB as a chromogen. Endogenous peroxidase was inactivated by incubating sections in a solution of 0.3% hydrogen peroxide in PBS for 30 min. Brain sections were washed in PBS, blocked for 1 h at room temperature with 1% BSA, 5% FBS, and 0.2% Triton X-100 (Sigma-Aldrich) in PBS, and subsequently incubated with rabbit polyclonal antibody against Caspase 3 (catalog 9661, Cell Signaling, 1:50). Finally, brain sections were incubated with avidin–biotin complex using Elite Vectastain kit (Vector Laboratories). Chromogen reactions were performed with DAB (SigmaFAST DAB, Sigma-Aldrich) and 0.003% H_2O_2 for 10 min. Once washed, sections were mounted on glass slides and after dried were coverslipped using FluorSave (Calbiochem).

Image Acquisition

Transmitted light images were acquired using a microscope (Eclipse TE200, Nikon) with DFC310FX camera (Leica Microsystems GmbH) using Leica Application Suite (v4.1). Sections were photographed with Plan 4× dry objective lens (NA = 0.1) and insets with Plan S-Fluor 40× dry objective lens (NA = 0.90, Nikon) at room temperature.

Quantitative Real-Time PCR (qRT-PCR)

Total RNA was extracted from hippocampi of adult mouse brains using a Speedtools total RNA Extraction Kit (Biotools). Briefly, animals were sacrificed by cervical dislocation and the hippocampi were immediately dissected and frozen using dry ice to procedure with total RNA isolation according to the manufacturer's instruction. After digestion with TURBO DNase (Ambion), 1 μg of total RNA was reverse transcribed with 6 μg of random primers, 350 μM dNTPs and M-MLV reverse transcriptase (all from Invitrogen). qRT-PCR reaction mixtures containing DNA Master SYBR Green I mix (Applied Biosystems) were incubated at 95°C for 20 s followed by 40 PCR cycles (95°C for 1 s and 60°C for 20 s) in a StepOnePlus Real-Time PCR System (Applied Biosystems). Specific primers for *Entpd1* were 5′-AAAGCCATGCAGTGCCTTTG-3′, 5′-GCAAGGACTCTTTGGCTTTAGC-3′; for *Entpd2* were 5′-AGCTACGCAAATGACCCTTC-3′; 5′-TGGAGTGCTGGCATATCTGTC-3′; for *Entpd3* were 5′-AGGTGGCTTCTGTGTTTGAC-3′, 5′-AACCTTGGGCTGGTAAATGC-3′; for *Enpp1* were 5′-AAAGGCCGCTGCTTTGAAAG-3′, 5′-ACCGCACCTGAATTTGTTGC-3′; for *Enpp2* were 5′-ACCTTCCCAAACGTT

TGCAC-3′, 5′-AGGTTTCCTTGCAACATGCC-3′; for *Enpp3* were 5′-ATGACGTGCACCTCAACAAG-3′, 5′-ATTGCCGTTA GCCAAATCGG-3′. Expression levels of mRNA were represented as $2^{-\Delta\Delta Ct}$, where average cycle threshold (Ct) was obtained from triplicates of each sample. First, ΔCt means normalization to parallel amplification of GAPDH as endogenous control. Next, ΔΔCt means normalization to the average of corresponding controls.

In Vivo Seizure Induction and Recording

First, WT or TNAP+/− mice were anesthetized using isoflurane (3–5%) and maintained normothermic by means of a feedback controlled heat blanket (Harvard Apparatus, Ltd., Kent, United Kingdom). Mice were then placed in a stereotaxic frame, and three partial craniotomies were performed to affix cortical skull-mounted EEG electrodes (Bilaney Consultants, Ltd., Sevenoaks, United Kingdom). EEG was recorded using a Grass Comet XL digital EEG (Medivent, Ltd., Lucan, Ireland) at bandwidth 1–70 Hz (Notch filter was set to 50 Hz) and Sampling rate +800 Hz. A guide cannula was affixed (coordinates from Bregma: AP = 0.4 mm; L = 0.95 mm) and the entire skull assembly was fixed in place with dental cement. Baseline EEG was recorded for at least 10 min, and then an injection cannula was lowered through the guide cannula for i.c.v. injection of 2 μL vehicle or 0.5 M ATP at 10 s/μL (Sigma-Aldrich). Mice were monitored up to 2 h after ATP injection. Automated EEG frequency analysis was performed by uploading EEG into Labchart7 software (ADInstruments, Ltd., Oxford, United Kingdom).

CSF Acquisition and ATP Measurement

Briefly, mice were anesthetized with isoflurane diluted in a 50% O_2 and placed in a stereotaxic frame with the head forming a nearly 135° angle with the body. Mice were kept under anesthesia during the surgery. The CSF of WT and TNAP+/− mice was collected from the cisterna magna with a pulled capillary. Blood vessels were carefully avoided when penetrating the dura mater with the capillary tube to prevent contamination from plasma proteins. CSF was placed in a tube with 100 μM ARL 67156, a competitive inhibitor of ecto-ATPases (Levesque et al., 2007) and immediately frozen on dry ice to further determine the ATP concentration.

The nucleotide concentration in the CSF was measured using ENLITEN® rLuciferase/Luciferin reagent (Promega) according to the manufacturer's protocol. Briefly, 1 μL CSF from WT or TNAP+/− mice was transferred to wells of a 96-well plate placed on ice. The 96-well plate was set in a FLUOstar OPTIMA Microplate Luminometer (BMG LABTECH GmbH), and 100 μL of rLuciferase/Luciferin reagent was automatically injected into each well at room temperature.

Western Blot

Total protein extracts from hippocampus and cortex of adult and neonatal mouse brains were lysed and homogenized mechanically for 1 h at 4°C in lysis buffer containing 20 mM Hepes, 100 mM NaCl, 50 mM NaF, 5 mM EDTA, 5 mM Na_3VO_4 (all salts from Sigma-Aldrich), 1% Triton X-100, okadaic acid (Calbiochem), and Complete TM Protease Inhibitor Cocktail Tablets (Roche Diagnostics GmbH), pH 7.4. Protein quantity was detected using Bradford Protein Assay (Bio-Rad), and equal amounts of protein were used for Western blot analysis. Separation of the proteins was performed on 10 or 12% SDS-PAGE gels. Immunotransference was carried out in nitrocellulose membranes (Amersham Biosciences). The PBS-buffer containing 0.1% (v/v) Tween-20 (PBS-T) and 5% non-fat dried milk was used as a blocking medium for 1 h at room temperature. Incubation with antibodies was performed overnight at 4°C at the dilutions specified in parentheses: goat anti-Pannexin-1 antibody (catalog SC49695, Santa Cruz Biotechnology, 1:100), mouse anti-connexin 32 antibody (catalog 13-8200, Life Technologies, 1:100), mouse anti-connexin 43 antibody (catalog 13-8300, Life Technologies, 1:100), rabbit anti-VNUT (catalog PA5-63312, Thermo Fisher Scientific, 1:50), rabbit anti-VNUT (catalog ABN110; Millipore, Billerica, MA, United States 1:500) or rabbit anti-GAPDH (catalog G9545, Sigma-Aldrich, 1:40.000). The membranes were washed for 10 min with PBS-T three times, and incubated with secondary antibodies rabbit anti-goat, goat anti-rabbit or anti-mouse IgGs coupled to horse-radish peroxidase (HRP, Amersham GE Healthcare) for 1 h at room temperature used at 1:1000, 1:1000, or 1:5000, respectively. Protein bands were visualized by ECL Pro chemiluminescence (Amersham GE Healthcare). Protein expression was standardized by the expression of GAPDH from the same experiment. Gel band images densities were captured using ImageQuant LAS 500 (GE Healthcare Life Sciences) and analyzed using ImageJ software (v1.47d, NIH, Bethesda, MD, United States), without applying any background subtraction. In the figures, the representative Western blot images show only the quantified bands. Full size images are presented in Supplementary Figure 5.

Immunofluorescence Studies

For confocal microscopy, animals were transcardially perfused with 4% PFA for 10 min, post-fixed, and cryoprotected in 30% sucrose before sectioning. Tissue slices were washed in PBS and treated with blocking solution containing 5% FBS, 1% BSA, and 0.2% Triton X-100 in PBS buffer. After that, samples were incubated with primary antibodies diluted in blocking solution. After washing, sections were incubated with fluorescent-tagged secondary antibodies to be counterstained with DAPI (Thermo Fisher) and mounted in FluorSave (Merck Millipore) later. The following primary antibodies were used at the indicated dilutions: goat anti-Pannexin1 (catalog SC49695, Santa Cruz Biotechnology, 1:50), mouse anti-NeuN 1:100, mouse anti-GFAP 1:200 (Sigma-Aldrich). Donkey anti-mouse or anti-goat secondary antibodies, conjugated with Alexa 488 or 647 (Life Technologies, Madrid, Spain) were used at 1:500. Confocal images were acquired with a TCS SPE Confocal microscope equipped with four laser lines (405, 488, 561, and 653 nm) using a X63 oil objective (Leica Microsystems, Wetzlar, Germany) using the Leica software LAS AF v2.2.1 software (Leica Microsystems).

Statistical Analysis

Data are shown as mean values ± SEM. The numbers of mice per group or genotype used in each experiment are annotated in the corresponding figure legends as n. All experiments

shown were reproduced 3–5 times independently. Figures and statistical analyses were generated using GraphPad Prism 6 (GraphPad Software). Results were analyzed by un-paired Student's *t*-tests. The statistical test used and *p*-values are indicated in each figure legend. $p < 0.05$ was considered statistically significant. $^{*}p < 0.05$, $^{**}p < 0.01$, and ns, not significant.

RESULTS

TNAP+/− Brain Shows Reduced Alkaline Phosphatase Activity

We first sought evidence that the decreased genetic load of TNAP in heterozygous mice is associated with lower cerebral TNAP activity. Therefore, we performed TNAP enzymatic assays in parasagittal brain slices using WT and TNAP+/− mice. We observed high levels of TNAP activity in most structures of the adult WT brain including the neocortex, hippocampus and thalamus among others, except in the cerebellum. As expected, all these structures displayed lower alkaline phosphatase activity in TNAP+/− mice than in their corresponding WT littermates (**Figure 1A**, upper panels). As previously described, images at higher magnifications also revealed, in both genotypes, a high presence of catalytic activity associated with blood vessels of various calibers (Vorbrodt et al., 1986; Langer et al., 2008). Focusing on the hippocampus, we observed a significant decreased activity in the microvessels from TNAP+/− mice, and even clearer in their parenchyma (**Figure 1A**, lower panels and **Figure 1B**). These findings confirm TNAP+/− mice are a hypomorphic model for TNAP activity in the brain.

Increased Susceptibility of TNAP+/− Mice to ATP-Induced Electrographic Seizures

Recent work from our group has demonstrated that the i.c.v. administration of ATP induces seizures in adult WT and TNAP+/− mice by activating P2X7R. Accordingly, both the pharmacological blockage and the genetic depletion of P2X7R prevented ATP-induced seizures (Sebastián-Serrano et al., 2016). Here, we sought to extend these earlier findings by testing directly the response of TNAP+/− mice to an intracerebral injection of ATP to mimic a pathologic event such as cell death or prolonged seizure activity. We found that the i.c.v. administration of 2 μl of 0.5 M ATP induced a more prolonged and intense single seizure in TNAP+/− than in WT mice (**Figure 2A**). The average time of convulsive seizures was 14.2 ± 8.1 s in WT mice ($n = 7$) and 81.0 ± 41.9 s in TNAP+/− mice ($n = 5$) ($p < 0.05$), similar as previously reported (Sebastián-Serrano et al., 2016). The analysis of the mean power frequency of ATP-evoked seizures revealed that although slightly higher in WT mice, there was no significant difference between both groups (WT = 9.92 ± 1.5 Hz and TNAP 12.95 ± 4.01 Hz, $p = 0.47$, by Student's two-tailed *t*-test $n = 3$ WT and 5 TNAP+/− mice).

Decreased ATP Concentration in the CSF of TNAP+/− Mice

Despite their high susceptibility to ATP-induced seizures, TNAP+/− mice do not display spontaneous seizures (Waymire et al., 1995; Narisawa et al., 1997). In order to evaluate if TNAP+/− mice develop any compensatory mechanisms suppressing the development of spontaneous seizures, we decided to analyze the extracellular levels of ATP. To this end, we collected samples of the CSF from the cisterna magna of WT and TNAP+/− mice. Extracellular ATP levels were measured using rLuciferase/Luciferin reagent. Surprisingly, we found ATP levels were significantly lower in TNAP+/− mice when compared WT mice (57.41 ± 12% relative to WT) (**Figure 2B**).

Normal Physiological Cell Death in TNAP+/− Mice

Because under pathological conditions cell death is an important source responsible for large increases in extracellular ATP, we decided to analyze whether decreased extracellular ATP levels in TNAP +/− brains was associated with lower cellular mortality. To evaluate this point, we performed immunohistochemical assays against caspase-3, an indicator of apoptosis. Occasionally, we found a few positive cells with active caspase-3 in the hippocampus of both genotypes (**Figure 3A**), however, we did not detect any significant differences both in the total number (**Figure 3B**) or distribution (**Figure 3C**) of caspase-3 positive cells between both genotypes. Similar results were observed in cerebral cortex (Supplementary Figure 1).

TNAP+/− Mice Present Reduced Hippocampal Ecto-ATPase Activity

Next, we wondered whether the decreased alkaline phosphatase activity observed in TNAP heterozygous mice was compensated by changes in the expression of other ectonucleotidases. To answer this question, we measured messenger RNA levels of the main CNS ectonucleotidases capable of hydrolyzing extracellular nucleotide triphosphates. Specifically, we focused on surface-located members of E-NTPDase and E-NPP families encoded respectively by the genes *Entpd* and *Enpp* (Zimmermann, 2006). The results showed that WT and TNAP+/− mice present similar mRNA levels of the different E-NTPDases and E-NPPs analyzed (**Figure 4A**). Accordingly, the lower ecto-ATPase activity does not appear to prompt compensatory gene expression responses in other nucleotidases (**Figures 4B,C**).

Reduced Panx1 Protein Levels in the Brain of TNAP+/− Mice

Next, to determinate if the observed reduction in ATP levels was related with an altered exocytotic release of this nucleotide, we decided to measure protein levels of VNUT responsible for the storage of ATP in secretory vesicles (Sawada et al., 2008). Lysates from hippocampal and cortical samples were subjected to immunoblotting assays using specific antibodies against VNUT protein. Western blot analysis using the polyclonal antibody anti-VNUT PA5-63312 from Thermo Fisher showed that VNUT protein levels were similar between WT and

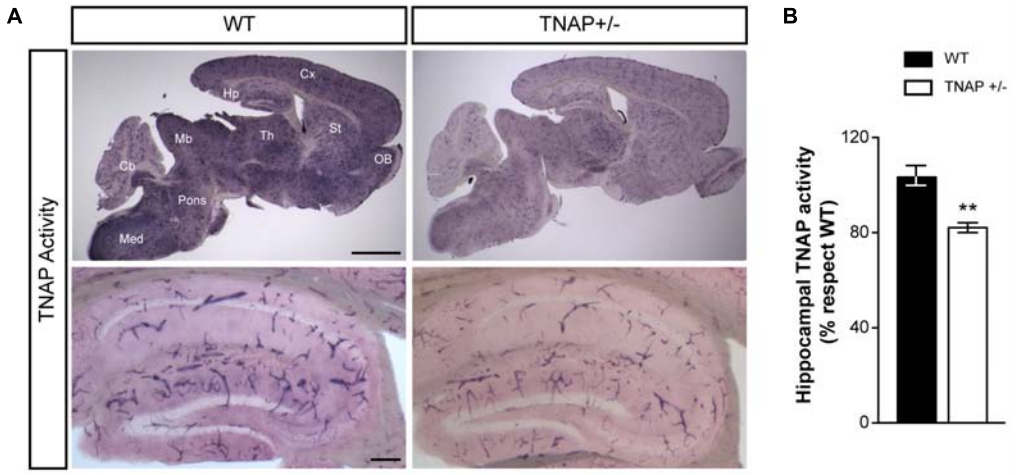

FIGURE 1 | TNAP+/– brain presents reduced alkaline phosphatase activity. **(A)** TNAP enzymatic assays on brain slices shows an overall (upper panels) and a hippocampal (lower panels) decrease of alkaline phosphatase activity in TNAP+/– mice compared with WT. Cx, neocortex; Hp, hippocampus; Th, thalamus; St, striatum; OB, olfactory bulbs; Mb, midbrain; Cb, cerebellum; Med, medulla. Scale bars: 2 mm (upper panels) and 200 μm (lower panels). **(B)** Graph shows quantification of the hippocampal TNAP activity (n = 6 mice per genotype; sections = 3 per mouse). The 100% value corresponds to the BCIP/NBT precipitated amount detected in the hippocampus of WT mice. Data are given as means ± SEM, $^{**}p < 0.01$, using unpaired Student's t-test.

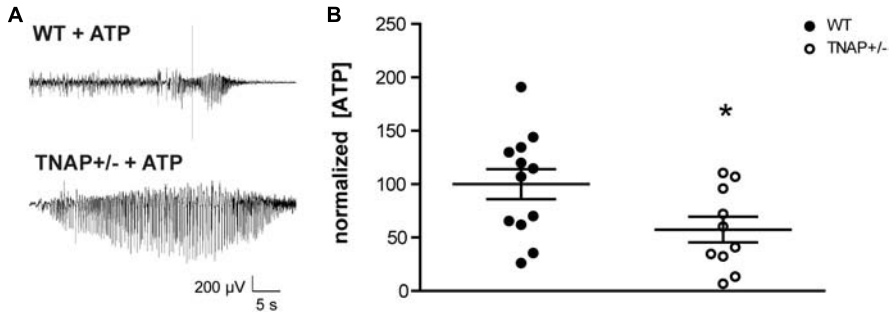

FIGURE 2 | TNAP+/– CSF present lower levels of ATP. **(A)** Representative example of EEG trace recorded showing high frequency high amplitude spiking during ATP-induced seizures in WT and TNAP+/– mice. **(B)** ATP concentrations were measured in CSF samples collected from mice (n = 12 WT and n = 10 TNAP+/–) using a commercially available bioluminescence kit. The 100% value corresponds to 6.63 ± 1.78 pmol/μL of ATP detected in the CSF. Data are given as means ± SEM, $^{*}p < 0.05$, using unpaired Student's t-test.

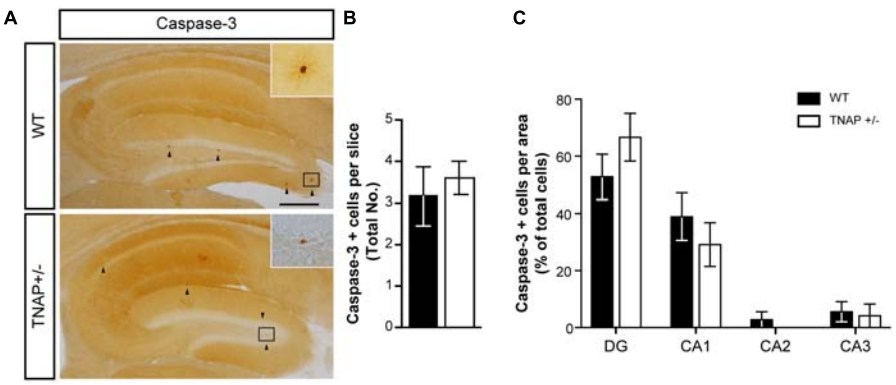

FIGURE 3 | Unaltered physiological cell death in TNAP+/– mice. **(A)** Image showing caspase-3 immunoreactivity in the hippocampus of WT and TNAP+/– mice. Inset shows detail of caspase-3 positive cells. Black arrowheads indicate samples of caspase-3 positive cells. Scale bar: 200 μm. **(B)** Total number of caspase-3 positive cells and **(C)** their distribution throughout the hippocampus (n = 6 mice per genotype; sections = 3 per mouse). Data are given as means ± SEM.

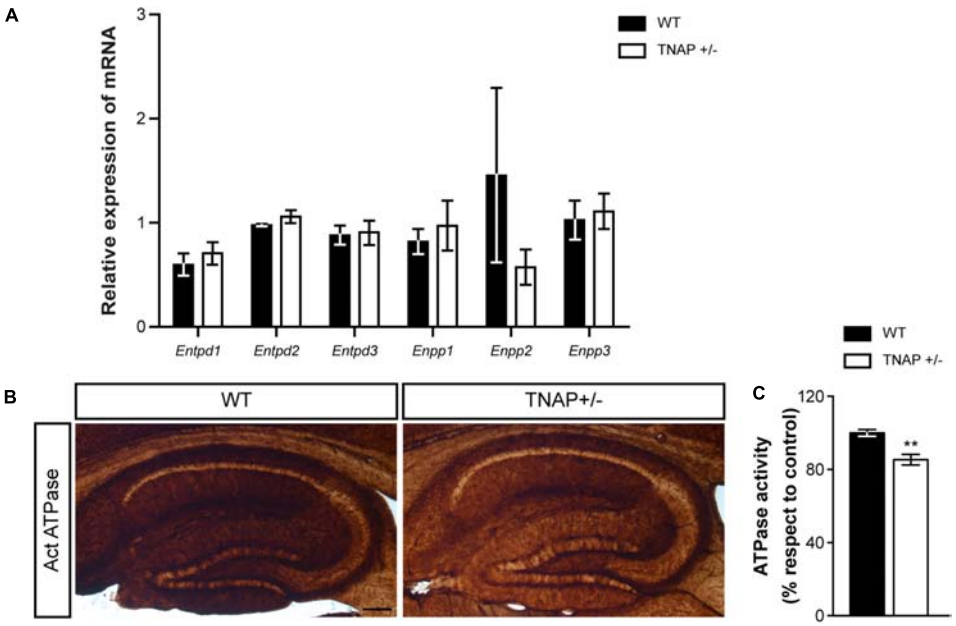

FIGURE 4 | TNAP+/– brain presents diminished ecto-ATPase activity. **(A)** Lack of upregulation of other CNS ectonucleotidases in TNAP+/– mice as revealed by qRT-PCR. The graph represents quantification of the relative abundance of *Entpd1*, *Entpd2*, *Entpd3*, *Enpp1*, *Enpp2,* and *Enpp3* mRNA from the hippocampus of WT and TNAP+/– mice (n = 6 per genotype). **(B)** Enzyme histochemical reaction products in parasagittal sections using ATP as a substrate for visualizing ecto-ATPase activity. Images show a more intense staining in the hippocampus of WT mice when compared to TNAP+/–. Scale bar: 200 μm. **(C)** Graph shows quantification of the hippocampal ATPase activity (n = 4 mice per genotype; sections = 3 per mouse). The 100% value corresponds to the ATPase activity detected in the hippocampus of WT mice. Data are given as means ± SEM, $^{**}p < 0.01$, using unpaired Student's t-test.

TNAP+/− mice both in the hippocampus and cerebral cortex (**Figure 5A**). Similar results were obtained using the polyclonal antibody against VNUT ABN110 from Millipore (Supplementary Figure 2).

We next considered changes to non-exocytotic mechanisms in the TNAP+/− mice. Neural cells, in response to a variety of different stimuli, are also capable of releasing ATP by non-secretory mechanisms involving mainly membrane channels. To explore if the decrease in ATP levels detected in TNAP+/− mice is the result of reduced expression of these channels we measured the levels of connexin 32 and 43 hemichannels, the principal connexins involved in the ATP release in oligodendrocytes and astrocytes respectively (Nagy and Rash, 2000). Hippocampal expression of both connexins was similar between TNAP+/− and WT mice (**Figure 5B**). Similar results were observed in the cerebral cortex (**Figure 5B**).

Finally, because Panx1 is a protein forming hemichannels that can release extracellular ATP in a non-secretory manner (Huang et al., 2007; Chekeni et al., 2010), we decided to explore Panx1 levels in both genotypes. It should be noted that Panx1 is an extensively glycosylated protein, showing multiple specific bands when performing western blotting (Supplementary Figure 4) (Penuela et al., 2007). Hippocampal and cortical Panx1 levels were lower in TNAP+/− mice than in their corresponding WT littermates (**Figure 5C**). Double immunofluorescence using specific neuronal (NeuN) and astroglial (GFAP) markers revealed that a reduction in Panx1 expression took mainly place in neurons (**Figures 6A,B**). This finding suggests there is a select deficit in the non-secretory ATP release pathway that may underlie the lower extracellular ATP concentration found in TNAP+/− mice. Because in previous work we reported that TNAP−/− mice presented higher extracellular ATP levels in the CNS than their WT littermates (Sebastián-Serrano et al., 2016), we decided to measure their Panx1 levels. Since TNAP−/− mice died around the postnatal day 10, we measured the Panx1 levels in cortical samples obtained from neonatal TNAP−/− and TNAP+/− mice at postnatal day 9. Unexpectedly, results revealed that both TNAP−/− and TNAP+/− mice showed similar Panx1 levels than those observed in their WT littermates (Supplementary Figure 3).

DISCUSSION

In the current study, we confirm that the brains from adult TNAP+/− mice show an overall decrease in alkaline phosphatase activity. Unexpectedly, these mice displayed lower extracellular ATP levels in the CSF than those detected in their corresponding WT littermates. This decrease was neither compensated by changes in the expression or increased activity of other ectonucleotidases nor by a decreased expression of VNUT, which could have down-regulated the exocytotic ATP release. In addition, no alterations in cell death was detected between genotypes. Regarding the proteins related to the non-exocytotic release of ATP, we did not find alterations in the expression levels of the main connexins expressed in glial cells

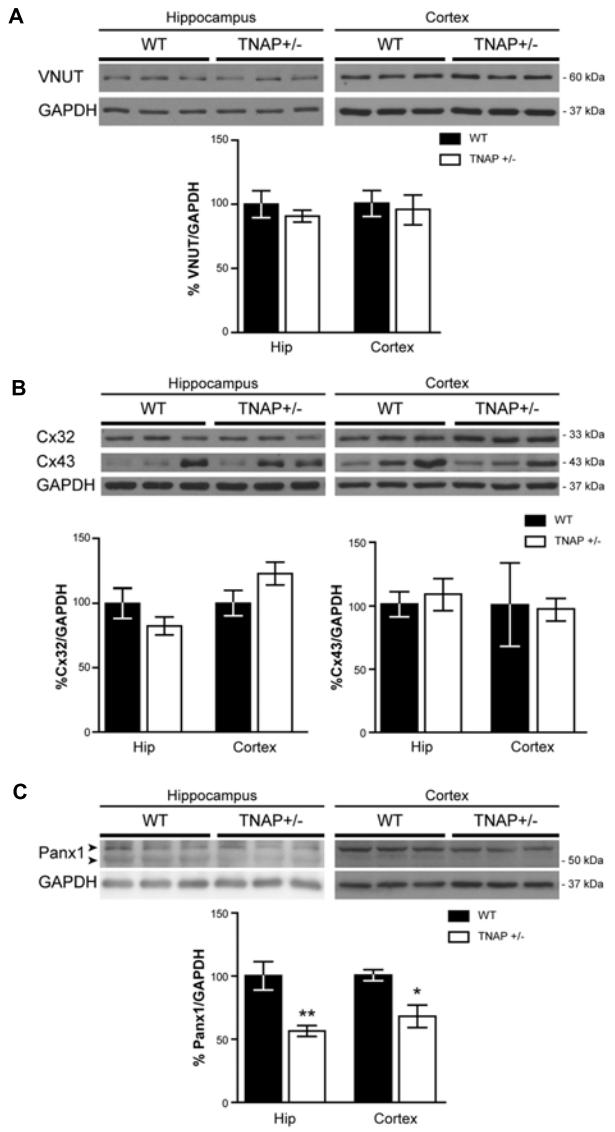

FIGURE 5 | Panx1 is downregulated in TNAP+/– hippocampus. Representative Western blot and quantification of the protein expression of **(A)** VNUT, **(B)**, connexin 32 (Cx32) and connexin 43 (Cx43) and **(C)** Panx1 ($n = 4$ WT and $n = 5$ TNAP+/–). Data are normalized to the expression levels of GAPDH "housekeeping" gene. Data are given as means ± SEM, $^{*}p < 0.05$ and $^{**}p < 0.01$, using unpaired Student's *t*-test.

(Nagy and Rash, 2000). However, a significant decrease in the protein levels of Panx1 was observed in TNAP+/− mice. Because Panx1, a single-membrane, large-conductance channel (Sosinsky et al., 2011) has been widely related to the non-exocytotic ATP release (Heinrich et al., 2012; Prochnow et al., 2012; Wicki-Stordeur et al., 2012), our results suggest that this adjustment may be a compensative mechanism of adult TNAP+/− mice to regulate the brain extracellular ATP levels (Engel et al., 2012; Sebastián-Serrano et al., 2015, 2016). Nevertheless, because other channels have also been related with the non-vesicular ATP release from astrocytes, such as maxi-chloride channels (Liu et al., 2008), additional studies are necessary to evaluate their possible contribution in the regulation of extracellular ATP levels in TNAP+/− mice.

Over the past years, several lines of evidence have suggested that Panx1 plays a key role in cellular epileptogenesis. For example, increased expression of this channel protein has been found in surgically resected cortex of patients with temporal lobe epilepsy (Jiang et al., 2013). Notably, enhanced Panx1 mRNA expression is positively correlated with seizure frequency (Li et al., 2017). Moreover, areas with high Panx1 expression are regions that become hyperexcitable in experimental models of epilepsy (Leung and Wu, 2006). These results strongly suggest that this protein is involved in the generation of epileptic events. Studies have also supported anticonvulsant functions. Silencing expression of Panx1 was reported to increase susceptibility to seizures induced by muscarinic acetylcholine receptor activation (Kim and Kang, 2011). In addition, data also showed that the ingestion of the Panx1 blocker Mefloquine resulted in convulsions in humans with a prior history of seizures (Bem et al., 1992). Nevertheless, other groups suggested a pro-seizure role of this channel based on the anticonvulsive consequences of its pharmacological blockade. Pharmacological inhibition of Panx1 decreased the spiking amplitude of the epileptiform burst activity induced by activating NMDA receptors under Mg^{2+}-free conditions in the hippocampus (Thompson et al., 2008) and prevented both the ATP release and the neuronal oscillations induced by the activation of metabotropic glutamate receptors in hippocampus (Lopatar et al., 2015) and cerebral cortex (Cepeda et al., 2015). In addition, genetic depletion of Panx1 results in the abolition of epileptiform behavior in mice exposed to kainic acid (Santiago et al., 2011). Although the reduction of Panx1 expression observed in TNAP+/− mice is not necessarily associated with a loss of function, its downregulation via interference RNA or its pharmacological blockage might contribute to regulate the basal ATP levels decreasing the non-vesicular extracellular ATP release.

In previous work, we have demonstrated that ATP-induced seizures are mediated through the P2X7R activation (Engel et al., 2012; Sebastián-Serrano et al., 2016). We established that the TNAP−/− mice reduce, at early ages, their neuronal P2X7R levels which may be a compensatory mechanism to counteract the development of spontaneous seizures induced by the increased extracellular ATP levels in the absence of this ectoenzyme (Sebastián-Serrano et al., 2016). In the present study, we found that adult TNAP+/− mice show a significant decrease of the TNAP function resulting in a reduced ecto-ATPase activity in the brain. Interestingly, although they show similar P2X7R levels than their WT littermates, do not develop spontaneous seizures and are more susceptible to ATP-induced seizures than WT mice (Sebastián-Serrano et al., 2016). Because we found that TNAP+/− mice have lower ATP levels in the CSF than their WT littermates, we reasoned that, besides P2X7R, factors regulating extracellular ATP levels might take part in the molecular mechanisms underlying the seizures associated with HPP. The analysis of the main elements involved in ATP release revealed that TNAP+/− mice only have significantly reduced the expression of Panx1. Altogether, these data suggest

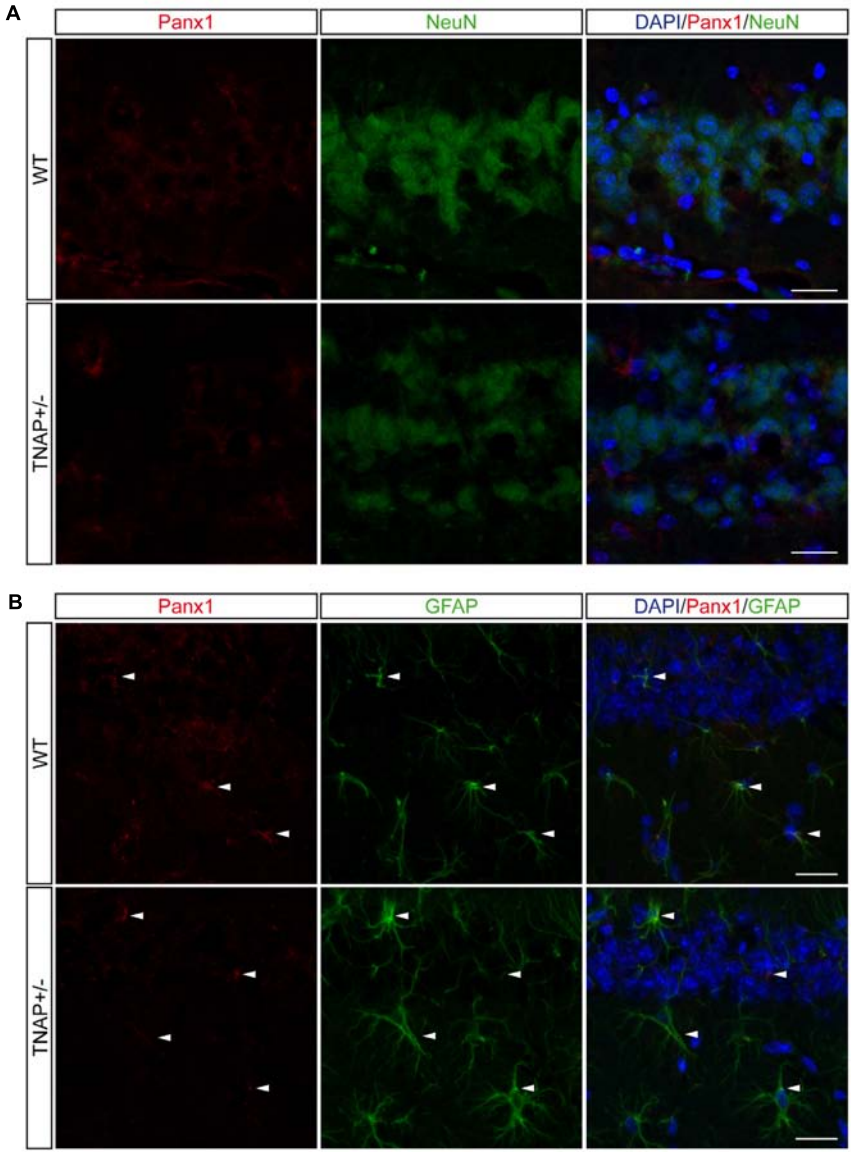

FIGURE 6 | Location of Panx1 in the hippocampus. Representative images of hippocampal parasagittal sections from TNAP+/– and WT mice co-stained with an antibody against pannexin-1 (red channel) and **(A)** neuronal marker NeuN (green channel) or **(B)** astroglial marker GFAP (green channel) and counterstained with nuclear marker DAPI. White arrowheads point to double stained astrocytes. Scale bar: 50 μm.

that alterations in TNAP activity may be compensated by different molecular mechanisms depending on its severity. So, with a partial decrease of TNAP activity, the alteration in the ATP basal levels caused by deficient ATP clearance may be balanced by decreasing the Panx1 levels. Where there is a complete lack of TNAP activity, the subsequent increase in the extracellular ATP levels induces spontaneous seizures and requires more extensive compensatory mechanisms with greater adverse outcomes as changes to P2X7R levels. Based on this hypothesis, we can postulate that although TNAP+/− and WT mice show similar expression of P2X7R, the low ATPase activity of TNAP+/− mice would contribute to extend the half-life of extracellular ATP. This event might contribute to increase the susceptibility to seizures induced by the addition of exogenous ATP. Therefore, it is reasonable to think that during growth, TNAP+/− mice reduce the expression of the Panx1 as a compensatory mechanism to reduce the basal levels of extracellular ATP, which would contribute to avoiding the seizures associated. In addition, it has been described that during the brain maturation both P2X7R and Panx1 undergo changes in location and function (Prochnow et al., 2012; Miras-Portugal et al., 2017), so we cannot discard an age-dependent component. Supporting the presence of an age-dependent factor involved in the molecular mechanism underlying the down-regulation of Panx1 neither TNAP−/− nor TNAP+/− mice showed a reduction of Panx1 levels at early ages.

So, the short life expectancy of TNAP−/− mice would avoid they may develop the compensative down-regulation of Panx1. However, additional studies should be done to elucidate this hypothesis.

In summary, here we demonstrate that adult TNAP+/− mice present reduced alkaline phosphatase activity in the brain. This decrease correlates with apparent compensatory changes in CSF extracellular ATP levels, at least in part, by diminution in Panx1 protein. The lack of spontaneous seizures in TNAP+/− mice point to the molecular mechanisms underlying the release of extracellular ATP as a new avenue for the therapeutic intervention of HPP-related seizures.

AUTHOR CONTRIBUTIONS

ÁS-S prepared protein extract, realized Western blot, immunohistochemistry, TNAP activity test, RT-qPCRs, ATP measurement, participated in experimental design, in the interpretation of the work and wrote the manuscript. LdD-G performed Western blot of hemichannels, ecto-ATPase activity assay, and revised the manuscript. TE performed *in vivo* seizure induction and recording and revised the manuscript. DH revised the manuscript. MD-H performed CSF acquisition and ATP measurement, participated in the experimental design, in the interpretation of the results, wrote the manuscript and also provided the financial support for the work.

FUNDING

This work was supported by funding from Spanish Ministry of Science and Education BFU2012-31195 European Union project H2020-MSCA-ITN-2017 number 766124 to MD-H and from Universidad Complutense of Madrid (UCM)-Santander Central Hispano Bank PR41/17-21014 to MD-H. ÁS-S was hired by BFU2012-31195 grant and LdD-G has an UCM pre-doctoral fellowship supervised by MD-H. DH and TE were supported by Science Foundation Ireland grant 16/RC/3948.

ACKNOWLEDGMENTS

We thank Prof. Jose Luis Millan for the kind gift of TNAP+/− mice, Dr. Carmen Pérez-Díaz for her technical support in obtaining CSF samples and Prof. Pablo Pelegrin and Dr. Gonzalo de la Rosa for the kind gift of spleen samples from Panx-1 knockout mice.

SUPPLEMENTARY MATERIAL

The Supplementary Material for this article can be found online at: https://www.frontiersin.org/articles/10.3389/fphar.2018.00170/full#supplementary-material

REFERENCES

Bem, J. L., Kerr, L., and Stuerchler, D. (1992). Mefloquine prophylaxis: an overview of spontaneous reports of severe psychiatric reactions and convulsions. *J. Trop. Med. Hyg.* 95, 167–179.

Burnstock, G. (2013). Introduction to purinergic signalling in the brain. *Adv. Exp. Med. Biol.* 986, 1–12. doi: 10.1007/978-94-007-4719-7_1

Burnstock, G. (2016). An introduction to the roles of purinergic signalling in neurodegeneration, neuroprotection and neuroregeneration. *Neuropharmacology* 104, 4–17. doi: 10.1016/j.neuropharm.2015.05.031

Cepeda, C., Chang, J. W., Owens, G. C., Huynh, M. N., Chen, J. Y., Tran, C., et al. (2015). In Rasmussen encephalitis, hemichannels associated with microglial activation are linked to cortical pyramidal neuron coupling: a possible mechanism for cellular hyperexcitability. *CNS Neurosci. Ther.* 21, 152–163. doi: 10.1111/cns.12352

Chekeni, F. B., Elliott, M. R., Sandilos, J. K., Walk, S. F., Kinchen, J. M., Lazarowski, E. R., et al. (2010). Pannexin 1 channels mediate 'find-me' signal release and membrane permeability during apoptosis. *Nature* 467, 863–867. doi: 10.1038/nature09413

Dubyak, G. R. (2006). "ATP release mechanisms," in *Edited Monograph: Nucleotides and Regulation of Bone Cell Function*, eds G. Burnstock, and T. R. Arnett (Boca Raton, FL: Taylor & Francis), 99–158. doi: 10.1201/9781420005059.ch5

Engel, T., Gomez-Villafuertes, R., Tanaka, K., Mesuret, G., Sanz-Rodriguez, A., Garcia-Huerta, P., et al. (2012). Seizure suppression and neuroprotection by targeting the purinergic P2X7 receptor during status epilepticus in mice. *FASEB J.* 26, 1616–1628. doi: 10.1096/fj.11-196089

Gampe, K., Stefani, J., Hammer, K., Brendel, P., Potzsch, A., Enikolopov, G., et al. (2015). NTPDase2 and purinergic signaling control progenitor cell proliferation in neurogenic niches of the adult mouse brain. *Stem Cells* 33, 253–264. doi: 10.1002/stem.1846

Heinrich, A., Ando, R. D., Turi, G., Rozsa, B., and Sperlagh, B. (2012). K^+ depolarization evokes ATP, adenosine and glutamate release from glia in rat hippocampus: a microelectrode biosensor study. *Br. J. Pharmacol.* 167, 1003–1020. doi: 10.1111/j.1476-5381.2012.01932.x

Huang, Y. J., Maruyama, Y., Dvoryanchikov, G., Pereira, E., Chaudhari, N., and Roper, S. D. (2007). The role of pannexin 1 hemichannels in ATP release and cell-cell communication in mouse taste buds. *Proc. Natl. Acad. Sci. U.S.A.* 104, 6436–6441. doi: 10.1073/pnas.0611280104

Jiang, T., Long, H., Ma, Y., Long, L., Li, Y., Li, F., et al. (2013). Altered expression of pannexin proteins in patients with temporal lobe epilepsy. *Mol. Med. Rep.* 8, 1801–1806. doi: 10.3892/mmr.2013.1739

Kim, J. E., and Kang, T. C. (2011). The P2X7 receptor-pannexin-1 complex decreases muscarinic acetylcholine receptor-mediated seizure susceptibility in mice. *J. Clin. Invest.* 121, 2037–2047. doi: 10.1172/JCI44818

Langer, D., Hammer, K., Koszalka, P., Schrader, J., Robson, S., and Zimmermann, H. (2008). Distribution of ectonucleotidases in the rodent brain revisited. *Cell Tissue Res.* 334, 199–217. doi: 10.1007/s00441-008-0681-x

Lazarowski, E. R., Sesma, J. I., Seminario-Vidal, L., and Kreda, S. M. (2011). Molecular mechanisms of purine and pyrimidine nucleotide release. *Adv. Pharmacol.* 61, 221–261. doi: 10.1016/B978-0-12-385526-8.00008-4

Leung, L. S., and Wu, K. (2006). Epilepsy-based changes in hippocampal excitability: causes and effects. *Adv. Neurol.* 97, 63–68.

Levesque, S. A., Lavoie, E. G., Lecka, J., Bigonnesse, F., and Sevigny, J. (2007). Specificity of the ecto-ATPase inhibitor ARL 67156 on human and mouse ectonucleotidases. *Br. J. Pharmacol.* 152, 141–150. doi: 10.1038/sj.bjp.0707361

Li, S., Zang, Z., He, J., Chen, X., Yu, S., Pei, Y., et al. (2017). Expression of pannexin 1 and 2 in cortical lesions from intractable epilepsy patients with focal cortical dysplasia. *Oncotarget* 8, 6883–6895. doi: 10.18632/oncotarget.14317

Liu, H. T., Toychiev, A. H., Takahashi, N., Sabirov, R. Z., and Okada, Y. (2008). Maxi-anion channel as a candidate pathway for osmosensitive ATP release from mouse astrocytes in primary culture. *Cell Res.* 18, 558–565. doi: 10.1038/cr.2008.49

Lopatar, J., Dale, N., and Frenguelli, B. G. (2015). Pannexin-1-mediated ATP release from area CA3 drives mGlu5-dependent neuronal oscillations. *Neuropharmacology* 93, 219–228. doi: 10.1016/j.neuropharm.2015.01.014

Millan, J. L. (2006). Alkaline Phosphatases : structure, substrate specificity and functional relatedness to other members of a large superfamily of enzymes. *Purinergic Signal.* 2, 335–341. doi: 10.1007/s11302-005-5435-6

Millan, J. L., and Whyte, M. P. (2016). Alkaline Phosphatase and Hypophosphatasia. *Calcif. Tissue Int.* 98, 398–416. doi: 10.1007/s00223-015-0079-1

Miras-Portugal, M. T., Sebastián-Serrano, Á., de Diego García, L., and Díaz-Hernández, M. (2017). Neuronal P2X7 receptor: involvement in neuronal physiology and pathology. *J. Neurosci.* 37, 7063–7072. doi: 10.1523/JNEUROSCI.3104-16.2017

Nagy, J. I., and Rash, J. E. (2000). Connexins and gap junctions of astrocytes and oligodendrocytes in the CNS. *Brain Res. Brain Res. Rev.* 32, 29–44. doi: 10.1016/S0165-0173(99)00066-1

Narisawa, S., Frohlander, N., and Millan, J. L. (1997). Inactivation of two mouse alkaline phosphatase genes and establishment of a model of infantile hypophosphatasia. *Dev. Dyn.* 208, 432–446. doi: 10.1002/(SICI)1097-0177(199703)208:3<432::AID-AJA13>3.0.CO;2-1

Narisawa, S., Wennberg, C., and Millan, J. L. (2001). Abnormal vitamin B6 metabolism in alkaline phosphatase knock-out mice causes multiple abnormalities, but not the impaired bone mineralization. *J. Pathol.* 193, 125–133. doi: 10.1002/1096-9896(2000)9999:9999<::AID-PATH722>3.0.CO;2-Y

Penuela, S., Bhalla, R., Gong, X. Q., Cowan, K. N., Celetti, S. J., Cowan, B. J., et al. (2007). Pannexin 1 and pannexin 3 are glycoproteins that exhibit many distinct characteristics from the connexin family of gap junction proteins. *J. Cell Sci.* 120, 3772–3783. doi: 10.1242/jcs.009514

Prochnow, N., Abdulazim, A., Kurtenbach, S., Wildforster, V., Dvoriantchikova, G., Hanske, J., et al. (2012). Pannexin1 stabilizes synaptic plasticity and is needed for learning. *PLoS One* 7:e51767. doi: 10.1371/journal.pone.0051767

Rodrigues, R. J., Tome, A. R., and Cunha, R. A. (2015). ATP as a multi-target danger signal in the brain. *Front. Neurosci.* 9:148. doi: 10.3389/fnins.2015.00148

Santiago, M. F., Veliskova, J., Patel, N. K., Lutz, S. E., Caille, D., Charollais, A., et al. (2011). Targeting pannexin1 improves seizure outcome. *PLoS One* 6:e25178. doi: 10.1371/journal.pone.0025178

Sawada, K., Echigo, N., Juge, N., Miyaji, T., Otsuka, M., Omote, H., et al. (2008). Identification of a vesicular nucleotide transporter. *Proc. Natl. Acad. Sci. U.S.A.* 105, 5683–5686. doi: 10.1073/pnas.0800141105

Scemes, E., Suadicani, S. O., Dahl, G., and Spray, D. C. (2007). Connexin and pannexin mediated cell-cell communication. *Neuron Glia Biol.* 3, 199–208. doi: 10.1017/S1740925X08000069

Sebastián-Serrano, Á., de Diego-García, L., Martinez-Frailes, C., Avila, J., Zimmermann, H., Millan, J. L., et al. (2015). Tissue-nonspecific alkaline phosphatase regulates purinergic transmission in the central nervous system during development and disease. *Comput. Struct. Biotechnol. J.* 13, 95–100. doi: 10.1016/j.csbj.2014.12.004

Sebastián-Serrano, Á., Engel, T., de Diego-García, L., Olivos-Ore, L. A., Arribas-Blazquez, M., Martinez-Frailes, C., et al. (2016). Neurodevelopmental alterations and seizures developed by mouse model of infantile hypophosphatasia are associated with purinergic signalling deregulation. *Hum. Mol. Genet.* 25, 4143–4156. doi: 10.1093/hmg/ddw248

Sosinsky, G. E., Boassa, D., Dermietzel, R., Duffy, H. S., Laird, D. W., Macvicar, B., et al. (2011). Pannexin channels are not gap junction hemichannels. *Channels* 5, 193–197. doi: 10.4161/chan.5.3.15765

Thompson, R. J., Jackson, M. F., Olah, M. E., Rungta, R. L., Hines, D. J., Beazely, M. A., et al. (2008). Activation of pannexin-1 hemichannels augments aberrant bursting in the hippocampus. *Science* 322, 1555–1559. doi: 10.1126/science.1165209

Vorbrodt, A. W., Lossinsky, A. S., and Wisniewski, H. M. (1986). Localization of alkaline phosphatase activity in endothelia of developing and mature mouse blood-brain barrier. *Dev. Neurosci.* 8, 1–13. doi: 10.1159/000112236

Waymire, K. G., Mahuren, J. D., Jaje, J. M., Guilarte, T. R., Coburn, S. P., and Macgregor, G. R. (1995). Mice lacking tissue non-specific alkaline phosphatase die from seizures due to defective metabolism of vitamin B-6. *Nat. Genet.* 11, 45–51. doi: 10.1038/ng0995-45

Whyte, M. P., Zhang, F., Wenkert, D., Mcalister, W. H., Mack, K. E., Benigno, M. C., et al. (2015). Hypophosphatasia: validation and expansion of the clinical nosology for children from 25 years experience with 173 pediatric patients. *Bone* 75, 229–239. doi: 10.1016/j.bone.2015.02.022

Wicki-Stordeur, L. E., Dzugalo, A. D., Swansburg, R. M., Suits, J. M., and Swayne, L. A. (2012). Pannexin 1 regulates postnatal neural stem and progenitor cell proliferation. *Neural Dev.* 7:11. doi: 10.1186/1749-8104-7-11

Zimmermann, H. (2006). Ectonucleotidases in the nervous system. *Novartis Found. Symp.* 276, 113–128. doi: 10.1002/9780470032244.ch10

Conflict of Interest Statement: The authors declare that the research was conducted in the absence of any commercial or financial relationships that could be construed as a potential conflict of interest.

frontiers in Pharmacology

ORIGINAL RESEARCH
published: 01 March 2018
doi: 10.3389/fphar.2018.00153

Unveiling the Role of Ecto-5′-Nucleotidase/CD73 in Astrocyte Migration by Using Pharmacological Tools

Marija Adzic[1,2] *and Nadezda Nedeljkovic*[1]*

[1] *Department of General Physiology and Biophysics, Institute for Physiology and Biochemistry, Faculty of Biology, University of Belgrade, Belgrade, Serbia,* [2] *Centre for Laser Microscopy, Institute for Physiology and Biochemistry, Faculty of Biology, University of Belgrade, Belgrade, Serbia*

CD73 is a bifunctional glycosylphosphatidylinositol (GPI)-anchored membrane protein which functions as ecto-5′-nucleotidase and a membrane receptor for extracellular matrix protein (ECM). A large body of evidence demonstrates a critical involvement of altered purine metabolism and particularly, increased expression of CD73 in a number of human disorders, including cancer and immunodeficiency. Massive up-regulation of CD73 was also found in reactive astrocytes in several experimental models of human neuropathologies. In all the pathological contexts studied so far, the increased expression of CD73 has been associated with the altered ability of cells to adhere and/or migrate. Thus, we hypothesized that increased expression of CD73 in reactive astrocytes has a role in the process of astrocyte adhesion and migration. In the present study, the involvement of CD73 in astrocyte migration was investigated in the scratch wound assay (SW), using primary astrocyte culture prepared from neonatal rat cortex. The cultures were treated with one of the following pharmacological inhibitors which preferentially target individual functions of CD73: (a) α,β-methylene ADP (APCP), which inhibits the catalytic activity of CD73 (b) polyclonal anti-CD73 antibodies, which bind to the internal epitope of CD73 molecule and mask their surface exposure and (c) small interfering CD73-RNA (siCD73), which silences the expression of CD73 gene. It was concluded that approaches that reduce surface expression of CD73 increase migration velocity and promote wound closure in the scratch wound assay, while inhibition of the enzyme activity by APCP induces redistribution of CD73 molecules at the cell surface, thus indirectly affecting cell adhesion and migration. Application of anti-CD73 antibodies induces a decrease in CD73 activity and membrane expression, through CD73 molecules shedding and their release to the culture media. In addition, all applied pharmacological inhibitors differentially affect other aspects of astrocyte function *in vitro,* including reduced cell proliferation, altered expression of adenosine receptors and increased expression of ERK1/2. Altogether these data imply that CD73 participates in cell adhesion/migration and transmits extracellular signals through interactions with ECM.

Keywords: ecto-5′-nucleotidase/CD73, reactive astrocytes, cell adhesion, migration, scratch wound assay

OPEN ACCESS

Edited by:
Francisco Ciruela,
Universitat de Barcelona, Spain

Reviewed by:
Carla Cicala,
University of Naples Federico II, Italy
Gourav Roy Choudhury,
Texas Biomedical Research Institute, United States

***Correspondence:**
Nadezda Nedeljkovic
nnedel@bio.bg.ac.rs

Specialty section:
This article was submitted to Experimental Pharmacology and Drug Discovery, a section of the journal Frontiers in Pharmacology

Received: *16 November 2017*
Accepted: *13 February 2018*
Published: *01 March 2018*

Citation:
Adzic M and Nedeljkovic N (2018) Unveiling the Role of Ecto-5′-Nucleotidase/CD73 in Astrocyte Migration by Using Pharmacological Tools. Front. Pharmacol. 9:153. doi: 10.3389/fphar.2018.00153

INTRODUCTION

Ecto-5′-nucleotidase, known as CD73 (eNT; E.C. 3.1.3.5) is Zn^{2+}-binding membrane enzyme with its active site facing the extracellular compartment (Zimmermann, 1992; Zimmermann et al., 2012). The enzyme is capable to dephosphorylate several ribo- and deoxyribonucleoside 5′-monophosphates to their corresponding nucleosides (Zimmermann et al., 2012), whereby 5′-adenosine monophosphate (AMP) is the most efficiently hydrolyzed substrate (Bianchi and Spychala, 2003). The enzyme has a broad tissue distribution, being expressed in many cell types, including subpopulations of T and B lymphocytes and in a number of tumor cells (Antonioli et al., 2013a). Thus, as the main source of extracellular adenosine in all tissues, it is of a major pharmacological interest.

The functional CD73 molecule comprises two identical subunits, tethered by non-covalent bonds and anchored to the outer leaflet of plasma membrane via glycosylphosphatidylinositol (GPI) anchor (Naito and Lowenstein, 1981; Ogata et al., 1990; Strater, 2006). Each enzyme monomer comprises 576 amino residues, organized in one flexible α-helical domain interposed between N- and C-terminal domains. Two 26-amino acid signal peptides in the N-terminal domains coordinate binding of two Zn^{2+} ions required for the catalytic activity, while two opposing C-terminal domains provide a binding site for AMP (Strater, 2006). Structure-function analysis revealed that a transition of the molecule between open and closed conformational states is required for the catalytic activity (Knofel and Strater, 2001; Knapp et al., 2012). The activity is competitively inhibited by adenosine diphosphate (ADP) (Cunha, 2001) or its analog, α,β-methylene ADP (APCP), which is the most potent CD73 inhibitor known to date. Mature CD73 contains four (human and mouse) or five (rat) *N*-glycosylation sites that can be completely or partially modified with a complex mixture of glycans (Zimmermann, 1992). As a result, in different tissues and cell types, CD73 occurs in several glycoforms, which differ in their apparent molecular weight (60–80 kDa) and sensitivity to lectins (Vogel et al., 1991; Zimmermann, 1992; Navarro et al., 1998). While bulk CD73 is membrane-bound glycoprotein attached to the cell surface via GPI anchor, the enzyme may be shed from the membrane by phosphatidylinositol-specific phospholipase or by proteolytic cleavage, to give rise to the soluble variant which retains its catalytic activity (Heuts et al., 2012). The soluble CD73 constitutes an important auxiliary system for maintaining extracellular nucleotide concentrations in blood and body fluids (Yegutkin, 2008; Heuts et al., 2012; Laketa et al., 2015).

CD73 has two major functions (Zimmermann et al., 2012). The first is a generation of extracellular adenosine from AMP, which derives from adenosine triphosphate (ATP) or nicotinamide dinucleotide (NAD+) released in the extracellular space. The nucleotides are crucially involved in cellular energy metabolism, but they also function as signaling molecules, after being secreted across cell membranes (Ziegler, 2000; Grahnert et al., 2011). In a response to diverse noxious stimuli in the brain, ATP and NAD+ are massively released out of cells, where they act as danger-associated molecular patterns (DAMPs) involved in an initiation of the immune reaction. Following their action at specific P2 purinoceptors (Abbracchio et al., 2006; Khakh and North, 2012), ATP and NAD+ are hydrolyzed to AMP by catalytic actions of ecto-nucleoside triphosphate diphosphohydrolase 1 (NTPDase1/CD39) (Zimmermann et al., 2012; Yegutkin, 2014) and nucleotide pyrophosphatase/phosphodiesterase 1 (NPP1/CD38) (Horenstein et al., 2013) respectively, thereby providing the substrate for CD73. Adenosine generated from AMP acts at G-protein coupled P1 purinoceptors, functionally linked to inhibition (A_1, A_3) or stimulation (A_2A, A_2B) of adenylate cyclase (Fredholm et al., 2001). Resulting adenosine is implicated in a broad range of physiological processes, including cell growth, differentiation and immune-suppression (Schwaninger et al., 1997; Hasko and Cronstein, 2004). In other words, extracellular pathways for a degradation of two danger signals, ATP and NAD+, converge toward CD73 and culminate in the formation of adenosine, which, in turn, exhibits strong tissue protective and anti-inflammatory actions (Antonioli et al., 2013b). Besides generation of adenosine, CD73 functions as a membrane receptor for extracellular matrix molecules (ECM), tenascin C, fibronectin and laminin (Stochaj et al., 1990; Olmo et al., 1992; Sadej et al., 2008). Interactions between cell adhesion molecules (CAM) and ECM play the key role in a regulation of cell adhesion, growth, migration, and differentiation, indicating that CD73 may participate in a control of these processes in both normal and neoplastic cells (Sadej et al., 2008).

Studies in a large number of human disorders demonstrate important role of CD73 in the immunity and cell communication (Schetinger et al., 2007; Deaglio and Robson, 2011; Ghiringhelli et al., 2012; Antonioli et al., 2013a,b; Gao et al., 2014) and highlight its potential as a pharmacologic target for immunomodulation and cancer treatment (Corbelini et al., 2015; Antonioli et al., 2016, 2017). Significant up-regulation of CD73 gene expression by reactive astrocytes was demonstrated in several experimental models of human neuropathologies, including ischemia (Braun et al., 1998), temporal lobe epilepsy (Bonan et al., 2000, Bonan, 2012), traumatic brain injury (Nedeljkovic et al., 2006; Bjelobaba et al., 2011), amyotrophic lateral sclerosis (Gandelman et al., 2010), experimental autoimmune encephalomyelitis (EAE) (Lavrnja et al., 2015) and glioma (Xu et al., 2013). In such conditions, astrocytes develop reactive phenotype, characterized by cellular hypertrophy and processes elongation (Sofroniew, 2009), they migrate to the area of tissue injury, where they interact with fibro-meningeal and $NG2^+$ glial cells, release cytokines and deposit ECM to form a glial scar (Oberheim et al., 2008, 2012; Wiese et al., 2012; Wanner et al., 2013). Among many classes of molecules directly involved in different aspects of the altered cellular activity (Sofroniew, 2009; Wiese et al., 2012), reactive astrocytes massively increase the expression of CD73, both *in vivo* (Braun et al., 1998; Bonan et al., 2000; Nedeljkovic et al., 2006; Lavrnja et al., 2009, 2015; Gandelman et al., 2010; Bjelobaba et al., 2011; Bonan, 2012) and *in vitro* (Fenoglio et al., 1997; Bavaresco et al., 2008; Brisevac et al., 2012, 2015). The expression switch for CD73, however, does not turn on

immediately, but in days following the initial tissue damage. Thus, in the model of stab brain injury *in vivo*, the contribution of $CD73^+$ astrocytes to a total number of $GFAP^+$ astrocytes gradually increases, reaching the maximum 14 days after the injury, when the patterns of CD73 and GFAP expression in reactive astrocytes completely overlap (Bjelobaba et al., 2011). The similar sustained pattern of CD73 expression is observed in EAE, where individual $CD73^+$ astrocytes appear just at the peak of the symptomatic phase of the illness and their number continues to increase toward the end of the disease, in apparently recovered animals (Lavrnja et al., 2015). Thus, delayed expression of CD73 may be an important part of the complex molecular phenotype of reactive astrocytes in different neuropathologies. The local production of adenosine by CD73 and the consequent activation of A_1R may account for numerous immunosuppressive actions of adenosine, such as reduced proliferation and enhanced protection of astrocytes from cell death (Ciccarelli et al., 1994, 2007; Tsutsui et al., 2004; Bjorklund et al., 2008).

Given that up-regulation of CD73 by reactive astrocytes represents a common phenomenon in neurological disorders associated with neuroinflammation, we suggest that CD73 might participate in a specific cellular activity performed by reactive astrocytes during course of reactive gliosis. Regarding the dual role of CD73 and its sustained up-regulation in neuroinflammatory conditions, we hypothesized that CD73 plays a role in the ability of reactive astrocytes to establish cell-ECM or cell–cell contacts that strengthen their ability to adhere to the substrate. Thus, we have applied diverse pharmacological tools to inhibit CD73 activity, to mask its surface exposure or to knock-down its membrane expression in cultured astrocytes, in order to study the involvement of CD73 in the cell migration in a scratch wound assay *in vitro*. We have found that approaches that reduce the number of CD73 molecules at the cell surface, either by application of anti-CD73 antibodies or CD73 gene knockdown, promote astrocytes migration *in vitro*. We have also demonstrated that application of anti-CD73 antibodies induces CD73 shedding from the cell membrane and activation of a downstream ERK1/2-mediated signaling, which implies physiological relevance of this interaction and a potential mechanism for CD73 regulation by its natural ligands *in vivo*.

MATERIALS AND METHODS

Chemicals

Glucose, poly-L-lysine (PLL), Trypsin, EDTA, Triton^{TM} X-100, adenosine (Ado), adenosine 5′-triphosphate disodium salt hydrate (ATP), adenosine 5′-diphosphate sodium salt hydrate (ADP), adenosine 5′-monophosphate sodium salt hydrate (AMP), adenosine 5′-(α,β-methylene) diphosphate (APCP), bovine serum albumin (BSA), normal donkey serum (NDS), paraformaldehyde (PFA), protease inhibitor cocktail and Mowiol bedding medium were all purchased from Sigma–Aldrich (St. Louis, MO, United States). Leibovitz's L-15 Medium, Penicillin/Streptomycin, Fetal Bovine serum (FBS), Dulbecco's modified Eagles's medium (DMEM), Opti-MEM (Reduced Serum Media) and Lipofectamine 2000 were obtained from Gibco. Small interfering RNA (siRNA) probes were purchased from Thermo Fisher Scientific (Carlsbad, CA, United States). 4,6-Diamidino-2-phenylindole (DAPI) was purchased from Molecular probes (Eugene, OR, United States). Immobilon Western Chemiluminescent HRP Substrate (Cat. #7632365) was obtained from Merck (KGaA, Darmstadt, Germany). Micro BCA Protein Assay Kit was purchased from (Thermo Fisher Scientific, Rockford, IL, United States).

Animals

One to 2-day old rat male pups of Wistar strain from the local colony were used for primary cortical astrocyte culture preparation. The animal procedures were performed in compliance with European Communities Council Directive (2010/63/EU) and Serbian Laboratory Animal Science Association for the protection of animals used for experimental and the scientific purposes and were approved by the Ethics Committee of the Faculty of Biology, University of Belgrade. Authorization reference number EK-BF-2016/05.

Primary Astrocyte Culture

Cerebral cortices were dissected and meninges were thoroughly removed in ice-cold phosphate–buffered saline (PBS). The cortices were mechanically dissociated by gentle pipetting under sterile conditions in Leibovitz's L-15 isolating medium supplemented with 2 mM L-glutamine, 100 IU/ml penicillin, 0.1 mg/ml streptomycin, and 0.1% BSA. After two centrifuge/washing steps at 500 × *g* for 4 min, cell suspension was passed through ø 0.8 mm and ø 0.6 mm sterile needles, to remove residual tissue aggregates. Additional centrifugation step at 500 × *g* for 4 min was followed by cells resuspension in Dulbecco's modified Eagle's medium with the addition of 10% heat-inactivated FBS, 25 mmol/l glucose, 2 mmol/l L-glutamine, 1 mmol/l sodium pyruvate, 100 IU/ml penicillin and 100 μg/ml streptomycin. Cells were subsequently seeded in tissue culture flasks for adherent cells and grown at 37°C in a humified incubator with 5% CO_2/95% air. Culture medium was replaced 1 day after the isolation and then every other day until cultures were 80–90% confluent. Primary microglia and oligodendrocytes were removed by vigorous shaking at 400 rpm for 16–20 h on a plate shaker (PerkinElmer, Turku, Finland) and additional mechanical washing using a 1-ml pipette if needed. Adherent primary astrocytes were washed with PBS, trypsinized (0.25% trypsin and 0.02% EDTA) and replated on new dishes at a density of 1.5×10^4 cells/cm^2 and maintained to reach confluence. Each cell culture was prepared from a single animal cortex. A total of 21 animals were used in the study.

Treatments

After reaching the near confluence, cells were synchronized by shifting the serum concentration to 0.5% FBS for 24 h prior the experiment. A scratch wound was made in astrocyte monolayer, afterward the primary pharmacological treatments were applied. The following primary treatments dissolved in standard medium with 10% FBS were applied: (a) 100 μM APCP;

(b) goat polyclonal anti-CD73 IgG (Santa Cruz Biotechnologies; # *v*-20; 1:500); (c) siCD73-RNA (50 nM). Dilutions of the pharmacological treatments were chosen in separate experiments, as those which block and/or inhibit CD73, without affecting astrocyte viability (**Supplementary Figure S1A**). ATP, ADP, AMP, and adenosine were applied at 1 mM concentration, separately or 30 min after the primary treatment (APCP or the anti-CD73 antibody). The 1 mM concentration of ATP was chosen based on its ability to induce up-regulation of CD73 (Brisevac et al., 2015) and strong activation of cortical astrocytes (Adzic et al., 2017) and given that the nucleotide is rapidly metabolized by ectonucleotidases to the downstream nucleotides and adenosine as a final product, the later were applied in the same concentration.

Stock solutions of ATP, ADP, AMP, adenosine (100 mM) and APCP (10 mM) were prepared in sterile water and kept at −20°C until use. The final concentration of the nucleotides was adjusted with normal medium.

siCD73 Gene Silencing

CD73 gene knockdown was induced by small interfering RNA-mediated gene silencing. Cells (2×10^4 cells/cm^2) were grown on the 35-mm Petri dishes. After reaching near confluence cells were transfected with siRNA duplexes (Thermo Fisher Scientific). The optimum concentration of 50 nM siRNA was determined in the separate dose-response experiment (**Supplementary Figure S1B**). For each siRNA probe, 50 nM siRNA and 5 μl Lipofectamine 2000 were dissolved in 150 μl Opti-MEM in separate tubes, incubated 5–10 min at room temperature (RT) and after mixing the two components, left for another 20 min. Aliquot of 300 μl of the complex was added to each Petri dish. Transfection was carried out for 8 h in 10% FBS supplemented DMEM (without Penicillin/Streptomycin). The medium was changed to standard growing medium (complete DMEM) and cells were left in standard conditions up to 48 h to increase the efficiency of transfection. The scratch wound assay and the treatments were performed 48 h after the transfection, isolation of total RNA was performed after additional 4 h, while all other tests and analysis were performed 72 h after the transfection.

The efficiency of transfection was validated by performing a positive and a negative control of transfection. The cells transfected with a siRNA sequence corresponding to the coding region of GADPH gene served as a positive control of transfection, while cells transfected with non-specific siRNA duplex which did not affect any target gene was used as a negative control of transfection (siCTR). The cells were processed 48 and 72 h after the transfection to determine the expression of the target genes at the mRNA and protein levels, whereas the normalized values obtained in siCTR were defined as 100% and used as a reference. In cells transfected with siGAPDH, the expression of GAPDH gene was considerably silenced at mRNA (10.3%) and protein levels (12.1%) with respect to siCTR. In culture transfected with siCD73, the expression of GAPDH gene was unaffected, whereas the expression of CD73, at mRNA and the protein levels, was reduced to about 51 and 36% relative to control, respectively.

Scratch Wound Assay

Astrocytes were seeded at a density of 2×10^4 cells/cm^2 on the 35-mm Petri dishes for adherent cells and were maintained until reaching near confluence. Wound healing assay was performed by the method of Kornyei et al. (2000), as previously described (Adzic et al., 2017). A wound was made in astrocyte monolayer, by scraping the bottom of the dish with a sterile 200-μl pipette tip. Three to four scratches were made per each Petri dish in a defined geometry (**Supplementary Table S1**). The treatment was applied to the cultures immediately after the wound was made and the cultures were further maintained in normal growth medium. Up to 16 random fields per each dish were captured at 0 h time on Carl Zeiss AxioObserver A1 inverted microscope (A-Plan 10× objective) by EM512 CCD Digital Camera System (Evolve, Photometrics). Consecutive images of selected microscopic fields were then captured at the time points of interest (4, 8, 12, 24, and 48 h) and stored as digitalized data. Wound area (μm^2) and wound width (μm) were determined using ImageJ software package for each frame and time point. The wound closure (%) under the control and treatment conditions was assessed by expressing the closed wound area at each time point as a percentage of the initial wound area (0 h). Data are expressed as mean closed area (% ± SEM), from $n \geq 7$ separate culture preparations. The values of mean closed wound area were plotted as a function of time and fitted to the logistic growth curve (Origin 8.0) to generate kinetic parameters, maximum closure velocity V_{max} (% closure/h) and slope of linear growth phase (s, %/h). The slope of the linear growth phase (%/h) was used to calculate cell front displacement (μm/h).

Immunofluorescence and Confocal Microscopy

Astrocyte grown on glass coverslips (15 mm) were subjected to SW and treated as described. Twenty-four hours after the treatment, cells were prefixed in 4% PFA and blocked (1 h, RT) with a solution containing 10% NDS and 2% BSA in 0.01 M PBS. After the overnight incubation at +4°C with primary rabbit anti-rat CD73 antibodies (in 1% NDS and 1% BSA in 0.01 M PBS), cells were washed and incubated with secondary donkey anti-rabbit Cy3 IgG antibodies (2 h, RT). Cells were permeabilized with 0.01% Triton X-100 (15 min, RT) and subjected to the same blocking procedure. In the following round, cells were incubated with mouse anti-rat GFAP antibodies (1 h, RT) and secondary donkey anti-mouse Cy2 IgG antibodies (2 h, RT). Finally, nuclei were counterstained with DAPI (10 min, RT) and the cells were mounted on microscope slides with Mowiol solution. Incubation with the appropriate rabbit pre-immune serum instead of the primary anti-CD73 antibody resulted in the absence of any specific reaction.

Images of microscopic fields were captured with the confocal laser-scanning microscope (LSM 510, Carl Zeiss GmbH, Jena, Germany) using Ar Multi-line (457, 478, 488, and 514 nm) and HeNe (543 nm) lasers using 63× DIC oil objective and monochrome camera AxioCam ICm1camera (Carl Zeiss GmbH, Germany). Images were quantified using ImageJ software

by calculating corrected total cell fluorescence (CTCF) for each frame using the following formula: CTCF = Integrated Density − (Area of selected cell × Mean fluorescence of background readings). The results present mean integrated fluorescence density ± SEM, from 15 frames for each treatment ($n = 3$ separate culture preparations, 5 frames per coverslip).

For Ki67/DAPI fluorescence staining, cells were fixed and permeabilized with 0.05% Triton X-100 and then blocked in 5% BSA in 0.01M PBS. Primary rabbit anti-Ki67 antibodies were applied overnight in 2% BSA at +4°C, followed by the incubation with the secondary donkey anti-rabbit Cy3 antibody for 2 h, on RT. The total nuclei were stained with DAPI (1:4000, for 10 min, on RT). Coverslips were mounted on microscopic slides with Mowiol solution. Images of microscopic fields were captured with Carl Zeiss Axio Observer A1 inverted epifluorescence microscope (A-Plan 10× objective) by EM512 CCD Digital Camera System (Evolve, Photometrics). Incubation without primary antibodies resulted in the absence of a specific reaction. The results are expressed as the percent of $Ki67^+$ cells in total cell number (DAPI), determined from $n = 2$ separate culture preparations, and 5–7 frames/coverslip.

Isolation of Cell Lysates and Separation of Culture Media

Astrocytes (2×10^4 cells/cm^2) were seeded on 60-mm diameter Petri dishes. After reaching confluence, cells were subjected to SW and treated as described. For the isolation of total proteins, cells were collected using warm 0.01 M PBS, centrifuged for 5 min at 500 × *g* and then re-suspended in 500 μl of cold RIPA lysis buffer, supplemented with 0.5% w/v protease inhibitor cocktail. The suspension was kept on ice for 30 min and subsequently centrifuged at 10000 × *g* for 10 min, at 4°C (Beckman, JA-20). The supernatant was carefully separated from the pellet, and the protein concentration was determined using BCA protein assay kit, according to manufacturer's instruction. Culture media were removed and centrifuged for 10 min at 500 × *g* (Beckman, TA-10) to pellet residual cells. The supernatant was collected and used detection of soluble CD73 by dot blot procedure.

Western Blot and Dot Blot Analysis

Samples were diluted in the 6× Laemmli sample buffer [375 mM Tris-HCl, pH 6.8, 12% sodium dodecyl sulfate (SDS), 60% (w/v) glycerol, 0.03% bromophenol blue], and the proteins prepared under reducing conditions were resolved on 4/12% SDS-PAGE gels. Proteins were electrotransferred to a PVDF support membrane (Immobilon-P transfer membrane, Millipore) and the membranes were blocked with 5% BSA in Tris buffer saline/Tween 20 (TBST). The overnight incubation with primary rabbit anti-rat CD73 antibodies (at 4°C), was followed by 2-h incubation with the appropriate secondary HRP-conjugated antibody. Support membranes were washed several times in TBST, and the bands were visualized with the use of ECL solution (Immobilon Western Chemiluminescent HRP Substrate, #7632365, Millipore) on a Chemi Doc-It imaging system (UVP, Upland, CA, United States).

The presence of soluble CD73 in culture media was detected by spotting 300-μl aliquots of culture media on PVDF support membrane (Immobilon-P transfer membrane, Millipore), through a vacuum-based Minifold dot blot apparatus (Schleicher & Schuell Inc., Keene, N.H.). The support membrane was blocked with 5% BSA in TBST and probed either with secondary donkey anti-goat HRP-conjugated IgG antibodies, or by a set of primary rabbit anti-rat CD73 and donkey anti-rabbit HRP conjugated IgG, followed by a visualization procedure, using ECL solution. Blots were washed in TBST and the chemiluminescent signal was detected on Chemi Doc-It imaging system (UVP, Upland, CA, United States). Media collected from $n = 4$ separate cultures were used in the analysis.

A list of used primary and secondary antibodies used for immunofluorescence, Western blotting, and dot blotting procedure is given in **Table 1**.

Quantitative Real-Time PCR

Astrocytes were seeded in 6-well plates at 2×10^4 cells/cm^2 density. After reaching near confluence (∼90%), the cultures were subjected to SW and treated as described. Four hours after the treatments, total RNA was extracted in TRIzol and RNA concentration and the purity were determined by measuring the absorbance at 260 nm and 260 nm/280 nm and 260 nm/230 nm ratios, respectively. A volume equivalent of 1 μg of total RNA was used to generate cDNA (High Capacity cDNA Reverse Transcription Kit, Applied Biosystems, Foster City, CA, United States), used for real-time PCR analysis (QuantStudio™ 3 Real-Time PCR System, Applied Biosystems, Foster City, CA, United States). The reaction mixture contained 2 μl cDNA (10 ng/μl), 5 μl QTM SYBR Green PCR Master Mix (Applied Biosystems, Foster City, CA, United States), 0.5 μl primers (100 pmol/μl) and 2 μl RNase-free water (UltraPure, Invitrogen, Germany). Amplification was carried out under the following conditions: 10 min of enzyme activation at 95°C, 40 cycles of 15 s denaturation at 95°C, 30 s annealing at 64°C, 30 s amplification at 72°C and 5 s fluorescence measurements at 72°C. Relative target gene expression was calculated by the $2^{-\Delta Ct}$ method, using GAPDH gene as internal gene control. In transfection studies, actin was used as the internal control. Melting curves and gel electrophoresis of the PCR products were routinely performed to determine this specificity of the PCR reaction (not shown). Primer sequences are listed in **Table 2**. Results present mean target gene expression (relative to GAPDH) ± SEM, from *n* separate determinations performed in duplicate.

5′-AMP Phosphohydrolase Assay and Free Phosphate Determination

Astrocytes were seeded on 24-well plate, at a density of 6×10^4 cells per well. After reaching near confluence, cultures were subjected to SW and treated as described. Cells were washed 3 × 5 min with phosphate-free medium (117 mM NaCl, 5.3 mM KCl, 1.8 mM $MgCl_2$, 26 mM $NaHCO_3$, 10 mM glucose, pH 7.4) to eliminate cell debris and free phosphates. 5′-AMP phosphohydrolase activity was assayed by determining free phosphates, liberated as a result of the enzyme reaction.

TABLE 1 | List of primary and secondary antibodies.

Antibody selectivity	Source and clonality	Dilution and application	Manufacturer	RRID
CD73	Goat, *pc*	1:500, T	Santa Cruz (V-20), sc-14682	AB_2154099
CD73	Rabbit, *mc*	1:1500, WB	Cell Signaling (D7F9A), #13160	AB_2716625
CD73	Rabbit, *pc*	1:100, IF	ectonucleotidases-ab.com, Cat# [rNu-9L(l_4,l_5)]	
GFAP	Mouse, *mc*	1:200 IF	Sigma–Aldrich, G-3893	AB_477010
GFAP	Rabbit, *pc*	1:10000 WB	DAKO, Z0334	AB_10013382
Ki67	Rabbit, *pc*	1:500, IF	Abcam, ab15580	AB_443209
p44/42 MAPK	Rabbit, *mc*	1:1000, WB	Cell Signaling, #4695	AB_390779
GAPDH	Goat, *pc*	1:1000, WB	Santa Cruz (V-18), sc-20357	AB_641107
Anti-goat HRP-conjugated IgG	Donkey, *pc*	1:10000, WB, DB	Santa Cruz, sc-2020	AB_631728
Anti-rabbit HRP-conjugated IgG	Donkey, *pc*	1:10000, WB, DB	Santa Cruz, sc-2305	AB_641180
Anti-rabbit IgG Cy3	Donkey, *pc*	1:500 IF	Jackson ImmunoResearch, 711-165-152	AB_2307443
Anti-mouse IgG Cy2	Donkey, *pc*	1:500 IF	Jackson ImmunoResearch, 715-225-151	AB_2340827

T, anti-CD73 blockade; WB, western blot; DB, dot blot; IF, immunofluorescence; pc, polyclonal; mc, monoclonal.

The reaction was initiated by adding 240 μl of 1 mM AMP (in phosphate-free medium) to each well and the plates were incubated at 37°C for 30 min. The reaction was stopped by transferring the reaction volume to tubes already containing 24 μl ice-cold 3 mM PCA. Enzymatic hydrolysis of AMP and a level of inorganic phosphates liberated as a result of the enzymatic reaction were determined by the malachite green assay method, using KH_2PO_4 as a standard. The content of free phosphates liberated by non-enzymatic hydrolysis of AMP was corrected by assaying the activity in the reaction mixture without AMP and adding the substrate to the reaction volume after the addition of PCA. A contribution of tissue non-specific alkaline phosphatase (TNAP) to 5′-AMP phosphohydrolase activity was determined by assaying 5′-AMP hydrolysis in the presence of TNAP inhibitor levamisole (100–300 μM). Total protein content was determined by adding 100 μl of RIPA buffer to each well and using Micro BCA Protein Assay Kit (Thermo Fisher Scientific, Rockford, IL, United States), according to manufacturer instructions.

Free phosphate concentration was detected by a malachite green assay (Baykov et al., 1988). Aliquots (20 μl) of a working solution (0.1% of malachite green in 20% H_2SO_4, 7.5% ammonium molybdate and 11% Tween 20 in a ratio 10:2.5:0.2) were added to 80-μl aliquots of the reaction mixtures. The absorbance was measured at 620 nm and the amount free phosphates (Pi) liberates as a result of enzyme reaction was corrected for the non-enzymatic hydrolysis and presented as mean specific activity (nmol Pi/mg/min) ± SEM, from *n* separate culture preparations, performed in sextuplicate.

TABLE 2 | List of primer pairs for rtPCR.

Target gene	Forward	Reverse
Nt5e/CD73	CAAATCTGCCTCTGGAAAGC	ACCTTCCAGAAGGACCCTGT
Adora1	GTGATTTGGGCTGTGAAGGT	GAGCTCTGGGTGAGGATGAG
Adora2a	TGCAGAACGTCACCAACTTC	CAAAACAGGCGAAGAAGAGG
Adora2b	CGTCCCGCTCAGGTATAAAG	CCAGGAAAGGAGTCAGTCCA
Adora3	TTCTTGTTTGCCTTGTGCTG	AGGGTTCATCATGGAGTTCG
GAPDH	TGGACCTCATGGCCTACAT	GGATGGAATTGTGAGGGAGA
HPRT	GGTCCATTCCTATGACTGTAG	CAATCAAGACGTTCTTTCCAGTT

Data Analysis

Raw data from the scratch wound assay were plotted as a function of time and fitted to the logistic growth curve using OriginPro8 SR0 software package (v8.0724, OriginLab Corporation, Northampton, MA, United States). Parameters of migration (maximum wound closure and slope of linear growth phase were derived as a logistic growth curve parameters. Comparison between means was performed by one-way ANOVA, followed by Tukey's *post hoc* test and the differences were considered significant at the level of $p < 0.05$). Data are presented as mean ± SEM (from *n* separate cell culture preparations).

RESULTS

Characterization of Primary Culture System

In the present study, the role of CD73 in astrocyte adhesion and migration was investigated in the scratch wound assay using primary astrocyte culture prepared from neonatal rat cortex. The validity of the chosen cell model has been demonstrated by assessing the expression and function of CD73 in a confluent astrocytes monolayer, prior to (Intact) and after creating the scratch wound (SW). To avoid variations in CD73 levels due to differences in cell density, cell cycle, and culturing conditions, the measurements have been always done under the same conditions, described in section "Materials and Methods." The cells in intact astrocyte monolayer expressed 5′-AMP phosphohydrolyzing activity at the level comparable to other rat primary astrocyte cultures (Bavaresco et al., 2008; Brisevac et al., 2012). After creating the wound, the abundance of CD73-mRNA increased more than twofold (223.3 ± 5.1%, $p < 0.01$; **Figure 1A**) in SW when compared to intact culture. The increase in CD73 gene expression was accompanied by an increase in total CD73 protein abundance (**Figures 1B,C**) and 5′-AMP

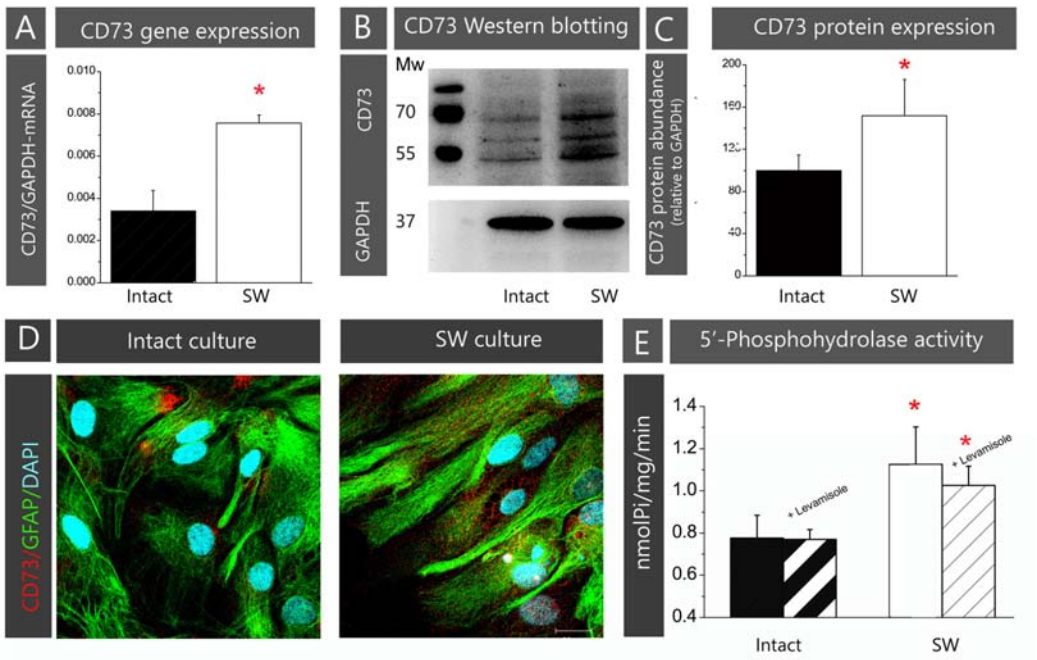

FIGURE 1 | Validation of primary astrocytes culture model. The contents of CD73 in astrocyte cultures prior to (intact) or after creating the scratch wound (SW) were analyzed at mRNA, protein and functional level. **(A)** Expression of CD73 gene was determined by rt-PCR. Bars represent mean ± SEM of CD73-mRNA abundance relative to GAPDH, determined in $n = 3$ separate intact (*black bar*) and SW (*white bar*) culture preparation. **(B)** The abundance of CD73 protein was analyzed by Western blotting, after resolving whole cell lysates proteins on SDS-PAGE and probing the support membrane with the anti-CD73 antibodies (1:1500 in TBST; Cell Signaling, US). The antibodies recognized three protein bands on blots, with molecular weights of ∼69, 61, and 55 kDa. **(C)** Relative abundance of CD73 protein in each sample was assessed by measuring combined optical density of all bands in each lane by using ImageJ and by expressing the value relative to the optical density of GAPDH band in the same lane. The value obtained for intact culture was arbitrarily defined as 100% and was used as a reference (*black bar*). The bars represent mean CD73 relative protein abundance (% ± SEM) from $n = 3$ separate culture preparations. **(D)** Representative confocal images showing cell morphology and membrane topography of CD73 in confluent astrocyte monolayer (*left*) and cultures subjected to scratch wound (*right*). The images were obtained by double immunofluorescence labeling for CD73 (*red fluorescence*) and GFAP (*green fluorescence*) and nuclear counterstaining with DAPI (*blue fluorescence*). Scale bar = 25 μm. **(E)** The level of 5′-AMP phosphohydrolase activity in whole cell culture (*black bars*) and SW (*white bars*) cultures, determined in assay conditions as described in section "Materials and Methods." Levamisole (100 μM) was used as the alkaline phosphatase inhibitor (*striped bars*). The bars represent mean activity (nmol Pi/mg/min) ± SEM, from $n = 3$ separate culture preparations performed in sextuplicate. Significance inside the graphs: * denotes significance at $p < 0.05$ in respect to intact culture.

phosphohydrolase activity (**Figure 1E**). Three protein bands were seen on Western blots, corresponding to glycosylated (∼69 and 61 kDa) and non-glycosylated (∼55 kDa) protein forms, with a combined abundance significantly higher in SW (151.6 ± 34.2%, $p < 0.05$) than in intact culture. Surface expression of CD73 was visualized by double CD73/GFAP-immunofluorescence labeling (**Figure 1D**). The cells in confluent monolayer displayed usual morphology *in vitro*, characterized by polygonal cell bodies with inconspicuous processes. The immunoreaction (*ir*) corresponding to CD73 is found in clusters at the corners of the polygonal cell bodies. In SW, the cells lining the wound edge developed protoplasmic processes extending to the wound area. These processes exhibited stronger GFAP-immunoreactivity, while fine punctuate CD73-*ir* was distributed all around the cells. Finally, the level of 5′-AMP phosphohydrolase activity was significantly higher in SW culture (1.13 ± 0.18 nmol Pi/mg/min, $p < 0.05$) than in intact culture (0.78 ± 0.11 nmol Pi/mg/min). The 5′-AMP hydrolyzing activities in intact and SW cultures were insensitive to alkaline phosphatase inhibitor levamisole, indicating that the activity belonged to CD73 (**Figure 1E**).

To confirm that the injury-induced upregulation of CD73 is associated with the reactive phenotype of cultured astrocytes, intact cells were activated by applying inflammatory mediators bacterial endotoxin LPS (100 ng/ml) or proinflammatory cytokine IL-1β (10 ng/ml) and the expression of CD73 was measured by immunofluorescence and by 5′-AMP phosphohydrolase assay after 24 h. Both proinflammatory mediators induced significant increase in surface expression of CD73 and upregulation of 5′-AMP phosphohydrolase activity in respect to non-treated control cells (**Supplementary Figure S2**).

Reduced Cell Surface Expression of CD73 Promotes Wound Closure in Primary Astrocyte Culture

The scratch wound assay was used to study astrocyte migration *in vitro*. The images were captured immediately after creating the wound (0 h) and at 4-h intervals during 48 h (**Supplementary Figure S3A**) and the remaining wound area at each time point was measured and expressed as a percentage of initial wound area

(at 0 h). The values were plotted vs. time and the curve was used to calculate the slope of linear growth phase (**Supplementary Figure S3B**). The percentage of the initial wound area covered between two consecutive time-points was used to calculate the velocity of wound closure (%/h), whereas cell front displacement was calculated as a displacement of the leading edge during 24 h (μm/h) (**Supplementary Figure S3C**).

To assess the role of CD73 in astrocyte migration, cell cultures were treated with one of the following pharmacological inhibitors of CD73: (1) anti-CD73 antibodies (goat polyclonal IgG, Santa Cruz Biotechnologies; # *v*-20; 1:500 in full growing medium), with epitope mapping within the internal region of CD73 molecule; (2) non-hydrolyzable ADP analog (100 μM α,β methylene ADP – APCP), which binds to the active site and inhibits CD73 catalytic activity, and (3) CD73 small interfering RNA (siCD73), which induces CD73 gene knockdown by neutralizing CD73-mRNA. The parameters of cell motility obtained in the scratch wound assays in SW conditions and in the presence of the inhibitors are given in **Table 3**.

As shown in **Figure 2**, treatment with anti-CD73 antibodies increased the velocity of wound closure (**Figures 2A,B**) and promoted cell front displacement (**Figure 2C**), resulting in a complete wound area covered after 24 h (**Figures 2A–D**). Treatment with APCP, however, did not produce any apparent effect on the wound closure velocity, which was reflected in the kinetic parameters comparable to those obtained for SW. Cells with CD73 gene silencing exhibited higher velocity of a wound closure and larger wound area covered after 48 h when compared to cells transfected with non-specific siRNA (siCTR). Transfected cultures were tested in the migration assay 48 h post-transfection when the existing pool of CD73 protein and transient knock-down of CD73-mRNA were still sustained at the level of about 50%. Based on the data obtained with different pharmacological inhibitors of CD73, it was concluded that approaches that reduce expression or exposure of CD73 molecules at cell surface increase migration velocity and promote wound closure in the scratch wound assay.

Exogenous Adenosine Does Not Affect the Motility of Astrocytes in the Scratch Wound Assay

The results of the previous set of scratch wound assays did not show any apparent effect of APCP on astrocyte migration. Since APCP inhibits the 5′-AMP phosphohydrolase activity of CD73, the finding further implies the lack of adenosine involvement in astrocyte migration. However, one could not exclude the possibility that APCP partially inhibits CD73, leaving the remaining activity sufficient to generate adenosine. Therefore, next set of migration assays was performed in the presence of exogenously added adenosine and short-lived nucleotides AMP, ADP, and ATP, which are efficiently converted to adenosine by ectonucleotidases action. The ability of the purine molecules to affect migration was tested in SW culture (**Figure 3A**) and in the cultures treated with the inhibitors (**Figures 3B,C**). While the addition of adenosine, AMP, and ADP notably slowed down wound closure in SW culture, the addition of ATP increased cell front displacement (**Figure 3A** and **Table 3**). When the same purine molecules were applied to cultures treated with APCP (**Figure 3B**) or anti-CD73 antibodies (**Figure 3C**), none of them induced any effect on astrocyte migration. Based on the findings presented in **Figures 2**, **3**, it was concluded that although exogenous adenosine did not revert the stimulative effects of anti-CD73 antibodies and siCD73, it decreased migration velocity in SW culture, i.e., in cultures with intact CD73 function.

The Pharmacological Inhibitors Suppress Cell Proliferation

Astrocytes in the scratch wound assay typically increase cell proliferation. To assess whether an enhanced proliferation

TABLE 3 | Cell motility parameters.

	V_{max} (% coverage/h)	Slope of linear growth phase (% coverage/h)	Cell front displacement velocity (μm/h)
Control	3.43 ± 0.52	3.11 ± 0.19	12.73 ± 0.77
Anti-CD73 Ab	4.56 ± 0.35*	4.31 ± 0.20*	17.66 ± 0.80*
Anti-CD73 Ab + Ado	4.44 ± 0.48	3.88 ± 0.26	15.89 ± 0.04
Anti-CD73 Ab + AMP	4.04 ± 0.40	3.73 ± 0.45	14.05 ± 0.84
Anti-CD73 Ab + ATP	3.96 ± 0.28	3.83 ± 0.18*	15.69 ± 0.75*
α,β-methylene ADP	3.27 ± 0.37	2.94 ± 0.26	12.04 ± 1.06
α,β-methylene ADP + Ado	3.34 ± 0.28	2.72 ± 0.25	11.40 ± 1.01
α,β-methylene ADP + AMP	3.71 ± 0.14	3.29 ± 0.14	13.48 ± 0.57
α,β-methylene ADP + ATP	3.82 ± 0.61	2.58 ± 0.24	11.57 ± 0.98
Ado	2.92 ± 0.21*	2.68 ± 0.17*	10.99 ± 0.68*
AMP	2.25 ± 0.08	1.98 ± 0.41*	8.11 ± 1.68*
ADP	1.99 ± 0.41*	2.18 ± 0.23*	8.93 ± 0.94*
ATP	3.14 ± 0.25	3.74 ± 0.18*	15.33 ± 0.76*
siCTR	1.61 ± 0.27	1.63 ± 0.20	6.68 ± 0.82
siCD73	3.31 ± 0.62*	2.34 ± 0.06*	9.58 ± 0.24*

**Significance at $p < 0.05$ in respect to control SW.*

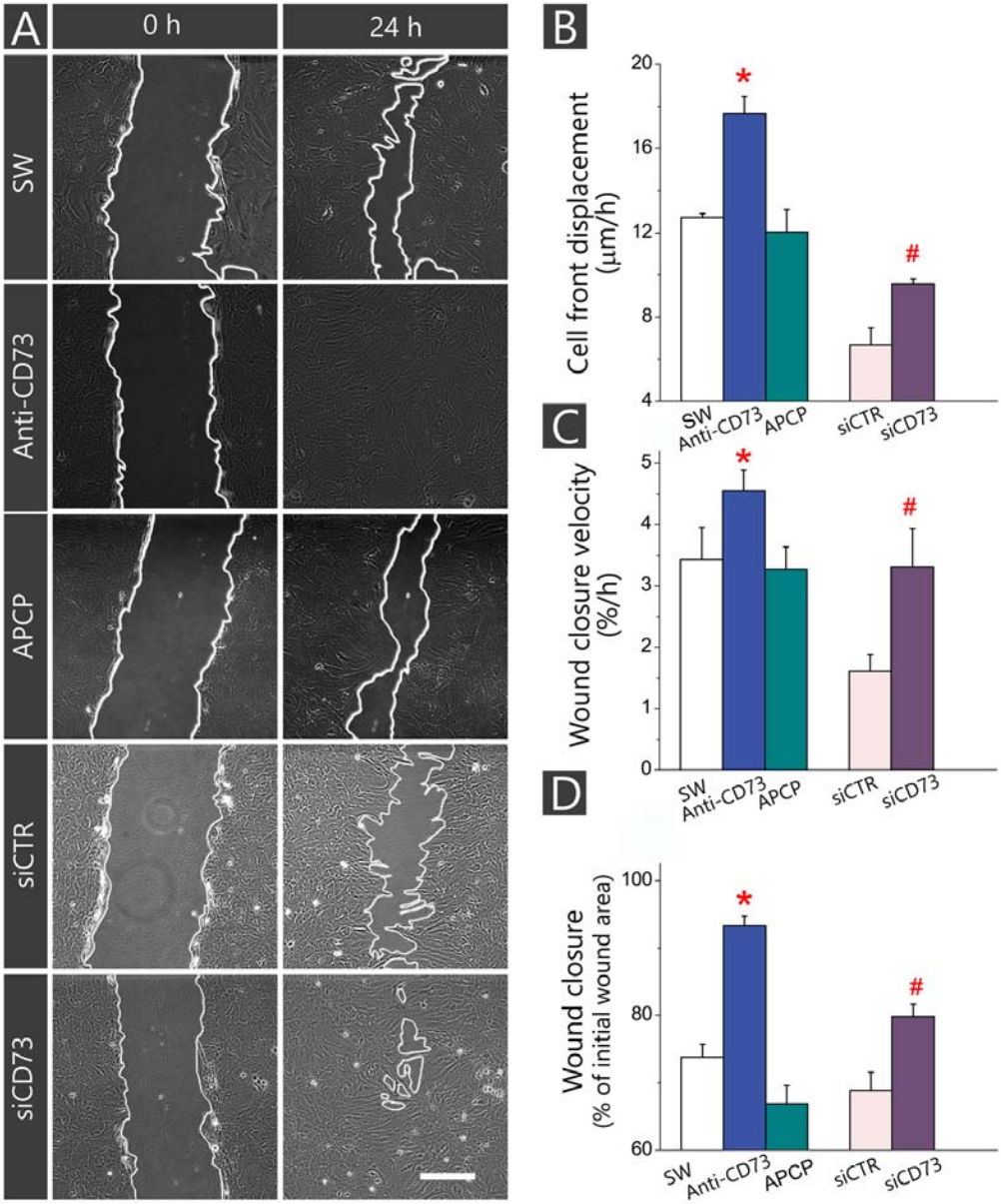

FIGURE 2 | Influence of different pharmacological inhibitors of CD73 on kinetics of astrocyte migration *in vitro*. Astrocytes were grown to confluence in normal FBS and wound was made by scraping the bottom of the dish with a sterile 200-μl pipette tip. The cultures were treated with anti-CD73 antibodies and APCP and the effects on the migration were compared with non-treated SW culture. In culture transfected with siCD73, negative control of the transfection was culture transfected with non-specific siRNA duplex (siCTR). **(A)** Representative images of defined microscopic fields taken at 0 and 24 after creating the wound in cultures treated with different pharmacological inhibitors of CD73. Digitalized images were captured and analyzed in 4-h intervals during 48 h. Scale bar = 100 μm. **(B–D)** Kinetic parameters of cell migration, cell front displacement **(B)**, wound closure velocity **(C)** and wound closure **(D)** obtained in cultures treated with anti-CD73 antibodies (*blue*), APCP (*green*) or transfected with siCD73 (*magenta*). Bars represent means (±SEM) determined from 6 to 8 microscopic fields captured per each dish in $n \geq 7$ independent culture preparations for anti-CD73 antibodies and APCP treatments and $n = 3$ for siCD73 transfection analysis. Significance inside the graphs: * denotes significance at $p < 0.05$ in respect to SW; # denotes significance at $p < 0.001$ in respect to siCTR.

contributes to the stimulating effect observed in cultures treated with anti-CD73 antibodies and siCD73, we next assessed cell proliferation by means of Ki-67/DAPI double fluorescence (**Figure 4**). Cells in the confluent culture proliferated at very low rate (∼2%), while cells adjacent to a scratch wound increased proliferation almost 10-fold (26.2 ± 1.5%, $p < 0.01$). In cultures treated with anti-CD73 antibodies (19.8 ± 1.0%, $p < 0.001$) and APCP (18.0 ± 1.2%, $p < 0.001$) cell proliferation decreased significantly in respect to SW, whereas in cells transfected with siCD73 cell proliferation was at the level of siCTR, but significantly lower than in non-treated control (9.9 ± 0.8%, $p < 0.001$). All applied

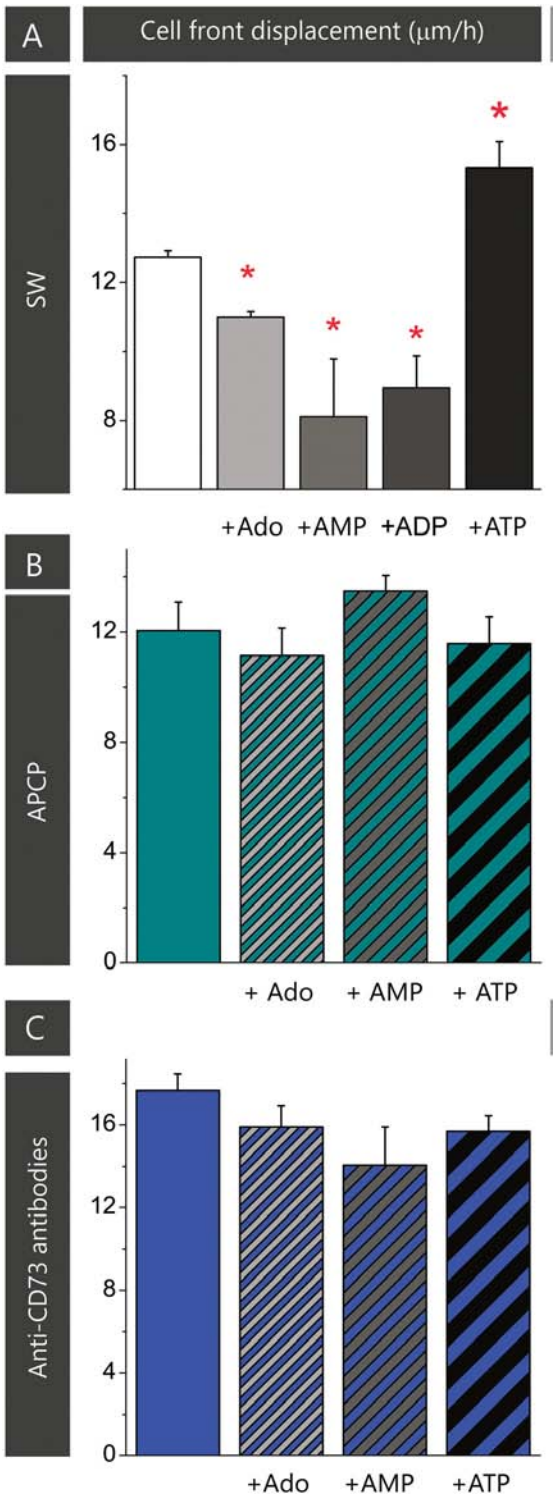

FIGURE 3 | Effect of adenosine on astrocyte migration. Effect of adenosine and adenine nucleotides on astrocyte migration in SW culture **(A)**. Effect of adenosine, AMP and ATP on cell motility in the scratch wound assay in cultures treated with APCP **(B)** and anti-CD73 **(C)**. Bars represent means (±SEM) determined from 6 to 8 microscopic fields captured per each dish in $n \geq 7$ independent culture preparations. Significance inside the graph: * denotes significance at $p < 0.05$ in respect to SW.

pharmacological inhibitors exhibit anti-proliferative effect, hence they do not contribute to astrocyte migration by enhancing cell proliferation.

Targeting CD73 With Pharmacological Inhibitors Alter the Expression Levels of Transcripts Encoding Adenosine Receptors

To enlighten an involvement of adenosine-mediated signaling in astrocyte migration, we next determined the expression levels of transcripts encoding adenosine receptors in cultures treated with the pharmacological inhibitors in the absence and presence of adenosine. As it is shown in **Table 4**, applied inhibitors distinctively affect the expression of P1 receptors, in a way that anti-CD73 antibodies significantly up-regulated the expression of A_{2A} and A_{2B} receptor subtypes and downregulated the expression of A_3 receptor subtype. On the other hand, APCP selectively decreased the expression of A_1R and the effect was prevented with the addition of adenosine. Adenosine alone altered the expression of A_2R receptor subtypes.

Pharmacological Inhibitors Decrease CD73 Activity, but Distinctly Affect Its Membrane Abundance in Cultured Astrocytes

CD73 functions as phosphohydrolase which hydrolyzes 5′-AMP to adenosine. To assess to what extent applied inhibitors interfere with CD73-mediated hydrolysis, we assayed 5′-AMP phosphohydrolase in live cells treated with different inhibitors (**Figure 5A**). The activity was significantly lower in cultures treated with APCP (0.58 ± 0.11 nmol Pi/mg/min; $p < 0.05$) and anti-CD73 antibodies (0.69 ± 0.05 nmol Pi/mg/min; $p < 0.001$) than in SW (1.13 ± 0.18 nmol Pi/mg/min). Expectedly, CD73 gene silencing notably decreased 5′-AMP phosphohydrolase activity (0.42 ± 0.04 nmol Pi/mg/min; $p < 0.001$) in cells transfected with siCD73 in respect to siCTR (0.76 ± 0.02 nmol Pi/mg/min). Obtained data imply that all pharmacological inhibitors interfere with CD73 activity, yet the stimulating effect on astrocyte migration was obtained only in the cultures with a reduced surface expression of CD73.

The decrease in the enzyme activity might be due to direct catalytic inhibition of the existing enzyme molecules, or to a reduced number of enzyme molecules expressed at the cell surface. Thus, we further determined CD73 protein content in whole cell lysates by Western blotting (**Figure 5B**). As shown in **Figures 5B,C**, the abundance of CD73 protein was considerably lower in cells treated with anti-CD73 antibodies and siCD73 in respect to the corresponding controls. On the other hand, the abundance of CD73 protein in cells treated with APCP remained comparable to SW. These findings lead us to conclude that the reduced CD73 activity in cells treated with anti-CD73 antibodies was due to a lesser number of the protein molecules expressed at the cell surface, whereas the reduced CD73 activity in cells treated with APCP, was due to the catalytic inhibition of the enzyme, with no apparent influence on the enzyme protein abundance.

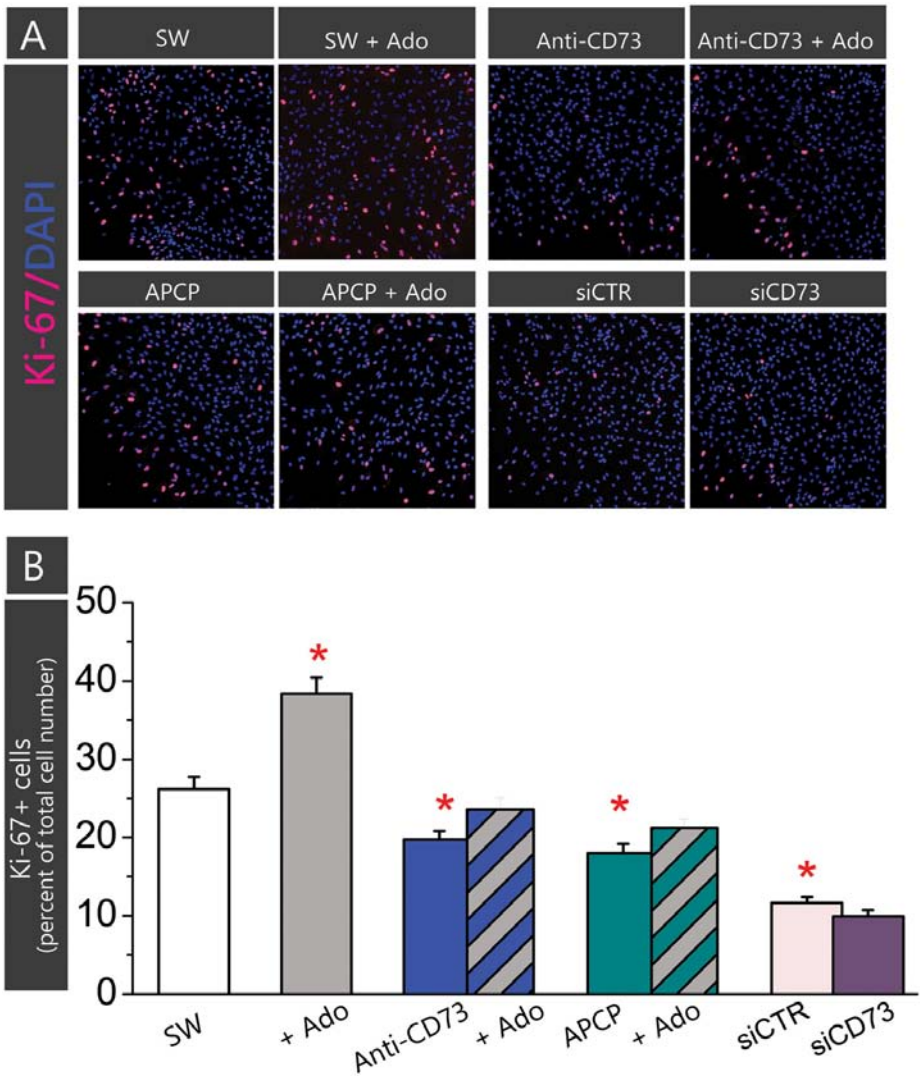

FIGURE 4 | Effect of pharmacological inhibitors on cell proliferation. Cell proliferation was determined in astrocytes subjected to scratch wound and treatment with APCP or anti-CD73 in the presence or absence of exogenous adenosine, and in the culture transfected with siCD73 or siCTR and subjected to scratch wound. Cells in SW culture were kept without any treatment. Cell proliferation was determined by fluorescence labeling for $Ki67^+$, which labels only dividing nuclei and $DAPI^+$, which labels all cell nuclei. **(A)** Representative images of Ki-67/DAPI staining. The cultures were fixed 24 h after the treatment. **(B)** The percentage of proliferating cells in total cell number in the same field ($Ki\text{-}67^+/DAPI^+$) was counted using ImageJ. Bars present mean percentage of proliferating cells (±SEM), determined in two separate culture preparations, 5–7 frames per each treatment per multiple coverslips. Significance inside the graph: * denotes significance at $p < 0.05$ in respect to SW.

TABLE 4 | Expression levels of transcripts encoding adenosine receptors.

	Target/GAPDH-mRNA abundance relative to SW (100%)				
Target	**+Ado**	**+Anti-CD73**	**+Anti-CD73 + Ado**	**+APCP**	**+APCP + Ado**
A_1R	90.7 ± 11.8	117.7 ± 19.4	87.6 ± 10.6	52.4 ± 19.7*	151.3 ± 10.1$^{\#}$
$A_{2A}R$	50.7 ± 31.6*	389.3 ± 20.3*	286.8 ± 12.8*	90.2 ± 9.1	96.4 ± 20.0
$A_{2B}R$	147.1 ± 18.8	804.3 ± 44.4*	674.9 ± 65.5*	112.8 ± 27.4	139.2 ± 19.2
A_3R	77.6 ± 36.5	21.1 ± 10.1	117.0 ± 28.4	111.2 ± 43.4	222.2 ± 67.7

*Results present mean % ± SEM, from n = 2 separate determinations performed twice in duplicate. *$p < 0.05$ in respect to control SW. $^{\#}p < 0.05$ in respect to SW + treatment (APCP or Anti-CD73).*

Ligation of Anti-CD73 Antibodies Induces Topographical Redistribution and Decrease in the Number of CD73 Molecules at the Cell Surface

Subcellular localization of CD73 in cultures treated with different pharmacological inhibitors was analyzed by double immunofluorescence staining for CD73 and GFAP (**Figure 6**). Based on the microscopic evaluation (**Figures 6A–L**) and distribution of total pixel immunofluorescence intensity (**Figures 6M,N**), we observed two types of astrocyte response to pharmacological inhibitors, depending on a cell distance from the wound edge. Cells lining the wound edge, irrespective of the treatment, developed protoplasmic processes extending toward the wound area (**Figures 6A,C,E**). The processes were densely labeled for GFAP, while fine punctuate CD73-*ir* was dispersed around the surface (**Figures 6B,D,F**). The overall CD73 fluorescence intensity, however, differed considerably depending on a treatment, being significantly lower in culture treated with anti-CD73 antibodies (66.2 ± 22.8%, $p < 0.01$) in respect to SW or APCP-treated culture (130.3 ± 27.1%, $p = 0.58$) (**Figure 6M**). The second type of the response was observed at 1–3 cell-row distance from the wound edge (**Figures 6G–L**). Again, irrespective of the treatment, the cells had the appearance of densely packed aggregates with strong immunoreaction for GFAP. However, in SW and APCP-treated cultures, the bulk CD73-*ir* was accumulated at few focal points at the cell surface (**Figures 6D,E**), whereas in the cells treated with anti-CD73 antibodies, the CD73-*ir* was dispersed over the cell surface (**Figure 6F**). However, the overall CD73 immunofluorescence intensities at the cells away from the wound edge were similar in all cultures. Aforementioned changes in the expression pattern of CD73 occurred without significant reorganization of the GFAP filament network or apparent changes in GFAP protein abundance (**Supplementary Figure S4**), both in the cells at the wound edge (**Figures 6A,C,E**) and in the cells away from the wound (**Figures 6G,I,K**).

Ligation of Anti-CD73 Antibodies Induces CD73 Molecule Shedding

Cleavage of a protein ectodomain is a common mechanism for ectoprotein regulation. To assess if anti-CD73 antibodies induce CD73 shedding, the presence of the soluble protein was tested in culture media, collected 24 h after the addition of the pharmacological blockades (**Figure 7A**). The culture media were first probed with secondary antibodies (donkey anti-goat IgG), matching the primary antibodies used for the pharmacological blockade (goat anti-rat CD73 IgG). Next, culture media were probed with another set of primary (rabbit anti-rat CD73 IgG; Cell Signaling) and matching secondary antibodies (Donkey anti-rabbit IgG, Invitrogen). As seen in **Figure 6A**, in both cases, soluble CD73 molecules were detected only in the media obtained from cultures treated with anti-CD73 antibodies. These findings imply that ligation of anti-CD73 antibodies with cell surface CD73 triggers a mechanism responsible for a GPI cleavage and CD73 molecule shedding.

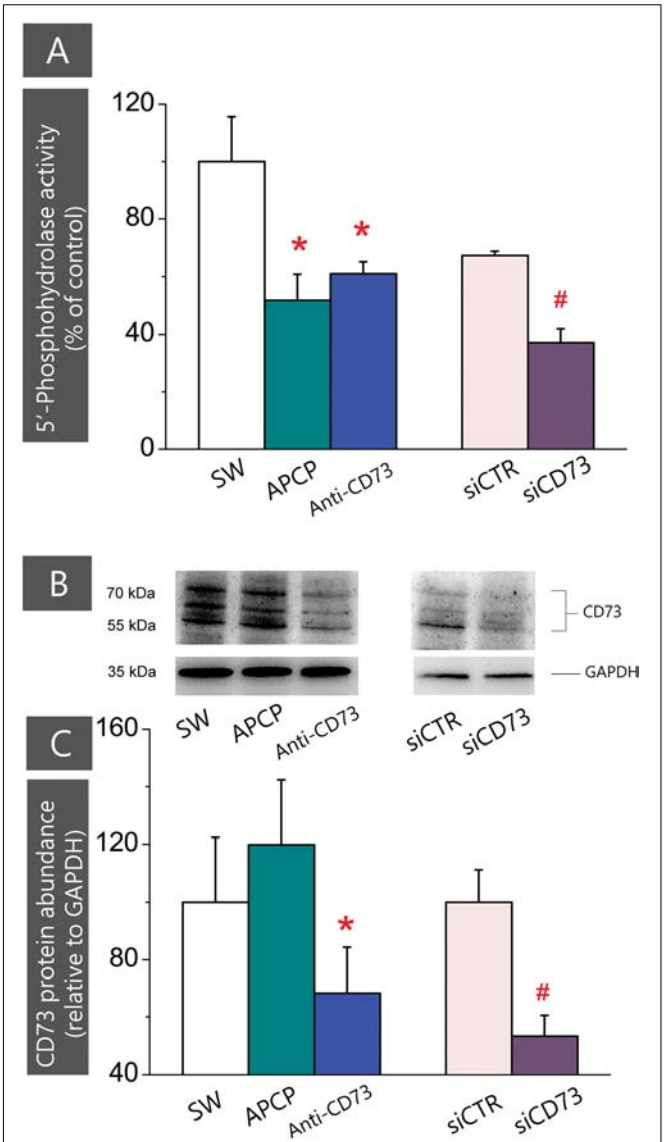

FIGURE 5 | Expression of CD73 in cultures treated with different pharmacological inhibitors. **(A)** 5′-AMP phosphohydrolase activity was assayed in whole cells, after subjecting the cultures to scratch wound and treatment with APCP (*green*), anti-CD73 antibodies (*blue*) and siCD73 (*magenta*). Bars represent mean relative phospohydrolase activity (%) ± SEM, from $n = 7$ independent determinations performed in sextuplicate. * denotes significance at $p < 0.01$ in respect to SW activity (1.13 ± 0.18 nmol Pi/mg/min); #denotes significance at $p < 0.05$ in respect to siCTR activity (0.76 ± 0.02 nmol Pi/mg/min). **(B)** Representative Western blot of whole cell lysates obtained from cultures treated with different pharmacological inhibitors. Blots were probed with anti-CD73 antibodies (1:1500 in TBST; Cell Signaling, US) or anti-GAPDH antibodies. **(C)** Abundance of CD73 protein relative to GAPDH (%) ± SEM, from $n = 3$ independent determinations. CD73/GAPDH ratio obtained for SW was arbitrarily defined as 100% and used as reference. Significance level inside the graph: * denotes significance at $p < 0.05$ in respect to SW; #denotes $p < 0.05$ in respect to siCTR.

To test whether the interaction between anti-CD73 antibodies and CD73 molecule may induce a signaling event, we examined the expression of ERK1/2 by Western blot analysis (**Figure 7B**).

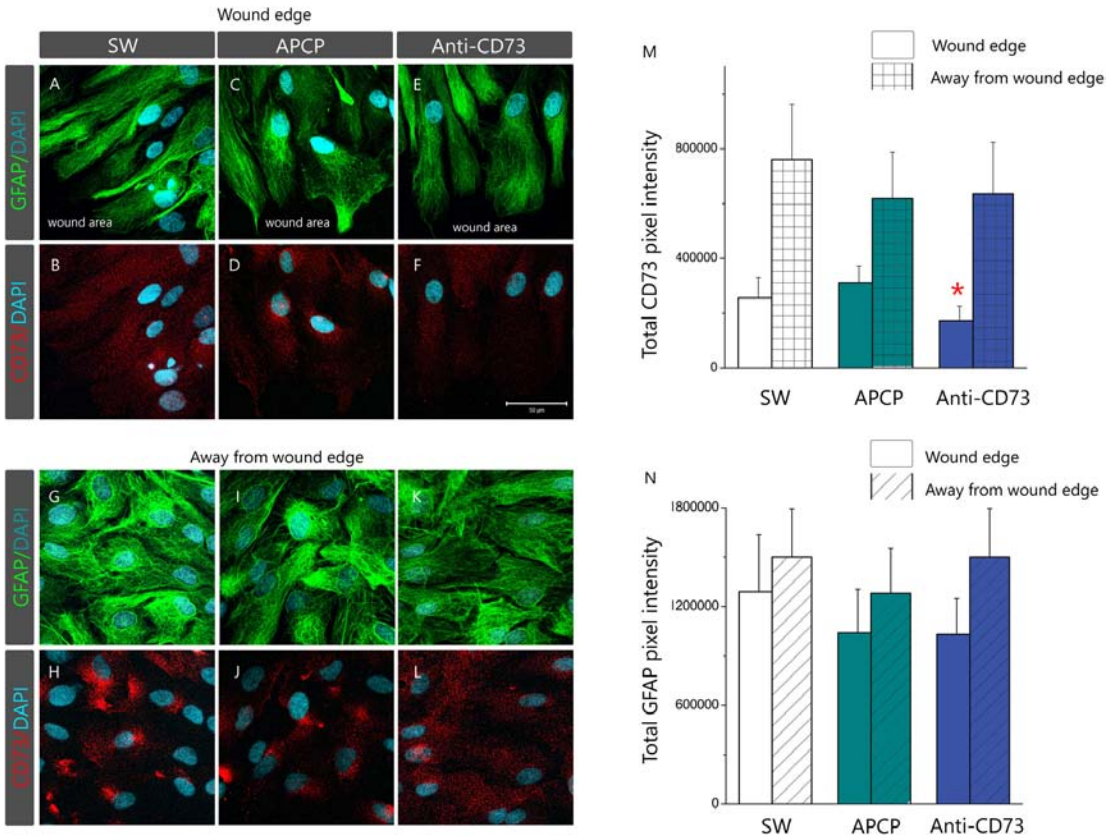

FIGURE 6 | Membrane topography of CD73. Confocal images of astrocyte cultures immunostained for CD73 (*red fluorescence*) and GFAP (*green fluorescence*) and counterstained for DAPI (*blue fluorescence*). Micrographs show astrocytes in SW culture and cultures treated with APCP and anti-CD73 antibodies at the wound edge **(A–F)** and at 1–3 cell-row distance away from the wound edge **(G–L)**. Scale bar at $F = 50$ μm applicable to all micrographs. **(H)** Relative immunofluorescence intensity corresponding to CD73 **(M)** and GFAP **(N)** quantified using the ImageJ software. The results present mean integrated fluorescence density ± SEM, from two separate culture preparations and total 15 frames per treatment. * denotes $p < 0.05$ in respect to SW.

The expression levels of ERK1/2 increased in cells treated with anti-CD73 antibodies and APCP, whereas the levels were not altered in cells with CD73 gene silencing. These findings imply that a direct interference with CD73 molecule may trigger an intracellular signaling, further implying that CD73 participation in cell adhesion/migration depends on both the catalytic action and the adhesive properties of CD73.

DISCUSSION

Several experimental models of human neuropathologies studied so far demonstrate that reactive astrocytes express significantly higher level of CD73 compared to their normal counterparts (Braun et al., 1998; Bonan et al., 2000; Nedeljkovic et al., 2006, 2008; Lavrnja et al., 2009, 2015; Gandelman et al., 2010; Bjelobaba et al., 2011; Bonan, 2012). This finding is confirmed *in vitro* in the present study, by demonstrating that reactive astrocytes, irrespective of the triggering stimuli, i.e., scratch wound, LPS or IL-1β, strongly upregulate the expression and activity of CD73. However, temporal analysis of the expression *in vivo* reveals that the increase in CD73 by reactive astrocytes lags behind the increase in GFAP, and that the overall CD73 abundance peaks at fully developed reactive astrocytes already occupying the site of injury (Nedeljkovic et al., 2006; Bjelobaba et al., 2011; Lavrnja et al., 2015). While studies in human and rat glioma and medulloblastoma cell lines *in vitro* also demonstrate significantly higher levels of CD73 compared to normal astrocytes (Wink et al., 2003; Cappellari et al., 2012, 2015; Xu et al., 2013), closer analysis reveals that CD73 differentiates primary tumor cell lines, which express CD73, from metastatic cell lines which do not express the enzyme (Cappellari et al., 2012). Thus, we hypothesized that one of the roles of CD73 in astrocytes might be to act as a docking molecule which facilitates adhesion of non-migrating cells to the lamina, whereas mobile astrocytes, which move toward the site of injury, decrease the protein expression. Given the dual roles of CD73, to generate adenosine and to interact with ECM, in the present study the hypothesis has been tested by assaying migration of primary astrocytes in the presence of different pharmacological inhibitors which selectively target individual functions of CD73.

The major findings of our study are the following: (a) pharmacological inhibitors which block or reduce membrane exposure of CD73, decrease cell proliferation and increase

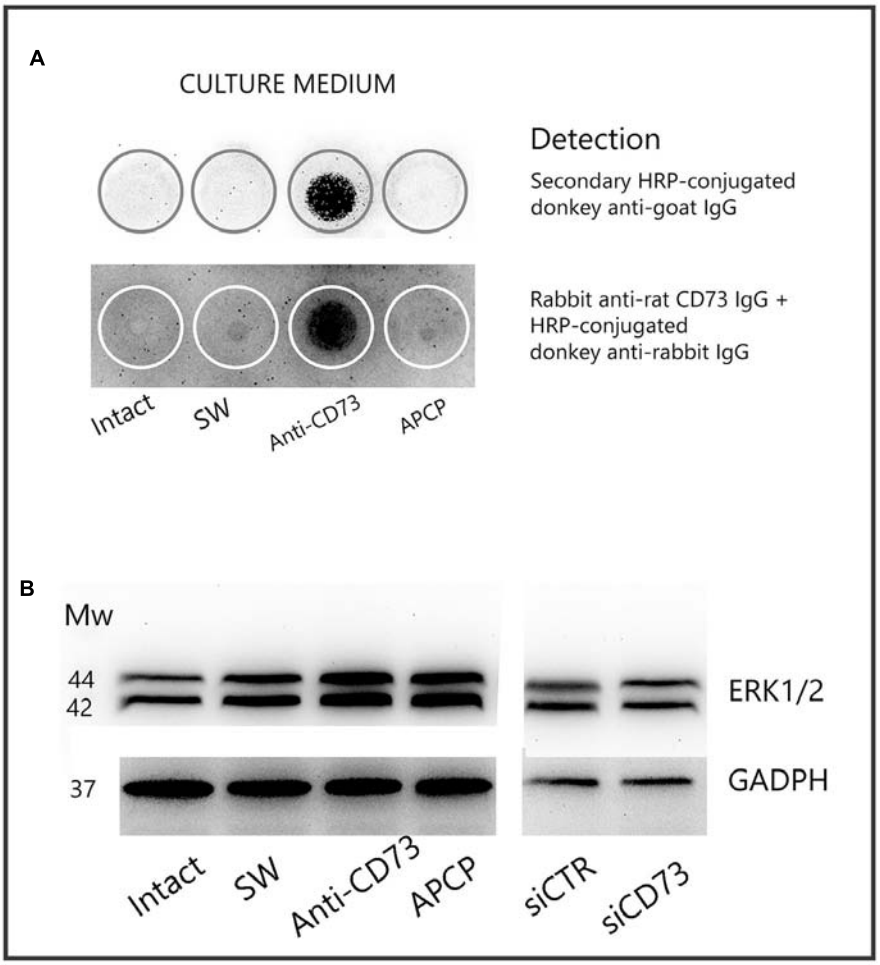

FIGURE 7 | CD73 shedding. **(A)** Detection of soluble CD73 in culture media collected 24 h after the addition of the pharmacological inhibitors. Culture media were analyzed for presence of CD73 by dot blot, using either secondary IgG antibody or another set of anti-CD73 primary and matching secondary antibodies, as described in section "Materials and Methods." Media from $n = 4$ separate cultures were used in the analysis. **(B)** Expression level of ERK1/2 in whole cell lysates obtained from cultures treated with different pharmacological inhibitors, detected by Western blotting using ERK1/2-specific antibodies.

cell migration *in vitro*, but do not affect organization of the intermediate filament network, nor decrease expression of GFAP; (b) ligation of anti-CD73 antibodies induces shedding of CD73 and the release of soluble CD73 in the culture media, and (c) the pharmacological targeting of CD73 triggers intracellular signaling events, indicating that CD73 may function as a membrane receptor which transmits activation signals into the cells. The evidence for the first notion is based on the findings that astrocytes treated with anti-CD73 antibodies or with siCD73 increase migration velocity in the scratch wound assay, while cells treated with APCP do not change migration velocity in respect to non-treated SW culture. The notion is also supported by a recent study showing that knockdown of CD73 in tumor cell lines more efficiently prevents cell adhesion to ECM than inhibition of CD73 activity with APCP (Zhi et al., 2007). Although these data together imply that adenosine has no part in astrocyte migration *in vitro*, analysis of adenosine effects in SW culture revealed that the nucleoside increased cell proliferation and reduced migration velocity in culture with functional CD73, thus indicating that CD73 and adenosine affect astrocyte migration by mutually complementing mechanisms.

It has been demonstrated that cells subjected to scratch wound increase cell proliferation (Lampugnani, 1999; Kornyei et al., 2000), whereas the cell proliferation positively correlates with CD73 expression in many different tumor cell lines, including glioma (Turnay et al., 1989; Christensen et al., 1996; Ciccarelli et al., 2000; Ohana et al., 2001; Bavaresco et al., 2008; Gao et al., 2017). Cell proliferation and CD73 expression are interconnected through TCF/LEF binding site in the regulatory region of CD73 gene, which is the nuclear target of Wnt pathway (Synnestvedt et al., 2002; Spychala and Kitajewski, 2004). This explains why factors that inhibit CD73 activity depress cell proliferation and vice versa (Andree et al., 1987; Bavaresco et al., 2008), which represent the basis for new and promising therapeutic options for cancer treatment (Antonioli et al., 2016). Our results are in agreement with the potential

role of CD73 as a proliferative factor since all applied CD73 inhibitors considerably reduce cell proliferation demonstrating that the stimulatory effects of anti-CD73 antibodies and siCD73 on astrocyte migration, at least *in vitro*, cannot be attributed to increased cell proliferation.

Cell migration is a multi-step process based on a specificity of interactions and a fine balance between cell–cell and cell-substratum interactions. Involvement of several families of CAM and ECM in cell migration and adhesion is well described (Ridley et al., 2003; Wang et al., 2008), while the role of CD73 is less clear and more contradictory (Zhi et al., 2007; Wang et al., 2008; Andrade et al., 2011). Studies in normal and neoplastic cell lines have demonstrated that CD73 specifically binds tenascin C, laminin, and fibronectin (Stochaj et al., 1990; Sadej et al., 2008), with different outcomes regarding its catalytic activity and cell adhesiveness. While tenascin C strongly inhibits CD73 catalytic activity and promotes cell migration (Sadej et al., 2008), fibronectin and laminin strengthen cell adhesion, while either increasing or not affecting the activity (Olmo et al., 1992; Mehul et al., 1993). Tenascin C triggers intracellular signaling pathways, including Rho-mediated, Wnt, and FAK signaling, the latter being responsible for disruption of cell adhesion to fibronectin (Brosicke and Faissner, 2015). Thus, data suggest the possibility of CD73 playing a role in interactions between activated cells and ECM, whereas the interaction with a particular ligand determines whether the cell will adhere, migrate or completely detach. Cells actively produce ECM components and create their own extracellular environment, which in turn critically determine the cell behavior (Geiger et al., 2009). Thus, in physiological conditions, the content of tenascin C in adult brain tissue is very low and one can speculate that cell adhesion and domain organization of quiescent astrocytes are strengthened by interactions between CD73 and fibronectin. In conditions of brain injury *in vivo*, reactive astrocytes deposit large amounts of tenascin C (Wiese et al., 2012; Brosicke and Faissner, 2015) and actively change their microenvironment, which becomes more permissive for astrocyte migration, at least in part, through the altered interactions between CD73 and ECM.

The second major finding of our study is that the binding of anti-CD73 antibodies triggers CD73 molecules to shed from astrocyte membrane. Several recent studies demonstrating the potential of anti-CD73 antibodies in immunomodulation and cancer treatment, also show that specific anti-CD73 antibodies trigger CD73 to internalize (Terp et al., 2013), to shed from the membrane (this study, Airas et al., 2000; Geoghegan et al., 2016) or to remain intact (Airas et al., 1997; Sadej et al., 2006; Sadej and Skladanowski, 2012; Terp et al., 2013; Geoghegan et al., 2016), indicating that the effect may be epitope specific. Thus, it is possible that binding of anti-CD73 antibodies, depending on the exact epitope, mimics the engagement of CD73 with its natural ligands to induce CD73 shedding. Upon ligand binding, CD73 may interact with other membrane proteins, cytoskeleton components and intracellular pathways to promote stronger adhesion or migration due to internalization or shedding (Sadej et al., 2006; Terp et al., 2013). The physiological relevance of this interaction is reflected in the evidence that the interference with the CD73 molecules, by APCP or by anti-CD73 antibodies, increased the expression level of ERK1/2 in our cell culture. In the conditions *in vivo*, this scenario may be much more complex and the functional links between CD73, ECM, and intracellular signaling events have yet to be established.

Beyond these considerations, several studies demonstrate functional differences of CD73 in different cells and tissues, such as discrepancy between CD73 protein level and enzyme activity (Christensen et al., 1996; Airas et al., 1997; Cunha, 2001; Nedeljkovic et al., 2006; Stanojević et al., 2011; Brisevac et al., 2012; Lavrnja et al., 2015) or susceptibility of CD73 to ECM and lectins (Olmo et al., 1992; Mehul et al., 1993; Airas et al., 1997; Navarro et al., 1998). Data regarding the involvement of CD73 in tumor growth, invasiveness and metastasis in different tumor cell lines are even more contradictory (Antonioli et al., 2016). Since CD73 has no structural isoforms (Zimmermann, 1992), these functional variations are exhibited by CD73 molecules which are identical at protein, mRNA and cDNA level (Airas et al., 1995) but differ in their carbohydrate content. Based on the carbohydrate content, CD73 may be classified as a high-mannose type, complex carbohydrates type and hybrid type, which contains both complex carbohydrates and sialic acid residues (Meflah et al., 1984; van den Bosch et al., 1986, 1988; Wada et al., 1986; Baron and Luzio, 1987). As it is quite clear that the differences in glycosylation may be responsible for the variations found in apparent molecular weight of CD73 isolated from different sources (Turnay et al., 1989; Olmo et al., 1992; Zimmermann, 1992; Navarro et al., 1998; Grkovic et al., 2014; Lavrnja et al., 2015), it has been increasingly evident that the variations in glycan content may be responsible for the functional differences of CD73 found in different cell types and tissues. Since glycans are charged molecules, changes in the carbohydrate composition of CD73 or incorporation of negatively charged sialic acid molecules (Meflah et al., 1984), may significantly affect membrane charge density and thus cell behavior. Indeed, some earlier and recent studies demonstrate that the post-translational modifications of CD73 and alterations in the carbohydrate content may be responsible for a short-term (Vogel et al., 1991; Schoen and Kreutzberg, 1994; Lavrnja et al., 2015) and long term (Grkovic et al., 2014) regulation of CD73 functions, including its role in cell adhesion and migration. All these data point out that the regulation of CD73 by cells is a very complex mechanism, and include transcriptional and post-translational modification, together with cell-specific and tissue-specific regulators that have yet to be established.

Taken together, our results demonstrate that CD73 participates in process of astrocyte adhesion and migration, whereas both the interaction of CD73 with select ECM and the generation of adenosine may affect underlying mechanism involved in migration and adhesion. In our study, all applied pharmacological inhibitors affected certain aspect of astrocyte behavior *in vitro*; inhibition of CD73 catalytic activity did not directly affect the kinetics of a wound closure, but it decreased cell proliferation and altered the expression level of the A_1R receptor,

both effects being antagonized by the addition of adenosine. Ligation of anti-CD73 antibodies inhibited CD73 catalytic activity, decreased cell proliferation, increased migration velocity and significantly up-regulated the expression of the $A_{2A}R$ and $A_{2B}R$ of astrocytes *in vitro*, all effects being induced by CD73 molecules shedding. Both approaches altered the expression level of ERK1/2, implying that CD73 may act as a membrane receptor for the extracellular signals transmitting through interactions with ECM. Given the fact that reactive astrocytes, as well as glioma cells are highly migratory cells which express significantly higher levels of CD73 compared to their normal counterparts, it is of major scientific, clinical and pharmacological interest to discover how CD73 affects cells migration, and what is the underlying migration mechanism in the activated cells.

DATA ACCESSIBILITY

Following tools, software and databases were used: Image analyses were conducted using *ImageJ* (http://imagej.nih.gov/ij/download.html; **RRID:SCR_ 003070**). Statistical analysis was performed using Origin 8.0 Software package (http://www.originlab.com/index.aspx?go=PRODUCTS/Origin; **RRID:SCR_014212**).

AUTHOR CONTRIBUTIONS

Animal handling, cell culture preparation, treatments, rt-PCR, enzyme assay, Western blot, dot blot, immunocytochemistry and confocal microscopy imaging, cell proliferation assay, scratch wound assay were peformed by MA. Morphometric analyses: NN. Data analyses and interpretation: NN. Writing of article: NN and MA. Figure preparation: NN. Final approval of version to be published: MA and NN. Conceived and designed: NN.

FUNDING

This study was entirely supported by Ministry of Education, Science and Technological Development of the Republic of Serbia No. III41014.

ACKNOWLEDGMENTS

This study is a part of MA doctoral thesis. The authors thank Dr. J. Sévigny, Centre de recherche du CHU de Québec, Québec, Canada for a kind gift of ecto-5′-nucleotidase/CD73 antibodies [rNu-9L(I4,I5)].

SUPPLEMENTARY MATERIAL

The Supplementary Material for this article can be found online at: https://www.frontiersin.org/articles/10.3389/fphar.2018.00153/full#supplementary-material

FIGURE S1 | Concentrations of pharmacological inhibitors were chosen based on their ability to block CD73, without affecting astrocyte viability. **(A)** Cells were incubated for 24 h with APCP (50–300 μM) or anti-CD73 antibodies (1:1000 to 1:250 dilution), and 5′-AMP phosphohydrolase was assayed as described. **(B)** Optimal concentration of siCD73 for transfection analysis was determined based on the ability to induce efficient transfection and inhibition of CD73 gene expression via RNA interference. There was no significant change in cell viability within applied concentrations of the inhibitors.

FIGURE S2 | Expression of CD73 in cultures treated with LPS or IL-1β. **(A)** Confocal images of astrocyte cultures immunostained for CD73 (*red fluorescence*) and GFAP (*green fluorescence*) and counterstained for DAPI (*blue fluorescence*). Micrographs show astrocytes in control intact culture and intact cultures treated with 100 ng/ml LPS or 10 ng/ml IL-1β. Scale bar = 50 μm. **(B)** Relative immunofluorescence intensity corresponding to CD73, quantified using the ImageJ software. The results present mean integrated fluorescence density ± SEM, from five microscopic frames captured from one culture preparation. * denotes $p < 0.05$ in respect to control. **(C)** 5′-AMP phosphohydrolase activity assayed in whole cells, after treating the cultures with 100 ng/ml LPS or 10 ng/ml IL-1β for 24 h Bars represent mean phosphohydrolase activity (nmol Pi/mg/min) ± SEM, from $n = 3$ determinations performed in triplicate. * denotes significance at $p < 0.05$ in respect to control.

FIGURE S3 | Kinetics of wound closure in a primary astrocyte culture. Astrocytes were grown to confluence in normal FBS and wound was made by scraping the bottom of the dish with a sterile 200-μl pipette tip. **(A)** Representative images of defined microscopic fields taken at 0–48 h after creating the wound. Scale bar = 200 μm. **(B)** Digitalized images were analyzed in ImageJ and the values of % covered area (in respect to initial wound area) at each time point were plotted vs. time to generate a growth curve. **(C)** The wound area (% of initial wound area) covered between two consecutive time-points was used to calculate the velocity of wound closure (%/h).

FIGURE S4 | Representative Western blot of whole cell lysates obtained from cultures treated with different pharmacological inhibitors. Blots were probed with anti-GFAP antibodies (1:10000 in TBST) and visualized with the use of ECL solution on a Chemi Doc-It imaging system.

TABLE S1 | The scratch wound assay, although very powerful to investigate cell dynamics, suffers from several disadvantages, as you pointed in your next comment. Being aware of the limitation, we performed scratching according to different geometrical patterns in distinct culture dishes, to ensure more favorable ratio between activated and non-affected cells. The number of scratches per culture dish depended on a dish diameter and type of measurements. In general, for fluorescence microscopy and visualization procedures, three scratches surrounded by several-cell wide area of intact cells were applied, whereas for the expression analysis, 5–8 scratches per dish were applied, according to the following table.

REFERENCES

Abbracchio, M. P., Burnstock, G., Boeynaems, J. M., Barnard, E. A., Boyer, J. L., Kennedy, C., et al. (2006). International union of pharmacology LVIII: update on the P2Y G protein-coupled nucleotide receptors: from molecular mechanisms and pathophysiology to therapy. *Pharmacol. Rev.* 58, 281–341. doi: 10.1124/pr.58.3.3

Adzic, M., Stevanovic, I., Josipovic, N., Laketa, D., Lavrnja, I., Bjelobaba, I. M., et al. (2017). Extracellular ATP induces graded reactive response of astrocytes and strengthens their antioxidative defense in vitro. *J. Neurosci. Res.* 95, 1053–1066. doi: 10.1002/jnr.23950

Airas, L., Hellman, J., Salmi, M., Bono, P., Puurunen, T., Smith, D. J., et al. (1995). CD73 is involved in lymphocyte binding to the endothelium: characterization of lymphocyte-vascular adhesion protein 2 identifies

it as CD73. *J. Exp. Med.* 182, 1603–1608. doi: 10.1084/jem.182.5.1603

Airas, L., Niemela, J., and Jalkanen, S. (2000). CD73 engagement promotes lymphocyte binding to endothelial cells via a lymphocyte function-associated antigen-1-dependent mechanism. *J. Immunol.* 165, 5411–5417. doi: 10.4049/jimmunol.165.10.5411

Airas, L., Niemela, J., Salmi, M., Puurunen, T., Smith, D. J., and Jalkanen, S. (1997). Differential regulation and function of CD73, a glycosyl-phosphatidylinositol-linked 70-kD adhesion molecule, on lymphocytes and endothelial cells. *J. Cell Biol.* 136, 421–431. doi: 10.1083/jcb.136.2.421

Andrade, C. M., Lopez, P. L., Noronha, B. T., Wink, M. R., Borojevic, R., Margis, R., et al. (2011). Ecto-5′-nucleotidase/CD73 knockdown increases cell migration and mRNA level of collagen I in a hepatic stellate cell line. *Cell Tissue Res.* 344, 279–286. doi: 10.1007/s00441-011-1140-7

Andree, T., Gutensohn, W., and Kummer, U. (1987). Is ecto-5′-nucleotidase essential for stimulation of human lymphocytes? Evidence against a role of the enzyme as mitogenic lectin receptor. *Immunobiology* 175, 214–225. doi: 10.1016/s0171-2985(87)80030-x

Antonioli, L., Blandizzi, C., Pacher, P., and Hasko, G. (2013a). Immunity, inflammation and cancer: a leading role for adenosine. *Nat. Rev. Cancer* 13, 842–857. doi: 10.1038/nrc3613

Antonioli, L., Novitskiy, S. V., Sachsenmeier, K. F., Fornai, M., Blandizzi, C., and Hasko, G. (2017). Switching off CD73: a way to boost the activity of conventional and targeted antineoplastic therapies. *Drug Discov. Today* 22, 1686–1696. doi: 10.1016/j.drudis.2017.06.005

Antonioli, L., Pacher, P., Vizi, E. S., and Hasko, G. (2013b). CD39 and CD73 in immunity and inflammation. *Trends Mol. Med.* 19, 355–367. doi: 10.1016/j.molmed.2013.03.005

Antonioli, L., Yegutkin, G. G., Pacher, P., Blandizzi, C., and Hasko, G. (2016). Anti-CD73 in cancer immunotherapy: awakening new opportunities. *Trends Cancer* 2, 95–109. doi: 10.1016/j.trecan.2016.01.003

Baron, M. D., and Luzio, J. P. (1987). The synthesis and turnover of 5′-nucleotidase in primary cultured hepatocytes. *Biochim. Biophys. Acta* 927, 81–85. doi: 10.1016/0167-4889(87)90068-1

Bavaresco, L., Bernardi, A., Braganhol, E., Cappellari, A. R., Rockenbach, L., Farias, P. F., et al. (2008). The role of ecto-5′-nucleotidase/CD73 in glioma cell line proliferation. *Mol. Cell. Biochem* 319, 61–68. doi: 10.1007/s11010-008-9877-3

Baykov, A. A., Evtushenko, O. A., and Avaeva, S. M. (1988). A malachite green procedure for orthophosphate determination and its use in alkaline phosphatase-based enzyme immunoassay. *Anal. Biochem.* 171, 266–270. doi: 10.1016/0003-2697(88)90484-8

Bianchi, V., and Spychala, J. (2003). Mammalian 5′-nucleotidases. *J. Biol. Chem.* 278, 46195–46198. doi: 10.1074/jbc.R300032200

Bjelobaba, I., Parabucki, A., Lavrnja, I., Stojkov, D., Dacic, S., Pekovic, S., et al. (2011). Dynamic changes in the expression pattern of ecto-5′-nucleotidase in the rat model of cortical stab injury. *J. Neurosci. Res.* 89, 862–873. doi: 10.1002/jnr.22599

Bjorklund, O., Shang, M., Tonazzini, I., Dare, E., and Fredholm, B. B. (2008). Adenosine A1 and A3 receptors protect astrocytes from hypoxic damage. *Eur. J. Pharmacol.* 596, 6–13. doi: 10.1016/j.ejphar.2008.08.002

Bonan, C. D. (2012). Ectonucleotidases and nucleotide/nucleoside transporters as pharmacological targets for neurological disorders. *CNS Neurol. Disord. Drug Targets* 11, 739–750. doi: 10.2174/187152712803581092

Bonan, C. D., Walz, R., Pereira, G. S., Worm, P. V., Battastini, A. M., Cavalheiro, E. A., et al. (2000). Changes in synaptosomal ectonucleotidase activities in two rat models of temporal lobe epilepsy. *Epilepsy Res.* 39, 229–238. doi: 10.1016/S0920-1211(00)00095-4

Braun, N., Zhu, Y., Krieglstein, J., Culmsee, C., and Zimmermann, H. (1998). Upregulation of the enzyme chain hydrolyzing extracellular ATP after transient forebrain ischemia in the rat. *J. Neurosci.* 18, 4891–4900.

Brisevac, D., Adzic, M., Laketa, D., Parabucki, A., Milosevic, M., Lavrnja, I., et al. (2015). Extracellular ATP selectively upregulates ecto-nucleoside triphosphate diphosphohydrolase 2 and ecto-5′-nucleotidase by rat cortical astrocytes in vitro. *J. Mol. Neurosci.* 57, 452–462. doi: 10.1007/s12031-015-0601-y

Brisevac, D., Bjelobaba, I., Bajic, A., Clarner, T., Stojiljkovic, M., Beyer, C., et al. (2012). Regulation of ecto-5′-nucleotidase (CD73) in cultured cortical astrocytes by different inflammatory factors. *Neurochem. Int.* 61, 681–688. doi: 10.1016/j.neuint.2012.06.017

Brosicke, N., and Faissner, A. (2015). Role of tenascins in the ECM of gliomas. *Cell Adh. Migr.* 9, 131–140. doi: 10.1080/19336918.2014.1000071

Cappellari, A. R., Pillat, M. M., Souza, H. D., Dietrich, F., Oliveira, F. H., Figueiro, F., et al. (2015). Ecto-5′-nucleotidase overexpression reduces tumor growth in a Xenograph Medulloblastoma model. *PLoS One* 10:e0140996. doi: 10.1371/journal.pone.0140996

Cappellari, A. R., Rockenbach, L., Dietrich, F., Clarimundo, V., Glaser, T., Braganhol, E., et al. (2012). Characterization of ectonucleotidases in human medulloblastoma cell lines: ecto-5′NT/CD73 in metastasis as potential prognostic factor. *PLoS One* 7:e47468. doi: 10.1371/journal.pone.0047468

Christensen, L. D., Andersen, V., and Ryder, L. (1996). Decreased number of CD73 (ecto-5′-nucleotidase) molecules on lymphocytes from patients with primary immunoglobulin deficiencies. Correlation between number of CD73 molecules and T-lymphocyte function in vitro. *Scand. J. Immunol.* 44, 62–70. doi: 10.1046/j.1365-3083.1996.d01-281.x

Ciccarelli, R., D'Alimonte, I., Ballerini, P., D'Auro, M., Nargi, E., Buccella, S., et al. (2007). Molecular signalling mediating the protective effect of A1 adenosine and mGlu3 metabotropic glutamate receptor activation against apoptosis by oxygen/glucose deprivation in cultured astrocytes. *Mol. Pharmacol.* 71, 1369–1380. doi: 10.1124/mol.106.031617

Ciccarelli, R., Di Iorio, P., Ballerini, P., Ambrosini, G., Giuliani, P., Tiboni, G. M., et al. (1994). Effects of exogenous ATP and related analogues on the proliferation rate of dissociated primary cultures of rat astrocytes. *J. Neurosci. Res.* 39, 556–566. doi: 10.1002/jnr.490390507

Ciccarelli, R., Di Iorio, P., D'Alimonte, I., Giuliani, P., Florio, T., Caciagli, F., et al. (2000). Cultured astrocyte proliferation induced by extracellular guanosine involves endogenous adenosine and is raised by the co-presence of microglia. *Glia* 29, 202–211. doi: 10.1002/(SICI)1098-1136(20000201)29:3<202::AID-GLIA2>3.0.CO;2-C

Corbelini, P. F., Figueiro, F., das Neves, G. M., Andrade, S., Kawano, D. F., Oliveira Battastini, A. M., et al. (2015). Insights into Ecto-5′-nucleotidase as a new target for cancer therapy: a medicinal chemistry study. *Curr. Med. Chem.* 22, 1776–1792. doi: 10.2174/0929867322666150408112615

Cunha, R. A. (2001). Regulation of the ecto-nucleotidase pathway in rat hippocampal nerve terminals. *Neurochem. Res.* 26, 979–991. doi: 10.1023/A:1012392719601

Deaglio, S., and Robson, S. C. (2011). Ectonucleotidases as regulators of purinergic signaling in thrombosis, inflammation, and immunity. *Adv. Pharmacol.* 61, 301–332. doi: 10.1016/b978-0-12-385526-8.00010-2

Fenoglio, C., Necchi, D., Civallero, M., Ceroni, M., and Nano, R. (1997). Cytochemical demonstration of nitric oxide synthase and 5′ nucleotidase in human glioblastoma. *Anticancer Res.* 17, 2507–2511.

Fredholm, B. B., IJzerman, A. P., Jacobson, K. A., Klotz, K. N., and Linden, J. (2001). International Union of Pharmacology. XXV. Nomenclature and classification of adenosine receptors. *Pharmacol. Rev.* 53, 527–552.

Gandelman, M., Peluffo, H., Beckman, J. S., Cassina, P., and Barbeito, L. (2010). Extracellular ATP and the P2X7 receptor in astrocyte-mediated motor neuron death: implications for amyotrophic lateral sclerosis. *J. Neuroinflammation* 7:33. doi: 10.1186/1742-2094-7-33

Gao, Z. W., Dong, K., and Zhang, H. Z. (2014). The roles of CD73 in cancer. *Biomed. Res. Int.* 2014:460654. doi: 10.1155/2014/460654

Gao, Z. W., Wang, H. P., Lin, F., Wang, X., Long, M., Zhang, H. Z., et al. (2017). CD73 promotes proliferation and migration of human cervical cancer cells independent of its enzyme activity. *BMC Cancer* 17:135. doi: 10.1186/s12885-017-3128-5

Geiger, B., Spatz, J. P., and Bershadsky, A. D. (2009). Environmental sensing through focal adhesions. *Nat. Rev. Mol. Cell Biol.* 10, 21–33. doi: 10.1038/nrm2593

Geoghegan, J. C., Diedrich, G., Lu, X., Rosenthal, K., Sachsenmeier, K. F., Wu, H., et al. (2016). Inhibition of CD73 AMP hydrolysis by a therapeutic antibody with a dual, non-competitive mechanism of action. *MAbs* 8, 454–467. doi: 10.1080/19420862.2016.1143182

Ghiringhelli, F., Bruchard, M., Chalmin, F., and Rebe, C. (2012). Production of adenosine by ectonucleotidases: a key factor in tumor immunoescape. *J. Biomed. Biotechnol.* 2012:473712. doi: 10.1155/2012/473712

Grahnert, A., Grahnert, A., Klein, C., Schilling, E., Wehrhahn, J., and Hauschildt, S. (2011). Review: NAD +: a modulator of immune functions. *Innate Immun.* 17, 212–233. doi: 10.1177/1753425910361989

Grkovic, I., Bjelobaba, I., Nedeljkovic, N., Mitrovic, N., Drakulic, D., Stanojlovic, M., et al. (2014). Developmental increase in ecto-5′-nucleotidase activity overlaps with appearance of two immunologically distinct enzyme isoforms in rat hippocampal synaptic plasma membranes. *J. Mol. Neurosci.* 54, 109–118. doi: 10.1007/s12031-014-0256-0

Hasko, G., and Cronstein, B. N. (2004). Adenosine: an endogenous regulator of innate immunity. *Trends Immunol.* 25, 33–39. doi: 10.1016/j.it.2003.11.003

Heuts, D. P., Weissenborn, M. J., Olkhov, R. V., Shaw, A. M., Gummadova, J., Levy, C., et al. (2012). Crystal structure of a soluble form of human CD73 with ecto-5′-nucleotidase activity. *Chembiochem* 13, 2384–2391. doi: 10.1002/cbic.201200426

Horenstein, A. L., Chillemi, A., Zaccarello, G., Bruzzone, S., Quarona, V., Zito, A., et al. (2013). A CD38/CD203a/CD73 ectoenzymatic pathway independent of CD39 drives a novel adenosinergic loop in human T lymphocytes. *Oncoimmunology* 2:e26246. doi: 10.4161/onci.26246

Khakh, B. S., and North, R. A. (2012). Neuromodulation by extracellular ATP and P2X receptors in the CNS. *Neuron* 76, 51–69. doi: 10.1016/j.neuron.2012.09.024

Knapp, K., Zebisch, M., Pippel, J., El-Tayeb, A., Muller, C. E., and Strater, N. (2012). Crystal structure of the human ecto-5′-nucleotidase (CD73): insights into the regulation of purinergic signaling. *Structure* 20, 2161–2173. doi: 10.1016/j.str.2012.10.001

Knofel, T., and Strater, N. (2001). E. coli 5′-nucleotidase undergoes a hinge-bending domain rotation resembling a ball-and-socket motion. *J. Mol. Biol.* 309, 255–266. doi: 10.1006/jmbi.2001.4657

Kornyei, Z., Czirok, A., Vicsek, T., and Madarasz, E. (2000). Proliferative and migratory responses of astrocytes to in vitro injury. *J. Neurosci. Res.* 61, 421–429. doi: 10.1002/1097-4547(20000815)61:4<421::aid-jnr8<3.0.co;2-4

Laketa, D., Savic, J., Bjelobaba, I., Lavrnja, I., Vasic, V., Stojiljkovic, M., et al. (2015). Brain injury alters ectonucleotidase activities and adenine nucleotide levels in rat serum. *J. Med. Biochem.* 34, 215–222. doi: 10.2478/jomb-2014-0025

Lampugnani, M. G. (1999). Cell migration into a wounded area in vitro. *Methods Mol. Biol.* 96, 177–182. doi: 10.1385/1-59259-258-9:177

Lavrnja, I., Bjelobaba, I., Stojiljkovic, M., Pekovic, S., Mostarica-Stojkovic, M., Stosic-Grujicic, S., et al. (2009). Time-course changes in ectonucleotidase activities during experimental autoimmune encephalomyelitis. *Neurochem. Int.* 55, 193–198. doi: 10.1016/j.neuint.2009.02.013

Lavrnja, I., Laketa, D., Savic, D., Bozic, I., Bjelobaba, I., Pekovic, S., et al. (2015). Expression of a second ecto-5′-nucleotidase variant besides the usual protein in symptomatic phase of experimental autoimmune encephalomyelitis. *J. Mol. Neurosci.* 55, 898–911. doi: 10.1007/s12031-014-0445-x

Meflah, K., Bernard, S., and Massoulie, J. (1984). Interactions with lectins indicate differences in the carbohydrate composition of the membrane-bound enzymes acetylcholinesterase and 5′-nucleotidase in different cell types. *Biochimie* 66, 59–69. doi: 10.1016/0300-9084(84)90192-5

Mehul, B., Aubery, M., Mannherz, H. G., and Codogno, P. (1993). Dual mechanism of laminin modulation of ecto-5′-nucleotidase activity. *J. Cell. Biochem.* 52, 266–274. doi: 10.1002/jcb.240520303

Naito, Y., and Lowenstein, J. M. (1981). 5′-Nucleotidase from rat heart. *Biochemistry* 20, 5188–5194. doi: 10.1021/bi00521a014

Navarro, J. M., Olmo, N., Turnay, J., Lopez-Conejo, M. T., and Lizarbe, M. A. (1998). Ecto-5′-nucleotidase from a human colon adenocarcinoma cell line. Correlation between enzyme activity and levels in intact cells. *Mol. Cell. Biochem.* 187, 121–131. doi: 10.1023/A:1006808232059

Nedeljkovic, N., Bjelobaba, I., Lavrnja, I., Stojkov, D., Pekovic, S., Rakic, L., et al. (2008). Early temporal changes in ecto-nucleotidase activity after cortical stab injury in rat. *Neurochem. Res.* 33, 873–879. doi: 10.1007/s11064-007-9529-0

Nedeljkovic, N., Bjelobaba, I., Subasic, S., Lavrnja, I., Pekovic, S., Stojkov, D., et al. (2006). Up-regulation of ectonucleotidase activity after cortical stab injury in rats. *Cell Biol. Int.* 30, 541–546. doi: 10.1016/j.cellbi.2006.03.001

Oberheim, N. A., Goldman, S. A., and Nedergaard, M. (2012). Heterogeneity of astrocytic form and function. *Methods Mol. Biol.* 814, 23–45. doi: 10.1007/978-1-61779-452-0_3

Oberheim, N. A., Tian, G. F., Han, X., Peng, W., Takano, T., Ransom, B., et al. (2008). Loss of astrocytic domain organization in the epileptic brain. *J. Neurosci.* 28, 3264–3276. doi: 10.1523/jneurosci.4980-07.2008

Ogata, S., Hayashi, Y., Misumi, Y., and Ikehara, Y. (1990). Membrane-anchoring domain of rat liver 5′-nucleotidase: identification of the COOH-terminal serine-523 covalently attached with a glycolipid. *Biochemistry* 29, 7923–7927. doi: 10.1021/bi00486a021

Ohana, G., Bar-Yehuda, S., Barer, F., and Fishman, P. (2001). Differential effect of adenosine on tumor and normal cell growth: focus on the A3 adenosine receptor. *J. Cell. Physiol.* 186, 19–23. doi: 10.1002/1097-4652(200101)186:1<19::aid-jcp1011<3.0.co;2-3

Olmo, N., Turnay, J., Risse, G., Deutzmann, R., von der Mark, K., and Lizarbe, M. A. (1992). Modulation of 5′-nucleotidase activity in plasma membranes and intact cells by the extracellular matrix proteins laminin and fibronectin. *Biochem. J.* 282(Pt 1), 181–188. doi: 10.1042/bj2820181

Ridley, A. J., Schwartz, M. A., Burridge, K., Firtel, R. A., Ginsberg, M. H., Borisy, G., et al. (2003). Cell migration: integrating signals from front to back. *Science* 302, 1704–1709. doi: 10.1126/science.1092053

Sadej, R., Inai, K., Rajfur, Z., Ostapkowicz, A., Kohler, J., Skladanowski, A. C., et al. (2008). Tenascin C interacts with ecto-5′-nucleotidase (eN) and regulates adenosine generation in cancer cells. *Biochim. Biophys. Acta* 1782, 35–40. doi: 10.1016/j.bbadis.2007.11.001

Sadej, R., and Skladanowski, A. C. (2012). Dual, enzymatic and non-enzymatic, function of ecto-5′-nucleotidase (eN, CD73) in migration and invasion of A375 melanoma cells. *Acta Biochim. Pol.* 59, 647–652.

Sadej, R., Spychala, J., and Skladanowski, A. C. (2006). Expression of ecto-5′-nucleotidase (eN, CD73) in cell lines from various stages of human melanoma. *Melanoma Res.* 16, 213–222. doi: 10.1097/01.cmr.0000215030.69823.11

Schetinger, M. R., Morsch, V. M., Bonan, C. D., and Wyse, A. T. (2007). NTPDase and 5′-nucleotidase activities in physiological and disease conditions: new perspectives for human health. *Biofactors* 31, 77–98. doi: 10.1002/biof.5520310205

Schoen, S. W., and Kreutzberg, G. W. (1994). Synaptic 5′-nucleotidase activity reflects lesion-induced sprouting within the adult rat dentate gyrus. *Exp. Neurol.* 127, 106–118. doi: 10.1006/exnr.1994.1084

Schwaninger, M., Neher, M., Viegas, E., Schneider, A., and Spranger, M. (1997). Stimulation of interleukin-6 secretion and gene transcription in primary astrocytes by adenosine. *J. Neurochem.* 69, 1145–1150. doi: 10.1046/j.1471-4159.1997.69031145.x

Sofroniew, M. V. (2009). Molecular dissection of reactive astrogliosis and glial scar formation. *Trends Neurosci.* 32, 638–647. doi: 10.1016/j.tins.2009.08.002

Spychala, J., and Kitajewski, J. (2004). Wnt and beta-catenin signaling target the expression of ecto-5′-nucleotidase and increase extracellular adenosine generation. *Exp. Cell Res.* 296, 99–108. doi: 10.1016/j.yexcr.2003.11.001

Stanojević, I., Bjelobaba, I., Nedeljković, N., Drakulić, D., Petrović, S., Stojiljković, M., et al. (2011). Ontogenetic profile of ecto-5′-nucleotidase in rat brain synaptic plasma membranes. *Int. J. Dev. Neurosci.* 29, 397–403. doi: 10.1016/j.ijdevneu.2011.03.003

Stochaj, U., Richter, H., and Mannherz, H. G. (1990). Chicken gizzard 5′-nucleotidase is a receptor for the extracellular matrix component fibronectin. *Eur. J. Cell Biol.* 51, 335–338.

Strater, N. (2006). Ecto-5′-nucleotidase: structure function relationships. *Purinergic Signal.* 2, 343–350. doi: 10.1007/s11302-006-9000-8

Synnestvedt, K., Furuta, G. T., Comerford, K. M., Louis, N., Karhausen, J., Eltzschig, H. K., et al. (2002). Ecto-5′-nucleotidase (CD73) regulation by hypoxia-inducible factor-1 mediates permeability changes in intestinal epithelia. *J. Clin. Invest.* 110, 993–1002. doi: 10.1172/jci15337

Terp, M. G., Olesen, K. A., Arnspang, E. C., Lund, R. R., Lagerholm, B. C., Ditzel, H. J., et al. (2013). Anti-human CD73 monoclonal antibody inhibits metastasis formation in human breast cancer by inducing clustering and internalization of CD73 expressed on the surface of cancer cells. *J. Immunol.* 191, 4165–4173. doi: 10.4049/jimmunol.1301274

Tsutsui, S., Schnermann, J., Noorbakhsh, F., Henry, S., Yong, V. W., Winston, B. W., et al. (2004). A1 adenosine receptor upregulation and activation attenuates neuroinflammation and demyelination in a model of multiple sclerosis. *J. Neurosci.* 24, 1521–1529. doi: 10.1523/jneurosci.4271-03.2004

Turnay, J., Olmo, N., Risse, G., von der Mark, K., and Lizarbe, M. A. (1989). 5-nucleotidase activity in cultured cell lines. Effect of different assay conditions and correlation with cell proliferation. *In Vitro Cell. Dev. Biol.* 25, 1055–1061. doi: 10.1007/BF02624141

van den Bosch, R., Geuze, H. J., du Maine, A. P., and Strous, G. J. (1986). Transport and metabolism of 5′-nucleotidase in a rat hepatoma cell line. *Eur. J. Biochem.* 160, 49–54. doi: 10.1111/j.1432-1033.1986.tb09938.x

van den Bosch, R. A., du Maine, A. P., Geuze, H. J., van der Ende, A., and Strous, G. J. (1988). Recycling of 5′-nucleotidase in a rat hepatoma cell line. *Embo J.* 7, 3345–3351.

Vogel, M., Kowalewski, H. J., Zimmermann, H., Janetzko, A., Margolis, R. U., and Wollny, H. E. (1991). Association of the HNK-1 epitope with 5′-nucleotidase from Torpedo marmorata (electric ray) electric organ. *Biochem. J.* 278(Pt 1), 199–202. doi: 10.1042/bj2780199

Wada, I., Himeno, M., Furuno, K., and Kato, K. (1986). Biosynthesis and intracellular transport of rat liver 5′-nucleotidase. *J. Biol. Chem.* 261, 2222–2227.

Wang, L., Zhou, X., Zhou, T., Ma, D., Chen, S., Zhi, X., et al. (2008). Ecto-5′-nucleotidase promotes invasion, migration and adhesion of human breast cancer cells. *J. Cancer Res. Clin. Oncol.* 134, 365–372. doi: 10.1007/s00432-007-0292-z

Wanner, I. B., Anderson, M. A., Song, B., Levine, J., Fernandez, A., Gray-Thompson, Z., et al. (2013). Glial scar borders are formed by newly proliferated, elongated astrocytes that interact to corral inflammatory and fibrotic cells via STAT3-dependent mechanisms after spinal cord injury. *J. Neurosci.* 33, 12870–12886. doi: 10.1523/jneurosci.2121-13.2013

Wiese, S., Karus, M., and Faissner, A. (2012). Astrocytes as a source for extracellular matrix molecules and cytokines. *Front. Pharmacol.* 3:120. doi: 10.3389/fphar.2012.00120

Wink, M. R., Lenz, G., Braganhol, E., Tamajusuku, A. S., Schwartsmann, G., Sarkis, J. J., et al. (2003). Altered extracellular ATP, ADP and AMP catabolism in glioma cell lines. *Cancer Lett.* 198, 211–218. doi: 10.1016/S0304-3835(03)00308-2

Xu, S., Shao, Q. Q., Sun, J. T., Yang, N., Xie, Q., Wang, D. H., et al. (2013). Synergy between the ectoenzymes CD39 and CD73 contributes to adenosinergic immunosuppression in human malignant gliomas. *Neuro Oncol.* 15, 1160–1172. doi: 10.1093/neuonc/not067

Yegutkin, G. G. (2008). Nucleotide- and nucleoside-converting ectoenzymes: important modulators of purinergic signalling cascade. *Biochim. Biophys. Acta* 1783, 673–694. doi: 10.1016/j.bbamcr.2008.01.024

Yegutkin, G. G. (2014). Enzymes involved in metabolism of extracellular nucleotides and nucleosides: functional implications and measurement of activities. *Crit. Rev. Biochem. Mol. Biol.* 49, 473–497. doi: 10.3109/10409238.2014.953627

Zhi, X., Chen, S., Zhou, P., Shao, Z., Wang, L., Ou, Z., et al. (2007). RNA interference of ecto-5′-nucleotidase (CD73) inhibits human breast cancer cell growth and invasion. *Clin. Exp. Metastasis* 24, 439–448. doi: 10.1007/s10585-007-9081-y

Ziegler, M. (2000). New functions of a long-known molecule. Emerging roles of NAD in cellular signaling. *Eur. J. Biochem.* 267, 1550–1564. doi: 10.1046/j.1432-1327.2000.01187.x

Zimmermann, H. (1992). 5′-Nucleotidase: molecular structure and functional aspects. *Biochem. J.* 285(Pt 2), 345–365. doi: 10.1042/bj2850345

Zimmermann, H., Zebisch, M., and Strater, N. (2012). Cellular function and molecular structure of ecto-nucleotidases. *Purinergic Signal.* 8, 437–502. doi: 10.1007/s11302-012-9309-4

Conflict of Interest Statement: The authors declare that the research was conducted in the absence of any commercial or financial relationships that could be construed as a potential conflict of interest.

frontiers in Pharmacology

ORIGINAL RESEARCH
published: 28 February 2018
doi: 10.3389/fphar.2018.00149

$P2Y_6$ Receptors Regulate CXCL10 Expression and Secretion in Mouse Intestinal Epithelial Cells

*Mabrouka Salem[1,2], Alain Tremblay[2], Julie Pelletier[2], Bernard Robaye[3] and Jean Sévigny[1,2]**

[1] Département de Microbiologie-Infectiologie et d'Immunologie, Faculté de Médecine, Université Laval, Québec City, QC, Canada, [2] Centre de Recherche du CHU de Québec – Université Laval, Québec City, QC, Canada, [3] Institut de Recherche Interdisciplinaire en Biologie Humaine et Moléculaire, Université Libre de Bruxelles, Gosselies, Belgium

In this study, we investigated the role of extracellular nucleotides in chemokine (KC, MIP-2, MCP-1, and CXCL10) expression and secretion by murine primary intestinal epithelial cells (IECs) with a focus on $P2Y_6$ receptors. qRT-PCR experiments showed that $P2Y_6$ was the dominant nucleotide receptor expressed in mouse IEC. In addition, the $P2Y_6$ ligand UDP induced expression and secretion of CXCL10. For the other studies, we took advantage of mice deficient in $P2Y_6$ (*P2ry6*$^{-/-}$). Similar expression levels of $P2Y_1$, $P2Y_2$, P2X2, P2X4, and A_{2A} were detected in *P2ry6*$^{-/-}$ and WT IEC. Agonists of TLR3 (poly(I:C)), TLR4 (LPS), $P2Y_1$, and $P2Y_2$ increased the expression and secretion of CXCL10 more prominently in *P2ry6*$^{-/-}$ IEC than in WT IEC. CXCL10 expression and secretion induced by poly(I:C) in both *P2ry6*$^{-/-}$ and WT IEC were inhibited by general P2 antagonists (suramin and Reactive-Blue-2), by apyrase, and by specific antagonists of $P2Y_1$, $P2Y_2$, $P2Y_6$ (only in WT), and P2X4. Neither adenosine nor an A_{2A} antagonist had an effect on CXCL10 expression and secretion. Macrophage chemotaxis was induced by the supernatant of poly(I:C)-treated IEC which was consistent with the level of CXCL10 secreted. Finally, the non-nucleotide agonist FGF2 induced MMP9 mRNA expression also at a higher level in *P2ry6*$^{-/-}$ IEC than in WT IEC. In conclusion, extracellular nucleotides regulate CXCL10 expression and secretion by IEC. In the absence of $P2Y_6$, these effects are modulated by other P2 receptors also present on IEC. These data suggest that the presence of $P2Y_6$ regulates chemokine secretion and may also regulate IEC homeostasis.

Keywords: intestinal epithelial cells (IEC), $P2Y_6$, CXCL10, TLR, nucleotides

OPEN ACCESS

Edited by:
Kenneth A. Jacobson, National Institutes of Health (NIH), United States

Reviewed by:
Fernando Ochoa-Cortes, Universidad Autónoma de San Luis Potosí, Mexico
Markus Neurath, Universitätsklinikum Erlangen, Germany
Robin Mark Howard Rumney, University of Portsmouth, United Kingdom

***Correspondence:**
Jean Sévigny
jean.sevigny@crchudequebec.ulaval.ca

Specialty section:
This article was submitted to Experimental Pharmacology and Drug Discovery, a section of the journal Frontiers in Pharmacology

Received: *16 November 2017*
Accepted: *13 February 2018*
Published: *28 February 2018*

Citation:
Salem M, Tremblay A, Pelletier J, Robaye B and Sévigny J (2018) $P2Y_6$ Receptors Regulate CXCL10 Expression and Secretion in Mouse Intestinal Epithelial Cells. Front. Pharmacol. 9:149. doi: 10.3389/fphar.2018.00149

INTRODUCTION

Dysregulation of immune response is an important contributor to inflammatory bowel diseases in which the epithelium plays central functions. The intestine is bordered by intestinal epithelial cells (IECs) that represent the first line of defense against environmental pathogens. In addition to acting as a physical barrier to prevent passage of luminal contents, IECs are crucial for maintaining intestinal homeostasis. For example, IECs express a wide range of pattern-recognition receptors (PRRs), including Toll-like receptors (TLRs) that are activated by pathogen-associated molecular patterns (PAMPs) (Qureshi and Medzhitov, 2003; Medzhitov, 2007). The activation of these receptors results in the activation of innate immune responses, inducing the expression

of pro-inflammatory cytokines, chemokines, and antimicrobial peptides (Fritz et al., 2006; Artis, 2008).

Once injured, or upon mechanical stimulation, epithelial cells such as bronchial and IECs release danger signals such as nucleotides which include adenosine triphosphate (ATP), uridine triphosphate (UTP), and their derivatives (Hazama et al., 1999; Braunstein et al., 2001; Vitiello et al., 2012). These molecules can alert the immune system by initiating tissue inflammation via the activation of plasma membrane P2 receptors (Lazarowski et al., 2003; Kukulski et al., 2011). Based on their structure and distinct signal-transduction mechanism, P2 receptors are divided into P2X (P2X1-7) and P2Y ($P2Y_{1,2,4,6,11,12,13,14}$) subfamilies (Abbracchio et al., 2006). Among the P2YR receptor subtypes, $P2Y_6$ is known as a pro-inflammatory receptor which is specifically activated by UDP in human and by UTP and UDP in mouse (Kauffenstein et al., 2010). Several reports suggested an important role of $P2Y_6$ receptors in modulating cellular responses to inflammation. $P2Y_6$ participates in the regulation of TLR1/2-induced IL-8 secretion from monocytes and, as a consequence, in neutrophil migration (Ben Yebdri et al., 2009). In microglia and astrocytes, $P2Y_6$ activation results in the regulation of CCL2 expression (Kim et al., 2011). Moreover, its activation results in the amplification of chemokine secretion induced by lipopolysaccharide (LPS) in the monocytic cell line (THP-1) and in human and mouse monocytes/macrophages (Warny et al., 2001; Kukulski et al., 2007; Bar et al., 2008).

In the context of the gastrointestinal tract, $P2Y_6$ receptors were reported to be strongly expressed by colonic epithelial cells in biopsies from patients with inflammatory bowel disease (Grbic et al., 2008). It was also shown that colonic epithelial cell lines challenged by TNF stimulation, to mimic an inflammatory stress, release UDP which activates $P2Y_6$ receptor and mediates production of CXCL8 (Grbic et al., 2008). There are also some reports that show increase of chemokine expression in IEC lines upon bacterial infection or stimulation with TNF-α or IL-1α (Jung et al., 1995; Yang et al., 1997) in which it is not excluded that $P2Y_6$ may participate.

Other studies suggest that CXCL10 has a strong association with inflammatory diseases and particularly with intestinal inflammation (Laragione et al., 2011; Bondar et al., 2014). In humans, CXCL10 is constitutively expressed by colonic epithelial cells (Dwinell et al., 2001) and it is permanently over-expressed in patients with ulcerative colitis (UC) and Crohn's disease (CD) (Uguccioni et al., 1999; Ostvik et al., 2013; Singh et al., 2016). CXCL10 is a chemoattractant for activated T cells and monocytes (Suzuki et al., 2007; Zhao et al., 2017). It was shown that CXCL10, by binding to CXCR3 receptors, is responsible for Th1 cell differentiation and trafficking into both, the epithelium and the lamina propria of inflamed colons (Uguccioni et al., 1999; Suzuki et al., 2007). Additionally, CXCL10 is responsible for macrophage chemotaxis in murine models of inflammation: non-alcoholic steatohepatitis and puromycin aminonucleoside nephrosis (Petrovic-Djergovic et al., 2015; Tomita et al., 2016).

Giving the fact that the expression of $P2Y_6$ receptor by IEC is increased in inflammatory condition and in biopsies of patients with intestinal inflammation and that it contributes to chemokine release such as CXCL8, we hypothesized that $P2Y_6$ receptor plays a role in the secretion of chemokines by IEC and in immune cell migration to the epithelium. We addressed this hypothesis here with primary IEC cultures from mice deficient in the expression of $P2Y_6$ receptor. We observed that extracellular nucleotides, via the activation of $P2Y_6$ and also of other P2 receptors, regulate the expression and secretion of CXCL10. In addition, our results also show that IEC deficient for $P2Y_6$ respond more vigorously to stimulation with several ligands activating other nucleotide receptors as well as a non-nucleotide receptor. In other words, these data suggest that $P2Y_6$ activation not only activates the synthesis and release of a chemokine but that the presence of $P2Y_6$ also maintains a proper state of activation of these cells, preventing them from overstimulation by several stimuli.

MATERIALS AND METHODS

Reagents and Chemicals

Suramin and Reactive-Blue-2 (RB-2) were obtained from MP Biomedical (Santa Ana, CA, United States). DMEM/F12, advanced DMEM/F12, HEPES, L-glutamine, penicillin, streptomycin, FBS, Dulbecco's PBS, apyrase, formyl-methionine-leucyl-phenylalanine (FMLP), LPSs, adenosine 5'-triphosphate (ATP), adenosine 5'-diphosphate (ADP), uridine 5'-triphosphate (UTP), uridine 5'-diphosphate (UDP), adenosine, Zm 241385, and fibroblast growth factor 2 (FGF2) were purchased from Sigma–Aldrich (Oakville, ON, Canada). Collagenase type I, SuperScript III, gentamicin, B-27 and N-2 supplements, polyinosinic–polycytidylic acid [poly(I:C)], EDTA, and TRIzol were obtained from Invitrogen (Carlsbad, CA, United States). Collagen type I was purchased from BD Bioscience (San Jose, CA, United States). Y-27632, mrEGF, Wnt-3a, and R-spondin were purchased from R&D Systems (Minneapolis, MN, United States). Noggin and M-CSF were purchased from PeproTech (QC, Canada). SYBR Green and DNAseI were from Roche Diagnostics (Indianapolis, IN, United States). Flagellin was obtained from InvivoGen (San Diego, CA, United States). Oligo(dt)18 was obtained from Fisher Scientific (Ottawa, ON, Canada). MRS 2500, MRS 2179, MRS 2578, AR-C 118925XX, PSB 1114, and 5-BDBD were purchased from Tocris Bioscience (Minneapolis, MN, United States).

Animals

All experiments were conducted according to the Canadian Council on Animal Care and the protocols were approved by the Animal Care Committee of Laval University. Adult male C57Bl/6 mice 8–12 weeks (Charles River, Pointe-Claire, QC, Canada) were used as control. *P2ry6*$^{-/-}$ mice were bred at our animal facility in CHUL. Previously to the experiments presented in this paper, $P2Y_6$-deficient mice obtained from B. Robaye (Université Libre de Bruxelles, Belgium) (Bar et al., 2008) were backcrossed 10 times with C57Bl/6 mice from Charles River. A few backcrosses with WT females were performed to ascertain that the mitochondrial DNA is the same in mutant and control mice. Animals were maintained in a specific pathogen-free environment in a temperature-controlled room (21°C) on a 12-h/12-h light and dark cycle and given unrestricted access to

standard diet and tap water. Mice were allowed to acclimate to these conditions for at least 7 days before experimentation.

Intestinal Epithelial Cell Isolation

Primary IECs were isolated from WT and *P2ry6*$^{-/-}$ mice according to Moon et al. (2014) and Graves et al. (2014) with minor modifications as detailed below. Briefly, the longitudinal muscle layer was removed and the colonic tissue was washed with ice-cold Mg^{2+} and Ca^{2+} free salt solution (PBS). Obtained tissue was incubated with 75 U ml^{-1} collagenase type V for 30 min and the reaction was stopped with Dulbecco's modified Eagles medium (DMEM/F12) containing 10% v/v fetal bovine serum (FBS), L-glutamine, HEPES, N-2 supplement, B-27 supplement, and antibiotics as before. The digestion mixture was filtered through a 70-μm mesh and the effluent containing crypts was centrifuged twice at 50 × *g* for 5 min at 4°C. The remaining pellet comprising isolated intestinal crypts was suspended in complete growth media DMEM/F12 advance containing 50 ng/ml mrEGF, 1 μg/ml R-spondin, 100 ng/ml noggin, and 5 ng/ml Wnt-3a in the presence of 10 μM Y-27632 as an anoikis inhibitor. The suspended crypts were then plated in a 24-well plate coated with type I collagen at a density of 1000 crypts/well. Cells were incubated at 37°C in a 5% CO_2 incubator. The media was replaced 48 h later without Y-27632 and the epithelial cells from the crypts were allowed to grow to confluence for 2 days to obtain a monolayer of differentiated IEC. The cells were either collected for qPCR or stimulated as detailed below.

IEC Stimulation

Intestinal epithelial cells were stimulated for 5 (for qPCR experiments) or 24 h (for ELISA experiments) with the ultrapure TLR agonists poly(I:C) [TLR3] (10 μg/ml), LPS [TLR4] (100 ng/ml), flagellin [TLR5] (100 ng/ml), or with the nucleotide ATP, ADP, UTP, UDP, or adenosine all at the concentration of 100 μM. In some experiments, IEC culture was stimulated with poly(I:C) in the presence of general P2 receptor blockers added 20 min before stimulation, suramin (100 μM), RB-2 (100 μM), apyrase (2 U/ml), or in the presence of specific antagonist of $P2Y_1$, $P2Y_2$, $P2Y_6$, P2X4, or A_{2A} receptor (as described in the legend of the figures).

Quantitative Real-Time PCR (qRT-PCR) and ELISA

RNA extraction, cDNA synthesis, and quantification were performed as described previously with some modifications (Bahrami et al., 2014). Briefly, total RNA from stimulated or unstimulated IEC monolayer was extracted with TRIzol then quantified with a Quant-iT RNA BR Assay Kit and Qubit Fluorometer. The cDNA was synthesized with SuperScript III from 1 μg of total RNA with oligo (dT)18 as the primer, according to the instructions of the manufacturer (Invitrogen, Carlsbad, CA, United States). Primers specific for the differentiation marker villin, for the ectonucleotidases, and for P2X, P2Y, and P1 receptors were either designed by us and synthetized by Invitrogen (Carlsbad, CA, United States) or purchased from Qiagen (Toronto, ON, Canada), as detailed in **Table 1**. SYBR Green Supermix was used for qRT-PCR. For the negative controls, water was used as template. Standard curves were used to determine mRNA transcript copy number in individual reactions. GAPDH or actin was used to normalize RNA quantities between samples.

Supernatants from IEC stimulated for 24 h were centrifuged (1000 × *g*, 10 min, 4°C) to discard the detached cells. The supernatants were collected and frozen at −80°C until determination of cytokine concentrations by ELISA Kits (R&D Systems, Minneapolis, MN, United States), following the manufacturers' instructions.

Isolation and Preparation of Murine Bone Marrow Macrophages

Murine macrophages were isolated as described before (Cho et al., 2012) with some modifications. Briefly, bone marrow-derived monocytes were isolated from tibia and femur harvested from mice. Cells were flushed out with PBS containing 1% FBS then filtered through a 70-μm cell strainer. The single cell suspension was centrifuged 10 min at 500 × *g* then resuspended in macrophage complete media [DMEM/F12 medium supplemented with 10% (v/v) FBS, 100 U/ml penicillin, 100 mg/ml streptomycin, 10 mM L-glutamine, and 10 ng/ml M-CSF]. Cells were seeded on 24-well plates (10^6 cells per well) and incubated at 37°C in a 5% CO_2 atmosphere. Four days after seeding the cells, an extra 5 ml of fresh macrophage complete medium was added per plate and incubated for an additional 3 days to get adherent cells constituted of approximately 95% macrophages. To obtain bone marrow-derived macrophages (BMDM), the cell supernatant was discarded and the attached cells were washed with 10 ml of sterile PBS. Then, cell stripper non-enzymatic cell dissociation solution (D-PBS containing 1 mM EDTA) was added to each dish and incubated 5 min at 37°C. This solution contains the divalent cation chelator EDTA that gently dislodges adherent cells as an alternative to trypsin. After detachment of macrophages from the plate, an equal volume of cold DMEM/F12-10 medium was added to the wells then cells were centrifuged at 400 × *g* for 10 min at 4°C. The cells were counted then used for chemotaxis assay.

In Vitro Chemotaxis Assay

Macrophage chemotaxis was carried out in a Boyden chambers as described before (Cho et al., 2012) with some modifications. Briefly, cell culture inserts (5 μm pore size) were used to form dual compartments (chambers) in a 24-well culture plate (Corning-Costar, Lowell, MA, United States). Macrophages prepared as described above (10^6 cells in 0.2 ml of DMEM/F12–5% FBS) were loaded in the upper chamber and their migration was initiated with IEC supernatant prepared as above or with FMLP (10 μM) as a positive control, added to the bottom chamber. Cell migration was carried out for 24 h at 37°C and 5% CO_2. The migrated macrophages were collected from the bottom chambers and counted with a hemocytometer, as detailed in previous studies (Vereyken et al., 2011; Unver et al., 2015). Basal macrophage migration observed in the absence of IEC

TABLE 1 | qRT-PCR primers.

Gene	Forward primer	Reverse primer	Amplicon (bp)
Vil1	Qiagen	Qiagen	135
Alpi	Qiagen	Qiagen	113
Gapdh	AACTTTGGCATTGTGGAAGG	ACA CAT TGG GGG TAG GAA CA	223
Actb	AGCCATGTACGTAGCCATCC	CTC TCA GCT GTG GTG GTG AA	228
Entpdl	AGC TGC CCC TTA TGG AAG AT	TCA GTC CCA CAG CAA TCA AA	123
Entpd2	TTC CTG GGA TGT CAG GTC TC	GTC TCT GGT GCT TGC CTT TC	132
Entpd3	ACC TGT CCC GTG CTT AAA TG	AGA CAG AGT GAA GCC CCT GA	183
Entpdl7	Qiagen	Qiagen	91
Entpd8	CCC TTA TGA ACC CCT GAC CT	AAT CCA ACC ACA GGC TCT TG	292
NtT5e/CD73	CAG GAA ATC CAC CTT CCA AA	AAC CTT CAG GTA GCC CAG GT	128
P2ry1	TCG-TGT-CTC-CAT-TCT-GCT-TG	CGA CAG GGT TTA TGC CAC TT	218
P2ry2	TGA CGA CTC AAG ACG GAC AG	GTC CCC TAC AGC TCC CCT AC	108
P2ry4	AGACGGGCCTGATGTGTATC	AGG TTC ACA TGC CCT GTA CC	126
P2ry6	GGT-AGC-GCT-GGA-AGC-TAA-TG	TTT CAA GCG ACT GCT GCT AA	308
P2ry12	GGC-AGC-CTT-GAG-TGT-TCT-TC	ATA ACG TGC TAC CCG ACC TG	130
P2ry13	ATA-GAG-AAC-CGG-GAA-CAG-CA	CAA AAC AAA GCT GAT GCT CG	115
P2ry14	TTT TGT CGT CTG CTT TGT GC	GCA GCC GAG AGT AGC AGA GT	135
P2rx1	CAA CTG TGT GCC CTT CAA TG	GGT ACC ATT CAC CTC CTC CA	114
Pr2x2	GCT GGG CTT CAT TGT AGA GC	CCT GTC CAT GCA CAA TAA CG	281
P2rx3	ATT TCC TCA AAG GGG CTG AT	GTT CTG CAG CCC AAG GAT AA	204
P2rx4	CAC AAC GTG TCT CCT GGC TA	GCC TTT CCA AAC ACG ATG AT	125
P2rx5	CTG TCA CTT CAG CTC CAC CA	TTT GTT GTC CAG ACG GTT GA	196
P2rx6	TCA CCC GCT AAC CCT GTT AC	TAG TCC CGC TGA AGC TTT GT	242
P2rx7	AAT CGG TGT GTT TCC TTT GG	CCG GGT GAC TTT GTT TGT CT	165
Adora 1	GTG ATT TGG GCT GTG AAG GT	AGT AGG TCT GTG GCC CAA TG	142
Adora2a	TCA ACA GCA ACC TGC AGA AC	GGC TGA AGA TGG AAC TCT GC	186
Adora2b	TCT GGC CTT TTG GAG AAG AA	TTT CCG GAA TCA ATT CAA GC	246
Adora3	TGT GGA GGG AGT CTC GTC TT	TCC TTC TGT TCC CCA CAT TC	97

supernatant was <20% of that induced with IEC supernatant and was subtracted from the data presented in the figures.

Statistical Analysis

Results are expressed as mean ± SEM. The statistical differences between mean values were assessed by two-way ANOVA followed by Bonferroni test using graph-prism software. All results were considered statistically significant at $p < 0.05$ (one symbol), $p < 0.01$ (two symbols), or $p < 0.001$ (three symbols). The symbol (*) was used to compare responses from *P2ry6*$^{-/-}$ IEC with those from WT IEC. The symbol (#) was used to compare responses from stimulated IEC with those from non-stimulated IEC. The symbol (¶) was used to compare responses from poly(I:C)-treated IEC in the presence of inhibitors or antagonist with those from IEC treated with poly(I:C) alone.

RESULTS

$P2Y_6$ Receptor Is the Major Nucleotide Receptor Expressed in IEC

We first evaluated the expression of P2 receptors in primary IECs isolated from WT colon. $P2Y_6$ was the nucleotide receptor with the highest mRNA expression in these cells ($13 \times 10^5 \pm 1.7 \times 10^5$ copies/μg of cDNA) followed by $P2Y_1$ ($9.5 \times 10^5 \pm 1.4 \times 10^5$ copies/μg of cDNA). There were also lower gene expressions of $P2Y_2$ ($1.2 \times 10^5 \pm 0.1 \times 10^5$ copies/μg of cDNA), P2X2 ($1.37 \times 10^5 \pm 0.22 \times 10^5$ copies/μg cDNA), P2X4 ($2.2 \times 10^5 \pm 0.11 \times 10^5$ copies/μg cDNA), and A_{2A} ($2.1 \times 10^5 \pm 0.5 \times 10^5$ copies/μg cDNA) compared to the gene expression of $P2Y_6$ receptor (**Figures 1A,B,E**).

Characterization of *P2ry6*$^{-/-}$ IEC

Our main hypothesis is that $P2Y_6$ receptors regulate functions of IEC related to inflammation. To address this, we used IEC isolated from mice deficient for the expression of $P2Y_6$ receptor (*P2ry6*$^{-/-}$). Microscopic observation of IEC and trypan blue staining did not show any apparent differences in the growth and differentiation of WT and *P2ry6*$^{-/-}$ IEC (data not shown). In addition, IEC of both genotypes exhibited similar levels of mRNA of the IEC differentiation markers villin and intestinal alkaline phosphatase (ALPi) before and after differentiation. Before differentiation, the expression of villin and ALPi genes was below $0.04 \times 10^6 \pm 0.002 \times 10^6$ and $0.02 \times 10^6 \pm 0.003 \times 10^6$ copies/μg of cDNA, respectively (data not shown), for both WT and *P2ry6*$^{-/-}$ IEC. After differentiation, the expression of these markers was as expected dramatically increased, over $1 \times 10^6 \pm 0.02 \times 10^6$ and

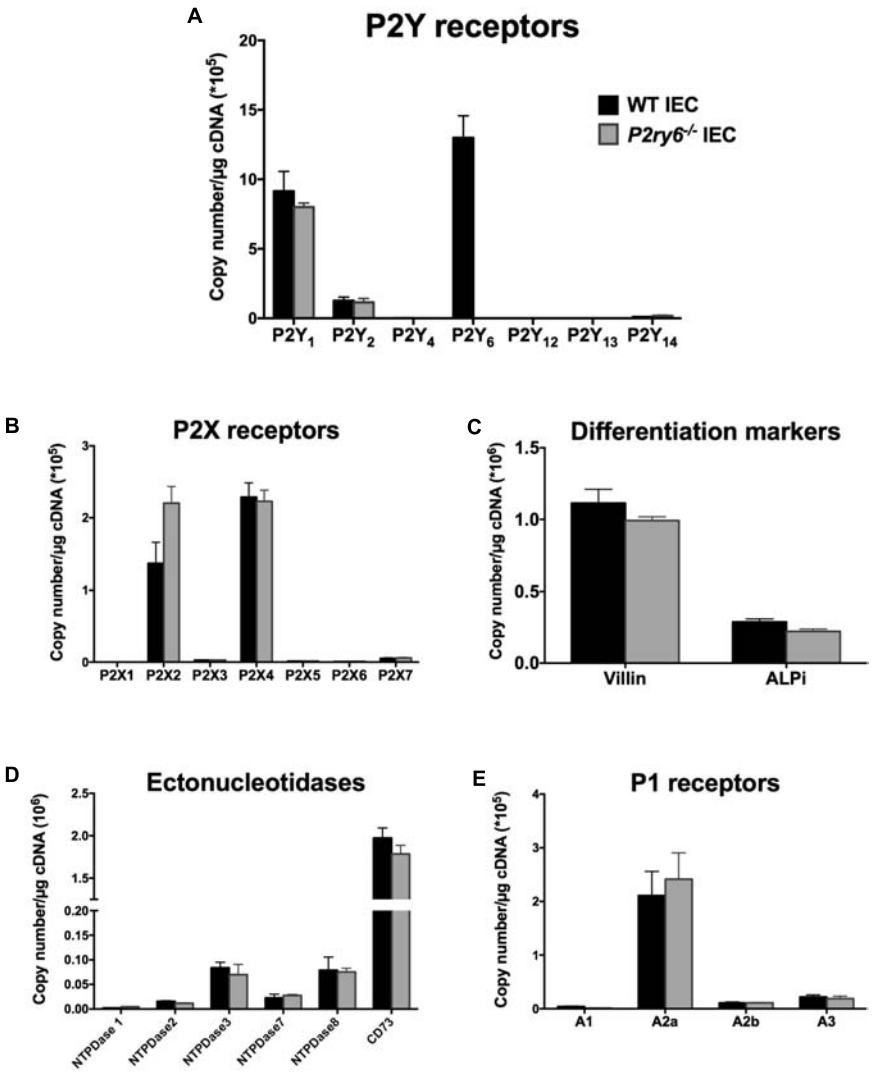

FIGURE 1 | Characterization of primary IEC cultures. IECs were prepared and cultured as mentioned in the section "Materials and Methods" to obtain a monolayer of differentiated cells. RNA was isolated and the expression of P2Y receptors **(A)**, P2X receptors **(B)**, the differentiated epithelial cell markers villin and ALPi **(C)**, ectonucleotidases **(D)**, and P1 receptors **(E)** were analyzed by qRT-PCR. Data are normalized to GAPDH mRNA level. Data presented are the mean ± SEM of three independent experiments each with cells pooled from three mice.

$0.28 \times 10^6 \pm 0.01 \times 10^6$ copies/µg of cDNA for villin and ALPi, respectively, for both genotypes as measured by qRT-PCR (**Figure 1C**).

We then compared the expression of the receptors and enzymes involved in nucleotide signaling in WT and *P2ry6*$^{-/-}$ IEC primary cultures. Aside $P2Y_6$, we noted similar expression of all P2Y and P2X receptors at the gene level in IEC from both genotypes (**Figures 1A,B**) as well as of the plasma membrane-bound NTPDases and ecto-5'-nucleotidase (CD73) (**Figure 1D**). It is noteworthy that these ectonucleotidases not only hydrolyse the agonists of P2 receptors but also generate adenosine which activates P1 receptors. The analysis of P1 receptor expression reveals an important gene expression of the adenosine A_{2A} receptor ($2.1 \times 10^5 \pm 0.4 \times 10^5$ for WT IEC and $2.5 \times 10^5 \pm 0.4 \times 10^5$ for *P2ry6*$^{-/-}$ IEC) and nearly no expression of the other P1 receptors, in both WT and *P2ry6*$^{-/-}$ IEC, which was in the order of 2×10^5 copies/µg of cDNA (**Figure 1E**). Aside $P2Y_6$, the minor variations in the expression of the genes tested in **Figure 1** between WT and *P2ry6*$^{-/-}$ IEC were all not significantly different.

Together, these data show that *P2ry6*$^{-/-}$ IECs are similar to WT IEC in all aspects analyzed, including gene expression of enzymes and receptors involved in nucleotide signaling, except, obviously, for the gene expression of $P2Y_6$. We therefore used these cells to investigate the role of $P2Y_6$ receptor in functions of IEC related to immune responses. More specifically, we investigated the implication of $P2Y_6$ on IEC stimulated with TLR agonists to explore the contribution of this receptor in responses to PAMP.

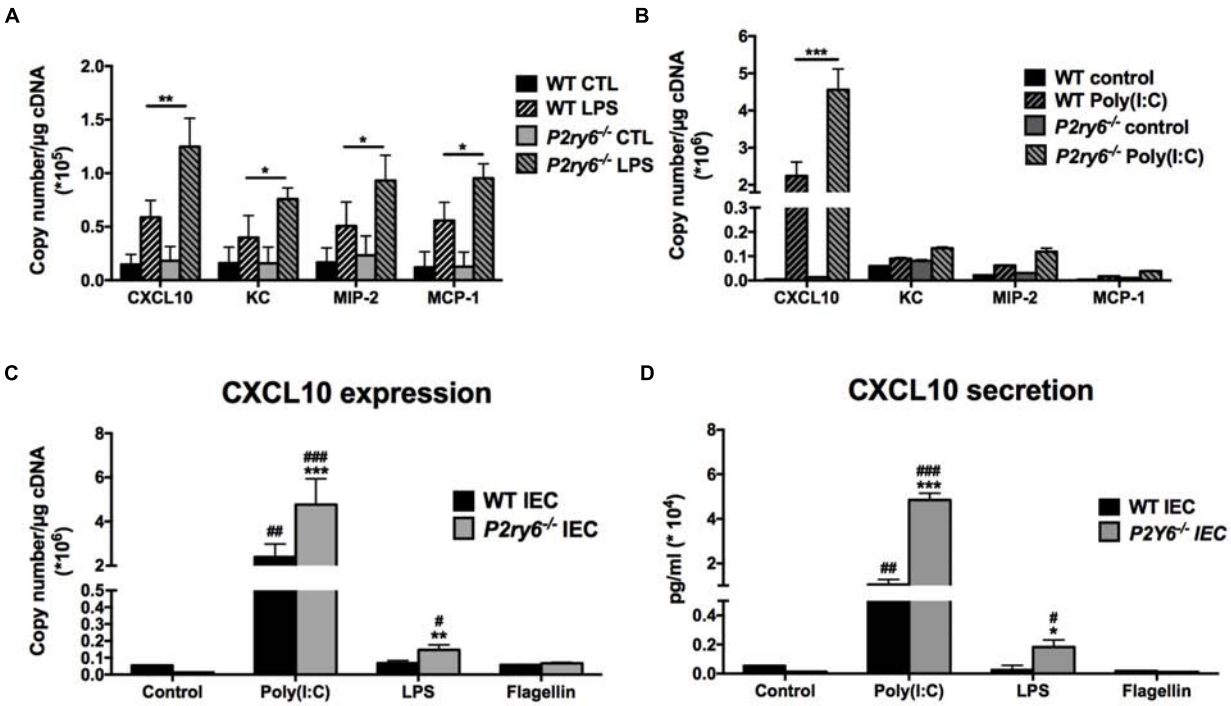

FIGURE 2 | CXCL10 expression and secretion are increased in primary *P2ry6*$^{-/-}$ IEC stimulated by a TLR3 ligand. **(A,B)** Primary IEC from WT or *P2ry6*$^{-/-}$ mice was stimulated with LPS (0.1 µg/ml) **(A)** or poly(I:C) (10 µg/ml) **(B)** for 5 h then the expression of CXCL10, KC, MIP-2, and MCP-1 was analyzed by qRT-PCR. **(C,D)** Quantification of CXCL10 expression by qRT-PCR (**C**) and secretion by ELISA (**D**) in WT and *P2ry6*$^{-/-}$ IEC stimulated with poly(I:C) (10 µg/ml), LPS (0.1 µg/ml), or flagellin (0.1 µg/ml) for 5 (qRT-PCR) or 24 h (ELISA), respectively. Data were normalized to GAPDH mRNA levels. Data presented are the mean ± SEM of five independent experiments for qRT-PCR and three independent experiments for ELISA, each with cells pooled from three mice. $^{***}p < 0.001$ compared to WT IEC. $^{\#\#}p < 0.01$, $^{\#\#\#}p < 0.01$, poly(I:C) stimulated IEC compared to non-stimulated IEC.

CXCL10 Expression and Secretion Are Augmented in *P2ry6*$^{-/-}$ IEC Stimulated by Poly(I:C)

We previously observed that the activation of $P2Y_6$ was necessary to trigger the secretion of CXCL8 from human monocytes stimulated with TLR-2 ligand (Ben Yebdri et al., 2009). Moreover, $P2Y_6$ activation increased CXCL8 secretion in the colonic tumor cell line Caco-2/15 (Grbic et al., 2008). Therefore, we hypothesized that in the absence of $P2Y_6$ in IEC, chemokine secretion would be decreased upon TLR stimulation.

Intestinal epithelial cells express several TLRs at varying levels (Graves et al., 2014). The most important TLR receptors expressed in IEC lines, and which can affect the immune response, are TLR3, TLR4, and TLR5 (Bambou et al., 2004; Graves et al., 2014). We first investigated whether these TLRs induce chemokine expression in primary murine WT IEC and in IEC deficient for the expression of $P2Y_6$. IECs were stimulated with the TLR agonists poly(I:C) (to activate TLR3), LPS (TLR4), and FLA-ST (TLR5). The expression of the chemokines KC, MIP-2, MCP-1, and CXCL10, known to be expressed by IEC in inflammatory conditions (Yang et al., 1997; Dwinell et al., 2001), was assessed by qRT-PCR.

The stimulation of primary IEC with LPS increased the expression of the four tested chemokines in both WT and *P2ry6*$^{-/-}$ cells. The expression of KC, MIP-2, MCP-1, and CXCL10 was significantly increased in *P2ry6*$^{-/-}$ IEC ($0.75 \times 10^5 \pm 0.05 \times 10^5$, $0.93 \times 10^5 \pm 0.2 \times 10^5$, $0.95 \times 10^5 \pm 0.1 \times 10^5$, and $1.3 \times 10^5 \pm 0.2 \times 10^5$ copies/µg of cDNA, respectively) when compared to WT IEC treated with LPS ($0.39 \times 10^5 \pm 0.15 \times 10^5$, $p < 0.05$; $0.5 \times 10^5 \pm 0.2 \times 10^5$, $p < 0.05$; $0.55 \times 10^5 \pm 0.18 \times 10^5$, $p < 0.05$, and $0.58 \times 10^5 \pm 0.1 \times 10^5$, $p < 0.01$, copies per µg of cDNA). CXCL10 was the highest chemokine expressed in both WT and *P2ry6*$^{-/-}$ IEC (**Figure 2A**). The TLR3 agonist poly(I:C) also induced the expression of CXCL10 but more strongly [40-fold more than with LPS: 45×10^5 and 1.3×10^5 copies/µg of cDNA for poly(I:C) and LPS stimulation, respectively) (**Figures 2A,B**). As for LPS, poly(I:C) induced an increased expression and secretion of CXCL10 more prominently in *P2ry6*$^{-/-}$ IEC than in WT IEC. The gene expression of CXCL10 was $4.5 \times 10^6 \pm 0.5 \times 10^6$ and $2.4 \times 10^6 \pm 0.4 \times 10^6$, $p < 0.001$, copies/µg of cDNA in *P2ry6*$^{-/-}$ IEC and WT IEC, respectively. These data correlated with CXCL10 secretion which were $5.3 \times 10^4 \pm 0.3 \times 10^4$ and $1.8 \times 10^4 \pm 0.2 \times 10^4$ pg/ml, $p < 0.001$, in the supernatant of *P2ry6*$^{-/-}$ IEC and WT IEC, respectively (**Figures 2B–D**). Stimulation with the purified flagellin FLA-ST showed low mRNA expression of the same chemokines (KC, MIP-2, and MCP-1) in both WT and

P2ry6$^{-/-}$ IEC (data not shown). We noted also low mRNA expression and protein secretion of CXCL10 in comparison with LPS and poly(I:C). The gene expression of CXCL10 was $0.08 \times 10^6 \pm 0.001 \times 10^6$ copies/μg of cDNA in both *P2ry6*$^{-/-}$ IEC and WT IEC while for CXCL10 secretion was 250 ± 10 pg/ml in the supernatant of both *P2ry6*$^{-/-}$ IEC and WT IEC (**Figures 2C,D**). These data show that murine primary IEC stimulated with the TLR-3 agonist poly(I:C) expressed high level of CXCL10 and that this production was more pronounced in the absence of $P2Y_6$ receptor.

Extracellular Nucleotides Are Involved in Poly(I:C)-Induced CXCL10 Release by IEC

In previous studies, we observed that the expression and secretion of the chemokine IL-8 induced by TLR2 and TLR4 activation required the concomitant activation of the nucleotide receptors $P2Y_2$ and $P2Y_6$ in human monocytes (Ben Yebdri et al., 2009). Therefore, we were not expecting that the expression of the chemokines tested here would be increased in *P2ry6*$^{-/-}$ IEC as we observed for the four chemokines tested (**Figure 2**).

We then investigated whether extracellular nucleotides and their receptors played a role in TLR3-induced CXCL10 expression and secretion in both WT and *P2ry6*$^{-/-}$ IEC. As seen in **Figure 3A**, IEC stimulated with poly(I:C), in the presence of the nucleotide scavenger apyrase or of the general P2 receptor antagonists suramin or RB-2, expressed much less CXCL10 mRNA level in both WT and *P2ry6*$^{-/-}$ IEC. For WT IEC, CXCL10 gene expression was reduced from $2.4 \times 10^6 \pm 0.7 \times 10^6$ to $0.81 \times 10^6 \pm 0.29 \times 10^6$, $p < 0.001$; to $0.88 \times 10^6 \pm 0.14 \times 10^6$, $p < 0.001$ or to $0.9 \times 10^6 \pm 0.15 \times 10^6$, $p < 0.001$, copies/μg of cDNA in the presence of apyrase, suramin, or RB-2, respectively. For *P2ry6*$^{-/-}$ IEC, CXCL10 gene expression was reduced from $5.0 \times 10^6 \pm 1.3 \times 10^6$ to $1.62 \times 10^6 \pm 0.002 \times 10^6$, $p < 0.001$; to $2.22 \times 10^6 \pm 0.001 \times 10^6$, $p < 0.001$ or to $1.33 \times 10^6 \pm 0.005 \times 10^6$, $p < 0.001$, copies/μg of cDNA in the presence of apyrase, suramin, or RB-2, respectively. Similar data were obtained at the protein level (**Figure 3B**). These data suggest that nucleotides participate in the regulation of TLR3-induced CXCL10 expression and secretion in IEC.

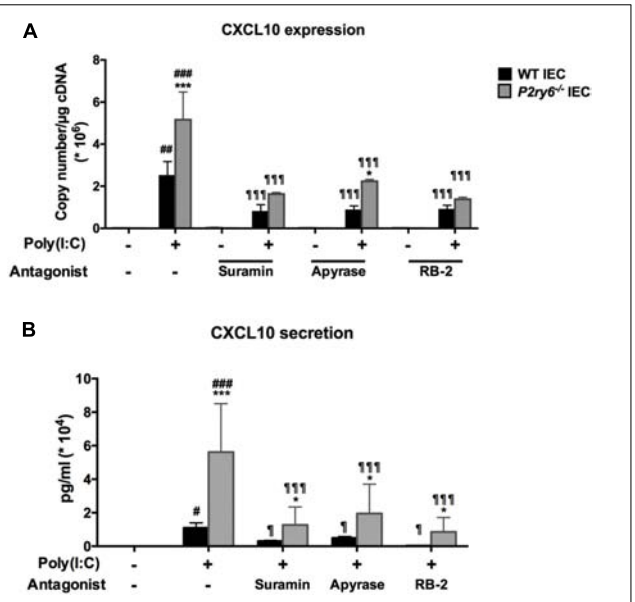

FIGURE 3 | The TLR3 ligand poly(I:C) induces CXCL10 expression and secretion from IEC in a nucleotide-dependent manner. IECs were stimulated with poly(I:C) (10 μg/ml) for 5 h for qRT-PCR, or 24 h for ELISA, in the presence of the P2 blockers suramin (0.1 mM), RB-2 (0.1 mM), or apyrase (2 U/ml) added 20 min before stimulation. The CXCL10 expression **(A)** and secretion **(B)** were measured by qRT-PCR and ELISA, respectively. For qRT-PCR, data were normalized to actin mRNA levels. Data presented are the mean ± SEM of three independent experiments, each with cells pooled from three mice. One symbol $p < 0.05$, two symbols $p < 0.01$, and three symbols $p < 0.001$. *, stimulated IEC from *P2ry6*$^{-/-}$ mice compared with WT; #, poly(I:C) stimulated IEC compared with non-stimulated IEC; and ¶, treated IEC in presence of inhibitors compared with poly(I:C) alone.

Supernatants from Poly(I:C)-Stimulated IEC Induce Macrophage Migration *in Vitro*

CXCL10 directs the chemotaxis of lymphocytes and macrophages. This can be observed *in vivo* when these cells migrate to an inflammatory site (Haemmerle et al., 2013; Zhao et al., 2017). We then questioned whether the supernatant of poly(I:C)-stimulated IEC, which contained significant amount of CXCL10 (**Figure 3B**), induced macrophage migration. Macrophage migration was assessed with a modified Boyden chamber system. The kinetics of cell migration presented in **Figure 4A** show that the supernatants of *P2ry6*$^{-/-}$ IEC stimulated with poly(I:C) recruited significantly more macrophages ($5.8 \times 10^5 \pm 0.3 \times 10^5$) than did the supernatants of poly(I:C)-stimulated WT IEC ($2.1 \times 10^5 \pm 0.1 \times 10^5$) (60 vs. 20% of the macrophages added to the upper chamber had migrated to the lower chamber, respectively). This observation is in agreement with the higher concentration of CXCL10 measured in these supernatants. Note that we cannot exclude that other components and chemokines present in supernatants could also be implicated in this macrophage chemotaxis.

Then, we tested whether the inhibition of nucleotide signaling in poly(I:C)-treated IEC by apyrase or general P2 antagonists would diminish the ability of these cell supernatants to attract macrophages to the lower chamber. As shown in **Figure 4B**, the supernatants of both WT and *P2ry6*$^{-/-}$ IEC stimulated with poly(I:C) in the presence of apyrase, suramin, or RB-2 recruited significantly fewer macrophages than did the supernatants of the cells stimulated in the absence of P2 blockers. Macrophage migration was reduced by about 94, 86, and 75% with supernatants from either WT or *P2ry6*$^{-/-}$ IEC stimulated with poly(I:C) in the presence of suramin, apyrase, or RB-2, respectively. For example, the supernatant of *P2ry6*$^{-/-}$ IEC stimulated with poly(I:C) alone induced the migration of $6.28 \times 10^5 \pm 0.28 \times 10^5$ macrophages which was reduced to $0.42 \times 10^5 \pm 0.57 \times 10^5$, $0.85 \times 10^5 \pm 0.14 \times 10^5$, or $1.42 \times 10^5 \pm 0.14 \times 10^5$ macrophages when the IECs

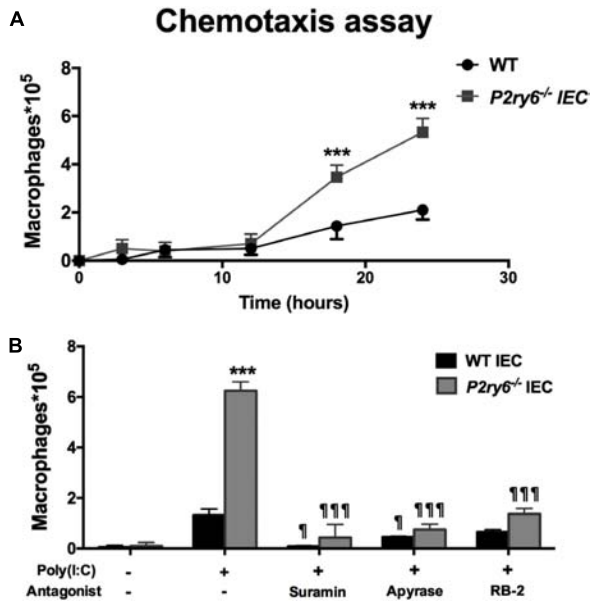

FIGURE 4 | Supernatants from poly(I:C) stimulated IEC induce macrophage migration in a nucleotide-dependant manner. **(A)** Time course of bone marrow macrophage chemotaxis in Boyden chambers. The supernatant from poly(I:C)-treated WT or *P2ry6*$^{-/-}$ *IEC* was added to the bottom chamber and 10^6 BMDMs were applied to the upper chamber and allowed to migrate for 24 h. The migrated macrophages to the bottom chamber were counted with a hemocytometer and the measurements were reported on the *Y*-axis. Data presented are the mean ± SEM of three independent experiments, each with cells pooled from two mice. **(B)** Different IEC monolayers were preincubated for 20 min with the indicated P2 blockers or apyrase, at the same concentration as in **Figure 3**, prior stimulation with poly(I:C) for 24 h. These supernatants were added to the bottom chamber and macrophage chemotaxis was carried out for 24 h. Data presented are the mean ± SEM of four independent experiments, each with cells pooled from two mice. One symbol $p < 0.05$; three symbols $p < 0.001$. *, stimulated IEC from *P2ry6*$^{-/-}$ mice compared with WT and ¶, treated IEC in the presence of inhibitors compared with poly(I:C) alone.

were stimulated in the presence of suramin, apyrase, or RB-2, respectively. The *p*-values corresponding to these data are significant and are presented in **Figure 4B**.

These data show that supernatant of IEC stimulated with poly(I:C) induced macrophage migration (**Figure 4**) which correlated with the amount of CXCL10 detected in the supernatant of poly(I:C)-stimulated IEC in the presence/absence of P2 blockers (**Figure 3B**).

Several P2 Receptors Are Involved in CXCL10 Expression and Secretion Induced by Poly(I:C) in *P2ry6*$^{-/-}$ IEC

We then tested the involvement of different P2 receptors in the responses described above in both *P2ry6*$^{-/-}$ and WT IEC. We first stimulated these cells with P1 and P2 receptor agonists. The natural ligand ATP, ADP, and UTP increased mRNA expression of CXCL10 in IEC from both, WT and *P2ry6*$^{-/-}$ mice. Again the increase of expression was more prominent in *P2ry6*$^{-/-}$ IEC (**Figure 5A**). The mRNA expression of CXCL10 was $13.0 \times 10^3 \pm 0.4 \times 10^3$ and $7.35 \times 10^3 \pm 0.58 \times 10^3$, $p < 0.01$, copies/μg of cDNA in *P2ry6*$^{-/-}$ and WT IEC, respectively, when stimulated with ATP. When IECs were stimulated with ADP, it was $14.7 \times 10^3 \pm 0.3 \times 10^3$ and $8.2 \times 10^3 \pm 1.2 \times 10^3$, $p < 0.01$, copies/μg of cDNA for *P2ry6*$^{-/-}$ and WT IEC, respectively. In addition, the specific agonist of $P2Y_1$ (MRS 2365) and of $P2Y_2$ (PSB1114) induced CXCL10 mRNA expression in *P2ry6*$^{-/-}$ IEC more prominently than in WT IEC ($16.2 \times 10^3 \pm 1.5 \times 10^3$ vs. $5.9 \times 10^3 \pm 0.9 \times 10^3$, $p < 0.001$, copies/μg of cDNA in the presence of MRS 2365 and $11.8 \times 10^3 \pm 0.3 \times 10^3$ vs. $6.2 \times 10^3 \pm 1.6 \times 10^3$, $p < 0.01$, copies/μg of cDNA in the presence of PSB1114. UDP, the specific agonist of $P2Y_6$, also induced CXCL10 expression in WT IEC ($8.5 \times 10^3 \pm 1.1 \times 10^3$ copies/μg of cDNA) compared to control IEC ($3.6 \times 10^3 \pm 0.1 \times 10^3$ copies/μg of cDNA) (**Figure 5A**), which suggest that $P2Y_6$ receptor plays a proinflammatory role in WT IEC. The *p*-value of UDP stimulation is significant and is presented in **Figure 5A**.

As expected, UDP did not induce any response in *P2ry6*$^{-/-}$ IEC confirming the specificity of the assay (**Figure 5A**). In contrast, adenosine failed to induce a response in IEC of both WT and *P2ry6*$^{-/-}$ mice (**Figure 5A**). Finally, **Figure 5B** shows that the CXCL10 protein level was in agreement with the level of expression detected in **Figure 5A**.

The candidate P2Y receptors expressed on IEC $P2Y_1$, $P2Y_2$, and $P2Y_6$ as well as P2X4 and A_{2A} were tested with specific antagonists. MRS 2500 and MRS 2179 were used to block $P2Y_1$, AR-C 118925XX to block $P2Y_2$, MRS 2578 for $P2Y_6$ receptor, 5-BDBD to prevent P2X4 activation, and Zm 241385 to block A_{2A} receptor. With the exception of the A_{2A} antagonist, all other selective and specific antagonists tested diminished CXCL10 mRNA expression in IEC upon stimulation with poly(I:C) (**Figure 5C**). For example, for *P2ry6*$^{-/-}$ IEC, CXCL10 mRNA expression decreased from $4.3 \times 10^6 \pm 0.8 \times 10^6$ copies/μg of cDNA in IEC stimulated only with poly(I:C) to $0.45 \times 10^6 \pm 0.08 \times 10^6$, $p < 0.001$; $0.54 \times 10^6 \pm 0.05 \times 10^6$, $p < 0.001$; or $0.18 \times 10^6 \pm 0.01 \times 10^6$, $p < 0.001$, copies/μg of cDNA in the presence of MRS 2179, AR-C, or BDBD, respectively. No significant differences were noted between the responses produced by WT and *P2ry6*$^{-/-}$ IEC in the presence of these antagonists except for $P2Y_1$ and $P2Y_6$ antagonists (**Figure 5C**). MRS 2578 did not affect significantly CXCL10 expression in *P2ry6*$^{-/-}$ IEC showing the specificity of the assay. The nucleotide receptor P2X2 was not tested due to the lack of specific antagonists commercially available. We therefore cannot exclude that this receptor might also have an effect in CXCL10 expression. The A_{2A} antagonist had no effect on CXCL10 expression in either WT or *P2ry6*$^{-/-}$ IEC (**Figure 5C**), which is in agreement with the absence of effect of adenosine on CXCL10 expression (**Figure 5A**). Similar data were obtained for all these antagonists at the protein level (**Figure 5D**).

These data suggest that several nucleotide receptors are involved in poly(I:C) stimulation and that these receptors are more stimulated in the absence of $P2Y_6$ receptor in *P2ry6*$^{-/-}$ *IEC*.

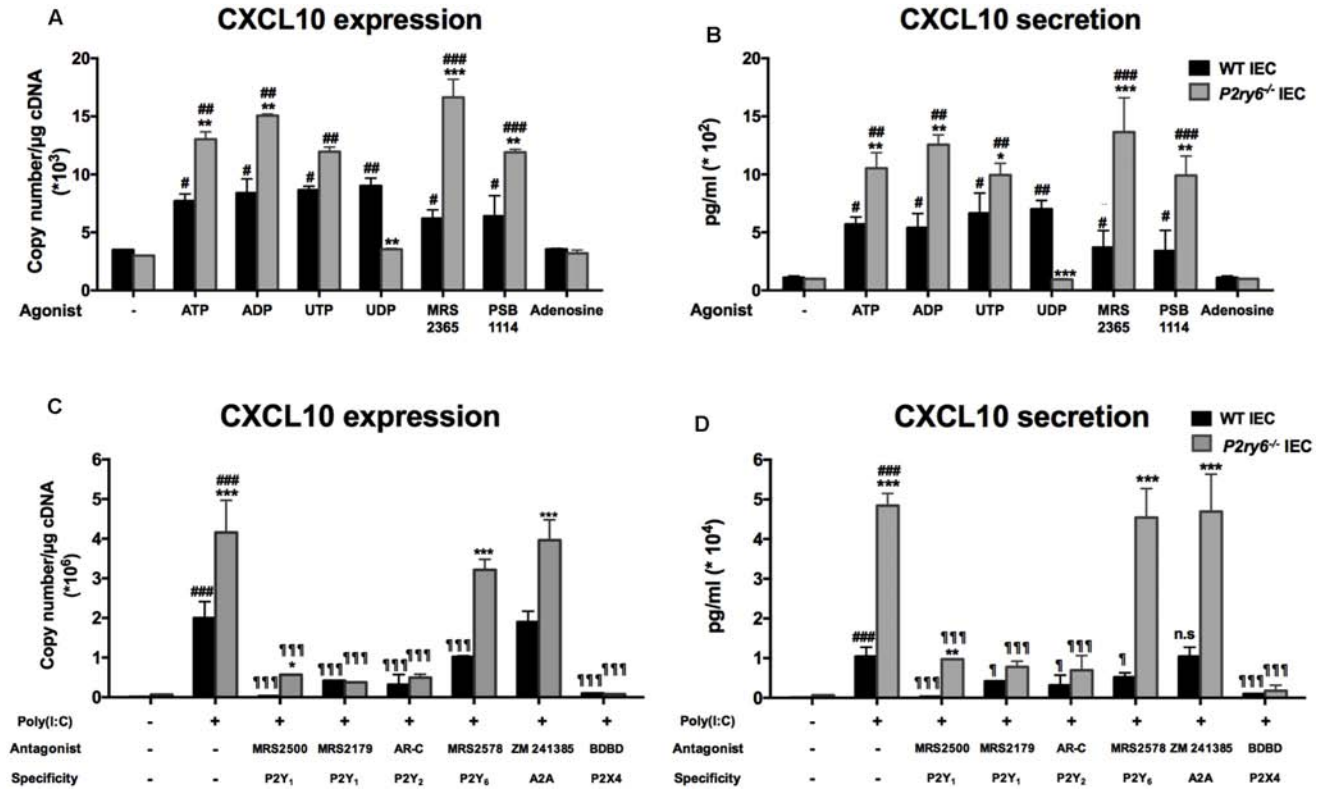

FIGURE 5 | $P2Y_6$ modulates nucleotide signaling-dependent CXCL10 expression and secretion from IEC. **(A,B)** IECs were stimulated either with nucleotides (ATP, ADP, UTP, or UDP) or adenosine (100 µM), or with specific agonist of $P2Y_1$ (MRS 2365; 1 µM) or $P2Y_2$ (PSB 114; 0.5 µM) receptors. Five or 24 h later the expression **(A)** or the secretion **(B)** of CXCL10 was evaluated by qRT-PCR and ELISA, respectively. **(C,D)** IECs were treated with poly(I:C) in the absence or presence of P receptor antagonists then CXCL10 expression **(C)** and secretion **(D)** were evaluated by qRT-PCR (5 h after the beginning of stimulation) and ELISA (24 h later), respectively. The antagonists used were MRS 2500 (5 µM) or MRS 2179 (0.15 µM) for $P2Y_1$, AR-C 118925XX (2 µM) for $P2Y_2$, MRS 2578 (1 µM) for $P2Y_6$, or BDBD (100 µM) for P2X4, and Zm 241385 (10 nM) for A_{2A} receptor. Data are normalized to actin mRNA levels. Data presented are the mean ± SEM of five independent experiments for qRT-PCR and of three independent experiments for ELISA, each with cells pooled from three mice. One symbol $p < 0.05$; two symbols $p < 0.01$; three symbols $p < 0.001$. *, stimulated IEC from *P2ry6*$^{-/-}$ mice compared with WT; #, poly(I:C) stimulated IEC compared with non-stimulated IEC; ¶, treated IEC in the presence of antagonists compared with poly(I:C) alone.

FGF2 Signaling Pathway Is Upregulated in *P2ry6*$^{-/-}$ IEC

Given that there is no difference in the expression of P2 receptors and ectonucleotidases in WT and *P2ry6*$^{-/-}$ *IEC*, we questioned whether the "primed" stimulation in *P2ry6*$^{-/-}$ *IEC* was specific for nucleotide signaling or if it was also affecting other pathways not dependant on nucleotides. FGF2 stimulation for 6 h is known to induce the secretion of MMP-9 from mouse primary IECs (Song et al., 2015). While the stimulation of WT mouse IEC with FGF2 induced the expected gene expression of MMP-9 ($0.67 \times 10^4 \pm 0.02 \times 10^4$, $p < 0.05$, copies/µg of cDNA), this response was significantly increased in *P2ry6*$^{-/-}$ *IEC* ($1.58 \times 10^4 \pm 0.07 \times 10^4$, $p < 0.01$, copies/µg of cDNA) (**Figure 6**).

DISCUSSION

In this study, we provide evidence that extracellular nucleotides regulate chemokine expression and secretion in primary IEC from mouse. We found that $P2Y_6$ was the major nucleotide receptor expressed by primary IEC. We noted also the expression of $P2Y_1$, $P2Y_2$, P2X2, P2X4, and of the adenosine receptor A_{2A} in IEC. Previous studies also showed the presence of $P2Y_6$ in Caco2/15 and IEC-6, which are human and rat intestinal cell lines, respectively (Grbic et al., 2008; Nakamura et al., 2013).

We next investigated the role of nucleotides in chemokine secretion by IEC and the implication of $P2Y_6$ in this function. The activation of $P2Y_6$ receptor with its specific agonist UDP led to a significant increase of CXCL10 expression and secretion in WT IEC. These data are in line with other studies which showed that $P2Y_6$ had proinflammatory functions such as the induction of expression and secretion of proinflammatory cytokines and chemokines (Grbic et al., 2008; Ben Yebdri et al., 2009; Hao et al., 2014).

For the following studies, we purified primary IEC from *P2ry6*$^{-/-}$ mice to verify whether these cells could still release CXCL10 in the absence of $P2Y_6$. To mimic inflammatory conditions, we used TLR activation as stimuli as mounting evidences suggest that their activation is often, if not always,

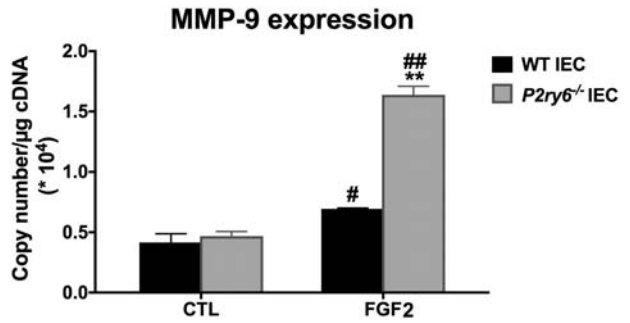

FIGURE 6 | MMP9 gene expression induced by FGF2 is increased in *P2ry6*$^{-/-}$ IEC. MMP-9 mRNA level in IEC stimulated with FGF2 (10 ng/ml) for 6 h was analyzed by qRT-PCR. Data were normalized to GAPDH mRNA levels. Data presented are the mean ± SEM of three independent experiments, each with cells pooled from three mice. One symbol $p < 0.05$; two symbols $p < 0.01$. *, stimulated IEC from *P2ry6*$^{-/-}$ mice compared with WT; #, FGF2 stimulated IEC compared with non-stimulated IEC.

associated with the release of nucleotides from affected cells (Yin et al., 2007; Ben Yebdri et al., 2009; Kukulski et al., 2010; Ivison et al., 2011). This process is important as extracellular nucleotides, by activating P2 receptors, have been shown to be necessary for the optimal proinflammatory effects induced by TLR activation. In this study, we found that TLR3 and TLR4 stimulation led to an up-regulation of CXCL10 expression from IEC. The other chemokines tested, KC, MIP-2, and MCP-1, also followed this tendency with an expression level much lower than that of CXCL10. The group of Proost et al. (2003) has reported an increased expression of CXCL10 in fibroblasts and peripheral blood mononuclear cells upon stimulation by TLR3 ligand and IFN-gamma.

The TLR3 stimulation with poly(I:C) led to high CXCL10 secretion from IEC of both genotypes (WT and *P2ry6*$^{-/-}$). The inhibition of this response by general P2 blockers suggests that nucleotides are implicated in these responses. We then further studied the implication of nucleotide signaling in this process. First, the activation of each P2 receptor expressed by IEC, but not P1 receptor, resulted in a significant increase of CXCL10 expression and secretion. CXCL10 expression and secretion induced by a TLR3 agonist were decreased in the presence of the general P2 receptor antagonists suramin and RB-2, and also by the nucleotide scavenger apyrase in both WT and *P2ry6*$^{-/-}$ IEC (**Figure 3**). In all the experiments above, the level of CXCL10 measured correlated with the level of macrophage chemotaxis reported in **Figure 4**.

These data suggest that nucleotides play a key role in inducing chemokine expression and secretion by IEC under PAMP stimulation and that several P2 receptors are involved in this response. In agreement with these results, we and others have shown that extracellular nucleotides are implicated in chemokine expression and cell migration. In addition, Kukulski et al. (2010) showed that nucleotides and P2 receptors were required for IL-8 to induce neutrophil migration. In agreement with the above observations, nucleotide hydrolysis by ectoenzymes controlled IL-8 production in the colonic human cell line HT-29 (Bahrami et al., 2014). In addition to these observations, Ivison et al. (2011) demonstrated that ATP regulated the inflammatory response to flagellin via TLR5 activation in immortalized human IEC.

One surprising observation presented in this paper was that IEC that do not express $P2Y_6$ induced greater levels of chemokines expression in response to TLR agonists, suggesting that the presence of $P2Y_6$ negatively regulates the reactivity of other receptors at the surface of IEC. Indeed, we observed that in the absence of $P2Y_6$, other P2 receptors expressed on IEC such as $P2Y_1$ and $P2Y_2$ induced a stronger response than what was measured in WT IEC that express $P2Y_6$ normally. It is noteworthy to mention that genes of all nucleotide receptors were expressed at similar levels in both WT and *P2ry6*$^{-/-}$ IEC excluding a compensatory mechanism involving a greater expression of another P2 receptor in *P2ry6*$^{-/-}$ IEC. It is noteworthy that the pharmacological inhibition of $P2Y_6$ activation in WT IEC did not reproduce the stimulatory effect of *p2ry6* gene deletion on the expression and secretion of CXCL10. The $P2Y_6$ antagonist reduced the poly(I:C)-stimulated expression and secretion of CXCL10. Pharmacological inhibition and gene targeting differ in that, while the MRS 2578 effect is punctual, that of gene deletion is permanent. It is possible that despite the fact that *P2ry6*$^{-/-}$ and WT IEC are equally differentiated, *P2ry6*$^{-/-}$ IEC respond more vigorously to stimulation because $P2Y_6$ receptors regulate the expression of the component of TLR3 signaling pathway. The examination of this hypothesis is beyond the scope of the present study and will be investigated subsequently.

As the activation of several P2 receptors seemed to be regulated by the presence of $P2Y_6$, we questioned whether this effect also affected pathways independent of nucleotide signaling. Indeed, FGF2 stimulation induced a greater gene expression of MMP-9 in *P2ry6*$^{-/-}$ IEC than in WT IEC (**Figure 6**). Altogether, these data suggest that the presence of $P2Y_6$ regulates the activation of multiple receptors at the surface of IEC in a general manner which may affect the homeostasis of the cells.

Another explanation could be that $P2Y_6$ triggers not only a signaling pathway which controlled positively chemokine production but also a negative loop to prevent overstimulation of the cells. The interaction between intracellular signaling of P2X and P2Y receptors has already been observed in several cell types (Erb and Weisman, 2012). For example, crosstalk between P2 receptors has previously been reported by Bernier et al. (2013) who showed that P2X4 activation is controlled by $P2Y_6$ in microglia possibly through depletion of membrane phosphoinositide resulting from phospholipase C activation by $P2Y_6$. In a human osteoblast cell line (Jorgensen et al., 1997), Ihara et al. (2005) observed that the activation of P2X4, P2X5, and P2X6 with ATP resulted in IL-6 secretion and that this response was inhibited by the antagonist of P2Y receptors. Activation of human $P2Y_1$ and $P2Y_2$ receptors has been shown to potentiate subsequent function-mediated Ca^{2+} signaling which is related to P2X function (Bowler et al., 1999).

As mentioned above, we also observed that CXCL10 expression was decreased in the presence of P2X4, $P2Y_1$, and $P2Y_2$ antagonists in both WT and *P2ry6*$^{-/-}$ IEC. The blockade of an important part of the response by an antagonist of a

single-nucleotide receptor may suggest a complex function of nucleotides in cytokine expression in IEC. The fact that these receptors are coupled to different pathways may partly explain this observation. $P2Y_1$ is coupled to G_q protein, $P2Y_2$ is coupled to G_0, $P2Y_6$ to $Gq/_{11}$ (Okada et al., 2002; Ando et al., 2010; Harden et al., 2010; Ishida et al., 2013) while P2X4 is a ligand-gated ion channel (North, 2002). The co-stimulation of different nucleotide receptors to get a function has been well documented in platelets which express $P2Y_1$, $P2Y_{12}$, and P2X1 receptors (Daniel et al., 1998; Jin et al., 1998). The co-stimulation of $P2Y_1$ and $P2Y_{12}$ by the same agonist ADP is necessary to induce platelet activation. While $P2Y_1$ is coupled to phospholipase C, $P2Y_{12}$ is linked with the inhibition of adenylyl cyclase. If one of these two pathways is blocked, there will be no platelet activation (Jin and Kunapuli, 1998).

It is noteworthy that a cross talk between P2Y receptors and P2X receptor ion channels has also been noted in *Xenopus* oocytes. In these cells, P2X1 receptor activated by ATP led to a transient inward current that is rapidly desensitized by ATP itself (Rettinger and Schmalzing, 2003). Interestingly, the co-expression and co-activation of either $P2Y_1$ or $P2Y_2$ inhibit P2X1 receptor desensitization. The mechanism of P2Y receptor-mediated inhibition of P2X1 receptor desensitization does not appear to involve direct phosphorylation of the P2X1 receptor but does involve protein kinase activity, perhaps mediated by an accessory protein (Jones et al., 2014). Although these mechanisms cannot be shared completely with the data presented here in IEC, it still shows that nucleotide signaling is complex and that several nucleotide receptors may often be needed to control specific effects.

CONCLUSION

The data presented in this study support the view that nucleotide signaling can contribute to leukocyte recruitment to the intestinal epithelium via CXCL10 secretion by IEC. This mechanism involves $P2Y_6$. The results presented here also show that $P2Y_1$, $P2Y_2$, and P2X4 also regulate CXCL10 secretion in these cells, especially in the absence of $P2Y_6$. Indeed, in $P2ry6^{-/-}$ IEC, activation of nucleotide receptors induced a stronger expression and secretion of the chemokine CXCL10 when compared to WT IEC. The $P2ry6^{-/-}$ IEC also responded more vigorously to a non-nucleotide receptor as demonstrated with FGF2 that induced a stronger expression of MMP9 gene in the $P2ry6^{-/-}$ IEC. Therefore, $P2Y_6$ receptors may not only induce effects such as chemokine release but may also act as a regulator of IEC homeostasis by preventing these cells to over react to various stimuli.

AUTHOR CONTRIBUTIONS

MS conceived the proposal study design, performed all the experiments, analyzed the data, and wrote the first draft of the manuscript. AT helped MS to perform epithelial cell culture and qRT-PCR experiments. JP took care of mice reproduction. BR provided $P2Y_6$-deficient mice and helped with the analysis of the data and with manuscript writing. JS supervised the study.

FUNDING

This work was supported by grants to JS from the Canadian Institutes of Health Research (CIHR; MOP-102472 and MOP-93683) and from the *Fondation du CHU de Québec*. MS was a recipient of a scholarship from the *Fonds de Recherche du Québec-Santé* (FRQS) and JS of a "Chercheur National" Scholarship award from the FRQS.

ACKNOWLEDGMENTS

We thank Dr. Paul Naccache from the CRCHU de Québec – Université Laval (QC, Canada) for his help with the writing of the manuscript and for helpful discussions.

REFERENCES

Abbracchio, M. P., Burnstock, G., Boeynaems, J. M., Barnard, E. A., Boyer, J. L., Kennedy, C., et al. (2006). International Union of Pharmacology LVIII: update on the P2Y G protein-coupled nucleotide receptors: from molecular mechanisms and pathophysiology to therapy. *Pharmacol. Rev.* 58, 281–341. doi: 10.1124/pr.58.3.3

Ando, R. D., Mehesz, B., Gyires, K., Illes, P., and Sperlagh, B. (2010). A comparative analysis of the activity of ligands acting at P2X and P2Y receptor subtypes in models of neuropathic, acute and inflammatory pain. *Br. J. Pharmacol.* 159, 1106–1117. doi: 10.1111/j.1476-5381.2009.00596.x

Artis, D. (2008). Epithelial-cell recognition of commensal bacteria and maintenance of immune homeostasis in the gut. *Nat. Rev. Immunol.* 8, 411–420. doi: 10.1038/nri2316

Bahrami, F., Kukulski, F., Lecka, J., Tremblay, A., Pelletier, J., Rockenbach, L., et al. (2014). Purine-metabolizing ectoenzymes control IL-8 production in human colon HT-29 cells. *Mediators Inflamm.* 2014:879895. doi: 10.1155/2014/879895

Bambou, J. C., Giraud, A., Menard, S., Begue, B., Rakotobe, S., Heyman, M., et al. (2004). *In vitro* and *ex vivo* activation of the TLR5 signaling pathway in intestinal epithelial cells by a commensal *Escherichia coli* strain. *J. Biol. Chem.* 279, 42984–42992. doi: 10.1074/jbc.M405410200

Bar, I., Guns, P. J., Metallo, J., Cammarata, D., Wilkin, F., Boeynams, J. M., et al. (2008). Knockout mice reveal a role for P2Y6 receptor in macrophages, endothelial cells, and vascular smooth muscle cells. *Mol. Pharmacol.* 74, 777–784. doi: 10.1124/mol.108.046904

Ben Yebdri, F., Kukulski, F., Tremblay, A., and Sevigny, J. (2009). Concomitant activation of P2Y(2) and P2Y(6) receptors on monocytes is required for TLR1/2-induced neutrophil migration by regulating IL-8 secretion. *Eur. J. Immunol.* 39, 2885–2894. doi: 10.1002/eji.200939347

Bernier, L. P., Ase, A. R., Boue-Grabot, E., and Seguela, P. (2013). Inhibition of P2X4 function by P2Y6 UDP receptors in microglia. *Glia* 61, 2038–2049. doi: 10.1002/glia.22574

Bondar, C., Araya, R. E., Guzman, L., Rua, E. C., Chopita, N., and Chirdo, F. G. (2014). Role of Cxcr3/Cxcl10 axis in immune cell recruitment into the small intestine in celiac disease. *PLoS One* 9:e89068. doi: 10.1371/journal.pone.0089068

Bowler, W. B., Dixon, C. J., Halleux, C., Maier, R., Bilbe, G., Fraser, W. D., et al. (1999). Signaling in human osteoblasts by extracellular nucleotides. Their weak induction of the c-fos proto-oncogene via Ca2+ mobilization is strongly potentiated by a parathyroid hormone/camp-dependent protein kinase pathway independently of mitogen-activated protein kinase. *J. Biol. Chem.* 274, 14315–14324. doi: 10.1074/jbc.274.20.14315

Braunstein, G. M., Roman, R. M., Clancy, J. P., Kudlow, B. A., Taylor, A. L., Shylonsky, V. G., et al. (2001). Cystic fibrosis transmembrane conductance regulator facilitates ATP release by stimulating a separate ATP release channel for autocrine control of cell volume regulation. *J. Biol. Chem.* 276, 6621–6630. doi: 10.1074/jbc.M005893200

Cho, H. J., Jung, J. I., Lim, D. Y., Kwon, G. T., Her, S., Park, J. H., et al. (2012). Bone marrow-derived, alternatively activated macrophages enhance solid tumor growth and lung metastasis of mammary carcinoma cells in a Balb/C mouse orthotopic model. *Breast Cancer Res.* 14:R81. doi: 10.1186/bcr3195

Daniel, J. L., Dangelmaier, C., Jin, J., Ashby, B., Smith, J. B., and Kunapuli, S. P. (1998). Molecular basis for ADP-induced platelet activation. I. Evidence for three distinct ADP receptors on human platelets. *J. Biol. Chem.* 273, 2024–2029. doi: 10.1074/jbc.273.4.2024

Dwinell, M. B., Lugering, N., Eckmann, L., and Kagnoff, M. F. (2001). Regulated production of interferon-inducible T-cell chemoattractants by human intestinal epithelial cells. *Gastroenterology* 120, 49–59. doi: 10.1053/gast.2001.20914

Erb, L., and Weisman, G. A. (2012). Coupling of P2Y receptors to G proteins and other signaling pathways. *Wiley Interdiscip. Rev. Membr. Transp. Signal.* 1, 789–803. doi: 10.1002/wmts.62

Fritz, J. H., Ferrero, R. L., Philpott, D. J., and Girardin, S. E. (2006). Nod-like proteins in immunity, inflammation and disease. *Nat. Immunol.* 7, 1250–1257. doi: 10.1038/ni1412

Graves, C. L., Harden, S. W., Lapato, M., Nelson, M., Amador, B., Sorenson, H., et al. (2014). A method for high purity intestinal epithelial cell culture from adult human and murine tissues for the investigation of innate immune function. *J. Immunol. Methods* 414, 20–31. doi: 10.1016/j.jim.2014.08.002

Grbic, D. M., Degagne, E., Langlois, C., Dupuis, A. A., and Gendron, F. P. (2008). Intestinal inflammation increases the expression of the P2Y6 receptor on epithelial cells and the release of CXC chemokine ligand 8 by UDP. *J. Immunol.* 180, 2659–2668. doi: 10.4049/jimmunol.180.4.2659

Haemmerle, M., Keller, T., Egger, G., Schachner, H., Steiner, C. W., Stokic, D., et al. (2013). Enhanced lymph vessel density, remodeling, and inflammation are reflected by gene expression signatures in dermal lymphatic endothelial cells in type 2 diabetes. *Diabetes Metab. Res. Rev.* 62, 2509–2529. doi: 10.2337/db12-0844

Hao, Y., Liang, J. F., Chow, A. W., Cheung, W. T., and Ko, W. H. (2014). P2Y6 receptor-mediated proinflammatory signaling in human bronchial epithelia. *PLoS One* 9:e106235. doi: 10.1371/journal.pone.0106235

Harden, T. K., Sesma, J. I., Fricks, I. P., and Lazarowski, E. R. (2010). Signalling and pharmacological properties of the P2Y receptor. *Acta Physiol.* 199, 149–160. doi: 10.1111/j.1748-1716.2010.02116.x

Hazama, A., Shimizu, T., Ando-Akatsuka, Y., Hayashi, S., Tanaka, S., Maeno, E., et al. (1999). Swelling-induced, CFTR-independent ATP release from a human epithelial cell line: lack of correlation with volume-sensitive cl(-) channels. *J. Gen. Physiol.* 114, 525–533. doi: 10.1085/jgp.114.4.525

Ihara, H., Hirukawa, K., Goto, S., and Togari, A. (2005). ATP-stimulated interleukin-6 synthesis through P2Y receptors on human osteoblasts. *Biochem. Biophys. Res. Commun.* 326, 329–334. doi: 10.1016/j.bbrc.2004.11.037

Ishida, K., Matsumoto, T., Taguchi, K., Kamata, K., and Kobayashi, T. (2013). Mechanisms underlying reduced P2Y(1) -receptor-mediated relaxation in superior mesenteric arteries from long-term streptozotocin-induced diabetic rats. *Acta Physiol.* 207, 130–141. doi: 10.1111/j.1748-1716.2012.02469.x

Ivison, S. M., Himmel, M. E., Mayer, M., Yao, Y., Kifayet, A., Levings, M. K., et al. (2011). The stress signal extracellular ATP modulates antiflagellin immune responses in intestinal epithelial cells. *Inflamm. Bowel Dis.* 17, 319–333. doi: 10.1002/ibd.21428

Jin, J., Daniel, J. L., and Kunapuli, S. P. (1998). Molecular basis for ADP-induced platelet activation. II. The P2Y1 receptor mediates ADP-induced intracellular calcium mobilization and shape change in platelets. *J. Biol. Chem.* 273, 2030–2034. doi: 10.1074/jbc.273.4.2030

Jin, J., and Kunapuli, S. P. (1998). Coactivation of two different G protein-coupled receptors is essential for ADP-induced platelet aggregation. *Proc. Natl. Acad. Sci. U.S.A.* 95, 8070–8074. doi: 10.1073/pnas.95.14.8070

Jones, S., Evans, R. J., and Mahaut-Smith, M. P. (2014). Ca2+ influx through P2X1 receptors amplifies P2Y1 receptor-evoked Ca2+ signaling and ADP-evoked platelet aggregation. *Mol. Pharmacol.* 86, 243–251. doi: 10.1124/mol.114.092528

Jorgensen, N. R., Geist, S. T., Civitelli, R., and Steinberg, T. H. (1997). ATP- and gap junction-dependent intercellular calcium signaling in osteoblastic cells. *J. Cell Biol.* 139, 497–506. doi: 10.1083/jcb.139.2.497

Jung, H. C., Eckmann, L., Yang, S. K., Panja, A., Fierer, J., Morzycka-Wroblewska, E., et al. (1995). A distinct array of proinflammatory cytokines is expressed in human colon epithelial cells in response to bacterial invasion. *J. Clin. Invest.* 95, 55–65. doi: 10.1172/JCI117676

Kauffenstein, G., Furstenau, C. R., D'orleans-Juste, P., and Sevigny, J. (2010). The ecto-nucleotidase Ntpdase1 differentially regulates P2Y1 and P2Y2 receptor-dependent vasorelaxation. *Br. J. Pharmacol.* 159, 576–585. doi: 10.1111/j.1476-5381.2009.00566.x

Kim, B., Jeong, H. K., Kim, J. H., Lee, S. Y., Jou, I., and Joe, E. H. (2011). Uridine 5'-diphosphate induces chemokine expression in microglia and astrocytes through activation of the P2Y6 receptor. *J. Immunol.* 186, 3701–3709. doi: 10.4049/jimmunol.1000212

Kukulski, F., Ben Yebdri, F., Bahrami, F., Fausther, M., Tremblay, A., and Sevigny, J. (2010). Endothelial P2Y2 receptor regulates LPS-induced neutrophil transendothelial migration in vitro. *Mol. Immunol.* 47, 991–999. doi: 10.1016/j.molimm.2009.11.020

Kukulski, F., Ben Yebdri, F., Lefebvre, J., Warny, M., Tessier, P. A., and Sevigny, J. (2007). Extracellular nucleotides mediate LPS-induced neutrophil migration in vitro and in vivo. *J. Leukoc. Biol.* 81, 1269–1275. doi: 10.1189/jlb.1206758

Kukulski, F., Levesque, S. A., and Sevigny, J. (2011). Impact of ectoenzymes on p2 and p1 receptor signaling. *Adv. Pharmacol.* 61, 263–299. doi: 10.1016/B978-0-12-385526-8.00009-6

Laragione, T., Brenner, M., Sherry, B., and Gulko, P. S. (2011). Cxcl10 and its receptor Cxcr3 regulate synovial fibroblast invasion in rheumatoid arthritis. *Arthritis Rheum.* 63, 3274–3283. doi: 10.1002/art.30573

Lazarowski, E. R., Boucher, R. C., and Harden, T. K. (2003). Mechanisms of release of nucleotides and integration of their action as P2X- and P2Y-receptor activating molecules. *Mol. Pharmacol.* 64, 785–795. doi: 10.1124/mol.64.4.785

Medzhitov, R. (2007). TLR-mediated innate immune recognition. *Semin. Immunol.* 19, 1–2. doi: 10.1016/j.smim.2007.02.001

Moon, C., Vandussen, K. L., Miyoshi, H., and Stappenbeck, T. S. (2014). Development of a primary mouse intestinal epithelial cell monolayer culture system to evaluate factors that modulate IgA transcytosis. *Mucosal Immunol.* 7, 818–828. doi: 10.1038/mi.2013.98

Nakamura, T., Murata, T., Hori, M., and Ozaki, H. (2013). UDP induces intestinal epithelial migration via the P2Y6 receptor. *Br. J. Pharmacol.* 170, 883–892. doi: 10.1111/bph.12334

North, R. A. (2002). Molecular physiology of P2X receptors. *Physiol. Rev.* 82, 1013–1067. doi: 10.1152/physrev.00015.2002

Okada, M., Nakagawa, T., Minami, M., and Satoh, M. (2002). Analgesic effects of intrathecal administration of P2Y nucleotide receptor agonists UTP and UDP in normal and neuropathic pain model rats. *J. Pharmacol. Exp. Ther.* 303, 66–73. doi: 10.1124/jpet.102.036079

Ostvik, A. E., Granlund, A. V., Bugge, M., Nilsen, N. J., Torp, S. H., Waldum, H. L., et al. (2013). Enhanced expression of Cxcl10 in inflammatory bowel disease: potential role of mucosal Toll-like receptor 3 stimulation. *Inflamm. Bowel Dis.* 19, 265–274. doi: 10.1002/ibd.23034

Petrovic-Djergovic, D., Popovic, M., Chittiprol, S., Cortado, H., Ransom, R. F., and Partida-Sanchez, S. (2015). Cxcl10 induces the recruitment of monocyte-derived macrophages into kidney, which aggravate puromycin aminonucleoside nephrosis. *Clin. Exp. Immunol.* 180, 305–315. doi: 10.1111/cei.12579

Proost, P., Vynckier, A. K., Mahieu, F., Put, W., Grillet, B., Struyf, S., et al. (2003). Microbial Toll-like receptor ligands differentially regulate Cxcl10/IP-10 expression in fibroblasts and mononuclear leukocytes in synergy with IFN-gamma and provide a mechanism for enhanced synovial chemokine levels in septic arthritis. *Eur. J. Immunol.* 33, 3146–3153. doi: 10.1002/eji.200324136

Qureshi, S., and Medzhitov, R. (2003). Toll-like receptors and their role in experimental models of microbial infection. *Genes Immun.* 4, 87–94. doi: 10.1038/sj.gene.6363937

Rettinger, J., and Schmalzing, G. (2003). Activation and desensitization of the recombinant P2X1 receptor at nanomolar ATP concentrations. *J. Gen. Physiol.* 121, 451–461. doi: 10.1085/jgp.200208730

Singh, U. P., Singh, N. P., Murphy, E. A., Price, R. L., Fayad, R., Nagarkatti, M., et al. (2016). Chemokine and cytokine levels in inflammatory bowel disease patients. *Cytokine* 77, 44–49. doi: 10.1016/j.cyto.2015.10.008

Song, X., Dai, D., He, X., Zhu, S., Yao, Y., Gao, H., et al. (2015). Growth factor FGF2 cooperates with interleukin-17 to repair intestinal epithelial damage. *Immunity* 43, 488–501. doi: 10.1016/j.immuni.2015.06.024

Suzuki, K., Kawauchi, Y., Palaniyandi, S. S., Veeraveedu, P. T., Fujii, M., Yamagiwa, S., et al. (2007). Blockade of interferon-gamma-inducible protein-10 attenuates chronic experimental colitis by blocking cellular trafficking and protecting intestinal epithelial cells. *Pathol. Int.* 57, 413–420. doi: 10.1111/j.1440-1827.2007.02117.x

Tomita, K., Freeman, B. L., Bronk, S. F., Lebrasseur, N. K., White, T. A., Hirsova, P., et al. (2016). Cxcl10-mediates macrophage, but not other innate immune cells-associated inflammation in murine nonalcoholic steatohepatitis. *Sci. Rep.* 6:28786. doi: 10.1038/srep28786

Uguccioni, M., Gionchetti, P., Robbiani, D. F., Rizzello, F., Peruzzo, S., Campieri, M., et al. (1999). Increased expression of IP-10, IL-8, MCP-1, and MCP-3 in ulcerative colitis. *Am. J. Pathol.* 155, 331–336. doi: 10.1016/S0002-9440(10)65128-0

Unver, N., Esendagli, G., Yilmaz, G., and Guc, D. (2015). Cxcl7-induced macrophage infiltration in lung tumor is independent of Cxcr2 expression: Cxcl7-induced macrophage chemotaxis in LLC tumors. *Cytokine* 75, 330–337. doi: 10.1016/j.cyto.2015.07.018

Vereyken, E. J., Heijnen, P. D., Baron, W., De Vries, E. H., Dijkstra, C. D., and Teunissen, C. E. (2011). Classically and alternatively activated bone marrow derived macrophages differ in cytoskeletal functions and migration towards specific CNS cell types. *J. Neuroinflammation* 8:58. doi: 10.1186/1742-2094-8-58

Vitiello, L., Gorini, S., Rosano, G., and La Sala, A. (2012). Immunoregulation through extracellular nucleotides. *Blood* 120, 511–518. doi: 10.1182/blood-2012-01-406496

Warny, M., Aboudola, S., Robson, S. C., Sevigny, J., Communi, D., Soltoff, S. P., et al. (2001). P2Y(6) nucleotide receptor mediates monocyte interleukin-8 production in response to UDP or lipopolysaccharide. *J. Biol. Chem.* 276, 26051–26056. doi: 10.1074/jbc.M102568200

Yang, S. K., Eckmann, L., Panja, A., and Kagnoff, M. F. (1997). Differential and regulated expression of C-X-C, C-C, and C-chemokines by human colon epithelial cells. *Gastroenterology* 113, 1214–1223. doi: 10.1053/gast.1997.v113.pm9322516

Yin, J., Xu, K., Zhang, J., Kumar, A., and Yu, F. S. (2007). Wound-induced ATP release and EGF receptor activation in epithelial cells. *J. Cell Sci.* 120, 815–825. doi: 10.1242/jcs.03389

Zhao, Q., Kim, T., Pang, J., Sun, W., Yang, X., Wang, J., et al. (2017). A novel function of cxcl10 in mediating monocyte production of proinflammatory cytokines. *J. Leukoc. Biol.* 102, 1271–1280. doi: 10.1189/jlb.5A0717-302

Conflict of Interest Statement: The authors declare that the research was conducted in the absence of any commercial or financial relationships that could be construed as a potential conflict of interest.

frontiers in Pharmacology

ORIGINAL RESEARCH
published: 21 February 2018
doi: 10.3389/fphar.2018.00110

Uncovering the Signaling Pathway behind Extracellular Guanine-Induced Activation of NO System: New Perspectives in Memory-Related Disorders

Mariachiara Zuccarini[1,2†], Patricia Giuliani[1,2†], Monica Frinchi[3], Giuseppa Mudò[3], Rosa Maria Serio[4], Natale Belluardo[3], Silvana Buccella[1,2], Marzia Carluccio[1,2], Daniele F. Condorelli[5], Francesco Caciagli[1,2*], Renata Ciccarelli[1,2] and Patrizia Di Iorio[1,2]*

[1] Department of Medical, Oral and Biotechnological Sciences, Università degli Studi "G. d'Annunzio" Chieti-Pescara, Chieti, Italy, [2] Aging Research Center, Ce.S.I., "G. d'Annunzio" University Foundation, Chieti, Italy, [3] Department of Experimental Biomedicine and Clinical Neurosciences, University of Palermo, Palermo, Italy, [4] Department of Biological, Chemical and Pharmaceutical Sciences and Technologies (STEBICEF), University of Palermo, Palermo, Italy, [5] Department of Bio-Medical Sciences, University of Catania, Catania, Italy

OPEN ACCESS

Edited by:
Kenneth A. Jacobson,
National Institutes of Health (NIH),
United States

Reviewed by:
Martina Schmidt,
University of Groningen, Netherlands
Fabio Tascedda,
University of Modena and Reggio Emilia, Italy

***Correspondence:**
Francesco Caciagli
francesco.caciagli@unich.it
Mariachiara Zuccarini
mariachiara.zuccarini@unich.it

† These authors are co-first authors.

Specialty section:
This article was submitted to Experimental Pharmacology and Drug Discovery, a section of the journal Frontiers in Pharmacology

Received: 15 November 2017
Accepted: 31 January 2018
Published: 21 February 2018

Citation:
Zuccarini M, Giuliani P, Frinchi M, Mudò G, Serio RM, Belluardo N, Buccella S, Carluccio M, Condorelli DF, Caciagli F, Ciccarelli R, and Di Iorio P (2018) Uncovering the Signaling Pathway behind Extracellular Guanine-Induced Activation of NO System: New Perspectives in Memory-Related Disorders. Front. Pharmacol. 9:110. doi: 10.3389/fphar.2018.00110

Mounting evidence suggests that the guanine-based purines stand out as key player in cell metabolism and in several models of neurodegenerative disorders, such as Parkinson's and Alzheimer's diseases. Guanosine (GUO) and guanine (GUA) are extracellular signaling molecules derived from the breakdown of the correspondent nucleotide, GTP, and their intracellular and extracellular levels are regulated by the fine-tuned activity of two major enzymes, purine nucleoside phosphorylase (PNP) and guanine deaminase (GDA). Noteworthy, GUO and GUA, seem to play opposite roles in the modulation of cognitive functions, such as learning and memory. Indeed GUO, despite exerting neuroprotective, anti-apoptotic and neurotrophic effects, causes a decay of cognitive activities, whereas GUA administration in rats results in working memory improvement (prevented by L-NAME pre-treatment). This study was designed to investigate, in a model of SH-SY5Y neuroblastoma cell line, the signal transduction pathway activated by extracellular GUA. Altogether, our results showed that: (i) in addition to an enhanced phosphorylation of ASK1, p38 and JNK, likely linked to a non-massive and transient ROS production, the PKB/NO/sGC/cGMP/PKG/ERK cascade seems to be the main signaling pathway elicited by extracellular GUA; (ii) the activation of this pathway occurs in a pertussis-toxin sensitive manner, thus suggesting the involvement of a putative G protein coupled receptor; (iii) the GUA-induced NO production, strongly reduced by cell pre-treatment with L-NAME, is negatively modulated by the EPAC-cAMP-CaMKII pathway, which causes the over-expression of GDA that, in turn, reduces the levels of GUA. These molecular mechanisms activated by GUA may be useful to support our previous observation showing that GUA improves learning and memory functions through the stimulation of NO signaling pathway, and underscore the therapeutic potential of oral administration of guanine for treating memory-related disorders.

Keywords: guanine, L-NAME, nitric oxide, cGMP, ERK, SH-SY5Y cell line

INTRODUCTION

Guanine-based purines are known to play crucial role in the modulation of neurotransmission and neuropathologies (Ciccarelli et al., 2001; Boison, 2011; Bettio et al., 2016; Di Liberto et al., 2016). In particular, the purine nucleoside Guanosine (GUO), which is mostly released from astrocytes under pathological conditions (i.e., hypoxic or hypoglycemic stress), is thought to exert both neurotrophic and neuroprotective effects (Di Iorio et al., 2001, 2004; Giuliani et al., 2012, 2015; Lanznaster et al., 2016); indeed, it oversees neuronal development and synaptic activity, and protects neuronal and glial cells against oxidative stress and excitotoxicity (Neary, 1996; Schmidt et al., 2007; Tarozzi et al., 2010; Quincozes-Santos et al., 2014; Bellaver et al., 2015; Ribeiro, 2016; Thomaz et al., 2016). Furthermore, in rats, GUO administration during pre-training displays amnesic effect on inhibitory avoidance task (Roesler et al., 2000; Vinadé et al., 2004; Saute et al., 2006). At present, much less is known about the effects that Guanine (GUA) exerts in the central nervous system. Intracellular GUA derives from guanosine triphosphate (GTP) breakdown and represents the starting point of reactions deputed to maintain intracellular levels of GTP (purine salvage pathway). When intracellular levels of GUA are excessive, it may be transported outside the cells by specific transmembrane nucleobases transporters, although most of the extracellular GUA derives from the breakdown of the released GTP and it is generated by GUO in a reaction catalyzed by the purine nucleoside phosphorylase (PNP) (Rathbone et al., 2008; Giuliani et al., 2016, 2017; Peña-Altamira et al., 2017). On the contrary, GUA degradation to xanthine (Xan) is mediated by Guanine deaminase (GDA) or cypin (Miyamoto et al., 1982), which has been regarded as one of the "intrinsic factors" that regulate dendrite morphology together with the small GTPases RhoA, Rac1, the β-catenin (Yu and Malenka, 2004), PSD-95 (Charych et al., 2006) and the calcium/calmodulin-dependent protein kinase II (CAMKII) (Fink et al., 2003). CaMKII is a synaptic signaling molecule that plays a crucial role during long-term memory formation (Lucchesi et al., 2011) and its endogenous inhibitors CaMK2N1 and CaMK2N2 are highly expressed during memory consolidation (Lepicard et al., 2006). Cyclic AMP-CREB axis is implicated in learning and memory processes and has been shown to activate CaMKII.

In a previous work (Giuliani et al., 2012), we reported the effects of GUO and GUA on learning and memory in a model of passive avoidance task in rats. In that study, the oral administration of GUO exerted amnesic activity on inhibitory avoidance task and was unable to prevent the amnesic effect caused by *N*-omega-nitro-l-arginine methyl ester (L-NAME), a non-specific NOS inhibitor known to reduce the capability of treated animals to acquire or retain information in several learning tasks. Conversely, the administration of GUA counteracted the L-NAME-mediated amnesic effects, by increasing the step-through latency either when it was given in the learning phase or during the memory consolidation phase.

In addition to GUO and GUA, another guanine-based purine has been correlated to changes in memory processes, namely cyclic guanosine monophosphate (cGMP), which exerts memory-enhancing effect through the modulation of NMDA receptors and the glutamate-nitric oxide (NO) pathway (Cabrera-Pastor et al., 2016) or via NOS-soluble guanylyl cyclase (sGC)-cGMP- protein kinase G (PKG) pathway (Friebe and Koesling, 2003; Boess et al., 2004; Masood et al., 2009; Bollen et al., 2014; Lueptow et al., 2015). Noteworthy, there is a large body of evidence confirming the existence of a cross-talk between NO and ERK signaling pathways during memory formation and learning processes (Moosavi et al., 2014). Indeed, it has been shown that ERK represents a crucial downstream mediator of NO in the brain (Chien et al., 2008) and that the blockage of NO-cGMP-PKG prevents the activation of ERK mediated by high-frequency stimulation-(HFS) (Ping and Schafe, 2010).

Based on the above mentioned mnesic effects elicited, *in vivo*, by GUA, and several findings showing that NO-cGMP-PKG-ERK signaling pathway is positively correlated with enhancement of memory formation (Adams and Sweatt, 2002; Davis and Laroche, 2006; Giovannini, 2006; Philips et al., 2007; Chien et al., 2008; Adaikkan and Rosenblum, 2012), in this study we aimed to:

(a) verify, by using human neuroblastoma cell line SH-SY5Y, if cGMP and NO-PKG-ERK signaling pathway resulted to be activated upon cell exposure to GUA;
(b) assess whether the activation of this signaling pathway may involve the extracellular GUA interaction with a new putative receptor.

MATERIALS AND METHODS

Materials and Chemicals

The human neuroblastoma cell line SH-SY5Y was purchased from European Collection of Authenticated Cell Culture (ECACC, Salisbury, United Kingdom); Guanine, Guanosine, Nutrient Mixture F-12 Ham, Minimum Essential Medium Eagle (MEM), Non-Essential Amino Acids (NEAA), L-Glutamine, Trypsin-EDTA, Pertussis toxin from Bordetella pertussis (PTX), 3-Isobutyl-1-methylxanthine (IBMX), ᵻ[1,2,4]Oxadiazolo[4,3-a]quinoxalin-1-one (ODQ), 8-(4-Chlorophenylthio)-2′-*O*-methyladenosine 3′,5′-cyclic monophosphate monosodium hydrate (8-pCPT-2′-O-Me-cAMP), N-[2-[N-(4-Chlorocinnamyl)-*N*-methylaminomethyl]phenyl]-N-(2-hydroxyethyl)-4-methoxybenzenesulfonamide phosphate salt, N-[2-[[3-(4′-Chlorophenyl)-2-propenyl]methylamino]methyl]phenyl]-*N*-(2-hydroxyethyl)-4′-methoxybenzenesulfonamide phosphate salt (KN-93), Propentofylline, S-(4-Nitrobenzyl)-6-thioinosine (NBTI), 2′,7′-Dichlorofluorescin diacetate (H2DCF-DA), dimethylsulfoxide (DMSO), Ionomycin, trypsin/EDTA, EDTA, EGTA, HEPES, Phosphate Buffer Solution (PBS), dithiothreitol (DTT), NADPH, calmodulin, CaCl2, tetrahydrobiopterin and the cationic exchange resin Dowex AG50WX-8, *N*-(1-naphthylethylenediamine) dihydrochloride, were purchased from Sigma (Milan, Italy); NG-Nitro-L-arginine methyl ester hydrochloride (L-NAME), MSC 20329644, GF109203X, 10-DEBC hydrochloride, Dipyridamole and LY 294002 hydrochloride were purchased from Tocris (Milan, Italy); Penicillin-streptomycin and Heat-inactivated fetal bovine

serum (FBS) were purchased from Gibco® (Thermo Fischer Scientific, Monza, Italy); Phospho-ASK1, Phospho-p38 MAPK, Phospho-SAPK/JNK, Phospho-PKC (pan), Phospho-Akt, Phospho-p44/42 MAPK (Erk1/2), β-Actin, secondary anti-rabbit IgG HRP-linked antibody were purchased from Cell Signaling Technology (Cell Signaling, Leiden, Netherlands); PNP and Guanase Deaminase antibodies were purchased from Novus Biologicals (Space Import-Export, Milan, Italy).

Cell Culture

The human neuroblastoma cells, SH-SY5Y, were cultured in 75 cm^2 flasks in a 1:1 mixture of F-12 nutrient mixture (Ham 12) and Eagle's MEM (EBSS) supplemented with 2 mM Glutamine, 1% Non-Essential Amino Acids (NEAA), 15% Foetal Bovine Serum (FBS) and 100 units/mL penicillin and 100 μg/mL streptomycin and maintained at 37°C in 5% CO2, humified air.

For the evaluation of PNP and GDA release, cell medium was removed and replaced by serum free-medium and maintained in humified atmosphere, 5% CO2, 37°C. At the end of the experiment, aliquots (2 mL) of the culture medium were collected, placed in suitable devices (Amikon Ultra 2 mL, cutoff 10 K, Merck Millipore, Germany) and centrifuged following the manufacturer's instruction, in order to concentrate culture media containing the enzymes.

For the evaluation of purine release, cell medium was removed and replaced with Krebs-HEPES buffer (15 m M HEPES, pH 7.4, 120 mM NaCl, 4 mM KCl, 1.2 mM $MgSO_4$, 1 mM $CaCl_2$), and 10 mM D-glucose oxygenated (95% O2/5% CO2). After 30 min, the cells were incubated for further 30 min with the same buffer containing 2.5 μM GUO combined with 0.675 μM of [3H]GUO (specific activity 5.3 Ci/mmol; Movarek Biochemicals). At the end of this incubation period, cells were washed twice with unlabeled Krebs-HEPES buffer and maintained in this medium in standard condition (37°C, 5% CO2). When used, purine uptake inhibitors were added to Krebs-HEPES just after the incubation with labeled GUO. At the end of the experiment, an aliquot of the culture medium was collected and immediately heat-inactivated for 5 min at 70°C to avoid any further enzymatic degradation of the released purine. Samples were, then, centrifuged, filtered with 0.2 μm filters (Millipore, Vimodrone, Italy) and stored at 80°C before HPLC analysis.

For Immunoblot assays, SH-SY5Y cells were subcultured in 100 × 20-mm Petri Dishes (BD Falcon) at a seeding density of 2×10^5 per dish (for each sample two dishes were pulled together) and grown until 80% confluence. Before all experiments, cells were starved for 24 h in medium containing 0.1% FBS.

HPLC Method for the Evaluation of Purine Levels in the Extracellular Milieu

According to the method previously described (Giuliani et al., 2012, 2017), purines were measured by an Agilent 1100 series HPLC system (Agilent Technologies, Santa Clara, CA, United States), by using, for the separation of the compounds, a reverse phase analytical column (LiChrospher 100 RP-18 5 μm in LiChroCART 125-4, Merck) and a 15-min linear gradient [from 100% of buffer A (60 mM KH_2PO_4 and 5 mM tetrabutylammonium phosphate, pH 6.0) to 100% solvent B (30% methanol plus 70% buffer A)] at a flow rate of 1.5 mL/min. The detection of unlabeled compounds was achieved using a Diode Array Detector (Agilent Technologies, Santa Clara, CA, United States) with wavelength set at 254 nm for all the substances except Uric Acid (UAc), which was 290 nm. Released purines were identified and quantified by comparison with pure external standards. Since many purine compounds are present in the extracellular milieu at concentrations below the UV detection limit, the HPLC system was equipped with an online radiochemical detector (FLO-ONE 500 TR, Packard Instruments) for the concurrent measurement of radiolabeled purine present in the outflow from the Diode Array Detector, in order to improve the sensibility of the analysis. Thus, the HPLC effluent was mixed with the liquid scintillation cocktail (Ultima-FloM, Perkin-Elmer) at a flow ratio of 2:1 and passed through a 500 μL detector flow cell. Radiochromatograms were integrated and each radioactive peak was quantified.

Measurement of Enzyme Activity in the Extracellular Milieu

PNP activity was measured in an assay buffer containing 50 mM HEPES, pH 7.0, 50 mM inorganic phosphate (Pi), used as co-substrate, and 200 μM GUO used as substrate, whereas the mixture used to evaluate GDA activity consisted of 100 mM TrisHCl pH 8 plus 200 μM GUA used as substrate. These enzymatic reactions were started by adding aliquot of the concentrated extracellular culture medium. The mixtures were then incubated by shaking at 37°C for 15 min, to evaluate PNP activity, and for 60 min, to determine GDA activity. The reactions were stopped by heating the mixture at 70°C for 5 min and the precipitated proteins were removed by centrifugation. The enzyme activity was determined by quantifying the rate of conversion of GUO to GUA, for PNP, or the conversion of GUA to XAN for GDA, using the HPLCmethod previously described (Giuliani et al., 2016). In this case, the Agilent HPLC was equipped with a thermostated column compartment, a diode array detector, and a fluorescence detector (Agilent Technologies). Briefly, separation was achieved using a Phenomenex Kinetex pentafluorophenyl analytical column (5 μm pore size, 100 Å particle size, 250 × 4.6 mm; Phenomenex INC) at 35°C. Separation was carried out with a 15-min non-linear gradient elution (flow rate 1 mL/min) using a mobile phase composed of 0.1% (v/v) formic acid in water (solution A) and methanol (solution B). The fluorescent GUO and GUA were monitored at an excitation wavelength of 260 nm and an emission wavelength of 375 nm, whereas for the non-fluorescent compounds, i.e., XAN and UAc, the UV detector was set at 254 and 290 nm respectively. Allsubstances were identified and quantified by comparison with pure external standards. Enzyme activity was expressed as Unit (U) present in the total medium, being 1 U of enzyme the amount of enzyme that converts 1 μmole of substrateinto product per min.

Cell Viability Assay

Cell death was monitored by using the CytoTox-96 assay (Promega Italia, Milan, Italy) that allows to evaluate the lactate dehydrogenase (LDH) activity. The assay is based on a 30-min coupled enzymatic assay, catalyzed by released LDH, which results in conversion of a tetrazolium salt, 2-p-(iodophenyl)-3-(p-nitrophenyl)-5-phenyltetrazolium chloride (INT), into a red formazan product. SH-SY5Y cells were seeded in 96-well plates at 5×10^3 cells/well of confluence and incubated for 2 days. For all samples, the cell culture medium was replaced with Krebs-HEPES buffer (15 mM HEPES, pH 7.4, 120 mM NaCl, 4 mM KCl, 1.2 mM $MgSO_4$, 1 mM $CaCl_2$) with or without 50 μM GUA (0–12 h). At the end of exposure, the Lysis solution was added for 45 min to control wells for the determination of maximum LDH release. Afterward, 50 μL of collected media were transferred to a fresh 96-well (enzymatic assay) plate, together with 50 μL of Substrate buffer containing 0.7 mM *p*-iodonitrotetrazolium Violet, 50 mM L-lactic acid, 0.3 mM phenazine methoxysulfate, 0.4 mM NAD and 0.2 M Tris-HCl pH 8.0. Finally, the plate was protected from light and incubated for 30 min at RT. The absorbance was recorded at 490 nm of wavelength in a microplate reader after adding the Stop Solution. LDH activity was expressed as the proportion of LDH released into the culture medium compared to the total amount of LDH present in cells lysates and calculated as follows: (medium absorbance value – white absorbance value)/(medium absorbance + lysate absorbance) × 100.

Immunoblot

SH-SY5Y cells were seeded overnight onto 100 mm Petri Dishes (BD Falcon) at 2.0×10^5 cells/dish in 6 mL of 1:1 mixture of F-12 nutrient mixture (Ham 12) and Eagle's MEM (EBSS) supplemented with 2 mM Glutamine, 1% Non Essential Amino Acids (NEAA), 15% Foetal Bovine Serum (FBS) and 100 units/mL penicillin and 100 μg/mL streptomycin. After 24-h starvation, cells were submitted to different treatments in MEM supplemented with 0.5% FBS and 1% Penicillin/Streptomycin. After treatment, cells were washed twice with ice cold 1× PBS (Sigma–Aldrich), lysed with RIPA Buffer (Sigma–Aldrich) containing 150 mM NaCl, 10 mM EDTA, 1% NP40, 0.5% deoxycholic acid, 0.1% SDS, and 50 mM Tris, pH 7.5, supplemented with 1% Protease Inhibitor Cocktail (Sigma–Aldrich), scraped off, pulled, and clarified by centrifugation at 12.500 × *g* for 20 min, 4°C. Before performing Immunoblot, a sample buffer (5× Laemmli buffer with 10% mercaptoethanol) was added to melted lysates 1:4. Protein concentrations were obtained using the Bio-Rad Protein Assay (Bio-Rad Laboratories, Hercules, CA, United States) based on the Bradford method. An equal amount of 50–70 μg of protein was resolved by 10% sodium dodecyl sulfate–polyacrylamide gel electrophoresis (SDS-PAGE). The resolved proteins were transferred onto a nitrocellulose membrane and then incubated with blocking buffer 1× TBS containing 0.1% Tween-20 (TBST) and 3% BSA or 5% non-fat dry milk for 2 h, RT, and subsequently probed with specific primary antibody at 4°C, overnight. After washing with TBST, the membrane was further probed with corresponding horseradish peroxidase (HRP)-conjugated secondary antibodies at RT for 1 h. Membranes were finally washed, before subjecting them to ECL Plus Immunoblot Detection Reagent (Amersham, GE Healthcare). The immunoreactive bands were visualized under a chemiluminescence detection system (UVItec, Cambridge, United Kingdom). Band intensity data were obtained using Quantity One software (Bio-Rad Laboratories). Blotting membranes were stripped and re-probed with anti-actin antibody as equal loading control. Estimates of phosphorylated proteins are presented as densitometric ratios, normalized to the corresponding total protein content. Apart from PNP antibody (1:500), all primary antibodies [Phospho-ASK1 (Ser83), Phospho-p38 MAPK (Thr180/Tyr182), Phospho-SAPK/JNK (Thr183/Tyr185), Phospho-PKC (Ser660), Phospho-Akt (Thr450), Phospho-p44/42 MAPK (Erk1/2) (Thr202/Tyr204), Guanase Deaminase, β-Actin] were diluted 1:1000 in 3% BSA/1× TBS/0.1% Tween 20 or 2.5% non-fat dry milk/1× TBS/0.1% Tween 20. The secondary antibody was used at 1:2500 dilution in 3% BSA/1× TBS/0.1% Tween 20 or 2.5% non-fat dry milk/1× TBS/0.1% Tween 20.

Measurement of Cellular Reactive Oxygen Species (ROS)

The amount of intracellular reactive oxygen species (ROS) was measured by using the probe H_2DCF-DA (Ha et al., 1997), which diffuses into the cells and is oxidized to the green fluorescent compound 2′,7′-dichlorofluorescein (DCF) upon reaction with intracellular hydrogen peroxide or low-molecular-weight hydroperoxides. Cells were seeded at 1×10^6 cells/well in 6-well culture plates and incubated overnight. After exposure to different concentration of GUA for 30 min, cells were incubated with 5 μM H_2DCF-DA for 30 min, in the dark, at 37°C. At the end of incubation, the cells were washed with PBS and fluorescence was measured at an excitation wavelength of 480 nm and an emission wavelength of 540 nm in a fluorescence microplate reader (Thermo Fischer Scientific, Monza, Italy). ROS production was determined by analyzing DCF fluorescence normalized for total protein content. The fluorescence intensity was proportional to the amount of ROS produced by cells.

Determination of Nitric Oxide Synthase (NOS) Activity

Nitric oxide synthase activity was measured from the conversion of L-[3 H]-arginine to L-[3 H]-citrulline based on the method of Bredt et al. (1991) with modifications. SH-SY5Y cells were grown overnight in 6-well plates. After 24-h starvation, cells were exposed for 30 min to 50 μM GUA, 5 μM L-NAME or 2 μM Ionomycin, the latter used as positive control. When used in combination, L-NAME was administered 15 min before cell exposure to GUA or Ionomycin. Thereafter, cells were washed three times with ice-cold 1X PBS, scraped in 1X PBS containing 1 mM EDTA, and centrifuged for 10 min at 1200 *g*. The pellets were resuspended in a reaction buffer containing 50 mM Hepes, 1 mM EDTA, 1mM DTT (pH 7.2) and sonicated on ice with two 10 s bursts. The reaction was started by addition to samples of reaction mixture [1 mM NADPH, 1 nmol/l calmodulin,

A

Levels of Guanine-based purines in the cytosol of SH-SY5Y cells (nmoles/10^5 cells)

	GTP	GUO	GUA	XAN	UAc
Control	2.86 ± 0.511	0.33 ± 0.062	0.22 ± 0.052	0.05 ± 0.112	0.05 ± 0.093
Uptake Inhibitors	2.59 ± 0.431	0.30 ± 0.044	0.15 ± 0.042	0.04 ± 0.082	0.06 ± 0.104

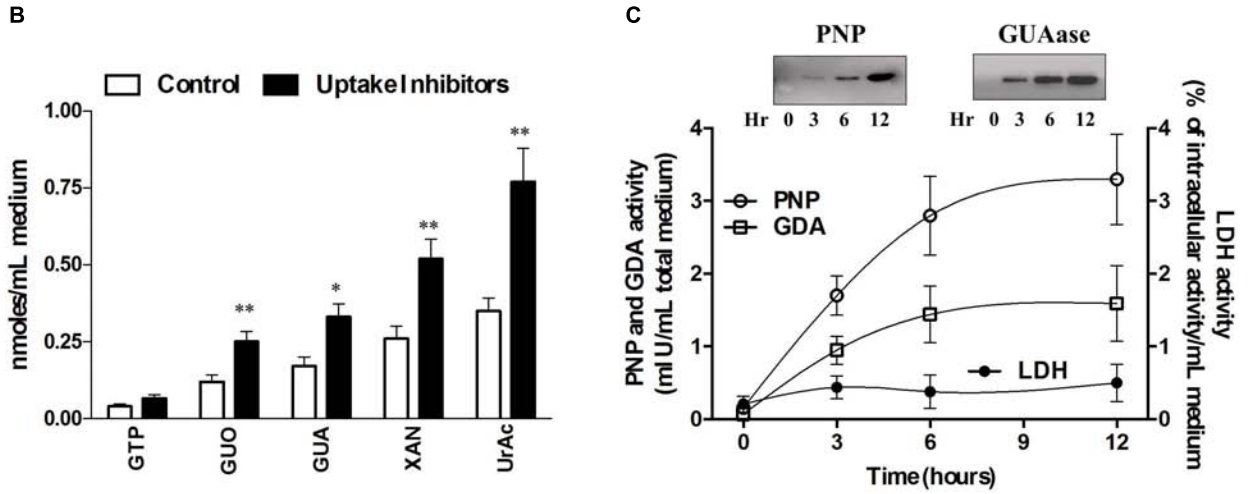

FIGURE 1 | SH-SY5Y neuroblastoma cells release guanine-based purines, PNP and GDA in the culture medium. **(A)** HPLC analysis of intracellular levels of Guanine-based purines in SH-SY5Y cells. **(B)** HPLC analysis of extracellular levels of guanine-based purines at rest (control) and in the presence of the inhibitors of cell uptake. SH-SY5Y were incubated with 2.5 μM guanosine (GUO) combined with 0.675 μM of [3H]GUO, the latter used as tracer. Values are expressed as nmoles/mL of culture medium, and represent the mean ± SEM of five independent experiments. $*p < 0.05$; $**p < 0.01$: statistical significance versus untreated cells (control) (Student's *t*-test). **(C)** Evaluation of the presence and activity of purine nucleoside phosphorylase (PNP) and guanine deaminase (GDA) in the culture medium of SH-SY5Y cells. (C1) Representative Immunoblots of PNP and GDA expression in SH-SY5Y culture medium. After 24 h incubation, SH-SY5Y cell culture medium was collected after 3, 6, and 12 h, concentrated and analyzed for PNP and GDA expression. (C2) HPLC analysis of PNP and GDA activity evaluated up to 12 h. PNP activity was assayed by using 200 μM guanosine (GUO) as substrate plus 50 mM Pi as co-substrate for 15 min at 37°C, whereas GDA activity was measured by using 100 mM TrisHCl pH 8 plus 200 μM GUA as substrate for 60 min at 37°C. Values are expressed as milli-International Units (mIU) of enzyme per total culture medium and represent the mean ± SEM of three independent experiments, run in duplicate. (C3) Evaluation of cell viability of SH-SY5Y cells by LDH assay. Values are expressed as the percentage of the intracellular LDH activity that was determined after cell lysis, and represent the mean ± SEM of five different experiments.

1.25 mM CaCl2, 3 μM tetrahydrobiopterin, 2.5 μCi/μl of L-[3H]arginine (Perkin Elmer, Boston, MA, United States, specific activity 42.6 Ci/mmol), unlabelled arginine]. After an incubation of 15 min at 37°C, the assay was stopped by adding 20 mM Hepes-Na containing 2 mM EDTA and 2 mM EGTA (pH 5.5), and the reaction mixture was applied to 2-ml columns of Dowex AG50WX-8 (Na+ form), which were eluted with 4 ml of water. The radioactivity corresponding to the [3H]-citrulline was measured by liquid scintillation analyzer (Tris-Carb 2100 TR, Perkin Elmer) and normalized for extract protein content determined with Bradford method. NOS activity was expressed as pmoles citrulline/min/mg cell protein.

Statistical Analysis

Data are represented as means ± standard error of mean (SEM). Comparisons among experimental groups were performed by Student *t*-test or by two-way ANOVA followed by Sidak's multiple comparisons test using GraphPad Prism 6.01 (San Diego, CA, United States), as indicated. Statistical difference was accepted when $P < 0.05$. All experiments were performed at least three times.

RESULTS

The Levels of Guanine-Based Purines in SH-SY5Y Culture Media Are Controlled by Specific Nucleobase and Nucleoside Transporters and by the Presence of Purine-Converting Enzymes

A hallmark of several neurodegenerative diseases is the activation of neuronal and glial cells and the following induction of oxidative stress and neuronal toxicity. In the attempt to investigate neuronal response to GUA exposure, we used SH-SY5Y, a human derived neuroblastoma cell, which has been often used as a model to study molecular mechanisms associated to ROS production, apoptosis and amyloid-β-induced neuronal toxicity in Alzheimer's disease (Tarozzi et al., 2010; Ali-Rahmani et al., 2014; Puangmalai et al., 2017; Modi et al., 2017).

We firstly measured both the intracellular and extracellular levels of purines in cultured SH-SY5Y cells, in resting conditions. In the SH-SH5Y lysates, the levels of Guanine-based nucleotides prevailed over the correspondent nucleobases and the inhibition of the uptake, performed by treating cell culture with a cocktail

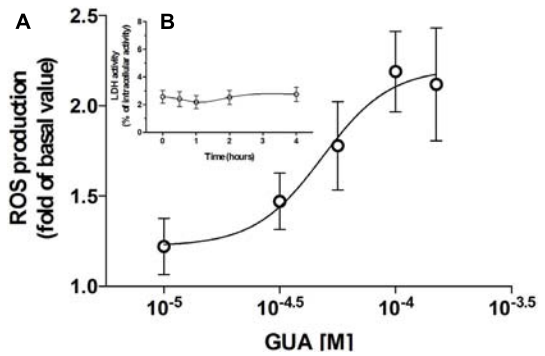

FIGURE 2 | Guanine (GUA) induces ROS production in SH-SY5Y neuroblastoma cells in a dose-dependent manner. **(A)** SH-SY5Y cells were incubated for 30 min with different concentrations of GUA (0–100 μM). The levels of ROS are presented as folds of control and represent the mean ± SEM of five different experiments. **(B)** Evaluation of cell viability of SH-SY5Y cells exposed to 50 μM GUA up to 4 h. Values are expressed as the percentage of the intracellular LDH activity that was determined after cell lysis and represent the mean ± SEM of five different experiments.

of inhibitors of nucleoside and nucleobase transmembrane transporters (100 μM propentofylline, 10 μM NBTI, 10 μM dypiridamole) did not caused any significant effect (**Figure 1A**). An opposite trend was observed in the culture medium, wherein the uptake inhibitors significantly increased extracellular levels of GUA, Xan and UAc [two-way ANOVA analysis and Sidak's multiple comparisons test: $P < 0{,}005$] (**Figure 1B**). This suggested that the levels of extracellular guanine-based purines depended both on the balance between nucleotide release and nucleoside uptake and on the presence, in the culture medium, of extracellular purine-converting enzymes. Indeed, by using Immunoblot analysis and HPLC for the measurement of the enzyme activities (Giuliani et al., 2017), we confirmed the presence in the culture medium of PNP and GDA (**Figure 1C**). Both the enzymes tended to accumulate in the culture medium over the time (from 2 up to 12 h) following a similar trend even though at different levels (PNP amount was about 7–10 fold higher than GDA). This event was not associated with significant cell damage or death, as demonstrated by the constant and minor presence of LDH, measured during the same period in the culture media (**Figure 1C**).

Guanine Increases ASK1, p38, JNK, PKC and PKB Phosphorylation and This Effect Is Prevented, Except for PKB, by Cell Treatment with a Cocktail of Inhibitors of the Uptake

Cell exposure to exogenous GUA, for 30 min, elicited a non-massive and dose-dependent production of ROS. This occurred without any significant collateral LDH production (**Figure 2**). A similar effect has been found in different glial cells (astrocytes or microglial cells, data not shown), wherein ROS production seemed to be even greater than that elicited in SH-SY5Y cells. The ROS production has been often associated with an increased phosphorylation of ASK1, p38 and JNK (Shen and Liu, 2006; Jiang et al., 2017) and it has been reported that the inhibition of c-Jun N-terminal Kinase (JNK) in SH-SY5Y cells, prevented 6-Hydroxydopamine-induced ROS production and toxicity (Feng et al., 2013). Based on this evidence, we investigated which signaling transduction pathways were involved in GUA-induced effect. SH-SY5Y cells were exposed to 50 μM GUA, the half maximal effective concentration, for 10 min, and the expression of p-ASK1, p-p38, p-JNK, PKC and PKB was analyzed by Immunoblot. The short-term exposure of cells to GUA significantly increased the phosphorylation of all the mentioned kinases. The two-way ANOVA analysis of their expression showed an effect of cell exposure to GUA [$F_{(1,12)} = 27.53$, $P = 0.0002$ for p-ASK1; $F_{(1,12)} = 16.89$, $P = 0.0014$ for p-38; $F_{(1,12)} = 41.35$, $P = 0.0001$ for p-JNK; $F_{(1,12)} = 16.09$, $P = 0.0017$ for PKC and $F_{(1,12)} = 27.07$, $P = 0.0002$ for PKB] (**Figures 3A,B**). Cell pre-treatment with the previously mentioned cocktail of inhibitors of both nucleoside and nucleobase transmembrane transporters, 30 min before cell exposure to GUA, did not modify the basal phosphorylation level of all kinases but strongly reduced GUA-induced phosphorylation of ASK1, p38, JNK and PKC, [two-way ANOVA: $F_{(1,12)} = 4.77$, $P = 0.045$ for p-ASK1; $F_{(1,12)} = 13.07$, $P = 0.0035$ for p-JNK; $F_{(1,12)} = 7.20$, $P = 0.019$ for PKC with interaction values between factors of $F_{(1,12)} = 13.86$, $P = 0.0029$; $F_{(1,12)} = 15.51$, $P = 0.002$ and $F_{(1,12)} = 22.49$, $P = 0.0005$, respectively], revealing that the effect of GUA on these pathways was mainly intracellular (**Figures 3A,B**). Conversely, GUA-induced phosphorylation of PKB was not modified, [two-way ANOVA: $F_{(1,12)} = 0.6131$, $P = 0.4488$ and no effect of the interaction between both factors $F_{(1,12)} = 0.01$, $P = 0.9212$], thus suggesting that the activation of this pathway mainly depends on the extracellular activity of GUA (**Figure 3C**).

PI3K-PKB-ERK Is the Main Signaling Pathway Activated by Extracellular GUA in SH-SY5Y Cells

Due to the evidence that ERK stands out as a key player in the modulation of several memory processes (Giovannini, 2006) and that, in different experimental models, it represents the downstream effector of ROS-induced phosphorylation of ASK1, p38 and JNK (Lee and Cheong, 2017), we sought to determine the relevance of each of these pathways on GUA-induced effect, by selectively blocking ASK1 or PKC, two upstream kinases in ERK signaling. Immunoblot analysis of p-ERK1/2 expression revealed that GUA elicited a dose-dependent phosphorylation of ERK (10-100 μM), [two-way ANOVA analysis and Sidak's multiple comparisons test: $P < 0{,}005$ for GUA 50 and 100 μM] and the time course [two-way ANOVA analysis: $F_{(1,24)} = 74.57$, $P < 0{,}0001$ with interaction values between factors of $F_{(2,24)} = 5.053$, $P = 0.0147$] showed that the maximum effect of the purine base was achieved in 10 min and decreased after 30 min (**Figure 4**). The inhibition of ASK1 or PKC by cell pre-treatment with 10 μM MSC2032964A or 1 μM GF109203X for

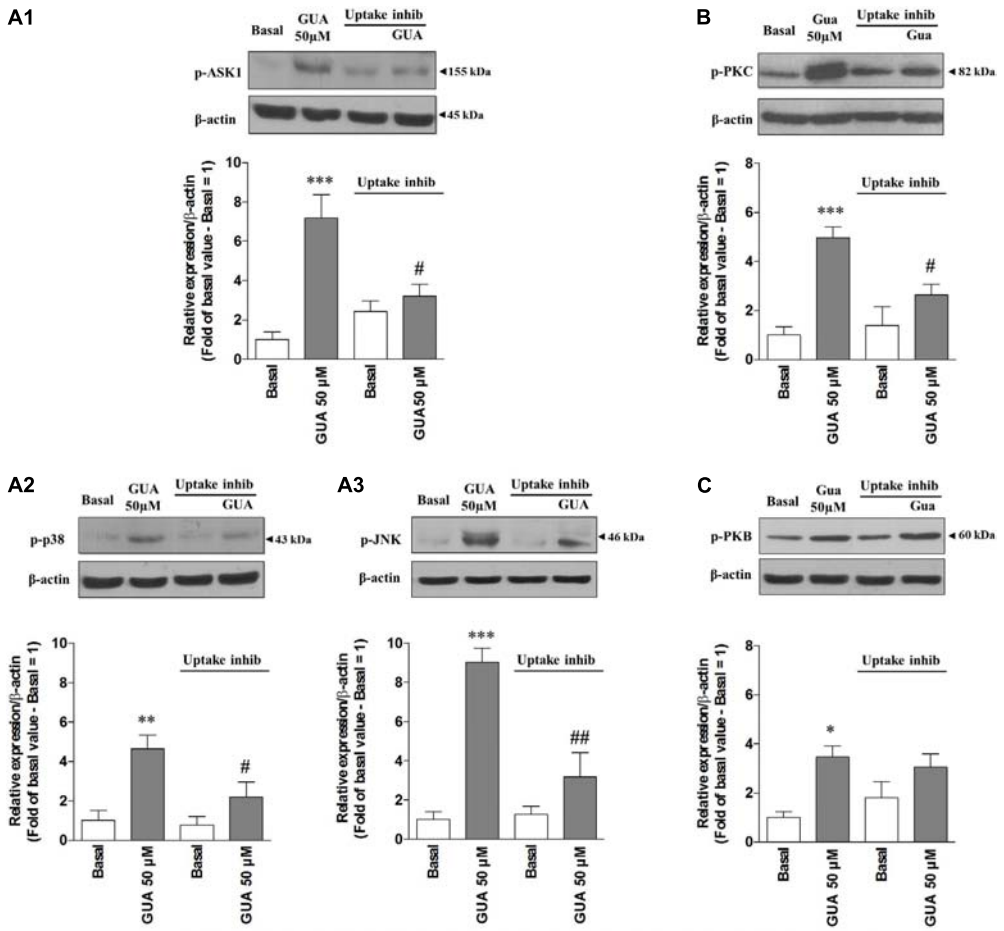

FIGURE 3 | Guanine induces ASK1, p38, JNK, PKC and PKB phosphorylation in SH-SY5Y neuroblastoma cells. SH-SY5Y cells were cultured for 24 h and incubated for 10 min with 50 μM GUA, in the absence or presence of a cocktail of inhibitors of both nucleoside and nucleobase transmembrane transporters (100 μM Propentofylline, 10 μM NBTI, 10 μM Dypiridamole). Representative Immunoblot analysis of **(A1)** p-ASK1 (Thr845), **(A2)** p-p38, **(A3)** p-JNK, **(B)** PKC, **(C)** p-PKB, with the respective β-actin as loading control, and the correspondent quantitative data of densitometric analysis. Each column represents the mean ± SEM of four independent experiments, and it is expressed as relative protein expression normalized to β-actin. Student's *t*-test: $^{*}P < 0.05$, $^{**}P < 0.01$, $^{***}P < 0.001$, vs. untreated cells (Basal); $\#P < 0.05$, $\#\#P < 0.01$, vs. GUA-treated cells.

30 min, respectively, did not affect basal ERK phosphorylation, and only in part reduced that induced by GUA [two-way ANOVA: GUA effect $F_{(1,16)} = 4.543$, $P < 0.0489$, ASK1 inhibitor effect $F_{(1,16)} = 37.66$, $P < 0.0001$ with interaction values between factors of $F_{(3,32)} = 4.449$, $P = 0.0499$; GUA effect $F_{(1,16)} = 3.220$, $P < 0.0917$, PKC inhibitor effect $F_{(1,16)} = 39.35$, $P < 0.0001$ with interaction values between factors of $F_{(3,32)} = 4.504$, $P = 0.0498$]. Conversely, the inhibition of PKB by cell pre-treatment with 10 μM 10-DEBC dihydrochloride, as well as the inhibition of the upstream PI3K by 25 μM LY294002, did not modify the basal p-ERK expression and strongly reduced that elicited by GUA [two-way ANOVA: GUA effect $F_{(1,16)} = 10.84$, $P < 0.0046$, 10-DEBC effect $F_{(1,16)} = 22.53$, $P < 0.0002$ with interaction values between factors of $F_{(3,32)} = 13.82$, $P = 0.0019$; GUA effect $F_{(1,16)} = 6.456$, $P < 0.0218$, LY294002 effect $F_{(1,16)} = 20.12$, $P < 0.0004$ with interaction values between factors of $F_{(3,32)} = 8.564$, $P = 0.0098$] (**Figures 5A,B**). This suggests that, in SH-SY5Y cells, PI3-PKB-ERK signaling cascade is likely the main pathway activated by extracellular GUA.

GUA Activates PKB-ERK Signaling Pathway in a Pertussis-Toxin Sensitive Manner

We, then, inquired whether GUA effect may be ascribed to an eventual interaction with a new putative receptor. For this purpose, SH-SY5Y cells were treated for 4 h with 200 ng/mL Pertussis Toxin (PTX), a specific inhibitor of Gi/Go-proteins, and the expression of p-ERK 1/2 was analyzed by Immunoblot. PTX did not affect basal ERK1/2 phosphorylation but significantly reduced that induced by GUA [two-way ANOVA: $F_{(1,16)} = 9.795$, $P = 0.0065$ with interaction values between factors of $F_{(1,16)} = 16.09$, $P = 0.0010$], thus supporting the involvement of a G_i protein-coupled receptor in the effect of GUA (**Figure 5C**).

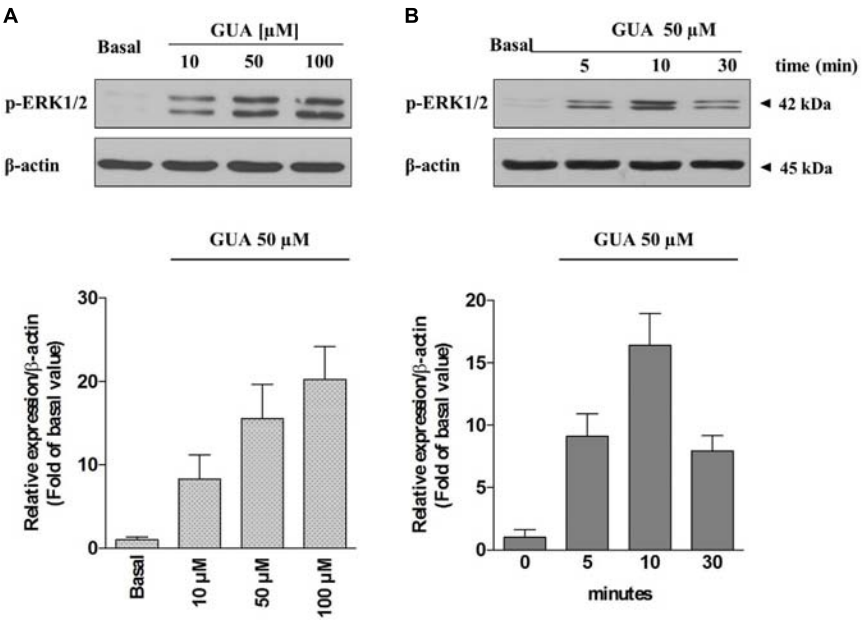

FIGURE 4 | Guanine induces ERK1 phosphorylation in SH-SY5Y neuroblastoma cells in a dose-dependent manner. Representative Immunoblot analysis of ERK1/2 expression in SH-SY5Y cells, with β-actin as loading control, and the correspondent quantitative data of densitometric analysis. **(A)** Cells were cultured for 24 h and exposed for 10 min to different concentrations of GUA (0–100 μM). **(B)** The time course of activation of ERK1/2 induced by GUA. Cells were cultured for 24 h and exposed to 50 μM GUA for different time points (0–30 min). Each column represents the mean ± SEM of at least four independent experiments, and it is expressed as relative protein expression normalized to β-actin.

Extracellular GUA Stimulates the PI3K-PKB Phosphorylation and NO Production and Activates the Downstream sGC-cGMP-PKG-ERK Pathway

Nitric oxide (NO) is known to induce ERK phosphorylation via sGC-cGMP-PKG pathway, (Prickaerts et al., 2001; Suvarna and O'Donnell, 2002; Boess et al., 2004; Rutten et al., 2007; Chien et al., 2008; Masood et al., 2009; Xu et al., 2013; Bollen et al., 2014; Matsumoto et al., 2016). Hence, we evaluated the involvement of NO system on GUA-induced ERK phosphorylation, by selectively blocking every step of this cascade and by analyzing p-ERK1/2 expression by Immunoblot. As expected, phosphodiesterase inhibitor, 10 μM IBMX, strongly enhanced GUA-induced ERK phosphorylation [two-way ANOVA: IBMX effect $F_{(1,16)} = 67.23$, $P < 0.0001$]. Most importantly, NOS inhibitor, 1 mM L-NAME, completely prevented ERK1/2 phosphorylation elicited by GUA [two-way ANOVA: L-NAME effect $F_{(1,16)} = 16.82$, $P < 0.0008$]. The cell co-treatment with IBMX and L-NAME partially restored GUA-induced ERK phosphorylation, thus confirming the presence of other pathways converging on cGMP activation. The sGC inhibitor, 10 μM ODQ, likewise L-NAME, completely abrogated GUA-mediated ERK phosphorylation [two-way ANOVA: ODQ effect $F_{(1,16)} = 25.33$, $P < 0.0001$]. Of note, among the possible pathways involved in the PKB-ERK signaling, extracellular GUA stimulates the PI3K-PKB phosphorylation and NO production, thus evoking the downstream activation of sGC-cGMP-PKG pathway (**Figure 6**). Corroborating with these findings, PDE inhibitors have been shown to improve cognitive skills and memory formation in rodents (Reneerkens et al., 2009). The mechanism likely involves the induction of cAMP-protein kinase A (PKA)-cAMP responsive element-binding protein (CREB) and cGMP-PKG-CREB signaling pathways (Rutten et al., 2007), which are both associated with late-phase of Long-Term Potentiation (LTP).

The Activation of the cAMP-Epac-CaMKII Pathway Influences NOS Activity

In an attempt to investigate whether the activation of collateral signaling pathway was able to affect the NO-sGC-cGMP-PKG-ERK cascade, we examined the possible role of cAMP-Epac-CaMKII pathway. CaMKII (Ca^{2+}/calmodulin-dependent protein kinases II) is highly expressed in hippocamapal neurons and is involved in the glutamate-mediated LTP phase, wherein two major events occur: (i) Ca^{2+} enters the cell through NMDA channels and activates CaMKII that, in turn, recruits AMPA receptors to the plasma membrane; (ii) Ca^{2+} increases cAMP that activates ERK signaling (Giovannini, 2006; Miyamoto, 2006).

It has been recently proposed that extracellular cGMP regulates the glutamate-NO-cGMP pathway in a learning task, and this modulation resulted to be biphasic and relied on an inverse correlation between CaMKII and NOS activity (Moosavi et al., 2014; Cabrera-Pastor et al., 2016).

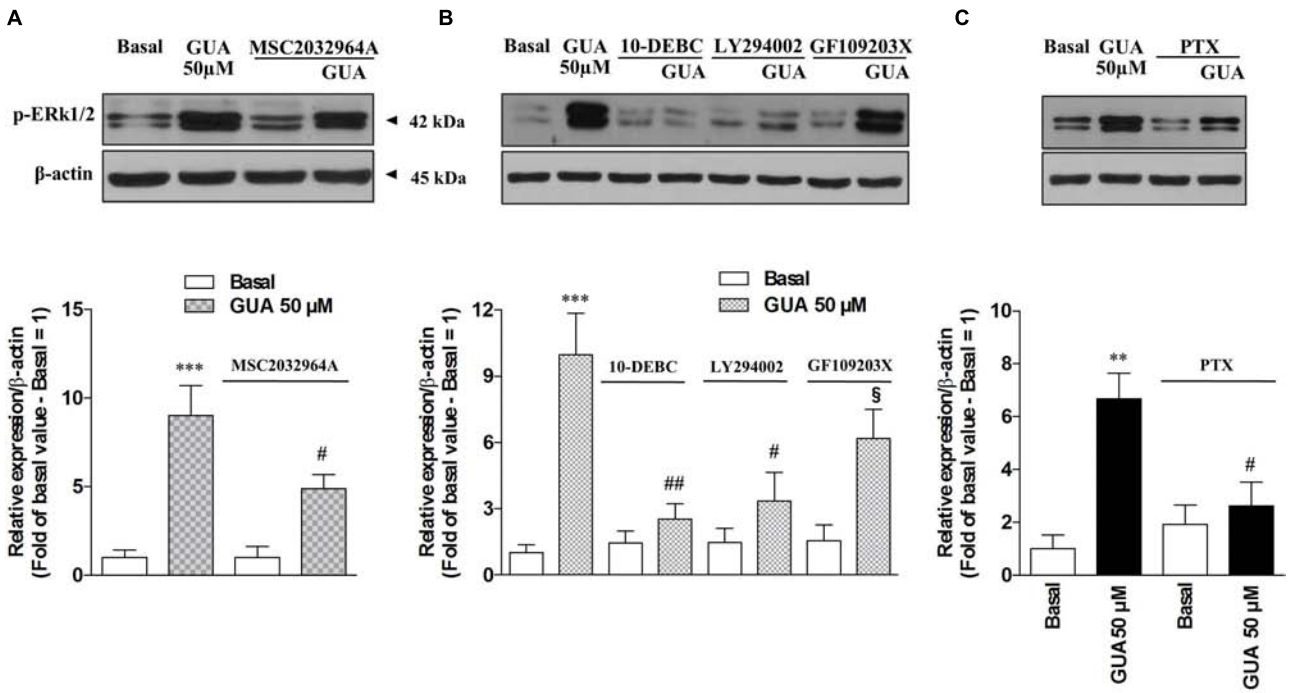

FIGURE 5 | Guanine induces ERK1 phosphorylation in SH-SY5Y neuroblastoma cells via PI3K-PKB-ERK signaling pathway in a PTX-sensitive manner. Representative Immunoblot analysis of ERK1/2 expression in SH-SY5Y cells, with β-actin as loading control, and the correspondent quantitative data of densitometric analysis. Cells were cultured for 24 h and exposed for 10 min **(A,B)** or for 4 h **(C)** to 50 μM GUA, in the absence or presence of **(A)** ASK1 inhibitor, 10 μM MSC2032964A, **(B)** PKC inhibitor (1 μM GF109203X), PKB inhibitor (10 μM 10-DEBC dihydrochloride), PI3K inhibitor (25 μM LY294002), **(C)** 200 ng/mL Pertussis Toxin (PTX.) Each column represents the mean ± SEM of at least four independent experiments, and it is expressed as relative protein expression normalized to β-actin. Student's *t*-test: $^{*}P < 0.05$, $^{**}P < 0.01$, $^{***}P < 0.001$, vs. untreated cells (Basal); $^{\#}P < 0.05$, $^{\#\#}P < 0.01$, vs. GUA-treated cells, §$P < 0.05$, vs. GUA- and GF109203X-treated cells.

In our study, Immunoblot analysis of p-ERK showed that 2,5 μM 8-CPT-cAMP, an EPAC specific cAMP analog, inhibited GUA-induced ERK phosphorylation [two-way ANOVA: effect of 8-CPT-cAMP $F_{(1,16)} = 18.16$, $P < 0.0006$], although this result has to be further elucidated by using an EPAC-specific inhibitor. The inhibitor of CaMKII, 20 μM KN-93, caused an opposite effect and significantly enhanced p-ERK expression [two-way ANOVA: effect of KN-93 $F_{(1,16)} = 30.80$, $P < 0.0001$] (**Figure 6**). Therefore, we hypothesized that the functional interplay between NOS activity and CaMKII phosphorylation, observed in our experimental model, might have similar features to the above-mentioned glutamate-NO-cGMP pathway.

GUA Enhances NO Production in SH-SY5Y Cells and Pre-treatment with L-NAME Prevents This Effect

Finally, in order to compare the present data with those previously obtained *in vivo* (Giuliani et al., 2012), wherein L-NAME was able to prevent the GUA-mediated mnesic effect, we evaluated the effects of GUA on NO production. Cell exposure to 50 μM GUA for 30 min significantly increased NO production [two-way ANOVA: GUA effect $F_{(1,16)} = 6.451$, $P < 0.0218$, L-NAME effect $F_{(1,16)} = 6.451$, $P < 0.0218$ with interaction values between factors of $F_{(1,16)} = 4.681$, $P = 0.0460$] (**Figure 7**). A similar effect has been obtained when SH-SY5Y cells were challenged with 2 μM ionomycin, a calcium ionophore that induces NO production mainly via mobilization of intracellular Ca^{2+} [two-way ANOVA: GUA effect $F_{(1,16)} = 5.523$, $P < 0.0319$, ionomycin effect $F_{(1,16)} = 5.523$, $P < 0.0319$ with interaction values between factors of $F_{(1,16)} = 4.190$, $P = 0.0575$]. Cell pre-treatment (15 min before exposure to GUA or ionomycin) with 5 μM L-NAME, which *per se* did not affect the NO production of SH-SY5Y cells, strongly reduced the NO production induced by either GUA or ionomycin (**Figure 7**).

DISCUSSION

This work provides new insights on the transduction pathways involved in neuronal plasticity, in particular on the putative mechanism responsible of GUA-induced mnesic effects.

The major findings of the present study, performed in a model of neuronal-like cells (SH-SY5Y cells), are the following: (i) in resting condition, GUA is present in the intercellular milieu and derives from GTP breakdown, promoted by the activity of purine-converting enzymes (i.e., PNP and GDA) released in the culture medium; (ii) the inhibition of specific nucleoside and nucleobase transmembrane transporters enhances the extracellular levels of GUO, GUA and XAN;

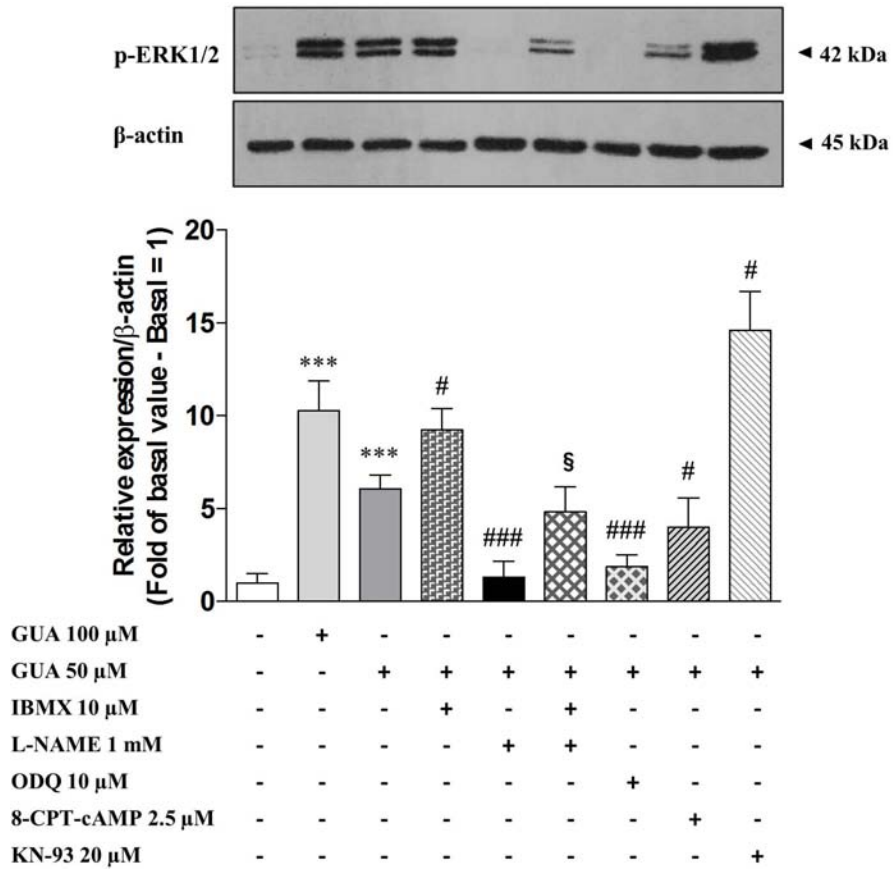

FIGURE 6 | Guanine activates sGC-cGMP-PKG-ERK signaling pathway in SH-SY5Y neuroblastoma cells. Representative Immunoblot analysis of ERK1/2 expression in SH-SY5Y cells, with β-actin as loading control, and the correspondent quantitative data of densitometric analysis. Cells were cultured for 24 h and exposed for 30 min to 100 μM GUA, 50 μM GUA, a phosphodiesterase inhibitor (10 μM IBMX), a NOS inhibitor (1 mM L-NAME), a sGC inhibitor (10 μM ODQ), an EPAC specific cAMP analog (2,5 μM 8-CPT-cAMP), a CaMKII inhibitor (20 μM KN-93). Each column represents the mean ± SEM of at least three independent experiments, and it is expressed as relative protein expression normalized to β-actin. Student's *t*-test: $^{***}P < 0.001$, vs. untreated cells (Basal); $^{\#}P < 0.05$, $^{\#\#\#}P < 0.001$, vs. GUA-treated cells, $^{\S}P < 0.05$, vs. GUA- and L-NAME-treated cells.

(iii) the addition of GUA to the culture medium caused a non-massive and dose-dependent production of ROS, and promotes the phosphorylation of ASK1, p38, JNK, PKC and PKB; (iv) extracellular GUA stimulates the PI3K-PKB phosphorylation and NO production, and activates the downstream sGC-cGMP-PKG-ERK pathway in a pertussis-toxin sensitive manner; (v) GUA-induced NO production is negatively modulated by the EPAC-cAMP-CAMKII pathway.

To better understand the results of this study, it has to be emphasized that, both *in vitro* and *in vivo* (Rathbone et al., 2008; Giuliani et al., 2012), the system of the extracellular guanine-based purines, together with a physiological and concerted activity of the enzymes regulating their metabolism (in particular PNP and GDA), is basically oriented to generate an higher amount of GUA rather than GUO or XAN; moreover, GUA stimulates the cGMP formation through NO production, which is known to modulate a broad range of effects in the CNS, such as neuronal development and synaptic plasticity (Prast and Philippu, 2001).

The evidence of the involvement of NO-cGMP pathway in some forms of learning and memory has been worked out by many authors (Erceg et al., 2005; Piedrafita et al., 2007; Ben Aissa et al., 2016; Cabrera-Pastor et al., 2016; Zhou et al., 2017). In several brain areas (i.e., hippocampus, cerebellum and striatum), increased levels of cGMP seemed to improve learning and memory consolidation, mainly during early stages of memory formation (immediately after training). This data is confirmed by full amnesia for inhibitory avoidance task when rats were treated with LY 83583, a soluble guanylate cyclase inhibitor, immediately after training (Bernabeu et al., 1997). However, not all signal transduction pathways, leading to cGMP formation, cause beneficial effects on cognitive functions. For example, cGMP has been found to mediate the stimulation of dendritic number and branching as well as the neurite elongation. This event likely occurs as a consequence of an interplay between cGMP and the activity of extrinsic/external factors such as neurotrophins (Tian et al., 2017) that, usually, stimulate cAMP formation. Cyclic nucleotides are differently involved in the memory consolidation process, since it has

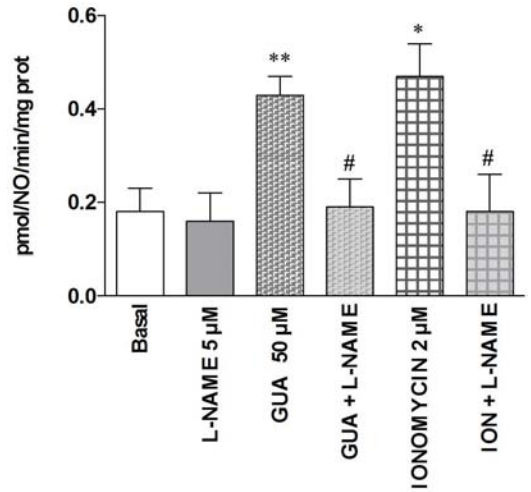

FIGURE 7 | Guanine increases NO production in SH-SY5Y neuroblastoma cells. SH-SY5Y cells were treated for 30 min with 5 μM L-NAME or 50 μM GUA (alone or in combination), 2 μM ionomycin (ION), alone or in combination with 5 μM L-NAME. NOS activity was determined by the conversion of L-[3H]-arginine into L-[3H]-citrulline and expressed as pmol/NO/min/mg prot tot. Data were expressed as means ± SEM of four different experiments. Student's *t*-test: $^{*}P < 0.05$, $^{**}P < 0.01$, vs. untreated cells (Basal); $^{\#}P < 0.05$, vs. GUA-treated cells.

been reported that cGMP regulates the early consolidation phase, whereas cAMP is implicated in late processes of memory formation (Izquierdo et al., 2006; Rutten et al., 2007; Bollen et al., 2014). In this functional interplay, a significant role seems to be played by the guanine-based purines, in particular by GUO and GUA. Indeed, several studies reported that GUO causes memory impairment (Roesler et al., 2000; Vinadé et al., 2003, 2004) but, at the same time and sinergistically with NGF, it promotes neurite outgrowth in PC12 cells via activation of heme-oxygenase and cGMP formation (Gysbers and Rathbone, 1996; Bau et al., 2005; Tomaselli et al., 2005). Cell exposure to neurotrophic factors such as NGF, for more than 24 h, promotes the phosphorylation of PKC-Ras-MAPK (Kumar et al., 2005) and, in turn, increases the mRNA levels of GDA, responsible of GUA degradation (Rathbone et al., 1999). This enzyme favors dendrite branching and elongation by directly binding tubulin heterodimers, thus promoting the microtubule assembly via cytoskeletal rearrangement (Akum et al., 2004). Therefore, the synergistic activity of neurotrophins with agents promoting neuritogenesis, such as GUO, explains why the neurogenic activity of GUO, despite being linked to an increased cGMP formation, is associated with an amnesic effect. Conversely, GUA promotes the early stages of memory formation in rats (Giuliani et al., 2012) and its effect seems to be linked to the NO-cGMP signaling pathway. In line with it, we observed that L-NAME prevented memory consolidation caused by the administration of GUA *in vivo*, in a model of passive avoidance task (Giuliani et al., 2012). In the same study, the administration of GUA, 15 min before treatment with L-NAME, prevented the amnesic effect of the NOS inhibitor.

The involvement of the NO-cGMP-PKG-ERK signaling pathway in synaptic plasticity has been extensively reported (Chien et al., 2008; Ota et al., 2010; Bartus et al., 2013; Matsumoto et al., 2016). However, the role of NO in each step of learning appears controversial and it might be task-dependent. ERK cascade is positively implicated in the development of fear conditioning, conditioned taste aversion memory, spatial memory, step-down inhibitory avoidance and object recognition memory (Giovannini, 2006; Chen et al., 2017; Vithayathil et al., 2017). In our study, this pathway resulted to be activated upon cell exposure to GUA. Specifically, extracellular GUA stimulated the PI3K-PKB phosphorylation and NO production, and activated the downstream sGC-cGMP-PKG-ERK pathway. It is feasible that GUA-induced ROS production, with the subsequent phosphorylation of ASK1, p38 and JNK, may contribute to the cGMP formation trough other pathways than NO, as confirmed by our data, wherein, in cells pre-treated with L-NAME, the inhibition of phosphodiesterases caused a limited increase in GUA-induced ERK1/2 phosphorylation.

Noteworthy, if the role of cGMP in learning and memory is important, much more valuable is that its mnesic effect is mediated by NO production. Indeed, the increase of the intracellular levels of cGMP induced by GUO, through the activation of HEME-oxygenase and independent of the NO production, is important for the dendrite and neurite outgrowth but it is associated with amnesia (Vinadé et al., 2004; Bau et al., 2005).

We, then, took into account the existence of a more complex network, wherein the NO production is eventually under the control of other molecular mechanisms and, among them, we investigated the EPAC-CAMKII system. CaMKII has a prominent role in memory formation (LTM) (Tan, 2007; Takao et al., 2010; Giese and Mizuno, 2013; Nakamura et al., 2017). For this purpose, we took advantage of a recent study, where they showed that the activation of CAMKII, upon stimulation of NMDA receptors, inhibits the production of NO that functions as a retrograde signal able to modulate the glutamatergic system (Cabrera-Pastor et al., 2016). Noteworthy, in our model, the activity of GUA was similar to that of glutamate, since we observed that the stimulation of the EPAC-CAMKII pathway inhibited the NO-mediated phosphorylation of ERK1/2 induced by GUA. The blockage of this pathway by using a CaMKII inhibitor, KN-93, amplified GUA effect. Consistent with it, two endogenous CaMKII inhibitors (CaMK2N1 and CaMK2N2) have been shown to prevent memory loss after retrieval (Vigil et al., 2017). However, it should be pointed out that the influence exerted by CaMKII on the phosphorylation of ERK is not univocal. Indeed, it has been reported that: (i) in vascular smooth muscle cells the CaMKII inhibitor KN-93 caused an H_2O_2-mediated reduction of ERK1/2 and PKB phosphorylation (Robison et al., 2007; Bouallegue et al., 2009); (ii) the presynaptic injection of a CaMKII inhibitor blocked LTP and neurotransmitter release induced by either the NO donor or the PKG activator (Feil and Kleppisch, 2008).

Finally, we speculated that the extracellular effect of GUA may be mediated by a membrane receptor at present not well identified. In this study, cell treatment with pertussis toxin

strongly reduced the GUA-evoked ERK1/2 phosphorylation, thus indicating that this putative new GUA receptor is likely coupled with Gi/o proteins.

Guanine-based purines, in particular GUO, seems to bind to metabotropic receptors and many of their effects are mediated through G-protein-dependent signaling pathways; it has been shown, for instance, that the pertussis toxin-mediated inhibition of Gi/Go-protein reverses some of the effects of GUO on cell viability and glutamate uptake in hippocampal slices (Traversa et al., 2003; Dal-Cim et al., 2012, 2013).

Several years ago, our group found a specific [3H]-guanosine binding site in rat brain membranes, compatible with an unknown G protein-coupled receptor (Traversa et al., 2002, 2003; Di Liberto et al., 2012; Grillo et al., 2012). In order to provide insight into the characteristics of the binding site, we evaluated the relative abilities of purine analogs to displace [3H]GUO. Binding data revealed that all the adenine-based purines as well as GTP, GDP and GMP were ineffective in displacing [3H]GUO. The 6-Thio-GUO or 6-keto-GUO derivatives resulted to be as effective as GUO in displacing [3H]GUO. On the contrary, the binding affinity was strongly reduced when the 6-amino or 2-amino derivatives were assayed.

These findings seem to be compatible with a membrane binding site, expressed in the rat brain, which, in addition to GUO, may interact with GUA, although with a lower affinity. At present, we are carrying out a study to individuate and functionally characterize this new putative receptor.

At the same time, it cannot be excluded an interaction of GUA with another receptor functionally different from G protein-coupled receptors. Indeed, it is well known that compounds that are structurally very similar to GUO and GUA represent the main agonists of several Toll-like receptors (i.e., TLR9, 7 and 8) (Lee et al., 2003; Yu et al., 2017).

In this context, it has been recently reported that the stimulation of some subtypes of Toll-Like receptors (TLR9, 7 and 8) in microglial cells leads to cognitive improvements and ameliorates the vascular amyloid pathology in triple transgenic mice expressing human Swedish K670N/M671L and vasculotropic Dutch/Iowa E693Q/D694N mutations and exhibiting early cerebral microvascular accumulation of Aβ (Scholtzova et al., 2017). Interestingly, some guanine-based purines and their modified derivatives have been recently recognized as endogenous ligands for TLRs, especially 7 and 9 subtypes (Shibata et al., 2016; Abdul-Cader et al., 2017). In this regard, in order to eliminate the effects potentially mediated by TLRs, in our study we used cultured SH-SY5Y cells, wherein the expression of TLR 7/8 and 9 is not reported in literature.

CONCLUSION

Targeting NO-cGMP-PKG-ERK signaling pathway may represent an interesting approach for the development of new drugs in the treatment of memory dysfunctions occurring in neurodegenerative and psychiatric diseases, among others Alzheimer's disease and dementia. Initial promising findings in this direction have been reported regarding the use of PDE inhibitors (Kumar and Singh, 2017; Prickaerts et al., 2017) or sGC stimulator (Montfort et al., 2017) in the treatment of neuroinflammatory and neuropathological conditions.

It is plausible to expect that, beyond the above-mentioned guanine-derivatives, the administration of GUA itself (Giuliani et al., 2012), due to its long half-life *in vivo*, may elicit molecular changes that underlie synaptic alterations and memory formation through a putative receptor that could represent a new pharmacological target. This may serve the purpose of avoiding a major challenge, that is to discriminate the numerous downstream effectors ensuing the activation of NO-cGMP-ERK signaling pathway, thus bypassing the sophisticated network of different and multifunctional protein kinases.

AUTHOR CONTRIBUTIONS

All authors listed have made a substantial, direct and intellectual contribution to the work, and approved it for publication.

FUNDING

This study was partially supported by funds to PDI from the Italian Ministry of Education, University and Research (MIUR).

REFERENCES

Abdul-Cader, M. S., Ahmed-Hassan, H., Amarasinghe, A., Nagy, E., Sharif, S., and Abdul-Careem, M. F. (2017). Toll-like receptor (TLR)21 signalling-mediated antiviral response against avian influenza virus infection correlates with macrophage recruitment and nitric oxide production. *J. Gen. Virol.* 98, 1209–1223. doi: 10.1099/jgv.0.000787

Adaikkan, C., and Rosenblum, K. (2012). The role of protein phosphorylation in the gustatory cortex and amygdala during taste learning. *Exp. Neurobiol.* 21, 37–51. doi: 10.5607/en.2012.21.2.37

Adams, J. P., and Sweatt, J. D. (2002). Molecular psychology: roles for the ERK MAP kinase cascade in memory. *Annu. Rev. Pharmacol. Toxicol.* 42, 135–163. doi: 10.1146/annurev.pharmtox.42.082701.145401

Akum, B. F., Chen, M., Gunderson, S. I., Riefler, G. M., Scerri-Hansen, M. M., and Firestein, B. L. (2004). Cypin regulates dendrite patterning in hippocampal neurons by promoting microtubule assembly. *Nat. Neurosci.* 7, 145–152. doi: 10.1038/nn1179

Ali-Rahmani, F., Grigson, P. S., Lee, S., Neely, E., Connor, J. R., and Schengrund, C. L. (2014). H63D mutation in hemochromatosis alters cholesterol metabolism and induces memory impairment. *Neurobiol. Aging* 35, 1511.e1–1511.e12. doi: 10.1016/j.neurobiolaging.2013.12.014

Bartus, K., Pigott, B., and Garthwaite, J. (2013). Cellular targets of nitric oxide in the hippocampus. *PLoS One* 8:e57292. doi: 10.1371/journal.pone.0057292

Bau, C., Middlemiss, P. J., Hindley, S., Jiang, S., Ciccarelli, R., Caciagli, F., et al. (2005). Guanosine stimulates neurite outgrowth in PC12 cells via activation of heme oxygenase and cyclic GMP. *Purinergic Signal.* 1, 161–172. doi: 10.1007/s11302-005-6214-0

Bellaver, B., Souza, D. G., Bobermin, L. D., Goncalves, C. A., Souza, D. O., and Quincozes-Santos, A. (2015). Guanosine inhibits LPS-induced pro-inflammatory response and oxidative stress in hippocampal astrocytes through the heme oxygenase-1 pathway. *Purinergic Signal.* 11, 571–580. doi: 10.1007/s11302-015-9475-2

Ben Aissa, M., Lee, S. H., Bennett, B. M., and Thatcher, G. R. (2016). Targeting NO/cGMP signaling in the CNS for neurodegeneration and

Alzheimer's disease. *Curr. Med. Chem.* 23, 2770–2788. doi: 10.2174/0929867323666160812145454

Bernabeu, R., Schroder, N., Quevedo, J., Cammarota, M., Izquierdo, I., and Medina, J. H. (1997). Further evidence for the involvement of a hippocampal cGMP/cGMP-dependent protein kinase cascade in memory consolidation. *Neuroreport* 8, 2221–2224. doi: 10.1097/00001756-199707070-00026

Bettio, L. E., Gil-Mohapel, J., and Rodrigues, A. L. (2016). Guanosine and its role in neuropathologies. *Purinergic Signal.* 12, 411–426. doi: 10.1007/s11302-016-9509-4

Boess, F. G., Hendrix, M., van der Staay, F. J., Erb, C., Schreiber, R., van Staveren, W., et al. (2004). Inhibition of phosphodiesterase 2 increases neuronal cGMP, synaptic plasticity and memory performance. *Neuropharmacology* 47, 1081–1092. doi: 10.1016/j.neuropharm.2004.07.040

Boison, D. (2011). Modulators of nucleoside metabolism in the therapy of brain diseases. *Curr. Top. Med. Chem.* 11, 1068–1086. doi: 10.2174/156802611795347609

Bollen, E., Puzzo, D., Rutten, K., Privitera, L., De Vry, J., Vanmierlo, T., et al. (2014). Improved long-term memory via enhancing cGMP-PKG signaling requires cAMP-PKA signaling. *Neuropsychopharmacology* 39, 2497–2505. doi: 10.1038/npp.2014.106

Bouallegue, A., Pandey, N. R., and Srivastava, A. K. (2009). CaMKII knockdown attenuates H2O2-induced phosphorylation of ERK1/2, PKB/Akt, and IGF-1R in vascular smooth muscle cells. *Free Radic. Biol. Med.* 47, 858–866. doi: 10.1016/j.freeradbiomed.2009.06.022

Bredt, D. S., Hwang, P. M., Glatt, C. E., Lowenstein, C., Reed, R. R., and Snyder, S. H. (1991). Cloned and expressed nitric oxide synthase structurally resembles cytochrome P-450 reductase. *Nature* 351, 714–718. doi: 10.1038/351714a0

Cabrera-Pastor, A., Malaguarnera, M., Taoro-Gonzalez, L., Llansola, M., and Felipo, V. (2016). Extracellular cGMP modulates learning biphasically by modulating glycine receptors, CaMKII and glutamate-nitric oxide-cGMP pathway. *Sci. Rep.* 6:33124. doi: 10.1038/srep33124

Charych, E. I., Akum, B. F., Goldberg, J. S., Jörnsten, R. J., Rongo, C., Zheng, J. Q., et al. (2006). Activity-independent regulation of dendrite patterning by postsynaptic density protein PSD-95. *J. Neurosci.* 26, 10164–10176. doi: 10.1523/JNEUROSCI.2379-06.2006

Chen, X., Wang, X., Tang, L., Wang, J., Shen, C., Liu, J., et al. (2017). Nhe5 deficiency enhances learning and memory via upregulating Bdnf/TrkB signaling in mice. *Am. J. Med. Genet. B Neuropsychiatr. Genet.* 174, 828–838. doi: 10.1002/ajmg.b.32600

Chien, W. L., Liang, K. C., and Fu, W. M. (2008). Enhancement of active shuttle avoidance response by the NO-cGMP-PKG activator YC-1. *Eur. J. Pharmacol.* 590, 233–240. doi: 10.1016/j.ejphar.2008.06.040

Ciccarelli, R., Ballerini, P., Sabatino, G., Rathbone, M. P., D'Onofrio, M., Caciagli, F., et al. (2001). Involvement of astrocytes in purine-mediated reparative processes in the brain. *Int. J. Dev. Neurosci.* 19, 395–414. doi: 10.1016/S0736-5748(00)00084-8

Dal-Cim, T., Ludka, F. K., Martins, W. C., Reginato, C., Parada, E., Egea, J., et al. (2013). Guanosine controls inflammatory pathways to afford neuroprotection of hippocampal slices under oxygen and glucose deprivation conditions. *J. Neurochem.* 126, 437–450. doi: 10.1111/jnc.12324

Dal-Cim, T., Molz, S., Egea, J., Parada, E., Romero, A., Budni, J., et al. (2012). Guanosine protects human neuroblastoma SH-SY5Y cells against mitochondrial oxidative stress by inducing heme oxigenase-1 via PI3K/Akt/GSK-3beta pathway. *Neurochem. Int.* 61, 397–404. doi: 10.1016/j.neuint.2012.05.021

Davis, S., and Laroche, S. (2006). Mitogen-activated protein kinase/extracellular regulated kinase signalling and memory stabilization: a review. *Genes Brain Behav.* 5, 61–72. doi: 10.1111/j.1601-183X.2006.00230.x

Di Iorio, P., Ballerini, P., Traversa, U., Nicoletti, F., D'Alimonte, I., Kleywegt, S., et al. (2004). The antiapoptotic effect of guanosine is mediated by the activation of the PI 3-kinase/AKT/PKB pathway in cultured rat astrocytes. *Glia* 46, 356–368. doi: 10.1002/glia.20002

Di Iorio, P., Caciagli, F., Giuliani, P., Ballerini, P., Ciccarelli, R., Sperling, O., et al. (2001). Purine nucleosides protect injured neurons and stimulate neuronal regeneration by intracellular and membrane receptor-mediated mechanisms. *Drug Dev. Res.* 52, 303–315. doi: 10.1002/ddr.1128

Di Liberto, V., Garozzo, R., Grillo, M., Mudo, G., Caciagli, F., Condorelli, D. F., et al. (2012). Identification of GPR23/LPA4 as a candidate G protein-coupled receptor for guanosine. *Acta Physiol.* 206(Suppl. 692):O.16. doi: 10.1089/adt.2009.0261

Di Liberto, V., Mudò, G., Garozzo, R., Frinchi, M., Fernandez-Dueñas, V., Di Iorio, P., et al. (2016). The guanine-based purinergic system: the tale of an orphan neuromodulation. *Front. Pharmacol.* 7:158. doi: 10.3389/fphar.2016.00158

Erceg, S., Monfort, P., Hernández-Viadel, M., Rodrigo, R., Montoliu, C., and Felipo, V. (2005). Oral administration of sildenafil restores learning ability in rats with hyperammonemia and with portacaval shunts. *Hepatology* 41, 299–306. doi: 10.1002/hep.20565

Feil, R., and Kleppisch, T. (2008). NO/cGMP-dependent modulation of synaptic transmission. *Handb. Exp. Pharmacol.* 184, 529–560. doi: 10.1007/978-3-540-74805-2_16

Feng, Y., Chambers, J. W., Iqbal, S., Koenig, M., Park, H., Cherry, C., et al. (2013). A small molecule bidentate-binding dual inhibitor probe of the LRRK2 and JNK kinases. *ACS Chem. Biol.* 8, 1747–1754. doi: 10.1021/cb3006165

Fink, C. C., Bayer, K. U., Myers, J. W., Ferrell, J. E. Jr., Schulman, H., and Meyer, T. (2003). Selective regulation of neurite extension and synapse formation by the beta but not the alpha isoform of CaMKII. *Neuron* 39, 283–297. doi: 10.1016/S0896-6273(03)00428-8

Friebe, A., and Koesling, D. (2003). Regulation of nitric oxide-sensitive guanylyl cyclase. *Circ. Res.* 93, 96–105. doi: 10.1161/01.RES.0000082524.34487.31

Giese, K. P., and Mizuno, K. (2013). The roles of protein kinases in learning and memory. *Learn. Mem.* 20, 540–552. doi: 10.1101/lm.028449.112

Giovannini, M. G. (2006). The role of the extracellular signal-regulated kinase pathway in memory encoding. *Rev. Neurosci.* 17, 619–634. doi: 10.1515/REVNEURO.2006.17.6.619

Giuliani, P., Ballerini, P., Buccella, S., Ciccarelli, R., Rathbone, M. P., Romano, S., et al. (2015). Guanosine protects glial cells against 6-hydroxydopamine toxicity. *Adv. Exp. Med. Biol.* 837, 23–33. doi: 10.1007/5584_2014_73

Giuliani, P., Buccella, S., Ballerini, P., Ciccarelli, R., D'Alimonte, I., Cicchitti, S., et al. (2012). Guanine-based purines modulate the effect of L-NAME on learning and memory in rats. *Panminerva Med.* 54, 53–58.

Giuliani, P., Zuccarini, M., Buccella, S., Pena-Altamira, L. E., Polazzi, E., Virgili, M., et al. (2017). Evidence for purine nucleoside phosphorylase (PNP) release from rat C6 glioma cells. *J. Neurochem.* 141, 208–221. doi: 10.1111/jnc.14004

Giuliani, P., Zuccarini, M., Buccella, S., Rossini, M., D'Alimonte, I., Ciccarelli, R., et al. (2016). Development of a new HPLC method using fluorescence detection without derivatization for determining purine nucleoside phosphorylase activity in human plasma. *J. Chromatogr. B Analyt. Technol. Biomed. Life Sci.* 1009–1010, 114–121. doi: 10.1016/j.jchromb.2015.12.012

Grillo, M., di Liberto, V., Garozzo, R., Mudo, G., Caciagli, F., Condorelli, D. F., et al. (2012). Brain expression and 3H-guanosine binding analysis of novel G protein- coupled receptor for guanosine (GPR23/LPA4). *Acta Physiol.* 206(Suppl. 692):P4.19.

Gysbers, J. W., and Rathbone, M. P. (1996). Neurite outgrowth in PC12 cells is enhanced by guanosine through both cAMP-dependent and -independent mechanisms. *Neurosci. Lett.* 220, 175–178. doi: 10.1016/S0304-3940(96)13253-5

Ha, H. C., Woster, P. M., Yager, J. D., and Casero, R. A. (1997). The role of polyamine catabolism in polyamine analogue-induced programmed cell death. *Proc. Natl. Acad. Sci. U.S.A.* 94, 11557–11562. doi: 10.1073/pnas.94.21.11557

Izquierdo, I., Bevilaqua, L. R., Rossato, J. I., Bonini, J. S., Medina, J. H., and Cammarota, M. (2006). Different molecular cascades in different sites of the brain control memory consolidation. *Trends Neurosci.* 29, 496–505. doi: 10.1016/j.tins.2006.07.005

Jiang, W., Chen, Y., Li, B., and Gao, S. (2017). DBA-induced caspase-3-dependent apoptosis occurs through mitochondrial translocation of cyt-c in the rat hippocampus. *Mol. Biosyst.* 3, 1863–1873. doi: 10.1039/c7mb00246g

Kumar, A., and Singh, N. (2017). Inhibitor of phosphodiestearse-4 improves memory deficits, oxidative stress, neuroinflammation and neuropathological alterations in mouse models of dementia of Alzheimer's type. *Biomed. Pharmacother.* 88, 698–707. doi: 10.1016/j.biopha.2017.01.059

Kumar, V., Zhang, M. X., Swank, M. W., Kunz, J., and Wu, G. Y. (2005). Regulation of dendritic morphogenesis by Ras–PI3K–Akt–mTOR and Ras–MAPK signaling pathways. *J. Neurosci.* 25, 11288–11299. doi: 10.1523/JNEUROSCI.2284-05.2005

Lanznaster, D., Dal-Cim, T., Piermartiri, T. C. B., and Tasca, C. I. (2016). Guanosine: a neuromodulator with therapeutic potential in brain disorders. *Aging Dis.* 7, 657–679. doi: 10.14336/AD.2016.0208

Lee, D. S., and Cheong, S. H. (2017). Taurine have neuroprotective activity against oxidative damage-induced HT22 cell death through heme oxygenase-1 pathway. *Adv. Exp. Med. Biol.* 975, 159–171. doi: 10.1007/978-94-024-1079-2_14

Lee, J., Chuang, T. H., Redecke, V., She, L., Pitha, P. M., Carson, D. A., et al. (2003). Molecular basis for the immunostimulatory activity of guanine nucleoside analogs: activation of Toll-like receptor 7. *Proc. Natl. Acad. Sci. U.S.A.* 100, 6646–6651. doi: 10.1073/pnas.0631696100

Lepicard, E. M., Mizuno, K., Antunes-Martins, A., von Hertzen, L. S., and Giese, K. P. (2006). An endogenous inhibitor of calcium/calmodulin-dependent kinase II is up-regulated during consolidation of fear memory. *Eur. J. Neurosci.* 23, 3063–3070. doi: 10.1111/j.1460-9568.2006.04830.x

Lucchesi, W., Mizuno, K., and Giese, K. P. (2011). Novel insights into CaMKII function and regulation during memory formation. *Brain Res. Bull.* 85, 2–8. doi: 10.1016/j.brainresbull.2010.10.009

Lueptow, L. M., Zhan, C. G., and O'Donnell, J. M. (2015). Cyclic GMP–mediated memory enhancement in the object recognition test by inhibitors of phosphodiesterase-2 in mice. *Psychopharmacology* 233, 447–456. doi: 10.1007/s00213-015-4129-1

Masood, A., Huang, Y., Hajjhussein, H., Xiao, L., Li, H., Wang, W., et al. (2009). Anxiolytic effects of phosphodiesterase-2 inhibitors associated with increased cGMP signaling. *J. Pharmacol. Exp. Ther.* 331, 690–699. doi: 10.1124/jpet.109.156729

Matsumoto, Y., Matsumoto, C. S., Takahashi, T., and Mizunami, M. (2016). Activation of NO-cGMP signaling rescues age-related memory impairment in crickets. *Front. Behav. Neurosci.* 10:166. doi: 10.3389/fnbeh.2016.00166

Miyamoto, E. (2006). Molecular mechanism of neuronal plasticity: induction and maintenance of long-term potentiation in the hippocampus. *J. Pharmacol. Sci.* 100, 433–442. doi: 10.1254/jphs.CPJ06007X

Miyamoto, S., Ogawa, H., Shiraki, H., and Nakagawa, H. (1982). Guanine deaminase from rat brain. Purification, characteristics, and contribution to ammoniagenesis in the brain. *J. Biochem.* 91, 167–176. doi: 10.1093/oxfordjournals.jbchem.a133673

Modi, K. K., Jana, A., Ghosh, S., Watson, R., and Pahan, K. (2017). A physically-modified saline suppresses neuronal apoptosis, attenuates tau phosphorylation and protects memory in an animal model of Alzheimer's disease. *PLoS One* 12:e0180602. doi: 10.1371/journal.pone.0103606

Montfort, W. R., Wales, J. A., and Weichsel, A. (2017). Structure and activation of soluble guanylyl cyclase, the nitric oxide sensor. *Antioxid. Redox Signal.* 26, 107–121. doi: 10.1089/ars.2016.6693

Moosavi, M., Abbasi, L., Zarifkar, A., and Rastegar, K. (2014). The role of nitric oxide in spatial memory stages, hippocampal ERK and CaMKII phosphorylation. *Pharmacol. Biochem. Behav.* 122, 164–172. doi: 10.1016/j.pbb.2014.03.021

Nakamura, T. Y., Nakao, S., Nakajo, Y., Takahashi, J. C., Wakabayashi, S., and Yanamoto, H. (2017). Possible signaling pathways mediating neuronal calcium sensor-1-dependent spatial learning and memory in mice. *PLoS One* 12:e0170829. doi: 10.1371/journal.pone.0170829

Neary, J. T. (1996). Trophic actions of extracellular nucleotides and nucleosides on glial and neuronal cells. *Trends Neurosci.* 19, 13–18. doi: 10.1016/0166-2236(96)81861-3

Ota, K. T., Monsey, M. S., Wu, M. S., Young, G. J., and Schafe, G. E. (2010). Synaptic plasticity and NO-cGMP-PKG signaling coordinately regulate ERK-driven gene expression in the lateral amygdala and in the auditory thalamus following Pavlovian fear conditioning. *Learn. Mem.* 17, 221–235. doi: 10.1101/lm.1592510

Peña-Altamira, L. E., Polazzi, E., Giuliani, P., Beraudi, A., Massenzio, F., Mengoni, I., et al. (2017). Release of soluble and vesicular purine nucleoside phosphorylase from rat astrocytes and microglia induced by pro-inflammatory stimulation with extracellular ATP via P2X7 receptors. *Neurochem. Int.* doi: 10.1016/j.neuint.2017.10.010 [Epub ahead of print].

Philips, G. T., Tzvetkova, E. I., and Carew, T. J. (2007). Transient mitogen-activated protein kinase activation is confined to a narrow temporal window required for the induction of two-trial long-term memory in *Aplysia*. *J. Neurosci.* 27, 13701–13705. doi: 10.1523/JNEUROSCI.4262-07.2007

Piedrafita, B., Cauli, O., Montoliu, C., and Felipo, V. (2007). The function of the glutamate-nitric oxide-cGMP pathway in brain in vivo and learning ability decrease in parallel in mature compared with young rats. *Learn. Mem.* 14, 254–258. doi: 10.1101/lm.541307

Ping, J., and Schafe, G. E. (2010). The NO-cGMP-PKG signaling pathway coordinately regulates ERK and ERK-driven gene expression at pre- and postsynaptic sites following LTP-inducing stimulation of thalamo-amygdala synapses. *Neural Plast.* 2010:540940. doi: 10.1155/2010/540940

Prast, H., and Philippu, A. (2001). Nitric oxide as modulator of neuronal function. *Prog. Neurobiol.* 64, 51–68. doi: 10.1016/S0301-0082(00)00044-7

Prickaerts, J., de Vente, J., Honig, W., Steinbusch, H. W. M., and Blokland, A. (2001). cGMP, but not cAMP, in rat hippocampus is involved in early stages of object memory consolidation. *Eur. J. Pharmacol.* 436, 83–87. doi: 10.1016/S0014-2999(01)01614-4

Prickaerts, J., Heckman, P. R. A., and Blokland, A. (2017). Investigational phosphodiesterase inhibitors in phase I and phase II clinical trials for Alzheimer's disease. *Expert Opin. Investig. Drugs* 26, 1033–1048. doi: 10.1080/13543784.2017.1364360

Puangmalai, N., Thangnipon, W., Soi-Ampornkul, R., Suwanna, N., Tuchinda, P., and Nobsathian, S. (2017). Neuroprotection of N-benzylcinnamide on scopolamine-induced cholinergic dysfunction in human SH-SY5Y neuroblastoma cells. *Neural Regen. Res.* 12, 1492–1498. doi: 10.4103/1673-5374.215262

Quincozes-Santos, A., Bobermin, L. D., Souza, D. G., Bellaver, B., Goncalves, C. A., and Souza, D. O. (2014). Guanosine protects C6 astroglial cells against azide-induced oxidative damage: a putative role of heme-oxygenase 1. *J. Neurochem.* 130, 61–74. doi: 10.1111/jnc.12694

Rathbone, M., Pilutti, L., Caciagli, F., and Jiang, S. (2008). Neurotrophic effects of extracellular guanosine. *Nucleosides Nucleotides Nucleic Acids* 27, 666–672. doi: 10.1080/15257770802143913

Rathbone, M. P., Middlemiss, P. J., Gysbers, J. W., Andrew, C., Herman, M. A., Reed, J. K., et al. (1999). Trophic effects of purines in neurons and glial cells. *Prog. Neurobiol.* 59, 663–690. doi: 10.1016/S0301-0082(99)00017-9

Reneerkens, O. A. H., Rutten, K., Steinbusch, H. W. M., Blokland, A., and Prickaerts, J. (2009). Selective phosphodiesterase inhibitors: a promising target for cognition enhancement. *Psychopharmacology* 202, 419–443. doi: 10.1007/s00213-008-1273-x

Ribeiro, F. (2016). Purine nucleosides in neuroregeneration and neuroprotection. *Neuropharmacology* 104, 226–242. doi: 10.1016/j.neuropharm.2015.11.006

Robison, A. J., Winder, D. G., Colbran, R. J., and Bartlett, R. K. (2007). Oxidation of calmodulin alters activation and regulation of CaMKII. *Biochem. Biophys. Res. Commun.* 356, 97–101. doi: 10.1016/j.bbrc.2007.02.087

Roesler, R., Vianna, M. R., Lara, D. R., Izquierdo, I., Schmidt, A. P., and Souza, D. O. (2000). Guanosine impairs inhibitory avoidance performance in rats. *Neuroreport* 11, 2537–2540. doi: 10.1097/00001756-200008030-00038

Rutten, K., Prickaerts, J., Hendrix, M., van der Staay, F. J., Şik, A., and Blokland, A. (2007). Time-dependent involvement of cAMP and cGMP in consolidation of object memory: studies using selective phosphodiesterase type 2, 4 and 5 inhibitors. *Eur. J. Pharmacol.* 558, 107–112. doi: 10.1016/j.ejphar.2006.11.041

Saute, J. A., da Silveira, L. E., Soares, F. A., Martini, L. H., Souza, D. O., and Ganzella, M. (2006). Amnesic effect of GMP depends on its conversion to guanosine. *Neurobiol. Learn. Mem.* 85, 206–212. doi: 10.1016/j.nlm.2005.10.006

Schmidt, A. P., Lara, D. R., and Souza, D. O. (2007). Proposal of a guanine-based purinergic system in the mammalian central nervous system. *Pharmacol. Ther.* 116, 401–416. doi: 10.1016/j.pharmthera.2007.07.004

Scholtzova, H., Do, E., Dhakal, S., Sun, Y., Liu, S., Mehta, P. D., et al. (2017). Innate immunity stimulation via toll-like receptor 9 ameliorates vascular amyloid pathology in Tg-SwDI mice with associated cognitive benefits. *J. Neurosci.* 37, 936–959. doi: 10.1523/JNEUROSCI.1967-16.2016

Shen, H. M., and Liu, Z. G. (2006). JNK signaling pathway is a key modulator in cell death mediated by reactive oxygen and nitrogen species. *Free Radic. Biol. Med.* 40, 928–939. doi: 10.1016/j.freeradbiomed.2005.10.056

Shibata, T., Ohto, U., Nomura, S., Kibata, K., Motoi, Y., Zhang, Y., et al. (2016). Guanosine and its modified derivatives are endogenous ligands for TLR7. *Int. Immunol.* 28, 211–222. doi: 10.1093/intimm/dxv062

Suvarna, N. U., and O'Donnell, J. M. (2002). Hydrolysis of N-methyl-D-aspartate receptor-stimulated cAMP and cGMP by PDE4 and PDE2 phosphodiesterases

in primary neuronal cultures of rat cerebral cortex and hippocampus. *J. Pharmacol. Exp. Ther.* 302, 249–256. doi: 10.1124/jpet.302.1.249

Takao, K., Tanda, K., Nakamura, K., Kasahara, J., Nakao, K., Katsuki, M., et al. (2010). Comprehensive behavioral analysis of calcium/calmodulin-dependent protein kinase IV knockout mice. *PLoS One* 5:e9460. doi: 10.1371/journal.pone.0009460

Tan, S. E. (2007). Roles of hippocampal nitric oxide and calcium/calmodulin-dependent protein kinase II in inhibitory avoidance learning in rats. *Behav. Pharmacol.* 18, 29–38. doi: 10.1097/FBP.0b013e3280142636

Tarozzi, A., Merlicco, A., Morroni, F., Bolondi, C., Di Iorio, P., Ciccarelli, R., et al. (2010). Guanosine protects human neuroblastoma cells from oxidative stress and toxicity induced by amyloid-beta peptide oligomers. *J. Biol. Regul. Homeost. Agents* 24, 297–306.

Thomaz, D. T., Dal-Cim, T. A., Martins, V. C., Cunha, M. P., Lanznaster, D., de Bem, A. F., et al. (2016). Guanosine prevents nitroxidative stress and recovers mitochondrial membrane potential disruption in hippocampal slices subjected to oxygen/glucose deprivation. *Purinergic Signal.* 12, 707–718. doi: 10.1007/s11302-016-9534-3

Tian, X., Yan, H., Li, J., Wu, S., Wang, J., and Fan, L. (2017). Neurotrophin promotes neurite outgrowth by inhibiting Rif GTPase activation downstream of MAPKs and PI3K signaling. *Int. J. Mol. Sci.* 18:148. doi: 10.3390/ijms18010148

Tomaselli, B., Podhraski, V., Heftberger, V., Bock, G., and Baier-Bitterlich, G. (2005). Purine nucleoside-mediated protection of chemical hypoxia-induced neuronal injuries involves p42/44 MAPK activation. *Neurochem. Int.* 46, 513–521. doi: 10.1016/j.neuint.2005.02.003

Traversa, U., Bombi, G., Camaioni, E., Macchiarulo, A., Costantino, G., Palmieri, C., et al. (2003). Rat brain guanosine binding site. Biological studies and pseudo- receptor construction. *Bioorg. Med. Chem.* 11, 5417–5425. doi: 10.1016/j.bmc.2003.09.043

Traversa, U., Bombi, G., Di Iorio, P., Ciccarelli, R., Werstiuk, E. S., and Rathbone, M. P. (2002). Specific [^{3}H]-guanosine binding sites in rat brain membranes. *Br. J. Pharmacol.* 135, 969–976. doi: 10.1038/sj.bjp.0704542

Vigil, F. A., Mizuno, K., Lucchesi, W., Valls-Comamala, V., and Giese, K. P. (2017). Prevention of long-term memory loss after retrieval by an endogenous CaMKII inhibitor. *Sci. Rep.* 7:4040. doi: 10.1038/s41598-017-04355-8

Vinadé, E. R., Izquierdo, I., Lara, D. R., Schmidt, A. P., and Souza, D. O. (2004). Oral administration of guanosine impairs inhibitory avoidance performance in rats and mice. *Neurobiol. Learn. Mem.* 81, 137–143. doi: 10.1016/j.nlm.2003.12.003

Vinadé, E. R., Schmidt, A. P., Frizzo, M. E., Izquierdo, I., Elisabetsky, E., and Souza, D. O. (2003). Chronically administered guanosine is anticonvulsant, amnesic and anxiolytic in mice. *Brain Res.* 977, 97–102. doi: 10.1016/S0006-8993(03)02769-0

Vithayathil, J., Pucilowska, J., Friel, D., and Landreth, G. E. (2017). Chronic impairment of ERK signaling in glutamatergic neurons of the forebrain does not affect spatial memory retention and LTP in the same manner as acute blockade of the ERK pathway. *Hippocampus* 27, 1239–1249. doi: 10.1002/hipo.22769

Xu, Y., Pan, J., Chen, L., Zhang, C., Sun, J., Li, J., et al. (2013). Phosphodiesterase-2 inhibitor reverses corticosterone-induced neurotoxicity and related behavioural changes via cGMP/PKG dependent pathway. *Int. J. Neuropsychopharmacol.* 16, 835–847. doi: 10.1017/S146114571200065X

Yu, C., An, M., Li, M., and Liu, H. (2017). Immunostimulatory properties of lipid modified CpG oligonucleotides. *Mol. Pharm.* 14, 2815–2823. doi: 10.1021/acs.molpharmaceut.7b00335

Yu, X., and Malenka, R. C. (2004). Multiple functions for the cadherin/catenin complex during neuronal development. *Neuropharmacology* 47, 779–786. doi: 10.1016/j.neuropharm.2004.07.031

Zhou, X. Y., Zhang, F., Ying, C. J., Chen, J., Chen, L., Dong, J., et al. (2017). Inhibition of iNOS alleviates cognitive deficits and depression in diabetic mice through downregulating the NO/sGC/cGMP/PKG signal pathway. *Behav. Brain Res.* 322, 70–82. doi: 10.1016/j.bbr.2016.12.046

Conflict of Interest Statement: The authors declare that the research was conducted in the absence of any commercial or financial relationships that could be construed as a potential conflict of interest.

frontiers in Pharmacology

ORIGINAL RESEARCH
published: 15 February 2018
doi: 10.3389/fphar.2018.00079

Long-term Treatment with Low-Dose Caffeine Worsens BPSD-Like Profile in 3xTg-AD Mice Model of Alzheimer's Disease and Affects Mice with Normal Aging

*Raquel Baeta-Corral[1,2], Björn Johansson[3,4] and Lydia Giménez-Llort[1,2]**

[1] Institut de Neurociències, Universitat Autònoma de Barcelona, Barcelona, Spain, [2] Department of Psychiatry and Forensic Medicine, Universitat Autònoma de Barcelona, Barcelona, Spain, [3] Department of Molecular Medicine and Surgery, Karolinska Institutet, Solna, Sweden, [4] Department of Geriatrics, Karolinska University Hospital, Solna, Sweden

Coffee or caffeine has recently been suggested as prophylaxis for dementia. Although memory problems are hallmarks of Alzheimer's disease, this dementia is also characterized by neuropsychiatric symptoms called Behavioral and Psychological Symptoms of Dementia (BPSD). The impact of preventive/therapeutic strategies on both cognitive and non-cognitive symptoms can be addressed in the 3xTg-AD mice, since they exhibit cognitive but also BPSD-like profiles. Here, we studied the long-term effects of a low dose of caffeine in male 3xTg-AD mice and as compared to age-matched non-transgenic (NTg) counterparts with normal aging. Animals were treated (water or caffeine in drinking water) from adulthood (6 months of age) until middle-aged (13 months of age), that in 3xTg-AD mice correspond to onset of cognitive impairment and advanced stages, respectively. The low caffeine dosing used (0.3 mg/ml) was previously found to give a plasma concentration profile in mice roughly equivalent to that of a human coffee drinker. There were significant effects of caffeine on most behavioral variables, especially those related to neophobia and other anxiety-like behaviors, emotionality, and cognitive flexibility. The 3xTg-AD and NTg mice were differently influenced by caffeine. Overall, the increase of neophobia and other anxiety-related behaviors resulted in an exacerbation of BPSD-like profile in 3xTg-AD mice. Learning and memory, strongly influenced by anxiety in 3xTg-AD mice, got little benefit from caffeine, only shown after a detailed analysis of navigation strategies. The worsened pattern in NTg mice and the use of search strategies in 3xTg-AD mice make both groups more similar. Circadian motor activity showed genotype differences, which were found to be enhanced by caffeine. Selective effects of caffeine on NTg were found in the modulation of behaviors related to emotional profile and risk assessment. Caffeine normalized splenomegaly of 3xTg-AD mice, a physical indicator of their impaired peripheral immune system, and trended to increase their corticosterone levels. Our observations of adverse caffeine effects in an Alzheimer's disease model together with previous clinical observations suggest that an exacerbation of BPSD-like symptoms may partly interfere with the beneficial cognitive effects of caffeine. These results are relevant when coffee-derived new potential treatments for dementia are to be devised and tested.

Keywords: aging, anxiety, memory, NPS, BPSD, circadian activity, translational, long-term effects

OPEN ACCESS

Edited by:
Francisco Ciruela, University of Barcelona, Spain

Reviewed by:
Maria Grazia Morgese, University of Foggia, Italy
Tommaso Cassano, University of Foggia, Italy

****Correspondence:***
Lydia Giménez-Llort
lidia.gimenez@uab.cat

Specialty section:
This article was submitted to Experimental Pharmacology and Drug Discovery, a section of the journal Frontiers in Pharmacology

Received: *16 November 2017*
Accepted: *24 January 2018*
Published: *15 February 2018*

Citation:
Baeta-Corral R, Johansson B and Giménez-Llort L (2018) Long-term Treatment with Low-Dose Caffeine Worsens BPSD-Like Profile in 3xTg-AD Mice Model of Alzheimer's Disease and Affects Mice with Normal Aging. Front. Pharmacol. 9:79. doi: 10.3389/fphar.2018.00079

INTRODUCTION

Caffeine, a non-selective A1 and A2A receptor antagonist, is one of the most consumed drugs all over the world. The average consumption of caffeine in humans is around 300–400 mg/day (three to four cups of coffee) and its effects in several physiological functions, such as locomotion, sleep, and cardiovascular function, depend on the dose and duration of the consumption (Fredholm et al., 1999, 2017; Fredholm, 2007). A large part of the cognitive enhancing properties of caffeine is due to its indirect action on arousal, mood, and concentration (reviewed by Nehlig, 2010). Thus, low doses of caffeine (20–200 mg/day) have been associated with positive effects on subjective mood: wellbeing, confidence, motivation, alert, security, efficiency, concentration, and desire for socialization (see Griffiths et al., 1990; Silverman et al., 1994). In this low range, caffeine (up to 300–400 mg) has also a stimulating action with biphasic motor effects (Fredholm et al., 1999). However, restraint from moderate or high intake of coffee (more than four cups a day) is recommended due to negative effects of caffeine on pregnancy, risk of osteoporosis, cardiovascular problems, anxiety, sleep disturbances, and alterations in physiological functions such as locomotion (Fredholm et al., 1999; Johansson et al., 2001; Giménez-Llort et al., 2005; Fredholm, 2007; Hermansen et al., 2012).

In the last decade, a neuroprotective role of caffeine and other compounds of coffee such as theophylline has been postulated and it is of a growing interest (Maia and de Mendonça, 2002; Chen et al., 2010; Eskelinen and Kivipelto, 2010; Cao et al., 2012). For instance, the study "Cardiovascular Risk Factors, Aging and Dementia" (Eskelinen et al., 2009) indicated that consumption of three to five cups of coffee daily average age of the population is associated in 65% of cases, with a lower risk of developing dementia in the future. Although the whole complexity of aging process is still unknown, the use of caffeine to treat cognitive deficits associated with natural aging and those in Alzheimer's disease is foreseen as promising. With that, a substantial number of studies have been published suggesting preventive effects of coffee or caffeine on Alzheimer's disease (e.g., Arendash et al., 2006; Solfrizzi et al., 2015; Kolahdouzan and Hamadeh, 2017; Oñatibia-Astibia et al., 2017; Wierzejska, 2017).

The role of caffeine as a possible protective agent is supported by the pharmacological action of caffeine blocking adenosine A2A receptors, which show an aberrant expression and function in aging and related diseases (Marques et al., 2011). At the experimental level, long-term caffeine treatment has been demonstrated to ameliorate cognitive impairment in animal models of Alzheimer disease: βA-injection mouse models (Dall'Igna et al., 2007; Canas et al., 2009) and transgenic mouse models including APP (Arendash et al., 2006; Cao et al., 2009; Chu et al., 2012), APP/PS1 (Cao et al., 2011; Han et al., 2013), and more recently in a tau transgenic model (Laurent et al., 2014). Most importantly, because among the underlying mechanisms the reduction of amyloid beta production is postulated (Arendash et al., 2006). Interestingly, age-like HPA-axis dysfunction has been related to overactivation of caffeine-binding adenosine A2A receptors in rats mimicking the upregulation found in the forebrain of aged and AD patients, and their direct regulatory action on glucocorticoid receptor function (Batalha et al., 2016).

The main clinical manifestation of dementia is a decline in cognitive function. However, neuropsychiatric symptoms (NPS) are quite prevalent among the patients since early stages of Alzheimer's disease (Reisberg et al., 1987) and show a clear trend toward increasing their frequency with the progress of the disease (Piccininni et al., 2005). The symptoms, also referred as "Behavioral and Psychological Symptoms of Dementia" (BPSD), may include depression, apathy, hallucinations, delusions, agitation, aggression, and sleep disturbances. This wide array of NPS or BPSD is considered a strong source of distress and burden for AD patients and caregivers. The treatment of these NPS is a major challenge (Wang et al., 2016) as it is the understanding of the pathophysiology underlying their comorbidity in Alzheimer's disease (e.g., reviewed by Corrêa-Velloso et al., 2018). At the experimental level, research in animal models of Alzheimer's disease has focused on the cognitive deficits while few of them have also considered their non-cognitive profile (reviewed by Giménez-Llort et al., 2007). Since 2006, our laboratory has been devoted to characterize the cognitive but also the non-cognitive symptoms (i.e., anxiety, phobias, bizarre behaviors, hyperactivity, disinhibition, apathy and motivation, persistence of behaviors, and diurnal rhythm disturbances) in the homozygous 3xTg-AD mice created by LaFerla (Oddo et al., 2003). As we have consistently reported (e.g., Giménez-Llort et al., 2006, 2008, 2010; Baeta-Corral and Giménez-Llort, 2014, 2015; Torres-Lista and Giménez-Llort, 2014, 2015; Manuel et al., 2016), these animals show a noticeable BPSD-like profile. Recently, depressive-like profile has also been reported in the 3xTg-AD mice (Romano et al., 2015), early symptoms bearing some resemblance to bipolar disorder have also been noticed (Corrêa-Velloso et al., 2018), and the effects of preventive/therapeutical strategies on such BPSD-like symptoms have began to be studied (García-Mesa et al., 2011, 2012; Blázquez et al., 2014; Cañete et al., 2015; Torres-Lista and Giménez-Llort, 2015; Sabogal-Guáqueta et al., 2017).

In our focus of interest, the 3xTg-AD mice and their non-transgenic (NTg) counterparts with normal aging may be useful to investigate whether the aging process or the presence of an anxiety-like BPSD profile may modify the output of the potential therapeutic benefits of caffeine. The effects of caffeine on sensorimotor performance (open field, balance beam, string agility) and anxiety level [elevated plus-maze (EPM)] have been addressed by Arendash and Cao (2010), in the APP_{Swe} mice. In the present work, we explored the effects of a long-term (7 months) chronic treatment with a very low oral dose of caffeine (0.3 mg/kg) starting at the adulthood until the middle age (from 6 to 13 months of age) of 3xTg-AD mice, and as compared to age-matched NTg mice. In the transgenic mice, these ages correspond to the onset and advanced stages of the disease, respectively (Oddo et al., 2003). Since adenosine receptors are involved in neuronal but also non-neuronal mechanisms, including immunoendocrine responses, the effects of chronic treatment were assessed on sensorimotor functions, physiology [body weight (BW), circadian motor activity, and survival], immunoendocrine system (spleen size and corticosterone), and behavior (exploratory activity, bizarre movements, emotional

and anxiety-like behaviors, risk assessment, visual perceptual learning, and reference spatial learning and memory). The effects of caffeine on other BPSD such as apathy/depression were indirectly monitored by means of opposed behaviors [exploration in the activity tests (ACT), floating in the Morris water maze (MWM)] and tests [hole-board (HB) for novelty seeking, cue learning with a visual platform in the water maze].

MATERIALS AND METHODS

Animals

Homozygous triple-transgenic 3xTg-AD mice harboring $PS1/_{M146V}$, APP_{Swe}, and tau_{P301L} transgenes were genetically engineered at the University of California, Irvine, as previously described (Oddo et al., 2003). Briefly, two independent transgenes (encoding human APP_{Swe} and human tau_{P301L}, both under control of the mouse Thy1.2 regulatory element) were co-injected into single-cell embryos harvested from homozygous mutant PS1M146V knock-in (PS1KI) mice. The PS1 knock-in mice were originally generated as a hybrid C57BL/6 x 129.

Thirty-eight 6-month-old 3xTg-AD mice and C57BL/6 x 129 mice from 15 l of a breeding program that was established in our laboratory at the Medical Psychology Unit, Universitat Autònoma de Barcelona, were used in this study. All the animals were housed three to four per cage and maintained (Makrolon, 35 × 35 × 25 cm) under standard laboratory conditions (12 h light:dark, cycle starting at 8:00 h, food and water available *ad libitum*, 22 ± 2°C, 50–60% humidity). The circadian activity was recorded during one whole light–dark (LD) period, and the rest of the tests from 9:00 to 13:00 h.

This study was carried out in accordance with the recommendations of Animals in Research: Reporting In Vivo Experiments (ARRIVE) guidelines developed by the NC3Rs (Kilkenny et al., 2010) and the Spanish legislation on "Protection of Animals Used for Experimental and Other Scientific Purposes" and the European Communities Council Directive (2010/63/EU) on this subject. The protocol CEEAH 2481/DMAH 8700 entitled "Risk factors and preventive/therapeutical strategies in Alzheimer's disease: studies in triple-transgenic 3xTg-AD mice" was approved by Departament de Medi Ambient i Habitatge, Generalitat de Catalunya.

Caffeine Treatment

Mice were allowed to consume *ad libitum* either drinking water or caffeinated drinking water at 0.3 mg/ml (Sigma, St. Louis, MO, United States) beginning at 6 months of age, considered the age of onset of cognitive symptoms in this animal model. The experimental design consisted in the following groups: NTg vehicle, NTg caffeine, Tg vehicle, and Tg caffeine (n = 8–10, in each group). Caffeine treatment was continued throughout behavioral testing until the end of the experiment (13 months of age).

It has been previously confirmed that this treatment regimen leads to a 1.5 mg daily dose in a mouse and it is equivalent to an approximately 500 mg daily caffeine intake (approximately five cups of coffee) by a human (Johansson et al., 1996; Arendash et al., 2006). A plasma concentration of caffeine about 30 μM (*circa* three cups of coffee daily) has been recommended to probe the beneficial effects of caffeine on cognition (Costenla et al., 2010).

Behavioral Assessments

The effects of the chronic caffeine treatment on physical and behavioral profile of 3xTg-AD mice and their NTg counterparts were assessed at 13 months of age, considered advanced stages of disease in this animal model. The battery of behavioral tests consisted in the evaluation of sensorimotor functions and a series of classical unconditioned tasks measuring locomotion and exploratory activity, anxiety-like behaviors, and cognitive functions.

Day 1. Corner Test (CT) and Open-Field (OF) Test

Neophobia was evaluated in the corner test (CT) for 30 s. Animals were individually placed in the center of a clean standard home cage, filled with wood shave bedding. Number of corners visited, latency to realize the first rearing, and the number of rearings were recorded.

Immediately after the CT, mice were placed in the center of an open field (homemade woodwork, white box, 50 × 50 × 20 cm) and observed for 5 min. The temporal profile of the following sequence of behavioral events was recorded: duration of freezing behavior, latency to leave the central square and that of entering the peripheral ring, as well as latency and total duration of self-grooming behavior. Horizontal (crossings of 10 × 10 cm squares) and vertical (rearings with a wall support) locomotor activities were also measured. Bizarre behaviors observed in this test were also measured according to the previous reported criterion (Baeta-Corral and Giménez-Llort, 2014). During the tests, defecation boli and urination were also recorded.

Day 2. Hole-Board (HB) Test

Mice were placed in the center of the apparatus (woodwork white box of 32 × 32 × 32 cm) with four holes (3 cm diameter) equally spaced in the floor of the HB. In the exploratory behavior, non-goal-directed (rearings) and goal-directed (head-dips) exploratory activities were measured for 5 min. Moreover, the time spent head-dipping, the latencies of first movement, first dipping, and to explore the four different holes (this last one was established as criterion of the four holes exploration) were also measured. Repetition of already visited holes before reaching the criterion was considered as errors and the total number was measured. Defecation boli were also recorded.

Day 3. Dark–Light Box (DLB) Test

The dark–light box (DLB) test (Panlab, S.L., Barcelona, Spain) consists of a two-compartment box (black and dark, 27 × 18 × 27 cm; white and illuminated 20 W, 27 × 27 × 27 cm) connected by an opening (7 × 7 cm). The mice were placed into the dark compartment and observed for 5 min. Latency to enter into the lit compartment (all four paws criterion), number of entries, total time spent, and distance covered as well as number of rearings and groomings in this compartment were noted. Risk assessment was measured by means of the latency and number

of stretch attendances toward the lit area. Defecation boli and urination in each of both compartments were measured.

Day 4. Elevated Plus-Maze (EPM) Test

The plus-maze (woodwork, black Plexiglass) consisted of two enclosed arms (EAs, 30.3 × 5.3 × 15 cm, transparent walls) and two open arms (OAs, 30.3 × 5 cm) forming a square cross with a 5.3 × 5 cm square center piece. The apparatus was elevated 40 cm above the floor. The animal was placed in the center of the plus-maze facing one of the OAs. The number of entries (all four paws criterion) into OA and EA, the time spent in each arm, and defecation boli were recorded for 5 min. The anxiety index TOA/(TOA+TEA) was calculated as time in the OA/(time in the OA + time in the EA).

Day 5. T-Maze (TM) Test

The apparatus consists in a T-shaped maze (two short arms of 25 × 8 cm and a long arm of 30 × 8 cm). The working memory paradigm assessed in the T-maze (TM) consisted in two consecutive trials: one forced choice in the first trial and one free choice (recall trial) in the second trial, with a 90-s intertrial interval. In the forced choice, only one of the arms according to a random order and contrabalanced in each group was accessible. The animal was placed inside the "vertical" arm of the maze with its head facing the end wall and it was allowed to explore the maze. After spending 20 s in the accessible arm, the animal was put back into the home cage starting box. This 20 s period was established as the learning criterion. In the recall trial, the animal was allowed to explore the maze in a free choice trial where both arms were accessible. The arm chosen by the mice and the time spent in each arm during the free choice was recorded. The choice of the already visited arm in the previous trial before exploring the arm that was inaccessible was considered as an error and the total number was calculated. Also the time spent to explore the three arms of the maze was recorded. Finally, defecation boli and urination were also recorded.

Day 6. Marble Test (MB)

The procedure for marble test (MB) was adopted with minor modifications from that originally described by Broekkamp et al. (1986). Mice were placed individually in a standard home cage (Macrolon, 35 × 35 × 25 cm). The cage contained six glass marbles (dimensions 1 × 1 × 1 cm) evenly spaced making a triangle (three rows of three, two, and one marbles per row only in the left area of the cage) on a 5-cm thick layer of sawdust. The mice were left in the cage with marbles for a 30-min period after which the test was terminated by removing the mice and counting the number of marbles: intact (the number of marbles untouched), rotated (the number of marbles rotated 90° or 180°), half-buried (the number of marbles at least ½ buried by sawdust), and buried (the number of marbles 100% buried by sawdust).

Day 7. Body Weight (BW) and Sensorimotor Functions (SMT)

The physical condition of the mice was evaluated by their BW and sensorimotor functions. Visual reflex and posterior legs extension reflex were measured three times by holding the animal by its tail and slowly lowering it toward a black surface. Motor coordination and equilibrium were assessed twice (20-s trials) in two consecutive rod tasks of increasing difficulty. The distance covered and the latency to fall off a wooden (1.3 cm wide) and a metal wire (1 cm diameter) rod (both, 1 m long) were recorded. The hanger test was used to measure prehensibility and motor coordination by the distance covered and the number of elements of support and the latency to fall. The animal was allowed to cling with its forepaws from the middle of a horizontal wire (2 mm diameter, 40 cm length, divided into eight 5 cm segments) for two trials of 5 s. A third trial of 60 s was used to complement these measures with that of muscle strength or resistance. All the apparatus were suspended 40 cm above a padded table.

Days 8–15. Circadian Motor Activity Test (ACT)

Three mice per day were tested for 23 consecutive hours (beginning at 15.00 h, periods of 30 min) in a multicage activity meter system (three cages simultaneously, Actitrack, Panlab, S.L., Barcelona, Spain) set to measure spontaneous locomotor activity. Each testing cage (Macrolon, 35.3 × 35.3 × 25 cm) contained clean sawdust and had food and water available. Weight of animals was recorded before and after the test. Food intake (FI) also was measured.

Days 16–21. Morris Water Maze (MWM) Test

Animals were tested for spatial learning and memory in the MWM test consisting of 1 day of cue learning and 4 days of place learning for spatial reference memory, followed by one probe trial. Mice were trained to locate a hidden platform (7 cm diameter, 1 cm below the water surface) in a circular pool for mice (Intex Recreation Corp., Long Beach, CA, United States; 91 cm diameter, 40 cm height, 25°C opaque water), located in a completely black painted 6 m^2 test room. Mice failing to find the platform were placed on it for 10 s, the same period as the successful animals. The protocol (Giménez-Llort et al., 2007) was used as follows: 1 day of cue learning, 4 days of place learning followed by a probe trial.

Cue learning with a visible platform

On the first day, the animals were tested for the cue learning of a visual platform consisting of four trials in 1 day. In each trial, the mouse was gently released (facing the wall) from one randomly selected starting point (E or W) and allowed to swim until it escaped onto the platform, elevated 1 cm above the water level in the N position and indicated by a visible striped flag (5.3 × 8.3 × 15 cm). Extra maze cues were absent in the black painted walls of the room.

Place learning with a hidden platform

On the following day, the place learning task consisted of four trial sessions per day for 4 days with trials spaced 30 min apart. The mouse was gently released (facing the wall) from one randomly selected starting point (E or W, as these are equidistant from the target) and allowed to swim until escaped onto the hidden platform which was now located in the middle of the S quadrant. Mice that failed to find the platform within 60 s were placed on it for 10 s, the same period as was allowed for the

successful animals. White geometric figures, one hung on each wall of the room, were used as external visual clues.

Probe trial

One hour thirty minutes after the last trial of the place learning task, the platform was removed from the maze and the mice performed a "probe trial" of 60 s to evaluate their spatial memory for the platform position.

Quantitative and qualitative analyses

Behavior was evaluated by both direct observation and analysis of videotape-recorded images. Variables of time (escape latency, quadrant preference), distance covered, and swimming speed were analyzed in all the trials of the tasks. The escape latency was readily measured with a stopwatch by an observer unaware of the animal's genotype and confirmed during the subsequent video-tracking analysis. A video camera placed above the water maze recorded the animal's behavior and thereafter an automated system (Smart, Panlab S.L., Barcelona, Spain) enabled computerized measurement of the distance traveled by the animal during the trials. The swimming speed (cm/s) of the mice during each trial was calculated. In the probe trial, the time spent in each of the four quadrants, the distance traveled along them, and the number of crossings over the removed platform position (annulus crossings) were also measured retrospectively by means of the automated video-tracking analysis.

Finally, the swim paths for each mouse in each trial of the cue learning task, place learning task, and probe trial were analyzed following the swimming strategies described by Janus (2004) and classified according to three criteria: the objective (non-search behaviors, namely floating and circling, vs. search strategies), the direction (goal-directed vs. non-goal-directed strategies), and the variety (single vs. mixed strategies) (see Baeta-Corral and Giménez-Llort, 2015).

Survival and Immunoendocrine Status

Mortality was recorded from 6 to 13 months of age. The effects of caffeine on the neuroimmunoendocrine status (Giménez-Llort et al., 2014) were monitored by means of the levels of corticosterone and the size (weight in milligram) and relative size (% vs. BW) of the spleen (Giménez-Llort et al., 2008). Splenomegaly was used as a physical indicator of the altered status of the peripheral immune system in 3xTg-AD mice (Giménez-Llort et al., 2012; Marchese et al., 2014).

Mice were sacrificed and samples of about 0.5 ml of whole trunk blood were collected into heparinized tubes and centrifugated immediately at 10,000 × *g* for 2 min. The plasma obtained was stored at −20°C. Corticosterone content (nanogram per milliliter) was analyzed using a commercial kit (Corticosterone EIA Immunodiagnostic Systems Ltd., Boldon, United Kingdom) and ELISA EMS Reader MF V.29.-0.

Statistics

Statistical analyses were performed using SPSS 17.0 software. All data are presented as mean ± SEM or percentage. To evaluate the effects of genotype and caffeine treatment a 2 × 2 factorial analysis design was applied. Differences were studied through Multivariate General Lineal model analysis, followed by *post hoc* Duncan's test comparisons. $P < 0.05$ was taken as statistically significant.

RESULTS

Figures 1–7 summarize the behavioral phenotype exhibited by male 3xTg-AD and NTg at 13 months of age and the effects of caffeine on these behaviors.

Corner Test (CT)

Genotype and treatment effects were found in the CT (**Figures 1A–C**). Horizontal locomotor activity measured by number of corners visited was reduced in the 3xTg-AD mice [G, $F(1,30) = 4.760$; $p < 0.05$] as compared to the NTg animals. Vertical activity was influenced by caffeine, with treated animals showing higher latencies to perform a first rearing [T, $F(1,30) = 4.676$; $p < 0.05$] and a reduction in the total number of rearings [T, $F(1,30) = 4.571$; $p < 0.05$].

Open-Field Test

Genotype differences were found in the ethogram (**Figure 1D**), the behavioral sequence of events, pointing out to increased thigmotaxis. 3xTg-AD animals spent more time leaving the center of the apparatus [G, $t(1,14) = -2.785$; $p < 0.05$] and arriving at the periphery [G, $F(1,30) = 4.366$; $p < 0.05$]. Caffeine increased the time spent in the center in NTg+caff animals whereas it was reduced in the 3xTg-AD group [GxT, $F(1,30) = 4.936$; $p < 0.05$]. Once the animals arrived to the periphery, self-grooming behavior was delayed in time in NTg+caff mice as compared to their control group [T, $F(1,30) = 7.158$; $p < 0.05$ and GxT, $F(1,30) = 8.194$; $p < 0.01$] although the total duration of self-grooming (NTg-Veh: 2.25 s ± 0.48; NTg-Caff: 1.00 s ± 0.50; Tg-Veh: 1.50 s ± 0.50; Tg-Caff: 1.75 s ± 0.52) was not modified.

Regarding the locomotor activity (**Figures 1E–H**), 3xTg-AD mice showed a reduced number of crossings as compared to NTg animals [G, $F(1,30) = 12.132$; $p < 0.01$]. Moreover, caffeine had a bidirectional effect increasing this horizontal component in the NTg genotype whereas reducing it in the 3xTg-AD treated animals [minute 4; GxT, $F(1,30) = 8.994$; $p < 0.01$]. In the vertical activity, 3xTg-AD mice showed a reduced number of rearings as compared to the NTg mice [G, $F(1,30) = 10.944$ $p < 0.01$]. No stereotyped rearing was observed in NTg mice (NTg-Veh: none) and their presence was scarce in the other groups (NTg-Caff: 0.33 ± 0.30; Tg-Veh: 0.17 ± 0.10; Tg-Caff: 1.25 s ± 0.90).

Finally, the NTg+caff group showed an increase in defecation behavior whereas it was reduced in the 3xTg-AD+caff group [(NTg-Veh: 2.00 s ± 0.20; NTg-Caff: 3.50 ± 0.20; Tg-Veh: 3.67 ± 1.0; Tg-Caff: 2.50 ± 0.62) GxT, $F(1,30) = 4.681$; $p < 0.05$].

Hole-Board Test

Significant changes in the exploratory activity were detected in the HB test (**Figures 2A–D**) All groups showed similar latencies in the first movement and to explore the first hole. The reduction in the exploratory activity in the 3xTg-AD groups was the most significant difference observed in this test [G, $F(1,30) = 13.492$;

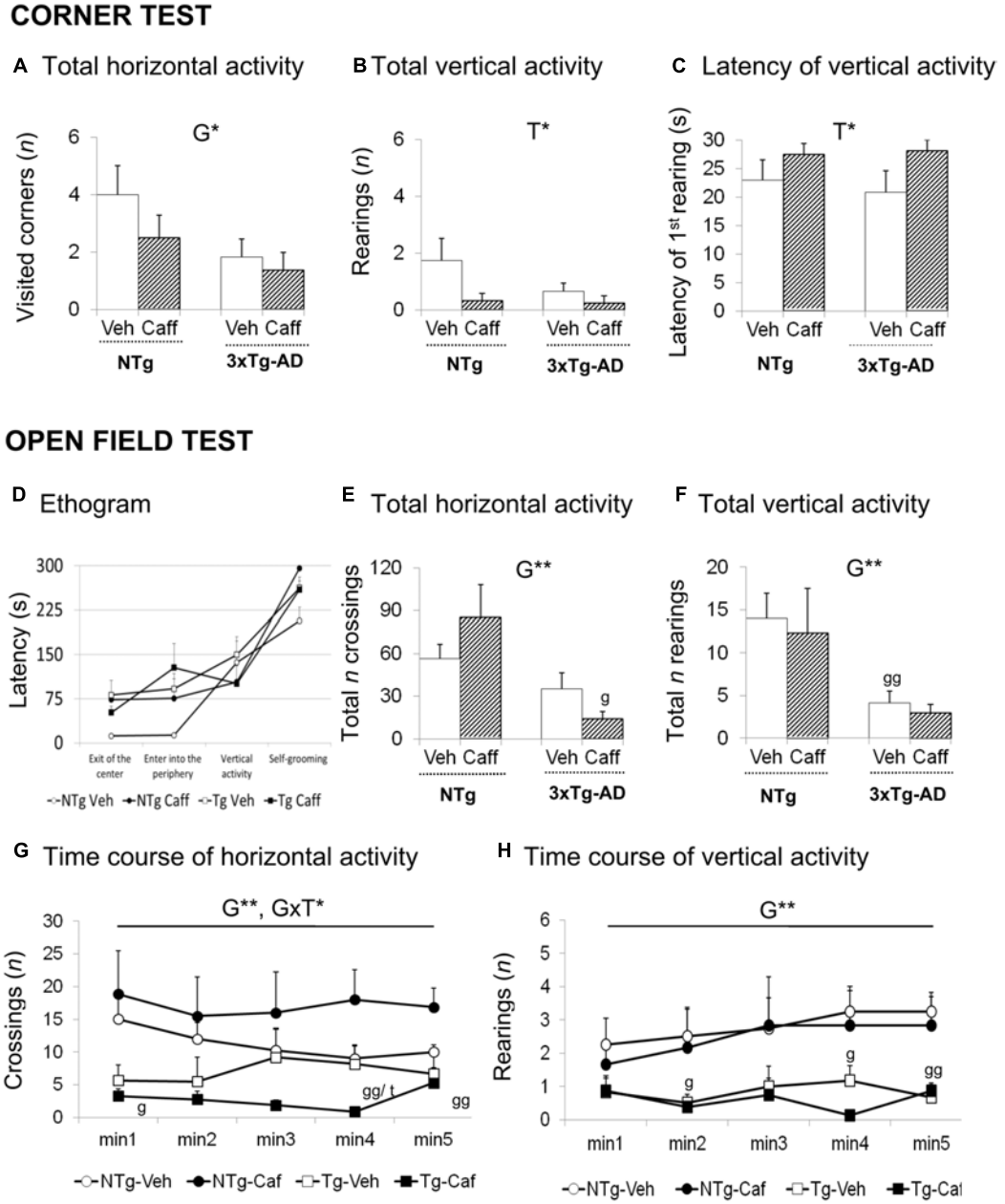

FIGURE 1 | Effects of chronic caffeine treatment assessed in NTg and 3xTg-AD mice at 13-months of age in the corner (CT) and open-field (OF) tests. Horizontal **(A)** and vertical **(B,C)** activities in the corner test. Ethogram **(D)**, horizontal **(E,G)**, and vertical **(F,H)** activities in the OF test. Data are expressed by mean ± SEM. Veh, vehicle; Caff, caffeine. The text at the top of each graph refers to the *p*-values of the 2 × 2 ANOVA: G, genotype effect; T, treatment effect; GxT, genotype × treatment interaction; $^{*}p < 0.05$, $^{**}p < 0.01$, $^{***}p < 0.001$. *Post hoc* comparisons are shown in the graphs as: g $p < 0.05$, gg $p < 0.01$ vs. the corresponding NTg group; $^{*}p < 0.05$, $^{**}p < 0.01$, $^{***}p < 0.001$ vs. the corresponding non-treated group.

$p < 0.001$]. Treatment reduced vertical activity in both genotypes [T, $F(1,30) = 5.290$; $p < 0.05$]. The 3xTg-AD groups performed more head dippings [G, $F(1,30) = 4.750$; $p < 0.05$] and total time spent in this activity was higher as compared to the NTg groups [G, $F(1.30) = 4.818$; $p < 0.05$]. Hundred percent of the 3xTg-AD groups reached the criterion of the four holes exploration [G, $t(1,14) = -3.055$; $p < 0.05$] and faster than NTg groups [G, $F(1,30) = 4.893$ $p < 0.05$]. Independently of the genotype, caffeine reduced the percentage of animals that reached the criterion [T, $F(1,30) = 11.904$; $p < 0.01$]. Moreover, the treatment increased the number of errors in the 3xTg-AD genotype whereas it was reduced in the NTg+caff animals [GxT, $F(1,30) = 5.652$; $p < 0.05$].

Grooming behavior was advanced in time in 3xTg-AD the spent more time on it [G, $F(1,30) = 7.649$; $p < 0.01$ and G, $F(1,30) = 7.179$; $p < 0.05$, respectively]. Finally, caffeine reduced

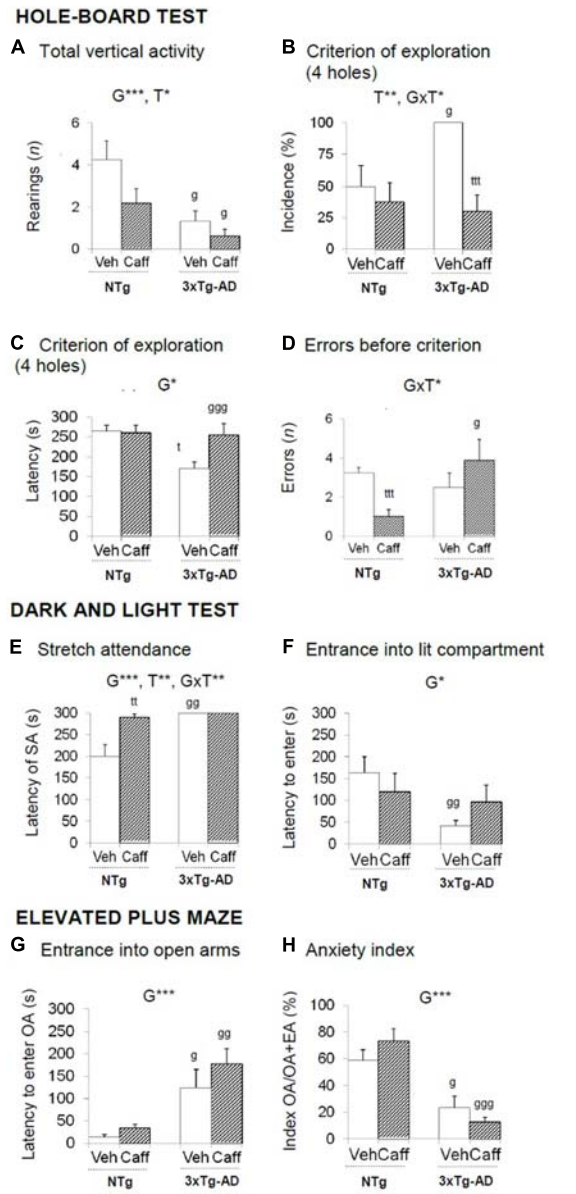

FIGURE 2 | Effects of chronic caffeine treatment assessed in the HB, DLB, and EPM tests in NTg and 3xTg-AD mice at 13 months of age. Data are expressed as mean ± SEM. **(A–H)** Behavioral variables (as indicated) of the hole-board test **(A–D)**, the dark and light test **(E,F)** and the elevated plus maze **(D–H)**. The text at the top of each graph refers to the *p*-values of the 2 × 2 ANOVA: G, genotype effect; T, treatment effect; GxT, genotype × treatment interaction; *$p < 0.05$, **$p < 0.01$, ***$p < 0.001$. *Post hoc* comparisons are shown in the graphs as: g $p < 0.05$, gg $p < 0.01$ vs. the corresponding NTg group; *$p < 0.05$, **$p < 0.01$, ***$p < 0.001$ vs. the corresponding non-treated group. SA, stretch attendance.

the number of defecation boli [T, $F(1,30) = 5.457$; $p < 0.05$] especially in the 3xTg-AD mice [GxT, $F(1,30) = 6.365$; $p < 0.05$].

Dark–Light Box Test

Stretch attendance activity (**Figures 2E,F**) was present in NTg but not in 3xTg-AD mice [G, $F(1,30) = 17.690$; $p < 0.001$] and caffeine increased the latency of stretch attendance in the NTg mice [T, $F(1,30) = 11.842$; $p < 0.01$ and GxT, $F(1,30) = 11.842$; $p < 0.01$].

The incidence of animals that entered into the lit area ranged 50–70% in the NTg mice and increased to the 90–100% in the 3xTg-AD mice [G, $F(1,30) = 9.098$; $p < 0.01$]. The disinhibitory behavior of the 3xTg-AD groups was shown as a reduced latency to enter into the lit area [**Figure 4B**; G, $F(1,30) = 4.859$; $p < 0.05$], more than double of crossings between the two compartments [G, $t(1,14) = -3.049$; $p < 0.01$], and less time into the lit area [G, $F(1,30) = 4.158$; $p < 0.05$].

Finally, a genotype and a genotype × treatment interaction effect was found in total defecation [G, $F(1,30) = 4.158$; $p < 0.05$ and GxT, $F(1,30) = 6.794$; $p < 0.05$, respectively].

Elevated Plus Maze

The latency to enter into the OA [G, $F(1,30) = 20.029$; $p < 0.001$] and the anxiety index TOA/(TOA+TEA) [G, $F(1,30) = 43.619$; $p < 0.001$] indicated that 3xTg-AD animals were more anxious than NTg mice (**Figures 2G,H**). All groups showed a similar number of entries in all the arms and the central piece [all $Fs(1,30) < 3.583$; $p > 0.068$, n.s.]. A genotype and a genotype × treatment interaction effects were found in defecation behavior [G, $F(1,30) = 4.536$; $p < 0.05$ and GxT, $F(1,30) = 6.648$; $p < 0.05$, respectively].

T-Maze Test

In the forced trial, 3xTg-AD groups spent less time to reach the intersection point of the TM [G, $F(1,30) = 5.729$; $p < 0.05$] and to reach the criterion of the 20 s exploration [G, $F(1,30) = 56.375$; $p < 0.05$]. In the recall, the number of errors before choosing the unexplored arm in the previous trial was lower in the 3xTg-AD genotype [G, $F(1,30) = 6.111$; $p < 0.05$]. However, 3xTg-AD-treated animals reduced their efficiency to explore both arms since they spent more time to reach the goal [GxT, $F(1,30) = 4.188$; $p < 0.05$] (**Figures 3A–D**).

Marble Test

The 3xTg-AD mice buried a higher number of marbles [G, $F(1,28) = 20.802$; $p < 0.001$] whereas NTg animals left them intact [G, $F(1,28) = 8.660$; $p < 0.01$]. Caffeine reduced the number of marbles buried in the 3xTg-AD genotype [GxT, $F(1,28) = 5.565$; $p < 0.05$] (**Figure 3E**).

Body Weight and Sensorimotor Functions

At 6 months of age, before the treatment was started, the 3xTg-AD mice were overweighed (+20.26%) [t, $F(1,32) = -5.603$, $p < 0.000$]. The genotype effect was maintained till the end of the treatment (+20.09%) [G, $F(1,30) = 68.826$; $p < 0.001$].

At 13 months of age, the genotype × treatment interaction effects [GxT, $F(1,30) = 7.383$; $p < 0.05$] pointed out a reduction of the BW induced by caffeine in the 3xTg-AD animals (Duncan's test, $p < 0.05$ vs. 3xTg-AD+veh group) but the treatment did not correct the overweight of 3xTg-AD mice (Duncan's test, $p < 0.05$ vs. NTg+caff).

In the sensory-motor functions, no deficits were found in the reflexes assessed, with all the animals obtaining the maximum score. In the wood rod test, most animals petrified (no distance

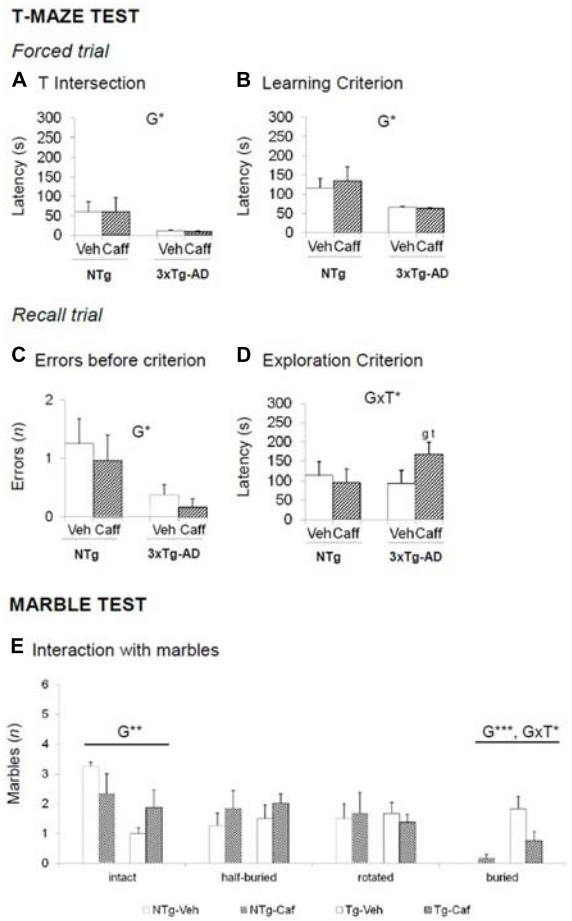

FIGURE 3 | Effects of chronic caffeine treatment assessed in NTg and 3xTg-AD mice at 13 months of age in the T-maze (TM) and marble (MB) tests. **(A–E)** Behavioral variables (as indicated) of the T-maze test **(A–D)** and the marble test **(E)**. Data are expressed by mean ± SEM. Veh, vehicle; Caff, caffeine. The text at the top of each graph refers to the *p*-values of the 2 × 2 ANOVA: G, genotype effect; T, treatment effect: GxT, genotype × treatment interaction; $*p < 0.05$, $**p < 0.01$, $***p < 0.001$. *Post hoc* comparisons are shown in the graphs as: g $p < 0.05$, gg $p < 0.0$l vs. the corresponding NTg group: $*p < 0.059$, $**p < 0.01$, $***p < 0.001$ vs. the corresponding non-treated group.

covered) and this response determined a high latency to fall. Still, 3xTg-AD mice exhibited longer latencies to fall than NTg animals [G, $F(1,30) = 12.037$; $p < 0.01$]. Caffeine increased the latency to fall in the NTg genotype [T, $F(1,30) = 4.841$; $p < 0.05$]. When the complexity of the task was increased (metal wire test) all groups showed worse equilibrium, but no differences were found between the groups neither in the latency to fall nor in the distance covered. In the Hanger test, the 5 s trial showed genotype-dependent differences in the latency to fall [G, $F(1,30) = 7.879$; $p < 0.01$]. This effect was confirmed in the 60 s trial [G, $F(1,30) = 6.561$; $p < 0.05$] (**Figures 4A–E**).

Circadian Motor Activity Test

A circadian temporal course was found in the 23 h motor activity period studied [t, $F(23,690) = 29.732$; $p < 0.001$] that differed between genotype [txG, $F(23,690) = 4.570$; $p < 0.001$], treatment [txT, $F(23,690) = 5.360$; $p < 0.001$], and the interaction between these two factors [txGxT, $F(23,690) = 2.858$; $p < 0.001$] (**Figure 5A**). During the first hour of habituation, time [t, $F(11,330) = 78.341$; $p < 0.001$] and genotype [G, $F(11,330) = 9.395$; $p < 0.01$] effects were found. Besides, "time × genotype" [txG, $F(11,330) = 7.984$; $p < 0.001$], "time × treatment" [txT, $F(11,330) = 2.591$; $p < 0.01$], and "time × genotype × treatment" [txGxT, $F(11,330) = 4.083$; $p < 0.001$] interaction effects were found (**Figure 5B**) with treated 3xTg-AD mice showing a reduced locomotor activity as compared to their non-treated group.

3xTg-AD+veh mice showed a reduced total motor activity [G, $t(1,15) = 6.591$; $p < 0.01$]. Caffeine increased the overall spontaneous motor activity along a 23-h LD period in the 3xTg-AD genotype [**Figure 5C**; GxT, $F(1,30) = 11.525$; $p < 0.01$], and more significantly, during the dark cycle [**Figure 5E**; $F(1,30) = 15.311$; $p < 0.001$].

Morris Water Maze Test

Figures 6A–C illustrate the "day-by-day" (left panel) and "trial-by-trial" (right panels) acquisition curves.

In the cue learning task (**Figure 6A**, CUE), genotype and treatment effects were found, with 3xTg-AD mice reaching the visible platform faster than NTg [G, $F(1,30) = 17.727$; $p < 0.001$]. Independently of the genotype, treated animals spent more time [T, $F(1,30) = 30.891$; $p < 0.001$] and showed longer distance covered [T, $F(1,30) = 28.171$; $p < 0.001$] to find the platform than non-treated mice. 3xTg-AD mice showed an increased swimming speed [G, $F(1,30) = 68.397$; $p < 0.001$] and caffeine increased the swimming speed in both treated groups [T, $F(1,30) = 5.394$; $p < 0.05$].

In the place learning task (PT), when the cue was removed and the platform was hidden, animals exhibited a different genotype- and treatment-dependent acquisition curves, with 3xTg-AD animals finding faster the hidden platform along the 4 days of the test [G, $F(1,30) = 6.920$; $p < 0.05$]. Caffeine increased the time spent [T, $F(1,30) = 11.449$; $p < 0.01$] and the distance covered [T, $F(1,30) = 15.566$; $p < 0.001$] to reach the platform as compared to their non-treated groups. Swimming speed showed a consistent genotype effect [G, $F(1,30) = 21.239$; $p < 0.001$]. Caffeine modified the swimming speed in an opposite manner, since it was increased in the NTg and reduced in the 3xTg-AD animals [GxT, $F(1,30) = 9.540$; $p < 0.05$].

"Trial-by-trial" analysis revealed that time, genotype, and treatment factors frequently showed mutual interactions [**Figures 6A–C**, right panels; RMA, $F(3,90) > 2.984$; $p < 0.05$]. Between all the differences found, it is interesting to note that caffeine effects were found both in long-term (T1) and short-term (T3 and T4) memory trials. The acquisition level achieved at the end of the place task (distance PT4 and PT4.4) was similar in all the groups [G and T, $F(1,30) < 1.631$; $p > 0.05$, n.s.].

In the probe trial (**Figure 6D**), all the groups showed similar ability to distinguish the platform quadrant during the place task [all ANOVAs, $F(3,28) > 25.522$; $p < 0.001$] despite the NTg+caff group did it with one or two lower scale [all ANOVAs, $F(3,28) > 3.667$; $p < 0.05$].

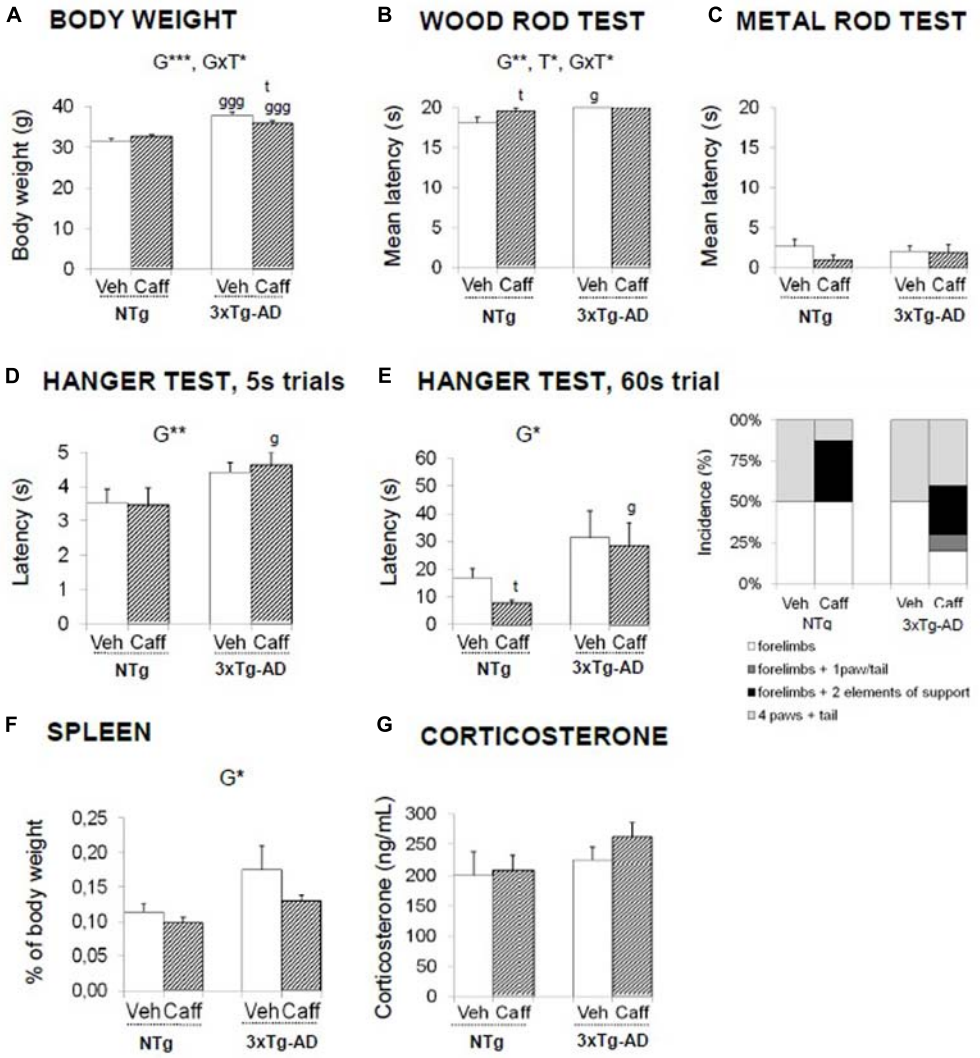

FIGURE 4 | Effects of chronic caffeine treatment on body weight, sensorimotor functions, percentage of weight of spleen, and plasmatic corticosterone levels in NTg and 3xTg-AD mice at 13 months of age. **(A)** Body weight and **(B–G)** behavioral variables (as indicated) on the wood rod test **(B)**, metal rod test **(C)** and the two hanger tests **(D,E)**. The relative weight of spleen **(F)** and corticosterone levels **(G)**. Data are expressed by mean ± SEM or percentage (%). Veh, vehicle; Caff, caffeine. The text at the top of each graph refers to the *p*-values of the 2 × 2 ANOVA: G, genotype effect; T, treatment effect; GxT, genotype × treatment interaction; $^{*}p < 0.05$, $^{**}p < 0.01$, $^{***}p < 0.001$. *Post hoc* comparisons are shown in the graphs as: g $p < 0.05$, gg $p < 0.01$ vs. the corresponding NTg group; $^{*}p < 0.05$, $^{**}p < 0.01$, $^{***}p < 0.001$ vs. the corresponding non-treated group.

Qualitative analysis of the non-search behaviors and search strategies allowed to find caffeine effects (**Figure 7**) based on the distinctive characteristics of both genotypes: presence of floating and the use of "single-" and "goal-directed" strategies in the NTg genotype in contrast to "circling" and "mixed" and "non-goal-directed" strategies in the 3xTg-AD mice. Caffeine modified these swimming patterns, reducing differences between genotypes. Thus, the NTg+caff group showed a higher proportion of "mixed" and "non-goal-directed" strategies whereas the 3xTg-AD group showed more "single-" and "goal-directed" strategies.

Moreover, in the cue learning task, caffeine reduced the incidence of floating [T, $F(1,30) = 7.660$; $p < 0.01$] and increased the incidence of "thigmotaxis" (test exacte de Fisher; $p < 0.05$) in both treated groups.

In the probe trial, all the vehicle animals (100%) swam "directly" to the platform quadrant during the place task, whereas nearly 50% of the 3xTg-AD+caff animals used "random search." When the animals failed to find the platform, NTg+veh mice alternated different strategies. In contrast, 3xTg-AD mice persisted in their behavior. A higher variety of strategies was shown by both genotypes of treated animals.

Survival and Immunoendocrine Status

All NTg+veh mice survived until the age of 13 months, whereas the survival rate in the 3xTg-AD+veh and

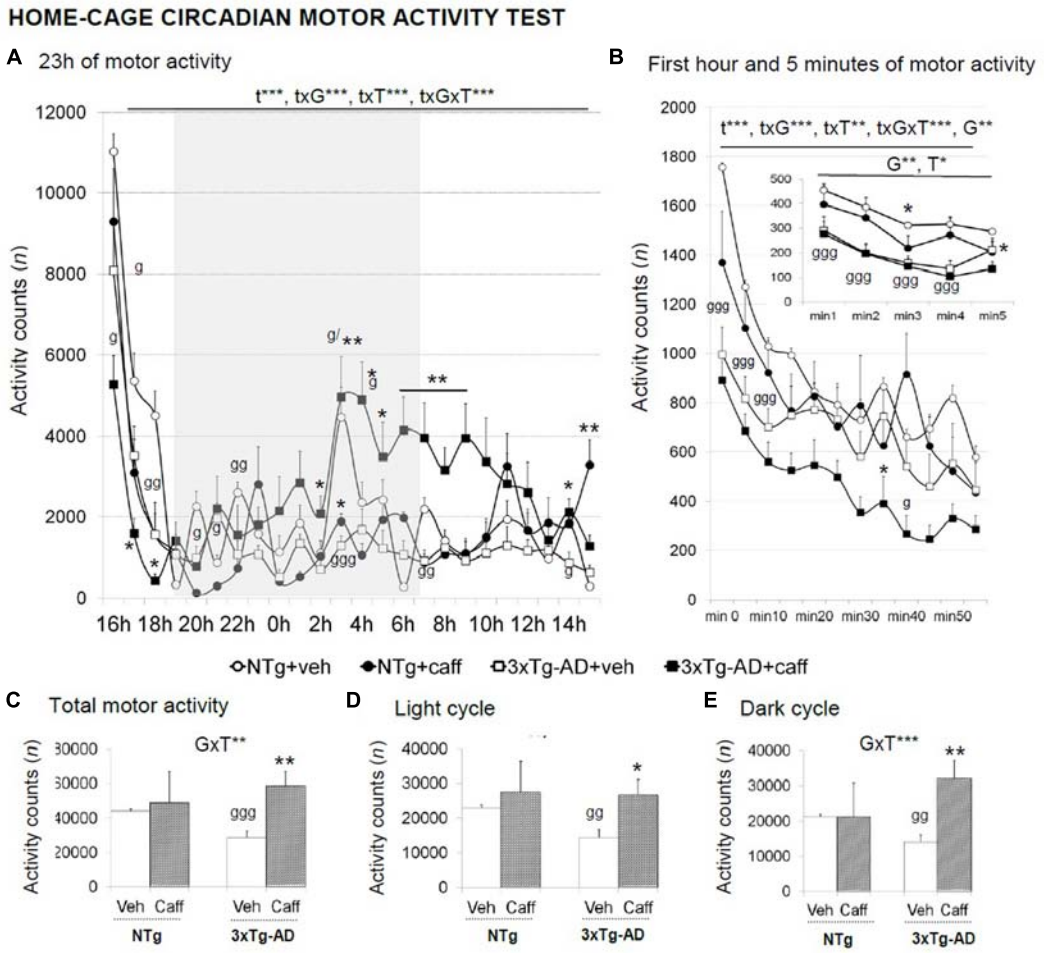

FIGURE 5 | Effects of chronic caffeine treatment in the home-cage on circadian motor activity in NTg and 3xTg-AD mice at 13 months of age. Data are expressed by mean ± SEM or percentage (%). Veh, vehicle: Caff, caffeine. The vertical axis shows motor activity counts during the time intervals of the 23 h continuous recording **(A)**, 1-min intervals (right-hand graphs) during a period of l h **(B)**, or 5-min intervals (inset of **B**). Total activity counts during the 23 h **(C)**, the light **(D)**, and the dark **(E)** cycles are detailed. Data are expressed by mean ± SEM. The text at the top of each graph refers to the *p*-values of the 2 × 2 ANOVA: G, genotype effect; GxT, genotype × treatment interaction; t, time effect; txG, time × genotype interaction; txT, time × treatment interaction; $*p < 0.05$, $**p < 0.01$, $***p < 0.001$. *Post hoc* comparisons are shown in the graphs as: g $p < 0.05$, gg $p < 0.01$, ggg $p < 0.00$l vs. the corresponding NTg group; $*p < 0.05$ vs. the corresponding non-treated group.

NTg+caff groups of the same age decreased to 80%. However, the differences were not significant when analyzed statistically.

The weight of the spleen was increased in 3xTg-AD mice [G, $F(1,30) = 6.549$; $p < 0.05$]. In the treated groups, caffeine showed a tendency to reduce the weight of the spleen [T, $F(1,30) = 2.721$; $p = 0.109$, n.s.]. In 3xTg-AD+caff mice, this reduction was sufficient to restore the normal weight of the spleen [G, $t(1,16) = -1.145$; $p = 0.269$, n.s. vs. the control group NTg+veh] (**Figure 4F**).

Corticosterone levels showed slight increases due to genotype [G, $F(1,30) = 1.983$; $p = 0.169$, n.s.] that did not reach statistical significance. If any, treatment [T, $F(1,30) = 0.728$; $p = 0.400$, n.s., GxT, $F(1,30) = 0.311$, $p = 0.400$, n.s.] slightly trend to increase corticosterone levels in 3xTg-AD+caff mice.

DISCUSSION

This study analyzes, in a translational scenario, the long-term effects of a chronic low dose of caffeine started at the onset of disease (6 months of age) in 3xTg-AD mice, an animal model for Alzheimer's disease characterized by cognitive but also BPSD-like profile (Giménez-Llort et al., 2006). The behavioral effects were assessed at advanced stages (13 month of age) when both amyloid and tau pathologies are present (Oddo et al., 2003). At this age, we have consistently reported that survival male 3xTg-AD mice starts to be compromised (Giménez-Llort et al., 2008, 2010; García-Mesa et al., 2016; Torres-Lista et al., 2017). Effects were compared to age-matched NTg mice with normal aging, that according to the background strain represent overcoming the middle age. The results showed significant effects of caffeine in most of the variables, especially those related to neophobia

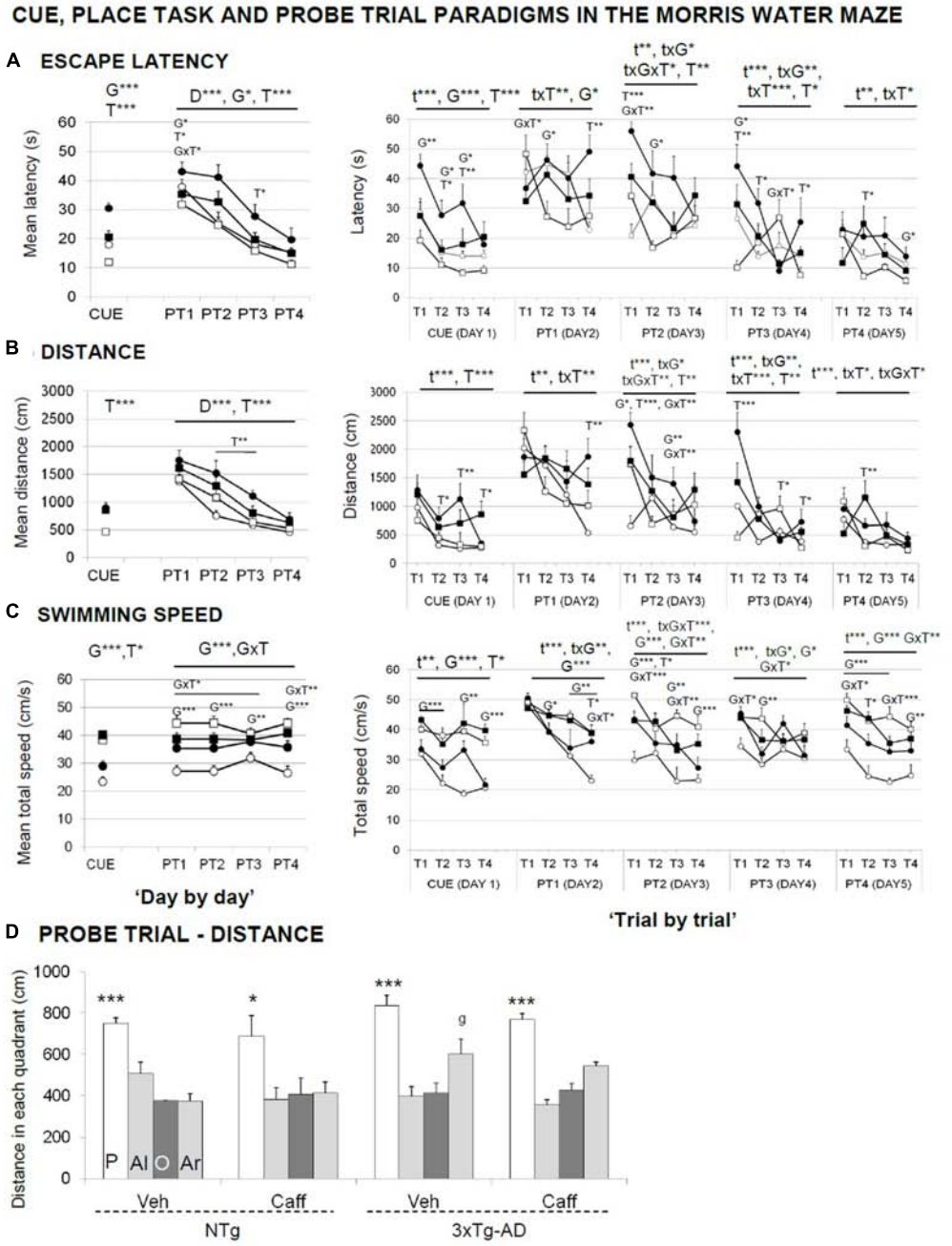

FIGURE 6 | Effects of chronic caffeine treatment assessed in the CUE and PT, place learning tasks, and the probe trial of the Morris water maze test in NTg and 3xTg-AD mice at 13 months of age. Data are expressed by mean ± SEM in the cue and learning tasks **(A–C)** and by distance covered in the platform (P), adjacent left (Al), opposite (O), and adjacent right (Ar) quadrants **(D)**. ANOVA 2 × 2: G, genotype effect; T, treatment effect; GxT, genotype × treatment interaction; $*p < 0.05$, $**p < 0.01$, $***p < 0.001$. *Post hoc*: g $p < 0.05$ vs. the NTg group. ANOVA, $*p < 0.05$, $***p < 0.001$ P vs. all quadrants.

and other anxiety-like behaviors, emotionality, and cognitive flexibility. Thus, anxiogenic effects were seen in middle-aged animals and that effect, in the 3xTg-AD model, resulted in an aggravation of its BPSD-like pattern. The groups treated with caffeine did not improve their long-term memory until they completed the behavioral spatial reference memory paradigm in the water maze, and the short-term memory, in any case, was disadvantaged. It was only in the second time interval of the probe trial, where the 3xTg-AD group treated with caffeine was able to use search strategies similar to those exhibited by both groups of NTg mice. In addition, the behavioral analysis pointed at distinct genotype-dependent functional capacity of caffeine-treated animals to meet task-dependent performance demands. Thus, selective effects of caffeine for the 3xTg-AD genotype were

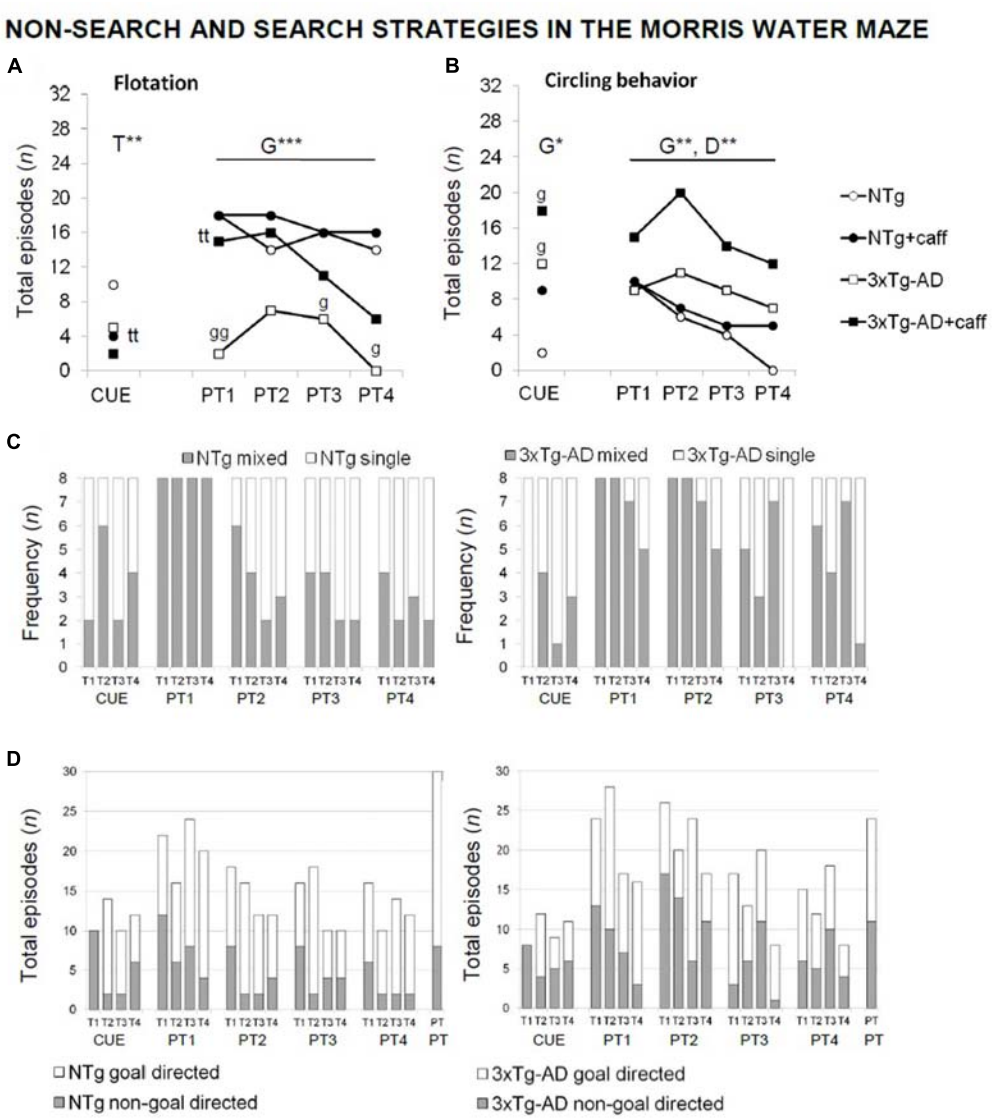

FIGURE 7 | Qualitative analysis of the non-search and search strategies assessed "trial by trial" in the paradigms of the MWM test in NTg and 3xTg-AD mice at 13 months of age. Flotation behavior **(A)**, circling **(B)**, single vs. mixed strategies **(C)**, and goal- vs. non-goal-directed strategies **(D)**. Data are expressed by frequency or total number of episodes (*n*). RMA: G, genotype effect; D, day effect; $*p < 0.05$, $**p < 0.01$. *Post hoc*: $*p < 0.05$, $**p <$ 0.0l vs. the corresponding NTg group.

observed in the increase of the circadian motor activity and the reduction of body and spleen weights, indicators of the functional and neuroimmune status. Caffeine also exerted bidirectional effects: stimulating motor activity in NTg mice in the open-field (OF) test but reducing it in the 3xTg-AD; increasing the emotionality of NTg mice and decreasing it in the 3xTg-AD in the OF, EPM, and HB; and finally, modifying the navigation strategies in the learning tasks of the MWM, making them more similar.

The anxiogenic effects induced by caffeine were observed, in general, as an increase of neophobia and the anxious profile. In the NTg genotype, the reduction in the exploratory behavior in CT, the increased latency to reach the protected areas (thigmotaxis) in the OF, and the delay in the risk assessment activity in the DLB demonstrated these anxiogenic effects. The increase in defecation observed in the NTg+caff group suggests an increased emotionality induced by caffeine. These results agree with those obtained in animals treated with high doses of caffeine, which were more emotionally reactive and showed more immobility, defecation, and urination than control animals (Anderson and Hughes, 2008). In 3xTg-AD animals, increased anxiety profile induced by chronic caffeine treatment led to a worsening BPSD pattern, where the behavioral response varied depending on the level of anxiety that each test involves. In this regard, direct exposure to an open and illuminated field caused a reduction in motor activity, almost completely. Conversely, in mild stressful environments such as the case of the motor ACT, the anxious response was reflected as an increase in the hyperactive pattern characteristic of 3xTg-AD animals

(Giménez-Llort et al., 2007). In the cue learning task of the MWM, this increase of the hyperactivity pattern induced by caffeine was also observed as an increase in the swimming speed as compared to the 3xTg-AD+veh group, that may explain the reduction of floating behavior. The stimulating effects of caffeine at the motor level were observed in NTg animals as an increase in the number of crossings in the OF and the swimming speed in the learning tasks of the MWM. As expected (i.e., Nehlig et al., 1992), this stimulatory effect of the horizontal motor activity was in decrement to the vertical activity, considered the variable that better reflects the exploratory behavior *per se* (Colorado et al., 2006). Therefore, caffeine exerted its effects increasing hyperactivity (locomotion) and reducing vertical exploratory behavior.

As introduced before, here it is interesting to note that a depressive-like profile paired to monoaminergic alterations has been recently reported in the 3xTg-AD mice using two models of stress-coping behavior (FST, Porsolt forced swim test, and Tail suspension test) and with an anhedonia test such as the sucrose preference test (Romano et al., 2015). In the current study, the effects of caffeine on behavioral despair were not directly addressed, i.e., using the forced swim test in order to avoid carry on effects on the MWM. Also, because in our hands 3xTg-AD mice showed a persistence of behaviors in the FST that interfered with the interpretation of the performances (Torres-Lista and Giménez-Llort, 2014, 2015). Instead, the presence of immobility (floating) was taken into account in all the trials in the maze (as described in Baeta-Corral and Giménez-Llort, 2015) and the "Cue learning with a visible platform" was a specific paradigm used to control lack of motivation as well as sensorimotor differences. Besides, the effect of caffeine on other variables such as exploration in the ACTs and more specifically the performance in the HB test for novelty seeking was among the studied behaviors as opposed to the expression of apathy/depressive symptoms.

Regarding sensorimotor functions, the results obtained in the balance of 3xTg-AD mice cannot exclude the presence of a false positive, since the innate fear of heights made that group showing more petrifaction (i.e., genotype 3xTg-AD treated with caffeine) were those that stayed longer on the rod. This is in agreement with prior results obtained at the same age, in female 3xTg-AD mice (Giménez-Llort et al., 2007). In contrast, in NTg animals that roam the rod, caffeine improved balance but worsened muscle resistance in this genotype. Similar results were also obtained by our laboratory in the behavioral assessment A_1 receptor knockout mice (Giménez-Llort et al., 2002), a genetic strategy to emulate the chronic effects of caffeine (Johansson et al., 2001).

It has been shown that chronic caffeine treatment prevents weight gain in rodents that were fed a high fat diet (Moy and McNay, 2013). In the present work, the long-term treatment with a low dose of caffeine modified, but not corrected, the overweight of 3xTg-AD mice. We have already shown that overweight is a characteristic of the Spanish colony of 3xTg-AD mice, since onset of disease (Giménez-Llort et al., 2010), it is related to a higher relative contribution of white adipose tissue (WAT) (Giménez-Llort et al., 2010; García-Mesa et al., 2011, 2012) and could not be corrected by health strategies such as forced (Giménez-Llort et al., 2010) or voluntary exercise (García-Mesa et al., 2011). In the present work, the increase in the nocturnal activity found in 3xTg-AD+caff mice could explain their weight loss.

The MWM showed that the increased latency, distance, and speed that chronic caffeine indiscriminately exerts over both genotypes in the cue learning task does not correspond to the expected cognitive effects, quite the contrary. In the first experience in the maze, the benefits attributed to caffeine improving attention (Griffiths et al., 1990), did not confer any advantage to the animals in this learning task, considered as a visual perceptive learning. In the following three trials for short-term memory, the effects were also contrary to those expected, since caffeine increased the distance covered to reach the platform. In the second paradigm, the place learning task, increased speed in the NTg group and decreased in the 3xTg-AD could emulate stimulant and depressant effects of low and high doses of caffeine, respectively (Fredholm et al., 1999). Thus, the chronic low-dose (0.3 mg/kg) acted exhilarating swimming speed in the NTg group, while in 3xTg-AD mice – which consistently show a higher speed than NTg animals – the reduction induced by caffeine may be the result of a depressant drug effect. Although it seems that caffeine improved short-term memory because it did so in a pair of trials, this fact could be considered exceptional in the face of nine trials in which the effects of caffeine involved a significantly worse execution. At the end of this task, all experimental groups reached the same level of acquisition and in the probe trial, conducted after 1 h 30 min, all of them also showed the same ability to remember the position of the final platform. Still, the NTg+caff group did so with one or two lower orders of magnitude. Considering that in the first trials of everyday, quantitative values between NTg and 3xTg-AD were more distinct, it is likely that a 24-h probe trial would have been more suitable to detect cognitive differences. In general, quantitative results show that, under these experimental conditions, cognitive outcomes were strongly conditioned by the genotype differences in swimming speed or the hyperactive profile shown in our 3xTg-AD colony.

The anxiogenic conditions that the MWM represents for mice were also reflected in the high level of floating observed in NTg animals and the sustained increase in the speed of 3xTg-AD mice. As we have extensively discussed in a precedent report' (Baeta-Corral and Giménez-Llort, 2015), this means that in this colony of 3xTg-AD mice, the MWM may probably not be specific to assess hippocampal-dependent cognitive deficits related to spatial memory, as in other models for AD (i.e., Arendash et al., 2009). In this mice model, the MWM may involve the assessment of cognition under anxiogenic conditions and therefore the measurement of emotional memory depending on limbic system. Therefore, the anxiogenic effects of caffeine may have counteracted the potential cognitive effects in both visual perceptive (cue learning task) and spatial (place learning task) learning and memory tasks. The fact that the acquisition curve of the 3xTg-AD animals showed an even better performance than NTg mice reminds us of the results obtained in this colony of animals in the conditioned fear test (España et al., 2010). In that work, not only the 3xTg-AD model but also APP_{Swe} and

APP_{Swe}/ind models showed an enhanced contextual conditioned fear response that was dependent on their respective levels of accumulation of βA in the basolateral amygdala.

The possible masking that the presence of flotation could exert on the measures of latency and distance was also considered. The analysis of these variables including the time invested in flotation indicated that results did not differ from those obtained when the total floating time was excluded. Regarding this "non-search behavior," caffeine reduced the incidence of floating in the cue learning task in both genotypes. This action could be explained by its effects increasing attention or motivation in this learning and memory visual perceptive task. The effects of increasing the incidence of "thigmotaxis," that is a non-goal-directed swimming around the wall of the pool, would be consistent with the horizontal locomotor hyperactivity induced by caffeine in the OF.

In order to better understand the results shown in the MWM, we analyzed the swimming strategies developed along the different trials of the three paradigms (Baeta-Corral and Giménez-Llort, 2015). The detailed analysis of strategies unveiled traits that allowed to distinguish both genotypes: single- and goal-directed strategies in NTg animals but mixed and non-goal-directed in the 3xTg-AD ones. In the present work, caffeine decreased genotype differences in learning and memory tests, because the NTg-treated animals showed mixed and non-goal-directed strategies and, conversely, the 3xTg-AD exhibited single- and goal-directed strategies attributed to a normal pattern. Therefore, behaviors that were previously easy discriminated, now were more similar.

In the probe trial, two intervals could be distinguished: the first section of navigation until the animals arrive to the previous location of the platform, and the remaining interval in which the animals could look for it or not in a new location. While in the first interval, all animals, 3xTg-AD and NTg, swam directly to the platform, caffeine treatment reduced in 50% the use of this strategy in the 3xTg-AD+caff group. In the second interval could be hypothesized that the animals are facing a problem similar to the first day of the place task, with the exception that now there have already fulfilled the acquisition process. Here, the 3xTg-AD mice showed a poor cognitive flexibility using steadily a single strategy, which could be considered an inefficient response to solve this situation. Interestingly, we have reported poor cognitive flexibility shown as persistence of behaviors in the forced swim test at more advanced stages of disease (17 months of age) (Torres-Lista and Giménez-Llort, 2014). In this sense, it is important to note that caffeine increased the variety of strategies in the 3xTg-AD group suggesting improved cognitive integration processes that may be taking part in the resolution of the problem.

Regarding mortality data in this study, the number of animals is far from the minimum necessary to reliably assess the degree of survival and the effects of caffeine on it. Still, what our results suggest is that the data are congruent with the increased vulnerability of male 3xTg-AD mice at neuroimunoendocrine level, that could explain an important 40% of mortality at 12–13 months of age (Giménez-Llort et al., 2008) that can reach 100% at 15 month of age (García-Mesa et al., 2016). The observed mortality in the NTg+caff group would be in agreement with the reduced survival curve we reported in A_1 knockout mice (Giménez-Llort et al., 2002). While health benefits of caffeine and coffee are increasingly recognized, there are also notable reports of adverse effects of especially high-dose caffeine (Jain et al., 2017), including a case report of psychotic symptoms in a patient with dementia (Golden et al., 2015). The neurochemical scenario produced by long-term loss of A1 and A2a receptor function has been addressed in A1 (Johansson et al., 2001) and A2a (Ledent et al., 1997) knockout mice. Perhaps adverse effects can be sufficiently avoided by partial receptor blockade by low doses. Already now, there is reason to consider caffeine intake in patients with BPSD and its reduction in difficult-to-treat cases.

Since our first report (Giménez-Llort et al., 2008) proposing gender-specific immunoendocrine aging in 3xTg-AD mice, we have consistently reported that simple measures of weight and relative weight of peripheral organs indicate splenomegaly and thymus involution in this AD model. Both are considered physical indicators of peripheral immunological system aging (reviewed by Giménez-Llort et al., 2012) and impaired neuroimmunoendocrine crosstalk in AD (Giménez-Llort et al., 2014). More recently other laboratories have worked on this issue and successfully demonstrated the validity of splenomegaly as part of the autoimmune manifestations in the 3xTg-AD model (Marchese et al., 2014). In the present work, relative spleen size was slightly modulated by caffeine in both genotypes, a modulatory effect enough to restore the normal weight of the spleen in the 3xTg-AD mice. This suggests that in the 3xTg-AD+caff group, there could be an improvement in the deregulation of this network that recently has been described as relevant in AD (Giménez-Llort et al., 2014).

At the endocrine level, slight increases of corticosterone were observed due to genotype and treatment, without reaching statistical significance. This trend would be in agreement with our first report on the increase of glucocorticoid levels in male 3xTg-AD mice at more advanced stages of disease, concomitantly to increased anxiety and peripheral immune dysfunction (Giménez-Llort et al., 2008). Stress-like patterns of increased corticosterone secretion and decreased thyrotropin are described among the neuroendocrine effects of caffeine, while chronic treatment is known to induce tolerance to these effects (Spindel et al., 1983).

Immunomodulatory effects of caffeine by the decrease of cytokines (Frost-Meyer and Logomarsino, 2012) have also been proposed to contribute to neuroprotection, e.g., in Alzheimer's disease (Horrigan et al., 2006). A better balance between pro- and anti-inflammatory cytokines in favor of anti-inflammation is also posed as the main hypothesis to explain the effects of caffeine reducing the inflammatory processes in severe life-threatening conditions (Bessler et al., 2012). Further experiments addressing the effects of chronic caffeine on peripheral cytokine levels will help to better elucidate its actions on the impaired neuro-immune system in AD.

CONCLUSION

The present results provide evidence of the adverse effects of caffeine in 3xTg-AD mice with a BPSD-like profile that raises

the concern for its general recommendation to AD patients. These results confirm that caffeine, despite its everyday use and relative lack of government regulation, is a potent compound with multifaceted effects. Our study adds to the evidence for caffeine and other adenosine-receptor blockers have distinct physiological effects. Some ways to deal with these multi-effects are to optimize the dose, to use active substances in coffee other than caffeine, and to use synthetic drugs modeled after caffeine, such as subtype-selective adenosine receptor antagonists, rather caffeine itself. We speculate that over a chronic treatment with caffeine, the exacerbation of anxiety-like BPSD symptoms may partially interfere with the beneficial cognitive effects to the extent that they can be in the opposite direction.

AUTHOR CONTRIBUTIONS

LG-L the concept development, the study design, the study conduct, and the data collection. RB-C data analysis. RB-C and LG-L data interpretation and drafting the manuscript. BJ scientific discussions and critical revision of the manuscript and figures content. All authors approved final version of the manuscript. LG-L and BJ supported for financial resources.

FUNDING

The work received support by Instituto de Salud Carlos III, ISC3 PI10/00283 Spain, UAB GE260804. BJ received support by the Åhlén Foundation and the Stockholm County Council (ALF 20170190). RB-C received a predoctoral grant FI-DGR (2012FI_B1 00198) from Secretaria d'Universitats i Recerca, Departament d'Economia i Coneixement, Generalitat de Catalunya. We thank Ismael Álvarez-Montón for his assistance in the chronic caffeine treatment. The animals used in the present study came from the colony of homozygous 3xTg-AD and wild-type NTg mice established by Dr. LG-L at the Universitat Autònoma de Barcelona, Spain, from progenitors kindly provided by Prof. Frank M. LaFerla, Department of Neurobiology and Behavior, University of California, Irvine, Irvine, CA, United States.

REFERENCES

Anderson, N. L., and Hughes, R. N. (2008). Increased emotional reactivity in rats following exposure to caffeine during adolescence. *Neurotoxicol. Teratol.* 30, 195–201. doi: 10.1016/j.ntt.2008.02.002

Arendash, G. W., and Cao, C. (2010). Caffeine and coffee as therapeutics against Alzheimer's disease. *J. Alzheimers Dis.* 20(Suppl. 1), S117–S126. doi: 10.3233/JAD-2010-091249

Arendash, G. W., Mori, T., Cao, C., Mamcarz, M., Runfeldt, M., Dickson, A., et al. (2009). Caffeine reverses cognitive impairment and decreases brain amyloid-beta levels in aged Alzheimer's disease mice. *J. Alzheimers Dis.* 17, 661–680. doi: 10.3233/JAD-2009-1087

Arendash, G. W., Schleif, W., Rezai-Zadeh, K., Jackson, E. K., Zacharia, L. C., Cracchiolo, J. R., et al. (2006). Caffeine protects Alzheimer's mice against cognitive impairment and reduces brain beta-amyloid production. *Neuroscience* 142, 941–952. doi: 10.1016/j.neuroscience.2006.07.021

Baeta-Corral, R., and Giménez-Llort, L. (2014). Bizarre behaviors and risk assessment in 3xTg-AD mice at early stages of the disease. *Behav. Brain Res.* 258, 97–105. doi: 10.1016/j.bbr.2013.10.017

Baeta-Corral, R., and Giménez-Llort, L. (2015). Persistent hyperactivity and distinctive strategy features in the Morris water maze in 3xTg-AD mice at advanced stages of disease. *Behav. Neurosci.* 129, 129–137. doi: 10.1037/bne0000027

Batalha, V. L., Ferreira, D. G., Coelho, J. E., Valadas, J. S., Gomes, R., Temido-Ferreira, M., et al. (2016). The caffeine-binding adenosine A2A receptor induces age-like HPA-axis dysfunction by targeting glucocorticoid receptor function. *Sci. Rep.* 6:31493. doi: 10.1038/srep31493

Bessler, H., Salman, H., Bergman, M., and Djaldetti, M. (2012). Caffeine alters cytokine secretion by PBMC induced by colon cancer cells. *Cancer Invest.* 30, 87–91. doi: 10.3109/07357907.2011.636113

Blázquez, G., Cañete, T., Tobeña, A., Giménez-Llort, L., and Fernández-Teruel, A. (2014). Cognitive and emotional profiles of aged Alzheimer's disease (3 × TgAD) mice: effects of environmental enrichment and sexual dimorphism. *Behav. Brain Res.* 268, 185–201. doi: 10.1016/j.bbr.2014.04.008

Broekkamp, C. L., Rijk, H. W., Joly-Gelouin, D., and Lloyd, K. L. (1986). Major tranquillizers can be distinguished from minor tranquillizers on the basis of effects on marble burying and swim-induced grooming in mice. *Eur. J. Pharmacol.* 126, 223–229. doi: 10.1016/0014-2999(86)90051-8

Canas, P. M., Porciúncula, L. O., Cunha, G. M., Silva, C. G., Machado, N. J., Oliveira, J. M., et al. (2009). Adenosine A2A receptor blockade prevents synaptotoxicity and memory dysfunction caused by beta-amyloid peptides via p38 mitogen-activated protein kinase pathway. *J. Neurosci.* 29, 14741–14751. doi: 10.1523/JNEUROSCI.3728-09.2009

Cañete, T., Blázquez, G., Tobeña, A., Giménez-Llort, L., and Fernández-Teruel, A. (2015). Cognitive and emotional alterations in young Alzheimer's disease (3xTgAD) mice: effects of neonatal handling stimulation and sexual dimorphism. *Behav. Brain Res.* 281, 156–171. doi: 10.1016/j.bbr.2014.11.004

Cao, C., Cirrito, J. R., Lin, X., Wang, L., Verges, D. K., Dickson, A., et al. (2009). Caffeine suppresses amyloid-beta levels in plasma and brain of Alzheimer's disease transgenic mice. *J. Alzheimers Dis.* 17, 681–697. doi: 10.3233/JAD-2009-1071

Cao, C., Loewenstein, D. A., Lin, X., Zhang, C., Wang, L., Duara, R., et al. (2012). High blood caffeine levels in MCI linked to lack of progression to dementia. *J. Alzheimers Dis.* 30, 559–572. doi: 10.3233/JAD-2012-111781

Cao, C., Wang, L., Lin, X., Mamcarz, M., Zhang, C., Bai, G., et al. (2011). Caffeine synergizes with another coffee component to increase plasma GCSF: linkage to cognitive benefits in Alzheimer's mice. *J. Alzheimers Dis.* 25, 323–335. doi: 10.3233/JAD-2011-110110

Chen, J. F., Yu, L., Shen, H. Y., He, J. C., Wang, X., and Zheng, R. (2010). What knock-out animals tell us about the effects of caffeine. *J. Alzheimers Dis.* 20(Suppl. 1), S17–S24. doi: 10.3233/JAD-2010-1403

Chu, Y. F., Chang, W. H., Black, R. M., Liu, J. R., Sompol, P., Chen, Y., et al. (2012). Crude caffeine reduces memory impairment and amyloid β(1-42) levels in an Alzheimer's mouse model. *Food Chem.* 135, 2095–2102. doi: 10.1016/j.foodchem.2012.04.148

Colorado, R. A., Shumake, J., Conejo, N. M., Gonzalez-Pardo, H., and Gonzalez-Lima, F. (2006). Effects of maternal separation, early handling, and standard facility rearing on orienting and impulsive behavior of adolescent rats. *Behav. Processes* 71, 51–58. doi: 10.1016/j.beproc.2005.09.007

Corrêa-Velloso, J. C., Gonçalves, M. C. B., Naaldijka, Y., Oliveira-Giacomelli, A., Pillat, M. M., and Ulrich, H. (2018). Pathophysiology in the comorbidity of Bipolar Disorder and Alzheimer's disease: pharmacological and stem cell approaches. *Prog. Neuropsychopharmacol. Biol. Psychiatry* 80, 34–53. doi: 10.1016/j.pnpbp.2017.04.033

Costenla, A. R., Cunha, R. A., and de Mendonca, A. (2010). Caffeine, adenosine receptors, and synaptic plasticity. *J. Alzheimers Dis.* 20(Suppl. 1), S25–S34. doi: 10.3233/JAD-2010-091384

Dall'Igna, O. P., Fett, P., Gomes, M. W., Souza, D. O., Cunha, R. A., and Lara, D. R. (2007). Caffeine and adenosine A_{2a} receptor antagonists prevent beta-amyloid (25-35)-induced cognitive deficits in mice. *Exp. Neurol.* 203, 241–245. doi: 10.1016/j.expneurol.2006.08.008

Eskelinen, M. H., and Kivipelto, M. (2010). Caffeine as a protective factor in dementia and Alzheimer's disease. *J. Alzheimers Dis.* 20(Suppl. 1), S167–S174. doi: 10.3233/JAD-2010-1404

Eskelinen, M. H., Ngandu, T., Tuomilehto, J., Soininen, H., and Kivipelto, M. (2009). Midlife coffee and tea drinking and the risk of late-life dementia: a population-based CAIDE study. *J. Alzheimers Dis.* 16, 85–91. doi: 10.3233/JAD-2009-0920

España, J., Valero, J., Miñano-Molina, A. J., Masgrau, R., Martín, E., Guardia-Laguarta, C., et al. (2010). beta-Amyloid disrupts activity-dependent gene transcription required for memory through the CREB coactivator CRTC1. *J. Neurosci.* 30, 9402–9410. doi: 10.1523/JNEUROSCI.2154-10.2010

Fredholm, B. B. (2007). Adenosine, an endogenous distress signal, modulates tissue damage and repair. *Cell Death Differ.* 14, 1315–1323. doi: 10.1038/sj.cdd.4402132

Fredholm, B. B., Bättig, K., Holmen, J., Nehlig, A., and Zvartau, E. E. (1999). Actions of caffeine in the brain with special reference to factors that contribute to its widespread use. *Pharmacol. Rev.* 51, 83–133.

Fredholm, B. B., Yang, J., and Wang, Y. (2017). Molecular aspects of medicine low, but not high, dose caffeine is a readily available probe for adenosine actions. *Mol. Aspects Med.* 55, 20–25. doi: 10.1016/j.mam.2016.11.011

Frost-Meyer, N. J., and Logomarsino, J. V. (2012). Impact of coffee components on inflammatory markers: a review. *J. Funct. Foods* 4, 819–830. doi: 10.1016/j.jff.2012.05.010

García-Mesa, Y., Colie, S., Corpas, R., Cristòfol, R., Comellas, F., Nebreda, A. R., et al. (2016). Oxidative stress is a central target for physical exercise neuroprotection against pathological brain aging. *J. Gerontol. A Biol. Sci. Med. Sci.* 71, 40–49. doi: 10.1093/gerona/glv005

García-Mesa, Y., Giménez-Llort, L., López, L. C., Venegas, C., Cristòfol, R., Escames, G., et al. (2012). Melatonin plus physical exercise are highly neuroprotective in the 3xTg-AD mouse. *Neurobiol. Aging* 33, 1124.e13–1124.e29. doi: 10.1016/j.neurobiolaging.2011.11.016

García-Mesa, Y., Lopez-Ramos, J. C., Gimenez-Llort, L., Revilla, S., Guerra, R., Gruart, A., et al. (2011). Physical exercise protects against Alzheimer's disease in 3xTg-AD mice. *J. Alzheimers Dis.* 24, 421–454. doi: 10.3233/JAD-2011-101635

Giménez-Llort, L., Arranz, L., Maté, I., and De la Fuente, M. (2008). Gender-specific neuroimmunoendocrine aging in a triple-transgenic3xTgAD mouse model for Alzheimer's disease and its relation with longevity. *Neuroimmunomodulation* 15, 331–343. doi: 10.1159/000156475

Giménez-Llort, L., Blázquez, G., Cañete, T., Johansson, B., Oddo, S., Tobeña, A., et al. (2007). Modeling behavioral and neuronal symptoms of Alzheimer's disease in mice: a role for intraneuronal amyloid. *Neurosci. Biobehav. Rev.* 31, 125–147. doi: 10.1016/j.neubiorev.2006.07.007

Giménez-Llort, L., Blázquez, G., Cañete, T., Rosa, R., Vivó, M., Oddo, S., et al. (2006). "Modeling neuropsychiatric symptoms of Alzheimer's disease dementia in 3xTg-AD mice," in *Alzheimer's Disease: New Advances*, eds K. Iqbal, B. Winblad, and J. Avila (Pianoro: Medimond SRL), 513–516.

Giménez-Llort, L., Fernandez-Teruel, A., Escorihuela, R. M., Fredholm, B. B., Tobena, A., Pekny, M., et al. (2002). Mice lacking the adenosine A1 receptor are anxious and aggressive, but are normal learners with reduced muscle strength and survival rate. *Eur. J. Neurosci.* 16, 547–550. doi: 10.1046/j.1460-9568.2002.02122.x

Giménez-Llort, L., Garcia, Y., Buccieri, K., Revilla, S., Sunol, C., Cristofol, R., et al. (2010). Gender-specific neuroimmunoendocrine response to treadmill exercise in 3xTg-AD mice. *Int. J. Alzheimers Dis.* 2010:128354. doi: 10.4061/2010/128354

Giménez-Llort, L., Masino, S. A., Diao, L., Fernandez-Teruel, A., Tobena, A., Halldner, L., et al. (2005). Mice lacking the adenosine A1 receptor have normal spatial learning and plasticity in the CA1 region of the hippocampus, but they habituate more slowly. *Synapse* 57, 8–16. doi: 10.1002/syn.20146

Giménez-Llort, L., Maté, I., Manassra, R., Vida, C., and De la Fuente, M. (2012). Peripheral immune system and neuroimmune communication impairment in a mouse model of Alzheimer's disease. *Ann. N. Y. Acad. Sci.* 1262, 74–84. doi: 10.1111/j.1749-6632.2012.06639.x

Giménez-Llort, L., Torres-Lista, V., and De la Fuente, M. (2014). Crosstalk between behavior and immune system during the prodromal stages of Alzheimer's disease. *Curr. Pharm. Des.* 20, 4723–4732. doi: 10.2174/1381612820666140130205500

Golden, L. E., Sassoon, P., and Cáceda, R. (2015). A case report of late onset psychosis with dementia and aspirin and caffeine addiction. *Schizophr. Res.* 168, 591–592. doi: 10.1016/j.schres.2015.08.021

Griffiths, R. R., Evans, S. M., Heishman, S. J., Preston, K. L., Sannerud, C. A., Wolf, B., et al. (1990). Low-dose caffeine discrimination in humans. *J. Pharmacol. Exp. Ther.* 252, 970–978.

Han, K., Jia, N., Li, J., Yang, L., and Min, L. Q. (2013). Chronic caffeine treatment reverses memory impairment and the expression of brain BNDF and TrkB in the PS1/APP double transgenic mouse model of Alzheimer's disease. *Mol. Med. Rep.* 8, 737–740. doi: 10.3892/mmr.2013.1601

Hermansen, K., Krogholm, K. S., Bech, B. H., Dragsted, L. O., Hyldstrup, L., Jørgensen, K., et al. (2012). Coffee can protect against disease. *Ugeskr. Laeger* 174, 2293–2297.

Horrigan, L. A., Kelly, J. P., and Connor, T. J. (2006). Immunomodulatory effects of caffeine: friend or foe? *Pharmacol. Ther.* 111, 877–892. doi: 10.1016/j.pharmthera.2006.02.002

Jain, S., Srivastava, A. S., Verma, R. P., and Maggu, G. (2017). Caffeine addiction: need for awareness and research and regulatory measures. *Asian J. Psychiatry* doi: 10.1016/j.ajp.2017.01.008 [Epub ahead of print].

Janus, C. (2004). Search strategies used by *APP* transgenic mice during navigation in the Morris water maze. *Learn. Mem.* 11, 337–346. doi: 10.1101/lm.70104

Johansson, B., Georgiev, V., Kuosmanen, T., and Fredholm, B. B. (1996). Long-term treatment with some methylxanthines decreases the susceptibility to bicuculline- and pentylenetetrazol-induced seizures in mice. Relationship to c-fos expression and receptor binding. *Eur. J. Neurosci.* 8, 2447–2458. doi: 10.1111/j.1460-9568.1996.tb01539.x

Johansson, B., Halldner, L., Dunwiddie, T. V., Masino, S. A., Poelchen, W., Giménez-Llort, L., et al. (2001). Hyperalgesia, anxiety, and decreased hypoxic neuroprotection in mice lacking the adenosine A1 receptor. *Proc. Natl. Acad. Sci. U.S.A.* 98, 9407–9412. doi: 10.1073/pnas.161292398

Kilkenny, C., Browne, W. J., Cuthill, I. C., Emerson, M., and Altman, D. G. (2010). Improving bioscience research reporting: the ARRIVE guidelines for reporting animal research. *PLOS Biol.* 8:e1000412. doi: 10.1371/journal.pbio.1000412

Kolahdouzan, M., and Hamadeh, M. J. (2017). The neuroprotective effects of caffeine in neurodegenerative diseases. *CNS Neurosci. Ther.* 23, 272–290. doi: 10.1111/cns.12684

Laurent, C., Eddarkaoui, S., Derisbourg, M., Leboucher, A., Demeyer, D., Carrier, S., et al. (2014). Beneficial effects of caffeine in a transgenic model of Alzheimer's disease-like tau pathology. *Neurobiol. Aging* 35, 2079–2090. doi: 10.1016/j.neurobiolaging.2014.03.027

Ledent, C., Vaugeois, J. M., Schiffmann, S. N., Pedrazzini, T., El Yacoubi, M., Vanderhaeghen, J. J., et al. (1997). Aggressiveness, hypoalgesia and high blood pressure in mice lacking the adenosine A2a receptor. *Nature* 388, 674–678. doi: 10.1038/41771

Maia, L., and de Mendonça, A. (2002). Does caffeine intake protect from Alzheimer's disease? *Eur. J. Neurol.* 9, 377–382.

Manuel, I., Lombardero, L., LaFerla, F. M., Giménez-Llort, L., and Rodríguez-Puertas, R. (2016). Activity of muscarinic, galanin and cannabinoid receptors in the prodromal and advanced stages in the triple transgenic mice model of Alzheimer's disease. *Neuroscience* 329, 284–293. doi: 10.1016/j.neuroscience.2016.05.012

Marchese, M., Cowan, D., Head, E., Ma, D., Karimi, K., Ashthorpe, V., et al. (2014). Autoimmune manifestations in the 3xTg-AD model of Alzheimer's disease. *J. Alzheimers Dis.* 39, 191–210. doi: 10.3233/JAD-131490

Marques, S., Batalha, V. L., Lopes, L. V., and Outeiro, T. F. (2011). Modulating Alzheimer's disease through caffeine: a putative link to epigenetics. *J. Alzheimers Dis.* 24(Suppl. 2), 161–171. doi: 10.3233/JAD-2011-110032

Moy, G. A., and McNay, E. C. (2013). Caffeine prevents weight gain and cognitive impairment caused by a high-fat diet while elevating hippocampal BDNF. *Physiol. Behav.* 109, 69–74. doi: 10.1016/j.physbeh.2012.11.008

Nehlig, A. (2010). Is caffeine a cognitive enhancer? *J. Alzheimers Dis.* 20(Suppl. 1), S85–S94. doi: 10.3233/JAD-2010-091315

Nehlig, A., Daval, J. L., and Debry, G. (1992). Caffeine and the central nervous system: mechanisms of action, biochemical, metabolic and psychostimulant effects. *Brain Res. Brain Res. Rev.* 17, 139–170. doi: 10.1016/0165-0173(92)90012-B

Oddo, S., Caccamo, A., Shepherd, J. D., Murphy, M. P., Golde, T. E., Kayed, R., et al. (2003). Triple-transgenic model of Alzheimer's disease with plaques and tangles: intracellular Aβ and synaptic dysfunction. *Neuron* 39, 409–421. doi: 10.1016/S0896-6273(03)00434-3

Oñatibia-Astibia, A., Franco, R., and Martínez-Pinilla, E. (2017). Health benefits of methylxanthines in neurodegenerative diseases. *Mol. Nutr. Food Res.* 61:1600670. doi: 10.1002/mnfr.201600670

Piccininni, M., Di Carlo, A., Baldereschi, M., Zaccara, G., and Inzitari, D. (2005). Behavioral and psychological symptoms in Alzheimer's disease: frequency and relationship with duration and severity of the disease. *Dement. Geriatr. Cogn. Disord.* 19, 276–281. doi: 10.1159/000084552

Reisberg, B., Borenstein, J., Salob, S. P., Ferris, S. H., Franssen, E., and Georgotas, A. (1987). Behavioral symptoms in Alzheimer's disease: phenomenology and treatment. *J. Clin. Psychiatry* 48(Suppl.), 9–15.

Romano, A., Pace, L., Tempesta, B., Lavecchia, A. M., Macheda, T., Bedse, G., et al. (2015). Depressive-like behavior is paired to monoaminergic alteration in a murine model of Alzheimer's disease. *Int. J. Neuropsychopharmacol.* 18:yu020. doi: 10.1093/ijnp/pyu020

Sabogal-Guáqueta, A.-M., Carrillo-Hormaz, L., Osorio, E., and Cardona-Gómez, G. P. (2017). Effects of biflavonoids from *Garcinia madruno* on a triple transgenic mouse model of Alzheimer's disease. *Pharmacol. Res.* doi: 10.1016/j.phrs.2017.12.002 [Epub ahead of print].

Silverman, K., Mumford, G. K., and Griffiths, R. R. (1994). A procedure for studying the within-session onset of human drug discrimination. *J. Exp. Anal. Behav.* 61, 181–189. doi: 10.1901/jeab.1994.61-181

Solfrizzi, V., Panza, F., Imbimbo, B. P., D'Introno, A., Galluzzof, L., Gandin, C., et al. (2015). Coffee consumption habits and the risk of mild cognitive impairment: the Italian longitudinal study on aging. *J. Alzheimers Dis.* 47, 889–899. doi: 10.3233/JAD-150333

Spindel, E., Griffith, L., and Wurtman, R. J. (1983). Neuroendocrine effects of caffeine. II. Effects on thyrotropin and corticosterone secretion. *J. Pharmacol. Exp. Ther.* 225, 346–350.

Torres-Lista, V., de la Fuente, M., and Giménez-Llort, L. (2017). Survival curves and behavioral profiles of female 3xTg-AD mice surviving to 18-months of age as compared to mice with normal aging. *J. Alzheimers Dis. Rep.* 1, 47–57. doi: 10.3233/ADR-170011

Torres-Lista, V., and Giménez-Llort, L. (2014). Persistence of behaviours in the Forced Swim Test in 3xTg-AD mice at advanced stages of disease. *Behav. Processes* 106, 118–121. doi: 10.1016/j.beproc.2014.05.001

Torres-Lista, V., and Giménez-Llort, L. (2015). Early postnatal handling and environmental enrichment improve the behavioral responses of 17-month-old 3xTg-AD and non-transgenic mice in the Forced Swim Test in a gender-dependent manner. *Behav. Processes* 120, 120–127. doi: 10.1016/j.beproc.2015.09.011

Wang, F., Feng, T. Y., Yang, S., Preter, M., Zhou, J., and Wang, X. (2016). Drug therapy for behavioral, and psychological symptoms of dementia. *Curr. Neuropharmacol.* 14, 307–313. doi: 10.2174/1570159X14666151208114232

Wierzejska, R. (2017). Can coffee consumption lower the risk of Alzheimer's disease and Parkinson's disease? A literature review. *Arch. Med. Sci.* 13, 507–514. doi: 10.5114/aoms.2016.63599

Conflict of Interest Statement: The authors declare that the research was conducted in the absence of any commercial or financial relationships that could be construed as a potential conflict of interest.

frontiers in Pharmacology

ORIGINAL RESEARCH
published: 15 February 2018
doi: 10.3389/fphar.2018.00106

Molecular Evidence of Adenosine Deaminase Linking Adenosine A_{2A} Receptor and CD26 Proteins

*Estefanía Moreno[1,2,3], Júlia Canet[1,2,3], Eduard Gracia[1,2,3], Carme Lluís[1,2,3], Josefa Mallol[1,2,3], Enric I. Canela[1,2,3], Antoni Cortés[1,2,3] and Vicent Casadó[1,2,3]**

[1] Department of Biochemistry and Molecular Biomedicine, Faculty of Biology, University of Barcelona, Barcelona, Spain, [2] Institute of Biomedicine of the University of Barcelona (IBUB), Barcelona, Spain, [3] Centro de Investigación Biomédica en Red sobre Enfermedades Neurodegenerativas, Madrid, Spain

Adenosine is an endogenous purine nucleoside that acts in all living systems as a homeostatic network regulator through many pathways, which are adenosine receptor (AR)-dependent and -independent. From a metabolic point of view, adenosine deaminase (ADA) is an essential protein in the regulation of the total intracellular and extracellular adenosine in a tissue. In addition to its cytosolic localization, ADA is also expressed as an ecto-enzyme on the surface of different cells. Dipeptidyl peptidase IV (CD26) and some ARs act as binding proteins for extracellular ADA in humans. Since CD26 and ARs interact with ADA at opposite sites, we have investigated if ADA can function as a cell-to-cell communication molecule by bridging the anchoring molecules CD26 and $A_{2A}R$ present on the surfaces of the interacting cells. By combining site-directed mutagenesis of ADA amino acids involved in binding to $A_{2A}R$ and a modification of the bioluminescence resonance energy transfer (BRET) technique that allows detection of interactions between two proteins expressed in different cell populations with low steric hindrance (NanoBRET), we show direct evidence of the specific formation of trimeric complexes CD26-ADA-$A_{2A}R$ involving two cells. By dynamic mass redistribution assays and ligand binding experiments, we also demonstrate that $A_{2A}R$-NanoLuc fusion proteins are functional. The existence of this ternary complex is in good agreement with the hypothesis that ADA could bridge T-cells (expressing CD26) and dendritic cells (expressing $A_{2A}R$). This is a new metabolic function for ecto-ADA that, being a single chain protein, it has been considered as an example of moonlighting protein, because it performs more than one functional role (as a catalyst, a costimulator, an allosteric modulator and a cell-to-cell connector) without partitioning these functions in different subunits.

Keywords: adenosine deaminase, adenosine A_{2A} receptor, bioluminescence resonance energy transfer, CD26, dipeptidyl peptidase IV, moonlighting protein, protein–protein interaction

OPEN ACCESS

Edited by:
Kenneth A. Jacobson, National Institutes of Health (NIH), United States

Reviewed by:
Oscar J. Cordero, Universidade de Santiago de Compostela, Spain
Claudia Martini, University of Pisa, Italy
Paul Proost, Rega Institute for Medical Research, KU Leuven, Belgium

****Correspondence:***
Vicent Casadó
vcasado@ub.edu

Specialty section:
This article was submitted to Experimental Pharmacology and Drug Discovery, a section of the journal Frontiers in Pharmacology

Received: *09 November 2017*
Accepted: *30 January 2018*
Published: *15 February 2018*

Citation:
Moreno E, Canet J, Gracia E, Lluís C, Mallol J, Canela EI, Cortés A and Casadó V (2018) Molecular Evidence of Adenosine Deaminase Linking Adenosine A_{2A} Receptor and CD26 Proteins. Front. Pharmacol. 9:106. doi: 10.3389/fphar.2018.00106

INTRODUCTION

Many proteins interact with other proteins or are organized into macromolecular complexes, in which multiple components work together to perform different cellular processes (Petschnigg et al., 2012). Transient protein-protein interactions are composed of relatively weak interactions and they perform essential functional roles in biological systems, notably in regulating the dynamic

of biological networks (Maleki et al., 2013; Tsuji et al., 2015; Cigler et al., 2017). Investigation of protein–protein interactions of the membrane proteins is of special interest, as they have pivotal roles in cellular processes, they are major targets for the development of new therapeutics and they are often directly linked to human diseases (Petschnigg et al., 2012; Bourgaux and Couvreur, 2014; Jazayeri et al., 2015; Yin and Flynn, 2016; Saraon et al., 2017; Shrivastava et al., 2017). An example of these interactions is that established by the enzyme adenosine deaminase with different proteins (Cortés et al., 2015). Fluorescence resonance energy transfer (FRET) and bioluminescence resonance energy transfer (BRET) are biophysical techniques widely used to analyze direct protein–protein interactions that take place in living cells as well as conformational changes within proteins or molecular complexes (Ciruela, 2008; Kimura et al., 2010; Kim et al., 2011; Lohse et al., 2012; Deriziotis et al., 2014; Brown et al., 2015; Mo and Fu, 2016; Corbel et al., 2017).

Adenosine deaminase (ADA, EC 3.5.4.4) catalyzes the irreversible deamination of adenosine or 2′-deoxyadenosine to inosine or 2-deoxyinosine, respectively. In humans, there are two different enzymes, which are designated ADA1, from here ADA, and ADA2. ADA is a monomeric enzyme that plays a central role in purine metabolism (He et al., 2015; Kutryb-Zajac et al., 2016). Interest in ADA function increased after the discovery that about 15% of inherited immunodeficiencies are caused by mutations in the ADA gene that lead to a loss of function of this protein (Buckley, 2004). This set of disorders is known as severe combined immunodeficiency (SCID), characterized by dysfunction of the T, B, and natural killers (NK) cells and severe lymphopenia. The absence of ADA activity causes lymph-toxic deoxyadenosine triphosphate accumulation that results in apoptosis in immature thymocytes (Buckley, 2004; Shaw et al., 2017; Turel et al., 2017). Different crystal structures of ADA have been obtained, containing a tightly bound Zn^{2+} that is essential for the stability and the catalytic function of the native protein (Wilson et al., 1991; Cooper et al., 1997; Wang and Quiocho, 1998; Kinoshita et al., 2005; Niu et al., 2010; Khare et al., 2012; Bottari et al., 2014; Grosskopf et al., 2017). ADA is a cytosolic enzyme localized in many human tissues, being the lymphoid system (lymph nodes, spleen and thymus) where the highest levels are found (Beyazit et al., 2012; Maiuolo et al., 2016). In the case of ADA2, Zavialov and Engström (2005) showed that the abundance of this enzyme in human tissues is low and that the gene encoding ADA2 is part of a new family of adenosine deaminase growth factors. Likewise, the same authors reported the structure of ADA2, revealing striking differences with ADA both in their global structures and in the arrangement of their catalytic centers (Zavialov et al., 2010).

It has been demonstrated that ADA can also be expressed as an ecto-enzyme on the surface of several cell types, such us lymphocytes (Martín et al., 1995; Blackburn and Kellems, 2005), erythrocytes (Da Silva et al., 2013), dendritic cells (Pacheco et al., 2005; Desrosiers et al., 2007; Casanova et al., 2012), endothelial and epithelial cells (Ginés et al., 2002; Eltzschig et al., 2006), fibroblasts (Torvinen et al., 2002), platelets (Souza Vdo et al., 2012) and neurons (Ruiz et al., 2000; Hawryluk et al., 2012). Up to now, dipeptidyl peptidase IV (DPPIV, EC3.4.14.5, also known as CD26) and some adenosine receptors (ARs), as A_1R, $A_{2A}R$, and $A_{2B}R$, serve as binding proteins for extracellular ADA in humans (Beckenkamp et al., 2016; Arin et al., 2017). The cluster differentiation antigen CD26, is a ubiquitously expressed multifunctional cell surface serine protease that cleaves dipeptides from the N-terminal end of oligopeptides and smaller peptides with either L-Ala or L-Pro in the penultimate position (Gorrell, 2005; Zhong et al., 2015a; Klemann et al., 2016; Mortier et al., 2016).

Human CD26 is a homodimeric integral membrane type II glycoprotein which is anchored through its signal peptide. The large C-terminal of the extracellular component of CD26 contains an α/β-hydrolase domain and an eight-blade β-propeller domain, that is open and consists of two subdomains responsible for the glycosylation-rich and cysteine-rich regions, respectively. ADA, caveolin-1 and many monoclonal anti-CD26 antibodies bind to the glycosylation-rich domain, while plasminogen, fibronectin, collagen and streptokinase bind to the cysteine-rich region (Klemann et al., 2016). The catalytic region of CD26 is responsible for the enzymatic activity on its natural substrates, including incretins, such as glucagon-like peptide-1 and glucose-dependent insulinotropic peptide, neuropeptides, chemokines, and a few growth factors and cytokines leading to their inactivation and/or degradation (Larrinaga et al., 2015; Zhong et al., 2015b; Mortier et al., 2016). Moreover, a soluble monomeric form of CD26 has been reported in plasma and other body fluids, which enhances the effect of stimulant agents on T-cell proliferation independently of both the enzymatic activity and the ADA-binding ability of CD26 (Yu et al., 2011; Zhong et al., 2015a).

CD26 has been implicated in a variety of pathologies, including rheumatoid arthritis, autoimmune diseases, HIV infection and different types of cancers and CNS tumors (Yu et al., 2006; Songok et al., 2010; Havre et al., 2013; Cordero et al., 2015; Larrinaga et al., 2015; Klemann et al., 2016; Mortier et al., 2016; Beckers et al., 2017; Lee et al., 2017). CD26 has a number of non-enzymatic functions via interactions with several proteins, for instance, ADA, caveolin-1, streptokinase, tyrosine phosphatase, collagen, fibronectin, CD45, chemokine receptor CXCR4, plasminogen type 2, the HIV gp120 protein and the human coronavirus MERS-CoV spike protein (Lambeir et al., 2003; Havre et al., 2008; Fan et al., 2012; Lu et al., 2013; Zhong et al., 2015a; Baerts et al., 2015; Kanno et al., 2016; Xin et al., 2017). As an adhesion molecule, CD26 could facilitate adhesion, migration and metastasis of tumor cells by binding to the extracellular matrix proteins fibronectin and collagen (see Mortier et al., 2016).

The second type of ADA anchoring proteins on the cell surface are the A_1R (Ciruela et al., 1996; Saura et al., 1996; Sun et al., 2005; Gracia et al., 2008, 2013b), the $A_{2A}R$ (Gracia et al., 2011, 2013a) and the $A_{2B}R$ (Herrera et al., 2001; Antonioli et al., 2014; Arin et al., 2015, 2017), which are members of the family A of G-protein coupled receptors (GPCRs) (Fredholm et al., 2011). A_1R is coupled to $G_{i/o}$ proteins, while $A_{2A}R$ and $A_{2B}R$ are coupled to $G_{s/olf}$ proteins. A_1Rs inhibit adenylyl cyclase activity through the activation of a G-protein that is sensitive to pertussis toxin, therefore reducing the intracellular levels of cyclic AMP.

In contrast, $A_{2A}R$ and $A_{2B}R$ have a stimulatory effect on adenylyl cyclase activity increasing cyclic AMP levels, with the consequent PKA activation and CREB phosphorylation. The activation of $A_{2A}R$ can also activate protein kinase C (PKC), through cyclic AMP-dependent and -independent mechanisms (Jacobson and Gao, 2006; Sheth et al., 2014; Cortés et al., 2015; Leiva et al., 2017). A_1R and $A_{2A}R$ are high affinity receptors with activity in the low to middle nanomolar range whereas $A_{2B}R$ has a substantially lower affinity for adenosine (micromolar) (Borea et al., 2015). All ARs are widely expressed and are involved in multiple biological functions, both in physiological and pathological conditions (Chen et al., 2013), including sleep regulation (Lazarus et al., 2017), cardioprotection (Gile and Eckle, 2016), renal function (Welch, 2015), lipolysis (Leiva et al., 2017), immune function (Cekic and Linden, 2016), angiogenesis (Du et al., 2015), as well as ischemia-reperfusion injury (Sharma et al., 2016), inflammation (Cronstein and Sitkovsky, 2017) and neurodegenerative disorders (Huang et al., 2017; Stockwell et al., 2017).

Since CD26 and ARs interact with ADA at opposite sites (Weihofen et al., 2004; Fan et al., 2012; Gracia et al., 2013a), in the present paper we have investigated if ADA could function as a cell-to-cell communication molecule by bridging the anchoring molecules CD26 and $A_{2A}R$ present on the surfaces of the interacting cells. We have used a modification of the BRET technique that allows detection of interactions between two proteins expressed in different cell populations with low steric hindrance (NanoBRET) (Machleidt et al., 2015; Mo and Fu, 2016). The results obtained confirm that the cloned $A_{2A}R$-NanoLuc and CD26-YFP constructs express correctly in HEK cells and can form with ecto-ADA oligomeric complexes which can be of metabolic relevance *in vivo*.

MATERIALS AND METHODS

Expression Vectors and Fusion Proteins

Human cDNAs for $A_{2A}R$, NMDAR1A or CD26 protein, cloned into pcDNA3.1, were amplified without their stop codons using sense and antisense primers harboring: EcoRI and KpnI sites to clone $A_{2A}R$ in pRluc-N1 vector (p*Rluc*-N1; PerkinElmer, Wellesley, MA, United States), KpnI and BamHI sites to clone $A_{2A}R$ or EcoRI and NotI to clone NMDAR1A in Nluc vector (*NanoLuc* Promega, Madison, WI, United States) and EcoRI and KpnI to clone CD26 or HindIII and BamHI to clone NMDAR1A in pEYFP-N1 vector (enhanced yellow variant of GFP; Clontech, Heidelberg, Germany). Amplified fragments were subcloned to be in-frame with restriction sites of pRluc-N1, Nluc or pEYFP-N1 vectors to provide plasmids that express proteins fused to YFP on the C-terminal end (CD26-YFP) or on the N-terminal end (NMDAR1A-YFP) or protein fused to Rluc on the C-terminal end ($A_{2A}R$-Rluc) or Nluc on the N-terminal end (NMDAR1A-Nluc, $A_{2A}R$-Nluc) with and without spacer (GTAGTGCCA). It was observed that all fusion proteins showed a similar membrane distribution as naïve receptors, and fusion of bioluminescent protein to receptor did not modify receptor function as determined by ERK assays. Plasmid pZC11-containing TAC-promoted wild-type human ADA or Leu58Ala or Leu62Ala ADA mutants cDNA were used as previously indicated (Gracia et al., 2013a).

Antibodies and Purified Proteins

Human-specific monoclonal antibody (mAb) against CD26, TA5.9-CC1-4C8 directed against the ADA-binding epitope on CD26 was previously characterized (Blanco et al., 2000; Pacheco et al., 2005; Martinez-Navio et al., 2009; Casanova et al., 2012). Albumin was purchased from Sigma–Aldrich (St. Louis, MI, United States). Bovine ADA was purchased from Roche (Basel, Switzerland).

Bacterial Strains and Vector

Escherichia coli SΦ3834, a multiple auxotroph (rpsL, Dadduid-man, metB, guaA, uraA: Tn 10) with a deletion of add (bacterial ADA gene), and plasmid pZC11-containing TAC-promoted wild-type human ADA cDNA (Chang et al., 1991) and Leu58Ala and Leu62Ala ADA mutants cDNA were used (Gracia et al., 2013a). Overnight cultures of pZC11-hADA transformants of SΦ3834 were inoculated into the appropriate volume of Luria-Bertani (LB) medium supplemented with carbenicillin (200 μg/ml) and tetracycline (18.75 μg/ml) (Sigma–Aldrich). Cells were grown with shaking at 37°C until an $A_{600\,nm} = 1.0$ and then were harvested and frozen at −80°C (Richard et al., 2002; Gracia et al., 2008).

Partial Purification of ADA

Recombinant wild-type and ADA mutants were partially purified from 500 ml cultures of *E. coli* SΦ3834 cells, and transformed with the plasmid pZC11 containing the cDNA of ADA, according to Gracia et al. (2013a). Briefly, cell pellets were resuspended at 4°C in 5 ml of lysis buffer. The suspensión was cooled on ice, and sonicated for 24 s × 20 s at 15% intensity in a sonifier (Branson Ultrasonics Corp., Danbury, CT, United States). The homogenate was centrifuged at 105,000 × *g* for 60 min, and protamine sulfate (Sigma–Aldrich) was slowly added up to a final concentration of 2 mg/ml. After 60 min of constant stirring, the suspension was again centrifuged, and the supernatant was desalted with a PD10 (GE Healthcare) gel filtration column, preequilibrated with 50 mM, pH 7.4, Tris-HCl buffer, and stored at 4°C for their immediate use.

Enzyme Activity and Kinetic Parameters of ADA

Adenosine deaminase activity was determined at 25°C with 0.1 mM adenosine as substrate in 50 mM Tris-HCl buffer, pH 7.4, as previously reported (Gracia et al., 2013a). The decrease in the absorbance at 265 nm ($\Delta\varepsilon = 7800\ M^{-1}\ cm^{-1}$) was monitored in an Ultrospec 3300 pro spectrophotometer (Biochrom Ltd., Cambridge, United Kingdom) with 1-ml cuvettes. One unit (U) of ADA activity is defined as the amount of enzyme required to hydrolyze 1 μmol of adenosine per minute in the assay conditions. Steady-state kinetic measurements were performed in 50 mM Tris-HCl buffer (pH 7.4) using a concentration range of adenosine from 10 μM to 1 mM and a constant enzyme concentration. Inhibition studies were carried out by monitoring

the hydrolysis rates of adenosine in the presence of constant concentrations of purine riboside (from 5 μM to 0.5 mM; Sigma–Aldrich) (Gracia et al., 2013a). In all cases, a minimum of four replicates for each single experimental point were performed. Kinetic parameters were obtained by fitting the data to the appropriate rate equations, using a non-linear regression software (Grafit, Erithacus Software, Surrey, United Kingdom).

Cell Culture and Transient Transfection

Human embryonic kidney (HEK-293T) cells obtained from ATCC were grown in Dulbecco's modified Eagle's medium (DMEM) (Gibco) supplemented with 100 μg/ml sodium pyruvate, 2 mM L-glutamine, 100 U/ml penicillin/streptomycin, essential medium non-essential amino acids solution (1/100) and 5% (v/v) heat inactivated fetal bovine serum (all from Invitrogen, Paisley, United Kingdom) and were maintained at 37°C in an atmosphere with 5% CO_2. Cells growing in 6-well dishes were transiently transfected with the corresponding protein cDNA by the polyethylenimine method (Sigma–Aldrich). Cells were incubated with the corresponding cDNA together with polyethylenimine (5.47 mM in nitrogen residues) and 150 mM NaCl in a serum-starved medium. After 4 h, the medium was renewed and 48 h after transfection, cells were washed twice in quick succession in HBSS [containing 137 NaCl, 5 KCl, 1.26 $CaCl_2$, 0.4 $MgSO_4$, 0.5 $MgCl_2$, 0.34 Na_2HPO_4, 0.44 KH_2PO_4, 10 HEPES, pH 7.4, in mM], supplemented with 10 mM glucose, detached, and resuspended in the same buffer. Protein concentration was determined using the Bradford assay (Bio-Rad, Munich, Germany), in order to control cell number.

Immunodetection Assays

Cells were fixed in 4% paraformaldehyde for 15 min and washed with PBS containing 20 mM glycine (buffer A) to quench the aldehyde groups. Then, cells were permeabilized with buffer A containing 0.2% Triton X-100 for 5 min, and treated with 1% of BSA in PBS. After 1 h at room temperature, cells were labeled with the primary mouse anti-$A_{2A}R$ antibody (1:200; Millipore, Darmstadt, Germany; cat #05-717) for 1 h to detect $A_{2A}R$–Nluc, washed, and stained with the secondary goat anti-mouse Alexa Fluor 488 (1:300; Invitrogen, Paisley, United Kingdom; cat #A-11001). The specificity of this antibody for immunocytofluorescence studies has been previously reported by Moreno et al. (2017a). CD26-YFP fused to YFP protein was detected by its fluorescence properties. The samples were rinsed several times and mounted with 30% Mowiol (Calbiochem) as reported by Moreno et al. (2017b). Samples were observed in a Leica SP2 confocal microscope.

ERK Phosphorylation Assay

HEK-293T cells expressing $A_{2A}R$ were cultured in serum-free medium for 16 h before the addition of any agent. Cells were treated at 25°C with 100 nM CGS 21680 (Sigma–Aldrich) for 10 min and rinsed with ice-cold PBS. Cells were lysed by ice-cold lysis buffer (1% Triton X-100, 150 mM NaCl, 50 mM Tris-HCl pH 7.4, 50 mM NaF, 45 mM β-glycerophosphate, 20 mM phenyl-arsine oxide, 0.4 mM $NaVO_4$ and protease inhibitor cocktail). The cellular debris was removed by centrifugation at 13,000 × *g* for 5 min at 4°C and the protein was quantified by the bicinchoninic acid method using bovine serum albumin as standard. The level of ERK 1/2 phosphorylation was determined in equivalent amounts of protein (10 μg) separated by electrophoresis on 7.5% SDS polyacrylamide gel and transferred onto PVDF-FL membranes, according to Gracia et al. (2013b). Odyssey blocking buffer (LI-COR Biosciences, Lincoln, NE, United States) was used for 90 min. Membranes were then probed with a mixture of a mouse anti-phospho-ERK 1/2 antibody (1:2500, Sigma) and rabbit anti-ERK 1/2 antibody (1:40,000, Sigma) for 2–3 h. Bands were visualized after 1 h incubation with a mixture of IRDye 800 (anti-mouse) antibody (1:10,000, Sigma) and IRDye 680 (anti-rabbit) antibody (1:10,000, Sigma) and scanned by the Odyssey infrared scanner (LICOR Biosciences, Lincoln, NE, United States). Bands densities were quantified and the level of phosphorylated ERK 1/2 isoforms was normalized according to the total ERK 1/2 protein bands (Gracia et al., 2013b).

Dynamic Mass Redistribution (DMR) Assays

The cell signaling signature was determined using an EnSpire® Multimode Plate Reader (PerkinElmer, Waltham, MA, United States) by a label-free technology. Refractive waveguide grating optical biosensors, integrated into 384-well microplates, allow the measurement of changes in local optical density in a detecting zone up to 150 nm above the surface of the sensor. Cellular mass movements induced after activation of the receptors are detected by illuminating the lower part of the biosensor with polychromatic light, determining changes in wavelength of the reflected monochromatic light, which are a sensitive function of the refractive index. The magnitude of this wavelength shift (in picometers) is directly proportional to the amount of DMR (Viñals et al., 2015). The assay was carried out according to Viñals et al. (2015); briefly, 24 h before the assay, cells were seeded in 384-well sensor microplates at a density of 10,000–12,000 cells per well, with 30 μl growth medium and were cultured for 24 h (37°C, 5% CO_2) until reaching 70–80% confluent monolayers. For the assay, cells were washed twice with assay buffer (HBSS with 20 mM HEPES, pH 7.15) and incubated for 2 h in 30 μl per well of assay-buffer with 0.1% DMSO in the reader at 24°C. Then, the sensor plate was scanned and a baseline optical signature was recorded before adding 10 μl of receptor agonist dissolved in assay buffer containing 0.1% DMSO. DMR responses were monitored for at least 5,000 s and kinetic results were analyzed using the EnSpire Workstation software v 4.10.

Determination of cAMP Concentration

cAMP production was determined according to Viñals et al. (2015), using a homogeneous time-resolved fluorescence energy transfer (HTRF) assay with the Lance Ultra cAMP kit (PerkinElmer, Waltham). We first established the optimal cell density to obtain an appropriate TR-FRET signal within the dynamic range of a standard cAMP curve. This was done by measuring the basal and activated TR-FRET signal using different

cell densities. Cells (1,000 cells/well) growing at 25°C in white ProxiPlate 384-well microplates (PerkinElmer) with a medium containing 50 μM zardaverine were stimulated with 100 nM CGS 21680 (Sigma–Aldrich) for 10 min or treated with vehicle. Fluorescence at 665 nm was analyzed on a PHERAstar Flagship microplate reader equipped with an HTRF optical module (BMG Lab technologies, Offenburg, Germany).

Nano Bioluminescence Resonance Energy Transfer (NanoBRET) between Two Proteins Expressed in Two Different Cell Populations

HEK-293T cells were transiently transfected with the corresponding donor o acceptor, 48 h after transfection, cells expressing the donor were mixed with HEK-293 cells expressing the acceptor. Cells were incubated 10 min with HBSS without shaking in the presence or in the absence of wild-type ADA, albumin, TA5.9-CC1-4C8 antibody or Leu58Ala and Leu62Ala ADA mutants. Protein-YFP expression was quantified by distributing cells (20 μg protein, around 4000 cells/well) in 96-well microplates (black plates with a transparent bottom) and fluorescence was read at 400 nm in a Fluo Star Optima Fluorimeter (BMG Labtechnologies), equipped with a high-energy xenon flash lamp, using a 10 nm bandwidth excitation filter. Protein fluorescence expression was determined as fluorescence of the sample minus the fluorescence of cells expressing Nluc alone. For NanoBRET measurements, the equivalent of 20 μg of mixed cells were distributed in 96-well microplates (Corning 3600, white plates; Sigma) and 5 μM of coelenterazine H (Molecular Probes, Eugene, OR) was added. After 1 min, readings were collected using a Mithras LB 940 late reader (Berthold Technologies) that allows the integration of the signals detected in the short-wavelength filter at 440–500 nm and the long-wavelength filter at 510–590 nm. To quantify receptor-Nluc expression, bioluminescence readings were also performed after 10 min of adding 5 μM of coelenterazine H. Fluorescence and bioluminescence of each sample were measured before every experiment to confirm similar donor expressions (approximately 120,000 bioluminescence units per 20 μg of protein) while acceptor expression (25,000 fluorescence units per 20 μg of protein). The net BRET was defined as [(long-wavelength emission)/(short-wavelength emission)]-Cf where Cf corresponds to [(long-wavelength emission)/(short-wavelength emission)] for the receptor-Nluc expressed alone in the same experiment. BRET is expressed as milliBRET units (mBU).

Cell Membranes Preparation and Radioligand Binding Experiments

Human embryonic kidney cells transfected with $A_{2A}R$ non-fused or fused to Nluc-spacer were disrupted with a Polytron homogenizer (PTA 20 TS rotor, setting 3; Kinematica, Basel, Switzerland) for three 5 s-periods in 10 volumes of 50 mM Tris–HCl buffer, pH 7.4 containing a proteinase inhibitor cocktail. Cell debris was removed by centrifugation at 1,000 × *g* (5 min, 4°C) and membranes were obtained by centrifugation at 105,000 × *g* (40 min, 4°C). The pellet was resuspended and re-centrifuged under the same conditions and was stored at −80°C. Membranes were washed once more as described above and resuspended in 50 mM Tris–HCl buffer, pH 7.4 containing 10 mM $MgCl_2$. Membrane protein was quantified by the bicinchoninic acid method (Pierce Chemical Co., Rockford, IL, United States) using bovine serum albumin dilutions as standard. For $A_{2A}R$ competition-binding assays, membrane suspensions (0.2 mg of protein/ml) were incubated for 2 h at 25°C with a constant free concentration of 2.2 nM of the $A_{2A}R$ antagonist [^{3}H]ZM 241385 (50 Ci/mmol; American Radiolabeled Chemicals, St. Louis, MO, United States) and increasing concentrations of unlabelled ZM 241385 (Tocris, Ellisville, MO, United States), in the absence or in the presence of bovine ADA. In dose-response curves of ADA, membranes were also incubated with 2.2 nM [^{3}H]ZM 241385 and with increasing concentrations of bovine ADA. In all cases, non-specific binding was determined in the presence of 10 μM of unlabelled ZM 241385. Free and membrane-bound ligands were separated by rapid filtration of 500 μl aliquots in a cell harvester (Brandel, Gaithersburg, MD, United States) through Whatman GF/C filters embedded in 0.3% polyethylenimine that were subsequently washed for 5 s with 5 ml of ice-cold 50 mM Tris-HCl buffer. The filters were incubated overnight with 10 ml of Ultima Gold MV scintillation cocktail (PerkinElmer) at room temperature and radioactivity counts were determined using a Tri-Carb 2800 TR scintillation counter (PerkinElmer) with a mean efficiency of 62%.

Data were analyzed according to the 'two-state dimer model.' This model assumes GPCR dimers as a main functional unit and provides a more robust analysis of parameters obtained from saturation and competition experiments with orthosteric ligands, as compared with the commonly used 'two-independent-site model' (Casadó et al., 2007, 2009a,b). In competition experiments the model analyzes the interactions of the radioligand with a competing ligand and it provides the affinity of the competing ligand for the first protomer in the unoccupied dimer (K_{DB1}) and the affinity of the competing ligand for the second protomer when the first protomer is already occupied by the competing ligand (K_{DB2}). Radioligand competition curves were analyzed by non-linear regression using the commercial Grafit software (Erithacus Software, Surrey, United Kingdom). To calculate the macroscopic equilibrium dissociation constants from competition experiments, the following general equation 1 must be applied:

$$A_{bound} = \frac{(K_{DA2}\,A + 2A^2 + \frac{K_{DA2}A\,B}{K_{DAB}})\,R_T}{K_{DA1}\,K_{DA2} + K_{DA2}\,A + A^2 + \frac{K_{DA2}\,A\,B}{K_{DAB}} + \frac{K_{DA1}\,K_{DA2}\,B}{K_{DB1}} + \frac{K_{DA1}\,K_{DA2}\,B^2}{K_{DB1}\,K_{DB2}}} \quad (1)$$

where *A* represents the radioligand concentration, *B* the assayed competing compound concentration, K_{Dn} the equilibrium dissociation constant of the first or second binding of *A* or *B* to the dimer, and K_{DAB} the hybrid allosteric modulation between *A* and *B*. For *A* and *B* being the same non-cooperative ligand, the

equation 1 can be simplified to equation 2 (Gracia et al., 2013b):

$$A_{bound} = \frac{(4K_{DA1}\,A + 2A^2 + A\,B)\,R_T}{4K_{DA1}^2 + 4K_{DA1}\,A + A^2 + A\,B + 4K_{DA1}\,B + B^2} \quad (2)$$

RESULTS

Expression and Characterization of $A_{2A}R$ and CD26 Fusion Proteins

The aim of this paper is to investigate the ADA-mediated molecular interaction between $A_{2A}R$ expressed in the membrane of one cell and CD26 expressed in the membrane of another cell by the NanoBioluminiscence Resonance Energy Transfer (NanoBRET) technique. This biophysical technique has been extensively validated to analyze direct protein–protein interactions occurring in living cells. For any approximation based in transfer of energy it is necessary a donor, a protein fused to the enzyme NanoLuc (Nluc) and an acceptor, a protein fused to the fluorescent protein YFP. Here we used $A_{2A}R$ fused to Nluc ($A_{2A}R$-Nluc) or to Nluc with a spacer ($A_{2A}R$-Nluc-spacer) and CD26 fused to YFP (CD26-YFP). To detect NanoBRET with a donor in one cell and an acceptor in another cell is necessary that fusion proteins are placed at the extracellular space. One of the main drawbacks in this case is that the bioluminescent protein fused at the N-terminus of $A_{2A}R$ could disturb the expression and/or the ligand binding to the receptor giving a non-functional receptor or block the unknown ADA binding site of the receptor. We have used the enzyme Nluc to improve protein translocation of fused complexes and to reduce the volume of the bioluminescent enzyme fused to $A_{2A}R$. Moreover, the "combination of greater light intensity with improved spectral resolution results in substantially increased detection sensitivity and dynamic range over current BRET technologies" (Machleidt et al., 2015). In the case of CD26, the binding domain of ADA has been described previously (Weihofen et al., 2004), and given that it is located in a middle area of the extracellular domain, the binding of ADA to CD26 should not be hindered by the binding of the YFP protein at the C-terminal end of CD26. Taken this into account, we first characterized the fusion proteins.

HEK-293T cells were transfected with increasing concentrations of cDNA for $A_{2A}R$-Nluc or $A_{2A}R$-Nluc-spacer or with increasing concentrations of cDNA for non-fused $A_{2A}R$ as negative control or $A_{2A}R$-Rluc fused at the C-terminal domain as positive control and bioluminescence was measured (**Figure 1A**). All fusion proteins were expressed and $A_{2A}R$-Nluc-spacer was significantly better expressed compared to $A_{2A}R$-Nluc, reaching expression values similar to the ones obtained for common Rluc fused at the C-terminus domain of $A_{2A}R$ (**Figure 1A**). HEK-293T cells were also transfected with increasing concentrations of cDNA for CD26-YFP or non-fused CD26 as negative control and fluorescence was measured (**Figure 1B**). We observed that the fusion protein was expressed. Next we tested by confocal microscopy that $A_{2A}R$-Nluc-spacer (**Figure 1C**) and CD26-YFP (**Figure 1D**) showed a plasma membrane distribution as expected.

To evaluate the functional characteristics of the $A_{2A}R$ constructs we measured the global cellular response using the DMR label-free assay. This technique detects agonist-induced changes in light diffraction in the bottom 150 nm of a cell monolayer (see section "Materials and Methods"). HEK-293T cells were transfected with cDNA corresponding to $A_{2A}R$-Nluc (**Figure 2A**), $A_{2A}R$-Nluc-spacer (**Figure 2B**), or $A_{2A}R$-Rluc (**Figure 2C**). Cells were stimulated with increasing concentrations of the $A_{2A}R$ agonist CGS 21680, and DMR signal was obtained against time. From DMR curves (**Figures 2A–C**) it is observed that $A_{2A}R$-Nluc-spacer gives higher signaling than $A_{2A}R$-Nluc and the signal was similar to the one obtained for common $A_{2A}R$-Rluc construction (**Figures 2A–C**). The lost of functionality of $A_{2A}R$-Nluc respect to the $A_{2A}R$-Rluc indicates that the fused Nluc probably disturbs the agonist binding; thus, introducing the spacer between $A_{2A}R$ N-terminal and Nluc, that allows Nluc moving away from the membrane surface, not only favors the fusion protein expression (see **Figure 1A**) but also ligand binding and the corresponding signaling. Moreover, we checked if agonist activation of $A_{2A}R$-Nluc-spacer was able to induce second messengers as naïve receptors. To do this, HEK-293T cells were transfected with cDNA corresponding to $A_{2A}R$-Nluc-spacer or $A_{2A}R$-Rluc or $A_{2A}R$ as controls. Cells were stimulated with $A_{2A}R$ agonist CGS 21680 (100 nM) and ERK 1/2 phosphorylation and cAMP production were determined. We detected similar extend of ERK 1/2 phosphorylation (**Figure 2D**) and similar cAMP accumulation (**Figure 2E**) in all cells, showing that $A_{2A}R$-Nluc-spacer is fully functional. According to this, the $A_{2A}R$-Nluc-spacer was selected for further studies.

ADA Binding to $A_{2A}R$ Fusion Protein

One characteristic of $A_{2A}R$ is their ability to bound extracellular ADA. It has been described that ADA increases the receptor ligand binding affinity and potentiates the receptor functionality (Gracia et al., 2011). Here we analyzed the ability of ADA to bind and modulate $A_{2A}R$-Nluc-spacer fusion protein. We first determined if ADA increases the affinity parameters of antagonist binding to $A_{2A}R$-Nluc-spacer. Ligand binding was analyzed using membranes from HEK-293T cells transfected with cDNA corresponding to $A_{2A}R$-Nluc-spacer. Competition experiments with the $A_{2A}R$ antagonist [^{3}H]ZM 241385 were performed with increasing concentrations of unlabelled ZM 241385 from 0.001 nM to 10 μM in the absence or in the presence of 1 μg/ml bovine ADA. All curves (**Figure 3A**) are monophasic ($D_C = 0$), according to the non-cooperative behavior expected for a $A_{2A}R$ ligand binding (Gracia et al., 2011). Moreover, in the presence of ADA, the competition curve of $A_{2A}R$ antagonist shifts to the left, indicating an increase in the affinity. The equilibrium binding parameters obtained according to equation (2) (see section "Materials and Methods") from curves in **Figure 3A** are shown in **Table 1**. When membranes of HEK-293T cells, transfected with cDNA from $A_{2A}R$ fused or not to NanoLuc-spacer, were incubated with increasing concentrations of ADA (from 0.1 ng/ml to 10 μg/ml) and with the radiolabeled $A_{2A}R$ antagonist, ADA enhanced in a

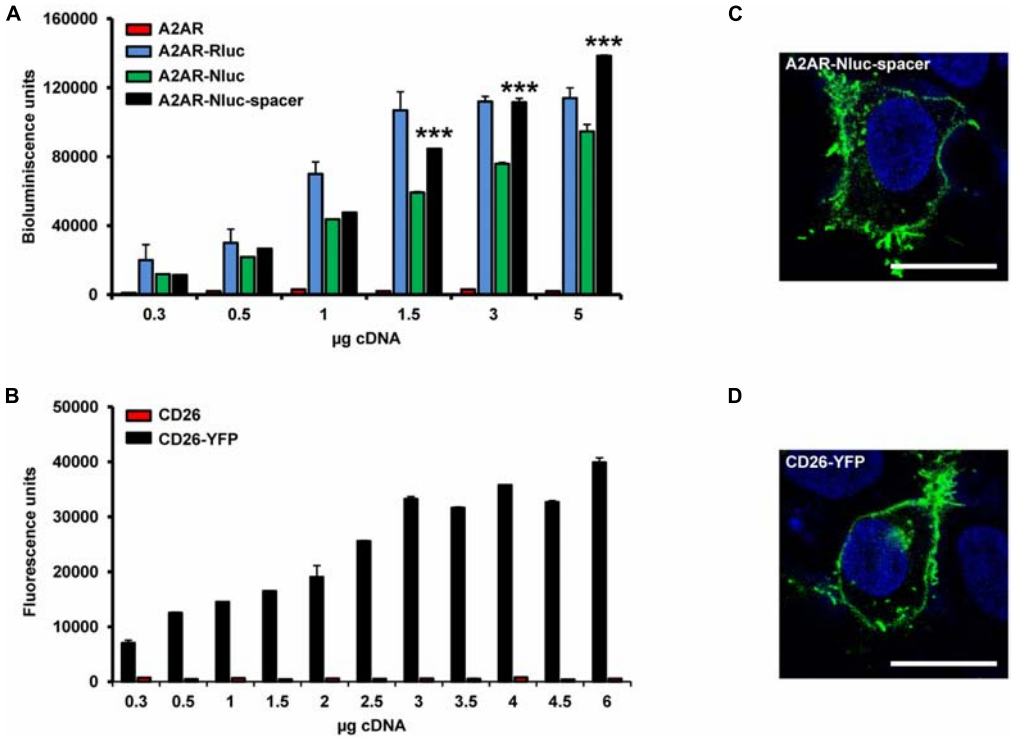

FIGURE 1 | Expression of $A_{2A}R$ and CD26 fusion proteins. **(A)** Bioluminescence assays were performed in HEK-293T cells transfected with increasing concentrations of fusion protein cDNA corresponding to $A_{2A}R$ (red), $A_{2A}R$-Rluc fused on the C-terminal end (blue), $A_{2A}R$-Nluc fused on the N-terminal (green) or $A_{2A}R$-Nluc-spacer fused on the N-terminal end (black) on the N-terminal end. Results are given in relative bioluminescence units by subtracting the value of non-transfected cells and represent mean ± SEM (n = 6). Statistical significance was calculated by one-way ANOVA followed by a Bonferroni multiple comparison *post hoc* test; ***$p < 0.001$ against $A_{2A}R$-Nluc. **(B)** Fluorescence assays were performed in HEK-293T cells transfected with increasing concentrations of CD26 (red) or CD26-YFP fused on the C-terminal end (black). Results are given in relative fluorescence units by subtracting the value of non-transfected cells and represent mean ± SEM (n = 10). **(C,D)** Confocal microscopy images from immunofluorescence experiments using HEK-293T cells transfected with 0.75 µg of $A_{2A}R$-Nluc-spacer fused on the N-terminal end **(C)** or 1 µg of CD26-YFP fused on the C-terminal end **(D)** are shown. Immunocytofluorescence experiments were carried out with anti-$A_{2A}R$ primary antibody (1:100; Millipore) and goat anti-mouse Alexa Fluor 488 (1:300; Invitrogen) as secondary antibody. YFP-fused proteins were identified by their own fluorescence. $A_{2A}R$-Nluc-spacer and CD26-YFP are labeled in green. Nuclei are colored in blue by DAPI staining. Scale bar: 20 µM.

dose-dependent manner the antagonist binding to both $A_{2A}R$ non-fused and fused to NanoLuc-spacer (**Figure 3B**). The EC_{50} values obtained with the two proteins are not significantly different (see **Table 1**). These results indicate that ADA can also bind to $A_{2A}R$-Nluc-spacer and significantly increases antagonist affinity. It point out that ADA exerts positive modulation on the antagonist binding to $A_{2A}R$-Nluc-spacer similar to the one obtained for the naïve $A_{2A}R$ (**Figure 3B**; and see Gracia et al., 2011, 2013a).

To investigate if ADA binding to $A_{2A}R$-Nluc-spacer also increases the receptor functionality, DMR label-free assays were performed in HEK-293T cells transfected with cDNA corresponding to $A_{2A}R$-Nluc-spacer. Cells were not treated or treated with ADA and were stimulated with increasing concentrations of $A_{2A}R$ agonist CGS 21680. DMR signal was measured against time. From DMR curves, the response at 3000 s was calculated and plotted as a function of CGS 21680 concentrations used (**Figure 3C**). As in ligand binding experiments, it is observed a significantly increase in the response in the presence of ADA. This indicates that ADA exerts positive modulation on the $A_{2A}R$-Nluc-spacer signaling similar to the one reported for the naïve receptor (Gracia et al., 2011).

ADA Mediates Cell to Cell Contact by Simultaneous Binding to $A_{2A}R$ and CD26

To investigate if ADA can induce cell to cell contacts by simultaneous binding to $A_{2A}R$ in one and to CD26 in another cell, NanoBRET experiments between cells expressing the NanoBRET donor and cells expressing the NanoBRET acceptor were performed. $A_{2A}R$-Nluc-spacer and CD26-YFP cDNA were transfected separately into different cells. Both cell populations were mixed in the presence and absence of ADA and were allowed to sediment rapidly to facilitate their proximity. If the interaction occurs, the energy transfer between $A_{2A}R$-Nluc-spacer and CD26-YFP could subsequently take place and it could be detected as NanoBRET signal. HEK-293T cells were transfected with increasing concentrations of cDNA corresponding to $A_{2A}R$-Nluc-spacer or CD26-YFP and those samples showing approximately 120.000 bioluminescence units and 25.000 fluorescence units were chosen to perform NanoBRET experiments. Equal number of transfected cells from

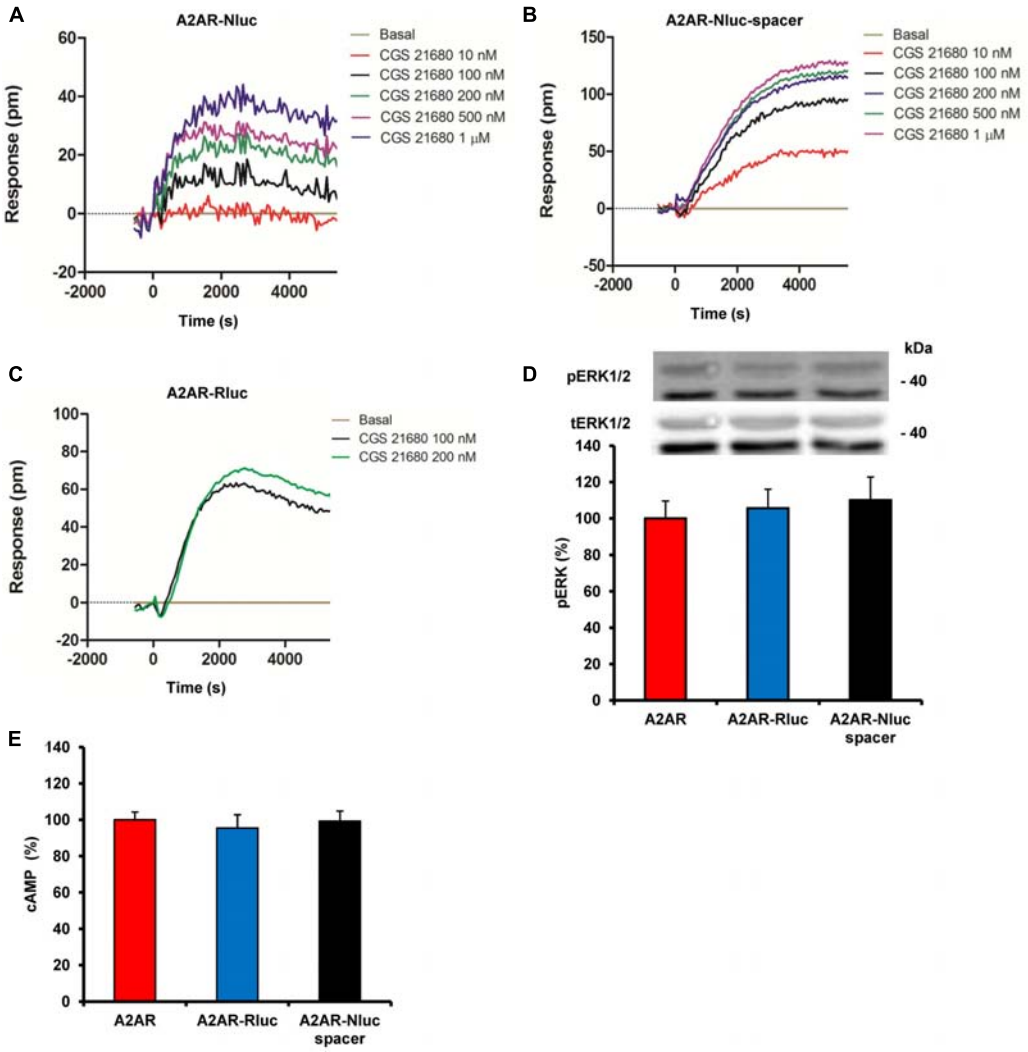

FIGURE 2 | Functional characterization of $A_{2A}R$ fusion proteins. **(A–C)** DMR assays were performed in HEK-293T cells transfected with cDNA (1.5 μg) corresponding to $A_{2A}R$-Nluc **(A)** or $A_{2A}R$-Nluc-spacer **(B)** both fused on the N-terminal end or $A_{2A}R$-Rluc fused on the C-terminal end **(C)**. Cells were stimulated with vehicle (basal) or with increasing concentrations of the $A_{2A}R$ agonist CGS 21680. The resulting shifts of reflected light wavelength (pm) were monitored over time. Each panel is a representative experiment of $n = 3$ different experiments. Each curve is the mean of a representative optical trace experiment carried out in quadruplicates. **(D,E)** ERK1/2 phosphorylation **(D)** and cAMP production **(E)** were determined in cells transfected with the cDNA (1.5 μg) corresponding to $A_{2A}R$, $A_{2A}R$-Rluc fused on the C-terminal end or $A_{2A}R$-Nluc-spacer fused on the N-terminal end. Cells were stimulated with 100 nM CGS 21680 for 10 min. Results are given as percentage respect cells expressing only $A_{2A}R$. Values are expressed as means ± SEM ($n = 4$). **(D)** A representative western blot is shown at the top of the panel and in **(E)** 100% represents 80–100 pmols of cAMP/10^6 cells.

both types was mixed as well as $A_{2A}R$-Nluc-spacer expressing cells and non-transfected cell or CD26-YFP expressing cells and non-transfected cell as controls and cells were incubated with increasing bovine ADA concentrations, before NanoBRET detection. As shown in **Figure 4A**, we only obtained positive NanoBRET signal in the presence of 1 and 3 μg/ml of ADA, which points out that CD26 and $A_{2A}R$ are in close proximity. It is interesting to note that at higher concentrations of ADA (10 μg/ml) the energy transfer decreased. This could be due to the fact that an excess of ADA could saturate the $A_{2A}R$ on cells expressing them as well as saturating CD26 protein on the other cells, thereby when both cell types approach, ADA cannot act as a bridge between $A_{2A}R$ and CD26, avoiding energy transfer (see schemes in **Figure 4A**, top panels). The results shown in **Figure 4A** show that ADA bridges CD26 and $A_{2A}R$ in a narrow range of concentrations, and the optimal ADA concentration required to observe the ternary complex is around 1–3 μg/ml. This is in agreement with the affinity constants of ADA to bind to these two proteins. It has been reported that the affinity of ^{125}I-ADA by CD26 is around 18 nM (Gonzalez-Gronow et al., 2004) (equivalent to 0.7 μg/ml), and its affinity by A_1R is around 230 nM (Saura et al., 1996) (equivalent to 9 μg/ml). These values indicate that first ADA binds to CD26 and then to AR, so that a balance of ADA concentrations occurs between the bars of

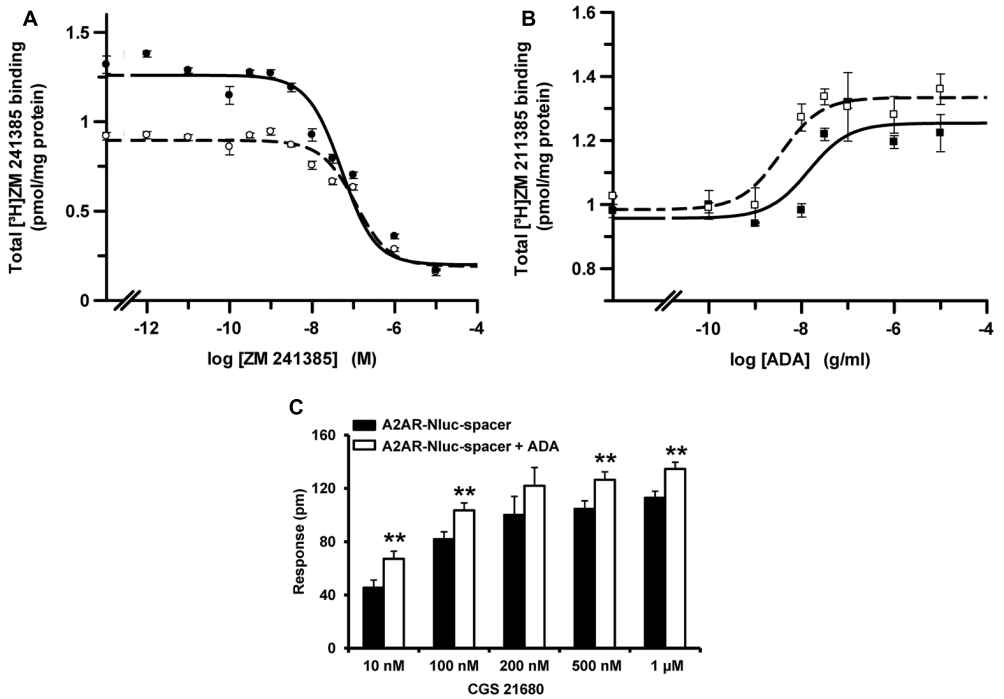

FIGURE 3 | Effect of bovine ADA binding on $A_{2A}R$. **(A)** Competition experiments of 2.2 nM [^{3}H]ZM 241385 binding in the presence of increasing concentrations of unlabeled ZM 241385, in the absence (○) or in the presence (●) of 1 μg/ml of ADA were performed using membranes from HEK-293T cells transfected with $A_{2A}R$-Nluc-spacer cDNA (1.5 μg). **(B)** Dose-response effect of ADA on 2.2 nM [^{3}H]ZM 241385 binding to membranes from HEK-293T cells transfected with cDNA (1.5 μg) corresponding to $A_{2A}R$-Nluc-spacer (■) or $A_{2A}R$ (□). Data are mean ± SD from a representative experiment (n = 3) performed in triplicate. **(C)** DMR assays were performed in HEK-293T cells transfected with $A_{2A}R$-Nluc-spacer cDNA (1.5 μg). Cells were stimulated with increasing CGS 21680 concentrations in the presence (white columns) or in the absence (black columns) of ADA (1 μg/ml). Values are mean ± SEM (n = 4) and are expressed as shift at 3000 s of reflected light wavelength (pm) over basal obtained from the corresponding DMR curves. Statistical significance was calculated by one-way ANOVA followed by a Bonferroni multiple comparison *post hoc* test; $^{**}p < 0.01$ against samples without ADA.

TABLE 1 | Effect of adenosine deaminase (ADA) on binding of $A_{2A}R$ antagonist [^{3}H]ZM 241385.

Binding experiment			ADA	Parameters[a]		
Assay type	**Increasing effector**	**Transfected AR**	**1 μg/ml**	**K_{DA1}[b]**	**D_C[c]**	**EC_{50}[d]**
Competition	ZM 241385	$A_{2A}R$-Nluc-spacer	−	90 ± 20	0	
		$A_{2A}R$-Nluc-spacer	+	30 ± 10**	0	
Dose-response	Bovine ADA	$A_{2A}R$-Nluc-spacer				14 ± 8
		$A_{2A}R$				4 ± 2

Competition curves with ZM 241385 in the absence (–) or the presence (+) of bovine ADA and dose-response curves with bovine ADA were carried out as described in section "Materials and Methods," using membranes of transfected HEK-293T cells. [a]Values are mean ± SD of three independent experiments performed in triplicate. [b]K_{DA1} (nM) is the equilibrium dissociation constant of the binding of the radioligand to the first protomer in the dimer. [c]D_C is the dimer cooperativity index for the binding of the radioligand. Note that when $D_C = 0$ the radioligand is non-cooperative and $K_{DA2} = 4K_{DA1}$. [d]EC_{50} (ng/ml) is the concentration of ADA providing half-maximal increase in radioligand binding. $^{**}P < 0.01$ against control without ADA; statistical differences were evaluated using Student's t-test.

0.1 and 10 μg/ml in **Figure 4A** to form a trimeric complex, where ADA has enough concentration to bridge CD26 and AR, but higher concentrations shift the equilibrium toward dimeric ADA-CD26 and ADA-AR complexes.

To determine the specificity of this interaction, equal number of HEK-293T cells transfected with $A_{2A}R$-Nluc-spacer (expressing 120.000 bioluminescence units) were mixed with HEK-293T cells transfected with CD26-YFP (expressing 25.000 fluorescence units) and were incubated with medium (0), with 1 μg/ml bovine ADA, with 1 μg/ml albumin as non-specific protein or with bovine ADA plus 0.3 μg/ml of the human-specific mAb against CD26, TA5.9-CC1-4C8, which is directed against the ADA-binding epitope on CD26 and blocks ADA binding to CD26 (Blanco et al., 2000; Pacheco et al., 2005; Martinez-Navio et al., 2009; Casanova et al., 2012). In these cells, positive NanoBRET signal was only significantly detected in the presence of ADA but not in the presence of albumin or ADA plus TA5.9-CC1-4C8 (**Figure 4B**), showing that ADA specifically mediates $A_{2A}R$-CD26 interaction between different cells. Moreover, when HEK-293T cells transfected with $A_{2A}R$-Nluc-spacer or with

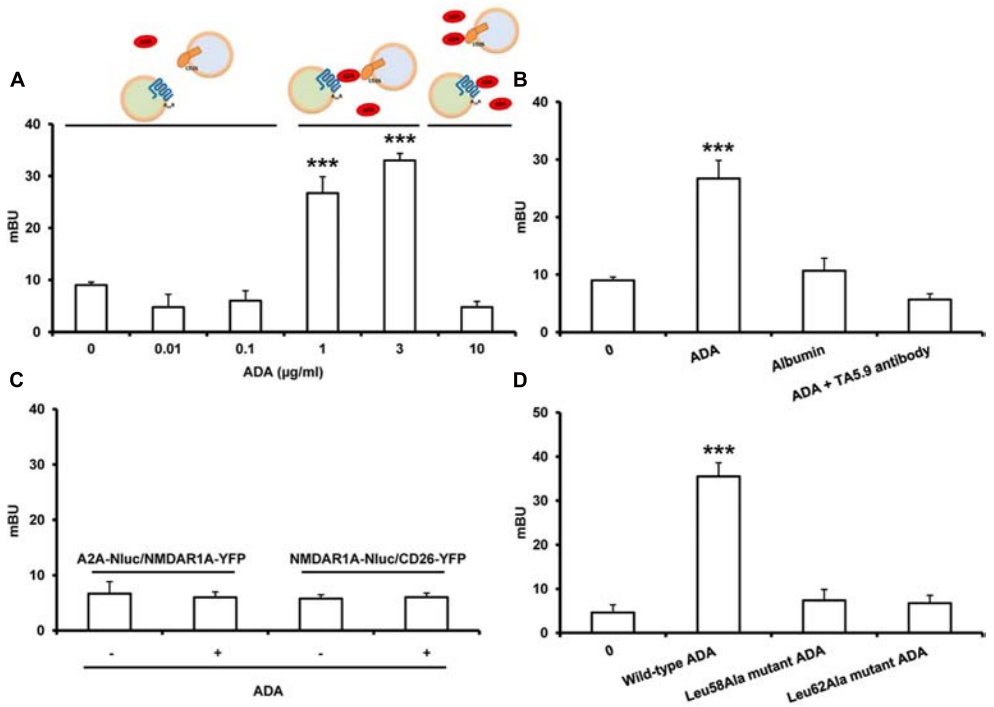

FIGURE 4 | NanoBRET between A_{2A}R-Nluc and CD26-YFP expressed in different cells. HEK-293T cells transfected with 1.5 μg of A_{2A}R-Nluc-spacer cDNA **(A–D)** or NMDAR1A-Nluc **(C)** were mixed with HEK-293T cells transfected with 2 μg of CD26-YFP cDNA **(A–D)** or 2 μg of NMDAR1A-YFP cDNA **(C)**. Cells were incubated 10 min without shaking with HBSS in the absence or in the presence of increasing concentrations of ADA (from 0.01 to 10 μg/ml) **(A)**, in the presence or in the absence of 1 μg/ml of bovine ADA **(B,C)**, bovine albumin (1 μg/ml) **(B)**, human-specific mAb against CD26, TA5.9-CC1-4C8 (0.3 μg/ml) **(B)** or in the presence or in the absence of human wild-type ADA, Leu58Ala mutant ADA or Leu62Ala mutant ADA, all at 1 μg/ml **(D)**, previously to BRET detection. Both fluorescence and luminescence of each sample were measured before every experiment to confirm similar donor expressions (approximately 120.000 bioluminescence units) and similar acceptor expression (25.000 fluorescence units). BRET is expressed as milliBRET units (mBU = net BRET × 1000) and is means ± SEM of 3–4 different experiments grouped as a function of the amount of BRET acceptor. Statistical significance was calculated by one way ANOVA followed by a Dunnett's multiple comparison *post hoc* test; ***$p < 0.001$ compared with the corresponding untreated cells. At the top of the **(A)**, a schematic representation of the effect of different ADA concentrations on the interaction between A_{2A}R-Nluc-spacer and CD26-YFP is shown.

NMDAR1A-Nluc (both expressing 120.000 bioluminescence units) were mixed with HEK-293T cells transfected with the metabotropic glutamate receptor subunit NMDAR1A-YFP or with CD26-YFP (both expressing 25.000 fluorescence units), respectively, as negative controls, none NanoBRET signal was detected in the absence or in the presence of ADA (**Figure 4C**) again demonstrating the specificity of the interaction.

We previously reported that ADA mutations nearly to the catalytic site that reduce the enzymatic activity, as Leu58Ala and Leu62Ala ADA mutants, also reduce the capacity of ADA to interact with A_{2A}R. For these mutants, "changes detected on both k_{cat} and K_M values indicate that both the substrate affinity and the maximum velocity were decreased, suggesting that these mutations alter the structure of the catalytic pocket" (Gracia et al., 2013a). This was corroborated by much greater value obtained for these mutants in the affinity of the competitive structural analog purine riboside, compared to the wild type (**Table 2**). The specific enzyme activity of Leu58Ala and Leu62Ala ADA mutants is highly reduced respect to the wild-type enzyme and both mutants are unable to significantly affect agonist binding to A_{2A}R (**Table 2** and Gracia et al., 2013a). Here we tested if these ADA mutants are able to induce NanoBRET signal between A_{2A}R-Nluc-spacer expressing cells and CD26-YFP expressing cells. HEK-293T cells transfected with A_{2A}R-Nluc-spacer (expressing 120.000 bioluminescence units) were mixed with HEK-293T cells transfected with CD26-YFP (expressing 25.000 fluorescence units) and were incubated with medium (0), with human wild-type ADA or with Leu58Ala or Leu62Ala ADA mutants previously to detect the NanoBRET signal. Positive NanoBRET signal was not detected with Leu58Ala or Leu62Ala ADA mutants, whilst NanoBRET was significantly detected with wild-type ADA (**Figure 4D**). All these results show that ADA could act as a bridge simultaneously interacting with A_{2A}R and CD26 expressed in different cells, and allowing cell-cell contacts as schematized in **Figure 5**.

DISCUSSION

Intracellular adenosine is an important intermediary metabolite, which acts as a piece in the assembly of nucleic acids and as a component of the molecule that provides the biological energy ATP (Chen et al., 2013). On the other hand, extracellular adenosine plays an important role in intercellular signaling

TABLE 2 | Comparison of steady-state kinetic and agonist binding parameters of wild-type and representative ADA mutants.

Enzyme	Specific activity (μmol min^{-1} mg^{-1})[#]	k_{cat}/K_M (M^{-1} s^{-1})[&]	K_i (PR) (μM)[&]	Δ [^{3}H]CGS 21680 binding (%)[&]	EC50 (ng/ml)[&$]
WT	3 ± 1	7.3×10^6	13 ± 2	88 ± 10	7 ± 3
L58A	ND	0.051×10^6	>1000**	0**	>1500**
L62A	ND	0.074×10^6	>1000**	0**	>1500**

*Wild-type and mutant enzymes were partially purified as indicated in Materials and Methods. WT, control wild-type ADA; PR, purine riboside; ND, not detected. [#]Specific activity was determined using the substrate concentration that gives V_{max}, and protein concentration was measured by the bicinchoninic acid method. [&]Data adapted from Gracia et al. (2013a). [$]$EC_{50}$ value is the amount of wild-type or mutant ADA that is able to produce the 50% of the maximum increase in [^{3}H]CGS 21680 binding to $A_{2A}R$. Values are mean ± SEM of three separate experiments. **P < 0.01 against WT; statistical differences were evaluated using one-way ANOVA followed by a Dunnett's multiple comparison post hoc test.*

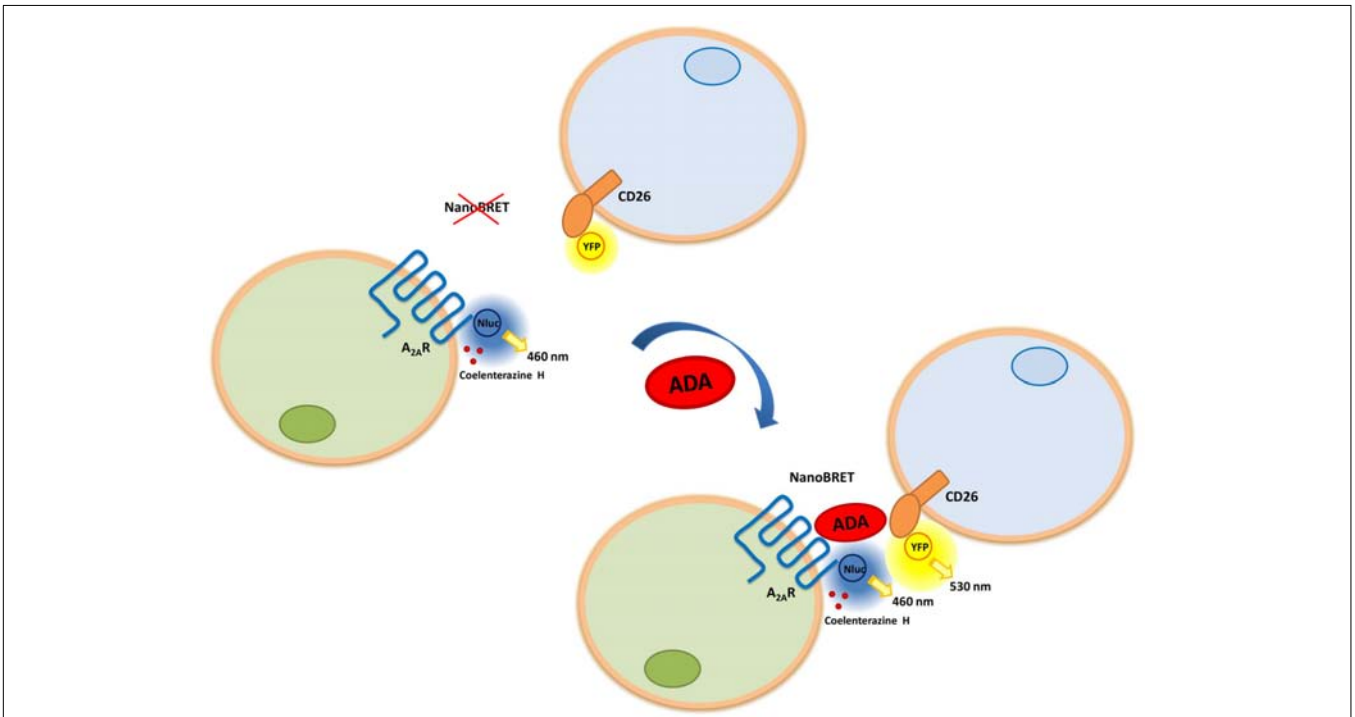

FIGURE 5 | Adenosine deaminase linking $A_{2A}R$ and CD26 expressed in different cells. Schematic representation of the effect of ADA on the NanoBRET between $A_{2A}R$-Nluc-spacer (on the N-terminal end) acting as a donor and CD26-YFP (on the C-terminal domain) acting as an acceptor. $A_{2A}R$ adenosine receptor (blue), in the absence (left) or in the presence (right) of ADA (red) and CD26 protein (orange), are represented as complexes between cell membranes of different cell types. In the NanoBRET process between $A_{2A}R$-Nluc-spacer expressing cells and CD26-YFP expressing cells, the catalysis of the substrate coelenterazine H emits at 460 nm, allowing YFP excitation and concomitant emission at 530 nm. For simplicity, $A_{2A}R$ and CD26 are not represented as homodimeric proteins.

by binding to ARs on the cell surface. This affects various physiological functions, such as cardiovascular, neurological, and immunological systems (Ohta, 2016). Most of the extracellular adenosine comes from the release and metabolism of adenine nucleotides such as ATP after several stimuli, which include inflammation, mechanical stress, tissue injury and osmotic challenge (Sun and Huang, 2016). This extracellular adenosine is degraded by ecto-ADA, which requires cell-surface anchoring proteins to stay joined to the plasma membrane. To date, four ADA-binding proteins have been described: the multifunctional CD26 protein, and the subtypes A_1R, $A_{2A}R$ and $A_{2B}R$ of ARs.

Weihofen et al. (2004) crystallized the complex constituted by bovine ADA and human CD26 ectodomain and showed that each CD26 dimer binds two ADA molecules. In this structure two different interactions contribute to stabilize the CD26/ADA complex. In one, the Ile287-Asp297 loop A of CD26 and the Arg76-Ala91 helix α1 of ADA interact; in the other, the Asp331-Gln344 loop B of CD26 interacts with the Pro126-Asp143 helix α2 of ADA (see **Figure 6** and Cortés et al., 2015). Moreover, the crystal structure shows the intermolecular links in a highly amphiphilic interface that contributes to the CD26/ADA complex formation and also stabilizes the binding interface, where two hydrophobic loops protruding from the β-propeller domain of CD26 interact with two hydrophilic and strongly charged α-helices of ADA. This results in a very high percentage of charged residues that are involved in this protein–protein interaction (Weihofen et al., 2004). On the other hand, in this complex, ADA does not block the active site of CD26 and conversely, binding of CD26 does not block the active site of ADA; this indicates that CD26 and ADA remain catalytically

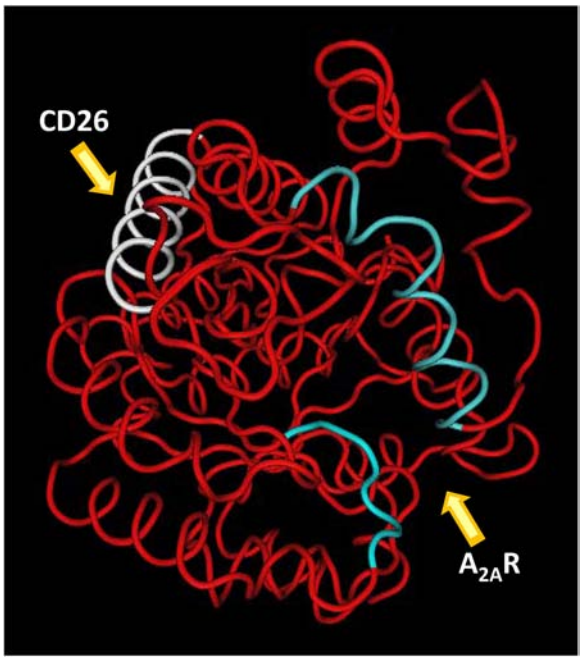

FIGURE 6 | Representation of ADA regions involved in the interaction with $A_{2A}R$ and CD26. ADA in red (MMDBID:75950) was drawn with Cn3D4.1 program (http://www.ncbi.nlm.nih.gov). Helix α-1 (portion P55-I72) and loop (G184-P189) of $A_{2A}R$ binding site are in blue; helix α-2 (CD26 binding site, P126-D143) is in white.

active upon the complex formation (Weihofen et al., 2004; Fan et al., 2012). It has been reported that the CD26/ADA complex is selectively expressed on Hodgkin's and ALK-positive anaplastic large cell lymphomas (Kameoka et al., 2006). Likewise, Mandapathil et al. (2012) showed ADA activity and CD26 expression in T_{reg} cells and $CD4^+$ T_{eff} cells in patients with neck and head squamous cell carcinoma. All these results put these proteins in the focus of immunological regulation and point out that the costimulatory activity of ADA could be relevant in a variety of immunological diseases (Martinez-Navio et al., 2011; Casanova et al., 2012; Anz et al., 2014; Cortés et al., 2015; Klemann et al., 2016; Naval-Macabuhay et al., 2016; Wagner et al., 2016; Aliyari Serej et al., 2017).

It has been also reported that the binding of ADA to CD26 can be relevant in the regulation of lymphocyte and epithelia cell adhesion (Ginés et al., 2002). The ability of cells to adhere to one another is a fundamental property in the evolution of multicellularity. Adhesion between two different cell types is "a complex phenomenon that requires a variety of extracellular matrix (ECM) components and proteins on the surface of the interacting cells" (Ginés et al., 2002). In this mechanism, apart from cell adhesion molecules, many other soluble cell mediators such as cytokines and components of the tissue matrix such as collagen, fibronectin, etc. play a crucial role (Akiyama, 1996; Golias et al., 2011; Horwitz, 2012; Loeser, 2014). Cell adhesion links one cell to another and to the ECM, and also allows extracellular information to be integrated with the main intracellular signaling pathways. Cell adhesion is also essential in cell communication and regulation and "becomes of fundamental importance in the development and maintenance of tissues" (Khalili and Ahmad, 2015). Ginés et al. (2002) hypothesized that the ADA-CD26 module would be important for the interaction of lymphocytes with epithelial and other cell types expressing ecto-ADA in the first steps of cell to cell recognition, and it would subsequently contribute, by signaling, to the engagement of the mechanism required to change integrins over to their active conformations in T cells (Baker et al., 2009; Zhang and Wang, 2012; Moretti et al., 2013; Meli et al., 2016).

Adenosine receptors A_1R, $A_{2A}R$, and $A_{2B}R$ are the second type of ecto-ADA binding proteins (see section "Introduction"). Among these receptors, $A_{2A}Rs$ are highly expressed in spleen, thymus, blood platelets, striatum, olfactory tubercle and expressed to a lesser extent in the heart, lung, blood vessels and other brain regions including cortex and hippocampus (Cunha et al., 1997; Chen et al., 2013; Cortés et al., 2015; Stockwell et al., 2017). $A_{2A}Rs$ are expressed on most immune cells, including T cells, NK and invariant natural killer T cells, DCs, macrophages, monocytes, mast cells, eosinophils and B cells (Cekic and Linden, 2016). The $A_{2A}R$ is recognized as mediating major adenosine anti-inflammatory activity (Welihinda and Amento, 2014) and is involved in various metabolic and pathological states including sleep regulation, ischemia-reperfusion injury, inflammation and autoimmune diseases and neurodegenerative disorders (Borea et al., 2016; Sharma et al., 2016; Lazarus et al., 2017; Stockwell et al., 2017). Likewise, $A_{2A}R$ is responsible for most of the known immunoregulatory effects of adenosine in the immune system and is a molecule crucially involved in CNS autoimmunity (Ingwersen et al., 2016).

Bioluminescence resonance energy transfer has provided much of the evidence supporting GPCRs oligomerization. Angers et al. (2000) used this technique in HEK-293 cells to demonstrate that human beta-2 adrenergic receptors form constitutive homodimers. We and others demonstrated that A_1R and $A_{2A}R$ are expressed as homodimers or higher-order oligomers, which are the functional species *ex vivo* or in transfected cells (Ciruela et al., 1995; Canals et al., 2004; Briddon et al., 2008; Gandia et al., 2008; Vidi et al., 2008; Namba et al., 2010; Gracia et al., 2011, 2013b; Casadó-Anguera et al., 2016; Navarro et al., 2016). For both receptors, enzymatically active or Hg^{2+}-inactivated ADA increases the signaling and the receptor affinity by a protein–protein interaction. ADA acts as an allosteric modulator of A_1R and $A_{2A}R$, altering their quaternary structure and, consequently, their pharmacological and functional characteristics (Ciruela et al., 1996; Saura et al., 1996; Sarrió et al., 2000; Sun et al., 2005; Gracia et al., 2008, 2011, 2013b). The ADA-induced molecular rearrangement in the corresponding receptor structure, demonstrated by BRET experiments, is in good agreement with the ADA-promoted increase in agonist-induced signaling and ligand affinity for both A_1R and $A_{2A}R$. These results suggest that ADA can exert "a finely tuned modulation of adenosine neuroregulation that may have important implications for the function of neuronal ARs" (Cortés et al., 2015).

In the last decade, the only high-resolution information available for the ARs comes from structures of A_{2A}Rs complexes with several agonists, antagonists, an inverse agonist and an engineered G protein (Jaakola et al., 2008; Doré et al., 2011; Lebon et al., 2011, 2015; Xu et al., 2011; Congreve et al., 2012; Liu et al., 2012; Hino et al., 2012; Carpenter et al., 2016; Segala et al., 2016; Cheng et al., 2017; Sun et al., 2017). These structures can facilitate the discovery of more effective and selective A_{2A}R ligands and have provide a detailed molecular understanding of the receptor function and the conformational landscape between the agonist and the antagonist states of this receptor (Bertheleme et al., 2014; Cheng et al., 2017). By a combination of computational docking simulations and molecular dynamics simulations between the crystal structures of human ADA and human A_{2A}R, we demonstrated that the putative molecular regions of ADA involved in the interaction with the A_{2A}R were opposed to the ADA domains interacting with CD26 (see above) (Gracia et al., 2013a). We now demonstrate a direct molecular interaction between ARs, specifically A_{2A}R, and CD26 bound by ADA, using biophysical techniques. To achieve this goal it is necessary an energy transfer at the extracellular level between two transmembrane proteins that only happens when they are linked by ADA. We have taken advantage of a variant of the BRET assay in which, using fusion proteins of the Nluc enzyme, both the translocation of the N-terminal fusion protein and the steric hindrance are improved (Machleidt et al., 2015; Mo and Fu, 2016). This is compatible with a macromolecular complex in which A_{2A}R and CD26 are bridged by ADA (see **Figure 5**), in a narrow range of ADA concentrations around the binding affinity values (Saura et al., 1996; Gonzalez-Gronow et al., 2004), and showing a peak pattern, instead of a saturable pattern. Lower concentrations are insufficient to bridge the trimer and higher ADA concentrations favor the dimeric ADA-CD26 and ADA-A_{2A}R complexes (see **Figure 4A**, top panels). Soluble CD26 could interfere with this role of ADA in many pathological conditions, such as obesity and several viral infections, where its concentration is highly increased, but not in healthy physiological conditions, where its concentration (up to 4 nM) is much lower than its affinity for ADA (see Yu et al., 2011). Because A_{2A}R and CD26 are homodimers (see above), their protein arrangement is probably more complex, with two ADA molecules linking the two homodimers.

Gracia et al. (2013a) highlighted the contribution of the 55–65, 114–118, 155–158, and 184–189 amino acidic segments of ADA to the A_{2A}R/ADA interface. The 55–65 stretch interacts with the extracellular loop 2 of the receptor whereas the 184–189 stretch interacts with the N-terminus of the A_{2A}R (see **Figure 6**). Moreover, these two stretches constitute the structural gate to the catalytic site of ADA in the tertiary structure of this enzyme, which can take different conformations: the closed and the open forms (Wilson et al., 1991; Kinoshita et al., 2005). In the absence of the substrate adenosine, ADA adopts the open form, whereas in complexes with adenine-based substrate analogs it adopts the closed form, which indicates that it is obtained after the binding of the substrate (Cortés et al., 2015; Maiuolo et al., 2016). Since ADA can increase the binding of the ligand to ARs in the absence of adenosine, it was suggested that the open form, and not the closed one, is able to bind to A_{2A}R (Gracia et al., 2013a; Cortés et al., 2015). In fact, using alanine scanning mutagenesis we showed that the two amino acid regions that participate in the structural gate of the active site pocket (the α-1 helix 55–65 and the 184–189 loop) play a central role in ADA catalysis and/or ADA-induced modulation of agonist binding to A_{2A}R (Gracia et al., 2013a). In particular, we showed that mutations of the hydrophobic residues Leu58 and Leu62 produce a 100-fold decrease of the catalytic efficiency (see **Table 2**), because they decrease both the maximum velocity and the substrate affinity. This suggests that hydrophobicity may help to maintain the control of the catalysis and the affinity for adenosine (Gracia et al., 2013a). Moreover, when we performed experiments with increasing concentrations of these ADA mutants to determine the amount of enzyme able to produce an increase of the 50% of the maximum agonist (CGS) binding (EC_{50} values), we obtained a very big increase (>200-fold) in the EC_{50} values of Leu58 and Leu62 with respect to the ADA wild type (see **Table 2**). These results point out that the α-1 helix is an important ADA domain involved in the allosteric modulation of the A_{2A}R. For this reason, in our results, NanoBRET is abolished when these mutants are used to link cell populations with A_{2A}R and with CD26.

Besides the existence of the binary complexes between ADA-ARs and ADA-CD26, higher order protein aggregates containing both ARs and ADA have been postulated. In that sense, Franco et al. (1997, 1998) suggested that ecto-ADA may participate in cell to cell contacts (CD26/ADA/CD26; CD26/ADA/A_1R and A_1R/ADA/A_1R) which can be of relevance in neural functionality and development. Later, Torvinen et al. (2002) proposed the existence of functional trimeric complexes formed by ADA and A_1R and dopamine D_1 receptors in cortical neurons and that their aggregation can be modulated by both adenosine and dopamine. Likewise, by acting as a bridge between A_{2B}R on DCs and CD26 on T cells, by forming an "immunological synapse" (Pacheco et al., 2005; Franco et al., 2007), ADA acts as a costimulatory molecule in T-cell-DC co-cultures enhancing Th-1/pro-inflammatory cytokine secretion, T-cell proliferation, and T-$CD4^+$ cell activation, memory, and $Foxp3^+$ generation in healthy subjects, but also in subjects infected with HIV (Martinez-Navio et al., 2011; Casanova et al., 2012). Our results with NanoBRET assays reinforce these hypotheses and extend them to the formation of CD26/ADA/A_{2A}R complexes, where ecto-ADA anchored to CD26 could direct the interaction between T cells and ARs-containing cells, such as neurons, DCs, and so on. Future studies demonstrating adhesion between cells promoted by ADA (e.g., DCs and T-cells) under physiological conditions, and analyzing how this ternary complex affects the function of the three proteins involved, will be necessary.

CONCLUSION

In this study, using biophysical techniques we demonstrate the possibility of formation of the ternary complex CD26/ADA/A_{2A}R. This molecular interaction is specific, as

it is abolished by a human-specific mAb against CD26, TA5.9-CC1-4C8, or by ADA mutants (Leu58Ala and Leu62Ala) with highly reduced capacity to interact with $A_{2A}R$. The bridge in the ternary complex is neither produced by a non-specific protein as albumin or between $A_{2A}R$ and another membrane protein different of CD26, as NMDA receptor, newly showing the specificity of the ADA-linked proteins. In that ternary complex, ADA can act as a bridge that interacts simultaneously with $A_{2A}R$ and CD26 expressed in different cells. This fact could allow a physiological cell-cell adhesion between, for example, DCs or neurons that express $A_{2A}R$ (Fredholm et al., 2005; Cekic and Linden, 2016) and T cells that express CD26 (Klemann et al., 2016). This would add a new metabolic function for ecto-ADA, that being a single chain protein it has been considered as an example of moonlighting protein (Cortés et al., 2015). This is because it performs more than one functional role (Copley, 2012, 2014; Jeffery, 2014, 2015, 2016; Chapple and Brun, 2015): (1) as a catalyst that degrades adenosine; (2) as a costimulatory molecule promoting T-cell differentiation and proliferation by interacting with CD26; (3) as an allosteric modulator of A_1R and $A_{2A}R$, without portioning these functions in different subunits; and (4), as a bridge, forming cell-to-cell contacts, as described in the present study.

AUTHOR CONTRIBUTIONS

EM, JC, EG, AC, and VC performed the experiments and analyzed the data. EM, JM, CL, AC, and VC designed the experiments. EM, EG, EC, AC, and VC wrote the manuscript.

FUNDING

This work was supported by Spanish "Ministerio de Economía y Competitividad" and European Regional Development Funds of the European Union (SAF2014-54840-R), "Centro de Investigación Biomédica en Red sobre Enfermedades Neurodegenerativas, CIBERNED" (Grant CB06/05/0064), and "Fundació La Marató de TV3" (Grant 20140610).

REFERENCES

Akiyama, S. K. (1996). Integrins in cell adhesion and signaling. *Hum. Cell* 9, 181–186.

Aliyari Serej, Z., Ebrahimi Kalan, A., Mehdipour, A., and Nozad Charoudeh, H. (2017). Regulation and roles of CD26/DPPIV in hematopoiesis and diseases. *Biomed. Pharmacother.* 91, 88–94. doi: 10.1016/j.biopha.2017.04.074

Angers, S., Salahpour, A., Joly, E., Hilairet, S., Chelsky, D., Dennis, M., et al. (2000). Detection of beta 2-adrenergic receptor dimerization in living cells using bioluminescence resonance energy transfer (BRET). *Proc. Natl. Acad. Sci. U.S.A.* 97, 3684–3689. doi: 10.1073/pnas.060590697

Antonioli, L., Fornai, M., Awwad, O., Giustarini, G., Pellegrini, C., Tuccori, M., et al. (2014). Role of the A_{2B} receptor-adenosine deaminase complex in colonic dysmotility associated with bowel inflammation in rats. *Br. J. Pharmacol.* 171, 1314–1329. doi: 10.1111/bph.12539

Anz, D., Kruger, S., Haubner, S., Rapp, M., Bourquin, C., and Endres, S. (2014). The dipeptidylpeptidase-IV inhibitors sitagliptin, vildagliptin and saxagliptin do not impair innate and adaptive immune responses. *Diabetes Obes. Metab.* 16, 569–572. doi: 10.1111/dom.12246

Arin, R. M., Vallejo, A. I., Rueda, Y., Fresnedo, O., and Ochoa, B. (2015). The A2B adenosine receptor colocalizes with adenosine deaminase in resting parietal cells from gastric mucosa. *Biochemistry (Mosc.)* 80, 120–125. doi: 10.1134/S0006297915010149

Arin, R. M., Vallejo, A. I., Rueda, Y., Fresnedo, O., and Ochoa, B. (2017). Expression of adenosine A_{2B} receptor and adenosine deaminase in rabbit gastric mucosa ECL cells. *Molecules* 22:E625. doi: 10.3390/molecules22040625

Baerts, L., Glorie, L., Maho, W., Eelen, A., Verhulst, A., D'Haese, P., et al. (2015). Potential impact of sitagliptin on collagen-derived dipeptides in diabetic osteoporosis. *Pharmacol. Res.* 100, 336–340. doi: 10.1016/j.phrs.2015.08.023

Baker, R. G., Hsu, C. J., Lee, D., Jordan, M. S., Maltzman, J. S., Hammer, D. A., et al. (2009). The adapter protein SLP-76 mediates "outside-in" integrin signaling and function in T cells. *Mol. Cell. Biol.* 29, 5578–5589. doi: 10.1128/MCB.00283-09

Beckenkamp, A., Davies, S., Willig, J. B., and Buffon, A. (2016). DPPIV/CD26: a tumor suppressor or a marker of malignancy? *Tumour Biol.* 37, 7059–7073. doi: 10.1007/s13277-016-5005-2

Beckers, P. A. J., Gielis, J. F., Van Schil, P. E., and Adriaensen, D. (2017). Lung ischemia reperfusion injury: the therapeutic role of dipeptidyl peptidase 4 inhibition. *Ann. Transl. Med.* 5:129. doi: 10.21037/atm.2017.01.41

Bertheleme, N., Strege, A., Bunting, S. E., Dowel, S. J., and Byrne, B. (2014). Arginine 199 and leucine 208 have key roles in the control of adenosine A_{2A} receptor signaling function. *PLOS ONE* 9:e89613. doi: 10.1371/journal.pone.0089613

Beyazit, Y., Koklu, S., Tas, A., Purnak, T., Sayilir, A., Kurt, M., et al. (2012). Serum adenosine deaminase activity as a predictor of disease severity in ulcerative colitis. *J. Crohns Colitis* 6, 102–107. doi: 10.1016/j.crohns.2011.07.010

Blackburn, M. R., and Kellems, R. E. (2005). Adenosine deaminase deficiency: metabolic basis of immune deficiency and pulmonary inflammation. *Adv. Immunol.* 86, 1–41.

Blanco, J., Valenzuela, A., Herrera, C., Lluís, C., Hovanessian, A. G., and Franco, R. (2000). The HIV-1 gp120 inhibits the binding of adenosine deaminase to CD26 by a mechanism modulated by CD4 and CXCR4 expression. *FEBS Lett.* 477, 123–128.

Borea, P. A., Gessi, S., Merighi, S., and Varani, K. (2016). Adenosine as a multi-signalling guardian angel in human diseases: when, where and how does it exert its protective effects? *Trends Pharmacol. Sci.* 37, 419–434. doi: 10.1016/j.tips.2016.02.006

Borea, P. A., Varani, K., Vincenzi, F., Baraldi, P. G., Tabrizi, M. A., Merighi, S., et al. (2015). The A_3 adenosine receptor: history and perspectives. *Pharmacol. Rev.* 67, 74–102. doi: 10.1124/pr.113.008540

Bottari, N. B., Baldissera, M. D., Oliveira, C. B., Duarte, T., Duarte, M. M., Leal, M. L., et al. (2014). Effect of zinc supplementation on E-ADA activity, seric zinc, and cytokines levels of *Trypanosoma evansi* infected Wistar rats. *Microb. Pathog.* 74, 15–19. doi: 10.1016/j.micpath.2014.06.004

Bourgaux, C., and Couvreur, P. (2014). Interactions of anticancer drugs with biomembranes: what can we learn from model membranes? *J. Control. Release* 190, 127–138. doi: 10.1016/j.jconrel.2014.05.012

Briddon, S. J., Gandía, J., Amaral, O. B., Ferré, S., Lluís, C., Franco, R., et al. (2008). Plasma membrane diffusion of G protein-coupled receptor oligomers. *Biochim. Biophys. Acta* 1783, 2262–2268. doi: 10.1016/j.bbamcr.2008.07.006

Brown, N. E., Blumer, J. B., and Hepler, J. R. (2015). Bioluminescence resonance energy transfer to detect protein-protein interactions in live cells. *Methods Mol. Biol.* 1278, 457–465.

Buckley, R. H. (2004). Molecular defects in human severe combined immunodeficiency and approaches to immune reconstitution. *Annu. Rev. Immunol.* 22, 625–655. doi: 10.1146/annurev.immunol.22.012703.104614

Canals, M., Burgueño, J., Marcellino, D., Cabello, N., Canela, E. I., Mallol, J., et al. (2004). Homodimerization of adenosine A_{2A} receptors: qualitative and quantitative assessment by fluorescence and bioluminescence energy transfer. *J. Neurochem.* 88, 726–734.

Carpenter, B., Nehmé, R., Warne, T., Leslie, A. G., and Tate, C. G. (2016). Structure of the adenosine A_{2A} receptor bound to an engineered G protein. *Nature* 536, 104–107. doi: 10.1038/nature18966

Casadó, V., Cortés, A., Ciruela, F., Mallol, J., Ferré, S., Lluis, C., et al. (2007). Old and new ways to calculate the affinity of agonists and antagonists interacting

with G-protein-coupled monomeric and dimeric receptors: the receptor-dimer cooperativity index. *Pharmacol. Ther.* 116, 343–354. doi: 10.1016/j.pharmthera.2007.05.010

Casadó, V., Cortés, A., Mallol, J., Pérez-Capote, K., Ferré, S., Lluis, C., et al. (2009a). GPCR homomers and heteromers: a better choice as targets for drug development than GPCR monomers? *Pharmacol. Ther.* 124, 248–257. doi: 10.1016/j.pharmthera.2009.07.005

Casadó, V., Ferrada, C., Bonaventura, J., Gracia, E., Mallol, J., Canela, E. I., et al. (2009b). Useful pharmacological parameters for G-protein-coupled receptor homodimers obtained from competition experiments. Agonist-antagonist binding modulation. *Biochem. Pharmacol.* 78, 1456–1463. doi: 10.1016/j.bcp.2009.07.012

Casadó-Anguera, V., Bonaventura, J., Moreno, E., Navarro, G., Cortés, A., Ferré, S., et al. (2016). Evidence for the heterotetrameric structure of the adenosine A_{2A} receptor-dopamine D2 receptor complex. *Biochem. Soc. Trans.* 44, 595–600. doi: 10.1042/BST20150276

Casanova, V., Naval-Macabuhay, I., Massanella, M., Rodríguez-García, M., Blanco, J., Gatell, J. M., et al. (2012). Adenosine deaminase enhances the immunogenicity of human dendritic cells from healthy and HIV-infected individuals. *PLOS ONE* 7:e51287. doi: 10.1371/journal.pone.0051287

Cekic, C., and Linden, J. (2016). Purinergic regulation of the immune system. *Nat. Rev. Immunol.* 16, 177–192. doi: 10.1038/nri.2016.4

Chang, Z. Y., Nygaard, P., Chinault, A. C., and Kellems, R. E. (1991). Deduced amino acid sequence of *Escherichia coli* adenosine deaminase reveals evolutionarily conserved amino acid residues: implications for catalytic function. *Biochemistry* 30, 2273–2280.

Chapple, C. E., and Brun, C. (2015). Redefining protein moonlighting. *Oncotarget* 6, 16812–16813. doi: 10.18632/oncotarget.4793

Chen, J. F., Eltzschig, H. K., and Fredholm, B. B. (2013). Adenosine receptors as drug targets–what are the challenges? *Nat. Rev. Drug Discov.* 12, 265–286. doi: 10.1038/nrd3955

Cheng, R. K. Y., Segala, E., Robertson, N., Deflorian, F., Doré, A. S., Errey, J. C., et al. (2017). Structures of human A_1 and A_{2A} adenosine receptors with xanthines reveal determinants of selectivity. *Structure* 25, 1275–1285. doi: 10.1016/j.str.2017.06.012

Cigler, M., Müller, T. G., Horn-Ghetko, D., von Wrisberg, M. K., Fottner, M., and Goody, R. S. (2017). Proximity-triggered covalent stabilization of low-affinity protein complexes in vitro and in vivo. *Angew. Chem. Int. Ed. Engl.* 56, 15737–15741. doi: 10.1002/anie.201706927

Ciruela, F. (2008). Fluorescence based methods in the study of protein-protein interactions in living cells. *Curr. Opin. Biotechnol.* 19, 338–343. doi: 10.1016/j.copbio.2008.06.003

Ciruela, F., Casadó, V., Mallol, J., Canela, E. I., Lluis, C., and Franco, R. (1995). Immunological identification of A1 adenosine receptors in brain cortex. *J. Neurosci. Res.* 42, 818–828. doi: 10.1002/jnr.490420610

Ciruela, F., Saura, C., Canela, E. I., Mallol, J., Lluis, C., and Franco, R. (1996). Adenosine deaminase affects ligand-induced signalling by interacting with cell surface adenosine receptors. *FEBS Lett.* 380, 219–223.

Congreve, M., Andrews, S. P., Doré, A. S., Hollenstein, K., Hurrell, E., Langmead, C. J., et al. (2012). Discovery of 1,2,4-triazine derivatives as adenosine A_{2A} antagonists using structure based drug design. *J. Med. Chem.* 55, 1898–1903. doi: 10.1021/jm201376w

Cooper, B. F., Sideraki, V., Wilson, D. K., Dominguez, D. Y., Clark, S. W., Quiocho, F. A., et al. (1997). The role of divalent cations in structure and function of murine adenosine deaminase. *Protein Sci.* 6, 1031–1037. doi: 10.1002/pro.5560060509

Copley, S. D. (2012). Moonlighting is mainstream: paradigm adjustment required. *Bioessays* 34, 578–588. doi: 10.1002/bies.201100191

Copley, S. D. (2014). An evolutionary perspective on protein moonlighting. *Biochem. Soc. Trans.* 42, 1684–1691. doi: 10.1042/BST20140245

Corbel, C., Sartini, S., Levati, E., Colas, P., Maillet, L., Couturier, C., et al. (2017). Screening for protein-protein interaction inhibitors using a bioluminescence resonance energy transfer (BRET)-based assay in yeast. *SLAS Discov.* 22, 751–759. doi: 10.1177/2472555216689530

Cordero, O. J., Varela-Calviño, R., López-González, T., Calviño-Sampedro, C., Viñuela, J. E., Mouriño, C., et al. (2015). CD26 expression on T helper populations and sCD26 serum levels in patients with rheumatoid arthritis. *PLOS ONE* 10:e0131992. doi: 10.1371/journal.pone.0131992

Cortés, A., Gracia, E., Moreno, E., Mallol, J., Lluís, C., Canela, E. I., et al. (2015). Moonlighting adenosine deaminase: a target protein for drug development. *Med. Res. Rev.* 35, 85–125. doi: 10.1002/med.21324

Cronstein, B. N., and Sitkovsky, M. (2017). Adenosine and adenosine receptors in the pathogenesis and treatment of rheumatic diseases. *Nat. Rev. Rheumatol.* 13, 41–51. doi: 10.1038/nrrheum.2016.178

Cunha, R. A., Constantino, M. D., and Ribeiro, J. A. (1997). ZM241385 is an antagonist of the facilitatory responses produced by the A_{2A} adenosine receptor agonists CGS21680 and HENECA in the rat hippocampus. *Br. J. Pharmacol.* 122, 1279–1284.

Da Silva, A. S., Schafer, A. S., Aires, A. R., Tonin, A. A., Pimentel, V. C., Oliveira, C. B., et al. (2013). E-ADA activity in erythrocytes of lambs experimentally infected with *Haemonchus contortus* and its possible functional correlations with anemia. *Res. Vet. Sci.* 95, 1026–1030. doi: 10.1016/j.rvsc.2013.07.008

Deriziotis, P., Graham, S. A., Estruch, S. B., and Fisher, S. E. (2014). Investigating protein-protein interactions in live cells using bioluminescence resonance energy transfer. *J. Vis. Exp.* 87:e51438. doi: 10.3791/51438

Desrosiers, M. D., Cembrola, K. M., Fakir, M. J., Stephens, L. A., Jama, F. M., Shameli, A., et al. (2007). Adenosine deamination sustains dendritic cell activation in inflammation. *J. Immunol.* 179, 1884–1892.

Doré, A. S., Robertson, N., Errey, J. C., Ng, I., Hollenstein, K., Tehan, B., et al. (2011). Structure of the adenosine A_{2A} receptor in complex with ZM241385 and the xanthines XAC and caffeine. *Structure* 19, 1283–1293. doi: 10.1016/j.str.2011.06.014

Du, X., Ou, X., Song, T., Zhang, W., Cong, F., Zhang, S., et al. (2015). Adenosine A_{2B} receptor stimulates angiogenesis by inducing VEGF and eNOS in human microvascular endothelial cells. *Exp. Biol. Med.* 240, 1472–1479. doi: 10.1177/1535370215584939

Eltzschig, H. K., Faigle, M., Knapp, S., Karhausen, J., Ibla, J., Rosenberger, P., et al. (2006). Endothelial catabolism of extracellular adenosine during hypoxia: the role of surface adenosine deaminase and CD26. *Blood* 108, 1602–1610. doi: 10.1182/blood-2006-02-001016

Fan, H., Tansi, F. L., Weihofen, W. A., Böttcher, C., Hu, J., and Martinez, J. (2012). Molecular mechanism and structural basis of interactions of dipeptidyl peptidase IV with adenosine deaminase and human immunodeficiency virus type-1 transcription transactivator. *Eur. J. Cell Biol.* 91, 265–273. doi: 10.1016/j.ejcb.2011.06.001

Franco, R., Casadó, V., Ciruela, F., Saura, C., Mallol, J., Canela, E. I., et al. (1997). Cell surface adenosine deaminase: much more than an ectoenzyme. *Prog. Neurobiol.* 52, 283–294.

Franco, R., Pacheco, R., Gatell, J. M., Gallart, T., and Lluis, C. (2007). Enzymatic and extraenzymatic role of adenosine deaminase 1 in T-cell-dendritic cell contacts and in alterations of the immune function. *Crit. Rev. Immunol.* 27, 495–509.

Franco, R., Valenzuela, A., Lluis, C., and Blanco, J. (1998). Enzymatic and extraenzymatic role of ecto-adenosine deaminase in lymphocytes. *Immunol. Rev.* 161, 27–42.

Fredholm, B. B., Chen, J. F., Cunha, R. A., Svenningsson, P., and Vaugeois, J. M. (2005). Adenosine and brain function. *Int. Rev. Neurobiol.* 63, 191–270. doi: 10.1016/S0074-7742(05)63007-3

Fredholm, B. B., IJzerman, A. P., Jacobson, K. A., Linden, J., and Müller, C. E. (2011). International union of basic and clinical pharmacology. LXXXI. Nomenclature and classification of adenosine receptors–an update. *Pharmacol. Rev.* 63, 1–34. doi: 10.1124/pr.110.003285

Gandia, J., Galino, J., Amaral, O. B., Soriano, A., Lluís, C., Franco, R., et al. (2008). Detection of higher-order G protein-coupled receptor oligomers by a combined BRET-BiFC technique. *FEBS Lett.* 582, 2979–2984. doi: 10.1016/j.febslet.2008.07.045

Gile, J., and Eckle, T. (2016). ADORA2b signaling in cardioprotection. *J. Nat. Sci.* 2:e222.

Ginés, S., Mariño, M., Mallol, J., Canela, E. I., Morimoto, C., Callebaut, C., et al. (2002). Regulation of epithelial and lymphocyte cell adhesion by adenosine deaminase-CD26 interaction. *Biochem. J.* 361, 203–209.

Golias, C., Batistatou, A., Bablekos, G., Charalabopoulos, A., Peschos, D., Mitsopoulos, P., et al. (2011). Physiology and pathophysiology of selectins, integrins, and IgSF cell adhesion molecules focusing on inflammation.

A paradigm model on infectious endocarditis. *Cell Commun. Adhes.* 18, 19–32. doi: 10.3109/15419061.2011.606381

Gonzalez-Gronow, M., Hershfield, M. S., Arredondo-Vega, F. X., and Pizzo, S. V. (2004). Cell surface adenosine deaminase binds and stimulates plasminogen activation on 1-LN human prostate cancer cells. *J. Biol. Chem.* 279, 20993–20998.

Gorrell, M. D. (2005). Dipeptidyl peptidase IV and related enzymes in cell biology and liver disorders. *Clin. Sci.* 108, 277–292. doi: 10.1042/CS20040302

Gracia, E., Cortés, A., Meana, J. J., García-Sevilla, J., Herhsfield, M. S., Canela, E. I., et al. (2008). Human adenosine deaminase as an allosteric modulator of human A_1 adenosine receptor: abolishment of negative cooperativity for [^{3}H](R)-pia binding to the caudate nucleus. *J. Neurochem.* 107, 161–170. doi: 10.1111/j.1471-4159.2008.05602.x

Gracia, E., Farré, D., Cortés, A., Ferrer-Costa, C., Orozco, M., Mallol, J., et al. (2013a). The catalytic site structural gate of adenosine deaminase allosterically modulates ligand binding to adenosine receptors. *FASEB J.* 27, 1048–1061. doi: 10.1096/fj.12-212621

Gracia, E., Moreno, E., Cortés, A., Lluís, C., Mallol, J., McCormick, P. J., et al. (2013b). Homodimerization of adenosine A_1 receptors in brain cortex explains the biphasic effects of caffeine. *Neuropharmacology* 71, 56–69. doi: 10.1016/j.neuropharm.2013.03.005

Gracia, E., Pérez-Capote, K., Moreno, E., Barkešová, J., Mallol, J., Lluís, C., et al. (2011). A_{2A} adenosine receptor ligand binding and signalling is allosterically modulated by adenosine deaminase. *Biochem. J.* 435, 701–709. doi: 10.1042/BJ20101749

Grosskopf, H. M., Schwertz, C. I., Machado, G., Bottari, N. B., da Silva, E. S., Gabriel, M. E., et al. (2017). Cattle naturally infected by *Eurytrema coelomaticum*: relation between adenosine deaminase activity and zinc levels. *Res. Vet. Sci.* 110, 79–84. doi: 10.1016/j.rvsc.2016.10.016

Havre, P. A., Abe, M., Urasaki, Y., Ohnuma, K., Morimoto, C., and Dang, N. H. (2008). The role of CD26/dipeptidyl peptidase IV in cancer. *Front. Biosci.* 13, 1634–1645.

Havre, P. A., Dang, L. H., Ohnuma, K., Iwata, S., Morimoto, C., and Dang, N. H. (2013). CD26 expression on T-anaplastic large cell lymphoma (ALCL) line Karpas 299 is associated with increased expression of versican and MT1-MMP and enhanced adhesion. *BMC Cancer* 13:517. doi: 10.1186/1471-2407-13-517

Hawryluk, J. M., Ferrari, L. L., Keating, S. A., and Arrigoni, E. (2012). Adenosine inhibits glutamatergic input to basal forebrain cholinergic neurons. *J. Neurophysiol.* 107, 2769–2781. doi: 10.1152/jn.00528.2011

He, T., Brocca-Cofano, E., Gillespie, D. G., Xu, C., Stock, J. L., Ma, D., et al. (2015). Critical role for the adenosine pathway in controlling simian immunodeficiency virus-related immune activation and inflammation in gut mucosal tissues. *J. Virol.* 89, 9616–9630. doi: 10.1128/JVI.01196-15

Herrera, C., Casadó, V., Ciruela, F., Schofield, P., Mallol, J., Lluis, C., et al. (2001). Adenosine A_{2B} receptors behave as an alternative anchoring protein for cell surface adenosine deaminase in lymphocytes and cultured cells. *Mol. Pharmacol.* 59, 127–134.

Hino, T., Arakawa, T., Iwanari, H., Yurugi-Kobayashi, T., Ikeda-Suno, C., Nakada-Nakura, Y., et al. (2012). G-protein-coupled receptor inactivation by an allosteric inverse-agonist antibody. *Nature* 482, 237–240. doi: 10.1038/nature10750

Horwitz, A. R. (2012). The origins of the molecular era of adhesion research. *Nat. Rev. Mol. Cell Biol.* 13, 805–811. doi: 10.1038/nrm3473

Huang, Y., Todd, N., and Thathiah, A. (2017). The role of GPCRs in neurodegenerative diseases: avenues for therapeutic intervention. *Curr. Opin. Pharmacol.* 32, 96–110. doi: 10.1016/j.coph.2017.02.001

Ingwersen, J., Wingerath, B., Graf, J., Lepka, K., Hofrichter, M., Schröter, F., et al. (2016). Dual roles of the adenosine A2a receptor in autoimmune neuroinflammation. *J. Neuroinflammation* 13:48. doi: 10.1186/s12974-016-0512-z

Jaakola, V. P., Griffith, M. T., Hanson, M. A., Cherezov, V., Chien, E. Y., Lane, J. R., et al. (2008). The 2.6 angstrom crystal structure of a human A_{2A} adenosine receptor bound to an antagonist. *Science* 322, 1211–1217. doi: 10.1126/science.1164772

Jacobson, K. A., and Gao, Z. G. (2006). Adenosine receptors as therapeutic targets. *Nat. Rev. Drug Discov.* 5, 247–264. doi: 10.1038/nrd1983

Jazayeri, A., Dias, J. M., and Marshall, F. H. (2015). From G Protein-coupled receptor structure resolution to rational drug design. *J. Biol. Chem.* 290, 19489–19495. doi: 10.1074/jbc.R115.668251

Jeffery, C. J. (2014). An introduction to protein moonlighting. *Biochem. Soc. Trans.* 42, 1679–1683. doi: 10.1042/BST20140226

Jeffery, C. J. (2015). Why study moonlighting proteins? *Front. Genet.* 6:211. doi: 10.3389/fgene.2015.00211

Jeffery, C. J. (2016). Protein species and moonlighting proteins: very small changes in a protein's covalent structure can change its biochemical function. *J. Proteomics* 134, 19–24. doi: 10.1016/j.jprot.2015.10.003

Kameoka, J., Ichinohasama, R., Inoue, H., Yamamoto, J., Yokoyama, H., Tomiya, Y., et al. (2006). CD26, together with cell surface adenosine deaminase, is selectively expressed on ALK-positive, but not on ALK-negative, anaplastic large cell lymphoma and Hodgkin's lymphoma. *Leuk. Lymphoma* 47, 2181–2188. doi: 10.1080/10428190600773396

Kanno, Y., Sakai, A., Miyashita, M., Tsuchida, K., and Matsuo, O. (2016). Plasminogen deficiency is associated with improved glucose tolerance, and lower DPP-4 activity. *Diabetes Res. Clin. Pract.* 120, 190–193. doi: 10.1016/j.diabres.2016.08.007

Khalili, A. A., and Ahmad, M. R. (2015). A review of cell adhesion studies for biomedical and biological applications. *Int. J. Mol. Sci.* 16, 18149–18184. doi: 10.3390/ijms160818149

Khare, S. D., Kipnis, Y., Greisen, P. Jr., Takeuchi, R., Ashani, Y., Goldsmith, M., et al. (2012). Computational redesign of a mononuclear zinc metalloenzyme for organophosphate hydrolysis. *Nat. Chem. Biol.* 8, 294–300. doi: 10.1038/nchembio.777

Kim, J., Lee, J., Kwon, D., Lee, H., and Grailhe, R. (2011). A comparative analysis of resonance energy transfer methods for Alzheimer related protein-protein interactions in living cells. *Mol. Biosyst.* 7, 2991–2996. doi: 10.1039/c1mb05279a

Kimura, T., Hiraoka, K., Kasahara, N., and Logg, C. R. (2010). Optimization of enzyme-substrate pairing for bioluminescence imaging of gene transfer using *Renilla* and *Gaussia* luciferases. *J. Gene Med.* 12, 528–537. doi: 10.1002/jgm.1463

Kinoshita, T., Nakanishi, I., Terasaka, T., Kuno, M., Seki, N., Warizaya, M., et al. (2005). Structural basis of compound recognition by adenosine deaminase. *Biochemistry* 44, 10562–10569. doi: 10.1021/bi050529e

Klemann, C., Wagner, L., Stephan, M., and von Hörsten, S. (2016). Cut to the chase: a review of CD26/dipeptidyl peptidase-4's (DPP4) entanglement in the immune system. *Clin. Exp. Immunol.* 185, 1–21. doi: 10.1111/cei.12781

Kutryb-Zajac, B., Mateuszuk, L., Zukowska, P., Jasztal, A., Zabielska, M. A., and Toczek, M. (2016). Increased activity of vascular adenosine deaminase in atherosclerosis and therapeutic potential of its inhibition. *Cardiovasc. Res.* 112, 590–605. doi: 10.1093/cvr/cvw203

Lambeir, A. M., Durinx, C., Scharpe, S., and De Meester, I. (2003). Dipeptidyl-peptidase IV from bench to bedside: an update on structural properties, functions, and clinical aspects of the enzyme DPP IV. *Crit. Rev. Clin. Lab. Sci.* 40, 209–294. doi: 10.1080/713609354

Larrinaga, G., Perez, I., Sanz, B., Beitia, M., Errarte, P., and Fernández, A. (2015). Dipeptidyl-peptidase IV activity is correlated with colorectal cancer prognosis. *PLOS ONE* 10:e0119436. doi: 10.1371/journal.pone.0119436

Lazarus, M., Chen, J. F., Huang, Z. L., Urade, Y., and Fredholm, B. B. (2017). Adenosine and sleep. *Handb. Exp. Pharmacol.* 7, 238–245. doi: 10.1007/164_2017_36

Lebon, G., Edwards, P. C., Leslie, A. G., and Tate, C. G. (2015). Molecular determinants of CGS21680 binding to the human adenosine A_{2A} receptor. *Mol. Pharmacol.* 87, 907–915. doi: 10.1124/mol.114.097360

Lebon, G., Warne, T., Edwards, P. C., Bennett, K., Langmead, C. J., Leslie, A. G., et al. (2011). Agonist-bound adenosine A_{2A} receptor structures reveal common features of GPCR activation. *Nature* 474, 521–525. doi: 10.1038/nature10136

Lee, J. J., Wang, T. Y., Liu, C. L., Chien, M. N., Chen, M. J., Hsu, Y. C., et al. (2017). Dipeptidyl peptidase IV as a prognostic marker and therapeutic target in papillary thyroid carcinoma. *J. Clin. Endocrinol. Metab.* 102, 2930–2940. doi: 10.1210/jc.2017-00346

Leiva, A., Guzmán-Gutiérrez, E., Contreras-Duarte, S., Fuenzalida, B., Cantin, C., Carvajal, L., et al. (2017). Adenosine receptors: modulators of lipid availability that are controlled by lipid levels. *Mol. Aspects Med.* 55, 26–44. doi: 10.1016/j.mam.2017.01.007

Liu, W., Chun, E., Thompson, A. A., Chubukov, P., Xu, F., Katritch, V., et al. (2012). Structural basis for allosteric regulation of GPCRs by sodium ions. *Science* 337, 232–236. doi: 10.1126/science.1219218

Loeser, R. F. (2014). Integrins and chondrocyte-matrix interactions in articular cartilage. *Matrix Biol.* 39, 11–16. doi: 10.1016/j.matbio.2014.08.007

Lohse, M. J., Nuber, S., and Hoffmann, C. (2012). Fluorescence/bioluminescence resonance energy transfer techniques to study G-protein-coupled receptor activation and signaling. *Pharmacol. Rev.* 64, 299–336. doi: 10.1124/pr.110.004309

Lu, G., Hu, Y., Wang, Q., Qi, J., Gao, F., Li, Y., et al. (2013). Molecular basis of binding between novel human coronavirus MERS-CoV and its receptor CD26. *Nature* 500, 227–231. doi: 10.1038/nature12328

Machleidt, T., Woodroofe, C. C., Schwinn, M. K., Méndez, J., Robers, M. B., Zimmerman, K., et al. (2015). NanoBRET-A novel BRET platform for the analysis of protein-protein interactions. *ACS Chem. Biol.* 10, 1797–1804. doi: 10.1021/acschembio.5b00143

Maiuolo, J., Oppedisano, F., Gratteri, S., Muscoli, C., and Mollace, V. (2016). Regulation of uric acid metabolism and excretion. *Int. J. Cardiol.* 213, 8–14. doi: 10.1016/j.ijcard.2015.08.109

Maleki, M., Vasudev, G., and Rueda, L. (2013). The role of electrostatic energy in prediction of oblígate protein-protein interactions. *Proteome Sci.* 11(Suppl. 1):S11. doi: 10.1186/1477-5956-11-S1-S11

Mandapathil, M., Szczepanski, M., Harasymczuk, M., Ren, J., Cheng, D., Jackson, E. K., et al. (2012). CD26 expression and adenosine deaminase activity in regulatory T cells (Treg) and $CD4^+$ T effector cells in patients with head and neck squamous cell carcinoma. *Oncoimmunology* 1, 659–669. doi: 10.4161/onci.20387

Martín, M., Huguet, J., Centelles, J. J., and Franco, R. (1995). Expression of ecto-adenosine deaminase and CD26 in human T cells triggered by the TCR-CD3 complex. Possible role of adenosine deaminase as costimulatory molecule. *J. Immunol.* 155, 4630–4643.

Martinez-Navio, J. M., Casanova, V., Pacheco, R., Naval-Macabuhay, I., Climent, N., Garcia, F., et al. (2011). Adenosine deaminase potentiates the generation of effector, memory, and regulatory $CD4^+$ T cells. *J. Leukoc. Biol.* 89, 127–136. doi: 10.1189/jlb.1009696

Martinez-Navio, J. M., Climent, N., Pacheco, R., Garcia, F., Plana, M., Nomdedeu, M., et al. (2009). Immunological dysfunction in HIV-1-infected individuals caused by impairment of adenosine deaminase-induced costimulation of -cell activation. *Immunology* 128, 393–404. doi: 10.1111/j.1365-2567.2009.03121.x

Meli, A. P., Fontés, G., Avery, D. T., Leddon, S. A., Tam, M., Elliot, M., et al. (2016). The integrin LFA-1 controls T follicular helper cell generation and maintenance. *Immunity* 45, 831–846. doi: 10.1016/j.immuni.2016.09.018

Mo, X. L., and Fu, H. (2016). BRET: NanoLuc-based bioluminescence resonance energy transfer platform to monitor protein-protein interactions in live cells. *Methods Mol. Biol.* 1439, 263–271. doi: 10.1007/978-1-4939-3673-1_17

Moreno, E., Chiarlone, A., Medrano, M., Puigdellívol, M., Bibic, L., Howell, L. A., et al. (2017a). Singular location and signaling profile of adenosine A_{2A} cannabinoid CB1 receptor heteromers in the dorsal striatum. *Neuropsychopharmacology* doi: 10.1038/npp.2017.12 [Epub ahead of print]

Moreno, E., Quiroz, C., Rea, W., Cai, N. S., Mallol, J., Cortés, A., et al. (2017b). Functional μ-opioid-galanin receptor heteromers in the ventral tegmental area. *J. Neurosci.* 37, 1176–1186. doi: 10.1523/JNEUROSCI.2442-16.2016

Moretti, F. A., Moser, M., Lyck, R., Abadier, M., Ruppert, R., Engelhardt, B., et al. (2013). Kindlin-3 regulates integrin activation and adhesion reinforcement of effector T cells. *Proc. Natl. Acad. Sci. U.S.A.* 110, 17005–17010. doi: 10.1073/pnas.1316032110

Mortier, A., Gouwy, M., Van Damme, J., Proost, P., and Struyf, S. (2016). CD26/dipeptidylpeptidase IV-chemokine interactions: double-edged regulation of inflammation and tumor biology. *J. Leukoc. Biol.* 99, 955–969. doi: 10.1189/jlb.3MR0915-401R

Namba, K., Suzuki, T., and Nakata, H. (2010). Immunogold electron microscopic evidence of *in situ* formation of homo- and heteromeric purinergic adenosine A_1 and $P2Y_2$ receptors in rat brain. *BMC Res. Notes* 3:323. doi: 10.1186/1756-0500-3-323

Naval-Macabuhay, I., Casanova, V., Navarro, G., García, F., León, A., Miralles, L., et al. (2016). Adenosine deaminase regulates Treg expression in autologous T cell-dendritic cell cocultures from patients infected with HIV-1. *J. Leukoc. Biol.* 99, 349–359. doi: 10.1189/jlb.3A1214-580RR

Navarro, G., Cordomí, A., Zelman-Femiak, M., Brugarolas, M., Moreno, E., Aguinaga, D., et al. (2016). Quaternary structure of a G-protein-coupled receptor heterotetramer in complex with Gi and Gs. *BMC Biol.* 14:26. doi: 10.1186/s12915-016-0247-4

Niu, W., Shu, Q., Chen, Z., Mathews, S., Di Cera, E., and Frieden, C. (2010). The role of Zn^{2+} on the structure and stability of murine adenosine deaminase. *J. Phys. Chem. B* 114, 16156–16165. doi: 10.1021/jp106041v

Ohta, A. (2016). A metabolic immune checkpoint: adenosine in tumor microenvironment. *Front. Immunol.* 7:109. doi: 10.3389/fimmu.2016.00109

Pacheco, R., Martinez-Navio, J. M., Lejeune, M., Climent, N., Oliva, H., Gatell, J. M., et al. (2005). CD26, adenosine deaminase, and adenosine receptors mediate costimulatory signals in the immunological synapse. *Proc. Natl. Acad. Sci. U.S.A.* 102, 9583–9588. doi: 10.1073/pnas.0501050102

Petschnigg, J., Wong, V., Snider, J., and Stagljar, I. (2012). Investigation of membrane protein interactions using the split-ubiquitin membrane yeast two-hybrid system. *Methods Mol. Biol.* 812, 225–244. doi: 10.1007/978-1-61779-455-1_13

Richard, E., Alam, S. M., Arredondo-Vega, F. X., Patel, D. D., and Hershfield, M. S. (2002). Clustered charged amino acids of human adenosine deaminase comprise a functional epitope for binding the adenosine deaminase complexing protein CD26/dipeptidyl peptidase IV. *J. Biol. Chem.* 277, 19720–19726. doi: 10.1074/jbc.M111901200

Ruiz, M. A., Escriche, M., Lluis, C., Franco, R., Martín, M., Andrés, A., et al. (2000). Adenosine A_1 receptor in cultured neurons from rat cerebral cortex: colocalization with adenosine deaminase. *J. Neurochem.* 75, 656–664.

Saraon, P., Grozavu, I., Lim, S. H., Snider, J., Yao, Z., and Stagljar, I. (2017). Detecting membrane protein-protein interactions using the mammalian membrane two-hybrid (MaMTH) assay. *Curr. Protoc. Chem. Biol.* 9, 38–54. doi: 10.1002/cpch.15

Sarrió, S., Casadó, V., Escriche, M., Ciruela, F., Mallol, J., Canela, E. I., et al. (2000). The heat shock cognate protein hsc73 assembles with A_1 adenosine receptors to form functional modules in the cell membrane. *Mol. Cell. Biol.* 20, 5164–5174.

Saura, C., Ciruela, F., Casadó, V., Canela, E. I., Mallol, J., Lluis, C., et al. (1996). Adenosine deaminase interacts with A_1 adenosine receptors in pig brain cortical membranes. *J. Neurochem.* 66, 1675–1682.

Segala, E., Guo, D., Cheng, R. K., Bortolato, A., Deflorian, F., Doré, A. S., et al. (2016). Controlling the dissociation of ligands from the adenosine A_{2A} receptor through modulation of salt bridge strength. *J. Med. Chem.* 59, 6470–6479. doi: 10.1021/acs.jmedchem.6b00653

Sharma, A. K., LaPar, D. J., Stone, M. L., Zhao, Y., Mehta, C. K., Kron, I. L., et al. (2016). NOX2 Activation of natural killer T cells is blocked by the adenosine A_{2A} receptor to inhibit lung ischemia-reperfusion injury. *Am. J. Respir. Crit. Care Med.* 193, 988–999. doi: 10.1164/rccm.201506-1253OC

Shaw, K. L., Garabedian, E., Mishra, S., Barman, P., Davila, A., Carbonaro, D., et al. (2017). Clinical efficacy of gene-modified stem cells in adenosine deaminase-deficient immunodeficiency. *J. Clin. Invest.* 127, 1689–1699. doi: 10.1172/JCI90367

Sheth, S., Brito, R., Mukherjea, D., Rybak, L. P., and Ramkumar, V. (2014). Adenosine receptors: expression, function and regulation. *Int. J. Mol. Sci.* 15, 2024–2052. doi: 10.3390/ijms15022024

Shrivastava, A. N., Aperia, A., Melki, R., and Triller, A. (2017). Physico-pathologic mechanisms involved in neurodegeneration: misfolded protein-plasma membrane interactions. *Neuron* 95, 33–50. doi: 10.1016/j.neuron.2017.05.026

Songok, E. M., Osero, B., McKinnon, L., Rono, M. K., Apidi, W., Matey, E. J., et al. (2010). CD26/dipeptidyl peptidase IV (CD26/DPPIV) is highly expressed in peripheral blood of HIV-1 exposed uninfected female sex workers. *Virol. J.* 7:343. doi: 10.1186/1743-422X-7-343

Souza Vdo, C., Schlemmer, K. B., Noal, C. B., Jaques, J. A., Bagatini, M. D., Pimentel, V. C., et al. (2012). Purinergic system ecto-enzymes participate in the thromboregulation of patients with indeterminate form of Chagas disease. *Purinergic Signal.* 8, 753–762. doi: 10.1007/s11302-012-9322-7

Stockwell, J., Jakova, E., and Cayabyab, F. S. (2017). Adenosine A_1 and A_{2A} receptors in the brain: current research and their role in neurodegeneration. *Molecules* 22:E676. doi: 10.3390/molecules22040676

Sun, B., Bachhawat, P., Chu, M. L., Wood, M., Ceska, T., Sands, Z. A., et al. (2017). Crystal structure of the adenosine A_{2A} receptor bound to an antagonist reveals a potential allosteric pocket. *Proc. Natl. Acad. Sci. U.S.A.* 114, 2066–2071. doi: 10.1073/pnas.1621423114

Sun, W. C., Cao, Y., Jin, L., Wang, L. Z., Meng, F., and Zhu, X. Z. (2005). Modulating effect of adenosine deaminase on function of adenosine A_1 receptors. *Acta Pharmacol. Sin.* 26, 160–165. doi: 10.1111/j.1745-7254.2005.00524.x

Sun, Y., and Huang, P. (2016). Adenosine A_{2B} receptor: from cell biology to human diseases. *Front. Chem.* 4:37. doi: 10.3389/fchem.2016.00037

Torvinen, M., Gines, S., Hillion, J., Latini, S., Canals, M., Ciruela, F., et al. (2002). Interactions among adenosine deaminase, adenosine A_1 receptors and dopamine D_1 receptors in stably cotransfected fibroblast cells and neurons. *Neuroscience* 113, 709–719.

Tsuji, G., Okiyama, N., Villarroel, V. A., and Katz, S. I. (2015). Histone deacetylase 6 inhibition impairs effector CD8 T-cell functions during skin inflammation. *J. Allergy Clin. Immunol.* 135, 1228–1239. doi: 10.1016/j.jaci.2014.10.002

Turel, O., Aygun, D., Kardas, M., Torun, E., Hershfield, M., and Camcıoglu, Y. (2017). A case of severe combined immunodeficiency caused by adenosine deaminase deficiency with a new mutation. *Pediatr. Neonatol.* doi: 10.1016/j.pedneo.2016.10.008 [Epub ahead of print]

Vidi, P. A., Chen, J., Irudayaraj, J. M., and Watts, V. J. (2008). Adenosine A_{2A} receptors assemble into higher-order oligomers at the plasma membrane. *FEBS Lett.* 582, 3985–3990. doi: 10.1016/j.febslet.2008.09.062

Viñals, X., Moreno, E., Lanfumey, L., Cordomí, A., Pastor, A., de La Torre, R., et al. (2015). Cognitive impairment induced by delta9-tetrahydrocannabinol occurs through heteromers between cannabinoid CB1 and serotonin 5-HT2A receptors. *PLOS Biol.* 9:e1002194. doi: 10.1371/journal.pbio.1002194

Wagner, L., Klemann, C., Stephan, M., and von Hörsten, S. (2016). Unravelling the immunological roles of dipeptidyl peptidase 4 (DPP4) activity and/or structure homologue (DASH) proteins. *Clin. Exp. Immunol.* 184, 265–283. doi: 10.1111/cei.12757

Wang, Z., and Quiocho, F. A. (1998). Complexes of adenosine deaminase with two potent inhibitors: X-ray structures in four independent molecules at pH of maximum activity. *Biochemistry* 37, 8314–8324. doi: 10.1021/bi980324o

Weihofen, W. A., Liu, J., Reutter, W., Saenger, W., and Fan, H. (2004). Crystal structure of CD26/dipeptidyl-peptidase IV in complex with adenosine deaminase reveals a highly amphiphilic interface. *J. Biol. Chem.* 279, 43330–43335. doi: 10.1074/jbc.M405001200

Welch, W. J. (2015). Adenosine, type 1 receptors: role in proximal tubule Na^+ reabsorption. *Acta Physiol.* 213, 242–248. doi: 10.1111/apha.12413

Welihinda, A. A., and Amento, E. P. (2014). Positive allosteric modulation of the adenosine A_{2A} receptor attenuates inflammation. *J. Inflamm.* 11:37. doi: 10.1186/s12950-014-0037-0

Wilson, D. K., Rudolph, F. B., and Quiocho, F. A. (1991). Atomic structure of adenosine deaminase complexed with a transition-state analog: understanding catalysis and immunodeficiency mutations. *Science* 252, 1278–1284.

Xin, Y., Wang, X., Zhu, M., Qu, M., Bogari, M., Lin, L., et al. (2017). Expansion of CD26 positive fibroblast population promotes keloid progression. *Exp. Cell Res.* 356, 104–113. doi: 10.1016/j.yexcr.2017.04.021

Xu, F., Wu, H., Katritch, V., Han, G. W., Jacobson, K. A., Gao, Z. G., et al. (2011). Structure of an agonist-bound human A_{2A} adenosine receptor. *Science* 332, 322–327. doi: 10.1126/science.1202793

Yin, H., and Flynn, A. D. (2016). Drugging membrane protein interactions. *Annu. Rev. Biomed. Eng.* 18, 51–76. doi: 10.1146/annurev-bioeng-092115-025322

Yu, D. M., Slaitini, L., Gysbers, V., Riekhoff, A. G., Kähne, T., Knott, H. M., et al. (2011). Soluble CD26/dipeptidyl peptidase IV enhances human lymphocyte proliferation *in vitro* independent of dipeptidyl peptidase enzyme activity and adenosine deaminase binding. *Scand. J. Immunol.* 73, 102–111. doi: 10.1111/j.1365-3083.2010.02488.x

Yu, D. M., Wang, X. M., McCaughan, G. W., and Gorrell, M. D. (2006). Extraenzymatic functions of the dipeptidyl peptidase IV-related proteins DP8 and DP9 in cell adhesion, migration and apoptosis. *FEBS J.* 273, 2447–2460. doi: 10.1111/j.1742-4658.2006.05253.x

Zavialov, A. V., and Engström, A. (2005). Human ADA2 belongs to a new family of growth factors with adenosine deaminase activity. *Biochem. J.* 391, 51–57. doi: 10.1042/BJ20050683

Zavialov, A. V., Yu, X., Spillmann, D., Lauvau, G., and Zavialov, A. V. (2010). Structural basis for the growth factor activity of human adenosine deaminase ADA2. *J. Biol. Chem.* 285, 12367–12377. doi: 10.1074/jbc.M109.083527

Zhang, Y., and Wang, H. (2012). Integrin signalling and function in immune cells. *Immunology* 135, 268–275. doi: 10.1111/j.1365-2567.2011.03549.x

Zhong, J., Gong, Q., Goud, A., Srinivasamaharaj, S., and Rajagopalan, S. (2015a). Recent advances in dipeptidyl-peptidase-4 inhibition therapy: lessons from the bench and clinical trials. *J. Diabetes Res.* 2015:606031. doi: 10.1155/2015/606031

Zhong, J., Maiseyeu, A., Davis, S. N., and Rajagopalan, S. (2015b). DPP4 in cardiometabolic disease: recent insights from the laboratory and clinical trials of DPP4 inhibition. *Circ. Res.* 116, 1491–1504. doi: 10.1161/CIRCRESAHA.116.305665

Conflict of Interest Statement: The authors declare that the research was conducted in the absence of any commercial or financial relationships that could be construed as a potential conflict of interest.

frontiers in Pharmacology

REVIEW
published: 06 February 2018
doi: 10.3389/fphar.2018.00052

The P2X7 Receptor in Inflammatory Diseases: Angel or Demon?

*Luiz E. B. Savio[1], Paola de Andrade Mello[2], Cleide Gonçalves da Silva[3] and Robson Coutinho-Silva[1]**

[1] Laboratory of Immunophysiology, Biophysics Institute Carlos Chagas Filho, Federal University of Rio de Janeiro, Rio de Janeiro, Brazil, [2] Division of Gastroenterology, Department of Medicine, Beth Israel Deaconess Medical Center, Harvard Medical School, Harvard University, Boston, MA, United States, [3] Division of Vascular Surgery, Department of Surgery, Center for Vascular Biology Research, Beth Israel Deaconess Medical Center, Harvard Medical School, Boston, MA, United States

Under physiological conditions, adenosine triphosphate (ATP) is present at low levels in the extracellular milieu, being massively released by stressed or dying cells. Once outside the cells, ATP and related nucleotides/nucleoside generated by ectonucleotidases mediate a high evolutionary conserved signaling system: the purinergic signaling, which is involved in a variety of pathological conditions, including inflammatory diseases. Extracellular ATP has been considered an endogenous adjuvant that can initiate inflammation by acting as a danger signal through the activation of purinergic type 2 receptors—P2 receptors (P2Y G-protein coupled receptors and P2X ligand-gated ion channels). Among the P2 receptors, the P2X7 receptor is the most extensively studied from an immunological perspective, being involved in both innate and adaptive immune responses. P2X7 receptor activation induces large-scale ATP release via its intrinsic ability to form a membrane pore or in association with pannexin hemichannels, boosting purinergic signaling. ATP acting via P2X7 receptor is the second signal to the inflammasome activation, inducing both maturation and release of pro-inflammatory cytokines, such as IL-1β and IL-18, and the production of reactive nitrogen and oxygen species. Furthermore, the P2X7 receptor is involved in caspases activation, as well as in apoptosis induction. During adaptive immune response, P2X7 receptor modulates the balance between the generation of T helper type 17 (Th17) and T regulatory (Treg) lymphocytes. Therefore, this receptor is involved in several inflammatory pathological conditions. In infectious diseases and cancer, P2X7 receptor can have different and contrasting effects, being an angel or a demon depending on its level of activation, cell studied, type of pathogen, and severity of infection. In neuroinflammatory and neurodegenerative diseases, P2X7 upregulation and function appears to contribute to disease progression. In this review, we deeply discuss P2X7 receptor dual function and its pharmacological modulation in the context of different pathologies, and we also highlight the P2X7 receptor as a potential target to treat inflammatory related diseases.

Keywords: purinergic signaling, extracellular ATP, inflammation, macrophages, lymphocytes, neurodegenerative diseases, inflammatory disease, sepsis

OPEN ACCESS

Edited by:
Francisco Ciruela, University of Barcelona, Spain

Reviewed by:
Talia H. Swartz, Icahn School of Medicine at Mount Sinai, United States
Elena Adinolfi, University of Ferrara, Italy

****Correspondence:***
Robson Coutinho-Silva
rcsilva@biof.ufrj.br

Specialty section:
This article was submitted to Experimental Pharmacology and Drug Discovery, a section of the journal Frontiers in Pharmacology

Received: *31 October 2017*
Accepted: *15 January 2018*
Published: *06 February 2018*

Citation:
Savio LEB, de Andrade Mello P, da Silva CG and Coutinho-Silva R (2018) The P2X7 Receptor in Inflammatory Diseases: Angel or Demon? Front. Pharmacol. 9:52. doi: 10.3389/fphar.2018.00052

INTRODUCTION

Adenosine triphosphate (ATP) has long been known as the intracellular energy currency molecule of the cell. Under physiological conditions, extracellular ATP (eATP) is present at low levels (nanomolar range). However, this phosphate compound can be released by stressed, injured, or dying cells, reaching high concentrations (hundred micromolar) in the extracellular milieu (Pellegatti et al., 2008; Wilhelm et al., 2010). Once outside the cells, ATP and its metabolites (ADP, AMP, and adenosine) generated by the action of ecto-enzymes—named ectonucleotidases—mediate a high evolutionary conserved signaling system: the Purinergic Signaling (Burnstock and Verkhratsky, 2009; Verkhratsky and Burnstock, 2014).

Purinergic Signaling was first reported in the 1920s by Drury and Szent-Gyorgyi, when the effects of adenine compounds in the circulatory system of mammals were described (Drury and Szent-Gyorgyi, 1929). In the 1950s, studies showed that ATP was released from sensory nerves (Holton and Holton, 1954; Holton, 1959), but only in the 1970s, adenine compounds were recognized as signaling molecules thanks to Geoffrey Burnstock's studies (Burnstock et al., 1970, 1972; Burnstock, 1972). Interestingly, the first article reporting the effects of eATP in immune cells also dates back to the 1970s (Dahlquist and Diamant, 1970). In their paper, Dahlquist and Diamant (1970) described that eATP induces histamine release from mast cells. Further studies involving these same cells have led to the discovery of a specific receptor for eATP, later identified as the P2X7 receptor subtype (Cockcroft and Gomperts, 1980). Since then, especially in the last three decades, eATP-P2X7 receptor signaling has become one of the most studied pathways in infectious and inflammatory diseases.

P2X7 receptor is a ligand-gated ion channel belonging to the purinergic type 2 receptor family (P2). P2 receptor family comprises the P2Y G protein–coupled receptors ($P2Y_{1,2,4,6,11-14}$) and P2X receptors (P2X1–7), which are ligand-gated ion channels (Ralevic and Burnstock, 1998; Abbracchio et al., 2006). P2X7 is the most extensively studied receptor subtype from an immunological perspective. Its sustained stimulation by millimolar concentrations of eATP, triggers non-selective pore formation, which allows the passage of molecules of up to 900 Da, Na^+ and Ca^{2+} influx and K^+ efflux resulting in changes in the ionic homeostasis of the cell (Coutinho-Silva and Persechini, 1997). In addition, P2X7 receptor can initiate the release of large-scale intracellular ATP via its intrinsic pore formation ability or in association with pannexin hemichannels, therefore boosting purinergic signaling and inflammation (Pelegrin and Surprenant, 2006).

Several other functions have been attributed to P2X7 receptor in innate and adaptive immune responses. It is widely expressed by different immune cells including monocytes, macrophages, neutrophils, lymphocytes, mast cells, among others (reviewed in Lenertz et al., 2011; Jacob et al., 2013; Idzko et al., 2014; Morandini et al., 2014b). During innate immune response, damage-associated molecular patterns (DAMPs) or pathogen-associated molecular pattern (PAMPs) activate pattern recognition receptors (PRRs) (i.e., Toll-like receptors—TLRs) inducing ATP release, which in turn can activate P2X7 receptor (Cohen et al., 2013). In addition, TLR-mediated NF-κB pathway activation act as the first signal promoting the transcription of several genes encoding inflammatory mediators including pro-IL-1β and inflammasome components, such as NLRP3 and ASC. P2X7 receptor stimulation represents the second signal to inflammasome activation by triggering K^+ efflux, inflammasome assembly, and subsequent caspase-1 activation. The later, in turn, processes pro-IL-1β to its mature form which is able to be released then (Ferrari et al., 1997, 2006; Qu et al., 2007; Ting et al., 2008; Di Virgilio et al., 2017). P2X7 receptor also promotes IL-6 release in a Ca^{2+}-dependent mechanism (Shieh et al., 2014). Moreover, P2X7 receptor stimulates the production of free radicals (Cruz et al., 2007; Hewinson and Mackenzie, 2007; Hung et al., 2013) and it is involved in the activation of caspases and phospholipases (Coutinho-Silva et al., 2003b; Kahlenberg et al., 2005; Costa-Junior et al., 2011), as well as in cell cycle regulation and apoptosis (Coutinho-Silva et al., 1999; Bianco et al., 2006). P2X7 receptor also modulates intracellular signaling pathways, such as MyD88/NF-κB, PI3K/Akt/mTOR, and the activation of mitogen-activated protein kinase (MAPK) pathway proteins (MEK, ERK 1/2) (Bradford and Soltoff, 2002; Skaper et al., 2010; Liu et al., 2011; Bian et al., 2013; Savio et al., 2017a).

During adaptive immune response, P2X7 receptor is directly involved in T cell activation. Indeed, ATP-P2X7 receptor signaling is required for TCR-mediated calcium influx and IL-2 production. The blockading of P2X7 receptor-mediated calcium influx inhibited T cell activation (Yip et al., 2009). Moreover, P2X7 receptor modulates the balance between the generation of T helper type 17 (Th17) and T regulatory (Treg) lymphocytes (Schenk et al., 2011; Cekic and Linden, 2016). ATP-P2X7 receptor signaling decreases the suppressive activity and viability of Treg cells and favors the polarization of T cells into Th17 cells (Schenk et al., 2011). In addition, P2X7 receptor's blockade facilitates the conversion of naive $CD4^+$ T cells into Treg cells (Schenk et al., 2011).

Taking into account its crucial role in immune response, it is expected that an imbalance in P2X7 receptor activation may favor several pathological conditions including infectious, inflammatory, and neurodegenerative diseases, as well as cancer. Up until now, several studies have pointed different and contrasting effects for P2X7 receptor, whose activation may be able to either potentiate or ameliorate disease progression. In this review, we discuss P2X7 receptor's dual function and its pharmacological modulation in the context of different pathologies, as well as highlight its potential use as a therapeutic target for the treatment of inflammatory related diseases.

P2X7 RECEPTOR AGONISTS, ANTAGONISTS, AND KNOCKOUT MICE—IMPORTANT CONSIDERATIONS

To date, no specific agonist for P2X7 receptor has been described (De Marchi et al., 2016). The endogenous P2X7 receptor ligand, eATP itself, has distinct effects on P2X7 activation depending

on its concentration at the active site (Steinberg and Silverstein, 1987; Virginio et al., 1999; Hibell et al., 2000). As a rule, high eATP concentrations (in the millimolar range—EC50≥ 100 μM) are required to activate P2X7 receptor (Surprenant et al., 1996; Bianchi et al., 1999; Donnelly-Roberts et al., 2009). While high micromolar levels of ATP stimulates P2X7 receptor to form a cation-selective channel, prolonged exposure to millimolar levels trigger a nonselective large cytolytic pore conformation, allowing the passage of 900 Da molecules through the plasma membrane (Steinberg and Silverstein, 1987; Virginio et al., 1999; North, 2002). eATP is readily metabolized by extracellular ectonucleotidases, dropping initially high eATP levels to much lower levels (nanomolar to low micromolar), wherein it can activate other P2X subtypes (De Marchi et al., 2016). In this context, the non-hydrolyzable derivative ATP substrate, ATPγS, is a better alternative for studies involving P2 receptor activation. The benzoyl ester of ATP, BzATP, is far the most potent P2X7 agonist available, being ∼10–30 times more potent than ATP—with a low micromolar EC50 for the human receptor (Surprenant et al., 1996; Bianchi et al., 1999). However, it can also activate other P2X subtypes (such as P2X1 and P2X3) and it is metabolized to other adenine derivatives (De Marchi et al., 2016). Besides lack of specificity, differences in agonist potency across mammalian species are also an aggravating factor for studies involving P2X7 receptor (Hibell et al., 2000).

Several molecules have been developed to block P2X7 receptor activity (De Marchi et al., 2016). They can be subdivided into orthosteric ligands—binding the receptor within the ATP-binding cavity—and allosteric ligands—binding the receptor at sites, other than the ATP-binding cavity, and decreasing the effect of the endogenous ligand ATP (De Marchi et al., 2016). The first group is represented by suramin or suramin-like derivatives, ATP derivatives (TNP-ATP, periodate-oxidized ATP [oATP]), tetrazole derivatives (A438079, A839977), and cyanoguanidine derivatives (A740003, A804598) (De Marchi et al., 2016). Among them, tetrazole and cyanoguanidine derivatives present the highest potency and selectivity for P2X7 receptor vs. other P2X and P2Y receptors (Honore et al., 2006; Nelson et al., 2006; Carroll et al., 2007; Donnelly-Roberts et al., 2009; Adinolfi et al., 2015; Amoroso et al., 2015). Their IC50 values vary according to the compound and the mammalian species: A438079 IC50 is 0.13 and 0.32 μM at the human and rat P2X7 receptors (Nelson et al., 2006; Donnelly-Roberts et al., 2009), A839977 IC50 is 0.02–0.150 μM at recombinant human, rat, and mouse P2X7 receptors (Florjancic et al., 2008; Honore et al., 2009; Friedle et al., 2010), A740003 IC50 is 0.040 and 0.020 μM at human and rat P2X7 receptor (Honore et al., 2006; Adinolfi et al., 2015; Amoroso et al., 2015), and A804598 IC50 is 0.0109, 0.0099, and 0.0089 μM at the human, rat, and mouse P2X7 receptors, respectively (Donnelly-Roberts et al., 2009). Unlike the tetrazole and cyanoguanidine derivatives, ATP derivatives (TNP-ATP and oATP) are potent P2X7 receptor antagonist at high micromolar levels and can interact with other P2X receptors (Di Virgilio, 2003; De Marchi et al., 2016). Moreover, besides being an irreversible P2X7 antagonist (Easterbrook-Smith et al., 1976), oATP itself appears to exert anti-inflammatory effects, modulating the immune response independently of P2X7 blockage (Beigi et al., 2003; Di Virgilio, 2003; Figliuolo et al., 2014). In this way, experiments using oATP to evaluate P2X7 role in inflammatory diseases should be carefully analyzed.

The second group of P2X7 blocking molecules is represented by a class of synthetic negative allosteric modulators such as Brilliant Blue G (BBG), AZD9056, KN-62, AZ-11645373, AZ-10606120, GW791343, GSK314181A, GSK1482160, CE-224,535, AFC-5128, JNJ-479655, and EVT-401 (Guile et al., 2009; Friedle et al., 2010; Kaczmarek-Hájek et al., 2012; Alves et al., 2013; North and Jarvis, 2013; Mehta et al., 2014). Even though these compounds present nanomolar/micromolar potency at the P2X7 receptor, they can still interact with other P2X receptors' allosteric binding sites. For example, BBG have been widely used as a selective antagonist for P2X7 receptor, but it can also block P2X1, P2X4, and sodium channels (Jiang et al., 2000; Seyffert et al., 2004; Jo and Bean, 2011). Therefore, divergent and unexpected results found in P2X7 receptor studies might be attributed to different experimental settings where diverse agonist/antagonist drugs with different affinity and specificity were used and hence should be critically analyzed.

Regarding P2X7 receptor knockout (P2X7 KO) mice, at least two strains are currently commercially available. One, generated by GlaxoSmithKline, in which the *lacZ* gene and neomycin cassette (Neo) were inserted into exon 1, and the second, from Pfizer (commercially available from The Jackson Laboratory), which has a Neo insertion in exon 13—exon coding for the long C–terminal cytoplasmic tail (Sikora et al., 1999; Solle et al., 2001). However, the identification of P2X7 splice variants revealed that both knockout mice express P2X7 receptor on T cells, whereas DCs, macrophages, and neurons do not (Taylor et al., 2009; Masin et al., 2012). Although both P2X7 KO mice express P2X7 receptor on T cells, only P2X7 KO mice from GlaxoSmithKline have a functional P2X7 receptor in these cells (Taylor et al., 2009). T cells obtained from Pfizer P2X7 KO mice did not respond to BzATP stimulation, while lymphocytes from GlaxoSmithKline P2X7 KO mice showed high levels of P2X7 activity in comparison to wild type (WT) mice (Taylor et al., 2009).

Taken together, these reports indicate that studies using GlaxoSmithKline KO mice for evaluating P2X7 receptor relevance in an immunological context should be carefully analyzed considering the tissue specific expression of a functional P2X7 protein in T cells.

P2X7 RECEPTOR IN INFECTIOUS DISEASES—ANGEL OR DEMON DEPENDING ON THE TYPE OF PATHOGEN, VIRULENCE, AND SEVERITY OF INFECTION

In response to viral, bacterial, fungal, and protozoa infection, ATP is released from immune and non-immune cells. Subsequent activation of the ATP-gated P2X7 receptor has been implicated in the pathophysiology of several infectious diseases through modulation of innate and adaptive immune responses (Coutinho-Silva and Ojcius, 2012; Morandini et al., 2014b; Savio and Coutinho-Silva, 2016; Di Virgilio et al., 2017). Interestingly, P2X7 receptor activation can generate both beneficial and deleterious effects depending on the type of

pathogen, virulence, and severity of infection (**Figure 1**). In the next sections, both positive and negative effects of P2X7 receptor activation are discussed. In addition, the effects of P2X7 receptor pharmacological inhibition or genetic deletion in infectious disease are summarized in **Table 1**.

P2X7 Receptor in Viral Infections

Host macrophages and L929 cells secrete ATP by exocytosis and/or pannexin channels in response to viral infections (Zhang et al., 2017). Extracellular ATP, acting via P2X7 receptor, regulates immune responses against several types of viruses. ATP-P2X7 signaling decreases viral replication and consequently protects bone marrow-derived macrophages (BMDM), macrophage cells line RAW 264.7, and HEK 293T cells from cell death mediated by vesicular stomatitis virus (VSV) infection *in vitro*. This happens by inducing IFN-β secretion via activation of P38/JNK/ATF-2 signaling pathways (Zhang et al., 2017). *In vivo*, ATP treatment reduces viral replication and improves survival of VSV-infected

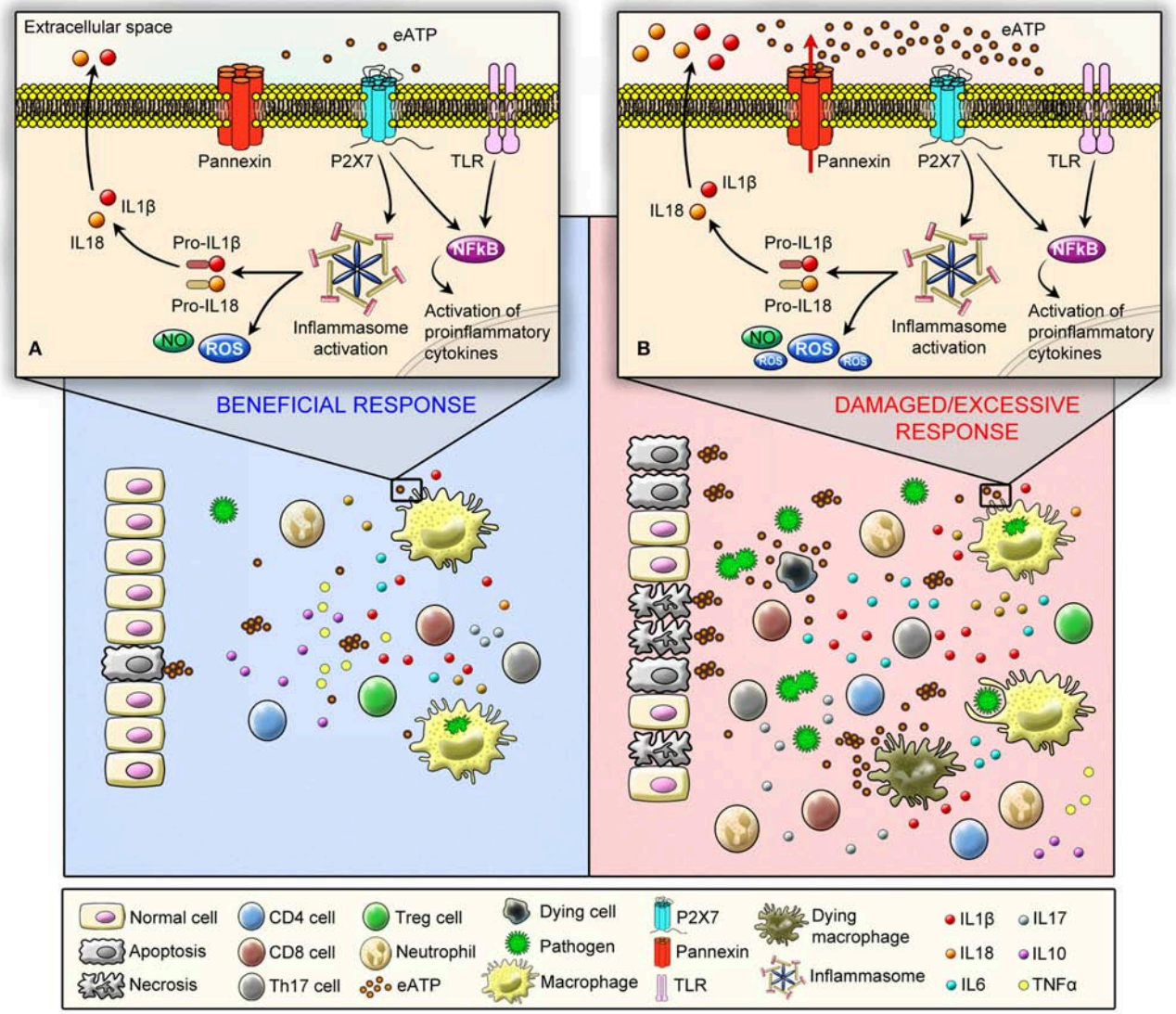

FIGURE 1 | Schematic illustration showing P2X7 receptor protective (angel) and deleterious (demon) effects in immune responses against pathogens. The recognition of pathogen-associated molecular pattern (PAMPs) by Pattern Recognition Receptors (PRRs) can induce ATP release, which activates P2X7 receptor. As a consequence, P2X7 receptor activation induces ATP release—chiefly via pannexin hemichannels—boosting inflammation. **(A)** At a molecular level (upper panel) P2X7 receptor beneficial effects are mediated by the stimulation of microbicidal mechanisms and production of inflammatory mediators in phagocytic cells, such as ROS, NO, and interleukins. P2X7 receptor acts as a second signal for NLRP3 inflammasome activation and IL-1β release. In addition, at a cellular level (low panel) P2X7 receptor is involved in the activation of effector T cells, and it favors the polarization of T cells into Th17 cells and decreases the suppressive activity and viability of Tregs. **(B)** On the other hand, P2X7 can act as a demon depending on the type of pathogen, virulence, and severity of infection by inducing an excessive production and release of inflammatory mediators (upper panel) coupled to a high incidence of apoptotic and necrotic cell death due the release of large amounts of ATP (low panel), which results in sustained P2X7 receptor activation, leading to a self-sustained pro-inflammatory deleterious cycle.

TABLE 1 | Protective or deleterious effects of P2X7 receptor pharmacological inhibition or genetic deletion in infectious disease.

Pathogen or PAMP	Pharmacological inhibitor or genetic deletion	Effect	Inflammatory mediator or immune cell involved	References
VIRAL INFECTIONS				
Vesicular stomatitis virus	P2X7 KO mice	Deleterious	↓IFN-β ↑viral replication	Zhang et al., 2017
Adenoviral vectors	oATP, A438079, P2X7 KO mice	Protective	↓IL-1β, IL-6, NO, and neutrophil infiltration	Lee et al., 2012
Influenza virus	P2X7 KO mice	Protective	↓INF-γ, TNF-α, IL-6, and neutrophil infiltration	Leyva-Grado et al., 2017
HIV viral proteins in brain cells	oATP, A438079, BBG, suramin	Protective	↓ NF-κB activation, TNF-α, IL-1β, ROS, NO, MCP-1, and neuronal damage	Tewari et al., 2015; Chen et al., 2016
HIV	PPADS, suramin	Protective	↓ HIV-1 fusion $CD4^+$ cells	Swartz et al., 2014
HIV	oATP, A740003, BBG, and suramin	Protective	↓ HIV replication in macrophages	Hazleton et al., 2012
BACTERIAL INFECTIONS				
C. trachomatis	P2X7 KO mice	Deleterious	↓IL-1β ↑ bacterial burden	Darville et al., 2007
P. gingivalis	P2X7 KO mice	Deleterious	↓IFN-γ, IL-17	Ramos-Junior et al., 2015
M. tuberculosis				
• H37RV	P2X7 KO mice	Deleterious	↑ Treg ↑ bacterial burden	Santos et al., 2013
• Beijing 1471 or MP287/03	P2X7 KO mice	Protective	↓IL-1β and INF-γ ↓ bacterial burden	Amaral et al., 2014
M. bovis	P2X7 KO mice	Protective	↓immature-like myeloid cells ↓ bacterial burden	Bomfim et al., 2017
Sepsis				
• Endotoxic shock (LPS)	P2X7 KO mice	Protective	↑ survival ↓cytotoxicity	Yang et al., 2015
• CLP model	A438079, P2X7 KO mice	Protective	↓IL-1β, CXCL1 and CX3CL1 ↑ survival	Wang et al., 2015a
• CLP model	A740003	Protective	↓ p-NF-κB, IL-1β, IL-6,	Wu et al., 2017a
• CLP model	P2X7 KO mice, BBG	Protective	↓p-NF-κB, IL-1β, IL-6, NO, ALT, and neutrophil infiltration ↑ survival	Santana et al., 2015 Savio et al., 2017a Savio et al., 2017b
• CLP model	P2X7 KO mice, oATP	Deleterious	↑ IL-1β, IL-6, TNF-α and bacterial burden ↓ survival	Csóka et al., 2015a
FUNGAL INFECTIONS				
C. albicans	KN-62	Deleterious	↓DC activation, PGE2	Xu et al., 2016
P. brasiliensis	P2X7 KO mice	Deleterious	↓Th17/Th1 response ↑ fungal burden	Feriotti et al., 2017
PROTOZOA INFECTIONS				
L. amazonensis	P2X7 KO mice, A740003	Deleterious	↓ IL-1β and LTB4	Chaves et al., 2014
L. amazonensis	P2X7 KO mice	Deleterious	↑IFN-γ ↓ IL-17, IL-12, and TGF-β ↑parasitic load	Figliuolo et al., 2017a
T. gondii	P2X7 KO mice	Deleterious	↓TNF-α ↓survival	Miller et al., 2011
T. gondii	P2X7 KO mice	Deleterious	↓IFN-γ, TNF-α, IL-6,$CD4^+$ cells ↑parasitic load	Huang et al., 2017

(Continued)

TABLE 1 | Continued

Pathogen or PAMP	Pharmacological inhibitor or genetic deletion	Effect	Inflammatory mediator or immune cell involved	References
T. gondii	P2X7 KO mice	Deleterious	↓ IL-1β, IL-12, TNF-α, and IFN-γ ↑parasitic load	Corrêa et al., 2017
T. gondii	P2X7 KO mice	Deleterious	↓ IL-1β and ROS ↑parasitic load	Moreira-Souza et al., 2017
T. cruzi	P2X7 KO mice	Deleterious	↑ mast cells	Meuser-Batista et al., 2011
P. chabaudi	P2X7 KO mice	Deleterious	↓Th1 response	Salles et al., 2017
E. histolytica	oATP, KN-62	Deleterious	↓ IL-1β	Mortimer et al., 2015
HELMINTH INFECTIONS				
H. polygyrus	BBG	Deleterious	↓Mast cell activation ↓IL-13	Shimokawa et al., 2017
S. mansoni	P2X7 KO	Deleterious	↑TGF-β1 ↓ survival	Oliveira et al., 2014

WT mice. This antiviral effect is not observed in P2X7 KO mice (Zhang et al., 2017). Additionally, activation of P2X7 receptor is crucial to control infection of human monocytes by dengue virus-2 (Corrêa et al., 2016). Those findings suggest an important role for this receptor in restraining viral replication and infection. On the other hand, P2X7 receptor activation boosts inflammation and potentially contributes to an exacerbated immune response, depending on the virulence and severity of the infection. In this context, Lee et al. (2012) showed that genetic deletion or pharmacological inhibition of P2X7 receptor improves survival in a mouse model of acute respiratory distress syndrome induced by intranasal administration of replication deficient adenoviral vectors. Improved outcome observed in these settings correlated with decreased production of inflammatory mediators (i.e., IL-1β and IL-6) and reduced neutrophil infiltration (Lee et al., 2012). Similar results were observed in P2X7 KO mice infected with a lethal dose of influenza virus (Leyva-Grado et al., 2017).

A role for extracellular ATP and P2X7 receptor in human immunodeficiency virus (HIV) infection has also been reported (Barat et al., 2008; Swartz et al., 2014, 2015; Graziano et al., 2015). Broad-spectrum P2 receptor antagonists, such as PPADS and suramin, significantly inhibit HIV-1 membrane fusion in $CD4^+$ cells (Swartz et al., 2014, 2015). In addition, P2X7 inhibitors oATP, A740003, BBG, and suramin decrease HIV replication in human macrophages (Hazleton et al., 2012). Graziano et al. (2015) showed that ATP induces the release of HIV-1 virions derived from virus containing compartments (subcellular vacuoles), present in monocyte-derived macrophages. P2X7 receptor blockade with A438079 prevented eATP-induced release of virions from monocyte-derived macrophages and D-U1 cells, a chronically HIV-1infected promonocytic cell line. Imipramine, an inhibitor of ceramide formation, also blocked virions release from these cells, suggesting that P2X7 activation stimulates ceramide production, thus favoring the formation of exosomes containing HIV-1 virions. Therefore, targeting P2X7 receptor might be a suitable therapeutic strategy to eliminate HIV-1 reservoirs in individuals receiving combination antiretroviral therapy (cART) (Graziano et al., 2015).

Evidence supporting the involvement of P2X7 receptor in the deleterious effects caused by HIV-1 infection in the central nervous system (CNS) has also been described (Swartz et al., 2015). After primary infection, HIV virus invades the CNS, resulting in neuroinflammation and neurodegeneration. Viral proteins and inflammatory factors produced during the immune response against HIV induce blood-brain barrier (BBB) dysfunction and activate glial cells. BBB dysfunction facilitates transmigration of infected monocytes and $CD4^+$ T cells, further propagating infection and inflammation within the CNS. The HIV viral protein called transactivator of transcription (Tat) is described as an important neurotoxin detected in the CNS of HIV-1 infected subjects and it is responsible for triggering P2X7 receptor overexpression in human astrocytes and to promote neuroinflammation (Tewari et al., 2015). Tat enhances the expression of monocyte chemoattractant protein 1 (MCP-1) in human astrocytes in a P2X7-dependent manner (Tewari et al., 2015). In addition, the glycoprotein gp120 (gp120)—an HIV envelope glycoprotein—increases P2X7 receptor expression in BV2 microglia cells (Chen et al., 2016) and in hippocampus of rats (Liu et al., 2017). Pretreatment with BBG has prevented NF-κB activation and production of inflammatory mediators induced by gp120 in BV2 cells (Chen et al., 2016), suggesting a key role for P2X7 receptor in HIV-induced glial cells activation and brain damage.

These findings support the contribution of P2X7 receptor in viral infections promoting protective and deleterious effects depending on viral strain and severity of the infection, which makes the use of P2X7 receptor pharmacological blockers or activators a challenging task on these settings.

P2X7 Receptor in Bacterial Infections

In the 90's, Humphreys and Dubyak (1996) published one of the first reports describing the enhancement of P2X7 receptor-mediated cell responses, such as membrane permeability and Ca^{2+} influx, in response to lipopolysaccharide (LPS). Currently, it is well-documented that TLRs activation by bacterial products, such as LPS, induces ATP release from immune cells, modulating inflammatory responses (Coutinho-Silva and Ojcius, 2012; Cohen et al., 2013; Morandini et al., 2014b; Di Virgilio et al., 2017). The role of P2X7 receptor in activation of microbicidal mechanisms and production of inflammatory mediators in phagocytic cells, as well as modulation of adaptive immune responses to bacterial infection, have been extensively studied (Coutinho-Silva and Ojcius, 2012; Morandini et al., 2014b; Di Virgilio et al., 2017). In this section, we highlight the role of this purinergic receptor in some important bacterial diseases, including Chlamydia disease, Tuberculosis, Periodontitis, and in bacterial Sepsis.

Chlamydiae Infections

Chlamydiae are obligatory intracellular pathogenic bacteria that infect epithelial cells and macrophages. Chlamydiae can evade host defense mechanisms mainly by inhibiting phagosome–lysosome fusion and acidification (Herweg and Rudel, 2016; Pettengill et al., 2016). Interestingly, ATP, acting through P2X7 receptor, decreases bacterial load in macrophages and epithelial cells infected with different Chlamydia species and strains (Coutinho-Silva et al., 2001b, 2003b; Darville et al., 2007) by overriding Chlamydiae's evasion mechanisms. P2X7 receptor activation in Chlamydia-infected macrophages induces phospholipase D activation, intracellular Ca^{+2} mobilization, and subsequent phagolysosome formation and acidification (Coutinho-Silva et al., 2003b). P2X7 genetic deletion increased inflammation in the endocervix, oviduct, and mesosalpingeal tissues in a model of Chlamydia vaginal infection, making P2X7 KO mice more susceptible to infection than wild-type mice (Darville et al., 2007). In addition, P2X7 receptor is important for NLRP3 inflammasome activation and IL-1β secretion, which contributes to an efficient immune response against Chlamydiae infections (Abdul-Sater et al., 2010; He et al., 2010; Shimada et al., 2011; Nagarajan et al., 2012). Therefore, these reports suggest a role for P2X7 receptor in the control of Chlamydiae infections by increasing the microbicidal mechanisms in infected cells and the immune response against these bacteria.

Porphyromonas gingivalis Infection

The importance of P2X7 receptor in the immune response against bacteria involved in the pathogenesis of periodontitis, such as *Porphyromonas gingivalis*, has been explored over the last decade (reviewed in Almeida-da-Silva et al., 2016). *P. gingivalis* is an intracellular bacteria member of the polymicrobial dental biofilm community, which is involved in the pathogenesis of periodontitis. *P. gingivalis* infection induces ATP secretion from macrophage-derived THP-1 cells. Released ATP, in turn, activates P2X7 receptor, which is crucial for K^+ efflux and NLRP3 inflammasome activation, inducing IL-1β secretion and pyroptotic cell death (Park et al., 2014). P2X7/P2X4 receptors are also required for ROS-mediated NLRP3 inflammasome formation and IL-1β secretion in *P. gingivalis*-infected gingival epithelial cells (Choi et al., 2013; Hung et al., 2013).

However, *P. gingivalis* has an ATP-consuming enzyme called nucleoside diphosphate kinase (NDK), a strategy to subvert these microbicidal mechanisms triggered by P2X7 receptor activation. When secreted, NDK metabolizes eATP, inhibiting ATP/P2X7 receptor-mediated ROS production and apoptosis of gingival epithelial cells (Yilmaz et al., 2008; Choi et al., 2013). Moreover, *P. gingivalis* fimbriae impair P2X7-dependent IL-1β secretion in murine macrophages (Morandini et al., 2014a).

Finally, Ramos-Junior et al. (2015) showed the importance of this receptor for the adaptive immune response during *P. gingivalis* infection by using P2X7 receptor deficient mice. Draining lymph node cells from P2X7 KO mice produced less IL-17 and IFN-γ compared to cells from WT-infected mice (Ramos-Junior et al., 2015). Therefore, P2X7 receptor seems to be a potential target for the development of new strategies to treat periodontitis. Additional detailed information regarding the role of P2X7 receptor and inflammasomes in *P. gingivalis* can be found in a recent review (Almeida-da-Silva et al., 2016).

Mycobacterial Infections

P2X7 receptor expression increases in peripheral blood mononuclear cells from patients with tuberculosis (Franco-Martínez et al., 2006). Also, P2X7 receptor's loss-of-function polymorphisms have been linked to an increased susceptibility to pulmonary (Sharma et al., 2010; Areeshi et al., 2015; Wu et al., 2015; Shamsi et al., 2016) and extra-pulmonary tuberculosis (Fernando et al., 2007; Sharma et al., 2010; Ben-Selma et al., 2011; Singla et al., 2012). This elevated susceptibility was correlated with an impaired capacity of macrophages to eliminate the bacillus (Fernando et al., 2007).

Molloy et al. (1994) showed for the first time that eATP is able to induce mycobacterial killing in infected human monocytes. Several subsequent studies described that eATP, acting via P2X7 receptor, induces mycobacterial killing in infected macrophages by mechanisms which are dependent on phospholipase D activation and apoptosis of infected cells (Kusner and Adams, 2000; Fairbairn et al., 2001; Placido et al., 2006). Interestingly, *in vivo* studies have shown that the susceptibility of P2X7 KO mice to mycobacterium infection depends on the strains, virulence and severity of the infection. Santos et al. (2013) reported that P2X7 deficient mice were more susceptible to mycobacterium infection when exposed to a high dose of the common laboratory strain H37Rv. On the other hand, P2X7 KO mice infected with hypervirulent strains (Beijing1471 or MP287/03) were less susceptible to infection than WT mice (Amaral et al., 2014).

The reduced susceptibility of P2X7 KO mice is verified because hypervirulent mycobacteria lead to macrophage death by necrosis in a P2X7 receptor-dependent manner increasing the bacillus release. So, the deleterious effects of P2X7 receptor observed in hypervirulent mycobacteria infection may be related to a vicious cycle where high eATP amounts are released by damaged cells, exacerbating inflammation, lung damage, and bacillus spreading (Amaral et al., 2014). Bomfim et al. (2017)

recently showed that bone marrow-derived cells expressing P2X7 receptor have a critical role in promoting progression of severe tuberculosis. Therefore, P2X7 receptor is a key player in the modulation of immune responses against mycobacterium infections presenting protective or deleterious effects depending on mycobacterial strains.

Bacterial Sepsis

Sepsis is the leading cause of death in intensive care units worldwide and represents a major public health issue. During this life-threatening condition, the body's unfettered inflammatory response to a pathogen, commonly bacteria, triggers a cascade of events, which culminate in death by multiple organ failure (Singer, 2016). Plasma ATP levels increase in sepsis, suggesting a possible role for this pro-inflammatory molecule in the development of excessive systemic inflammation, characteristic of the disease (Cauwels et al., 2014; Sumi et al., 2014). The potential role of ATP and purinergic signaling in the pathophysiology of sepsis has been explored in humans and different animal models over the last few years (Haskó et al., 2011; Vuaden et al., 2011; Cauwels et al., 2014; Sumi et al., 2014; Csóka et al., 2015a,b; Ledderose et al., 2016; Savio et al., 2017a).

Two putative genotypes composed of five functional P2X7 receptor single nucleotide polymorphisms (SNPs) have been identified in patients with sepsis (Geistlinger et al., 2012). In the sequence, P2X7 functionality tests in dendritic cells isolated from healthy individuals that carry the same SNPs previously identified in septic patients were performed. These tests revealed an improved P2X7 receptor functionality, characterizing those as gain-of-function SNPs with deleterious effects in sepsis (Geistlinger et al., 2012). Animal models support this assumption by demonstrating that P2X7 receptor contributes to the production of inflammatory cytokines and exacerbates inflammatory response in sepsis (Santana et al., 2015; Wang et al., 2015a; Yang et al., 2015; Savio et al., 2017a,b; Wu et al., 2017a). P2X7 receptor genetic deletion improved survival rate by 30% as compared to septic WT mice (Santana et al., 2015). Similarly, Wang et al. (2015a) reported that A438079-treated WT mice or P2X7 KO mice showed a significant reduction in the mortality rate (50%) in a sepsis model of cecal ligation puncture (CLP) surgery.

Moreover, systemic administration of BzATP increases inflammation, while the systemic blockade of P2X7 receptor with A740003 decreases levels of serum and intestinal mucosal pro-inflammatory cytokines after CLP (Wu et al., 2017a). The reduced inflammatory response in A740003-treated mice protects them against sepsis-induced intestinal barrier disruption (Wu et al., 2017a). BBG treatment has also been shown to improve outcomes in sepsis. We recently showed that BBG improves survival, reduces cytokine production, activation of inflammatory signaling pathways, and liver injury in CLP-induced sepsis (Savio et al., 2017a). Accordingly, BBG-treated mice showed significantly lower production of inflammatory mediators, such as IL-1β and TNF-α, as well as a tendency toward better survival rate after intravenously administration of a uropathogenic α-haemolysin producing *E. coli* strain (ARD6) (Greve et al., 2017).

Other studies suggest that P2X7 receptor activation might be protective in sepsis by enhancing macrophage's ability to kill bacteria, and increasing secretion of IgM by B1 cells lymphocytes (Proietti et al., 2014; Csóka et al., 2015a). Intriguingly, Csóka et al. (Csóka et al., 2015a) showed higher levels of inflammatory chemokines and cytokines and increased mortality rate in P2X7 KO mice after sepsis by CLP compared to WT mice. Csóka et al. (2015a) also demonstrated increased cytokine levels in septic mice treated with oATP (an irreversible non-specific P2X7 antagonist), conflicting with several reports conferring anti-inflammatory properties to oATP by inhibition of P2X7 receptor, and other inflammatory signaling pathways (i.e., MyD88/NF-kB) and cytokine production *in vitro* and in models of autoimmune disease (Beigi et al., 2003; Vergani et al., 2013a,b; Savio et al., 2017a).

As in Csòka's findings, Greve et al. (2017) also showed increased susceptibility of P2X7 KO mice from GlaxoSmithKline (Brentford, UK)—mice that express a functional P2X7 protein in T cells—to a severe model of sepsis, in which mice received a high dose (165 million) of ARD6 *E. coli* strain intravenously. However, no significant differences were observed in bacterial load and plasma TNF-α, keratinocyte chemoattractant (KC), IL-1β and IL-6 between P2X7 KO and WT mice, 2.5 h after injection of a high dose of ARD6. Surprisingly, increased levels of IL-1β and IL-6, but not KC and TNF-α were reported in P2X7 KO mice injected with a low dose (41 million) of ARD6. The authors propose that the higher production of IL-1β in P2X7 KO receptor mice occurs via a non-canonical caspase8-dependent mechanism (Greve et al., 2017).

Finally, opposing results regarding the P2X7 receptor in sepsis could be related to differences in the mice microbiome, bacterial virulence, and severity of the infection. Although the P2X7 receptor may be relevant to bacterial control, morbidity, and mortality in this complex disease are related to onset of shock and hemodynamic compromise with multiple organ dysfunction and failure due to the excessive, unfettered inflammation in response to a pathogen. Since studies in humans and animal models have shown that P2X7 receptor contributes to the exacerbated inflammatory response, the use of P2X7 receptor inhibitors in addition to the antibiotic therapy seems to be a promising therapeutic strategy for sepsis management.

P2X7 Receptor in Fungal Infections

A limited number of studies have explored the role of P2X7 receptor in fungal infections. Perez-Flores et al. (2016) reported that P2X7 receptor in J774 cells functions as a scavenger receptor for bacteria but not yeast. P2X7 receptor is not required for NLRP3 activation and IL-1β secretion during *Candida albicans* infection, an opportunistic fungal pathogen. *In vitro*, P2X7 KO and WT macrophages secreted similar levels of IL-1β in response to *C. albicans* infection (Hise et al., 2009).

On the other hand, Xu et al. (2016) showed that invariant natural killer T (iNKT) cells interact with DC and release ATP, which activates P2X7 receptor in DC. P2X7 receptor activation in DC induces secretion of prostaglandin E2 (PGE2) stimulating neutrophil recruitment and controlling *C. albicans* infection. P2X7 deficient mice were more susceptible to pulmonary

paracoccidioidomycosis, a disease caused by the dimorphic fungus *Paracoccidioides brasiliensis* (Feriotti et al., 2017). P2X7 receptor is crucial for the induction of an efficient Th1/Th17 immune response against *P. brasiliensis* in an NLRP3-dependent manner (Feriotti et al., 2017). Although P2X7 receptor may contribute to immune responses against certain fungal infections, further studies evaluating the relevance of pharmacological manipulation of P2X7 receptor in this field are necessary.

P2X7 Receptor in Protozoa Infections

Over the last decade, our laboratory has been exploring the role of P2X7 receptor in Leishmaniasis, a neglected tropical disease caused by a parasite of the genus Leishmania (Alvar et al., 2012). P2X7 receptor expression is upregulated in *Leishmania amazonensis*-infected macrophages and its activation reduces parasitic load in these cells (Chaves et al., 2009). Mechanistically, we demonstrated that activation of P2X7 receptor in infected macrophages reduces parasitic load via leukotriene B4 (LTB4) production (Chaves et al., 2009, 2014). Moreover, macrophage infection with *L. amazonensis* induced P2X7 receptor-mediated membrane permeabilization to anionic dye molecules, while it strongly decreased the uptake of cationic dyes (Marques-da-Silva et al., 2011). Interestingly, oATP affects parasite integrity and macrophage function by inhibiting the attachment/entrance of *L. amazonensis* promastigotes in a P2X7 receptor-independent manner (Figliuolo et al., 2014).

Recently, we showed that P2X7 receptor modulates the balance between inflammation and parasite control through a series of *in vivo* experiments where we infect P2X7 KO and WT mice with *L. amazonensis*. In a mouse model where subcutaneous *L. amazonensis* infection is induced by subcutaneous injection of the parasite in the footpad, genetic deletion of P2X7 receptor resulted in increased cell infiltration, higher IFN-γ levels, and low concentrations of IL-17 and TGF-β in the footpad, suggesting an excessive pro-inflammatory response. In addition to that, $CD4^+$ and $CD8^+$ T cells from infected P2X7 KO mice exhibited higher proliferative capacity than cells from infected WT mice (Figliuolo et al., 2017a). P2X7 KO mice were more susceptible to *L. amazonensis* infection showing increased lesion size and parasitic load (Figliuolo et al., 2017a). Increased susceptibility of P2X7 KO mice to *L. amazonensis* might be related to the role of P2X7 receptor in controlling T cell proliferation by inducing apoptosis. P2X7 KO mice showed an excessive $CD4^+$ T cell proliferation which has a pathogenic role in leishmaniasis (Figliuolo et al., 2017a). Thus, P2X7 receptor is crucial for the immune response during leishmaniasis by regulating both innate and adaptive immunity.

P2X7 receptor also plays a key role in the microbicidal mechanisms that control infection by *Toxoplasma gondii,* a protozoan parasite that infects most species of warm-blooded animals causing toxoplasmosis. P2X7 receptor activation in *T. gondii* infected macrophages mediates pathogen elimination through ROS production and acidification of the parasitophorous vacuole (Corrêa et al., 2010; Lees et al., 2010). Mechanistically, we recently showed that P2X7 receptor controls *T. gondii* infection *via* ROS generated from NADPH oxidase, while IL-1β stimulates mitochondrial ROS production (Moreira-Souza et al., 2017). In intestinal epithelial cells, P2X7 receptor induces production of cytokines and chemokines that contribute to host immune response against *T. gondii* infection (Huang et al., 2017). P2X7 KO mice showed increased susceptibility to toxoplasmosis characterized by an impaired production of pro-inflammatory cytokines (IL-1β, IL-12, TNF-α, and IFN-γ) and increased tissue damage and parasitic load (Miller et al., 2011, 2015; Corrêa et al., 2017; Huang et al., 2017). Accordingly, loss-of-function SNPs in the human P2X7 receptor gene have been directly associated with increased susceptibility to toxoplasmosis by generating less functional proteins (Jamieson et al., 2010). Therefore, P2X7 receptor functionality is crucial to mount an efficient immune response against *T. gondii* infection.

P2X7 receptor relevance in the pathophysiology of Chagas disease or American trypanosomiasis, a tropical disease caused by the parasite *Trypanosoma cruzi,* has also been explored. By mechanisms still unknown, this parasite potentiates P2X7 receptor sensitivity to ATP, increasing plasma membrane permeabilization, calcium signaling, and death of $CD4^+/CD8^+$ double positive thymocytes during the atrophy phase of disease in a murine model (Mantuano-Barradas et al., 2003). Nevertheless, experiments performed with P2X7 KO mice suggested that this receptor might not be critically involved in *T. cruzi*-mediated thymus atrophy (Cascabulho et al., 2008). On the other hand, P2X7 KO mice showed an increased migration of mast cells toward the inflamed heart, which may compromise the innate immune response against *T. cruzi* (Meuser-Batista et al., 2011). Importantly, P2X7 receptor expression and functionality is not altered in peripheral lymphocytes from patients with Chagas Disease (Souza et al., 2017).

The role of P2X7 receptor in Malaria, a blood disease caused by the plasmodium parasite transmitted by the Anopheles mosquito, has also been explored since plasmodium-infected erythrocytes release large amounts of ATP (Akkaya et al., 2009). Extracellular ATP increases Ca^{2+} levels in *P. falciparum* modulating parasite invasion. Interestingly, treatment with pam P2 inhibitor suramin or apyrase before infection significantly reduces invasion of red blood cells by *P. falciparum* (Levano-Garcia et al., 2010). Recently, we have shown that ATP released by rupture of infected erythrocytes activates P2X7 receptor in $CD4^+$ T inducing a Th1 immune response during blood-stage *Plasmodium chabaudi* malaria. P2X7 receptor deficient mice were more susceptible to plasmodium infection due to an impaired Th1 immune response (Salles et al., 2017). Therefore, P2X7 receptor is important for the development of an efficient immune response against plasmodium infection.

Finally, Mortimer et al. (2015) described that infection by *Entamoeba histolytica,* an extracellular human parasite that causes intestinal and extra-intestinal amebiasis, induces $\alpha_5\beta_1$ integrin activation and ATP release through pannexin-1 channels activating P2X7 receptor and, consequently, NLRP3 inflammasome in macrophages. These results highlight the role of ATP-P2X7-NLRP3 inflammasome axis in the inflammatory immune response during amebiasis.

Overall, these data support a role for ATP-P2X7 receptor in boosting the immune system against the protozoa infections. Nevertheless, peculiarities of each parasite infection

should be considered when developing pharmacological treatments targeting P2X7 receptor during protozoan infections.

P2X7 Receptor in Helminth Infections

Helminths are worm-like parasites that currently infect more than 1 billion people worldwide (Hotez et al., 2014). These worms usually induce a type 2 immune response, increasing susceptibility to infections by other lethal pathogen, being a serious socioeconomic problem in developing countries (Cortés et al., 2017).

P2X7 receptor has been implicated in the immune response against helminth parasites. Recently, Shimokawa et al. (2017) showed that P2X7 receptor activated by ATP released from intestinal epithelial cells induces the production of IL-33 by mast cells, which is crucial for induction of IL-13-producing group 2 innate lymphoid cells and clearance of helminth infections. In addition, soluble products derived from Trichuris *suis* (a type of helminth) downregulated P2X7 receptor expression in DC and macrophages. Co-stimulation of DC and macrophages with LPS and *T. suis* soluble products caused lower levels of IL-1β compared to LPS-primed cells, indicating a reduction in the activation state and inflammatory response of human macrophages (Ottow et al., 2014).

Purinergic signaling is also altered during Schistosomiasis, a chronic inflammatory disease caused by blood fluke worms belonging to the genus Schistosoma (Oliveira et al., 2013, 2014, 2016; Silva, 2016). P2X7 receptor functionality, as assessed by ATP-mediated Ca^{2+} influx and cell permeabilization, is reduced in mesenteric endothelial cells (Oliveira et al., 2013) and peritoneal macrophages from *S. mansoni* infected mice. This reduction is caused by increased TGF-β1 levels, which can reduce P2X7 receptor cell surface expression (Oliveira et al., 2014). Moreover, P2X7 KO mice infected with *S. mansoni* died 60 days after the infection, while no death was observed in *S. mansoni*-infected WT mice (Oliveira et al., 2014), suggesting that this receptor is crucial for an efficient immune response against this worm.

Taken together, these reports showed that helminth infections downregulate P2X7 functionality and expression. Since this receptor is crucial for controlling these infections, the use of P2X7 agonists could be a therapeutic strategy to boost the immune response against these worms.

P2X7 RECEPTOR IN INFLAMMATORY DISEASE—A DEMON VIA EXACERBATION OF THE INFLAMMATORY STATE

P2X7 receptor is involved in several physiological and pathological conditions in different body systems by modulating cellular responses in immune and non-immune cells in a variety of disease (Burnstock, 2017b). In this section, we discuss the role of P2X7 receptor in inflammatory disease, including the respiratory tract, gut, liver, and renal diseases as well as in diabetes.

P2X7 Receptor in Respiratory Tract Diseases

Purinergic signaling modulates important physiological processes in the airways. P2 purinergic receptors are expressed in different cells present in the respiratory system, such as type I alveolar epithelial cells, pulmonary endothelial cells, and resident immune cells (Mishra et al., 2011; Burnstock et al., 2012). Mishra et al. (2011) reported that P2X7 receptor activation with BzATP increases surfactant secretion in primary cultures of alveolar epithelial cells. However, this effect was blocked by BBG treatment. In addition, P2X7 KO mice showed impaired surfactant secretion in response to hyperventilation, highlighting the physiological importance of this receptor in lung homeostasis (Mishra et al., 2011).

However, P2X7 receptor hyperactivation has been implicated in the pathogenesis of a variety of respiratory diseases, including pulmonary hypertension, asthma, chronic obstructive pulmonary disease, acute lung injury, and pulmonary fibrosis (reviewed in Burnstock et al., 2012; Gentile et al., 2015). Increased ATP concentrations were detected in bronchoalveolar fluid of patients with idiopathic pulmonary fibrosis as well as in the bronchoalveolar space of mice subjected to a model of lung inflammation induced by LPS (Riteau et al., 2010) or cigarette smoking (Baxter et al., 2014).

Once released in the extracellular medium during lung injury, eATP acts as a danger signal through activation of P2X7 receptor, inducing alveolar macrophage activation and secretion of IL-1β (Riteau et al., 2010; Wang et al., 2015b; Galam et al., 2016) and IL-1α (Dagvadorj et al., 2015), and neutrophil recruitment (Riteau et al., 2010; Monção-Ribeiro et al., 2011; Baxter et al., 2014; Dagvadorj et al., 2015; Wang et al., 2015b; Mishra et al., 2016). The activation of P2X7 receptor increases markers of tissue fibrosis, such as lung collagen content and tissue inhibitor of matrix metalloproteinase-1 (TIMP-1) during lung injury (Riteau et al., 2010; Monção-Ribeiro et al., 2011). All these deleterious effects were attenuated in P2X7 KO mice (Riteau et al., 2010; Monção-Ribeiro et al., 2011; Baxter et al., 2014; Dagvadorj et al., 2015; Galam et al., 2016) or pharmacological inhibition of P2X7 receptor with A438079 (Wang et al., 2015b), BBG (Wang et al., 2015b), and suramin, a broad spectrum P2 receptor antagonist (Riteau et al., 2010).

Experiments performed *in vitro* co-cultures of human lung epithelial and macrophage cell lines suggest that P2X7 receptor also participates in lung inflammation triggered by nanoparticles such as SiO2 and TiO2, through the induction of inflammasome activation and IL-1β secretion (Dekali et al., 2013). Moreover, Monção-Ribeiro et al. (2014) showed that P2X7 receptor activation contributes to silica-induced lung fibrosis. P2X7 receptor deficient or BBG-treated mice showed diminished lung inflammation and fibrosis, as well as improved pulmonary function after silica instillation (Monção-Ribeiro et al., 2014). Therefore, P2X7 receptor contributes to lung inflammation and fibrosis, being an attractive therapeutic target to treat diseases of the respiratory tract.

P2X7 Receptor in Gut Disease

Several reports have described the participation of purinergic signaling in pathophysiological mechanism of gut diseases (reviewed in Burnstock, 2016; Longhi et al., 2017). P2X7 receptor expression and functionality have been characterized in different gut compartments (de Campos et al., 2012), and shown to be upregulated in colon of patients with Crohn's disease (CD) (Neves et al., 2014).

Rodent animal models of inflammatory bowel disease have shown that activation of P2X7 receptor induces death of enteric neurons and intestinal inflammation by activation of mast cells in the gut, leading to intestinal motility disorders (Gulbransen et al., 2012; Kurashima et al., 2012; Antonioli et al., 2014; Matsukawa et al., 2016). In this context, pharmacological inhibition of P2X7 receptor by BBG (Marques et al., 2014), A438079 (Wan et al., 2016), and A740003 (Marques et al., 2014; Figliuolo et al., 2017b) in animal models of inflammatory bowel disease showed beneficial effects attenuating the inflammatory response in the colon. Likewise, genetic deletion of P2X7 receptor protects mice against chemically induced colitis (Neves et al., 2014; Figliuolo et al., 2017b). Mechanistically, we recently demonstrated that eATP, released from damaged cells or pathogenic bacteria, contributes to chemically-induced colitis by triggering P2X7 receptor-mediated Treg cell death (Figliuolo et al., 2017b). P2X7 receptor deletion increases the expression of CD103, an integrin involved in T lymphocytes addressing the intestinal epithelium, in mesenteric lymph nodes of mice with 2,4,6-Trinitrobenzenesulfonic acid solution (TNBS)-induced colitis. In this model, Treg cells leave the mesenteric lymph nodes and migrate to lamina propria in greater numbers in P2X7 receptor KO than WT mice. Increased number of activated Treg cells, leading to higher levels of anti-inflammatory cytokines, such as IL 10 and TGF-β, in the lamina propria of P2X7 receptor KO mice protects them against experimental colitis (Figliuolo et al., 2017b).

In contrast, studies reported by Hashimoto-Hill et al. (2017), using a different model of colitis induced by *Citrobacter rodentium* infection, suggest a protective role for upregulation of P2X7 receptor expression in the gut. In their studies, retinoic acid-induced P2X7 receptor expression in $CD4^+$ effector T cells in the intestine, by activation of the intragenic enhancer region of the P2X7 receptor mouse gene, inhibited excessive expansion of Th1 and Th17 cells in the intestine during colitis (Hashimoto-Hill et al., 2017).

Taken together, these reports support the involvement of P2X7 receptor in inflammatory mechanisms underlying inflammatory bowel diseases. Interestingly, a clinical trial evaluating the effects of a selective orally active inhibitor of the P2X7 receptor (AZD9056) showed beneficial effects in patients with moderate-to-severe Crohn's Disease (Eser et al., 2015). Therefore, this receptor seems to be a suitable therapeutic target to treat gut disease.

P2X7 Receptor in Liver Disease

Purinergic signaling has been implicated in liver inflammation (Vaughn et al., 2012). Particularly, the P2X7 receptor is involved in oxidative and inflammatory mechanisms, as well as fibrogenesis, by inducing activation of Kupffer cells and hepatic stellate cells in several liver diseases (Vaughn et al., 2012). P2X7 receptor blockade with A438079 attenuates mouse CCl_4-induced liver fibrosis (Huang et al., 2014). BBG or oATP treatment also reduces the production of inflammatory mediators, activation of inflammatory signaling pathways and liver fibrosis in a model of bile duct ligation-induced cirrhosis (Tung et al., 2015).

Savio et al. (2017a) reported that P2X7 receptor blockade with BBG protects mice against sepsis-induced liver injury by decreasing activation of inflammatory signaling pathways, cytokine production, and apoptosis of sinusoidal cells. Pretreatment with BBG, followed by administration of celastrol, a pentacyclic triterpene isolated from plants with anti-inflammatory activity, also protects the liver from acetaminophen-induced liver injury by reducing inflammation and oxidative damage (Abdelaziz et al., 2017). In a model of carbon tetrachloride-induced steatohepatitis in obese mice, P2X7 receptor mediates oxidative and inflammatory events in the liver by NADPH oxidase-dependent mechanisms. P2X7 receptor is required for NADPH oxidase activation by inducing the expression of the p47 phox subunit and p47 phox binding to the membrane subunit, gp91 phox, suggesting that P2X7 receptor is involved in oxidative damage in liver disease (Chatterjee et al., 2012). According to Das et al. (2013) this receptor is also crucial for oxidative stress-mediated autophagy, inflammation, and fibrosis in liver during experimental non-alcoholic steatohepatitis in P2X7 KO mice (Das et al., 2013).

P2X7 receptor also contributes to acetaminophen hepatotoxicity in mice (Hoque et al., 2012) and to hepatic stellate cell activation and liver fibrogenesis via NLRP3 inflammasome and PKC/GSK3β pathways (Jiang et al., 2017; Wu et al., 2017b). P2X7 receptor stimulation by BzATP induced the expression of inflammatory mediators and proteins related to fibrosis development, such as collagen I, in hepatic stellate cells treated with acetaldehyde. These effects were attenuated by P2X7 receptor inhibition with A438079 (Wu et al., 2017b). Therefore, P2X7 receptor blockade might be an innovative therapeutic avenue to limit the activation of Kupffer and hepatic stellate cells, and, consequently, the inflammation and fibrogenesis in liver diseases.

P2X7 Receptor in Diabetes

Purinergic signaling has been studied in pancreas physiology and pathophysiology since the 1960's, when Rodrigue-Candela et al. (1963) showed that ATP induces secretion of insulin in rabbit pancreas slices. Currently, the role of several purinergic receptors and ectonucleotidases in pancreas physiology and diabetes is widely accepted (Burnstock and Novak, 2012, 2013). Specifically, P2X7 receptor has been implicated in diabetes development and pathology (Coutinho-Silva et al., 2007; Burnstock and Novak, 2013). Polymorphisms in P2X7 receptor gene have been associated with altered glucose homeostasis in both mice and humans (Todd et al., 2015). In rat and mice, P2X7 receptor is expressed in α cells, but not in β or δ cells, an expression pattern that remains unchanged during aging or after streptozotocin (STZ) administration (Coutinho-Silva et al., 2001a, 2003a). Besides that, P2X7 receptor-mediated apoptosis is increased in

fibroblasts from type 2 diabetes patients (Solini et al., 2004) and in human fibroblasts exposed to high glucose levels (Solini et al., 2000). In addition, osteoblast function is impaired in a P2X7-dependent manner after high glucose exposure (Seref-Ferlengez et al., 2016). Interestingly, Weitz et al. (2017) recently showed that high glucose levels also induce ATP secretion from β cells triggering the activation of pancreatic islet-resident macrophages.

Using P2X7 receptor deficient mice, Glas et al. (2009) reported that these mice subjected to a high-fat/high-sucrose diet have diminished insulin secretion and glucose tolerance correlated with an elevated number of apoptotic β cells. However, Chen et al. (2011) reported that P2X7 genetic deletion did not alter type 1 diabetes development in non-obese mice, while Vieira et al. (2016) showed that P2X7 KO mice are resistant to STZ-induced type 1 diabetes induction. No increase in blood glucose and a decrease in insulin-positive cells were reported in STZ-treated P2X7 KO mice in comparison to WT counterparts and an analysis of pancreatic lymph nodes showed a diminished inflammatory response in diabetic P2X7 KO mice. Finally, BBG treatment also prevented the STZ-induced diabetes (Vieira et al., 2016). Therefore, P2X7 receptor seems to be implicated in diabetes types 1 and 2.

P2X7 receptor also appears to be involved in diabetes-related comorbidities, including cardiovascular alterations, diabetic retinopathy, and kidney injury (Burnstock and Novak, 2013). P2X7 receptor expression is increased in renal biopsy sections from diabetic patients (Rodrigues et al., 2014; Menzies et al., 2017a) and in the kidney of STZ-induced diabetic rats contributing to diabetic nephropathy pathogenesis. P2X7 receptor blockade with AZ11657312 (Menzies et al., 2017a), aerobic training or N-acetylcysteine administration attenuated diabetes related kidney injury (Rodrigues et al., 2014). Therefore, these results suggest that P2X7 receptor is involved in the development of diabetes and associated comorbidities.

P2X7 Receptor in Kidney Disease

Purinergic signaling exerts crucial physiological effects on renal function, controlling both vascular contractility and tubular function (recently reviewed in Menzies et al., 2017b). eATP released by renal cells regulates renal homeostasis through activation of P2 purinergic receptors present in non-hematopoietic renal cells as well as infiltrating immune cells (Koo et al., 2017; Menzies et al., 2017b). Thus, an imbalance on purinergic receptors activation, as well as in ectonucleotidases activity, contributes to kidney diseases (Vuaden et al., 2012; Franco et al., 2015).

Uncontrolled activation of P2X receptors, mainly P2X7 receptor, has been shown to play a critical role in the inflammatory reactions observed in renal diseases, contributing to renal glomerular, tubular, and vascular damage (Gonçalves et al., 2006; Deplano et al., 2013; Solini et al., 2013; Franco et al., 2015). This assumption is supported by the fact that, in a healthy kidney, P2X7 receptor is weakly expressed in podocytes, endothelial cells, mesanglial cells, and tubular epithelial cells, while its levels become upregulated after injury (Gonçalves et al., 2006; Solini et al., 2013; Burnstock et al., 2014; Rodrigues et al., 2014; Franco et al., 2015).

In the same way, infiltrated inflammatory cells such as macrophages, DCs, and T cells increase their P2X7 receptor expression after renal damage (Ji et al., 2012a,b; Deplano et al., 2013; Koo et al., 2017). It is now clear that activation of P2X7 receptor promotes pathologic inflammation in several experimental models of renal diseases, such as glomerulonephritis (Deplano et al., 2013), diabetic nephropathy (Solini et al., 2013; Rodrigues et al., 2014), tubulointerstitial nephritis (Gonçalves et al., 2006), hypertensive nephropathy (Franco et al., 2015), acute kidney injury (Koo et al., 2017), and chronic kidney injury (Granata et al., 2015) via activation of NLPR3 inflammasome and consequent release of inflammatory cytokine, such as IL-1β and IL-18. Moreover, this receptor participates in the production of interstitial collagen, contributing to renal fibrosis (Gonçalves et al., 2006; Koo et al., 2017). Therefore, blocking P2X7 receptor activation may be a potential strategy to prevent or ameliorate renal damage. In fact, several studies have demonstrated a protective effect of P2X7 receptor antagonism (with BBG, oATP, AZ10606120, A-438079, and AZ11657312) or its genetic deletion in animal models of renal injury due, primarily, to anti-inflammatory actions (Gonçalves et al., 2006; Ji et al., 2012a,b; Deplano et al., 2013; Solini et al., 2013; Menzies et al., 2015; Yan et al., 2015; Koo et al., 2017).

In this sense, P2X7 receptor appears to be an attractive therapeutic target to reduce inflammation in renal diseases. Unfortunately, recent clinical trials failed to demonstrate a beneficial effect for P2X7 receptor antagonists in several inflammatory illnesses (Arulkumaran et al., 2011; Menzies et al., 2017b). Additional detailed information regarding P2X7 receptor role in renal disease and its potential use as a new target in renal disease therapy can be found in a recent review (Menzies et al., 2017b).

P2X7 Receptor in Cardiovascular Disease

Purinergic signaling and P2X7 receptor also play a key role in cardiovascular physiology and pathophysiology. P2X7 receptor shows deleterious effects in cardiovascular disease by promoting inflammation, thrombosis, and endothelial dysfunction (Burnstock, 2017a). Additional detailed information can be accessed in an excellent recent review by Burnstock (2017a).

P2X7 RECEPTOR IN CANCER—ANGEL OR DEMON DEPENDING ON ITS LEVEL OF ACTIVATION AND CELL TYPE STUDIED

Despite recent advances in research and care, cancer is still a major public health problem worldwide and it is the second leading cause of death in the United States (Siegel et al., 2017). Recent research has granted both pro- and anti-carcinogenic properties to eATP in tumor biology. The definitive effect of eATP will depend on its concentration in the tumor intersticium, the panel of P2 receptor subtypes expressed by the tumor

core and the levels of the ectonucleotidades expressed by immune, tumor, and stromal cells (Di Virgilio, 2012). Increased metabolism of eATP by CD39 and CD73 sequential enzymatic activity generates adenosine in the tumor microenvironment (TME), which is a potent immunosuppressive mediator and promotes cancer cell growth (Ohta et al., 2006; Deaglio et al., 2007; Mello et al., 2017b).

Particularly, P2X7 receptor activation has been linked to conflicting effects on carcinogenesis, being beneficial in certain circumstances and injurious in others (Roger et al., 2015). In order to facilitate the understanding of P2X7 receptor role in tumor progression, we will divide this following sections according to its effect on tumor cells (pro-tumoral and anti-tumoral) and immune infiltrated cells, highlighting P2X7 receptor impact on the tumor-host interaction and its inhibition/activation as a new therapeutic target potential in cancer.

P2X7 Receptor Basal Stimulation in Tumor Cells—Pro-tumoral Activities

Growing body of evidence indicates that P2X7 receptor plays a central role in tumorigenesis (Adinolfi et al., 2009, 2012; Tafani et al., 2011; Amoroso et al., 2015). P2X7 inhibition, either by silencing or pharmacological blockade, restrained tumor progression, and metastasis while P2X7 overexpression accelerated it (Jelassi et al., 2011; Adinolfi et al., 2012). Moreover, high expression levels of P2X7 receptor have been found in many malignant human tumors, including leukemia (Adinolfi et al., 2002; Zhang et al., 2004; Chong et al., 2010), melanoma (Deli et al., 2007), neuroblastoma (Raffaghello et al., 2006), pancreatic adenocarcinoma (Giannuzzo et al., 2015), esophageal carcinoma (Santos et al., 2017), papillary thyroid carcinoma (Kwon et al., 2014), renal cell carcinoma (Liu et al., 2015), breast cancer (Tan et al., 2015), prostate cancer (Ghalali et al., 2014), colorectal cancer (Qian et al., 2017), and head and neck cancer (Bae et al., 2017).

It is now consensus that under conditions of low-intensity basal stimulation, P2X7 receptor has a potent pro-growth activity, contributing to tumor progression (Di Virgilio, 2012). P2X7 stimulation results in increased oxidative phosphorylation and aerobic glycolysis, both events leading to an overall enhancement in the total cellular ATP content (Adinolfi et al., 2005; Amoroso et al., 2012) and consequent proliferative advantage (Di Virgilio, 2016). P2X7 receptor activates several intracellular growth promoting pathways, such as NFATc1, ERK, PI3K/Akt, and HIF-1α (Jacques-Silva et al., 2004; Tafani et al., 2011; Adinolfi et al., 2012; Amoroso et al., 2012, 2015). It also triggers the release of vascular endothelial growth factor (VEGF) (Hill et al., 2010; Adinolfi et al., 2012), tissue factor and matrix metalloproteinases (Gu and Wiley, 2006), contributing to tumor growth, angiogenesis, invasiveness, and metastasis spreading. P2X7 receptor role in tumor metastasis is also supported by the fact that its silencing leads to reduced expression of genes linked to epithelial/mesenchymal transition such as Snail, E-cadherin, Claudin-1, IL-8, and MMP-3 (Qiu et al., 2014).

Generally, the P2X7 receptor exhibits striking oncogene-like features, being therefore a potential target in cancer therapy. Many studies using P2X7 inhibitors and antagonist have rendered promising results, reducing cancer growth or spreading in preclinical animal models of colon cancer (Adinolfi et al., 2012), breast cancer (Jelassi et al., 2011; Park et al., 2016), ovarian cancer (Vázquez-Cuevas et al., 2014), pancreatic ductal adenocarcinoma (Giannuzzo et al., 2016), neuroblastoma (Amoroso et al., 2015), melanoma (Adinolfi et al., 2012, 2015), glioma (Ryu et al., 2011), and mesothelioma (Amoroso et al., 2016). The pharmacological molecules used to block P2X7 in those studies were administrated either intratumorally or systemically and included oATP (Adinolfi et al., 2012; Hattori and Gouaux, 2012), BBG (Vázquez-Cuevas et al., 2014), AZ10606120 (Adinolfi et al., 2012, 2015; Amoroso et al., 2015, 2016; Giannuzzo et al., 2016), A740003 (Adinolfi et al., 2015; Amoroso et al., 2015), A438079 (Jelassi et al., 2011), Antraquinone emodin (Jelassi et al., 2013), novel 1-Piperidinylimidazole based antagonists (Park et al., 2016), and P2X7 blocking antibodies (Ren et al., 2010). Many pharmaceutical companies are attempting to develop a clinical candidate targeting P2X7 receptor and various scaffolds have been disclosed (Park and Kim, 2017). A recent clinical trial in phase I, which used an anti-P2X7 antibody, provided significant data to support its use as a safe and tolerable topical therapy for basal cell carcinoma (BCC) (Gilbert et al., 2017). According to this study, 65% of patients responded to the treatment, having a significant reduction in the lesion area.

Considering P2X7 receptor role in promoting tumor angiogenesis via increased HIF1α activity and VEGF secretion (Adinolfi et al., 2012; Amoroso et al., 2012, 2015), it is tempting to say that the use of antagonists of P2X7 in association with anti-angiogenic drugs would surge synergistic effects in controlling tumorigenesis. In fact, administration of the VEGF antagonist Avastin strongly inhibits growth of P2X7-expressing tumors *in vivo* (Adinolfi et al., 2012).

Although outcomes of pre-clinical and clinical studies are exciting, novel P2X7-targeted strategy would only be feasible in tumors that overexpress this receptor, as tumors with low or no P2X7 expression showed slight response to P2X7 blocking therapy in preclinical models (Adinolfi et al., 2012).

P2X7 Receptor Over-Activation in Tumor Cells—Anti-tumoral Activities

Overstimulation of P2X7 receptor with high levels of exogenous ATP in order to produce tumor cell death is a longstanding observation and it was demonstrated in many types of cancer, such as colon cancer (Bian et al., 2013; Mello et al., 2017a), prostate cancer (Shabbir et al., 2008), cervical cancer (Wang et al., 2004; Mello et al., 2014), endometrial cancer (Li et al., 2006), melanoma (White et al., 2009; Feng et al., 2011; Bian et al., 2013), squamous cell carcinomas (Deli and Csernoch, 2008), and glioma (Tamajusuku et al., 2010; Gehring et al., 2012, 2015), among others. However, despite its promising results in preclinical models, clinical trials have failed to demonstrate a potent anti-cancer effect for eATP administration in patients,

with an improvement of the quality of life being the only positive effect observed (Agteresch et al., 2003; Beijer et al., 2009, 2010).

This lack of effect in patients might be explained by the fact that both tumor and other cells in the TME are resistant to the high ATP concentrations usually present in this inflammatory setting (Bianchi et al., 2014). The mechanism enrolled in such refractoriness to ATP stimulation has not been completely understood yet, but it appears to resultfrom P2X7 receptor uncoupling from intracellular death pathways, at least in some types of cancer (Raffaghello et al., 2006). Therefore, finding strategies to enhance eATP-P2X7 signaling in the TME by boosting P2X7 functional responses might be a better approach to overcome cancer cell death escape in those cases where P2X7 receptor is less responsive.

We have recently demonstrated that hyperthermia is a suitable strategy to augment ATP-elicited P2X7 functionality, thereby maximizing tumor cell death (Mello et al., 2017a). Hyperthermia alters plasma membrane fluidity facilitating P2X7 receptor pore opening and dilatation upon ATP stimulation resulting in increased colon cancer cell death. Moreover, when combined with cisplatin or mitomycin C, hyperthermia, and eATP potentiate chemotherapy cytotoxicity, enhancing the therapeutic efficacy of conventional cancer treatments. Likewise hyperthermia, shock wave and photodynamic therapy alter cells membrane permeability via ATP-P2X7 signaling, boosting hydrophilic drugs intake, and cell death induction (Pacheco et al., 2016; Qi et al., 2016). P2X7 receptor activation also modulates radiotherapy-killing activity (Gehring et al., 2012, 2015).

According to Gering et al. eATP-P2X7 signaling acts synergistically with radiotherapy potentiating glioma cell death (Gehring et al., 2012, 2015). Moreover, silencing of P2X7 receptor in animal model of glioblastoma prevented response to radiation, reinforcing that functional P2X7 receptor expression is essential for an efficient radiotherapy response in gliomas *in vivo* (Gehring et al., 2015). These studies combined bring a different approach in relation to the use of eATP-P2X7 signaling intervention, specifically regarding its property to increase plasma membrane permeability to boost the efficacy of other anti-cancer modalities. Importantly, this strategy would only be applicable to tumor cells expressing the P2X7(A) splice variant, which is the well-characterized full-length receptor capable of inducing pore formation and apoptosis (Rassendren et al., 1997). So far, both functional and non-functional splice variants have been described for the human P2X7 receptor (Cheewatrakoolpong et al., 2005; Feng et al., 2006a,b). The truncated P2X7(B) variant is a functional ion channel with a dominant positive effect, however it lacks the ability to form the large non-selective conductance pore (Giuliani et al., 2014). Differently, the non-functional splice variant P2X7(J) exerts a dominant negative effect (Feng et al., 2006a,b). In these settings, tumor cells predominantly expressing truncated/defective P2X7 receptor variant might fail to undergo cell pore formation and death even with agonist stimulus (Cheewatrakoolpong et al., 2005; Skarratt et al., 2005; Feng et al., 2006a,b).

P2X7 Receptor in Tumor-Associated Immune Cells

The TME is composed of different subsets of immune cells that interact with tumor cells to enable tumor growth and progression (de Visser et al., 2006; Hanahan and Weinberg, 2011). In this inflammatory microenvironment, accumulated eATP activates P2X7 receptor highly expressed in monocytes, macrophages, DCs, lymphocytes, and myeloid-derived suppressor cells (MDSCs), modulating the immune response against tumors (Fernando et al., 1999; Gudipaty et al., 2003; Idzko et al., 2014). In this scenario, P2X7 receptor activation on DCs is crucial for the anti-immune response (Ghiringhelli et al., 2009; Aymeric et al., 2010). Engagement of P2X7 receptor triggers NLRP3 inflammasome activation and IL-1β release with consequent stimulation of $CD8^+$ and $CD4^+$ mediated anti-tumor responses. This signaling is particularly important for the induction of immunogenic cell death after radiotherapy and some chemotherapeutic agents, dictating the efficacy of those treatments (Zitvogel et al., 2008; Ghiringhelli et al., 2009; Aymeric et al., 2010). Moreover, two studies showed that expression of P2X7 receptor by host immune cells has a fundamental role in restraining tumor growth and metastatic spreading (Adinolfi et al., 2015; Hofman et al., 2015). Accordingly, tumors implanted in P2X7 KO mice grow faster, lack inflammatory infiltrate—such as neutrophils, lymphocytes, and macrophages—and metastasize more readily. Furthermore, plasma and intratumoral levels of IL-1β and VEGF were significantly lower in P2X7 KO compared to WT strains (Adinolfi et al., 2015).

P2X7 receptor appears to hinder tumor growth by promoting DC/tumor cell interaction, cytokine release, chemotaxis, and infiltration of immune cells in the TME (Adinolfi et al., 2015; Di Virgilio, 2016). It also stimulates the release of immunosuppressive factors from MDSCs (Bianchi et al., 2014), and modulates macrophages to the M2-immunosuppressive phenotype, preventing tumor cell attack by natural killer and T cells (Noy and Pollard, 2014; Bergamin et al., 2015). In this complex scenario, the prevalence of one of those conflicting inflammatory responses will dictate whether a tumor will grow and metastasize or will be successfully hindered by the immune system (Hanahan and Weinberg, 2011; Di Virgilio, 2016). In fact, the observation that systemic administration of pharmacologic P2X7 receptor antagonist strongly inhibits tumor growth in immune-competent mice (Adinolfi et al., 2012, 2015), suggests that blocking P2X7 receptor is more beneficial for cancer regression. Evidence supporting this assumption comes from the fact that, in tumors overexpressing P2X7 receptor, such as neuroblastoma, the anti-tumoral effect of P2X7 antagonists is more pronounced in immune-competent than in immune-compromised (nude/nude) mice, indicating an additional contribution of the immune response against tumor in the former case (Amoroso et al., 2015; Di Virgilio and Adinolfi, 2017). This effect could be partially attributed to blockade of P2X7 receptor expressed by suppressor immune cells (i.e., MDSCs and M2-macrophages), restoring the anti-tumor immune response.

Therefore, targeting eATP/adenosine signaling is a promising strategy to increase anti-tumor immunity in the TME and many researchers have pointed the blockage of this signaling as the next generation of cancer immunotherapy (Allard et al., 2017; Mello et al., 2017b). Considering the diversity of cells, the complexity of signaling, and the contradictory effect of P2X7 receptor in the TME, the application of P2X7 receptor-blocking therapy to restrain tumor growth and boost the anti-tumor immunity will only be feasible after our complete understanding of its role in the host-tumor interaction.

P2X7 RECEPTOR ACTIVATION IN NEURODEGENERATIVE DISORDERS—A DEMON VIA EXACERBATION OF NEUROINFLAMMATION

In the brain, extracellular nucleotides, mainly ATP, act as signaling molecules mediating neuron-neuron and neuron-glia communication through activation of ionotropic (P2X) and metabotropic (P2Y) purinergic receptors (Cisneros-Mejorado et al., 2015). P2X7 receptor is widely distributed in the brain (Yu et al., 2008) and it is abundantly expressed in microglia and neurons, as well as in other glial cells such as oligodendrocytes and astrocytes (Yu et al., 2008). P2X7 receptor plays a key physiologic role on neural axonal growth and modulation of neurotransmitter release from presynaptic terminals, where it is prominently present (Sperlágh et al., 2002; Alloisio et al., 2008). Its brief stimulation also induces non-cytotoxic glial activation. However, in pathologic situations, even mild perturbations, ATP can be released in large amounts from neurons and activated glial cells, as well as from dying cells at the site of injury, dramatically increasing eATP levels. Repeated and prolonged activation of P2X7 receptor by high levels of eATP induces formation of large non-selective membrane pores, in addition to the typical Ca^{+2} influx and K^{+} efflux through non-selective cationic channels, initiating a cascade of pro-inflammatory and pro-apoptotic events that culminate in cell death. In addition, P2X7 receptor pores may be a route of glutamate and ATP efflux from glia and neurons, further fueling inflammation and cytotoxicity (Di Virgilio et al., 2001; Liang and Schwiebert, 2005).

Neuroinflammation and gliosis are the most prominent aspects in the pathophysiology of many neurodegenerative diseases. Increasing evidence suggests that deregulated expression and activation of P2X7 receptor is an underlying key mechanism in the pathogenesis and progression of many pathological states of central nervous system (CNS), particularly due to its regulatory role in glial activation, integrity, and survival. Activation of P2X7 receptor signaling in microglia induces inflammasome formation, releases pro-inflammatory cytokines (IL-1β, IL-18, and TNFα) and reactive oxygen species such asROS, particularly superoxide (Parvathenani et al., 2003), which induces activation of NFκB signaling, upregulation of pro-inflammatory, and pro-apoptotic genes. This willresult in death of surrounding cells, including neurons (Parvathenani et al., 2003). ATP released from dying cells perpetuates the inflammatory and degenerative cycle.

This cascade of events has been proposed as a common pathological mechanism to many CNS diseases where an initial perturbation, either mechanical, inflammatory, cytotoxic or infectious, induces increased in eATP, triggering P2X7 receptor-dependent inflammatory and pro-apoptotic cascade. If that holds true, such deleterious effects commonly present in neurodegenerative diseases could potentially be manageable by antagonists of P2X7 receptor, irrespective of the primary cause.

In fact, extensive body of work has demonstrated the involvement of P2X7 receptor activation not only in microglia but also in neurons, oligodendrocytes, and astrocytes, in the development of multiple CNS disorders including Traumatic Brain Injury, Parkinson's disease, Alzheimer's disease, ischemia, epilepsy, Huntington's disease, and Multiple Sclerosis. In the next sections, we will focus on the role of P2X7 receptor in the development and possible treatment of the neurodegenerative disorders that most heavily affect patients worldwide: Alzheimer's disease (AD), Parkinson's disease (PD), Huntington's disease (HD), and Multiple Sclerosis (MS). A detailed coverage of the physiologic role of P2X7 receptor in the brain, as well as its role in other CNS disorders, is available in recent reviews (Sperlágh and Illes, 2014; Tewari and Seth, 2015; De Marchi et al., 2016).

Role of P2X7 Receptor in Alzheimer's Disease (AD)

According to the latest World Alzheimer Report from the Alzheimer's Disease (AD) International (an international federation of Alzheimer associations around the world), 46 million people are living with AD or a related dementia, being more than 10 million people only in the United States ("World Alzheimer Report 2016 | Alzheimer's Disease International" 2017). AD is a progressive form of dementia characterized by increasing neuronal loss, mainly in cortex and hippocampus. Neuropathological hallmarks of this disease are the presence of neurofibrillary tangles, formed by the accumulation of intracellular inclusions of hyperphosphorylated tau protein, and the deposition of extracellular plaques of amyloid-β peptides (Aβ) (Koffie et al., 2012; Pooler et al., 2014).

AD pathogenesis is complex and it has not been completely understood yet. Aβ production and aggregation is still considered to be at the origin of AD pathology, while Aβ-induced microglia activation is believed to contribute to disease progression through secretion of pro-inflammatory mediators and cytotoxic agents (Hardy and Selkoe, 2002). Protein post-translation modifications that promote inflammation, specifically the ureido degenerative protein modification arginine citrullination and lysine carbamylation, have been also associated with initiation and progression of dementia and AD. Interestingly, Gallart-Palau et al. (2017) have demonstrated presence of P2X7 receptor modified by a dementia-specific citrulline residue in soluble brain proteome of AD. However, the contribution of this post-translational modification to P2X7 receptor's activity remains to be demonstrated. Upregulation of P2X7 receptor was observed in the brain of AD patients, as well as in the hippocampus of animal models of AD such as Tg2576 transgenic mice and rats following intrahippocampal Aβ injection. In both cases, P2X7

receptor brain expression was concentrated in areas of high Aβ plaques density and co-localized with activated microglia, identifying microglial P2X7 receptor as another player in the pathogenesis of AD (Parvathenani et al., 2003; McLarnon et al., 2006). More recently, *in vitro* autoradiography quantification of brain slices incubated with a potent iodinated radiotracer for P2X7 receptor, [^{123}I]TZ6019, demonstrated higher binding in brains from P301C tau transgenic mice, a tauopathy mouse model of AD, compared to control (Jin et al., 2017). While the cause of increased P2X7 receptor in AD is still unknown, studies performed in human fetal microglia demonstrated a significant two-fold upregulation in P2X7 receptor expression following *in vitro* treatment with Aβ, suggesting a direct effect of this peptide on P2X7 receptor expression (McLarnon et al., 2006).

Aβ also induces ATP release from microglia (Kim et al., 2007). Released ATP, acting in an autocrine/paracrine manner, further augments microglial activation, and likely contributes to neuronal death (Rampe et al., 2004; Kim et al., 2007; Sanz et al., 2009). Furthermore, due to its potent chemoattractant properties, higher eATP levels contribute to the high density of activated microglia surrounding Aβ plaques, a common finding in the brain of AD patients. Most interestingly, the inability of Aβ to activate P2X7 receptor deficient microglia suggests a fundamental role for this receptor in microglial activation induced by Aβ (Sanz et al., 2009). Supporting this assumption, P2X7 receptor blockade with antagonists or P2X7 receptor silencing prevented Aβ-induced pro-inflammatory signaling in microglia (McLarnon et al., 2006; Ryu and McLarnon, 2008). Silencing of P2X7 receptor also enhanced Aβ phagocytosis by microglia, an important mechanism for Aβ clearance (Ni et al., 2013).

A possible involvement for P2X7 receptor in modulating amyloid precursor protein (APP) processing and Aβ peptides production has also been proposed (Delarasse et al., 2011; León-Otegui et al., 2011; Miras-Portugal et al., 2015). APP, a transmembrane protein present in neurons and glia, can be processed by α- and β-secretases, followed by sequential cleavage by γ secretases to produce soluble APPα (sAPPα) and amyloidβ (Aβ) fragments, respectively. While both pathways of APP processing occur in the CNS, in a healthy brain, APP is preferentially processed by α-secretases (non-amyloidogenic process), precluding the formation of Aβ and resulting in sAPPα accumulation, which has been shown to have neurotrophic and neuroprotective properties. However, in AD brain, for reasons still unknown, APP cleavage by β-secretases is more pronounced, resulting in accumulation of Aβ peptides in senile plaques (Murphy and LeVine, 2010). While the protective role of activation of P2Y2 receptor in inducing the non-amyloidogenic possessing of APP is well-established (Camden et al., 2005; Kong et al., 2009), the contribution of P2X7 receptor is debatable.

Delarasse et al. (2011) performed studies using human and mouse neuroblastoma cell lines that constitutively express APP and a functional P2X7 receptor. They showed that these cells release APP fragments when stimulated with both ATP and high levels of BzATP. Interestingly, APP fragments were secreted mostly as sAPPα while Aβ was undetectable, suggesting that P2X7 receptor activation promotes APP cleavage predominantly via α-secretase pathway. Moreover, this effect was abolished by both P2X7 receptor siRNA and pre-treatment with P2X7 receptor pharmacologic inhibitors, further validating the involvement of P2X7 receptor signaling in promoting sAPPα release. These results were also replicated in mouse primary astrocytes and neural progenitor cells, as well as in human neuroblastoma cells. In these cells, ATP increased sAPPα secretion in wild type cells, but failed to do so in P2X7 receptor knockout cells. This non-amyloidogenic APP cleavage induced by P2X7 receptor activation was mediated by metalloproteases, via activation of an ERK1/2, P38, and JNK signaling pathway, independently from typical P2X7 receptor induced Ca^{+2} influx (Delarasse et al., 2011). Such results suggest a protective effect of P2X7 receptor on APP processing, contradicting the initial claims of a deleterious role for P2X7 receptor activation in AD.

Follow up studies using the same mouse neuroblastoma cells cited above, but applying a different methodology for quantification of APP fragments, challenged those controversial findings. Accordingly, two independent studies demonstrated that BzATP-induced P2X7 receptor activation leads to decreased α-secretase activity, which was prevented by P2X7 receptor antagonists and P2X7 receptor siRNA (León-Otegui et al., 2011; Miras-Portugal et al., 2015).

In agreement with these findings, studies performed in J20 mice, an *in vivo* model of AD in which Aβ senile plaques develop spontaneously, demonstrated decreased Aβ plaques in hippocampus of AD animals upon treatment with P2X7 receptor antagonist BBG. This effect was attributed to a shift toward APP metabolism by α-secretase via reduction of GSK3 activity (Diaz-Hernandez et al., 2012), an enzyme known to phosphorylate specific AAP domains, making it more suitable to be processed into Aβ.

Altogether, those studies suggest that modulation of microglia functions, as well as regulation of APP processing by P2X7 receptor antagonists, may be a promising therapeutic strategy in the management of AD.

Role of P2X7 Receptor in Parkinson's Disease

Parkinson's disease (PD) is a motor illness clinically characterized by bradykinesia, rigidity, postural instability, and tremor at rest, caused by progressive impairment of the striatal dopaminergic system that evolves to loss of dopaminergic (DA) neurons in the substantia nigra. While the mechanisms enrolled in PD development are still not completely understood, a growing body of evidence shows that chronic neuroinflammation and excessive microglia activation strongly contribute to degeneration of DA neurons within the substantia nigra and striatum of PD patients (Durrenberger et al., 2012). Oligomerization and accumulation of α-Synuclein (ASN) is also believed to be an important player in the pathophysiology of PD. ASN mediates neurotoxicity by inducing deregulation of dopaminergic and glutamatergic neurotransmission and by activating microglia, with subsequent production of pro-inflammatory molecules and reactive oxygen species (Stefanis, 2012). Interestingly, ASN also binds and activates P2X7 receptor in microglia and this interaction appears

to be key to ASN-induced microglia ROS production, as it is partially reduced in P2X7 receptor knockdown cells (Jiang et al., 2015). Additionally, ASN stimulates P2X7 receptor transcription (Jiang et al., 2015), which might explain, at least in part, the P2X7 upregulation observed in brains of patients with PD (Durrenberger et al., 2012).

In vivo indication of a possible involvement of P2X7 receptor in the nigrostriatal degeneration first appeared in studies using the 6-OHDA rat model of PD. In this animal model, destruction of DA neurons is induced by unilateral intranigral injection of a DA selective neurotoxin 6-hydroxydopamine (6-OHDA). This leads to marked reduction of dopamine levels and nigrostriatal lesions that are accompanied by microgliosis, as typically found in autopsy of PD patients, culminating in the development of motor symptoms, closely mimicking the human disease. Administration of selective P2X7 receptor antagonists ameliorated motor and memory deficit, and significantly attenuated 6-OHDA-induced microgliosis (Marcellino et al., 2010; Carmo et al., 2014; Ferrazoli et al., 2017; Kumar et al., 2017), suggesting a pro-inflammatory role for P2X7 receptor signaling via microglia activation in PD. In addition, P2X7 receptor antagonists significantly ameliorated 6-OHDA-induced decrease in mitochondrial respiration, as well as increase in oxidative stress and mitochondrial-linked apoptosis, adding preservation of mitochondrial function and integrity to the protective mechanisms of P2X7 receptor antagonists in PD (Kumar et al., 2017).

While the evidence supporting the involvement of P2X7 receptor in PD neuroinflammation is strong, whether direct activation of neuronal P2X7 receptor is responsible for PD neurodegeneration has been subject of discussion. Sensitivity of dopaminergic neurons to ATP- and 6-OHDA-induced cytotoxicity via activation of P2X7 receptor has been demonstrated *in vitro* (Jun et al., 2007; Carmo et al., 2014). Along the same lines, *in vitro* studies performed in neuroblastoma SH-SY5Y cells demonstrated that extracellular ASN directly activates P2X7 receptor to induced ATP release, contributing to neuronal toxicity in PD (Wilkaniec et al., 2017). However, the association between activation of neuronal P2X7 receptor and DA neuronal loss *in vivo* remains to be proven. Intranigral injection of P2X7 receptor antagonist A438079 attenuated depletion of striatal dopamine stores but it did not affect loss of dopaminergic cells in the 6-OHDA PD model (Marcellino et al., 2010). Similarly, genetic deletion and pharmacologic inhibition of P2X7 receptor failed to promote neuroprotection in a mouse model of PD induced by administration of the dopaminergic neurotoxin MPTP (Hracskó et al., 2011).

On the other hand, BBG treatment significantly prevented and even reversed loss of DA neurons in 6-OHDA-treated animals, as evaluated by striatal content of tyrosine hydroxylase (TH) (Carmo et al., 2014; Ferrazoli et al., 2017), the limiting enzyme in the production of dopamine often used a surrogate for number of DA neurons. Additional work done in an endotoxin-induced model of PD confirmed the neuroprotective properties of BBG. As in the rat 6-OHDA model, brain of LPS-treated mice showed high levels of P2X7 receptor expressing activated microglia in the substantia nigra that was, once again, reduced by selective inhibition of the P2X7 receptor by BBG. Lower microglia activation correlated with marked protection of DA neurons from LPS-induced cytotoxicity, as assessed by number of TH^+ cells (Wang et al., 2017).

Collectively, those studies strongly support the hypothesis that P2X7-induced microglia activation is involved in PD pathology. However, they fail to demonstrate whether neuroprotection conferred by P2X7 receptor antagonistic results solely from inhibition of microgliosis or from direct effect on neuronal P2X7 receptor. Using the current immunohistochemistry tools, P2X7 receptor expression was showed to co-localize with nigrostriatal glia in animal models of PD, not neurons. Brain analysis of the recently generate, conditional humanized P2X7 receptor mice confirmed the expression of P2X7 receptor in all major non-neuronal lineages throughout the brain (astrocytes, microglia and oligodendrocytes), as well as glutamatergic pyramidal neurons of the hippocampus (Metzger et al., 2017), further questioning the existence of these receptors in DA neurons.

Role of P2X7 Receptor in Multiple Sclerosis (MS)

Multiple sclerosis (MS) is an immune-mediated, chronic degenerative disease of the CNS, characterized by inflammatory focal lesions in both white and gray matter, immune cell infiltration, loss of oligodendrocytes, and axonal damage, leading to demyelinization and neuronal death. Clinically, patients present neurological deficit including sensory disturbances, lack of motor coordination, and visual impairment (Lucchinetti et al., 2011). An autoimmune inflammatory reaction to myelin is believed to be the triggering event in the pathogenesis of MS, with genetic and environmental factors strongly contributing to disease susceptibility (Kidd, 2001; Stys, 2010). Due to the highly inflammatory nature of MS, a link between P2X7 receptor activation and MS development has been proposed.

While MS is seen most traditionally as a "white matter" disease, with loss of oligodendrocytes and damage to myelin being the core of its pathology, the involvement of other cell types such as neurons and glia on the development of this disease has also been recognized. In fact, increased in P2X7 receptor expression has been reported in oligodendrocytes, neurons and glia of MS patients.

Early post mortem studies have revealed high P2X7 expression in astrocytes and activated microglia in the brain and spinal cord of MS patients (Narcisse et al., 2005; Yiangou et al., 2006). Deregulated P2X7 expression seems to precede the symptomatology of the disease, as increased P2X7 levels are present in normal appearing optic nerve samples of MS patients (Matute et al., 2007), suggesting that deregulated P2X7 signaling might be a risk factor associated with early lesion development of MS.

A better understanding of the kinetics of P2X7 receptor expression in MS is provided by studies performed with rat models of experimental autoimmune encephalomyelitis (EAE). EAE is the most common rodent model used to study the molecular mechanisms responsible for the development of inflammation and progressive demyelination characteristics

of MS (Tsunoda and Fujinami, 1996). In this model, EAE symptoms start 7 days following immunization. Full-blown symptomatology, characterized by paralysis of tail, hind limbs, and loss of reflexes, develops at 10 days. The disease spontaneously resolves by 15 days following initial immunization.

Temporal analysis of P2X7 receptor expression and its relation to disease progression showed biphasic increase on P2X7 receptor expression in the brain of EAE rats, which was most evident in the frontal motor and somatosensory cortical areas, with higher intensity in the deep cortical layers. Upregulation of P2X7 receptor occurred in astroglia cells at very early stage, when animals were still asymptomatic (Grygorowicz et al., 2010). P2X7 receptor upregulation in neurons and oligodentrocytes occurred later, corresponding to a moment of maximal neurological symptoms, and then decreases to base line levels during the recovery phase (Matute et al., 2007).

Such kinetics indicates that P2X7 receptor-induced cytokine release by glia likely contributes to the inflammatory milieu established very early in the disease development. Higher expression of P2X7 receptor in neurons and olygodendrocytes in the acute phase of the disease, corresponding to a peak in inflammatory cytokine levels and cells death, further intensifies the cytotoxic effects of P2X7 receptor signaling in these cells, contributing to progressive inflammation and degeneration in EAE. Interestingly, total P2X7 receptor levels remained high in the brain of EAE rats even 20 days after immunization and it correlates to increased levels of glial fibrillary acidic protein (GAFP), a marker of astrocyte activation, suggesting a role for P2X7 receptor activation in the sustained astrocytosis that is observed in the advanced stages of the disease, in both EAE and MS, despite clinical recovery (Holley et al., 2003; Grygorowicz et al., 2011). A study performed in brain samples from MS patients has shown up-regulation of P2X7 receptor on astrocytes in the parenchyma of frontal cortex from secondary progressive MS patients, validating the animal findings (Amadio et al., 2017).

Increased P2X7 receptor expression correlates with higher P2X7 receptor signaling in MS. Supporting this assumption, *in vitro* and *in vivo* animal studies have shown that enhanced ATP signaling via P2X7 receptor activation leads to oligodendrocytes excitotoxicity and death, resulting in tissue damage that highly resembles MS lesions. Moreover, administration of P2X7 receptor antagonist to EAE rats significantly decreases astrogliosis, reduces demyelination, and improves neurological symptoms (Matute et al., 2007; Grygorowicz et al., 2016). These findings reinforce eATP-P2X7 signaling as a key factor contributing to MS pathology and the potential use of P2X7 pharmacological blockers to prevent or ameliorate MS symptoms.

Interestingly, temporal analysis of P2X7 receptor expression and activity in myeloid cells in MS patients demonstrated that P2X7 receptor is present but inhibited on peripheral monocytes during the acute phase, while totally absent from microglia/macrophages during the secondary progressive phase. This possibly granted these cells increased survival and further contributed to neuroinflammation in both phases of the disease (Amadio et al., 2017).

Several independent European and Australasian case-control cohort discovery studies have identified a significant association of a rare, loss-of-function, minor allele frequency P2X7 receptor single nucleotide gene polymorphism (SNP), rs28360457, coding for Arg307Gln with protection against MS. The same European cohort also demonstrated a significant association of gain-of-function haplotype in P2X7 receptor with increased risk of MS. Functional studies using monocytes of normal subjects heterozygous carriers of rs28360457 revealed dominant negative effects on pore formation and downstream pro-inflammatory effects, while monocytes harboring the gain-of-function haplotype showed receptor activity two-fold higher than controls (Gu et al., 2015). In addition, a Spanish case-control association study found increased frequency of a gain-of-function SNP, rs17525809, in MS patients compared to control (Oyanguren-Desez et al., 2011). Altogether, the mentioned studies strengthen the hypothesis that P2X7 receptor's gene variants may play a major role in the pathogenesis of MS. Such data also reinforce P2X7 receptor increased expression and functionality as an important feature in MS disease.

Role of P2X7 Receptor in Huntington's Disease (HD)

Huntington's disease is an inherited neurodegenerative disorder caused by a CAG triplet-repeat expansion coding for a polyglutamine (polyQ) sequence in the N-terminal region of the huntingtin (HTT) protein, leading to progressive degeneration of nerve cells in the brain, predominantly in the cortex and striatum. Clinically, patients present progressive cognitive decline, motor, and psychological dysfunction. The molecular mechanisms behind HTT toxicity are still under investigation, but recent studies have suggested a possible role for ATP and P2X7 receptor activation in the pathophysiology of HD.

Increased mRNA and protein levels of P2X7 receptor were described in the brain of two distinct genetic mouse models of HD (Tet/HD94 and R6/1) as compared to WT mice (Díaz-Hernández et al., 2009). In both animal models, P2X7 receptor protein levels were increased at the onset of the motor impairment, and occurred in axonal processes of cortical neurons projecting to the striatum, particularly at the level of synaptic terminals. Moreover, aging related decline of P2X7 receptor levels in striatum that normally occurs in WT mice was less prominent or totally absent in HD mice. Increased synaptic P2X7 receptor expression correlated with modified calcium flux in response to BzATP in synaptosomes isolated from HD mice vs. control WT, suggesting altered P2X7 function in HD synaptic terminal. This may explain the increased sensitivity to BzATP-induced apoptosis in mutant-HTT-expressing primary cortical neurons in culture, which was prevented by BBG (Díaz-Hernández et al., 2009). However, how mutant HTT expression modulates P2X7 receptor levels remains unknown.

Supporting evidence for the involvement of P2X7 receptor in HD onset and development comes from the fact that BBG treatment prevented body weight loss and deterioration of motor coordination of R6/1 mouse model of HD as compared to vehicle-treated HD mice.This protective effect might be

correlated with lower caspase-3 activation in neurons (Díaz-Hernández et al., 2009). Interestingly, P2X7 receptor inhibition was only beneficial when BBG was administered at the age that immediately preceded symptom onset, and had no significant effect when used at earlier ages. This data suggests that a therapy using P2X7 antagonists might be successful only when administered at more advanced stages of the disease, when P2X7 receptor expression is already altered. An important note, despite several reports of the anti-inflammatory effects of P2X7 receptor antagonists in microglia, BBG did not affect reactive gliosis in this HD model (Díaz-Hernández et al., 2009).

Collectively, all those studies support the hypothesis that upregulated expression and function of P2X7 receptor contribute to the pathogenesis of several neuroinflammatory and neurodegenerative diseases, and identify P2X7 receptor as a potential druggable therapeutic target.

BRAIN PERMEABLE P2X7 RECEPTOR PHARMACOLOGICAL INHIBITORS

The development of CNS-permeable P2X7 receptor antagonists has been at the center of intense efforts in the pharmaceutical industry in the last 15 years, a task that has been quite challenging due to poor molecular stability and pharmacokinetic properties. Availability of P2X7 ligands and inhibitors suitable for *in vivo* studies is limited. Despite that, several *in vivo* studies have shown benefits of P2X7 receptor antagonists in animal models of neurodenegerative diseases.

BBG is the P2X7 antagonist most used in animal models of brain disease due to its ability to efficiently cross the blood-brain-barrier (BBB) and infiltrate the brain parenchyma. Intraperitoneal administration of 54.5 mg/kg of BBG results in 200 nM of this compound in the brain in mice, a concentration that is within the range of IC_{50} of BBG to antagonize P2X7 receptor (10–200 nM) and bellow the DL50 by one order magnitude. BBG efficiency in improving disease outcomes has been repeatedly reported in mice models of HD, AD, PD, and epilepsy. However, it is less efficient at antagonizing P2X7 receptor in human than rodents (Jiang et al., 2000). In addition to BBG, the P2X7 receptor blocker A438079 can also cross the BBB, but its use in animal studies has been restricted due to its short half-life (1.02 h) and limited bioavailability (19%) (Nelson et al., 2006). Such pharmacokinetic properties make A438079 inappropriate for chronic applications or clinical purposes. (Díaz-Hernández et al., 2009; Marcellino et al., 2010).

While several classes of specific P2X7 receptor inhibitors have been developed lately, only few of them can efficiently cross the BBB. Despite this progress, finding a potent, selective and CNS penetrable P2X7 receptor inhibitor with acceptable pharmacokinetics (PK), particularly clearance, is still challenging academic researchers and pharmaceutical companies.

In 2010, Pfizer developed a potent P2X7 receptor antagonist (IC_{50} 27 nM), 2-chloro-N-((4,4-difluoro-1-hydroxycyclohexyl)methyl)-5-(5-fluoropyrimidin-2-yl)benzamide, which is an improved version of 2-chlorobenzamide template previously disclosed by AstraZeneca (Guile et al., 2009). This compound showed excellent CNS penetrability, with a brain/plasma ratio of 1.3, in addition to better PK properties when tested in rats: clearance of 3.3 mL/min/kg, 4.6 h half-life and high oral bioavailability of 84% (Chen et al., 2010).

Three years later, Janssen Research and Development released preclinical studies using two newly developed P2X7 receptor antagonists (Letavic et al., 2013). Both compounds demonstrated high potency across different species and reached high levels in the animal's brain. They were also able to successfully reduce signs of neuroinflammation, epilepsy, and seizure, as well as improve behavior in animal models of schizophrenia, hyperactivity, and social stress. However, their compounds had poor PK properties, making them unsuited to further clinical applications (Letavic et al., 2017).

Researchers from The University of Sydney and University of South Australia have recently discovered a new adamantly-cyanoguanidine hybrid compound (O'Brien-Brown et al., 2017). This new hybrid molecule combined two promising classes of P2X7 receptor antagonist as to retain desirable characteristics of each category, i.e., good pharmacokinetic properties of truncated cyanoguanidines scaffold reported by Abbott Laboratories and high potency and selectivity of the adamantyl amide moiety disclosed by AstraZeneca. Using structure-activity studies (SAR) and *in vitro* measurement of P2X7 receptor activity, they identified two promising P2X7 receptor antagonist candidates (IC50 $<$ 50 nM). Unfortunately, the compound identified as having the best druggability, a 3-pyridyl analog, showed poor PK in mice, with a fast clearance (117 mL/min.kg) and extremely short half-life (0.22 h), making it unsuitable for human clinical studies (O'Brien-Brown et al., 2017). While brain levels of the compound were not measured, indirect evidence for CNS penetrability and inhibition of P2X7 receptor *in vivo* was provided by improvement in scape-oriented behavior in forced swimming test (FST), a test designed to evaluate depressive behavior in mice, following administration of the compound. This observation agrees with previous FST studies performed in P2X7 KO mice (Boucher et al., 2011).

Janssen Research & Development has also been working on a series of modification substitutions of the 4-methyl-6,7-dihydro-4H-triazolo[4,5-c] pyridine core in order to develop a P2X7 receptor antagonist suitable for clinical use (Letavic et al., 2017). *In vivo* studies in rats and dogs using the most promising candidate among those modified molecules have shown efficient inhibition of IL-1β release in the brain, with no significant clinical or metabolic side-effects even at the highest administered doses. Based on such performance on PK, efficacy and safety test in animals, Jansen has moved to its first steps in clinical development of their compound and safety tests in healthy volunteers are on their way (Letavic et al., 2017). Their newly developed compound demonstrated very low clearance across several species, including non-human primates, and high bioavailability, which predicted human clearance of 0.6 mL/kg and half-life of 29 h.

Despite all advances in the development of CNS penetrable P2X7 receptor antagonist and promising preclinical evidence, no clinical trial using P2X7 antagonists for treatment CNS disorders

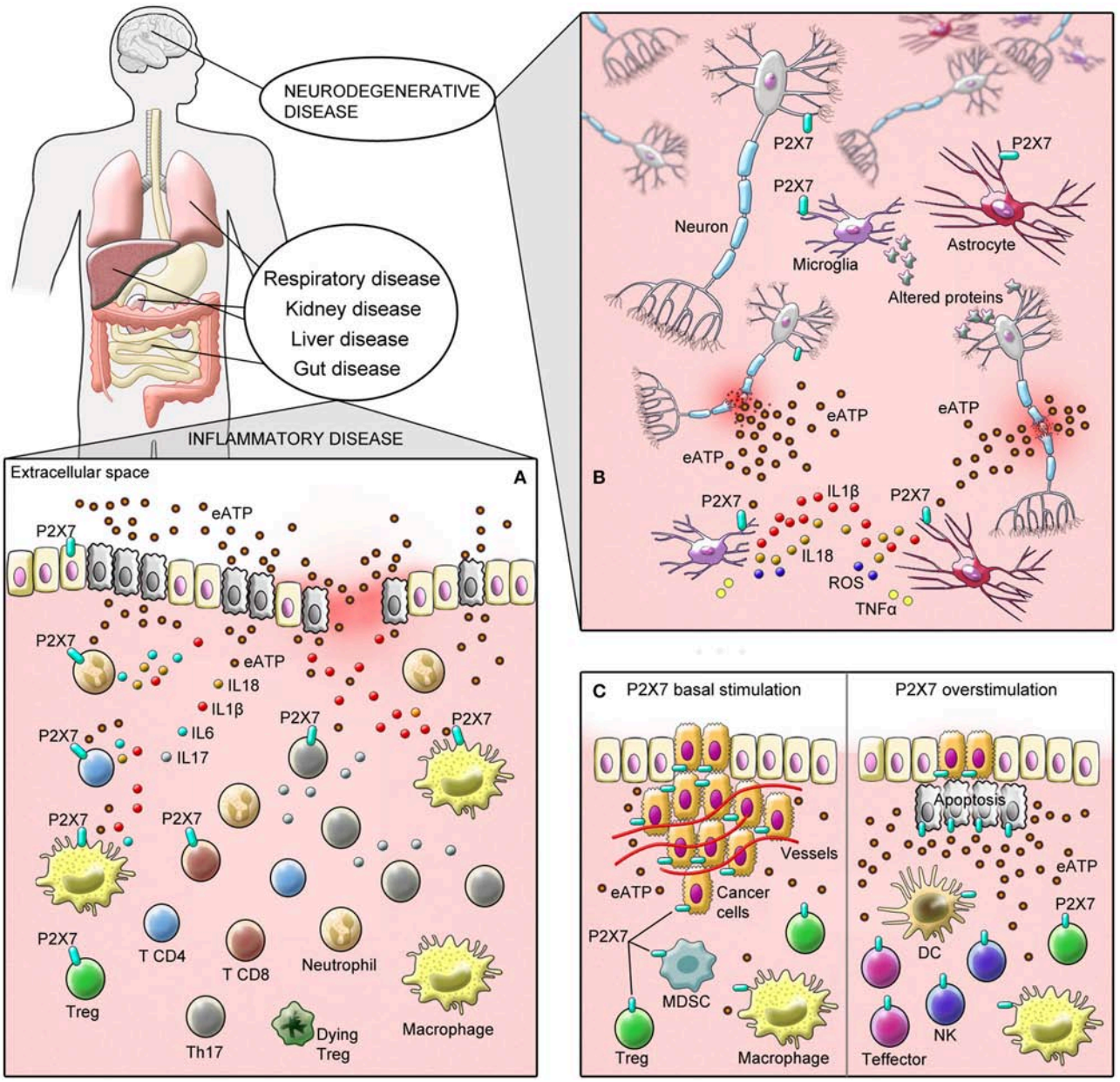

FIGURE 2 | Schematic illustration showing P2X7 receptor deleterious (demon) effects in inflammatory and neurodegenerative disease. **(A)** ATP can be released from injured immune and non-immune cells activating P2X7 receptor. As a consequence, P2X7 receptor activation induces large-scale ATP release—chiefly via pannexin hemichannels—acting as a start point to inflammation. In this scenario, P2X7 activation contributes to the pathogenesis of several inflammatory diseases by activating intracellular signaling pathways and stimulating the production of pro-inflammatory mediators (i.e., ROS, NO, chemokines, and cytokines). In addition, P2X7 receptor induces T cell activation, decreases the suppressive activity and viability of Treg cells and favors the polarization of T cells into Th17 cells promoting inflammation and cell death. **(B)** Likewise, microglial P2X7 receptor activation in neurodegenerative diseases induces inflammasome activation and release of pro-inflammatory cytokines and ROS, leading to the activation of NF-κB signaling, upregulation of pro-inflammatory and pro-apoptotic genes, and death of surrounding cells, including neurons. ATP released from dying cells perpetuates the inflammatory and degenerative cycle, at least in part, via P2X7 receptor. **(C)** P2X7 receptor activation has been linked to conflicting effects on carcinogenesis, being able to exert either pro-tumoral (demon) or anti-tumoral (angel) effects depending on its level of activation and cell type studied. Left: Pro-tumoral effects are associated with P2X7 receptor basal stimulation in tumor cells as well as its activation in immunussupresive cells such as MDSCs and M2-macrophages. Right: On the other hand, anti-tumoral effects can be trigger by P2X7 overstimulation with high levels of exogenous ATP in tumor cells, resulting in membrane pore formation and cell death through apoptosis. In this inflammatory context, eATP accumulation also activates P2X7 receptor highly expressed in DCs, T effectors, NK, and macrophages, boosting the immune response against tumors.

have been conducted to date. GlaxoSmithKline completed a phase I clinical trial to evaluate safety and pharmacodynamics of its pyroglutamate-based P2X7 inhibitor GSK1482160, intended for the treatment of pain and inflammation. Interestingly, this compound has good CNS penetration (B/P ∼0.5). However, while no major safety issues were observed, conclusions from phase I clinical trial led to the discontinuation of the study (Ali et al., 2013). In fact, only three other P2X7 receptor antagonists have been used in clinical trials. In 2009, Pfizer completed a Phase 2a, Randomized, Double-Blind, Placebo-Controlled clinical trial to evaluate the compound CE-224,535 for the treatment of signs and symptoms of rheumatoid arthritis (Stock et al., 2012). Few years later, AstraZeneca performed a phase IIa study and subsequently in a phase IIb clinical trial to assess the effects of AZD9056 on the symptoms of rheumatoid arthritis as well. Unfortunately, despite encouraging results regarding safety, all trial failed to demonstrate efficacy of the compounds in the treatment of RA (Keystone et al., 2012).

CONCLUSION

P2X7 is a multifaceted receptor involved in several physiological and pathological conditions in different body systems by modulating cellular responses in immune and non-immune cells. In infectious inflammatory disease and cancer, P2X7 receptor can have different and contrasting effects, being an angel or a demon depending on its level of activation, cell studied, and type of pathogen.

Overall, ATP-P2X7 receptor signaling boosts the immune system in the context of pathogen infections, activates microbicidal mechanisms, and induces the production of inflammatory mediators in phagocytic cells, as well as modulates adaptive immune responses. Nevertheless, P2X7 receptor activation can generate both protective and deleterious responses depending on the type of pathogen, virulence, and severity of infection. The activation of this ATP-gated ion channel shows deleterious effects during infections by hypervirulent pathogens, inducing severe inflammation and necrotic cell death, release of large amounts of ATP, which results in sustained P2X7 receptor activation, leading to a self-sustained pro-inflammatory cycle (**Figure 1**).

Likewise, increased expression and prolonged activation of P2X7 receptor contribute to the pathogenesis of several inflammatory and neurodegenerative diseases. In the context of these pathologies, P2X7 receptor acts as a start point to initiate inflammation and promotes disease progression by regulating T cell adaptive immune responses. Initially, it can be activated by ATP released from both injured immune and non-immune cells. As a consequence, P2X7 induces large-scale ATP release, boosting inflammation and purinergic signaling. Upon activation, P2X7 triggers intracellular signaling pathways, stimulates the production of pro-inflammatory mediators (i.e., ROS, NO, chemokines, and cytokines), and, consequently, promotes the migration of immune cells to the inflammatory site. In addition, P2X7 receptor induces T cell activation, decreases the suppressive activity and viability of Treg cells and favors the polarization of T cells into Th17 cells, promoting inflammation and cell death (**Figure 2**). Therefore, P2X7 receptor pharmacological inhibition or genetic deletion in different inflammatory models completely abrogates or significantly attenuates inflammation and disease progression.

Finally, the outcomes of studies—aimed at understanding P2X7 pharmacology and using P2X7 receptor agonists, antagonists, and P2X7 KO mice—should be carefully analyzed and discussed in order to accurately bring up the biology and relevance of this receptor in the context of inflammatory and infectious diseases. In addition, peculiarities of each parasite infection and inflammatory disease should be considered when developing pharmacological treatments targeting P2X7 receptor.

AUTHOR CONTRIBUTIONS

LS, PdA, CdS, and RC-S wrote the article. All authors contributed to the study conception and design, and critically revised the manuscript.

ACKNOWLEDGMENTS

This work was supported by funds from the Conselho Nacional de Desenvolvimento Cientifico e Tecnológico do Brasil (CNPq), Coordenação de Aperfeiçoamento de Pessoal de Nível Superior (CAPES), and Fundação de Amparo à Pesquisa do Estado do Rio de Janeiro (FAPERJ – Pós-doutorado Nota 10 Edital 05/2016).

REFERENCES

Abbracchio, M. P., Burnstock, G., Boeynaems, J. M., Barnard, E. A., Boyer, J. L., Kennedy, C., et al. (2006). International Union of Pharmacology LVIII: update on the P2Y G protein-coupled nucleotide receptors: from molecular mechanisms and pathophysiology to therapy. *Pharmacol. Rev.* 58, 281–341. doi: 10.1124/pr.58.3.3

Abdelaziz, H. A., Shaker, M. E., Hamed, M. F., and Gameil, N. M. (2017). Repression of acetaminophen-induced hepatotoxicity by a combination of celastrol and brilliant blue G. *Toxicol. Lett.* 275, 6–18. doi: 10.1016/j.toxlet.2017.04.012

Abdul-Sater, A. A., Saïd-Sadier, N., Padilla, E. V., and Ojcius, D. M. (2010). Chlamydial infection of monocytes stimulates IL-1β secretion through activation of the NLRP3 inflammasome. *Microbes Infect.* 12, 652–661. doi: 10.1016/j.micinf.2010.04.008

Adinolfi, E., Callegari, M. G., Cirillo, M., Pinton, P., Giorgi, C., Cavagna, D., et al. (2009). Expression of the P2X7 receptor increases the $Ca2^{+}$ content of the endoplasmic reticulum, activates NFATc1, and protects from apoptosis. *J. Biol. Chem.* 284, 10120–10128. doi: 10.1074/jbc.M805805200

Adinolfi, E., Callegari, M. G., Ferrari, D., Bolognesi, C., Minelli, M., Wieckowski, M. R., et al. (2005). Basal activation of the P2X7 ATP receptor elevates mitochondrial calcium and potential, increases cellular ATP levels, and promotes serum-independent growth. *Mol. Biol. Cell* 16, 3260–3272. doi: 10.1091/mbc.E04-11-1025

Adinolfi, E., Capece, M., Franceschini, A., Falzoni, S., Giuliani, A. L., Rotondo, A., et al. (2015). Accelerated tumor progression in mice lacking the ATP receptor P2X7. *Cancer Res.* 75, 635–644. doi: 10.1158/0008-5472.CAN-14-1259

Adinolfi, E., Melchiorri, L., Falzoni, S., Chiozzi, P., Morelli, A., Tieghi, A., et al. (2002). P2X7 receptor expression in evolutive and indolent forms of chronic B lymphocytic leukemia. *Blood* 99, 706–708. doi: 10.1182/blood.V99.2.706

Adinolfi, E., Raffaghello, L., Giuliani, A. L., Cavazzini, L., Capece, M., Chiozzi, P., et al. (2012). Expression of P2X7 receptor increases *in vivo* tumor growth. *Cancer Res.* 72, 2957–2969. doi: 10.1158/0008-5472.CAN-11-1947

Amadio, S., Parisi, C., Piras, E., Fabbrizio, P., Apolloni, S., Montilli, C., et al. (2017). Modulation of P2X7 receptor during inflammation in multiple sclerosis. *Front. Immunol.* 8:1529. doi: 10.3389/fimmu.2017.01529

Agteresch, H. J., Burgers, S. A., van der Gaast, A., Wilson, J. H., and Dagnelie, P. C. (2003). Randomized clinical trial of adenosine 5′-triphosphate on tumor growth and survival in advanced lung cancer patients. *Anticancer Drugs* 14, 639–644. doi: 10.1097/00001813-200309000-00009

Akkaya, C., Shumilina, E., Bobballa, D., Brand, V. B., Mahmud, H., Lang, F., et al. (2009). The *Plasmodium falciparum*-induced anion channel of human erythrocytes is an ATP-release pathway. *Pflugers Arch.* 457, 1035–1047. doi: 10.1007/s00424-008-0572-8

Ali, Z., Laurijssens, B., Ostenfeld, T., McHugh, S., Stylianou, A., Scott-Stevens, P., et al. (2013). Pharmacokinetic and pharmacodynamic profiling of a P2X7 receptor allosteric modulator GSK1482160 in healthy human subjects. *Br. J. Clin. Pharmacol.* 75, 197–207. doi: 10.1111/j.1365-2125.2012.04320.x

Allard, B., Longhi, M. S., Robson, S. C., and Stagg, J. (2017). The ectonucleotidases CD39 and CD73: novel checkpoint inhibitor targets. *Immunol. Rev.* 276, 121–144. doi: 10.1111/imr.12528

Alloisio, S., Cervetto, C., Passalacqua, M., Barbieri, R., Maura, G., Nobile, M., et al. (2008). Functional evidence for presynaptic P2X7 receptors in adult rat cerebrocortical nerve terminals. *FEBS Lett.* 582, 3948–3953. doi: 10.1016/j.febslet.2008.10.041

Almeida-da-Silva, C. L., Morandini, A. C., Ulrich, H., Ojcius, D. M., and Coutinho-Silva, R. (2016). Purinergic signaling during *Porphyromonas gingivalis* infection. *Biomed. J.* 39, 251–260. doi: 10.1016/j.bj.2016.08.003

Alvar, J., Velez, I. D., Bern, C., Herrero, M., Desjeux, P., Cano, J., et al. (2012). Leishmaniasis worldwide and global estimates of its incidence. *PLoS ONE* 7:e35671. doi: 10.1371/journal.pone.0035671

Alves, L. A., Bezerra, R. J., Faria, R. X., Ferreira, L. G., and da Silva Frutuoso, V. (2013). Physiological roles and potential therapeutic applications of the P2X7 receptor in inflammation and pain. *Molecules* 18, 10953–10972. doi: 10.3390/molecules180910953

Amaral, E. P., Ribeiro, S. C., Lanes, V. R., Almeida, F. M., de Andrade, M. R., Bomfim, C. C., et al. (2014). Pulmonary infection with hypervirulent Mycobacteria reveals a crucial role for the P2X7 receptor in aggressive forms of tuberculosis. *PLoS Pathog.* 10:e1004188. doi: 10.1371/journal.ppat.1004188

Amoroso, F., Capece, M., Rotondo, A., Cangelosi, D., Ferracin, M., Franceschini, A., et al. (2015). The P2X7 receptor is a key modulator of the PI3K/GSK3β/VEGF signaling network: evidence in experimental neuroblastoma. *Oncogene* 34, 5240–5251. doi: 10.1038/onc.2014.444

Amoroso, F., Falzoni, S., Adinolfi, E., Ferrari, D., and Di Virgilio, F. (2012). The P2X7 receptor is a key modulator of aerobic glycolysis. *Cell Death Dis.* 3:e370. doi: 10.1038/cddis.2012.105

Amoroso, F., Salaro, E., Falzoni, S., Chiozzi, P., Giuliani, A. L., Cavallesco, G., et al. (2016). P2X7 targeting inhibits growth of human mesothelioma. *Oncotarget* 7, 49664–49676. doi: 10.18632/oncotarget.10430

Antonioli, L., Giron, M. C., Colucci, R., Pellegrini, C., Sacco, D., Caputi, V., et al. (2014). Involvement of the P2X7 purinergic receptor in colonic motor dysfunction associated with bowel inflammation in rats. *PLoS ONE* 9:e116253. doi: 10.1371/journal.pone.0116253

Areeshi, M. Y., Mandal, R. K., Dar, S., Wahid, M., Khan, M. E., Panda, A. K., et al. (2015). P2X71513 A>C polymorphism confers increased risk of extrapulmonary tuberculosis: a meta-analysis of case-control studies. *Curr. Genomics* 17, 450–458. doi: 10.2174/1389202917666160513104737

Arulkumaran, N., Unwin, R. J., and Tam, F. W. (2011). A potential therapeutic role for P2X7 receptor (P2X7R) antagonists in the treatment of inflammatory diseases. *Expert Opin. Investig. Drugs* 20, 897–915. doi: 10.1517/13543784.2011.578068

Aymeric, L., Apetoh, L., Ghiringhelli, F., Tesniere, A., Martins, I., Kroemer, G., et al. (2010). Tumor cell death and ATP release prime dendritic cells and efficient anticancer immunity. *Cancer Res.* 70, 855–858. doi: 10.1158/0008-5472.CAN-09-3566

Bae, J. Y., Lee, S. W., Shin, Y. H., Lee, J. H., Jahng, J. W., and Park, K. (2017). P2X7 receptor and NLRP3 inflammasome activation in head and neck cancer. *Oncotarget* 8, 48972–48982 doi: 10.18632/oncotarget.16903

Barat, C., Gilbert, C., Imbeault, M., and Tremblay, M. J. (2008). Extracellular ATP reduces HIV-1 transfer from immature dendritic cells to $CD4^+$ T lymphocytes. *Retrovirology* 5:30. doi: 10.1186/1742-4690-5-30

Baxter, M., Eltom, S., Dekkak, B., Yew-Booth, L., Dubuis, E. D., Maher, S. A., et al. (2014). Role of transient receptor potential and pannexin channels in cigarette smoke-triggered ATP release in the lung. *Thorax* 69, 1080–1089. doi: 10.1136/thoraxjnl-2014-205467

Beigi, R. D., Kertesy, S. B., Aquilina, G., and Dubyak, G. R. (2003). Oxidized ATP (oATP) attenuates proinflammatory signaling via P2 receptor-independent mechanisms. *Br. J. Pharmacol.* 140, 507–519. doi: 10.1038/sj.bjp.0705470

Beijer, S., Hupperets, P. S., van den Borne, B. E., Eussen, S. R., van Henten, A. M., de van den Beuken-van Everdingen, G. A., et al. (2009). Effect of adenosine 5′-triphosphate infusions on the nutritional status and survival of preterminal cancer patients. *Anticancer. Drugs* 20, 625–633. doi: 10.1097/CAD.0b013e32832d4f22

Beijer, S., Hupperets, P. S., van den Borne, B. E., Wijckmans, N. E., Spreeuwenberg, C., van den Brandt, P. A., et al. (2010). Randomized clinical trial on the effects of adenosine 5′-triphosphate infusions on quality of life, functional status, and fatigue in preterminal cancer patients. *J. Pain Symptom Manage.* 40, 520–530. doi: 10.1016/j.jpainsymman.2010.01.023

Ben-Selma, W., Ben-Kahla, I., Boukadida, J., and Harizi, H. (2011). Contribution of the P2X7 1513A/C loss-of-function polymorphism to extrapulmonary tuberculosis susceptibility in Tunisian populations. *FEMS Immunol. Med. Microbiol.* 63, 65–72. doi: 10.1111/j.1574-695X.2011.00824.x

Bergamin, L. S., Braganhol, E., Figueiro, F., Casali, E. A., Zanin, R. F., Sevigny, J., et al. (2015). Involvement of purinergic system in the release of cytokines by macrophages exposed to glioma-conditioned medium. *J. Cell. Biochem.* 116, 721–729. doi: 10.1002/jcb.25018

Bian, S., Sun, X., Bai, A., Zhang, C., Li, L., Enjyoji, K., et al. (2013). P2X7 integrates PI3K/AKT and AMPK-PRAS40-mTOR signaling pathways to mediate tumor cell death. *PLoS ONE* 8:e60184. doi: 10.1371/journal.pone.0060184

Bianco, F., Ceruti, S., Colombo, A., Fumagalli, M., Ferrari, D., Pizzirani, C., et al. (2006). A role for P2X7 in microglial proliferation. *J. Neurochem.* 99, 745–758. doi: 10.1111/j.1471-4159.2006.04101.x

Bianchi, B. R., Lynch, K. J., Touma, E., Niforatos, W., Burgard, E. C., Alexander, K. M., et al. (1999). Pharmacological characterization of recombinant human and rat P2X receptor subtypes. *Eur. J. Pharmacol.* 376, 127–138. doi: 10.1016/S0014-2999(99)00350-7

Bianchi, G., Vuerich, M., Pellegatti, P., Marimpietri, D., Emionite, L., Marigo, I., et al. (2014). ATP/P2X7 axis modulates myeloid-derived suppressor cell functions in neuroblastoma microenvironment. *Cell Death Dis.* 5:e1135. doi: 10.1038/cddis.2014.109

Bomfim, C. C. B., Amaral, E. P., Cassado, A. D. A., Salles, E. M., do Nascimento, R. S., Lasunskaia, E., et al. (2017). P2X7 receptor in bone marrow-derived cells aggravates tuberculosis caused by hypervirulent *Mycobacterium bovis*. *Front. Immunol.* 8:435. doi: 10.3389/fimmu.2017.00435

Boucher, A. A., Arnold, J. C., Hunt, G. E., Spiro, A., Spencer, J., Brown, C., et al. (2011). Resilience and reduced c-Fos expression in P2X7 receptor knockout mice exposed to repeated forced swim test. *Neuroscience* 189, 170–177. doi: 10.1016/j.neuroscience.2011.05.049

Bradford, M. D., and Soltoff, S. P. (2002). P2X7 receptors activate protein kinase D and p42/p44 mitogen-activated protein kinase (MAPK) downstream of protein kinase C. *Biochem. J.* 366, 745–755. doi: 10.1042/bj20020358

Burnstock, G. (1972). Purinergic nerves. *Pharmacol. Rev.* 24, 509–581.

Burnstock, G. (2016). Purinergic signalling in the gut. *Adv. Exp. Med. Biol.* 891, 91–112. doi: 10.1007/978-3-319-27592-5_10

Burnstock, G. (2017a). Purinergic signaling in the cardiovascular system. *Circ. Res.* 120, 207–228. doi: 10.1161/CIRCRESAHA.116.309726

Burnstock, G. (2017b). Purinergic signalling: therapeutic developments. *Front. Pharmacol.* 8:661. doi: 10.3389/fphar.2017.00661

Burnstock, G., and Novak, I. (2012). Purinergic signalling in the pancreas in health and disease. *J. Endocrinol.* 213, 123–141. doi: 10.1530/JOE-11-0434

Burnstock, G., and Novak, I. (2013). Purinergic signalling and diabetes. *Purinergic Signal.* 9, 307–324. doi: 10.1007/s11302-013-9359-2

Burnstock, G., and Verkhratsky, A. (2009). Evolutionary origins of the purinergic signalling system. *Acta Physiol.* 195, 415–447. doi: 10.1111/j.1748-1716.2009.01957.x

Burnstock, G., Brouns, I., Adriaensen, D., and Timmermans, J. P. (2012). Purinergic signaling in the airways. *Pharmacol. Rev.* 64, 834–868. doi: 10.1124/pr.111.005389

Burnstock, G., Campbell, G., Satchell, D., and Smythe, A. (1970). Evidence that adenosine triphosphate or a related nucleotide is the transmitter substance released by non-adrenergic inhibitory nerves in the gut. *Br. J. Pharmacol.* 40, 668–688. doi: 10.1111/j.1476-5381.1970.tb10646.x

Burnstock, G., Evans, L. C., and Bailey, M. A. (2014). Purinergic signalling in the kidney in health and disease. *Purinergic Signal.* 10, 71–101. doi: 10.1007/s11302-013-9400-5

Burnstock, G., Satchell, D. G., and Smythe, A. (1972). A comparison of the excitatory and inhibitory effects of non-adrenergic, non-cholinergic nerve stimulation and exogenously applied ATP on a variety of smooth muscle preparations from different vertebrate species. *Br. J. Pharmacol.* 46, 234–242. doi: 10.1111/j.1476-5381.1972.tb06868.x

Camden, J. M., Schrader, A. M., Camden, R. E., Gonzalez, F. A., Erb, L., Seye, C. I., et al. (2005). P2Y2 nucleotide receptors enhance alpha-secretase-dependent amyloid precursor protein processing. *J. Biol. Chem.* 280, 18696–18702. doi: 10.1074/jbc.M500219200

Carmo, M. R., Menezes, A. P., Nunes, A. C., Pliassova, A., Rolo, A. P., Palmeira, C. M., et al. (2014). The P2X7 receptor antagonist brilliant blue G attenuates contralateral rotations in a rat model of Parkinsonism through a combined control of synaptotoxicity, neurotoxicity and gliosis. *Neuropharmacology* 81, 142–152. doi: 10.1016/j.neuropharm.2014.01.045

Carroll, W. A., Kalvin, D. M., Perez, M. A., Florjancic, A. S., Wang, Y., Donnelly-Roberts, D. L., et al. (2007). Novel and potent 3-(2,3-dichlorophenyl)-4-(benzyl)-4H-1,2,4-triazole P2X7 antagonists. *Bioorg. Med. Chem. Lett.* 17, 4044–4048. doi: 10.1016/j.bmcl.2007.04.075

Cascabulho, C. M., Menna-Barreto, R. F., Coutinho-Silva, R., Persechini, P. M., and Henriques-Pons, A. (2008). P2X7 modulatory web in *Trypanosoma cruzi* infection. *Parasitol. Res.* 103, 829–838. doi: 10.1007/s00436-008-1063-8

Cauwels, A., Rogge, E., Vandendriessche, B., Shiva, S., and Brouckaert, P. (2014). Extracellular ATP drives systemic inflammation, tissue damage and mortality. *Cell Death Dis.* 5:e1102. doi: 10.1038/cddis.2014.70

Cekic, C., and Linden, J. (2016). Purinergic regulation of the immune system. *Nat. Rev. Immunol.* 16, 177–192. doi: 10.1038/nri.2016.4

Chatterjee, S., Rana, R., Corbett, J., Kadiiska, M. B., Goldstein, J., and Mason, R. P. (2012). P2X7 receptor-NADPH oxidase axis mediates protein radical formation and Kupffer cell activation in carbon tetrachloride-mediated steatohepatitis in obese mice. *Free Radic. Biol. Med.* 52, 1666–1679. doi: 10.1016/j.freeradbiomed.2012.02.010

Chaves, M. M., Marques-da-Silva, C., Monteiro, A. P., Canetti, C., and Coutinho-Silva, R. (2014). Leukotriene B4 modulates P2X7 receptor-mediated *Leishmania amazonensis* elimination in murine macrophages. *J. Immunol.* 192, 4765–4773. doi: 10.4049/jimmunol.1301058

Chaves, S. P., Torres-Santos, E. C., Marques, C., Figliuolo, V. R., Persechini, P. M., Coutinho-Silva, R., et al. (2009). Modulation of P2X(7) purinergic receptor in macrophages by *Leishmania amazonensis* and its role in parasite elimination. *Microbes Infect.* 11, 842–849. doi: 10.1016/j.micinf.2009.05.001

Cheewatrakoolpong, B., Gilchrest, H., Anthes, J. C., and Greenfeder, S. (2005). Identification and characterization of splice variants of the human P2X7 ATP channel. *Biochem. Biophys. Res. Commun.* 332, 17–27. doi: 10.1016/j.bbrc.2005.04.087

Chen, Q., Wu, H., Qin, S., Liu, C., Chen, Y., Yang, Y., et al. (2016). The P2X7 receptor involved in gp120-induced cell injury in BV2 microglia. *Inflammation* 39, 1814–1826. doi: 10.1007/s10753-016-0417-0

Chen, X., Pierce, B., Naing, W., Grapperhaus, M. L., and Phillion, D. P. (2010). Discovery of 2-chloro-N-((4,4-difluoro-1-hydroxycyclohexyl)methyl)-5-(5-fluoropyrimidin-2-yl)b enzamide as a potent and CNS penetrable P2X7 receptor antagonist. *Bioorg. Med. Chem. Lett.* 20, 3107–3111. doi: 10.1016/j.bmcl.2010.03.094

Chen, Y. G., Scheuplein, F., Driver, J. P., Hewes, A. A., Reifsnyder, P. C., Leiter, E. H., et al. (2011). Testing the role of P2X7 receptors in the development of type 1 diabetes in nonobese diabetic mice. *J. Immunol.* 186, 4278–4284. doi: 10.4049/jimmunol.1003733

Choi, C. H., Spooner, R., DeGuzman, J., Koutouzis, T., Ojcius, D. M., and Yilmaz, O. (2013). Porphyromonas gingivalis-nucleoside-diphosphate-kinase inhibits ATP-induced reactive-oxygen-species via P2X7 receptor/NADPH-oxidase signalling and contributes to persistence. *Cell. Microbiol.* 15, 961–976. doi: 10.1111/cmi.12089

Chong, J. H., Zheng, G. G., Zhu, X. F., Guo, Y., Wang, L., Ma, C. H., et al. (2010). Abnormal expression of P2X family receptors in Chinese pediatric acute leukemias. *Biochem. Biophys. Res. Commun.* 391, 498–504. doi: 10.1016/j.bbrc.2009.11.087

Cisneros-Mejorado, A., Perez-Samartin, A., Gottlieb, M., and Matute, C. (2015). ATP signaling in brain: release, excitotoxicity and potential therapeutic targets. *Cell. Mol. Neurobiol.* 35, 1–6. doi: 10.1007/s10571-014-0092-3

Cockcroft, S., and Gomperts, B. D. (1980). The ATP4- receptor of rat mast cells. *Biochem. J.* 188, 789–798. doi: 10.1042/bj1880789

Cohen, H. B., Briggs, K. T., Marino, J. P., Ravid, K., Robson, S. C., and Mosser, D. M. (2013). TLR stimulation initiates a CD39-based autoregulatory mechanism that limits macrophage inflammatory responses. *Blood* 122, 1935–1945. doi: 10.1182/blood-2013-04-496216

Corrêa, G., Almeida, L. C., Moreira-Souza, A. C., Savio, L. E., Takiya, C. M., Marques-da-Silva, C., et al. (2017). Inflammatory early events associated to the role of P2X7 receptor in acute murine toxoplasmosis. *Immunobiology* 222, 676–683. doi: 10.1016/j.imbio.2016.12.007

Corrêa, G., de A Lindenberg C., Fernandes-Santos, C., Gandini, M., Petitinga, P. F., Coutinho-Silva, R., et al. (2016). The purinergic receptor P2X7 role in control of Dengue virus-2 infection and cytokine/chemokine production in infected human monocytes. *Immunobiology* 221, 794–802. doi: 10.1016/j.imbio.2016.02.003

Corrêa, G., Marques da, S. C., de Abreu Moreira-Souza, A. C., Vommaro, R. C., and Coutinho-Silva, R. (2010). Activation of the P2X(7) receptor triggers the elimination of *Toxoplasma gondii* tachyzoites from infected macrophages. *Microbes Infect.* 12, 497–504. doi: 10.1016/j.micinf.2010.03.004

Cortés, A., Muñoz-Antoli, C., Esteban, J. G., and Toledo, R. (2017). Th2 and Th1 responses: clear and hidden sides of immunity against intestinal Helminths. *Trends Parasitol.* 33, 678–693. doi: 10.1016/j.pt.2017.05.004

Costa-Junior, H. M., Marques-da-Silva, C., Vieira, F. S., Moncao-Ribeiro, L. C., and Coutinho-Silva, R. (2011). Lipid metabolism modulation by the P2X7 receptor in the immune system and during the course of infection: new insights into the old view. *Purinergic Signal.* 7, 381–392. doi: 10.1007/s11302-011-9255-6

Coutinho-Silva, R., Persechini, P. M., Bisaggio, R. D., Perfettini, J. L., Neto, A. C., Kanellopoulos, J. M., et al. (1999). P2Z/P2X7 receptor-dependent apoptosis of dendritic cells. *Am. J. Physiol.* 276, C1139–C1147. doi: 10.1152/ajpcell.1999.276.5.C1139

Coutinho-Silva, R., and Ojcius, D. M. (2012). Role of extracellular nucleotides in the immune response against intracellular bacteria and protozoan parasites. *Microbes Infect.* 14, 1271–1277. doi: 10.1016/j.micinf.2012.05.009

Coutinho-Silva, R., and Persechini, P. M. (1997). P2Z purinoceptor-associated pores induced by extracellular ATP in macrophages and J774 cells. *Am. J. Physiol.* 273, C1793–C1800. doi: 10.1152/ajpcell.1997.273.6.C1793

Coutinho-Silva, R., Parsons, M., Robson, T., and Burnstock, G. (2001a). Changes in expression of P2 receptors in rat and mouse pancreas during development and ageing. *Cell Tissue Res.* 306, 373–383. doi: 10.1007/s004410100458

Coutinho-Silva, R., Parsons, M., Robson, T., Lincoln, J., and Burnstock, G. (2003a). P2X and P2Y purinoceptor expression in pancreas from streptozotocin-diabetic rats. *Mol. Cell. Endocrinol.* 204, 141–154. doi: 10.1016/S0303-7207(03)00003-0

Coutinho-Silva, R., Perfettini, J. L., Persechini, P. M., Dautry-Varsat, A., and Ojcius, D. M. (2001b). Modulation of P2Z/P2X(7) receptor activity in macrophages infected with *Chlamydia psittaci*. *Am. J. Physiol. Cell Physiol.* 280, C81–C89. doi: 10.1152/ajpcell.2001.280.1.C81

Coutinho-Silva, R., Robson, T., Beales, P. E., and Burnstock, G. (2007). Changes in expression of P2X7 receptors in NOD mouse pancreas during the development of diabetes. *Autoimmunity* 40, 108–116. doi: 10.1080/08916930601118841

Coutinho-Silva, R., Stahl, L., Raymond, M. N., Jungas, T., Verbeke, P., Burnstock, G., et al. (2003b). Inhibition of chlamydial infectious activity due to P2X7R-dependent phospholipase D activation. *Immunity* 19, 403–412. doi: 10.1016/S1074-7613(03)00235-8

Cruz, C. M., Rinna, A., Forman, H. J., Ventura, A. L., Persechini, P. M., and Ojcius, D. M. (2007). ATP activates a reactive oxygen species-dependent oxidative

stress response and secretion of proinflammatory cytokines in macrophages. *J. Biol. Chem.* 282, 2871–2879. doi: 10.1074/jbc.M608083200

Csóka, B., Németh, Z. H., Toro, G., Idzko, M., Zech, A., Koscso, B., et al. (2015a). Extracellular ATP protects against sepsis through macrophage P2X7 purinergic receptors by enhancing intracellular bacterial killing. *FASEB J.* 29, 3626–3637. doi: 10.1096/fj.15-272450

Csóka, B., Nemeth, Z. H., Toro, G., Koscso, B., Kokai, E., Robson, S. C., et al. (2015b). CD39 improves survival in microbial sepsis by attenuating systemic inflammation. *FASEB J.* 29, 25–36. doi: 10.1096/fj.14-253567

Dagvadorj, J., Shimada, K., Chen, S., Jones, H. D., Tumurkhuu, G., Zhang, W., et al. (2015). Lipopolysaccharide induces alveolar macrophage necrosis via CD14 and the P2X7 receptor leading to Interleukin-1alpha release. *Immunity* 42, 640–653. doi: 10.1016/j.immuni.2015.03.007

Dahlquist, R., and Diamant, B. (1970). Further observations on ATP-induced histamine release from rat mast cells. *Acta Pharmacol. Toxicol.* 28, 43.

Darville, T., Welter-Stahl, L., Cruz, C., Sater, A. A., Andrews, C. W. Jr., and Ojcius, D. M. (2007). Effect of the purinergic receptor P2X7 on Chlamydia infection in cervical epithelial cells and vaginally infected mice. *J. Immunol.* 179, 3707–3714. doi: 10.4049/jimmunol.179.6.3707

Das, S., Seth, R. K., Kumar, A., Kadiiska, M. B., Michelotti, G., Diehl, A. M., et al. (2013). Purinergic receptor X7 is a key modulator of metabolic oxidative stress-mediated autophagy and inflammation in experimental nonalcoholic steatohepatitis. *Am. J. Physiol. Gastrointest. Liver Physiol.* 305, G950–G963. doi: 10.1152/ajpgi.00235.2013

de Campos, N. E., Marques-da-Silva, C., Corrêa, G., Castelo-Branco, M. T., de Souza, H. S., and Coutinho-Silva, R. (2012). Characterizing the presence and sensitivity of the P2X7 receptor in different compartments of the gut. *J. Innate Immun.* 4, 529–541. doi: 10.1159/000336628

De Marchi, E., Orioli, E., Dal, B. D., and Adinolfi, E. (2016). P2X7 receptor as a therapeutic target. *Adv. Protein Chem. Struct. Biol.* 104, 39–79. doi: 10.1016/bs.apcsb.2015.11.004

de Visser, K. E., Eichten, A., and Coussens, L. M. (2006). Paradoxical roles of the immune system during cancer development. *Nat. Rev. Cancer* 6, 24–37. doi: 10.1038/nrc1782

Deaglio, S., Dwyer, K. M., Gao, W., Friedman, D., Usheva, A., Erat, A., et al. (2007). Adenosine generation catalyzed by CD39 and CD73 expressed on regulatory T cells mediates immune suppression. *J. Exp. Med.* 204, 1257–1265. doi: 10.1084/jem.20062512

Dekali, S., Divetain, A., Kortulewski, T., Vanbaelinghem, J., Gamez, C., Rogerieux, F., et al. (2013). Cell cooperation and role of the P2X(7) receptor in pulmonary inflammation induced by nanoparticles. *Nanotoxicology* 7, 1302–1314. doi: 10.3109/17435390.2012.735269

Delarasse, C., Auger, R., Gonnord, P., Fontaine, B., and Kanellopoulos, J. M. (2011). The purinergic receptor P2X7 triggers alpha-secretase-dependent processing of the amyloid precursor protein. *J. Biol. Chem.* 286, 2596–2606. doi: 10.1074/jbc.M110.200618

Deli, T., and Csernoch, L. (2008). Extracellular ATP and cancer: an overview with special reference to P2 purinergic receptors. *Pathol. Oncol. Res.* 14, 219–231. doi: 10.1007/s12253-008-9071-7

Deli, T., Varga, N., Adam, A., Kenessey, I., Raso, E., Puskas, L. G., et al. (2007). Functional genomics of calcium channels in human melanoma cells. *Int. J. Cancer* 121, 55–65. doi: 10.1002/ijc.22621

Deplano, S., Cook, H. T., Russell, R., Franchi, L., Schneiter, S., Bhangal, G., et al. (2013). P2X7 receptor-mediated Nlrp3-inflammasome activation is a genetic determinant of macrophage-dependent crescentic glomerulonephritis. *J. Leukoc. Biol.* 93, 127–134. doi: 10.1189/jlb.0612284

Di Virgilio, F. (2003). Novel data point to a broader mechanism of action of oxidized ATP: the P2X7 receptor is not the only target. *Br. J. Pharmacol.* 140, 441–443. doi: 10.1038/sj.bjp.0705469

Di Virgilio, F. (2012). Purines, purinergic receptors, and cancer. *Cancer Res.* 72, 5441–5447. doi: 10.1158/0008-5472.CAN-12-1600

Di Virgilio, F. (2016). P2RX7: a receptor with a split personality in inflammation and cancer. *Mol. Cell Oncol.* 3:e1010937. doi: 10.1080/23723556.2015.1010937

Di Virgilio, F., and Adinolfi, E. (2017). Extracellular purines, purinergic receptors and tumor growth. *Oncogene* 36, 293–303. doi: 10.1038/onc.2016.206

Di Virgilio, F., Chiozzi, P., Ferrari, D., Falzoni, S., Sanz, J. M., Morelli, A., et al. (2001). Nucleotide receptors: an emerging family of regulatory molecules in blood cells. *Blood* 97, 587–600. doi: 10.1182/blood.V97.3.587

Di Virgilio, F., Dal, B. D., Sarti, A. C., Giuliani, A. L., and Falzoni, S. (2017). The P2X7 receptor in infection and inflammation. *Immunity* 47, 15–31. doi: 10.1016/j.immuni.2017.06.020

Diaz-Hernandez, J. I., Gomez-Villafuertes, R., Leon-Otegui, M., Hontecillas-Prieto, L., Del, P. A., Trejo, J. L., et al. (2012). *In vivo* P2X7 inhibition reduces amyloid plaques in Alzheimer's disease through GSK3β and secretases. *Neurobiol. Aging* 33, 1816–1828. doi: 10.1016/j.neurobiolaging.2011.09.040

Díaz-Hernández, M., Diez-Zaera, M., Sanchez-Nogueiro, J., Gomez-Villafuertes, R., Canals, J. M., Alberch, J., et al. (2009). Altered P2X7-receptor level and function in mouse models of Huntington's disease and therapeutic efficacy of antagonist administration. *FASEB J.* 23, 1893–1906. doi: 10.1096/fj.08-122275

Donnelly-Roberts, D. L., Namovic, M. T., Han, P., and Jarvis, M. F. (2009). Mammalian P2X7 receptor pharmacology: comparison of recombinant mouse, rat and human P2X7 receptors. *Br. J. Pharmacol.* 157, 1203–1214. doi: 10.1111/j.1476-5381.2009.00233.x

Drury, A. N., and Szent-Gyorgyi, A. (1929). The physiological activity of adenine compounds with especial reference to their action upon the mammalian heart. *J. Physiol.* 68, 213–237. doi: 10.1113/jphysiol.1929.sp002608

Durrenberger, P. F., Grunblatt, E., Fernando, F. S., Monoranu, C. M., Evans, J., Riederer, P., et al. (2012). Inflammatory pathways in Parkinson's disease; a BNE microarray study. *Parkinsons Dis.* 2012:214714. doi: 10.1155/2012/214714

Easterbrook-Smith, S. B., Wallace, J. C., and Keech, D. B. (1976). Pyruvate carboxylase: affinity labelling of the magnesium adenosine triphosphate binding site. *Eur. J. Biochem.* 62, 125–130. doi: 10.1111/j.1432-1033.1976.tb10105.x

Eser, A., Colombel, J. F., Rutgeerts, P., Vermeire, S., Vogelsang, H., Braddock, M., et al. (2015). Safety and efficacy of an oral inhibitor of the purinergic receptor P2X7 in adult patients with moderately to severely active Crohn's disease: a randomized placebo-controlled, double-blind, phase IIa study. *Inflamm. Bowel Dis.* 21, 2247–2253. doi: 10.1097/MIB.0000000000000514

Fairbairn, I. P., Stober, C. B., Kumararatne, D. S., and Lammas, D. A. (2001). ATP-mediated killing of intracellular mycobacteria by macrophages is a P2X(7)-dependent process inducing bacterial death by phagosome-lysosome fusion. *J. Immunol.* 167, 3300–3307. doi: 10.4049/jimmunol.167.6.3300

Feng, L., Sun, X., Csizmadia, E., Han, L., Bian, S., Murakami, T., et al. (2011). Vascular CD39/ENTPD1 directly promotes tumor cell growth by scavenging extracellular adenosine triphosphate. *Neoplasia* 13, 206–216. doi: 10.1593/neo.101332

Feng, Y. H., Li, X., Wang, L., Zhou, L., and Gorodeski, G. I. (2006a). A truncated P2X7 receptor variant (P2X7-j) endogenously expressed in cervical cancer cells antagonizes the full-length P2X7 receptor through hetero-oligomerization. *J. Biol. Chem.* 281, 17228–17237. doi: 10.1074/jbc.M602999200

Feng, Y. H., Li, X., Zeng, R., and Gorodeski, G. I. (2006b). Endogenously expressed truncated P2X7 receptor lacking the C-terminus is preferentially upregulated in epithelial cancer cells and fails to mediate ligand-induced pore formation and apoptosis. *Nucleosides Nucleotides Nucleic Acids* 25, 1271–1276. doi: 10.1080/15257770600890921

Feriotti, C., de Araujo, E. F., Loures, F. V., da Costa, T. A., Galdino, N. A. L., Zamboni, D. S., et al. (2017). NOD-like receptor P3 inflammasome controls protective Th1/Th17 immunity against pulmonary paracoccidioidomycosis. *Front. Immunol.* 8:786. doi: 10.3389/fimmu.2017.00786

Fernando, K. C., Gargett, C. E., and Wiley, J. S. (1999). Activation of the P2Z/P2X7 receptor in human lymphocytes produces a delayed permeability lesion: involvement of phospholipase D. *Arch. Biochem. Biophys.* 362, 197–202. doi: 10.1006/abbi.1998.1045

Fernando, S. L., Saunders, B. M., Sluyter, R., Skarratt, K. K., Goldberg, H., Marks, G. B., et al. (2007). A polymorphism in the P2X7 gene increases susceptibility to extrapulmonary tuberculosis. *Am. J. Respir. Crit. Care Med.* 175, 360–366. doi: 10.1164/rccm.200607-970OC

Ferrari, D., Chiozzi, P., Falzoni, S., Dal, S. M., Melchiorri, L., Baricordi, O. R., et al. (1997). Extracellular ATP triggers IL-1 β release by activating the purinergic P2Z receptor of human macrophages. *J. Immunol.* 159, 1451–1458.

Ferrari, D., Pizzirani, C., Adinolfi, E., Lemoli, R. M., Curti, A., Idzko, M., et al. (2006). The P2X7 receptor: a key player in IL-1 processing and release. *J. Immunol.* 176, 3877–3883. doi: 10.4049/jimmunol.176.7.3877

Ferrazoli, E. G., de Souza, H. D., Nascimento, I. C., Oliveira-Giacomelli, A., Schwindt, T. T., Britto, L. R., et al. (2017). Brilliant blue, G., but not fenofibrate,

treatment reverts hemiparkinsonian behavior and restores dopamine levels in an animal model of Parkinson's disease. *Cell Transplant.* 26, 669–677. doi: 10.3727/096368917X695227

Figliuolo, V. R., Chaves, S. P., Santoro, G. F., Coutinho, C. M., Meyer-Fernandes, J. R., Rossi-Bergmann, B., et al. (2014). Periodate-oxidized ATP modulates macrophage functions during infection with *Leishmania amazonensis*. *Cytometry A* 85, 588–600. doi: 10.1002/cyto.a.22449

Figliuolo, V. R., Chaves, S. P., Savio, L. E. B., Thorstenberg, M. L. P., Machado, S. E., Takiya, C. M., et al. (2017a). The role of the P2X7 receptor in murine cutaneous leishmaniasis: aspects of inflammation and parasite control. *Purinergic Signal.* 13, 143–152. doi: 10.1007/s11302-016-9544-1

Figliuolo, V. R., Savio, L. E. B., Safya, H., Nanini, H., Bernardazzi, C., Abalo, A., et al. (2017b). P2X7 receptor promotes intestinal inflammation in chemically induced colitis and triggers death of mucosal regulatory T cells. *Biochim. Biophys. Acta* 1863, 1183–1194. doi: 10.1016/j.bbadis.2017.03.004

Florjancic, A. S., Peddi, S., Perez-Medrano, A., Li, B., Namovic, M. T., Grayson, G., et al. (2008). Synthesis and *in vitro* activity of 1-(2,3-dichlorophenyl)-N-(pyridin-3-ylmethyl)-1H-1,2,4-triazol-5-amine and 4-(2,3-dichlorophenyl)-N-(pyridin-3-ylmethyl)-4H-1,2,4-triazol-3-amine P2X7 antagonists. *Bioorg. Med. Chem. Lett.* 18, 2089–2092. doi: 10.1016/j.bmcl.2008.01.095

Franco, M., Bautista-Perez, R., and Perez-Mendez, O. (2015). Purinergic receptors in tubulointerstitial inflammatory cells: a pathophysiological mechanism of salt-sensitive hypertension. *Acta Physiol.* 214, 75–87. doi: 10.1111/apha.12471

Franco-Martínez, S., Nino-Moreno, P., Bernal-Silva, S., Baranda, L., Rocha-Meza, M., Portales-Cervantes, L., et al. (2006). Expression and function of the purinergic receptor P2X7 in patients with pulmonary tuberculosis. *Clin. Exp. Immunol.* 146, 253–261. doi: 10.1111/j.1365-2249.2006.03213.x

Friedle, S. A., Curet, M. A., and Watters, J. J. (2010). Recent patents on novel P2X(7) receptor antagonists and their potential for reducing central nervous system inflammation. *Recent Pat. CNS Drug Discov.* 5, 35–45. doi: 10.2174/157488910789753530

Galam, L., Rajan, A., Failla, A., Soundararajan, R., Lockey, R. F., and Kolliputi, N. (2016). Deletion of P2X7 attenuates hyperoxia-induced acute lung injury via inflammasome suppression. *Am. J. Physiol. Lung Cell. Mol. Physiol.* 310, L572–L581. doi: 10.1152/ajplung.00417.2015

Gallart-Palau, X., Serra, A., Lee, B. S. T., Guo, X., and Sze, S. K. (2017). Brain ureido degenerative protein modifications are associated with neuroinflammation and proteinopathy in Alzheimer's disease with cerebrovascular disease. *J. Neuroinflammation* 14:175 doi: 10.1186/s12974-017-0946-y

Gehring, M. P., Kipper, F., Nicoletti, N. F., Sperotto, N. D., Zanin, R., Tamajusuku, A. S., et al. (2015). P2X7 receptor as predictor gene for glioma radiosensitivity and median survival. *Int. J. Biochem. Cell Biol.* 68, 92–100. doi: 10.1016/j.biocel.2015.09.001

Gehring, M. P., Pereira, T. C., Zanin, R. F., Borges, M. C., Braga, F. A., Battastini, A. M., et al. (2012). P2X7 receptor activation leads to increased cell death in a radiosensitive human glioma cell line. *Purinergic Signal.* 8, 729–739. doi: 10.1007/s11302-012-9319-2

Geistlinger, J., Du, W., Groll, J., Liu, F., Hoegel, J., Foehr, K. J., et al. (2012). P2RX7 genotype association in severe sepsis identified by a novel multi-individual array for rapid screening and replication of risk SNPs. *Clin. Chim. Acta* 413, 39–47. doi: 10.1016/j.cca.2011.05.023

Gentile, D., Natale, M., Lazzerini, P. E., Capecchi, P. L., and Laghi-Pasini, F. (2015). The role of P2X7 receptors in tissue fibrosis: a brief review. *Purinergic Signal.* 11, 435–440. doi: 10.1007/s11302-015-9466-3

Ghalali, A., Wiklund, F., Zheng, H., Stenius, U., and Hogberg, J. (2014). Atorvastatin prevents ATP-driven invasiveness via P2X7 and EHBP1 signaling in PTEN-expressing prostate cancer cells. *Carcinogenesis* 35, 1547–1555. doi: 10.1093/carcin/bgu019

Ghiringhelli, F., Apetoh, L., Tesniere, A., Aymeric, L., Ma, Y., Ortiz, C., et al. (2009). Activation of the NLRP3 inflammasome in dendritic cells induces IL-1β-dependent adaptive immunity against tumors. *Nat. Med.* 15, 1170–1178. doi: 10.1038/nm.2028

Giannuzzo, A., Pedersen, S. F., and Novak, I. (2015). The P2X7 receptor regulates cell survival, migration and invasion of pancreatic ductal adenocarcinoma cells. *Mol. Cancer* 14:203. doi: 10.1186/s12943-015-0472-4

Giannuzzo, A., Saccomano, M., Napp, J., Ellegaard, M., Alves, F., and Novak, I. (2016). Targeting of the P2X7 receptor in pancreatic cancer and stellate cells. *Int. J. Cancer* 139, 2540–2552. doi: 10.1002/ijc.30380

Gilbert, S. M., Gidley, B. A., Glazer, S., Barden, J. A., Glazer, A., Teh, L. C., et al. (2017). A phase I clinical trial demonstrates that nfP2X7 -targeted antibodies provide a novel, safe and tolerable topical therapy for basal cell carcinoma. *Br. J. Dermatol.* 177, 117–124. doi: 10.1111/bjd.15364

Glas, R., Sauter, N. S., Schulthess, F. T., Shu, L., Oberholzer, J., and Maedler, K. (2009). Purinergic P2X7 receptors regulate secretion of interleukin-1 receptor antagonist and β cell function and survival. *Diabetologia* 52, 1579–1588. doi: 10.1007/s00125-009-1349-0

Gonçalves, R. G., Gabrich, L., Rosario, A. Jr., Takiya, C. M., Ferreira, M. L., Chiarini, L. B., et al. (2006). The role of purinergic P2X7 receptors in the inflammation and fibrosis of unilateral ureteral obstruction in mice. *Kidney Int.* 70, 1599–1606. doi: 10.1038/sj.ki.5001804

Granata, S., Masola, V., Zoratti, E., Scupoli, M. T., Baruzzi, A., Messa, M., et al. (2015). NLRP3 inflammasome activation in dialyzed chronic kidney disease patients. *PLoS ONE* 10:e0122272. doi: 10.1371/journal.pone.0122272

Graziano, F., Desdouits, M., Garzetti, L., Podini, P., Alfano, M., Rubartelli, A., et al. (2015). Extracellular ATP induces the rapid release of HIV-1 from virus containing compartments of human macrophages. *Proc. Natl. Acad. Sci. U.S.A.* 112, E3265–E3273. doi: 10.1073/pnas.1500656112

Greve, A. S., Skals, M., Fagerberg, S. K., Tonnus, W., Ellermann-Eriksen, S., Evans, R. J., et al. (2017). P2X1, P2X4, and P2X7 receptor knock out mice expose differential outcome of sepsis induced by alpha-haemolysin producing *Escherichia coli*. *Front. Cell. Infect. Microbiol.* 7:113. doi: 10.3389/fcimb.2017.00113

Grygorowicz, T., Struzynska, L., Sulkowski, G., Chalimoniuk, M., and Sulejczak, D. (2010). Temporal expression of P2X7 purinergic receptor during the course of experimental autoimmune encephalomyelitis. *Neurochem. Int.* 57, 823–829. doi: 10.1016/j.neuint.2010.08.021

Grygorowicz, T., Sulejczak, D., and Struzynska, L. (2011). Expression of purinergic P2X7 receptor in rat brain during the symptomatic phase of experimental autoimmune encephalomyelitis and after recovery of neurological deficits. *Acta Neurobiol. Exp* 71, 65–73.

Grygorowicz, T., Welniak-Kaminska, M., and Struzynska, L. (2016). Early P2X7R-related astrogliosis in autoimmune encephalomyelitis. *Mol. Cell. Neurosci.* 74, 1–9. doi: 10.1016/j.mcn.2016.02.003

Gu, B. J., and Wiley, J. S. (2006). Rapid ATP-induced release of matrix metalloproteinase 9 is mediated by the P2X7 receptor. *Blood* 107, 4946–4953. doi: 10.1182/blood-2005-07-2994

Gu, B. J., Field, J., Dutertre, S., Ou, A., Kilpatrick, T. J., Lechner-Scott, J., et al. (2015). A rare P2X7 variant Arg307Gln with absent pore formation function protects against neuroinflammation in multiple sclerosis. *Hum. Mol. Genet.* 24, 5644–5654. doi: 10.1093/hmg/ddv278

Gudipaty, L., Munetz, J., Verhoef, P. A., and Dubyak, G. R. (2003). Essential role for Ca2+ in regulation of IL-1β secretion by P2X7 nucleotide receptor in monocytes, macrophages, and HEK-293 cells. *Am. J. Physiol. Cell Physiol.* 285, C286–C299. doi: 10.1152/ajpcell.00070.2003

Guile, S. D., Alcaraz, L., Birkinshaw, T. N., Bowers, K. C., Ebden, M. R., Furber, M., et al. (2009). Antagonists of the P2X(7) receptor. From lead identification to drug development. *J. Med. Chem.* 52, 3123–3141. doi: 10.1021/jm801528x

Giuliani, A. L., Colognesi, D., Ricco, T., Roncato, C., Capece, M., Amoroso, F., et al. (2014). Trophic activity of human P2X7 receptor isoforms A and B in osteosarcoma. *PLoS ONE* 9:e107224. doi: 10.1371/journal.pone.0107224

Gulbransen, B. D., Bashashati, M., Hirota, S. A., Gui, X., Roberts, J. A., MacDonald, J. A., et al. (2012). Activation of neuronal P2X7 receptor-pannexin-1 mediates death of enteric neurons during colitis. *Nat. Med.* 18, 600–604. doi: 10.1038/nm.2679

Hanahan, D., and Weinberg, R. A. (2011). Hallmarks of cancer: the next generation. *Cell* 144, 646–674. doi: 10.1016/j.cell.2011.02.013

Hardy, J., and Selkoe, D. J. (2002). The amyloid hypothesis of Alzheimer's disease: progress and problems on the road to therapeutics. *Science* 297, 353–356. doi: 10.1126/science.1072994

Hashimoto-Hill, S., Friesen, L., Kim, M., and Kim, C. H. (2017). Contraction of intestinal effector T cells by retinoic acid-induced purinergic receptor P2X7. *Mucosal Immunol.* 10, 912–923. doi: 10.1038/mi.2016.109

Haskó, G., Csóka, B., Koscsó, B., Chandra, R., Pacher, P., Thompson, L. F., et al. (2011). Ecto-5′-nucleotidase (CD73) decreases mortality and organ injury in sepsis. *J. Immunol.* 187, 4256–4267. doi: 10.4049/jimmunol.1003379

Hattori, M., and Gouaux, E. (2012). Molecular mechanism of ATP binding and ion channel activation in P2X receptors. *Nature* 485, 207–212. doi: 10.1038/nature11010

Hazleton, J. E., Berman, J. W., and Eugenin, E. A. (2012). Purinergic receptors are required for HIV-1 infection of primary human macrophages. *J. Immunol.* 188, 4488–4495. doi: 10.4049/jimmunol.1102482

He, X., Mekasha, S., Mavrogiorgos, N., Fitzgerald, K. A., Lien, E., and Ingalls, R. R. (2010). Inflammation and fibrosis during *Chlamydia pneumoniae* infection is regulated by IL-1 and the NLRP3/ASC inflammasome. *J. Immunol.* 184, 5743–5754. doi: 10.4049/jimmunol.0903937

Herweg, J. A., and Rudel, T. (2016). Interaction of *Chlamydiae* with human macrophages. *FEBS J.* 283, 608–618. doi: 10.1111/febs.13609

Hewinson, J., and Mackenzie, A. B. (2007). P2X(7) receptor-mediated reactive oxygen and nitrogen species formation: from receptor to generators. *Biochem. Soc. Trans.* 35, 1168–1170. doi: 10.1042/BST0351168

Hibell, A. D., Kidd, E. J., Chessell, I. P., Humphrey, P. P., and Michel, A. D. (2000). Apparent species differences in the kinetic properties of P2X(7) receptors. *Br. J. Pharmacol.* 130, 167–173. doi: 10.1038/sj.bjp.0703302

Hill, L. M., Gavala, M. L., Lenertz, L. Y., and Bertics, P. J. (2010). Extracellular ATP may contribute to tissue repair by rapidly stimulating purinergic receptor X7-dependent vascular endothelial growth factor release from primary human monocytes. *J. Immunol.* 185, 3028–3034. doi: 10.4049/jimmunol.1001298

Hise, A. G., Tomalka, J., Ganesan, S., Patel, K., Hall, B. A., Brown, G. D., et al. (2009). An essential role for the NLRP3 inflammasome in host defense against the human fungal pathogen *Candida albicans*. *Cell Host Microbe* 5, 487–497. doi: 10.1016/j.chom.2009.05.002

Hofman, P., Cherfils-Vicini, J., Bazin, M., Ilie, M., Juhel, T., Hebuterne, X., et al. (2015). Genetic and pharmacological inactivation of the purinergic P2RX7 receptor dampens inflammation but increases tumor incidence in a mouse model of colitis-associated cancer. *Cancer Res.* 75, 835–845. doi: 10.1158/0008-5472.CAN-14-1778

Holley, J. E., Gveric, D., Newcombe, J., Cuzner, M. L., and Gutowski, N. J. (2003). Astrocyte characterization in the multiple sclerosis glial scar. *Neuropathol. Appl. Neurobiol.* 29, 434–444. doi: 10.1046/j.1365-2990.2003.00491.x

Holton, F. A., and Holton, P. (1954). The capillary dilator substances in dry powders of spinal roots; a possible role of adenosine triphosphate in chemical transmission from nerve endings. *J. Physiol.* 126, 124–140. doi: 10.1113/jphysiol.1954.sp005198

Holton, P. (1959). The liberation of adenosine triphosphate on antidromic stimulation of sensory nerves. *J. Physiol.* 145, 494–504. doi: 10.1113/jphysiol.1959.sp006157

Honore, P., Donnelly-Roberts, D., Namovic, M. T., Hsieh, G., Zhu, C. Z., Mikusa, J. P., et al. (2006). A-740003 [N-(1-{[(cyanoimino)(5-quinolinylamino) methyl]amino}-2,2-dimethylpropyl)-2-(3,4-dimethoxyphenyl)acetamide], a novel and selective P2X7 receptor antagonist, dose-dependently reduces neuropathic pain in the rat. *J. Pharmacol. Exp. Ther.* 319, 1376–1385. doi: 10.1124/jpet.106.111559

Honore, P., Donnelly-Roberts, D., Namovic, M., Zhong, C., Wade, C., Chandran, P., et al. (2009). The antihyperalgesic activity of a selective P2X7 receptor antagonist, A-839977, is lost in IL-1alphaβ knockout mice. *Behav. Brain Res.* 204, 77–81. doi: 10.1016/j.bbr.2009.05.018

Hoque, R., Sohail, M. A., Salhanick, S., Malik, A. F., Ghani, A., Robson, S. C., et al. (2012). P2X7 receptor-mediated purinergic signaling promotes liver injury in acetaminophen hepatotoxicity in mice. *Am. J. Physiol. Gastrointest. Liver Physiol.* 302, G1171–G1179. doi: 10.1152/ajpgi.00352.2011

Hotez, P. J., Alvarado, M., Basanez, M. G., Bolliger, I., Bourne, R., Boussinesq, M., et al. (2014). The global burden of disease study 2010: interpretation and implications for the neglected tropical diseases. *PLoS Negl. Trop. Dis.* 8:e2865. doi: 10.1371/journal.pntd.0002865

Hracskó, Z., Baranyi, M., Csolle, C., Goloncser, F., Madarasz, E., Kittel, A., et al. (2011). Lack of neuroprotection in the absence of P2X7 receptors in toxin-induced animal models of Parkinson's disease. *Mol. Neurodegener.* 6:28. doi: 10.1186/1750-1326-6-28

Huang, C., Yu, W., Cui, H., Wang, Y., Zhang, L., Han, F., et al. (2014). P2X7 blockade attenuates mouse liver fibrosis. *Mol. Med. Rep.* 9, 57–62. doi: 10.3892/mmr.2013.1807

Huang, S. W., Walker, C., Pennock, J., Else, K., Muller, W., Daniels, M. J., et al. (2017). P2X7 receptor-dependent tuning of gut epithelial responses to infection. *Immunol. Cell Biol.* 95, 178–188. doi: 10.1038/icb.2016.75

Humphreys, B. D., and Dubyak, G. R. (1996). Induction of the P2z/P2X7 nucleotide receptor and associated phospholipase D activity by lipopolysaccharide and IFN-γ in the human THP-1 monocytic cell line. *J. Immunol.* 157, 5627–5637.

Hung, S. C., Choi, C. H., Said-Sadier, N., Johnson, L., Atanasova, K. R., Sellami, H., et al. (2013). P2X4 assembles with P2X7 and pannexin-1 in gingival epithelial cells and modulates ATP-induced reactive oxygen species production and inflammasome activation. *PLoS ONE* 8:e70210. doi: 10.1371/journal.pone.0070210

Idzko, M., Ferrari, D., and Eltzschig, H. K. (2014). Nucleotide signalling during inflammation. *Nature* 509, 310–317. doi: 10.1038/nature13085

Jacob, F., Perez, N. C., Bachert, C., and Van, C. K. (2013). Purinergic signaling in inflammatory cells: P2 receptor expression, functional effects, and modulation of inflammatory responses. *Purinergic Signal.* 9, 285–306. doi: 10.1007/s11302-013-9357-4

Jacques-Silva, M. C., Rodnight, R., Lenz, G., Liao, Z., Kong, Q., Tran, M., et al. (2004). P2X7 receptors stimulate AKT phosphorylation in astrocytes. *Br. J. Pharmacol.* 141, 1106–1117. doi: 10.1038/sj.bjp.0705685

Jamieson, S. E., Peixoto-Rangel, A. L., Hargrave, A. C., Roubaix, L. A., Mui, E. J., Boulter, N. R., et al. (2010). Evidence for associations between the purinergic receptor P2X(7) (P2RX7) and toxoplasmosis. *Genes Immun.* 11, 374–383. doi: 10.1038/gene.2010.31

Jelassi, B., Anchelin, M., Chamouton, J., Cayuela, M. L., Clarysse, L., Li, J., et al. (2013). Anthraquinone emodin inhibits human cancer cell invasiveness by antagonizing P2X7 receptors. *Carcinogenesis* 34, 1487–1496. doi: 10.1093/carcin/bgt099

Jelassi, B., Chantome, A., Alcaraz-Perez, F., Baroja-Mazo, A., Cayuela, M. L., Pelegrin, P., et al. (2011). P2X(7) receptor activation enhances SK3 channels-and cystein cathepsin-dependent cancer cells invasiveness. *Oncogene* 30, 2108–2122. doi: 10.1038/onc.2010.593

Ji, X., Naito, Y., Hirokawa, G., Weng, H., Hiura, Y., Takahashi, R., et al. (2012a). P2X(7) receptor antagonism attenuates the hypertension and renal injury in Dahl salt-sensitive rats. *Hypertens. Res.* 35, 173–179. doi: 10.1038/hr.2011.153

Ji, X., Naito, Y., Weng, H., Endo, K., Ma, X., and Iwai, N. (2012b). P2X7 deficiency attenuates hypertension and renal injury in deoxycorticosterone acetate-salt hypertension. *Am. J. Physiol. Renal Physiol.* 303, F1207–F1215. doi: 10.1152/ajprenal.00051.2012

Jiang, L. H., Mackenzie, A. B., North, R. A., and Surprenant, A. (2000). Brilliant blue G selectively blocks ATP-gated rat P2X(7) receptors. *Mol. Pharmacol.* 58, 82–88. doi: 10.1124/mol.58.1.82

Jiang, S., Zhang, Y., Zheng, J. H., Li, X., Yao, Y. L., Wu, Y. L., et al. (2017). Potentiation of hepatic stellate cell activation by extracellular ATP is dependent on P2X7R-mediated NLRP3 inflammasome activation. *Pharmacol. Res.* 117, 82–93. doi: 10.1016/j.phrs.2016.11.040

Jiang, T., Hoekstra, J., Heng, X., Kang, W., Ding, J., Liu, J., et al. (2015). P2X7 receptor is critical in alpha-synuclein–mediated microglial NADPH oxidase activation. *Neurobiol. Aging* 36, 2304–2318. doi: 10.1016/j.neurobiolaging.2015.03.015

Jin, H., Han, J., Resing, D., Liu, H., Yue, X., Miller, R. L., et al. (2017). Synthesis and *in vitro* characterization of a P2X7 radioligand [(123)I]TZ6019 and its response to neuroinflammatory in a mouse model of Alzheimer disease. *Eur. J. Pharmacol.* 820, 8–17. doi: 10.1016/j.ejphar.2017.12.006

Jo, S., and Bean, B. P. (2011). Inhibition of neuronal voltage-gated sodium channels by brilliant blue G. *Mol. Pharmacol.* 80, 247–257. doi: 10.1124/mol.110.070276

Jun, D. J., Kim, J., Jung, S. Y., Song, R., Noh, J. H., Park, Y. S., et al. (2007). Extracellular ATP mediates necrotic cell swelling in SN4741 dopaminergic neurons through P2X7 receptors. *J. Biol. Chem.* 282, 37350–37358. doi: 10.1074/jbc.M707915200

Kaczmarek-Hájek, K., Lorinczi, E., Hausmann, R., and Nicke, A. (2012). Molecular and functional properties of P2X receptors–recent progress and persisting challenges. *Purinergic Signal.* 8, 375–417. doi: 10.1007/s11302-012-9314-7

Kahlenberg, J. M., Lundberg, K. C., Kertesy, S. B., Qu, Y., and Dubyak, G. R. (2005). Potentiation of caspase-1 activation by the P2X7 receptor is dependent on TLR signals and requires NF-kappaB-driven protein synthesis. *J. Immunol.* 175, 7611–7622. doi: 10.4049/jimmunol.175.11.7611

Keystone, E. C., Wang, M. M., Layton, M., Hollis, S., McInnes, I. B., and D1520C00001 Study Team (2012). Clinical evaluation of the efficacy of the P2X7 purinergic receptor antagonist AZD9056 on the signs and symptoms of rheumatoid arthritis in patients with active disease despite treatment with methotrexate or sulphasalazine. *Ann. Rheum. Dis.* 71, 1630–1635. doi: 10.1136/annrheumdis-2011-143578

Kidd, P. M. (2001). Multiple sclerosis, an autoimmune inflammatory disease: prospects for its integrative management. *Altern. Med. Rev.* 6, 540–566.

Kim, S. Y., Moon, J. H., Lee, H. G., Kim, S. U., and Lee, Y. B. (2007). ATP released from β-amyloid-stimulated microglia induces reactive oxygen species production in an autocrine fashion. *Exp. Mol. Med.* 39, 820–827. doi: 10.1038/emm.2007.89

Koffie, R. M., Hashimoto, T., Tai, H. C., Kay, K. R., Serrano-Pozo, A., Joyner, D., et al. (2012). Apolipoprotein E4 effects in Alzheimer's disease are mediated by synaptotoxic oligomeric amyloid-β. *Brain* 135, 2155–2168. doi: 10.1093/brain/aws127

Kong, Q., Peterson, T. S., Baker, O., Stanley, E., Camden, J., Seye, C. I., et al. (2009). Interleukin-1β enhances nucleotide-induced and alpha-secretase-dependent amyloid precursor protein processing in rat primary cortical neurons via up-regulation of the P2Y(2) receptor. *J. Neurochem.* 109, 1300–1310. doi: 10.1111/j.1471-4159.2009.06048.x

Koo, T. Y., Lee, J. G., Yan, J. J., Jang, J. Y., Ju, K. D., Han, M., et al. (2017). The P2X7 receptor antagonist, oxidized adenosine triphosphate, ameliorates renal ischemia-reperfusion injury by expansion of regulatory T cells. *Kidney Int.* 92, 415–431. doi: 10.1016/j.kint.2017.01.031

Kumar, S., Mishra, A., and Krishnamurthy, S. (2017). Purinergic antagonism prevents mitochondrial dysfunction and behavioral deficits associated with dopaminergic toxicity induced by 6-OHDA in rats. *Neurochem. Res.* 42, 3414–3430. doi: 10.1007/s11064-017-2383-9

Kurashima, Y., Amiya, T., Nochi, T., Fujisawa, K., Haraguchi, T., Iba, H., et al. (2012). Extracellular ATP mediates mast cell-dependent intestinal inflammation through P2X7 purinoceptors. *Nat. Commun.* 3:1034. doi: 10.1038/ncomms2023

Kusner, D. J., and Adams, J. (2000). ATP-induced killing of virulent *Mycobacterium tuberculosis* within human macrophages requires phospholipase D. *J. Immunol.* 164, 379–388. doi: 10.4049/jimmunol.164.1.379

Kwon, J. H., Nam, E. S., Shin, H. S., Cho, S. J., Park, H. R., and Kwon, M. J. (2014). P2X7 receptor expression in coexistence of papillary thyroid carcinoma with Hashimoto's thyroiditis. *Korean J. Pathol.* 48, 30–35. doi: 10.4132/KoreanJPathol.2014.48.1.30

Ledderose, C., Bao, Y., Kondo, Y., Fakhari, M., Slubowski, C., Zhang, J., et al. (2016). Purinergic signaling and the immune response in Sepsis: a review. *Clin. Ther.* 38, 1054–1065. doi: 10.1016/j.clinthera.2016.04.002

Lee, B. H., Hwang, D. M., Palaniyar, N., Grinstein, S., Philpott, D. J., and Hu, J. (2012). Activation of P2X(7) receptor by ATP plays an important role in regulating inflammatory responses during acute viral infection. *PLoS ONE* 7:e35812. doi: 10.1371/journal.pone.0035812

Lees, M. P., Fuller, S. J., McLeod, R., Boulter, N. R., Miller, C. M., Zakrzewski, A. M., et al. (2010). P2X7 receptor-mediated killing of an intracellular parasite, *Toxoplasma gondii*, by human and murine macrophages. *J. Immunol.* 184, 7040–7046. doi: 10.4049/jimmunol.1000012

Lenertz, L. Y., Gavala, M. L., Zhu, Y., and Bertics, P. J. (2011). Transcriptional control mechanisms associated with the nucleotide receptor P2X7, a critical regulator of immunologic, osteogenic, and neurologic functions. *Immunol. Res.* 50, 22–38. doi: 10.1007/s12026-011-8203-4

León-Otegui, M., Gomez-Villafuertes, R., Diaz-Hernandez, J. I., Diaz-Hernandez, M., Miras-Portugal, M. T., and Gualix, J. (2011). Opposite effects of P2X7 and P2Y2 nucleotide receptors on alpha-secretase-dependent APP processing in Neuro-2a cells. *FEBS Lett.* 585, 2255–2262. doi: 10.1016/j.febslet.2011.05.048

Letavic, M. A., Savall, B. M., Allison, B. D., Aluisio, L., Andres, J. I., De, A. M., et al. (2017). 4-Methyl-6,7-dihydro-4H-triazolo[4,5-c]pyridine-based P2X7 receptor antagonists: optimization of pharmacokinetic properties leading to the identification of a clinical candidate. *J. Med. Chem.* 60, 4559–4572. doi: 10.1021/acs.jmedchem.7b00408

Letavic, M. A., Lord, B., Bischoff, F., Hawryluk, N. A., Pieters, S., Rech, J. C., et al. (2013). Synthesis and pharmacological characterization of two novel, brain penetrating P2X7 antagonists. *ACS Med. Chem. Lett.* 4, 419–422. doi: 10.1021/ml400040v

Levano-Garcia, J., Dluzewski, A. R., Markus, R. P., and Garcia, C. R. (2010). Purinergic signalling is involved in the malaria parasite *Plasmodium falciparum* invasion to red blood cells. *Purinergic Signal.* 6, 365–372. doi: 10.1007/s11302-010-9202-y

Leyva-Grado, V. H., Ermler, M. E., Schotsaert, M., Gonzalez, M. G., Gillespie, V., Lim, J. K., et al. (2017). Contribution of the Purinergic receptor P2X7 to development of lung immunopathology during influenza virus infection. *MBio*. 8:e00229-17. doi: 10.1128/mBio.00229-17

Li, X., Zhou, L., Feng, Y. H., Abdul-Karim, F. W., and Gorodeski, G. I. (2006). The P2X7 receptor: a novel biomarker of uterine epithelial cancers. *Cancer Epidemiol. Biomarkers Prev.* 15, 1906–1913. doi: 10.1158/1055-9965.EPI-06-0407

Liang, L., and Schwiebert, E. M. (2005). Large pore formation uniquely associated with P2X7 purinergic receptor channels. Focus on "Are second messengers crucial for opening the pore associated with P2X7 receptor?" *Am. J. Physiol. Cell Physiol.* 288, C240–C242. doi: 10.1152/ajpcell.00532.2004

Liu, Y., Chen, G. Q., Liu, B. Y., Chen, Q., Qian, Y. M., Qin, S. S., et al. (2017). P2X7 receptor in the hippocampus is involved in gp120-induced cognitive dysfunction. *Genet. Mol. Res.* 16, 1–12. doi: 10.4238/gmr16019356

Liu, Y., Xiao, Y., and Li, Z. (2011). P2X7 receptor positively regulates MyD88-dependent NF-kappaB activation. *Cytokine* 55, 229–236. doi: 10.1016/j.cyto.2011.05.003

Liu, Z., Liu, Y., Xu, L., An, H., Chang, Y., Yang, Y., et al. (2015). P2X7 receptor predicts postoperative cancer-specific survival of patients with clear-cell renal cell carcinoma. *Cancer Sci.* 106, 1224–1231. doi: 10.1111/cas.12736

Longhi, M. S., Moss, A., Jiang, Z. G., and Robson, S. C. (2017). Purinergic signaling during intestinal inflammation. *J. Mol. Med.* 95, 915–925. doi: 10.1007/s00109-017-1545-1

Lucchinetti, C. F., Popescu, B. F., Bunyan, R. F., Moll, N. M., Roemer, S. F., Lassmann, H., et al. (2011). Inflammatory cortical demyelination in early multiple sclerosis. *N. Engl. J. Med.* 365, 2188–2197. doi: 10.1056/NEJMoa1100648

Mantuano-Barradas, M., Henriques-Pons, A., Araujo-Jorge, T. C., Di Virgilio, F., Coutinho-Silva, R., and Persechini, P. M. (2003). Extracellular ATP induces cell death in CD4+/CD8+ double-positive thymocytes in mice infected with *Trypanosoma cruzi*. *Microbes Infect.* 5, 1363–1371. doi: 10.1016/j.micinf.2003.09.017

Marcellino, D., Suarez-Boomgaard, D., Sanchez-Reina, M. D., Aguirre, J. A., Yoshitake, T., Yoshitake, S., et al. (2010). On the role of P2X(7) receptors in dopamine nerve cell degeneration in a rat model of Parkinson's disease: studies with the P2X(7) receptor antagonist A-438079. *J. Neural. Transm.* 117, 681–687. doi: 10.1007/s00702-010-0400-0

Marques, C. C., Castelo-Branco, M. T., Pacheco, R. G., Buongusto, F., do Rosário, A. Jr., Schanaider, A., et al. (2014). Prophylactic systemic P2X7 receptor blockade prevents experimental colitis. *Biochim. Biophys. Acta* 1842, 65–78. doi: 10.1016/j.bbadis.2013.10.012

Marques-da-Silva, C., Chaves, M. M., Rodrigues, J. C., Corte-Real, S., Coutinho-Silva, R., and Persechini, P. M. (2011). Differential modulation of ATP-induced P2X7-associated permeabilities to cations and anions of macrophages by infection with *Leishmania amazonensis*. *PLoS ONE* 6:e25356. doi: 10.1371/journal.pone.0025356

Masin, M., Young, C., Lim, K., Barnes, S. J., Xu, X. J., Marschall, V., et al. (2012). Expression, assembly and function of novel C-terminal truncated variants of the mouse P2X7 receptor: re-evaluation of P2X7 knockouts. *Br. J. Pharmacol.* 165, 978–993. doi: 10.1111/j.1476-5381.2011.01624.x

Matsukawa, T., Izawa, K., Isobe, M., Takahashi, M., Maehara, A., Yamanishi, Y., et al. (2016). Ceramide-CD300f binding suppresses experimental colitis by inhibiting ATP-mediated mast cell activation. *Gut* 65, 777–787. doi: 10.1136/gutjnl-2014-308900

Matute, C., Torre, I., Perez-Cerda, F., Perez-Samartin, A., Alberdi, E., Etxebarria, E., et al. (2007). P2X(7) receptor blockade prevents ATP excitotoxicity in oligodendrocytes and ameliorates experimental autoimmune encephalomyelitis. *J. Neurosci.* 27, 9525–9533. doi: 10.1523/JNEUROSCI.0579-07.2007

McLarnon, J. G., Ryu, J. K., Walker, D. G., and Choi, H. B. (2006). Upregulated expression of purinergic P2X(7) receptor in Alzheimer

disease and amyloid-β peptide-treated microglia and in peptide-injected rat hippocampus. *J. Neuropathol. Exp. Neurol.* 65, 1090–1097. doi: 10.1097/01.jnen.0000240470.97295.d3

Mehta, N., Kaur, M., Singh, M., Chand, S., Vyas, B., Silakari, P., et al. (2014). Purinergic receptor P2X(7): a novel target for anti-inflammatory therapy. *Bioorg. Med. Chem.* 22, 54–88. doi: 10.1016/j.bmc.2013.10.054

Mello, P. A., Bian, S., Savio, L. E. B., Zhang, H., Zhang, J., Junger, W., et al. (2017a). Hyperthermia and associated changes in membrane fluidity potentiate P2X7 activation to promote tumor cell death. *Oncotarget* 8, 67254–67268. doi: 10.18632/oncotarget.18595

Mello, P. A., Coutinho-Silva, R., and Savio, L. E. B. (2017b). Multifaceted effects of extracellular ATP and adenosine in the tumor-host interaction and therapeutic perspectives. *Front. Immunol.* 8:1526. doi: 10.3389/fimmu.2017.01526

Mello, P. A., Filippi-Chiela, E. C., Nascimento, J., Beckenkamp, A., Santana, D. B., Kipper, F., et al. (2014). Adenosine uptake is the major effector of extracellular ATP toxicity in human cervical cancer cells. *Mol. Biol. Cell* 25, 2905–2918. doi: 10.1091/mbc.E14-01-0042

Menzies, R. I., Booth, J. W. R., Mullins, J. J., Bailey, M. A., Tam, F. W. K., Norman, J. T., et al. (2017a). Hyperglycemia-induced renal P2X7 receptor activation enhances diabetes-related injury. *EBioMedicine* 19, 73–83. doi: 10.1016/j.ebiom.2017.04.011

Menzies, R. I., Howarth, A. R., Unwin, R. J., Tam, F. W., Mullins, J. J., and Bailey, M. A. (2015). Inhibition of the purinergic P2X7 receptor improves renal perfusion in angiotensin-II-infused rats. *Kidney Int.* 88, 1079–1087. doi: 10.1038/ki.2015.182

Menzies, R. I., Tam, F. W., Unwin, R. J., and Bailey, M. A. (2017b). Purinergic signaling in kidney disease. *Kidney Int.* 91, 315–323. doi: 10.1016/j.kint.2016.08.029

Metzger, M. W., Walser, S. M., Aprile-Garcia, F., Dedic, N., Chen, A., Holsboer, F., et al. (2017). Genetically dissecting P2rx7 expression within the central nervous system using conditional humanized mice. *Purinergic Signal.* 13, 153–170. doi: 10.1007/s11302-016-9546-z

Meuser-Batista, M., Correa, J. R., Carvalho, V. F., de Carvalho Britto, C. F., Moreira, O. C., Batista, M. M., et al. (2011). Mast cell function and death in *Trypanosoma cruzi* infection. *Am. J. Pathol.* 179, 1894–1904. doi: 10.1016/j.ajpath.2011.06.014

Miller, C. M., Zakrzewski, A. M., Ikin, R. J., Boulter, N. R., Katrib, M., Lees, M. P., et al. (2011). Dysregulation of the inflammatory response to the parasite, *Toxoplasma gondii*, in P2X7 receptor-deficient mice. *Int. J. Parasitol.* 41, 301–308. doi: 10.1016/j.ijpara.2010.10.001

Miller, C. M., Zakrzewski, A. M., Robinson, D. P., Fuller, S. J., Walker, R. A., Ikin, R. J., et al. (2015). Lack of a functioning P2X7 receptor leads to increased susceptibility to toxoplasmic ileitis. *PLoS ONE* 10:e0129048. doi: 10.1371/journal.pone.0129048

Miras-Portugal, M. T., Diaz-Hernandez, J. I., Gomez-Villafuertes, R., Diaz-Hernandez, M., Artalejo, A. R., and Gualix, J. (2015). Role of P2X7 and P2Y2 receptors on alpha-secretase-dependent APP processing: control of amyloid plaques formation "*in vivo*" by P2X7 receptor. *Comput. Struct. Biotechnol. J.* 13, 176–181. doi: 10.1016/j.csbj.2015.02.005

Mishra, A., Chintagari, N. R., Guo, Y., Weng, T., Su, L., and Liu, L. (2011). Purinergic P2X7 receptor regulates lung surfactant secretion in a paracrine manner. *J. Cell Sci.* 124, 657–668. doi: 10.1242/jcs.066977

Mishra, A., Guo, Y., Zhang, L., More, S., Weng, T., Chintagari, N. R., et al. (2016). A critical role for P2X7 receptor-induced VCAM-1 shedding and neutrophil infiltration during acute lung injury. *J. Immunol.* 197, 2828–2837. doi: 10.4049/jimmunol.1501041

Molloy, A., Laochumroonvorapong, P., and Kaplan, G. (1994). Apoptosis, but not necrosis, of infected monocytes is coupled with killing of intracellular bacillus Calmette-Guerin. *J. Exp. Med.* 180, 1499–1509. doi: 10.1084/jem.180.4.1499

Monção-Ribeiro, L. C., Cagido, V. R., Lima-Murad, G., Santana, P. T., Riva, D. R., Borojevic, R., et al. (2011). Lipopolysaccharide-induced lung injury: role of P2X7 receptor. *Respir. Physiol. Neurobiol.* 179, 314–325. doi: 10.1016/j.resp.2011.09.015

Monção-Ribeiro, L. C., Faffe, D. S., Santana, P. T., Vieira, F. S., da Graca, C. L., Marques-da-Silva, C., et al. (2014). P2X7 receptor modulates inflammatory and functional pulmonary changes induced by silica. *PLoS ONE* 9:e110185. doi: 10.1371/journal.pone.0110185

Morandini, A. C., Ramos-Junior, E. S., Potempa, J., Nguyen, K. A., Oliveira, A. C., Bellio, M., et al. (2014a). *Porphyromonas gingivalis* fimbriae dampen P2X7-dependent interleukin-1β secretion. *J. Innate Immun.* 6, 831–845. doi: 10.1159/000363338

Morandini, A. C., Savio, L. E., and Coutinho-Silva, R. (2014b). The role of P2X7 receptor in infectious inflammatory diseases and the influence of ectonucleotidases. *Biomed. J.* 37, 169–177. doi: 10.4103/2319-4170.127803

Moreira-Souza, A. C. A., Almeida-da-Silva, C. L. C, Rangel, T. P., Rocha, G. C, Bellio, M., Zamboni, D. S., et al. (2017). The P2X7 receptor mediates *Toxoplasma gondii* control in macrophages through canonical NLRP3 inflammasome activation and reactive oxygen species production. *Front. Immunol.* 8:1257. doi: 10.3389/fimmu.2017.01257

Mortimer, L., Moreau, F., Cornick, S., and Chadee, K. (2015). The NLRP3 inflammasome is a pathogen sensor for invasive *Entamoeba histolytica* via activation of alpha5β1 Integrin at the Macrophage-Amebae intercellular junction. *PLoS Pathog.* 11:e1004887. doi: 10.1371/journal.ppat.1004887

Murphy, M. P., and LeVine, H. III. (2010). Alzheimer's disease and the amyloid-β peptide. *J. Alzheimers. Dis.* 19, 311–323. doi: 10.3233/JAD-2010-1221

Nagarajan, U. M., Sikes, J. D., Yeruva, L., and Prantner, D. (2012). Significant role of IL-1 signaling, but limited role of inflammasome activation, in oviduct pathology during *Chlamydia muridarum* genital infection. *J. Immunol.* 188, 2866–2875. doi: 10.4049/jimmunol.1103461

Narcisse, L., Scemes, E., Zhao, Y., Lee, S. C., and Brosnan, C. F. (2005). The cytokine IL-1β transiently enhances P2X7 receptor expression and function in human astrocytes. *Glia* 49, 245–258. doi: 10.1002/glia.20110

Nelson, D. W., Gregg, R. J., Kort, M. E., Perez-Medrano, A., Voight, E. A., Wang, Y., et al. (2006). Structure-activity relationship studies on a series of novel, substituted 1-benzyl-5-phenyltetrazole P2X7 antagonists. *J. Med. Chem.* 49, 3659–3666. doi: 10.1021/jm051202e

Neves, A. R., Castelo-Branco, M. T., Figliuolo, V. R., Bernardazzi, C., Buongusto, F., Yoshimoto, A., et al. (2014). Overexpression of ATP-activated P2X7 receptors in the intestinal mucosa is implicated in the pathogenesis of Crohn's disease. *Inflamm. Bowel Dis.* 20, 444–457. doi: 10.1097/01.MIB.0000441201.10454.06

Ni, J., Wang, P., Zhang, J., Chen, W., and Gu, L. (2013). Silencing of the P2X(7) receptor enhances amyloid-β phagocytosis by microglia. *Biochem. Biophys. Res. Commun.* 434, 363–369. doi: 10.1016/j.bbrc.2013.03.079

North, R. A. (2002). Molecular physiology of P2X receptors. *Physiol. Rev.* 82, 1013–1067. doi: 10.1152/physrev.00015.2002

North, R. A., and Jarvis, M. F. (2013). P2X receptors as drug targets. *Mol. Pharmacol.* 83, 759–769. doi: 10.1124/mol.112.083758

Noy, R., and Pollard, J. W. (2014). Tumor-associated macrophages: from mechanisms to therapy. *Immunity* 41, 49–61. doi: 10.1016/j.immuni.2014.06.010

O'Brien-Brown, J., Jackson, A., Reekie, T. A., Barron, M. L., Werry, E. L., Schiavini, P., et al. (2017). Discovery and pharmacological evaluation of a novel series of adamantyl cyanoguanidines as P2X7 receptor antagonists. *Eur. J. Med. Chem.* 130, 433–439. doi: 10.1016/j.ejmech.2017.02.060

Ohta, A., Gorelik, E., Prasad, S. J., Ronchese, F., Lukashev, D., Wong, M. K., et al. (2006). A2A adenosine receptor protects tumors from antitumor T cells. *Proc. Natl. Acad. Sci. U.S.A.* 103, 13132–13137. doi: 10.1073/pnas.0605251103

Oliveira, S. D., Coutinho-Silva, R., and Silva, C. L. (2013). Endothelial P2X7 receptors' expression is reduced by schistosomiasis. *Purinergic Signal.* 9, 81–89. doi: 10.1007/s11302-012-9332-5

Oliveira, S. D., Nanini, H. F., Savio, L. E., Waghabi, M. C., Silva, C. L., and Coutinho-Silva, R. (2014). Macrophage P2X7 receptor function is reduced during schistosomiasis: putative role of TGF- β1. *Mediators Inflamm.* 2014:134974. doi: 10.1155/2014/134974

Oliveira, S. D., Oliveira, N. F., Meyer-Fernandes, J. R., Savio, L. E., Ornelas, F. G., Ferreira, Z. S., et al. (2016). Increased expression of NTPDases 2 and 3 in mesenteric endothelial cells during schistosomiasis favors leukocyte adhesion through P2Y1 receptors. *Vascul. Pharmacol.* 82, 66–72. doi: 10.1016/j.vph.2016.02.005

Ottow, M. K., Klaver, E. J., van der Pouw Kraan, T. C., Heijnen, P. D., Laan, L. C., Kringel, H., et al. (2014). The helminth *Trichuris suis* suppresses TLR4-induced inflammatory responses in human macrophages. *Genes Immun.* 15, 477–486. doi: 10.1038/gene.2014.38

Oyanguren-Desez, O., Rodriguez-Antiguedad, A., Villoslada, P., Domercq, M., Alberdi, E., and Matute, C. (2011). Gain-of-function of P2X7 receptor gene variants in multiple sclerosis. *Cell Calcium* 50, 468–472. doi: 10.1016/j.ceca.2011.08.002

Pacheco, P. A., Ferreira, L. B., Mendonca, L., Ferreira, D. N., Salles, J. P., Faria, R. X., et al. (2016). P2X7 receptor as a novel drug delivery system to increase the entrance of hydrophilic drugs into cells during photodynamic therapy. *J. Bioenerg. Biomembr.* 48, 397–411. doi: 10.1007/s10863-016-9668-6

Park, E., Na, H. S., Song, Y. R., Shin, S. Y., Kim, Y. M., and Chung, J. (2014). Activation of NLRP3 and AIM2 inflammasomes by *Porphyromonas gingivalis* infection. *Infect. Immun.* 82, 112–123. doi: 10.1128/IAI.00862-13

Park, J. H., and Kim, Y. C. (2017). P2X7 receptor antagonists: a patent review (2010–2015). *Expert Opin. Ther. Pat.* 27, 257–267. doi: 10.1080/13543776.2017.1246538

Park, J. H., Williams, D. R., Lee, J. H., Lee, S. D., Lee, J. H., Ko, H., et al. (2016). Potent suppressive effects of 1-piperidinylimidazole based novel P2X7 receptor antagonists on cancer cell migration and invasion. *J. Med. Chem.* 59, 7410–7430. doi: 10.1021/acs.jmedchem.5b01690

Parvathenani, L. K., Tertyshnikova, S., Greco, C. R., Roberts, S. B., Robertson, B., and Posmantur, R. (2003). P2X7 mediates superoxide production in primary microglia and is up-regulated in a transgenic mouse model of Alzheimer's disease. *J. Biol. Chem.* 278, 13309–13317. doi: 10.1074/jbc.M209478200

Pelegrin, P., and Surprenant, A. (2006). Pannexin-1 mediates large pore formation and interleukin-1β release by the ATP-gated P2X7 receptor. *EMBO J.* 25, 5071–5082. doi: 10.1038/sj.emboj.7601378

Pellegatti, P., Raffaghello, L., Bianchi, G., Piccardi, F., Pistoia, V., and Di Virgilio, F. (2008). Increased level of extracellular ATP at tumor sites: *in vivo* imaging with plasma membrane luciferase. *PLoS ONE* 3:e2599. doi: 10.1371/journal.pone.0002599

Perez-Flores, G., Hernandez-Silva, C., Gutierrez-Escobedo, G., De Las, P. A., Castano, I., Arreola, J., et al. (2016). P2X7 from j774 murine macrophages acts as a scavenger receptor for bacteria but not yeast. *Biochem. Biophys. Res. Commun.* 481, 19–24. doi: 10.1016/j.bbrc.2016.11.027

Pettengill, M. A., Abdul-Sater, A., Coutinho-Silva, R., and Ojcius, D. M. (2016). Danger signals, inflammasomes, and the intricate intracellular lives of chlamydiae. *Biomed. J.* 39, 306–315. doi: 10.1016/j.bj.2016.07.001

Placido, R., Auricchio, G., Falzoni, S., Battistini, L., Colizzi, V., Brunetti, E., et al. (2006). P2X(7) purinergic receptors and extracellular ATP mediate apoptosis of human monocytes/macrophages infected with *Mycobacterium tuberculosis* reducing the intracellular bacterial viability. *Cell. Immunol.* 244, 10–18. doi: 10.1016/j.cellimm.2007.02.001

Pooler, A. M., Noble, W., and Hanger, D. P. (2014). A role for tau at the synapse in Alzheimer's disease pathogenesis. *Neuropharmacology* 76(Pt A), 1–8. doi: 10.1016/j.neuropharm.2013.09.018

Proietti, M., Cornacchione, V., Rezzonico, J. T., Romagnani, A., Faliti, C. E., Perruzza, L., et al. (2014). ATP-gated ionotropic P2X7 receptor controls follicular T helper cell numbers in Peyer's patches to promote host-microbiota mutualism. *Immunity* 41, 789–801. doi: 10.1016/j.immuni.2014.10.010

Qi, B., Yu, T., Wang, C., Wang, T., Yao, J., Zhang, X., et al. (2016). Shock wave-induced ATP release from osteosarcoma U2OS cells promotes cellular uptake and cytotoxicity of methotrexate. *J. Exp. Clin. Cancer Res.* 35, 161. doi: 10.1186/s13046-016-0437-5

Qian, F., Xiao, J., Hu, B., Sun, N., Yin, W., and Zhu, J. (2017). High expression of P2X7R is an independent postoperative indicator of poor prognosis in colorectal cancer. *Hum. Pathol.* 64, 61–68. doi: 10.1016/j.humpath.2017.03.019

Qiu, Y., Li, W. H., Zhang, H. Q., Liu, Y., Tian, X. X., and Fang, W. G. (2014). P2X7 mediates ATP-driven invasiveness in prostate cancer cells. *PLoS ONE* 9:e114371. doi: 10.1371/journal.pone.0114371

Qu, Y., Franchi, L., Nunez, G., and Dubyak, G. R. (2007). Nonclassical IL-1 β secretion stimulated by P2X7 receptors is dependent on inflammasome activation and correlated with exosome release in murine macrophages. *J. Immunol.* 179, 1913–1925. doi: 10.4049/jimmunol.179.3.1913

Raffaghello, L., Chiozzi, P., Falzoni, S., Di Virgilio, F., and Pistoia, V. (2006). The P2X7 receptor sustains the growth of human neuroblastoma cells through a substance P-dependent mechanism. *Cancer Res.* 66, 907–914. doi: 10.1158/0008-5472.CAN-05-3185

Ralevic, V., and Burnstock, G. (1998). Receptors for purines and pyrimidines. *Pharmacol. Rev.* 50, 413–492.

Ramos-Junior, E. S., Morandini, A. C., Almeida-da-Silva, C. L., Franco, E. J., Potempa, J., Nguyen, K. A., et al. (2015). A dual role for P2X7 receptor during *Porphyromonas gingivalis* infection. *J. Dent. Res.* 94, 1233–1242. doi: 10.1177/0022034515593465

Rampe, D., Wang, L., and Ringheim, G. E. (2004). P2X7 receptor modulation of β-amyloid- and LPS-induced cytokine secretion from human macrophages and microglia. *J. Neuroimmunol.* 147, 56–61. doi: 10.1016/j.jneuroim.2003.10.014

Rassendren, F., Buell, G. N., Virginio, C., Collo, G., North, R. A., and Surprenant, A. (1997). The permeabilizing ATP receptor, P2X7. Cloning and expression of a human cDNA. *J. Biol. Chem.* 272, 5482–5486. doi: 10.1074/jbc.272.9.5482

Ren, S., Zhang, Y., Wang, Y., Lui, Y., Wei, W., Huang, X., et al. (2010). Targeting P2X(7) receptor inhibits the metastasis of murine P388D1 lymphoid neoplasm cells to lymph nodes. *Cell Biol. Int.* 34, 1205–1211. doi: 10.1042/CBI20090428

Riteau, N., Gasse, P., Fauconnier, L., Gombault, A., Couegnat, M., Fick, L., et al. (2010). Extracellular ATP is a danger signal activating P2X7 receptor in lung inflammation and fibrosis. *Am. J. Respir. Crit. Care Med.* 182, 774–783. doi: 10.1164/rccm.201003-0359OC

Rodrigue-Candela, J. L., Martin-Hernandez, D., and Castilla-Cortazar, T. (1963). Stimulation of insulin secretion *in vitro* by adenosine triphosphate. *Nature* 197:1304. doi: 10.1038/1971304a0

Rodrigues, A. M., Bergamaschi, C. T., Fernandes, M. J., Paredes-Gamero, E. J., Buri, M. V., Ferreira, A. T., et al. (2014). P2X(7) receptor in the kidneys of diabetic rats submitted to aerobic training or to N-acetylcysteine supplementation [corrected]. *PLoS ONE* 9:e97452. doi: 10.1371/journal.pone.0097452

Roger, S., Jelassi, B., Couillin, I., Pelegrin, P., Besson, P., and Jiang, L. H. (2015). Understanding the roles of the P2X7 receptor in solid tumour progression and therapeutic perspectives. *Biochim. Biophys. Acta* 1848, 2584–2602. doi: 10.1016/j.bbamem.2014.10.029

Ryu, J. K., and McLarnon, J. G. (2008). Block of purinergic P2X(7) receptor is neuroprotective in an animal model of Alzheimer's disease. *Neuroreport* 19, 1715–1719. doi: 10.1097/WNR.0b013e3283179333

Ryu, J. K., Jantaratnotai, N., Serrano-Perez, M. C., McGeer, P. L., and McLarnon, J. G. (2011). Block of purinergic P2X7R inhibits tumor growth in a C6 glioma brain tumor animal model. *J. Neuropathol. Exp. Neurol.* 70, 13–22. doi: 10.1097/NEN.0b013e318201d4d4

Salles, É. M., Menezes, M. N., Siqueira, R., Silva, H. B. D., Amaral, E. P., Castillo-Mendez, S. I., et al. (2017). P2X7 receptor drives Th1 cell differentiation and controls the follicular helper T cell population to protect against *Plasmodium chabaudi* malaria. *PLoS Pathog.* 13:e1006595. doi: 10.1371/journal.ppat.1006595

Santana, P. T., Benjamim, C. F., Martinez, C. G., Kurtenbach, E., Takiya, C. M., and Coutinho-Silva, R. (2015). The P2X7 receptor contributes to the development of the exacerbated inflammatory response associated with sepsis. *J. Innate Immun.* 7, 417–427. doi: 10.1159/000371388

Santos, A. A. Jr., Cappellari, A. R., de Marchi, F. O., Gehring, M. P., Zaparte, A., Brandao, C. A., et al. (2017). Potential role of P2X7R in esophageal squamous cell carcinoma proliferation. *Purinergic Signal.* 13, 279–292. doi: 10.1007/s11302-017-9559-2

Santos, A. A. Jr., Rodrigues-Junior, V., Zanin, R. F., Borges, T. J., Bonorino, C., Coutinho-Silva, R., et al. (2013). Implication of purinergic P2X7 receptor in M. tuberculosis infection and host interaction mechanisms: a mouse model study. *Immunobiology* 218, 1104–1112. doi: 10.1016/j.imbio.2013.03.003

Sanz, J. M., Chiozzi, P., Ferrari, D., Colaianna, M., Idzko, M., Falzoni, S., et al. (2009). Activation of microglia by amyloid {β} requires P2X7 receptor expression. *J. Immunol.* 182, 4378–4385. doi: 10.4049/jimmunol.0803612

Savio, L. E. B., de Andrade, M. P., Figliuolo, V. R., de Avelar Almeida, T. F., Santana, P. T., Oliveira, S. D. S., et al. (2017a). CD39 limits P2X7 receptor inflammatory signaling and attenuates sepsis-induced liver injury. *J. Hepatol.* 67, 716–726. doi: 10.1016/j.jhep.2017.05.021

Savio, L. E., and Coutinho-Silva, R. (2016). Purinergic signaling in infection and autoimmune disease. *Biomed. J.* 39, 304–305. doi: 10.1016/j.bj.2016.09.002

Savio, L. E., Andrade, M. G., de Andrade, M. P., Santana, P. T., Moreira-Souza, A. C., Kolling, J. et al. (2017b). P2X7 receptor signaling contributes to sepsis-associated brain dysfunction. *Mol. Neurobiol.* 54, 6459–6470. doi: 10.1007/s12035-016-0168-9

Schenk, U., Frascoli, M., Proietti, M., Geffers, R., Traggiai, E., Buer, J., et al. (2011). ATP inhibits the generation and function of regulatory T cells

through the activation of purinergic P2X receptors. *Sci Signal.* 4:ra12. doi: 10.1126/scisignal.2001270

Seref-Ferlengez, Z., Maung, S., Schaffler, M. B., Spray, D. C., Suadicani, S. O., and Thi, M. M. (2016). P2X7R-Panx1 complex impairs bone mechanosignaling under high glucose levels associated with type-1 diabetes. *PLoS ONE* 11:e0155107. doi: 10.1371/journal.pone.0155107

Seyffert, C., Schmalzing, G., and Markwardt, F. (2004). Dissecting individual current components of co-expressed human P2X1 and P2X7 receptors. *Curr. Top. Med. Chem.* 4, 1719–1730. doi: 10.2174/1568026043387160

Shabbir, M., Thompson, C., Jarmulowiczc, M., Mikhailidis, D., and Burnstock, G. (2008). Effect of extracellular ATP on the growth of hormone-refractory prostate cancer *in vivo*. *BJU Int.* 102, 108–112. doi: 10.1111/j.1464-410X.2008.07578.x

Shamsi, M., Zolfaghari, M. R., and Farnia, P. (2016). Association of IFN-γ and P2X7 receptor gene polymorphisms in susceptibility to tuberculosis among Iranian Patients. *Acta Microbiol. Immunol. Hung.* 63, 93–101. doi: 10.1556/030.63.2016.1.7

Sharma, S., Kumar, V., Khosla, R., Kajal, N., Sarin, B., and Sehajpal, P. (2010). Association of P2X7 receptor +1513 (A–>C) polymorphism with tuberculosis in a Punjabi population. *Int. J. Tuberc. Lung Dis.* 14, 1159–1163.

Shieh, C. H., Heinrich, A., Serchov, T., van Calker. D., and Biber, K. (2014). P2X7-dependent, but differentially regulated release of IL-6, CCL2, and TNF-alpha in cultured mouse microglia. *Glia* 62, 592–607. doi: 10.1002/glia.22628

Shimada, K., Crother, T. R., Karlin, J., Chen, S., Chiba, N., Ramanujan, V. K., et al. (2011). Caspase-1 dependent IL-1β secretion is critical for host defense in a mouse model of *Chlamydia pneumoniae* lung infection. *PLoS ONE* 6:e21477. doi: 10.1371/journal.pone.0021477

Shimokawa, C., Kanaya, T., Hachisuka, M., Ishiwata, K., Hisaeda, H., Kurashima, Y., et al. (2017). Mast cells are crucial for induction of group 2 innate lymphoid cells and clearance of Helminth infections. *Immunity* 46, 863–874. doi: 10.1016/j.immuni.2017.04.017

Siegel, R. L., Miller, K. D., and Jemal, A. (2017). Cancer statistics, 2017. *CA Cancer J. Clin.* 67, 7–30. doi: 10.3322/caac.21387

Sikora, A., Liu, J., Brosnan, C., Buell, G., Chessel, I., and Bloom, B. R. (1999). Cutting edge: purinergic signaling regulates radical-mediated bacterial killing mechanisms in macrophages through a P2X7-independent mechanism. *J. Immunol.* 163, 558–561.

Silva, C. L. (2016). Purinergic signaling in schistosomal infection. *Biomed. J.* 39, 316–325. doi: 10.1016/j.bj.2016.06.006

Singer, M. (2016). The new sepsis consensus definitions (Sepsis-3): the good, the not-so-bad, and the actually-quite-pretty. *Intensive Care Med.* 42, 2027–2029. doi: 10.1007/s00134-016-4600-4

Singla, N., Gupta, D., Joshi, A., Batra, N., and Singh, J. (2012). Genetic polymorphisms in the P2X7 gene and its association with susceptibility to tuberculosis. *Int. J. Tuberc. Lung Dis.* 16, 224–229. doi: 10.5588/ijtld.11.0076

Skaper, S. D., Debetto, P., and Giusti, P. (2010). The P2X7 purinergic receptor: from physiology to neurological disorders. *FASEB J.* 24, 337–345. doi: 10.1096/fj.09-138883

Skarratt, K. K., Fuller, S. J., Sluyter, R., Dao-Ung, L. P., Gu, B. J., and Wiley, J. S. (2005). A 5′ intronic splice site polymorphism leads to a null allele of the P2X7 gene in 1-2% of the Caucasian population. *FEBS Lett.* 579, 2675–2678. doi: 10.1016/j.febslet.2005.03.091

Solini, A., Chiozzi, P., Falzoni, S., Morelli, A., Fellin, R., and Di Virgilio, F. (2000). High glucose modulates P2X7 receptor-mediated function in human primary fibroblasts. *Diabetologia* 43, 1248–1256. doi: 10.1007/s001250051520

Solini, A., Chiozzi, P., Morelli, A., Adinolfi, E., Rizzo, R., Baricordi, O. R., et al. (2004). Enhanced P2X7 activity in human fibroblasts from diabetic patients: a possible pathogenetic mechanism for vascular damage in diabetes. *Arterioscler. Thromb. Vasc. Biol.* 24, 1240–1245. doi: 10.1161/01.ATV.0000133193.11078.c0

Solini, A., Menini, S., Rossi, C., Ricci, C., Santini, E., Blasetti, F. C., et al. (2013). The purinergic 2X7 receptor participates in renal inflammation and injury induced by high-fat diet: possible role of NLRP3 inflammasome activation. *J. Pathol.* 231, 342–353. doi: 10.1002/path.4237

Solle, M., Labasi, J., Perregaux, D. G., Stam, E., Petrushova, N., Koller, B. H., et al. (2001). Altered cytokine production in mice lacking P2X(7) receptors. *J. Biol. Chem.* 276, 125–132. doi: 10.1074/jbc.M006781200

Souza, V. D., Dos Santos, J. T., Cabral, F. L., Barbisan, F., Azevedo, M. I., Dias Carli, L. F., et al. (2017). Evaluation of P2X7 receptor expression in peripheral lymphocytes and immune profile from patients with indeterminate form of Chagas disease. *Microb. Pathog.* 104, 32–38. doi: 10.1016/j.micpath.2017.01.002

Sperlágh, B., and Illes, P. (2014). P2X7 receptor: an emerging target in central nervous system diseases. *Trends Pharmacol. Sci.* 35, 537–547. doi: 10.1016/j.tips.2014.08.002

Sperlágh, B., Kofalvi, A., Deuchars, J., Atkinson, L., Milligan, C. J., Buckley, N. J., et al. (2002). Involvement of P2X7 receptors in the regulation of neurotransmitter release in the rat hippocampus. *J. Neurochem.* 81, 1196–1211. doi: 10.1046/j.1471-4159.2002.00920.x

Stefanis, L. (2012). alpha-Synuclein in Parkinson's disease. *Cold Spring Harb. Perspect. Med.* 2:a009399. doi: 10.1101/cshperspect.a009399

Steinberg, T. H., and Silverstein, S. C. (1987). Extracellular. *J. Biol. Chem.* 262, 3118–3122.

Stock, T. C., Bloom, B. J., Wei, N., Ishaq, S., Park, W., Wang, X., et al. (2012). Efficacy and safety of CE-224,535, an antagonist of P2X7 receptor, in treatment of patients with rheumatoid arthritis inadequately controlled by methotrexate. *J. Rheumatol.* 39, 720–727. doi: 10.3899/jrheum.110874

Stys, P. K. (2010). Multiple sclerosis: autoimmune disease or autoimmune reaction? *Can. J. Neurol. Sci.* 37(Suppl. 2), S16–S23. doi: 10.1017/S0317167100022393

Sumi, Y., Woehrle, T., Chen, Y., Bao, Y., Li, X., Yao, Y., et al. (2014). Plasma ATP is required for neutrophil activation in a mouse sepsis model. *Shock* 42, 142–147. doi: 10.1097/SHK.0000000000000180

Surprenant, A., Rassendren, F., Kawashima, E., North, R. A., and Buell, G. (1996). The cytolytic P2Z receptor for extracellular ATP identified as a P2X receptor (P2X7). *Science* 272, 735–738. doi: 10.1126/science.272.5262.735

Swartz, T. H., Dubyak, G. R., and Chen, B. K. (2015). Purinergic receptors: key mediators of HIV-1 infection and inflammation. *Front. Immunol.* 6:585. doi: 10.3389/fimmu.2015.00585

Swartz, T. H., Esposito, A. M., Durham, N. D., Hartmann, B. M., and Chen, B. K. (2014). P2X-selective purinergic antagonists are strong inhibitors of HIV-1 fusion during both cell-to-cell and cell-free infection. *J. Virol.* 88, 11504–11515. doi: 10.1128/JVI.01158-14

Tafani, M., Schito, L., Pellegrini, L., Villanova, L., Marfe, G., Anwar, T., et al. (2011). Hypoxia-increased RAGE and P2X7R expression regulates tumor cell invasion through phosphorylation of Erk1/2 and Akt and nuclear translocation of NF-{kappa}B. *Carcinogenesis* 32, 1167–1175. doi: 10.1093/carcin/bgr101

Tamajusuku, A. S., Villodre, E. S., Paulus, R., Coutinho-Silva, R., Battasstini, A. M., Wink, M. R., et al. (2010). Characterization of ATP-induced cell death in the GL261 mouse glioma. *J. Cell. Biochem.* 109, 983–991. doi: 10.1002/jcb.22478

Tan, C., Han, L. I., Zou, L., Luo, C., Liu, A., Sheng, X., et al. (2015). Expression of P2X7R in breast cancer tissue and the induction of apoptosis by the gene-specific shRNA in MCF-7 cells. *Exp. Ther. Med.* 10, 1472–1478. doi: 10.3892/etm.2015.2705

Taylor, S. R., Gonzalez-Begne, M., Sojka, D. K., Richardson, J. C., Sheardown, S. A., Harrison, S. M., et al. (2009). Lymphocytes from P2X7-deficient mice exhibit enhanced P2X7 responses. *J. Leukoc. Biol.* 85, 978–986. doi: 10.1189/jlb.0408251

Tewari, M., and Seth, P. (2015). Emerging role of P2X7 receptors in CNS health and disease. *Ageing Res. Rev.* 24, 328–342. doi: 10.1016/j.arr.2015.10.001

Tewari, M., Monika, Varghse, R. K., Menon, M., and Seth, P. (2015). Astrocytes mediate HIV-1 Tat-induced neuronal damage via ligand-gated ion channel P2X7R. *J. Neurochem.* 132, 464–476. doi: 10.1111/jnc.12953

Ting, J. P., Willingham, S. B., and Bergstralh, D. T. (2008). NLRs at the intersection of cell death and immunity. *Nat. Rev. Immunol.* 8, 372–379. doi: 10.1038/nri2296

Todd, J. N., Poon, W., Lyssenko, V., Groop, L., Nichols, B., Wilmot, M., et al. (2015). Variation in glucose homeostasis traits associated with P2RX7 polymorphisms in mice and humans. *J. Clin. Endocrinol. Metab.* 100, E688–E696. doi: 10.1210/jc.2014-4160

Tsunoda, I., and Fujinami, R. S. (1996). Two models for multiple sclerosis: experimental allergic encephalomyelitis and Theiler's murine encephalomyelitis virus. *J. Neuropathol. Exp. Neurol.* 55, 673–686. doi: 10.1097/00005072-199606000-00001

Tung, H. C., Lee, F. Y., Wang, S. S., Tsai, M. H., Lee, J. Y., Huo, T. I., et al. (2015). The beneficial effects of P2X7 antagonism in rats with bile duct ligation-induced cirrhosis. *PLoS ONE* 10:e0124654. doi: 10.1371/journal.pone.0124654

Vaughn, B. P., Robson, S. C., and Burnstock, G. (2012). Pathological roles of purinergic signaling in the liver. *J. Hepatol.* 57, 916–920. doi: 10.1016/j.jhep.2012.06.008

Vázquez-Cuevas, F. G., Martinez-Ramirez, A. S., Robles-Martinez, L., Garay, E., Garcia-Carranca, A., Perez-Montiel, D., et al. (2014). Paracrine stimulation of P2X7 receptor by ATP activates a proliferative pathway in ovarian carcinoma cells. *J. Cell. Biochem.* 115, 1955–1966. doi: 10.1002/jcb.24867

Vergani, A., Fotino, C., D'Addio, F., Tezza, S., Podetta, M., Gatti, F., et al. (2013a). Effect of the purinergic inhibitor oxidized ATP in a model of islet allograft rejection. *Diabetes* 62, 1665–1675. doi: 10.2337/db12-0242

Vergani, A., Tezza, S., D'Addio, F., Fotino, C., Liu, K., Niewczas, M., et al. (2013b). Long-term heart transplant survival by targeting the ionotropic purinergic receptor P2X7. *Circulation* 127, 463–475. doi: 10.1161/CIRCULATIONAHA.112.123653

Verkhratsky, A., and Burnstock, G. (2014). Biology of purinergic signalling: its ancient evolutionary roots, its omnipresence and its multiple functional significance. *Bioessays* 36, 697–705. doi: 10.1002/bies.201400024

Vieira, F. S., Nanini, H. F., Takiya, C. M., and Coutinho-Silva, R. (2016). P2X7 receptor knockout prevents streptozotocin-induced type 1 diabetes in mice. *Mol. Cell. Endocrinol.* 419, 148–157. doi: 10.1016/j.mce.2015.10.008

Virginio, C., MacKenzie, A., North, R. A., and Surprenant, A. (1999). Kinetics of cell lysis, dye uptake and permeability changes in cells expressing the rat P2X7 receptor. *J. Physiol.* 519(Pt 2), 335–346. doi: 10.1111/j.1469-7793.1999.0335m.x

Vuaden, F. C., Savio, L. E., Bastos, C. M., Bogo, M. R., and Bonan, C. D. (2011). Adenosine A(2A) receptor agonist (CGS-21680) prevents endotoxin-induced effects on nucleotidase activities in mouse lymphocytes. *Eur. J. Pharmacol.* 651, 212–217. doi: 10.1016/j.ejphar.2010.11.003

Vuaden, F. C., Savio, L. E., Ramos, D. B., Casali, E. A., Bogo, M. R., and Bonan, C. D. (2012). Endotoxin-induced effects on nucleotide catabolism in mouse kidney. *Eur. J. Pharmacol.* 674, 422–429. doi: 10.1016/j.ejphar.2011.11.002

Wan, P., Liu, X., Xiong, Y., Ren, Y., Chen, J., Lu, N., et al. (2016). Extracellular ATP mediates inflammatory responses in colitis via P2 x 7 receptor signaling. *Sci. Rep.* 6:19108. doi: 10.1038/srep19108

Wang, H., Hong, L. J., Huang, J. Y., Jiang, Q., Tao, R. R., Tan, C., et al. (2015a). P2RX7 sensitizes Mac-1/ICAM-1-dependent leukocyte-endothelial adhesion and promotes neurovascular injury during septic encephalopathy. *Cell Res.* 25, 674–690. doi: 10.1038/cr.2015.61

Wang, Q., Wang, L., Feng, Y. H., Li, X., Zeng, R., and Gorodeski, G. I. (2004). P2X7 receptor-mediated apoptosis of human cervical epithelial cells. *Am. J. Physiol. Cell Physiol.* 287, C1349–C1358. doi: 10.1152/ajpcell.00256.2004

Wang, S., Zhao, J., Wang, H., Liang, Y., Yang, N., and Huang, Y. (2015b). Blockage of P2X7 attenuates acute lung injury in mice by inhibiting NLRP3 inflammasome. *Int. Immunopharmacol.* 27, 38–45. doi: 10.1016/j.intimp.2015.04.035

Wang, X. H., Xie, X., Luo, X. G., Shang, H., and He, Z. Y. (2017). Inhibiting purinergic P2X7 receptors with the antagonist brilliant blue G is neuroprotective in an intranigral lipopolysaccharide animal model of Parkinson's disease. *Mol. Med. Rep.* 15, 768–776. doi: 10.3892/mmr.2016.6070

Weitz, J. R., Makhmutova, M., Almaca, J., Stertmann, J., Aamodt, K., Brissova, M., et al. (2017). Mouse pancreatic islet macrophages use locally released ATP to monitor β cell activity. *Diabetologia* 61, 182–192. doi: 10.1007/s00125-017-4416-y

White, N., Knight, G. E., Butler, P. E., and Burnstock, G. (2009). An *in vivo* model of melanoma: treatment with ATP. *Purinergic Signal.* 5, 327–333. doi: 10.1007/s11302-009-9156-0

Wilhelm, K., Ganesan, J., Muller, T., Durr, C., Grimm, M., Beilhack, A., et al. (2010). Graft-versus-host disease is enhanced by extracellular ATP activating P2X7R. *Nat. Med.* 16, 1434–1438. doi: 10.1038/nm.2242

Wilkaniec, A., Gassowska, M., Czapski, G. A., Cieślik, M., Sulkowski, G., and Adamczyk, A. (2017). P2X7 receptor-pannexin 1 interaction mediates extracellular alpha-synuclein-induced ATP release in neuroblastoma SH-SY5Y cells. *Purinergic Signal.* 13, 347–361. doi: 10.1007/s11302-017-9567-2

Wu, J., Lu, L., Zhang, L., Ding, Y., Wu, F., Zuo, W., et al. (2015). Single nucleotide polymorphisms in P2X7 gene are associated with serum immunoglobulin G responses to *Mycobacterium tuberculosis* in tuberculosis patients. *Dis. Markers* 2015:671272. doi: 10.1155/2015/671272

Wu, X., Ren, J., Chen, G., Wu, L., Song, X., Li, G., et al. (2017a). Systemic blockade of P2X7 receptor protects against sepsis-induced intestinal barrier disruption. *Sci. Rep.* 7:4364. doi: 10.1038/s41598-017-04231-5

Wu, X., Wang, Y., Wang, S., Xu, R., and Lv, X. (2017b). Purinergic P2X7 receptor mediates acetaldehyde-induced hepatic stellate cells activation via PKC-dependent GSK3β pathway. *Int. Immunopharmacol.* 43, 164–171. doi: 10.1016/j.intimp.2016.12.017

Xu, X., Pocock, G. M., Sharma, A., Peery, S. L., Fites, J. S., Felley, L., et al. (2016). Human iNKT cells promote protective inflammation by inducing oscillating purinergic signaling in monocyte-derived DCs. *Cell Rep.* 16, 3273–3285. doi: 10.1016/j.celrep.2016.08.061

Yan, Y., Bai, J., Zhou, X., Tang, J., Jiang, C., Tolbert, E., et al. (2015). P2X7 receptor inhibition protects against ischemic acute kidney injury in mice. *Am. J. Physiol. Cell Physiol.* 308, C463–C472. doi: 10.1152/ajpcell.00245.2014

Yang, D., He, Y., Munoz-Planillo, R., Liu, Q., and Nunez, G. (2015). Caspase-11 requires the pannexin-1 channel and the Purinergic P2X7 pore to mediate pyroptosis and endotoxic shock. *Immunity* 43, 923–932. doi: 10.1016/j.immuni.2015.10.009

Yiangou, Y., Facer, P., Durrenberger, P., Chessell, I. P., Naylor, A., Bountra, C., et al. (2006). COX-2, CB2 and P2X7-immunoreactivities are increased in activated microglial cells/macrophages of multiple sclerosis and amyotrophic lateral sclerosis spinal cord. *BMC Neurol.* 6:12. doi: 10.1186/1471-2377-6-12

Yilmaz, O., Yao, L., Maeda, K., Rose, T. M., Lewis, E. L., Duman, M., et al. (2008). ATP scavenging by the intracellular pathogen *Porphyromonas gingivalis* inhibits P2X7-mediated host-cell apoptosis. *Cell. Microbiol.* 10, 863–875. doi: 10.1111/j.1462-5822.2007.01089.x

Yip, L., Woehrle, T., Corriden, R., Hirsh, M., Chen, Y., Inoue, Y., et al. (2009). Autocrine regulation of T-cell activation by ATP release and P2X7 receptors. *FASEB J.* 23, 1685–1693. doi: 10.1096/fj.08-126458

Yu, Y., Ugawa, S., Ueda, T., Ishida, Y., Inoue, K., Kyaw, N. A., et al. (2008). Cellular localization of P2X7 receptor mRNA in the rat brain. *Brain Res.* 1194, 45–55. doi: 10.1016/j.brainres.2007.11.064

Zhang, C., He, H., Wang, L., Zhang, N., Huang, H., Xiong, Q., et al. (2017). Virus-triggered ATP release limits viral replication through facilitating IFN-β production in a P2X7-dependent manner. *J. Immunol.* 199, 1372–1381. doi: 10.4049/jimmunol.1700187

Zhang, X. J., Zheng, G. G., Ma, X. T., Yang, Y. H., Li, G., Rao, Q., et al. (2004). Expression of P2X7 in human hematopoietic cell lines and leukemia patients. *Leuk. Res.* 28, 1313–1322. doi: 10.1016/j.leukres.2004.04.001

Zitvogel, L., Apetoh, L., Ghiringhelli, F., and Kroemer, G. (2008). Immunological aspects of cancer chemotherapy. *Nat. Rev. Immunol.* 8, 59–73. doi: 10.1038/nri2216

Conflict of Interest Statement: The authors declare that the research was conducted in the absence of any commercial or financial relationships that could be construed as a potential conflict of interest.

frontiers in Pharmacology

HYPOTHESIS AND THEORY
published: 02 February 2018
doi: 10.3389/fphar.2018.00058

The Molecular Determinants of Small-Molecule Ligand Binding at P2X Receptors

Gaia Pasqualetto[1], *Andrea Brancale*[1] *and Mark T. Young*[2]*

[1] School of Pharmacy and Pharmaceutical Sciences, Cardiff University, Cardiff, United Kingdom, [2] School of Biosciences, Cardiff University, Cardiff, United Kingdom

P2X receptors are trimeric eukaryotic ATP-gated cation channels. Extracellular ATP—their physiological ligand—is released as a neurotransmitter and in conditions of cell damage such as inflammation, and substantial evidence implicates P2X receptors in diseases including neuropathic pain, cancer, and arthritis. In 2009, the first P2X crystal structure, *Danio rerio* P2X4 in the *apo*- state, was published, and this was followed in 2012 by the ATP-bound structure. These structures transformed our understanding of the conformational changes induced by ATP binding and the mechanism of ligand specificity, and enabled homology modeling of mammalian P2X receptors for ligand docking and rational design of receptor modulators. P2X receptors are attractive drug targets, and a wide array of potent, subtype-selective modulators (mostly antagonists) have been developed. In 2016, crystal structures of human P2X3 in complex with the competitive antagonists TNP-ATP and A-317491, and *Ailuropoda melanoleuca* P2X7 in complex with a series of allosteric antagonists were published, giving fascinating insights into the mechanism of channel antagonism. In this article we not only summarize current understanding of small-molecule modulator binding at P2X receptors, but also use this information in combination with previously published structure-function data and molecular docking experiments, to hypothesize a role for the dorsal fin loop region in differential ATP potency, and describe novel, testable binding conformations for both the semi-selective synthetic P2X7 agonist 2′-(3′)-O-(4-benzoyl)benzoyl ATP (BzATP), and the P2X4-selective positive allosteric modulator ivermectin. We find that the distal benzoyl group of BzATP lies in close proximity to Lys-127, a residue previously implicated in BzATP binding to P2X7, potentially explaining the increased potency of BzATP at rat P2X7 receptors. We also present molecular docking of ivermectin to rat P2X4 receptors, illustrating a plausible binding conformation between the first and second transmembrane domains which not only tallies with previous mutagenesis studies, but would also likely have the effect of stabilizing the open channel structure, consistent with the mode of action of this positive allosteric modulator. From our docking simulations and analysis of sequence homology we propose a series of mutations likely to confer ivermectin sensitivity to human P2X1.

Keywords: P2X, ligand binding, molecular modeling, structure-function, ion channel

OPEN ACCESS

Edited by:
Kenneth A. Jacobson, National Institutes of Health (NIH), United States

Reviewed by:
Samuel J. Fountain, University of East Anglia, United Kingdom
Lin-Hua Jiang, University of Leeds, United Kingdom

***Correspondence:**
Mark T. Young
Youngmt@cardiff.ac.uk

Specialty section:
This article was submitted to Experimental Pharmacology and Drug Discovery, a section of the journal Frontiers in Pharmacology

Received: *17 November 2017*
Accepted: *17 January 2018*
Published: *02 February 2018*

Citation:
Pasqualetto G, Brancale A and Young MT (2018) The Molecular Determinants of Small-Molecule Ligand Binding at P2X Receptors. Front. Pharmacol. 9:58. doi: 10.3389/fphar.2018.00058

INTRODUCTION

In recent years, our understanding of the relationship between the structure and the function of the ATP-gated P2X receptor family of ion channels has been transformed by a series of crystal structures, from the first structure of a P2X receptor, that of *Danio rerio* P2X4.1 (zfP2X4) in the *apo*-state, published in 2009 (Kawate et al., 2009), via structures of zfP2X4 bound to ATP (Hattori and Gouaux, 2012), a Gulf Coast tick (*Amblyomma maculatum*) P2X structure (Kasuya et al., 2016), human P2X3 in the *apo*-, ATP- and antagonist-bound states (Mansoor et al., 2016), zfP2X4 bound to the partial agonist CTP (Kasuya et al., 2017a), to the most recently determined structures of giant panda (*Ailuropoda melanoleuca*) P2X7 (Karasawa and Kawate, 2016) and chicken P2X7 (Kasuya et al., 2017b). These impressive achievements, along with their enabling of the interpretation of a large body of prior mutagenesis data (reviewed in Chataigneau et al., 2013; Jiang et al., 2013; Alves et al., 2014; Samways et al., 2014; Grimes and Young, 2015; Habermacher et al., 2016; Kawate, 2017), have led to significant breakthroughs in our understanding of channel architecture, ligand binding, and the mechanisms of channel opening, desensitization and both orthosteric and allosteric antagonism. In addition, the availability of structural data has allowed for the construction and testing of molecular models of those human receptors which still lack direct high-resolution structural data (Alves et al., 2014; Ahmadi et al., 2015; Caseley et al., 2015, 2016; Farmer et al., 2015; Fryatt et al., 2016), paving the way for mutational analysis to elucidate antagonist binding sites (Farmer et al., 2015; Allsopp et al., 2017), and structure-aided drug design (Ahmadi et al., 2015; Caseley et al., 2015, 2016).

P2X receptors play wide-ranging physiological roles and are important in health and disease progression (North, 2016); for this reason they have been significant targets for the pharmaceutical industry (Burnstock, 2017). The functional unit of the P2X receptor is a trimer, and seven P2X receptor subtypes are found in mammals (numbered P2X1-P2X7), which can form a variety of both homo-and hetero-trimeric receptors, which display subtly different pharmacological properties and tissue distribution (North, 2016). Developing potent, subtype-selective P2X receptor modulators has been a slow process, but several such compounds are now available (Bartlett et al., 2014; Burnstock, 2017), including the P2X7 antagonists CE-224,535 (Stock et al., 2012) and AZD9056 (McInnes et al., 2007; Keystone et al., 2012; Eser et al., 2015), and the P2X3 antagonist AF-219 (Abdulqawi et al., 2015), which have been used in clinical trials for rheumatoid arthritis, Crohn's disease and chronic cough, respectively. The majority of developed compounds are antagonists; at present there are no truly subtype-selective P2X receptor agonists available, although α,β-methylene ATP shows selectivity for P2X1 and P2X3 receptors, and BzATP is partially selective for P2X7 receptors (North, 2002). One compound, the anti-helminthic drug ivermectin, has also been reported to be a selective (in terms of P2X receptors) positive allosteric modulator of P2X4 receptors (Khakh et al., 1999). For the majority of known P2X modulators, their binding sites have not yet been elucidated. However, the recent crystal structures of human P2X3 in complex with the orthosteric antagonists A-317491 and trinitrophenyl-ATP (TNP-ATP) (Mansoor et al., 2016), chicken P2X7 in complex with TNP-ATP (Kasuya et al., 2017b), and panda P2X7 in complex with a series of allosteric antagonists including A-740003 (Karasawa and Kawate, 2016) have given valuable insight into the binding modes and mechanism of antagonism of these compounds.

In this article our aim is to describe our current understanding of small-molecule modulator binding to P2X receptors, and use this data in conjunction with molecular docking experiments to develop novel hypotheses for the involvement of the dorsal fin region in altered agonist potency at P2X7 receptors, and how the P2X7-selective agonist BzATP and the P2X4 positive allosteric modulator ivermectin bind to their respective receptor subtypes. We first focus on the currently available crystal structures of P2X receptors, highlighting which portions of the receptor they cover, and how they are related by amino-acid sequence identity. We briefly discuss the conformational changes induced by ATP binding, before analyzing the orthosteric binding sites in zfP2X4, human P2X3, gulf coast tick P2X, and chicken P2X7, and the allosteric binding site in panda P2X7. Finally, we build upon published data from structure-function experiments, using molecular docking simulations to hypothesize how the P2X7 agonist BzATP may be able to bind more effectively than ATP at the rat isoform of this receptor by interacting with Lys-127 adjacent to the ATP binding pocket, and how ivermectin may stabilize the open state of rat P2X4 receptors by binding between the first and second transmembrane domains.

MODULATOR BINDING IN P2X RECEPTOR CRYSTAL STRUCTURES

Analysis of Solved P2X Structures

To date, high-resolution structural data has been obtained for a total of six different P2X receptor constructs, including an NMR structure of the isolated head domain of rat P2X4 (Igawa et al., 2015), and crystal structures of zfP2X4 (Kawate et al., 2009; Hattori and Gouaux, 2012; Kasuya et al., 2017a), Gulf Coast tick P2X (Kasuya et al., 2016), human P2X3 (Mansoor et al., 2016), panda P2X7 (Karasawa and Kawate, 2016), and chicken P2X7 (Kasuya et al., 2017b). Each available entry in the Protein Data Bank is listed in **Table 1**, along with the state in which the crystal structure was determined and its reported resolution. It is important to note that none of these structures represents the native, full-length receptor; the regions of protein sequence encompassed by each representative structure are shown in comparison to the full-length human P2X receptors in **Figure 1A**, and the percentage sequence coverage compared to each human P2X receptor shown in **Figure 1B**. All "crystal constructs" are truncated to some degree at both the N- and C-termini (and indeed the N- and C-termini of the crystal constructs are often not observed in the crystal structures due to their inherent flexibility), and all (apart from human P2X3) bear point mutations. The effects of these truncations and/or mutations on protein function are significant in some cases; the original zfP2X4 *apo*-state crystal structure was significantly

TABLE 1 | List of P2X receptor structures (PDB codes) solved to date.

PDB ID	Resolution (Å)	P2X subtype (Species)	State (ligand)
2BP5	2.8	P2X4 (rat)	n/a
2RUP	*	P2X4 (rat)	n/a
3H9V	3.1	P2X4 (zebrafish)	Apo
3I5D	3.46	P2X4 (zebrafish)	Apo
4DW0	2.9	P2X4 (zebrafish)	Apo
4DW1	2.8	P2X4 (zebrafish)	Bound (ATP)
5F1C	2.9	P2X (Gulf Coast tick)	Bound (ATP)
5SVJ	2.98	P2X3 (human)	Apo
5SVK	2.77	P2X3 (human)	Bound (ATP); open
5SVL	2.9	P2X3 (human)	Bound (ATP); desensitized
5SVM	3.09	P2X3 (human)	Bound (2-methylthio-ATP); desensitized
5SVP	3.3	P2X3 (human)	Bound (2-methylthio-ATP); desensitzed
5SVQ	3.25	P2X3 (human)	Bound (TNP-ATP)
5SVR	3.13	P2X3 (human)	Bound (A-317491)
5SVS	4.03	P2X3 (human)	Apo
5SVT	3.79	P2X3 (human)	apo
5U1L	3.4	P2X7 (giant panda)	Apo
5U1U	3.6	P2X7 (giant panda)	Bound (A740003)
5U1V	3.4	P2X7 (giant panda)	Bound (A804598)
5U1W	3.5	P2X7 (giant panda)	Bound (AZ10606120)
5U1X	3.2	P2X7 (giant panda)	Bound (JNJ47965567)
5U1Y	3.3	P2X7 (giant panda)	Bound (GW791343)
5U2H	3.9	P2X7 (giant panda)	Bound (ATP, A804598)
5WZY	2.8	P2X4 (zebrafish)	Bound (CTP)
5XW6	3.1	P2X7 (chicken)	Bound (TNP-ATP)

*All structures were solved using X-ray diffraction except 2RUP (marked with *), which was obtained using NMR. n/a refers to sequences with <60 amino acids.*NMR structure.*

impaired in ion channel function (Kawate et al., 2009; Young, 2010), the Gulf Coast tick P2X construct, while still able to bind ATP, did not form a functional ion channel (Kasuya et al., 2016), and the chicken P2X7 construct, while still able to bind TNP-ATP, was also non-functional (Kasuya et al., 2017b). However, later zfP2X4 constructs (used to elucidate new *apo*-state and ATP-bound state structures) displayed channel function approaching that of the native receptor (Hattori and Gouaux, 2012), and human P2X3 constructs were fully functional compared to wild-type receptors (Mansoor et al., 2016). The amino-acid sequence identities between the full-length human P2X receptors and the crystal constructs (**Figure 1C**) demonstrate that these structures are very useful as templates for homology modeling with the human receptors that lack crystal structures, due to the high degree of similarity between them.

The Conformational Change Induced by ATP Binding

The conformational changes induced by the binding of ATP (and the partial agonist CTP) have been captured in the crystal structures of zfP2X4 (Hattori and Gouaux, 2012; Kasuya et al., 2017a) and human P2X3 (Mansoor et al., 2016). These changes are vital for the agonist-induced gating of the cation channel, and while not central to the focus of this article, are discussed briefly here. For a detailed treatment of the structural basis for the activation of P2X receptors see (Kawate, 2017). Using the *apo*- and ATP-bound zfP2X4 crystal structures as a guide (Hattori and Gouaux, 2012), ATP binding into its pocket in a cleft between subunits (**Figure 2**, center panel) induces movements in the extracellular domain of the receptor (**Figure 2**, right panel), leading to the upward movement of the dorsal fin domain and the closure of the head region around the ATP binding site, and the downward movement of the left flipper domain. This in turn leads to movement in the lower body of the extracellular domain, which has the effect of moving the second transmembrane domain (which lines the channel) relative to the first transmembrane domain (**Figure 2**, left panel), opening the channel in a manner similar to a camera iris. In the recent ATP-bound human P2X3 crystal structure (Mansoor et al., 2016), the center of the second transmembrane domain is observed to transition from an α-helix to a 3_{10} helix, which may stabilize channel opening.

The Orthosteric Binding Site

Prior to the availability of P2X receptor crystal structures complexed with ATP, several conserved amino-acids critical for ligand binding were identified in a series of key structure-function experiments (reviewed in Browne et al., 2010; Young, 2010), and these residues were demonstrated to line a pocket between receptor subunits in the extracellular domain in the first P2X crystal structure, *apo*-zfP2X4 (Kawate et al., 2009). ATP-bound structures are now available for zfP2X4 (Hattori and Gouaux, 2012), Gulf Coast tick P2X (Kasuya et al., 2016), and human P2X3 [also obtained in the presence of the agonist 2-methylthio-ATP (Mansoor et al., 2016) (**Figures 3A–D**); they display near-identical U-shaped conformations. Of critical importance for agonist activity are the polar interactions with the γ-phosphate and the adenine ring; P2X receptors are not activated by ADP [although tethering of ligands to one binding site of P2X7 has been shown to alter the specificity of other binding sites in the same receptor, enabling further activation by ADP and CTP (Browne and North, 2013)]. P2X receptors display selectivity for purines over pyrimidines, but CTP is a partial agonist at some P2X receptors, including zfP2X4 (Kasuya et al., 2017a). In the crystal structure of CTP-bound zfP2X4 (**Figure 3E**), a hydrogen bond is observed between the N-4 atom of cytosine and the main chain of Thr-189 (zfP2X4 numbering), and an additional hydrogen bond is formed between the O-2 atom of the cytosine ring and the sidechain of Arg-143. This enables the CTP to adopt a similar conformation to that of ATP, even though the pyrimidine ring is smaller. Another point of note in all 5 agonist-bound structures is the close proximity between the γ-phosphate oxygen and the 2′-hydroxyl group of the ribose, which may give rise to hydrogen-bond formation. This hydrogen bond may be very important for maintaining the stability of the ATP molecule in the P2X receptor orthosteric binding site, as suggested by recent molecular dynamics simulations and the observation that 2′-deoxy-ATP is a poor agonist at

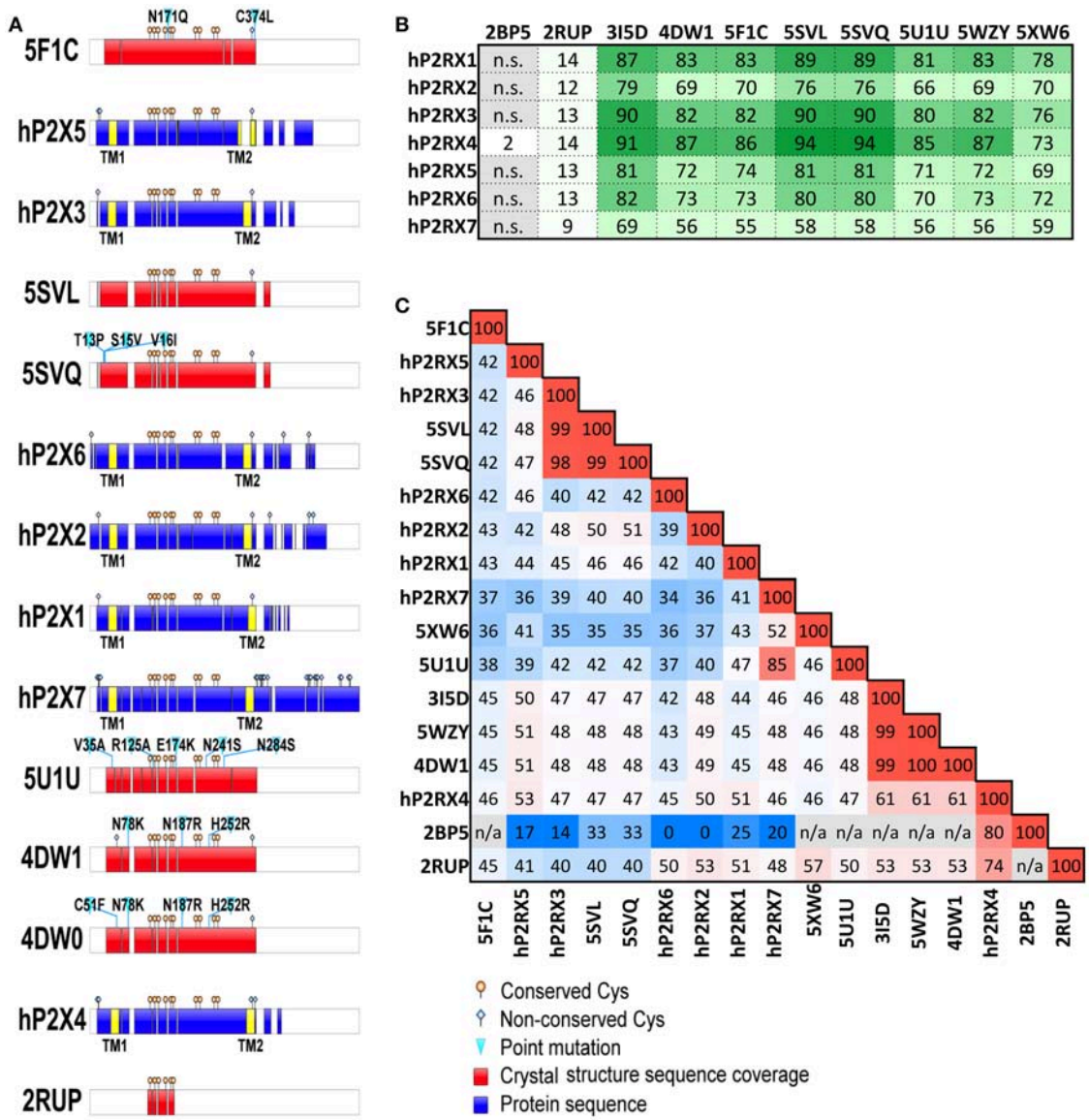

FIGURE 1 | Published P2X receptor constructs; sequence coverage and amino-acid identity. **(A)** Graphical representation of coverage of human P2Xs sequence by crystal structures showing aligned domains. Transmembrane domains (TM) highlighted in yellow; white sections represent gaps. 4DW0 was represented separately to highlight the presence and location of an additional mutation compared to 4DW1. The graphical representation of 5XW6 (chicken P2X7 structure) is not shown. **(B)** Percentage coverage of human P2X receptor sequences by each crystal structure, calculated using BlastP. **(C)** Amino-acid identity matrix of human P2X receptor sequences and sequences listed in **Table 1** (values in percentage; blue for lowest identity, red for highest identity, n/a for non-alignable sequences). Sequences of human P2X (hP2X) receptors were retrieved from UniProt database (Uniprot IDs: P51575, hP2RX1; Q9UBL9, hP2RX2; P56373, hP2RX3; Q99571, hP2RX4; Q93086, hP2RX5; O15547, hP2RX6; Q99572, hP2RX7) and aligned with PDB sequences using ClustalW. Sequences with more than 99.5% identity were grouped together under a single PDB ID for clarity (e.g., 5SVL with 5SVM and 5SVP; 5SVQ with 5SVJ, 5SVK, 5SVR, 5SVT and 5SVS; 4DW1 with 4DW0 and 3H9V; 5U1U with 5U1L, 5U1V, 5U1W, 5U1X, 5U1Y and 5U2H).

human P2X1 receptors in contrast to 3′-deoxy-ATP (Fryatt et al., 2016). Structures of human P2X3 determined in complex with the orthosteric antagonists TNP-ATP (**Figure 3G**) and A-317491 (**Figure 3H**) (Mansoor et al., 2016), and chicken P2X7 in complex with TNP-ATP (**Figure 3F**) (Kasuya et al., 2017b) give a fascinating insight into the molecular basis for competitive antagonism at these receptors. Somewhat surprisingly, when bound to human P2X3 TNP-ATP adopts a strikingly different conformation to that of ATP; although the γ-phosphate is in a broadly similar position, the molecule adopts a Y-shaped conformation, making a hydrophobic interaction deep in the cleft between subunits that ATP does not access (**Figure 3G**). This Y-shaped conformation and deeper binding is also observed for A-317419 (**Figure 3H**), and the effect is to prevent the upward movement of the dorsal fin domain, precluding the closure of the binding cleft that is a prerequisite for channel opening (Mansoor

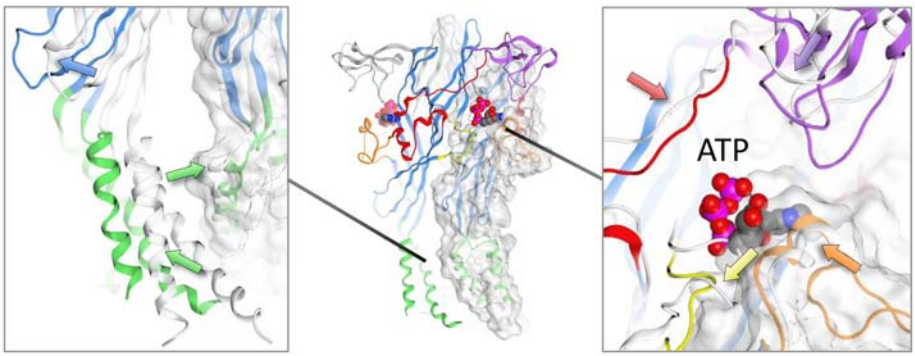

FIGURE 2 | Conformational changes observed in zebrafish crystal structure upon ATP binding. Structures shown are zfP2X4; PDB IDs: 4DW0 (*apo*), and 4DW1 (ATP-bound). Arrows show the trajectories of the backbone rearrangement. The *apo*-structure is presented in white ribbons while the ATP-bound structure follows the canonical domain coloring scheme (green, transmembrane domains; blue, lower and upper body; purple, head domain; orange, dorsal fin; red, right flipper; yellow, left flipper). Detail of transmembrane region and the ATP-binding pocket are shown in the left and right panels, respectively.

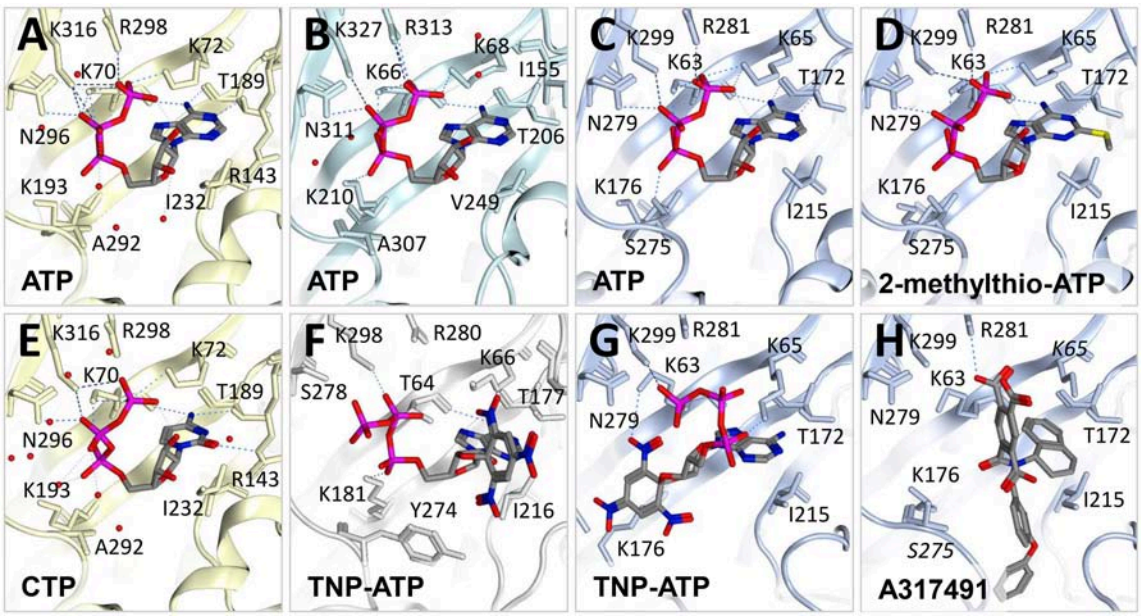

FIGURE 3 | Molecular determinants of orthosteric binding. Crystal structures of zebrafish P2X4 (light yellow ribbon) bound to **(A)** ATP (PDB ID: 4DW1) and **(E)** CTP (5WZY). Water molecules are shown as red dots. **(B)** Gulf coast tick crystal structure (in light cyan ribbon) in the presence of ATP (5F1C). Human P2X3 crystal structures (light blue ribbon) bound to **(C)** ATP (5SVK), **(D)** 2-methylthio-ATP (5SVP), **(G)** TNP-ATP (5SVQ) and **(H)** A317491 (5SVR). **(F)** Crystal structure of chicken P2X7 (gray ribbon) in the presence of TNP-ATP (5XW6). H-bond interactions are displayed with dotted lines. Only residues in close proximity to the ligand are labeled. Note that crystal structure data relative to the ATP binding site is incomplete in **(G)** where the loop containing S275 is missing from the PDB file and in **(F)** where K65 and S275 (labeled in italics) have missing atoms. Figures were made using Molecular Operating Environment (MOE).

et al., 2016). In chicken P2X7, the TNP-ATP conformation is markedly different to that observed in human P2X3 (**Figure 3F**). The adenine ring and ribose adopt similar conformations to that observed for ATP in other P2X receptor crystal structure, but the position of the TNP moiety is altered (contacting the head and dorsal fin domains, rather than buried in the body domain as observed in human P2X3), and the phosphate chains display an extended conformation (Kasuya et al., 2017b). Kasuya et al. used molecular dynamics simulations to conclude that, while TNP-ATP binding to chicken P2X7 induces initial conformational changes similar to those which might be expected for ATP, the TNP moiety prevents downward movement of the head domain induced by cleft closure of the ATP binding pocket and consequently prevents activation of the receptor (Kasuya et al., 2017b). We propose that the observation of different binding conformations for TNP-ATP in P2X3 and P2X7 subtypes may well reflect the 1,000-fold difference in potency of TNP-ATP at P2X3 and P2X7 receptors [$IC_{50} \sim 1$ nM for P2X3 (North, 2002) and 3.55 μM for chicken P2X7 (Kasuya et al., 2017b)], suggesting that a competitive antagonist which can bind deeper into the cleft

between subunits may well be significantly more potent than one which prevents movement of the head domain.

An Allosteric Binding Site in P2X7

The P2X7 receptor, with its wide-ranging proposed physiological roles in inflammatory disease, cancer, neurological disorders (Bartlett et al., 2014; Roger et al., 2015; Pevarello et al., 2017) and, most recently, metabolic disease (Arguin et al., 2017), has been a focus within the pharmaceutical industry and several potent and selective P2X7 antagonists have been developed (Park and Kim, 2017). Many of these were thought to be orthosteric, but painstaking and elegant recent work by Alsopp et al, using structure-function and molecular modeling (Allsopp et al., 2017), and by Karasawa and Kawate, using functional assay and crystallization of giant panda P2X7 in complex with a series of P2X7 antagonists (Karasawa and Kawate, 2016) has clearly demonstrated that these compounds bind to an allosteric site in the extracellular domain distinct from the ATP binding pocket (**Figure 4A**). Crystals were obtained in complex with AZ10606120, GW791343, JNJ47965567, A740003, and A804598 (**Figures 4B–F**). Comparison of the binding of these compounds shows either an elongated conformation which appears to extend across subunits (AZ10606120, GW791343, JNJ47965567), or a more compact conformation making a polar interaction between A740003 and A804598 and the side-chain of Lys-110. In all cases extensive hydrophobic interactions are observed in a pocket delineated by Phe-95, Phe-103, Met-105, Phe-293, and Tyr-295 (panda P2X7 numbering). The discovery of this new allosteric binding pocket in P2X7 (and the availability of the crystal structure as a modeling template) should greatly facilitate the structure-aided design of new allosteric P2X7 antagonists; it may also be possible to exploit this pocket in other receptor subtypes to develop antagonists with increased subtype selectivity.

Comparison of the Dorsal Fin Loops in P2X3, P2X4, and P2X7

P2X receptor subtypes display substantial differences in relative ATP potency. For example, ATP EC_{50} values for human P2X3, human P2X4, and human P2X7 have been reported as 0.13, 7.4, and 720 μM (in low divalent cation-containing solution), respectively (Garcia-Guzman et al., 1997; Neelands et al., 2003; Stokes et al., 2006). Particularly striking is the >1,000-fold lower ATP potency observed at P2X7 receptors compared to other subtypes. Lower potency could be either due to reduced agonist affinity, or reduced ability of the agonist to effect a response (efficacy, here considered as the ability of the agonist to induce a conformational change in the receptor). Because the residues important for binding ATP in P2X receptors and the overall shape of the ATP binding pocket are well-conserved across subtypes, we hypothesize that lower ATP potency observed at P2X7 receptors may result from reduced efficacy. There are a number of regions of sequence difference between P2X7 and the other subtypes which could be responsible for differences in

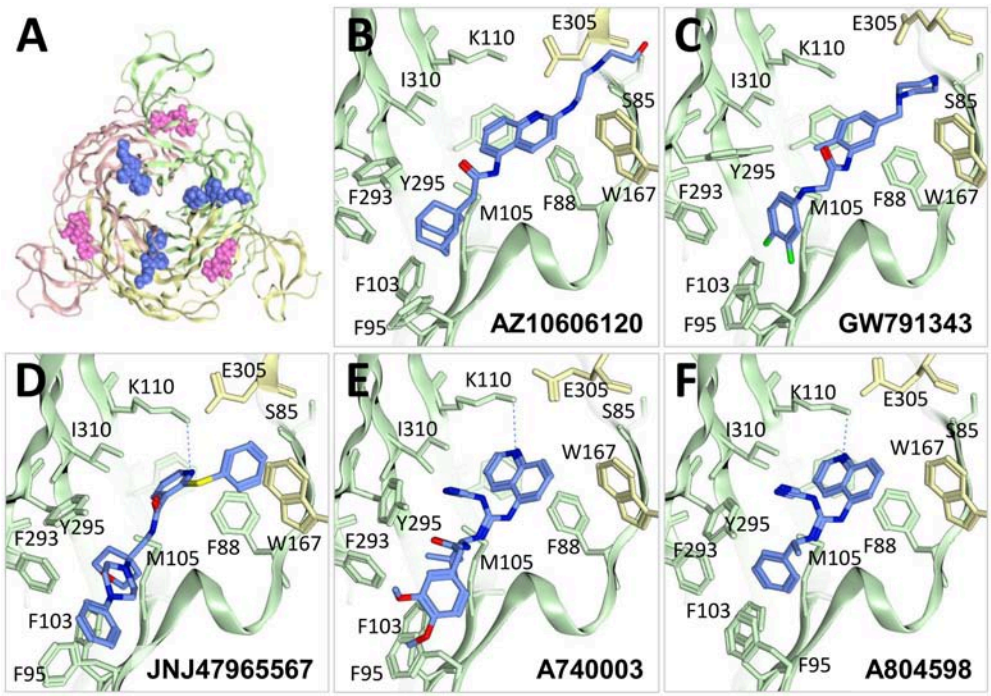

FIGURE 4 | Allosteric antagonists bound to P2X7. **(A)** Top view of giant panda P2X7 crystal structure (PDB ID: 5U1W) bound to AZ10606120 antagonist (blue). ATP (pink) was superposed to highlight the difference between the location of the allosteric pocket and the ATP-binding site. Crystal structures of giant panda bound to **(B)** AZ10606120 (5U1W), **(C)** GW791343 (5U1Y), **(D)** JNJ47965567 (5U1X), **(E)** A740003 (5U1U) and **(F)** A804598 (5U1V) showing residues near the allosteric antagonist colored according to **(A)**. F108 is not labeled for clarity. Figures were made using MOE.

efficacy, but multiple sequence alignment of receptor subtypes shows a clear candidate; the dorsal fin loop (**Figure 5A**). This loop moves upward on ATP binding (Hattori and Gouaux, 2012; Mansoor et al., 2016), and P2X7 subtypes bear a 4 amino-acid deletion in this region, substantially changing its conformation in P2X7 compared to P2X3 and P2X4, both in complex with ATP (**Figure 5B**) and TNP-ATP (**Figure 5C**). It is interesting to note that while the dorsal fin conformation in human P2X3 bound to ATP and TNP-ATP is markedly different (compare **Figures 5B,C**), suggesting a lack of movement of the dorsal fin in the antagonist-bound structure, the conformation of this region in P2X7 is less affected. One reason for this may be that, in chick P2X7, TNP-ATP adopts a similar conformation to ATP, and so a conformational change in the dorsal fin region has taken place in this structure (unfortunately the corresponding *apo*-structure is not available for comparison). An alternative hypothesis is that the shorter dorsal fin loop in P2X7 does not undergo the extensive conformational change seen in P2X3, effectively limiting the degree of conformational change that occurs in P2X7 upon ATP binding, and thus lowering the efficacy of ATP. One way to test this hypothesis would be to replace the dorsal fin loop region in P2X7 with that of another subtype (and *vice versa*) and testing the effects of this substitution on ATP EC_{50}. It should be noted that the conformation of the dorsal fin region of each crystal structure may be affected by crystal contacts in the unit cell of the crystals used for structure determination, and also that these regions of the protein are likely to be dynamic and mobile, and may be capable of

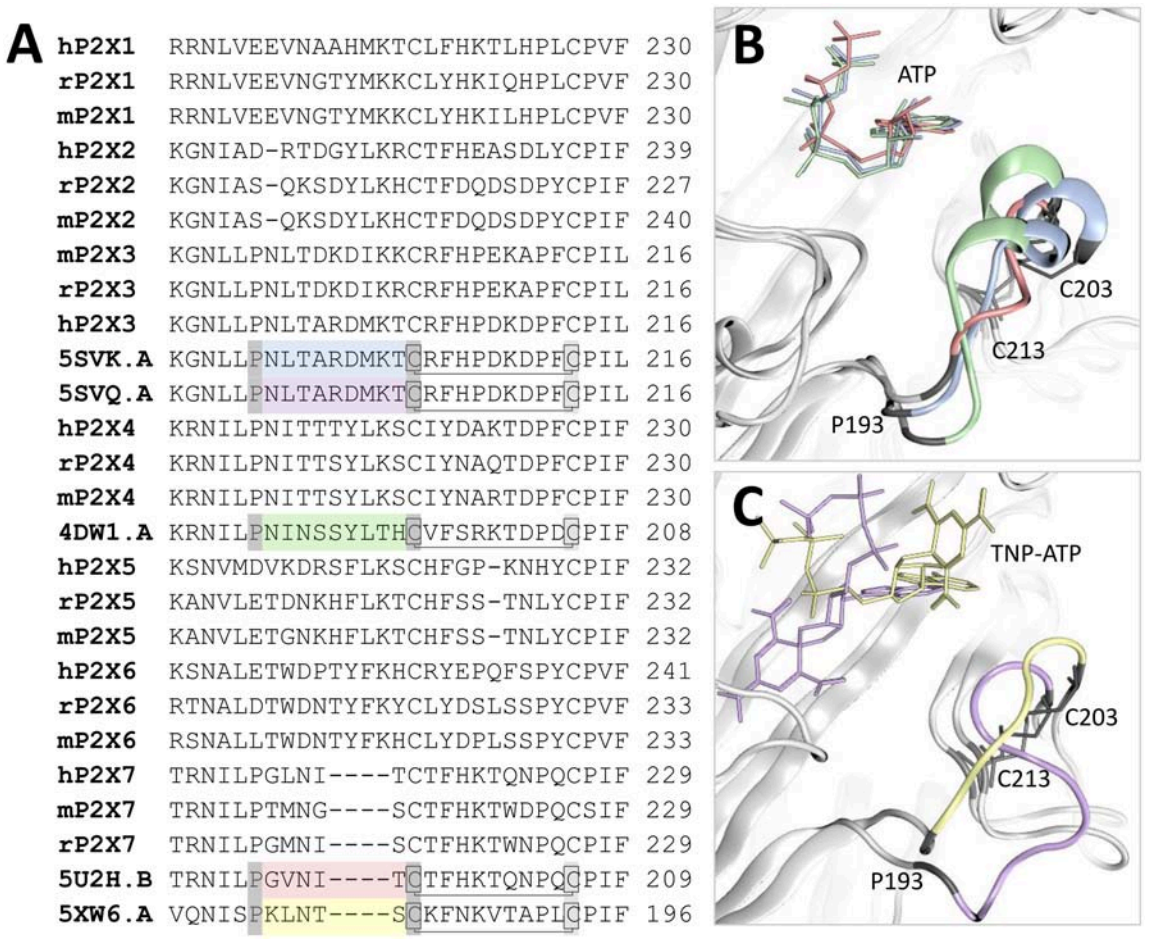

FIGURE 5 | Comparison of the dorsal fin loop structure in P2X3, P2X4, and P2X7. **(A)** Sequence alignment of mouse (m), rat (r), and human (h) P2X receptors with crystal structures bound to either ATP (hP2X3, 5SVK.A; zfP2X4, 4DW1.A; panda P2X7, 5U2H.B) or TNP-ATP (hP2X3, 5SVQ.A; chick P2X7, 5XW6.A). For each crystal structure the dorsal fin region is shown in a different color corresponding to those displayed in **(B,C)** (blue for hP2X3-ATP, purple for hP2X3-TNP-ATP, green for zfP2X4-ATP, pink for panda P2X7-ATP and yellow for chick P2X7-TNP-ATP), and the amino-acid residues at the loop boundaries are shown in dark gray boxes. The conserved disulfide bond is shown with a line. **(B)** Comparison of the ATP-bound structures of hP2X3, zfP2X4, and panda P2X7 with the dorsal fin loop shown in blue, purple, and pink respectively. The shorter dorsal fin region of P2X7 leads to a significantly altered loop conformation which may affect the ability of the receptor to effect conformational change following ATP binding. **(C)** Comparison of the TNP-ATP-bound structures of hP2X3 and chick P2X7 with the dorsal fin loop shown in purple and yellow respectively. The disulfide bond is indicated with gray lines. The dorsal fin loop conformation of hP2X3 is significantly altered compared to that observed in the ATP-bound structure, suggesting that the conformational change has not taken place.

adopting a range of conformations in either *apo*- or ligand-bound states.

MODELING MODULATOR BINDING

The Semi-selective P2X7 Agonist BzATP

BzATP is a synthetic ATP derivative with a benzoylbenzoyl moiety linked to either the 2′ or the 3′ oxygen of ribose. Commercially available BzATP preparations are a mixture of the two isomers and to our knowledge, it is not known whether just one or both isomers have activity at P2X7 receptors. Some initial studies describe the application of the 3′ isomer, but this may be because the original paper describing BzATP synthesis reported it as the 3′ isomer (Williams and Coleman, 1982). However, later synthesis and characterization using similar methods reported a mixture of 3′ and 2′ isomers in a 60:40 ratio (Mahmood et al., 1987). BzATP is more potent than ATP at the P2X7 receptor, and this attribute can be used as pharmacological evidence to support functional expression of P2X7 receptors. However, it is important to note that BzATP is also a full agonist at P2Y receptors (Boyer and Harden, 1989), a partial agonist at P2X4 receptors (Bowler et al., 2003), and an agonist at P2X1, P2X2, and P2X5 receptors (Evans et al., 1995; Bo et al., 2003), meaning that claims of physiological roles for P2X7 receptors based on BzATP-induced responses must be treated with some caution. However, at P2X7 receptors, BzATP is significantly more potent than ATP (∼30-fold at rat P2X7 compared to 4-fold at mouse P2X7, Young et al., 2007) and elicits larger whole-cell responses (Surprenant et al., 1996). It has previously been demonstrated that BzATP potency in rat P2X7 is governed by Lys-127 (the mutation A127K in mouse P2X7 significantly increases BzATP potency relative to ATP), and suggested that the side-chain of this residue might be able to form a π-cation interaction with one of the benzene rings of BzATP (Young et al., 2007). To test this hypothesis, we docked both isomers of BzATP into the ATP binding site of a molecular model of mouse P2X7 bearing the A127K mutation (**Figure 6**). Docking of 2′-BzATP reproduced a strikingly similar conformation to that of ATP (**Figure 6A**). Approximate positions of the phosphate chains and adenine moiety were preserved; however the ribose of BzATP was translated relative to ATP, presumably to accommodate the benzoylbenzoyl moiety. Docking of 3′-BzATP (**Figure 6B**) was less satisfactory; although the positions of the adenine and ribose were well-conserved, the position of the critical γ-phosphate was not. Strikingly, in both conformations, the benzene ring most distant from the ribose was positioned very near to Lys-127, suggesting that formation of a π-cation interaction is plausible. In summary, our docking suggests not only that the original molecular hypothesis for enhanced BzATP potency at rat P2X7 (Young et al., 2007) may be correct, but also that the 2′ isomer of BzATP should possess greater activity at P2X7 receptors than the 3′ isomer. Testing this hypothesis

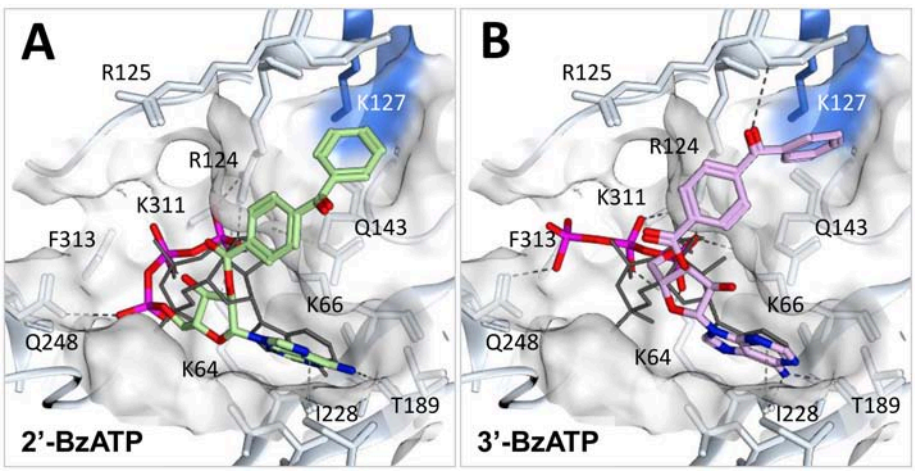

FIGURE 6 | Docking of BzATP into mouse P2X7 A127K. A mouse P2X7 homology model (Uniprot sequence: Q9Z1M0, which was modified to obtain the A127K mutation) was generated using Molecular Operating Environment (MOE) software (MOE 2014.10; Chemical Computing Group ULC, 1010 Sherbooke St. West, Suite #910, Montreal, QC, Canada, H3A 2R7, 2018). The sequences of mouse P2X7 receptor and 5U2H.pdb [chain B; retrieved from RCSB Protein Data Bank (http://www.rcsb.org)] were aligned and the trimeric system was prepared by adding hydrogens and calculating partial charges according to the AMBER10:EHT forcefield. The MOE Built-in homology modeling tool was then used with default settings to make the model, maintaining ATP molecules in the environment and enabling the induced-fit option. As per default settings, the final model was refined after the generation of 10 intermediate models. Schrödinger Suite was employed for all the docking simulations and their preprocessing. In brief, the model was prepared, checked and parameterized with Protein Preparation Wizard (Schrödinger Suite 2015-1, Protein Preparation Wizard; Epik, Schrödinger, LLC, New York, NY; Impact, Schrödinger, LLC, New York, NY; Prime, Schrödinger, LLC, New York, NY). The two isomers of BzATP were built using the MOE Builder tool then preprocessed with LigPrep (Schrödinger, LLC, New York, NY) employing the OPLS_2005 force field and Epik to generate ionization states at pH 7.0 ± 2.0. Docking of the ligands in the competitive binding site was performed using Glide extra precision (release 2015-1, Glide, Schrödinger, LLC, New York, NY) within a box of 38Å^3, using superposed ATP as the centroid of the box. **(A)** 2′-BzATP (green) and **(B)** 3′-BzATP (lilac) compared to the superposed ATP crystal conformation (dark gray lines). The surface of the pocket is represented in white, the surface of the shallow pocket where the Lys-127 residue is located near the benzoyl group is represented in blue. H-bond interactions are shown in dark gray dotted lines, hydrophobic interactions in green dotted lines.

would require the selective purification of 2′- and 3′-BzATP isomers.

The P2X4 Positive Allosteric Modulator Ivermectin

P2X4 receptors play an important role in the central nervous system (CNS) in the modulation of neuroinflammation and neuropathic pain, and are important CNS drug targets (Stokes et al., 2017). Ivermectin (**Figure 7A**) is an anti-helminthic drug used in veterinary medicine, and in humans to treat river blindness (onchocerciasis) (Zemkova et al., 2014). It kills nematodes by activating glutamate-gated chloride channels and has been shown to affect the activity of several other ligand-gated ion channels, including glycine receptors, γ-amino butyric acid (GABA) receptors, nicotinic acetylcholine receptors, and P2X4 receptors (Zemkova et al., 2014; Chen and Kubo, 2017). The mode of action of ivermectin on the cys-loop ligand-gated ion channel family has been structurally characterized; ivermectin is known to bind between transmembrane domains, stabilizing the channel open state (Hibbs and Gouaux, 2011). In this way ivermectin acts as a positive allosteric modulator. It is currently unknown how ivermectin binds to P2X4 receptors, but it is known that ivermectin exerts two effects on P2X4; it causes an increase in maximum current amplitude (this effect occurs at relatively low concentrations of ivermectin and has an EC_{50} of 0.25 μM), and at it slows receptor deactivation by stabilizing the open conformation of the channel (this effect occurs at relatively high concentrations of ivermectin and has an EC_{50} of 2 μM) (Priel and Silberberg, 2004). The dual effects of ivermectin potentially suggest two (or more) binding modes, but it is plausible to assume that it may stabilize the open conformation of P2X4 by a similar mechanism to that observed in cys-loop receptors. Indeed, a series of mutagenesis and structure-function experiments have been conducted in order to determine amino-acid residues important for the effects of ivermectin at P2X4 receptors (Silberberg et al., 2007; Samways et al., 2012; Tvrdonova et al., 2014), reviewed in (Chen and Kubo, 2017) and the majority of these residues are clustered toward the upper (extracellular side of the membrane) and central portions of the first transmembrane domain, and the central and lower portions of the second transmembrane domain (**Figure 7B**). Using these amino-acids as a reference, we were able to dock ivermectin B1a into a molecular model of rat P2X4 between the first and second transmembrane domains from adjacent subunits (**Figure 7B**). In our docking simulation the ivermectin molecule is positioned with the hydrogenated benzofuran moiety toward the intracellular face of the membrane, forming hydrophobic interactions with Leu-345 and Val-348 near the bottom of the second transmembrane domain of one subunit (colored blue in **Figures 7C,D**). The disaccharide moiety (dioleandrose) is positioned near the extracellular face, forming hydrophobic interactions with Tyr-42, Trp-46, and Val-47 at the top of the first transmembrane domain, and a hydrogen bond between the hydroxyl group of the distal oleandrose and the oxygen atom of the side-chain of Asn-338 near the top of the second transmembrane domain of the adjacent subunit (colored green in **Figures 7C,D**). This means that ivermectin is interacting with the bottom of the second transmembrane domain in one subunit, and the top of both the first and second transmembrane domains in the adjacent subunit, which would have the effect of stabilizing the channel in the open state following activation by ATP. It is important to note that this conformation does not preclude ivermectin from binding to the other two equivalent binding sites in the trimer.

In order to understand why ivermectin is capable of potentiating current responses at some P2X receptor subtypes but not others, we aligned the transmembrane domain sequences of human, rat, and mouse P2X1, P2X1, P2X3, P2X4, and P2X7, along with those of *Schistosoma mansoni* P2X (Agboh et al., 2004) and *Hypsibius dujardini* P2X (Bavan et al., 2009), also shown to be sensitive to ivermectin (**Figure 7E**). The ivermectin-sensitive receptor subtypes are grouped together in a yellow box (**Figure 7E**). It should be noted that ivermectin sensitivity has been reported in human P2X7 (but not mouse P2X7) in whole-cell patch clap experiments on transfected human cells (Norenberg et al., 2012); however, a recent study on human P2X7 expressed in *Xenopus* oocytes observed no potentiation (Schneider et al., 2017). In **Figure 7E**, amino-acid residues identical to rat P2X4 are colored in gray, amino-acids conserved across all subtypes are in gray boxes, and amino-acids conserved in subtypes where ivermectin is active are shown in blue. Red boxes highlight the amino-acid residues where substitution with tryptophan significantly reduced ivermectin activity in rat P2X4 (Silberberg et al., 2007). Of the nine amino-acids implicated in ivermectin action by tryptophan mutagenesis, seven are within 4.5 Å of the ivermectin molecule in our dock (green and blue arrows indicate residues in close proximity in **Figure 7E**), showing a good correlation between our docking simulation and experimental data. In our docking simulation we observed a hydrogen bond between the sidechain of Asn-338 and the oleandrose moiety of ivermectin (**Figures 7C,D**, large blue arrowhead in **Figure 7E**). Interestingly, the rat P2X4 mutant N338W retained ivermectin sensitivity (Silberberg et al., 2007). We explored this by modeling ivermectin binding to the rat P2X4 N338W mutant, finding that ivermectin was still able to make an H-arene interaction with the tryptophan (data not shown). We hypothesize that mutating this residue to one incapable of forming H-bonds (such as Ile or Leu) should significantly impair the ability of ivermectin to potentiate current responses at rat P2X4. Analysis of sequence conservation across the transmembrane domains suggests that the P2X1 subtype is most similar to the ivermectin-sensitive subtypes. While it may not be possible to confer ivermectin sensitivity to another subtype with one point mutation, we suggest that a combination of the mutations F33N, T333I, T334N, I341L, and F342L in human P2X1 may confer ivermectin sensitivity to this receptor subtype.

In summary, our docking simulation explains the ability of ivermectin to stabilize the open state of P2X4 receptors, and hints at the amino-acid residues important for the subtype-specific effects of ivermectin; furthermore, our docking should permit the rational design of smaller lipophilic molecules which specifically target sub-regions of the putative ivermectin binding site in

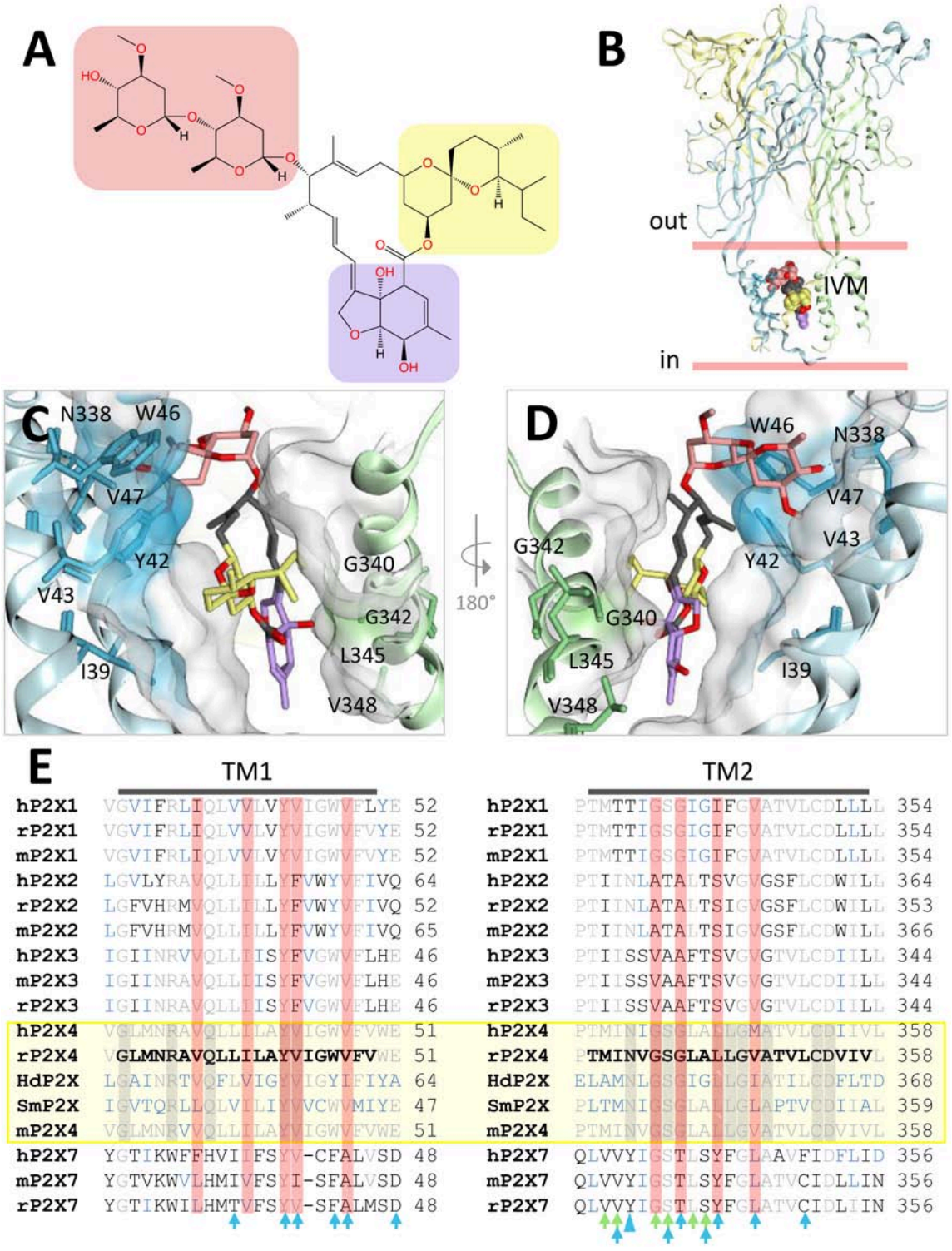

FIGURE 7 | Docking of ivermectin (IVM) in the predicted allosteric binding site of the rat P2X4 homology model. A rat P2X4 homology model (Uniprot sequence: P51577) was built using MOE with 4DW1 structure as a template and prepared for docking with Protein Preparation Wizard (see **Figure 6**). Docking was performed within a box of 35Å^3 located at the level of the transmembrane domain using the coordinates of a previously identified pocket [with Site Finder (MOE)] as the centroid of the box. **(A)** Chemical structure of ivermectin B1a, highlighting the dioleandrose (disaccharide) (salmon), spiroketal (yellow), and hydrogenated benzofuran (purple). **(B)** Location of the predicted IVM binding site in rat P2X4. The membrane bilayer is delimited by red lines. IVM atoms are colored according to **(A)** while the receptor is represented in ribbons, each color representing a different subunit. **(C)** Detail of IVM conformation docked between two subunits, using the same color scheme as in

(Continued)

FIGURE 7 | (A). The residues close to the IVM pose and identified to be important in IVM activity (see text) are shown and colored according to the receptor subunit. The surface of the receptor is shown in white; colored areas correspond to the highlighted residues. **(D)** 180° rotation of the IVM pose displayed in **(C)**. The third subunit (yellow in **B**) is omitted for clarity. **(E)** Sequence alignment of the transmembrane (TM) domains of human (h), rat (r), mouse (m), *Schistosoma mansoni* (Sm), and *Hypsibius dujardini* (Hd) P2X receptor sequences. Amino-acids identical to those found in rP2X4 are colored in gray. Receptors sensitive to IVM are shown in a yellow box, and residues conserved across all subtypes are encapsulated in gray boxes. Residues colored blue are those which are conserved in P2X receptor subtypes where IVM is active. Residues in red boxes are those identified by Silberberg et al. to significantly reduce IVM activity when mutated to tryptophan (Silberberg et al., 2007). Blue and green arrows indicate the amino-acid residues within a distance of 4.5Å of IVM in our rP2X4-IVM dock; arrows are colored according to the receptor subunit involved in the interaction (same color scheme as **A**). The large blue arrow head indicates Asn-338, which in our docking simulation forms an H-bond with the oleandrose moiety of IVM.

P2X4. It is important to note that Glu-51, located in the lateral ion-access portal just above the transmembrane domains and conserved in P2X1 and P2X3 receptors (shown in **Figure 7E**), has also been implicated in the action of ivermectin (Samways et al., 2012). We did not observe an interaction between ivermectin and Glu-51 in our docking simulation; it is possible that the region including and surrounding Glu-51 may contribute to a second ivermectin binding site, which may explain the dual actions of ivermectin on P2X4 receptors. Finally, we note that, as our manuscript was at the proof stage, a molecular dock of P2X4 bound to ivermectin was published (Latapiat et al., 2017) which appears to adopt a similar conformation to that shown in our docking simulation.

CONCLUDING REMARKS

This article demonstrates how the growing collection of P2X receptor crystal structures, from different species and subtypes, in complex with orthosteric agonists and both orthosteric and allosteric antagonists, has not only transformed our understanding of how small molecule modulators bind to and influence P2X receptor function, but also has enabled us to effectively model novel binding conformations for other ligands based on the available molecular evidence. We have been able to compare the binding of ATP at zfP2X4, Gulf Coast tick P2X and human P2X3, and to analyze the molecular basis for competitive and non-competitive antagonism at human P2X3 and panda and chicken P2X7. The orthosteric antagonist binding site in P2X7 may well be a valid target for future structure-based drug design in other receptor subtypes in order to develop subtype-selective antagonists. We have analyzed the difference in conformation of the dorsal fin loop between P2X7 and P2X3 and P2X4, hypothesizing that the shorter loop in P2X7 may affect the degree of conformational change induced by ATP binding, and hence the efficacy of the agonist. Using molecular modeling and docking experiments, we have been able to propose plausible and testable binding conformations for the agonist BzATP at P2X7, and the positive allosteric modulator ivermectin at rat P2X4, hypothesizing that the 2′ isomer of BzATP should be more potent than the 3′ isomer, and outlining a series of mutations which may confer ivermectin sensitivity onto P2X1 receptors. While a comprehensive structural basis for subtype-specific differences in agonist potency is still lacking, it is to be hoped that structures of P2X1 and P2X2 receptor subtypes, where the majority of structure-function studies have been conducted, will be solved in the near future, giving new insights into ligand binding and a better context to previously published data.

AUTHOR CONTRIBUTIONS

GP and AB: Performed and analyzed ligand docking experiments; GP: Prepared the Figures, MY: Wrote the manuscript; GP, AB, and MY: Edited the manuscript.

FUNDING

This work was supported by a Life Sciences Research Network Wales Ph.D. studentship award to GP (Project NRN-507962).

REFERENCES

Abdulqawi, R., Dockry, R., Holt, K., Layton, G., McCarthy, B. G., Ford, A. P., et al. (2015). P2X3 receptor antagonist (AF-219) in refractory chronic cough: a randomised, double-blind, placebo-controlled phase 2 study. *Lancet* 385, 1198–1205. doi: 10.1016/S0140-6736(14)61255-1

Agboh, K. C., Webb, T. E., Evans, R. J., and Ennion, S. J. (2004). Functional characterization of a P2X receptor from *Schistosoma mansoni*. *J. Biol. Chem.* 279, 41650–41657. doi: 10.1074/jbc.M408203200

Ahmadi, M., Nowroozi, A., and Shahlaei, M. (2015). Constructing an atomic-resolution model of human P2X7 receptor followed by pharmacophore modeling to identify potential inhibitors. *J. Mol. Graph. Model.* 61, 243–261. doi: 10.1016/j.jmgm.2015.08.005

Allsopp, R. C., Dayl, S., Schmid, R., and Evans, R. J. (2017). Unique residues in the ATP gated human P2X7 receptor define a novel allosteric binding pocket for the selective antagonist AZ10606120. *Sci. Rep.* 7:725. doi: 10.1038/s41598-017-00732-5

Alves, L. A., da Silva, J. H., Ferreira, D. N., Fidalgo-Neto, A. A., Teixeira, P. C., de Souza, C. A., et al. (2014). Structural and molecular modeling features of P2X receptors. *Int. J. Mol. Sci.* 15, 4531–4549. doi: 10.3390/ijms15034531

Arguin, G., Bourzac, J. F., Placet, M., Molle, C. M., Paquette, M., Beaudoin, J. F., et al. (2017). The loss of P2X7 receptor expression leads to increase intestinal glucose transit and hepatic steatosis. *Sci. Rep.* 7:12917. doi: 10.1038/s41598-017-13300-8

Bartlett, R., Stokes, L., and Sluyter, R. (2014). The P2X7 receptor channel: recent developments and the use of P2X7 antagonists in models of disease. *Pharmacol. Rev.* 66, 638–675. doi: 10.1124/pr.113.008003

Bavan, S., Straub, V. A., Blaxter, M. L., and Ennion, S. J. (2009). A P2X receptor from the tardigrade species *Hypsibius dujardini* with fast kinetics and sensitivity to zinc and copper. *BMC Evol. Biol.* 9:17. doi: 10.1186/1471-2148-9-17

Bo, X., Jiang, L. H., Wilson, H. L., Kim, M., Burnstock, G., Surprenant, A., et al. (2003). Pharmacological and biophysical properties of the human P2X5 receptor. *Mol. Pharmacol.* 63, 1407–1416. doi: 10.1124/mol.63.6.1407

Bowler, J. W., Bailey, R. J., North, R. A., and Surprenant, A. (2003). P2X4, P2Y1 and P2Y2 receptors on rat alveolar macrophages. *Br. J. Pharmacol.* 140, 567–575. doi: 10.1038/sj.bjp.0705459

Boyer, J. L., and Harden, T. K. (1989). Irreversible activation of phospholipase C-coupled P2Y-purinergic receptors by 3'-O-(4-benzoyl)benzoyl adenosine 5'-triphosphate. *Mol. Pharmacol.* 36, 831–835.

Browne, L. E., Jiang, L. H., and North, R. A. (2010). New structure enlivens interest in P2X receptors. *Trends Pharmacol. Sci.* 31, 229–237. doi: 10.1016/j.tips.2010.02.004

Browne, L. E., and North, R. A. (2013). P2X receptor intermediate activation states have altered nucleotide selectivity. *J. Neurosci.* 33, 14801–14808. doi: 10.1523/JNEUROSCI.2022-13.2013

Burnstock, G. (2017). Purinergic signalling: therapeutic developments. *Front. Pharmacol.* 8:661. doi: 10.3389/fphar.2017.00661

Caseley, E. A., Muench, S. P., Baldwin, S. A., Simmons, K., Fishwick, C. W., and Jiang, L. H. (2015). Docking of competitive inhibitors to the P2X7 receptor family reveals key differences responsible for changes in response between rat and human. *Bioorg. Med. Chem. Lett.* 25, 3164–3167. doi: 10.1016/j.bmcl.2015.06.001

Caseley, E. A., Muench, S. P., Fishwick, C. W., and Jiang, L. H. (2016). Structure-based identification and characterisation of structurally novel human P2X7 receptor antagonists. *Biochem. Pharmacol.* 116, 130–139. doi: 10.1016/j.bcp.2016.07.020

Chataigneau, T., Lemoine, D., and Grutter, T. (2013). Exploring the ATP-binding site of P2X receptors. *Front. Cell. Neurosci.* 7:273. doi: 10.3389/fncel.2013.00273

Chen, I. S., and Kubo, Y. (2017). Ivermectin and its target molecules: shared and unique modulation mechanisms of ion channels and receptors by ivermectin. *J. Physiol.* 595, 5895–5912. doi: 10.1113/JP275236

Eser, A., Colombel, J. F., Rutgeerts, P., Vermeire, S., Vogelsang, H., Braddock, M., et al. (2015). Safety and efficacy of an oral inhibitor of the purinergic receptor P2X7 in adult patients with moderately to severely active crohn's disease: a randomized placebo-controlled, double-blind, phase iia study. *Inflamm. Bowel Dis.* 21, 2247–2253. doi: 10.1097/MIB.0000000000000514

Evans, R. J., Lewis, C., Buell, G., Valera, S., North, R. A., and Surprenant, A. (1995). Pharmacological characterization of heterologously expressed ATP-gated cation channels (P2x purinoceptors). *Mol. Pharmacol.* 48, 178–183.

Farmer, L. K., Schmid, R., and Evans, R. J. (2015). Use of chimeras, point mutants, and molecular modeling to map the antagonist-binding site of 4,4′,4″,4‴-(carbonylbis-(imino-5,1,3-benzenetriylbis(carbonylimino)))tetrakisb enzene-1,3-disulfonic acid (NF449) at P2X1 receptors for ATP. *J. Biol. Chem.* 290, 1559–1569. doi: 10.1074/jbc.M114.592246

Fryatt, A. G., Dayl, S., Cullis, P. M., Schmid, R., and Evans, R. J. (2016). Mechanistic insights from resolving ligand-dependent kinetics of conformational changes at ATP-gated P2X1R ion channels. *Sci. Rep.* 6:32918. doi: 10.1038/srep32918

Garcia-Guzman, M., Soto, F., Gomez-Hernandez, J. M., Lund, P. E., and Stühmer, W. (1997). Characterization of recombinant human P2X4 receptor reveals pharmacological differences to the rat homologue. *Mol. Pharmacol.* 51, 109–118. doi: 10.1124/mol.51.1.109

Grimes, L., and Young, M. T. (2015). Purinergic P2X receptors: structural and functional features depicted by X-ray and molecular modelling studies. *Curr. Med. Chem.* 22, 783–798. doi: 10.2174/0929867321999141212131457

Habermacher, C., Dunning, K., Chataigneau, T., and Grutter, T. (2016). Molecular structure and function of P2X receptors. *Neuropharmacology* 104, 18–30. doi: 10.1016/j.neuropharm.2015.07.032

Hattori, M., and Gouaux, E. (2012). Molecular mechanism of ATP binding and ion channel activation in P2X receptors. *Nature* 485, 207–212. doi: 10.1038/nature11010

Hibbs, R. E., and Gouaux, E. (2011). Principles of activation and permeation in an anion-selective Cys-loop receptor. *Nature* 474, 54–60. doi: 10.1038/nature10139

Igawa, T., Abe, Y., Tsuda, M., Inoue, K., and Ueda, T. (2015). Solution structure of the rat P2X4 receptor head domain involved in inhibitory metal binding. *FEBS Lett.* 589, 680–686. doi: 10.1016/j.febslet.2015.01.034

Jiang, R., Taly, A., and Grutter, T. (2013). Moving through the gate in ATP-activated P2X receptors. *Trends Biochem. Sci.* 38, 20–29. doi: 10.1016/j.tibs.2012.10.006

Karasawa, A., and Kawate, T. (2016). Structural basis for subtype-specific inhibition of the P2X7 receptor. *Elife* 5:e22153. doi: 10.7554/eLife.22153

Kasuya, G., Fujiwara, Y., Takemoto, M., Dohmae, N., Nakada-Nakura, Y., Ishitani, R., et al. (2016). Structural Insights into divalent cation modulations of ATP-Gated P2X receptor channels. *Cell Rep.* 14, 932–944. doi: 10.1016/j.celrep.2015.12.087

Kasuya, G., Fujiwara, Y., Tsukamoto, H., Morinaga, S., Ryu, S., Touhara, K., et al. (2017a). Structural insights into the nucleotide base specificity of P2X receptors. *Sci. Rep.* 7:45208. doi: 10.1038/srep45208

Kasuya, G., Yamaura, T., Ma, X. B., Nakamura, R., Takemoto, M., Nagumo, H., et al. (2017b). Structural insights into the competitive inhibition of the ATP-gated P2X receptor channel. *Nat. Commun.* 8:876. doi: 10.1038/s41467-017-00887-9

Kawate, T. (2017). P2X receptor activation. *Adv. Exp. Med. Biol.* 1051, 55–69. doi: 10.1007/5584_2017_55

Kawate, T., Michel, J. C., Birdsong, W. T., and Gouaux, E. (2009). Crystal structure of the ATP-gated P2X4 ion channel in the closed state. *Nature* 460, 592–598. doi: 10.1038/nature08198

Keystone, E. C., Wang, M. M., Layton, M., Hollis, S., and McInnes, I. B. (2012). Clinical evaluation of the efficacy of the P2X7 purinergic receptor antagonist AZD9056 on the signs and symptoms of rheumatoid arthritis in patients with active disease despite treatment with methotrexate or sulphasalazine. *Ann. Rheum. Dis.* 71, 1630–1635. doi: 10.1136/annrheumdis-2011-143578

Khakh, B. S., Proctor, W. R., Dunwiddie, T. V., Labarca, C., and Lester, H. A. (1999). Allosteric control of gating and kinetics at P2X(4) receptor channels. *J. Neurosci.* 19, 7289–7299.

Latapiat, V., Rodríguez, F. E., Godoy, F., Montenegro, F. A., Barrera, N. P., and Huidobro-Toro, J. P. (2017). P2X4 receptor *in Silico* and electrophysiological approaches reveal insights of ivermectin and zinc allosteric modulation. *Front. Pharmacol.* 8:918. doi: 10.3389/fphar.2017.00918

Mahmood, R., Cremo, C., Nakamaye, K. L., and Yount, R. G. (1987). The interaction and photolabeling of myosin subfragment 1 with 3'(2')-O-(4-benzoyl)benzoyladenosine 5'-triphosphate. *J. Biol. Chem.* 262, 14479–14486.

Mansoor, S. E., Lü, W., Oosterheert, W., Shekhar, M., Tajkhorshid, E., and Gouaux, E. (2016). X-ray structures define human P2X(3) receptor gating cycle and antagonist action. *Nature* 538, 66–71. doi: 10.1038/nature19367

McInnes, I. B., Snell, N. J., Perrett, J. H., Parmar, H., Wang, M. M., and Astbury, C. (2007). "Results of a Phase II clinical trial of a novel P2X7 receptor antagonist, AZD9056, in patients with active rheumatoid arthritis (CREATE study)," in *ARHP Annual Scientific Meeting, Presentation 2085.*

Neelands, T. R., Burgard, E. C., Uchic, M. E., McDonald, H. A., Niforatos, W., Faltynek, C. R., et al. (2003). 2', 3'-O-(2,4,6,trinitrophenyl)-ATP and A-317491 are competitive antagonists at a slowly desensitizing chimeric human P2X3 receptor. *Br. J. Pharmacol.* 140, 202–210. doi: 10.1038/sj.bjp.0705411

Norenberg, W., Sobottka, H., Hempel, C., Plotz, T., Fischer, W., Schmalzing, G., et al. (2012). Positive allosteric modulation by ivermectin of human but not murine P2X7 receptors. *Br. J. Pharmacol.* 167, 48–66. doi: 10.1111/j.1476-5381.2012.01987.x

North, R. A. (2002). Molecular physiology of P2X receptors. *Physiol. Rev.* 82, 1013–1067. doi: 10.1152/physrev.00015.2002

North, R. A. (2016). P2X receptors. *Philos. Trans. R. Soc. Lond. B. Biol. Sci.* 371:20150427. doi: 10.1098/rstb.2015.0427

Park, J. H., and Kim, Y. C. (2017). P2X7 receptor antagonists: a patent review (2010-2015). *Expert Opin. Ther. Pat.* 27, 257–267. doi: 10.1080/13543776.2017.1246538

Pevarello, P., Bovolenta, S., Tarroni, P., Za, L., Severi, E., Torino, D., et al. (2017). P2X7 antagonists for CNS indications: recent patent disclosures. *Pharm. Pat. Anal.* 6, 61–76. doi: 10.4155/ppa-2016-0044

Priel, A., and Silberberg, S. D. (2004). Mechanism of ivermectin facilitation of human P2X4 receptor channels. *J. Gen. Physiol.* 123, 281–293. doi: 10.1085/jgp.200308986

Roger, S., Jelassi, B., Couillin, I., Pelegrin, P., Besson, P., and Jiang, L. H. (2015). Understanding the roles of the P2X7 receptor in solid tumour progression and therapeutic perspectives. *Biochim. Biophys. Acta* 1848, 2584–2602. doi: 10.1016/j.bbamem.2014.10.029

Samways, D. S., Khakh, B. S., and Egan, T. M. (2012). Allosteric modulation of Ca2+ flux in ligand-gated cation channel (P2X4) by actions on lateral portals. *J. Biol. Chem.* 287, 7594–7602. doi: 10.1074/jbc.M111.322461

Samways, D. S., Li, Z., and Egan, T. M. (2014). Principles and properties of ion flow in P2X receptors. *Front. Cell. Neurosci.* 8:6. doi: 10.3389/fncel.2014.00006

Schneider, M., Prudic, K., Pippel, A., Klapperstück, M., Braam, U., Müller, C. E., et al. (2017). Interaction of purinergic P2X4 and P2X7 receptor subunits. *Front. Pharmacol.* 8:60. doi: 10.3389/fphar.2017.00860

Silberberg, S. D., Li, M., and Swartz, K. J. (2007). Ivermectin Interaction with transmembrane helices reveals widespread rearrangements during opening of P2X receptor channels. *Neuron* 54, 263–274. doi: 10.1016/j.neuron.2007.03.020

Stock, T. C., Bloom, B. J., Wei, N., Ishaq, S., Park, W., Wang, X., et al. (2012). Efficacy and safety of CE-224,535, an antagonist of P2X7 receptor, in treatment of patients with rheumatoid arthritis inadequately controlled by methotrexate. *J. Rheumatol.* 39, 720–727. doi: 10.3899/jrheum.110874

Stokes, L., Jiang, L. H., Alcaraz, L., Bent, J., Bowers, K., Fagura, M., et al. (2006). Characterization of a selective and potent antagonist of human P2X(7) receptors, AZ11645373. *Br. J. Pharmacol.* 149, 880–887. doi: 10.1038/sj.bjp.0706933

Stokes, L., Layhadi, J. A., Bibic, L., Dhuna, K., and Fountain, S. J. (2017). P2X4 Receptor Function in the Nervous System and Current Breakthroughs in Pharmacology. *Front. Pharmacol.* 8:291. doi: 10.3389/fphar.2017.00291

Surprenant, A., Rassendren, F., Kawashima, E., North, R. A., and Buell, G. (1996). The cytolytic P2Z receptor for extracellular ATP identified as a P2X receptor (P2X7). *Science* 272, 735–738. doi: 10.1126/science.272.5262.735

Tvrdonova, V., Rokic, M. B., Stojilkovic, S. S., and Zemkova, H. (2014). Identification of functionally important residues of the rat P2X4 receptor by alanine scanning mutagenesis of the dorsal fin and left flipper domains. *PLoS ONE* 9:e112902. doi: 10.1371/journal.pone.0112902

Williams, N., and Coleman, P. S. (1982). Exploring the adenine nucleotide binding sites on mitochondrial F1-ATPase with a new photoaffinity probe, 3'-O-(4-benzoyl)benzoyl adenosine 5'-triphosphate. *J. Biol. Chem.* 257, 2834–2841.

Young, M. T. (2010). P2X receptors: dawn of the post-structure era. *Trends Biochem. Sci.* 35, 83–90. doi: 10.1016/j.tibs.2009.09.006

Young, M. T., Pelegrin, P., and Surprenant, A. (2007). Amino acid residues in the P2X7 receptor that mediate differential sensitivity to ATP and BzATP. *Mol. Pharmacol.* 71, 92–100. doi: 10.1124/mol.106.030163

Zemkova, H., Tvrdonova, V., Bhattacharya, A., and Jindrichova, M. (2014). Allosteric modulation of ligand gated ion channels by ivermectin. *Physi. Res.* 63(Suppl. 1), S215–S224.

Conflict of Interest Statement: The authors declare that the research was conducted in the absence of any commercial or financial relationships that could be construed as a potential conflict of interest.

frontiers in Pharmacology

REVIEW
published: 01 February 2018
doi: 10.3389/fphar.2018.00039

Non-nucleotide Agonists Triggering P2X7 Receptor Activation and Pore Formation

Francesco Di Virgilio, Anna L. Giuliani, Valentina Vultaggio-Poma, Simonetta Falzoni and Alba C. Sarti*

Department of Morphology, Surgery and Experimental Medicine, University of Ferrara, Ferrara, Italy

The P2X7 receptor (P2X7R) is a ligand-gated plasma membrane ion channel belonging to the P2X receptor subfamily activated by extracellular nucleotides. General consensus holds that the physiological (and maybe the only) agonist is ATP. However, scattered evidence generated over the last several years suggests that ATP might not be the only agonist, especially at inflammatory sites. Solid data show that NAD^+ covalently modifies the P2X7R of mouse T lymphocytes, thus lowering the ATP threshold for activation. Other structurally unrelated agents have been reported to activate the P2X7R via a poorly understood mechanism of action: (a) the antibiotic polymyxin B, possibly a positive allosteric P2X7R modulator, (b) the bactericidal peptide LL-37, (c) the amyloidogenic β peptide, and (d) serum amyloid A. Some agents, such as Alu-RNA, have been suggested to activate the P2X7R acting on the intracellular N- or C-terminal domains. Mode of P2X7R activation by these non-nucleotide ligands is as yet unknown; however, these observations raise the intriguing question of how these different non-nucleotide ligands may co-operate with ATP at inflammatory or tumor sites. New information obtained from the cloning and characterization of the P2X7R from exotic mammalian species (e.g., giant panda) and data from recent patch-clamp studies are strongly accelerating our understanding of P2X7R mode of operation, and may provide hints to the mechanism of activation of P2X7R by non-nucleotide ligands.

Keywords: P2X7 receptor, extracellular ATP, inflammation, cathelicidin, polymyxin B

OPEN ACCESS

Edited by:
Kenneth A. Jacobson, National Institutes of Health (NIH), United States

Reviewed by:
Szilvia Benkö, University of Debrecen, Hungary
Claudia Lucia Martins Silva, Universidade Federal do Rio de Janeiro, Brazil
Henning Ulrich, University of São Paulo, Brazil

****Correspondence:***
Francesco Di Virgilio
fdv@unife.it

Specialty section:
This article was submitted to Experimental Pharmacology and Drug Discovery, a section of the journal Frontiers in Pharmacology

Received: *14 November 2017*
Accepted: *12 January 2018*
Published: *01 February 2018*

Citation:
Di Virgilio F, Giuliani AL, Vultaggio-Poma V, Falzoni S and Sarti AC (2018) Non-nucleotide Agonists Triggering P2X7 Receptor Activation and Pore Formation. Front. Pharmacol. 9:39. doi: 10.3389/fphar.2018.00039

INTRODUCTION

The P2X7 receptor (P2X7R) belongs to the ionotropic P2X receptor subfamily (Burnstock, 2006). It was previously known as P2Z, and when first characterized in rat mast cells, it was named the "ATP^{4-} receptor" (Cockcroft and Gomperts, 1980). Identification of the mast cell receptor with the P2X7R cloned by Surprenant et al. (1996) has been questioned on the basis of the widely different apparent Kds for ATP of these receptors, but the functional features are very similar and therefore suggestive that the "ATP^{4-} receptors" and the P2X7R are one and the same molecule. Following experiments have shown that human mast cells express P2X7R-like non-desensitizing currents (Wareham et al., 2009). P2X7R expression and function was also documented in mouse mast cells (Kurashima et al., 2012). Reason for the very high affinity for ATP of the rat mast cell ATP^{4-} receptor is not obvious. For sure, in the original experiments by Bastien Gomperts the ATP Kd was measured in the absence of divalent cations (Ca^{2+} and Mg^{2+}), thus it refers to the fully dissociated nucleotide species, and it is well known that threshold for P2X7R activation is lower

in the absence of divalent cations. It is also worth mentioning that to our knowledge no analysis of P2X7R expression and function was ever repeated in the same experimental model used by Gomperts, i.e., mast cells obtained by peritoneal lavage of rats pre-immunized with ovalbumin or with antigens from the helminth parasite *Nippostrongylus brasiliensis* (Cockcroft and Gomperts, 1979, 1980). It is therefore possible that P2X7R affinity, and therefore ATP threshold for P2X7R activation, in sensitized mast cells is much higher than in unprimed cells, as shown by the reported up-regulation of this receptor in bronchial alveolar lavage (BAL) macrophages and eosinophils from asthmatic patients (Muller et al., 2011). Eosinophils from asthmatic patients are also more prone to release reactive oxygen species when challenged with the selective P2X7R agonist benzoyl ATP. There is evidence that during infection and inflammation P2X7R affinity is modulated by agents acting on the extracellular domain or at as yet unidentified intracellular residues (Rissiek et al., 2015; Yang et al., 2015). This raises the issue of whether shift in P2X7R activity may naturally occur under pathophysiological conditions, thus permitting P2X7R activation at much lower ATP concentrations. The low affinity of the P2X7R for ATP has been a contentious issue ever since the functional and pharmacological identification and cloning, to the point that its pathophysiological relevance was questioned. On the other hand, it has been argued that the low affinity for ATP is indeed a safe-guard mechanism because it prevents its unwanted stimulation: P2X7R activation in an improper situation may trigger release of potentially injurious inflammatory mediators (e.g., reactive oxygen species, ROS, or IL-1β), or may even precipitate cytotoxicity. In fact, while the ATP concentration in the healthy interstitial tissue is extremely low, i.e., in the nanomolar range, at inflammatory sites it can be as high as a few hundred micromoles/liter (Morciano et al., 2017). Therefore, it is assumed that under physiological conditions the P2X7R should be mostly silent. However, even at the ATP-rich inflammatory sites, with an *in vitro* Kd for ATP of about 0.5–1.0 mM, probability for the P2X7R to be activated is very low. Thus, asking if other agonists besides ATP are active at the P2X7R, or whether physiological positive allosteric modulators may help to lower the activation threshold is not unjustified. On the other hand, given the large repertoire of nucleotide receptors with widely different affinity expressed by most cells, it is likely that even at tumor and inflammatory sites a variable response is generated in the presence of ATP concentrations that may range from the high nano to the low micromolar level.

GENETICS OF THE P2X7R

The human *P2RX7* gene is located on chromosome 12q24.31, in the proximity of the *P2RX4* gene located at 12.q24.32. Mouse *P2rx7* and *P2rx4* genes are both located on chromosome 5. Close proximity of *P2RX7* and *P2RX4* may suggest an origin by gene duplication (Di Virgilio et al., 2017). Ten, or nine according to a more recent re-evaluation (Sluyter, 2017), splice variants of the human and four of the mouse P2X7 subunit are known. The canonical full-length variant, whether human or mouse, is named P2X7A, while the most common human splice variant, referred to as P2X7B, is a truncated form lacking the last 249 COOH terminal amino acids (aa) and incorporating 18 extra aa after residue 346 (Cheewatrakoolpong et al., 2005). Receptor made by P2X7B assembly retains channel functions but lacks ability to generate the non-selective, large conductance pore considered to be the functional signature of P2X7R. P2X7A and P2X7B may co-assemble on the plasma membrane generating a heterotrimeric receptor with distinct functional properties (Adinolfi et al., 2010). Thus, P2X7B might be considered an "endogenous" modulator of P2X7R activity. Two mouse variants, the natural P2X7k variant, and an artificial hybrid variant occurring in the P2X7-KO mouse originated at Pfizer, have attracted interest because they may escape inactivation in the commonly used P2X7-KO mice (the Pfizer and the Glaxo mice) (Kaczmarek-Hajek et al., 2012). Whether they are also present in a third P2X7-KO mouse described in the literature is not known (Basso et al., 2009). Several loss- or gain-of-function single-nucleotide polymorphisms (SNPs) have been described in the human P2X7 (Di Virgilio et al., 2017; Sluyter, 2017). Combination of these SNPs generates complex haplotypes that affect P2X7R functions, and make basically impossible to predict P2X7R activity on the basis of the mere identification of one SNP. Most interesting SNPs are the loss-of-function rs3751143 1513A>C SNP, which causes replacement of glutamate 496 with alanine (E496A), and the gain-of-function rs208294 489C>T, that causes replacement of histidine 155 with tyrosine (H155Y) (Gu et al., 2001; Cabrini et al., 2005). Additional polymorphisms described in the P2X7 subunit and variably associated to disease susceptibility are: (a) rs17525809, causing replacement of a valine with an alanine (V76A), (b) rs28360447, causing replacement of a glycine with an arginine (G150R), (c) rs7958311, causing replacement of an arginine with an histidine (R270H), (d) rs28360457, that causes replacement of an arginine with glutamine (R307Q), (e) rs1718119, that causes replacement of an alanine with a threonine (A348T), (f) rs2230911, causing replacement of a threonine with a serine (T357S), (g) rs2230912, causing replacement of a glutamine with an arginine (Q460R), (h) rs2230913, causing replacement of a histidine with a glutamine (H521Q), and (i) rs1653624, causing replacement of an isoleucine with an asparagine (I568N) (Wiley et al., 2011; **Table 1**).

TABLE 1 | Most common human P2X7 single-nucleotide polymorphisms.

dbSNP ID	Amino acid substitution	Effect on P2X7 function
rsl7525809	V76A	Loss
rs28360447	G150R	Loss
rs208294	H155Y	Gain
rs7958311	R270H	Loss
rs28360457	R307Q	Loss
rs1718119	A348T	Gain
rs2230911	T357S	Loss
rs2230912	Q460R	Loss
rs3751143	E496A	Loss
rs2230913	H521Q	Neutral
rs1653624	I568N	Loss

From Wiley et al. (2011), Di Virgilio et al. (2017), and Sluyter (2017).

The most relevant mouse SNP is the P451L missense mutation that changes a proline to a leucine at position 451 (Adriouch et al., 2002). This mutation is constitutively present in C57Black/6, DBA, and C3H strains, while the common laboratory Balb/c strain harbors the P451 allele. The L451 allele reduces P2X7R functions via an as yet undetermined mechanism and has been associated with reduced bone strength and density, and impaired glucose homeostasis (Syberg et al., 2012; Todd et al., 2015).

RECENT PROGRESS IN UNDERSTANDING P2X7R STRUCTURE AND FUNCTION

A mammalian P2X7 subunit deleted of the terminal 240 C-terminal residues (356 aa) from *Ailuropoda melanoleuca* (giant panda) has been crystalized, allowing 3-D reconstruction of the trimeric receptor and identification of the ATP-binding pocket and of allosteric sites (Karasawa and Kawate, 2016). This 3-D reconstruction has allowed identification of the ion pathway through the receptor and of a possible mechanism for allosteric inhibition. Due to the persistent inability to crystallize the full-length P2X7 subunit, i.e., including the long COOH terminal tail, structural modeling has provided no hints as to the molecular mechanism underlying the large and non-selective increase in permeability associated to sustained activation of the P2X7R (the enigmatic P2X7R "macropore"). Nevertheless, analysis of the panda P2X7 subunit, which is 605 aa long, and 85% identical to the human P2X7 subunit, may help decipher the molecular basis of the large permeability increases associated to P2X7R activation (Karasawa and Kawate, 2016; Karasawa et al., 2017).

A solid dogma in this field is that the carboxyl terminal extension of the P2X7 subunit is absolutely needed to support "macropore" formation (Surprenant et al., 1996; Adinolfi et al., 2010), therefore it is assumed that truncated forms of the P2X7 will be of little help to investigate the molecular basis of such a peculiar process. However, it is possible that even a defective P2X7 subunit might provide interesting hints, if properly "interrogated," and if the answers it offers are placed in the proper context. An example of this is the recent paper by Kawate colleagues in which permeability features of the truncated panda P2X7R were investigated in a model system allowing a controlled modulation of the lipid composition of the bilayer in which the receptor was reconstituted (Karasawa et al., 2017). In this regard, information stemming from the analysis of P2X7R activation by non-nucleotide ligands may well complement those generated by investigation of truncated P2X7Rs, and might provide clues to the molecular mechanism of "macropore" formation.

Interest on P2X7R stimulants alternative to nucleotides originated from the finding that some agents (see below) strongly synergize with ATP to stimulate P2X7R-mediated uptake of low MW fluorescent dyes (such as ethidium bromide) (Ferrari et al., 2004), or even induce dye uptake via a P2X7R made by the assembly of carboxyl-terminal truncated P2X7 subunits (P2X7ΔC) in the absence of co-stimulation with ATP (Tomasinsig et al., 2008). This is rather peculiar because homotrimers made by the assembly of subunits lacking the COOH tail (e.g., P2X7B) are generally assumed to be unable to generate the "macropore." The molecular identity of the pathway underlying "macropore" formation is a contentious issue. Two main hypothesis have been put forward: (1) the P2X7R itself undergoes dilatation during prolonged stimulation, thus transitioning from a cation-selective channel to a non-selective, large conductance pore (Surprenant et al., 1996); (2) the P2X7R itself is a cation-selective channel, intrinsically unable to mediate uptake of high MW aqueous solutes; however, when overstimulated it may recruit additional and yet to identify accessory protein(s) responsible for "macropore" formation (Pelegrin and Surprenant, 2006; Di Virgilio et al., 2017). A variant of the "dilatation hypothesis" holds that overstimulation of the P2X7R might allow recruitment of additional P2X7 subunits (a shift from the canonical trimeric to a hexameric stoichiometry), thus allowing generation of a larger permeation pathway (Ferrari et al., 2004; Di Virgilio et al., 2017; **Figure 1**).

THE ATP-BINDING POCKET AND THE ALLOSTERIC SITE

Some of the agents showed to potentiate ATP-mediated P2X7R activation, as well as some widely used inhibitors, are thought to be allosteric modulators. The ATP-binding site is contributed by two adjacent subunits. Structural analysis revealed three equivalent ATP-binding sites at the interface of each of the three couples of adjacent subunit contact surfaces (Karasawa and Kawate, 2016). The ATP-binding pocket is unique to P2X receptors and bears no similarity to all other ATP-binding sites known. Seven positively charged aa and two hydrophobic residues line the ATP-binding pocket (Jiang et al., 2000; Di Virgilio et al., 2017). Remarkable is the presence of four lysins (Lys64, Lys66, Lys193, and Lys311) which might explain the exquisite sensitivity to P2X7R inhibition by oxidized ATP, a dialdehyde reagent that forms Schiff bases with unprotonated lysins (Murgia et al., 1993). Lack in the P2X7 subunit of a key residue (Ile 217), which is on the contrary present in the ATP-binding pocket of the zebrafish P2X4, might explain lower ATP sensitivity of the P2X7R and higher potency of BzATP (Jiang et al., 2013). Sequence and structural analysis suggests a restricted access and a limited size of the ATP-binding pocket, which might explain why several hydrophilic agonists of other P2XRs are weakly active or fully inactive at the P2X7R.

An allosteric-binding site in a pocket made by two adjacent subunits, close and juxtaposed to the ATP-binding site, was identified (**Figure 2**). Occupancy of this site prevents conformational changes associated to P2X7R activation and therefore might hinder movements of P2X7R subunits necessary to allow opening of the ion-conducting pathway (Karasawa and Kawate, 2016). Such an allosteric-binding pocket is absent in P2X4Rs and P2X3Rs, thus highlighting the possibility to develop receptor-selective drugs. Very interestingly, the allosteric site narrows upon ATP binding, thus preventing binding and effect of the allosteric inhibitors. This observation may

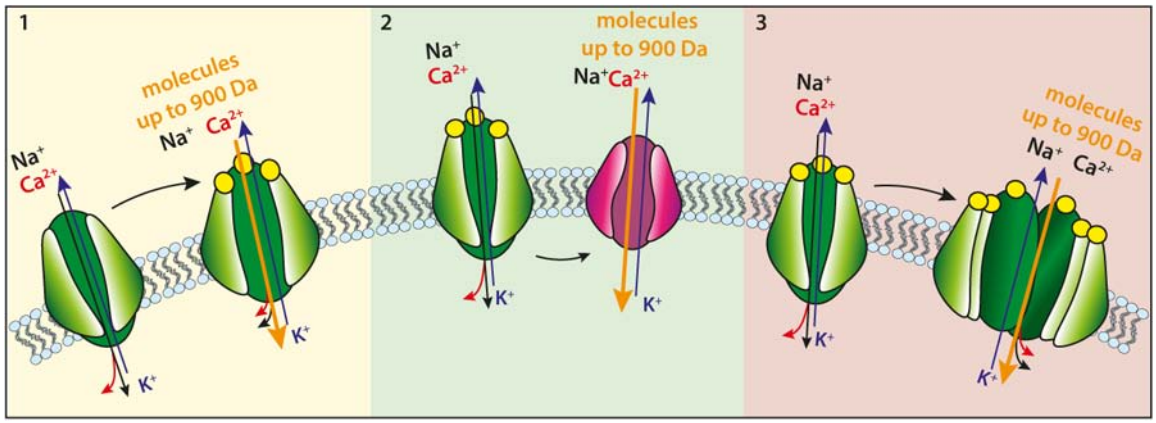

FIGURE 1 | Proposed mechanisms for P2X7R-mediated uptake of molecular solutes up to 900 Da MW. **(1)** Upon sustained or repetitive stimulation with ATP (yellow circles) the P2X7R pore undergoes dilatation to form a high conductance (possibly non-selective) large pore (the macropore); **(2)** activation of the P2X7R recruits in an as yet undefined fashion an accessory molecule (red) that forms the conduit responsible for large aqueous solute uptake; **(3)** sustained or repetitive stimulation of the P2X7R triggers recruitment of additional P2X7 subunits that allow formation of the macropore.

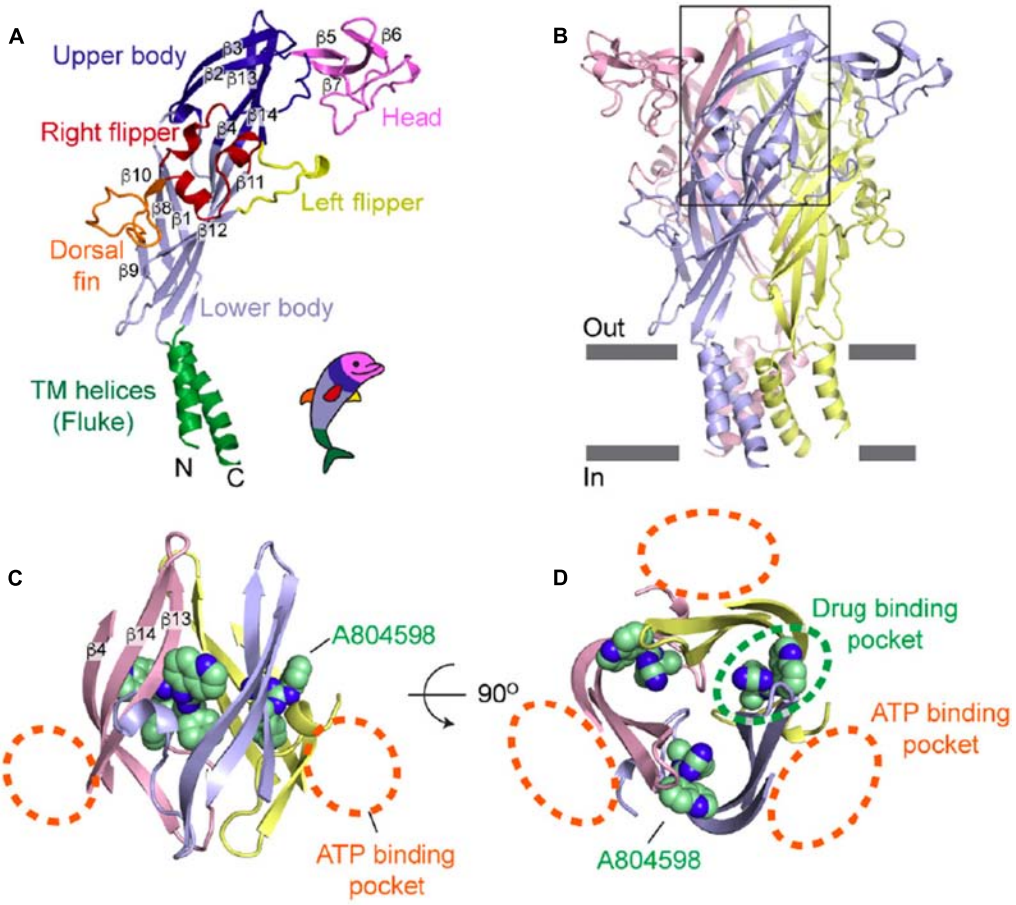

FIGURE 2 | Visualization of the drug-binding pocket of the P2X7R. **(A)** Schematic rendition of the P2X7 subunit in the "dolphin-like" shape. **(B)** Representation of the trimeric panda P2X7R viewed from the side. The black rectangle indicates the approximate location of the area where the ATP-binding pocket and the putative allosteric site are located. **(C)** Side view of the area located in the extracellular domain exhibiting A804598 and ATP-binding pockets (orange dashed lines). **(D)** Top view of the panda P2X7 structure showing the ATP-binding pockets (orange dashed lines) and the drug-binding pocket (green dashed line). Reprinted from Karasawa and Kawate (2016) with permission.

have important translational implications since it may indicate that in the presence of high concentrations of extracellular ATP this allosteric site will not be accessible, and therefore allosteric P2X7R inhibitors will not be efficacious. This might be a serious inconvenient for the treatment of chronic inflammatory diseases as accumulating evidence shows that ATP may reach a concentration of several hundred micromoles/liter at inflammatory sites (Di Virgilio et al., 2017). Thus, albeit the action of competitive antagonists also depends on the ambient ATP concentration, in the end high affinity competitive antagonists could show higher efficacy than negative allosteric modulators in conditions of high extracellular concentrations of ATP, and might be better suited for the development of P2X7R blockers with higher therapeutic efficacy. Finally, structural analysis did not address the site and possible mechanism of action of agents suggested to be "positive" allosteric modulators, e.g., the antibiotic polymyxin B (Ferrari et al., 2004).

MODULATION OF P2X7R PERMEABILITY

Permeability features and low ATP affinity of the P2X7R were a puzzle from the very beginning, to the point that many wondered whether this receptor had any physiological relevance. Nowadays the pathophysiological role of the P2X7R is well established, especially in the context of the immune response. Even the high threshold for activation is not anymore seen as an insurmountable obstacle, since there is now ample evidence that the extracellular ATP concentration can reach hundreds of micromole/liter at inflammatory and tumor sites. However, it has been often wondered whether ATP was indeed the only physiological agonist at the P2X7R, and whether other factors released in the context of pathophysiological responses might synergize with ATP, or even replace it. Or alternatively, the plasma membrane microenvironment might modulate permeability through the P2X7R.

Targeting of the P2X7R to lipid rafts has been shown in several cell systems (Garcia-Marcos et al., 2006a,b; Gonnord et al., 2009; Weinhold et al., 2010), a finding coherent with palmitoylation of several cysteine residues in the COOH tail (Gonnord et al., 2009). Palmitoylation is a reversible post-translational modification assumed to be a plasma membrane localization signal. Covalent modification of protein domains increases the overall hydrophobicity and enhances membrane–protein interaction. For P2X1, P2X2, and P2X4 receptors, reduction of the cholesterol plasma membrane content with methyl-β-cyclodextrin caused inhibition of channel activation (Murrell-Lagnado, 2017), while P2X7R activity was strongly potentiated (Robinson et al., 2014). Kawate colleagues investigated in detail the effect of membrane lipids on P2X7R function, confirming that cholesterol strongly inhibited the P2X7R, and highlighting a facilitating effect of palmitoyl-oleoyl-glycero-phosphoglycerol and of sphingomyelin (Karasawa et al., 2017). These authors went further to identify the mechanism of action of cholesterol suggesting that changes in membrane fluidity are not involved, while on the contrary cholesterol is likely to interact with the transmembrane domains. The effect of the cholesterol content on P2X7R permeability is striking as reconstitution of a truncated form of the panda P2X7R in cholesterol-free liposomes promotes ATP-stimulated fluorescent dye uptake (Karasawa et al., 2017). These latter findings have an additional important implication: they might help shed light on the identity of the "macropore." Based on current measurements performed in the presence of charge-carrying cations of different sizes it was postulated that formation of the "macropore" is a late event following P2X7R activation, likely due to dilatation of the early cation-selective channel. However, recent electrophysiology experiments clearly showed that the P2X7R exhibits an immediate permeability to large organic cations ($NMDG^+$ or spermidine), and that no channel dilatation occurs even during prolonged (30 min) stimulation with ATP (Harkat et al., 2017; Pippel et al., 2017). These findings rule out one of the mechanisms thought to underlay macropore formation, and tilt the balance toward the alternative mechanism that postulate recruitment of an accessory "pore-forming" molecule. However, all attempts so far carried out to identify this hypothetical P2X7R-associated permeability pathway have failed (Di Virgilio et al., 2017). Data by Kawate's group now give further impetus to the hypothesis that gating of the P2X7R opens a permeability pathway (the "macropore") intrinsic to the receptor through which cationic fluorescent dyes such as Yo-Pro may permeate the plasma membrane (Karasawa et al., 2017). Similar data documenting Yo-Pro influx were also reported for another member of the P2X family, the P2X2R, by Harkat et al. (2017). On the contrary, we are still left with the unsolved issue of the permeation of anionic fluorescent dyes such as Lucifer yellow (MW 457) or fura-2-free acid (MW 832). Electrophysiological analysis has repeatedly shown that the P2X7R channel is highly selective for cations; thus, it is unclear how anions might permeate. On the other hand if, as currently thought, the P2X7R macropore has no intrinsic selectivity barrier, both cations and anions should be freely permeant.

In principle, Kawate's group experiments might also rescue the "pore-dilatation" hypothesis because changing the lipid microenvironment of the P2X7R might modulate permeability in such a way to allow a graded increase in pore size. Thus, inability of patch-clamp analysis to document pore dilatation might simply be due to the specific constraints imposed on one side by the transfected cells (e.g., *Xenopus* oocytes), and on the other by the technique (e.g., isolation of individual plasma membrane patches) that might perturb phospholipid mobility in the vicinity of the P2X7R. However, in absence of an experimental proof of these hypotheses, we must stick to the hard data highlighting a discrepancy between description of P2X7R permeability features provided by electrophysiology and cell biology. Electrophysiology and cell biology evidence might be reconciled by assuming that the "macropore" is a separate entity from the P2X7R, i.e., an accessory molecule recruited upon P2X7R activation. This accessory molecule has been long searched for, and general consensus now points to pannexin-1 as the most likely candidate (Pelegrin and Surprenant, 2006). However, the finding that cells from pannexin-1-deficient mouse exhibit basically normal P2X7R-dependent permeability changes casts doubts on pannexin-1 role (Qu et al., 2011; Alberto et al., 2013).

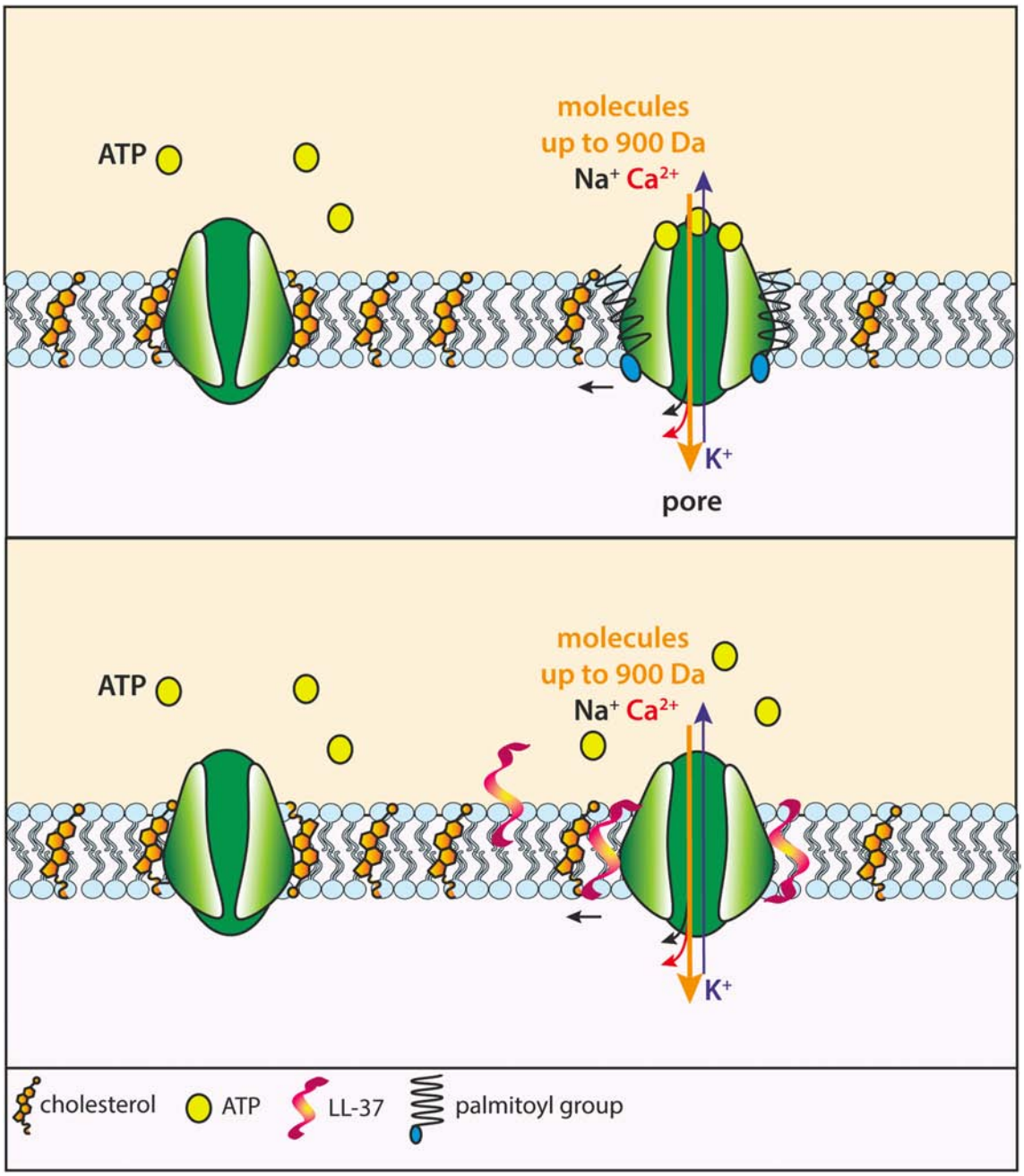

FIGURE 3 | Proposed mechanism of facilitation of macropore formation by the COOH tail of P2X7 subunits and hypothetical mechanism of action of the bactericidal peptide LL-37. The COOH tail of P2X7 subunits harbors several cysteines that can be palmitoylated. Upon ATP binding to P2X7R, palmitoylation increases interaction of the COOH tail with the plasma membrane in the vicinity of the P2X7 TM2, thus relieving the inhibitory effect of cholesterol, thus allowing opening of the macropore **(Upper)**. The LL-37 peptide inserts into the plasma membrane in the vicinity of the P2X7R and repels cholesterol away from the receptor, thus removing its inhibitory action **(Lower)**.

EXTRACELLULAR ATP MIGHT NOT BE THE ONLY AGONIST

Over the time, other agonists, nucleotides such as NAD, or completely unrelated agents such as cathelicidins, have been suggested to activate the P2X7R. The best documented example of a "non-ATP" agonist case is NAD^+ in mouse cells. Mouse cells express the plasma membrane enzyme ADP-ribosyltransferase (ARTC2.2) that catalyzes transfer of an ADP-ribose moiety from NAD^+ to arginine 125, close to the ATP-binding pocket of the P2X7R (Seman et al., 2003). ADP ribosylation (being a covalent modification) causes a long-lasting activation of

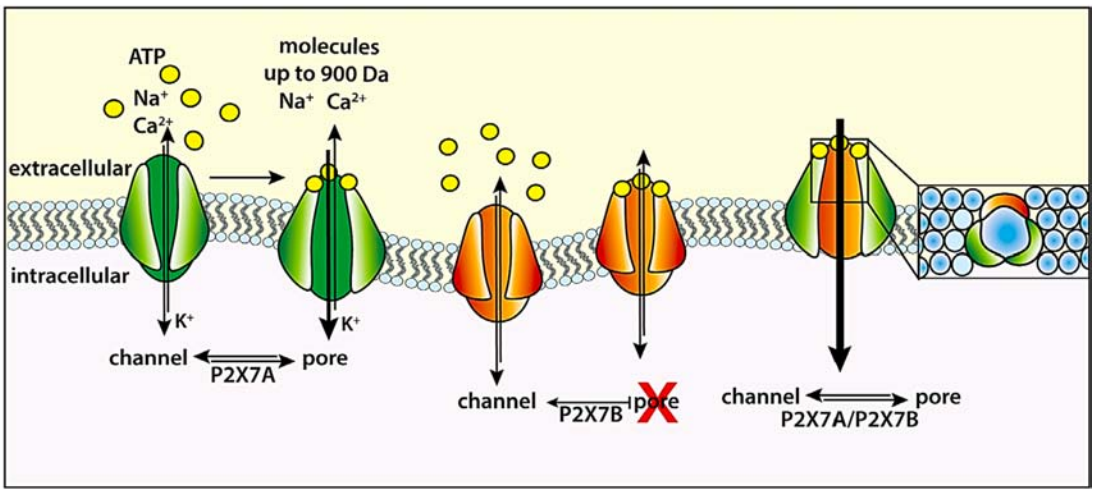

FIGURE 4 | The P2X7B as an endogenous modulator of the P2X7R. The P2X7R formed by full-length P2X7 subunits (green) can function as both an ion channel and a large conductance pore (macropore). The truncated P2X7B (orange) is unable to generate the macropore. The P2X7B can assemble with P2X7A to form a heterotrimeric P2X7A/P2X7B (green and orange) receptor that sustains higher Ca^{2+} influx and ethidium bromide uptake compared to the homotrimeric P2X7A receptor (Adinolfi et al., 2010).

mouse P2X7R which can be reversed by the NAD^+-degrading enzyme ecto-NAD^+-glycohydrolase (CD38). It is not entirely clear whether NAD^+ is a true P2X7R agonist or whether it lowers the activation threshold for ATP, thus sensitizing the P2X7R to autocrine/paracrine-released ATP. Anyway, since an increased NAD^+ content has been shown at inflammatory sites (Adriouch et al., 2007), it is likely that NAD^+ has a role in the pathophysiological mechanism of P2X7R activation. Of the four splice variants expressed in the mouse, the P2X7k subunit preferentially expressed by T lymphocytes is the most sensitive to ADP-ribosylation (Rissiek et al., 2015).

A few non-nucleotide agonists are reported to activate the P2X7R (Di Virgilio et al., 2017). Given the structural constraints set by the ATP-binding pocket, it is likely that these agents either stimulate the P2X7R secondarily to ATP release, or act as positive allosteric effectors. The amyloidogenic β peptides Aβ 1–42 or Aβ 25–35 trigger several P2X7R-associated responses in mouse microglia, such as Ca^{2+} influx and ethidium bromide uptake, cell rounding and swelling, IL-1β release, and cytotoxicity (Sanz et al., 2009). All such responses are abrogated by P2X7R blockade, and are absent in microglia cells isolated from P2X7R-deficient mice. The finding that amyloid β also triggers ATP release from microglia, and that amyloid β-dependent permeabilization of microglia plasma membrane is abrogated by co-incubation in the presence of apyrase, might suggest that P2X7R activation is secondary to ATP release. However, two findings are at odd with this interpretation: firstly, amyloid β-stimulated ATP release is inhibited by pre-treatment with oxidized ATP and absent in microglia from P2X7-deficient mice; secondly, addition of amyloid β strongly potentiates ATP-dependent cytotoxicity (Sanz et al., 2009). Lack of ATP release in the absence of a functional P2X7R might suggest that the P2X7R itself is a pathway for ATP release, or alternatively that amyloid β directly stimulates the P2X7R. Furthermore, potentiation of ATP-dependent cytotoxicity by amyloid β is unlikely due to further ATP release since it occurs in the presence of maximally stimulatory ATP concentrations. It cannot be excluded that amyloid β acts as a positive allosteric modulator that lowers the activation threshold for ATP. The inhibitory effect of apyrase on amyloid β-stimulated P2X7R activation can also be re-interpreted along these lines, since amyloid β would be ineffective in the absence of the physiological ATP ligand. The P2X7R is currently heavily investigated as a druggable target for the treatment of neurological pathologies, Alzheimer's diseases included, albeit no P2X7R-targeting drugs have yet been taken to clinical trials for central nervous system diseases (Di Virgilio et al., 2009; Bhattacharya and Biber, 2016). Activation of the P2X7R by amyloid β suggests the possible use of P2X7R blockers to treat Alzheimer's and other neurological diseases.

Besides amyloid β, serum amyloid A (SAA) has also been suggested to directly stimulate the P2X7R (Niemi et al., 2011). However, in these experiments IL-1β release from human macrophages was used as readout, which is a rather indirect measurement of P2X7R activation. Rather surprisingly, IL-1β release was not inhibited by treatment with apyrase, but in fact enhanced. These findings suggest that SAA does not induce ATP release, but rather directly interacts with the P2X7R. However, it is not clear why apyrase treatment increased SAA efficacy.

More interesting is the activity of the bactericidal peptide cathelicidin LL-37. Cathelicidins are a family of endogenous antimicrobial peptides found in mammals where they are either constitutively expressed or induced following injury and inflammation (Frohm et al., 1997; Dorschner et al., 2001). LL-37 is the only cathelicidin present in humans where it is stored within granulocytes, lymphocytes, macrophages, and epithelial cells. It was originally shown by Wewers colleagues that LL-37 activates the P2X7R of human monocytes thus causing YO-Pro

uptake and IL-1β release (Elssner et al., 2004). LL-37-stimulated effects could be blocked by P2X7R antagonists and, despite LL-37 stimulation induced some ATP release, were independent of ATP release. As a follow up to these studies, we showed that LL-37 triggered Ca^{2+} influx and ethidium bromide uptake in HEK293 cells transfected with the human P2X7R (Tomasinsig et al., 2008). LL-37 stimulation replicated the growth-promoting effect described as a result of low-level, tonic, stimulation of the P2X7R (Adinolfi et al., 2005) as it promoted proliferation of mouse NIH3T3 fibroblasts or P2X7R-transfected HEK293 cells, but not of wild-type, P2X7R-less HEK293 cells (Tomasinsig et al., 2008). Even more intriguing is the effect of LL-37 in HEK293 transfected with the rat P2X7 construct truncated at position 415 (P2X7ΔC). This truncated subunit assembles into a receptor that supports cation fluxes but is unable to form the non-selective macropore (Surprenant et al., 1996). Incubation in the presence of LL-37 allowed formation of the non-selective macropore even in HEK293 cells transfected with the defective P2X7ΔC subunits (**Figure 3**).

LL-37 can be considered an endogenous antibiotic. Another antibiotic of bacterial origin, polymyxin B, derived from the bacterium *Bacillus polymyxa*, also acts as a positive allosteric P2X7R modulator (Ferrari et al., 2004, 2007). Polymyxin B potentiates P2X7R-dependent Ca^{2+} uptake, plasma membrane permeabilization, and cytotoxicity in mouse and human macrophages and in HEK293 and erythroleukemia K562 cells transfected with the P2X7R. Incubation in the presence of polymyxin B also potentiated ATP-stimulated cytotoxicity in leukemic B lymphocytes. Polymyxin B might be a tool for the investigation of the pathway for P2X7R-dependent fluorescent dye uptake. Several years ago we showed that co-incubation in the presence of this antibiotic and ATP induces the appearance of a 440-kDa band in western blots stained with anti-P2X7 antibodies (Ferrari et al., 2004). We interpreted this band as a higher order aggregation form (hexamer?) of the P2X7 subunit. In the same blots we also detected a 220 band, possibly related to the canonical trimer.

Gating of the P2X7R may be triggered by agonists acting on the cytoplasmic side. We reported several years ago that macrophage activation by lipopolysaccharide (LPS), the paradigmatic bacterial endotoxin, involves ATP release and P2X7R activation (Ferrari et al., 1997). Recently, a study by Nunez and coworkers has provided an intracellular mechanism to explain this effect by showing that cytoplasmic LPS lowers the threshold of P2X7R activation, sensitizing this receptor to ambient ATP concentrations, and thus triggering P2X7R-dependent responses (Yang et al., 2015). P2X7R modulation by cytoplasmic agents is also supported by the finding that Alu-RNA accumulation in the cytoplasm can activate P2X7R independently of ATP release (Fowler et al., 2014).

Activity of the P2X7R macropore can be also affected by changing the splice variants expressed. It is well known that 10, or 9 according to some authors (Sluyter, 2017), human P2X7 splice variants are present, P2X7A being the canonical full-length monomer (Di Virgilio et al., 2017). A common variant is the truncated P2X7B isoform. The receptor resulting from P2X7B monomer assembly shows ion channel activity but no macropore function. However, co-expression of P2X7B together with P2X7A leads to formation of a functional P2X7A–P2X7B heterotrimeric receptor that shows enhanced macropore function compared to the homotrimeric P2X7A receptor. The heterotrimeric P2X7A–P2X7B receptor shows higher affinity for ATP or BzATP, and an enhanced capability to support cell energy metabolism and proliferation (**Figure 4**).

CONCLUSION

Ever since its molecular cloning and functional characterization it was assumed that the only physiologically relevant agonist of the P2X7R was extracellular ATP. Accruing evidence from various laboratories now shows that other factors may gate this receptor thus revealing an entirely novel and exciting scenario where multiple agents produced during inflammation may converge on this receptor to trigger release of pro-inflammatory factors and even cytotoxic reactions. Furthermore, novel data suggest that permeability through the P2X7R can also be modulated from the inside of the cell, albeit the mechanism involved is utterly unknown. Finally, resolution of the 3-D structure of the full-length receptor, i.e., COOH tail included, will certainly bring novel exciting information on the mechanism underlying P2X7R permeability changes.

AUTHOR CONTRIBUTIONS

FDV delineated the outlines, wrote a section, and edited the whole review. ALG wrote a section in the review and contributed to others. VV-P wrote a section of the review. SF wrote a section on the review. ACS wrote a section, contributed to overall writing of the review, and took responsibility for iconography.

FUNDING

FDV was supported by grants from the Italian Association for Cancer Research (Nos. IG 13025 and IG 18581), the Ministry of Health of Italy (No. RF-2011-02348435), and institutional funds from the University of Ferrara.

REFERENCES

Adinolfi, E., Callegari, M. G., Ferrari, D., Bolognesi, C., Minelli, M., Wieckowski, M. R., et al. (2005). Basal activation of the P2X7 ATP receptor elevates mitochondrial calcium and potential, increases cellular ATP levels, and promotes serum-independent growth. *Mol. Biol. Cell* 16, 3260–3272. doi: 10.1091/mbc.E04-11-1025

Adinolfi, E., Cirillo, M., Woltersdorf, R., Falzoni, S., Chiozzi, P., Pellegatti, P., et al. (2010). Trophic activity of a naturally occurring truncated isoform of the P2X7 receptor. *FASEB J.* 24, 3393–3404. doi: 10.1096/fj.09-153601

Adriouch, S., Dox, C., Welge, V., Seman, M., Koch-Nolte, F., and Haag, F. (2002). Cutting edge: a natural P451L mutation in the cytoplasmic domain impairs the function of the mouse P2X7 receptor. *J. Immunol.* 169, 4108–4112. doi: 10.4049/jimmunol.169.8.4108

Adriouch, S., Hubert, S., Pechberty, S., Koch-Nolte, F., Haag, F., and Seman, M. (2007). NAD^+ released during inflammation participates in T cell homeostasis by inducing ART2-mediated death of naive T cells in vivo. *J. Immunol.* 179, 186–194. doi: 10.4049/jimmunol.179.1.186

Alberto, A. V., Faria, R. X., Couto, C. G., Ferreira, L. G., Souza, C. A., Teixeira, P. C., et al. (2013). Is pannexin the pore associated with the P2X7 receptor? *Naunyn Schmiedebergs Arch. Pharmacol.* 386, 775–787. doi: 10.1007/s00210-013-0868-x

Basso, A. M., Bratcher, N. A., Harris, R. R., Jarvis, M. F., Decker, M. W., and Rueter, L. E. (2009). Behavioral profile of P2X7 receptor knockout mice in animal models of depression and anxiety: relevance for neuropsychiatric disorders. *Behav. Brain Res.* 198, 83–90. doi: 10.1016/j.bbr.2008.10.018

Bhattacharya, A., and Biber, K. (2016). The microglial ATP-gated ion channel P2X7 as a CNS drug target. *Glia.* 64, 1772–1787. doi: 10.1002/glia.23001

Burnstock, G. (2006). Pathophysiology and therapeutic potential of purinergic signaling. *Pharmacol. Rev.* 58, 58–86. doi: 10.1124/pr.58.1.5

Cabrini, G., Falzoni, S., Forchap, S. L., Pellegatti, P., Balboni, A., Agostini, P., et al. (2005). A His-155 to Tyr polymorphism confers gain-of-function to the human P2X7 receptor of human leukemic lymphocytes. *J. Immunol.* 175, 82–89. doi: 10.4049/jimmunol.175.1.82

Cheewatrakoolpong, B., Gilchrest, H., Anthes, J. C., and Greenfeder, S. (2005). Identification and characterization of splice variants of the human P2X7 ATP channel. *Biochem. Biophys. Res. Commun.* 332, 17–27. doi: 10.1016/j.bbrc.2005.04.087

Cockcroft, S., and Gomperts, B. D. (1979). ATP induces nucleotide permeability in rat mast cells. *Nature* 279, 541–542. doi: 10.1038/279541a0

Cockcroft, S., and Gomperts, B. D. (1980). The ATP4- receptor of rat mast cells. *Biochem. J.* 188, 789–798. doi: 10.1042/bj1880789

Di Virgilio, F., Ceruti, S., Bramanti, P., and Abbracchio, M. P. (2009). Purinergic signalling in inflammation of the central nervous system. *Trends Neurosci.* 32, 79–87. doi: 10.1016/j.tins.2008.11.003

Di Virgilio, F., Dal Ben, D., Sarti, A. C., Giuliani, A. L., and Falzoni, S. (2017). The P2X7 receptor in infection and inflammation. *Immunity* 47, 15–31. doi: 10.1016/j.immuni.2017.06.020

Dorschner, R. A., Pestonjamasp, V. K., Tamakuwala, S., Ohtake, T., Rudisill, J., Nizet, V., et al. (2001). Cutaneous injury induces the release of cathelicidin antimicrobial peptides active against group A *Streptococcus*. *J. Invest. Dermatol.* 117, 91–97. doi: 10.1046/j.1523-1747.2001.01340.x

Elssner, A., Duncan, M., Gavrilin, M., and Wewers, M. D. (2004). A novel P2X7 receptor activator, the human cathelicidin-derived peptide LL37, induces IL-1 beta processing and release. *J. Immunol.* 172, 4987–4994. doi: 10.4049/jimmunol.172.8.4987

Ferrari, D., Chiozzi, P., Falzoni, S., Hanau, S., and Di Virgilio, F. (1997). Purinergic modulation of interleukin-1 beta release from microglial cells stimulated with bacterial endotoxin. *J. Exp. Med.* 185, 579–582. doi: 10.1084/jem.185.3.579

Ferrari, D., Pizzirani, C., Adinolfi, E., Forchap, S., Sitta, B., Turchet, L., et al. (2004). The antibiotic polymyxin B modulates P2X7 receptor function. *J. Immunol.* 173, 4652–4660. doi: 10.4049/jimmunol.173.7.4652

Ferrari, D., Pizzirani, C., Gulinelli, S., Callegari, G., Chiozzi, P., Idzko, M., et al. (2007). Modulation of P2X7 receptor functions by polymyxin B: crucial role of the hydrophobic tail of the antibiotic molecule. *Br. J. Pharmacol.* 150, 445–454. doi: 10.1038/sj.bjp.0706994

Fowler, B. J., Gelfand, B. D., Kim, Y., Kerur, N., Tarallo, V., Hirano, Y., et al. (2014). Nucleoside reverse transcriptase inhibitors possess intrinsic anti-inflammatory activity. *Science* 346, 1000–1003. doi: 10.1126/science.1261754

Frohm, M., Agerberth, B., Ahangari, G., Stahle-Backdahl, M., Liden, S., Wigzell, H., et al. (1997). The expression of the gene coding for the antibacterial peptide LL-37 is induced in human keratinocytes during inflammatory disorders. *J. Biol. Chem.* 272, 15258–15263. doi: 10.1074/jbc.272.24.15258

Garcia-Marcos, M., Pochet, S., Marino, A., and Dehaye, J. P. (2006a). P2X7 and phospholipid signalling: the search of the "missing link" in epithelial cells. *Cell. Signal.* 18, 2098–2104.

Garcia-Marcos, M., Pochet, S., Tandel, S., Fontanils, U., Astigarraga, E., Fernandez-Gonzalez, J. A., et al. (2006b). Characterization and comparison of raft-like membranes isolated by two different methods from rat submandibular gland cells. *Biochim. Biophys. Acta.* 1758, 796–806.

Gonnord, P., Delarasse, C., Auger, R., Benihoud, K., Prigent, M., Cuif, M. H., et al. (2009). Palmitoylation of the P2X7 receptor, an ATP-gated channel, controls its expression and association with lipid rafts. *FASEB J.* 23, 795–805. doi: 10.1096/fj.08-114637

Gu, B. J., Zhang, W., Worthington, R. A., Sluyter, R., Dao-Ung, P., Petrou, S., et al. (2001). A Glu-496 to Ala polymorphism leads to loss of function of the human P2X7 receptor. *J. Biol. Chem.* 276, 11135–11142. doi: 10.1074/jbc.M010353200

Harkat, M., Peverini, L., Cerdan, A. H., Dunning, K., Beudez, J., Martz, A., et al. (2017). On the permeation of large organic cations through the pore of ATP-gated P2X receptors. *Proc. Natl. Acad. Sci. U. S. A.* 114, E3786–E3795. doi: 10.1073/pnas.1701379114

Jiang, L. H., Baldwin, J. M., Roger, S., and Baldwin, S. A. (2013). Insights into the molecular mechanisms underlying mammalian P2X7 receptor functions and contributions in diseases, revealed by structural modeling and single nucleotide polymorphisms. *Front. Pharmacol.* 4:55. doi: 10.3389/fphar.2013.00055

Jiang, L. H., Rassendren, F., Surprenant, A., and North, R. A. (2000). Identification of amino acid residues contributing to the ATP-binding site of a purinergic P2X receptor. *J. Biol. Chem.* 275, 34190–34196. doi: 10.1074/jbc.M005481200

Kaczmarek-Hajek, K., Lorinczi, E., Hausmann, R., and Nicke, A. (2012). Molecular and functional properties of P2X receptors–recent progress and persisting challenges. *Purinergic. Signal.* 8, 375–417. doi: 10.1007/s11302-012-9314-7

Karasawa, A., and Kawate, T. (2016). Structural basis for subtype-specific inhibition of the P2X7 receptor. *eLife* 5, :e22153. doi: 10.7554/eLife.22153

Karasawa, A., Michalski, K., Mikhelzon, P., and Kawate, T. (2017). The P2X7 receptor forms a dye-permeable pore independent of its intracellular domain but dependent on membrane lipid composition. *eLife* 6, :e31186. doi: 10.7554/eLife.31186

Kurashima, Y., Amiya, T., Nochi, T., Fujisawa, K., Haraguchi, T., Iba, H., et al. (2012). Extracellular ATP mediates mast cell-dependent intestinal inflammation through P2X7 purinoceptors. *Nat. Commun.* 3:1034. doi: 10.1038/ncomms2023

Morciano, G., Sarti, A. C., Marchi, S., Missiroli, S., Falzoni, S., Raffaghello, L., et al. (2017). Use of luciferase probes to measure ATP in living cells and animals. *Nat. Protoc.* 12, 1542–1562. doi: 10.1038/nprot.2017.052

Muller, T., Vieira, R. P., Grimm, M., Durk, T., Cicko, S., Zeiser, R., et al. (2011). A potential role for P2X7R in allergic airway inflammation in mice and humans. *Am. J. Respir. Cell Mol. Biol.* 44, 456–464. doi: 10.1165/rcmb.2010-0129OC

Murgia, M., Hanau, S., Pizzo, P., Rippa, M., and Di Virgilio, F. (1993). Oxidized ATP. An irreversible inhibitor of the macrophage purinergic P2Z receptor. *J. Biol. Chem.* 268, 8199–8203.

Murrell-Lagnado, R. D. (2017). Regulation of P2X purinergic receptor signaling by cholesterol. *Curr. Top. Membr.* 80, 211–232. doi: 10.1016/bs.ctm.2017.05.004

Niemi, K., Teirila, L., Lappalainen, J., Rajamaki, K., Baumann, M. H., Oorni, K., et al. (2011). Serum amyloid A activates the NLRP3 inflammasome via P2X7 receptor and a cathepsin B-sensitive pathway. *J. Immunol.* 186, 6119–6128. doi: 10.4049/jimmunol.1002843

Pelegrin, P., and Surprenant, A. (2006). Pannexin-1 mediates large pore formation and interleukin-1beta release by the ATP-gated P2X7 receptor. *EMBO J.* 25, 5071–5082. doi: 10.1038/sj.emboj.7601378

Pippel, A., Stolz, M., Woltersdorf, R., Kless, A., Schmalzing, G., and Markwardt, F. (2017). Localization of the gate and selectivity filter of the full-length P2X7 receptor. *Proc. Natl. Acad. Sci. U. S. A.* 114, E2156–E2165. doi: 10.1073/pnas.1610414114

Qu, Y., Misaghi, S., Newton, K., Gilmour, L. L., Louie, S., Cupp, J. E., et al. (2011). Pannexin-1 is required for ATP release during apoptosis but not for inflammasome activation. *J. Immunol.* 186, 6553–6561. doi: 10.4049/jimmunol.1100478

Rissiek, B., Haag, F., Boyer, O., Koch-Nolte, F., and Adriouch, S. (2015). P2X7 on mouse T cells: one channel, many functions. *Front. Immunol.* 6:204. doi: 10.3389/fimmu.2015.00204

Robinson, L. E., Shridar, M., Smith, P., and Murrell-Lagnado, R. D. (2014). Plasma membrane cholesterol as a regulator of human and rodent P2X7 receptor activation and sensitization. *J. Biol. Chem.* 289, 31983–31994. doi: 10.1074/jbc.M114.574699

Sanz, J. M., Chiozzi, P., Ferrari, D., Colaianna, M., Idzko, M., Falzoni, S., et al. (2009). Activation of microglia by amyloid {beta} requires P2X7 receptor expression. *J. Immunol.* 182, 4378–4385. doi: 10.4049/jimmunol.0803612

Seman, M., Adriouch, S., Scheuplein, F., Krebs, C., Freese, D., Glowacki, G., et al. (2003). NAD-induced T cell death: ADP-ribosylation of cell surface proteins by ART2 activates the cytolytic P2X7 purinoceptor. *Immunity* 19, 571–582. doi: 10.1016/S1074-7613(03)00266-8

Sluyter, R. (2017). The P2X7 receptor. *Adv. Exp. Med. Biol.* 1051, 17–53. doi: 10.1007/5584_2017_59

Surprenant, A., Rassendren, F., Kawashima, E., North, R. A., and Buell, G. (1996). The cytolytic P2Z receptor for extracellular ATP identified as a P2X receptor (P2X7). *Science* 272, 735–738. doi: 10.1126/science.272.5262.735

Syberg, S., Schwarz, P., Petersen, S., Steinberg, T. H., Jensen, J. E., Teilmann, J., et al. (2012). Association between P2X7 receptor polymorphisms and bone status in mice. *J. Osteoporos.* 2012, :637986. doi: 10.1155/2012/637986

Todd, J. N., Poon, W., Lyssenko, V., Groop, L., Nichols, B., Wilmot, M., et al. (2015). Variation in glucose homeostasis traits associated with P2RX7 polymorphisms in mice and humans. *J. Clin. Endocrinol. Metab.* 100, E688–E696. doi: 10.1210/jc.2014-4160

Tomasinsig, L., Pizzirani, C., Skerlavaj, B., Pellegatti, P., Gulinelli, S., Tossi, A., et al. (2008). The human cathelicidin LL-37 modulates the activities of the P2X7 receptor in a structure-dependent manner. *J. Biol. Chem.* 283, 30471–30481. doi: 10.1074/jbc.M802185200

Wareham, K., Vial, C., Wykes, R. C., Bradding, P., and Seward, E. P. (2009). Functional evidence for the expression of P2X1, P2X4 and P2X7 receptors in human lung mast cells. *Br. J. Pharmacol.* 157, 1215–1224. doi: 10.1111/j.1476-5381.2009.00287.x

Weinhold, K., Krause-Buchholz, U., Rodel, G., Kasper, M., and Barth, K. (2010). Interaction and interrelation of P2X7 and P2X4 receptor complexes in mouse lung epithelial cells. *Cell Mol. Life Sci.* 67, 2631–2642. doi: 10.1007/s00018-010-0355-1

Wiley, J. S., Sluyter, R., Gu, B. J., Stokes, L., and Fuller, S. J. (2011). The human P2X7 receptor and its role in innate immunity. *Tissue Antigens* 78, 321–332. doi: 10.1111/j.1399-0039.2011.01780.x

Yang, D., He, Y., Munoz-Planillo, R., Liu, Q., and Nunez, G. (2015). Caspase-11 requires the pannexin-1 channel and the purinergic P2X7 pore to mediate pyroptosis and endotoxic shock. *Immunity* 43, 923–932. doi: 10.1016/j.immuni.2015.10.009

Conflict of Interest Statement: FDV is a member of the Scientific Advisory Board of Biosceptre, Ltd., a UK-based biotech company involved in the development of P2X7R-targeted therapeutics.

The other authors declare that the research was conducted in the absence of any commercial or financial relationships that could be construed as a potential conflict of interest.

frontiers in Pharmacology

MINI REVIEW
published: 01 February 2018
doi: 10.3389/fphar.2018.00030

Recent Advances in CNS P2X7 Physiology and Pharmacology: Focus on Neuropsychiatric Disorders

*Anindya Bhattacharya**

Neuroscience Therapeutic Area, Janssen Research and Development, LLC, San Diego, CA, United States

The ATP-gated P2X7 ion channel is an abundant microglial protein in the CNS that plays an important pathological role in executing ATP-driven danger signal transduction. Emerging data has generated scientific interest and excitement around targeting the P2X7 ion channel as a potential drug target for CNS disorders. Over the past years, a wealth of data has been published on CNS P2X7 biology, in particular the role of P2X7 in microglial cells, and *in vivo* effects of brain-penetrant P2X7 antagonists. Likewise, significant progress has been made around the medicinal chemistry of CNS P2X7 ligands, as antagonists for *in vivo* target validation in models of CNS diseases, to identification of two clinical compounds (JNJ-54175446 and JNJ-55308942) and finally, discovery of P2X7 PET ligands. This review is an attempt to bring together the current understanding of P2X7 in the CNS with a focus on P2X7 as a drug target in neuropsychiatric disorders.

Keywords: P2X7, microglia, depression, IL-1beta, schizophrenia, bipolar disorder, neuroinflammation, neuropsychiatry

OPEN ACCESS

Edited by:
Kenneth A. Jacobson, National Institutes of Health (NIH), United States

Reviewed by:
Hendra Gunosewoyo, Curtin University, Australia
Carlos De Torre, IMIB-Arrixaca, Spain

***Correspondence:**
Anindya Bhattacharya
abhatta2@its.jnj.com

Specialty section:
This article was submitted to Experimental Pharmacology and Drug Discovery, a section of the journal Frontiers in Pharmacology

Received: *13 October 2017*
Accepted: *10 January 2018*
Published: *01 February 2018*

Citation:
Bhattacharya A (2018) Recent Advances in CNS P2X7 Physiology and Pharmacology: Focus on Neuropsychiatric Disorders. Front. Pharmacol. 9:30. doi: 10.3389/fphar.2018.00030

INTRODUCTION

P2X7 is an ATP-gated ion channel; activation of the ion channel by ATP leads to opening of the pore causing non-selective flux of Ca^{2+}, Na^{+}, and K^{+} ions (Bartlett et al., 2014). In addition to the non-selective cation conductance, P2X7 channel opening under constant stimulation to ATP is believed to form a "macro-pore," the function of which has remained elusive; pharmacologically, there is no antagonist or modulator of P2X7 that selectively disrupts the macro-pore and as such the physiological relevance of the macro-pore has been debated and recently challenged (Pippel et al., 2017). In addition to ion flux, the best studied downstream function of P2X7 is the release of pro-inflammatory cytokines, IL-1β and IL-18 (He et al., 2017) that functions through the recruitment of the NLRP3 inflammasome complex (Giuliani et al., 2017). Since P2X7 is abundantly expressed in blood cells, IL-1β release in the blood has been used as a biomarker of P2X7 activity and has been used in both preclinical and clinical assessment of target engagement (Stock et al., 2012; Letavic et al., 2017). Although the P2X7-dependent NLRP3-mediated IL-1β release is the best characterized signature of P2X7 activity *in vivo*, there are numerous other physiological endpoints (pyroptosis, membrane blebbing shedding of cell surface proteins, microvesicle/exosome release to even modulation of synaptic events), some or all of which may contribute to P2X7-driven pathology (Bartlett et al., 2014). P2X7 function is even modulated by cholesterol and other membrane lipids (Karasawa et al., 2017). Within the CNS P2X7 is abundantly expressed in microglial cells (Bhattacharya and Biber, 2016) and P2X7 activation causes IL-1β (and IL-18) release, neuroinflammation, and microglial activation (Monif et al., 2010;

Bhattacharya et al., 2013; He et al., 2017). In addition to microglia, astrocytes and oligodendrocytes also express this ion channel subtype in the CNS; the expression of P2X7 in CNS neurons is inconsistent and sometimes controversial (Illes et al., 2017). Even though P2X7 expression is abundant in microglia (and in peripheral immune cells), the channel is "silent" under normal physiology where ATP concentrations do not reach high micromolar levels to activate the ion channel (Bhattacharya and Biber, 2016). As such, from a drug discovery perspective, P2X7 is an ideal drug target as antagonism of a silent channel by true neutral antagonists would not cause any serious target mediated (adverse) effects, i.e., antagonism will only elicit when the channel is activated by high ATP concentrations (i.e., on-demand activation, danger signal), which is believed to be achieved during pathology of neuroinflammatory disorders of the CNS such as stroke, epilepsy, multiple sclerosis, chronic neurodegenerative, and neuropsychiatric diseases. There have been several excellent and comprehensive review articles on P2X7 highlighting the biology, genetics, and disease relevance (Bartlett et al., 2014; Sperlagh and Illes, 2014; De Marchi et al., 2016; Park and Kim, 2017); for this mini-review, the focus is entirely on the role of CNS P2X7 in neuropsychiatry, with an emphasis on pharmacology and medicinal chemistry of brain-penetrant P2X7 antagonists including the identification of the two CNS P2X7 clinical compounds, JNJ-54175446 and JNJ-55308942 (see later).

ROLE OF P2X7 IN NEUROPSYCHIATRIC DISORDERS

Chronic inflammation is one of the core underpinnings of many diseases; relatively recent scientific literature over the past few years points to the role of peripheral and central inflammation in neuropsychiatric diseases (Leighton et al., 2017; Wetsman, 2017). With the relatively recent discovery of CNS lymphatics in the meningeal tissue that drains CSF into deep cervical nodes (Louveau et al., 2015), and emerging science supporting the possibility of compromised blood–brain, blood–CSF, blood–choroid plexus barriers in chronic diseases of the CNS, the role of immune cells and their signaling partners in CNS pathophysiology are beginning to be thoroughly appreciated (Wohleb et al., 2016). As has happened in the space of immuno-oncology, there is a now a growing body of scientific literature that supports a role of immunology in neuropsychiatry, the emerging discipline of neuroimmunopsychiatry (Bhattacharya et al., 2016). Perhaps, it is not a mere coincidence that several inflammatory disorders are co-morbid with depression, bipolar disorder, and schizophrenia (Miller et al., 2017). This has been supported by immune-related gene enrichment in patients (Jansen et al., 2016; Leday et al., 2018).

Within the CNS, microglia are considered as innate immune cells and one of consequences of activated microglia results in neuroinflammation as defined by the release of several pro-inflammatory cytokines including IL-1β . This cytokine is present at higher levels in plasma, CSF, and postmortem brain tissue of individuals with mood disorders (Söderlund et al., 2011; Jones and Thomsen, 2013). This cytokine has been linked with geriatric depression and postpartum depression as well (Corwin et al., 2008; Diniz et al., 2010). In animal models of stress-induced depression, it was shown that IL-1β signaling was critical to the development of depression-like phenotype (Koo and Duman, 2009). Due to this body of data it is reasonable to hypothesize that targeting P2X7, upstream of NLRP3 and IL-1β signaling, with CNS penetrable P2X7 antagonists would be beneficial for treating mood disorders. As such, there is a growing body of literature that strengthens the role of P2X7-IL-1β pathway in mood disorders including depression and bipolar disorder (Chrovian et al., 2014; Stokes et al., 2015; Bhattacharya and Biber, 2016; Bhattacharya and Drevets, 2017). Some of the key data supporting the role of P2X7 in models of depression, mania, and schizophrenia is discussed below.

P2X7 activation produces microglial activation (Monif et al., 2010). Microglial activation has been clinically demonstrated in depression, bipolar disorder, and schizophrenia by use of PET ligands designed to target TSPO, a mitochondrial protein used as a surrogate of microglial activation (Mondelli et al., 2017). As such, it is plausible that P2X7 plays a role in the etiology of neuropsychiatric diseases, maybe in a subset of patients with neuroinflammation. Recently, P2X7 has come to the light as a potential molecular player in schizophrenia (Kovanyi et al., 2016). This is not surprising given the role of microglia and neuroinflammation in schizophrenia (Laskaris et al., 2016). For depression and bipolar disorder, there is even more growing genetic evidence of P2X7, although the penetrance and frequency of the SNPs to disease susceptibility and protection is not clearly understood. It is perhaps not surprising that the data is equivocal, clouded with both positive and negative associations (Barden et al., 2006; Lucae et al., 2006; Hejjas et al., 2009; Backlund et al., 2011, 2012; Soronen et al., 2011; Halmai et al., 2013). One of the most reported P2X7 SNP is rs2230912. The rs2230912-G allele is known to exhibit a gain-of-function for IL-1β release from human monocytes (Stokes et al., 2010). A recent meta-analysis was reported for rs2230912 and the authors concluded strong association of rs2230912 with depression and bipolar disorder (Czamara et al., 2017), although negative association meta-analysis also exists for this particular SNP (Feng et al., 2014). In addition to rs2230912, there are additional SNPs on the *p2rx7* gene (rs1718119, rs3751143, rs1653624) that may shed additional insight into the role of P2X7 SNPs and disease susceptibility; perhaps, more detailed haplotype analysis is needed to understand the relationship between allelic variation, function (IL-1β release), and disease protection and/or susceptibility. In addition to the human genetic literature, emerging science in animal models of despair and anhedonia has been supportive of the P2X7 hypothesis of mood disorders. Several groups have demonstrated an anti-depressant and anti-manic phenotype of P2X7 knockout mice (Basso et al., 2009; Boucher et al., 2011; Csolle et al., 2013a,b; Wilkinson et al., 2014). Whether the knockout phenotypes, in particular the acute despair like behaviors seen in forced swim immobility measurements, can be robustly recapitulated in rodents with pharmacological specificity remains to be seen as it is not clear how ATP would activate central P2X7 channels in an

acute stressful setting. Where P2X7 probably plays a more significant role is in chronic settings of stress, where IL-1β-driven microglial activation and neuroinflammation has been shown to upregulate and P2X7 antagonism may be efficacious. In line with this hypothesis, in a model of sucrose consumption that is reflective of hedonic behavior, pharmacological antagonism of P2X7 restored the deficit observed in drinking sucrose-water (anhedonia) either under chronic stress or by systemic administration of lipopolysaccharides (LPS) (Csolle et al., 2013b). Consistent with these observations, recent data with P2X7 selective, brain-penetrant antagonists demonstrated efficacy in chronic models of stress (Lovenberg et al., 2015; Iwata et al., 2016; Yue et al., 2017); these findings point to a pathway of stress mediated ATP-driven activation of P2X7–NLRP3–IL-1β pathway, leading to microglial activation (pro-inflammatory) and neuroinflammation. A recent study demonstrated enhanced IL-1β release in the brain, upregulation of P2X7 mRNA, and microglial activation in a chronic stress paradigm (Tan et al., 2017). Chronic stress is known to contribute to clinical depression (Calcia et al., 2016) and as such there is hope that P2X7 antagonists with good CNS penetration and drug likeliness will proceed into clinical testing as novel mechanisms for mood disorders. There is also a recent publication indicating the role of P2X7 channels in modulating stress-mediated spine density downregulation and P2X7 knock out mice are protective from this decrease in spine density (Otrokocsi et al., 2017). In addition to depression, blockade of P2X7 may be useful as mood stabilizer in bipolar disorder (Gubert et al., 2014). P2X7 antagonism was efficacious in amphetamine-induced sensitization of hyperactivity (Bhattacharya et al., 2013; Lord et al., 2014), and similar phenotypes were observed in P2X7 knockout mice (Gubert et al., 2014). Taken together, the body of emerging data suggests a potential therapeutic utility of brain-penetrant P2X7 antagonists in mood disorders, especially targeting treatment resistant patient sub-populations or as an adjunct to current pharmacotherapy for efficacy maintenance.

P2X7 PHARMACOLOGY: BRAIN-PENETRANT ANTAGONISTS

Significant progress has been made toward identification of brain-penetrant P2X7 antagonists. This spans medicinal chemistry efforts from identification of tool molecules to selection of brain-penetrant clinical candidates JNJ-54175446 (Letavic et al., 2017) and JNJ-55308942 (Chrovian et al., 2017). Unlike the Pfizer and AstraZeneca clinical compounds (**Figure 1**), the Janssen molecules retain rodent activity providing the discovery team to develop robust target engagement assays to drive the chemistry program; in addition, rodent activity provided the team with an opportunity to test the molecules in rodent models of disease, an important missing link in the prior two clinical compounds (CE-224,535 and AZD-9056). Medicinal chemistry efforts toward identification of brain-penetrant P2X7 ligands in the industry are summarized in **Figure 2**. The Pfizer molecule (compound 7f) was reported to be drug like with a low clearance, long half-life in rats,

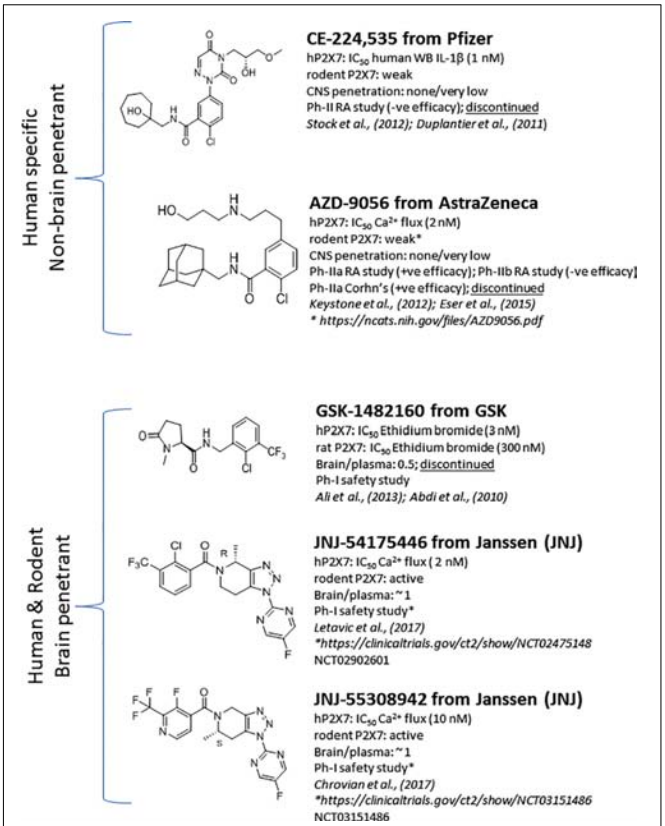

FIGURE 1 | P2X7 antagonists that transitioned into clinical development.

and good CNS exposure (brain/plasma of 1.3) (Chen et al., 2010). Medicinal chemistry groups at Abbott Laboratories (now Abbvie) and GlaxoSmithKline (GSK) were the pioneers in discovering scaffolds with both rodent potency and low-moderate CNS permeability (Nelson et al., 2006; Beswick et al., 2010; Chen et al., 2010). The group at Janssen has published several papers disclosing P2X7 antagonists with excellent brain penetration (**Figure 2**) and focusing on brain P2X7-mediated pharmacodynamic endpoints (Bhattacharya et al., 2013; Letavic et al., 2013; Lord et al., 2014; Savall et al., 2015). JNJ-47965567 and JNJ-42253432 demonstrated activity at rodent and human P2X7, had good rat pharmacokinetic profiles, and excellent brain penetration when dosed subcutaneously to allow for >80% brain P2X7 occupancy, as judged by *ex vivo* autoradiography in rat brain slices. Docking studies with JNJ-47965567 reveal an allosteric binding site (Karasawa and Kawate, 2016). More recently, Janssen disclosed several additional classes of P2X7 antagonists, beginning with a series of fused 1,2,3-triazoles. A closer look at the nuances of adding the methyl substituents to the 1,2,4-triazolopyrazine core revealed a strong enantiomeric preference of the P2X7 ion channel. Chiral separation and ultimately enantioselective synthesis demonstrated the (S)-7-methyl derivative (human IC_{50} of 7.7 ± 2.6 nM and rat IC_{50} of 8.0 ± 2.9 nM) was highly favored over the (R)-8-methyl derivative devoid of any significant P2X7 activity (human IC_{50} of 1560 nM and rat IC_{50} of 2240 nM). JNJ-54140515 was

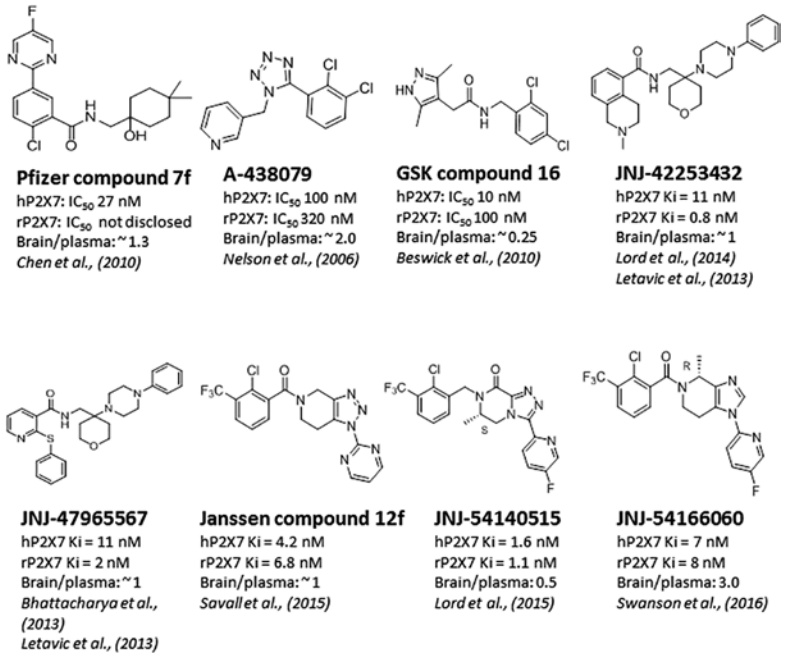

FIGURE 2 | Brain-penetrant P2X7 antagonists.

discovered from this series and was shown to readily cross the blood–brain barrier facilitating the high level of brain P2X7 occupancy. In addition to good *in vivo* properties, this ligand was highly selective and was tritiated to produce a radioligand for P2X7 (Lord et al., 2015). JNJ-54166060 was discovered from an imidazopyridine scaffold (Swanson et al., 2016) and was shown to have a significant brain/plasma ratio of close to 3. Although the brain concentrations were approximately threefold greater than plasma levels, free plasma and free brain concentrations were similar after correcting for brain binding (1.5% free) and plasma protein binding (5.5% free). The compound demonstrated an ED_{50} of 2.3 mg/kg oral dose.

The discovery of the clinical compound JNJ-54175446 (**Figure 1**; NCT02902601) and JNJ-55308942 (**Figure 1**; NCT03151486) is described in detail by Letavic et al. (2017) and Chrovian et al. (2017). JNJ-54175446 is a high affinity (and potency) P2X7 antagonist that displays pharmacology at recombinant human, rat, mouse, macaque, and dog P2X7. In native systems, this compound displayed P2X7 pharmacology as well: it blocked P2X7-dependent IL-1β release in human blood and displayed binding to rat, dog, and human brain sections. Target engagement in rat brain was demonstrated for JNJ-54175446 utilizing *ex vivo* autoradiography. The molecule showed dose-dependent brain P2X7 occupancy with an ED_{50} of 0.46 mg/kg, which corresponded to plasma EC_{50} of 105 ng/ml. This compound efficiently crossed into the brain compartment with a brain/plasma ratio of approximately 1.1 in rat. JNJ-54175446 demonstrated robust and sustained P2X7 brain occupancy in the rat following a 10 mg/kg oral dose (>80% occupancy for 24 h). Consistent with rat brain target engagement, the compound did attenuate brain IL-1β release, as measured by microdialysis. When the molecule was dosed in a higher species (i.e., dog), JNJ-54175446 also bound to dog brain P2X7, and blocked dog blood IL-1β release, providing a model of both central and peripheral target engagement in one

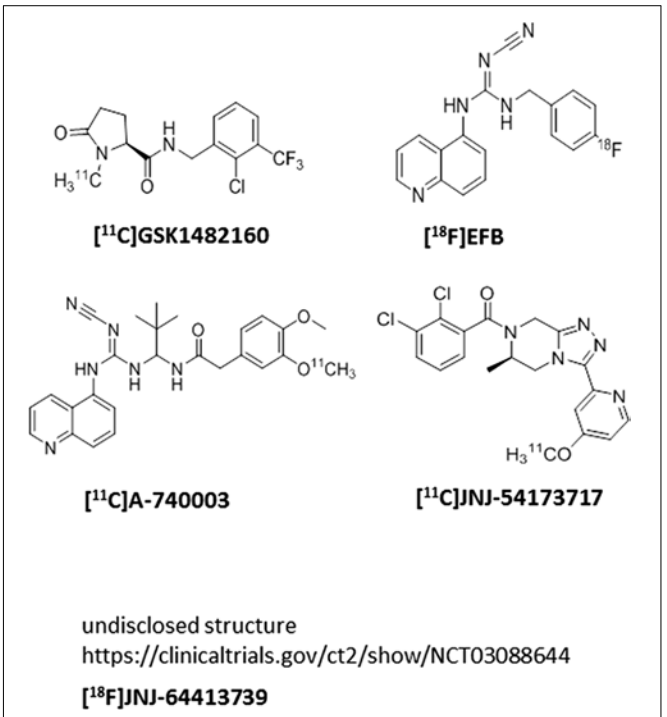

FIGURE 3 | P2X7 PET ligands.

species. This data highlights the fact that blood IL-1β can be used as a biomarker, and may be a surrogate for central target engagement in the absence of a PET ligand. As has been described later on, there are several P2X7 PET ligands that should enable human target engagement (i.e., human brain P2X7) studies. Given the excellent target engagement data in rats and dogs, JNJ-54175446 was profiled further to enrich clinical candidacy data package including toxicity and cardiovascular safety studies. JNJ-55308942, has been chosen as the second P2X7 antagonist from Janssen to enter clinical trials, as a back-up to JNJ-54175446. While maintaining the superior P2X7 pharmacology of the lead molecule, JNJ-55308942 provides significant improvement in solubility and protein binding properties (i.e., increased free fraction). JNJ-55308942 showed excellent P2X7 receptor occupancy in the hippocampus of rats, demonstrating a low ED_{50} of 0.07 mg/kg. The compound also demonstrated good tolerability margins in preclinical species, as well as an acceptable cardiovascular safety profile *in vivo*.

In addition to Janssen's efforts, several other companies (Affectis, Axxam, Actelion, Lundbeck) have published patents on brain-penetrant P2X7 scaffolds (Park and Kim, 2017). Both Lundbeck and Axxam Pharmaceuticals published patents disclosing CNS-penetrant P2X7 antagonists, with Axxam entering into a collaborative agreement with Alzheimer's drug discovery foundation to understand the role of centrally penetrant P2X7 antagonists in Alzheimer's. Lastly, AFC-5128 is a brain-penetrant P2X7 antagonist from Affectis Pharmaceuticals that is being pushed for neuropathic pain and multiple sclerosis indications (company website).

P2X7 PET LIGANDS

Several P2X7 PET ligands have been described in the literature recently (**Figure 3**); there are two clinical utilities of P2X7 PET ligands that cross the blood–brain barrier: (a) the PET ligands can be used as a probe to measure central target occupancy of the clinical compound being developed for a CNS indication; (b) since P2X7 activation is related to microglial activation, P2X7 PET ligands can potentially be used as central biomarkers of assessing microglial activation in diseases accompanying neuroinflammation such as mood disorders, schizophrenia, epilepsy, multiple sclerosis, and others. Our team has disclosed a [^{11}C]-labeled P2X7 PET ligand (JNJ-54173717), where it was shown that P2X7 overexpression can be detected under basal and overexpressed conditions and the PET signal was blocked by competition with cold P2X7 ligands in a dose-dependent manner in rats (Ory et al., 2016). A second P2X7 PET ligand, with [^{18}F] label (JNJ-64413739), has been recently described at the American College of Neuropsychopharmacology conference (December, 2017) where it was elegantly demonstrated that JNJ-54175446 (i.e., the clinical compound shown in **Figure 1**) was able to displace [^{18}F]JNJ-64413739 PET signal in healthy human subjects in a dose-dependent manner (NCT03088644). Similarly, the [^{11}C]GSK1482160 PET signal in the brain of LPS challenged rats was also blocked by a cold P2X7 antagonist, demonstrating specificity of the PET signal to P2X7 (Territo et al., 2017). In addition to [^{18}F]JNJ-64413739, [^{11}C]JNJ-54173717, and [11C]GSK1482160, two other groups have disclosed P2X7 PET ligands ([^{11}C]A-7400003 and [^{18}F]-EFB), albeit with no data to support P2X7 specificity of the brain signal (Janssen et al., 2014; Fantoni et al., 2017). The field has made significant progress in discovery of brain-penetrant P2X7 antagonists in recent years. Molecules such as JNJ-54175446 will now need to be tested in clinical settings to find efficacy signals in psychiatric disorders; persistent and prudent drug developmental paradigms, out-of-box thinking, challenging the status-quo, may result in a P2X7 therapeutic that will benefit patients suffering from life-changing CNS disorders.

CONCLUSION AND PERSPECTIVES

The unmet medical need in neuropsychiatry is staggering; it is clear from existing clinical data that "one pill fits all" strategy has not worked. Patients suffering from depression, bipolar disorder, and schizophrenia may have neuroinflammatory causality of the disease, and not every patient carries similar inflammatory disease burden. While there are patients that will benefit from existing pharmacotherapy, a huge sub-population of patients will respond better to therapies that address the underlying cause of the disease and the hope is CNS P2X7 antagonists in clinical trials will advance into proof of concept studies either as monotherapy or as adjunctives for neuropsychiatric disorders.

AUTHOR CONTRIBUTIONS

AB conceived the topic for the mini-review and wrote the draft of the manuscript.

ACKNOWLEDGMENTS

The author acknowledges the contribution of Devin Swanson and Michael Letavic for providing feedback on the manuscript.

REFERENCES

Abdi, M. H., Beswick, P. J., Billinton, A., Chambers, L. J., Charlton, A., Collins, S. D., et al. (2010). Discovery and structure–activity relationships of a series of pyroglutamic acid amide antagonists of the $P2X_7$ receptor. *Bioorg. Med. Chem. Lett.* 20, 5080–5084. doi: 10.1016/j.bmcl.2010.07.033

Ali, Z., Laurijssens, B., Ostenfeld, T., McHugh, S., Stylianou, A., Scott-Stevens, P., et al. (2013). Pharmacokinetic and pharmacodynamic profiling of a P2X7 receptor allosteric modulator GSK1482160 in healthy human subjects. *Br. J. Clin. Pharmacol.* 75, 197–207. doi: 10.1111/j.1365-2125.2012.04320.x

Backlund, L., Lavebratt, C., Frisen, L., Nikamo, P., Hukic Sudic, D., Traskman-Bendz, L., et al. (2012). P2RX7: expression responds to sleep deprivation and associates with rapid cycling in bipolar disorder type 1. *PLOS ONE* 7:e43057. doi: 10.1371/journal.pone.0043057

Backlund, L., Nikamo, P., Hukic, D. S., Ek, I. R., Traskman-Bendz, L., Landen, M., et al. (2011). Cognitive manic symptoms associated with the P2RX7 gene in

bipolar disorder. *Bipolar Disord.* 13, 500–508. doi: 10.1111/j.1399-5618.2011.00952.x

Barden, N., Harvey, M., Gagne, B., Shink, E., Tremblay, M., Raymond, C., et al. (2006). Analysis of single nucleotide polymorphisms in genes in the chromosome 12Q24.*31* region points to P2RX7 as a susceptibility gene to bipolar affective disorder. *Am. J. Med. Genet B Neuropsychiatr. Genet.* 141B, 374–382.

Bartlett, R., Stokes, L., and Sluyter, R. (2014). The P2X7 receptor channel: recent developments and the use of P2X7 antagonists in models of disease. *Pharmacol. Rev.* 66, 638–675. doi: 10.1124/pr.113.008003

Basso, A. M., Bratcher, N. A., Harris, R. R., Jarvis, M. F., Decker, M. W., and Rueter, L. E. (2009). Behavioral profile of P2X7 receptor knockout mice in animal models of depression and anxiety: relevance for neuropsychiatric disorders. *Behav. Brain Res.* 198, 83–90. doi: 10.1016/j.bbr.2008.10.018

Beswick, P. J., Billinton, A., Chambers, L. J., Dean, D. K., Fonfria, E., Gleave, R. J., et al. (2010). Structure-activity relationships and in vivo activity of (1H-pyrazol-4-yl) acetamide antagonists of the P2X(7) receptor. *Bioorg. Med. Chem. Lett.* 20, 4653–4656. doi: 10.1016/j.bmcl.2010.05.107

Bhattacharya, A., and Biber, K. (2016). The microglial ATP-gated ion channel P2X7 as a CNS drug target. *Glia* 64, 1772–1787. doi: 10.1002/glia.23001

Bhattacharya, A., Derecki, N. C., Lovenberg, T. W., and Drevets, W. C. (2016). Role of neuro-immunological factors in the pathophysiology of mood disorders. *Psychopharmacology* 233, 1623–1636. doi: 10.1007/s00213-016-4214-0

Bhattacharya, A., and Drevets, W. C. (2017). Role of neuro-immunological factors in the pathophysiology of mood disorders: implications for novel therapeutics for treatment resistant depression. *Curr. Top. Behav. Neurosci.* 31, 339–356. doi: 10.1007/7854_2016_43

Bhattacharya, A., Wang, Q., Ao, H., Shoblock, J. R., Lord, B., Aluisio, L., et al. (2013). Pharmacological characterization of a novel centrally permeable P2X7 receptor antagonist: JNJ-47965567. *Br. J. Pharmacol.* 170, 624–640. doi: 10.1111/bph.12314

Boucher, A. A., Arnold, J. C., Hunt, G. E., Spiro, A., Spencer, J., Brown, C., et al. (2011). Resilience and reduced c-Fos expression in P2X7 receptor knockout mice exposed to repeated forced swim test. *Neuroscience* 189, 170–177. doi: 10.1016/j.neuroscience.2011.05.049

Calcia, M. A., Bonsall, D. R., Bloomfield, P. S., Selvaraj, S., Barichello, T., and Howes, O. D. (2016). Stress and neuroinflammation: a systematic review of the effects of stress on microglia and the implications for mental illness. *Psychopharmacology* 233, 1637–1650. doi: 10.1007/s00213-016-4218-9

Chen, X., Pierce, B., Naing, W., Grapperhaus, M. L., and Phillion, D. P. (2010). Discovery of 2-chloro-N-((4,4-difluoro-1-hydroxycyclohexyl)methyl)-5-(5-fluoropyrimidin-2-yl)b enzamide as a potent and CNS penetrable P2X7 receptor antagonist. *Bioorg. Med. Chem. Lett.* 20, 3107–3111. doi: 10.1016/j.bmcl.2010.03.094

Chrovian, C. C., Rech, J. C., Bhattacharya, A., and Letavic, M. A. (2014). P2X7 antagonists as potential therapeutic agents for the treatment of CNS disorders. *Progr. Med. Chem.* 53, 65–100. doi: 10.1016/B978-0-444-63380-4.00002-0

Chrovian, C. C., Soyode-Johnson, A., Peterson, A. A., Gelin, C. F., Deng, X., Dvorak, C. A., et al. (2017). A dipolar cycloaddition reaction to access 6-methyl-4,5,6,7-tetrahydro-1H-[1,2,3]triazolo[4,5-c]pyridines enables the discovery synthesis and preclinical profiling of a P2X7 antagonist clinical candidate. *J. Med. Chem.* 61, 207–223. doi: 10.1021/acs.jmedchem.7b01279

Corwin, E. J., Johnston, N., and Pugh, L. (2008). Symptoms of postpartum depression associated with elevated levels of interleukin-1 beta during the first month postpartum. *Biol. Res. Nurs.* 10, 128–133. doi: 10.1177/1099800408323220

Csolle, C., Ando, R. D., Kittel, A., Goloncser, F., Baranyi, M., Soproni, K., et al. (2013a). The absence of P2X7 receptors (P2rx7) on non-haematopoietic cells leads to selective alteration in mood-related behaviour with dysregulated gene expression and stress reactivity in mice. *Int. J. Neuropsychopharmacol.* 16, 213–233. doi: 10.1017/S1461145711001933

Csolle, C., Baranyi, M., Zsilla, G., Kittel, A., Goloncser, F., Illes, P., et al. (2013b). Neurochemical changes in the mouse hippocampus underlying the antidepressant effect of genetic deletion of P2X7 receptors. *PLOS ONE* 8:e66547. doi: 10.1371/journal.pone.0066547

Czamara, D., Muller-Myhsok, B., and Lucae, S. (2017). The P2RX7 polymorphism rs2230912 is associated with depression: a meta-analysis. *Progr. Neuro Psychopharmacol. Biol. Psychiatry* doi: 10.1016/j.pnpbp.2017.11.003 [Epub ahead of print].

De Marchi, E., Orioli, E., Dal Ben, D., and Adinolfi, E. (2016). P2X7 receptor as a therapeutic target. *Adv. Protein Chem. Struct. Biol.* 104, 39–79. doi: 10.1016/bs.apcsb.2015.11.004

Diniz, B. S., Teixeira, A. L., Talib, L., Gattaz, W. F., and Forlenza, O. V. (2010). Interleukin-1β serum levels is increased in antidepressant-free elderly depressed patients. *Am. J. Geriatr. Psychiatry* 18, 172–176. doi: 10.1097/JGP.0b013e3181c2947f

Duplantier, A. J., Dombroski, M. A., Subramanyam, C., Beaulieu, A. M., Chang, S. P., Gabel, C. A., et al. (2011). Optimization of the physicochemical and pharmacokinetic attributes in a 6-azauracil series of $P2X_7$ receptor antagonists leading to the discovery of the clinical candidate CE-224,535. *Bioorg. Med. Chem. Lett.* 21, 3708–3711. doi: 10.1016/j.bmcl.2011.04.077

Eser, A., Colombel, J.-F., Rutgeerts, P., Vermeire, S., Vogelsang, H., Braddock, M., et al. (2015). Safety and Efficacy of an oral inhibitor of the purinergic receptor $P2X_7$ in adult patients with moderately to severely active crohn's disease: a randomized placebo-controlled, double-blind, phase IIa study. *Inflamm. Bowel Dis.* 21, 2247–2253. doi: 10.1097/MIB.0000000000000514

Fantoni, E. R., Dal Ben, D., Falzoni, S., Di Virgilio, F., Lovestone, S., and Gee, A. (2017). Design, synthesis and evaluation in an LPS rodent model of neuroinflammation of a novel 18F-labelled PET tracer targeting P2X7. *EJNMMI Res.* 7:31. doi: 10.1186/s13550-017-0275-2

Feng, W. P., Zhang, B., Li, W., and Liu, J. (2014). Lack of association of P2RX7 gene rs2230912 polymorphism with mood disorders: a meta-analysis. *PLOS ONE* 9:e88575. doi: 10.1371/journal.pone.0088575

Giuliani, A. L., Sarti, A. C., Falzoni, S., and Di Virgilio, F. (2017). The P2X7 receptor-interleukin-1 liaison. *Front. Pharmacol.* 8:123. doi: 10.3389/fphar.2017.00123

Gubert, C., Fries, G. R., Pfaffenseller, B., Ferrari, P., Coutinho-Silva, R., Morrone, F. B., et al. (2014). Role of P2X7 receptor in an animal model of mania induced by D-amphetamine. *Mol. Neurobiol.* 53, 611–620. doi: 10.1007/s12035-014-9031-z

Halmai, Z., Dome, P., Vereczkei, A., Abdul-Rahman, O., Szekely, A., Gonda, X., et al. (2013). Associations between depression severity and purinergic receptor P2RX7 gene polymorphisms. *J. Affect. Disord.* 150, 104–109. doi: 10.1016/j.jad.2013.02.033

He, Y., Taylor, N., Fourgeaud, L., and Bhattacharya, A. (2017). The role of microglial P2X7: modulation of cell death and cytokine release. *J. Neuroinflammat.* 14:135. doi: 10.1186/s12974-017-0904-8

Hejjas, K., Szekely, A., Domotor, E., Halmai, Z., Balogh, G., Schilling, B., et al. (2009). Association between depression and the Gln460Arg polymorphism of P2RX7 gene: a dimensional approach. *Am. J. Med. Genet. B Neuropsychiatr. Genet.* 150B, 295–299. doi: 10.1002/ajmg.b.30799

Illes, P., Khan, T. M., and Rubini, P. (2017). Neuronal P2X7 receptors revisited: do they really exist? *J. Neurosci.* 37, 7049–7062. doi: 10.1523/JNEUROSCI.3103-16.2017

Iwata, M., Ota, K. T., Li, X.-Y., Sakaue, F., Li, N., Dutheil, S., et al. (2016). Psychological stress activates the inflammasome via release of ATP and stimulation of the P2X7 receptor. *Biol. Psychiatry* 80, 12–22. doi: 10.1016/j.biopsych.2015.11.026

Jansen, R., Penninx, B. W., Madar, V., Xia, K., Milaneschi, Y., Hottenga, J. J., et al. (2016). Gene expression in major depressive disorder. *Mol. Psychiatry* 21, 339-47. doi: 10.1038/mp.2015.57

Janssen, B., Vugts, D. J., Funke, U., Spaans, A., Schuit, R. C., Kooijman, E., et al. (2014). Synthesis and initial preclinical evaluation of the P2X7 receptor antagonist [(1)(1)C]A-740003 as a novel tracer of neuroinflammation. *J. Labelled Comp. Radiopharm.* 57, 509–516. doi: 10.1002/jlcr.3206

Jones, K. A., and Thomsen, C. (2013). The role of the innate immune system in psychiatric disorders. *Mol. Cell. Neurosci.* 53, 52–62. doi: 10.1016/j.mcn.2012.10.002

Karasawa, A., and Kawate, T. (2016). Structural basis for subtype-specific inhibition of the P2X7 receptor. *eLife* 5:e22153. doi: 10.7554/eLife.22153

Karasawa, A., Michalski, K., Mikhelzon, P., and Kawate, T. (2017). The P2X7 receptor forms a dye-permeable pore independent of its intracellular domain but dependent on membrane lipid composition. *eLife* 6:e31186. doi: 10.7554/eLife.31186

Keystone, E. C., Wang, M. M., Layton, M., Hollis, S., McInnes, I. B., and Team, D. C. S. (2012). Clinical evaluation of the efficacy of the P2X7 purinergic receptor antagonist AZD9056 on the signs and symptoms of rheumatoid

arthritis in patients with active disease despite treatment with methotrexate or sulphasalazine. *Ann. Rheumat. Dis.* 71, 1630–1635.

Koo, J. W., and Duman, R. S. (2009). Evidence for IL-1 receptor blockade as a therapeutic strategy for the treatment of depression. *Curr. Opin. Investig. Drugs* 10, 664–671.

Kovanyi, B., Csolle, C., Calovi, S., Hanuska, A., Kato, E., Koles, L., et al. (2016). The role of P2X7 receptors in a rodent PCP-induced schizophrenia model. *Sci. Rep.* 6:36680. doi: 10.1038/srep36680

Laskaris, L. E., Di Biase, M. A., Everall, I., Chana, G., Christopoulos, A., Skafidas, E., et al. (2016). Microglial activation and progressive brain changes in schizophrenia. *Br. J. Pharmacol.* 173, 666–680. doi: 10.1111/bph.13364

Leday, G. G. R., Vertes, P. E., Richardson, S., Greene, J. R., Regan, T., Khan, S., et al. (2018). Replicable and coupled changes in innate and adaptive immune gene expression in two case-control studies of blood microarrays in major depressive disorder. *Biol. Psychiatry* 83, 70–80. doi: 10.1016/j.biopsych.2017.01.021

Leighton, S. P., Nerurkar, L., Krishnadas, R., Johnman, C., Graham, G. J., and Cavanagh, J. (2017). Chemokines in depression in health and in inflammatory illness: a systematic review and meta-analysis. *Mol. Psychiatry* 23, 48–58. doi: 10.1038/mp.2017.205

Letavic, M. A., Lord, B., Bischoff, F., Hawryluk, N. A., Pieters, S., Rech, J. C., et al. (2013). Synthesis and pharmacological characterization of two novel, brain penetrating P2X7 antagonists. *ACS Med. Chem. Lett.* 4, 419–422. doi: 10.1021/ml400040v

Letavic, M. A., Savall, B. M., Allison, B. D., Aluisio, L., Andres, J. I., De Angelis, M., et al. (2017). 4-Methyl-6,7-dihydro-4H-triazolo[4,5-c]pyridine-based P2X7 receptor antagonists: optimization of pharmacokinetic properties leading to the identification of a clinical candidate. *J. Med. Chem.* 60, 4559–4572. doi: 10.1021/acs.jmedchem.7b00408

Lord, B., Aluisio, L., Shoblock, J. R., Neff, R. A., Varlinskaya, E. I., Ceusters, M., et al. (2014). Pharmacology of a novel central nervous system-penetrant P2X7 antagonist JNJ-42253432. *J. Pharmacol. Exp. Ther.* 351, 628–641. doi: 10.1124/jpet.114.218487

Lord, B., Ameriks, M. K., Wang, Q., Fourgeaud, L., Vliegen, M., Verluyten, W., et al. (2015). A novel radioligand for the ATP-gated ion channel P2X7: [3H] JNJ-54232334. *Eur. J. Pharmacol.* 765, 551–559. doi: 10.1016/j.ejphar.2015.09.026

Louveau, A., Smirnov, I., Keyes, T. J., Eccles, J. D., Rouhani, S. J., Peske, J. D., et al. (2015). Structural and functional features of central nervous system lymphatic vessels. *Nature* 523, 337–341. doi: 10.1038/nature14432

Lovenberg, T., Aluisio, L., Ceusters, M., Letavic, M., and Bhattacharya, A. (2015). "Characterization of P2X7 antagonists in the rodent brain: promise for a novel mechanism of action for mood disorder?," in *Proceedings of the CINP Thematic Meeting on Stress, Inflammation and Depression: Focus on Novel Antidepressant Targets*, Dublin.

Lucae, S., Salyakina, D., Barden, N., Harvey, M., Gagne, B., Labbe, M., et al. (2006). P2RX7, a gene coding for a purinergic ligand-gated ion channel, is associated with major depressive disorder. *Hum. Mol. Genet.* 15, 2438–2445. doi: 10.1093/hmg/ddl166

Miller, A. H., Haroon, E., and Felger, J. C. (2017). Therapeutic implications of brain-immune interactions: treatment in translation. *Neuropsychopharmacology* 42, 334–359. doi: 10.1038/npp.2016.167

Mondelli, V., Vernon, A. C., Turkheimer, F., Dazzan, P., and Pariante, C. M. (2017). Brain microglia in psychiatric disorders. *Lancet Psychiatry* 4, 563–572. doi: 10.1016/S2215-0366(17)30101-3

Monif, M., Burnstock, G., and Williams, D. A. (2010). Microglia: proliferation and activation driven by the P2X7 receptor. *Int. J. Biochem. Cell Biol.* 42, 1753–1756. doi: 10.1016/j.biocel.2010.06.021

Nelson, D. W., Gregg, R. J., Kort, M. E., Perez-Medrano, A., Voight, E. A., Wang, Y., et al. (2006). Structure-activity relationship studies on a series of novel, substituted 1-benzyl-5-phenyltetrazole P2X7 antagonists. *J. Med. Chem.* 49, 3659–3666. doi: 10.1021/jm051202e

Ory, D., Celen, S., Gijsbers, R., Van Den Haute, C., Postnov, A., Koole, M., et al. (2016). Preclinical Evaluation of a P2X7 receptor-selective radiotracer: PET studies in a rat model with local overexpression of the human P2X7 receptor and in nonhuman primates. *J. Nucl. Med.* 57, 1436–1441. doi: 10.2967/jnumed.115.169995

Otrokocsi, L., Kittel, A., and Sperlagh, B. (2017). P2X7 receptors drive spine synapse plasticity in the learned helplessness model of depression. *Int. J. Neuropsychopharmacol.* 20, 813–822. doi: 10.1093/ijnp/pyx046

Park, J. H., and Kim, Y. C. (2017). P2X7 receptor antagonists: a patent review (2010-2015). *Exp. Opin. Therap. Patents* 27, 257–267. doi: 10.1080/13543776.2017.1246538

Pippel, A., Stolz, M., Woltersdorf, R., Kless, A., Schmalzing, G., and Markwardt, F. (2017). Localization of the gate and selectivity filter of the full-length P2X7 receptor. *Proc. Natl. Acad. Sci. U.S.A.* 114, E2156–E2165. doi: 10.1073/pnas.1610414114

Savall, B. M., Wu, D., De Angelis, M., Carruthers, N. I., Ao, H., Wang, Q., et al. (2015). Synthesis, SAR, and pharmacological characterization of brain penetrant P2X7 receptor antagonists. *ACS Med. Chem. Lett.* 6, 671–676. doi: 10.1021/acsmedchemlett.5b00089

Söderlund, J., Olsson, S. K., Samuelsson, M., Walther-Jallow, L., Johansson, C., Erhardt, S., et al. (2011). Elevation of cerebrospinal fluid interleukin-1ß in bipolar disorder. *J. Psychiatry Neurosci.* 36, 114–118. doi: 10.1503/jpn.100080

Soronen, P., Mantere, O., Melartin, T., Suominen, K., Vuorilehto, M., Rytsala, H., et al. (2011). *P2RX7* gene is associated consistently with mood disorders and predicts clinical outcome in three clinical cohorts. *Am. J. Med. Genet. B Neuropsychiat. Genet.* 156B, 435–447. doi: 10.1002/ajmg.b.31179

Sperlagh, B., and Illes, P. (2014). P2X7 receptor: an emerging target in central nervous system diseases. *Trends Pharmacol. Sci.* 35, 537–547. doi: 10.1016/j.tips.2014.08.002

Stock, T. C., Bloom, B. J., Wei, N., Ishaq, S., Park, W., Wang, X., et al. (2012). Efficacy and safety of CE-224,535, an antagonist of P2X7 receptor, in treatment of patients with rheumatoid arthritis inadequately controlled by methotrexate. *J. Rheumatol.* 39, 720–727. doi: 10.3899/jrheum.110874

Stokes, L., Fuller, S. J., Sluyter, R., Skarratt, K. K., Gu, B. J., and Wiley, J. S. (2010). Two haplotypes of the P2X(7) receptor containing the Ala-348 to Thr polymorphism exhibit a gain-of-function effect and enhanced interleukin-1beta secretion. *FASEB J.* 24, 2916–2927. doi: 10.1096/fj.09-150862

Stokes, L., Spencer, S. J., and Jenkins, T. A. (2015). Understanding the role of P2X7 in affective disorders-are glial cells the major players? *Front. Cell. Neurosci.* 9:258. doi: 10.3389/fncel.2015.00258

Swanson, D. M., Savall, B. M., Coe, K. J., Schoetens, F., Koudriakova, T., Skaptason, J., et al. (2016). Identification of (R)-(2-Chloro-3-(trifluoromethyl) phenyl)(1-(5-fluoropyridin-2-yl)-4-methyl-6,7-di hydro-1H-imidazo[4,5-c]pyridin-5(4H)-yl)methanone (JNJ 54166060), a Small Molecule Antagonist of the P2X7 receptor. *J. Med. Chem.* 59, 8535–8548. doi: 10.1021/acs.jmedchem.6b00989

Tan, S., Wang, Y., Chen, K., Long, Z., and Zou, J. (2017). Ketamine alleviates depressive-like behaviors via down-regulating inflammatory cytokines induced by chronic restraint stress in mice. *Biol. Pharmaceut. Bull.* 40, 1260–1267. doi: 10.1248/bpb.b17-00131

Territo, P. R., Meyer, J. A., Peters, J. S., Riley, A. A., McCarthy, B. P., Gao, M., et al. (2017). Characterization of 11C-GSK1482160 for targeting the P2X7 receptor as a biomarker for neuroinflammation. *J. Nuclear Med.* 58, 458–465. doi: 10.2967/jnumed.116.181354

Wetsman, N. (2017). Inflammatory illness: why the next wave of antidepressants may target the immune system. *Nat. Med.* 23, 1009–1011. doi: 10.1038/nm0917-1009

Wilkinson, S. M., Gunosewoyo, H., Barron, M. L., Boucher, A., McDonnell, M., Turner, P., et al. (2014). The first CNS-active carborane: a novel P2X7 receptor antagonist with antidepressant activity. *ACS Chem. Neurosci.* 5, 335–339. doi: 10.1021/cn500054n

Wohleb, E. S., Franklin, T., Iwata, M., and Duman, R. S. (2016). Integrating neuroimmune systems in the neurobiology of depression. *Nat. Rev. Neurosci.* 17, 497–511. doi: 10.1038/nrn.2016.69

Yue, N., Huang, H., Zhu, X., Han, Q., Wang, Y., Li, B., et al. (2017). Activation of P2X7 receptor and NLRP3 inflammasome assembly in hippocampal glial cells mediates chronic stress-induced depressive-like behaviors. *J. Neuroinflammation* 14:102. doi: 10.1186/s12974-017-0865-y

Conflict of Interest Statement: The author is a full-time employee of Johnson & Johnson.

frontiers in Pharmacology

ORIGINAL RESEARCH
published: 31 January 2018
doi: 10.3389/fphar.2018.00054

The A_{2B} Adenosine Receptor Modulates the Epithelial–Mesenchymal Transition through the Balance of cAMP/PKA and MAPK/ERK Pathway Activation in Human Epithelial Lung Cells

Chiara Giacomelli[1], Simona Daniele[1], Chiara Romei[2,3], Laura Tavanti[4], Tommaso Neri[2], Ilaria Piano[1], Alessandro Celi[2], Claudia Martini[1] and Maria L. Trincavelli[1]*

[1] Department of Pharmacy, University of Pisa, Pisa, Italy, [2] Department of Surgical, Medical and Molecular Pathology and Critical Care Medicine, University of Pisa, Pisa, Italy, [3] Radiology Unit, University Hospital of Pisa, Pisa, Italy, [4] Pneumology Unit, Cardio-Thoracic Department, University Hospital of Pisa, Pisa, Italy

OPEN ACCESS

Edited by:
Francisco Ciruela, University of Barcelona, Spain

Reviewed by:
Rodrigo A. Cunha, University of Coimbra, Portugal
Aline Appert-Collin, URCA, France

***Correspondence:**
Claudia Martini
claudia.martini@unipi.it

Specialty section:
This article was submitted to Experimental Pharmacology and Drug Discovery, a section of the journal Frontiers in Pharmacology

Received: *04 October 2017*
Accepted: *15 January 2018*
Published: *31 January 2018*

Citation:
Giacomelli C, Daniele S, Romei C, Tavanti L, Neri T, Piano I, Celi A, Martini C and Trincavelli ML (2018) The A_{2B} Adenosine Receptor Modulates the Epithelial–Mesenchymal Transition through the Balance of cAMP/PKA and MAPK/ERK Pathway Activation in Human Epithelial Lung Cells. Front. Pharmacol. 9:54. doi: 10.3389/fphar.2018.00054

The epithelial-mesenchymal transition (EMT) is a complex process in which cell phenotype switches from the epithelial to mesenchymal one. The deregulations of this process have been related with the occurrence of different diseases such as lung cancer and fibrosis. In the last decade, several efforts have been devoted in understanding the mechanisms that trigger and sustain this transition process. Adenosine is a purinergic signaling molecule that has been involved in the onset and progression of chronic lung diseases and cancer through the A_{2B} adenosine receptor subtype activation, too. However, the relationship between A_{2B}AR and EMT has not been investigated, yet. Herein, the A_{2B}AR characterization was carried out in human epithelial lung cells. Moreover, the effects of receptor activation on EMT were investigated in the absence and presence of transforming growth factor-beta (TGF-β1), which has been known to promote the transition. The A_{2B}AR activation alone decreased and increased the expression of epithelial markers (E-cadherin) and the mesenchymal one (Vimentin, N-cadherin), respectively, nevertheless a complete EMT was not observed. Surprisingly, the receptor activation counteracted the EMT induced by TGF-β1. Several intracellular pathways regulate the EMT: high levels of cAMP and ERK1/2 phosphorylation has been demonstrated to counteract and promote the transition, respectively. The A_{2B}AR stimulation was able to modulated these two pathways, cAMP/PKA and MAPK/ERK, shifting the fine balance toward activation or inhibition of EMT. In fact, using a selective PKA inhibitor, which blocks the cAMP pathway, the A_{2B}AR-mediated EMT promotion were exacerbated, and conversely the selective inhibition of MAPK/ERK counteracted the receptor-induced transition. These results highlighted the A_{2B}AR as one of the receptors involved in the modulation of EMT process. Nevertheless, its activation is not enough to trigger a complete transition, its ability to affect different intracellular pathways

could represent a mechanism at the basis of EMT maintenance/inhibition based on the extracellular microenvironment. Despite further investigations are needed, herein for the first time the A_{2B}AR has been related to the EMT process, and therefore to the different EMT-related pathologies.

Keywords: adenosine A_{2B} receptor, epithelial mesenchymal transition, lung, MAPK-ERK, cAMP-PKA, transforming growth factor-β1

INTRODUCTION

The epithelial-mesenchymal transition (EMT) is an evolutionarily conserved biochemical process in which cells undergo conversion from an epithelial to a mesenchymal phenotype. The EMT is characterized by the loss of the epithelial cell–cell adhesion molecule CDH1 (E-cadherin), and/or a concomitant gain of mesenchymal markers such as CDH2 (N-cadherin), VIM (Vimentin), and/or αSMA (alpha-smooth muscle actin) (Nieto et al., 2016; Singh et al., 2017). EMT is a Janus-faced process due to its pivotal role in embryogenesis and wound healing and in the development of chronic pathologies, such as fibrosis and cancer (Lamouille et al., 2014).

The EMT process has been widely correlated with lung embryogenesis (Lee et al., 2006) and cancer (Sung et al., 2016; Legras et al., 2017), but it has only recently been linked to chronic human lung and airway diseases such as chronic obstructive pulmonary disease (COPD) and idiopathic pulmonary fibrosis (IPF) (Willis et al., 2006; Sohal and Walters, 2013; Jonsdottir et al., 2015; Jolly et al., 2017). In fact, it has been proposed that alveolar epithelial cells (AECs), undergoing EMT (De Maio et al., 2012; Yamaguchi et al., 2017) or partial EMT (Morbini et al., 2011), are a source of extracellular matrix-producing fibroblasts/myofibroblasts. It has been widely accepted that several soluble factors such as, growth factors [fibroblast growth factor (FGF), epidermal growth factor (EGF)] and inflammatory cytokines (transforming growth factor-beta (TGF-β1), interleukin-6 (Il-6), tumor necrosis factor-alpha (TNF-α), could trigger and promote the EMT (Nieto et al., 2016; Suarez-Carmona et al., 2017). In the lung, attention has been focused on TGF-β1, which has been found to promote AEC differentiation (Yang et al., 2014; Shi et al., 2016) and the aggressiveness of cancer cells (Sakuma, 2017).

Adenosine is a soluble factor involved in physiological processes; however, after tissue injury, its levels rise to micromolar concentration promoting anti-inflammatory action (Ohta and Sitkovsky, 2001). Recently, a correlation between the increase in adenosine levels and the EMT process has been reported (Guillén-Gómez et al., 2012; Lu and Insel, 2014; Gao et al., 2016). Adenosine binds to four specific cell membrane G-protein-coupled receptors (GPCRs) known as adenosine receptors (ARs): A_1, A_{2A}, A_{2B}, and A_3. In this context, great attention has been focused on the purine receptor involvement in the EMT process. Only a few studies have correlated the EMT and purinergic receptors P2X and P2Y, such as P2X7, P2Y2, P2Y6, and P2Y12 (review in Martínez-Ramírez et al., 2017). Furthermore, some evidence has correlated the adenosine receptor A_{2A} with the transition (Xiao et al., 2013). However, no evidence has been reported on the role of the A_{2B}AR subtype in the trigger or modulation of induced-EMT.

The A_{2B}AR subtype has been recently linked to cancer aggressiveness (Mittal et al., 2016; Sepúlveda et al., 2016) and fibrotic processes of the heart (Ryzhov et al., 2014; Phosri et al., 2017), kidney (Roberts et al., 2014; Wilkinson et al., 2016) and lung (Zhou et al., 2011; Karmouty-Quintana et al., 2012; Karmouty-Quintana et al., 2013). A_{2B}AR couples to $G_{\alpha s}$ proteins, resulting in the activation of adenylyl cyclase (AC) and an increase in intracellular cyclic AMP (cAMP) levels that subsequently activate protein kinase A (PKA) (Schulte and Fredholm, 2003; Sun and Huang, 2016). However, A_{2B}AR can also coupled to the G_q-PLC pathway and induces the activation of mitogen-activated protein kinase (MAPK) (Schulte and Fredholm, 2003; Sun and Huang, 2016). In fact, A_{2B}AR induces the phosphorylation of ERK1/2 in human umbilical vein endothelial cells (HUVECs) (Fang and Olah, 2007), human mast cell line (MHC-1 cells) (Feoktistov et al., 1999), and human retinal endothelial cells (HRECs) (Grant et al., 2001). The cAMP role in EMT promotion/blockade is debatable. Pattabiraman et al. (2016) reported that a PKA activator could lead to a mesenchymal-epithelial transition as previously reported by Boucher et al. (2005). Furthermore, the increase in the cAMP intracellular levels, induced by forskolin or phosphodiesterase inhibitors, as well as the administration of a PKA activator counteracts the EMT induced by TGF-β1 (Zhang et al., 2006a,b; Nadella et al., 2008; Lambers et al., 2015). By contrast, other evidence has been reported regarding the positive role of cAMP and PKA in the induction of EMT (Shaikh et al., 2012). Conversely, it has been widely accepted that ERK phosphorylation is one of the mechanisms that promotes the EMT program (Singh et al., 2017). In fact, ERK activation is one of the Smad-independent events that is necessary for TGF-β-mediated EMT (Gui et al., 2012; O'Connor and Gomez, 2014).

Therefore, in the present study, the effects of A_{2B}AR stimulation on EMT was investigated in human lung epithelial cells. Particularly, the role of this adenosine receptor subtype in directly modulating the epithelial-mesenchymal markers under physiological or inflammatory conditions (TGF-β1) was analyzed. Furthermore, the intracellular pathways activated by A_{2B}AR, cAMP/PKA, and MAPK/ERK, involved in EMT, were explored.

MATERIALS AND METHODS

Material and Reagents

Human type II alveolar epithelial cells (A549, American Type Culture Collection, CCL-195), were kindly provided

by Dr. R. Danesi, University of Pisa, Pisa, Italy. The chemicals 2-[6-amino-3,5-dicyano-4-[4-(cyclopropylmethoxy) phenyl]pyridin-2-ylsulfanyl] acetamide (BAY 60-6583) and N-(4-acetylphenyl)-2-[4-(2,3,6,7-tetrahydro-2,6-dioxo-1,3-dipropyl-1H-purin-8-yl)phenoxy]-acetamide (MRS1706) were purchased from Tocris Bioscience (Bristol, United Kingdom). The RNeasy minikit was obtained from Qiagen. The Script cDNA synthesis kit was furnished by Bio-Rad s.r.l. Fluocycle II SYBR was from Euroclone (Milan, Italy). TGF-β1 was purchased from Sigma–Aldrich. All other reagents were obtained from standard commercial sources and were of the highest commercially available grade

Cell Culture

Human type II alveolar epithelial cells (A549) were maintained in DMEM-F12 containing 10% FBS, 2 mM L-glutamine, 100 U/ml penicillin and 100 μg/ml streptomycin at 37°C in a humidified 5% CO^2 atmosphere. For the different experiments, cultures of cells were maintained in serum-free DMEM for 8 h prior to stimulation with cytokines or other reagents.

RNA Extraction and Real-Time RT-PCR Analysis

A549 cells were untreated or treated with DMSO (CTRL) or BAY 60-6583 (100 nM) in the absence or presence of TGF-β1 (10 ng/ml) and MRS 1706 (1 μM) for the indicated time. At the end of treatments, cells were collected, and total RNA was extracted using Rneasy®Mini Kit (Qiagen, Hilden, Germany) as previously reported (Da Pozzo et al., 2014); residual DNA was removed using RNase free DNAse set (#79254, Qiagen, Hilden, Germany). The RNA purity was checked measuring the A260/280 ratio. cDNA synthesis was performed with 400 ng of RNA using i-Script cDNA synthesis kit (BioRad, Hercules, CA, United States) following manufacturer's instructions. Real-time RT-PCR reactions consisted of 25 μL Fluocycle®II SYBR® (Euroclone, Milan, Italy), 1.0 μL of both 10 μM forward and reverse primers, 2.5 μL cDNA (100 ng), and 20.5 μL of H_2O. All reactions were performed for 40 cycles using the following temperature profiles: 98°C for 30 s (initial denaturation); 55°C for 30 s (annealing); and 72°C for 3 s (extension). The primer sequences were listed in **Table 1**. When possible, the primers used were designed to span intron/exon boundaries and the β-actin was used as the housekeeping gene. The mRNA levels for each sample were normalized against β-actin mRNA levels, and the relative expression was calculated by using a Ct value. PCR specificity was determined by both the melting curve analysis and gel electrophoresis.

Western Blotting Analysis

A549 cells (3.5×10^4 cell/cm^2) were maintained untreated or treated with DMSO (CTRL) or BAY 60-6583 (100 nM) in the absence or presence of TGF-β1 (10 ng/ml) and MRS 1706 (1 μM) for 48 h. At the end 200 μl RIPA buffer were added for 60 min at 4°C to lyse the cells. Fifty microgram of total proteins was diluted in Laemmli solution, resolved by SDS-PAGE (7.5%), transferred to PVDF membranes and probed overnight at 4°C with primary anti-A_1AR (diluted 1:200, sc-28995; Santa Cruz Biotechnology), anti-A_{2A}AR (diluted 1:200, sc-13937; Santa Cruz Biotechnology), anti-A_{2B}AR (diluted 1:150, sc-28996; Santa Cruz Biotechnology), anti-A_3AR (diluted 1:200, sc-13938; Santa Cruz Biotechnology), anti-E-cadherin antibody (diluted 1:200; sc-7870; Santa Cruz Biotechnology), anti-N-cadherin antibody (diluted 1:200; sc-7939; Santa Cruz Biotechnology) anti-Vimentin (diluted 1:1000, #5741; Cell Signaling Technology) or β-actin antibody (diluted 1:1000; MAB1501, Merck KGaA, Darmstadt, Germany). The primary antibody was detected using appropriate secondary antibody. The peroxidase was detected using a chemiluminescent substrate (ECL, Perkin Elmer), and the images were acquired by photographic film or by LAS4010 (GE Health Care Europe, Uppsala, Sweden). Immunoreactive bands were quantified performing a densitometric analysis with Image J Software (version 1.41; Bethesda, MD, United States).

Immunofluorescence Analysis

A549 cells were seeded at 3.5×10^4 cell/cm^2 in chamber slide (BD Biosciences, San Jose, CA, United States). After treatment, cells were fixed in 2% paraformaldheyde in 0.1 M phosphate buffer, washed three times with PBS, rinsed, and blocked for 45 min with PBS containing 0.1% Triton-X 100 and 1% BSA. After washing, cells were incubated overnight at 4°C with mouse monoclonal anti-β-actin antibody (diluted 1:500; MAB1501, Merck KGaA, Darmstadt, Germany) or a rabbit polyclonal anti-A_{2B}AR (diluted 1:100, sc-28996; Santa Cruz Biotechnology) primary antibodies diluted in PBS containing 0.03% Triton-X 100 and 1% BSA overnight at 4°C. After washing, to visualize the staining, cells were incubated with Alexa Fluor 488- and Alexa Fluor 568-labeled goat anti-mouse (1:500) or anti-rabbit (1:500) antibodies for 2 h at room temperature. Then slides were covered with Vectashield conjugated with DAPI (Vector Laboratories, Burlingame, CA, United States). Images were obtained with a Nikon Ni-E microscope, using a 20× objective with 1.45 NA and a recommended pinhole size of less than 1.0 mm, and equipped with digital camera Nikon Mod.DS-Ri2. The images were processed with ImageJ software.

Cell Viability Assay

A549 cells were seeded at a density of 3×10^3 cells/well in a black, clear bottom PerkinElmer 96-well CellCarrier™ microplate (#6005550). After 24 h, the cells were starved for 8 h with non-complete medium; then, cells were treated with different concentrations of BAY 60-6583 (0.5 nM–1 μM) or TGF-β1 (5–20 ng/ml) alone or in combination for 48 or 72 h. Following the treatment period, cells were imaged with the EnSight™ multimode plate reader equipped with well-imaging module, and Kaleido Data Acquisition and Analysis Software. Brightfield images were taken before and 48 or 72 h after treatments to allow for a Cell Count comparison between both time points. The cell count was determined using the pre-defined Brightfield Cell Count algorithm provided by the Kaleido software. Cell with a mean area ≥100 μm^2 were counted. Data were normalized

TABLE 1 | Primers used for real-time RT-PCR.

Gene	Primer nucleotide sequences	Product size (base pairs)	Annealing temperature
ADORA1	FOR: 5′-TCCCTCTCCGGTACAAGATG -3′ REV: 5′-GCTGCTTGCGGATTAGGTAG-3′	300 bp	55°C
ADORA2A	FOR: 5′-TCTTCAGTCTCCTGGCCATC-3′ REV: 5′-TCCAACCTAGCATGGGAGTC-3′	156 bp	55°C
ADORA2B	FOR: 5′-TCCATCTTCAGCCTTCTGGC -3′ REV: 5′-AAAGGCAAGGACCCAGAGGA-3′	129 bp	55°C
ADORA3	FOR: 5′-CAGCAAAGCGTCAACTCGTGC -3′ REV: 5′-CAAACGGGAGAAGCAGAGGAAC-3′	118 bp	55°C
CDH1	FOR: 5′-AGGGGTTAAGCACAACAGCA-3′ REV: 5′-GGGGGCTTCATTCACATCCA-3′'	395 bp	55°C
Vimentin	FOR: 5′-CTCTTCCAAACTTTTCCTCCC-3′ REV: 5′-AGTTTCGTTGATAACCTGTCC-3′	134 bp	55°C
CDH2	FOR: 5′-AGGGGACCTTTTCCTCAAGA-3′ REV: 5′-CAATGTCAATGGGGTTCTCC-3′	246 bp	55°C
ZEB1	FOR: 5′-CCCTTGAAAGTGATCCAGCCA-3′ REV: 5′-AGACCCAGAGTGTGAGAAGCG-3′	354 bp	55°C
Snail	FOR: 5′-AAGATGCACATCCGAAGCCA-3′ REV: 5′-CATTCGGGAGAAGGTCCGAG-3′	237 bp	55°C
Slug	FOR: 5′-TGGTTGCTTCAAGGACACAT-3′ REV: 5′-GTTGCAGTGAGGGCAAGAA-3′	66 bp	55°C
TWIST	FOR: 5′-ACGAGCTGGACTCCAAGATG-3′ REV: 5′-CACGCCCTGTTTCTTTGAAT-3′	290 bp	55°C
β-actin	FOR: 5′-GCACTCTTCCAGCCTTCCTTCC-3′ REV: 5′-GAGCCGCCGATCCACACG-3′	254 bp	55°C

to the cell count at t_0 and expressed as the number of cell per well.

cAMP Quantification

A549 cells were seeded at a density of 3×10^3 cells/well in a black, clear bottom PerkinElmer 96-well CellCarrier^{TM} microplate (#6005550). After 24 h, the cells were starved for 8 h with non-complete medium; then, cells were treated with different concentrations of BAY 60-6583 (0.1 nM–1 μM) in the absence or presence of TGF-β1 (10 ng/ml) in 100 μl of non-complete medium for 48 h. Cells were imaged with the EnSight^{TM} multimode plate reader. The desensitization experiments were performed incubating the cells with BAY 60-6583 (100 nM) in the presence or absence of TGF-β1 (10 ng/ml) for 48 h. At the end the medium was changed and cells were treated with different concentrations of BAY 60-6583 (0.1 nM–1 μM) for 15 min. Then, cells were lysed with 50 μl of 1X lysis buffer (PerkinElmer, #AL003C) supplemented with protease inhibitors and phosphatase inhibitors for 10 min with gentle shaking. Lysates were either tested immediately in AlphaLISA assays or frozen at –80°C for later testing. cAMP levels were quantified using cAMP AlphaLISA kit (PerkinElmer, #AL312) following manufacturer's instructions. Standard curves for each AlphaLISA immunoassay were performed in the same diluent as the samples being tested (1X lysis buffer with supplements) using the recombinant standards provided in each kit. Curves were plotted with a sigmoidal concentration-response curve with variable slope. Quantitation of protein levels in cellular assays were interpolated off their respective standard curves.

MAPK (Mitogen-Activated Phosphorylation Kinase) Assays

A549 cells were seeded at a density of 3×10^3 cells/well in 96 multi-well plate. After 24 h, the cells were starved for 8 h with non-complete medium; then, cells were treated with BAY 60-6583 (100 nM) in the absence or presence of TGF-β1 (10 ng/ml) and MRS1706 (1 μM) for 5 min, 30 min, 6, 24, and 48 h. In some experiments, before incubation with BAY 60-6583 or TGF-β1, cells were pre-treated for 30 min with PD98059 (1 μM) (MEK, inhibitor). At the end of treatments, cells were fixed with 4% formaldehyde to preserve activation of specific protein modification. Levels of total and phosphorylated extracellular signal-regulated kinases (ERK1/2) were determined by ELISA assays, as previously reported (Giacomelli et al., 2015). Briefly, the cells were washed three times with wash buffer (0.1% Triton X-100 in PBS) and 100 μl of quenching buffer (1% H_2O_2; 0.1% sodium azide in wash buffer) was added and incubation was protracted for other 20 min. The cells were washed with PBS twice, and then 100 μl of blocking solution (1% BSA; 0.1% Triton X-100 in PBS) was added for 60 min. After blocking, cells were washed three times with wash buffer and the specific primary antibodies (anti-phospho ERK1/2, 1:500, sc-7383 Santa Cruz Biotechnology; anti-ERK1/2, 1:500, #4695 Cell Signaling Technology) were added on at 4°C. Subsequent incubation with secondary HRP-conjugated antibodies and developing solution allowed a colorimetric quantification of total and phosphorylated levels. Blanks were obtained by treating cells in the absence of the primary antibody. The relative number of cells in each well was then determined using Crystal Violet solution. The results were calculated by subtracting the mean background from the values

obtained from each test condition; values were normalized to the number of cells in each well, and were expressed as the percentage of untreated cells (basal).

Quantification of E-cad and N-cad Proteins

A549 cells were seeded at a density of 3×10^3 cells/well in a black, clear bottom PerkinElmer 96-well CellCarrier™ microplate (#6005550). After 24 h, the cells were starved for 8 h with non-complete medium; then, cells were treated with different concentrations of BAY 60-6583 (0.1 nM–1 μM) in the absence or presence of TGF-β1 (10 ng/ml) in 100 μl of non-complete medium for 48 h. In some experiments, before incubation with BAY 60-6583 or TGF-β1, cells were pre-treated for 30 min with PD98059 (1 μM, MEK, inhibitor), H89 (100 nM, PKA inhibitor) or 8-Br-cAMP (100 nM–1 μM, cAMP analog & PKA activator). Then, cells were imaged with the EnSight™ multimode plate reader. After imaging, cells were lysed with 50 μl of 1X lysis buffer (PerkinElmer, #AL003C) supplemented with protease inhibitors and phosphatase inhibitors for 10 min with gentle shaking. E-cad were quantified using E-cadherin AlphaLISA kit (PerkinElmer, #AL370), and N-cad were quantified using N-cadherin AlphaLISA kit (PerkinElmer, #AL379) following the manufacturer's instructions. Standard curves for each AlphaLISA immunoassay were performed in the same diluents as the samples being tested (1X lysis buffer with supplements), using the recombinant standards provided in each kit. Curves were plotted with a sigmoidal concentration-response curve with variable slope. Quantitation of protein levels in cellular assays were interpolated off their respective standard curves.

Statistical Analysis

The Graph-Pad Prism program (GraphPad Software Inc., San Diego, CA, United States) was used for data analysis and graphic presentation. All data are the mean ± SEM of at least three different experiments. Statistical analysis was performed by one-way analysis of variance (ANOVA) with Dunnett *post hoc* analysis to compare the data to the control, or two-way ANOVA with Bonferroni correction and two-sided tests for multiple comparisons. EC_{50} values were reported as mean of the values obtained in at least three independent experiments performed in duplicate ± SEM. $P \leq 0.05$ was considered statistically significant.

RESULTS

Adenosine Receptor Expression in Human Epithelial Lung Cells and Its Modulation by TGF-β1

The A549 human alveolar epithelial cells have been widely used to study the fibrotic process in the lung and related EMT mechanism (Kim et al., 2007; Ji et al., 2016). Furthermore, these cells were maintained in serum-free medium to increase the epithelial phenotype (Dong et al., 2014).

First, the expression of the AR subtypes in A549 cells was evaluated after incubation in serum-free medium for 48 h (**Figure 1A**). All the ARs were expressed under this condition, and the A_{2B}AR subtype was the most expressed with a fold change of approximately 200 (**Figure 1A**).

TGF-β1 has been reported to affect the expression of several proteins (Zhang, 2017); thus, the effects of cytokine treatment on AR expression were evaluated (**Figures 1B–D**). Challenging the A549 cells for 48 h with increasing concentrations of TGF-β1 (5–20 ng/ml) modified the expression of the different adenosine subtypes. Particularly, A_1AR expression was significantly increased when a high concentration of TGF-β1 was used; conversely, A_{2A} and A_3 receptor expression was slightly decreased when increased concentration of the cytokine was applied. Regarding A_{2B}AR expression, low concentrations of TGF-β1 (5 or 10 ng/ml) were not sufficient to modify the receptor expression; by contrast, a higher concentration of the cytokine significantly decreased its expression. In this light, further experiments were performed using a maximum concentration of the cytokine of 10 ng/ml for 48 h to minimize the change in the receptor expression.

TGF-β1 Effects on A_{2B}AR Functionality and Lung Cell Growth

A_{2B}AR stimulation or blockade has been correlated to different levels of cell proliferation depending on the cell type and culture condition (Phosri et al., 2017; Zhou et al., 2017). Thus, the effects of A_{2B}AR stimulation in the absence or presence of TGF-β1 were evaluated in the lung cells (**Figure 2**). The selective agonist BAY 60-6583 was used to stimulate selectively the A_{2B}AR subtype. The compound could slightly increase the cell proliferation when used at low concentration (50–100 nM) for 48 or 72 h treatment (**Figure 2A**), conversely, it produced a decrease in proliferation when used at a high concentration (1 μM), with a significant effect after 72 h of treatment (13970 ± 488 n° of cells CTRL, 11038 ± 816 n° of cells BAY; $P \leq 0.05$). TGF-β1 alone presented a hormetic concentration-response course: the lower concentration possessed positive effects on cell proliferation that are lost at higher concentrations (**Figure 2B**). The combined treatment with BAY 60-6583 and TGF-β1 for 48 h did not significantly affect the cell proliferation (**Figure 2C**). These data confirmed the diverse role of A_{2B}AR in the cell proliferative mechanism. Based on such results, further experiments were then performed using BAY 60-6583 at a concentration (100 nM) not affecting significantly the A549 cell proliferation.

Next, the effect of cytokine treatment on A_{2B}AR functionality was evaluated by measuring the agonist-mediated cAMP production (**Figure 2D**). The potency of BAY 60-6583 was in the nanomolar range ($EC_{50} = 17.2 \pm 2.5$ nM), as derived by agonist concentration-response curves, it is a value comparable to that described for the same agonist in transfected cells (**Figure 2D**) (Trincavelli et al., 2014). The presence of TGF-β1 did not significantly affect the agonist potency ($EC_{50} = 10.0 \pm 1.8$ nM), even if the maximal effect of BAY in the production of cAMP was slightly increased ($E_{max} = 4.3$ pmol – TGF-β1; $E_{max} = 5.8$ pmol + TGF-β1, $P = 0.0565$) even if it was

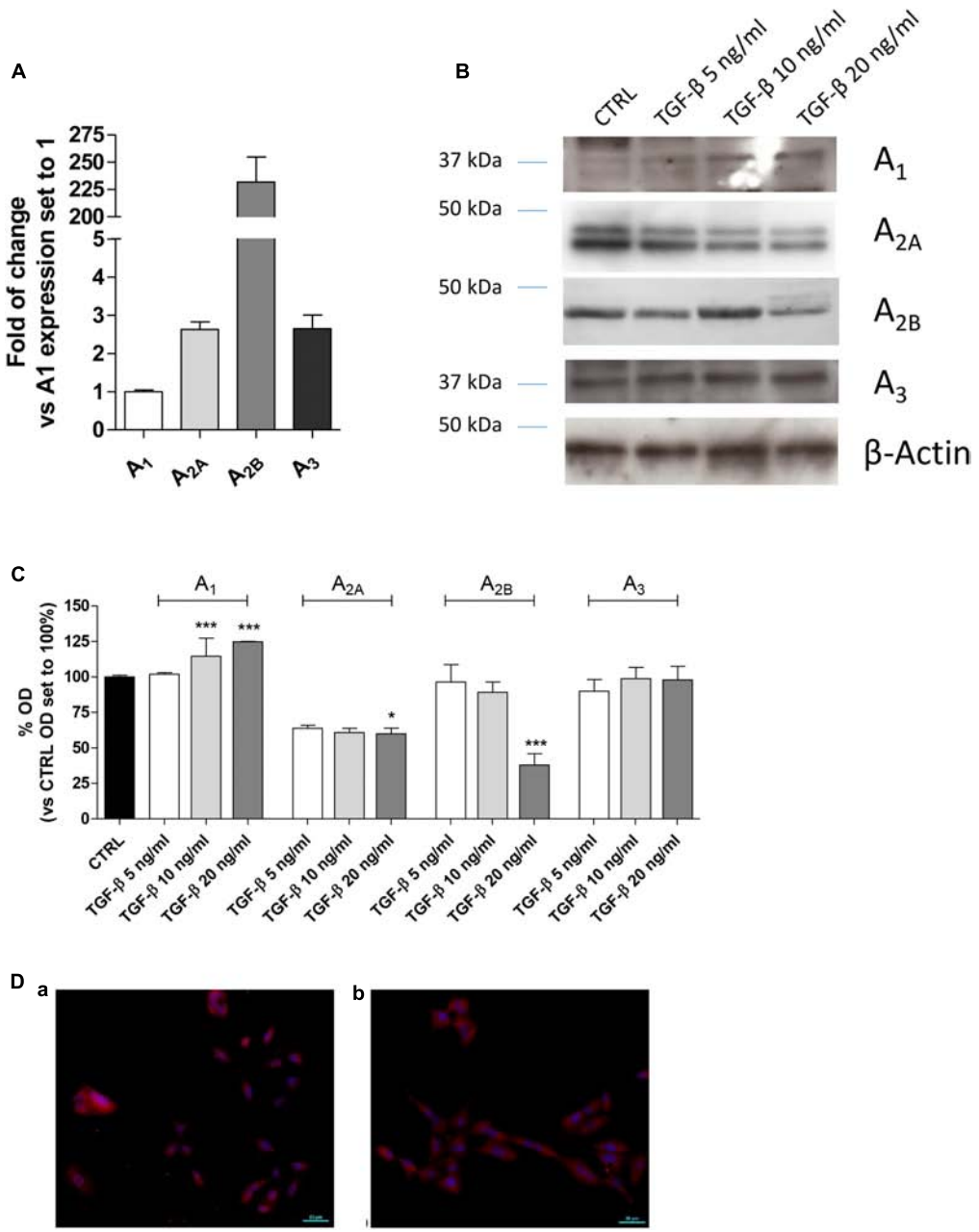

FIGURE 1 | Expression of ARs in A549 cells and their modulation in the presence of TGF-β1. **(A)** A549 cells were maintained in serum-free medium for 48 h. Next, real-time RT-PCR analysis of A_1, A_{2A}, A_{2B}, and A_3 adenosine receptors was performed. The data were expressed as the fold change vs. A_1AR expression, which was set to 1 and are the mean values ± SEM of three different experiments. **(B,C)** A549 cells were treated with different concentrations of TGF-β1 for 48 h, and the levels of AR subtypes were evaluated by Western blotting. One representative Western blot is presented **(C)**. The bar graph **(D)** shows the densitometric analysis of the Western blot performed using the ImageJ program. Cells were maintained in serum-free medium for 48 h in the absence (a) or presence (b) of TGF-β1. Next, cells were fixed and stained with anti-β actin and visualized with goat anti-rabbit Alexa Fluor 568 (red). Nuclei were counterstained with DAPI (blue). The data are presented as the means of three different experiments. The significance of the differences was determined by one-way ANOVA, followed by Dunnett's *post hoc* test: $^*P \leq 0.05$, $^{***}P \leq 0.001$ vs. the CTRL.

not statistically significant. These results are in accordance with the effect of other cytokines on A_{2B}AR functionality (Daniele et al., 2017); in fact, TNF-α has been demonstrated to increase A_{2B}AR coupling to the G_s protein (Daniele et al., 2017).

In parallel, the BAY-induced ERK phosphorylation was evaluated in order to further assess the A_{2B}AR functionality (**Figure 2E**). The agonist was able to produce a concentration-dependent increase of pERK with a potency in the sub-micromolar range of ($EC_{50} = 114.8 \pm 24.5$ nM).

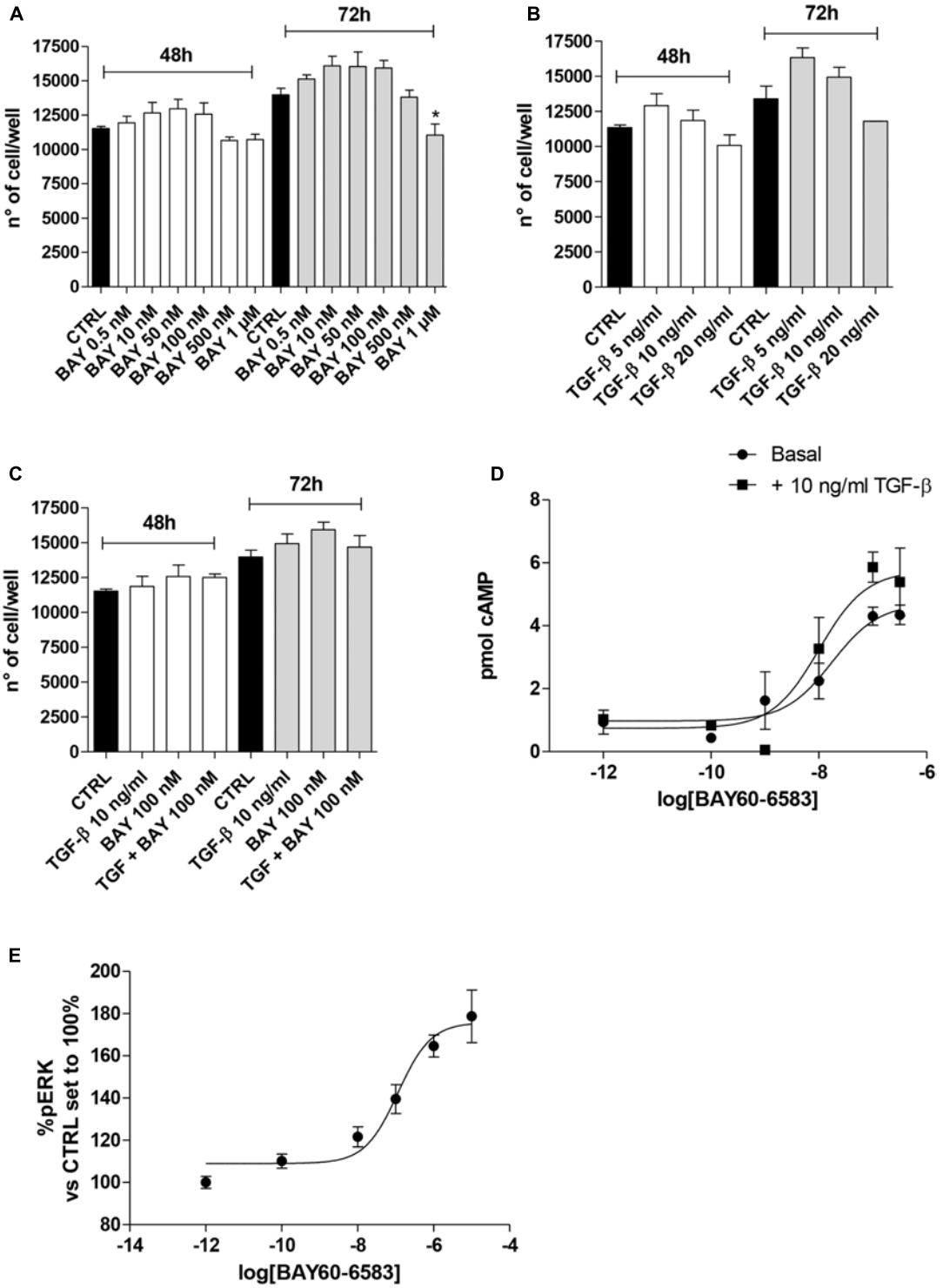

FIGURE 2 | Effects of BAY 60-6583 and TGF-β1 on cell proliferation and cAMP accumulation. A549 cells were treated in serum-free medium with different concentrations of BAY 60-6583 (0.5 nM–1 μM) and TGF-β1 (5–20 ng/ml), alone or in combination, for 48 h **(A–C)**. At the end of the treatments, the cell numbers were counted. The data were expressed as cell number per well, and they were presented as the mean values ± SEM of three independent experiments, each performed in duplicate. The significance of the differences was determined by one-way ANOVA, followed by Dunnett's *post hoc* test: $^*P \leq 0.05$ vs. the CTRL. **(D)** A549 cells were maintained in the absence or presence of TGF-β1 (10 ng/ml) for 48 h. Next, cells were challenged with increasing concentrations of BAY 60-6583, and cAMP production was quantified. **(E)** A549 cells were treated with different concentrations of BAY 60-6583 for 5 min and the levels of pERK were quantified. The data were expressed as pmol of cAMP and are the mean values ± SEM of three independent experiments, each performed in duplicate.

Effects of A_{2B}AR Stimulation on EMT Markers in the Absence or Presence of TGF-β1

Typically, the EMT process is triggered and maintained by the action of different cytokines and extracellular stimuli that, through the activation of specific intracellular pathways, modify the expression of several proteins (Nieto et al., 2016). A549 cells were treated for 48 h with the A_{2B}AR agonist alone or in the presence of TGF-β1 (10 ng/ml), which has been reported to induce EMT (Kawata et al., 2012). First, a morphological analysis of the cells was performed (**Figures 3A,B**). TGF-β1 treatment induced a change in cell morphology: most of the A549 cells, which normally display an oval shape, showed an elongated shape with a fibroblast-like appearance. Surprisingly, cells challenged with the A_{2B}AR agonist lead to a partial morphological change, with only some cells presenting an elongated shape, suggesting the induction of partial EMT.

The morphological changes, which are characteristic of cells undergoing EMT, are accompanied by a shift in the expression of epithelial genes to a mesenchymal gene repertoire (Nieto et al., 2016). Accordingly, challenging cells with TGF-β1 modified the expression of EMT markers, leading to a significant increase in the expression of the mesenchymal markers, Vimentin and N-cadherin (128.8 ± 6.5, $P \leq 0.01$, and 162.7 ± 3.8% $P \leq 0.001$ vs. CTRL, respectively; **Figures 3C,D**) and a concomitant decrease in the expression of the epithelial marker E-cadherin (6.7 ± 2.5% $P \leq 0.001$ vs. CTRL; **Figures 3C,D**). The data were confirmed at the gene expression level by real-time RT-PCR analysis of E-cadherin (CDH1), Vimentin, and N-cadherin (CHD2) expression (**Figure 3E**).

A_{2B}AR stimulation was able to slightly decrease the expression of E-cad protein (**Figures 3C,D**) and increase the expression of a mesenchymal marker (N-cad, 119.8 ± 0.6% vs. CTRL; $P \leq 0.05$). These effects are in accordance with the effects elicited by BAY on epithelial/mesenchymal gene transcription. Conversely, A_{2B}AR activation in the presence of TGF-β1 produced an opposite effect, significantly counteracting the induced EMT (**Figures 3C–E**). These effects were almost completely counteracted by concomitant treatment with the A_{2B}AR selective inverse agonist MRS 1706 (1 μM), demonstrating that they were mediated specifically by A_{2B}AR. The treatment with MRS 1706 alone was not able to significantly modify the expression of mesenchymal and epithelial markers in the absence or presence of TGF-β1 demonstrating that the adenosine in the medium was not sufficient to induce a basal A_{2B}AR activation.

Effects of A_{2B}AR Modulation on EMT Major Transcription Factors (EMT-TFs)

The modulation of classical EMT centers on the transcriptional control of different transcription factors: Snail (SNAI1), Slug (SNAI2), ZEB1 and TWIST (Nieto et al., 2016). To gain insight into the mechanisms by which A_{2B}AR affects E-cadherin deficiency alone and in TGF-β1-induced A549 cells, the expression levels of the EMT-TFs were examined using real-time RT-qPCR (**Figure 4**).

A549 cells expressed Snail and Slug at low levels (Supplementary Figure 1), in accordance with the high expression of E-cad (**Figure 2**). Treatment with TGF-β1 for 48 h changed the expression pattern of these genes (**Figure 4A**), with a significant increase in ZEB1 (1.57 ± 0.13-fold; $P \leq 0.05$), Slug (2.63 ± 0.25-fold; $P \leq 0.001$), in accordance with the literature data (Ji et al., 2016). Next, the effects of A_{2B}AR stimulation (BAY 60-6583) or blockade (MRS 1706) were evaluated (**Figure 4B**). The MRS alone could not modify the expression of EMT-TFs, highlighting that the endogenous activation of the receptor was not sufficient to modify the related-EMT gene expression. Conversely, A_{2B}AR activation modified the gene repertoire, producing a significant increase in the Slug expression (1.65 ± 0.16-fold; $P \leq 0.05$). These data are in accordance with the effects of A_{2B}AR activation on epithelial/mesenchymal markers (**Figure 3**).

Next, the role of A_{2B}AR stimulation on EMT-TF was evaluated in the presence of TGF-β1 (**Figure 4C**). As expected, the A_{2B}AR activation counteracted the effects of cytokine treatment, with a significant decrease in ZEB1 and Slug expression. When the A_{2B}AR inverse agonist was applied, the TGF-β1-induced decrease in gene expression was completely counteracted, demonstrating that these effects were mediated by A_{2B}AR.

The Balance of cAMP Production and MAPK/ERK Activation Orchestrates the A_{2B}AR Effects on EMT

A_{2B}AR couples to $G_{\alpha s}$ proteins, leading to an increase in intracellular cAMP, and to the G_q-PLC pathway, which induces the activation of the MAPK/ERK pathway (Schulte and Fredholm, 2003; Sun and Huang, 2016). Thus, activation of these two intracellular signaling pathways were investigated following A_{2B}AR stimulation, in the absence or presence of TGF-β1 (**Figure 5**). MRS 1706 alone did not affect the activation of the two pathways, demonstrating that the adenosine levels in our cellular model were not sufficient to activate the receptor. BAY was able to increase the intracellular cAMP concentration (**Figure 5A**), and significantly enhance ERK1/2 phosphorylation (178.9 ± 10.5% vs. CTRL, $P \leq 0.05$; **Figure 5B**), producing transient activation of these kinases (**Figure 5C**). The effects evoked by A_{2B}AR stimulation were almost completely reversed by the A_{2B}AR inverse agonist MRS1706, demonstrating the specific involvement of the A_{2B}AR subtype. As expected, TGF-β1 did not produce a significant increase in the cAMP levels (**Figure 5A**); conversely, it was able to significantly increase ERK1/2 phosphorylation (341.7 ± 16.2% vs. CTRL, $P \leq 0.001$; **Figure 5B**). Both BAY and TGF-β1 induced transient activation of ERK1/2 but with different kinetics; whereas ERK phosphorylation induced by BAY peaked within 30 min and then returned to the basal value within 6 h, TGF-β1 caused a more sustained ERK activation up to 48 h of cell treatment (48 h, 155.2 ± 7.8%, TGF-β1; 85.3 ± 8.8%, BAY; $P \leq 0.05$; **Figure 5C**). These data highlighted a difference in the final reorganization of the intracellular pathways activated by the cytokine and the receptor.

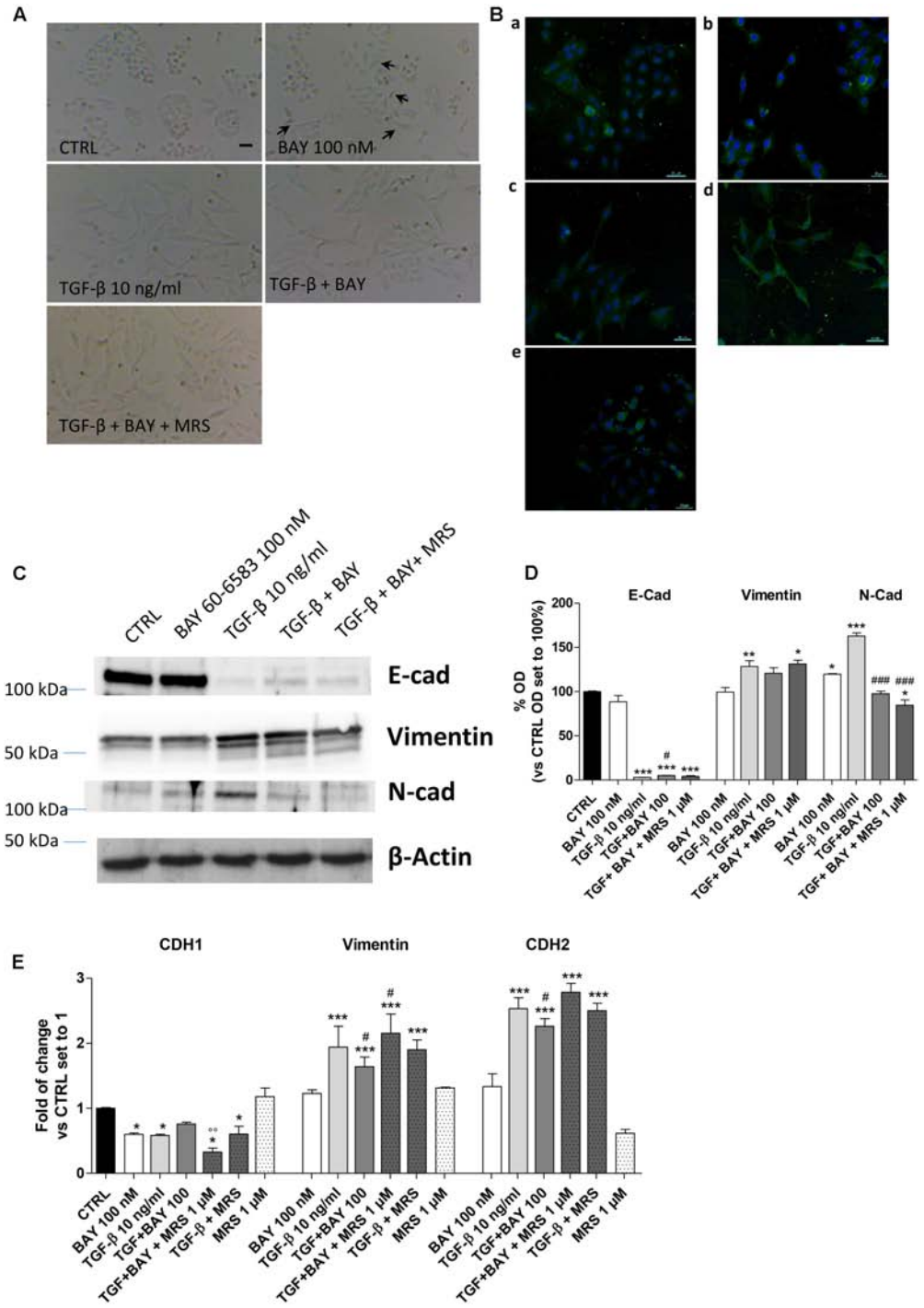

FIGURE 3 | A_{2B}AR stimulation affects EMT markers and decreases TGF-β1-induced EMT. A549 cells were treated with BAY 60-6583 (100 nM) in the absence or presence of TGF-β1 (10 ng/ml) for 48 h. When indicated, the A_{2B}AR inverse agonist, MRS 1706 (1 μM), was applied. **(A)** At the end of the incubation times, representative images were taken. Scale bar = 100 μm. **(B)** Cells treated as above were fixed and stained with anti-β actin and visualized with goat anti-mouse AlexaFluo 488 (green). Nuclei were counterstained with DAPI (blue). **(C,D)** A549 cells were treated as described above, and the levels of the EMT markers E-cad, Vimentin and N-cad were evaluated by Western blotting. One representative Western Blot is presented **(C)**. The bar graph **(D)** shows the densitometric analysis of the Western blot performed using the ImageJ program. The data are presented as the means of three different experiments. **(E)** Real-time RT-PCR analysis of the same EMT markers were performed. The data were expressed as the fold change vs. the CTRL levels, which were set to 1 and are the mean values ± SEM of three different experiments each performed in duplicate. The significance of the differences was determined by one-way ANOVA, followed by Dunnett's *post hoc* test or two-way ANOVA with Bonferroni correction and two-sided tests for multiple comparisons. $^{*}P \leq 0.05$, $^{**}P \leq 0.01$, $^{***}P \leq 0.001$ vs. the CTRL; $^{\#}P \leq 0.05$, $^{\#\#\#}P \leq 0.001$ vs. TGF-β1 alone; $^{\circ\circ}P \leq 0.01$ vs. TGF-β1 + BAY.

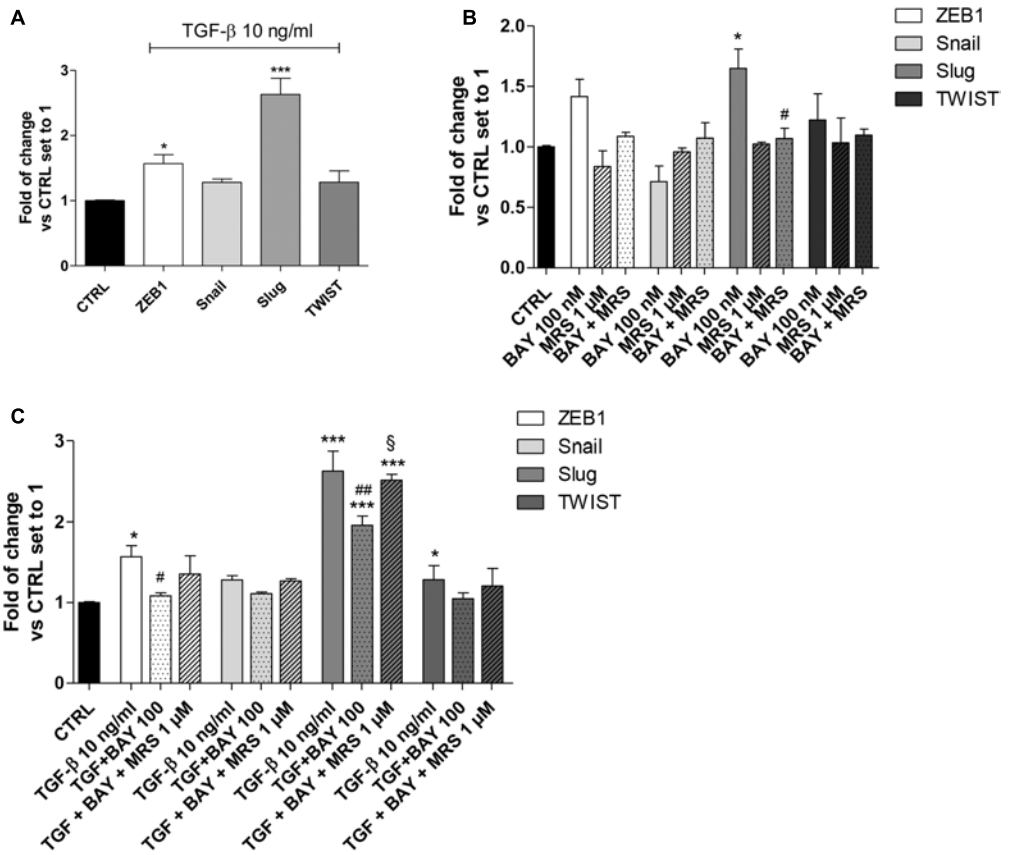

FIGURE 4 | A_{2B}AR activation of EMT transcription factors. **(A)** A549 cells were treated with TGF-β1 (10 ng/ml) for 48 h. At the end of the incubation, real-time RT-PCR analysis of the transcription factors that act as master regulators of EMT (ZEB1, Snail, Slug, TWIST) was performed. **(B,C)** A549 cells were treated with BAY 60-6583 (100 nM) in the absence or presence of TGF-β1 (10 ng/ml) for 48 h. When indicated, the A_{2B}AR inverse agonist MRS 1706 (1 μM) was applied. At the end of the incubation, real-time RT-PCR analysis of the transcription factors that act as master regulators of EMT (ZEB1, Snail, Slug, TWIST) was performed. The data were expressed as the fold change vs. the CTRL levels, which were set to 1 and are the mean values ± SEM of three different experiments, each performed in duplicate. The significance of the differences was determined by one-way ANOVA, followed by Bonferroni's *post hoc* test or two-way ANOVA with Bonferroni correction and two-sided tests for multiple comparisons. $^{*}P \leq 0.05$, $^{***}P \leq 0.001$ vs. the CTRL; $^{\#}P \leq 0.05$, $^{\#\#}P \leq 0.01$ vs. TGF-β1 alone; $^{\S}P \leq 0.05$ vs. the TGF-β1 + BAY.

When A_{2B}AR was activated in the presence of TGF-β1, the receptor activation produced a significant increase in the intracellular cAMP concentration (56.4 ± 1.9 nM, CTRL; 96.6 ± 5.3 nM, TGF-β1 + BAY $P \leq 0.01$; **Figure 5A**). This effect was in accordance with the slight increase in A_{2B}AR functionality that was noticed in the presence of the cytokine (**Figure 2D**). Regarding pERK1/2, the co-treatment led to a modest decrease in phosphorylation. The BAY activities on cAMP and pERK1/2 were most completely counteracted by cell pre-incubation with the A_{2B}AR inverse agonist MRS1706. Finally, TGF-β1 and BAY did not affect the amount of total ERK (Supplementary Figure 2).

To elucidate if the different activation of cAMP and ERK pathway in the presence of the cytokine, could be related to A_{2B}AR desensitization, the functionality of the receptor was evaluated after 48 h of cell treatment in the absence or presence of BAY and TGF-β1 alone or in combination (**Figure 5D**). In the basal condition (48 h without treatment), A_{2B}AR maintained its functional response. The cell treatment with BAY (100 nM) for 48 h induced the desensitization of the A_{2B} receptor (219.9 ± 7.7% in Basal condition; 113.3 ± 13.6% in BAY pre-treated cells; $P \leq 0.001$). Cytokine alone was not able to significantly interfere on the receptor desensitization. Interestingly, when cells were treated with BAY in the presence of TGF-β1 for 48 h, the desensitization of the receptor was partially impaired (164.2 ± 8.7%; $P \leq 0.01$).

cAMP/PKA Regulation of EMT Markers in Human Epithelial Cells

The role of the cAMP pathway in EMT is controversial, depending on the cell type, the nature of the EMT inducers and maximum levels of the intracellular cAMP obtained (Weng et al., 2015). Thus, the effects of different levels of cAMP on EMT markers in our cellular model were investigated using the cAMP analog Br-cAMP (8-bromoadenosine 3′,5′-cyclic monophosphate) as the PKA activator (**Figure 6**). Br-cAMP (100 nm–1 μM) induced a concentration-dependent increase in the intracellular cAMP levels (**Figure 6A**). Surprisingly, different

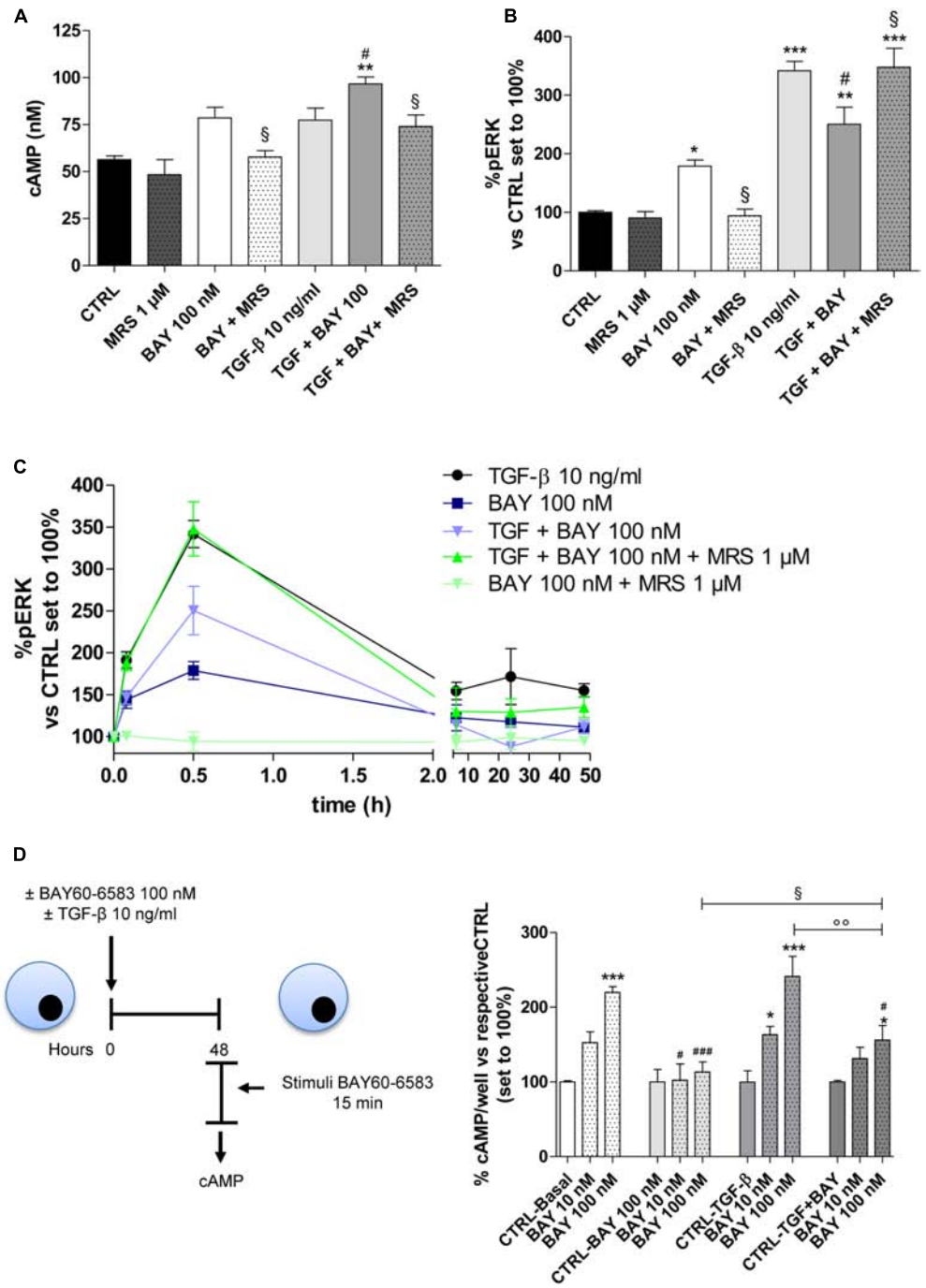

FIGURE 5 | Effects of BAY 60-6583 and TGF-β1 on cAMP accumulation and ERK 1/2 phosphorylation. **(A)** A549 cells were treated with BAY 60-6583 (100 nM) in the absence or presence of TGF-β1 (10 ng/ml) for 48 h. When indicated, the A_{2B}AR inverse agonist, MRS 1706 (1 μM), was applied. At the end of the treatment, the cAMP production was quantified. The data were expressed as cAMP concentrations and were presented as mean values ± SEM of three independent experiments, each performed in duplicate. **(B,C)** Cells treated as above for different time (30 min-48 h), were fixed, and ERK 1/2 phosphorylation was measured by immunoenzymatic assay. **(B)** ERK 1/2 phosphorylation after 30 min of treatment. **(C)** Time-course of ERK 1/2 phosphorylation in A549 cells. The data were expressed as the percentage versus untreated cells (CTRL) set to 100% ± SEM of at least three different experiments performed in duplicate. $^{*}P \leq 0.05$, $^{**}P \leq 0.01$, $^{***}P \leq 0.001$ vs. the CTRL; $^{\#}P \leq 0.05$ vs. TGF-β1 alone; $^{\S}P \leq 0.05$ vs. the TGF-β1 + BAY. **(D)** Cells were treated with BAY 60-6583 (100 nM) in the absence or presence of TGF-β1 (10 ng/ml) for 48 h. After extensive washing, cells were treated for 15 min with different concentrations of BAY60-6583. Next, intracellular cAMP levels were evaluated. The data were expressed as the percentage versus untreated cells (CTRL-Basal) set to 100% ± SEM of at least three different experiments performed in duplicate. $^{*}P \leq 0.05$, $^{***}P \leq 0.001$ vs. the CTRL-Basal; $^{\#}P \leq 0.05$, $^{\#\#\#}P \leq 0.001$ vs. respective basal condition. The significance of the differences was determined by one-way ANOVA, followed by Dunnett's *post hoc* test or two-way ANOVA with Bonferroni correction and two-sided tests for multiple comparisons.

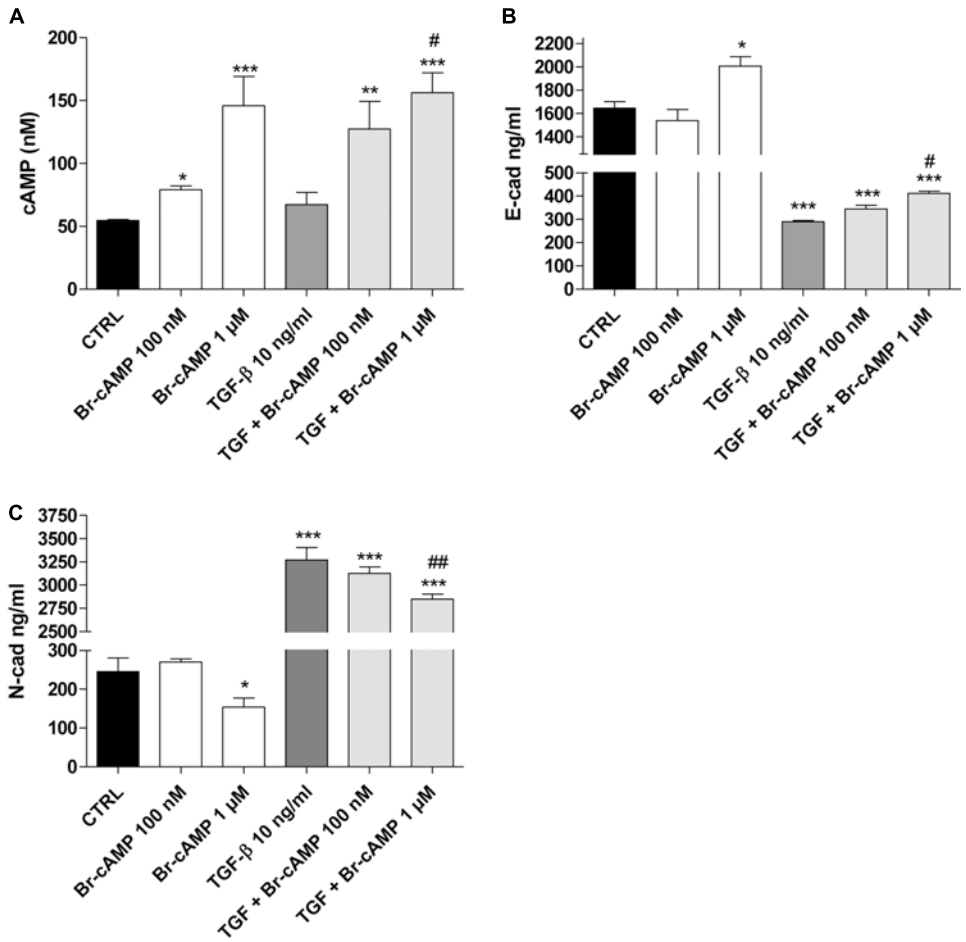

FIGURE 6 | Effect of the cAMP pathway on E-cadherin and N-cadherin expression. A549 cells were treated with Br-cAMP (100 nm–1 μM) in the absence or presence of TGF-β1 (10 ng/ml) for 48 h. **(A)** At the end of the treatment, cAMP production was quantified. The data were expressed as cAMP concentrations and are presented as mean values ± SEM of three independent experiments, each performed in duplicate. Cells treated as above were lysed, and the expression of E-cadherin **(B)** or N-cadherin **(C)** was quantified using AlphaLISA kits. The data were expressed as E-cadherin and N-cadherin concentrations (ng/ml) and are presented as mean values ± SEM of three independent experiments, each performed in duplicate. The significance of the differences was determined by two-way ANOVA with Bonferroni correction and two-sided tests for multiple comparisons. $^{*}P \leq 0.05$, $^{**}P \leq 0.01$, $^{***}P \leq 0.001$ vs. the CTRL; $^{\#}P \leq 0.05$, $^{\#\#}P \leq 0.01$, vs. TGF-β1 alone.

concentrations of the activator caused opposite effects on E-cad (**Figure 6B**) and N-cad (**Figure 6C**) expression. A high Br-cAMP concentration increased E-cad and decreased N-cad expression. A low Br-cAMP concentration (100 nM) was sufficient to determine a modest decrease of E-cad (1646 ± 56 ng/ml, CTRL; 1540 ± 93 ng/ml, Br-cAMP; **Figure 6B**) and an increase of N-cad (246 ± 35 ng/ml, CTRL; 270 ± 8 ng/ml, Br-cAMP; **Figure 6C**) even if these variations were not statistically significant. When TGF-β1 and BAY were used simultaneously, the activator produced higher cAMP levels and a concentration-dependent increase in E-cad and decrease in N-cad.

These data demonstrate that, in our cellular model, when the cAMP was increased up to high concentrations, it could negatively affect the EMT process. Conversely, when cAMP levels remained low, it seems to mediate the opposite effects, promoting a slight decrease in epithelial markers and an increase in the mesenchymal markers. This controversial nature of the cAMP analogue on the EMT process is in accordance with the recent data reported by Zuccarini et al. (2017).

The cAMP/PKA-MAPK/ERK Balance in the A_{2B}AR Modulation of EMT Markers and EMT-TFs

Nevertheless, high levels of cAMP counteract EMT, and ERK phosphorylation mediated by MAPK activation has been demonstrated to promote EMT (Singh et al., 2017). Thus, the ability of A_{2B}AR to modify the amounts of both pERK and of cAMP could be a possible mechanism by which the receptor agonist affects epithelial/mesenchymal markers. In this respect, the involvement of A_{2B}AR in the regulation of EMT markers and transcription factors was investigated in the presence of PKA inhibitor (H89, 100 nM) and a mitogen-activated protein kinase inhibitor (PD98059, 1 μM) (**Figure 7**, Supplementary

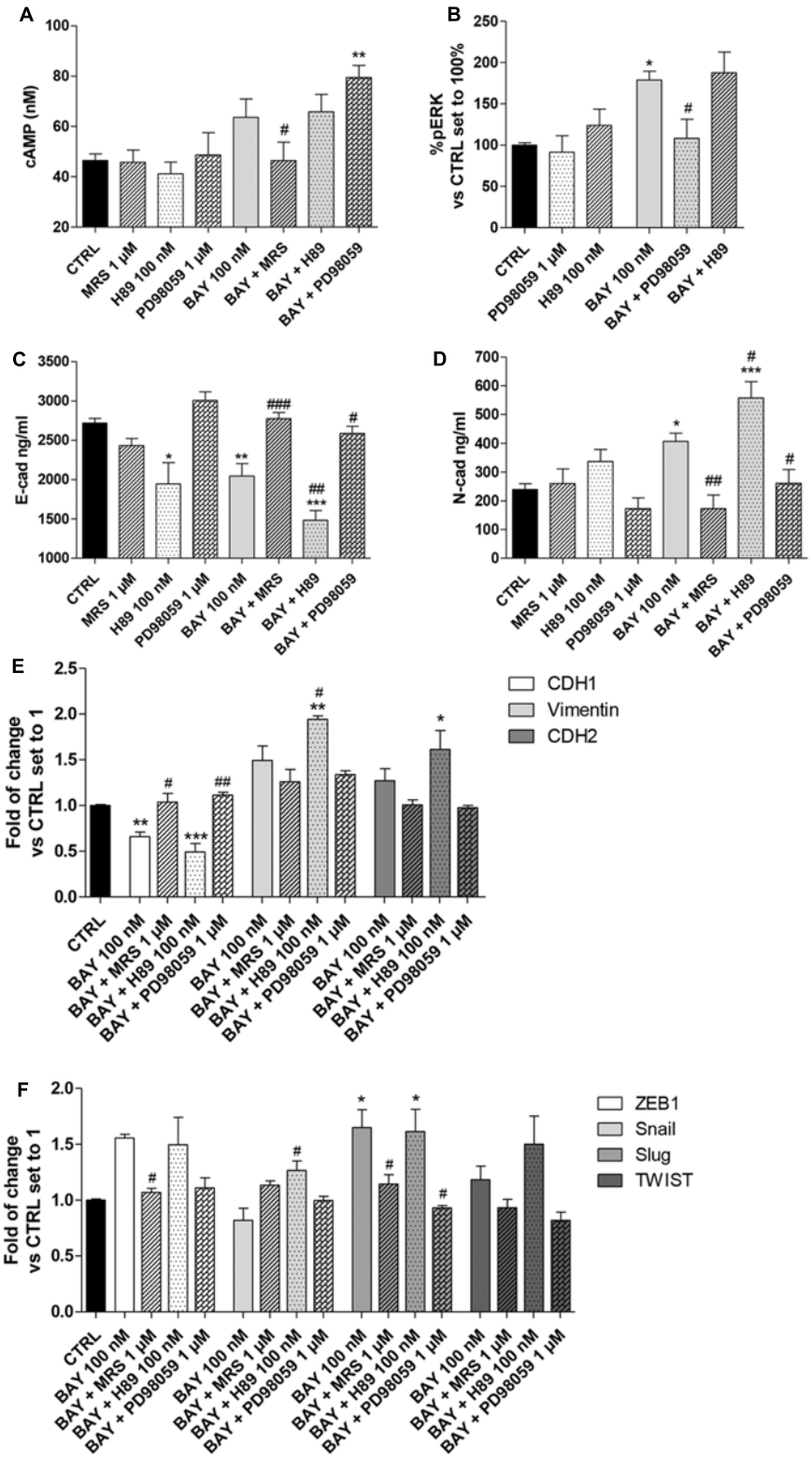

FIGURE 7 | Effect of cAMP and ERK1/2 phosphorylation blockade on A_{2B}AR-mediated changes in EMT markers. A549 cells were treated with BAY 60-6583 (100 nM) in the absence or presence of MRS 1706 (1 μM), PKA inhibitor H89 (100 nM) or MEK1/2 inhibitor PD98059 (1 μM) for 48 h. When indicated, the antagonist and inhibitor were applied 30 min before treatment with BAY 60-6583. **(A)** At the end of the treatment, cAMP production was quantified. The data were expressed as cAMP concentrations and are the mean values ± SEM of three independent experiments, each performed in duplicate. **(B)** Cells were treated as above

(Continued)

FIGURE 7 | Continued
and ERK 1/2 phosphorylation was evaluated after 30 min of treatment. The data were expressed as the percentage versus untreated cells (CTRL) set to 100% ± SEM of at least three different experiments performed in duplicate. Cells treated as above were lysed, and the expression of E-cadherin **(C)** or N-cadherin **(D)** were quantified using AlphaLISA kits. The data were expressed as E-cadherin and N-cadherin concentrations (ng/ml) and are the mean values ± SEM of three independent experiments, each performed in duplicate. The significance of the differences was determined by one-way ANOVA, followed by Dunnett's *post hoc* test or two-way ANOVA with Bonferroni correction and two-sided tests for multiple comparisons. $^{*}P \leq 0.05$, $^{**}P \leq 0.01$, $^{***}P \leq 0.001$ vs. the CTRL; $^{\#}P \leq 0.05$, $^{\#\#}P \leq 0.01$, $^{\#\#\#}P \leq 0.001$ vs. BAY alone. **(E,F)** Cells were treated as above and real-time RT-PCR analysis of EMT markers (E-cad, N-cad and Vimentin) **(E)**, and EMT transcription factors (ZEB1, Snail, Slug, TWIST) **(F)** was performed. The data were expressed as the fold change vs. the CTRL levels, which were set to 1 and are the mean values ± SEM of three different experiments each performed in duplicate. The significance of the differences was determined by one-way ANOVA, followed by Dunnett's *post hoc* test or two-way ANOVA with Bonferroni correction and two-sided tests for multiple comparisons. $^{*}P \leq 0.05$, $^{**}P \leq 0.01$, $^{***}P \leq 0.001$ vs. the CTRL; $^{\#}P \leq 0.05$, $^{\#\#}P \leq 0.01$ vs. BAY alone.

Figure 3). The BAY-mediated increase in the intracellular cAMP levels was not affected by H89 treatment (**Figure 7A**); conversely, PD98059 was able to block BAY-mediated ERK phosphorylation (**Figure 7B**). In this respect, the inhibitors were used to unveil the involvement of the two signaling pathways in A_{2B}AR mediated triggering of EMT.

BAY decreased the protein density of E-cad and increased that of the N-cad one; these effects were lost in the presence of the inverse agonist MRS 1706, in accordance with the abovementioned data (**Figure 3**). The ability of BAY to decrease the expression of E-cad was augmented by pretreatment with the PKA inhibitor (2718 ± 58 ng/ml, CTRL; 2045 ± 157 ng/ml, BAY; $P \leq 0.01$; 1483 ± 122 ng/ml, BAY + H89; $P \leq 0.001$ vs. CTRL, $P \leq 0.01$ vs BAY, **Figure 7C**). Similarly, A_{2B}AR mediated increase in N-cad was enhanced when the cAMP/PKA axis was abrogated (239 ± 20 ng/ml, CTRL; 406 ± 29 ng/ml, BAY; $P \leq 0.05$; 558 ± 72 ng/ml, BAY + H89; $P \leq 0.001$ vs. CTRL, $P \leq 0.05$ vs BAY; **Figure 7D**). These effects highlighted that cAMP, through PKA activation, could partially antagonize A_{2B}AR-mediated EMT induction. When the MEK inhibitor was used, the changes induced by A_{2B}AR stimulation were almost completely counteracted, restoring the basal conditions (E-cad, 2586 ± 90 ng/ml, BAY + PD98059; $P \leq 0.05$ vs BAY; N-cad, 260 ± 49 ng/ml, BAY + PD89059; $P \leq 0.05$ vs BAY, **Figures 7C,D**). These results are in accordance with the effects of the inhibitor treatments on A_{2B}AR-mediated alteration of the expression of CDH1, CDH2 and vimentin genes (**Figure 7E**).

Finally, the modulation of the EMT-TF gene expression by BAY was evaluated in the presence of H89 and PD98059. Similarly, regarding the EMT markers, the PKA inhibitor slightly exacerbated the A_{2B}AR-mediated effects; conversely, the MEK inhibitor counteracted the BAY-mediated increase in gene expression. The PD98059 activity was more pronounced on Slug expression, causing a significant decrease of gene expression (1.65 ± 0.16-fold, BAY; 1.61 ± 0.20-fold, BAY + H89; 0.93 ± 0.09-fold vs. CTRL, BAY + PD98059; $P \leq 0.05$). These data are consistent with the reported role of ERK phosphorylation in the induction of Slug expression (Choi et al., 2007; Joannes et al., 2014).

DISCUSSION

Adenosine receptors (ARs) have attracted great attention as possible targets to control the EMT process in pathologies such as fibrosis and cancer (Lu and Insel, 2014). However, among the AR subtypes, no data have been reported that correlate A_{2B}AR activation with EMT in epithelial cells. In this respect, herein, we report for the first time the ability of A_{2B}AR activation to promote EMT or contrast the effects of the extracellular inducer, TGF-β1, in human lung epithelial cells. Furthermore, the ability of the receptor activation to modulate two signaling pathways involved in EMT, cAMP/PKA, and MAPK/ERK, was demonstrated as a possible mechanism explaining the different effects mediated by A_{2B}AR stimulation in different extracellular microenvironment (**Figure 8**).

Human carcinoma epithelial lung cells (A549) were maintained under serum deprivation, a condition that has been demonstrated to amplify the epithelial phenotype (Dong et al., 2014). Although all the ARs are expressed in epithelial lung cells, the A_{2B} receptor subtype was demonstrated to be the most represented, as previously reported (Roman et al., 2006). Challenging these cells with TGF-β1 produced a marked change in the phenotype through the simultaneous decrease in epithelial markers (E-cad) and increase in mesenchymal markers (N-cad). In accordance with the literature (Kawata et al., 2012), these data demonstrated the suitability of the model to study the A_{2B}AR involvement in the EMT process.

A_{2B}AR stimulation modified the expression of epithelial/mesenchymal markers with a low but significant amplitude. Surprisingly, the same receptor could counteract the EMT induction mediated by TGF-β1. These opposite effects elicited by A_{2B}AR stimulation in lung cells reflect the well documented debated role of this receptor in the onset and progression of different pathologies. The receptor activation has been reported to protect the lungs and other tissues from inflammation and acute injury (Eckle et al., 2008; Davies et al., 2014; Hoegl et al., 2015). By contrast, other evidence has been reported concerning the A_{2B}AR-mediated pro-fibrotic effects and promotion of cancer development (Karmouty-Quintana et al., 2012; Huerter et al., 2016; Sepúlveda et al., 2016). Furthermore, Zhou et al. (2011) have shown that A_{2B}AR genetic removal slightly affects acute lung injury but reduces lung fibrosis, supporting a pro-fibrotic role for this receptor.

In our study, the A_{2B}AR selective agonist regulated the gene transcription of different EMT-transcription factors (EMT-TFs). EMT is a complex process regulated by the orchestration of several transcription factors. Among these EMT-TFs, ZEB1, Snail and Slug (SNAI2) are the major transcription factors involved in the promotion of the EMT process in A549 cells,

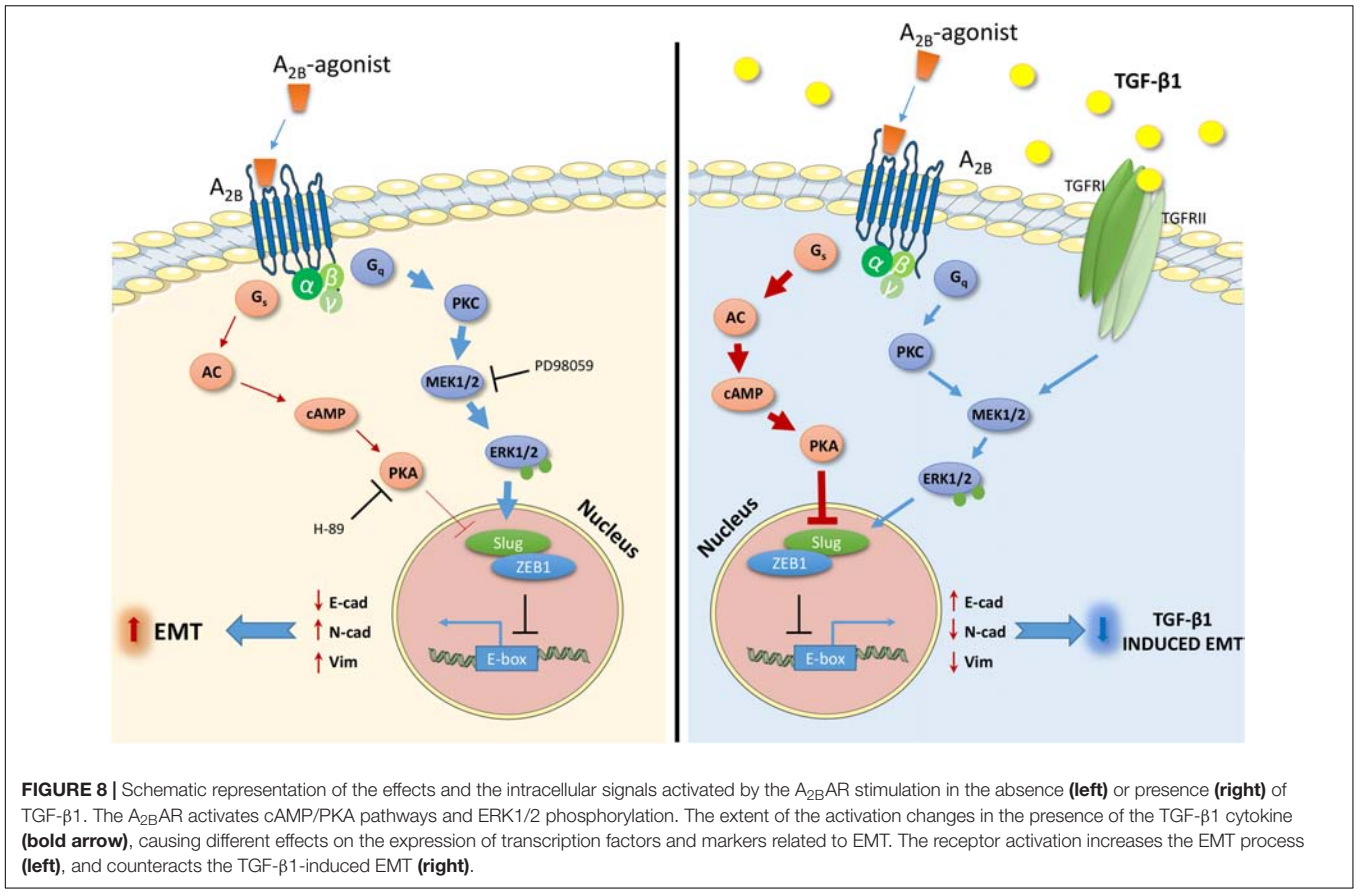

FIGURE 8 | Schematic representation of the effects and the intracellular signals activated by the A_{2B}AR stimulation in the absence **(left)** or presence **(right)** of TGF-β1. The A_{2B}AR activates cAMP/PKA pathways and ERK1/2 phosphorylation. The extent of the activation changes in the presence of the TGF-β1 cytokine **(bold arrow)**, causing different effects on the expression of transcription factors and markers related to EMT. The receptor activation increases the EMT process **(left)**, and counteracts the TGF-β1-induced EMT **(right)**.

as previously reported (Ji et al., 2016). A_{2B}AR stimulation did not affect significantly the expression of Snail and TWIST, other master genes of EMT. However, A_{2B}AR activation modulate the expression of Slug and, to a lesser extent, that of ZEB1, which are commonly considered the major actors in myofibroblast differentiation and fibrogenesis (Lamouille et al., 2014). Furthermore, Slug expression has been correlated to direct repression of E-cadherin expression (Choi et al., 2007). This evidence was in accordance with the increase in E-cadherin induced by A_{2B}AR stimulation.

The EMT-TFs are regulated by the activation of different intracellular pathways, which in turn regulate the balance between the epithelial and mesenchymal markers. ERK1/2, GSK3β, p38, STAT3, and cAMP are only few of all the proteins involved in the promotion/inhibition of EMT (Nieto et al., 2016). In our cellular model, activation of the cAMP/PKA axis promoted opposite effects depending on the levels of intracellular the cAMP. Low concentrations led to a slight promotion or no effects on epithelial/mesenchymal markers; conversely, high levels of cAMP could counteract EMT progression. In accordance with our results, it has been reported that cAMP/PKA activation could exert opposite effects on EMT (Zhang et al., 2006a,b; Nadella et al., 2008; Shaikh et al., 2012; Lambers et al., 2015) that could be ascribed to the different cell models, type of EMT inducer and maximum levels of intracellular cAMP obtained (Weng et al., 2015).

A_{2B}AR activation increases the intracellular cAMP levels and promotes the phosphorylation of ERK 1/2 (Grant et al., 2001; Zhou et al., 2017). In this respect, we hypothesize that the controversial role of A_{2B}AR in promoting EMT or reversing TGF-β1-induced EMT could be ascribed to the different balance of the intracellular pathways activated. The activation of other GPCRs coupled to different G proteins has been reported to elicit opposite effects on EMT. Zhang et al. (2016) have demonstrated that norepinephrine, which activates G_s protein, induces the epithelial-mesenchymal transition in A549 cells; similarly, the P2X7 stimulation, which activates the PI3K/Akt and ERK1/2 signaling pathways, promotes the mesenchymal phenotype in epithelial renal cells (Zuccarini et al., 2017). A_{2A}ARs have been reported to modify the epithelial/mesenchymal phenotype in renal cells by downregulating TGF-β1-induced EMT (Zuccarini et al., 2017) in accordance with the effects elicited by A_{2B}AR activation in our cellular model when the cytokine was present. TGF-β1 activates both Smad signaling and non-Smad signaling including the ERK pathway, critically regulating EMT (Xie et al., 2004). A_{2B}AR stimulation could counteract cytokine-induced EMT, reducing the transition progression. These effects were correlated with a robust increase in cAMP production and with a concomitant decrease in ERK phosphorylation. In this respect, we could speculate that the increase in the cAMP, mediated by A_{2B}AR activation, could counteract the cytokine-mediated effects on EMT. This is in accordance with the ability of other

G_s coupled receptors (i.e., A_{2A}AR) or cAMP inducers (i.e., forskolin, 8-Br-cAMP) to prevent TGF-β1-mediated EMT (Zhang et al., 2006a,b; Zuccarini et al., 2017). It should also be considered that cAMP/PKA has a negative effect on TGF-β induced pERK 1/2, but only when the cytokine downstream pathways are highly expressed (Weng et al., 2015). This mechanism could explain the reduction in ERK1/2 phosphorylation in the presence of the A_{2B}AR agonist.

The modulation of cAMP production and ERK phosphorylation could be affected by internalization or desensitization processes of the receptor. Several GPCRs employ a variety of signaling mechanisms to exert their functions. The production of second messengers, such as cAMP, is the results of the receptor-G protein coupling. However, other signals produced in conjunction with, or even independent of heterotrimeric G protein could be activated. It is well known that the arrestins, a family of four GPCR-binding proteins originally described for their role in the GPCR desensitization, have been found to interact with Src family kinases and to serve as scaffolds for activation of ERK1/2 and c-Jun N-terminal kinase 3 mitogen-activated protein kinases (Ferguson, 2001; Luttrell, 2005; Lee et al., 2008). Thus, the desensitization could represent a mechanism to maintain the activation of G-protein independent pathways. The activation of the A_{2B}AR for long time produced the desensitization of the receptor. This may be another mechanism through which A_{2B}AR mediate the ERK phosphorylation favoring the EMT traits. Conversely, the TGF-β1 was able to reduce the agonist-induced A_{2B}AR desensitization, maintaining the ability of A_{2B}AR to produce cAMP that negatively affected EMT process. These data could better highlight the controversial role of A_{2B}AR in the EMT. In different pathological status in which adenosine raise to micromolar concentration, the extracellular microenvironment and the localization of the receptor could interfere with the levels of the activated intracellular signaling shifting the balance in favor of or against the EMT.

In our cellular model, A_{2B}AR activation was able to induce partial EMT; however, it was not sufficient to promote a complete epithelial-mesenchymal transformation of the lung cells. The involvement of the cAMP/PKA and MAPK/ERK signaling pathways was demonstrated by the use of selective inhibitors. The EMT traits, in the presence of A_{2B}AR agonist was enhanced by PKA inhibition and decreased by the ERK1/2 phosphorylation blockade. Furthermore, the pretreatment with a PKA inhibitor did not enhance receptor effects on TF expression. Conversely, the presence of the MEK inhibitor completely counteracted the A_{2B}-mediated increase in Slug and ZEB1 gene expression, demonstrating the involvement of MAPK/ERK pathway activation in A_{2B}AR-mediated EMT induction.

CONCLUSION

For the first time, these results highlight the possibility that A_{2B}AR is one of the numerous receptors that could be involved in EMT regulation. Although the expression of the other adenosine receptor subtypes are low, in physiological condition the involvement of all the AR in the EMT regulation could not be excluded. A_{2B}AR activation is not enough to trigger a complete transition; it can affect the expression of the epithelial and mesenchymal markers promoting EMT traits. These effects are related to the ability of A_{2B}AR to modify the balance between cAMP/PKA and MAPK/ERK activation. The presence of extracellular cytokines that activate the transition could change the balance and levels of these two intracellular pathways, shifting the effects exerted by the receptor stimulation on EMT trigger and maintenance. Thus, the A_{2B}AR seems to act as an EMT regulator rather than a main actor in the EMT induction. Although the EMT is a complex machinery and further investigation are needed to better elucidate the effects of adenosine and the contribution of the other AR subtypes in physiopathological conditions, herein, for the first time, the A_{2B}AR was shown to be related to the EMT process, highlighting its potential role as pharmacological target in EMT-related pathologies.

AUTHOR CONTRIBUTIONS

CG designed and performed the biological experiments. CG, SD, and MT. analyzed the data and wrote the manuscript. IP performed the immunofluorescence analysis. CR, LT, and TN contributed to the experimental work. MT, AC, and CM designed the study and played a key role as project supervisor. MT and CM coordinated the project. All the authors contributed to and approved the final manuscript.

FUNDING

This work was financially supported by the Italian Ministry of Education (Project of National Research Interest PRIN 2015, 2015E8EMCM_007).

SUPPLEMENTARY MATERIAL

The Supplementary Material for this article can be found online at: https://www.frontiersin.org/articles/10.3389/fphar.2018.00054/full#supplementary-material

REFERENCES

Boucher, M. J., Laprise, P., and Rivard, N. (2005). Cyclic AMP-dependent protein kinase A negatively modulates adherens junction integrity and differentiation of intestinal epithelial cells. *J. Cell. Physiol.* 202, 178–190. doi: 10.1002/jcp.20104

Choi, J., Park, S. Y., and Joo, C. K. (2007). Transforming growth factor-beta1 represses E-cadherin production via slug expression in lens epithelial cells. *Invest. Ophthalmol. Vis. Sci.* 48, 2708–2718. doi: 10.1167/iovs.06-0639

Da Pozzo, E., La Pietra, V., Cosimelli, B., Da Settimo, F., Giacomelli, C., Marinelli, L., et al. (2014). p53 functional inhibitors behaving like pifithrin-β counteract the Alzheimer peptide non-β-amyloid component effects in human SH-SY5Y cells. *ACS Chem. Neurosci.* 5, 390–399. doi: 10.1021/cn4002208

Daniele, S., Natali, L., Giacomelli, C., Campiglia, P., Novellino, E., Martini, C., et al. (2017). Osteogenesis is improved by low tumor necrosis factor alpha concentration through the modulation of Gs-coupled receptor signals. *Mol. Cell. Biol.* 37:e00442-16. doi: 10.1128/MCB.00442-16

Davies, J., Karmouty-Quintana, H., Le, T. T., Chen, N. Y., Weng, T., Luo, F., et al. (2014). Adenosine promotes vascular barrier function in hyperoxic lung injury. *Physiol. Rep.* 2:e12155. doi: 10.14814/phy2.12155

De Maio, L., Buckley, S. T., Krishnaveni, M. S., Flodby, P., Dubourd, M., Banfalvi, A., et al. (2012). Ligand-independent transforming growth factor-β type I receptor signalling mediates type I collagen-induced epithelial-mesenchymal transition. *J. Pathol.* 226, 633–644. doi: 10.1002/path.3016

Dong, S., Khoo, A., Wei, J., Bowser, R. K., Weathington, N. M., Xiao, S., et al. (2014). Serum starvation regulates E-cadherin upregulation via activation of c-Src in non-small-cell lung cancer A549 cells. *Am. J. Physiol. Cell Physiol.* 307, C893–C899. doi: 10.1152/ajpcell.00132.2014

Eckle, T., Grenz, A., Laucher, S., and Eltzschig, H. K. (2008). A2B adenosine receptor signaling attenuates acute lung injury by enhancing alveolar fluid clearance in mice. *J. Clin. Invest.* 118, 3301–3315. doi: 10.1172/JCI34203

Fang, Y., and Olah, M. E. (2007). Cyclic AMP-dependent, protein kinase A-independent activation of extracellular signal-regulated kinase 1/2 following adenosine receptor stimulation in human umbilical vein endothelial cells: role of exchange protein activated by cAMP 1 (Epac1). *J. Pharmacol. Exp. Ther.* 322, 1189–1200. doi: 10.1124/jpet.107.119933

Feoktistov, I., Goldstein, A. E., and Biaggioni, I. (1999). Role of p38 mitogen-activated protein kinase and extracellular signal-regulated protein kinase kinase in adenosine A2B receptor-mediated interleukin-8 production in human mast cells. *Mol. Pharmacol.* 55, 726–734.

Ferguson, S. S. (2001). Evolving concepts in G protein-coupled receptor endocytosis: the role in receptor desensitization and signaling. *Pharmacol. Rev.* 53, 1–24.

Gao, Z. W., Wang, H. P., Dong, K., Lin, F., Wang, X., and Zhang, H. Z. (2016). Adenosine inhibits migration, invasion and induces apoptosis of human cervical cancer cells. *Neoplasma* 63, 201–207. doi: 10.4149/204_150723N407

Giacomelli, C., Trincavelli, M. L., Satriano, C., Hansson, Ö, La Mendola, D., Rizzarelli, E., et al. (2015). ♦Copper (II) ions modulate Angiogenin activity in human endothelial cells. *Int. J. Biochem. Cell Biol.* 60, 185–196. doi: 10.1016/j.biocel.2015.01.005

Grant, M. B., Davis, M. I., Caballero, S., Feoktistov, I., Biaggioni, I., and Belardinelli, L. (2001). Proliferation, migration, and ERK activation in human retinal endothelial cells through A(2B) adenosine receptor stimulation. *Invest. Ophthalmol. Vis. Sci.* 42, 2068–2073.

Gui, T., Sun, Y., Shimokado, A., and Muragaki, Y. (2012). The roles of mitogen-activated protein kinase pathways in TGF-β-induced epithelial-mesenchymal transition. *J. Signal Transduct.* 2012:289243. doi: 10.1155/2012/289243

Guillén-Gómez, E., Pinilla-Macua, I., Pérez-Torras, S., Choi, D. S., Arce, Y., Ballarín, J. A., et al. (2012). New role of the human equilibrative nucleoside transporter 1 (hENT1) in epithelial-to-mesenchymal transition in renal tubular cells. *J. Cell Physiol.* 227, 1521–1528. doi: 10.1002/jcp.22869

Hoegl, S., Brodsky, K. S., Blackburn, M. R., Karmouty-Quintana, H., Zwissler, B., and Eltzschig, H. K. (2015). Alveolar epithelial A2B adenosine receptors in pulmonary protection during acute lung injury. *J. Immunol.* 195, 1815–1824. doi: 10.4049/jimmunol.1401957

Huerter, M. E., Sharma, A. K., Zhao, Y., Charles, E. J., Kron, I. L., and Laubach, V. E. (2016). Attenuation of pulmonary ischemia-reperfusion injury by adenosine A2B receptor antagonism. *Ann. Thorac. Surg.* 102, 385–393. doi: 10.1016/j.athoracsur.2016.02.060

Ji, Y., Dou, Y. N., Zhao, Q. W., Zhang, J. Z., Yang, Y., Wang, T., et al. (2016). Paeoniflorin suppresses TGF-β mediated epithelial-mesenchymal transition in pulmonary fibrosis through a Smad-dependent pathway. *Acta Pharmacol. Sin.* 37, 794–804. doi: 10.1038/aps.2016.36

Joannes, A., Grelet, S., Duca, L., Gilles, C., Kileztky, C., Dalstein, V., et al. (2014). Fhit regulates EMT targets through an EGFR/Src/ERK/Slug signaling axis in human bronchial cells. *Mol. Cancer Res.* 12, 775–783. doi: 10.1158/1541-7786.MCR-13-0386-T

Jolly, M. K., Ward, C., Eapen, M. S., Myers, S., Hallgren, O., Levine, H., et al. (2017). Epithelial-mesenchymal transition, a spectrum of states: role in lung development, homeostasis, and disease. *Dev. Dyn.* doi: 10.1002/dvdy.24541 [Epub ahead of print].

Jonsdottir, H. R., Arason, A. J., Palsson, R., Franzdottir, S. R., Gudbjartsson, T., Isaksson, H. J., et al. (2015). Basal cells of the human airways acquire mesenchymal traits in idiopathic pulmonary fibrosis and in culture. *Lab. Invest.* 95, 1418–1428. doi: 10.1038/labinvest.2015.114

Karmouty-Quintana, H., Weng, T., Garcia-Morales, L. J., Chen, N. Y., Pedroza, M., Zhong, H., et al. (2013). Adenosine A2B receptor and hyaluronan modulate pulmonary hypertension associated with chronic obstructive pulmonary disease. *Am. J. Respir. Cell Mol. Biol.* 49, 1038–1047. doi: 10.1165/rcmb.2013-0089OC

Karmouty-Quintana, H., Zhong, H., Acero, L., Weng, T., Melicoff, E., West, J. D., et al. (2012). The A2B adenosine receptor modulates pulmonary hypertension associated with interstitial lung disease. *FASEB J.* 26, 2546–2557. doi: 10.1096/fj.11-200907

Kawata, M., Koinuma, D., Ogami, T., Umezawa, K., Iwata, C., Watabe, T., et al. (2012). TGF-β-induced epithelial-mesenchymal transition of A549 lung adenocarcinoma cells is enhanced by pro-inflammatory cytokines derived from RAW 264.7 macrophage cells. *J. Biochem.* 151, 205–216. doi: 10.1093/jb/mvr136

Kim, J. H., Jang, Y. S., Eom, K. S., Hwang, Y. I., Kang, H. R., Jang, S. H., et al. (2007). Transforming growth factor beta1 induces epithelial-to-mesenchymal transition of A549 cells. *J. Korean Med. Sci.* 22, 898–904. doi: 10.3346/jkms.2007.22.5.898

Lambers, C., Costa, L., Ying, Q., Zhong, J., Lardinois, D., Dekan, G., et al. (2015). Aclidinium bromide combined with formoterol inhibits remodeling parameters in lung epithelial cells through cAMP. *Pharmacol. Res.* 102, 310–318. doi: 10.1016/j.phrs.2015.09.010

Lamouille, S., Xu, J., and Derynck, R. (2014). Molecular mechanisms of epithelial-mesenchymal transition. *Nat. Rev. Mol. Cell Biol.* 15, 178–196. doi: 10.1038/nrm3758

Lee, J. M., Dedhar, S., Kalluri, R., and Thompson, E. W. (2006). The epithelial-mesenchymal transition: new insights in signaling, development, and disease. *J. Cell Biol.* 172, 973–981. doi: 10.1083/jcb.200601018

Lee, M. H., El-Shewy, H. M., Luttrell, D. K., and Luttrell, L. M. (2008). Role of beta-arrestin-mediated desensitization and signaling in the control of angiotensin AT1a receptor-stimulated transcription. *J. Biol. Chem.* 283, 2088–2097. doi: 10.1074/jbc.M706892200

Legras, A., Pécuchet, N., Imbeaud, S., Pallier, K., Didelot, A., Roussel, H., et al. (2017). Epithelial-to-mesenchymal transition and MicroRNAs in lung cancer. *Cancers* 9:E101. doi: 10.3390/cancers9080101

Lu, D., and Insel, P. A. (2014). Cellular mechanisms of tissue fibrosis. 6. Purinergic signaling and response in fibroblasts and tissue fibrosis. *Am. J. Physiol. Cell Physiol.* 306, C779–C788. doi: 10.1152/ajpcell.00381.2013

Luttrell, L. M. (2005). Composition and function of g protein-coupled receptor signalsomes controlling mitogen-activated protein kinase activity. *J. Mol. Neurosci.* 26, 253–264. doi: 10.1385/JMN:26:2-3:253

Martínez-Ramírez, A. S., Díaz-Muñoz, M., Butanda-Ochoa, A., and Vázquez-Cuevas, F. G. (2017). Nucleotides and nucleoside signaling in the regulation of the epithelium to mesenchymal transition (EMT). *Purinergic Signal.* 13, 1–12. doi: 10.1007/s11302-016-9550-3

Mittal, D., Sinha, D., Barkauskas, D., Young, A., Kalimutho, M., Stannard, K., et al. (2016). Adenosine 2B receptor expression on cancer cells promotes metastasis. *Cancer Res.* 76, 4372–4382. doi: 10.1158/0008-5472.CAN-16-0544

Morbini, P., Inghilleri, S., Campo, I., Oggionni, T., Zorzetto, M., and Luisetti, M. (2011). Incomplete expression of epithelial-mesenchymal transition markers in idiopathic pulmonary fibrosis. *Pathol. Res. Pract.* 207, 559–567. doi: 10.1016/j.prp.2011.06.006

Nadella, K. S., Jones, G. N., Trimboli, A., Stratakis, C. A., Leone, G., and Kirschner, L. S. (2008). Targeted deletion of Prkar1a reveals a role for protein kinase A in mesenchymal-to-epithelial transition. *Cancer Res.* 68, 2671–2677. doi: 10.1158/0008-5472.CAN-07-6002

Nieto, M. A., Huang, R. Y., Jackson, R. A., and Thiery, J. P. (2016). EMT: 2016. *Cell* 166, 21–45. doi: 10.1016/j.cell.2016.06.028

O'Connor, J. W., and Gomez, E. W. (2014). Biomechanics of TGFβ-induced epithelial-mesenchymal transition: implications for fibrosis and cancer. *Clin. Transl. Med.* 3:23. doi: 10.1186/2001-1326-3-23

Ohta, A., and Sitkovsky, M. (2001). Role of G-protein-coupled adenosine receptors in downregulation of inflammation and protection from tissue damage. *Nature* 414, 916–920. doi: 10.1038/414916a

Pattabiraman, D. R., Bierie, B., Kober, K. I., Thiru, P., Krall, J. A., Zill, C., et al. (2016). Activation of PKA leads to mesenchymal-to-epithelial transition and loss of tumor-initiating ability. *Science* 351:aad3680. doi: 10.1126/science.aad3680

Phosri, S., Arieyawong, A., Bunrukchai, K., Parichatikanond, W., Nishimura, A., Nishida, M., et al. (2017). Stimulation of Adenosine A_{2B} receptor inhibits endothelin-1-induced cardiac fibroblast proliferation and α-smooth muscle actin synthesis through the cAMP/Epac/PI3K/Akt-signaling pathway. *Front. Pharmacol.* 8:428. doi: 10.3389/fphar.2017.00428

Roberts, V. S., Cowan, P. J., Alexander, S. I., Robson, S. C., and Dwyer, K. M. (2014). The role of adenosine receptors A2A and A2B signaling in renal fibrosis. *Kidney Int.* 86, 685–692. doi: 10.1038/ki.2014.244

Roman, J., Rivera, H. N., Roser-Page, S., Sitaraman, S. V., and Ritzenthaler, J. D. (2006). Adenosine induces fibronectin expression in lung epithelial cells: implications for airway remodeling. *Am. J. Physiol. Lung Cell. Mol. Physiol.* 290, L317–L325. doi: 10.1152/ajplung.00118.2005

Ryzhov, S., Sung, B. H., Zhang, Q., Weaver, A., Gumina, R. J., Biaggioni, I., et al. (2014). Role of adenosine A2B receptor signaling in contribution of cardiac mesenchymal stem-like cells to myocardial scar formation. *Purinergic Signal.* 10, 477–486. doi: 10.1007/s11302-014-9410-y

Sakuma, Y. (2017). Epithelial-to-mesenchymal transition and its role in EGFR-mutant lung adenocarcinoma and idiopathic pulmonary fibrosis. *Pathol. Int.* 67, 379–388. doi: 10.1111/pin.12553

Schulte, G., and Fredholm, B. B. (2003). Signalling from adenosine receptors to mitogen-activated protein kinases. *Cell. Signal.* 15, 813–827. doi: 10.1016/S0898-6568(03)00058-5

Sepúlveda, C., Palomo, I., and Fuentes, E. (2016). Role of adenosine A2b receptor overexpression in tumor progression. *Life Sci.* 166, 92–99. doi: 10.1016/j.lfs.2016.10.008

Shaikh, D., Zhou, Q., Chen, T., Ibe, J. C., Raj, J. U., and Zhou, G. (2012). cAMP-dependent protein kinase is essential for hypoxia-mediated epithelial-mesenchymal transition, migration, and invasion in lung cancer cells. *Cell. Signal.* 24, 2396–2406. doi: 10.1016/j.cellsig.2012.08.007

Shi, L., Dong, N., Fang, X., and Wang, X. (2016). Regulatory mechanisms of TGF-β1-induced fibrogenesis of human alveolar epithelial cells. *J. Cell Mol. Med.* 20, 2183–2193. doi: 10.1111/jcmm.12918

Singh, M., Yelle, N., Venugopal, C., and Singh, S. K. (2017). EMT: mechanisms and therapeutic implications. *Pharmacol. Ther.* doi: 10.1016/j.pharmthera.2017.08.009 [Epub ahead of print].

Sohal, S. S., and Walters, E. H. (2013). Role of epithelial mesenchymal transition (EMT) in chronic obstructive pulmonary disease (COPD). *Respir. Res.* 14:120. doi: 10.1186/1465-9921-14-120

Suarez-Carmona, M., Lesage, J., Cataldo, D., and Gilles, C. (2017). EMT and inflammation: inseparable actors of cancer progression. *Mol. Oncol.* 11, 805–823. doi: 10.1002/1878-0261.12095

Sun, Y., and Huang, P. (2016). Adenosine A2B receptor: from cell biology to human diseases. *Front. Chem.* 4:37. doi: 10.3389/fchem.2016.00037

Sung, W. J., Kim, H., and Park, K. K. (2016). The biological role of epithelial-mesenchymal transition in lung cancer (Review). *Oncol. Rep.* 36, 1199–1206. doi: 10.3892/or.2016.4964

Trincavelli, M. L., Giacomelli, C., Daniele, S., Taliani, S., Cosimelli, B., Laneri, S., et al. (2014). Allosteric modulators of human A_{2B} adenosine receptor. *Biochim. Biophys. Acta* 1840, 1194–1203. doi: 10.1016/j.bbagen.2013.12.021

Weng, L., Wang, W., Su, X., Huang, Y., Su, L., Liu, M., et al. (2015). The effect of cAMP-PKA activation on TGF-β1-induced profibrotic signaling. *Cell Physiol. Biochem.* 36, 1911–1927. doi: 10.1159/000430160

Wilkinson, P. F., Farrell, F. X., Morel, D., Law, W., and Murphy, S. (2016). Adenosine signaling increases proinflammatory and profibrotic mediators through activation of a functional adenosine 2B receptor in renal fibroblasts. *Ann. Clin. Lab. Sci.* 46, 339–345.

Willis, B. C., duBois, R. M., and Borok, Z. (2006). Epithelial origin of myofibroblasts during fibrosis in the lung. *Proc. Am. Thorac. Soc.* 3, 377–382. doi: 10.1513/pats.200601-004TK

Xiao, H., Shen, H. Y., Liu, W., Xiong, R. P., Li, P., Meng, G., et al. (2013). Adenosine A2A receptor: a target for regulating renal interstitial fibrosis in obstructive nephropathy. *PLOS ONE* 8:e60173. doi: 10.1371/journal.pone.0060173

Xie, L., Law, B. K., Chytil, A. M., Brown, K. A., Aakre, M. E., and Moses, H. L. (2004). Activation of the Erk pathway is required for TGF-beta1-induced EMT *in vitro*. *Neoplasia* 6, 603–610. doi: 10.1593/neo.04241

Yamaguchi, M., Hirai, S., Tanaka, Y., Sumi, T., Miyajima, M., Mishina, T., et al. (2017). Fibroblastic foci, covered with alveolar epithelia exhibiting epithelial-mesenchymal transition, destroy alveolar septa by disrupting blood flow in idiopathic pulmonary fibrosis. *Lab. Invest.* 97, 232–242. doi: 10.1038/labinvest.2016.135

Yang, J., Velikoff, M., Canalis, E., Horowitz, J. C., and Kim, K. K. (2014). Activated alveolar epithelial cells initiate fibrosis through autocrine and paracrine secretion of connective tissue growth factor. *Am. J. Physiol. Lung Cell. Mol. Physiol.* 306, L786–L796. doi: 10.1152/ajplung.00243.2013

Zhang, A., Dong, Z., and Yang, T. (2006a). Prostaglandin D2 inhibits TGF-beta1-induced epithelial-to-mesenchymal transition in MDCK cells. *Am. J. Physiol. Renal Physiol.* 291, F1332–F1342. doi: 10.1152/ajprenal.00131.2006

Zhang, A., Wang, M. H., Dong, Z., and Yang, T. (2006b). Prostaglandin E2 is a potent inhibitor of epithelial-to-mesenchymal transition: interaction with hepatocyte growth factor. *Am. J. Physiol. Renal Physiol.* 291, F1323–F1331. doi: 10.1152/ajprenal.00480.2005

Zhang, J., Deng, Y. T., Liu, J., Wang, Y. Q., Yi, T. W., Huang, B. Y., et al. (2016). Norepinephrine induced epithelial-mesenchymal transition in HT-29 and A549 cells in vitro. *J. Cancer Res. Clin. Oncol.* 142, 423–435. doi: 10.1007/s00432-015-2044-9

Zhang, Y. E. (2017). Non-Smad signaling pathways of the TGF-β family. *Cold Spring Harb. Perspect. Biol.* 9:a022129. doi: 10.1101/cshperspect.a022129

Zhou, Y., Chu, X., Deng, F., Tong, L., Tong, G., Yi, Y., et al. (2017). The adenosine A2b receptor promotes tumor progression of bladder urothelial carcinoma by enhancing MAPK signaling pathway. *Oncotarget* 8, 48755–48768. doi: 10.18632/oncotarget.17835

Zhou, Y., Schneider, D. J., Morschl, E., Song, L., Pedroza, M., Karmouty-Quintana, H., et al. (2011). Distinct roles for the A2B adenosine receptor in acute and chronic stages of bleomycin-induced lung injury. *J. Immunol.* 186, 1097–1106. doi: 10.4049/jimmunol.1002907

Zuccarini, M., Giuliani, P., Buccella, S., Di Liberto, V., Mudò, G., Belluardo, N., et al. (2017). Modulation of the TGF-β1-induced epithelial to mesenchymal transition (EMT) mediated by P1 and P2 purine receptors in MDCK cells. *Purinergic Signal.* 13, 429–442. doi: 10.1007/s11302-017-9571-6

Conflict of Interest Statement: The authors declare that the research was conducted in the absence of any commercial or financial relationships that could be construed as a potential conflict of interest.

frontiers in Pharmacology

REVIEW
published: 30 January 2018
doi: 10.3389/fphar.2018.00037

Biology of Platelet Purinergic Receptors and Implications for Platelet Heterogeneity

Milka Koupenova[1] and Katya Ravid[2]**

[1] Department of Medicine, Division of Cardiovascular Medicine, University of Massachusetts Medical School, Worcester, MA, United States, [2] Departments of Medicine and Biochemistry and Whitaker Cardiovascular Institute, Boston University School of Medicine, Boston, MA, United States

Platelets are small anucleated cells present only in mammals. Platelets mediate intravascular hemostatic balance, prevent interstitial bleeding, and have a major role in thrombosis. Activation of platelet purinergic receptors is instrumental in initiation of hemostasis and formation of the hemostatic plug, although this activation process becomes problematic in pathological settings of thrombosis. This review briefly outlines the roles and function of currently known platelet purinergic receptors (P1 and P2) in the setting of hemostasis and thrombosis. Additionally, we discuss recent novel studies on purinergic receptor distribution according to heterogeneous platelet size, and the possible implication of this distribution on hemostatic function.

Keywords: platelets, purinergic receptors, ATP, ADP, adenosine

OPEN ACCESS

Edited by:
Kenneth A. Jacobson, National Institutes of Health (NIH), United States

Reviewed by:
Alvin H. Schmaier, Case Western Reserve University, United States
Martyn P. Mahaut-Smith, University of Leicester, United Kingdom

****Correspondence:***
Milka Koupenova
milka.koupenova@umassmed.edu
Katya Ravid
kravid@bu.edu

Specialty section:
This article was submitted to Experimental Pharmacology and Drug Discovery, a section of the journal Frontiers in Pharmacology

Received: *20 November 2017*
Accepted: *12 January 2018*
Published: *30 January 2018*

Citation:
Koupenova M and Ravid K (2018) Biology of Platelet Purinergic Receptors and Implications for Platelet Heterogeneity. Front. Pharmacol. 9:37. doi: 10.3389/fphar.2018.00037

INTRODUCTION

Adenine nucleosides and nucleotides accumulate in the circulation under various pathological conditions and can initiate and mediate the response to cell damage, hypoxia, and inflammation (Koupenova and Ravid, 2013). Additionally, adenosine diphosphate (ADP) and adenosine triphosphate (ATP) are released from dense-granules during platelet activation and propagate platelet–platelet interactions, ultimately leading to three-dimensional plug formation that seals endothelial damage (McNicol and Israels, 1999; Koupenova and Ravid, 2013; Koupenova et al., 2017). Adenosine, in turn, is not known to be present in platelets but is generated in the extracellular space from ATP and ADP by two ectonucleotidases, CD39 (ENTPD1) and CD73 (NT5E) (reviewed in Koupenova and Ravid, 2013), that are present on endothelial and platelet surfaces (Koziak et al., 1999; Castilhos et al., 2016).

Two major classes of receptors mediate the physiological effect of adenosine and adenosine phosphates. These are the P1 and P2 purinergic receptors, classified based on their preference for adenosine (P1) or adenosine phosphates (P2). The P1 purinergic receptors include four G-protein-coupled receptors, two that activate adenylate cyclase [Adora2A (A2aAR) and Adora2b (A2bAR)] and generate cyclic AMP (cAMP), and two that inhibit adenylate cyclase [AdoraA1 (A1AR) and AdoraA3 (A3AR)] and decrease cAMP. The P2 purinergic receptor group is subdivided further into two groups that, in platelets, are represented by receptors activated by ATP (P2X1) and receptors activated by ADP (P2Y1 and P2Y12). P2Y1 and P2Y12 are G-protein-coupled receptors, while P2X1 is a ligand-gated ion channel receptor (Jacobson et al., 2006; Cattaneo, 2007). Adenosine and adenosine phosphates play a central role in regulating platelet behavior during hemostasis and thrombosis, as ADP induces platelet activation, while adenosine, for the most

part, inhibits it. ATP, in turn, can initiate platelet activation through the P2X1 receptor and inhibit ADP-mediated activation when acting as an antagonist on the P2Y receptors (Cattaneo, 2007). The potential explanation as to why platelets have both ATP and ADP receptors is that all of the purinergic receptors are necessary for establishing a balanced regulation of hemostasis or thrombus formation, depending on the intensity of vessel injury. Nucleotides released from damaged cells may occupy platelet P2 receptors and initiate shape change (via P2X receptors) and aggregation (via P2Y12 and P2Y1 receptor). The level of ADP-mediated P2Y12 or P2Y1 receptor activation can be controlled by ATP. Conversion of ATP and ADP (by CD39/CD73) to adenosine provides a second level of regulation that controls propagation of the hemostatic plaque by inhibiting activation through the A2 ARs. Deeper damage of the vessel leads to an increase in platelet aggregation response (collagen- or tissue factor-mediated) in order to prevent leakage into the interstitial tissue. This simplified explanation, however, is complicated by the fact that platelets are a heterogeneous population (as discussed in the last section of this review) and there is differential expression of distinct purinergic receptors based on size and function. In this review, we will focus on the role of purinergic receptors in platelet function and their distribution according to platelet heterogeneity.

PURINERGIC RECEPTORS IN HEMOSTASIS

Recent *in vivo* studies have further clarified the complex interactions and agonist distribution in the formation of three-dimensional platelet arrangement during hemostasis. According to this newly elucidated model, the hemostatic plug is composed of a core and an outer shell through which platelets are differentially activated. The stringent plug architecture consists of a platelet activation gradient with the most activated platelets in the core of the clot, surrounded by less activated platelets in the outer shell region. Fibrin deposition is localized distinctly at the base of the core in the extravascular space before hemostasis is achieved (Stalker et al., 2013; Tomaiuolo et al., 2017). The inner core of the hemostatic plug is packed tightly with degranulated platelets that are P-selectin positive. The outer shell is composed of loosely packed platelets that do not express P-selectin, and there is little to no fibrin present.

Although stable, the outer shell is porous and permeable to plasma solutes. Consistent with the platelet activation distribution gradient, there is a distinct distribution of platelet agonists throughout the hemostatic plug. The core of the plug contains a high concentration of thrombin (factor IIa) and, as the plug becomes more porous, a gradient of ADP and thromboxane A2 (TxA2) develops (Stalker et al., 2013; Tomaiuolo et al., 2017). The porous outer shell of the thrombus allows for recruitment of leukocytes necessary for injury repair or pathogen elimination. An increase in thrombin leads to PAR4 cleavage, consequently leading to leukocyte recruitment and migration to the damaged endothelium (Kaplan et al., 2015). Leukocyte recruitment, in turn, is limited by binding of thrombin to platelet GP1bα that can reduce platelet activation. Additionally, fibrin deposition in the thrombus physically inhibits leukocyte migration (Kaplan et al., 2015). The distinct distribution of P-selectin expressing platelets in the core vs. P-selectin-negative platelets in the shell suggests a possibility for a specific distribution of different platelet subpopulations throughout the hemostatic plug, according to their function in the interaction with either damaged endothelium or circulating leukocytes.

PLATELETS AND P2 RECEPTORS

ATP Receptors in Platelets

The P2X1 receptor is a ligand-gated ion channel receptor (Sun et al., 1998) that is activated by ATP and inhibited by ADP. Binding of ATP to the P2X1 receptor leads to calcium influx into platelets (Rolf et al., 2001; Mahaut-Smith, 2012) which consequently results in a transient change of platelet shape, platelet degranulation, pseudopodia formation, and platelet activation (Rolf et al., 2001; Toth-Zsamboki et al., 2003; Mahaut-Smith, 2012). P2X1 receptor activation by ATP alone does not mediate platelet aggregation; however, it can amplify ADP-mediated aggregation through the platelet-P2Y1 receptor (Jones et al., 2014). Furthermore, during early stages of vessel damage, in the presence of a low concentration of collagen, ATP contributes to increased aggregation through the P2X1 receptor (Oury et al., 2001). Similarly, P2X1 receptors can amplify thrombin-mediated platelet aggregation through protease-activated receptor 1 (PAR1) at low levels of thrombin (Erhardt et al., 2006). Importantly, in the presence of collagen or pathogenic stimuli, endothelial inhibitors (such as prostacyclins) are unable to completely inhibit calcium-mediated platelet aggregation partially due to activation of P2X1 receptor by ATP (Fung et al., 2012).

Intracellularly, P2X1 activation leads to MAPK/ERK2 pathway signaling that contributes to myosin light chain (MLC) phosphorylation and propagation of collagen-mediated platelet secretion (Toth-Zsamboki et al., 2003). During high shear stress, ATP-activated P2X1 also contributes to platelet-induced aggregation by MLC-mediated cytoskeletal rearrangements (Oury et al., 2004). P2X1 activation by ATP can also contribute to platelet secretion of TxA2 and enhance TxA2-mediated platelet aggregation (Huang et al., 2014). Additionally, in cases of a co-stimulatory role with P2Y1 signaling, P2X1 increases the influx of calcium and amplifies the consequent calcium signaling through P2Y1 and other $G_{\alpha q}$-coupled platelet receptors (Jones et al., 2014). Therefore, at sites of vascular injury, intensity of the platelet response can be regulated by the availability of various forms of adenosine phosphates.

Murine platelets lacking the P2X1 receptor exhibit decreased collagen-induced aggregation and adhesion (Hechler et al., 2003a). Furthermore, these platelets show diminished thrombus growth on collagen-coated slides, particularly at higher shear stress (Hechler et al., 2003a). Overall, P2X1 activation seems to be important at high shear stress and low agonist concentration, suggesting that ATP contributes to platelet aggregation at the

initial stages of platelet attachment to damaged endothelium, particularly in the arteries.

ADP Receptors in Platelets

P2Y12 and P2Y1 receptors are G-protein-coupled receptors activated by ADP and inhibited by ATP. With respect to adenine nucleotide-mediated aggregation in platelets, the ADP-activated P2Y12 receptor is the most important receptor. P2Y12 was first discovered in 2001 (Hollopeter et al., 2001), and it can couple to the $G_{\alpha i}$ subunit leading to the inhibition of adenylyl cyclase that mediates the conversion of ATP to cAMP (Hollopeter et al., 2001; Cattaneo, 2007; Hechler and Gachet, 2011). Consequently, the overall levels of cAMP can be decreased which may lead to an increase in platelet activation state. One of the mechanisms by which cAMP reduces platelet aggregation involves activation of protein kinase A (PKA) which leads to the phosphorylation and inhibition of inositol 1,4,5-triphosphate (IP3) receptor-mediated increase of calcium from the dense tubular system; reduced levels of cAMP have the opposite effect on IP3 and consequently increase intracellular calcium (Quinton and Dean, 1992; Tertyshnikova and Fein, 1998). In addition to coupling through $G_{\alpha i}$ and inhibition of adenylyl cyclase, ADP-mediated activation of P2Y12 receptors leads to activation of PI-3 kinase (PI-3K) through $G_{\beta\gamma}$ (Shankar et al., 2004). It is now understood that the P2Y12 receptor contributes to the ADP-mediated calcium response (by P2Y1) in platelets by activating PI-3K, in addition to simultaneously inhibiting adenylyl cyclase, i.e., by reducing cAMP levels (Hardy et al., 2004). Importantly, ADP activation through $G_{\alpha i}$-coupled P2Y12 receptors and the consequent RAP1 activation is critical for GPIIb/IIIa integrin-mediated platelet aggregation (Larson et al., 2003; Stefanini and Bergmeier, 2017). The P2Y12, but not P2Y1 receptor is required for sustained activation of RAP1 (Ras-related protein 1). P2Y12 is necessary for the formation of a shear-resistant hemostatic plug which is mediated by locally secreted ADP from platelets (Larson et al., 2003; Stolla et al., 2011b; Stefanini and Bergmeier, 2017). RAP1 activation is also dependent on guanine exchange factor (GEF), proteins RapGEF and RAS guanyl releasing protein 2 (RASGRP2), that are regulated by intracellular calcium signaling and by inhibition from the GTP-ase activating protein Ras GTPase-activating protein 3 (RASA3) (Stolla et al., 2011a; Stefanini and Bergmeier, 2017). ADP-activated P2Y1 receptor, on the other hand, does not affect cAMP levels (Fabre et al., 1999), couples to the $G_{\alpha q}$ subunit leading to the activation of phospholipase C (PLC) (Cattaneo, 2007; Hechler and Gachet, 2011). In platelets, PLC activation leads to a cascade of molecular signaling events that result in increased levels of cytosolic calcium, particularly from the dense tubular system. Interestingly, the P2Y1 receptor is able to activate Src kinase and consequently establish negative regulation over P2Y12 signaling through PI-3K (Hardy et al., 2004). This suggests that for ADP-mediated calcium signaling in platelets, P2Y12 and P2Y1 receptors cross-communicate to establish a controlled response to vascular damage; the P2Y12 receptor contributes to the absolutely required P2Y1-mediated calcium response by activating PI-3K and reducing cAMP levels, while the P2Y1 receptor inhibits PI-3K by coupling with Src kinase (Hardy et al., 2004). Thus, now it is understood that, in addition to ADP activation of platelets through two different molecular signaling mechanisms in which platelet activation by P2Y1 leads to rapid shape change and reversible aggregation while P2Y12 activation induces sustained platelet aggregation but without a shape change (Cattaneo, 2007; Hechler and Gachet, 2011), there is also a synergy between these receptors at the level of calcium signaling (Hardy et al., 2004). Importantly, other platelet G-protein-coupled receptor signaling through $G_{\alpha q}$ and contribution to the overall calcium pool can further synergize with ADP receptors and affect platelet function. Detailed reviews of platelet P2 signaling and synergy at calcium regulation can be found elsewhere (Dorsam and Kunapuli, 2004; Cattaneo, 2007; Varga-Szabo et al., 2009; Hechler and Gachet, 2011; Stefanini and Bergmeier, 2017).

It is important to mention that the role of ADP secreted from platelet dense-granules is to amplify the aggregation signal induced by other strong platelet agonists (such as TxA2), assuring stable platelet aggregation. Conversely, coordinated signaling involving activation of the P2Y12 and P2Y1 ADP receptors and integrin GPIIb/IIIa can mediate TxA2 generation (Jin et al., 2002). This multifactorial ADP receptors–TxA2 axis in platelets is important for thrombus growth and stabilization. Interestingly, patients deficient only in P2Y12 receptors have unaffected TxA2 production (Cattaneo et al., 1992, 2000), suggesting an important requirement of the two ADP receptors for proper hemostasis.

Studies utilizing murine platelets deficient in P2Y1 receptor showed that these platelets lack shape change and are prone to decreased aggregation in response to high concentrations of ADP (Fabre et al., 1999; Leon et al., 1999). However, P2Y1-deficient platelets had strongly impaired aggregation at low concentrations of ADP or collagen (Leon et al., 1999), suggesting that the P2Y1 receptor contributes to the overall ADP-mediated platelet aggregation and responses to other agonists. On the other hand, platelet overexpression of the P2Y1 receptor induces platelet hyperactivity (Hechler et al., 2003b). Bleeding time of mice deficient in this receptor is increased and they are protected from collagen- or ADP-induced thromboembolism (Fabre et al., 1999; Leon et al., 1999), suggesting that P2Y1 mediates ADP–platelet aggregation effects *in vivo*. Studies utilizing a murine model deficient in P2Y12 (Andre et al., 2003) in the context of the mesenteric artery injury model, support the observation that this receptor mediates platelet adhesion and activation, in addition to mediating the growth and stability of the thrombus. Consistently, *in vivo* antagonism of the P2Y12 receptor in rabbits reduces the size of the initial thrombus in injured mesenteric arterioles. However, in this study utilizing P2Y12 antagonists, AR-C69931 MX or clopidogrel (vs. genetic elimination), the stability of the thrombus was not affected by P2Y12 and the formation of the hemostatic plug was also not affected (van Gestel et al., 2003).

There are various reasons as to why a genetic deletion may lead to a different outcome than pharmacological inhibition in growth and stability of the thrombus. An inhibitor can vary in binding affinity for the receptor, reversibility, availability at specific sites, and off-target effects, as compared to a complete lack of receptor expression. Genetic deletion, on the other hand, can lead to elimination not only of the gene of interest but

can also alter levels of other genes that may be transcriptionally regulated by the particular gene. Finally, since human and murine platelets exhibit differences in content, the differences in pharmacological inhibition vs. deletion can additionally be related to species variability. Regardless, although an antagonist may not completely inhibit the action of P2Y12 or account for other functions of P2 receptors, it is clear that inhibition of P2Y12 can be beneficial in limiting thrombus growth in arterial thrombosis and secondary prevention of ischemia (Andre et al., 2003; van Gestel et al., 2003).

PLATELETS AND P1 RECEPTORS

Adenosine Receptors in Platelets

In addition to P2 receptors, platelets express functional P1 purinergic receptors on their surfaces. As mentioned earlier, P1 purinergic receptors are activated by adenosine at various concentrations that may be generated by ATP/ADP hydrolysis. In addition, an increase in levels of nucleotides, and consequent adenosine generation, can occur during inflammation, cell damage during infection, or other cardiovascular pathologies (Fredholm, 2007; Koupenova and Ravid, 2013). Human and murine platelets express functional cAMP-increasing P1 receptors A2aAR and A2bAR (Ledent et al., 1997; Yang et al., 2010), but are not known to have functional cAMP-inhibiting P1 receptors A1AR and A3AR. It is noteworthy that A1AR mRNA has been detected by qRT-PCR (Amisten et al., 2008) but significant expression was not detected by sequencing in more recent studies (Rowley et al., 2011; Clancy et al., 2017). An increased level of intracellular cAMP, in turn, inhibits platelet aggregation/function.

Among the A2 adenosine receptors, A2aAR has the highest affinity for adenosine and is the major adenosine receptor expressed in platelets that mediates inhibition of platelet aggregation. A2aAR is a G-protein-coupled receptor that couples with $G_{\alpha s}$ and activates adenylyl cyclase (Koupenova et al., 2012). A2aAR mediates platelet function through increasing cAMP levels (Yang et al., 2010), and by inhibiting the rise of thrombin-mediated increase in intracellular calcium levels (Paul et al., 1990). Both of these effects on intracellular second messengers in platelets are presumed to be mediated by the action of adenylyl cyclase (Paul et al., 1990). It is now understood that the inhibitory effect of cAMP on platelet aggregation involves complex regulation of diverging signaling pathways. Intracellularly, cAMP affects calcium signaling by inhibiting PLC-mediated diacylglycerol (DAG) and inositol triphosphate formation, by inhibiting protein kinase C directly or indirectly through reduction of DAG level, or by affecting actin polymerization through phosphorylation of the β-subunit of the glycoprotein receptor GPIb (Fox and Berndt, 1989; Schwarz et al., 2001; Varga-Szabo et al., 2009). In addition to inhibiting platelet aggregation in human blood, activation of A2aAR by specific agonists leads to a reduction in P-selectin expression on the platelet cell surface, as a result of TxA2 or ADP stimulation. This is followed by a greater than 50% reduction in platelet–monocyte aggregate formation (Linden et al., 2008). This suggests that the A2aAR has the potential to mediate the impact of prothrombotic agonists during hemostasis and thrombosis as a fast responder.

Studies utilizing platelets from A2aAR null mice have confirmed that inhibition of platelet aggregation is mediated by this receptor, as platelets without A2aAR have an increased aggregation potential and are not affected by any concentration of the adenosine receptor (non-specific) agonist, 5′-*N*-ethylcarboxamidoadenosine (NECA) (Ledent et al., 1997). Similarly, inhibition of A2aAR by caffeine, a non-specific adenosine receptor antagonist, also leads to decreased aggregation potential of human platelets (Varani et al., 1999, 2000). However, chronic intake of caffeine leads to a desensitization effect on aggregation, possibly mediated by increased upregulation of A2aAR (or A2bAR) on the platelet surface (Varani et al., 1999, 2000).

Although platelets have a large density of A2aAR, they also contain A2bARs. Similarly to A2aAR, A2bAR is a G-protein receptor that couples to $G_{\alpha s}$ (Koupenova et al., 2012), but can also couple to $G_{\alpha q}$ (Feoktistov et al., 1994; Linden et al., 1999; Gao et al., 2017) and, in some cells, to $G_{\alpha i}$ (Gao et al., 2017). Importantly, in different cells, A2bAR can couple to the same pathways through different G-proteins possibly depending on specific intracellular G-protein signatures (Gao et al., 2017). In cells of the same type, A2bAR can also couple to $G_{\alpha s}$ or $G_{\alpha i}$ leading to activation of opposing or synergistic signaling pathways (Gao et al., 2017), suggesting that these adenosine receptors have the ability to balance different signaling mechanisms in different cell types. Contrary to the other P1 receptors, A2bAR is a low affinity receptor that requires the concentration of adenosine to be higher than 10 μM (reviewed in Koupenova and Ravid, 2013). Additionally, A2bAR is an inducible receptor, the expression of which is known to be upregulated under inflammation, stress, or vascular injury (Yang et al., 2006, 2008, 2010; St. Hilaire et al., 2008). Since platelets are anucleate cells, increase in A2bAR expression most likely occurs in the platelet precursors, the megakaryocytes (MK). The low affinity for adenosine, the inducibility of A2bAR expression, and the promiscuous coupling with downstream G-proteins suggest that this receptor may play an instrumental role in platelet function during chronic inflammation and pathophysiological conditions.

Recent sequencing studies show that mRNA expression of A2bAR in human platelets is almost sixfold lower than A2aAR (**Table 1**) (Rowley et al., 2011). Murine platelets lacking A2bAR have reduced cAMP levels and are prone to increased ADP- or collagen-mediated aggregation (Yang et al., 2010). Additionally, A2bAR increases the inhibition of ADP-mediated aggregation of platelets isolated from LPS-injected animals (Yang et al., 2010). Elimination of A2bAR also leads to increased platelet expression of the P2Y1 receptor (Yang et al., 2010), and P2Y1 activation, as mentioned before, leads to an increase in intracellular calcium levels (Cattaneo, 2007; Hechler and Gachet, 2011). This suggests that the absence of A2bAR can have a stimulatory effect on platelet aggregation through simultaneous reduction of cAMP and increase in calcium levels. A2bAR signaling could be particularly important over prolonged periods of inflammation or injury.

TABLE 1 | Platelet purinergic receptors assessed by RNA sequencing of healthy human or murine platelets.

Purinergic receptor	Nucleotide/ nucleoside	G-Protein coupling	Effect on platelet cAMP	Effect on platelet calcium	*Large human* platelets (Clancy et al., 2017) (FPKM)	*Small human* platelets (Clancy et al., 2017) (FPKM)	*All human* platelets (Rowley et al., 2011) (RPKM)	*All murine* platelets (Rowley et al., 2011) (RPKM)
P1 Purinergic receptors								
A1AR	Ado	$G_{\alpha i}$	–	–	0	0	0.05	0
A3AR	Ado	$G_{\alpha i}$	–	–	0	1.80	0.08	1.86
A2aAR	Ado	$G_{\alpha s}$	↑	–	0	2.23	31.80	0.36
A2bAR	Ado	$G_{\alpha s}$	↑	–	0	0	5.37	0
P2 Purinergic receptors								
P2X1	ATP	Ion-gated channel	–	↑	4.21	1.55	90.79	630.06
P2Y1	ADP	$G_{\alpha q}$	–	↑	0	0	12.53	30.56
P2Y12	ADP	$G_{\alpha i}$	↓	–	13.19	1.77	73.75	1044.24

The two studies summarized here included healthy human donors and isolated platelets by sorting [large and small platelets (Clancy et al., 2017)] or by centrifugation followed by leukocyte depletion (Rowley et al., 2011). The human cohorts, methods of platelet isolation, and RNA extractions are described in Rowley et al. (2011) and Clancy et al. (2017). Mice sequencing data represent RNA transcripts in platelets from male and female C57BL/6 murine models (Rowley et al., 2011). Of note: The data summarized here are derived from platelets from two human male donors (large and small platelets) and from one male and one female donor (data in "all platelet" column). Data validation is required in various individuals of different ages and sexes in order to establish a broader distribution profile of purinergic receptors. cAMP, cyclic AMP; FPKM, fragments per kilobase of transcript per million mapped reads; RPKM, reads per kilobase of transcript per million mapped reads; Ado, Adenosine; ATP, adenosine triphosphate; ADP, adenosine diphosphate.

PURINERGIC RECEPTORS AND PLATELET HETEROGENEITY

Circulating platelets are anucleate cell fragments originating from their bone marrow precursor, the MK. Human platelets are not a homogeneous population, but vary in size (2–5 μm) and content. RNA sequencing shows that platelets may contain as many as 9500 different transcripts (Rowley et al., 2011; Bray et al., 2013; Clancy et al., 2017), most of which are prepackaged from the MK. Additionally, platelets uptake transcripts and transcript fragments from circulating cells and the endothelium (Clancy et al., 2017). The heterogeneous size of platelets (Thon and Italiano, 2012) is hypothesized to be a result of platelets losing their contents into the circulation as they age; hence, large platelets are also referred to as "immature" and small platelets are referred to as "mature" (Penington and Streatfield, 1975; Penington et al., 1976a,b). Alternatively, in the late 1970s, it was proposed that platelets vary in density and structure depending on ploidy of the MK from which platelets are originating. Low ploidy MKs produce less hemostatically active platelets while high ploidy MKs produce hemostatically functional platelets (Penington and Streatfield, 1975; Penington et al., 1976a,b). Direct experimental evidence is limited for each of these hypotheses and it is possible that both of these explanations are valid. Studies have shown that large (immature) platelets are highly hemostatically active while small (mature) platelets are less hemostatically functional (Thompson et al., 1984; Guthikonda et al., 2008). It is noteworthy that the predominant size of platelets in a healthy individual lies somewhere in between (Clancy et al., 2017). In patients with acute coronary syndrome (developing early stent thrombosis) there is a baseline platelet size increase predicting platelet reactivity (Huczek et al., 2010). A population study performed with patients after non-cardiac surgery has provided evidence that large platelets may be a novel biomarker for adverse cardiovascular events (Anetsberger et al., 2017).

Sequencing studies have addressed the overall platelet mRNA transcriptome of the entire platelet population (Rowley et al., 2011) and that of small and large platelets sorted from the blood of healthy human donors (Clancy et al., 2017). Of note, in platelets there is a reported mismatch between mRNA and protein expression (Burkhart et al., 2012) that can be partially justified by the ability of platelets to uptake mRNA transcripts (Clancy et al., 2017). However, in cases when both proteins and transcripts are detectable in platelets, there is strong evidence that mRNA and the corresponding protein expression are correlated (Rowley and Weyrich, 2013). Large platelets (sorted as 10% of the entire platelet population) have transcripts associated with classical platelet functions, such as platelet activation/aggregation, hemostasis, and wound healing (Clancy et al., 2017). Small platelets show a distinct and more diverse platelet transcriptome as compared to large platelets, and those transcripts are more involved in platelet-immune cell interactions and apoptosis (Clancy et al., 2017). For instance, small platelets contain distinct transcripts that are associated with activation, proliferation and differentiation of T- and B-lymphocytes (Clancy et al., 2017). Consistent with the hemostatic role of large platelets and their contribution to aggregation, transcripts for the P2 purinergic receptors, P2Y12 and P2X1, seem to be present at higher levels in this platelet population (**Table 1**). mRNA from the inhibitory P1 receptor A2aAR is distinctly located in small platelets, similar to P1 A3AR (**Table 1**). The function of platelet-A3AR is unclear. On the other hand, sequencing of the entire platelet population, that includes platelets of all sizes, shows the presence of all four P1 purinergic receptors with the inhibitory A2aAR and A2bAR receptors in the highest proportions (**Table 1**). Interestingly, P2Y1 is detected

only in the mixed, non-sorted platelet population, but not in the large or small platelet subpopulations. There is a possibility that the P2Y1 receptor is present on platelets which compose the rest of the platelet population that was not included in the large/small platelet sorting, or P2Y1 was not detected due to low expression levels in each group or in these particular donors. The two sequencing studies also agree on transcripts for other P2 purinergic receptors such as P2X5, P2Y10, and P2Y13 that have not been previously reported to be present in platelets or to have a functional role. Distinct signatures of purinergic receptors in different platelet subpopulations suggests that the architecture of the hemostatic plug may involve platelets of heterogeneous size and function. Large platelets may be predominantly located at the core while small platelets may be located (together with the large) in the shell (**Figure 1**). Since small platelets have more immune transcripts and are less hemostatically active, their presence may allow for direct interactions with immune cells inside of the shell of the thrombus. The mechanism by which MKs mediate this diverse distribution of distinct transcripts in platelets according to size and function is still controversial.

CONCLUSION AND FUTURE DIRECTIONS

The distinct distribution of purinergic receptor types across different platelet sizes may provide a new approach to

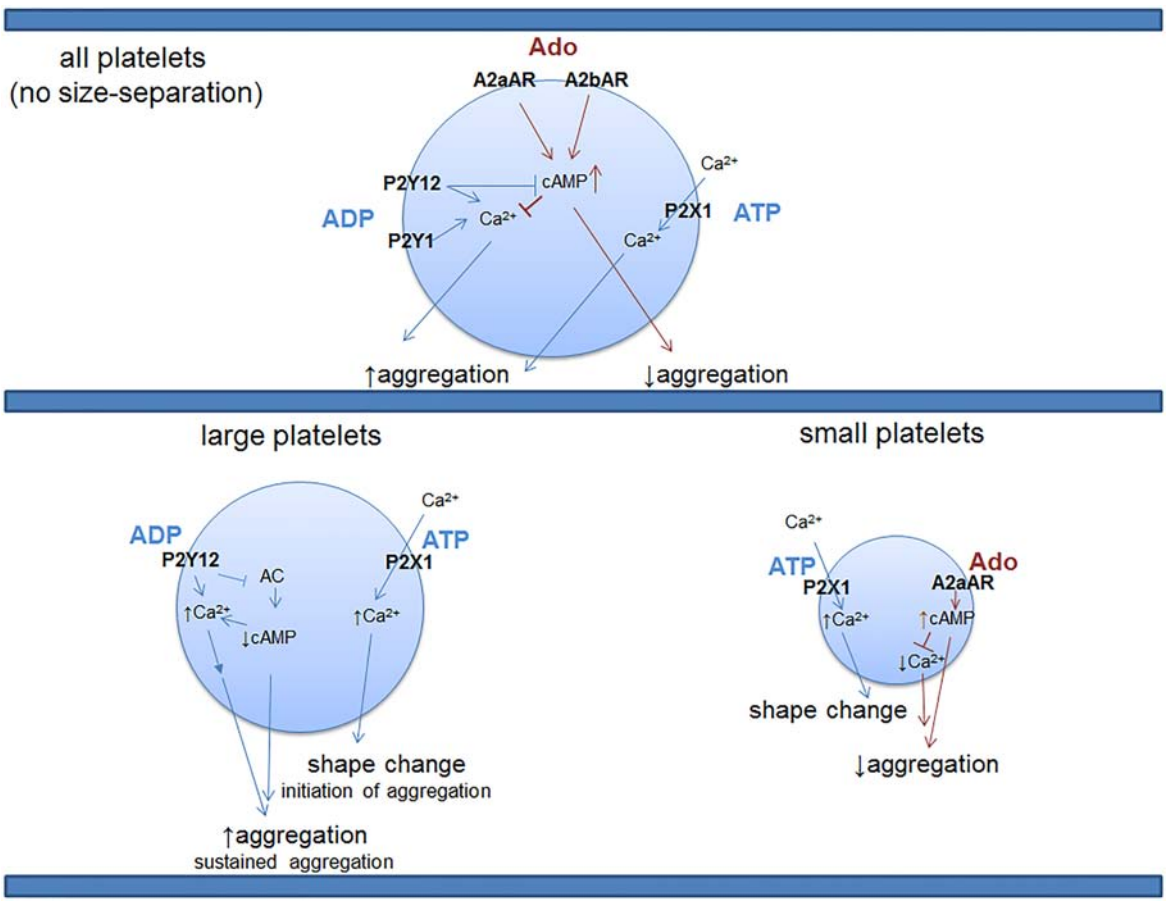

FIGURE 1 | Distribution of purinergic receptor transcripts with known function in the entire platelet population vs. large and small platelets. Platelets are a heterogeneous population of various sizes. Large platelets are highly hemostatically active while small ones are known to be much less active in hemostasis (Thompson et al., 1984; Guthikonda et al., 2008). RNA sequencing studies shown in **Table 1** suggest differential distribution of purinergic receptors across platelets of different sizes, providing a provocative hypothesis related to potential functional differences in hemostasis when activated by adenine nucleosides and nucleotides, depending on platelet size. Future protein studies will be needed to test this contention. P2X1 is a ligand-gated ion channel that requires binding of ATP for influx of calcium; the rest of the P2 and P1 receptors in platelets are G-protein-coupled receptors. Of note, with the sensitivity of the above method of detection, P2Y1 or A2bAR transcripts are not found in the small or large platelets; however, these receptors for ADP or adenosine (respectively) are detected in the entire platelet population, suggesting a differential expression level in different platelet populations, possibly necessary for an extra layer of control over platelet function. These findings further encourage future examination of the receptors at protein and functional levels in different platelet populations. It is not known, however, if all of the purinergic receptors depicted in the top (or bottom) panel can be expressed on the same platelet, if there is differential signature of co-expression or if there is a mix of both of these possibilities. Ado, adenosine; ATP, adenosine triphosphate; ADP, adenosine diphosphate; cAMP, cyclic adenosine monophosphate; AC, adenylate cyclase.

purinergic signaling manipulation in order to establish effective antithrombotic therapies. The platelet mRNA profile may have a broader impact on overall platelet function, and proposes an explanation of previously identified functional differences between small and large platelets, with increased mean platelet volume being historically associated with increased hemostatic potential. It remains unclear, however, if within the sophisticated architecture of the thrombus there is a distinct arrangement of platelets with differential expression of purinergic or immune receptors. Perhaps, big platelets are primarily responsible for the formation of the core of the hemostatic plug since they predominantly contain transcripts related to the hemostatic function of platelets, such as the P2 receptors. Small platelets in turn contain more immune transcripts. These cells may need to communicate with both aggregated platelets and leukocytes and may be located in the porous shell of the hemostatic plaque. In that sense, it would be necessary for small platelets to be less prone to aggregation and hence express only purinergic receptors for shape change (P2X1) and reduction of aggregation (A2ARs). It is also not completely clear if platelet heterogeneity increases as a function of pathological conditions, thereby changing the balance between P2/P1 receptors and limiting the beneficial effect of current therapies.

It would be important to test these receptors at protein and agonist functional levels in the different platelet subpopulations. Additionally, future studies are necessary to elucidate the complex cross-communication of purinergic receptors in the hemostatic plug as a function of platelet heterogeneity and to determine if there is a functional presence of the other ADP/ATP receptors that were detected at mRNA level. These future findings may provide additional pharmacological targets in the management of thrombus growth and stability in patients.

AUTHOR CONTRIBUTIONS

MK and KR co-wrote and edited this review article.

FUNDING

This work was supported by AHA Award 16SDG30450001 (to MK) and the Thrombosis and Hemostasis Affinity Research Collaborative and the Evans Center for Interdisciplinary Biomedical Research at Boston University School of Medicine (to KR). KR is an Established Investigator with the American Heart Association.

ACKNOWLEDGMENTS

We apologize to all whose work was not cited due to limited space.

REFERENCES

Amisten, S., Braun, O. O., Bengtsson, A., and Erlinge, D. (2008). Gene expression profiling for the identification of G-protein coupled receptors in human platelets. *Thromb. Res.* 122, 47–57.

Andre, P., Delaney, S. M., Larocca, T., Vincent, D., Deguzman, F., Jurek, M., et al. (2003). P2Y12 regulates platelet adhesion/activation, thrombus growth, and thrombus stability in injured arteries. *J. Clin. Invest.* 112, 398–406.

Anetsberger, A., Blobner, M., Haller, B., Schmid, S., Umgelter, K., Hager, T., et al. (2017). Immature platelets as a novel biomarker for adverse cardiovascular events in patients after non-cardiac surgery. *Thromb. Haemost.* 117, 1887–1895. doi: 10.1160/TH16-10-0804

Bray, P. F., Mckenzie, S. E., Edelstein, L. C., Nagalla, S., Delgrosso, K., Ertel, A., et al. (2013). The complex transcriptional landscape of the anucleate human platelet. *BMC Genomics* 14:1. doi: 10.1186/1471-2164-14-1

Burkhart, J. M., Vaudel, M., Gambaryan, S., Radau, S., Walter, U., Martens, L., et al. (2012). The first comprehensive and quantitative analysis of human platelet protein composition allows the comparative analysis of structural and functional pathways. *Blood* 120, e73–82. doi: 10.1182/blood-2012-04-416594

Castilhos, L. G., Doleski, P. H., Adefegha, S. A., Becker, L. V., Ruchel, J. B., and Leal, D. B. (2016). Altered E-NTPDase/E-ADA activities and CD39 expression in platelets of sickle cell anemia patients. *Biomed. Pharmacother.* 79, 241–246. doi: 10.1016/j.biopha.2016.02.009

Cattaneo, M. (2007). Platelet P2 receptors: old and new targets for antithrombotic drugs. *Expert Rev. Cardiovasc. Ther.* 5, 45–55.

Cattaneo, M., Lecchi, A., Lombardi, R., Gachet, C., and Zighetti, M. L. (2000). Platelets from a patient heterozygous for the defect of P2CYC receptors for ADP have a secretion defect despite normal thromboxane A2 production and normal granule stores: further evidence that some cases of platelet 'primary secretion defect' are heterozygous for a defect of P2CYC receptors. *Arterioscler. Thromb. Vasc. Biol.* 20, E101–E106.

Cattaneo, M., Lecchi, A., Randi, A. M., Mcgregor, J. L., and Mannucci, P. M. (1992). Identification of a new congenital defect of platelet function characterized by severe impairment of platelet responses to adenosine diphosphate. *Blood* 80, 2787–2796.

Clancy, L., Beaulieu, L. M., Tanriverdi, K., and Freedman, J. E. (2017). The role of RNA uptake in platelet heterogeneity. *Thromb. Haemost.* 117, 948–961. doi: 10.1160/TH16-11-0873

Dorsam, R. T., and Kunapuli, S. P. (2004). Central role of the P2Y12 receptor in platelet activation. *J. Clin. Invest.* 113, 340–345.

Erhardt, J. A., Toomey, J. R., Douglas, S. A., and Johns, D. G. (2006). P2X1 stimulation promotes thrombin receptor-mediated platelet aggregation. *J. Thromb. Haemost.* 4, 882–890.

Fabre, J. E., Nguyen, M., Latour, A., Keifer, J. A., Audoly, L. P., Coffman, T. M., et al. (1999). Decreased platelet aggregation, increased bleeding time and resistance to thromboembolism in P2Y1-deficient mice. *Nat. Med.* 5, 1199–1202.

Feoktistov, I., Murray, J. J., and Biaggioni, I. (1994). Positive modulation of intracellular Ca2+ levels by adenosine A2b receptors, prostacyclin, and prostaglandin E1 via a cholera toxin-sensitive mechanism in human erythroleukemia cells. *Mol. Pharmacol.* 45, 1160–1167.

Fox, J. E., and Berndt, M. C. (1989). Cyclic AMP-dependent phosphorylation of glycoprotein Ib inhibits collagen-induced polymerization of actin in platelets. *J. Biol. Chem.* 264, 9520–9526.

Fredholm, B. B. (2007). Adenosine, an endogenous distress signal, modulates tissue damage and repair. *Cell Death Differ.* 14, 1315–1323.

Fung, C. Y., Jones, S., Ntrakwah, A., Naseem, K. M., Farndale, R. W., and Mahaut-Smith, M. P. (2012). Platelet Ca(2+) responses coupled to glycoprotein VI and Toll-like receptors persist in the presence of endothelial-derived inhibitors: roles for secondary activation of P2X1 receptors and release from intracellular Ca(2+) stores. *Blood* 119, 3613–3621. doi: 10.1182/blood-2011-10-386052

Gao, Z. G., Inoue, A., and Jacobson, K. A. (2017). On the G protein-coupling selectivity of the native A2B adenosine receptor. *Biochem. Pharmacol.* doi: 10.1016/j.bcp.2017.12.003 [Epub ahead of print].

Guthikonda, S., Alviar, C. L., Vaduganathan, M., Arikan, M., Tellez, A., Delao, T., et al. (2008). Role of reticulated platelets and platelet size heterogeneity on

platelet activity after dual antiplatelet therapy with aspirin and clopidogrel in patients with stable coronary artery disease. *J. Am. Coll. Cardiol.* 52, 743–749. doi: 10.1016/j.jacc.2008.05.031

Hardy, A. R., Jones, M. L., Mundell, S. J., and Poole, A. W. (2004). Reciprocal cross-talk between P2Y1 and P2Y12 receptors at the level of calcium signaling in human platelets. *Blood* 104, 1745–1752.

Hechler, B., and Gachet, C. (2011). P2 receptors and platelet function. *Purinergic Signal.* 7, 293–303. doi: 10.1007/s11302-011-9247-6

Hechler, B., Lenain, N., Marchese, P., Vial, C., Heim, V., Freund, M., et al. (2003a). A role of the fast ATP-gated P2X1 cation channel in thrombosis of small arteries *in vivo*. *J. Exp. Med.* 198, 661–667.

Hechler, B., Zhang, Y., Eckly, A., Cazenave, J. P., Gachet, C., and Ravid, K. (2003b). Lineage-specific overexpression of the P2Y1 receptor induces platelet hyper-reactivity in transgenic mice. *J. Thromb. Haemost.* 1, 155–163.

Hollopeter, G., Jantzen, H. M., Vincent, D., Li, G., England, L., Ramakrishnan, V., et al. (2001). Identification of the platelet ADP receptor targeted by antithrombotic drugs. *Nature* 409, 202–207.

Huang, Z., Liu, P., Zhu, L., Li, N., and Hu, H. (2014). P2X1-initiated p38 signalling enhances thromboxane A2-induced platelet secretion and aggregation. *Thromb. Haemost.* 112, 142–150. doi: 10.1160/TH13-09-0726

Huczek, Z., Filipiak, K. J., Kochman, J., Michalak, M., Roik, M., Piatkowski, R., et al. (2010). Baseline platelet size is increased in patients with acute coronary syndromes developing early stent thrombosis and predicts future residual platelet reactivity. A case-control study. *Thromb. Res.* 125, 406–412. doi: 10.1016/j.thromres.2009.09.003

Jacobson, K. A., Costanzi, S., Joshi, B. V., Besada, P., Shin, D. H., Ko, H., et al. (2006). Agonists and antagonists for P2 receptors. *Novartis Found. Symp.* 276, 58–281.

Jin, J., Quinton, T. M., Zhang, J., Rittenhouse, S. E., and Kunapuli, S. P. (2002). Adenosine diphosphate (ADP)-induced thromboxane A(2) generation in human platelets requires coordinated signaling through integrin alpha(IIb)beta(3) and ADP receptors. *Blood* 99, 193–198.

Jones, S., Evans, R. J., and Mahaut-Smith, M. P. (2014). Ca2+ influx through P2X1 receptors amplifies P2Y1 receptor-evoked Ca2+ signaling and ADP-evoked platelet aggregation. *Mol. Pharmacol.* 86, 243–251. doi: 10.1124/mol.114.092528

Kaplan, Z. S., Zarpellon, A., Alwis, I., Yuan, Y., Mcfadyen, J., Ghasemzadeh, M., et al. (2015). Thrombin-dependent intravascular leukocyte trafficking regulated by fibrin and the platelet receptors GPIb and PAR4. *Nat. Commun.* 6:7835. doi: 10.1038/ncomms8835

Koupenova, M., Johnston-Cox, H., and Ravid, K. (2012). Regulation of atherosclerosis and associated risk factors by adenosine and adenosine receptors. *Curr. Atheroscler. Rep.* 14, 460–468. doi: 10.1007/s11883-012-0263-y

Koupenova, M., Kehrel, B. E., Corkrey, H. A., and Freedman, J. E. (2017). Thrombosis and platelets: an update. *Eur. Heart J.* 38, 785–791. doi: 10.1093/eurheartj/ehw550

Koupenova, M., and Ravid, K. (2013). Adenosine, adenosine receptors and their role in glucose homeostasis and lipid metabolism. *J. Cell Physiol.* doi: 10.1002/jcp.24352 [Epub ahead of print].

Koziak, K., Sevigny, J., Robson, S. C., Siegel, J. B., and Kaczmarek, E. (1999). Analysis of CD39/ATP diphosphohydrolase (ATPDase) expression in endothelial cells, platelets and leukocytes. *Thromb. Haemost.* 82, 1538–1544.

Larson, M. K., Chen, H., Kahn, M. L., Taylor, A. M., Fabre, J. E., Mortensen, R. M., et al. (2003). Identification of P2Y12-dependent and -independent mechanisms of glycoprotein VI-mediated Rap1 activation in platelets. *Blood* 101, 1409–1415.

Ledent, C., Vaugeois, J. M., Schiffmann, S. N., Pedrazzini, T., El Yacoubi, M., Vanderhaeghen, J. J., et al. (1997). Aggressiveness, hypoalgesia and high blood pressure in mice lacking the adenosine A2a receptor. *Nature* 388, 674–678.

Leon, C., Hechler, B., Freund, M., Eckly, A., Vial, C., Ohlmann, P., et al. (1999). Defective platelet aggregation and increased resistance to thrombosis in purinergic P2Y(1) receptor-null mice. *J. Clin. Invest.* 104, 1731–1737.

Linden, J., Thai, T., Figler, H., Jin, X., and Robeva, A. S. (1999). Characterization of human A(2B) adenosine receptors: radioligand binding, western blotting, and coupling to G(q) in human embryonic kidney 293 cells and HMC-1 mast cells. *Mol. Pharmacol.* 56, 705–713.

Linden, M. D., Barnard, M. R., Frelinger, A. L., Michelson, A. D., and Przyklenk, K. (2008). Effect of adenosine A2 receptor stimulation on platelet activation-aggregation: differences between canine and human models. *Thromb. Res.* 121, 689–698.

Mahaut-Smith, M. P. (2012). The unique contribution of ion channels to platelet and megakaryocyte function. *J. Thromb. Haemost.* 10, 1722–1732. doi: 10.1111/j.1538-7836.2012.04837.x

McNicol, A., and Israels, S. J. (1999). Platelet dense granules: structure, function and implications for haemostasis. *Thromb. Res.* 95, 1–18.

Oury, C., Sticker, E., Cornelissen, H., De Vos, R., Vermylen, J., and Hoylaerts, M. F. (2004). ATP augments von Willebrand factor-dependent shear-induced platelet aggregation through Ca2+-calmodulin and myosin light chain kinase activation. *J. Biol. Chem.* 279, 26266–26273.

Oury, C., Toth-Zsamboki, E., Thys, C., Tytgat, J., Vermylen, J., and Hoylaerts, M. F. (2001). The ATP-gated P2X1 ion channel acts as a positive regulator of platelet responses to collagen. *Thromb. Haemost.* 86, 1264–1271.

Paul, S., Feoktistov, I., Hollister, A. S., Robertson, D., and Biaggioni, I. (1990). Adenosine inhibits the rise in intracellular calcium and platelet aggregation produced by thrombin: evidence that both effects are coupled to adenylate cyclase. *Mol. Pharmacol.* 37, 870–875.

Penington, D. G., Lee, N. L., Roxburgh, A. E., and Mcgready, J. R. (1976a). Platelet density and size: the interpretation of heterogeneity. *Br. J. Haematol.* 34, 365–376.

Penington, D. G., and Streatfield, K. (1975). Heterogeneity of megakaryocytes and platelets. *Ser. Haematol.* 8, 22–48.

Penington, D. G., Streatfield, K., and Roxburgh, A. E. (1976b). Megakaryocytes and the heterogeneity of circulating platelets. *Br. J. Haematol.* 34, 639–653.

Quinton, T. M., and Dean, W. L. (1992). Cyclic AMP-dependent phosphorylation of the inositol-1,4,5-trisphosphate receptor inhibits Ca2+ release from platelet membranes. *Biochem. Biophys. Res. Commun.* 184, 893–899.

Rolf, M. G., Brearley, C. A., and Mahaut-Smith, M. P. (2001). Platelet shape change evoked by selective activation of P2X1 purinoceptors with alpha,beta-methylene ATP. *Thromb. Haemost.* 85, 303–308.

Rowley, J. W., Oler, A. J., Tolley, N. D., Hunter, B. N., Low, E. N., Nix, D. A., et al. (2011). Genome-wide RNA-seq analysis of human and mouse platelet transcriptomes. *Blood* 118, e101–e111. doi: 10.1182/blood-2011-03-339705

Rowley, J. W., and Weyrich, A. S. (2013). Coordinate expression of transcripts and proteins in platelets. *Blood* 121, 5255–5256.

Schwarz, U. R., Walter, U., and Eigenthaler, M. (2001). Taming platelets with cyclic nucleotides. *Biochem. Pharmacol.* 62, 1153–1161.

Shankar, H., Murugappan, S., Kim, S., Jin, J., Ding, Z., Wickman, K., et al. (2004). Role of G protein-gated inwardly rectifying potassium channels in P2Y12 receptor-mediated platelet functional responses. *Blood* 104, 1335–1343.

St. Hilaire, C., Koupenova, M., Carroll, S. H., Smith, B. D., and Ravid, K. (2008). TNF-alpha upregulates the A2B adenosine receptor gene: The role of NAD(P)H oxidase 4. *Biochem. Biophys. Res. Commun.* 375, 292–296. doi: 10.1016/j.bbrc.2008.07.059

Stalker, T. J., Traxler, E. A., Wu, J., Wannemacher, K. M., Cermignano, S. L., Voronov, R., et al. (2013). Hierarchical organization in the hemostatic response and its relationship to the platelet-signaling network. *Blood* 121, 1875–1885. doi: 10.1182/blood-2012-09-457739

Stefanini, L., and Bergmeier, W. (2017). Negative regulators of platelet activation and adhesion. *J. Thromb. Haemost.* doi: 10.1111/jth.13910 [Epub ahead of print].

Stolla, M., Stefanini, L., Andre, P., Ouellette, T. D., Reilly, M. P., Mckenzie, S. E., et al. (2011a). CalDAG-GEFI deficiency protects mice in a novel model of Fcgamma RIIA-mediated thrombosis and thrombocytopenia. *Blood* 118, 1113–1120. doi: 10.1182/blood-2011-03-342352

Stolla, M., Stefanini, L., Roden, R. C., Chavez, M., Hirsch, J., Greene, T., et al. (2011b). The kinetics of alphaIIbbeta3 activation determines the size and stability of thrombi in mice: implications for antiplatelet therapy. *Blood* 117, 1005–1013. doi: 10.1182/blood-2010-07-297713

Sun, B., Li, J., Okahara, K., and Kambayashi, J. (1998). P2X1 purinoceptor in human platelets. Molecular cloning and functional characterization after heterologous expression. *J. Biol. Chem.* 273, 11544–11547.

Tertyshnikova, S., and Fein, A. (1998). Inhibition of inositol 1,4,5-trisphosphate-induced Ca2+ release by cAMP-dependent protein kinase in a living cell. *Proc. Natl. Acad. Sci. U.S.A.* 95, 1613–1617.

Thompson, C. B., Jakubowski, J. A., Quinn, P. G., Deykin, D., and Valeri, C. R. (1984). Platelet size and age determine platelet function independently. *Blood* 63, 1372–1375.

Thon, J. N., and Italiano, J. E. Jr. (2012). Does size matter in platelet production? *Blood* 120, 1552–1561. doi: 10.1182/blood-2012-04-408724

Tomaiuolo, M., Brass, L. F., and Stalker, T. J. (2017). Regulation of platelet activation and coagulation and its role in vascular injury and arterial thrombosis. *Interv. Cardiol. Clin.* 6, 1–12. doi: 10.1016/j.iccl.2016.08.001

Toth-Zsamboki, E., Oury, C., Cornelissen, H., De Vos, R., Vermylen, J., and Hoylaerts, M. F. (2003). P2X1-mediated ERK2 activation amplifies the collagen-induced platelet secretion by enhancing myosin light chain kinase activation. *J. Biol. Chem.* 278, 46661–46667.

van Gestel, M. A., Heemskerk, J. W., Slaaf, D. W., Heijnen, V. V., Reneman, R. S., and Oude Egbrink, M. G. (2003). *In vivo* blockade of platelet ADP receptor P2Y12 reduces embolus and thrombus formation but not thrombus stability. *Arterioscler. Thromb. Vasc. Biol.* 23, 518–523.

Varani, K., Portaluppi, F., Gessi, S., Merighi, S., Ongini, E., Belardinelli, L., et al. (2000). Dose and time effects of caffeine intake on human platelet adenosine A(2A) receptors : functional and biochemical aspects. *Circulation* 102, 285–289.

Varani, K., Portaluppi, F., Merighi, S., Ongini, E., Belardinelli, L., and Borea, P. A. (1999). Caffeine alters A2A adenosine receptors and their function in human platelets. *Circulation* 99, 2499–2502.

Varga-Szabo, D., Braun, A., and Nieswandt, B. (2009). Calcium signaling in platelets. *J. Thromb. Haemost.* 7, 1057–1066. doi: 10.1111/j.1538-7836.2009.03455.x

Yang, D., Chen, H., Koupenova, M., Carroll, S. H., Eliades, A., Freedman, J. E., et al. (2010). A new role for the A2b adenosine receptor in regulating platelet function. *J. Thromb. Haemost.* 8, 817–827. doi: 10.1111/j.1538-7836.2010.03769.x

Yang, D., Koupenova, M., Mccrann, D. J., Kopeikina, K. J., Kagan, H. M., Schreiber, B. M., et al. (2008). The A2b adenosine receptor protects against vascular injury. *Proc. Natl. Acad. Sci. U.S.A.* 105, 792–796. doi: 10.1073/pnas.0705563105

Yang, D., Zhang, Y., Nguyen, H. G., Koupenova, M., Chauhan, A. K., Makitalo, M., et al. (2006). The A2B adenosine receptor protects against inflammation and excessive vascular adhesion. *J. Clin. Invest.* 116, 1913–1923.

Conflict of Interest Statement: The authors declare that the research was conducted in the absence of any commercial or financial relationships that could be construed as a potential conflict of interest.

frontiers in Pharmacology

ORIGINAL RESEARCH
published: 24 January 2018
doi: 10.3389/fphar.2018.00016

Elevated Pressure Changes the Purinergic System of Microglial Cells

*Ana C. Rodrigues-Neves[1,2], Inês D. Aires[1,2], Joana Vindeirinho[2,3], Raquel Boia[1,2], Maria H. Madeira[1,2], Francisco Q. Gonçalves[2,3], Rodrigo A. Cunha[2,3,4], Paulo F. Santos[1,2,5], António F. Ambrósio[1,2,4,6] and Ana R. Santiago[1,2,4,6]**

[1] Coimbra Institute for Clinical and Biomedical Research (iCBR), Faculty of Medicine, University of Coimbra, Coimbra, Portugal, [2] CNC.IBILI Consortium, University of Coimbra, Coimbra, Portugal, [3] Center for Neuroscience and Cell Biology, University of Coimbra, Coimbra, Portugal, [4] Faculty of Medicine, University of Coimbra, Coimbra, Portugal, [5] Department of Life Sciences, Faculty of Sciences and Technology, University of Coimbra, Coimbra, Portugal, [6] Association for Innovation and Biomedical Research on Light and Image, Coimbra, Portugal

Glaucoma is the second cause of blindness worldwide and is characterized by the degeneration of retinal ganglion cells (RGCs) and optic nerve atrophy. Increased microglia reactivity is an early event in glaucoma that may precede the loss of RGCs, suggesting that microglia and neuroinflammation are involved in the pathophysiology of this disease. Although global changes of the purinergic system have been reported in experimental and human glaucoma, it is not known if this is due to alterations of the purinergic system of microglial cells, the resident immune cells of the central nervous system. We now studied if elevated hydrostatic pressure (EHP), mimicking ocular hypertension, changed the extracellular levels of ATP and adenosine and the expression, density and activity of enzymes, transporters and receptors defining the purinergic system. The exposure of the murine microglial BV-2 cell line to EHP increased the extracellular levels of ATP and adenosine, increased the density of ecto-nucleoside triphosphate diphosphohydrolase 1 (E-NTPDase1, CD39) and decreased the density of the equilibrative nucleotide transporter 2 as well as the activity of adenosine deaminase. The expression of adenosine A_1 receptor also decreased, but the adenosine A_3 receptor was not affected. Notably, ATP and adenosine selectively control migration rather than phagocytosis, both bolstered by EHP. The results show that the purinergic system is altered in microglia in conditions of elevated pressure. Understanding the impact of elevated pressure on the purinergic system will help to unravel the mechanisms underlying inflammation and neurodegeneration associated with glaucoma.

Keywords: purinergic system, ATP, adenosine, microglia, elevated pressure, glaucoma

OPEN ACCESS

Edited by:
Francisco Ciruela, University of Barcelona, Spain

Reviewed by:
Rodrigo Pacheco, Universidad Andrés Bello, Chile
Claire H. Mitchell, University of Pennsylvania, United States

***Correspondence:**
Ana R. Santiago
asantiago@fmed.uc.pt

Specialty section:
This article was submitted to Experimental Pharmacology and Drug Discovery, a section of the journal Frontiers in Pharmacology

Received: *17 October 2017*
Accepted: *05 January 2018*
Published: *24 January 2018*

Citation:
Rodrigues-Neves AC, Aires ID, Vindeirinho J, Boia R, Madeira MH, Gonçalves FQ, Cunha RA, Santos PF, Ambrósio AF and Santiago AR (2018) Elevated Pressure Changes the Purinergic System of Microglial Cells. Front. Pharmacol. 9:16. doi: 10.3389/fphar.2018.00016

INTRODUCTION

Glaucoma is a multifactorial degenerative disease characterized by the progressive loss of retinal ganglion cells (RGCs) and optic nerve fibers that leads to vision loss (Casson et al., 2012). Elevated intraocular pressure (IOP) is the most common risk factor of glaucoma and the current treatments are based on lowering the IOP (Cohen and Pasquale, 2014). However, some patients still progress to blindness despite successful control of IOP (Song et al., 2015), suggesting that the control of IOP is not sufficient to prevent RGC loss (Levin et al., 2017).

Microglial cells are the immunocompetent cells of the central nervous system (CNS). Under resting conditions, microglial cells are ramified and constantly monitor their surrounding environment. However, after an insult, microglia change their morphology and become reactive, migrate toward the lesion site, release pro-inflammatory mediators and phagocyte cell debris (Ransohoff and Perry, 2009). Sustained microglia-mediated neuroinflammation is associated with several retinal neurodegenerative diseases, namely glaucoma (Madeira et al., 2015a). Exacerbated microglia reactivity has been detected early in experimental models of glaucoma, even before RGC death (Bosco et al., 2011, 2015), suggesting that the modulation of microglia reactivity may attenuate disease progression.

Purine nucleotides are, among others, primordial mediators of cell-to-cell communication (Burnstock and Verkhratsky, 2009; Verkhratsky and Burnstock, 2014). Particularly, purines control several functions of microglia, such as chemotaxis, phagocytosis, and cytokine and chemokine release (reviewed in Di Virgilio et al., 2009). In pathological conditions, neurons, astrocytes and microglia release ATP and adenosine to the extracellular space (Sperlágh and Illes, 2007; Rodrigues et al., 2015). The ratio between the release and the removal, by enzymatic degradation and uptake, determines the extracellular levels of ATP and adenosine. ATP has been postulated to be released by vesicular exocytosis, carrier-mediated release, cytolytic release and through channels and membrane pores (Ballerini et al., 2002; Cook and McCleskey, 2002; Stout et al., 2002; Sperlágh and Illes, 2007; Gajardo-Gomez et al., 2016). Adenosine is considered to be generated by the breakdown of ATP through the actions of NTPDase (CD39) and ecto-5′-nucleotidase (CD73) (Yegutkin, 2008; Cunha, 2016), but it can also be released on its own (Sperlágh and Illes, 2007). The extracellular levels of adenosine are regulated by equilibrative nucleoside transporters (ENTs), that mediate the bidirectional adenosine transport, or through concentrative transporters (CNTs), that mediate the influx of adenosine (Yegutkin, 2008; Melani et al., 2012). Moreover, adenosine can be metabolized into adenosine monophosphate (AMP) by adenosine kinase (ADK) or into inosine by adenosine deaminase (ADA).

There are indications that the purinergic system is altered in glaucoma, as heralded by the increased levels of ATP detected in the aqueous humor of patients with glaucoma (Zhang et al., 2007; Li et al., 2011) and in experimental models of the disease (Resta et al., 2007; Reigada et al., 2008). Since microglial cells have a role in the pathophysiology of glaucoma and the purinergic system in microglial cells has been demonstrated to play a critical role in controlling inflammation and immune response in several models of neurological diseases (reviewed in Harry, 2013), we now studied the impact of elevated pressure in the set-up of the purinergic system in microglia and also assessed the role of ATP and adenosine in mediating the effects of elevated pressure in microglia phagocytosis and motility.

Abbreviations: A_1R, adenosine A_1 receptor; $A_{2A}R$, adenosine A_{2A} receptor; $A_{2B}R$, adenosine A_{2B} receptor; A_3R, adenosine A_3 receptor; ADA, adenosine deaminase; ADK, adenosine kinase; ADP, adenosine di-phosphate; AMP, adenosine monophosphate; ATP, adenosine triphosphate; BCA, bicinchoninic acid; BSA, bovine serum albumin; CD73, ecto-5′-nucleotidase; CNS, central nervous system; CNT, concentrative nucleoside transporter; ECF, chemi-fluorescence; ECL, Chemiluminescence; EHP, elevated hydrostatic pressure; ENT, equilibrative nucleoside transporter; E-NTPDase1/CD39, ecto-nucleoside triphosphate diphosphohydrolase 1; FBS, fetal bovine serum; HPLC, high-performance liquid chromatography; IOP, intraocular pressure; NBMPR, S-(4-nitrobenzyl)-6-thioinosine; PFA, paraformaldehyde; RGCs, retinal ganglion cells; RPMI, Roswell Park Memorial Institute; SDS, sodium dodecyl sulfate; TRITC, tetramethylrhodamine B isothiocyanate; VNUT, nucleotide transporter.

MATERIALS AND METHODS

Microglial Cell Culture

The immortalized murine BV-2 microglia cell line was cultured in Roswell Park Memorial Institute (RPMI) medium, supplemented with 10% fetal bovine serum (FBS) and 1% of antibiotics (penicillin 100 U/ml, streptomycin 100 μg/ml) and maintained at 37°C under a humidified atmosphere with 5% CO_2. For experiments, cells were cultured in RPMI with 2% FBS and 1% antibiotics at a density of 6×10^3 cells/cm^2 in 6-well-plates or at density of 1×10^4 cells/cm^2 in 12-well-plates.

Cells were exposed to elevated hydrostatic pressure (EHP, 70 mmHg above atmospheric pressure) for 4 or 24 h, as previously described (Madeira et al., 2016). Control cultures were kept in a standard incubator at atmospheric pressure.

ATP Quantification

The extracellular levels of ATP were measured with a luciferin-luciferase assay kit, as previously described (Cunha et al., 2000; Madeira et al., 2015b). Briefly, cell culture supernatants were collected and stored at −80°C until used. Cells were collected and protein concentration was determined by the bicinchoninic acid (BCA) method (Pierce Biotechnology). Supernatants were quickly defrosted and incubated with ATP assay mix (Sigma-Aldrich) in an opaque 96-well plate. ATP levels were measured using a VICTOR multilabel plate reader (Perkin Elmer). The ATP concentration in each sample was determined by interpolation with a standard curve obtained from an ATP stock solution and was normalized to the amount of protein. Results are presented as percentage of control.

Adenosine Quantification

The extracellular levels of adenosine were quantified using high-performance liquid chromatography (HPLC), as previously described (Vindeirinho et al., 2013). Briefly, cell supernatants were analyzed in Beckman-System Gold HPLC apparatus, with a computer controlled 126 Binary Pump Model using a 166 Variable UV detector (detection at 254 nm) and a Lichrospher 100 RP-18 (5 mm) column from Merck. An isocratic elution with 10 mM phosphate buffer (NaH_2PO_4; pH 6.0) and 14% methanol was performed with a flow rate of 1.5 ml/min. Adenosine was quantified by considering the retention time and absorption spectra, and then comparing with the standard curve. Results are presented as percentage of control.

Measurement of AMP Dephosphorylation

BV-2 microglial cells were washed with warm reaction buffer (in mM: 2 $MgCl_2$, 125 NaCl, 1 KCl, 10 glucose, 10 HEPES; pH 7.4), and then incubated with 2 mM adenosine monophosphate

(AMP; Sigma-Aldrich) for 40 min at 37°C. The medium was collected to quantify the free inorganic phosphate, as a measurement of AMP degradation with the Malachite Green Phosphate Assay kit, following the instructions provided by the manufacturer (Cayman Chemicals). Inorganic free phosphate was detected by spectrophotometry (620–630 nm). Results are presented as fold-change of control.

Measurement of ADA Activity

BV-2 cells were washed twice with ice-cold phosphate-buffered saline (PBS, in mM: 137 NaCl, 2.7 KCl, 10 Na_2HPO_4, 1.8 KH_2PO_4, pH 7.4) and lysed in 50 mM Tris-HCl (pH 7.2), supplemented with complete mini protease inhibitor cocktail tablets (Roche). The enzymatic activity of ADA was measured following the instructions provided by the manufacturer (Diazyme). Results were normalized to the amount of protein quantified by the BCA method, and are presented as percentage of control.

Western Blotting

BV-2 cells were washed twice with ice-cold PBS at 4°C. Cells were lysed in radioimmunoprecipitation assay buffer [RIPA, in mM: 50 Tris HCl, pH 7.4; 150 NaCl; 5 EDTA; 1% Triton X-100; 0.5% sodium deoxycholate; 0.1% sodium dodecyl sulfate (SDS)] supplemented with complete mini protease inhibitor cocktail tablets and 1 mM of dithiothreitol (DTT) at 4°C. Samples were denatured by adding 6x concentrated sample buffer (0.5 M Tris, 30% glycerol, 10% SDS, 0.6 M DTT, 0.012% bromophenol blue) and heating for 5 min at 95°C. When blotting for CD39, cells were lysed in non-reduced conditions.

Samples were separated in SDS-polyacrylamide gel electrophoresis (SDS-PAGE) and transferred onto PVDF membranes (Millipore). The membranes were blocked with 5% milk and then were incubated with the antibodies indicated in **Table 1**. Immunoreactive bands were visualized using Enhanced Chemi-Fluorescence system (ECF; GE Healthcare) on a Storm device (Molecular Dynamics, GE Healthcare) or with Enhance Chemiluminescence system (ECL; Bio-Rad) on a Versadoc (Bio-Rad). Digital quantification of band intensity was performed using Quantity One software (Bio-Rad). The membranes were reprobed for glyceraldehyde 3-phosphate dehydrogenase (GAPDH) to control for similar amounts of protein.

Immunocytochemistry

Cells were washed with ice-cold PBS and fixed using 4% of paraformaldehyde (PFA) with 4% sucrose for 10 min at room temperature (RT). After fixation, the cells were washed with PBS and permeabilized during 5 min with 1% Triton X-100 in PBS. Then, cells were blocked with 3% of bovine serum albumin (BSA; NZYtech) and 0.2% Tween-20 in PBS for 1 h at RT to prevent the non-specific binding. Afterwards, cells were incubated with the primary antibody diluted in the blocking solution for 90 min at RT (**Table 2**). After washing, the cells were incubated with the secondary antibody in the same solution for 1 h at RT in the dark. Then, cells were rinsed with PBS. Nuclei were stained with 4′,6-diamidino-2-phenylindole (DAPI 1:2,000; Molecular Probes, Life Technologies) and F-actin was stained with phalloidin conjugated to Tetramethylrhodamine B isothiocyanate (TRITC, 1:500; Sigma-Aldrich). Upon rising with PBS, the coverslips were mounted in glycergel mounting medium and observed with a fluorescence microscope (Axio Observer.Z1), using a LD Plan-Neofluar 40x/0.6 Korr Ph2 M27 objective.

Representative images were acquired with a confocal microscope (LSM 710, Zeiss) on an Axio Observer.Z1 microscope using Plan-Apochromat 63x/1.40 Oil Dic M27 objective.

TABLE 1 | List of primary antibodies used in Western blotting.

Primary antibody	Dilution	Protein (μg)	Molecular weight (kDa)	Supplier
Anti-A_1R	1:500	30	37	Thermo Fisher Scientific
Anti-A_3R	1:100	60	44	Santa Cruz Biotechnology
Anti-ADA	1:100	60	41	Santa Cruz Biotechnology
Anti-ADK	1:100	60	48/38	Santa Cruz Biotechnology
Anti-CNT2	1:100	60	72	Santa Cruz Biotechnology
Anti-CD39	1:100	70	~70	Ectonucleotidases-ab
Anti-ENT2	1:100	40	50-55	Santa Cruz Biotechnology
Anti-GAPDH	1:5000	–	37	Abcam

TABLE 2 | List of primary antibodies used in immunocytochemistry.

Primary antibody	Dilution	Supplier
A_1R	1:250	Thermo Fisher Scientific
A_3R	1:50	Santa Cruz Biotechnology

Boyden Chamber Migration Assay

BV-2 cells were cultured in serum-free medium for 24 h before the experiment. Then, cells were plated in transwell cell culture inserts (8.0 μm pore diameter; Merck Millipore) in RPMI with 2% FBS and 1% antibiotics. Cells were incubated with apyrase (30 U/mL) and ADA (1 U/mL) followed by exposure to EHP for 4 h. At the end of the experiment, cells were washed with warm PBS and the cells in upper side of the insert were removed with a cotton swab. After fixation with 4% PFA with 4% sucrose during 10 min, the nuclei were stained with DAPI (1:2,000). The membranes were mounted in glass slides with glycergel mounting medium, and the preparations were observed with a fluorescence microscope (Axio Observer.Z1) using a N-Achroplan 5x/0.15 M27 objective. Five random images per sample were acquired. The number of cells in the bottom side of the insert (the cells that migrated) was counted and the results were expressed as percentage of control.

Phagocytosis Assay

BV-2 cells were plated in RPMI with 2% FBS and 1% antibiotics and exposed to EHP for 24 h. Cells were incubated with apyrase (30 U/mL) and ADA (1 U/mL) 2 h before the end of the experiment. One hour before the end of the experiment, BV-2 cells were incubated with 0.025% fluorescent beads at 37°C. Then, cells were washed with warm PBS and fixed with 4%

PFA with 4% sucrose. BV-2 cells were stained with TRITC-conjugated phalloidin (1:500; Sigma-Aldrich) and nuclei were stained with DAPI (1:2,000). Cells were observed with a confocal microscope (LSM 710, Zeiss) using a Plan-Apochromat 20x/0.8 M27 objective and five random fields were acquired from each condition. The total number of cells in each field, the number of cells with incorporated beads and the number of fluorescent beads phagocytized by each cell were counted. The phagocytic efficiency was calculated:

$$Phagocytic\ efficiency\ (\%) = \frac{(1 \times x1 + 2 \times x2 + 3 \times x3 + n \times xn)}{total\ number\ of\ cells} \times 100\%$$

where xn represents the number of cells containing n microspheres ($n = 1, 2, 3 \ldots$ up to a maximum of 6 points for more than 5 microspheres ingested per each cell).

Statistical Analysis

Results are presented as mean ± SEM. The number of independent experiments is indicated in each bar. Statistical analysis was performed using GraphPad Prism Version 6 (GraphPad Software). The normality of the data was assessed with Shapiro-Wilk test. Data was analyzed using the non-parametric Kruskall-Wallis test, followed by Dunn's multiple comparison test. Differences were considered significant for $p < 0.05$.

RESULTS

Microglial cells are endowed with the machinery of the purinergic system (Sperlágh and Illes, 2007; Castellano et al., 2016). We now assessed how the purinergic system of microglial cells is altered after challenging the microglial cells in a pressure chamber to mimic elevated IOP.

Elevated Hydrostatic Pressure Increases Extracellular Levels of ATP and Adenosine

BV-2 cells were exposed to elevated pressure for 4 and 24 h and the levels of ATP (**Figure 1A**) and adenosine (**Figure 1B**) were quantified in cell culture medium supernatants. The exposure of microglia to EHP for 4 and 24 h increased the extracellular levels of ATP to 233.1 ± 49.9% ($p < 0.01$) and 187.9 ± 33.4% of control, respectively, and the adenosine levels to 124.1 ± 9.6% and 131.9 ± 9.6% of the control ($p < 0.05$), respectively.

Elevated Hydrostatic Pressure Increases CD39 but Does Not Affect AMP Catabolism

Adenosine can be formed through the hydrolysis of adenine nucleotides [ATP, adenosine di-phosphate (ADP) and AMP] by a cascade of ectonucleotidases, including CD39 and CD73 that are expressed in several cell types, including microglia (Haskó et al., 2005).

Here, we addressed whether EHP could affect the expression of CD39 as well as AMP catabolism, both involved in adenosine formation through ATP hydrolysis. CD73 was not detected in BV-2 cells either by qPCR or Western blot (data not shown). The protein levels of CD39 significantly increased in BV-2 cells exposed to EHP for 4 and 24 h (147.3 ± 23.1% and 128.6 ± 11.0% of the control, respectively; $p < 0.05$; **Figure 2A**), which is in agreement with the previous proposal that CD39 might be a potential indicator of increased extracellular levels of ATP in retina cells (Lu et al., 2007). However, the dephosphorylation of AMP into adenosine was not altered in BV-2 cells exposed to 4 h EHP (1.0 ± 1 fold-change; **Figure 2B**).

Elevated Hydrostatic Pressure Impairs the Activity of ADA, but Not the Protein Levels of ADA and ADK

Adenosine can be removed from the extracellular space by degradation into inosine mediated by ADA, while the intracellular the removal of adenosine also occurs by the conversion into AMP mediated by adenosine kinase (Yegutkin, 2008).

The exposure of microglial cells to EHP for 4 and 24 h did not affect the protein levels of ADA and ADK (**Figures 3A,C**). Nevertheless, the activity of ADA (**Figure 3B**) significantly decreased in microglia exposed to EHP for 24 h to 67.9 ± 10.2% of the control ($p < 0.05$).

Elevated Hydrostatic Pressure Decreases ENT2 but Does Not Change CNT2 Protein Levels

Extracellular adenosine levels are typically regulated by nucleoside transporters or metabolism (Latini and Pedata, 2001). Hence, we also evaluated the impact of EHP exposure on the expression of nucleoside transporters ENT1, ENT2, and CNT2 in BV-2 cells.

ENT1 was not detected by Western blot (data not shown). The protein levels of ENT2 in BV-2 microglia exposed to EHP for 4 h were similar to the control. However, exposure to EHP for 24 h significantly decreased the protein levels of ENT2 in microglia (46.5 ± 9.6% of the control; $p < 0.05$; **Figure 4A**). The protein levels of CNT2 were not altered in BV-2 cells exposed to EHP (83.8 ± 13.5% and 105.2 ± 10.0% of the control, for 4 and 24 h, respectively; **Figure 4B**).

Elevated Hydrostatic Pressure Changes the Expression and Density of A_1R but Not A_3R

The actions of adenosine are dependent on the activation of the adenosine receptors. We evaluated the impact of EHP on the expression of A_1R and A_3R receptors in BV-2 microglial cells.

The exposure of BV-2 cells to EHP, for 4 and 24 h, decreased the protein levels of A_1R to 64.5 ± 15.6% and 45.9 ± 4.2% ($p < 0.05$) of the control, respectively, as assessed by Western blot (**Figure 5A**). As we previously reported (Lopes et al., 2003), Western blot for A_3R yields three bands but we quantified the more intense 44 kDa that corresponds to the expected molecular weight of A_3R. This analysis revealed that the protein levels of A_3R (**Figure 5B**) did not change in microglial cells upon exposure

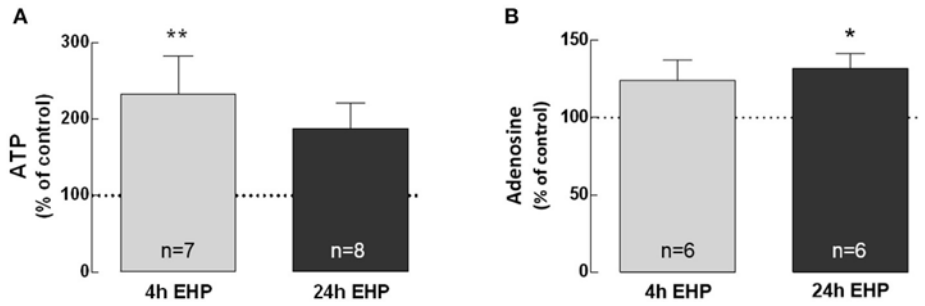

FIGURE 1 | Elevated hydrostatic pressure increases extracellular levels of ATP and adenosine. The levels of extracellular ATP **(A)** and adenosine **(B)** were quantified in cell supernatants. Results were normalized to the amount of protein in each sample and are expressed as percentage of the control. *$p < 0.05$, **$p < 0.01$, different from control; Kruskal-Wallis test, followed by Dunn's multiple comparison test.

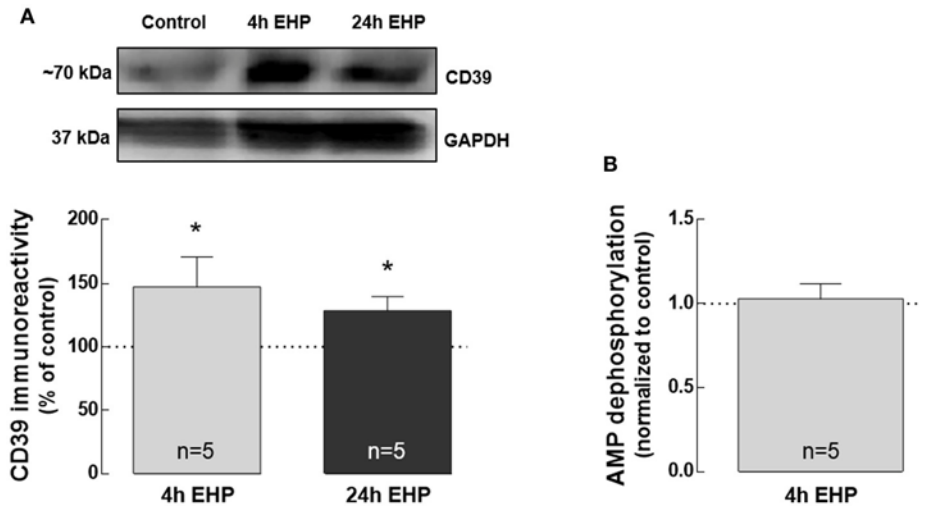

FIGURE 2 | Elevated hydrostatic pressure increases CD39 but does not affect AMP catabolism. Total BV-2 cell extracts were assayed for CD39 **(A)** by Western blot. Representative images for CD39 and GAPDH (loading control) are presented above the graph. Results are expressed as percentage of control. **(B)** AMP dephosphorylation was evaluated by the malachite green phosphate assay in cell supernatants. Results are expressed as fold change of control. *$p < 0.05$, different from control; Kruskal-Wallis test, followed by Dunn's multiple comparison test.

to EHP for 4 and 24 h (97.4 ± 17.2% and 124.0 ± 27.8% of the control, respectively).

The effects of EHP on the immunoreactivity of A_1R and A_3R were also assessed by immunocytochemistry in microglia (**Figures 5C,D**). In microglial cells exposed to EHP, A_1R immunoreactivity decreased when compared with the control, whereas the A_3R immunoreactivity was similar to the control, supporting the results obtained by Western blotting.

ATP and Adenosine Mediate Microglia Migration Induced by Elevated Hydrostatic Pressure

A feature of reactive microglia is their ability to migrate toward the site of injury, where they release pro-inflammatory mediators and phagocyte cell debris (Karlstetter et al., 2010). Although the role of the purinergic system in microglia chemotaxis is well established (Honda et al., 2001; Davalos et al., 2005; Wu et al., 2007), the contribution of ATP and adenosine to the motility of microglia in conditions of elevated pressure it still unknown. Therefore, we evaluated whether EHP could affect microglia migration and if ATP and adenosine affected this process (**Figure 6**). When microglial cells were exposed to EHP for 4 h, the number of microglia that migrated to the bottom side of the transwell significantly increased to 220.5 ± 22.8% of the control ($p < 0.05$). The treatment of BV-2 cells with 30 U/ml apyrase, to remove the extracellular ATP, prevented the effect of EHP in microglia migration (98.0 ± 10.4% of the control; $p < 0.01$ compared with EHP). BV-2 cells were also pre-treated with 1 U/ml ADA, to remove the extracellular adenosine. The removal of extracellular adenosine also prevented the migration of microglial cells to the bottom side of the membrane elicited by EHP (115.5 ± 19.2% of the control, $p < 0.01$ compared with EHP). This strict dependency on extracellular ATP and adenosine for the increased migration of microglia upon EHP is also an important control to exclude the possibility that migration in

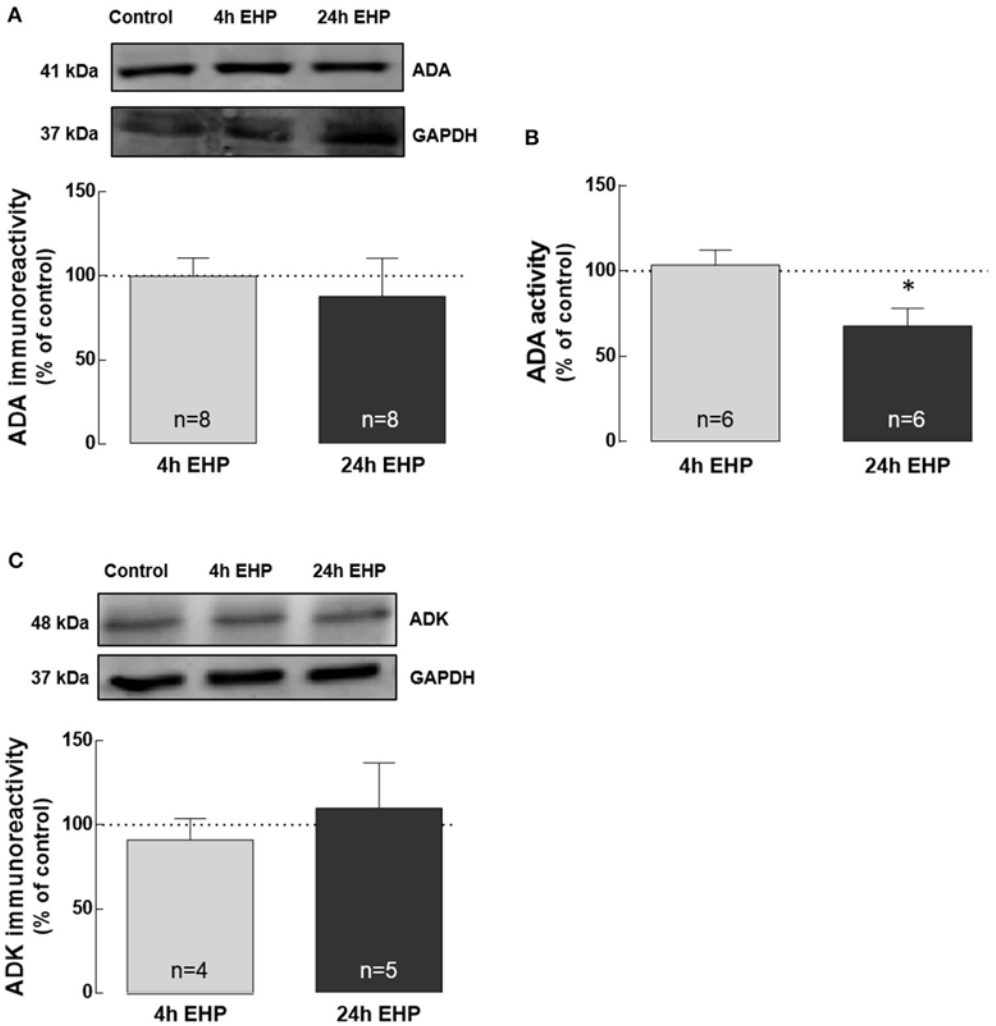

FIGURE 3 | Elevated hydrostatic pressure impairs the activity of ADA, but not the protein levels of ADA and ADK. Total BV-2 cell extracts were assayed for ADA by Western blot **(A)** and enzymatic activity **(B)** as well as for ADK by Western blot **(C)**. Representative images for ADA, ADK and GAPDH (loading control) are presented above the graphs **(A**,**C)**. Results are expressed as percentage of control. *$p < 0.05$, different from control; Kruskal-Wallis test, followed by Dunn's multiple comparison test.

EHP conditions might result from cells that were just pushed through the pores.

ATP and Adenosine Do Not Contribute to the Increase of Phagocytic Efficiency in Microglia Induced by Elevated Hydrostatic Pressure

Increased phagocytic efficiency is a feature of reactive microglia (Kettenmann et al., 2011). The contribution of adenosine and ATP to the phagocytic efficiency of microglia upon exposure to EHP was assessed by incubating microglia with fluorescent microbeads (**Figure 7**). The phagocytic efficiency of microglia exposed to EHP increased by nearly 200% when compared with control cells (from 13 ± 2% in control conditions to 25 ± 3% under EHP; $p < 0.01$). Incubation with apyrase (30 U/ml) and ADA (1 U/ml) was unable to decrease the phagocytic efficiency in cells under EHP (23 ± 2% and 19 ± 3%, respectively).

DISCUSSION

The purinergic system is a controller of inflammation (reviewed in Di Virgilio et al., 2009) and microglia-mediated neuroinflammation contributes to the pathogenesis of glaucoma (reviewed in Madeira et al., 2015a). Here, we show for the first time that elevated pressure modifies the purinergic system of BV-2 microglial cells, altering the levels of ATP and adenosine, as well as enzymes responsible for the maintenance of purine levels, which we showed to regulate the EHP-induced microglial cell migration.

EHP increased the extracellular levels of ATP in BV-2 cells, without increasing cell death (data not shown), indicating that

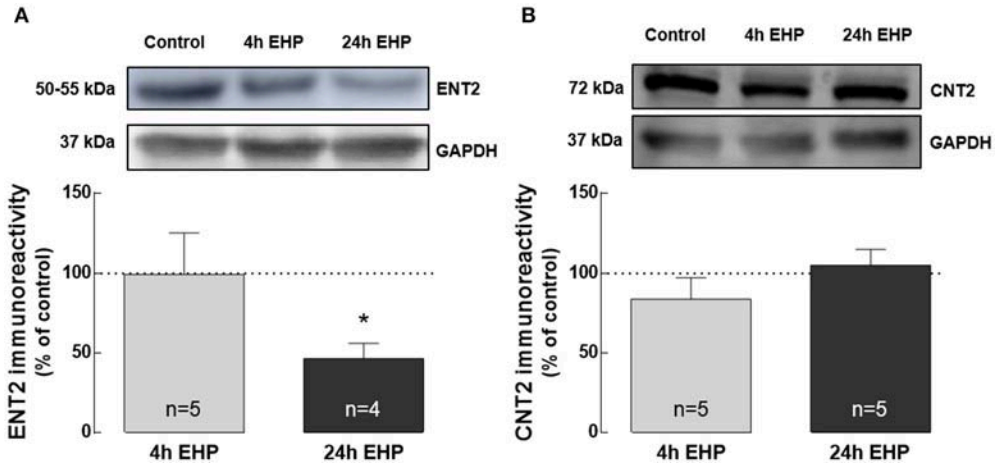

FIGURE 4 | Elevated hydrostatic pressure decreases ENT2 but does not change CNT2 protein levels. Total BV-2 cell extracts were assayed for ENT2 **(A)** and CNT2 **(B)** by Western blot. Representative images for ENT2, CNT2, and GAPDH (loading control) are presented above the graphs. Results are expressed as percentage of control. *$p < 0.05$, different from control; Kruskal-Wallis test, followed by Dunn's multiple comparison test.

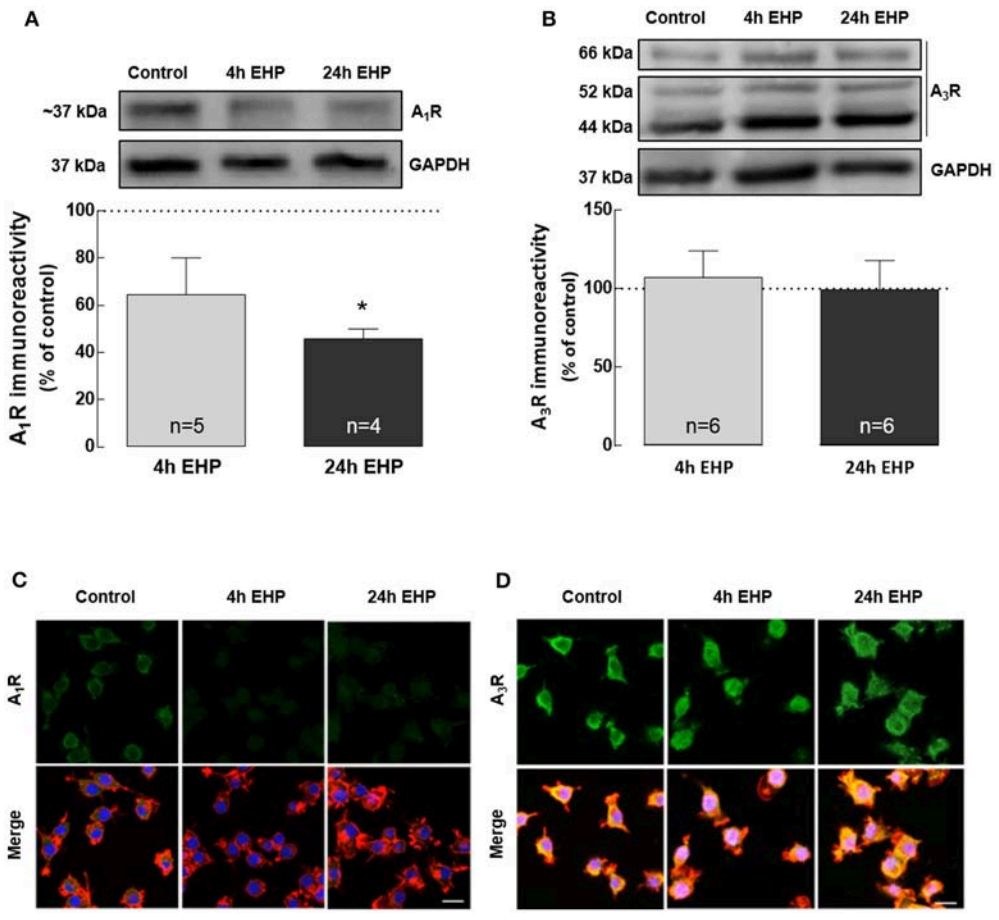

FIGURE 5 | Elevated hydrostatic pressure changes the expression and density of A_1R but not A_3R. Total BV-2 cell extracts were assayed for A_1R **(A)** and A_3R **(B)** by Western blot. Representative images for A_1R, A_3R and GAPDH (loading control) are presented above the graphs. Results are expressed as percentage of control. Cells were immunolabelled with anti-A_1R (green) **(C)** or anti-A_3R (green) **(D)** antibodies. Phalloidin (red) staining was used to visualize cells. Nuclei were counterstained with DAPI (blue). Scale bar: 20 μm. *$p < 0.05$, different from control; Kruskal-Wallis test, followed by Dunn's multiple comparison test.

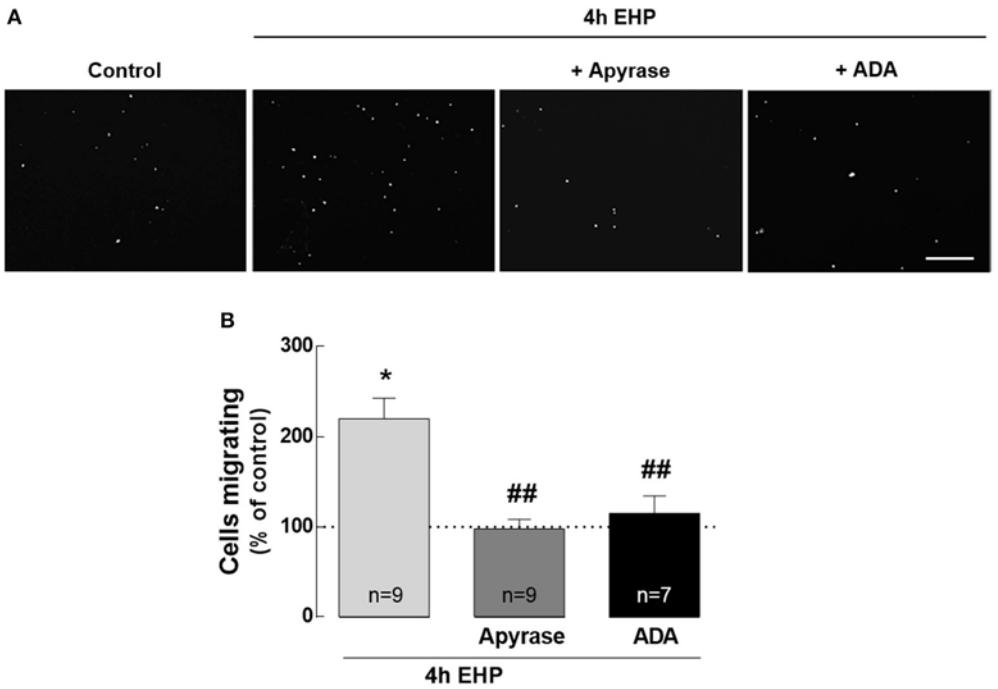

FIGURE 6 | ATP and adenosine mediate microglia migration induced by elevated hydrostatic pressure. Cell migration was assessed with the Boyden chamber migration assay. The cell nuclei in the bottom surface of the Transwell were observed after DAPI staining **(A)** and the number of migrated BV-2 cells was counted. **(B)** Results are expressed as percentage of control. Scale bar: 100 μm. $^{*}p < 0.05$, different from control; $^{\#\#}p < 0.01$, different from 4 h EHP; Kruskal-Wallis test, followed by Dunn's multiple comparison test.

ATP released from these cells occurs by a non-lytic mechanism. Several reports have demonstrated the ability of microglia to release ATP under different conditions (Ferrari et al., 1997; Imura et al., 2013; Shinozaki et al., 2014; George et al., 2015). Indeed, microglia are endowed with the nucleotide transporter (VNUT) that transports cytosolic ATP into vesicles (Sawada et al., 2008) and the genetic deletion of VNUT impairs ATP release from microglia (Shinozaki et al., 2014). Other mechanisms mediate the release of ATP in microglia, namely, the carrier-mediated release (Ballerini et al., 2002), pannexins and/or hemi-channels (Gajardo-Gomez et al., 2016), as well as the cytolytic release (Sperlágh and Illes, 2007).

Increased ATP and adenosine levels have been reported in the aqueous humor of glaucoma patients (Daines et al., 2003; Zhang et al., 2007; Li et al., 2011), implicating the purinergic system in the pathophysiology of glaucoma. Increased ATP levels have been also documented in the retinas of animal models of glaucoma (Lu et al., 2015; Pérez de Lara et al., 2015) and in the vitreous of bovine eyecup preparations subjected to elevated pressure (Reigada et al., 2008). Moreover, we have recently reported that elevated pressure increases extracellular ATP in rat retinal organotypic cultures (Madeira et al., 2015b). In the retinal eyecup and organotypic models it is not possible to identify which cells release ATP, even though several cells are potential sources of extracellular ATP, such as neurons, astrocytes, Müller cells, and microglia (Rodrigues et al., 2015). Astrocytes, for instance, can release ATP when subjected to chronic mechanical strain (Beckel et al., 2014). Under mechanical strain, NLRP3 inflammasome is activated in the retina and astrocytes, due to the upregulation of IL-1β expression, which depends on ATP (released from pannexin hemichannels) and P_2X_7 receptor stimulation (Albalawi et al., 2017).

The levels of extracellular adenosine were increased in BV-2 microglia exposed to elevated pressure. Extracellular adenosine can arise from the direct release of adenosine into the extracellular space, or by ATP hydrolysis through ecto-enzymes (Yegutkin, 2008; Cunha, 2016), involving the conversion of ATP or ADP into AMP by CD39, followed by AMP dephosphorylation into adenosine by ecto-5′-nucleotidase (Ecto5′NTase, CD73). Increased expression of NTPDase1 in the posterior eye of rat, mouse, and primate models of glaucoma has been demonstrated (Lu et al., 2015), which is in line with our findings of increased CD39 protein levels in BV-2 cells under elevated pressure. Indeed, NTPDase1 was already proposed as an index for increased ATP levels under pathological conditions (Lu et al., 2007). However, AMP dephosphorylation in microglial cells was not altered by elevated pressure. In addition, we were unable to detect CD73, which is in accordance with a recent study that reported the absence of CD73 expression in the BV-2 cell line (Murphy et al., 2017). Importantly, other enzymes, such as alkaline phosphatase, widely distributed in cell surface, can also degrade ATP, ADP, and AMP into adenosine (Zimmermann, 2006; Yegutkin, 2008; Vardy et al., 2012), and may be responsible for the conversion of extracellular AMP into adenosine in these cells. The half-life of extracellular adenosine may be regulated by extracellular adenosine deaminase (Ecto-ADA) that irreversibly

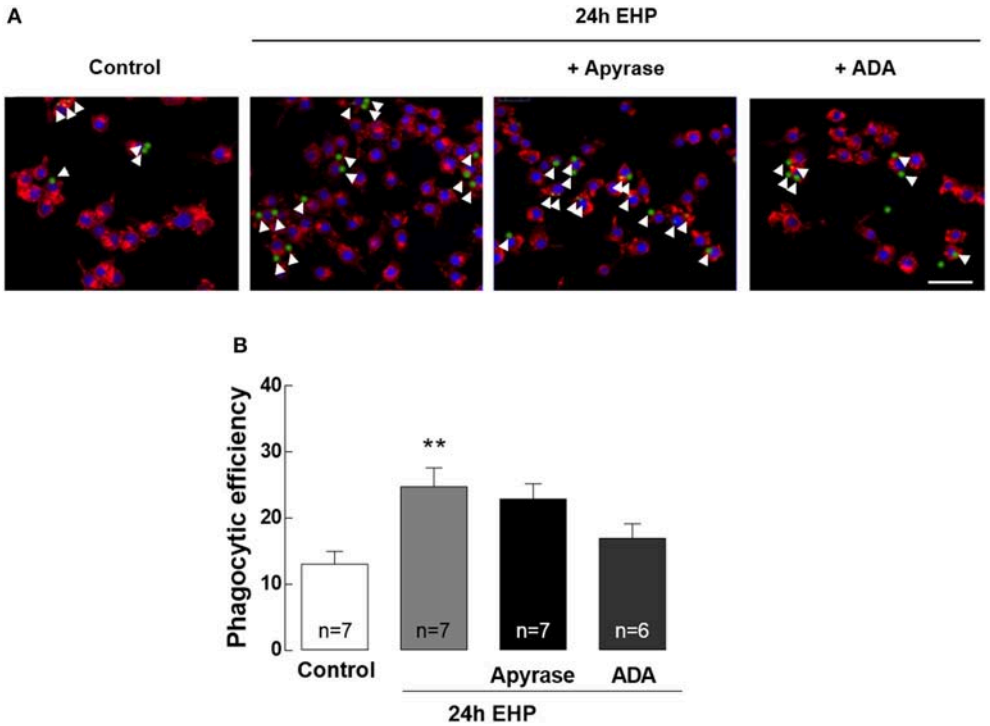

FIGURE 7 | ATP and adenosine do not contribute to the increase of phagocytic efficiency in microglia induced by elevated hydrostatic pressure. Phagocytosis was assessed using fluorescent microbeads. **(A)** Representative images of BV-2 cells stained with phalloidin (red) with incorporated beads (green). Nuclei were counterstained with DAPI (blue). Arrowheads show some beads engulfed by microglia. **(B)** Phagocytic efficiency. Scale bar: 50 μm. $^{**}p < 0.01$, different from control; Kruskal-Wallis test, followed by Dunn's multiple comparison test.

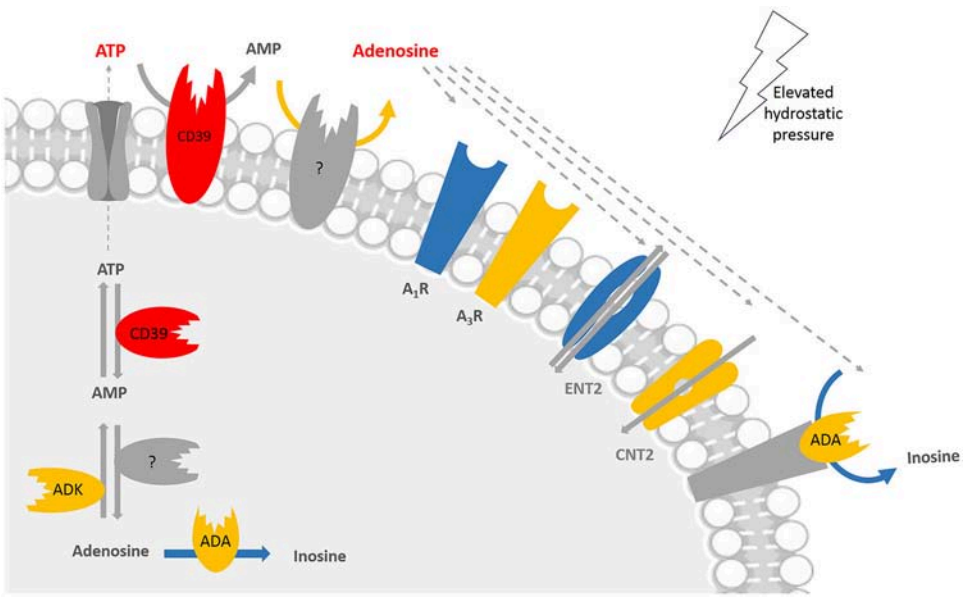

FIGURE 8 | Main alterations in the purinergic system of microglial cells in conditions of elevated pressure. The exposure of microglial cells to elevated pressure changes several players of the purinergic system in microglia, including enzymes, receptors, and transporters. Color code: red means increased levels, expression, or density; blue means decreased expression, density, or activity; and yellow means no changes at elevated pressure when compared with control pressure. Taking into account the lack of CD73 in BV-2 cells, the enzyme responsible for converting AMP into adenosine was not identified; it could be for instance alkaline phosphatase (AP), but we did not assess it experimentally. Adenosine triphosphate (ATP), adenosine monophosphate (AMP), adenosine deaminase (ADA), adenosine kinase (ADK), adenosine A_1 receptor (A_1R), adenosine A_3 receptor (A_3R), concentrative nucleoside transporter 2 (CNT2), equilibrative nucleoside transporter 2 (ENT2).

deaminates adenosine into inosine (Regateiro et al., 2013). Although no alterations were detected in the protein levels of ADA, the activity of this enzyme was decreased in cells exposed to elevated pressure, probably as a result of an allosteric modulation of ADA (Levine and Ginsburg, 2013), which we did not experimentally confirmed. This may explain the increase in extracellular adenosine levels. No changes were found in the protein levels of ADK (which converts intracellularly adenosine into AMP). Notably, this enzyme becomes easily saturated with basal concentrations of adenosine (Dunwiddie and Masino, 2001; Latini and Pedata, 2001), which prompts hypothesizing that ADK mostly controls basal levels of adenosine, but does not contribute to these increased levels of adenosine during elevated pressure.

Apart from metabolism, adenosine can also be cleared from the extracellular space by nucleoside transporters (Latini and Pedata, 2001). There are two types of adenosine transporters: equilibrative nucleoside transporters (ENTs) 1-4 and concentrative nucleoside transporters (CNTs) 1–3. Adenosine follows a concentrative gradient through ENTs, while CNTs transport nucleosides against the gradient (Thorn and Jarvis, 1996). ENTs are blocked by S-(4-nitrobenzyl)-6-thioinosine (NBMPR). In EOC-20 murine microglial cell line and in RAW264.7 macrophage cells, the majority of the adenosine transport is NBMPR-sensitive and insensitive to sodium removal, suggesting that ENTs are the primary transporters functioning in microglia (Carrier et al., 2006), where the presence of ENTs other than 1 and 2 has never been described. The decrease of ENT2 density in microglia caused by exposure to elevated pressure may affect the removal of adenosine from the extracellular space.

Adenosine mediates its actions by means of activation of G protein-coupled receptors named A_1R, $A_{2A}R$, $A_{2B}R$, and A_3R (Fredholm et al., 2001). All adenosine receptors have been described in microglial cells and microglia cell lines (Hammarberg et al., 2003; van Calker and Biber, 2005; Dare et al., 2007; Beckel et al., 2016). It is well documented that under brain noxious conditions, A_1Rs are downregulated with a concomitant increase in $A_{2A}R$ density (reviewed in Cunha, 2005). Accordingly, we found that EHP caused A_1R down-regulation in microglia and in previous reports, we demonstrated the up-regulation of $A_{2A}R$ in microglial cells triggered by elevated pressure (Madeira et al., 2015b, 2016). The downregulation of A_1R may result from the exposure of the receptor to an excessive amount of adenosine that results in ligand-induced internalization of the receptor (Ciruela et al., 1997; Coelho et al., 2006).

The purinergic system regulates several functions of microglial cells, such as cell process extension and retraction, migration, proliferation, and phagocytosis (Davalos et al., 2005; Koizumi et al., 2007; Gomes et al., 2013; Matyash et al., 2017). Microglia migration increased under elevated pressure, and this process appears to be mediated by ATP and adenosine. Cell migration can occur by three mechanisms: basal motility (in the absence of a chemical stimulus), chemokinesis (random motility in response to a chemical stimulus), and chemotaxis (migration toward and dependent of a chemical gradient; Wilkinson, 1998; Miller and Stella, 2009). ATP is a known microglial chemotactic agent (Honda et al., 2001; Davalos et al., 2005; Wu et al., 2007) acting on P_2Y_{12} and P_2X_4 receptors (Honda et al., 2001; Haynes et al., 2006). In addition to chemotaxis, ATP can mediate migration by chemokinesis (Miller and Stella, 2009). Moreover, adenosine may also play a role although it stills remains to be determined which adenosine receptor might bolster microglia chemotaxis: in fact $A_{2A}Rs$ are responsible for microglia retraction (Orr et al., 2009), whereas it was proposed that the activation of A_3R is required for ADP-induced P_2Y_{12}-mediated migration of microglia (Ohsawa et al., 2012).

Phagocytosis is a crucial function of microglia both in the surveillance and in reactive states (Mandrekar et al., 2009; Karlstetter et al., 2014; Scheiblich and Bicker, 2016). Elevated pressure increased microglia phagocytosis, but extracellular ATP and adenosine failed to prevent the increased phagocytosis, indicating that ATP and adenosine do not control this microglial function under elevated pressure conditions. In addition, ATP and adenosine *per se* did not change the phagocytic efficiency under basal conditions (data not shown). Others reported that the dual activation of P1 and P2 are mandatory for both migration and phagocytic capacity of microglial cells (Bulavina et al., 2013), which is not in total accordance with our results. Therefore, we cannot discard the possibility that the synergistic action of ATP and adenosine could be pivotal in phagocytosis, during elevated pressure conditions.

Our data showed for the first time that elevated pressure impaired the purinergic system of microglial cells (**Figure 8**) and this could interfere with microglial functions under elevated pressure. While it is important to keep in mind that an *in vitro* model of elevated pressure is an over-simplified model of glaucoma and that the BV-2 microglia cell line has particularities different from endogenous microglia in their native environment, the present results still pave the way to better appreciate the purinergic system in microglial cells as a putative target to be further considered for the management of glaucoma.

AUTHOR CONTRIBUTIONS

AR-N, IA, and AS conceived and designed the experiments; AR-N, IA, JV, and FG performed the experiments; AR-N, IA, JV, RB, MM, FG, RC, PS, AA, and AS analyzed and interpreted the results; RC, PS, AA, and AS contributed with reagents, materials, analysis tools; AR-N wrote the first draft of the manuscript and all authors have read and approved the final version.

FUNDING

This work was supported by FCT, Portugal (Project PTDC/BIM-MEC/0913/2012 and Strategic Projects PEst-C/SAU/UI3282/2013 and UID/NEU/04539/2013), FEDER-COMPETE (POCI-01-0145-FEDER-007440), Centro 2020 Regional Operational Programme (CENTRO-01-0145-FEDER-000008: BrainHealth 2020).

ACKNOWLEDGMENTS

The authors acknowledge Prof. Sancha Santos, Faculty of Pharmacy, University of Coimbra, for the help with the HPLC equipment.

REFERENCES

Albalawi, F., Lu, W., Beckel, J. M., Lim, J. C., McCaughey, S. A., and Mitchell, C. H. (2017). The P2X7 receptor primes IL-1β and the NLRP3 inflammasome in astrocytes exposed to mechanical strain. *Front. Cell. Neurosci.* 11:227. doi: 10.3389/fncel.2017.00227

Ballerini, P., Di Iorio, P., Ciccarelli, R., Nargi, E., D'Alimonte, I., Traversa, U., et al. (2002). Glial cells express multiple ATP binding cassette proteins which are involved in ATP release. *Neuroreport* 13, 1789–1792. doi: 10.1097/00001756-200210070-00019

Beckel, J. M., Argall, A. J., Lim, J. C., Xia, J., Lu, W., Coffey, E. E., et al. (2014). Mechanosensitive release of adenosine 5′-triphosphate through pannexin channels and mechanosensitive upregulation of pannexin channels in optic nerve head astrocytes: a mechanism for purinergic involvement in chronic strain. *Glia* 62, 1486–1501. doi: 10.1002/glia.22695

Beckel, J. M., Lu, W., Civan, M. M., and Mitchell, C. H. (2016). Treatment of retinal disorders with purinergic drugs: beyond receptors. *J. Ocul. Pharmacol. Ther.* 32, 488–489. doi: 10.1089/jop.2016.29020.jbe

Bosco, A., Romero, C. O., Breen, K. T., Chagovetz, A. A., Steele, M. R., Ambati, B. K., et al. (2015). Neurodegeneration severity is anticipated by early microglia alterations monitored *in vivo* in a mouse model of chronic glaucoma. *Dis. Model. Mech.* 8, 443–455. doi: 10.1242/dmm.018788

Bosco, A., Steele, M. R., and Vetter, M. L. (2011). Early microglia activation in a mouse model of chronic glaucoma. *J. Comp. Neurol.* 519, 599–620. doi: 10.1002/cne.22516

Bulavina, L., Szulzewsky, F., Rocha, A., Krabbe, G., Robson, S. C., Matyash, V., et al. (2013). NTPDase1 activity attenuates microglial phagocytosis. *Purinergic Signal.* 9, 199–205. doi: 10.1007/s11302-012-9339-y

Burnstock, G., and Verkhratsky, A. (2009). Evolutionary origins of the purinergic signalling system. *Acta Physiol.* 195, 415–447. doi: 10.1111/j.1748-1716.2009.01957.x

Carrier, E. J., Auchampach, J. A., and Hillard, C. J. (2006). Inhibition of an equilibrative nucleoside transporter by cannabidiol: a mechanism of cannabinoid immunosuppression. *Proc. Natl. Acad. Sci. U.S.A.* 103, 7895–7900. doi: 10.1073/pnas.0511232103

Casson, R. J., Chidlow, G., Wood, J. P., Crowston, J. G., and Goldberg, I. (2012). Definition of glaucoma: clinical and experimental concepts. *Clin. Exp. Ophthalmol.* 40, 341–349. doi: 10.1111/j.1442-9071.2012.02773.x

Castellano, B., Bosch-Queralt, M., Almolda, B., Villacampa, N., and González, B. (2016). Purine signaling and microglial wrapping. *Adv. Exp. Med. Biol.* 949, 147–165. doi: 10.1007/978-3-319-40764-7_7

Ciruela, F., Saura, C., Canela, E. I., Mallol, J., Lluís C., and Franco, R. (1997). Ligand-induced phosphorylation, clustering, and desensitization of A1 adenosine receptors. *Mol. Pharmacol.* 52, 788–797. doi: 10.1124/mol.52.5.788

Coelho, J. E., Rebola, N., Fragata, I., Ribeiro, J. A., de Mendonça, A., and Cunha, R. A. (2006). Hypoxia-induced desensitization and internalization of adenosine A1 receptors in the rat hippocampus. *Neuroscience* 138, 1195–1203. doi: 10.1016/j.neuroscience.2005.12.012

Cohen, L. P., and Pasquale, L. R. (2014). Clinical characteristics and current treatment of glaucoma. *Cold Spring Harb. Perspect. Med.* 4:a017236. doi: 10.1101/cshperspect.a017236

Cook, S. P., and McCleskey, E. W. (2002). Cell damage excites nociceptors through release of cytosolic ATP. *Pain* 95, 41–47. doi: 10.1016/S0304-3959(01)00372-4

Cunha, R. A. (2005). Neuroprotection by adenosine in the brain: from A(1) receptor activation to A (2A) receptor blockade. *Purinergic Signal.* 1, 111–134. doi: 10.1007/s11302-005-0649-1

Cunha, R. A. (2016). How does adenosine control neuronal dysfunction and neurodegeneration? *J. Neurochem.* 139, 1019–1055. doi: 10.1111/jnc.13724

Cunha, R. A., Almeida, T., and Ribeiro, J. A. (2000). Modification by arachidonic acid of extracellular adenosine metabolism and neuromodulatory action in the rat hippocampus. *J. Biol. Chem.* 275, 37572–37581. doi: 10.1074/jbc.M003011200

Daines, B. S., Kent, A. R., McAleer, M. S., and Crosson, C. E. (2003). Intraocular adenosine levels in normal and ocular-hypertensive patients. *J. Ocul. Pharmacol. Ther.* 19, 113–119. doi: 10.1089/108076803321637645

Daré, E., Schulte, G., Karovic, O., Hammarberg, C., and Fredholm, B. B. (2007). Modulation of glial cell functions by adenosine receptors. *Physiol. Behav.* 92, 15–20. doi: 10.1016/j.physbeh.2007.05.031

Davalos, D., Grutzendler, J., Yang, G., Kim, J. V., Zuo, Y., Jung, S., et al. (2005). ATP mediates rapid microglial response to local brain injury *in vivo*. *Nat. Neurosci.* 8, 752–758. doi: 10.1038/nn1472

Di Virgilio, F., Ceruti, S., Bramanti, P., and Abbracchio, M. P. (2009). Purinergic signalling in inflammation of the central nervous system. *Trends Neurosci.* 32, 79–87. doi: 10.1016/j.tins.2008.11.003

Dunwiddie, T. V., and Masino, S. A. (2001). The role and regulation of adenosine in the central nervous system. *Annu. Rev. Neurosci.* 24, 31–55. doi: 10.1146/annurev.neuro.24.1.31

Ferrari, D., Chiozzi, P., Falzoni, S., Dal Susino, M., Collo, G., Buell, G., et al. (1997). ATP-mediated cytotoxicity in microglial cells. *Neuropharmacology* 36, 1295–1301. doi: 10.1016/S0028-3908(97)00137-8

Fredholm, B. B., IJzerman, A. P., Jacobson, K. A., Klotz, K. N., and Linden, J. (2001). International Union of Pharmacology. XXV. Nomenclature and classification of adenosine receptors. *Pharmacol. Rev.* 53, 527–552.

Gajardo-Gómez, R., Labra, V. C., and Orellana, J. A. (2016). Connexins and pannexins: new insights into microglial functions and dysfunctions. *Front. Mol. Neurosci.* 9:86. doi: 10.3389/fnmol.2016.00086

George, J., Gonçalves, F. Q., Cristovao, G., Rodrigues, L., Meyer Fernandes, J. R., Goncalves, T., et al. (2015). Different danger signals differently impact on microglial proliferation through alterations of ATP release and extracellular metabolism. *Glia* 63, 1636–1645. doi: 10.1002/glia.22833

Gomes, C., Ferreira, R., George, J., Sanches, R., Rodrigues, D. I., Gonçalves, N., et al. (2013). Activation of microglial cells triggers a release of brain-derived neurotrophic factor (BDNF) inducing their proliferation in an adenosine A2A receptor-dependent manner: A2A receptor blockade prevents BDNF release and proliferation of microglia. *J. Neuroinflammation* 10:16. doi: 10.1186/1742-2094-10-16

Hammarberg, C., Schulte, G., and Fredholm, B. B. (2003). Evidence for functional adenosine A3 receptors in microglia cells. *J. Neurochem.* 86, 1051–1054. doi: 10.1046/j.1471-4159.2003.01919.x

Harry, G. J. (2013). Microglia during development and aging. *Pharmacol. Ther.* 139, 313–326. doi: 10.1016/j.pharmthera.2013.04.013

Haskó, G., Pacher, P., Vizi, E. S., and Illes, P. (2005). Adenosine receptor signaling in the brain immune system. *Trends Pharmacol. Sci.* 26, 511–516. doi: 10.1016/j.tips.2005.08.004

Haynes, S. E., Hollopeter, G., Yang, G., Kurpius, D., Dailey, M. E., Gan, W. B., et al. (2006). The P2Y12 receptor regulates microglial activation by extracellular nucleotides. *Nat. Neurosci.* 9, 1512–1519. doi: 10.1038/nn1805

Honda, S., Sasaki, Y., Ohsawa, K., Imai, Y., Nakamura, Y., Inoue, K., et al. (2001). Extracellular ATP or ADP induce chemotaxis of cultured microglia through Gi/o-coupled P2Y receptors. *J. Neurosci.* 21, 1975–1982.

Imura, Y., Morizawa, Y., Komatsu, R., Shibata, K., Shinozaki, Y., Kasai, H., et al. (2013). Microglia release ATP by exocytosis. *Glia* 61, 1320–1330. doi: 10.1002/glia.22517

Karlstetter, M., Ebert, S., and Langmann, T. (2010). Microglia in the healthy and degenerating retina: insights from novel mouse models. *Immunobiology* 215, 685–691. doi: 10.1016/j.imbio.2010.05.010

Karlstetter, M., Nothdurfter, C., Aslanidis, A., Moeller, K., Horn, F., Scholz, R., et al. (2014). Translocator protein (18 kDa) (TSPO) is expressed in reactive retinal microglia and modulates microglial inflammation and phagocytosis. *J. Neuroinflammation* 11:3. doi: 10.1186/1742-2094-11-3

Kettenmann, H., Hanisch, U. K., Noda, M., and Verkhratsky, A. (2011). Physiology of microglia. *Physiol. Rev.* 91, 461–553. doi: 10.1152/physrev.00011.2010

Koizumi, S., Shigemoto-Mogami, Y., Nasu-Tada, K., Shinozaki, Y., Ohsawa, K., Tsuda, M., et al. (2007). UDP acting at P2Y6 receptors is a mediator of microglial phagocytosis. *Nature* 446, 1091–1095. doi: 10.1038/nature05704

Latini, S., and Pedata, F. (2001). Adenosine in the central nervous system: release mechanisms and extracellular concentrations. *J. Neurochem.* 79, 463–484. doi: 10.1046/j.1471-4159.2001.00607.x

Levin, L. A., Crowe, M. E., Quigley, H. A., Lasker/IRRF Initiative on Astrocytes and Glaucomatous Neurodegeneration Participants (2017). Neuroprotection for glaucoma: requirements for clinical translation. *Exp. Eye Res.* 157, 34–37. doi: 10.1016/j.exer.2016.12.005

Levine, R. L., and Ginsburg, A. (2013). *Modulation by Molecular Interactions—Current Topics in Cellular Regulation*. London: Academic press.

Li, A., Zhang, X., Zheng, D., Ge, J., Laties, A. M., and Mitchell, C. H. (2011). Sustained elevation of extracellular ATP in aqueous humor from humans with primary chronic angle-closure glaucoma. *Exp. Eye Res.* 93, 528–533. doi: 10.1016/j.exer.2011.06.020

Lopes, L. V., Rebola, N., Pinheiro, P. C., Richardson, P. J., Oliveira, C. R., and Cunha, R. A. (2003). Adenosine A3 receptors are located in neurons of the rat hippocampus. *Neuroreport* 14, 1645–1648. doi: 10.1097/00001756-200308260-00021

Lu, W., Hu, H., Sévigny, J., Gabelt, B. T., Kaufman, P. L., Johnson, E. C., et al. (2015). Rat, mouse, and primate models of chronic glaucoma show sustained elevation of extracellular ATP and altered purinergic signaling in the posterior eye. *Invest. Ophthalmol. Vis. Sci.* 56, 3075–3083. doi: 10.1167/iovs.14-15891

Lu, W., Reigada, D., Sévigny, J., and Mitchell, C. H. (2007). Stimulation of the P2Y1 receptor up-regulates nucleoside-triphosphate diphosphohydrolase-1 in human retinal pigment epithelial cells. *J. Pharmacol. Exp. Ther.* 323, 157–164. doi: 10.1124/jpet.107.124545

Madeira, M. H., Boia, R., Elvas, F., Martins, T., Cunha, R. A., Ambrósio, A. F., et al. (2016). Selective A2A receptor antagonist prevents microglia-mediated neuroinflammation and protects retinal ganglion cells from high intraocular pressure-induced transient ischemic injury. *Transl. Res.* 169, 112–128. doi: 10.1016/j.trsl.2015.11.005

Madeira, M. H., Boia, R., Santos, P. F., Ambrósio, A. F., and Santiago, A. R. (2015a). Contribution of microglia-mediated neuroinflammation to retinal degenerative diseases. *Mediators Inflamm.* 2015:673090. doi: 10.1155/2015/673090

Madeira, M. H., Elvas, F., Boia, R., Gonçalves, F. Q., Cunha, R. A., Ambrósio, A. F., et al. (2015b). Adenosine A2AR blockade prevents neuroinflammation-induced death of retinal ganglion cells caused by elevated pressure. *J. Neuroinflammation* 12:115. doi: 10.1186/s12974-015-0333-5

Mandrekar, S., Jiang, Q., Lee, C. Y., Koenigsknecht-Talboo, J., Holtzman, D. M., and Landreth, G. E. (2009). Microglia mediate the clearance of soluble Abeta through fluid phase macropinocytosis. *J. Neurosci.* 29, 4252–4262. doi: 10.1523/JNEUROSCI.5572-08.2009

Matyash, M., Zabiegalov, O., Wendt, S., Matyash, V., and Kettenmann, H. (2017). The adenosine generating enzymes CD39/CD73 control microglial processes ramification in the mouse brain. *PLoS ONE* 12:e0175012. doi: 10.1371/journal.pone.0175012

Melani, A., Corti, F., Stephan, H., Müller, C. E., Donati, C., Bruni, P., et al. (2012). Ecto-ATPase inhibition: ATP and adenosine release under physiological and ischemic *in vivo* conditions in the rat striatum. *Exp. Neurol.* 233, 193–204. doi: 10.1016/j.expneurol.2011.09.036

Miller, A. M., and Stella, N. (2009). Microglial cell migration stimulated by ATP and C5a involve distinct molecular mechanisms: quantification of migration by a novel near-infrared method. *Glia* 57, 875–883. doi: 10.1002/glia.20813

Murphy, P. S., Wang, J., Bhagwat, S. P., Munger, J. C., Janssen, W. J., Wright, T. W., et al. (2017). CD73 regulates anti-inflammatory signaling between apoptotic cells and endotoxin-conditioned tissue macrophages. *Cell Death Differ.* 24, 559–570. doi: 10.1038/cdd.2016.159

Ohsawa, K., Sanagi, T., Nakamura, Y., Suzuki, E., Inoue, K., and Kohsaka, S. (2012). Adenosine A3 receptor is involved in ADP-induced microglial process extension and migration. *J. Neurochem.* 121, 217–227. doi: 10.1111/j.1471-4159.2012.07693.x

Orr, A. G., Orr, A. L., Li, X. J., Gross, R. E., and Traynelis, S. F. (2009). Adenosine A(2A) receptor mediates microglial process retraction. *Nat. Neurosci.* 12, 872–878. doi: 10.1038/nn.2341

Pérez de Lara, M. J., Guzmán-Aránguez, A., de la Villa, P., Díaz-Hernández, J. I., Miras-Portugal, M. T., and Pintor, J. (2015). Increased levels of extracellular ATP in glaucomatous retinas: possible role of the vesicular nucleotide transporter during the development of the pathology. *Mol. Vis.* 21, 1060–1070.

Ransohoff, R. M., and Perry, V. H. (2009). Microglial physiology: unique stimuli, specialized responses. *Annu. Rev. Immunol.* 27, 119–145. doi: 10.1146/annurev.immunol.021908.132528

Regateiro, F. S., Cobbold, S. P., and Waldmann, H. (2013). CD73 and adenosine generation in the creation of regulatory microenvironments. *Clin. Exp. Immunol.* 171, 1–7. doi: 10.1111/j.1365-2249.2012.04623.x

Reigada, D., Lu, W., Zhang, M., and Mitchell, C. H. (2008). Elevated pressure triggers a physiological release of ATP from the retina:possible role for pannexin hemichannels. *Neuroscience* 157, 396–404. doi: 10.1016/j.neuroscience.2008.08.036

Resta, V., Novelli, E., Vozzi, G., Scarpa, C., Caleo, M., Ahluwalia, A., et al. (2007). Acute retinal ganglion cell injury caused by intraocular pressure spikes is mediated by endogenous extracellular ATP. *Eur. J. Neurosci.* 25, 2741–2754. doi: 10.1111/j.1460-9568.2007.05528.x

Rodrigues, R. J., Tomé, A. R., and Cunha, R. A. (2015). ATP as a multi-target danger signal in the brain. *Front. Neurosci.* 9:148. doi: 10.3389/fnins.2015.00148

Sawada, K., Echigo, N., Juge, N., Miyaji, T., Otsuka, M., Omote, H., et al. (2008). Identification of a vesicular nucleotide transporter. *Proc. Natl. Acad. Sci. U.S.A.* 105, 5683–5686. doi: 10.1073/pnas.0800141105

Scheiblich, H., and Bicker, G. (2016). Nitric oxide regulates antagonistically phagocytic and neurite outgrowth inhibiting capacities of microglia. *Dev. Neurobiol.* 76, 566–584. doi: 10.1002/dneu.22333

Shinozaki, Y., Nomura, M., Iwatsuki, K., Moriyama, Y., Gachet, C., and Koizumi, S. (2014). Microglia trigger astrocyte-mediated neuroprotection via purinergic gliotransmission. *Sci. Rep.* 4:4329. doi: 10.1038/srep04329

Song, W., Huang, P., and Zhang, C. (2015). Neuroprotective therapies for glaucoma. *Drug Des. Devel. Ther.* 9, 1469–1479. doi: 10.2147/DDDT.S80594

Sperlágh, B., and Illes, P. (2007). Purinergic modulation of microglial cell activation. *Purinergic Signal.* 3, 117–127. doi: 10.1007/s11302-006-9043-x

Stout, C. E., Costantin, J. L., Naus, C. C., and Charles, A. C. (2002). Intercellular calcium signaling in astrocytes via ATP release through connexin hemichannels. *J. Biol. Chem.* 277, 10482–10488. doi: 10.1074/jbc.M109902200

Thorn, J. A., and Jarvis, S. M. (1996). Adenosine transporters. *Gen. Pharmacol.* 27, 613–620. doi: 10.1016/0306-3623(95)02053-5

van Calker, D., and Biber, K. (2005). The role of glial adenosine receptors in neural resilience and the neurobiology of mood disorders. *Neurochem. Res.* 30, 1205–1217. doi: 10.1007/s11064-005-8792-1

Vardy, E. R., Kellett, K. A., Cocklin, S. L., and Hooper, N. M. (2012). Alkaline phosphatase is increased in both brain and plasma in Alzheimer's disease. *Neurodegener. Dis.* 9, 31–37. doi: 10.1159/000329722

Verkhratsky, A., and Burnstock, G. (2014). Biology of purinergic signalling: its ancient evolutionary roots, its omnipresence and its multiple functional significance. *Bioessays* 36, 697–705. doi: 10.1002/bies.201400024

Vindeirinho, J., Costa, G. N., Correia, M. B., Cavadas, C., and Santos, P. F. (2013). Effect of diabetes/hyperglycemia on the rat retinal adenosinergic system. *PLoS ONE* 8:e67499. doi: 10.1371/journal.pone.0067499

Wilkinson, P. C. (1998). Assays of leukocyte locomotion and chemotaxis. *J. Immunol. Methods* 216, 139–153. doi: 10.1016/S0022-1759(98)00075-1

Wu, L. J., Vadakkan, K. I., and Zhuo, M. (2007). ATP-induced chemotaxis of microglial processes requires P2Y receptor-activated initiation of outward potassium currents. *Glia* 55, 810–821. doi: 10.1002/glia.20500

Yegutkin, G. G. (2008). Nucleotide- and nucleoside-converting ectoenzymes: important modulators of purinergic signalling cascade. *Biochim. Biophys. Acta* 1783, 673–694. doi: 10.1016/j.bbamcr.2008.01.024

Zhang, X., Li, A., Ge, J., Reigada, D., Laties, A. M., and Mitchell, C. H. (2007). Acute increase of intraocular pressure releases ATP into the anterior chamber. *Exp. Eye Res.* 85, 637–643. doi: 10.1016/j.exer.2007.07.016

Zimmermann, H. (2006). Ectonucleotidases in the nervous system. *Novartis Found Symp.* 276, 113–128. discussion: 128–130, 233–117, 275–181. doi: 10.1002/9780470032244.ch10

Conflict of Interest Statement: The authors declare that the research was conducted in the absence of any commercial or financial relationships that could be construed as a potential conflict of interest.

frontiers in Pharmacology

ORIGINAL RESEARCH
published: 22 January 2018
doi: 10.3389/fphar.2018.00013

Phenotyping of Mice with Heart Specific Overexpression of A_{2A}-Adenosine Receptors: Evidence for Cardioprotective Effects of A_{2A}-Adenosine Receptors

Peter Boknik[1], Katharina Drzewiecki[1], John Eskandar[1], Ulrich Gergs[2], Stephanie Grote-Wessels[1], Larissa Fabritz[3], Paulus Kirchhof[3], Frank U. Müller[1], Frank Stümpel[1], Wilhelm Schmitz[1], Norbert Zimmermann[4], Uwe Kirchhefer[1] and Joachim Neumann[2]**

[1] *Institut für Pharmakologie und Toxikologie, Universitätsklinikum Münster, Westfälische Wilhelms-Universität, Münster, Germany,* [2] *Institut für Pharmakologie und Toxikologie, Medizinische Fakultät, Martin-Luther-Universität Halle-Wittenberg, Halle, Germany,* [3] *Centre for Cardiovascular Sciences, University of Birmingham, Birmingham, United Kingdom,* [4] *Bundesinstitut für Arzneimittel und Medizinprodukte, Bonn, Germany*

OPEN ACCESS

Edited by:
Francisco Ciruela, University of Barcelona, Spain

Reviewed by:
Jason N. Peart, Griffith University, Australia
Andrew F. James, University of Bristol, United Kingdom

***Correspondence:**
Joachim Neumann
joachim.neumann@medizin.uni-halle.de
Ulrich Gergs
ulrich.gergs@medizin.uni-halle.de

Specialty section:
This article was submitted to Experimental Pharmacology and Drug Discovery, a section of the journal Frontiers in Pharmacology

Received: *06 November 2017*
Accepted: *05 January 2018*
Published: *22 January 2018*

Citation:
Boknik P, Drzewiecki K, Eskandar J, Gergs U, Grote-Wessels S, Fabritz L, Kirchhof P, Müller FU, Stümpel F, Schmitz W, Zimmermann N, Kirchhefer U and Neumann J (2018) Phenotyping of Mice with Heart Specific Overexpression of A_{2A}-Adenosine Receptors: Evidence for Cardioprotective Effects of A_{2A}-Adenosine Receptors. Front. Pharmacol. 9:13. doi: 10.3389/fphar.2018.00013

Background: Adenosine can be produced in the heart and acts on cardiac adenosine receptors. One of these receptors is the A_{2A}-adenosine receptor (A_{2A}-AR).

Methods and Results: To better understand its role in cardiac function, we generated and characterized mice (A_{2A}-TG) which overexpress the human A_{2A}-AR in cardiomyocytes. In isolated atrial preparations from A_{2A}-TG but not from WT, CGS 21680, an A_{2A}-AR agonist, exerted positive inotropic and chronotropic effects. In ventricular preparations from A_{2A}-TG but not WT, CGS 21680 increased the cAMP content and the phosphorylation state of phospholamban and of the inhibitory subunit of troponin in A_{2A}-TG but not WT. Protein expression of phospholamban, SERCA, triadin, and junctin was unchanged in A_{2A}-TG compared to WT. Protein expression of the α-subunit of the stimulatory G-protein was lower in A_{2A}-TG than in WT but expression of the α-subunit of the inhibitory G-protein was higher in A_{2A}-TG than in WT. While basal hemodynamic parameters like left intraventricular pressure and echocardiographic parameters like the systolic diameter of the interventricular septum were higher in A_{2A}-TG than in WT, after β-adrenergic stimulation these differences disappeared. Interestingly, A_{2A}-TG hearts sustained global ischemia better than WT.

Conclusion: We have successfully generated transgenic mice with cardiospecific overexpression of a functional A_{2A}-AR. This receptor is able to increase cardiac function *per se* and after receptor stimulation. It is speculated that this receptor may be useful to sustain contractility in failing human hearts and upon ischemia and reperfusion.

Keywords: A_{2A}-adenosine receptor, contractility, ischemia, reperfusion, protein phosphorylation

INTRODUCTION

Adenosine elicits multiple effects in the human body. These include effects on cardiac function that have been studied for many years and some effects of adenosine including the downstream signaling mechanisms are similar to those of vagal stimulation. For example, the negative chronotropic effect on the sinus node, the negative dromotropic effect on the AV-node, and the negative inotropic effect in atrial tissue of adenosine (Shryock and Belardinelli, 1997). Extracellular adenosine acts on A_1-, A_2-, and A_3-adenosine receptors (AR). Typically, A_1-AR inhibits and A_2-AR stimulates adenylyl cyclase activities (Olsson and Pearson, 1990). The A_{2A}-AR was the first of the P_1-purinoceptor family to be cloned (Libert et al., 1989).

The negative inotropic effects of adenosine in the rat atrium were mediated by inhibition of adenylyl cyclase activity followed by a decreased cAMP content (Linden et al., 1985). But in guinea pig atrium, no adenosine-induced decrease in cAMP content was found (Böhm et al., 1984). Here, the negative inotropic effect of adenosine was inhibited by pertussis toxin (Böhm et al., 1986) and therefore mediated by a pertussis toxin-sensitive G-protein. Probably, an enhanced conductance of potassium in the sarcolemma was involved (Belardinelli and Isenberg, 1983). However, the activation of protein phosphatases has also been suggested (Gupta et al., 1993a,b).

In contrast, in the ventricle of most species, adenosine is nearly ineffective to influence force of contraction but via activation of A_1-adenosine receptors, it can decrease the effects of β-adrenergic stimulation or in other words the inotropic effects of cAMP-elevating agents are decreased by adenosine [for example forskolin or phosphodiesterase inhibitors; rat (Dobson, 1978, 1983) or guinea pig (Böhm et al., 1984; Brückner et al., 1985)]. Adenosine can also provoke relaxation of the vasculature via activation of A_{2A}-AR on smooth muscle cells [human coronaries (Makujina et al., 1992)].

Adenosine is produced in cardiomyocytes and its release there is markedly enhanced during β-adrenergic stimulation, ischemia, or necrosis. In the clinic, adenosine and its precursor ATP can be used to stop supraventricular arrhythmias and therefore, the effects of adenosine in the mammalian heart are of clinical relevance and should be further investigated. It is controversial and may be species dependent (or method dependent) whether A_{2A}-AR is functional (increase in cAMP, increase in contractility) in the mammalian heart: some reported a lack of effect [rat (Shryock et al., 1993), guinea-pig (Boknik et al., 1997), rabbit (Kilpatrick et al., 2002)] whereas other reported a functional response [mouse (Morrison et al., 2006), rat (Monahan et al., 2000)].

It is important to note, that A_{2A}-receptors in human hearts have been detected on the protein level (Marala and Mustafa, 1998). Moreover, work in isolated perfused A_{2A}-KO (constitutive deletion) mouse hearts clearly established that CGS 21680 a classical A_{2A}-receptor agonist was selective: only in WT hearts CGS 21680 (up to 1 μM) increased contractility but not in hearts from A_{2A}-KO mice (Ledent et al., 1997). However, under basal conditions (no CGS 21680 given) contractility of WT and KO were not different (Ledent et al., 1997; Ashton et al., 2017), suggesting that CGS 21680 is an appropriate tool to assess A_{2A} function in mice. Moreover, there is evidence that A_{2A}-receptor stimulation can protect the heart against reperfusion injury [e.g., rat (Cargnoni et al., 1999)].

As part of our long-standing effort to characterize all known adenosine receptors in the mammalian heart, we report here on the generation and phenotyping of a novel transgenic mouse model in which we successfully expressed an inotropically active A_{2A}-AR. We used this model to study reperfusion injury in the isolated perfused heart. A progress report of this work has appeared as abstract (Grote-Wessels et al., 2007).

MATERIALS AND METHODS

Isolation of A_{2A}-Receptor cDNA and Generation of Transgenic Mice

The investigation conforms to the *Guide for the Care and Use of Laboratory Animals* published by the National Research Council (2011). Animals were handled and maintained to according to approved protocols of the animal welfare committee of the University of Münster, Germany.

The PCR generated human A_{2A}-AR cDNA fragment containing a 3′ and 5′ engineered *NotI* digestion site was inserted into a mouse cardiac α-myosin heavy chain promoter expression cassette via *NotI*. The orientation of the cDNA was confirmed by sequencing. The A_{2A}-AR cDNA promoter construct was digested with NruI and purified by a cesium chloride gradient centrifugation for injection into the pronuclei of single-cell fertilized mouse embryos. Generation of transgenic (A_{2A}-TG) mice was performed by standard procedures (mouse strain: FVB/N). One transgenic line overexpressing the A_{2A}-AR under the control of the α-myosin heavy chain (MHC) promoter was established, which was investigated in the present study. Genotypes were identified by PCR analyses of tail-tip DNA using the following primers 5′-acaaagcaggcgatgaag-3′ and 5′-acccttaccccacatagacc-3′. For the reverse transcription 4 μg RNA and random primers were used (Transcriptor High Fidelity cDNA Synthesis Kit, Roche Applied Science, Mannheim, Germany). The PCR reaction was performed using the Ampliqon Taq DNA polymerase (Biomol, Hamburg, Germany) according to the manufacturer's instructions. For all experiments, 12–30 weeks old A_{2A}-TG mice and WT littermates of both sexes were used.

Western Blot Analysis

Homogenates from ventricular tissue samples were prepared in 300 μl of 10 mM $NaHCO_3$ and 100 μl 20% SDS. Crude extracts were incubated at 25°C for 30 min before centrifugation to remove debris and thereafter, the supernatants (= homogenates) were separated and stored at −20°C until further use. Western blot analysis was performed as previously described (Gergs et al., 2004). Briefly, aliquots of 100 μg of protein were loaded per lane and finally, bands were detected using enhanced chemifluorescence (ECF, GE Healthcare, Munich, Germany) together with a Storm™ PhosphorImager (GE Healthcare, Munich, Germany). Following primary antibodies were used

in this study: polyclonal rabbit anti calsequestrin, monoclonal mouse anti SERCA2a, polyclonal rabbit anti triadin, and polyclonal rabbit anti junctin (all kindly provided by L.R. Jones, Indianapolis, IN, United States), monoclonal mouse anti PLB (A-1, Badrilla, Leeds, United Kingdom), polyclonal rabbit anti phospho-PLB (antibodies were raised against PLB-peptide phosphorylated at serine-16 or at threonine-17, Badrilla, Leeds, United Kingdom). The characteristics and use of these antibodies has been reported repeatedly by our group (Kirchhefer et al., 2002). The antibodies against TnI and phosphor-TnI were obtained from GE Healthcare (Freiburg, Germany), the antibodies against α-subunits of Gi-protein and Gs-protein were purchased from Calbiochem (Darmstadt, Germany).

Histological Analysis

Hearts were fixed in buffered 4% formaldehyde and embedded in paraffin. Four micron sections were mounted on polylysine microslides, dewaxed in xylene, rehydrated in sequential decreasing alcohol concentrations and pre-treated in Tris/EDTA-buffer, pH 9 in a pressure cooker for antigen retrieval. After blocking endogenous mouse IgG with Fab Fragment of goat IgG directed against mouse IgG (100 $\mu g\ mL^{-1}$, Dianova, Hamburg, Germany) for 1 h at room temperature and washing slides were incubated with mouse primary monoclonal antibody to A_{2A}-AR (clone 7F6-G5-A2, 5 $\mu g\ ml^{-1}$, Upstate, NY, United States). For detection a goat-anti-mouse antibody conjugated to Alexa Fluor 594 (1:300, Dianova, Hamburg, Germany) was used. Finally, samples were counterstained for approximately 15 s with DAPI and mounted with Vectashield (Vector Laboratories, Burlingame, CA, United States). For imaging a Zeiss Axiophot2 microscope was used, separate color images (blue for DAPI, red for Alexa 594) were merged by AxioVision multichannel image processing (Carl Zeiss Vision GmbH, Germany). Images shown are representative of at least five independent experiments, which gave similar results (Buchwalow et al., 2004).

Echocardiography

Echocardiography in spontaneously breathing mice was performed under anesthesia with 1.5% isoflurane as described previously (Gergs et al., 2010).

Left-Ventricular Catheterization

Mice were anesthetized by i.p. injection of avertin (2,2,2-tribromoethanol, Sigma–Aldrich) in 2% solution at a dose of 400 $mg\ kg^{-1}$ bodyweight and placed on a controlled heating pad (Föhr Medical Instruments, Seeheim-Ober Beerbach, Germany) in supine position. Additional doses of avertin (each 10% of the initial dose) were applied during experiments if appropriate to maintain depth of anesthesia. A miniature pressure-volume catheter (model SPR-839, Millar Instruments, Houston, TX, United States) was inserted via the right carotid artery and placed in the left ventricle. Increasing doses of dobutamine were administered into the cannulated left external jugular vein using an automated syringe pump (B. Braun, Melsungen, Germany). Data were recorded using the MPVS-400 system (Millar Instruments) and Chart5 software (ADInstruments, Bella Vista, NSW, Australia). At the end of experiments, animals were euthanized by avertin overdose, and hearts were excised, weighed, and stored at −80°C until further examination. Hemodynamic data were analyzed using Chart5 software (ADInstruments) and PVAN software (Millar Instruments).

Isolation of Cardiomyocytes

Ventricular cardiomyocytes were isolated using a published protocol (Kirchhefer et al., 2002). In brief, hearts were perfused for 5 min at 2 $ml\ min^{-1}$ with a Ca^{2+}-free solution (solution A) composed of (in mM) 140 NaCl, 5.8 KCl, 0.5 KH_2PO_4, 0.4 NaH_2PO_4, 0.9 $MgSO_4$, 10 HEPES, 11.1 glucose (pH 7.1). Thereafter, hearts were perfused for 30 min with solution A supplemented with 0.2 $mg\ ml^{-1}$ collagenase (type D, Roche Molecular Biochemicals) and the Ca^{2+} concentration was gradually increased during digestion. After enzymatic digestion, the hearts were perfused for 10 min with solution A and ventricles were cut into several pieces before myocytes were separated by filtration through a nylon mesh.

Stimulation of Cardiomyocytes

To avoid the interference from endogenous adenosine, adenosine deaminase (5 units/ml) was present under all experimental conditions. In order to get an insight into the signaling via A_{2A}-AR we used the following highly selective antagonists for pre-incubation: 1 μM DPCPX (A_1-AR antagonist) or 1 μM ZM 241385 (A_{2A}-AR antagonist). For subsequent stimulation activity 1 μM CGS 21680 [A_{2A}-AR agonist (Boknik et al., 2009)] or isoproterenol was added for 10 min at 37°C. After denaturation with 0.1 M HCl at 95°C and centrifugation the supernatant was stored at −20°C for cAMP quantification and the pellet was dissolved in 0.1 M NaOH for subsequent determination of the protein concentration by the assay according to Bradford. For determination of the phosphorylation state the incubation was terminated by adding SDS solution according to Laemmli and samples were subjected SDS PAGE and Western Blotting.

Contractile Function

Mice were anesthetized by i.p. injection of pentobarbital sodium (50 $mg\ kg^{-1}$) and hearts were excised. Right and left atria were dissected from isolated A_{2A}-AR transgenic and wild type (WT) mice hearts and mounted in an organ bath. Left atrial preparations were continuously electrically stimulated (field stimulation) with each impulse consisting of 1 Hz, with a voltage of 10–15% above threshold and 5 ms duration. Right atrial preparations were allowed to contract spontaneously. The bathing solution contained (in mM) NaCl 119.8, KCl 5.4, $CaCl_2$ 1.8, $MgCl_2$ 1.05, NaH_2PO_4 0.42, $NaHCO_3$ 22.6, Na_2EDTA 0.05, ascorbic acid 0.28 and glucose 5.0, continuously gassed with 95% O_2 and 5% CO_2 and maintained at 35°C resulting in a pH of 7.4. Signals detected via an isometric force transducer were amplified and continuously recorded. CGS 21680, ZM 241385or isoproterenol (1 μM each) were cumulatively applied with approximately 20 min for each compound. Contraction experiments were performed after addition of adenosine deaminase (1 $\mu g\ ml^{-1}$) and DPCPX (1 μM) to avoid interference from endogenous adenosine or A_1 adenosine receptor activation.

Langendorff-Perfused Hearts

Heart preparations were utilized as described previously (Kirchhefer et al., 2014). Mice were anesthetized intraperitoneally with 2.0 g kg^{-1} body weight urethane and treated with 1.5 units of heparin. The hearts were removed from the opened chest, immediately attached by the aorta to a 20-gauge cannula, and perfused retrogradely under constant pressure of 50 mmHg with oxygenized Krebs-Henseleit buffer (37.4°C) containing 118 mM NaCl, 25 mM $NaHCO_3$, 0.5 mM Na-EDTA, 4.7 mM KCl, 1.2 mM KH_2PO_4, 1.2 mM $MgSO_4$, 2.5 mM $CaCl_2$, and 11 mM glucose in an isolated heart system (Hugo Sachs Elektronik, March-Hugstetten, Germany). The heart preparations were allowed to equilibrate for 30 min before measurements. Hearts were stimulated at 8 Hz and heart rate, aortic pressure, and LV pressure were measured and monitored continuously. The first derivative of LV pressure (+dP/dt and −dP/dt) was calculated (ISOHEART Software, Hugo Sachs Elektronik). To generate global ischemia, the perfusion was stopped for 20 min (or 40 and 60 min, respectively) and thereafter the hearts were reperfused for 40 min.

Quantification of cAMP

Measurements of intracellular cAMP levels were performed by using the Biotrak direct enzyme immunoassay (GE Healthcare, Amersham, Chalfont St. Giles, United Kingdom) according to the manufacturer's instructions. The cAMP containing supernatant was acetylated (1:40 with acetylation reagent, 1 volume acetic anhydride + 2 volume triethylamine), and divided into the donkey anti-rabbit IgG coated wells of a microtiter plate prefilled with anti-cAMP serum. Competition between unlabeled cAMP in the sample and a fixed quantity of peroxidase-labeled cAMP, for a limited number of binding sites on the cAMP specific antibody allowed quantification of intracellular cAMP.

Radioligand Binding Experiments

Freshly obtained ventricular tissue was manually minced in small slices. Homogenization was performed at 4°C with Polytron (PT-MR 3000, Kinematica, Lucerne, Switzerland) three times for 30 s at the speed of 20,000 rpm in buffer A, containing sucrose 250 mM, histidine 30 mM (pH = 7.4) and thereafter using Virsonic 100 (VirTis, Gardiner, NY, United States) for 2 s. This suspension was centrifuged for 10 min at 1,500 × *g* and 4°C (Varifuge 3.0R, Heraeus, Hanau, Germany). The supernatant was centrifuged at 45,000 × *g* (Beckman Avanti J-20XP, Beckman Coulter, Palo Alto, CA, United States). The resulting supernatant was stored at −20°C. The pellet was resuspended in buffer B, containing KCl 600 mM, histidine 30 nM (pH = 7.0) and again centrifuged for 45 min at 64,000 × *g*. The pellet was resuspended in 250 µl buffer C, containing sucrose 250 mM, histidine 10 mM (pH = 7.0) and stored at −80°C until it was used for ligand binding experiments.

The density of A_{2A}-AR was determined using [^{3}H]-CGS 21680. Membrane proteins were diluted to the concentration of 2 µg $µl^{-1}$. The binding assays contained 40 µg of membranes in A_{2A}-TG and 400 µg in WT and in addition 8 nmol of [^{3}H]-CGS 21680 in a final volume of 200 µl (A_{2A}-TG) and 2 ml (WT), which contained also 10 U ml^{-1} adenosine deaminase. Unspecific binding was determined by addition of 1 µM ZM 241385. Binding assay was performed by incubation at 37°C for 90 min. Initially, the experiments for time dependency of ligand association were performed for 15–120 min. Furthermore, protein linearity was measured in the range of 20–120 µg protein. In order to determine B_{max} and K_D 16 increasing concentrations of [^{3}H]-CGS 21680 from 0.1 to 20 nM were used. For assessment of the specificity of radioligand binding incubations in the presence of the A_1-AR antagonist PSB36 (100 nM) as well as of the A_3-AR antagonist MRS1220 were performed. Incubations were terminated by filtration (filter type GF/52, Schleicher und Schuell, Dassel, Germany). Radioactivity bound to the filters was determined by adding 5 ml scintillation fluid (Ultima Gold, Perkin Elmer, Rodgau, Germany) in a counter (Canberra Packard 1600TR, Dreieich, Germany).

Data Analysis

Data shown are means ± SE. Statistical significance was estimated by analysis of variance followed by Bonferroni's *t*-test or using the χ^2-test as appropriate. A *p*-value < 0.05 was considered as significant.

Drugs and Materials

All other chemicals were of analytical grade. Deionized water was used throughout the experiments. Stock solutions were freshly prepared daily.

RESULTS

A_{2A}-AR Overexpression

In transgenic mice which overexpress the A_{2A}-AR, we noted that the A_{2A}-AR could be detected on the protein level for the following reasons. First of all, using very sensitive radioligand binding experiments, we could detect binding of the [^{3}H]-labeled A_{2A}-AR-agonist CGS 21680 samples form A_{2A}-TG hearts. This binding of [^{3}H]-labeled A_{2A}-AR-agonist CGS 21680 could be almost completely blocked by addition of the (non-radioactively labeled) A_{2A}-AR-antagonist ZM 241385, whereas (non-radioactively labeled) A_1-AR-antagonist PSB36 or (non-radioactively labeled) A_3-AR-antagonist MRS 1220 did not affect the binding of [^{3}H]-CGS 21680. Interestingly, under the same experimental conditions used in samples from A_{2A}-TG heart, no specific binding of A_{2A}-AR using the [^{3}H]-labeled A_{2A}-AR-agonist CGS 21680 could be established in samples of the hearts from WT littermates (**Figure 1A**). Secondly, the A_{2A}-AR could be visualized using immunohistology in A_{2A}-TG hearts. We tentatively identified the localization of the receptor in A_{2A}-TG to the vicinity of the sarcolemma (**Figure 1B**). Relative heart weight, an established parameter of cardiac hypertrophy, did not differ in whole hearts, ventricles or right atria between A_{2A}-TG and WT (**Table 1**). These data exclude a cardiac hypertrophy of A_{2A}-AR hearts at the two time points studied.

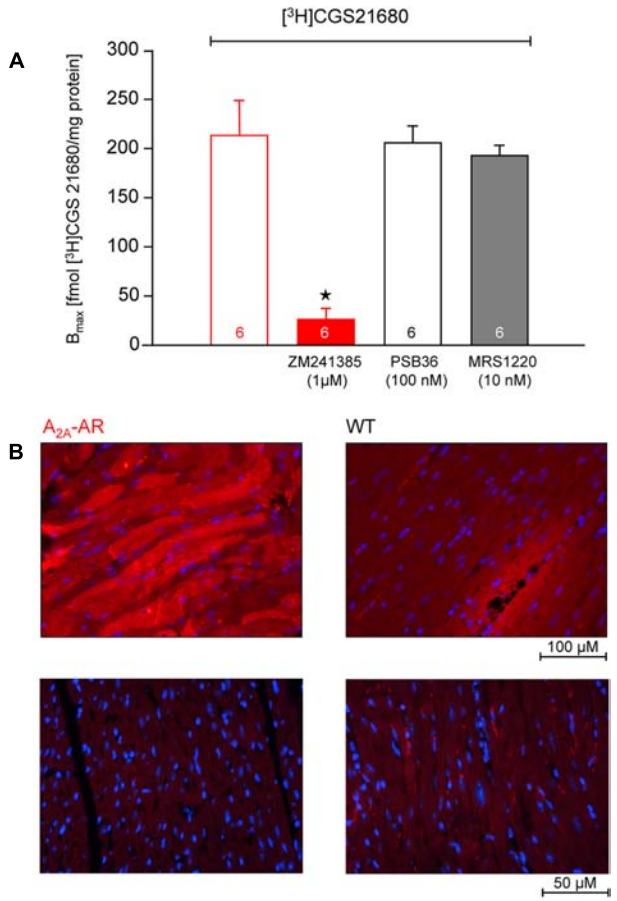

FIGURE 1 | (A) Radioligand binding studies in membrane fraction of A_{2A}-AR-overexpressing animals. The experiments were performed as described in Section "Materials and Methods." The binding of [^{3}H]-labeled A_{2A}-AR-agonist CGS 21680 could be almost completely blocked by addition of A_{2A}-AR-antagonist ZM 241385, whereas A_1-AR-antagonist PSB36 and A_3-AR-antagonist MRS 1220 did not affect the binding of [^{3}H]-CGS 21680. No specific binding was detectable in membrane fraction from WT animals. **(B)** Immunohistological staining of ventricular tissue from A_{2A}-AR-overexpressing and wild type (WT) animals. A_{2A}-AR was visualized using a monoclonal antibody against A_{2A}-AR and goat anti-mouse antibody conjugated to Alexa Fluor 594 (red, upper row). The nuclei were counterstained using DAPI (blue). Note staining of cardiomyocytes from A_{2A}-AR animals, mainly in the vicinity of the sarcolemma. Lower row: negative controls with omission of the primary antibody. *$p < 0.05$ vs. [^{3}H]-CGS 21680 alone.

Expression of Sarcoplasmic and G Proteins

The expression of CSQ (calsequestrin), SERCA [sarcoplasmic reticulum (SR) Ca^{2+} ATPase 2a], and triadin and junctin (both proteins located to the junctional SR), were unchanged between WT and A_{2A}-TG. However, PLB (phospholamban) expression was tentatively but not significantly increased in A_{2A}-TG and is currently regarded as unchanged. Interestingly, at weeks 12 and 30 the expression of Gsα was lower in A_{2A}-TG compared to WT ventricles (**Table 2**). On the opposite note, in ventricle from 30 weeks of A_{2A}-TG mice an increase of Giα proteins was detected, but not at age 12 weeks or in atrial preparations (**Table 2**).

TABLE 1 | Relative weight [with regard to body weight (BW)] of whole hearts (HW/BW), ventricles (V/BW), right atria (RA/BW) and left atria (LA/BW) in wild type (WT) and A_{2A}-AR overexpressing animals at the age of 12 and 30 weeks.

	12 weeks		30 weeks	
	WT ($n = 65$)	**A_{2A}-AR ($n = 51$)**	**WT ($n = 32$)**	**A_{2A}-AR ($n = 36$)**
HW/BW (mg/g)	4.79 ± 0.06	4.73 ± 0.06	4.88 ± 0.07	4.89 ± 0.11
V/BW (mg/g)	4.08 ± 0.04	4.03 ± 0.06	4.05 ± 0.05	4.11 ± 0.02
RA/BW (mg/g)	0.37 ± 0.01	0.38 ± 0.01	0.38 ± 0.01	0.41 ± 0.02
LA/BW (mg/g)	0.18 ± 0.01	0.15 ± 0.02	0.17 ± 0.01	0.17 ± 0.01

No significant differences were noted between WT and A_{2A}-AR overexpressing animals.

TABLE 2 | Expression of cardiac regulatory proteins in ventricles of wild type (WT) and A_{2A}-AR overexpressing animals at the age of 12 and 30 weeks.

	12 weeks		30 weeks	
	WT	**A_{2A}-AR**	**WT**	**A_{2A}-AR**
CSQ	100 ± 11	100 ± 11	100 ± 7	89 ± 5
Gsα	100 ± 6	64 ± 4*	100 ± 7	66 ± 6*
Giα	100 ± 11	109 ± 10	100 ± 10	148 ± 13*
JCN	100 ± 15	99 ± 15	100 ± 9	109 ± 11
PLB	100 ± 15	148 ± 23	100 ± 11	140 ± 16
SERCA	100 ± 16	119 ± 20	100 ± 10	125 ± 11
TRD	100 ± 16	100 ± 15	100 ± 6	120 ± 19

*Data are given as % of expression in corresponding WT animals (n = 6 each). CSQ, calsequestrin; Gsα, α-subunit of stimulatory G protein; Giα, α-subunit of inhibitory G protein; JCN, junctin; PLB, phospholamban; SERCA, sarcoendoplasmatic Ca^{2+}-ATP-ase; TRD, triadin. *$p < 0.05$ vs. corresponding WT.*

Receptor Signaling

The A_{2A}-AR agonist CGS 21680 concentration-dependently increased the cAMP content in ventricular cardiomyocytes from A_{2A}-TG but not in WT cardiomyocytes (**Figure 2A**). The increase in cAMP content in the presence of 1 μM CGS 21680 under these conditions was similar to the response of a maximum effective concentration (1 μM) of the β-adrenoceptor agonist isoproterenol (**Figure 2B**). These findings are consistent with the fact that we measured a concentration dependent effect of CGS 21680 on phospholamban phosphorylation in isolated ventricular cardiomyocytes from A_{2A}-TG but not WT hearts (**Figure 2C**). We used in these experiments adenosine deaminase (ADA) that is an enzyme that rapidly degrades adenosine to inosine. Inosine is not an agonist at adenosine receptors. The inclusion of ADA was, in our hands, crucial in order to detect changes in protein phosphorylation (see **Figure 2** in Gupta et al., 1993a). Importantly, we also noted a similar increase in isoproterenol-induced phospholamban phosphorylation in cardiomyocytes from A_{2A}-TG and WT (**Figure 2D**). Moreover, it is noteworthy that the maximum increase in phospholamban phosphorylation was similar in WT in the presence of isoproterenol vs. CGS 21680 in A_{2A}-TG cardiomyocytes (**Figure 2D**). In addition, we also

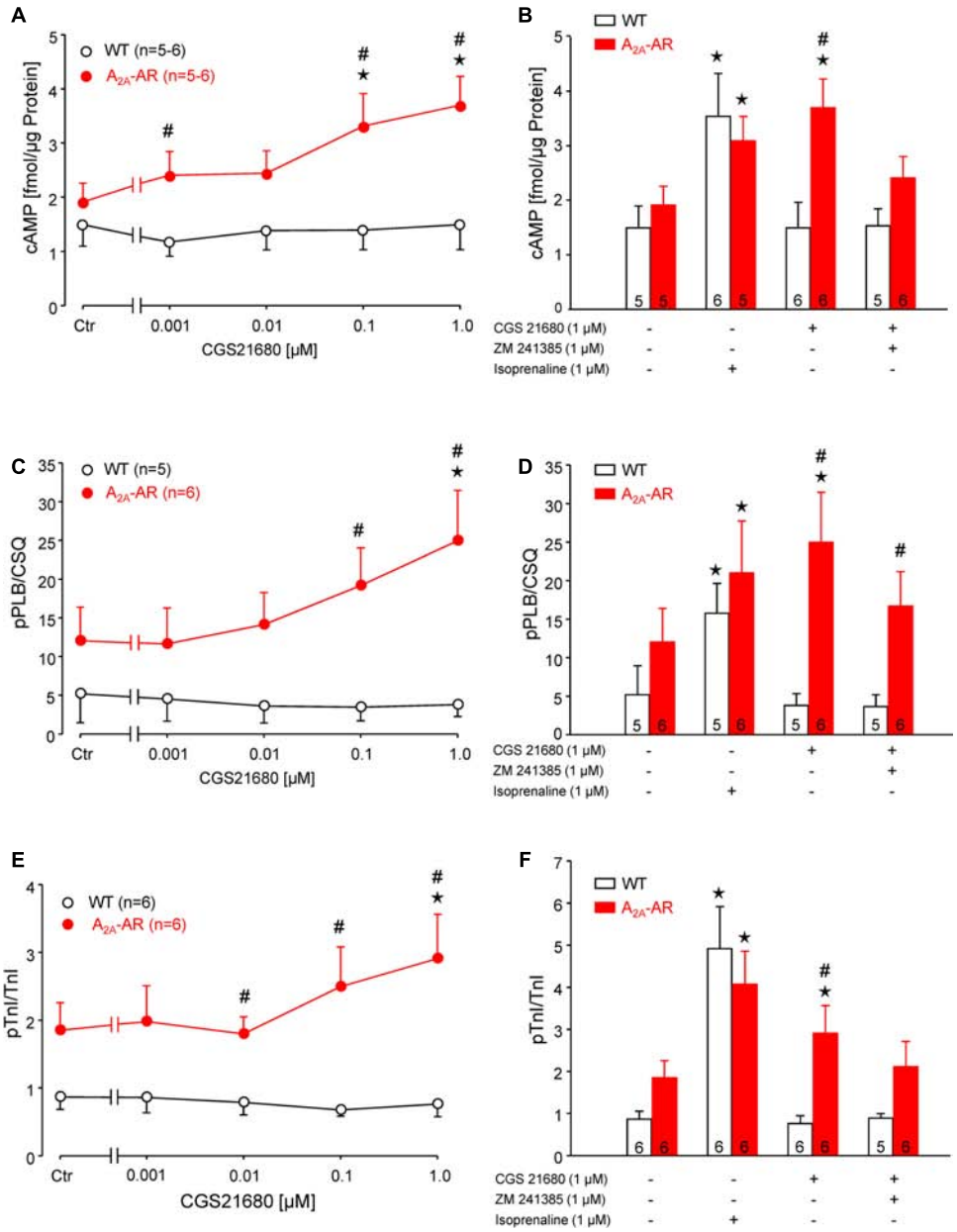

FIGURE 2 | (A,B) cAMP content in isolated ventricular cardiomyocytes from WT and A_{2A}-AR-overexpressing animals. cAMP content was determined by Biotrak direct Enzymimmunoassay. Note concentration dependent increase of cAMP content by A_{2A}-AR agonist CGS 21680 in A_{2A}-AR cardiomyocytes **(A)**; this effect could be completely blocked by A_{2A}-AR antagonist ZM 241385. The effect of β-adrenoceptor agonist isoproterenol on cAMP content did not differ between WT and A_{2A}-AR **(B)**. **(C,D)** Phosphorylation of phospholamban at serine-16 (pPLB). **(E,F)** Phosphorylation of the inhibitory subunit of troponin (pTnI). The phosphorylation state of PLB and TnI was assessed by phosphorylation specific antibodies. The signals obtained using phosphorylation specific antibodies were normalized to the corresponding protein expression. Note concentration dependent increase of pPLB **(C)** and pTnI **(E)** by A_{2A}-AR agonist CGS 21680 in A_{2A}-AR cardiomyocytes; these effects were abolished by A_{2A}-AR antagonist ZM 241385. The effects of isoproterenol on protein phosphorylation were comparable in WT and A_{2A}-AR **(D,F)**. $^{*}p < 0.05$ vs. Ctr; $^{\#}p < 0.05$ vs. WT.

noted a similar increase in CGS 21680-induced phosphorylation of troponin I in ventricular cardiomyocytes from A_{2A}-TG hearts but not from WT hearts (**Figure 2E**). Likewise, it is notable that isoproterenol increased the phosphorylation of troponin I not only in A_{2A}-TG cardiomyocytes but also WT cardiomyocytes (**Figure 2F**). Furthermore, the maximum increase in TnI phosphorylation was similar in WT in the presence of isoproterenol vs. CGS 21680 in A_{2A}-TG myocytes (**Figure 2F**). Moreover, the increase of cAMP-content and protein phosphorylation in A_{2A}-TG in the presence of the A_{2A}-AR agonist CGS 21680 could be attenuated by the additional presence of the A_{2A}-AR antagonist ZM 241385 (**Figure 2**, bar diagrams).

TABLE 3 | Basal force of contraction (FOC) in electrically driven left atria and basal beating rate (BR) in spontaneously beating right atria at the age of 12 and 30 weeks in wild type (WT) and A_{2A}-AR overexpressing animals.

	12 weeks		30 weeks	
	WT	A_{2A}-AR	WT	A_{2A}-AR
FOC (mN)	2.49 ± 0.25 (19)	2.91 ± 0.25 (23)	3.23 ± 0.23 (19)	3.69 ± 0.20$^{\#}$ (25)
BR (bpm)	441 ± 12 (12)	469 ± 22 (8)	410 ± 27 (11)	496 ± 16* (10)

*The measurements were performed after preincubation with adenosine deaminase (30 min, 1 μg/ml) to avoid interference from endogenous adenosine. Numbers of atria are given in parentheses. *$p < 0.05$ vs. corresponding WT; $^{\#}p < 0.05$ vs. A_{2A}-AR at the age of 12 weeks.*

Contractility

The mean values of developed tension under basal conditions (no exogenous pharmacological stimulation) in electrically driven left atrial preparations (12 and 30 weeks) were higher at both ages in A_{2A}-TG than WT but did not gain statistical significance (**Table 3**). However, basal beating rate in A_{2A}-TG was higher than in WT (30 weeks **Table 3**) Contractile studies in the organ bath were performed in the additional presence of the A_1-AR antagonist DPCPX (Neumann et al., 1989). This was done in order to exclude possible interference of any residual adenosine released from cells with the A_1-AR (stimulation of A_1-AR in the atrium exerts negative inotropic and negative chronotropic effects [mouse (Boknik et al., 1997)]. At weeks 12 and 30, the A_{2A}-AR agonist CGS 21680 (1 μM) increased force of contraction in electrically stimulated A_{2A}-TG left atrial preparations but not in electrically stimulated WT atrial preparations (**Figure 3A**). In electrically stimulated A_{2A}-TG left atrial preparations, the positive inotropic effects of CGS 21680 (1 μM) were attenuated by the A_{2A}-AR antagonist ZM 241385 (1 μM, **Figure 3A**). Similarly, 1 μM CGS 21680 was able to increase the beating rate at 12 and 30 weeks in spontaneously beating A_{2A}-TG right atrial preparations but not in spontaneously beating WT right atrial preparations (**Figure 3B**). This increase in beating rate in spontaneously beating A_{2A}-TG right atrial preparations was attenuated by the A_{2A}-AR antagonist ZM 241385 (1 μM, **Figure 3B**).

β-Adrenergic Stimulation

In A_{2A}-TG and WT, invasively left ventricular function was assessed by a catheter while drug was continuously infused with a syringe pump into the jugular vein. The increase of the beating rate to infusion of dobutamine (a clinically used β-adrenoceptor agonist) was similar in A_{2A}-TG and WT (**Figure 4A**). Basal left +dP/dT was higher in A_{2A}-TG compared to WT animals (**Figure 4B**). However, in WT, dobutamine increased +dP/dT to a higher extent than in A_{2A}-TG (**Figure 4B**). In subsequent echocardiographic studies, basal heart rate and interventricular systolic septum thickness were increased in A_{2A}-TG compared to WT. However, the effects of β-adrenoceptor agonist isoproterenol on both parameters were comparable between WT and A_{2A}-TG animals (**Figure 5**).

Ischemia/Reperfusion Experiments

Global ischemia was induced in paced (8 Hz) isolated Langendorff-perfused hearts by complete stop of the perfusion. Hearts were paced because differences in heart rate, alone, might influence contractility. Basal heart rates before pacing amounted to 421.5 ± 14.5 bpm for WT and 467.8 ± 11.7 bpm for TG ($p < 0.05$ vs. WT, $n = 5$–7). During global ischemia (20 min duration), contractile response (here +dP/dt) rapidly stopped (**Figure 6A**). Protective effects were smaller but also present after 40 and 60 min of global ischemia and reperfusion (**Figures 6B,C**). Notably, basal rates of pressure development were higher in A_{2A}-TG than in WT (6,097.3 ± 213.9 mmHg/s vs. 3,657.7 ± 144.7 mmHg/s, $p < 0.05$ vs. WT, $n = 5$–7). Upon reperfusion, cardiac contractile response gradually resumed and relative similar pressure values were reached as before the ischemia in A_{2A}-TG and WT (**Figure 7A**). It is noteworthy that diastolic function is quite sensitive to ischemia in A_{2A}-TG (**Figure 7B**) and the increase in diastolic pressure and its normalization as well as increase and normalization of rates of pressure development were sensitive to 100 nM SCH 442416, an A_{2A}-AR antagonist (**Figures 7A,B**). Moreover, CGS 21680 was able to hasten and elevate the percentile restoration of ventricular + dP/dT (**Figure 7C**).

DISCUSSION

In case of β-adrenergic stimulation and hypoxia, the amount of extracellular adenosine increases in the coronary system (Bardenheuer et al., 1987). Adenosine concentrations are much higher in cardiomyocytes compared to in the extracellular space. Thus, there is a huge concentration gradient for adenosine across the cell membrane and if for example during a myocardial infarction a necrosis occurs, a large amount of adenosine can be released from dying cardiomyocytes.

Adenosine can be a degradation product of ATP but it can also be produced *de novo*. Finally, adenosine deaminases are responsible for metabolizing and thus inactivating adenosine. Adenosine acts via adenosine receptors. All adenosine receptors are a subgroup of *P*-purinoceptors which are separated further into P_1 - or P_2 -purinoceptors (Shryock and Belardinelli, 1997; Burnstock, 2017). P_1-purinoceptors are more sensitive to adenosine than to ATP, the opposite holds true for P_2-purinoceptors (Shryock and Belardinelli, 1997; Burnstock, 2017).

We succeeded in expressing exogenous A_{2A}-AR in cardiomyocytes: importantly we can only detect radioligand binding to the A_{2A}-AR in the A_{2A}-TG heart but not in WT heart. None of the biochemical or physiological parameters studied in an integrated and fairly complete approach supports the functional presence of A_{2A}-AR in WT myocytes, e.g., A_{2A}-AR agonists did not increase cAMP, protein phosphorylation, beating rate or force of contraction in cardiomyocytes or isolated cardiac preparation from WT mouse hearts. In contrast, a selective A_{2A}-AR agonist CGS 21680 increased cAMP content, protein phosphorylation and contractility in A_{2A}-TG preparations.

In genetically modified hearts, homeostatic changes in the expression of other genes occur (Engelhardt et al., 2001;

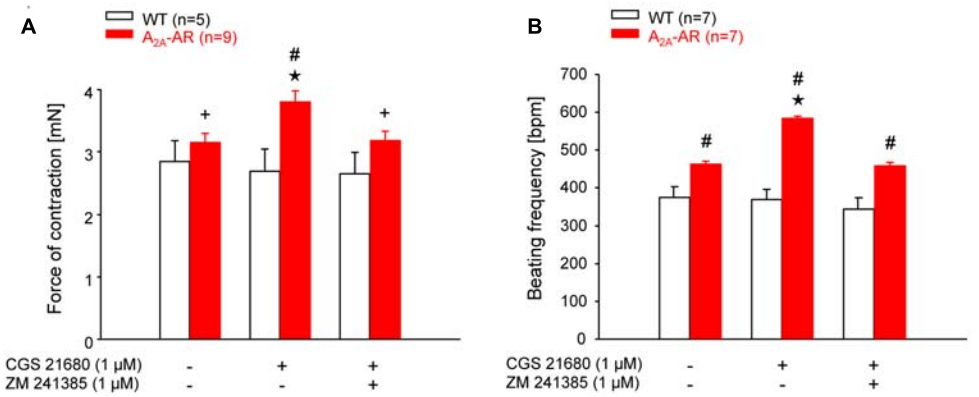

FIGURE 3 | (A) Force of contraction (FOC) in isolated electrically driven left atria. **(B)** Beating frequency (BF) in isolated spontaneously beating right atria. The contraction experiments were performed in the presence of A_1-AR antagonist DPCPX (1 µM). Note the higher basal BF and the increase of FOC and BF by A_{2A}-AR agonist CGS 21680 in atria of A_{2A}-AR overexpressing animals. These effects were abolished in the presence of A_{2A}-AR antagonist ZM 241385. $^{*}p < 0.05$ vs. Ctr; $^{\#}p < 0.05$ vs. WT; $^{+}p < 0.05$ vs. CGS 21680 alone.

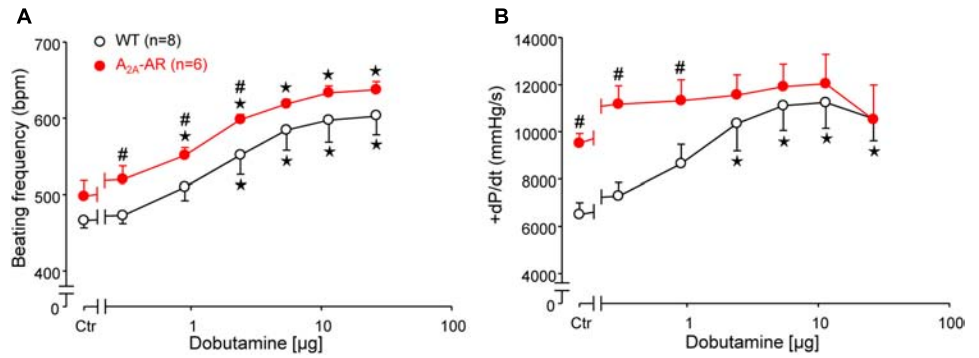

FIGURE 4 | Hemodynamic parameters assessed by left ventricular catheterization in anesthetized WT and A_{2A}-AR overexpressing animals as described in Section "Materials and Methods." Effects of dobutamine on beating frequency (BF, **A**) and maximum rate of left ventricular pressure development (+dP/dt, **B**). Note the higher basal +dP/dt and the lack of dobutamine effect on +dP/dt in A_{2A}-AR overexpressing animals. $^{*}p < 0.05$ vs. Ctr; $^{\#}p < 0.05$ vs. WT.

Lankford et al., 2002). Similar homoeostatic gene changes are plausible in the present transgenic model. Hence, we interpret the decrease in Gs as a protection against persistent basal activity of the A_{2A}-AR leading to chronic elevation of AC activity and cAMP levels. Likewise, it is tempting to assume that the increased Gi levels in order to decrease cAMP levels to normal levels. The unchanged expression of main Ca^{2+} handling proteins of the SR facilitates the interpretation of our contractile data and may be seen in light of our previous work where we studied the function of for example triadin or junctin overexpressing mice (Kirchhefer et al., 2001, 2003, 2004a,b, 2006, 2007; Buchwalow et al., 2004; Kirchhof et al., 2007).

There are a number of studies *in vitro* and *in vivo* showing the overexpression of a Gs coupled receptor *per se* can increase the coupling of receptor and cAMP accumulation. This can result in increased basal effects of the generated cAMP and manifests itself in an increase in basal cAMP and/or increase in PLB phosphorylation, increased basal contraction in left atrial preparations (or intact catheterized hearts of on echocardiography) and/or increased beating rate in isolated right atrial preparation (or in isolated perfused hearts or catheterized hearts of echocardiography). We reported this chain of events before for $5HT_4$ receptor overexpressing mice (Gergs et al., 2013). In part these alterations are present in this mouse model like an increase in basal beating rate (isolated atrial preparations, catheterized hearts, echocardiography).

The continuous stimulation of cAMP content by the overexpressed A_{2A}-AR might explain why higher beating rates are noted in 30 week old A_{2A}-TG right atrial preparations. It is possible that the compensatory mechanisms detected and discussed above lose their effectiveness at this age (but note that they are apparently sufficient to keep parameters in the range of WT at age 12 weeks).

Our interpretation of a functional A_{2A}-AR expression (or overexpression, depending on data interpretation) is supported by the fact that an A_{2A}-AR agonist increases force in left atrial preparations and beating rate in isolated right atrial preparations. Consistent with this the inotropic and chronotropic effects could be reduced by an appropriate antagonist.

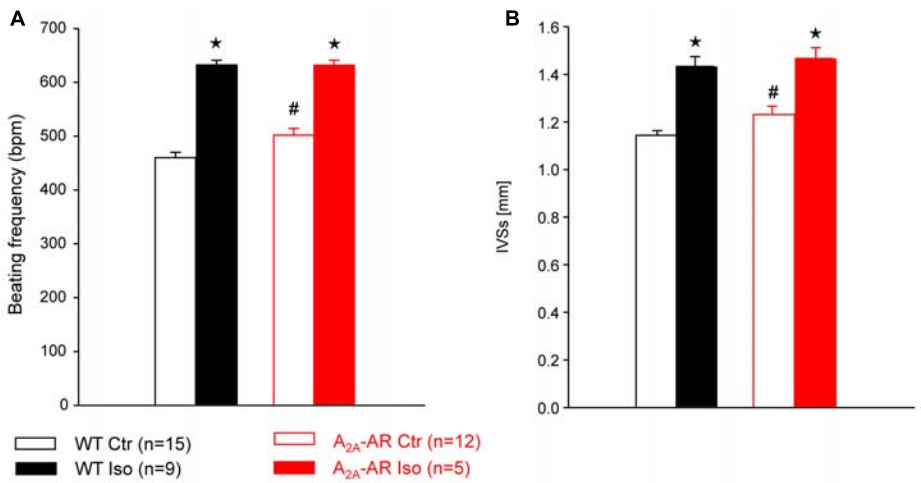

FIGURE 5 | Hemodynamic parameters assessed by Doppler echocardiography in anesthetized WT and A_{2A}-AR overexpressing animals. Note the increased basal beating frequency **(A)** and interventricular systolic septum thickness (IVSs, **B**) in A_{2A}-AR overexpressing animals. The effects of β-adrenoceptor agonist isoproterenol on both parameters were comparable between WT and A_{2A}-AR overexpressing animals. $^{*}p < 0.05$ vs. Ctr; $^{\#}p < 0.05$ vs. WT.

Others have shown that A_1-AR overexpression as well as A_3-AR receptor overexpression can protect cardiac contractility against short term ischemia [preconditioning (Matherne et al., 1997; Black et al., 2002)].

Others have reported before on a constitutive (Chan et al., 2008) or inducible overexpression (Hamad et al., 2010) of the human A_{2A}-receptor in the mouse heart. Our data confirm but also extend this previous work: like us they noted an increase in the heart rate in TG.

In contrast to our data they noted cardiac hypertrophy (**Table 1**; Chan et al., 2008). Similar to Chan et al. (2008) we detected histologically A_{2A}-AR overexpression in myocytes, increased expression of A_{2A}-AR in Western Blots, and increased levels of Giα and increased basal contractility (in invasive left ventricular measurements prior to any drug application). We extend those data (besides that we used a similar but not identical promoter to drive cardiomyocyte specific overexpression) by describing a reduced expression of Gs in TG, studying isolated atrial preparations (elucidation the regional cardiac effects of A_{2A}-AR-overexpression) and by studying the signal transduction in more detail. We concur with their data that cAMP (they measured adenylyl cyclase activity) is not increased in TG under basal conditions and therefore basal phosphorylation state of TnI and phospholamban was not enhanced (which they did not measure). We further extend their work by showing that the overexpressed A_{2A}-receptor exhibits the expected pharmacology: namely the A_{2A}-AR agonist CGS 21680 concentration dependently increased cAMP content in TG (but not WT) and likewise, probably by stimulating the activity of PKA, leads to increased phosphorylation state of phospholamban on its PKA sensitive phosphorylation site and in increased phosphorylation state addition of TnI.

While the group of Feldman elegantly used their model to study *in vivo* functional interaction of A_{1A} coexpression with A_{2A}-receptors (Chan et al., 2008), the protective role of A_{2A} in pressure overload (aortic banding: Hamad et al., 2012) or protection against the cardiodepressant role of chronic Adriamycin treatment (Hamad et al., 2010), we used our model to initiate a first study on the putative protective role of A_{2A}-overexpression in reperfusion of the heart, which to the best of our knowledge has not been studied before, while a protective role of A_{2A}-AR in other species using pharmacological stimulation has been described. We would argue that overexpression of the receptor adds substantially on our mechanistically knowledge in reperfusion injury because, pharmacological stimulation will not allow delineating which cells are involved in a putative protective effect of A_{2A}-receptors: they are expressed (at least functionally) not only in cardiomyocytes but also in cardiac endothelial cells and smooth muscle cells. Hence, any effect we observe in perfused hearts (in the absence of drug application) is probably due to the action of endogenously produced adenosine on the human A_{2A}-AR in cardiomyocytes. Another advantage of our approach (compared to other reports, e.g., Jordan et al., 1997) is that we used isolated buffer perfused hence A_{2A}-receptors in the blood cannot confound our data (which can occur, see, Yang et al., 2005). Others have failed to see any effect of A_{2A}-KO vs. WT in isolated perfused heart on reperfusion injury (Zhan et al., 2011, review: McIntosh and Lasley, 2012). Based on our data, we would argue that it might be due to the loss of A_{2A} not only in cardiomyocytes (which we would predict to be deleterious) but also on endothelial, smooth muscle and fibroblasts (for review cell specific expression of A_{2A}-AR, e.g., McIntosh and Lasley, 2012). It would be interesting to generate and study reperfusion in mice with cardiomyocytes specific A_{2A}-AR KO.

Finally, the data on ischemia may suggest that the A_{2A}-AR may play a protective role of this receptor in ischemia. It might be speculated that alterations of this receptor occur physiologically in myocardial ischemia (for instance during infarction and

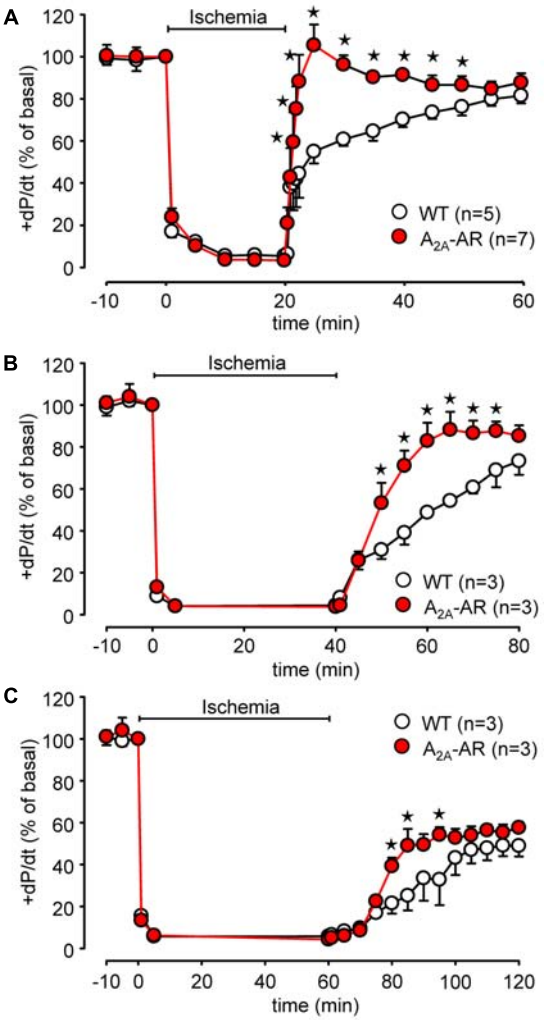

FIGURE 6 | Comparison of 20 min **(A)**, 40 min **(B)**, and 60 min **(C)** of global ischemia in isolated Langendorff-perfused hearts from WT and A_{2A}-AR overexpressing animals. Maximum rate of left ventricular pressure development (+dP/dt) is presented as % of basal value. $^{*}p < 0.05$ vs. WT.

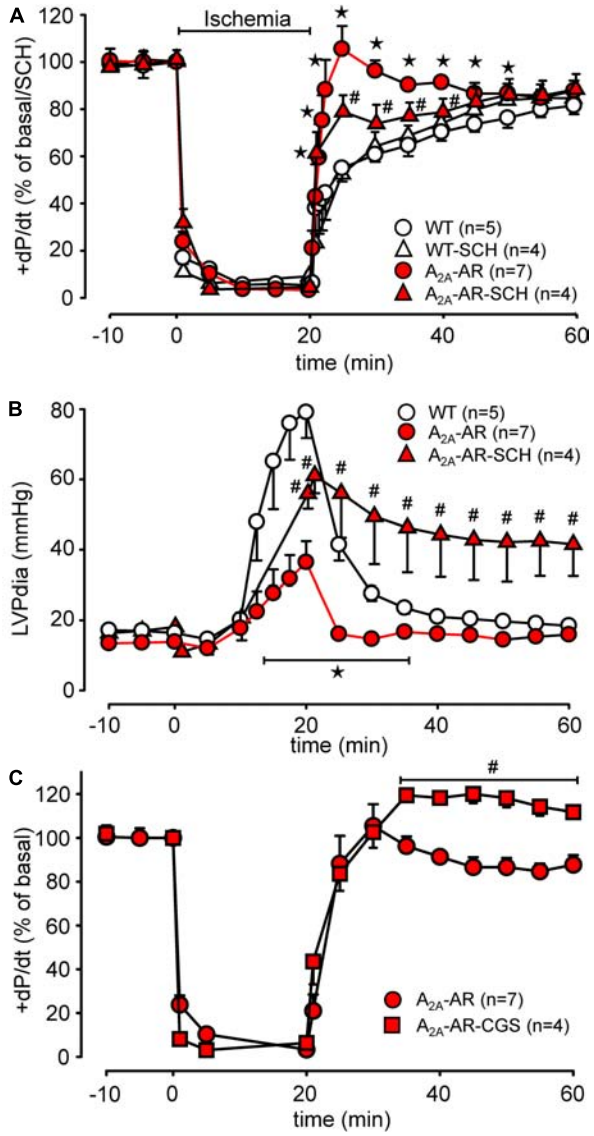

FIGURE 7 | Hemodynamic parameters during global ischemia with subsequent reperfusion assessed in isolated Langendorff-perfused hearts from WT and A_{2A}-AR overexpressing animals. **(A)** Maximum rate of left ventricular pressure development (+dP/dt) as % of basal value with and without the A_{2A}-AR antagonist SCH 442416 (SCH, 100 nM). **(B)** Left ventricular end diastolic pressure with and without the A_{2A}-AR antagonist SCH 442416 (SCH, 100 nM). **(C)** Effect of A_{2A}-AR agonist CGS 21680 (1 μM) administered during reperfusion on +dP/dt in A_{2A}-AR overexpressing hearts. Note the higher basal +dP/dt, markedly prolonged time to ischemic contracture as well as the additional effect of A_{2A}-AR agonist CGS 21680 on the +dP/dt in A_{2A}-AR overexpressing hearts during reperfusion. $^{*}p < 0.05$ vs. WT; $^{\#}p < 0.05$ vs. A_{2A}-AR.

stenting of the vessel). These receptors may therefore be a target for pharmacological treatment of reperfusion injury. However, more detailed studies are called for and are expected with interest.

Moreover, one can ask whether this model has (patho)-physiological relevance. In this regard it might be of interest that during ischemia in isolated perfused hearts the expression of A_{2A}-AR increases (Morrison et al., 2006). A_{2A} agonists like regadenoson are clinically used to detect latent ischemia in patients (Cerqueira et al., 2008).

Study Limitations

Furthermore, the direct comparison with the human situation is not easy. In earlier work, we reported that adenosine can in some atrial samples from patients exert a positive inotropic effect (Gergs et al., 2009). However, the effect was A_1 receptor mediated. We have not been able to perform similar experiments in human ventricular tissue (for lack of material at our institutions). However, some years ago we reported at least an increase in the mRNA of A_{2A}-AR in failing human ventricular samples compared to non-failing (Stein et al., 1998). Thus, it is tempting to speculate that A_{2A}-AR may sustain contractility in end stage human heart failure. Hence, A_{2A}-AR may serve a physiological

role in humans and, as shown for adenoviral expression of adenylate cyclase, genetic manipulation of A_{2A}-AR may offer a novel venue for treating human heart failure.

CONCLUSION

We describe a transgenic mouse with A_{2A}-AR overexpression to cardiomyocytes using the established alpha myosin heavy chain promoter. Moreover, transgenic A_{2A}-AR is functional after drug-induced stimulation to increase force and beating rate in mouse hearts or mouse heart preparations and the transgenic A_{2A}-AR can protect the mouse heart against ischemia.

AUTHOR CONTRIBUTIONS

KD, JE, SG-W, LF, FS, and UK performed the research. PB, FM, WS, and JN designed the research study. PB, PK, NZ, UK, and JN analyzed the data. PB, UG, and JN wrote the paper.

ACKNOWLEDGMENTS

This work was supported by the Bundesinstitut für Arzneimittel und Medizinprodukte. We acknowledge the financial support of the Open Access Publication Fund of the Martin Luther University Halle-Wittenberg.

REFERENCES

Ashton, K. J., Reichelt, M. E., Mustafa, S. J., Teng, B., Ledent, C., Delbridge, L. M., et al. (2017). Transcriptomic effects of adenosine 2A receptor deletion in healthy and endotoxemic murine myocardium. *Purinergic Signal.* 13, 27–49. doi: 10.1007/s11302-016-9536-1

Bardenheuer, H., Whelton, B., and Sparks, H. V. (1987). Adenosine release by the isolated guinea pig heart in response to isoproterenol, acetylcholine, and acidosis: the minimal role of vascular endothelium. *Circ. Res.* 61, 594–600. doi: 10.1161/01.RES.61.4.594

Belardinelli, L., and Isenberg, G. (1983). Isolated atrial myocytes: adenosine and acetylcholine increase potassium conductance. *Am. J. Physiol. Heart Circ. Physiol.* 244, H734–H737. doi: 10.1152/ajpheart.1983.244.5.H734

Black, R. G., Guo, Y., Ge, Z. D., Murphree, S. S., Prabhu, S. D., Jones, W. K., et al. (2002). Gene dosage-dependent effects of cardiac-specific overexpression of the A_3 adenosine receptor. *Circ. Res.* 91, 165–172. doi: 10.1161/01.RES.0000028007.91385.EE

Böhm, M., Brückner, R., Hackbarth, I., Haubitz, B., Linhart, R., Meyer, W., et al. (1984). Adenosine inhibition of catecholamine-induced increase in force of contraction in guinea-pig atrial and ventricular heart preparations. Evidence against a cyclic AMP- and cyclic GMP-dependent effect. *J. Pharmacol. Exp. Ther.* 230, 483–492.

Böhm, M., Brückner, R., Neumann, J., Schmitz, W., Scholz, H., and Starbatty, J. (1986). Role of guanine nucleotide-binding protein in the regulation by adenosine of cardiac potassium conductance and force of contraction. Evaluation with pertussis toxin. *Naunyn Schmiedebergs Arch. Pharmacol.* 332, 403–405.

Boknik, P., Grote-Wessels, S., Barteska, G., Jiang, M., Müller, F. U., Schmitz, W., et al. (2009). Genetic disruption of G proteins, Gi2α or Goα, does not abolish inotropic and chronotropic effects of stimulating muscarinic cholinoceptors in atrium. *Br. J. Pharmacol.* 158, 1557–1564. doi: 10.1111/j.1476-5381.2009.00441.x

Boknik, P., Neumann, J., Schmitz, W., Scholz, H., and Wenzlaff, H. (1997). Characterization of biochemical effects of CGS 21680C, an A2-adenosine receptor agonist, in the mammalian ventricle. *J. Cardiovasc. Pharmacol.* 30, 750–758. doi: 10.1097/00005344-199712000-00009

Brückner, R., Fenner, A., Meyer, W., Nobis, T. M., Schmitz, W., and Scholz, H. (1985). Cardiac effects of adenosine and adenosine analogs in guinea-pig atrial and ventricular preparations: evidence against a role of cyclic AMP and cyclic GMP. *J. Pharmacol. Exp. Ther.* 234, 766–774.

Buchwalow, I. B., Podzuweit, T., Samoilova, V. E., Wellner, M., Haller, H., Grote, S., et al. (2004). An in situ evidence for autocrine function of NO in the vasculature. *Nitric Oxide* 10, 203–212. doi: 10.1016/j.niox.2004.04.004

Burnstock, G. (2017). Purinergic signaling in the cardiovascular system. *Circ. Res.* 120, 207–228. doi: 10.1161/CIRCRESAHA.116.309726

Cargnoni, A., Ceconi, C., Boraso, A., Bernocchi, P., Monopoli, A., Curello, S., et al. (1999). Role of A2A receptor in the modulation of myocardial reperfusion damage. *J. Cardiovasc. Pharmacol.* 33, 883–893. doi: 10.1097/00005344-199906000-00008

Cerqueira, M. D., Nguyen, P., Staehr, P., Underwood, S. R., Iskandrian, A. E., and ADVANCE-MPI Trial Investigators. (2008). Effects of age, gender, obesity, and diabetes on the efficacy and safety of the selective A2A agonist regadenoson versus adenosine in myocardial perfusion imaging integrated ADVANCE-MPI trial results. *JACC Cardiovasc. Imaging* 1, 307–316. doi: 10.1016/j.jcmg.2008.02.003

Chan, T. O., Funakoshi, H., Song, J., Zhang, X. Q., Wang, J., Chung, P. H., et al. (2008). Cardiac-restricted overexpression of the A(2A)-adenosine receptor in FVB mice transiently increases contractile performance and rescues the heart failure phenotype in mice overexpressing the A(1)-adenosine receptor. *Clin. Transl. Sci.* 1, 126–133. doi: 10.1111/j.1752-8062.2008.00027.x

Dobson, J. G. (1978). Reduction by adenosine of the isoproterenol-induced increase in cyclic adenosine 3-monophosphate formation and glycogen phosphorylase activity in rat heart muscle. *Circ. Res.* 43, 785–792. doi: 10.1161/01.RES.43.5.785

Dobson, J. G. (1983). Mechanism of adenosine inhibition of catecholamine-induced responses in heart. *Circ. Res.* 52, 151–160. doi: 10.1161/01.RES.52.2.151

Engelhardt, S., Boknik, P., Keller, U., Neumann, J., Lohse, M. J., and Hein, L. (2001). Early impairment of calcium handling and altered expression of junction in hearts of mice overexpressing the b1-adrenergic receptor. *FASEB J.* 15, 2718–2720.

Gergs, U., Baumann, M., Böckler, A., Buchwalow, I. B., Ebelt, H., Fabritz, L., et al. (2010). Cardiac overexpression of the human 5-HT4 receptor in mice. *Am. J. Physiol. Heart Circ. Physiol.* 299, H788-H798. doi: 10.1152/ajpheart.00691.2009

Gergs, U., Böckler, A., Ebelt, H., Hauptmann, S., Keller, N., Otto, V., et al. (2013). Human 5-HT4 receptor stimulation in atria of transgenic mice. *Naunyn Schmiedebergs Arch. Pharmacol.* 386, 357–367. doi: 10.1007/s00210-013-0831-x

Gergs, U., Boknik, P., Buchwalow, I., Fabritz, L., Matus, M., Justus, I., et al. (2004). Overexpression of the catalytic subunit of protein phosphatase 2A impairs cardiac function. *J. Biol. Chem.* 279, 40827–40834. doi: 10.1074/jbc.M405770200

Gergs, U., Boknik, P., Schmitz, W., Simm, A., Silber, R. E., and Neumann, J. (2009). A positive inotropic effect of adenosine in cardiac preparations of right atria from diseased human hearts. *Naunyn Schmiedebergs Arch. Pharmacol.* 379, 533–540. doi: 10.1007/s00210-008-0374-8

Grote-Wessels, S., Buchwalow, I., Fabritz, L., Zimmermann, N., Schmitz, W., Müller, F. U., et al. (2007). Functional studies in mice overexpressing A2A adenosine receptors in the heart. *Arch. Pharmacol.* 375(Suppl. 1), 59.

Gupta, R. C., Neumann, J., Durant, P., and Watanabe, A. M. (1993a). A1-adenosine receptor-mediated inhibition of isoproterenol-stimulated protein phosphorylation in ventricular myocytes. Evidence against a cAMP-dependent effect. *Circ. Res.* 72, 65–74.

Gupta, R. C., Neumann, J., and Watanabe, A. M. (1993b). Comparison of adenosine and muscarinic receptor-mediated effects on protein phosphatase inhibitor-1 activity in the heart. *J. Pharmacol. Exp. Ther.* 266, 16–22.

Hamad, E. A., Li, X., Song, J., Zhang, X. Q., Myers, V., Funakoshi, H., et al. (2010). Effects of cardiac-restricted overexpression of the A(2A) adenosine receptor on adriamycin-induced cardiotoxicity. *Am. J. Physiol. Heart Circ. Physiol.* 298, H1738–H1747. doi: 10.1152/ajpheart.00688.2009

Hamad, E. A., Zhu, W., Chan, T. O., Myers, V., Gao, E., Li, X., et al. (2012). Cardioprotection of controlled and cardiac-specific over-expression of A(2A)-adenosine receptor in the pressure overload. *PLOS ONE* 7:e39919. doi: 10.1371/journal.pone.0039919

Jordan, J. E., Zhao, Z. Q., Sato, H., Taft, S., and Vinten-Johansen, J. (1997). Adenosine A2 receptor activation attenuates reperfusion injury by inhibiting neutrophil accumulation, superoxide generation and coronary endothelial adherence. *J. Pharmacol. Exp. Ther.* 280, 301–309.

Kilpatrick, E. L., Narayan, P., Mentzer, R. M. Jr., and Lasley, R. D. (2002). Cardiac myocyte adenosine A_{2A} receptor activation fails to alter cAMP or contractility: role of receptor localization. *Am. J. Physiol. Heart Circ. Physiol.* 282, H1035–H1040. doi: 10.1152/ajpheart.00808.2001

Kirchhefer, U., Baba, H. A., Hanske, G., Jones, L. R., Kirchhof, P., Schmitz, W., et al. (2004a). Age-dependent biochemical and contractile properties in atrium of transgenic mice overexpressing junction. *Am. J. Physiol. Heart Circ. Physiol.* 287, H2216-H2225.

Kirchhefer, U., Baba, H. A., Kobayashi, Y. M., Jones, L. R., Schmitz, W., and Neumann, J. (2002). Altered function in atrium of transgenic mice overexpressing triadin 1. *Am. J. Physiol. Heart Circ. Physiol.* 283, H1334-H1343. doi: 10.1152/ajpheart.00937.2001

Kirchhefer, U., Brekle, C., Eskandar, J., Isensee, G., Kucerová, D., Müller, F. U., et al. (2014). Cardiac function is regulated by B56α-mediated targeting of protein phosphatase 2A (PP2A) to contractile relevant substrates. *J. Biol. Chem.* 289, 33862–33873. doi: 10.1074/jbc.M114.598938

Kirchhefer, U., Hanske, G., Jones, L. R., Justus, I., Kaestner, L., Lipp, P., et al. (2006). Overexpression of junction causes adaptive changes in cardiac myocyte Ca2+ signaling. *Cell Calcium* 39, 131–142. doi: 10.1016/j.ceca.2005.10.004

Kirchhefer, U., Jones, L. R., Begrow, F., Boknik, P., Hein, L., Lohse, M. J., et al. (2004b). Transgenic triadin 1 overexpression alters SR Ca2+ handling and leads to a blunted contractile response to β-adrenergic agonists. *Cardiovasc. Res.* 62, 122–134.

Kirchhefer, U., Klimas, J., Baba, H. A., Buchwalow, I. B., Fabritz, L., Hüls, M., et al. (2007). Triadin is a critical determinant of cellular Ca cycling and contractility in the heart. *Am. J. Physiol. Heart Circ. Physiol.* 293, H3165-H3174. doi: 10.1152/ajpheart.00799.2007

Kirchhefer, U., Neumann, J., Baba, H. A., Begrow, F., Kobayashi, Y. M., Reinke, U., et al. (2001). Cardiac hypertrophy and impaired relaxation in transgenic mice overexpressing triadin 1. *J. Biol. Chem.* 276, 4142–4149. doi: 10.1074/jbc.M006443200

Kirchhefer, U., Neumann, J., Bers, D. M., Buchwalow, I. B., Fabritz, L., Hanske, G., et al. (2003). Impaired relaxation in transgenic mice overexpressing junction. *Cardiovasc. Res.* 59, 369–379. doi: 10.1016/S0008-6363(03)00432-2

Kirchhof, P., Klimas, J., Fabritz, L., Zwiener, M., Jones, L. R., Schäfers, M., et al. (2007). Stress and high heart rate provoke ventricular tachycardia in mice expressing triadin. *J. Mol. Cell. Cardiol.* 42, 962–971. doi: 10.1016/j.yjmcc.2007.02.012

Lankford, A. R., Byford, A. M., Ashton, K. J., French, B. A., Lee, J. K., Headrick, J. P., et al. (2002). Gene expression profile of mouse myocardium with transgenic overexpression of A_1 adenosine receptors. *Physiol. Genomics* 11, 81–89. doi: 10.1152/physiolgenomics.00008.2002

Ledent, C., Vaugeois, J. M., Schiffmann, S. N., Pedrazzini, T., El Yacoubi, M., Vanderhaeghen, J. J., et al. (1997). Aggressiveness, hypoalgesia and high blood pressure in mice lacking the adenosine A_{2A} receptor. *Nature* 388, 674–678. doi: 10.1038/41771

Libert, F., Parmentier, M., Lefort, A., Dinsart, C., van Sande, J., Maenhaut, C., et al. (1989). Selective amplification and cloning of four new members of the G protein-coupled receptor family. *Science* 244, 569–572. doi: 10.1126/science.2541503

Linden, J., Hollen, C. E., and Patel, A. (1985). The mechanism by which adenosine and cholinergic agents reduce contractility in rat myocardium. Correlation with cyclic adenosine monophosphate and receptor densities. *Circ. Res.* 56, 728–735. doi: 10.1161/01.RES.56.5.728

Makujina, S. R., Sabouni, M. H., Bhatia, S., Douglas, F. L., and Mustafa, S. J. (1992). Vasodilatory effects of adenosine A2 receptor agonists CGS 21680 and CGS 22492 in human vasculature. *Eur. J. Pharmacol.* 221, 243–247. doi: 10.1016/0014-2999(92)90708-C

Marala, R. B., and Mustafa, S. J. (1998). Immunological characterization of adenosine A_{2A}receptors in human and porcine cardiovascular tissues. *J. Pharmacol. Exp. Ther.* 286, 1051–1057.

Matherne, G. P., Linden, J., Byford, A. M., Gauthier, N. S., and Headrick, J. P. (1997). Transgenic A_1 adenosine receptor overexpression increases myocardial resistance to ischemia. *Proc. Natl. Acad. Sci. U.S.A.* 94, 6541–6546. doi: 10.1073/pnas.94.12.6541

McIntosh, V. J., and Lasley, R. D. (2012). Adenosine receptor-mediated cardioprotection: are all 4 subtypes required or redundant? *J. Cardiovasc. Pharmacol. Ther.* 17, 21–33. doi: 10.1177/1074248410396877

Monahan, T. S., Sawmiller, D. R., Fenton, R. A., and Dobson, J. G. Jr. (2000). Adenosine A(2a)-receptor activation increases contractility in isolated perfused hearts. *Am. J. Physiol. Heart Circ. Physiol.* 279, H1472–H1481.

Morrison, R. R., Teng, B., Oldenburg, P. J., Katwa, L. C., Schnermann, J. B., and Mustafa, S. J. (2006). Effects of targeted deletion of A_1 adenosine receptors on postischemic cardiac function and expression of adenosine receptor subtypes. *Am. J. Physiol. Heart Circ. Physiol.* 291, H1875–H1882. doi: 10.1152/ajpheart.00158.2005

National Research Council. (2011). *Guide for the Care and Use of Laboratory Animals*, 8th Edn. Washington, DC: The National Academies Press.

Neumann, J., Schmitz, W., Scholz, H., and Stein, B. (1989). Effects of adenosine analogues on contractile response and CAMP content in guinea-pig isolated ventricular myocytes. *Naunyn Schmiedebergs Arch. Pharmacol.* 340, 689–695.

Olsson, R. A., and Pearson, J. D. (1990). Cardiovascular purinoceptors. *Physiol. Rev.* 70, 761–845. doi: 10.1152/physrev.1990.70.3.761

Shryock, J., Song, Y., Wang, D., Baker, S. P., Olsson, R. A., and Belardinelli, L. (1993). Selective A2-adenosine receptor agonists do not alter action potential duration, twitch shortening, or cAMP accumulation in guinea pig, rat, or rabbit isolated ventricular myocytes. *Circ. Res.* 72, 194–205. doi: 10.1161/01.RES.72.1.194

Shryock, J. C., and Belardinelli, L. (1997). Adenosine and adenosine receptors in the cardiovascular system: biochemistry, physiology, and pharmacology. *Am. J. Cardiol.* 79, 2–10. doi: 10.1016/S0002-9149(97)00256-7

Stein, B., Kiehn, J., and Neumann, J. (1998). "Regulation of adenosine receptor subtypes and dysfunction in human heart failure," in *Cardiovascular Biology of Purines*, eds G. Burnstock, J. G. Dobson Jr., B. T. Liang, and J. Linden (Dordrecht: Kluwer Academic Publishers), 108–125.

Yang, Z., Day, Y. J., Toufektsian, M. C., Ramos, S. I., Marshall, M., Wang, X. Q., et al. (2005). Infarct-sparing effect of A_{2A}-adenosine receptor activation is due primarily to its action on lymphocytes. *Circulation* 111, 2190–2197. doi: 10.1161/01.CIR.0000163586.62253.A5

Zhan, E., McIntosh, V. J., and Lasley, R. D. (2011). Adenosine A_{2A} and A_{2B} receptors are both required for adenosine A_1 receptor-mediated cardioprotection. *Am. J. Physiol. Heart Circ. Physiol.* 301, H1183–H1189. doi: 10.1152/ajpheart.00264.2011

Conflict of Interest Statement: The authors declare that the research was conducted in the absence of any commercial or financial relationships that could be construed as a potential conflict of interest.

frontiers in Pharmacology

ORIGINAL RESEARCH
published: 10 January 2018
doi: 10.3389/fphar.2017.00986

Adenine Nucleotides Attenuate Murine T Cell Activation Induced by Concanavalin A or T Cell Receptor Stimulation

*Yuria Shinohara and Mitsutoshi Tsukimoto**

Department of Radiation Biosciences, Faculty of Pharmaceutical Sciences, Tokyo University of Science, Chiba, Japan

Extracellular ATP and its metabolites affect various cellular immune responses, including T cell function, but there are apparently conflicting reports concerning the effects of adenine nucleotides on T cells. For example, it has been reported that ATP-mediated activation of P2 receptor is involved in T cell activation; activation of adenosine receptors suppresses T cell function; and 1 mM ATP induces T cell death via activation of P2X7 receptor. Therefore, in this work we investigated in detail the effects of 100–250 μM ATP, ADP, or AMP on murine T cell activation. First, an *in vitro* study showed that pretreatment of murine splenic T cells with 100–250 μM ATP, ADP, or AMP significantly suppressed the concanavalin A (ConA)-induced release of cytokines, including IL-2. This suppression was not due to induction of cell death via the P2X7 receptor or to an immunosuppressive effect of adenosine. ATP attenuated the expression of CD25, and decreased the cell proliferation ability of activated T cells. The release of IL-2 by ConA-stimulated lymphocytes was suppressed by post-treatment with ATP, as well as by pretreatment. These results suggest that exogenous ATP suppresses the activation of T cells. Secondly, we evaluated the effect of ATP in a ConA-treated mice. Treatment with ATP attenuated the increase of IL-2 concentration in the blood. Overall, these results suggest that adenine nucleotides might have potential as supplemental therapeutic agents for T cell-mediated immune diseases, by suppressing T cell activation.

Keywords: ATP, T cell, purinergic receptor, inflammation, IL-2, concanavalin A, T cell receptor

OPEN ACCESS

Edited by:
Francisco Ciruela,
University of Barcelona, Spain

Reviewed by:
Hai Li,
Shanghai Jiao Tong University, China
Urs Christen,
Goethe University Frankfurt, Germany

***Correspondence:**
Mitsutoshi Tsukimoto
tsukim@rs.noda.tus.ac.jp

Specialty section:
This article was submitted to Experimental Pharmacology and Drug Discovery, a section of the journal Frontiers in Pharmacology

Received: *07 November 2017*
Accepted: *22 December 2017*
Published: *10 January 2018*

Citation:
Shinohara Y and Tsukimoto M (2018) Adenine Nucleotides Attenuate Murine T Cell Activation Induced by Concanavalin A or T Cell Receptor Stimulation. Front. Pharmacol. 8:986. doi: 10.3389/fphar.2017.00986

INTRODUCTION

Activation of T cells by MAPKs induces various responses necessary for immune function. There are three major MAPK pathways that operate in T-cells (Rincon et al., 2000a,b; Gong et al., 2001), involving c-Jun NH2-terminal kinase, extracellular signal regulatory protein kinase (ERK) (Fischer et al., 2005; Zhang and Dong, 2005), and p38 MAPK. Activation of these MAPKs results in nuclear translocation and promoter binding of transcription factors, and results in gene expression of a number of mediators involved in the inflammatory response (Marshall et al., 1995; Whitehurst and Geppert, 1996). Elevated intracellular Ca^{2+} ion concentration is also essential for T cell activation.

Abbreviations: 2-MeS-ADP, 2-(methylthio)adenosine 5′-diphosphate trisodium salt hydrate; ATP-γS, adenosine 5′-O-(3-thiotriphosphate); BrdU, 5-bromodeoxyuridine; BzATP, 2′(3′)-O-(4-benzoylbenzoyl)adenosine 5′-triphosphate triethylammonium salt; ConA, concanavalin A; ERK, extracellular signal-regulated kinase; IL, interleukin; LDH, lactate dehydrogenase; mAb, monoclonal antibody; MAPK, mitogen-activated protein kinase; TCR, T cell receptor.

In lymphocytes, calcium release-activated calcium channels open in response to calcium depletion of the endoplasmic reticulum and increase the intracellular Ca^{2+} concentration (Oh-hora, 2009), thereby activating expression of numerous cytokine genes (Gallo et al., 2006). In particular, the production of IL-2 and the induction of CD25 (IL-2 receptor α chain) expression (Kondo et al., 1993; Nelson et al., 1994) are involved in T cell activation and proliferation (Nelson et al., 1994; Lin and Leonard, 1997). Pathological activation of T cells plays an important role in autoimmune diseases, including multiple sclerosis, rheumatoid arthritis, and autoimmune hepatitis.

Concanavalin A (ConA) is a plant lectin isolated from *Canavalia ensiformis* (jack bean) seeds that binds to various glycosyl proteins and to α-D-mannose residues on glycolipids. It induces mitogenic activity of T lymphocytes and has various bioactivities (Lei and Chang, 2009). Treatment of mice with ConA increased production of inflammatory cytokines such as IL-2, IL-4, IL-6, IL-10, IL-12, TNF-α, and IFN-γ (Sass et al., 2002).

ATP is released from various types of cells into the extracellular compartment. ATP and its metabolites, such as ATP, ADP, AMP and adenosine, regulate various physiological effects via the ligand-gated ion channel P2X receptor and the metabotropic G protein-coupled P2Y receptor (Burnstock, 2009; Burnstock and Boeynaems, 2014). Previous studies have demonstrated that P2X, P2Y, and adenosine receptors play roles in both TCR stimulation-induced and hypertonic stress-induced T cell activation (Yip et al., 2007; Woehrle et al., 2010). Many researchers, including our group, have reported involvement of extracellular ATP and purinergic receptors in these actions, showing that extracellular ATP induces T cell activation via P2X7, P2X4, and P2Y6 receptors (Schenk et al., 2008; Tsukimoto et al., 2009; Yip et al., 2009; Tokunaga et al., 2010; Woehrle et al., 2010). However, the inhibitory effect of ATP and its metabolites on T cell activation is still not completely understood. It was reported that activation of P2X7 receptor by ATP (0.5–1 mM) induces T cell death (Chused et al., 1996; Tsukimoto et al., 2006). On the other hand, 250 nM ATP induces T cell proliferation, cytokine release, and molecular adhesion (Trabanelli et al., 2012). Another report indicated that ATP suppresses T cell proliferation (Weiler et al., 2016). That is, the functions of ATP appear to depend on its concentration. Thus, a detailed understanding of the effects of exogenously added adenine nucleotides on T cells is very important for the elucidation of T cell functions. Although adenosine is well known to inhibit T cell function via activation of adenosine receptor, it is poorly soluble in water, whereas ATP is very soluble, and shows very low cytotoxicity. Thus, if ATP can suppress T cell activation, sustained intravenous injection of ATP in patients with immune disease or graft-versus-host disease might be a promising candidate for supplemental treatment of their disease.

In this study, we found that activation of murine T cells is suppressed by ATP, as well as by its metabolites, ADP and AMP. ATP inhibited the production of inflammatory cytokine IL-2 at both the mRNA and protein levels, as well as expression of CD25 and activation-associated T cell proliferation. In addition, intravenous administration of ATP into mice suppressed ConA-induced elevation of serum IL-2 level in mice. These results suggest that combination of ATP with existing treatment modalities might be beneficial in patients with T cell mediated-immune diseases.

MATERIALS AND METHODS

Reagents

Concanavalin A (ConA) were purchased from Sigma–Aldrich. Anti-CD3ε mAb was purchased from R&D Systems (United States). Anti-CD28 mAb was from eBioscience (United States). ATP, ADP, and adenosine were from Sigma (United States). PPADS, BDBD, MRS2578, SCH442416, PSB36, MRS3777, A438079, CGS15943, PSB603, and MRS2111 were from Tocris Bioscience (United Kingdom). Suramin and oxATP were purchased from Sigma–Aldrich. NF449 was from Abcam (United Kingdom). Adenosine 5′-[γ-thio]triphosphate tetralithium salt (ATP-γ-S), α,β-methyleneadenosine 5′-triphosphate lithium salt (α,β-Me-ATP), BzATP, α,β-methyleneadenosine 5′-diphosphate sodium salt (α,β-Me-ADP), and 2-methylthioadenosine diphosphate trisodium salt (2-MeS-ADP) were purchased from Sigma–Aldrich. Anti-ERK1/2 mAb and anti-phospho-ERK 1/2 (Thr^{202}/Tyr^{204}) mAb and other secondary Abs were obtained from Cell Signaling Technology (United States). All other chemicals used were of the highest purity available.

Animals

Male BALB/c mice (21.6 ± 1.04 g) were purchased from Sankyo Labo Service (Japan) and used at 6 weeks of age. They were housed in plastic cages with paper chip bedding and bred in rooms kept at a temperature of 23 ± 2°C and a relative humidity of 55 ± 10% under a 12 h light–dark cycle. They were allowed free access to tap water and normal diet, CE-2 (CLEA Co. Ltd.). The mice were treated and handled according to the Guiding Principles for the Care and Use of Laboratory Animals of the Japanese Pharmacological Society and with the approval of Tokyo University of Science's Institutional Animal Care and Use Committee (permit numbers S17007 and S17010).

Preparation of Splenic Lymphocytes

Splenocytes were isolated from the spleen of BALB/c mice, and were purified by means of hemolysis. Cells were washed twice with complete RPMI1640 medium and re-suspended in RPMI1640-based buffer (Tsukimoto et al., 2006). To remove adherent cells such as macrophages and dendritic cells, splenocytes were incubated for 1.5 h in a plastic cell culture plate for 1 h in an atmosphere of 5% CO_2/95% air at 37°C. Non-adherent cells, mainly lymphocytes, were collected and washed once with RPMI1640-based buffer.

Cytokine Production

Splenocytes (6.0×10^6 cells/well) were stimulated with ConA (5 μg/mL) in a 96-well cell culture plate in RPMI 1640 medium containing 10% heat-inactivated FBS, 100 units/ml of penicillin, and 100 μg/ml of streptomycin in an atmosphere of 5% CO_2, 95% air at 37°C. For TCR stimulation, splenocytes were incubated

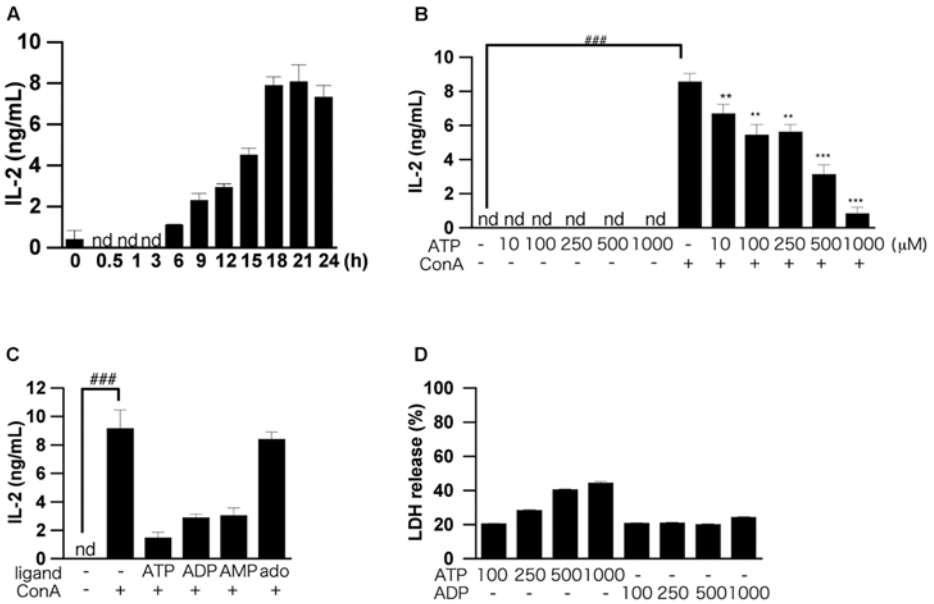

FIGURE 1 | Effects of ATP on ConA-induced IL-2 production by splenic lymphocytes isolated from BALB/c mice. **(A)** Splenic lymphocytes were stimulated with 50 μg/mL ConA and incubated for the indicated times. The concentration of IL-2 released into the culture medium was measured by means of ELISA. **(B)** Lymphocytes were pre-incubated with various concentrations of ATP (10, 50, 100, 250, and 500 μM) for 30 min, and then stimulated with 50 μg/mL ConA for 24 h. **(C)** Lymphocytes were pre-incubated with 250 μM ATP, ADP, AMP, and adenosine (ado) for 30 min, and then stimulated with 50 μg/mL ConA for 24 h. **(D)** Cell damage after incubation of lymphocytes with ATP or ADP (100, 250, and 500 μM) for 1 h was measured by LDH assay. Each value represents the mean ± SE ($n = 4$). Significant difference between the vehicle control group and the ConA-treated group in the absence of ATP or other ligand is indicated by $^{###}P < 0.001$. Significant differences between the ConA-treated, ATP-untreated group and the ConA-treated, ATP-treated groups is indicated by $^{***}P < 0.001$ and $^{**}P < 0.01$. Each figure is representative of several independent experiments.

with anti-CD28 mAb (0.5 mg/ml) (eBioscience, San Diego, CA, United States) in a 96-well plastic cell culture plate, coated with anti-CD3ε mAb (5 μg/ml) (R&D Systems, Minneapolis, MN, United States), in RPMI1640 medium containing 10% FBS in an atmosphere of 5% CO_2/95% air at 37°C. After incubation, the culture supernatant was harvested for determination of IL-2 and IL-6. The concentrations of IL-2, IL-6, and IL-17 were measured by means of ELISA as described below. Wells of a 96-well plate were coated with purified anti-mouse IL-2 (1:500) (eBioscience) and IL-6 (1:500) (eBioscience) IL-17 mAb. The plate was incubated overnight at 4°C, then washed with PBS containing 0.05% Tween-20, and non-specific binding was blocked with PBS containing 1% BSA for 1 h at room temperature. The plate was washed again, and the culture supernatant was added. After 2 h at room temperature, the plate was washed again, and biotin-conjugated anti-mouse IL-2 (1:1000) (eBioscience) and IL-6 (1:500) (eBioscience) IL-17 mAb were added for 1 h at room temperature. The plate was further washed, and Streptavidin, Peroxidase Conjugated, Solution (Wako) was added. The plate was washed, 3,3′,5,5′-tetramethylbenzidine was added, and incubation was continued for several minutes. The reaction was stopped by adding 5 N H_2SO_4. The absorbance at 450 nm (contrast wavelength: 570 nm) was measured. Standard curves were established with recombinant mouse IL-2 (31–2000 pg/mL), IL-6 (31–2000 pg/mL), or IL-17 (31–2000 pg/mL), and the concentrations of IL-2 and IL-6 were estimated from the standard curves. IFN-γ, IL-4, TNF-α production was determined with mouse IFN-γ, IL-4, TNF-α Quantikine ELISA kits (R&D Systems) according to the manufacturer's instructions.

Evaluation of Cell Damage

Cell damage was quantified in terms of released LDH activity (Tsukimoto et al., 2006). Splenocytes were incubated with adenine nucleotides for 1 h, and the culture supernatants were collected. Release of LDH into the cell culture supernatant was quantified with a Cytotoxicity Detection Kit (Roche Applied Science, Penzberg, Germany), according to the supplied instructions. LDH release is expressed as a percentage of the total content determined after lysing an equal amount of cells with 1% Triton X-100.

Flow Cytometry

Splenocytes (6.0×10^6 cells/well) were stimulated with ConA (5 μg/mL) in a 6-well plate in RPMI 1640 medium containing 10% heat-inactivated FBS, 100 units/ml of penicillin, and 100 μg/ml of streptomycin in an atmosphere of 5% CO_2, 95% air at 37°C for 24 h. Splenocytes (5×10^5 cells) were collected by centrifugation (4°C at 300 × *g*) and the supernatant was discarded. The cell pellet was washed twice with RPMI1640-based buffer and re-suspended in the same buffer. FITC rat anti-mouse CD4 (1 μL) (BD Pharmingen) and PE-conjugated anti-mouse CD25 (1 μL) (TOMBO) were added to 50 μL of the cell suspension and the mixture was incubated at room temperature for 30 min in the dark. The cells were then washed twice

in RPMI1640-based buffer and immediately subjected to flow cytometry (FACSCalibur Flow Cytometer, Becton, Dickinson and Co., United States)

Cell Proliferation Assay

Splenocyte proliferation was assessed by detection of bromodeoxyuridine (BrdU) uptake using the Cell Proliferation ELISA, BrdU (colorimetric) (Roche) according to the manufacturer's protocol. Briefly, splenocytes (4×10^5 cells) were seeded into 96-well plates in RPMI 1640 medium containing 10% heat-inactivated FBS, 100 units/ml of penicillin, and 100 μg/ml of streptomycin and labeled with BrdU (Roche) for 24 h. After centrifugation (10°C at 300 *g*), removal of the supernatant, and drying of the cells with a hair-dryer for about 15 min, 200 μL FixDenat reagent was added. The cells were incubated at room temperature for 30 min, then the FixDenat solution was washed out. The cells were incubated with peroxidase-conjugated anti-BrdU solution and the amount of incorporated BrdU was determined. The absorbance was measured with an ELISA plate reader (450 nm).

Immunoblotting

Concanavalin A-stimulated murine splenocytes (1.0×10^7 cells) were lysed, and the lysate was taken up in sample buffer (25% glycerin, 1% SDS, 62.5 mm Tris-Cl, 10 mm dithiothreitol) and boiled for 10 min. Aliquots of samples were analyzed by SDS–PAGE and transferred to a polyvinylidene difluoride membrane. The membrane was incubated at 4°C overnight with blocking buffer (10 mM Tris–HCl, 100 mM NaCl, 0.1% Tween 20, 1% BSA, pH 7.5), and then with rabbit mAb against phospho-ERK 1/2 (1:1000) or ERK 1/2 (1:1000) (Cell Signaling Technology, Beverly, MA, United States) at 4°C overnight. The membranes were washed four times with TBST, then incubated with goat horseradish peroxidase-conjugated anti-rabbit IgG Ab (1:20,000) (Cell Signaling Technology) for 1.5 h at room temperature. The membrane was further washed with TBST, and specific proteins were visualized by using ImmunoStar®LD (Wako). Western blotting detection reagents were from LI-COR, and bands were analyzed with Image Studio 4.0 for C-DiGit Scanner (LI-COR).

Measurement of IL-2 mRNA Expression

Total RNA was extracted from lymphocytes, and first-strand cDNA was synthesized with PrimeScript Reverse Transcriptase (Takata Bio). The cDNA was used as a template for real-time PCR analysis: reactions were performed in a CFX Connect Real-Time System (Bio-Rad). RT2-qPCR® primer assay for mouse IL-2 was purchased from Qiagen. Glyceraldehyde-3-phosphate dehydrogenase mRNA was determined as a positive control. Each sample was assayed in a 20 μL amplification reaction mixture, containing cDNA, primers and 2× KAPA SYBR® FAST qPCR Master Mix (Kapa Biosystems). The samples were incubated at 95°C 1 min, then amplification was carried out for 40 cycles (each cycle, 95°C for 3 s, annealing at 60°C 30 s), followed by incubation at 95°C 1 min. Fluorescent products were detected at the last step of each cycle. The obtained values were within the linear range of the standard curve and were normalized to glyceraldehyde-3-phosphate dehydrogenase mRNA expression.

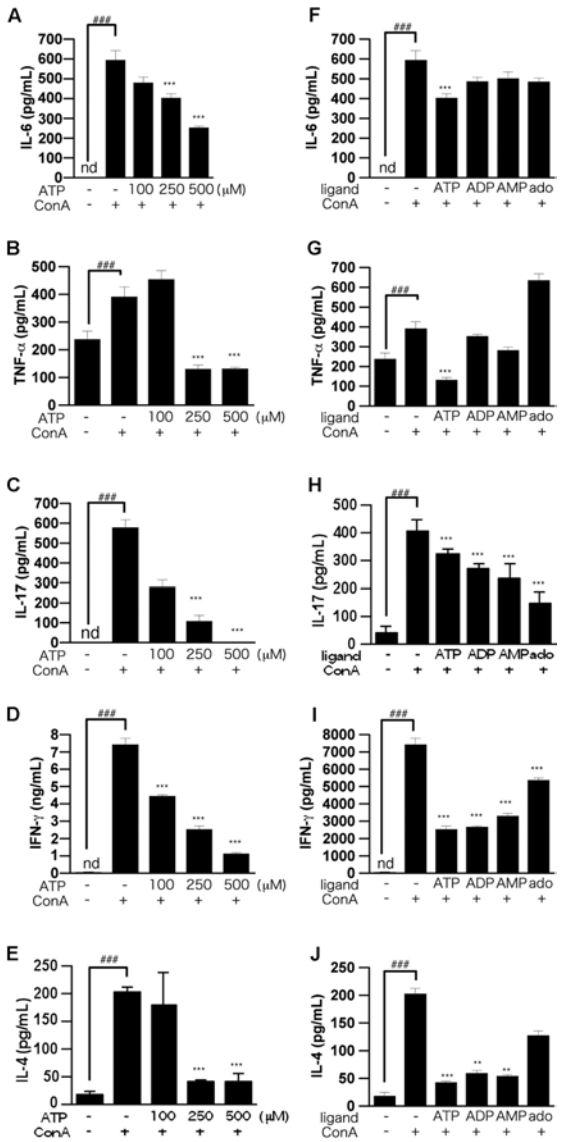

FIGURE 2 | Effects of ATP on ConA-induced production of pro-inflammatory cytokines by splenic lymphocytes isolated from BALB/c mice. **(A–E)** Lymphocytes were pre-incubated with various concentrations of ATP (100, 250, or 500 μM), and then stimulated with 50 μg/mL ConA for 24 h. **(F–J)** Lymphocytes were pre-incubated with 250 μM ATP, ADP, AMP, or adenosine, and then stimulated with 50 μg/mL ConA for 24 h. Concentrations of IL-6 **(A,F)**, TNF-α **(B,G)**, IL-17 **(C,H)**, IFN-γ **(D,I)**, or IL-4 **(E,J)** in the culture medium were measured by ELISA. Each value represents the mean ± SE ($n = 4$). Significant difference between the vehicle control group and the ConA-treated group in the absence of ATP or other ligand is indicated by $^{###}P < 0.001$. Significant differences between the ConA-treated, ATP-untreated group and the ConA-treated, ATP (or other ligand)-treated groups is indicated by $^{***}P < 0.001$ and $^{**}P < 0.01$. Each figure is representative of several independent experiments.

Measurement of Intracellular IL-2 Protein

Splenocytes (1.0×10^7 cells/mL) in a 6-well plate were stimulated with ConA (5 μg/mL) in RPMI 1640 medium containing 10% heat-inactivated FBS, 100 units/ml of penicillin, and 100 μg/ml

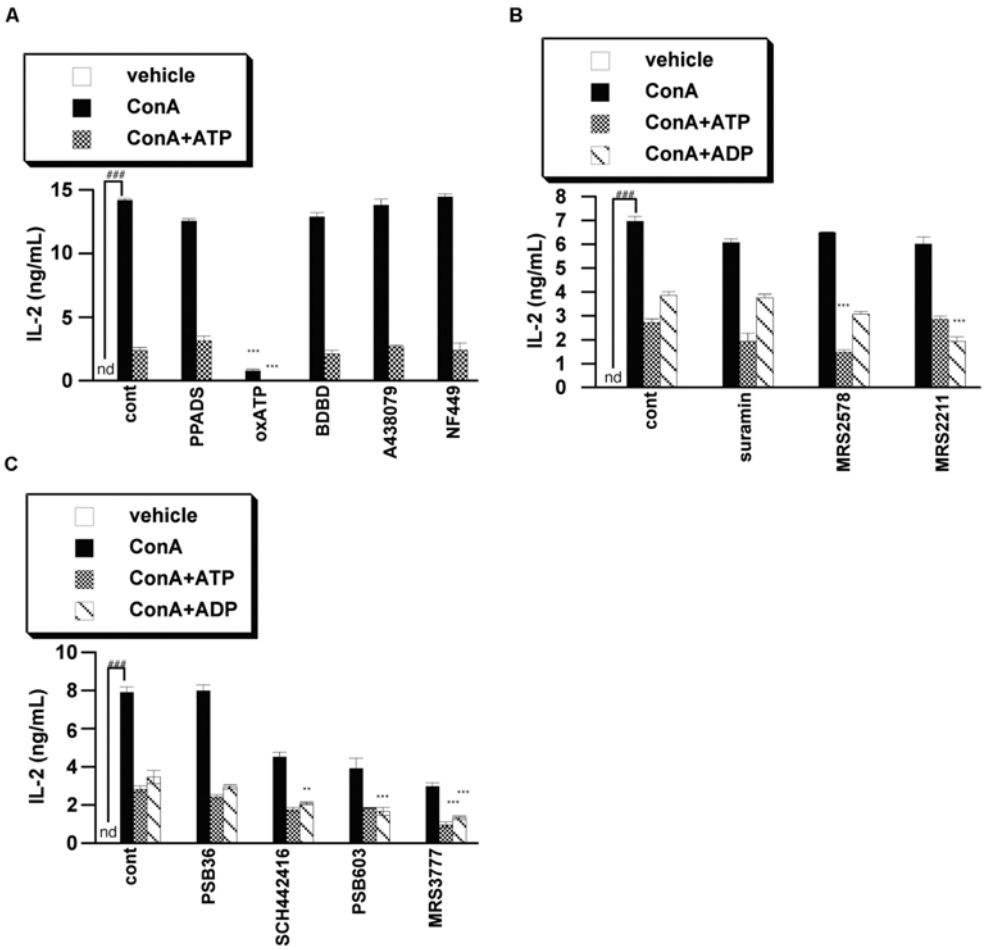

FIGURE 3 | Effects of purinergic receptor antagonists on IL-2 secretion from activated splenic lymphocytes. Lymphocytes were pre-incubated with 250 μM ATP or ADP and with a P2X receptor inhibitor [PPADS (100 μM), oxATP (300 μM), BDBD (10 μM), A438079 (50 μM), NF449 (10 μM)] **(A)**, P2Y receptor inhibitor [suramin (100 μM), MRS2578 (10 μM), MRS2211 (100 μM)] **(B)**, or adenosine receptor inhibitor PSB36 (5 μM), SCH442416 (10 μM), PSB603 (10 μM), or MRS3777(10 μM) **(C)**, and then stimulated with 50 μg/mL ConA for 24 h. Concentrations of IL-2 in the culture medium were measured by ELISA. Significant difference between the vehicle control group and the ConA-treated group in the absence of ligand and inhibitor is indicated by $^{\#\#\#}P < 0.001$. Significant differences between ConA-treated, inhibitor-untreated control (cont) groups and the corresponding inhibitor-treated groups are indicated by $^{***}P < 0.001$ and $^{**}P < 0.01$. Each value represents the mean ± SE ($n = 4$). Each figure is representative of several independent experiments.

of streptomycin in an atmosphere of 5% CO_2, 95% air at 37°C. After incubation, the supernatant was discarded. The cells were lysed in 1 M HEPES-NaOH, 10% Triton/PBS, 0.5 M EDTA, pH 8.0, 1% protease inhibitor for 30 min at 4°C, followed by centrifugation at 300 × *g* (at 4°C). IL-2 protein in the culture supernatant was measured by means of ELISA, as described above.

Treatment with ConA into Mice

BALB/c mice were injected intravenously (*i.v.*) with 400 μg of ConA in 100 μL PBS, or with 100 μL PBS as a control. After ConA treatment, blood samples were collected. They were centrifuged at 5,000 × *g* for 10 min at 4°C, and the separated serum was stored at −80°C until analysis. Serum concentrations of IL-2 and IL-6 were determined by means of ELISA as described above.

Statistics

Results are expressed as mean ± SE. The statistical significance of differences between control and other groups was calculated by using Dunnett's test with the Instat version 3.0 statistical package (GraphPad Software, San Diego, CA, United States). The criterion of significance was set at $P < 0.05$.

RESULTS

Effect of ATP on Release of Inflammatory Cytokines from ConA-Stimulated Splenocytes

In our previous study, we found that production of IL-2, an inflammatory cytokine, in splenocytes of BALB/c mice was increased dose-dependently by ConA, and was maximum at

1–10 μg/mL ConA. Here, using ConA (5 μg/mL), we found that production of IL-2 increased time-dependently up to 24 h after ConA addition (**Figure 1A**). These results suggest that ConA directly induces IL-2 production in murine splenocytes. In the following experiments, assays of IL-2 secretion were all conducted at 24 h after stimulation with 5 μg/mL of ConA.

We first examined the dose dependence of the effect of exogenously added ATP on IL-2 production by splenocytes. Pretreatment with more than 100 μM ATP significantly suppressed production of IL-2 (**Figure 1B**). Next, we examined the effects of ATP, ADP, AMP, and adenosine on the ConA-induced IL-2 production. As shown in **Figure 1C**, treatment with ATP, ADP, and AMP suppressed the ConA-induced increase of IL-2 secretion at 24 h, although adenosine was ineffective. UTP and UDP did not suppress IL-2 production (data not shown).

The results of LDH assays showed that ATP concentration-dependently induced cell death, whereas ADP was not cytotoxic (**Figure 1D**). That is, the suppression of IL-2 production by 250 μM ATP might not be due to cytotoxicity mediated by activation of the P2X7 receptor (Tsukimoto et al., 2006). Also, production of IL-6, TNF-α, IL-17, IFN-γ, and IL-4, as well as IL-2, by ConA-stimulated lymphocytes was suppressed by ATP treatment (**Figures 2A–J**).

Antagonists of Purinergic Receptors Did Not Block ATP-Induced Suppression of T Cell Activation

We next examined whether purinergic receptors are involved in the ATP-induced suppression of IL-2 release by using of a variety of purinergic receptor antagonists. We found that antagonists of P2X receptors, including P2X7 receptor, did not block ATP-induced suppression of IL-2 release, suggesting that P2X receptors are not involved in the effect of ATP. On the other hand, P2Y6 antagonists (MRS2578), P2Y13 antagonists (MRS2211) and A3 antagonists (MRS3777) enhanced the suppression of IL-2 release by ATP or ADP, indicating that activation of these receptors by ATP contributes to the induction of IL-2 release, rather than inhibition of IL-2 release (**Figures 3A–C**). It seems likely that the suppression of IL-2 release from lymphocytes by ATP might be mediated by factor(s) other than purinergic receptors.

ATP Treatment Suppressed CD25 Expression and Cell Proliferation after ConA Stimulation

T cells up-regulate activation markers such as CD25 during T cell activation (Malek and Bayer, 2004), and activation of IL-2 receptor by IL-2 triggers a signaling cascade leading to T cell proliferation and further IL-2 production (Kim and Leonard, 2002). As expected, we found that CD25-positive CD4 T cells in ConA-stimulated lymphocytes were significantly reduced by adenine nucleotides (**Figure 4A**). To investigate the effect of ATP on T cell proliferation, we employed BrdU incorporation assay. The incorporation of BrdU into ATP-treated lymphocytes was significantly lower than that into untreated lymphocytes (**Figure 4B**).

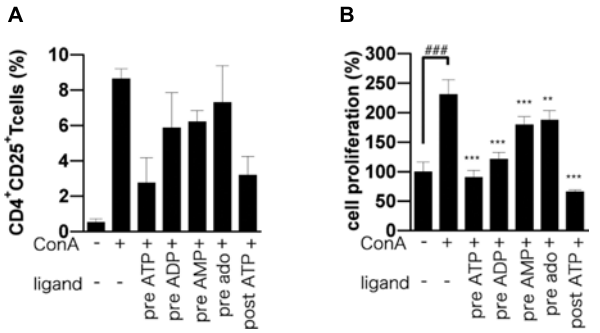

FIGURE 4 | Effect of adenine nucleotides on expression of CD25 and proliferation of BrdU-labeled cells. Lymphocytes were pre-incubated for 30 min with 250 μM ATP, ADP, AMP, or adenosine before ConA treatment or post-incubated with ATP at 30 min after ConA treatment. **(A)** Cells were incubated for 24 h with ConA. The lymphocytes were stained with PE-conjugated anti-CD25 mAb and FITC-conjugated anti-CD4 mAb. The percentage of $CD4^+$ $CD25^+$ cells was analyzed by flow cytometry. **(B)** Cells were incubated for 21 h with ConA. Lymphocyte proliferation was determined by BrdU cell proliferation assay. Each value represents the mean ± SE ($n = 4$). Significant difference between the vehicle control group and the ConA-treated group in the absence of ATP or other ligand is indicated by $^{###}P < 0.001$. Significant differences between ConA-treated groups without ligand treatment and the corresponding groups given the indicated ligand treatment are indicated by $^{***}P < 0.001$ and $^{**}P < 0.01$. **(A)** Represents three independent experiments and **(B)** represents two independent experiments.

Post-treatment with ATP Also Suppressed IL-2 Release from T Cells Activated by ConA or TCR

To confirm whether the suppressive effect of ATP is dependent on the nature of the T cell activation stimulus, we examined IL-2 release from TCR-activated splenic lymphocytes. As shown in **Figure 5A**, treatment with ATP suppressed the increase of IL-2 secretion at 24 h after stimulation of splenocytes with TCR or ConA. To clarify whether ATP is also effective on prestimulated T cells, we treated splenocytes with adenine nucleotides after ConA stimulation. They proved effective in suppressing IL-2 release when applied up to 9 h after ConA or TCR stimulation (**Figures 5B–I**).

Effect of ATP on IL-2 mRNA Expression and the ERK1/2 Pathway in Activated T Cells

IL-2 mRNA was increased in murine lymphocytes 3 h after ConA stimulation. We examined whether ATP and their metabolites affected this increase of IL-2 mRNA. Indeed, ATP or ADP significantly suppressed the increase of IL-2 mRNA (**Figure 6A**). However, the suppressive effect of AMP or adenosine was less than that of ATP or ADP. We also measured the intracellular IL-2 protein level in lymphocytes by ELISA. The IL-2 protein level was decreased by treatment with adenine nucleotides (**Figure 6B**). In order to investigate the signaling pathway involved into suppression of ConA-induced IL-2 release by ATP, phosphorylation of ERK were measured (**Figure 6C**).

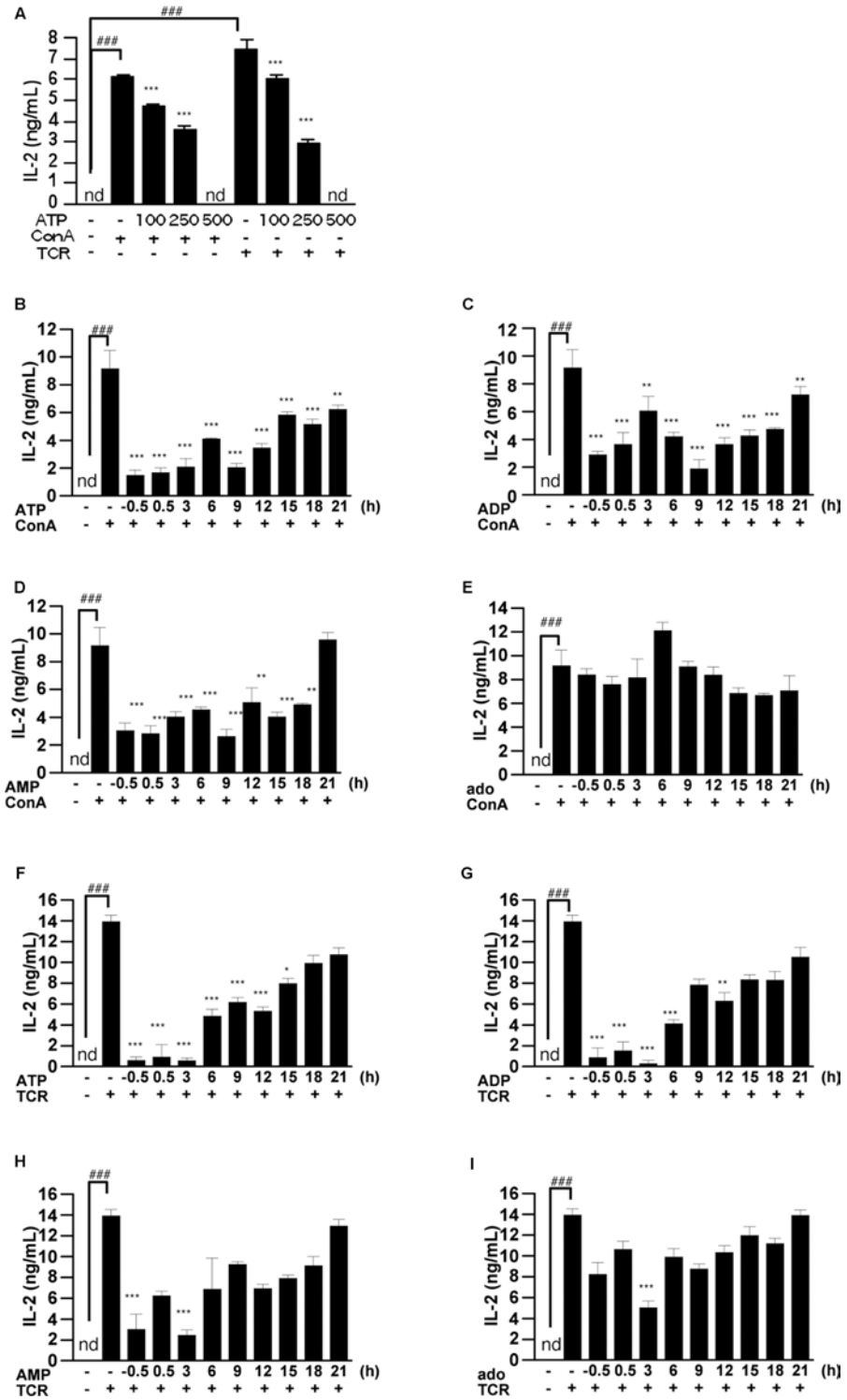

FIGURE 5 | Effect of ATP, ADP, AMP, and adenosine on already activated T cells. **(A)** Lymphocytes were pre-incubated with ATP (100, 250, and 500 μM), and then stimulated with 50 μg/mL ConA or with plate-bound anti CD3ε mAb and soluble anti CD28 mAb for 24 h. Concentrations of IL-2 in the culture medium were measured by ELISA. **(B–I)** Lymphocytes were post-treated with ATP, ADP, AMP, and adenosine at the indicated time points after treatment with 50 μg/mL ConA **(B–E)** or with plate-bound anti CD3ε mAb and soluble anti CD28 mAb **(F–I)**. Cells were incubated for 24 h with ConA or the antibodies. Concentrations of IL-2 in the culture medium were measured by means of ELISA. Each value represents the mean ± SE (n = 4). Significant difference between the vehicle control group or the vehicle plus TCR group and the corresponding ConA-treated group in the absence of ligand is indicated by $^{###}P < 0.001$. Significant differences between ConA-treated groups without ligand treatment and the corresponding groups given the indicated ligand treatment are indicated by $^{***}P < 0.001$ and $^{**}P < 0.01$. Each figure is representative of several independent experiments.

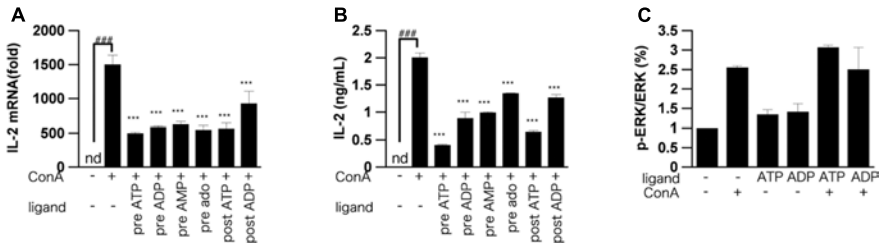

FIGURE 6 | Effect of ATP, ADP, AMP and adenosine on IL-2 expression. Lymphocytes were pre-incubated or post-incubated with ATP, ADP, AMP, or adenosine, and then stimulated with 50 μg/mL ConA for 3 h **(A)**, 6 h **(B)**, or 5 min **(C)**. **(A)** IL-2 mRNA level in lymphocytes was measured by real-time RT-PCR analysis. **(B)**, Intracellular protein level of IL-2 was measured by means of ELISA. **(C)** Lymphocytes were lyzed and analyzed by western blotting for phospho-ERK1/2 and total ERK1/2. Each value represents the mean ± SE (n = 4). Significant difference between the vehicle control group and the ConA-treated group in the absence of ATP and ADP is indicated by $^{###}P < 0.001$. Significant differences between ConA-treated groups without ligand treatment and the corresponding groups given the indicated ligand treatment are indicated by $^{***}P < 0.001$. **(A,B)** Represent two independent experiments and **(C)** represents three independent experiments.

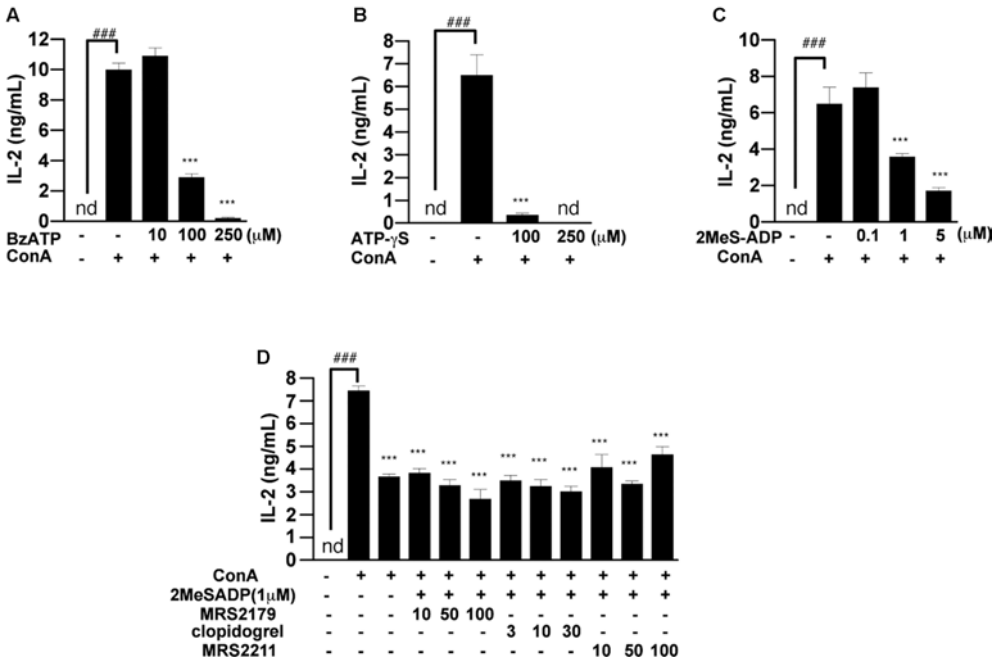

FIGURE 7 | Effects of non-hydrolyzable ATP and ADP analog on ConA-induced IL-2 production. **(A)** Lymphocytes were pre-incubated with various concentrations of Bz-ATP **(A)**, ATP-γS **(B)**, and 2-MeS-ADP **(C)**. **(D)** Lymphocytes were pre-incubated with 1 μM 2-MeS-ADP and with MRS2179, clopidogrel, or MRS2211. Then, the lymphocytes were stimulated with 50 μg/mL ConA for 24 h. Concentrations of IL-2 in the culture medium were measured by means of ELISA. Each value represents the mean ± SE (n = 4). Significant difference between the vehicle control group and the ConA-treated group in the absence of any ligand is indicated by $^{###}P < 0.001$. Significant differences between the ConA-treated group without any ligand treatment and the corresponding ConA-treated groups given the indicated ligand treatment are indicated by $^{***}P < 0.001$. Each figure is representative of several experiments.

ATP did not affect the ConA-evoked phosphorylation of ERK1/2.

Inhibitory Effect of ATP and ADP Analogs on IL-2 Release

To investigate what is the largest contributor to suppression of IL-2 release among ATP and its metabolites, we examined the effects of non-hydrolyzable ATP and ADP analogs (ATP-γS, BzATP, and 2-MeS-ADP) on IL-2 production. Bz-ATP and ATP-γS suppressed the ConA-induced increase of IL-2 secretion at 24 h, like ATP (**Figures 7A,B**). However, the reason why BzATP suppressed IL-2 release is presumably that BzATP-induced activation of the P2X7 receptor resulted in induction of cell death. On the other hand, the addition of 2-MeS-ADP had a potent inhibitory effect on IL-2 production (**Figure 7C**), suggesting that ADP is important for suppression of T cell activation. 2-MeS-ADP is known to have high affinities for the P2Y1, P2Y12, P2Y13 receptors (Macfarlane et al., 1983; Sak and Webb, 2002; Zhang et al., 2002). We therefore examined the effects of P2Y1, P2Y12, and P2Y13 receptor antagonists (MRS2179, clopidogrel, and MRS2211, respectively) on 2-MeS-ADP-induced

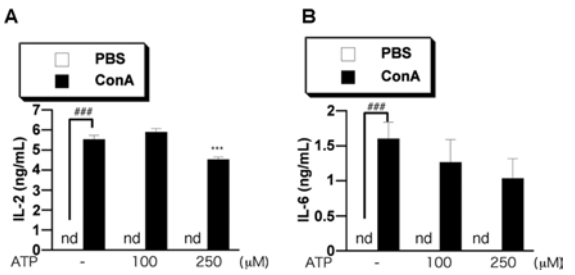

FIGURE 8 | Treatment with ATP attenuates ConA-induced cytokine production *in vivo*. BALB/c mice (n = 5/group) were pretreated with PBS or ATP (100 or 250 μM) at 2 h before treatment with ConA. Mice were injected with ConA (400 μg of ConA in 100 μL PBS) via the tail vein. Serum samples were collected at 3 h **(A,B)** after the ConA injection. Serum IL-2 **(A)** and IL-6 **(B)** concentrations were determined as described in the text. Significant difference between the vehicle control group and the ConA-treated group in the absence of any ligand is indicated by $^{###}P < 0.001$. Significant differences between the ConA-treated group without any ligand treatment and the corresponding ConA-treated groups given the indicated ligand treatment are indicated by $^{***}P < 0.001$.

suppression of IL-2 release. However, these antagonists had no effect (**Figure 7D**).

Intravenous Administration of ATP Reduced Serum Pro-inflammatory Cytokine Levels

Finally, we investigated the effect of ATP on the elevation of cytokines in blood of ConA-treated mice. We measured the levels of IL-2 and IL-6 in serum by ELISA. We previously confirmed that the levels of IL-2 and IL-6 were increased at 3–12 h after ConA injection, but then decreased until 24 h (data not shown). We examined the effect of ATP on the increase of proinflammatory cytokines in serum at 3 h after ConA injection into BALB/c mice. Pretreatment with 250 μM ATP suppressed the increase of serum IL-2 and tended to suppress IL-6 (**Figures 8A,B**), suggesting that ATP would suppress activation of immune cells including T cells *in vivo*.

DISCUSSION

T cells are activated and release inflammatory cytokines including IL-2 in response to stimulation with ConA. We found that the IL-2 release from ConA-activated T cells was suppressed by treatment with ATP. Specifically, we found that pretreatment with more than 100 μM ATP significantly and dose-dependently suppressed production of IL-2 by ConA-treated splenic lymphocytes of BALB/c mice. Further, the suppression of IL-2 production by 250 μM ATP did not appear to be due to cytotoxicity mediated by activation of P2X7 receptor (Di Virgilio et al., 1998; Tsukimoto et al., 2006). Our data show that ATP also suppressed the ConA-induced release of other cytokines (IL-6, IL-17, TNF-α, IFN-γ, and IL-4) from T cells.

Previous studies have demonstrated that P2X, P2Y, and adenosine receptors play important roles in the regulation of T cell activation (Lappas et al., 2005; Yip et al., 2007; Woehrle et al., 2010). We pharmacologically investigated the contribution of P2 receptors to the suppression of T cell activation, in order to determine whether purinergic receptors are involved in the suppression of IL-2 release. We found that antagonists of P2X receptors did not block ATP-induced suppression of IL-2 release, suggesting that P2X receptors were not involved in the effect of ATP. However, P2Y6 antagonist (MRS2578), P2Y13 antagonist (MRS2211) and A3 antagonist (MRS3777) strongly suppressed IL-2 release upon co-treatment with ATP or ADP. That is, we found that activation of these receptors by ATP contributes to induction of IL-2 release, rather than inhibition of IL-2 release. Thus, suppression of IL-2 release from lymphocytes by ATP might be mediated by other factor(s).

When T cells are activated, they express CD25 and produce IL-2, both of which are involved in T cell growth and proliferation (Morgan et al., 1976). Our results show that DNA replication monitored in terms of BrdU incorporation was greatly reduced by pretreatment with ATP and ADP, compared with AMP and adenosine. We also confirmed that ConA stimulation increased CD25 expression in T cells and that ATP and its metabolites suppressed the ConA-induced CD25 expression. In other words, it appears that ATP and ADP can suppress T cell proliferation and activation.

Pretreatment with ATP also suppressed the TCR-induced increase of IL-2 secretion at 24 h, as was the case for ConA stimulation. Even when ATP, ADP, AMP, and adenosine were added after ConA or TCR stimulation, ATP and ADP were effective in suppressing IL-2 release. In other words, ATP and ADP might have inhibitory functions on already activated T cells. Furthermore, pretreatment with ATP and ADP caused a marked reduction of ConA-induced IL-2 mRNA expression and intracellular protein levels. In order to investigate which intracellular signals are involved in the suppression of ConA-induced IL-2 release by ATP treatment, we measured phosphorylation of ERK1/2. Responses to stimuli such as TCR are mediated by MAPK, and MAPKs are involved in T cell activation and proliferation by activating various downstream factors. MAPKs play important roles in T cell activation, proliferation, and differentiation into Th1 or Th2 (Dong et al., 2002; Huang and Wange, 2004). Among MAPKs, ERK consists of two species, ERK 1 and 2, with molecular weights of 42 and 44 kDa, respectively. No significant suppression of ERK1/2 phosphorylation by ATP was observed after ConA stimulation in T cells, suggesting that ATP may affect pathways other than ERK1/2.

The inhibitory effect of ATP on ConA-induced IL-2 release was mimicked by non-hydrolyzable ATP and ADP analogs, ATP-γ-S, BzATP, and 2-MeS-ADP. The results of pretreatment with ATP-γS and BzATP were similar to those of pretreatment with ATP. But, since BzATP is known to be a P2X7 receptor agonist, it seems likely that the cell death induced by 250 μM BzATP was due to activation of P2X7 receptor. Since the addition of 2-MeS-ADP had a potent inhibitory effect on the production of IL-2, ADP seems to have an important role in the suppression of T cell activation. Pre-treatment with P2Y1, P2Y12, and P2Y13 antagonists before treatment with 2-MeS-ADP did not cause any significant change of IL-2 production compared with

2-MeS-ADP treatment alone. These results suggest that ADP may have a novel immunosuppressive effect, not mediated by P2Y1, P2Y12, or P2Y13 receptors.

There is some evidence that guanosine administration reduces brain damage and has an anti-inflammatory action (Ciccarelli et al., 2001), possibly via cAMP accumulation and activation of PI3K/Akt. It has also been reported that addition of deoxyguanosine triphosphate (dGTP), guanosine triphosphate (GTP) and guanosine inhibits T-cell proliferation, though the mechanisms involved remain unknown (Weiler et al., 2016). Thus, it is possible that new receptors activated by GDPs or ATP might be involved in the effects observed in the present study.

T cell activation plays an important role in autoimmune inflammatory diseases, such as rheumatoid arthritis, multiple sclerosis, and autoimmune hepatitis. Currently, adrenocortical hormone and immunosuppressants are mainly used for treatment of autoimmune diseases. However, adrenocortical hormone therapy causes serious side effects such as weight gain, osteoporosis, weakness of the skin and hair, abuse, diabetes, hypertension, cataracts, glaucoma, anxiety, and confusion. Immunosuppressive agents also cause serious side effects such as decreased leucocytes, nausea, vomiting, liver disorder, pancreatitis, and promotion of cancer growth. Therefore, a new treatment approach is urgently needed. Our present findings suggested that ATP or ADP might be useful for this purpose. Our preliminary data implicates that treatment with ATP tended to suppress the elevations of serum liver damage markers (glutamic oxaloacetic transaminase and glutamic pyruvic transaminase levels) in ConA-treated mice which is known as an autoimmune hepatitis model (Tiegs et al., 1992) (data not shown), suggesting that pretreatment with ATP might attenuate the acute liver damage, though the effect of ATP on actual liver damage should be carefully evaluated by liver histology in the mice in future study. ATP might at least have potential as a supplemental drug in the treatment of immune diseases, possibly allowing a reduction in the administered dose of the main treatment agent(s) and thereby potentially reducing the incidence or severity of side effects. Since ATP is an endogenous energy source, it should be safe to use as a supplemental treatment, though further studies would be needed to confirm its efficacy, and to optimize treatment concentration and schedule. Also, the target molecule for this action of adenine nucleotides is still unknown, and it will be important to identify it.

AUTHOR CONTRIBUTIONS

YS contributed to the acquisition of data for this work. MT contributed to the conception and design of the work. Both YS and MT contributed to the analysis and interpretation of data for the work, and wrote the paper.

ACKNOWLEDGMENTS

The authors thank Ms. Yuki Ninomiya for her technical support and Prof. Sei-ichi Tanuma for his kind support.

REFERENCES

Burnstock, G. (2009). Purinergic signalling: past, present and future. *Braz. J. Med. Biol. Res.* 42, 3–8.

Burnstock, G., and Boeynaems, J. (2014). Purinergic signalling and immune cells. *Purinergic Signal.* 10, 529–564. doi: 10.1007/s11302-014-9427-2

Chused, T. M., Apasov, S., and Sitkovsky, M. (1996). Murine T lymphocytes modulate activity of an ATP-activated P2Z-type purinoceptor during differentiation. *J. Immunol.* 157, 1371–1380.

Ciccarelli, R., Ballerini, P., Sabatino, G., Rathbone, M. P., D'Onofrio, M., Caciagli, F., et al. (2001). Involvement of astrocytes in purine-mediated reparative processes in the brain. *Int. J. Dev. Neurosci.* 19, 395–414. doi: 10.1016/S0736-5748(00)00084-8

Di Virgilio, F., Chiozzi, P., Falzoni, S., Ferrari, D., Sanz, J. M., Venketaraman, V., et al. (1998). Cytolytic P2X purinoceptors. *Cell Death Differ.* 5, 191–199. doi: 10.1038/sj.cdd.4400341

Dong, C., Davis, R. J., and Flavell, R. A. (2002). MAP kinases in the immune response. *Annu. Rev. Immunol.* 20, 55–72. doi: 10.1146/annurev.immunol.20.091301.131133

Fischer, A. M., Katayama, C. D., Pagès, G., Pouysségur, J., Hedrick, S. M., Adachi, S., et al. (2005). The role of erk1 and erk2 in multiple stages of T cell development. *Immunity* 23, 431–443. doi: 10.1016/j.immuni.2005.08.013

Gallo, E. M., Canté-Barrett, K., and Crabtree, G. R. (2006). Lymphocyte calcium signaling from membrane to nucleus. *Nat. Immunol.* 7, 25–32. doi: 10.1038/ni1295

Gong, Q., Cheng, A. M., Akk, A. M., Alberola-Ila, J., Gong, G., Pawson, T., et al. (2001). Disruption of T cell signaling networks and development by Grb2 haploid insufficiency. *Nat. Immunol.* 2, 29–36. doi: 10.1038/83134

Huang, Y., and Wange, R. L. (2004). T cell receptor signaling: beyond complex complexes. *J. Biol. Chem.* 279, 28827–28830. doi: 10.1074/jbc.R400012200

Kim, H.-P., and Leonard, W. J. (2002). The basis for TCR-mediated regulation of the IL-2 receptor alpha chain gene: role of widely separated regulatory elements. *EMBO J.* 21, 3051–3059. doi: 10.1093/emboj/cdf321

Kondo, M., Takeshita, T., Ishii, N., Nakamura, M., Watanabe, S., Arai, K., et al. (1993). Sharing of the interleukin-2 (IL-2) receptor gamma chain between receptors for IL-2 and IL-4. *Science* 262, 1874–1877. doi: 10.1126/science.8266076

Lappas, C. M., Rieger, J. M., and Linden, J. (2005). A2A Adenosine receptor induction inhibits IFN-γ production in murine CD4+ T cells. *J. Immunol.* 174, 1073–1080. doi: 10.4049/jimmunol.174.2.1073

Lei, H.-Y., and Chang, C.-P. (2009). Lectin of concanavalin A as an anti-hepatoma therapeutic agent. *J. Biomed. Sci.* 16:10. doi: 10.1186/1423-0127-16-10

Lin, J. X., and Leonard, W. J. (1997). Signaling from the IL-2 receptor to the nucleus. *Cytokine Growth Factor Rev.* 8, 313–332. doi: 10.1016/S1359-6101(97)00021-X

Macfarlane, D. E., Srivastava, P. C., and Mills, D. C. (1983). 2-Methylthioadenosine[beta-32P]diphosphate. An agonist and radioligand for the receptor that inhibits the accumulation of cyclic AMP in intact blood platelets. *J. Clin. Invest.* 71, 420–428. doi: 10.1172/JCI110786

Malek, T. R., and Bayer, A. L. (2004). Tolerance, not immunity, crucially depends on IL-2. *Nat. Rev. Immunol.* 4, 665–674. doi: 10.1038/nri1435

Marshall, C. J., Alessi, D., Saito, Y., Campbell, D., Cohen, P., Sithanandam, G., et al. (1995). Specificity of receptor tyrosine kinase signaling: transient versus sustained extracellular signal-regulated kinase activation. *Cell* 80, 179–185. doi: 10.1016/0092-8674(95)90401-8

Morgan, D. A., Ruscetti, F. W., and Gallo, R. (1976). Selective in vitro growth of T lymphocytes from normal human bone marrows. *Science* 193, 1007–1008. doi: 10.1126/science.181845

Nelson, B. H., Lord, J. D., and Greenberg, P. D. (1994). Cytoplasmic domains of the interleukin-2 receptor β and γ chains mediate the signal for T-cell proliferation. *Nature* 369, 333–336. doi: 10.1038/369333a0

Oh-hora, M. (2009). Calcium signaling in the development and function of T-lineage cells. *Immunol. Rev.* 231, 210–224. doi: 10.1111/j.1600-065X.2009.00819.x

Rincon, M., Conze, D., Weiss, L., Diehl, N. L., Fortner, K. A., Yang, D., et al. (2000a). Do T cells care about the mitogen-activated protein kinase signalling pathways? *Immunol. Cell Biol.* 78, 166–175. doi: 10.1046/j.1440-1711.2000.00900.x

Rincon, M., Flavell, R. A., and Davis, R. A. (2000b). The JNK and P38 MAP kinase signaling pathways in T cell–mediated immune responses. *Free Radic. Biol. Med.* 28, 1328–1337. doi: 10.1016/S0891-5849(00)00219-7

Sak, K., and Webb, T. E. (2002). A retrospective of recombinant P2Y receptor subtypes and their pharmacology. *Arch. Biochem. Biophys.* 397, 131–136. doi: 10.1006/abbi.2001.2616

Sass, G., Heinlein, S., Agli, A., Bang, R., Schümann, J., and Tiegs, G. (2002). Cytokine expression in three mouse models of experimental hepatitis. *Cytokine* 19, 115–120. doi: 10.1006/cyto.2002.1948

Schenk, U., Westendorf, A. M., Radaelli, E., Casati, A., Ferro, M., Fumagalli, M., et al. (2008). Purinergic control of T cell activation by ATP released through pannexin-1 hemichannels. *Sci. Signal.* 1:ra6. doi: 10.1126/scisignal.1160583

Tiegs, G., Hentschel, J., and Wendel, A. (1992). A T cell-dependent experimental liver injury in mice inducible by concanavalin A. *J. Clin. Invest.* 90, 196–203. doi: 10.1172/JCI115836

Tokunaga, A., Tsukimoto, M., Harada, H., Moriyama, Y., and Kojima, S. (2010). Involvement of SLC17A9-dependent vesicular exocytosis in the mechanism of ATP release during T cell activation. *J. Biol. Chem.* 285, 17406–17416. doi: 10.1074/jbc.M110.112417

Trabanelli, S., Ocadlíková, D., Gulinelli, S., Curti, A., Salvestrini, V., Vieira, R., et al. (2012). Extracellular ATP exerts opposite effects on activated and regulatory $CD4^+$ T cells via purinergic P2 receptor activation. *J. Immunol.* 189, 1303–1310. doi: 10.4049/jimmunol.1103800

Tsukimoto, M., Maehata, M., Harada, H., Ikari, A., Takagi, K., and Degawa, M. (2006). P2X7 receptor-dependent cell death is modulated during murine T cell maturation and mediated by dual signaling pathways. *J. Immunol.* 177, 2842–2850. doi: 10.4049/jimmunol.177.5.2842

Tsukimoto, M., Tokunaga, A., Harada, H., and Kojima, S. (2009). Blockade of murine T cell activation by antagonists of P2Y6 and P2X7 receptors. *Biochem. Biophys. Res. Commun.* 384, 512–518. doi: 10.1016/j.bbrc.2009.05.011

Weiler, M., Schmetzer, H., Braeu, M., and Buhmann, R. (2016). Inhibitory effect of extracellular purine nucleotide and nucleoside concentrations on T cell proliferation. *Exp. Cell Res.* 349, 1–14. doi: 10.1016/j.yexcr.2016.05.017

Whitehurst, C. E., and Geppert, T. D. (1996). MEK1 and the extracellular signal-regulated kinases are required for the stimulation of IL-2 gene transcription in T cells. *J. Immunol.* 156, 1020–1029.

Woehrle, T., Yip, L., Elkhal, A., Sumi, Y., Chen, Y., Yao, Y., et al. (2010). Pannexin-1 hemichannel-mediated ATP release together with P2X1 and P2X4 receptors regulate T-cell activation at the immune synapse. *Blood* 116, 3475–3484. doi: 10.1182/blood-2010-04-277707

Yip, L., Cheung, C. W., Corriden, R., Chen, Y., Insel, P. A., and Junger, W. G. (2007). Hypertonic stress regulates T-cell function by the opposing actions of extracellular adenosine triphosphate and adenosine. *Shock* 27, 242–250. doi: 10.1097/01.shk.0000245014.96419.3a

Yip, L., Woehrle, T., Corriden, R., Hirsh, M., Chen, Y., Inoue, Y., et al. (2009). Autocrine regulation of T-cell activation by ATP release and P2X7 receptors. *FASEB J.* 23, 1685–1693. doi: 10.1096/fj.08-126458

Zhang, F. L., Luo, L., Gustafson, E., Palmer, K., Qiao, X., Fan, X., et al. (2002). P2Y(13): identification and characterization of a novel Galphai-coupled ADP receptor from human and mouse. *J. Pharmacol. Exp. Ther.* 301, 705–713. doi: 10.1124/jpet.301.2.705

Zhang, Y. L., and Dong, C. (2005). MAP kinases in immune responses. *Cell. Mol. Immunol.* 2, 20–27.

Conflict of Interest Statement: The authors declare that the research was conducted in the absence of any commercial or financial relationships that could be construed as a potential conflict of interest.

frontiers in Pharmacology

REVIEW
published: 10 January 2018
doi: 10.3389/fphar.2017.00985

The Role of Adenosine Receptors in Psychostimulant Addiction

Inmaculada Ballesteros-Yáñez[1], Carlos A. Castillo[2], Stefania Merighi[3]* and Stefania Gessi[3]*

[1] Department of Inorganic and Organic Chemistry and Biochemistry, School of Medicine, University of Castilla-La Mancha, Ciudad Real, Spain, [2] Department of Nursing, Physiotherapy and Occupational Therapy, School of Nursing and Physiotherapy, University of Castilla-La Mancha, Toledo, Spain, [3] Department of Medical Sciences, Pharmacology Section, University of Ferrara, Ferrara, Italy

Adenosine receptors (AR) are a family of G-protein coupled receptors, comprised of four members, named A_1, A_{2A}, A_{2B}, and A_3 receptors, found widely distributed in almost all human body tissues and organs. To date, they are known to participate in a large variety of physiopathological responses, which include vasodilation, pain, and inflammation. In particular, in the central nervous system (CNS), adenosine acts as a neuromodulator, exerting different functions depending on the type of AR and consequent cellular signaling involved. In terms of molecular pathways and second messengers involved, A_1 and A_3 receptors inhibit adenylyl cyclase (AC), through $G_{i/o}$ proteins, while A_{2A} and A_{2B} receptors stimulate it through G_s proteins. In the CNS, A_1 receptors are widely distributed in the cortex, hippocampus, and cerebellum, A_{2A} receptors are localized mainly in the striatum and olfactory bulb, while A_{2B} and A_3 receptors are found at low levels of expression. In addition, AR are able to form heteromers, both among themselves (e.g., A_1/A_{2A}), as well as with other subtypes (e.g., A_{2A}/D_2), opening a whole range of possibilities in the field of the pharmacology of AR. Nowadays, we know that adenosine, by acting on adenosine A_1 and A_{2A} receptors, is known to antagonistically modulate dopaminergic neurotransmission and therefore reward systems, being A_1 receptors colocalized in heteromeric complexes with D_1 receptors, and A_{2A} receptors with D_2 receptors. This review documents the present state of knowledge of the contribution of AR, particularly A_1 and A_{2A}, to psychostimulants-mediated effects, including locomotor activity, discrimination, seeking and reward, and discuss their therapeutic relevance to psychostimulant addiction. Studies presented in this review reinforce the potential of A_1 agonists as an effective strategy to counteract psychostimulant-induced effects. Furthermore, different experimental data support the hypothesis that A_{2A}/D_2 heterodimers are partly responsible for the psychomotor and reinforcing effects of psychostimulant drugs, such as cocaine and amphetamine, and the stimulation of A_{2A} receptor is proposed as a potential therapeutic target for the treatment of drug addiction. The overall analysis of presented data provide evidence that excitatory modulation of A_1 and A_{2A} receptors constitute promising tools to counteract psychostimulants addiction.

Keywords: Adenosine A_1 receptors, Adenosine A_{2A} receptors, amphetamines, cocaine, dopamine, psychostimulants, behavioral effects, striatum

OPEN ACCESS

Edited by:
Francisco Ciruela, University of Barcelona, Spain

Reviewed by:
Olga Valverde, Pompeu Fabra University, Spain
Ester Aso, Bellvitge University Hospital, Spain

****Correspondence:***
Carlos A. Castillo
carlosa.castillo@uclm.es
Stefania Merighi
stefania.merighi@unife.it

Specialty section:
This article was submitted to Experimental Pharmacology and Drug Discovery, a section of the journal Frontiers in Pharmacology

Received: *17 October 2017*
Accepted: *22 December 2017*
Published: *10 January 2018*

Citation:
Ballesteros-Yáñez I, Castillo CA, Merighi S and Gessi S (2018) The Role of Adenosine Receptors in Psychostimulant Addiction. Front. Pharmacol. 8:985. doi: 10.3389/fphar.2017.00985

INTRODUCTION

Drug addiction is a complex chronic cognitive disorder characterized by drug seeking and compulsive use, which is difficult to control despite its harmful consequences. According to DSM-5 (American Psychiatric Association, 2013), which is used to define mental disorders in epidemiologic studies, it is now accepted that the criteria used to clinically define the terms *abuse* and *dependence* should be combined to form a new category known as *Substance use disorders*, including *craving* as a new criterion to increase diagnostic accuracy (Hasin et al., 2013). In terms of epidemiology, drug addiction is currently a global health problem, as can be deduced from comparison of data obtained from the Global Burden of Diseases Study between 1990 and 2015. For the period 1990–2015, global exposure to drug use increased by 30.2% for both sexes. In addition, by 2015 drug use was a major risk factor for early death and disability in developed countries like the United States, Canada, Australia, and the United Kingdom, being the 5th leading global risk factor for men and the 12th for women (GBD 2015 Risk Factors Collaborators, 2016).

Psychostimulants are a broad class of drugs whose effects include increases in arousal, wakefulness, cardiovascular stimulation, vigilance, and attention, and which constitute one of the most abused classes of prohibited drugs in the world, including as representative examples cocaine and amphetamine-like molecules (Chesworth et al., 2016). According to the 2017 report of the European Monitoring Centre for Drugs and Drug Addiction (European Monitoring Centre for Drugs and Drug Addiction, 2017), it was estimated that in the year 2016, the global annual prevalence among Europeans aged 15 or over was 3.5 million users of cocaine, 2.7 million users of MDMA and 1.8 million users of amphetamines which corresponds to 1.0, 0.8, and 0.5% of the European adults, respectively, which occasional consumed mentioned psychostimulants during 2016.

To date, the therapies developed to manage drug addiction are inadequate and unsatisfactory, and many scientists around the world are focusing on new strategies to improve them. Even though numerous aspects of this phenomenon are not well understood, the neurochemical mechanism common to all drugs causing abuse in humans is the increase of the neurotransmitter dopamine (DA) released from the ventral tegmental area (VTA), to a region in the mesocorticolimbic part of the brain, like the nucleus accumbens (NAc) and the prefrontal cortex (Filip et al., 2012; Morales and Margolis, 2017). This, in turn, increases the physiological reward and reinforcement mechanisms (Nestler and Landsman, 2001). This point is particularly important because DA not only mediates the effects of acute rewarding, but is also thought to be involved in the increased motivation to consume psychostimulants in psychostimulant abusers (Volkow et al., 2012). Furthermore, abuse of psychostimulants may induce changes in brain regions not only with relevance for addictive behavior, but may also promote long-term adverse consequences in areas related to memory and cognition (Nyberg, 2014). In addition, relapse into drug use after abstinence has been attributed to exposure to cues, stress or re-exposure to the drug itself that induce drug craving; the incubation of craving being a common phenomenon reported for most drugs of abuse, including psychostimulants, that may last from the beginning of abstinence for extended periods of time. Although little is known about the molecular mechanisms that lead to the incubation of craving during drug abstinence, vulnerability to relapse correlates with changes in the activity and structure of neurons from the limbic and frontal cortical circuitry, induced by the drug use (Pickens et al., 2011; Wolf, 2016).

The repeated ingestion of psychostimulants, as for most substances with marked abuse potential, shares one of the following two common features consistently reported in the literature: on the one hand, psychostimulants, by blocking molecular reuptake, enhance the extracellular neurotransmitter concentration in the synapses of monoaminergic neurons (Cooper et al., 1996; Rothman and Baumann, 2003; Wood et al., 2014); on the other hand, psychostimulants increase DA release in the NAc, a critical area for the reward circuit (Preedy, 2016). There is a growing body of scientific evidence demonstrating that psychostimulants affect dopaminergic neurons in the limbic reward system, and that this effect underlies addiction to stimulants (Siciliano et al., 2015).

Adenosine, an ubiquitous endogenous nucleoside, has been implicated in the reward-related behavior, and represents a novel and interesting target to interfere with it, as a consequence of its modulatory function on neurotransmission exerted by DA, glutamate and acetylcholine (Linden, 2001; Cunha, 2005; Gomes et al., 2011; Lopes et al., 2011; Borea et al., 2016; Burnstock, 2017; Jacobson et al., 2017). Interestingly, adenosine levels are modified following acute or chronic consumption of drugs of abuse and psychostimulants (Hack and Christie, 2003; Brown and Short, 2008; Filip et al., 2012), suggesting that a better comprehension of adenosine signaling in the brain during addiction may open new pharmacological frontiers to explore potential treatments in preclinical studies and clinical trials over the next years (Stone, 1981; Clark and Dar, 1989; Krauss et al., 1993; Bonci and Williams, 1996; Salem and Hope, 1999). The question of whether adenosine signaling can be used as a potential therapy in abuse disorders remains to be answered. Therefore, the goal of this review is to discuss current scientific evidence based on animal models of psychostimulant addiction, and to suggest promising candidates in the search for pharmacological interventions. We will include, when available, the effects of adenosine receptor (AR) ligands on the complex process of behavior related to psychostimulant consumption, seeking, withdrawal, craving and relapse, and we will restrict our discussion to what we can consider psychostimulant drugs, namely cocaine and amphetamine-like molecules.

BRAIN CIRCUITRY AND ADENOSINE RECEPTOR INTERACTIONS

The main brain circuitry associated with addiction is distributed across multiple areas. This circuitry is associated with the three stages of the addiction cycle (Koob and Volkow, 2010). The reinforcing effects in an initial binge/intoxication stage are mediated by DA and opioid neurotransmission, and depend

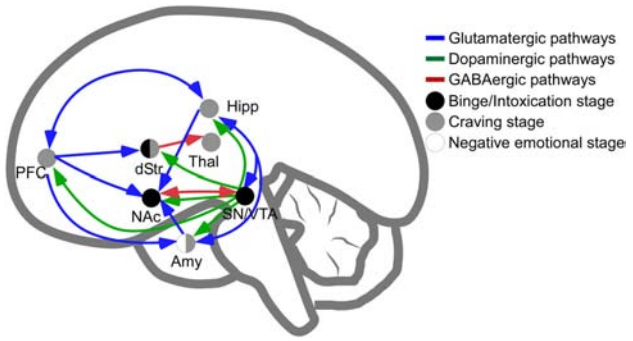

FIGURE 1 | Schematic representation of pathways involved in intoxication, withdrawal and craving stages of addiction. Release of dopamine in the nucleus accumbens is a common feature of psychostimulants reinforcement at initial stages of psychostimulants intake (dots in black are regions directly involved in binge and intoxication). The negative emotional stage of withdrawal appears to be related to the activation of amygdala (dots in white are regions directly involved in negative emotional stage) and, finally, the latter stage of psychostimulant addiction, craving, depends on prefrontal cortex, amygdala and hippocampal activities (dots in gray). In blue, glutamatergic pathways; in green, dopaminergic pathways; in red, GABAergic connections. NAc, Nucleus Accumbens; Amy, Amygdala; dStr, dorsal Striatum; Hipp, Hippocampus; PFC, Prefrontal Cortex; SN/VTA, Substantia Nigra and Ventral Tegmental Area; Thal, Thalamus.

on modifications in the VTA and striatum (particularly NAc). The negative emotional stage of withdrawal may be due to activation of the amygdala with norepinephrine, dynorphin and corticotropin-releasing factor. The third stage, craving, depends on the prefrontal cortex, amygdala and hippocampus, and glutamate is the major neurotransmitter involved (reviewed in Kelley and Berridge, 2002; Koob and Volkow, 2010; Kim et al., 2017; **Figure 1**). The NAc acts as a hub of convergence from the different regions, and it has been considered a key element in the neuronal circuitry of drug addiction. This nucleus is composed of two distinct populations of medium spiny neurons (MSN) with different levels of dopamine D_1 and D_2 receptors and projections (direct and indirect basal ganglia pathways), which are positively and negatively coupled to cyclic adenosine monophosphate (cAMP)/protein kinase A (PKA) signaling, respectively. Striatonigral MSN (direct pathway) send substantia P and dynorphin projections to substantia nigra/VTA and globus pallidus interna, and are enriched with dopamine D_1 receptors. Striatopallidal MSN (indirect pathway) send enkephalin projections to globus pallidus externa and are enriched with dopamine D_2 receptors (Lobo, 2009). Taking together several studies using different approaches such as analysis of psychiatric disorders, transgenic mice, neuropharmacology and optogenetic techniques, it has been possible to postulate an integrative representation of the synaptic connections in NAc and the neurotransmitter systems (Silberberg and Bolam, 2015; **Figure 2**).

Adenosine acts in the central nervous system (CNS) as a neuromodulator, with DA neurotransmission being one of its targets. The modulation of dopaminergic activity is mediated by two main subtypes of AR, being the antagonist of DA receptors. Specifically, A_1 receptors colocalize with D_1 receptors, and A_{2A} receptors with D_2 receptors in heteromeric complexes (Fuxe et al., 2010). Building on this rationale, the case of A_{2A} receptors is particularly important when we are studying the effects of drugs of abuse, for reasons that have been extensively reviewed previously (Hack and Christie, 2003; Brown and Short, 2008; Filip et al., 2012), and that we only briefly enumerate here. First, A_{2A} receptors are highly expressed in the striatum, a key brain nucleus for the reward circuitry, and A_{2A} are crucial receptors, modulating behavioral responses induced by drugs of abuse (Ferré et al., 2007); indeed, their genetic deletion in mice results in a selective decrease of locomotor responses to cocaine and amphetamine (Chen et al., 2000). Furthermore, A_{2A} receptors are able to form heteromers with other adenosine subtypes, resulting in, e.g., the A_1/A_{2A} heteromer (Ferré et al., 2008a), and also with families of receptors relevant for the treatment of some neuropsychiatric disorders and drug addiction, producing, e.g., $A_{2A}/mGlu_5$ (Ferré et al., 2002), A_{2A}/D_2 (Ferré et al., 2008b; Bonaventura et al., 2015), and A_{2A}/CB_1 receptor heteromers (Tebano et al., 2012). This spectrum of interaction opens a wide range of possibilities in the field of AR pharmacology (Casadó et al., 2009). Interestingly, the oligomer formed by $A_{2A}/mGlu_5/D_2$ receptors confers to the A_{2A} subtype the ability to modulate the effects of psychostimulants in striatal neurons, through the balance of GABAergic, dopaminergic and glutamatergic signaling (Cabello et al., 2009; Kniazeff et al., 2011). The modulation of dopaminergic and glutamatergic signaling by A_{2A} receptors has been particularly important in the field of psychiatric disorders, as DA and glutamate are two key players in the processing of moods, which could also be very relevant in drug addiction-related disorders (Cunha et al., 2008).

ADENOSINE RECEPTORS OVERVIEW

Adenosine Metabolism and Adenosine Receptors Structure

In the CNS, extracellular adenosine exists in basal conditions, and its concentration may increase under pathological situations, including hypoxia, ischemia or cell injury. Adenosine is produced by different mechanisms, including metabolism of ATP released from neurons or glial cells. Specifically, ATP undergoes dephosphorylation to ADP and AMP by the activity of particular enzymes named ectonucleoside triphosphate diphosphohydrolase (CD39), and to adenosine through a specific ecto-5′-nucleotidase (CD73) enzyme (Drury and Szent-Györgyi, 1929). Alternatively, adenosine may derive from hydrolysis of intracellular AMP through a cytoplasmic 5′-nucleotidase, or S-adenosyl-homocysteine (SAH) by SAH hydrolase, and may be released through facilitated diffusion, using bi-directional equilibrative nucleoside transporters (ENT) (Dunwiddie, 1985; Ledent et al., 1997; Ribeiro, 1999; Hack and Christie, 2003). Under resting conditions, extra- and intra-cellular levels of adenosine are very similar, but in pathophysiological states (inflammation, ischemia, and hypoxia), characterized by high levels of this nucleoside, transport through ENTs is the main mechanism responsible for extracellular adenosine removal.

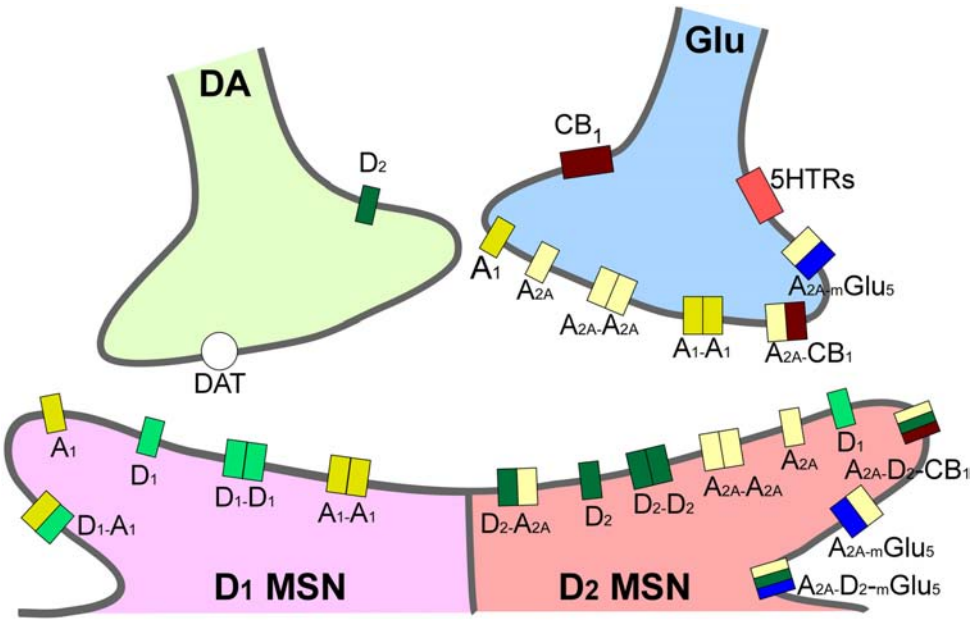

FIGURE 2 | Integrative scheme of reward circuit in striatum with focus on adenosine and dopamine receptors and their interactions. A_1 and A_{2A} receptors are located pre- and post-synaptically forming homo-, heterodimers and oligomers in the dendritic spines of medium spiny neurons in striatum (MSN). Glutamatergic input from cortex and dopaminergic input from ventral tegmental area project to both MSNs expressing D_1-like and MSNs expressing D_2-like dopamine receptors. A_{2A}, adenosine 2A receptors; CB_1, endocannabinoid CB_1 receptors; DAT, dopamine active transporters; D_1, dopamine D_1 receptors; D_2, dopamine D_2 receptors; $mGlu_5$, metabotropic glutamate subtype 5 receptors; 5HTRs, serotonin receptors.

Inside the cell, adenosine is deaminated to inosine through adenosine deaminase (ADA), or phosphorylated to AMP by adenosine kinase (AK). These enzymes display different affinities for adenosine, with AK more affine than ADA; thus in physiologic conditions adenosine is preferentially transformed to AMP, whilst in pathological states predominantly to inosine, a process which occurs also in the extracellular milieu (Godinho et al., 2015; Borea et al., 2016).

Adenosine affects several functions in the body, exerting its physiological effects through regulation of four G-protein coupled receptors (GPCRs) named A_1, A_{2A}, A_{2B}, and A_3, characterized by different affinities for adenosine, tissue distribution, and coupling with effector systems. They have been cloned and pharmacologically characterized in different species, presenting a sequence homology of around 80–95%, except for A_3 receptors which vary depending on species and show a variance of 30% in amino-acid composition between human and rat. The A_3 receptor, in contrast to other AR, was the first to be isolated and then pharmacologically characterized (Meyerhof et al., 1991). All AR show a common structure, characterized by seven transmembrane domains connected by three intracellular and extracellular domains (Fredholm et al., 2000). At the extracellular level, the N-terminus presents specific glycosylation sites, while at the intracellular side, the C-terminus contains phosphorylation and palmitoylation sites, important for receptor desensitization. The A_{2A} receptor has a longer C-terminus tail constituted by 122 amino acids, whereas A_1, A_{2B}, and A_3 receptors' C-terminal domains comprise 30–40 amino acids (Fredholm et al., 2001). Recently, important crystallization results have determined the structures of human A_1 and A_{2A} receptors, thus allowing better drug design for A_1 and A_{2A} receptor-selective ligands (Jaakola et al., 2008; Lebon et al., 2011; Xu et al., 2011; Carpenter et al., 2016; Glukhova et al., 2017; Sun et al., 2017). In the case of A_3 receptors, structure-based molecular modeling techniques have led to the rational design of potent A_3 receptor-selective ligands (Ciancetta and Jacobson, 2017). Furthermore, AR may be present in the cell membrane in homomer isolated forms or in heteromers and oligomers, providing another possibility of intervention for drug development (Cabello et al., 2009). Specifically, the ability of AR to interact with many other receptors, such as A_{2A}/D_2 receptor heterodimers located in the striatum (represented in **Figure 2**), means they play a pivotal role in the modulation and integration of neurotransmission, and may be targeted by drugs for the treatment of neurological diseases, including drug addiction (Chen et al., 2013).

Adenosine Receptors: Distribution, Signal Transduction, and Function

AR are widely distributed in almost all organ and tissues, spanning brain, heart, lung, liver, kidney, bone, eye, skin, joints, and blood cells, suggesting that these proteins are potentially able to affect almost every physiological function (Peleli et al., 2017).

Specifically, as for the presence of each AR subtype in CNS, the A_1 receptor is mainly present in the cortex, hippocampus, cerebellum, nerve terminals, spinal cord, and glia (Chen et al., 2013). This wide range of locations reflects the multitude of physiological effects orchestrated by it, including inhibition

of neurotransmitter release, reduction of neuronal excitability, sedation, anticonvulsant and anxiolytic effects, analgesia and regulation of sleep (Stenberg et al., 2003; Gessi et al., 2011; Sawynok, 2016; Vincenzi et al., 2016a,b; Varani et al., 2017). These effects are mediated through A_1 receptors coupling to G_i/G_o proteins, inhibition of AC, activation of phospholipase-C (PLC)β and, particularly in neurons, activation of potassium channels and deactivation of Q-, P-, and N-type Ca^{2+} channels. They also modulate mitogen-activated protein kinases (MAPK) with important functional effects (Schulte and Fredholm, 2003).

The A_{2A} receptor is highly expressed in the striatum, mainly present in GABAergic striatopallidal neurons, corticostriatal glutamatergic terminals, and cholinergic interneurons, but it is also detectable in the olfactory tubercle, cerebral cortex, hippocampus, neurons, and glial cells, where it induces excitotoxicity by affecting release of glutamate, activation of glia and infiltration of immune cells from the periphery, through blood brain barrier passage (Fuxe et al., 2003, 2007b; de Lera Ruiz et al., 2014). The A_{2A} receptor generally couples to G_s proteins to increase cAMP levels, but in the brain it stimulates G_{olf}, a specific G_s protein in neurons also associated with AC (Kull et al., 2000), which is supposed to have a prominent role as a mediator of the locomotor effects of some psychostimulant drugs (Hervé et al., 2001). The signaling cascade starting from cAMP and PKA regulates different proteins such as cAMP responsive element binding protein (CREB) and DA- and cAMP-regulated phosphoprotein (DARPP-32) (Preti et al., 2015), which is also involved in the responses to psychostimulant drugs (Engmann et al., 2015). CREB phosphorylation then increases transcription of immediate early genes such as c-fos and other genes like preproenkephalin (Ferré, 2008). In addition, the A_{2A} receptor, with its long C-terminus, could also bind to different accessory proteins like D_2 receptors, ADP-ribosylation factor nucleotide site opener (ARNO), α-actinin, translin-associated protein X (TRAX) and ubiquitin-specific protease (USP4). A_{2A} receptor activation may also trigger the Ras/Raf-1/MEK/ERK pathway through PKA-dependent or independent mechanisms (Schulte and Fredholm, 2003).

A_{2B} receptors are present in astrocytes, neurons, and microglia, but their role in the CNS is less well characterized in comparison to the other AR subtypes. As for the effector systems, it activates G_s proteins/cAMP/PKA phosphorylation. Furthermore, the A_{2B} receptor stimulates an increase in G_q protein/PLC/Ca^{2+}, while modulating ion channels through βγ subunits. Coupling to MAPK has been also reported (Merighi et al., 2017).

Finally, for A_3 receptors, a low level of expression has been detected in the brain, in which it was detected in the cortex, thalamus and hypothalamus, hippocampus, motor nerve terminals, retinal ganglion cells, pial and intracerebral arteries and glia (Borea et al., 2015; Jacobson et al., 2017). The A_3 receptor couples to G_i proteins and decreases cAMP levels, whilst through G_q proteins or $G_{\beta\gamma}$ subunits, it stimulates PLC and increase Ca^{2+} concentration. In addition, a pathway presenting RhoA, a monomeric G-protein and PLD, is relevant for the neuroprotection effects of A_3 receptors. Inhibition of the transcription hypoxia-inducible factor (HIF-1) has been reported in astrocytes with neuromodulatory effects through MAPK and Akt modulation (Gessi et al., 2013). Interestingly, the reduction of neuroinflammation has been related to analgesia (Janes et al., 2014).

PSYCHOSTIMULANTS AND ADENOSINE RECEPTORS

In this section, we will describe the current state of knowledge about how adenosine signaling can interfere with common addictive psychostimulant consumption, focusing on data obtained from animal, particularly murine, models and from human studies. Animal models not only give us useful information on the pathophysiological mechanisms of psychostimulant drugs intake that are not accessible to study in human subjects but also provide an useful tool to assay pharmacological approaches to explore potential treatments before develop clinical trials. Certainly, although animal models may produce similar responses to those observed in humans, all the paradigms used in them for drug addiction research imply a lower degree of complexity than that observed in human drug addiction. Nowadays, more complex animal models have been developed to include some behavioral responses observed in human addictions, such as social peer influences in drug intake (Moser et al., 2011; Ross et al., 2015; Strickland and Smith, 2015). Nevertheless, in the last part of this section, information obtained from human studies is also provided and the actual information regarding this issue is discussed.

Psychostimulants can be classified into two broad categories depending on the mechanism by which DA levels are increased; namely, amphetamines (AMPH) behave as DA releasers, while cocaine acts to inhibit DA reuptake trough the inhibition of the DA active transporter (DAT) (Siciliano et al., 2015). In addition to the increase in levels of DA in the striatum, AMPH and cocaine are able to induce an increase in norepinephrine (NE), by blocking NE transporter (NET), while only cocaine also increases serotonin, by inhibiting serotonin transporter (SERT) (Phillips et al., 2014; Zwartsen et al., 2017).

Cocaine is extracted from coca leaves, mainly in South America where the coca plant is commonly grown. Despite being the most widely used illicit narcotic drug, cocaine has been used for centuries (if not millennia) for medical and cultural purposes (Johanson and Fischman, 1989). Although cocaine may be illegally distributed in several forms, mainly cocaine hydrochloride but also cocaine sulfate or crystalized as "crack," the physiological and psychoactive effects of cocaine in different forms are similar (Hatsukami and Fischman, 1996).

The family of "amphetamines" or amphetamine-like psychostimulants includes a wide range of compounds which can be synthetized based on chemical substitutions of the original structure of alpha-methylphenethylamine. AMPH and methamphetamine (S(+)-methylamphetamine, METH) are the most studied compounds of the family, but other well-known psychostimulants in this family include methylphenidate,

MDMA (3,4-methylenedioxymethamphetamine, "ecstasy"), ephedrine and cathinone (synthetic derivatives of which are known as "bath salts") (Sulzer et al., 2005). Specifically, although cathinones have a synthetic profile similar to AMPH, their mechanism of action is rather similar to that of cocaine, being potent DAT inhibitors (López-Arnau et al., 2017). On the other hand, MDMA, in addition to inhibiting NET and DAT, is both a substrate for SERTs and an inhibitor of them, with an IC_{50} in the micromolar range, thus differentiating its behavior from that of AMPH, which is unable to affect SERTs (Rudnick and Wall, 1992; Baumann et al., 2005; Zwartsen et al., 2017). Although AMPH and METH have similar pharmacokinetics, they differ in their pharmacodynamic properties, with METH inducing DA release in the NAc more efficiently than AMPH (Goodwin et al., 2009). AMPH and METH have been studied for a long time, but their neurobiology remains largely unknown with discrepancies in the literature between pharmacological and genetic-based experiments.

As for psychostimulants-induced changes in AR expression in brain areas only few scientific reports have been reported. Specifically, during a study of cocaine withdrawal and its relationship with sleep architecture, Yang et al. (2011) reported that A_1 receptor expression in the hippocampus of rats was reduced after 14 days of withdrawal, A_{2A} receptor density was increased on withdrawal-day 8 and 14, while the A_{2B} receptors remained unchanged. Other findings provide neurochemical evidence that after 10 days of cocaine self-administration, an up-regulation of functional A_{2A} receptors in the NAc of rats was induced that returned to baseline expression levels after 7 days of drug withdrawal (Marcellino et al., 2007). In a study of the motivational mechanisms after cocaine self-administration and extinction, it was reported that, in the dorsal striatum of Wistar rats, there was an increase in the affinity of A_{2A} receptors during maintenance and an increase in A_{2A} receptor density after extinction from cocaine self-administration (Frankowska et al., 2013). Nevertheless, using a paradigm of escalating administration of cocaine dose ("binge") and subsequent withdrawal, the density of adenosine A_1 and A_{2A} receptors in various brain nuclei of Fischer rats was not different nor in chronic cocaine-treated rats or in the long-term withdrawn rats group (Bailey et al., 2005). Finally, rats trained to self-administer METH for 14 days showed selective altered expression of AR, with A_1 receptor levels increased in the NAc shell, caudate-putamen and prefrontal cortex, and A_{2A} receptors decreased in the NAc shell and raised in the amygdala (Kavanagh et al., 2015). Interestingly, it is well known that GPCR act as an oligomer, and indeed homodimers of A_{2A} and 5-HT1A receptors occur constitutively, and are further increased by agonists such as CGS 21680 and 8-OH-DPAT, or reduced by antagonists including SCH 58216 and methysergide, which could also contribute to psychostimulant addiction (Łukasiewicz, 2007).

Even though there are no consistent and complete studies about amphetamines- and cocaine-induced changes in AR expression in brain areas, a prominent role in the modulation of psychostimulant addiction attributed to adenosine is mediated through the activation of AR by complex mechanisms, affecting various aspects of this phenomenon including locomotor activity, discrimination, seeking behavior and reward.

Studies in Animal Models

Although the interactions between adenosine and DA in the striatum were previously known, the role of AR in AMPH-induced locomotor responses was first characterized only at the end of the last century. Turgeon et al. (1996) demonstrated that, in Sprague-Dawley rats, AMPH-induced behavior could be pharmacologically modulated by pretreatment with CHA, an A_1 receptor agonist, or APEC, an A_{2A} receptor agonist, which reduced locomotor responses induced by acute AMPH exposure. However, only the A_{2A} receptor agonist inhibited c-Fos immunoreactivity, induced by AMPH, in striatum and NAc. In the case of METH, the experimental paradigm used to determine the role of AR in METH-mediated effects was METH-induced toxicity. In these studies, administration of the A_1 agonist CPA attenuated the METH-provoked neurochemical tyrosine hydroxylase changes in Swiss-Webster mice (Delle Donne and Sonsalla, 1994) while, in other experimental models, represented by Wistar rats, both CPA and CGS 21680, an A_{2A} receptor agonist, were able to attenuate METH-mediated DA release in the striatum (Gołembiowska and Zylewska, 1998a). In terms of METH-induced locomotor responses, it was also reported that administration of CHA and CGS 21680 before acute METH exposure in Wistar rats was able to inhibit METH-induced hyperlocomotion (Shimazoe et al., 2000) but, interestingly, when those same agonists were tested to study METH-induced sensitization (which occurs after repeated intermittent drug administration), only CGS 21680 was able to inhibit METH-induced increase of locomotion while CHA had no effect (Shimazoe et al., 2000). In addition, the activation of A_{2A} receptors could also be the mechanism by which some herbal compounds, PAP9704 and ginsenoside herbal compounds, attenuate METH-induced hyperlocomotion and conditioned place preference in BALB/C AnNcrj mice as well as in C57BL/6 mice, respectively (Kwon et al., 2004; Shin et al., 2005). Furthermore, AMPH-induced stereotyped head movements in Wistar rats were attenuated in a dose-dependent manner with CGS 21680, poorly reduced when CPA was used and even potentiated when DMPX, an A_2 receptor antagonist, was used (Poleszak and Malec, 2000). Finally, it seemed that the inhibition of AMPH-induced stereotyped head movements, through activation of A_1 receptor, could depend on agonist properties, as Ribavirin, an A_1 receptor agonist, reduced AMPH-induced total locomotor activity but had no effects on stereotypic activity in Wistar rats (Janać et al., 2005). Relevant literature concerning the functional effects of AR ligands in psychostimulant-induced phenomena, with a focus on rodent models, are presented in **Supplementary Table S1**.

A complete study of AR and their relationship with cocaine-induced locomotion was carried out by Poleszak and Malec (2002b) at the beginning of this century. They reported that CPA and CGS 21680, decreased both cocaine- and AMPH-induced locomotor activity. The agonist doses required to inhibit the effect of AMPH were higher than those which were active in cocaine-induced hyperactivity, while the A_2

antagonist DMPX enhanced the effects of AMPH in Swiss mice (Poleszak and Malec, 2002b). Accordingly, the selective stimulation of A_{2A} receptors in Wistar rats using CGS 2160 reduced the cocaine-induced locomotor response, the locomotor response during the development of sensitization, and the expression of sensitization in a cocaine challenge dose, while blocking A_{2A} receptors with the antagonist MSX-3 induced the opposite effects in the three studied paradigms (Filip et al., 2006).

Genetic deletion of A_{2A} receptors (A_{2A} KO) in animal models of drug addiction provides a tool to understand the role of these receptors under certain circumstances by comparison to wild-type animals. Nevertheless, the results obtained using A_{2A} KO animals on cocaine-, AMPH-, and METH-induced behavioral responses seem contradictory. In this sense, it was reported that in 129-Steel and hybrid C57BL/6 × 129-Steel mice, A_{2A} KO attenuated cocaine-induced locomotor stimulation (Chen et al., 2000). Similar experiments, performed to demonstrate the effects of A_{2A} genetic deletion with independence of the genetic background, were reproduced later in pure 129-Steel mice resulting in missed AMPH-induced locomotor sensitization (Chen et al., 2003). Accordingly, similar results were obtained when hybrid C57BL/6 × 129-Steel animals were used to generate tissue-specific A_{2A} KO animals, where deletion of forebrain A_{2A} receptors was carried out, which showed a loss of AMPH-mediated locomotor response (Bastia et al., 2005). In contrast, in CD1 background mice, it was reported that there were no differences in the cocaine-induced locomotor activity, sensitization and conditioned place preference between A_{2A} KO animals and their littermates (Soria et al., 2006). Authors only found a lower rate of cocaine self-administration and motivation as well as lower efficacy of cocaine reinforcing effects in A_{2A} KO mice (Soria et al., 2006). Interestingly, Soria et al. (2006) concluded with the hypothesis that separate neuronal substrates could mediate cocaine-induced locomotor effects and self-administration in an operant behavior paradigm. In order to corroborate this hypothesis, Shen et al. (2008) designed two different KO animals to distinguish between striatal versus non-striatal cocaine-mediated effects. In these experiments, cocaine-induced locomotor activity was enhanced in striatum-specific A_{2A} KO mice (A_{2A} receptors were deleted in striatal neurons) but attenuated in forebrain-specific A_{2A} KO mice (A_{2A} receptors were deleted in the neurons of striatum, cerebral cortex, and hippocampus). In addition, pharmacological inactivation (using KW6002, an A_{2A} receptor antagonist with preferential affinity for post-synaptic A_{2A} binding sites) of extra-striatal A_{2A} receptors in striatum-specific A_{2A} KO mice attenuated cocaine-induced hyperlocomotion, while the same antagonist enhanced cocaine-induced hyperlocomotion in the wild-type mice, reflecting the antagonism between striatal A_{2A} receptors and extra-striatal A_{2A} receptors (Shen et al., 2008). Finally, in CD1 A_{2A} KO mice, a lesser increase in DA levels after acute cocaine exposure was reported while locomotor activity was further increased in A_{2A} KO mice in comparison to wild-type littermates (Wells et al., 2012). The genetic models derived from the manipulation of AR, and their effect on the interaction of AR with psychostimulants, are presented in **Supplementary Table S2**.

Interestingly, there is some research available about the role of A_3 receptors in modulation of AMPH- and METH-mediated actions. METH-induced DA release was measured in the rat striatum using APNEA, a putative A_3 receptor agonist, which has a biphasic effect when perfused locally to the striatum via microdialysis. At the lower concentration studied, APNEA induced a decrease in DA outflow, but at the higher concentration studied, a clear increase in DA outflow was reported, which led researchers to conclude that the activation of A_3 receptors exerts a rather toxic effect on DA neurons (Gołembiowska and Zylewska, 1998b). Nevertheless, when the A_3 receptor was genetically deleted, it was reported that the resultant mice were much more sensitive to the toxic actions of METH, including Iba-1, caspase 3, TNF-α, and vesicular monoamine transport 2 (VMAT) increased expression (Shen et al., 2011), and also presented reduced AMPH-induced locomotor response (Björklund et al., 2008).

Adenosine receptors modulate psychostimulant-induced discriminative-stimulus effects, as A_1 and A_{2A} receptors antagonists (CPT and MSX-3 or DMPX, respectively) partially mimicked the discriminative-stimulus effects of METH, by increasing the levels of drug-lever selection, and potentiating the discriminative-stimulus actions of METH, as shown by significant leftward shifts of the METH dose-response curve, behaving like psychostimulant drugs (Munzar et al., 2002; Justinova et al., 2003). Surprisingly, CPA and CGS 21680 also shifted the dose-response curve to the left for cocaine, but not for METH, suggesting that A_1 and A_{2A} receptors have different influences on the discriminative-stimulus effects of METH and cocaine in Sprague-Dawley rats (Justinova et al., 2003).

Another relevant aspect in drug addiction which is strongly influenced by AR is the seeking behavior. In terms of the effect of A_1 agonists, CPA microinfusions in the NAc of Sprague-Dawley rats inhibited cocaine seeking behavior (Hobson et al., 2013). On the other hand, treatment with A_{2A} agonists such as NECA or CGS 21680 reduced the number of cocaine infusions self-administrated by rats, mainly due to an increase in the latency for the first cocaine infusion (Knapp et al., 2001). Accordingly, the activation of A_{2A} receptors, using CGS 21680, antagonized the reinstatement of cocaine seeking in Sprague-Dawley rats (Bachtell and Self, 2009). In addition, it was reported that A_{2A} receptor blockade, using CGS15943, increased cocaine-seeking in a dose-dependent manner and also reinstated cocaine-seeking, functioning as an intravenous reinforcer, in baboons (Weerts and Griffiths, 2003). The effects of activation and blockade of A_{2A} receptors, using CGS 21680 and MSX-3, respectively, were also tested in Sprague-Dawley rats trained to press a lever for cocaine. Pretreatment with intra-NAc core microinjections of CGS 21680 reduced cocaine-induced reinstatement, while MSX-3 exacerbated it (O'Neill et al., 2012). Similar results were obtained in Sprague-Dawley rats, where intra-NAc microinjections of CPA and CGS 21680 inhibited the expression of cocaine sensitization, and microinjections of ABT-702 and DCF (AK and ADA

inhibitors, respectively) blocked cocaine sensitization (Hobson et al., 2012). Interestingly, A_{2A} receptor activation (with CGS 21680) in Wistar rats was able to affect food seeking with a similar potency to that observed for cocaine seeking, whilst A_{2A} receptor antagonists increased cocaine-, but not food-, seeking behavior, suggesting that possibly a differential expression of A_{2A} receptors occurs in striatopallidal GABAergic neurons involved in cocaine and food seeking (Wydra et al., 2015). In contrast, it was reported that although the activation of A_1 (using CPA) and A_{2A} (using CGS 21680) receptors impaired initial extinction responding, the blockade of presynaptic A_{2A} receptors using SCH 442416 produced persistent impairment of cocaine-induced seeking in Sprague-Dawley rats (O'Neill et al., 2014).

As reported in **Supplementary Table S1**, the vast majority of studies have focused exclusively on males. Nevertheless, there is a large amount of literature concerning the differences in drug-mediated effects between males and females (for a recent review see Lynch, 2017). Although the focus of the present review is on the relationship between AR and psychostimulants, sex differences will be briefly commented upon to provide a fuller picture of the problem of addiction. In this regard, it has been reported that female rats self-administer higher levels of cocaine or METH, and escalate intake faster than males during extended daily psychostimulant access (Roth and Carroll, 2004; Reichel et al., 2012). Females also require shorter periods of time to show increased motivation to obtain cocaine (Lynch and Taylor, 2004). In addition, following short access self-administration, females show markedly higher levels of METH seeking (Ruda-Kucerova et al., 2015), and females present increased cocaine-seeking behavior during cocaine withdrawal (up to 6 months) compared to males (Kerstetter et al., 2008). Sex-dependent responses to AR's ligands have also been reported in Sprague-Dawley rats using ATL444, a novel A_{2A}/A_1 receptor antagonist, in studies of motivation for cocaine. In these experiments, it was reported that ATL444 treatment acutely increased motivation for cocaine in females but, in males, induced a long-term decrease in motivation for cocaine (Doyle et al., 2012). Finally, one interesting more recent study, evaluating the effects of A_{2A} receptor deletion on schizophrenia, found that AMPH induced a lower hyperlocomotion response in male CD1 A_{2A} KO mice at 120–170 min, in comparison to wild type AMPH-treated mice; this effect was observed to a major extent in female CD1 A_{2A} KO mice at 70–180 min, in comparison to wild type AMPH-treated mice (Moscoso-Castro et al., 2016).

Rewarding effects induced by AMPH and METH have mainly been evaluated using conditioned place preference procedures. In this way, Poleszak and Malec (2003) proved that CPA and, under certain conditions, CGS 21680, reduced the development of AMPH-induced conditioned place preference in Wistar rats; however, only CGS 21680 was able to decrease the expression of METH-induced conditioned place preference. In addition, ginseng saponins reduced the METH-induced circling behavior and conditioned place preference in C57BL/6 mice, via activation of the A_{2A} receptor, as this reduction was reversed in a dose-dependent manner using the A_{2A} receptor antagonist CSC. Interestingly, reduction of AP-1 DNA binding activity and proenkephalin gene expression induced by METH exposure were reduced by CSC (Shin et al., 2005). Furthermore, C57BL/6J mice with D_2 receptors knocked down in the NAc core have been reported to exhibit a reduction in METH-induced locomotion, as in other paradigms (locomotor sensitization and conditioned place preference) after repeated METH-treatment, suggesting that D_2 receptors are necessary mediators for the development of METH-induced rewarding effects (Miyamoto et al., 2014). Thus, the antagonism between A_{2A} and D_2 receptors further supports the conclusion that the activation of A_{2A} receptors could be a promising way to counteract AMPH- and METH-induced rewarding effects.

A series of experiments to increase our understanding of the role of A_1 and A_{2A} receptors in METH-induced behavior were designed by Kavanagh et al. (2015), reporting that the initial METH-mediated rewarding effects may be tempered by A_1 or A_{2A} receptor activation in a model of rat self-administration. Therefore, they found that in Sprague-Dawley rats, the stimulation of A_1 receptors using CPA reduced METH self-administration, and that the stimulation of both A_1 and A_{2A} receptors (using CPA and CGS 21680, respectively) reduced METH-induced place preference (Kavanagh et al., 2015). These results suggest that, taking into account the antagonism of A_1/D_1 and A_{2A}/D_2 heteromers, both A_1 and A_{2A} agonists will be useful to reduce METH-induced behaviors during the initial exposures to METH but, when METH exposures are more prolonged, the modulation of AR renders only the A_1 agonist powerful enough to counteract the rewarding properties of METH. Accordingly, A_{2A} KO animals (CD1 background) were less sensitive to METH rewarding properties, as METH exposure did not induce conditioned place preference in those animals and, although METH-self administration was not altered, the motivation to self-administer METH was reduced when compared with wild-type (Chesworth et al., 2016).

Finally, the important role of AR as possible pharmacological tools to treat psychostimulant addiction has also been tested in animal models using other members of the amphetamine family, albeit to a lesser extent. Specifically, it was demonstrated that SCH 58261, but not DPCPX, increased MDMA-induced hyperthermia (Vanattou-Saïfoudine et al., 2010) but, conversely, DPCPX, but not SCH 58261, enhanced MDMA-induced DA release from striatal slices (Vanattou-Saïfoudine et al., 2011). Accordingly, the blockade of A_1 or A_{2A} receptors using DPCPX or KW 6002, respectively, in mouse striatum increased the MDMA-mediated release of DA and 5-HT (Górska and Gołembiowska, 2015). In contrast to these pharmacological experiments, when A_{2A} receptors were knocked down in a CD1 background model, MDMA-mediated reinforcement was dramatically decreased (although locomotor response was not altered) compared to wild-type littermates (Ruiz-Medina et al., 2011), suggesting that the lack of A_{2A} receptors will increase resistance to psychostimulant rewarding properties.

Human Studies

The genomic era has provided the opportunity to study human polymorphisms and so to provide a tool to design

personalized treatments according to observed mutations. Recent meta-analysis of case-control studies of psychostimulant users (cocaine, AMPH, and METH) have revealed that there is a general down-regulation of the dopaminergic system, as in psychostimulant users there is a decrease in DA release, in DA transporter availability, and also in the levels of D_2 and D_3 receptors, concluding that DA function is down-regulated both pre- and post-synaptically. This suggests that restoring DA function must be an important goal in the treatment of psychostimulant abusers (Ashok et al., 2017). Due to the antagonistic relationship between dopaminergic function and AR, some authors have studied the relationship between A_1 and A_{2A} gene polymorphisms and susceptibility to psychostimulant consumption/addiction. Most relevant human studies are presented in **Supplementary Table S3**.

The first study designed to discern the influence of A_1 and A_{2A} gene (ADORA1 and ADORA2A, respectively) polymorphisms on inter-individual variability in AMPH response was carried out by Hohoff et al. (2005). Using a sample of 99 healthy volunteers (50 men and 49 women), who received AMPH or a placebo, the authors reported that two ADORA2A polymorphisms (1976C/T and 2592C/T_{ins}) were associated with increases in reported anxiety by participants after AMPH consumption (Hohoff et al., 2005). Nevertheless, these results should be regarded with caution, as the same research group could not reproduce them using the same methodology for a larger sample of individuals (Hart et al., 2013). In addition, a study by Kobayashi et al. (2010) searching for the relationship between ADORA2A variations and susceptibility to METH dependence/psychosis reported that, in a population of 171 Japanese METH dependent/psychotic patients (compared to 229 control subjects), six ADORA2A polymorphisms were found. The authors reported that only one single nucleotide polymorphism (SNP) of the A_{2A} receptor gene was significantly associated with a subgroup of female patients (METH dependent/psychotic) that consumed only METH and no other psychostimulants or drugs (Kobayashi et al., 2010). Interestingly, that SNP was 1976C/T (rs5751876), the same that Hohoff et al. (2005) associated with anxiety after AMPH consumption, and this SNP is a synonymous variant, meaning that it cannot include amino acid substitutions. Finally, in the same Japanese population as the previous study, seven ADORA1 SNPs were identified but none was specific to any subgroup of METH dependent/psychotic patients, which would suggest that ADORA1 polymorphisms would make little or no contribution to METH vulnerability (Kobayashi et al., 2011); however, further research is needed to confirm this supposition. In addition, caffeine-induced anxiety has also been associated with ADORA2A 1976C/T polymorphism in a sample of 102 individuals (Childs et al., 2008), although other ADORA2A polymorphisms (such as 1976TT) also seem to be related to caffeine-induced anxiety, and could also influence predominantly women vulnerable to anxiety (Domschke et al., 2012; Gajewska et al., 2013).

Despite the huge amount of evidence that connects AR with psychostimulant-mediated actions, the translation of this knowledge to the clinic has been quite slow in comparison with other areas. A few reasons related to particular characteristics of AR could be that AR receptors are widely distributed, not only in the CNS but throughout the human body, with adenosine signaling responsible for the regulation of a broad spectrum of physiologic and pathologic actions (for a more detailed discussion see Müller and Jacobson, 2011; Chen et al., 2013). For this reason, it is experimentally difficult to demonstrate the clinical effectiveness and safety of an AR ligand. Therefore, only two clinical studies (registered in website[1]) have studied psychostimulant dependence and its link with AR (**Supplementary Table S3**). One of these compared the responses of volunteers to acute caffeine (150 and 300 mg), AMPH (20 mg) and placebo between 13 cocaine users and 10 healthy control subjects (NCT00733993). The main target of the trial was to study caffeine-mediated effects in cocaine users. Nevertheless, although caffeine and AMPH produced a series of differential results across the cocaine and control groups, these outcomes were not systematic, perhaps due to limitations of the study itself (Lane et al., 2014). On the other hand, the effect of an acute dose (100 mg) of the A_{2A} antagonist SYN115 was studied to elucidate the effects of this antagonist on brain function and behavior in a group of cocaine-dependent volunteers (NCT00783276). Some subjective effects (consistent with stimulation) were induced by SYN115 administration in cocaine users (Lane et al., 2012). Furthermore, the administration of SYN115 to cocaine-dependent volunteers increased brain activation in the orbitofrontal cortex, insula, and superior and middle temporal pole, as measured by fMRI while the participants were performing working memory tasks; this suggests that the blockade of A_{2A} receptors could mitigate cocaine-associated neurobehavioral deficits (Moeller et al., 2012). In addition, no clinically significant adverse cardiovascular events were reported by the volunteers in either study (Lane et al., 2012; Moeller et al., 2012).

Finally, epidemiological and preclinical data demonstrate that gender differences exist for the three phases of drug abuse (represented in **Figure 1**). The pattern of gender differences establishes that women have lower prevalence of drug use disorders involving both licit and illicit drugs (including alcohol, sedatives, cannabis, tranquilizers, opioids, hallucinogens, and cocaine use disorders). Nevertheless, women that begin to self-administer drugs, even at lower doses than men do, escalate faster to addiction and present higher rates of relapse compared to men. These gender differences can be interpreted in terms of sociocultural factors as well as biological/physiological factors (reviewed in Lynch, 2006; Lev-Ran et al., 2013; Bobzean et al., 2014; Becker and Koob, 2016). Men and women also differ markedly in terms of psychostimulant use/abuse. For example for METH consumption, women tend to begin METH use at earlier ages and seem more dependent on METH consumption than men, although women do suffer a decreased degree of toxicity and respond better to treatment (Dluzen and Liu, 2008). In addition, women present more severe problems related to cocaine intake, beginning to use cocaine at earlier ages,

[1] ClinicalTrials.gov

and some pharmacological treatments for drug addiction have poor outcomes among women compared to men (Kennedy et al., 2013; DeVito et al., 2014). Several pathophysiological studies have demonstrated that the reinforcing effect of cocaine is strongly influenced by the female hormonal cycle; in fact, some authors suggest that gender differences in addiction are due to differences in the reinforcement pathways of neural systems induced by ovarian hormones (Anker and Carroll, 2011; Bobzean et al., 2014). These findings highlight the importance of taking gender into account when analyzing psychostimulant use, and designing prevention programs and personalized treatment programs.

MECHANISMS OF ADENOSINE RECEPTOR-MEDIATED PATHWAYS IN DRUG ADDICTION

As noted in previous sections, it has been reported that AR interact in an antagonistic way with DA receptors, A_1 receptors being colocalized in heteromeric complexes with D_1 receptors, and A_{2A} receptors with D_2 receptors, counteracting DA-induced behavioral effects (Ferré et al., 1997; Ginés et al., 2000; Hillion et al., 2002; Fuxe et al., 2007a). Specifically, the stimulation of striatal D_2 receptors is responsible for the locomotor, sensitizing and rewarding effects of drugs of abuse such as cocaine and amphetamines, and A_{2A} receptor stimulation counteracts them (Heffner et al., 1989; Popoli et al., 1994; Rimondini et al., 1997; Poleszak and Malec, 2000, 2002a; Shimazoe et al., 2000; Knapp et al., 2001; Bachtell and Self, 2009; Jastrzêbska et al., 2014; Johnson and Lovinger, 2016). In general, the process of addiction depends on an increase in DA neurotransmission in the striatum and an activation of its receptors. Specifically, cocaine induces its effects by indirectly increasing DA levels and directly activating D_2 receptors (Fuxe et al., 2007a; Ferraro et al., 2012), thus enhancing dopaminergic signaling. The DA receptors most involved are of the D_2 subtype, as demonstrated by their persistent striatal decrease following drug detoxification, and their induction of relapse as a consequence of chronic drug administration.

Interestingly, A_{2A} and D_2 receptors are co-expressed in the striatum, forming heteroceptors, especially in the GABAergic striatopallidal neurons, where A_{2A} receptor activation increases GABA release and counteracts the effects induced by D_2 receptors. These receptors may be linked to each other in two opposite ways. On the one hand, these receptor subtypes may form heteromers, causing antagonistic interactions between A_{2A} receptors and D_2 receptors at the AC level, related to $G_{s/olf}$ and G_i type V AC signaling. On the other hand, at the membrane level, A_{2A} receptor activation exerts a counterbalancing effect to D_2 receptor stimulation, by reducing its affinity for DA and decreasing functional effects induced by D_2 receptor stimulation (Ferré et al., 1991, 1994). In support of this relationship, transgenic animal models overexpressing A_{2A} receptors in the brain showed reduced D_2 receptors in the striatum. Accordingly, A_{2A} receptor activation decreases behavioral responses to psychostimulants, indicating that the A_{2A} receptor may represent a novel drug target for the treatment of drug addiction. In particular, A_{2A} receptor stimulation decreases cocaine reward and seeking behavior, by reducing D_2 agonist affinity (Pintsuk et al., 2016). In the context of the antagonistic interaction between A_{2A}/D_2 receptors, it has also been reported that the D_2 receptor, through coupling to G_i, inhibits A_{2A} receptor-mediated cAMP/PKA signaling, and thus CREB phosphorylation and c-fos expression (Pinna et al., 1997; Kull et al., 2000; Hillion et al., 2002). However, synergistic A_{2A} and D_2 receptor interaction has been revealed, again at the AC level in the striatum, linked to the overexpression of activator of G protein (AGS3) and $G_{s/olf}$ and G_i type II/IV AC pathway. This relationship becomes important when AGS3 is upregulated, such as during ethanol consumption, and withdrawal from cocaine, ethanol or morphine, because its activity stabilizes and inhibits the GDP-bound form of G_i, at the same time increasing the $\beta\gamma$-dependent effect of $G_{s/olf}$ protein, producing a strong increase in cAMP-PKA signaling. Even though in the striatum the first A_{2A}/D_2 antagonistic relationship is predominant, due to the higher distribution of AC V, when AGS3 is upregulated, such as during chronic exposure to addictive drugs, the synergistic interaction between A_{2A} and D_2 receptors becomes relevant, suggesting that A_{2A} receptor antagonists may represent a class of drug to combat addiction and relapse (Ferré et al., 2008b). In addition, neuroprotection exerted by A_{2A} receptor agonists seemed to be mediated by an increase in nuclear factor-κB (Kermanian et al., 2012, 2013; Soleimani et al., 2012).

Furthermore, neuromodulation of neuronal networks by systemic A_{2A} receptor activation inhibits the reward and motivational properties of cocaine targeting A_{2A}/D_2 heteroreceptors in the striatopallidal GABA pathway. Microdialysis studies have related this effect to their increase and reduction of GABAergic and dopaminergic transmissions, respectively, in the NAc, as a consequence of an antagonistic A_{2A}/D_2 interaction, both at the membrane cell surface and at the intra-cellular level (Fuxe et al., 2007a; Trifilieff et al., 2011; Franco et al., 2013; Wydra et al., 2015; Borroto-Escuela et al., 2017). A_{2A}/D_2 heteromers involved in reward mechanisms reside in GABAergic neurons of the ventral striatopallidal area that are responsible for rewarding, motivational and seeking effects induced by cocaine, as well as by food (Wydra et al., 2013). However, both systemic treatment with an A_{2A} receptor antagonist and its direct injection into the NAc reduced relapse in heroin-addicted rats and prevented DA increases in the NAc shell induced by tetrahydrocannabinol (THC), but not those mediated by cocaine (Yao et al., 2006; Justinova et al., 2011). Furthermore, A_{2A} receptor antagonists alone may behave like psychostimulants by triggering cocaine-seeking behavior, thus decreasing their utility in the treatment of drug-dependence. Indeed, some findings on the addictive properties of A_{2A} receptor antagonists have reported that they substituted for cocaine in baboons (Weerts and Griffiths, 2003), also inducing conditioned place preference (Harper et al., 2006) and restored cocaine-seeking behaviors in rats (O'Neill et al., 2014). In addition, the blockade of A_{2A} receptors increased DA in the striatal network in cocaine-dependent subjects, which resulted in major

prefrontal cortex stimulation (Moeller et al., 2012). However, in rats trained to self-administer heroin, the administration of A_{2A} antagonists eliminated reinstatement (Yao et al., 2006), opening the possibility of using A_{2A} antagonists as therapeutic ligands in the management of abstinence in the addiction of some drugs. The effect of cocaine exposure in fetal brains and the modulation of DA and adenosine effects have also been addressed; specifically, from E8 to E14 embryonic days, cocaine treatment induced changes in DA and adenosine signaling which increased basal cAMP levels in the striatum and cerebral cortex. This effect could be reverted by blocking A_{2A} receptors (using SCH58261), suggesting that A_{2A} receptors could be considered good candidates as targets to treat prenatal cocaine exposure-related syndromes. Indeed, D_2 and A_{2A} receptors counterbalance each other's effects in the embryonic brain in a similar manner to what happens in the mature brain (Kubrusly and Bhide, 2010).

A_{2A} receptors, independent of their interaction with D_2 receptors in A_{2A}/D_2 heteromers, are also present in other complexes with $mGlu_5$ and CB_1 in striatal GABAergic neurons, as well as with A_1, $mGlu_5$, and CB_1 in striatal glutamatergic terminals (**Figure 2**), that may be involved in the modulation of reward, exerting an important role in the regulation of dopaminergic and glutamatergic effects in addiction (Kalivas and Volkow, 2011; Cahill et al., 2014; Zhang et al., 2014; Johnson and Lovinger, 2016). In this sense, the blockade of A_{2A} receptors increased cocaine-mediated locomotor effects through the activation of CB_1 receptors in rat striatum (Tozzi et al., 2012). It has also been demonstrated that an interaction between A_{2A} receptors and metabotropic glutamate 5 receptors ($mGlu_5$) in the striatum avoided METH-, but not cocaine-, induced hyperactivity and rewarding behavior, making a combined antagonism of A_{2A} and $mGlu_5$ receptors in the therapy of METH addiction possible (Wright et al., 2016). Accordingly, the influence of adenosine on glutamatergic transmission in the striatal region has been reported (Fuxe et al., 2008). Finally, it was reported that the functions and pharmacology of extra-striatal A_{2A} receptors must also be taken into account (Shen et al., 2008), although their function could not be totally extrapolated from the available data for striatal A_{2A} receptors. In this sense, the apparent controversial data obtained from pharmacological studies and genetic approaches using KO animals (presented in **Supplementary Tables S1**, **S2**) must be carefully exposed as the genetic background effects in A_{2A} KO animals may invalidate them as a model to study A_{2A} receptors (Filip et al., 2012). To conclude, the exploitation of the full potential of AR as drug targets will not only necessitate a full comprehension of AR-mediated mechanisms, but will also require the availability of ligands which let us distinguish among the different receptor populations discussed in this paper (Popoli and Pepponi, 2012).

MISUSE OF LEGAL PSYCHOSTIMULANTS

The consumption of legal psychostimulants has increased over recent years. For example, the misuse of prescribed psychostimulants, which are approved for the treatment of attention deficit hyperactivity disorder, for weight control or for the treatment of narcolepsy (Phillips et al., 2014), both by the patients themselves, and by non-affected individuals, based on misconceptions or simple lack of knowledge of the associated risks, is becoming more and more common nowadays (Lakhan and Kirchgessner, 2012; McHugh et al., 2015). This has been the case for methylphenidate consumption among college students as a study aid to enhance their academic performance (Maier et al., 2013; Webb et al., 2013; Vrecko, 2015). Although their use as a study aid is not the only reason why these substances are consumed (Drazdowski, 2016), this is one historically significant example, with reports of the use of amphetamines as study aids dating back to 1937 (Strohl, 2011).

In addition, caffeine, which is the most consumed psychoactive drug in the world, could also be of particular importance when addressing psychostimulant or drug addiction-related problems. Indeed, caffeine is commonly found as an adulterant in the preparation of illicit drugs (Prieto et al., 2016) and in energy drinks consumed in combination with alcohol or other psychostimulants (Reissig et al., 2009; Vanattou-Saïfoudine et al., 2012; Ferré, 2016). Interestingly, both acute and chronic adverse effects rise following concurrent consumption of caffeine and psychostimulant drugs. Specifically, caffeine worsens the psychostimulant's toxicity by increasing hyperthermia, cardiotoxicity, and seizures, as well as influencing the stimulatory, discriminative, and reinforcing effects of psychostimulant drugs. These effects have been investigated for the cases of MDMA and cocaine ingested with caffeine (Comer and Carroll, 1996; Kuzmin et al., 1999; Vanattou-Saïfoudine et al., 2012; Górska et al., 2017). The molecular mechanism underlying the action of caffeine is the antagonism of AR, with A_1 and A_{2A} subtypes the most involved. Indeed, it has been reported that caffeine induces increased DA release through A_1 receptor blockade (Okada et al., 1997). More recently, findings by Ferré (2016) attribute caffeine potentiation of the psychomotor activating and reinforcing effects of psychostimulants to the existence of A_{2A}/D_2 heteromers, where the antagonism of A_{2A} receptors by caffeine reverts the inhibitory brake exerted by adenosine on D_2 receptor signaling. Therefore, as ingestion of caffeine with cocaine and MDMA can significantly alter the drug-induced effects, understanding the molecular mechanisms underpinning this interaction will help to define correct approaches for the management of these side effects and toxicity.

CONCLUDING REMARKS AND FUTURE PROSPECTS

Although the A_{2A} receptor has been far more extensively studied (refer to **Supplementary Table S1** for summary), some papers considered in this review do highlight the role of A_1 receptor activation to modulate psychostimulant-mediated effects. The properties of A_1 agonists, mainly CPA, as anxiolytics have been previously reported in mice lacking A_1 receptors (Giménez-Llort et al., 2002), in animal models of cocaine or alcohol consumption (Prediger et al., 2006; Hobson et al., 2013; O'Neill et al., 2014),

and in classical behavioral studies (Jain et al., 1995). In this sense, electrophysiological studies in basolateral amygdala reported that application of CPA inhibits excitatory postsynaptic currents and glutamate release (Rau et al., 2014). This evidence, and the experiments reported in this review, will make A_1 receptor signaling an important target for the development of novel pharmacological treatments for the common anxiety-like disorders reported during the process of drug-seeking and withdrawal, and as such will produce lasting changes in relapse susceptibility.

Evidence for the role of A_{2A} receptors in psychostimulant-mediated effects seems to be somewhat contradictory between different pharmacological studies, experimental models tested (particularly self-administration vs. experimenter-administration) and genetic approaches using A_{2A} KO animals (refer to **Supplementary Table S2** for more detail). However, the overall analysis of the presented data indicates that excitatory modulation of GPCR heteroreceptor complexes, in this case A_{2A}/D_2 heteroreceptors using A_{2A} agonists, is a promising tool to counteract psychostimulant-induced effects. Indeed, a prominent role in the modulation of psychostimulant addiction attributed to adenosine is mediated through A_{2A} activation by complex mechanisms, affecting various aspects of this phenomenon including locomotor activity, discrimination, seeking behavior and reward.

In this review, we have discussed current scientific evidence mainly based on animal models of psychostimulant addiction, and suggested promising candidates in the search for pharmacological interventions. This is particularly important because, nowadays, the main treatments against psychostimulant addiction are focused on behavioral interventions (Phillips et al., 2014), while AR pharmacology could be a powerful weapon to modify the neurochemical alterations that occur during psychostimulant addiction. AR are widely distributed in the CNS where they mediate a myriad of functions and interact with other neurotransmitter systems, which provides an opportunity to modulate specific complex brain functions. In addition, selective ligands are available for the different AR subtypes, which increase the chances to achieve nuclei-specific modulation, representing a pharmacological opportunity to control addictive psychostimulant consumption and health-related problems. Certainly, identifying strategies to fully understand AR signaling in drug addiction may provide insight into the factors contributing to consumption/craving/relapse of abused psychostimulants, thus revealing novel therapeutic approaches. We suggest that efforts could be made in three main aspects of adenosine pharmacology affecting psychostimulant addiction. Firstly, we have stated in this review that there is broad experimental evidence that pharmacological stimulation of A_1 and A_{2A} receptors may counteract the effects induced by psychostimulants of abuse, but it is also important to highlight that approaches including a combination of AR drugs, like A_1/A_{2A} ligands, may help form a more robust strategy when AR are the basis of pharmacological interventions. Secondly, as stated in Section "Mechanisms of Adenosine Receptor-Mediated Pathways in Drug Addiction," due to the ability of AR to form homomers, heteromers and oligomers, it is mandatory to obtain specific ligands capable of discriminating among those different receptor populations. Thirdly, due to the lack of information concerning the effects consequent to alcohol and psychostimulant co-abuse, which is very common in drug addiction (Althobaiti and Sari, 2016; Barrett et al., 2016; Sánchez-López et al., 2017), it would be of particular interest to investigate the role of AR in those interactions.

AUTHOR CONTRIBUTIONS

CC developed the original idea. SG and CC designed the review. IB-Y and SG prepared the images. SG and CC prepared the tables. CC and SM edited and reviewed the final version of the article. All listed authors contributed to writing the article.

FUNDING

This work was supported by Universidad de Castilla-La Mancha (GI20174050).

ACKNOWLEDGMENTS

IB-Y and CC would like to thank Prof. Mario Durán (UCLM) and Prof. Emilio Ambrosio (UNED) for their generosity and kind advice.

SUPPLEMENTARY MATERIAL

The Supplementary Material for this article can be found online at: https://www.frontiersin.org/articles/10.3389/fphar.2017.00985/full#supplementary-material

TABLE S1 | The role of adenosine receptor (AR)'s ligands in psychostimulant-induced effects upon behavior and function. The most relevant animal studies on the interaction between adenosine and psychostimulants are shown. Arrows represent decrease (↓) and increase (↑). When adenosine ligands induced no effect, the symbol "≈" is used. Although PAP9704 and ginsenosides are not ligands of AR, the effects of those ligands are reported in this table as authors suggests that their biological effects are mediated by AR.

TABLE S2 | Genetic manipulation of AR in murine models and psychostimulant-induced effects. Genetic models derived from the manipulation of AR used to explore the interaction between adenosine and psychostimulants are shown. Arrows represent decrease (↓) and increase (↑). The symbol "≈" is used to indicate no difference between the genetic model and the wild-type animal (*Unless other comparison is stated).

TABLE S3 | Most relevant human clinical studies targeting AR. Ordered by publication date, most relevant clinical studies carried out in humans targeting the relationship between AR and psychostimulant addiction are shown. For each reference it is described the type of study, the number of subjects enrolled and its main objective and results. The number of the clinical trial is provided for the studies registered at ClinicalTrials.gov.

REFERENCES

Althobaiti, Y. S., and Sari, Y. (2016). Alcohol Interactions with psychostimulants: an overview of animal and human studies. *J. Addict. Res. Ther.* 7:281. doi: 10.4172/2155-6105.1000281

American Psychiatric Association (2013). *Diagnostic and Statistical Manual of Mental Disorders, DSM-5*, 5th Edn. Delhi: CBS Publishers & Distributors. doi: 10.1176/appi.books.9780890425596

Anker, J. J., and Carroll, M. E. (2011). Females are more vulnerable to drug abuse than males: evidence from preclinical studies and the role of ovarian hormones. *Curr. Top. Behav. Neurosci.* 8, 73–96. doi: 10.1007/7854_2010_93

Ashok, A. H., Mizuno, Y., Volkow, N. D., and Howes, O. D. (2017). Association of stimulant use with dopaminergic alterations in users of cocaine, amphetamine, or methamphetamine: a systematic review and meta-analysis. *JAMA Psychiatry* 74, 511–519. doi: 10.1001/jamapsychiatry.2017.0135

Bachtell, R. K., and Self, D. W. (2009). Effects of adenosine A2A receptor stimulation on cocaine-seeking behavior in rats. *Psychopharmacology* 206, 469–478. doi: 10.1007/s00213-009-1624-2

Bailey, A., Gianotti, R., Ho, A., and Kreek, M. J. (2005). Persistent upregulation of mu-opioid, but not adenosine, receptors in brains of long-term withdrawn escalating dose "binge" cocaine-treated rats. *Synapse* 57, 160–166. doi: 10.1002/syn.20168

Barrett, S. P., Jemcov, A., and Darredeau, C. (2016). Patterns and effects of alcohol and psychostimulant co-administration: a brief review of pharmacological considerations and subjective responses. *Curr. Addict. Rep.* 3, 138–143. doi: 10.1007/s40429-016-0080-4

Bastia, E., Xu, Y.-H., Scibelli, A. C., Day, Y.-J., Linden, J., Chen, J.-F., et al. (2005). A crucial role for forebrain adenosine A(2A) receptors in amphetamine sensitization. *Neuropsychopharmacology* 30, 891–900. doi: 10.1038/sj.npp.1300630

Baumann, M. H., Clark, R. D., Budzynski, A. G., Partilla, J. S., Blough, B. E., and Rothman, R. B. (2005). N-substituted piperazines abused by humans mimic the molecular mechanism of 3,4-methylenedioxymethamphetamine (MDMA, or 'Ecstasy'). *Neuropsychopharmacology* 30, 550–560. doi: 10.1038/sj.npp.1300585

Becker, J. B., and Koob, G. F. (2016). Sex differences in animal models: focus on addiction. *Pharmacol. Rev.* 68, 242–263. doi: 10.1124/pr.115.011163

Björklund, O., Halldner-Henriksson, L., Yang, J., Eriksson, T. M., Jacobson, M. A., Daré, E., et al. (2008). Decreased behavioral activation following caffeine, amphetamine and darkness in A3 adenosine receptor knock-out mice. *Physiol. Behav.* 95, 668–676. doi: 10.1016/j.physbeh.2008.09.018

Bobzean, S. A. M., DeNobrega, A. K., and Perrotti, L. I. (2014). Sex differences in the neurobiology of drug addiction. *Exp. Neurol.* 259, 64–74. doi: 10.1016/j.expneurol.2014.01.022

Bonaventura, J., Navarro, G., Casadó-Anguera, V., Azdad, K., Rea, W., Moreno, E., et al. (2015). Allosteric interactions between agonists and antagonists within the adenosine A2A receptor-dopamine D2 receptor heterotetramer. *Proc. Natl. Acad. Sci. U.S.A.* 112, E3609–E3618. doi: 10.1073/pnas.1507704112

Bonci, A., and Williams, J. T. (1996). A common mechanism mediates long-term changes in synaptic transmission after chronic cocaine and morphine. *Neuron* 16, 631–639. doi: 10.1016/S0896-6273(00)80082-3

Borea, P. A., Gessi, S., Merighi, S., and Varani, K. (2016). Adenosine as a multi-signalling guardian angel in human diseases: when, where and how does it exert its protective effects? *Trends Pharmacol. Sci.* 37, 419–434. doi: 10.1016/j.tips.2016.02.006

Borea, P. A., Varani, K., Vincenzi, F., Baraldi, P. G., Tabrizi, M. A., Merighi, S., et al. (2015). The A3 adenosine receptor: history and perspectives. *Pharmacol. Rev.* 67, 74–102. doi: 10.1124/pr.113.008540

Borroto-Escuela, D. O., Carlsson, J., Ambrogini, P., Narváez, M., Wydra, K., Tarakanov, A. O., et al. (2017). Understanding the role of GPCR heteroreceptor complexes in modulating the brain networks in health and disease. *Front. Cell. Neurosci.* 11:37. doi: 10.3389/fncel.2017.00037

Brown, R. M., and Short, J. L. (2008). Adenosine A(2A) receptors and their role in drug addiction. *J. Pharm. Pharmacol.* 60, 1409–1430. doi: 10.1211/jpp/60.11.0001

Burnstock, G. (2017). Purinergic signalling: therapeutic developments. *Front. Pharmacol.* 8:661. doi: 10.3389/fphar.2017.00661

Cabello, N., Gandía, J., Bertarelli, D. C. G., Watanabe, M., Lluís, C., Franco, R., et al. (2009). Metabotropic glutamate type 5, dopamine D2 and adenosine A2a receptors form higher-order oligomers in living cells. *J. Neurochem.* 109, 1497–1507. doi: 10.1111/j.1471-4159.2009.06078.x

Cahill, E., Salery, M., Vanhoutte, P., and Caboche, J. (2014). Convergence of dopamine and glutamate signaling onto striatal ERK activation in response to drugs of abuse. *Front. Pharmacol.* 4:172. doi: 10.3389/fphar.2013.00172

Carpenter, B., Nehmé, R., Warne, T., Leslie, A. G. W., and Tate, C. G. (2016). Structure of the adenosine A(2A) receptor bound to an engineered G protein. *Nature* 536, 104–107. doi: 10.1038/nature18966

Casadó, V., Cortés, A., Mallol, J., Pérez-Capote, K., Ferré, S., Lluis, C., et al. (2009). GPCR homomers and heteromers: a better choice as targets for drug development than GPCR monomers? *Pharmacol. Ther.* 124, 248–257. doi: 10.1016/j.pharmthera.2009.07.005

Chen, J. F., Beilstein, M., Xu, Y. H., Turner, T. J., Moratalla, R., Standaert, D. G., et al. (2000). Selective attenuation of psychostimulant-induced behavioral responses in mice lacking A(2A) adenosine receptors. *Neuroscience* 97, 195–204. doi: 10.1016/S0306-4522(99)00604-1

Chen, J.-F., Eltzschig, H. K., and Fredholm, B. B. (2013). Adenosine receptors as drug targets–what are the challenges? *Nat. Rev. Drug Discov.* 12, 265–286. doi: 10.1038/nrd3955

Chen, J.-F., Moratalla, R., Yu, L., Martin, A. B., Xu, K., Bastia, E., et al. (2003). Inactivation of adenosine A2A receptors selectively attenuates amphetamine-induced behavioral sensitization. *Neuropsychopharmacology* 28, 1086–1095. doi: 10.1038/sj.npp.1300152

Chesworth, R., Brown, R. M., Kim, J. H., Ledent, C., and Lawrence, A. J. (2016). Adenosine 2A receptors modulate reward behaviours for methamphetamine. *Addict. Biol.* 21, 407–421. doi: 10.1111/adb.12225

Childs, E., Hohoff, C., Deckert, J., Xu, K., Badner, J., and de Wit, H. (2008). Association between ADORA2A and DRD2 polymorphisms and caffeine-induced anxiety. *Neuropsychopharmacology* 33, 2791–2800. doi: 10.1038/npp.2008.17

Ciancetta, A., and Jacobson, K. A. (2017). Structural probing and molecular modeling of the A3 adenosine receptor: a focus on agonist binding. *Molecules* 22:E449. doi: 10.3390/molecules22030449

Clark, M., and Dar, M. S. (1989). Effect of acute ethanol on release of endogenous adenosine from rat cerebellar synaptosomes. *J. Neurochem.* 52, 1859–1865. doi: 10.1111/j.1471-4159.1989.tb07268.x

Comer, S. D., and Carroll, M. E. (1996). Oral caffeine pretreatment produced modest increases in smoked cocaine self-administration in rhesus monkeys. *Psychopharmacology* 126, 281–285. doi: 10.1007/BF02247378

Cooper, J. R., Bloom, F. E., and Roth, R. H. (1996). *The Biochemical Basis of Neuropharmacology*, 7th Edn. New York, NY: Oxford University Press.

Cunha, R. A. (2005). Neuroprotection by adenosine in the brain: from A(1) receptor activation to A (2A) receptor blockade. *Purinergic Signal.* 1, 111–134. doi: 10.1007/s11302-005-0649-1

Cunha, R. A., Ferré, S., Vaugeois, J.-M., and Chen, J.-F. (2008). Potential therapeutic interest of adenosine A2A receptors in psychiatric disorders. *Curr. Pharm. Des.* 14, 1512–1524. doi: 10.2174/138161208784480090

de Lera Ruiz, M., Lim, Y.-H., and Zheng, J. (2014). Adenosine A2A receptor as a drug discovery target. *J. Med. Chem.* 57, 3623–3650. doi: 10.1021/jm4011669

Delle Donne, K. T., and Sonsalla, P. K. (1994). Protection against methamphetamine-induced neurotoxicity to neostriatal dopaminergic neurons by adenosine receptor activation. *J. Pharmacol. Exp. Ther.* 271, 1320–1326.

DeVito, E. E., Babuscio, T. A., Nich, C., Ball, S. A., and Carroll, K. M. (2014). Gender differences in clinical outcomes for cocaine dependence: randomized clinical trials of behavioral therapy and disulfiram. *Drug Alcohol Depend.* 145, 156–167. doi: 10.1016/j.drugalcdep.2014.10.007

Dluzen, D. E., and Liu, B. (2008). Gender differences in methamphetamine use and responses: a review. *Gend. Med.* 5, 24–35. doi: 10.1016/S1550-8579(08)80005-8

Domschke, K., Gajewska, A., Winter, B., Herrmann, M. J., Warrings, B., Mühlberger, A., et al. (2012). ADORA2A Gene variation, caffeine, and emotional processing: a multi-level interaction on startle reflex. *Neuropsychopharmacology* 37, 759–769. doi: 10.1038/npp.2011.253

Doyle, S. E., Breslin, F. J., Rieger, J. M., Beauglehole, A., and Lynch, W. J. (2012). Time and sex-dependent effects of an adenosine A2A/A1 receptor antagonist on motivation to self-administer cocaine in rats. *Pharmacol. Biochem. Behav.* 102, 257–263. doi: 10.1016/j.pbb.2012.05.001

Drazdowski, T. K. (2016). A systematic review of the motivations for the non-medical use of prescription drugs in young adults. *Drug Alcohol Depend.* 162, 3–25. doi: 10.1016/j.drugalcdep.2016.01.011

Drury, A. N., and Szent-Györgyi, A. (1929). The physiological activity of adenine compounds with especial reference to their action upon the mammalian heart. *J. Physiol.* 68, 213–237. doi: 10.1113/jphysiol.1929.sp002608

Dunwiddie, T. V. (1985). The physiological role of adenosine in the central nervous system. *Int. Rev. Neurobiol.* 27, 63–139. doi: 10.1016/S0074-7742(08)60556-5

Engmann, O., Giralt, A., Gervasi, N., Marion-Poll, L., Gasmi, L., Filhol, O., et al. (2015). DARPP-32 interaction with adducin may mediate rapid environmental effects on striatal neurons. *Nat. Commun.* 6:10099. doi: 10.1038/ncomms10099

European Monitoring Centre for Drugs and Drug Addiction (2017). *European Drug Report 2017: Trends and Developments*. Luxembourg: Publications Office of the European Union.

Ferraro, L., Frankowska, M., Marcellino, D., Zaniewska, M., Beggiato, S., Filip, M., et al. (2012). A novel mechanism of cocaine to enhance dopamine d2-like receptor mediated neurochemical and behavioral effects. An in vivo and in vitro study. *Neuropsychopharmacology* 37, 1856–1866. doi: 10.1038/npp.2012.33

Ferré, S. (2008). An update on the mechanisms of the psychostimulant effects of caffeine. *J. Neurochem.* 105, 1067–1079. doi: 10.1111/j.1471-4159.2007.05196.x

Ferré, S. (2016). Mechanisms of the psychostimulant effects of caffeine: implications for substance use disorders. *Psychopharmacology* 233, 1963–1979. doi: 10.1007/s00213-016-4212-2

Ferré, S., Ciruela, F., Borycz, J., Solinas, M., Quarta, D., Antoniou, K., et al. (2008a). Adenosine A1-A2A receptor heteromers: new targets for caffeine in the brain. *Front. Biosci.* 13, 2391–2399.

Ferré, S., Diamond, I., Goldberg, S. R., Yao, L., Hourani, S. M. O., Huang, Z. L., et al. (2007). Adenosine A2A receptors in ventral striatum, hypothalamus and nociceptive circuitry. Implications for drug addiction, sleep and pain. *Prog. Neurobiol.* 83, 332–347. doi: 10.1016/j.pneurobio.2007.04.002

Ferré, S., Fredholm, B. B., Morelli, M., Popoli, P., and Fuxe, K. (1997). Adenosine-dopamine receptor-receptor interactions as an integrative mechanism in the basal ganglia. *Trends Neurosci.* 20, 482–487. doi: 10.1016/S0166-2236(97)01096-5

Ferré, S., Karcz-Kubicha, M., Hope, B. T., Popoli, P., Burgueño, J., Gutiérrez, M. A., et al. (2002). Synergistic interaction between adenosine A2A and glutamate mGlu5 receptors: implications for striatal neuronal function. *Proc. Natl. Acad. Sci. U.S.A.* 99, 11940–11945. doi: 10.1073/pnas.172393799

Ferré, S., O'Connor, W. T., Snaprud, P., Ungerstedt, U., and Fuxe, K. (1994). Antagonistic interaction between adenosine A2A receptors and dopamine D2 receptors in the ventral striopallidal system. Implications for the treatment of schizophrenia. *Neuroscience* 63, 765–773. doi: 10.1016/0306-4522(94)90521-5

Ferré, S., Quiroz, C., Woods, A. S., Cunha, R., Popoli, P., Ciruela, F., et al. (2008b). An update on adenosine A2A-dopamine D2 receptor interactions: implications for the function of G protein-coupled receptors. *Curr. Pharm. Des.* 14, 1468–1474.

Ferré, S., von Euler, G., Johansson, B., Fredholm, B. B., and Fuxe, K. (1991). Stimulation of high-affinity adenosine A2 receptors decreases the affinity of dopamine D2 receptors in rat striatal membranes. *Proc. Natl. Acad. Sci. U.S.A.* 88, 7238–7241. doi: 10.1073/pnas.88.16.7238

Filip, M., Frankowska, M., Zaniewska, M., Przegaliński, E., Müller, C. E., Agnati, L., et al. (2006). Involvement of adenosine A2A and dopamine receptors in the locomotor and sensitizing effects of cocaine. *Brain Res.* 1077, 67–80. doi: 10.1016/j.brainres.2006.01.038

Filip, M., Zaniewska, M., Frankowska, M., Wydra, K., and Fuxe, K. (2012). The importance of the adenosine A2A receptor-dopamine D(2) receptor interaction in drug addiction. *Curr. Med. Chem.* 19, 317–355. doi: 10.2174/092986712803414231

Franco, R., Martínez-Pinilla, E., Ricobaraza, A., and McCormick, P. J. (2013). Challenges in the development of heteromer-GPCR-based drugs. *Prog. Mol. Biol. Transl. Sci.* 117, 143–162. doi: 10.1016/B978-0-12-386931-9.00006-4

Frankowska, M., Marcellino, D., Adamczyk, P., Filip, M., and Fuxe, K. (2013). Effects of cocaine self-administration and extinction on D2 -like and A2A receptor recognition and D2 -like/Gi protein coupling in rat striatum. *Addict. Biol.* 18, 455–466. doi: 10.1111/j.1369-1600.2012.00452.x

Fredholm, B. B., Arslan, G., Halldner, L., Kull, B., Schulte, G., and Wasserman, W. (2000). Structure and function of adenosine receptors and their genes. *Naunyn Schmiedebergs Arch. Pharmacol.* 362, 364–374.

Fredholm, B. B., IJzerman, A. P., Jacobson, K. A., Klotz, K. N., and Linden, J. (2001). International union of pharmacology. XXV. Nomenclature and classification of adenosine receptors. *Pharmacol. Rev.* 53, 527–552.

Fuxe, K., Agnati, L. F., Jacobsen, K., Hillion, J., Canals, M., Torvinen, M., et al. (2003). Receptor heteromerization in adenosine A2A receptor signaling: relevance for striatal function and Parkinson's disease. *Neurology* 61, S19–S23. doi: 10.1212/01.WNL.0000095206.44418.5C

Fuxe, K., Ferré, S., Genedani, S., Franco, R., and Agnati, L. F. (2007a). Adenosine receptor-dopamine receptor interactions in the basal ganglia and their relevance for brain function. *Physiol. Behav.* 92, 210–217. doi: 10.1016/j.physbeh.2007.05.034

Fuxe, K., Marcellino, D., Borroto-Escuela, D. O., Guescini, M., Fernández-Dueñas, V., Tanganelli, S., et al. (2010). Adenosine-dopamine interactions in the pathophysiology and treatment of CNS disorders. *CNS Neurosci. Ther.* 16, e18–e42. doi: 10.1111/j.1755-5949.2009.00126.x

Fuxe, K., Marcellino, D., Genedani, S., and Agnati, L. (2007b). Adenosine A(2A) receptors, dopamine D(2) receptors and their interactions in Parkinson's disease. *Mov. Disord.* 22, 1990–2017. doi: 10.1002/mds.21440

Fuxe, K., Marcellino, D., Rivera, A., Diaz-Cabiale, Z., Filip, M., Gago, B., et al. (2008). Receptor-receptor interactions within receptor mosaics. Impact on neuropsychopharmacology. *Brain Res. Rev.* 58, 415–452. doi: 10.1016/j.brainresrev.2007.11.007

Gajewska, A., Blumenthal, T. D., Winter, B., Herrmann, M. J., Conzelmann, A., Mühlberger, A., et al. (2013). Effects of ADORA2A gene variation and caffeine on prepulse inhibition: a multi-level risk model of anxiety. *Prog. Neuropsychopharmacol. Biol. Psychiatry* 40, 115–121. doi: 10.1016/j.pnpbp.2012.08.008

GBD 2015 Risk Factors Collaborators (2016). Global, regional, and national comparative risk assessment of 79 behavioural, environmental and occupational, and metabolic risks or clusters of risks, 1990-2015: a systematic analysis for the Global Burden of Disease Study 2015. *Lancet* 388, 1659–1724. doi: 10.1016/S0140-6736(16)31679-8

Gessi, S., Merighi, S., Fazzi, D., Stefanelli, A., Varani, K., and Borea, P. A. (2011). Adenosine receptor targeting in health and disease. *Expert Opin. Investig. Drugs* 20, 1591–1609. doi: 10.1517/13543784.2011.627853

Gessi, S., Merighi, S., Stefanelli, A., Fazzi, D., Varani, K., and Borea, P. A. (2013). A(1) and A(3) adenosine receptors inhibit LPS-induced hypoxia-inducible factor-1 accumulation in murine astrocytes. *Pharmacol. Res.* 76, 157–170. doi: 10.1016/j.phrs.2013.08.002

Giménez-Llort, L., Fernández-Teruel, A., Escorihuela, R. M., Fredholm, B. B., Tobeña, A., Pekny, M., et al. (2002). Mice lacking the adenosine A1 receptor are anxious and aggressive, but are normal learners with reduced muscle strength and survival rate. *Eur. J. Neurosci.* 16, 547–550. doi: 10.1046/j.1460-9568.2002.02122.x

Ginés, S., Hillion, J., Torvinen, M., Le Crom, S., Casadó, V., Canela, E. I., et al. (2000). Dopamine D1 and adenosine A1 receptors form functionally interacting heteromeric complexes. *Proc. Natl. Acad. Sci. U.S.A.* 97, 8606–8611. doi: 10.1073/pnas.150241097

Glukhova, A., Thal, D. M., Nguyen, A. T., Vecchio, E. A., Jörg, M., Scammells, P. J., et al. (2017). Structure of the adenosine A1 receptor reveals the basis for subtype selectivity. *Cell* 168, 867.e13–877.e13. doi: 10.1016/j.cell.2017.01.042

Godinho, R. O., Duarte, T., and Pacini, E. S. A. (2015). New perspectives in signaling mediated by receptors coupled to stimulatory G protein: the emerging significance of cAMP efflux and extracellular cAMP-adenosine pathway. *Front. Pharmacol.* 6:58. doi: 10.3389/fphar.2015.00058

Gołembiowska, K., and Zylewska, A. (1998a). Agonists of A1 and A2A adenosine receptors attenuate methamphetamine-induced overflow of dopamine in rat striatum. *Brain Res.* 806, 202–209.

Gołembiowska, K., and Zylewska, A. (1998b). N6-2-(4-aminophenyl) ethyladenosine (APNEA), a putative adenosine A3 receptor agonist, enhances methamphetamine-induced dopamine outflow in rat striatum. *Pol. J. Pharmacol.* 50, 299–305.

Gomes, C. V., Kaster, M. P., Tomé, A. R., Agostinho, P. M., and Cunha, R. A. (2011). Adenosine receptors and brain diseases: neuroprotection and neurodegeneration. *Biochim. Biophys. Acta* 1808, 1380–1399. doi: 10.1016/j.bbamem.2010.12.001

Goodwin, J. S., Larson, G. A., Swant, J., Sen, N., Javitch, J. A., Zahniser, N. R., et al. (2009). Amphetamine and methamphetamine differentially affect dopamine transporters in vitro and in vivo. *J. Biol. Chem.* 284, 2978–2989. doi: 10.1074/jbc.M805298200

Górska, A. M., and Gołembiowska, K. (2015). The role of adenosine A1 and A2A receptors in the caffeine effect on MDMA-induced DA and 5-HT release in the mouse striatum. *Neurotox. Res.* 27, 229–245. doi: 10.1007/s12640-014-9501-0

Górska, A. M., Kamińska, K., Wawrzczak-Bargieła, A., Costa, G., Morelli, M., Przewłocki, R., et al. (2017). Neurochemical and neurotoxic effects of MDMA (ecstasy) and caffeine after chronic combined administration in mice. *Neurotox. Res.* doi: 10.1007/s12640-017-9831-9 [Epub ahead of print].

Hack, S. P., and Christie, M. J. (2003). Adaptations in adenosine signaling in drug dependence: therapeutic implications. *Crit. Rev. Neurobiol.* 15, 235–274. doi: 10.1615/CritRevNeurobiol.v15.i34.30

Harper, L. K., Beckett, S. R., Marsden, C. A., McCreary, A. C., and Alexander, S. P. H. (2006). Effects of the A 2A adenosine receptor antagonist KW6002 in the nucleus accumbens in vitro and in vivo. *Pharmacol. Biochem. Behav.* 83, 114–121. doi: 10.1016/j.pbb.2005.12.014

Hart, A. B., de Wit, H., and Palmer, A. A. (2013). Candidate gene studies of a promising intermediate phenotype: failure to replicate. *Neuropsychopharmacology* 38, 802–816. doi: 10.1038/npp.2012.245

Hasin, D. S., O'Brien, C. P., Auriacombe, M., Borges, G., Bucholz, K., Budney, A., et al. (2013). DSM-5 criteria for substance use disorders: recommendations and rationale. *Am. J. Psychiatry* 170, 834–851. doi: 10.1176/appi.ajp.2013.12060782

Hatsukami, D. K., and Fischman, M. W. (1996). Crack cocaine and cocaine hydrochloride: are the differences myth or reality? *JAMA* 276, 1580–1588. doi: 10.1001/jama.1996.03540190052029

Heffner, T. G., Wiley, J. N., Williams, A. E., Bruns, R. F., Coughenour, L. L., and Downs, D. A. (1989). Comparison of the behavioral effects of adenosine agonists and dopamine antagonists in mice. *Psychopharmacology* 98, 31–37. doi: 10.1007/BF00442002

Hervé, D., Le Moine, C., Corvol, J. C., Belluscio, L., Ledent, C., Fienberg, A. A., et al. (2001). Galpha(olf) levels are regulated by receptor usage and control dopamine and adenosine action in the striatum. *J. Neurosci.* 21, 4390–4399.

Hillion, J., Canals, M., Torvinen, M., Casado, V., Scott, R., Terasmaa, A., et al. (2002). Coaggregation, cointernalization, and codesensitization of adenosine A2A receptors and dopamine D2 receptors. *J. Biol. Chem.* 277, 18091–18097. doi: 10.1074/jbc.M107731200

Hobson, B. D., Merritt, K. E., and Bachtell, R. K. (2012). Stimulation of adenosine receptors in the nucleus accumbens reverses the expression of cocaine sensitization and cross-sensitization to dopamine D2 receptors in rats. *Neuropharmacology* 63, 1172–1181. doi: 10.1016/j.neuropharm.2012.06.038

Hobson, B. D., O'Neill, C. E., Levis, S. C., Monteggia, L. M., Neve, R. L., Self, D. W., et al. (2013). Adenosine A1 and dopamine d1 receptor regulation of AMPA receptor phosphorylation and cocaine-seeking behavior. *Neuropsychopharmacology* 38, 1974–1983. doi: 10.1038/npp.2013.96

Hohoff, C., McDonald, J. M., Baune, B. T., Cook, E. H., Deckert, J., and de Wit, H. (2005). Interindividual variation in anxiety response to amphetamine: possible role for adenosine A2A receptor gene variants. *Am. J. Med. Genet. B Neuropsychiatr. Genet.* 139B, 42–44. doi: 10.1002/ajmg.b.30228

Jaakola, V.-P., Griffith, M. T., Hanson, M. A., Cherezov, V., Chien, E. Y. T., Lane, J. R., et al. (2008). The 2.6 angstrom crystal structure of a human A2A adenosine receptor bound to an antagonist. *Science* 322, 1211–1217. doi: 10.1126/science.1164772

Jacobson, K. A., Merighi, S., Varani, K., Borea, P. A., Baraldi, S., Aghazadeh Tabrizi, M., et al. (2017). A3 adenosine receptors as modulators of inflammation: from medicinal chemistry to therapy. *Med. Res. Rev.* doi: 10.1002/med.21456 [Epub ahead of print].

Jain, N., Kemp, N., Adeyemo, O., Buchanan, P., and Stone, T. W. (1995). Anxiolytic activity of adenosine receptor activation in mice. *Br. J. Pharmacol.* 116, 2127–2133. doi: 10.1111/j.1476-5381.1995.tb16421.x

Janać, B., Pesić, V., Peković, S., Rakić, L., and Stojiljković, M. (2005). Different effects of adenosine A1 agonist ribavirin on amphetamine-induced total locomotor and stereotypic activities in rats. *Ann. N. Y. Acad. Sci.* 1048, 396–399. doi: 10.1196/annals.1342.048

Janes, K., Esposito, E., Doyle, T., Cuzzocrea, S., Tosh, D. K., Jacobson, K. A., et al. (2014). A3 adenosine receptor agonist prevents the development of paclitaxel-induced neuropathic pain by modulating spinal glial-restricted redox-dependent signaling pathways. *Pain* 155, 2560–2567. doi: 10.1016/j.pain.2014.09.016

Jastrzêbska, J., Nowak, E., Smaga, I., Bystrowska, B., Frankowska, M., Bader, M., et al. (2014). Adenosine (A)(2A)receptor modulation of nicotine-induced locomotor sensitization. A pharmacological and transgenic approach. *Neuropharmacology* 81, 318–326. doi: 10.1016/j.neuropharm.2014.03.002

Johanson, C. E., and Fischman, M. W. (1989). The pharmacology of cocaine related to its abuse. *Pharmacol. Rev.* 41, 3–52.

Johnson, K. A., and Lovinger, D. M. (2016). Presynaptic G protein-coupled receptors: gatekeepers of addiction? *Front. Cell. Neurosci.* 10:264. doi: 10.3389/fncel.2016.00264

Justinova, Z., Ferré, S., Redhi, G. H., Mascia, P., Stroik, J., Quarta, D., et al. (2011). Reinforcing and neurochemical effects of cannabinoid CB1 receptor agonists, but not cocaine, are altered by an adenosine A2A receptor antagonist. *Addict. Biol.* 16, 405–415. doi: 10.1111/j.1369-1600.2010.00258.x

Justinova, Z., Ferré, S., Segal, P. N., Antoniou, K., Solinas, M., Pappas, L. A., et al. (2003). Involvement of adenosine A1 and A2A receptors in the adenosinergic modulation of the discriminative-stimulus effects of cocaine and methamphetamine in rats. *J. Pharmacol. Exp. Ther.* 307, 977–986. doi: 10.1124/jpet.103.056762

Kalivas, P. W., and Volkow, N. D. (2011). New medications for drug addiction hiding in glutamatergic neuroplasticity. *Mol. Psychiatry* 16, 974–986. doi: 10.1038/mp.2011.46

Kavanagh, K. A., Schreiner, D. C., Levis, S. C., O'Neill, C. E., and Bachtell, R. K. (2015). Role of adenosine receptor subtypes in methamphetamine reward and reinforcement. *Neuropharmacology* 89, 265–273. doi: 10.1016/j.neuropharm.2014.09.030

Kelley, A. E., and Berridge, K. C. (2002). The neuroscience of natural rewards: relevance to addictive drugs. *J. Neurosci.* 22, 3306–3311.

Kennedy, A. P., Epstein, D. H., Phillips, K. A., and Preston, K. L. (2013). Sex differences in cocaine/heroin users: drug-use triggers and craving in daily life. *Drug Alcohol Depend.* 132, 29–37. doi: 10.1016/j.drugalcdep.2012.12.025

Kermanian, F., Mehdizadeh, M., Soleimani, M., Ebrahimzadeh Bideskan, A. R., Asadi-Shekaari, M., Kheradmand, H., et al. (2012). The role of adenosine receptor agonist and antagonist on Hippocampal MDMA detrimental effects; a structural and behavioral study. *Metab. Brain Dis.* 27, 459–469. doi: 10.1007/s11011-012-9334-6

Kermanian, F., Soleimani, M., Ebrahimzadeh, A., Haghir, H., and Mehdizadeh, M. (2013). Effects of adenosine A2a receptor agonist and antagonist on hippocampal nuclear factor-kB expression preceded by MDMA toxicity. *Metab. Brain Dis.* 28, 45–52. doi: 10.1007/s11011-012-9366-y

Kerstetter, K. A., Aguilar, V. R., Parrish, A. B., and Kippin, T. E. (2008). Protracted time-dependent increases in cocaine-seeking behavior during cocaine withdrawal in female relative to male rats. *Psychopharmacology* 198, 63–75. doi: 10.1007/s00213-008-1089-8

Kim, H. J., Lee, J. H., Yun, K., and Kim, J.-H. (2017). Alterations in striatal circuits underlying addiction-like behaviors. *Mol. Cells* 40, 379–385. doi: 10.14348/molcells.2017.0088

Knapp, C. M., Foye, M. M., Cottam, N., Ciraulo, D. A., and Kornetsky, C. (2001). Adenosine agonists CGS 21680 and NECA inhibit the initiation of cocaine self-administration. *Pharmacol. Biochem. Behav.* 68, 797–803. doi: 10.1016/S0091-3057(01)00486-5

Kniazeff, J., Prézeau, L., Rondard, P., Pin, J.-P., and Goudet, C. (2011). Dimers and beyond: the functional puzzles of class C GPCRs. *Pharmacol. Ther.* 130, 9–25. doi: 10.1016/j.pharmthera.2011.01.006

Kobayashi, H., Ujike, H., Iwata, N., Inada, T., Yamada, M., Sekine, Y., et al. (2010). The adenosine A2A receptor is associated with methamphetamine dependence/psychosis in the Japanese population. *Behav. Brain Funct.* 6:50. doi: 10.1186/1744-9081-6-50

Kobayashi, H., Ujike, H., Iwata, N., Inada, T., Yamada, M., Sekine, Y., et al. (2011). Association analysis of the adenosine A1 receptor gene

polymorphisms in patients with methamphetamine dependence/psychosis. *Curr. Neuropharmacol.* 9, 137–142. doi: 10.2174/157015911795016958

Koob, G. F., and Volkow, N. D. (2010). Neurocircuitry of addiction. *Neuropsychopharmacology* 35, 217–238. doi: 10.1038/npp.2009.110

Krauss, S. W., Ghirnikar, R. B., Diamond, I., and Gordon, A. S. (1993). Inhibition of adenosine uptake by ethanol is specific for one class of nucleoside transporters. *Mol. Pharmacol.* 44, 1021–1026.

Kubrusly, R. C. C., and Bhide, P. G. (2010). Cocaine exposure modulates dopamine and adenosine signaling in the fetal brain. *Neuropharmacology* 58, 436–443. doi: 10.1016/j.neuropharm.2009.09.007

Kull, B., Svenningsson, P., and Fredholm, B. B. (2000). Adenosine A(2A) receptors are colocalized with and activate g(olf) in rat striatum. *Mol. Pharmacol.* 58, 771–777.

Kuzmin, A., Johansson, B., Zvartau, E. E., and Fredholm, B. B. (1999). Caffeine, acting on adenosine A(1) receptors, prevents the extinction of cocaine-seeking behavior in mice. *J. Pharmacol. Exp. Ther.* 290, 535–542.

Kwon, Y. S., Nabeshima, T., Shin, E.-J., Chun, W., Jhoo, J. H., Jhoo, W.-K., et al. (2004). PAP 9704, a Korean herbal medicine attenuates methamphetamine-induced hyperlocomotion via adenosine A2A receptor stimulation in mice. *Biol. Pharm. Bull.* 27, 906–909. doi: 10.1248/bpb.27.906

Lakhan, S. E., and Kirchgessner, A. (2012). Prescription stimulants in individuals with and without attention deficit hyperactivity disorder: misuse, cognitive impact, and adverse effects. *Brain Behav.* 2, 661–677. doi: 10.1002/brb3.78

Lane, S., Green, C., Steinberg, J., Ma, L., Schmitz, J., Rathnayaka, N., et al. (2012). Cardiovascular and subjective effects of the novel adenosine A(2A) receptor antagonist SYN115 in cocaine dependent individuals. *J. Addict. Res. Ther.* S1:009. doi: 10.4172/2155-6105.S1-009

Lane, S. D., Green, C. E., Schmitz, J. M., Rathnayaka, N., Fang, W. B., Ferré, S., et al. (2014). Comparison of caffeine and d-amphetamine in cocaine-dependent subjects: differential outcomes on subjective and cardiovascular effects, reward learning, and salivary paraxanthine. *J. Addict. Res. Ther.* 5:176. doi: 10.4172/2155-6105.1000176

Lebon, G., Warne, T., Edwards, P. C., Bennett, K., Langmead, C. J., Leslie, A. G. W., et al. (2011). Agonist-bound adenosine A2A receptor structures reveal common features of GPCR activation. *Nature* 474, 521–525. doi: 10.1038/nature10136

Ledent, C., Vaugeois, J. M., Schiffmann, S. N., Pedrazzini, T., El Yacoubi, M., Vanderhaeghen, J. J., et al. (1997). Aggressiveness, hypoalgesia and high blood pressure in mice lacking the adenosine A2a receptor. *Nature* 388, 674–678. doi: 10.1038/41771

Lev-Ran, S., Le Strat, Y., Imtiaz, S., Rehm, J., and Le Foll, B. (2013). Gender differences in prevalence of substance use disorders among individuals with lifetime exposure to substances: results from a large representative sample. *Am. J. Addict.* 22, 7–13. doi: 10.1111/j.1521-0391.2013.00321.x

Linden, J. (2001). Molecular approach to adenosine receptors: receptor-mediated mechanisms of tissue protection. *Annu. Rev. Pharmacol. Toxicol.* 41, 775–787. doi: 10.1146/annurev.pharmtox.41.1.775

Lobo, M. (2009). Molecular profiling of striatonigral and striatopallidal medium spiny neurons past, present, and future. *Int. Rev. Neurobiol.* 89, 1–35. doi: 10.1016/S0074-7742(09)89001-6

Lopes, L. V., Sebastião, A. M., and Ribeiro, J. A. (2011). Adenosine and related drugs in brain diseases: present and future in clinical trials. *Curr. Top. Med. Chem.* 11, 1087–1101. doi: 10.2174/156802611795347591

López-Arnau, R., Luján, M. A., Duart-Castells, L., Pubill, D., Camarasa, J., Valverde, O., et al. (2017). Exposure of adolescent mice to 3,4-methylenedioxypyrovalerone increases the psychostimulant, rewarding and reinforcing effects of cocaine in adulthood. *Br. J. Pharmacol.* 174, 1161–1173. doi: 10.1111/bph.13771

Łukasiewicz, S., Błasiak, E., Faron-Górecka, A., Polit, A., Tworzydło, M., Górecki, A., et al. (2007). Fluorescence studies of homooligomerization of adenosine A2A and serotonin 5-HT1A receptors reveal the specificity of receptor interactions in the plasma membrane. *Pharmacol. Rep.* 59, 379–392.

Lynch, W. J. (2006). Sex differences in vulnerability to drug self-administration. *Exp. Clin. Psychopharmacol.* 14, 34–41. doi: 10.1037/1064-1297.14.1.34

Lynch, W. J. (2017). Modeling the development of drug addiction in male and female animals. *Pharmacol. Biochem. Behav.* doi: 10.1016/j.pbb.2017.06.006 [Epub ahead of print].

Lynch, W. J., and Taylor, J. R. (2004). Sex differences in the behavioral effects of 24-h/day access to cocaine under a discrete trial procedure. *Neuropsychopharmacology* 29, 943–951. doi: 10.1038/sj.npp.1300389

Maier, L. J., Liechti, M. E., Herzig, F., and Schaub, M. P. (2013). To dope or not to dope: neuroenhancement with prescription drugs and drugs of abuse among Swiss University students. *PLOS ONE* 8:e77967. doi: 10.1371/journal.pone.0077967

Marcellino, D., Roberts, D. C. S., Navarro, G., Filip, M., Agnati, L., Lluís, C., et al. (2007). Increase in A2A receptors in the nucleus accumbens after extended cocaine self-administration and its disappearance after cocaine withdrawal. *Brain Res.* 1143, 208–220. doi: 10.1016/j.brainres.2007.01.079

McHugh, R. K., Nielsen, S., and Weiss, R. D. (2015). Prescription drug abuse: from epidemiology to public policy. *J. Subst. Abuse Treat.* 48, 1–7. doi: 10.1016/j.jsat.2014.08.004

Merighi, S., Bencivenni, S., Vincenzi, F., Varani, K., Borea, P. A., and Gessi, S. (2017). A2B adenosine receptors stimulate IL-6 production in primary murine microglia through p38 MAPK kinase pathway. *Pharmacol. Res.* 117, 9–19. doi: 10.1016/j.phrs.2016.11.024

Meyerhof, W., Müller-Brechlin, R., and Richter, D. (1991). Molecular cloning of a novel putative G-protein coupled receptor expressed during rat spermiogenesis. *FEBS Lett.* 284, 155–160. doi: 10.1016/0014-5793(91)80674-R

Miyamoto, Y., Iida, A., Sato, K., Muramatsu, S., and Nitta, A. (2014). Knockdown of dopamine D2 receptors in the nucleus accumbens core suppresses methamphetamine-induced behaviors and signal transduction in mice. *Int. J. Neuropsychopharmacol.* 18:yu038. doi: 10.1093/ijnp/pyu038

Moeller, F. G., Steinberg, J. L., Lane, S. D., Kjome, K. L., Ma, L., Ferré, S., et al. (2012). Increased orbitofrontal brain activation after administration of a selective adenosine A(2A) antagonist in cocaine dependent subjects. *Front. Psychiatry* 3:44. doi: 10.3389/fpsyt.2012.00044

Morales, M., and Margolis, E. B. (2017). Ventral tegmental area: cellular heterogeneity, connectivity and behaviour. *Nat. Rev. Neurosci.* 18, 73–85. doi: 10.1038/nrn.2016.165

Moscoso-Castro, M., Gracia-Rubio, I., Ciruela, F., and Valverde, O. (2016). Genetic blockade of adenosine A2A receptors induces cognitive impairments and anatomical changes related to psychotic symptoms in mice. *Eur. Neuropsychopharmacol.* 26, 1227–1240. doi: 10.1016/j.euroneuro.2016.04.003

Moser, P., Wolinsky, T., Duxon, M., and Porsolt, R. D. (2011). How good are current approaches to nonclinical evaluation of abuse and dependence? *J. Pharmacol. Exp. Ther.* 336, 588–595. doi: 10.1124/jpet.110.169979

Müller, C. E., and Jacobson, K. A. (2011). Recent developments in adenosine receptor ligands and their potential as novel drugs. *Biochim. Biophys. Acta* 1808, 1290–1308. doi: 10.1016/j.bbamem.2010.12.017

Munzar, P., Justinova, Z., Kutkat, S. W., Ferré, S., and Goldberg, S. R. (2002). Adenosinergic modulation of the discriminative-stimulus effects of methamphetamine in rats. *Psychopharmacology* 161, 348–355. doi: 10.1007/s00213-002-1075-5

Nestler, E. J., and Landsman, D. (2001). Learning about addiction from the genome. *Nature* 409, 834–835. doi: 10.1038/35057015

Nyberg, F. (2014). Structural plasticity of the brain to psychostimulant use. *Neuropharmacology* 87, 115–124. doi: 10.1016/j.neuropharm.2014.07.004

Okada, M., Kiryu, K., Kawata, Y., Mizuno, K., Wada, K., Tasaki, H., et al. (1997). Determination of the effects of caffeine and carbamazepine on striatal dopamine release by in vivo microdialysis. *Eur. J. Pharmacol.* 321, 181–188. doi: 10.1016/S0014-2999(96)00938-7

O'Neill, C. E., Hobson, B. D., Levis, S. C., and Bachtell, R. K. (2014). Persistent reduction of cocaine seeking by pharmacological manipulation of adenosine A1 and A 2A receptors during extinction training in rats. *Psychopharmacology* 231, 3179–3188. doi: 10.1007/s00213-014-3489-2

O'Neill, C. E., LeTendre, M. L., and Bachtell, R. K. (2012). Adenosine A2A receptors in the nucleus accumbens bi-directionally alter cocaine seeking in rats. *Neuropsychopharmacology* 37, 1245–1256. doi: 10.1038/npp.2011.312

Peleli, M., Fredholm, B. B., Sobrevia, L., and Carlström, M. (2017). Pharmacological targeting of adenosine receptor signaling. *Mol. Aspects Med.* 55, 4–8. doi: 10.1016/j.mam.2016.12.002

Phillips, K. A., Epstein, D. H., and Preston, K. L. (2014). Psychostimulant addiction treatment. *Neuropharmacology* 87, 150–160. doi: 10.1016/j.neuropharm.2014.04.002

Pickens, C. L., Airavaara, M., Theberge, F., Fanous, S., Hope, B. T., and Shaham, Y. (2011). Neurobiology of the incubation of drug craving. *Trends Neurosci.* 34, 411–420. doi: 10.1016/j.tins.2011.06.001

Pinna, A., Wardas, J., Cristalli, G., and Morelli, M. (1997). Adenosine A2A receptor agonists increase Fos-like immunoreactivity in mesolimbic areas. *Brain Res.* 759, 41–49. doi: 10.1016/S0006-8993(97)00214-X

Pintsuk, J., Borroto-Escuela, D. O., Pomierny, B., Wydra, K., Zaniewska, M., Filip, M., et al. (2016). Cocaine self-administration differentially affects allosteric A2A-D2 receptor-receptor interactions in the striatum. Relevance for cocaine use disorder. *Pharmacol. Biochem. Behav.* 144, 85–91. doi: 10.1016/j.pbb.2016.03.004

Poleszak, E., and Malec, D. (2000). Influence of adenosine receptor agonists and antagonists on amphetamine-induced stereotypy in rats. *Pol. J. Pharmacol.* 52, 423–429.

Poleszak, E., and Malec, D. (2002a). Adenosine receptor ligands and cocaine in conditioned place preference (CPP) test in rats. *Pol. J. Pharmacol.* 54, 119–126.

Poleszak, E., and Malec, D. (2002b). Cocaine-induced hyperactivity is more influenced by adenosine receptor agonists than amphetamine-induced hyperactivity. *Pol. J. Pharmacol.* 54, 359–366.

Poleszak, E., and Malec, D. (2003). Effects of adenosine receptor agonists and antagonists in amphetamine-induced conditioned place preference test in rats. *Pol. J. Pharmacol.* 55, 319–326.

Popoli, P., and Pepponi, R. (2012). Potential therapeutic relevance of adenosine A2B and A2A receptors in the central nervous system. *CNS Neurol. Disord. Drug Targets* 11, 664–674. doi: 10.2174/18715271280358 1100

Popoli, P., Pèzzola, A., and de Carolis, A. S. (1994). Modulation of striatal adenosine A1 and A2 receptors induces rotational behaviour in response to dopaminergic stimulation in intact rats. *Eur. J. Pharmacol.* 257, 21–25. doi: 10.1016/0014-2999(94)90689-0

Prediger, R. D. S., da Silva, G. E., Batista, L. C., Bittencourt, A. L., and Takahashi, R. N. (2006). Activation of adenosine A1 receptors reduces anxiety-like behavior during acute ethanol withdrawal (hangover) in mice. *Neuropsychopharmacology* 31, 2210–2220. doi: 10.1038/sj.npp.1301001

Preedy, V. R. (2016). *Neuropathology of Drug Addictions and Substance Misuse: General Processes and Mechanisms, Prescription Medications, Caffeine and Areca, Polydrug Misuse, Emerging Addictions and Non-Drug Addictions*, Vol. 3. Cambridge, MA: Academic Press.

Preti, D., Baraldi, P. G., Moorman, A. R., Borea, P. A., and Varani, K. (2015). History and perspectives of A2A adenosine receptor antagonists as potential therapeutic agents. *Med. Res. Rev.* 35, 790–848. doi: 10.1002/med.21344

Prieto, J. P., Scorza, C., Serra, G. P., Perra, V., Galvalisi, M., Abin-Carriquiry, J. A., et al. (2016). Caffeine, a common active adulterant of cocaine, enhances the reinforcing effect of cocaine and its motivational value. *Psychopharmacology* 233, 2879–2889. doi: 10.1007/s00213-016-4320-z

Rau, A. R., Ariwodola, O. J., and Weiner, J. L. (2014). Presynaptic adenosine A1 receptors modulate excitatory transmission in the rat basolateral amygdala. *Neuropharmacology* 77, 465–474. doi: 10.1016/j.neuropharm.2013.10.029

Reichel, C. M., Chan, C. H., Ghee, S. M., and See, R. E. (2012). Sex differences in escalation of methamphetamine self-administration: cognitive and motivational consequences in rats. *Psychopharmacology* 223, 371–380. doi: 10.1007/s00213-012-2727-8

Reissig, C. J., Strain, E. C., and Griffiths, R. R. (2009). Caffeinated energy drinks—A growing problem. *Drug Alcohol Depend.* 99, 1–10. doi: 10.1016/j.drugalcdep.2008.08.001

Ribeiro, J. A. (1999). Adenosine A2A receptor interactions with receptors for other neurotransmitters and neuromodulators. *Eur. J. Pharmacol.* 375, 101–113. doi: 10.1016/S0014-2999(99)00230-7

Rimondini, R., Ferré, S., Ogren, S. O., and Fuxe, K. (1997). Adenosine A2A agonists: a potential new type of atypical antipsychotic. *Neuropsychopharmacology* 17, 82–91. doi: 10.1016/S0893-133X(97)00033-X

Ross, E. J., Graham, D. L., Money, K. M., and Stanwood, G. D. (2015). Developmental consequences of fetal exposure to drugs: what we know and what we still must learn. *Neuropsychopharmacology* 40, 61–87. doi: 10.1038/npp.2014.147

Roth, M. E., and Carroll, M. E. (2004). Sex differences in the escalation of intravenous cocaine intake following long- or short-access to cocaine self-administration. *Pharmacol. Biochem. Behav.* 78, 199–207. doi: 10.1016/j.pbb.2004.03.018

Rothman, R. B., and Baumann, M. H. (2003). Monoamine transporters and psychostimulant drugs. *Eur. J. Pharmacol.* 479, 23–40. doi: 10.1016/j.ejphar.2003.08.054

Ruda-Kucerova, J., Amchova, P., Babinska, Z., Dusek, L., Micale, V., and Sulcova, A. (2015). Sex differences in the reinstatement of methamphetamine seeking after forced abstinence in sprague-dawley rats. *Front. Psychiatry* 6:91. doi: 10.3389/fpsyt.2015.00091

Rudnick, G., and Wall, S. C. (1992). The molecular mechanism of "ecstasy" [3,4-methylenedioxy-methamphetamine (MDMA)]: serotonin transporters are targets for MDMA-induced serotonin release. *Proc. Natl. Acad. Sci. U.S.A.* 89, 1817–1821. doi: 10.1073/pnas.89.5.1817

Ruiz-Medina, J., Ledent, C., Carretón, O., and Valverde, O. (2011). The A2a adenosine receptor modulates the reinforcement efficacy and neurotoxicity of MDMA. *J. Psychopharmacol.* 25, 550–564. doi: 10.1177/0269881110389210

Salem, A., and Hope, W. (1999). Role of endogenous adenosine in the expression of opiate withdrawal in rats. *Eur. J. Pharmacol.* 369, 39–42. doi: 10.1016/S0014-2999(99)00046-1

Sánchez-López, E., Marcos, A., Ambrosio, E., Mayboroda, O. A., Marina, M. L., and Crego, A. L. (2017). Investigation on the combined effect of cocaine and ethanol administration through a liquid chromatography-mass spectrometry metabolomics approach. *J. Pharm. Biomed. Anal.* 140, 313–321. doi: 10.1016/j.jpba.2017.03.061

Sawynok, J. (2016). Adenosine receptor targets for pain. *Neuroscience* 338, 1–18. doi: 10.1016/j.neuroscience.2015.10.031

Schulte, G., and Fredholm, B. B. (2003). Signalling from adenosine receptors to mitogen-activated protein kinases. *Cell. Signal.* 15, 813–827. doi: 10.1016/S0898-6568(03)00058-5

Shen, H., Luo, Y., Yu, S.-J., and Wang, Y. (2011). Enhanced neurodegeneration after a high dose of methamphetamine in adenosine A3 receptor null mutant mice. *Neuroscience* 194, 170–180. doi: 10.1016/j.neuroscience.2011.08.013

Shen, H.-Y., Coelho, J. E., Ohtsuka, N., Canas, P. M., Day, Y.-J., Huang, Q.-Y., et al. (2008). A critical role of the adenosine A2A receptor in extrastriatal neurons in modulating psychomotor activity as revealed by opposite phenotypes of striatum and forebrain A2A receptor knock-outs. *J. Neurosci.* 28, 2970–2975. doi: 10.1523/JNEUROSCI.5255-07.2008

Shimazoe, T., Yoshimatsu, A., Kawashimo, A., and Watanabe, S. (2000). Roles of adenosine A(1) and A(2A) receptors in the expression and development of methamphetamine-induced sensitization. *Eur. J. Pharmacol.* 388, 249–254. doi: 10.1016/S0014-2999(99)00899-7

Shin, E.-J., Nabeshima, T., Suh, H.-W., Jhoo, W.-K., Oh, K.-W., Lim, Y.-K., et al. (2005). Ginsenosides attenuate methamphetamine-induced behavioral side effects in mice via activation of adenosine A2A receptors: possible involvements of the striatal reduction in AP-1 DNA binding activity and proenkephalin gene expression. *Behav. Brain Res.* 158, 143–157. doi: 10.1016/j.bbr.2004.08.018

Siciliano, C. A., Calipari, E. S., Ferris, M. J., and Jones, S. R. (2015). Adaptations of presynaptic dopamine terminals induced by psychostimulant self-administration. *ACS Chem. Neurosci.* 6, 27–36. doi: 10.1021/cn500 2705

Silberberg, G., and Bolam, J. P. (2015). Local and afferent synaptic pathways in the striatal microcircuitry. *Curr. Opin. Neurobiol.* 33, 182–187. doi: 10.1016/j.conb.2015.05.002

Soleimani, M., Katebi, M., Alizadeh, A., Mohammadzadeh, F., and Mehdizadeh, M. (2012). The role of the A2A receptor in cell apoptosis caused by MDMA. *Cell J.* 14, 231–236.

Soria, G., Castañé, A., Ledent, C., Parmentier, M., Maldonado, R., and Valverde, O. (2006). The lack of A2A adenosine receptors diminishes the reinforcing efficacy of cocaine. *Neuropsychopharmacology* 31, 978–987. doi: 10.1038/sj.npp.1300876

Stenberg, D., Litonius, E., Halldner, L., Johansson, B., Fredholm, B. B., and Porkka-Heiskanen, T. (2003). Sleep and its homeostatic regulation in mice lacking the adenosine A1 receptor. *J. Sleep Res.* 12, 283–290. doi: 10.1046/j.0962-1105.2003.00367.x

Stone, T. W. (1981). The effects of morphine and methionine-enkephalin on the release of purines from cerebral cortex slices of rats and mice. *Br. J. Pharmacol.* 74, 171–176. doi: 10.1111/j.1476-5381.1981.tb09970.x

Strickland, J. C., and Smith, M. A. (2015). Animal models of social contact and drug self-administration. *Pharmacol. Biochem. Behav.* 136, 47–54. doi: 10.1016/j.pbb.2015.06.013

Strohl, M. P. (2011). Bradley's Benzedrine studies on children with behavioral disorders. *Yale J. Biol. Med.* 84, 27–33.

Sulzer, D., Sonders, M. S., Poulsen, N. W., and Galli, A. (2005). Mechanisms of neurotransmitter release by amphetamines: a review. *Prog. Neurobiol.* 75, 406–433. doi: 10.1016/j.pneurobio.2005.04.003

Sun, B., Bachhawat, P., Chu, M. L.-H., Wood, M., Ceska, T., Sands, Z. A., et al. (2017). Crystal structure of the adenosine A2A receptor bound to an antagonist reveals a potential allosteric pocket. *Proc. Natl. Acad. Sci. U.S.A.* 114, 2066–2071. doi: 10.1073/pnas.1621423114

Tebano, M. T., Martire, A., and Popoli, P. (2012). Adenosine A(2A)-cannabinoid CB(1) receptor interaction: an integrative mechanism in striatal glutamatergic neurotransmission. *Brain Res.* 1476, 108–118. doi: 10.1016/j.brainres.2012.04.051

Tozzi, A., de Iure, A., Marsili, V., Romano, R., Tantucci, M., Di Filippo, M., et al. (2012). A2A adenosine receptor antagonism enhances synaptic and motor effects of cocaine via CB1 cannabinoid receptor activation. *PLOS ONE* 7:e38312. doi: 10.1371/journal.pone.0038312

Trifilieff, P., Rives, M.-L., Urizar, E., Piskorowski, R. A., Vishwasrao, H. D., Castrillon, J., et al. (2011). Detection of antigen interactions ex vivo by proximity ligation assay: endogenous dopamine D2-adenosine A2A receptor complexes in the striatum. *Biotechniques* 51, 111–118. doi: 10.2144/000113719

Turgeon, S. M., Pollack, A. E., Schusheim, L., and Fink, J. S. (1996). Effects of selective adenosine A1 and A2a agonists on amphetamine-induced locomotion and c-Fos in striatum and nucleus accumbens. *Brain Res.* 707, 75–80. doi: 10.1016/0006-8993(95)01223-0

Vanattou-Saïfoudine, N., Gossen, A., Harkin, A., and Neuropsychopharmacology Research Group (2011). A role for adenosine A(1) receptor blockade in the ability of caffeine to promote MDMA "Ecstasy"-induced striatal dopamine release. *Eur. J. Pharmacol.* 650, 220–228. doi: 10.1016/j.ejphar.2010.10.012

Vanattou-Saïfoudine, N., McNamara, R., and Harkin, A. (2010). Mechanisms mediating the ability of caffeine to influence MDMA ('Ecstasy')-induced hyperthermia in rats. *Br. J. Pharmacol.* 160, 860–877. doi: 10.1111/j.1476-5381.2010.00660.x

Vanattou-Saïfoudine, N., McNamara, R., and Harkin, A. (2012). Caffeine provokes adverse interactions with 3,4-methylenedioxymethamphetamine (MDMA, 'ecstasy') and related psychostimulants: mechanisms and mediators. *Br. J. Pharmacol.* 167, 946–959. doi: 10.1111/j.1476-5381.2012.02065.x

Varani, K., Vincenzi, F., Merighi, S., Gessi, S., and Borea, P. A. (2017). Biochemical and pharmacological role of A1 adenosine receptors and their modulation as novel therapeutic strategy. *Adv. Exp. Med. Biol.* doi: 10.1007/5584_2017_61 [Epub ahead of print].

Vincenzi, F., Borea, P. A., and Varani, K. (2016a). Anxiolytic properties of A1 adenosine receptor PAMs. *Oncotarget* 8, 7216–7217. doi: 10.18632/oncotarget.13802

Vincenzi, F., Ravani, A., Pasquini, S., Merighi, S., Gessi, S., Romagnoli, R., et al. (2016b). Positive allosteric modulation of A1 adenosine receptors as a novel and promising therapeutic strategy for anxiety. *Neuropharmacology* 111, 283–292. doi: 10.1016/j.neuropharm.2016.09.015

Volkow, N. D., Wang, G.-J., Fowler, J. S., and Tomasi, D. (2012). Addiction circuitry in the human brain. *Annu. Rev. Pharmacol. Toxicol.* 52, 321–336. doi: 10.1146/annurev-pharmtox-010611-134625

Vrecko, S. (2015). Everyday drug diversions: a qualitative study of the illicit exchange and non-medical use of prescription stimulants on a university campus. *Soc. Sci. Med.* 131, 297–304. doi: 10.1016/j.socscimed.2014.10.016

Webb, J. R., Valasek, M. A., and North, C. S. (2013). Prevalence of stimulant use in a sample of US medical students. *Ann. Clin. Psychiatry* 25, 27–32.

Weerts, E. M., and Griffiths, R. R. (2003). The adenosine receptor antagonist CGS15943 reinstates cocaine-seeking behavior and maintains self-administration in baboons. *Psychopharmacology* 168, 155–163. doi: 10.1007/s00213-003-1410-5

Wells, L., Opacka-Juffry, J., Fisher, D., Ledent, C., Hourani, S., and Kitchen, I. (2012). In vivo dopaminergic and behavioral responses to acute cocaine are altered in adenosine A2A receptor knockout mice. *Synapse* 66, 383–390. doi: 10.1002/syn.21527

Wolf, M. E. (2016). Synaptic mechanisms underlying persistent cocaine craving. *Nat. Rev. Neurosci.* 17, 351–365. doi: 10.1038/nrn.2016.39

Wood, S., Sage, J. R., Shuman, T., and Anagnostaras, S. G. (2014). Psychostimulants and cognition: a continuum of behavioral and cognitive activation. *Pharmacol. Rev.* 66, 193–221. doi: 10.1124/pr.112.007054

Wright, S. R., Zanos, P., Georgiou, P., Yoo, J.-H., Ledent, C., Hourani, S. M., et al. (2016). A critical role of striatal A2A R-mGlu5 R interactions in modulating the psychomotor and drug-seeking effects of methamphetamine. *Addict. Biol.* 21, 811–825. doi: 10.1111/adb.12259

Wydra, K., Gołembiowska, K., Suder, A., Kamińska, K., Fuxe, K., and Filip, M. (2015). On the role of adenosine (A)2A receptors in cocaine-induced reward: a pharmacological and neurochemical analysis in rats. *Psychopharmacology* 232, 421–435. doi: 10.1007/s00213-014-3675-2

Wydra, K., Golembiowska, K., Zaniewska, M., Kamińska, K., Ferraro, L., Fuxe, K., et al. (2013). Accumbal and pallidal dopamine, glutamate and GABA overflow during cocaine self-administration and its extinction in rats. *Addict. Biol.* 18, 307–324. doi: 10.1111/adb.12031

Xu, F., Wu, H., Katritch, V., Han, G. W., Jacobson, K. A., Gao, Z.-G., et al. (2011). Structure of an agonist-bound human A2A adenosine receptor. *Science* 332, 322–327. doi: 10.1126/science.1202793

Yang, S.-L., Han, J.-Y., Kim, Y.-B., Nam, S.-Y., Song, S., Hong, J. T., et al. (2011). Increased non-rapid eye movement sleep by cocaine withdrawal: possible involvement of A2A receptors. *Arch. Pharm. Res.* 34, 281–287. doi: 10.1007/s12272-011-0214-0

Yao, L., McFarland, K., Fan, P., Jiang, Z., Ueda, T., and Diamond, I. (2006). Adenosine A2a blockade prevents synergy between mu-opiate and cannabinoid CB1 receptors and eliminates heroin-seeking behavior in addicted rats. *Proc. Natl. Acad. Sci. U.S.A.* 103, 7877–7882. doi: 10.1073/pnas.0602661103

Zhang, S., Jin, Y., Liu, X., Yang, L., Ge, Z. J., Wang, H., et al. (2014). Methamphetamine modulates glutamatergic synaptic transmission in rat primary cultured hippocampal neurons. *Brain Res.* 1582, 1–11. doi: 10.1016/j.brainres.2014.07.040

Zwartsen, A., Verboven, A. H. A., van Kleef, R. G. D. M., Wijnolts, F. M. J., Westerink, R. H. S., and Hondebrink, L. (2017). Measuring inhibition of monoamine reuptake transporters by new psychoactive substances (NPS) in real-time using a high-throughput, fluorescence-based assay. *Toxicol. In Vitro* 45, (Pt 1), 60–71. doi: 10.1016/j.tiv.2017.05.010

Conflict of Interest Statement: The authors declare that the research was conducted in the absence of any commercial or financial relationships that could be construed as a potential conflict of interest.

frontiers in Pharmacology

ORIGINAL RESEARCH
published: 04 January 2018
doi: 10.3389/fphar.2017.00899

Caffeine Controls Glutamatergic Synaptic Transmission and Pyramidal Neuron Excitability in Human Neocortex

*Amber Kerkhofs[1,2], Ana C. Xavier[2], Beatriz S. da Silva[3], Paula M. Canas[2], Sander Idema[4], Johannes C. Baayen[4], Samira G. Ferreira[2], Rodrigo A. Cunha[2,5] and Huibert D. Mansvelder[1]**

[1] Department of Integrative Neurophysiology, Center for Neurogenomics and Cognitive Research, Neuroscience Amsterdam, Vrije Universiteit Amsterdam, Amsterdam, Netherlands, [2] Center for Neuroscience and Cell Biology, University of Coimbra, Coimbra, Portugal, [3] Portuguese National Institute of Legal Medicine and Forensic Sciences, Coimbra, Portugal, [4] Department of Neurosurgery, Neuroscience Amsterdam, VU University Medical Center Amsterdam, Amsterdam, Netherlands, [5] Faculty of Medicine, University of Coimbra, Coimbra, Portugal

OPEN ACCESS

Edited by:
Francisco Ciruela, University of Barcelona, Spain

Reviewed by:
Carl Richard Lupica, National Institute on Drug Abuse (NIH), United States
David Blum, Institut National de la Santé et de la Recherche Médicale, France

***Correspondence:**
Huibert D. Mansvelder
h.d.mansvelder@vu.nl

Specialty section:
This article was submitted to Experimental Pharmacology and Drug Discovery, a section of the journal Frontiers in Pharmacology

Received: *03 September 2017*
Accepted: *27 November 2017*
Published: *04 January 2018*

Citation:
Kerkhofs A, Xavier AC, da Silva BS, Canas PM, Idema S, Baayen JC, Ferreira SG, Cunha RA and Mansvelder HD (2018) Caffeine Controls Glutamatergic Synaptic Transmission and Pyramidal Neuron Excitability in Human Neocortex. Front. Pharmacol. 8:899. doi: 10.3389/fphar.2017.00899

Caffeine is the most widely used psychoactive drug, bolstering attention and normalizing mood and cognition, all functions involving cerebral cortical circuits. Whereas studies in rodents showed that caffeine acts through the antagonism of inhibitory A_1 adenosine receptors (A_1R), neither the role of A_1R nor the impact of caffeine on human cortical neurons is known. We here provide the first characterization of the impact of realistic concentrations of caffeine experienced by moderate coffee drinkers (50 μM) on excitability of pyramidal neurons and excitatory synaptic transmission in the human temporal cortex. Moderate concentrations of caffeine disinhibited several of the inhibitory A_1R-mediated effects of adenosine, similar to previous observations in the rodent brain. Thus, caffeine restored the adenosine-induced decrease of both intrinsic membrane excitability and excitatory synaptic transmission in the human pyramidal neurons through antagonism of post-synaptic A_1R. Indeed, the A_1R-mediated effects of endogenous adenosine were more efficient to inhibit synaptic transmission than neuronal excitability. This was associated with a distinct affinity of caffeine for synaptic *versus* extra-synaptic human cortical A_1R, probably resulting from a different molecular organization of A_1R in human cortical synapses. These findings constitute the first neurophysiological description of the impact of caffeine on pyramidal neuron excitability and excitatory synaptic transmission in the human temporal cortex, providing adequate ground for the effects of caffeine on cognition in humans.

Keywords: caffeine, human neocortex, synapses, adenosine, A_1R, pyramidal neuron

INTRODUCTION

Coffee is the second most consumed beverage after water and its main constituent, caffeine, is the most widely consumed drug, improving attention and alertness, and normalizing mood and cognition (Fredholm et al., 1999; Smith, 2002). These central effects of caffeine result from the antagonism of adenosine receptors (Fredholm et al., 1999), in particular A_1 receptors (A_1R) and A_{2A} receptors ($A_{2A}R$), which are the main adenosine receptors in the brain

(Fredholm et al., 2005). Because of its hydrophobic properties, brain concentrations of caffeine are similar to plasma concentrations (McCall et al., 1982; Fredholm et al., 1999), in the range of 20–70 μM upon moderate intake (Thithapandha et al., 1972; Kaplan et al., 1990; Costenla et al., 2010). These concentrations trigger the maximal psychostimulant effects of caffeine (Bruce et al., 1986). Careful consideration of caffeine concentration is important since most effects of caffeine are bell-shaped, being a psychostimulant with neuroprotective actions at moderate doses and a depressant with deleterious effects at higher doses (Rogers and Dernoncourt, 1998; Smith, 2002; Doepker et al., 2016).

Moderate doses of caffeine antagonize adenosine receptors (Daly et al., 1981; El Yacoubi et al., 2000; Karcz-Kubicha et al., 2003; Huang et al., 2005; Yang et al., 2009; Simões et al., 2016), whereas higher caffeine concentrations act on other targets such as the inhibition of phosphodiesterases, the modification of $GABA_A$ receptor function or the release of calcium from intracellular calcium stores (Lopez et al., 1989; McPherson et al., 1991; Fredholm et al., 1999; Boswell-Smith et al., 2006). These are likely associated with the toxic effects of caffeine (Yu et al., 2009). Since A_1R are inhibitory, reducing excitatory synaptic transmission and neuronal excitability (Dunwiddie and Masino, 2001), whereas $A_{2A}R$ are mostly excitatory, facilitating synaptic plasticity processes (Cunha, 2016), it is assumed that the neurostimulant effect of caffeine mostly results from the partial antagonism of A_1R whereas the neuroprotective effects of caffeine may results from limiting excessive $A_{2A}R$ activation (Ferré, 2008; Cunha, 2016). The role of A_1R in the cerebral cortex has mostly been studied in rodents, where A_1R are mostly located at synapses (Tetzlaff et al., 1987; Rebola et al., 2003), in particular at excitatory rather than at inhibitory synapses (e.g., Rombo et al., 2015). At excitatory synapses, A_1R depress synaptic transmission and neuronal excitability through a combined presynaptic action decreasing glutamate release, post-synaptic actions decreasing the activation of glutamate receptors and voltage-sensitive calcium channels (de Mendonça et al., 1995; Klishin et al., 1995) as well as extra-synaptic actions through a decrease of neuronal excitability by controlling potassium rectifier channels (Greene et al., 1985), after-hyperpolarization potentials (Haas and Greene, 1984) and HCN (Li et al., 2011). Both *in vivo* and *in vitro* studies in rodents concluded that the inhibitory effect of A_1R predominantly results from the presynaptic inhibition of glutamate release (Phillis et al., 1979; Thompson et al., 1992).

Despite the clear effects of caffeine in human subjects on cortical regions resulting in alterations of vigilance, mood, and cognition (Smith, 2002; Doepker et al., 2016), the functional impact of caffeine on neuronal excitability and information flow in the human cerebral cortex is not yet characterized. On a molecular level, moderate doses of caffeine affect A_1R binding (Boulenger et al., 1982) and occupancy in human cortical neurons (Elmenhorst et al., 2012; Paul et al., 2014). While studies in rodents revealed an ability of caffeine to partially antagonize some A_1R-mediated effects (Phillis et al., 1979; Qi et al., 2016), responses in the human cortical network might differ as A_1R have clear inter-species differences, typified by a lower density (Boulenger et al., 1982; Dodd et al., 1986; Fastbom et al., 1987; Svenningsson et al., 1997), a higher affinity for agonists and a lower affinity for antagonists in human *versus* rodent cerebral cortex (Murphy and Snyder, 1982; Ferkany et al., 1986; Maemoto et al., 1997). Therefore, we here delineate the synaptic and subsynaptic localization of A_1R in the human cerebral cortex, and test how A_1R affect neuronal excitability and excitatory synaptic transmission. We report how caffeine at realistic concentrations reached in the brain parenchyma and experienced by coffee consumers after 1–2 cups of coffee, affects these neuronal and synaptic A_1R actions in human neocortex.

MATERIALS AND METHODS

Human Samples

All procedures on human brain resection material that had to be removed for the surgical treatment of deeper brain structures were performed with the approval of the Medical Ethical Committee of the VU University Medical Centre, written informed consent by patients involved, and in accordance with Dutch license procedures and the declaration of Helsinki, as previously described (Verhoog et al., 2016). Human brain samples were also collected at autopsies, performed at the Instituto Nacional de Medicina Legal e Ciências Forenses, which approved all procedures according to the rules of the European Consortium of Nervous Tissues: BrainNet Europe II, to protect the identity of individual donors, as previously described (Pliássova et al., 2016).

Membrane Preparation and Binding Assays

Total membranes and synaptic membranes (from a synaptosomal preparation) were obtained by isopicnic and gradient centrifugations of homogenized brain tissue, as previously described (Rebola et al., 2005; Pliássova et al., 2016). To determine the enrichment and basic binding characteristics of A_1R in cortical synapses, we compared saturation binding isotherms of the selective A_1R antagonist ^{3}H-DPCPX (0.1–10 nM; specific activity of 102.1 Ci/mmol; from DuPont NEN) in total and synaptosomal membranes (72–164 μg) incubated for 2 h incubation at room temperature in a buffer containing 50 mM Tris, 1 mM EDTA, 2 mM EGTA, pH 7.4, with adenosine deaminase (4 U/ml, Roche) before filtration through Whatman GF/C filters (Millipore), as previously described (Rebola et al., 2003; Coelho et al., 2006). To estimate the binding affinity of caffeine, we carried out displacement curves of ^{3}H-DPCPX binding with caffeine (0.1–300 μM; from Sigma), as previously described (Coelho et al., 2006). Results are expressed as specific binding, determined by subtraction of the non-specific binding, which was measured in the presence of 2 μM 8-{4-[(2-aminoethyl)amino]carbonylmethyloxyphenyl}xanthine (XAC, a mixed $A_1R/A_{2A}R$ antagonist; from Tocris) and normalized per amount of protein (bicinchoninic acid assay). To derive the binding parameters from saturation curves (K_D and B_{max} values) the data were fitted by a rectangular hyperbola using

the GraphPad Prism software. For displacement binding curves, IC_{50} values were converted to K_i values by non-linear fitting of the semi-logarithmic curves derived from the competitions curves.

Subsynaptic Fractionation and Western Blot Analysis

To separate the extrasynaptic (non-active) zone, presynaptic active zone and post-synaptic fractions from synaptosomes, we used a fractionation method previously described in detail (Rebola et al., 2005; Canas and Cunha, 2016). The efficiency of separation is based on the segregation of different markers in the several fractions: SNAP-25 in the presynaptic active zone, PSD-95 in the post-synaptic density and synaptophysin outside the active zone (extrasynaptic fraction). Western blot analysis was performed with a rabbit anti-A_1R antibody (1:500, Thermo Scientific), as previously described (Rebola et al., 2003).

Human Brain Slice Preparation and Electrophysiological Recordings

Human brain slices were derived from resected tissue obtained from patients suffering from mild-to severe forms of epilepsy ($n = 6$, of which 5 were diagnosed with meso-temporal epilepsia, 1 with dysplasia; average age 44.8 ± 10.0). All obtained tissue is derived from the temporal lobe area ($n = 6$), away from the focal area of the epilepsy. Slices were prepared as described previously (Testa-Silva et al., 2014; Verhoog et al., 2016). Briefly, blocks of resected cortical tissue were transported to the laboratory in carbogen-saturated (95% O_2, 5% CO_2 at pH 7.4) ice-cold choline-based slicing solution containing (in mM): 110 choline chloride, 11.6 sodium ascorbate, 2.5 KCl, 1.3 NaH_2PO_4, 7 $MgCl_2$, 0.5 $CaCl_2$, 26 $NaHCO_3$, 10 glucose. Cortical slices (350–400 μm) were prepared in the same ice-cold solution as used for transport, and then transferred to holding chambers with artificial cerebrospinal fluid (aCSF) containing (in mM) 125 NaCl, 3 KCl, 1.25 NaH_2PO_4, 1 $MgSO_4$, 2 $CaCl_2$, 26 $NaHCO_3$, 10 glucose. Here, they were stored for 30 min at 34°C and subsequently at room temperature for at least 1 h before recording.

Following recovery, recordings from cells in deeper layers of the human temporal cortex were made in oxygenated aCSF (flow rate of 2–3 ml/min, 32°C). Whole-cell patch-clamp recordings were made with borosilicate glass pipettes (3–6 MΩ) filled with an intracellular solution containing (in mM): 111 K-gluconate, 8 KCl, 10 HEPES, 4 Mg-ATP, 10 K_2HPO_4, 0.4 GTP, 0.2 EGTA. Biocytin (0.5%) was added to all solutions for *post hoc* cell identification, and osmolarity was adjusted to 290–295 mOsm. Pyramidal neurons were visualized with differential interference contrast microscopy, selected based on their large and pyramidal shape and further identified by their spike profile. During recordings, cells were kept at a holding potential close to −70 mV. Recordings were made using MultiClamp 700 A/B amplifiers (Axon Instruments, Sunnyvale, CA, United States), sampling at 10 kHz and low-pass filtering at 3–4 kHz. Recordings were digitized with an Axon Digidata 1440A and acquired using pClamp software (Axon). Acquired data were stored for off-line analysis.

To characterize the electrophysiological properties of pyramidal neurons, we used a step protocol to calculate the input resistance (Rin) as the slope of the linear fit through the current–voltage relationship in 10 pA steps. The membrane time constant was obtained by fitting a single exponential function to the membrane potential deflection in response to a −50 pA current injection. The sag was calculated as the percentage of the difference between transient and stable membrane potentials to a hyperpolarization amplitude of −10 mV after injecting a negative current. The rheobase was defined as the minimal current amplitude of 1 s duration that resulted in the first action potential (AP). Analysis of spike waveforms was performed on single APs elicited by depolarizing threshold current pulses. The AP half-width was defined as the spike width at its half amplitude. To study synaptic transmission, we evaluated spontaneous events that were detected using MiniAnalysis software. The average amplitude and frequency of excitatory post-synaptic potentials (EPSPs) was determined over a time span of 5 min.

The tested drugs, adenosine (20 μM, Sigma), caffeine (50 μM, Sigma) or DPCPX (100 nM, Tocris), were used in concentrations previously tested in rodent preparations (Cunha et al., 1998; Sebastião et al., 2000; Costenla et al., 2010) and were dissolved in aCSF at the desired concentration and bath applied during the experiments.

Morphological Analysis

After recording, slices were fixed at 4°C for at least 24 h in 100 mM phosphate buffer saline containing 4% paraformaldehyde (pH 7.4), for subsequent neuronal visualization and reconstruction as previously described (Mohan et al., 2015). Slices containing biocytin-filled neuronal pairs were processed using a protocol described previously (Mohan et al., 2015). Slices were incubated in 0.1% Triton X-100 solution containing avidin biotinylated horseradish peroxidase (ABC-Elite; Camon); subsequently, they were reacted using 3,3-diaminobenzidine as a chromogen under visual control until the dendritic and axonal arborization was clearly visible (usually after 2–4 min). Slices were dehydrated and then mounted on slides, embedded in Mowiol and enclosed with a thin coverslip.

Biocytin-labeled neurons were examined under the light microscope. Representative pairs were photographed at low magnification to document the dendritic and axonal arborization. Subsequently, neurons were reconstructed with the aid of Neurolucida software (MicroBright Field).

Statistical Analysis

Data are means ± SEM. Paired Student's *t*-test or Wilcoxon signed-rank test ($n < 10$) was used for statistical comparisons between two groups and one-way ANOVA followed by *post hoc* Tukey's test for statistical comparisons among multiple groups. The normality of the distribution of values was determined by the Kolmogorov–Smirnov test. Statistical significance was set at $p < 0.05$.

RESULTS

Synaptic Localization of A_1R in the Human Cerebral Cortex

To define if A_1R were enriched in synapses of the human cerebral cortex, as occurs in rodents (Tetzlaff et al., 1987; Rebola et al., 2003), we compared the binding density of the previously validated selective A_1R antagonist ^{3}H-DPCPX (Svenningsson et al., 1997) in membranes from synaptosomes (purified synapses) and in total membranes (mostly representing non-synaptic neuronal and astrocytic membranes) from human neocortical tissue. **Figure 1A** shows that the binding density of A_1R was larger in synaptosomal membranes (B_{max} = 755 ± 22 fmol/mg protein, n = 5) than in total membranes (B_{max} = 421 ± 17 fmol/mg protein, n = 5; $p < 0.001$ *versus* synaptosomal membranes; unpaired Student's t-test).

Interestingly, ^{3}H-DPCPX displayed a higher affinity to bind A_1R in synaptosomal membranes (K_D = 2.68 nM, 95% confidence interval: 2.12–3.24 nM, n = 5) than in total membranes (K_D = 4.58 nM, 95% confidence interval: 3.69–5.46 nM, n = 5; p = 0.0079 *versus* synaptosomal membranes; unpaired Student's t-test). These different binding properties of synaptic *versus* extra-synaptic A_1R in the human cerebral cortex were confirmed by the different apparent affinity of caffeine for these two populations of A_1R. In fact, competition curves of ^{3}H-DPCPX binding by caffeine (a non-selective adenosine receptor antagonist; Daly et al., 1981) showed that caffeine displaced ^{3}H-DPCPX binding with greater efficiency in synaptosomal membranes (K_i = 11.53 μM, 95% confidence interval: 7.89–15.17 μM, n = 5) than in total membranes (K_i = 33.02 μM, 95% confidence interval: 25.18–40.86 μM, n = 5; p = 0.0079 *versus* synaptosomal membranes; unpaired Student's t-test) (**Figure 1B**). This is suggestive of a possible difference in human cerebral cortical synaptic and extra-synaptic membranes of the homo- or heterodimerization of A_1R, which has been shown to affect the binding of caffeine and A_1R antagonists (Ciruela et al., 2006; Gracia et al., 2013).

We further detailed the localization of A_1R within human cerebral cortical synapses. Using different subsynaptic fractions prepared from synaptosomes of the human temporal cortex, we concluded that A_1R are present in all the subsynaptic fractions on somatodendritic (post-synaptic) and axon terminal (presynaptic) compartments, inside and outside the presynaptic active zone and post-synaptic density (**Figure 1C** and Supplementary Figure S1). Such a widespread distribution predicts a complex role for the A_1R in the control of synaptic communication in the human cerebral cortex.

Adenosine Effects on Intrinsic Membrane Properties of Pyramidal Neurons Are Mediated by A_1R

Adenosine, at non-toxic concentrations (i.e., in low μM range), is known to affect intrinsic membrane properties of layers 2–3 and layer 5 pyramidal neurons in the rodent cerebral cortex through the activation of A_1R (Phillis et al., 1979; van Aerde et al., 2015). Since A_1R activation also controls excitability in the human brain (Klaft et al., 2016) by still undefined mechanisms, we first characterized the effect of exogenous adenosine application on membrane properties of pyramidal neurons in the human temporal cortex (**Figure 2A**). On average, adenosine (20–100 μM) did not decrease the resting membrane potential (RMP; control: −67.2 ± 2.3 mV; adenosine: −67.2 ± 3.4 mV; difference: 0.01 ± 3.7 mV, n = 12, paired t-test: p = 0.99), while it did lower the input resistance (R_{input}; control: 45.9 ± 16.7 MΩ; adenosine: 40.4 ± 14.5 MΩ; difference: 5.5 ± 6.5 MΩ, n = 12, paired t-test: p = 0.01; **Figures 2C,F**) and increased the current injection needed before firing of the first AP, expressed as the rheobase value (Rheobase; control: 251.7 ± 130.5 pA; adenosine: 344.5 ± 149.9 pA; difference: 92.8 ± 45.0 pA, n = 12, paired t-test: $p < 0.0001$; **Figures 2B,E**). Altogether these changes lead to a decreased neuronal excitability and a need for a larger input to fire an AP. Furthermore, adenosine decreased the voltage sag (Sag; control: 2.1 ± 1.2 mV; adenosine: 1.6 ± 1.1 mV; difference: 0.45 ± 0.44 mV, n = 12, paired t-test: p = 0.003; **Figures 2D,G**), reflecting an adenosine-induced partial block of HCN channels, as described in rodents (Li et al., 2011). These effects of adenosine were not seen at 5 μM and were concentration-dependent in the range of 20–100 μM.

The effects of adenosine on membrane intrinsic properties were due to A_1R activation, since the selective A_1R antagonist DPCPX (100 nM) blocked the effects of adenosine on the rheobase (DPCPX: 275.0 ± 125.5 pA; DPCPX+adenosine: 293.6 ± 120.4 pA; difference: 16.4 ± 25.0 pA, n = 7, paired t-test: p = 0.13; **Figures 2B,E**), input resistance (DPCPX: 42.2 ± 20.5 MΩ; DPCPX+adenosine: 33.0 ± 12.9 MΩ; difference: 2.2 ± 5.5 MΩ, n = 7, paired t-test: p = 0.33; **Figures 2C,F**), and sag (DPCPX: 2.3 ± 1.2 mV; DPCPX+adenosine: 2.5 ± 0.6 mV; difference: 0.1 ± 0.6 mV, n = 7, paired t-test: p = 0.72; **Figures 2D,G**). By itself, DPCPX (100 nM) did not significantly alter these membrane properties: rheobase (control: 350.0 ± 151.2 pA; DPCPX: 275.0 ± 125.5 pA; difference 75.0 ± 133.8 pA, n = 8, paired t-test: p = 0.16; **Figures 2B,E**), Input resistance (control: 44.4 ± 22.7 MΩ; DPCPX: 42.2 ± 20.5 MΩ; difference: 0.2 ± 5.8 MΩ, n = 8, paired t-test: p = 0.92; **Figures 2C,F**) or sag (control: 2.1 ± 0.7 mV; DPCPX: 2.3 ± 1.2 mV; difference: 0.3 ± 0.6 mV, n = 8, paired t-test: p = 0.17; **Figures 2D,G**). This indicates the lack of a constitutive effect of endogenous adenosine on the A_1R controlling membrane intrinsic properties of pyramidal neurons in human cortical slices.

Caffeine Does Not Modify Intrinsic Membrane Properties of Pyramidal Neurons

As with DPCPX, there were no effects of caffeine (50 μM) by itself on intrinsic membrane properties of pyramidal neurons in human temporal-cortical slices. The rheobase (control: 192.9 ± 73.4 pA; caffeine: 196.4 ± 69.8 pA; difference 18.2 ± 72.9 pA, n = 11, paired t-test: p = 0.42; **Figures 2B,E**), input resistance (control: 67.5 ± 21.0 MΩ; caffeine: 68.2 ± 16.3 MΩ; difference: 4.1 ± 10.3 MΩ, n = 11, paired t-test: p = 0.21; **Figures 2C,F**) and sag were unaltered (control: 1.4 ± 0.7 mV;

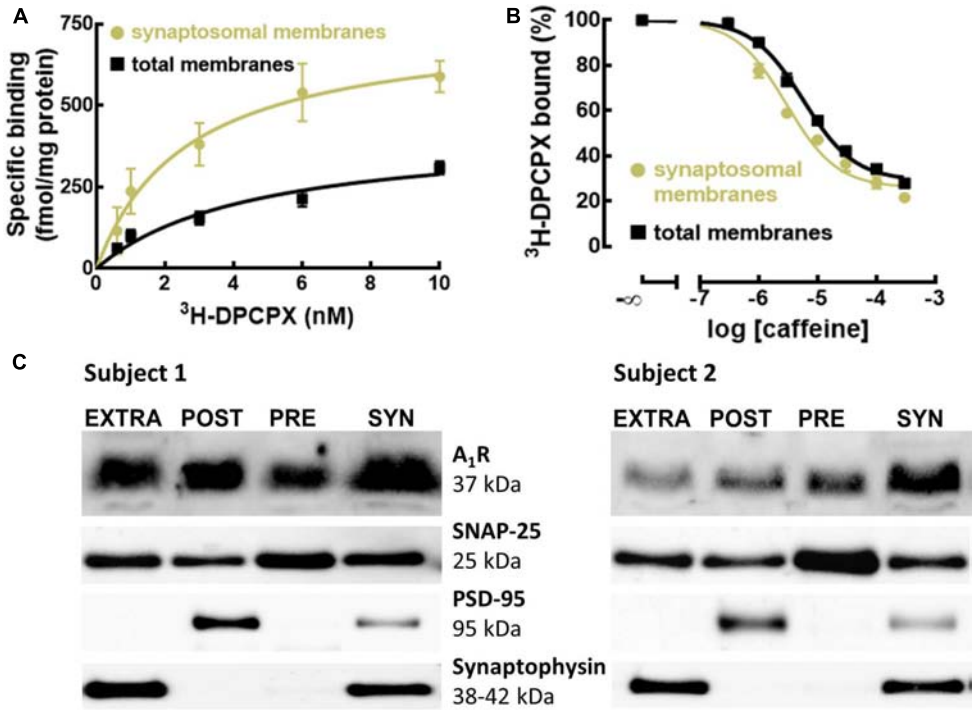

FIGURE 1 | A_1R are enriched and evenly distributed in human cortical synapses, and have greater affinity for caffeine and selective A_1R antagonist compared to extra-synaptic A_1R. **(A)** The selective A_1R antagonist ^{3}H-DPCPX binds with greater affinity and to a larger number of A_1R in synaptosomal compared to total membranes of the human temporal cortex. Data are mean ± SEM of five subjects. **(B)** Caffeine has a greater affinity to displace the binding of the selective A_1R antagonist ^{3}H-DPCPX (2 nM) from synaptosomal compared to total membranes of the human temporal cortex. Data are mean ± SEM of five subjects. **(C)** Western blots of subsynaptic fractions prepared from synaptosomes (SYN) showing the subsynaptic distribution of A_1R in the human temporal cortex (n = 2). A_1R are present in all the subsynaptic fractions, outside (EXTRA) and inside the presynaptic active zone (PRE) and post-synaptic density (POST).

caffeine: 1.6 ± 0.8 mV; difference: 0.3 ± 0.6 mV, n = 11, paired t-test: p = 0.12; **Figures 2D,G**). Since the selective A_1R antagonist DPCPX had no effect by itself and thereby ruled out constitutive activation of A_1R in human cortical slices, the lack of a direct effect of caffeine on intrinsic membrane properties suggests that A_{2A}R are also not constitutively altering intrinsic membrane properties in human pyramidal neurons *in vitro* (reviewed in Cunha, 2016).

We next tested if concentrations of caffeine reached in the brain parenchyma by moderate coffee drinkers (50 μM) could effectively antagonize the A_1R-mediated control of the intrinsic membrane properties of pyramidal neurons. The effect of exogenously applied adenosine on the rheobase was still observed in the presence of caffeine (50 μM). Thus, when adenosine (20 μM) was added in the presence of caffeine (50 μM), the rheobase increased significantly (control: 192.9 ± 73.4 pA; caffeine+adenosine: 318.2 ± 110.8 pA; difference: 116.4 ± 108.7 pA, n = 11, paired t-test: p = 0.005; **Figures 2B,E**). In contrast, caffeine partially blocked the effects of adenosine on the input resistance (control: 67.5 ± 21.0 MΩ; caffeine+adenosine: 55.8 ± 13.6 MΩ; difference: 4.1 ± 10.3 MΩ, n = 11, paired t-test: p = 0.21; **Figures 2C,F**) and voltage sag (control: 1.4 ± 0.7 mV; caffeine+adenosine: 1.3 ± 0.5 mV; difference: 0.3 ± 0.7 mV, n = 11, paired t-test: p = 0.12; **Figures 2D,G**). This indicates that caffeine concentrations experienced by coffee drinkers can interfere with effects of adenosine on the intrinsic membrane properties of pyramidal neurons in human neocortex.

Adenosine Controls Synaptic Transmission through A_1R

The impact of caffeine on cerebral cortical-mediated behavioral responses may also result from its ability to control glutamatergic synaptic transmission, as observed in rodents (Phillis et al., 1979; Thompson et al., 1992; Costenla et al., 2010; Qi et al., 2016). To evaluate the effect of caffeine on glutamatergic synaptic transmission in the human neocortex, we made whole-cell recordings of large deeper-layer pyramidal neurons of the human temporal cortex and recorded spontaneous excitatory transmission. Adenosine (20 μM) significantly decreased both the amplitude of excitatory events (control: 41.7 ± 10.6 pA; adenosine: 38.1 ± 6.6 pA; difference: 3.9 ± 4.9 pA, n = 10, paired t-test: p = 0.03, **Figures 3D,E**) as well as the frequency of excitatory events (control: 1.8 ± 1.6 Hz; adenosine: 0.6 ± 0.5 Hz; difference: 1.2 ± 1.4 Hz; n = 10, paired t-test: p = 0.02; **Figure 3A**). Both effects were reversible upon washout of adenosine (**Figure 3E**; EPSC amplitude: wash-out: 43.6 ± 12.2 pA; difference vs. adenosine: 5.8 ± 6.6 pA; n = 10, paired t-test: p = 0.02; EPSC frequency: wash-out: 2.8 ± 2.2 Hz; difference vs. adenosine: 2.1 ± 1.8 Hz; n = 9, paired t-test: p = 0.009). The effects

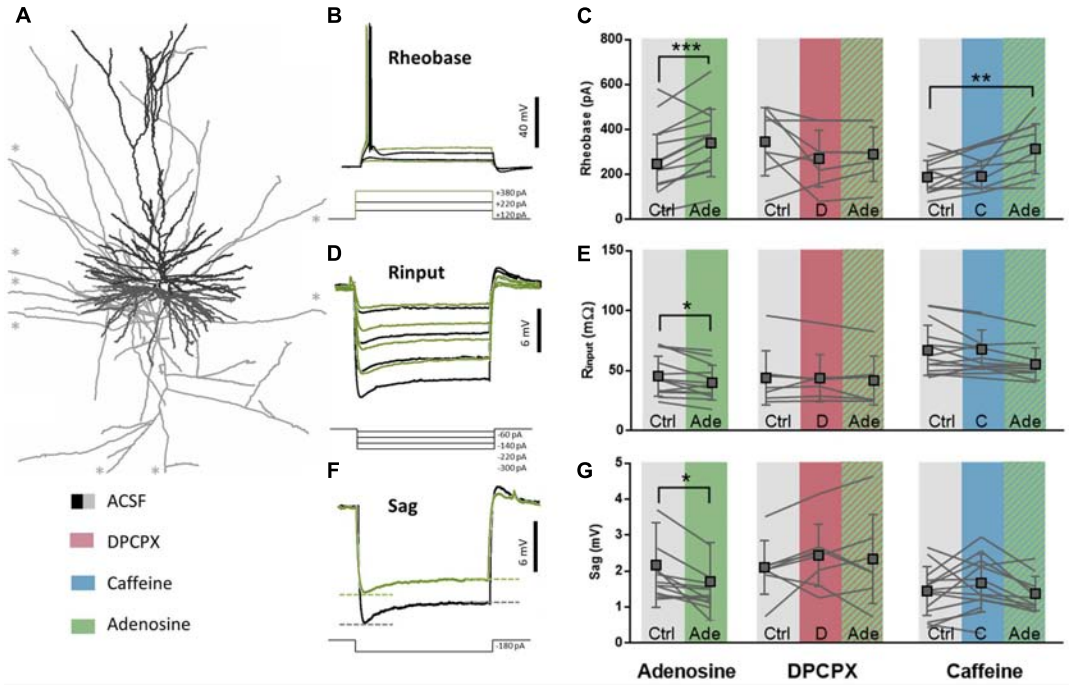

FIGURE 2 | A_1R-mediated effects on intrinsic membrane properties are moderately affected by caffeine. **(A)** Biocytin reconstruction of deeper layer pyramidal neuron from slice of human temporal cortex showing dendritic (black) and axonal (gray) branches. *Axonal branches stretch longer than could be depicted here. **(B,E)** Rheobase value of pyramidal neurons increased after adenosine application (20–100 μM, green, **E**, left panel). This effect was blocked by pre-incubation of DPCPX (100 nM, red, **E**, middle panel), but still occurred when caffeine was pre-incubated (50 μM, blue, **E**, right panel). Paired *t*-test comparing adenosine (20–100 μM) to ACSF condition: $^{**}p < 0.01$; $^{***}p < 0.001$. Boxes depict average ± SD. **(C,F)** Input resistance of pyramidal neurons decreased after adenosine application (20–100 μM, **F**, left panel). Both DPCPX (100 nM, red, **F**, middle panel) and caffeine (50 μM, **F**, blue, right panel) inhibited adenosine-induced effects (striped green). Paired *t*-test comparing adenosine (20–100 μM) to ACSF condition: $^{*}p < 0.05$. Boxes depict average ± SD. **(D,G)** The sag of hyperpolarization-activated cationic depolarizing current (I_h) decreased after adenosine application (20–100 μM, **G**, left panel). Both DPCPX (100 nM, red, **G**, middle panel) and caffeine (50 μM, blue, **G**, right panel) inhibited adenosine-induced effects (striped green). Paired *t*-test comparing adenosine (20–100 μM) to ACSF condition: $^{*}p < 0.05$. Boxes depict average ± SD.

of adenosine were mediated by A_1R, since the selective A_1R antagonist DPCPX (100 nM) blunted the effect of exogenously added adenosine (20 μM) on frequency (control: 2.0 ± 1.8 Hz; DPCPX+adenosine: 1.9 ± 1.2 Hz; difference: 0.1 ± 0.9 Hz; $n = 6$, paired *t*-test: $p = 0.77$; **Figure 3B**) and amplitude of excitatory post-synaptic events (control: 41.8 ± 12.9 pA; DPCPX+adenosine: 51.7 ± 30.0 pA; difference: 9.7 ± 17.2 pA, $n = 7$, paired *t*-test: $p = 0.18$; **Figure 3F**). DPCPX (100 nM) by itself increased the frequency (control: 2.0 ± 1.8 Hz; DPCPX: 3.0 ± 2.0 Hz; difference: 1.1 ± 0.6 Hz; $n = 6$, paired *t*-test: $p = 0.01$; **Figure 3B**) but not the amplitude of excitatory synaptic events (control: 41.8 ± 12.9 pA; DPCPX: 49.8 ± 24.9 pA; difference: 8.0 ± 13.0 pA, $n = 8$, paired *t*-test: $p = 0.13$; **Figure 3F**), which may suggest a constitutive activity of presynaptic A_1R inhibiting synaptic release of glutamate.

We next investigated the effect of caffeine concentrations experienced by most coffee drinkers (50 μM) on synaptic transmission in the presence of adenosine. Caffeine (50 μM) blocked the effect of adenosine (20 μM) on the amplitude of spontaneous excitatory events which indicates a post-synaptic effect of caffeine (control: 38.9 ± 10.3 pA; caffeine+adenosine: 36.7 ± 11.5 pA; difference: 2.1 ± 8.9 pA, $n = 9$, paired *t*-test: $p = 0.49$; **Figure 3G**), but did not prevent the effect of adenosine on the frequency of spontaneous events (control: 1.1 ± 0.7 Hz; caffeine+adenosine: 0.2 ± 0.1 Hz; difference: 0.9 ± 0.7 Hz; $n = 9$, paired *t*-test: $p = 0.007$; **Figure 3C**). Similar to the adenosine-only group, effects of adenosine in the case of pre-incubated caffeine could be washed out (wash-out: 0.5 ± 0.4 pA; difference vs. adenosine: 0.3 ± 0.3 pA; $n = 8$, paired *t*-test: $p = 0.04$; **Figure 3C**). In contrast to DPCPX, caffeine (50 μM) by itself had no effect on spontaneous glutamatergic synaptic transmission. It did not modify the amplitude (control: 38.9 ± 10.3 pA; caffeine: 40.1 ± 12.9 pA; difference: 1.1 ± 0.6 pA, $n = 9$, paired *t*-test: $p = 0.59$; **Figure 3G**) or frequency of spontaneous excitatory post-synaptic events (control: 1.1 ± 0.7 Hz; caffeine: 0.6 ± 0.2 Hz; difference: 0.5 ± 0.7 Hz; $n = 9$, paired *t*-test: $p = 0.06$; **Figure 3C**). This may suggest that, in contrast to DPCPX, moderate concentrations of caffeine are not sufficient to interfere with constitutive activity of presynaptic A_1R. Together, our findings show that caffeine concentrations experienced by coffee drinkers interfere with adenosine signaling when there is an additional adenosine load, allowing to restore excitatory synaptic transmission and pyramidal neuron excitability in the human neocortex.

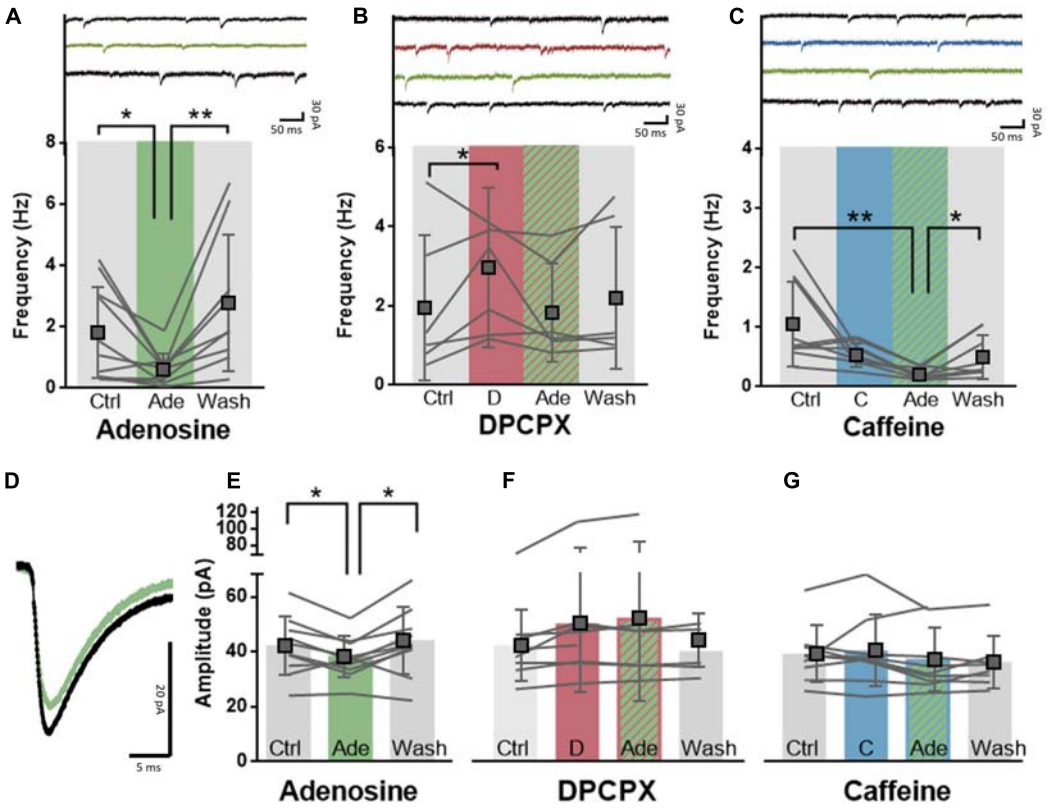

FIGURE 3 | A_1R-mediated effects of adenosine on synaptic transmission are post-synaptically blocked by caffeine. **(A)** Adenosine (20 μM, green) significantly decreased the frequency of excitatory events onto pyramidal neurons in a reversible manner. Paired *t*-test comparing adenosine (20 μM) to ACSF condition: $^*p < 0.05$; $^{**}p < 0.01$. Boxes depict average ± SD. **(B)** Direct application of DPCPX (100 nM, red) significantly increased the frequency of excitatory events and blocked adenosine-induced inhibition (green). Paired *t*-test comparing DPCPX (100 nM) to ACSF condition: $^*p < 0.05$. Boxes depict average ± SD. **(C)** Caffeine pre-incubation (50 μM, blue) did not affect the potency of adenosine (20 μM, green) to decrease the frequency of excitatory events onto pyramidal neurons. Wash-out of adenosine and caffeine restored the frequency of events. Paired *t*-test comparing adenosine (20 μM) to ACSF condition: $^*p < 0.05$; $^{**}p < 0.01$. Boxes depict average ± SD. **(D)** Example trace of the average effect of adenosine application onto the amplitude of excitatory events onto a pyramidal neuron. **(E–G)** Adenosine (20 μM, green) significantly decreased the amplitude of excitatory events onto pyramidal neurons in a reversible manner **(E)**. Pre-incubation with either DPCPX (100 nM, red, **F**) or caffeine (50 μM, blue, **G**) completely abolished this effect. Paired *t*-test comparing adenosine (20 μM) to ACSF control/wash-out condition: $^*p < 0.05$.

DISCUSSION

In this study, we provide the first characterization of the impact of caffeine concentrations experienced by moderate coffee drinkers (50 μM) on neuronal excitability in pyramidal neurons and excitatory synapses of the human temporal cortex. Caffeine had a larger affinity for synaptic A_1R compared to extra-synaptic A_1R in the human temporal cortex, which contrasts with the affinity profile of caffeine in the rodent cortex; this difference probably results from a different molecular organization of A_1R within human cortical synapses compared to rodent cortical synapses. Caffeine interfered with several of the inhibitory A_1R-mediated effects of adenosine in the human cortex, similar to previous observations in the rodent brain. Caffeine blunted the effects of adenosine on intrinsic membrane properties and prevented the amplitude reduction of excitatory synaptic transmission through antagonistic actions at post-synaptic A_1R.

A distinct interaction of caffeine with A_1R in the human cerebral cortex compared with rodent cortex is in agreement with several previous studies describing differences of binding properties of brain A_1R between humans and different animal models (Boulenger et al., 1982; Murphy and Snyder, 1982; Dodd et al., 1986; Ferkany et al., 1986; Fastbom et al., 1987; Maemoto et al., 1997; Svenningsson et al., 1997). Our results confirmed previous evidence that the binding density of A_1R in the temporal cortex is lower in humans compared to mice or rats (Boulenger et al., 1982; Dodd et al., 1986; Fastbom et al., 1987; Svenningsson et al., 1997). We also confirmed previous evidence that human A_1R display a different affinity for xanthine-based selective antagonists, which tend to have lower affinity in humans compared to rodents (Murphy and Snyder, 1982; Ferkany et al., 1986; Maemoto et al., 1997). Despite these different pharmacological properties, human A_1R seem to exert an overall inhibitory effect in the cerebral cortex that is similar to that observed

in rodents: in fact, the exogenous administration of adenosine decreased the excitability of pyramidal neurons in the human temporal cortex in a manner similar to the inhibition previously reported to occur through A_1R activation in the cerebral cortex of rodents (Phillis et al., 1979; Li et al., 2011). In rodents (Thompson et al., 1992), tonic adenosine inhibition is dominated by a A_1R-mediated inhibition of excitatory transmission. In human neocortex, both intrinsic membrane properties of pyramidal neurons as well as excitatory synaptic transmission received by these neurons, were inhibited by somatodendritic post-synaptic A_1R. Whether one of these mechanisms dominates effects of adenosine on cortical overall excitability in human neocortex cannot be concluded based on our present results. We did find a high density of A_1R in human cortical synapses, both at somatodendritic (post-synaptic) and axon terminals (presynaptic) compartments, as well as a greater affinity for DPCPX of synaptic A_1R in comparison with extra-synaptic A_1R, which may point to a stronger control of synaptic transmission by A_1R. Since one of the few factors that has been documented to regulate the affinity of A_1R for antagonists is their relative homomerization (Gracia et al., 2013) or heteromerization (Ciruela et al., 2006), the present findings are suggestive of a different molecular arrangement of A_1R in synapses of the human cerebral cortex.

To characterize the impact of caffeine on human cortical neurons, we used a concentration of caffeine within the range of concentrations reached by caffeine in the brain parenchyma upon moderate consumption of caffeine (20–70 μM) (Thithapandha et al., 1972; Kaplan et al., 1990; Costenla et al., 2010; Duarte et al., 2012; Silva et al., 2013), which are similar to plasma concentrations of caffeine that cause maximal psycho-activating responses in humans (Bruce et al., 1986). Many studies have described neuronal effects of caffeine using high millimolar or submillimolar concentrations of caffeine (Lee et al., 1987; Martin and Buno, 2003; Margineanu and Klitgaard, 2004; Vyleta and Smith, 2008; Grigoryan et al., 2012), which represent toxic effects of caffeine found in extreme cases of caffeinism (Gilliland and Andress, 1981). Using concentrations of caffeine realistic for normal human consumption, we found that caffeine only targets inhibitory A_1R, since caffeine mimics the effects of DPCPX. This is in agreement with PET imaging studies that documented a decreased occupancy of cortical A_1R in subjects consuming caffeine (Elmenhorst et al., 2012; Paul et al., 2014). Importantly, we now report that caffeine displays a greater affinity for synaptic A_1R compared to extra-synaptic A_1R. This may suggest that synaptic A_1R are more strongly affected by caffeine and that interference with inhibitory effects of adenosine on transmission at excitatory synapses is a major effect in the human cerebral cortex. In contrast to effects in rodent neocortex, we find that effects of caffeine in human cortical neurons interfered both with adenosine effects on neuronal excitability and excitatory synaptic transmission through post-synaptic A_1R, while in rodents, caffeine mostly controls synaptic transmission through presynaptic A_1R and affect the release of excitatory neurotransmitters (Phillis et al., 1979; Greene et al., 1985). Nevertheless, also in rodent neocortex, caffeine can exert a post-synaptic effect (Greene et al., 1985; Simons et al., 2011) in accordance with the ability of post-synaptic A_1R to induce robust responses in rodent cortical neurons (van Aerde et al., 2015; Qi et al., 2016). Differences in effects of caffeine in human and rodent neocortex may result from the previously discussed different molecular organization of A_1R or to a different subsynaptic distribution of A_1R in rodent and human cortical synapses; thus, A_1R seem to be more abundant presynaptically in rodent synapses (Tetzlaff et al., 1987; Rebola et al., 2003), whereas we find here in human neocortex an even distribution of A_1R in all subsynaptic fractions.

For our experiments, we used neocortical tissue derived from epileptic patients that underwent surgery for treatment of deeper brain structures. Although the resected tissue was from regions outside the focal area of epilepsy or tumor, and was not part of the disease, our observations could be affected by disease and medication history. Earlier, adenosine A_1R density was shown to be up- or downregulated in surrounding neocortical areas of patients suffering from temporal lobe epilepsy (Angelatou et al., 1993; Glass et al., 1996) and adenosine A_1R agonists are explored as therapeutic targets to treat epilepsy (Boison, 2016). Therefore, the possibility that epileptic conditions affect the adenosine neuromodulation system in the cerebral cortex (Rebola et al., 2005) should be considered as a factor influencing the presently reported effects of caffeine. However, the impact of caffeine in epileptic conditions is still largely unclear (Dworetzky et al., 2010; Samsonsen et al., 2013) and seems to be more evident in the developing than in the mature brain (e.g., Tchekalarova et al., 2006), with reports of proconvulsant (e.g., Chu, 1981) and anticonvulsant effects of caffeine (e.g., Rigoulot et al., 2003). It is also important to keep in mind that the present study focused on the human temporal cortex and it remains to be confirmed if the effects of caffeine are similar in other cortical regions, although both the density of A_1R and the occupancy of A_1R by caffeine seem to be similar in different cortical areas (Svenningsson et al., 1997; Diukova et al., 2012; Elmenhorst et al., 2012; Park et al., 2014).

The present characterization of the effects of a physiological concentration of caffeine (50 μM) on the human temporal cortex provides an important insight in the subtle effects of cortical exposure to human caffeine consumption. By acting mainly post-synaptically, caffeine is able to counteract adenosine-induced inhibition of the received excitatory signal. This provides a mechanism to explain the enhancement by caffeine on human cognition (Borota et al., 2014), which is not readily observed in adult rodents (e.g., Dall'Igna et al., 2007; Duarte et al., 2012; Espinosa et al., 2013; Kaster et al., 2015; reviewed in Cunha and Agostinho, 2010), where caffeine intake mostly normalizes rather than bolsters learning and memory performance. Thus, these findings provide the first neurophysiological description of the impact of caffeine on excitatory synaptic transmission in the human temporal cortex, providing adequate ground for the effects of caffeine in normal consumption amounts on cognition in humans.

AUTHOR CONTRIBUTIONS

AK, HM, RC, and SF designed the research; AK, AX, BdS, and PC performed the experiments; RC performed the research; JCB and SI provided the resources; AK, HM, and RC wrote the manuscript. All authors commented on the manuscript.

FUNDING

Supported by Maratona da Saúde, Santa Casa da Misericórdia, GAI-FMUC and Banco Santander-Totta, NARSAD, Erasmus Mundus Joint Doctorate grant (ENC-Network) and ERDF, through Centro 2020 (project CENTRO-01-0145-FEDER-000008:BrainHealth 2020), and through FCT (projects POCI-01-0145-FEDER-007440 and PTDC/NEU-NMC/4154/2016) to RC. HM received funding for this work from the Netherlands Organization for Scientific Research (NWO; VICI grant), ERC StG "BrainSignals," EU H2020 Framework Programme (agreement no. 604102 "Human Brain Project") and the EU 7th framework program (EU MSCA-ITN CognitionNet FP7-PEOPLE-2013-ITN 607508).

ACKNOWLEDGMENTS

We thank Anton Pieneman, Eline Mertens, and Christiaan de Kock for histology and Neurolucida reconstructions. We thank Hans Lodder for technical assistance.

SUPPLEMENTARY MATERIAL

The Supplementary Material for this article can be found online at: https://www.frontiersin.org/articles/10.3389/fphar.2017.00899/full#supplementary-material

REFERENCES

Angelatou, F., Pagonopoulou, O., Maraziotis, T., Olivier, A., Villemeure, J. G., Avoli, M., et al. (1993). Upregulation of A1 adenosine receptors in human temporal lobe epilepsy: a quantitative autoradiographic study. *Neurosci. Lett.* 163, 11–14. doi: 10.1016/0304-3940(93)90217-9

Boison, D. (2016). Adenosinergic signaling in epilepsy. *Neuropharmacology* 104, 131–139. doi: 10.1016/j.neuropharm.2015.08.046

Borota, D., Murray, E., Keceli, G., Chang, A., Watabe, J. M., Ly, M., et al. (2014). Post-study caffeine administration enhances memory consolidation in humans. *Nat. Neurosci.* 17, 201–203. doi: 10.1038/nn.3623

Boswell-Smith, V., Spina, D., and Page, C. P. (2006). Phosphodiesterase inhibitors. *Br. J. Pharmacol.* 147(Suppl. 1), S252–S257. doi: 10.1038/sj.bjp.0706495

Boulenger, J. P., Patel, J., and Marangos, P. J. (1982). Effects of caffeine and theophylline on adenosine and benzodiazepine receptors in human brain. *Neurosci. Lett.* 30, 161–166. doi: 10.1016/0304-3940(82)90290-7

Bruce, M., Scott, N., Lader, M., and Marks, V. (1986). The psychopharmacological and electrophysiological effects of single doses of caffeine in healthy human subjects. *Br. J. Clin. Pharmacol.* 22, 81–87. doi: 10.1111/j.1365-2125.1986.tb02883.x

Canas, P. M., and Cunha, R. A. (2016). "Subsynaptic membrane fractionation," in *Receptor and Ion Channel Detection in the Brain*, Vol. 110, eds R. Luján and F. Ciruela (New York, NY: Humana Press), 31–37. doi: 10.1007/978-1-4939-3064-7_3

Chu, N. S. (1981). Caffeine- and aminophylline-induced seizures. *Epilepsia* 22, 85–94. doi: 10.1111/j.1528-1157.1981.tb04335.x

Ciruela, F., Casadó, V., Rodrigues, R. J., Luján, R., Burgueño, J., Canals, M., et al. (2006). Presynaptic control of striatal glutamatergic neurotransmission by adenosine A1-A2A receptor heteromers. *J. Neurosci.* 26, 2080–2087. doi: 10.1523/JNEUROSCI.3574-05.2006

Coelho, J. E., Rebola, N., Fragata, I., Ribeiro, J. A., de Mendonça, A., and Cunha, R. A. (2006). Hypoxia-induced desensitization and internalization of adenosine A1 receptors in the rat hippocampus. *Neuroscience* 138, 1195–1203. doi: 10.1016/j.neuroscience.2005.12.012

Costenla, A. R., Cunha, R. A., and de Mendonça, A. (2010). Caffeine, adenosine receptors, and synaptic plasticity. *J. Alzheimers Dis.* 20(Suppl. 1), S25–S34. doi: 10.3233/JAD-2010-091384

Cunha, R. A. (2016). How does adenosine control neuronal dysfunction and neurodegeneration? *J. Neurochem.* 139, 1019–1055. doi: 10.1111/jnc.13724

Cunha, R. A., and Agostinho, P. M. (2010). Chronic caffeine consumption prevents memory disturbance in different animal models of memory decline. *J. Alzheimers Dis.* 20(Suppl. 1), S95–S116. doi: 10.3233/JAD-2010-1408

Cunha, R. A., Sebastião, A. M., and Ribeiro, J. A. (1998). Inhibition by ATP of hippocampal synaptic transmission requires localized extracellular catabolism by ecto-nucleotidases into adenosine and channeling to adenosine A1 receptors. *J. Neurosci.* 18, 1987–1995.

Dall'Igna, O. P., Fett, P., Gomes, M. W., Souza, D. O., Cunha, R. A., and Lara, D. R. (2007). Caffeine and adenosine A2a receptor antagonists prevent beta-amyloid (25-35)-induced cognitive deficits in mice. *Exp. Neurol.* 203, 241–245. doi: 10.1016/j.expneurol.2006.08.008

Daly, J. W., Bruns, R. F., and Snyder, S. H. (1981). Adenosine receptors in the central nervous system: relationship to the central actions of methylxanthines. *Life Sci.* 28, 2083–2097. doi: 10.1016/0024-3205(81)90614-7

de Mendonça, A., Sebastião, A. M., and Ribeiro, J. A. (1995). Inhibition of NMDA receptor-mediated currents in isolated rat hippocampal neurones by adenosine A1 receptor activation. *Neuroreport* 6, 1097–1100. doi: 10.1097/00001756-199505300-00006

Diukova, A., Ware, J., Smith, J. E., Evans, C. J., Murphy, K., Rogers, P. J., et al. (2012). Separating neural and vascular effects of caffeine using simultaneous EEG-FMRI: differential effects of caffeine on cognitive and sensorimotor brain responses. *Neuroimage* 62, 239–249. doi: 10.1016/j.neuroimage.2012.04.041

Dodd, P. R., Watson, W. E., and Johnston, G. A. (1986). Adenosine receptors in post-mortem human cerebral cortex and the effect of carbamazepine. *Clin. Exp. Pharmacol. Physiol.* 13, 711–722. doi: 10.1111/j.1440-1681.1986.tb02412.x

Doepker, C., Lieberman, H. R., Smith, A. P., Peck, J. D., El-Sohemy, A., and Welsh, B. T. (2016). Caffeine: friend or foe? *Annu. Rev. Food Sci. Technol.* 7, 117–137. doi: 10.1146/annurev-food-041715-033243

Duarte, J. M., Agostinho, P. M., Carvalho, R. A., and Cunha, R. A. (2012). Caffeine consumption prevents diabetes-induced memory impairment and synaptotoxicity in the hippocampus of NONcZNO10/LTJ mice. *PLOS ONE* 7:e21899. doi: 10.1371/journal.pone.0021899

Dunwiddie, T. V., and Masino, S. A. (2001). The role and regulation of adenosine in the central nervous system. *Annu. Rev. Neurosci.* 24, 31–55. doi: 10.1146/annurev.neuro.24.1.31

Dworetzky, B. A., Bromfield, E. B., Townsend, M. K., and Kang, J. H. (2010). A prospective study of smoking, caffeine, and alcohol as risk factors for seizures or epilepsy in young adult women: data from the Nurses' Health Study II. *Epilepsia* 51, 198–205. doi: 10.1111/j.1528-1167.2009.02268.x

El Yacoubi, M., Ledent, C., Menard, J. F., Parmentier, M., Costentin, J., and Vaugeois, J. M. (2000). The stimulant effects of caffeine on locomotor behaviour in mice are mediated through its blockade of adenosine A2A receptors. *Br. J. Pharmacol.* 129, 1465–1473. doi: 10.1038/sj.bjp.0703170

Elmenhorst, D., Meyer, P. T., Matusch, A., Winz, O. H., and Bauer, A. (2012). Caffeine occupancy of human cerebral A1 adenosine receptors: in vivo quantification with 18F-CPFPX and PET. *J. Nucl. Med.* 53, 1723–1729. doi: 10.2967/jnumed.112.105114

Espinosa, J., Rocha, A., Nunes, F., Costa, M. S., Schein, V., Kazlauckas, V., et al. (2013). Caffeine consumption prevents memory impairment, neuronal damage, and adenosine A2A receptors upregulation in the hippocampus of a rat model of sporadic dementia. *J. Alzheimers Dis.* 34, 509–518. doi: 10.3233/JAD-111982

Fastbom, J., Pazos, A., Probst, A., and Palacios, J. M. (1987). Adenosine A1 receptors in the human brain: a quantitative autoradiographic study. *Neuroscience* 22, 827–839. doi: 10.1016/0306-4522(87)92962-9

Ferkany, J. W., Valentine, H. L., Stone, G. A., and Williams, M. (1986). Adenosine A1 receptors in mammalian brain: species differences in their interactions with agonists and antagonists. *Drug Dev. Res.* 9, 85–93. doi: 10.1002/ddr.430090202

Ferré, S. (2008). An update on the mechanisms of the psychostimulant effects of caffeine. *J. Neurochem.* 105, 1067–1079. doi: 10.1111/j.1471-4159.2007.05196.x

Fredholm, B. B., Bättig, K., Holmén, J., Nehlig, A., and Zvartau, E. E. (1999). Actions of caffeine in the brain with special reference to factors that contribute to its widespread use. *Pharmacol. Rev.* 51, 83–133.

Fredholm, B. B., Chen, J. F., Cunha, R. A., Svenningsson, P., and Vaugeois, J. M. (2005). Adenosine and brain function. *Int. Rev. Neurobiol.* 63, 191–270. doi: 10.1016/S0074-7742(05)63007-3

Gilliland, K., and Andress, D. (1981). Ad lib caffeine consumption, symptoms of caffeinism, and academic performance. *Am. J. Psychiatry* 138, 512–514. doi: 10.1176/ajp.138.4.512

Glass, M., Faull, R. L., Bullock, J. Y., Jansen, K., Mee, E. W., Walker, E. B., et al. (1996). Loss of A1 adenosine receptors in human temporal lobe epilepsy. *Brain Res.* 710, 56–68. doi: 10.1016/0006-8993(95)01313-X

Gracia, E., Moreno, E., Cortés, A., Lluís, C., Mallol, J., McCormick, P. J., et al. (2013). Homodimerization of adenosine A1 receptors in brain cortex explains the biphasic effects of caffeine. *Neuropharmacology* 71, 56–69. doi: 10.1016/j.neuropharm.2013.03.005

Greene, R. W., Haas, H. L., and Hermann, A. (1985). Effects of caffeine on hippocampal pyramidal cells in vitro. *Br. J. Pharmacol.* 85, 163–169. doi: 10.1111/j.1476-5381.1985.tb08843.x

Grigoryan, G., Korkotian, E., and Segal, M. (2012). Selective facilitation of LTP in the ventral hippocampus by calcium stores. *Hippocampus* 22, 1635–1644. doi: 10.1002/hipo.22000

Haas, H. L., and Greene, R. W. (1984). Adenosine enhances afterhyperpolarization and accommodation in hippocampal pyramidal cells. *Pflugers Arch.* 402, 244–247. doi: 10.1007/BF00585506

Huang, Z. L., Qu, W. M., Eguchi, N., Chen, J. F., Schwarzschild, M. A., Fredholm, B. B., et al. (2005). Adenosine A2A, but not A1, receptors mediate the arousal effect of caffeine. *Nat. Neurosci.* 8, 858–859. doi: 10.1038/nn1491

Kaplan, G. B., Tai, N. T., Greenblatt, D. J., and Shader, R. I. (1990). Caffeine-induced behavioural stimulation is dose- and concentration-dependent. *Br. J. Pharmacol.* 100, 435–440. doi: 10.1111/j.1476-5381.1990.tb15824.x

Karcz-Kubicha, M., Antoniou, K., Terasmaa, A., Quarta, D., Solinas, M., Justinova, Z., et al. (2003). Involvement of adenosine A1 and A2A receptors in the motor effects of caffeine after its acute and chronic administration. *Neuropsychopharmacology* 28, 1281–1291. doi: 10.1038/sj.npp.1300167

Kaster, M. P., Machado, N. J., Silva, H. B., Nunes, A., Ardais, A. P., Santana, M., et al. (2015). Caffeine acts through neuronal adenosine A2A receptors to prevent mood and memory dysfunction triggered by chronic stress. *Proc. Natl. Acad. Sci. U.S.A.* 112, 7833–7838. doi: 10.1073/pnas.1423088112

Klaft, Z. J., Hollnagel, J. O., Salar, S., Calişkan, G., Schulz, S. B., Schneider, U. C., et al. (2016). Adenosine A1 receptor-mediated suppression of carbamazepine-resistant seizure-like events in human neocortical slices. *Epilepsia* 57, 746–756. doi: 10.1111/epi.13360

Klishin, A., Tsintsadze, T., Lozovaya, N., and Krishtal, O. (1995). Latent N-methyl-D-aspartate receptors in the recurrent excitatory pathway between hippocampal CA1 pyramidal neurons: Ca^{2+}-dependent activation by blocking A1 adenosine receptors. *Proc. Natl. Acad. Sci. U.S.A.* 92, 12431–12435. doi: 10.1073/pnas.92.26.12431

Lee, W. L., Anwyl, R., and Rowan, M. (1987). Caffeine inhibits post-tetanic potentiation but does not alter long-term potentiation in the rat hippocampal slice. *Brain Res.* 426, 250–256. doi: 10.1016/0006-8993(87)90879-1

Li, Y., Fan, S., Yan, J., Li, B., Chen, F., Xia, J., et al. (2011). Adenosine modulates the excitability of layer II stellate neurons in entorhinal cortex through A1 receptors. *Hippocampus* 21, 265–280. doi: 10.1002/hipo.20745

Lopez, F., Miller, L. G., Greenblatt, D. J., Kaplan, G. B., and Shader, R. I. (1989). Interaction of caffeine with the GABAA receptor complex: alterations in receptor function but not ligand binding. *Eur. J. Pharmacol.* 172, 453–459. doi: 10.1016/0922-4106(89)90028-X

Maemoto, T., Finlayson, K., Olverman, H. J., Akahane, A., Horton, R. W., and Butcher, S. P. (1997). Species differences in brain adenosine A1 receptor pharmacology revealed by use of xanthine and pyrazolopyridine based antagonists. *Br. J. Pharmacol.* 122, 1202–1208. doi: 10.1038/sj.bjp.0701465

Margineanu, D. G., and Klitgaard, H. (2004). Caffeine-induced epileptiform field potentials in rat hippocampal slices: a pharmacological characterization. *Neuropharmacology* 47, 926–934. doi: 10.1016/j.neuropharm.2004.06.014

Martin, E. D., and Buno, W. (2003). Caffeine-mediated presynaptic long-term potentiation in hippocampal CA1 pyramidal neurons. *J. Neurophysiol.* 89, 3029–3038. doi: 10.1152/jn.00601.2002

McCall, A. L., Millington, W. R., and Wurtman, R. J. (1982). Blood-brain barrier transport of caffeine: dose-related restriction of adenine transport. *Life Sci.* 31, 2709–2715. doi: 10.1016/0024-3205(82)90715-9

McPherson, P. S., Kim, Y. K., Valdivia, H., Knudson, C. M., Takekura, H., Franzini-Armstrong, C., et al. (1991). The brain ryanodine receptor: a caffeine-sensitive calcium release channel. *Neuron* 7, 17–25. doi: 10.1016/0896-6273(91)90070-G

Mohan, H., Verhoog, M. B., Doreswamy, K. K., Eyal, G., Aardse, R., Lodder, B. N., et al. (2015). Dendritic and axonal architecture of individual pyramidal neurons across layers of adult human neocortex. *Cereb. Cortex* 25, 4839–4853. doi: 10.1093/cercor/bhv188

Murphy, K. M., and Snyder, S. H. (1982). Heterogeneity of adenosine A1 receptor binding in brain tissue. *Mol. Pharmacol.* 22, 250–257.

Park, C. A., Kang, C. K., Son, Y. D., Choi, E. J., Kim, S. H., Oh, S. T., et al. (2014). The effects of caffeine ingestion on cortical areas: functional imaging study. *Magn. Reson. Imaging* 32, 366–371. doi: 10.1016/j.mri.2013.12.018

Paul, S., Khanapur, S., Sijbesma, J. W., Ishiwata, K., Elsinga, P. H., Meerlo, P., et al. (2014). Use of 11C-MPDX and PET to study adenosine A1 receptor occupancy by nonradioactive agonists and antagonists. *J. Nucl. Med.* 55, 315–320. doi: 10.2967/jnumed.113.130294

Phillis, J. W., Edstrom, J. P., Kostopoulos, G. K., and Kirkpatrick, J. R. (1979). Effects of adenosine and adenine nucleotides on synaptic transmission in the cerebral cortex. *Can. J. Physiol. Pharmacol.* 57, 1289–1312. doi: 10.1139/y79-194

Pliássova, A., Canas, P. M., Xavier, A. C., da Silva, B. S., Cunha, R. A., and Agostinho, P. (2016). Age-related changes in the synaptic density of amyloid-β protein precursor and secretases in the human cerebral cortex. *J. Alzheimers Dis.* 52, 1209–1214. doi: 10.3233/JAD-160213

Qi, G., van Aerde, K., Abel, T., and Feldmeyer, D. (2016). Adenosine differentially modulates synaptic transmission of excitatory and inhibitory microcircuits in layer 4 of rat barrel cortex. *Cereb. Cortex* 27, 4411–4422. doi: 10.1093/cercor/bhw243

Rebola, N., Pinheiro, P. C., Oliveira, C. R., Malva, J. O., and Cunha, R. A. (2003). Subcellular localization of adenosine A1 receptors in nerve terminals and synapses of the rat hippocampus. *Brain Res.* 987, 49–58. doi: 10.1016/S0006-8993(03)03247-5

Rebola, N., Porciúncula, L. O., Lopes, L. V., Oliveira, C. R., Soares-da-Silva, P., and Cunha, R. A. (2005). Long-term effect of convulsive behavior on the density of adenosine A1 and A2A receptors in the rat cerebral cortex. *Epilepsia* 46(Suppl. 5), 159–165. doi: 10.1111/j.1528-1167.2005.01026.x

Rigoulot, M. A., Leroy, C., Koning, E., Ferrandon, A., and Nehlig, A. (2003). Prolonged low-dose caffeine exposure protects against hippocampal damage but not against the occurrence of epilepsy in the lithium-pilocarpine model in the rat. *Epilepsia* 44, 529–535. doi: 10.1046/j.1528-1157.2003.50502.x

Rogers, P. J., and Dernoncourt, C. (1998). Regular caffeine consumption: a balance of adverse and beneficial effects for mood and psychomotor performance. *Pharmacol. Biochem. Behav.* 59, 1039–1045. doi: 10.1016/S0091-3057(97)00515-7

Rombo, D. M., Newton, K., Nissen, W., Badurek, S., Horn, J. M., Minichiello, L., et al. (2015). Synaptic mechanisms of adenosine A2A receptor-mediated hyperexcitability in the hippocampus. *Hippocampus* 25, 566–580. doi: 10.1002/hipo.22392

Samsonsen, C., Bråthen, G., Reimers, A., Helde, G., and Brodtkorb, E. (2013). Is dietary caffeine involved in seizure precipitation? *Epilepsy Behav.* 28, 147–150. doi: 10.1016/j.yebeh.2013.05.003

Sebastião, A. M., Cunha, R. A., de Mendonça, A., and Ribeiro, J. A. (2000). Modification of adenosine modulation of synaptic transmission in the hippocampus of aged rats. *Br. J. Pharmacol.* 131, 1629–1634. doi: 10.1038/sj.bjp.0703736

Silva, C. G., Métin, C., Fazeli, W., Machado, N. J., Darmopil, S., Launay, P. S., et al. (2013). Adenosine receptor antagonists including caffeine alter fetal brain development in mice. *Sci. Transl. Med.* 5:197ra104. doi: 10.1126/scitranslmed.3006258

Simões, A. P., Machado, N. J., Gonçalves, N., Kaster, M. P., Simões, A. T., Nunes, A., et al. (2016). Adenosine A2A receptors in the amygdala control synaptic plasticity and contextual fear memory. *Neuropsychopharmacology* 41, 2862–2871. doi: 10.1038/npp.2016.98

Simons, S. B., Caruana, D. A., Zhao, M., and Dudek, S. M. (2011). Caffeine-induced synaptic potentiation in hippocampal CA2 neurons. *Nat. Neurosci.* 15, 23–25. doi: 10.1038/nn.2962

Smith, A. (2002). Effects of caffeine on human behavior. *Food Chem. Toxicol.* 40, 1243–1255. doi: 10.1016/S0278-6915(02)00096-0

Svenningsson, P., Hall, H., Sedvall, G., and Fredholm, B. B. (1997). Distribution of adenosine receptors in the postmortem human brain: an extended autoradiographic study. *Synapse* 27, 322–335. doi: 10.1002/(SICI)1098-2396(199712)27:4<322::AID-SYN6>3.0.CO;2-E

Tchekalarova, J., Kubová, H., and Mares, P. (2006). Biphasic effect of chronic postnatal caffeine treatment on cortical epileptic afterdischarges during ontogeny in rats. *Brain Res.* 1082, 43–49. doi: 10.1016/j.brainres.2006.01.067

Testa-Silva, G., Verhoog, M. B., Linaro, D., de Kock, C. P., Baayen, J. C., Meredith, R. M., et al. (2014). High bandwidth synaptic communication and frequency tracking in human neocortex. *PLOS Biol.* 12:e1002007. doi: 10.1371/journal.pbio.1002007

Tetzlaff, W., Schubert, P., and Kreutzberg, G. W. (1987). Synaptic and extrasynaptic localization of adenosine binding sites in the rat hippocampus. *Neuroscience* 21, 869–875. doi: 10.1016/0306-4522(87)90043-1

Thithapandha, A., Maling, H. M., and Gillette, J. R. (1972). Effects of caffeine and theophylline on activity of rats in relation to brain xanthine concentrations. *Proc. Soc. Exp. Biol. Med.* 139, 582–586. doi: 10.3181/00379727-139-36191

Thompson, S. M., Haas, H. L., and Gähwiler, B. H. (1992). Comparison of the actions of adenosine at pre- and postsynaptic receptors in the rat hippocampus in vitro. *J. Physiol.* 451, 347–363. doi: 10.1113/jphysiol.1992.sp019168

van Aerde, K. I., Qi, G., and Feldmeyer, D. (2015). Cell type-specific effects of adenosine on cortical neurons. *Cereb. Cortex* 25, 772–787. doi: 10.1093/cercor/bht274

Verhoog, M. B., Obermayer, J., Kortleven, C. A., Wilbers, R., Wester, J., Baayen, J. C., et al. (2016). Layer-specific cholinergic control of human and mouse cortical synaptic plasticity. *Nat. Commun.* 7:12826. doi: 10.1038/ncomms12826

Vyleta, N. P., and Smith, S. M. (2008). Fast inhibition of glutamate-activated currents by caffeine. *PLOS ONE* 3:e3155. doi: 10.1371/journal.pone.0003155

Yang, J. N., Chen, J. F., and Fredholm, B. B. (2009). Physiological roles of A1 and A2A adenosine receptors in regulating heart rate, body temperature, and locomotion as revealed using knockout mice and caffeine. *Am. J. Physiol.* 296, H1141–H1149. doi: 10.1152/ajpheart.00754.2008

Yu, L., Coelho, J. E., Zhang, X., Fu, Y., Tillman, A., Karaoz, U., et al. (2009). Uncovering multiple molecular targets for caffeine using a drug target validation strategy combining A2A receptor knockout mice with microarray profiling. *Physiol. Genomics* 37, 199–210. doi: 10.1152/physiolgenomics.90353.2008

Conflict of Interest Statement: RC is a scientific consultant for the Institute for Scientific Information on Coffee.

The other authors declare that the research was conducted in the absence of any commercial or financial relationships that could be construed as a potential conflict of interest.

frontiers in Pharmacology

ORIGINAL RESEARCH
published: 22 December 2017
doi: 10.3389/fphar.2017.00951

Specific Temporal Distribution and Subcellular Localization of a Functional Vesicular Nucleotide Transporter (VNUT) in Cerebellar Granule Neurons

Aida Menéndez-Méndez[1,2,3], Juan I. Díaz-Hernández[1,2,3], Felipe Ortega[1,2,3], Javier Gualix[1,2,3], Rosa Gómez-Villafuertes[1,2,3] and María T. Miras-Portugal[1,2,3]**

[1] Department of Biochemistry and Molecular Biology, Faculty of Veterinary, Complutense University of Madrid, Madrid, Spain, [2] University Institute of Neurochemistry Research (IUIN), Complutense University of Madrid, Madrid, Spain, [3] Instituto de Investigación Sanitaria del Hospital Clínico San Carlos, Madrid, Spain

OPEN ACCESS

Edited by:
Francisco Ciruela,
University of Barcelona, Spain

Reviewed by:
Marçal Pastor-Anglada,
University of Barcelona, Spain
Arun Chaudhury,
GIM Foundation, United States

***Correspondence:**
Rosa Gómez-Villafuertes
marosa@ucm.es;
marosa@vet.ucm.es
María T. Miras-Portugal
mtmiras@ucm.es;
mtmiras@vet.ucm.es

Specialty section:
This article was submitted to Experimental Pharmacology and Drug Discovery, a section of the journal Frontiers in Pharmacology

Received: 25 October 2017
Accepted: 15 December 2017
Published: 22 December 2017

Citation:
Menéndez-Méndez A, Díaz-Hernández JI, Ortega F, Gualix J, Gómez-Villafuertes R and Miras-Portugal MT (2017) Specific Temporal Distribution and Subcellular Localization of a Functional Vesicular Nucleotide Transporter (VNUT) in Cerebellar Granule Neurons. Front. Pharmacol. 8:951. doi: 10.3389/fphar.2017.00951

Adenosine triphosphate (ATP) is an important extracellular neurotransmitter that participates in several critical processes like cell differentiation, neuroprotection or axon guidance. Prior to its exocytosis, ATP must be stored in secretory vesicles, a process that is mediated by the Vesicular Nucleotide Transporter (VNUT). This transporter has been identified as the product of the SLC17A9 gene and it is prominently expressed in discrete brain areas, including the cerebellum. The main population of cerebellar neurons, the glutamatergic granule neurons, depends on purinergic signaling to trigger neuroprotective responses. However, while nucleotide receptors like P2X7 and P2Y13 are known to be involved in neuroprotection, the mechanisms that regulate ATP release in relation to such events are less clearly understood. In this work, we demonstrate that cerebellar granule cells express a functional VNUT that is involved in the regulation of ATP exocytosis. Numerous vesicles loaded with this nucleotide can be detected in these granule cells and are staining by the fluorescent ATP-marker, quinacrine. High potassium stimulation reduces quinacrine fluorescence in granule cells, indicating they release ATP via calcium dependent exocytosis. Specific subcellular markers were used to assess the localization of VNUT in granule cells, and the transporter was detected in both the axonal and somatodendritic compartments, most predominantly in the latter. However, co-localization with the specific lysosomal marker LAMP-1 indicated that VNUT can also be found in non-synaptic vesicles, such as lysosomes. Interestingly, the weak co-localization between VNUT and VGLUT1 suggests that the ATP and glutamate vesicle pools are segregated, as also observed in the cerebellar cortex. During post-natal cerebellar development, VNUT is found in granule cell precursors, co-localizing with markers of immature cells like doublecortin, suggesting that this transporter may be implicated in the initial stages of granule cell development.

Keywords: VNUT, granule cells, cerebellum, ATP exocytosis, VGLUT1, GCPs

INTRODUCTION

Extracellular adenosine triphosphate (ATP) and nucleotide analogs influence essential activities in the nervous system, acting through both G protein-coupled P2Y receptors and ionotropic P2X receptors (for review see (Burnstock, 2006, 2013). ATP is mainly released from neural cells by an exocytotic process (Gutierrez-Martin et al., 2011), which requires a previous storage into secretory vesicles (SVs), a process mediated by a specific vesicular transporter. Depending on the cell type and the environmental conditions, ATP release may also be driven by connexins and pannexins, large-pore ion and metabolite channels (for review see (Baroja-Mazo et al., 2013).

Vesicular neurotransmitter transporters (VNTs) drive the storage of specific soluble compounds in SVs, a crucial step in neurotransmission. Vesicles containing more than one neurotransmitter require specific VNTs for each of them. The abundance of ATP in secretory granules opens new horizons in neurotransmission and the term co-transmission was coined by Burnstock (1976, 2004) 40 years ago in reference to such complexity. Initially, the storage of different nucleotides in the same catecholaminergic chromaffin granules was reported, and then further confirmed in cholinergic and other storage vesicles (reviewed by Winkler and Westhead, 1980; Volknandt and Zimmermann, 1986). The vesicular monoamine transporter (VMAT1) was the first VNT to be isolated from a rat leukemia cell line cDNA library (Erickson et al., 1992). The existence of an active vesicular nucleotide transporter (VNUT) was first inferred from its kinetic parameters, exhibiting a mnemonic saturation profile and low specificity, capable of transporting a variety of nucleotides at intravesicular concentrations close to 150 mM (Bankston and Guidotti, 1996; Gualix et al., 1996, 1999a). The VNUT was identified as a product of the *SLC17A9* gene (Sawada et al., 2008), a member of the anion solute carrier transporters 17 family (SLC17) that includes other VNTs, such as the three vesicular glutamate transporter isoforms (VGLUT1, VGLUT2 and VGLUT3). Recently, the role of VNUT has been studied extensively in chromaffin granules from the adrenal medulla, assessing catecholamine storage and granule release (Estevez-Herrera et al., 2016). Moreover, co-localization of VNUT and the vesicular acetylcholine transporter (VAChT) has been reported in cholinergic vesicles from the electroplaque of *Torpedo californica* (Li and Harlow, 2014), and in other types of secretory granules (Haanes and Novak, 2010).

Immunohistochemical studies in the brain have demonstrated that VNUT is not homogeneously expressed in all cell subtypes and anatomical structures, rather it is particularly abundant in the mouse cerebellar cortex (Larsson et al., 2012). Among the different cell populations that constitute the cerebellum, granule neurons in the granular layer of adults is the most numerous cell subtype. Cerebellar granule neurons are glutamatergic cells that express high levels of VGLUT1 (Hallberg et al., 2006). The axons from these neurons ascend to the molecular layer, where they bifurcate to form the parallel fibers that connect with the dendritic tree of Purkinje cells (Ramón y Cajal, 1889, 1904, 1995; Cerminara et al., 2015). Primary cultures of cerebellar granule neurons are widely used to study neurotransmission, as these cells can develop the morphological, biochemical and electrophysiological characteristics of mature neurons *in vitro*. Indeed, they express a variety of functional P2Y and P2X nucleotide receptors, making them a suitable model to study the purinergic system (Hervas et al., 2003, 2005; Leon et al., 2006; Sanchez-Nogueiro et al., 2009, 2014).

The maturation of granule cells in culture is accompanied by time-dependent changes in the expression and activity of purinergic receptors (Sanz et al., 1996; Hervas et al., 2003). We previously reported that activation of either P2X3 or P2X7 receptors induces an increase in cytosolic Ca^{2+} in cerebellar granule neurons, resulting in the exocytotic release of glutamate and the subsequent enhancement of synapsin-1 phosphorylation (Leon et al., 2006, 2008). In addition, both the $P2Y_{13}$ and P2X7 receptors in granule neurons are involved in neuroprotection (Ortega et al., 2009; Ortega et al., 2010, 2011; Morente et al., 2014; Miras-Portugal et al., 2016). Despite the obvious importance of the purinergic system in the pathophysiological context of granule cells, there is currently no information concerning vesicular ATP storage and its relationship with VNUT expression. Moreover, granule neuron development occurs in the context of the cerebellar structure, and thus, it would be relevant to study the presence and evolution of VNUT in a more physiological context.

In the present work, we analyzed the vesicular release of ATP from primary cultures of cerebellar granule cells, studying the involvement of VNUT in this process and the effect of its inhibition. The distribution of VNUT was compared to that of VGLUT1 *in vitro* and *in vivo*, assessing both the subcellular location and temporal evolution during neuronal maturation. Our findings shed light on the ATPergic and glutamatergic nature of cerebellar granule neurons.

MATERIALS AND METHODS

Ethics Statement

All animal procedures were carried out at the Complutense University of Madrid in accordance with European and Spanish regulations (2010/63/EU; RD1201/2005; RD 53/2013), and following the guidelines of the International Council for the Laboratory Animal Science. The C57BL/6 mice used in these studies were obtained in-house. The protocols employed were approved by the Committee for Animal Experiments at the Complutense University of Madrid and by the Committee for Animal Ethics of the Regional Government of Madrid.

Cerebellar Granule Cells Culture

Primary cultures of cerebellar granule cells were prepared using a modified version of the procedure described by Pons et al. (2001). Briefly, the cerebellum was dissected out from postnatal day 5 mice and dissociated with the Papain Dissociation System (Worthington Biochemical, Lakewood, NJ, United States). Neurons were plated onto coverslips at a density of 120,000 cells/cm^2 or in culture plates pre-coated with poly-L-lysine (10 μg/ml; Biochrom, Berlin, Germany) and they were maintained at 37°C in a humidified atmosphere containing 5% CO_2 and in Neurobasal medium (Life Technologies,

Gaithersburg, MD, United States) supplemented with 2% B27, 25 mM KCl, 1% GlutaMAX™, 100 U/ml penicillin and 0.1 mg/ml streptomycin. The antimitotic drug cytosine arabinoside (AraC, 10 μM) was added to the culture medium to avoid the proliferation of non-neuronal cells.

RT-PCR and Quantitative Real-Time PCR

Total RNA was obtained from cultured granule cells using a SpeedTools Total RNA Extraction kit (Biotools), following the manufacturer's instructions. After purification, the total RNA was quantified and 1 μg was reversed transcribed using M-MLV reverse transcriptase, 6 μg of random primers and 350 μM dNTPs (all from Thermo Fisher Scientific). Quantitative real-time PCR (qPCR) reactions were performed in final volume of 25 μl using the LuminoCt qPCR Ready Mix (Sigma–Aldrich), 5 μl of the cDNA synthesized previously and 1.25 μl of specific commercial TaqMan® gene expression assays for mouse: VGLUT1 (Mm00812886_m1), VNUT (Mm00805914_m1), the housekeeping gene glyceraldehyde 3-phospate dehydrogenase (GAPDH, Mm99999915_g1), all from Applied Biosystems. The qPCR assays were carried out using a StepOnePlus Real-Time PCR System (Applied Biosystems) as follows: denaturation at 95°C for 20 s, followed by 40 cycles of 95°C for 1 s and 60°C for 20 s. As indicated, the expression of each gene was normalized to that of the endogenous housekeeping gene GAPDH amplified in parallel.

Western Blotting

Granule cells or cerebellar tissues were lysed and homogenized for 1 h at 4°C in lysis buffer (pH 7.4) containing 50 mM Tris-HCl, 150 mM NaCl, 1% Nonidet P40 and Complete™ Protease Inhibitor Cocktail Tablets (Roche Diagnostics GmbH). The cell lysate was then centrifuged at 16,000 × g for 9 min and the supernatants collected. Protein extracts were resolved on 10% SDS-PAGE gels and transferred to nitrocellulose membranes, which were then blocked for 1 h at RT (∼25°C) with 3% BSA in TBS (10 mM Tris, 137 mM NaCl, 2.7 mM KCl, 5 mM Na_2HPO_4, 1.4 mM KH_2PO_4 and 0.1% Tween [pH 7.5]). The membranes were probed with primary antibodies raised against VNUT (1:500, MBL), anti-VGLUT1 (1:7500, Synaptic Systems) and GAPDH (1:10,000, Sigma Aldrich). Antibody binding was detected by ECL chemiluminescence (Amersham GE Healthcare), and images were captured with ImageQuant LAS 500 (GE Healthcare Life Sciences) and analyzed using ImageQuant TL.

Immunofluorescence

Granule cells cultured on coverslips in 35 mm dishes were fixed for 15 min with 4% paraformaldehyde (PFA) and then rinsed with PBS twice for 10 min. For immunofluorescence studies of the cerebellum, the extracted brains were fixed in 4% PFA for 24 h, cryoprotected in 30% sucrose, embedded in O.C.T. (Sakura Finetek), and cryosections (30 μM) were obtained in the sagittal plane on a Leica CM1950 cryostat. Afterward, coverslips or cryosections were blocked and permeabilized for 1h at RT with blocking solution (0.1% Triton X-100, 5% FBS and 10% BSA in PBS). The coverslips or sections were then incubated overnight at 4°C with the corresponding primary antibodies: rabbit anti-VNUT (1:100, MBL), mouse anti-βIII-tubulin (1:1000, Promega), mouse anti-VGLUT1 (1:500, Synaptic Systems), mouse anti-synaptophysin (1:500, Sigma–Aldrich), chicken anti-MAP2 (1:1000, Abcam), guinea pig anti-DCX (1:500, Millipore), mouse anti-Math1 (1:250, Abcam), mouse anti-LAMP-1 (1:50, ThermoFisher Scientific), and mouse anti-SMI 312 (1:500, Abcam). The following day, the cells or sections were washed three times with PBS and incubated with the corresponding fluorescent-tagged secondary antibodies for 1 h at RT: Alexa fluor 594® donkey anti-rabbit, Alexa fluor 488® goat anti-mouse, Alexa fluor 647® goat anti-mouse (all from Thermo Fisher Scientific), Cy™5 donkey anti-guinea pig, and FITC donkey anti-chicken (both from Jackson ImmunoResearch). The nuclei were counterstained with 4′, 6-diamidino-2-phenylindole (DAPI, Thermo Fisher Scientific) and the coverslips or sections were finally mounted on glass slides using FluoroSave™ Reagent (Calbiochem). When antibodies against VNUT and Math1 were used on cerebellar sections, streptavidin-biotin amplification of the fluorescence signal was used. Images were acquired on a Leica TCS SPE confocal microscope using the 40X and 63X W/IR objectives.

Fluorescent Labeling of Vesicular ATP

Quinacrine [4-*N*-(6-chloro-2-methoxyacridin-9-yl)-1-*N*,1-*N*-diethylpentane-1,4-diamine] was used to visualize vesicular ATP, a fluorescent dye widely used to detect ATP-enriched vesicles (Gutierrez-Martin et al., 2011). Quinacrine staining was carried out by incubating granule cells for 15 min at 37°C in Locke's buffer (140 mM NaCl, 4.5 mM KCl, 2.5 mM $CaCl_2$, 1.2 mM KH_2PO_4, 1.2 mM $MgSO_4$, 5.5 mM glucose and 10 mM HEPES [pH 7.4]) containing 4 μM quinacrine (Sigma–Aldrich). Time-lapse studies were performed with an Olympus IX81 inverted microscope equipped with a 100X, 1.45 NA, oil-immersion objective. Images were acquired every 200 ms with a Hamamatsu C9100 EM-CCD digital camera (Hamamatsu) controlled by CellR software (Olympus). Vesicular fusion and release into the extracellular space was observed as a rapid loss of the quinacrine signal. During the assays, cells were continuously perfused with Locke's buffer at a rate of 1.5 ml/min at 37°C. Perfusion was gravity-driven and solution exchange was performed by manually operating electronic valves of a VC-6 drug application system (Warner Instruments). Images were processed using the ImageJ free software v.1.50i (National Institutes of Health, Bethesda, MD, United States).

ATP Release

Adenosine triphosphate release was measured using the ENLITEN® rLuciferase/Luciferin reagent (Promega). Granule cells were maintained for 30 min at 37°C in Mg^{2+}-free Locke's buffer containing 100 μM ARL67156, a competitive inhibitor of ecto-ATPases (Levesque et al., 2007), and subsequently, 50 μl of extracellular medium was collected to measure the basal ATP levels. The cells were then stimulated with 10 μM ionomycin and after 5 min, 50 μl of the extracellular medium was collected to measure ATP concentration after stimulation. The samples were centrifuged at 600 × *g* for 5 min at 4°C

and 10 μl of supernatant were transferred onto 96-well plate placed on ice. When indicated, cells were incubated with 2 μM Evans Blue (Sigma–Aldrich) for 1 h (Loiola and Ventura, 2011). The plate was then situated in a FLUOstar OPTIMA Microplate Luminometer (BMG LABTECH GmbH) and 100 μl of rLuciferase/Luciferin reagent was automatically injected into each well at RT. The ATP concentration was estimated by interpolation from a linear standard curve.

Statistical Analysis

The data shown are mean values ± standard error of the mean (s.e.m) and all independent experiments shown were reproduced 3–6 times. The figures were generated and the statistical analyses performed using GraphPad Prism 6 (GraphPad Software). The results were analyzed using an unpaired Student's *t*-tests or ANOVA with Dunnet's Multiple Comparisons test. A p-value ≤ 0.05 was considered statistically significant.

RESULTS

Cerebellar Granule Cells Express Native Functional VNUT

The expression of a variety of functional P2Y and P2X nucleotide receptors in primary cultures of cerebellar granule cells was already reported (Hervas et al., 2003, 2005; Leon et al., 2006; Sanchez-Nogueiro et al., 2009, 2014). In order to investigate the presence of native VNUT in granule neurons, western blot and immunofluorescence studies were performed. Unless specified otherwise, all experiments were carried out at day 7 *in vitro* coinciding with the peak of synaptogenesis in these cultured neurons (Mundy et al., 2008; Juranek et al., 2013). In western blots of total protein extracts from granule cells, a 60 kDa band was detected (**Figure 1A**) that is consistent with the molecular size of the VNUT protein (Sawada et al., 2008). The specificity of this band was confirmed using specific neutralizing peptides (data not shown). When immunocytofluorescence studies were performed on PFA-fixed cells using antibodies against VNUT and βIII-tubulin (**Figure 1B**), VNUT was widely expressed in granule cells displaying a characteristic punctuate staining of VNTs. The functionality of VNUT was also confirmed through the capacity of granule cells to release ATP in a calcium-dependent manner. Using the sensitive luciferin-luciferase assay to quantify ATP in the extracellular medium, the Ca^{2+}-selective ionophore ionomycin produced a significant increase of extracellular ATP relative to the basal unstimulated state (**Figure 1C**). The kinetics of ATP release reflected a rapid mechanism, completed within seconds of stimulation and suggestive of calcium-dependent exocytosis. The participation of VNUT in vesicular ATP storage was confirmed using Evans Blue, a VNUT inhibitor (Sawada et al., 2008), which reduced the net release of ATP induced by ionomycin (**Figure 1C**). Remarkably, although Evans Blue was the most effective VNUT inhibitor available, previous studies in synaptic vesicles isolated from rat brain demonstrated that Evans Blue behaved only as a partial inhibitor of ATP release (Gualix et al., 1999b). Likewise, it is important to consider that inhibition of VNUT affects only the subsequent ATP transport and not the ATP stored prior to the treatment, which will be eventually released after ionomycin stimulation. The co-localization of VNUT and the vesicular protein synaptophysin further supported the exocytotic nature of ATP release (**Figure 1D**). Interestingly, co-localization of VNUT and synaptophysin immunostaining was not complete, indicating that VNUT may also be located in another type of storage vesicle or subcellular structure.

Purinergic Receptor Activation Triggers the Release of ATP-Enriched Vesicles in Granule Cells

Many neuronal and non-neuronal cells release ATP in a controlled manner. Indeed, an autoregulated mechanism of ATP release has been reported where P2X7 receptor activation not only triggers ATP exocytosis but also, it profoundly modifies secretory vesicle dynamics in N2a neuroblastoma cells (Gutierrez-Martin et al., 2011). To assess whether similar autoregulation occurs in granule cells, we visualized exocytosis of single ATP-enriched vesicles from granule neurons after activation of purinergic receptors using fluorescence microscopy. Quinacrine is an acidophilic antimalarial drug that binds to intracellular ATP stored in vesicles and that was used as a fluorescent marker to detect the exocytosis of releasable ATP-enriched vesicles (Orriss et al., 2009; Liu et al., 2016). Granule cells contained abundant quinacrine-labeled vesicles and such punctate staining was not only evident throughout the soma but also, in cell prolongations (**Figure 2A**). Changes in fluorescence of single vesicles were analyzed under basal conditions and during ATP (1 mM) administration (**Figure 2B**). This ATP concentration was selected in order to trigger P2X7 receptors, which requires such a high concentration of ATP. As expected, ATP stimulation was followed by a reduction in the number of quinacrine fluorescence puncta (**Figure 2B**). Moreover, the abrupt time course of fluorescence loss in several regions of interest (ROIs) with quinacrine-stained vesicles reflected vesicular fusion with the plasma membrane and quinacrine release into the extracellular medium (**Figure 2B**). A parallel control assay was performed in which the cells were depolarized with 30 mM KCl, which produced a comparable release of quinacrine-stained vesicles (**Figure 2C**). These observations demonstrate that ATP-mediated activation of purinergic receptors can induce vesicular ATP release in cerebellar granule neurons.

Subcellular Distribution of the VNUT in Cerebellar Granule Cells

Given the morphological complexity of cerebellar granule cells in culture, we assessed the co-localization of VNUT with specific subcellular markers to define its distribution. When immunofluorescence was performed with antibodies against the somatodendritic marker microtubule-associated protein 2 (MAP2) and the pan-axonal neurofilament marker (SMI 312), VNUT co-localized with both these subcellular markers, indicating that this vesicular transporter exists both pre- and

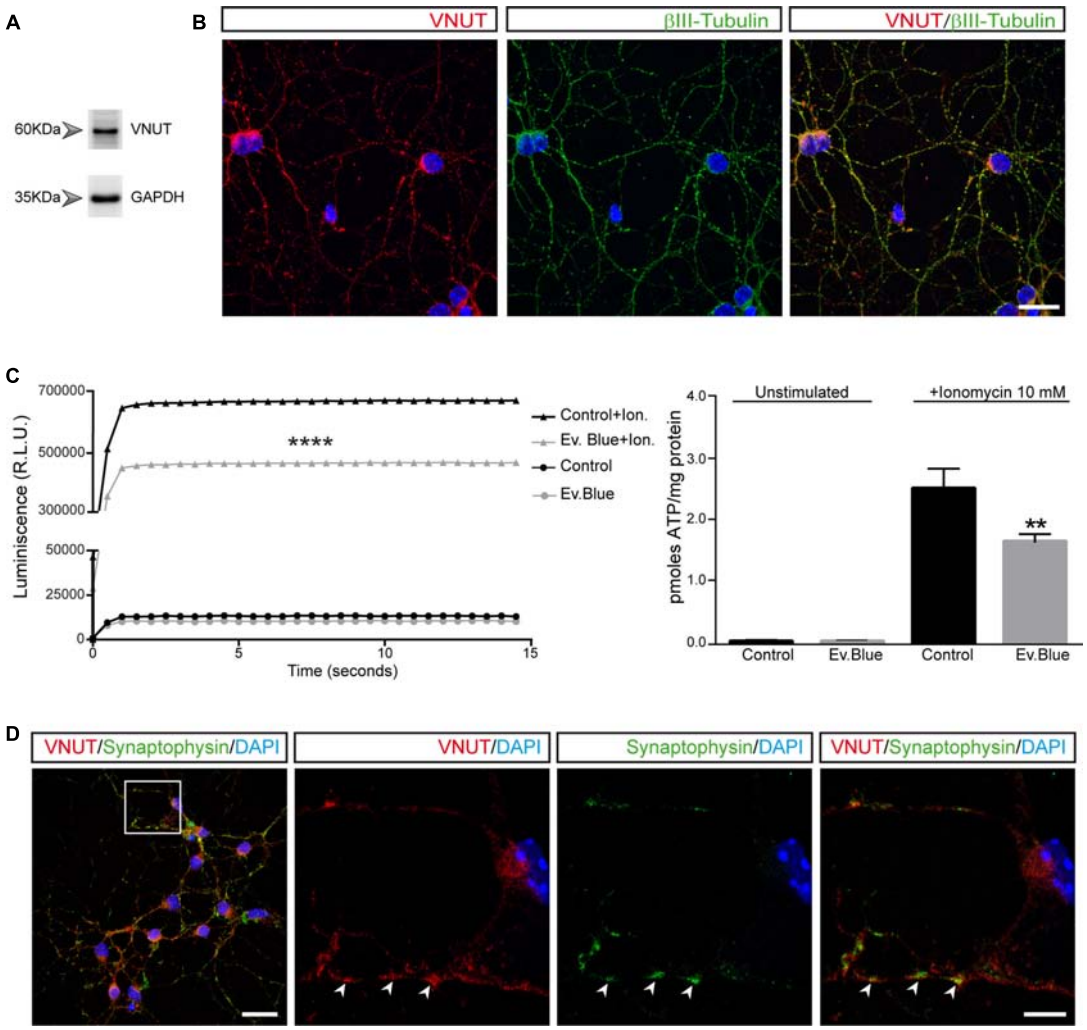

FIGURE 1 | Vesicular nucleotide transporter (VNUT) is expressed by cultured cerebellar granule cells. Identification of VNUT in granule cells by western blotting **(A)** and immunofluorescence **(B)**. Cells were stained with antibodies against VNUT (red) and βIII-tubulin (green). Scale bar: 20 μm. **(C)** ATP release to the extracellular medium by granule cells. The graph shows the luminescence values of cells maintained in the presence or absence of Evans Blue (2 μM) and stimulated with ionomycin (10 μM) or left unstimulated. The right graph represents the pmoles of ATP released per mg of protein in the different experimental conditions. The values represent the mean ±SEM (n = 3: $^{**}p<0.01$, $^{****}p<0.0001$, unpaired Student's t-test). **(D)** Representative confocal microscopy images of the immunostaining of granule cell neurons for VNUT (red) and synaptophysin (green). The nuclei are counterstained with DAPI (blue). Scale bar: 20 μm. The inset represents a 4x magnification of the cell indicated. The arrows indicate the most prominent VNUT and synaptophysin positive vesicles. Scale bar: 5 μm.

post-synaptically in granule neurons (**Figure 3A**). However, VNUT co-localized more intensely with MAP-2 than with SMI 312, suggesting that this vesicular transporter might be more strongly expressed post-synaptically. To confirm the presence of VNUT in dendrites, double immunofluorescence was performed with antibodies against VNUT and the postsynaptic density protein 95 (PSD-95) (**Figure 3B**). Both these proteins clearly co-localized, confirming that VNUT is located post-synaptically in granule neurons. The abundance of VNUT in the soma of granule cells suggested that this vesicular transporter is actively synthesized and packaged in earlier structures for further subcellular transportation, for instance into storage vesicles. Notably, VNUT expression has previously been reported in lysosomes (Shin et al., 2012; Jung et al., 2013; Oya et al., 2013; Cao et al., 2014) and interestingly, the clear co-localization in certain cytosolic areas of antibody staining for VNUT and the lysosomal marker LAMP-1 (**Figure 3C**), confirmed the presence of VNUT in lysosomes.

Distribution and Time-Dependent Expression of VNUT and VGLUT1 in Primary Cultures of Cerebellar Granule Neurons

The glutamatergic phenotype of cerebellar granule cells reflects the storage and release of glutamate as a classic neurotransmitter, which requires the expression of VGLUTs, of which VGLUT1 is the most abundant isoform. Thus, we compared the

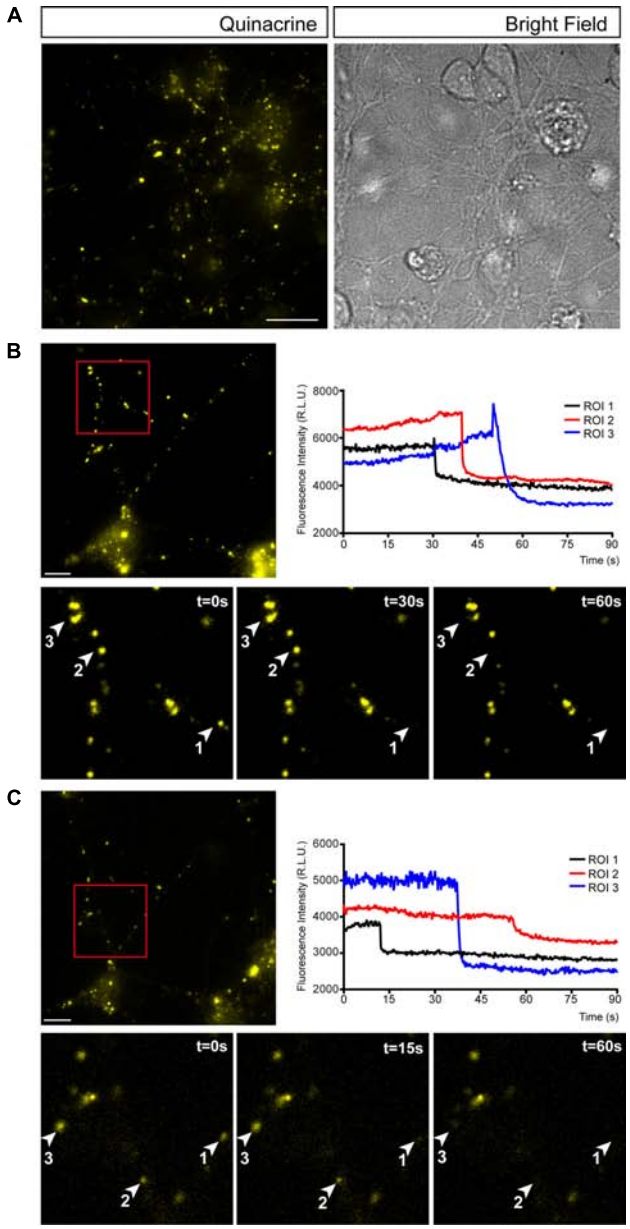

FIGURE 2 | Cerebellar granule cells release ATP through by exocytosis. **(A)** Representative micrographs of granule cells stained with quinacrine (pseudo colored in yellow). Bright field image of the same area is showed on the right. Vesicular ATP release after stimulation with 1 mm ATP **(B)** or 30 mM KCl **(C)**. In each panel, the upper image corresponds to the micrograph representing quinacrine staining before stimulation. Scale bar: 5 μm. Insets represent sequential images of quinacrine-loaded vesicles showing the time course of the changes in fluorescence within a ROI during a 60 s stimulation with ATP **(B)** or KCl **(C)**. Graphical representation of the changes in fluorescence intensity corresponding to the selected ROIs during stimulation with ATP **(B)** or KCl **(C)**.

subcellular distribution and time-dependent expression of this transporter and VNUT. Interestingly, the dense and abundant co-localization of VNUT and MAP2 was not accompanied by a similar co-localization between VGLUT1 and MAP2, which rarely coincided in dendritic regions (**Figure 4**). By contrast, while VNUT and SMI 312 co-localized sparsely in some prolongations, the co-localization of staining for SMI 312 and VGLUT1 was dense an almost complete (**Figure 4**).

Double immunofluorescence was performed to determine whether VNUT and VGLUT1 coincide in the same vesicles and very few vesicles containing VGLUT1 were stained for VNUT, with most expressing only one of these vesicular transporters (**Figure 5A**). Thus, cerebellar granule cells appeared to contain segregated populations of secretory vesicles that store either ATP or glutamate. However, it should be remembered that these studies were performed *in vitro*, in primary cultures of granule neurons and, the expression of each transporter may vary during the maturation of the cells in culture. Thus, we analyzed the transcriptional and protein time-course of VNUT and VGLUT1 expression in these cultures from days 1 to 10 *in vitro*. While VNUT mRNA expression could be detected from the first day of culture and it gradually increased over the following days (**Figure 5B**), VGLUT1 expression was not evident until day 4 *in vitro*, although it increased strongly on the following days (**Figure 5C**). The detection of both these vesicular transporters in western blots correlated well with their mRNA expression (**Figure 5D**), consistent with the maturation of the culture and the establishment of synaptic contacts by granule cells *in vitro* and the development of a functional synaptic machinery. Cerebellar extracts from P15 or adult mice were used as positive control of both transporters (**Figure 5E**).

Presence and Distribution of VNUT in the Mouse Cerebellar Cortex

The aforementioned results in primary cultures of cerebellar granule cells suggested the existence of different vesicular pools preferentially containing either VNUT or VGLUT1, with a few vesicles exhibiting both transporters. To assess whether this distribution reflects the situation in the mouse cerebellum, this tissue was immunostained with antibodies against both vesicular transporters. In slices of the postnatal day 15 (P15) mouse cerebellum, both vesicular transporters were located in the molecular and the granular layers of the cerebellar cortex (**Figures 6A,B**). While VGLUT1 was found in the axons and soma of granule cells located in the molecular and granular layers, respectively (**Figure 6B**), VNUT was also observed in the Purkinje layer surrounding the soma of Purkinje neurons (**Figure 6B**). Although these vesicular transporters exhibited distinct distributions, confocal images with orthogonal views showed a few examples of co-localization between VNUT and VGLUT1 in both the molecular (ML) and granular (GL) layers (**Figures 6C,D**).

The presence of VNUT early in primary cultures of granule cells obtained from P5 mice (**Figures 1B**, **5B,D**) raised the question as to how such expression varied during cerebellar development. It is well known that the cortical layers of the cerebellum are not defined at P5 and that secondary proliferation niches containing granule cell precursors (GCPs) can be found (Altman, 1972; Espinosa and Luo, 2008). Moreover, at this time

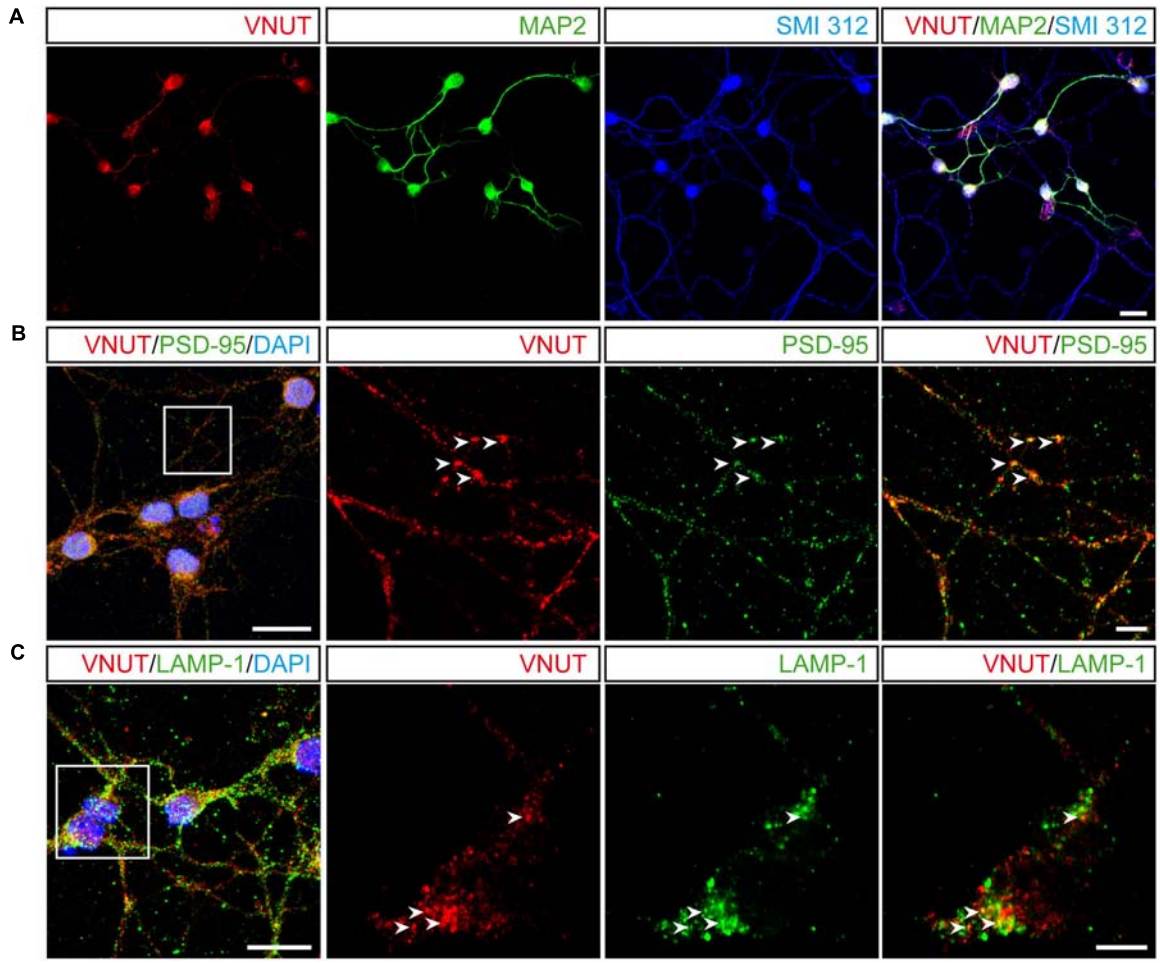

FIGURE 3 | Subcellular localization of VNUT in cerebellar granule cells. **(A)** Representative confocal images showing the immunofluorescence for VNUT (red), MAP2 (green) and SMI 312 (blue). Scale bar: 20 μm. **(B)** Confocal images of double immunofluorescence for VNUT (red) and PSD95 (green). Scale bar: 15 μm. Insets represents higher magnifications to show the co-localization (yellow) of VNUT (red) and PSD95 (green). Arrowheads indicated co-localized immunostaining for the two proteins. Scale bar: 5 μm. **(C)** Representative confocal images of double immunofluorescence for VNUT (red) and LAMP-1 (green). Scale bar: 15 μm. Insets represents higher magnifications to show co-localization (yellow) of VNUT (red) and LAMP-1 (green). The arrowheads indicate co-localization of the immunostaining for the two proteins. Scale bar: 5 μm.

immature granule cells are migrating from the external granular layer (EGL) to the internal granular layer (IGL), where they will reach their final location (Altman and Bayer, 1997). At P5, VNUT staining in cerebellar slices was stronger and more widely distributed (**Figures 7A,A′**) than at P15 stage (**Figure 7E**). To characterize the specific populations expressing VNUT during development, we used an antibody against Math1 to identify GCPs, a transcription factor of the bHLH (basic helix-loop-helix) class that is essential for the proper development of cerebellar granule layer (Ben-Arie et al., 1997), and an antibody against the microtubule-associated protein doublecortin (DCX) to recognize neuroblasts and immature neurons (**Figure 7**). At P5, VNUT and Math1 co-localized in the cerebellum (**Figures 7D,D′**), confirming that GCPs express VNUT during their postnatal development. Moreover, in certain regions of the IGL, VNUT, Math1 and DCX co-localization was also observed (**Figures 7D,D′**). Hence, the onset of VNUT expression appears to commence early in cerebellar development, and it is expressed by neuronal progenitors like GCPs and immature neurons that have not fully differentiated. Alternatively, Math1 and DCX expression was weaker at P15 due to the development of the cerebellum (**Figures 7E–H**), although VNUT persisted at this stage and it was found in several cerebellar layers, yet mainly in the ML. These results correlate with our observations *in vitro*, whereby VNUT is expressed from the first day of cerebellar granule cell culture, when neurons are still immature, persisting once the neurons have matured and established functional synapses.

DISCUSSION

The present study confirms that the VNUT, is functionally expressed in primary cultures of cerebellar granule neurons, its

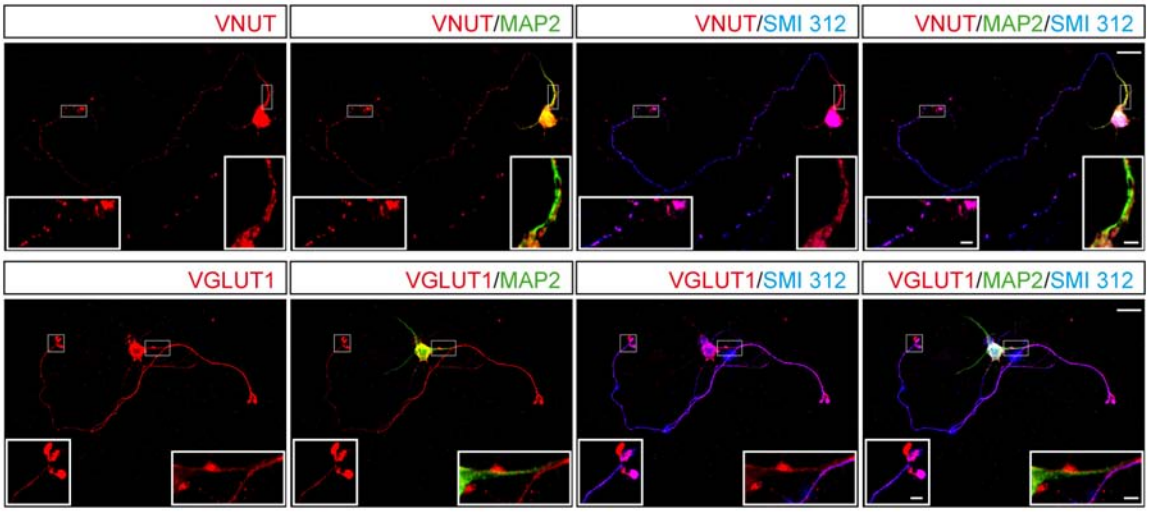

FIGURE 4 | Distribution of VNUT or VGLUT1 in a single cerebellar granule cell. Representative confocal images showing the immunostaining for MAP2 (green), SMI 312 (blue) and either VNUT (red, upper panels) or VGLUT1 (red, lower panels). Scale bar: 15 μm. The insets represent higher magnifications of the somatodendritic or axonal compartments. Scale bar: 2.5 μm.

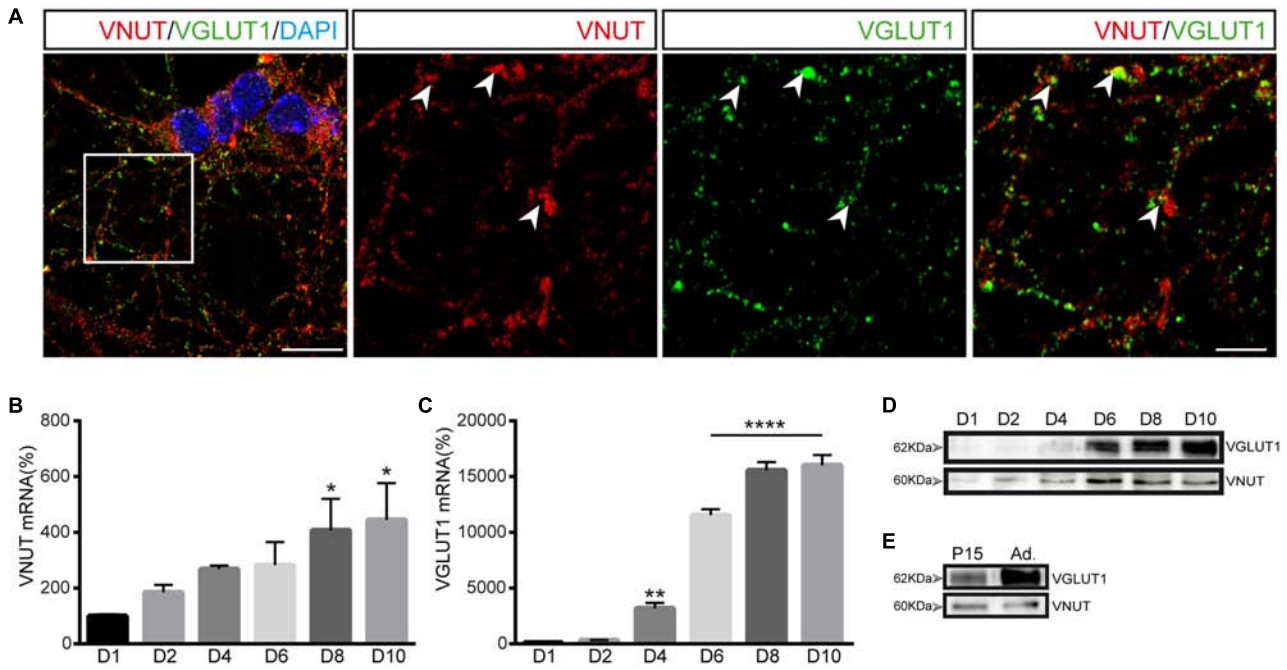

FIGURE 5 | Expression of VNUT and VGLUT1 in cerebellar granule cells. **(A)** Representative confocal images showing double immunofluorescence for VNUT (red) and VGLUT1 (green). The nuclei were counterstained with DAPI (blue). Scale bar: 12 μm. Right panels represent a higher magnification to show the immunostaining for each vesicular transporter. The arrowheads indicate co-localization of the immunoreactivity for VNUT and VGLUT1. Immunofluorescence was performed on day 7 *in vitro*. Scale bar: 5 μm. VNUT **(B)** and VGLUT1 **(C)** mRNA levels analyzed by qPCR of cerebellar granule cells after different days of the culture. The values represent the mean ±SEM (n = 3: *p<0.05, **p<0.01, ***p<0.001, ANOVA with Dunnet test with respect to day 1). **(D)** Western blots of the total protein (10 μg) in cell lysates after different times in culture. **(E)** Western blot of total protein extracts from cerebellum used as positive control of VNUT and VGLUT1 expression.

expression varying as the cell cultures mature *in vitro* and it is distributed in presynaptic and postsynaptic vesicles in these neurons. Moreover, we demonstrate that VNUT is expressed very early in the cerebellar granule neuronal lineage, both *in vitro* and *in vivo*. Together, these results imply that VNUT potentially contributes to the postnatal development of granule cells in the cerebellar cortex, a role that will be challenging to define.

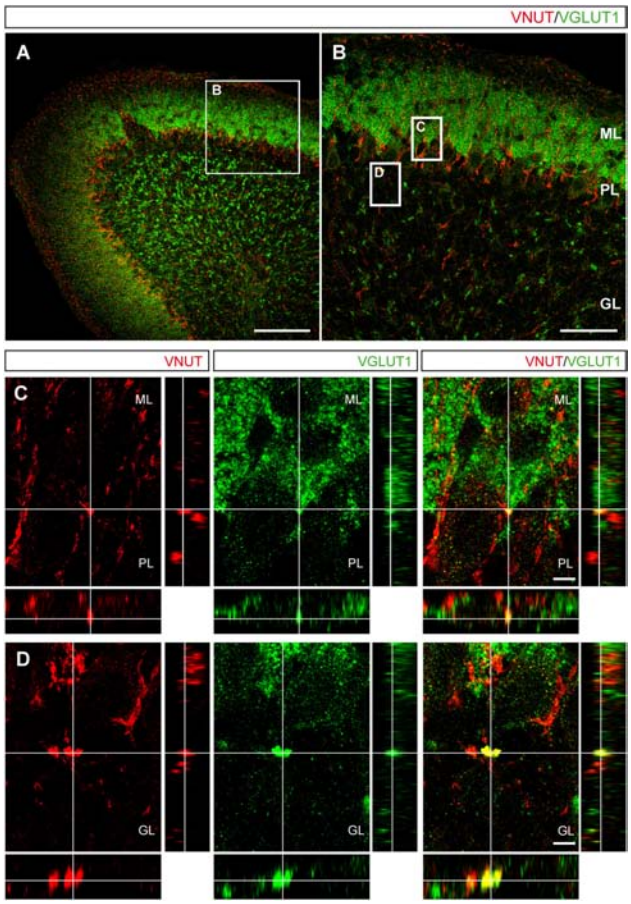

FIGURE 6 | Localization of VNUT and VGLUT1 in the mouse cerebellar cortex. **(A)** Representative micrograph of a section of the P15 cerebellum immunostained for VNUT (red) and VGLUT1 (green). Scale bar: 100 μm. **(B)** Higher magnification of the selected region in **(A)** showing the three cerebellar layers. Scale bar: 50 μm. The insets are shown in the lower panels. **(C,D)** Orthogonal sections. Selected z-scanning series of images showing double labeling for VNUT and VGLUT1, representing the three planes of view for one point, as indicated by the crossed dashed lines. Scale bar: 10 μm. ML, Molecular Layer; PL, Purkinje Layer; GL, Granular Layer.

Extracellular nucleotides play an essential role in cellular signaling, acting through purinergic receptors, and in neural tissues, extracellular ATP is involved in physiological processes like synaptic transmission, proliferation, differentiation or axonal elongation (Diaz-Hernandez et al., 2008; Gomez-Villafuertes et al., 2009; Diez-Zaera et al., 2011). In physio-pathological conditions including neuropathic pain, psychiatric disorders or epileptic seizures, enhanced P2 receptor expression has been reported, such as P2X4 or P2X7 (Tsuda et al., 2003; Beggs et al., 2012; Henshall et al., 2013; Sperlagh and Illes, 2014). Thus, the levels of extracellular nucleotides must be tightly controlled in order to only activate specific purinergic receptors when necessary. This tight regulation mainly focuses on controlling the release and the removal of nucleotides from the extracellular space. In terms of extracellular nucleotide removal, these compounds can be rapidly hydrolyzed to the last product adenosine, subsequently transported and incorporated to the cellular nucleotide pool (Rotllan and Miras Portugal, 1985; Miras-Portugal et al., 1986; Sen et al., 1998; Zimmermann et al., 2012; Gomez-Villafuertes et al., 2014; Pastor-Anglada and Perez-Torras, 2015).

By contrast, the exocytotic release of ATP and other nucleotides depends on VNUT activity, which links the intra- and extracellular steps of ATP signaling. Although its existence and kinetic parameters were described long ago (Bankston and Guidotti, 1996; Gualix et al., 1996, 1999a), not until recently was VNUT cloned (Sawada et al., 2008). VNUT is heterogeneously expressed in distinct cell subtypes and structures in the murine brain, being particularly abundant in cerebellar cortex (Larsson et al., 2012). However, little is known about its specific subcellular distribution and function within the complex cyto-architecture of the cerebellum.

Among the different neuronal subtypes that make up the cerebellum, granule cells are the most abundant. Purinergic signaling seems to play an important role in these cells, since they not only strongly express different purinergic receptors but also, VNUT (Larsson et al., 2012). Primary cultures of granule cells represent a suitable model to understand basic neurobiological processes. For instance, depolarization of these glutamatergic neurons through the activation of P2X3 or P2X7 receptors can induce glutamate release (Leon et al., 2008). However, as mentioned previously, there is nothing known about the role of VNUT in this cell model, although the data presented here clarifies some relevant issues. First, VNUT appears to co-localize with the vesicular marker synaptophysin in these cells and in addition, granule cells appear to release ATP by exocytosis. As inhibiting VNUT reduces the net release of ATP, VNUT is clearly involved in the vesicular storage of ATP as indicated elsewhere (Gualix et al., 1999a,b; Sawada et al., 2008).

We previously showed that activation of P2X7 receptors by ATP evokes the release of this nucleotide in neuroblastoma N2a cells (Gutierrez-Martin et al., 2011), and here we demonstrate a similar phenomenon occurs in cerebellar granule cells. Quinacrine loading highlighted the large number of acidic fluorescent vesicles that store ATP in cerebellar granule cells, and ATP stimulation induced an abrupt loss of fluorescence due to exocytosis. Hence, ATP appears to induce its own release in granule cells, an effect that could be mediated by P2X7 receptors since they require high ATP concentrations to be activated (Gutierrez-Martin et al., 2011). Depolarization induced by KCl also confirms the existence of a vesicular mechanism for ATP release, although it does not produce complete loss of quinacrine-loaded vesicles. This may indicate that not all the quinacrine-loaded vesicles belong to the ready releasable pool close to the plasma membrane or that these vesicles are not secretory ones. This latter possibility was confirmed by immunofluorescence assays with the lysosomal marker LAMP-1, whereby quinacrine-loaded vesicles that do not respond to the increase in intracellular calcium could be "conventional" lysosomes that accumulate high concentrations of ATP (Li et al., 2008). Moreover, VNUT does not fully co-localize with synaptophysin, indicating that the vesicular

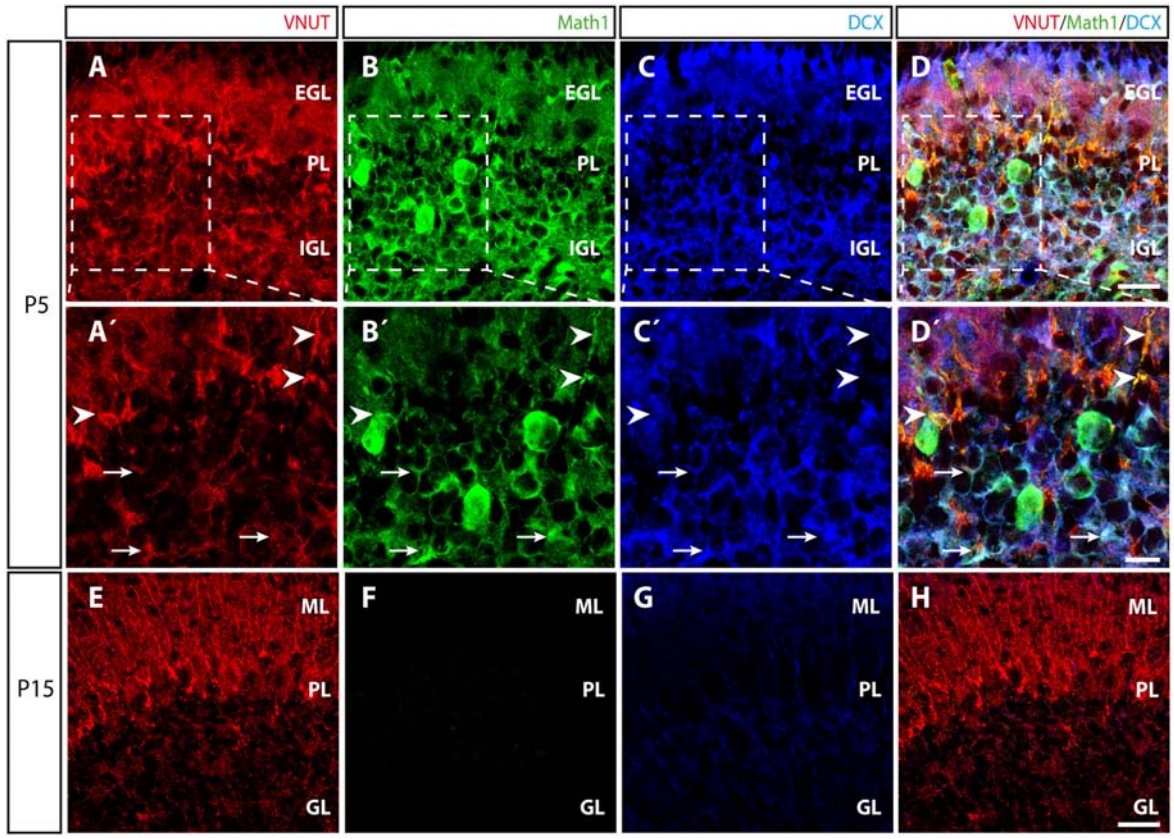

FIGURE 7 | Distribution of VNUT during the postnatal development of the cerebellar cortex. **(A–D)** Representative confocal images of P5 cerebellar sections showing triple immunofluorescence for VNUT (red), Math1 (a marker of committed GCPs) (green) and DCX (a marker of immature neurons) (blue), and the overlaid image. Scale bar: 20 μm. **(A′–D′)** Higher magnification of the selected region at P5 in which the arrowheads indicate the co-localization of the immunoreactivity for VNUT and Math1. The arrows indicate the co-localization of VNUT, Math1 and DCX immunostaining. Scale bar: 10 μm. **(E–H)** Representative micrographs of P15 cerebellar sections showing triple immunofluorescence for VNUT (red), Math1 (green) and DCX, (blue) and the overlaid images. Scale bar: 20 μm. EGL, External Granular Layer; PL, Purkinje Layer; IGL, Internal Granular Layer; ML, Molecular Layer; GL, Granular Layer.

transporter is present in non-synaptic vesicles. Indeed, VNUT has been identified in lysosomes of different cellular lineages (Shin et al., 2012; Oya et al., 2013; Cao et al., 2014), including sensory neurons (Jung et al., 2013). Lysosomes are best known for their role in protein degradation during autophagy and phagocytosis, yet they may also be involved in regulated exocytosis, acting as secretory vesicles (Blott and Griffiths, 2002; Li et al., 2008). Moreover, lysosomes can store large amounts of ATP and release it through exocytosis (Zhang et al., 2007; Pryazhnikov and Khiroug, 2008; Dou et al., 2012). In terms of cerebellar granule cells, the co-localization between VNUT and LAMP-1 confirmed the presence of this vesicular transporter in lysosomes, suggesting that these neurons can store ATP in lysosomes, and even release it from these vesicles by exocytosis.

Several studies of vesicular ATP release at central synapses suggest that ATP comes from a different pool of vesicles that is not synchronized either with GABA or glutamate release (for review see Pankratov et al., 2006). To assess whether cerebellar granule cells that release ATP and glutamate, and that express both VNUT and VGLUT1, also have a specific pool of ATP-containing vesicles, the distribution of both vesicular transporters was studied. When compared with the somatodendritic marker MAP2 and the neurofilament axonal marker SMI 312, VNUT was clearly present in both pre- and postsynaptic areas. By contrast, VGLUT1 was mainly seen to co-localize with the axonal marker and it was barely present in the somatodendritic regions. On the other hand, co-localization of VNUT and PSD-95 confirmed the transporter's presence in postsynaptic domains, suggesting that exocytosis of ATP could be bi-directional at synaptic contacts. Accordingly, the ATP released in the synaptic cleft can activate both pre- and postsynaptic purinergic receptors. At the presynaptic level, P2X receptor activation induces or enhances neurotransmitter release (Gu and MacDermott, 1997; Khakh and Henderson, 1998; Nakatsuka and Gu, 2001; Khakh et al., 2003; Rodrigues et al., 2005; Sperlagh et al., 2007; Khakh, 2009), whereas P2Y receptor activation mainly dampens neurotransmitter release (Rodrigues et al., 2005). Additionally, activation of postsynaptic P2X receptors may induce AMPA receptor internalization at the dendrites (Pougnet et al., 2014), modulating synaptic transmission. Presynaptic modulation by

ATP could originate from different sources, the terminal itself and neighboring nerve terminals or astrocytes. Moreover, the postsynaptic location of VNUT in granule cells suggests an additional source of ATP through its release from dendrites. VNUT was previously found in postsynaptic dendrites of dentate gyrus and hippocampal CA1 neurons (Larsson et al., 2012). The possibility that dendritic spines might be able to release ATP indicates that they might modulate presynaptic release of neurotransmitters through a retrograde mechanism. Exocytotic release of ATP and glutamate from granule cells can occur simultaneously, although they may be stored in different vesicle pools, as reflected by the segregated distribution of VNUT and VGLUT1. Indeed, co-localization between these vesicular transporters was rare after 7 days *in vitro*, although the expression of VNUT and VGLUT1 increased as the granule cell cultures mature, consistent with the establishment of synaptic contacts that require the corresponding synaptic machinery. Nevertheless, VNUT expression by these cells was detected very early, from their first day in culture.

As the granule cells culture were obtained at an early postnatal developmental stage, it is possible that the expression of VNUT and VGLUT1is distinct in the native tissue. Thus, the distribution of both vesicular transporters was analyzed in sagittal sections of the cerebral cortex at P15 stage, when VGLUT expression increases significantly (Boulland et al., 2004). The two vesicular transporters exhibited a clear non-overlapping distribution, with scarce co-localization, which was consistent with the results obtained in granule cell cultures. In fact, while the two transporters are located in both the molecular and granule layer of the cerebellar cortex, VNUT-staining was stronger in the molecular stratum. On the other hand, VNUT was also located around the soma of Purkinje cells, suggesting an important role of purinergic signaling in controlling GABAergic transmission (Casel et al., 2005). Indeed, it has already been demonstrated that P2X receptors can elicit Ca^{2+} responses in primary cultures of Purkinje cells (Mateo et al., 1998).

The evolution of VNUT expression in the mouse cerebellum was assessed from the immature postnatal P5–P15 stage. As the cerebellar layers are not well defined at P5 and granule cells are still migrating from the external to the internal granular layer, this appears to be a good model to correlate VNUT expression with that of the essential specific factors, Math1 and DCX. Math1 is a master gene that specifies the cerebellar granule neuron lineage and it is expressed in the committed GCPs (Ben-Arie et al., 1997; Srivastava et al., 2013), whereas DCX is a microtubule-associated protein that identifies neuronal precursors and immature neurons (Brown et al., 2003). In accordance with its early expression *in vitro*, VNUT was expressed abundantly at P5, and it co-localized with both Math1 and DCX, suggesting that it is expressed by GCPs and the immature neurons migrating from the external to the internal granular layer of the cerebellum. During the subsequent development of the cerebellum, committed granule cells become mature granule neurons between P5 and P15, as confirmed by the absence of Math1 and the dramatic reduction in DCX. Nevertheless, VNUT remains prominently expressed in the molecular and granule layer, highlighting the relevance of VNUT during the commitment and differentiation of cerebellar granule neurons.

There is now increasing evidence implicating VNUT in both physiological and pathological processes in neural tissues. For instance, VNUT helps regulate neuronal differentiation of neuroblastoma N2a cells (Menendez-Mendez et al., 2015) Moreover, during the development of glaucoma, there is a direct correlation between enhanced VNUT expression in the intern plexiform layers of the retina and an increase in extracellular ATP (Perez de Lara et al., 2015). More recently it was proposed that VNUT-dependent ATP release from spinal cord dorsal root neurons might originate neuropathic pain in mice (Masuda et al., 2016). Furthermore, clodronate was identified as a novel inhibitor of VNUT for the treatment of neuropathic and inflammatory pain, opening up new therapeutic possibilities for other pathologies (Kato et al., 2013, 2017).

In summary, we have characterized the subcellular localization and activity of VNUT during the maturation of cerebellar granule neurons *in vitro*. The correlation between these findings and the situation in the cerebellum *in vivo* raises exciting new questions that should be addressed in the near future.

AUTHOR CONTRIBUTIONS

AM-M designed, performed the majority of experiments and wrote the manuscript. JD-H designed and supervised the experiments. FO designed, performed the experiments and wrote the manuscript. JG designed and supervised the experiments. RG-V and MM-P was designed, supervised the experiments and wrote the manuscript.

FUNDING

This work was funded by the Spanish Ministerio de Economía y Competitividad (MINECO, BFU 2014-53654-P) and the "Red de Excelencia Consolider-Ingenio Spanish Ion Channel Initiative" (BFU2015-70067REDC); by the Comunidad de Madrid (BRADE-CM S2013/ICE-2958); UCM-Santander (PR26/16-18B-3) and by a Fundación Ramón Areces Grant (PR2018/16-02). AM-M is a recipient of a contract from the MINECO, BFU 2014-53654-P. FO acknowledges the Ramon y Cajal Program of the Spanish Ministry of Economy and Competitiveness (MEC: RYC-2013-13290).

ACKNOWLEDGMENT

The authors are grateful to Dr. Mark Sefton for his help in the preparation of this manuscript.

REFERENCES

Altman, J. (1972). Postnatal development of the cerebellar cortex in the rat. I. The external germinal layer and the transitional molecular layer. *J. Comp. Neurol.* 145, 353–397. doi: 10.1002/cne.901450305

Altman, J., and Bayer, S. A. (1997). *Development of the Cerebellar System in Relation to its Evolution, Structure and Function*. Boca Raton, FL: CRC.

Bankston, L. A., and Guidotti, G. (1996). Characterization of ATP transport into chromaffin granule ghosts. Synergy of ATP and serotonin accumulation in chromaffin granule ghosts. *J. Biol. Chem.* 271, 17132–17138. doi: 10.1074/jbc.271.29.17132

Baroja-Mazo, A., Barbera-Cremades, M., and Pelegrin, P. (2013). The participation of plasma membrane hemichannels to purinergic signaling. *Biochim. Biophys. Acta* 1828, 79–93. doi: 10.1016/j.bbamem.2012.01.002

Beggs, S., Trang, T., and Salter, M. W. (2012). P2X4R+ microglia drive neuropathic pain. *Nat. Neurosci.* 15, 1068–1073. doi: 10.1038/nn.3155

Ben-Arie, N., Bellen, H. J., Armstrong, D. L., McCall, A. E., Gordadze, P. R., Guo, Q., et al. (1997). Math1 is essential for genesis of cerebellar granule neurons. *Nature* 390, 169–172. doi: 10.1038/36579

Blott, E. J., and Griffiths, G. M. (2002). Secretory lysosomes. *Nat. Rev. Mol. Cell Biol.* 3, 122–131. doi: 10.1038/nrm732

Boulland, J. L., Qureshi, T., Seal, R. P., Rafiki, A., Gundersen, V., Bergersen, L. H., et al. (2004). Expression of the vesicular glutamate transporters during development indicates the widespread corelease of multiple neurotransmitters. *J. Comp. Neurol.* 480, 264–280. doi: 10.1002/cne.20354

Brown, J. P., Couillard-Despres, S., Cooper-Kuhn, C. M., Winkler, J., Aigner, L., and Kuhn, H. G. (2003). Transient expression of doublecortin during adult neurogenesis. *J. Comp. Neurol.* 467, 1–10. doi: 10.1002/cne.10874

Burnstock, G. (1976). Do some nerve cells release more than one transmitter? *Neuroscience* 1, 239–248.

Burnstock, G. (2004). Cotransmission. *Curr. Opin. Pharmacol.* 4, 47–52. doi: 10.1016/j.coph.2003.08.001

Burnstock, G. (2006). Historical review: ATP as a neurotransmitter. *Trends Pharmacol. Sci.* 27, 166–176. doi: 10.1016/j.tips.2006.01.005

Burnstock, G. (2013). Introduction to purinergic signalling in the brain. *Adv. Exp. Med. Biol.* 986, 1–12. doi: 10.1007/978-94-007-4719-7_1

Cao, Q., Zhao, K., Zhong, X. Z., Zou, Y., Yu, H., Huang, P., et al. (2014). SLC17A9 protein functions as a lysosomal ATP transporter and regulates cell viability. *J. Biol. Chem.* 289, 23189–23199. doi: 10.1074/jbc.M114.567107

Casel, D., Brockhaus, J., and Deitmer, J. W. (2005). Enhancement of spontaneous synaptic activity in rat Purkinje neurones by ATP during development. *J. Physiol.* 568(Pt 1), 111–122. doi: 10.1113/jphysiol.2005.091371

Cerminara, N. L., Lang, E. J., Sillitoe, R. V., and Apps, R. (2015). Redefining the cerebellar cortex as an assembly of non-uniform Purkinje cell microcircuits. *Nat. Rev. Neurosci.* 16, 79–93. doi: 10.1038/nrn3886

Diaz-Hernandez, M., del Puerto, A., Diaz-Hernandez, J. I., Diez-Zaera, M., Lucas, J. J., Garrido, J. J., et al. (2008). Inhibition of the ATP-gated P2X7 receptor promotes axonal growth and branching in cultured hippocampal neurons. *J. Cell Sci.* 121(Pt 22), 3717–3728. doi: 10.1242/jcs.034082

Diez-Zaera, M., Diaz-Hernandez, J. I., Hernandez-Alvarez, E., Zimmermann, H., Diaz-Hernandez, M., and Miras-Portugal, M. T. (2011). Tissue-nonspecific alkaline phosphatase promotes axonal growth of hippocampal neurons. *Mol. Biol. Cell* 22, 1014–1024. doi: 10.1091/mbc.E10-09-0740

Dou, Y., Wu, H. J., Li, H. Q., Qin, S., Wang, Y. E., Li, J., et al. (2012). Microglial migration mediated by ATP-induced ATP release from lysosomes. *Cell Res.* 22, 1022–1033. doi: 10.1038/cr.2012.10

Erickson, J. D., Eiden, L. E., and Hoffman, B. J. (1992). Expression cloning of a reserpine-sensitive vesicular monoamine transporter. *Proc. Natl. Acad. Sci. U.S.A.* 89, 10993–10997. doi: 10.1073/pnas.89.22.10993

Espinosa, J. S., and Luo, L. (2008). Timing neurogenesis and differentiation: insights from quantitative clonal analyses of cerebellar granule cells. *J. Neurosci.* 28, 2301–2312. doi: 10.1523/JNEUROSCI.5157-07.2008

Estevez-Herrera, J., Dominguez, N., Pardo, M. R., Gonzalez-Santana, A., Westhead, E. W., Borges, R., et al. (2016). ATP: The crucial component of secretory vesicles. *Proc. Natl. Acad. Sci. U.S.A.* 113, E4098–E4106. doi: 10.1073/pnas.1600690113

Gomez-Villafuertes, R., del Puerto, A., Diaz-Hernandez, M., Bustillo, D., Diaz-Hernandez, J. I., Huerta, P. G., et al. (2009). Ca2+/calmodulin-dependent kinase II signalling cascade mediates P2X7 receptor-dependent inhibition of neuritogenesis in neuroblastoma cells. *FEBS J.* 276, 5307–5325. doi: 10.1111/j.1742-4658.2009.07228.x

Gomez-Villafuertes, R., Pintor, J., Miras-Portugal, M. T., and Gualix, J. (2014). Ectonucleotide pyrophosphatase/phosphodiesterase activity in Neuro-2a neuroblastoma cells: changes in expression associated with neuronal differentiation. *J. Neurochem.* 131, 290–302. doi: 10.1111/jnc.12794

Gu, J. G., and MacDermott, A. B. (1997). Activation of ATP P2X receptors elicits glutamate release from sensory neuron synapses. *Nature* 389, 749–753. doi: 10.1038/39639

Gualix, J., Abal, M., Pintor, J., Garcia-Carmona, F., and Miras-Portugal, M. T. (1996). Nucleotide vesicular transporter of bovine chromaffin granules. Evidence for a mnemonic regulation. *J. Biol. Chem.* 271, 1957–1965. doi: 10.1074/jbc.271.4.1957

Gualix, J., Alvarez, A. M., Pintor, J., and Miras-Portugal, M. T. (1999a). Studies of chromaffin granule functioning by flow cytometry: transport of fluorescent epsilon-ATP and granular size increase induced by ATP. *Receptors Channels* 6, 449–461.

Gualix, J., Pintor, J., and Miras-Portugal, M. T. (1999b). Characterization of nucleotide transport into rat brain synaptic vesicles. *J. Neurochem.* 73, 1098–1104.

Gutierrez-Martin, Y., Bustillo, D., Gomez-Villafuertes, R., Sanchez-Nogueiro, J., Torregrosa-Hetland, C., Binz, T., et al. (2011). P2X7 receptors trigger ATP exocytosis and modify secretory vesicle dynamics in neuroblastoma cells. *J. Biol. Chem.* 286, 11370–11381. doi: 10.1074/jbc.M110.139410

Haanes, K. A., and Novak, I. (2010). ATP storage and uptake by isolated pancreatic zymogen granules. *Biochem. J.* 429, 303–311. doi: 10.1042/BJ20091337

Hallberg, O. E., Bogen, I. L., Reistad, T., Haug, K. H., Wright, M. S., Fonnum, F., et al. (2006). Differential development of vesicular glutamate transporters in brain: an in vitro study of cerebellar granule cells. *Neurochem. Int.* 48, 579–585. doi: 10.1016/j.neuint.2005.12.027

Henshall, D. C., Diaz-Hernandez, M., Miras-Portugal, M. T., and Engel, T. (2013). P2X receptors as targets for the treatment of status epilepticus. *Front. Cell Neurosci.* 7:237. doi: 10.3389/fncel.2013.00237

Hervas, C., Perez-Sen, R., and Miras-Portugal, M. T. (2003). Coexpression of functional P2X and P2Y nucleotide receptors in single cerebellar granule cells. *J. Neurosci. Res.* 73, 384–399. doi: 10.1002/jnr.10676

Hervas, C., Perez-Sen, R., and Miras-Portugal, M. T. (2005). Presence of diverse functional P2X receptors in rat cerebellar synaptic terminals. *Biochem. Pharmacol.* 70, 770–785. doi: 10.1016/j.bcp.2005.05.033

Jung, J., Shin, Y. H., Konishi, H., Lee, S. J., and Kiyama, H. (2013). Possible ATP release through lysosomal exocytosis from primary sensory neurons. *Biochem. Biophys. Res. Commun.* 430, 488–493. doi: 10.1016/j.bbrc.2012.12.009

Juranek, J. K., Mukherjee, K., Siddiqui, T. J., Kaplan, B. J., Li, J. Y., Ahnert-Hilger, G., et al. (2013). Active zone protein expression changes at the key stages of cerebellar cortex neurogenesis in the rat. *Acta Histochem.* 115, 616–625. doi: 10.1016/j.acthis.2013.01.003

Kato, Y., Hiasa, M., Ichikawa, R., Hasuzawa, N., Kadowaki, A., Iwatsuki, K., et al. (2017). Identification of a vesicular ATP release inhibitor for the treatment of neuropathic and inflammatory pain. *Proc. Natl. Acad. Sci. U.S.A.* doi: 10.1073/pnas.1704847114 [Epub ahead of print].

Kato, Y., Omote, H., and Miyaji, T. (2013). Inhibitors of ATP release inhibit vesicular nucleotide transporter. *Biol. Pharm. Bull.* 36, 1688–1691. doi: 10.1248/bpb.b13-00544

Khakh, B. S. (2009). ATP-gated P2X receptors on excitatory nerve terminals onto interneurons initiate a form of asynchronous glutamate release. *Neuropharmacology* 56, 216–222. doi: 10.1016/j.neuropharm.2008.06.011

Khakh, B. S., Gittermann, D., Cockayne, D. A., and Jones, A. (2003). ATP modulation of excitatory synapses onto interneurons. *J. Neurosci.* 23, 7426–7437.

Khakh, B. S., and Henderson, G. (1998). ATP receptor-mediated enhancement of fast excitatory neurotransmitter release in the brain. *Mol. Pharmacol.* 54, 372–378.

Larsson, M., Sawada, K., Morland, C., Hiasa, M., Ormel, L., Moriyama, Y., et al. (2012). Functional and anatomical identification of a vesicular transporter mediating neuronal ATP release. *Cereb. Cortex* 22, 1203–1214. doi: 10.1093/cercor/bhr203

Leon, D., Hervas, C., and Miras-Portugal, M. T. (2006). P2Y1 and P2X7 receptors induce calcium/calmodulin-dependent protein kinase II phosphorylation in cerebellar granule neurons. *Eur. J. Neurosci.* 23, 2999–3013. doi: 10.1111/j.1460-9568.2006.04832.x

Leon, D., Sanchez-Nogueiro, J., Marin-Garcia, P., and Miras-Portugal, M. A. (2008). Glutamate release and synapsin-I phosphorylation induced by P2X7 receptors activation in cerebellar granule neurons. *Neurochem. Int.* 52, 1148–1159. doi: 10.1016/j.neuint.2007.12.004

Levesque, S. A., Lavoie, E. G., Lecka, J., Bigonnesse, F., and Sevigny, J. (2007). Specificity of the ecto-ATPase inhibitor ARL 67156 on human and mouse ectonucleotidases. *Br. J. Pharmacol.* 152, 141–150. doi: 10.1038/sj.bjp.0707361

Li, D., Ropert, N., Koulakoff, A., Giaume, C., and Oheim, M. (2008). Lysosomes are the major vesicular compartment undergoing Ca2+-regulated exocytosis from cortical astrocytes. *J. Neurosci.* 28, 7648–7658. doi: 10.1523/JNEUROSCI.0744-08.2008

Li, H., and Harlow, M. L. (2014). Individual synaptic vesicles from the electroplaque of *Torpedo californica*, a classic cholinergic synapse, also contain transporters for glutamate and ATP. *Physiol. Rep.* 2:e00206. doi: 10.1002/phy2.206

Liu, J., Liu, W., and Yang, J. (2016). ATP-containing vesicles in stria vascular marginal cell cytoplasms in neonatal rat cochlea are lysosomes. *Sci. Rep.* 6:20903. doi: 10.1038/srep20903

Loiola, E. C., and Ventura, A. L. (2011). Release of ATP from avian Muller glia cells in culture. *Neurochem. Int.* 58, 414–422. doi: 10.1016/j.neuint.2010.12.019

Masuda, T., Ozono, Y., Mikuriya, S., Kohro, Y., Tozaki-Saitoh, H., Iwatsuki, K., et al. (2016). Dorsal horn neurons release extracellular ATP in a VNUT-dependent manner that underlies neuropathic pain. *Nat. Commun.* 7:12529. doi: 10.1038/ncomms12529

Mateo, J., Garcia-Lecea, M., Miras-Portugal, M. T., and Castro, E. (1998). Ca2+ signals mediated by P2X-type purinoceptors in cultured cerebellar Purkinje cells. *J. Neurosci.* 18, 1704–1712.

Menendez-Mendez, A., Diaz-Hernandez, J. I., and Miras-Portugal, M. T. (2015). The vesicular nucleotide transporter (VNUT) is involved in the extracellular ATP effect on neuronal differentiation. *Purinergic Signal.* 11, 239–249. doi: 10.1007/s11302-015-9449-4

Miras-Portugal, M. T., Gomez-Villafuertes, R., Gualix, J., Diaz-Hernandez, J. I., Artalejo, A. R., Ortega, F., et al. (2016). Nucleotides in neuroregeneration and neuroprotection. *Neuropharmacology* 104, 243–254. doi: 10.1016/j.neuropharm.2015.09.002

Miras-Portugal, M. T., Torres, M., Rotllan, P., and Aunis, D. (1986). Adenosine transport in bovine chromaffin cells in culture. *J. Biol. Chem.* 261, 1712–1719.

Morente, V., Perez-Sen, R., Ortega, F., Huerta-Cepas, J., Delicado, E. G., and Miras-Portugal, M. T. (2014). Neuroprotection elicited by P2Y13 receptors against genotoxic stress by inducing DUSP2 expression and MAPK signaling recovery. *Biochim. Biophys. Acta* 1843, 1886–1898. doi: 10.1016/j.bbamcr.2014.05.004

Mundy, W. R., Robinette, B., Radio, N. M., and Freudenrich, T. M. (2008). Protein biomarkers associated with growth and synaptogenesis in a cell culture model of neuronal development. *Toxicology* 249, 220–229. doi: 10.1016/j.tox.2008.05.012

Nakatsuka, T., and Gu, J. G. (2001). ATP P2X receptor-mediated enhancement of glutamate release and evoked EPSCs in dorsal horn neurons of the rat spinal cord. *J. Neurosci.* 21, 6522–6531.

Orriss, I. R., Knight, G. E., Utting, J. C., Taylor, S. E., Burnstock, G., and Arnett, T. R. (2009). Hypoxia stimulates vesicular ATP release from rat osteoblasts. *J. Cell. Physiol.* 220, 155–162. doi: 10.1002/jcp.21745

Ortega, F., Perez-Sen, R., Delicado, E. G., and Miras-Portugal, M. T. (2009). P2X7 nucleotide receptor is coupled to GSK-3 inhibition and neuroprotection in cerebellar granule neurons. *Neurotox. Res.* 15, 193–204. doi: 10.1007/s12640-009-9020-6

Ortega, F., Perez-Sen, R., Delicado, E. G., and Teresa Miras-Portugal, M. (2011). ERK1/2 activation is involved in the neuroprotective action of P2Y13 and P2X7 receptors against glutamate excitotoxicity in cerebellar granule neurons. *Neuropharmacology* 61, 1210–1221. doi: 10.1016/j.neuropharm.2011.07.010

Ortega, F., Perez-Sen, R., Morente, V., Delicado, E. G., and Miras-Portugal, M. T. (2010). P2X7, NMDA and BDNF receptors converge on GSK3 phosphorylation and cooperate to promote survival in cerebellar granule neurons. *Cell Mol. Life Sci.* 67, 1723–1733. doi: 10.1007/s00018-010-0278-x

Oya, M., Kitaguchi, T., Yanagihara, Y., Numano, R., Kakeyama, M., Ikematsu, K., et al. (2013). Vesicular nucleotide transporter is involved in ATP storage of secretory lysosomes in astrocytes. *Biochem. Biophys. Res. Commun.* 438, 145–151. doi: 10.1016/j.bbrc.2013.07.043

Pankratov, Y., Lalo, U., Verkhratsky, A., and North, R. A. (2006). Vesicular release of ATP at central synapses. *Pflugers Arch.* 452, 589–597. doi: 10.1007/s00424-006-0061-x

Pastor-Anglada, M., and Perez-Torras, S. (2015). Nucleoside transporter proteins as biomarkers of drug responsiveness and drug targets. *Front. Pharmacol.* 6:13. doi: 10.3389/fphar.2015.00013

Perez de Lara, M. J., Guzman-Aranguez, A., de la Villa, P., Diaz-Hernandez, J. I, Miras-Portugal, M. T., and Pintor, J. (2015). Increased levels of extracellular ATP in glaucomatous retinas: possible role of the vesicular nucleotide transporter during the development of the pathology. *Mol. Vis.* 21, 1060–1070.

Pons, S., Trejo, J. L., Martinez-Morales, J. R., and Marti, E. (2001). Vitronectin regulates Sonic hedgehog activity during cerebellum development through CREB phosphorylation. *Development* 128, 1481–1492.

Pougnet, J. T., Toulme, E., Martinez, A., Choquet, D., Hosy, E., and Boue-Grabot, E. (2014). ATP P2X receptors downregulate AMPA receptor trafficking and postsynaptic efficacy in hippocampal neurons. *Neuron* 83, 417–430. doi: 10.1016/j.neuron.2014.06.005

Pryazhnikov, E., and Khiroug, L. (2008). Sub-micromolar increase in [Ca(2+)](i) triggers delayed exocytosis of ATP in cultured astrocytes. *Glia* 56, 38–49. doi: 10.1002/glia.20590

Ramón y Cajal, S. (1889). Sobre las fibras nerviosas de la capa granulosa del cerebelo. *Rev. Trim. Histol. Norm. Patol.* 1, 107–118.

Ramón y Cajal, S. (1904). *Textura del Sistema Nervioso del Hombre y de Los Vertebrados: Estudios Sobre el Plan Estructural y Composición Histológical de Los Centros Nerviosos Adicionados de Consideraciones Fisiológicas Fundadas en Los Nuevos Descubrimientos*. Madrid: Moya.

Ramón y Cajal, S. (1995). *Histology of the Nervous System of Man and Vertebrates*. New York, NY: Oxford University Press.

Rodrigues, R. J., Almeida, T., Richardson, P. J., Oliveira, C. R., and Cunha, R. A. (2005). Dual presynaptic control by ATP of glutamate release via facilitatory P2X1, P2X2/3, and P2X3 and inhibitory P2Y1, P2Y2, and/or P2Y4 receptors in the rat hippocampus. *J. Neurosci.* 25, 6286–6295. doi: 10.1523/JNEUROSCI.0628-05.2005

Rotllan, P., and Miras Portugal, M. T. (1985). Adenosine kinase from bovine adrenal medulla. *Eur. J. Biochem.* 151, 365–371. doi: 10.1111/j.1432-1033.1985.tb09110.x

Sanchez-Nogueiro, J., Marin-Garcia, P., Bustillo, D., Olivos-Ore, L. A., Miras-Portugal, M. T., and Artalejo, A. R. (2014). Subcellular distribution and early signalling events of P2X7 receptors from mouse cerebellar granule neurons. *Eur. J. Pharmacol.* 744, 190–202. doi: 10.1016/j.ejphar.2014.10.036

Sanchez-Nogueiro, J., Marin-Garcia, P., Leon, D., Leon-Otegui, M., Salas, E., Gomez-Villafuertes, R., et al. (2009). Axodendritic fibres of mouse cerebellar granule neurons exhibit a diversity of functional P2X receptors. *Neurochem. Int.* 55, 671–682. doi: 10.1016/j.neuint.2009.06.009

Sanz, J. M., Vendite, D., Fernandez, M., Andres, A., and Ros, M. (1996). Adenosine A1 receptors in cultured cerebellar granule cells: role of endogenous adenosine. *J. Neurochem.* 67, 1469–1477. doi: 10.1046/j.1471-4159.1996.67041469.x

Sawada, K., Echigo, N., Juge, N., Miyaji, T., Otsuka, M., Omote, H., et al. (2008). Identification of a vesicular nucleotide transporter. *Proc. Natl. Acad. Sci. U.S.A.* 105, 5683–5686. doi: 10.1073/pnas.0800141105

Sen, R. P., Delicado, E. G., Alvarez, A., Brocklebank, A. M., Wiley, J. S., and Miras-Portugal, M. T. (1998). Flow cytometric studies of nucleoside transport regulation in single chromaffin cells. *FEBS Lett.* 422, 368–372. doi: 10.1016/S0014-5793(98)00047-7

Shin, Y. H., Lee, S. J., and Jung, J. (2012). Secretion of ATP from Schwann cells through lysosomal exocytosis during Wallerian degeneration. *Biochem. Biophys. Res. Commun.* 429, 163–167. doi: 10.1016/j.bbrc.2012.10.121

Sperlagh, B., Heinrich, A., and Csolle, C. (2007). P2 receptor-mediated modulation of neurotransmitter release-an update. *Purinergic Signal.* 3, 269–284. doi: 10.1007/s11302-007-9080-0

Sperlagh, B., and Illes, P. (2014). P2X7 receptor: an emerging target in central nervous system diseases. *Trends Pharmacol. Sci.* 35, 537–547. doi: 10.1016/j.tips.2014.08.002

Srivastava, R., Kumar, M., Peineau, S., Csaba, Z., Mani, S., Gressens, P., et al. (2013). Conditional induction of Math1 specifies embryonic stem cells to

cerebellar granule neuron lineage and promotes differentiation into mature granule neurons. *Stem Cells* 31, 652–665. doi: 10.1002/stem.1295

Tsuda, M., Shigemoto-Mogami, Y., Koizumi, S., Mizokoshi, A., Kohsaka, S., Salter, M. W., et al. (2003). P2X4 receptors induced in spinal microglia gate tactile allodynia after nerve injury. *Nature* 424, 778–783. doi: 10.1038/nature 01786

Volknandt, W., and Zimmermann, H. (1986). Acetylcholine, ATP, and proteoglycan are common to synaptic vesicles isolated from the electric organs of electric eel and electric catfish as well as from rat diaphragm. *J. Neurochem.* 47, 1449–1462. doi: 10.1111/j.1471-4159.1986.tb0 0778.x

Winkler, H., and Westhead, E. (1980). The molecular organization of adrenal chromaffin granules. *Neuroscience* 5, 1803–1823. doi: 10.1016/0306-4522(80) 90031-7

Zhang, Z., Chen, G., Zhou, W., Song, A., Xu, T., Luo, Q., et al. (2007). Regulated ATP release from astrocytes through lysosome exocytosis. *Nat. Cell Biol.* 9, 945–953. doi: 10.1038/ncb1620

Zimmermann, H., Zebisch, M., and Strater, N. (2012). Cellular function and molecular structure of ecto-nucleotidases. *Purinergic Signal.* 8, 437–502. doi: 10.1007/s11302-012-9309-4

Conflict of Interest Statement: The authors declare that the research was conducted in the absence of any commercial or financial relationships that could be construed as a potential conflict of interest.

The reviewer MP-A and handling editor declared their shared affiliation.

frontiers in Pharmacology

MINI REVIEW
published: 22 December 2017
doi: 10.3389/fphar.2017.00932

Adenosine in the Thymus

*Krisztina Köröskényi[1,2], Gergely Joós[1,2] and Zsuzsa Szondy[1,2]**

[1] Department of Biochemistry and Molecular Biology, Faculty of Medicine, University of Debrecen, Debrecen, Hungary,
[2] Department of Basic Medical Sciences of Dental Faculty, University of Debrecen, Debrecen, Hungary

Adenosine is an ancient extracellular signaling molecule that regulates various biological functions via activating four G-protein-coupled receptors, A_1, A_{2A}, A_{2B}, and A_3 adenosine receptors. As such, several studies have highlighted a role for adenosine signaling in affecting the T cell development in the thymus. Recent studies indicate that adenosine is produced in the context of apoptotic thymocyte clearance. This review critically discusses the involvement of adenosine and its receptors in the complex interplay that exists between the developing thymocytes and the thymic macrophages which engulf the apoptotic cells. This crosstalk contributes to the effective and immunologically silent removal of apoptotic thymocytes, as well as affects the TCR-driven T-cell selection processes.

Keywords: efferocytosis, adenosine, thymocyte, apoptosis, T cell selection

OPEN ACCESS

Edited by:
Kenneth A. Jacobson, National Institutes of Health (NIH), United States

Reviewed by:
Celio Geraldo Freire De Lima, Universidade Federal do Rio de Janeiro, Brazil
Philippe Saas, INSERM UMR1098 Interactions Hôte-Greffon-Tumeur and Ingénierie Cellulaire et Génique, France

***Correspondence:**
Zsuzsa Szondy
szondy@med.unideb.hu

Specialty section:
This article was submitted to Experimental Pharmacology and Drug Discovery, a section of the journal Frontiers in Pharmacology

Received: *18 October 2017*
Accepted: *11 December 2017*
Published: *22 December 2017*

Citation:
Köröskényi K, Joós G and Szondy Z (2017) Adenosine in the Thymus. Front. Pharmacol. 8:932. doi: 10.3389/fphar.2017.00932

INTRODUCTION

Generation of immunocompetent T lymphocytes from bone marrow-derived $CD4^-CD8^-$ double negative progenitors takes place in the thymus. This process occurs through a series of differentiation and selection steps (Bommhardt et al., 2004) leading via apoptosis to the removal of 95% of thymocytes produced with improper TCR. T-cell differentiation is unique in a sense that it is not a cell-autonomous process, but depends on signals provided by fibroblasts, thymic epithelial cells, macrophages, dendritic cells, and endothelial cells that surround the developing thymocytes (Petrie and Zuniga-Pflucker, 2007). Among these cells thymic epithelial cells play the major role in shaping the T cell repertoire by presenting self-antigens on their cell surface (Alexandropoulos and Danzi, 2012), while thymic $F4/80^+$ macrophages are the main cleaners of the constantly produced dying cells (Surh and Sprent, 1994). While generally tissue resident macrophages are originated from the yolk sac (Gomez et al., 2015), part of the thymic macrophages seem to be differentiated from the hematopoietic stem cells (Haymaker et al., 2012) or even from T cell progenitors (Esashi et al., 2004) in the bone marrow.

At the beginning of differentiation, $CD4^-CD8^-$ progenitor cells rearrange their TCR β gene locus to produce a pre-TCR complex. Subsequently, thymocytes divide rapidly, become $CD4^+CD8^+$ DP thymocytes, then they rearrange their TCRα chain as well. Those thymocytes, which successfully generate a functional α chain replace the pre-TCR with mature TCRαβ and continue to differentiate $CD4^+CD8^+$ $TCR\alpha\beta^{low}$ cells (Hernandez et al., 2010). The TCR of these thymocytes is able to interact with self-peptides presented on major histocompatibility complex molecules of thymic non-lymphoid cells. Their destiny will be decided by the strength of the TCRαβ

Abbreviations: ADA, adenosine deaminase; ADO, adenosine; AR, adenosine receptor; CO, carbon monoxide; DP, double positive; MAPK, mitogen-activated protein kinase; NPP, nucleotide pyrophosphatase/phosphodiesterase; NECA, *N*-ethyl-carboxamidoadenosine; 8-PT, 8-phenyl-theophylline; PGE_2, prostaglandin E_2; TCR, T-cell receptor; TG2, transglutaminase 2; TGF-β, transforming growth factor-β; T_{reg}, regulatory T cell; tT_{reg}, thymic regulatory T cell.

signal generated during this interaction. Cells receiving a TCRαβ signal of intermediate strength continue to differentiate into $CD4^+$ or $CD8^+$ $TCR\alpha\beta^{high}$ single positive thymocytes, leave the thymic cortex and complete their maturation in the thymic medulla, while those, which are exposed to a strong TCRαβ signal, are eliminated by activation-induced apoptosis, a major mechanism for generating self-tolerance (Kisielow and von Boehmer, 1995). A few percent of thymocytes that have TCR specificities for higher affinity ligands than that of the conventional $CD4^+$ T cells (Moran et al., 2011) are diverted into $CD4^+CD25^+FoxP3^+$ tT_{reg}, which induce peripheral tolerance by silencing excessive peripheral immune responses, thus prevent autoimmunity (Benoist and Mathis, 2012). The remaining 90% of the DP thymocytes express TCRs, which cannot interact with peptide-loaded self-major histocompatibility molecules, thus in the absence of TCR-driven cell survival signals they undergo a default apoptosis cell death pathway named "death by neglect."

Increasing evidence indicate that molecules produced by macrophages during the constant engulfment of apoptotic cells generate a thymic milieu for the developing thymocytes that affect the TCR-determined cell selection processes. These molecules are produced primarily not to regulate thymic selection processes, rather they are needed for the macrophages themselves. Thus, in response to the chemotactic signals produced by dying thymocytes, macrophages release ATP that contributes to their migration to the apoptotic site (Kronlage et al., 2010). Following apoptotic cell phagocytosis, they release TGF-β and prostaglandin E_2 (PGE_2) to prevent their pro-inflammatory cytokine production in an autocrine manner (Fadok et al., 1998). During degrading hem containing proteins, they also produce CO as a result of hem oxygenase-I action (Gemsa et al., 1973). And finally, macrophages also produce retinoids in an engulfment-dependent manner (Garabuczi et al., 2013) that regulate their own phagocytic capacity (Sarang et al., 2014). However, DP thymocytes express receptors for the macrophage-released molecules, such as ATP, PGE_2, TGF-β, CO or retinoids (Cillie et al., 1983; Suzuki et al., 1991; Szondy et al., 1997; Levéen et al., 2005; Tsukimoto et al., 2006; Dzhagalov et al., 2007), and respond to them with an outcome that depends on the simultaneous TCR signaling. Thus, all these molecules were shown to induce or enhance thymocyte death in the absence of TCR signaling (Szondy et al., 2012). Macrophage-derived retinoids and TGF-β also synergize in the induction of TG2 (Fésüs and Szondy, 2005) in apoptotic thymocytes (Garabuczi et al., 2013). TG2 in dying cells contributes to the formation of a chemotactic signal for macrophage recruitment (Nishiura et al., 1998), prevents the leakage of the harmful cell content (Piredda et al., 1997) and facilitates the exposure of phosphatidylserine, the main important apoptotic cell recognition signal for macrophages (Sarang et al., 2007). On the other hand, in the presence of TCR signaling retinoids inhibit TCR-mediated cell death in a dose-dependent manner, thus regulate the threshold of negative selection (Szondy et al., 1998; Szegezdi et al., 2003; Sarang et al., 2013), while TGF-βplays such a determining role in the formation of tT_{reg} cells, that no tT_{reg} cells can be detected in the thymus until apoptosis and the consequent engulfment-dependent TGF-β production is induced (Liu et al., 2008; Konkel et al., 2014; Chen and Konkel, 2015).

The fact that adenosine is also produced in the thymus and affects thymic selection processes was discovered after it was found that ADA deficiency leads to adenosine accumulation and severe T cell deficiency (Apasov et al., 2000).

ADENOSINE

Adenosine is an intra- and extracellularly produced purine nucleoside, which concentration is strictly controlled due to its intense and diverse biological effects. Intracellularly, it can be produced by three main pathways: (a) decomposition of adenine nucleotides (ATP, ADP, AMP) by ATPases, ATPase and cellular 5′ nucleotidase (c5′-NT); (b) hydrolysis of *S*-Adenosyl-L-homocysteine by its hydrolase; (c) phosphodiesterase-mediated degradation of cAMP (Park and Gupta, 2012). Intracellularly ADO can be converted to inosine by ADA and later on to uric acid (da Rocha Lapa et al., 2014). It also can be shifted back to the nucleotide pool in the form of AMP by ADO kinase (Ramakers et al., 2011). Finally, it can be transported to the extracellular space by specific transporters (Antonioli et al., 2014). The extracellular ADO concentration is lower than 1 μM (30–200 nM) under physiological conditions, but it can reach extremely high levels (>100 μM) during inflammation and hypoxia (Haskó and Cronstein, 2004). The waste majority of extracellular ADO is formed extracellularly from ATP, which is transported out from various cells via exocytosis, co-release or ion channels (Chen et al., 2013; Antonioli et al., 2014). Extracellular ATP then undergoes a two-step hydrolysis. The rate limiting step in extracellular ADO formation is catalyzed by either ecto-nucleoside triphosphate diphosphohydrolases, such as CD39 that phosphohydrolyses ATP, and less efficiently ADP, in a Ca^{2+}- and Mg^{2+}-dependent fashion, to yield AMP (Heine et al., 2001), or by members of the ecto-nucleotide pyrophosphatase/phosphodiesterase family, such as NPP1 and 3, which are also located on the cell surface, but produce AMP directly (Stefan et al., 2006). AMP in turn, is rapidly degraded to ADO by soluble or membrane-bound ecto-5′-nucleotidases, such as CD73 (da Rocha Lapa et al., 2014). The effect of extracellular ADO is terminated by the decomposition of ADO by ecto-ADA or by the uptake into the surrounding cells through equilibrative nucleoside transporters (Liu and Xia, 2015).

THE DIFFERENT ADENOSINE RECEPTORS

The regulatory effects of ADO, are almost exclusively mediated by the activation of its plasma membrane-associated receptors (ADO receptors) (Fredholm et al., 2001) which are expressed in a cell type specific manner. All of the four ARs (A_1R, $A_{2A}R$, $A_{2B}R$, A_3R) belong to the large family of seven-transmembrane receptors, also known as G-protein-coupled receptors (Fredholm et al., 2001). Physiological ADO levels activate A_1R, $A_{2A}R$, and

A_3R receptor subtypes (K_i = 100–300 nM for human receptors). $A_{2B}Rs$ (K_i = 15 μM for human $A_{2B}R$) are activated only during pathological conditions (e.g., hypoxia, inflammation) (Haskó et al., 2007; Eltzschig, 2009; Dubyak, 2012). The duration and magnitude of the ADO's effect are influenced by a number of processes including intra- and extracellular production of ADO, transport, cellular uptake, degradation, receptor density, as well as the activity of receptors and signaling molecules (Eltzschig, 2009; Chen et al., 2013). In general, ARs affecting intracellular cAMP levels are involved in the regulation of a large scale of biological processes (Liu and Xia, 2015). In addition, all of the four ARs can activate different types of MAPKs (p38, ERK1/2, JNK) (Antonioli et al., 2014). Further AR downstream effectors include phospholipase C, ion channels, phosphoinositide 3-kinase and protein kinase B, nitric oxide, reactive oxygen species, and lipid mediators (Liu and Xia, 2015). Like other G-protein-coupled receptors, ARs tend to form homo- and heterodimers as well as oligomers (Chen et al., 2013). With the formation of such complexes, the range of signaling pathways and biological processes controlled by ARs is further broadened.

ADENOSINE METABOLISM AND ADENOSINE RECEPTORS IN THE THYMUS

Studies in our laboratory have found that neither macrophages nor apoptotic thymocytes produce detectable amount of ADO, if they are cultured alone, but ADO is produced during the apoptotic cell engulfment indicating that ADO is an additional molecule which appears in the thymic milieu in an engulfment-dependent manner (Köröskényi et al., 2011). Apoptotic cells release adenine nucleotides via pannexin channels (Chekeni et al., 2010; Yamaguchi et al., 2014), which open in a caspase-dependent manner (Sandilos et al., 2012). In addition, thymocytes release ATP also via a pannexin channel-independent manner, when they undergo secondary necrosis (Sándor et al., 2017). CD39 is constitutively expressed in the thymus and is associated primarily with macrophages and tT_{reg} cells (Antonioli et al., 2013), while thymocytes express NPP1 (Petersen et al., 2007). Thus in the thymic cortex, where apoptotic thymocytes and macrophages are present in close proximity, both cell types can contribute to the extracellular degradation of ATP to AMP. In accordance, high amount of AMP was detected in the culture of dying thymocytes (Yamaguchi et al., 2014). However, while CD73 and prostatic acid phosphatase are expressed by macrophages (Eichin et al., 2015), in thymocytes CD73 expression is differentiation-dependent: it is virtually absent in cortical thymocytes, but becomes upregulated in the medullary ones (Resta et al., 1997, 1998). Thus in the thymic cortex, where the majority of improper thymocytes die, ADO formation must be fully dependent on the CD73 activity of macrophages. Indeed, in the context of dying thymocytes and engulfing macrophages ADO production was confirmed *in vitro* to be fully dependent on the CD73 activity of macrophages (Yamaguchi et al., 2014; Sándor et al., 2017). The endogenous CD73 activity of macrophages is so high in the thymus that even if CD73 expression is artificially upregulated in thymocytes, the *in vivo* thymic ADO levels do not change (Resta et al., 1997). The extracellular ADO concentrations in the thymus, however, are determined by the thymocyte ADA activities as well, and ADA activity was found to be extraordinarily high in cortical thymocytes, while to be strongly downregulated in the medullary ones (Chechik et al., 1981; Ma et al., 1982). These observations indicate that either ADO concentrations are kept lower in the cortical zone, where most of the positive selection takes place, while are higher in the medullary zone, where selected thymocytes mature further and also undergo negative selection. Alternatively, since in the medullary zone the rate of apoptosis, consequently the rate of ATP release is lower, thymocyte cell surface CD73 expression and the low thymocyte surface ADA activity together maintain the sufficient ADO levels around the thymocyte ARs. Loss of ADA activity in ADA deficient patients is associated with increased ADO levels in the thymus, which thus affect primarily the cortical

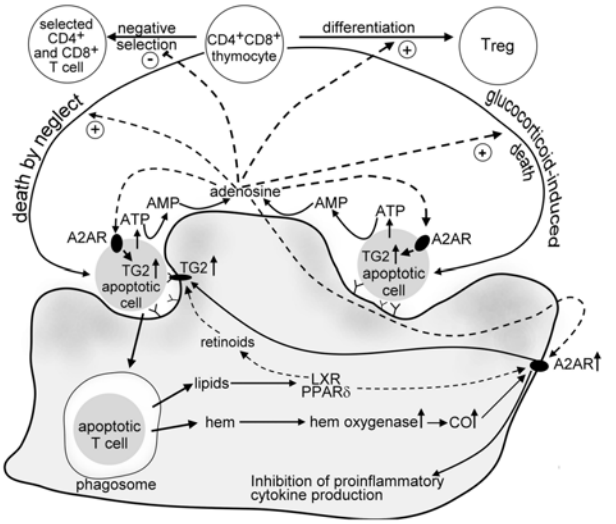

FIGURE 1 | Suggested crosstalk between developing thymocytes and engulfing macrophages in the thymus involving adenosine. Dying thymocytes release ATP via caspase-regulated pannexin channels. ATP is then fast degraded to AMP by cell surface ATP degrading enzymes of thymocytes and macrophages, and to adenosine by CD73 expressed on the macrophage cell surface. ADO acting on thymocyte adenosine A_{2A} receptors induces "death by neglect" alone or promotes the glucocorticoid-induced death of DP thymocytes. In addition, it interferes with the negative selection of thymocytes that have TCR specificities with intermediate affinity for self-antigens, thus promote positive selection. ADO is also required for the tTreg formation. In dying thymocytes ADO enhances the intracellular expression of TG2, an apoptosis-related protein that promotes fast recognition of apoptotic cells by macrophages. In macrophages ADO activates adenosine A_{2A} receptors, the expression of which is strongly induced following apoptotic cell uptake. The mechanism involves both hem oxygenase and the lipid sensing peroxisome proliferator activating receptor δand liver X receptor that are triggered by the fatty acid and oxysterol content of the engulfed apoptotic cells, respectively. A_{2A} adenosine receptor signaling in macrophages prevents neutrophil chemokine formation and might also contribute to the apoptotic cell lipid content-induced upregulation of cell surface TG2. TG2 in macrophages acts as a phagocyte coreceptor for the proper phagocytosis of apoptotic cells, and contributes to the activation of latent TGF-β, an anti-inflammatory cytokine released by the engulfing macrophages.

thymocytes (Resta and Thompson, 1997). ADA, however, is responsible for the degradation of deoxyadenosine as well, thus low ADA activities in the cortex might promote formation of the intracellular dATP and consequently proliferation of cortical thymocytes (Sandberg, 1983). ARs are expressed already by the T-lymphopoietic and monocytopoietic cells as well, and both of them express all the four ARs. While, however, in the T-lymphopoietic lineage the expression of A_{2A}Rs dominates, in the monocytopoietic cells all the A_{2A}, A_{2B}, and A_3 receptors are highly expressed subtypes (Streitová et al., 2010). However, as thymic apoptosis is initiated in the developing thymus and phagocytosis follows, engulfing macrophages upregulate their A_{2A}Rs (Köröskényi et al., 2011), while downregulate the A_3 ones (Duró et al., 2014). Upregulation of the A_{2A}Rs is engulfment-dependent in macrophages, and involves both lipid sensing transcription factors and CO produced via the hem oxygenase reaction (Haschemi et al., 2007; Köröskényi et al., 2011).

EFFECT OF ADENOSINE ON THE T CELL DEVELOPMENT

Early studies on fetal thymic organ cultures conducted in the presence of the ADO agonist 5′-(*N*-ethyl)-carboxamidoadenosine, and the AR antagonist 8-phenyl-theophylline (8-PT) indicated that ARs influence the development of thymocytes, since administration of both compounds resulted in a decreased thymocyte cell number (Hamad, 1997). Results obtained with 8-PT were concluded in a way that ADO is required for proper thymocyte development, while results obtained with NECA indicated that higher concentrations of it induce thymocyte death. 8-PT is, however, not only an AR antagonist, but acts also as a potent inhibitor of cAMP phosphodiesterase. Thus, it can induce elevations in the intracellular cAMP levels (Nicholson and Wilke, 1989), and a consequent loss of thymocyte cell number due to cAMP-induced thymocyte death (McConkey et al., 1990). Thus 8-PT could decrease the thymocyte cell number by inducing apoptosis, rather than ADO being required generally for thymocyte differentiation. In accordance, loss of A_{2A}Rs, the dominant thymocyte AR subtype, does not affect the number and the distribution of various thymocyte populations in mice (Kiss et al., 2006), despite of the fact that the expression of other ARs remained unchanged (Lukashev et al., 2003). ADO is, however, constantly produced in the cortical layer of the thymus, and can contribute to the apoptosis of neglected thymocytes similar to other signaling molecules that are also produced by macrophages in an engulfment-dependent manner (Szondy et al., 2012). The ADO-induced death of mouse thymocytes is strongly dependent on the A_{2A}Rs, as in A_{2A}R null thymocytes ADO fails to induce significant cell death (Kiss et al., 2006). The ADO-dependent death in mouse thymocytes is mediated via cAMP and cAMP-dependent protein kinase (Armstrong et al., 2001; Kiss et al., 2006) and involves upregulation of Bim, a BH3-only pro-apoptotic member of the Bcl-2 protein family (Kiss et al., 2006). In human thymocytes, on the other hand, ADO induces a Ca^{2+}-dependent death (Szondy, 1994). ADO also promotes the glucocorticoid-induced death of neglected thymocytes (McConkey et al., 1993), and together with the engulfing macrophage-produced retinoids and TGF-β, also contributes to the upregulation of TG2 in the dying cells (Sándor et al., 2016, 2017). Thus, engulfing macrophage-produced apoptosis-promoting molecules, including ADO, appearing in the cortical thymic milieu cooperate in both the fast killing of thymocytes, which express useless TCRs, and in the upregulation of their TG2 expression. These signals together are so crucial for the upregulation of TG2 *in vivo* that *in vitro,* though thymocytes die upon exposure to apoptotic stimuli, they cannot upregulate the expression of the protein (Szegezdi et al., 2000). Several molecules, which induce apoptosis of neglected thymocytes, also interfere with the TCR-mediated signaling pathways and inhibit negative selection in a dose dependent manner (Ashwell et al., 1996; Szondy et al., 1998; Szegezdi et al., 2003). For glucocorticoids, it has been demonstrated that this way these molecules determine the TCR avidity thresholds that determine whether developing thymocytes survive or die, and therefore help to mold the antigen-specific T cell repertoire (Ashwell et al., 1996). Interestingly, ADO has also been reported to interfere with the TCR-induced signaling pathways and negative selection via interfering with the CD3 ζ chain phosphorylation (Apasov et al., 2000). Thus ADO, similar to glucocorticoids and retinoids, might affect the TCR avidity thresholds in a dose dependent manner. And finally, development of tT_{reg} cells have been shown to be dependent on engulfing macrophage-derived TGF-β (Konkel et al., 2014; Chen and Konkel, 2015). Interestingly, both retinoids (Mucida et al., 2007) and ADO (Ohta and Sitkovsky, 2014) promote the TGF-β-dependent development of T_{reg} cells in the periphery. In CD73/prostatic acid phosphatase double knock out mice, where the extracellular ADO levels are low, the tT_{reg} cell production was found to be impaired (Yegutkin et al., 2014) indicating the involvement of ADO also in the tT_{reg} cell differentiation.

EFFECT OF ADENOSINE ON THE ENGULFMENT-RELATED PROCESSES OF THE MACROPHAGE

Apoptotic cells release find me signals for macrophages so that the macrophages could find them efficiently. In the thymic cortex the apoptosis sensitive DP thymocytes are in strong interaction with the cortical macrophages forming clusters with them (Rezzani et al., 2008). Thus, the removal of the constantly appearing apoptotic cells might not require chemotactic migration of macrophages. When, however, a large amount of DP thymocytes die, additional macrophages migrate through vessels into the thymus, and enter the cortical region, where most of the apoptosis takes place (Odaka and Mizouchi, 2002). In macrophages a purinergic autocrine signaling functions to amplify and translate chemotactic signals into directional motility (Kronlage et al., 2010). Upon sensing chemotactic signals, macrophages release ATP at the leading edge of the cell, which is then degraded to ADP, AMP, and ADO. Loss of either adenosine A_3R or A_{2B}R receptor function blocks the

chemotactic migration of macrophages toward the apoptotic cells (Joós et al., 2017). The involvement of AR subtype in the control of chemotactic navigation, however, might be macrophage type specific, since peritoneal tissue resident macrophages express both receptors at high levels, while in monocyte-derived macrophages the expression of the adenosine A_{2B}R dominates. In accordance, loss of A_3Rs affects the apoptotic cell removal in the peritoneal cavity, but has no effect on the thymic apoptotic cell removal *in vivo* (Joós et al., 2017). ADO has no effect on the phagocytosis of apoptotic cells (Köröskényi et al., 2011; Duró et al., 2014), but it might contribute to the apoptotic cell-induced upregulation of cell surface TG2 (Szondy et al., 2003; Rébé et al., 2009; Sarang et al., 2014) which acts as a phagocytosis coreceptor in macrophages (Tóth et al., 2009) and contributes to the activation of TGF-β released in latent form (Nunes et al., 1997). ADO is also required to maintain the immunologically silent removal of apoptotic cells. In the absence of A_{2A}R signaling KC and macrophage inflammatory protein-2 neutrophil chemokines are released by engulfing macrophages (Köröskényi et al., 2011). During the engulfment of apoptotic cells several anti-inflammatory mechanisms are activated to prevent the production of pro-inflammatory cytokines (Trahtemberg and Mevorach, 2017). Many of them act via inhibiting nuclear factor kappa-light-chain-enhancer of activated B cells (NF-κB) transcriptional activity which plays a key role in the induction of inflammatory cytokine genes (Baeuerle and Henkel, 1994), or via inducing the production of TGF-β or IL-10 (Szondy et al., 2017). ADO signaling was also shown to interfere with the NF-κB function by inhibiting its nuclear translocation, DNA binding and transcriptional activity (Xia et al., 2000; Majumdar and Aggarwal, 2003; Lukashev et al., 2004) and to induce IL-10 (Németh et al., 2005). In addition, A_{2A}R signaling prevents nitrogen monoxide formation in engulfing macrophages (Köröskényi et al., 2011) and enhances the expression of dual specific phosphatase, which interferes the MAPK signaling pathways known to contribute also to the pro-inflammatory cytokine expression (Köröskényi et al., 2016).

A_3Rs, on the other hand, were found to promote apoptotic cell uptake-induced neutrophil chemoattractant formation (Duró et al., 2014). Since A_3Rs are downregulated during engulfment, while the expression of A_{2A}Rs is induced, the immune silencing signaling of ADO acting via the upregulated A_{2A}Rs dominate during phagocytosis of apoptotic cells.

CONCLUSION

Increasing evidence indicate that macrophages engulfing apoptotic cells respond to the chemotactic signals released by apoptotic cells, to the apoptotic cell engagement and to the apoptotic cell uptake with producing various molecules, such as ATP, IL-10, TGF-β, CO, prostaglandin E_2, retinoids, and also ADO. These molecules together regulate either the phagocytic activity of macrophages and/or contribute to the immunologically silent removal of apoptotic cells. However, they might play also additional roles in the maintenance of tissue homeostasis, and this role vary from tissue to tissue. The data presented in this review indicate that in the thymus ADO in an interplay with other engulfing macrophage-derived molecules might contribute to the thymocyte selection processes (**Figure 1**).

AUTHOR CONTRIBUTIONS

All authors listed have made a substantial, direct and intellectual contribution to the work, and approved it for publication.

ACKNOWLEDGMENTS

This study was supported by the National Research, Development and Innovation Office (124244) and by the GINOP-2.3.2-15-2016-00006 project (co-financed by the European Union and the European Regional Development Fund).

REFERENCES

Alexandropoulos, K., and Danzi, N. M. (2012). Thymic epithelial cells: antigen presenting cells that regulate T cell repertoire and tolerance development. *Immunol. Res.* 54, 177–190. doi: 10.1007/s12026-012-8301-y

Antonioli, L., Csóka, B., Fornai, M., Colucci, R., Kókai, E., Blandizzi, C., et al. (2014). Adenosine and inflammation: what's new on the horizon? *Drug Discov. Today* 19, 1051–1068. doi: 10.1016/j.drudis.2014.02.010

Antonioli, L., Pacher, P., Vizi, E. S., and Haskó, G. (2013). CD39 and CD73 in immunity and inflammation. *Trends Mol. Med.* 19, 355–367. doi: 10.1016/j.molmed.2013.03.005

Apasov, S., Chen, J. F., Smith, P., and Sitkovsky, M. (2000). A(2A) receptor dependent and A(2A) receptor independent effects of extracellular adenosine on murine thymocytes in conditions of adenosine deaminase deficiency. *Blood* 95, 3859–3867.

Armstrong, J. M., Chen, J. F., Schwarzschild, M. A., Apasov, S., Smith, P. T., Caldwell, C., et al. (2001). Gene dose effect reveals no Gs-coupled A2A adenosine receptor reserve in murine T-lymphocytes: studies of cells from A2A-receptor-gene-deficient mice. *Biochem. J.* 354, 123–130. doi: 10.1042/bj3540123

Ashwell, J. D., King, L. B., and Vacchio, M. S. (1996). Cross-talk between the T cell antigen receptor and the glucocorticoid receptor regulates thymocyte development. *Stem Cells* 14, 490–500. doi: 10.1002/stem.140490

Baeuerle, P. A., and Henkel, T. (1994). Function and activation of NF-kappa B in the immune system. *Annu. Rev. Immunol.* 12, 141–179. doi: 10.1146/annurev.iy.12.040194.001041

Benoist, C., and Mathis, D. (2012). Treg cells, life history, and diversity. *Cold Spring Harb. Perspect. Biol.* 4:a007021. doi: 10.1101/cshperspect.a007021

Bommhardt, U., Beyer, M., Hünig, T., and Reichardt, H. M. (2004). Molecular and cellular mechanisms of T cell development. *Cell. Mol. Life Sci.* 61, 263–280. doi: 10.1007/s00018-003-3224-3

Chechik, B. E., Schrader, W. P., and Minowada, J. (1981). An immunomorphologic study of adenosine deaminase distribution in human thymus tissue, normal lymphocytes, and hematopoietic cell lines. *J. Immunol.* 126, 1003–1007.

Chekeni, F. B., Elliott, M. R., Sandilos, J. K., Walk, S. F., Kinchen, J. M., Lazarowski, E. R., et al. (2010). Pannexin 1 channels mediate 'find-me' signal release and membrane permeability during apoptosis. *Nature* 467, 863–867. doi: 10.1038/nature09413

Chen, J. F., Eltzschig, H. K., and Fredholm, B. B. (2013). Adenosine receptors as drug targets–what are the challenges? *Nat. Rev. Drug Discov.* 12, 265–286. doi: 10.1038/nrd3955

Chen, W., and Konkel, J. E. (2015). Development of thymic Foxp3(+) regulatory T cells: TGF-β matters. *Eur. J. Immunol.* 45, 958–965. doi: 10.1002/eji.201444999

Cillie, Y., Deviller, P., and Beteuel, H. (1983). Guanylate cyclase activity of human lymphocytes from peripheral blood, thymus, and tonsils. A comparative study. *Enzyme* 129, 86–92. doi: 10.1159/000469612

da Rocha Lapa, F., Macedo, S. J. Jr., Cerutti, M. L., and Santos, A. R. (2014). "Pharmacology of Adenosine Receptors and Their Signaling Role in Immunity and Inflammation. in *Pharmacology and Therapeutics*, ed. S. J. T. Gowder (Rijeka: InTech), 85–130. doi: 10.5772/57206

Dubyak, G. R. (2012). Function without form: an ongoing search for maxi-anion channel proteins. Focus on "Maxi-anion channel and pannexin 1 hemichannel constitute separate pathways for swelling-induced ATP release in murine L929 fibrosarcoma cells". *Am. J. Physiol. Cell Physiol.* 303, C913–C915. doi: 10.1152/ajpcell.00285.2012

Duró, E., Pallai, A., Köröskényi, K., Sarang, Z., and Szondy, Z. (2014). Adenosine A3 receptors negatively regulate the engulfment-dependent apoptotic cell suppression of inflammation. *Immunol. Lett.* 162, 292–301. doi: 10.1016/j.imlet.2014.06.014

Dzhagalov, I., Chambon, P., and He, Y. W. (2007). Regulation of CD8+ T lymphocyte effector function and macrophage inflammatory cytokine production by retinoic acid receptor γ. *J. Immunol.* 178, 2113–2121. doi: 10.4049/jimmunol.178.4.2113

Eichin, D., Laurila, J. P., Jalkanen, S., and Salmi, M. (2015). CD73 Activity is dispensable for the polarization of M2 macrophages. *PLOS ONE* 10:e0134721. doi: 10.1371/journal.pone.0134721

Eltzschig, H. K. (2009). Adenosine: an old drug newly discovered. *Anesthesiology* 111, 904–915. doi: 10.1097/ALN.0b013e3181b060f2

Esashi, E., Ito, H., Ishihara, K., Hirano, T., Koyasu, S., and Miyajima, A. (2004). Development of CD4+ macrophages from intrathymic T cell progenitors is induced by thymic epithelial cells. *J. Immunol.* 173, 4360–4367. doi: 10.4049/jimmunol.173.7.4360

Fadok, V. A., Bratton, D. L., Konowal, A., Freed, P. W., Westcott, J. Y., and Henson, P. M. (1998). Macrophages that have ingested apoptotic cells in vitro inhibit proinflammatory cytokine production through autocrine/paracrine mechanisms involving TGF-beta, PGE2, and PAF. *J. Clin. Invest.* 101, 890–898. doi: 10.1172/JCI1112

Fésüs, L., and Szondy, Z. (2005). Transglutaminase 2 in the balance of cell death and survival. *FEBS Lett.* 579, 3297–3302. doi: 10.1016/j.febslet.2005.03.063

Fredholm, B. B., IJzerman, A. P., Jacobson, K. A., Klotz, K. N., and Linden, J. (2001). International Union of Pharmacology. XXV. Nomenclature and classification of adenosine receptors. *Pharmacol. Rev.* 53, 527–552.

Garabuczi, É, Kiss, B., Felszeghy, S., Tsay, G. J., Fésüs, L., and Szondy, Z. (2013). Retinoids produced by macrophages engulfing apoptotic cells contribute to the appearance of transglutaminase 2 in apoptotic thymocytes. *Amino Acids* 44, 235–244. doi: 10.1007/s00726-011-1119-4

Gemsa, C., Woo, C. H., Fudenberg, H. H., and Schmid, R. (1973). Erythrocyte catabolism by macrophages in vitro. The effect of hydrocortisone on erythrophagocytosis and on the induction of heme oxygenase. *J. Clin. Invest.* 52, 812–822. doi: 10.1172/JCI107245

Gomez, P. E., Klapproth, K., Schulz, C., Busch, K., Azzoni, E., Crozet, L., et al. (2015). Tissue-resident macrophages originate from yolk-sac-derived erythro-myeloid progenitors. *Nature* 518, 547–551. doi: 10.1038/nature13989

Hamad, M. (1997). The role of adenosine receptor engagement in murine fetal thymocyte development. *APMIS* 107, 896–902. doi: 10.1111/j.1699-0463.1999.tb01489.x

Haschemi, A., Wagner, O., Marculescu, R., Wegiel, B., Robson, S. C., Gagliani, N., et al. (2007). Cross-regulation of carbon monoxide and the adenosine A2A receptor in macrophages. *J. Immunol.* 178, 5921–5929. doi: 10.4049/jimmunol.178.9.5921

Haskó, G., and Cronstein, B. N. (2004). Adenosine: an endogenous regulator of innate immunity. *Trends Immunol.* 25, 33–39. doi: 10.1016/j.it.2003.11.003

Haskó, G., Pacher, P., Deitch, E. A., and Vizi, E. S. (2007). Shaping of monocyte and macrophage function by adenosine receptors. *Pharmacol. Ther.* 113, 264–275. doi: 10.1016/j.pharmthera.2006.08.003

Haymaker, C. L., Guloglu, F. B., Cascio, J. A., Hardaway, J. C., Dhakal, M., Wan, X., et al. (2012). Bone marrow-derived IL-13Rα1-positive thymic progenitors are restricted to the myeloid lineage. *J. Immunol.* 188, 3208–3216. doi: 10.4049/jimmunol.1103316

Heine, P., Braun, N., Sévigny, J., Robson, S. C., Servos, J., and Zimmermann, H. (2001). The C-terminal cysteine-rich region dictates specific catalytic properties in chimeras of the ectonucleotidases NTPDase1 and NTPDase2. *Eur. J. Biochem.* 268, 364–373. doi: 10.1046/j.1432-1033.2001.01896.x

Hernandez, J. B., Newton, R. H., and Walsh, C. M. (2010). Life and death in the thymus - cell death signaling during T cell development. *Curr. Opin. Cell Biol.* 22, 865–871. doi: 10.1016/j.ceb.2010.08.003

Joós, G., Jákim, J., Kiss, B., Szamosi, R., Papp, T., Felszeghy, S., et al. (2017). Involvement of adenosine A3 receptors in the chemotactic navigation of macrophages towards apoptotic cells. *Immunol. Lett.* 183, 62–72. doi: 10.1016/j.imlet.2017.02.002

Kisielow, P., and von Boehmer, H. (1995). Development and selection of T cells: facts and puzzles. *Adv. Immunol.* 58, 87–209.

Kiss, I., Oskolás, H., Tóth, R., Bouillet, P., Tóth, K., Fülöp, A., et al. (2006). Adenosine A2A receptor-mediated cell death of mouse thymocytes involves adenylate cyclase and Bim and is negatively regulated by Nur77. *Eur. J. Immunol.* 36, 1559–1571. doi: 10.1002/eji.200535334

Konkel, J. E., Jin, W., Abbatiello, B., Grainger, J. R., and Chen, W. (2014). Thymocyte apoptosis drives the intrathymic generation of regulatory T cells. *Proc. Natl. Acad. Sci. U.S.A.* 111, E465–E473. doi: 10.1073/pnas.1320319111

Köröskényi, K., Duró, E., Pallai, A., Sarang, Z., Kloor, D., Ucker, D. S., et al. (2011). Involvement of adenosine A2A receptors in engulfment-dependent apoptotic cell suppression of inflammation. *J. Immunol.* 186, 7144–7155. doi: 10.4049/jimmunol.1002284

Köröskényi, K., Kiss, B., and Szondy, Z. (2016). Adenosine A2A receptor signaling attenuates LPS-induced pro-inflammatory cytokine formation of mouse macrophages by inducing the expression of DUSP1. *Biochim. Biophys. Acta* 1863, 1461–1471. doi: 10.1016/j.bbamcr.2016.04.003

Kronlage, M., Song, J., Sorokin, L., Isfort, K., Schwerdtle, T., Leipziger, J., et al. (2010). Autocrine purinergic receptor signaling is essential for macrophage chemotaxis. *Sci. Signal.* 3:ra555. doi: 10.1126/scisignal.2000588

Levéen, P., Carlsén, M., Makowska, A., Oddsson, S., Larsson, J., Goumans, M. J., et al. (2005). TGF-beta type II receptor-deficient thymocytes develop normally but demonstrate increased CD8+ proliferation in vivo. *Blood* 106, 4234–4240. doi: 10.1182/blood-2005-05-1871

Liu, H., and Xia, Y. J. (2015). Beneficial and detrimental role of adenosine signaling in diseases and therapy. *J. Appl. Physiol.* 119, 1173–1182. doi: 10.1152/japplphysiol.00350.2015

Liu, Y., Zhang, P., Li, J., Kulkarni, A. B., Perruche, S., and Chen, W. (2008). A critical function for TGF-beta signaling in the development of natural CD4+CD25+Foxp3+ regulatory T cells. *Nat. Immunol.* 9, 632–640. doi: 10.1038/ni.1607

Lukashev, D. E., Ohta, A., Apasov, S., Chen, J. F., and Sitkovsky, M. (2004). Cutting edge: physiological attenuation of proinflammatory transcription by the Gs protein-coupled A2a adenosine receptor in vivo. *J. Immunol.* 173, 21–24. doi: 10.4049/jimmunol.173.1.21

Lukashev, D. E., Smith, P. T., Caldwell, C. C., Ohta, A., Apasov, S. G., and Sitkovsky, M. V. (2003). Analysis of A2a receptor-deficient mice reveals no significant compensatory increases in the expression of A2b, A1, and A3 adenosine receptors in lymphoid organs. *Biochem. Pharmacol.* 65, 2081–2090. doi: 10.1016/S0006-2952(03)00158-8

Ma, D. D., Sylwestrowicz, T. A., Granger, S., Massaia, M., Franks, R., Janossy, G., et al. (1982). Distribution of terminal deoxynucleotidyl transferase and purine degradative and synthetic enzymes in subpopulations of human thymocytes. *J. Immunol.* 129, 1430–1435.

Majumdar, S., and Aggarwal, B. B. (2003). Adenosine suppresses activation of nuclear factor-κB selectively induced by tumor necrosis factor in different cell types. *Oncogene* 22, 1206–1218. doi: 10.1038/sj.onc.1206184

McConkey, D. J., Orrenius, S., and Jondal, M. (1990). Agents that elevate cAMP stimulate DNA fragmentation in thymocytes. *J. Immunol.* 145, 1227–1230.

McConkey, D. J., Orrenius, S., Okret, S., and Jondal, M. (1993). Cyclic AMP potentiates glucocorticoid-induced endogenous endonuclease activation in thymocytes. *FASEB J.* 7, 580–585.

Moran, A. E., Holzapfel, K. L., Xing, Y., Cunningham, R. L., Maltzman, J. S., Punt, J., et al. (2011). T cell receptor signal strength in Treg and iNKT cell development demonstrated by a novel fluorescent reporter mouse. *J. Exp. Med.* 208, 1279–1289. doi: 10.1084/jem.20110308

Mucida, D., Park, Y., Kim, G., Turovskaya, O., Scott, I., Kronenberg, M., et al. (2007). Reciprocal TH17 and regulatory T cell differentiation mediated by retinoic acid. *Science* 317, 256–260. doi: 10.1126/science.1145697

Németh, Z. H., Lutz, C. S., Csóka, B., Deitch, E. A., Leibovich, S. J., Gause, W. C., et al. (2005). Adenosine augments IL-10 production by macrophages through an A2B receptor-mediated posttranscriptional mechanism. *J. Immunol.* 175, 8260–8270. doi: 10.4049/jimmunol.175.12.8260

Nicholson, C. D., and Wilke, R. (1989). 8-phenyltheophylline as an inhibitor of cyclic AMP hydrolysis by cyclic nucleotide phosphodiesterase. *J. Auton. Pharmacol.* 9, 159–165. doi: 10.1111/j.1474-8673.1989.tb00207.x

Nishiura, H., Shibuya, Y., and Yamamoto, T. (1998). S19 ribosomal protein cross-linked dimer causes monocyte-predominant infiltration by means of molecular mimicry to complement C5a. *Lab. Invest.* 78, 1615–1623.

Nunes, I., Gleizes, P. E., Metz, C. N., and Rifkin, D. B. (1997). Latent transforming growth factor-beta binding protein domains involved in activation and transglutaminase-dependent cross-linking of latent transforming growth factor-beta. *J. Cell Biol.* 136, 1151–1163. doi: 10.1083/jcb.136.5.1151

Odaka, C. M., and Mizouchi, T. (2002). Macrophages are involved in DNA degradation of apoptotic cells in murine thymus after administration of hydrocortisone. *Cell Death. Differ.* 9, 104–112. doi: 10.1038/sj.cdd.4400941

Ohta, A., and Sitkovsky, M. (2014). Extracellular adenosine-mediated modulation of regulatory T cells. *Front. Immunol.* 5:304. doi: 10.3389/fimmu.2014.00304

Park, J., and Gupta, R. S. (2012). "Adenosine Metabolism, Adenosine Kinase, and Evolution, Adenosine," in *Adenosine*, eds S. Masino and D. Boison (New York, NY: Springer), 23–54.

Petersen, C. B., Nygård, A. B., Viuff, B., Fredholm, M., Aasted, B., and Salomonsen, J. (2007). Porcine ecto-nucleotide pyrophosphatase/phosphodiesterase 1 (NPP1/CD203a): cloning, transcription, expression, mapping, and identification of an NPP1/CD203a epitope for swine workshop cluster 9 (SWC9) monoclonal antibodies. *Dev. Comp. Immunol.* 31, 618–631. doi: 10.1016/j.dci.2006.08.012

Petrie, H. T., and Zuniga-Pflucker, J. C. (2007). Zoned out: functional mapping of stromal signaling microenvironments in the thymus. *Annu. Rev. Immunol.* 25, 649–679. doi: 10.1146/annurev.immunol.23.021704.115715

Piredda, L., Amendola, A., Colizzi, V., Davies, P. J., Farrace, M. G., Fraziano, M., et al. (1997). Lack of 'tissue' transglutaminase protein cross-linking leads to leakage of macromolecules from dying cells: relationship to development of autoimmunity in MRLIpr/Ipr mice. *Cell Death Differ.* 4, 463–472. doi: 10.1038/sj.cdd.4400267

Ramakers, B. P., Riksen, N. P., van der Hoeven, J. G., Smits, P., and Pickkers, P. (2011). Modulation of innate immunity by adenosine receptor stimulation. *Shock* 36, 208–215. doi: 10.1097/SHK.0b013e318225aee4

Rébé, C., Raveneau, M., Chevriaux, A., Lakomy, D., Sberna, A. L., Costa, A., et al. (2009). Induction of transglutaminase 2 by a liver X receptor/retinoic acid receptor alpha pathway increases the clearance of apoptotic cells by human macrophages. *Circ. Res.* 105, 393–401. doi: 10.1161/CIRCRESAHA.109.201855

Resta, R., Hooker, S. W., Laurent, A. B., Jamshedur Rahman, S. M., Franklin, M., Knudsen, T. B., et al. (1997). Insights into thymic purine metabolism. *J. Clin. Invest.* 99, 676–683. doi: 10.1172/JCI119211

Resta, R., and Thompson, L. F. (1997). SCID: the role of adenosine deaminase deficiency. *Immunol. Today* 18, 371–374. doi: 10.1016/S0167-5699(97)01047-5

Resta, R., Yamashita, Y., and Thompson, L. F. (1998). Ecto-enzyme and signaling functions of lymphocyte CD73. *Immunol. Rev.* 161, 95–109. doi: 10.1111/j.1600-065X.1998.tb01574.x

Rezzani, R., Bonomini, F., and Rodella, L. F. (2008). Histochemical and molecular overview of the thymus as site for T-cells development. *Prog. Histochem. Cytochem.* 43, 73–120. doi: 10.1016/j.proghi.2008.03.001

Sandberg, G. (1983). Regulation of thymocyte proliferation by endogenous adenosine and adenosine deaminase. *Int. J. Immunopharmacol.* 5, 259–265. doi: 10.1016/0192-0561(83)90027-9

Sandilos, J. K., Chiu, Y. H., Chekeni, F. B., Armstrong, A. J., Walk, S. F., Ravichandran, K. S., et al. (2012). Pannexin 1, an ATP release channel, is activated by caspase cleavage of its pore-associated C-terminal autoinhibitory region. *J. Biol. Chem.* 287, 11303–11311. doi: 10.1074/jbc.M111.323378

Sándor, K., Daniel, B., Kiss, B., Kovács, F., and Szondy, Z. (2016). Transcriptional control of transglutaminase 2 expression in mouse apoptotic thymocytes. *Biochim. Biophys. Acta* 1859, 964–974. doi: 10.1016/j.bbagrm.2016.05.011

Sándor, K., Pallai, A., Duró, E., Legendre, P., Couillin, I., Sághy, T., et al. (2017). Adenosine produced from adenine nucleotides through an interaction between apoptotic cells and engulfing macrophages contributes to the appearance of transglutaminase 2 in dying thymocytes. *Amino Acids* 49, 671–681. doi: 10.1007/s00726-016-2257-5

Sarang, Z., Garabuczi, É, Joós, G., Kiss, B., Tóth, K., Rühl, R., et al. (2013). Macrophages engulfing apoptotic thymocytes produce retinoids to promote selection, differentiation, removal and replacement of double positive thymocytes. *Immunobiology* 218, 1354–1360. doi: 10.1016/j.imbio.2013.06.009

Sarang, Z., Joós, G., Garabuczi, E., Rühl, R., Gregory, C. D., and Szondy, Z. (2014). Macrophages engulfing apoptotic cells produce non-classical retinoids to enhance their phagocytic capacity. *J. Immunol.* 192, 5730–5738. doi: 10.4049/jimmunol.1400284

Sarang, Z., Mádi, A., Koy, C., Varga, S., Glocker, M. O., Ucker, D. S., et al. (2007). Tissue transglutaminase (TG2) facilitates phosphatidylserine exposure and calpain activity in calcium-induced death of erythrocytes. *Cell Death Differ.* 14, 1842–1844. doi: 10.1038/sj.cdd.4402193

Stefan, C., Jansen, S., and Bollen, M. (2006). Modulation of purinergic signaling by NPP-type ectophosphodiesterases. *Purinergic Signal.* 2, 361–370. doi: 10.1007/s11302-005-5303-4

Streitová, D., Sefc, L., Savvulidi, F., Pospísil, M., Holá, J., and Hofer, M. (2010). Adenosine A(1), A(2a), A(2b), and A(3) receptors in hematopoiesis. 1. Expression of receptor mRNA in four mouse hematopoietic precursor cells. *Physiol. Res.* 59, 133–137.

Surh, C. D., and Sprent, J. (1994). T-cell apoptosis detected in situ during positive and negative selection in the thymus. *Nature* 372, 100–103. doi: 10.1038/372100a0

Suzuki, K., Tadakuma, T., and Kizaki, H. (1991). Modulation of thymocyte apoptosis by isoproterenol and prostaglandin E2. *Cell. Immunol.* 134, 235–240. doi: 10.1016/0008-8749(91)90346-D

Szegezdi, E., Kiss, I., Simon, A., Blaskó, B., Reichert, U., Michel, S., et al. (2003). Ligation of retinoic acid receptor alpha regulates negative selection of thymocytes by inhibiting both DNA binding of nur77 and synthesis of bim. *J. Immunol.* 170, 3588–3594. doi: 10.4049/jimmunol.170.7.3577

Szegezdi, E., Szondy, Z., Nagy, L., Nemes, Z., Friis, R. R., Davies, P. J., et al. (2000). Apoptosis-linked in vivo regulation of the tissue transglutaminase gene promoter. *Cell Death Differ.* 7, 1225–1233. doi: 10.1038/sj.cdd.4400751

Szondy, Z. (1994). Adenosine stimulates DNA fragmentation in human thymocytes by Ca(2+)-mediated mechanisms. *Biochem. J.* 304(Pt 3), 877–885.

Szondy, Z., Garabuczi, E., Tóth, K., Kiss, B., and Köröskényi, K. (2012). Thymocyte death by neglect: contribution of engulfing macrophages. *Eur. J. Immunol.* 42, 1662–1667. doi: 10.1002/eji.201142338

Szondy, Z., Reichert, U., Bernardon, J. M., Michel, S., Tóth, R., Ancian, P., et al. (1997). Induction of apoptosis by retinoids and retinoic acid receptor gamma-selective compounds in mouse thymocytes through a novel apoptosis pathway. *Mol. Pharmacol.* 51, 972–982.

Szondy, Z., Reichert, U., Bernardon, J. M., Michel, S., Tóth, R., Karászi, E., et al. (1998). Inhibition of activation-induced apoptosis of thymocytes by all-trans- and 9-cis-retinoic acid is mediated via retinoic acid receptor alpha. *Biochem. J.* 331, 767–774. doi: 10.1042/bj3310767

Szondy, Z., Sarang, Z., Kiss, B., Garabuczi, É, and Köröskényi, K. (2017). Anti-inflammatory mechanisms triggered by apoptotic cells during their clearance. *Front. Immunol.* 8:909. doi: 10.3389/fimmu.2017.00909

Szondy, Z., Sarang, Z., Molnar, P., Nemeth, T., Piacentini, M., Mastroberardino, P. G., et al. (2003). Transglutaminase 2-/- mice reveal a phagocytosis-associated crosstalk between macrophages and apoptotic cells. *Proc. Natl. Acad. Sci. U.S.A.* 100, 7812–7817. doi: 10.1073/pnas.0832466100

Tóth, B., Garabuczi, E., Sarang, Z., Vereb, G., Vámosi, G., Aeschlimann, D., et al. (2009). Transglutaminase 2 is needed for the formation of an efficient phagocyte portal in macrophages engulfing apoptotic cells. *J. Immunol.* 182, 2084–2092. doi: 10.4049/jimmunol.0803444

Trahtemberg, U., and Mevorach, D. (2017). Apoptotic cells induced signaling for immune homeostasis in macrophages and dendritic cells. *Front. Immunol.* 8:1356. doi: 10.3389/fimmu.2017.01356

Tsukimoto, M., Maehata, M., Harada, H., Ikari, A., Takagi, K., and Degawa, M. (2006). P2X7 receptor-dependent cell death is modulated during murine T cell maturation and mediated by dual signaling pathways. *J. Immunol.* 177, 2842–2850. doi: 10.4049/jimmunol.177.5.2842

Xia, D., Wang, F., and Parmely, M. J. (2000). Inhibition of nuclear factor-kappab activation in mouse macrophages and the RAW264.7 cell line by a synthetic adenyl carbocyclic nucleoside. *Biochem. Pharmacol.* 60, 717–727. doi: 10.1016/S0006-2952(00)00367-1

Yamaguchi, H., Maruyama, T., Urade, Y., and Nagata, S. (2014). Immunosuppression via adenosine receptor activation by adenosine monophosphate released from apoptotic cells. *Elife* 3:e02172. doi: 10.7554/eLife.02172

Yegutkin, G. G., Auvinen, K., Karikoski, M., Rantakari, P., Gerke, H., Elima, K., et al. (2014). Consequences of the lack of CD73 and prostatic acid phosphatase in the lymphoid organs. *Mediators Inflamm.* 2014:485743. doi: 10.1155/2014/485743

Conflict of Interest Statement: The authors declare that the research was conducted in the absence of any commercial or financial relationships that could be construed as a potential conflict of interest.

frontiers in Pharmacology

REVIEW
published: 22 December 2017
doi: 10.3389/fphar.2017.00947

Purinergic Signaling in Mast Cell Degranulation and Asthma

Zhan-Guo Gao and Kenneth A. Jacobson**

Molecular Recognition Section, Laboratory of Bioorganic Chemistry, National Institute of Diabetes and Digestive and Kidney Diseases, National Institutes of Health, Bethesda, MD, United States

Mast cells are responsible for the majority of allergic conditions. It was originally thought that almost all allergic events were mediated directly only via the high-affinity immunoglobulin E receptors. However, recent evidence showed that many other receptors, such as G protein-coupled receptors and ligand-gated ion channels, are also directly involved in mast cell degranulation, the release of inflammatory mediators such as histamine, serine proteases, leukotrienes, heparin, and serotonin. These mediators are responsible for the symptoms in allergic conditions such as allergic asthma. In recent years, it has been realized that purinergic signaling, induced via the activation of G protein-coupled adenosine receptors and P2Y nucleotide receptors, as well as by ATP-gated P2X receptors, plays a significant role in mast cell degranulation. Both adenosine and ATP can induce degranulation and bronchoconstriction on their own and synergistically with allergens. All three classes of receptors, adenosine, P2X and P2Y are involved in tracheal mucus secretion. This review will summarize the currently available knowledge on the role of purinergic signaling in mast cell degranulation and its most relevant disease, asthma.

Keywords: purinergic signaling, adenosine receptors, P2Y receptors, P2X receptors, mast cell degranulation, asthma, allergy, bronchoconstriction

OPEN ACCESS

Edited by:
Vsevolod V. Gurevich,
Vanderbilt University, United States

Reviewed by:
Kempuraj Duraisamy,
University of Missouri, United States
Silvia Bulfone-Paus,
University of Manchester, United Kingdom
Vanesa Esteban,
Instituto de Investigación Sanitaria de la Fundación Jiménez Díaz, Spain

****Correspondence:***
Zhan-Guo Gao
zg21o@nih.gov
Kenneth A. Jacobson
kennethJ@niddk.nih.gov;
kajacobs@helix.nih.gov

Specialty section:
This article was submitted to Experimental Pharmacology and Drug Discovery, a section of the journal Frontiers in Pharmacology

Received: *16 October 2017*
Accepted: *14 December 2017*
Published: *22 December 2017*

Citation:
Gao Z-G and Jacobson KA (2017) Purinergic Signaling in Mast Cell Degranulation and Asthma. Front. Pharmacol. 8:947. doi: 10.3389/fphar.2017.00947

INTRODUCTION

It is known that purinergic signaling is involved in various immune responses (Cekic and Linden, 2016; Cronstein and Sitkovsky, 2017). However, its role in mast cell degranulation, which leads to hypersensitivity reactions in response to environmental factors, is not fully understood. There are three subfamilies of receptors, 7 P2X receptor (P2XR) subunits (combined into functional trimeric channels), 8 P2Y receptors (P2YRs) and 4 adenosine receptors (ARs), that respond to purine nucleosides and purine (or pyrimidine) nucleotides (Jacobson and Gao, 2006; Chen et al., 2013; Burnstock and Boeynaems, 2014). Adenosine 5′-triphosphate (ATP, compound 3 in **Figure 1**) is abundant in mast cells, stored in granules and secreted upon activation. ATP acts via P2X receptors (P2XRs), which are ligand-gated cation channels, to induce mast cell degranulation (Bulanova and Bulfone-Paus, 2010). In general, ATP is considered a major damage-associated molecular pattern molecule (DAMP) in the immune system, and one of its principle mechanisms is by activating the P2X7R (Di Virgilio and Vuerich, 2015). Other nucleotides, such as adenosine 5′-diphosphate (ADP) 2, uridine 5′-diphosphate (UDP) 5, uridine 5′-triphosphate (UTP) 6, Up4A 7 and UDP-glucose (UDPG) 8, act mainly via P2Y receptors which are coupled to G proteins (Jacobson et al., 2015; Gao et al., 2010a,b, 2013). Purine nucleosides, especially adenosine 9, released under stress conditions, are demonstrated to be involved in many allergic conditions, particularly,

the pathogenesis of asthma and the subsequent chronic obstructive pulmonary diseases (COPD) (Adriaensen and Timmermans, 2004; Barnes, 2011). Both adenosine and allergens can cause bronchoconstriction (Cushley et al., 1984; Rafferty et al., 1987; Fozard, 2003; Hua et al., 2013b). Adenosine 5′-monophosphate (AMP) 1 also induces bronchoconstriction in asthmatic patients, and this compound, which forms adenosine *in situ*, is used in inhalation challenge testing (Isogai et al., 2017). Additionally, adenosine, ATP, and allergens can induce mast cell degranulation independently or synergistically (Nunomura et al., 2010; Hua et al., 2013a).

AR antagonists, theophylline 21 and enprofylline 25, have long been used in the clinic, particularly for asthma (Schultze-Werninghaus and Meier-Sydow, 1982). The mechanism of action of these xanthines was initially thought to be via the inhibition of phosphodiesterases (PDEs), and they are now considered to also act via the antagonism of one or several subtypes of ARs (Marquardt et al., 1978; Pauwels and Joos, 1995; Fozard, 2003; Barnes, 2011). It should be noted that adenosine-induced bronchodilation is possibly mediated via the A_{2B}AR, whereas bronchoconstriction occurs via the A_1AR. Antagonism of the A_1AR causes bronchodilation, while blockade of the A_{2B}AR causes bronchoconstriction (which will be discussed later). The simple methylxanthines, e.g., theophylline, often antagonize both A_1 and A_{2B}ARs thus producing a mixed effect, although the overall effect is bronchodilation in most cases. It should also be kept in mind that inhibition of PDE3 and PDE4 should produce a net effect similar to that of activation of the A_{2B}AR, i.e., elevation of 3′,5′-cyclic adenosine monophosphate (cAMP) levels in smooth muscle cells. However, upon examination of the dose response curves for action of simple xanthines, the antagonism of ARs begins to occur at lower concentrations than PDE inhibition (Daly and Fredholm, 1998). An increase in cAMP leads to activation of protein kinase A (PKA) and exchange protein directly activated by cAMP (EPAC), which phosphorylate target proteins, leading to the modulation of myosin activity and eventually relaxation of smooth muscle. The A_{2B}AR is also known to induce intracellular Ca^{2+} mobilization in many types of cells including smooth muscle cells leading to the relaxation of tracheal smooth muscle, which is often independent of Gs-protein and cAMP. It is important to understand the physiological roles and the signaling mechanisms involved in order to develop purinergic agonists and antagonists with appropriate selectivity and efficacy. Several P2YRs, e.g., $P2Y_{13}$ and $P2Y_{14}$, (Gao et al., 2010a,b, 2013) and P2XRs, e.g., P2X4 and P2X7 (Yoshida et al., 2017), are also recently demonstrated to be mediators and/or potentiators of mast cell degranulation.

This review will first summarize the currently available knowledge related to the role of adenosine, P2Y and P2X receptors in mast cell degranulation. We will then analyze the therapeutic rationale and potential mechanisms of AR, P2Y, and P2X receptor ligands in asthma, particularly in bronchoconstriction and tracheal mucus secretion. Methylxanthines, e.g., theophylline 21, enprofylline 25, and

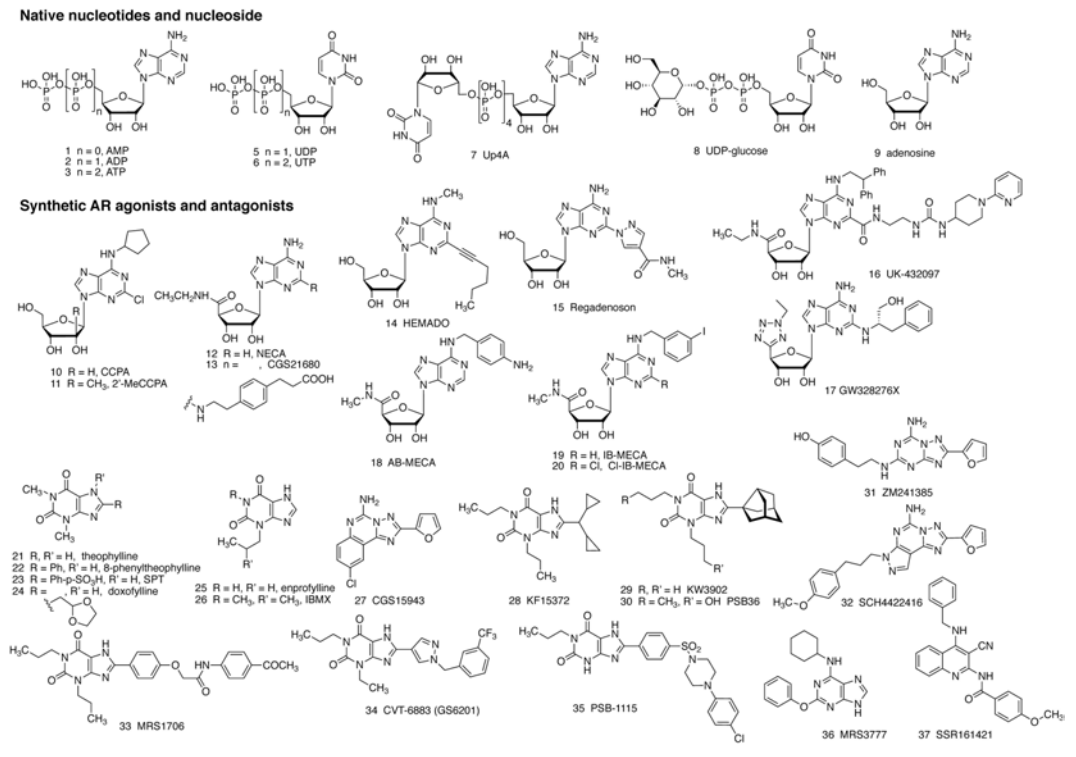

FIGURE 1 | Structure of native agonists of the purinergic receptors, including both P2Rs (1–8) and ARs (9), and structures of agonist (10–20) and antagonist (21–37) ligands developed for the ARs, as described in the text. Compounds 24 – 26 inhibit PDEs, but are weaker in inhibiting ARs.

doxofylline 24 are used in asthmatics for the alleviation of bronchoconstriction and trachea mucus secretion (Barnes, 2011). Two inhaled, selective AR ligands with anti-inflammatory actions, i.e., A_{2A}AR agonist UK432097 16 (for COPD) and mixed A_{2A}AR agonist/A_3AR antagonist GW328267X 17 (for asthma and allergic rhinitis) failed to show efficacy in clinical trials, but there were complicating pharmacokinetic factors (Mantell et al., 2010). Selective A_{2B}AR antagonist CVT-6883 34 was under development for asthma (Zablocki et al., 2005). $P2Y_2$R agonists uridine 5′-triphosphate 6 (UTP) and INS365 (compound 39 in **Figure 2**) have been in clinical trials for patients with cough due to its potential in airway mucus clearance (Noone et al., 1999; Kellerman, 2002). Orally active P2X3R antagonist MK-7264 49 (gefapixant, AF-219) is under clinical investigation for the treatment of idiopathic chronic cough, asthma, pulmonary fibrosis and other conditions (clinicaltrials.gov) [accessed October 15, 2017]. Thus, all three sub-families of receptors activated by purine nucleosides or nucleotides, are potential targets for asthma and some other allergic conditions.

REVIEW CONTENTS: ROLES OF FOUR AR SUBTYPES IN MAST CELL DEGRANULATION, MUCUS SECRETION AND BRONCHOCONSTRICTION

It has been known for decades that inhaled adenosine induces bronchoconstriction in asthmatics and COPD patients, but not in non-asthmatics (Cushley et al., 1984). Exercise-induced asthma is often accompanied by increases in plasma adenosine (Fozard, 2003). Both adenosine deaminase (ADA) and AR antagonist theophylline 21 can block adenosine-induced bronchial hyperresponsiveness (Rothstein, 1980). However, it is still not fully understood which AR subtype is actually involved in the antiasthmatic effects of methylxanthines (Barnes, 2011). It is important to establish the precise roles of adenosine and AR subtypes in mast cell degranulation, bronchoconstriction and mucus secretion, and develop appropriate AR subtype-selective agonists/antagonists for asthma and COPD.

IN VITRO STUDIES OF DEGRANULATION USING MAST CELL LINES

RBL-2H3 Cells

RBL-2H3 rat basophilic cells are a useful model for studies of degranulation. Ali et al. (1990) have shown that a non-selective adenosine agonist, NECA 12, acts synergistically with antigen in RBL-2H3 mast-like cells via a novel AR in a pertussis toxin (PTX)-sensitive manner. This novel AR was later cloned and defined as A_3AR (Zhou et al., 1992). Collado-Escobar et al. (1990) reported that the widely used glucocorticoid dexamethasone down-regulates IgE-receptor-mediated signals but up-regulates A_3AR-mediated signals in RBL-2H3 cells, suggesting A_3AR involvement in inflammation and mast cell function. Ramkumar et al. (1995) showed later that dexamethasone increases the expression of both A_3AR and G proteins in RBL-2H3 cells which contributes to the enhanced response to adenosine. Jin et al. (1997) reported that, in addition to adenosine, inosine, which was known to bind to the rat A_3AR (Jacobson et al., 2017), also stimulates degranulation in RBL-2H3 cells. Thus, results from these earlier studies suggest that adenosine and its analogs, acting via the A_3AR, can stimulate degranulation on their own, enhance the effect of antigen to stimulate degranulation via FcεRI receptor, and may offset the anti-inflammatory effects of glucocorticoids, such as dexamethasone, suggesting the anti-allergic potential of the A_3AR antagonists.

However, unlike the results from studies using RBL-2H3 cells, Auchampach et al. (1997) showed that in canine mast cells which express A_1AR, A_{2B}AR, and A_3AR, degranulation is mediated by the A_{2B}AR, rather than the A_3 or A_1ARs. NECA-stimulated degranulation is not PTX-sensitive and is blocked by enprofylline 25, a slightly A_{2B}AR selective antagonist (K_i = 7 or 4.7 or 19.8 μM at human A_{2B}AR), with weaker effects on human A_1AR (42 μM), A_{2A}AR (32 μM), and A_3AR (65 μM) (Müller and Jacobson, 2011). Auchampach et al. (1997) suggest that A_1AR and A_3AR might involve a mast cell function other than degranulation in this specific cell type. However, there was no further report since then on the role of the A_{2B}AR in canine mast cell degranulation.

HMC-1 and LAD2 Human Mast Cell Lines

Two human mast cell lines, HMC-1 (Butterfield et al., 1988) and LAD2 (Kirshenbaum et al., 2003), have been used for the study of mast cell function. HMC-1 cell line is often not considered as a good model for studying mast cell degranulation due to the low expression level of high-affinity IgE receptor (Guhl et al., 2010), but it has some other mast cell functions. Feoktistov and Biaggioni (1995) demonstrated that HMC-1 cells express both A_{2A} and A_{2B}ARs. NECA 12, but not A_{2A}AR-selective agonist CGS21680 13, induced interleukin (IL)-8 production in HMC-1 mast cells in an enprofylline-sensitive manner, suggesting a possible role of the A_{2B}AR in mast cell function. In the simulated tumor microenvironment, contact with cancer cells induces HMC-1 cells to upregulate IL8 secretion, and this effect is dependent on released adenosine activating the A_3AR (Gorzalczany et al., 2017).

The LAD2 cell line can be used as a model for the study of mast cell degranulation. LAD2 cells highly express FcεRIα and FcεRIγ, and antigens can induce a robust release of histamine (Guhl et al., 2010). It is suggested that connective tissue-type and mucosal-type mast cells are developed via distinct pathways, and tryptase/chymase expression can be considered as an indication of the maturity of mast cells (Ma et al., 2008; Guhl et al., 2010). Guhl et al. (2010) reported that tryptase and chymase expression is low in LAD2 cells in comparison to that in the primary skin mast cells, although much higher than in HMC-1 cells. Nevertheless, Leung et al. (2014) were able to examine the role of ARs in degranulation of human LAD2 mast cells, which express A_{2A}, A_{2B}, and A_3 but not A_1ARs. The non-selective agonist NECA alone induced a small but significant stimulation of β-hexosaminidase (β-hex) release. Further, NECA increased both antigen and C3a-stimulated degranulation. The authors suggested that more than one AR subtype is involved

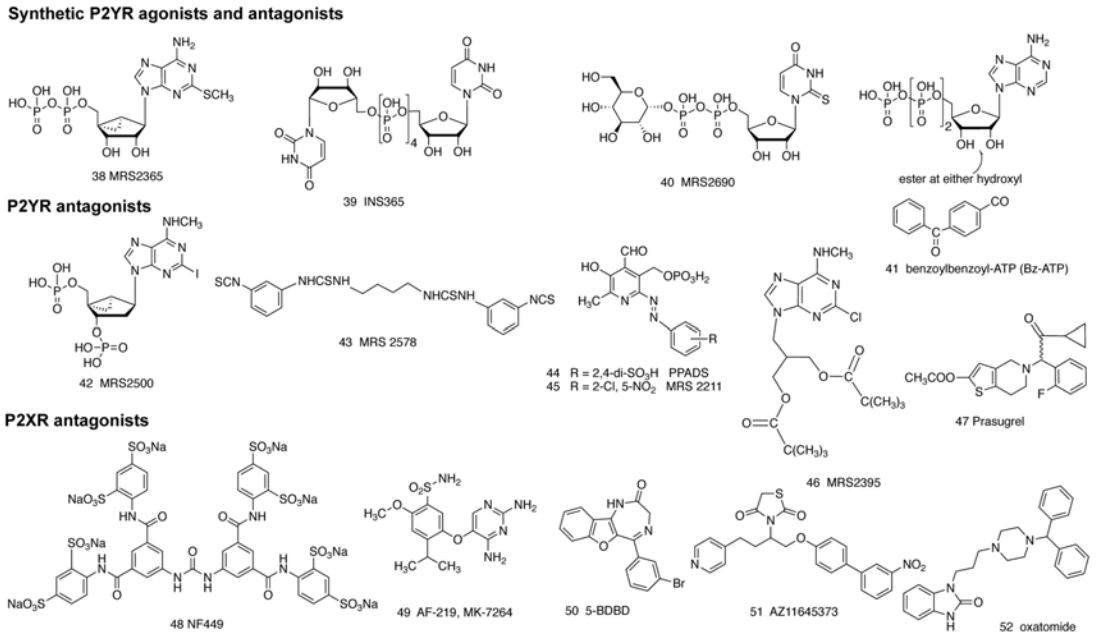

FIGURE 2 | Structure of various synthetic agonist (38–41) and antagonist (42–52) ligands for the P2YRs and P2XRs, as described in the text. Compound 52 was introduced as an antihistamine and later found to block the P2X7R.

in degranulation. Thus, there is a difference in AR expression profile and roles of ARs in various types of mast cells. Receptor expression level may play a critical role in mast cell activation and release of both newly synthesized cytokines and chemokines and stored mediators that are implicated in mast cell mediated allergic and inflammatory reactions in asthma. It seems that the differences between LAD2 and HMC-1 in terms of degranulation are mainly related to the expression level of FCεRI, tryptase and chymase, and to a much lesser extent related to histamine content or c-Kit expression (Guhl et al., 2010). The role of adenosine to induce or enhance degranulation may also be related to the AR expression in various types of mast cells. The use of primary mast cells is needed for the characterization of the roles of various ARs.

IN VITRO STUDIES OF DEGRANULATION USING PRIMARY MAST CELLS

Murine Primary Mast Cells

The role of adenosine receptors in mast cells degranulation was first reported in primary rat mast cells (Marquardt et al., 1978). Both adenosine and inosine were found to potentiate degranulation (Marquardt et al., 1978). Theophylline, at concentrations of 1–100 μM, blocks the potentiating effect of adenosine without affecting other mast cell functions (Marquardt et al., 1978), suggesting that the beneficial effects of theophylline in bronchial asthma is possibly via an AR subtype, but it is not clear if the A_3AR is involved, as methylxanthines are weak at the rat or mouse A_3AR (Jacobson and Gao, 2006). Möller et al. (2003) reported that activation of bone marrow derived mouse mast cells (BMMC) with NECA caused the release of β-hex, although to a lesser extent than antigen-induced release via FcεRI. The specific AR subtype involved in degranulation was not reported in that study, although A_1AR expression and survival was found enhanced upon FcεRI activation. Nunomura et al. (2010) suggested a mechanism of synergistic degranulation response in BMMC is via FcεRI and ARs. The FcεRI beta-chain (FcRbeta) was found to be a critical element in a synergistic mast cell degranulation response through FcεRI and ARs. Furthermore, phosphoinositide 3-kinase (PI3K)-signaling through FcRbeta immunoreceptor tyrosine-based activation motifs (ITAM) is a crucial participant in augmentation of FcεRI-mediated degranulation by adenosine, although the specific AR subtype involved in degranulation was not investigated. Leung et al. (2014) also found that NECA enhanced antigen-induced degranulation in BMMC. Zhong et al. (2003) established primary murine lung mast cell cultures and demonstrated the expression of A_{2A}, A_{2B}, and A_3 ARs on murine lung mast cells. The authors suggest that the A_3AR plays an important role in adenosine-mediated murine lung mast cell degranulation. Thus, adenosine or its analogs are clearly demonstrated to induce and/or enhance degranulation in primary murine mast cells, although it remains to be established if one AR or multiple AR subtypes are involved.

Human Primary Mast Cells

Gomez et al. (2011) reported FcεRI-induced degranulation is different in primary human lung and skin mast cells after exposure to adenosine. Human lung mast cells were found to express the A_3AR threefold higher than human skin mast cells. Low concentrations of adenosine or an A_3AR agonist was found to potentiate FcεRI-induced degranulation of human lung

mast cells but not that of skin mast cells, in a PTX-dependent way. The authors suggest that A_3AR, as a potentiator of FcεRI-induced degranulation, may involve a bronchoconstrictive response to adenosine in asthmatics, but not dermatologic allergy responses. The results also suggested that the AR expression level is related to the extent of AR-mediated degranulation. Yip et al. (2011) reported the dual and opposing modulation by A_1 and A_{2B}ARs of anti-IgE induced histamine release from primary human mast cells derived from progenitor stem cells. By using multiple selective AR agonists (CCPA 10, A_1; 2′-MeCCPA 11, A_1; HEMADO 14, A_{2A}; Cl-IB-MECA 20, A_3) and antagonists (PSB-36 30, A_1; SCH442416 32, A_{2A}; MRS1706 33, A_{2B}; PSB-1115 35, A_{2B}; MRS3777 36, A_3), the authors showed that inhibition of human mast cell activation is a mechanism for A_1AR antagonists, but not A_{2B}AR antagonists. Hua et al. (2011) found that IL-4, a cytokine that is involved in airway inflammation, increased expression of the A_{2B}AR in human umbilical cord blood-derived mast cells. The authors suggest that Th2 cytokines in the asthmatic lung may upregulate AR expression on airway mast cells to promote increased responsiveness to adenosine, which may explain at least in part why asthmatic lungs are more sensitive to adenosine than normal lungs or skin. Thus, results from primary human mast cells indicate that multiple AR subtypes are possibly involved in degranulation. The A_3AR and possibly A_1AR induce and/or potentiate, whereas the A_{2B}AR may inhibit degranulation in human mast cells. Thus, results from primary human mast cells are not completely consistent with those from cell lines, such as LAD2, HMC-1, or canine mast cells, especially concerning the role of the A_{2B}AR. It is also noted that from the aspect of degranulation, the A_1AR and A_{2A}AR most likely are not major players, although isolated reports suggest in certain cell types A_1AR plays a contributory role. The A_{2A}AR, a largely anti-inflammatory AR, may be involved in many mast cell functions other than degranulation.

IN VIVO STUDIES OF DEGRANULATION

In addition to the studies from mast cell lines and primary mast cells described above, by studying vasoconstriction of hamster cheek pouch arterioles, Shepherd et al. (1996) showed that both adenosine and its metabolite, inosine, can cause vasoconstriction *in vivo* by stimulation of mast cell degranulation via the hamster A_3AR. Reeves et al. (1997) reported that the A_3AR promotes degranulation of rat mast cells both *in vitro* and *in vivo*. Fozard et al. (1996) studied A_3AR activation in anesthetized Sprague-Dawley rats (using SPT 23 at a dose that blocks rat A_1, A_{2A} and A_{2B} ARs, but not A_3). The authors suggest that the A_3AR activation results in rapid mast cell degranulation, which plays a key role in A_3AR-mediated hypotension in rat. Thus, the role of the A_3AR in mast cell degranulation *in vivo* in rodents is consistent with findings from RBL-2H3 cells and primary murine mast cells. However, concerning the effects of dexamethasone, Hannon et al. (2002) reported that adenosine-induced mast cell degranulation in rat *in vivo* is suppressed by dexamethasone, which is in contrast to the findings by using RBL-2H3 cells (Collado-Escobar et al., 1990), suggesting potentially both pro- and anti-inflammatory roles of the A_3AR.

In an effort to study the role of the A_3AR in mast cell degranulation and development of A_3AR antagonists for allergic conditions especially for asthma (to evaluate the pharmacological effects of human A_3AR antagonists in mice or rats), Yamano et al. (2005) generated A_3AR-humanized mice, in which the mouse A_3AR gene was replaced by its human homolog, the authors found that human A_3AR can activate intracellular Ca^{2+} mobilization but not the mouse PI3K-γ signaling pathway. Antigen-dependent degranulation was not potentiated by the A_3AR agonist in the mast cells from A_3AR-humanized mice, suggesting the complexity of the A_3AR signaling and function in mast cells and in different species. The use of A_3AR agonists 19 and 20 in clinical trials has not revealed any serious adverse effects (Jacobson et al., 2017).

The role of the A_3AR in mast cell degranulation and inflammation has been explored using A_3AR knockout (KO) mice. Salvatore et al. (2000) demonstrated that adenosine and the A_3AR agonist, Cl-IB-MECA 20, potentiate antigen-dependent degranulation of BMMCs from wild-type (WT) but not A_3AR(−/−) mice, as measured by β-hex release. The authors also showed that A_3AR plays a role in both pro- and anti-inflammatory responses. Tilley et al. (2003) identified A_3AR- and mast cell-dependent and -independent components of adenosine-mediated airway responsiveness in mice. The authors indicate that mouse airway responses to aerosolized adenosine are largely dependent on A_3AR activation with a significant contribution from mast cells, and that activation of additional ARs on other cell types may also contribute to adenosine-induced airway responsiveness *in vivo*. Tilley et al. (2000) showed that both adenosine and inosine increase cutaneous vasopermeability by activating A_3AR on mast cells. Using mice deficient in the A_3AR, the authors showed that increases in cutaneous vascular permeability induced by adenosine or its metabolite inosine are mediated through the A_3AR. Also, adenosine does not increase vascular permeability in mast cell-deficient mice. This response is independent of activation of FcεRI, by antigen, as adenosine is also increases permeability in FcεRI beta-chain-deficient mice. Highly specific A_3AR agonists caused hypothermia in mice via peripheral mast cell degranulation, although the body temperature reduction was dependent on a central histamine H_1 receptor (Carlin et al., 2016). This study made use of AR KO mice (A_1AR, A_3AR and combined A_1AR/A_3AR), a non-brain-penetrant A_3AR agonist and mast cell depletion. Thus, *in vivo* studies suggest a role of the A_3AR in degranulation, independent of antigen activation of the high-affinity IgE receptor. In addition to using A_3AR KO mice, Zhong et al. (2003) showed that lung mast cells in ADA-deficient mice degranulated robustly with the elevated adenosine present. ADA prevented the accumulation of lung adenosine as well as mast cell degranulation, suggesting that this process was dependent on elevated lung adenosine levels. Consistent with this, treatment of ADA-deficient mice with non-selective AR antagonists attenuated degranulation by 30–40%. These studies are consistent with the ability of adenosine generated *in vivo* to activate ARs and thereby enhance lung mast cell degranulation. Thus, the role of the A_3AR in mast

cell degranulation has been well established. However, there has not been report about the role of the A_3AR in asthmatic patients, although *in vitro* studies in human mast cells suggested a role. This could be partly due to the fact that other events beyond degranulation, such as bronchoconstriction and trachea mucus secretion need more immediate attention for patients with asthma and are possibly more related to the A_1 and A_{2B}AR mechanisms, which will be discussed later in this manuscript.

Concerning the role of AR subtypes other than the A_3AR in mast cell degranulation, the A_{2B}AR is the most studied. In a variety of studies including in primary human or mouse mast cells and in receptor KO mice, the A_{2B}AR has been demonstrated to inhibit rather than mediate mast cell degranulation. Yip et al. (2011) reported that activation of the human mast cell A_{2B}AR inhibits anti-IgE induced release of histamine, while A_1AR agonists potentiated mast cell activation. Hua et al. (2007) reported that mice deficient in the A_{2B}AR showed enhanced mast cell activation. Basal levels of cAMP were reduced in BMMCs from A_{2B}AR KO mice and the influx of extracellular calcium through store-operated calcium channels following antigen activation was increased. A_{2B}AR KO mice also are more sensitive to IgE-mediated anaphylaxis. The authors suggest that the A_{2B}AR can act in concert to attenuate mast cell responsiveness following antigen exposure. Thus, A_{2B}AR agonists rather than antagonists can be considered as a therapy for asthma. Hua et al. (2013a) reported that the two Gs-coupled A_{2A} and A_{2B}ARs differentially limit antigen-induced mast cell activation. By comparing mast cell responses of mice with various combinations of AR KOs, they showed that AR agonists can modulate mast cell degranulation and induction of cytokine production both *in vitro* and *in vivo*. A_{2B}AR was identified as the principal subtype attenuating mast cell degranulation; however, both A_{2A} and A_{2B}AR need to be activated to inhibit cytokine synthesis.

Zaynagetdinov et al. (2010) reported that, unlike the role of the A_{2B}AR in acute inflammation, genetic deletion of A_{2B}AR reduced allergen-induced chronic pulmonary inflammation, accompanied by fewer bronchoalveolar lavage eosinophils and lower peribronchial eosinophilic infiltration. Allergen-induced IL-4 release in airways was observed in WT, but not in A_{2B}AR KO mice. Ryzhov et al. (2008b) demonstrated that BMMCs in A_{2B}AR KO mice display two distinct phenotypes. One effect is enhanced antigen-induced degranulation, consistent with an inhibitory role of A_{2B}AR in degranulation as reported by Hua et al. (2013a). The other effect observed in A_{2B}AR KO mice is loss of NECA-induced increases of IL-13 leading to vascular endothelial growth factor (VEGF) secretion. However, Ryzhov et al. (2008a), by using A_{2B}AR KO mice, demonstrated that A_{2B}AR upregulates the proinflammatory cytokine IL-6. Thus, it seems A_{2B}AR activation can induce secretion of several proinflammatory cytokines, which apparently contradicts an anti-inflammatory role for the A_{2B}AR. Indeed, it has been proposed that an A_{2B}AR antagonist rather than agonist would be suitable for potential use in asthma, based on the findings that A_{2B}AR induced IL-8 secretion by an enprofylline-sensitive mechanism in HMC-1 cells (Feoktistov and Biaggioni, 1995), a mast cell line that does not degranulate but has some other mast cell functions. The A_{2B}AR is involved in degranulation of canine BR mastocytoma cells which can be blocked by enprofylline (Auchampach et al., 1997). However, this conclusion needs to be examined more carefully, considering the fact that A_{2B}AR activation inhibits degranulation in primary human and murine mast cells. Inhibition of PDEs (Barnes, 2011) and activation of histone deacetylase (HDAC) (Barnes, 2011) are often described as a major mechanism for methylxanthines in the treatment of asthma. The inhibition of the A_{2B}AR probably produces side effects rather than a desired therapeutic effect.

The role of the A_{2A}AR in mast cell degranulation was explored in a number of earlier studies. Hughes (1984) showed that adenosine and NECA can either inhibit or potentiate IgE-dependent histamine release by human lung mast cells in suspension, depending on the time sequence. However, the A_{2B}AR and A_3AR had not yet been cloned or defined at that time, thus it is not clear which specific AR is involved in inhibition or enhancement. Lohse et al. (1987) showed that adenosine and its analogs enhance the release of histamine from rat peritoneal mast cells. The authors suggest that an A_2 AR is involved in adenosine-induced enhancement of histamine release, but it is not clear if it is through the A_{2A}AR or A_{2B}AR, as the AR subtypes were not yet defined. Marquardt et al. (1994) showed that A_{2A}AR is not involved in BMMC degranulation, as an A_{2A}AR-specific agonist failed to enhance mast cell mediator release. Gomez et al. (2013) showed that adenosine specifically inhibited FcεRI but not through the A_{2A}AR. Rork et al. (2008) reported that A_{2A}AR activation in the isolated, perfused mouse heart inhibits degranulation of resident cardiac mast cells to limit the extent of infarction. The authors found that CGS21680 significantly reduced mast cell degranulation in WT but not in A_{2A}AR KO mice. Suzuki et al. (1998) suggested that adenosine acts via the A_{2A}AR to inhibit FcεRI-mediated release of tryptase from primary human mast cells, as this inhibitory effect can be mimicked by CGS21680 and blocked by A_{2A}AR/A_{2B}AR antagonist ZM241385 31.

In summary, of the 4 ARs in mast cell degranulation, it seems that A_1AR plays a minor role, and A_{2A}AR, although overall anti-inflammatory, either does not have an effect or plays an inhibitory role in mast cell degranulation. However, A_{2B}AR has prominent proinflammatory and anti-inflammatory roles depending what is measured. A_{2B}AR may induce proinflammatory cytokines from some types of cells but inhibit mast cell degranulation both in human and murine mast cells, both *in vitro* and *in vivo*, although isolated studies of mast cell showed that it may also cause degranulation (e.g., in canine mast cells, Auchampach et al., 1997). The A_3AR has also been demonstrated to be both pro- and anti-inflammatory. However, in terms of its role in mast cell degranulation, most pieces of evidence suggest that A_3AR mediates mast cell degranulation, but in a species-dependent fashion (Carlin et al., 2016). Thus, A_{2B}AR and A_3AR, which inhibits and stimulates, respectively, are the two major AR subtypes involved in mast cell degranulation. Additionally, ARs are also involved in the function of other granulocytes such as neutrophils, basophils, and eosinophils, which are also related to release of inflammatory mediators albeit to a lesser extent compared with mast cells (Barletta et al., 2012), but this is not the main focus of the current review.

Asthma and COPD are probably the most relevant conditions related to adenosine release and subsequent AR activation that are primarily initiated by mast cell degranulation, which is followed by bronchoconstriction and mucus secretion. We have mainly examined the role of ARs in mast cell degranulation in the above sections. We will then summarize and analyze the roles of 4 ARs in the mucus secretion and bronchoconstriction in the following sections.

ROLE OF ARs IN MUCUS SECRETION

Although the mechanisms of action are still debatable, methylxanthines, such as theophylline and enprofylline, have been used for asthma treatment for almost a century presumably due to their effect on mast cell degranulation, bronchoconstriction and airway mucus clearance. Mucus hypersecretion is an important contributor to airway obstruction. The action of methylxanthines on mucus clearance may complement their effects on mast cell degranulation and bronchoconstriction in asthmatic patients (Wanner, 1985; Ziment, 1987; Wang et al., 2016); the mechanism of methylxanthines have been proposed to be via PDEs, HDAC, and ARs (Barnes, 2011). In an earlier study, Wagner et al. (1996) reported effects of several xanthines as PDE inhibitors, i.e., theophylline 21, enprofylline 25, and 3-isobutyl-1-methylxanthine 26 (IBMX), on tracheal mucus secretion in rat and found that they stimulate mucus secretion with EC_{50} values of 690, 400, and 46 μM, respectively. This may suggest a possible mechanism as mixed PDE inhibition and AR antagonism, or interpreted as the antagonism of multiple ARs, as methylxanthines are non-selective AR antagonists. As will be discussed in the following sections, blockade of the A_1AR and A_{2B}AR may have a respective positive and negative impact on trachea mucus clearance. Increasing attentions have been paid on the roles of ARs in mucus clearance in recent years including the use of KO animals, although the role of individual AR subtypes is still controversial. In the following section, we briefly summarize the roles of ARs in mucus clearance.

McNamara et al. (2004) showed that mucin 2 (MUC2) expression increased in response to adenosine in cultured airway epithelial cells. The authors suggest that adenosine in combination with inflammatory cytokines stimulates asthmatic airway mucin production. The results were consistent with suggested use of antagonists of A_1AR, calcium-activated chloride channel regulator 1 (CLCA1), and epidermal growth factor receptor (EGFR) in asthma treatment. A_1AR antagonists contribute to airway mucus clearance. Mohsenin et al. (2007) showed that genetic ablation of the A_{2A}AR in ADA-deficient mice enhanced pulmonary inflammation, mucin production, and angiogenesis. Thus, A_{2A}AR agonists should contribute to airway clearance. Rollins et al. (2008) demonstrated that activation of the A_{2B}AR contributes to mucus clearance. Hua et al. (2013b) showed that adenosine increased mucus clearance via both A_{2A} and A_{2B} ARs. In both A_3AR KO mice (Young et al., 2006) and ADA-deficient mice (Young et al., 2004), A_3AR activation increases airway mucin secretion in response to allergen challenge. In summary, A_{2A} and A_{2B}AR agonists or A_1 and A_3AR antagonists may contribute to trachea mucus clearance.

ROLES OF ARs IN BRONCHOCONSTRICTION

As methylxanthines can inhibit PDEs, activate HDAC (i.e., theophylline), and activate ryanodine receptors, as well as antagonize ARs, many of their therapeutic effects in asthma, especially their use against bronchoconstriction, have often been ascribed to non-adenosine mechanisms, such as the inhibition of PDEs (Barnes, 2011). Theophylline's therapeutic effect has been suggested to be due to the activation of HDAC (Donnelly and Rogers, 2003).

Inhaled adenosine induces bronchoconstriction in asthmatic patients but not in healthy subjects (Cushley et al., 1984; Rorke and Holgate, 2002). Theophylline was found more potent in blocking adenosine-induced than histamine-induced bronchoconstriction suggesting most likely an AR- but not PDE-mediated mechanism. It seems that adenosine-induced bronchoconstriction of isolated sensitized lung tissues is via the release of three mediators, i.e., histamine, cyclooxygenase products and leukotrienes (Martin and Broadley, 2002), as none of the mediators alone is responsible for the constriction. Fozard (2010) summarized apparent contradictions about the role the A_3AR in bronchoconstriction, using sensitized Brown Norway rats. Alfieri et al. (2012) found that A_1AR expression on smooth muscle cells is increased on bronchi of sensitized Wistar rats challenged with allergen, suggesting that the A_1AR is responsible for bronchial hyperresponsiveness to adenosine. Hua et al. (2007) demonstrated that adenosine-induced bronchoconstriction in mice is mediated via the A_1AR. Ponnoth et al. (2010) demonstrated using allergic WT and A_1AR KO mice that this receptor is systemically proinflammatory and increases airway hyperresponsiveness. Use of DNA antisense against the A_1AR in a rabbit model of asthma suggested that receptor subtype may promote bronchoconstriction (Nyce and Metzger, 1997). Two A_1AR antagonists, KF15372 28 and KW3902 29 significantly inhibited the NECA-induced bronchoconstriction in an *in vivo* rat model. Pauwels and Joos (1995) showed that the A_1AR is possibly involved in adenosine-induced bronchoconstriction based on the order of bronchoconstrictor potency of adenosine analogs. Mikus et al. (2013) examined the effects of a novel A_3AR antagonist, SSR161421 37 on bronchoconstriction. In ovalbumin presensitized guinea pigs, SSR161421 (IV or PO) inhibited antigen-induced contractions in isolated tracheal muscles that were enhanced by agonist AB-MECA 18 and also reduced bronchoconstriction *in vivo*. In addition to blocking AR agonist-induced enhancement, SSR161421 significantly decreased antigen-induced contraction. However, this compound has not been extensively evaluated in other models. Thus, antagonists of the A_1AR and possibly the A_3AR may be beneficial for treatment of bronchoconstriction.

TABLE 1 | Roles of ARs, P2XRs and P2YRs in mast cell degranulation, bronchoconstriction and airway mucus secretion.

Receptor	Mast cell degranulation	Bronchial contraction	Tracheal mucus secretion	Reference
A_1	ND	+	+	McNamara et al., 2004; Ponnoth et al., 2010
A_{2A}	ND (–)	ND	–	Rollins et al., 2008
A_{2B}	–	–	–	Breschi et al., 2007; Hua et al., 2007, 2013b; Yip et al., 2011;
A_3	+	+	+	Young et al., 2006; Gomez et al., 2011
$P2Y_2$	ND	ND	+	Kellerman, 2002; Donnelly and Rogers, 2003
$P2Y_{13}$	+	ND	ND	Gao et al., 2010a
$P2Y_{14}$	+	ND	ND	Gao et al., 2010b; Gao et al., 2013
$P2X_4$	+	+	+	Nagaoka et al., 2009; Chen et al., 2016; Yoshida et al., 2017
$P2X_7$	+	ND	ND	Wareham and Seward, 2016; Yoshida et al., 2017

+, induce; –, inhibit. ND, not clearly demonstrated (see complete reference list for more information). ATP can induce mast cell degranulation, mucus secretion, and bronchoconstriction, which are reported in many publications, but the roles of specific receptor subtypes involved have not been unambiguously demonstrated so far except for P2X4 and P2X7. The specific roles of $P2Y_1$, $P2Y_2$, $P2Y_4$, $P2Y_6$, $P2Y_{11}$, $P2Y_{12}$, P2X1, P2X2, P2X3, P2X5, and P2X6 receptors in degranulation have not yet been unambiguously demonstrated in mast cells, although many of them are involved in some other mast cell functions and functions of many other types of immune and non-immune cells.

Pauwels and Joos (1995) demonstrated the lack of bronchoconstriction activity of CGS21680 13, and suggested that the A_{2A}AR is not involved in adenosine-induced bronchoconstriction. The A_{2A}AR-selective antagonist KF17837 (structure not shown) had no activity on adenosine-induced bronchoconstriction. Regadenoson 15 has been demonstrated to be safe to use in patients with mild to moderate COPD and asthma, although it is recommended that Regadenoson should be avoided in patients with severe bronchial asthma at this time (Golzar and Doukky, 2014). A_{2A}AR agonist Binodenoson (structure not shown) was also shown to be well tolerated in humans without significant bronchoconstriction or pulmonary consequences (Murray et al., 2009). Thus, A_{2A}AR does not seem to play a major role in adenosine-induced bronchoconstriction. Breschi et al. (2007) characterized the role of ARs in the contractility modulation of guinea-pig airway smooth muscle in normal and pathological settings. The authors found that the non-selective agonist NECA 12, relaxed tracheal muscles in preparations from normal and sensitized animals that were pre-exposed to histamine to induce contraction, and this effect was completely blocked by an A_{2B}AR antagonist, MRS1706 33. Administration of NECA or adenosine to normal animals inhibited histamine-mediated bronchoconstriction. Adenosine plasma levels were demonstrated significantly higher in sensitized than normal animals. The authors suggest that the A_{2B}AR is responsible for the relaxing effects of adenosine on guinea-pig airways. A_{2B}AR, but not A_{2A}AR activation contributes to the relaxing of adenosine-induced bronchoconstriction. Thus, development of selective A_{2B}AR agonists are a potential future direction for the treatment of asthma.

In summary, all four AR subtypes are to some extent involved in three aspects related to asthma, mast cell degranulation, trachea mucus secretion, and bronchoconstriction. To develop drugs for asthma and COPD, it is important to consider ligands with appropriate agonist or antagonist activity and subtype selectivity at certain AR subtypes, e.g., compounds with A_{2B}AR agonist and A_1AR antagonist activity. Although not yet available, allosteric A_{2B}AR agonist modulators in theory could be potentially be a novel attractive therapy for asthma, due to the site- or event- specific nature of allosteric modulators. Also, as adenosine is a ubiquitous bronchoconstrictor, the prevention of adenosine accumulation in airways by modulators of ADA, AK and adenosine transporters should also be considered as future anti-asthmatic therapy. The importance of ARs in asthma was also highlighted by a recent report that the inhalation of a novel glucocorticoid receptor agonist GW870086X (structure not shown) protects against adenosine-induced bronchoconstriction in asthma (Leaker et al., 2015). Both methylxanthines and glucocorticoids have been suggested to act via HDAC, one of the converging points for inflammation control. Also, although not reviewed in this manuscript, both adenosine and allergen may regulate immune response via other types including T cells (Erdmann et al., 2005; Mukherjee and Zhang, 2011). In human asthma, initial exposure to allergen or adenosine may induce T cell-dependent stimulation or inhibition of the immune response mediating the production of IgE and cytokines. Subsequent allergen exposure may then activate mast cells to release histamine and leukotrienes.

P2YRs

P2YRs in Mast Cell Degranulation

Several P2Y receptor subtypes have recently been demonstrated to be mediators of mast cell degranulation. Jaffar and Pearce (1990) showed that ATP-induced release of prostaglandin D2 and histamine from rat serosal mast cells was inhibited by antagonists of both P2X and P2Y receptors. Schulman et al. (1999) suggested that ATP-enhanced histamine release from human lung mast cells are possibly via the $P2Y_1$ and $P2Y_2$ receptors. However, Lee et al. (2001) suggested that ATP-induced histamine release in rat peritoneal mast cells is via a P2X receptor rather than a P2Y subtype. UDPG 8, a glycosyl donor in the biosynthesis of carbohydrates, acting at the $P2Y_{14}$R was first identified as a mediator of degranulation in RBL-2H3 mast cells as indicated by β-hex release (Gao et al., 2010b), suggesting a potential novel

therapeutic target for allergic conditions. The role of $P2Y_{14}R$ was further confirmed using human LAD2 mast cells (Gao et al., 2013). All eight P2YRs were expressed at variable levels in LAD2 cells. Gene expression levels of ADP receptors, $P2Y_1$, $P2Y_{12}$, and $P2Y_{13}$Rs, are similar, but it seems only $P2Y_{13}$ plays a major role in degranulation. Although $P2Y_{11}$ and $P2Y_4$Rs are highly expressed (three–fivefold of $P2Y_1R$), they do not seem to have a role in degranulation. Both UDPG 8 and MRS2690 40, enhanced C3a-induced β-hex release, which was inhibited by a $P2Y_{14}$ antagonist, specific $P2Y_{14}R$ siRNA and PTX, suggesting a role of $P2Y_{14}R$ activation in promoting human mast cell degranulation. The involvement of $P2Y_1$ and $P2Y_6$Rs in degranulation is negligible. The enhancement by ADP and ATP appears mediated via multiple receptors. In a separate study using RBL-2H3 cells it was demonstrated that, both $P2Y_1$ and $P2Y_{13}$Rs are highly expressed. Native agonist ADP was two orders of magnitude less potent than the $P2Y_1$-selective agonist MRS2365 38 in inducing intracellular Ca^{2+} mobilization; however, ADP reached the same maximal efficacy as MRS2365. ADP-induced β-hex release was PTX-sensitive and antagonized by a selective antagonist of the $P2Y_{13}R$, i.e., MRS2211 45, but not by MRS2500 42. This pharmacological profile suggested a mechanism dependent on Gi-coupled $P2Y_{13}R$ but not a Gq-coupled $P2Y_1R$. ADP-mediated intracellular calcium mobilization and β-hex release were found to be via $P2Y_1$ and $P2Y_{13}$Rs, respectively, indicating selective $P2Y_{13}R$ antagonists might be useful as therapeutic agents for various allergic conditions. (Gao et al., 2010a). Gendaszewska-Darmach et al. (2016) recently showed that nucleoside 5′-O-monophosphorothioates are weak antagonists of the $P2Y_{14}R$ and blocked antigen-induced RBL-2H3 mast cell degranulation enhanced by UDPG. Hundreds of genetic variants are thought to contribute to asthma risk by modulating gene expression. Ferreira et al. (2017), using gene-based analysis, identifies four putative novel asthma risk genes, two of which are P2Y receptors, $P2Y_{13}R$ and $P2Y_{14}R$, highlighted the importance of these two receptors. In a recent study, although not the focus of the present review and not in mast cells, Nakano et al. (2017) showed that uridine 5′-diphosphate (UDP) promoted IgE-dependent degranulation, blocked by antagonist MRS2578 43, suggesting inhibition of $P2Y_6R$ may also be a potential anti-asthma therapy.

P2YRs in Bronchoconstriction

Flores-Soto et al. (2011) suggested that ATP induces tracheal muscle contraction indirectly via epithelial P2Y receptors and prostaglandins release. Basoglu et al. (2017) found that adenosine, AMP and ATP all induced bronchoconstriction in asthmatic patients, but via different mechanisms, i.e., their respective ARs and P2Y and/or P2X receptors. Lussana et al. (2015) examined the role of the $P2Y_{12}R$ in asthmatic patients, and suggested that the $P2Y_{12}R$ antagonist prodrug prasugrel 40 may reduce the bronchial inflammatory burden, and thus may contribute to asthma treatment. Leukotriene antagonists montelukast and pranlukast have been demonstrated to antagonize the $P2Y_6R$ (Mamedova et al., 2005). Brüser et al. (2017) recently reported that prostaglandin $(PGE)_2$-glycerol ester acts as an agonist at the $P2Y_6R$, further suggesting a potential role of the $P2Y_6R$ in asthma.

P2YRs in Mucus Secretion

In asthma and COPD, airway mucus hypersecretion typically leads to mucostasis and plugging of the airways by mucus. ATP release in the airways is known to be elevated in COPD, and has been demonstrated to exacerbate inflammation by activating P2Y or P2X receptors. Sabater et al. (1999) showed that inhaled $P2Y_2R$ agonists can increase lung mucus clearance in sheep. The purinoceptor $P2Y_2R$ agonist diquafosol (INS365 39) has been in clinical trials to increase mucus clearance (Kellerman, 2002; Donnelly and Rogers, 2003). Button et al. (2013) reported that changes in mechanical strain is regulated by ATP and adenosine acting via P2YRs or ARs proportional to mucus hydration in airway epithelia. Shishikura et al. (2016) showed that the extracellular ATP increases MUC5AC expression and release, mainly as an autocrine agonist of the $P2Y_2R$. Shirasaki et al. (2015) used MRS2395 46, an uncharged $P2Y_{12}R$ antagonist, to partially inhibit the LTE4-induced release of MUC5AC protein in the airway. The authors suggest that role of LTE4 in allergic mucus secretion partially might involve activation of $P2Y_{12}R$. $P2Y_1R$ immunoreactivity was found within the respiratory epithelium and submucosal glandular tissue. $P2Y_2R$ immunoreactivity was localized to the mucus-secreting cells within the vomeronasal organ (VNO) (Gayle and Burnstock, 2005). Lau et al. (2011) showed that three leukotriene antagonists, i.e., montelukast, pranlukast, and zafirlukast, inhibit $P2Y_6R$ agonist UDP-induced ion transport in human bronchial epithelia. Thus, several P2YR subtypes play a role in mucus secretion.

In summary, multiple subtypes of P2YRs are potentially involved in degranulation, bronchoconstriction and mucus secretion. It is important to develop appropriate P2YR-selective ligands targeting all three functions related to asthma.

P2XRs

P2XRs in Degranulation

Rossi et al. (1992) reported interactions between high-affinity IgE receptors and ATP receptors on immature murine mast cells. Both antigen and ATP had significant effects on intracellular calcium in cells. Wareham et al. (2009) demonstrated that three subtypes of ATP receptors, P2X1, P2X4, and P2X7Rs, were identified in both the LAD2 human mast cell line and in primary human lung mast cells. Yoshida et al. (2017) studied the role of ATP in degranulation using BMMC cells, and found that both P2X4 and P2X7Rs are involved in the regulation of BMMC degranulation. P2X7R but not P2Y4 activation induced degranulation on its own. Activation of the P2X4R significantly potentiated the degranulation induced by antigen, although it does not induce degranulation on its own. Interestingly, ATP synergistically enhanced A_3AR mediated degranulation. Thus, ATP and adenosine may induce or enhance degranulation via multiple targets synergistically. It is suggested that P2X7R antagonists are potentially attractive anti-allergic agent (Yoshida et al., 2015). Interestingly, the antihistamine oxatomide 45 has been reported to act as a P2X7R antagonist (Yoshida et al., 2015), suggesting potentially dual antagonism. Wareham

and Seward (2016) showed that P2X7R activation in human mast cells by either ATP or BzATP 41 induces pronounced increases in intracellular calcium and degranulation, which are inhibited by the selective P2X7R antagonist AZ11645373 51, or by removing extracellular calcium. P2X1R activation in human mast cells also induces calcium influx, which is significantly inhibited by antagonists PPADS 44 and NF449 48. P2X1R activation does not trigger degranulation by itself. The authors indicate that P2X7R, compared with P2X1R and P2X4R, may play a more significant role in contributing to the degranulation of mast cells. Additionally, a role of the P2X3R has also been demonstrated in murine mast cells (Bulanova et al., 2009).

P2XRs in Bronchoconstriction

The role of ATP and P2X receptors in bronchoconstriction has been extensively studied (Basoglu et al., 2005; Weigand et al., 2012; Pelleg et al., 2016). ATP plays a major role in obstructive airway diseases (Pelleg et al., 2016). Studies in animal models and in COPD and asthma patients have detected increased ATP release in the lungs, which can affect multiple surrounding cell types to increase inflammation, bronchoconstriction, and cough (Pelleg et al., 2016). Most of these effects of ATP are mediated by P2X and/or P2Y receptors. It has recently been reported that P2X3R antagonists are promising for the alleviation of chronic cough (Pelleg et al., 2016). Basoglu et al. (2017) found that ATP and adenosine have opposite effects on capsaicin challenge in asthmatic patients. Asthmatic patients showed hypersensitivity to AMP and ATP, but AMP does not mimic the effects of ATP and the effects of ATP are not mediated by adenosine, suggesting adenosine and ATP act via ARs and P2X receptors, respectively. Gui et al. (2011) showed that the dinucleotide Up4A-induced tracheal contraction was blocked by a P2X antagonist diinosine pentaphosphate (structure not shown). Montaño et al. (2013) found that ATP-induced contraction of tracheas from guinea pigs was potentiated by pretreatment with histamine, but blocked by antagonists of P2X and P2YRs, and inhibitors of COX-1 and COX-2. Oguma et al. (2007) found that ATP, via the P2X receptor, increased the sensitivity of other inducers to induce contraction of airway smooth muscle. Nagaoka et al. (2009) demonstrated that the P2X4R is involved in the contraction of airway smooth muscle cells.

P2XRs in Trachea Mucus Secretion

The mucociliary system in the body is responsible for clearing inhaled particles and pathogens from the airways, one of the most potent of which is extracellular ATP which acts by releasing calcium ions from internal stores via the P2YRs and by activating calcium influx via the P2XRs. Several P2XRs were found localized to various tissue types present within the nasal cavity. P2X3R immunoreactivity was localized in the primary olfactory neurons located both in the olfactory epithelium and VNO and also on subepithelial nerve fibers in the respiratory region. P2X5R was found in the squamous, respiratory and olfactory epithelial cells of the rat nasal mucosa. P2X7R was also expressed in epithelial cells, suggesting an association with epithelial turnover (Gayle and Burnstock, 2005). ATP signaling has been demonstrated to be critical in maintaining proper mucus hydration of airways (Button et al., 2013). Excessive sodium salt is known to exacerbate chronic coughing. Ma et al. (1999) show that, in airway ciliated cells, extracellular sodium ions specifically and competitively inhibit an ATP-gated channel that is permeable to calcium ions, and thereby attenuate ATP-induced ciliary motility. The authors suggest that mucus clearance might be improved in chronic bronchitis and asthma by decreasing the sodium concentration of the airway surface. Chen et al. (2016) investigated the effects of P2X4R in a murine experimental asthma model, and suggested that ATP-P2X4R signaling may not only contribute to airway inflammation, but it may also contribute to airway remodeling in allergic asthma. ATP was found to enhance the allergic reaction, which was attenuated by the P2X4R antagonist, 5-BDBD 50 (Chen et al., 2016).

Thus, several P2XRs are involved in mast cell degranulation, mucus secretion, and bronchoconstriction. ATP, acting at the P2X7R may induce degranulation its own, and synergize with adenosine and allergen, suggesting a critical role in asthma.

The roles of adenosine, P2X and P2Y receptors have been extensively investigated in both immune and non-immune cells (Jacobson and Gao, 2006; Chen et al., 2013; Burnstock and Boeynaems, 2014; Jacobson et al., 2015). Interactions among receptors for nucleosides, nucleotides, and other allergic mediators in immune and non-immune cells have been explored. For example, Pinheiro et al. (2013) showed that histamine induced release of ATP from human subcutaneous fibroblasts. Oguma et al. (2007) showed that ATP enhanced the methacholine-induced contractile response in airway smooth muscle. Montaño et al. (2013) found that ATP-induced tracheal contraction was potentiated by histamine and blocked by inhibitors of COX-1 and COX-2.

Although asthma is the major disease most relevant to the purinergic signaling, other allergic conditions have also been reported to be related to purinergic signaling. For example, Weber et al. (2010) demonstrated that the P2X7R is essential for extracellular ATP release in the response of skin to allergen exposure. Thus, P2X7R antagonists might be considered for the prevention of allergic contact dermatitis.

CONCLUSION

Despite the many current asthma and COPD therapies, all drugs have some drawbacks. For example, long acting β-adrenergic agonists were suggested not to be used alone in patients with asthma (Billington et al., 2017). In addition, asthma in a significant proportion of patients remains uncontrolled; thus, more novel and newer drugs are needed for its treatment. All four AR subtypes, and several P2XR and P2YR subtypes are involved in mast cell degranulation, bronchoconstriction, and tracheal mucus secretion (**Table 1**). There are opportunities to develop appropriate ligands for the treatment of asthma by targeting one or several of these three classes of receptors. Adenosine and ATP both can induce degranulation by themselves and enhance antigen-induced degranulation, suggesting a critical role in asthmatics. Compounds with A_{2B}AR agonist activity or

A_1AR and A_3AR antagonist activity, and agonists of $P2Y_2R$ or antagonists of $P2Y_{13}R$, $P2Y_{14}R$, P2X3R, P2X4R, and P2X7R should be beneficial for the treatment of asthma. Also, in addition to receptors, targeting purinergic degradation cascade, such as ADA, AK and nucleotidases, could also be an attractive approach to controlling mast cell degranulation, mucus secretion, and bronchodilation. Finally, considering the mechanisms of action, it seems that selective A_{2B}AR agonists, A_1AR and/or possibly A_3AR antagonists, methylxanthines that lack A_{2A} and A_{2B} antagonist activity, and P2X7R antagonists should be particularly useful for the treatment of asthma.

AUTHOR CONTRIBUTIONS

Both authors listed have made a substantial, direct and intellectual contribution to the work, and approved it for publication.

ACKNOWLEDGMENT

We acknowledge funding from the NIDDK Intramural Research Program (No. ZIADK031117).

REFERENCES

Adriaensen, D., and Timmermans, J. P. (2004). Purinergic signalling in the lung: important in asthma and COPD? *Curr. Opin. Pharmacol.* 4, 207–214. doi: 10.1016/j.coph.2004.01.010

Alfieri, A., Parisi, A., Maione, F., Grassia, G., Morello, S., Ialenti, A., et al. (2012). Hyperresponsiveness to adenosine in sensitized Wistar rats over-expressing A1 receptor. *Eur. J. Pharmacol.* 695, 120–125. doi: 10.1016/j.ejphar.2012.09.002

Ali, H., Cunha-Melo, J. R., Saul, W. F., and Beaven, M. A. (1990). Activation of phospholipase C via adenosine receptors provides synergistic signals for secretion in antigen-stimulated RBL-2H3 cells. Evidence for a novel adenosine receptor. *J. Biol. Chem.* 265, 745–753.

Auchampach, J. A., Jin, X., Wan, T. C., Caughey, G. H., and Linden, J. (1997). Canine mast cell adenosine receptors: cloning and expression of the A3 receptor and evidence that degranulation is mediated by the A2B receptor. *Mol. Pharmacol.* 52, 846–860. doi: 10.1124/mol.52.5.846

Barletta, K. E., Ley, K., and Mehrad, B. (2012). Regulation of neutrophil function by adenosine. *Arterioscler. Thromb. Vasc. Biol.* 32, 856–864. doi: 10.1161/ATVBAHA.111.226845

Barnes, P. J. (2011). Biochemical basis of asthma therapy. *J. Biol. Chem.* 286, 32899–32905. doi: 10.1074/jbc.R110.206466

Basoglu, O. K., Pelleg, A., Essilfie-Quaye, S., Brindicci, C., Barnes, P. J., and Kharitonov, S. A. (2005). Effects of aerosolized adenosine 5′-triphosphate vs adenosine 5′-monophosphate on dyspnea and airway caliber in healthy nonsmokers and patients with asthma. *Chest* 128, 1905–1909. doi: 10.1378/chest.128.4.1905

Basoglu, O. K., Pelleg, A., Kharitonov, S. A., and Barnes, P. J. (2017). Contrasting effects of ATP and adenosine on capsaicin challenge in asthmatic patients. *Pulm. Pharmacol. Ther.* 45, 13–18. doi: 10.1016/j.pupt.2017.04.004

Billington, C. K., Penn, R. B., and Hall, I. P. (2017). β2 agonists. *Handb. Exp. Pharmacol.* 237, 23–40. doi: 10.1007/164_2016_64

Breschi, M. C., Blandizzi, C., Fogli, S., Martinelli, C., Adinolfi, B., Calderone, V., et al. (2007). In vivo adenosine A2B receptor desensitization in guinea-pig airway smooth muscle: implications for asthma. *Eur. J. Pharmacol.* 575, 149–157. doi: 10.1016/j.ejphar.2007.07.051

Brüser, A., Zimmermann, A., Crews, B. C., Sliwoski, G., Meiler, J., König, G. M., et al. (2017). Prostaglandin E2 glyceryl ester is an endogenous agonist of the nucleotide receptor P2Y6. *Sci. Rep.* 7:2380. doi: 10.1038/s41598-017-02414-8

Bulanova, E., Budagian, V., Orinska, Z., Koch-Nolte, F., Haag, F., and Bulfone-Paus, S. (2009). ATP induces P2X7 receptor-independent cytokine and chemokine expression through P2X1 and P2X3 receptors in murine mast cells. *J. Leukoc. Biol.* 85, 692–702. doi: 10.1189/jlb.0808470

Bulanova, E., and Bulfone-Paus, S. (2010). P2 receptor-mediated signaling in mast cell biology. *Purinergic Signal.* 6, 3–17. doi: 10.1007/s11302-009-9173-z

Burnstock, G., and Boeynaems, J. M. (2014). Purinergic signalling and immune cells. *Purinergic Signal.* 10, 529–564. doi: 10.1007/s11302-014-9427-2

Butterfield, J. H., Weiler, D., Dewald, G., and Gleich, G. J. (1988). Establishment of an immature mast cell line from a patient with mast cell leukemia. *Leuk. Res.* 12, 345–355. doi: 10.1016/0145-2126(88)90050-1

Button, B., Okada, S. F., Frederick, C. B., Thelin, W. R., and Boucher, R. C. (2013). Mechanosensitive ATP release maintains proper mucus hydration of airways. *Sci. Signal.* 6:ra46. doi: 10.1126/scisignal.2003755

Carlin, J. L., Tosh, D. K., Xiao, C., Piñol, R. A., Chen, Z., Salvemini, D., et al. (2016). Peripheral adenosine A3 receptor activation causes regulated hypothermia in mice that is dependent on central histamine H1 receptors. *J. Pharmacol. Exp. Ther.* 356, 474–482. doi: 10.1124/jpet.115.229872

Cekic, C., and Linden, J. (2016). Purinergic regulation of the immune system. *Nat. Rev. Immunol.* 16, 177–192. doi: 10.1038/nri.2016.4

Chen, H., Xia, Q., Feng, X., Cao, F., Yu, H., Song, Y., et al. (2016). Effect of P2X4R on airway inflammation and airway remodeling in allergic airway challenge in mice. *Mol. Med. Rep.* 13, 697–704. doi: 10.3892/mmr.2015.4622

Chen, J. F., Eltzschig, H. K., and Fredholm, B. B. (2013). Adenosine receptors as drug targets - what are the challenges? *Nat. Rev. Drug Discov.* 12, 265–286. doi: 10.1038/nrd3955

Collado-Escobar, D., Cunha-Melo, J. R., and Beaven, M. A. (1990). Treatment with dexamethasone down-regulates IgE-receptor-mediated signals and up-regulates adenosine-receptor-mediated signals in a rat mast cell (RBL-2H3) line. *J. Immunol.* 144, 244–250.

Cronstein, B. N., and Sitkovsky, M. (2017). Adenosine and adenosine receptors in the pathogenesis and treatment of rheumatic diseases. *Nat. Rev. Rheumatol.* 13, 41–51. doi: 10.1038/nrrheum.2016.178

Cushley, M. J., Tattersfield, A. E., and Holgate, S. T. (1984). Adenosine-induced bronchoconstriction in asthma. Antagonism by inhaled theophylline. *Am. Rev. Respir. Dis.* 129, 380–384.

Daly, J. W., and Fredholm, B. B. (1998). Caffeine–an atypical drug of dependence. *Drug Alcohol Depend.* 51, 199–206. doi: 10.1016/S0376-8716(98)00077-5

Di Virgilio, F., and Vuerich, M. (2015). Purinergic signaling in the immune system. *Auton. Neurosci.* 191, 117–123. doi: 10.1016/j.autneu.2015.04.011

Donnelly, L. E., and Rogers, D. F. (2003). Therapy for chronic obstructive pulmonary disease in the 21st century. *Drugs* 63, 1973–1998. doi: 10.2165/00003495-200363190-00002

Erdmann, A. E., Gao, Z. G., Jung, U., Foley, J., Borenstein, T., Jacobson, K. A., et al. (2005). Activation of Th1 and Tc1 Cell A2A adenosine receptors directly inhibits IL-2 secretion in vitro and IL-2 driven expansion in vivo. *Blood* 105, 4707–4714. doi: 10.1182/blood-2004-04-1407

Feoktistov, I., and Biaggioni, I. (1995). Adenosine A2b receptors evoke interleukin-8 secretion in human mast cells. An enprofylline-sensitive mechanism with implications for asthma. *J. Clin. Invest.* 96, 1979–1986. doi: 10.1172/JCI118245

Ferreira, M. A., Jansen, R., Willemsen, G., Penninx, B., Bain, L. M., Vicente, C. T., et al. (2017). Gene-based analysis of regulatory variants identifies 4 putative novel asthma risk genes related to nucleotide synthesis and signaling. *J. Allergy Clin. Immunol.* 139, 1148–1157. doi: 10.1016/j.jaci.2016.07.017

Flores-Soto, E., Carbajal, V., Reyes-García, J., García-Hernández, L. M., Figueroa, A., Checa, M., et al. (2011). In airways ATP refills sarcoplasmic reticulum via P2X smooth muscle receptors and induces contraction through P2Y epithelial receptors. *Pflugers Arch.* 461, 261–275. doi: 10.1007/s00424-010-0886-1

Fozard, J. R. (2003). The case for a role for adenosine in asthma: almost convincing? *Curr. Opin. Pharmacol.* 3, 264–269. doi: 10.1016/S1471-4892(03)00039-0

Fozard, J. R. (2010). "From hypertension (+) to asthma: interactions with the adenosine A3 receptor from a personal perspective," in *A3 Adenosine Receptors from Cell Biology to Pharmacology and Therapeutics*, ed. P. A. Borea (Dordrecht: Springer Science+Business Media BV), 3–26. doi: 10.1007/978-90-481-3144-0_1

Fozard, J. R., Pfannkuche, H. J., and Schuurman, H. J. (1996). Mast cell degranulation following adenosine A3 receptor activation in rats. *Eur. J. Pharmacol.* 298, 293–297. doi: 10.1016/0014-2999(95)00822-5

Gao, Z. G., Ding, Y., and Jacobson, K. A. (2010a). P2Y13 receptor is responsible for ADP-mediated degranulation in RBL-2H3 rat mast cells. *Pharmacol. Res.* 62, 500–505. doi: 10.1016/j.phrs.2010.08.003

Gao, Z. G., Ding, Y., and Jacobson, K. A. (2010b). UDP-glucose acting at P2Y14 receptors is a mediator of mast cell degranulation. *Biochem. Pharmacol.* 79, 873–879. doi: 10.1016/j.bcp.2009.10.024

Gao, Z. G., Wei, Q., Jayasekara, M. P., and Jacobson, K. A. (2013). The role of P2Y14 and other P2Y receptors in degranulation of human LAD2 mast cells. *Purinergic Signal.* 9, 31–40. doi: 10.1007/s11302-012-9325-4

Gayle, S., and Burnstock, G. (2005). Immunolocalisation of P2X and P2Y nucleotide receptors in the rat nasal mucosa. *Cell Tissue Res.* 319, 27–36. doi: 10.1007/s00441-004-0979-2

Gendaszewska-Darmach, E., Wêgłowska, E., Walczak-Drzewiecka, A., and Karaś, K. (2016). Nucleoside 5′-O-monophosphorothioates as modulators of the P2Y14 receptor and mast cell degranulation. *Oncotarget* 7, 69358–69370. doi: 10.18632/oncotarget.12541

Golzar, Y., and Doukky, R. (2014). Regadenoson use in patients with chronic obstructive pulmonary disease: the state of current knowledge. *Int. J. Chron. Obstruct. Pulmon. Dis.* 9, 129–137. doi: 10.2147/COPD.S56879

Gomez, G., Nardone, V., Lotfi-Emran, S., Zhao, W., and Schwartz, L. B. (2013). Intracellular adenosine inhibits IgE-dependent degranulation of human skin mast cells. *J. Clin. Immunol.* 33, 1349–1359. doi: 10.1007/s10875-013-9950-x

Gomez, G., Zhao, W., and Schwartz, L. B. (2011). Disparity in FcεRI-induced degranulation of primary human lung and skin mast cells exposed to adenosine. *J. Clin. Immunol.* 31, 479–487. doi: 10.1007/s10875-011-9517-7

Gorzalczany, Y., Akiva, E., Klein, O., Merimsky, O., and Sagi-Eisenberg, R. (2017). Mast cells are directly activated by contact with cancer cells by a mechanism involving autocrine formation of adenosine and autocrine/paracrine signaling of the adenosine A3 receptor. *Cancer Lett.* 397, 23–32. doi: 10.1016/j.canlet.2017.03.026

Guhl, S., Babina, M., Neou, A., Zuberbier, T., and Artuc, M. (2010). Mast cell lines HMC-1 and LAD2 in comparison with mature human skin mast cells–drastically reduced levels of tryptase and chymase in mast cell lines. *Exp. Dermatol.* 19, 845–847. doi: 10.1111/j.1600-0625.2010.01103.x

Gui, Y., Wang, Z., Sun, X., Walsh, M. P., Li, J. J., Gao, J., et al. (2011). Uridine adenosine tetraphosphate induces contraction of airway smooth muscle. *Am. J. Physiol. Lung Cell. Mol. Physiol.* 301, L789–L794. doi: 10.1152/ajplung.00203.2011

Hannon, J. P., Tigani, B., Schuurman, H. J., and Fozard, J. R. (2002). Suppression of adenosine A3 receptor-mediated hypotension and mast cell degranulation in the rat by dexamethasone. *J. Pharmacol. Exp. Ther.* 302, 725–730. doi: 10.1124/jpet.102.035790

Hua, X., Chason, K. D., Jania, C., Acosta, T., Ledent, C., and Tilley, S. L. (2013a). Gs-coupled adenosine receptors differentially limit antigen-induced mast cell activation. *J. Pharmacol. Exp. Ther.* 344, 426–435. doi: 10.1124/jpet.112.198978

Hua, X., Chason, K. D., Patel, J. Y., Naselsky, W. C., and Tilley, S. L. (2011). IL-4 amplifies the pro-inflammatory effect of adenosine in human mast cells by changing expression levels of adenosine receptors. *PLOS ONE* 6:e24947. doi: 10.1371/journal.pone.0024947

Hua, X., Erikson, C. J., Chason, K. D., Rosebrock, C. N., Deshpande, D. A., Penn, R. B., et al. (2007). Involvement of A1 adenosine receptors and neural pathways in adenosine-induced bronchoconstriction in mice. *Am. J. Physiol. Lung Cell. Mol. Physiol.* 293, L25–L32. doi: 10.1152/ajplung.00058.2007

Hua, X., Naselsky, W. C., Bennett, W. D., Ledent, C., Senior, B. A., and Tilley, S. L. (2013b). Adenosine increases nasal mucociliary clearance rate in mice through A2A and A2B adenosine receptors. *Laryngoscope* 123, 306–310. doi: 10.1002/lary.23586

Hughes, P. J. (1984). Adenosine inhibits and potentiates IgE-dependent histamine release from human lung mast cells by an A2-purinoceptor mediated mechanism. *Biochem. Pharmacol.* 33, 3847–3852. doi: 10.1016/0006-2952(84)90050-9

Isogai, S., Niwa, Y., Yatsuya, H., Hayashi, M., Yamamoto, N., Okamura, T., et al. (2017). Increased airway hyperresponsiveness to adenosine in patients with aspirin intolerant asthma. *Allergol. Int.* 66, 360–362. doi: 10.1016/j.alit.2016.10.001

Jacobson, K. A., and Gao, Z. G. (2006). Adenosine receptors as therapeutic targets. *Nat. Rev. Drug Discov.* 5, 247–264. doi: 10.1038/nrd1983

Jacobson, K. A., Merighi, S., Varani, K., Borea, P. A., Baraldi, S., Tabrizi, M. A., et al. (2017). A3 adenosine receptors as modulators of inflammation: from medicinal chemistry to therapy. *Med. Res. Rev.* doi: 10.1002/med.21456 [Epub ahead of print].

Jacobson, K. A., Paoletta, S., Katritch, V., Wu, B., Gao, Z. G., Zhao, Q., et al. (2015). Nucleotides acting at P2Y receptors: connecting structure and function. *Mol. Pharmacol.* 88, 220–230. doi: 10.1124/mol.114.095711

Jaffar, Z. H., and Pearce, F. L. (1990). Histamine secretion from mast cells stimulated with ATP. *Agents Actions* 30, 64–66. doi: 10.1007/BF01968999

Jin, X., Shepherd, R. K., Duling, B. R., and Linden, J. (1997). Inosine binds to A3 adenosine receptors and stimulates mast cell degranulation. *J. Clin. Invest.* 100, 2849–2857. doi: 10.1172/JCI119833

Kellerman, D. J. (2002). P2Y2 receptor agonists: a new class of medication targeted at improved mucociliary clearance. *Chest* 121(Suppl. 5), 201S–205S. doi: 10.1378/chest.121.5_suppl.201S

Kirshenbaum, A. S., Akin, C., Wu, Y., Rottem, M., Goff, J. P., Beaven, M. A., et al. (2003). Characterization of novel stem cell factor responsive human mast cell lines LAD 1 and 2 established from a patient with mast cell sarcoma/leukemia; activation following aggregation of FcepsilonRI or FcgammaRI. *Leuk. Res.* 27, 677–682. doi: 10.1016/S0145-2126(02)00343-0

Lau, W. K., Chow, A. W., Au, S. C., and Ko, W. H. (2011). Differential inhibitory effects of CysLT1 receptor antagonists on P2Y6 receptor-mediated signaling and ion transport in human bronchial epithelia. *PLOS ONE* 6:e22363. doi: 10.1371/journal.pone.0022363

Leaker, B. R., O'Connor, B., Singh, D., and Barnes, P. J. (2015). The novel inhaled glucocorticoid receptor agonist GW870086X protects against adenosine-induced bronchoconstriction in asthma. *Allergy Clin. Immunol.* 136, 501–502. doi: 10.1016/j.jaci.2015.01.034

Lee, Y. H., Lee, S. J., Seo, M. H., Kim, C. J., and Sim, S. S. (2001). ATP-induced histamine release is in part related to phospholipase A2-mediated arachidonic acid metabolism in rat peritoneal mast cells. *Arch. Pharm. Res.* 24, 552–556. doi: 10.1007/BF02975164

Leung, C. T., Li, A., Banerjee, J., Gao, Z. G., Kambayashi, T., Jacobson, K. A., et al. (2014). The role of activated adenosine receptors in degranulation of human LAD2 mast cells. *Purinergic Signal.* 10, 465–475. doi: 10.1007/s11302-014-9409-4

Lohse, M. J., Maurer, K., Gensheimer, H. P., and Schwabe, U. (1987). Dual actions of adenosine on rat peritoneal mast cells. *Naunyn Schmiedebergs Arch. Pharmacol.* 335, 555–560.

Lussana, F., Di Marco, F., Terraneo, S., Parati, M., Razzari, C., Scavone, M., et al. (2015). Effect of prasugrel in patients with asthma: results of PRINA, a randomized, double-blind, placebo-controlled, cross-over study. *J. Thromb. Haemost.* 13, 136–141. doi: 10.1111/jth.12779

Ma, F., Kambe, N., Wang, D., Shinoda, G., Fujino, H., Umeda, K., et al. (2008). Direct development of functionally mature tryptase/chymase double-positive connective tissue-type mast cells from primate embryonic stem cells. *Stem Cells* 26, 706–714. doi: 10.1634/stemcells.2007-0348

Ma, W., Korngreen, A., Uzlaner, N., Priel, Z., and Silberberg, S. D. (1999). Extracellular sodium regulates airway ciliary motility by inhibiting a P2X receptor. *Nature* 400, 894–897. doi: 10.1038/23743

Mamedova, L., Capra, V., Accomazzo, M. R., Gao, Z. G., Ferrario, S., Fumagalli, M., et al. (2005). CysLT1 leukotriene receptor antagonists inhibit the effects of nucleotides acting at P2Y receptors. *Biochem. Pharmacol.* 71, 115–125. doi: 10.1016/j.bcp.2005.10.003

Mantell, S., Jones, R., and Trevethick, M. (2010). Design and application of locally delivered agonists of the adenosine A2A receptor. *Expert Rev. Clin. Pharmacol.* 3, 55–72. doi: 10.1586/ecp.09.57

Marquardt, D. L., Parker, C. W., and Sullivan, T. J. (1978). Potentiation of mast cell mediator release by adenosine. *J. Immunol.* 120, 871–878.

Marquardt, D. L., Walker, L. L., and Heinemann, S. (1994). Cloning of two adenosine receptor subtypes from mouse bone marrow-derived mast cells. *J. Immunol.* 152, 4508–4515.

Martin, T. J., and Broadley, K. J. (2002). Mediators of adenosine- and ovalbumen-induced bronchoconstriction of sensitized guinea-pig isolated airways. *Eur. J. Pharmacol.* 451, 89–99. doi: 10.1016/S0014-2999(02)02197-0

McNamara, N., Gallup, M., Khong, A., Sucher, A., Maltseva, I., Fahy, J., et al. (2004). Adenosine up-regulation of the mucin gene, MUC2, in asthma. *FASEB J.* 18, 1770–1772.

Mikus, E. G., Szeredi, J., Boer, K., Tímári, G., Finet, M., Aranyi, P., et al. (2013). Evaluation of SSR161421, a novel orally active adenosine A3 receptor antagonist on pharmacology models. *Eur. J. Pharmacol.* 699, 172–179. doi: 10.1016/j.ejphar.2012.11.049

Mohsenin, A., Mi, T., Xia, Y., Kellems, R. E., Chen, J. F., and Blackburn, M. R. (2007). Genetic removal of the A2A adenosine receptor enhances pulmonary inflammation, mucin production, and angiogenesis in adenosine deaminase-deficient mice. *Am. J. Physiol. Lung Cell. Mol. Physiol.* 293, L753–L761. doi: 10.1152/ajplung.00187.2007

Möller, C., Xiang, Z., and Nilsson, G. (2003). Activation of mast cells by immunoglobulin E-receptor cross-linkage, but not through adenosine receptors, induces A1 expression and promotes survival. *Clin. Exp. Allergy* 33, 1135–1140. doi: 10.1046/j.1365-2222.2003.01728.x

Montaño, L. M., Carbajal, V., Vargas, M. H., García-Hernández, L. M., Díaz-Hernández, V., Checa, M., et al. (2013). Histamine, carbachol, and serotonin induce hyperresponsiveness to ATP in guinea pig tracheas: involvement of COX-2 pathway. *Pflugers Arch.* 465, 1171–1179. doi: 10.1007/s00424-013-1253-9

Mukherjee, A. B., and Zhang, Z. (2011). Allergic asthma: influence of genetic and environmental factors. *J. Biol. Chem.* 286, 32883–32889. doi: 10.1074/jbc.R110.197046

Müller, C. E., and Jacobson, K. A. (2011). "Xanthines as adenosine receptor antagonists," in *Methylxanthines: Handbook of Experimental Pharmacology*, Vol. 200 (Berlin: Springer), 151–199. doi: 10.1007/978-3-642-13443-2_6

Murray, J. J., Weiler, J. M., Schwartz, L. B., Busse, W. W., Katial, R. K., Lockey, R. F., et al. (2009). Safety of binodenoson, a selective adenosine A2A receptor agonist vasodilator pharmacological stress agent, in healthy subjects with mild intermittent asthma. *Circ. Cardiovasc. Imaging* 2, 492–498. doi: 10.1161/CIRCIMAGING.108.817932

Nagaoka, M., Nara, M., Tamada, T., Kume, H., Oguma, T., Kikuchi, T., et al. (2009). Regulation of adenosine 5′-triphosphate (ATP)-gated P2X4 receptors on tracheal smooth muscle cells. *Respir. Physiol. Neurobiol.* 166, 61–67. doi: 10.1016/j.resp.2009.02.002

Nakano, M., Ito, K., Yuno, T., Soma, N., Aburakawa, S., Kasai, K., et al. (2017). UDP/P2Y6 receptor signaling regulates IgE-dependent degranulation in human basophils. *Allergol. Int.* 66, 574–580. doi: 10.1016/j.alit.2017.02.014

Noone, P. G., Bennett, W. D., Regnis, J. A., Zeman, K. L., Carson, J. L., King, M., et al. (1999). Effect of aerosolized uridine-5′-triphosphate on airway clearance with cough in patients with primary ciliary dyskinesia. *Am. J. Respir. Crit. Care Med.* 160, 144–149. doi: 10.1164/ajrccm.160.1.9806146

Nunomura, S., Gon, Y., Yoshimaru, T., Kashiwakura, J., Kawakami, T., and Ra, C. (2010). FcepsilonRI beta-chain ITAM amplifies PI3K-signaling to ensure synergistic degranulation response via FcepsilonRI and adenosine receptors. *Eur. J. Immunol.* 40, 1205–1217. doi: 10.1002/eji.200939651

Nyce, J. W., and Metzger, W. J. (1997). DNA antisense therapy for asthma in an animal model. *Nature* 385, 721–725. doi: 10.1038/385721a0

Oguma, T., Ito, S., Kondo, M., Makino, Y., Shimokata, K., Honjo, H., et al. (2007). Roles of P2X receptors and Ca^{2+} sensitization in extracellular adenosine triphosphate-induced hyperresponsiveness in airway smooth muscle. *Clin. Exp. Allergy* 37, 893–900. doi: 10.1111/j.1365-2222.2007.02719.x

Pauwels, R. A., and Joos, G. F. (1995). Characterization of the adenosine receptors in the airways. *Arch. Int. Pharmacodyn. Ther.* 329, 151–160.

Pelleg, A., Schulman, E. S., and Barnes, P. J. (2016). Extracellular adenosine 5′-triphosphate in obstructive airway diseases. *Chest* 150, 908–915. doi: 10.1016/j.chest.2016.06.045

Pinheiro, A. R., Paramos-de-Carvalho, D., Certal, M., Costa, M. A., Costa, C., Magalhães-Cardoso, M. T., et al. (2013). Histamine induces ATP release from human subcutaneous fibroblasts, via pannexin-1 hemichannels, leading to Ca^{2+} mobilization and cell proliferation. *J. Biol. Chem.* 288, 27571–27583. doi: 10.1074/jbc.M113.460865

Ponnoth, D. S., Nadeem, A., Tilley, S., and Mustafa, S. J. (2010). Involvement of A1 adenosine receptors in altered vascular responses and inflammation in an allergic mouse model of asthma. *Am. J. Physiol. Heart Circ. Physiol.* 299, H81–H87. doi: 10.1152/ajpheart.01090.2009

Rafferty, P., Beasley, R., Southgate, P., and Holgate, S. (1987). The role of histamine in allergen and adenosine-induced bronchoconstriction. *Int. Arch. Allergy Appl. Immunol.* 82, 292–294. doi: 10.1159/000234210

Ramkumar, V., Wilson, M., Dhanraj, D. N., Gettys, T. W., and Ali, H. (1995). Dexamethasone up-regulates A3 adenosine receptors in rat basophilic leukemia (RBL-2H3) cells. *J. Immunol.* 154, 5436–5443.

Reeves, J. J., Jones, C. A., Sheehan, M. J., Vardey, C. J., and Whelan, C. J. (1997). Adenosine A3 receptors promote degranulation of rat mast cells both in vitro and in vivo. *Inflamm. Res.* 46, 180–184. doi: 10.1007/s000110050169

Rollins, B. M., Burn, M., Coakley, R. D., Chambers, L. A., Hirsh, A. J., Clunes, M. T., et al. (2008). A2B adenosine receptors regulate the mucus clearance component of the lung's innate defense system. *Am. J. Respir. Cell Mol. Biol.* 39, 190–197. doi: 10.1165/rcmb.2007-0450OC

Rork, T. H., Wallace, K. L., Kennedy, D. P., Marshall, M. A., Lankford, A. R., and Linden, J. (2008). Adenosine A2A receptor activation reduces infarct size in the isolated, perfused mouse heart by inhibiting resident cardiac mast cell degranulation. *Am. J. Physiol. Heart Circ. Physiol.* 295, H1825–H1833. doi: 10.1152/ajpheart.495.2008

Rorke, S., and Holgate, S. T. (2002). Targeting adenosine receptors: novel therapeutic targets in asthma and chronic obstructive pulmonary disease. *Am. J. Respir. Med.* 1, 99–105. doi: 10.1007/BF03256599

Rossi, G. L., Yen, A., and Barrett, K. E. (1992). IgE and adenosine 5′ triphosphate receptors on immature murine mast cells are functionally linked to signal transduction mechanisms. *J. Allergy Clin. Immunol.* 90, 765–771. doi: 10.1016/0091-6749(92)90100-G

Rothstein, R. J. (1980). Intravenous theophylline therapy in asthma: a clinical update. *Ann. Emerg. Med.* 9, 327–330. doi: 10.1016/S0196-0644(80)80070-9

Ryzhov, S., Zaynagetdinov, R., Goldstein, A. E., Novitskiy, S. V., Blackburn, M. R., Biaggioni, I., et al. (2008a). Effect of A2B adenosine receptor gene ablation on adenosine-dependent regulation of proinflammatory cytokines. *J. Pharmacol. Exp. Ther.* 324, 694–700.

Ryzhov, S., Zaynagetdinov, R., Goldstein, A. E., Novitskiy, S. V., Dikov, M. M., Blackburn, M. R., et al. (2008b). Effect of A2B adenosine receptor gene ablation on proinflammatory adenosine signaling in mast cells. *J. Immunol.* 180, 7212–7220.

Sabater, J. R., Mao, Y. M., Shaffer, C., James, M. K., O'Riordan, T. G., and Abraham, W. M. (1999). Aerosolization of P2Y2-receptor agonists enhances mucociliary clearance in sheep. *J. Appl. Physiol.* 87, 2191–2196.

Salvatore, C. A., Tilley, S. L., Latour, A. M., Fletcher, D. S., Koller, B. H., and Jacobson, M. A. (2000). Disruption of the A3 adenosine receptor gene in mice and its effect on stimulated inflammatory cells. *J. Biol. Chem.* 275, 4429–4434. doi: 10.1074/jbc.275.6.4429

Schulman, E. S., Glaum, M. C., Post, T., Wang, Y., Raible, D. G., Mohanty, J., et al. (1999). ATP modulates anti-IgE-induced release of histamine from human lung mast cells. *Am. J. Respir. Cell Mol. Biol.* 20, 530–537. doi: 10.1165/ajrcmb.20.3.3387

Schultze-Werninghaus, G., and Meier-Sydow, J. (1982). The clinical and pharmacological history of theophylline: first report on the bronchospasmolytic action in man by S. R. Hirsch in Frankfurt (Main) 1922. *Clin. Allergy* 12, 211–215. doi: 10.1111/j.1365-2222.1982.tb01641.x

Shepherd, R. K., Linden, J., and Duling, B. R. (1996). Adenosine-induced vasoconstriction in vivo. Role of the mast cell and A3 adenosine receptor. *Circ. Res.* 78, 627–634. doi: 10.1161/01.RES.78.4.627

Shirasaki, H., Kanaizumi, E., Seki, N., and Himi, T. (2015). Leukotriene E4 induces MUC5AC release from human airway epithelial NCI-H292 cells. *Allergol. Int.* 64, 169–174. doi: 10.1016/j.alit.2014.11.002

Shishikura, Y., Koarai, A., Aizawa, H., Yamaya, M., Sugiura, H., Watanabe, M., et al. (2016). Extracellular ATP is involved in dsRNA-induced MUC5AC production via P2Y2R in human airway epithelium. *Respir. Res.* 17:121. doi: 10.1186/s12931-016-0438-0

Suzuki, H., Takei, M., Nakahata, T., and Fukamachi, H. (1998). Inhibitory effect of adenosine on degranulation of human cultured mast cells upon cross-linking

of Fc epsilon RI. *Biochem. Biophys. Res. Commun.* 242, 697–702. doi: 10.1006/bbrc.1997.8040

Tilley, S. L., Tsai, M., Williams, C. M., Wang, Z. S., Erikson, C. J., Galli, S. J., et al. (2003). Identification of A3 receptor- and mast cell-dependent and -independent components of adenosine-mediated airway responsiveness in mice. *J. Immunol.* 171, 331–337. doi: 10.4049/jimmunol.171.1.331

Tilley, S. L., Wagoner, V. A., Salvatore, C. A., Jacobson, M. A., and Koller, B. H. (2000). Adenosine and inosine increase cutaneous vasopermeability by activating A_3 receptors on mast cells. *J. Clin. Invest.* 105, 361–367. doi: 10.1172/JCI8253

Wagner, U., Bredenbröker, D., Fehmann, H. C., Schwarz, F., Schudt, C., and Von Wichert, P. (1996). Effects of selective and non-selective phosphodiesterase inhibitors on tracheal mucus secretion in the rat. *Eur. J. Pharmacol.* 298, 265–270. doi: 10.1016/0014-2999(95)00794-6

Wang, S., Xiong, L., Deng, X., Zhou, Q., Li, C., Ren, W., et al. (2016). Effect of aminophylline and simvastatin on airway inflammation and mucus hypersecretion in rats with chronic obstructive pulmonary disease. *Zhong Nan Da Xue Xue Bao Yi Xue Ban* 41, 37–43. doi: 10.11817/j.issn.1672-7347.2016.01.006

Wanner, A. (1985). Effects of methylxanthines on airway mucociliary function. *Am. J. Med.* 79, 16–21. doi: 10.1016/0002-9343(85)90082-8

Wareham, K., Vial, C., Wykes, R. C., Bradding, P., and Seward, E. P. (2009). Functional evidence for the expression of P2X1, P2X4 and P2X7 receptors in human lung mast cells. *Br. J. Pharmacol.* 157, 1215–1224. doi: 10.1111/j.1476-5381.2009.00287.x

Wareham, K. J., and Seward, E. P. (2016). P2X7 receptors induce degranulation in human mast cells. *Purinergic Signal.* 12, 235–246. doi: 10.1007/s11302-016-9497-4

Weber, F. C., Esser, P. R., Müller, T., Ganesan, J., Pellegatti, P., Simon, M. M., et al. (2010). Lack of the purinergic receptor P2X7 results in resistance to contact hypersensitivity. *J. Exp. Med.* 207, 2609–2619. doi: 10.1084/jem.20092489

Weigand, L. A., Ford, A. P., and Undem, B. J. (2012). A role for ATP in bronchoconstriction-induced activation of guinea pig vagal intrapulmonary C-fibres. *J. Physiol.* 590, 4109–4120. doi: 10.1113/jphysiol.2012.233460

Yamano, K., Inoue, M., Masaki, S., Saki, M., Ichimura, M., and Satoh, M. (2005). Human adenosine A3 receptor leads to intracellular Ca^{2+} mobilization but is insufficient to activate the signaling pathway via phosphoinositide 3-kinase gamma in mice. *Biochem. Pharmacol.* 70, 1487–1496. doi: 10.1016/j.bcp.2005.08.003

Yip, K. H., Lau, H. Y., and Wise, H. (2011). Reciprocal modulation of anti-IgE induced histamine release from human mast cells by A1 and A2B adenosine receptors. *Br. J. Pharmacol.* 164, 807–819. doi: 10.1111/j.1476-5381.2011.01446.x

Yoshida, K., Ito, M., and Matsuoka, I. (2015). P2X7 receptor antagonist activity of the anti-allergic agent oxatomide. *Eur. J. Pharmacol.* 767, 41–51. doi: 10.1016/j.ejphar.2015.10.002

Yoshida, K., Ito, M., and Matsuoka, I. (2017). Divergent regulatory roles of extracellular ATP in the degranulation response of mouse bone marrow-derived mast cells. *Int. Immunopharmacol.* 43, 99–107. doi: 10.1016/j.intimp.2016.12.014

Young, H. W., Molina, J. G., Dimina, D., Zhong, H., Jacobson, M., Chan, L. N., et al. (2004). A3 adenosine receptor signaling contributes to airway inflammation and mucus production in adenosine deaminase-deficient mice. *J. Immunol.* 173, 1380–1389. doi: 10.4049/jimmunol.173.2.1380

Young, H. W., Sun, C. X., Evans, C. M., Dickey, B. F., and Blackburn, M. R. (2006). A3 adenosine receptor signaling contributes to airway mucin secretion after allergen challenge. *Am. J. Respir. Cell Mol. Biol.* 35, 549–558. doi: 10.1165/rcmb.2006-0060OC

Zablocki, J., Kalla, R., Perry, T., Palle, V., Varkhedkar, V., Xiao, D., et al. (2005). The discovery of a selective, high affinity A2B adenosine receptor antagonist for the potential treatment of asthma. *Bioorg. Med. Chem.* 15, 609–612. doi: 10.1016/j.ejmech.2017.04.014

Zaynagetdinov, R., Ryzhov, S., Goldstein, A. E., Yin, H., Novitskiy, S. V., Goleniewska, K., et al. (2010). Attenuation of chronic pulmonary inflammation in A2B Adenosine receptor knockout mice. *Am. J. Respir. Cell Mol. Biol.* 42, 564–571. doi: 10.1165/rcmb.2008-0391OC

Zhong, H., Shlykov, S. G., Molina, J. G., Sanborn, B. M., Jacobson, M. A., Tilley, S. L., et al. (2003). Activation of murine lung mast cells by the adenosine A3 receptor. *J. Immunol.* 171, 338–345. doi: 10.4049/jimmunol.171.1.338

Zhou, Q. Y., Li, C., Olah, M. E., Johnson, R. A., Stiles, G. L., and Civelli, O. (1992). Molecular cloning and characterization of an adenosine receptor: the A3 adenosine receptor. *Proc. Natl. Acad. Sci. U.S.A.* 89, 7432–7436. doi: 10.1073/pnas.89.16.7432

Ziment, I. (1987). Theophylline and mucociliary clearance. *Chest* 92(Suppl. 1), 38S–43S. doi: 10.1378/chest.92.1_Supplement.38S

Conflict of Interest Statement: The authors declare that the research was conducted in the absence of any commercial or financial relationships that could be construed as a potential conflict of interest.

frontiers in Pharmacology

ORIGINAL RESEARCH
published: 22 December 2017
doi: 10.3389/fphar.2017.00937

Prostaglandin E_2 Impairs $P2Y_2/P2Y_4$ Receptor Signaling in Cerebellar Astrocytes via EP3 Receptors

*Lucía Paniagua-Herranz, Juan C. Gil-Redondo, Mª José Queipo, Silvia González-Ramos†, Lisardo Boscá†, Raquel Pérez-Sen, Mª Teresa Miras-Portugal and Esmerilda G. Delicado**

Departamento de Bioquímica y Biología Molecular IV, Facultad de Veterinaria, Instituto Universitario de Investigación en Neuroquímica, Instituto de Investigación Sanitaria del Hospital Clínico San Carlos, Universidad Complutense Madrid, Madrid, Spain

Prostaglandin E_2 (PGE_2) is an important bioactive lipid that accumulates after tissue damage or inflammation due to the rapid expression of cyclooxygenase 2. PGE_2 activates specific G-protein coupled EP receptors and it mediates pro- or anti-inflammatory actions depending on the cell-context. Nucleotides can also be released in these situations and they even contribute to PGE_2 production. We previously described the selective impairment of P2Y nucleotide signaling by PGE_2 in macrophages and fibroblasts, an effect independent of prostaglandin receptors but that involved protein kinase C (PKC) and protein kinase D (PKD) activation. Considering that macrophages and fibroblasts influence inflammatory responses and tissue remodeling, a similar mechanism involving P2Y signaling could occur in astrocytes in response to neuroinflammation and brain repair. We analyzed here the modulation of cellular responses involving $P2Y_2/P2Y_4$ receptors by PGE_2 in rat cerebellar astrocytes. We demonstrate that PGE_2 inhibits intracellular calcium responses elicited by UTP in individual cells and that inhibiting this P2Y signaling impairs the astrocyte migration elicited by this nucleotide. Activation of EP3 receptors by PGE_2 not only impairs the calcium responses but also, the extracellular regulated kinases (ERK) and Akt phosphorylation induced by UTP. However, PGE_2 requires epidermal growth factor receptor (EGFR) transactivation in order to dampen P2Y signaling. In addition, these effects of PGE_2 also occur in a pro-inflammatory context, as evident in astrocytes stimulated with bacterial lipopolysaccharide (LPS). While we continue to investigate the intracellular mechanisms responsible for the inhibition of UTP responses, the involvement of novel PKC and PKD in cerebellar astrocytes cannot be excluded, kinases that could promote the internalization of P2Y receptors in fibroblasts.

Keywords: astrocytes, calcium, EP receptors, nucleotide receptor, P2Y receptors, PGE_2

Edited by:
Francisco Ciruela, University of Barcelona, Spain

Reviewed by:
Tycho Hoogland, Erasmus University Rotterdam, Netherlands
Chuang Wang, Ningbo University, China

****Correspondence:***
Esmerilda G. Delicado
esmerild@ucm.es

†Present address:
Silvia González-Ramos, Instituto de Investigaciones Biomédicas Alberto Sols, Centro Mixto del Consejo Superior de Investigaciones Científicas, Universidad Autónoma de Madrid, Madrid, Spain
Lisardo Boscá, Instituto de Investigaciones Biomédicas Alberto Sols, Centro Mixto del Consejo Superior de Investigaciones Científicas, Universidad Autónoma de Madrid, Madrid, Spain; Departamento de Bioquímica y Biología Molecular IV, Facultad de Veterinaria, Universidad Complutense Madrid, Madrid, Spain

Specialty section:
This article was submitted to Experimental Pharmacology and Drug Discovery, a section of the journal Frontiers in Pharmacology

Received: *16 October 2017*
Accepted: *11 December 2017*
Published: *22 December 2017*

Citation:
Paniagua-Herranz L, Gil-Redondo JC, Queipo MJ, González-Ramos S, Boscá L, Pérez-Sen R, Miras-Portugal MT and Delicado EG (2017) Prostaglandin E_2 Impairs $P2Y_2/P2Y_4$ Receptor Signaling in Cerebellar Astrocytes via EP3 Receptors. Front. Pharmacol. 8:937. doi: 10.3389/fphar.2017.00937

Abbreviations: $[Ca^{2+}]_i$, intracellular free calcium concentration; DMEM, Dulbecco's modified Eagle's medium; EGF, epidermal growth factor; EGFR, epidermal growth factor receptor; ERK, extracellular signal regulated kinases; FCS, fetal calf serum; GPCRs, G protein-coupled receptors; GAPDH, glyceraldehyde-3-phosphate dehydrogenase; LPS, lipopolysaccharide; MEK, mitogen extracellular activated kinases; NGF, nerve growth factor; PI-3 kinase, phosphatidylinositol-4,5-bisphosphate 3-kinase; nPKC, novel protein kinase C; PKD, protein kinase D; PPADS, pyridoxal phosphate-6-azophenyl-2′,4′-disulfonic acid; PGs, prostaglandins; PGE_2, prostaglandin E_2.

INTRODUCTION

Prostaglandins are bioactive lipids produced through the metabolism of arachidonic acid by cyclooxygenase and they play important modulatory roles throughout the body (Sugimoto and Narumiya, 2007). Both COX-1 and COX-2 display cyclooxygenase activity, which are constitutive and inducible enzymes, respectively (Smith et al., 2000). These enzymes convert the arachidonic acid released following phospholipase A_2 (PLA_2) activation from membrane lipids into PGH_2, the precursor of both PGs and thromboxanes. One of the principal activators of PLA_2 is intracellular calcium, which brings arachidonic acid production under the control of multiple extracellular signals, including extracellular nucleotides (Zonta et al., 2003). PGE_2 is one of the most studied PGs, and not only is it the most widely found in different animal species (including humans) but it also exhibits the most versatile actions. Through specific membrane receptors, PGE_2 fulfills many physiological functions, such as gastrointestinal mucosa protection or labor, as well as participating in pathological events like inflammation or fever. Indeed, the cyclooxygenase enzymes have been widely explored in anti-inflammatory therapies, although the majority of COX inhibitors display side effects due to COX-1 inhibition, mainly gastrointestinal bleeding and renal toxicity (Dannhardt and Kiefer, 2001; Dwivedi et al., 2015).

Prostaglandin E_2 activates specific GPCRs, named EP receptors. Four different EP receptor subtypes have been identified, EP1–EP4, which differ in the signal transduction pathways they use, their distribution and the regulation of their expression (St-Jacques and Ma, 2016). The EP1 receptor is mainly coupled to Gq proteins and its stimulation induces intracellular calcium responses. By contrast, the EP2 and EP4 receptors are coupled to Gs proteins and they produce an accumulation of cAMP, whereas the EP3 receptor is mainly coupled to Gi proteins and it provokes a decrease in the cAMP produced in response to Gs-protein coupled receptor stimulation. There are three EP3 splice variants (α, β, and γ), each of which contains a distinct C-terminal tail of 30, 26, and 29 amino acids, respectively. These isoforms all have similar ligand binding properties but they activate different signal transduction pathways. Indeed, the EP3 variants not only couple to Gi proteins but also, to Gq proteins, Rho or even adenylate cyclase. In addition, some effects of PGE_2 are exert independently of EP receptors and other intracellular targets have even been proposed (Traves et al., 2013).

Extracellular nucleotides are also important extracellular messengers (Burnstock, 2006; Miras-Portugal et al., 2016). Nucleotides can be released from living cells under basal conditions and their release is enhanced by cell stressors, including mechanical stress, hypoxia, viral infection or pro-apoptotic stimuli. Nucleotides are stored in secretory vesicles along with biogenic amines and other neurotransmitters, and they are released by exocytosis (Lazarowski et al., 2011). Once in the extracellular space, nucleotides interact with specific membrane nucleotide receptors, which are classified in two main types: the ionotropic P2X receptors and the metabotropic P2Y receptors. Seven P2X nucleotide receptors have been identified and they are trimeric ATP-activated ion channels that are permeable to Na^+, K^+, and Ca^{2+} (North, 2016). Metabotropic P2Y receptors belong to the superfamily of GPCRs and unlike P2X receptors, they can be activated by adenine and/or uridine nucleotides (ATP, ADP, UTP, and UDP) and nucleotide sugars (UDP-glucose). Eight subtypes of P2Y receptors have been identified that have been classified in two main subfamilies according to their pharmacology, signal transduction and structure (Costanzi et al., 2004; von Kugelgen and Hoffmann, 2016). The first of these is coupled to Gq proteins and phospholipase C (PLC), and it includes the $P2Y_1$, $P2Y_2$, $P2Y_4$, $P2Y_6$, and $P2Y_{11}$ receptors. By contrast, the second one is linked to Gi/Go proteins and it includes the $P2Y_{12}$, $P2Y_{13}$, and $P2Y_{14}$ receptors. However, like other GPCRs, P2Y receptors are promiscuous and additional G protein linkages have been described (Erb and Weisman, 2012). P2X and P2Y receptors are co-expressed throughout the body, and they play important roles in the vascular system, in immune defense and in the nervous system. The extracellular concentration of nucleotides is controlled by a family of ectoenzymes that catalyze the hydrolysis of nucleotides, generating their corresponding diphosphate nucleotides and ultimately, nucleosides. These nucleosides are then taken back up by the cells via nucleoside transporters.

Both, PGE_2 and nucleotides have beneficial or detrimental effects depending on the cell context, and the duration of PGE_2 production or nucleotide release. Furthermore, they can co-exist in the extracellular milieu under physiological and pathological conditions. As mentioned previously, nucleotides can influence PGE_2 production and *vice versa*, PGE_2 may regulate nucleotide activity (Chen and Lin, 2000; Zonta et al., 2003; Ito and Matsuoka, 2008, 2015). In this regard, we previously showed that PGE_2 inhibited P2Y responses in macrophages, particularly those mediated by P2Y receptors sensitive to purine and pyrimidine nucleotides, the metabotropic $P2Y_2$, $P2Y_4$, and $P2Y_6$ receptors. The selective impairment of P2Y signaling by PGE_2 appears to be independent of EP receptors, involving the activation of nPKC and PKD, and with functional implications for the biological responses of macrophages due to the influence on their metabolism and migration. Such interactions take place in thioglycollate-elicited and alternative macrophages, which could contribute to the resolution phase of inflammation (Traves et al., 2013). The same cross-talk between PGE_2 and P2Y signaling has been described in murine fibroblasts, suggesting that macrophages and fibroblasts contribute to the regulation of inflammatory responses and tissue damage repair through aligned mechanisms associated with P2Y signaling. Such cross-talk may open new avenues to develop future anti-inflammatory therapies (Pimentel-Santillana et al., 2014).

In an attempt to investigate whether PGE_2 would modulate nucleotide P2Y responses in the nervous system we decided to analyze this interaction in astrocytes. Thanks to their strategic location in close proximity with neurons and endothelial cells, astrocytes regulate cerebral blood flow to metabolic demands, PGE_2 being one of the first described mediators of cerebral vasodilation (Ellis et al., 1979; Takano et al., 2006). Astrocytes are also able to detect danger signals, secrete cytokines, and activate adaptive defense [see excellent reviews (Sofroniew, 2015; Colombo and Farina, 2016)]. Moreover, the typical hallmark

of brain injury is the upregulation of the astrocyte marker, the glial fibrillary acidic protein (GFAP), as consequence of astrocyte proliferation and the glial scar formation. The impact of astrocytes activity on tissue homeostasis is ambivalent, it may exacerbate inflammatory responses and tissue damage, or promote immunosuppression and tissue repair, depending on timing and context. *In vivo* studies performed in disease models of brain or spinal cord injury and experimental autoimmune encephalomyelitis (EAE) have revealed that the loss of reactive astrocytes during the early phases of injury results in exacerbation of clinical signs, motor deficits, scar disorganization, demyelination and neuronal death. By contrast, astrocyte depletion during chronic phase of EAE ameliorates disease and reduces leukocyte infiltration into nervous system. Recently, it has been described that astrocytes also respond to proinflammatory stimuli with the intense production of PGE_2, adapting cerebral blood flow to neuro-inflammatory demands (Font-Nieves et al., 2012; Howarth et al., 2017).

Astrocytes represent a heterogeneous cell population in terms of their ability to respond to neuroligands linked to calcium mobilization and they are also able to selectively discriminate between the activities of different pathways that use the same neurotransmitter. However, native and cultured astrocytes from different brain areas, cortical, hippocampal and cerebellar astrocytes are sensitive to nucleotides given that they co-express P2Y and P2X nucleotide receptors (Neary et al., 2004; Domercq et al., 2006; Fujita et al., 2009; Peterson et al., 2010; Oliveira et al., 2011). The present study was performed on cultured cerebellar astrocytes, because they constitute a homogeneous cell population that exhibited functional P2Y nucleotide receptors, especially those we are interested, the $P2Y_2$ and $P2Y_4$ receptors sensitive to adenine and pyrimidine nucleotide (ATP/UTP). In previous studies we demonstrated that metabotropic ATP calcium responses were submitted to a fine regulation by growth factors (EGF/NGF) and signals coupled to Gs stimulation, such as noradrenaline and adenosine, which would suggest the importance to maintain purinergic tone. Using different approaches we found that PGE_2 inhibits $P2Y_2/P2Y_4$ signaling in rat cerebellar astrocytes. Indeed, PGE_2 reduced UTP calcium responses and intracellular signaling cascades activated by this nucleotide, as well as preventing UTP-induced cell migration. In astrocytes, the PGE_2 effect appeared to be mediated by EP3 receptors and was also observed in LPS-treated cells.

MATERIALS AND METHODS

Chemicals, Materials, and Antibodies

Papain was purchased from Worthington (Lake Wood, NJ, United States), FCS from Invitrogen and Fura-2 from Molecular Probes (Life Technologies, Barcelona, Spain). Culture flasks, Plastic Petri dishes and transwell chambers with 8 μm pore transparent PET membrane inserts were supplied by Falcon Becton Dickinson Labware (Franklin Lakes, NJ, United States). Antibiotics, DMEM, UTP, and AG1478 were purchased from Sigma Aldrich (St. Louis, MO, United States). PGE_2, and the EP agonists and antagonists, were from Cayman Chemical (Ann Arbor, MI, United States), while LY294002 was from Calbiochem Co. (San Diego, CA, United States). Specific antibodies against phosphor-ERK1/2 (Tyr^{204}), ERK2, phosphor-Akt (Thr^{308}) and Akt were purchased from Santa Cruz Biotechnology (Santa Cruz, CA, United States), and anti-COX-2 was from Abcam (Cambridge, United Kingdom). Antibodies against P2Y receptors, $P2Y_2$ and $P2Y_4$ receptors, and those against the EP3 receptor were from Alomone Labs (Jerusalem BioPark, Israel), while antibodies against GAPDH were purchased from Cell Signaling Technology (Beverly, MA, United States). Secondary horseradish peroxidase-conjugated anti-mouse and anti-rabbit antibodies (Dako, Denmark) were used here. All other reagents not specified were routinely supplied by Sigma, Merck (Darmstadt, Germany) or Roche Diagnostics SL (Barcelona, Spain).

Experimental Animals

All the experiments were carried out at the Complutense University of Madrid (Madrid, Spain) following the International Council for Laboratory Animal Science guidelines (ICLAS). All the procedures were approved by both the Animal Ethics Committee of the Complutense University and the Regional Authorities in Madrid (Area of Animal Protection), according to the Spanish Royal Decree RD53/2013 and the European Directive 2010/63/UE on the protection of animals used for scientific purposes. The assays were designed to minimize the number of animals used while maintaining statistical validity.

Astrocyte Cultures

Primary cultures of astrocytes were prepared as described previously with some modifications (Jimenez et al., 1999). Briefly, the cerebellum from Wistar rat pups (P7) was removed aseptically, digested with papain and cerebellar cells were resuspended in DMEM containing 10% FCS (v/v), 25 mM glucose, 2 mM glutamine, 100 U/ml penicillin, 100 μg/ml streptomycin, and 2.5 μg/ml amphotericin. The cells were plated in culture flasks at density of 70,000 cells/cm^2 and they were maintained in culture until reaching confluence (approximately 10–12 days), replacing the medium every 3–4 days. Cultures were depleted of microglial cells by orbital shaking and finally, the astrocytes were detached from the culture flasks by trypsin treatment and seeded onto culture plates. For microfluorometry experiments, astrocytes were plated onto glass coverslips in 35 mm Petri dishes at 50,000 cells/cm^2 and for Western blotting, cells were plated onto Petri dishes at a density of 35,000 cells/cm^2. Astrocytes were routinely used 48 h after plating.

Fura-2 Microfluorimetry and Calcium Imaging

Calcium imaging experiments were carried out essentially as described previously (Carrasquero et al., 2005). Astrocytes attached to coverslips were incubated in Locke's solution (composition in mM: 140 NaCl, 4.5 KCl, 2.5 $CaCl_2$, 1.2 KH_2PO_4, 1.2 $MgSO_4$, 5.5 glucose, 10 HEPES pH 7.4) supplemented with 1 mg/mL bovine serum albumin (BSA) and loaded with 5–7 μM fura-2/AM for 45 min at 37°C. Once washed in fresh

Locke's solution, a coverslip was placed in a small superfusion chamber and the cells were imaged on a NIKON TE-200 microscope equipped with a Plan Fluor 20X/0.5 objective. Cells were continuously superfused with Locke's medium at a rate of 1.5 mL/min, and agonists were usually applied for 20 s by switching the superfusion solution with the aid of WC-8 valve controller (Warner Instruments). Cells were illuminated at 340 and 380 nm, and the emitted light was isolated with a dichroic mirror (430 nm) and a 510 nm band-pass filter (Omega Optical). Images were obtained with an ORCA-ER C 47 42-80 camera (Hamamatsu City, Japan) controlled by MetaFluor 6.2r and PC software (Universal Imaging, Corp., Cambridge, United Kingdom). The exposure time was 100 ms and the wavelength of incoming light was changed from 340 to 380 nm in less than 5 ms. Fluorescence images were acquired at a sampling frequency of 2 Hz and processed by averaging signals from small elliptical regions within individual cells. Background signals were subtracted from each wavelength and the F_{340}/F_{380} fluorescence ratio was calculated. Fluorescence ratio increases represent $[Ca^{2+}]_i$ changes. The quantification of the responses was made by measuring the magnitude of the initial transients. Data are represented as the percentage of the control responses elicited by an UTP challenge in the same experimental conditions (each individual cell).

Migration Assays

Astrocytes were detached from the culture flasks and they were suspended in DMEM supplemented with 1% FCS. The lower chambers of Transwell 6-well culture plates were filled with 3 mL DMEM containing UTP (as indicated), and with an 8 μm membrane insert placed into the wells, a 1 mL cell suspension containing 300,000 cells was added to the upper chamber. After 18 h at 37°C in a 5% CO_2 incubator, the cells in the upper chambers were removed by scraping the membranes with a cotton swab, while the cells attached to the bottom of the membranes were fixed with 4% paraformaldehyde for 15 min, washed with PBS and stained with the nuclear marker, DAPI. The cells were visualized under a microscope and counted in five random fields. They cells attached to the bottom of the membrane represented those that had migrated from the upper to lower chamber in response to nucleotide stimulation.

In Vitro Wound Healing

Astrocytes detached from culture flasks were seeded onto Petri dishes in complete culture medium and they were maintained in the incubator to form a confluent monolayer (48 h after plating). A wound was made by scraping a conventional yellow pipette tip across the monolayer and the cells were then washed with culture medium, replacing the medium with fresh DMEM plus 1% FCS and with the addition of the nucleotide or another effector to induce migration. After 24 h at 37°C in a 5% CO_2 incubator, the cells were fixed with paraformaldehyde as described above and their nucleus was stained with DAPI.

Cell Treatments and Lysate Preparations

Cells were stimulated in Locke's solution and where indicated, the astrocytes were preincubated in the presence or absence of effectors, antagonists or inhibitors prior to stimulation with the nucleotide UTP. Controls were systematically used with the corresponding vehicle alone (DMSO always at a concentration <2%), in which cell viability was not significantly affected. Incubations were stopped by removing the incubation medium and lysing the cells in cold lysis buffer (20 mM MOPS pH 7.2, 50 mM NaF, 40 mM β-glycerophosphate, 1 mM sodium orthovanadate, 5 mM EDTA, 2 mM EGTA, 0.5% Triton X-100, 1 mM PMSF, and a protease inhibitor cocktail).

Western Blotting

Total cellular lysates (15–30 μg protein) were resolved in SDS–PAGE gels and transferred to PVDF membranes. The membranes were probed overnight at 4°C with primary antibodies in either TBS 0.1% with Tween-20 containing low-fat milk powder (5%, w/v), and then for 1 h at room temperature with the secondary antibodies. Antibodies were used at following dilutions: anti-phosphor-ERK1/2, anti-ERK2 (1:1000), anti-phosphor Akt and Akt (1:1000), anti-COX-2 (1:500), anti-$P2Y_2$ and anti-$P2Y_4$ (1:200), anti-EP3 receptors (1:200), and anti-mouse and anti-rabbit horseradish peroxidase-conjugated secondary antibodies (1:2000 and 1:1000, respectively). Specific protein bands were visualized by ECL (Western Lighting ECL PRO kit, Perkin Elmer, Madrid, Spain), and chemiluminescence images were taken with the ImageQuant LAS 500® image system and quantified by densitometry using ImageQuantTL software.

Statistical Analysis

The results are expressed as the means ± SEM calculated from at least three experiments performed on cells from different cultures. When multiple comparisons were made, one-way analysis of variance was used and Dunnett's post-test analysis was applied only when a significant ($p < 0.05$) effect was indicated by the one-way analysis of variance (GraphPad Prism 5; GraphPad Software, Inc., San Diego, CA, United States).

RESULTS

PGE_2 Modulates Metabotropic ATP Calcium Responses in Individual Cerebellar Astrocytes

Cerebellar astrocytes co-express several subtypes of P2Y metabotropic nucleotide receptors (Jimenez et al., 2000), and metabotropic calcium responses to ATP mediated by $P2Y_2/P2Y_4$ nucleotide receptors were evident in the entire astrocyte population, in which ATP and UTP were equipotent. To examine the modulatory role of PGE_2 on P2Y signaling in cerebellar astrocytes, we investigated the effect of this prostaglandin on UTP induced calcium responses. We did not use ATP, because cerebellar astrocytes also express ATP sensitive P2X7 receptors (Carrasquero et al., 2009). As expected all the cells tested responded to the UTP challenge (100 μM) by increasing their intracellular calcium $[Ca^{2+}]_i$, which peaked ($\Delta F_{340}/F_{380}$ of 0.73 ± 0.02 relative to the basal levels between

0.3 and 0.5; n = 327 cells) and then returned to the basal level within the first 20 s of stimulation (**Figure 1A**). These cells also responded to a second UTP challenge with similar calcium transients, the magnitude of which was reduced by 10%. It is known that EP1 receptors couple to Gq proteins and EP2 receptor stimulation promotes calcium responses in rat cortical astrocytes (Di Cesare et al., 2006). Thus, before analyzing the modulatory role of PGE_2 on UTP calcium responses, cells were challenged with PGE_2 (1 μM) alone, which did not evoke any increase in $[Ca^{2+}]_i$. Cells were also insensitive to stimulation with 6,16-Dimethylprostaglandin E_2, a synthetic analog that resists metabolism and that has a prolonged half-life *in vivo* (results not shown). These results indicated that cerebellar astrocytes did not express functional EP1 receptors, although they did not rule out the presence of functional EP2/EP4 receptors coupled to adenylate cyclase activation. PGE_2 inhibited UTP calcium responses (**Figure 1B**) and preincubation with PGE_2 (1 μM, 5 min) dampened the calcium responses elicited by 100 μM UTP, the maximal effective concentration. This inhibition was observed in all the cells tested and the magnitude of the initial Ca^{2+} transient was reduced by a 40%. Nevertheless, the effect of preincubation with PGE_2 was not necessary due to the simultaneous co-stimulation of astrocytes with PGE_2 and UTP reduced the calcium responses triggered by the nucleotide alone by 35%. These results were consistent with the regulatory influence of PGE_2 on P2Y signaling evident in macrophages and fibroblasts (Ito and Matsuoka, 2008; Traves et al., 2013; Pimentel-Santillana et al., 2014).

The presence of EP2/EP4 receptors coupled to Gs proteins in cerebellar astrocytes was analyzed indirectly, assessing whether UTP-mediated responses could be enhanced by PGE_2 (**Figure 2**). We previously reported an important cross-talk between Gs-coupled receptors and P2Y nucleotide receptors in these glial cells (Jimenez et al., 1999). Indeed, the activation of A_{2B} adenosine receptors, or other signals coupled to adenylate cyclase stimulation, strongly potentiated the metabotropic calcium responses to nucleotides. Co-stimulation of astrocytes with adenosine (10 μM) and ATP (1 μM, ineffective when administered alone) elicited $[Ca^{2+}]_i$ transients that represented 60% of the maximal calcium response elicited by ATP/UTP (100 μM). This potentiation was parallel to but independent of cAMP accumulation, suggesting the involvement of βγ subunits released upon Gs stimulation. Co-stimulation of astrocytes with PGE_2 and ineffective concentrations of UTP (1 μM) did not evoke any signals (**Figure 2**), and no signal was observed after preincubation with PGE_2 and simultaneous co-stimulation with UTP (1 μM). Hence, cerebellar astrocytes do not appear to express functional EP2/EP4 receptors and if they are present, they were unable to modulate UTP calcium responses in the same way as other signals coupled to adenylate cyclase activation.

Having excluded the participation of EP1 and EP2/EP4 receptors in the inhibitory effect of PGE_2 on the calcium responses to UTP, we assessed the involvement of EP3 receptors in this effect (**Figure 3**). The EP3 agonist sulprostone is a synthetic analog of PGE_2 that is resistant to metabolism and it reproduced the effect of PGE_2 (**Figure 4A**). Stimulation with UTP (100 μM) after preincubation with sulprostone (30 nM, 5 min) dampened the calcium responses, which reached 57.44% of the control responses. Likewise, co-stimulation with sulprostone and UTP resulted in calcium responses that reached 61.71% of the control UTP responses. These findings supported the involvement of EP3 receptors in this phenomenon. In fact, EP3 receptors were detected in Western blots, although assays carried out with an EP3 receptor antagonist, L798106 ((2E)-*N*-[(5-bromo-2-methoxyphenyl) sulfonyl]-3-[2-(2-naphthalenylmethyl) phenyl]-2-propenamide), proved inconclusive. This antagonist did not modify the basal calcium levels but it did depress the calcium responses to UTP by 40% (**Figure 4B**). Moreover, pretreatment of astrocytes with L798106 prior to their stimulation with PGE_2 or sulprostone did not prevent their inhibitory effects. Thus, despite the detection of EP3 receptors in Western blots (**Figure 8**), their involvement in the regulatory effect of PGE_2 remained unclear. Indeed, we suggest that L798106 might be interacting with P2Y receptors given its similar structure to non-selective antagonists of nucleotide receptors, such as PPADS or suramin (Ho et al., 1995; Communi et al., 1996; Jimenez et al., 2000).

PGE_2 Impairs the Cell Migration Induced by UTP in Cerebellar Astrocytes

We next examined whether PGE_2 modulated the migration of cerebellar astrocytes induced by UTP, as reported in macrophages and fibroblasts (Pimentel-Santillana et al., 2014). In both assays used, transwell migration and wound-healing, PGE_2 attenuated the migration of astrocytes induced by UTP (**Figure 5**). When UTP (100 μM) was added to the lower transwell chamber of cell culture dishes containing membrane inserts, transmembrane chemotactic migration of astrocytes was enhanced (**Figure 5A**). However, preincubation of cells with PGE_2 (1 μM, 5 min) prior to their introduction into the upper chamber diminished their migration under control conditions and that induced by the nucleotide by 45%. UTP-induced chemotaxis was also prevented by U0126 (**Figure 5A**), an inhibitor of MEK, which indicated that ERK activation was required for cell migration. In wound-healing migration assays, PGE_2 completely prevented cell migration in control conditions (without additional exogenous nucleotide), as well as that induced by the nucleotide (**Figure 5B**). In this case, prostaglandin was included in the fresh medium added after the cells were washed to remove cell debris.

Characterization of the Intracellular Mechanism Used by PGE_2 to Modulate the Responses to UTP

The impact of PGE_2 on the intracellular signaling cascades triggered by UTP was analyzed to further study the mechanism through which PGE_2 modulates UTP responses. The ERK1/2 and PI3-kinase/Akt proteins are known to play relevant roles in nucleotide signaling and cell migration (Brambilla et al., 2002; Jimenez et al., 2002; Neary et al., 2004). Indeed, stimulation

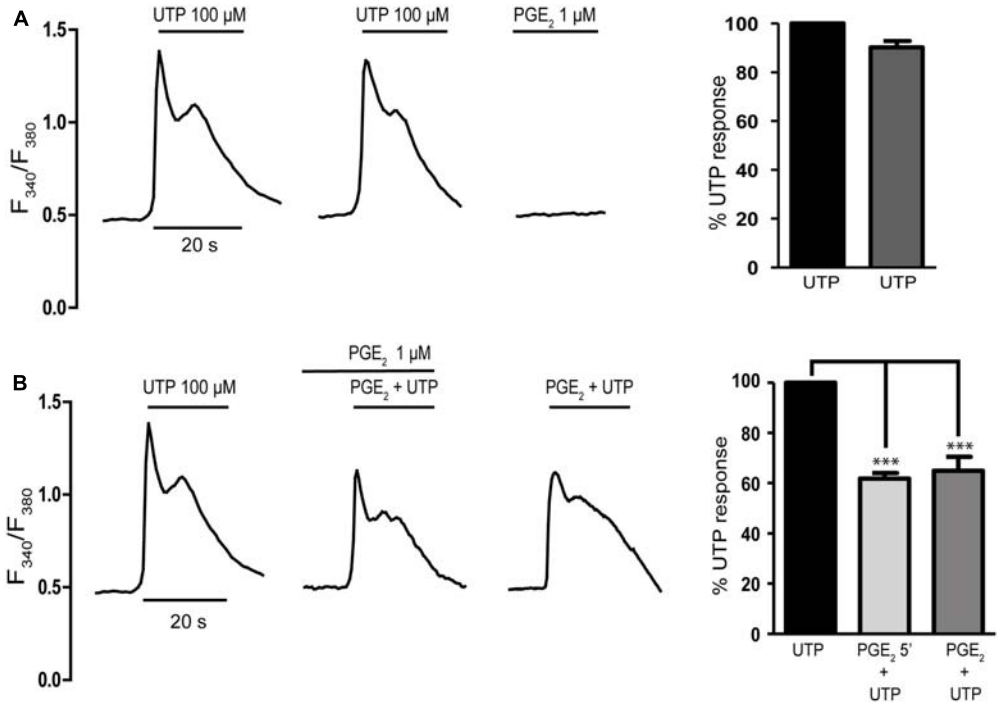

FIGURE 1 | Prostaglandin E_2 (PGE2) inhibits UTP calcium responses in rat cerebellar astrocytes. **(A)** Typical traces of calcium responses induced by 100 μM UTP in individual astrocytes. Cells loaded with fura-2 were challenged with the nucleotide or PGE_2 (1 μM) and calcium responses were recorded as described in the Section "Materials and Methods." **(B)** Effect of PGE_2 on UTP calcium responses. Astrocytes were incubated in the presence or absence of PGE_2 (1 μM) and subsequently stimulated with UTP (100 μM), again in the presence or absence of PGE_2. Typical recordings are shown and the graphs show the quantification of the responses, obtained by measuring the magnitude of the initial transients. The data are presented as the percentage of the control responses elicited by UTP and the values are the means ± SEM (n = 327 cells from four different cultures). ***$p < 0.0001$ according to one way analysis of variance and Dunnett's post-test.

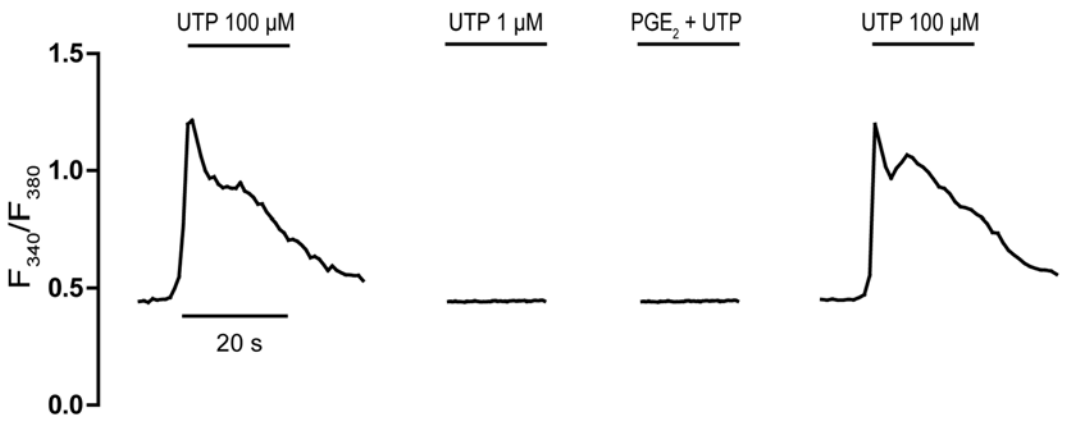

FIGURE 2 | Effect of PGE_2 on an ineffective UTP challenge. Astrocytes were stimulated with UTP (100 μM) or an ineffective concentration of UTP (1 μM), alone or in conjunction with PGE_2 (1 μM), and the calcium responses were recorded as described in Section "Materials and Methods."

of astrocytes with UTP (100 μM) induced a remarkable increase in the phosphorylation of ERK1/2 (a fourfold to eightfold increase over basal levels) and of the Akt protein (a twofold increase over basal levels: **Figure 6**). Pretreatment of astrocytes with PGE_2 (1 μM) reduced the ERK and Akt phosphorylation induced by UTP 35 and 40%, respectively. Stimulating astrocytes with PGE_2 alone had no significant effect on ERK phosphorylation but it did dampen the phosphorylation of Akt. The inhibitory effects of PGE_2 were also reproduced by sulprostone. Preincubation with the prostanoids was not necessary, and similar effects were observed after co-stimulation with PGE_2/sulprostone and the nucleotide (results not shown). The extent of inhibition is consistent with the changes in the calcium responses observed.

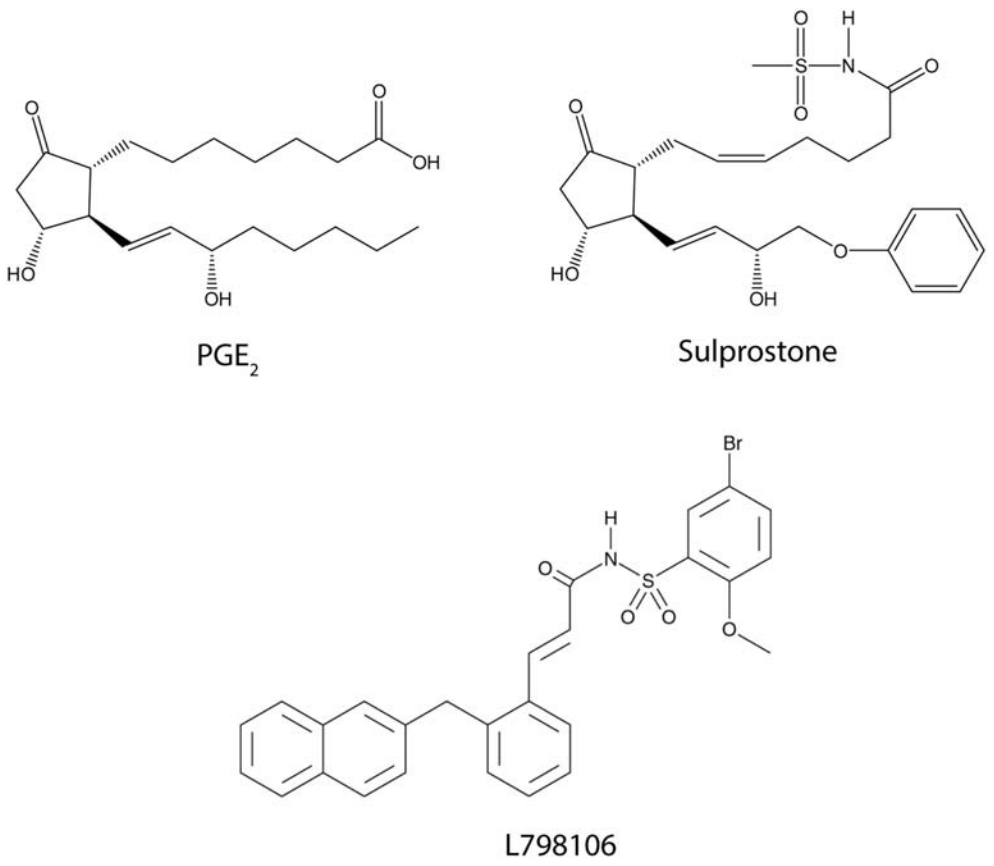

FIGURE 3 | The structure of agonists and antagonists of EP3 receptors.

EGFR Is Required for PGE_2 to Modulate UTP-Induced ERK1/2 and PI3-K/Akt Activation

The EGF receptor plays a key role in the intracellular signaling cascades triggered by GPCRs, including $P2Y_2$ receptors (Liu et al., 2004). To determine whether EGFR activation was required for the activation of ERK and/or Akt by the nucleotide, or for the modulatory effect of PGE_2, the influence of an EGFR tyrosine kinase inhibitor was tested, AG1478. Interestingly, pretreatment of cells with AG1478 (1 μM) for 20 min reduced the basal phosphorylation of the two kinases, although it did not affect the UTP-induced ERK and Akt phosphorylation (**Figure 7**). Nevertheless, the EGFR inhibitor impaired the regulatory effect of PGE_2, indicating that EGFR transactivation was required for the effect of the prostaglandin. Moreover, inhibition of PI3K with LY294002 (50 μM, 20 min) not only reduced the basal phosphorylation of ERK but it also prevented the regulatory effect of PGE_2, although like the EGFR inhibitor it did not affect UTP-induced ERK phosphorylation. Thus, PGE_2 could regulate ERK and Akt activation by a mechanism dependent on the transactivation of the EGFR and PI3K kinase, which would also support the involvement of EP3 receptors. To clearly demonstrate the possible implication of these receptors, more comprehensive studies will be necessary that take into account the different splice variants of these receptors described.

Modulation of UTP-Induced ERK1/2 and PI3-K/Akt Activation by PGE_2 in Astrocytes Activated with LPS

To determine whether the modulation of PGE_2 might be relevant to neuroinflammation and pathological conditions, we investigated the cross-talk between PGE_2 and nucleotides in astrocytes treated with LPS, a toll-like receptor (TLR) ligand. Pretreatment with LPS (10 ng/mL, 24 h) did not affect either UTP-induced ERK phosphorylation or the modulatory effect of PGE_2 (**Figure 8A**). UTP-induced ERK activation was higher (a 7.98-fold increase over unstimulated cells) than that observed in untreated cells (4.5-fold increase over basal levels) in the same experimental conditions, while PGE_2 decreased UTP-induced ERK activation by 55%. Pretreatment of astrocytes with LPS notably increased the basal levels of the Akt phosphorylation and it diminished UTP-induced Akt phosphorylation by 55% (**Figure 8B**). In addition, PGE_2 prevented Akt activation induced by the nucleotide. LPS induced strong expression of COX-2 (twofold over basal) but it did not significantly modify the levels of $P2Y_2$/$P2Y_4$ receptors in cerebellar astrocytes. Note that as reported previously, the $P2Y_2$ receptor is more abundant in these

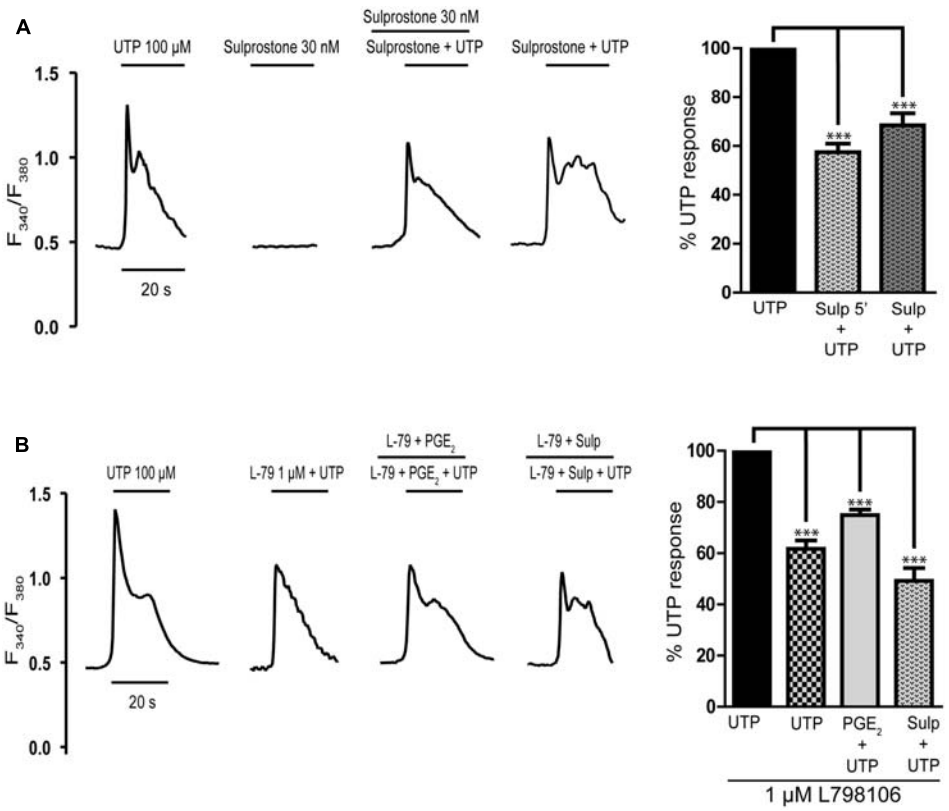

FIGURE 4 | Effects of EP3 receptor ligands on UTP calcium responses in rat cerebellar astrocytes. **(A)** Sulprostone dampened the UTP calcium responses. Astrocytes were stimulated with UTP (100 μM), 30 nM Sulprostone or both these agonists, and the calcium responses were recorded. Where indicated, the cells were pre-incubated with sulprostone for 5 min before UTP stimulation. **(B)** Effect of L798106, an antagonist of EP3 receptors, on the calcium responses elicited by UTP and on PGE_2 modulation. Where indicated, cells were pre-incubated with L798106 (1 μM) or with L798106 and PGE_2/sulprostone, prior to stimulation with the nucleotide. Typical calcium traces are shown, and the graphs represent the quantification of the responses obtained as described in **Figure 1** and presented as the means ± SEM (n = 227 cells from three different cultures). ***$p < 0.0001$ according to one way analysis of variance and Dunnett's post-test.

cells than the $P2Y_4$ receptor. Nevertheless, LPS also increased the levels of EP3 receptors (twofold to threefold increase over basal levels) (**Figure 8C**).

DISCUSSION

The current study was carried out on cultured rat cerebellar astrocytes, a good model to address the regulation of nucleotide P2Y receptors. We previously characterized the function of the different P2Y receptors present in individual astrocytes by microfluorimetry using fura-2 (Jimenez et al., 2000). We found that all astrocytes in our cultures were sensitive to ATP/UTP stimulation, which provoked a metabotropic calcium response. Furthermore, the metabotropic ATP calcium responses mediated by $P2Y_2$/$P2Y_4$ receptors were modulated by other agonists of the purinergic system, such as adenosine, the final product of extracellular nucleotide degradation, and the dinucleotide Ap_5A, which is also stored in secretory vesicles and that has potentiating activity (Jimenez et al., 1999, 2002; Delicado et al., 2005). Similar effects were observed with signals that activated Gs-coupled receptors and with EGF. Here we identified another mechanism that regulates the metabotropic calcium responses to ATP and we demonstrate that PGE_2 inhibits UTP signaling in cerebellar astrocytes, not only impairing intracellular calcium mobilization but also dampening ERK activation, activation of the PI3K/Akt axis, and impairing cell migration (**Figure 9**).

The effect of PGE_2 on UTP driven calcium responses was also evaluated at the single cell level. The fact that PGE_2 modulation was observed in all the cells tested suggests universal and homogenous expression of the $P2Y_2$/$P2Y_4$ receptors of UTP in these glial cells, although it also indicated that a specific target for PGE_2 might be present in these cells. In fact, although, most of the studies were performed on cell populations, the 40% inhibition displayed by PGE_2 was similar to that obtained in individual cells. Although glial cells had more $P2Y_2$ and $P2Y_4$ receptors than murine macrophages, the inhibitory effect of PGE_2 on UTP calcium responses in astrocytes was weaker than that found in macrophages and fibroblasts, in which it accounted for 60–70% inhibition (Traves et al., 2013). Nevertheless, the data gathered here indicate astrocytes are another cell type involved in tissue remodeling, in which PGE_2 negatively modulates UTP and/or ATP responses, in addition to macrophages and fibroblasts.

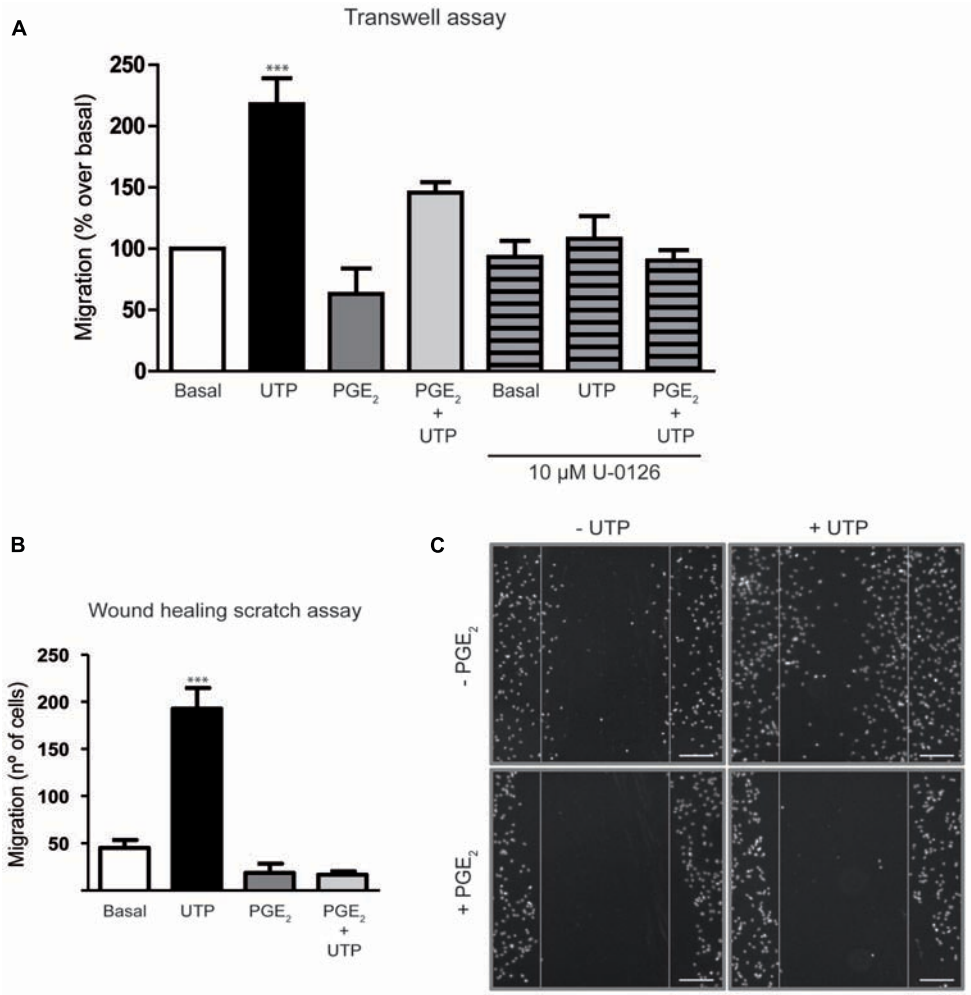

FIGURE 5 | Prostaglandin E_2 impairs rat cerebellar astrocyte migration. **(A)** The capacity of astrocytes to migrate in the Transwell assay. Cells were added to the upper chamber of transwell plates with inserts (8 μm porous), with UTP (100 μM) in the lower chamber as a chemoattractant. The cells were preincubated in the presence or absence of PGE_2 (1 μM) for 5 min prior to being placed on the insert. After 18 h, cell migration was determined as described in Section "Materials and Methods." Similar experiments were carried out with cells pretreated for 20 min with U0126 (10 μM). **(B)** *In vitro* wound-healing assay. Wound-healing experiments were carried out after inducing a standard wound in an astrocyte monolayer, washing with PBS and analyzing cell replenishment after 24 h. Where indicated the cells were preincubated with PGE_2 (1 μM) for 5 min prior to UTP (100 μM) stimulation. **(C)** Representative images of cell nuclei revealed with DAPI staining in a wound-healing experiment (Magnification 10X). Scale bar = 200 μm. The results are expressed as the means ± SEM of migrating (%) or invading cells (number of cells) with respect to that obtained in control conditions, in the absence of any effectors. ***$p < 0.0001$ according to one way analysis of variance and Dunnett's post-test.

Considering that co-stimulation of astrocytes with PGE_2 and UTP reproduced the inhibitory effect observed in cells previously exposed to PGE_2, and intracellular calcium mobilization is one of the first steps of the intracellular cascades triggered by GPCRs, the target/s of PGE_2 might be located at the plasma membrane. This raises the question as to whether the activity of PGE_2 is mediated by EP receptors, and what might be the intracellular mechanism and the final target of PGE_2 used to impair the responses to UTP. Moreover, it raises interest in the physiological implications of the cross-talk between PGE_2 and P2Y nucleotide receptors in these glial cells. Focusing on the possible interaction of PGE_2 with EP receptors, all four subtypes of EP receptors (EP1–EP4) have been described in the brain, and they are present in neurons and glial cells (Sang et al., 2005; Di Cesare et al., 2006; Kunori et al., 2011). The presence of functional EP1 receptors in cerebellar astrocytes was ruled out as PGE_2 and its analogs did not induce calcium responses. These findings contrast to those of astrocytes isolated from other brain sites, such as the hippocampus and cortex (Bezzi et al., 1998; Di Cesare et al., 2006). Rat cortical astrocytes were sensitive to PGE_2 (1 μM) challenges, EP1, EP2/EP4, and EP3 receptors evoking calcium responses heterogeneously in the astrocyte population. Moreover, in cortical astrocytes, calcium responses mediated by EP2/EP4 receptors were reproduced by isoproterenol, a β-agonist, and forskolin, a direct adenylate cyclase activator (Di Cesare et al., 2006). In cerebellar astrocytes neither isoproterenol nor forskolin triggered calcium responses

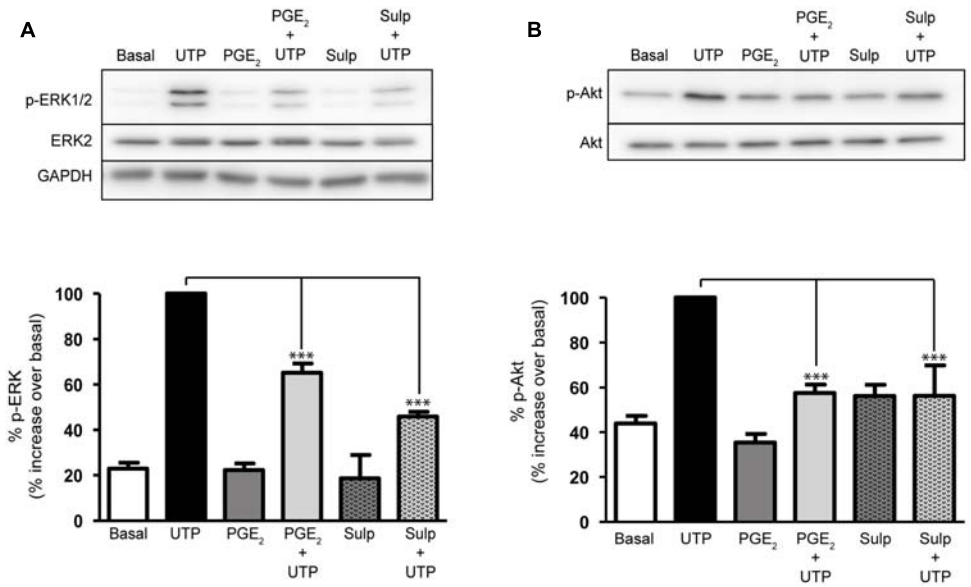

FIGURE 6 | Prostaglandin E_2 modulation on ERK and Akt activation elicited by UTP. Astrocytes were stimulated for 5 min with UTP (100 μM), PGE_2 (1 μM) or Sulprostone (30 nM), and the phosphorylated and non-phosphorylated forms of ERK1/2 **(A)** and **(B)** Akt proteins present in total lysates were assessed in Western blots. Where indicated the cells were preincubated with PGE_2 or sulprostone for 5 min prior to stimulation with the nucleotide. The blots shown are representative of independent experiments and GAPDH was used as an internal loading control. The values are the means ± SEM from 24 independent experiments performed on different cultures and the data is presented relative to the phosphorylation elicited by UTP (100 μM) in each individual experiment. ***$p < 0.0001$.

(Jimenez et al., 1999), whereas extracellular signals coupled to adenylate cyclase stimulation strongly potentiated metabotropic ATP calcium responses. This potentiation was parallel to but independent of cAMP accumulation, suggesting the involvement of βγ subunits released after Gs stimulation. The data reported here indicated that PGE_2 was unable to potentiate UTP calcium responses, suggesting that EP2/EP4 receptors were neither present nor involved in the inhibitory effect of PGE_2, although their presence cannot been ruled out. PGE2 has been shown to evoke calcium responses and potentiated glutamate-induced calcium signaling in astrocytes from the OVLT (organum vasculosum laminae terminals) and MnPO (median preoptic nucleus), contributing to the manifestation of fever (Simm et al., 2016).

The effects of PGE_2 in cerebellar astrocytes could be mediated by EP3 receptors, as they were detected by immunobloting and sulprostone reproduced all the modulatory roles of the prostaglandin (**Figure 9**). Sulprostone was even more potent than PGE_2 in reducing UTP-induced ERK activation, and this EP3 agonist slightly increased ERK phosphorylation in unstimulated cells and prevented UTP-induced Akt phosphorylation. The expression of EP3 receptors increased following exposure to LPS, consistent with the increase in these receptors in astrocytes and microglia after ischemic stroke (Han et al., 2016). Nevertheless, the actions of the two agonists assayed, the physiological and the synthetic PGE_2 analog, were not reversed by the EP3 receptor antagonist, L798106, which depressed UTP calcium responses. However, L79829 might also interact with P2 nucleotide receptors, acting as a non-competitive antagonist. The interaction of PGE_2 with EP3 receptors could induce Gi/o protein recruitment, a mechanism possibly responsible for the inhibition of UTP calcium responses. In cerebellar astrocytes, metabotropic calcium responses and ERK activation induced by the nucleotide were sensitive to PTX (Carrasquero, 2008), and PGE_2 abolished the PTX-sensitive component of UTP calcium responses. Thus, an effect on G protein recruitment could also account for the reduction of ERK activation by PGE_2 and sulprostone described previously. To identify the target and the pathway involved in the modulation of UTP responses by PGE_2, we extended the signaling studies to the PI3K/Akt axis that plays a key role in the nervous system, in development, neuroprotection, proliferation and cancer (Ortega et al., 2008, 2009; Fransson et al., 2013). As expected, UTP induced Akt phosphorylation, agreeing with data reported in rat cortical astrocytes (Jacques-Silva et al., 2004). Moreover, PGE_2 decreased both the basal phosphorylation of Akt and that Akt induced by the nucleotide.

The PI3K axis can be activated by Gi/o-proteins and/or the transactivation of tyrosine kinase receptors that are also present in cortical and cerebellar astrocytes, including EGF and NGF receptors (Lenz et al., 2001; Jimenez et al., 2002; Delicado et al., 2005). The treatment of astrocytes with AG1478 reduces the basal phosphorylation of ERKs and Akt, revealing that EGFR transactivation lies upstream of these kinases. This may not be surprising as the cells are cultured with FCS, although this did not affect the ERK phosphorylation induced by UTP, which was even higher than that obtained in control conditions, nor Akt phosphorylation. AG1478 strongly impeded the modulatory action of PGE_2, suggesting that transactivation of EGFR is one step of the intracellular mechanism triggered by the PGE_2, opening new roles for the EGFR in rat

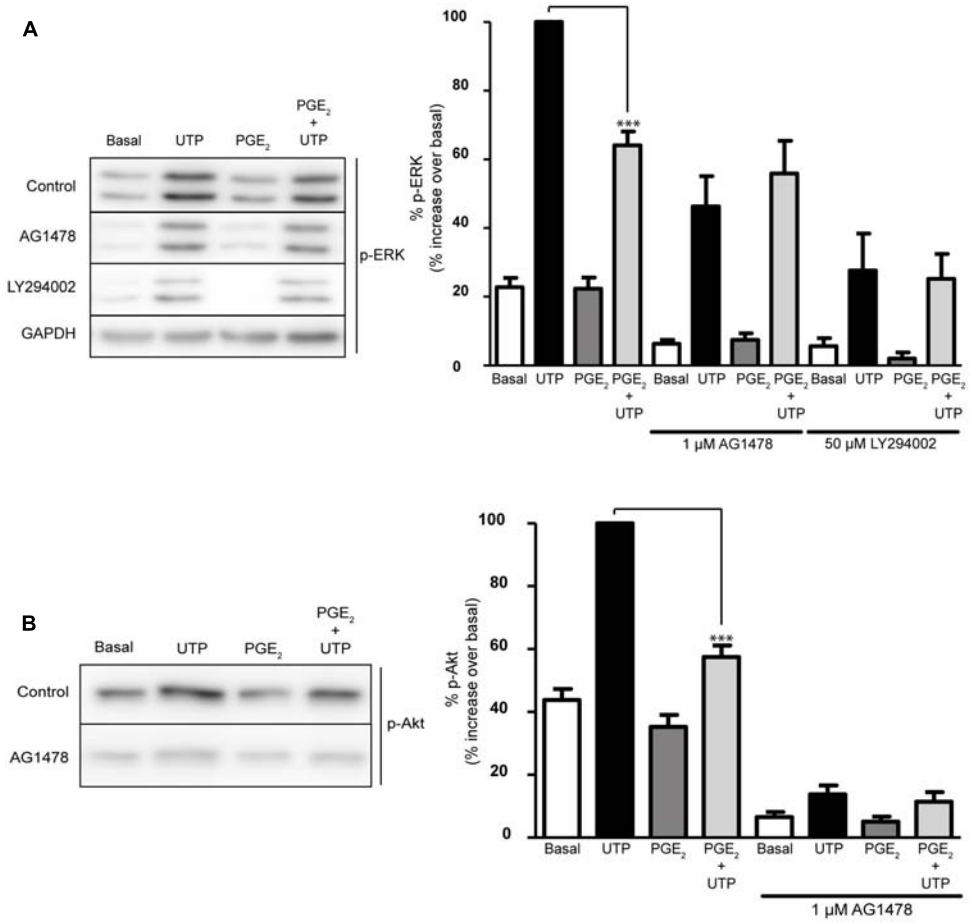

FIGURE 7 | Modulation of UTP-induced ERK1/2 and PI3-K/Akt activation by PGE_2 is dependent on EGFR and PI3K activation. Astrocytes were preincubated for 20 min in the presence or absence of AG1478 (1 μM) or LY294002 (50 μM) prior to stimulation with UTP (100 μM) for 5 min, and the p-ERK1/2 **(A)** and p-Akt **(B)** in the total lysates was detected in Western blots. Where indicated, the cells were treated with PGE_2 (1 μM) for 5 min prior to stimulation with the nucleotide. The blots shown are representative of independent experiments and GAPDH was used as an internal loading control. GAPDH blot corresponding to that obtained in the presence of AG1478. The values are the means ± SEM from five independent experiments performed on different cultures and the results are presented as the phosphorylation relative to that elicited by UTP (100 μM) in each individual experiment. ***$p < 0.0001$.

cerebellar astrocytes. It was clearly demonstrated that EGFR participates in the inhibition of UTP responses displayed by PGE_2 when high nucleotide concentrations accompany PGE_2 in the extracellular milieu. However, when the nucleotide levels diminish EGFR can contribute to the maintenance of the actions of nucleotides, as EGF potentiated previously ineffective UTP/ATP concentrations.

Subsequent studies with LY294002 revealed that PI3K inhibition has similar effects to EGFR inhibition, which would make it interesting to explore the targets of Akt. More than 50 substrates have been identified for this protein, the phosphorylation of which might positively or negatively modulate their functions, alter their subcellular localization, or modify their stability (Liao and Hung, 2010). One of the most relevant substrates is glycogen synthase kinase 3 (GSK3), which regulates cell metabolism and survival in the nervous system (Bhat et al., 2004). Unpublished results (not shown) indicate that GSK3 is also phosphorylated in astrocytes after UTP stimulation to a similar extent as Akt, although PGE_2 only reduced UTP-induced phosphorylation by 20%. GSK3 is a well-known negative regulator of the enzyme responsible for the glycogen synthesis, glycogen synthase. Glycogen is mainly synthesized and accumulated in astrocytes, and it is mobilized and transformed into lactate to be supplied for neurons in situations of hypoxia or upon demand (Suzuki et al., 2011).

PI3K might also interact with some PKC isoforms regulating their activation. Some PKC isoforms present in cerebellar astrocytes can interact with this kinase, such as PKC-α, -δ, and -ζ identified in cortical astrocytes (Chen and Chen, 1996). In neuroblastoma cells, the atypical PKC-ζ dampened Akt phosphorylation, thereby providing a negative feedback loop to regulate P2X7 expression (Gomez-Villafuertes et al., 2015). In cerebellar astrocytes, it could be responsible for decreasing GSK3 phosphorylation, although we did not find evidence of an involvement of PKC-ζ in this phenomenon. The involvement of other PKC isoforms cannot be ruled out and nPKC could

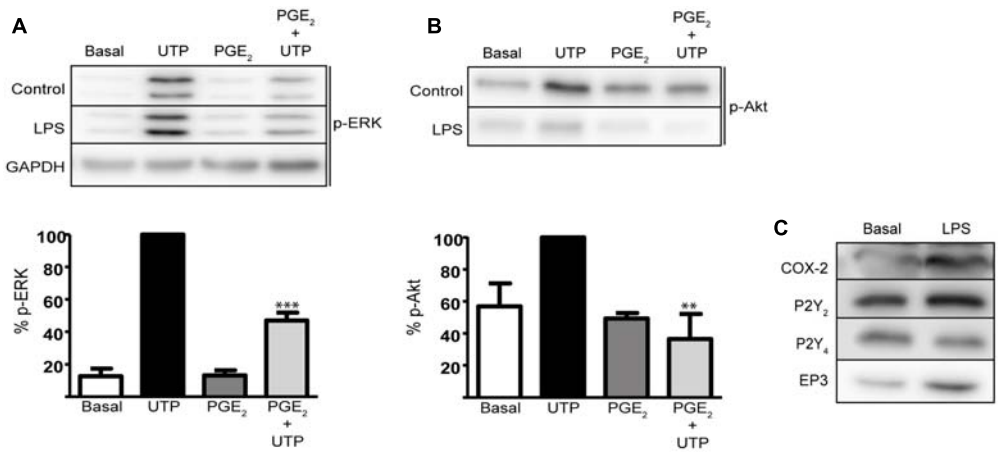

FIGURE 8 | Prostaglandin E_2 modulates UTP-induced ERK1/2 and PI3-K/Akt activation in astrocytes activated with LPS. Astrocytes were incubated in the presence or absence of LPS (10 ng/ml) for 24 h prior to analyzing the modulatory effect of PGE_2 on the increase in p-ERK1/2 **(A)** and p-Akt **(B)** induced by UTP (see **Figure 6**). The Western blots are representative of independent experiments and GAPDH was used as an internal loading control. The values are the means ± SEM from three independent experiments performed on different cultures and the results are expressed relative to the UTP response in each individual experiment. **(C)** LPS induced COX-2 and EP3 receptor expression in rat cerebellar astrocytes. The presence of COX-2, P2Y2R, P2Y4R, and EP3R proteins was detected in Western blots of total cell lysates. ***$p < 0.0001$, **$p < 0.001$.

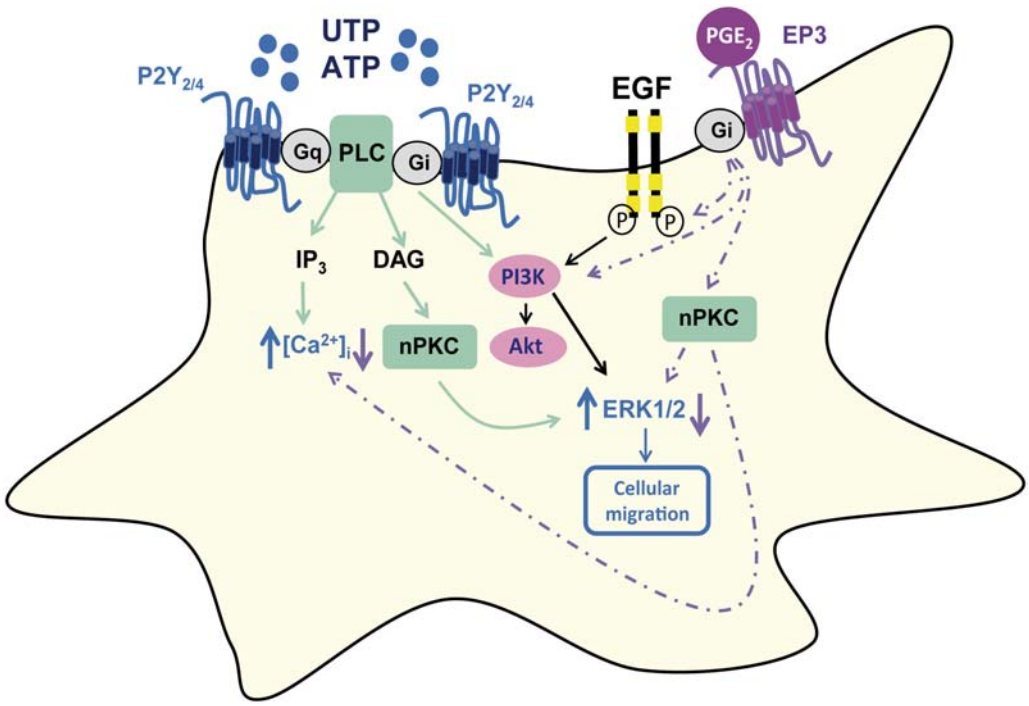

FIGURE 9 | Schematic representation of PGE_2 modulation of UTP signaling in rat cerebellar astrocytes. PGE_2 dampened the calcium responses induced by UTP stimulation of $P2Y_2/P2Y_4$, as well as reducing the UTP-induced ERK and Akt activation, and cell migration. The effect of PGE_2 was dependent on EP3 receptor interactions, and it involved EGFR transactivation and PI3K activity, although the involvement of nPKC could be not excluded.

be responsible for the phosphorylation of $P2Y_2/P2Y_4$ receptors, which could be internalized to dampen the calcium responses. Moreover, DAG production/nPKC activation may be required for nucleotides to drive ERK activity in these glial cells, particularly as UTP-P2Y receptors were sensitive to feedback inhibition by PKC (Jimenez et al., 2000; Flores et al., 2005). In fact, in astrocytes in which nPKC was down-regulated by prolonged exposure to phorbol dibutyrate (PDBu) the UTP calcium responses were stronger than those obtained in control cells (results not shown). In macrophages and fibroblasts, the effect of PGE_2 was dependent

on PKC and PKD activation, although it was also independent of EP receptors (Traves et al., 2013; Pimentel-Santillana et al., 2014).

Physiological Implications

This study aimed to explore the cross-talk between PGE_2 and UTP-sensitive P2Y receptors in cerebellar astrocytes. We found that PGE_2 negatively modulated UTP responses, as reported previously in macrophages and fibroblasts. However, there were two differences inasmuch as the effect of PGE_2 appeared to be dependent on EP3 receptors and also, it was observed in LPS treated cells. In macrophages the interaction took place in thioglycollate-elicited and alternative macrophages (M2), but not in macrophages activated with the endotoxin (M1). While the metabolic changes that occur during macrophage activation and the transition from M1 to M2 phenotype have been largely explored (Rodriguez-Prados et al., 2010; Traves et al., 2012), this is not the case for astrocytes activated with LPS. Nevertheless, macrophages and astrocytes share some metabolic features and they are constitutively glycolytic (Bolanos, 2016). Hence, it will be very interesting to investigate the metabolic implications of the cross-talk reported in cerebellar astrocytes, both in control conditions and in LPS-treated astrocytes, and the intracellular targets of the endotoxin. The negative effects of PGE_2 on UTP signaling could contribute to limit excessive astrogliosis, which could represent part of the adaptive mechanism to neuroinflammation. Several studies have indicated that both P2Y and P2X receptors are upregulated in the astrogliosis process involving ERK and Akt activation (Franke et al., 2001; Neary et al., 2005; Franke and Illes, 2014). We are developing studies to determine whether $P2Y_2$/$P2Y_4$ receptors are upregulated after prolonged treatment with the endotoxin and whether they can be down-regulated by PGE_2.

AUTHOR CONTRIBUTIONS

ED, LB, and RP-S designed experiments; LP-H, JG-R, MQ, and SG-R performed experiments; ED, RP-S, and MM-P wrote the manuscript; LP-H, JG-R, and MQ made illustrations and generated figures; MM-P and ED directed the project.

FUNDING

This work was funded by the Spanish Ministerio de Economía y Competitividad (MINECO, BFU 2014-53654-P and SAF2014-5249R) and the "Red de Excelencia Consolider-Ingenio Spanish Ion Channel Initiative" (BFU2015-70067REDC); by the Comunidad de Madrid (BRADE-CM S2013/ICE-2958), and by a Fundación Ramón Areces Grants (PR2018/16-02 and OTR02670). LP-H is a recipient of a grant from the European Social Fund through the Youth Employment and the Youth Employment Initiative, JG-R is the recipient of a FPI fellowship and MQ is the recipient of a FPU fellowship.

ACKNOWLEDGMENT

The authors are grateful to Dr. Mark Sefton for his revision of the manuscript.

REFERENCES

Bezzi, P., Carmignoto, G., Pasti, L., Vesce, S., Rossi, D., Rizzini, B. L., et al. (1998). Prostaglandins stimulate calcium-dependent glutamate release in astrocytes. *Nature* 391, 281–285. doi: 10.1038/34651

Bhat, R. V., Budd Haeberlein, S. L., and Avila, J. (2004). Glycogen synthase kinase 3: a drug target for CNS therapies. *J. Neurochem.* 89, 1313–1317. doi: 10.1111/j.1471-4159.2004.02422.x

Bolanos, J. P. (2016). Bioenergetics and redox adaptations of astrocytes to neuronal activity. *J. Neurochem.* 139(Suppl. 2), 115–125. doi: 10.1111/jnc.13486

Brambilla, R., Neary, J. T., Cattabeni, F., Cottini, L., D'Ippolito, G., Schiller, P. C., et al. (2002). Induction of COX-2 and reactive gliosis by P2Y receptors in rat cortical astrocytes is dependent on ERK1/2 but independent of calcium signalling. *J. Neurochem.* 83, 1285–1296. doi: 10.1046/j.1471-4159.2002.01239.x

Burnstock, G. (2006). Purinergic signalling. *Br. J. Pharmacol.* 147(Suppl. 1), S172–S181. doi: 10.1038/sj.bjp.0706429

Carrasquero, L. (2008). *Cascadas de Señalización Activadas por Nucleótidos en Astrocitos de Cerebelo de Rata: Receptores P2X y P2Y Implicados*. Ph.D. Tesis, Universidad Complutense de Madrid, Madrid.

Carrasquero, L. M., Delicado, E. G., Bustillo, D., Gutierrez-Martin, Y., Artalejo, A. R., and Miras-Portugal, M. T. (2009). P2X7 and P2Y13 purinergic receptors mediate intracellular calcium responses to BzATP in rat cerebellar astrocytes. *J. Neurochem.* 110, 879–889. doi: 10.1111/j.1471-4159.2009.06179.x

Carrasquero, L. M., Delicado, E. G., Jimenez, A. I., Perez-Sen, R., and Miras-Portugal, M. T. (2005). Cerebellar astrocytes co-express several ADP receptors. Presence of functional P2Y(13)-like receptors. *Purinergic Signal.* 1, 153–159. doi: 10.1007/s11302-005-6211-3

Chen, B. C., and Lin, W. W. (2000). Pyrimidinoceptor potentiation of macrophage PGE(2) release involved in the induction of nitric oxide synthase. *Br. J. Pharmacol.* 130, 777–786. doi: 10.1038/sj.bjp.0703375

Chen, C. C., and Chen, W. C. (1996). ATP-evoked inositol phosphates formation through activation of P2U purinergic receptors in cultured astrocytes: regulation by PKC subtypes alpha, delta, and theta. *Glia* 17, 63–71. doi: 10.1002/(SICI)1098-1136(199605)17:1<63::AID-GLIA6>3.0.CO;2-8

Colombo, E., and Farina, C. (2016). Astrocytes: key regulators of neuroinflammation. *Trends Immunol.* 37, 608–620. doi: 10.1016/j.it.2016.06.006

Communi, D., Motte, S., Boeynaems, J. M., and Pirotton, S. (1996). Pharmacological characterization of the human P2Y4 receptor. *Eur. J. Pharmacol.* 317, 383–389. doi: 10.1016/S0014-2999(96)00740-6

Costanzi, S., Mamedova, L., Gao, Z. G., and Jacobson, K. A. (2004). Architecture of P2Y nucleotide receptors: structural comparison based on sequence analysis, mutagenesis, and homology modeling. *J. Med. Chem.* 47, 5393–5404. doi: 10.1021/jm049914c

Dannhardt, G., and Kiefer, W. (2001). Cyclooxygenase inhibitors–current status and future prospects. *Eur. J. Med. Chem.* 36, 109–126. doi: 10.1016/S0223-5234(01)01197-7

Delicado, E. G., Jimenez, A. I., Carrasquero, L. M., Castro, E., and Miras-Portugal, M. T. (2005). Cross-talk among epidermal growth factor, Ap(5)A, and nucleotide receptors causing enhanced ATP Ca(2+) signaling involves extracellular kinase activation in cerebellar astrocytes. *J. Neurosci. Res.* 81, 789–796. doi: 10.1002/jnr.20609

Di Cesare, A., Del Piccolo, P., Zacchetti, D., and Grohovaz, F. (2006). EP2 receptor stimulation promotes calcium responses in astrocytes via activation of the adenylyl cyclase pathway. *Cell. Mol. Life Sci.* 63, 2546–2553. doi: 10.1007/s00018-006-6262-9

Domercq, M., Brambilla, L., Pilati, E., Marchaland, J., Volterra, A., and Bezzi, P. (2006). P2Y1 receptor-evoked glutamate exocytosis from astrocytes: control by tumor necrosis factor-alpha and prostaglandins. *J. Biol. Chem.* 281, 30684–30696. doi: 10.1074/jbc.M606429200

Dwivedi, A. K., Gurjar, V., Kumar, S., and Singh, N. (2015). Molecular basis for nonspecificity of nonsteroidal anti-inflammatory drugs (NSAIDs). *Drug Discov. Today* 20, 863–873. doi: 10.1016/j.drudis.2015.03.004

Ellis, E. F., Wei, E. P., and Kontos, H. A. (1979). Vasodilation of cat cerebral arterioles by prostaglandins D2, E2, G2, and I2. *Am. J. Physiol.* 237, H381–H385.

Erb, L., and Weisman, G. A. (2012). Coupling of P2Y receptors to G proteins and other signaling pathways. *Wiley Interdiscip. Rev. Membr. Transp. Signal.* 1, 789–803. doi: 10.1002/wmts.62

Flores, R. V., Hernandez-Perez, M. G., Aquino, E., Garrad, R. C., Weisman, G. A., and Gonzalez, F. A. (2005). Agonist-induced phosphorylation and desensitization of the P2Y2 nucleotide receptor. *Mol. Cell. Biochem.* 280, 35–45. doi: 10.1007/s11010-005-8050-5

Font-Nieves, M., Sans-Fons, M. G., Gorina, R., Bonfill-Teixidor, E., Salas-Perdomo, A., Marquez-Kisinousky, L., et al. (2012). Induction of COX-2 enzyme and down-regulation of COX-1 expression by lipopolysaccharide (LPS) control prostaglandin E2 production in astrocytes. *J. Biol. Chem.* 287, 6454–6468. doi: 10.1074/jbc.M111.327874

Franke, H., and Illes, P. (2014). Nucleotide signaling in astrogliosis. *Neurosci. Lett.* 565, 14–22. doi: 10.1016/j.neulet.2013.09.056

Franke, H., Krugel, U., Schmidt, R., Grosche, J., Reichenbach, A., and Illes, P. (2001). P2 receptor-types involved in astrogliosis in vivo. *Br. J. Pharmacol.* 134, 1180–1189. doi: 10.1038/sj.bjp.0704353

Fransson, S., Abel, F., Kogner, P., Martinsson, T., and Ejeskar, K. (2013). Stage-dependent expression of PI3K/Aktpathway genes in neuroblastoma. *Int. J. Oncol.* 42, 609–616. doi: 10.3892/ijo.2012.1732

Fujita, T., Tozaki-Saitoh, H., and Inoue, K. (2009). P2Y1 receptor signaling enhances neuroprotection by astrocytes against oxidative stress via IL-6 release in hippocampal cultures. *Glia* 57, 244–257. doi: 10.1002/glia.20749

Gomez-Villafuertes, R., Garcia-Huerta, P., Diaz-Hernandez, J. I., and Miras-Portugal, M. T. (2015). PI3K/Akt signaling pathway triggers P2X7 receptor expression as a pro-survival factor of neuroblastoma cells under limiting growth conditions. *Sci. Rep.* 5:18417. doi: 10.1038/srep18417

Han, X., Lan, X., Li, Q., Gao, Y., Zhu, W., Cheng, T., et al. (2016). Inhibition of prostaglandin E2 receptor EP3 mitigates thrombin-induced brain injury. *J. Cereb. Blood Flow Metab.* 36, 1059–1074. doi: 10.1177/0271678X15606462

Ho, C., Hicks, J., and Salter, M. W. (1995). A novel P2-purinoceptor expressed by a subpopulation of astrocytes from the dorsal spinal cord of the rat. *Br. J. Pharmacol.* 116, 2909–2918. doi: 10.1111/j.1476-5381.1995.tb15944.x

Howarth, C., Sutherland, B., Choi, H. B., Martin, C., Lind, B. L., Khennouf, L., et al. (2017). A critical role for astrocytes in hypercapnic vasodilation in brain. *J. Neurosci.* 37, 2403–2414. doi: 10.1523/JNEUROSCI.0005-16.2016

Ito, M., and Matsuoka, I. (2008). Regulation of purinergic signaling by prostaglandin E2 in murine macrophages. *J. Pharmacol. Sci.* 107, 443–450. doi: 10.1254/jphs.08087FP

Ito, M., and Matsuoka, I. (2015). Inhibition of P2Y6 receptor-mediated phospholipase C activation and Ca(2+) signalling by prostaglandin E2 in J774 murine macrophages. *Eur. J. Pharmacol.* 749, 124–132. doi: 10.1016/j.ejphar.2014.12.024

Jacques-Silva, M. C., Rodnight, R., Lenz, G., Liao, Z., Kong, Q., Tran, M., et al. (2004). P2X7 receptors stimulate AKT phosphorylation in astrocytes. *Br. J. Pharmacol.* 141, 1106–1117. doi: 10.1038/sj.bjp.0705685

Jimenez, A. I., Castro, E., Communi, D., Boeynaems, J. M., Delicado, E. G., and Miras-Portugal, M. T. (2000). Coexpression of several types of metabotropic nucleotide receptors in single cerebellar astrocytes. *J. Neurochem.* 75, 2071–2079. doi: 10.1046/j.1471-4159.2000.0752071.x

Jimenez, A. I., Castro, E., Delicado, E. G., and Miras-Portugal, M. T. (2002). Specific diadenosine pentaphosphate receptor coupled to extracellular regulated kinases in cerebellar astrocytes. *J. Neurochem.* 83, 299–308. doi: 10.1046/j.1471-4159.2002.01111.x

Jimenez, A. I., Castro, E., Mirabet, M., Franco, R., Delicado, E. G., and Miras-Portugal, M. T. (1999). Potentiation of ATP calcium responses by A2B receptor stimulation and other signals coupled to Gs proteins in type-1 cerebellar astrocytes. *Glia* 26, 119–128. doi: 10.1002/(SICI)1098-1136(199904)26:2<119::AID-GLIA3>3.0.CO;2-D

Kunori, S., Matsumura, S., Okuda-Ashitaka, E., Katano, T., Audoly, L. P., Urade, Y., et al. (2011). A novel role of prostaglandin E2 in neuropathic pain: blockade of microglial migration in the spinal cord. *Glia* 59, 208–218. doi: 10.1002/glia.21090

Lazarowski, E. R., Sesma, J. I., Seminario-Vidal, L., and Kreda, S. M. (2011). Molecular mechanisms of purine and pyrimidine nucleotide release. *Adv. Pharmacol.* 61, 221–261. doi: 10.1016/B978-0-12-385526-8.00008-4

Lenz, G., Goncalves, D., Luo, Z., Avruch, J., Rodnight, R., and Neary, J. T. (2001). Extracellular ATP stimulates an inhibitory pathway towards growth factor-induced cRaf-1 and MEKK activation in astrocyte cultures. *J. Neurochem.* 77, 1001–1009. doi: 10.1046/j.1471-4159.2001.00299.x

Liao, Y., and Hung, M. C. (2010). Physiological regulation of Akt activity and stability. *Am. J. Transl. Res.* 2, 19–42.

Liu, J., Liao, Z., Camden, J., Griffin, K. D., Garrad, R. C., Santiago-Perez, L. I., et al. (2004). Src homology 3 binding sites in the P2Y2 nucleotide receptor interact with Src and regulate activities of Src, proline-rich tyrosine kinase 2, and growth factor receptors. *J. Biol. Chem.* 279, 8212–8218. doi: 10.1074/jbc.M312230200

Miras-Portugal, M. T., Gomez-Villafuertes, R., Gualix, J., Diaz-Hernandez, J. I., Artalejo, A. R., Ortega, F., et al. (2016). Nucleotides in neuroregeneration and neuroprotection. *Neuropharmacology* 104, 243–254. doi: 10.1016/j.neuropharm.2015.09.002

Neary, J. T., Kang, Y., and Shi, Y. F. (2004). Signaling from nucleotide receptors to protein kinase cascades in astrocytes. *Neurochem. Res.* 29, 2037–2042. doi: 10.1007/s11064-004-6876-y

Neary, J. T., Kang, Y., Tran, M., and Feld, J. (2005). Traumatic injury activates protein kinase B/Akt in cultured astrocytes: role of extracellular ATP and P2 purinergic receptors. *J. Neurotrauma* 22, 491–500. doi: 10.1089/neu.2005.22.491

North, R. A. (2016). P2X receptors. *Philos. Trans. R. Soc. Lond. B Biol. Sci.* 371: 20150427. doi: 10.1098/rstb.2015.0427

Oliveira, J. F., Riedel, T., Leichsenring, A., Heine, C., Franke, H., Krugel, U., et al. (2011). Rodent cortical astroglia express in situ functional P2X7 receptors sensing pathologically high ATP concentrations. *Cereb. Cortex* 21, 806–820. doi: 10.1093/cercor/bhq154

Ortega, F., Perez-Sen, R., Delicado, E. G., and Miras-Portugal, M. T. (2009). P2X7 nucleotide receptor is coupled to GSK-3 inhibition and neuroprotection in cerebellar granule neurons. *Neurotox. Res.* 15, 193–204. doi: 10.1007/s12640-009-9020-6

Ortega, F., Perez-Sen, R., and Miras-Portugal, M. T. (2008). Gi-coupled P2Y-ADP receptor mediates GSK-3 phosphorylation and beta-catenin nuclear translocation in granule neurons. *J. Neurochem.* 104, 62–73. doi: 10.1111/j.1471-4159.2007.05021.x

Peterson, T. S., Camden, J. M., Wang, Y., Seye, C. I., Wood, W. G., Sun, G. Y., et al. (2010). P2Y2 nucleotide receptor-mediated responses in brain cells. *Mol. Neurobiol.* 41, 356–366. doi: 10.1007/s12035-010-8115-7

Pimentel-Santillana, M., Traves, P. G., Perez-Sen, R., Delicado, E. G., Martin-Sanz, P., Miras-Portugal, M. T., et al. (2014). Sustained release of prostaglandin E(2) in fibroblasts expressing ectopically cyclooxygenase 2 impairs P2Y-dependent Ca(2)(+)-mobilization. *Mediators Inflamm.* 2014:832103. doi: 10.1155/2014/832103

Rodriguez-Prados, J. C., Traves, P. G., Cuenca, J., Rico, D., Aragones, J., Martin-Sanz, P., et al. (2010). Substrate fate in activated macrophages: a comparison between innate, classic, and alternative activation. *J. Immunol.* 185, 605–614. doi: 10.4049/jimmunol.0901698

Sang, N., Zhang, J., Marcheselli, V., Bazan, N. G., and Chen, C. (2005). Postsynaptically synthesized prostaglandin E2 (PGE2) modulates hippocampal synaptic transmission via a presynaptic PGE2 EP2 receptor. *J. Neurosci.* 25, 9858–9870. doi: 10.1523/JNEUROSCI.2392-05.2005

Simm, B., Ott, D., Pollatzek, E., Murgott, J., Gerstberger, R., Rummel, C., et al. (2016). Effects of prostaglandin E2 on cells cultured from the rat organum vasculosum laminae terminalis and median preoptic nucleus. *Neuroscience* 313, 23–35. doi: 10.1016/j.neuroscience.2015.11.034

Smith, W. L., DeWitt, D. L., and Garavito, R. M. (2000). Cyclooxygenases: structural, cellular, and molecular biology. *Annu. Rev. Biochem.* 69, 145–182. doi: 10.1146/annurev.biochem.69.1.145

Sofroniew, M. V. (2015). Astrocyte barriers to neurotoxic inflammation. *Nat. Rev. Neurosci.* 16, 249–263. doi: 10.1038/nrn3898

St-Jacques, B., and Ma, W. (2016). Preferred recycling pathway by internalized PGE2 EP4 receptor following agonist stimulation in cultured dorsal root ganglion neurons contributes to enhanced EP4 receptor sensitivity. *Neuroscience* 326, 56–68. doi: 10.1016/j.neuroscience.2016.04.005

Sugimoto, Y., and Narumiya, S. (2007). Prostaglandin E receptors. *J. Biol. Chem.* 282, 11613–11617. doi: 10.1074/jbc.R600038200

Suzuki, A., Stern, S. A., Bozdagi, O., Huntley, G. W., Walker, R. H., Magistretti, P. J., et al. (2011). Astrocyte-neuron lactate transport is required for long-term memory formation. *Cell* 144, 810–823. doi: 10.1016/j.cell.2011.02.018

Takano, T., Tian, G. F., Peng, W., Lou, N., Libionka, W., Han, X., et al. (2006). Astrocyte-mediated control of cerebral blood flow. *Nat. Neurosci.* 9, 260–267. doi: 10.1038/nn1623

Traves, P. G., de Atauri, P., Marin, S., Pimentel-Santillana, M., Rodriguez-Prados, J. C., Marin de Mas, I., et al. (2012). Relevance of the MEK/ERK signaling pathway in the metabolism of activated macrophages: a metabolomic approach. *J. Immunol.* 188, 1402–1410. doi: 10.4049/jimmunol.1101781

Traves, P. G., Pimentel-Santillana, M., Carrasquero, L. M., Perez-Sen, R., Delicado, E. G., Luque, A., et al. (2013). Selective impairment of P2Y signaling by prostaglandin E2 in macrophages: implications for Ca2+-dependent responses. *J. Immunol.* 190, 4226–4235. doi: 10.4049/jimmunol.1203029

von Kugelgen, I., and Hoffmann, K. (2016). Pharmacology and structure of P2Y receptors. *Neuropharmacology* 104, 50–61. doi: 10.1016/j.neuropharm.2015.10.030

Zonta, M., Sebelin, A., Gobbo, S., Fellin, T., Pozzan, T., and Carmignoto, G. (2003). Glutamate-mediated cytosolic calcium oscillations regulate a pulsatile prostaglandin release from cultured rat astrocytes. *J. Physiol.* 553, 407–414. doi: 10.1113/jphysiol.2003.046706

Conflict of Interest Statement: The authors declare that the research was conducted in the absence of any commercial or financial relationships that could be construed as a potential conflict of interest.

frontiers in Pharmacology

REVIEW
published: 19 December 2017
doi: 10.3389/fphar.2017.00941

Pathophysiological Role of Purines and Pyrimidines in Neurodevelopment: Unveiling New Pharmacological Approaches to Congenital Brain Diseases

*Marta Fumagalli, Davide Lecca, Maria P. Abbracchio and Stefania Ceruti**

Laboratory of Molecular and Cellular Pharmacology of Purinergic Transmission, Department of Pharmacological and Biomolecular Sciences, Università degli Studi di Milano, Milan, Italy

OPEN ACCESS

Edited by:
Kenneth A. Jacobson, National Institutes of Health (NIH), United States

Reviewed by:
Alexej Verkhratsky, University of Manchester, United Kingdom
Michal Mielcarek, Imperial College London, United Kingdom
H. A. (Buz) Jinnah, Emory University, United States

***Correspondence:**
Stefania Ceruti
stefania.ceruti@unimi.it

Specialty section:
This article was submitted to Experimental Pharmacology and Drug Discovery, a section of the journal Frontiers in Pharmacology

Received: *19 October 2017*
Accepted: *11 December 2017*
Published: *19 December 2017*

Citation:
Fumagalli M, Lecca D, Abbracchio MP and Ceruti S (2017) Pathophysiological Role of Purines and Pyrimidines in Neurodevelopment: Unveiling New Pharmacological Approaches to Congenital Brain Diseases. Front. Pharmacol. 8:941. doi: 10.3389/fphar.2017.00941

In recent years, a substantial body of evidence has emerged demonstrating that purine and pyrimidine synthesis and metabolism play major roles in controlling embryonic and fetal development and organogenesis. Dynamic and time-dependent changes in the expression of purine metabolizing enzymes (such as ectonucleotidases and adenosine deaminase) represent a key checkpoint for the correct sequential generation of the different signaling molecules, that in turn activate their specific membrane receptors. In neurodevelopment, Ca^{2+} release from radial glia mediated by $P2Y_1$ purinergic receptors is fundamental to allow neuroblast migration along radial glia processes, and their correct positioning in the different layers of the developing neocortex. Moreover, ATP is involved in the development of synaptic transmission and contributes to the establishment of functional neuronal networks in the developing brain. Additionally, several purinergic receptors (spanning from adenosine to P2X and P2Y receptor subtypes) are differentially expressed by neural stem cells, depending on their maturation stage, and their activation tightly regulates cell proliferation and differentiation to either neurons or glial cells, as well as their correct colonization of the developing telencephalon. The purinergic control of neurodevelopment is not limited to prenatal life, but is maintained in postnatal life, when it plays fundamental roles in controlling oligodendrocyte maturation from precursors and their terminal differentiation to fully myelinating cells. Based on the above-mentioned and other literature evidence, it is now increasingly clear that any defect altering the tight regulation of purinergic transmission and of purine and pyrimidine metabolism during pre- and post-natal brain development may translate into functional deficits, which could be at the basis of severe pathologies characterized by mental retardation or other disturbances. This can occur either at the level of the recruitment and/or signaling of specific nucleotide or nucleoside receptors or through genetic alterations in key steps of the purine salvage pathway. In this review, we have provided a critical analysis of what is currently known on the pathophysiological role of purines and pyrimidines during brain development with the aim of unveiling new future strategies for pharmacological intervention in different neurodevelopmental disorders.

Keywords: neurodevelopmental disorders, purine metabolism, enzyme deficiencies, adenosine, purine salvage pathway, P2X7 receptors

CONTRIBUTION OF PURINERGIC TRANSMISSION TO THE DEVELOPMENT OF THE CENTRAL NERVOUS SYSTEM

Neural development is a complex highly orchestrated process involving genetic, epigenetic, and environmental events that are crucial for shaping the architecture of the growing brain. Proliferation and migration of glia and neurons, followed by naturally occurring cell death of damaged or unnecessary cells, formation of synapses, myelination of axons, and generation of neuronal connections are indeed critically controlled by intrinsic and environmental factors at each stage during development (Stiles and Jernigan, 2010).

Purine and pyrimidine nucleotides are essential precursors for nucleic acid synthesis, but their functions are not limited to this. Purines act as metabolic signals, provide energy, control cell growth, are part of essential coenzymes, contribute to sugar transport and donate phosphate groups in phosphorylation reactions (Jankowski et al., 2005; Handford et al., 2006). Pyrimidines are involved in polysaccharide and phospholipid biosynthesis, detoxification processes, and in protein and lipid glycosylation (Lecca and Ceruti, 2008; Löffler et al., 2015). The nervous tissue produces huge amount of ATP, which is mainly employed to provide energy for membrane active pumps, such as Na^+/K^+ ATPase, and is fundamental to sustain synaptic transmission and the cooperation between neurons and glial cells (Bélanger et al., 2011; Micheli et al., 2011; Harris et al., 2012).

In the central nervous system (CNS), some purines serve more specialized roles, not only in neurons, but also in glial cells. Over the last 40 years it has been progressively understood that extracellular nucleotides exert many of their functions through the activation of ligand-gated P2X channels (the P2X1-7 subtypes) and of G protein-coupled P2Y receptors (the $P2Y_{1,2,4,6,11,12,13,14}$ subtypes; Abbracchio et al., 2006). Also, purine nucleosides exert receptor-mediated actions in all mammalian tissues and systems, including the brain. The vast majority of available data are focused on adenosine which activates 4 G protein-coupled receptors (the $A_{1,2A,2B,3}$ subtypes; Fredholm et al., 2011), collectively referred to as P1 receptors. An increasing body of evidence is now also pointing to specific effects of extracellular guanosine in modulating brain functions (for review, see Di Liberto et al., 2016). Nevertheless, the identification and cloning of guanosine receptor have failed so far. Overall, despite the presence of pyrimidine signaling molecules acting on the $P2Y_{2,4,6,14}$ receptor subtypes (von Kügelgen and Hoffmann, 2016) and on the P2Y-like receptor GPR17 (see section Involvement of the Purinergic System in Brain Alterations Observed in Down Syndrome), this system is referred to as the "purinergic system" (Burnstock, 2017). P1 and P2 receptors are widely expressed throughout the body, where they exert a variety of physiological functions, including neurotransmission (Burnstock, 2017). Some specific subtypes are also crucially involved in controlling brain development.

P2Y Receptors in CNS Development

The first hints of a specific role for purinergic receptor signaling during development came from studies in *Xenopus*, where ATP degradation to ADP by E-NTPDase-2 in the anterior neural plate, with subsequent activation of the $P2Y_1$ receptor subtype, leads to the induction of *Pax6, Rx1,* and *Six3* genes. These genes encode for transcription factors collectively referred to as eye field transcription factors (EFTF), and are fundamental to promote and sustain eye development (Massè et al., 2007). Altering purinergic signaling, by either overexpressing or downregulating some of the molecular components of this pathway, leads to abnormal eye development, thus confirming the crucial role of extracellular nucleotides during tissue generation and cell specification in embryos.

Data have been further confirmed and expanded to the mammalian brain, where it has been demonstrated that the expression of specific P2Y receptor subtypes is plastic and tightly controlled at different embryonic stages, and correlates with their recruitment in controlling brain development (Oliveira et al., 2016). For example, $P2Y_1$ receptor-mediated calcium signaling is fundamental for the specification of the cortical layers. At this stage of development, daughter cells derived from neural precursors located in the ventricular/subventricular zone start their migration toward their final localization in the developing cortex where they differentiate to either neurons or astrocytes (Pino et al., 2017). Radial glial cells, a peculiar type of glial cells, act as both neuronal progenitors in the ventricular/subventricular zone through their asymmetric division and as "guiding sign" for migrating cells. In fact, their long radial process extends up to the subpial surface, and constitute a "highway" for migrating cells to find their final localization in the correct cortical layer (Ulrich et al., 2012; **Figure 1**).

Extracellular nucleotides control both radial glial cell proliferation and migration of developing neuroblasts and glial cells. In fact, a paracrine ATP signaling is established through its degradation to ADP and activation of $P2Y_1$ receptors, leading to the generation of $[Ca^{2+}]_i$ waves that propagate through hemichannel and gap junctions, thereby synchronizing cell cycle and migration (Weissman et al., 2004; Lecca et al., 2016; **Figure 1**). In turn, calcium waves amplify ATP release accompanied by other neurotransmitters and growth factors, which further contribute to drive neural precursor migration toward developing cortical layers, where they terminally differentiate to neurons or glial cells (Ulrich et al., 2012).

Furthermore, extracellular ATP acts as one of the main activity-dependent axonal signal and activates P2 receptors on oligodendrocyte precursors cells (OPCs), which generate mature oligodendrocytes during early post-natal development (Fields and Stevens, 2000). ATP and uracil nucleotides interact with growth factors to trigger specific intracellular pathways that regulate OPC proliferation, migration, terminal maturation, and myelination (Fumagalli et al., 2016).

Neurotransmitters and growth factors released by migrating cells and radial glia are also fundamental for driving neuronal

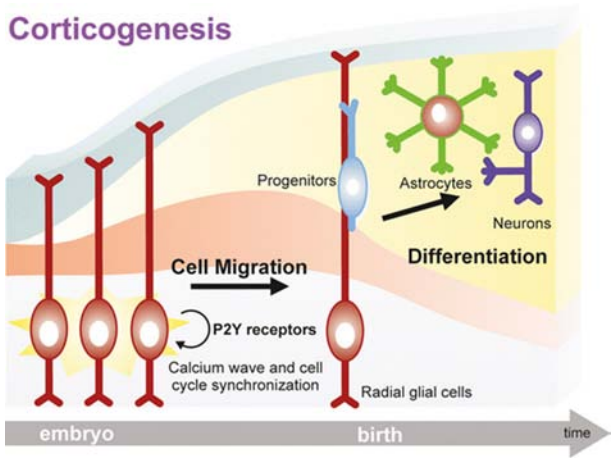

FIGURE 1 | A key role for purinergic receptors in cell cycle synchronization and progenitor migration during CNS development. Radial glia cells originate from neuroepithelial cells after the onset of neurogenesis, and they bear two essential functions: (i) act as neural progenitor cells, and (ii) provide a scaffold for migration and organization of the cortex structure. Following activation of purinergic receptors, mostly P2Y subtypes, calcium waves sustain cell cycle progression of migrating precursors, which are synchronized with neighboring radial glial cells thanks to a sustained paracrine ATP release. Progenitors eventually mature into neurons and astrocytes organizing the cortical structure. Neurogenesis and gliogenesis initiated by purinergic signaling in the embryonic brain continue during postnatal development. Reproduced from Ulrich et al. (2012) with permission (license # 4213050265596) from Springer.

differentiation and maturation, and for neurite extension and myelination. As recently elegantly reviewed (Heine et al., 2016), the purinergic system is crucially involved also in these later stages of neuronal development, thanks to the recruitment of several receptor subtypes, activated by either nucleotides or adenosine. For example, both purine $P2Y_{1,13}$ and pyrimidine $P2Y_2$ receptor subtypes have been positively correlated to neurite elongation, with the latter specifically linked to the α_V integrin/Rho/ROCK pathway (del Puerto et al., 2012; Peterson et al., 2013). A significant contribution to these events is also provided by astrocytes, and the purinergic system is also directly involved in controlling their functions (Buffo et al., 2010; Heine et al., 2016).

Neurogenesis and gliogenesis initiated by purinergic signaling in the embryonic brain continue during postnatal development, and the ventricular/subventricular zone is recognized in the adult brain as neurogenic niche, together with the subgranular layer of the hippocampus (Boda et al., 2017). *In vitro* and *in vivo* studies have demonstrated that the ADP-responsive $P2Y_1$ receptor subtype endures in its role of modulator of precursor cell proliferation and differentiation throughout life (Suyama et al., 2012; Boccazzi et al., 2014). Several other P2Y (and also P2X) receptor subtypes have been found expressed in the adult neurogenic niches (Mishra et al., 2006; Stafford et al., 2007; Grimm et al., 2009), and could therefore contribute to modulate neural precursor cell proliferation, differentiation, and recruitment following brain injury, in an often-unsatisfactory attempt to damage repair.

The Elusive Role of P2X7 Receptor in Controlling Neuronal Functions

Although for many years the expression of P2X7 receptor in adult brain has been confined to glial cells (i.e., astrocytes and microglia), a lively debate is currently open on its expression by adult neurons, with arguments both in favor and against this statement (Illes et al., 2017; Miras-Portugal et al., 2017). What is now widely accepted is that P2X7 is highly expressed by neuroblasts and neural precursors during brain development, where it inhibits cell proliferation and neurite outgrowth, but promotes neuronal differentiation (Heine et al., 2016; Oliveira et al., 2016). Interestingly, recent data point for a new role of $P2X7^+$ neuroblasts which also express high levels of doublecortin, the typical marker of developing neurons (Boda et al., 2017). These cells are in fact endowed with the peculiar ability to phagocyte surrounding cells dying by programmed cell death well before brain colonization by specialized phagocytes, such as microglia/macrophages (Gu et al., 2015; Lovelace et al., 2015; **Figure 2**). Based on these data, since programmed cell death is a fundamental process during brain development and shaping, leading to the elimination of unnecessary, damaged, or exceeding cells, a new fundamental role for P2X7-mediated purinergic signaling during embryonal life is now emerging.

Contribution of Adenosine P1 Receptors to Neurodevelopment and Neuromodulation

Adenosine has been shown to dramatically affect embryonic development as well. In fact, it is directly involved in the elimination of interdigital membranes, in the apoptotic death of clones of autoreactive lymphocytes in the thymus, and in the morphogenetic outgrowth of vertebrate limb buds (Jacobson et al., 1999). Moreover, the adenosine catabolizing enzyme adenosine deaminase (ADA) is expressed at high levels in the placenta, and its pharmacological inhibition disrupts fetal development (Knudsen et al., 1992), thus suggesting that developing tissues and organs are highly sensitive to increased adenosine concentrations. A direct link with the activation of specific P1 receptor subtypes has not been demonstrated; it is more likely that non-receptor mediated effects are involved in this pro-apoptotic and toxic actions of adenosine, as already demonstrated in ADA deficiency and in other disorders (see below; Jacobson et al., 1999). Additionally, in the developing brain the expression of adenosine kinase, the enzyme responsible for the rephosphorylation of adenosine to nucleotides, is switched from neurons during life *in utero* to exclusive astrocytic expression along with progressive brain maturation (Studer et al., 2006). It is therefore clear that a tight control of adenosine levels is fundamental for brain development and neural plasticity (Boison et al., 2012). A role for adenosine in promoting neurite outgrowth through the A_{2A} receptor subtype (Heine et al., 2016), and in fostering the differentiation of OPCs and their ability of myelinate axons (Butt et al., 2014) has been also highlighted.

Adenosine is involved in the regulation of several signaling pathways in CNS (Boison, 2008), acting as a neuromodulator through multiple mechanisms, including the control of neurotransmitter release, or via regulatory effects on glial

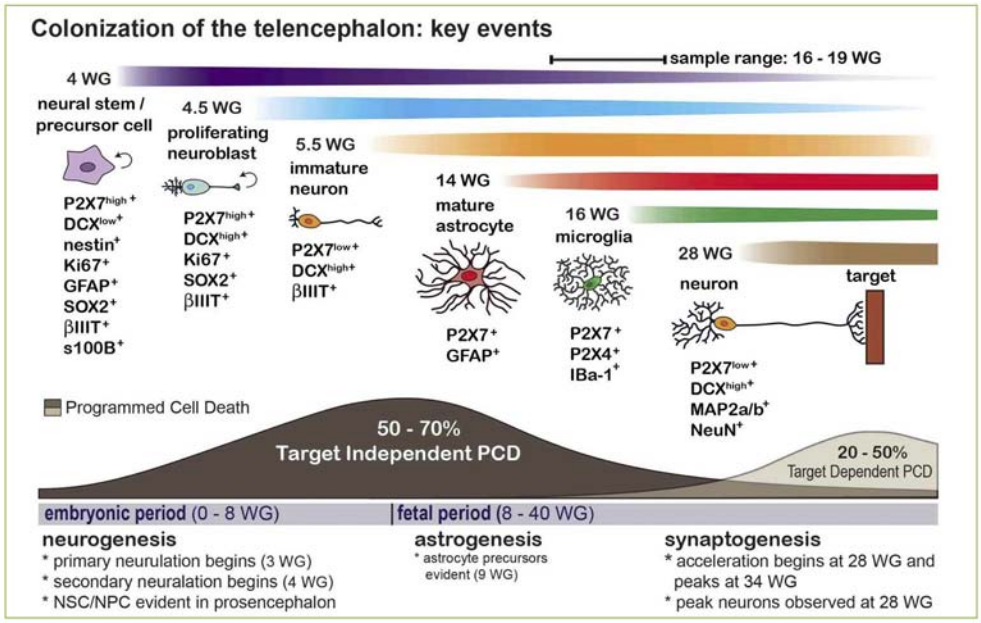

FIGURE 2 | Expression and phagocytic roles for the P2X7 receptor in the developing human CNS and its contribution to Programmed Cell Death (PCD). The scheme indicates that naturally occurring PCD is fundamental in CNS development, due to cell overproduction. It can be divided into: (i) target-independent PCD of proliferating neural stem/precursor cells or neuroblasts, and (ii) target-dependent PCD of postmitotic neurons after establishing synaptic contact with their targets. The phagocytosis and elimination of dead precursors (∼50–70% is eliminated by target-independent PCD prior to maturation) is mediated via the scavenger receptor P2X7 expressed by surrounding neurobalsts. The colonization of the developing CNS parenchyma by professional phagocytes (i.e., microglia/macrophages) or the full maturation of astrocytes occurs after 14–15 weeks of gestation (WG). Reproduced from Gu et al. (2015) under a Creative Commons (CC) license.

cells (Boison et al., 2010, 2012). As extensively reviewed elsewhere (Fredholm et al., 2005), activation of A_1 receptors inhibits the release of neurotrasmitters, such as dopamine and glutamate, and decreases neural excitability by inducing post-synaptic hyperpolarization. Conversely, A_{2A} receptors promote neurotransmitter release. Based on these interactions with glutamatergic and dopaminergic neurotransmission, a role for adenosine in neurodevelopmental defects at the basis of schizophrenia has been proposed (Lara and Souza, 2000; Lewis and Levitt, 2002; see section The Adenosine Dysfunction Hypothesis in Neurodevelopment). A role for A_{2B} and A_3 adenosine receptors (both expressed in brain) in neural development still remains to be unveiled.

NEURODEVELOPMENTAL DISORDERS ASSOCIATED TO ALTERATIONS IN PURINE AND PYRIMIDINE METABOLISM

Defects in Nucleotide Metabolism

Purine *de novo* biosynthesis is a complex, energy-expensive process. As depicted in **Figure 3**, it begins with the formation of phosphoribosyl pyrophosphate (PRPP) and leads to the first fully formed nucleotide, inosine 5′-monophosphate (IMP), which can be subsequently converted into either AMP or GMP (Kelley and Andersson, 2014). PRPP is also utilized to convert the nucleobase orotic acid into uridine monophosphate (UMP), the first step of the biosynthesis of pyrimidines. Alternatively, intracellular nucleosides coming from the diet or from the dephosphorylation of endogenous nucleotides can be recycled by the salvage pathway. The catabolism of residual free bases generates uric acid in case of purines, and β-alanine and β-aminoisobutyric acid in case of pyrimidines to be excreted as end products. Both *de novo* and salvage pathways are feedback-regulated by their end products, whereas purine catabolism is mostly regulated by substrate availability (Micheli et al., 2011). Only 10–30% of the free purines generated by intracellular metabolism are degraded or excreted (Torres and Puig, 2007), thus highlighting the importance of nucleotide salvage, which is fundamental in brain tissues; in addition, salvaged IMP from the liver is transported by erythrocytes to the brain and other tissues, where it is released for conversion to ATP or GTP (Ipata et al., 2011).

Considering the crucial roles of purines, pyrimidines, and their derivatives in brain development (see section Contribution of Purinergic Transmission to the Development of the Central Nervous System), it is evident that alterations in their synthesis, catabolism, and concentrations may lead to significant functional consequences. Inborn errors in purine metabolism are usually rare, and characterized by the absence or abnormal concentrations of purine nucleotides in cells, or by the presence of toxic intermediates in body fluids. At present, more than 35 enzyme defects of nucleotide synthesis, salvage, and catabolism of both purines and pyrimidines have been identified, some of which are associated with serious clinical consequences during development (**Table 1**; for review see Micheli et al., 2011). These disorders, previously considered as pediatric diseases, are

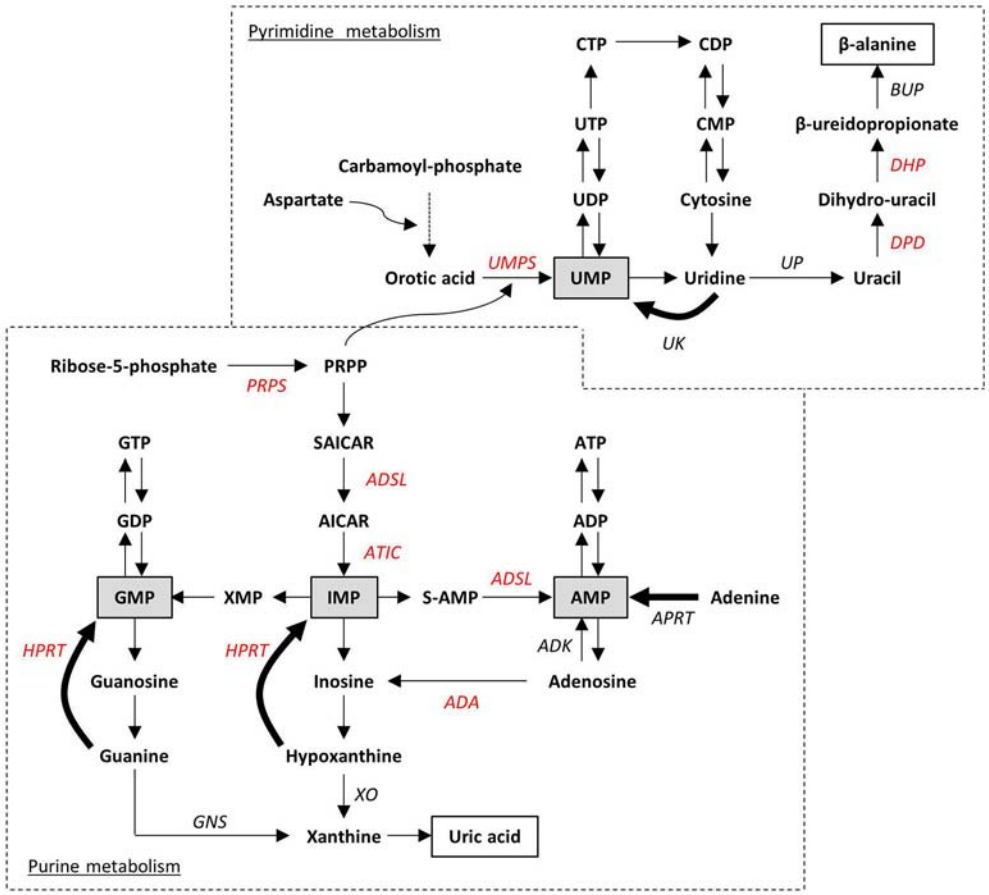

FIGURE 3 | Schematic representation of purine and pyrimidine metabolism. Ribose-5-phosphate and carbamoyl-phosphate are the starting points of the two *de novo* biosynthesis pathways. Salvage pathways are indicated with bold arrows. Monophosphate intermediates, representing the link between *de novo* biosynthesis and salvage pathways, are highlighted in gray boxes. End-products of purine and pyrimidine catabolism (i.e., uric acid and β-alanine) are in white boxes. Impairment at any enzymatic step can lead to inborn disorders. Enzymes whose altered functions have already been associated to the neurodevelopmental disorders described in the text are indicated in red. ADA, Adenosine deaminase; ADK, Adenosine kinase; ADSL, adenylosuccinate lyase; APRT, adenine phosphorybosyl-transferase; ATIC, AICA-ribotidetransformylase/IMP cyclohydrolase; BUP, β-ureidopropionase; DHP, dihydropyrimidinase; DPD, dihydropyrimidine dehydrogenase; GNS, guanase; HPRT, hypoxanthine-guanine phosphorybosyl-transferase; PRPP, 5-phosphorybosyl-1-pyrophosphate; PRPS, PRPP synthetase; S-AMP, adenylosuccinate; SAICAR: succinylaminoimidazole carboxamide ribotide; XO, xanthine oxydase; UK, uridine kinase; UMPS, UMP synthetase; UP, uridine phosphorylase.

now increasingly recognized in adults with milder phenotypes. Although purines and pyrimidines are essential in all tissues, the clinical outcomes of these disorders often suggest that the CNS is more seriously affected than other organs.

In the following paragraphs, we will introduce some of these disorders, focusing on the possible links between enzyme alterations during development and their neurological outcomes.

Defects in Purine *de Novo* Biosynthesis and Catabolism

PRPP synthetases (PRPS) catalyze PRPP synthesis from Mg-ATP and ribose-5-phosphate, and represent the first step in purine synthesis. Modulation of PRPS1 activity by its substrates, inhibitors (ADP and GDP), activators (Mg^{2+} and organic phosphate), and end-products determines the intracellular levels of PRPP, an essential cofactor for both *de novo* biosynthesis and salvage pathway (see section Defects in Nucleotide Metabolism; **Figure 3**; Micheli et al., 2011). Thus, defects in PRPS have serious consequences for several essential processes, such as nucleic acid synthesis, cellular metabolism, and signaling (de Brouwer et al., 2010).

Three isoforms of PRPS have been identified in humans, two of which are expressed in the brain: PRPS1 and PRPS2. In particular, altered activity of PRPS1 was associated to several distinct diseases. The most characterized is enzyme superactivity resulting from point mutations affecting the allosteric regions that regulate the enzyme switching off. Purine overproduction leads to hyperuricemia, and patients often show increased hypoxanthine and xanthine levels in cerebrospinal fluid (Torres et al., 2016). However, low purine nucleotide, in particular GTP, levels are observed, since the deregulated enzyme is also unstable and becomes inactive in anucleated or post-mitotic cells, such as erythrocytes and brain cells, in which the enzyme turnover is low or absent. Neurological outcomes include mental retardation,

TABLE 1 | Description of the most relevant pathologies where an involvement of purines and pyrimidines in neurodevelopmental alterations has been hypothesized or demonstrated.

Disease	Causes and incidence	Symptoms	References
ADA deficiency (ADA-SCID)	Autosomal recessive mutation in the ADA gene (20q13.12). Estimated incidence 1:200,000-1,000,000.	• Severe immunodeficiency • Seizures • Autistic behaviors	Bottini et al., 2001; Micheli et al., 2011
ADSL deficiency	Autosomal recessive mutation in the ADSL gene (22q13.1). Enzyme deficiency leads to accumulation of toxic derivatives of adenosine in body fluids. Rare disorder (80 patients worldwide).	• Developmental delay • Seizures • Hypotonia • Autistic features • Brain atrophy	Micheli et al., 2011; Jinnah et al., 2013
ATIC deficiency	Autosomal recessive mutation in the ATIC gene (2q35). Accumulation of toxic derivatives of adenosine in body fluids. One single case with complete deficiency of the ATIC enzyme was described.	• Intellectual disabilities • Blindness • Epilepsy	Marie et al., 2004
Autism spectrum disorder	Still to be clarified. The concurrence of genetic and environmental factors has been suggested. It manifests in the first 36 months of life. Estimated incidence 30-60:10,000.	• Impairments in social communication and interactions • Stereotyped repetitive behaviors • Affective instability	Voineagu et al., 2011; Lauritsen, 2013
Dihydropyrimidinase (DHP) deficiency	Autosomal recessive mutation in the DPYS gene (8q22). 11 cases with complete DHP absence have been described. Heterozygous subjects are asymptomatic and show some of the described symptoms upon 5-FU administration (pharmacogenetic syndrome).	• Developmental delay • Epilepsy	van Kuilenburg et al., 2003, 2010; Micheli et al., 2011
Dihydropyrimidine dehydrogenase (DPD) deficiency	Autosomal recessive mutation in the DPYD gene (1p21.3). Full or partial DPD deficiency is estimated to be present in about 3%-5% of the population. Most of them are asymptomatic. Some of the severe outcomes were observed upon administration of 5-FU (pharmacogenetic syndrome).	• Seizures • Motor and mental retardation • Autistic features • Gastroenteric disorders • Myelosuppression, myelopathy	van Kuilenburg et al., 2003
Down Syndrome (DS)	Trisomy of chromosome 21 leading to the aberrant overexpression of genes and miRNAs. Incidence: 1:700, 1:1,000 live births.	• Broad clinical spectrum • Platelet disorders • Cardiac alterations • Mental retardation • Accelerated aging with early deposition of β-amyloid-plaques and Alzheimer's-like features	Dierssen, 2012
Hereditary orotic aciduria (UMPS deficiency)	Autosomal recessive mutation in the UMPS gene (3q21). Rare disorder (20 cases worldwide).	• Orotic aciduria, crystalluria, • Megaloblastic anemia, immunodeficiency • Developmental delay • Motor impairment, hypotonia	Wortmann et al., 2017
Hypophosphatasia	Hypomorphic mutations in the *ALPL* gene, encoding TNAP Estimated incidence: 1/100.000.	• Rickets • Osteomalacia • Seizures	Whyte, 2010; Sebastián-Serrano et al., 2016
Lesch-Nyhan syndrome	X-linked mutation in the HPRT1 gene (Xq26.2-q26.3), producing a defective form of the enzyme. Uric acid precipitates in the body fluids. Alteration in dopamine levels, in particular in basal ganglia. Estimated incidence 1:500,000 (affects only males).	• Hyperuricemia, nephrolithiasis, gout • Dystonia, choreoathetosis, extrapyramidal symptoms • Intellectual disability, self-injurious behavior	Wong et al., 1996; Ceballos-Picot et al., 2009; Jinnah et al., 2013
PRPP synthetase 1 (PRPS1)-deficiency	X-linked point mutation in the PRPS1 gene, with partial or complete loss of enzymatic activity. The most severe outcome is Arts syndrome. Extremely rare.	• Developmental delay • Hypotonia, ataxia, hearing impairment, optic atrophy, peripheral neuropathy • Premature death due to recurrent infections	Duley et al., 2011

(Continued)

TABLE 1 | Continued

Disease	Causes and incidence	Symptoms	References
PRPS1-superactivation	X-linked point mutation in the PRPS1 gene (Xq22.4), leading to increased enzymatic activity in cells with high RNA/protein turnover. Conversely, the mutated enzyme is unstable in neural cells and erythrocytes, where very low residual activity was found. Rare disorder (30 families worldwide).	• Cognitive impairment • Ataxia • Hypotonia • Sensorineural deafness • Hyperuricemia, gout, kidney failure	Duley et al., 2011
Schizophrenia	Chronic and severe mental disorder with a typical onset in late adolescence or early adulthood. Caused by a combination of genetic susceptibility and environmental perturbations. Estimated incidence: 1.5:10,000.	• Positive symptoms: visual or auditory hallucinations • Negative symptoms: apathy, anhedonia and alogia • Cognitive symptoms: altered ability to think clearly and to sustain attention	Lewis and Levitt, 2002; McGrath et al., 2008

early-onset hypotonia, ataxia, delayed motor development, sensorineural deafness, and optic atrophy (de Brouwer et al., 2010). Interestingly, similar neurological symptoms are observed in patients affected by Arts syndrome, a severe disease in which a missense mutation completely inactivates PRPS1 (Duley et al., 2011). Other mutations in the same enzyme are associated to sensorineural symptoms (e.g., neuropathy, deafness) not directly related to specific defects in neurodevelopment. There is no univocal explanation of the variety of neurological symptoms, but increased oxypurine production and GTP depletion in the CNS could play an important role (de Brouwer et al., 2010).

The last steps of purine *de novo* biosynthesis (see **Figure 3**) require the sequential activity of two enzymes: adenosylosuccinate lyase (ADSL) and AICAR transformylase/IMP cyclohydrolase (ATIC). ADSL catalyzes both the conversion of succinylaminoimidazole carboxamide ribotide (SAICA-R) into AICA-ribotide (AICAR), and of adenylosuccinate (S-AMP) to AMP. Altered function of ADSL leads to the accumulation of succinyl-purines in body fluids, mainly in cerebrospinal fluid and urines, with consequent neurotoxic effects (Jinnah et al., 2013). The clinical manifestations of mutations in this enzyme are very diverse and include psychomotor retardation, seizures, and autistic features. The ratio between S-adenosine (a toxic intermediate produced by dephosphorylation of S-AMP) and SAICAR is inversely proportional to the onset and severity of symptoms.

ATIC deficiency, described in one single case, also leads to the formation of toxic intermediates, mainly AICAR and its ribosides (called ZMP, ZDP, and ZTP), with mental retardation, epilepsy, brachycephaly, dysmorphic features, and blindness (Marie et al., 2004). In this patient, erytrocyte ATP and AMP concentration was lowered by 60%, but no significant changes in other nucleotides were observed. AICAR is neurotoxic in undifferentiated neuroblastoma cells and triggers apoptosis, and shows a marked inhibition of carbohydrate and lipid metabolism in the liver through the activation of AMP-dependent protein kinase (AMPK; Garcia-Gil et al., 2006). ATIC deficiency and consequent depletion of purines could be particularly relevant during embryonic development and organogenesis, when *de novo* synthesis is more important. This consideration may be true for several other defects in purine and pyrimidine metabolism in which the link with some neurological features are not fully clarified.

Dysfunction in ADA, the enzyme catalyzing the deamination of adenosine to inosine (see section Contribution of Purinergic Transmission to the Development of the Central Nervous System), is correlated to a severe combined immunodeficiency (named ADA-SCID). Accumulation of adenosine affects physiological methylation reactions, induces apoptosis of thymic lymphocytes and inhibits ribonucleotide reductase, thus interfering with DNA synthesis and repair (Joachims et al., 2008); these effects could explain the immunological impairment observed in ADA-deficient patients. Neurological symptoms, such as seizures and autistic behaviors, usually absent in early infancy and increasing in severity with age, were also described. Interestingly, reduced ADA activity has been reported in the serum of autistic children, in association with a polymorphism in the ADA gene (Bottini et al., 2001). *In vivo* studies in animal models support the hypothesis of adenosine toxicity during embryonal life, similarly to what observed in lymphocytes (see above). Both receptor-mediated and receptor-independent mechanisms have been demonstrated to be at the basis of adenosine toxicity (Jacobson et al., 1999). When specific receptor subtypes are involved, high adenosine levels may either overactivate or inhibit cAMP signaling, thus starting a cascade of events that leads to impaired neurotransmission (see also section The Adenosine Dysfunction Hypothesis in Neurodevelopment).

These examples of alterations in purine biosynthesis and catabolism clearly highlight how the blockade of the same pathway can have distinct neurological outcomes. In some of these disorders the concentration of purine nucleotides in body fluids is only slightly changed, probably due to supply by the salvage pathway.

Deficiencies in the Purine Salvage Pathway

The hypoxantine-guanine phosphoribosyl transferase (HPRT) enzyme catalyzes the reutilization of hypoxantine and guanine in the energetically favorable synthesis of the nucleotides IMP and GMP, respectively, (see bold arrows in **Figure 3**). Any mutation in the human *HPRT1* gene, located on the X chromosome, produces defective forms of the enzyme that are unable to recycle nucleotides; thus, accelerated *de novo* biosynthesis is

stimulated as a result of the accumulation of PRPP and reduced inhibition by end-products (Deutsch et al., 2005). This unbalance causes overproduction of uric acid that can precipitate in body fluids with subsequent hyperuricemia, nephrolithiasis, and gout. The most severe disorder associated with a very low residual HPRT activity is Lesch-Nyhan syndrome, also characterized by motor impairment, with dystonia and extrapyramidal symptoms, intellectual disabilities, and dramatic compulsive self-mutilation such as biting digits, lips, or buccal mucosa (Nguyen and Nyhan, 2016). Treatment with allopurinol, an inhibitor of xanthine oxidase, reduces plasma concentrations of uric acid, with no effect on neurological symptoms (Deutsch et al., 2005), suggesting that in the brain more complex metabolic mechanisms are involved.

Although the pathogenesis of neurological and neurobehavioral manifestations is not clearly understood, several pieces of evidence support the idea that HRPT deficiency strongly influences early development of dopaminergic neurons (Ceballos-Picot et al., 2009; Kang et al., 2011). Post mortem brains from Lesch-Nyhan subjects did not show any morphological abnormality or signs of degeneration (Del Bigio and Halliday, 2007; Göttle et al., 2014). However, voxel-based morphometry imaging revealed a significant reduction of brain volumes in Lesch-Nyhan patients, likely due to developmental deficits, in particular in clusters of white matter including the nigrostriatal dopamine pathway (Schretlen et al., 2015). Moreover, positron emission tomography and autopsy studies showed a 60–90% reduction in both dopamine levels and dopamine uptake in basal ganglia of patients (Wong et al., 1996). In accordance, neurochemical analysis revealed alterations of brain neurotransmitters, with decreased dopaminergic synapses in the striatum (Visser et al., 2000). All these changes were consistent with the extrapyramidal symptoms of the syndrome.

Several authors have tried to explain the molecular link between the altered purine metabolism and neuronal development. It has been recently hypothesized that the excess in hypoxantine concentrations is the trigger for subsequent neurochemical abnormalities (Torres et al., 2016). Indeed, normal neurons are very efficient in consuming almost all the hypoxanthine synthesized from nucleotide catabolism and they release virtually no hypoxanthine into the culture medium. Due to feedback enzyme regulation, defective salvage is counterbalanced by an increased *de novo* purine synthesis. HPRT-deficient rat neuroblastoma cell line B103, used as an experimental *in vitro* model of the disease, showed normal excretion of xanthine, but hypoxanthine is not recycled to IMP, leading to a 15-fold increase in extracellular hypoxanthine excretion (Pelled et al., 1999). These abnormal concentrations of hypoxantine, in turn, diminish adenosine uptake into the cells by a competitive mechanism through equilibrative nucleoside transporters (Prior et al., 2007) and increase extracellular adenosine concentrations, thus prolonging the activation of its receptors. As mentioned above, one of the main effects of adenosine in the CNS is the inhibition of neurotransmitter release through the A_1 receptor subtype, with decreased neural excitability by post-synaptic hyperpolarization. However, adenosine can also induce opposite effects through the A_{2A} receptor (Fredholm et al., 2005). These receptor subtypes are expressed in different areas of the developing brain, and their timely recruitment regulates a correct integration between excitatory and inhibitory processes. It is likely that in Lesch-Nyhan syndrome excitatory A_{2A}-mediated signaling is predominant compared to A_1-mediated inhibitory effects. Thus, alterations in adenosine levels generate an imbalance in neurotransmission, that could be responsible for some of the symptoms observed in patients, including aggressive and self-injurious behaviors. Moreover, in post mitotic neurons hypoxanthine also increases the expression of the adenosine A_{2A}, dopamine D1, and serotonin 5-HT_7 receptors further potentiating their signaling (Torres and Puig, 2015).

Neurodevelopmental Diseases and Pyrimidine Metabolism

Ten defects in pyrimidine metabolism have been described, but their incidence is probably underestimated (Balasubramaniam et al., 2014). As for purines, pyrimidine-based compounds are ubiquitous, and this may explain the clinical heterogeneity of the symptoms of the deficiency of specific enzymes. Clinical manifestations include unexplained anemia, delayed development, seizures, neonatal fitting, microcephaly, mental retardation, and dysmorphic features.

The typical disorder of pyrimidine metabolism is orotic aciduria, known as a megaloblastic anemia accompanied by renal impairment, due to a deficiency in uridine monophosphate synthetase (UMPS; see **Figure 3**), a bifunctional enzyme in the *de novo* pyrimidine synthesis. The first reaction catalyzes the conversion of orotate to orotidine monophosphate, thanks to orotate phosphoribosyltransferase (OPRT) activity. In the second step, orotidine decarboxylase (ODC) generates UMP. Very high orotate levels (up to 400-fold compared to control subjects) are found in urine and plasma of patients suffering from the disease (Wortmann et al., 2017). Children with UMPS deficiency have a strong pyrimidine starvation and, if untreated, can develop growth retardation, intellectual disability, and epilepsy.

Interestingly, pyrimidine nucleotide starvation can be partially rescued by exogenous administration of uridine (see section Toward a Purinergic-Based Therapy for Congenital Neurodevelopmental Disorders?). Indeed, dietary pyrimidines (mainly cytosine and uracil derivatives) are able to pass into the circulation, where they are salvaged starting from their nucleosides (cytidine and uridine, respectively). Conversely, most purines do not enter the bloodstream as they are converted to uric acid during their transit across the small intestine (Duley et al., 2011). Uridine has been utilized in clinics as an anticonvulsant in the treatment of autism-associated seizures (Kovács et al., 2014).

A small number of patients show specific enzymatic deficiencies in the catabolic pathways for pyrimidines, mostly showing with mental retardation, seizures, or both. In this case, toxic accumulation of pyrimidines and their metabolites were found. Dihydropirimidine dehydrogenase (DPD) catalyzes the first step of the catabolism of pyrimidine bases, i.e., the reduction of uracil and thymine to dihydrouracil and dihydrothymine, respectively. Point mutations in the DPYD gene

lead to a defective enzyme that, in homozygous subjects, results in thymine-uraciluria. Complete DPD-deficiency is associated to convulsions, motor, and mental retardation in the most severe forms, with autistic features and NMR evidence of severe delay in brain myelination (Enns et al., 2004). Usually, psychomotor development is normal at birth, but progressively worsens during the first years of life with speech retardation and various degrees of developmental delay (van Kuilenburg et al., 2010). Heterozygous subjects are usually asymptomatic, but can show gastroenteric disorders, myelosuppression, cerebellar ataxia, mental deterioration, and myelopathy if treated with the DPD substrate 5-fluorouracil (5-FU), a pyrimidine analog widely used as antineoplastic drug. In fact, enzyme deficiency prevents the degradation of 5-FU, whose accumulation quickly reaches toxic concentrations (van Kuilenburg et al., 2003).

The second enzyme of pyrimidine catabolism is dihydropirimidinase (DHP), responsible for the reversible hydrolysis of dihydrouracil and dihydrothymine coming from the previous step to N-carbamyl-β-alanine and N-carbamyl-β-aminoisobutyric acid, respectively. DHP is expressed in liver and kidney, whereas no activity was found in brain. However, DHP-deficient subjects can show strong neurological manifestations similar to those observed in DPD deficiency, including the pharmacogenetic syndrome induced by 5-FU. In fact, toxic accumulation of dihydropyrimidines was found not only in blood, but also in cerebrospinal fluid, thus confirming that these metabolites cross the blood-brain barrier (van Kuilenburg et al., 2003).

Defects in Purine Metabolism and Abnormal Brain Development: The Case of Tissue Non-specific Alkaline Phosphatase (TNAP)

As highlighted in section Contribution of Purinergic Transmission to the Development of the Central Nervous System, during CNS development both extracellular nucleotides and nucleosides are directly involved in the timely and accurate modulation of neural precursor proliferation, migration, and differentiation. Among the various metabolic pathways leading to increased adenosine concentrations, a tight control of the enzymatic processes driving adenine nucleotide dephosphorylation is therefore mandatory to guarantee the correct balance between these two classes of signaling molecules.

Among enzymes involved in nucleotide catabolism, tissue non-specific alkaline phosphatase (TNAP) is peculiarly expressed in mineralizing bones, in the kidney, and in the CNS (Sebastián-Serrano et al., 2015). The main function of TNAP is to hydrolyze extracellular inorganic pyrophosphate (PPi), a potent mineralization inhibitor, thus enabling the deposition of hydroxyapatite in bones and teeth (Sebastián-Serrano et al., 2015). Additionally, TNAP is highly expressed at early stages of CNS development when proliferation of neural precursors and migration of their progeny toward their final position in the brain take place (see also Contribution of Purinergic Transmission to the Development of the Central Nervous System). Specifically, strong TNAP activity is observed at embryonic day 14 in the ventricular/subventricular zone where neural precursors are located and reside until adulthood (Langer et al., 2007). The direct role of TNAP in proliferation and differentiation processes during CNS development is still elusive, but it has now become evident that purinergic signaling plays a fundamental role in modulating proliferation, differentiation and migration capacity of neural precursors and of newborn neurons and glia cells (see Contribution of Purinergic Transmission to the Development of the Central Nervous System; Suyama et al., 2012; Boccazzi et al., 2014). Moreover, purinergic signaling is also crucially involved in axon guidance and growth and in the establishment of correct synaptic contacts, and high TNAP activity has also been documented at the stages of intensive synaptic generation and plasticity (Sebastián-Serrano et al., 2015). Based on TNAP ability to fine-tune the balance between extracellular nucleotides and nucleosides, it is therefore conceivable that this enzyme might be crucially involved in controlling the delicate phases of the building of the correct brain architecture, and in modulating the activation of specific purinergic receptors.

TNAP can also dephosphorylate pyridoxal-5′-phosphate (PLP, the active form of vitamin B6) to pyridoxal, which in turn enters the cytoplasm where it is rephosphorylated and acts as cofactor for the synthesis of enzymes involved in the metabolism of various neurotransmitters (e.g., GABA, serotonin; Amadasi et al., 2007).

Based on the above-mentioned localization and activities of TNAP, it can be speculated that defects in its expression would lead to significant pathological outcomes. In fact, hypomorphic mutations in the *ALPL* gene encoding TNAP lead to accumulation of PPi in the extracellular matrix with deficits in bone mineralization, causing hypophosphatasia, a heritable form of rickets in children or osteomalacia in adults (**Table 1**; Whyte, 2010). Although the exact consequences of these mutations on brain development have not been clarified yet, TNAP knock-out mice show abnormalities in myelination and synaptogenesis (Hanics et al., 2012), and subjects with hypophosphatasia suffer from seizures (Whyte, 2010), thus indicating defects in neurotransmission and/or in neurodevelopment (Fonta et al., 2015). Recent data have now started to link these defects and clinical manifestations to altered purinergic transmission, with the first demonstration of a direct involvement of an aberrant P2X7 activation in the alterations of hippocampal and cortex structure and in the development of seizures in TNAP$^{-/-}$ mice, due to high ATP concentrations as a consequence of reduced TNAP activity (Sebastián-Serrano et al., 2016). This observation would greatly help the development of possible new pharmacological approaches to the pathology.

OTHER DISORDERS POTENTIALLY DUE TO ABNORMALITIES OF PURINE NEUROMODULATION DURING DEVELOPMENT

Involvement of the Purinergic System in Brain Alterations Observed in Down Syndrome

Down Syndrome (DS) represents the most typical example of genetic disorder associated to mental retardation. Trisomy of

chromosome 21 leads to the pathological overexpression of various gene products and miRNAs, but also to additional alterations spanning from the deregulation of non-coding DNA, the abnormal expression of non-HSA21 (non-*Homo sapiens* autosome 21) genes and epigenetic modifications (for review see Dierssen, 2012). These genetic abnormalities lead to a consequent dysregulation of related biochemical pathways in all tissues (**Table 1**; Spellman et al., 2013), but the most relevant alterations are localized in the brain, with consequent moderate to severe mental retardation (Dierssen, 2012). The most evident anatomical correlates of mental retardation in DS children and fetuses are brain hypoplasia and hypocellularity, leading to a decreased brain size (Rachidi and Lopes, 2008). Consistent with this observation, many groups have detected an impaired proliferation of neural precursors and reduction in neurogenesis in the developing neocortex, hippocampus, and cerebellum of mouse models of DS and of DS fetuses (Contestabile et al., 2007, 2009; Guidi et al., 2008). In the adult brain the above-mentioned modifications also translate in reduced spine density and impaired synaptic plasticity, paralleled by profound alterations in several neurotransmitter pathways (i.e., GABA, glutamate, serotonin etc.), with a consequent imbalance between excitatory and inhibitory neurotransmission mostly in the hippocampus (Dierssen, 2012). Additionally, amyloid precursor protein (APP) is triplicated in DS and it is believed to contribute to neurodevelopmental alterations and to trigger the development of Alzheimer-like pathology in DS adults (Stagni et al., 2017). As extensively reviewed elsewhere (Stagni et al., 2017), various biochemical pathways have been causally associated to the impairment of neurogenesis and the consequent shift in cell destiny leading to reduced neurons and increased percentage of astrocytes.

The first, and up to now the only available, hint of altered purinergic signaling in DS came indirectly from the observation that lack of sortin nexin 27 (SNX27), a PDZ-containing protein of the endosome-associated retromer complex controlling the trafficking of several proteins (Carlton et al., 2005), leads to severe impairment of brain functions, including cognitive manifestations mimicking those observed in DS (Wang et al., 2013, 2014). Additionally, SNX27 is down-regulated in Ts65Dn mice, the most common mouse model of DS, as a consequence of the hyperexpression of miR-155 which is physiologically responsible for its degradation (Wang et al., 2013, 2014). Our research group got interested in SNX27 while searching for the biochemical pathways responsible for the membrane-to-cytosol recycling or intracellular degradation of the G protein-coupled P2Y-like receptor GPR17. GPR17 responds to both extracellular uracil nucleotides (UDP, UDP-glucose) and cysteinyl-leukotrienes (Ciana et al., 2006). GPR17 is highly expressed by cells of the oligodendrocyte lineage, specifically during the transition from OPCs to immature oligodendrocytes. After this stage, GPR17 expression must be down-regulated to promote the generation of fully myelinating mature cells (Lecca et al., 2008; Chen et al., 2009; Boda et al., 2011; Ceruti et al., 2011; Fumagalli et al., 2011, 2015). In agreement with these findings, forced overexpression of GPR17 during late stages of differentiation leads to defective myelination *in vitro* and *in vivo*, whereas *in vivo* GPR17 knock-out accelerates oligodendrocyte myelination (Chen et al., 2009). Based on these data, we evaluated the possible involvement of SNX27 in the fine-tuned regulation of GPR17 membrane expression, and demonstrated that the endocytic trafficking of the receptor is mediated by the interaction of a type I PDZ-binding motif located at its C-terminus with SNX27. Additionally, SNX27 knock-down *in vitro* reduced GPR17 plasma membrane recycling in differentiating oligodendrocytes while fostering their terminal maturation (Meraviglia et al., 2016). When analyzing the brains of Ts65Dn mice, we observed that trisomy-linked down-regulation of SNX27 was paralleled by decreased GPR17 expression and increased number of mature oligodendrocytes, which, however, fail in reaching full maturation, eventually leading to brain hypomyelination (Meraviglia et al., 2016; **Figure 4**).

We therefore speculate that altered GPR17 signaling and oligodendrocyte maturation, with consequent defective axon myelination, could contribute to the overall brain pathological phenotype of DS, both in terms of brain structure and functions.

New Perspectives for the Identification of Causative Genes Involved in Mental Retardation: The Example of PANX1

The availability of innovative and automated strategies to evaluate the presence of gene variants and mutations is accelerating our comprehension of the genetic alterations at the basis of rare or sporadic pathological phenotypes, such as some forms of mental retardation. The discovery of the first patient bearing a homozygous Pannexin 1 (Panx1) loss-of-function gene variant associated with multisystem dysfunction and intellectual disability has been recently published (Shao et al., 2016). Panx1 is a membrane channel allowing the passage of ions and small molecules, among which ATP is one of the most common (Boyce and Swayne, 2017). In the CNS, Panx1 is highly expressed by developing and mature neurons, and contributes to brain development, maturation, and to synaptic plasticity (Wicki-Stordeur et al., 2016). Thus, reduced ATP release in the presence of mutated Panx1 could lead to defective purinergic transmission which in turn could be responsible for alterations in brain structures and mental retardation. It is worth mentioning that a close relationship has been demonstrated between Panx1 and the P2X7 receptor subtype, which is crucially involved in brain development (see Contribution of Purinergic Transmission to the Development of the Central Nervous System). Data demonstrate that the two proteins can physically interact (Boyce and Swayne, 2017) and that ATP released through Panx1 in the microenvironment of P2X7 receptor ultimately leads to its activation. Defects in this signaling pathway can therefore have profound impact on brain development during embryonic and fetal life and on intellectual functions after birth.

Maternal Immune Activation and Neurodevelopmental Abnormalities: The Role of Purinergic Signaling

It is now increasingly recognized that inflammation is a crucial contributor to an altered fetal brain development (Hagberg et al.,

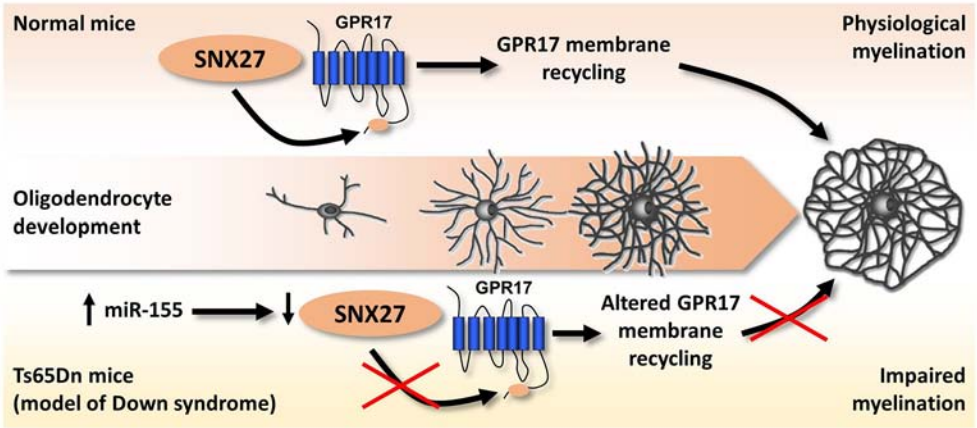

FIGURE 4 | Altered SNX27/GPR17 interaction and impaired myelination in a mouse model of DS. During physiological oligodendrocyte maturation, GPR17 must be downregulated at a specific step of oligodendrocyte differentiation to allow the transition from mature to fully myelinating cells. SNX27 promotes and controls oligodendrocyte maturation, by guiding the membrane recycling and degradation of GPR17 receptor through the binding to a type I PDZ-binding motif located at its C-terminus. In the brains of Ts65Dn mice (an animal model of DS), trisomic miR-155 leads to SNX27 degradation, which in turn dysregulates GPR17 membrane expression leading to its precocious downregulation. We hypothesize that this event is crucially related to the altered pattern of myelination observed in Ts65Dn mouse brains, with reduced expression of myelin proteins, which could significantly affect cognitive functions. See text and Meraviglia et al. (2016) for details.

2015). In particular, epidemiological studies have shown that maternal infection is an important environmental risk factor for neurodevelopmental disorders (Boksa, 2010). In preclinical animal models, perinatal infection has been indeed reported to cause maternal immune activation (also called mIA) that is associated with later appearance of autism spectrum disorder, and schizophrenia by altering fetal brain development at critical periods of pregnancy (Knuesel et al., 2014; Estes and McAllister, 2016; **Table 1**).

Although the initial prenatal insult alone may not be enough for clinical manifestation in human, many studies have focused on animal models of maternal infection to investigate the causal chain of events linking immune exposure and genetic predisposition, to neurodevelopmental abnormalities, as extensively reviewed elsewhere (Knuesel et al., 2014). Maternal infection is mainly mimicked by exposing pregnant rats to either LPS, or the inflammatory viral mimetic polyinosinic:polycytidylic acid (poly I:C) in the gestational period or by direct intrauterin administration of LPS (Cai et al., 2000; Bell and Hallenbeck, 2002). Immune mediators (cytokines and chemokines), reactive oxygen or nitrogen species, excitotoxicity, mitochondrial impairment, and altered vascular integrity have been described to be critical contributors to abnormal brain development in the offspring after maternal immune activation (Hagberg et al., 2015). In particular, microglial priming and elevation of maternal pro-inflammatory cytokines (i.e., TNF-α, IL-6, IL1-β) have been casually linked to dysregulation of fundamental neurodevelopment programs (Vargas et al., 2005; Morgan et al., 2010; Upthegrove et al., 2014). In this respect, members of the nucleotide-binding domain-like receptor (NLR) protein family act as inflammasome sensors, and mediate the translation of maternal immune activation to pathologically relevant neurodevelopmental abnormalities. Inflammasomes critically control different aspects of innate immunity, including the release of pro-inflammatory cytokines that induce and sustain the inflammatory response (Latz et al., 2013). The NLRP3 inflammasome is one of the major signaling routes that mediates the shift from innate immune activation to inflammation in response to different pathogenic or endogenous danger signals, including ATP (de Torre-Minguela et al., 2017). ATP-dependent stimulation of P2X7 receptors indeed promotes inflammasome activation, leading to caspase-1 cleavage and release of mature IL1-β (Ferrari et al., 2006; Di Virgilio et al., 2017). In line with this, recent data have demonstrated that both genetic deletion and the pharmacological inhibition of P2X7 receptors mitigate schizophrenia-like behavioral changes in a phencyclidine-induced rodent model of schizophrenia (Koványi et al., 2016).

Another study has revealed the critical role of P2X7 receptor in affecting astrocyte-neuron cross-talk after LPS prenatal exposure. The infection during gestation triggers the release of ATP from astrocytes via Cx43 and Panx1 unopposed channel, resulting in increased neuronal death mediated by P2X7 receptors and Panx1 channels (Avendano et al., 2015).

Maternal inflammation induced by perinatal infections can also result in preterm infants (Hagberg et al., 2012). Diffuse perinatal white matter injuries, including periventricular leukomalacia caused by ischemic damage, are the most common type of brain injury in preterm infants. Pathological demyelination and impaired oligodendrocyte maturation are known to cause cerebral palsy, and cognitive, behavioral, and sensory deficits as well as psychological problems later in life (van Tilborg et al., 2016). As detailed in section Toward a Purinergic-Based Therapy for Congenital Neurodevelopmental Disorders?, administration of UDP-glucose, acting on different purinergic receptors, has proven successful in improving the survival of newly generated oligodendrocytes in neonatal rats with ischemic

TABLE 2 | Purine- and pyrimidine-based pharmacological approaches to modulate congenital neurodevelopmental disorders and their functional outcomes.

Neurodevelopmental disorder	Approach	Target receptor(s)	Effects	References
Autism spectrum disorder	Suramin (SAT-1 translational pilot study)	P2 receptors	↑ language and social interactions ↓ repetitive behaviors	Naviaux et al., 2017
	Ketogenic diet	Mainly A_1 receptors (increased activity)	↑ cognition, mood, behavior and social life	Masino et al., 2011b, 2013
HPRT deficiency	SAM	None	↓ self-injurious behavior	Chen et al., 2014
Ischemic periventricular leukomalacia	UDP-glucose	Activation of $P2Y_{14}$ and GPR17 receptors	↑ proliferation and differentiation to mature oligodendrocytes of glial progenitors in the subventricular zone	Mao et al., 2012; Li et al., 2015
PRPS1-related disorders (including Arts syndrome)	SAM	None	↓ neurological symptoms	de Brouwer et al., 2010
Schizophrenia	Strategies to upregulate extracellular adenosine (see text)	Mainly A_1 receptors (increased activity)	↓ psychotic symptoms	Shen et al., 2012
	JNJ-47965567	Block of P2X7 receptor	↑ of social interactions (phencyclidine-induced schizophrenia)	Koványi et al., 2016
UMPS deficiency	UMP and CMP administration	None	↓ neurological and non-neurological symptoms	Nyhan, 2005

periventricular leukomalacia (Mao et al., 2012; Li et al., 2015; **Table 2**).

Interestingly, another approach targeting purinergic receptors with suramin has been reported to correct the autism spectrum disorder-like phenotype and to restore normal social behavior in a maternal immune activation murine model of autism-like behaviors using polyI:C exposure, and in the Fragile X (*Fmr1* knockout) model (Naviaux et al., 2013, 2015; **Table 2**). These effects have been ascribed to the capability of the anti-purinergic treatment to normalize the expression of two purinergic receptors ($P2Y_2$ and P2X7) and the phosphorylation of ERK1, ERK2, and CAMKII, all of which modulate purinergic signaling. In addition, suramin has been reported to correct the concentrations of some altered purine metabolites (9 out of 11, including ATP and allantoin) in the plasma of mice subjected to maternal immune activation (Naviaux et al., 2013, 2014, 2015). Metabolomic studies have also revealed similar alterations in the purine and pyrimidine metabolite profile in human biofluids (urines and plasma) of children suffering from autism spectrum disorder (Gevi et al., 2016). Moreover, purinergic signaling in the brain has been identified as one of the top-regulated gene expression pathways correlated with abnormal behaviors in children with autism spectrum disorder suggesting a key role of purines in driving a cell danger response in these disorders (Ginsberg et al., 2012).

Although the molecular basis of the altered purine metabolism in murine models of autism spectrum disorder still remains to be elucidated, these data suggest that metabolic pathways that synthesize and catabolize purines are critical regulatory elements in autism spectrum disorder, in accordance with their increasingly recognized role in promoting other neurodevelopmental and behavioral abnormalities (Micheli et al., 2011, see sections Defects in Nucleotide Metabolism and Toward a Purinergic-Based Therapy for Congenital Neurodevelopmental Disorders?).

THE ADENOSINE DYSFUNCTION HYPOTHESIS IN NEURODEVELOPMENT

Interestingly, as elegantly summarized in a previously published review (Boison et al., 2012), it has been proposed that dysfunctions in normal adenosine homeostasis during critical early brain development may have important consequences on the formation of neuronal circuitries, thus contributing to the neurodevelopment alterations at the basis of schizophrenia (Lara and Souza, 2000; Lara et al., 2006). In particular, abnormal adenosine levels (consequent to brain insults, such as hypoxia, seizures, infections, and trauma, eventually leading to ATP breakdown or due to altered control exerted by adenosine kinase; Cunha, 2001; Dunwiddie and Masino, 2001; Boison et al., 2010) have been described to induce primary brain changes. In line with these observations, administration of an A_1 adenosine receptor agonist immediately after birth leads to ventricular enlargement and widespread gray and white matter alterations (Turner et al., 2002), paralleled by a reduction in A_1 receptor density. Furthermore, magnetic resonance imaging (MRI) studies in schizophrenic patients have revealed diffuse gray and white matter changes (Davis et al., 2003), that could be also related to early adenosine alterations. Interestingly, in the

immature brain adenosine in mostly toxic to axons, which is in agreement with high neuronal density and reduced arborization in schizophrenic brain (Davis et al., 2003). These events would lead to deficit of adenosine-mediated inhibitory actions due to a partial loss of A_1 receptors, which has been proposed to increase brain vulnerability to damage in the adulthood. In fact, it results in increased basal dopaminergic activity, due to attenuation of the tonic inhibition of dopamine release, leading to positive symptoms of the pathology (e.g., hallucinations), and in augmented vulnerability to excitotoxic glutamate in mature brain. On these bases, pharmacological treatments enhancing adenosine activity could be effective for symptoms control in schizophrenia (Shen et al., 2012; see section Toward a Purinergic-Based Therapy for Congenital Neurodevelopmental Disorders?).

Of note, several studies have also shown that adenosine plays a key role in reducing multiple behavioral symptoms of autism (Tanimura et al., 2010; Masino et al., 2011a), based on the well-established role of this purine nucleoside as anti-convulsant, sleep-promoter and anxiolytic (Ribeiro et al., 2002; see section Toward a Purinergic-Based Therapy for Congenital Neurodevelopmental Disorders? and **Table 2**).

TOWARD A PURINERGIC-BASED THERAPY FOR CONGENITAL NEURODEVELOPMENTAL DISORDERS?

Overall, the above-mentioned evidence suggests that purinergic signaling is directly involved in many neurodevelopmental alterations that eventually lead to severe congenital disorders. In the case of exclusively genetic pathologies, the ideal strategy would be to fully restore the deficits by gene therapy. This has been successfully obtained for children affected by ADA-SCID (see section Defects in Purine *De Novo* Biosynthesis and Catabolism), by unconditioned hematopoietic stem cell transplant (Ferrua and Aiuti, 2017), due to the predominant peripheral manifestations of the pathology. To date, the correction of neurodevelopment defects through genetic *in utero* manipulation of defective pathways is still a matter of debate, also due to significant ethical issues. Thus, when modifications in enzyme and receptor activity are involved, acting pharmacologically after birth to restore defective functions can represent an innovative and feasible strategy to alleviate the symptoms.

One possibility is the dietary administration of the end-products of defective pathways. Concerning diseases linked to altered nucleotide and nucleoside metabolism (see section Neurodevelopmental Disorders Associated to Alterations in Purine and Pyrimidine Metabolism), depletion of the purine nucleotide pools observed in patients completely lacking PRPS1 or having some residual enzyme activity induces a significant ATP starvation, that results in a strong energy impairment in neurons. Ideally, direct brain administration of adenosine would be the best therapeutic strategy, as it is efficiently salvaged to corresponding nucleotides by adenosine kinase. Unfortunately, as already mentioned (see section Neurodevelopmental Diseases and Pyrimidine Metabolism), dietary adenosine itself is not absorbed by the intestine, but S-adenosylmethionine (SAM) can function as cargo to cross both the gut and the blood-brain barriers; accordingly, it has been already successfully used to treat some cases of Arts syndrome (see section Defects in Purine *de Novo* Biosynthesis and Catabolism; de Brouwer et al., 2010). Moreover, SAM has been demonstrated to reduce self-injurious behavior in children with HPRT deficiency (Chen et al., 2014). The main risk of SAM administration is the possible generation of homocysteine with consequent vascular toxicity. Thus, its extensive use in clinics should be carefully evaluated.

UMP and CMP administration was reported to have a therapeutic effect in subjects with UMPS deficiency, likely due to dephosphorylation to their respective nucleosides, able to cross the plasma membrane. Uridine supplementation was also shown to provide a good source for salvage to UMP, displaying remarkable effects on both neurological and non-neurological symptoms and even complete remission in patients with pyrimidine deficiency (Nyhan, 2005). Conversely, uracil was ineffective.

Based on the known role of purines in promoting myelination (see section Contribution of Purinergic Transmission to the development of the Central Nervous System), the presence of congenital white matter abnormalities is suggestive of alterations of specific purinergic signaling pathways. Of note, the long-term prognosis of neonatal rats with cerebral white matter injury due to ischemic periventricular leukomalacia (see section Maternal Immune Activation and Neurodevelopmental Abnormalities: the Role of Purinergic Signaling) was significantly improved by the intraperitoneal injection of UDP-glucose, an endogenous agonist acting on different purinergic receptor subtypes, including GPR17 receptor (a key determinant of oligodendrocyte maturation and differentiation; see section Involvement of the Purinergic System in Brain Alterations Observed in Down Syndrome). UDP-glucose stimulated the proliferation of glial progenitor cells derived from both the ventricular/subventricular zone and white matter, promoted their differentiation into mature oligodendrocytes, and raised the survival rate of newly generated glial cells (Mao et al., 2012; Li et al., 2015). Based on the observed dysfunctions in the pattern of myelination accompanied by reduced GPR17 expression in brains from a mouse model of DS (see section Involvement of the Purinergic System in Brain Alterations Observed in Down Syndrome), it can be speculated that the pharmacological manipulation of this receptor could prove effective in reducing DS-linked intellectual disabilities.

Autism spectrum disorder is currently lacking pharmacological approaches, also due to the wide range of associated symptoms and clinical manifestations. Based on the promising findings on a mouse model of the disease (see section Maternal Immune Activation and Neurodevelopmental Abnormalities: the Role of Purinergic Signaling), a recent small, phase I/II, randomized clinical trial has been carried out to examine the safety and activity of a single intravenous low-dose of suramin in children with autism spectrum disorder D. The Suramin Autism Treatment-1 (called SAT-1) was a double-blind, placebo controlled, translational pilot study that

showed improvements in language, and social interaction and decreased repetitive behaviors (Naviaux et al., 2017). Despite some limitations of this study, included its small size and the suboptimal timing of the outcome measurements, and the need to confirm the results in a larger number of children (Naviaux et al., 2017), the SAT-1 trial highlighted suramin as an encouraging innovative approach for autism spectrum disorder therapy.

Furthermore, results from diverse clinical trials have shown that a ketogenic diet (a high fat, low carbohydrate, adequate protein formula which promotes the use of ketones, rather than glucose, for energy production) can improve cognition, mood, behavior, and social life in autism spectrum disorder patients. Interestingly, these positive effects have been also ascribed to an augmented action of adenosine at A_1 receptors, leading to opening of K^+ channels and membrane hyperpolarization/reduced excitability (Kawamura et al., 2010; Masino et al., 2011b). Currently, two independent studies on the effects of an intermittent ketogenic diet on the behavior of children with autism spectrum disorder have been performed, and results indicated that the most significant improvements were noticed in patients showing only mild autistic behavior (Herbert and Buckley, 2013; Masino et al., 2013).

Likewise, patients affected by schizophrenia would benefit from increased adenosine receptor activity (see section The Adenosine Dysfunction Hypothesis in Neurodevelopment). Promising strategies to upregulate extracellular adenosine are represented by the inhibition of adenosine kinase (e.g., with direct inhibitors, ketogenic diet that downregulate the enzyme, or allopurinol and dipyridamole, which augment extracellular adenosine by inhibiting its degradation and reuptake) and by the use of brain implants of adenosine-releasing cells (Shen et al., 2012).

It is therefore evident that encouraging attempts to pharmacologically target the purinergic system in disorders associated to neurodevelopment have been already performed (see **Table 2** for summary). Future research should now move to different directions: (i) to implement the knowledge on the physiological role played by purines/pyrimidines in controlling and promoting CNS development (see section Contribution of Purinergic Transmission to the Development of the Central Nervous System); (ii) to highlight the contribution to altered neurodevelopmental stages of dysfunction/mutations of specific enzymes or receptor subtypes and of their cross-talk [e.g., the TNAP enzyme and the P2X7-Pax1 complex; see sections Defects in Purine Metabolism and Abnormal Brain Development: the Case of Tissue Non Specific Alkaline Phosphatase (TNAP) and New Perspectives for the Identification of Causative Genes Involved in Mental Retardation: the Example of PANX1]; (iii) to foster the design and synthesis of more selective, potent, and brain permeable ligands, and their evaluation in pre-clinical animal models of the diseases. The goal to cure congenital neurodevelopmental disorders through the purinergic system will be only achieved thanks to the collaborations of different and complementary scientific expertizes, including neuroscience, neurobiology, genetics, physiology, neuropharmacology, and medicinal chemistry.

AUTHOR CONTRIBUTIONS

All authors listed have made a substantial, direct and intellectual contribution to the work, and approved it for publication.

FUNDING

This work was supported by: Fondazione AriSLA, Milan, Italy (grant number GPR17ALS to MF); Merck_Serono Grant for Multiple Sclerosis Innovation (grant number GMSI-2015 to MF as participant); Università degli Studi di Milano, piano di sostegno alla Ricerca 2015/2017, linea 2—AZIONE A to MF and to DL; Fondazione Italiana Sclerosi Multipla (FISM; grant number 2013/R/1 to MA).

REFERENCES

Abbracchio, M. P., Burnstock, G., Boeynaems, J. M., Barnard, E. A., Boyer, J. L., Kennedy, C., et al. (2006). International Union of Pharmacology LVIII: update on the P2Y G protein-coupled nucleotide receptors: from molecular mechanisms and pathophysiology to therapy. *Pharmacol. Rev.* 58, 281–341. doi: 10.1124/pr.58.3.3

Amadasi, A., Bertoldi, M., Contestabile, R., Bettati, S., Cellini, B., di Salvo, M. L., et al. (2007). Pyridoxal 5′-phosphate enzymes as targets for therapeutic agents. *Curr. Med. Chem.* 14, 1291–1324. doi: 10.2174/092986707780597899

Avendano, B. C., Montero, T. D., Chavez, C. E., von Bernhardi, R., and Orellana, J. A. (2015). Prenatal exposure to inflammatory conditions increases Cx43 and Panx1 unopposed channel opening and activation of astrocytes in the offspring effect on neuronal survival. *Glia*. 63, 2058–2072. doi: 10.1002/glia.22877

Balasubramaniam, S., Duley, J. A., and Christodoulou, J. (2014). Inborn errors of pyrimidine metabolism: clinical update and therapy. *J. Inherit. Metab. Dis.* 37, 687–698. doi: 10.1007/s10545-014-9742-3

Bélanger, M., Allaman, I., and Magistretti, P. (2011). Brain energy metabolism: focus on astrocyte-neuron metabolic cooperation. *Cell Metab.* 14, 724–738. doi: 10.1016/j.cmet.2011.08.016

Bell, M. J., and Hallenbeck, J. M. (2002). Effects of intrauterine inflammation on developing rat brain. *J. Neurosci. Res.* 70, 570–579. doi: 10.1002/jnr.10423

Boccazzi, M., Rolando, C., Abbracchio, M. P., Buffo, A., and Ceruti, S. (2014). Purines regulate adult brain subventricular zone cell functions: contribution of reactive astrocytes. *Glia* 62, 428–439. doi: 10.1002/glia.22614

Boda, E., Nato, G., and Buffo, A. (2017). Emerging pharmacological approaches to promote neurogenesis from endogenous glial cells. *Biochem. Pharmacol.* 141, 23–41. doi: 10.1016/j.bcp.2017.06.129

Boda, E., Viganò, F., Rosa, P., Fumagalli, M., Labat-Gest, V., Tempia, F., et al. (2011). The GPR17 receptor in NG2 expressing cells: focus on *in vivo* cell maturation and participation in acute trauma and chronic damage. *Glia* 59, 1958–1973. doi: 10.1002/glia.21237

Boison, D. (2008). Adenosine as a neuromodulator in neurological diseases. *Curr. Opin. Pharmacol.* 8, 2–7. doi: 10.1016/j.coph.2007.09.002

Boison, D., Chen, J. F., and Fredholm, B. B. (2010). Adenosine signaling and function in glial cells. *Cell Death Differ.* 17, 1071–1082. doi: 10.1038/cdd.2009.131

Boison, D., Singer, P., Shen, H. Y., Feldon, J., and Yee, B. K. (2012). Adenosine hypothesis of schizophrenia—opportunities for pharmacotherapy. *Neuropharmacology* 62, 1527–1543. doi: 10.1016/j.neuropharm.2011.01.048

Boksa, P. (2010). Effects of prenatal infection on brain development and behavior: a review of findings from animal models. *Brain Behav. Immun*. 24, 881–897. doi: 10.1016/j.bbi.2010.03.005

Bottini, N., De Luca, D., Saccucci, P., Fiumara, A., Elia, M., Porfirio, M. C., et al. (2001). Autism: evidence of association with adenosine deaminase genetic polymorphism. *Neurogenetics* 3, 111–113. doi: 10.1007/s100480000104

Boyce, A. K. J., and Swayne, L. A. (2017). P2X7 receptor cross-talk regulates ATP-induced pannexin 1 internalization. *Biochem. J*. 474, 2133–2144. doi: 10.1042/BCJ20170257

Buffo, A., Rolando, C., and Ceruti, S. (2010). Astrocytes in the damaged brain: molecular and cellular insights into their reactive response and healing potential. *Biochem. Pharmacol*. 79, 77–89. doi: 10.1016/j.bcp.2009.09.014

Burnstock, G. (2017). Purinergic signaling: therapeutic developments. *Front. Pharmacol*. 8:661. doi: 10.3389/fphar.2017.00661

Butt, A. M., Fern, R. F., and Matute, C. (2014). Neurotransmitter signaling in white matter. *Glia* 62, 1762–1779. doi: 10.1002/glia.22674

Cai, Z., Pan, Z. L., Pang, Y., Evans, O. B., and Rhodes, P. G. (2000). Cytokine induction in fetal rat brains and brain injury in neonatal rats after maternal lipopolysaccharide administration. *Pediatr. Res*. 47, 64–72. doi: 10.1203/00006450-200001000-00013

Carlton, J., Bujny, M., Rutherford, A., and Cullen, P. (2005). Sorting nexins – unifying trends and new perspectives. *Traffic* 6, 75–82. doi: 10.1111/j.1600-0854.2005.00260.x

Ceballos-Picot, I., Mockel, L., Potier, M. C., Dauphinot, L., Shirley, T. L., Torero-Ibad, R., et al. (2009). Hypoxanthine-guanine phosphoribosyl transferase regulates early developmental programming of dopamine neurons: implications for Lesch-Nyhan disease pathogenesis. *Hum. Mol. Genet*. 18, 2317–2327. doi: 10.1093/hmg/ddp164

Ceruti, S., Viganò, F., Boda, E., Ferrario, S., Magni, G., Boccazzi, M., et al. (2011). Expression of the new P2Y-like receptor GPR17 during oligodendrocyte precursor cell maturation regulates sensitivity to ATP- induced death. *Glia* 59, 363–378. doi: 10.1002/glia.21107

Chen, B. C., Balasubramaniam, S., McGown, I. N., O'Neill, J. P., Chng, G. S., Keng, W. T., et al. (2014). Treatment of Lesch-Nyhan disease with S-adenosylmethionine: experience with five young Malaysians, including a girl. *Brain Dev*. 36, 593–600. doi: 10.1016/j.braindev.2013.08.013

Chen, Y., Wu, H., Wang, S., Koito, H., Li, J., Ye, F., et al. (2009). The oligodendrocyte-specific G protein-coupled receptor GPR17 is a cell-intrinsic timer of myelination. *Nat. Neurosci*. 12, 1398–1406. doi: 10.1038/nn.2410

Ciana, P., Fumagalli, M., Trincavelli, M. L., Verderio, C., Rosa, P., Lecca, D., et al. (2006). The orphan receptor GPR17 identified as a new dual uracil nucleotides/cysteinyl-leukotrienes receptor. *Embo J*. 25, 4615–4627. doi: 10.1038/sj.emboj.7601341

Contestabile, A., Fila, T., Bartesaghi, R., and Ciani, E. (2009). Cell cycle elongation impairs proliferation of cerebellar granule cell precursors in the Ts65Dn mouse, an animal model for down syndrome. *Brain Pathol*. 19, 224–237. doi: 10.1111/j.1750-3639.2008.00168.x

Contestabile, A., Fila, T., Ceccarelli, C., Bonasoni, P., Bonapace, L., Santini, D., et al. (2007). Cell cycle alteration and decreased cell proliferation in the hippocampal dentate gyrus and in the neocortical germinal matrix of fetuses with down syndrome and in Ts65Dn mice. *Hippocampus* 17, 665–678. doi: 10.1002/hipo.20308

Cunha, R. A. (2001). Adenosine as a neuromodulator and as a homeostatic regulator in the nervous system: different roles, different sources and different receptors. *Neurochem. Int*. 2, 107–125. doi: 10.1016/S0197-0186(00)00034-6

Davis, K. L., Stewart, D. G., Friedman, J. I., Buchsbaum, M., Harvey, P. D., Hof, P. R., et al. (2003). White matter changes in schizophrenia: evidence for myelin-related dysfunction. *Arch. Gen. Psychiatry* 5, 443–456. doi: 10.1001/archpsyc.60.5.443

de Brouwer, A. P., van Bokhoven, H., Nabuurs, S. B., Arts, W. F., Christodoulou, J., and Duley, J. (2010). PRPS1 mutations: four distinct syndromes and potential treatment. *Am. J. Hum. Genet*. 86, 506–518. doi: 10.1016/j.ajhg.2010.02.024

de Torre-Minguela, C., Mesa Del Castillo, P., and Pelegrín, P. (2017). The NLRP3 and pyrin inflammasomes: implications in the pathophysiology of autoinflammatory diseases. *Front. Immunol*. 27:43. doi: 10.3389/fimmu.2017.00043

Del Bigio, M. R., and Halliday, W. C. (2007). Multifocal atrophy of cerebellar internal granular neurons in lesch-nyhan disease: case reports and review. *J. Neuropathol. Exp. Neurol*. 66, 346–353. doi: 10.1097/nen.0b013e31805 15319

del Puerto, A., Díaz-Hern andez, J. I., Tapia, M., Gomez-Villafuertes, R., Benitez, M. J., Zhang, J., et al. (2012). Adenylate cyclase 5 coordinates the action of ADP, P2Y1, P2Y13 and ATP- gated P2X7 receptors on axonal elongation. *J. Cell Sci*. 125, 176–188. doi: 10.1242/jcs.091736

Deutsch, S. I., Long, K. D., Rosse, R. B., Mastropaolo, J., and Eller, J. (2005). Hypothesized deficiency of guanine-based purines may contribute to abnormalities of neurodevelopment, neuromodulation, and neurotransmission in Lesch-Nyhan syndrome. *Clin. Neuropharmacol*. 28, 28–37. doi: 10.1097/01.wnf.0000152043.36198.25

Di Liberto, V., Mudò, G., Garozzo, R., Frinchi, M., Fernandez-Dueñas, V., Di Iorio, P., et al. (2016). The guanine-based purinergic system: the tale of an orphan neuromodulation. *Front. Pharmacol*. 7:158. doi: 10.3389/fphar.2016.00158

Di Virgilio, F., Dal Ben, D., Sarti, A. C., Giuliani, A. L., and Falzoni, S. (2017). The P2X7 receptor in infection and inflammation. *Immunity* 47, 15–31. doi: 10.1016/j.immuni.2017.06.020

Dierssen, M. (2012). Down syndrome: the brain in trisomic mode. *Nat. Rev. Neurosci*. 13, 844–858. doi: 10.1038/nrn3314

Duley, J. A., Christodoulou, J., and de Brouwer, A. P. (2011). The PRPP synthetase spectrum: what does it demonstrate about nucleotide syndromes? *Nucleosides Nucleotides Nucleic Acids* 30, 1129–1139. doi: 10.1080/15257770.2011.591747

Dunwiddie, T. V., and Masino, S. A. (2001). The role and regulation of adenosine in the central nervous system. *Annu. Rev. Neurosci*. 24, 31–55. doi: 10.1146/annurev.neuro.24.1.31

Enns, G. M., Barkovich, A. J., van Kuilenburg, A. B., Manning, M., Sanger, T., Witt, D. R., et al. (2004). Head imaging abnormalities in dihydropyrimidine dehydrogenase deficiency. *J. Inherit. Metab. Dis*. 27, 513–522. doi: 10.1023/B:BOLI.0000037350.24142.d5

Estes, M. L., and McAllister, A. K. (2016). Maternal immune activation: implications for neuropsychiatric disorders. *Science* 353, 772–777. doi: 10.1126/science.aag3194

Ferrari, D., Pizzirani, C., Adinolfi, E., Lemoli, R. M., Curti, A., Idzko, M., et al. (2006). The P2X7 receptor: a key player in IL-1 processing and release. *J. Immunol*. 176, 3877–3883. doi: 10.4049/jimmunol.176.7.3877

Ferrua, F., and Aiuti, A. (2017). Twenty-five years of gene therapy for ADA-SCID: from bubble babies to an approved drug. *Hum. Gene Ther*. 28, 972–981. doi: 10.1089/hum.2017.175

Fields, R. D., and Stevens, B. (2000). ATP: an extracellular signaling molecule between neurons and glia. *Trends Neurosci*. 23, 625–633. doi: 10.1016/S0166-2236(00)01674-X

Fonta, C., Barone, P., Rodriguez Martinez, L., and Négyessy, L. (2015). Rediscovering TNAP in the brain: a major role in regulating the function and development of the cerebral cortex. *Subcell. Biochem*. 76, 85–106. doi: 10.1007/978-94-017-7197-9_5

Fredholm, B. B., Chen, J. F., Cunha, R. A., Svenningsson, P., and Vaugeois, J. M. (2005). Adenosine and brain function. *Int. Rev. Neurobiol*. 63, 191–270. doi: 10.1016/S0074-7742(05)63007-3

Fredholm, B. B., IJzerman, A. P., Jacobson, K. A., Linden, J., and Müller, C. E. (2011). International union of basic and clinical pharmacology. LXXXI. Nomenclature and classification of adenosine receptors–an update. *Pharmacol. Rev*. 63, 1–34. doi: 10.1124/pr.110.003285

Fumagalli, M., Bonfanti, E., Daniele, S., Zappelli, E., Lecca, D., Martini, C., et al. (2015). The ubiquitin ligase Mdm2 controls oligodendrocyte maturation by interwining mTor with G protein-coupled receptor kinase 2 in the regulation of GPR17 receptor desensitization. *Glia* 63, 2327–2339. doi: 10.1002/glia.22896

Fumagalli, M., Daniele, S., Lecca, D., Lee, P. R., Parravicini, C., Fields, R. D., et al. (2011). Phenotypic changes, signaling pathway, and functional correlates of GPR17-expressing neural precursor cells during oligodendrocyte differentiation. *J. Biol. Chem*. 286, 10593–10604. doi: 10.1074/jbc.M110.162867

Fumagalli, M., Lecca, D., and Abbracchio, M. P. (2016). CNS remyelination as a novel reparative approach to neurodegenerative diseases: the roles of purinergic signaling and the P2Y-like receptor GPR17. *Neuropharmacology* 104, 82–93. doi: 10.1016/j.neuropharm.2015.10.005

Garcia-Gil, M., Bertini, F., Pesi, R., Voccoli, V., Tozzi, M. G., and Camici, M. (2006). 5′-Amino-4-imidazolecarboxamide riboside induces apoptosis in human neuroblastoma cells via the mitochondrial pathway. *Nucleosides Nucleotides Nucleic Acids* 25, 1265–1270. doi: 10.1080/15257770600890905

Gevi, F., Zolla, L., Gabriele, S., and Persico, A. M. (2016). Urinary metabolomics of young Italian autistic children supports abnormal tryptophan and purine metabolism. *Mol. Autism* 7:47. doi: 10.1186/s13229-016-0109-5

Ginsberg, M. R., Rubin, R. A., Falcone, T., Ting, A. H., and Natowicz, M. R. (2012). Brain transcriptional and epigenetic associations with autism. *PLoS ONE* 7:e44736. doi: 10.1371/journal.pone.0044736

Göttle, M., Prudente, C. N., Fu, R., Sutcliffe, D., Pang, H., Cooper, D., et al. (2014). Loss of dopamine phenotype among midbrain neurons in Lesch-Nyhan disease. *Ann. Neurol.* 76, 95–107. doi: 10.1002/ana.24191

Grimm, I., Messemer, N., Stanke, M., Gachet, C., and Zimmermann, H. (2009). Coordinate pathways for nucleotide and EGF signaling in cultured adult neural progenitor cells. *J. Cell Sci.* 122, 2524–2533. doi: 10.1242/jcs.044891

Gu, B. J., Lovelace, M. D., Weible II, M. W., Allen, D. G., Eamegdool, S. S., Chan-Ling, T., et al. (2015). P2X7 is an archaic scavenger receptor recognizing apoptotic neuroblasts in early human neurogenesis. *Receptor Clin. Invest.* 2:e699. doi: 10.14800/rci.699

Guidi, S., Bonasoni, P., Ceccarelli, C., Santini, D., Gualtieri, F., Ciani, E., et al. (2008). Neurogenesis impairment and increased cell death reduce total neuron number in the hippocampal region of fetuses with down syndrome. *Brain Pathol.* 18, 180–197. doi: 10.1111/j.1750-3639.2007.00113.x

Hagberg, H., Gressens, P., and Mallard, C. (2012). Inflammation during fetal and neonatal life: implications for neurologic and neuropsychiatric disease in children and adults. *Ann. Neurol.* 71, 444–457. doi: 10.1002/ana.22620

Hagberg, H., Mallard, C., Ferriero, D. M., Vannucci, S. J., Levison, S. W., Vexler, Z. S., et al. (2015). The role of inflammation in perinatal brain injury. *Nat. Rev. Neurol.* 11, 192–208. doi: 10.1038/nrneurol.2015.13

Handford, M., Rodriguez-Furlán, C., and Orellana, A. (2006). Nucleotide-sugar transporters: structure, function and roles *in vivo*. *Braz. J. Med. Biol. Res.* 39, 1149–1158. doi: 10.1590/S0100-879X2006000900002

Hanics, J., Barna, J., Xiao, J., Millán, J. L., Fonta, C., and Négyessy, L. (2012). Ablation of TNAP function compromises myelination and synaptogenesis in the mouse brain. *Cell. Tissue Res.* 349, 459–471. doi: 10.1007/s00441-012-1455-z

Harris, J. J., Jolivet, R., and Attwell, D. (2012). Synaptic energy use and supply. *Neuron* 75, 762–777. doi: 10.1016/j.neuron.2012.08.019

Heine, C., Sygnecka, K., and Franke, H. (2016). Purines in neurite growth and astroglia activation. *Neuropharmacology*. 104, 255–271. doi: 10.1016/j.neuropharm.2015.10.022

Herbert, M. R., and Buckley, J. A. (2013). Autism and dietary therapy: case report and review of the literature. *J. Child. Neurol.* 28, 975–982. doi: 10.1177/0883073813488668

Illes, P., Khan, T. M., and Rubini, P. (2017). Neuronal P2X7 receptors revisited: do they really exist? *J. Neurosci.* 37, 7049–7062. doi: 10.1523/JNEUROSCI.3103-16.2017

Ipata, P. L., Camici, M., Micheli, V., and Tozz, M. G. (2011). Metabolic network of nucleosides in the brain. *Curr. Top. Med. Chem.* 11, 909–922. doi: 10.2174/156802611795347555

Jacobson, K. A., Hoffmann, C., Cattabeni, F., and Abbracchio, M. P. (1999). Adenosine-induced cell death: evidence for receptor-mediated signalling. *Apoptosis* 4, 197–211. doi: 10.1023/A:1009666707307

Jankowski, V., Tölle, M., Vanholder, R., Schönfelder, G., van der Giet, M., Henning, L., et al. (2005). Uridine adenosine tetraphosphate: a novel endothelium-derived vasoconstrictive factor. *Nat. Med.* 11, 223–227. doi: 10.1038/nm1188

Jinnah, H. A., Sabina, R. L., and Van Den Berghe, G. (2013). Metabolic disorders of purine metabolism affecting the nervous system. *Handb. Clin. Neurol.* 113, 1827–1836. doi: 10.1016/B978-0-444-59565-2.00052-6

Joachims, M. L., Marble, P. A., Laurent, A. B., Pastuszko, P., Paliotta, M., Blackburn, M. R., et al. (2008). Restoration of adenosine deaminase-deficient human thymocyte development *in vitro* by inhibition of deoxynucleoside kinases. *J. Immunol.* 181, 8153–8161. doi: 10.4049/jimmunol.181.11.8153

Kang, T. H., Guibinga, G. H., Jinnah, H. A., and Friedmann, T. (2011). HPRT deficiency coordinately dysregulates canonical Wnt and presenilin-1 signaling: a neuro-developmental regulatory role for a housekeeping gene? *PLoS ONE* 6:e16572. doi: 10.1371/journal.pone.0016572

Kawamura, M. Jr., Ruskin, D. N., and Masino, S. A. (2010). Metabolic autocrine regulation of neurons involves cooperation among pannexin hemichannels, adenosine receptors and channels. *J. Neurosci.* 30, 3886–3895. doi: 10.1523/JNEUROSCI.0055-10.2010

Kelley, R. E., and Andersson, H. C. (2014). Disorders of purines and pyrimidines. *Handb. Clin. Neurol.* 120, 827–838. doi: 10.1016/B978-0-7020-4087-0.00055-3

Knudsen, T. B., Winters, R. S., Otey, S. K., Blackburn, M. R., Airhart, M. J., Church, J. K., et al. (1992). Effects of (R)-deoxycoformycin (pentostatin) on intrauterine nucleoside catabolism and embryo viability in the pregnant mouse. *Teratology* 45, 91–103. doi: 10.1002/tera.1420450109

Knuesel, I., Chicha, L., Britschgi, M., Schobel, S. A., Bodmer, M., Hellings, J. A., et al. (2014). Maternal immune activation and abnormal brain development across CNS disorders. *Nat. Rev. Neurol.* 10, 643–660. doi: 10.1038/nrneurol.2014.187

Kovács, Z., Kékesi, K. A., Juhász, G., and Dobolyi, Á. (2014). The antiepileptic potential of nucleosides. *Curr. Med. Chem.* 21, 788–821. doi: 10.2174/13816128196661311191545O5

Koványi, B., Csölle, C., Calovi, S., Hanuska, A., Kató, E., Köles, L., et al. (2016). The role of P2X7 receptors in a rodent PCP-induced schizophrenia model. *Sci. Rep.* 6:36680. doi: 10.1038/srep36680

Langer, D., Ikehara, Y., Takebayashi, H., Hawkes, R., and Zimmermann, H. (2007). The ectonucleotidases alkaline phosphatase and nucleoside triphosphate diphosphohydrolase 2 are associated with subsets of progenitor cell populations in the mouse embryonic, postnatal and adult neurogenic zones. *Neuroscience* 150, 863–879. doi: 10.1016/j.neuroscience.2007.07.064

Lara, D. R., and Souza, D. O. (2000). Schizophrenia: a purinergic hypothesis. *Med. Hypotheses* 54, 157–166. doi: 10.1054/mehy.1999.0003

Lara, D. R., Dall'Igna, O. P., Ghisolfi, E. S., and Brunstein, M. G. (2006). Involvement of adenosine in the neurobiology of schizophrenia and its therapeutic implications. *Prog. Neuropsychopharmacol. Biol. Psychiatry*. 30, 617–629. doi: 10.1016/j.pnpbp.2006.02.002

Latz, E., Xiao, T. S., and Stutz, A. (2013). Activation and regulation of the inflammasomes. *Nat. Rev. Immunol.* 13, 397–411. doi: 10.1038/nri3452

Lauritsen, M. B. (2013). Autism spectrum disorders. *Eur. Child. Adolesc. Psychiatry* 22, S37–S42. doi: 10.1007/s00787-012-0359-5

Lecca, D., and Ceruti, S. (2008). Uracil nucleotides: from metabolic intermediates to neuroprotection and neuroinflammation. *Biochem. Pharmacol.* 75, 1869–1881. doi: 10.1016/j.bcp.2007.12.009

Lecca, D., Fumagalli, M., Ceruti, S., and Abbracchio, M. P. (2016). Intertwining extracellular nucleotides and their receptors with Ca^{2+} in determining adult neural stem cell survival, proliferation and final fate. *Philos. Trans. R. Soc. Lond. B. Biol. Sci.* 371:20150433. doi: 10.1098/rstb.2015.0433

Lecca, D., Trincavelli, M. L., Gelosa, P., Sironi, L., Ciana, P., Fumagalli, M., et al. (2008). The recently identified P2Y-like receptor GPR17 is a sensor of brain damage and a new target for brain repair. *PLoS ONE* 3:e3579. doi: 10.1371/journal.pone.0003579

Lewis, D. A., and Levitt, P. (2002). Schizophrenia as a disorder of neurodevelopment. *Annu. Rev. Neurosci.* 25, 409–432. doi: 10.1146/annurev.neuro.25.112701.142754

Li, W. J., Mao, F. X., Chen, H. J., Qian, L. H., and Buzby, J. S. (2015). Treatment with UDP-glucose, GDNF, and memantine promotes SVZ and white matter self-repair by endogenous glial progenitor cells in neonatal rats with ischemic PVL. *Neuroscience* 284, 444–458. doi: 10.1016/j.neuroscience.2014.10.012

Löffler, M., Carrey, E. A., and Zameitat, E. (2015). Orotic acid, more than just an intermediate of pyrimidine *de novo* synthesis. *J. Genet. Genomics* 42, 207–219. doi: 10.1016/j.jgg.2015.04.001

Lovelace, M. D., Gu, B. J., Eamegdool, S. S., Weible, M. W. II., Wiley, J. S., Allen, D. G., et al. (2015). P2X7 receptors mediate innate phagocytosis by human neural precursor cells and neuroblasts. *Stem Cells* 33, 526–541. doi: 10.1002/stem.1864

Mao, F. X., Li, W. J., Chen, H. J., Qian, L. H., and Buzby, J. S. (2012). Periventricular leukomalacia long-term prognosis may be improved by treatment with UDP-glucose, GDNF, and memantine in neonatal rats. *Brain Res.* 1486, 112–120. doi: 10.1016/j.brainres.2012.09.033

Marie, S., Heron, B., Bitoun, P., Timmerman, T., Van Den Berghe, G., and Vincent, M. F. (2004). AICA-ribosiduria: a novel, neurologically devastating inborn error of purine biosynthesis caused by mutation of ATIC. *Am. J. Hum. Genet.* 74, 1276–1281. doi: 10.1086/421475

Masino, S. A., Kawamura, M. Jr., Cote, J. L., Williams, R. B., and Ruskin, D. N. (2013). Adenosine and autism: a spectrum of opportunities. *Neuropharmacology* 68, 116–121. doi: 10.1016/j.neuropharm.2012.08.013

Masino, S. A., Kawamura, M. Jr., Plotkin, L. M., Svedova, J., DiMario, F. J. Jr, and Eigsti, I.-E. (2011a). The relationship between the neuromodulator adenosine and behavioral symptoms of autism. *Neurosci. Lett.* 500, 1–5. doi: 10.1016/j.neulet.2011.06.007

Masino, S. A., Li, T., Theofilas, P., Ruskin, D. N., Fredholm, B. B., Geiger, J. D., et al. (2011b). A ketogenic diet suppresses seizures in mice through adenosine Areceptors. *J. Clin. Invest.* 121, 2679–2683. doi: 10.1172/JCI57813

Massè, K., Bhamra, S., Eason, R., Dale, N., and Jones, E. A. (2007). Purine-mediated signalling triggers eye development. *Nature* 449, 1058–1062. doi: 10.1038/nature06189

McGrath, J., Saha, S., Chant, D., and Welham, J. (2008). Schizophrenia: a concise overview of incidence, prevalence, and mortality. *Epidemiol. Rev.* 30, 67–76. doi: 10.1093/epirev/mxn001

Meraviglia, V., Ulivi, A. F., Boccazzi, M., Valenza, F., Fratangeli, A., Passafaro, M., et al. (2016). SNX27, a protein involved in down syndrome, regulates GPR17 trafficking and oligodendrocyte differentiation. *Glia* 64, 1437–1460. doi: 10.1002/glia.23015

Micheli, V., Camici, M., Tozzi, M. G., Ipata, P. L., Sestini, S., Bertelli, M., et al. (2011). Neurological disorders of purine and pyrimidine metabolism. *Curr. Top. Med. Chem.* 11, 923–947. doi: 10.2174/156802611795347645

Miras-Portugal, M. T., Sebastián-S errano, Á., de Diego García, L., and Díaz-Hernández, M. (2017). Neuronal P2X7 receptor: involvement in neuronal physiology and pathology. *J. Neurosci.* 37, 7063–7072. doi: 10.1523/JNEUROSCI.3104-16.2017

Mishra, S. K., Braun, N., Shukla, V., Füllgrabe, M., Schomerus, C., Korf, H-W., et al. (2006). Extra- cellular nucleotide signaling in adult neural stem cells: synergism with growth factor-mediated cellular proliferation. *Development* 133, 675–684. doi: 10.1242/dev.02233

Morgan, J. T., Chana, G., Pardo, C. A., Achim, C., Semenderferi, K., and Courchesbe, E. (2010). Microglial activation and increased microglial density observed in the dorsolateral prefrontal cortex in autism. *Biol. Psychiatry* 68, 368–376. doi: 10.1016/j.biopsych.2010.05.024

Naviaux, J. C., Schuchbauer, M. A., Li, K., Wang, L., Risbrough, V. B., Powell, S. B., et al. (2014). Reversal of autism-like behaviors and metabolism in adult mice with single-dose antipurinergic therapy. *Transl. Psychiatry* 4:e400. doi: 10.1038/tp.2014.33

Naviaux, J. C., Wang, L., Li, K., Bright, A. T., Alaynick, W. A., Williams, K. R., et al. (2015). Antipurinergic therapy corrects the autism-like features in the Fragile X (Fmr1 knockout) mouse model. *Mol. Autism* 6:1. doi: 10.1186/2040-2392-6-1

Naviaux, R. K., Curtis, B., Li, K., Naviaux, J. C., Bright, A. T., and Reiner, G. E. (2017). Low-dose suramin in autism spectrum disorder: a small, phase I/II, randomized clinical trial. *Ann. Clin. Transl. Neurol.* 4, 491–505. doi: 10.1002/acn3.424

Naviaux, R. K., Zolkipli, Z., Wang, L., Nakayama, T., Naviaux, J. C., Le, T. P., et al. (2013). Antipurinergic therapy corrects the autism-like features in the poly(IC) mouse model. *PLoS ONE* 3:e57380. doi: 10.1371/journal.pone.0057380

Nguyen, K. V., and Nyhan, W. L. (2016). Mutation in the Human HPRT1 Gene and the Lesch-nyhan syndrome. *Nucleosides Nucleotides Nucleic Acids*. 35, 426–433. doi: 10.1080/15257770.2015.1098660

Nyhan, W. L. (2005). Disorders of purine and pyrimidine metabolism. *Mol. Genet. Metab.* 86, 25–33. doi: 10.1016/j.ymgme.2005.07.027

Oliveira, Á., Illes, P., and Ulrich, H. (2016). Purinergic receptors in embryonic and adult neurogenesis. *Neuropharmacology* 104, 272–281. doi: 10.1016/j.neuropharm.2015.10.008

Pelled, D., Sperling, O., and Zoref-Shani, E. (1999). Abnormal purine and pyrimidine nucleotide content in primary astroglia cultures from hypoxanthine-guanine phosphoribosyltransferase-deficient transgenic mice. *J. Neurochem.* 72, 1139–1145. doi: 10.1046/j.1471-4159.1999.0721139.x

Peterson, T. S., Thebeau, C. N., Ajit, D., Camden, J. M., Woods, L. T., Wood, W. G., et al. (2013). Up-regulation and activation of the P2Y2 nucleotide receptor mediate neurite extension in IL-1β-treated mouse primary cortical neurons. *J. Neurochem.* 125, 885–896. doi: 10.1111/jnc.12252

Pino, A., Fumagalli, G., Bifari, F., and Decimo, I. (2017). New neurons in adult brain: distribution, molecular mechanisms and therapies. *Biochem. Pharmacol.* 141, 4–22. doi: 10.1016/j.bcp.2017.07.003

Prior, C., Torres, R. J., and Puig, J. G. (2007). Hypoxanthine decreases equilibrative type of adenosine transport in lymphocytes from Lesch-Nyhan patients. *Eur. J. Clin. Invest.* 37, 905–911. doi: 10.1111/j.1365-2362.2007.01869.x

Rachidi, M., and Lopes, C. (2008). Mental retardation and associated neurological dysfunctions in down syndrome: a consequence of dysregulation in critical chromosome 21 genes and associated molecular pathways. *Eur. J. Paediatr. Neurol.* 12, 168–182. doi: 10.1016/j.ejpn.2007.08.010

Ribeiro, J. A., Sebastião, A. M., and de Mendonça, A. (2002). Adenosine receptors in the nervous system: pathophysiological implications. *Prog. Neurobiol.* 68, 377–392. doi: 10.1016/S0301-0082(02)00155-7

Schretlen, D. J., Varvaris, M., Vannorsdall, T. D., Gordon, B., Harris, J. C., and Jinnah, H. A. (2015). Brain white matter volume abnormalities in Lesch-Nyhan disease and its variants. *Neurology* 84, 190–196. doi: 10.1212/WNL.0000000000001128

Sebastián-Serrano, Á., de Diego-García, L., Martínez-Frailes, C., Ávila, J., Zimmermann, H., Millán, J. L., et al. (2015). Tissue-nonspecific alkaline phosphatase regulates purinergic transmission in the central nervous system during development and disease. *Comput. Struct. Biotechnol.* 13, 95–100. doi: 10.1016/j.csbj.2014.12.004

Sebastián-Serrano, Á., Engel, T., de Diego-García, L., Olivos-Oré, L. A., Arribas-Blázquez, M., Martínez-Frailes, C., et al. (2016). Neurodevelopmental alterations and seizures developed by mouse model of infantile hypophosphatasia are associated with purinergic signalling deregulation. *Hum. Mol. Genet.* 25, 4143–4156. doi: 10.1093/hmg/ddw248

Shao, Q., Lindstrom, K., Shi, R., Kelly, J., Schroeder, A., Juusola, J., et al. (2016). A germline variant in the PANX1 gene has reduced channel function and is associated with multisystem dysfunction. *J. Biol. Chem.* 291, 12432–12443. doi: 10.1074/jbc.M116.717934

Shen, H. Y., Singer, P., Lytle, N., Wei, C. J., Lan, J. Q., Williams-Karnesky, R. L., et al. (2012). Adenosine augmentation ameliorates psychotic and cognitive endophenotypes of schizophrenia. *J. Clin. Invest.* 122, 2567–2577. doi: 10.1172/JCI62378

Spellman, C., Ahmed, M. M., Dubach, D., and Gardiner, K. J. (2013). Expression of trisomic proteins in down syndrome model systems. *Gene* 512, 219–225. doi: 10.1016/j.gene.2012.10.051

Stafford, M. R., Bartlett, P. F., and Adams, D. J. (2007). Purinergic receptor activation inhibits mitogen-stimulated proliferation in primary neurospheres from the adult mouse subventricular zone. *Mol. Cell. Neurosci.* 35, 535–548. doi: 10.1016/j.mcn.2007.04.013

Stagni, F., Giacomini, A., Emili, M., Guidi, S., and Bartesaghi, R. (2017). Neurogenesis impairment: An early developmental defect in down syndrome. *Free Radic. Biol. Med.* doi: 10.1016/j.freeradbiomed.2017.07.026. [Epub ahead of print].

Stiles, J., and Jernigan, T. L. (2010). The basics of brain development. *Neuropsychol. Rev.* 20, 327–348. doi: 10.1007/s11065-010-9148-4

Studer, F. E., Fedele, D. E., Marowsky, A., Schwerdel, C., Wernli, K., Vogt, K., et al. (2006). Shift of adenosine kinase expression from neurons to astrocytes during postnatal development suggests dual functionality of the enzyme. *Neuroscience* 142, 125–137. doi: 10.1016/j.neuroscience.2006.06.016

Suyama, S., Sunabori, T., Kanki, H., Sawamoto, K., Gachet, C., Koizumi, S., et al. (2012). Purinergic signaling promotes proliferation of adult mouse subventricular zone cells. *J. Neurosci.* 32, 9238–9247. doi: 10.1523/JNEUROSCI.4001-11.2012

Tanimura, Y., Vaziri, S., and Lewis, M. H. (2010). Indirect basal ganglia pathway mediation of repetitive behavior: attenuation by adenosine receptor agonists. *Behav. Brain Res.* 210, 116–122. doi: 10.1016/j.bbr.2010.02.030

Torres, R. J., and Puig, J. G. (2007). Hypoxanthine-guanine phosophoribosyltransferase (HPRT) deficiency: Lesch-Nyhan syndrome. *Orphanet J. Rare Dis.* 2:48. doi: 10.1186/1750-1172-2-48

Torres, R. J., and Puig, J. G. (2015). Hypoxanthine deregulates genes involved in early neuronal development. Implications in Lesch-Nyhan disease pathogenesis. *J. Inherit. Metab. Dis.* 38, 1109–1118. doi: 10.1007/s10545-015-9854-4

Torres, R. J., Prior, C., Garcia, M. G., and Puig, J. G. (2016). A review of the implication of hypoxanthine excess in the physiopathology of Lesch-Nyhan disease. *Nucleosides Nucleotides Nucleic Acids* 35, 507–516. doi: 10.1080/15257770.2016.1147579

Turner, C. P., Yan, H., Schwartz, M., Othman, T., and Rivkees, S. A. (2002). A1 adenosine receptor activation induces ventriculomegaly and white matter loss. *Neuroreport* 13, 1199–1204 doi: 10.1097/00001756-200207020-00026

Ulrich, H., Abbracchio, M. P., and Burnstock, G. (2012). Extrinsic purinergic regulation of neural stem/progenitor cells: implications for CNS development and repair. *Stem Cell Rev*. 8, 755–767. doi: 10.1007/s12015-012-9372-9

Upthegrove, R., Manzanares-Teson, N., and Barnes, N. M. (2014). Cytokine function in medication-naive first episode psychosis: a systematic review and meta-analysis. *Schizophr. Res*. 155, 101–108. doi: 10.1016/j.schres.2014.03.005

van Kuilenburg, A. B., Dobritzsch, D., Meijer, J., Meinsma, R., Benoist, J. F., Assmann, B., et al. (2010). Dihydropyrimidinase deficiency: phenotype, genotype and structural consequences in 17 patients. *Biochim. Biophys. Acta* 1802, 639–648. doi: 10.1016/j.bbadis.2010.03.013

van Kuilenburg, A. B., Meinsma, R., Zonnenberg, B. A., Zoetekouw, L., Baas, F., Matsuda, K., et al. (2003). Dihydropyrimidinase deficiency and severe 5-fluorouracil toxicity. *Clin. Cancer Res*. 9, 4363–4367.

van Tilborg, E., Heijnen, C. J., Benders, M. J., van Bel, F., Fleiss, B., Gressens, P., et al. (2016). Impaired oligodendrocyte maturation in preterm infants: potential therapeutic targets. *Prog. Neurobiol*. 136, 28–49. doi: 10.1016/j.pneurobio.2015.11.002

Vargas, D. L., Nascimbene, C., Krishnan, C., Zimmerman, A. W., and Pardo, C. A. (2005). Neuroglial activation and neuroinflammation in the brain of patients with autism. *Ann. Neurol*. 57, 67–81. doi: 10.1002/ana.20315

Visser, J. E., Bär, P. R., and Jinnah, H. A. (2000). Lesch-Nyhan disease and the basal ganglia. *Brain Res. Brain Res. Rev*. 32, 449–475. doi: 10.1016/S0165-0173(99)00094-6

Voineagu, I., Wang, X., Johnston, P., Lowe, J. K., Tian, Y., Horvath, S., et al. (2011). Transcriptomic analysis of autistic brain reveals convergent molecular pathology. *Nature* 474, 380–384. doi: 10.1038/nature10110

von Kügelgen, I., and Hoffmann, K. (2016). Pharmacology and structure of P2Y receptors. *Neuropharmacol*. 104, 50–61. doi: 10.1016/j.neuropharm.2015.10.030

Wang, X., Huang, T., Zhao, Y., Zheng, Q., Thompson, R. C., Bu, G., et al. (2014). Sorting nexin 27 regulates Aβ production through modulating γ-secretase activity. *Cell Rep*. 9, 1023–1033. doi: 10.1016/j.celrep.2014.09.037

Wang, X., Zhao, Y., Zhang, X., Badie, H., Zhou, Y., Mu, Y., et al. (2013). Loss of sorting nexin 27 contributes to excitatory synaptic dysfunction by modulating glutamate receptor recycling in down's syndrome. *Nat. Med*. 19, 473–481. doi: 10.1038/nm.3117

Weissman, T. A., Riquelme, P. A., Ivic, L., Flint, A. C., and Kriegstein, A. R. (2004). Calcium waves propagate through radial glial cells and modulate proliferation in the developing neocortex. *Neuron* 43, 647– 661. doi: 10.1016/j.neuron.2004.08.015

Whyte, M. P. (2010). Physiological role of alkaline phosphatase explored in hypophosphatasia. *Ann. N.Y. Acad. Sci*. 1192, 190–200. doi: 10.1111/j.1749-6632.2010.05387.x

Wicki-Stordeur, L. E., Sanchez-Arias, J. C., Dhaliwal, J., Carmona-Wagner, E. O., Shestopalov, V. I., Lagace, D. C., et al. (2016). Pannexin 1 differentially affects neural precursor cell maintenance in the ventricular zone and peri-infarct cortex. *J. Neurosci*. 36, 1203–1210. doi: 10.1523/JNEUROSCI.0436-15.2016

Wong, D. F., Harris, J. C., Naidu, S., Yokoi, F., Marenco, S., Dannals, R. F., et al. (1996). Dopamine transporters are markedly reduced in Lesch-Nyhan disease *in vivo*. *Proc. Natl. Acad. Sci. U.S.A*. 93, 5539–5543. doi: 10.1073/pnas.93.11.5539

Wortmann, S. B., Chen, M. A., Colombo, R., Pontoglio, A., Alhaddad, B., Botto, L. D., et al. (2017). Mild orotic aciduria in UMPS heterozygotes: a metabolic finding without clinical consequences. *J. Inherit. Metab. Dis*. 40, 423–431. doi: 10.1007/s10545-017-0015-9

Conflict of Interest Statement: The authors declare that the research was conducted in the absence of any commercial or financial relationships that could be construed as a potential conflict of interest.

frontiers in Pharmacology

ORIGINAL RESEARCH
published: 18 December 2017
doi: 10.3389/fphar.2017.00914

Increased Number of Circulating CD8/CD26 T Cells in the Blood of Duchenne Muscular Dystrophy Patients Is Associated with Augmented Binding of Adenosine Deaminase and Higher Muscular Strength Scores

Jonathan H. Soslow[1], Larry W. Markham[1,2], W. Bryan Burnette[3], Cristi L. Galindo[2], Igor Feoktistov[2], Frank J. Raucci Jr.[1], Bruce M. Damon[4], Douglas B. Sawyer[5,6] and Sergey Ryzhov[6]**

[1] Thomas P. Graham Jr. Division of Pediatric Cardiology, Department of Pediatrics, Vanderbilt University Medical Center, Nashville, TN, United States, [2] Division of Cardiovascular Medicine, Department of Medicine, Vanderbilt University Medical Center, Nashville, TN, United States, [3] Division of Pediatric Neurology, Department of Pediatrics, Vanderbilt University Medical Center, Nashville, TN, United States, [4] Departments of Radiology and Radiological Sciences, Molecular Physiology and Biophysics, and Biomedical Engineering, Vanderbilt University Medical Center, Nashville, TN, United States, [5] Maine Medical Center, Portland, ME, United States, [6] Maine Medical Center Research Institute, Scarborough, ME, United States

Duchenne muscular dystrophy (DMD) is an X-linked disorder that leads to cardiac and skeletal myopathy. The complex immune activation in boys with DMD is incompletely understood. To better understand the contribution of the immune system into the progression of DMD, we performed a systematic characterization of immune cell subpopulations obtained from peripheral blood of DMD subjects and control donors. We found that the number of CD8 cells expressing CD26 (also known as adenosine deaminase complexing protein 2) was increased in DMD subjects compared to control. No differences, however, were found in the levels of circulating factors associated with pro-inflammatory activation of CD8/CD26 cells, such as tumor necrosis factor-α (TNFα), granzyme B, and interferon-γ (IFNγ). The number of CD8/CD26 cells correlated directly with quantitative muscle testing (QMT) in DMD subjects. Since CD26 mediates binding of adenosine deaminase (ADA) to the T cell surface, we tested ADA-binding capacity of CD8/CD26 cells and the activity of bound ADA. We found that mononuclear cells (MNC) obtained from DMD subjects with an increased number of CD8/CD26 T cells had a greater capacity to bind ADA. In addition, these MNC demonstrated increased hydrolytic deamination of adenosine to inosine. Altogether, our data demonstrated that (1) an increased number of circulating CD8/CD26 T cells is associated with preservation of muscle strength in DMD subjects, and (2) CD8/CD26 T cells from DMD subjects mediated degradation of adenosine by adenosine deaminase. These results support a role for T cells in slowing the decline in skeletal muscle function, and a need for further investigation into contribution of CD8/CD26 T cells in the regulation of chronic inflammation associated with DMD.

Keywords: Duchenne muscular dystrophy, immune response, T cells, adenosine deaminase, adenosine

OPEN ACCESS

Edited by:
Francisco Ciruela, University of Barcelona, Spain

Reviewed by:
Giulia Maria Camerino, Università degli studi di Bari Aldo Moro, Italy
Erick Omar Hernandez-Ochoa, University of Maryland, Baltimore, United States
Francisco Altamirano, University of Texas Southwestern Medical Center, United States

***Correspondence:**
Jonathan H. Soslow
jonathan.h.soslow@vanderbilt.edu
Sergey Ryzhov
sryzhov@mmc.org

Specialty section:
This article was submitted to Experimental Pharmacology and Drug Discovery, a section of the journal Frontiers in Pharmacology

Received: *19 September 2017*
Accepted: *30 November 2017*
Published: *18 December 2017*

Citation:
Soslow JH, Markham LW, Burnette WB, Galindo CL, Feoktistov I, Raucci FJ Jr., Damon BM, Sawyer DB and Ryzhov S (2017) Increased Number of Circulating CD8/CD26 T Cells in the Blood of Duchenne Muscular Dystrophy Patients Is Associated with Augmented Binding of Adenosine Deaminase and Higher Muscular Strength Scores. Front. Pharmacol. 8:914. doi: 10.3389/fphar.2017.00914

INTRODUCTION

Duchenne muscular dystrophy (DMD) is an X-linked disorder caused by a mutation in the DMD gene, which encodes the protein dystrophin. Affecting 1 in 4,700 male births, DMD results in both cardiac and skeletal myopathy (Dooley et al., 2010). While the genetic cause of DMD is known, the underlying pathophysiology of disease is incompletely understood. Dystrophin exists along the inner surface of the plasma membrane. It is a major component of the dystrophin-glycoprotein complex (DGC), which acts as a structural link between the extracellular matrix and the cytoskeleton and also possesses cell-signaling properties (Carlson, 1998; Cohn and Campbell, 2000; Rando, 2001; Lapidos et al., 2004). The loss of dystrophin in boys with DMD disrupts the DGC and leads to destabilization of the sarcolemma, setting off a complex cascade of inflammation and immune response (Rosenberg et al., 2015). The inflammatory response, combined with calcium dysregulation, causes cycles of skeletal muscle necrosis and regeneration with eventual fibro-fatty infiltration (Carlson, 1998; Cohn and Campbell, 2000; Guiraud and Davies, 2017).

Different subpopulations of immune cells, including monocytes/macrophages, lymphocytes, eosinophils, and natural killer cells, have been found in muscles of DMD patients (Arahata and Engel, 1984; Martin et al., 2014) and dystrophin-deficient animals (Cai et al., 2000; Vetrone et al., 2009). Importantly, different subpopulations of immune cells modulate either skeletal muscle damage or repair. Thus, IFN-γ, predominantly produced from pro-inflammatory T cells, leads to suppression of M2 macrophage polarization and muscle cell proliferation (Villalta et al., 2011). In contrast, regulatory T cells (Tregs) produce IL-10 and contribute to muscle regeneration in mdx mice (Burzyn et al., 2013; Villalta et al., 2014). While immunosuppression can potentially abrogate muscle damage, it also runs the risk of suppressing immunologic repair mechanisms. Corticosteroids, which suppress inflammation and immune response, significantly delay DMD loss of skeletal muscle strength and function, but their exact mechanism remains unclear (Mendell et al., 1989; Fenichel et al., 1991; Griggs et al., 1991; Wong and Christopher, 2002; Flanigan et al., 2013; Guglieri et al., 2017). Other immunosuppressive regimens have had only limited success (Griggs et al., 1993; Kissel et al., 1993; Kirschner et al., 2010); azathioprine, for example, demonstrated a similar decrease of mononuclear infiltrates in skeletal muscle compared with corticosteroids, but no significant improvement in muscle strength (Kissel et al., 1993). The failure of some immunosuppressive medications reflects the complex role of the immune system in DMD and necessitates improved understanding of the underlying immunologic mechanisms. Identification of subpopulations of immune cells associated with the prevention of skeletal muscle damage could help in the discovery of novel, targeted therapies for prevention of DMD progression.

The goals of this project were to further explore the complex immune activation found in boys with DMD by performing systematic characterization of immune cell subpopulations obtained from peripheral blood of DMD subjects and control donors. We report for the first time that the number of CD8 cells, expressing CD26, is increased in DMD subjects compared to control donors. CD26, a cell surface glycoprotein, is known as an ADA-anchoring protein. To examine the role of CD8/CD26 T cells, we investigated the relationships between subsets of CD8 T cells and clinical parameters used to assess progression of DMD, and determined capacity of mononuclear cells to bind ADA and produce inosine in DMD subjects with increased numbers of CD8/CD26 cells.

METHODS

Enrollment

This research protocol was approved by the Vanderbilt Institutional Review Board. The study was completed between 2012 and 2014. In accordance with the Declaration of Helsinki, participants 18 years of age and older signed informed written consent forms for the study. For those under 18 years of age, parents, or legal guardians signed informed written consents and participants signed age-appropriate informed written assent forms. DMD patients were recruited as part of a study evaluating cardiac function from the multidisciplinary Neuromuscular-Cardiology Clinic. DMD patients were over 7 years of age and the diagnosis was confirmed by either skeletal muscle biopsy or the presence of a dystrophin mutation and skeletal muscle phenotype. Healthy controls 8–18 years of age were enrolled prior to a clinically indicated treadmill test. Exclusion criteria were: (1) abnormal treadmill test, (2) presence or concern for structural or functional cardiovascular disease (congenital heart disease, cardiomyopathy, or any secondary cardiovascular disease), (3) abnormal echocardiogram, (4) arrhythmia or clinical concern for arrhythmia.

Study Procedures

Pertinent clinical data were collected from the electronic medical record for all participants with DMD. For the control participants, screening was performed prior to enrollment to assess suitability, including comprehensive questioning on past and family medical history.

Blood Collection and Analysis

Venous blood (10 ml) was collected from DMD and control subjects using BD Vacutainer EDTA tubes. The total number of white blood cells (WBC) was determined after erythrocyte lysis with ammonium chloride lysing solution (150 mM NH_4CI, 10 mM $NaHCO_3$, and 1 mM EDTA, pH 7.4). Mononuclear cells (MNC) were isolated from blood on Ficoll-Paque™ Premium gradient (GE Healthcare Life Sciences, Uppsala, Sweden) within 4–6 h of drawing and cryopreserved in fetal calf serum/ dimethyl sulfoxide (9:1) using a slow temperature-lowering method (Mr. Frosty polyethylene vial holder). Cells were stored in liquid nitrogen for ≥1 week before thawing. Viability and recovery were measured using 4′,6-diamidino-2-phenylindole (DAPI) exclusion.

Flow Cytometric Analysis

Flow cytometry experiments were performed as previously described (Ryzhov et al., 2017) with modifications. In brief, WBC or MNC were resuspended at the concentration of 10^6 cell/ml

and treated with Human TruStain FcX™ (Biolegend, San Diego, CA) to prevent non-specific binding followed by incubation with relevant antibodies for 25 min at 4°C. Cell-surface antigens were stained with FITC-conjugated anti-human CD3 (UCHT1), PE-conjugated CD26 (BA5b), PeCy7-conjugated CD14 (HCD14) and CD8 (HIT8a), HLA-DR-PeCy5 (L243), CD4-APC (OKT4), CD19-APC/Cy7 (HIB19), and CD16-APC/Cy7 (3G8) antibodies (all from BioLegend, San Diego, CA). Data acquisition was performed on MacsQuant Analyzer 10 (Miltenyi Biotec., Inc.).

Flow cytometry data were analyzed using WinList 5.0 software and presented in one of two ways: (1) histograms, which measure only a single parameter (e.g., expression of specific protein) or (2) dot plots, which compare two parameters simultaneously on a two-dimensional scatter plot. Axes show the number of cells (cell count) or represent fluorescence intensity (5-decade logarithmic scale) corresponded to the level of specific marker expression. Both histograms and dot plots were used to determine percentage of cells expressing specific marker using rectangular, quadrant, or freehand tools. Number of cells within specific subpopulation was calculated from total cell number and percent of corresponding cell subpopulation. Gates were set using fluorescent minus one controls or isotype-matched control IgGs. Only viable cells were analyzed. Viable and non-viable cells were distinguished using DAPI.

Analysis of Circulating TNFα, Granzyme B, and IFNγ

Blood plasma was prepared and stored as previously described (Swiger et al., 2016). Plasma levels of TNFα, IFNγ, and granzyme B were measured using enzyme-linked immunosorbent assay kits (all are from Bio-techne/R&D Systems).

Binding of Adenosine Deaminase

Human recombinant ADA (7048-AD-010, Bio-techne/ R&D Systems) at the final concentration of 5 μg/ml was incubated with 3×10^5 mononuclear cells for 30 min in a CO_2 incubator. Cells were washed twice with PBS/2 mM EDTA and the percentage of ADA-bound cells was determined using biotinylated anti-ADA antibody (ab34677, Abcam) in combination with Streptavidin-Phycoerythrin (Biolegend).

Analysis of Adenosine Deaminase Activity

After binding of ADA to the cell surface, mononuclear cells were washed twice with PBS/2 mM EDTA and resuspended in Dulbecco's Phosphate-buffered solution at the concentration of 5×10^4 cells/ml. Cells were incubated in the absence or presence of 10 μM adenosine (Sigma) for 20 min in a CO_2 incubator. The reaction was stopped by adding perchloric acid to the final concentration of 0.5 M. Supernatant was used to determine adenosine deamination to inosine using RayBio® Inosine Assay kit (Ray Biotech, Inc). Protein concentration was determined using BCA protein assay (ThermoFisher Scientific).

Skeletal Muscle Strength Assessment

Quantitative muscle testing (QMT) was performed by a single investigator (WBB) in participants with DMD as previously described (Posner et al., 2016). QMT is an objective, reproducible method for assessing skeletal muscle strength (Mathur et al., 2010; Lerario et al., 2012; Connolly et al., 2015). In brief, a dynamometer was used to assess total upper extremity strength, which was calculated by summing the flexion and extension values for the right and left elbows. Total lower extremity strength was calculated by summing flexion and extension values for both knees. The total QMT score was calculated as the sum of the total upper and lower extremity QMTs. All but 4 QMT measurements were performed the same day as the blood draw and none were performed longer than 3 months from the blood draw. One patient did not have QMT measured.

Echocardiography

Echocardiograms were performed by 1 of 4 research sonographers with experience in imaging patients with DMD. Whenever possible, echocardiograms were performed supine. Post-processing included assessment of left ventricular (LV) function using fractional shortening (FS) measured from 2-dimensional images and 5/6 area length left ventricular ejection fraction (LVEF), as previously described(Lopez et al., 2010; Lang et al., 2015); these echocardiographic measures have the best accuracy and reproducibility for LV function in patients with DMD (Soslow et al., 2016). Echocardiograms were interpreted by a single investigator (JHS).

Statistical Analysis

Data were analyzed with GraphPad Prism 4.0 (GraphPad Software Inc., San Diego, CA). Normally distributed variables are expressed as mean ± SEM. Comparisons between two groups were performed using two-tailed unpaired *t*-tests. Data are expressed as median values when distributions are skewed. For variables with skewed distributions, pairwise comparisons of median values were examined using Mann–Whitney test. For continuous variables, correlation analysis was performed using a Pearson (normal distribution) or Spearman (skewed distribution correlation). A P-value < 0.05 was considered significant.

RESULTS

A total of 20 DMD participants and 10 controls were analyzed. There was no significant difference in age between DMD and controls (**Table 1**). As expected, controls were taller than DMD participants. There were 4 females enrolled in the control cohort; all DMD participants were male. DMD participants had decreased LVEF and FS compared with controls (49% ± 12 vs. 61% ± 5 and 26% ± 9 vs. 39% ± 4, $p = 0.007$ and $p = 0.001$, respectively). A total of 11 DMD participants (55%) had abnormal LV systolic function defined as FS < 28% or LVEF < 55%. Two DMD participants (10%) were ambulatory. The median total QMT was 55 pounds (interquartile range 39, 105) for DMD patients.

Number of CD8 T Cells Is Increased in DMD Subjects

To determine if DMD is associated with changes in systemic inflammatory response, we performed a flow cytometric analysis of lymphocyte and monocyte subpopulations in peripheral blood

TABLE 1 | Demographics and characteristics of study subjects.

	Control ($N = 10$)	DMD ($N = 20$)	p-value
Age	14.4 (12.5, 16.3)	14.2 (12.0, 16.1)	0.965
Male gender	60%	100%	0.002
Height (cm)	170 (154, 174)	151 (139, 160)	0.015
Weight (kg)	65 (52, 85)	55 (40, 60)	0.131
Race			0.136
Caucasian	6 (60%)	17 (85%)	
African American	2 (20%)	2 (10%)	
Asian	0	1 (5%)	
Mixed	0	0	
Unknown	2 (20%)	0	
Hispanic	1 (10%)	3 (15%)	0.864
Ambulatory	0	2 (10%)	
Total quantitative muscle testing (QMT) (pounds)	Not tested	55 (39, 105)	
Arm QMT (pounds)	Not tested	18 (11.5, 39.5)	
Leg QMT (pounds)	Not tested	34.5 (27.5, 69)	
Current Medications:			
Corticosteroid	0	16 (80%)	
Angiotensin converting enzyme inhibitor	0	13 (65%)	
Angiotensin receptor blocker	0	5 (25%)	
Beta-blocker	0	7 (35%)	
Aldosterone inhibitor	0	0	

Data presented as the median with interquartile range in parentheses or the total number of patients with percent of patients in parentheses. DMD, Duchenne muscular dystrophy.

obtained from DMD subjects and control donors. **Figure 1** illustrates our gating strategy to define subpopulations of lymphocytes and monocytes within population of CD45 positive, viable cells (**Figures 1A,B**). We identified phenotypically distinct cell subpopulations corresponding to CD3 T lymphocytes and CD19 B lymphocytes (**Figure 1C**). The subpopulation of CD3 T cells was further analyzed for CD4 and CD8 T cell subsets (**Figure 1D**). Subsets of $CD14^{pos}CD16^{neg}$ and $CD14^{pos}CD16^{pos}$ cells were identified within HLA-DR positive cells as shown in **Figures 1E,F**. Our analysis revealed that the total number of WBC was not different between the two groups (**Figure 1G**). However, the number of CD8 T cells was significantly increased in DMD subjects compared to controls. No differences were found in other subpopulations of WBC, including CD3/CD4, CD19 cells and subsets of monocytes (**Figures 1G,H**).

Subset of CD8 Cells Expressing CD26, but Not CD71 or CD28, Is Increased in DMD Subjects

To determine whether or not changes in the number of CD8 T cells are also accompanied by T cell activation, we initially performed characterization of cell surface markers, including CD26, CD71, and CD28, which are associated with CD8 activation (Morimoto and Schlossman, 1998; Ohnuma et al., 2008). We found that the subset of CD8 positive cells expressing CD26 was increased in DMD subjects (**Figure 2A**). Further analysis revealed the presence of several subsets of CD8/CD26 cells, including $CD26^{high}$, $CD26^{int}$, and $CD26^{neg}$ (**Figure 2B**). The major subset of CD8/CD26 cells was represented by $CD8/CD26^{int}$ cells and was significantly increased in DMD vs. control subjects (**Figure 2C**). There were no differences in minor subsets of $CD8/CD26^{neg}$ and $CD8/CD26^{high}$ cells (**Figures 2D,E**), or in the number of CD8/CD71 and CD8/CD28 T cells (**Figures 2F,G**) between DMD and control subjects.

Interestingly, we found an increase in the number of $CD8/CD26^{int}$ cells in subjects taking corticosteroids (0.21 ± 0.07 vs. 0.12 ± 0.04, $p = 0.047$). However, the uneven cohort size ($n = 16$ vs. $n = 4$, subjects taking vs. not taking corticosteroids, **Table 1**) necessitates further validation of this positive correlation between corticosteroids and $CD8/CD26^{int}$ cells. There were no differences noted in subjects on or off angiotensin converting enzyme inhibitors or angiotensin receptor blockers. Subjects taking beta-blockers had a decrease in a minor subpopulation of $CD8/CD26^{high}$ T cells (0.02 ± 0.01 vs. 0.06 ± 0.04, $p = 0.008$).

The Levels of Pro-inflammatory Factors Secreted by CD8/CD26 Cells Are Not Increased in DMD Subjects

It has been recently shown that CD26 is involved in activation of CD8 T cells and stimulation of TNFα, granzyme B and IFNγ production (Hatano et al., 2013). To determine if the increased number of CD8/CD26 cells is associated with higher levels of pro-inflammatory factors, we measured TNFα, granzyme B, and IFNγ in plasma samples. As shown in **Figure 3**, no differences were found in the levels of pro-inflammatory factors between DMD and control subjects.

The Number of CD8/CD26 Cells Is Associated with Higher Muscle Strength Scores

To further characterize the role of CD8/CD26 T cells in DMD subjects, we performed a correlation analysis to examine the association of these cells with clinical parameters of skeletal muscle function (QMT) and heart function (echocardiogram derived FS and LVEF). A positive correlation was found between the number of CD8/CD26 cells and the QMT score in DMD subjects ($r_p = 0.489$, $p = 0.028$; **Figure 4A**). In contrast, no significant correlations were found between CD8/CD71, CD8/CD28 subsets (**Figures 4B,C**), or CD3/CD8 subsets (**Figure 4D**), indicating the potential significance of CD26 for maintenance of muscle strength. No statistically significant correlations were identified between subsets of CD8 cells and FS or LVEF in DMD subjects (Supplementary Table 1).

The Presence of an Increased Number of CD8/CD26 Cells Is Associated with Higher ADA-Binding Capacity and Deamination of Adenosine to Inosine

In addition to being a marker of T cell activation, CD26 binds adenosine deaminase to the T cell surface. To determine if

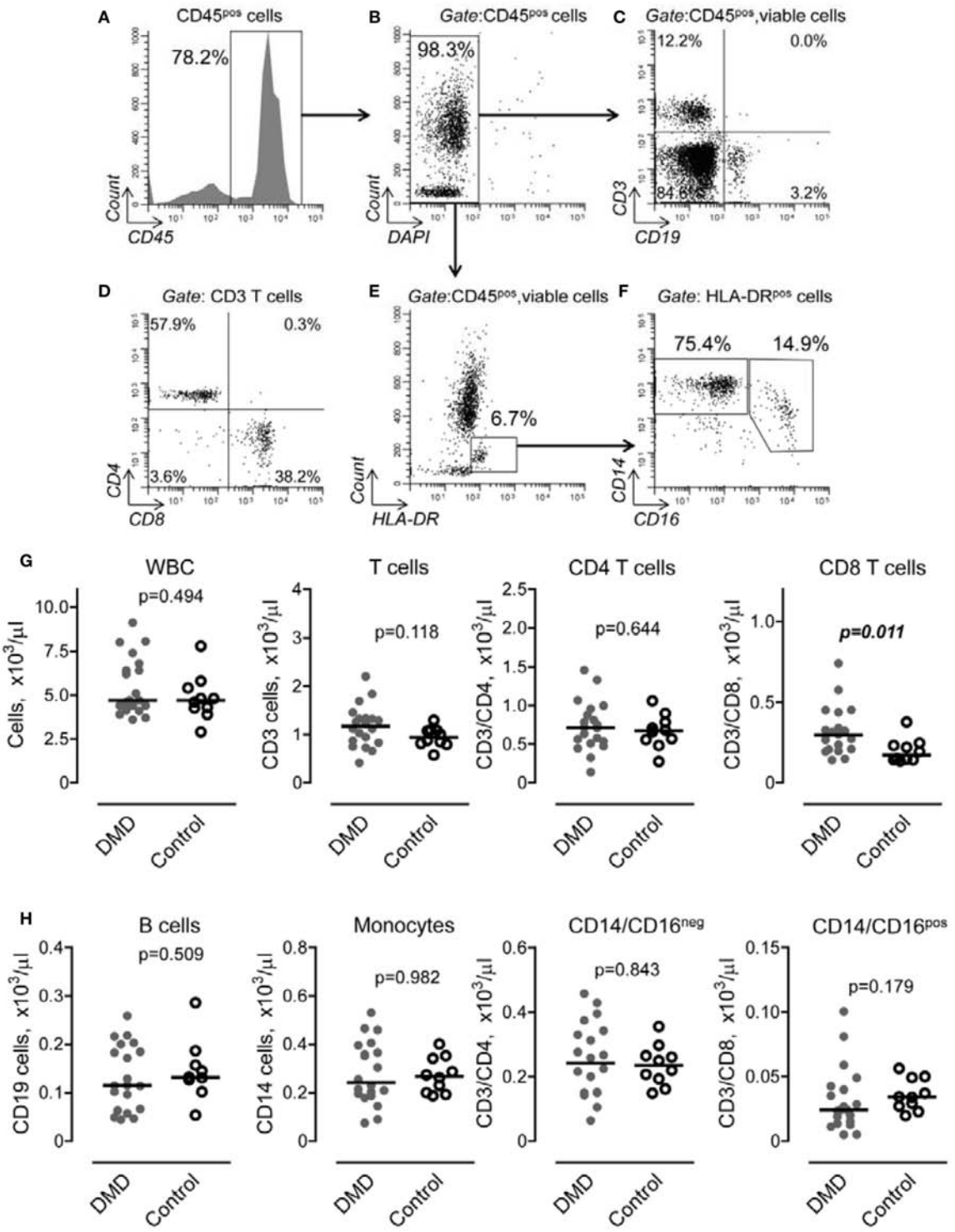

FIGURE 1 | Gating strategy and flow cytometric analysis of peripheral blood lymphocytes and monocytes in Duchenne muscular dystrophy (DMD) and control subjects. **(A,B)** CD45 positive **(A)**, viable **(B)** cells were *initially* gated to *exclude non-lysed erythrocytes and dead cells from analysis.* **(C)** Subpopulation of T lymphocytes (*upper left quadrant*) and B lymphocytes (*lower right quadrant*) were distinguished by expression of CD3 and CD19 cell markers. **(D)** Subsets of CD4 (*upper left quadrant*) and CD8 (*lower right quadrant*) were determined within CD3 positive subpopulation. **(E)** Monocytes were defined as HLA-DR positive/SSA intermediate cells (*rectangular gate*). **(F)** Subpopulation of $CD14^{pos}CD16^{neg}$ and $CD14^{pos}CD16^{pos}$ monocytes were determined within HLA-DR positive/SSA intermediate cells. Representative dot plots are shown. **(G,H)** Number of cell subpopulation was calculated from total cell number and percent of corresponding cell subpopulation defined as shown in **(A–F)**. Data are presented as scatter dot plots and the horizontal line indicates the median values. Differences between DMD ($n = 20$) and control ($n = 0$) subjects were examined using Mann–Whitney *U*-test. *P*-values are indicated.

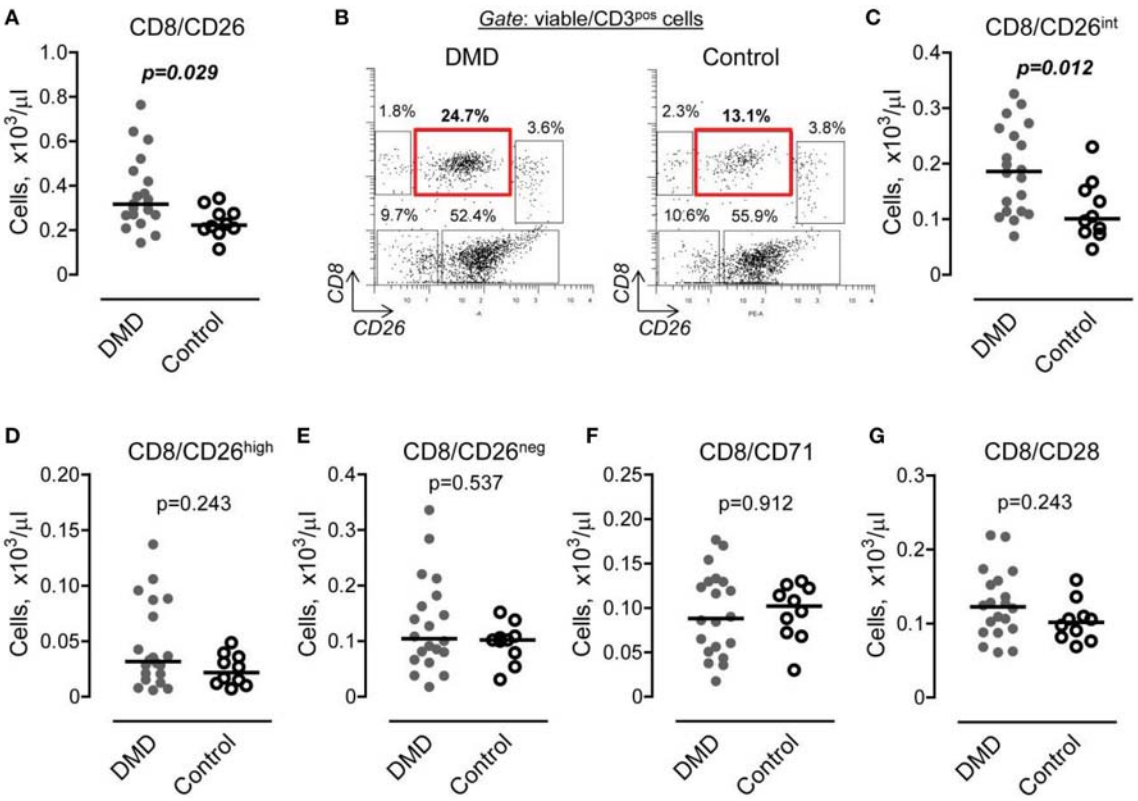

FIGURE 2 | The number of CD8 cells expressing CD26 is increased in Duchenne muscular dystrophy (DMD) subjects. **(A)** Graphical representation of flow cytometry data demonstrating the number of CD8 T cells expressing CD26 in DMD ($n = 20$) and control ($n = 10$) subjects. *Horizontal lines indicate median values. Mann-Whitney U-test.* **(B)** Representative flow cytometric dot plots showing three subsets of CD8 cells, CD26 negative (upper left gate), CD26 intermediate (upper middle gate), and CD26 high (upper right gate) in DMD ($n = 20$) and control ($n = 10$) subjects. **(C–E)** Number of CD8 cells characterized by the absence or presence of CD26 expression (**C**, *intermediate subset*; **D**, *high subset*; and **E**, *negative subset*) was calculated from total number of CD3 cells and percent of corresponding subset. *Horizontal lines indicate median values. Mann-Whitney U-test*. **(F,G)** Graphical representation of flow cytometry data showing the number of CD8 cells expressing CD71 **(F)** and CD28 **(G)**. *Horizontal lines indicate medians. Mann-Whitney U-test.*

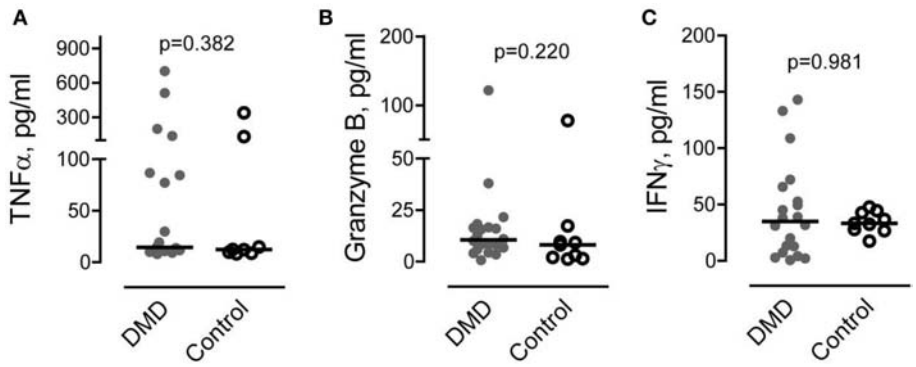

FIGURE 3 | Levels of circulating cytotoxic factors associated with CD8 cell activation. **(A–C)** Tumor necrosis factor alpha (TNFα) **(A)**, granzyme B **(B)** and interferon gamma (IFNγ) **(C)** were measured in plasma obtained from Duchenne muscular dystrophy (DMD) ($n = 20$) and control ($n = 10$) subjects as described in Methods. Mann-Whitney *U* test. *P* values are indicated.

the increased number of CD8/CD26 cells is associated with a higher binding of ADA to the T cell surface, we first divided DMD subjects into two subgroups, with high and low numbers of CD8/CD26, based on the median value of number of CD8/CD26 cells as shown in **Figure 5A**. Then, we analyzed the capability of MNC, obtained from the peripheral blood of

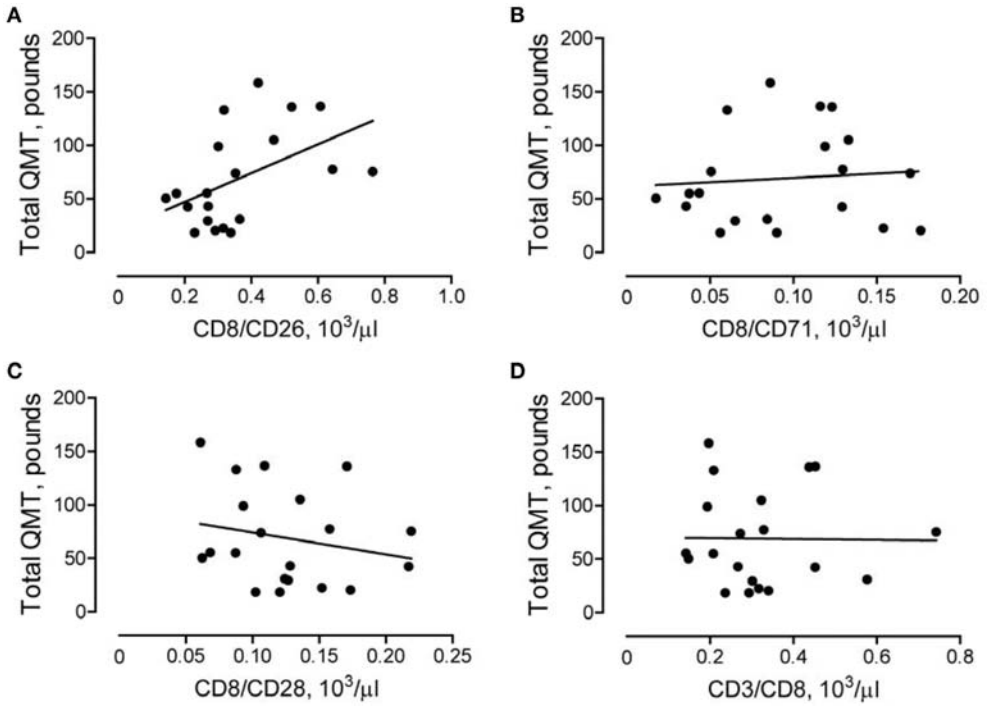

FIGURE 4 | Association between number of CD8/CD26 cells and skeletal muscle strength. Quantitative muscle testing (QMT) was performed as described in Methods. The correlations between QMT and number of CD8/CD26 cells (**A**, $r_p = 0.489$, $\boldsymbol{p = 0.028}$), number of CD8/CD71 cells (**B**, $r_p = 0.085$, $p = 0.719$), CD8/CD28 cells (**C**, $r_p = -0.211$, $p = 0.371$), and CD3/CD8 cells (**D**, $r_p = -0.013$, $p = 0.956$) in Duchenne muscular dystrophy (DMD) subjects ($n = 20$).

DMD subjects, to bind ADA. No differences were found in the total number of isolated MNC and CD3 T cells between the two subgroups (**Figures 5B,C**). After incubation of MNC in the absence or presence of recombinant human adenosine deaminase, the number of cells that bound ADA was determined using flow cytometry as shown in **Figures 5D,E**. Only CD3 T cells, but not other subpopulations of MNC, were able to bind ADA. Our analysis revealed that both percent (data not shown) and number of T cells characterized by the capability to bind ADA (ADA positive cells) was significantly higher in the subgroup of CD8/CD26^{high} compared to CD8/CD26^{low} DMD subjects (**Figure 5F**). To determine the functional significance of increased binding of ADA to T cells, we tested adenosine deaminase activities of MNC, incubated with ADA, in two subgroups of DMD subjects. Our data demonstrated that the level of inosine accumulation was significantly higher in the subgroup of DMD subjects with higher number of CD8/CD26 cells (**Figure 5G**). Thus, our data indicate that CD26 mediates binding of ADA to T cells and that the increased number of CD8/CD26 cells is associated with a higher capability of adenosine deamination to inosine in DMD subjects.

DISCUSSION

The immune system plays dual roles in DMD, contributing to both progression of muscle degeneration (Wehling-Henricks et al., 2008; Villalta et al., 2011) and promotion of muscle repair (Tidball et al., 2014). Animal models of muscular dystrophy reinforce this duality and demonstrate the different, sometimes diametrically opposed, effects of immune system activation (Farini et al., 2007; Villalta et al., 2009, 2014). In the current study, we investigated the association between subpopulations of immune cells and muscle strength in DMD. Our main findings are that the number of CD8 T cells expressing CD26 is increased in DMD subjects and associated with a higher muscle strength score.

DMD is characterized by intramuscular infiltration of immune cells, including T cells (Spencer and Tidball, 2001). Studies in mdx mice have shown that T cells may be involved in promotion of muscle fibrosis and eosinophilia (Cai et al., 2000; Farini et al., 2007). However, the contribution of specific subsets of CD8/CD26 cells was not determined in those studies. CD26 has been previously characterized as a co-activation marker of both CD4 and CD8 (Morimoto and Schlossman, 1998). Co-stimulation of CD8 cells with anti-CD3 and anti-CD26 resulted in the upregulation of cytotoxic factors, such as granzyme B, TNFα, and IFNγ (Hatano et al., 2013). Our studies show that the levels of these factors are similar in DMD and control subjects, suggesting no pro-inflammatory activation associated with the increased number of CD8/CD26 cells. We also found that among the three subsets of CD8/CD26 cells, only the number of CD8/CD26^{int} was significantly increased. It has been previously shown that CD8/CD26^{int} cells represent the subset of naive or central memory T cells, while both CD8/CD26^{high} and

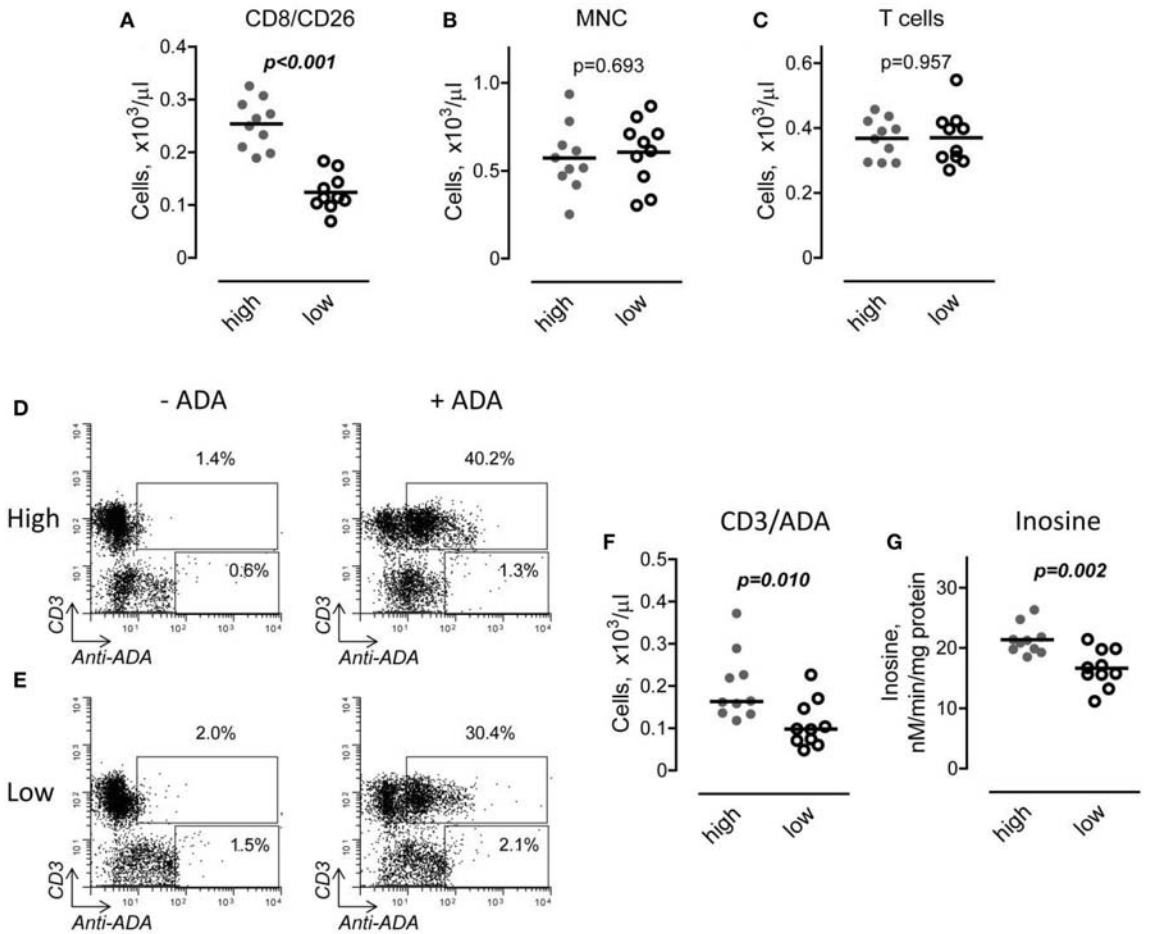

FIGURE 5 | Interaction of adenosine deaminase (ADA) with CD26 in Duchenne muscular dystrophy (DMD) subjects with high and low number of CD8/CD26 cells. **(A)** DMD subjects were divided into two subgroups based on the median value of number of CD8/CD26 cells. Horizontal line indicates mean value. Unpaired *t*-test. **(B,C)** Number of mononuclear cells (MNC) **(B)** and CD3 positive T cells **(C)** in subgroups with high ($n = 10$) and low ($n = 10$) number of CD8/CD26 cells after isolation of MNC using Ficoll-Paque density gradient. Unpaired *t*-test. **(D,E)** Representative flow cytometric dot plots showing percent of cells which bind recombinant ADA in subgroups of subjects with high **(D)** and low **(E)** number of CD8/CD26 cells. **(F)** Graphical representation of flow cytometric data on number of cells which bind ADA. **(G)** ADA activity in MNC cell suspensions obtained from DMD subjects with high and low number of CD8/CD26 cells. Unpaired *t*-test.

CD8/CD26^{neg} bore activated cell phenotypes (Ibegbu et al., 2009; Hatano et al., 2013). Interestingly, IL-15, which is involved in the maintenance and expansion of naïve CD8 T cells (Wallace et al., 2006), has also been shown to improve muscle strength in mdx mice (Harcourt et al., 2005).

Besides its involvement in T cells activation, CD26 serves as a receptor for ADA (Kameoka et al., 1993). There is no evidence of a direct immunomodulatory effect of ADA bound to CD26 in T cells. However, ADA may regulate immune and inflammatory responses through prevention of endogenous adenosine accumulation (Morimoto and Schlossman, 1998) and activation of purinergic receptors involved in inflammation and fibrosis (Gazzerro et al., 2015). The endogenous level of adenosine is increased in the muscles of DMD subjects (Castro-Gago et al., 1987; Camiña et al., 1995). It has been shown that adenosine can induce apoptosis in myogenic cells (Rufini et al., 1997; Ceruti et al., 2000). However, the role of adenosine in the regulation of inflammation and progression of DMD has not been well-characterized. Adenosine has been shown to promote differentiation of Th17 cells and production of proinflammatory IL-17 (Wilson et al., 2011). The intramuscular level of IL-17 mRNA is increased and correlates to muscle inflammation in subjects with DMD (De Pasquale et al., 2012). It has also been shown that early stages of DMD are associated with low intramuscular levels of ADA activity (Kar and Pearson, 1973). These findings suggest that adenosine accumulation may be an important regulator of inflammation-mediated muscle damage in DMD. We found that binding of ADA to T cells was higher in DMD subjects with an increased number of CD8/CD26 cells and associated with a higher rate of adenosine deamination to inosine and higher muscle strength score. It is possible that the positive correlation between CD8/CD26 cells and muscle strength could be explained by an increased intramuscular level of ADA bound to T cells, which is contributing to prevention

of adenosine accumulation and muscle protection. Measurement of adenosine levels in blood and tissue samples from DMD subjects is necessary to directly address the involvement of adenosinergic mechanisms in effects mediated by CD8/CD26 T cells. It should be noted, however, that the determination of adenosine concentration *in vivo* is not simple. The short half-life of adenosine in peripheral blood (Möser et al., 1989) and massive release of adenosine triphosphate during sampling procedures (Macey et al., 2002) contribute to falsely elevated levels of adenosine. While these problems can be ameliorated with a freeze-clamping technique at the time of blood collection (Chen et al., 2013), this was not performed during the collection of samples in the current study.

Inosine exhibits anti-inflammatory properties, which include inhibition of cytokine and chemokine release from activated macrophages (Haskó et al., 2000; Garcia Soriano et al., 2001) and attenuation of TNFα production from LPS stimulated human neutrophils (Marton et al., 2001). Enhanced levels of inosine due to ADA-dependent deamination of adenosine to inosine in subjects with an increased number of CD8/CD26 cells may also contribute to muscle protection from invading inflammatory cells. However, the specific role of inosine in DMD has not been investigated.

The role of CD8 T cells in muscle regeneration has been recently demonstrated in a mouse model of cardiotoxin-induced injury (Zhang et al., 2014). In this model, genetic depletion of CD8 resulted in reduced chemokine ligand 2 production by T cells and impaired recruitment of macrophages into muscles. Monocytes and macrophages represent predominant subpopulations of intramuscular leukocytes (Honda et al., 1990; Brigitte et al., 2010) and can contribute to muscle protection through suppression of M1 macrophage-mediated cytotoxicity (Villalta et al., 2009). In the current study, we found that the number of CD8 T cells is increased in DMD subjects. However, no association was identified between CD8 T cells and monocytes in peripheral blood. Further study will help to determine if CD8 T cells induce intramuscular accumulation of pro-regenerative monocytes and macrophages in DMD human subjects.

In summary, our study shows that the number of CD8/CD26 T cells positively correlates to muscle strength in DMD. The binding of ADA to T cells and deamination of adenosine to inosine by MNC were significantly increased in subjects with a higher number of CD8/CD26 cells. We speculate that CD8/CD26 cells, acting through binding and delivery of ADA to skeletal muscles, may contribute to the prevention of adenosine accumulation and muscle protection. ADA-dependent regulation of adenosinergic signaling may represent a new therapeutic option to prevent loss of muscle strength and improve quality of life of patients with DMD.

AUTHOR CONTRIBUTIONS

JS, SR, and DS: designed the study and interpreted the data; JS, DS, BD, and LM: helped organize the study, including recruitment, consent, and blood collection from subjects; SR, IF, CG, WB, LM, BD, FR, and JS: analyzed clinical and lab data; IF and CG: assisted with lab work and data analysis; JS and SR: wrote the manuscript, which was critically reviewed by DS, IF, FR, WB, BD and LM.

ACKNOWLEDGMENTS

This work was supported by the National Institute of General Medical Sciences (P30GM106391, Phase III COBRE in Stem Cell Biology and Regenerative Medicine Progenitor Cell Analysis Core Facility and P30GM103392 and Phase III COBRE in Vascular Biology). This work was supported by American Heart Association Grant 13CRP14530007 (JS) and 15GRNT25760035 (IF). Research reported in this publication was supported by the National Heart, Lung, and Blood Institute of the National Institutes of Health under Award Number K23HL123938 (Bethesda, MD) (JS) and K01HL121045 (CG). The content is solely the responsibility of the authors and does not necessarily represent the official views of the National Institutes of Health. The project was supported by the National Center for Research Resources, Grant UL1 RR024975-01, and is now at the National Center for Advancing Translational Sciences, Grant 2 UL1 TR000445-06 (Bethesda, MD). The content is solely the responsibility of the authors and does not necessarily represent the official views of the NIH. This project was supported by the Fighting Duchenne Foundation and the Fight DMD/Jonah & Emory Discovery Grant (Nashville, TN) (LM).

SUPPLEMENTARY MATERIAL

The Supplementary Material for this article can be found online at: https://www.frontiersin.org/articles/10.3389/fphar.2017.00914/full#supplementary-material

REFERENCES

Arahata, K., and Engel, A. G. (1984). Monoclonal antibody analysis of mononuclear cells in myopathies. I: Quantitation of subsets according to diagnosis and sites of accumulation and demonstration and counts of muscle fibers invaded by T cells. *Ann. Neurol.* 16, 193–208. doi: 10.1002/ana.410160206

Brigitte, M., Schilte, C., Plonquet, A., Baba-Amer, Y., Henri, A., Charlier, C., et al. (2010). Muscle resident macrophages control the immune cell reaction in a mouse model of notexin-induced myoinjury. *Arthritis Rheum.* 62, 268–279. doi: 10.1002/art.27183

Burzyn, D., Kuswanto, W., Kolodin, D., Shadrach, J. L., Cerletti, M., Jang, Y., et al. (2013). A special population of regulatory T cells potentiates muscle repair. *Cell* 155, 1282–1295. doi: 10.1016/j.cell.2013.10.054

Cai, B., Spencer, M. J., Nakamura, G., Tseng-Ong, L., and Tidball, J. G. (2000). Eosinophilia of dystrophin-deficient muscle is promoted by perforin-mediated cytotoxicity by T cell effectors. *Am. J. Pathol.* 156, 1789–1796. doi: 10.1016/S0002-9440(10)65050-X

Camiña, F., Novo-Rodriguez, M. I., Rodriguez-Segade, S., and Castro-Gago, M. (1995). Purine and carnitine metabolism in muscle of patients with Duchenne muscular dystrophy. *Clin. Chim. Acta* 243, 151–164. doi: 10.1016/0009-8981(95)06164-9

Carlson, C. G. (1998). The dystrophinopathies: an alternative to the structural hypothesis. *Neurobiol. Dis.* 5, 3–15. doi: 10.1006/nbdi.1998.0188

Castro-Gago, M., Lojo, S., Novo, I., del Rio, R., Peña, J., and Rodriguez-Segade, S. (1987). Effects of chronic allopurinol therapy on purine metabolism in Duchenne muscular dystrophy. *Biochem. Biophys. Res. Commun.* 147, 152–157. doi: 10.1016/S0006-291X(87)80100-6

Ceruti, S., Giammarioli, A. M., Camurri, A., Falzano, L., Rufini, S., Frank, C., et al. (2000). Adenosine- and 2-chloro-adenosine-induced cytopathic effects on myoblastic cells and myotubes: involvement of different intracellular mechanisms. *Neuromuscul. Disord.* 10, 436–446. doi: 10.1016/S0960-8966(00)00118-8

Chen, J. F., Eltzschig, H. K., and Fredholm, B. B. (2013). Adenosine receptors as drug targets–what are the challenges? *Nat. Rev. Drug Discov.* 12, 265–286. doi: 10.1038/nrd3955

Cohn, R. D., and Campbell, K. P. (2000). Molecular basis of muscular dystrophies. *Muscle Nerve* 23, 1456–1471. doi: 10.1002/1097-4598(200010)23:10<1456::AID-MUS2>3.0.CO;2-T

Connolly, A. M., Malkus, E. C., Mendell, J. R., Flanigan, K. M., Miller, J. P., Schierbecker, J. R., et al. (2015). Outcome reliability in non-ambulatory boys/men with Duchenne muscular dystrophy. *Muscle Nerve* 51, 522–532. doi: 10.1002/mus.24346

De Pasquale, L., D'Amico, A., Verardo, M., Petrini, S., Bertini, E., and De Benedetti, F. (2012). Increased muscle expression of interleukin-17 in Duchenne muscular dystrophy. *Neurology* 78, 1309–1314. doi: 10.1212/WNL.0b013e31825 18302

Dooley, J., Gordon, K. E., Dodds, L., and MacSween, J. (2010). Duchenne muscular dystrophy: a 30-year population-based incidence study. *Clin. Pediatr.* 49, 177–179. doi: 10.1177/0009922809347777

Farini, A., Meregalli, M., Belicchi, M., Battistelli, M., Parolini, D., D'Antona, G., et al. (2007). T and B lymphocyte depletion has a marked effect on the fibrosis of dystrophic skeletal muscles in the scid/mdx mouse. *J. Pathol.* 213, 229–238. doi: 10.1002/path.2213

Fenichel, G. M., Mendell, J. R., Moxley, R. T. III, Griggs, R. C., Brooke, M. H., Miller, J. P., et al. (1991). A comparison of daily and alternate-day prednisone therapy in the treatment of Duchenne muscular dystrophy. *Arch. Neurol.* 48, 575–579. doi: 10.1001/archneur.1991.00530180027012

Flanigan, K. M., Campbell, K., Viollet, L., Wang, W., Gomez, A. M., Walker, C. M., et al. (2013). Anti-dystrophin T cell responses in Duchenne muscular dystrophy: prevalence and a glucocorticoid treatment effect. *Hum. Gene Ther.* 24, 797–806. doi: 10.1089/hum.2013.092

Garcia Soriano, F., Liaudet, L., Marton, A., Haskó, G., Batista Lorigados, C., Deitch, E. A., et al. (2001). Inosine improves gut permeability and vascular reactivity in endotoxic shock. *Crit. Care Med.* 29, 703–708. doi: 10.1097/00003246-200104000-00001

Gazzerro, E., Baldassari, S., Assereto, S., Fruscione, F., Pistorio, A., Panicucci, C., et al. (2015). Enhancement of muscle T regulatory cells and improvement of muscular dystrophic process in mdx mice by blockade of extracellular ATP/P2X axis. *Am. J. Pathol.* 185, 3349–3360. doi: 10.1016/j.ajpath.2015.08.010

Griggs, R. C., Moxley, R. T. III, Mendell, J. R., Fenichel, G. M., Brooke, M. H., Pestronk, A., et al. (1991). Prednisone in Duchenne dystrophy. A randomized, controlled trial defining the time course and dose response. Clinical investigation of duchenne dystrophy group. *Arch. Neurol.* 48, 383–388. doi: 10.1001/archneur.1991.00530160047012

Griggs, R. C., Moxley, R. T. III, Mendell, J. R., Fenichel, G. M., Brooke, M. H., Pestronk, A., et al. (1993). Duchenne dystrophy: randomized, controlled trial of prednisone (18 months) and azathioprine (12 months). *Neurology* 43(3 Pt 1), 520–527. doi: 10.1212/WNL.43.3_Part_1.520

Guglieri, M., Bushby, K., McDermott, M. P., Hart, K. A., Tawil, R., Martens, W. B., et al. (2017). Developing standardized corticosteroid treatment for Duchenne muscular dystrophy. *Contemp. Clin. Trials* 58, 34–39. doi: 10.1016/j.cct.2017.04.008

Guiraud, S., and Davies, K. E. (2017). Pharmacological advances for treatment in Duchenne muscular dystrophy. *Curr. Opin. Pharmacol.* 34, 36–48. doi: 10.1016/j.coph.2017.04.002

Harcourt, L. J., Holmes, A. G., Gregorevic, P., Schertzer, J. D., Stupka, N., Plant, D. R., et al. (2005). Interleukin-15 administration improves diaphragm muscle pathology and function in dystrophic mdx mice. *Am. J. Pathol.* 166, 1131–1141. doi: 10.1016/S0002-9440(10)62333-4

Haskó, G., Kuhel, D. G., Németh, Z. H., Mabley, J. G., Stachlewitz, R. F., Virág, L., et al. (2000). Inosine inhibits inflammatory cytokine production by a posttranscriptional mechanism and protects against endotoxin-induced shock. *J. Immunol.* 164, 1013–1019. doi: 10.4049/jimmunol.164.2.1013

Hatano, R., Ohnuma, K., Yamamoto, J., Dang, N. H., and Morimoto, C. (2013). CD26-mediated co-stimulation in human CD8(+) T cells provokes effector function via pro-inflammatory cytokine production. *Immunology* 138, 165–172. doi: 10.1111/imm.12028

Honda, H., Kimura, H., and Rostami, A. (1990). Demonstration and phenotypic characterization of resident macrophages in rat skeletal muscle. *Immunology* 70, 272–277.

Ibegbu, C. C., Xu, Y. X., Fillos, D., Radziewicz, H., Grakoui, A., and Kourtis, A. P. (2009). Differential expression of CD26 on virus-specific CD8(+) T cells during active, latent and resolved infection. *Immunology* 126, 346–353. doi: 10.1111/j.1365-2567.2008.02899.x

Kameoka, J., Tanaka, T., Nojima, Y., Schlossman, S. F., and Morimoto, C. (1993). Direct association of adenosine deaminase with a T cell activation antigen, CD26. *Science* 261, 466–469. doi: 10.1126/science.8101391

Kar, N. C., and Pearson, C. M. (1973). Muscle adenylic acid deaminase activity. Selective decrease in early-onset Duchenne muscular dystrophy. *Neurology* 23, 478–482. doi: 10.1212/WNL.23.5.478

Kirschner, J., Schessl, J., Schara, U., Reitter, B., Stettner, G. M., Hobbiebrunken, E., et al. (2010). Treatment of Duchenne muscular dystrophy with ciclosporin A: a randomised, double-blind, placebo-controlled multicentre trial. *Lancet Neurol.* 9, 1053–1059. doi: 10.1016/S1474-4422(10)70196-4

Kissel, J. T., Lynn, D. J., Rammohan, K. W., Klein, J. P., Griggs, R. C., Moxley, R. T. III, et al. (1993). Mononuclear cell analysis of muscle biopsies in prednisone- and azathioprine-treated Duchenne muscular dystrophy. *Neurology* 43(3 Pt 1), 532–536. doi: 10.1212/WNL.43.3_Part_1.532

Lang, R. M., Badano, L. P., Mor-Avi, V., Afilalo, J., Armstrong, A., Ernande, L., et al. (2015). Recommendations for cardiac chamber quantification by echocardiography in adults: an update from the American Society of echocardiography and the European association of cardiovascular imaging. *Eur. Heart J. Cardiovasc. Imaging* 16, 233–270. doi: 10.1093/ehjci/jev014

Lapidos, K. A., Kakkar, R., and McNally, E. M. (2004). The dystrophin glycoprotein complex: signaling strength and integrity for the sarcolemma. *Circ. Res.* 94, 1023–1031. doi: 10.1161/01.RES.0000126574.61061.25

Lerario, A., Bonfiglio, S., Sormani, M., Tettamanti, A., Marktel, S., Napolitano, S., et al. (2012). Quantitative muscle strength assessment in duchenne muscular dystrophy: longitudinal study and correlation with functional measures. *BMC Neurol.* 12:91. doi: 10.1186/1471-2377-12-91

Lopez, L., Colan, S. D., Frommelt, P. C., Ensing, G. J., Kendall, K., Younoszai, A. K., et al. (2010). Recommendations for quantification methods during the performance of a pediatric echocardiogram: a report from the pediatric measurements writing group of the American society of echocardiography pediatric and congenital heart disease council. *J. Am. Soc. Echocardiogr.* 23, 465–495; quiz: 576–577. doi: 10.1016/j.echo.2010.03.019

Macey, M., Azam, U., McCarthy, D., Webb, L., Chapman, E. S., Okrongly, D., et al. (2002). Evaluation of the anticoagulants EDTA and citrate, theophylline, adenosine, and dipyridamole (CTAD) for assessing platelet activation on the ADVIA 120 hematology system. *Clin. Chem.* 48(6 Pt 1), 891–899.

Martin, P. T., Golden, B., Okerblom, J., Camboni, M., Chandrasekharan, K., Xu, R., et al. (2014). A comparative study of N-glycolylneuraminic acid (Neu5Gc) and cytotoxic T cell (CT) carbohydrate expression in normal and dystrophin-deficient dog and human skeletal muscle. *PLoS ONE* 9:e88226. doi: 10.1371/journal.pone.0088226

Marton, A., Pacher, P., Murthy, K. G., Németh, Z. H., Haskó, G., and Szabó, C. (2001). Anti-inflammatory effects of inosine in human monocytes, neutrophils and epithelial cells *in vitro*. *Int. J. Mol. Med.* 8, 617–621. doi: 10.3892/ijmm.8.6.617

Mathur, S., Lott, D. J., Senesac, C., Germain, S. A., Vohra, R. S., Sweeney, H. L., et al. (2010). Age-related differences in lower-limb muscle cross-sectional area and torque production in boys with Duchenne muscular dystrophy. *Arch. Phys. Med. Rehabil.* 91, 1051–1058. doi: 10.1016/j.apmr.2010.03.024

Mendell, J. R., Moxley, R. T., Griggs, R. C., Brooke, M. H., Fenichel, G. M., Miller, J. P., et al. (1989). Randomized, double-blind six-month trial of prednisone in Duchenne's muscular dystrophy. *N. Engl. J. Med.* 320, 1592–1597. doi: 10.1056/NEJM198906153202405

Morimoto, C., and Schlossman, S. F. (1998). The structure and function of CD26 in the T-cell immune response. *Immunol. Rev.* 161, 55–70. doi: 10.1111/j.1600-065X.1998.tb01571.x

Möser, G. H., Schrader, J., and Deussen, A. (1989). Turnover of adenosine in plasma of human and dog blood. *Am. J. Physiol.* 256(4 Pt 1),C799–C806.

Ohnuma, K., Takahashi, N., Yamochi, T., Hosono, O., Dang, N. H., and Morimoto, C. (2008). Role of CD26/dipeptidyl peptidase IV in human T cell activation and function. *Front. Biosci.* 13, 2299–2310. doi: 10.2741/2844

Posner, A. D., Soslow, J. H., Burnette, W. B., Bian, A., Shintani, A., Sawyer, D. B., et al. (2016). The correlation of skeletal and cardiac muscle dysfunction in Duchenne muscular dystrophy. *J. Neuromusc. Dis.* 3, 91–99. doi: 10.3233/JND-150132

Rando, T. A. (2001). The dystrophin-glycoprotein complex, cellular signaling, and the regulation of cell survival in the muscular dystrophies. *Muscle Nerve* 24, 1575–1594. doi: 10.1002/mus.1192

Rosenberg, A. S., Puig, M., Nagaraju, K., Hoffman, E. P., Villalta, S. A., Rao, V. A., et al. (2015). Immune-mediated pathology in Duchenne muscular dystrophy. *Sci. Transl. Med.* 7:299rv4. doi: 10.1126/scitranslmed.aaa7322

Rufini, S., Rainaldi, G., Abbracchio, M. P., Fiorentini, C., Capri, M., Franceschi, C., et al. (1997). Actin cytoskeleton as a target for 2-chloro adenosine: evidence for induction of apoptosis in C2C12 myoblastic cells. *Biochem. Biophys. Res. Commun.* 238, 361–366. doi: 10.1006/bbrc.1997.7287

Ryzhov, S., Matafonov, A., Galindo, C. L., Zhang, Q., Tran, T. L., Lenihan, D. J., et al. (2017). ERBB signaling attenuates proinflammatory activation of nonclassical monocytes. *Am. J. Physiol. Heart Circ. Physiol.* 312, H907–H918. doi: 10.1152/ajpheart.00486.2016

Soslow, J. H., Xu, M., Slaughter, J. C., Stanley, M., Crum, K., Markham, L. W., et al. (2016). Evaluation of echocardiographic measures of left ventricular function in patients with Duchenne muscular dystrophy: assessment of reproducibility and comparison to cardiac magnetic resonance imaging. *J. Am. Soc. Echocardiogr.* 29, 983–991. doi: 10.1016/j.echo.2016.07.001

Spencer, M. J., and Tidball, J. G. (2001). Do immune cells promote the pathology of dystrophin-deficient myopathies? *Neuromuscul. Disord.* 11, 556–564. doi: 10.1016/S0960-8966(01)00198-5

Swiger, K. J., Friedman, E. A., Brittain, E. L., Tomasek, K. A., Huang, S., Su, Y. R., et al. (2016). Plasma hepatocyte growth factor is a novel marker of AL cardiac amyloidosis. *Amyloid* 23, 242–248. doi: 10.1080/13506129.2016.1242480

Tidball, J. G., Dorshkind, K., and Wehling-Henricks, M. (2014). Shared signaling systems in myeloid cell-mediated muscle regeneration. *Development* 141, 1184–1196. doi: 10.1242/dev.098285

Vetrone, S. A., Montecino-Rodriguez, E., Kudryashova, E., Kramerova, I., Hoffman, E. P., Liu, S. D., et al. (2009). Osteopontin promotes fibrosis in dystrophic mouse muscle by modulating immune cell subsets and intramuscular TGF-beta. *J. Clin. Invest.* 119, 1583–1594. doi: 10.1172/JCI 37662

Villalta, S. A., Deng, B., Rinaldi, C., Wehling-Henricks, M., and Tidball, J. G. (2011). IFN-gamma promotes muscle damage in the mdx mouse model of Duchenne muscular dystrophy by suppressing M2 macrophage activation and inhibiting muscle cell proliferation. *J. Immunol.* 187, 5419–5428. doi: 10.4049/jimmunol.1101267

Villalta, S. A., Nguyen, H. X., Deng, B., Gotoh, T., and Tidball, J. G. (2009). Shifts in macrophage phenotypes and macrophage competition for arginine metabolism affect the severity of muscle pathology in muscular dystrophy. *Hum. Mol. Genet.* 18, 482–496. doi: 10.1093/hmg/ddn376

Villalta, S. A., Rosenthal, W., Martinez, L., Kaur, A., Sparwasser, T., Tidball, J. G., et al. (2014). Regulatory T cells suppress muscle inflammation and injury in muscular dystrophy. *Sci. Transl. Med.* 6:258ra142. doi: 10.1126/scitranslmed.3009925

Wallace, D. L., Berard, M., Soares, M. V., Oldham, J., Cook, J. E., Akbar, A. N., et al. (2006). Prolonged exposure of naive CD8+ T cells to interleukin-7 or interleukin-15 stimulates proliferation without differentiation or loss of telomere length. *Immunology* 119, 243–253. doi: 10.1111/j.1365-2567.2006.02429.x

Wehling-Henricks, M., Sokolow, S., Lee, J. J., Myung, K. H., Villalta, S. A., and Tidball, J. G. (2008). Major basic protein-1 promotes fibrosis of dystrophic muscle and attenuates the cellular immune response in muscular dystrophy. *Hum. Mol. Genet.* 17, 2280–2292. doi: 10.1093/hmg/ddn129

Wilson, J. M., Kurtz, C. C., Black, S. G., Ross, W. G., Alam, M. S., Linden, J., et al. (2011). The A2B adenosine receptor promotes Th17 differentiation via stimulation of dendritic cell IL-6. *J. Immunol.* 186, 6746–6752. doi: 10.4049/jimmunol.1100117

Wong, B. L., and Christopher, C. (2002). Corticosteroids in Duchenne muscular dystrophy: a reappraisal. *J. Child Neurol.* 17, 183–190. doi: 10.1177/088307380201700306

Zhang, J., Xiao, Z., Qu, C., Cui, W., Wang, X., and Du, J. (2014). CD8 T cells are involved in skeletal muscle regeneration through facilitating MCP-1 secretion and Gr1(high) macrophage infiltration. *J. Immunol.* 193, 5149–5160. doi: 10.4049/jimmunol.1303486

Conflict of Interest Statement: The authors declare that the research was conducted in the absence of any commercial or financial relationships that could be construed as a potential conflict of interest.

frontiers in Pharmacology

ORIGINAL RESEARCH
published: 18 December 2017
doi: 10.3389/fphar.2017.00903

Age-Related Decrease in Male Extra-Striatal Adenosine A_1 Receptors Measured Using ^{11}C-MPDX PET

Masahiro Mishina[1,2,3], Yuichi Kimura[2,4], Muneyuki Sakata[2], Kenji Ishii[2], Keiichi Oda[2,5], Jun Toyohara[2], Kazumi Kimura[3] and Kiichi Ishiwata[2,6,7]*

[1] Department of Neuro-pathophysiological Imaging, Graduate School of Medicine, Nippon Medical School, Tokyo, Japan, [2] Research Team for Neuroimaging, Tokyo Metropolitan Institute of Gerontology, Tokyo, Japan, [3] Department of Neurological Science, Graduate School of Medicine, Nippon Medical School, Tokyo, Japan, [4] Department of Computational Systems Biology, Faculty of Biology-Oriented Science and Technology, Kindai University, Kinokawa, Japan, [5] Department of Radiological Technology, Faculty of Health Sciences, Hokkaido University of Science, Sapporo, Japan, [6] Institute of Cyclotron and Drug Discovery Research, Southern TOHOKU Research Institute for Neuroscience, Koriyama, Japan, [7] Department of Biofunctional Imaging, Fukushima Medical University, Fukushima, Japan

Adenosine A_1 receptors (A_1Rs) are widely distributed throughout the entire human brain, while adenosine A_{2A} receptors (A_{2A}Rs) are present in dopamine-rich areas of the brain, such as the basal ganglia. A past study using autoradiography reported a reduced binding ability of A_1R in the striatum of old rats. We developed positron emission tomography (PET) ligands for mapping the adenosine receptors and we successfully visualized the A_1Rs using 8-dicyclopropylmethyl-1-^{11}C-methyl-3-propylxanthine (^{11}C-MPDX). We previously reported that the density of A_1Rs decreased with age in the human striatum, although we could not observe an age-related change in A_{2A}Rs. The aim of this study was to investigate the age-related change of the density of A_1Rs in the thalamus and cerebral cortices of healthy participants using ^{11}C-MPDX PET. We recruited eight young (22.0 ± 1.7 years) and nine elderly healthy male volunteers (65.7 ± 8.0 years). A dynamic series of decay-corrected PET scans was performed for 60 min starting with the injection of ^{11}C-MPDX. We placed the circular regions of interest of 10 mm in diameter in ^{11}C-MPDX PET images. The values for the binding potential (BP_{ND}) of ^{11}C-MPDX in the thalamus, and frontal, temporal, occipital, and parietal cortices were calculated using a graphical analysis, wherein the reference region was the cerebellum. BP_{ND} of ^{11}C-MPDX was significantly lower in elderly participants than young participants in the thalamus, and frontal, temporal, occipital, and parietal cortices. In the human brain, we could observe the age-related decrease in the distribution of A_1Rs.

Keywords: adenosine A_1 receptor, aging, positron emission tomography, humans, cerebral cortex, thalamus

OPEN ACCESS

Edited by:
Francisco Ciruela, University of Barcelona, Spain

Reviewed by:
Vittoria Colotta, University of Florence, Italy
Elena Martín-García, Pompeu Fabra University, Spain

****Correspondence:***
Masahiro Mishina
mishina@nms.ac.jp

Specialty section:
This article was submitted to Experimental Pharmacology and Drug Discovery, a section of the journal Frontiers in Pharmacology

Received: *30 August 2017*
Accepted: *28 November 2017*
Published: *18 December 2017*

Citation:
Mishina M, Kimura Y, Sakata M, Ishii K, Oda K, Toyohara J, Kimura K and Ishiwata K (2017) Age-Related Decrease in Male Extra-Striatal Adenosine A_1 Receptors Measured Using ^{11}C-MPDX PET. Front. Pharmacol. 8:903. doi: 10.3389/fphar.2017.00903

INTRODUCTION

Medical development has increased the average human lifespan (Vaupel, 2010). Cognitive functions such as memory often decline as humans age (van Geldorp et al., 2015), and aging is the major risk factor for Alzheimer's disease (Fjell et al., 2014a). Human brain becomes atrophied with the aging (Fjell et al., 2014b), although brain atrophy remains mild in some elderly people

called "superager" or "successful aging" whose cognitive functions remain intact with age (Depp and Jeste, 2006; Harrison et al., 2012; Sun et al., 2016).

Neuronal systems responsible for brain function are known to decline with age (Morrison and Baxter, 2012). In the human brain, neuroimaging studies revealed that endogenous dopamine, and dopamine transporter, D_1 and D_2 receptors and aromatic L-amino acid decarboxylase decrease with age (Suhara et al., 1991; Reeves et al., 2002; Ishibashi et al., 2009), while monoamine oxidase B increases with age (Reeves et al., 2002). Such age-related decrease has also been reported in the cholinergic, glutamatergic and γ-aminobutyric acid (GABA)ergic systems (Segovia et al., 2001; Rissman et al., 2007; Schliebs and Arendt, 2011).

In the adenosinergic system, animal studies reported that the age-related changes differ in the subtypes: adenosine A_1 (A_1R) and A_{2A} receptors ($A_{2A}R$) (Cunha et al., 1995, 2001; Lopes et al., 1999; Rebola et al., 2003; Meerlo et al., 2004). We developed ligands for positron emission tomography (PET) to map the adenosine receptors, and successfully visualized the A_1Rs using 8-dicyclopropylmethyl-1-^{11}C-methyl-3-propylxanthine (^{11}C-MPDX, **Figure 1**) (Fukumitsu et al., 2005) and the $A_{2A}Rs$ using [7-methyl-^{11}C]-(*E*)-8-(3,4,5-trimethoxystyryl)-1,3,7-trimethylxanthine (^{11}C-TMSX) (Ishiwata et al., 2000a,b, 2002). Using ^{11}C-MPDX and ^{11}C-TMSX PET, we previously reported that the density of A_1Rs decreased with age in the human striatum, although we could not observe an age-related change in $A_{2A}Rs$ (Mishina et al., 2012). In order to compare A_1R and $A_{2A}R$, we did not study the density of A_1Rs other than striatum in the past paper (Mishina et al., 2012). Because $A_{2A}Rs$ are enriched in the striatum (Fredholm and Svenningsson, 2003; Mishina et al., 2007), while A_1Rs are widely distributed throughout the entire human brain (Fukumitsu et al., 2005). Another human PET study reported that the binding ability of ^{18}F-8-cyclopentyl-3-(3-fluoropropyl)-1-propylxanthine (^{18}F-CPFPX), an A_1R ligand, was negatively correlated with age in the cerebral cortices and thalamus in addition to the striatum (Meyer et al., 2007). The A_1Rs in the cerebral cortex are thought to help regulate the GABAergic and glutamatergic systems (Albasanz et al., 2002; Cunha-Reis et al., 2008; Ferreira et al., 2014), while A_1Rs in the striatum are mainly responsible for the regulation of the D_1 receptor in medium spiny neurons (Ferre et al., 1994; Yabuuchi et al., 2006). We hypothesized that the A_1Rs may decrease with age in the thalamus and cerebral cortices. The aim of this study was to investigate the age-related change in the density of A_1Rs in the thalamus and cerebral cortices of healthy participants using ^{11}C-MPDX PET.

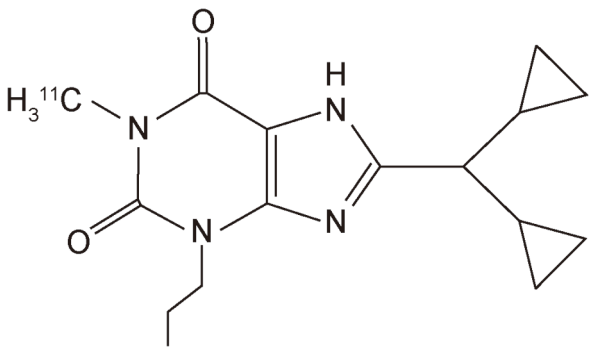

FIGURE 1 | Chemical structures of ^{11}C-MPDX.

MATERIALS AND METHODS

Participants

We recruited eight young healthy (mean age ± standard deviation [SD], 22.0 ± 1.7 years, age range, 20–25 years) and nine elderly male volunteers (65.7 ± 8.0 years, age range, 51–77 years). The participants were all Japanese and right-handed. None of the participants had a history of neurological diseases or any abnormalities upon physical or neurological examinations. Additionally, none took any medications known to affect the brain function or had a history of alcoholism. They had no medical history of bronchial asthma, and did not regularly use theophylline, a nonselective A_1R and $A_{2A}R$ antagonist.

This study was approved by the Ethics Committee of Tokyo Metropolitan Institute of Gerontology. Written, informed consent was obtained from all participants in this study.

Magnetic Resonance Imaging (MRI)

MRI was performed in the Tokyo Metropolitan Geriatric Hospital with three-dimensional spoiled gradient-recalled echo (SPGR) imaging and a SIGNA 1.5 Tesla machine (General Electric, Waukesha, WI, United States). The MRI images validated that the participants had no neurological diseases, such as stroke or brain tumors, and were used as a reference for placing the regions of interest (ROIs) on the PET images.

PET Measurements

Positron emission tomography was performed in the Positron Medical Center, Tokyo Metropolitan Institute of Gerontology with a SET-2400W PET scanner (Shimadzu, Kyoto, Japan). The scanner had an axial field-of-view of 20 cm, acquired 63 slices at a center-to-center interval of 3.125 mm, and had a spatial resolution of 4.4 mm full width at half maximum (FWHM) and a z-axis resolution of 6.5 mm FWHM (Fujiwara et al., 1997). All participants were asked to abstain from caffeinated beverages, such as tea and coffee, and foods containing chocolate, for 12 h prior to undergoing the ^{11}C-MPDX PET, because caffeine is a non-selective adenosine receptor antagonist (Statland and Demas, 1980). ^{11}C-MPDX was prepared as described previously (Fukumitsu et al., 2005). To obtain an attenuation map to correct for photon attenuation, an 8-min transmission scan with a rotating ^{68}Ga/^{68}Ge line source was recorded before the radiotracer injection. Starting at the time of injection, a dynamic series of decay-corrected PET scans was performed for 60 min in a two-dimensional scanning mode. The injected dose of ^{11}C-MPDX was 639 ± 77 MBq (16.0 ± 11.6 nmol). Specific activity at the time of injection ranged from 14.6 to 129.5 TBq/mmol (59.5 ± 36.8 TBq/mmol). The total number of frames was 27 and the frame arrangements were 6 × 10 s, 3 × 30 s, 5 × 1 min, 5 × 2.5 min, and 8 × 5 min.

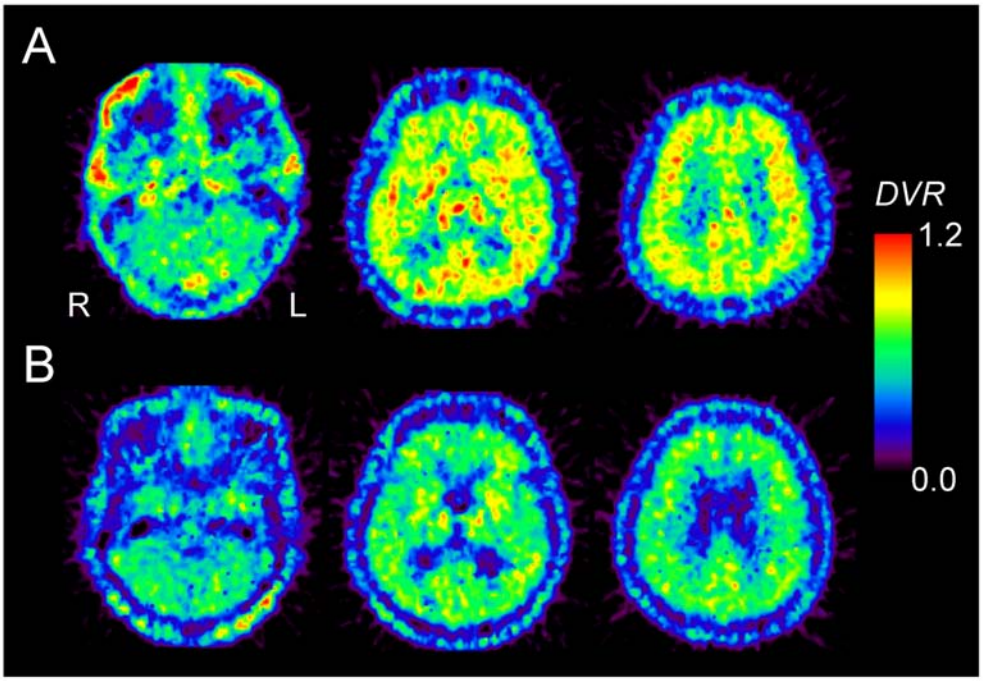

FIGURE 2 | ^{11}C-MPDX PET images for a 22-year-old male subject **(A)** and a 77-year-old male subject **(B)**. The pixel values for the PET images of ^{11}C-MPDX are visualized as the distribution volume ratio (*DVR*), because the brain anatomy is unclear in the BP_{ND} images of ^{11}C-MPDX. Note that we use the values for the binding potential (BP_{ND}) in the kinetic analysis for ^{11}C-MPDX PET in **Figures 3** and **4**.

Image Processing

Image analyses were carried out with the medical image processing software Dr. View/Linux R2.5 (AJS, Tokyo, Japan) implemented in CentOS 5.4 (The CentOS Project[1]) and Parallels Desktop 5.0.9344 (Parallels Holdings, Renton, WA, United States).

We generated early images, which were considered similar to images for cerebral blood flow, by summing frames from 0 to 10 min (Mishina et al., 2000). The MRI image was three-dimensionally registered to the early image of each participant. The early images and the registered MRI images were used as references for placing each ROI on the PET images from the dynamic scans. Circular ROIs with 10 mm in diameter were placed bilaterally on the PET images over the thalamus, frontal, temporal, occipital, and parietal cortex. We also placed the circular ROI over the cerebellar hemisphere as a reference region for kinetic analysis. Averaged tissue time activity curves (tTACs) were derived from the dynamic data and ROI, and data were used to calculate the standardized uptake value.

Kinetic analyses of the tTACs were performed using programs implemented on MATLAB version 7.04 (The Mathworks, Natick, MA, United States) and a General Kinetic Modeling Tool in PMOD 3.0 (PMOD Technologies, Zurich, Switzerland). The values for the binding potential (BP_{ND}) of ^{11}C-MPDX (Kimura et al., 2004) in the regions were calculated using an averaged tTAC and a graphical analysis with the cerebellum as the reference region (Logan, 2003), where the k_2 of the reference region was 0.23/min that was the averaged k_2 as presented in the **Table 1** of a past paper (Kimura et al., 2004) and the starting time for the analysis was 10 min after the administration. We confirmed that the BP_{ND} of ^{11}C-MPDX was suitable for evaluating the distribution of A_1Rs (Kimura et al., 2004).

Statistical Analysis

Statistical computations were performed using the software package JMP Pro version 13.2.0 (SAS Institute, Cary, NC, United States). If the variance had a significant difference between young and elderly groups with Bartlett's test, Welch's t-test were used to compare the BP_{ND} of ^{11}C-MPDX. If not, unpaired *t*-tests were used instead. We also used the regression analysis to compare the age with the BP_{ND} of participants. The level of significance was set at $p < 0.05$.

RESULTS

Figure 2 shows representative ^{11}C-MPDX PET images. BP_{ND} of ^{11}C-MPDX was significantly smaller in elderly participants than young participants in the thalamus (young *vs.* elderly; 0.43 ± 0.07 *vs.* 0.33 ± 0.06, $p < 0.01$; unpaired *t*-test), frontal (0.19 ± 0.04 *vs.* 0.12 ± 0.04, $p < 0.001$; unpaired *t*-test), temporal (0.29 ± 0.05 *vs.* 0.21 ± 0.06, $p < 0.05$; unpaired *t*-test), occipital (0.31 ± 0.05 *vs.* 0.23 ± 0.06, $p < 0.05$; unpaired *t*-test), and parietal cortices (0.27 ± 0.05 *vs.* 0.20 ± 0.06, $p < 0.05$; unpaired *t*-test, **Figure 3**).

[1]http://www.centos.org/

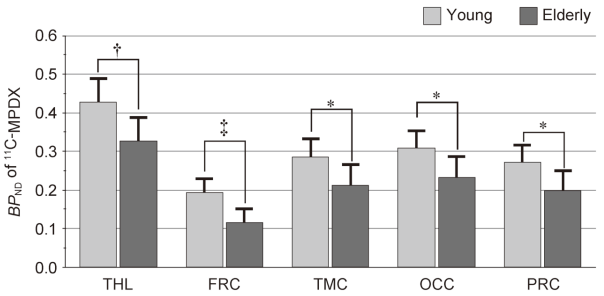

FIGURE 3 | BP_{ND} of ^{11}C-MPDX in the young and elderly participants. BP_{ND} of ^{11}C-MPDX was significantly smaller in elderly participants than young participants in the thalamus, frontal, temporal, occipital, and parietal cortex. THL, thalamus; FRC, frontal cortex; TMC, temporal cortex; OCC, occipital cortex; PRC, parietal cortex. $^*p < 0.05$, $^†p < 0.01$, $^‡p < 0.001$, unpaired *t*-test.

Regression analyses also showed that the BP_{ND} of ^{11}C-MPDX was negatively correlated with age in the thalamus ($R^2 = 0.458$; $p < 0.005$, **Figure 4A**), and frontal ($R^2 = 0.500$; $p < 0.005$, **Figure 4B**), temporal ($R^2 = 0.402$; $p < 0.01$, **Figure 4C**), occipital ($R^2 = 0.338$; $p < 0.05$, **Figure 4D**), and parietal cortices ($R^2 = 0.349$; $p < 0.05$, **Figure 4E**).

DISCUSSION

In the human thalamus and cerebral cortices, we observed an age-related decrease of the BP_{ND} of ^{11}C-MPDX, which is in line with previous findings in the striatum (Mishina et al., 2012). Two reasons are considered to have reduced the BP_{ND} of ^{11}C-MPDX, namely (1) reduced binding site and (2) increased endogenous adenosine. If the concentration of extracellular adenosine is increased, the estimated apparent BP_{ND} using ^{11}C-MPDX is decreased by competition at the A_1R between endogenous adenosine and ^{11}C-MPDX. Extracellular adenosine levels in the striatum were not affected by age (Burnstock and Dale, 2015), although no data are available on adenosine in the cerebral cortex. In addition, the affinity of ^{11}C-MPDX is higher than that of adenosine (Noguchi et al., 1997; Müller and Jacobson, 2011; Mishina and Ishiwata, 2014). These findings weaken the counter-hypothesis that the age-related decrease in the BP_{ND} of ^{11}C-MPDX involved an increase in adenosine. Therefore, the results involved an age-related decrease in A_1Rs in the human brain.

Some studies have revealed differences in age-related changes between A_1Rs and A_{2A}Rs (Burnstock and Dale, 2015). The age-related changes vary in different brain regions. Cunha et al. (1995) studied age-related changes in rats, using [^{3}H]2-[4-(2-p-carboxyethyl)phenylamino]-5′-*N*-ethylcarboxamidoadenosine (^{3}H-CGS 21680) for A_1Rs and [^{3}H]-1,3-dipropyl-8-cyclopentylxanthine (^{3}H-DPCPX) for A_{2A}Rs. In their study, A_1Rs were decreased in the cerebral cortex and hippocampus, but A_{2A}Rs were increased only in the cerebral cortex of aged rats. No significant changes were observed in A_1R of the striatum and in A_{2A}R of both the hippocampus and the striatum. An autoradiography study using [^{3}H]N6-cyclohexyladenosine demonstrated that there was an age-dependent reduction in A_1Rs in most of the brain areas of rats, but that the degree of the reduction varied among regions (Meerlo et al., 2004). Efficiency of A_{2A}Rs to modulate synaptic transmission in the hippocampus was decreased in aged rats (Sebastiao et al., 2000), although the efficiency of A_{2A}Rs was

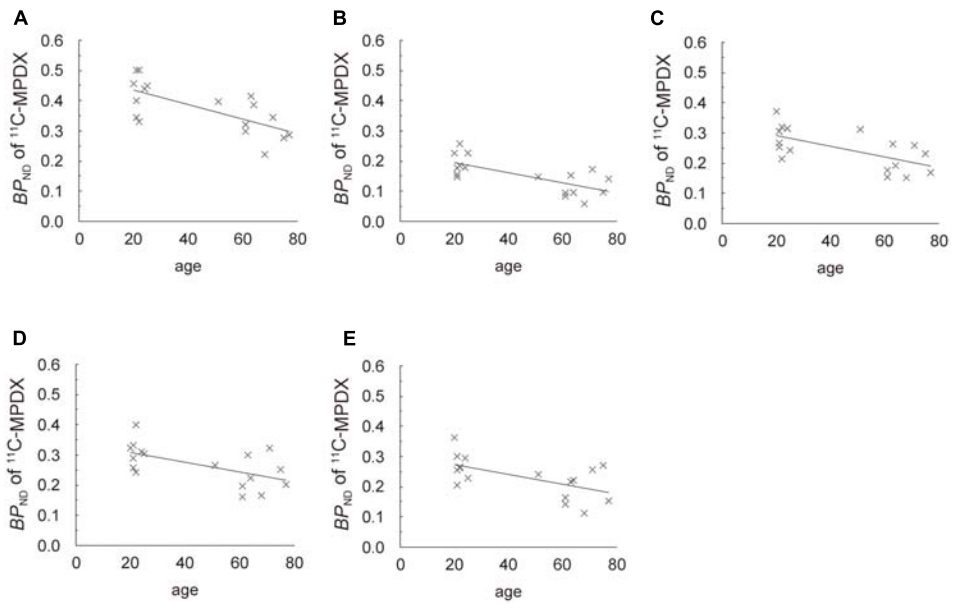

FIGURE 4 | Scattergrams of age *vs.* BP_{ND} of ^{11}C-MPDX. BP_{ND} of ^{11}C-MPDX was negatively correlated with age in the thalamus **(A)**, and frontal **(B)**, temporal **(C)**, occipital **(D)**, and parietal cortices **(E)**.

increased by aging (Lopes et al., 1999; Rebola et al., 2003). It seems that there are age-related changes in the balance between inhibitory A_1R- and excitatory A_{2A}R-mediated actions.

A limitation the lack of data on participants' daily sleep state. A_1R and A_{2A}R play an important role in regulating sleep (Basheer et al., 2000; Scammell et al., 2001; Urade et al., 2003; Elmenhorst et al., 2007; Oishi et al., 2008). Some studies showed that sleep deprivation increased A_1R (Basheer et al., 2000; Elmenhorst et al., 2007). Another study suggested that endogenous adenosine suppressed the histaminergic system via A_1R to promote non-rapid eye movement sleep (Oishi et al., 2008). Many elderly people are suffering from insomnia (Dijk et al., 2000; Ohayon et al., 2004; Colrain, 2011). The age-related changes to A_1R may be associated with insomnia in elderly people.

Another limitation of this study was the lack of data on participants' daily caffeine intake. In this study, we restricted caffeine consumption in the 12 h prior to performing PET scans, because caffeine is a non-selective adenosine receptor antagonist. Many elderly Japanese people habitually drink green tea after meals (Kuriyama et al., 2006), although the overall caffeine consumption is attributed more to coffee than to tea in Japan (Fredholm et al., 1999). Animal studies reported that chronic administration of caffeine increases the density of adenosine receptors (Green and Stiles, 1986; Nehlig et al., 1992; Li et al., 2008), although human data are sparse. Another limitation the lack of data on participants' daily sleep state. Adenosine is involved in circadian rhythm and sleep (Bjorness and Greene, 2009), and adenosine inhibits the arousal system via A_1R and induces sleep (Oishi et al., 2008). Elderly people often have sleep disorders. Further studies are needed to reveal the relationship between chronic caffeine consumption and A_1R density.

Our study was only comprised of males. A post-mortem study reported adenosine level in the cerebral cortex was higher in male than in female (Kovacs et al., 2010). However, some papers showed that there was no significant gender effect on A_1Rs in the human brain (Ulas et al., 1993; Glass et al., 1996; Meyer et al., 2007).

AUTHOR CONTRIBUTIONS

MM wrote the first draft of the manuscript. MM, KeI, KO, JT, and KiI performed PET examinations. YK and MS performed kinetic analyses. KK and KiI supervised the study. All authors reviewed, commented on, and approved the final report.

ACKNOWLEDGMENTS

This work was funded by Grants-in-Aid for Scientific Research (B) No. 16390348, (B) No. 20390334, (C) No. 17590901, (C) No. 20591033, and (C) No. 23591287 from the Japan Society for the Promotion of Science.

REFERENCES

Albasanz, J. L., Leon, D., Ruiz, M. A., Fernandez, M., and Martin, M. (2002). Adenosine A1 receptor agonist treatment up-regulates rat brain metabotropic glutamate receptors. *Biochim. Biophys. Acta* 1593, 69–75. doi: 10.1016/S0167-4889(02)00330-0

Basheer, R., Porkka-Heiskanen, T., Strecker, R. E., Thakkar, M. M., and McCarley, R. W. (2000). Adenosine as a biological signal mediating sleepiness following prolonged wakefulness. *Biol. Signals Recept.* 9, 319–327. doi: 10.1159/000014655

Bjorness, T. E., and Greene, R. W. (2009). Adenosine and sleep. *Curr. Neuropharmacol.* 7, 238–245. doi: 10.2174/157015909789152182

Burnstock, G., and Dale, N. (2015). Purinergic signalling during development and ageing. *Purinergic Signal.* 11, 277–305. doi: 10.1007/s11302-015-9452-9

Colrain, I. M. (2011). Sleep and the brain. *Neuropsychol. Rev.* 21, 1–4. doi: 10.1007/s11065-011-9156-z

Cunha, R. A., Constantino, M. C., Sebastiao, A. M., and Ribeiro, J. A. (1995). Modification of A1 and A2a adenosine receptor binding in aged striatum, hippocampus and cortex of the rat. *Neuroreport* 6, 1583–1588. doi: 10.1097/00001756-199507310-00029

Cunha, R. A., Constantino, M. D., Fonseca, E., and Ribeiro, J. A. (2001). Age-dependent decrease in adenosine A1 receptor binding sites in the rat brain. Effect of cis unsaturated free fatty acids. *Eur. J. Biochem.* 268, 2939–2947. doi: 10.1046/j.1432-1327.2001.02183.x

Cunha-Reis, D., Ribeiro, J. A., and Sebastiao, A. M. (2008). A_1 and A_{2A} receptor activation by endogenous adenosine is required for VIP enhancement of K^+-evoked [^{3}H]-GABA release from rat hippocampal nerve terminals. *Neurosci. Lett.* 430, 207–212. doi: 10.1016/j.neulet.2007.10.037

Depp, C. A., and Jeste, D. V. (2006). Definitions and predictors of successful aging: a comprehensive review of larger quantitative studies. *Am. J. Geriatr. Psychiatry* 14, 6–20. doi: 10.1097/01.JGP.0000192501.03069.bc

Dijk, D. J., Duffy, J. F., and Czeisler, C. A. (2000). Contribution of circadian physiology and sleep homeostasis to age-related changes in human sleep. *Chronobiol. Int.* 17, 285–311. doi: 10.1081/CBI-100101049

Elmenhorst, D., Meyer, P. T., Winz, O. H., Matusch, A., Ermert, J., Coenen, H. H., et al. (2007). Sleep deprivation increases A1 adenosine receptor binding in the human brain: a positron emission tomography study. *J. Neurosci.* 27, 2410–2415. doi: 10.1523/JNEUROSCI.5066-06.2007

Ferre, S., Popoli, P., Gimenez-Llort, L., Finnman, U. B., Martinez, E., Scotti de Carolis, A., et al. (1994). Postsynaptic antagonistic interaction between adenosine A1 and dopamine D1 receptors. *Neuroreport* 6, 73–76. doi: 10.1097/00001756-199412300-00020

Ferreira, D. D., Stutz, B., de Mello, F. G., Reis, R. A., and Kubrusly, R. C. (2014). Caffeine potentiates the release of GABA mediated by NMDA receptor activation: involvement of A1 adenosine receptors. *Neuroscience* 281, 208–215. doi: 10.1016/j.neuroscience.2014.09.060

Fjell, A. M., McEvoy, L., Holland, D., Dale, A. M., Walhovd, K. B., and Alzheimer's Disease Neuroimaging Initiative (2014a). What is normal in normal aging? Effects of aging, amyloid and Alzheimer's disease on the cerebral cortex and the hippocampus. *Prog. Neurobiol.* 117, 20–40. doi: 10.1016/j.pneurobio.2014.02.004

Fjell, A. M., Westlye, L. T., Grydeland, H., Amlien, I., Espeseth, T., Reinvang, I., et al. (2014b). Accelerating cortical thinning: unique to dementia or universal in aging? *Cereb. Cortex* 24, 919–934. doi: 10.1093/cercor/bhs379

Fredholm, B. B., Battig, K., Holmen, J., Nehlig, A., and Zvartau, E. E. (1999). Actions of caffeine in the brain with special reference to factors that contribute to its widespread use. *Pharmacol. Rev.* 51, 83–133.

Fredholm, B. B., and Svenningsson, P. (2003). Adenosine-dopamine interactions: development of a concept and some comments on therapeutic possibilities. *Neurology* 61(11 Suppl. 6), S5–S9. doi: 10.1212/01.WNL.0000095204.89871.FF

Fujiwara, T., Watanuki, S., Yamamoto, S., Miyake, M., Seo, S., Itoh, M., et al. (1997). Performance evaluation of a large axial field-of-view PET scanner: SET-2400W. *Ann. Nucl. Med.* 11, 307–313. doi: 10.1007/BF03165298

Fukumitsu, N., Ishii, K., Kimura, Y., Oda, K., Sasaki, T., Mori, Y., et al. (2005). Adenosine A1 receptor mapping of the human brain by PET with 8-dicyclopropylmethyl-1-11C-methyl-3-propylxanthine. *J. Nucl. Med.* 46, 32–37.

Glass, M., Faull, R. L., Bullock, J. Y., Jansen, K., Mee, E. W., Walker, E. B., et al. (1996). Loss of A1 adenosine receptors in human temporal lobe epilepsy. *Brain Res.* 710, 56–68. doi: 10.1016/0006-8993(95)01313-X

Green, R. M., and Stiles, G. L. (1986). Chronic caffeine ingestion sensitizes the A1 adenosine receptor-adenylate cyclase system in rat cerebral cortex. *J. Clin. Invest.* 77, 222–227. doi: 10.1172/JCI112280

Harrison, T. M., Weintraub, S., Mesulam, M. M., and Rogalski, E. (2012). Superior memory and higher cortical volumes in unusually successful cognitive aging. *J. Int. Neuropsychol. Soc.* 18, 1081–1085. doi: 10.1017/S1355617712000847

Ishibashi, K., Ishii, K., Oda, K., Kawasaki, K., Mizusawa, H., and Ishiwata, K. (2009). Regional analysis of age-related decline in dopamine transporters and dopamine D2-like receptors in human striatum. *Synapse* 63, 282–290. doi: 10.1002/syn.20603

Ishiwata, K., Noguchi, J., Wakabayashi, S., Shimada, J., Ogi, N., Nariai, T., et al. (2000a). 11C-labeled KF18446: a potential central nervous system adenosine A2A receptor ligand. *J. Nucl. Med.* 41, 345–354.

Ishiwata, K., Ogi, N., Shimada, J., Nonaka, H., Tanaka, A., Suzuki, F., et al. (2000b). Further characterization of a CNS adenosine A2A receptor ligand [11C]KF18446 with in vitro autoradiography and in vivo tissue uptake. *Ann. Nucl. Med.* 14, 81–89.

Ishiwata, K., Ogi, N., Hayakawa, N., Oda, K., Nagaoka, T., Toyama, H., et al. (2002). Adenosine A2A receptor imaging with [11C]KF18446 PET in the rat brain after quinolinic acid lesion: comparison with the dopamine receptor imaging. *Ann. Nucl. Med.* 16, 467–475. doi: 10.1007/BF02988643

Kimura, Y., Ishii, K., Fukumitsu, N., Oda, K., Sasaki, T., Kawamura, K., et al. (2004). Quantitative analysis of adenosine A1 receptors in human brain using positron emission tomography and [1-methyl-11C]8-dicyclopropylmethyl-1-methyl-3-propylxanthine. *Nucl. Med. Biol.* 31, 975–981. doi: 10.1016/j.nucmedbio.2004.06.005

Kovacs, Z., Juhasz, G., Dobolyi, A., Bobest, M., Papp, V., Takats, L., et al. (2010). Gender- and age-dependent changes in nucleoside levels in the cerebral cortex and white matter of the human brain. *Brain Res. Bull.* 81, 579–584. doi: 10.1016/j.brainresbull.2009.10.010

Kuriyama, S., Shimazu, T., Ohmori, K., Kikuchi, N., Nakaya, N., Nishino, Y., et al. (2006). Green tea consumption and mortality due to cardiovascular disease, cancer, and all causes in Japan: the Ohsaki study. *JAMA* 296, 1255–1265. doi: 10.1001/jama.296.10.1255

Li, W., Dai, S., An, J., Li, P., Chen, X., Xiong, R., et al. (2008). Chronic but not acute treatment with caffeine attenuates traumatic brain injury in the mouse cortical impact model. *Neuroscience* 151, 1198–1207. doi: 10.1016/j.neuroscience.2007.11.020

Logan, J. (2003). A review of graphical methods for tracer studies and strategies to reduce bias. *Nucl. Med. Biol.* 30, 833–844. doi: 10.1016/S0969-8051(03)00114-8

Lopes, L. V., Cunha, R. A., and Ribeiro, J. A. (1999). Increase in the number, G protein coupling, and efficiency of facilitatory adenosine A2A receptors in the limbic cortex, but not striatum, of aged rats. *J. Neurochem.* 73, 1733–1738. doi: 10.1046/j.1471-4159.1999.731733.x

Meerlo, P., Roman, V., Farkas, E., Keijser, J. N., Nyakas, C., and Luiten, P. G. (2004). Ageing-related decline in adenosine A1 receptor binding in the rat brain: an autoradiographic study. *J. Neurosci. Res.* 78, 742–748. doi: 10.1002/jnr.20314

Meyer, P. T., Elmenhorst, D., Boy, C., Winz, O., Matusch, A., Zilles, K., et al. (2007). Effect of aging on cerebral A1 adenosine receptors: a [18F]CPFPX PET study in humans. *Neurobiol. Aging* 28, 1914–1924. doi: 10.1016/j.neurobiolaging.2006.08.005

Mishina, M., and Ishiwata, K. (2014). Adenosine receptor PET imaging in human brain. *Int. Rev. Neurobiol.* 119, 51–69. doi: 10.1016/B978-0-12-801022-8.00002-7

Mishina, M., Ishiwata, K., Kimura, Y., Naganawa, M., Oda, K., Kobayashi, S., et al. (2007). Evaluation of distribution of adenosine A2A receptors in normal human brain measured with [^{11}C]TMSX PET. *Synapse* 61, 778–784. doi: 10.1002/syn.20423

Mishina, M., Kimura, Y., Naganawa, M., Ishii, K., Oda, K., Sakata, M., et al. (2012). Differential effects of age on human striatal adenosine A1 and A2A receptors. *Synapse* 66, 832–839. doi: 10.1002/syn.21573

Mishina, M., Senda, M., Kimura, Y., Toyama, H., Ishiwata, K., Ohyama, M., et al. (2000). Intrasubject correlation between static scan and distribution volume images for [^{11}C]flumazenil PET. *Ann. Nucl. Med.* 14, 193–198. doi: 10.1007/BF02987859

Morrison, J. H., and Baxter, M. G. (2012). The ageing cortical synapse: hallmarks and implications for cognitive decline. *Nat. Rev. Neurosci.* 13, 240–250. doi: 10.1038/nrn3200

Müller, C. E., and Jacobson, K. A. (2011). Recent developments in adenosine receptor ligands and their potential as novel drugs. *Biochim. Biophys. Acta* 1808, 1290–1308. doi: 10.1016/j.bbamem.2010.12.017

Nehlig, A., Daval, J. L., and Debry, G. (1992). Caffeine and the central nervous system: mechanisms of action, biochemical, metabolic and psychostimulant effects. *Brain Res. Brain Res. Rev.* 17, 139–170. doi: 10.1016/0165-0173(92)90012-B

Noguchi, J., Ishiwata, K., Furuta, R., Simada, J., Kiyosawa, M., Ishii, S., et al. (1997). Evaluation of carbon-11 labeled KF15372 and its ethyl and methyl derivatives as a potential CNS adenosine A1 receptor ligand. *Nucl. Med. Biol.* 24, 53–59. doi: 10.1016/S0969-8051(96)00161-8

Ohayon, M. M., Carskadon, M. A., Guilleminault, C., and Vitiello, M. V. (2004). Meta-analysis of quantitative sleep parameters from childhood to old age in healthy individuals: developing normative sleep values across the human lifespan. *Sleep* 27, 1255–1273. doi: 10.1093/sleep/27.7.1255

Oishi, Y., Huang, Z. L., Fredholm, B. B., Urade, Y., and Hayaishi, O. (2008). Adenosine in the tuberomammillary nucleus inhibits the histaminergic system via A1 receptors and promotes non-rapid eye movement sleep. *Proc. Natl. Acad. Sci. U.S.A.* 105, 19992–19997. doi: 10.1073/pnas.0810926105

Rebola, N., Sebastiao, A. M., de Mendonca, A., Oliveira, C. R., Ribeiro, J. A., and Cunha, R. A. (2003). Enhanced adenosine A2A receptor facilitation of synaptic transmission in the hippocampus of aged rats. *J. Neurophysiol.* 90, 1295–1303. doi: 10.1152/jn.00896.2002

Reeves, S., Bench, C., and Howard, R. (2002). Ageing and the nigrostriatal dopaminergic system. *Int. J. Geriatr. Psychiatry* 17, 359–370. doi: 10.1002/gps.606

Rissman, R. A., De Blas, A. L., and Armstrong, D. M. (2007). GABAA receptors in aging and Alzheimer's disease. *J. Neurochem.* 103, 1285–1292. doi: 10.1111/j.1471-4159.2007.04832.x

Scammell, T. E., Gerashchenko, D. Y., Mochizuki, T., McCarthy, M. T., Estabrooke, I. V., Sears, C. A., et al. (2001). An adenosine A2a agonist increases sleep and induces Fos in ventrolateral preoptic neurons. *Neuroscience* 107, 653–663. doi: 10.1016/S0306-4522(01)00383-9

Schliebs, R., and Arendt, T. (2011). The cholinergic system in aging and neuronal degeneration. *Behav. Brain Res.* 221, 555–563. doi: 10.1016/j.bbr.2010.11.058

Sebastiao, A. M., Cunha, R. A., de Mendonca, A., and Ribeiro, J. A. (2000). Modification of adenosine modulation of synaptic transmission in the hippocampus of aged rats. *Br. J. Pharmacol.* 131, 1629–1634. doi: 10.1038/sj.bjp.0703736

Segovia, G., Porras, A., Del Arco, A., and Mora, F. (2001). Glutamatergic neurotransmission in aging: a critical perspective. *Mech. Ageing Dev.* 122, 1–29. doi: 10.1016/S0047-6374(00)00225-6

Statland, B. E., and Demas, T. J. (1980). Serum caffeine half-lives. Healthy subjects vs. patients having alcoholic hepatic disease. *Am. J. Clin. Pathol.* 73, 390–393. doi: 10.1093/ajcp/73.3.390

Suhara, T., Fukuda, H., Inoue, O., Itoh, T., Suzuki, K., Yamasaki, T., et al. (1991). Age-related changes in human D1 dopamine receptors measured by positron emission tomography. *Psychopharmacology* 103, 41–45. doi: 10.1007/BF02244071

Sun, F. W., Stepanovic, M. R., Andreano, J., Barrett, L. F., Touroutoglou, A., and Dickerson, B. C. (2016). Youthful brains in older adults: preserved neuroanatomy in the default mode and salience networks contributes to youthful memory in superaging. *J. Neurosci.* 36, 9659–9668. doi: 10.1523/JNEUROSCI.1492-16.2016

Ulas, J., Brunner, L. C., Nguyen, L., and Cotman, C. W. (1993). Reduced density of adenosine A1 receptors and preserved coupling of adenosine A1 receptors to G proteins in Alzheimer hippocampus: a quantitative autoradiographic study. *Neuroscience* 52, 843–854. doi: 10.1016/0306-4522(93)90533-L

Urade, Y., Eguchi, N., Qu, W. M., Sakata, M., Huang, Z. L., Chen, J. F., et al. (2003). Sleep regulation in adenosine A2A receptor-deficient mice. *Neurology* 61(11 Suppl. 6), S94–S96. doi: 10.1212/01.WNL.0000095222.41066.5E

van Geldorp, B., Heringa, S. M., van den Berg, E., Olde Rikkert, M. G., Biessels, G. J., and Kessels, R. P. (2015). Working memory binding and episodic memory formation in aging, mild cognitive impairment, and Alzheimer's dementia. *J. Clin. Exp. Neuropsychol.* 37, 538–548. doi: 10.1080/13803395.2015.1037722

Vaupel, J. W. (2010). Biodemography of human ageing. *Nature* 464, 536–542. doi: 10.1038/nature08984

Yabuuchi, K., Kuroiwa, M., Shuto, T., Sotogaku, N., Snyder, G. L., Higashi, H., et al. (2006). Role of adenosine A1 receptors in the modulation of dopamine D1 and adenosine A2A receptor signaling in the neostriatum. *Neuroscience* 141, 19–25. doi: 10.1016/j.neuroscience.2006.04.047

Conflict of Interest Statement: The authors declare that the research was conducted in the absence of any commercial or financial relationships that could be construed as a potential conflict of interest.

frontiers in Pharmacology

ORIGINAL RESEARCH
published: 15 December 2017
doi: 10.3389/fphar.2017.00918

P2X4 Receptor *in Silico* and Electrophysiological Approaches Reveal Insights of Ivermectin and Zinc Allosteric Modulation

*Verónica Latapiat[1], Felipe E. Rodríguez[1], Francisca Godoy[2], Felipe A. Montenegro[2], Nelson P. Barrera[2] and Juan P. Huidobro-Toro[1,3]**

[1] Laboratorio de Farmacología de Nucleótidos, Departamento de Biología, Facultad de Química y Biología, Estación Central, Universidad de Santiago de Chile, Santiago, Chile, [2] Departamento de Fisiología, Facultad de Ciencias Biológicas, Pontificia Universidad Católica de Chile, Santiago, Chile, [3] Centro Desarrollo de Nanociencia y Nanotecnología, CEDENNA, Estación Central, Universidad de Santiago de Chile, Santiago, Chile

OPEN ACCESS

Edited by:
Francisco Ciruela, University of Barcelona, Spain

Reviewed by:
Antonio R. Artalejo, Complutense University of Madrid, Spain
Dietmar Krautwurst, German Research Centre for Food Chemistry (LG), Germany

***Correspondence:**
Juan P. Huidobro-Toro
juan.garcia-huidobro@usach.cl

Specialty section:
This article was submitted to Experimental Pharmacology and Drug Discovery, a section of the journal Frontiers in Pharmacology

Received: *15 September 2017*
Accepted: *01 December 2017*
Published: *15 December 2017*

Citation:
Latapiat V, Rodríguez FE, Godoy F, Montenegro FA, Barrera NP and Huidobro-Toro JP (2017) P2X4 Receptor in Silico and Electrophysiological Approaches Reveal Insights of Ivermectin and Zinc Allosteric Modulation. Front. Pharmacol. 8:918. doi: 10.3389/fphar.2017.00918

Protein allosteric modulation is a pillar of metabolic regulatory mechanisms; this concept has been extended to include ion channel regulation. P2XRs are ligand-gated channels activated by extracellular ATP, sensitive to trace metals and other chemicals. By combining *in silico* calculations with electrophysiological recordings, we investigated the molecular basis of P2X4R modulation by Zn(II) and ivermectin, an antiparasite drug currently used in veterinary medicine. To this aim, docking studies, molecular dynamics simulations and non-bonded energy calculations for the P2X4R in the apo and holo states or in the presence of ivermectin and/or Zn(II) were accomplished. Based on the crystallized *Danio rerio* P2X4R, the rat P2X4R, P2X2R, and P2X7R structures were modeled, to determine ivermectin binding localization. Calculations revealed that its allosteric site is restricted to transmembrane domains of the P2X4R; the role of Y42 and W46 plus S341 and non-polar residues were revealed as essential, and are not present in the homologous P2X2R or P2X7R transmembrane domains. This finding was confirmed by preferential binding conformations and electrophysiological data, revealing P2X4R modulator specificity. Zn(II) acts in the P2X4R extracellular domain neighboring the SS3 bridge. Molecular dynamics in the different P2X4R states revealed allosterism-induced stability. Pore and lateral fenestration measurements of the P2X4R showed conformational changes in the presence of both modulators compatible with a larger opening of the extracellular vestibule. Electrophysiological studies demonstrated additive effects in the ATP-gated currents by joint applications of ivermectin plus Zn(II). The C132A P2X4R mutant was insensitive to Zn(II); but IVM caused a 4.9 ± 0.7-fold increase in the ATP-evoked currents. Likewise, the simultaneous application of both modulators elicited a 7.1 ± 1.7-fold increase in the ATP-gated current. Moreover, the C126A P2X4R mutant evoked similar ATP-gated currents comparable to those of wild-type P2X4R. Finally, a P2X4/2R chimera did not respond to IVM but Zn(II) elicited a 2.7 ± 0.6-fold increase in the ATP-gated current. The application of IVM plus Zn(II) evoked a 2.7 ± 0.9-fold

increase in the ATP-gated currents. In summary, allosteric modulators caused additive ATP-gated currents; consistent with lateral fenestration enlargement. Energy calculations demonstrated a favorable transition of the holo receptor state following both allosteric modulators binding, as expected for allosteric interactions.

Keywords: P2X4R, positive allosteric modulation, ivermectin, Zn(II), molecular docking, molecular dynamics, independent allosteric modulator sites

INTRODUCTION

P2XRs are ATP-gated ionotropic channels; seven different clones are known which form functional channels as homo- and heterotrimers (Nicke et al., 1998; Barrera et al., 2005; Marquez-Klaka et al., 2007). Each subunit has two membrane domains and a large extracellular loop comprising 10 conserved cysteines to form five intersubunit disulphide bonds (Kawate et al., 2009). These receptor sets firmly established the extracellular role of nucleotides as novel signal molecules implicated in physiological and pathophysiological conditions including transmitter function in sympathetic co-transmission, the pain pathway, gliotransmission, epithelia and endothelial cell signaling, platelet aggregation, urinary reflex, smooth muscle contractility, bone physiology, among other roles (Burnstock, 2007; Köles et al., 2007; Coddou et al., 2011).

Upon ATP binding to its orthosteric site, conformational changes occur in the region linking the extracellular domain with the transmembrane (TM) helices, and the three lateral portals known as "lateral fenestrations", which reach 8 Å in diameter in the holo state (Jiang et al., 2013). Analysis of the crystallized P2X4R structure (Hattori and Gouaux, 2012) revealed two possible cation pathways in the holo state via lateral fenestrations, or the central pore pathway lined by negatively charged residues. Recent experiments based on accessibility studies and on electrostatic energy calculations convincingly demonstrated that ions gain access to the P2X4R pore mainly through the three lateral fenestrations (Kawate et al., 2011; Samways et al., 2011, 2012; Roberts et al., 2012).

P2XRs, like other ionic ligand-gated channels, are modulated by several endogenous compounds, including trace metals such as Zn(II) or Cu(II) (Coddou et al., 2003b, 2005; Huidobro-Toro et al., 2008). Zn(II) is stored in synaptic vesicles. Upon electrical depolarization, a fraction of the stored metal may be released to the synaptic cleft (Kardos et al., 1989; Kay, 2006; Kay and Tóth, 2006) to modify neurotransmission (Peralta and Huidobro-Toro, 2016). Therefore, the final response due to the activation of the ATP-gated channels depends not only on the concentration of ATP, but also on the presence of allosteric modulators in the synapse. Since P2XR channels do not contain a linear metal binding motif, we hypothesized that the metal binding site forms after receptor protein folding, exposing the three-dimensional metal binding site. In the P2X4R, the specific role of C132 and H140 were identified related to the coordination of Zn(II) and Cu(II), respectively (Acuña-Castillo et al., 2000; Coddou et al., 2003a, 2007; Lorca et al., 2005; Huidobro-Toro et al., 2008), which are critical as structural elements to understand receptor topology and its molecular basis of allosteric modulation (Cully et al., 1994; Vassilatis et al., 1997; Adelsberger et al., 2000). Ivermectin (IVM), a semisynthetic macrocyclic lactone derived from *Streptomycetes avermectilis* is an antiparasite amply used in veterinary medicine (Omura and Crump, 2004; Geary, 2005). IVM has multiple ionic channel targets (including glutamate and nicotinic receptors), but in parasites it appears to paralyze nematodes by intensifying GABA-A-mediated peripheral nerve transmission. Several reports also indicate that IVM facilitates selectively P2X4R-mediated ATP-gated currents (Khakh et al., 1999; Priel and Silberberg, 2004). In the absence of IVM, this channel activates and deactivates rapidly, does not show transition from the open to dilated states, desensitizes completely at a moderate rate, and recovers only fractionally during washout. IVM treatment triggers a larger ATP-dependent current in a concentration and time-dependent manner, and slows receptor desensitization during sustained ATP applications and receptor deactivation. Rescuing the receptor from desensitization temporally coincides with pore dilation, and the dilated channel can be reactivated after ATP washout (Khakh et al., 1999; Priel and Silberberg, 2004; Jelínková et al., 2006; Zemkova et al., 2015). The spatial location of the IVM binding site has not yet been addressed in the context of the recent crystal structures of a zP2X4R in an apo, closed channel state (Kawate et al., 2009), and holo, open state, with ATP bound crystals (Hattori and Gouaux, 2012). The molecular mechanism of IVM action is related to an allosteric interaction that involves both TM helices at the protein-lipid interface during the opening of the P2X4R pore (Jelínková et al., 2006; Jelinkova et al., 2008; Silberberg et al., 2007; Zemkova et al., 2007). Mutations of nonpolar residues in the lower part of TM1 and TM2 helices apparently did not disturb IVM affinity, but rather the efficacy with which IVM potentiates the receptor. Additionally, the three-dimensional models of the IVM and TM1 fragment of P2X4R suggest that these residues might be accessible simultaneously by large IVM concentrations. In agreement with this information, none of the single mutants in this region fully eliminated IVM effects on current amplitude and the rate of deactivation (Silberberg et al., 2007; Jelinkova et al., 2008; Zemkova et al., 2014). Using molecular docking, W46, and W50 in TM1 plus D331, M336 in TM2 were identified as sites for IVM binding, while residues N338, S341, G342, L346, G347, A349, and I356 all belonging to the P2X4R TM2 which were supposed to play a role in IVM modulation (Silberberg et al., 2007; Jelinkova et al., 2008). Interestingly, these sites are located at the bottom of the P2X4R lateral fenestrations. However, the conformational changes induced by P2X4R positive allosteric modulators such as IVM or Zn(II) remain to be understood in detail.

We hypothesized that IVM and Zn(II) modulate independently the P2X4R by binding at separate sites that may cause additive or even synergistic effects when applied in a concomitant manner. To this aim, we combined *in silico* methods with electrophysiological protocols, to describe how and where these modulators elicit P2X4R positive allosterism. Based on P2X4R models, docking studies, and molecular dynamics (MD) simulations, pore and lateral fenestrations analysis and non-bonded energy were calculated. We assessed the mode of action of these modulators by studying the nature of the interaction in several P2X4R mutants and a P2X4/2R chimera. MD simulations of P2X4R bound to allosteric modulators are consistent with the opening of a larger upper extracellular vestibule and receptor lateral fenestrations, revealing the energetically favorable state transition induced by allosterism. The present report shows how receptor structural determinants provide pharmacodynamically relevant molecular insights to identify allosteric regulatory mechanisms.

MATERIALS AND METHODS

Molecular Modeling of Rat P2XRs

While rat P2X4R shares a 62% sequence identity with the open/closed state, *Danio rerio* P2X4R X-ray diffraction structure (PDB ID: 3I5D, Kawate et al., 2009; PDB ID: 4DW1, Hattori and Gouaux, 2012), P2X2R shares a 48% sequence identity with open state *D. rerio* P2X4R X-ray diffraction structure (PDB ID: 4DW1, Hattori and Gouaux, 2012), and P2X7R shares a 76% sequence identity with open state *Ailuropoda melanoleuca* P2X7R X-ray diffraction structure (PDB ID:5U2H, Karasawa and Kawate, 2016). Using these reference structures, we built homology models of P2X4R holo, P2X4R apo, P2X2R holo and P2X7R holo states, via Modeller v 9.10 software (Sali and Blundell, 1993). Final Modeler models were chosen based on model quality using the DOPE (Discrete Optimized Protein Energy) method (Shen and Sali, 2006), a statistical potential optimized for model assessment. Models were further assessed by RAMPAGE (Lovell et al., 2002) through Ramachandran plots for residue distribution in favored, allowed, and outlier regions. The energetic quality of three-dimensional models was verified by ProSA (Protein Structure Analysis) (Wiederstein and Sippl, 2007) to calculate an overall quality score of the predicted structures.

The rat P2X4R models were embedded into a phosphatidylcholine (POPC) lipid bilayer in a water box; hydrated systems were neutralized with 150 mM NaCl. The all-atom systems were subjected to MD simulations under periodic bordering conditions and isobaric-isothermal ensemble (NPT). The full systems were minimized using NAMD 2.9 software (Phillips et al., 2005) for 50,000 time-step minimization and subsequently equilibrated for 5 ns.

Molecular Docking of P2XRs with IVM

Homology minimized models of the rat P2X4 apo, P2X4R, P2X2R, and P2X7R holo states were used in docking simulations to identify IVM binding sites. The molecular docking procedure used Autodock software (Morris et al., 2009) employing the Lamarckian genetic algorithm (Morris et al., 1998). ATP and IVM structures were obtained from the Pubchem database (Kim et al., 2016). P2XR models were prepared using Autodock with grid size for ATP: 126 Å×126 Å×126 Å, and IVM: 120 Å×120 Å×80 Å). ATP and IVM binding sites were defined from known P2XR structures (PDB ID: 4DW1, Hattori and Gouaux, 2012; Popova et al., 2013). The rat P2XRs were kept rigid and ligands set flexible to rotate and explore the most probable binding poses. The search was done with 100 dockings with four repetitions per complex.

MD Simulations of Allosteric Modulators Bound to P2X4Rs

Six systems were considered: P2X4R apo; P2X4R holo; P2X4R holo with IVM; P2X4R holo with Zn(II), and P2X4R holo with IVM plus Zn(II). MD simulations were performed with the CHARMM (Brooks et al., 2009) force field protocol, and each molecular complex was embedded into a 140 × 140 Å POPC lipid bilayer in a water box of the TIP3P water model (Jorgensen et al., 1983). The hydrated system was neutralized with 150 mM NaCl. The system was submitted to an MD simulation under periodic bordering conditions, NPT ensemble, and 300 K temperature. The full system was minimized by NAMD 2.9 software (Phillips et al., 2005) for 50,000 minimization steps, 5 ns thermodynamic equilibration, and 35 ns of production dynamics.

Pore Radius and Lateral Fenestration Measurements of P2XRs Bound to Allosteric Modulators

After MD simulations of each system, the HOLE program (Smart et al., 1996) was used to determine P2X4R channel pore dimensions, considering the last 10 ns of trajectory simulation (see above). Lateral fenestration length was measured between Cα of D58 residues (Jiang et al., 2013) in adjacent receptor subunits. Similarly, the upper region of lateral fenestration was calculated using the distance between Cα of V323 and S62 residues from adjacent subunits.

Non-bonded Energy Calculations for P2X4R Bound to Allosteric Modulators

Non-bonded energy ($E_{Non-bonded} = E_{van\ der\ Walls} + E_{Electrostatic}$) (Levitt, 2001) was used to determine whether the reactions are energetically favorable (non-bonded energy of products lower than the energy of reactants) or not at constant pressure and temperature (Thauer et al., 1977). Non-bonded energy difference ($\Delta E_{protein}$), between the apo and holo state of P2X4R was calculated in the presence of allosteric modulators using the last 10 ns of the simulation trajectory (total simulation time 40 ns).

Protocols Characterizing P2XR Expression

Oocyte Microinjection and P2XR Expression in *Xenopus laevis*

Stage 5–6 *Xenopus laevis* oocytes were manually defolliculated and incubated for 15 min with 1 mg/mL collagenase 1A. Separate sets of oocytes were injected intranuclearly with 3–5 ng cDNA for wild type (wt) rat P2X4R, P2X2R, or P2X7Rs, Cys-mutated P2X4R,and the P2X4/2R chimera receptor. Non-injected oocytes did not evoke currents upon exogenous ATP applications. Each protocol was replicated in at least 4-5 different oocytes attained from separate oocyte batches from separate *X. laevis* frogs. The

animals were carefully handled before, during, and after surgery; in accordance with the principles of the Helsinki declaration on animal welfare and our Faculty and University ethical procedures. All protocols regarding oocyte microinjections were approved by the Universidad de Santiago Ethical Committee as well as by the local Faculty Ethical Committee (protocol code 471-2017). Injected oocytes were stored at 12°C for 36–48 h in Barth's incubation solution containing (mM): 88 NaCl; 1 KCl; 2.4 $NaHCO_3$; 10 HEPES; 0.82 $MgSO_4$; 0.33 $Ca(NO_3)_2$; 0.91 $CaCl_2$; pH 7.5 supplemented with 10 IU/L penicillin/10 mg streptomycin, and 2 mM pyruvate. On the testing day, oocytes were clamped at −70 mV using the two-electrode voltage-clamp configuration with an OC-725C clamper (Warner Instruments Corp., Hamden, CT, USA). The 1 μM ATP-gated currents were recorded following regular 10 s nucleotide applications, which were repeated at regular 10-min intervals. Recovery of control ATP-gated currents was always assessed. ATP, Zn(II) and the IVM stock solution in DMSO were dissolved in Barth's media and perfused to the oocyte using a pump operating at constant flow (2 mL/min). Control DMSO experiments were performed to rule out a possible solvent effect. The procedure for oocyte dissection and P2XR expression followed the Acuña-Castillo et al. (2007) or Coddou et al. (2007) detailed protocols.

Modulator Action of IVM and Zn(II) in wt P2XRs

To examine the IVM specificity as a P2XR modulator, oocytes expressing the rat P2X4, P2X2, or P2X7R were tested by application of 3 μM ATP preincubated with 3 μM IVM for 3 min, following the Silberberg et al. (2007) protocol. IVM was dissolved in DMSO; the final dilution was less than 0.1%, a vehicle concentration that did not affect ATP-evoked currents of control oocytes. In all protocols, full reversal of the IVM effect was mandatory prior to assessing a following IVM concentration. Recovery of the basal ATP-gated currents was assessed comparing the magnitude of ATP-gated currents every 8–10 min. The same protocol was followed using oocytes administered with P2X2R and P2X7Rs. The results are expressed as the fold-increase in the ATP-evoked currents.

To assess the nature of the metal modulator action, 10 μM Zn(II) was always pre-applied for 1 min before 1 μM ATP applications. Reversal of the metal modulator effect was always checked by comparing the ATP-evoked currents in the same oocyte after prolonged metal washout. The results are expressed as the fold-increase in the ATP-evoked currents. To confirm the results observed in oocytes, identical protocols were performed with HEK 293 cells expressing the wt P2X4R. To this end, 3 μM IVM or 10 μM Zn(II) pre-applications were performed for 3 min or 1 min prior to the 1 μM ATP application.

Joint Application of IVM and Zn(II) in wt P2XRs

The same oocyte was used to assess the action of both modulators applied simultaneously: 3 μM IVM was first applied, followed 2 min later by a 1 min pre-application of 10 μM Zn(II). One minute later, oocytes were challenged with 1 μM ATP. As controls, the same oocytes were previously tested separately with either 3 μM IVM or 10 μM Zn(II). Experiments where one of the modulators showed a statistically weak response were discarded, reducing experimental variability (2/48 cases). The results are expressed as the fold-increase of the 1 μM ATP-evoked currents. Oocyte findings were confirmed in HEK293 cells expressing the wt P2X4R.

Experiments with P2X4R Mutants and P2X4/2R Chimera

Similar protocols as described previously were performed in oocytes injected with the following P2X4R mutants: C132A, C126A or the P2X4/2R chimera. C126A and C132A mutated P2X4Rs and chimeric P2X4/2R. Mutants were synthetized as reported by Coddou et al. (2007); the P2X4/2R chimera contained the extracellular domain of the P2X4R but the membrane and intracellular domains of the P2X2R (He et al., 2003). This chimera was a personal contribution of Dr. S. Stojilkovic (National Institute of Health, Bethesda, USA) for this particular study. We next examined the relevance of the Zn(II) and IVM potentiation in oocytes injected with either C126A or C132A P2X4R mutants. For this purpose, we recorded the currents gated by 1 μM ATP, and ATP in the presence of either 10 μM Zn(II) or 3 μM IVM, or both modulators co-applied. Reversibility of the two modulator s' effects was mandatory prior to continuing with the protocol. All experiments tested the action of both modulators on the same oocyte.

Chimeric receptors: Protocols first examined the magnitude of the 3 μM ATP-gated currents in oocytes and HEK cells, respectively, in the presence of either 10 μM Zn(II) or 3 μM IVM alone. Next, we assessed the ATP-gated currents exposed to both modulators applied simultaneously in the same cell. These protocols were examined in oocytes as well as in HEK cells.

HEK 293 Cell Transfection and Electrophysiological Recordings of P2X4R wt and Chimeras

HEK 293 cells were stably transfected with 1 μg cDNA for the wt P2X4R or the P2X4/2R chimera. Cells were grown in DMEM media to 80% confluence on 35-mm culture dishes and incubated with the cDNA mixed with 10 μL of Lipofectamine 2000 in 1 mL of serum freemedia (Opti-MEM, Invitrogen, Carlsbad, California, USA). The P2X positive colonies were selected with G 418 during at least 2 weeks.

Whole-cell ATP-gated currents were recorded from single HEK 293 cells using an Axopatch 200B amplifier (Axon Instruments, Foster City, CA). Patch pipettes (2–4 megohm) were filled as follows (mM): 150 CsCl, 10 tetraethylammonium chloride, 10 EGTA, 10 HEPES, pH 7.3, and 275–285 mOsm; pH was adjusted with CsOH (Coddou et al., 2003a). The recording chamber was perfused with a solution containing (mM): 150 NaCl, 1 $CaCl_2$, 1 $MgCl_2$, 10 glucose, and 10 HEPES. Only cells with membrane potential more negative than −55 mV, access resistance <10 MΩ, and input resistance >00 MΩ were assessed. ATP-gated currents were assessed recording at a holding potential of −80 mV. Responses were digitized at a frequency of 10 kHz and analyzed using the pCLAMP 8 from Axon Instruments (Foster City, CA). All protocols were conducted at room temperature (22–25°C).

Drugs and Chemicals

ATP as the trisodium salt, zinc chloride, tetraethylammonium chloride, EGTA, HEPES, and penicillin-streptomycin were purchased from Sigma Chemicals (St. Louis, MO, USA). Lipofectamine 2000 was purchased from Invitrogen. G-418 sulfate was obtained from Calbiochem (San Diego, CA, USA). The salts used to prepare the incubation media were obtained from Sigma-Aldrich or Merck (Darmstadt, Germany). Triple-distilled water with minimal electro conductivity was produced locally; its trace metal contamination was less than 0.1 μM.

Statistical Data Analysis and Expression of Electrophysiological Results

Non-parametric analyses were performed as appropriate (Kruskal-Wallis Friedman or Mann-Whitney tests); we previously determined the convenience of nonparametric analysis procedures (Theodorson-Norheim, 1987) for statistical evaluations of oocyte studies. Significance was set at $p < 0.05$, (*).

ATP-gated currents are always expressed as the fold-increase in the ATP-evoked response (normalized current) when comparing the control ATP-gated currents with that elicited in the same oocyte or HEK cell, in the presence of either Zn(II), IVM, or both modulators applied jointly.

RESULTS

IVM Selectivity as an Allosteric P2X4R Modulator

Based on the rat P2X4R model, the TM residues, previously proposed by Popova et al. (2013) to interact with IVM, were aligned with those present in the P2X2R and P2X7R to ascertain the role of IVM allosteric modulation. While Y42 is conserved in these three P2XRs, W46 was only found in the P2X4R. In addition, two single residue replacements were observed among the P2XRs. W46 in P2X4R was replaced by Y46 (P2X2R) and F46 (P2X7R), while W50 in P2X4R was replaced by V50 (P2X2R) and S50 (P2X7R) (**Table 1**). Moreover, we determined the free energies of transfer from water to ethanol (Nozaki and Tanford, 1971; von Heijne and Blomberg, 1979), and we also examined the hydrophobicity score of amino acid side chains/backbone localized in the extracellular area immediately close to the TM domain. These calculations determined the hydrophobic environment related to the IVM putative TM domain allosteric binding site. In agreement with this proposal, P2X4R showed the highest hydrophobic score (−33.75 kcal/mol) followed by P2X7R (−40.55 kcal/mol) and the P2X2R (−53.8 kcal/mol), data confirming the physicochemical characteristics favoring IVM access to its binding site. A graphical representation of this data is given in **Supplementary Figure 1**.

Following the P2XRs alignment, the molecular docking studies at the allosteric binding site provided the binding probability to this site versus other non-related sites in the close P2XR vicinity. Docking analysis revealed that IVM has a 62% higher probability of binding to the described P2X4R allosteric site ($p < 0.05$) compared to other sites in the TM region. Moreover, the probability of IVM binding to a similar site in the P2X2R was significantly lower (48%) and even less in the P2X7R (18%). Furthermore, the probability of IVM binding to other sites was 52 and 82% for the P2X2R and P2X7R respectively (**Figure 1A**). Based on these findings, graphical representations of the preferred binding mode of IVM to the three P2XRs examined are shown in **Figure 1B**. The docking of IVM to P2X4R involves π-π stacking interactions with Y42 and W46 in the TM1 domain, plus hydrogen bonding to S341 in the TM2 domain. Moreover, W46 and W50 clearly show a π-π interaction which influences the aromatic ring orientation, a finding not observed in P2X2R or P2X7R at the analogous binding place (**Table 1**, **Figure 1B**). The calculated IVM binding energy for its P2X4R binding site was −6.85 kcal/mol.

TABLE 1 | Alignment of transmembrane P2X4R, P2X2R, and P2X7R rat sequences.

	Receptor	Sequence
TM1		42 46 50
	ratP2X4R	28VGLMNRAVQLLILAYVIGWVFVWEKGY54
	ratP2X2R	28LGFVHRMVQLLILLYFVWYVFIVQKSY54
	ratP2X7R	28YGTIKWILHMTVFSYVS-FALMSDKLY53
TM2		336 341 349
	ratP2X4R	331DIIPTVINVGSGLALLGVATVLCDVIVL358
	ratP2X2R	331SLIPTIINLATALTSIGVGSFLCDWILL358
	ratP2X7R	331DIIQLVVYIGSTLSYFGLATVCIDLIIN358

Key amino acids previously reported to participate in P2X4R IVM modulation are written in red, showing the coincidence with the present residues obtained by molecular docking (gray boxes). The corresponding residues in P2X2R and P2X7R, enumerated from the alignment with the P2XR sequence, are shown in orange.

Consistent with bioinformatics, electrophysiological recordings of ATP-gated currents in P2XRs showed that only the P2X4R was positively modulated by IVM (**Figure 1C**). Interestingly, although a 48% probability of IVM binding to the P2X2R putative allosteric binding site was determined and the hydrophobic environment seems compatible with an IVM chemical nature (**Table 1**, **Supplementary Figure 1**), it was not enough to trigger an ATP-gated current, reflecting the IVM selectivity for the P2X4R. Altogether this set of evidence leads us to firmly propose the structural bases for IVM P2X4R selectivity.

MD simulations revealed that π-π stacking interactions were maintained at the expected 5 Å distance throughout the simulation time, and hydrogen bonding of IVM to D331 oscillates between 2.5 and 5 Å, indicative of dynamic hydrogen bonding fluctuations. Calculations are also consistent with a relative conserved distance of 3–5 Å between IVM and S341, which at 28 ns shows an abrupt reduction of the distance to approximate 2.5 Å, stabilizing the hydrogen bond with IVM (**Figure 2**).

The Zn(II) Modulator Site

IVM and Zn(II) interact on separate binding sites (**Figure 3A**) and elicit biological responses. C132 in the P2X4R extracellular

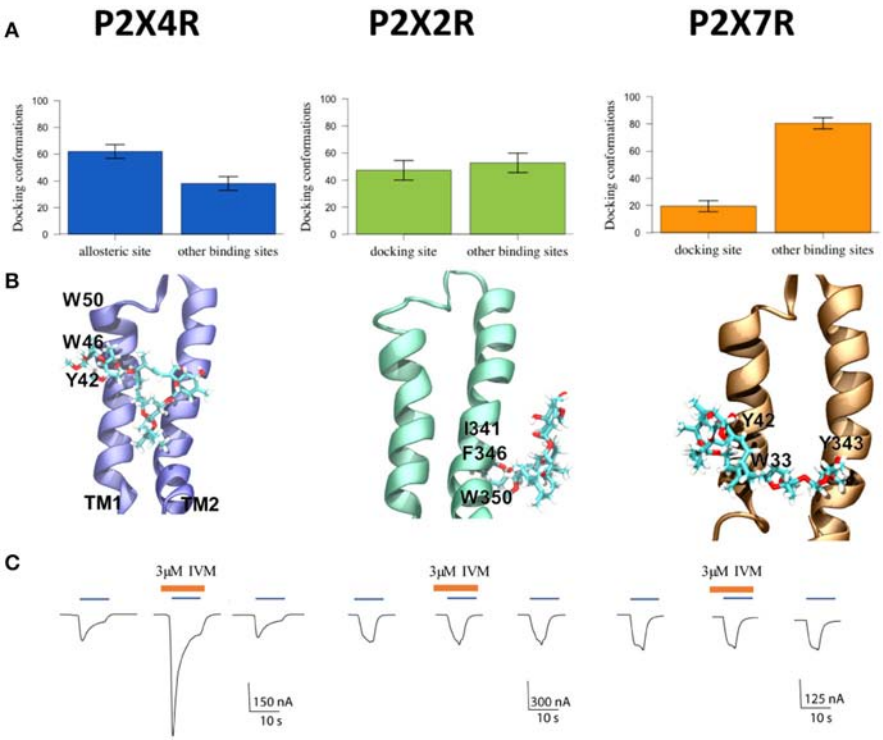

FIGURE 1 | Characterization of P2XR-IVM binding specificity by *in silico* and electrophysiological approaches. **(A)** Number of conformations obtained by molecular docking of IVM to rat P2X4R, P2X2R, and P2X7R. **(B)** Representative best energy conformation of IVM docking with the three P2XRs studied; lowest IVM P2X2R binding energy to other sites not analogous to the allosteric site in the P2X4R. IVM binding showed interaction with I341, F346, and W350 residues. In the case of P2X7R, IVM docking interacted with Y42, W33, and Y343. **(C)** Representative recordings of 1 μM ATP-gated currents in *Xenopus laevis* oocytes pretreated with 3 μM IVM (brown line) for 3 min prior to 1 μM ATP addition (blue line) in separate oocytes, each expressing P2X4R, or P2X2R, or P2X7R, respectively. Calibration scales are different for each oocyte-evoked currents during 10 s. *$p < 0.05$ between the allosteric or docking and other binding sites. #$p < 0.05$ between the allosteric site in the P2X4R and putative docking sites in the P2X2R or the P2X7R.

domain was previously identified as a key residue involved in Zn(II) modulation (Coddou et al., 2007). To further characterize the role of C132 in a wt and the C132A P2X4R mutant, we studied the stability of P2X4R Zn(II) based on the distance between C132 and the Zn atom. MD simulations showed that a single Zn(II) positioned at 5 Å from the wt P2X4R C132 sulfur atom (SS3), maintained its position at a distance of less 8–10 Å during 40 ns. In the case of the C132A mutant, Zn(II) was also placed at 5 Å from an alanine C_β. Simulations show that the carbon distance was maintained only for the first 6 ns (**Figure 3B**); thereafter the Zn(II) suffered a sudden separation reaching a distance of 16–18 Å that was maintained for the next 35 ns. As negative control, a Zn(II) ion positioned in the extracellular domain at 8 Å from C132 sulfur showed a steady distancing from the P2X4R, reaching distances greater than 80 Å after 40 ns.

Pore Radius and Lateral Fenestration Dimensions of P2XRs Bound to IVM, to Zn(II), and to both Modulators

In agreement with the findings that IVM and Zn(II) interact at separate binding sites and elicit differential biological responses, we searched for structural changes in the pore size. To this end, a HOLE trajectory analysis of P2X4R apo, and holo systems with one or both modulators bound were performed.

P2X4R in the presence of ATP plus Zn(II) and IVM resulted in an enlargement of the upper part of the extracellular vestibule (7.97 ± 0.01 Å, $p < 0.05$), compared to the holo P2X4R which is 6.03 ± 0.3 Å (**Table 2**, **Figure 4A**). When the P2X4R is activated by ATP plus Zn(II) or ATP plus IVM, the calculated size of the upper vestibular portion of the pore size was significantly smaller, 6.93 ± 0.2 Å and 7.03 ± 0.3 Å, respectively ($p < 0.05$). Altogether, these results support a metal-induced enlargement of the pore radius and lateral fenestration by the allosteric modulator permitting a larger intracellular ionic flux. This fact is supported by electrophysiological findings, ATP-gated currents were increased 15.1 ± 3.7-fold ($n = 4$) by 10 μM Zn(II) and 6.9 ± 1.2 fold ($n = 5$) by 3 μM IVM. When both modulators were applied jointly (IVM pre-applied for 3 min and Zn(II) for 1 min prior to the 1 μM ATP challenge), a 30.8 ± 5.5-fold increase of the ATP-gated current was observed ($p < 0.01$ compared to either modulator alone). Representative recordings are shown in **Figure 4B**. Regarding the P2X4R holo system, the lateral fenestration at the membrane interphase was increased 4 Å after binding of both modulators, while Zn(II) and IVM applied separately only triggered an increase of 1 Å and 2 Å, respectively (**Figure 5**). Similarly, concomitant experiments

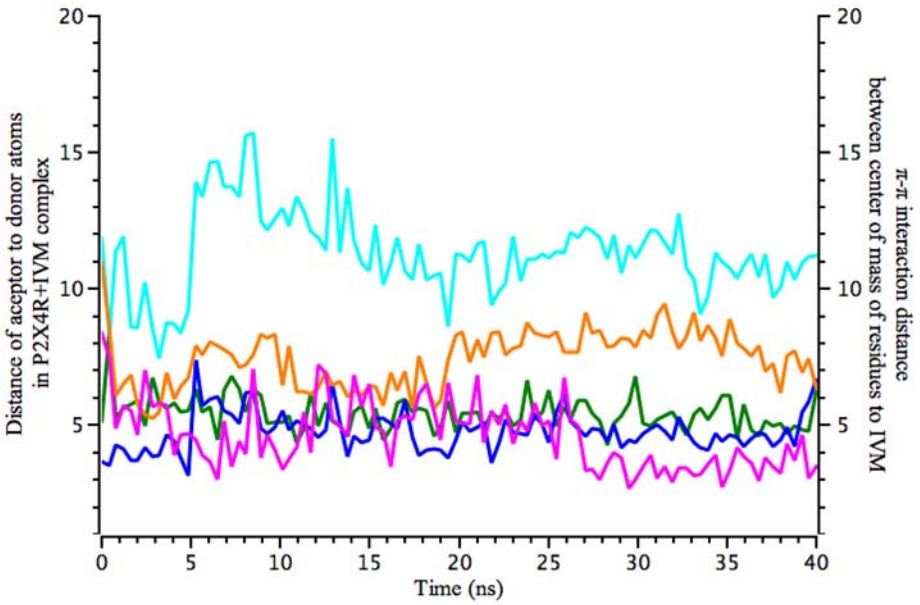

FIGURE 2 | Molecular dynamics calculations show the distance of IVM interaction with P2X4R. Calculated 40 ns MD simulations of IVM interaction with the holo P2X4R. Left y-axis plots the distance (in Å) between acceptor to donor atoms (hydrogen bonds), calculated between O1 of S341 (magenta) with O4 of IVM, and O1 of D331 (orange) with O12 of IVM. Right y-axis refers to possible π-π stacking interactions between W50 (blue sky), W46 (blue), and Y42 (green), calculated between center of mass of the aromatic residues and IVM atoms.

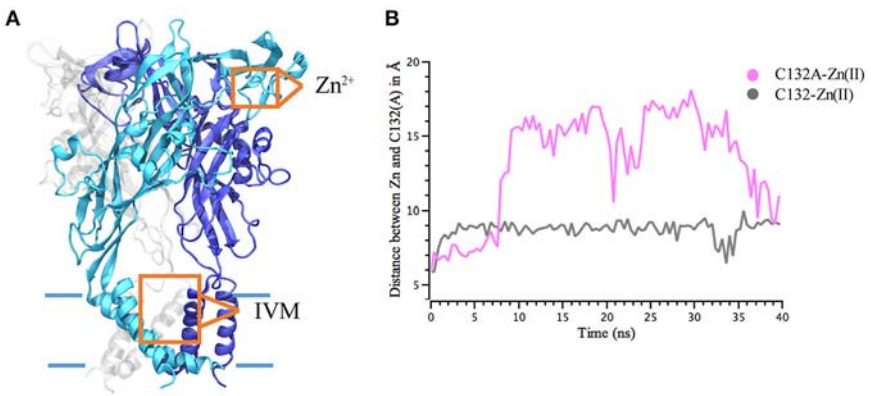

FIGURE 3 | Interaction distance between Zn(II) and P2X4R calculated through molecular dynamics simulations. Calculated 40 ns MD simulations of Zn(II) interaction with the P2X4R holo. **(A)** Model of P2X4R showing the putative Zn(II) site in the extracellular domain and IVM binding site in the TM region. **(B)** Distance between Zn(II) and S atom of C132wt P2X4R (gray) or Cβ of the C132A mutated P2X4R (pink).

TABLE 2 | Radius of P2X4R pore in the apo, holo, and holo plus allosteric modulators; (values are expressed as the mean ±standard deviation; values in Å).

P2X4R compartment	P2X4 apo	P2X4 holo	P2X4 holo IVM	P2X4 holo Zn(II)	P2X4 holo IVM Zn(II)
Upper vestibule	2.10 ± 0.19	1.83 ± 0.21	1.24 ± 0.28	1.34 ± 0.22	1.28 ± 0.20
Upper extracellular vestibule	5.95 ± 0.09	6.03 ± 0.30*	7.03 ± 0.26*	6.93 ± 0.15*	7.96 ± 0.01*
Extracellular vestibule	7.21 ± 0.23	9.27 ± 0.27*	8.45 ± 0.59	8.11 ± 0.58	8.40 ± 0.64
Intracellular vestibule	0.28 ± 0.07*	0.88 ± 0.1*	0.97 ± 0.28	0.86 ± 0.34	0.80 ± 0.28

*Radius values were calculated following HOLE program analysis during the last 10 ns of the MD simulations lasting 30–40 ns (or 40–50 ns when allosteric modulators were present). The minimum radius of the upper vestibule was calculated, the maximum radius of the extracellular vestibule was also calculated as the minimum value of the intracellular vestibule (*p < 0.05 compared to P2X4R apo state).*

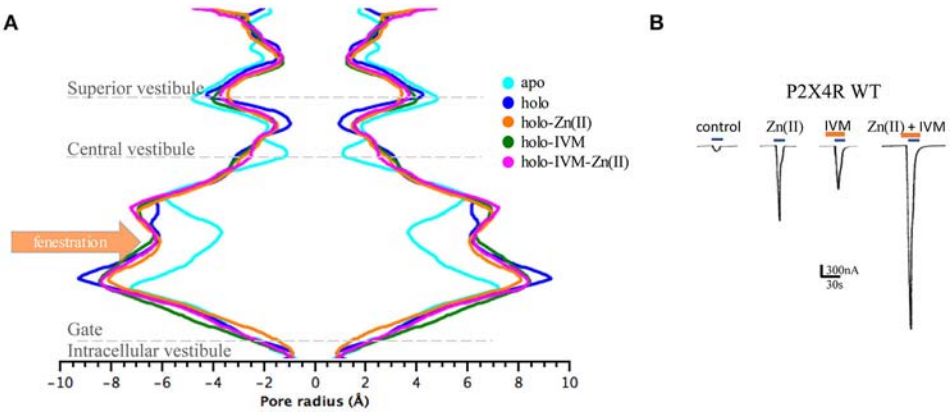

FIGURE 4 | Allosteric modulators induced changes in the pore radius of the extracellular P2X4R vestibule in different states of the P2X4R. **(A)** Pore dimensions obtained during the last 10 ns MD simulations of the P2X4R in apo or holo state, holo with Zn(II) or with IVM, and the holo P2X4R with both IVM and Zn(II), along the vestibular portions of the P2X4R. **(B)** Representative tracings obtained in a single oocyte expressing the wt P2X4R following 1 μM ATP-evoked currents in the absence of modulators, and following incubation with either 10 μM Zn(II), 3 μM IVM, or the joint application of IVM plus Zn(II). In all cases 1 μM ATP-evoked currents were recorded (blue rectangles), while IVM applications are shown in brown rectangles.

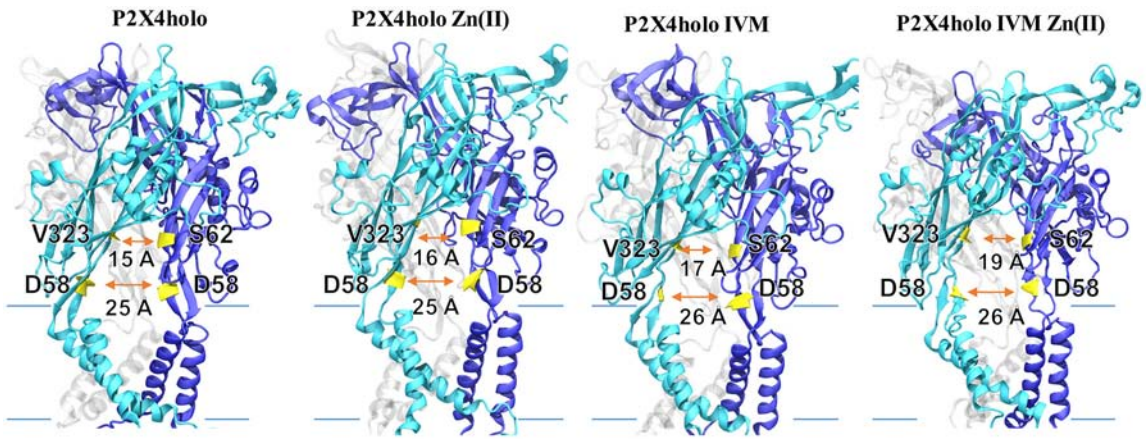

FIGURE 5 | Lateral fenestration dimension of P2X4R in different states. Models represent the P2X4R holo state with either Zn(II), IVM, or both bound. Lateral fenestration size was calculated in the apo as well as the holo state, holo in the presence of Zn(II) or IVM, or holo plus IVM and Zn(II). Backbone distance between D58 with its corresponding D58 in the adjacent P2X4R subunit was considered. Likewise, the backbone distances between V323 with S62 in the adjacent subunit were determined. Lateral fenestration dimensions are expressed in Å.

on P2X4R transfected HEK cells, 10 μM Zn(II) alone doubled ($n = 9$) and IVM tripled the ATP-evoked currents ($n = 6$); the joint application of these modulators resulted in an almost 4-fold larger current ($n = 6$, data not shown). Taken together, both *in silico* and electrophysiological results are consistent with an additive effect rather than a strong synergic allosteric interaction.

Non-bonded Energy Calculations of the Different P2X4R States with and without ATP and Modulators

We calculated energy changes elicited by the P2X4R transition steps from apo to its holo state as well as IVM and/or Zn(II) binding complexes, and the difference in non-binding energies elicited by ATP and modulator binding was examined. The apo to holo state transition is favored by the energy change of −2222 kcal/mol. Likewise, the sequence of IVM binding to the holo P2X4R is energetically more favorable compared to the apo P2X4R binding (−3383 vs. −3090 kcal/mol, **Figure 6**). In addition, our calculations indicated that Zn(II) causes transitions requiring more energy than IVM, leading to a more favorable and stable P2X4R conformation in the presence of IVM. Based on these calculations, we inferred that Zn(II), due to its lower molecular weight and charge, has fewer degrees of freedom compared to IVM, leading to an increased P2X4R dynamic movement. Energy calculations for the different transitions are consistent with the following sequence of steps accounting for P2X4R modulation: 1. Apo to holo transition; 2. Holo P2X4R IVM complex; 3. Holo P2X4R Zn(II) IVM. These favorable

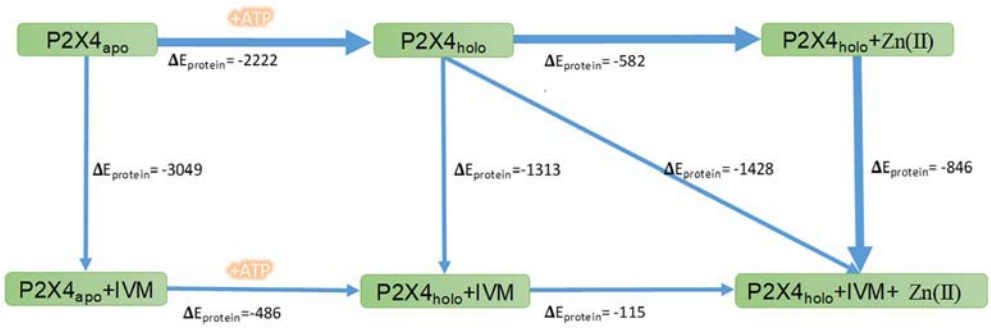

FIGURE 6 | Non-bonded energy determination of the P2X4R in different states. Numbers indicate the changes in non-bonded energies, expressed as kcal/mol, of the whole wtP2X4R ($\Delta E_{protein}$) in the different conformational complexes of the P2X4R. The rectangles indicate P2X4R states in the apo or holo state alone or following allosteric modulator binding. The arrows refer to the transition between the different states. The thicker blue lines indicate the favored P2X4R transitions after allosteric modulator binding.

P2X4R transitions are shown by the thicker black arrows represented in **Figure 6.**

Studies with the P2X4R C132A Mutant and a P2X4/2R Chimera

Based on docking and MD simulations we predicted that the P2X4R C132A mutant, should be insensitive to the allosteric action of Zn(II), while it should preserve the modulator action of IVM. As an electrophysiological control for this protocol, we examined the P2X4R-C126A mutant, since a structurally equivalent mutation, P2X4R-C132A, is located in close vicinity. Parallel studies proved that the Zn(II)-induced potentiation of the receptor activity was retained (Coddou et al., 2007). The data confirmed that the C132A mutant is not sensitive to the modulator action of Zn(II), since it failed to modify the 1 μM ATP-gated current compared to the wt (**Figure 7A**). In contrast, Zn(II) applications to the C126A mutant increased 11.6 ± 1.5-fold the ATP-gated current (**Figure 7B**). Moreover, and in support of our contention, 3 μM IVM increased the ATP-evoked currents 4.9 ± 0.7–fold ($n = 10$) and 7.3 ± 0.5-fold ($n = 8$) in the C132A and C126A mutants, respectively, values which are not statistically significant between them. The joint application of Zn(II) plus IVM resulted in a 7.1 ± 1.7-fold increase of the ATP-evoked currents ($n = 9$, **Figure 7B**), a value not statistically different from that elicited by IVM alone, while in the C126A mutant the increase in the ATP-gated current was 31.9 ± 4.1-fold (**Figure 7B**), confirming that both modulators act at separate and apparently independent allosteric modulator sites and that the joint action of both modulators elicited additive effects.

As a proof of concept, we took advantage of a P2X4/2R chimera constituted by the extracellular P2X4R domain and the TM plus intracellular P2X2R domains. Based on the *in silico* studies, we again predicted, that this construct should be insensitive to IVM. Electrophysiological findings showed that 10 μM Zn(II) application increased 2.7 ± 0.6-fold ($n = 5$, p-value < 0.001) the 1 μM ATP-gated current, a value which is significantly less than that observed in the wt P2X4R (**Figure 4B**). Prominently, and as anticipated, the chimera was insensitive to 3 μM IVM (1.1 ± 0.1-fold increase, $n = 5$); the joint application of both IVM plus Zn(II) did not increase further the magnitude of the ATP-gated currents (2.7 ± 0.9-fold, $n = 3$, $p < 0.05$). These results were confirmed in HEK cells expressing the P2X4/2R chimera; almost identical values were attained for IVM and the joint application of IVM plus Zn(II) (1.55 ± 0.1 ($n = 3$) and 1.4 ± 0.2 ($n = 4$), respectively. Although experimental values of the currents recorded from HEK cells were slightly reduced in magnitude, the results agree with a general picture compatible with the proposed hypothesis that guided this study.

DISCUSSION

The present set of results revealed the advantages of using complementary approaches to study the mechanisms of action of P2X4R allosteric modulators. MD simulations allowed the visualization of the most likely initial conformational changes occurring in the receptor by allosteric interactions, whose interpretation benefits from prior pharmacological investigations using site-directed mutagenesis on P2XRs (Coddou et al., 2007), and in particular benefits from the results with the P2X4/2R chimera in the present study.

Our data strongly suggest that the IVM and Zn(II) allosteric binding sites are distinct and operate by separate mechanisms. The joint application of IVM plus Zn(II), each acting at its specific allosteric site, caused additive rather than synergic effects. Moreover, bioinformatics concurred to identify the Zn(II) allosteric site, which is localized in the extracellular receptor domain, at a site not totally identified as yet, but in the near vicinity of C132 comprising the SS3 receptor bond. In contrast, the IVM site, as previously proposed, is restricted to the P2X4R TM domain. This paper provides precise docking studies identifying details of the IVM binding site characteristics, in agreement with the hypothesis that IVM is inserted between two neighboring TM domain of the P2X4R subunits and restricts molecular rearrangement in the TM domains involved in channel gating. A similar finding was reported for the Cys-loop receptor family of ligand-gated ion channels (Hibbs and Gouaux, 2011),

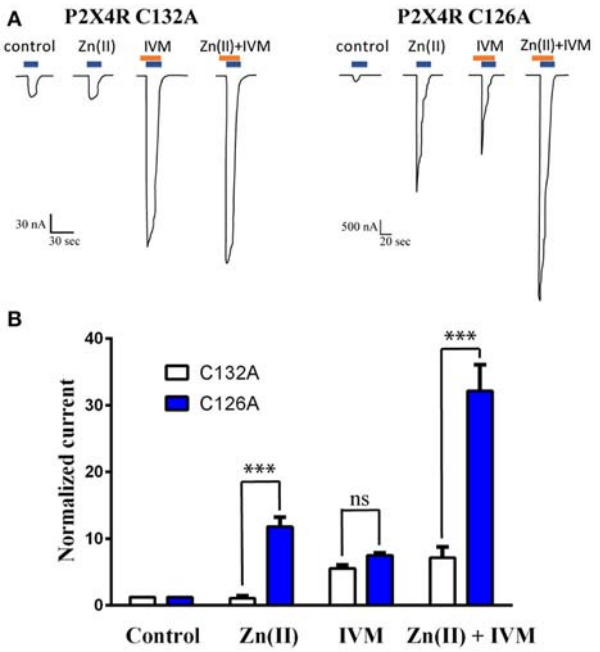

FIGURE 7 | Loss of Zn(II) modulator activity in the C132A P2X4R mutant but not the C126A mutant. **(A)** Representative recordings of 1 μM ATP-gated currents in two P2X4R mutants (C132A and C126A) in the absence or presence of 10 μM Zn(II), 3 μM IVM and joint application of Zn(II) plus IVM. ATP and IVM applications are represented by blue and brown rectangles, respectively. Each set of recordings is derived from a single oocyte expressing either the C132A or the C126A mutants. **(B)** Statistical analyses of a set of 5 separate oocytes expressing the C132A mutant (open bars) and 4 oocytes expressing the C126A mutant (closed bars) (***$p < 0.001$); ns (not statistically significant).

showing functional commonalities of allosteric regulation among other ionic channel families.

To address and compare IVM selectivity for the P2X4R, we conducted parallel calculations on the P2X2R or the P2X7Rs. Based on the sequence alignment of these P2XRs, plus the IVM docking studies, we concluded that TM1 plays a critical role in the interaction, highlighting hydrophobic and stacking interactions with Y42 and W46 plus a minor role of W50. These interactions assisted the positioning of IVM at this site, creating a non-polar environment for the drug entry to this binding pocket essential for IVM activity (Jelínková et al., 2006). The interaction is further stabilized by hydrogen bonding to S341 of the adjacent subunit and other residues with less propensity for hydrogen bonding, a bond that occurs relatively late in time compared to the hydrophobic forces. The immediate environment of this P2X4R area, in the vicinity of the lateral fenestration (**Supplementary Figure 1**), is relatively hydrophobic in nature, a finding supported by IVM hydrophobicity (log P = 5.83, Viswanadhan et al., 1989). Additionally, the P2X4/2R chimera construct was insensitive to IVM, a result that correlates with the in silico studies. Moreover, mutation of four amino acids of the lateral fenestration, Y195, F198, F200, and F330, altered the ability of IVM to sensitize P2X4R to ATP, revealing their contribution to the channel function and deactivation effect (Gao et al., 2015). Although docking studies revealed a 62% probability of IVM binding at this specific site, we are aware that 38% of non-specific interactions are also formed. This binding dominance to a preferred site is in marked contrast with the P2X7R docking results, where non-specific binding is close to 82%. Although the binding probability is almost half in the P2X2R, electrophysiological results consistently demonstrated that the P2X2R is not IVM-modulated. We infer that neither IVM binding to TM1 aromatic residues nor the possible hydrogen bonding to P2X2R or P2X7R TM2 residues confer enough stability compatible with eliciting the correct conformational change related to the allosteric modulation.

Considering the trimer nature of P2X4R, it has not escaped our interest to determine whether three IVM molecules bind to the receptor. It was our working hypothesis that at a given IVM concentration range, all three allosteric receptor sites should be occupied. To this end, longer dynamics are critical to investigate whether all three IVM molecules reach and stabilize the P2X4R at the same time or whether this occurs gradually, suggesting binding cooperativity, where the first IVM binding facilitates the subsequent binding of the next IVM molecule. This proposal is supported by the Markov model presented by Zemkova et al. (2015). A similar argument could be argued for the binding of Zn(II) to its allosteric site in the extracellular P2X4R domain. In the case of the metal, this is even more attractive, since its allosteric site is distant from the pore. Energy determinations indicated that Zn(II), in contrast to IVM, evidenced a larger standard deviation of the non-bonded electrostatic energies derived from the MD studies. The latter might be indicative that Zn(II) elicited a favorable electrostatic component in the ionic flux to intracellular compartment (V. Latapiat et al., data not shown). Taken together, these findings validate the result obtained with the C132A P2X4R mutant insensitive to the allosteric action of Zn(II), but that preserve the modulating action by IVM. This result is different from those observed with C126A, confirming the predominant role of C132 in the Zn(II) allosterism. In addition, it also supports that the joint action of both modulators is additive, as will be discussed in the next.

An exciting issue analyzed in this investigation refers to the pore size widening by allosteric modulators, an enterprise worth bioinformatics analysis. Present studies consistently showed that ATP opened the pore and lateral fenestrations, but not the intracellular vestibule, which in the case of P2XRs is directly associated with the ion flux to a larger extent than the central pore (Kawate et al., 2009). Both IVM and Zn(II) enlarged the upper region of the extracellular vestibule, but only within a 1 Å width (**Table 2**), an amount which was increased to 2 Å by the joint application of both modulators, an issue that was further supported by an additional experiment. A classical biophysical approach to explore pore size consists in replacing sodium by N-methyl D glucamine, a charged molecule with a radius 4–5 times larger than Na^+. Preliminary experiments showed that the sodium replacement by the N-methyl D glucamine abolished the ATP-induced currents in oocytes injected with wt P2X4R, a reversible effect since ATP-gated currents were 100% recovered after sodium substitution. Moreover, addition of 3 μM

IVM plus 10 μM Zn(II) did not elicit an ATP-gated current (F. Peralta, unpublished observations). This result confirms the bioinformatics calculations indicating that the pore opening did not permit pore enlargement to 4.5 Å radius, which is incompatible with N-methyl D glucamine diffusion through the ATP channel.

A most enlightening aspect of the combined bioinformatics plus electrophysiological assays confronts the non-bonded energy calculations of the changes occurring by allosteric modulators bound to apo or holo states of the P2X4R. Apo to holo transition is necessary to cause lateral fenestration opening that allows the entrance of IVM to its binding site. Once the holo state is present, the calculations indicate that the most favorable transition energy corresponds to the IVM binding, which is in agreement with the electrophysiological procedure testing the joint modulator application, where IVM is pre-incubated with Zn(II). This could indicate a much greater influence of the hydrophobic energy of the IVM binding the TM region rather than a more electrostatic role of the Zn(II) binding site. The electrophysiological experiments showed that IVM needs to be pre-incubated 3 min prior to ATP addition, a time needed for IVM to reach the vicinity of the lateral fenestration. The concentration response curves of P2X4R revealed that not only 10 and 30 s pretreatments with IVM increased ATP sensitivity, but they also increased the maximum current amplitude evoked by ATP (Mackay et al., 2017). In agreement with this, molecular docking of IVM to the apo P2X4R showed less than 5% binding to its allosteric site. On the other hand, Zn(II) as a modulator does not require pre-incubation, probably due to the fact that its binding site is easily accessible from the extracellular space and does not require the holo P2X4R state. Since the intracellular vestibular size was not significantly an increased by these modulators, the increased ion currents observed experimentally imply either an increased probability of pore opening or a modulator-induced stabilization of the open state channel dynamics.

In summary, the combination of bioinformatics tools plus pharmacological protocols successfully assisted a comprehensive understanding of the mechanism of P2X4R modulation by allosteric modulators. Three main conclusions highlight the perspectives posed by the present findings. (1) The molecular basis that account for the IVM P2X4R specificity compared to the related P2XRs family members. (2) The link of molecular pharmacology with structural biology, via the elucidation of the precise IVM allosteric site and the partial assignment of the Zn(II) site. (3) Channel pore dynamics and lateral fenestration enlargement by the allosteric modulators Zn(II) and IVM as a requirement for the increased ion flux, contrasting with the central pore expansion characteristic of Cys loop ligand-gated ion channels. Altogether, the combination of these methodologies allows visualizing the molecular events that support allosteric modulation, adding novel implications to the foundations of molecular pharmacology.

AUTHOR CONTRIBUTIONS

VL: designed and performed in-silico experiments, analyzed data, and wrote the paper. FR and FG: performed in-vitro experiments and analyzed data. FM: analyzed in-silico data and wrote the paper. NB: analyzed data and wrote the paper; JH-T: supervised the investigation, analyzed data, and wrote the paper.

ACKNOWLEDGMENTS

To Dr. Stanko Stojilkovic from the Endocrinology and Reproduction Research Branch NICHD, National Institute of Health (NIH, Bethesda, USA) for P2X4/2R chimera and Dr. J. F. Codocedo for the HEK cell experiments expressing the chimera. Dr. F. Rodríguez holds an intramural DICYT postdoctoral fellowship from the Universidad de Santiago de Chile (021643GT-postdoc). FONDECYT grants 114-1132 and 117-0842, funded the senior author (JH-T), while Newton Picarte PCI-DPI Conicyt grant 20140080 funded Prof N. Barrera's Lab. Partial funding was also derived from CEDENNA (Centre for the Development of Nanoscience and Nanotechnology), grant FB 0807. Additional funds from the supercomputing infrastructure of the NLHPC (ECM-02, Powered@NLHPC) allowed part of this study. To Samy Atala for English editing.

SUPPLEMENTARY MATERIAL

The Supplementary Material for this article can be found online at: https://www.frontiersin.org/articles/10.3389/fphar.2017.00918/full#supplementary-material

Supplementary Figure 1 | Grafical representation of hydrophobic environment related to the IVM putative TM domain allosteric binding site in P2XRs based on free energies of transfer from water to ethanol.

REFERENCES

Acuña-Castillo, C., Coddou, C., Bull, P., Brito, J., and Huidobro-Toro, J. P. (2007). Differential role of extracellular histidines in copper, zinc, magnesium and proton modulation of the P2X7 purinergic receptor. *J. Neurochem.* 101, 17–26. doi: 10.1111/j.1471-4159.2006.04343.x

Acuña-Castillo, C., Morales, B., and Huidobro-Toro, J. P. (2000). Zinc and copper modulate differentially the P2X4 receptor. *J. Neurochem.* 74, 1529–1537. doi: 10.1046/j.1471-4159.2000.0741529.x

Adelsberger, H., Lepier, A., and Dudel, J. (2000). Activation of rat recombinant alpha(1)beta(2)gamma(2S) GABA(A) receptor by the insecticide ivermectin. *Eur. J. Pharmacol.* 394, 163–170. doi: 10.1016/S0014-2999(00)00164-3

Barrera, N. P., Ormond, S. J., Henderson, R. M., Murrell-Lagnado, R. D., and Edwardson, J. M. (2005). Atomic force microscopy imaging demonstrates that P2X2 receptors are trimers but that P2X6 receptor subunits do not oligomerize. *J. Biol. Chem.* 280, 10759–10765. doi: 10.1074/jbc.M412265200

Brooks, B. R., Brooks, C. L., Mackerell, A. D., Nilsson, L., and Petrella, R. J. (2009). CHARMM: the biomolecular simulation program. *J. Comput. Chem.* 30, 1545–1614. doi: 10.1002/jcc.21287

Burnstock, G. (2007). Purine and pyrimidine receptors. *Cell. Mol. Life Sci.* 64, 1471–1483. doi: 10.1007/s00018-007-6497-0

Coddou, C., Acuña-Castillo, C., Bull, P., and Huidobro-Toro, J. P. (2007). Dissecting the facilitator and inhibitor allosteric metal sites of the P2X4 receptor channel: critical roles of CYS132 for zinc potentiation

and ASP138 for cooper inhibition. *J. Biol. Chem.* 282, 36879–36886. doi: 10.1074/jbc.M706925200

Coddou, C., Lorca, R. A., Acuña-Castillo, C., Grauso, M., Rassendren, F., and Huidobro-Toro, J. P. (2005). Heavy metals modulate the activity of the purinergic P2X4 receptor. *Toxicol. Appl. Pharmacol.* 202, 121–131. doi: 10.1016/j.taap.2004.06.015

Coddou, C., Morales, B., Gonzalez, J., Grauso, M., Gordillo, F., Bull, P., et al. (2003a). Histidine 140 plays a key role in the inhibitory modulation of the P2X4 nucleotide receptor by copper but not zinc. *J. Biol. Chem.* 278, 36777–36785. doi: 10.1074/jbc.M305177200

Coddou, C., Morales, B., and Huidobro-Toro, J. P. (2003b). Neuromodulator role of zinc and copper during prolonged ATP applications to P2X4 purinoceptors. *Eur. J. Pharmacol.* 472, 49–56. doi: 10.1016/S0014-2999(03)01864-8

Coddou, C., Yan, Z., Obsil, T., Huidobro-Toro, J. P., and Stojilkovic, S. S. (2011). Activation and regulation of purinergic P2X receptor Channels. *Pharmacol. Rev.* 63, 641–683. doi: 10.1124/pr.110.003129

Cully, D. F., Vassilatis, D. K., Liu, K. K., Paress, P. S., Van der Ploeg, L. H., Schaeffer, J. M., et al. (1994). Cloning of an avermectin-sensitive glutamate-gated chloride channel from *Caenorhabditis elegans*. *Nature* 371, 707–711. doi: 10.1038/371707a0

Gao, C., Yu, Q., Xu, H., Zhang, L., Liu, J., Jie, Y., et al. (2015). Roles of the lateral fenestration residues of the P2X(4) receptor that contribute to the channel function and the deactivation effect of ivermectin. *Purinergic Signal.* 11, 229–238. doi: 10.1007/s11302-015-9448-5

Geary, T. G. (2005). Ivermectin 20 years on: maturation of a wonder drug. *Trends Parasitol.* 21, 530–532. doi: 10.1016/j.pt.2005.08.014

Hattori, M., and Gouaux, E. (2012). Molecular mechanism of ATP binding and ion channel activation in P2X receptors. *Nature* 485, 207–212. doi: 10.1038/nature11010

He, M. L., Zemkova, H., and Stojilkovic, S. S. (2003). Dependence of purinergic P2X receptor activity on ectodomain structure. *J. Biol. Chem.* 278, 10182–10188. doi: 10.1074/jbc.M209094200

Hibbs, R. E., and Gouaux, E. (2011). Principles of activation and permeation in an anion-selective Cys-loop receptor. *Nature* 474, 54–60. doi: 10.1038/nature10139

Huidobro-Toro, J. P., Lorca, R. A., and Coddou, C. (2008). Trace metals in the brain: allosteric modulators of ligand-gated receptor channels, the case of ATP-gated P2X receptors. *Eur. Biophys. J.* 37, 301–314. doi: 10.1007/s00249-007-0230-7

Jelinkova, I., Vavra, V., Jindrichova, M., Obsil, T., Zemkova, H. W., Zemkova, H., et al. (2008). Identification of P2X4 receptor transmembrane residues contributing to channel gating and interaction with ivermectin. *Pflugers Arch.* 456, 939–950. doi: 10.1007/s00424-008-0450-4

Jelínková, I., Yan, Z., Liang, Z., Moonat, S., Teisinger, J., Stojilkovic, S. S. et al. (2006). Identification of P2X4 receptor-specific residues contributing to the ivermectin effects on channel deactivation. *Biochem. Biophys. Res. Commun.* 349, 619–625. doi: 10.1016/j.bbrc.2006.08.084

Jiang, R., Taly, A., and Grutter, T. (2013). Moving through the gate in ATP- activated P2X receptors. *Trends Biochem. Sci.* 38, 20–29. doi: 10.1016/j.tibs.2012.10.006

Jorgensen, W. L., Chandrasekha, R. J., Madura, J. D., Impey, R. W., and Klein, M. I. (1983). Comparison of simple potential functions for simulating liquid water. *J. Chem. Phys.* 79, 926–935. doi: 10.1063/1.445869

Karasawa, A., and Kawate, T. (2016). Structural basis for subtype-specific inhibition of the P2X7 receptor. *Elife* 5:e22153. doi: 10.7554/eLife.22153

Kardos, J., Kovács, I., Hajós, F., Kálman, M., and Simonyi, M. (1989). Nerve endings from rat brain tissue release copper upon depolarization. A possible role in regulating neuronal excitability. *Neurosci. Lett.* 103, 139–144. doi: 10.1016/0304-3940(89)90565-X

Kawate, T., Michel, J. C., Birdsong, W. T., and Gouaux, E. (2009). Crystal structure of the ATP-gated P2X(4) ion channel in the closed state. *Nature* 460, 592–598. doi: 10.1038/nature08198

Kawate, T., Robertson, J. L., Li, M., Silberberg, S. D., and Swartz, K. J. (2011). Ion access pathway to the transmembrane pore in P2X receptor channels. *J. Gen. Physiol.* 137, 579–590. doi: 10.1085/jgp.201010593

Kay, A. R. (2006). Imaging synaptic zinc: promises and perils. *Trends Neurosci.* 29, 200–206. doi: 10.1016/j.tins.2006.02.004

Kay, A. R., and Tóth, K. (2006). The influence of location of a fluorescent zinc-probe in brain slices on its response to synaptic activation. *J. Neurophysiol.* 95, 1949–1956. doi: 10.1152/jn.00959.2005

Khakh, B. S., Bao, X. R., Labarca, C., and Lester, H. A. (1999). Neuronal P2X transmitter- gated cation channels change their ion selectivity in seconds. *Nat. Neurosci.* 2, 322–330. doi: 10.1038/7233

Kim, S., Thiessen, P. A., Bolton, E. E., Chen, J., Fu, G., Gindulyte, A., et al. (2016). PubChem substance and compound databases. *Nucleic Acids Res.* 44, D1202–D1213. doi: 10.1093/nar/gkv951

Köles, L., Fürst, S., and Illes, P. (2007). Purine ionotropic (P2X) receptors. *Curr. Pharm. Des.* 2368–2384. doi: 10.2174/138161207781368747

Levitt, M. (2001). The birth of computational structural. *Nat. Struct. Biol.* 8, 392–393. doi: 10.1038/87545

Lorca, R. A., Coddou, C., Gazitúa, M. C., Bull, P., Arredondo, C., and Huidobro-Toro, J. P. (2005). Extracellular histidine residues identify common structural determinants in the copper/zinc P2X2 receptor modulation. *J. Neurochem.* 95, 499–512. doi: 10.1111/j.1471-4159.2005.03387.x

Lovell, S. C., Davis, I. W., Arendall, W. B. III., de Bakker, P. I. W., Word, J. M., Prisant, M. G., et al. (2002). Structure validation by Calpha geometry: phi, psi and Cβ deviation. *Proteins* 50, 437–450. doi: 10.1002/prot.10286

Mackay, L., Zemkova, H., Stojilkovic, S. S., Sherman, A., and Khadra, A. (2017). Deciphering the regulation of P2X4 receptor channel gating by ivermectin using Markov models. *PLoS Comput. Biol.* 13:e1005643 doi: 10.1371/journal.pcbi.1005643

Marquez-Klaka, B., Rettinger, J., Bhargava, Y., Eisele, T., and Nicke, A. (2007). Identification of an intersubunit cross-link between substituted cysteine residues located in the putative ATP binding site of the P2X1 receptor. *J. Neurosci.* 27, 1456–1466. doi: 10.1523/JNEUROSCI.3105-06.2007

Morris, G. M., Goodsell, D. S., Halliday, R. S., Huey, R., and Hart, W. E. (1998). Automated docking using a Lamarckian genetic algorithm and an empirical free energy function. *J. Comput. Chem.* 19, 1639–1662 doi: 10.1002/(SICI)1096-987X(19981115)19:14<1639::AID-JCC10>3.0.CO;2-B

Morris, G. M., Huey, R., Lindstrom, W., Sanner, M. F., Belew, R. K., Goodsell, D. S., et al. (2009). Autodock4 and AutoDockTools4: automated docking with selective receptor flexibility. *J. Comput. Chem.* 16, 2785–2791. doi: 10.1002/jcc.21256

Nicke, A., Bäumert, H. G., Rettinger, J., Eichele, A., Lambrecht, G., Mutschler, E., et al. (1998). P2X1 and P2X3 receptors form stable trimers: a novel structural motif of ligand-gated ion channels. *EMBO J.* 17, 3016–3028. doi: 10.1093/emboj/17.11.3016

Nozaki, Y., and Tanford, C. (1971). The solubility of amino acids and two glycine peptides in aqueous ethanol and dioxane solutions. establishment of a hydrophobicity scale. *J. Biol. Chem.* 246, 2211–2217.

Omura, S., and Crump, A. (2004). The life and times of ivermectin - a success story. *Nat. Rev. Microbiol.* 2, 984–989. doi: 10.1038/nrmicro1048

Peralta, F. A., and Huidobro-Toro, J. P. (2016). Zinc as allosteric ion channel modulator: ionotropic receptors as metalloproteins. *Int. J. Mol. Sci.* 17:E1059. doi: 10.3390/ijms17071059

Phillips, J. C., Braun, R., Wang, W., Gumbart, J., Tajkhorshid, E., Villa, E, et al. (2005). Scalable molecular dynamics with NAMD. *J. Comput. Chem.* 26, 1781–1802. doi: 10.1002/ jcc.20289

Popova, M., Trudell, J., Li, K., Alkana, R., Davies, D., and Asatryan, L. (2013). Tryptophan 46 is a site for ethanol and ivermectin action in P2X4 receptors. *Purinergic Signal.* 9, 621–632. doi: 10.1007/s11302-013-9373-4

Priel, A., and Silberberg, S. D. (2004). Mechanism of ivermectin facilitation of human P2X4 receptor channels. *J. Gen. Physiol.* 123, 281–293. doi: 10.1085/jgp.200308986

Roberts, J. A., Allsoppa, R. C., El Ajouz, S., Vial, C., Schmid, R., Young, M. T. (2012). Agonist binding evokes extensive conformational changes in the extracellular domain of the ATP- gated human P2X1 receptor ion channel. *Proc. Natl. Acad. Sci. U.S.A.* 109, 4663–4667. doi: 10.1073/pnas.1201872109

Sali, A., and Blundell, T. L. (1993). Comparative protein modelling by satisfaction of spatial restraints. *J. Mol. Biol.* 234, 779–815. doi: 10.1006/jmbi.1993.1626

Samways, D. S. K., Khakh, B. S., Dutertre, S., and Egan, T. M. (2011). Preferential use of unobstructed lateral portals as the access route to the pore of human

ATP-gated ion channels (P2X receptors). *Proc. Natl. Acad. Sci. U.S.A.* 108, 13800–13805. doi: 10.1073/pnas.1017550108

Samways, D. S., Khakh, B. S., and Egan, T. M. (2012). Allosteric modulation of Ca2+ flux in ligand-gated cation channel (P2X4) by actions on lateral portals. *J. Biol. Chem.* 287, 7594–7602. doi: 10.1074/jbc.M111.322461

Shen, M. Y., and Sali, A. (2006). Statistical potential for assessment and prediction of protein structures. *Protein Sci.* 15, 2507–2524. doi: 10.1110/ps.062416606

Silberberg, S. D., Li, M., and Swartz, K. J. (2007). Ivermectin interaction with transmembrane helices reveals widespread rearrangements during opening of P2X receptor channels. *Neuron* 54, 263–274. doi: 10.1016/j.neuron.2007.03.020

Smart, O. S., Neduvelil, J. G., Wang, X., Wallace, B. A., and Sansom, M. S. (1996). HOLE: a program for the analysis of the pore dimensions of ion channel structural models. *J. Mol. Graph.* 14, 354–360. doi: 10.1016/S0263-7855(97)00009-X

Thauer, R. K., Jungermann, K., and Decker, K. (1977). Energy conservation in chemotrophic anaerobic bacteria. *Bacteriol. Rev.* 41, 100–180.

Theodorson-Norheim, E. (1987). Friedman and quade tests: BASIC computer program to perform nonparametric two-way analysis of variance and multiple comparisons of several related samples. *Comput. Biol. Med.* 17, 85–99. doi: 10.1016/0010-4825(87)90003-5

Vassilatis, D. K., Arena, J. P., Plasterk, R. H., Wilkinson, H. A., Schaeffer, J. M., Cully, D. F., et al. (1997). Genetic and biochemical evidence for a novel avermectin-sensitive chloride channel in *Caenorhabditis elegans*. Isolation and characterization. *J. Biol. Chem.* 272, 33167–33174. doi: 10.1074/jbc.272.52.33167

Viswanadhan, V. N., Ghose, A. K., Revankar, G. R., and Robins, R. K. (1989). Atomic physicochemical parameters for three dimensional structure directed quantitative structure-activity relationships. 4. Additional parameters for hydrophobic and dispersive interactions and their application for an automated superposition of certain naturally occurring nucleoside antibiotics. *J. Chem. Inf. Comput. Sci.* 29, 163–172. doi: 10.1021/ci00063a006

von Heijne, G., and Blomberg, C. (1979). Trans-membrane translocation of proteins. The direct transfer model. *Eur. J. Biochem.* 97, 175–181. doi: 10.1111/j.1432-1033.1979.tb13100.x

Wiederstein, M., and Sippl, M. J. (2007). ProSA-web: interactive web service for the recognition of errors in three-dimensional structures of proteins. *Nucleic Acids Res.* 35, W407–W410. doi: 10.1093/nar/gkm290

Zemkova, H., Khadra, A., Rokic, M. B., Tvrdonova, V., Sherman, A., and Stojilkovic, S. S. (2015). Allosteric regulation of the P2X4 receptor channel pore dilation. *Pflugers Arch.* 467, 713–726. doi: 10.1007/s00424-014-1546-7

Zemkova, H., Tvrdonova, V., Bhattacharya, A., and Jindrichova, M. (2014). Allosteric modulation of ligand gated ion channels by ivermectin. *Physiol. Res.* 63(Suppl. 1), S215–S224.

Zemkova, H., Yan, Z., Liang, Z., Jelinkova, I., Tomic, M., and Stojilkovic, S. S. (2007). Role of aromatic and charged ectodomain residues in the P2X(4) receptor functions. *J Neurochem.* 102, 1139–1150. doi: 10.1111/j.1471-4159.2007.04616.x

Conflict of Interest Statement: The authors declare that the research was conducted in the absence of any commercial or financial relationships that could be construed as a potential conflict of interest.

frontiers in Pharmacology

REVIEW
published: 14 December 2017
doi: 10.3389/fphar.2017.00898

Human Adenosine A_{2A} Receptor: Molecular Mechanism of Ligand Binding and Activation

Byron Carpenter[1]* *and Guillaume Lebon*[2]*

[1] Warwick Integrative Synthetic Biology Centre, School of Life Sciences, University of Warwick, Coventry, United Kingdom, [2] Institut de Génomique Fonctionnelle, Neuroscience Department, UMR CNRS 5203, INSERM U1191, Université de Montpellier, Montpellier, France

Adenosine receptors (ARs) comprise the P1 class of purinergic receptors and belong to the largest family of integral membrane proteins in the human genome, the G protein-coupled receptors (GPCRs). ARs are classified into four subtypes, A_1, A_{2A}, A_{2B}, and A_3, which are all activated by extracellular adenosine, and play central roles in a broad range of physiological processes, including sleep regulation, angiogenesis and modulation of the immune system. ARs are potential therapeutic targets in a variety of pathophysiological conditions, including sleep disorders, cancer, and dementia, which has made them important targets for structural biology. Over a decade of research and innovation has culminated with the publication of more than 30 crystal structures of the human adenosine A_{2A} receptor (A_{2A}R), making it one of the best structurally characterized GPCRs at the atomic level. In this review we analyze the structural data reported for A_{2A}R that described for the first time the binding of mode of antagonists, including newly developed drug candidates, synthetic and endogenous agonists, sodium ions and an engineered G protein. These structures have revealed the key conformational changes induced upon agonist and G protein binding that are central to signal transduction by A_{2A}R, and have highlighted both similarities and differences in the activation mechanism of this receptor compared to other class A GPCRs. Finally, comparison of A_{2A}R with the recently solved structures of A_1R has provided the first structural insight into the molecular determinants of ligand binding specificity in different AR subtypes.

Keywords: GPCR, adenosine, structural biology, G protein, drugs, x-ray diffraction

Key Concepts

1. **A_{2A}R crystallization: selection of different conformational states**
   Structure determination of A_{2A}R required the application of novel protein engineering techniques to lock the receptor in defined conformational states and facilitate the growth of crystals that diffract to high resolution.
2. **Structural determinants of A_{2A}R ligand binding and selectivity**
   The atomic resolution structural features of A_{2A}R that dictate which ligands it can bind and whether the ligands act as agonists, to promote signaling, or antagonists, to block signaling.
3. **Ligand-induced activation of A_{2A}R**
   The molecular changes that are induced in A_{2A}R by agonist binding, which facilitate G protein coupling and ultimately signal transduction.
4. **Structural diversity of the adenosine receptor family**
   The difference in the primary and ternary structure between the four AR subtypes that is ultimately responsible for their ligand-binding specificity and pharmacological profiles.

OPEN ACCESS

Edited by:
Kenneth A. Jacobson, National Institutes of Health (NIH), United States

Reviewed by:
Fei Xu, ShanghaiTech University, China
Kate White, University of Southern California, United States

***Correspondence:**
Byron Carpenter
b.carpenter@warwick.ac.uk
Guillaume Lebon
glebon@igf.cnrs.fr

Specialty section:
This article was submitted to Experimental Pharmacology and Drug Discovery, a section of the journal Frontiers in Pharmacology

Received: *24 October 2017*
Accepted: *24 November 2017*
Published: *14 December 2017*

Citation:
Carpenter B and Lebon G (2017) Human Adenosine A_{2A} Receptor: Molecular Mechanism of Ligand Binding and Activation. Front. Pharmacol. 8:898. doi: 10.3389/fphar.2017.00898

INTRODUCTION

Purinergic signaling is predominantly mediated by extracellular purine nucleosides and nucleotides, including adenosine and adenosine triphosphate (ATP), but also by purine bases such as caffeine and xanthine. Purinergic receptors are integral membrane protein that are divided into three classes, P1 (better known as adenosine receptors), P2Y, and P2X (Burnstock, 2006). Both P1 and P2Y receptors belong to the G protein-coupled receptor (GPCR) family, whereas P2X receptors are ATP-gated ion channels. Adenosine receptors (ARs) are divided into four subtypes, A_1, A_{2A}, A_{2B}, and A_3 (Fredholm et al., 2001), which are broadly expressed in the central nervous system as well as peripheral tissues of the cardiovascular, respiratory, renal, and immune systems (Fredholm et al., 2001, 2011). Extracellular adenosine is the endogenous agonist for all ARs, however differences in the adenosine binding affinity, tissue distribution, expression level and G protein coupling preference between the subtypes gives each a distinct signaling profile (Cieslak et al., 2008; Fredholm, 2014). A_1R and A_3R predominantly activate heterotrimeric G proteins belonging to the $G\alpha_{i/o}$ family, which inhibit cAMP production by adenylate cyclase, in contrast $A_{2A}R$ and $A_{2B}R$ predominantly activate $G\alpha_s$ family members, which stimulate cAMP production (Jacobson and Gao, 2006). G protein $\beta\gamma$ subunits also contribute to signaling through the mitogen-activated protein kinase (MAPK) and phospholipase C (PLC) pathways (Jacobson and Gao, 2006). ARs mediate the general cytoprotective functions associated with extracellular adenosine, with some of the key physiological processes regulated by individual subtypes being: sleep, vasoconstriction and inhibition of neurotransmitter release by A_1R; sleep, angiogenesis, and immunosuppression by $A_{2A}R$; vascular integrity and myocardial preconditioning by $A_{2B}R$; mast cell regulation and myocardial preconditioning by A_3R (Fredholm et al., 2011).

ARs have been proposed as potential targets in a wide variety of pathophysiological conditions, including arrhythmia, ischemia, sleep disorders, pain, dementia, Parkinson's, renal failure, asthma, type 2 diabetes, glaucoma, inflammation, and cancer (Jacobson and Gao, 2006; Cieslak et al., 2008; Sawynok, 2016). However, one of the challenges of therapeutic intervention has been targeting individual AR subtypes with sufficient specificity to limit off-target side effects (Chen et al., 2013). Medicinal chemistry approaches have been used to develop an array of compounds that exhibit improved subtype specificity (Müller and Jacobson, 2011), but very few have been approved for clinical use, due in part to the persistence of undesirable side effects (Chen et al., 2013; Glukhova et al., 2017). Further improvements in subtype specificity, coupled with the development of allosteric modulators (Gentry et al., 2015) that bind outside the orthosteric site, and biased ligands (Kenakin and Christopoulos, 2013) that can target a distinct signaling pathway associated with an individual AR subtype, may help to eliminate side effects entirely. Structure-based drug design, which involves *in silico* screening of vast compound libraries against experimentally determined receptor structures, offers huge potential for the development of a new generation of highly selective orthosteric, allosteric, and biased ligands, however, the difficulty of crystallizing GPCRs has, until recently, hindered this approach (Jazayeri et al., 2015).

Structure determination of GPCRs is notoriously challenging due to their conformationally dynamic nature and poor thermostability when extracted from the plasma membrane. During the past decade crystallization strategies have been developed that have revolutionized the structural biology of GPCRs, these include protein engineering approaches, such as fusion proteins (Cherezov et al., 2007; Chun et al., 2012), antibodies (Rasmussen et al., 2007, 2011a) and conformational thermostabilization (Magnani et al., 2008; Serrano-Vega et al., 2008; Shibata et al., 2009), as well as technical developments, such as the lipidic cubic phase (LCP) (Landau and Rosenbusch, 1996; Caffrey, 2015). Human $A_{2A}R$ has been at the forefront of this revolution and is now one of the best structurally characterized GPCRs, with more than 30 structures deposited in the protein data bank (PDB; **Table 1**). It is the only receptor for which structures of three distinct activation states have been reported, namely the inactive conformation bound to an antagonist or inverse agonist (Jaakola et al., 2008), an intermediate-active conformation bound to an agonist (Lebon et al., 2011b; Xu et al., 2011), and the active conformation bound to both an agonist and engineered G protein (Carpenter et al., 2016). Crystallization of the other AR subtypes has proved more difficult and it is only during the past year that structures of A_1R have been published (Cheng et al., 2017; Glukhova et al., 2017). Significantly, these have provided the first atomic resolution insight in to the molecular determinants of ligand binding specificity in different AR subtypes.

In this review we consolidate and analyze all of the structural information published during the past decade, which provides a near complete picture of $A_{2A}R$ activation. We compare the binding mode of antagonists, including the widely consumed stimulant caffeine (Doré et al., 2011; Cheng et al., 2017), and agonists, including the endogenous ligand adenosine (Lebon et al., 2011b). We highlight the agonist-induced conformational changes that activate $A_{2A}R$ (Lebon et al., 2011b; Xu et al., 2011), and the cooperative conformational changes induced by G protein coupling (Carpenter et al., 2016). Finally, we compare $A_{2A}R$ with the recently solved structures of A_1R (Cheng et al., 2017; Glukhova et al., 2017) and discuss the current evidence for the molecular basis of ligand binding specificity in different AR subtypes.

$A_{2A}R$ CRYSTALLIZATION: SELECTION OF DIFFERENT CONFORMATIONAL STATES

GPCRs are challenging targets for structural studies for three main reasons. First, flexibility and conformationally dynamics play a central role in receptor activation by maintaining a dynamic equilibrium between different conformational states (Kobilka and Deupi, 2007). Ligand binding is often insufficient to trap the receptor in a distinct conformation (Manglik et al., 2015; Ye et al., 2016), which can perturb the growth of crystals that diffract to high resolution (Cherezov et al., 2007; Warne et al., 2008; Tate and Schertler, 2009). Second,

TABLE 1 | Adenosine receptor X-ray crystal structures.

Receptor subtype	Conformational state	Ligand class	Ligand name	Fusion protein	Thermostabilized	Binding partner	Resolution (Å)	PDB code	References
A_1	Inactive	Antagonist	DU172[a]	BRIL	No	None	3.2	5UEN	Glukhova et al., 2017
	Inactive	Antagonist	PSB36	BRIL	Yes	None	3.3	5N2S	Cheng et al., 2017
A_{2A}	Inactive	Inverse agonist	ZM241385	T4L	No	None	2.6	3EML	Jaakola et al., 2008
	Inactive	Inverse agonist	ZM241385	None	Yes	None	3.3	3PWH	Doré et al., 2011
	Inactive	Antagonist	XAC	None	Yes	None	3.3	3REY	Doré et al., 2011
	Inactive	Antagonist	Caffeine	None	Yes	None	3.6	3RFM	Doré et al., 2011
	Inactive	Inverse agonist	ZM241385	BRIL	No	None	1.8	4EIY	Liu et al., 2012
	Inactive	Antagonist	T4G[b]	None	Yes	None	3.3	3UZA	Congreve et al., 2012
	Inactive	Antagonist	T4E[b]	None	Yes	None	3.3	3UZC	Congreve et al., 2012
	Inactive	Inverse agonist	ZM241385	None	No	Fab2823	2.7	3VG9	Hino et al., 2012
	Inactive	Inverse agonist	ZM241385	None	No	Fab2823	3.1	3VGA	Hino et al., 2012
	Inactive	Inverse agonist	ZM241385	BRIL	Yes	None	1.7	5IU4	Segala et al., 2016
	Inactive	Antagonist	6DY[b]	BRIL	Yes	None	1.9	5IU7	Segala et al., 2016
	Inactive	Antagonist	6DZ[b]	BRIL	Yes	None	2.0	5IU8	Segala et al., 2016
	Inactive	Antagonist	6DX[b]	BRIL	Yes	None	2.2	5IUA	Segala et al., 2016
	Inactive	Antagonist	6DV[b]	BRIL	Yes	None	2.1	5IUB	Segala et al., 2016
	Inactive	Inverse agonist	ZM241385	BRIL	No	None	2.5	5K2A	Batyuk et al., 2016
	Inactive	Inverse agonist	ZM241385	BRIL	No	None	2.5	5K2B	Batyuk et al., 2016
	Inactive	Inverse agonist	ZM241385	BRIL	No	None	1.9	5K2C	Batyuk et al., 2016
	Inactive	Inverse agonist	ZM241385	BRIL	No	None	1.9	5K2D	Batyuk et al., 2016
	Inactive	Inverse agonist	ZM241385	BRIL	No	None	2.8	5JTB	Melnikov et al., 2017
	Inactive	Antagonist	8D1[b]	BRIL	No	None	3.5	5UIG	Sun et al., 2017
	Inactive	Inverse agonist	ZM241385	BRIL	No	None	3.2	5UVI	Martin-Garcia et al., 2017
	Inactive	Antagonist	Caffeine	BRIL	Yes	None	2.1	5MZP	Cheng et al., 2017
	Inactive	Antagonist	Theophylline	BRIL	Yes	None	2.0	5MZJ	Cheng et al., 2017
	Inactive	Antagonist	PSB36	BRIL	Yes	None	2.8	5N2R	Cheng et al., 2017
	Inactive	Inverse agonist	ZM241385	BRIL	Yes	None	2.1	5NLX	Weinert et al., 2017
	Inactive	Inverse agonist	ZM241385	BRIL	Yes	None	2.0	5NM2	Weinert et al., 2017
	Inactive	Inverse agonist	ZM241385	BRIL	Yes	None	1.7	5NM4	Weinert et al., 2017
	Intermediate-active	Agonist	UK-432097	T4L	No	None	2.7	3QAK	Xu et al., 2011
	Intermediate-active	Agonist	Adenosine	None	Yes	None	3.0	2YDO	Lebon et al., 2011b
	Intermediate-active	Agonist	NECA	None	Yes	None	2.6	2YDV	Lebon et al., 2011b
	Intermediate-active	Agonist	CGS21680	None	Yes	None	2.6	4UG2	Lebon et al., 2015
	Intermediate-active	Agonist	CGS21680	None	Yes	None	2.6	4UHR	Lebon et al., 2015
	Active	Agonist	NECA	None	No	Mini-G_S	3.4	5G53	Carpenter et al., 2016

[a] *Covalently bound antagonist.*
[b] *Ligand nomenclature as used in the PDB.*

GPCRs are highly unstable upon extraction from the membrane by detergent solubilization, which makes purification of the receptors both technically challenging and inefficient (Serrano-Vega et al., 2008). Third, class A receptors are compact proteins that typically have only minimal hydrophilic surface area capable of forming crystal contacts. Structure determination of virtually all GPCRs, including $A_{2A}R$, has therefore required the development of novel protein engineering strategies (discussed below), crystallization techniques, including LCP (Landau and Rosenbusch, 1996; Xu et al., 2011; Caffrey, 2015), and data collection methods, including the use of micrometer-sized X-ray beams (Moukhametzianov et al., 2008) or serial crystallography (Weinert et al., 2017), in order to obtain well-diffracting crystals and collect high resolution diffraction data.

The first structure of $A_{2A}R$ was solved bound to the inverse agonist ZM241385 at 2.6 Å resolution (Jaakola et al., 2008). This structure was facilitated by a combined approach of using a high affinity ligand, which locks the receptor in its inactive state, and by replacing the third intracellular loop (ICL3) with a T4 lysozyme (T4L) fusion protein (Rosenbaum et al., 2007), which increases the hydrophilic surface area available for crystal contact formation (**Figure 1A**). This fusion protein strategy was subsequently modified to utilize apocytochrome b_{562}RIL (BRIL) instead of T4L (Liu et al., 2012), which resulted in the solution of seven additional structures of $A_{2A}R$ bound to ZM241385 ranging in resolution from 3.2 to 1.8 Å (Liu et al., 2012; Batyuk et al., 2016; Martin-Garcia et al., 2017; Melnikov et al., 2017), and one structure bound to the

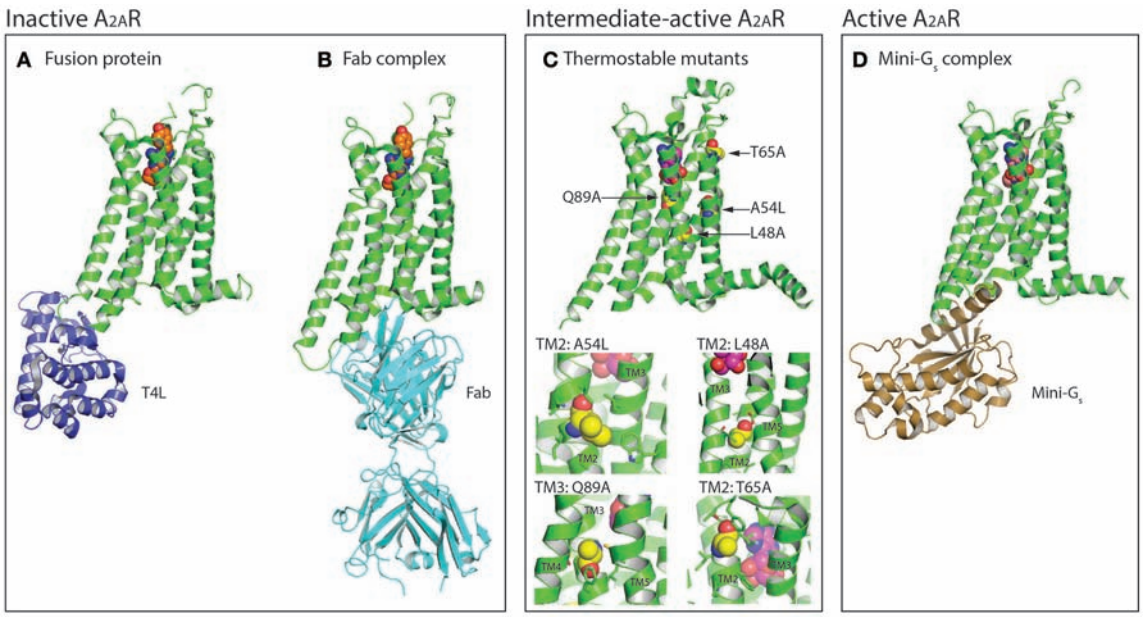

FIGURE 1 | Protein engineering strategies used for the selection and crystallization of distinct $A_{2A}R$ conformations. **(A)** Crystal structure of $A_{2A}R$ (colored green) in the inactive conformation bound to the inverse agonist ZM241385 (shown as spheres, carbon atoms colored orange) with T4 lysozyme (T4L; colored blue) fused between the intracellular ends of H5 and H6 (PDB: 3EML) (Jaakola et al., 2008). The T4L fusion protein has also been substituted with apocytochrome b_{562}RIL (BRIL; not shown) (Liu et al., 2012). **(B)** Structure of $A_{2A}R$ in the inactive conformation bound to ZM241385 (shown as spheres, carbon atoms colored orange) and an antibody F_{ab} fragment (colored cyan) that acts as an intracellular inverse agonist (PDB: 3VG9 and 3VGA) (Hino et al., 2012). **(C)** Crystal structure of thermostabilized $A_{2A}R$-GL26 in the intermediate-active conformation bound to the agonist adenosine (shown as spheres, carbon atoms colored magenta), the four thermostabilizing mutations ($L48A^{2.46}$, $A54L^{2.52}$, $T65A^{2.63}$, and $Q89A^{3.37}$) are shown as spheres and their carbon atoms colored yellow (PDB: 2YDO) (Lebon et al., 2011b). In the expanded view the residues with which the thermostabilizing mutations interact (distance < 4 Å) are shown as sticks. Conformational thermostabilization has facilitated the crystallization of $A_{2A}R$ in both the agonist- and antagonist- bound conformations. **(D)** Structure of $A_{2A}R$ in the active conformation bound to NECA (shown as spheres, carbon atoms colored light pink) and an engineered G protein mini-G_S (colored brown; PDB: 5G53) (Carpenter et al., 2016). Figures were prepared using PyMOL (PyMOL™ Molecular Graphics System, Version 1.8.6.0).

antagonist 8D1 (Sun et al., 2017) (**Table 1**). Conformational thermostabilization, which utilizes alanine scanning mutagenesis to identify point mutations that stabilize the receptor in a particular conformational state and increase its thermostability in detergent (Magnani et al., 2008, 2016), was also applied to solve the structure of $A_{2A}R$ bound to ZM241385 (Doré et al., 2011). The construct $A_{2A}R$-StaR2 contained eight thermostabilizing mutations ($A54L^{2.52}$, $T88A^{3.36}$, $R107A^{3.55}$, $K122^{4.43}$, $L202A^{5.63}$, $L235A^{6.37}$, $V239A^{6.41}$, and $S277A^{7.42}$; superscripts refer to Ballesteros–Weinstein numbering) (Ballesteros and Weinstein, 1995) that increased the stability of the receptor in the detergent dodecylmaltoside (DDM) by ∼18°C. $A_{2A}R$-StaR2 has since been crystallized bound to four different antagonists XAC, caffeine, T4G and T4E (Doré et al., 2011; Congreve et al., 2012). Conformational thermostabilization has also been used in combination with a BRIL fusion protein to facilitate the crystallization of $A_{2A}R$ bound to the antagonists 6DY, 6DZ, 6DX, 6DV, ZM241385, caffeine, theophylline, and PSB36 (Segala et al., 2016; Cheng et al., 2017). Furthermore, ZM241385-bound $A_{2A}R$ has been co-crystallized in complex with an antibody F_{ab} fragment (Fab2823), which acts as an intracellular inverse agonist locking the receptor in its inactive conformation, and also helps to increase the hydrophilic protein surface available for crystal contact formation (**Figure 1B**) (Hino et al., 2012).

The first agonist bound structure of $A_{2A}R$ was solved in complex with the synthetic agonist UK-432097, using the T4L fusion strategy (Xu et al., 2011). This ligand is large, approximately three times the molecular weight of adenosine, and imparts a significant increase in thermostability to the receptor. Crystallization of $A_{2A}R$ bound to smaller less stabilizing agonists required the application of the conformational thermostabilization methodology (**Figure 1C**). In this case the receptor was thermostabilized in the presence of the agonist NECA, and four mutations ($L48A^{2.46}$, $A54L^{2.52}$, $T65A^{2.63}$, and $Q89A^{3.37}$) were combined in the final construct ($A_{2A}R$-GL26) (Lebon et al., 2011a). The stability of $A_{2A}R$-GL26 was ∼16°C higher than the wild type receptor in DDM, which facilitated structure determination of the receptor in complex with the small agonists adenosine and NECA (Lebon et al., 2011b), as well as the larger CGS21680 (Lebon et al., 2015). All four agonist-bound structures adopted a conformation that was different from the inactive state, but that did not fully resemble the active state of the β_2 adrenergic receptor (β_2AR) in complex with heterotrimeric G_s (Rasmussen et al., 2011b), this conformation was therefore defined as the intermediate-active state (Lebon et al., 2011b). Interestingly, the high affinity agonist UK-432097 was sufficiently stabilizing to allow the crystallization of non-thermostabilized $A_{2A}R$ in the intermediate-active state. This is likely due to

the large size of the ligand, which results in it forming more extensive molecular contacts with the receptor, in particular UK-432097 forms four additional direct hydrogen bonds with $A_{2A}R$ compared to adenosine. In the case of small low affinity agonists, such as adenosine, conformational thermostabilization was absolutely necessary to facilitate structured determination.

The agonist-bound $A_{2A}R$ structures exhibited some characteristics of the active receptor (Lebon et al., 2012), however stabilizing the fully active conformation requires simultaneous binding of the agonist and G protein or a functional mimetic (Rasmussen et al., 2011a,b). Co-crystallization of GPCRs in complex with heterotrimeric G proteins is the ideal case for characterizing receptors in their active state, however this approach is challenging, due in part to the large size and conformationally dynamic nature of the G protein (Westfield et al., 2011). The development of nanobodies that act as surrogates of heterotrimeric G proteins has proved to be a powerful approach to crystallize receptors in their active conformation (Steyaert and Kobilka, 2011), however the disadvantage of this method is that nanobodies do not recapitulate the native GPCR–G protein interface. Structure determination of $A_{2A}R$ in its active conformation was achieved using a recently developed minimal G protein, which is composed of a single engineered domain from the $G\alpha_s$ subunit (**Figure 1D**) (Carpenter and Tate, 2016, 2017b,c). This mini G protein (mini-G_s) sufficiently stabilized NECA-bound $A_{2A}R$ in its fully active conformation to facilitate crystallization and structure determination at 3.4 Å resolution (Carpenter et al., 2016). This approach has now been applied to most heterotrimeric G proteins (Nehmé et al., 2017) and should play an important role solving high-resolution structures of other GPCRs in their active state (Strege et al., 2017).

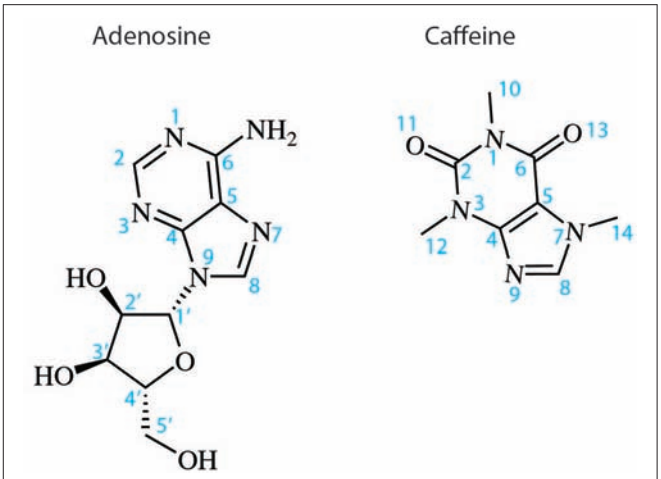

FIGURE 2 | Two dimensional structures of the endogenous $A_{2A}R$ agonist adenosine and the naturally occurring antagonist caffeine. The atom numbering indicated is used in the text to describe the binding of these ligands and their derivatives to $A_{2A}R$.

STRUCTURAL DETERMINANTS OF $A_{2A}R$ LIGAND BINDING AND SELECTIVITY

The orthosteric binding site of $A_{2A}R$ can be defined by the residues involved in binding the endogenous agonist adenosine and the naturally occurring antagonist caffeine (see **Figure 2** for the ligand structures and atom numbering, and **Table 2** for $A_{2A}R$-ligand contacts). Adenosine and caffeine share a common xanthine moiety that in both cases establishes van der Waals interactions with $M177^{5.38}$, $M270^{7.35}$ and $I274^{7.39}$, and a π-stacking interaction with the aromatic ring of F168, which is part of the helical portion of extracellular loop 2 (ECL2; **Figures 3**, **4**) (Doré et al., 2011; Lebon et al., 2011b; Cheng et al., 2017). $N253^{6.55}$ forms hydrogen bonds with either the amine groups at positions C6 and N7 of the adenine moiety of adenosine (Lebon et al., 2011b) or O11/O13 from the xanthine heterocycle of caffeine, for which two distinct binding orientations have been observed (Cheng et al., 2017). The ribose moiety of adenosine forms van der Waals interactions with $V84^{3.32}$, $L85^{3.33}$, $T88^{3.36}$, $W246^{6.48}$, and $L249^{6.51}$; these residues form similar contacts with many antagonist. The main difference between the adenosine- and caffeine-binding modes is the formation of hydrogen bonds from the hydroxyl groups at positions C2 and C3 of the ribose moiety of adenosine to $S277^{7.42}$ and $H278^{7.43}$. The recent high-resolution structure of $A_{2A}R$ bound to caffeine (2.10 Å) did reveal a water-mediated contact between $H278^{7.43}$ and O11 of caffeine (Cheng et al., 2017). However, the presence of this water molecule highlights the difference in the distance between these atoms compared to the adenosine-bound state, where a direct interaction is observed. This distance is reduced concomitantly with the conformational changes in H3 and H7 associated with agonist binding to the receptor (**Figure 5**) (Lebon et al., 2012). All agonists that have been co-crystallized with $A_{2A}R$ engage H3 through $T88^{3.36}$ and H7 through $S277^{7.42}$/$H278^{7.43}$ (**Table 2**). Some antagonists do interact with either $T88^{3.36}$ or $S277^{7.42}$/$H278^{7.43}$, but never at the same time, which suggests that the simultaneous engagement of these residues in H3 and H7 may be a key determinant of agonist activity.

Structures of $A_{2A}R$ have been solved in complex with three high-affinity synthetic agonists NECA, CGS21680 and UK-432097 (Lebon et al., 2011b, 2015; Xu et al., 2011). These agonists share a core adenosine moiety, the binding mode of which is very similar to adenosine itself, with the ribose group establishing hydrogen bonds with $S277^{7.42}$ and $H278^{7.43}$. For all three ligands the N-ethylcarboxyamido tail at position C5′ of the ribose ring extends deep into the binding pocket. The nitrogen and oxygen atoms form polar contacts with $T88^{3.36}$ and $H250^{6.52}$, respectively, and the substituent is further stabilized by van der Waals interactions with $N181^{5.42}$, $W246^{6.48}$ and to a lesser extent $Q/A^{3.37}$. In contrast, the OH group at this position of adenosine interacts with $N181^{5.42}$ and $H250^{6.52}$ through water-mediated interactions and $M177^{5.38}$ through a van der Waals interaction. The major difference between the binding mode of these agonists can be seen in the extracellular loops of the receptor. NECA and adenosine are both stabilized by a hydrogen bond with $E169^{ECL2}$ (Lebon et al., 2011b); this residue also forms a salt bridge with $H264^{ECL3}$, which closes the top of the binding

TABLE 2 | A_{2A}R-ligand interactions.

Secondary structure element	A_{2A}R residue	Ligand (agonist/antagonist)															
		Adenosine (2YDO)	NECA (2YDV)	CGS21680 (4UG2)	UK-432097 (3QAK)	Caffeine (5MZP)	Theophylline (5MZJ)	ZM241385 (3EML)	T4G (3UZA)	T4E (3UZC)	XAC (3REY)	6DX (5IUA)	6DZ (5IU8)	6DY (5IU7)	6DV (5IUB)	PSB36 (5N2R)	8D1 (5UIG)
H1	Y9																
H2	A63																
	I66																
	S67																
H3	A81																
	V84																
	L85																
	T/A88																
	Q/A89																
	I92																
ECL2	L167																
	F168																
	E169																
	M174																
H5	M177																
	N181																
H6	W246																
	L249																
	H250																
	I252																
	N253																
	T256																
ECL3	H264																
	A265																
H7	P266																
	L267																
	M270																
	Y271																
	I274																
	S/A277																
	H278																

A_{2A}R residues that directly interact with each ligand (distances < 4 Å) are indicated by filled cells and colored according to the ligand type with which they interact (agonists only, red; antagonists only, blue; both agonists and antagonists, gray). Residues F168^{ECL2}, M177$^{5.38}$, L249$^{6.51}$, N253$^{6.55}$ and I274$^{7.39}$ interact with all agonists and antagonists for which structures have been solved and are indicated by filled cells colored green. T88$^{3.36}$ interacts with all agonists for which structures have been solved and is a key residue in agonist-induced receptor activation, however since it also interacts with the antagonist 8D1 (discussed in the text) it is indicated by hatched cells colored red. The secondary structure element in which each residue is located is shown in the left hand column (H, transmembrane helix; ECL, extracellular loop). The PDB codes of the A_{2A}R structures used for analysis are shown in parentheses next to each ligand. Note that several of the A_{2A}R structures contain thermostabilizing mutations, including T88A/S277A (caffeine, theophylline, T4G, T4E, XAC, 6DX, 6DZ, 6DY, 6DV, PSB36) and Q89A (adenosine, NECA and CGS21680).

pocket and is known to affect ligand binding kinetics (Guo et al., 2016; Segala et al., 2016). CGS21680 takes advantage of similar hydrogen bond between the amine group at position C6 of adenine moiety and E169^{ECL2} (Lebon et al., 2015). The larger (2-carboxyethyl)phenylethylamino substituent at the C2 position protrudes outside the binding pocket and is stabilized by van der Waals interactions with E169^{ECL2}, H264^{ECL3}, and L267$^{7.32}$ as well as a hydrogen bond with S67$^{2.65}$. As a consequence, the extracellular end of H2 is displaced inward compared to other agonist-bound structures, reducing the volume of the binding pocket. UK-432097 has two substituents on the adenine moiety, that make it an even larger molecule than CGS21680. The consequence is that the bulky 2-(3-[1-(pyridine-2-yl)piperidin-4-yl]ureido)ethylcarboxamido substitution at position C2 displaces ECL3 away from the binding pocket, which induces rotamer changes in E169^{ECL2} and H264^{ECL3} and breaks the salt bridge between these side chains (Xu et al., 2011). The urea group forms two hydrogen bonds with E169^{ECL2} as

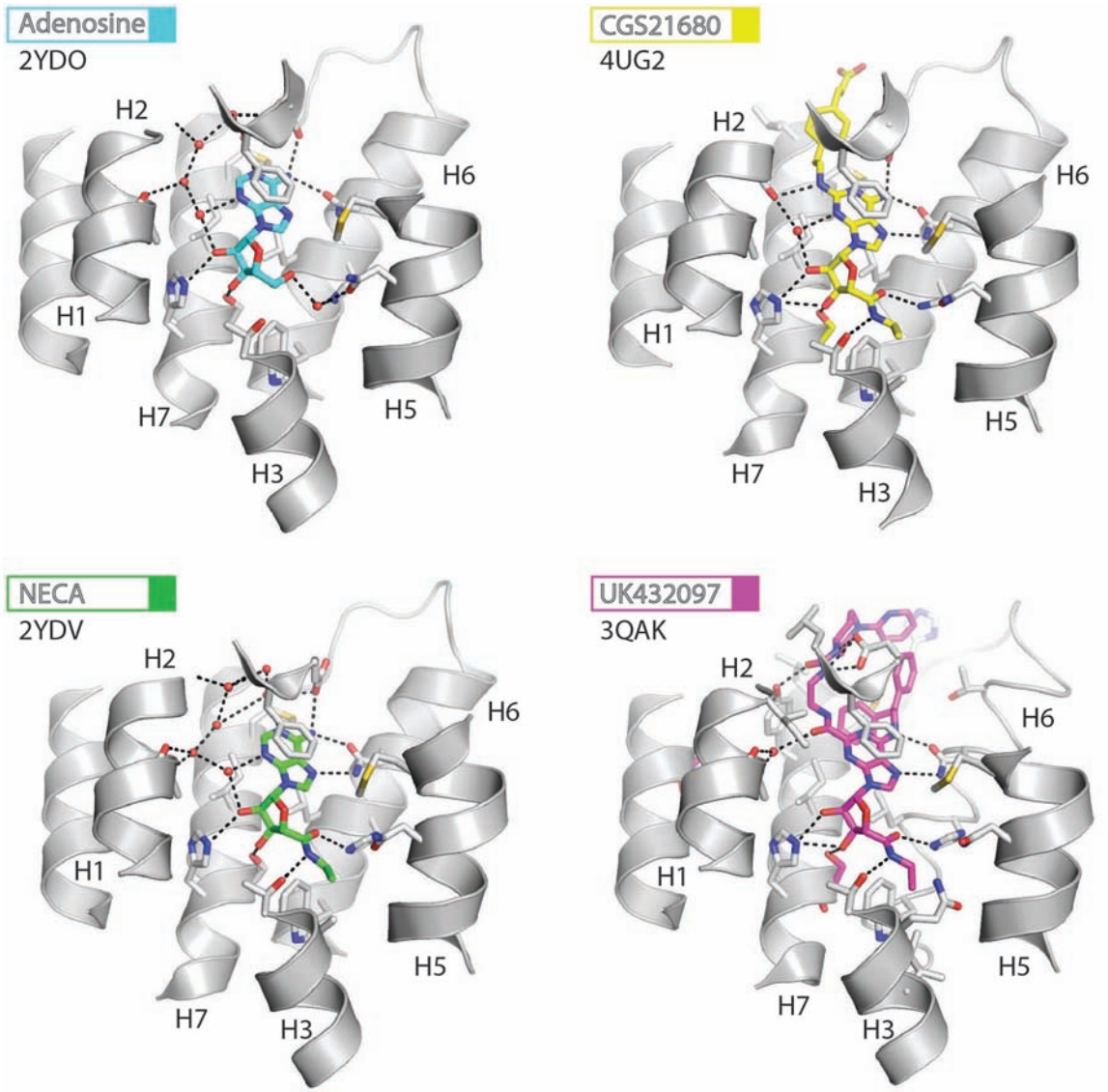

FIGURE 3 | High-resolution view of the agonist-binding site of human $A_{2A}R$. Four different agonists have been co-crystallized with $A_{2A}R$ in the intermediate-active conformation. The receptor is shown as cartoons and colored gray, residues and side chains that interact with the ligand are shown as sticks and colored by element (carbon, gray; nitrogen, blue; oxygen, red; sulfur, yellow). The ligands are shown as sticks and their carbon atoms are colored to match their labels, PDB codes are shown in the figure. Polar contacts are represented as dashed lines and water molecules are shown as red spheres.

well as a hydrogen bond and van der Waals interactions with $Y271^{7.36}$ on its opposite side. The pyridinyl-piperidine group, which extends furthest from the binding pocket, is stabilized by van der Waals interactions with $L267^{7.32}$ and $H264^{ECL3}$.

Like agonists, antagonists can exploit subsidiary binding sites by expanding their contact surface outside the orthosteric binding pocket. Starting with ZM241385, the trizolotriazine ring occupies the orthosteric binding site, and is surrounded by $F168^{ECL2}$, $L249^{6.51}$, $M270^{7.35}$, $I274^{7.39}$. Two residues, $E169^{ECL2}$ and $N253^{6.55}$, form hydrogen bonds with the amine group of the ZM241385 heterocycle and an additional hydrogen bond is established between $N253^{6.55}$ and the oxygen of the furan ring. The formation of van der Waals interactions with $M177^{5.38}$, $W246^{6.48}$, $L249^{6.51}$, and $H250^{6.52}$ stabilize H5 and H6 against the furan ring. ZM241385 explores the chemical space outside the orthosteric site by taking advantage of the cavity on the extracellular surface of the receptor. Two distinct orientations have been observed for the phenol ring of ZM241385, in the first conformation the salt bridge between $E169^{ECL2}$ and $H264^{ECL3}$ is intact and the phenol ring forms van der Waals interactions with $H264^{ECL3}$, $L267^{7.32}$ and $M270^{7.35}$ (Jaakola et al., 2008). Interestingly, the phenylethylamine group of ZM241385 adopts a binding mode similar to the (2-carboxyethyl)phenylethylamino

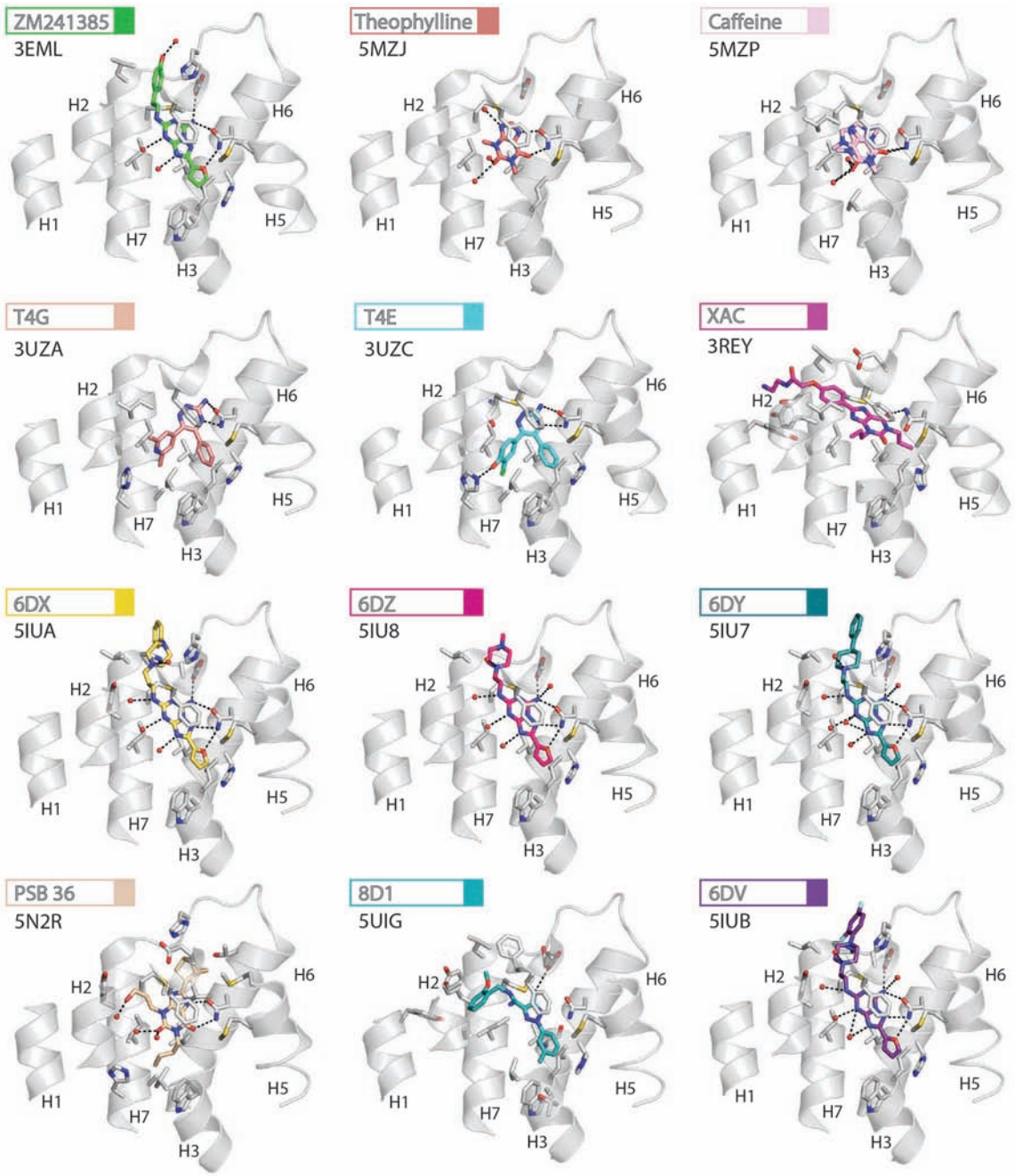

FIGURE 4 | High-resolution view of the antagonist- or inverse agonist- binding site of human $A_{2A}R$. Twelve different antagonists or inverse agonists have been co-crystallized with $A_{2A}R$, in the inactive conformation. The receptor is shown as cartoons and colored gray, residues and side chains that interact with the ligand are shown as sticks and colored by element (carbon, gray; nitrogen, blue; oxygen, red; sulfur, yellow). The ligands are shown as sticks and their carbon atoms are colored to match their labels, PDB codes are shown in the figure. Polar contacts are represented as dashed lines and water molecules are shown as red spheres. Note that for caffeine the two distinct binding orientations that were observed in the structure are overlaid.

substituent of CGS21680 (Lebon et al., 2015). The second conformation was observed in a thermostabilized receptor structure where the salt bridge between $E169^{ECL2}$ and $H264^{ECL3}$ is broken (Doré et al., 2011). In this case the phenol moiety is pointing toward H1 and H2 engaging $S67^{2.65}$, $Y271^{7.36}$, and $I274^{7.39}$ through van der Waals interactions and $A63^{2.61}$ through a hydrogen bond. Both $Y9^{1.35}$ and $Y271^{7.36}$ sidechains adopt different rotamers in order to accommodate the phenol substituent in this pose, demonstrating that this subsidiary pocket is conformationally malleable. The xanthine derivative

XAC occupies the orthosteric pocket with the xanthine ring adopting a similar position to caffeine and the trizolotriazine heterocycle of ZM241385 (Doré et al., 2011). However, the xanthine core is branched at position N1 and N3; the N3 propyl substituent forms van der Waals interactions with $I66^{2.64}$ and $A81^{3.29}$ that are not observed for ZM241385. On the extracellular surface of the receptor the phenoxy-acetamide tail of XAC adopts a pose that is similar to the phenol group of ZM241385 in the thermostabilized receptor structure and is engaged by $S67^{2.65}$, $L267^{7.32}$, $M270^{7.35}$, $Y271^{7.36}$, and $I274^{7.39}$. However, none of these interactions are unique to XAC since they are all observed for ZM241385 in either of its two poses. The recent structure of 8D1 (also known as compound-1) bound to $A_{2A}R$ provides another example of a ligand that exploits this subsidiary binding site (Sun et al., 2017). The methoxy phenyl substituent of 8D1 occupies the extracellular pocket formed by $Y9^{1.35}$, $A63^{2.61}$, $I66^{2.64}$, $S67^{2.65}$, $L267^{7.32}$, $M270^{7.35}$, $Y271^{7.36}$, and $I274^{7.39}$ in a similar way to XAC and ZM241385. In this case a unique interaction is observed between 8D1 and $Y9^{1.35}$ that is not observed for any other ligand (**Table 2**). Thus, several different ligands and chemical substituents have been shown to take advantage of the subsidiary binding pocket located between H1, H2, and H7 on the extracellular surface of the receptor.

Cavities identified from high-resolution crystal structures provide valuable information for structure-based drug discovery. This can be best illustrated by the study of Congreve et al. who have reported the discovery of 1,2,4-triazine derivatives as $A_{2A}R$ antagonists by exploiting structural data (Congreve et al., 2012). The authors optimized a series of compounds and hypothesized that 1,2,4-triazine derivatives may occupy the same area of the binding pocket as the ribose moiety of agonists. Solution of the corresponding ligand–receptor structures showed that the triazine ring of T4E or T4G sits in a pocket similar to other ligands, and forms van der Waals interactions with $F168^{ECL2}$ and two hydrogen bonds with $N253^{6.55}$. The phenol substituent forms van der Waals interactions with $L85^{3.33}$, $M177^{5.38}$, $W246^{6.48}$ $L249^{6.51}$, and $H250^{6.52}$. As predicted the dimethyl-pyridine group of T4G occupies the ribose pocket and the phenolic hydroxyl group of T4E establishes a hydrogen bond with $H278^{7.43}$, but importantly the ligands retain their antagonistic properties.

Crystallographic studies have also highlighted the role that ECL2 and ECL3 play in ligand binding, specifically the effect of the salt bridge between $E169^{ECL2}$ and $H264^{ECL3}$ (Lebon et al., 2015; Guo et al., 2016; Segala et al., 2016). These two residue as well as the salt bridge that they form, stabilize several ligands in the binding pocket, as described above for ZM241385. The phenol ring of the ZM241385 has recently been replaced by a set of larger substitutions and their structures have been solved in complex with $A_{2A}R$ at high resolution (Segala et al., 2016). The substitutions were reported to affect the residence time of the ligands, with the ligand 6DV (also known as 12x) displaying the slowest off-rate. This observation is also in agreement with the agonist-bound structures where the salt bridge closes the binding site for adenosine, NECA and CGS21680 (Lebon et al., 2011b, 2015). Mutation of either $E169^{ECL2}$ or $H264^{ECL3}$ has been shown to impair the potency of NECA whereas only mutation of $H264^{ECL3}$ affected CGS21680 (Lebon et al., 2015). The lower potency of agonists on these mutant receptors might be a consequence of a faster off-rate in absence of the salt bridge, however it appears that the stabilizing effect of the salt bridge can be compensated for by extended molecular contact formed by large molecules, such as CGS21680.

LIGAND-INDUCED ACTIVATION OF $A_{2A}R$

GPCRs exist in dynamic equilibrium between several discrete conformational states that are separated by energy barriers (Manglik et al., 2015; Ye et al., 2016). The inactive and active states are well-conserved between GPCRs (Rosenbaum et al., 2009; Carpenter and Tate, 2017a), however a number of intermediate conformations have been identified that appear to be more divergent (Lebon et al., 2011b; Xu et al., 2011; White et al., 2012; Manglik et al., 2015; Ye et al., 2016). Agonist binding to the receptor is one of the key events required to overcome the energy barrier of activation and increase occupancy of the conformational state(s) that are capable of binding heterotrimeric G proteins (Manglik et al., 2015; Ye et al., 2016; Prosser et al., 2017). $A_{2A}R$ is one of the only receptors for which an intermediate-active agonist-bound state has been crystallized (Lebon et al., 2011b; Xu et al., 2011). This structure has provided unique insight into the molecular changes that occur during two key activation events, namely agonist-induced transition from the inactive to intermediate-active state and G protein-induced transition from the intermediate-active to active state. The structures used for comparison are the inactive state bound to the inverse agonist ZM241385 (Doré et al., 2011; Liu et al., 2012), the intermediate-active state bound to the agonist NECA (Lebon et al., 2011b) and the active state bound to NECA and mini-G_s (Carpenter et al., 2016), see **Figure 5**. Agonist binding to $A_{2A}R$ triggers a series of conformational changes, most notably within the ligand-binding pocket and on the intracellular side of the receptor (**Figure 5A**). In the ligand binding pocket the most significant changes are a 2 Å translocation of H3 along its axis that is necessary to prevent steric clashes of $V84^{3.32}$ and $L85^{3.33}$ with NECA, the formation of contacts between the ribose moiety of the agonist and residues $S277^{7.42}$ and $H278^{7.43}$ in H7 that are completely absent in the inverse agonist-bound state, and an inward bulge in H5 that disrupts the local helix geometry and shifts $C185^{5.46}$ toward the core of the receptor by 4 Å (Lebon et al., 2011b). Notably, the bulge in H5 has a knock-on effect on the position of $H250^{6.52}$, which is shifted toward the ligand by 2 Å, a movement that would be sterically forbidden if the inverse agonist were bound (Lebon et al., 2011b, 2012; Xu et al., 2011). This bulge is also observed in other GPCR structures suggesting it is one of the key event in activation (Venkatakrishnan et al., 2013). Agonist binding causes only subtle conformational changes on the extracellular side of the receptor, including 1-2 Å inward shifts in the ends of H1, H2, and H3. More significant changes are observed on the intracellular side, which are thought to prime the receptor for G protein coupling (Venkatakrishnan et al., 2016), specifically combined rotations and lateral movements in

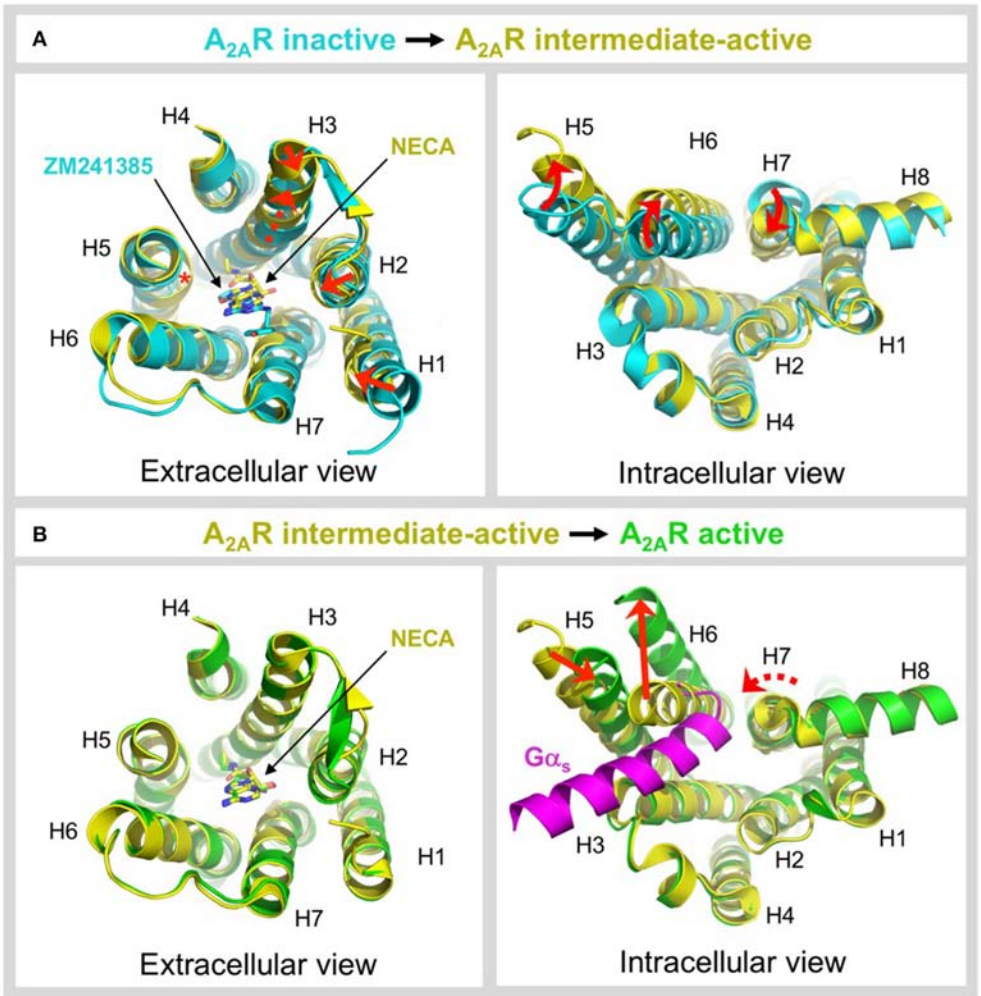

FIGURE 5 | Ligand-induced activation of $A_{2A}R$. **(A)** Conformational changes associated with agonist-induced transition from the inactive state (colored cyan) to the intermediate-active state (colored yellow; PDB: 2YDV) (Lebon et al., 2011b). Two different inactive state structures were used for the alignments, the extracellular view uses 4EIY (Liu et al., 2012) because it is the highest resolution non-thermostabilized structure available, the intracellular view uses 3PWH (Doré et al., 2011) because it was crystallized without a fusion protein in ICL3. The extracellular view shows the 1–2 Å inward shifts in the ends of H1, H2, and H3 (indicated by a red arrows), the 2 Å translocation of H3 along its axis (indicated by a dashed red arrow), and the inward bulge in H5 (indicated by a red asterisk). The inverse agonist ZM241385 (colored cyan) and agonist NECA (colored yellow) are shown as sticks. The intracellular view shows the combined rotational and lateral movements in H5, H6, and H7 (indicated by curved red arrows). H5 and H6 are displaced outwards by 7 and 5 Å, respectively, while H7 moves inwards in by 4 Å. **(B)** Conformational changes associated with G protein-induced transition from the intermediate-active state (colored yellow; PDB: 2YDV) (Lebon et al., 2011b) to the active state (colored green; PDB: 5G53) (Carpenter et al., 2016). No significant changes are observed on the extracellular side of the receptor, and the position of NECA (shown as sticks) is essentially identical in both states (Carpenter et al., 2016). On the intracellular side of the receptor an outward movement of H6 by 14 Å (indicated by a red arrow) is required to accommodate binding of mini-G_s (colored magenta). H5 moves inwards by 5 Å (indicated by a red arrow) and forms direct contacts the α5 helix of mini-G_s. H7 undergoes a rotation, without significant lateral movement (indicated by a curved and dashed red arrow), which reorients the H7-H8 boundary to interact with the C-terminus of mini-G_s (Carpenter et al., 2016). Note that for clarity, ECL2 has been omitted from the extracellular view of all alignments.

the cytoplasmic ends of H5, H6, and H7, outwards by 7 and 5 Å for H5 and H6, respectively, and inwards by 4 Å for H7 (**Figure 5A**) (Lebon et al., 2011b; Xu et al., 2011). The ionic lock between $R102^{3.50}$ and $E228^{6.30}$, which is often engaged in inactive GPCR structures, is broken by the reorientation of H6.

Sodium ions (Na^+) act as negative allosteric modulators of many class A GPCRs, typically stabilizing the ligand-free and antagonist-bound states, thereby imposing an energy barrier on receptor activation (Katritch et al., 2014). The high-resolution model of $A_{2A}R$ in its inactive state was the first GPCR structure to reveal the mode of Na^+ binding (Liu et al., 2012). In $A_{2A}R$ the Na^+-binding pocket is composed of residues $D52^{2.50}$, $S91^{3.39}$, $T88^{3.36}$, $W246^{6.48}$, $N280^{7.45}$, and $S281^{7.46}$; both $D52^{2.50}$ and $S91^{3.39}$ form direct polar interactions with Na^+, whereas interactions with the other residues are mediated through a network of ordered water molecules (Liu et al., 2012; Gutiérrez-de-Terán et al., 2013). The conformational

changes induced by agonist binding, particularly the rotation and inward shift of H7 and the outward shift of H6, cause the Na^+-binding pocket to collapse, potentiating the displacement of Na^+, thereby allowing the agonist to overcome the negative allosteric effect of Na^+ and activate the receptor (Gutiérrez-de-Terán et al., 2013). Interestingly, the intermediate-active conformation is not observed in crystal structures of agonist-bound β_1AR (Warne et al., 2011) or β_2AR (Rosenbaum et al., 2011). Recent ^{19}F nuclear magnetic resonance (^{19}F NMR) studies have confirmed the existence of an additional active-like state in A_{2A}R compared to β_2AR (Manglik et al., 2015; Ye et al., 2016; Prosser et al., 2017), which may correlate with the intermediate-active conformation observed in the crystal structures, thus highlighting differences in the energy landscape of activation between these receptors.

In contrast to the widely distributed effects of agonist binding, G protein-induced conformational changes are confined to the intracellular side of the receptor (**Figure 5B**). G protein coupling has been reported to increase the agonist-binding affinity of A_{2A}R between 10- and 40-fold (Murphree et al., 2002; Carpenter et al., 2016), yet it is striking that the conformation of the residues in the ligand-binding pocket and the position of the agonist are essentially identical in both the intermediate-active and active states (Carpenter et al., 2016). The most likely explanation is that in the intermediate-active structure the ligand-binding pocket has already adopted the high-affinity conformation (Carpenter et al., 2016). However, it cannot be discounted that the relatively small increase in the agonist-binding affinity of A_{2A}R does not result from direct changes to the ligand-binding pocket, for example, a reduction in the conformational dynamics of the receptor caused by G protein binding could decrease the off-rate of the agonist, thus increasing its affinity (Carpenter and Tate, 2017a). On the intracellular side of the receptor the pivotal event is a 14 Å outward movement of the cytoplasmic end of H6 to accommodate binding of the α5 helix from mini-G_s. The outward movement of H6 triggers both a 5 Å inward movement of H5, positioning it to interact with the α5 helix of the G protein, and a rotation within H7 that reorients the H7-H8 boundary to form extensive contacts with the C-terminus of mini-G_s (Carpenter et al., 2016). These helix movements also result in reorientation of R102$^{3.50}$, Y197$^{5.58}$, and Y288$^{7.53}$ side chains within the core of the receptor, which likely stabilizes the active state, and which is one of the signatures of a GPCR in its active conformation (Carpenter and Tate, 2017a). It is clear that the intermediate-active state of A_{2A}R is incompatible with G protein binding in its final orientation, i.e., that observed in the A_{2A}R–mini-G_s structure (Carpenter et al., 2016), due to a large sterically forbidden clash between the α5 helix of mini-G_s and H6 of the receptor (**Figure 5B**). However, it is possible that the intermediate-active state of A_{2A}R may be responsible for recognition of the G protein through an initial docking interaction, before cooperative conformational changes trigger nucleotide dissociation from the G protein and drive the receptor into its active conformation (Rasmussen et al., 2011b; Flock et al., 2015; Carpenter et al., 2016).

STRUCTURAL DIVERSITY OF THE ADENOSINE RECEPTOR FAMILY

The amino acid sequence of the four AR subtypes is relatively poorly conserved, A_{2A}R shares only 49, 56, and 39% identity with A_1R, A_{2B}R, and A_3R, respectively (aligned over residues 1-312 of A_{2A}R). This means that, despite there being a wealth of structural data available for A_{2A}R, it has proved challenging to homology model other AR subtypes with sufficient accuracy for structure-based drug design applications (Glukhova et al., 2017). It is only during the past year that structures of an AR other than A_{2A}R have been published, namely two structures of A_1R bound to the xanthine antagonists DU172 (Glukhova et al., 2017) and PSB36 (Cheng et al., 2017). The two A_1R structures are closely related and align with an RMSD of 0.6 Å (over 235 Cα atoms), they also align well with the ZM241385-bound structure of A_{2A}R (Liu et al., 2012), with RMSDs of 0.8 Å (over 238 Cα atoms) and 1.0 Å (over 234 Cα atoms) for the DU172- and PSB36- bound structures, respectively. The intracellular side of both A_1R structures strongly resemble the ZM241385-bound A_{2A}R structure (3PWH), which was crystallized without a fusion protein in ICL3 (Doré et al., 2011), and the ionic lock between residues R105$^{3.50}$ and E229$^{6.30}$ is engaged in both cases (Cheng et al., 2017; Glukhova et al., 2017). The organization of the sodium-binding site is also well-conserved between A_1R and A_{2A}R, which supports mutagenesis data that indicated the negative allosteric effect of sodium on A_1R was mediated through this site (Barbhaiya et al., 1996), although neither A_1R structure was of sufficient resolution to conclusively model the sodium ion.

The most striking differences between A_1R and A_{2A}R are the conformational variations in extracellular ends of H1, H2, H3, and H7 and the orientation of ECL2. In the DU172-bound structure H3 is displaced inwards by 4 Å, and H1, H2, and H7 are displaced outwards by 5, 4, and 4 Å, respectively (**Figure 6A**). The outward movements in H1, H2, and H7 are required to accommodate the benzene sulfonate group of DU172, which is covalently linked to Y271$^{7.36}$, and result in both the expansion of the orthosteric site and the formation of a secondary allosteric pocket (Glukhova et al., 2017). Direct comparison of A_1R and A_{2A}R bound to PSB36, which does not contain the benzene sulfonate substituent, also reveals a partial expansion of the orthosteric pocket (Cheng et al., 2017), indicating that this region of A_1R is indeed more conformationally malleable than that of A_{2A}R. Intriguingly, it has been suggested that the conformational rearrangements in H1, H2, and H3 in A_1R may be a direct result of the different disulphide bond structure of ECL2 (Glukhova et al., 2017). In both A_1R structures ECL2 adopts a similar conformation, which is different from that observed in any of the published A_{2A}R structures (**Figure 6B**). The helical segment in ECL2 of A_1R is extended by five residues and is positioned almost perpendicular to the transmembrane helices, compared to the near parallel arrangement in A_{2A}R (Cheng et al., 2017; Glukhova et al., 2017). There is only a single disulphide bond in ECL2 of A_1R compared to three within the same region of A_{2A}R, which results in it adopting an extended conformation (**Figure 6B**). This appears to reduce conformational constraints

on the extracellular ends of H2 and H3 allowing them to be displaced outwards, which in turn influences the positioning of H1. The displacement of H7 may also be linked to structural divergence in the extracellular loops, in this case a single amino acid truncation in ECL3 of A_1R has been proposed to induce the outward tilt observed in the structures (Cheng et al., 2017; Glukhova et al., 2017).

What do these structures tell us about the molecular determinants of ligand-binding specificity in different AR subtypes? First, sequence differences in the binding pocket do not appear to be the main determinant of ligand-binding specificity in ARs. The orthosteric binding pocket of A_1R and $A_{2A}R$ in the PSB36-bound structures differ by only four residues $V62^{2.57}$, $N70^{2.65}$, $E170^{ECL2}$, and $T270^{7.35}$ (corresponding to $A59^{2.57}$, $S67^{2.65}$, $L170^{ECL2}$, and $M270^{7.35}$ in $A_{2A}R$), and of these, only $T/M270^{7.35}$ form direct contacts with the ligand (Cheng et al., 2017). Mutagenesis studies have shown that residue $270^{7.35}$ is important in ligand-binding specificity, introducing the T270M mutation into A_1R resulted in decreased binding affinity of A_1R-specific ligands and increased binding affinity of $A_{2A}R$-specific ligands, the reverse effect was observed when the M270T mutation was introduced into $A_{2A}R$ (Cheng et al., 2017; Glukhova et al., 2017). However, the positioning of this residue on the extracellular end of H7, at the perimeter of the binding pocket, suggests its main role is to act as a "gatekeeper" that regulates ligand access to the orthosteric site (Glukhova et al., 2017). Second, the topology of the binding pocket appears to play a central role in ligand-binding specificity. As described above the disulphide bond structure of ECL1 and ECL2 in A_1R increases mobility in H1, H2 and H3, which causes an expansion of the binding pocket that is required to accommodate the benzene sulfonate group of the A_1R-selective ligand DU172 (**Figure 6A**) (Glukhova et al., 2017). Binding pocket topology is also the predominant factor in the differential binding modes of PSB36 between A_1R and $A_{2A}R$ (**Figure 6C**). PSB36 binds 2 Å deeper in the orthosteric pocket of A_1R due to the presence of a channel between H3, H5 and H6 that can accommodate the butyl substituent at position N1 of the xanthine core (**Figure 6C**) (Cheng et al., 2017). This channel is created by a 2 Å displacement of $L88^{3.34}$ in A_1R that appears to be the result of an upstream proline residue ($P86^{3.31}$), which is located outside the binding pocket, distorting the helix geometry in this region of H3. A proline at this position is unique to A_1R and helps to explain why substitutions at position N1 of the xanthine core contribute to A_1R selectivity (Cheng et al., 2017). Thus, the amino acid sequence both inside and outside the ligand-binding site, the extracellular loop structure and the topology of the binding pocket play interconnected roles in governing the ligand binding affinity and kinetics that are ultimately responsible for the functional selectivity of AR subtypes.

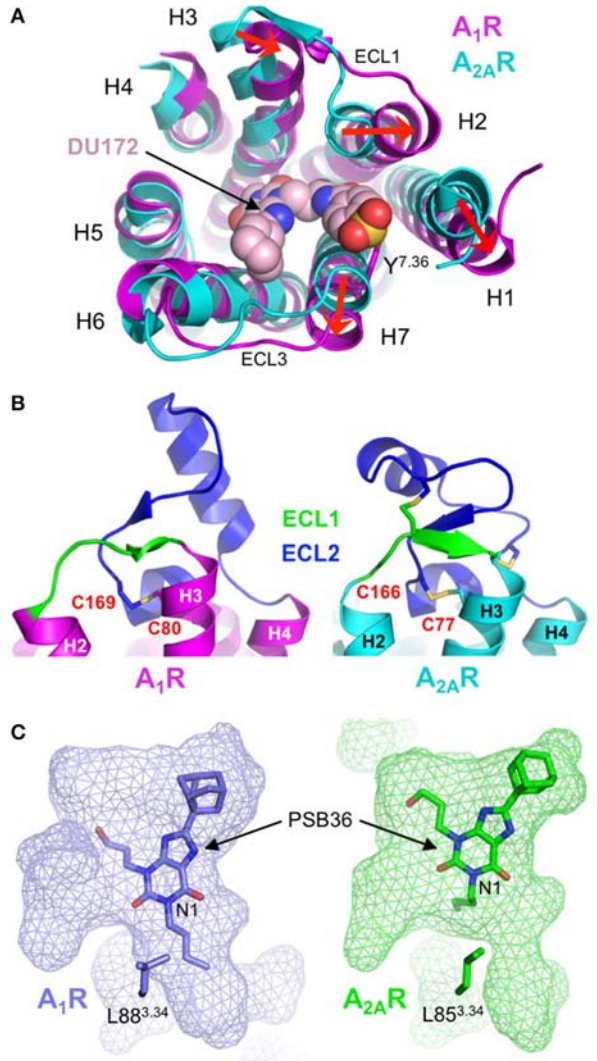

FIGURE 6 | Structural diversity of the adenosine receptor family. **(A)** Extracellular view of the conformational differences between DU172-bound A_1R (colored magenta; PDB: 5UEN) (Glukhova et al., 2017) and ZM241385-bound $A_{2A}R$ (colored cyan; PDB: 4EIY) (Liu et al., 2012). The extracellular ends of H1, H2 and H7 are displaced outwards by 5, 4, and 4 Å, respectively and H3 is displaced inwards by 4 Å (indicated by red arrows). The antagonist DU172 (shown as spheres) is covalently attached to $Y271^{7.36}$ (shown as sticks) through a benzene sulfonate linkage. Note that for clarity, ECL2 has been omitted from the alignment. **(B)** Differential conformations of ECL1 (colored green) and ECL2 (colored blue) in A_1R (colored magenta; PDB: 5UEN) (Glukhova et al., 2017) and $A_{2A}R$ (colored cyan; PDB: 4EIY) (Liu et al., 2012), disulphide bonds are shown as sticks. In A_1R ECL2 adopts an extended conformation that is stabilized by a single disulphide bond ($C80^{3.25}$-$C169^{ECL2}$). In contrast, ECL2 from $A_{2A}R$ adopts a compact conformation that is stabilized by three disulphide bond, one of which ($C77^{3.25}$-$C166^{ECL2}$) is conserved in A_1R. **(C)** Surface representation of the ligand-binding pocket (rendered as semi-transparent mesh) in A_1R (colored blue; PDB: 5N2R) (Cheng et al., 2017) and $A_{2A}R$ (colored green; PDB: 5N2S) (Cheng et al., 2017), which highlights differences in both the topology of the orthosteric site and the binding orientation of PSB36 (shown as sticks). The butyl substituent at position N1 of the xanthine core of PSB36 fits into a channel between H3, H5, and H6 in A_1R, this channel is constricted in $A_{2A}R$ due to the different orientation of $L85^{3.34}$ (shown as sticks), which results in the ligand binding in a different orientation.

CONCLUSION

A decade of research and innovation has culminated in the crystallization of more than 30 structures of human $A_{2A}R$ in complex with one inverse agonist, 11 antagonists and four agonists, as well as an engineered G protein. These

structures represent the inactive, intermediate-active and active conformational states, and $A_{2A}R$ remains the only receptor for which this complete series of structures has been reported. Most of the structure were obtained using high affinity ligands, such as ZM241385, XAC, NECA, UK-432097, CGS21680. However, the application of conformational thermostabilization has also facilitated structure determination of the receptor in complex with lower affinity ligands, including the endogenous agonist adenosine and the natural plant-derived antagonists caffeine and theophylline. Structural characterization of the ligand-binding pocket of $A_{2A}R$ has provide novel insight into the binding modes of different classes of ligands; the ribose moiety has been identified as a key component of agonists that helps to stabilize the intermediate-active state before the receptor can adopt the fully active conformation upon G protein coupling. The chemical diversity of compounds co-crystallized with $A_{2A}R$ has also revealed how some ligands can exploit subsidiary binding sites on the extracellular surface of the receptor, as exemplified by the antagonists XAC, ZM241385, 8D1, T4G, and T4E and agonists CGS21680 and UK-432097.

High-resolution structures have not only provided a clear picture of the ligand-binding pocket, but have also highlighted the impact of receptor flexibility, notably in ECL2 and ECL3, on the mode and kinetics of ligand binding. Furthermore, the recently solved structures of A_1R revealed that binding pocket topology and extracellular loop structure are two of the most important factors affecting the ligand binding specificity of different AR subtypes. These observations highlight the challenges of homology modeling GPCRs, since differential extracellular loop structures, global helix movements and changes in binding pocket topology are more difficult to model than amino acid substitutions within the orthosteric site. Thus, continued efforts to experimentally determine structures of all four AR subtypes in the three distinct activation states are essential to maximize the potential of structure based drug design for this family of receptors. Interestingly, despite the fact that all ARs are known to signal through G protein-independent pathways, no biased ligands have thus far been reported for $A_{2A}R$ (Verzijl and Ijzerman, 2011). Functional selectivity has now been observed in A_1R, $A_{2B}R$, and A_3R (Gao et al., 2014; Baltos et al., 2016a,b), which suggests that biased ligands could also be developed for $A_{2A}R$. However, it is also possible that subtle differences in the energy landscape and mechanism of $A_{2A}R$ activation may mean that biased signaling is less pronounced for this receptor. Therefore, at present $A_{2A}R$ is not an ideal model for studying functional selectivity, however structural insight from other GPCRs that have been co-crystallized with biased agonists, such as β_1AR (Warne et al., 2012), may yet help to facilitate the design biased ligands for $A_{2A}R$.

Finally, how will the wealth of high-quality structural data reported for $A_{2A}R$ shape the future of drug development for this receptor? Structural based design has already been used to develop novel $A_{2A}R$ antagonists, including a 1,2,4-triazine derivative that is a preclinical candidate for the treatment of Parkinson's disease (Congreve et al., 2012). Further application of this approach will likely result in the identification of additional novel compounds, both agonists and antagonists, and will also facilitate the derivatization and optimization of existing ligands. The identification of the subsidiary binding pocket on the extracellular surface of $A_{2A}R$ is an important step toward the design of allosteric modulators. Exploitation of this pocket has thus far been achieved using orthosteric ligands with large substituents that extend outside the orthosteric site, however in the future it may also be possible to target this region using purely allosteric ligands. Such compounds have the potential to modulate the properties of orthosteric ligands, and could thus be used to fine tune adenosine signaling through individual AR subtypes.

AUTHOR CONTRIBUTIONS

All authors listed have made a substantial, direct, and intellectual contribution to the work, and approved it for publication.

ACKNOWLEDGMENTS

BC was supported by funding from a BBSRC/EPSRC grant awarded to WISB (BB/M017982/1). GL was supported by the ATIP-AVENIR program, the CNRS, INSERM and Montpellier University. We thank Chris Tate for comments on the manuscript.

REFERENCES

Ballesteros, J. A., and Weinstein, H. (1995). Integrated methods for the construction of three-dimensional models and computational probing of structure-function relations in G protein-coupled receptors. *Methods Neurosci.* 25, 366–428. doi: 10.1016/S1043-9471(05)80049-7

Baltos, J. A., Gregory, K. J., White, P. J., Sexton, P. M., Christopoulos, A., and May, L. T. (2016a). Quantification of adenosine A(1) receptor biased agonism: implications for drug discovery. *Biochem. Pharmacol.* 99, 101–112. doi: 10.1016/j.bcp.2015

Baltos, J. A., Paoletta, S., Nguyen, A. T., Gregory, K. J., Tosh, D. K., Christopoulos, A., et al. (2016b). Structure-activity analysis of biased agonism at the human Adenosine A3 receptor. *Mol. Pharmacol.* 90, 12–22. doi: 10.1124/mol.116.103283

Barbhaiya, H., McClain, R., Ijzerman, A., and Rivkees, S. A. (1996). Site-directed mutagenesis of the human A1 adenosine receptor: influences of acidic and hydroxy residues in the first four transmembrane domains on ligand binding. *Mol. Pharmacol.* 50, 1635–1642.

Batyuk, A., Galli, L., Ishchenko, A., Han, G. W., Gati, C., Popov, P. A., et al. (2016). Native phasing of x-ray free-electron laser data for a G protein-coupled receptor. *Sci. Adv.* 2:e1600292. doi: 10.1126/sciadv.1600292

Burnstock, G. (2006). Purinergic signalling. *Br. J. Pharmacol.* 147(Suppl. 1), S172–S181. doi: 10.1038/sj.bjp.0706429

Caffrey, M. (2015). A comprehensive review of the lipid cubic phase or in meso method for crystallizing membrane and soluble proteins and complexes. *Acta Crystallogr. F Struct. Biol. Commun.* 71(Pt. 1), 3–18. doi: 10.1107/S2053230X14026843

Carpenter, B., and Tate, C. G. (2016). Engineering a minimal G protein to facilitate crystallisation of G protein-coupled receptors in their active conformation. *Protein Eng. Des. Sel.* 29, 583–594. doi: 10.1093/protein/gzw049

Carpenter, B., and Tate, C. G. (2017a). Active state structures of G protein-coupled receptors highlight the similarities and differences in the G protein and arrestin coupling interfaces. *Curr. Opin. Struct. Biol.* 45, 124–132. doi: 10.1016/j.sbi.2017.04.010

Carpenter, B., and Tate, C. G. (2017b). Expression and purification of mini G proteins from *Escherichia coli*. *Bio Protoc.* 7:e2235. doi: 10.21769/BioProtoc.2235

Carpenter, B., and Tate, C. G. (2017c). Expression, purification and crystallisation of the Adenosine A_{2A} receptor bound to an engineered mini G protein. *Bio Protoc.* 7:e2234. doi: 10.21769/BioProtoc.2234

Carpenter, B., Nehmé, R., Warne, T., Leslie, A. G., and Tate, C. G. (2016). Structure of the adenosine A_{2A} receptor bound to an engineered G protein. *Nature* 536, 104–107. doi: 10.1038/nature18966

Chen, J. F., Eltzschig, H. K., and Fredholm, B. B. (2013). Adenosine receptors as drug targets–what are the challenges? *Nat. Rev. Drug Discov.* 12, 265–286. doi: 10.1038/nrd3955

Cheng, R. K. Y., Segala, E., Robertson, N., Deflorian, F., Doré, A. S., Errey, J. C., et al. (2017). Structures of human A_1 and A_{2A} adenosine receptors with xanthines reveal determinants of selectivity. *Structure* 25:e1274. doi: 10.1016/j.str.2017.06.012

Cherezov, V., Rosenbaum, D. M., Hanson, M. A., Rasmussen, S. G., Thian, F. S., Kobilka, T. S., et al. (2007). High-resolution crystal structure of an engineered human beta2-adrenergic G protein-coupled receptor. *Science* 318, 1258–1265. doi: 10.1126/science.1150577

Chun, E., Thompson, A. A., Liu, W., Roth, C. B., Griffith, M. T., Katritch, V., et al. (2012). Fusion partner toolchest for the stabilization and crystallization of G protein-coupled receptors. *Structure* 20, 967–976. doi: 10.1016/j.str.2012.04.010

Cieslak, M., Komoszynski, M., and Wojtczak, A. (2008). Adenosine A(2A) receptors in Parkinson's disease treatment. *Purinergic Signal.* 4, 305–312. doi: 10.1007/s11302-008-9100-8

Congreve, M., Andrews, S. P., Doré, A. S., Hollenstein, K., Hurrell, E., Langmead, C. J., et al. (2012). Discovery of 1,2,4-triazine derivatives as adenosine A_{2A} antagonists using structure based drug design. *J. Med. Chem.* 55, 1898–1903. doi: 10.1021/jm201376w

Doré, A. S., Robertson, N., Errey, J. C., Ng, I., Hollenstein, K., Tehan, B., et al. (2011). Structure of the adenosine A_{2A} receptor in complex with ZM241385 and the xanthines XAC and caffeine. *Structure* 19, 1283–1293. doi: 10.1016/j.str.2011.06.014

Flock, T., Ravarani, C. N. J., Sun, D., Venkatakrishnan, A. J., Kayikci, M., Tate, C. G., et al. (2015). Universal allosteric mechanism for Galpha activation by GPCRs. *Nature* 524, 173–179. doi: 10.1038/nature14663

Fredholm, B. B. (2014). Adenosine–a physiological or pathophysiological agent? *J. Mol. Med.* 92, 201–206. doi: 10.1007/s00109-013-1101-6

Fredholm, B. B., IJzerman, A. P., Klotz, K. N., and Linden, J. (2001). International Union of Pharmacology. XXV. Nomenclature and classification of adenosine receptors. *Pharmacol. Rev.* 53, 527–552.

Fredholm, B. B., IJzerman, A. P., Jacobson, K. A., Linden, J., and Müller, C. E. (2011). International union of basic and clinical pharmacology. LXXXI. nomenclature and classification of adenosine receptors–an update. *Pharmacol. Rev.* 63, 1–34. doi: 10.1124/pr.110.003285

Gao, Z. G., Balasubramanian, R., Kiselev, E., Wei, Q., and Jacobson, K. A. (2014). Probing biased/partial agonism at the G protein-coupled A_{2B} adenosine receptor. *Biochem. Pharmacol.* 90, 297–306. doi: 10.1016/j.bcp.2014.05.008

Gentry, P. R., Sexton, P. M., and Christopoulos, A. (2015). Novel allosteric modulators of G Protein-coupled receptors. *J. Biol. Chem.* 290, 19478–19488. doi: 10.1074/jbc.R115.662759

Glukhova, A., Thal, D. M., Nguyen, A. T., Vecchio, E. A., Jörg, M., Scammells, P. J., et al. (2017). Structure of the Adenosine A1 Receptor reveals the basis for subtype selectivity. *Cell* 168, 867–877.e813. doi: 10.1016/j.cell.2017.01.042

Guo, D., Pan, A. C., Dror, R. O., Mocking, T., Liu, R., Heitman, L. H., et al. (2016). Molecular basis of ligand dissociation from the Adenosine A_{2A} receptor. *Mol. Pharmacol.* 89, 485–491. doi: 10.1124/mol.115.102657

Gutiérrez-de-Terán, H., Massink, A., Rodríguez, D., Liu, W., Han, G. W., Joseph, J. S., et al. (2013). The role of a sodium ion binding site in the allosteric modulation of the A_{2A} adenosine G protein-coupled receptor. *Structure* 21, 2175–2185. doi: 10.1016/j.str.2013.09.020

Hino, T., Arakawa, T., Iwanari, H., Yurugi-Kobayashi, T., Ikeda-Suno, C., Nakada-Nakura, Y., et al. (2012). G-protein-coupled receptor inactivation by an allosteric inverse-agonist antibody. *Nature* 482, 237–240. doi: 10.1038/nature10750

Jaakola, V. P., Griffith, M. T., Hanson, M. A., Cherezov, V., Chien, E. Y., Lane, J. R., et al. (2008). The 2.6 angstrom crystal structure of a human A_{2A} adenosine receptor bound to an antagonist. *Science* 322, 1211–1217. doi: 10.1126/science.1164772

Jacobson, K. A., and Gao, Z. G. (2006). Adenosine receptors as therapeutic targets. *Nat. Rev. Drug Discov.* 5, 247–264. doi: 10.1038/nrd1983

Jazayeri, A., Dias, J. M., and Marshall, F. H. (2015). From G protein-coupled receptor structure resolution to rational drug design. *J. Biol. Chem.* 290, 19489–19495. doi: 10.1074/jbc.R115.668251

Katritch, V., Fenalti, G., Abola, E. E., Roth, B. L., Cherezov, V., and Stevens, R. C. (2014). Allosteric sodium in class A GPCR signaling. *Trends Biochem. Sci.* 39, 233–244. doi: 10.1016/j.tibs.2014.03.002

Kenakin, T., and Christopoulos, A. (2013). Signalling bias in new drug discovery: detection, quantification and therapeutic impact. *Nat. Rev. Drug Discov.* 12, 205–216. doi: 10.1038/nrd3954

Kobilka, B. K., and Deupi, X. (2007). Conformational complexity of G-protein-coupled receptors. *Trends Pharmacol. Sci.* 28, 397–406. doi: 10.1016/j.tips.2007.06.003

Landau, E. M., and Rosenbusch, J. P. (1996). Lipidic cubic phases: a novel concept for the crystallization of membrane proteins. *Proc. Natl. Acad. Sci. U.S.A.* 93, 14532–14535. doi: 10.1073/pnas.93.25.14532

Lebon, G., Bennett, K., Jazayeri, A., and Tate, C. G. (2011a). Thermostabilisation of an agonist-bound conformation of the human adenosine A_{2A} receptor. *J. Mol. Biol.* 409, 298–310. doi: 10.1016/j.jmb.2011.03.075.

Lebon, G., Edwards, P. C., Leslie, A. G., and Tate, C. G. (2015). Molecular determinants of CGS21680 binding to the human Adenosine A_{2A} receptor. *Mol. Pharmacol.* 87, 907–915. doi: 10.1124/mol.114.097360

Lebon, G., Warne, T., and Tate, C. G. (2012). Agonist-bound structures of G protein-coupled receptors. *Curr. Opin. Struct. Biol.* 22, 482–490. doi: 10.1016/j.sbi.2012.03.007

Lebon, G., Warne, T., Edwards, P. C., Bennett, K., Langmead, C. J., Leslie, A. G., et al. (2011b). Agonist-bound adenosine A_{2A} receptor structures reveal common features of GPCR activation. *Nature* 474, 521–525. doi: 10.1038/nature10136

Liu, W., Chun, E., Thompson, A. A., Chubukov, P., Xu, F., Katritch, V., et al. (2012). Structural basis for allosteric regulation of GPCRs by sodium ions. *Science* 337, 232–236. doi: 10.1126/science.1219218

Magnani, F., Serrano-Vega, M. J., Shibata, Y., Abdul-Hussein, S., Lebon, G., Miller-Gallacher, J., et al. (2016). A mutagenesis and screening strategy to generate optimally thermostabilized membrane proteins for structural studies. *Nat. Protoc.* 11, 1554–1571. doi: 10.1038/nprot.2016.088

Magnani, F., Shibata, Y., Serrano-Vega, M. J., and Tate, C. G. (2008). Co-evolving stability and conformational homogeneity of the human adenosine A_{2A} receptor. *Proc. Natl. Acad. Sci. U.S.A.* 105, 10744–10749. doi: 10.1073/pnas.0804396105

Manglik, A., Kim, T. H., Masureel, M., Altenbach, C., Yang, Z., Hilger, D., et al. (2015). Structural insights into the dynamic process of beta2-Adrenergic receptor signaling. *Cell* 161, 1101–1111. doi: 10.1016/j.cell.2015.04.043

Martin-Garcia, J. M., Conrad, C. E., Nelson, G., Stander, N., Zatsepin, N. A., Zook, J., et al. (2017). Serial millisecond crystallography of membrane and soluble protein microcrystals using synchrotron radiation. *IUCrJ* 4, 439–454. doi: 10.1107/S205225251700570X

Melnikov, I., Polovinkin, V., Kovalev, K., Gushchin, I., Shevtsov, M., Shevchenko, V., et al. (2017). Fast iodide-SAD phasing for high-throughput membrane protein structure determination. *Sci. Adv.* 3:e1602952. doi: 10.1126/sciadv.1602952

Moukhametzianov, R., Burghammer, M., Edwards, P. C., Petitdemange, S., Popov, D., Fransen, M., et al. (2008). Protein crystallography with a micrometre-sized synchrotron-radiation beam. *Acta Crystallogr. D Biol. Crystallogr.* 64(Pt. 2), 158–166. doi: 10.1107/S090744490705812X

Müller, C. E., and Jacobson, K. A. (2011). Recent developments in adenosine receptor ligands and their potential as novel drugs. *Biochim. Biophys. Acta* 1808, 1290–1308. doi: 10.1016/j.bbamem.2010.12.017

Murphree, L. J., Marshall, M. A., Rieger, J. M., MacDonald, T. L., and Linden, J. (2002). Human A_{2A} adenosine receptors: high-affinity agonist binding to receptor-G protein complexes containing Gbeta(4). *Mol. Pharmacol.* 61, 455–462. doi: 10.1124/mol.61.2.455

Nehmé, R., Carpenter, B., Singhal, A., Strege, A., Edwards, P. C., White, C. F., et al. (2017). Mini-G proteins: novel tools for studying GPCRs in their active conformation. *PLoS ONE* 12:e0175642. doi: 10.1371/journal.pone.0175642

Prosser, R. S., Ye, L., Pandey, A., and Orazietti, A. (2017). Activation processes in ligand-activated G protein-coupled receptors: a case study of the adenosine A_{2A} receptor. *Bioessays* 39:1700072. doi: 10.1002/bies.201700072

Rasmussen, S. G., Choi, H. J., Fung, J. J., Pardon, E., Casarosa, P., Chae, P. S., et al. (2011a). Structure of a nanobody-stabilized active state of the beta(2) adrenoceptor. *Nature* 469, 175–180. doi: 10.1038/nature09648

Rasmussen, S. G., Choi, H. J., Rosenbaum, D. M., Kobilka, T. S., Thian, F. S., Edwards, P. C., et al. (2007). Crystal structure of the human beta2 adrenergic G-protein-coupled receptor. *Nature* 450, 383–387. doi: 10.1038/nature06325

Rasmussen, S. G., DeVree, B. T., Zou, Y., Kruse, A. C., Chung, K. Y., Kobilka, T. S., et al. (2011b). Crystal structure of the beta2 adrenergic receptor-Gs protein complex. *Nature* 477, 549–555. doi: 10.1038/nature10361.

Rosenbaum, D. M., Cherezov, V., Hanson, M. A., Rasmussen, S. G., Thian, F. S., Kobilka, T. S., et al. (2007). GPCR engineering yields high-resolution structural insights into beta2-adrenergic receptor function. *Science* 318, 1266–1273. doi: 10.1126/science.1150609

Rosenbaum, D. M., Rasmussen, S. G., and Kobilka, B. K. (2009). The structure and function of G-protein-coupled receptors. *Nature* 459, 356–363. doi: 10.1038/nature08144.

Rosenbaum, D. M., Zhang, C., Lyons, J. A., Holl, R., Aragao, D., Arlow, D. H., et al. (2011). Structure and function of an irreversible agonist-beta(2) adrenoceptor complex. *Nature* 469, 236–240. doi: 10.1038/nature09665.

Sawynok, J. (2016). Adenosine receptor targets for pain. *Neuroscience* 338, 1–18. doi: 10.1016/j.neuroscience.2015.10.031

Segala, E., Guo, D., Cheng, R. K., Bortolato, A., Deflorian, F., Doré, A. S., et al. (2016). Controlling the dissociation of ligands from the Adenosine A_{2A} receptor through modulation of salt bridge strength. *J. Med. Chem.* 59, 6470–6479. doi: 10.1021/acs.jmedchem.6b00653

Serrano-Vega, M. J., Magnani, F., Shibata, Y., and Tate, C. G. (2008). Conformational thermostabilization of the beta1-adrenergic receptor in a detergent-resistant form. *Proc. Natl. Acad. Sci. U.S.A.* 105, 877–882. doi: 10.1073/pnas.0711253105

Shibata, Y., White, J. F., Serrano-Vega, M. J., Magnani, F., Aloia, A. L., Grisshammer, R., et al. (2009). Thermostabilization of the neurotensin receptor NTS1. *J. Mol. Biol.* 390, 262–277. doi: 10.1016/j.jmb.2009.04.068

Steyaert, J., and Kobilka, B. K. (2011). Nanobody stabilization of G protein-coupled receptor conformational states. *Curr. Opin. Struct. Biol.* 21, 567–572. doi: 10.1016/j.sbi.2011.06.011

Strege, A., Carpenter, B., Edwards, P. C., and Tate, C. G. (2017). Strategy for the thermostabilization of an agonist-bound GPCR coupled to a G protein. *Methods Enzymol.* 594, 243–264. doi: 10.1016/bs.mie.2017.05.014

Sun, B., Bachhawat, P., Chu, M. L., Wood, M., Ceska, T., Sands, Z. A., et al. (2017). Crystal structure of the adenosine A_{2A} receptor bound to an antagonist reveals a potential allosteric pocket. *Proc. Natl. Acad. Sci. U.S.A.* 114, 2066–2071. doi: 10.1073/pnas.1621423114

Tate, C. G., and Schertler, G. F. (2009). Engineering G protein-coupled receptors to facilitate their structure determination. *Curr. Opin. Struct. Biol.* 19, 386–395. doi: 10.1016/j.sbi.2009.07.004

Venkatakrishnan, A. J., Deupi, X., Lebon, G., Heydenreich, F. M., Flock, T., Miljus, T., et al. (2016). Diverse activation pathways in class A GPCRs converge near the G-protein-coupling region. *Nature* 536, 484–487. doi: 10.1038/nature19107

Venkatakrishnan, A. J., Deupi, X., Lebon, G., Tate, C. G., Schertler, G. F., and Babu, M. M. (2013). Molecular signatures of G-protein-coupled receptors. *Nature* 494, 185–194. doi: 10.1038/nature11896

Verzijl, D., and Ijzerman, A. P. (2011). Functional selectivity of adenosine receptor ligands. *Purinergic Signal.* 7, 171–192. doi: 10.1007/s11302-011-9232-0

Warne, T., Edwards, P. C., Leslie, A. G., and Tate, C. G. (2012). Crystal structures of a stabilized beta1-adrenoceptor bound to the biased agonists bucindolol and carvedilol. *Structure* 20, 841–849. doi: 10.1016/j.str.2012.03.014

Warne, T., Moukhametzianov, R., Baker, J. G., Nehmé, R., Edwards, P. C., Leslie, A. G., et al. (2011). The structural basis for agonist and partial agonist action on a beta(1)-adrenergic receptor. *Nature* 469, 241–244. doi: 10.1038/nature09746

Warne, T., Serrano-Vega, M. J., Baker, J. G., Moukhametzianov, R., Edwards, P. C., Henderson, R., et al. (2008). Structure of a β_1-adrenergic G-protein-coupled receptor. *Nature* 454, 486–491. doi: 10.1038/nature07101

Weinert, T., Olieric, N., Cheng, R., Brünle, S., James, D., Ozerov, D., et al. (2017). Serial millisecond crystallography for routine room-temperature structure determination at synchrotrons. *Nat. Commun.* 8:542. doi: 10.1038/s41467-017-00630-4

Westfield, G. H., Rasmussen, S. G., Su, M., Dutta, S., DeVree, B. T., Chung, K. Y., et al. (2011). Structural flexibility of the G alpha s alpha-helical domain in the β_2-adrenoceptor Gs complex. *Proc. Natl. Acad. Sci. U.S.A.* 108, 16086–16091. doi: 10.1073/pnas.1113645108

White, J. F., Noinaj, N., Shibata, Y., Love, J., Kloss, B., Xu, F., et al. (2012). Structure of the agonist-bound neurotensin receptor. *Nature* 490, 508–513. doi: 10.1038/nature11558

Xu, F., Wu, H., Katritch, V., Han, G. W., Jacobson, K. A., Gao, Z. G., et al. (2011). Structure of an agonist-bound human A_{2A} adenosine receptor. *Science* 332, 322–327. doi: 10.1126/science.1202793

Ye, L., Van Eps, N., Zimmer, M., Ernst, O. P., and Prosser, R. S. (2016). Activation of the A_{2A} adenosine G-protein-coupled receptor by conformational selection. *Nature* 533, 265–268. doi: 10.1038/nature17668

Conflict of Interest Statement: The authors declare that the research was conducted in the absence of any commercial or financial relationships that could be construed as a potential conflict of interest.

frontiers in Pharmacology

ORIGINAL RESEARCH
published: 13 December 2017
doi: 10.3389/fphar.2017.00908

A Non-imaging High Throughput Approach to Chemical Library Screening at the Unmodified Adenosine-A_3 Receptor in Living Cells

Maria Augusta Arruda[1,2,3†], *Leigh A. Stoddart*[1,2†], *Karolina Gherbi*[1,2], *Stephen J. Briddon*[1,2*], *Barrie Kellam*[4] *and Stephen J. Hill*[1,2*]

[1] *Division of Physiology, Pharmacology and Neuroscience, School of Life Sciences, Medical School, Queen's Medical Centre, University of Nottingham, Nottingham, United Kingdom,* [2] *Centre of Membrane Proteins and Receptors, University of Birmingham and University of Nottingham, The Midlands, United Kingdom,* [3] *Vice-Diretoria de Ensino, Pesquisa e Inovacao, Farmanguinhos, Fiocruz, Rio de Janeiro, Brazil,* [4] *Centre for Biomolecular Sciences, School of Pharmacy, University of Nottingham, Nottingham, United Kingdom*

OPEN ACCESS

Edited by:
Kenneth A. Jacobson, National Institutes of Health (NIH), United States

Reviewed by:
Vittoria Colotta, University of Florence, Italy
Eddy Sotelo, Universidade de Santiago de Compostela, Spain

****Correspondence:***
Stephen J. Briddon
stephen.briddon@nottingham.ac.uk
Stephen J. Hill
stephen.hill@nottingham.ac.uk

[†] *These authors have contributed equally to this work.*

Specialty section:
This article was submitted to Experimental Pharmacology and Drug Discovery, a section of the journal Frontiers in Pharmacology

Received: *17 October 2017*
Accepted: *28 November 2017*
Published: *13 December 2017*

Citation:
Arruda MA, Stoddart LA, Gherbi K, Briddon SJ, Kellam B and Hill SJ (2017) A Non-imaging High Throughput Approach to Chemical Library Screening at the Unmodified Adenosine-A_3 Receptor in Living Cells. Front. Pharmacol. 8:908. doi: 10.3389/fphar.2017.00908

Recent advances in fluorescent ligand technology have enabled the study of G protein-coupled receptors in their native environment without the need for genetic modification such as addition of N-terminal fluorescent or bioluminescent tags. Here, we have used a non-imaging plate reader (PHERAstar FS) to monitor the binding of fluorescent ligands to the human adenosine-A_3 receptor (A_3AR; CA200645 and AV039), stably expressed in CHO-K1 cells. To verify that this method was suitable for the study of other GPCRs, assays at the human adenosine-A_1 receptor, and β_1 and β_2 adrenoceptors (β_1AR and β_2AR; BODIPY-TMR-CGP-12177) were also carried out. Affinity values determined for the binding of the fluorescent ligands CA200645 and AV039 to A_3AR for a range of classical adenosine receptor antagonists were consistent with A_3AR pharmacology and correlated well ($R^2 = 0.94$) with equivalent data obtained using a confocal imaging plate reader (ImageXpress Ultra). The binding of BODIPY-TMR-CGP-12177 to the β_1AR was potently inhibited by low concentrations of the β_1-selective antagonist CGP 20712A (pK_i 9.68) but not by the β_2-selective antagonist ICI 118551(pK_i 7.40). Furthermore, in experiments conducted in CHO K1 cells expressing the β_2AR this affinity order was reversed with ICI 118551 showing the highest affinity (pK_i 8.73) and CGP20712A (pK_i 5.68) the lowest affinity. To determine whether the faster data acquisition of the non-imaging plate reader (~3 min per 96-well plate) was suitable for high throughput screening (HTS), we screened the LOPAC library for inhibitors of the binding of CA200645 to the A_3AR. From the initial 1,263 compounds evaluated, 67 hits (defined as those that inhibited the total binding of 25 nM CA200645 by ≥40%) were identified. All compounds within the library that had medium to high affinity for the A_3AR (pK_i ≥6) were successfully identified. We found three novel compounds in the library that displayed unexpected sub-micromolar affinity for the A_3AR. These were K114 (pK_i 6.43), retinoic acid *p*-hydroxyanilide (pK_i 6.13) and SU 6556 (pK_i 6.17). Molecular docking of these latter three LOPAC library members

provided a plausible set of binding poses within the vicinity of the established orthosteric A_3AR binding pocket. A plate reader based library screening using an untagged receptor is therefore possible using fluorescent ligand opening the possibility of its use in compound screening at natively expressed receptors.

Keywords: adenosine receptors, fluorescent ligands, adenosine A_3 receptor, high throughput screening, LOPAC library

INTRODUCTION

G protein-coupled receptors (GPCRs) represent the largest family of cell surface receptors and account for approximately 4% of the entire protein-coding human genome. There are approximately 700 separate GPCRs of which over 300 are non-olfactory receptors (Kuder and Kieć-Kononowicz, 2014). Based on sequence homology, five distinct families of non-olfactory receptors have been proposed: Family A/Rhodopsin, Family B/secretin, Adhesion GPCRs, Family C/Glutamate, and Family F/frizzled (Guo et al., 2012). Family A contains the largest number of the non-olfactory GPCRs including many of the most widely studied receptors, each of which acts to translate extracellular signals into intracellular effects by activating both heterotrimeric G protein-dependent and -independent signaling cascades (Castro et al., 2005; Guo et al., 2012). Importantly, these family A GPCRs are also currently targeted by a large number of clinically used drugs and are validated targets for a significant number of drug discovery programmes.

Adenosine is one biological transmitter which plays a vital homeostatic role and acts via a family of Class A GPCRs comprising four distinct subtypes: namely the adenosine-A_1 receptor (A_1AR), A_{2A}AR, A_{2B}AR, and A_3AR (Fredholm et al., 2011). Both the A_1AR and A_3ARs inhibit intracellular cAMP formation by activating inhibitory G_i proteins, whilst the A_{2A}AR and A_{2B}ARs generally stimulate cAMP formation via stimulatory G_s proteins. Adenosine-mediated signaling has been implicated in a number of pathological states. For instance, the signaling pathways regulated by these receptors can promote angiogenesis (Headrick et al., 2013) and reduce inflammation (Antonioli et al., 2014). Within this family, the A_3AR is a promising molecular target for the control of a range of pathological conditions including cancer (Montinaro et al., 2013; Nakamura et al., 2015; Cao et al., 2017; Joshaghani et al., 2017), inflammation (Cohen et al., 2014; Yoshida et al., 2017), autoimmune diseases (Ravani et al., 2017), ischaemia (Mulloy et al., 2013; González-Fernández et al., 2014; Hussain et al., 2014; Ohana et al., 2016) and chronic neuropathic pain (Little et al., 2015; Tosh et al., 2015), making it an important target for drug development (Borea et al., 2015). As a consequence, identifying new screening methods for discovery of novel chemical scaffolds which bind to the A_3AR would be beneficial.

With this in mind, it is of note that recent advances in fluorescent ligand technology have enabled unlabeled GPCRs to be studied in their native environment without any need for genetic modification through the addition of a bioluminescent or fluorescent tag. For instance fluorescent ligands have been used to study various aspects of GPCR pharmacology including ligand binding, receptor-ligand kinetics, receptor localization and trafficking (Stoddart et al., 2015b). Of particular relevance to purinergic drug discovery, Stoddart et al. (2012) developed a competitive binding assay for the human A_3AR and A_1AR in live cells, using a high content screening (HCS) platform that allowed the screening of small fragment libraries. This assay system was also used to validate the pharmacology of A_3AR selective compounds that were identified from virtual screening of homology models (Ranganathan et al., 2015). However, a disadvantage of this technique is that it involves the acquisition and analysis of a large number of images which can impose severe time, data handling and storage limitations at the early stages of drug discovery, particularly in hit discovery, when very large libraries (>100,000 compounds) are used in initial screening campaigns (Tomasch et al., 2012). In this work, we show that such a competitive fluorescent based binding screen is possible on a higher throughput, non-imaging-based platform using two structurally unrelated fluorescent antagonists. The suitability of this assay for higher throughput screens has been demonstrated by screening a library of pharmacological active compounds (LOPAC) against the native human A_3AR in living cells, with a view to identifying potential novel scaffolds for A_3AR ligands.

RESULTS

Comparison of High Content (HCS) and High Throughput (HTS) Screening Platforms for Measuring Competition Binding to the A_3AR

As previously described, competition binding assays have been performed on cells expressing the wild type human A_3AR using the fluorescent adenosine receptor antagonist CA200645 by automated image acquisition using an ImageXpress (IX) Ultra confocal imaging plate reader (Stoddart et al., 2012). In order to see if this method could be translated into a faster non-imaging format, we directly compared HCS and plate reader based CA200645 binding by sequentially reading the same samples on the PHERAstar FS (BMG technologies) then the IX Ultra. As shown in the IX Ultra plate image in **Figure 1A**, binding of 25 nM CA200645 was clearly detected, and was subsequently displaced by increasing concentrations of competing (unlabeled) antagonists. The same 96-well plate was also measured on a standard non-imaging fluorescence plate reader (PHERAstar FS), with 81 separate repeat reads per well to take into account variation in cell density, and a similar pattern of fluorescence was observed (**Figure 1B**). The montage images from both instruments show that the

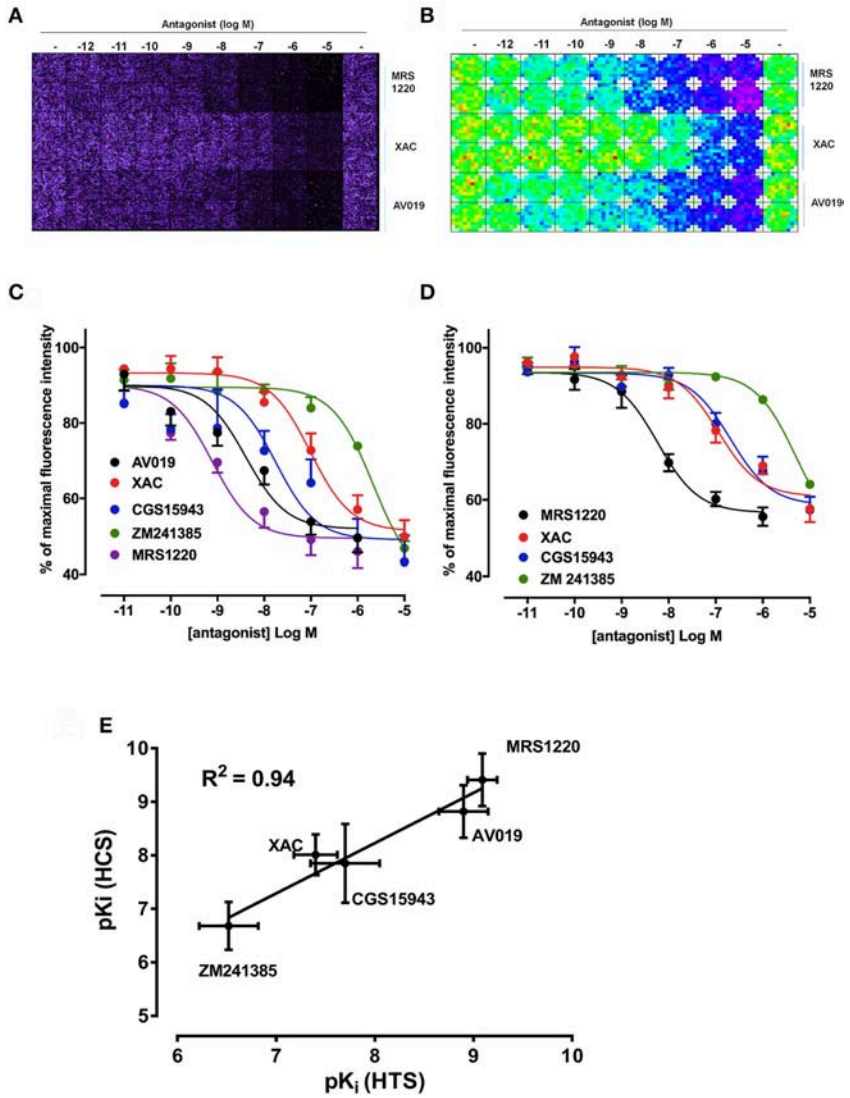

FIGURE 1 | Competition binding at the A_3AR using fluorescent ligands. CHO cells expressing the A_3AR were incubated with 25 nM CA200645 and increasing concentrations of MRS1220, XAC, or AV019. **(A)** Four images per well were obtained on the IX Ultra confocal plate reader and resulting images shown as a montage. **(B)** Montage fluorescence intensity measurement of the same plate obtained using the FS PHERAstar where blue, green, yellow and red pixels represents increasing intensity of fluorescence. **(C)** Competition curves at the A_3AR generated from the total fluorescence intensity measured on the PHERAstar FS microplate reader for five adenosine receptor antagonists. **(D)** CHO A_3AR cells were incubated with increasing concentrations of antagonist and 5 nM AV039 for 1 h, 37°C, washed and fluorescence intensity assessed using the PHERAstar FS. **(E)** Correlation between pKi values obtained using the IX Ultra (high content screening; HCS) and the PHERAstar FS (high throughput screening; HTS) for the data obtained using CA200645 as fluorescent ligand. Data were normalized to the maximal intensity observed per experiment and each data point represents the mean ± SEM from *n* number of experiments (See **Table 1**) performed in triplicate.

high affinity A_3AR antagonist MRS1220, AV019 (compound 1 in Vernall et al., 2012) and the non-selective adenosine receptor antagonist xanthine amine congener (XAC) caused a concentration-dependent reduction in the fluorescence intensity observed with 25 nM CA200645 alone. Competition binding curves were generated from the quantified data (**Figure 1C**), and pK_i values for the five adenosine receptor antagonists obtained, which were comparable to values reported in the literature (**Table 1**). Comparison of the affinity values from the HTS platform (PHERAstar) to those from the HCS platform (IX Ultra) showed a high degree of correlation ($R^2 = 0.94$) (**Figure 1E**) and we have previously shown that affinity values obtained from the HCS platform correlated well with values obtained in a functional assay (Stoddart et al., 2012). In addition to the XAC based fluorescent ligand CA200645, a structurally distinct and highly selective fluorescent A_3AR antagonist was also used (AV039; compound 19 in Vernall et al., 2012). As with CA200645, using 5 nM AV039 as label, competition binding experiments measured on the PHERAstar FS produced the expected rank order of antagonist affinity for the A_3AR (**Figure 1D**, **Table 1**).

TABLE 1 | Affinity of compounds measured at the A_1AR and A_3AR: Affinity values from the PHERAstar HTS assay for unlabeled ligands measured on CHO cells expressing the A_3AR or the A_1AR using 25 nM CA200645 or 5 nM AV039.

	A_3AR				Literature values	A_1AR		Literature values
	CA200645		AV039			CA200645		
	pK_i	*n*	pK_i	*n*		pK_i	*n*	
MRS1220	9.30 ± 0.32	5	9.21 ± 0.12	6	9.02	7.35 ± 0.19	5	7.14
AV019	8.82 ± 0.28	4	ND	–	8.51	ND	–	5.93
XAC	8.06 ± 0.16	5	8.04 ± 0.22	4	7.85	7.70 ± 0.08	4	7.54
CGS15943	7.91 ± 0.20	3	7.91 ± 0.01	3	8.18	8.35 ± 0.16	3	8.95
ZM241385	6.63 ± 0.20	3	6.32 ± 0.28	3	6.74	6.54 ± 0.04	3	6.68

Values represent mean ± SEM from n number of experiments performed in triplicate. ND, Not determined. Literature values for both A_3AR and A_1AR taken from Stoddart et al. (2012).

Application to A_1AR and β-Adrenoceptors

To verify that the experimental approach used for the A_3AR was suitable for the study of other GPCRs, we conducted the same experimental design with CA200645 on CHO cells expressing the human A_1AR, since this fluorescent ligand also binds with high affinity to this receptor (Stoddart et al., 2012). This is important, since being able to screen for compound selectivity is an important aspect of developing a screening methodology. As with the A_3AR, a clear concentration-dependent decrease in fluorescence intensity was detected on the HTS plate reader in the presence of four different adenosine receptor antagonists (**Figure 2A**). The affinity values from these data were consistent with A_1AR pharmacology with CGS 15943 showing the highest affinity and MRS1220 exhibiting a lower affinity than at the A_3AR. In addition, ZM241385, an A_{2A}AR selective antagonist showed the expected low affinity at the A_1AR (**Table 1**).

The confocal based fluorescent ligand binding assay has also been recently applied to study the pharmacology of the β_1AR using BODIPY-TMR labeled CGP 12177 (BODIPY-TMR-CGP; Gherbi et al., 2014) and we therefore also tested whether ligand binding to the β_1AR and β_2AR could also be monitored using the HTS platform in order to develop a counter screen for the A_3AR. As shown in **Figure 2B**, in CHO cells expressing either the β_1AR or β_2AR, binding of BODIPY-TMR-CGP could be clearly detected, and clear competition binding was observed with all three βAR ligands at both receptors. Importantly, the β_1AR selective antagonist CGP 20712A displayed the highest affinity at the β_1AR and the β_2AR selective antagonist ICI 118551 the lowest (**Table 2**), whilst this rank order was reversed at the β_2AR, with ICI 118551 showing the highest affinity and CGP20712A the lowest affinity (**Figure 2C**, **Table 2**).

Screening of a Focused Library of Pharmacologically Active Ligands at the A_3AR

To determine whether the HTS version of the competitive fluorescent binding assay was suitable for the screening of large compound libraries, we chose to screen the Library of Pharmacologically Active Compounds (LOPAC) against the A_3AR. The LOPAC library is considered to be a recognized standard for assay validation as it is based on an extensive number of bioactive compounds. Many of these are known to affect targets involved in adenosine receptor signaling (Iturrioz et al., 2010). CHO cells expressing the A_3AR were grown to confluency in 96-well plates and incubated with a single concentration (10 μM) of the known A_3AR antagonist MRS1220 as a positive control or one of the 1,263 compounds (10 μM) from the LOPAC library and CA200645 (25 nM) and the fluorescence intensity of each well determined on the PHERAstar FS plate reader as described in *Experimental Procedures*. Hits were defined as those compounds which inhibited the binding of CA200645 by >40%, and of the initial 1263 compounds evaluated, 67 hits were identified (Supporting Information Table 1, **Figure 3**, **Table 3**). Inhibition data for all the compounds tested in the initial screen can be found in Supporting Information Table 1. Among the hits, all the compounds within the library with medium to high affinity for the A_3AR ($pK_i \geq 6$; **Figure 3**, **Table 3**) were identified along with four low affinity adenosine-related molecules (1,3-dipropyl-8-*p*-sulfophenylxanthine, DMPX, etazolate hydrochloride and 2-phenylaminoadenosine; **Table 3**). This confirmed the utility of this approach to identify compounds with known A_3AR binding affinity. Importantly, the assay Z' factor was 0.47 ± 0.03 (mean ± SEM, $n = 97$), demonstrating its suitability for screening larger libraries in living cells.

Ten hits from the initial screen which demonstrated the biggest inhibition of CA200645 binding to the A_3AR were investigated further and full inhibition curves for each compound were generated. We were unable to further test reactive blue 2 (position 4 in the full screen) as it is currently not available commercially. As shown in **Figure 4**, **Table 4**, four of the top ten compounds showed low- to sub-micromolar affinity for the A_3AR. As expected the adenosine receptor antagonist CGS15943 displaced the binding of CA200645 at both the A_3AR and A_1AR in a concentration-dependent manner with the expected affinity (**Figure 4**, **Table 1**). As CGS15943 was one of the top ten hits from the initial screen it was also tested in cells expressing the β_2AR and had no effect on the binding of BODIPY-TMR-CGP (**Figure 4**). Three further compounds, retinoic acid *p*-hydroxyanilide (fenretinide), K114 and SU 6656, were found to inhibit the binding of CA20065 to the A_3AR in a concentration-dependent manner with affinity values in the sub-micromolar range, roughly 10-fold

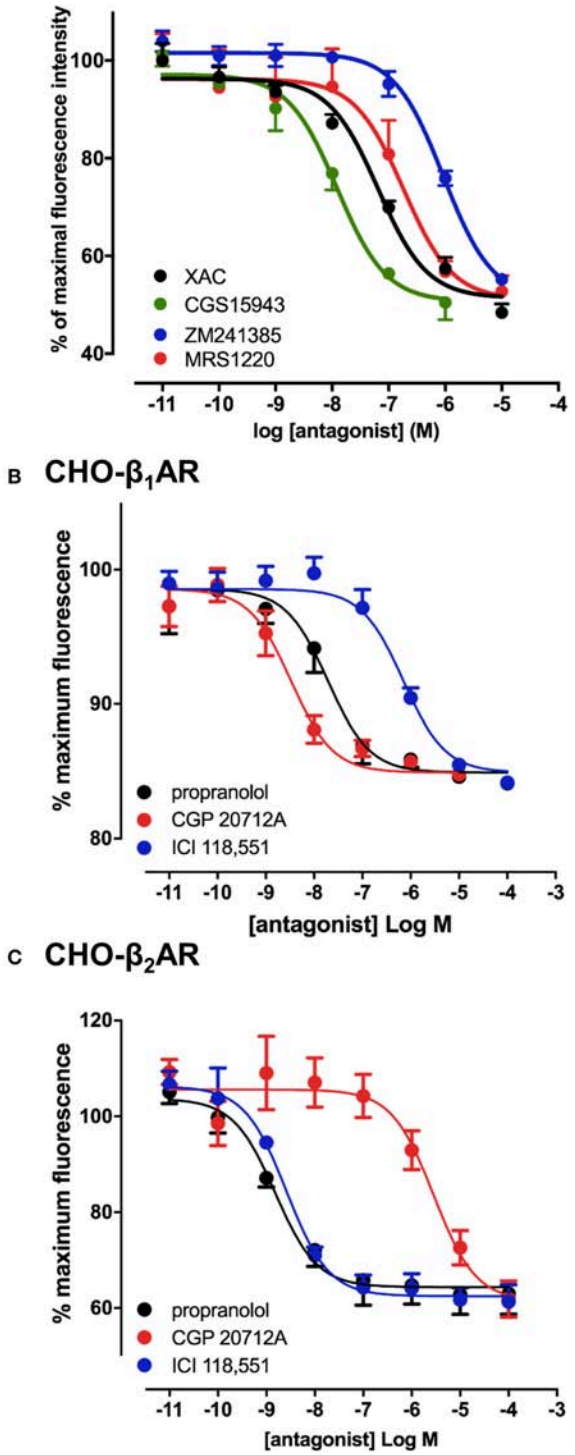

FIGURE 2 | Competition binding assays at the adenosine A_1 and β_1/β_2-adrenoceptors. CHO cell lines stably expressing A_1AR **(A)**, β_1AR **(B)** or the β_2AR **(C)** were incubated with 25 nM CA200645 (A_1AR) or 10 nM BODIPY-TMR-CGP (β_1AR and β_2AR), in the absence or the presence of increasing concentrations of antagonists. Fluorescence intensity in each well was monitored using the PHERAstar FS. Values are mean ± SEM from 3–6 independent experiments performed in triplicate.

TABLE 2 | Affinity of compounds measured at the β_1AR and β_2AR: Affinity values for β-adrenoceptor ligands measured in CHO cells expressing the β_1AR or the β_2AR using 10 nM of BODIPY-TMR-CGP in the HTS format fluorescent ligand binding assay.

	β_1AR		β_2AR	
	pK_i	*n*	pK_i	*n*
Propranolol	8.89 ± 0.16	3	9.00 ± 0.09	3
CGP 20712A	9.68 ± 0.12	3	5.68 ± 0.06	3
ICI 118,551	7.40 ± 0.03	3	8.73 ± 0.07	3

Values represent mean ± SEM from three experiments performed in triplicate.

lower than CGS15943 (**Figure 4**, **Table 4**). Five further hits (BIO, rottlerin, quercetin, PD173952 and kenpaullone) only displaced the binding of CA200645 at the highest concentration tested (10 μM), prohibiting an accurate affinity determination. For those four compounds showing micromolar affinity, the selectivity of their interaction with the A_3AR was determined by investigating their ability to bind to A_1AR and β_2AR. Both K114 and retinoic acid *p*-hydroxyanilide inhibited the binding of CA200645 at the A_1AR with similar affinity to that observed at the A_3AR. SU 6656 only inhibited binding at the highest concentration tested and the affinity was not calculated. None of the other compounds showed any measureable activity at the A_1AR. When tested in CHO cells expressing the β_2AR, no significant inhibition of BODIPY-TMR-CGP binding was observed for any of the 10 compounds screened but the control β_2AR antagonist propranolol had the expected affinity (pK_i = 8.72 ± 0.14, n = 3). There was an increase in fluorescence in the presence of 10 μM SU 6656 (128.4 ± 18.4%). However this was small compared to the increase seen with 10 nM BODIPY-TMR-CGP and the large increase in fluorescence in the presence of BIO (pEC_{50} = 5.84 ± 0.13). This is likely to be due to these compounds interfering with the BODIPY-TMR fluorescence signal, which was not observed when using the more red-shifted BODIPY 630/650 fluorophore in the A_1AR and A_3AR binding assays.

Molecular Modeling of Selected LOPAC Hits at the A_3AR

Using our previously established homology model of the human A_3AR (Vernall et al., 2013) we sought to investigate potential binding poses for the three sub-micromolar compounds (retinoic acid *p*-hydroxyanilide (fenretinide), K114 and SU 6656) identified in the LOPAC screen which did not have previous literature precedent for interacting with this receptor sub-type. Using the commercially available docking software, CLC Drug Discovery Workbench, ligand and receptor binding pocket preparation was followed by targeted ligand docking. The highest scoring docked poses for K114, SU 6656 and retinoic acid *p*-hydroxyanilide were selected and are illustrated in **Figure 5**. All three compounds were able to engage via plausible poses to the A_3R within the vicinity of the orthosteric binding pocket of this receptor.

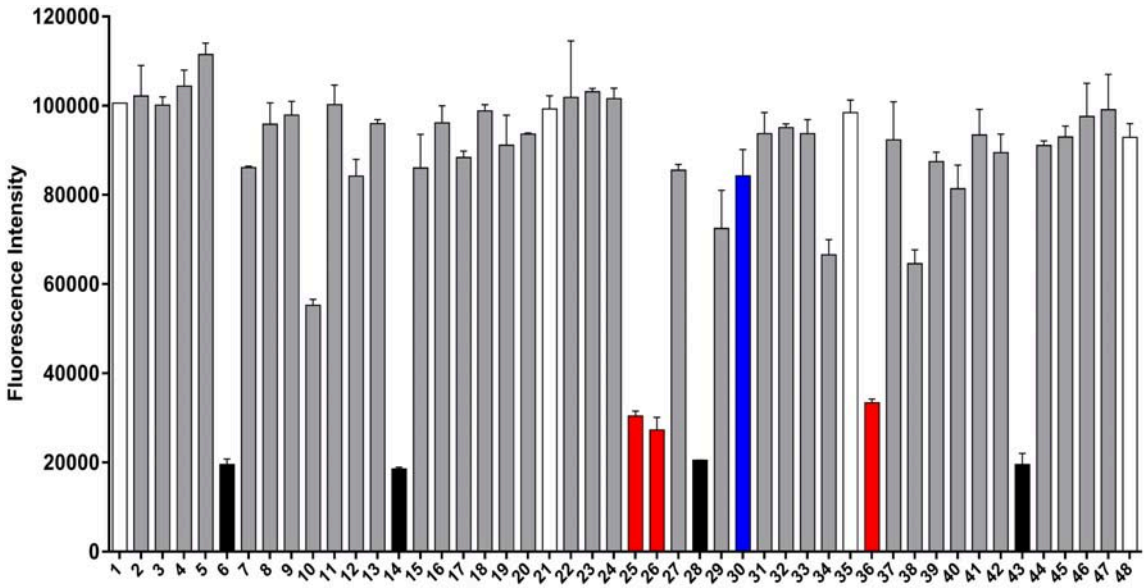

1. Basal
2. Amoxapine
3. 5'-Amino-5'-deoxyadenosine p-toluenesulfonate
4. Amiloride
5. 6-Aminohexanoic acid
6. MRS1220
7. Trovafloxacin mesylate
8. Antozoline
9. Aniracetam
10. 1-benzoyl-5-methoxy-2-methylindole-3-acetic acid
11. (±)-AMT hydrochloride
12. CBIQ
13. L-2-aminoadipic acid
14. MRS1220
15. 5-(N,N-hexamethylene)amiloride
16. L(-)-Norepinephrine bitartrate
17. Fulvestrant
18. 2-(Methylthio)adenosine 5'-diphosphate
19. Altretamine
20. Paroxetine
21. Basal
22. N-Acetyl-L-Cysteine
23. Benzamide
24.SKF-89145
25. **HEMADO**
26. **AS-252424**
27. (±)-p-Aminoglutethimide
28. MRS1220
29. Psora-4
30. Adenosine
31. Opipramol
32. AIDA
33. Allopurinol
34. SB 200646
35. Basal
36. N6-2-(4-Aminophenyl)ethyladenosine
37. Amsacrine
38. Lercanidipine
39. N-(4-Amino-2-chlorophenyl)phthalimide
40. Sildenafil
41.Azithromycin
42. S(-)-Atenolol
43. MRS1220
44. (±)-HA-966
45. Astaxanthin
46. L-Aspartic acid
47. Alaproclate
48.Basal

FIGURE 3 | Screening the LOPAC library against the A_3AR. Example of the data generated from one plate of compounds from the LOPAC library. Each plate contained 40 compounds (each at 10 μM final concentration) from the LOPAC library in duplicate along with four basal and four MRS1220 (10 μM) controls, also in duplicate. The fluorescence intensities obtained on the PHERAstar FS from this plate are shown as mean and range of duplicates with the hits highlighted in red and adenosine indicated in blue. The plate shown is a representative plate of one of the three experiments performed using these compounds and the inhibition data for all compounds screened can be found in Supporting Information Table 1.

DISCUSSION

Fluorescent ligands for GPCRs are a valuable tool in the study of multiple aspects of receptor pharmacology and they are a potential replacement for radiolabelled ligands in saturation and equilibrium binding studies to determine the affinity of labeled and unlabeled ligands (Stoddart et al., 2016). In this study, we aimed to further develop a previously described fluorescence based live cell binding assay that used a HCS system (Stoddart et al., 2012) to an assay that could be performed with un-tagged receptors on a HTS system. To this end, we chose the PHERAstar FS fluorescent plate reader since it allowed the determination of the optimal focal height for the fluorescence read and multiple scans per well. Use of the HTS system to obtain data resulted in a marked reduction in the time each 96-well plate took to process; from around 40 minutes per plate on the confocal HCS system for data collection and analysis to less than 3 minutes for the HTS system. This also produced a significant reduction in the amount of data that needed to be stored; 500 Mb per plate for HCS versus 160 Kb for HTS. Using the A_3AR as a model system, we demonstrated that the data generated on the HTS system was in close agreement to that obtained on the HCS system, validating this system as a higher throughput methodology that would be essential for screening large compound libraries using fluorescence-based binding assays in whole cells.

TABLE 3 | Known A_3AR ligands in the LOPAC library: Compounds within the LOPAC library that have known activity at adenosine receptors, their rank order in the full screen and the % of 25 nM CA200645 binding in the presence of 10 μM of these compounds.

Name	Agonist or antagonist	LOPAC description	% Total CA200645 binding	Rank
CGS 15943	Antagonist	Potent non-selective adenosine receptor antagonist	30.0 ± 3.0	9
2-Cl-IB-MECA	Agonist	A_3 adenosine receptor agonist	32.3 ± 6.1	12
IB-MECA	Agonist	Selective A_3 adenosine receptor agonist	36.3 ± 4.0	18
NECA	Agonist	Adenosine receptor agonist	38.1 ± 4.3	20
HEMADO	Agonist	A_3 adenosine receptor agonist	40.1 ± 10.5	24
APNEA	Agonist	Non-selective adenosine receptor agonist	41.0 ± 7.2	26
1,3-dipropyl-8-*p*-sulfophenylxanthine	Antagonist	Adenosine receptor antagonist (slight selectivity for A_1 over A_2)	42.3 ± 4.8	29
AB-MECA	Agonist	High affinity A_3 adenosine receptor agonist	49.5 ± 5.8	38
2-CADO	Agonist	Adenosine receptor agonist with selectivity for A_1 over A_2	51.0 ± 6.7	43
SCH 58261	Antagonist	A_{2A} adenosine receptor antagonist	52.2 ± 5.4	47
CV1808	Agonist	Selective A_2 adenosine receptor agonist	53.3 ± 19.9	56
DPCPX	Antagonist	Selective A1 adenosine receptor antagonist	56.3 ± 3.4	58
FSCPX	Antagonist	Irreversible A_1 adenosine receptor antagonist	57.5 ± 23.0	63
MRS 1523	Antagonist	Selective A_3 adenosine receptor antagonist in rat	58.3 ± 11.4	64

Various methods using fluorescent ligands to measure ligand binding at GPCRs have been recently developed, each using a different approaches to measure the fluorescence of the bound ligand, including flow cytometry (Young et al., 2005; Hara et al., 2009; Kozma et al., 2013), fluorescence polarization (Cornelius et al., 2009; Kecskes et al., 2010) and resonance energy transfer based systems (Zwier et al., 2010; Stoddart et al., 2015a). Each method has advantages and disadvantages, for instance ligand depletion (fluorescence polarization) and the need to tag the receptor of interest (BRET and FRET). One limitation of the simple fluorescent intensity measurement used in the system described here is the potential for a low signal/noise ratio as a result of high levels of non-specific binding and the use of whole cells. As this technique measures total well fluorescence intensity it will be affected by both high levels of non-specific membrane binding and also non-specific uptake of the fluorescent ligand into the cells. As an example of this, for the A_3AR the maximal reduction in the levels of CA200645 fluorescence measured in the presence of unlabeled ligands was 60% whilst that with BODIPY-TMR-CGP for the β_1AR was only 20% (**Figures 1C**, **2B**). This small signal/noise ratio for this ligand at the β_1AR has been observed previously (Gherbi et al., 2014), although it is notable that even under these conditions, the method described here still allowed us to generate robust data within this small signal/noise window. The proximity-based assays (e.g., NanoBRET; Stoddart et al., 2015a) overcome this issue but they obviously require genetic modification of the extracellular N-terminus of the receptor with a fluorescent or luminescent protein, which precludes their use on native receptors—a main aim of the assay developed in this study. What is also clear from this point of view, is that the limit of this signal to noise ratio is likely to be highly dependent on both the pharmacological and photophysical properties of the fluorescent ligand, as we have previously demonstrated (Vernall et al., 2013). To progress the use of this assay to use with endogenously expressed untagged receptors, consideration should also be given to fluorescent ligand selectivity in situations where multiple receptor subtypes are often co-expressed; this is particularly true for adenosine receptors. To this end, the demonstration that this assay also works with a highly A_3AR selective ligand, AV039 (Vernall et al., 2012) is important.

To demonstrate the utility of this assay system for compound screening, we investigated if we could identify known ligands for the A_3AR within a library of pharmacologically active compounds (LOPAC). Within the LOPAC library there were 37 compounds identified as ligands for adenosine receptors. For the 1,263 compounds screened, we defined a hit as a compound that inhibited more than 40% of the total CA200645 binding. Using these criteria, we identified 67 hits, of which 14 had previously described activity at adenosine receptors (**Table 3**). Of these, four were the known A_3R selective agonists, 2-Cl-IB-MECA (Gallo-Rodriguez et al., 1994), IB-MECA (Klotz et al., 1998), AB-MECA (Klotz et al., 1998) and HEMADO (Klotz et al., 2007), and the A_3R selective antagonist MRS1523 (Li et al., 1998). A further five compounds were known to be non-selective at this adenosine receptor subtype [CGS15943 (Ongini et al., 1999), NECA (Gao et al., 2004), APNEA (Gao et al., 2004), 2-CADO (van Galen et al., 1994) and 1,3-dipropyl-8-*p*-sulfophenylxanthine (Daly et al., 1985)]. The remaining four compounds were SCH 58261, CV1808, DPCPX and FSCPX. SCH 58261 is widely described as an A_{2A} selective and DPCPX as an A_1AR-selective antagonist, and both retain affinity in the μM range for the A_3AR (Ongini et al., 1999; Stoddart et al., 2012). FSCPX is an irreversible antagonist at the A_1AR (van Muijlwijk-Koezen et al., 2001) but to date it had not been tested at other adenosine receptor subtypes. Our data from this screen indicates that FSCPX is likely to retain activity at the A_3R at least in the low μM range and this is also true for CV1808 that has been described as an agonist at the A_{2A}AR (Dionisotti et al., 1997). A variety of different compounds that act at different (i.e., non-A_3AR) adenosine

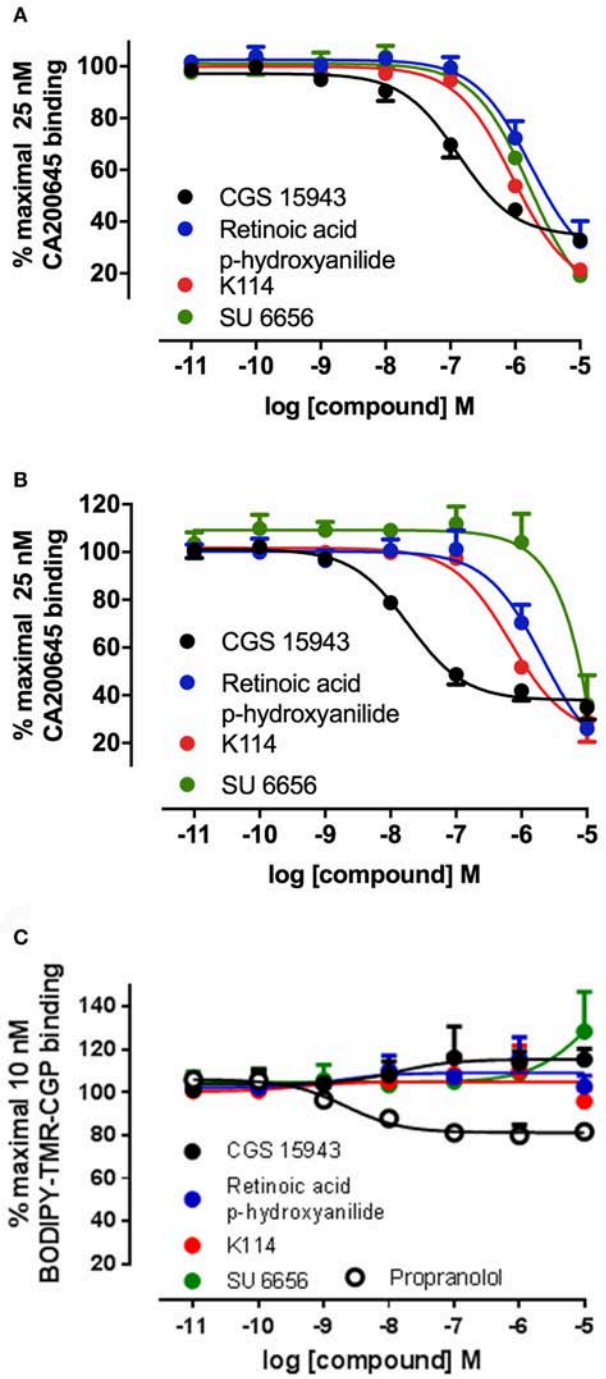

FIGURE 4 | Competition binding curves at the A_1AR, A_3AR, and β_2AR for three hits identified from the LOPAC library. CHO cell lines stably expressing A_1AR **(A)**, A_3AR **(B)**, or β_2AR **(C)** were incubated with 25 nM CA200645 (A_3AR and A_1AR) or 10 nM BODIPY-TMR-CGP (β_2AR) in the absence or in the presence of increasing concentrations of the indicated compounds. Values are mean ± SEM from three independent experiments performed in triplicate.

receptors were included in the library and as expected were not identified as hits in our screen (Supporting Information Table 1). These included A_1AR selective agonists and antagonists such as R-PIA (Klotz et al., 1998) and CPT (Dalpiaz et al., 1998), A_{2A}AR selective agonists and antagonists such as CGS 21680 (Klotz et al., 1998) and CSC (Jacobson et al., 1993), and the A_{2B}AR selective antagonist alloxazine (Ji et al., 2001). A variety of low affinity non-selective antagonists and agonists were also present in the library including adenosine, theophylline, caffeine and paraxanthine that have reported affinity at the A_3AR in the 13-100 μM range (Jacobson et al., 1999; Fredholm et al., 2001). Due to the concentration of CA200645 (25 nM) used in the primary screen only compounds with an affinity of <10 μM would be expected to be identified as a hit. Overall, the assay performed well at identifying all the compounds with known activity at the A_3AR.

We found three compounds in the library that displayed unexpected sub-micromolar affinity at the A_3AR (**Figure 4**, **Table 4**). These were K114, retinoic acid *p*-hydroxyanilide and SU 6556. K114 is used to identify amyloid lesions from Aβ peptide, α-synuclien and tau through an increase in its fluorescence upon binding to these lesions. It is has minimal fluorescence in aqueous solution and has emission maxima of 550 nm that is unlikely to interfere with the emission of BY630 at 650 nm (Crystal et al., 2003). In addition, the assay described here monitors a decrease in fluorescence in the presence of inhibitors that would mean it would be more likely to give false-negatives rather than false-positives. Retinoic acid *p*-hydroxyanilide, also known as fenretinide or 4-HPR, is an analog of retinoic acid and is a potential therapy in the treatment of cancer due to its ability to induce apoptosis (Wu et al., 2001). It is possible that it was causing apoptosis of the cells in our assay system leading to a concurrent decrease in fluorescence but as the presence of retinoic acid *p*-hydroxyanilide had no effect in cells expressing the β_2AR this is unlikely to be the case (**Figure 4**). SU6556 is a Src kinase inhibitor that has also been found to inhibit a variety of other kinases including Aurora C and AMPK (Bain et al., 2007). It also displayed slight selectivity for the A_3AR over A_1AR.

Docking of the sub-micromolar compounds identified in the LOPAC screen provided a plausible set of binding poses within the vicinity of the established orthosteric A_3AR binding pocket (**Figure 5**). K114 bound in a fully extended form with one of the terminal phenols optimally positioned to engage in a hydrogen bond interaction with the side-chain of Thr94. Meanwhile, the remaining vinyl-linked aromatic moieties pass through a hydrophobic channel created by Ile76, Val169, Leu90, Leu246, Ile249, Leu264, Ile268, and Phe168; the latter engaging via a face-to-face pi-stacking interaction. SU 6656 favored binding higher up in the orthosteric pocket with the 4,5,6,7-tetrahydroindolyl portion of the molecule engaging in a face-to-face interaction with Phe168, with the hydrophobic interactions predominating with Leu90, Val65, Ile268, and Leu246. Finally, retinoic acid *p*-hydroxyanilide displayed a binding pose passing through the same hydrophobic channel observed with K114. The 1,3,3-trimethylcyclohex-1-enyl region of the molecule was positioned deepest into the binding pocket engaging in hydrophobic interactions with residues Leu246, Ile249, Met177, and Phe168. The *p*-hydroxyanilde region of the molecule was positioned in such a way as to allow a face-to-edge interaction with Tyr265 at the top of transmembrane helix 7. With the predominance

TABLE 4 | Affinity of selected hits from the LOPAC library at the A_3AR, A_1AR, and β_2AR: Compounds were tested on CHO cells expressing the A_3AR, A_1AR, and β_2AR in the HTS format fluorescent ligand binding assay using 25 nM CA200645 as the tracer for A_3AR and A_1AR and 10 nM of BODIPY-TMR-CGP for β_2AR.

Position in primary screen	Compound	A_3AR	A_1AR	β_2AR
		pK_i	pK_i	% Total binding at 10 μM
2	SU 6656	6.17 ± 0.08	ND	128.4 ± 18.4
5	K114	6.43 ± 0.04	6.56 ± 0.11	95.8 ± 5.5
8	Retinoic acid p-hydroxyanilide	6.13 ± 0.18	6.04 ± 0.21	102.7 ± 5.1
9	CGS 15943	7.24 ± 0.14	8.14 ± 0.09	115.4 ± 5.0

Data represents mean ± SEM from three experiments performed in triplicate. ND, Not determined as accurate curve could not be generated.

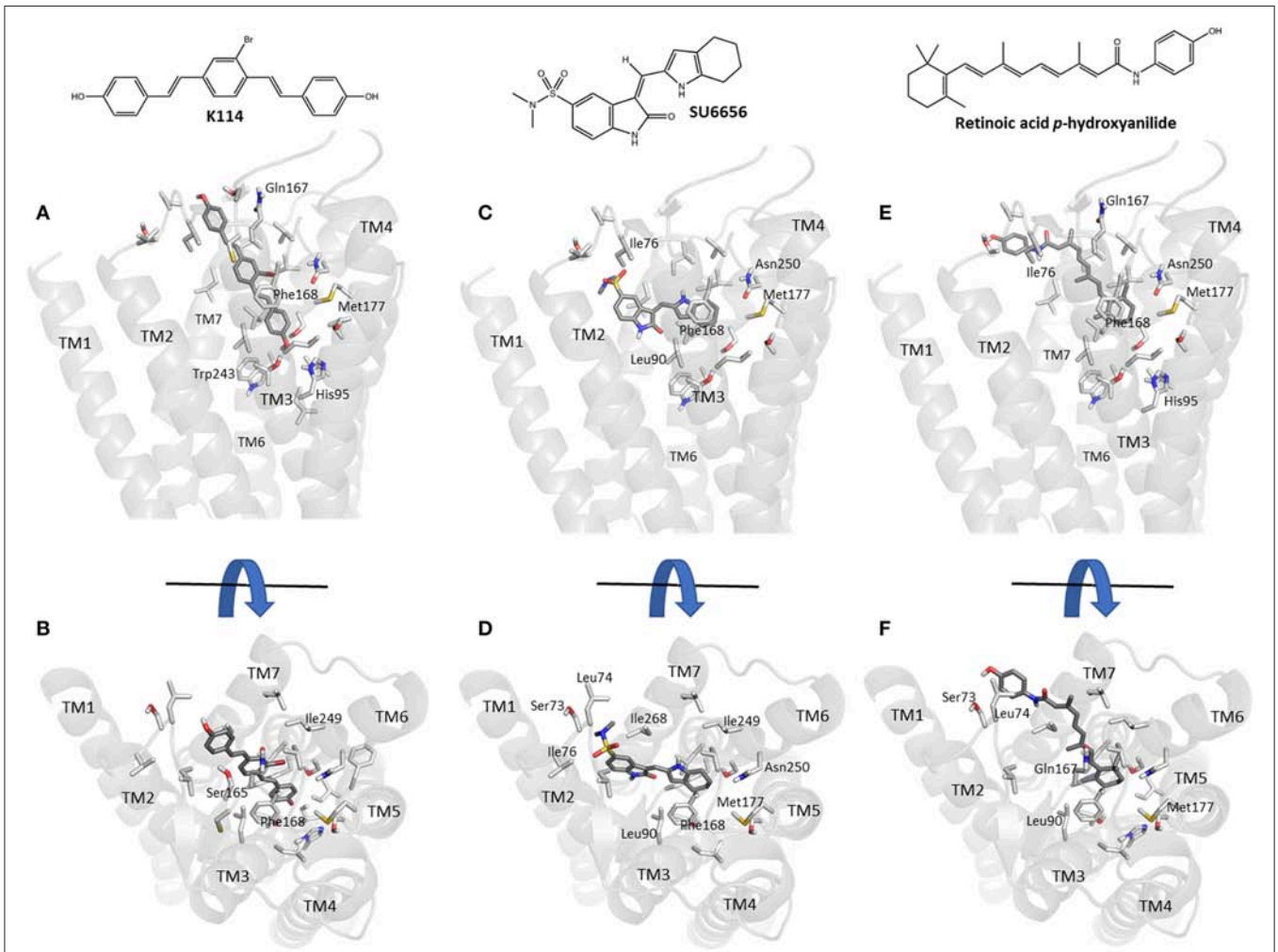

FIGURE 5 | Molecular modeling simulation of K114, SU 6656 and retinoic acid *p*-hydroxyanilide binding to the A_3AR. A side-on **(A,C,E)** and top-down **(B,D,F)** view of the top scoring binding poses for K114, SU 6656 and retinoic acid *p*-hydroxyanilide (dark gray liquorice coloring) respectively, bound into our previously reported A_3AR receptor homology model (Vernall et al., 2013). Previously identified amino acid side chain residues associated with the orthosteric binding pocket (Squarcialupi et al., 2013) are represented in light gray liquorice coloring and labeled alongside the TM loop regions for clarity.

of aromatic and hydrophobic interactions observed between the receptor and the three ligands discussed, this would seem to correlate well with the experimental binding affinities whilst also offering the potential to undertake productive modifications of these compounds to potentially enhance their overall binding interactions.

In conclusion, we have shown that a simple intensity based fluorescent ligand binding assay can be modified to work

in a potentially high throughput format, giving significant advances in both speed and data volume compared to previous high content versions. The assay allows screening of a small compound library in live cells, and can assess binding to the unmodified native receptors. The assays performed well under test conditions, identifying both known adenosine receptor ligands in a focused library as well as novel potential ligand scaffolds. Further work on establishing this assay to screen at endogenous A_3AR in a mixed receptor background will be important to allow subsequent screens to be performed under more physiological conditions.

EXPERIMENTAL PROCEDURES

Chemicals

Known GPCR antagonists were purchased from Tocris Bioscience and G418 was obtained from Invitrogen. Fetal calf serum was obtained from PAA Laboratories and L-glutamine from Lonza. All other biological reagents were obtained from Sigma-Aldrich. CA200645 was obtained from CellAura Technologies. BODIPY-TMR-CGP (BODIPY-TMR-(±)-CGP 12177) was purchased from Molecular Probes. AV039 and AV019 were synthesized in house as previously described (Vernall et al., 2012). The LOPAC library was obtained from Sigma-Aldrich.

Cell Culture

CHO-K1 cells stably expressing the human A_3AR (Vernall et al., 2012), β_1AR (Guo et al., 2012), β_2AR (Baker et al., 2002) or the human A_1AR (May et al., 2010) were maintained in DMEM/F12 medium containing 10% fetal calf serum and 2 mM L-glutamine at 37°C in a humidified atmosphere of air/CO_2 (19:1).

Fluorescence Competition Binding Assay

CHO cells stably expressing the A_3AR, A_1AR, β_1AR or β_2AR were seeded into the central 60 wells (for high content confocal analysis) or every well (high throughput analysis) of a 96-well clear-bottomed, black-walled plate (Greiner BioOne) and grown to confluency. On the day of experiment, normal growth medium was removed and cells washed twice with HEPES-buffered saline solution (HBSS; 10 mM HEPES, 10 mM glucose, 145 mM NaCl, 5 mM KCl, 1 mM $MgSO_4$, 2 mM sodium pyruvate, 1.3 mM $CaCl_2$, 1.5 mM $NaHCO_3$, pH 7.4) pre-warmed to 37°C. Fresh HBSS was added to each well followed by the addition of the required concentration of unlabeled compound and the respective fluorescent ligands (25 nM CA200645, 5 nM AV039 or 10 nM BODIPY-TMR-CGP). Cells were incubated for 1h at 37°C/5% CO_2. Buffer was then removed from each well, cells washed once in HBSS and fresh HBSS added at room temperature. Plates were then immediately subjected to high content or HTS analysis as detailed below.

High Content Screening

High content analysis was conducted as previously described (Stoddart et al., 2012). Briefly, plates were imaged using an ImageXpress Ultra confocal plate reader, which captured four central images per well using a Plan Fluor 40x NA0.6 extra-long working distance objective. CA200645 was excited at 635 nm and emission collected through a 640–685 nm band pass filter. Total image intensity was obtained using a modified multi-wavelength cell scoring algorithm within the MetaXpress software (MetaXpress 2.0, Molecular Devices).

High Throughput Screening

High throughput analysis was performed using a PHERAstar FS plate reader (BMG Technologies). Fluorescent intensity of each well was assessed by bottom scanning using the following optical modules: excitation 540 nm and emission 590 nm (for BODIPY-TMR-CGP-labeled cells), or excitation 630 nm and emission 650 nm (for the BY630 compounds CA200645 and AV039). Optimal focal height was determined automatically and total fluorescence intensity was assessed by taking 81 reads per well.

Screening of the LOPAC Library of Pharmacological Active Compounds

The LOPAC compound library contained 1263 compounds and each compound was provided as a pre-dissolved solution in 10 mM in DMSO. Compound plates containing 2 µl of compound per well were provided by the University of Nottingham Managed Compound Collection. Each plate contained 40 compounds from the LOPAC library together with positive and blank control samples. For the blank controls, 2 µl of DMSO was added per well and for the positive controls the A_3AR antagonist MRS1220 (10 µM final concentration) was used. The compounds were diluted to 100 µM in HBSS prior to assay. Each compound was tested in duplicate at a final concentration of 10 µM on three separate experimental days. Experiment was carried out as detailed above using the A_3AR expressing cell line and 25 nM CA200645 as the tracer ligand. Data were normalized on a per plate basis to the fluorescence observed in blank control wells.

The 67 compounds that inhibited by more than 40% the total binding of CA200645 compared to blank controls were classed as hits. From this list 16 compounds were selected for secondary screening to determine their IC_{50} values and binding affinity. This was achieved by investigating the effect of increasing concentrations of each inhibitor on the specific binding of 25 nM CA200645 or 10 nM BODIPY-TMR-CGP in cells expressing the A_3AR, A_1AR or β_2AR.

Molecular Modeling

Using our previously reported homology model of the human A_3AR (Vernall et al., 2013) and the CLC Drug Discovery Workbench software package (Version 3.0.2, Qiagen, Netherlands), the protein target was prepared with no water molecules present. Before setting up the docking experiments, the binding site was generated as a 13 Å sphere centered around the established orthosteric pocket. All small molecules were constructed using ChemDraw Professional 16.0 (CambridgeSoft, Cambridge, MA, USA) and imported into the docking programme using the Balloon PlugIn (http://users.abo.fi/mivainio/balloon) (Vainio and Johnson, 2007) to afford the lowest energy conformer for each ligand. During the docking process, each ligand underwent 1000

individual iterations, with the conformation of each ligand set as flexible, allowing full movement around all rotatable bonds, whilst the protein was held as a rigid structure. The best scoring pose for each ligand was returned using the $PLANTS_{PLP}$ algorithm to determine that docking score (Korb et al., 2009) and the best ranked compounds were selected and their binding residues observed using the CLC Drug Discovery Workbench visualization tool.

Data Analysis

Competition binding curves were fitted to the following equation using GraphPad Prism 5 (GraphPad Software):

$$\%\ inhibition\ of\ specific\ binding = \frac{100 \times [A]}{[A] + IC_{50}}$$

where [A] is the concentration of competing drug and IC_{50} is the molar concentration of ligand required to inhibit 50% of the specific binding of a fixed concentration [L] of the appropriate fluorescent ligand. The IC_{50} values obtained were converted to K_i values using the following equation:

$$K_i = \frac{IC_{50}}{1 + \frac{[L]}{K_D}}$$

where [L] is the concentration and K_D is the equilibrium dissociation constant of the fluorescent ligand. The K_D values for the fluorescent ligands used were 11.0 nM and 3.11 nM for CA200645 at the A_1AR and A_3AR respectively (Stoddart et al., 2012). K_D values for BODIPY-TMR-CGP were taken from Baker et al. (2003).

The Z′ values were calculated on a per plate basis using the following equation:

$$Z' = 1 - \frac{3(\sigma_p + \sigma_n)}{\mu_p - \mu_n}$$

where μ_p and σ_p are the mean and standard deviation from the control wells (DMSO only) and μ_n and σ_n are the mean and standard deviation from the MRS1220 treated wells.

AUTHOR CONTRIBUTIONS

SH, SB, and BK: Conceived the study; MA, LS, SB, BK, and SH: Participated in research design; MA and LS: Performed the experiments and data analysis; KG: Performed the beta receptor screening experiments and analyzed the data; BK: Performed the molecular docking studies; MA, LS, BK, SB, and SH: All wrote or contributed to the writing and editing of the manuscript.

ACKNOWLEDGMENTS

This work was supported by the Medical Research Council (grant numbers G0800006, MR/N020081/1).

SUPPLEMENTARY MATERIAL

The Supplementary Material for this article can be found online at: https://www.frontiersin.org/articles/10.3389/fphar.2017.00908/full#supplementary-material

REFERENCES

Antonioli, L., Csóka, B., Fornai, M., Colucci, R., Kókai, E., Blandizzi, C., et al. (2014). Adenosine and inflammation: what's new on the horizon? *Drug Discov. Today.* 19, 1051–1068. doi: 10.1016/j.drudis.2014.02.010

Bain, J., Plater, L., Elliott, M., Shpiro, N., Hastie, C. J., McLauchlan, H., et al. (2007). The selectivity of protein kinase inhibitors: a further update. *Biochem. J.* 408, 297–315. doi: 10.1042/BJ20070797

Baker, J. G., Hall, I. P., and Hill, S. J. (2002). Pharmacological characterization of CGP 12177 at the human beta(2)-adrenoceptor. *Br. J. Pharmacol.* 137, 400–408. doi: 10.1038/sj.bjp.0704855

Baker, J. G., Hall, I. P., and Hill, S. J. (2003). Pharmacology and direct visualisation of BODIPY-TMR-CGP: a long-acting fluorescent β2-adrenoceptor agonist. *Br. J. Pharmacol.* 139, 232–242. doi: 10.1038/sj.bjp.0705287

Borea, P. A., Varani, K., Vincenzi, F., Baraldi, P. G., Tabrizi, M. A., Merighi, S., et al. (2015). The A3 adenosine receptor: history and perspectives. *Pharmacol. Rev.* 67, 74–102. doi: 10.1124/pr.113.008540

Cao, H. L., Liu, Z. J., and Chang, Z. (2017). Cordycepin induces apoptosis in human bladder cancer cells via activation of A3 adenosine receptors. *Tumour Biol.* 39. doi: 10.1177/1010428317706915

Castro, M., Nikolaev, V. O., Palm, D., Lohse, M. J., and Vilardaga, J.-P. (2005). Turn-on switch in parathyroid hormone receptor by a two-step parathyroid hormone binding mechanism. *Proc. Natl. Acad. Sci. U.S.A.* 102, 16084–16089. doi: 10.1073/pnas.0503942102

Cohen, S., Barer, F., Bar-Yehuda, S., IJzerman, A. P., Jacobson, K. A., and Fishman, P. (2014). A_3 adenosine receptor allosteric modulator induces an anti-inflammatory effect: *in vivo* studies and molecular mechanism of action. *Mediators Inflamm.* 2014:708746. doi: 10.1155/2014/708746

Cornelius, P., Lee, E., Lin, W., Wang, R., Werner, W., Brown, J. A., et al. (2009). Design, synthesis, and pharmacology of fluorescently labeled analogs of serotonin: application to screening of the 5-HT2C receptor. *J. Biomol. Screen.* 14, 360–370. doi: 10.1177/1087057109331804

Crystal, A. S., Giasson, B. I., Crowe, A., Kung, M. P., Zhuang, Z. P., Trojanowski, J. Q., et al. (2003). A comparison of amyloid fibrillogenesis using the novel fluorescent compound K114. *J. Neurochem.* 86, 1359–1368. doi: 10.1046/j.1471-4159.2003.01949.x

Dalpiaz, A., Townsend-Nicholson, A., Beukers, M. W., Schofield, P. R., and IJzerman, A. P. (1998). Thermodynamics of full agonist, partial agonist, and antagonist binding to wild-type and mutant adenosine A1 receptors. *Biochem. Pharmacol.* 56, 1437–1445.

Daly, J. W., Padgett, W., Shamim, M. T., Butts-Lamb, P., and Waters, J. (1985). 1,3-Dialkyl-8-(p-sulfophenyl)xanthines: potent water-soluble antagonists for A1- and A2-adenosine receptors. *J. Med. Chem.* 28, 487–492.

Dionisotti, S., Ongini, E., Zocchi, C., Kull, B., Arslan, G., and Fredholm, B. B. (1997). Characterization of human A2A adenosine receptors with the antagonist radioligand [3H]-SCH 58261. *Br. J. Pharmacol.* 121, 353–360.

Fredholm, B. B., IJzerman, A. P., Jacobson, K. A., Linden, J., and Müller, C. E. (2011). International Union of Basic And Clinical Pharmacology. *LXXXI. Nomenclature and classification of adenosine receptors–an update. Pharmacol. Rev.* 63, 1–34. doi: 10.1124/pr.110.003285

Fredholm, B. B., Irenius, E., Kull, B., and Schulte, G. (2001). Comparison of the potency of adenosine as an agonist at human adenosine receptors expressed in Chinese hamster ovary cells. *Biochem. Pharmacol.* 61, 443–448. doi: 10.1016/S0006-2952(00)00570-0

Gallo-Rodriguez, C., Ji, X. D., Melman, N., Siegman, B. D., Sanders, L. H., Orlina, J., et al. (1994). Structure-activity relationships of N6-benzyladenosine-5'-uronamides as A3-selective adenosine agonists. *J. Med. Chem.* 37, 636–646.

Gao, Z. G., Mamedova, L. K., Chen, P., and Jacobson, K. A. (2004). 2-Substituted adenosine derivatives: affinity and efficacy at four subtypes of human adenosine receptors. *Biochem. Pharmacol.* 68, 1985–1993. doi: 10.1016/j.bcp.2004.06.011

Gherbi, K., Briddon, S. J., and Hill, S. J. (2014). Detection of the secondary, low-affinity β1-adrenoceptor site in living cells using the fluorescent CGP 12177 derivative BODIPY-TMR-CGP. *Br. J. Pharmacol.* 171, 5431–5445. doi: 10.1111/bph.12858

González-Fernández, E., Sánchez-Gómez, M. V., Pérez-Samartín, A., Arellano, R. O., and Matute, C. (2014). A3 Adenosine receptors mediate oligodendrocyte death and ischemic damage to optic nerve. *Glia* 62, 199–216. doi: 10.1002/glia.22599

Guo, J., Song, L., Liu, M., and Mahon, M. J. (2012). Fluorescent ligand-directed co-localization of the parathyroid hormone 1 receptor with the brush-border scaffold complex of the proximal tubule reveals hormone-dependent changes in ezrin immunoreactivity consistent with inactivation. *Biochim. Biophys. Acta* 1823, 2243–2253. doi: 10.1016/j.bbamcr.2012.09.010

Hara, T., Hirasawa, A., Sun, Q., Koshimizu, T. A., Itsubo, C., Sadakane, K., et al. (2009). Flow cytometry-based binding assay for GPR40 (FFAR1; Free Fatty Acid Receptor 1). *Mol. Pharmacol.* 75, 85–91. doi: 10.1124/mol.108.052225

Headrick, J. P., Ashton, K. J., Rose'meyer, R. B., and Peart, J. N. (2013). Cardiovascular adenosine receptors: expression, actions and interactions. *Pharmacol. Ther.* 140, 92–111. doi: 10.1016/j.pharmthera.2013.06.002

Hussain, A., Gharanei, A. M., Nagra, A. S., and Maddock, H. L. (2014). Caspase inhibition via A3 adenosine receptors: a new cardioprotective mechanism against myocardial infarction. *Cardiovasc. Drugs Ther.* 28, 19–32. doi: 10.1007/s10557-013-6500-y

Iturrioz, X., Alvear-Perez, R., De Mota, N., Franchet, C., Guillier, F., Leroux, V., et al. (2010). Identification and pharmacological properties of E339-3D6, the first nonpeptidic apelin receptor agonist. *FASEB J.* 24, 1506–1517. doi: 10.1096/fj.09-140715

Jacobson, K. A., Gallo-Rodriguez, C., Melman, N., Fischer, B., Maillard, M., van Bergen, A., et al. (1993). Structure-activity relationships of 8-styrylxanthines as A2-selective adenosine antagonists. *J. Med. Chem.* 36, 1333–1342.

Jacobson, K. A., Ijzerman, A. P., and Linden, J. (1999). 1,3-dialkylxanthine derivatives having high potency as antagonists at human A2B adenosine receptors. *Drug Dev. Res.* 47, 45–53.

Ji, X., Kim, Y. C., Ahern, D. G., Linden, J., and Jacobson, K. A. (2001). [3H]MRS 1754, a selective antagonist radioligand for A(2B) adenosine receptors. *Biochem. Pharmacol.* 61, 657–663. doi: 10.1016/S0006-2952(01)00531-7

Joshaghani, H. R., Jafari, S. M., Aghaei, M., Panjehpour, M., and Abedi, H. (2017). A3 adenosine receptor agonist induce G1 cell cycle arrest via Cyclin, D., and cyclin-dependent kinase 4 pathways in OVCAR-3 and Caov-4 cell lines. *J. Cancer Res. Ther.* 13, 107–112. doi: 10.4103/0973-1482.199381

Kecskes, M., Kumar, T. S., Yoo, L., Gao, Z. G., and Jacobson, K. A. (2010). Novel Alexa Fluor-488 labeled antagonist of the A(2A) adenosine receptor: application to a fluorescence polarization-based receptor binding assay. *Biochem. Pharmacol.* 80, 506–511. doi: 10.1016/j.bcp.2010.04.027

Klotz, K.-N., Falgner, N., Kachler, S., Lambertucci, C., Vittori, S., Volpini, R., et al. (2007). [3H]HEMADO– a novel tritiated agonist selective for the human adenosine A3 receptor. *Eur. J. Pharmacol.* 556, 14–18. doi: 10.1016/j.ejphar.2006.10.048

Klotz, K. N., Hessling, J., Hegler, J., Owman, C., Kull, B., Fredholm, B. B., et al. (1998). Comparative pharmacology of human adenosine receptor subtypes - characterization of stably transfected receptors in CHO cells. *Naunyn-Schmiedebergs Arch. Pharmacol.* 357, 1–9.

Korb, O., Stutzle, T., and Exner, T. E. (2009). Empirical scoring functions for advanced protein-ligand docking with PLANTS. *J. Chem. Inf. Model.* 49, 84–96. doi: 10.1021/ci800298z

Kozma, E., Gizewski, E. T., Tosh, D. K., Squarcialupi, L., Auchampach, J. A., and Jacobson, K. A. (2013). Characterization by flow cytometry of fluorescent, selective agonist probes of the A(3) adenosine receptor. *Biochem. Pharmacol.* 85, 1171–1181. doi: 10.1016/j.bcp.2013.01.021

Kuder, K. J., and Kieć-Kononowicz, K. (2014). Fluorescent GPCR ligands as new tools in pharmacology-update, years 2008-early 2014. *Curr. Med. Chem.* 21, 3962–3975. doi: 10.2174/0929867321666140826120058

Li, A. H., Moro, S., Melman, N., Ji, X. D., and Jacobson, K. A. (1998). Structure-activity relationships and molecular modeling of 3,5-diacyl-2,4-dialkylpyridine derivatives as selective A(3) adenosine receptor antagonists. *J. Med. Chem.* 41, 3186–3201.

Little, J. W., Ford, A., Symons-Liguori, A. M., Chen, Z., Janes, K., Doyle, T., et al. (2015). Endogenous adenosine A3 receptor activation selectively alleviates persistent pain states. *Brain* 138, 28–35. doi: 10.1093/brain/awu330

May, L. T., Self, T. J., Briddon, S. J., and Hill, S. J. (2010). The effect of allosteric modulators on the kinetics of agonist-G protein-coupled receptor interactions in single living cells. *Mol. Pharmacol.* 78, 511–523. doi: 10.1124/mol.110.064493

Montinaro, A., Iannone, R., Pinto, A., and Morello, S. (2013). Adenosine receptors as potential targets in melanoma. *Pharmacol. Res.* 76, 34–40. doi: 10.1016/j.phrs.2013.07.002

Mulloy, D. P., Sharma, A. K., Fernandez, L. G., Zhao, Y., Lau, C. L., Kron, I. L., et al. (2013). Adenosine A3 receptor activation attenuates lung ischemia-reperfusion injury. *Ann. Thorac. Surg.* 95, 1762–1767. doi: 10.1016/j.athoracsur.2013.01.059

Nakamura, K., Shinozuka, K., and Yoshikawa, N. (2015). Anticancer and antimetastatic effects of cordycepin, an active component of *Cordyceps sinensis*. *J. Pharmacol. Sci.* 127, 53–56. doi: 10.1016/j.jphs.2014.09.001

Ohana, G., Cohen, S., Rath-Wolfson, L., and Fishman, P. (2016). A3 adenosine receptor agonist, CF102, protects against hepatic ischemia/reperfusion injury following partial hepatectomy. *Mol. Med. Rep.* 14, 4335–4341. doi: 10.3892/mmr.2016.5746

Ongini, E., Dionisotti, S., Gessi, S., Irenius, E., and Fredholm, B. B. (1999). Comparison of CGS 15943, ZM 241385 and SCH 58261 as antagonists at human adenosine receptors. *Naunyn-Schmiedeberg's Arch. Pharmacol.* 359, 7–10.

Ranganathan, A., Stoddart, L. A., Hill, S. J., and Carlsson, J. (2015). Fragment-based discovery of subtype-selective adenosine receptor ligands from homology models. *J. Med. Chem.* 58, 9578–9590. doi: 10.1021/acs.jmedchem.5b01120

Ravani, A., Vincenzi, F., Bortoluzzi, A., Padovan, M., Pasquini, S., Gessi, S., et al. (2017). Role and function of A(2A) and A_3 adenosine receptors in patients with ankylosing spondylitis, psoriatic arthritis and rheumatoid arthritis. *Int. J. Mol. Sci.* 18:E697. doi: 10.3390/ijms18040697

Squarcialupi, L., Colotta, V., Catarzi, D., Varano, F., Filacchioni, G., Varani, K., et al. (2013). 2-Arylpyrazolo[4,3-d]pyrimidin-7-amino derivatives as new potent and selective human A3 adenosine receptor antagonists. *Molecular modeling studies and pharmacological evaluation. J. Med. Chem.* 56, 2256–2269. doi: 10.1021/jm400068e

Stoddart, L. A., Johnstone, E. K., Wheal, A. J., Goulding, J., Robers, M. B., Machleidt, T., et al. (2015a). Application of BRET to monitor ligand binding to GPCRs. *Nat. Methods* 12, 661–663. doi: 10.1038/nmeth.3398

Stoddart, L. A., Kilpatrick, L. E., Briddon, S. J., and Hill, S. J. (2015b). Probing the pharmacology of G protein-coupled receptors with fluorescent ligands. *Neuropharmacology* 98, 48–57. doi: 10.1016/j.neuropharm.2015.04.033

Stoddart, L. A., Vernall, A. J., Denman, J. L., Briddon, S. J., Kellam, B., and Hill, S. J. (2012). Fragment screening at adenosine-A(3) receptors in living cells using a fluorescence-based binding assay. *Chem. Biol.* 19, 1105–1115. doi: 10.1016/j.chembiol.2012.07.014

Stoddart, L. A., White, C. W., Nguyen, K., Hill, S. J., and Pfleger, K. D. (2016). Fluorescence- and bioluminescence-based approaches to study GPCR ligand binding. *Br. J. Pharmacol.* 173, 3028–3037. doi: 10.1111/bph.13316

Tomasch, M., Schwed, J. S., Kuczka, K., Meyer Dos Santos, S., Harder, S., Nusing, R. M., et al. (2012). Fluorescent human EP3 receptor antagonists. *ACS Med. Chem. Lett.* 3, 774–779. doi: 10.1021/ml300191g

Tosh, D. K., Padia, J., Salvemini, D., and Jacobson, K. A. (2015). Efficient, large-scale synthesis and preclinical studies of MRS5698, a highly selective A3 adenosine receptor agonist that protects against chronic neuropathic pain. *Purinergic Signal.* 11, 371–387. doi: 10.1007/s11302-015-9459-2.

Vainio, M. J., and Johnson, M. S. (2007). Generating conformer ensembles using a multiobjective genetic algorithm. *J. Chem. Inf. Model.* 47, 2462–2474. doi: 10.1021/ci6005646

van Galen, P. J., van Bergen, A. H., Gallo-Rodriguez, C., Melman, N., Olah, M. E., IJzerman, I. J., et al. (1994). A binding site model and structure-activity relationships for the rat A3 adenosine receptor. *Mol. Pharmacol.* 45, 1101–1111.

van Muijlwijk-Koezen, J. E., Timmerman, H., van der Sluis, R. P., van de Stolpe, A. C., Menge, W. M., Beukers, M. W., et al. (2001). Synthesis and use of FSCPX, an irreversible adenosine A1 antagonist, as a 'receptor knock-down'

tool. *Bioorg. Med. Chem. Lett.* 11, 815–818. doi: 10.1016/S0960-894X(01)00069-5

Vernall, A. J., Stoddart, L. A., Briddon, S. J., Hill, S. J., and Kellam, B. (2012). Highly potent and selective fluorescent antagonists of the human adenosine A(3) receptor based on the 1,2,4-triazolo 4,3-a quinoxalin-1-one Scaffold. *J. Med. Chem.* 55, 1771–1782. doi: 10.1021/jm201722y

Vernall, A. J., Stoddart, L. A., Briddon, S. J., Ng, H. W., Laughton, C. A., Doughty, S. W., et al. (2013). Conversion of a non-selective adenosine receptor antagonist into A3-selective high affinity fluorescent probes using peptide-based linkers. *Org. Biomol. Chem.* 11, 5673–5682. doi: 10.1039/c3ob41221k

Wu, J. M., DiPietrantonio, A. M., and Hsieh, T. C. (2001). Mechanism of fenretinide (4-HPR)-induced cell death. *Apoptosis* 6, 377–388. doi: 10.1023/A:1011342220621

Yoshida, K., Ito, M., and Matsuoka, I. (2017). Divergent regulatory roles of extracellular ATP in the degranulation response of mouse bone marrow-derived mast cells. *Int. Immunopharmacol.* 43, 99–107. doi: 10.1016/j.intimp.2016.12.014

Young, S. M., Bologa, C., Prossnitz, E. R., Oprea, T. I., Sklar, L. A., and Edwards, B. S. (2005). High-throughput screening with HyperCyt (R) flow cytometry to detect small molecule formylpeptide receptor ligands. *J. Biomol. Screen.* 10, 374–382. doi: 10.1177/1087057105274532

Zwier, J. M., Roux, T., Cottet, M., Durroux, T., Douzon, S., Bdioui, S., et al. (2010). A fluorescent ligand-binding alternative using tag-lite (R) technology. *J. Biomol. Screen.* 15, 1248–1259. doi: 10.1177/1087057110384611

Conflict of Interest Statement: The authors declare that the research was conducted in the absence of any commercial or financial relationships that could be construed as a potential conflict of interest.

frontiers in Pharmacology

ORIGINAL RESEARCH
published: 13 December 2017
doi: 10.3389/fphar.2017.00910

ATP Modifies the Proteome of Extracellular Vesicles Released by Microglia and Influences Their Action on Astrocytes

Francesco Drago[1,2†], Marta Lombardi[3†], Ilaria Prada[4], Martina Gabrielli[4], Pooja Joshi[4], Dan Cojoc[5], Julien Franck[1], Isabelle Fournier[1], Jacopo Vizioli[1] and Claudia Verderio[3,4]*

[1] Univ. Lille, INSERM, U1192 – Protéomique Réponse Inflammatoire Spectrométrie de Masse – PRISM, Lille, France, [2] Fondazione Istituto Oncologico del Mediterraneo, Viagrande, Italy, [3] IRCCS Humanitas, Rozzano, Italy, [4] Institute of Neuroscience (CNR), Milan, Italy, [5] Institute of Materials (CNR), Trieste, Italy

OPEN ACCESS

Edited by:
Francisco Ciruela,
University of Barcelona, Spain

Reviewed by:
Amanda Sierra,
Achucarro Basque Center for Neuroscience, Spain
Felipe A. Court,
Universidad Mayor, Chile

***Correspondence:**
Claudia Verderio
c.verderio@in.cnr.it

[†] These authors have contributed equally to this work.

Specialty section:
This article was submitted to Experimental Pharmacology and Drug Discovery, a section of the journal Frontiers in Pharmacology

Received: 01 October 2017
Accepted: 29 November 2017
Published: 13 December 2017

Citation:
Drago F, Lombardi M, Prada I, Gabrielli M, Joshi P, Cojoc D, Franck J, Fournier I, Vizioli J and Verderio C (2017) ATP Modifies the Proteome of Extracellular Vesicles Released by Microglia and Influences Their Action on Astrocytes. Front. Pharmacol. 8:910. doi: 10.3389/fphar.2017.00910

Extracellular ATP is among molecules promoting microglia activation and inducing the release of extracellular vesicles (EVs), which are potent mediators of intercellular communication between microglia and the microenvironment. We previously showed that EVs produced under ATP stimulation (ATP-EVs) propagate a robust inflammatory reaction among astrocytes and microglia *in vitro* and in mice with subclinical neuroinflammation (Verderio et al., 2012). However, the proteome of EVs released upon ATP stimulation has not yet been elucidated. In this study we applied a label free proteomic approach to characterize the proteome of EVs released constitutively and during microglia activation with ATP. We show that ATP drives sorting in EVs of a set of proteins implicated in cell adhesion/extracellular matrix organization, autophagy-lysosomal pathway and cellular metabolism, that may influence the response of recipient astrocytes to EVs. These data provide new clues to molecular mechanisms involved in microglia response to ATP and in microglia signaling to the environment via EVs.

Keywords: ATP, microglia, extracellular vesicles, proteomics, astrocyte activation

INTRODUCTION

Microglia are essential components of the innate immune response in the brain. They are self-renewing, long-lived cells, and stem from a unique non-haematopoietic yolk-sac-derived cell lineage (Ginhoux et al., 2010). They are multitasking cells involved in various functions under physiological and pathological states, participating in synaptic refinement, phagocytosis or immunosurveillance (Casano and Peri, 2015). During brain development microglia regulate the formation and stability of dendritic spines and eliminate via phagocytosis redundant synapses, a process known as synaptic pruning (Paolicelli et al., 2011). This process involves the complement factors C1q and C3, which localize to redundant synapse, and C3 receptor, which triggers synaptic

Abbreviations: ATP-EVs, EVs produced from ATP-stimulated microglia, DAVID, Database for Annotation, Visualization, and Integrated Discovery, EVs, extracellular vesicles; ExoCarta, exosome network database; FA, formic acid; FDR, False discovery rates; GO, gene ontology; IAA, 3-indole acetic acid; KEGG, Kyoto Encyclopedia of Genes and Genome; LC-MS, liquid chromatography-mass spectrometry; MVs, microvesicles; NCE, normalized collision energy; PANTHER, Protein ANalysis THrough Evolutionary Relationships; PS, phosphatidylserine; TRPS, tunable resistive pulse sensing.

engulfment (Stevens et al., 2007). In the adult brain, microglia are critical for the maintenance of brain homeostasis and continuously move their processes to survey the surrounding territory (Davalos et al., 2005) (Nimmerjahn et al., 2005). In response to injury or infection, these highly dynamic cells proliferate and migrate to sites of injury, where they participate in mechanisms of injury but also in tissue repair.

Extracellular ATP is among molecules promoting microglia activation, proliferation, phagocytic function and guiding their migration toward damaged cells (Dou et al., 2012; Sieger et al., 2012; Domercq et al., 2013). ATP accumulates extracellularly at sites of injury or inflammation, being released from dead cells (Di Virgilio, 2007). By inducing further release of ATP from neighboring cells, the molecule establishes a long-range ATP gradient, that induces chemotaxis of remote microglia (Honda et al., 2001; Corriden and Insel, 2012; Casano et al., 2016).

Our previous evidence indicates that ATP, through activation of the ATP receptor P2X7, massively increases release of EVs from microglia (Bianco et al., 2005b, 2009). EVs are membrane vesicles released by all cells which contain a selection of donor cell components, including proteins, lipids and RNA, and serve as transfer vehicles for these molecules between cells. By exposing cell-type-specific adhesion receptors, EVs interact with specific cells and deliver complex "signals," playing a key role in cell-to-cell signaling. EVs have different sizes and subcellular origin. Quite large EVs bud from the plasma membrane (ectosomes, also called microvesicles or MVs) while small EVs result from exocytosis of multivesicular bodies (exosomes) (Cocucci and Meldolesi, 2015).

Extracellular vesicles released by ATP-stimulated microglia induce a robust inflammatory reaction in glial cells *in vitro* and propagate an inflammatory response among microglia in mice with subclinical neuroinflammation (Verderio et al., 2012). However, the action of ATP-EVs has never been compared to that of constitutive EVs nor the proteome of constitutive or ATP-EVs has been elucidated yet (Prada et al., 2013). To our knowledge, only one proteomic study has been performed on EVs derived from primary microglia. This work led to the identification of ∼45 proteins in exosomes released from microglia activated with the signaling protein Wnt3a but it did not identify any protein in constitutive exosomes (Hooper et al., 2012), thus limiting current knowledge of EV composition.

In this study we applied a label free proteomic approach to explore the changes in EV proteome induced by microglia activation with ATP. We also investigated how ATP stimulation impacts the response of recipient astrocytes to microglia-derived EVs. We found that ATP stimulation drives secretion via EVs of a set of proteins implicated in cell adhesion/extracellular matrix organization, in degradative pathways, and energy metabolism, and that ATP-EVs enhance the expression of few activation markers in target astrocytes. These data provide new clues to molecular mechanisms involved in microglia response to ATP and in their signaling to the environment.

MATERIALS AND METHODS

Animals

All the experimental procedures followed the guidelines established by the European Legislation (Directive 2010/63/EU) and the Italian Legislation (L.D. no 26/2014).

Primary Glial Culture and Stimulation

Mixed glial cell cultures, containing both astrocytes and microglial cells, were established from postnatal rat Sprague–Dawley pups (P2). Briefly, after dissection, hippocampi and cortices were dissociated by treatment with trypsin and DNase-I for 15 min at 37°C, followed by fragmentation with a fire-polished Pasteur pipette. Dissociated cells were plated on poly-L-lysine coated T75 flasks in minimal essential medium (E-MEM, Invitrogen) supplemented with 20% fetal bovine serum (Gibco, Life Technologies, Carlsbad, CA, United States) and glucose (5.5 g/L). To obtain a pure astrocyte monolayer, microglial cells were harvested from 7-days-old cultures by orbital shaking for 30 min at 1300 rpm. Astrocytes were trypsinised and re-plated onto poly-L-lysine-coated glass coverslips while shaken microglia were re-plated on poly-DL-ornithine-coated tissue culture dishes.

Recipient astrocytes were exposed to an amount of EVs produced by twice as many donor microglia (1:2 receiving cells to donor cells relative ratio). To reduce the level of activation, recipient astrocytes were pre-starved overnight in serum-free medium and kept in low (1%) serum medium during exposure to EVs. To minimize the activation of microglia, half of the medium in which microglia were kept after shaking from mixed glial cultures was replaced with fresh low (1%) serum medium. At the end of incubation, recipient astrocytes were washed and harvested with TRIZOL for RT-PCR analysis.

EV Isolation and Quantification

Extracellular vesicles released from 1×10^6 microglia constitutively or upon exposure to 1 mM ATP for 1h in KRH (125 mM NaCl, 5 mM KCl, 1.2 mM $MgSO_4$, 1.2 mM KH_2PO_4, 2 mM $CaCl_2$, 6 mM D-glucose, and 25 mM HEPES/NaOH, pH 7.4) were pelletted at 10K g (ectosome-enriched fraction) and 100K g (exosomes-enriched fraction) after pre-clearing from cells and debris as described previously (Gabrielli et al., 2015). TRPS, by qNano (Izon, Christchurch, New Zealand) was used to measure the size distribution and concentration of particles in 10 and 100K g pellets after re-suspension in 100 μl. TRPS is an impedance based method. A voltage is applied across a pore that is filled with electrolyte, resulting in an ionic current. As EVs cross the pore they briefly block the ionic current, creating a blockade event, which is proportional to EV volume. A reagent kit from Izon (Izon EV reagent kit) were used for both pre-treating the pore and suspending EVs in order to prevent EV binding to the pore or spontaneous EV aggregation. NP300 nanopore (150–600 nm diameter range; Izon) was used for MV sample analysis, while NP150 nanopore (85–300 nm diameter range; Izon) was used for exosome sample analysis. In each experiment, the same applied voltage, pressure and pore

stretch values were set for all MV/exosome sample recordings and relative calibration. Three pressure values per sample were used for multipressure analysis. CPC200 and CPC150 calibration particles (carboxylated polystyrene particles, supplied by Izon and diluted following manufacturer's instructions) were used as standards, for MV and exosome sample respectively. They were measured immediately before or after the experimental samples under identical conditions. Data acquisition and analysis were performed using Izon Control Suite software (version V3.2).

To deplete luminal cargo, EVs were broken by freeze and thaw and repelletted at 100K g for 1 h. To mask PS residues on the EV surface and avoid contact with recipient astrocytes, EVs were resuspended in annexin-V for 30 min, washed and repelleted. For biochemical fractionation of EVs, total lipids were extracted through the method previously described (Antonucci et al., 2012) with 2:1 (by volume) of chloroform and methanol. The lipid fraction was evaporated under a nitrogen stream, dried for 1 h at 50°C and resuspended in PBS at 40°C in order to obtain multilamellar vesicles. Small unilamellar vesicles were obtained by sonication, following the procedure of (Barenholz et al., 1977).

EV Proteomics

Extracellular vesicles released from 15×10^6 microglia constitutively or upon exposure to 1 mM ATP in MEM for 1h were centrifuged as above and frozen at −80°C. Dried samples were reconstituted with 20 μL of 50 mM bicarbonate buffer containing 50 mM DTT and 4% SDS. The samples were then loaded on 12% polyacrylamide gel and separated at 70 V for 15 min and then 120 V until the dye front entered in the separating gel at a distance of 1 cm. The gel was cut into pieces of 1 mm^3. Pieces were washed with 300 μl of distilled deionized water for 15 min, 300 μl of acetonitrile (ACN) for 15 min, and 300 μl of NH_4HCO_3 100 mM (pH 8) for 15 min. Then a mix of 300 μl of NH_4HCO_3/ACN (1:1, v/v) for 15 min and 300 μl of ACN for 5 min. Band pieces were dried in a Speedvac for 5 min. The reduction of cysteine residues was made with 50 μl of 10 mM of DTT in NH_4HCO_3 100 mM (pH 8). Pieces were incubated at 56°C for 1 h. Alkylation of cysteines was made with 50 μl of 50 mM of IAA in NH_4HCO_3 100 mM (pH 8). Pieces were incubated at room temperature in the dark for 30 min. Band pieces were washed a second time with 300 μl of NH_4HCO_3 100 mM (pH 8) for 15 min. Then a mix of 300 μl of NH_4HCO_3/ACN (1:1, v/v) for 15 min and 300 μl of ACN for 5 min. Band pieces were dried in a Speedvac for 5 min. A digestion of band pieces was made with trypsin (12.5 μg/ml) in NH_4HCO_3 20 mM (pH 8), enough to cover pieces. Pieces were incubated at 37°C overnight. Peptides were extracted on shaking platform with 50 μl of FA 1% two times for 20 min, then 150 μl of ACN for 10 min. The supernatant was transferred in new tube and dried with Speedvac.

The trypsin-digested protein extracts were reconstituted with 20 μl of 5% ACN/0.1% FA and injected on an EASY-nLC 1000 UPLC (Thermo Fisher Scientific) equipped with a 75 μm × 2 cm Acclaim PepMap 100 pre-column with nanoViper fittings and a 50 μm ID × 150 mm Acclaim PepMap RSLC analytical column (C18, particle size 2 μm, pore size 100 Å, Thermo Fisher Scientific). The peptides were eluted using a 2 h gradient of ACN starting from 5 to 30% over 120 min at a flow rate of 300 nl/min. The Q-Exactive instrument was set to acquire top 10 MS2. The survey scans were taken at 70,000 FWHM (at m/z 400) resolving power in positive mode and using a target of 3E6 and default charge state of +2. Unassigned and +1 charge states were rejected and dynamic exclusion was enabled for 20 s. The scan range was set to 300–1600 m/z. For the MS2, 1 microscan was obtained at 17,500 FWHM, isolation window of 4.0 m/z and a normalized collision energy (NCE) = 30 using a scan range between 200 and 2000 m/z.

Data Analysis

Protein tandem MS/MS data were processed using Proteome Discoverer 1.4 (Thermo Fisher Scientific). Peptides were identified by using the Sequest search engine, where target-decoy searches were performed against the *Rattus norvegicus* UniProt database (accessed March 4, 2014, 33,675 entries) combined with the 262 commonly detected contaminant databases. The parent and fragment mass tolerances were set at 10 ppm and 0.5 Da, respectively. The enzyme used was trypsin, and the maximum allowable cleavages were set to 2. Carbamidomethylation of cysteine was set as fixed modification while oxidation of methionine was set as variable modifications. FDR for the peptide and protein levels were both set at 0.01.

The data sets and Proteome Discoverer result files used for analysis were deposited at the ProteomeXchange Consortium[1] via the PRIDE partner repository with the data set identifier PXD007650 (For reviewer access only Username: reviewer86756@ebi.ac.uk; Password: 3qSILRLn).

Proteins were clustered in categories depending on their known main biological function using two different open source bioinformatics resources: DAVID Bioinformatics Resource 6.8[2] and PANTHER (Protein ANalysis THrough Evolutionary Relationships) database[3]. In both cases, the whole *Rattus norvegicus* genome was employed as background list. The analysis of cellular components and biological processes was performed in DAVID and selecting the GO terms for Cellular Component (GOTERM_CC_FAT) and for Biological Process (GOTERM_BP DIRECT). Molecular Function analysis was performed with AgBase Bioinformatics Resource 2.00[4] using the AgBase GO slim viewer Molecular Function. Pathway overrepresentation analysis was performed using DAVID bioinformatics resource and comparing the representation of the different KEGG[5] terms (KEGG_PATHWAY) to the expected pathway representation in rat. This analysis was coupled to the pathway enrichment analysis performed with PANTHER using the PANTHER Pathway keywords and exported as bar chart of representation percentages.

[1] http://proteomecentral.proteomexchange.org
[2] http://david.abcc.ncifcrf.gov
[3] http://www.pantherdb.org
[4] http://www.agbase.msstate.edu
[5] http://www.genome.jp/kegg

EV Delivery by Optical Manipulation

An IR laser beam (1064 nm, CW) for trapping was coupled into the optical path of an inverted microscope (Axiovert200M, Zeiss) through the right port of the microscope. The trapping beam was directed to the microscope lens (Zeiss 63X, NA 1.4) by the corresponding port mirror (100%) and the tube lens. Optical trapping and manipulation of EVs was performed following the approach previously described (Prada et al., 2016). Immediately before recording, ATP-EVs or constitutive EVs (100K g pellet) were added to in the temperature controlled recording chamber, where astrocytes plated on glass coverslips, were maintained in 400 µl of medium. As soon as an EV appeared in the recording field, it was trapped and positioned on a selected astrocyte by moving the cell stage horizontally and the microscope lens axially. After about 30 s from contact, the laser was switched off to prove EV-astrocyte interaction. During the experiments astrocytes were live imaged with a spinning disk confocal microscope (UltraVIEW acquisition system, Perkin Elmer Waltham, MA, United States) using a digital camera (High Sensitivity USB 3.0 CMOS Camera 1280 × 1024 Global Shutter Monochrome Sensor, Thorlabs, Newton, NJ, United States) at a frame rate of 2 Hz.

Reverse Transcriptase-Coupled PCR

Total RNA was isolated from rat primary astrocytes using Direct-zol™ RNA MiniPrep (Zymo Research) following the manufacturer's protocol. cDNA synthesis was performed using High Capacity cDNA Reverse Transcription Kit (Applied Biosystems) and Random Hexamers as primer. The resulting cDNAs were amplified using TaqMan® Gene Expression Assay (Applied Biosystems). The mRNA expression was normalized to the label of Rpl13 (Ribosomal Protein L13) mRNA.

Statistical Analysis

All data are presented as mean ± SE from the indicated number of independent experiments. Statistical analysis was performed using SigmaPlot 12.0 (Jandel Scientific, San Jose, CA, United States) software. After testing data for normal distribution, the appropriate statistical test has been used (see figure legends). Differences were considered significant when P was <0.05, $P < 0.01$ or $P < 0.001$ and they are indicated by one, two or three asterisks, respectively.

RESULTS

Constitutive and ATP-Induced EV Production from Rat Primary Microglia

Microglia are equipped with several ATP receptors (Farber and Kettenmann, 2006; Pocock and Kettenmann, 2007), including P2X7 receptor, a key determinant of cellular metabolism (Adinolfi et al., 2005), which massively increases release of EV (Bianco et al., 2005b). Among ATP receptors, P2Y12 is a key marker of adult microglia (Hickman et al., 2013; Butovsky et al., 2014) and is required for homeostatic activity and phagocytosis (Ohsawa et al., 2010; Preissler et al., 2015). In order to validate new-born rat primary microglia as a suitable system to characterize EVs secreted upon ATP stimulation we checked for the presence of P2Y12 as well as other homeostatic genes enriched in adult microglia (Gpr34, TGFβr1 and Tmem119) (Butovsky et al., 2014; Buttgereit et al., 2016; Matcovitch-Natan et al., 2016) and few metabolic genes in the cultures. We found that new-born microglia constitutively express P2Y12, Gpr34, TGFβr1, Tmem119 transcripts and respond to 1 mM ATP by upregulating P2Y12 (**Figure 1A**) and few metabolic genes (Supplementary Figure 1).

We next isolated by differential centrifugation quite large ectosomes (10,000 × g = 10K) and smaller exosomes (100,000 × g = 100K) from the medium conditioned by microglia either kept under resting conditions or exposed to ATP for 1 h, as previously described (Gabrielli et al., 2015). Our previous evidence indicates that 1 h stimulation with ATP does not induce cell damage or apoptosis (Bianco et al., 2005b). Accordingly, EVs isolated under ATP stimulation are not positive for apoptotic markers (Verderio et al., 2012) nor contaminated by intracellular organelles derived from damaged cells (Gabrielli et al., 2015). Quantification by TRPS confirmed the enrichment of quite large vesicles in the 10K pellet (mean diameter = 180.00 ± 26.41 nm) and of smaller vesicles in the 100K pellet (mean diameter = 111.97 ± 12.27 nm) (**Figure 1B**). It also revealed that stimulation with ATP increases production of exosomes but not ectosomes under stimulation for 1 h (**Figure 1C**).

Proteomic Analysis of Ectosomes and Exosomes Constitutively Released by Microglia

In order to determine the proteomic profile of microglia-derived EVs we used a LC-MS label free approach and analyzed four independent experiments. A total of 140 and 142 proteins were detected respectively in ectosomes and exosomes produced by unstimulated microglia, of which 69 proteins were common between the two vesicle populations (∼47% overlap) (**Figure 2A**). The set of proteins uniquely identified in ectosomes or exosomes along with common proteins are shown in Supplementary Table I. Matching with proteins collected in the exosome network database ExoCarta (and its compendium Vesiclepedia) showed that a large fraction of proteins (about 88%) were already described in EVs. When the top 100 exosomal proteins were considered, almost 15% were present in EVs secreted from microglia (Supplementary Table II). Among them we found two potent anti-inflammatory mediators, AnnexinA1 and AnnexinA2, which follow an unconventional secretory pathway. Other leaderless proteins were detected in EVs derived from unstimulated microglia, such as the microglial cell type specific protein Galectin-3 (Sharma et al., 2015), Enolase, HSP90 or GAPDH (Supplementary Table I), supporting a role for EVs in unconventional protein secretion.

Analysis of GO terms showed that the cellular component terms "extracellular region (part)," "membrane-bounded vesicles," "extracellular vesicles," and "extracellular exosome" are the highest enriched fractions (above 60%) of constitutive EVs

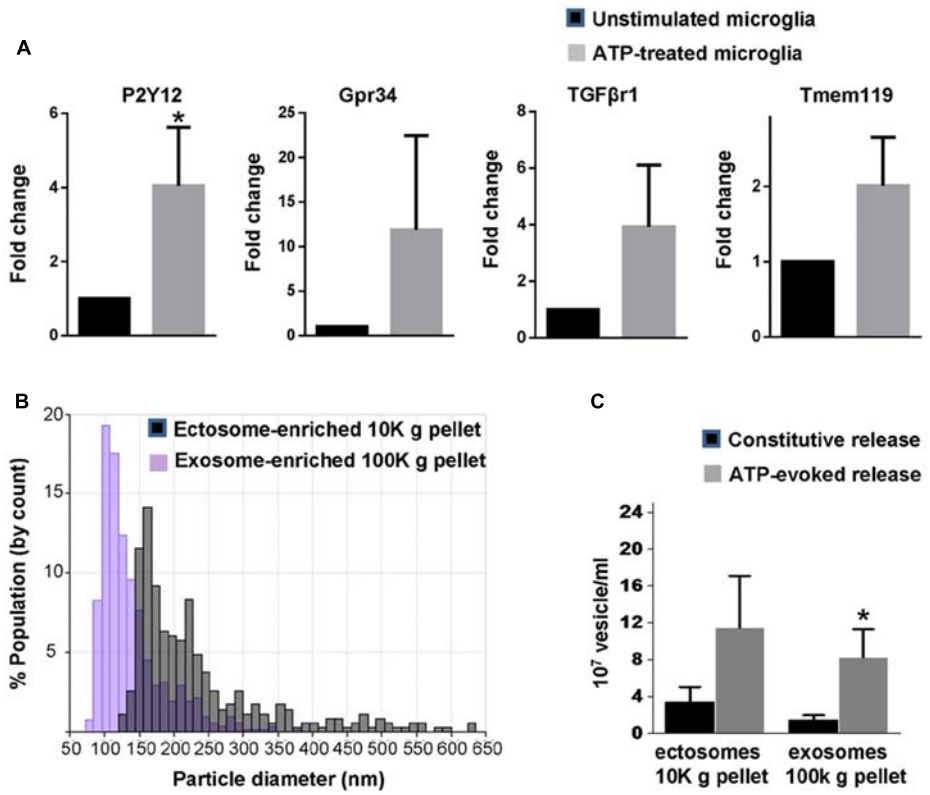

FIGURE 1 | Basal and ATP-induced production of EVs in primary rat microglia. **(A)** q-PCR analysis for the adult microglia markers P2Y12, Gpr34, TGFβr1 and Tmem119 in unstimulated rat primary microglia and in cells activated with 1 mM ATP for 1h (P2Y12: Mann–Whitney Rank Sum test $P = 0.029$; Gpr34: Mann–Whitney Rank Sum test $P = 0{,}343$, TGFβr1: Mann–Whitney Rank Sum test $P = 0{,}100$; Tmem119: Mann–Whitney Rank Sum test $P = 0.100$; $N = 3$). **(B)** Representative particle size distributions of ectosome-enriched 10 Kg pellet (gray) and exosome-enriched 100 Kg pellet (violet) analyzed using TRPS. The size distributions are shown as histograms with bin width 10 nm. **(C)** Histograms show the number of EVs released constitutively or under ATP from 1 million microglia, centrifuged and re-suspended in 100 μl of 0.1 μm-filtered Krebs-Ringer solution (ATP-ectosomes versus constitutive ectosomes Mann–Whitney Rank Sum Test $P = 0.182$; $N = 5$; ATP-exosomes versus constitutive exosomes, Mann-Whitney Rank Sum Test $P = 0.048$; $N = 3$).

(ectosomes and exosomes in total), followed by "cytosol" and "extracellular space," which is consistent with the vesicular and extracellular nature of EV proteins (**Figure 2B**). GO analysis of molecular functions showed that binding to protein and RNA/nucleotide are major categories, in line with adhesive properties of EVs and their content of genetic materials (**Figure 3A**). GO analysis of biological processes (Supplementary Table III) revealed terms related to response to compounds (∼32%), response to environmental changes (∼20%), cytoskeleton/motility (∼18%), protein folding and stabilization (∼15%), brain development (∼11%), innate immune response (∼11%), redox regulation (∼9%), and energy metabolism (∼8%) as predominant categories (**Figure 3B**). These functional categories reflect the surveying action of microglia and their role in brain development and homeostasis. Other important, albeit less abundant, functional categories included cell-cell adhesion (∼6%), fundamental for EV interaction with target cells, and autophagy-lysosomal pathway (∼7%) which, together with phagocytosis/endocytosis (4%), may reflect constitutive degradative activity of microglia (**Figure 3B** and Supplementary Table III). Twenty pathways were identified in constitutive EVs using the KEGG analysis. Among them "Phagosome," "Protein processing in endoplasmic reticulum," "Complement and coagulation cascades," "Antigen processing and presentation," "Lysosome," which further highlight the degradative potential of microglial EVs as well as their role in antigen presentation and immune response (**Figure 4A**). Moreover, panther GO pathway classification revealed "Cytoskeleton regulation by Rho GTPase" and "Inflammation-mediated by chemokine and cytokine signaling pathway" among more abundant pathways, in line with immune surveillance functions of microglia (**Figure 4B** and Supplementary Table IV).

Among proteins of constitutive EVs not previously reported in ExoCarta and Vesiclepedia we found IL-18 receptor, a molecule formerly described in microglia (Prinz and Hanisch, 1999), and other microglia-enriched proteins: the degradative enzyme lysozyme C, the solute carrier family 23 (Sharma et al., 2015) and the WASL-interacting protein family member 1 (Wipf1), a protein that plays a role in the reorganization of the actin cytoskeleton (Supplementary Table V). Furthermore, we detected the centrosomal protein Cep162, the cytosolic

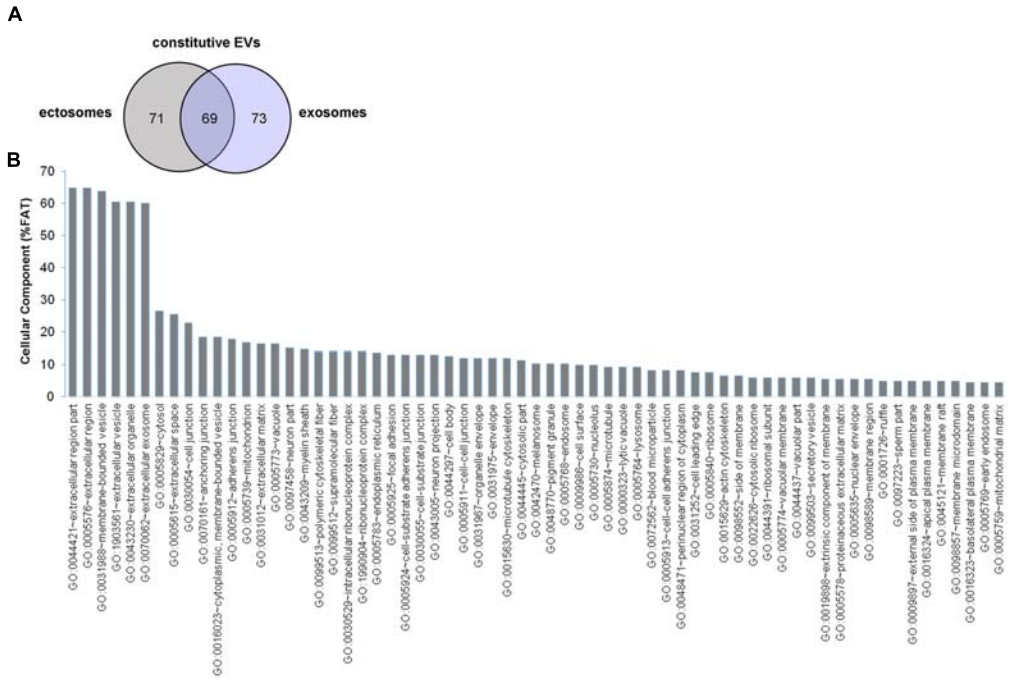

FIGURE 2 | Proteome of constitutive EVs released from microglia. **(A)** Venn diagram of the numerical values for common and unique proteins present in ectosomes (gray) and exosomes (violet). **(B)** Analysis of Cellular Component GO terms. The proteins detected in both ectosomes and exosomes-enriched fractions (total constitutive EV proteins) were grouped using GO terms related to cellular component analysis process using DAVID (Huang da et al., 2009). The graph shows the percentage of proteins identified by mass spectrometry that fall into designated GO category relative to the total number of proteins in the category. GO FAT was used to minimize the redundancy of general GO terms in the analysis. Categories with enrichment greater than 4% are shown.

enzyme G6PDX that participates in the pentose phosphate pathway and the reactive oxygen species-producing enzyme NADPH (nicotinamide adenine dinucleotide phosphate) oxidase 1, recently reported to mediate microglia-dependent synaptic dysfunction in experimental multiple sclerosis (Di Filippo et al., 2016), the Slingshot 3 phosphatase, a protein highly abundant in neurons but also present in microglia (Sharma et al., 2015), and the olfactory receptor Olr262, a G-coupled receptor, which is not expected to be functionally relevant in microglial cells (Supplementary Table V).

ATP Stimulation Modifies the Proteome of Microglia-Derived EVs

We next analyzed the proteome of EVs secreted by microglia upon ATP stimulation (ATP-EVs). 180 and 97 proteins were found in ectosomes and exosomes respectively, of which 48 proteins were common, confirming a significant overlap (∼40%) between the two vesicle populations (**Figure 5A** and Supplementary Table VI). Proteins uniquely identified in ectosomes or in exosomes released either constitutively or under ATP stimulation, are shown in **Table 1**. These proteins may represent ectosomal and exosomal markers for microglia-derived EVs.

No significant changes were detected in GO cellular component terms in ATP-EVs versus constitutive EVs (**Figure 5B**). However, we found substantial increases in GO biological process terms related to autophagy-lysosomal pathway (+129%), energy metabolism (+143%), cell adhesion (+100%) and phagocytosis and endocytosis (+100%), along with the appearance of new GO terms, including "Extracellular matrix" and "Apoptosis" (**Figure 5C** and Supplementary Table III). The fraction of proteins involved in redox regulation was reduced (−78%), while the fraction of proteins involved in response to compounds (∼31%), response to environmental changes (∼17%) and cytoskeleton/motility (∼19%) remained substantially unchanged (**Figure 5C** and Supplementary Table III). KEGG analysis confirmed the increase in degradative pathways ("Phagosome," "Lysosome") and cell adhesion pathways ("Gap-junction," "Focal adhesion" and "Adherens junction"). It also revealed an increase in "Antigen processing and presentation" and "Regulation of actin cytoskeleton" pathways with no significant changes in "Complement and coagulation cascades" pathway (**Figure 6A**). Importantly, KEGG analysis showed differences in energy metabolism, with the appearance of specific metabolic pathways, namely "Glycolysis/Gluconeogenesis," "Pyruvate metabolism," and "Arginine and proline metabolism" and increased fraction of proteins involved in "Pentose phosphate pathway" and "Carbon metabolism." Panther GO pathway classification confirmed major changes in metabolic pathways in ATP-EVs versus constitutive EVs, with a strong increase in "Glycolysis" and in "Pentose phosphate pathway" (+54% and +83% respectively) (**Figure 6B** and Supplementary Table IV), as well

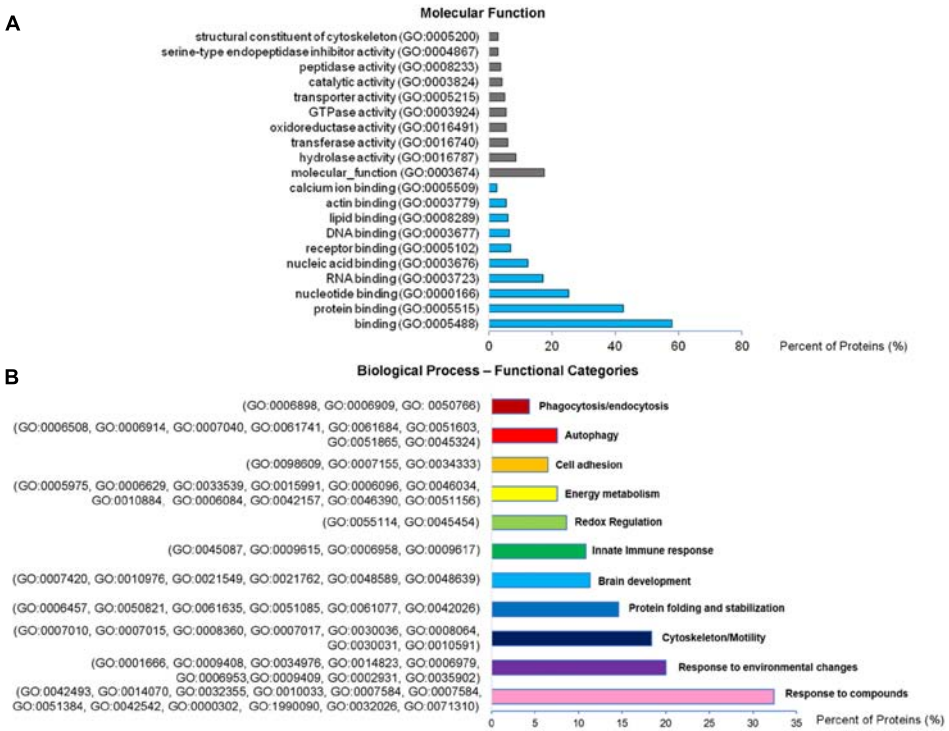

FIGURE 3 | Molecular function and Biological Process analysis of constitutive EVs. **(A)** Analysis of Molecular Function GO terms of total EV proteins. **(B)** Total EV proteins were grouped using (GO) terms related to Biological process analysis process using DAVID and shown in Supplementary Table III. Biological process GO terms falling into categories with similar/related function relevant in microglia were further clustered and shown in the column charts list.

as in "Cytoskeletal regulation by Rho GTPase" and "Integrin signaling pathway."

The complete list of proteins specifically associated to the ATP treatment (125 proteins), not present in constitutive EVs, are shown in Supplementary Table VII, of which 41 proteins are metabolic proteins.

ATP-EVs Have Stronger Impact on the Activation State of Recipient Astrocytes

Higher content of proteins involved in extracellular matrix organization and cell adhesion suggested that ATP-EVs might adhere stronger to target cells compared to constitutive EVs. In addition, more abundant representation of proteins involved in antigen presentation and in cellular metabolism suggested that ATP-EVs may have a greater influence on target cells. We addressed these hypotheses using rat primary astrocytes as recipient cells, which were previously shown by us to interact with microglia-derived EVs (Prada et al., 2016) and to be activated by ATP-EVs (Verderio et al., 2012).

We first quantified vesicle adhesion by delivering constitutive EVs or ATP-EVs to astrocytes by optical tweezers and monitoring EV-astrocyte contact by time-lapse microscopy (three independent experiments) (Prada et al., 2016). After addition to the cultures, EVs still suspended in the medium were trapped by the IR laser tweezers and kept in contact with astrocytes for 30 s. The trapping laser was then switched off to prove EV adhesion. We found that 42 ± 4.9% of ATP-EVs adhered to astrocytes ($n = 34$), while a significant smaller percentage (17 ± 5.5%) of constitutive EVs bound to the astrocyte surface ($n = 37$) (**Figure 7A**). Next we analyzed by q-PCR the expression of few activation markers in astrocytes exposed to constitutive EVs or ATP-EVs (ectosomes) derived from equal number of donor microglia for 48 h. A stronger upregulation of IL-1β, IL-6 and TNF-α was observed in astrocytes exposed to ATP-EVs compared to constitutive EVs, supporting a role for the proteins uniquely present in ATP-EVs in the response of recipient astrocytes (**Figure 7B**). Incubation of astrocytes with the same amount of ectosomes produced either constitutively or under ATP stimulation excluded that changes in ectosome production may account for the stronger response of astrocytes to ATP-EVs (Supplementary Figure 2).

We finally explored how ATP-EVs (ectosomes) modulate astrocyte activity. First, we pretreated ATP-EVs with Annexin-V to cloak PS residues on EV membrane and prevent EV-astrocyte contact (Prada et al., 2016). Untreated ATP-EVs were used as positive control. Cloaking PS abolished IL-6 and IL-10 induction in astrocytes, revealing that EV-astrocyte contact is necessary for astrocyte activation (**Figure 7C**). Second, ATP-EVs were broken by freeze and thaw and the surface components of EVs were separated from EV luminal cargo by ultracentrifugation, as previously defined (Antonucci et al., 2012). Broken EVs did not retain the capacity to activate astrocytes (**Figure 7C**). Finally, we extracted and sonicated lipids from ATP-EVs to

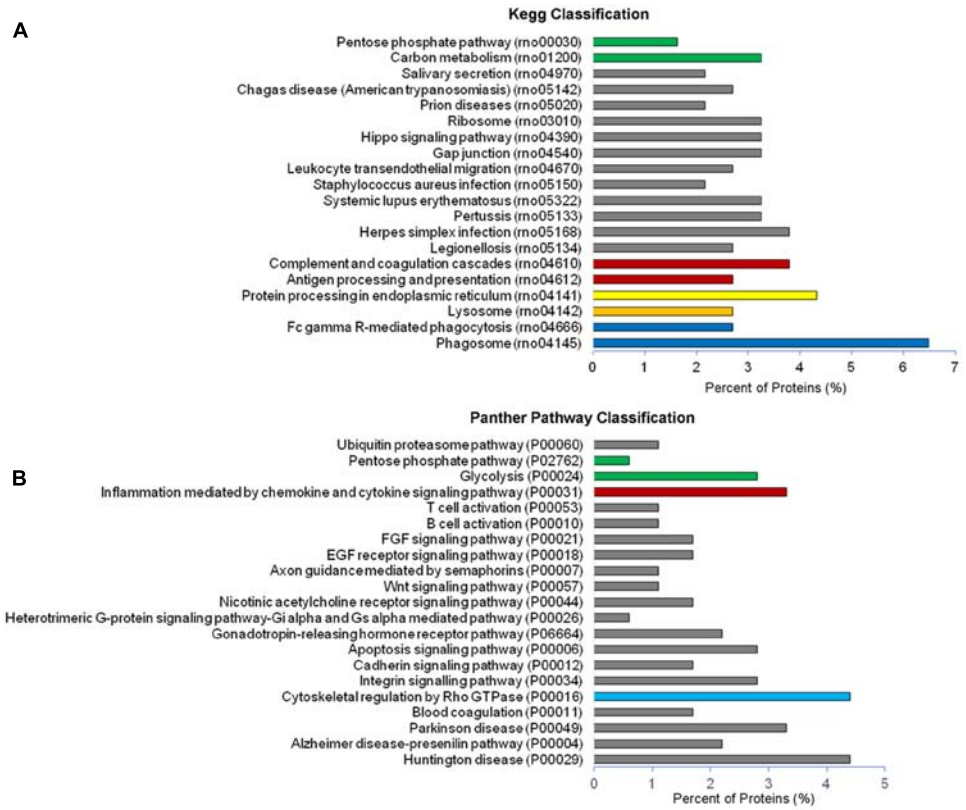

FIGURE 4 | Pathway analysis of constitutive EVs. **(A)** Histogram presentation of the KEGG pathway categories of total EVs. **(B)** Histogram presentation of panther GO term analysis of pathways.

obtain unilamellar lipid vesicles (Antonucci et al., 2012), which were delivered to astrocytes. We found that EV lipids did not induce significant alterations of astrocyte transcripts (**Figure 7C**). Collectively these findings revealed that the luminal cargo (proteins or RNA) of ATP-EVs is responsible for the astrocyte reaction.

DISCUSSION

We performed a comparative analysis of the protein composition of the two main populations of microglia-derived EVs, i.e., quite large ectosomes, shed from the plasma membrane, and smaller exosomes originating from the endosomal compartment (multivesicular bodies). Ectosomes were separated from exosomes using a classical differential ultracentrifugation protocol (Bianco et al., 2009; Gabrielli et al., 2015). As a source of EVs we used primary cultured microglia maintained *in vitro* in the absence of stimulus or exposed to ATP, a well-known molecule promoting microglia activation (Domercq et al., 2013) and increasing EV production (Bianco et al., 2005b) (Bianco et al., 2009). Of note, our microglial cultures express several ATP receptors including P2Y12, a key marker that distinguish microglia from peripheral monocytes and other immune cells (Butovsky et al., 2014). To avoid cell damage, we stimulated microglia with ATP for only 1h and isolated the EVs released into the extracellular medium during this time period. Due to the shortness of the protocol and the limited expansion of primary microglia, small vesicles batches could be generated, limiting detection of low abundant proteins and quantitative analysis of EV proteome. Despite these limitations, our proteomic analysis allowed the characterization of hundreds of proteins and provided new insights on the content of microglia-derived EVs and their potential to influence the response of recipient cells. Most importantly, it offered new clues on microglia response to ATP.

Ectosomes or Exosomes Contain Both Common and Unique Proteins

We found that exosomes and ectosomes, either constitutively released or under ATP stimulation, have a set of specific proteins but share a substantial fraction of proteins. This proteome overlap may derive, at least in part, from the isolation procedure used to collect EVs, which does not allow a precise separation of the vesicles. Accordingly, TRPS analysis showed that many ectosomes and exosomes have similar size, albeit peak sizes of the two vesicle fractions are distinct.

Among proteins present in ectosomes-enriched fraction we found 28 specific proteins of which Slingshot 3 phosphatase and ATP-dependent RNA helicase DDX25 were not described

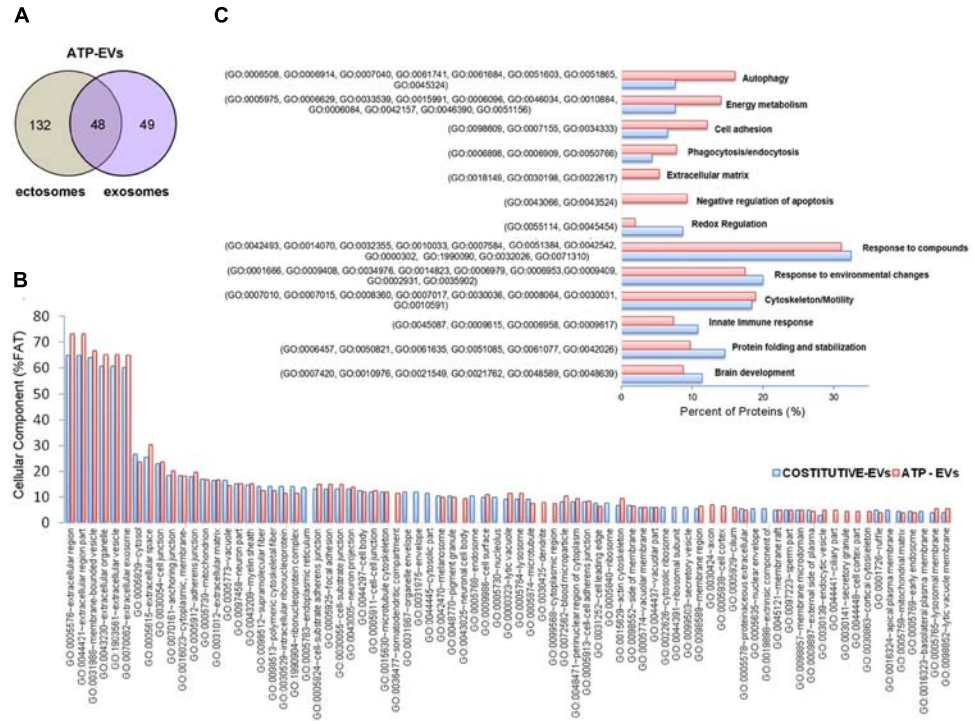

FIGURE 5 | Comparative analysis of the proteome of constitutive EVs and ATP-EVs. **(A)** Venn diagram of the numerical values for common and unique proteins present in ectosomes (gray) and exosomes (violet) produced by microglia upon ATP stimulation. **(B)** Analysis of Cellular Component GO terms of ATP-EV proteins (red) relative to constitutive EV proteins (blue) as in **Figure 2B**. The graphs show the percentage of proteins identified by mass spectrometry that fall into the designated category relative to the total number of protein in the category (% FAT). GO FAT was used to minimize the redundancy of general GO terms in the analysis. Categories with enrichment greater than 4% are shown. **(C)** Histograms representation of functional categories of ATP-EV proteins (red) relevant in microglia relative to constitutive EV proteins (blue) as in **Figure 3B**.

before in EVs (based on ExoCarta and Vesiclepedia). The two proteins may be used in future studies as selective markers of ectosomes released from microglia. With respect to exosome-specific proteins we found several C1q subunits.

Balanced Expression of Inflammatory and Protective Immune Proteins in Constitutive EVs

The proteome of constitutive EVs comprises many microglia-enriched or microglia-specific proteins, reflecting the proteome (and function) of parent cells (IL-18 receptor, Galectin-3, CD14, Lysozyme C, Ferritin, Hexosaminidase Subunit Beta, Wipfi, C1q). IL-18 receptor attenuates the release of pro-inflammatory cytokines (Prinz and Hanisch, 1999), while Galectin-3 sustains microglia activation in the brain, by acting as an endogenous ligand for TLR4 (Burguillos et al., 2015). CD14 acts as co-receptor for LPS. Lysozyme C plays a role in response against bacterial infection and Ferritin has antioxidative properties. Mutations of Hexosaminidase Subunit Beta (HexB) result in the neurodegenerative gangliosidosis Sandhoff disease (Hickman et al., 2013). Wipf1 plays a role in the reorganization of the actin cytoskeleton, which is crucial for the movement of microglial processes and phagocytosis. Finally, the complement factor C1q is released from microglia during brain development (Lui et al., 2016), localizes to inappropriate synapses and acts as a tag for synaptic pruning (Stevens et al., 2007; Stephan et al., 2012), although the mechanisms allowing synapses identification remain still unclear. The presence of C1q in constitutive exosomes suggests that they may serve as vehicles to deliver the complement factors to aberrant synapses. Selective delivery of C1q may be achieved through the interaction of exosomal and synaptic adhesion proteins. Galectin-3 (via integrins), AnnexinA2, Plectin, and Tyrosine 3-monooxygenase/tryptophan 5-monooxygenase activation protein zeta (Ywhaz) are among the exosomal proteins which might promote or stabilize contact between small vesicles and synapses. Importantly, EVs may have an intrinsic capacity to move to reach their synaptic target without the need for any moving fluid or passive transport, as previously suggested (Cvjetkovic et al., 2017), as they contain multiple proteins that regulate actin filament dynamics and reorganization (Cofilin-1, Coronin 1A, Tropomodulin 2, Plectin, Wipf1, Slingshot protein phosphatase 3).

Consistently with a possible role of microglial EVs in refinement of neuronal circuits, constitutive EVs also contain proteins involved in brain development (NSF attachment protein

TABLE 1 | Proteins uniquely identified in microglia-derived ectosomes or exosomes.

Markers for Microglia-derived EVs			
Ectosome-Markers		**Exosome-Markers**	
Entry ID	**Protein name**	**Entry ID**	**Protein name**
G3V6D3	ATP synthase subunit beta (Atp5b)	D3ZTH8	Uncharacterized protein (LOC689899)
G3V904	Phospholipase D family, member 4 (Pld4)	D4A6G6	Uncharacterized protein (LOC100362339)
M0R5A9	Uncharacterized protein (Dennd5b)	F1LIUW7	Myristoylated alanine-rich C-kinase substrate (Marcks)
M0RBJ7	Complement C3 (C3)	F7FEZ6/Q5I0M7	Heterogeneous nuclear ribonucleoprotein A1 (Hnrnpa2b1)
088797-2	Disabled homolog 2 (Dab2)	G3V7C6	Tubulin beta chain (Tubb4b)
P00564	Creatine kinase M-type (Ckm)	G3V7N9	Complement C1q subcomponent subunit B (C1qb)
P00787	Cathepsin B (Ctsb)	G3V8C3	Vimentin (Vim)
P04785	Protein disulfide-isomerase (P4hb)	P05370	Glucose-6-phosphate 1-dehydrogenase (G6pdx)
P10960	Prosaposin (Sulfated glycoprotein 1) (Psap)	P05982	NAD(P)H dehydrogenase 1 (Nqo1)
P11598	Protein disulfide-isomerase A3 (Pdia3)	P0CG51	Polyubiquitin-B (Ubb)
P12346	Serotransferrin (Tf)	P13471	40S ribosomal protein S14 (Rps14)
P17132/Q9JJ54	Heterogeneous nuclear ribonucleoprotein D0 (Hnrnpd)	P18588	Interferon-induced GTP-binding protein Mx1 (Mx1)
P24090	Alpha-2-HS-glycoprotein (Ahsg)	P31720	Complement C1q subcomponent subunit A (C1qa)
P62815	V-type proton ATPase subunit B, brain isoform (Atp6v1b2)	P31722	Complement C1q subcomponent subunit C (C1qc)
P68035	Actin, alpha cardiac muscle 1 (Actc1)	P45592	Cofilin-1 (Cfl1)
P70600-3	Protein-tyrosine kinase 2-beta (Ptk2b)	P62914	60S ribosomal protein L11 (Rpl11)
Q5FVQ0	Zinc transporter ZIP8 (Slc39a8)	P63039	60 kDa heat shock protein, mitochondrial (Hspd1)
Q5U1Y2	Ras-related C3 botulinum toxin substrate 2 (Rac2)	P85108	Tubulin beta-2A chain (Tubb2a)
Q5XIS1	Protein phosphatase Slingshot homolog 3 (Ssh3)	Q00715	Histone H2B type 1 (H2B1)
Q63081	Protein disulfide-isomerase A6 (Pdia6)	Q3MIE4	Synaptic vesicle membrane protein VAT-1 homolog (Vat1)
Q68FR6	Elongation factor 1-gamma (Eef1g)	Q4KLH6-2	Centrosomal protein of 162 kDa (Cep162)
Q6AXU4	E3 ubiquitin-protein ligase RNF181 (Rnf181)	Q5XI38	Lymphocyte cytosolic protein 1 (Lcp1)
Q6P0K8	Junction plakoglobin (Jup)	Q5XIN6	LETM1 and EF-hand domain-containing protein 1, mitochondrial (Letm1)
Q6P7C7	Transmembrane glycoprotein NMB (Gpnmb)	Q62667	Major vault protein (Mvp)
Q80ZA3	Alpha-2 antiplasmin (Serpinfl Dmrs91 rCG 34442)	Q63507	60S ribosomal protein L14 (Rpl14)
Q91ZN1	Coronin-1A (Coro1a)	Q6AYC4	Macrophage-capping protein (Capg)
Q9QY16-3	ATP-dependent RNA helicase DDX25 (Ddx25)	Q6AYZ1	Tubulin alpha-1C chain (Alpha-tubulin 6) (Tuba1c)
Q9R1T3	Cathepsin Z (Ctsz)	Q6URK4-2	Heterogeneous nuclear ribonucleoprotein A3 (Hnrnpa3)
		Q7TMC7	Ab2-417 (Cc1-8) (Tf)
		Q7TP54	Protein FAM65B (Fam65b)
		M0R5V7/Q6IE52	Murinoglobulin-2 (Mug2)

alpha, Dihydropyrimidinase-like 2 and Myristoylated alanine rich protein kinase C substrate), regulation of neuron projection (Serpin family F member 1), as well as lysosomal enzymes (Cathepsin Z, B and Phosphoinositide-3-kinase, regulatory subunit 4), which may mediate proteolysis and degradation of aberrant synapses. Further experiments are required to test this intriguing hypothesis, which goes beyond the aim of this study.

Exosome-associated C1q (and other immune proteins) may also play a key role in microglia-astrocyte signaling. Indeed C1q is one of the three essential microglial factors recently described to be responsible for the transformation of astrocytes from trophic to reactive cells (Liddelow et al., 2017). However, our q-PCR results show that constitutive EVs cause mild upregulation of inflammatory markers and also increase the expression of the pro-regenerative markers IL-10 and TGF-β in astrocytes, suggesting that the activity of the immune proteins may be balanced by protective molecules of EVs. Among them we have identified AnnexinA1, a potent anti-inflammatory agent, that downregulates the inflammatory response in experimental models of acute (Gastardelo et al., 2009; Girol et al., 2013), chronic (Oliani et al., 2008; Dalli et al., 2010), and systemic (Damazo et al., 2005) inflammation, and AnnexinA2, which facilitates release of anti-inflammatory cytokines and has a role in host defense against infection (Zhang et al., 2015). Both Annexins were recently detected in the secretome of pro-regenerative M2 macrophages, which promote resolution of inflammation (de Torre-Minguela et al., 2016) in association with PS externalization, a process linked to EV biogenesis (Turola et al., 2012). Together with our proteomic data, these previous findings suggest that Annexins exploit EVs to be released constitutively from immune cells and influence the biological activity of EVs.

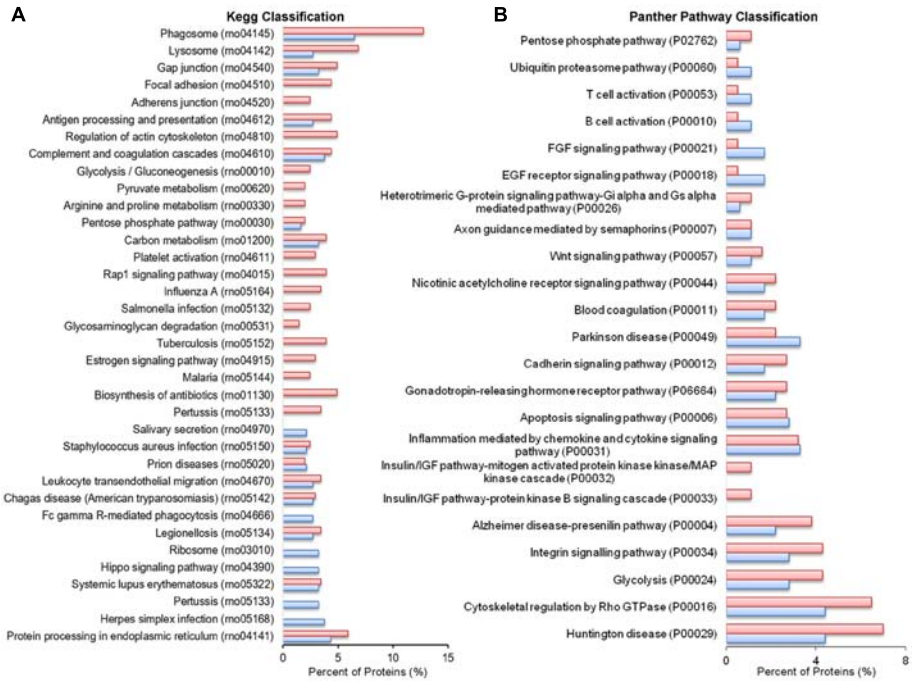

FIGURE 6 | Comparative pathway analysis of constitutive EVs and ATP-EVs. **(A)** Histogram presentation of the KEGG pathways in ATP-EVs (red) versus constitutive EVs (blue). **(B)** Histogram presentation of Panther GO term analysis of pathways in ATP–EVs (red) versus constitutive EVs (blue).

The Proteome of EVs Reflects Microglia Response to ATP

We provide evidence that the proteome of EVs released under ATP stimulation is largely distinct from that of constitutive vesicles.

We found a strong increase in the fraction of proteins associated to autophagy-lysosomal pathway. The Lysosomal-associated membrane protein 1 (Lamp1), Cathepsin D and C, Valosin-containing protein (Vcp) and CD68, a marker of microglial activation, were exclusively present in ATP-EVs. Increased content of degradative enzymes highlights the degradation potential of EVs released from ATP-stimulated microglia. It also reflects possible enhancement of degradative pathways in microglia to meet enhanced synaptic pruning in response to ATP. Importantly, several proteins uniquely detected in ATP-EVs may indeed facilitate C1q delivery to aberrant synapses via EVs and their consequent elimination. Proteins controlling extracellular matrix organization, such as Fibulin 1 (Fbln1), Cartilage oligomeric matrix protein (Comp), Plasminogen and the Matricellular proteins thrombospondin 1 and 4 may pave the way of ATP-EVs toward synapses, while Vinculin and Fermt3, proteins essential in the organization of focal adhesions, may enhance stabilization of the contact between ATP-EVs and synapses. The capping actin protein Capzb, Cap1 and ARP2 actin related protein might contribute to changes in EV morphology and motility (Prada et al., 2016; Cvjetkovic et al., 2017).

The largest difference between the proteome of ATP-EVs and constitutive EVs was related to proteins involved in cellular metabolism. More than 60% of ATP-EV metabolic proteins were not present in constitutive vesicles and "cell metabolism" was the most abundant pathway of ATP-EV specific proteins. They included several enzymes necessary for glycolysis (Glucose-6-phosphate isomerase -Gpi-), lactate production (Lactate dehydrogenase A -Ldha-, Malate dehydrogenase 2 -Mdh2-), the oxidative branch of the pentose phosphate pathway (Tranketolase), glutamine metabolism (Glutamate dehydrogenase 1) and fatty acid synthesis (Acetyl-CoA carboxylase beta -Acacb-). Collectively these changes may reflect an increase in microglia glycolysis and fatty acid synthesis, and in glutamine metabolism, which may serve to replenish levels of TCA cycle metabolites. Upregulation of mRNAs for the glycolytic enzyme PFKFB3, for glucose transporter SLC2A1 and for fatty acid enzyme Fasn in donor cells exposed to ATP is consistent with this possibility. This metabolic change may conserve/generate adequate pool of fatty acids for enabling membrane synthesis that is necessary to enhance routine ATP-dependent microglia behavior such as process scanning and phagocytic activity (Grabert et al., 2016). Metabolic enzymes (Enolase, Glyceraldehyde 3-phosphate dehydrogenase and Pyruvate kinase) were previously reported in exosomes constitutively released from N9 murine microglial cells (Potolicchio et al., 2005). However, their abundant expression likely reflected altered metabolism of the immortalized cell line.

Previous studies demonstrated that ectosome biogenesis evoked by ATP is calcium- and $P2X_7$ receptor- dependent (Bianco et al., 2005a; Pizzirani et al., 2007) and occurs from

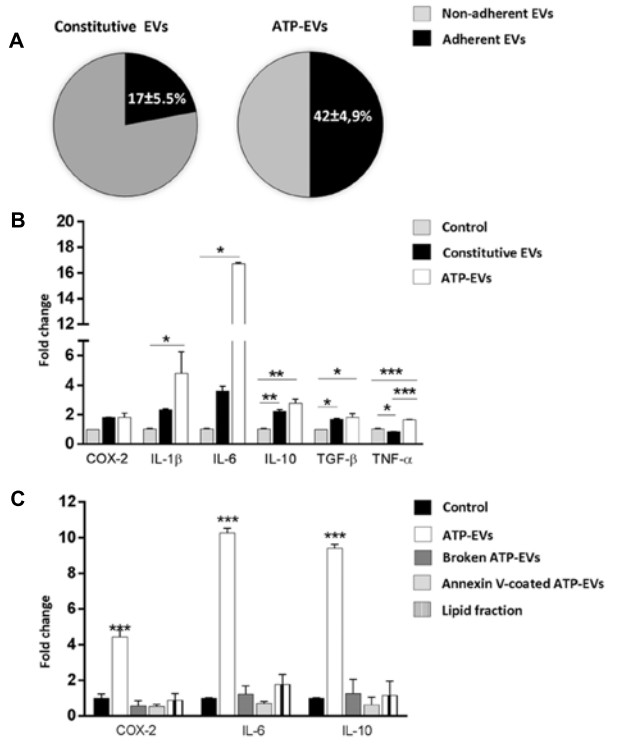

FIGURE 7 | ATP-EVs activate recipient astrocytes stronger. **(A)** Pie charts show the percentage of adhesion to astrocytes of constitutive EVs and ATP-EVs produced by microglia (Constitutive EVs versus ATP-EVs, unpaired *t*-test $P = 0.0278$; $N = 3$). **(B)** q-PCR for COX-2, IL-1β, IL-6, IL-10, TNF-α and TGF-β in astrocytes exposed to constitutive EVs or ATP-EVs for 48hr (COX2: Kruskal–Wallis One-way ANOVA $P = 0.071$; IL-1β: Kruskal–Wallis One-way ANOVA $P = 0.004$ followed by Dunn's multiple comparisons test; IL-6: Kruskal–Wallis One-way ANOVA $P = 0.004$, followed by Dunn's multiple comparisons test; IL-10: One-way ANOVA $P = 0.0014$ followed by Tukey's multiple comparisons test; TGF-β One-way ANOVA $P = 0{,}0143$ followed by Tukey's multiple comparisons test; TNF-α: One-way ANOVA $P = 0{,}0002$ followed by Tukey's multiple comparisons test; $N = 3$). **(C)** q-PCR for COX-2, IL-6, and IL-10 in control astrocytes, cells exposed for 48 h to intact ATP-EVs, broken ATP-EVs, ATP-EVs pre-incubated with annexin-V or EV lipids. (COX-2: One-way ANOVA $P < 0.0001$ Tukey's multiple comparisons test; IL-6: One-way ANOVA $P < 0.0001$ Tukey's multiple comparisons test; IL-10: One-way ANOVA $P < 0.0001$ Tukey's multiple comparisons test). Data are representative of three independent experiments.

specific plasma membrane domains, the lipid rafts, where $P2X_7$ receptor localizes (Bianco et al., 2009). Shedding typically involves a budding process, in which surface blebs selectively accumulate cellular constituents that are then packaged into MVs (Thomas and Salter, 2010). Following P2X7 receptor activation, cytoskeleton/membrane proteins interacting with the long cytoplasmic C-terminus of the receptor could be recruited and sorted into EVs, thus controlling the protein cargoes of ATP-EVs. Accordingly, we found that ATP-EVs contain cytoskeletal proteins and chaperones previously shown to interact with the P2X7 C-terminus (Kim et al., 2001; Gu et al., 2009). This sorting mechanism may be consistent with the proposed role of lipid rafts in setting up platforms to concentrate into MVs proteins destined to secretion (Del Conde et al., 2005).

Stronger Impact of ATP-EVs on Receiving Astrocytes

Here we show that EVs secreted from microglia under ATP stimulation have higher impact on the activation state of recipient astrocytes, compared to constitutive EVs, and that proteins (and/or RNAs) differentially sorted into the vesicle lumen under ATP stimulation rather than surface components account for the astrocyte reaction. However, how cargoes of ATP-EVs mediate astrocyte response and whether EV internalization is necessary for astrocyte activation still remains unknown. Importantly, ATP-EVs upregulate in astrocytes both the anti-inflammatory cytokine IL-10 and the pro-inflammatory cytokine IL-6, ruling out the acquisition of a detrimental phenotype.

Augmented sorting of metabolic enzymes in ATP-EVs opens the possibility that EVs may function as independent metabolic units (Iraci et al., 2017) and have the potential to increase sugar based energy outside mitochondria in recipient cells. In astrocytes glycolysis is stimulated by increased extracellular K+ (Bittner et al., 2011), following neuronal activity, and permits release of pyruvate or lactate to support axonal function. Thus, we can speculate that ATP-EVs, through astrocyte activation, may be beneficial to neurons and favor neuronal firing. However, further studies are necessary to verify the impact of ATP-EVs on astrocyte metabolism and to define the contribution of ATP-EV proteome in the metabolic changes, which are out of the scope of this study.

The presence in ATP-EVs of proteins promoting neurite outgrowth and synaptogenesis, i.e., Trombospondin 1 and 4 (Arber and Caroni, 1995; Eroglu et al., 2009) together with proteins which negatively regulate neuron apoptosis, suggest that microglia-derived EVs may also have direct protective action toward neurons. This is in agreement with previous evidence showing that exosomes produced by other glial cells, i.e., oligodendrocytes, enhance neuronal stress tolerance and promote neuronal survival (Fruhbeis et al., 2013; Frohlich et al., 2014).

ETHICS STATEMENT

All the experimental procedures followed the guidelines established by the European Legislation (Directive 2010/63/EU) and the Italian Legislation (L.D. no. 26/2014). It was also approved by the Italian Ministry of Health and the Bioethical Committee of the University of Milan.

AUTHOR CONTRIBUTIONS

FD performed LC-MS and data analysis, ML analyzed proteomic data and performed q-PCR analysis and optical tweezers experiments, IP isolated EV samples and contributed to the

study design, MG performed EV quantification by qNano. PJ established mixed glial cell cultures and primary microglia cultures and helped with EV isolation. DC supervised optical tweezer experiments. JF to proteomic analysis. IF supervised proteomic analysis. JV contributed to the study design and revised the text. CV supervised the whole work and wrote the manuscript. All authors revised and approved the final version of the manuscript.

FUNDING

This study was supported by FISM (grant 2016/R/30 to CV), by the ERA-NET NEURON JTC 2014 (Micromet project to CV), by GMSI 2015 (to CV), by ANR FUNMALDI (IF), by Région Nord-Pas de Calais ARCIR (IF), by SIRIC ONCOLille (IF), by Grant INCa-DGOS-Inserm 6041aa (IF), by the Ministère de l'Education Nationale, de l'Enseignement Supérieur et de la Recherche (JF, IF, JV) and by the Université de Lille (FD). MG was supported by a FISM Fellowship (2016/B/2) and FD by ANR Mimic Fellowship.

ACKNOWLEDGMENTS

The authors are grateful to E. Turola (University of Modena and Reggio Emilia), M. Baes (University of Leuven) and P. Giussani (University of Milan) for helpful discussion.

SUPPLEMENTARY MATERIAL

The Supplementary Material for this article can be found online at: https://www.frontiersin.org/articles/10.3389/fphar.2017.00910/full#supplementary-material

REFERENCES

Adinolfi, E., Pizzirani, C., Idzko, M., Panther, E., Norgauer, J., Di Virgilio, F., et al. (2005). P2X(7) receptor: death or life? *Purinergic Signal.* 1, 219–227. doi: 10.1007/s11302-005-6322-x

Antonucci, F., Turola, E., Riganti, L., Caleo, M., Gabrielli, M., Perrotta, C., et al. (2012). Microvesicles released from microglia stimulate synaptic activity via enhanced sphingolipid metabolism. *EMBO J.* 31, 1231–1240. doi: 10.1038/emboj.2011.489

Arber, S., and Caroni, P. (1995). Thrombospondin-4, an extracellular matrix protein expressed in the developing and adult nervous system promotes neurite outgrowth. *J. Cell Biol.* 131, 1083–1094. doi: 10.1083/jcb.131.4.1083

Barenholz, Y., Gibbes, D., Litman, B. J., Goll, J., Thompson, T. E., and Carlson, R. D. (1977). A simple method for the preparation of homogeneous phospholipid vesicles. *Biochemistry* 16, 2806–2810. doi: 10.1021/bi00631a035

Bianco, F., Fumagalli, M., Pravettoni, E., D'ambrosi, N., Volonte, C., Matteoli, M., et al. (2005a). Pathophysiological roles of extracellular nucleotides in glial cells: differential expression of purinergic receptors in resting and activated microglia. *Brain Res. Brain Res. Rev.* 48, 144–156. doi: 10.1016/j.brainresrev.2004.12.004

Bianco, F., Pravettoni, E., Colombo, A., Schenk, U., Moller, T., Matteoli, M., et al. (2005b). Astrocyte-derived ATP induces vesicle shedding and IL-1 beta release from microglia. *J. Immunol.* 174, 7268–7277.

Bianco, F., Perrotta, C., Novellino, L., Francolini, M., Riganti, L., Menna, E., et al. (2009). Acid sphingomyelinase activity triggers microparticle release from glial cells. *EMBO J.* 28, 1043–1054. doi: 10.1038/emboj.2009.45

Bittner, C. X., Valdebenito, R., Ruminot, I., Loaiza, A., Larenas, V., Sotelo-Hitschfeld, T., et al. (2011). Fast and reversible stimulation of astrocytic glycolysis by K+ and a delayed and persistent effect of glutamate. *J. Neurosci.* 31, 4709–4713. doi: 10.1523/JNEUROSCI.5311-10.2011

Burguillos, M. A., Svensson, M., Schulte, T., Boza-Serrano, A., Garcia-Quintanilla, A., Kavanagh, E., et al. (2015). Microglia-secreted galectin-3 acts as a toll-like receptor 4 ligand and contributes to microglial activation. *Cell Rep.* doi: 10.1016/j.celrep.2015.02.012 [Epub ahead of print],

Butovsky, O., Jedrychowski, M. P., Moore, C. S., Cialic, R., Lanser, A. J., Gabriely, G., et al. (2014). Identification of a unique TGF-beta-dependent molecular and functional signature in microglia. *Nat. Neurosci.* 17, 131–143. doi: 10.1038/nn.3599

Buttgereit, A., Lelios, I., Yu, X., Vrohlings, M., Krakoski, N. R., Gautier, E. L., et al. (2016). Sall1 is a transcriptional regulator defining microglia identity and function. *Nat. Immunol.* 17, 1397–1406. doi: 10.1038/ni.3585

Casano, A. M., Albert, M., and Peri, F. (2016). Developmental apoptosis mediates entry and positioning of microglia in the zebrafish brain. *Cell Rep.* 16, 897–906. doi: 10.1016/j.celrep.2016.06.033

Casano, A. M., and Peri, F. (2015). Microglia: multitasking specialists of the brain. *Dev. Cell* 32, 469–477. doi: 10.1016/j.devcel.2015.01.018

Cocucci, E., and Meldolesi, J. (2015). Ectosomes and exosomes: shedding the confusion between extracellular vesicles. *Trends Cell Biol.* 25, 364–372. doi: 10.1016/j.tcb.2015.01.004

Corriden, R., and Insel, P. A. (2012). New insights regarding the regulation of chemotaxis by nucleotides, adenosine, and their receptors. *Purinergic Signal.* 8, 587–598. doi: 10.1007/s11302-012-9311-x

Cvjetkovic, S. J., Jeremic, V. L., and Tiosavljevic, D. V. (2017). Knowledge and attitudes toward vaccination: a survey of Serbian students. *J. Infect. Public Health* 10, 649–656. doi: 10.1016/j.jiph.2017.05.008

Dalli, J., Rosignoli, G., Hayhoe, R. P., Edelman, A., and Perretti, M. (2010). CFTR inhibition provokes an inflammatory response associated with an imbalance of the annexin A1 pathway. *Am. J. Pathol.* 177, 176–186. doi: 10.2353/ajpath.2010.091149

Damazo, A. S., Yona, S., D'acquisto, F., Flower, R. J., Oliani, S. M., and Perretti, M. (2005). Critical protective role for annexin 1 gene expression in the endotoxemic murine microcirculation. *Am. J. Pathol.* 166, 1607–1617. doi: 10.1016/S0002-9440(10)62471-6

Davalos, D., Grutzendler, J., Yang, G., Kim, J. V., Zuo, Y., Jung, S., et al. (2005). ATP mediates rapid microglial response to local brain injury in vivo. *Nat. Neurosci.* 8, 752–758. doi: 10.1038/nn1472

de Torre-Minguela, C., Barbera-Cremades, M., Gomez, A. I., Martin-Sanchez, F., and Pelegrin, P. (2016). Macrophage activation and polarization modify P2X7 receptor secretome influencing the inflammatory process. *Sci. Rep.* 6:22586. doi: 10.1038/srep22586

Del Conde, I., Shrimpton, C. N., Thiagarajan, P., and Lopez, J. A. (2005). Tissue-factor-bearing microvesicles arise from lipid rafts and fuse with activated platelets to initiate coagulation. *Blood* 106, 1604–1611. doi: 10.1182/blood-2004-03-1095

Di Filippo, M., De Iure, A., Giampa, C., Chiasserini, D., Tozzi, A., Orvietani, P. L., et al. (2016). Persistent activation of microglia and NADPH oxidase [corrected] drive hippocampal dysfunction in experimental multiple sclerosis. *Sci. Rep.* 6:20926. doi: 10.1038/srep20926

Di Virgilio, F. (2007). Purinergic signalling in the immune system. A brief update. *Purinergic Signal.* 3, 1–3. doi: 10.1007/s11302-006-9048-5

Domercq, M., Vazquez-Villoldo, N., and Matute, C. (2013). Neurotransmitter signaling in the pathophysiology of microglia. *Front. Cell Neurosci.* 7:49. doi: 10.3389/fncel.2013.00049

Dou, Y., Wu, H. J., Li, H. Q., Qin, S., Wang, Y. E., Li, J., et al. (2012). Microglial migration mediated by ATP-induced ATP release from lysosomes. *Cell Res.* 22, 1022–1033. doi: 10.1038/cr.2012.10

Eroglu, C., Allen, N. J., Susman, M. W., O'rourke, N. A., Park, C. Y., Ozkan, E., et al. (2009). Gabapentin receptor alpha2delta-1 is a neuronal thrombospondin receptor responsible for excitatory CNS synaptogenesis. *Cell* 139, 380–392. doi: 10.1016/j.cell.2009.09.025

Farber, K., and Kettenmann, H. (2006). Purinergic signaling and microglia. *Pflugers. Arch.* 452, 615–621. doi: 10.1007/s11302-006-9048-5

Frohlich, D., Kuo, W. P., Fruhbeis, C., Sun, J. J., Zehendner, C. M., Luhmann, H. J., et al. (2014). Multifaceted effects of oligodendroglial exosomes on neurons: impact on neuronal firing rate, signal transduction and gene regulation. *Philos. Trans. R. Soc. Lond. B Biol. Sci.* 369:20130510. doi: 10.1098/rstb.2013.0510

Fruhbeis, C., Frohlich, D., Kuo, W. P., Amphornrat, J., Thilemann, S., Saab, A. S., et al. (2013). Neurotransmitter-triggered transfer of exosomes mediates oligodendrocyte-neuron communication. *PLOS Biol.* 11:e1001604. doi: 10.1371/journal.pbio.1001604

Gabrielli, M., Battista, N., Riganti, L., Prada, I., Antonucci, F., Cantone, L., et al. (2015). Active endocannabinoids are secreted on extracellular membrane vesicles. *EMBO Rep.* 16, 213–220. doi: 10.15252/embr.201439668

Gastardelo, T. S., Damazo, A. S., Dalli, J., Flower, R. J., Perretti, M., and Oliani, S. M. (2009). Functional and ultrastructural analysis of annexin A1 and its receptor in extravasating neutrophils during acute inflammation. *Am. J. Pathol.* 174, 177–183. doi: 10.2353/ajpath.2009.080342

Ginhoux, F., Greter, M., Leboeuf, M., Nandi, S., See, P., Gokhan, S., et al. (2010). Fate mapping analysis reveals that adult microglia derive from primitive macrophages. *Science* 330, 841–845. doi: 10.1126/science.1194637

Girol, A. P., Mimura, K. K., Drewes, C. C., Bolonheis, S. M., Solito, E., Farsky, S. H., et al. (2013). Anti-inflammatory mechanisms of the annexin A1 protein and its mimetic peptide Ac2-26 in models of ocular inflammation in vivo and in vitro. *J. Immunol.* 190, 5689–5701. doi: 10.4049/jimmunol.1202030

Grabert, K., Michoel, T., Karavolos, M. H., Clohisey, S., Baillie, J. K., Stevens, M. P., et al. (2016). Microglial brain region-dependent diversity and selective regional sensitivities to aging. *Nat. Neurosci.* 19, 504–516. doi: 10.1038/nn.4222

Gu, B. J., Rathsam, C., Stokes, L., Mcgeachie, A. B., and Wiley, J. S. (2009). Extracellular ATP dissociates nonmuscle myosin from P2X(7) complex: this dissociation regulates P2X(7) pore formation. *Am. J. Physiol. Cell Physiol.* 297, C430–C439. doi: 10.1152/ajpcell.00079.2009

Hickman, S. E., Kingery, N. D., Ohsumi, T. K., Borowsky, M. L., Wang, L. C., Means, T. K., et al. (2013). The microglial sensome revealed by direct RNA sequencing. *Nat. Neurosci.* 16, 1896–1905. doi: 10.1038/nn.3554

Honda, S., Sasaki, Y., Ohsawa, K., Imai, Y., Nakamura, Y., Inoue, K., et al. (2001). Extracellular ATP or ADP induce chemotaxis of cultured microglia through Gi/o-coupled P2Y receptors. *J. Neurosci.* 21, 1975–1982.

Hooper, C., Sainz-Fuertes, R., Lynham, S., Hye, A., Killick, R., Warley, A., et al. (2012). Wnt3a induces exosome secretion from primary cultured rat microglia. *BMC Neurosci.* 13:144. doi: 10.1186/1471-2202-13-144

Huang da, W., Sherman, B. T., and Lempicki, R. A. (2009). Systematic and integrative analysis of large gene lists using DAVID bioinformatics resources. *Nat. Protoc.* 4, 44–57. doi: 10.1038/nprot.2008.211

Iraci, N., Gaude, E., Leonardi, T., Costa, A. S. H., Cossetti, C., Peruzzotti-Jametti, L., et al. (2017). Extracellular vesicles are independent metabolic units with asparaginase activity. *Nat. Chem. Biol.* 13, 951–955. doi: 10.1038/nchembio.2422

Kim, M., Jiang, L. H., Wilson, H. L., North, R. A., and Surprenant, A. (2001). Proteomic and functional evidence for a P2X7 receptor signalling complex. *EMBO J.* 20, 6347–6358. doi: 10.1093/emboj/20.22.6347

Liddelow, S. A., Guttenplan, K. A., Clarke, L. E., Bennett, F. C., Bohlen, C. J., Schirmer, L., et al. (2017). Neurotoxic reactive astrocytes are induced by activated microglia. *Nature* 541, 481–487. doi: 10.1038/nature21029

Lui, H., Zhang, J., Makinson, S. R., Cahill, M. K., Kelley, K. W., Huang, H. Y., et al. (2016). Progranulin deficiency promotes circuit-specific synaptic pruning by microglia via complement activation. *Cell* 165, 921–935. doi: 10.1016/j.cell.2016.04.001

Matcovitch-Natan, O., Winter, D. R., Giladi, A., Vargas Aguilar, S., Spinrad, A., Sarrazin, S., et al. (2016). Microglia development follows a stepwise program to regulate brain homeostasis. *Science* 353:aad8670. doi: 10.1126/science.aad8670

Nimmerjahn, A., Kirchhoff, F., and Helmchen, F. (2005). Resting microglial cells are highly dynamic surveillants of brain parenchyma in vivo. *Science* 308, 1314–1318. doi: 10.1126/science.1110647

Ohsawa, K., Irino, Y., Sanagi, T., Nakamura, Y., Suzuki, E., Inoue, K., et al. (2010). P2Y12 receptor-mediated integrin-beta1 activation regulates microglial process extension induced by ATP. *Glia* 58, 790–801. doi: 10.1002/glia.20963

Oliani, S. M., Ciocca, G. A., Pimentel, T. A., Damazo, A. S., Gibbs, L., and Perretti, M. (2008). Fluctuation of annexin-A1 positive mast cells in chronic granulomatous inflammation. *Inflamm. Res.* 57, 450–456. doi: 10.1007/s00011-008-7222-7

Paolicelli, R. C., Bolasco, G., Pagani, F., Maggi, L., Scianni, M., Panzanelli, P., et al. (2011). Synaptic pruning by microglia is necessary for normal brain development. *Science* 333, 1456–1458. doi: 10.1126/science.1202529

Pizzirani, C., Ferrari, D., Chiozzi, P., Adinolfi, E., Sandona, D., Savaglio, E., et al. (2007). Stimulation of P2 receptors causes release of IL-1beta-loaded microvesicles from human dendritic cells. *Blood* 109, 3856–3864. doi: 10.1182/blood-2005-06-031377

Pocock, J. M., and Kettenmann, H. (2007). Neurotransmitter receptors on microglia. *Trends Neurosci.* 30, 527–535. doi: 10.1016/j.tins.2007.07.007

Potolicchio, I., Chitta, S., Xu, X., Fonseca, D., Crisi, G., Horejsi, V., et al. (2005). Conformational variation of surface class II MHC proteins during myeloid dendritic cell differentiation accompanies structural changes in lysosomal MIIC. *J. Immunol.* 175, 4935–4947. doi: 10.4049/jimmunol.175.8.4935

Prada, I., Amin, L., Furlan, R., Legname, G., Verderio, C., and Cojoc, D. (2016). A new approach to follow a single extracellular vesicle-cell interaction using optical tweezers. *Biotechniques* 60, 35–41. doi: 10.2144/000114371

Prada, I., Furlan, R., Matteoli, M., and Verderio, C. (2013). Classical and unconventional pathways of vesicular release in microglia. *Glia* 61, 1003–1017. doi: 10.1002/glia.22497

Preissler, J., Grosche, A., Lede, V., Le Duc, D., Krugel, K., Matyash, V., et al. (2015). Altered microglial phagocytosis in GPR34-deficient mice. *Glia* 63, 206–215. doi: 10.1002/glia.22744

Prinz, M., and Hanisch, U. K. (1999). Murine microglial cells produce and respond to interleukin-18. *J. Neurochem.* 72, 2215–2218. doi: 10.1046/j.1471-4159.1999.0722215.x

Sharma, K., Schmitt, S., Bergner, C. G., Tyanova, S., Kannaiyan, N., Manrique-Hoyos, N., et al. (2015). Cell type- and brain region-resolved mouse brain proteome. *Nat. Neurosci.* 18, 1819–1831. doi: 10.1038/nn.4160

Sieger, D., Moritz, C., Ziegenhals, T., Prykhozhij, S., and Peri, F. (2012). Long-range Ca2+ waves transmit brain-damage signals to microglia. *Dev. Cell* 22, 1138–1148. doi: 10.1016/j.devcel.2012.04.012

Stephan, A. H., Barres, B. A., and Stevens, B. (2012). The complement system: an unexpected role in synaptic pruning during development and disease. *Annu. Rev. Neurosci.* 35, 369–389. doi: 10.1146/annurev-neuro-061010-113810

Stevens, B., Allen, N. J., Vazquez, L. E., Howell, G. R., Christopherson, K. S., Nouri, N., et al. (2007). The classical complement cascade mediates CNS synapse elimination. *Cell* 131, 1164–1178. doi: 10.1016/j.cell.2007.10.036

Thomas, L. M., and Salter, R. D. (2010). Activation of macrophages by P2X7-induced microvesicles from myeloid cells is mediated by phospholipids and is partially dependent on TLR4. *J. Immunol.* 185, 3740–3749. doi: 10.4049/jimmunol.1001231

Turola, E., Furlan, R., Bianco, F., Matteoli, M., and Verderio, C. (2012). Microglial microvesicle secretion and intercellular signaling. *Front. Physiol.* 3:149. doi: 10.3389/fphys.2012.00149

Verderio, C., Muzio, L., Turola, E., Bergami, A., Novellino, L., Ruffini, F., et al. (2012). Myeloid microvesicles are a marker and therapeutic target for neuroinflammation. *Ann. Neurol.* 72, 610–624. doi: 10.1002/ana.23627

Zhang, S., Yu, M., Guo, Q., Li, R., Li, G., Tan, S., et al. (2015). Annexin A2 binds to endosomes and negatively regulates TLR4-triggered inflammatory responses via the TRAM-TRIF pathway. *Sci. Rep.* 5:15859. doi: 10.1038/srep15859

Conflict of Interest Statement: The authors declare that the research was conducted in the absence of any commercial or financial relationships that could be construed as a potential conflict of interest.

frontiers in Pharmacology

REVIEW
published: 12 December 2017
doi: 10.3389/fphar.2017.00913

Purines and Carotid Body: New Roles in Pathological Conditions

Silvia V. Conde, Emilia C. Monteiro and Joana F. Sacramento*

Centro de Estudos de Doenças Crónicas, NOVA Medical School – Faculdade de Ciências Médicas, Universidade NOVA de Lisboa, Lisboa, Portugal

It is known that adenosine and adenosine-5′-triphosphate (ATP) are excitatory mediators involved in carotid body (CB) hypoxic signaling. The CBs are peripheral chemoreceptors classically defined by O_2, CO_2, and pH sensors. When hypoxia activates the CB, it induces the release of neurotransmitters from chemoreceptor cells leading to an increase in the action potentials frequency at the carotid sinus nerve (CSN). This increase in the firing frequency of the CSN is integrated in the brainstem to induce cardiorespiratory compensatory responses. In the last decade several pathologies, as, hypertension, diabetes, obstructive sleep apnea and heart failure have been associated with CB overactivation. In the first section of the present manuscript we review in a concise manner fundamental aspects of purine metabolism. The second section is devoted to the role of purines on the hypoxic response of the CB, providing the state-of-the art for the presence of adenosine and ATP receptors in the CB; for the role of purines at presynaptic level in CB chemoreceptor cells, as well as, its metabolism and regulation; at postsynaptic level in the CSN activity; and on the ventilatory responses to hypoxia. Recently, we have showed that adenosine is involved in CB hypersensitization during chronic intermittent hypoxia (CIH), which mimics obstructive sleep apnea, since caffeine, a non-selective adenosine receptor antagonist that inhibits A_{2A} and A_{2B} adenosine receptors, decreased CSN chemosensory activity in animals subjected to CIH. Apart from this involvement of adenosine in CB sensitization in sleep apnea, it was recently found that P2X3 ATP receptor in the CB contributes to increased chemoreflex hypersensitivity and hypertension in spontaneously hypertension rats. Therefore the last section of this manuscript is devoted to review the recent findings on the role of purines in CB-mediated pathologies as hypertension, diabetes and sleep apnea emphasizing the potential clinical importance of modulating purines levels and action to treat pathologies associated with CB dysfunction.

Keywords: carotid body, adenosine, ATP, hypertension, chronic intermittent hypoxia, type 2 diabetes

OPEN ACCESS

Edited by:
Kenneth A. Jacobson, National Institutes of Health (NIH), United States

Reviewed by:
Eric Boué-Grabot, UMR5293 Institut des Maladies Neurodégénératives (IMN), France
Ana Paula Abdala, University of Bristol, United Kingdom

****Correspondence:***
Silvia V. Conde
silvia.conde@nms.unl.pt

Specialty section:
This article was submitted to Experimental Pharmacology and Drug Discovery, a section of the journal Frontiers in Pharmacology

Received: *17 October 2017*
Accepted: *29 November 2017*
Published: *12 December 2017*

Citation:
Conde SV, Monteiro EC and Sacramento JF (2017) Purines and Carotid Body: New Roles in Pathological Conditions. Front. Pharmacol. 8:913. doi: 10.3389/fphar.2017.00913

PURINES METABOLISM

From all purines, adenosine and adenosine-5′-triphosphate (ATP) are the only ones that are known to have a role in cell to cell communication and therefore they act extracellularly to mediate several biological effects via cell-surface receptors, the purine receptors. ATP has a fundamental intracellular role as universal source of energy for all living cells. The demonstration of its release into the extracellular space and the identification and localisation of specific receptors on target cells have been essential in establishing its extracellular physiological role. In the beginning of

the seventies, the purinergic neurotransmission was first proposed by Burnstock (1972). ATP was shown to be released from non-adrenergic, non-cholinergic nerves to signaling inhibitory enteric nerves in the guinea pig taenia coli and excitatory parasympathetic nerves in the urinary bladder (Burnstock et al., 1970, 1972). However, the concept of purinergic neurotransmission was only established in the nineties, when receptors for adenosine and ATP were cloned and sequenced (for a review see Ralevic and Burnstock, 1998). Short-term purinergic signaling was first described when ATP was identified as a cotransmitter with noradrenalin, acetylcholine and with substance P and calcitonin gene-related peptide (for a review see Burnstock, 2016) in the peripheral nervous system. Later ATP was shown to be a cotransmitter in neurons in the central nervous system (CNS), being co-released with GABA (Jo and Schlichter, 1999; Jo and Role, 2002) and Glutamate (Pankratov et al., 1999). Adenosine is a product of ATP catabolism, which can be used to resynthesize ATP itself. This mediator is an ubiquitous substance that is not stored or released as a classical neurotransmitter, being released by almost all cell types through nucleoside transporters (Fredholm et al., 2001). Intracellularly it has key roles in pathways as purinergic nucleic acid base synthesis, amino acid metabolism and modulation of cellular metabolic status (Conde et al., 2009). Extracellularly, adenosine modulates the activity of several systems at presynaptic level (inhibiting or facilitating neurotransmitters release), at postsynaptic or at non-synaptic level (e.g., modulating blood flow or the metabolism of sustentacular cells).

Metabolic Pathways of Adenosine Formation and Release

Adenosine is mostly formed by the catabolism of 5′adenosine phosphates (ATP, adenosine diphosphate – ADP and adenosine monophosphate – AMP). Intracellular adenosine production is mediated by an intracellular 5′-nucleotidase that dephosphorylates AMP (Schubert et al., 1979; Zimmermann et al., 1998) or by the hydrolysis of *S*-adenosylhomocysteine by *S*-adenosylhomocysteine hydrolase (Broch and Ueland, 1980) (**Figure 1**). Extracellular adenosine comes from ATP hydrolysis via 5′ectonucleotidases (Fredholm et al., 2001; Yegutkin, 2008) and by its intracellular production and release by nucleoside transport system (for a review see Conde et al., 2009). Another source of adenosine that is present extracellularly is cyclic AMP (cAMP) that can be released by secretory cells and converted by extracellular ectophosphodiesterases in AMP and then into adenosine by 5′-ectonucleotidases (Fredholm et al., 2001).

In contrast with other neurotransmitters, adenosine is not stored in synaptic vesicles or acts exclusively on synapses. Its release and uptake occurs through nucleoside transporters, which are constituted by two families: a Na^+ independent family and another one dependent of the same ion (Griffith and Jarvis, 1996). The Na^+ dependent-nucleoside transport system is concentrative, carrying nucleosides against a concentration gradient. The Na^+ independent-nucleoside transport system (equilibrative nucleoside transport system, ENT) is bi-directional and is formed by two different families (*es* and *ei*), classified based on their sensitivity to nitrobenzylthioinosine (NBTI). The *es* transport is inhibited by low nanomolar concentrations of NBTI, while *ei* transport requires micromolar concentrations to be inhibited (Griffith and Jarvis, 1996; Cass et al., 1998; Podgorska et al., 2005).

The major pathways of adenosine removal or degradation involve reactions catalyzed by two enzymes: adenosine kinase (AK) and adenosine deaminase (ADA) (Fredholm et al., 1999), which leads to the formation of inosine and AMP, respectively (Conde et al., 2009). ADA is mostly found in the intracellular space, however, it is also found in some extracellular compartments. This enzyme has relevance when adenosine concentrations are high (Arch and Newsholme, 1978) and alterations in its activity have been associated with several pathologies, such as *miastenia* gravis and diabetes mellitus (Hoshino et al., 1994; Oliveira et al., 2015).

Adenosine Receptors

Adenosine exerts is action through four different type of adenosine receptors coupled to G proteins A_1, A_{2A}, A_{2B}, and A_3 (Conde et al., 2009). These receptors are activated by different endogenous adenosine concentrations being the affinity for adenosine: $A_1 > A_{2A} > A_{2B} > A_3$. The adenosine that is available endogenously to activate these receptors is in equilibrium with the density of adenosine receptors at the site of action to help to control the different physiological responses to this nucleotide (Conde et al., 2009).

A_1 and A_2 adenosine receptors have been subdivided based on their capacity of inhibiting and stimulating adenylyl cyclase and therefore, their ability to decrease and increase the cAMP levels, respectively. In fact, A_1 and A_2 adenosine receptors are G_i and G_S-coupled receptors, respectively. The A_3 adenosine receptors are also coupled to G_i proteins (Fredholm et al., 2001). However, nowadays there are some evidences that adenosine receptors may activate signaling pathways via other G proteins, for example A_1 receptors are coupled preferentially to $G_{i1/2/3}$, but they can also be coupled to G_o. On the other hand, although A_{2A} and A_{2B} receptors preferentially activate G_S proteins, they can also activate G_{olf} and $G_{15/16}$, and G_q, respectively (Fredholm et al., 2001). A_3 receptors that activate $G_{i/o}$ proteins can also activate G_q (Conde et al., 2009). Apart from the activation of enzymes, the activation of G coupled proteins acts on ion channels. In addition it has been shown in hippocampal slices that A_1 adenosine receptors activate N, P, and Q-type Ca^{2+} channels (Wu and Saggau, 1994), several types of K^+ channels in cultured striatum mouse neurons (Trussell and Jackson, 1985) and also lead to the activation of phospholipase C (Fredholm et al., 2001). A_3 receptors seem to mediate the same effectors than A_1 receptors. The main second messenger involved in the activation of A_{2A} and A_{2B} receptors is cAMP, with the stimulation of these receptors originating an increase in cAMP intracellular levels, however, other actions, including

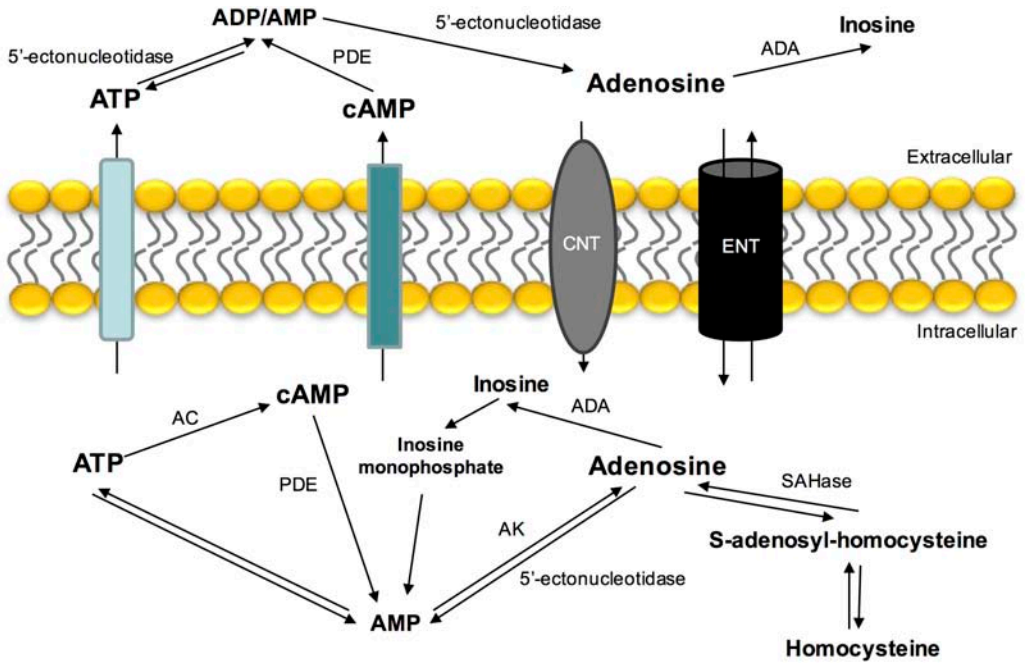

FIGURE 1 | Extra- and intracellular adenosine metabolism and nucleoside transporters that contribute to its release, uptake and production. ADA, adenosine deaminase; AC, adenylyl cyclase; AK, adenosine kinase; CNT, concentrative nucleoside transporter; ENT, equilibrative nucleoside transporter; PDE, phosphodiesterase; SAHase, *S*-adenosyl homocysteine hydrolase.

mobilization of intracellular calcium, have also been described (for a review see Fredholm et al., 2001).

Metabolic Pathways of ATP Formation and Release

Adenosine-5′-triphosphate is released from several cells in physiological conditions and/or pathophysiologically in response to hypoxia, inflammation, to mechanical stress and to some antagonists (Bodin and Burnstock, 2001; Burnstock, 2016). Classically, ATP was known to be released from nerve terminals by exocytosis, via Ca^{2+} dependent mechanisms (Zimmermann, 2016). However, apart from being released from nerve terminals it can be also released by glial cells such as astrocytes (Gordon et al., 2005) through ATP-binding-cassette transporters, surface-located hemichannels (connexin, pannexin) and plasmalemmal voltage-dependent anion channels (Zimmermann, 2016). Neuronal and glial ATP modulate postsynaptic strength though activation of postsynaptic P2X receptors (Gordon et al., 2005; Khakh and North, 2012; Pougnet et al., 2014, Neuron).

After released and exerting its action on its receptors, ATP must be removed from the synaptic clef, which is mainly performed by its breakdown by diverse types of ectonucleotidases. There are four large families of ectonucleotidase enzymes: ectonucleotide pyrophosphatase/phosphodiesterase (E-NPP), which hydrolyze ATP to AMP; ectonucleoside triphosphate diphosphohydrolase (E-NTDPase), which hydrolyze ATP to ADP or AMP; alkaline phosphatase which generate adenosine; and 5′-ectonucleotidase which hydrolyzed AMP to adenosine (Zimmermann et al., 2007; Knowles, 2011).

ATP Receptors

Adenosine-5′-triphosphate exerts its physiological actions by the activation of its receptors that have been divided in two families: P2X ionotropic ligand-gated ion channel receptors and P2Y metabotropic G-protein-coupled receptors (Abbracchio and Burnstock, 1994; Fredholm et al., 1994). Currently are described seven subtypes of P2X receptors ($P2X_1$–$P2X_7$) (Fredholm et al., 1994; Ralevic and Burnstock, 1998) and eight subtypes of P2Y receptors ($P2Y_1$, $P2Y_2$, $P2Y_4$, $P2Y_6$, $P2Y_{11}$, $P2Y_{12}$, $P2Y_{13}$, $P2Y_{14}$) (Burnstock and Knight, 2004).

The P2Y receptors are divided into two subgroups. $P2Y_1$, $P2Y_2$, $P2Y_4$, and $P2Y_6$ that activate G_q coupled proteins and phospholipase Cβ, leading to the formation of inositol 1,4,5-trisphosphate (IP3) which increases intracellular Ca^{2+}, and diacylglycerol which activates protein kinase C. In contrast, $P2Y_{12}$, $P2Y_{13}$, and $P2Y_{14}$ activate G_i, inhibiting adenylyl cyclase and decreasing intracellular cAMP levels. $P2Y_{11}$ receptor activates both Gq and Gs, which increases both intracellular Ca^{2+} and cAMP (Zimmermann, 2016). The seven P2X receptor subunits assemble to form trimeric homomers and often some combinations of trimeric heteromers (Lewis et al., 1995; Torres et al., 1999) that mediate rapid (within 10 ms) and selective permeability to Na^+, K^+, and Ca^{2+} ions (Khakh and North, 2006). This is in accordance with their role as mediators of ATP action as neurotransmitter or neuromodulator of fast synaptic transmission (Khakh and North, 2012; Boué-Grabot

and Pankratov, 2017) in both central and peripheral nervous systems. These P2X receptors can be located at pre-synaptic level (facilitating neurotransmitter release) and at post-synaptic level modulating synapse strength (for a review see North, 2016). In contrast, P2Y receptors, which involves coupling to G proteins and second-messenger systems present a slower onset of response (less than 100 ms) to ATP (for a review Ralevic and Burnstock, 1998).

ROLE OF PURINES ON THE HYPOXIC RESPONSE IN THE CAROTID BODY

The Carotid Bodies

The carotid bodies (CB) are paired chemoreceptors located in the bifurcation of the common carotid artery that are involved in the sensing of changes in arterial blood gasses such as hypoxia, hypercapnia, and acidosis. These stimuli generate action potentials at the CB sensitive nerve, the CSN, that are integrated in the brainstem to induce cardiorespiratory responses, to normalize blood gasses via hyperventilation (Gonzalez et al., 1994), and to regulate blood pressure and cardiac performance via activation of the sympathetic nervous system (Marshall, 1994).

The CB is organized into glomeruli, which are clusters of cells in close contact with a profuse network of capillaries and connective tissue. Each glomerulus contains chemoreceptor cells, also known as glomus or type I cells, which are derived of the neural crest and that are synaptically connected with the sensory nerve endings of the CSN (Gonzalez et al., 1994). Chemoreceptor cells contain several classical neurotransmitters as catecholamines (dopamine and norepinephrine), serotonin, acetylcholine, neuropeptides (substance P and enkephalins), but also contain ATP and adenosine (Gonzalez et al., 1994; Zhang et al., 2000; Rong et al., 2003; Buttigieg and Nurse, 2004; Conde and Monteiro, 2004; Conde et al., 2012a). Chemoreceptor/type I cells are enclosed by type II cells or sustentacular cells. It has been proposed that type II cells exhibit properties of stem cells that in response to hypoxia can proliferate and differentiate into new type I cells (Pardal et al., 2007).

Adenosine and ATP Receptors in the Carotid Body

The CB possesses receptors for both adenosine and ATP. The presence of A_1 receptors at the CB is not consensual. Rocher et al. (1999) described that A_1 receptors are present in rabbit CB chemoreceptor cells, since A_1 antagonists, DPCPX (10 μM) and 8-cyclopentyl-1,3-dimethylxantine (0.1 μM) prevented the inhibitory action of adenosine on L-type Ca^{2+} currents and on the release of catecholamines. A_1 receptors were also detected in the whole rat CB structure (Bairam et al., 2009). However, other authors described that A_1 receptors are absent in rat CB chemoreceptor cells (Gauda et al., 2000; Kobayashi et al., 2000) being present in the petrosal ganglion neurons that also express tyrosine hydroxylase (TH) mRNA (Gauda, 2002). The discrepancies described between the existence of A_1 receptors in the CB could be due to different receptor localization in the CB structures and due to the different species studied.

Among the different adenosine receptor subtypes, A_{2A} and A_{2B} receptors were the main receptors localized in the CB chemoreceptor cells. A_{2A} mRNA expression is developmentally regulated in the CB (Gauda et al., 2000) as it occurs with TH and dopamine D_2-receptors mRNAs (Gauda et al., 1996). The expression of A_{2A} receptors and their colocalization with TH in rat CB chemoreceptor cells have been demonstrated by immunocytochemistry (Gauda et al., 2000; Kobayashi et al., 2000). A_{2B} receptors were also present in rat CB chemoreceptor cells (Conde et al., 2006), as they colocalize with TH. Moreover, it was demonstrated, through the pharmacological decomposition of the effects of caffeine, a non-selective antagonist of adenosine receptors, on the CSN action potential frequency of discharge, that A_{2A} are also present post-synaptically on the CSN (Conde et al., 2006).

The expression of A_3 adenosine receptors was not detected in CB chemoreceptor cells (Kobayashi et al., 2000).

Regarding ATP receptors, McQueen and Ribeiro (1983) proposed for the first time the presence of P2 receptors in the cat CB based on experimental data obtained using the ATP analog, the αβ-methylene ATP. Later, the same authors concluded that P2X receptors were present in the rat CB, since P2X agonists activated the carotid chemoreceptor afferents (McQueen et al., 1998). In co-cultures of rat type I cells and petrosal ganglion cells $P2X_2$ receptors were present in the afferent terminals surrounding clusters of chemoreceptor cells, but not in chemoreceptor cells themselves, suggesting a post-synaptic localization (Zhang et al., 2000). One year later, a study from the same group showed that $P2X_3$ receptors were also present in chemoafferent CB neurons and that $P2X_2$ and $P2X_3$ colocalize in synaptic terminals opposed to chemoreceptors cells, forming a heterodimeric receptor (Prasad et al., 2001). In addition, in co-cultures of rat CB and glossopharyngeal neurons it has also been showed that glossopharyngeal neurons expressed at least four different subtypes of P2X receptors ($P2X_2$, $P2X_3$, $P2X_4$, and $P2X_7$) (Campanucci et al., 2006).

Apart from the presence of P2X ATP receptors, P2Y receptors were also described in the CB (Xu et al., 2003, 2005). In rat CB dissociated cells it has been shown that ATP triggers a transient rise in intracellular Ca^{2+} in type II cells, but not in type I cells, and that $P2Y_2$ receptors are localized in type II cells (Xu et al., 2003). Moreover, Xu et al. (2005) described the presence of $P2Y_1$ receptors in the CB since it was observed in CB type I dissociated cells that ATP suppressed the hypoxia-induced intracellular Ca^{2+} rise via the activation of $P2Y_1$ receptors being the order of purinoreceptor agonist potency in inhibiting the hypoxia response in agreement with the involvement of $P2Y_1$ receptors.

Adenosine Effects on Ventilation and on Carotid Sinus Nerve Activity

Adenosine increases ventilation in several species, and this effect was attributed to the activation of CB chemoreceptors. Studies performed in humans showed that adenosine increases

ventilation in a dose-dependent manner, an effect that is also dependent on the proximity of adenosine administration to the CB (Watt and Routledge, 1985; Watt et al., 1987), meaning that the effect is as higher as closer is adenosine administration from the CB. Consistent with the effect of adenosine in modulating ventilation via CB chemoreceptors, intra-arterially administration of adenosine in dog and cats showed that adenosine does not cross the blood brain barrier (Berne et al., 1974). Moreover, the effect of adenosine and its antagonists on ventilation in response to hypoxia was suggested to involve a mechanism of peripheral chemoreception, the CB, rather than effects on CNS (Maxwell et al., 1986, 1987). In humans, the intravenous infusion of adenosine, that is commercially available as antiarrhythmic, induces chest discomfort, hyperventilation and dyspnea, being these effects attributed to CB chemoreceptors activation (Watt and Routledge, 1985; Maxwell et al., 1986, 1987; Watt et al., 1987; Uematsu et al., 2000).

In the rat, intracarotid administration of adenosine and its analogs increased in a dose-dependent manner ventilation an effect abolished after CSN section (Monteiro and Ribeiro, 1987). This excitatory effect of adenosine on ventilation was mediated by A_2 receptors (Monteiro and Ribeiro, 1987; Ribeiro and Monteiro, 1991), and it seems that A_{2A} are responsible, at least in part, by this effect, since CGS21680, an A_{2A} selective agonist, increased ventilation in rats by 31% (Conde et al., 2009). A work performed in rhesus monkeys also supports the excitatory effect of adenosine on ventilation (Howell and Landrum, 1995). In this work, it was described that caffeine, a non-selective adenosine receptor antagonist, attenuated hypoxia-induced increases in ventilation when animals were exposed to 10% O_2 (Howell and Landrum, 1995). Furthermore, intracarotid administration of erythro-9-(2-hydroxy-3-nonyl) adenine (EHNA) and dipyridamole, inhibitors of adenosine deamination and uptake, respectively, leading to an increase in endogenous adenosine, emulated the excitatory effect of exogenous adenosine on ventilation (Monteiro and Ribeiro, 1989).

Besides, the demonstration of the role of adenosine on modulating ventilation via the CB, in McQueen and Ribeiro (1981) described for the first time that adenosine can stimulate the CSN chemosensory activity. This effect of adenosine on CSN chemosensory activity was mimicked by adenosine analogs and inhibited by theophylline and 8-phenyltheophylline, suggesting the presence and involvement of A_2 receptors (McQueen and Ribeiro, 1983, 1986). *In vitro* experiments in cats and rats corroborate these findings, since it was demonstrated that adenosine augments chemoreceptor discharge (Runold et al., 1990; Vandier et al., 1999), an effect that is dose dependent (Runold et al., 1990). Furthermore, McQueen and Ribeiro (1986) also described that intracarotid administration of 8-phenyltheophylline, an adenosine receptor antagonist, in the cat reduced the CB chemoreceptor response to hypoxia (10% O_2), which could indicate that adenosine released by the CB during hypoxia acts directly on nerve endings or as a modulator. These findings were supported by a previous work from the same group, where it was described an increase in CB chemoreceptor discharge in cat under normoxic conditions when adenosine uptake is inhibited by dipyridamole, suggesting that increases in the levels of endogenous adenosine cause chemoexcitation (McQueen and Ribeiro, 1983). In 2006, our group described that the CSN chemosensory activity elicited by hypoxia (5% O_2) is modulated by adenosine, an effect that is mediated by its action on both A_{2B} presynaptic receptors (25%) present in CB type I cells and A_{2A} postsynaptic receptors (30%) in CSN nerve endings (Conde et al., 2006).

Effects of ATP on Ventilation and Carotid Sinus Nerve Activity

The first evidence that ATP could affect ventilation was described by Anichkov and Belen'kii (1963), in a work that showed an increase in ventilation when ATP was administrated into the carotid bifurcation of decerebrated cats. Later, an autoradiographic study described the presence of ATP in the mouse CB (Kobayashi, 1976) and, nucleoside triphosphatase activity was detected in cat CB homogenates (Starlinger, 1982). Reyes et al. (2007) demonstrated in cats a dose-dependent excitatory effect of ATP on ventilation that was mediated through P2 receptors since the effect of ATP on ventilation was suppressed by suramin. Also, ATP and $P2X_2$ receptors are involved in the ventilatory responses to hypoxia mediated by the CB, since mice deficient in $P2X_2$ receptors exhibited a prominent diminished ventilatory response to hypoxia, being this effect inversely correlated with hypoxia intensity, meaning that the decrease in ventilation is higher when the PaO_2 decreases (Rong et al., 2003). In contrast, mice deficient in $P2X_3$ receptors subunit showed a response to hypoxia comparable with the response of wild-type animals (Rong et al., 2003), suggesting that the $P2X_3$ receptors that are also present in the CB do not mediate the ventilatory responses to hypoxia.

The results of ATP on ventilation are also consistent with the effect of ATP on CSN chemosensory activity. In the early 1950s, Jarisch et al. (1952) described an increase in CSN chemoreceptor discharge following an intracarotid administration of ATP. This excitatory effect of ATP on CSN chemoreceptor activity was also described by other *in vivo* and *in vitro* studies (Dontas, 1955; McQueen and Ribeiro, 1983; Ribeiro and McQueen, 1984; Spergel and Lahiri, 1993). Moreover, it was showed that this effect of ATP on CSN activity was dose-dependent (McQueen and Ribeiro, 1983; Alcayaga et al., 2000; Reyes et al., 2007; Soto et al., 2010) and due to ATP itself and not to its degradation into adenosine since the ATP agonists, βγ-methylene ATP promoted increases in the CSN chemoreceptor activity in cats (McQueen and Ribeiro, 1983; Reyes et al., 2007) and αβ-methylene ATP increased CSN discharges in rats (McQueen et al., 1998) and mice (Rong et al., 2003). Additionally, P2X receptor agonists induced rapid cardiorespiratory reflexes in anesthetized rat, suggesting the presence of this receptors in the rat CB (McQueen et al., 1998). These findings were supported by a work by Colin Nurse group (Zhang et al., 2000). They showed in a co-culture model of rat type I cell clusters and petrosal neurons that the application of suramin partially inhibited hypoxia-induced postsynaptic responses recorded in petrosal neurons (Zhang et al., 2000). In addition, both $P2X_2$ and $P2X_3$ receptor subunits were immunolocalized with petrosal afferent terminals in the rat

CB (Zhang et al., 2000; Prasad et al., 2001). Furthermore, Rong et al. (2003) not only showed that $P2X_2$ subunit are involved in the CB-mediated ventilatory responses to hypoxia, as herein described, but also showed a substantial decrease in the CSN responses to hypoxia in an *in vitro* CB-CSN preparation from mice deficient in $P2X_2$ subunits. Therefore, is now accepted that ATP is an excitatory neurotransmitter at the synapse between the CB and the CSN and that is involved in the CB response to hypoxia. However, the contribution of ATP for the hypoxic signaling in the CB is dependent on hypoxia intensity, with ATP having a more pronounced role in the response to high intensity hypoxias and adenosine with moderate hypoxias (Conde et al., 2012a), suggesting that the response to hypoxia in the CB are related with alterations in the ATP/adenosine metabolism.

While the effect of ATP in CB response to hypoxia is consensual, some controversy exists on the effect of ATP in fixing basal CSN activity. Zhang et al. (2000) described that suramin inhibited CSN basal activity. In contrast, our group reported that suramin did not modify CSN basal activity, which suggests that ATP is not the mediator involved in fixing the steady basal CSN chemosensory activity in adult rat (Conde et al., 2012a). These discrepancies could be related with developmental differences since the experiments performed by Zhang et al. (2000) were performed in postnatal 7- to 14-day-old rat pups. In fact, Niane et al. (2011) described a decrease in spontaneous CSN activity (80%) in newborn rats, an effect was constant across ages (4- to 21-day-old rats). However, previous studies of the same authors (Donnelly and Doyle, 1994) have shown that both basal and hypoxia-induced CSN activity increases with age. Additionally, Niane et al. (2011) showed by the use of a specific $P2X_3$ antagonist, A-317491, that in the CB from newborn rats, the $P2X_3$ receptor subunit plays a major role in the regulation of breathing under basal and hypoxic conditions, which is in contradiction with the results from Rong et al. (2003) in the mice. However, in both Zhang et al. (2000) and Niane et al. (2011) suramin was insufficient to fully promote inhibition of ventilation and the CSN chemosensory response to hypoxia suggesting that other excitatory co-transmitters are also involved (Fitzgerald, 2000; Iturriaga and Alcayaga, 2004; Zapata, 2007; Nurse, 2010; Conde et al., 2012a). Several authors have proposed the co-release of ATP-Acetylcholine, since the application of a mixture of nicotinic and purinergic antagonists completely suppress the CSN response to hypoxia (Zhang et al., 2000; Varas et al., 2003), however, Reyes et al. (2007) described that the perfusion of CB excised from cats with a mixture of nicotinic and purinergic antagonists was not able to eliminate the chemosensory response to hypoxia stimulation. Therefore, the hypothesis of the co-signaling of ATP-Acetylcholine in the CB remains controversial while the hypothesis of ATP-adenosine co-transmission gained many supporters.

ATP and Adenosine Release from Carotid Body

The first evidence for CB ATP release was a report describing a decrease in ATP content in the cat CB incubated with moderate hypoxia during 5 min or with cyanide, an inhibitor of the mitochondrial electron transport that induced a decrease in ATP and an increase in AMP content (Obeso et al., 1985, 1989). Also, rabbit CBs superfused during 15 min with cyanide or antimycin exhibit reduced ATP levels (Verna et al., 1990). In contrast with these results, it was observed that CB ATP levels were unchanged: (1) in cats exposed to hypoxia or hypercapnia (Acker and Starlinger, 1984); (2) in cat CBs incubated in the presence of dinitrophenol (Obeso et al., 1989), an uncoupler of oxidative phosphorylation that targets the mitochondria; (3) and in rabbit CBs superfused during 4–30 min with 10% O_2-equilibrated Krebs–Henseleit solution (Verna et al., 1990). Buttigieg and Nurse (2004), described that acute hypoxia evoked an increase in extracellular ATP in the whole CB, an effect that was inhibited by L-type Ca^{2+} channel blockers. In addition, observations from our group showed that adult rat CBs incubated in Tyrode solution equilibrated with different O_2 concentrations released higher concentrations of ATP when exposed to hypoxia (2% O_2 and 10% O_2) than when exposed to 20% O_2 and 95% O_2 (Conde and Monteiro, 2006). More recently, we showed that the release of ATP from rat CB is proportional with hypoxia intensity (Conde et al., 2012a) and that the increase in ATP release induced by hypoxia was completely prevented by removal of extracellular calcium and by a calcium chelating agent, suggesting that ATP released during hypoxia comes from a vesicular source through exocytosis (Conde and Monteiro, 2006; Conde et al., 2012a). Therefore, the signaling cascade between hypoxic signal and the release of ATP would be: (1) detection of hypoxia by an O_2 sensor (molecular identity unknown), (2) closure of K^+ channels, (3) opening of Ca^{2+} channels, (4) increase in intracellular calcium, (5) release of ATP by exocytosis (Gonzalez et al., 1994, 2010; Conde et al., 2012a).

Adenosine is also released from the CB. Our group showed that in adult rat CB adenosine is released in normoxic conditions, and its release augments in response to 10 and 30 min of moderate hypoxia (10% O_2) (Conde and Monteiro, 2004), but is not modified by hyperoxic exposure (95% O_2) (Conde and Monteiro, 2006). These experiments were performed under incubation of adenosine deaminase due to the short life-time of adenosine and to avoid its degradation. In contrast, the CB adenosine content was drastically reduced after 30 min of hypoxic exposure (Conde and Monteiro, 2004). Also, we have showed that approximately 40% of adenosine present extracellularly in the CB came from extracellular ATP degradation, both under normoxic and hypoxic conditions and that low pO(2) triggers adenosine efflux through the activation of NBTI-sensitive ENT. This effect was only apparent in hypoxia and when adenosine extracellular concentrations were reduced by the blockade of ecto-5′-nucleotidase (Conde and Monteiro, 2004).

Although we have showed that both ATP extracellular catabolism as well as release of adenosine *per se* through an NBTI-sensible ENT can account to the amount of adenosine present in the CB-CSN synapse, we cannot exclude another sources of extracellular adenosine, as cAMP. Even though several studies reported the role of cAMP in CB chemotransduction and/or chemotransmission (Nunes et al., 2014), the contribution of extracellular cAMP to extracellular adenosine has never been investigated in the CB. Additionally, other mechanisms, such as

inhibition of *S*-adenosylhomocysteine and adenosine deaminase, could be involved in adenosine production and release by the CB in normoxia and hypoxia.

Additionally, our group demonstrated that adenosine is preferentially released in response to moderate hypoxia (10% O_2) than in response to higher hypoxic intensities (2% O_2 and 5% O_2), while CB ATP release had a more pronounced role during high intensity hypoxias (Conde et al., 2012a). These findings were corroborated by electrophysiological data showing that ZM241385, in a concentration that block A_2 adenosine receptors (A_{2A} and A_{2B}, 300 nM), inhibits CSN chemosensory activity with higher efficacy in moderate hypoxia than in intense hypoxia (Conde et al., 2012a). Furthermore, it was also shown that during a high-intense hypoxia the main origin of extracellular adenosine is ATP catabolism, whereas at moderate hypoxia the main source of adenosine is its release *per se* by the ENT (Conde et al., 2012a). All together these findings showed that adenosine acting on the CB via A_{2A} and A_{2B} receptors together with ATP acting on P2X receptors are key neurotransmitters involved in hypoxic CB chemotransduction, depending the contribution of each neurotransmitter on the hypoxia intensity.

As previously described, the conversion of ATP to adenosine requires both membrane bound E-NTDPase and 5′-ectonucleotidases and, it was recently described that E-NTDPase2,3 are expressed prominently in the periphery of CB type I cells in the vicinity with CSN endings and that 5′-ectonucleotidase (CD73) is expressed in both types I and II cells (Salman et al., 2017). Holmes et al. (2017) recently showed that the inhibition of CD73 decreased the basal CSN activity and attenuated the responses to hypoxia. These authors also described that the *in vivo* inhibition of CD73 with AOPCP, blunted the hypoxic ventilatory response and reduced the elevation in the heart rate induced by hypoxia, showing that CD73 regulates peripheral chemoreceptor activity and the cardiorespiratory responses to hypoxia (Holmes et al., 2017). Additionally, it has been shown that under chronic hypobaric hypoxia an upregulation of E-NTDPase3 and CD73 was observed, while E-NTDPase2 was downregulated, suggesting that this differential regulation leading to alterations in purinergic adenosine and P2 receptors signaling, may contribute to CB plasticity during chronic hypoxia (Salman et al., 2017). These results together suggest a hypoxic modulation of purines metabolism at the CB that control the contribution of adenosine and ATP in CB chemotransduction both in basal conditions as well as in the responses to acute and chronic hypoxia.

Cellular Actions of Adenosine in the Carotid Body

At the moment, it is accepted that the chemoexcitatory effect of adenosine at the CB involves the activation of adenosine receptors and consequently the activation of cellular pathways activated by G-coupled receptors as well as alterations in cAMP and Ca^{2+} intracellular levels, cell depolarization among other events. There is a consensus that adenosine and its analogs increase cAMP levels in the rat (Monteiro et al., 1996; Conde et al., 2008) and rabbit CB (Chen et al., 1997). Hypoxia also induced an increase in cAMP in CB type I cells (Pérez-García et al., 1990; Wang et al., 1991) an effect that was potentiated by adenosine, since dipyridamole, an inhibitor of adenosine uptake, increased cAMP content in rabbit CB superfused with 5% O_2. This effect was blocked by A_2 adenosine receptors antagonists (Chen et al., 1997) meaning that A_2 receptors mediated the increase in cAMP produced by hypoxia. More recently, it was shown that this increase in cAMP levels evoked by adenosine is mostly mediated by the activation of A_{2B} adenosine receptors (Conde et al., 2008).

Another effector of cAMP is K^+ channels, and in fact K^+ channels are known to be modulated by the increase in cAMP levels induced by adenosine at the CB (López-López et al., 1993). López-López et al. (1993) showed that the application of a cAMP analog, dibutyryl cAMP, in isolated rabbit type I cells, decreased the amplitude of 4-aminopyridine-sensitive K^+ currents, an effect that is voltage independent. In contrast, Hatton and Peers (1996) demonstrated that dibutyryl cAMP (5 mM) and 8-bromo-cAMP (2 mM) were unable to modify K^+ current amplitudes in isolated rat type I cells. These discrepant results could be related with animal's age and with differences between the electrophysiological properties and responses to hypoxia of rabbit and rat type I cells (Peers and Buckler, 1995). Furthermore, Vandier et al. (1999) showed that adenosine decreased the amplitude of 4-aminopyridine-sensitive K^+ currents in isolated rat type I cells, an effect that is voltage independent and mainly Ca^{2+} dependent. However, a small but significant component of the current blocked by adenosine was Ca^{2+} dependent (Vandier et al., 1999). Additionally, in isolated rabbit type I cells, adenosine inhibits L-type Ca^{2+} channels and the release of catecholamines induced by hypoxia, an effect that was described to be mediated by A_1 adenosine receptors, since A_1 agonists and antagonists are capable of modulate Ca^{2+} currents (Rocher et al., 1999). Kobayashi et al. (2000) also described that adenosine inhibits voltage-dependent Ca^{2+} currents in isolated rat type I cells. However, this effect was attributed to A_{2A} adenosine receptors, since ZM241385, in a concentration that is specific for A_{2A} receptors (10 nM), abolished the effect of adenosine on Ca^{2+} currents (Kobayashi et al., 2000). This discrepancies as previously discussed could be attributed to differences between species. Additionally, adenosine attenuated the increase in intracellular Ca^{2+} evoked by hypoxia without changing the intracellular Ca^{2+} in cells exposed to normoxia (Kobayashi et al., 2000). In contrast, Xu et al. (2006) observed that adenosine via A_{2A} receptors elicited a rise in intracellular Ca^{2+}. The authors also described that this effect of adenosine on intracellular Ca^{2+} occurs through the action of adenosine on adenylate cyclase and protein kinase A pathways, which inhibits the TWIK-related acid-sensitive K^+-1 (TASK-1) channels, leading to depolarization and, therefore to Ca^{2+} entry via voltage-gated Ca^{2+} channels (VGCC) (Xu et al., 2006; Tse et al., 2012). However, the increase in the intracellular Ca^{2+} observed by Xu et al. (2006) may be insufficient to evoke the release of neurotransmitters, since it is much smaller than the increase that evokes the release of catecholamines from the rat CB (Vicario et al., 2000). Moreover, the block of A_{2A} adenosine receptors with SCH58261, a selective antagonist of A_{2A} receptors in the concentration used (5 nM), decreases hypoxia-evoked

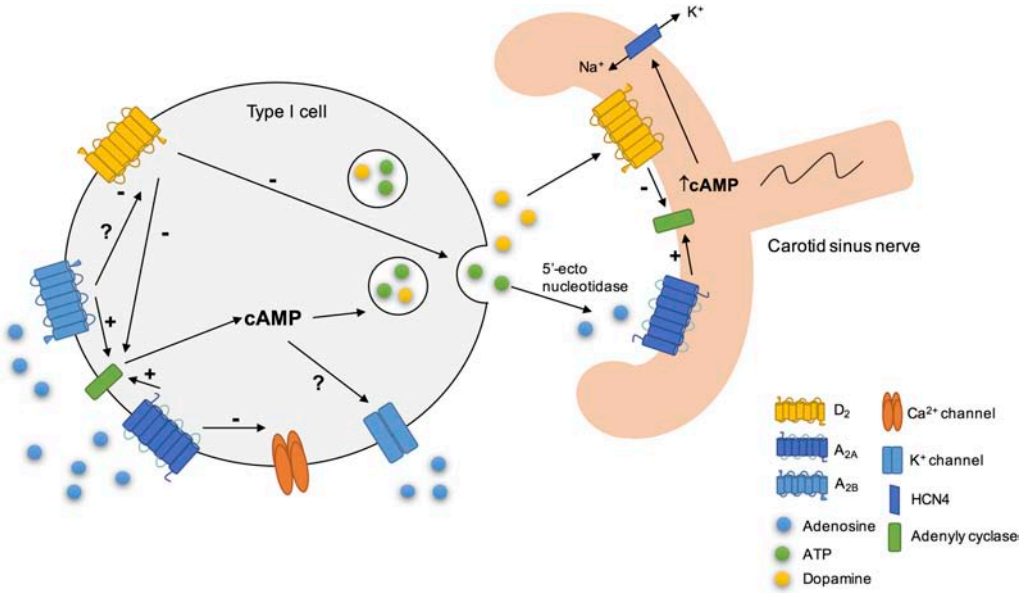

FIGURE 2 | Schematic representation of some of adenosine cellular actions on rat carotid body (CB). Adenosine increased cAMP content in type I cells via A_{2A} and A_{2B} action on adenylyl cyclase, leading to the release of neurotransmitters, as catecholamines (Conde et al., 2008). Additionally, its action on these receptors could modulate K^+ currents (López-López et al., 1993) for example by decreasing the amplitude of K^+ currents (Vandier et al., 1999) and inhibit the voltage-dependent Ca^{2+} currents in type I cells. During hypoxia, adenosine released *per se* through the equilibrative nucleoside transport system or generated by the extracellular breakdown of ATP by 5′-ectonucleotidases (Conde and Monteiro, 2004; Conde et al., 2012a; Salman et al., 2017), acts postsynaptically on A_{2A} receptors, leading to adenylyl cyclase activation and to an increase in cAMP, which stimulates HCN4-containing non-selective cation channels that mediate I_h, leading to an increase in membrane excitability. In contrast, dopamine exerts the opposite effect, leading to a decrease in petrosal membrane excitability (Zhang et al., 2017).

receptor potentials in rat type I cells (Nurse and Piskuric, 2013). The role of adenosine in modulating CB cells function in chronic hypoxia was also highlighted by the fact that the exposure of rat CB cultures to chronic hypoxia (2% O_2, 24 h) induced an augment in adenosine-evoked increases intracellular Ca^{2+} transients and catecholamine secretion from CB type I cells, an effect that is mediated by A_{2B} receptors (Livermore and Nurse, 2013). This pathway could contribute to CB sensitization during ventilatory acclimatization to hypoxia in animals and humans exposed to chronic hypoxia *in vivo* (Conde et al., 2009; Teppema and Dahan, 2010).

Adenosine also acts as a neuromodulator in CB chemoreceptor cells since it acts to modulate the release of other neurotransmitters. It has been showed that adenosine is involved in the release of catecholamines through the antagonist interaction between A_{2B} and dopamine D_2 receptors (Conde et al., 2008) (**Figure 2**). This interaction between A_{2B} and D_2 receptors in CB chemoreceptors cells is evident at adenylyl cyclase level, since D_2 agonists inhibited cAMP production in CB, an effect that is prevented by an A_{2B} receptor antagonist and occurs in basal conditions as well as hypoxia (Conde et al., 2008). However, an antagonistic interaction at the A_{2B}-D_2 receptor level, similar to that described in the CNS for A_{2A}-D_2 receptors (Fuxe et al., 2007) cannot be excluded. These results are in agreement with a previous work from Monteiro and Ribeiro (2000) that described an enhancement of the inhibitory effect of dopamine on ventilation induced by the intracarotid infusion of adenosine. Regarding the interactions between adenosine and dopamine at postsynaptic level, a recent work from Zhang et al. (2017) showed in co-culture of rat CB type I cells and sensory petrosal neurons that adenosine increases a hyperpolarization-activated cyclic nucleotide-gated (HCN) cation current I_h in chemosensory petrosal neurons through A_{2A} receptors, whereas dopamine had the opposite effect through D_2 receptors. The effect of adenosine on HCN cation current I_h seems to involve the activation of adenylyl cyclase and the increase in intracellular cAMP that in turn activates HCN4-containing non-selective cation channels that mediate I_h (Zhang et al., 2017). Moreover, the authors obtained evidence for a presynaptic role for adenosine acting via A_{2A} receptors during chemotransduction, since SCH58261 inhibited both hypoxia-induced presynaptic receptor potential and postsynaptic petrosal response (Zhang et al., 2017).

Cellular Actions of ATP in the Carotid Body

During hypoxia it was observed that rat chemoreceptors cells depolarized due to the closure of TASK1/3 background K^+ channels (Buckler, 2015) leading to the activation of extracellular Ca^{2+} entry via VGCCs triggering the release of several neurotransmitters from chemoreceptor cells, including ATP and adenosine (Buttigieg and Nurse, 2004; Conde and Monteiro, 2004; Conde et al., 2012a). In addition, it has been shown that ATP released by type I cells can induce a rise in intracellular Ca^{2+}

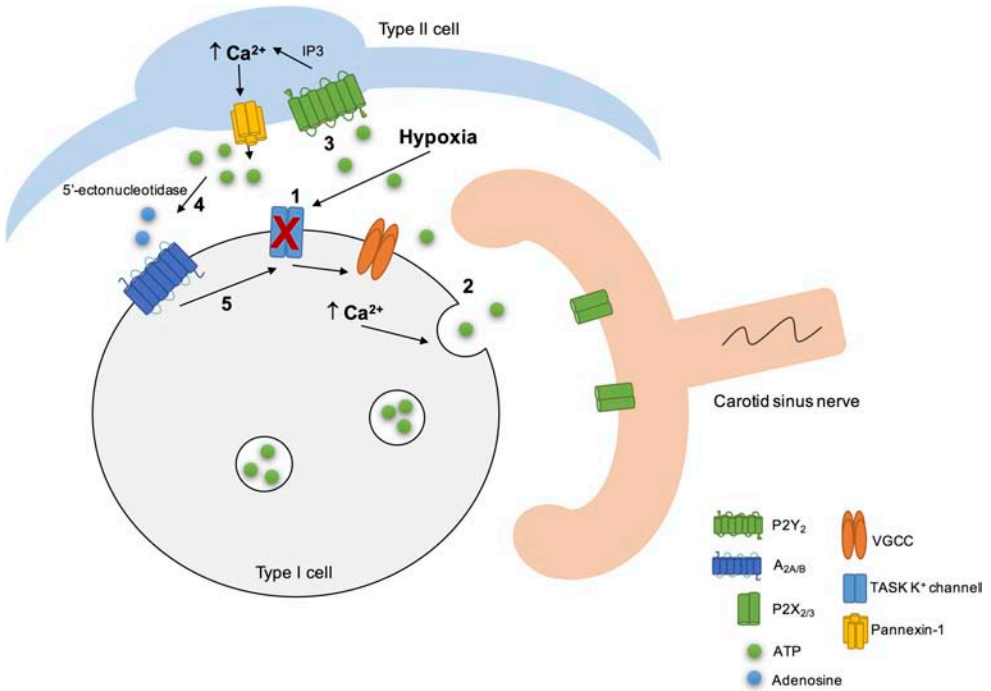

FIGURE 3 | Schematic representation of the CB "tripartite" synapse model proposed by Nurse and collaborators. Hypoxia induced type I cell depolarization through the inhibition of TASK1/3 K^+ channels (1), leading to Ca^{2+} entry via voltage-gated Ca^{2+} channels (VGCC) and to ATP release (2). ATP excites postsynaptic $P2X_{2/3}$ receptors on petrosal nerve terminal. ATP can also stimulate $P2Y_2$ receptors in adjacent type II cells (3), leading to the Ca^{2+} release from intracellular stores via inositol triphosphate (IP3) signaling pathways and opening of pannexin-1 channels. This results in ATP release that could be break down by extracellular 5'ectonucleotidase into adenosine (4) (Conde et al., 2012a; Salman et al., 2017). Adenosine stimulates A_{2A} adenosine receptors in type I cells, leading to the inhibition of TASK1/3 K^+ channels, that enhance type I cell depolarization (5) (Xu et al., 2005) and, therefore ATP release. It is not represented but hypoxia stimulates adenosine release *per se* from type I cells (Conde and Monteiro, 2004) and high levels of ATP could inhibit pannexin-1 channels in type II cells and inhibit the chemoreceptor function via $P2Y_1$ receptors, through a negative feedback mechanism. Adapted from Zhang et al. (2012), Nurse (2014), Murali and Nurse (2016).

in isolated type II cells (Xu et al., 2003; Tse et al., 2012), since the application of different purinoceptor agonists on dissociated cell cultures of types I and II CB showed that ATP acts on type II cells via $P2Y_2$ receptors subtype (Xu et al., 2003). Later, it was described that $P2Y_2$ receptors activation on type II cells lead to an increase in intracellular Ca^{2+} levels and to a prolonged membrane depolarization due to the opening of large-pore, pannexin-1 channels (Zhang et al., 2012). Moreover, it was also showed in co-cultures of dissociated CB cells and petrosal neurons that the selective activation of $P2Y_2$ receptors on type II cells can lead to ATP release through pannexin-1 channels, an effect that was reversibly inhibited by Panx-1 selective blocker, carbenoxolone (Zhang et al., 2012). These results lead to the authors to propose that CB type II cells may function as an ATP signal amplifier and therefore contribute to chemoexcitation through the mechanism of ATP-induced ATP release (Zhang et al., 2012).

More recently, Murali and Nurse (2016) suggested that the crosstalk between CB type I cells and type II cells during chemotransduction is mediated by purinergic signaling. In isolated rat chemoreceptor clusters, it was observed a delayed intracellular Ca^{2+} elevations in nearby type II cells that was promoted by type I cell depolarization induced by hypoxia, hypercapnia or high K^+, an effect blocked by the $P2Y_2$ antagonist suramin (Murali and Nurse, 2016). In contrast, when $P2Y_2$ receptors in type II cells were stimulated induced a delayed, secondary intracellular Ca^{2+} elevations in nearby type I cells, an effect that was blocked by inhibitors of pannexin-1 channels as well as by inhibitor of A_{2A} adenosine receptors and 5′-ectonucleotidase (Murali and Nurse, 2016). Therefore, this work demonstrated that the ATP released through pannexin-1 channels in type II cells and that is catabolized extracellularly by 5′-ectonucleotidase into adenosine is the principal source of adenosine mediating the crosstalk between types I and II cells (Murali and Nurse, 2016). The adenosine that is produced extracellularly then can stimulate A_{2A} receptors that are present in type I cells inducing the increase in intracellular Ca^{2+} (Xu et al., 2006; Tse et al., 2012; Nurse and Piskuric, 2013). On the postsynaptic side at the CSN nerve endings, adenosine could increase the CSN discharge through the activation of A_{2A} adenosine receptors on afferent nerve terminals (Conde et al., 2012a). However, since it was observed that even in the presence of AOPCP a residual Ca^{2+} response in type I cells persists, it cannot be excluded the possibility of type II cells via pannexin-1 channels directly release small amounts of adenosine (Murali and Nurse, 2016).

Adenosine-5′-triphosphate itself could also regulate its own extracellular levels at the synapse. High levels of extracellular

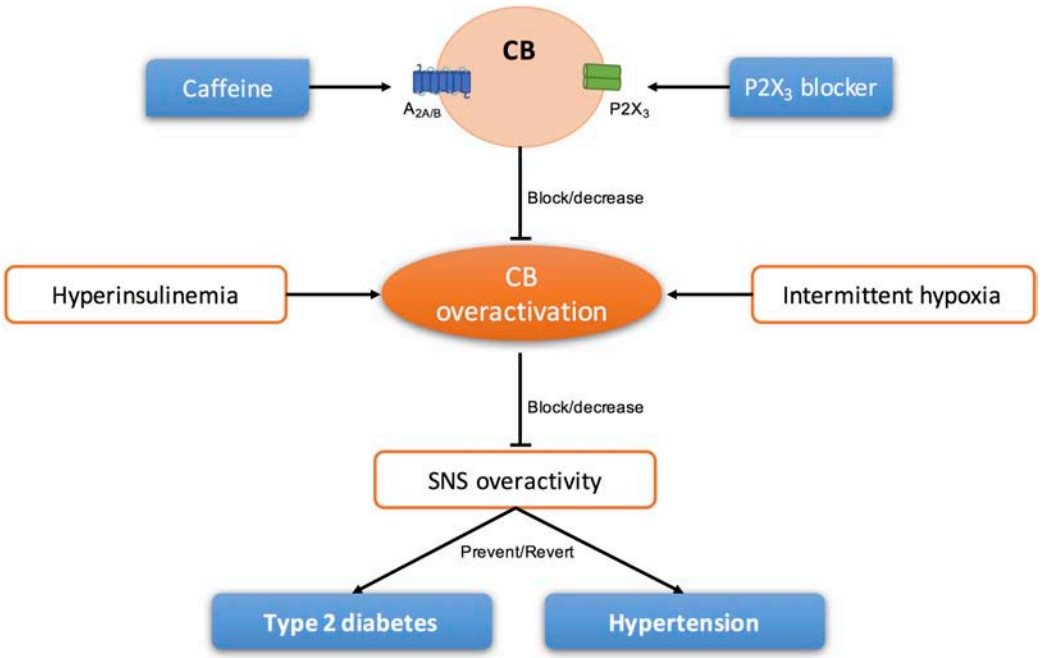

FIGURE 4 | Schematic representation of the modulation of purinergic systems to block/decrease the overactivation of CB present in sympathetic-mediated diseases, as type 2 diabetes and essential hypertension.

ATP could induce a negative feedback loop to inhibit pannexin-1 channels thereby regulating ATP release from type II cells (Dubyak, 2009). Additionally, high extracellular levels of ATP did not affect the resting intracellular Ca^{2+} (Xu et al., 2003) but strongly inhibited the hypoxia-induced elevation in intracellular Ca^{2+} in type I cells via a negative feedback mechanism involving $P2Y_1$ receptors (Xu et al., 2005; Tse et al., 2012). The mechanism behind this effect involved the closure of background conductance(s) other than TASK-like K^+, maxi-K or Na^+ channels (Xu et al., 2005; Tse et al., 2012). However, this negative feedback promoted by ATP on type I cells via $P2Y_1$ could be counteracted by the positive feedback action of adenosine on the presynaptic and/or postsynaptic side. All these findings about the purinergic signaling in the rat CB leads Colin Nurse group to propose a model of the CB "tripartite" synapse (**Figure 3**) (Zhang et al., 2012; Piskuric and Nurse, 2013; Nurse, 2014; Murali and Nurse, 2016).

ROLE OF PURINES IN CAROTID BODY-MEDIATED PATHOLOGIES

In the last years, several literature was published defending the idea that the CB could be a therapeutic target for the treatment of sympathetically mediated diseases, as CB activity seems to be increased and involved in the pathogenesis of these diseases (Paton et al., 2013; Iturriaga, 2017). Animal and human studies have suggested the use of unilateral and/or bilateral CB ablation for the treatment of essential hypertension and heart failure (Abdala et al., 2012; Niewinski et al., 2013, 2017; Fudim et al., 2015; Narkiewicz et al., 2016). However, knowing that the surgical resection of the CSN is prone to cause side effects (for a review see Iturriaga, 2017; Sacramento et al., 2017b) other approaches that do not permanently restrict carotid body (CB) function may be more appropriate in the long term. Therefore, modulation of purines levels and/or action could be a strategy to treat pathologies associated with CB dysfunction (**Figure 4**).

Type 2 Diabetes

In 2013, our group demonstrated for the first time that CB regulates peripheral insulin sensitivity and that CB overactivation is involved in the genesis of hypertension and insulin resistance induced by hypercaloric diets (Ribeiro et al., 2013), an effect that seems to be mediated by a sympathetic nervous system overactivation (Ribeiro et al., 2013; Sacramento et al., 2017b). Moreover, we also showed that insulin triggers CB activation, suggesting that hyperinsulinemia may be one of the stimulus responsible for CB overactivation leading to sympathetic nervous system overactivity that is associated with metabolic disturbances, such as type 2 diabetes (Ribeiro et al., 2013). In the same work, we described that bilateral CSN resection prevents the development of dysmetabolic changes induced by hypercaloric diets (Ribeiro et al., 2013) and more recently we have demonstrated that bilateral, but not unilateral CSN resection, restores insulin sensitivity and glucose homeostasis in prediabetes and type 2 diabetic rats (Sacramento et al., 2017a,b) suggesting that CB modulation could be used as a therapeutic approach.

Knowing that adenosine is one of the key neurotransmitters in the CB (Conde and Monteiro, 2004; Conde et al., 2012a) and that caffeine decreases CB activity acutely (Conde et al., 2006) and chronically (Conde et al., 2012c) by approximately 60%, it is expected that the overactivation of the CB seen in hypercaloric animal models could be decreased with long-term administration of caffeine. In fact, our group described that chronic caffeine intake prevents and reverted the increase in blood pressure and insulin resistance in hypercaloric animal models of prediabetes (Conde et al., 2012b). Additionally, epidemiological studies described that chronic caffeine consumption is associated with a significant lower risk of diabetes (van Dam and Hu, 2005; Ding et al., 2014). Therefore, it remains to prove that CB overactivation in hypercaloric animal models of diabetes is decreased in the presence of long-term caffeine treatment as well as the link caffeine-decreased CB activity- decreased sympathetic nervous system activity.

Obstructive Sleep Apnea

Chronic intermittent hypoxia (CIH), which is characterized by cyclic hypoxic episodes of short duration followed by normoxia, is a characteristic feature of obstructive sleep apnea, the most common form of sleep disorder. The CB has been proposed to be the link between the reflex increase in sympathetic nervous system activity and the blood pressure associated with obstructive sleep apnea due to CIH (Fletcher et al., 1992; Narkiewicz et al., 1999). In fact, an augment in peripheral CB drive in obstructive sleep apnea patients has been observed, since they showed an increase in ventilatory and cardiovascular reflex responses induced by acute hypoxia (Narkiewicz et al., 1999). This increase in CB drive has been showed to be due to CIH, since Peng et al. (2003) demonstrated that CIH induced a progressive increase in CSN activity with each hypoxic episode, remaining the baseline activity elevated approximately during 60 min after the last acute hypoxic stimuli, an effect called sensory long-term facilitation. These authors also suggested that sensory long-term facilitation contributes to the persistent increase in sympathetic nervous activity and blood pressure that is observed in obstructive sleep apnea, since the increase in CB sensory activity triggers sympathetic nerve discharge and an increase in blood pressure (Peng et al., 2003). Recently, our group showed that adenosine is one of the mediators involved in the sensitization of CB during CIH (Sacramento et al., 2015), since caffeine decreased basal and hypoxia-evoked (5% O_2) CSN chemosensory activity in rats subjected to 15 days of CIH (Sacramento et al., 2015). Moreover, it has been described that adenosine levels are augmented in obstructive sleep apnea patients (Lavie, 2003) suggesting a deregulation of adenosinergic system in sleep apnea patients. Therefore, the blockage of adenosine receptors in the CB or modulation of adenosine metabolism both in the CB and peripherally might be useful to treat some of the pathophysiological features of chronic obstructive sleep apnea.

Hypertension

Hypertension affects one-third of the human population and in the United States only 53% of those tacking antihypertensive medication have their condition controlled (Go et al., 2014). Furthermore, it is estimated that 14–16% of all patients with hypertension are resistant to antihypertensive medication and/or having poor compliance or tolerance to the medication (Achelrod et al., 2015). It is accepted that CB chemoreflex-evoked sympathetic activity responses are increased in human patients and animal models of systemic essential hypertension (Trzebski et al., 1982; Somers et al., 1988; Tan et al., 2010; Abdala et al., 2012; Siński et al., 2012) and therefore the CB has been proposed as a therapeutic target for the treatment of cardiovascular diseases. Accordingly, CB ablation was capable of control the development and maintenance of high blood pressure in spontaneously hypertensive rats and humans (Abdala et al., 2012; Narkiewicz et al., 2016). However, the effect of unilateral ablation CB in hypertensive patients has diminished efficacy 12 months after ablation, suggesting a compensation of the remaining CB (Narkiewicz et al., 2016), suggesting that other approaches are needed to modulate CB function in cardiovascular diseases. Pijacka et al. (2016) demonstrated an upregulation of the $P2X_3$ mRNA in the chemoreceptive petrosal sensory neurons of spontaneously hypertensive rats and that $P2X_3$ receptors are present in human CB from individuals with a medical history of hypertension. Moreover, it has also shown that a $P2X_3$ receptor antagonist is capable to decrease sympathetic activity and arterial pressure in spontaneously hypertensive rats, an effect that was absent in normotensive animals (Pijacka et al., 2016). All these data suggest that ATP is responsible for the CB hyperactivity and hyperreflexia seen in essential hypertension and that support the modulation of $P2X_3$ receptor as non-surgical a non-surgical strategy to control human hypertension. Although, apart from $P2X_3$ receptor, and knowing that $P2X_4$ receptors are expressed post-synaptically in the CB (Campanucci et al., 2006) and that they are involved in ventrolateral medulla control of the sympathetic autonomic function (Zoccal et al., 2011), we can postulate that modulation of $P2X_4$ receptors might be a therapeutic target for hypertension.

AUTHOR CONTRIBUTIONS

All authors listed have made a substantial, direct and intellectual contribution to the work, and approved it for publication.

ACKNOWLEDGMENT

JS is supported by Ph.D. Grant from the Portuguese Foundation for Science and Technology, PD/BD/105890/2014.

REFERENCES

Abbracchio, M. P., and Burnstock, G. (1994). Purinoceptors: Are there families of P2X and P2Y purinoceptors? *Pharmacol. Ther.* 64, 445–475. doi: 10.1016/0163-7258(94)00048-4

Abdala, A. P., McBryde, F. D., Marina, N., Hendy, E. B., Engelman, Z. J., Fudim, M., et al. (2012). Hypertension is critically dependent on the carotid body input in the spontaneously hypertensive rat. *J. Physiol.* 590, 4269–4277. doi: 10.1113/jphysiol.2012.237800

Achelrod, D., Wenzel, U., and Frey, S. (2015). Systematic review and meta-analysis of the prevalence of resistant hypertension in treated hypertensive populations. *Am. J. Hypertens.* 28, 355–361. doi: 10.1093/ajh/hpu151

Acker, H., and Starlinger, H. (1984). Adenosine triphosphate content in the cat carotid body under different arterial O_2 and CO_2 conditions. *Neurosci. Lett.* 50, 175–179. doi: 10.1016/0304-3940(84)90482-8

Alcayaga, J., Cerpa, V., Retamal, M., Arroyo, J., Iturriaga, R., and Zapata, P. (2000). Adenosine triphosphate-induced peripheral nerve discharges generated from the cat petrosal ganglion *in vitro*. *Neurosci. Lett.* 282, 185–188. doi: 10.1016/S0304-3940(00)00896-X

Anichkov, S. V., and Belen'kii, M. L. (1963). *Pharmacology of the Carotid Body Chemoreceptors*. Oxford: Pergamon Press Ltd.

Arch, J. R., and Newsholme, E. A. (1978). Activities and some properties of 5'-nucleotidase, adenosine kinase and adenosine deaminase in tissues from vertebrates and invertebrates in relation to the control of the concentration and the physiological role of adenosine. *Biochem. J.* 174, 965–977. doi: 10.1042/bj1740965

Bairam, A., Joseph, V., Lajeunesse, Y., and Kinkead, R. (2009). Altered expression of adenosine A1 and A2A receptors in the carotid body and nucleus tractus solitarius of adult male and female rats following neonatal caffeine treatment. *Brain Res.* 1287, 74–83. doi: 10.1016/j.brainres.2009.06.064

Berne, R. M., Rubio, R., and Curnish, R. R. (1974). Release of adenosine from ischemic brain: effect on cerebral vascular resistance and incorporation into cerebral adenine nucleotides. *Circ. Res.* 35, 262–271. doi: 10.1161/01.RES.35.2.262

Bodin, P., and Burnstock, G. (2001). Purinergic signalling: ATP release. *Neurochem. Res.* 26, 959–969. doi: 10.1023/A:1012388618693

Boué-Grabot, E., and Pankratov, Y. (2017). Modulation of central synapses by astrocyte-released ATP and postsynaptic P2X receptors. *Neural Plast.* 2017:454275. doi: 10.1155/2017/9454275

Broch, O. J., and Ueland, P. M. (1980). Regional and subcellular distribution of S-adenosylhomocysteine hydrolase in the adult rat brain. *J. Neurochem.* 35, 484–488. doi: 10.1111/j.1471-4159.1980.tb06291.x

Buckler, K. J. (2015). TASK channels in arterial chemoreceptors and their role in oxygen and acid sensing. *Pflugers Arch.* 467, 1013–1025. doi: 10.1007/s00424-015-1689-1

Burnstock, G. (1972). Purinergic nerves. *Pharmacol. Rev.* 24, 509–581.

Burnstock, G. (2016). Short- and long-term (trophic) purinergic signalling. *Philos. Trans. R. Soc. Lond. B. Biol. Sci.* 371:20150422. doi: 10.1098/rstb.2015.0422

Burnstock, G., Campbell, G., Satchell, D., and Smythe, A. (1970). Evidence that adenosine triphosphate or a related nucleotide is the transmitter substance released by non-adrenergic inhibitory nerves in the gut. *Br. J. Pharmacol.* 40, 668–688. doi: 10.1111/j.14765381.1997.tb06815.x

Burnstock, G., Dumsday, B., and Smythe, A. (1972). Atropine resistant excitation of the urinary bladder: the possibility of transmission via nerves releasing a purine nucleotide. *Br. J. Pharmacol.* 44, 451–461. doi: 10.1111/j.1476-5381.1972.tb07283.x

Burnstock, G., and Knight, G. E. (2004). Cellular distribution and functions of P2 receptor subtypes in different systems. *Int. Rev. Cytol.* 240, 31–304. doi: 10.1016/S0074-7696(04)40002-3

Buttigieg, J., and Nurse, C. A. (2004). Detection of hypoxia-evoked ATP release from chemoreceptor cells of the rat carotid body. *Biochem. Biophys. Res. Commun.* 322, 82–87. doi: 10.1016/j.bbrc.2004.07.081

Campanucci, V. A., Zhang, M., Vollmer, C., and Nurse, C. A. (2006). Expression of multiple P2X receptors by glossopharyngeal neurons projecting to rat carotid body O_2-chemoreceptors: role in nitric oxide-mediated efferent inhibition. *J. Neurosci.* 26, 9482–9493. doi: 10.1523/JNEUROSCI.1672-06.2006

Cass, C. E., Young, J. D., and Baldwin, S. A. (1998). Recent advances in the molecular biology of nucleoside transport of mammalian cells. *Biochem. Cell Biol.* 76, 761–770. doi: 10.1139/o98-095

Conde, S. V., Gonzalez, C., Batuca, J. R., Monteiro, E. C., and Obeso, A. (2008). An antagonistic interaction between A2B adenosine and D2 dopamine receptors modulates the function of rat carotid body chemoreceptor cells. *J. Neurochem.*107, 1369–1381. doi: 10.1111/j.1471-4159.2008.05704.x

Conde, S. V., and Monteiro, E. C. (2004). Hypoxia induces adenosine release from the rat carotid body. *J. Neurochem.* 89, 1148–1156. doi: 10.1111/j.1471-4159.2004.02380.x

Conde, S. V., and Monteiro, E. C., (2006). Profiles for ATP and adenosine release at the carotid body in response to O_2 concentrations. *Adv. Exp. Med. Biol.* 580, 179–184. doi: 10.1007/0-387-31311-7_27

Conde, S. V., Monteiro, E. C., Obeso, A., and Gonzalez, C. (2009). Adenosine in peripheral chemoreception: new insights into a historically overlooked molecule - invited article. *Adv. Exp. Med. Biol.* 648, 145–159. doi: 10.1007/978-90-481-2259-2_17

Conde, S. V., Monteiro, E. C., Rigual, R., Obeso, A., and Gonzalez, C. (2012a). Hypoxic intensity: a determinant for the contribution of ATP and adenosine to the genesis of carotid body chemosensory activity. *J. Appl. Physiol.* 112, 2002–2010. doi: 10.1152/japplphysiol.01617.2011

Conde, S. V., Nunes da Silva, T., Gonzalez, C., Mota Carmo, M., Monteiro, E. C., and Guarino, M. P. (2012b). Chronic caffeine intake decreases circulating catecholamines and prevents diet-induced insulin resistance and hypertension in rats. *Br. J. Nutr.* 107, 86–95. doi: 10.1017/S0007114511002406

Conde, S. V., Obeso, A., Vicario, I., Rigual, R., Rocher, A., and Gonzalez, C. (2006). Caffeine inhibition of rat carotid body chemoreceptors is mediated by A2A and A2B adenosine receptors. *J. Neurochem.* 98, 616–628. doi: 10.1111/j.1471-4159.2006.03912.x

Conde, S. V., Ribeiro, M. J., Obeso, A., Rigual, R., Monteiro, E. C., and Gonzalez, C. (2012c). Chronic caffeine intake in adult rat inhibits carotid body sensitization produced by chronic sustained hypoxia but maintains intact chemoreflex output. *Mol. Pharmacol.* 82, 1056–1065. doi: 10.1124/mol.112.081216

Chen, J., Dinger, B., and Fidone, S. J. (1997). cAMP production in rabbit carotid body: role of adenosine. *J. Appl. Physiol.* 82, 1771–1775.

Ding, M., Bhupathiraju, S. N., Chen, M., van Dam, R. M., and Hu, F. B. (2014). Caffeinated and decaffeinated coffee consumption and risk of type 2 diabetes: a systematic review and a dose-response meta-analysis. *Diabetes Care* 37, 569–586. doi: 10.2337/dc13-1203

Donnelly, D. F., and Doyle, T. P. (1994). Developmental changes in hypoxia-induced catecholamine release from rat carotid body, in vitro. *J. Physiol.* 475, 267–275. doi: 10.1113/jphysiol.1994.sp020067

Dontas, A. S. (1955). Effects of energy donors, metabolic inhibitors and substrates on chemoreceptor activity. *J. Pharmacol. Exp. Ther.* 115, 46–54.

Dubyak, G. R. (2009). Both sides now: multiple interactions of ATP with pannexin-1 hemichannels. Focus on "A permeant regulating its permeation pore: inhibition of pannexin 1 channels by ATP". *Am. J. Physiol. Cell. Physiol.* 296, C235–C241. doi: 10.1152/ajpcell.00639.2008

Fitzgerald, R. S. (2000). Oxygen and carotid body chemotransduction: the cholinergic hypothesis - a brief history and new evaluation. *Respir. Physiol.* 120, 89–104. doi: 10.1016/S0034-5687(00)00091-8

Fletcher, E. C., Lesske, J., Qian, W., Miller, C. C., and Unger, T. (1992). Repetitive, episodic hypoxia causes diurnal elevation of blood pressure in rats. *Hypertension* 19, 555–561. doi: 10.1161/01.HYP.19.6.555

Fredholm, B. B., Abbracchio, M. P., Burnstock, G., Daly, J. W., Harden, T. K., Jacobson, K. A., et al. (1994). Nomenclature and classification of purinoceptors. *Pharmacol. Rev.* 46, 143–156.

Fredholm, B. B., Bättig, K., Holmén, J., Nehlig, A., and Zvartau, E. E. (1999). Actions of caffeine in the brain with special reference to factors that contribute to its widespread use. *Pharmacol. Rev.* 51, 83–133.

Fredholm, B. B., IJzerman, A. P., Jacobson, K. A., Klotz, K. N., and Linden, J. (2001). International union of pharmacology. XXV. Nomenclature and classification of adenosine receptors. *Pharmacol. Rev.* 53, 527–552.

Fudim, M., Groom, K. L., Laffer, C. L., Netterville, J. L., Robertson, D., and Elijovich, F. (2015). Effects of carotid body tumor resection on the blood pressure of essential hypertensive patients. *J. Am. Soc. Hypertens.* 9, 435–442. doi: 10.1016/j.jash.2015.03.006

Fuxe, K., Canals, M., Torvinen, M., Marcellino, D., Terasmaa, A., Genedani, S., et al. (2007). Intramembrane receptor–receptor interactions: a novel principle in molecular medicine. *J. Neural. Transm.* 114, 49–75. doi: 10.1007/s00702-006-0589-0

Gauda, E. B. (2002). Gene expression in peripheral arterial chemoreceptors. *Microsc. Res. Tech*. 59, 153–167. doi: 10.1002/jemt.10190

Gauda, E. B., Bamford, O., and Gerfen, C. R. (1996). Developmental expression of tyrosine hydroxylase, D2-dopamine receptor and substance P genes in the carotid body of the rat. *Neuroscience* 75, 969–977. doi: 10.1016/0306-4522(96)00312-0

Gauda, E. B., Northington, F. J., Linden, J., and Rosin, D. L. (2000). Differential expression of A_{2a}, A_1-adenosine and D_2-dopamine receptor genes in rat peripheral arterial chemoreceptors during postnatal development. *Brain Res.* 28, 1–10. doi: 10.1016/S0006-8993(00)02314-3

Go, A. S., Mozaffarian, D., Roger, V. L., Benjamin, E. J., Berry, J. D., Blaha, M. J., et al. (2014). Executive summary: heart disease and stroke statistics–2014 update: a report from the American Heart Association. *Circulation* 129, 399–410. doi: 10.1161/01.cir.0000442015.53336.12

Gonzalez, C., Agapito, M. T., Rocher, A., Gomez-Niño, A., Rigual, R., Castañeda, J., et al. (2010). A revisit to O_2 sensing and transduction in the carotid body chemoreceptors in the context of reactive oxygen species biology. *Respir. Physiol. Neurobiol.* 174, 317–330. doi: 10.1016/j.resp.2010.09.002

Gonzalez, C., Almaraz, L., Obeso, A., and Rigual, R. (1994). Carotid body chemoreceptors: from natural stimuli to sensory discharges. *Physiol. Rev.* 74, 829–898.

Gordon, G. R., Baimoukhametova, D. V., Hewitt, S. A., Rajapaksha, W. R., Fisher, T. E., and Bains, J. S. (2005). Norepinephrine triggers release of glial ATP to increase postsynaptic efficacy. *Nat. Neurosci.* 8, 1078–1086. doi: 10.1038/nn1498

Griffith, D. A., and Jarvis, S. M. (1996). Nucleoside and nucleobase transport systems of mammalian cells. *Biochim. Biophys. Acta* 1286, 153–181. doi: 10.1016/S0304-4157(96)00008-1

Hatton, C. J., and Peers, C. (1996). Hypoxic inhibition of K^+ currents in isolated rat type I carotid body cells: evidence against the involvement of cyclic nucleotides. *Pflugers Arch.* 433, 129–135. doi: 10.1007/s004240050258

Holmes, A. P., Ray, C. J., Pearson, S. A., Coney, A. M., and Kumar, P. (2017). Ecto-5'-nucleotidase (CD73) regulates peripheral chemoreceptor activity and cardiorespiratory responses to hypoxia. *J. Physiol.* doi: 10.1113/JP274498 [Epub ahead of print].

Hoshino, T., Yamada, K., Masuoka, K., Tsuboi, I., Itoh, K., Nonaka, K., et al. (1994). Elevated adenosine deaminase activity in the serum of patients with diabetes mellitus. *Diabetes Res. Clin. Pract.* 25, 97–102. doi: 10.1016/0168-8227(94)90034-5

Howell, L. L., and Landrum, A. M. (1995). Attenuation of hypoxia-induced increases in ventilation by adenosine antagonists in rhesus monkeys. *Life Sci.* 57, 773–783. doi: 10.1016/0024-3205(95)02005-4

Iturriaga, R. (2017). Translating carotid body function into clinical medicine. *J. Physiol.* doi: 10.1113/JP275335 [Epub ahead of print].

Iturriaga, R., and Alcayaga, J. (2004). Neurotransmission in the carotid body: transmitters and modulators between glomus cells and petrosal ganglion nerve terminals. *Brain Res. Brain Res. Rev.* 47, 46–53. doi: 10.1016/j.brainresrev.2004.05.007

Jarisch, A., Landgren, S., Neil, E., and Zotterman, Y. (1952). Impulse activity in the carotid sinus nerve following intra-carotid injection of potassium chloride, veratrine, sodium citrate, adenosine-triphosphate and alpha-dinitrophenol. *Acta Physiol. Scand.* 25, 195–211. doi: 10.1111/j.1748-1716.1952.tb00872.x

Jo, Y. H., and Role, L. W. (2002). Coordinate release of ATP and GABA at in vitro synapses of lateral hypothalamic neurons. *J. Neurosci.* 22, 4794–4804.

Jo, Y. H., and Schlichter, R. (1999). Synaptic corelease of ATP and GABA in cultured spinal neurons. *Nat. Neurosci.* 2, 241–245. doi: 10.1038/6344

Khakh, B. S., and North, R. A. (2006). P2X receptors as cell-surface ATP sensors in health and disease. *Nature* 442, 527–532. doi: 10.1038/nature04886

Khakh, B. S., and North, R. A. (2012). Neuromodulation by extracellular ATP and P2X receptors in the CNS. *Neuron* 76, 51–69. doi: 10.1016/j.neuron.2012.09.024

Kobayashi, S. (1976). An autoradiographic study of the mouse carotid body using tritiated leucine dopa, dopamine and ATP with special reference to the chief cell as a paraneuron. *Arch. Histol. Jpn.* 39, 295–317. doi: 10.1679/aohc1950.39.295

Kobayashi, S., Conforti, L., and Millhorn, D. E. (2000). Gene expression and function of A2A receptor in the rat carotid body. *Am. J. Physiol. Lung Cell Mol. Physiol.* 279, L273–L282.

Knowles, A. F. (2011). The GDA1_CD39 superfamily: NTPDases with diverse functions. *Purinergic Signal.* 7, 21–45. doi: 10.1007/s11302-010-9214-7

Lavie, L. (2003). Obstructive sleep apnoea syndrome – an oxidative stress disorder. *Sleep Med. Rev.* 7, 35–51. doi: 10.1053/smrv.2002.0261

Lewis, C., Neidhart, S., Holy, C., North, R. A., Buell, G., and Surprenant, A. (1995). Coexpression of P2X2 and P2X3 receptor subunits can account for ATP-gated currents in sensory neurons. *Nature* 377, 432–435. doi: 10.1038/377432a0

Livermore, S., and Nurse, C. A. (2013). Enhanced adenosine A2b receptor signaling facilitates stimulus-induced catecholamine secretion in chronically hypoxic carotid body type I cells. *Am. J. Physiol. Cell Physiol.* 305, C739–C750. doi: 10.1152/ajpcell.00137.2013

López-López, J. R., De Luis, D. A., and Gonzalez, C. (1993). Properties of a transient K^+ current in chemoreceptor cells of rabbit carotid body. *J. Physiol.* 460, 15–32. doi: 10.1113/jphysiol.1993.sp019456

Marshall, J. M. (1994). Peripheral chemoreceptors and cardiovascular regulation. *Physiol. Rev.* 74, 543–594.

Maxwell, D., Fuller, R. W., Conradson, T. B., Dixon, C. M., Aber, V., Hughes, J. M., et al. (1987). Contrasting effects of two xanthines, theophylline and enprofylline, on the cardiorespiratory stimulation of infused adenosine in man. *Acta Physiol. Scand.* 131, 459–465. doi: 10.1111/j.1748-1716.1987.tb08262.x

Maxwell, D., Fuller, R. W., Nolop, K. B., Dixon, C. M., and Hughes, J. M. (1986). Effects of adenosine on ventilatory responses to hypoxia and hypercapnia in humans. *J. Appl. Physiol.* 61, 1762–1766.

McQueen, D. S., Bond, S. M., Moores, C., Chessell, I., Humphrey, P. P. A., and Dowd, E. (1998). Activation of P2Xreceptors for adenosine triphosphate evokes cardiorespiratory reflexes in anaesthetized rats. *J. Physiol.* 507, 843–855. doi: 10.1111/j.1469-7793.1998.843bs.x

McQueen, D. S., and Ribeiro, J. A. (1981). Effect of adenosine on carotid chemoreceptor activity in the cat. *Br. J. Pharmacol.* 74, 129–136. doi: 10.1111/j.1476-5381.1981.tb09964.x

McQueen, D. S., and Ribeiro, J. A. (1983). On the specificity and type of receptor involved in carotid body chemoreceptor activation by adenosine in the cat. *Br. J. Pharmacol.* 80, 347–354. doi: 10.1111/j.1476-5381.1983.tb10040.x

McQueen, D. S., and Ribeiro, J. A. (1986). Pharmacological characterization of the receptor involved in chemoexcitation induced by adenosine. *Br. J. Pharmacol.* 88, 615–620. doi: 10.1111/j.1476-5381.1986.tb10242.x

Monteiro, E. C., and Ribeiro, J. A. (1987). Ventilatory effects of adenosine mediated by carotid body chemoreceptors in the rat. *Naunyn Schmiedebergs Arch. Pharmacol.* 335, 143–148.

Monteiro, E. C., and Ribeiro, J. A. (1989). Adenosine deaminase and adenosine uptake inhibitions facilitate ventilation in rats. *Naunyn Schmiedebergs Arch. Pharmacol.* 340, 230–238.

Monteiro, E. C., and Ribeiro, J. A. (2000). Adenosine-dopamine interactions and ventilation mediated through carotid body chemoreceptors. *Adv. Exp. Med. Biol.* 475, 671–684. doi: 10.1007/0-306-46825-5_66

Monteiro, E. C., Vera-Cruz, P., Monteiro, T. C., and Silva e Sousa, M. A. (1996). Adenosine increases the cAMP content of the rat carotid body in vitro. *Adv. Exp. Med. Biol.* 410, 299–303. doi: 10.1007/978-1-4615-5891-0_45

Murali, S., and Nurse, C. A. (2016). Purinergic signalling mediates bidirectional crosstalk between chemoreceptor type I and glial-like type II cells of the rat carotid body. *J. Physiol.* 594, 391–406. doi: 10.1113/JP271494

Narkiewicz, K., Ratcliffe, L. E., Hart, E. C., Briant, L. J., Chrostowska, M., Wolf, J., et al. (2016). Unilateral carotid body resection in resistant hypertension: a safety and feasibility trial. *JACC Basic Transl. Sci.* 1, 313–324. doi: 10.1016/j.jacbts.2016.06.004

Narkiewicz, K., van de Borne, P. J., Pesek, C. A., Dyken, M. E., Montano, N., and Somers, V. K. (1999). Selective potentiation of peripheral chemore- flex sensitivity in obstructive sleep apnea. *Circulation* 99, 1183–1189. doi: 10.1161/01.CIR.99.9.1183

Niane, L. M., Donnelly, D. F., Joseph, V., and Bairam, A. (2011). Ventilatory and carotid body chemoreceptor responses to purinergic P2X receptor antagonists in newborn rats. *J. Appl. Physiol.* 110, 83–94. doi: 10.1152/japplphysiol.00871.2010

Niewinski, P., Janczak, D., Rucinski, A., Jazwiec, P., Sobotka, P. A., Engelman, Z. J., et al. (2013). Carotid body removal for treatment of chronic systolic heart failure. *Int. J. Cardiol.* 168, 2506–2509. doi: 10.1016/j.ijcard.2013.03.011

Niewinski, P., Janczak, D., Rucinski, A., Tubek, S., Engelman, Z. J., Piesiak, P., et al. (2017). Carotid body resection for sympathetic modulation in systolic heart failure: results from first-in-man study. *Eur. J. Heart Fail.* 19, 391–400. doi: 10.1002/ejhf.641

North, R. A. (2016). P2X receptors. *Philos. Trans. R. Soc. Lond. B Biol. Sci.* 371:20150427. doi: 10.1098/rstb.2015.0427

Nunes, A. R., Holmes, A. P., Conde, S. V., Gauda, E. B., and Monteiro, E. C. (2014). Revisiting cAMP signaling in the carotid body. *Front. Physiol.* 5:406. doi: 10.3389/fphys.2014.0040

Nurse, C. A. (2010). Neurotransmitter and neuromodulatory mechanisms at peripheral arterial chemoreceptors. *Exp. Physiol.* 95, 657–667. doi: 10.1113/expphysiol.2009.049312

Nurse, C. A. (2014). Synaptic and paracrine mechanisms at carotid body arterial chemoreceptors. *J. Physiol.* 592, 3419–3426. doi: 10.1113/jphysiol.2013.269829

Nurse, C. A., and Piskuric, N. A. (2013). Signal processing at mammalian carotid body chemoreceptors. *Semin. Cell Dev.* 24, 22–30. doi: 10.1016/j.semcdb.2012.09.006

Obeso, A., Almaraz, L., and González, C. (1985). Correlation between adenosine triphosphate levels, dopamine release and electrical activity in the carotid body: support for the metabolic hypothesis of chemoreception. *Brain Res.* 348, 64–68. doi: 10.1016/0006-8993(85)90360-9

Obeso, A., Almaraz, L., and González, C. (1989). Effects of cyanide and uncouplers on chemoreceptor activity and ATP content of the cat carotid body. *Brain Res.* 481, 250–257. doi: 10.1016/0006-8993(89)90801-9

Oliveira, L., Correia, A., Cristina Costa, A., Guerra-Gomes, S., Ferreirinha, F., Magalhães-Cardoso, M. T., et al. (2015). Deficits in endogenous adenosine formation by ecto-5'-nucleotidase/CD73 impair neuromuscular transmission and immune competence in experimental autoimmune myasthenia gravis. *Mediators Inflamm.* 2015:460610. doi: 10.1155/2015/460610

Pankratov, Y., Lalo, U., Castro, E., Miras-Portugal, M. T., and Krishtal, O. (1999). ATP receptor-mediated component of the excitatory synaptic transmission in the hippocampus. *Prog. Brain Res.* 120, 237–249. doi: 10.1016/S0079-6123(08)63559-1

Pardal, R., Ortega-Sáenz, P., Durán, R., and López-Barneo, J. (2007). Glia-like stem cells sustain physiologic neurogenesis in the adult mammalian carotid body. *Cell* 131, 364–377. doi: 10.1016/j.cell.2007.07.043

Paton, J. F., Sobotka, P. A., Fudim, M., Engelman, Z. J., Hart, E. C., McBryde, F. D., et al. (2013). The carotid body as a therapeutic target for the treatment of sympathetically mediated diseases. *Hypertension* 61, 5–13. doi: 10.1161/HYPERTENSIONAHA.111.00064

Peers, C., and Buckler, K. J. (1995). Transduction of chemostimuli by the type I carotid body cell. *J. Membr. Biol.* 144, 1–9. doi: 10.1007/BF00238411

Peng, Y. J., Overholt, J. L., Kline, D., Kumar, G. K., and Prabhakar, N. R. (2003). Induction of sensory long-term facilitation in the carotid body by intermittent hypoxia: implications for recurrent apneas. *Proc. Natl. Acad. Sci. U.S.A.* 100, 10073–10078. doi: 10.1073/pnas.1734109100

Pérez-García, M. T., Almaraz, L., and González, C. (1990). Effects of different types of stimulation on cyclic AMP content in the rabbit carotid body: functional significance. *J. Neurochem.* 55, 1287–1293. doi: 10.1111/j.1471-4159.1990.tb03137.x

Pijacka, W., Moraes, D. J., Ratcliffe, L. E., Nightingale, A. K., Hart, E. C., da Silva, M. P., et al. (2016). Purinergic receptors in the carotid body as a new drug target for controlling hypertension. *Nat. Med.* 22, 1151–1159. doi: 10.1038/nm.4173

Piskuric, N. A., and Nurse, C. A. (2013). Expanding role of ATP as a versatile messenger at carotid and aortic body chemoreceptors. *J. Physiol.* 591, 415–422. doi: 10.1113/jphysiol.2012.234377

Podgorska, M., Kocbuch, K., and Pawelczyk, T. (2005). Recent advances in studies on biochemical and structural properties of equilibrative and concentrative nucleoside transporters. *Act. Biochem. Pol.* 52, 749–758.

Pougnet, J. T., Toulme, E., Martinez, A., Choquet, D., Hosy, E., and Boué-Grabot, E. (2014). ATP P2X receptors downregulate AMPA receptor trafficking and postsynaptic efficacy in hippocampal neurons. *Neuron* 83, 417–430. doi: 10.1016/j.neuron.2014.06.005

Prasad, M., Fearon, I. M., Zhang, M., Laing, M., Vollmer, C., and Nurse, C. A. (2001). Expression of P2X2 and P2X3 receptor subunits in rat carotid body afferent neurones: role in chemosensory signalling. *J. Physiol.* 537, 667–677. doi: 10.1111/j.1469-7793.2001.00667.x

Ralevic, V., and Burnstock, G. (1998). Receptors for purines and pyrimidines. *Pharmacol. Rev.* 50, 413–492.

Reyes, E. P., Fernández, R., Larraín, C., and Zapata, P. (2007). Effects of combined cholinergic–purinergic block upon cat carotid body chemosensory activity and ventilatory chemoreflexes. *Respir. Physiol. Neurobiol.* 156, 23–32. doi: 10.1016/j.resp.2006.07.006

Ribeiro, J. A., and McQueen, D. S. (1984). "Effects of purines on carotid chemoreceptors", in *The Peripheral Arterial Chemoreceptors*, ed. D.J. Pallot (London: Croom Helm), 383–390.

Ribeiro, J. A., and Monteiro, E. C. (1991). On the adenosine receptor involved in the excitatory action of adenosine on respiration: ant- agonist profile. *Nucleosides Nucleotides* 10, 945–953. doi: 10.1080/07328319108047232

Ribeiro, M. J., Sacramento, J. F., Gonzalez, C., Guarino, M. P., Monteiro, E. C., and Conde, S. V. (2013). Carotid body denervation prevents the development of insulin resistance and hypertension induced by hypercaloric diets. *Diabetes Metab. Res. Rev.* 62, 2905–2916. doi: 10.2337/db12-1463

Rocher, A., Gonzalez, C., and Almaraz, L. (1999). Adenosine inhibits L-type Ca2+ currents and catecholamine release in the rabbit carotid body chemoreceptor cells. *Eur. J. Neurosci.* 11, 673–681. doi: 10.1046/j.1460-9568.1999.00470

Rong, W., Gourine, A. V., Cockayne, D. A., Xiang, Z., Ford, A. P., Spyer, K. M., et al. (2003). Pivotal role of nucleotide P2X2 receptor subunit of the ATP-gated ion channel mediating ventilatory responses to hypoxia. *J. Neurosci.* 23, 11315–11321.

Runold, M., Cherniack, N. S., and Prabhakar, N. R. (1990). Effect of adenosine on isolated and superfused cat carotid body activity. *Neurosci. Lett.* 113, 111–114. doi: 10.1016/0304-3940(90)90504-3

Sacramento, J. F., Chew, D. J., Melo, B. F., Donegá, M., Dopson, W., Guarino, M. P., et al. (2017a). Bioelectronic modulation of carotid sinus nerve activity in the rat: a potential therapeutic approach for type 2 diabetes. *Diabetologia* (in press).

Sacramento, J. F., Gonzalez, C., Gonzalez-Martin, M. C., and Conde, S. V. (2015). Adenosine receptor blockade by caffeine inhibits carotid sinus nerve chemosensory activity in chronic intermittent hypoxic animals. *Adv. Exp. Med. Biol.* 860, 133–137. doi: 10.1007/978-3-319-18440-1_15

Sacramento, J. F., Ribeiro, M. J., Rodrigues, T., Olea, E., Melo, B. F., Guarino, M. P., et al. (2017b). Functional abolition of carotid body activity restores insulin action and glucose homeostasis in rats: key roles for visceral adipose tissue and the liver. *Diabetologia* 60, 158–168. doi: 10.1007/s00125-016-4133-y

Salman, S., Vollmer, C., McClelland, G. B., and Nurse, C. A. (2017). Characterization of ectonucleotidase expression in the rat carotid body: regulation by chronic hypoxia. *Am. J. Physiol. Cell. Physiol.* 313, C274–C284. doi: 10.1152/ajpcell.00328.2016

Schubert, P., Komp W., and Kreutzberg, G. W. (1979). Correlation of 5 - nucleotidase activity and selective transneuronal transfer of adenosine in the hippocampus. *Brain Res.* 168, 419–424. doi: 10.1016/0006-8993(79)90186-0

Siński, M., Lewandowski, J., Przybylski, J., Bidiuk, J., Abramczyk, P., Ciarka, A., et al. (2012). Tonic activity of carotid body chemoreceptors contributes to the increased sympathetic drive in essential hypertension. *Hypertens. Res.* 35, 487–491. doi: 10.1038/hr.2011.209

Somers, V. K., Mark, A. L., and Abboud, F. M. (1988). Potentiation of sympathetic nerve responses to hypoxia in borderline hypertensive subjects. *Hypertension* 11, 608–612. doi: 10.1161/01.HYP.11.6.608

Soto, C. R., Ortiz, F. C., Vargas, R. V., Arroyo, J., and Alcayaga, J. (2010). Responses induced by acetylcholine and ATP in the rabbit petrosal ganglion. *Respir. Physiol. Neurobiol.* 172, 114–121. doi: 10.1016/j.resp.2010.05.003

Spergel, D., and Lahiri, S. (1993). Differential modulation by extracellular ATP of carotid chemosensory response. *J. Appl. Physiol.* 74, 3052–3056.

Starlinger, H. (1982). ATPases of the cat carotid body and of neighbouring ganglia. *Z. Naturforsch. C* 37, 532–539.

Tan, Z. Y., Lu, Y., Whiteis, C. A., Simms, A. E., Paton, J. F., and Chapleau, M. W., et al. (2010). Chemoreceptor hypersensitivity, sympathetic excitation, and overexpression of ASIC and TASK channels before the onset of hypertension in SHR. *Circ. Res.* 106, 536–545. doi: 10.1161/CIRCRESAHA.109.206946

Teppema, L. J., and Dahan, A. (2010). The ventilatory response to hypoxia in mammals: mechanisms, measurement, and analysis. *Physiol. Rev.* 90, 675–754. doi: 10.1152/physrev.00012.2009

Torres, G. E., Egan, T. M., and Voigt, M. M. (1999). Hetero-oligomeric assembly of P2X receptor subunits. Specificities exist with regard to possible partners. *J. Biol. Chem.* 274, 6653–6659. doi: 10.1074/jbc.274.10.6653

Trussell, L. O., and Jackson, M. B. (1985). Adenosine-activated potassium conductance in cultured striatal neurons. *Proc. Natl. Acad. Sci. U.S.A.* 82, 4857–4861. doi: 10.1073/pnas.82.14.4857

Trzebski, A., Ta, M., Zoltowski, M., and Przybylski, J. (1982). Increased sensitivity of the arterial chemoreceptor drive in young men with mild hypertension. *Cardiovasc. Res.* 16, 163–172.

Tse, A., Yan, L., Lee, A. K., and Tse, F. W. (2012). Autocrine and paracrine actions of ATP in rat carotid body. *Can. J. Physiol. Pharmacol.* 90, 705–711. doi: 10.1139/y2012-054

Uematsu, T., Kozawa, O., Matsuno, H., Niwa, M., Yoshikoshi, H., Oh-uchi, M., et al. (2000). Pharmacokinetics and tolerability of intravenous infusion of adenosine (SUNY4001) in healthy volunteers. *Br. J. Clin. Pharmacol.* 50, 177–181. doi: 10.1046/j.1365-2125.2000.00214.x

van Dam, R. M., and Hu, F. B. (2005). Coffee consumption and risk of type 2 diabetes: a systematic review. *JAMA* 294, 97–104. doi: 10.1001/jama.294.1.97

Vandier, C., Conway, A. F., Landauer, R. C., and Kumar, P. (1999). Presynaptic action of adenosine on a 4-aminopyridine-sensitive current in the rat carotid body. *J. Physiol.* 515, 419–429. doi: 10.1111/j.1469-7793.1999.419ac.x

Varas, R., Alcayaga, J., and Iturriaga, R. (2003). ACh and ATP mediate excitatory transmission in cat carotid identified chemoreceptor units in vitro. *Brain Res.* 988, 154–163. doi: 10.1016/S0006-8993(03)03366-3

Verna, A., Talib, N., Roumy, M., and Pradet, A. (1990). Effects of metabolic inhibitors and hypoxia on the ATP, ADP and AMP content of the rabbit carotid body in vitro: the metabolic hypothesis in question. *Neurosci. Lett.* 116, 156–161. doi: 10.1016/0304-3940(90)90402-U

Vicario, I., Obeso, A., Rocher, A., López-Lopez, J. R., and González, C. (2000). Intracellular Ca(2+) stores in chemoreceptor cells of the rabbit carotid body: significance for chemoreception. *Am. J. Physiol. Cell Physiol.* 279, 51–61.

Wang, W. J., Cheng, G. F., Yoshizaki, K., Dinger, B., and Fidone, S. (1991). The role of cyclic AMP in chemoreception in the rabbit carotid body. *Brain Res.* 540, 96–104. doi: 10.1016/0006-8993(91)90495-H

Watt, A. H., Reid, P. G., Stephens, M. R., and Routledge, P. A. (1987). Adenosine-induced respiratory stimulation in man depends on site of infusion. Evidence for an action on the carotid body. *Br. J. Clin. Pharmacol.* 23, 486–490. doi: 10.1111/j.1365-2125.1987.tb03081.x

Watt, A. H., and Routledge, P. A. (1985). Adenosine stimulates respiration in man. *Br. J. Pharmacol.* 20, 503–506. doi: 10.1111/j.1365-2125.1985.tb05108.x

Wu, L. G., and Saggau, P. (1994). Adenosine inhibits evoked synaptic transmission primarily by reducing presynaptic calcium influx in area CA1 of hippocampus. *Neuron* 12, 1139–1148. doi: 10.1016/0896-6273(94)90321-2

Xu, F., Xu, J., Tse, F. W., and Tse, A. (2006). Adenosine stimulates depolarization and rise in cytoplasmic [Ca2+] in type I cells of rat carotid bodies. *Am. J. Physiol. Cell Physiol.* 290, 1592–1598. doi: 10.1152/ajpcell.00546.2005

Xu, J., Tse, F. W., and Tse, A. (2003). ATP triggers intracellular Ca2+ release in type II cells of the rat carotid body. *J. Physiol.* 549, 739–747. doi: 10.1113/jphysiol.2003.039735

Xu, J., Xu, F., Tse, F. W., and Tse, A. (2005). ATP inhibits the hypoxia response in type I cells of rat carotid bodies. *J. Neurochem.* 92, 1419–1430. doi: 10.1111/j.1471-4159.2004.02978.x

Yegutkin, G. G. (2008). Nucleotide- and nucleoside-converting ectoenzymes: important modulators of purinergic signalling cascade. *Biochim. Biophys. Acta* 1783, 673–694. doi: 10.1016/j.bbamcr.2008.01.024

Zapata, P. (2007). Is ATP a suitable co-transmitter in carotid body arterial chemoreceptors? *Respir. Physiol. Neurobiol.* 157, 106–115. doi: 10.1016/j.resp.2007.01.002

Zhang, M., Piskuric, N. A., Vollmer, C., and Nurse, C. A. (2012). P2Y2 receptor activation opens pannexin-1 channels in rat carotid body type II cells: potential role in amplifying the neurotransmitter ATP. *J. Physiol.* 590, 4335–4350. doi: 10.1113/jphysiol.2012.236265

Zhang, M., Vollmer, C., and Nurse, C. A. (2017). Adenosine and dopamine oppositely modulate a hyperpolarization-activated current Ih in chemosensory neurons of the rat carotid body in co-culture. *J. Physiol.* doi: 10.1113/JP274743 [Epub ahead of print].

Zhang, M., Zhong, H., Vollmer, C., and Nurse, C. A. (2000). Co-release of ATP and ACh mediates hypoxic signalling at rat carotid body chemoreceptors *J. Physiol.* 525, 143–158. doi: 10.1111/j.1469-7793.2000.t01-1-00143.x

Zimmermann, H. (2016). Extracellular ATP and other nucleotides-ubiquitous triggers of intercellular messenger release. *Purinergic Signal.* 12, 25–57. doi: 10.1007/s11302-015-9483-2

Zimmermann, H., Braun, N., Kegel, B., and Heine, P. (1998). New insights into molecular structure and function of ectonucleotidases in the nervous system. *Neurochem. Int.* 32, 421–425. doi: 10.1016/S0197-0186(97)00126-5

Zimmermann, H., Mishra, S. K., Shukla, V., Langer, D., Gampe, K., Grimm, I., et al. (2007). Ecto-nucleotidases, molecular properties and functional impact. *An. R. Acad. Nac. Farm.* 73, 537–566.

Zoccal, D. B., Huidobro-Toro, J. P., and Machado, B. H. (2011). Chronic intermittent hypoxia augments sympatho-excitatory response to ATP but not to L-glutamate in the RVLM of rats. *Auton. Neurosci.* 165, 156–162. doi: 10.1016/j.autneu.2011.06.001

Conflict of Interest Statement: The authors declare that the research was conducted in the absence of any commercial or financial relationships that could be construed as a potential conflict of interest.

frontiers in Pharmacology

REVIEW
published: 04 December 2017
doi: 10.3389/fphar.2017.00858

Adenosine Receptors As Drug Targets for Treatment of Pulmonary Arterial Hypertension

*Allan K. N. Alencar, Guilherme C. Montes, Eliezer J. Barreiro, Roberto T. Sudo and Gisele Zapata-Sudo**

Programa de Pesquisa em Desenvolvimento de Fármacos, Instituto de Ciências Biomédicas, Universidade Federal do Rio de Janeiro, Rio de Janeiro, Brazil

Pulmonary arterial hypertension (PAH) is a clinical condition characterized by pulmonary arterial remodeling and vasoconstriction, which promote chronic vessel obstruction and elevation of pulmonary vascular resistance. Long-term right ventricular (RV) overload leads to RV dysfunction and failure, which are the main determinants of life expectancy in PAH subjects. Therapeutic options for PAH remain limited, despite the introduction of prostacyclin analogs, endothelin receptor antagonists, phosphodiesterase type 5 inhibitors, and soluble guanylyl cyclase stimulators within the last 15 years. Through addressing the pulmonary endothelial and smooth muscle cell dysfunctions associated with PAH, these interventions delay disease progression but do not offer a cure. Emerging approaches to improve treatment efficacy have focused on beneficial actions to both the pulmonary vasculature and myocardium, and several new targets have been investigated and validated in experimental PAH models. Herein, we review the effects of adenosine and adenosine receptors (A_1, A_{2A}, A_{2B}, and A_3) on the cardiovascular system, focusing on the A_{2A} receptor as a pharmacological target. This receptor induces pulmonary vascular and heart protection in experimental models, specifically models of PAH. Targeting the A_{2A} receptor could potentially serve as a novel and efficient approach for treating PAH and concomitant RV failure. A_{2A} receptor activation induces pulmonary endothelial nitric oxide synthesis, smooth muscle cell hyperpolarization, and vasodilation, with important antiproliferative activities through the inhibition of collagen deposition and vessel wall remodeling in the pulmonary arterioles. The pleiotropic potential of A_{2A} receptor activation is highlighted by its additional expression in the heart tissue, where it participates in the regulation of intracellular calcium handling and maintenance of heart chamber structure and function. In this way, the activation of A_{2A} receptor could prevent the production of a hypertrophic and dysfunctional phenotype in animal models of cardiovascular diseases.

Keywords: pulmonary arterial hypertension, cardiopulmonary system, adenosine receptors, cell proliferation, right ventricle dysfunction, pleiotropic effects

OPEN ACCESS

Edited by:
Kenneth A. Jacobson, National Institutes of Health (NIH), United States

Reviewed by:
Katia Varani, University of Ferrara, Italy
Paulo Correia-de-Sá, Universidade do Porto, Portugal

***Correspondence:**
Gisele Zapata-Sudo
gzsudo@oi.com.br

Specialty section:
This article was submitted to Experimental Pharmacology and Drug Discovery, a section of the journal Frontiers in Pharmacology

Received: *12 July 2017*
Accepted: *09 November 2017*
Published: *04 December 2017*

Citation:
Alencar AKN, Montes GC, Barreiro EJ, Sudo RT and Zapata-Sudo G (2017) Adenosine Receptors As Drug Targets for Treatment of Pulmonary Arterial Hypertension. Front. Pharmacol. 8:858. doi: 10.3389/fphar.2017.00858

INTRODUCTION

Pulmonary hypertension (PH) refers to a complex group of cardiopulmonary diseases that may lead to right-sided heart failure and reduced life expectancy (Galie et al., 2016). Pulmonary arterial hypertension (PAH) represents group 1 within the PH classification system (Simonneau et al., 2013). PAH is characterized by precapillary PH (i.e., mean pulmonary arterial pressure $\geq$ 25 mmHg

and normal pulmonary capillary wedge pressure $\leq$ 15 mmHg), as a consequence of exacerbated remodeling and hypertrophy of the walls of the pulmonary arteries (PAs) (Galie et al., 2016). The most severe form of PH, PAH has a prevalence of 15 cases per million adult population, incidence of 2.4 cases per million adult population per year (McGoon et al., 2013), and mean survival rate of 2.8 years in the absence of specific treatments (McGoon et al., 2013; Simonneau et al., 2013).

Current knowledge on PAH pathophysiology highlights microenvironmental changes in the pulmonary vessels as the initial cause of the disease. Crosstalk among endothelial cells (ECs), pulmonary arterial smooth muscle cells (PASMCs), myofibroblasts, pericytes, and circulating immunologic cells triggers PAH pathogenesis (Guignabert et al., 2015). Elevated pulmonary vascular resistance (PVR) causes insult to the right ventricular (RV) myocardium, with subsequent activation of neurohormonal, immunological, and mechanical-stretch signaling (Voelkel et al., 2006). The poor prognosis of PAH is mainly a consequence of long-term pressure overload in the RV chamber, which initially responds with adaptive myocardial hypertrophy. This response is followed by progressive contractile dysfunction, global heart failure, and premature death (Voelkel et al., 2006; Sztrymf et al., 2010).

Treatment of patients with PAH is palliative. Available agents include lung vasodilators, such as phosphodiesterase type 5 inhibitors, endothelin receptor antagonists, prostacyclin analogs, and guanylyl cyclase stimulators (Galie et al., 2016). Lung transplantation is an important strategy in eligible subjects with advanced PAH who are refractory to drug intervention (Galie et al., 2016). Current treatments of PAH simply control the intense PA vasoconstriction, but recent advances in understanding disease pathophysiology have driven efforts to develop new pharmacological strategies targeting the irreversible remodeling of the pulmonary vascular bed. Favorable actions in the hypertrophied and dysfunctional RV are required for better outcomes, and there is a clear need for pleiotropic targets with beneficial roles throughout the cardiopulmonary system (pulmonary vessel and cardiac cells).

Adenosine has a well-known pulmonary vasodilator effect with a rapid onset of action (Reeves et al., 1991; Nootens et al., 1995). Adenosine use is recommended as an alternative strategy in pulmonary vasoreactivity testing for identification of patients suitable for high-dose calcium channel blocker treatment (Galie et al., 2016). Patients suffering from PAH exhibit low adenosine levels in the pulmonary circulation, suggesting that this nucleoside plays a role in PAH pathophysiology. The reduction of the adenosine release on pulmonary vascular endothelium is consequent to the endothelial dysfunction that is present in PAH. Low levels in PAH may also be explained by increased activity of the adenosine deaminase in the pulmonary circulation (Saadjian et al., 1999), which was found in rats with hemolysis-associated pulmonary hypertension (Tofovic et al., 2009). However, clinical implications of the adenosine deaminase or its inhibitors in PAH remain unclear. Adenosine promotes various beneficial effects in the heart (Shryock and Belardinelli, 1997) and has been defined as a retaliatory metabolic product (Newby et al., 1985).

Long-term use of adenosine in PAH and RV failure has been limited by its extremely short half-life (Nootens et al., 1995) and adverse effects by non-selective activation of its four receptor subtypes. Nevertheless, adenosine receptors (ARs) promote multiple salutary actions in cardiac and vascular cells, including ECs, fibroblasts, and myocytes (McIntosh and Lasley, 2012; Headrick et al., 2013). Immune cells express ARs to respond to the modulatory effects of adenosine in an inflammatory environment (Hasko et al., 2008). Researchers from several fields are considering the possibility of targeting ARs as a therapeutic approach in various clinical conditions, including cerebral and cardiac diseases, sleep disorders, immune and inflammatory disorders, and cancer (Jacobson and Gao, 2006; Hasko et al., 2008; McIntosh and Lasley, 2012; Chen et al., 2013; Headrick et al., 2013).

This review compiles findings on the specific roles of each AR subtype in the cardiovascular system. The work focuses on AR activities in the small circulation, specifically in PAH pathogenesis, including the aberrant cellular proliferation and influx of inflammatory cells in and around various components of the vascular wall, as well as the distinct roles of ARs in RV cells. The main goal of this review is to answer an intriguing question: Does a specific AR exist that could be considered as a future target with pleiotropic potential in the whole cardiopulmonary system of patients with PAH?

PULMONARY VASCULAR CHANGES IN PAH

Before addressing the potential benefits of targeting specific ARs for the treatment of PAH, we must understand the intrinsic pathophysiological mechanisms of this disease. Dynamic interactions among cells in the pulmonary vascular bed are the main determinant of cellular behavior (e.g., proliferation, apoptosis, differentiation, migration, and survival) in PA walls. Abnormal cell communication can lead to development of PAH (Eddahibi et al., 2006; Xu and Mao, 2011; Guignabert and Dorfmuller, 2013; Guignabert et al., 2015). Crosstalk between PA cells is regulated through direct cell–cell contact and release of bioactive factors, such as EC-produced paracrine factors that influence the proliferation of PASMCs and fibroblasts (Eddahibi et al., 2006; Sakao et al., 2009; Amabile et al., 2013).

Below a cross-sectional diameter of 500 μm (lobular to intra-acinar level), the medial layer of the PAs is typically composed solely of smooth muscle cells (SMCs), due to loss of elastic fibers. Beyond this level, the PAs leave their adjacent airways and become barely muscularized precapillary arterioles (Guignabert and Dorfmuller, 2013). Vascular remodeling in the lungs of PAH patients initially begins in this type of arteriole and presents as PASMC hyperproliferation, underlining the importance of this cell type in PAH pathogenesis (Schermuly et al., 2011; Guignabert and Dorfmuller, 2013). Early lesions correspond to hypertrophic and hyperplastic PASMCs within the tunica media (Guignabert and Dorfmuller, 2013). The abnormal proliferation of PASMCs during PAH development occurs in response to the signaling of growth factors, including potent mitogens and chemoattractants

for vascular cells, which bind to and activate surface tyrosine kinase receptors (TKRs) (Schermuly et al., 2011).

Pulmonary ECs play a crucial role during the formation and maturation of blood vessels, producing and releasing growth factors that recruit and stabilize all vascular cells (Folkman and D'Amore, 1996; Hanahan, 1997). Eddahibi et al. (2006) showed that EC-induced PASMC growth was greater in tissues from PAH patients than from controls. Dysregulation of this process and excessive release of growth factors by ECs are intrinsic abnormalities linked to PAH pathogenesis. Indeed, abnormal communication between ECs and other vascular cells in PAH may occur due to loss-of-function of the endothelium.

Among different factors, bone morphogenic protein (BMP) signaling regulates pulmonary EC survival and differentiation (Teichert-Kuliszewska et al., 2006). Patients with PAH show abnormal BMP signaling, linked to mutations of bone morphogenetic protein receptor-2 (BMPR2) in ECs (Teichert-Kuliszewska et al., 2006). These mutations could lead to deleterious consequences in ECs and PASMCs. Loss of BMPR2 signaling in ECs may increase apoptosis in response to environmental stress and injury, particularly at the level of the distal PAs (Teichert-Kuliszewska et al., 2006). This apoptosis could be an initiating mechanism for PAH by leading to vessel obliteration due to degeneration of EC structures (Zhao et al., 2005). Excessive loss of ECs promotes the development of apoptosis-resistant and hyperproliferative ECs, which are characteristic features of later stages of PAH (Voelkel et al., 2002).

The initial trigger for pulmonary EC injury is unknown, although some events, such as shear stress, local inflammation, genetic predisposition, toxins, and reactive oxygen species (ROS)-induced cell damage, might be important inducers of endothelial dysfunction (Amabile et al., 2013). Exuberant proliferation of ECs leads to formation of plexiform lesions. These dynamic networks of vascular channels formed by the monoclonal proliferation of ECs (St Croix and Steinhorn, 2016) are a morphologic hallmark of severe PAH. A single plexiform lesion can occlude the entire length of an affected vessel (Cool et al., 1999). However, debate surrounds the functional importance of these lesions in the context of PAH, as it remains unclear if they have a role in disease progression or are simply a morphologic indicator of irreversible, end-stage disease (Tuder et al., 2007; Abe et al., 2010; Jonigk et al., 2011; St Croix and Steinhorn, 2016).

In PASMCs, signaling by BMPR2 is necessary for the control of cell proliferation and differentiation (Upton et al., 2008; Garcia de Vinuesa et al., 2016). Together with EC-induced cell proliferation and medial hypertrophy, BMPR2 mutations in PASMCs participate in the process of initiating or maintaining pulmonary vessel hypertrophy in PAH patients (Zhang et al., 2003).

Fibroblasts play important roles in PAH pathogenesis by responding to injury and chemoattraction via endothelium-derived growth factors. Rapid migration of fibroblasts to the injured vessel leads to formation of the neointimal layer and, most importantly, fibroblast transdifferentiation into other cell types, including myofibroblasts – an abnormal type of PASMC that contributes to muscularization of the distal vessels (Sartore et al., 2001; Sisbarro et al., 2005; Sakao et al., 2009).

Taken together, these findings indicate that any effect on BMPR2 signaling may trigger abnormal communication between ECs, PASMCs, and fibroblasts via growth factors. Subsequently, these growth factors trigger hyperproliferation and differentiation of cells, formation of plexiform lesions, obliteration and fibrosis of the vessels, and increases of PVR and pulmonary vascular pressure.

In an elegant review, Schermuly et al. (2011) summarized the growth factors that are most clearly implicated in PAH pathogenesis. The review showed increased signaling of the following molecules in injured pulmonary vascular cells: vascular endothelial growth factor (VEGF), transforming growth factor alpha and beta (TGF-α and TGF-β), platelet-derived growth factor (PDGF), and hepatocyte growth factor (HGF) (Schermuly et al., 2011). All of these growth factors bind to TKRs, resulting in multi-phosphorylation of tyrosine residues for the assembly of downstream signaling molecules that are recruited to the receptor and activated in response to agonist stimulation (Lemmon and Schlessinger, 2010). Subsets of intracellular signaling components influenced by growth factor receptor activation are intertwined in a complex network. Examples of intracellular molecules activated by TKRs are phosphoinositide 3-kinase (PI3K)/protein kinase B (Akt), mitogen-activated protein kinases (Ras/Raf/MAPK/ERK), protein kinase C (PKC), Janus kinase (JAK), signal transducer and activator of transcription (STAT), and cyclins (a family of proteins that control cell cycle progression by activating cyclin-dependent kinases) (Koledova and Khalil, 2006; Lemmon and Schlessinger, 2010).

Roles of TKRs and their antagonists in PAH have been reviewed, and cardiac safety issues of these molecules have been raised, especially in patients with heart disease that is intrinsically related to pulmonary vascular disease (Godinas et al., 2013). The large blockage spectrum and lack of selectivity of TKR antagonists would provide unexpected toxicities, including injury to the pulmonary vasculature. Furthermore, the benefit-to-risk ratio of available TKR antagonists is low in the context of PAH (Godinas et al., 2013). Thus, new approaches for PAH treatment should be aimed at ensuring a low toxicity profile, in addition to the high anti-proliferative efficacy.

Accumulating evidence shows that RhoA, a member of the Ras homolog gene family, and its downstream effectors, the Rho kinases (ROCKs), mediate the pathogenesis of PAH through their pro-proliferative contributions (Nagaoka et al., 2006; Guilluy et al., 2009; Connolly and Aaronson, 2011). ROCK downregulates expression of anti-proliferative molecules, leading to acceleration of cell cycle progression and vascular cell hyperproliferation (Laufs et al., 1999; Sawada et al., 2000). Distal muscularization of pulmonary vessels has been linked to amplification of the RhoA/ROCK pathway in PASMCs (Emerson et al., 1999; Fagan et al., 1999; Aznar and Lacal, 2001; Keil et al., 2002).

Another important factor involved in endothelium-smooth muscle interactions, serotonin makes a major contribution to PASMC hyperplasia in PAH (Eddahibi et al., 2006). Serotonin-mediated PASMC proliferation was greater in mice with

genetically mutated BMPR2 (Long et al., 2006). The BMP and serotonin mechanisms are convergent in PASMCs; both stimulate RhoA/ROCK signaling downstream for a pro-proliferative phenotype (Liu et al., 2009). These previous reports suggest that vascular cell proliferation induced by downstream growth factors could be attenuated, in part, through inhibition of RhoA/ROCK signaling.

The RhoA/ROCK pathway is of interest to pharmaceutical companies due to the pleiotropic effects of its inhibitors in numerous diseases (Feng et al., 2016). Fasudil is a ROCK inhibitor that has shown salutary effects in the cardiopulmonary system of PAH patients and in different experimental models of the disease. These effects derive from its anti-proliferative profile in the pulmonary vessels, which it achieves by reducing PVR and RV overload (Mouchaers et al., 2010; Raja, 2012; Fukumoto et al., 2013; Jiang et al., 2014; Xiao et al., 2015; Gupta et al., 2017). Nevertheless, the cardioprotective potential of this pharmacological modality is not completely clear, as the effect of fasudil on reducing PAH-related changes in the RV may be an indirect response of the lower afterload in the right heart chamber. In addition to the beneficial effects of ROCK inhibitors in the left heart (Demiryurek et al., 2005; Takeshima et al., 2012), their direct effects should be investigated in the RV cells, because the structures, hemodynamics, and functions of both ventricles are distinct.

Secondarily to the pro-proliferative phenotype in pulmonary vascular cells, damaged crosstalk between ECs and PASMCs can exacerbate PA vasoconstriction as a consequence of an imbalance in the production of endothelium-derived vasodilator [nitric oxide (NO) and prostacyclin] and constrictor factors (endothelin-1, serotonin, and angiotensin II). Crosstalk dysfunction is a pivotal element in the development and progression of the disease (Guignabert et al., 2015).

Furthermore, PAH is among many pathophysiologic conditions that are linked to inflammation (Schermuly et al., 2011). Inflammation has a pivotal role during development of PAH in humans and in animal models of the disease. Some patients with PAH present increased levels of tumor necrosis factor alpha (TNF-α), interleukins 12 and 6 (IL-12 and IL-6), and interferon-γ, associated with other inflammatory signals, such as plasma cell dyscrasia polyneuropathy. Induction of PAH in rodents by chronic hypoxia or monocrotaline leads to an increase in the number of inflammatory cells in the lungs (Minamino et al., 2001; Soon et al., 2010; Bi et al., 2013). Vascular and inflammatory cells are important local sources of cytokines and chemokines, which can trigger pulmonary vascular remodeling in PAH (Sutendra et al., 2011; Rabinovitch et al., 2014). Histopathological studies have demonstrated the presence of complement system components, autoantibodies, and inflammatory cells (neutrophils) in the vessel lumen, which can bind to the endothelium and may infiltrate the medial muscular layer. Inflammatory infiltrate in the neointimal layer is composed of T- and B-lymphocytes, with macrophages, mast cells, and dendritic cells present in the adventitial layer. Lymphoid follicles, characterized by T cells, B cells, and plasmacytoid dendritic cells (APCs), are found in the periadventitial space (Stacher et al., 2012; Rabinovitch et al., 2014). Thus, reversion of the pulmonary vessel injury in PAH requires an anti-inflammatory profile.

CARDIOVASCULAR FUNCTIONS OF ADENOSINE AND ITS RECEPTORS

Adenosine is a purine nucleoside that is widely distributed in all tissues. Structurally, adenosine is formed by the linking of adenine to a ribose sugar molecule. Synthesis of adenosine is increased after myocardial infarction (MI) (Daly, 1982; Hasko and Cronstein, 2004; Asakura et al., 2007; Hisatome, 2007). Adenosine is synthesized inside and outside the cells for immediate use and is not stored in vesicles for future release. For these reasons, this molecule is an autacoid, similar to several biological transmitters (Newby and Holmquist, 1981; Deussen et al., 1989; Deussen and Schrader, 1991; Decking et al., 1997; Zimmermann, 2000).

Extracellular production of adenosine depends on a cascade reaction initiated by ATP and ADP as substrates (Dunwiddie et al., 1997). ATP and ADP are converted to AMP by catalysis of ectonucleoside triphosphate diphosphohydrolases (NTPDases 1, 2, 3, and 8) on the cell surface, followed by AMP hydrolysis to adenosine by ecto-5′-nucleotidase (NTE5/CD73) (Ballard, 1970; Headrick and Willis, 1990; Decking et al., 1997; Bak and Ingwall, 1998; Gustafson and Kroll, 1998). Intracellular adenosine might be provided through other signaling processes. One of these events is the catabolism of ATP from stressed cells under hypoxia (Ham and Evans, 2012). This condition might be responsible for the perturbed recycling of adenosine and ATP, and the increased activity of specific phosphatases leads to excessive levels of adenosine (Spychala, 2000). Another source of intracellular adenosine is the cytosolic 5′-nucleotidase-mediated metabolism (dephosphorylation) of AMP, which is formed from the degradation of cyclic AMP (cAMP) by phosphodiesterases. Intracellular adenosine is also importantly generated by the conversion of *S*-adenosylhomocysteine to adenosine and homocysteine, catalyzed by *S*-adenosylhomocysteine hydrolase (Kloor and Osswald, 2004; Hermes et al., 2007; Antonioli et al., 2015).

Adenosine is converted, extra- or intracellularly, to inosine by adenosine deaminase (Ford et al., 2000; Singh and Sharma, 2000; Antonioli et al., 2012). Phosphorylation of adenosine to AMP by adenosine kinase reduces the intracellular concentration of adenosine (De Jong, 1977; Drabikowska et al., 1985; Pak et al., 1994; Boison, 2013). The adenosine concentration depends on two families of transmembrane proteins, concentrative and equilibrative nucleoside transporters, which facilitate the movement of nucleosides, nucleobases, and their analogs across the cell membrane. There are four isoforms of human equilibrative nucleoside transporters, but only ENT1 and ENT2 are expressed in tissues throughout the body (King et al., 2006; Playa et al., 2014). The adenosine transport process usually follows gradients from high to low concentration, with no energy spending (Chen et al., 2013). The extracellular adenosine concentration varies substantially between tissue types (Ramakers et al., 2008). The local adenosine concentration may

be increased from the nano- to the micromolar range, signaling tissue injury, by extreme pathophysiological cell activation (seizure) or insults due to ischemia, trauma, inflammation, or cancer (Fredholm et al., 2001; Linden, 2001; Flamand et al., 2006; Hasko et al., 2008; Antonioli et al., 2012, 2013; Hasko and Cronstein, 2013).

Drury and Szent-Gyorgyi (1929) described adenosine as a potent vasodilator-like molecule. In the cardiovascular system, adenosine offers protective effects against episodes of angina pectoris, preconditioning, and ischemia/reperfusion (I/R) injury (Olafsson et al., 1987; Lasley and Mentzer, 1992; Woolfson et al., 1996; Miura et al., 2000). Adenosine mediates its physiological effects on tissue regeneration and repair by binding to and activating a family of G-protein coupled receptors, denoted P1 purinoceptors and adenosine receptors A_1, A_{2A}, A_{2B}, and A_3 (Ralevic and Burnstock, 1998; Merighi et al., 2015), all expressed in the cardiovascular system (Headrick et al., 2013).

The transduction pathways involved in adenosine signaling through its receptors in the cardiovascular system are complex. A_1 receptor may couple to different G-proteins in order to regulate adenylyl cyclase (AC), phospholipase C (PLC), Ca^{2+} and K^+ channel functions, and possesses a high affinity for adenosine (Fredholm et al., 2000). When it is coupled to Gi protein it inhibits AC and modulates K^+ and Ca^{2+} channels activities. But it may also couple with Gs to activate AC, or with Gq/11 to stimulate PLC enzyme and, subsequently, the inositol triphosphate (IP_3) and diacylglycerol (DAG) production (Headrick et al., 2013). It was also described that A_1 receptor promotes K^+ efflux via $\beta\gamma$ subunit of G-protein inwardly rectifying channels (GIRK/$K_{IR}3$) (Kurachi et al., 1986; Kirsch et al., 1988; Belardinelli et al., 1995; Mubagwa and Flameng, 2001).

The A_{2A} receptor is very sensitive to adenosine (Fredholm et al., 2000). This receptor couples with Gs to activate AC and increase cAMP levels in the cardiovascular system and it interacts with A_1 receptor, dopamine D_2, metabotropic glutamate 5, NMDA and cannabinoid CB_1 receptor in other organs, but the specific functions and occurrence of such interactions remains unknown (Headrick et al., 2013).

Adenosine has the lowest affinity for the A_{2B} receptor subtype (Fredholm et al., 2000). A_{2B} signaling is mediated via Gs protein to stimulate AC activity, but it also may couple to Gq/11 protein to activate PLC (Headrick et al., 2013). It was reported that A_{2B} receptor might also modulate the arachidonic acid cascade (Donoso et al., 2005). Additionally, A_{2B} signaling can increase endothelial NO bioavailability with subsequent K_{ATP} channel opening in rodent vascular cells (Morrison et al., 2002; Hinschen et al., 2003). A_{2B} may also couple to p38-MAPK in coronary vessels (Teng et al., 2005).

The A_3 receptor is the newest subtype that was identified (Fredholm et al., 2000). Similarly to A_1 receptor, it can couple to Gi protein to inhibit AC activity, and also to Gq/11 to modulate PLC and Ca^{2+} intracellular handling (Headrick et al., 2013). Involvement of A_{2A} and A_{2B} receptor-mediated vasodilation has been reported in several vessels, including the muscular arteries [mesenteric (Hiley et al., 1995), renal (Rump et al., 1999), and coronary arteries (Flood and Headrick, 2001)] and elastic arteries, including the aorta of several species [guinea pigs (Stoggall and Shaw, 1990), rats (Prentice and Hourani, 1996), and hamsters (Prentice and Hourani, 2000)]. Adenosine relaxes precontracted isolated PA rings, an effect that probably occur via A_{2A} and A_{2B} receptor activation (El-Kashef et al., 1999). Some investigators have suggested that vascular relaxation in response to A_{2A} activation may be independent of ECs (Pearl, 1994), whereas others have shown substantial EC involvement (Martin and Potts, 1994). Resolving this controversy, researchers demonstrated that A_{2A} is located in both the vascular endothelium and vascular SMCs (Leal et al., 2008), and that its activation is involved in vasodilation (Lewis et al., 1994; Prentice and Hourani, 1996).

Activation of the Gs protein-coupled endothelial A_{2A} receptor triggers NO release by activating the AC-protein kinase A (PKA) pathway (Ikeda et al., 1997; Ray and Marshall, 2006). Activation of A_{2A} in vascular SMCs increases formation of cAMP and activation of PKA, which leads to phosphorylation and opening of potassium channels. This effect, in turn, causes hyperpolarization and vasodilatation (Ko et al., 2008). In contrast, the A_1 and A_3 receptors negatively modulate A_{2A-B} receptor-induced vasodilation (Talukder et al., 2002; Mustafa et al., 2009; Ponnoth et al., 2009). The A_1 receptor plays a negative role in regulating blood pressure, causes contraction of vascular smooth muscle, and decreases coronary blood flow (Ponnoth et al., 2009). These findings indicate that adenosine can act as a vasoconstrictor or a vasodilator, depending on its interaction with specific receptor subtypes, plasma levels, and tissue localization. Differences in the adenosine regulation of the pulmonary vascular tonus might be explained, in part, due to the higher affinity of this nucleoside for the A_1 receptor (promotes pulmonary vasoconstriction) than for A_{2B} receptor (promotes pulmonary vasodilation). Saadjian et al. (1999) have described a correlation of the progression of PH and the lower level of adenosine observed in patients. Low adenosine levels in lungs from PH patients are likely to stimulate A_1 more than A_{2B} receptors, thus contributing to the vasoconstriction in those subjects.

The pulmonary circulation is one of the few regions in the body where activation of ARs has a dual function (i.e., promoting both contraction and relaxation) that depends on the basal tone of the blood vessel (Cheng et al., 1996). In pulmonary vessels, A_1 receptors are stimulated under circumstances of low vasculature tone, thereby promoting vasoconstriction; when vessel tone is high, A_2 receptor subtypes are activated and promote vasodilation (Tabrizchi and Bedi, 2001). We can extrapolate these findings to the context of PAH. In terms of the induction of pulmonary vessel relaxation, ARs in the large PAs (vs. small arteries) were reported to be the A_{2B} subtype (vs. A_{2A} subtype) (Tabrizchi and Bedi, 2001). This information is relevant in the pathological environment of PAH, as the disease begins in the distal microvasculature. Thus, we may assume that activation of A_2 receptor subtypes in the pulmonary vessels could be targeted to reduce the extremely high vascular tone in PAH patients.

Pharmacological manipulation of adenosine signaling is of great interest for numerous cardiovascular conditions. Several potential agonists or antagonists of ARs are being

studied in experimental models of left ventricle (LV) ischemia and dysfunction and systemic hypertension. Whether the development of selective and potent ligands for ARs could be an interesting treatment alternative in the context of PAH and RV failure remains speculative.

ROLES OF ARs IN PROLIFERATION OF PULMONARY VESSEL CELLS

Repair of the pulmonary vessel cells in patients with PAH could be promoted by inhibition of the migration and/or proliferation of ECs, PASMCs, and/or fibroblasts. In this section, we describe recent findings for each AR subtype regarding their roles as targets to control PA wall remodeling and subsequent hypertrophy.

Several studies demonstrated the presence of ARs in lung in different species. For example, A_1, A_{2B}, and A_3 receptors were detected in rat airway SMCs (Michoud et al., 2002). In humans, levels of A_{2B} transcripts were the highest in bronchial SMCs; A_1 and A_{2A} transcripts were detected as well, but A_3 transcripts were below the detection limit (Zhong et al., 2004). Immunohistochemical analyses of human lung parenchyma demonstrated expression of A_{2A} and A_3 receptors in bronchiolar and alveolar epithelial cells, SMCs in bronchiolar and vessel walls, and ECs in the PAs (Varani et al., 2006). In contrast, A_{2B} receptor was expressed only in mast cells and macrophages, and A_1 receptor was expressed only in a few alveolar macrophages (Varani et al., 2006). Differences in AR expression between rodents and humans might be due to the cell- and tissue-specific effects of hypoxia on their expression (Fozard and Hannon, 2000).

Few studies have addressed specific roles of the A_1 receptor in the growth regulation of pulmonary vascular cells. This receptor subtype is down regulated in the pulmonary *vasa vasorum* ECs of calves with experimentally induced neonatal PH and in these cells the A_1 receptor activation leads to actin cytoskeletal remodeling and a barrier formation in *vasa vasorum*. A_1 activation in ECs could be targeted with the goal of reducing neovascularization and function of the *vasa vasorum*, indirectly contributing to the integrity of the pulmonary vasculature by preventing the triggering of inflammation (Umapathy et al., 2013). Nevertheless, A_1 receptor could be only a vascular bed-specific target for PAH in advanced stages, by blocking *vasa vasorum* expansion in large pulmonary vessels. Although the knowledge of the influence of A_1 receptor in animal model of PAH, this receptor is poorly expressed in human pulmonary vascular cells (Varani et al., 2006). Thus, it could be considered that A_1 receptor may not be relevant to the progression of HAP, but it is important further evaluation to characterize specific functions of this adenosine receptor subtype in the small lung vasculature from PAH patients, since in some pathological conditions the adenosine receptors pattern might be changed.

A_{2A} is the most well-described AR subtype in the pulmonary circulation and in the context of PAH. Using an A_{2A} receptor knockout (KO) mouse model, Xu et al. (2011) provided the first evidence of the critical contribution of A_{2A} to PAH development. At a postnatal age of 14–16 weeks, A_{2A} KO mice exhibited hemodynamic, histological, and ultrastructural characteristics suggestive of PAH. These changes included increases in RV systolic pressure, RV mass, and wall area and thickness, cellular proliferation in pulmonary resistance vessels, activation and hypertrophy of the PASMCs and ECs, and collagen deposition in the PA wall adventitia (Xu et al., 2011). The spontaneous PAH and altered PA remodeling were supported by the anatomical localization of A_{2A} in the vasculature, further demonstrating the functional activation of A_{2A} in ECs. These findings suggest that the effect of adenosine in PAH is likely mediated by the A_{2A} receptor in pulmonary vessels (Xu et al., 2011).

Recently, the same research group showed that A_{2A} KO mice exhibited key pathogenic characteristics of PAH, including muscularization of the pulmonary arterioles, PA remodeling, lumen narrowing, proliferation of pulmonary vascular ECs and SMCs, excessive hypertrophy of fibroblasts, and collagen deposition. A_{2A} KO mice overexpressed RhoA and ROCK mRNA and protein. As mentioned above, activation of RhoA/ROCK signaling may cause pulmonary vascular remodeling and development of PAH. Thus, this experimental study provides sufficient evidence for validation of the A_{2A} receptor as an anti-remodeling target in the pulmonary circulation (Shang et al., 2015). As such, this receptor may be a promising target for PAH therapy in the future (Antoniu, 2012). We agree with the authors on the need to confirm the specific downstream biochemical pathways that lead to inhibition of RhoA/ROCK signaling by A_{2A} receptor activation.

Salidroside, an active ingredient isolated from *Rhodiola rosea*, has multiple pharmacological activities, including anti-inflammatory, antioxidation, antistress, anticancer, and immune-enhancing effects. Salidroside effectively inhibited chronic hypoxia-induced PAH and PA remodeling by increasing A_{2A} expression and enhancing A_{2A}-related mitochondria-dependent apoptosis. The authors suggested that it could be targeted for reducing vessel wall remodeling and hypertrophy in PAH (Huang et al., 2015).

New compounds of the class *N*-acylhydrazones were designed and synthetized to act as agonists of AR. The lead compound for these new derivatives was named LASSBio-294, which showed beneficial activity in rat model of MI (Costa et al., 2010; da Silva et al., 2014) via activation of the A_{2A} receptor (da Silva et al., 2017). LASSBio-294 has shown low efficacy in the rat model of PAH (data not published) which leads to explore the influence of adding the methyl group in the *N*-acylhydrazone function as a chemical strategy to optimize its pharmacological properties. Thus, among the new series of methylated *N*-acylhydrazone derivatives, LASSBio-1359 ($EC_{50} = 6.6 \pm 1.7 \times 10^{-6}$ M) (Alencar et al., 2013) and LASSBio-1386 ($EC_{50} = 6.8 \pm 0.6 \times 10^{-6}$ M) (Alencar et al., 2014), showed a more potent vasodilator effect in rat PAs than LASSBio-294 ($EC_{50} = 7.0 \pm 0.7 \times 10^{-2}$ M). Those data reinforced the fact that the *N*-methyl group markedly changes the conformation of *N*-acylhydrazone function in the pulmonary vascular target. It was also previously described the importance of the presence of a small lipophilic group in substitution of the amide group of the *N*-acylhydrazone moiety to the increased cardiovascular effects (Silva et al., 2005).

Both compounds, LASSBio-1359 and LASSBio-1386, promoted PA vasodilation by the activation of the A_{2A} receptor, since their vascular effects were reduced by the selective antagonist of the A_{2A} receptor, ZM 241385 (Alencar et al., 2013, 2014). The binding assays for both substances confirmed their higher selectivity for the A_{2A} receptor subtype than for others (e.g., A_1, A_{2B}, and A_3). LASSBio-1359 (10 μM), significantly inhibited the binding of agonist to the A_{2A} receptor (CGS21680) by an average of 78.6%, while for other receptors it did not surpass 30% inhibition (Alencar et al., 2013). Furthermore, computational docking studies demonstrated how LASSBio-1359 and LASSBio-1386 might interact with the amino acid residues of the A_{2A} receptor crystal structure compared to the agonist CGS21680, supporting the fact that they were ligands of A_{2A} receptors (Alencar et al., 2013, 2014).

The involvement of the A_{2A} receptor in the regulation of cardiopulmonary physiology was investigated after administration of LASSBio-1359 and LASSBio-1386 in rats with monocrotaline-induced PAH (Alencar et al., 2013, 2014). Animals with monocrotaline-induced PAH, exhibited intense pulmonary microvessel remodeling and hypertrophy and when treated with LASSBio-1386 showed reductions of the proliferative changes in the pulmonary arterioles and pulmonary vascular remodeling. It was also observed a downregulation of the A_{2A} receptor in pulmonary tissue and RV tissue from rats with PAH (Alencar et al., 2014). Another A_{2A} receptor ligand, LASSBio-1359, induced pulmonary vascular relaxation and promoted recovery of endothelial function in PA rings from rats with PAH. Monocrotaline-induced PAH produced fibromuscular hypertrophy and hyperplasia in the arteriole walls which in turn increased the RV systolic pressure and led to RV hypertrophy. However, daily oral treatment with the A_{2A} agonist abolished the increased RV overload and reduced vessel wall hypertrophy. Importantly, LASSBio-1359 exhibited satisfactory efficacy through long-term oral administration regimens in the cardiopulmonary system of rats with PAH, with no side effects in the systemic circulation, such as hypotension or a compensatory increase in heart rate (Alencar et al., 2013).

Stimulation of the A_{2A} receptor effectively reduced neointimal layer formation in a murine model of carotid artery ligation (McPherson et al., 2001). Collagen deposition and wall thickening were increased in the adventitial layer of PA walls from A_{2A} KO mice (Xu et al., 2011). Therefore, we speculate that in addition to its anti-inflammatory effects (addressed later in this review), A_{2A} exhibits anti-remodeling activity in the pulmonary vascular bed, through which it can reduce fibroblast migration and transdifferentiation into myofibroblasts during PAH pathogenesis. This possibility was supported by our study showing that the A_{2A} receptor agonist LASSBio-1359 reduced collagen deposition in the pulmonary arterioles of PAH rats (Alencar et al., 2013). **Figure 1** shows an overview of the beneficial effects of A_{2A} receptor in the pathogenesis of PAH.

Of the four ARs, A_{2B} has emerged as the receptor that regulates many of the adenosine-driven remodeling responses seen in chronic lung diseases (Karmouty-Quintana et al., 2013b). Although there have been no studies of the A_{2B} receptor in *in vivo* animal models or clinical PAH, there have been some studies of its roles in PH due to lung fibrosis or chronic obstructive pulmonary disease (COPD).

Pulmonary hypertension is a common and deadly complication of interstitial lung disease (Behr and Ryu, 2008). Genetic removal of the A_{2B} receptor or treatment with its selective antagonist attenuated vascular remodeling in a mouse model of PH related to lung fibrosis. Karmouty-Quintana et al. (2012) proposed that A_{2B} receptor activation can promote the release of endothelin-1 and IL-6 from ECs and PASMCs, respectively, potentiating vessel wall remodeling and evolution to a PH phenotype. These authors later demonstrated an upregulation of the adenosine axis in lungs from patients with PH secondary to idiopathic pulmonary fibrosis, leading to enhanced accumulation of adenosine and expression of A_{2B}. The authors stated that, under acute conditions, hyperactivation of the A_{2B} receptor by adenosine is protective and leads to lung tissue repair. In humans with lung fibrosis, however, sustained activation of the receptor is deleterious and contributes to development of pulmonary vascular remodeling and PH (Garcia-Morales et al., 2016).

Varani et al. (2006) reported that the A_{2B} receptor is expressed only in mast and macrophage immunologic cells of human lung. Recently, researchers found that conditional deletion of the A_{2B} receptor from myeloid cells was able to alter the phenotype of macrophages and dampen the development of fibrosis in a mouse model of lung injury-induced PH. The authors suggested a role for A_{2B}-expressing myeloid cells as important regulators of fibrosis. These findings open the possibility of selectively blocking this AR subtype on macrophages as a novel therapeutic strategy for lung fibrosis and PH secondary to chronic lung diseases (Karmouty-Quintana et al., 2015).

Patients with COPD frequently develop PAH, characterized by extensive remodeling of the pulmonary vasculature due to increased proliferation of PASMCs and ECs, muscularization of previously non-muscular arteries, increased vascular tone, and formation of complex vascular lesions. Alveolar hypoxia, inflammation, and emphysema in patients with COPD contribute to remodeling, vasoconstriction, and reduction of the vascular bed (Chaouat et al., 2008). Patients with both COPD and PH present remodeled vessels, characterized by increased smooth muscle and collagen deposition. Patient lung sections had elevated A_{2B} transcript levels, which were significantly correlated with increased PA pressures. Findings from this study suggest a role for A_{2B} receptor antagonism as treatment for PH secondary to COPD (Karmouty-Quintana et al., 2013a).

On the other hand, in an *in vitro* model of cultured PASMCs under hypoxic conditions, Qian et al. (2013) showed that activation of the A_{2B} receptor induced antiproliferative effects. In another report, A_{2B} receptor stimulation counteracted PDGF-induced proliferation of human coronary SMCs through activating the exchange protein activated by cAMP (Mayer et al., 2011). Antiproliferative effects mediated by A_{2B} receptors have been observed in studies of rat and human aortic and pre-glomerular SMCs and in human coronary SMCs (Dubey et al., 1996, 1998, 2010; Jackson et al., 2010, 2011). In aortic-cultured

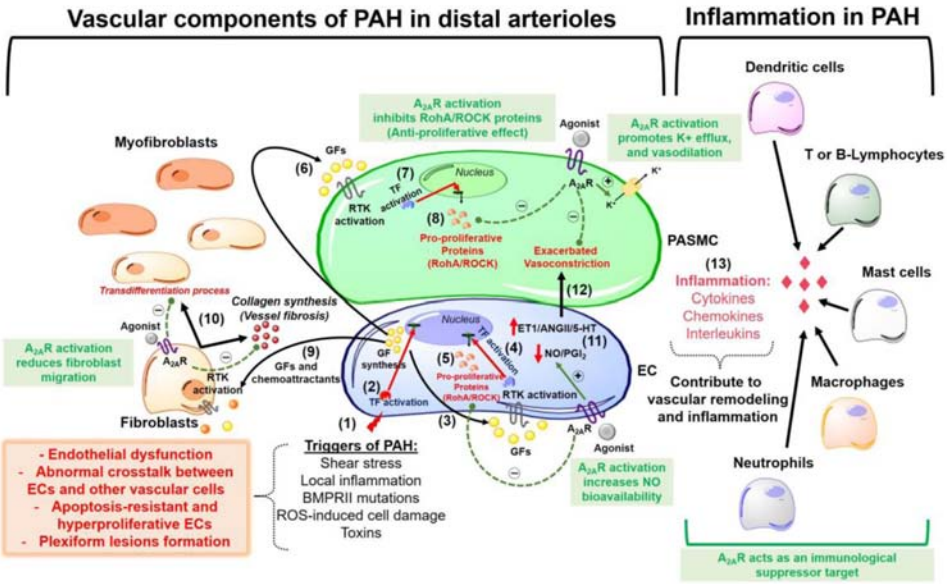

FIGURE 1 | Overview of pathophysiological mechanisms responsible for pulmonary arterial hypertension (PAH) development in lung pre-capillary arterioles. The beneficial effects of the adenosine A_{2A} receptor activation are highlighted in the green boxes. The events are sequentially numbered: (1) Triggers of PAH initially promote endothelial cells (EC) injury and dysfunction. The apoptosis-resistant ECs develop a hyperproliferative phenotype with a subsequent formation of obstructive plexiform lesions and this might be explained by (2) activation of transcription factors (TF) that promote a nuclear codification for an abnormal synthesis of growth factors (GF) and chemoattractants. (3) These GFs act activate receptors tyrosine kinase (RTK) in the ECs (autocrine signaling). (4) activation of RTK in ECs promotes gene transcription for the synthesis of (5) pro-proliferative proteins (e.g., RhoA/ROCK proteins). (6) ECs also release GFs that act in the pulmonary arterial smooth muscle cells (PASMC) triggering a paracrine signaling which is similar to what happens after activation of RTKs in ECs (steps 7 and 8) for the synthesis of pro-proliferative proteins. (9) Endothelial-derived chemoattractants and GFs also are responsible by fibroblasts migration and (10) collagen deposition (vessel wall fibrosis) with subsequent transdifferentiation into myofibroblasts. Other pathogenic characteristics of PAH are (11) increased endothelial production of vasoconstrictor molecules [endothelin-1 (ET-1), angiotensin II (AngII) and serotonin (5-HT)] and decreased release of vasodilators as nitric oxide (NO) and prostacyclin (PGI_2), an event that is responsible by the (12) exacerbated vasoconstriction in the disease progression. (13) An inflammatory environment is formed by recruitment of several immunological cells, all of which releasing molecules as cytokines, chemokines, and interleukins that contribute to vascular remodeling and lung vessel injury through inflammation. $A_{2A}R$, adenosine A_{2A} receptor; ROS, reactive oxygen species; RhoA/ROCK, pro-proliferative Rho kinases.

SMCs, the proliferation-inducing transcription factor B-Myb elevated endogenous A_{2B} receptor mRNA and receptor activity levels, which, in turn, decreased cell proliferation (St Hilaire et al., 2008). Accordingly, we assume that it would be of great importance to evaluate the specific roles of the A_{2B} receptor subtype and its agonists in both clinical and pre-clinical PAH experiments for further considerations about using this receptor as a target for the disease treatment. What would be an innovative strategy, antagonism or agonism of the A_{2B} receptor in PAH patients? This question might give a clue for the basic and clinical science about discovering any beneficial strategy concerning A_{2B} receptor for the treatment of PAH and its symptoms.

Regarding the specific roles of the A_3 receptor in the proliferation of pulmonary vessel cells in the context of PAH, we did not find consistent studies to discuss in this review. Nevertheless, experiments performed in aortas from A_3 receptor-deficient mice showed that this receptor has a role in increasing the proliferation of vascular SMCs (Jones et al., 2004). Another study demonstrated that A_3 receptor activation in cultured human coronary SMCs was coupled to SMC proliferation via activation of phospholipase C and MAPK, with subsequent induction of the early growth response proteins EGR2 and EGR3 (Hinze et al., 2012).

ROLES OF ARs IN INFLAMMATION

There is divergent information regarding the A_1 receptor in the inflammatory process. In several animal models of inflammation, A_1 receptor mediated anti-inflammatory effect (Liao et al., 2003; Lee et al., 2004; Tsutsui et al., 2004; Kim et al., 2008), however, A_1 receptor is also implicated with altered vascular response and systemic inflammation in an allergic mouse model of asthma (Ponnoth et al., 2010). Moreover, the block of A_1 receptor attenuated endotoxin-induced lung injury in cats (Neely et al., 1997). Immune cells appear to exert activity mediated by activation of the A_1 receptor because its activation may promote neutrophils adherence to endothelial cell and chemeotaxis (Barletta et al., 2012). Neutrophils are cells recruited to tissue in response to pathogen (host defense) or some inflammatory disease (Barletta et al., 2012). In early stage of inflammation the concentration of adenosine is low which may evoke neutrophil recruitment (Cronstein et al., 1990).

Evidences have suggested that anti-inflammatory effect via activation of A_{2A} receptor is a result of a positive stimulation of adenylate cyclase (AC) system with increased PKA levels and subsequently decrease NF-κB signaling through lower release of pro-inflammatory cytokines, such as TNF-α and IL-1β.

Moreover, to decrease the release of interleukins and chemokines, the A_{2A} receptors activation inhibits events that occur during an immune response such as antigen presentation, adhesion and trafficking cellular, cell proliferation (Milne and Palmer, 2011; Headrick et al., 2013; Geldenhuys et al., 2017). A_{2A} receptors are expressed in $CD4^+$ T lymphocytes cells which are inhibited in the heart after infarction of myocardium being the primarily target to A_{2A} agonist modulating a protective effect in heart (Yang et al., 2006). Furthermore, A_{2A} agonists reduce $CD3^+$ T lymphocytes and neutrophils which could inhibit the cellular adhesion consequently no transmigration across endothelial cell occurs (Yang et al., 2005; Hasko and Pacher, 2008; Barletta et al., 2012). Macrophage is a defense cell that can also migrate to inflammatory location and its regulation might be through adenosine receptor activation. There are two phenotypes of macrophage: phenotype 1 (M1) which is characterized by expression of several inflammatory cytokines (TNF-α, IL-1β, IL-6, and IL-12) and chemokines ensuring an inflammatory profile and phenotype 2 (M2) which controls inflammation and improves tissue healing. Stimulation of A_{2A} receptors might promote the change in the macrophage phenotype 1 to type 2 (Hasko and Cronstein, 2013; Cronstein and Sitkovsky, 2017) promoting reduction of inflammation.

The A_{2B} receptors are preferentially coupled to stimulatory G protein (Fredholm et al., 2001), but also couple to Gq protein leading to the regulation of intracellular calcium levels (Feoktistov and Biaggioni, 1997; Linden et al., 1999). Activation of A_{2B} receptors might mediate mast cell function, increasing degranulation and stimulation of IL-8 secretion (Feoktistov and Biaggioni, 1995, 1996, 1997). In addition, the A_{2B} receptors activation increases IL-6 production by pulmonary fibroblasts, leading to the formation of myofibroblasts that deposit extracellular matrix (Hasko et al., 2008). In contrast, A_{2B} receptors might modulate beneficial anti-inflammatory effect through the inhibition of neutrophils activity (Barletta et al., 2012). Similarly to A_{2A} receptors, A_{2B} receptors when stimulated produce a change in the macrophage profile from phenotype 1 to phenotype 2.

The A_3 receptors are widely expressed on immune cells and, upon binding their agonists, can activate phospholipase C and mediate inhibition of the PI3K/Akt and NF-kB signaling pathways to suppress production of TNF-α, IL-12, and IL-6 (Fishman et al., 2006, 2012; Varani et al., 2010b; Lee et al., 2011; Faas et al., 2017).

RV FAILURE IN PAH AND CARDIAC PROFILE OF ARs

In an important review, Voelkel et al. (2006) described the most relevant structural and functional changes to occur in the RV chamber subsequent to long-term pressure overload due to elevated PVR. The initial response of the right heart is myocardial remodeling and hypertrophy to compensate for the elevated postload, accompanied by progressive contractile dysfunction. Finally, the chamber dilates to allow compensatory preload and to maintain stroke volume despite the reduced systolic function. Patients may develop clinical evidence of RV failure, including elevated filling pressure, diastolic dysfunction, and reduced cardiac output. The LV develops diastolic dysfunction due to the increased size and pressure overload of the RV, such that PAH results in global heart failure (Voelkel et al., 2006). Maladaptive RV remodeling and subsequent hypertrophy might be accelerated by neurohormonal signaling, oxidative stress of cardiac cells, metabolic changes, and myocardial inflammation, which affect the cardiomyocytes, cardiac fibroblasts, and coronary vascular cells (Ryan and Archer, 2014). Thus, we propose that a cardioprotective target should be beneficial by acting throughout all of the cardiac cells.

In the heart, adenosine might modulate the growth and death of cardiomyocytes, cardiac fibroblasts, ECs and SMCs, as well as affect the extracellular matrix (Headrick et al., 2013). One important study evaluated the impact of chronic heart failure on the adenosine system and the effects of its stimulation on disease development in humans.

Patients with moderate heart failure who were treated with dipyridamole, an adenosine uptake inhibitor, exhibited reduced AR expression, increased adenosine levels, and symptom improvement (Asakura et al., 2007). Hence, disturbances of the adenosine system might contribute to development of chronic heart failure.

Although preclinical and clinical studies have shown benefits of activating the A_1 receptor in the context of LV dysfunction and failure (Ely and Berne, 1992; Headrick et al., 2003; Liao et al., 2003; Peart and Headrick, 2007; Chuo et al., 2016; Dinh et al., 2017), there is a lack of data regarding the effects of this receptor subtype in experimental models of PAH-induced RV impairment and global heart failure. We may discuss that the current unclear specific roles of this adenosine receptor subtype in the context of PAH should be the cause of researchers to consider it of low relevance.

Adenosine plays roles in the inflammatory process of LV heart failure. In cardiomyocytes from patients with LV heart failure, treatment with adenosine or the selective A_2 receptor agonist DPMA decreased TNF-α expression levels by 40% or 87%, respectively (Wagner et al., 1998). Activation of the A_{2A} receptor mediated the inflammatory process via activation of PKA, which, in turn, inhibited synthesis of proinflammatory molecules, such as TNF-α and IL-1β (Varani et al., 2010a; Impellizzeri et al., 2011).

The A_{2A} receptor is expressed in mast cells (Marquardt, 1994), neutrophils (Fredholm et al., 1996), and $CD4^+$ T cells (Koshiba et al., 1999). Xu et al. (1996) showed that adult rat ventricular myocytes express adenosine A_{2A} receptor messenger RNA and through an immunoblotting technique, it was demonstrated that they express A_{2A} receptor protein (Kilpatrick et al., 2002). Although numerous *in vivo* studies of the A_{2A} receptor implicate its anti-inflammatory effects, some studies have suggested that its cardioprotective activities could be due, at least in part, to direct myocardial effects (Woodiwiss et al., 1999; Monahan et al., 2000; Chandrasekera et al., 2010; McIntosh and Lasley, 2012). Constitutive overexpression of the A_{2A} receptor in young mice with LV dysfunction was associated with increases in cardiac contractility, heart rate, and LV mass (Chan et al., 2008).

Cardiac overexpression of the A_{2A} receptor showed protective effects by attenuating fibrosis and improving cardiac function in a mouse model of heart failure (Hamad et al., 2012). Another work showed that this receptor is expressed in cardiac fibroblasts, where it has an antifibrotic role (Sassi et al., 2014).

As addressed earlier in this review, our laboratory has synthesized two new molecules, LASSBio-1359 and LASSBio-1386, from the lead compound LASSBio-294. Using *in silico* approaches, we identified a putative docking pose of this compound class at the A_{2A} receptor. *In vitro* assays of all three compounds indicate A_{2A} receptor agonist activity, although second messenger assays and full binding curves were not performed. The compounds exhibited vascular benefits and cardioprotective activities when administered chronically in rats with MI-induced LV heart failure (Costa et al., 2010; da Silva et al., 2014, 2017) or PAH-induced RV heart failure (Alencar et al., 2013, 2014). LASSBio-294 was chronically administered to normotensive and spontaneous hypertensive rats 4 weeks after MI. In addition to showing inotropic and lusitropic activities, this drug decreased cardiac remodeling, reduced cell infiltration, and improved Ca^{2+} influx into the sarcoplasmic reticulum in two different studies (Costa et al., 2010; da Silva et al., 2017). In a third work, chronic administration of LASSBio-294 to rats 4 weeks after MI reduced exercise intolerance by recovering Ca^{2+} homeostasis in the skeletal muscle. LASSBio-294 prevented cellular infiltration into the skeletal muscle, similarly to what was described for cardiac muscle. We have proven that the beneficial effects of LASSBio-294 occur through its activation of the A_{2A} receptor (da Silva et al., 2017) in the cardiac and skeletal muscles (da Silva et al., 2014) and the subsequent increase of cAMP levels.

Given its salutary effects in animal models of left heart disease, we hypothesized that the A_{2A} receptor should show cardioprotective potential in both LV and RV tissues. We chronically administered our new adenosine A_{2A} agonists LASSBio-294 (data not published) LASSBio-1359 and LASSBio-1386 to rats with monocrotaline-induced RV failure (Alencar et al., 2013, 2014). Our new derivatives showed beneficial effects on the regulation of right heart physiology, as depicted by echocardiographic evaluations after long-term A_{2A} receptor activation (2 weeks of oral treatment with both substances) in monocrotaline-induced RV failure. Treatment of RV failure rats with LASSBio-1386 significantly improved their exercise capacity compared to control animals. Finally, we demonstrated, for the first time, that rats with RV failure had reduced A_{2A} receptor levels in RV tissue, which were correlated with reductions of SERCA2 content and Ca^{2+}-ATPase activity. Activation of SERCA2 is one of the most important processes to regulate cardiomyocyte relaxation (Katz, 2006). SERCA induces Ca^{2+} uptake from the cytosol to the sarcoplasmic reticulum lumen, activating cell relaxation and promoting restock of Ca^{2+} for the next cardiac contraction. Elevated SERCA2 activity and density lead to an increased potential for the next cardiac cycle (Periasamy and Huke, 2001). These findings suggest the beneficial effects of A_{2A} receptor-mediated signaling on global cardiac function. Using echocardiography, we confirmed the impairment of systolic function in PAH rats (Alencar et al., 2014). These data are consistent with previous reports showing an impaired pattern of this receptor in different experimental models of LV disease.

Additionally, we may discuss that the reduced expression of A_{2A} receptor in the cardiopulmonary tissues in rats with PAH-induced RV failure may be a consequence of the chronic state of the disease. Possibly, in earlier stage of PAH, the A_{2A} receptor expression could be unchanged or increased as a physiological compensatory mechanism. However, further studies are necessary to determine this receptor subtype levels during all stages of the disease in preclinical models. Despite the reduced expression of the A_{2A} receptor in the cardiopulmonary system on late stage of PAH, lower levels of the receptor were still detected and LASSBio-1359 and LASSBio-1386 could bind and activate these receptors, ameliorating PAH.

No study has investigated whether the A_{2B} receptor plays a role in RV function or in the pathophysiology of PAH-induced RV failure. However, this receptor is highly expressed in cardiac fibroblasts. Despite displaying antifibrotic potential in several *in vitro* studies, most *in vivo* animal models have described this receptor as being an inducer of cardiac remodeling and fibrosis. In their review, Vecchio et al. (2017) proposed that some proinflammatory mechanism may underlie this profibrotic activity of the A_{2B} receptor. A_{2B} receptor promoted a moderate increase in cardiac contractility in *ex vivo* mouse hearts (Chandrasekera et al., 2010). A later study showed that A_{2B} receptor prevented mitochondrial oxidative stress by decreasing superoxide generation, but its effects were simultaneously potentiated by activation of the A_{2A} receptor. Xu et al. (2017) concluded that the A_{2A} and A_{2B} receptors act together in the regulation of heart metabolism.

Given its high expression in mast cells, neutrophils, eosinophils, and other inflammatory cells, A_3 receptor has been speculated as a potential target for the treatment of ischemic conditions, glaucoma, asthma, arthritis, cancer, and other inflammation-related disorders (Gessi et al., 2008). Low-level expression of A_3 receptor in the heart provided effective protection against ischemic injury without detectable adverse effects, whereas overexpression led to development of dilated cardiomyopathy. Expression of this receptor was below the limits of detection of radioligand binding or northern blot (Black et al., 2002). Combined with the lack of works addressing the potential of A_3 receptor in PAH and RV failure, we do not have enough arguments to assume that the synthesis of new ligands for this adenosine target could represent a suitable strategy to treat the disease in the future.

CONCLUSION

Over the past 20 years, scientists in medicinal chemistry have generated agonists and antagonists with high affinity and high selectivity for human variants of each of the four ARs. Moreover, agonist and antagonist ligands containing positron-emitting radioisotopes have been developed to monitor the *in vivo* occupancy of ARs in humans (Muller and Jacobson, 2011; Chen et al., 2013). As such, the lack of selective ligands of ARs is

not a limiting factor for research and drug development, as has been the case for some other G-protein coupled receptors. Furthermore, researchers continue their efforts to develop novel adenosine ligands with refined structure-activity relationships, improved *in vivo* biodistribution, and tissue selectivity, which are crucial to druggability (Muller and Jacobson, 2011; Chen et al., 2013). A bigger problem in this process has been the broad distribution of the ARs. A possible approach for achieving tissue selectivity could be the use of partial agonists that would predominantly act where there are a high number of so-called "spare" receptors (Chen et al., 2013), as we also commented earlier in this review.

Advances in our understanding of the pathogenetic role of adenosine in PAH may soon be translated into effective treatment options. There is a complex interplay among the different distribution patterns and/or affinities of the four AR subtypes in specific cell types at different stages of disease. As such, combinations of selective antagonist/agonists for the different AR subtypes will likely be required to obtain reasonable clinical efficacy. Alternatively, controlling the factors involved in driving adenosine concentrations in tissue may be important.

Regarding the roles of A_1, A_{2B}, and A_3 adenosine receptor subtypes, with this review we are assuming the need of closely studying each one in specific pre-clinical models of PAH for further discussions on their use as targets to treat this deleterious cardiopulmonary disease in the clinical field.

Nevertheless, data discussed in this review indicate a role for the A_{2A} receptor in mediating beneficial effects, such as pulmonary vascular relaxation, reduction of pulmonary vessel and RV hypertrophy, amelioration of RV dysfunction, and exercise capacity, in rats with PAH. We have briefly described the importance of the adenosine system, specifically the A_{2A} receptor, as a new target for the treatment of PAH. Several factors remain to be explored. For example, global and local A_{2A} receptor function should be investigated in human PAH. The site of action of these drugs should be carefully determined through their administration to animals with cell-specific receptor deletions. Adenosine signaling and the effects of each drug over the specific disease course (e.g., acute and chronic stages of PAH and RV failure) should be carefully monitored in clinical studies. Finally, the possibility of combining direct A_{2A} receptor actions with drugs targeting other pathways and/or targets should be examined. Such explorations could uncover new therapeutic strategies, which are greatly needed for patients with PAH.

AUTHOR CONTRIBUTIONS

All authors listed have made a substantial, direct and intellectual contribution to the work, and approved it for publication.

ACKNOWLEDGMENTS

This work was supported by Conselho Nacional de Desenvolvimento Cientifico e Tecnológico (CNPq), Coordenação de Aperfeiçoamento de Pessoal de Nível Superior (CAPES), Programa de Apoio a Núcleos de Experiência (PRONEX), Fundação Carlos Chagas Filho de Amparo à Pesquisa do Estado do Rio de Janeiro (FAPERJ), Instituto Nacional de Ciência e Tecnologia INCT-INOFAR (Proc. 465249/2014-0).

REFERENCES

Abe, K., Toba, M., Alzoubi, A., Ito, M., Fagan, K. A., Cool, C. D., et al. (2010). Formation of plexiform lesions in experimental severe pulmonary arterial hypertension. *Circulation* 121, 2747–2754. doi: 10.1161/CIRCULATIONAHA.109.927681

Alencar, A. K., Pereira, S. L., da Silva, F. E., Mendes, L. V., Cunha Vdo, M., Lima, L. M., et al. (2014). N-acylhydrazone derivative ameliorates monocrotaline-induced pulmonary hypertension through the modulation of adenosine AA2R activity. *Int. J. Cardiol.* 173, 154–162. doi: 10.1016/j.ijcard.2014.02.022

Alencar, A. K., Pereira, S. L., Montagnoli, T. L., Maia, R. C., Kummerle, A. E., Landgraf, S. S., et al. (2013). Beneficial effects of a novel agonist of the adenosine A2A receptor on monocrotaline-induced pulmonary hypertension in rats. *Br. J. Pharmacol.* 169, 953–962. doi: 10.1111/bph.12193

Amabile, N., Guignabert, C., Montani, D., Yeghiazarians, Y., Boulanger, C. M., and Humbert, M. (2013). Cellular microparticles in the pathogenesis of pulmonary hypertension. *Eur. Respir. J.* 42, 272–279. doi: 10.1183/09031936.00087212

Antonioli, L., Blandizzi, C., Csoka, B., Pacher, P., and Hasko, G. (2015). Adenosine signalling in diabetes mellitus–pathophysiology and therapeutic considerations. *Nat. Rev. Endocrinol.* 11, 228–241. doi: 10.1038/nrendo.2015.10

Antonioli, L., Blandizzi, C., Pacher, P., and Hasko, G. (2013). Immunity, inflammation and cancer: a leading role for adenosine. *Nat. Rev. Cancer* 13, 842–857. doi: 10.1038/nrc3613

Antonioli, L., Colucci, R., La Motta, C., Tuccori, M., Awwad, O., Da Settimo, F., et al. (2012). Adenosine deaminase in the modulation of immune system and its potential as a novel target for treatment of inflammatory disorders. *Curr. Drug Targets* 13, 842–862. doi: 10.2174/138945012800564095

Antoniu, S. A. (2012). Targeting RhoA/ROCK pathway in pulmonary arterial hypertension. *Expert Opin. Ther. Targets* 16, 355–363. doi: 10.1517/14728222.2012.671811

Asakura, M., Asanuma, H., Kim, J., Liao, Y., Nakamaru, K., Fujita, M., et al. (2007). Impact of adenosine receptor signaling and metabolism on pathophysiology in patients with chronic heart failure. *Hypertens Res.* 30, 781–787. doi: 10.1291/hypres.30.781

Aznar, S., and Lacal, J. C. (2001). Rho signals to cell growth and apoptosis. *Cancer Lett* 165, 1–10. doi: 10.1016/S0304-3835(01)00412-8

Bak, M. I., and Ingwall, J. S. (1998). Regulation of cardiac AMP-specific 5′-nucleotidase during ischemia mediates ATP resynthesis on reflow. *Am. J. Physiol.* 274(4 Pt 1), C992–C1001.

Ballard, F. J. (1970). Adenine nucleotides and the adenylate kinase equilibrium in livers of foetal and newborn rats. *Biochem. J.* 117, 231–235. doi: 10.1042/bj1170231

Barletta, K. E., Ley, K., and Mehrad, B. (2012). Regulation of neutrophil function by adenosine. *Arterioscler. Thromb. Vasc. Biol.* 32, 856–864. doi: 10.1161/ATVBAHA.111.226845

Behr, J., and Ryu, J. H. (2008). Pulmonary hypertension in interstitial lung disease. *Eur. Respir. J.* 31, 1357–1367. doi: 10.1183/09031936.00171307

Belardinelli, L., Shryock, J. C., Song, Y., Wang, D., and Srinivas, M. (1995). Ionic basis of the electrophysiological actions of adenosine on cardiomyocytes. *FASEB J.* 9, 359–365.

Bi, L. Q., Zhu, R., Kong, H., Wu, S. L., Li, N., Zuo, X. R., et al. (2013). Ruscogenin attenuates monocrotaline-induced pulmonary hypertension in rats. *Int. Immunopharmacol.* 16, 7–16. doi: 10.1016/j.intimp.2013.03.010

Black, R. G. Jr., Guo, Y., Ge, Z. D., Murphree, S. S., Prabhu, S. D., Jones, W. K., et al. (2002). Gene dosage-dependent effects of cardiac-specific overexpression of the A3 adenosine receptor. *Circ. Res.* 91, 165–172. doi: 10.1161/01.RES.0000028007.91385.EE

Boison, D. (2013). Adenosine kinase: exploitation for therapeutic gain. *Pharmacol. Rev.* 65, 906–943. doi: 10.1124/pr.112.006361

Chan, T. O., Funakoshi, H., Song, J., Zhang, X. Q., Wang, J., Chung, P. H., et al. (2008). Cardiac-restricted overexpression of the A(2A)-adenosine receptor in FVB mice transiently increases contractile performance and rescues the heart failure phenotype in mice overexpressing the A(1)-adenosine receptor. *Clin. Transl. Sci.* 1, 126–133. doi: 10.1111/j.1752-8062.2008.00027.x

Chandrasekera, P. C., McIntosh, V. J., Cao, F. X., and Lasley, R. D. (2010). Differential effects of adenosine A2a and A2b receptors on cardiac contractility. *Am. J. Physiol. Heart Circ. Physiol.* 299, H2082–H2089. doi: 10.1152/ajpheart.00511.2010

Chaouat, A., Naeije, R., and Weitzenblum, E. (2008). Pulmonary hypertension in COPD. *Eur. Respir. J.* 32, 1371–1385. doi: 10.1183/09031936.00015608

Chen, J. F., Eltzschig, H. K., and Fredholm, B. B. (2013). Adenosine receptors as drug targets–what are the challenges? *Nat. Rev. Drug Discov.* 12, 265–286. doi: 10.1038/nrd3955

Cheng, D. Y., DeWitt, B. J., Suzuki, F., Neely, C. F., and Kadowitz, P. J. (1996). Adenosine A1 and A2 receptors mediate tone-dependent responses in feline pulmonary vascular bed. *Am. J. Physiol.* 270(1 Pt 2), H200–H207.

Chuo, C. H., Devine, S. M., Scammells, P. J., Krum, H., Christopoulos, A., May, L. T., et al. (2016). VCP746, a novel A1 adenosine receptor biased agonist, reduces hypertrophy in a rat neonatal cardiac myocyte model. *Clin. Exp. Pharmacol. Physiol* 43, 976–982. doi: 10.1111/1440-1681.12616

Connolly, M. J., and Aaronson, P. I. (2011). Key role of the RhoA/Rho kinase system in pulmonary hypertension. *Pulm. Pharmacol. Ther.* 24, 1–14. doi: 10.1016/j.pupt.2010.09.001

Cool, C. D., Stewart, J. S., Werahera, P., Miller, G. J., Williams, R. L., Voelkel, N. F., et al. (1999). Three-dimensional reconstruction of pulmonary arteries in plexiform pulmonary hypertension using cell-specific markers. Evidence for a dynamic and heterogeneous process of pulmonary endothelial cell growth. *Am. J. Pathol.* 155, 411–419. doi: 10.1016/S0002-9440(10)65137-1

Costa, D. G., da Silva, J. S., Kummerle, A. E., Sudo, R. T., Landgraf, S. S., Caruso-Neves, C., et al. (2010). LASSBio-294, A compound with inotropic and lusitropic activity, decreases cardiac remodeling and improves Ca(2)(+) influx into sarcoplasmic reticulum after myocardial infarction. *Am. J. Hypertens* 23, 1220–1227. doi: 10.1038/ajh.2010.157

Cronstein, B. N., Daguma, L., Nichols, D., Hutchison, A. J., and Williams, M. (1990). The adenosine/neutrophil paradox resolved: human neutrophils possess both A1 and A2 receptors that promote chemotaxis and inhibit O2 generation, respectively. *J. Clin. Invest.* 85, 1150–1157. doi: 10.1172/JCI114547

Cronstein, B. N., and Sitkovsky, M. (2017). Adenosine and adenosine receptors in the pathogenesis and treatment of rheumatic diseases. *Nat. Rev. Rheumatol.* 13, 41–51. doi: 10.1038/nrrheum.2016.178

da Silva, J. S., Gabriel-Costa, D., Sudo, R. T., Wang, H., Groban, L., Ferraz, E. B., et al. (2017). Adenosine A2A receptor agonist prevents cardiac remodeling and dysfunction in spontaneously hypertensive male rats after myocardial infarction. *Drug Des. Devel. Ther.* 11, 553–562. doi: 10.2147/DDDT.S113289

da Silva, J. S., Pereira, S. L., Maia Rdo, C., Landgraf, S. S., Caruso-Neves, C., Kummerle, A. E., et al. (2014). N-acylhydrazone improves exercise intolerance in rats submitted to myocardial infarction by the recovery of calcium homeostasis in skeletal muscle. *Life Sci* 94, 30–36. doi: 10.1016/j.lfs.2013.11.012

Daly, J. W. (1982). Adenosine receptors: targets for future drugs. *J. Med. Chem.* 25, 197–207. doi: 10.1021/jm00345a001

De Jong, J. W. (1977). Partial purification and properties of rat-heart adenosine kinase. *Arch. Int. Physiol. Biochim.* 85, 557–569. doi: 10.3109/13813457709069872

Decking, U. K., Schlieper, G., Kroll, K., and Schrader, J. (1997). Hypoxia-induced inhibition of adenosine kinase potentiates cardiac adenosine release. *Circ. Res.* 81, 154–164. doi: 10.1161/01.RES.81.2.154

Demiryurek, S., Kara, A. F., Celik, A., Babul, A., Tarakcioglu, M., and Demiryurek, A. T. (2005). Effects of fasudil, a Rho-kinase inhibitor, on myocardial preconditioning in anesthetized rats. *Eur. J. Pharmacol.* 527, 129–140. doi: 10.1016/j.ejphar.2005.10.018

Deussen, A., Lloyd, H. G., and Schrader, J. (1989). Contribution of S-adenosylhomocysteine to cardiac adenosine formation. *J. Mol. Cell Cardiol.* 21, 773–782. doi: 10.1016/0022-2828(89)90716-5

Deussen, A., and Schrader, J. (1991). Cardiac adenosine production is linked to myocardial pO2. *J. Mol. Cell Cardiol.* 23, 495–504. doi: 10.1016/0022-2828(91)90173-J

Dinh, W., Albrecht-Kupper, B., Gheorghiade, M., Voors, A. A., van der Laan, M., and Sabbah, H. N. (2017). Partial adenosine A1 agonist in heart failure. *Handb. Exp. Pharmacol.* 243, 177–203. doi: 10.1007/164_2016_83

Donoso, M. V., Lopez, R., Miranda, R., Briones, R., and Huidobro-Toro, J. P. (2005). A2B adenosine receptor mediates human chorionic vasoconstriction and signals through arachidonic acid cascade. *Am. J. Physiol. Heart Circ. Physiol.* 288, H2439–H2449. doi: 10.1152/ajpheart.00548.2004

Drabikowska, A. K., Halec, L., and Shugar, D. (1985). Purification and properties of adenosine kinase from rat liver: separation from deoxyadenosine kinase activity. *Z. Naturforsch. C* 40, 34–41.

Drury, A. N., and Szent-Gyorgyi, A. (1929). The physiological activity of adenine compounds with especial reference to their action upon the mammalian heart. *J. Physiol.* 68, 213–237. doi: 10.1113/jphysiol.1929.sp002608

Dubey, R. K., Gillespie, D. G., Mi, Z., and Jackson, E. K. (1998). Adenosine inhibits growth of human aortic smooth muscle cells via A2B receptors. *Hypertension* 31(1 Pt 2), 516–521. doi: 10.1161/01.HYP.31.1.516

Dubey, R. K., Gillespie, D. G., Osaka, K., Suzuki, F., and Jackson, E. K. (1996). Adenosine inhibits growth of rat aortic smooth muscle cells. Possible role of A2b receptor. *Hypertension* 27(3 Pt 2), 786–793. doi: 10.1161/01.HYP.27.3.786

Dubey, R. K., Rosselli, M., Gillespie, D. G., Mi, Z., and Jackson, E. K. (2010). Extracellular 3′,5′-cAMP-adenosine pathway inhibits glomerular mesangial cell growth. *J. Pharmacol. Exp. Ther.* 333, 808–815. doi: 10.1124/jpet.110.166371

Dunwiddie, T. V., Diao, L., and Proctor, W. R. (1997). Adenine nucleotides undergo rapid, quantitative conversion to adenosine in the extracellular space in rat hippocampus. *J. Neurosci.* 17, 7673–7682.

Eddahibi, S., Guignabert, C., Barlier-Mur, A. M., Dewachter, L., Fadel, E., Dartevelle, P., et al. (2006). Cross talk between endothelial and smooth muscle cells in pulmonary hypertension: critical role for serotonin-induced smooth muscle hyperplasia. *Circulation* 113, 1857–1864. doi: 10.1161/CIRCULATIONAHA.105.591321

El-Kashef, H., Elmazar, M. M., Al-Shabanah, O. A., and Al-Bekairi, A. M. (1999). Effect of adenosine on pulmonary circulation of rabbits. *Gen. Pharmacol.* 32, 307–313. doi: 10.1016/S0306-3623(98)00184-0

Ely, S. W., and Berne, R. M. (1992). Protective effects of adenosine in myocardial ischemia. *Circulation* 85, 893–904. doi: 10.1161/01.CIR.85.3.893

Emerson, M., Momi, S., Paul, W., Alberti, P. F., Page, C., and Gresele, P. (1999). Endogenous nitric oxide acts as a natural antithrombotic agent in vivo by inhibiting platelet aggregation in the pulmonary vasculature. *Thromb. Haemost.* 81, 961–966.

Faas, M.M., Saez, T., and de Vos, P. (2017). Extracellular ATP and adenosine: the Yin and Yang in immune responses? *Mol. Aspects Med.* 55, 9–19. doi: 10.1016/j.mam.2017.01.002

Fagan, K. A., Fouty, B. W., Tyler, R. C., Morris, K. G. Jr., Hepler, L. K., Sato, K., et al. (1999). The pulmonary circulation of homozygous or heterozygous eNOS-null mice is hyperresponsive to mild hypoxia. *J. Clin. Invest.* 103, 291–299. doi: 10.1172/JCI3862

Feng, Y., LoGrasso, P. V., Defert, O., and Li, R. (2016). Rho kinase (ROCK) inhibitors and their therapeutic potential. *J. Med. Chem.* 59, 2269–2300. doi: 10.1021/acs.jmedchem.5b00683

Feoktistov, I., and Biaggioni, I. (1995). Adenosine A2b receptors evoke interleukin-8 secretion in human mast cells. An enprofylline-sensitive mechanism with implications for asthma. *J. Clin. Invest.* 96, 1979–1986. doi: 10.1172/JCI118245

Feoktistov, I., and Biaggioni, I. (1996). Role of adenosine in asthma. *Drug Dev. Res.* 39, 333–336. doi: 10.1002/(SICI)1098-2299(199611/12)39:3/4<333::AID-DDR14>3.0.CO;2-2

Feoktistov, I., and Biaggioni, I. (1997). Adenosine A2B receptors. *Pharmacol. Rev.* 49, 381–402.

Fishman, P., Bar-Yehuda, S., Liang, B. T., and Jacobson, K. A. (2012). Pharmacological and therapeutic effects of A3 adenosine receptor agonists. *Drug Discov. Today* 17, 359–366. doi: 10.1016/j.drudis.2011.10.007

Fishman, P., Bar-Yehuda, S., Madi, L., Rath-Wolfson, L., Ochaion, A., Cohen, S., et al. (2006). The PI3K-NF-kappaB signal transduction pathway is involved in mediating the anti-inflammatory effect of IB-MECA in adjuvant-induced arthritis. *Arthritis Res. Ther.* 8:R33. doi: 10.1186/ar1887

Flamand, N., Lefebvre, J., Lapointe, G., Picard, S., Lemieux, L., Bourgoin, S. G., et al. (2006). Inhibition of platelet-activating factor biosynthesis by adenosine and histamine in human neutrophils: involvement of cPLA2alpha and reversal by lyso-PAF. *J. Leukoc. Biol.* 79, 1043–1051. doi: 10.1189/jlb.1005614

Flood, A., and Headrick, J. P. (2001). Functional characterization of coronary vascular adenosine receptors in the mouse. *Br. J. Pharmacol.* 133, 1063–1072. doi: 10.1038/sj.bjp.0704170

Folkman, J., and D'Amore, P. A. (1996). Blood vessel formation: what is its molecular basis? *Cell* 87, 1153–1155. doi: 10.1016/S0092-8674(00)81810-3

Ford, H. Jr., Dai, F., Mu, L., Siddiqui, M. A., Nicklaus, M. C., Anderson, L., et al. (2000). Adenosine deaminase prefers a distinct sugar ring conformation for binding and catalysis: kinetic and structural studies. *Biochemistry* 39, 2581–2592. doi: 10.1021/bi992112c

Fozard, J. R., and Hannon, J. P. (2000). Species differences in adenosine receptor-mediated bronchoconstrictor responses. *Clin. Exp. Allergy* 30, 1213–1220. doi: 10.1046/j.1365-2222.2000.00894.x

Fredholm, B. B., Arslan, G., Halldner, L., Kull, B., Schulte, G., and Wasserman, W. (2000). Structure and function of adenosine receptors and their genes. *Naunyn Schmiedebergs Arch. Pharmacol.* 362, 364–374. doi: 10.1007/s002100000313

Fredholm, B. B., IJzerman AP., Jacobson, K. A., Klotz, K. N., and Linden, J. (2001). International union of pharmacology. XXV. Nomenclature and classification of adenosine receptors. *Pharmacol. Rev.* 53, 527–552.

Fredholm, B. B., Zhang, Y., and van der Ploeg, I. (1996). Adenosine A2A receptors mediate the inhibitory effect of adenosine on formyl-Met-Leu-Phe-stimulated respiratory burst in neutrophil leucocytes. *Naunyn Schmiedebergs Arch. Pharmacol.* 354, 262–267. doi: 10.1007/BF00171056

Fukumoto, Y., Yamada, N., Matsubara, H., Mizoguchi, M., Uchino, K., Yao, A., et al. (2013). Double-blind, placebo-controlled clinical trial with a rho-kinase inhibitor in pulmonary arterial hypertension. *Circ. J.* 77, 2619–2625. doi: 10.1253/circj.CJ-13-0443

Galie, N., Humbert, M., Vachiery, J. L., Gibbs, S., Lang, I., Torbicki, A., et al. (2016). 2015 ESC/ERS guidelines for the diagnosis and treatment of pulmonary hypertension: the joint task force for the diagnosis and treatment of pulmonary hypertension of the European Society of Cardiology (ESC) and the European Respiratory Society (ERS): endorsed by: Association for European Paediatric and Congenital Cardiology (AEPC), International Society for Heart and Lung Transplantation (ISHLT). *Eur. Heart J.* 37, 67–119. doi: 10.1093/eurheartj/ehv317

Garcia de Vinuesa, A., Abdelilah-Seyfried, S., Knaus, P., Zwijsen, A., and Bailly, S. (2016). BMP signaling in vascular biology and dysfunction. *Cytokine Growth Factor Rev.* 27, 65–79. doi: 10.1016/j.cytogfr.2015.12.005

Garcia-Morales, L. J., Chen, N. Y., Weng, T., Luo, F., Davies, J., Philip, K., et al. (2016). Altered hypoxic-adenosine axis and metabolism in group III pulmonary hypertension. *Am. J. Respir. Cell Mol. Biol.* 54, 574–583. doi: 10.1165/rcmb.2015-0145OC

Geldenhuys, W. J., Hanif, A., Yun, J., and Nayeem, M. A. (2017). Exploring adenosine receptor ligands: potential role in the treatment of cardiovascular diseases. *Molecules* 22:E917. doi: 10.3390/molecules22060917.

Gessi, S., Merighi, S., Varani, K., Leung, E., Mac Lennan, S., and Borea, P. A. (2008). The A3 adenosine receptor: an enigmatic player in cell biology. *Pharmacol. Ther.* 117, 123–140. doi: 10.1016/j.pharmthera.2007.09.002

Godinas, L., Guignabert, C., Seferian, A., Perros, F., Bergot, E., Sibille, Y., et al. (2013). Tyrosine kinase inhibitors in pulmonary arterial hypertension: a double-edge sword? *Semin. Respir. Crit. Care Med.* 34, 714–724. doi: 10.1055/s-0033-1356494

Guignabert, C., and Dorfmuller, P. (2013). Pathology and pathobiology of pulmonary hypertension. *Semin. Respir. Crit. Care Med.* 34, 551–559. doi: 10.1055/s-0033-1356496

Guignabert, C., Tu, L., Girerd, B., Ricard, N., Huertas, A., Montani, D., et al. (2015). New molecular targets of pulmonary vascular remodeling in pulmonary arterial hypertension: importance of endothelial communication. *Chest* 147, 529–537. doi: 10.1378/chest.14-0862

Guilluy, C., Eddahibi, S., Agard, C., Guignabert, C., Izikki, M., Tu, L., et al. (2009). RhoA and Rho kinase activation in human pulmonary hypertension: role of 5-HT signaling. *Am. J. Respir. Crit. Care Med.* 179, 1151–1158. doi: 10.1164/rccm.200805-691OC

Gupta, N., Rashid, J., Nozik-Grayck, E., McMurtry, I. F., Stenmark, K. R., and Ahsan, F. (2017). Cocktail of superoxide dismutase and fasudil encapsulated in targeted liposomes slows PAH progression at a reduced dosing frequency. *Mol. Pharm* 14, 830–841. doi: 10.1021/acs.molpharmaceut.6b01061

Gustafson, L. A., and Kroll, K. (1998). Downregulation of 5′-nucleotidase in rabbit heart during coronary underperfusion. *Am. J. Physiol.* 274(2 Pt 2), H529–H538.

Ham, J., and Evans, B. A. (2012). An emerging role for adenosine and its receptors in bone homeostasis. *Front. Endocrinol.* 3:113. doi: 10.3389/fendo.2012.00113

Hamad, E. A., Zhu, W., Chan, T. O., Myers, V., Gao, E., Li, X., et al. (2012). Cardioprotection of controlled and cardiac-specific over-expression of A(2A)-adenosine receptor in the pressure overload. *PLOS ONE* 7:e39919. doi: 10.1371/journal.pone.0039919

Hanahan, D. (1997). Signaling vascular morphogenesis and maintenance. *Science* 277, 48–50. doi: 10.1126/science.277.5322.48

Hasko, G., and Cronstein, B. (2013). Regulation of inflammation by adenosine. *Front. Immunol.* 4:85. doi: 10.3389/fimmu.2013.00085

Hasko, G., and Cronstein, B. N. (2004). Adenosine: an endogenous regulator of innate immunity. *Trends Immunol.* 25, 33–39. doi: 10.1016/j.it.2003.11.003

Hasko, G., Linden, J., Cronstein, B., and Pacher, P. (2008). Adenosine receptors: therapeutic aspects for inflammatory and immune diseases. *Nat. Rev. Drug Discov.* 7, 759–770. doi: 10.1038/nrd2638

Hasko, G., and Pacher, P. (2008). A2A receptors in inflammation and injury: lessons learned from transgenic animals. *J. Leukoc. Biol.* 83, 447–455. doi: 10.1189/jlb.0607359

Headrick, J. P., Ashton, K. J., Rose'meyer, R. B., and Peart, J. N. (2013). Cardiovascular adenosine receptors: expression, actions and interactions. *Pharmacol. Ther.* 140, 92–111. doi: 10.1016/j.pharmthera.2013.06.002

Headrick, J. P., Hack, B., and Ashton, K. J. (2003). Acute adenosinergic cardioprotection in ischemic-reperfused hearts. *Am. J. Physiol. Heart Circ. Physiol.* 285, H1797–H1818. doi: 10.1152/ajpheart.00407.2003

Headrick, J. P., and Willis, R. J. (1990). Adenosine formation and energy metabolism: a 31P-NMR study in isolated rat heart. *Am. J. Physiol.* 258(3 Pt 2), H617–H624.

Hermes, M., Osswald, H., and Kloor, D. (2007). Role of S-adenosylhomocysteine hydrolase in adenosine-induced apoptosis in HepG2 cells. *Exp. Cell Res.* 313, 264–283. doi: 10.1016/j.yexcr.2006.10.003

Hiley, C. R., Bottrill, F. E., Warnock, J., and Richardson, P. J. (1995). Effects of pH on responses to adenosine, CGS 21680, carbachol and nitroprusside in the isolated perfused superior mesenteric arterial bed of the rat. *Br. J. Pharmacol.* 116, 2641–2646. doi: 10.1111/j.1476-5381.1995.tb17220.x

Hinschen, A. K., Rose'Meyer, R. B., and Headrick, J. P. (2003). Adenosine receptor subtypes mediating coronary vasodilation in rat hearts. *J. Cardiovasc. Pharmacol.* 41, 73–80. doi: 10.1097/00005344-200301000-00010

Hinze, A. V., Mayer, P., Harst, A., and von Kugelgen, I. (2012). Adenosine A(3) receptor-induced proliferation of primary human coronary smooth muscle cells involving the induction of early growth response genes. *J. Mol. Cell Cardiol.* 53, 639–645. doi: 10.1016/j.yjmcc.2012.08.003

Hisatome, I. (2007). Adenosine and cardioprotection in chronic heart failure: genes and protein expression. *Hypertens. Res.* 30, 757–758. doi: 10.1291/hypres.30.757

Huang, X., Zou, L., Yu, X., Chen, M., Guo, R., Cai, H., et al. (2015). Salidroside attenuates chronic hypoxia-induced pulmonary hypertension via adenosine A2a receptor related mitochondria-dependent apoptosis pathway. *J. Mol. Cell Cardiol.* 82, 153–166. doi: 10.1016/j.yjmcc.2015.03.005

Ikeda, U., Kurosaki, K., Ohya, K., and Shimada, K. (1997). Adenosine stimulates nitric oxide synthesis in vascular smooth muscle cells. *Cardiovasc. Res.* 35, 168–174. doi: 10.1016/S0008-6363(97)00068-0

Impellizzeri, D., Di Paola, R., Esposito, E., Mazzon, E., Paterniti, I., Melani, A., et al. (2011). CGS 21680, an agonist of the adenosine (A2A) receptor, decreases acute lung inflammation. *Eur. J. Pharmacol.* 668, 305–316. doi: 10.1016/j.ejphar.2011.06.049

Jackson, E. K., Ren, J., and Gillespie, D. G. (2011). 2′,3′-cAMP, 3′-AMP, and 2′-AMP inhibit human aortic and coronary vascular smooth muscle cell proliferation

via A2B receptors. *Am. J. Physiol. Heart Circ. Physiol.* 301, H391–H401. doi: 10.1152/ajpheart.00336.2011

Jackson, E. K., Ren, J., Gillespie, D. G., and Dubey, R. K. (2010). Extracellular 2,3-cyclic adenosine monophosphate is a potent inhibitor of preglomerular vascular smooth muscle cell and mesangial cell growth [corrected]. *Hypertension* 56, 151–158. doi: 10.1161/HYPERTENSIONAHA.110.152454

Jacobson, K. A., and Gao, Z. G. (2006). Adenosine receptors as therapeutic targets. *Nat. Rev. Drug Discov.* 5, 247–264. doi: 10.1038/nrd1983

Jiang, X., Wang, Y. F., Zhao, Q. H., Jiang, R., Wu, Y., Peng, F. H., et al. (2014). Acute hemodynamic response of infused fasudil in patients with pulmonary arterial hypertension: a randomized, controlled, crossover study. *Int. J. Cardiol.* 177, 61–65. doi: 10.1016/j.ijcard.2014.09.101

Jones, M. R., Zhao, Z., Sullivan, C. P., Schreiber, B. M., Stone, P. J., Toselli, P. A., et al. (2004). A(3) adenosine receptor deficiency does not influence atherogenesis. *J. Cell. Biochem.* 92, 1034–1043. doi: 10.1002/jcb.20122

Jonigk, D., Golpon, H., Bockmeyer, C. L., Maegel, L., Hoeper, M. M., Gottlieb, J., et al. (2011). Plexiform lesions in pulmonary arterial hypertension composition, architecture, and microenvironment. *Am. J. Pathol.* 179, 167–179. doi: 10.1016/j.ajpath.2011.03.040

Karmouty-Quintana, H., Philip, K., Acero, L. F., Chen, N. Y., Weng, T., Molina, J. G., et al. (2015). Deletion of ADORA2B from myeloid cells dampens lung fibrosis and pulmonary hypertension. *FASEB J.* 29, 50–60. doi: 10.1096/fj.14260182

Karmouty-Quintana, H., Weng, T., Garcia-Morales, L. J., Chen, N. Y., Pedroza, M., Zhong, H., et al. (2013a). Adenosine A2B receptor and hyaluronan modulate pulmonary hypertension associated with chronic obstructive pulmonary disease. *Am. J. Respir. Cell Mol. Biol.* 49, 1038–1047. doi: 10.1165/rcmb.2013-0089OC

Karmouty-Quintana, H., Xia, Y., and Blackburn, M. R. (2013b). Adenosine signaling during acute and chronic disease states. *J. Mol. Med.* 91, 173–181. doi: 10.1007/s00109-013-0997-1

Karmouty-Quintana, H., Zhong, H., Acero, L., Weng, T., Melicoff, E., West, J. D., et al. (2012). The A2B adenosine receptor modulates pulmonary hypertension associated with interstitial lung disease. *FASEB J.* 26, 2546–2557. doi: 10.1096/fj.11-200907

Katz, A. M. (2006). *Physiology of the Heart*. Philadelphia, PA: Lippincott Williams & Wilkins.

Keil, A., Blom, I. E., Goldschmeding, R., and Rupprecht, H. D. (2002). Nitric oxide down-regulates connective tissue growth factor in rat mesangial cells. *Kidney Int.* 62, 401–411. doi: 10.1046/j.1523-1755.2002.00462.x

Kilpatrick, E. L., Narayan, P., Mentzer, R. M. Jr., and Lasley, R. D. (2002). Cardiac myocyte adenosine A2a receptor activation fails to alter cAMP or contractility: role of receptor localization. *Am. J. Physiol. Heart Circ. Physiol.* 282, H1035–H1040. doi: 10.1152/ajpheart.00808.2001

Kim, J., Kim, M., Song, J. H., and Lee, H. T. (2008). Endogenous A1 adenosine receptors protect against hepatic ischemia reperfusion injury in mice. *Liver Transpl.* 14, 845–854. doi: 10.1002/lt.21432

King, A. E., Ackley, M. A., Cass, C. E., Young, J. D., and Baldwin, S. A. (2006). Nucleoside transporters: from scavengers to novel therapeutic targets. *Trends Pharmacol. Sci.* 27, 416–425. doi: 10.1016/j.tips.2006.06.004

Kirsch, G. E., Yatani, A., Codina, J., Birnbaumer, L., and Brown, A. M. (1988). Alpha-subunit of Gk activates atrial K+ channels of chick, rat, and guinea pig. *Am. J. Physiol.* 254(6 Pt 2), H1200–H1205.

Kloor, D., and Osswald, H. (2004). S-Adenosylhomocysteine hydrolase as a target for intracellular adenosine action. *Trends Pharmacol. Sci.* 25, 294–297. doi: 10.1016/j.tips.2004.04.004

Ko, E. A., Han, J., Jung, I. D., and Park, W. S. (2008). Physiological roles of K+ channels in vascular smooth muscle cells. *J. Smooth Muscle Res.* 44, 65–81. doi: 10.1540/jsmr.44.65

Koledova, V. V., and Khalil, R. A. (2006). Ca2+, calmodulin, and cyclins in vascular smooth muscle cell cycle. *Circ. Res.* 98, 1240–1243. doi: 10.1161/01.RES.0000225860.41648.63

Koshiba, M., Rosin, D. L., Hayashi, N., Linden, J., and Sitkovsky, M. V. (1999). Patterns of A2A extracellular adenosine receptor expression in different functional subsets of human peripheral T cells. Flow cytometry studies with anti-A2A receptor monoclonal antibodies. *Mol. Pharmacol.* 55, 614–624.

Kurachi, Y., Nakajima, T., and Sugimoto, T. (1986). On the mechanism of activation of muscarinic K+ channels by adenosine in isolated atrial cells: involvement of GTP-binding proteins. *Pflugers. Arch.* 407, 264–274. doi: 10.1007/BF00585301

Lasley, R. D., and Mentzer, R. M. Jr. (1992). Adenosine improves recovery of postischemic myocardial function via an adenosine A1 receptor mechanism. *Am. J. Physiol.* 263(5 Pt 2), H1460–H1465.

Laufs, U., Marra, D., Node, K., and Liao, J. K. (1999). 3-Hydroxy-3-methylglutaryl-CoA reductase inhibitors attenuate vascular smooth muscle proliferation by preventing rho GTPase-induced down-regulation of p27(Kip1). *J. Biol. Chem.* 274, 21926–21931. doi: 10.1074/jbc.274.31.21926

Leal, S., Sa, C., Goncalves, J., Fresco, P., and Diniz, C. (2008). Immunohistochemical characterization of adenosine receptors in rat aorta and tail arteries. *Microsc. Res. Tech.* 71, 703–709. doi: 10.1002/jemt.20609

Lee, H. S., Chung, H. J., Lee, H. W., Jeong, L. S., and Lee, S. K. (2011). Suppression of inflammation response by a novel A(3) adenosine receptor agonist thio-Cl-IB-MECA through inhibition of Akt and NF-kappaB signaling. *Immunobiology* 216, 997–1003. doi: 10.1016/j.imbio.2011.03.008

Lee, H. T., Gallos, G., Nasr, S. H., and Emala, C. W. (2004). A1 adenosine receptor activation inhibits inflammation, necrosis, and apoptosis after renal ischemia-reperfusion injury in mice. *J. Am. Soc. Nephrol.* 15, 102–111. doi: 10.1097/01.ASN.0000102474.68613.AE

Lemmon, M. A., and Schlessinger, J. (2010). Cell signaling by receptor tyrosine kinases. *Cell* 141, 1117–1134. doi: 10.1016/j.cell.2010.06.011

Lewis, C. D., Hourani, S. M., Long, C. J., and Collis, M. G. (1994). Characterization of adenosine receptors in the rat isolated aorta. *Gen. Pharmacol.* 25, 1381–1387. doi: 10.1016/0306-3623(94)90162-7

Liao, Y., Takashima, S., Asano, Y., Asakura, M., Ogai, A., Shintani, Y., et al. (2003). Activation of adenosine A1 receptor attenuates cardiac hypertrophy and prevents heart failure in murine left ventricular pressure-overload model. *Circ. Res.* 93, 759–766. doi: 10.1161/01.RES.0000094744.88220.62

Linden, J. (2001). Molecular approach to adenosine receptors: receptor-mediated mechanisms of tissue protection. *Annu. Rev. Pharmacol. Toxicol.* 41, 775–787. doi: 10.1146/annurev.pharmtox.41.1.775

Linden, J., Thai, T., Figler, H., Jin, X., and Robeva, A. S. (1999). Characterization of human A(2B) adenosine receptors: radioligand binding, western blotting, and coupling to G(q) in human embryonic kidney 293 cells and HMC-1 mast cells. *Mol. Pharmacol.* 56, 705–713.

Liu, Y., Ren, W., Warburton, R., Toksoz, D., and Fanburg, B. L. (2009). Serotonin induces Rho/ROCK-dependent activation of Smads 1/5/8 in pulmonary artery smooth muscle cells. *FASEB J.* 23, 2299–2306. doi: 10.1096/fj.08-127910

Long, L., MacLean, M. R., Jeffery, T. K., Morecroft, I., Yang, X., Rudarakanchana, N., et al. (2006). Serotonin increases susceptibility to pulmonary hypertension in BMPR2-deficient mice. *Circ. Res.* 98, 818–827. doi: 10.1161/01.RES.0000215809.47923.fd

Marquardt, D. L. (1994). Adenosine and other mast cell preformed mediators. *Allergy Proc.* 15, 125–127. doi: 10.2500/108854194778702883

Martin, P. L., and Potts, A. A. (1994). The endothelium of the rat renal artery plays an obligatory role in A2 adenosine receptor-mediated relaxation induced by 5′-N-ethylcarboxamidoadenosine and N6-cyclopentyladenosine. *J. Pharmacol. Exp. Ther.* 270, 893–899.

Mayer, P., Hinze, A. V., Harst, A., and von Kugelgen, I. (2011). A(2)B receptors mediate the induction of early genes and inhibition of arterial smooth muscle cell proliferation via Epac. *Cardiovasc. Res.* 90, 148–156. doi: 10.1093/cvr/cvq371

McGoon, M. D., Benza, R. L., Escribano-Subias, P., Jiang, X., Miller, D. P., Peacock, A. J., et al. (2013). Pulmonary arterial hypertension: epidemiology and registries. *J. Am. Coll. Cardiol.* 62(25 Suppl), D51–D59. doi: 10.1016/j.jacc.2013.10.023

McIntosh, V. J., and Lasley, R. D. (2012). Adenosine receptor-mediated cardioprotection: are all 4 subtypes required or redundant? *J. Cardiovasc. Pharmacol. Ther.* 17, 21–33. doi: 10.1177/1074248410396877

McPherson, J. A., Barringhaus, K. G., Bishop, G. G., Sanders, J. M., Rieger, J. M., Hesselbacher, S. E., et al. (2001). Adenosine A(2A) receptor stimulation reduces inflammation and neointimal growth in a murine carotid ligation model. *Arterioscler. Thromb. Vasc. Biol.* 21, 791–796. doi: 10.1161/01.ATV.21.5.791

Merighi, S., Borea, P. A., and Gessi, S. (2015). Adenosine receptors and diabetes: focus on the A2B adenosine receptor subtype. *Pharmacol. Res.* 99, 229–236. doi: 10.1016/j.phrs.2015.06.015

Michoud, M. C., Napolitano, G., Maghni, K., Govindaraju, V., Cogo, A., and Martin, J. G. (2002). Effects of extracellular triphosphate nucleotides and nucleosides on airway smooth muscle cell proliferation. *Am. J. Respir. Cell Mol. Biol.* 27, 732–738. doi: 10.1165/rcmb.4768

Milne, G. R., and Palmer, T. M. (2011). Anti-inflammatory and immunosuppressive effects of the A2A adenosine receptor. *ScientificWorldJournal* 11, 320–339. doi: 10.1100/tsw.2011.22

Minamino, T., Christou, H., Hsieh, C. M., Liu, Y., Dhawan, V., Abraham, N. G., et al. (2001). Targeted expression of heme oxygenase-1 prevents the pulmonary inflammatory and vascular responses to hypoxia. *Proc. Natl. Acad. Sci. U.S.A.* 98, 8798–8803. doi: 10.1073/pnas.161272598.

Miura, T., Liu, Y., Kita, H., Ogawa, T., and Shimamoto, K. (2000). Roles of mitochondrial ATP-sensitive K channels and PKC in anti-infarct tolerance afforded by adenosine A1 receptor activation. *J. Am. Coll. Cardiol.* 35, 238–245. doi: 10.1016/S0735-1097(99)00493-3

Monahan, T. S., Sawmiller, D. R., Fenton, R. A., and Dobson, J. G. Jr. (2000). Adenosine A(2a)-receptor activation increases contractility in isolated perfused hearts. *Am. J. Physiol. Heart Circ. Physiol.* 279, H1472–H1481.

Morrison, R. R., Talukder, M. A., Ledent, C., and Mustafa, S. J. (2002). Cardiac effects of adenosine in A(2A) receptor knockout hearts: uncovering A(2B) receptors. *Am. J. Physiol. Heart Circ. Physiol.* 282, H437–H444. doi: 10.1152/ajpheart.00723.2001

Mouchaers, K. T., Schalij, I., de Boer, M. A., Postmus, P. E., van Hinsbergh, V. W., van Nieuw Amerongen, G. P., et al. (2010). Fasudil reduces monocrotaline-induced pulmonary arterial hypertension: comparison with bosentan and sildenafil. *Eur. Respir. J.* 36, 800–807. doi: 10.1183/09031936.00130209

Mubagwa, K., and Flameng, W. (2001). Adenosine, adenosine receptors and myocardial protection: an updated overview. *Cardiovasc. Res.* 52, 25–39. doi: 10.1016/S0008-6363(01)00358-3

Muller, C. E., and Jacobson, K. A. (2011). Recent developments in adenosine receptor ligands and their potential as novel drugs. *Biochim. Biophys. Acta* 1808, 1290–1308. doi: 10.1016/j.bbamem.2010.12.017

Mustafa, S. J., Morrison, R. R., Teng, B., and Pelleg, A. (2009). Adenosine receptors and the heart: role in regulation of coronary blood flow and cardiac electrophysiology. *Handb. Exp. Pharmacol.* 193, 161–188. doi: 10.1007/978-3-540-89615-9_6

Nagaoka, T., Gebb, S. A., Karoor, V., Homma, N., Morris, K. G., McMurtry, I. F., et al. (2006). Involvement of RhoA/Rho kinase signaling in pulmonary hypertension of the fawn-hooded rat. *J. Appl. Physiol.* 100, 996–1002. doi: 10.1152/japplphysiol.01028.2005

Neely, C. F., Jin, J., and Keith, I. M. (1997). A1-adenosine receptor antagonists block endotoxin-induced lung injury. *Am. J. Physiol.* 272(2 Pt 1), L353–L361.

Newby, A. C., and Holmquist, C. A. (1981). Adenosine production inside rat polymorphonuclear leucocytes. *Biochem. J.* 200, 399–403. doi: 10.1042/bj2000399

Newby, A. C., Worku, Y., and Holmquist, C. A. (1985). Adenosine formation. Evidence for a direct biochemical link with energy metabolism. *Adv. Myocardiol.* 6, 273–284.

Nootens, M., Schrader, B., Kaufmann, E., Vestal, R., Long, W., and Rich, S. (1995). Comparative acute effects of adenosine and prostacyclin in primary pulmonary hypertension. *Chest* 107, 54–57. doi: 10.1378/chest.107.1.54

Olafsson, B., Forman, M. B., Puett, D. W., Pou, A., Cates, C. U., Friesinger, G. C., et al. (1987). Reduction of reperfusion injury in the canine preparation by intracoronary adenosine: importance of the endothelium and the no-reflow phenomenon. *Circulation* 76, 1135–1145. doi: 10.1161/01.CIR.76.5.1135

Pak, M. A., Haas, H. L., Decking, U. K., and Schrader, J. (1994). Inhibition of adenosine kinase increases endogenous adenosine and depresses neuronal activity in hippocampal slices. *Neuropharmacology* 33, 1049–1053. doi: 10.1016/0028-3908(94)90142-2

Pearl, R. G. (1994). Adenosine produces pulmonary vasodilation in the perfused rabbit lung via an adenosine A2 receptor. *Anesth. Analg.* 79, 46–51. doi: 10.1213/00000539-199407000-00010

Peart, J. N., and Headrick, J. P. (2007). Adenosinergic cardioprotection: multiple receptors, multiple pathways. *Pharmacol. Ther.* 114, 208–221. doi: 10.1016/j.pharmthera.2007.02.004

Periasamy, M., and Huke, S. (2001). SERCA pump level is a critical determinant of Ca(2+)homeostasis and cardiac contractility. *J. Mol. Cell Cardiol.* 33, 1053–1063. doi: 10.1006/jmcc.2001.1366

Playa, H., Lewis, T. A., Ting, A., Suh, B. C., Munoz, B., Matuza, R., et al. (2014). Dilazep analogues for the study of equilibrative nucleoside transporters 1 and 2 (ENT1 and ENT2). *Bioorg. Med. Chem. Lett.* 24, 5801–5804. doi: 10.1016/j.bmcl.2014.10.026

Ponnoth, D. S., Nadeem, A., Tilley, S., and Mustafa, S. J. (2010). Involvement of A1 adenosine receptors in altered vascular responses and inflammation in an allergic mouse model of asthma. *Am. J. Physiol. Heart Circ. Physiol.* 299, H81–H87. doi: 10.1152/ajpheart.01090.2009

Ponnoth, D. S., Sanjani, M. S., Ledent, C., Roush, K., Krahn, T., and Mustafa, S. J. (2009). Absence of adenosine-mediated aortic relaxation in A(2A) adenosine receptor knockout mice. *Am. J. Physiol. Heart Circ. Physiol.* 297, H1655–H1660. doi: 10.1152/ajpheart.00192.2009

Prentice, D. J., and Hourani, S. M. (1996). Activation of multiple sites by adenosine analogues in the rat isolated aorta. *Br. J. Pharmacol.* 118, 1509–1517. doi: 10.1111/j.1476-5381.1996.tb15567.x

Prentice, D. J., and Hourani, S. M. (2000). Characterisation of adenosine receptors mediating relaxation in hamster isolated aorta. *Naunyn Schmiedebergs Arch. Pharmacol.* 362, 427–434. doi: 10.1007/s002100000292

Qian, G., Cao, J., Chen, C., Wang, L., Huang, X., Ding, C., et al. (2013). Paeoniflorin inhibits pulmonary artery smooth muscle cells proliferation via upregulating A2B adenosine receptor in rat. *PLOS ONE* 8:e69141. doi: 10.1371/journal.pone.0069141

Rabinovitch, M., Guignabert, C., Humbert, M., and Nicolls, M. R. (2014). Inflammation and immunity in the pathogenesis of pulmonary arterial hypertension. *Circ. Res.* 115, 165–175. doi: 10.1161/CIRCRESAHA.113.301141

Raja, S. G. (2012). Evaluation of clinical efficacy of fasudil for the treatment of pulmonary arterial hypertension. *Recent Pat. Cardiovasc. Drug Discov.* 7, 100–104. doi: 10.2174/157489012801227238

Ralevic, V., and Burnstock, G. (1998). Receptors for purines and pyrimidines. *Pharmacol. Rev.* 50, 413–492.

Ramakers, B. P., Pickkers, P., Deussen, A., Rongen, G. A., van den Broek, P., van der Hoeven, J. G., et al. (2008). Measurement of the endogenous adenosine concentration in humans in vivo: methodological considerations. *Curr. Drug Metab.* 9, 679–685. doi: 10.2174/138920008786049249

Ray, C. J., and Marshall, J. M. (2006). The cellular mechanisms by which adenosine evokes release of nitric oxide from rat aortic endothelium. *J. Physiol.* 570(Pt 1), 85–96. doi: 10.1113/jphysiol.2005.099390

Reeves, J. T., Groves, B. M., and Weir, E. K. (1991). Adenosine and selective reduction of pulmonary vascular resistance in primary pulmonary hypertension. *Circulation* 84, 1437–1439. doi: 10.1161/01.CIR.84.3.1437

Rump, L. C., Jabbari, T. J., von Kugelgen, I., and Oberhauser, V. (1999). Adenosine mediates nitric-oxide-independent renal vasodilation by activation of A2A receptors. *J. Hypertens.* 17(12 Pt 2), 1987–1993. doi: 10.1097/00004872-199917121-00032

Ryan, J. J., and Archer, S. L. (2014). The right ventricle in pulmonary arterial hypertension: disorders of metabolism, angiogenesis and adrenergic signaling in right ventricular failure. *Circ. Res.* 115, 176–188. doi: 10.1161/CIRCRESAHA.113.301129

Saadjian, A. Y., Paganelli, F., Gaubert, M. L., Levy, S., and Guieu, R. P. (1999). Adenosine plasma concentration in pulmonary hypertension. *Cardiovasc. Res.* 43, 228–236. doi: 10.1016/S0008-6363(99)00059-0

Sakao, S., Tatsumi, K., and Voelkel, N. F. (2009). Endothelial cells and pulmonary arterial hypertension: apoptosis, proliferation, interaction and transdifferentiation. *Respir. Res.* 10:95. doi: 10.1186/1465-9921-10-95

Sartore, S., Chiavegato, A., Faggin, E., Franch, R., Puato, M., Ausoni, S., et al. (2001). Contribution of adventitial fibroblasts to neointima formation and vascular remodeling: from innocent bystander to active participant. *Circ. Res.* 89, 1111–1121. doi: 10.1161/hh2401.100844

Sassi, Y., Ahles, A., Truong, D. J., Baqi, Y., Lee, S. Y., Husse, B., et al. (2014). Cardiac myocyte-secreted cAMP exerts paracrine action via adenosine receptor activation. *J. Clin. Invest.* 124, 5385–5397. doi: 10.1172/JCI74349

Sawada, N., Itoh, H., Ueyama, K., Yamashita, J., Doi, K., Chun, T. H., et al. (2000). Inhibition of rho-associated kinase results in suppression of neointimal formation of balloon-injured arteries. *Circulation* 101, 2030–2033. doi: 10.1161/01.CIR.101.17.2030

Schermuly, R. T., Ghofrani, H. A., Wilkins, M. R., and Grimminger, F. (2011). Mechanisms of disease: pulmonary arterial hypertension. *Nat. Rev. Cardiol.* 8, 443–455. doi: 10.1038/nrcardio.2011.87

Shang, P., He, Z. Y., Chen, J. F., Huang, S. Y., Liu, B. H., Liu, H. X., et al. (2015). Absence of the adenosine A2A receptor confers pulmonary arterial hypertension through RhoA/ROCK signaling pathway in mice. *J. Cardiovasc. Pharmacol.* 66, 569–575. doi: 10.1097/FJC.0000000000000305

Shryock, J. C., and Belardinelli, L. (1997). Adenosine and adenosine receptors in the cardiovascular system: biochemistry, physiology, and pharmacology. *Am. J. Cardiol.* 79, 2–10. doi: 10.1016/S0002-9149(97)00256-7

Silva, A. G., Zapata-Sudo, G., Kummerle, A. E., Fraga, C. A., Barreiro, E. J., and Sudo, R. T. (2005). Synthesis and vasodilatory activity of new N-acylhydrazone derivatives, designed as LASSBio-294 analogues. *Bioorg. Med. Chem.* 13, 3431–3437. doi: 10.1016/j.bmc.2005.03.003

Simonneau, G., Gatzoulis, M. A., Adatia, I., Celermajer, D., Denton, C., Ghofrani, A., et al. (2013). Updated clinical classification of pulmonary hypertension. *J. Am. Coll. Cardiol.* 62(25 Suppl), D34–D41. doi: 10.1016/j.jacc.2013.10.029

Singh, L. S., and Sharma, R. (2000). Purification and characterization of intestinal adenosine deaminase from mice. *Mol. Cell. Biochem.* 204, 127–134. doi: 10.1023/A:1007087905192

Sisbarro, L., Ihida-Stansbury, K., Stevens, T., Bauer, N., McMurtry, I., and Jones, P. L. (2005). The extracellular matrix microenvironment specifies pulmonary endothelial cell identity: roles of tenascin-C and RhoA. *Chest* 128(6 Suppl), 564S. doi: 10.1378/chest.128.6_suppl.564S

Soon, E., Holmes, A. M., Treacy, C. M., Doughty, N. J., Southgate, L., Machado, R. D., et al. (2010). Elevated levels of inflammatory cytokines predict survival in idiopathic and familial pulmonary arterial hypertension. *Circulation* 122, 920–927. doi: 10.1161/CIRCULATIONAHA.109.933762

Spychala, J. (2000). Tumor-promoting functions of adenosine. *Pharmacol. Ther.* 87, 161–173. doi: 10.1016/S0163-7258(00)00053-X

St Croix, C. M., and Steinhorn, R. H. (2016). New Thoughts about the Origin of Plexiform Lesions. *Am. J. Respir. Crit. Care Med.* 193, 484–485. doi: 10.1164/rccm.201510-1959ED

St Hilaire, C., Yang, D., Schreiber, B. M., and Ravid, K. (2008). B-Myb regulates the A(2B) adenosine receptor in vascular smooth muscle cells. *J. Cell. Biochem.* 103, 1962–1974. doi: 10.1002/jcb.21586

Stacher, E., Graham, B. B., Hunt, J. M., Gandjeva, A., Groshong, S. D., McLaughlin, V. V., et al. (2012). Modern age pathology of pulmonary arterial hypertension. *Am. J. Respir. Crit. Care Med.* 186, 261–272. doi: 10.1164/rccm.201201-0164OC

Stoggall, S. M., and Shaw, J. S. (1990). The coexistence of adenosine A1 and A2 receptors in guinea-pig aorta. *Eur. J. Pharmacol.* 190, 329–335. doi: 10.1016/0014-2999(90)94197-6

Sutendra, G., Dromparis, P., Bonnet, S., Haromy, A., McMurtry, M. S., Bleackley, R. C., et al. (2011). Pyruvate dehydrogenase inhibition by the inflammatory cytokine TNFalpha contributes to the pathogenesis of pulmonary arterial hypertension. *J. Mol. Med.* 89, 771–783. doi: 10.1007/s00109-011-0762-2

Sztrymf, B., Souza, R., Bertoletti, L., Jais, X., Sitbon, O., Price, L. C., et al. (2010). Prognostic factors of acute heart failure in patients with pulmonary arterial hypertension. *Eur. Respir. J.* 35, 1286–1293. doi: 10.1183/09031936.00070209

Tabrizchi, R., and Bedi, S. (2001). Pharmacology of adenosine receptors in the vasculature. *Pharmacol. Ther.* 91, 133–147. doi: 10.1016/S0163-7258(01)00152-8

Takeshima, H., Kobayashi, N., Koguchi, W., Ishikawa, M., Sugiyama, F., and Ishimitsu, T. (2012). Cardioprotective effect of a combination of Rho-kinase inhibitor and p38 MAPK inhibitor on cardiovascular remodeling and oxidative stress in Dahl rats. *J. Atheroscler. Thromb.* 19, 326–336. doi: 10.5551/jat.11114

Talukder, M. A., Morrison, R. R., Jacobson, M. A., Jacobson, K. A., Ledent, C., and Mustafa, S. J. (2002). Targeted deletion of adenosine A(3) receptors augments adenosine-induced coronary flow in isolated mouse heart. *Am. J. Physiol. Heart Circ. Physiol.* 282, H2183–H2189. doi: 10.1152/ajpheart.00964.2001.

Teichert-Kuliszewska, K., Kutryk, M. J., Kuliszewski, M. A., Karoubi, G., Courtman, D. W., Zucco, L., et al. (2006). Bone morphogenetic protein receptor-2 signaling promotes pulmonary arterial endothelial cell survival: implications for loss-of-function mutations in the pathogenesis of pulmonary hypertension. *Circ. Res.* 98, 209–217. doi: 10.1161/01.RES.0000200180.01710.e6

Teng, B., Qin, W., Ansari, H. R., and Mustafa, S. J. (2005). Involvement of p38-mitogen-activated protein kinase in adenosine receptor-mediated relaxation of coronary artery. *Am. J. Physiol. Heart Circ. Physiol.* 288, H2574–H2580. doi: 10.1152/ajpheart.00912.2004

Tofovic, S. P., Jackson, E. K., and Rafikova, O. (2009). Adenosine deaminase-adenosine pathway in hemolysis-associated pulmonary hypertension. *Med. Hypotheses* 72, 713–719. doi: 10.1016/j.mehy.2008.12.043

Tsutsui, S., Schnermann, J., Noorbakhsh, F., Henry, S., Yong, V. W., Winston, B. W., et al. (2004). A1 adenosine receptor upregulation and activation attenuates neuroinflammation and demyelination in a model of multiple sclerosis. *J. Neurosci.* 24, 1521–1529. doi: 10.1523/JNEUROSCI.4271-03.2004

Tuder, R. M., Marecki, J. C., Richter, A., Fijalkowska, I., and Flores, S. (2007). Pathology of pulmonary hypertension. *Clin. Chest. Med.* 28, 23–42, vii. doi: 10.1016/j.ccm.2006.11.010.

Umapathy, S. N., Kaczmarek, E., Fatteh, N., Burns, N., Lucas, R., Stenmark, K. R., et al. (2013). Adenosine A1 receptors promote vasa vasorum endothelial cell barrier integrity via Gi and Akt-dependent actin cytoskeleton remodeling. *PLOS ONE* 8:e59733. doi: 10.1371/journal.pone.0059733

Upton, P. D., Long, L., Trembath, R. C., and Morrell, N. W. (2008). Functional characterization of bone morphogenetic protein binding sites and Smad1/5 activation in human vascular cells. *Mol. Pharmacol.* 73, 539–552. doi: 10.1124/mol.107.041673

Varani, K., Caramori, G., Vincenzi, F., Adcock, I., Casolari, P., Leung, E., et al. (2006). Alteration of adenosine receptors in patients with chronic obstructive pulmonary disease. *Am. J. Respir. Crit. Care Med.* 173, 398–406. doi: 10.1164/rccm.200506-869OC

Varani, K., Padovan, M., Govoni, M., Vincenzi, F., Trotta, F., and Borea, P. A. (2010a). The role of adenosine receptors in rheumatoid arthritis. *Autoimmun. Rev.* 10, 61–64. doi: 10.1016/j.autrev.2010.07.019

Varani, K., Vincenzi, F., Tosi, A., Targa, M., Masieri, F. F., Ongaro, A., et al. (2010b). Expression and functional role of adenosine receptors in regulating inflammatory responses in human synoviocytes. *Br. J. Pharmacol.* 160, 101–115. doi: 10.1111/j.1476-5381.2010.00667.x

Vecchio, E. A., White, P. J., and May, L. T. (2017). Targeting adenosine receptors for the treatment of cardiac fibrosis. *Front. Pharmacol.* 8:243. doi: 10.3389/fphar.2017.00243

Voelkel, N. F., Cool, C., Taraceviene-Stewart, L., Geraci, M. W., Yeager, M., Bull, T., et al. (2002). Janus face of vascular endothelial growth factor: the obligatory survival factor for lung vascular endothelium controls precapillary artery remodeling in severe pulmonary hypertension. *Crit. Care Med.* 30(5 Suppl), S251–S256. doi: 10.1097/00003246-200205001-00013

Voelkel, N. F., Quaife, R. A., Leinwand, L. A., Barst, R. J., McGoon, M. D., Meldrum, D. R., et al. (2006). Right ventricular function and failure: report of a National Heart, Lung, and Blood Institute working group on cellular and molecular mechanisms of right heart failure. *Circulation* 114, 1883–1891. doi: 10.1161/CIRCULATIONAHA.106.632208

Wagner, D. R., McTiernan, C., Sanders, V. J., and Feldman, A. M. (1998). Adenosine inhibits lipopolysaccharide-induced secretion of tumor necrosis factor-alpha in the failing human heart. *Circulation* 97, 521–524. doi: 10.1161/01.CIR.97.6.521

Woodiwiss, A. J., Honeyman, T. W., Fenton, R. A., and Dobson, J. G. Jr. (1999). Adenosine A2a-receptor activation enhances cardiomyocyte shortening via Ca2+-independent and -dependent mechanisms. *Am. J. Physiol.* 276(5 Pt 2), H1434–H1441.

Woolfson, R. G., Patel, V. C., and Yellon, D. M. (1996). Pre-conditioning with adenosine leads to concentration-dependent infarct size reduction in the isolated rabbit heart. *Cardiovasc. Res.* 31, 148–151. doi: 10.1016/S0008-6363(95)00185-9

Xiao, J. W., Zhu, X. Y., Wang, Q. G., Zhang, D. Z., Cui, C. S., Zhang, P., et al. (2015). Acute effects of Rho-kinase inhibitor fasudil on pulmonary arterial hypertension in patients with congenital heart defects. *Circ. J.* 79, 1342–1348. doi: 10.1253/circj.CJ-14-1015

Xu, H., Stein, B., and Liang, B. (1996). Characterization of a stimulatory adenosine A2a receptor in adult rat ventricular myocyte. *Am. J. Physiol.* 270(5 Pt 2), H1655–H1661.

Xu, J., Bian, X., Liu, Y., Hong, L., Teng, T., Sun, Y., et al. (2017). Adenosine A2 receptor activation ameliorates mitochondrial oxidative stress upon reperfusion through the posttranslational modification of NDUFV2 subunit of complex I in

the heart. *Free Radic. Biol. Med.* 106, 208–218. doi: 10.1016/j.freeradbiomed.2017.02.036.

Xu, M. H., Gong, Y. S., Su, M. S., Dai, Z. Y., Dai, S. S., Bao, S. Z., et al. (2011). Absence of the adenosine A2A receptor confers pulmonary arterial hypertension and increased pulmonary vascular remodeling in mice. *J. Vasc. Res.* 48, 171–183. doi: 10.1159/000316935

Xu, R., and Mao, J. H. (2011). Gene transcriptional networks integrate microenvironmental signals in human breast cancer. *Integr. Biol.* 3, 368–374. doi: 10.1039/c0ib00087f

Yang, Z., Day, Y. J., Toufektsian, M. C., Ramos, S. I., Marshall, M., Wang, X. Q., et al. (2005). Infarct-sparing effect of A2A-adenosine receptor activation is due primarily to its action on lymphocytes. *Circulation* 111, 2190–2197. doi: 10.1161/01.CIR.0000163586.62253.A5

Yang, Z., Day, Y. J., Toufektsian, M. C., Xu, Y., Ramos, S. I., Marshall, M. A., et al. (2006). Myocardial infarct-sparing effect of adenosine A2A receptor activation is due to its action on CD4+ T lymphocytes. *Circulation* 114, 2056–2064. doi: 10.1161/CIRCULATIONAHA.106.649244

Zhang, S., Fantozzi, I., Tigno, D. D., Yi, E. S., Platoshyn, O., Thistlethwaite, P. A., et al. (2003). Bone morphogenetic proteins induce apoptosis in human pulmonary vascular smooth muscle cells. *Am. J. Physiol. Lung. Cell Mol. Physiol.* 285, L740–L754. doi: 10.1152/ajplung.00284.2002

Zhao, Y. D., Courtman, D. W., Deng, Y., Kugathasan, L., Zhang, Q., and Stewart, D. J. (2005). Rescue of monocrotaline-induced pulmonary arterial hypertension using bone marrow-derived endothelial-like progenitor cells: efficacy of combined cell and eNOS gene therapy in established disease. *Circ. Res.* 96, 442–450. doi: 10.1161/01.RES.0000157672.70560.7b

Zhong, H., Belardinelli, L., Maa, T., Feoktistov, I., Biaggioni, I., and Zeng, D. (2004). A(2B) adenosine receptors increase cytokine release by bronchial smooth muscle cells. *Am. J. Respir. Cell Mol. Biol.* 30, 118–125. doi: 10.1165/rcmb.2003-0118OC

Zimmermann, H. (2000). Extracellular metabolism of ATP and other nucleotides. *Naunyn Schmiedebergs Arch. Pharmacol.* 362, 299–309. doi: 10.1007/s002100000309

Conflict of Interest Statement: The authors declare that the research was conducted in the absence of any commercial or financial relationships that could be construed as a potential conflict of interest.

frontiers in Pharmacology

ORIGINAL RESEARCH
published: 01 December 2017
doi: 10.3389/fphar.2017.00888

Inhibition of A_{2A} Adenosine Receptor Signaling in Cancer Cells Proliferation by the Novel Antagonist TP455

Stefania Gessi[1], Serena Bencivenni[1], Enrica Battistello[1], Fabrizio Vincenzi[1], Vittoria Colotta[2], Daniela Catarzi[2], Flavia Varano[2], Stefania Merighi[1], Pier Andrea Borea[1]* and Katia Varani[1]*

[1] Department of Medical Sciences, Pharmacology Section, University of Ferrara, Ferrara, Italy, [2] Department of Neuroscience, Psychology, Drug Research and Child Health, Pharmaceutical and Nutraceutical Section, University of Florence, Florence, Italy

OPEN ACCESS

Edited by:
Francisco Ciruela,
University of Barcelona, Spain

Reviewed by:
Luca Antonioli,
University of Pisa, Italy
Carla Cicala,
University of Naples Federico II, Italy

***Correspondence:**
Stefania Merighi
mhs@unife.it
Pier Andrea Borea
bpa@unife.it

Specialty section:
This article was submitted to Experimental Pharmacology and Drug Discovery, a section of the journal Frontiers in Pharmacology

Received: 12 September 2017
Accepted: 17 November 2017
Published: 01 December 2017

Citation:
Gessi S, Bencivenni S, Battistello E, Vincenzi F, Colotta V, Catarzi D, Varano F, Merighi S, Borea PA and Varani K (2017) Inhibition of A_{2A} Adenosine Receptor Signaling in Cancer Cells Proliferation by the Novel Antagonist TP455. Front. Pharmacol. 8:888. doi: 10.3389/fphar.2017.00888

Several evidences indicate that the ubiquitous nucleoside adenosine, acting through A_1, A_{2A}, A_{2B}, and A_3 receptor (AR) subtypes, plays crucial roles in tumor development. Adenosine has contrasting effects on cell proliferation depending on the engagement of different receptor subtypes in various tumors. The involvement of A_{2A}ARs in human A375 melanoma, as well as in human A549 lung and rat MRMT1 breast carcinoma proliferation has been evaluated in view of the availability of a novel A_{2A}AR antagonist, with high affinity and selectivity, named as 2-(2-furanyl)-N^5-(2-methoxybenzyl)[1,3]thiazolo[5,4-d]pyrimidine-5,7-diammine (TP455). Specifically, the signaling pathways triggered in the cancer cells of different origin and the antagonist effect of TP455 were investigated. The A_{2A}AR protein expression was evaluated through receptor binding assays. Furthermore, the effect of A_{2A}AR activation on cell proliferation at 24, 48 and 72 hours was studied. The selective A_{2A}AR agonist 2-*p*-(2-carboxyethyl)phenethylamino-5′-*N*-ethylcarboxamidoadenosine hydrochloride (CGS21680), concentration-dependently induced cell proliferation in A375, A549, and MRMT1 cancer cells and the effect was potently antagonized by the A_{2A}AR antagonist TP455, as well as by the reference A_{2A}AR blocker 4-(2-[7-amino-2-(2-furyl)[1,2,4]triazolo[2,3-a][1,3,5]triazin-5-ylamino]ethyl)phenol (ZM241385). As for the signaling pathway recruited in this response we demonstrated that, by using the specific inhibitors of signal transduction pathways, the effect of A_{2A}AR stimulation was induced through phospholipase C (PLC) and protein kinase C-delta (PKC-δ). In addition, we evaluated, through the AlphaScreen SureFire phospho(p) protein assay, the kinases enrolled by A_{2A}AR to stimulate cell proliferation and we found the involvement of protein kinase B (AKT), extracellular regulated kinases (ERK1/2), and c-Jun N-terminal kinases (JNKs). Indeed, we demonstrated that the CGS21680 stimulatory effect on kinases was strongly reduced in the presence of the new potent compound TP455, as well

as by ZM241385, confirming the role of the A_{2A}AR. In conclusion, the A_{2A}AR activation stimulates proliferation of A375, A549, and MRMT1 cancer cells and importantly TP455 reveals its capability to counteract this effect, suggesting selective A_{2A}AR antagonists as potential new therapeutics.

Keywords: A_{2A} adenosine receptor, cancer cell proliferation, intracellular signaling pathways, Drug Discovery and Therapy, receptor antagonist

INTRODUCTION

Adenosine, a ubiquitous purine nucleoside, is considered as an important modulator of tissue function, increasing its concentrations under adverse metabolic conditions. Adenosine is produced in the extracellular space through ATP degradation operated by specific ectoenzymes, named apyrase (CD39) and 5′-nucleotidase (CD73) and exerts its effects by recruitment of four G-protein-coupled A_1, A_{2A}, A_{2B}, and A_3 adenosine receptors (ARs) (Borea et al., 2016). A_1AR activation by interacting with Gi/Go proteins inhibits adenylyl cyclase (AC), regulates calcium and potassium channels, as well as phospholipase C (PLC). The A_{2A}AR couples to Gs/Golf proteins to activate AC thus increasing cAMP levels. The A_{2B} receptor, by recruiting Gs/Gq protein raises AC and activates PLC. Finally, the A_3AR interacts with Gi and Gq proteins inhibiting AC and stimulating PLC, respectively (Fredholm et al., 2011). In addition, in a cell type specific way, all adenosine receptors may also be linked to mitogen-activated protein kinases (MAPK), including extracellular signal-regulated kinase (ERK) 1/2, c-Jun-N-terminal kinase 1/2 (JNK1/2), and p38 MAPK kinase, crucial in the modulation of cell growth and death (Schulte and Fredholm, 2000). Indeed, an important role of adenosine in human cancerogenesis has been evidenced, as it regulates almost all the phases of cancer development including immunoescaping, cell proliferation, angiogenesis and metastasis, by recruiting different adenosine receptor subtypes (Antonioli et al., 2013a,b; Borea et al., 2017).

It is well established the relevance of immune cells in the fight against tumors and adenosine, that increases in hypoxic solid tumors, decreases the recognition of cancer cells by cytolytic T cells (Blay et al., 1997; Merighi et al., 2003; Muller-Haegele et al., 2014). Specifically, these cells are depressed by A_{2A}ARs with the final result of an increase in hypoxic tumor cell survival and immunoescaping as demonstrated in A_{2A}AR gene-deficient mice, having a much stronger antitumor immunity, rejection of established tumors and prolonged animal survival (Ohta et al., 2006; Sitkovsky et al., 2008; Young et al., 2016). Furthermore, A_{2A}ARs promote wound healing and angiogenesis and are able to increase also melanoma and breast cancer cell proliferation (Merighi et al., 2002; Etique et al., 2009; Koszałka et al., 2016; Perez-Aso et al., 2016). All these data support the importance of A_{2A}AR antagonists to combat tumor development.

Recently, a series of novel blockers, having the thiazolo[5,4-d]pyrimidine nucleus, showing an unprecedented high affinity for the A_{2A}AR and a behavior as antagonists and/or inverse agonists has been developed (Varano et al., 2016). With the availability of the novel compound 2-(2-furanyl)-N^5-(2-methoxybenzyl)[1,3]thiazolo[5,4-d]pyrimidine-5,7-diammine (TP455) (**Figure 1**), the involvement of A_{2A}ARs in human A375 melanoma, as well as in human A549 lung and rat MRMT1 breast carcinoma proliferation was evaluated. In addition, the signaling pathways triggered in the cancer cells of different origin and the antagonist effect of TP455 were investigated.

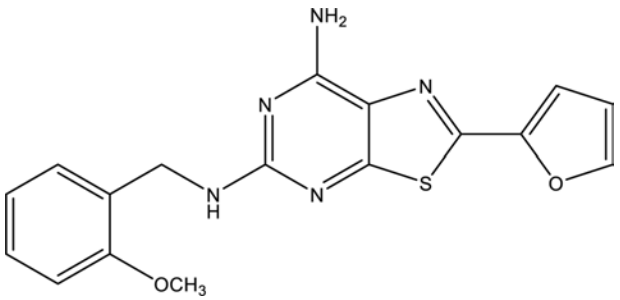

FIGURE 1 | Chemical structure of the A_{2A}AR antagonist/inverse agonist TP455 (2-(2-furanyl)-N^5-(2-methoxybenzyl)[1,3]thiazolo[5,4-d]pyrimidine-5,7-diammine).

Overall our data indicate that the A_{2A}AR activation stimulates proliferation of A375, A549, and MRMT1 cancer cells through ERK1/2, JNK1/2, and AKT downstream PLC and PKC-δ. Importantly, TP455 antagonizes this effect, adding a piece of evidence on the effects of selective A_{2A}AR antagonists on cancer development thus supporting their role as potential new anticancer drugs.

MATERIALS AND METHODS

The A_{2A}AR antagonist/inverse agonist TP455 was recently synthesized (compound 13 in Varano et al., 2016) and the chemical structure is shown in **Figure 1**. [^{3}H]-ZM 241385 was from PerkinElmer (Milan, Italy). 4-(2-[7-Amino-2-(2-furyl)[1,2,4]triazolo[2,3-a][1,3,5]triazin-5-ylamino]ethyl)phenol (ZM 241385) and 8-[4-[4-(4-Chlorophenzyl)piperazide-1-sulfonyl)phenyl]]-1-propylxanthine (PSB 603) were purchased from Tocris, Space Import–Export (Milan, Italy). 4- (4-Fluorophenyl)-2-(4-hydroxyphenyl)-5-(4-pyridyl)-1H-imidazole (SB202190) was purchased by Adipogen (Florence, Italy). D-3-Deoxy-2-*O*-methyl-myo-inositol 1-[(R)-2-methoxy-3-(octadecyloxy)propyl hydrogen phosphate] (SH5) and 1,9-Pyrazoloanthrone (SP600125) were from Enzo Life (Florence, Italy). 1-[6-[[(17β)-3-Methoxyestra-1,3,5(10)-trien-17-yl]amino]hexyl]-1H-pyrrole-2,5-dione (U73122) was from Cayman (Florence, Italy). 2-*p*-(2-Carboxyethyl)phenethylamino-5′-N-ethylcarboxamido-adenosine hydrochloride hydrate (CGS 21680), 5′-(*N*-Ethyl

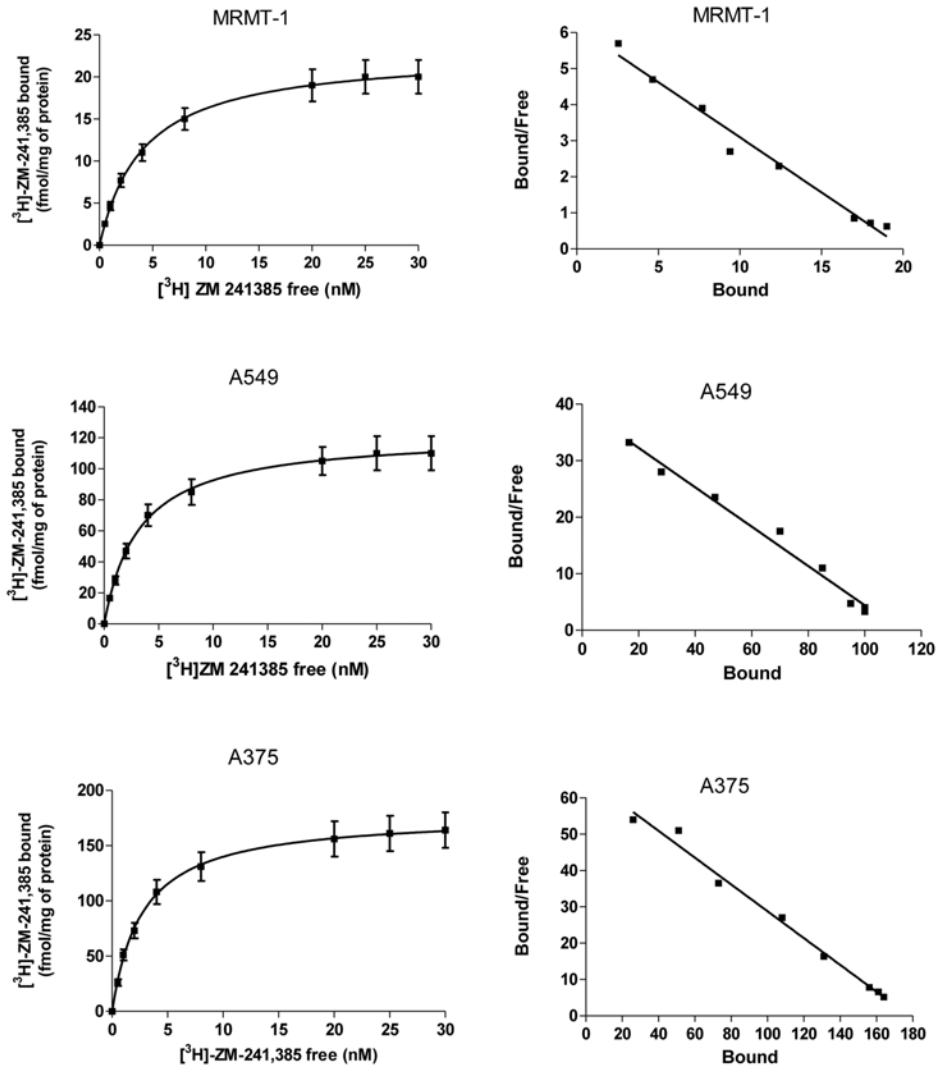

FIGURE 2 | Saturation curves of [^{3}H]-ZM 241385 binding in A375, A549, and MRMT-1 cell lines. Experiments were performed as described in Section "Materials and Methods". Values are the means and vertical lines SE of the mean of four separate experiments performed in triplicate. The Scatchard plots of the same data are shown.

carboxamido)adenosine (NECA), 1-[6-[(3-Acetyl-2,4,6-trihydroxy-5-methylphenyl)methyl]-5,7-dihydroxy-2,2-dimethyl-2H-1-benzopyran-8-yl]-3-phenyl-2-propen-1-one (Rottlerin) and 2-(2-Furanyl)-7-[3-(4-methoxyphenyl)propyl]-7H-pyrazolo[4,3-e][1,2,4]triazolo[1,5-c]pyrimidin-5-amine (SCH 442416) were purchased from Sigma (Milan, Italy). PKC-ε translocation inhibitor peptide was purchased by Calbiochem (Milan, Italy). AlphaScreen SureFire phospho(p)ERK1/2(Thr202/Tyr204), p-AKT1/2/3 (pThr308) and p-JNK1/3 (pThr183/Tyr185) assay kits, AlphaScreen® cAMP and DELFIA® Cell Proliferation kit were from PerkinElmer (Milan, Italy). Unless otherwise noted, all other reagents were purchased from Sigma (Milan, Italy).

Cell Culture Conditions

Tumoral cell lines A375 (human skin malignant melanoma), A549 (adenocarcinomic human alveolar basal epithelial cells) and rat cell line MRMT-1 (rat breast carcinoma cells) were purchased from ATCC and were grown adherently at 37°C in 5% CO_2/95% air. A375 and A549 were maintained in DMEM high glucose medium containing 10% fetal calf serum, penicillin (100 U/mL) and streptomycin (100 mg/mL) and MRMT-1 were grown in RPMI 1640 medium containing 10% fetal calf serum, penicillin (100 U/mL), streptomycin (100 mg/mL), and L-glutamine (2 mM). Adenosine receptor agonists and antagonists and inhibitors of kinases, were made up in dimethyl sulfoxide solution (DMSO) and then diluted in cell culture medium (0.1 max 0.2% of DMSO). An equal amount of DMSO was used in control cells (CTR).

Membrane Preparation

For membrane preparation the culture medium was removed. The cells were washed with PBS and scraped off 90 mm

TABLE 1 | Inhibition of [^{3}H]ZM241385 binding (Ki nM) by adenosine receptor agonists and antagonists in human A375 melanoma, A549 lung carcinoma, and rat MRMT-1 breast carcinoma membranes.

Compounds	A375 Ki (nM)	A549 Ki (nM)	MRMT-1 Ki (nM)
Agonists			
CGS21680	15 ± 1	16 ± 2	14 ± 1
NECA	6.65 ± 0.52	12 ± 1	9.33 ± 0.95
Cl-IB-MECA	694 ± 75	710 ± 89	500 ± 64
R-PIA	725 ± 78	670 ± 75	423 ± 52
Antagonists			
SCH58261	2.82 ± 0.32	3.15 ± 0.34	3.26 ± 0.43
ZM241385	2.23 ± 0.26	2.33 ± 0.24	2.47 ± 0.23
CGS15943	1.45 ± 0.18	1.66 ± 0.20	2.15 ± 0.34
TP455	0.0058 ± 0.0002	0.0053 ± 0.0003	0.0061 ± 0.0003

The data are expressed as mean ± SE.

diameter petri dishes in ice-cold hypotonic buffer (5 mM Tris–HCl, 2 mM EDTA, pH 7.4) (Gessi et al., 2007). The cell suspension was homogenized with Polytron and the homogenate was spun for 10 min at 1000 g. The supernatant was then centrifuged for 30 min at 100,000*g*. The membrane pellet was resuspended in 50 mM Tris HCl buffer pH 7.4, 10 mM $MgCl_2$. The protein concentration was determined according to a Bio-Rad method with BSA as a standard reference (Bradford, 1976). Then the suspension was frozen at −80°C.

Saturation and Competition Binding Experiments

Saturation binding experiments on A549, A375, and MRMT-1 cell membranes were performed by using [^{3}H]-ZM 241385 at different concentrations (0.1–30 nM), incubated with 100 μg of protein per assay of membrane suspension, for 1 h at 4°C. Competition experiments of [^{3}H]-ZM 241385 were performed in duplicate in test tubes containing the buffer, the membranes and different concentrations of A_{2A}ARs agonists and antagonists. Non-specific binding was defined as the binding in the presence of 1 μM ZM 241385 and was <32% of the total binding. At the end of the incubation, bound and free radioactivity were separated by filtering, in a Brandel cell harvester, the assay mixture through Whatman GF/B glass-fiber filters. The filter bound radioactivity was counted in a liquid Scintillation Counter Tri Carb Packard 2500 TR (Perkin-Elmer Life and Analytical Sciences, Boston, MA, United States).

AlphaScreen SureFire Assays

AlphaScreen SureFire phospho(p)ERK1/2(Thr202/Tyr204), pJNK1/3(pThr183/Tyr185), and p-AKT1/2/3 (pThr308) assay kits (Perkin Elmer, Milan, Italy) were utilized. Upon kinase phosphorylation and excitation at 680 nm, fluorescent signals at 615 nm are emitted. Cells were seeded in 100 μl culture medium into 96-well plates (30,000/well), and incubated at 37°C for 24 h. Cells were pretreated with various inhibitors and TP455 for 30 min. Then, receptors were maximally stimulated using 100 nM CGS 21680 and incubated for 5 min (ERK1/2, JNK1/2-MAPK) or 30 min (AKT) at 37°C. After agonist removal, lysis buffer was added, then donor and acceptor beads linked to specific anti-*p*-kinase- and anti-kinase-antibodies were dispensed, according to manufacturer instructions. Finally, fluorescent signals were detected through an Ensight Perkin Elmer-multimode plate reader (Perkin Elmer, Milan, Italy). Data were normalized to fold activation above basal *p*-kinase levels (=100). For inhibitor graphs, raw data were transformed into percentages relative to controls (basal level = 100%) in order to merge data from several experiments.

DELFIA Cell Proliferation Kit

The DELFIA assay was performed to determine cell proliferation according to the manufacturer's protocol from PerkinElmer (Milan, Italy). The assay is a time-resolved fluoroimmunoassay based on the incorporation of BrdU into newly synthesized DNA strands of proliferating cells cultured in microliter plates. Incorporated BrdU is detected using a europium labeled monoclonal antibody and the fluorescence measured is proportional to the DNA synthesis in the cell population of each well. A375, A549, and MRMT-1 cells were cultured over night at 1000 cells/well in a 96-well plate (at a final volume of 100 μl per well), agonists and antagonists were added and the cells were incubated for 30′ before addition of the BrdU-Labeling solution 10 μl/well. The cells were then cultured for 24, 48, or 72 h. At the end of the incubation period, cells were fixed (fix solution 100 μl/well), added with 100 μl/well of Anti-BrdU-Eu (0.5 μg/ml) and incubated for 120 min at room temperature. After four washes, 200 μl of DELFIA Inducer were added at room temperature for 15 min and the Eu-fluorescence was detected through an Ensight Perkin Elmer-multimode plate reader (Perkin Elmer, Milan, Italy). Two kinds of controls were performed: the blank where no cells were added to the well but only culture medium and the background where no BrdU was added to the wells.

Statistical Analysis

For saturation binding experiments, determination of receptor affinity (K_D) and receptor density (BMAX) was performed using the non-linear least-squares curve fitting program LIGAND (Munson and Rodbard, 1980). LIGAND was also used to determine inhibitory binding constant (Ki) values from the competition binding experiments. All values in the figures and text are expressed as mean ± standard error (SE) of three independent experiments. Data sets were examined by one-way analysis of variance (ANOVA) and Dunnett's test (when required). $^*P < 0.05$ was considered significant.

RESULTS

Saturation Studies

The expression of A_{2A}ARs in A375, A549, and MRMT-1 cells was determined performing saturation binding experiments with [^{3}H]-ZM 241385. The saturation curves of [^{3}H]-ZM 241385

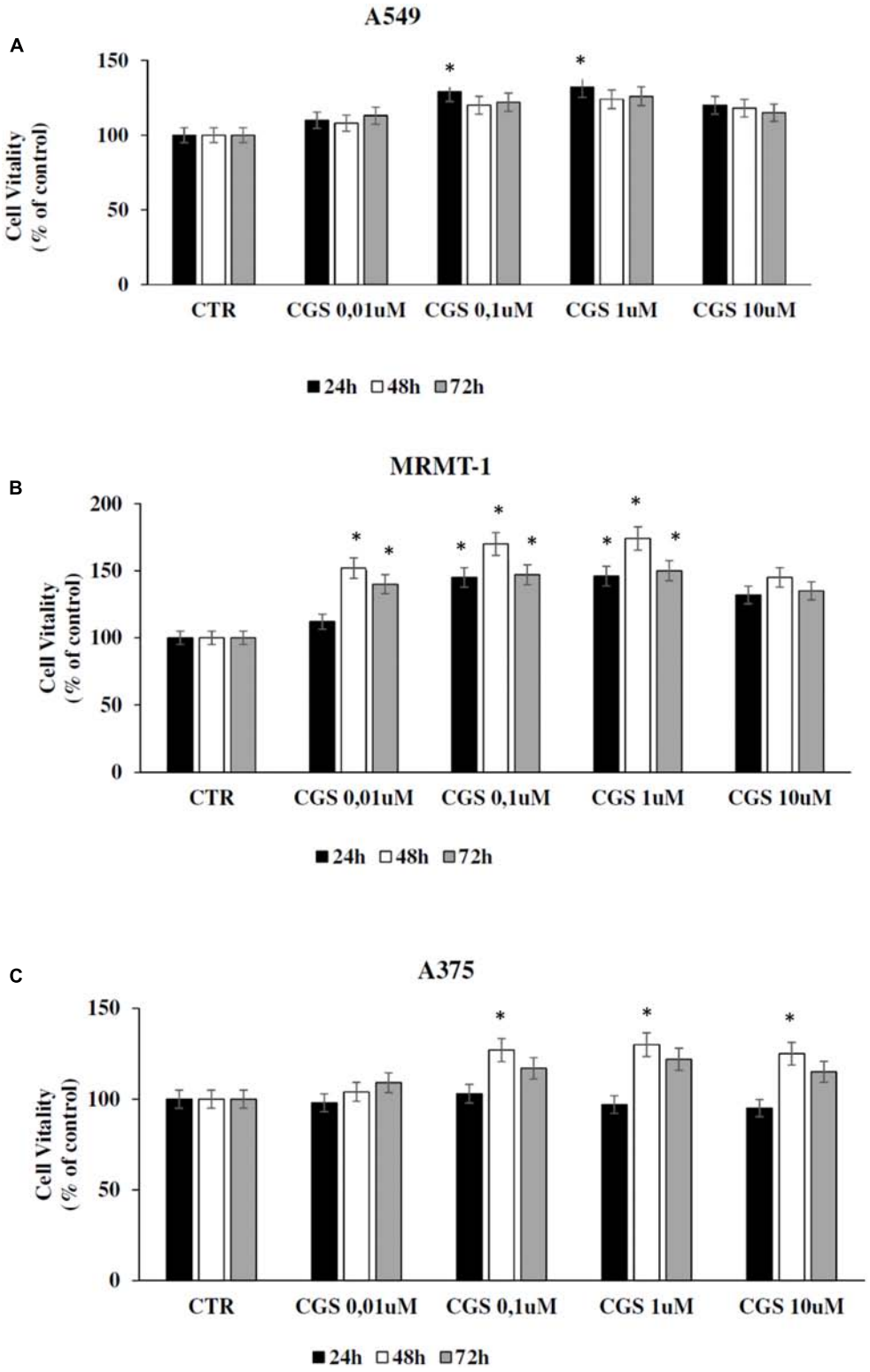

FIGURE 3 | Effect of CGS 21680 on cell proliferation in A549 **(A)**, MRMT-1 **(B)**, and A375 **(C)** cell lines. Cells were incubated in the presence of 0.01–10 μM CGS 21680 for 24, 48, and 72 h and cell proliferation was evaluated by DELFIA Cell Proliferation Kit. Solutions were made up in DMSO and then diluted in cell culture medium (0.1 max 0.2% of DMSO). An equal amount of DMSO was used in control cells (CTR). $^*P < 0.01$ compared with CTR. Means ± SE values from four experiments are shown. Analysis was by one way ANOVA, followed by Dunnett's test.

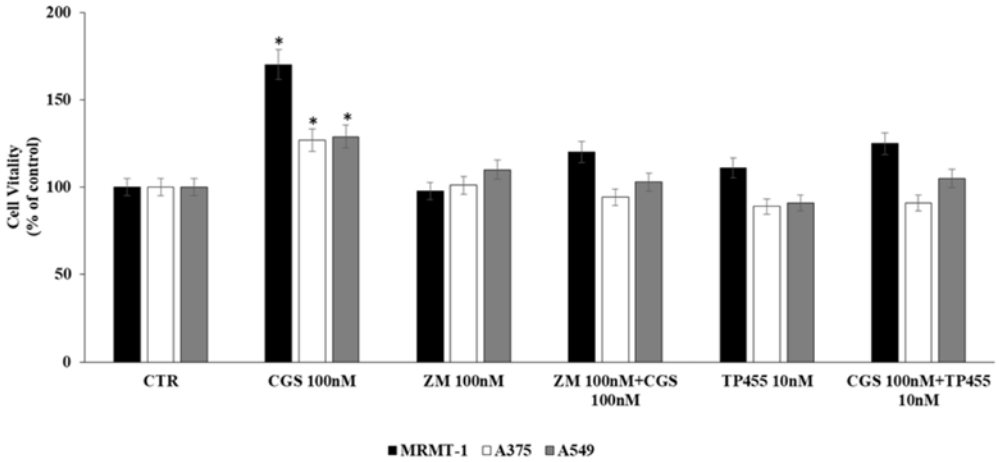

FIGURE 4 | Effect of 100 nM CGS 21680 on A375 and MRMT-1 cell viability (48 h) as well as in A549 (24 h) and antagonism by 100 nM ZM 241385 and 10 nM TP455 by DELFIA Cell Proliferation Kit. Solutions were made up in DMSO and then diluted in cell culture medium (0.1 max 0.2% of DMSO). An equal amount of DMSO was used in control cells (CTR) incubated for 24 h in case of A549 and 48 h in case of A375 and MRMT-1. $^*P < 0.01$ compared with CTR. Means ± SE values from four experiments are shown. Analysis was by one way ANOVA, followed by Dunnett's test.

binding, reported in **Figure 2**, show a K_D value of 2.75 ± 0.25, 2.98 ± 0.31 nM, 2.17 ± 0.18 nM, and a B_{max} of 178 ± 20, 110 ± 9, 21 ± 4 fmol $mg^{-1}$of protein in A375, A549, and MRMT-1 cells, respectively. The Scatchard plots in the insert are linear failing to show a significantly better fit to a two-site than to a one-site binding model, demonstrating that only one class of high affinity binding sites is present in our experimental conditions (Munson and Rodbard, 1980).

Competition Experiments

The affinity values of the examined ligands obtained in [^{3}H]-ZM 241385 competition binding experiments performed in A375, A549, and MRMT-1 cell membranes were determined, as shown in **Table 1**. The order of potency of the agonists was as follows: NECA > CGS 21680 > R-PIA = Cl-IB-MECA. The order of potency of the antagonists was as follows: TP455 > CGS15943 > ZM241385 > SCH58261. Specifically, the novel compound TP455 revealed a very good affinity for rat and human A_{2A}ARs with Ki value in the picomolar range in all the three cell lines investigated.

Increase in Cell Proliferation Induced by CGS 21680 in Cancer Cell Lines

The effect of A_{2A}ARs activation on tumor cell proliferation was evaluated in A549, MRMT-1, and A375 cancer cells. Specifically, the A_{2A}ARs selective agonist CGS21680 (10–100 nM) was applied to cancer cells for 24, 48, and 72 h of incubation before assessing proliferation. The results show that in A549 cells CGS 21680 slightly increased cell proliferation only when used at the concentration of 100 nM for 24 h and its effect was not more present after 48 and 72 h (**Figure 3A**). As for MRMT-1 cells the A_{2A}ARs agonist at 10 nM raised cell vitality after 48 and 72 h of treatment, while a significant stimulation was observed with CGS 21680 100 nM at all the time points investigated (**Figure 3B**). In A375 cells the stimulatory effect of cell proliferation A_{2A}ARs-dependent was revealed only at 48 h of treatment with CGS21680 100 nM (**Figure 3C**).

Antagonism of CGS 21680-Induced Cell Proliferation in Cancer Cell Lines by the New A_{2A}ARs Selective Antagonist TP455

In order to verify that the increase of cell proliferation induced by CGS21680 was mediated through A_{2A}ARs stimulation we antagonized its effect by using the standard antagonist ZM 241385. MRMT-1, A375 as well as A549 cells were pretreated for 30 min with 100 nM ZM 241385 before stimulation with 100 nM CGS21680 for 48 h with exception of A549 tested after 24 h. As shown in **Figure 4** this compound was able to completely block the agonist effect in all the cell lines studied, confirming the involvement of A_{2A}ARs in cancer cell proliferation. Therefore, the ability of the new selective and high affine A_{2A}ARs compound TP455 to revert cell proliferation induced by CGS21680 was investigated. Our results show that the increase in cell vitality CGS21680-dependent was antagonized by addition of 10 nM TP455 in all cancer cells, suggesting that this novel derivative behaves as an A_{2A}ARs antagonist (**Figure 4**). When tested alone 10 nM TP455 and 100 nM ZM 241385 did not alter cell proliferation, showing a behavior of pure A_{2A}AR antagonists (**Figure 4**).

Signaling Pathways Involved in Cell Proliferation Induced by CGS 21680 in Cancer Cell Lines

The involvement of PLC, AC, PKCε, and PKCδ in the increase of cell proliferation due to A_{2A}AR activation was investigated. Cells were incubated with U73122 (U73), SQ22,536 (SQ),

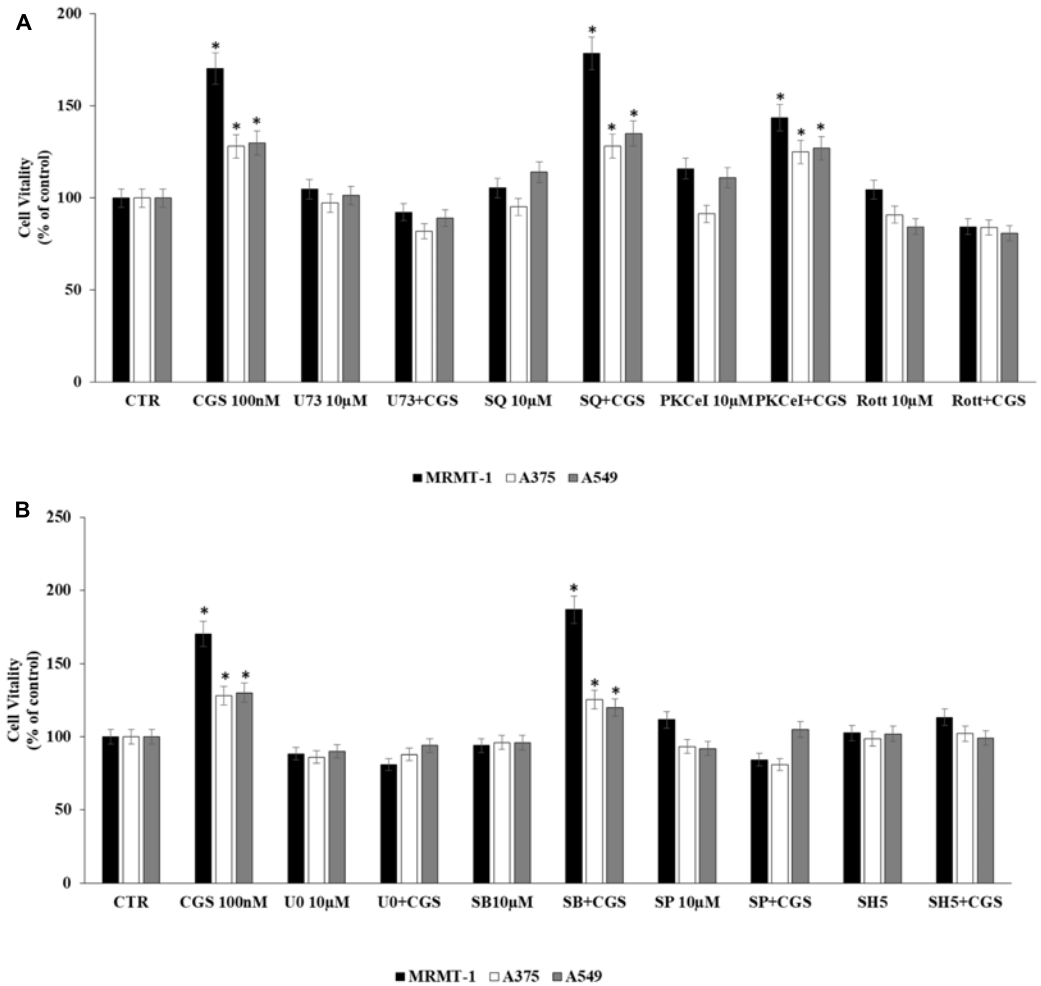

FIGURE 5 | Signaling pathways involved in cell proliferation induced by CGS 21680 in cancer cell lines. Effect of 100 nM CGS 21680 on A375, MRMT cell viability (48 h) as well as in A549 (24 h) and inhibition by 10 μM U73, SQ, PKCε-I, and Rott **(A)**, 10 μM SB202190 (SB), U0126 (U0), SP600125 (SP), and SH5 **(B)** by DELFIA Cell Proliferation Kit. Solutions were made up in DMSO and then diluted in cell culture medium (0.1 max 0.2% of DMSO). An equal amount of DMSO was used in control cells (CTR) incubated for 24 h in case of A549 and 48 h in case of A375 and MRMT-1. $^*P < 0.01$ compared with CTR. Means ± SE values from four experiments are shown. Analysis was by one way ANOVA, followed by Dunnett's test.

PKCε-translocation inhibitor peptide (PKCε-I), and rottlerin (Rott) as inhibitors of PLC, AC, PKCε, and PKCδ, respectively. MRMT-1, A375 as well as A549 cells were pretreated for 30 min with 10 μM inhibitors before stimulation with 100 nM CGS21680 for 48 h with exception of A549 tested after 24 h. All inhibitors alone did not significantly affect cell proliferation (**Figure 5A**). As shown in **Figure 5A** blockers of PLC and PKCδ were able to antagonize the stimulatory effect of 100 nM CGS21680, suggesting the involvement of these enzymes in the A_{2A}AR agonist effect, while inhibitors of AC and PKCε did not block the agonist effect.

In addition, to evaluate MAPK and AKT pathways involvement in A_{2A}AR-mediated cell proliferation, cells were pretreated for 30 min with 10 μM U0126, SB202190, SP600125, and SH5, inhibitors of ERK1/2, p38, JNK1/2 MAPK kinases and AKT, respectively, before exposure to 100 nM CGS 21680 for 48 h with exception of A549 tested after 24 h. All inhibitors alone did not significantly affect cell proliferation (**Figure 5B**). As shown in **Figure 5B**, U0126, SP600125, and SH5 strongly reduced the effect of CGS21680 on cell proliferation, whilst SB202190 did not. These results suggest the involvement of ERK1/2, JNK1/2 MAPK kinases, and AKT in the increase of cell proliferation mediated by A_{2A}AR activation.

Effect of CGS 21680 on ERK1/2, JNK MAPK Kinase, and AKT Phosphorylation

To confirm the role of ERK1/2, JNK1/2 MAPK kinases, and AKT in the increase of cell proliferation mediated by A_{2A}AR activation, kinases phosphorylation was assessed at 0–60 min in the absence and in the presence of 100 nM CGS 21680, as stimulator of A_{2A}ARs in MRMT-1, A375

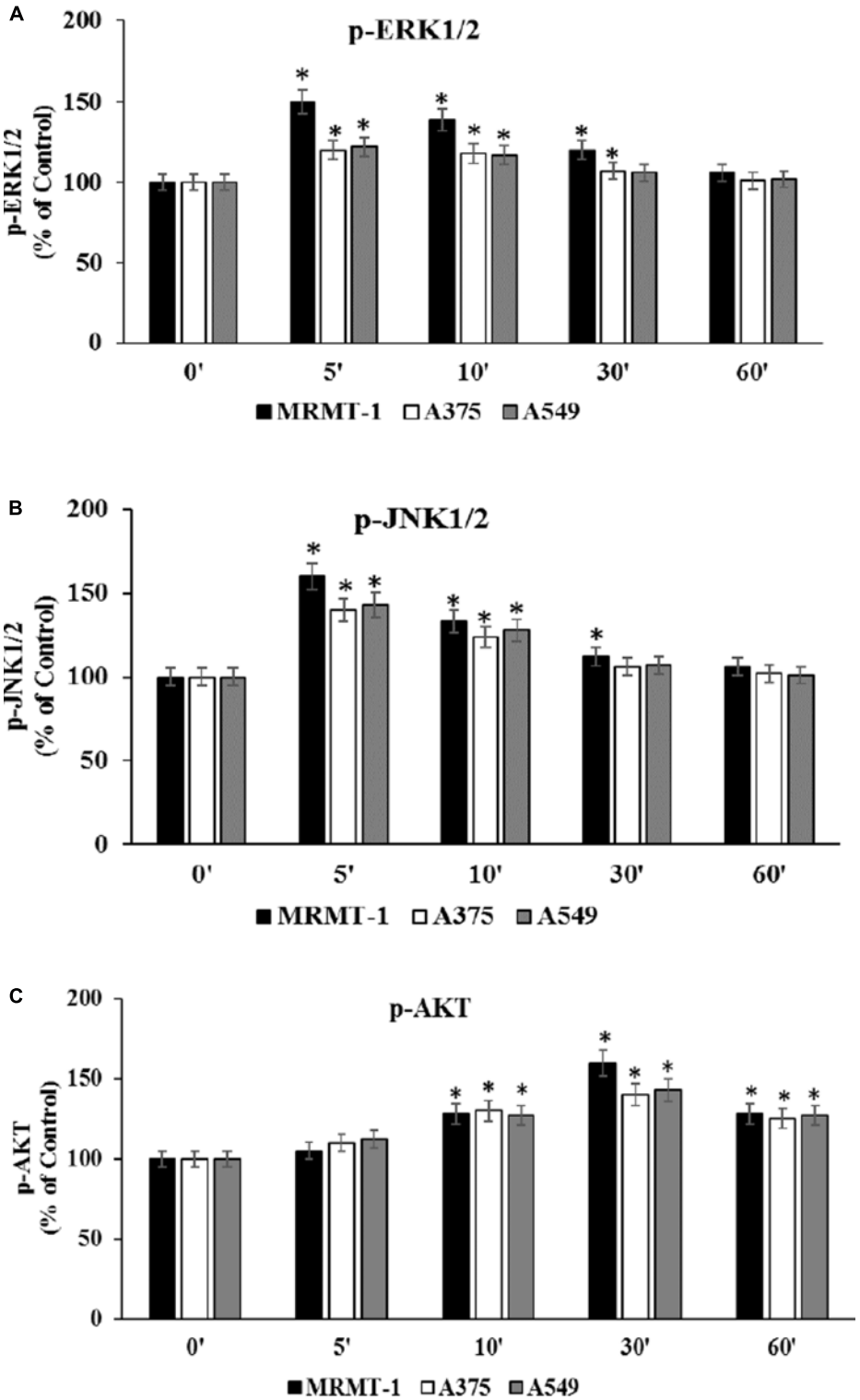

FIGURE 6 | Effect of CGS 21680 on pERK1/2, pJNK1/2 MAPK kinase, and pAKT activation. Cells were incubated in the presence of 100 nM CGS 21680 for 0, 5, 10, 30, and 60 min and pERK1/2 **(A)**, pJNK1/2 **(B)**, and pAKT **(C)** protein levels were evaluated by AlphaScreen SureFire pMAPK assays in MRMT-1, A375, and A549 cells. Solutions were made up in DMSO and then diluted in cell culture medium (0.1 max 0.2% of DMSO). An equal amount of DMSO was used in control cells (CTR). $^*P < 0.01$ compared with time 0. Means ± SE values from four experiments are shown. Analysis was by one-way ANOVA followed by Dunnett's test.

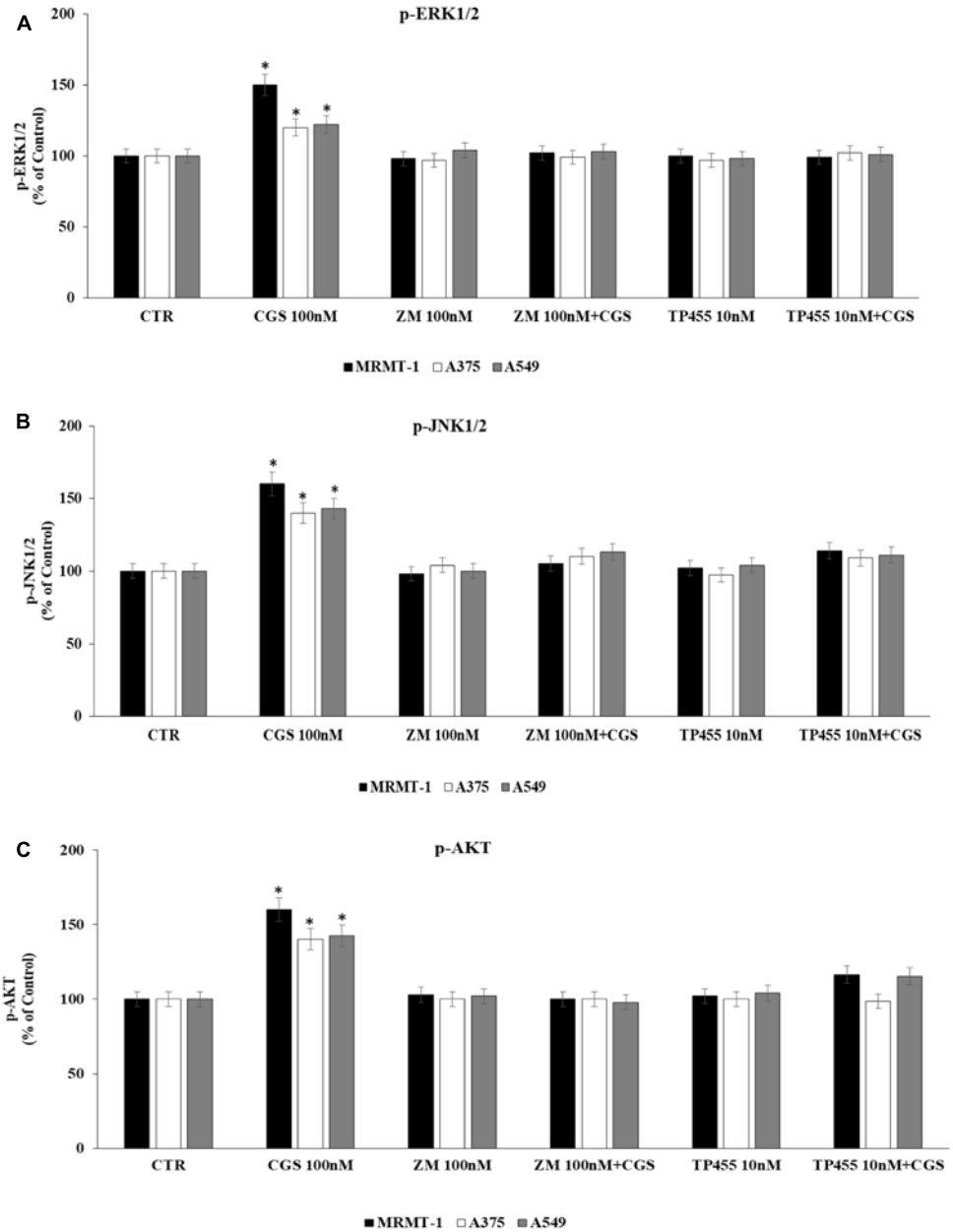

FIGURE 7 | Effect of antagonists on CGS 21680-dependent pERK1/2, pJNK MAPK kinase, and pAKT activation. MRMT-1, A375, and A549 cells in the absence or in the presence of 100 nM ZM 241385 and 10 nM TP455 were exposed to 100 nM CGS for 5 min or for 30 min and pERK1/2 **(A)**, pJNK **(B)**, and pAKT **(C)** protein levels were evaluated by AlphaScreen SureFire pMAPK assays respectively. Solutions were made up in DMSO and then diluted in cell culture medium (0.1 max 0.2% of DMSO). An equal amount of DMSO was used in control cells (CTR). $^*P < 0.01$ compared with CGS 21680 100 nM. Means ± SE values from four experiments are shown. Analysis was by one-way ANOVA followed by Dunnett's test.

and A549 cells (**Figures 6A–C**, respectively). ERK1/2 and JNK1/2 phosphorylation reached a maximal effect after 5 min of A_{2A}AR stimulation and disappeared at 60 min, while AKT phosphorylation started to increase after 10 min of treatment and decreased after 60 min. Furthermore, ERK1/2, JNK, and AKT phosphorylation were higher in MRMT-1 compared to A375 and A549 cells (**Figures 6A–C**, respectively).

Antagonism of CGS 21680-Induced ERK1/2, JNK1/2 MAPK Kinase and AKT Phosphorylation by the New A_{2A}ARs Selective Antagonist TP455

To evaluate whether stimulation of ERK1/2, JNK1/2, and AKT phosphorylation CGS21680-dependent was induced through A_{2A}AR activation we antagonized it by using the standard

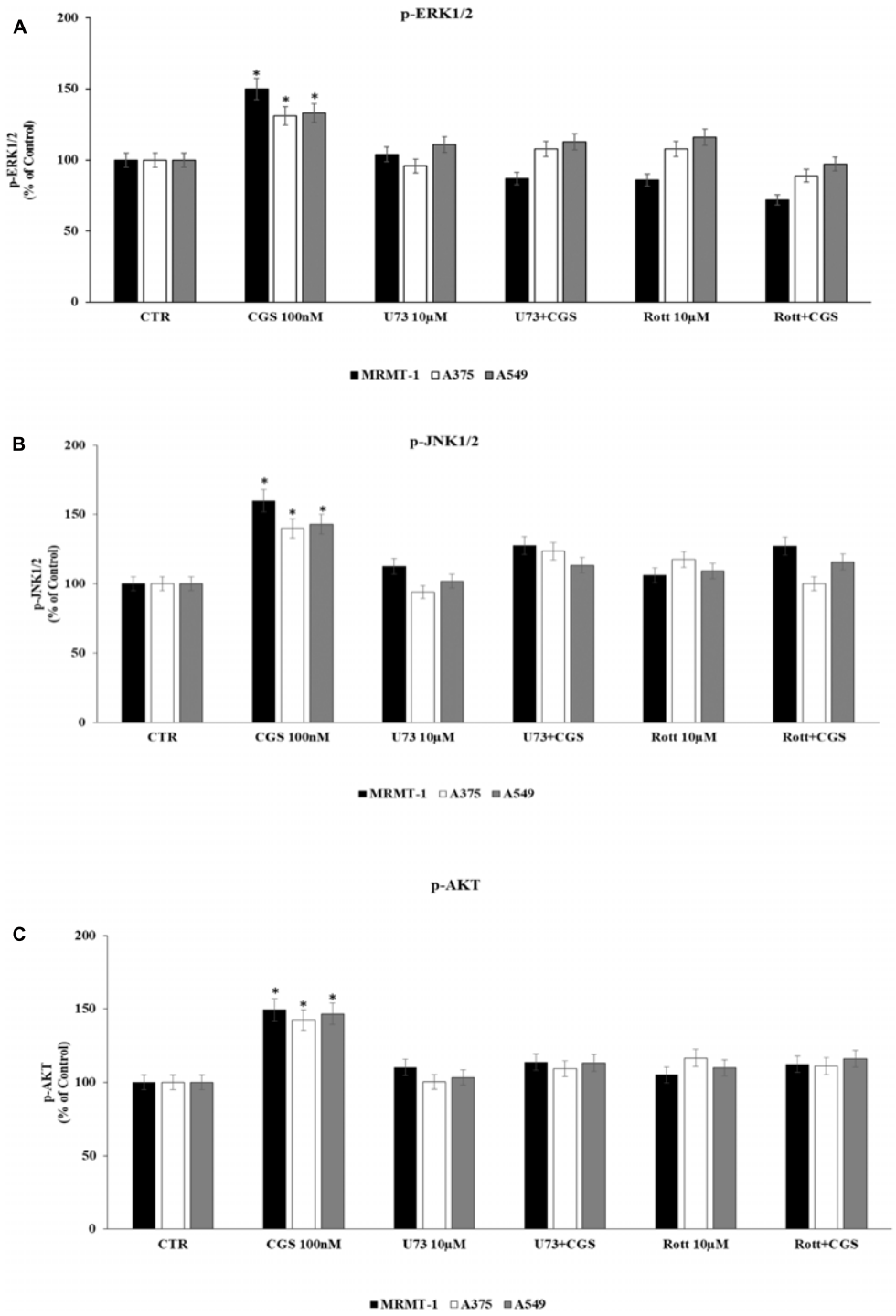

FIGURE 8 | Effect of 100 nM CGS 21680 on pERK1/2 **(A)**, pJNK1/2 **(B)**, and pAKT **(C)** protein levels in MRMT-1, A375 and A549 cells and antagonism by 10 μM U73122 (U73) and 10 μM rottlerin (Rott) evaluated by AlphaScreen SureFire pMAPK assays. Solutions were made up in DMSO and then diluted in cell culture medium (0.1 max 0.2% of DMSO). An equal amount of DMSO was used in control cells (CTR). $^*P < 0.01$ compared with CTR. Means ± SE values from four experiments are shown. Analysis was by one-way ANOVA followed by Dunnett's test.

antagonist ZM 241385. MRMT-1, A375, and A549 cells were pretreated for 30 min with 100 nM antagonist before stimulation with 100 nM CGS21680 for 5 (ERK1/2, JNK1/2) or 10 min (AKT) to assess kinases phosphorylation. As shown in **Figures 7A–C** the effect of CGS 21680 on ERK1/2, JNK1/2, and AKT phosphorylation, respectively, was completely

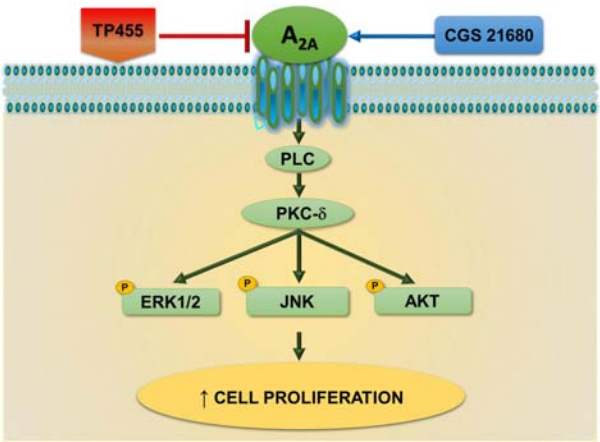

FIGURE 9 | A_{2A} adenosine receptors-triggered signal transduction cascade in cancer cells. CGS21680 agonist by activating A_{2A}ARs increases cell proliferation through a pathway dependent on PLC, PKCδ, pERK1/2, pJNK, and pAKT signaling. This effect is potently antagonized by the newly synthesized derivative TP455.

reverted by ZM 241385. In addition the ability of the A_{2A}AR antagonist TP455 to block kinases phosphorylation induced by CGS21680 was studied. Our results show that this effect was potently inhibited by pre-treatment for 30 min with 10 nM TP455 in MRMT-1, A375, and A549 cells (**Figures 7A–C**).

Characterization of ERK1/2, JNK1/2 MAPK Kinase, and AKT Signaling Cascade Triggered by CGS 21680 in Cancer Cell Lines

Finally, in order to deeply investigate the signaling cascade triggered by A_{2A}AR activation in the increase of ERK1/2, JNK1/2, and AKT phosphorylation, MRMT-1, A375, and A549 cells were incubated with PLC and PKCδ inhibitors before the exposure to 100 nM CGS 21680. Then ERK1/2, JNK1/2, and AKT phosphorylation status was examined. As reported in **Figure 8** phosphorylation of ERK1/2, JNK1/2, and AKT mediated by CGS21680 was strongly reduced in the presence of 10 μM U73 and Rott suggesting that PLC and PKCδ were upstream of ERK1/2, JNK1/2 and AKT (**Figures 8A–C**, respectively).

DISCUSSION

Several data in literature support an important role of adenosine in tumor development. Indeed, adenosine may act as both an anti- or pro-tumoral endogenous nucleoside depending on which adenosine receptor subtype is recruited (Borea et al., 2016, 2017). Specifically, as for the anti-tumoral effect, the main receptor subtype involved results the A_3AR for which the successful data obtained in preclinical studies lead to the development of A_3AR selective agonists, now under evaluation in clinical studies for the treatment of hepatocellular carcinoma (Stemmer et al., 2013; Jacobson et al., 2017). Instead, as for the protumoral effect, it is well established the enrollment of A_{2A}AR subtype in immune depression of anticancer response, in angiogenesis stimulation as well as in promotion of cancer cell migration, suggesting a role of A_{2A}ARs antagonists in the fight against cancer (Antonioli et al., 2013a,b, 2016). In addition, A_{2A}ARs have been suggested as regulators of cancer cell proliferation in melanoma and breast cancer, but the signaling pathways have not been deeply depicted (Merighi et al., 2002; Etique et al., 2009; Mediavilla-Varela et al., 2013).

In this study, we investigated the effect of A_{2A}AR activation in the modulation of cell proliferation in A375 melanoma, A549 lung and MRMT-1 breast carcinoma, the mechanisms involved and the efficacy of a novel antagonist to counteract A_{2A}AR effects on cell growth.

Our results show that A_{2A}ARs are expressed in all the three cancer cell lines investigated, with the following order of expression: A375 > A549 > MRMT-1 as evaluated through receptor binding experiments. In order to investigate the role of A_{2A}ARs in cancer growth we evaluated cancer cell proliferation, following the treatment with a selective A_{2A}AR agonist, and we found an increase of it, with a most significant effect in MRMT-1 cells. The mechanism involved does not affect AC or PKC-ε pathways but recruited PLC and PKC-δ stimulation. In addition, cell proliferation mediated by A_{2A}ARs was blocked by selective ERK1/2, JNK1/2, and AKT but not p38 inhibitors. Accordingly, phosphorylation of ERK1/2, JNK1/2, and AKT was significantly increased by A_{2A}ARs. It is interesting to note that ERK1/2, JNK1/2, and AKT activation by A_{2A}ARs depends on PLC and PKC- δ stimulation, as demonstrated through the block of kinases phosphorylation following treatment with PLC and PKC- δ inhibitors. These data suggest that PLC and PKC- δ are upstream ERK1/2, JNK1/2, and AKT in the signaling proliferative pathway induced by A_{2A}ARs.

These data are in agreement with other studies where A_{2A}AR activation was associated to an increase in cell growth such as A375 melanoma, MCF-7 breast and A549 lung carcinoma (Gessi et al., 2011). Specifically, in A375 cells the association of A_{2A}AR mediated cell proliferation with ERK1/2 has been already observed (Merighi et al., 2002). However, in A549 cell line, a direct increasing apoptotic effect, due to A_{2A}AR antagonist treatment was observed, even though the high concentration used in the reported study does not exclude the possible interaction with other receptors (Mediavilla-Varela et al., 2013). Therefore, the novelty of this work is to depict a novel signaling cascade involving the classical kinases ERK1/2, JNK1/2, and AKT downstream A_{2A}ARs, PLC, and PKC- δ, linked in the tumorigenic processes (**Figure 9**).

All the effects observed in this study, activated by the A_{2A}AR agonist, were reversed by the standard A_{2A}AR antagonist ZM241385, confirming the role of A_{2A}ARs in the signaling investigated. Importantly, the behavior of the novel compound TP455 similar to ZM241385, able to potently block A_{2A}AR-

induced cancer cell proliferation and kinase phosphorylation, indicates a role for it as a novel potent A_{2A}AR antagonist. Interestingly, this class of compounds is already under clinical development due to its anti-Parkinson therapeutic effects and is well known to be safe and well tolerated (Preti et al., 2015; Jazayeri et al., 2017).

Overall our data help to implement the knowledge concerning the signaling of A_{2A}ARs in cancer. However, to support the relevance of these receptors as novel targets in the therapy against cancer and the development of potent and selective antagonists, it will be important to evaluate whether A_{2A}ARs are also involved in normal cell proliferation and the signaling pathway enrolled.

AUTHOR CONTRIBUTIONS

SG and SM developed the original idea, designed the experiments and elaborated data. SB and EB performed experiments and prepared figures, KV and FaV elaborated data, FlV, DC, and VC edited and reviewed the final version of the article, PAB supervised the study. All listed authors contributed to article writing.

FUNDING

Grants supported by University of Ferrara.

REFERENCES

Antonioli, L., Blandizzi, C., Pacher, P., and Haskó, G. (2013a). Immunity, inflammation and cancer: a leading role for adenosine. *Nat. Rev. Cancer* 13, 842–57. doi: 10.1038/nrc3613

Antonioli, L., Blandizzi, C., Malavasi, F., Ferrari, D., and Haskó, G. (2016). Anti-CD73 immunotherapy: a viable way to reprogram the tumor microenvironment. *Oncoimmunology* 5:e1216292. doi: 10.1080/2162402X.2016.1216292

Antonioli, L., Pacher, P., Vizi, E. S., and Haskó, G. (2013b). CD39 and CD73 in immunity and inflammation. *Trends Mol. Med.* 19, 355–367. doi: 10.1016/j.molmed.2013.03.005

Blay, J., White, T. D., and Hoskin, D. W. (1997). The extracellular fluid of solid carcinomas contains immunosuppressive concentrations of adenosine. *Cancer Res.* 57, 2602–2605.

Borea, P. A., Gessi, S., Merighi, S., and Varani, K. (2016). Adenosine as a multi-signalling guardian angel in human diseases: when, where and how does it exert its protective effects. *Trends Pharmacol. Sci.* 37, 419–434. doi: 10.1016/j.tips.2016.02.006

Borea, P. A., Gessi, S., Merigh, S., Vincenzi, F., and Varani, K. (2017). Pathological overproduction: the bad side of adenosine. *Br. J. Pharmacol.* 174, 1945–1960. doi: 10.1111/bph.13763

Bradford, M. M. (1976). A rapid and sensitive method for the quantification of microgram quantities of protein utilizing the principle of protein dye-binding. *Anal. Biochem.* 72, 248–254. doi: 10.1016/0003-2697(76)90527-3

Etique, N., Grillier-Vuissoz, I., Lecomte, J., and Flament, S. (2009). Crosstalk between adenosine receptor (A2A isoform) and ERalpha mediates ethanol action in MCF-7 breast cancer cells. *Oncol. Rep.* 21, 977–981.

Fredholm, B. B., IJzerman, A. P., Jacobson, K. A., Linden, J., and Müller, C. E. (2011). International union of basic and clinical pharmacology. LXXXI. Nomenclature and classification of adenosine receptors–an update. *Pharmacol. Rev.* 63, 1–34. doi: 10.1124/pr.110.003285

Gessi, S., Merighi, S., Varani, K., Cattabriga, E., Benini, A., Mirandola, P., et al. (2007). Adenosine receptors in colon carcinoma tissues and colon tumoral cell lines: focus on the A3 adenosine subtype. *J. Cell. Physiol.* 211, 826–836. doi: 10.1002/jcp.20994

Gessi, S., Merighi, S., Sacchetto, V., Simioni, C., and Borea, P. A. (2011). Adenosine receptors and cancer. *Biochim. Biophys. Acta* 1808, 1400–1412. doi: 10.1016/j.bbamem.2010.09.020

Jacobson, K. A, Merighi, S., Varani, K., Borea, P. A., Baraldi, S., Aghazadeh tabrizi, M., et al. (2017). A3 Adenosine receptors as modulators of inflammation: from medicinal chemistry to therapy. *Med. Res. Rev.* doi: 10.1002/med.21456. [Epub ahead of print].

Jazayeri, A., Andrews, S. P., and Marshall, F. H. (2017). Structurally enabled discovery of adenosine A2A receptor antagonists. *Chem. Rev.* 117, 21–37. doi: 10.1021/acs.chemrev.6b00119

Koszałka, P., Gołuńska, M., Urban, A., Stasiłojć, G., Stanisławowski, M., Majewski, M., et al. (2016). Specific activation of A3, A2A and A1 adenosine receptors in CD73-Knockout mice affects B16F10 melanoma growth, neovascularization, angiogenesis and macrophage infiltration. *PLOS ONE* 11:e0151420. doi: 10.1371/journal.pone.0151420

Mediavilla-Varela, M., Luddy, K., Noyes, D., Khalil, F. K., Neuger, A. M., Soliman, H., et al. (2013). Antagonism of adenosine A2A receptor expressed by lung adenocarcinoma tumor cells and cancer associated fibroblasts inhibits their growth. *Cancer Biol. Ther.* 14, 860–868. doi: 10.4161/cbt.25643

Merighi, S., Mirandola, P., Varani, K., Gessi, S., Leung, E., Baraldi, P. G., et al. (2003). A glance at adenosine receptors: novel target for antitumor therapy. *Pharmacol. Ther.* 100, 31–48. doi: 10.1016/S0163-7258(03)00084-6

Merighi, S., Mirandola, P., Milani, D., Varani, K., Gessi, S., Klotz, K. N., et al. (2002). Adenosine receptors as mediators of both cell proliferation and cell death of cultured human melanoma cells. *J. Invest. Dermatol.* 119, 923–933. doi: 10.1046/j.1523-1747.2002.00111.x

Muller-Haegele, S., Muller, L., and Whiteside, T. L. (2014). Immunoregulatory activity of adenosine and its role in human cancer progression. *Expert Rev. Clin. Immunol.* 10, 897–914. doi: 10.1586/1744666X.2014.915739

Munson, P. J., and Rodbard, D. (1980). Ligand: a versatile computerized approach for the characterization of ligand binding systems. *Anal. Biochem.* 107, 220–239. doi: 10.1016/0003-2697(80)90515-1

Ohta, A., Gorelik, E., Prasad, S. J., Ronchese, F., Lukashev, D., Wong, M. K., et al. (2006). A2A adenosine receptor protects tumors from antitumor T-cells. *Proc. Natl. Acad. Sci. U.S.A.* 103, 13132–13137. doi: 10.1073/pnas.0605251103

Perez-Aso, M., Mediero, A., Low, Y. C., Levine, J., and Cronstein, B. N. (2016). Adenosine A2A receptor plays an important role in radiation-induced dermal injury. *FASEB J.* 30, 457–465. doi: 10.1096/fj.15-280388

Preti, D., Baraldi, P. G., Moorman, A. R., Borea, P. A., and Varani, K. (2015). History and perspectives of A2A adenosine receptor antagonists as potential therapeutic agents. *Med. Res. Rev.* 35, 790–848. doi: 10.1002/med.21344

Schulte, G., and Fredholm, B. B. (2000). Human adenosine A1, A2A, A2B, and A3 receptors expressed in Chinese hamster ovary cells all mediate the phosphorylation of extracellular-regulated kinase 1/2. *Mol. Pharmacol.* 58, 477–482.

Sitkovsky, M. V., Kjaergaard, J., Lukashev, D., and Ohta, A. (2008). Hypoxia-adenosinergic immunosuppression: tumor protection by T regulatory cells and cancerous tissue hypoxia. *Clin. Cancer Res.* 14, 5947–5952. doi: 10.1158/1078-0432.CCR-08-0229

Stemmer, S. M., Benjaminov, O., Medalia, G., Ciuraru, N. B., Silverman, M. H., Bar-Yehuda, S., et al. (2013). CF102 for the treatment of hepatocellular carcinoma:a

phase I/II, open-label, dose-escalation study. *Oncologist* 18, 25–26. doi: 10.1634/theoncologist.2012-0211

Varano, F., Catarzi, D., Vincenzi, F., Betti, M., Falsini, M., Ravani, A., et al. (2016). Design, synthesis, and pharmacological characterization of 2-(2-furanyl)thiazolo[5,4-d]pyrimidine-5,7-diamine derivatives: new highly potent A2A adenosine receptor inverse agonists with antinociceptive activity. *J. Med. Chem.* 59, 10564–10576. doi: 10.1021/acs.jmedchem.6b01068

Young, A., Ngiow, S. F., Barkauskas, D. S., Sult, E., Hay, C., Blake, S. J., et al. (2016). Co-inhibition of CD73 and A2AR adenosine signaling improves anti-tumor immune responses. *Cancer Cell* 30, 391–403. doi: 10.1016/j.ccell.2016.06.025

Conflict of Interest Statement: The authors declare that the research was conducted in the absence of any commercial or financial relationships that could be construed as a potential conflict of interest.

frontiers in Pharmacology

MINI REVIEW
published: 24 November 2017
doi: 10.3389/fphar.2017.00878

Purinergic Receptors in Adipose Tissue As Potential Targets in Metabolic Disorders

*Marco Tozzi and Ivana Novak**

Section for Cell Biology and Physiology, Department of Biology, University of Copenhagen, Copenhagen, Denmark

Extracellular nucleosides and nucleotides, such as adenosine and adenosine triphosphate (ATP), are involved in many physiological and pathological processes in adipose tissue (AT). It is becoming accepted that, in addition to the well-established sympathetic and hormonal system, purinergic receptors contribute significantly to regulation of adipocyte functions. Several receptor subtypes for both adenosine (P1) and ATP (P2X and P2Y) have been characterized in white adipocytes (WA) and brown adipocytes (BA). The effects mediated by adenosine and ATP on adipocytes are multiple and often differing, depending on specific receptors activated. Using a variety of agonists, antagonists and transgenic animals it has been demonstrated that adenosine and P2 receptors are involved in lipolysis, lipogenesis, adipokines secretion, glucose uptake, adipogenesis, cell proliferation, inflammation, and other processes. Given their central role in regulating many AT functions, purinergic receptors are considered potential therapeutic targets in different pathological conditions, such as obesity and type-2 diabetes. To achieve this goal, specific and potent P1 and P2 receptors activators and inhibitors are being developed and show promising results. However, more insight is needed into the function of P2 receptors in brown and beige adipocytes and their potential role in thermogenesis. This review aims at summarizing current knowledge on the patho-/physiological role of P1, P2X, and P2Y receptors in WA and BA and their potential exploitation for pharmacological intervention. Furthermore, we analyze impact of purinergic signaling in AT – in health and metabolic diseases.

Keywords: purinergic receptors, adenosine, ATP, adipocytes, obesity, type-2 diabetes, inflammation, adipose tissue

OPEN ACCESS

Edited by:
Francisco Ciruela,
University of Barcelona, Spain

Reviewed by:
Alessandro Bartolomucci,
University of Minnesota, United States
Gennady G. Yegutkin,
University of Turku, Finland

***Correspondence:**
Ivana Novak
inovak@bio.ku.dk

Specialty section:
This article was submitted to Experimental Pharmacology and Drug Discovery, a section of the journal Frontiers in Pharmacology

Received: *09 October 2017*
Accepted: *13 November 2017*
Published: *24 November 2017*

Citation:
Tozzi M and Novak I (2017) Purinergic Receptors in Adipose Tissue As Potential Targets in Metabolic Disorders. Front. Pharmacol. 8:878. doi: 10.3389/fphar.2017.00878

INTRODUCTION

Metabolic disorders, such as obesity, dyslipidemia, and hyperglycemia, are closely related to AT dysfunction, and indeed AT is considered one of the most promising therapeutic targets (Guilherme et al., 2008; Kusminski et al., 2016). AT is a metabolic and endocrine organ consisting mainly of adipocytes. In addition, AT contains other cell types collectively named SVF, which

Abbreviations: AT, adipose tissue; ADP, adenosine diphosphate; ATP, adenosine triphosphate; BA, brown adipocytes; BAT, brown adipose tissue; BzATP, 2′-3′-*O*-(4-benzoylbenzoyl)-ATP; cAMP, cyclic AMP; FFAs, free fatty acids; HFD, high fat diet; IL-, interleukin; KO, knockout; MSCs, mesenchymal stem cells; PAI-1, plasminogen activator inhibitor-1; PKA, protein kinase A; PLC, phospholipase C; SVF, stromal vascular fraction; TNFα, tumor necrosis factor-α; UCP1, uncoupling protein-1; UDP, uridine diphosphate; UTP, uridine triphosphate; VNUT, vesicular nucleotide transporter; WA, white adipocytes; WAT, white adipose tissue.

includes MSCs, preadipocytes, endothelial cells, fibroblasts, and a variety of immune cells such as macrophages and T regulatory cells. Mammals have two main types of AT: WAT comprises mainly of WA, which store excess energy as triglycerides; and BAT, characterized by mitochondria-rich adipocytes, which express UCP1 that enables dissipation of energy by production of heat. Within WAT, there are also UCP1-positive cells with thermogenic capacity called beige or brite (brown-in-white) adipocytes. Cold exposure or other specific factors can produce browning of WAT (Harms and Seale, 2013; Kim and Plutzky, 2016). WAT and BAT are innervated by the sympathetic nervous system that together with hormones and other factors regulates adipocyte function (Bulloch and Daly, 2014). Adipocytes are also regulated by nucleosides and nucleotides, such as adenosine and ATP.

Generally, ATP is released from sympathetic nerves (Burnstock, 2007) and this is also likely in AT (Gnad et al., 2014), though only sympathetic nerves innervating BAT were found to express the ATP transporter VNUT (Razzoli et al., 2016). Many other non-excitable cells, such as epithelial, glial, stromal, and immune cells release ATP in basal conditions (Corriden and Insel, 2010) and in response to various patho-/physiological stimuli (Junger, 2011; Novak, 2011; Lazarowski, 2012). Similarly, ATP could be released from adipocytes (Gnad et al., 2014; Adamson et al., 2015). The mechanism of ATP release is not extensively studied; so far one study suggests channel pannexin-1 (Adamson et al., 2015) and another vesicular-based mechanism (Razzoli et al., 2016). Other cells in AT could also release ATP, contributing to a purinergic cross-talk between different cells, but such signaling is yet to be explored. In the extracellular space ATP is hydrolyzed to adenosine by one or more ecto-nucleotidases belonging to four families: ecto-nucleoside triphosphate diphosphorylases (CD39 type), ecto-5′-nucleotidase (CD73 type), ecto-nucleotide pyrophosphatase/phosphodiesterases (NPP) and alkaline phosphatases (APs) (Zimmermann et al., 2012). Interestingly, one of the enzymes NPP2, also known as phospholipase D or autotaxin, is multifunctional and released by adipocytes, and up-regulated autotaxin expression correlates with obesity (Rancoule et al., 2014). Nevertheless, it is most often assumed that adipocytes can release adenosine, possibly through nucleoside transporters (Antonioli et al., 2008; Gnad et al., 2014).

Adenosine, ATP, and other nucleotides signal through purinergic receptors that operate in virtually all mammalian cells, and it can be disturbed in various diseases, including metabolic syndrome, and therefore is attractive for therapeutic targeting (Burnstock, 2013; Burnstock and Novak, 2013; Chen et al., 2013; Jacobson and Muller, 2016). Here, we summarize the current knowledge about (i) the expression and function of adenosine receptors (P1R) and P2 receptors (P2XR and P2YR) in white, brown, and possibly in beige adipocytes; (ii) their role in the onset and progression of metabolic disorders; and (iii) their potential as therapeutic targets. In some cases, it is difficult to dissect the contribution of purinergic signaling in adipocytes from the AT/whole body effects (Peleli and Carlstrom, 2017). This is because the SVF in AT and other organs express purinergic receptors, and various conditions (e.g., inflammation) and experimental set up (e.g., whole-body receptor KOs or systemic receptor modulators) will complicate interpretation of effects.

ADENOSINE RECEPTORS IN ADIPOSE TISSUE

Adenosine accumulates extracellularly in response to metabolic stress, tissue injury, hypoxia and inflammation and concentrations can range from nanomolar to micromolar in physiological and pathophysiological conditions, respectively (Fredholm, 2014). Adenosine can bind to four different G-protein-coupled receptors A_1, A_{2A}, A_{2B}, and A_3. A_1R and $A_{2A}R$ have high affinity for adenosine, while $A_{2B}R$ and A_3R have relatively lower affinity. A_1R and A_3R are coupled to $G_{i/o}$ proteins and their activation inhibits cAMP production and decreases PKA activity. $A_{2A}R$ and $A_{2B}R$ are coupled to $G_{s/olf}$ proteins and stimulate cAMP production, thus activating PKA. In addition, some adenosine receptors also activate PLC, Ca^{2+} signaling and mitogen-activated protein kinases (Fredholm et al., 2011).

Adenosine has a key role in regulating many patho-/physiological processes in AT and adipocytes (**Figure 1**). The most studied adenosine receptor is the A_1, identified in WAT of many species (Trost and Schwabe, 1981; Larrouy et al., 1991; Strong et al., 1993; Mersmann et al., 1997; Tatsis-Kotsidis and Erlanger, 1999). Using pharmacological tools and whole body A_1R KO mice, it was shown that activation of this receptor in rodents has anti-lipolytic effects mediated by inhibition of cAMP production and decrease in PKA and lipase activities (Fredholm, 1978; Schoelch et al., 2004; Dhalla et al., 2007a; Johansson et al., 2008). Rat WA are more responsive than BA to inhibition of lipolysis by the A_1R stimulators PIA and NECA (Saggerson and Jamal, 1990), probably due to higher expression of the receptor in WA (Gnad et al., 2014). A_1R activation also increases lipogenesis in mouse and rat WA (Johansson et al., 2008; Szkudelski et al., 2009). The A_1R is also implicated in adipogenesis (Gharibi et al., 2012) and leptin production in WA (Cheng et al., 2000; Rice et al., 2000). All these A_1R-mediated effects highlight the importance of adenosine signaling in AT, and predict impact on whole body metabolism. In accordance, A_1R KO mice have increased fat mass and body weight, and impaired glucose tolerance and insulin sensitivity (Faulhaber-Walter et al., 2011; Yang et al., 2015). In contrast, mice overexpressing the A_1R in AT are protected from obesity-induced insulin resistance (Dong et al., 2001).

Another fairly well studied receptor is the $A_{2B}R$, detected in adipocytes and SVF (Gnad et al., 2014). *In vitro* experiments on murine pre-osteoblast cell line expressing either human $A_{2B}R$ or A_1R showed that A_1R stimulated adipogenesis, while the $A_{2B}R$ inhibited both adipogenesis and lipogenesis, supporting osteoblastogenesis pathways (Gharibi et al., 2012). In *in vivo* experiments, $A_{2B}R$ expression seems to correlate with parameters of obesity, both in rodents and humans, and the receptor is upregulated in visceral AT of mice fed HFD (Johnston-Cox et al., 2012). Genetic KO of the receptor is also associated with metabolic disorders. Whole body $A_{2B}R$ KO led to AT

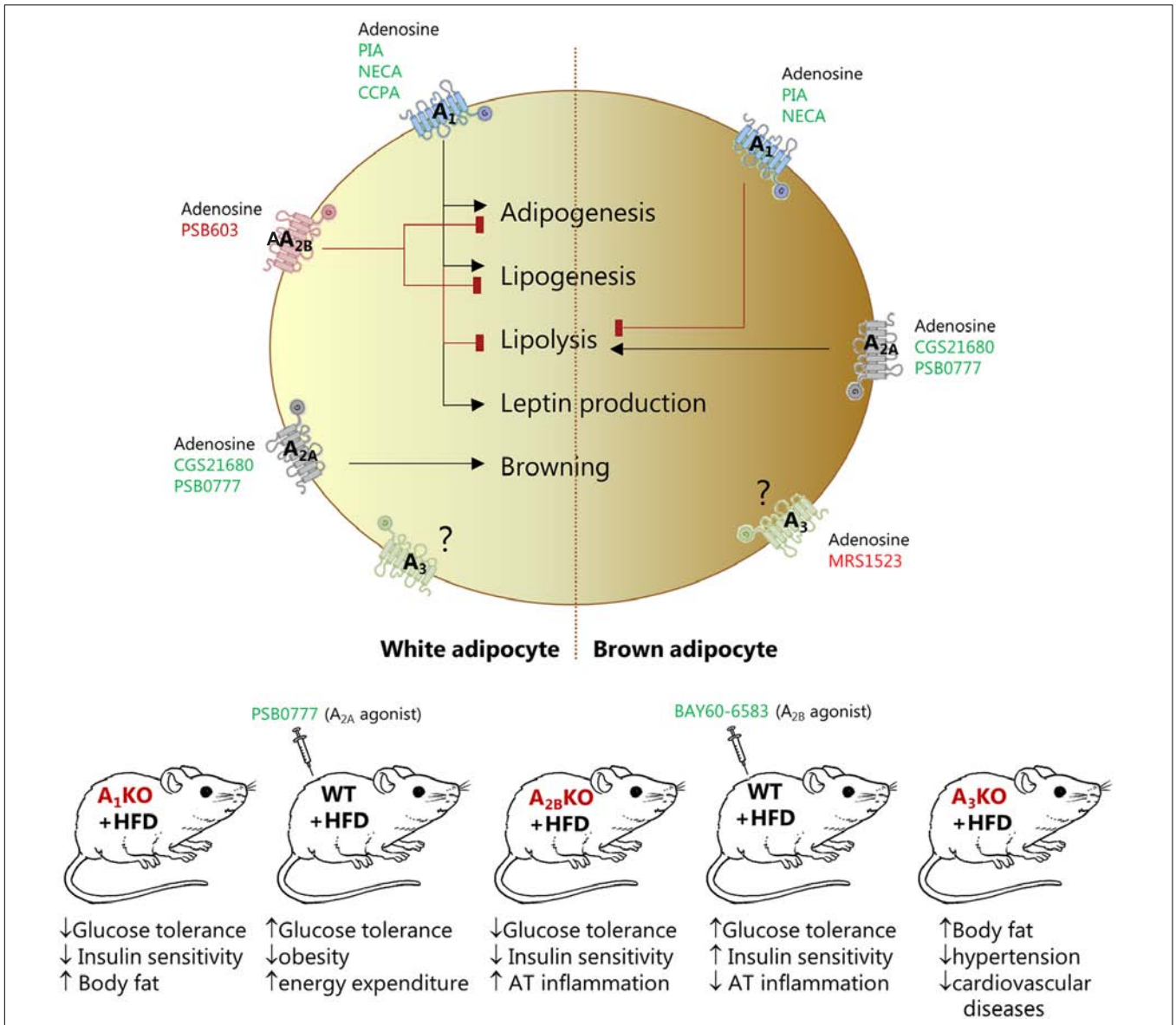

FIGURE 1 | Effect of pharmacological and genetic modulation of adenosine receptors in white (left) and brown (right) adipocytes and in various mouse models. The figure shows agonists (green), antagonists (red) and knockout animals (red) that have been used in the studies quoted in this review to address the function of the specific receptor.

inflammation, insulin resistance, impaired glucose and lipid metabolism in mice (Johnston-Cox et al., 2012; Csoka et al., 2014; Peleli et al., 2015). Importantly, systemic administration of the A_{2B} specific agonist BAY 60-6583, following HFD regime, lowered plasma glucose, insulin and IL-6 levels, and ameliorated type-2 diabetes in mice (Johnston-Cox et al., 2012). These animal studies and a recent study (Johnston-Cox et al., 2014) are interpreted mainly in terms of the A_{2B}R activation of WAT macrophage. Nevertheless, involvement of adipocyte A_{2B}R cannot be excluded.

The A_{2A}R may have a major role in BAT, where it is more abundantly expressed compared to WAT (Gnad et al., 2014). Early studies showed that adenosine inhibited lipolysis in BA from rat or hamster, probably via A_1R (Schimmel and McCarthy, 1984; Woodward and Saggerson, 1986). In contrast, recent work shows that adenosine and A_{2A}R agonists (CGS21680 or PSB-0777) activated lipolysis in human and murine BA, and to explain differences in the studies authors proposed species-related differential receptor expression (Gnad et al., 2014). Moreover, agonists used in this study increased energy expenditure, induced browning of WAT, improved glucose tolerance and protected C57Bl/6 mice from diet-induced obesity, thus revealing a promising thermogenic effect of adenosine. Similar effect on glucose homeostasis was reported for another A_{2A}R agonist CGS21680 administered to Swiss strain mice fed with HFD (DeOliveira et al., 2017). No alteration in body weight

or adiposity was detected, though decrease in some inflammatory markers was observed. The difference in animal obesity detected in the two studies could be due to different time regimes of drug treatment (8 weeks vs. 2 weeks), differences in strains of mice used (see below for comments on C57Bl/6 strain), or specificity of different $A_{2A}R$ agonists used.

There are only a few studies on A_3R in adipocytes/AT. Isolated human WA express higher levels of A_3R mRNA compared to BA. But inhibition of the receptor with MRS1523 had no significant effect on modulating lipolysis, at least in murine BA (Gnad et al., 2014). However, the A_3R KO mice had less abdominal and total body fat, and mice were protected from hypertension and cardiovascular diseases in the chronic kidney disease model tested (Yang et al., 2016).

Taken together, there is strong evidence that adipocytes express all types of adenosine receptors that regulate patho-/physiological processes (**Figure 1**). There is a consensus that A_1R regulates lipolysis and therefore FFAs levels, which play a significant role in the pathogenesis of insulin resistance, diabetes, and cardiovascular diseases (Dhalla et al., 2009; Antonioli et al., 2015). Several A_1R agonists, e.g., SDZWAG994 (Ishikawa et al., 1998), ARA (Zannikos et al., 2001), and RPR749 (Shah et al., 2004), have been clinically evaluated as anti-lipolytic agents for the treatment of hypertriglyceridemia and type-2 diabetes. Though, development of full A_1R agonists has been limited by (i) the debilitating side effects induced by the activation of the receptors in heart and kidney of animal models (Belardinelli et al., 1989; Wu et al., 2001); and (ii) a well-characterized desensitization of the receptor after repeated exposure to full agonists (Hoffman et al., 1986; Dhalla et al., 2007b). However, selective partial A_1R agonists, e.g., CPA and GS-9667 (CVT-3619), effectively lowered plasma FFA levels without detectable cardiovascular side effects in rodents and humans (Dhalla et al., 2007a,b). These effects were achieved by administering lower concentrations of these drugs, which acted predominantly on AT, as it has larger A_1R reserve compared to other tissues (i.e., atrioventricular node) (Staehr et al., 2013). Furthermore, given the role of the $A_{2B}R$ in glucose and lipid homeostasis, and AT inflammation, this receptor could be a promising target for the treatment of metabolic diseases. Finally, finding that activation of $A_{2A}R$ induces beiging of WA and activates BA (Gnad et al., 2014) may stimulate development of new pharmacological interventions for the treatment of obesity and metabolic disease.

PURINERGIC P2 RECEPTORS IN ADIPOSE TISSUE

In contrast to adenosine, patho-/physiological functions of ATP and other nucleotides have not been studied so extensively in AT. Tri- and di-nucleotides signal through P2R belonging to two main families: the ionotropic P2XRs and the metabotropic G-protein coupled P2YRs. The P2XRs (P2X1–7) are ligand-gated cation channels activated primarily by ATP (North, 2016). The P2YR subtypes can be stimulated by different endogenous nucleotides and most potent ones (in humans) are given in brackets. P2Y1R (ADP), P2Y2R (UTP), P2Y4R (UTP), P2Y6R (UDP) receptors couple to G_q proteins and thus activate PLC-β, mobilizing Ca^{2+} from intracellular stores. P2Y11R (ATP) couple in addition to G_s proteins increase cAMP, while P2Y12R (ADP), P2Y13R (ADP), and P2Y14R (UDP, UDP-glucose) couple to G_i proteins and inhibit cAMP formation (von Kugelgen and Hoffmann, 2016).

Early studies by Lee and Pappone (1997a,b) and Lee S.C. et al. (2005) used patch-clamp, Ca^{2+} imaging and mRNA analysis to fingerprint functional P2XRs and P2YRs in WA and BA. Here, we will focus on role of P2Rs in regulating multiple adipocyte-specific processes as summarized in **Figure 2**.

P2Rs regulate adipogenesis. Several studies used expression profiling and functional assays to describe that P2Y1R, P2Y2R or P2Y4R and P2Y11R positively affected adipogenic differentiation of stem cells derived from bone marrow or AT (Kawano et al., 2006; Zippel et al., 2012; Ciciarello et al., 2013; Li et al., 2016). In contrast, P2Y4R activation (UTP, MRS4062) inhibited cardiac AT-derived stem cells differentiation and P2Y4R KO mice developed bigger cardiac AT mass and higher expression of UCP1 (Lemaire et al., 2017). The opposite effect of P2Y4R in the mentioned studies could be related to the higher receptor expression in cardiac AT compared to other fat depots and/or beige/BA lineage in the cardiac tissue. Three other receptors have anti-adipogenic effects – P2Y13, P2Y14, and P2X7 (Zippel et al., 2012; Biver et al., 2013). Interestingly, P2X7R KO male mice had increased body weight, adipocyte hyperplasia in fat pads, and ectopic lipid accumulation in kidney, salivary glands, and pancreas (Beaucage et al., 2014). Other *in vitro* and *in vivo* studies indicate that the P2X7R stimulation directs differentiation of MSCs toward the osteoblast lineage rather than toward adipocytes (Li et al., 2015).

P2Rs are also implicated in lipid metabolism. One study on isolated rat WA shows that ATP, UTP, and BzATP, probably by activating different P2Rs, had dual effects – activated lipolysis and inhibited insulin-induced leptin production (Lee H. et al., 2005). In contrast, no lipolytic effect of ATP was found in a similar cellular model (Schodel et al., 2004). The explanation for these divergent results could be that the two studies used different ATP concentrations, thus affecting different palette of P2Rs. Furthermore, in the latter study on isolated WA, ATP stimulated lipogenesis but had no effect on glucose transport (Schodel et al., 2004).

The role of purinergic signaling in glucose uptake in adipocytes has been investigated in 1980s. Two studies showed that low concentrations of ATP inhibited insulin-stimulated glucose transport in rat fat cells (Chang and Cuatrecasas, 1974; Halperin et al., 1978), and it was assumed that extracellular ATP had direct inhibitory effect on the insulin receptor. More recently, it was shown that P2Y6R activation by UDP or MRS2957 increased GLUT-4 translocation and glucose uptake in primary WA and 3T3-L1 cells (Balasubramanian et al., 2014).

In addition to effects on adipogenesis, lipid metabolism, and glucose transport, P2Rs affect leptin and adiponectin production and secretion, but activation of different P2R subtypes might lead to opposite effects. ATP and BzATP reduced leptin mRNA levels and inhibited insulin-induced leptin secretion in rat WA (Lee H.

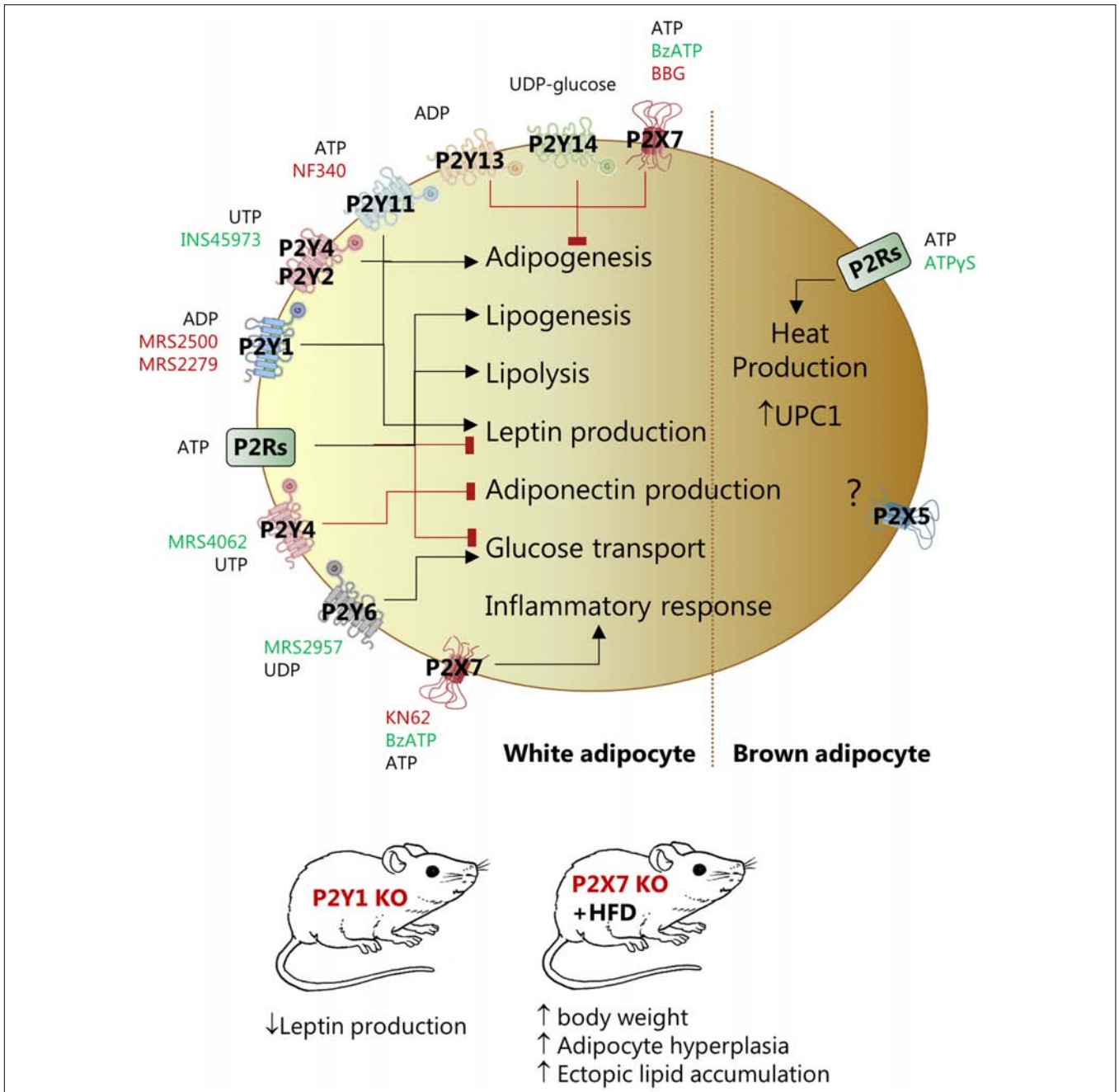

FIGURE 2 | Effect of pharmacological and genetic modulation of P2X and P2Y receptors in white (left) and brown (right) adipocytes and in various mouse models. The figure lists agonists (green), antagonists (red) and knockout animals (red) that have been used in the studies quoted in this review to address the function of the specific receptor.

et al., 2005). In another study, inhibition of P2Y1R by MRS2500 decreased leptin production under basal and insulin-stimulated conditions in isolated mouse WA (Laplante et al., 2010). Furthermore, the study showed that plasma leptin was lower in mice lacking P2Y1R, however, in mice on HFD the plasma leptin was enhanced and the inhibitory effect of receptor KO was not observed. Stimulation of P2Y4R by UTP or MRS4062 inhibited adiponectin expression and secretion in cardiac adipocytes and P2Y4R KO mice showed increased adiponectin secretion in hypoxia and a cardioprotective phenotype (Lemaire et al., 2017).

Adenosine triphosphate is generally considered as an inflammatory molecule (Idzko et al., 2014). Particularly the P2X7R mediates inflammation in AT. In primary adipocytes from rat epididymal fat, millimolar concentrations of ATP evoked inflammatory response and led to impaired insulin signaling and glucose uptake (Yu and Jin, 2010). Visceral and subcutaneous

human AT express functional P2X7R, which could be involved in release of inflammatory cytokines such as IL-6, TNFα, and PAI-1 (Madec et al., 2011). Interestingly, this study showed that P2X7R expression appeared to be high in adipocytes isolated from subjects affected by metabolic syndrome. The P2X7R and NLRP3 inflammasome expression and IL-1β secretion was elevated in metabolically unhealthy obese individuals and the receptor expression correlated with body mass index and metabolic syndrome scores (Pandolfi et al., 2015). Whether this was due to effects on adipocytes or infiltrating immune cells is not clear (Pandolfi et al., 2016). In contrast, an earlier study concluded that the P2X7R was not involved in obesity-associated inflammasome activation. This was based on the observation that P2X7R KO mice on the C57BL/6 background and fed on HFD were not protected from obesity, AT inflammation and associated metabolic abnormalities (Sun et al., 2012). The C57BL/6 mice though have a single nucleotide polymorphism in the P2X7R that compromises the immune response (Rissiek et al., 2015), which could explain discrepancies in inflammasome activation in the two studies.

Rodent BA, express several P2X and P2Y receptors and stimulation with ATP leads to exocytosis and heat production (Lee and Pappone, 1997a; Lee S.C. et al., 2005). In a more recent study, ATPγS, enhanced UCP1 expression and induced browning in BAT in conditions of low adaptive thermogenesis and b-adrenergic receptor KO mice (Razzoli et al., 2016). This effect is most likely exerted via more than one receptor and P2X5R, P2X7R, and P2Y12R are overexpressed in β-less BAT. Interestingly, P2X5R is proposed as a novel cell surface marker for beige and BA as its mRNA levels are markedly higher in mouse BAT compared to WAT and other tissues (Ussar et al., 2014). Furthermore, the P2X5R expression increased in both BAT and subcutaneous WAT upon chronic cold exposure, paralleling expression of UCP1 (Ussar et al., 2014; Garcia et al., 2016; Razzoli et al., 2016). However, mechanisms of P2X5R mediated effects in AT are unknown.

Taken together, there is good evidence that P2Rs affect a wide range of patho-/physiological processes in rodent and human AT. Many of these processes, e.g., lipid deposition, metabolism, endocrine activity, and inflammation, are deregulated during pathological states such as obesity and diabetes. However, P2Rs modulators have not yet been tested in clinical trials for treatment of metabolic disorders. Future research is still needed to dissect functions of P2R subtypes in adipocytes and AT before best P2R targets and drugs are selected.

CONCLUSION AND PERSPECTIVES

In this review, we discussed contribution of P1 and P2 receptors to modulation of AT functions and considered processes that may underlie their role in metabolic disorders. Several preclinical studies indicate that pharmacological manipulation of purinergic signaling in adipocytes and AT has interesting potential for treating metabolic disorders. However, translation of these findings into clinical trials will require more detailed knowledge about the role of extracellular ATP and adenosine in the onset and progression of obesity-related disorders, as well as about the basic physiology and pharmacology of purinergic receptors expressed in adipocytes and in AT. In this context, it will be necessary to: (i) know differential expression of adenosine and P2Rs in white, brown and beige adipocytes belonging to different fat depots (subcutaneous, visceral, cardiac etc.); (ii) clarify sources and concentrations of nucleotides/sides and modifying enzymes present in specific AT microenvironments; (iii) understand role of purinergic system in interplay between different cells in AT microenvironment and potential patho-/physiological conditions which may affect those.

AUTHOR CONTRIBUTIONS

MT wrote the draft and prepared figures. IN contributed to planning and writing of the review.

FUNDING

Work in our laboratory that inspired this review was funded by the Independent Research Fund Denmark/Natural Sciences (4002-00162B).

REFERENCES

Adamson, S. E., Meher, A. K., Chiu, Y. H., Sandilos, J. K., Oberholtzer, N. P., Walker, N. N., et al. (2015). Pannexin 1 is required for full activation of insulin-stimulated glucose uptake in adipocytes. *Mol. Metab.* 4, 610–618. doi: 10.1016/j.molmet.2015.06.009

Antonioli, L., Blandizzi, C., Csoka, B., Pacher, P., and Hasko, G. (2015). Adenosine signalling in diabetes mellitus–pathophysiology and therapeutic considerations. *Nat. Rev. Endocrinol.* 11, 228–241. doi: 10.1038/nrendo.2015.10

Antonioli, L., Fornai, M., Colucci, R., Ghisu, N., Tuccori, M., Del, T. M., et al. (2008). Regulation of enteric functions by adenosine: pathophysiological and pharmacological implications. *Pharmacol. Ther.* 120, 233–253. doi: 10.1016/j.pharmthera.2008.08.010

Balasubramanian, R., Robaye, B., Boeynaems, J. M., and Jacobson, K. A. (2014). Enhancement of glucose uptake in mouse skeletal muscle cells and adipocytes by P2Y6 receptor agonists. *PLOS ONE* 9:e116203. doi: 10.1371/journal.pone.0116203

Beaucage, K. L., Xiao, A., Pollmann, S. I., Grol, M. W., Beach, R. J., Holdsworth, D. W., et al. (2014). Loss of P2X7 nucleotide receptor function leads to abnormal fat distribution in mice. *Purinergic Signal.* 10, 291–304. doi: 10.1007/s11302-013-9388-x

Belardinelli, L., Linden, J., and Berne, R. M. (1989). The cardiac effects of adenosine. *Prog. Cardiovasc. Dis.* 32, 73–97. doi: 10.1016/0033-0620(89)90015-7

Biver, G., Wang, N., Gartland, A., Orriss, I., Arnett, T. R., Boeynaems, J. M., et al. (2013). Role of the P2Y13 receptor in the differentiation of bone marrow stromal cells into osteoblasts and adipocytes. *Stem Cells* 31, 2747–2758. doi: 10.1002/stem.1411

Bulloch, J. M., and Daly, C. J. (2014). Autonomic nerves and perivascular fat: interactive mechanisms. *Pharmacol. Ther.* 143, 61–73. doi: 10.1016/j.pharmthera.2014.02.005

Burnstock, G. (2007). Physiology and pathophysiology of purinergic neurotransmission. *Physiol. Rev.* 87, 659–797. doi: 10.1152/physrev.00043.2006

Burnstock, G. (2013). Purinergic signalling: pathophysiology and therapeutic potential. *Keio J. Med.* 62, 63–73. doi: 10.2302/kjm.2013-0003-RE

Burnstock, G., and Novak, I. (2013). Purinergic signalling and diabetes. *Purinergic Signal.* 9, 307–324. doi: 10.1007/s11302-013-9359-2

Chang, K. J., and Cuatrecasas, P. (1974). Adenosine triphosphate-dependent inhibition of insulin-stimulated glucose transport in fat cells. Possible role of membrane phosphorylation. *J. Biol. Chem.* 249, 3170–3180.

Chen, J. F., Eltzschig, H. K., and Fredholm, B. B. (2013). Adenosine receptors as drug targets–what are the challenges? *Nat. Rev. Drug Discov.* 12, 265–286. doi: 10.1038/nrd3955

Cheng, J. T., Liu, I. M., Chi, T. C., Shinozuka, K., Lu, F. H., Wu, T. J., et al. (2000). Role of adenosine in insulin-stimulated release of leptin from isolated white adipocytes of Wistar rats. *Diabetes Metab. Res. Rev.* 49, 20–24. doi: 10.2337/diabetes.49.1.20

Ciciarello, M., Zini, R., Rossi, L., Salvestrini, V., Ferrari, D., Manfredini, R., et al. (2013). Extracellular purines promote the differentiation of human bone marrow-derived mesenchymal stem cells to the osteogenic and adipogenic lineages. *Stem Cells Dev.* 22, 1097–1111. doi: 10.1089/scd.2012.0432

Corriden, R., and Insel, P. A. (2010). Basal release of ATP: an autocrine-paracrine mechanism for cell regulation. *Sci. Signal.* 3:re1. doi: 10.1126/scisignal.3104re1

Csoka, B., Koscso, B., Toro, G., Kokai, E., Virag, L., Nemeth, Z. H., et al. (2014). A2B adenosine receptors prevent insulin resistance by inhibiting adipose tissue inflammation via maintaining alternative macrophage activation. *Diabetes Metab. Res. Rev.* 63, 850–866. doi: 10.2337/db13-0573

DeOliveira, C. C., Paiva Caria, C. R., Ferreira Gotardo, E. M., Ribeiro, M. L., and Gambero, A. (2017). Role of A1 and A2A adenosine receptor agonists in adipose tissue inflammation induced by obesity in mice. *Eur. J. Pharmacol.* 799, 154–159. doi: 10.1016/j.ejphar.2017.02.017

Dhalla, A. K., Chisholm, J. W., Reaven, G. M., and Belardinelli, L. (2009). A1 adenosine receptor: role in diabetes and obesity. *Handb. Exp. Pharmacol.* 193, 271–295. doi: 10.1007/978-3-540-89615-9_9

Dhalla, A. K., Santikul, M., Smith, M., Wong, M. Y., Shryock, J. C., and Belardinelli, L. (2007a). Antilipolytic activity of a novel partial A1 adenosine receptor agonist devoid of cardiovascular effects: comparison with nicotinic acid. *J. Pharmacol. Exp. Ther.* 321, 327–333.

Dhalla, A. K., Wong, M. Y., Voshol, P. J., Belardinelli, L., and Reaven, G. M. (2007b). A1 adenosine receptor partial agonist lowers plasma FFA and improves insulin resistance induced by high-fat diet in rodents. *Am. J. Physiol. Endocrinol. Metab.* 292, E1358–E1363.

Dong, Q., Ginsberg, H. N., and Erlanger, B. F. (2001). Overexpression of the A1 adenosine receptor in adipose tissue protects mice from obesity-related insulin resistance. *Diabetes Obes. Metab.* 3, 360–366. doi: 10.1046/j.1463-1326.2001.00158.x

Faulhaber-Walter, R., Jou, W., Mizel, D., Li, L., Zhang, J., Kim, S. M., et al. (2011). Impaired glucose tolerance in the absence of adenosine A1 receptor signaling. *Diabetes Metab. Res. Rev.* 60, 2578–2587. doi: 10.2337/db11-0058

Fredholm, B. B. (1978). Effect of adenosine, adenosine analogues and drugs inhibiting adenosine inactivation on lipolysis in rat fat cells. *Acta Physiol. Scand.* 102, 191–198. doi: 10.1111/j.1748-1716.1978.tb06062.x

Fredholm, B. B. (2014). Adenosine–a physiological or pathophysiological agent? *J. Mol. Med. (Berl)* 92, 201–206. doi: 10.1007/s00109-013-1101-6

Fredholm, B. B., IJzerman, A. P., Jacobson, K. A., Linden, J., and Muller, C. E. (2011). International union of basic and clinical pharmacology. LXXXI. Nomenclature and classification of adenosine receptors–an update. *Pharmacol. Rev.* 63, 1–34. doi: 10.1124/pr.110.003285

Garcia, R. A., Roemmich, J. N., and Claycombe, K. J. (2016). Evaluation of markers of beige adipocytes in white adipose tissue of the mouse. *Nutr. Metab. (Lond).* 13:24. doi: 10.1186/s12986-016-0081-2

Gharibi, B., Abraham, A. A., Ham, J., and Evans, B. A. (2012). Contrasting effects of A1 and A2b adenosine receptors on adipogenesis. *Int. J. Obes. (Lond).* 36, 397–406. doi: 10.1038/ijo.2011.129

Gnad, T., Scheibler, S., von, K. I, Scheele, C., Kilic, A., Glode, A., et al. (2014). Adenosine activates brown adipose tissue and recruits beige adipocytes via A2A receptors. *Nature* 516, 395–399. doi: 10.1038/nature13816

Guilherme, A., Virbasius, J. V., Puri, V., and Czech, M. P. (2008). Adipocyte dysfunctions linking obesity to insulin resistance and type 2 diabetes. *Nat. Rev. Mol. Cell Biol.* 9, 367–377. doi: 10.1038/nrm2391

Halperin, M. L., Mak, M. L., and Taylor, W. M. (1978). Control of glucose transport in adipose tissue of the rat: role of insulin, ATP, and intracellular metabolites. *Can. J. Biochem.* 56, 708–712. doi: 10.1139/o78-106

Harms, M., and Seale, P. (2013). Brown and beige fat: development, function and therapeutic potential. *Nat. Med.* 19, 1252–1263. doi: 10.1038/nm.3361

Hoffman, B. B., Chang, H., Dall'Aglio, E., and Reaven, G. M. (1986). Desensitization of adenosine receptor-mediated inhibition of lipolysis. The mechanism involves the development of enhanced cyclic adenosine monophosphate accumulation in tolerant adipocytes. *J. Clin. Invest.* 78, 185–190. doi: 10.1172/JCI112550

Idzko, M., Ferrari, D., and Eltzschig, H. K. (2014). Nucleotide signalling during inflammation. *Nature* 509, 310–317. doi: 10.1038/nature13085

Ishikawa, J., Mitani, H., Bandoh, T., Kimura, M., Totsuka, T., and Hayashi, S. (1998). Hypoglycemic and hypotensive effects of 6-cyclohexyl-2′-O-methyl-adenosine, an adenosine A1 receptor agonist, in spontaneously hypertensive rat complicated with hyperglycemia. *Diabetes Res. Clin. Pract.* 39, 3–9. doi: 10.1016/S0168-8227(97)00116-2

Jacobson, K. A., and Muller, C. E. (2016). Medicinal chemistry of adenosine, P2Y and P2X receptors. *Neuropharmacology* 104, 31–49. doi: 10.1016/j.neuropharm.2015.12.001

Johansson, S. M., Lindgren, E., Yang, J. N., Herling, A. W., and Fredholm, B. B. (2008). Adenosine A1 receptors regulate lipolysis and lipogenesis in mouse adipose tissue-interactions with insulin. *Eur. J. Pharmacol.* 597, 92–101. doi: 10.1016/j.ejphar.2008.08.022

Johnston-Cox, H., Eisenstein, A. S., Koupenova, M., Carroll, S., and Ravid, K. (2014). The macrophage A2B adenosine receptor regulates tissue insulin sensitivity. *PLOS ONE* 9:e98775. doi: 10.1371/journal.pone.0098775

Johnston-Cox, H., Koupenova, M., Yang, D., Corkey, B., Gokce, N., Farb, M. G., et al. (2012). The A2b adenosine receptor modulates glucose homeostasis and obesity. *PLOS ONE* 7:e40584. doi: 10.1371/journal.pone.0040584

Junger, W. G. (2011). Immune cell regulation by autocrine purinergic signalling. *Nat. Rev. Immunol.* 11, 201–212. doi: 10.1038/nri2938

Kawano, S., Otsu, K., Kuruma, A., Shoji, S., Yanagida, E., Muto, Y., et al. (2006). ATP autocrine/paracrine signaling induces calcium oscillations and NFAT activation in human mesenchymal stem cells. *Cell Calcium* 39, 313–324. doi: 10.1016/j.ceca.2005.11.008

Kim, S. H., and Plutzky, J. (2016). Brown fat and browning for the treatment of obesity and related metabolic disorders. *Diabetes Metab. J.* 40, 12–21. doi: 10.4093/dmj.2016.40.1.12

Kusminski, C. M., Bickel, P. E., and Scherer, P. E. (2016). Targeting adipose tissue in the treatment of obesity-associated diabetes. *Nat. Rev. Drug Discov.* 15, 639–660. doi: 10.1038/nrd.2016.75

Laplante, M. A., Monassier, L., Freund, M., Bousquet, P., and Gachet, C. (2010). The purinergic P2Y1 receptor supports leptin secretion in adipose tissue. *Endocrinology* 151, 2060–2070. doi: 10.1210/en.2009-1134

Larrouy, D., Galitzky, J., and Lafontan, M. (1991). A1 adenosine receptors in the human fat cell: tissue distribution and regulation of radioligand binding. *Eur. J. Pharmacol.* 206, 139–147. doi: 10.1016/0922-4106(91)90022-A

Lazarowski, E. R. (2012). Vesicular and conductive mechanisms of nucleotide release. *Purinergic Signal.* 8, 359–373. doi: 10.1007/s11302-012-9304-9

Lee, H., Jun, D. J., Suh, B. C., Choi, B. H., Lee, J. H., Do, M. S., et al. (2005). Dual roles of P2 purinergic receptors in insulin-stimulated leptin production and lipolysis in differentiated rat white adipocytes. *J. Biol. Chem.* 280, 28556–28563. doi: 10.1074/jbc.M411253200

Lee, S. C., Vielhauer, N. S., Leaver, E. V., and Pappone, P. A. (2005). Differential regulation of ca(2+) signaling and membrane trafficking by multiple p2 receptors in brown adipocytes. *J. Membr. Biol.* 207, 131–142. doi: 10.1007/s00232-005-0808-x

Lee, S. C., and Pappone, P. A. (1997a). Effects of P2 purinergic receptor stimulation in brown adipocytes. *Am. J. Physiol.* 273(2 Pt 1), C679–C686.

Lee, S. C., and Pappone, P. A. (1997b). Membrane responses to extracellular ATP in rat isolated white adipocytes. *Pflugers Arch.* 434, 422–428. doi: 10.1007/s004240050416

Lemaire, A., Vanorle, M., Horckmans, M., di Pietrantonio, L., Clouet, S., Robaye, B., et al. (2017). Mouse P2Y4 nucleotide receptor is a negative regulator of cardiac adipose-derived stem cell differentiation and cardiac fat formation. *Stem Cells Dev.* 26, 363–373. doi: 10.1089/scd.2016.0166

Li, W., Li, G., Zhang, Y., Wei, S., Song, M., Wang, W., et al. (2015). Role of P2 x 7 receptor in the differentiation of bone marrow stromal cells into osteoblasts and adipocytes. *Exp. Cell Res.* 339, 367–379. doi: 10.1016/j.yexcr.2015.10.011

Li, W., Wei, S., Liu, C., Song, M., Wu, H., and Yang, Y. (2016). Regulation of the osteogenic and adipogenic differentiation of bone marrow-derived stromal cells by extracellular uridine triphosphate: the role of P2Y2 receptor and ERK1/2 signaling. *Int. J. Mol. Med.* 37, 63–73. doi: 10.3892/ijmm.2015.2400

Madec, S., Rossi, C., Chiarugi, M., Santini, E., Salvati, A., Ferrannini, E., et al. (2011). Adipocyte P2X7 receptors expression: a role in modulating inflammatory response in subjects with metabolic syndrome? *Atherosclerosis* 219, 552–558. doi: 10.1016/j.atherosclerosis.2011.09.012

Mersmann, H. J., Carey, G. B., and Smith, E. O. (1997). Adipose tissue beta-adrenergic and A1 adenosine receptors in suckling pigs. *J. Anim. Sci.* 75, 3161–3168. doi: 10.2527/1997.75123161x

North, R. A. (2016). P2X receptors. *Philos. Trans. R. Soc. Lond. B Biol. Sci.* 371:20150427. doi: 10.1098/rstb.2015.0427

Novak, I. (2011). Purinergic signalling in epithelial ion transport: regulation of secretion and absorption. *Acta Physiol. (Oxf).* 202, 501–522. doi: 10.1111/j.1748-1716.2010.02225.x

Pandolfi, J., Ferraro, A., Lerner, M., Serrano, J. R., Dueck, A., Fainboim, L., et al. (2015). Purinergic signaling modulates human visceral adipose inflammatory responses: implications in metabolically unhealthy obesity. *J. Leukoc. Biol.* 97, 941–949. doi: 10.1189/jlb.3A1214-626R

Pandolfi, J. B., Ferraro, A. A., Sananez, I., Gancedo, M. C., Baz, P., Billordo, L. A., et al. (2016). ATP-induced inflammation drives tissue-resident Th17 cells in metabolically unhealthy obesity. *J. Immunol.* 196, 3287–3296. doi: 10.4049/jimmunol.1502506

Peleli, M., and Carlstrom, M. (2017). Adenosine signaling in diabetes mellitus and associated cardiovascular and renal complications. *Mol. Aspects Med.* 55, 62–74. doi: 10.1016/j.mam.2016.12.001

Peleli, M., Hezel, M., Zollbrecht, C., Persson, A. E., Lundberg, J. O., Weitzberg, E., et al. (2015). In adenosine A2B knockouts acute treatment with inorganic nitrate improves glucose disposal, oxidative stress, and AMPK signaling in the liver. *Front. Physiol.* 6:222. doi: 10.3389/fphys.2015.00222

Rancoule, C., Dusaulcy, R., Treguer, K., Gres, S., Attane, C., and Saulnier-Blache, J. S. (2014). Involvement of autotaxin/lysophosphatidic acid signaling in obesity and impaired glucose homeostasis. *Biochimie* 96, 140–143. doi: 10.1016/j.biochi.2013.04.010

Razzoli, M., Frontini, A., Gurney, A., Mondini, E., Cubuk, C., Katz, L. S., et al. (2016). Stress-induced activation of brown adipose tissue prevents obesity in conditions of low adaptive thermogenesis. *Mol. Metab.* 5, 19–33. doi: 10.1016/j.molmet.2015.10.005

Rice, A. M., Fain, J. N., and Rivkees, S. A. (2000). A1 adenosine receptor activation increases adipocyte leptin secretion. *Endocrinology* 141, 1442–1445. doi: 10.1210/endo.141.4.7423

Rissiek, B., Haag, F., Boyer, O., Koch-Nolte, F., and Adriouch, S. (2015). P2X7 on mouse T cells: one channel, many functions. *Front. Immunol.* 6:204. doi: 10.3389/fimmu.2015.00204

Saggerson, E. D., and Jamal, Z. (1990). Differences in the properties of A1-type adenosine receptors in rat white and brown adipocytes. *Biochem. J.* 269, 157–161. doi: 10.1042/bj2690157

Schimmel, R. J., and McCarthy, L. (1984). Role of adenosine as an endogenous regulator of respiration in hamster brown adipocytes. *Am. J. Physiol.* 246(3 Pt 1), C301–C307.

Schodel, J., Weise, I., Klinger, R., and Schmidt, M. (2004). Stimulation of lipogenesis in rat adipocytes by ATP, a ligand for P2-receptors. *Biochem. Biophys. Res. Commun.* 321, 767–773. doi: 10.1016/j.bbrc.2004.06.179

Schoelch, C., Kuhlmann, J., Gossel, M., Mueller, G., Neumann-Haefelin, C., Belz, U., et al. (2004). Characterization of adenosine-A1 receptor-mediated antilipolysis in rats by tissue microdialysis, 1H-spectroscopy, and glucose clamp studies. *Diabetes Metab. Res. Rev.* 53, 1920–1926. doi: 10.2337/diabetes.53.7.1920

Shah, B., Rohatagi, S., Natarajan, C., Kirkesseli, S., Baybutt, R., and Jensen, B. K. (2004). Pharmacokinetics, pharmacodynamics, and safety of a lipid-lowering adenosine A1 agonist, RPR749, in healthy subjects. *Am. J. Ther.* 11, 175–189. doi: 10.1097/00045391-200405000-00005

Staehr, P. M., Dhalla, A. K., Zack, J., Wang, X., Ho, Y. L., Bingham, J., et al. (2013). Reduction of free fatty acids, safety, and pharmacokinetics of oral GS-9667, an A(1) adenosine receptor partial agonist. *J. Clin. Pharmacol.* 53, 385–392. doi: 10.1002/jcph.9

Strong, P., Anderson, R., Coates, J., Ellis, F., Evans, B., Gurden, M. F., et al. (1993). Suppression of non-esterified fatty acids and triacylglycerol in experimental animals by the adenosine analogue GR79236. *Clin. Sci. (Lond).* 84, 663–669. doi: 10.1042/cs0840663

Sun, S., Xia, S., Ji, Y., Kersten, S., and Qi, L. (2012). The ATP-P2X7 signaling axis is dispensable for obesity-associated inflammasome activation in adipose tissue. *Diabetes Metab. Res. Rev.* 61, 1471–1478. doi: 10.2337/db11-1389

Szkudelski, T., Szkudelska, K., and Nogowski, L. (2009). Effects of adenosine A1 receptor antagonism on lipogenesis and lipolysis in isolated rat adipocytes. *Physiol. Res.* 58, 863–871.

Tatsis-Kotsidis, I., and Erlanger, B. F. (1999). A1 adenosine receptor of human and mouse adipose tissues: cloning, expression, and characterization. *Biochem. Pharmacol.* 58, 1269–1277. doi: 10.1016/S0006-2952(99)00214-2

Trost, T., and Schwabe, U. (1981). Adenosine receptors in fat cells. Identification by (–)-N6-[3H]phenylisopropyladenosine binding. *Mol. Pharmacol.* 19, 228–235.

Ussar, S., Lee, K. Y., Dankel, S. N., Boucher, J., Haering, M. F., Kleinridders, A., et al. (2014). ASC-1, PAT2, and P2RX5 are cell surface markers for white, beige, and brown adipocytes. *Sci. Transl. Med.* 6:247ra103. doi: 10.1126/scitranslmed.3008490

von Kugelgen, I., and Hoffmann, K. (2016). Pharmacology and structure of P2Y receptors. *Neuropharmacology* 104, 50–61. doi: 10.1016/j.neuropharm.2015.10.030

Woodward, J. A., and Saggerson, E. D. (1986). Effect of adenosine deaminase, N6-phenylisopropyladenosine and hypothyroidism on the responsiveness of rat brown adipocytes to noradrenaline. *Biochem. J.* 238, 395–403. doi: 10.1042/bj2380395

Wu, L., Belardinelli, L., Zablocki, J. A., Palle, V., and Shryock, J. C. (2001). A partial agonist of the A(1)-adenosine receptor selectively slows AV conduction in guinea pig hearts. *Am. J. Physiol. Heart Circ. Physiol.* 280, H334–H343.

Yang, T., Gao, X., Sandberg, M., Zollbrecht, C., Zhang, X. M., Hezel, M., et al. (2015). Abrogation of adenosine A1 receptor signalling improves metabolic regulation in mice by modulating oxidative stress and inflammatory responses. *Diabetologia* 58, 1610–1620. doi: 10.1007/s00125-015-3570-3

Yang, T., Zollbrecht, C., Winerdal, M. E., Zhuge, Z., Zhang, X. M., Terrando, N., et al. (2016). Genetic abrogation of adenosine A3 receptor prevents uninephrectomy and high salt-induced hypertension. *J. Am. Heart Assoc.* 5:e003868. doi: 10.1161/JAHA.116.003868

Yu, Z., and Jin, T. (2010). Extracellular high dosages of adenosine triphosphate induce inflammatory response and insulin resistance in rat adipocytes. *Biochem. Biophys. Res. Commun.* 402, 455–460. doi: 10.1016/j.bbrc.2010.10.028

Zannikos, P. N., Rohatagi, S., and Jensen, B. K. (2001). Pharmacokinetic-pharmacodynamic modeling of the antilipolytic effects of an adenosine receptor agonist in healthy volunteers. *J. Clin. Pharmacol.* 41, 61–69. doi: 10.1177/00912700122009845

Zimmermann, H., Zebisch, M., and Strater, N. (2012). Cellular function and molecular structure of ecto-nucleotidases. *Purinergic Signal.* 8, 437–502. doi: 10.1007/s11302-012-9309-4

Zippel, N., Limbach, C. A., Ratajski, N., Urban, C., Luparello, C., Pansky, A., et al. (2012). Purinergic receptors influence the differentiation of human mesenchymal stem cells. *Stem Cells Dev.* 21, 884–900. doi: 10.1089/scd.2010.0576

Conflict of Interest Statement: The authors declare that the research was conducted in the absence of any commercial or financial relationships that could be construed as a potential conflict of interest.

The reviewer GY declared a past co-authorship with one of the authors IN to the handling Editor.

frontiers in Pharmacology

ORIGINAL RESEARCH
published: 22 November 2017
doi: 10.3389/fphar.2017.00860

Interaction of Purinergic P2X4 and P2X7 Receptor Subunits

Markus Schneider[1†], Kirsten Prudic[1†], Anja Pippel[1], Manuela Klapperstück[1], Ursula Braam[2], Christa E. Müller[3], Günther Schmalzing[2] and Fritz Markwardt[1]*

[1] Julius-Bernstein-Institute for Physiology, Martin-Luther-University, Halle, Germany, [2] Molecular Pharmacology, RWTH Aachen University, Aachen, Germany, [3] Pharmaceutical Institute, Pharmaceutical Chemistry I, University of Bonn, Bonn, Germany

P2X4 and P2X7 are members of the P2X receptor family, comprising seven isoforms (P2X1–P2X7) that form homo- and heterotrimeric non-specific cation channels gated by extracellular ATP. P2X4 and P2X7 are widely coexpressed, particularly in secretory epithelial cells and immune and inflammatory cells, and regulate inflammation and nociception. Although functional heteromerization has been established for P2X2 and P2X3 subunits expressed in sensory neurons, there are contradictory reports regarding a functional interaction between P2X4 and P2X7 subunits. To resolve this issue, we coexpressed P2X4 and P2X7 receptor subunits labeled with green (EGFP) and red (TagRFP) fluorescent proteins in *Xenopus laevis* oocytes and investigated a putative physical interaction between the fusion proteins by Förster resonance energy transfer (FRET). Coexpression of P2X4 and P2X7 subunits with EGFP and TagRFP located in the extracellular receptor domains led to significant FRET signals. Significant FRET signals were also measured between C-terminally fluorophore-labeled full-length $P2X4^{1-384}$ and C-terminally truncated fluorescent $P2X7^{1-408}$ subunits. We furthermore used the two-electrode voltage clamp technique to investigate whether human P2X4 and P2X7 receptors (hP2X4, hP2X7) functionally interact at the level of ATP-induced whole-cell currents. Concentration–response curves and effects of ivermectin (P2X4-potentiating drug) or BzATP (P2X7-specific agonist) were consistent with a model in which coexpressed hP2X4 and hP2X7 do not interact. Similarly, the effect of adding specific inhibitors of P2X4 (PSB-15417) or P2X7 (oATP, A438079) could be explained by a model in which only homomers exist, and that these are blocked by the respective antagonist. In conclusion, we show that P2X4 and P2X7 subunits can form heterotrimeric P2X4/P2X7 receptors. However, unlike observations for P2X2 and P2X3, coexpression of P2X4 and P2X7 subunits does not result in a novel electrophysiologically discriminable P2X receptor phenotype.

Keywords: P2X7, P2X4, voltage clamp, fluorescence, FRET, interaction, subunit

OPEN ACCESS

Edited by:
Kenneth A. Jacobson, National Institutes of Health (NIH), United States

Reviewed by:
Ichiro Maruyama, Okinawa Institute of Science and Technology, Japan
Dietmar Krautwurst, Leibniz Association (LG), Germany

***Correspondence:**
Fritz Markwardt
fritz.markwardt@medizin.uni-halle.de

† These authors have contributed equally to this work.

Specialty section:
This article was submitted to Experimental Pharmacology and Drug Discovery, a section of the journal Frontiers in Pharmacology

Received: *11 September 2017*
Accepted: *09 November 2017*
Published: *22 November 2017*

Citation:
Schneider M, Prudic K, Pippel A, Klapperstück M, Braam U, Müller CE, Schmalzing G and Markwardt F (2017) Interaction of Purinergic P2X4 and P2X7 Receptor Subunits. Front. Pharmacol. 8:860. doi: 10.3389/fphar.2017.00860

INTRODUCTION

P2X receptors are non-selective cation channels that are opened by extracellular ATP. The presence of ATP is considered a danger-associated signal (DAMP, danger-associated molecular pattern), because ATP is released from cells during damage, hypoxia, or cell membrane stretching (Di Virgilio, 2007; Praetorius and Leipziger, 2009). P2X receptors are homo- or heterotrimers that

assemble from a repertoire of seven possible subunits (P2X1–7) (Nicke et al., 1998; Aschrafi et al., 2004). All P2X subunits share similar membrane topology: intracellular N- and C-termini, two membrane-spanning domains (TM1 and TM2), and a large extracellular loop comprising the ATP binding site. The TM2 domains form the gate and the selectivity filter (Baconguis et al., 2013; Habermacher et al., 2015; Pippel et al., 2017). In addition to homotrimeric P2X receptors, P2X subunits can form heteromeric ion channels. The existence of P2X2/P2X3 heteromers in sensory neurons is well established (Lewis et al., 1995). A large number of other heteromers have been characterized in heterologous expression systems. However, their function in native tissue remains to be established (Saul et al., 2013).

The P2X4 and P2X7 subunit isoforms are widely coexpressed, particularly in secretory epithelial cells and cells of the immune and inflammatory system. The P2X7 subunit has the highest amino acid sequence similarity to the P2X4 subtype (Burnstock and Knight, 2004; Surprenant and North, 2008). Furthermore, the genes encoding both of these subunits colocalize on human chromosome 12, where they are separated by only 24 kbp (Craigie et al., 2013). P2X7 mRNA levels are reduced in P2X4 knockout mice, and vice versa (Craigie et al., 2013). In contrast, shRNA-mediated downregulation of P2X7 mRNA leads to increased P2X4 expression. Knockdown of P2X4 mRNA is reported to result in a compensatory increase in P2X7 protein expression (Weinhold et al., 2010).

Early co-immunoprecipitation studies of P2X subunit interactions excluded the interaction of P2X7 subunits with other subtypes (Torres et al., 1999), although later studies reported evidence of P2X4/P2X7 heteromerization (Guo et al., 2007). Subsequent investigations, however, have questioned the existence of P2X4/P2X7 heteromeric receptors (Nicke, 2008; Antonio et al., 2011; for reviews, see Craigie et al., 2013; Saul et al., 2013).

Here, we investigated physical and functional interactions P2X4 and P2X7 subunits heterologously expressed in *Xenopus* oocytes by measuring P2X4/P2X7-dependent Förster (or fluorescence) resonance energy transfer (FRET) signals and ion currents in *Xenopus* oocytes.

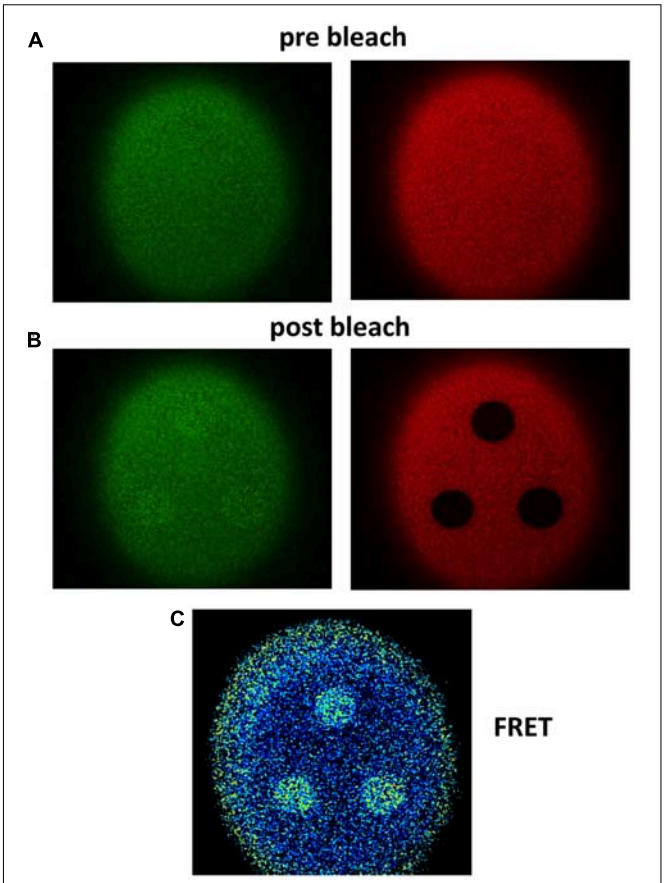

FIGURE 1 | Fluorescence signals before and after acceptor photobleaching. Example of Donor (GFP) recovery after acceptor (RFP) photobleaching for the P2X4 construct with a C-terminal tandem GFP-RFP label. **(A,B)** Pre-bleaching **(A)** and post-bleaching **(B)** fluorescence images were obtained as described in the Methods section using a confocal laser scanning microscope. The slightly increasing GFP fluorescence is shown on the left side and the RFP fluorescence, which is strongly decreased due to application of the maximal RFP exciting light for 1 min on the right side. **(C)** The FRET signal was calculated pointwise using the microscope software in the same manner as shown in **Figure 2**. A strong FRET signal is measured in areas of RFP bleaching. Blue pixels indicate low and yellow pixels high FE.

MATERIALS AND METHODS

Reagents

Unless otherwise stated, we purchased chemicals and molecular biology reagents from Sigma–Aldrich (Taufkirchen, Germany), Merck (Darmstadt, Germany), and New England Biolabs (Schwalbach, Germany). The novel hP2X4-selective antagonist PSB-15417 was provided by Prof. Christa Müller (Institute of Pharmaceutical Chemistry, University of Bonn, Germany) via Orion (Espoo, Finland).

Expression of hP2X4 and hP2X7 Subunits in *Xenopus laevis* Oocytes

The following oocyte expression plasmids encoding full-length human (h) and rat (r) subunits of ligand-gated ion channels were available from our previous work (reference sequence NCBI IDs and references in parenthesis): hP2X4 (ID: NP_002551.2, Rettinger et al., 2000); rP2X4 (ID: NP_113782.1, Aschrafi et al., 2004); hP2X7 (ID: NP_002553.3, Klapperstück et al., 2000), $hP2X7^{1-408}$ (C-terminally truncated by placing a premature TGA stop codon directly after the hP2X7 ^{408}H codon, Becker et al., 2008); and hGLYRA1 (ID: NP_000162.2, Büttner et al., 2001). We amplified full-length cDNA encoding the rat P2X7 subunit (ID: NP_062129.1) by RT-PCR from total rat brain RNA isolated using the RNA Clean System (Angewandte Gentechnologie Systeme, Heidelberg, Germany) and gene-specific primers (Supplementary Table 1) based on the published rP2X7 sequence (Surprenant et al., 1996). The PCR product was first inserted into the pGEM5 ZF(+) vector (X65308; Promega, Mannheim, Germany) by TA cloning (Kovalic et al., 1991) and then directionally subcloned it into the pNKS2 oocyte expression

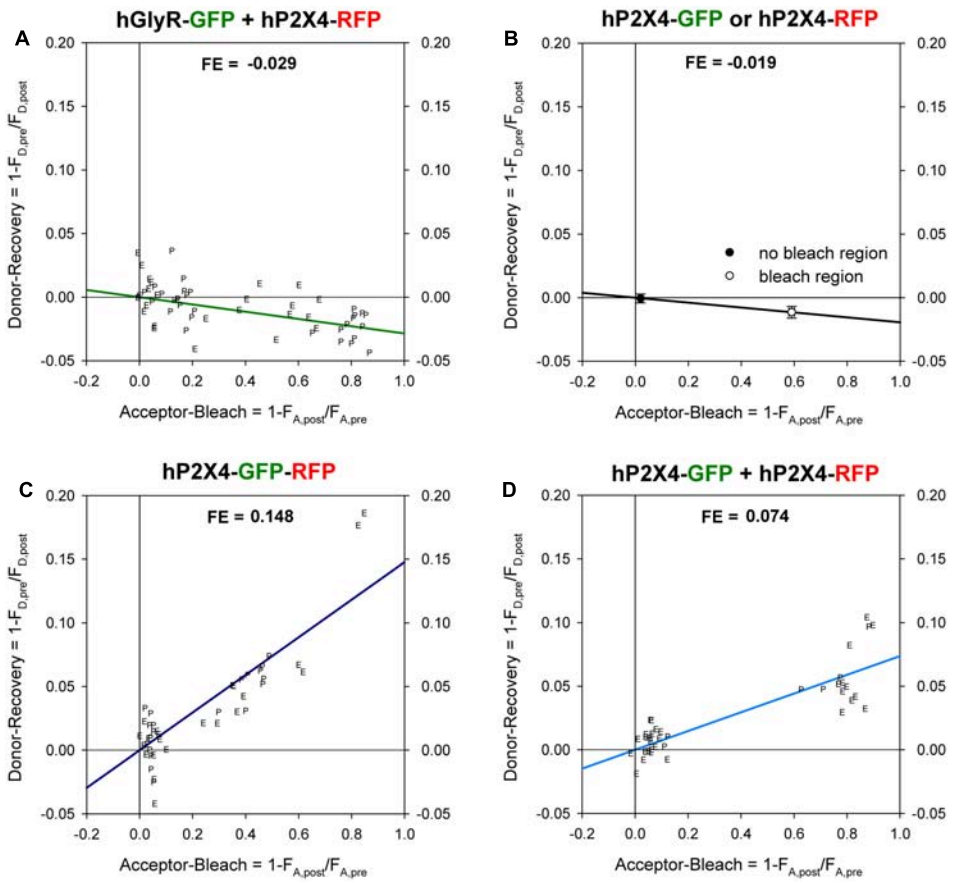

FIGURE 2 | Förster resonance energy transfer (FRET) between GFP- and RFP -labeled P2XR subunits measured with donor recovery by acceptor photobleaching. Measurements were made at the oocyte pole adjacent to the bottom of the recording chamber (P) or at the equator (E) of the oocytes, as shown in **Figure 1**. The degree of donor recovery was plotted against the degree of acceptor bleaching. FRET efficiency (FE) was obtained by extrapolating the linear regression line to complete acceptor bleaching (right hand *y*-axis). **(A)** Negative control: coexpression of C-terminally RFP-labeled hP2X4 with SP-GFP-GLYRA1. **(B)** In oocytes expressing either hP2X4-GFP or hP2X4-RFP, the mean changes in the donor (donor recovery) and acceptor fluorescence (acceptor bleach) were measured at bleached versus non-bleached areas. The decrease of the donor fluorescence in regions of acceptor bleach indicates a bleaching effect of the acceptor excitation light and leads to calculation of negative FE values. **(C)** Positive control: P2X4 protein with a C-terminal tandem GFP-RFP label. **(D)** Coexpression of C-terminally GFP- and RFP-labeled hP2X4 constructs. Mean fluorescence values were calculated from 50–60 regions of interests (ROIs) in 5–10 oocytes.

vector (Gloor et al., 1995) using *Aat*II and *Xba*I restriction sites introduced via PCR (underlined in Supplementary Table 1). We previously reported using the rP2X7-pNKS2 construct without describing its origin (Hausmann et al., 2006).

We obtained a synthetic gene encoding the *Caenorhabditis elegans* glutamate-gated chloride channel α (GluCl) optimized for crystallization ($GluCl_{cryst}$) (Hibbs and Gouaux, 2011) from ShineGene (Shanghai, China). This was subcloned into a Gateway-compatible pNKS2 vector (Stolz et al., 2015) using the Gateway cloning system (Invitrogen, Karlsruhe, Germany). We previously verified by blue native PAGE that ectopic $GluCl_{cryst}$ efficiently assembles into a homopentamer in *Xenopus laevis* oocytes (Dopychai et al., 2015). A plasmid harboring full-length cDNA for hTRPV2 (DNASU plasmid ID HsCD00045624) was obtained from the DNASU Plasmid Repository (The Biodesign Institute, Arizona State University, Tempe, AZ, United States) and subcloned using the Gateway system into the pNKS2 vector.

We generated fluorophore-labeled channel constructs with the enhanced green fluorescent protein or Tag red fluorescent protein (referred to as GFP or RFP throughout, respectively) located at the N-terminus (or ectodomain) or C-terminus (indicated by adding the name of the label (GFP or RFP) at the left (ectodomain) or right (C-terminus) of the fusion protein name). To N-terminally labeling hGLYRA1 (the human glycine receptor α1 subunit) with GFP, we first located the signal peptidase cleavage site at between codon position ^{28}A and ^{29}A using the SignalP 4.1 server[1] (Petersen et al., 2011). Next, we introduced unique *Nde*I and EcoR47III restriction sites using the QuikChange site-directed mutagenesis protocol (Stratagene, Heidelberg, Germany, (Braman et al., 1996) with primers O-1699/O-1700 (Supplementary Table 2). Finally, we PCR-amplified the full-length cDNA for GFP from the EGFP-N1 vector (Invitrogen, Karlsruhe, Germany) using

[1]http://www.cbs.dtu.dk/services/SignalP

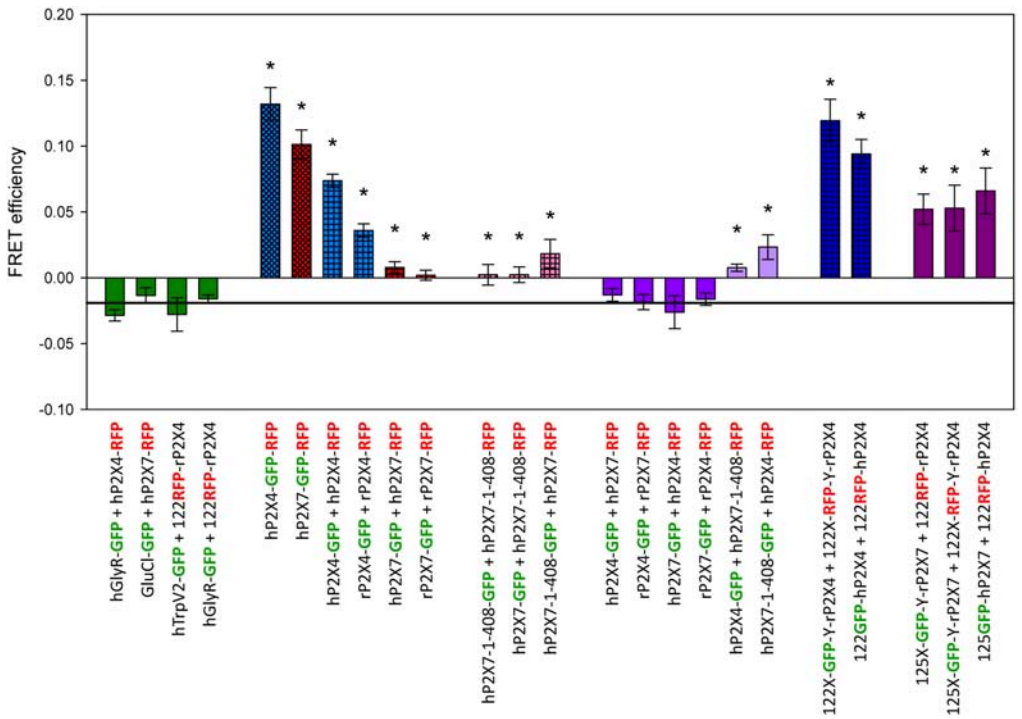

FIGURE 3 | Förster resonance energy transfer measurement of P2X4 and P2X7 subunit interactions. FRET efficiencies were calculated as described in **Figure 2**. Horizontal line represents GFP bleaching during acceptor bleaching leading to negative FE values of –0.019 (see **Figure 2B**). *, FRET efficiencies significantly larger than –0.019. Data are the means ± SEM from 12–20 oocytes. X and Y denote short, flexible linkers (-GAGA- and -AGAG-, respectively; single amino acid letter code) flanking the GFP or RFP moiety. The position of the fluorophore name indicates the position of the label in the P2X receptor fusion construct (i.e., P2X7-GFP indicates a C-terminal label). Bar colors: green = negative control, blue = P2X4 constructs, red = P2X7 constructs, pink = P2X4/P2X7 coexpression. Bar patterns: cross-hatched = tandem GFP-RFP label, checkered = positive controls.

primers O-1701/O-1702 (Supplementary Table 3), purified, and directionally cloned between *Nde*I and EcoR47III sites to construct the SP-GFP-hGLYRA1 vector (where SP indicates the position of the signal peptide). This construct encodes an additional alanine residue directly 5′ of the GFP moiety and is predicted by the SignalP 4.1 server to undergo signal peptidase cleavage at the same residues as wild type (wt) hGLYRA1.

We used the megaprimer method (Perez et al., 2006) for fluorescence labeling of all the other ion channel constructs (primers are listed in Supplementary Table 2). Single (GFP or RFP) or tandem (GFP-RFP) labels were added to the C-termini of ion channel constructs by in-frame fusion with full-length GFP and RFP sequences with the RFP sequence amplified from the TagRFP-N vector (Evrogen, Moscow, Russia). Likewise, we inserted GFP and RFP cDNA either singly or in tandem after *P2X4* codon 122 or *P2X7* codon 125. Our rational was that rP2X4 receptors containing a fluorescent pHluorin moiety after ^{122}K have previously been shown to function like wt-rP2X4 (Xu et al., 2014). A previous sequence alignment showed that rP2X4 ^{122}K (hP2X4 ^{122}A) corresponds to ^{125}R for both rP2X7 and hP2X7 (Kawate et al., 2009).

We synthesized capped cRNA using a modified method (Klapperstück et al., 2000) involving co-transcriptional incorporation of the anti-reverse cap analog ($m_2^{7,3'-O}$GpppG; NU-855; Jena Bioscience, Germany) to ensure the correct orientation at the ATG start codon of the cRNA (Grudzien-Nogalska et al., 2007; Stolz et al., 2015). We surgically isolated oocytes from tricaine-anesthetized *Xenopus laevis* (Xenopus Express, Vernassal, France) using sterile surgical techniques and defolliculated them with collagenase NB 4G (Serva, Heidelberg, Germany). We injected oocytes of Dumont stages V–VI individually with 5–50 ng *P2X4* and/or *P2X7* cRNA to obtain similar ATP-evoked current amplitudes mediated by the encoded P2X4 and P2X7 receptors. To optimize FRET efficiency (FE), we adjusted the amount of mRNA used to coexpress GFP- and RFP-labeled constructs to obtain higher fluorescence signals from channels labeled with GFP than with RFP (Ma et al., 2014). We incubated the oocytes at 19°C in sterilized frog Ringer solution (Mg/Ca-ORi: 100 mM NaCl, 2.5 mM KCl, 1 mM $MgCl_2$, 1 mM $CaCl_2$, and 10 mM HEPES, pH 7.4) supplemented with penicillin (100 U/ml) and streptomycin (100 µg/ml) or with gentamycin (50 µg/ml) (Flittiger et al., 2010). This study was carried out in accordance with the recommendations of the EC Directive 86/609/EEC for animal experimentation. The protocol was approved by the local animal welfare committee (reference no. 53a-42502/2–173; Magdeburg, Germany).

FRET Experiments

We measured fluorescence signals from human and rat P2X4 and P2X7 subunits labeled with GFP as the donor (excitation

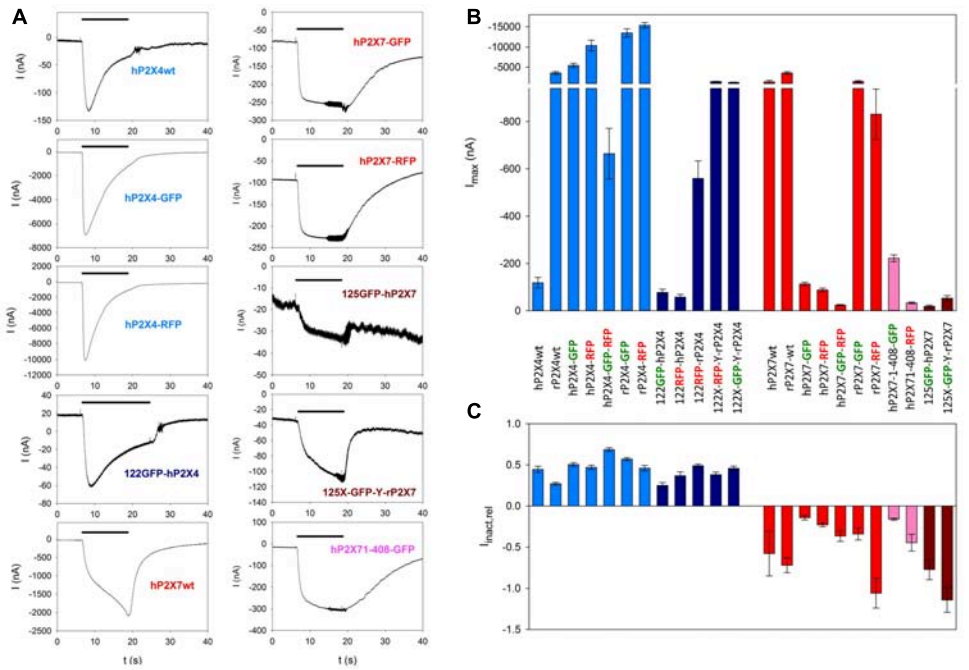

FIGURE 4 | Functional testing of fluorescence-labeled P2X4 and P2X7 constructs by two-electrode voltage clamp measurements. **(A)** Examples of current traces in oocytes expressing wildtype P2X4 (P2X4wt) of P2X7 (P2X7wt) or different fluorescence-labeled P2X4 and P2X7 constructs, as indicated. The colors of the construct names relate to the colors of the bars in **(B,C)**. **(B)** Maximal current amplitudes obtained during the application of 1 mM ATP for 6 s. **(C)** Kinetics of ion channel currents in oocytes expressing different labeled P2X constructs. The relative inactivation ($I_{inact,rel}$) was calculated as the amplitude of the current between 2 and 6 s after the application of 1 mM ATP normalized to the current amplitude at the 2 s time point. A decay in the current amplitude ($I_{inact,rel} > 0$) indicates desensitization (seen for all P2X4 constructs); an increase in current amplitude during this period ($I_{inact,rel} < 0$) was usually seen for P2X7 constructs and is of unknown origin. Bar colors: light blue = P2X4wt or C-terminally labeled constructs, dark blue = P2X4 constructs labeled within the extracelllar domain, red = P2X7wt or C-terminally labeled constructs, rosy = C-terminally truncated and labeled P2X7 constructs, dark red = P2X7 constructs labeled within the extracelllar domain. Data are the means ± SEM from 5–20 oocytes.

at 488 nm, emission at 500–550 nm) or RFP as the acceptor (excitation at 561 nm, emission at 570–650 nm) using a TCS SP5 spectral confocal laser scanning microscope (Leica Microsystems, Wetzlar, Germany) with a 20 × 0.5 HC PL Fluotar dry objective lens. We placed individual oocytes expressing the indicated constructs in a IBIDI μ-Slide 8-well chamber in oocyte Ringer solution (ORi: 100 mM NaCl, 2.5 mM KCl, 1 mM $MgCl_2$, 1 mM $CaCl_2$, and 5 mM HEPES, pH 7.4) and measured fluorescence signals from the oocyte pole adjacent to the chamber bottom or at the oocyte equator (which had similar FEs; **Figure 2**). Fluorescence signals from donor GFP and acceptor RFP labels were measured before and after acceptor photobleaching at 561 nm using Leica TCS SP5 software or FIJI[2].

Two-Electrode Voltage Clamp Electrophysiology

We performed the electrophysiological experiments at room temperature (~22°C) as previously described (Stolz et al., 2015). We accomplished rapid, reproducible solution exchange by using a small tube-like chamber (0.1 ml) combined with fast superfusion (75 μl/s). A set of computer-controlled magnetic valves combined with a modified U-tube technique permitted the bathing solutions to be changed in less than 1 s (Klapperstück et al., 2000). We recorded whole-cell membrane currents via the two-electrode voltage clamp method using 3 M KCl-filled microelectrodes (resistance range 0.8–1.2 MΩ). The currents were recorded and filtered at 100 Hz using an oocyte clamp amplifier (OC-725C; Hamden, CT, United States) and sampled at 85 Hz. We stored and analyzed the data on a personal computer using software written in our department (Superpatch 2000, SP-Analyzer by T. Böhm). Two or three days after cRNA injection, we superfused individual oocytes with ORi solution and impaled the voltage clamp electrodes. To measure currents induced by ATP^{4-}, the agonist of the P2X4 and P2X7 receptors (Klapperstück et al., 2001; Li et al., 2013), we switched the bathing solution to Ca^{2+}- and Mg^{2+}-free ORi (ORi0Ca0Mg: 100 mM NaCl, 2.5 mM KCl, 5 mM HEPES, and 0.1 mM flufenamic acid, pH 7.4) to prevent metal ion complexation of ATP^{4-}. We included flufenamic acid in the ORi0Ca0Mg solution to suppress the large inward conductance that develops in the absence of divalent ions (Kubick et al., 2011). Agonists and antagonists were diluted in the ORi0Ca0Mg solution, as indicated in the figures.

Data Analysis and Presentation

For approximations, statistical analysis, and presentation of the data we used SigmaPlot software (Systat Software).

[2]https://fiji.sc

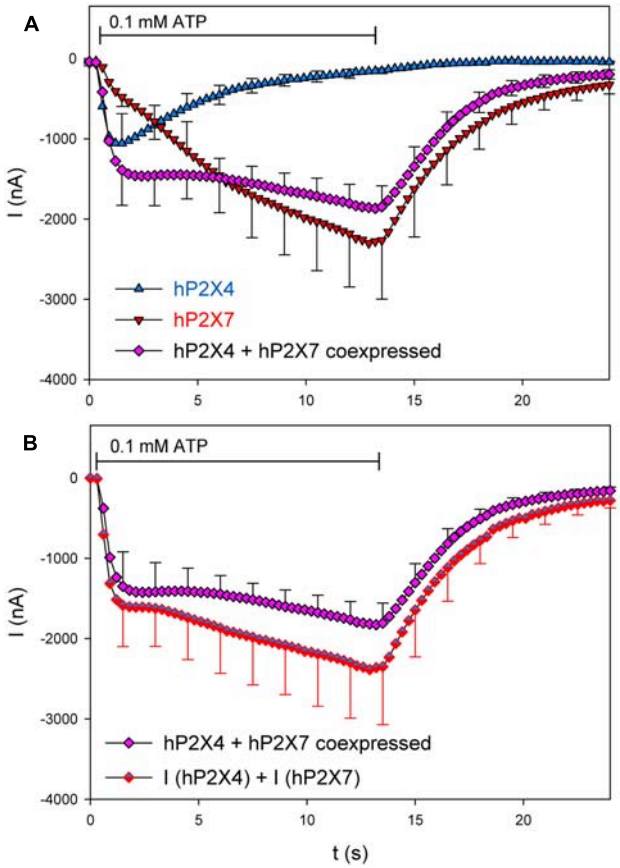

FIGURE 5 | Kinetics of ion channel currents in hP2X4/hP2X7-coexpressing oocytes. Two-electrode voltage clamp measurements of currents in *Xenopus* oocytes expressing hP2X4 and hP2X7 receptors were elicited by the application of 0.1 mM ATP. **(A)** Mean current traces were recorded from oocytes expressing hP2X4 or hP2X7 subunits alone or together, as indicated. **(B)** Mean currents in oocytes coexpressing hP2X4 and hP2X7 were compared with the sum of those in oocytes expressing hP2X4 or hP2X7 alone. The mean current amplitudes were not significantly different at any time point, indicating that P2X4/P2X7 heteromers with distinct current kinetics are not formed. Data are the means ± SD from five oocytes at each time point.

Statistical data were analyzed using one-way ANOVA. We tested the statistical significance of the differences between means using the Bonferroni multiple comparison *t*-test. The significance of the correlation coefficients was tested using the *t*-test. Statistical significance was set at *p*-value of <0.05.

RESULTS

FRET Demonstrates a Physical and Functional Interaction between P2X4 and P2X7

To investigate whether heteromerization occurs between P2X4 and P2X7 receptor subunits, we used the donor dequenching after acceptor photobleaching FRET quantification technique (Zheng, 2006; Ma et al., 2014). GFP- or RFP-dependent fluorescence was measured by laser scanning fluorimetry at the oocyte equator or at the oocyte pole in contact with the bottom of the recording chamber before (**Figure 1A**) and after (**Figure 1B**) photobleaching of the RFP-labeled acceptor construct. The FRET efficiency was visualized using the microscope software (**Figure 1C**) following quantitative evaluation (as demonstrated in **Figure 2**). The percentage increase in GFP fluorescence at different bleaching regions was calculated using Equation 1:

$$\text{Donor recovery} = 1 - F_{D,pre}/F_{D,post}$$

where $F_{D,pre}$ and $F_{D,post}$ are the mean fluorescence signals pre- and post-bleaching, respectively, for the donor GFP at bleached regions. The percentage increase in GFP fluorescence was plotted against the percentage decrease in RFP fluorescence, as calculated using Equation 2:

$$\text{Acceptor bleach} = 1 - F_{A,post}/F_{A,pre}$$

where $F_{A,pre}$ and $F_{A,post}$ are the mean pre- and post-bleaching fluorescence signals of the acceptor RFP. Extrapolation to 100% acceptor bleaching yielded the FE (Nashmi et al., 2003). FE values measured at the oocyte pole adjacent to the recording chamber were not significantly different from those measured at the oocyte equator (marked "P" and "E", respectively, in **Figure 2**).

Negative controls had negative FE values (**Figure 2A**) due to the reduction in GFP fluorescence during acceptor photobleaching (**Figure 2B**). A maximal FRET efficiency of 0.148 was measured in oocytes expressing the P2X4-GFP-RFP tandem by extrapolation of the regression line shown in **Figure 2C** to 1.0. A representative example of measurements of a positive control (i.e., oocytes coexpressing P2X4-GFP and P2X4-RFP subunits) is shown in **Figure 2D**.

Mean FRET measurements for different P2X4 and P2X7 constructs labeled with GFP or RFP are depicted in **Figure 3**. As negative controls, we coexpressed RFP-labeled P2X4 or P2X7 constructs with the tetrameric hTRPV2 channel, the pentameric human glycine receptor α1 hGLYRA1, or the pentameric invertebrate glutamate-gated chloride channel GluCl. FRET values for each of these combinations did not significantly differ from –0.019 (determined for the negative control example shown in **Figure 1**). The largest FRET signals were measured for the C-terminal tandemly labeled proteins hP2X4-GFP-RFP and hP2X7-GFP-RFP, and for the P2X4 constructs with single fluorescent labels in the extracellular domain (^{122}GFP-P2X4 + ^{122}RFP-P2X4). Robust FRET signals were also measured after coexpressing the C-terminally labeled positive controls P2X4-GFP and P2X4-RFP. Coexpression of P2X4-GFP with full-length P2X7-RFP did not result in significant FRET signals, but a significant FRET signal was obtained when C-terminally labeled truncated P2X7$^{1-408}$ and P2X4 were coexpressed. These values were similar to the FRET efficiencies measured after coexpression of C-terminally GFP- or RFP-labeled truncated hP2X7$^{1-408}$ with full-length P2X7-RFP or P2X7-GFP subunits, respectively. We consider these combinations as quasi-positive

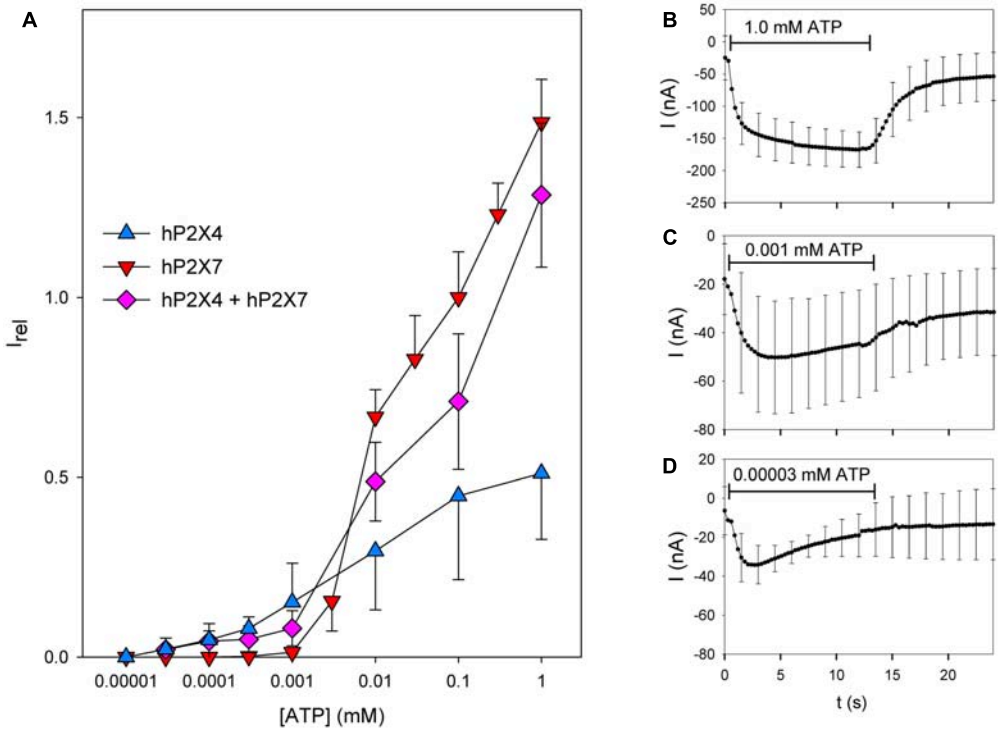

FIGURE 6 | Dependence on the ATP concentration of coexpressed hP2X4 and hP2X7 subunits. **(A)** Maximal current amplitudes in the presence of various ATP concentrations ([ATP]) were obtained by two-electrode voltage clamp measurements in oocytes expressing hP2X4 and/or hP2X7, as indicated. These amplitudes were measured during a 12 s lasting ATP application and normalized to the amplitude during a preceding application of 0.1 mM ATP to yield the relative current amplitude I_{rel}. I_{rel} values for hP2X4- or hP2X7-expressing oocytes are significantly different at all ATP concentrations. Current amplitudes of oocytes expressing hP2X4 + hP2X7 are significantly different from those of P2X7-expressing oocytes at 0.1–1 μM ATP and significantly different from those of P2X4-expressing oocytes at 0.01–1 mM ATP. Thus, the ATP concentration–response curve for hP2X4/hP2X7-coexpressing oocytes is dominated by the hP2X4 component at low ATP concentrations and by the P2X7 component at high ATP concentrations, arguing against a distinct P2X4/P2X7 phenotype regarding the agonist sensitivity. **(B–D)** Averaged current traces of different oocytes expressing hP2X4 and hP2X7, elicited by the second ATP application at the indicated concentrations. Data are the means ± SD from 4–10 oocytes.

controls because we previously showed that the truncated hP2X7 can co-assemble (i.e., physically interact) and function together with full-length hP2X7 receptor subunits (Becker et al., 2008). Much larger FRET signals were obtained for coexpressed P2X4 constructs with GFP or RFP located within the extracellular domain. Similarly, relatively higher FRET values were measured for P2X7 subunits with the GFP label located in the extracellular domain when coexpressed with P2X4 subunits with an extracellularly located RFP label. These results clearly indicate a close physical interaction between P2X4 and P2X7 subunits.

Next, we tested whether the significant FE values between GFP- and RFP-labeled subunits were due to non-specific FRET, i.e., interaction of homotrimeric P2X4 and P2X7 receptors. In this case, the FE should increase with higher levels of protein expression. However, the FE did not correlate with the strength of the fluorescence signal (Supplementary Figure 1).

Fluorophore-labeled P2X constructs formed functional ion channels (shown in **Figure 4**). Although the current amplitudes varied considerably depending on the presence and location of the fluorescent label (**Figures 4A,B**), the characteristics of P2X4-dependent (inactivating) and P2X7-dependent (slowly increasing) currents were retained (**Figures 4A,C**).

The Physical P2X4/P2X7 Interaction Is Not Associated with a Novel Functional Phenotype

Kinetics of Coexpressed hP2X4 and hP2X7 Receptor Subunits

We first tested whether coexpression changes the kinetics of hP2X4- and hP2X7-dependention channel currents. We therefore compared the mean ATP-induced currents in oocytes expressing hP2X4 and/or hP2X7 (**Figure 5A**). hP2X4-dependent currents displayed the typical inactivating behavior, leading to a peak current at about 1 s after ATP application. In contrast, currents in hP2X7-expressing oocytes showed the typical slowly activating non-saturating behavior during the 12 s of ATP application (Klapperstück et al., 2001; Stolz et al., 2015). In hP2X4/hP2X7-coexpressing oocytes, a peak ATP-induced

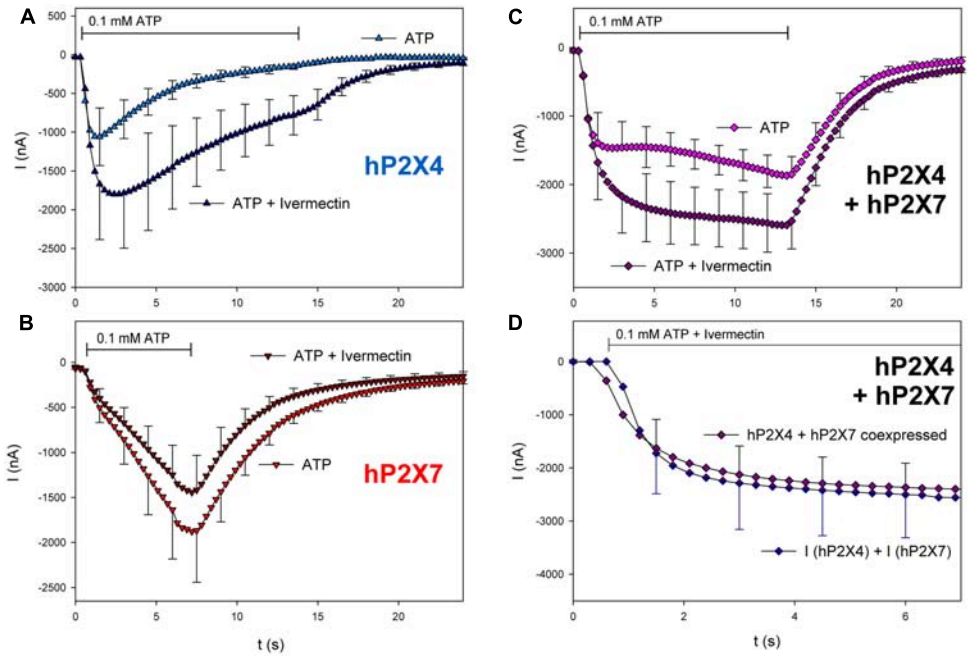

FIGURE 7 | Effect of ivermectin on ATP-induced currents of hP2X4/hP2X7-coexpressing oocytes. **(A–C)** Two-electrode voltage clamp measurements showing the effect of ivermectin (3 μM) on ATP-induced currents of oocytes expressing **(A)** hP2X4, **(B)** hP2X7, or **(C)** hP2X4 + hP2X7. Oocytes were incubated for 1 min with 3 μM ivermectin, and then with 3 μM ivermectin + 0.1 mM ATP. **(D)** Current amplitudes measured in P2X4/P2X7-coexpressing oocytes during ivermectin application were compared with the sum of the P2X4- and P2X7-dependent current amplitudes (as shown in parts **A**,**B**, respectively). Mean current amplitudes were not significantly different at any time point, indicating the lack of a distinct P2X4/P2X7 phenotype related to ivermectin. This may be explained by ivermectin affecting only homomeric P2X4 receptors. Data are the means ± SD from 4–6 oocytes.

current was barely detectable, and the slope of the slowly activating current was reduced compared with hP2X7-dependent currents. In **Figure 5B**, the current measured in hP2X4 and hP2X7 coexpressing oocytes is compared with the sum of the currents measured in oocytes expressing each protein alone. The Current amplitudes were not significantly different throughout the entire time course of ATP application and withdrawal. The simplest explanation for this observation is that hP2X4 and hP2X7 do not functionally interact in oocytes, and that the measured ATP-dependent current is simply the sum of the separate hP2X4- and hP2X7-dependent components.

ATP Dependence of Coexpressed hP2X4 and hP2X7 Receptor Subunits

We next investigated the ATP concentration dependency of the current in oocytes coexpressing hP2X4 and hP2X7 subunits (**Figure 6A**). As P2X4-dependent currents show long-lasting desensitization following ATP application, we normalized all maximal current amplitudes to the maximal current amplitude measured during a foregoing application of 0.1 mM ATP. The concentration–response curve for oocytes coexpressing hP2X4 and hP2X7 was located between the curves for those expressing hP2X4 or hP2X7 alone, indicating that hP2X4 is dominant at low ATP concentrations and hP2X7 is dominant at high ATP concentrations. At low ATP concentrations, the relative currents measured in oocytes coexpressing hP2X4 and hP2X7 were smaller than those in oocytes expressing hP2X4 only. This results from normalization to the current amplitudes evoked by 0.1 mM ATP. This ATP concentration evokes both hP2X4- and hP2X7-dependent currents, leading to a smaller relative current at ATP concentrations of 1–10 μM, although these are predominantly mediated by hP2X4. Similarly, at high ATP concentrations, the relative currents measured in hP2X4/hP2X7-coexpressing oocytes were smaller than those measured in oocytes expressing hP2X7 only. This also results from normalization to the first application of 0.1 mM ATP, where the hP2X4 component contributes. The hP2X4 component largely undergoes desensitization at the second ATP application, as shown in **Figures 6B–D**, where the mean currents measured in hP2X4/hP2X7-coexpressing oocytes at different ATP concentrations are displayed. At high ATP concentrations (**Figure 6B**), a slowly activating current, driven by the dominant hP2X7 component, was measured. In contrast, at very low ATP concentrations (**Figure 6D**), the inactivating current became apparent. At the intermediate ATP concentration of 1 μM (**Figure 6C**), hP2X4-and hP2X7-dependent currents were almost completely balanced, leading to almost constant current amplitudes over the 2–12 s time course of the ATP application.

Effect of P2X4 Modulators on Coexpressed hP2X4 and hP2X7 Receptor Subunits

We next investigated the pharmacologic phenotype of coexpressed hP2X4 and hP2X7 using subunit-specific

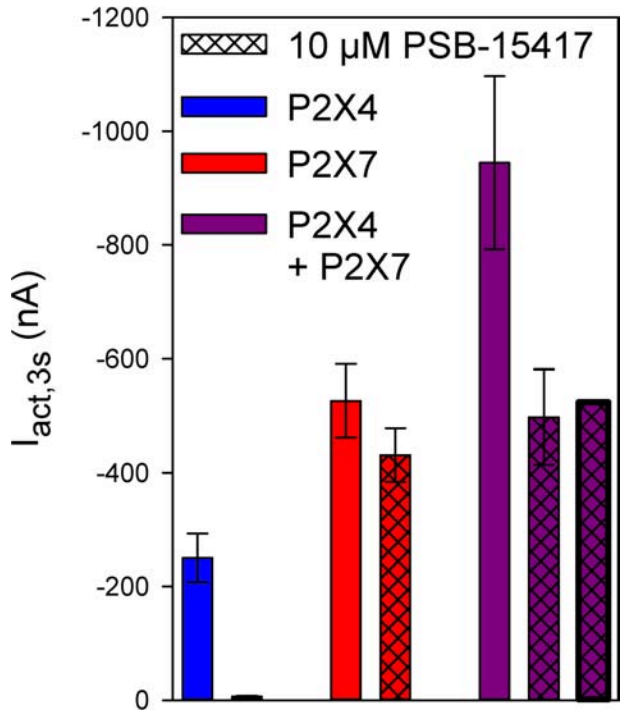

FIGURE 8 | Effect of PSB-14517 on ATP-induced currents of hP2X4/hP2X7-coexpressing oocytes. Two-electrode voltage clamp measurements showing ATP-induced current amplitudes ($I_{act,3s}$) at 3 s after the application of 0.1 mM ATP. The theoretical current remaining after PSB-14517 application to hP2X4/hP2X7-expressing oocytes (rightmost column) was calculated as described in Section "Results." The theoretical current amplitude was not significantly different from the measured value (next to rightmost column), indicating the lack of a distinct P2X4/P2X7 phenotype related to PSB-14517, which may be explained by PSB-14517 affecting only homomeric P2X4 receptors. Data are means ± SD from 4–11 oocytes.

activators and inhibitors. First, we investigated the effects of ivermectin, which potentiates P2X4-dependent ATP-induced ion currents (Priel and Silberberg, 2004). As shown in **Figure 7**, coapplication of ivermectin and ATP increased hP2X4-dependent currents (**Figure 7A**) but not hP2X7-dependent currents (**Figure 7B**). Currents in hP2X4/hP2X7-coexpressing oocytes were also stimulated by ivermectin (**Figure 7C**). However, the increased current amplitude was not significantly different from the sum of hP2X4- and hP2X7-dependent currents, as measured in oocytes expressing each P2X subtype.

Next, we measured the effect of adding PSB-15417, a P2X4 receptor-selective inhibitor. The addition of 10 µM PSB-15417 completely blocked hP2X4-mediated currents (**Figure 8**, column 1 vs. column 2), whereas hP2X7-dependent currents were reduced by only 18% (**Figure 8**, column 3 vs. column 4). To calculate the extent of PSB-15417 inhibition of hP2X4/hP2X7-coexpressed subunits, we assumed that in oocytes coexpressing hP2X4 and hP2X7 (**Figure 8**, column 5) 32% of the ATP-induced current resulted from P2X4 and 68% from P2X7, based on the amplitudes measured in oocytes expressing hP2X4 (**Figure 8**, column 1) or hP2X7 (**Figure 8**, column 3) alone and the fact that hP2X7-dependent currents do not undergo desensitization (**Figure 5**). By assuming that PSB-15417 has the same effect on hP2X4- and hP2X7-mediated currents in hP2X4/hP2X7-coexpressing oocytes as in oocytes expressing hP2X4 or hP2X7 alone (i.e., reduction by 100 or 18%, respectively), a theoretical value for the current remaining after applying PSB-15417 to hP2X4/hP2X7-coexpressing oocytes was calculated (**Figure 8**, column 7). This value was not significantly different from the measured value (**Figure 8**, column 6).

Effect of P2X7 Agonist and Antagonists on Coexpressed hP2X4 and hP2X7 Subunits

Oocytes expressing hP2X4, hP2X7, and hP2X4/hP2X7 were treated with the P2X7 agonist BzATP (**Figure 9**). As we expected from previous reports (von Kügelgen, 2008), 0.1 mM BzATP was less effective against hP2X4 compared with 0.1 mM ATP (**Figure 9A**). However, it was much more effective against hP2X7 than against hP2X4 (**Figure 9B**). The amplitude of the BzATP-stimulated current in hP2X4/hP2X7-coexpressing oocytes (**Figure 9C**) was equal to the sum of the current amplitudes measured in oocytes expressing either hP2X4 or hP2X7 alone (**Figure 9D**).

Next, we tested the effects of three different P2X7 antagonists/blockers on the currents in hP2X4/hP2X7-coexpressing oocytes. P2X7-dependent ion currents (North, 2002; Seyffert et al., 2004; Li et al., 2013) and Ca^{2+} signals (Pippel et al., 2015) are blocked by Mg^{2+} ions. Consistent with these findings, we found that Mg^{2+} coapplication reduces ATP-induced currents in hP2X7-expressing oocytes (**Figure 10B**) but not in those expressing hP2X4 (**Figure 10A**). The inhibitory effect of Mg^{2+} on hP2X4/hP2X7-coexpressing oocytes (**Figure 10C**) was equal to the sum of the separate effects of Mg^{2+} on hP2X4 and on hP2X7 (**Figure 10D**). The P2X7 antagonist oxidized ATP (oATP) (North, 2002; von Kügelgen, 2008) had qualitatively similar effects (**Figure 11**).

We investigated the effects of the P2X7-specific blocker A438079 (Nelson et al., 2006) using a protocol similar to the one used for PSB-15417 (**Figure 12**). As before, we normalized the amplitudes of the ATP-induced currents to those measured during a previous application of 0.1 mM ATP. Owing to hP2X4 desensitization, the amplitude of the second ATP-induced current was reduced by 70% on average (**Figure 12**, column 1 vs. column 2). Application of A438079 did not change this desensitization rate (**Figure 12**, column 3 vs. column 4), indicating a lack of effect on hP2X4. In contrast, P2X7-dependent currents did not display desensitization (**Figure 12**, column 5 vs. column 6). Considering 70% desensitization of hP2X4, the percentage of functional P2X4 in oocytes coexpressing P2X4 and P2X7 was calculated to be 20% (**Figure 12**, column 9 vs. column 10). By taking this into account, as well as the mean blocking effect of A438079 of 81% (**Figure 12**, column 7 vs.

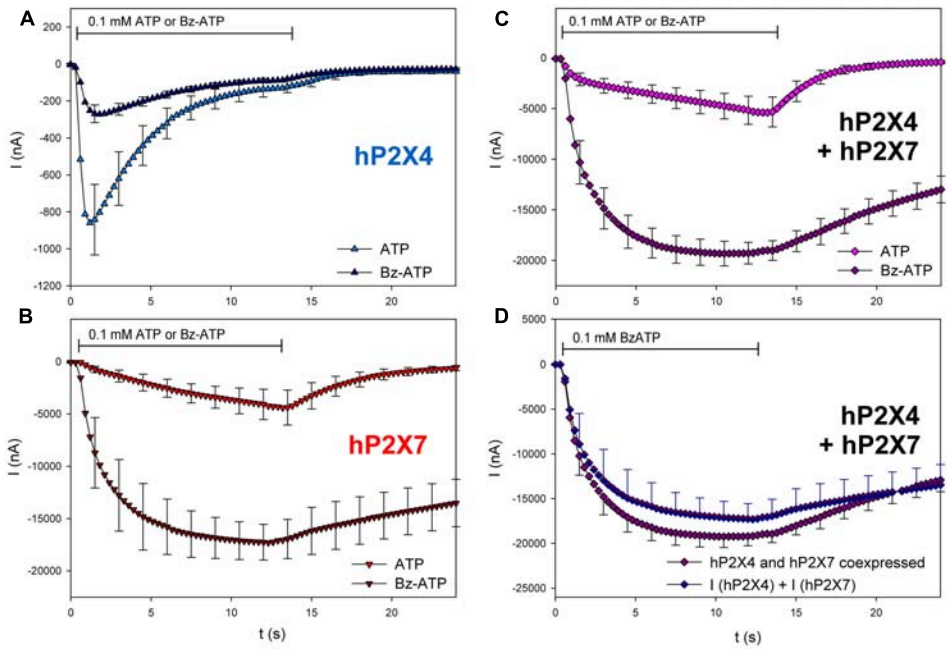

FIGURE 9 | Effect of BzATP on ATP-induced currents of hP2X4/hP2X7-coexpressing oocytes. **(A–C)** Two-electrode voltage clamp measurements showing the effect of BzATP on ATP-induced currents of oocytes expressing **(A)** hP2X4, **(B)** hP2X7, or **(C)** hP2X4 + hP2X7. **(D)** BzATP-induced currents measured in P2X4/P2X7-coexpressing oocytes were compared with the sum of P2X4- and P2X7-dependent current amplitudes (shown in parts **A**,**B**, respectively). Mean current amplitudes were not significantly different at any time point, indicating the lack of a distinct P2X4/P2X7 phenotype related to BzATP stimulation. means ± SD from 5–6 oocytes.

column 8), we calculated the ATP-induced current amplitude in hP2X4/hP2X7-coexpressing oocytes that was not blocked by A438079 (**Figure 12**, column 13). The calculated value for the amplitude was not significantly different from the measured value (**Figure 12**, column 12).

DISCUSSION

FRET as a Tool to Investigate Physical Interaction of P2X4 and P2X7 Receptor Subunits

Our FRET measurements indicate a close association between P2X4 and P2X7 receptor subunits. Furthermore, FRET values were similar to those of positive controls (coexpressed homomeric GFP- and RFP-labeled P2X4 or P2X7 constructs) when the fluorophore was incorporated within the extracellular loop. Similar FE values were obtained for homomers and heteromers, indicating an abundance of P2X4/P2X7 heteromers. We were unable to study several P2X4 and P2X7 constructs in which the label was incorporated within the extracellular domain because of their weak expression. For extracellularly labeled constructs with reasonable expression levels, FEs were much larger compared with the FEs of C-terminally fluorescence-labeled constructs. The differences in FRET efficiency are consistent with a model in which the fluorophore moiety has approximately the same relative distance from the (outer) membrane surface in both ectodomain-labeled P2X4 and P2X7 proteins. In C-terminally labeled constructs, the location of the fluorophore moiety relative to the (inner) membrane surface is strongly influenced by the length of the C-terminal tail, which is much shorter in the hP2X4 subunit (29 residues) than in the hP2X7 subunit (∼300 residues; see Supplementary Figures 2–27). Therefore, FE was very low or absent when C-terminally fluorescence-labeled P2X4 and P2X7 constructs were coexpressed. In contrast, coexpression of C-terminally labeled P2X4 and truncated $P2X7^{1-408}$ resulted in significant FE values. This indicates that the C-terminus is located far from the "trunk" of the P2X7 subunit (residues 1–408). Importantly, all of the sequence elements responsible for P2X subunit assembly are located within the ectodomain; therefore, C-terminal truncation does not affect trimerization (Duckwitz et al., 2006). We also previously reported that truncated $hP2X7^{1-408}$ subunits can assemble into functional trimers (Becker et al., 2008).

These findings contradict a previous FRET study of cyan fluorescent protein (CFP)-and yellow fluorescent protein (YFP)-labeled P2X proteins expressed in human embryonic kidney cells, which reported a larger FE for homomeric P2X7 than for homomeric P2X4 (Young et al., 2008). The authors concluded that longer rather than shorter P2X C-termini are more likely to interact. In another study using the same expression system, the P2X4/P2X7 interaction was investigated by measuring sensitized emissions of the acceptor YFP by Spectra-FRET (Perez-Flores et al., 2015). The authors reported that a significant FE for coexpressed P2X4/P2X7 was only obtained after activating the

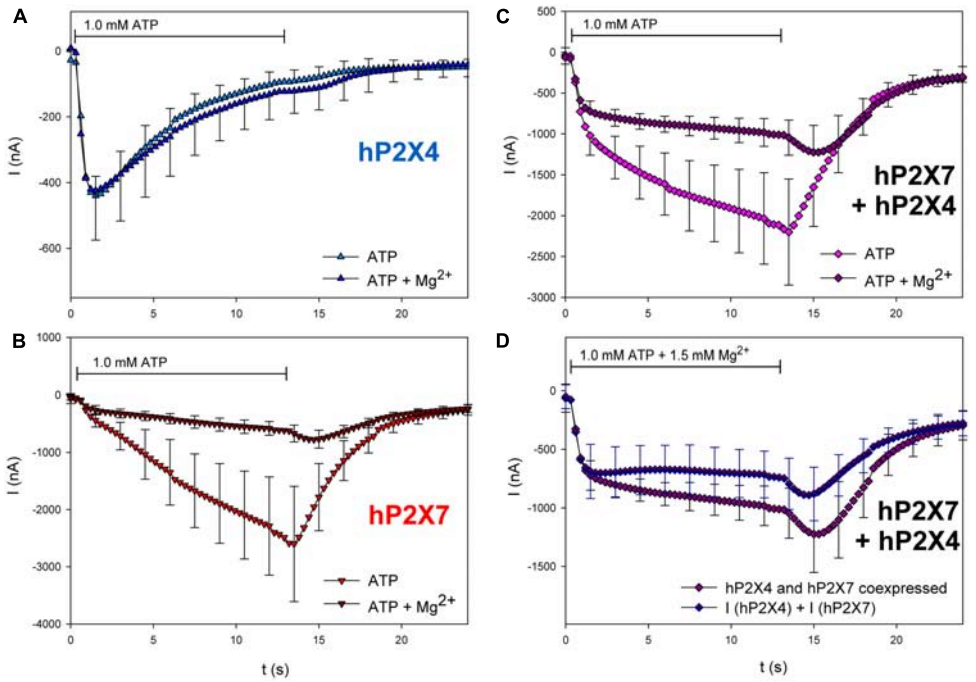

FIGURE 10 | Effect of Mg^{2+} on ATP-induced currents of hP2X4/hP2X7-coexpressing oocytes. **(A–C)** Two-electrode voltage clamp measurements showing the effect of Mg^{2+} on ATP-induced currents of oocytes expressing **(A)** hP2X4, **(B)** hP2X7, or **(C)** hP2X4 + hP2X7. **(D)** Currents induced by the coapplication of ATP and 1.5 mM Mg^{2+} measured in P2X4/P2X7-coexpressing oocytes were compared with the sum of P2X4- and P2X7-dependent current amplitudes (shown in parts **A**,**B**, respectively). Mean current amplitudes were not significantly different at any time point, indicating the lack of a distinct P2X4/P2X7 phenotype related to Mg^{2+} inhibition. Data are means ± SD from 4–6 oocytes.

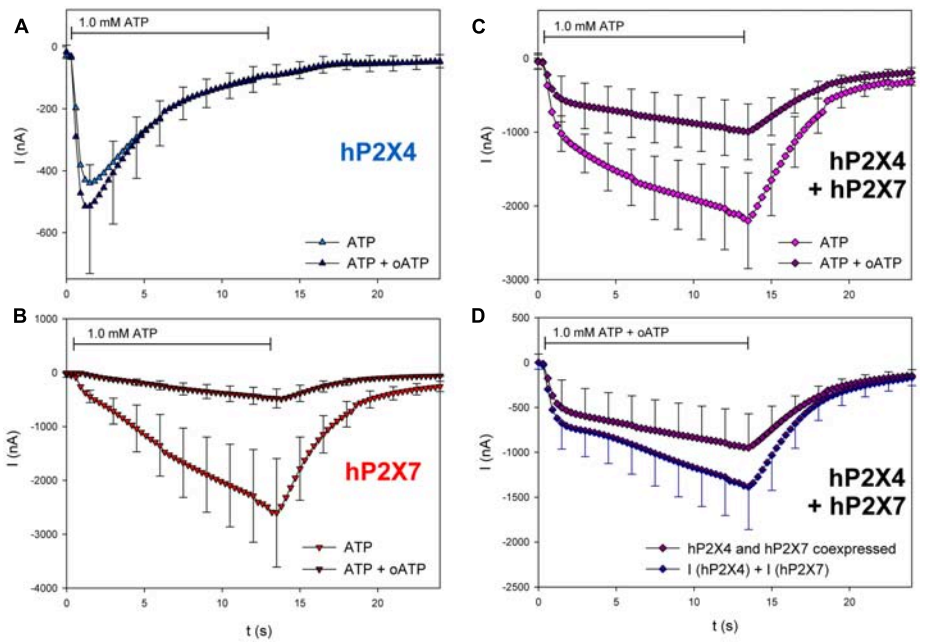

FIGURE 11 | Effect of oATP on ATP-induced currents of hP2X4/hP2X7-coexpressing oocytes. **(A–C)** Two-electrode voltage clamp measurements showing the effect of 3 h preincubation in 0.3 mM oATP on ATP-induced currents of oocytes expressing **(A)** hP2X4, **(B)** hP2X7, or **(C)** hP2X4 + hP2X7. **(D)** Currents induced by ATP after oATP preincubation in P2X4/P2X7-coexpressing oocytes were compared with the sum of P2X4- and P2X7-dependent current amplitudes (shown in parts **A**,**B**, respectively). Mean current amplitudes were not significantly different at any time point, indicating the lack of a distinct P2X4/P2X7 phenotype related to oATP antagonism. Data are the means ± SD from 4–5 oocytes.

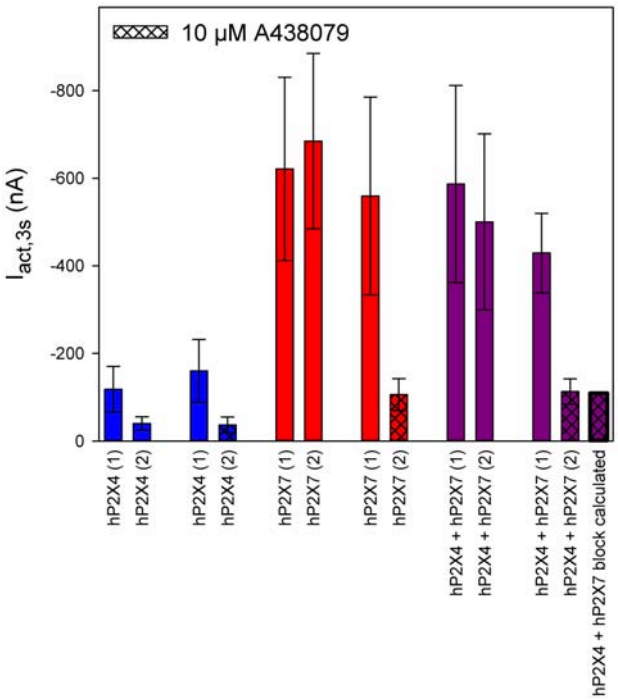

FIGURE 12 | Effect of the P2X7 antagonist A438079 on ATP-induced currents of hP2X4/hP2X7-coexpressing oocytes. Two-electrode voltage clamp measurements of ATP-induced current amplitudes ($I_{act,3s}$) at 3 s after the application of 0.1 mM ATP. Current amplitudes of the first and second ATP application are denoted (1) and (2), respectively. The theoretical current remaining after applying A438079 to P2X4/P2X7-expressing oocytes (rightmost column) was calculated as described in Section "Results." The theoretical current amplitude was not significantly different from the measured value (next to rightmost column), indicating the lack of a P2X4/P2X7 phenotype related to A438079, which may be explained by A438079 affecting only homomeric P2X7 receptors. Data are means ± SD from 4–11 oocytes.

P2X7 receptor with BzATP or high ATP concentrations. No measurable FE was obtained for truncated $P2X7^{1-418}$ constructs,. The reason for the discrepancies between these results and ours is unclear, but might be caused by differences in the choice of the expression system and the P2X constructs.

It is possible that P2X4 and P2X7 subunits interact not only as heteromers but also as homomers. Indications of close contact of P2X4 and P2X7 homomers have been reported (Boumechache et al., 2009; Weinhold et al., 2010). In contrast, atomic force microscopy measurements only rarely found dimers of distinct homotrimeric P2X4 and P2X7 receptors (Antonio et al., 2011). Although we cannot completely rule out the possibility of self-association for homotrimeric P2X4 and P2X7 receptors, in our FRET experiments, we consider it unlikely for the following reason. The probability of non-specific FRET signals is enhanced with increasing levels of subunit expression and diminished at low expression levels. However, we did not observe such a correlation (Supplementary Figure 1). It was calculated that non-specific bystander effects occur at a fluorescence molecule density of ≥2000 molecules/μm^2 (Clayton and Chattopadhyay, 2014). Given a surface area A of *Xenopus* oocytes of about 2×10^7 μm^2 (Lin-Moshier and Marchant, 2013), a single channel current amplitude i at −40 mV of ∼0.4 pA, an open probability P_o (1 mM ATP) of about 0.2 (Riedel et al., 2007), and a maximal P2X7-mediated whole-cell current I of 2000 nA (**Figure 4**), the molecule density $D = I/(iPoA) = 1.25$ molecules/μm^2 for fluorescence-labeled P2X7 receptors, or 3.75 P2X7 subunits/μm^2, far higher than the critical expression density for bystander FRET. Furthermore, the lack of FRET signals for our negative controls argue against non-specific FRET. The same line of argument holds against a possible non-specific interaction between GFP- and RFP-labeled constructs.

Do Coexpressed P2X4 and P2X7 Receptor Subunits Have a Distinct Electrophysiological Phenotype?

Our evidence for a physical interaction between P2X4 and P2X7 subunits within heteromers led us to investigate the functional consequences of this interaction by measuring hP2X4- and hP2X7-dependent ion currents in *Xenopus* oocytes. For this, we studied the current time course, the ATP concentration dependency of current amplitudes, and the effect of P2X4- or P2X7-specific drugs in P2X4/P2X7-coexpressing oocytes. For each parameter, the result could be explained by an additive effect of the individual hP2X4 and hP2X7 current components. Likewise, the simplest explanation for the time course of ATP-activated currents in hP2X4/hP2X7-coexpressing oocytes is that only homomeric hP2X4 and hP2X7 receptors are formed, with independent functions. Furthermore, the simplest explanation for the ATP concentration-dependence of currents in oocytes coexpressing hP2X4 and hP2X7 is that at low ATP concentrations (<10 µM) only hP2X4 receptors (with high ATP sensitivity) are activated, whereas at higher ATP concentrations additional hP2X7 receptor channels (with low ATP sensitivity) are opened. This explanation does not require the formation of P2X4/P2X7 heteromers with a distinct ATP concentration dependency. Similarly, the effects of P2X4- or P2X7-specific pharmacological agents in oocytes coexpressing hP2X4 and hP2X7 can be explained by their actions on homomers of the targeted subtype only.

The lack of a functional interaction is consistent with the functionally independent P2X4 and P2X7 phenotypes reported in rat cortical microglia (Visentin et al., 1999). In contrast, functional P2X4/P2X7 interactions have been reported in airway ciliated cells (Ma et al., 2006), macrophages (Babelova et al., 2009; Kawano et al., 2012a,b), dendritic cells (Sakaki et al., 2013), and gingival epithelial cells (Hung et al., 2013).

In the present study, it is difficult to reconcile evidence for a physical interaction in the form of heteromers, as demonstrated by the FRET measurements, with the lack of a new functional phenotype, as indicated by the electrophysiological recordings. A possible explanation is that heteromers exist, but the phenotype is either P2X4-like or P2X7-like. This might depend on the presence of a single P2X4 or P2X7 subunit driving the dominant phenotype or on which subunit is incorporated twice into the

trimer. Further study into the molecular mechanism of P2X receptor function is therefore necessary.

AUTHOR CONTRIBUTIONS

MS, KP, and AP performed experiments and evaluated data. MK designed study, performed experiments, evaluated data and critically read the manuscript. CM provided drugs and critically read the manuscript. UB made the P2X constructs. GS designed the study, evaluated data and wrote the manuscript. FM designed the study, performed experiments, evaluated data and wrote the manuscript.

FUNDING

We thank the Deutsche Forschungsgemeinschaft (Ma1581/15–3; Schm536/9–3) for financial support. Open access publishing was supported by the Publikationsfonds of the Martin-Luther University Halle.

ACKNOWLEDGMENTS

We thank Dr. Cora Büttner for cloning the P2X7 receptor subunit from rat brain RNA during her Ph.D. studies (1997–2001) at the Department of Pharmacology, Biocenter, Johann Wolfgang Goethe–University of Frankfurt.

SUPPLEMENTARY MATERIAL

The Supplementary Material for this article can be found online at: https://www.frontiersin.org/articles/10.3389/fphar.2017.00860/full#supplementary-material

REFERENCES

Antonio, L. S., Stewart, A. P., Xu, X. J., Varanda, W. A., Murrell-Lagnado, R. D., and Edwardson, J. M. (2011). P2X4 receptors interact with both P2X2 and P2X7 receptors in the form of homotrimers. *Br. J. Pharmacol.* 163, 1069–1077. doi: 10.1111/j.1476-5381.2011.01303.x

Aschrafi, A., Sadtler, S., Niculescu, C., Rettinger, J., and Schmalzing, G. (2004). Trimeric architecture of homomeric P2X2 and heteromeric P2X1+2 receptor subtypes. *J. Mol. Biol.* 342, 333–343. doi: 10.1016/j.jmb.2004.06.092

Babelova, A., Moreth, K., Tsalastra-Greul, W., Zeng-Brouwers, J., Eickelberg, O., Young, M. F., et al. (2009). Biglycan: a danger signal that activates the NLRP3 inflammasome via toll-like and P2X receptors. *J. Biol. Chem.* 284, 24035–24048. doi: 10.1074/jbc.M109.014266

Baconguis, I., Hattori, M., and Gouaux, E. (2013). Unanticipated parallels in architecture and mechanism between ATP-gated P2X receptors and acid sensing ion channels. *Curr. Opin. Struct. Biol.* 23, 277–284. doi: 10.1016/j.sbi.2013.04.005

Becker, D., Woltersdorf, R., Boldt, W., Schmitz, S., Braam, U., Schmalzing, G., et al. (2008). The P2X7 carboxyl tail is a regulatory module of P2X7 receptor channel activity. *J. Biol. Chem.* 283, 25725–25734. doi: 10.1074/jbc.M803855200

Boumechache, M., Masin, M., Edwardson, J. M., Gorecki, D. C., and Murrell-Lagnado, R. (2009). Analysis of assembly and trafficking of native P2X4 and P2X7 receptor complexes in rodent immune cells. *J. Biol. Chem.* 284, 13446–13454. doi: 10.1074/jbc.M901255200

Braman, J., Papworth, C., and Greener, A. (1996). Site-directed mutagenesis using double-stranded plasmid DNA templates. *Methods Mol. Biol.* 57, 31–44. doi: 10.1385/0-89603-332-5:31

Burnstock, G., and Knight, G. E. (2004). Cellular distribution and functions of P2 receptor subtypes in different systems. *Int. Rev. Cytol.* 240, 31–304. doi: 10.1016/S0074-7696(04)40002-3

Büttner, C., Sadtler, S., Leyendecker, A., Laube, B., Griffon, N., Betz, H., et al. (2001). Ubiquitination precedes internalization and proteolytic cleavage of plasma membrane-bound glycine receptors. *J. Biol. Chem.* 276, 42978–42985. doi: 10.1074/jbc.M102121200

Clayton, A. H., and Chattopadhyay, A. (2014). Taking care of bystander FRET in a crowded cell membrane environment. *Biophys. J.* 106, 1227–1228. doi: 10.1016/j.bpj.2014.02.004

Craigie, E., Birch, R. E., Unwin, R. J., and Wildman, S. S. (2013). The relationship between P2X4 and P2X7: a physiologically important interaction? *Front. Physiol.* 4:216. doi: 10.3389/fphys.2013.00216

Di Virgilio, F. (2007). Liaisons dangereuses: P2X7 and the inflammasome. *Trends Pharmacol. Sci.* 28, 465–472. doi: 10.1016/j.tips.2007.07.002

Dopychai, A., Pokam, C. F., and Schmalzing, G. (2015). Aromatic residues in the transmembrane helices play an essential role in the homopentameric assembly of the Glucl α. *Biophys. J.* 108:431a. doi: 10.1016/j.bpj.2014.11.2356

Duckwitz, W., Hausmann, R., Aschrafi, A., and Schmalzing, G. (2006). P2X5 subunit assembly requires scaffolding by the second transmembrane domain and a conserved aspartate. *J. Biol. Chem.* 281, 39561–39572. doi: 10.1074/jbc.M606113200

Flittiger, B., Klapperstück, M., Schmalzing, G., and Markwardt, F. (2010). Effects of protons on macroscopic and single-channel currents mediated by the human P2X7 receptor. *Biochim. Biophys. Acta Biomembr.* 1798, 947–957. doi: 10.1016/j.bbamem.2010.01.023

Gloor, S., Pongs, O., and Schmalzing, G. (1995). A vector for the synthesis of cRNAs encoding Myc epitope-tagged proteins in *Xenopus laevis* oocytes. *Gene* 160, 213–217. doi: 10.1016/0378-1119(95)00226-V

Grudzien-Nogalska, E., Stepinski, J., Jemielity, J., Zuberek, J., Stolarski, R., Rhoads, R. E., et al. (2007). Synthesis of anti-reverse cap analogs (ARCAs) and their applications in mRNA translation and stability. *Methods Enzymol.* 431, 203–227. doi: 10.1016/S0076-6879(07)31011-2

Guo, C., Masin, M., Qureshi, O. S., and Murrell-Lagnado, R. D. (2007). Evidence for functional P2X4/P2X7 heteromeric receptors. *Mol. Pharmacol.* 72, 1447–1456. doi: 10.1124/mol.107.035980

Habermacher, C., Dunning, K., Chataigneau, T., and Grutter, T. (2015). Molecular structure and function of P2X receptors. *Neuropharmacology* 104, 18–30. doi: 10.1016/j.neuropharm.2015.07.032

Hausmann, R., Rettinger, J., Gerevich, Z., Meis, S., Kassack, M. U., Illes, P., et al. (2006). The suramin analog 4,4′,4″,4‴-(carbonylbis(imino-5,1,3-benzenetriylbis (carbonylimino)))tetra-kis-benzenesulfonic acid (NF110) potently blocks P2X3 receptors: subtype selectivity is determined by location of sulfonic acid groups. *Mol. Pharmacol.* 69, 2058–2067. doi: 10.1124/mol.106.022665

Hibbs, R. E., and Gouaux, E. (2011). Principles of activation and permeation in an anion-selective Cys-loop receptor. *Nature* 474, 54–60. doi: 10.1038/nature10139

Hung, S. C., Choi, C. H., Said-Sadier, N., Johnson, L., Atanasova, K. R., Sellami, H., et al. (2013). P2X4 assembles with P2X7 and pannexin-1 in gingival epithelial cells and modulates ATP-induced reactive oxygen species production and inflammasome activation. *PLOS ONE* 8:e70210. doi: 10.1371/journal.pone.0070210

Kawano, A., Tsukimoto, M., Mori, D., Noguchi, T., Harada, H., Takenouchi, T., et al. (2012a). Regulation of P2X7-dependent inflammatory functions by P2X4 receptor in mouse macrophages. *Biochem. Biophys. Res. Commun.* 420, 102–107. doi: 10.1016/j.bbrc.2012.02.122

Kawano, A., Tsukimoto, M., Noguchi, T., Hotta, N., Harada, H., Takenouchi, T., et al. (2012b). Involvement of P2X4 receptor in P2X7 receptor-dependent cell

death of mouse macrophages. *Biochem. Biophys. Res. Commun.* 419, 374–380. doi: 10.1016/j.bbrc.2012.01.156

Kawate, T., Michel, J. C., Birdsong, W. T., and Gouaux, E. (2009). Crystal structure of the ATP-gated P2X4 ion channel in the closed state. *Nature* 460, 592–598. doi: 10.1038/nature08198

Klapperstück, M., Büttner, C., Böhm, T., Schmalzing, G., and Markwardt, F. (2000). Characteristics of P2X7 receptors from human B lymphocytes expressed in *Xenopus oocytes*. *Biochim. Biophys. Acta* 1467, 444–456. doi: 10.1016/S0005-2736(00)00245-5

Klapperstück, M., Büttner, C., Schmalzing, G., and Markwardt, F. (2001). Functional evidence of distinct ATP activation sites at the human P2X7 receptor. *J. Physiol. (Lond.)* 534, 25–35. doi: 10.1111/j.1469-7793.2001.00025.x

Kovalic, D., Kwak, J. H., and Weisblum, B. (1991). General method for direct cloning of DNA fragments generated by the polymerase chain reaction. *Nucleic Acids Res.* 19:4560. doi: 10.1093/nar/19.16.4560

Kubick, C., Schmalzing, G., and Markwardt, F. (2011). The effect of anions on the human P2X7 receptor. *Biochim. Biophys. Acta Biomembr.* 1808, 2913–2922. doi: 10.1016/j.bbamem.2011.08.017

Lewis, C., Neidhart, S., Holy, C., North, R. A., Buell, G., and Surprenant, A. (1995). Coexpression of P2X2 and P2X3 receptor subunits can account for ATP-gated currents in sensory neurons. *Nature* 377, 432–435. doi: 10.1038/377432a0

Li, M., Silberberg, S. D., and Swartz, K. J. (2013). Subtype-specific control of P2X receptor channel signaling by ATP and Mg2+. *Proc. Natl. Acad. Sci. U.S.A.* 110, E3455–E3463. doi: 10.1073/pnas.1308088110

Lin-Moshier, Y., and Marchant, J. S. (2013). The *Xenopus* oocyte: a single-cell model for studying Ca2+ signaling. *Cold Spring Harb. Protoc.* 2013:pdb.top066308. doi: 10.1101/pdb.top066308

Ma, L., Yang, F., and Zheng, J. (2014). Application of fluorescence resonance energy transfer in protein studies. *J. Mol. Struct.* 1077, 87–100. doi: 10.1016/j.molstruc.2013.12.071

Ma, W. Y., Korngreen, A., Weil, S., Cohen, E. B. T., Priel, A., Kuzin, L., et al. (2006). Pore properties and pharmacological features of the P2X receptor channel in airway ciliated cells. *J. Physiol.* 571, 503–517. doi: 10.1113/jphysiol.2005.103408

Nashmi, R., Dickinson, M. E., McKinney, S., Jareb, M., Labarca, C., Fraser, S. E., et al. (2003). Assembly of α4β2 nicotinic acetylcholine receptors assessed with functional fluorescently labeled subunits: effects of localization, trafficking, and nicotine-induced upregulation in clonal mammalian cells and in cultured midbrain neurons. *J. Neurosci.* 23, 11554–11567.

Nelson, D. W., Gregg, R. J., Kort, M. E., Perez-Medrano, A., Voight, E. A., Wang, Y., et al. (2006). Structure-activity relationship studies on a series of novel, substituted 1-benzyl-5-phenyltetrazole P2X7 antagonists. *J. Med. Chem.* 49, 3659–3666. doi: 10.1021/jm051202e

Nicke, A. (2008). Homotrimeric complexes are the dominant assembly state of native P2X7 subunits. *Biochem. Biophys. Res. Commun.* 377, 803–808. doi: 10.1016/j.bbrc.2008.10.042

Nicke, A., Bäumert, H. G., Rettinger, J., Eichele, A., Lambrecht, G., Mutschler, E., et al. (1998). P2X1 and P2X3 receptors form stable trimers: a novel structural motif of ligand-gated ion channels. *EMBO J.* 17, 3016–3028. doi: 10.1093/emboj/17.11.3016

North, R. A. (2002). Molecular physiology of P2X receptors. *Physiol. Rev.* 82, 1013–1067. doi: 10.1152/physrev.00015.2002

Perez, K., Yeam, I., Jahn, M. M., and Kang, B. C. (2006). Megaprimer-mediated domain swapping for construction of chimeric viruses. *J. Virol. Methods* 135, 254–262. doi: 10.1016/j.jviromet.2006.03.020

Perez-Flores, G., Levesque, S. A., Pacheco, J., Vaca, L., Lacroix, S., Perez-Cornejo, P., et al. (2015). The P2X7/P2X4 interaction shapes the purinergic response in murine macrophages. *Biochem. Biophys. Res. Commun.* 467, 484–490. doi: 10.1016/j.bbrc.2015.10.025

Petersen, T. N., Brunak, S., von, H. G., and Nielsen, H. (2011). SignalP 4.0: discriminating signal peptides from transmembrane regions. *Nat. Methods* 8, 785–786. doi: 10.1038/nmeth.1701

Pippel, A., Beßler, B., Klapperstück, M., and Markwardt, F. (2015). Inhibition of antigen receptor-dependent Ca2+ signals and NF-AT activation by P2X7 receptors in human B lymphocytes. *Cell Calcium* 57, 275–289. doi: 10.1016/j.ceca.2015.01.010

Pippel, A., Stolz, M., Woltersdorf, R., Kless, A., Schmalzing, G., and Markwardt, F. (2017). Localization of the gate and selectivity filter of the full-length P2X7 receptor. *Proc. Natl. Acad. Sci. U.S.A.* 114, E2156–E2165. doi: 10.1073/pnas.1610414114

Praetorius, H. A., and Leipziger, J. (2009). ATP release from non-excitable cells. *Purinergic Signal.* 5, 433–446. doi: 10.1007/s11302-009-9146-2

Priel, A., and Silberberg, S. D. (2004). Mechanism of ivermectin facilitation of human P2X4 receptor channels. *J. Gen. Physiol.* 123, 281–293. doi: 10.1085/jgp.200308986

Rettinger, J., Schmalzing, G., Damer, S., Müller, G., Nickel, P., and Lambrecht, G. (2000). The suramin analogue NF279 is a novel and potent antagonist selective for the P2X1 receptor. *Neuropharmacology* 39, 2044–2053. doi: 10.1016/S0028-3908(00)00022-8

Riedel, T., Lozinsky, I., Schmalzing, G., and Markwardt, F. (2007). Kinetics of P2X7 receptor-operated single channels currents. *Biophys. J.* 92, 2377–2391. doi: 10.1529/biophysj.106.091413

Sakaki, H., Fujiwaki, T., Tsukimoto, M., Kawano, A., Harada, H., and Kojima, S. (2013). P2X4 receptor regulates P2X7 receptor-dependent IL-1β and IL-18 release in mouse bone marrow-derived dendritic cells. *Biochem. Biophys. Res. Commun.* 432, 406–411. doi: 10.1016/j.bbrc.2013.01.135

Saul, A., Hausmann, R., Kless, A., and Nicke, A. (2013). Heteromeric assembly of P2X subunits. *Front. Cell Neurosci.* 7:250. doi: 10.3389/fncel.2013.00250

Seyffert, C., Schmalzing, G., and Markwardt, F. (2004). Dissecting individual current components of co-expressed human P2X1 and P2X7 receptors. *Curr. Top. Med. Chem.* 4, 1719–1730. doi: 10.2174/1568026043387160

Stolz, M., Klapperstück, M., Kendzierski, T., Detro-Dassen, S., Panning, A., Schmalzing, G., et al. (2015). Homodimeric anoctamin-1, but not homodimeric anoctamin-6, is activated by calcium increases mediated by the P2Y1 and P2X7 receptors. *Pflügers Arch.* 467, 2121–2140. doi: 10.1007/s00424-015-1687-3

Surprenant, A., and North, R. A. (2008). Signaling at purinergic P2X receptors. *Annu. Rev. Physiol.* 71, 333–359. doi: 10.1146/annurev.physiol.70.113006.100630

Surprenant, A., Rassendren, F., Kawashima, E., North, R. A., and Buell, G. (1996). The cytolytic P2Z receptor for extracellular ATP identified as a P2X receptor (P2X7). *Science* 272, 735–738. doi: 10.1126/science.272.5262.735

Torres, G. E., Egan, T. M., and Voigt, M. M. (1999). Hetero-oligomeric assembly of P2X receptor subunits. Specificities exist with regard to possible partners. *J. Biol. Chem.* 274, 6653–6659. doi: 10.1074/jbc.274.10.6653

Visentin, S., Renzi, M., Frank, C., Greco, A., and Levi, G. (1999). Two different ionotropic receptors are activated by ATP in rat microglia. *J. Physiol.* 519, 723–736. doi: 10.1111/j.1469-7793.1999.0723n.x

von Kügelgen, I. (2008). Pharmacology of mammalian P2X and P2Y receptors. *Biotrend Rev.* 3, 1–10.

Weinhold, K., Krause-Buchholz, U., Rodel, G., Kasper, M., and Barth, K. (2010). Interaction and interrelation of P2X7 and P2X4 receptor complexes in mouse lung epithelial cells. *Cell. Mol. Life Sci.* 67, 2631–2642. doi: 10.1007/s00018-010-0355-1

Xu, J., Chai, H., Ehinger, K., Egan, T. M., Srinivasan, R., Frick, M., et al. (2014). Imaging P2X4 receptor subcellular distribution, trafficking, and regulation using P2X4-pHluorin. *J. Gen. Physiol.* 144, 81–104. doi: 10.1085/jgp.201411169

Young, M. T., Fisher, J. A., Fountain, S. J., Ford, R. C., North, R. A., and Khakh, B. S. (2008). Molecular shape, architecture and size of P2X4 receptors determined using fluorescence resonance energy transfer and electron microscopy. *J. Biol. Chem.* 283, 26241–26251. doi: 10.1074/jbc.M804458200

Zheng, J. (2006). Spectroscopy-based quantitative fluorescence resonance energy transfer analysis. *Methods Mol. Biol.* 337, 65–77. doi: 10.1385/1-59745-095-2:65

Conflict of Interest Statement: The authors declare that the research was conducted in the absence of any commercial or financial relationships that could be construed as a potential conflict of interest.

frontiers in Pharmacology

ORIGINAL RESEARCH
published: 14 November 2017
doi: 10.3389/fphar.2017.00821

P2Y12 Receptor Antagonist, Clopidogrel, Does Not Contribute to Risk of Osteoporotic Fractures in Stroke Patients

Niklas R. Jørgensen[1,2,3], Peter Schwarz[1,4,5], Helle K. Iversen[5,6] and Peter Vestergaard[7]*

[1] Research Center for Ageing and Osteoporosis, Rigshospitalet, Copenhagen, Denmark, [2] Department of Clinical Biochemistry, Rigshospitalet, Copenhagen, Denmark, [3] Odense Patient Data Explorative Network, Odense University Hospital, Institute of Clinical Research, University of Southern Denmark, Odense, Denmark, [4] Department of Endocrinology, Rigshospitalet, Copenhagen, Denmark, [5] Faculty of Health Sciences, University of Copenhagen, Copenhagen, Denmark, [6] Stroke Unit, Department of Neurology, Rigshospitalet, Copenhagen, Denmark, [7] Departments of Clinical Medicine and Endocrinology, Aalborg University Hospital, Aalborg, Denmark

OPEN ACCESS

Edited by:
Kenneth A. Jacobson, National Institutes of Health (NIH), United States

Reviewed by:
Konstantinos Tziomalos, Aristotle University of Thessaloniki, Greece
Hector A. Cabrera-Fuentes, Justus-Liebig-Universität-Gießen, Germany
Alexander Kouzmenko, Alfaisal University, Saudi Arabia

***Correspondence:**
Niklas R. Jørgensen
niklas@dadlnet.dk

Specialty section:
This article was submitted to Experimental Pharmacology and Drug Discovery, a section of the journal Frontiers in Pharmacology

Received: *19 September 2017*
Accepted: *30 October 2017*
Published: *14 November 2017*

Citation:
Jørgensen NR, Schwarz P, Iversen HK and Vestergaard P (2017) P2Y12 Receptor Antagonist, Clopidogrel, Does Not Contribute to Risk of Osteoporotic Fractures in Stroke Patients. Front. Pharmacol. 8:821. doi: 10.3389/fphar.2017.00821

Background: Stroke is a leading cause of mortality and morbidity. It is associated with excessive bone loss and risk of fracture in stroke patients is high. The P2Y12R antagonist and platelet inhibitor, clopidogrel, is widely used for secondary prevention after a stroke. However, recent studies have shown that clopidogrel has negative effects on bone and that long-term clopidogrel use is associated with increased fracture risk. The purpose of the current study was therefore to investigate the association of clopidogrel treatment with risk of fractures in stroke and TIA patients.

Methods: The study was a cohort study including all subjects who were prescribed clopidogrel between 1996 and 2008 in Denmark (n = 77,503). Age- and gender matched controls (n = 232,510) were randomly selected from the background population. The study end-points were occurrence of stroke or TIA and occurrence of fracture. Clopidogrel use was primary exposure.

Results: Ischemic stroke increased risk of fracture by 50% while haemorrhagic stroke and TIA increased the risk by 30%. However, after adjusting for multiple confounders only patients with ischemic stroke and haemorrhagic stroke had increased fracture risk. Clopidogrel use was not associated with increased fracture risk in subjects with ischaemic stroke or TIA. In contrast, after adjusting for multiple confounders clopidogrel treatment was associated with a 10–35% reduced risk of fracture.

Conclusion: Patients with stroke have increased risk of osteoporotic fractures, but clopidogrel treatment does not increase fracture risk. In contrast, patients less adherent to the treatment have lower risk of fractures than non-users and patients with high adherence. However, based on the increased risk in stroke patients, clinicians should consider evaluation of bone status of these patients.

Keywords: stroke, antiplatelet therapy, osteoporosis, bone, fracture, P2Y12 receptor, clopidogrel

INTRODUCTION

Stroke is one of the leading causes of mortality and morbidity worldwide. In the surviving stroke patient the increased functional dependence and cognitive decline often leads to immobilization. Nearly 80–90% of all strokes occur in people over the age of 65, adding to the risk of osteoporosis in these patients (Truelsen et al., 2006). Balance is often impaired after a stroke increasing the risk of falls and in combination with immobilization and advanced age stroke patients have multiple risk factors for fractures. After a hemiplegic stroke, changes in bone metabolism occur already during the week following the stroke. Serum markers of bone formation are low and serum calcium and markers of bone resorption are increased and negatively correlated to the level of mobilization (Sato et al., 2000). Also, a high number of the patients had vitamin D deficiency, as only 27% had sufficient serum levels of vitamin D (Sato et al., 2000). Stroke patients with hemiparesis develop a significant bone loss during the first year after the stroke, primarily in the affected side and mainly in the humerus (loss in bone mineral density of 17.4% after 1 year) and the proximal femur (loss of 12.2%) (Ramnemark et al., 1999). Excessive bone loss is a clear risk factor of osteoporosis and subsequently fractures. A recent meta-analysis that included 13 cohorts of stroke survivors found a 50% increased risk of hip fracture in the stroke patients compared to healthy men and women of the same age (Yuan et al., 2016). In a Swedish cohort of stroke patients, the risk of fracture was 4% 1 year post-stroke, 15% after 5 years and 24% after 10 years (Ramnemark et al., 1998). Fractures occurred primarily after falls (84% of fractures) and mainly affected the paretic side in patients with paresis (Ramnemark et al., 1998). At least in younger individuals, no difference in fracture rates was found between stroke and TIA patients (Brown et al., 2008). Thus, post-stroke fractures may result from disuse hemiosteoporosis, hypovitaminosis D, and an increased risk of falls.

Treatment with platelet aggregation inhibitors has become the gold standard for secondary prevention of recurrent non-cardioembolic strokes after the initial episode, both in patients with ischaemic stroke and TIA (Kernan et al., 2014). Life-long treatment with the thienopyridine, clopidogrel, has become one of the standard treatments in patients suffering a stroke (Kernan et al., 2014). Clopidogrel inhibits platelet aggregation by irreversibly binding to the P2Y12 receptor, previously called the "platelet receptor."

Recent studies have shown that the P2Y12 receptor is expressed not only on platelets but also on bone cells. Clopidogrel inhibits the function of the bone forming osteoblasts (Syberg et al., 2012). Moreover, in a recent *in vivo* study mice treated with clopidogrel had reduced bone mass and -strength of approximately 20% (Syberg et al., 2012). Thus, clopidogrel induced severe osteoporosis in the animals. In addition, a large population-based register study including all patients having prescribed clopidogrel in Denmark between 1999 and 2008 confirmed the suspected negative effects of clopidogrel on bone, as the fracture risk was increased by 60% compared to non-clopidogrel users (Jørgensen et al., 2012). Thus, clopidogrel treatment has clear negative effects on bone.

As patients with ischaemic stroke and TIA are prescribed clopidogrel for the rest of their lives and as they are already susceptible to bone fractures, additional bone loss induced by clopidogrel treatment may therefore increase the risk even further. The aim of the present study was to evaluate the association between the platelet inhibitor clopidogrel and fracture incidence in stroke and TIA patients in a population-based nationwide case-control study.

MATERIALS AND METHODS

Study Design

The study was designed as a cohort study. All subjects who were prescribed clopidogrel during the years 1996 to 2008 in Denmark were included as exposed subjects ($n = 77{,}503$), and for each exposed subject three subjects of the same age (same birth year) and gender were randomly selected from the background population as controls ($n = 232{,}510$). The non-users were selected and matched on age- and gender to the users through an intensity sampling technique. As it is a register-based study, no approval from the Ethics Committee is necessary and Ethics approval was therefore not sought.

End-Points

The study end-points were occurrence of stroke or TIA and occurrence of any fracture succeeding the stroke or TIA (International Classification of Diseases (ICD) 10 codes: S02.0-S02.9, S07.0-S07.9, S12.0-S12.9, S22.0-S22.9, S32.0-S32.8, S42.0-S42.9, S52.0-S52.9, S62.0-S62.9, S72.0-S72.9, S82.0-S82.9, S92.0-S92.9), hip fracture (S72.0 and S72.1), forearm fracture (S52.5 and S52.6), and spine fracture (S12.0, S12.1, S12.2, S12.7, S12.8, S12.9, S22.0, S22.1, S32.0, S32.7, S32.8) between January 1st 1996 and December 31st 2008. The vertebral fractures included were clinical fractures collected from hospital records of patients, who were referred to emergency rooms or other departments and were diagnosed with a vertebral fracture.

Exposure Variables

Clopidogrel use was the primary exposure. Patterns of drug use were analyzed for the period from January 1st, 1996 to the date of fracture or corresponding dummy date among the non-users. Data were collected systematically and information on whether the drugs were used systematically or temporarily was included in the analyses of drug use via the Defined Daily Dose (DDD), using the dates of prescription. DDD is used according to the WHO definition, which is defined as the assumed average maintenance dose per day for a drug used for its main indication in adults. The other exposure variables were occurrence of (1) use of drugs known to be associated with fracture risk (corticosteroids), and (2) co-morbidities known to affect fracture risk (prior fracture Klotzbuecher et al., 2000) and alcoholism (Kanis et al., 2005). These factors were chosen as they were known to potentially

affect fracture risk, and were regarded as important potential confounders in a setting where many variables besides the main factor may influence the risk of fractures (confounding by indication). To analyze for confounding from use of other cardiovascular drugs these were also included (Rejnmark et al., 2005, 2006a,b).

Due to the imbalances in confounders typical for observational studies, extensive confounder control was performed including all the unevenly distributed known confounders: Charlson index, income, living alone or not, spironolactone use, use of bronchodilator drugs (proxy for smoking), use of drugs for smoking cessation (proxy for smoking), prior fracture, alcoholism, systemic corticosteroids, statin use, ACE use, ACE+diuretics use, combined alpha plus betablocker use, other diuretics use, betablocker use, betablocker plus other drug combined, calcium channel blocker, thiazide diuretics, loop diuretics, dipyridamole use, and acetylsalicylic use. The variables were entered into the statistical analysis and analyses for interaction were performed.

Information on bodyweight or body mass index (BMI) was not available.

Registers Used

The information on fracture occurrence, stroke and TIA as well as occurrence of other diseases, prior fractures, alcoholism came from two registers: (1) The National Hospital Discharge Register (Andersen et al., 1999), and (2) The Psychiatric Central Register (Munk-Jørgensen and Mortensen, 1997). These have been described in detail previously (Mosbech et al., 1995; Andersen et al., 1999; Vestergaard and Mosekilde, 2002; Jørgensen et al., 2012; Vestergaard et al., 2012; Grove et al., 2013).

The information on clopidogrel use came from The Danish Medicines Agency, who keeps a nationwide register of all drugs sold at pharmacies throughout the country from 1996 and onward (The National Pharmacological Database run by the Danish Medicines Agency[1]). Any drugs bought are registered with ATC code, dosage sold, and date of sale for the period January 1st 1996 to December 31st, 2008. Details about this have previously been published (Vestergaard et al., 2012).

It is possible to link these sources of information through the Central Person Register Number, which is a unique registration code given to every inhabitant, enabling registration on an individual basis.

The project was approved and controlled by the National Board of Health, the Danish Data Protection Agency, and the Directory board of the Psychiatric Central Register.

In Denmark almost all patients with fractures are managed in the hospital system (also including the emergency rooms) (Vestergaard et al., 2002), even fractures sustained abroad are registered upon return for insurance reasons. The capture of fractures is thus very high (Mosbech et al., 1995; Andersen et al., 1999). The validity of a fracture diagnosis is around 93% (Vestergaard and Mosekilde, 2002).

[1]http://www.dkma.dk

Statistical Analyses

Mean and standard deviation were used as descriptive statistics. Crude and adjusted hazard ratios (HRs), and 95% confidence intervals were calculated. Cox proportional hazard regression models were used to analyze the time to fracture in exposed vs. non-exposed subjects. The proportional hazard assumption was checked through inspection of survival plots. In addition, in the Cox regression models there was also tested for age and gender interaction. In order to avoid immortal time bias, patients are excluded from further risk analysis after subsequent stroke/TIA events.

Analyses were performed using STATA 9.0 (STATA Corp., College Station, TX, United States) and IBM SPSS 19.0 (SPSS Inc.).

RESULTS

Baseline Characteristics of Users and Non-users

Clopidogrel-treated and untreated controls were well matched for both gender and age and the baseline variables in the two groups are shown in **Table 1**. Not surprisingly, the fraction of individuals with prior cerebral incidents such as ischaemic and haemorrhagic stroke and TIA were significantly higher in the clopidogrel group than in the control group. Also, the fraction of individuals with other cardiovascular diseases (myocardial infarction, heart failure, atherosclerosis and angina pectoris) was significantly higher among clopidogrel-users than in non-users. Moreover, the proportion of subjects on prior statin, ACE inhibitors, beta blockers, diuretics and other anti-platelet inhibitors was higher amongst users than in controls (**Table 1**).

Fracture Risk of Cerebral Ischemic Events

The risk of fracture following TIA, ischaemic stroke and haemorrhagic stroke was calculated. A clear association between all three types of cerebral ischemic events and the risk of fracture was detected (**Table 2**). Ischemic stroke increased the risk of any fracture by approximately 50% while haemorrhagic stroke increased the risk by approximately 30%. Surprisingly, TIA also increased the risk of fracture to the same extent as haemorrhagic stroke. Even after adjusting for multiple confounders, a 14% increased risk of any fracture was seen in patients with ischaemic stroke and 19% increased risk of hip fractures was seen in patients with haemorrhagic stroke (**Table 3**).

As fracture risk is affected by gender, we stratified accordingly. Interestingly, increased risk of fractures was only seen in men, where it was significantly increased in men suffering ischaemic stroke (any fracture) and in men suffering haemorrhagic stroke (hip fracture) (**Table 4**).

Effect of Clopidogrel on Fracture Risk in Stroke Patients

We have previously shown that clopidogrel treatment increased fracture risk. Therefore, first we investigated whether clopidogrel

TABLE 1 | Baseline characteristics of clopidogrel users and non-users.

Parameter	Clopidogrel users (n = 77,503)	Non-users (n = 232,510)	P
Age (years, mean ± SD)	65.7 ± 12.7	65.7 ± 12.7	–
Men (number, %)	50,118 (64.7%)	150,354 (64.7%)	–
Women (number, %)	27,385 (35.3%)	82,156 (35.3%)	
Prior fracture	16,730 (21.6%)	47,795 (20.6%)	<0.01
Prior diagnosis of alcoholism	2,469 (3.2%)	6,562 (2.8%)	<0.01
Prior acute myocardial infarction	45,365 (58.5%)	10,709 (4.6%)	<0.01
Prior angina pectoris	53,523 (69.1%)	21,428 (9.2%)	<0.01
Prior heart failure	11,243 (14.5%)	8,129 (3.5%)	<0.01
Prior peripheral atherosclerosis	7,356 (9.5%)	7,193 (3.1%)	<0.01
Prior cerebral atherosclerosis	2,784 (3.6%)	2,900 (1.2%)	<0.01
Prior diabetes	10,863 (14.0%)	11,894 (5.1%)	<0.01
Prior atrial fibrillation	8,036 (10.4%)	12,080 (5.2%)	<0.01
Prior systemic corticosteroids	20,050 (25.9%)	47,067 (20.2%)	<0.01
Prior use of statins	30,345 (39.2%)	26,735 (11.5%)	<0.01
Prior ACE/ARB use	38,658 (49.9%)	46,380 (19.9%)	<0.01
Prior ACE/ARB plus diuretics use	6,529 (8.4%)	13,129 (5.6%)	<0.01
Prior combined alpha/beta blocker	2,897 (3.7%)	3,187 (1.4%)	<0.01
Prior use of other diuretics	8,737 (11.3%)	16,926 (7.3%)	<0.01
Prior use of betablockers	36,288 (46.8%)	43,114 (18.5%)	<0.01
Prior use of betablocker combinations	562 (0.7%)	1,249 (0.5%)	<0.01
Prior use of calcium antagonists	27,953 (36.1%)	41,744 (18.0%)	<0.01
Prior thiazide diuretic use	24,895 (32.1%)	53,675 (23.1%)	<0.01
Prior loop diuretic use	18,105 (23.4%)	31,725 (13.6%)	<0.01
Prior use of dipyridamole	8,123 (10.5%)	7,331 (3.2%)	<0.01
Prior use of low dose ASA	44,015 (56.8%)	54,610 (23.5%)	<0.01
Charlson index	2.1 ± 1.9	0.8 ± 1.5	<0.01
Income in index year (Danish crowns)	209,223 ± 315,460	224,149 ± 227,691	<0.01
Living with someone	29,030 (37.5%)	88,901 (38.2%)	<0.01
Bronchodilator drugs	23,900 (30.8%)	54,703 (23.5%)	<0.01
Drugs for smoking cessation	1,969 (2.5%)	2,240 (1.0%)	<0.01
Spironolactone	11,292 (14.6%)	11,889 (5.1%)	<0.01
Prior haemorrhagic stroke	924 (1.2%)	2,004 (0.9%)	<0.01
Prior ischemic stroke	7,227 (9.3%)	6,077 (2.6%)	<0.01
Prior TIA	5,573 (7.2%)	5,366 (2.3%)	<0.01

Figures are numbers and % or mean and standard deviation (SD). ACE: Angiotensin-converting enzyme inhibitor, ARB, angiotensin receptor blocker; ASA, acetylsalicylic acid.

TABLE 2 | The frequency and risk of any fracture are presented.

Crude relative risk	Any fracture IRR (95% CI)	Hip fracture IRR (95% CI)	Forearm fracture IRR (95% CI)	Spine fracture IRR (95% CI)
Clopidogrel	1.05 (1.02–1.09)**	1.00 (0.94–1.07)	1.03 (0.97–1.10)	1.13 (0.99–1.28)
TIA	1.28 (1.20–1.36)***	1.50 (1.32–1.71)*	1.18 (1.00–1.38)*	1.34 (1.00–1.79)*
Ischaemic stroke	1.54 (1.46–1.64)***	1.55 (1.24–1.92)*	1.15 (0.87–1.53)	1.80 (1.17–2.78)*
Haemorrhagic stroke	1.34 (1.18–1.51)***	2.17 (1.96–2.40)*	1.18 (1.03–1.36)*	1.73 (1.37–2.17)*
Previous fracture	2.41 (2.34–2.48)***	2.88 (2.72–3.04)*	2.33 (2.20–2.48)*	2.61 (2.33–2.93)*

*Risk of fracture is presented as crude relative risk and 95% confidence intervals in exposed individuals as compared to non-exposed (controls). Each individual row represents the risk of fracture of one exposure variable (e.g., clopidogrel) when adjusted for the other exposures. CI, confidence interval; IRR, incidence rate ratio; *Two-tailed $P < 0.05$, **Two-tailed $P < 0.01$, ***Two-tailed $P < 0.001$.*

treatment affected the fracture risk in the different categories of patients. In subjects with ischaemic stroke or TIA, no additional increase in fracture risk could be detected (**Figures 1A,B**). However, in subjects with haemorrhagic stroke, there was a striking change in fracture risk 6 years after the event. In clopidogrel-treated subjects, the risk leveled out and approached the risk in patients without stroke, while the risk in subjects not treated with clopidogrel increased dramatically (**Figure 1C**).

TABLE 3 | The risk of any fractures and of the three major groups of osteoporotic fractures (hip, forearm, and spine) is presented.

Crude relative risk	Any fracture HR (95% CI)	Hip fracture HR (95% CI)	Forearm fracture HR (95% CI)	Spine fracture HR (95% CI)
Clopidogrel	0.85 (0.82–0.88)*	0.65 (0.61–0.69)*	0.90 (0.84–0.97)*	0.77 (0.67–0.88)*
TIA	1.05 (0.98–1.13)	1.13 (0.99–1.30)	1.08 (0.91–1.28)	1.09 (0.81–1.48)
Ischaemic stroke	1.14 (1.07–1.21)*	1.02 (0.82–1.28)	0.98 (0.74–1.30)	1.12 (0.80–1.93)
Haemorrhagic stroke	1.04 (0.92–1.17)	1.19 (1.06–1.33)*	0.97 (0.84–1.13)	1.07 (0.84–1.38)

*Risk of fracture is presented as crude relative risk, hazard ratio adjusted for multiple confounders. Each individual row represents the risk of fracture of one exposure variable (e.g., clopidogrel) when adjusted for the other exposures. Multiple confounders: Prior alcoholism, prior fractures, Charlson index, income, living alone or not, spironolactone use, use of bronchodilator drugs (proxy for smoking), use of drugs for smoking cessation (proxy for smoking), systemic corticosteroids, statin use, ACE use, ACE + diuretics use, combined alpha plus betablocker use, other diuretics use, betablocker use, betablocker plus other drug combined, calcium channel blocker, thiazide diuretics, loop diuretics, dipyridamole use, and acetylsalicylic use. HR, Hazard Ratio; CI, Confidence Interval; TIA, Transitory Ischemic Attack. *Two-tailed $P < 0.05$.*

TABLE 4 | The risk of any fractures and of hip fractures stratified by gender is presented as crude relative risk, hazard ratio adjusted for multiple confounders.

Crude relative risk	Any fracture HR (95% CI)		Hip fracture HR (95% CI)	
	Men	Women	Men	Women
Clopidogrel	0.82 (0.78–0.87)*	0.88 (0.84–0.93)*	0.56 (0.51–0.62)*	0.74 (0.68–0.81)*
TIA	1.08 (0.98–1.20)	1.01 (0.92–1.10)	1.14 (0.92–1.40)	1.09 (0.91–1.30)
Ischaemic stroke	1.20 (1.09–1.31)*	1.08 (0.99–1.17)	1.11 (0.82–1.51)	0.94 (0.69–1.29)
Haemorrhagic stroke	1.04 (0.87–1.23)	1.06 (0.89–1.25)	1.35 (1.14–1.59)*	1.06 (0.91–1.23)

*Each individual row represents the risk of fracture of one exposure variable (e.g., clopidogrel) when adjusted for the other exposures. Multiple confounders: Prior alcoholism, prior fractures, Charlson index, income, living alone or not, spironolactone use, use of bronchodilator drugs (proxy for smoking), use of drugs for smoking cessation (proxy for smoking), systemic corticosteroids, statin use, ACE use, ACE + diuretics use, combined alpha plus betablocker use, other diuretics use, betablocker use, betablocker plus other drug combined, calcium channel blocker, thiazide diuretics, loop diuretics, dipyridamole use, and acetylsalicylic use. HR, Hazard Ratio; CI, Confidence Interval; TIA, Transitory Ischemic Attack. *Two-tailed $P < 0.05$.*

Interestingly, when adjusting for multiple confounders clopidogrel treatment was associated with a reduced risk of all fracture types evaluated with a reduction in fracture risk between 10 and 35% (**Table 3**). Moreover, men had a more pronounced reduction in fracture risk than women for both any fracture (HR: 0.82 vs. 0.88, men and women, respectively) and for hip fracture (HR: 0.56 vs. 0.74) (**Table 4**).

As previous studies have shown a dose-dependent biphasic association between clopidogrel and fracture risk, we next stratified according to dose expressed as DDD/day. For all fracture types evaluated, the fracture risk was reduced by 10–46%, when DDD/day < 0.80. In contrast, for doses 0.8 DDD/day, fracture risk was either unaltered (any fracture and spine fractures), marginally reduced (hip fractures) or marginally increased (forearm fractures) when compared to individuals who never used clopidogrel (**Table 5**). Again, when stratifying for gender, the risk reducing effect was more pronounced in men than in women and for hip fractures than for any fracture (**Table 6**).

DISCUSSION

In the present study, we observed a clear association between occurrence of stroke and risk of osteoporotic fractures. Moreover, we found that patients treated with the P2Y12 inhibitor, clopidogrel, overall had minimally affected fracture risk when compared to non-users. However, when stratifying for dosage and duration expressed as DDD/day, we found that the fracture risk was reduced by as much as 50% for less adherent patients while adherent patients treated with the recommended dose had the same fracture risk as non-users.

It is well known that immobilization following a stroke leads to increased bone resorption and decreased bone formation (Sato et al., 2000) and bone loss (Ramnemark et al., 1999). Excessive bone loss is a clear risk factor of osteoporosis and subsequently fractures. Also, stroke patients have a significantly increased incidence of falls, which aggravates the risk of osteoporotic fractures in these patients. A recent meta-analysis included 13 cohorts of stroke survivors and found a 50% increased risk of hip fracture in the stroke patients compared to men and women of the same age (Yuan et al., 2016). This corresponds well with our findings, where we see a 50% increase in risk in both any fracture and hip fracture in patients with ischaemic stroke, while the risk of spine fractures increase by as much as 80%. The increase in fracture risk is even higher in patients with haemorrhagic stroke, where risk of hip fractures is increased by as much as 120%. Hip fractures are especially serious in stroke patients, as hip fractures are associated with a high mortality, disability, loss of independence, and high medical costs.

Interestingly TIA was also associated with an increase in fracture risk of between 18 and 50%, but after adjusting for multiple confounders no increased fracture risk could be detected. In these patients, symptoms of the ischaemic attack would disappear within 24 h. However, TIA patients may have underlying common risk factors for fracture and stroke, or they might have minor, undetected neurological deficits after the TIA that affects balance and increases fall incidence as well as they

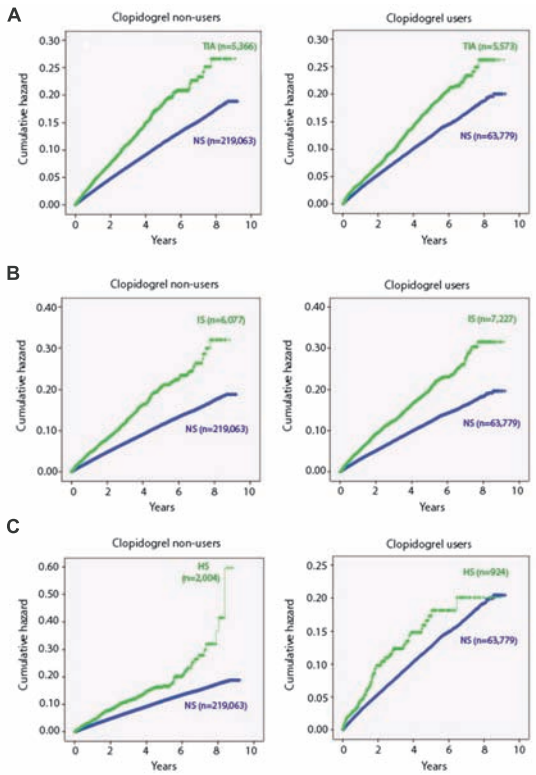

FIGURE 1 | Cumulative hazard of any fracture as a function of time in years since index event. Both transitory ischemic attack (TIA) **(A)** and ischaemic stroke (IS) **(B)** increase the risk of any fracture and the risk continues to increase during the years after the event. Clopidogrel treatment does not seem to further increase the fracture. In patients with haemorrhagic stroke (HS) there is also an increased risk of fractures **(C)**. Again, clopidogrel does not affect the fracture risk until 6 years after the event. After 6 years there is a striking increase in risk in non-clopidogrel treated patients, while the risk in clopidogrel-users levels out and equals the risk in non-stroke subjects. NS: non-stroke/non-TIA.

have an increased risk of developing more severe stroke at a later time point the clinician should still evaluate the fracture risk and bone health of these patients.

To our knowledge, this is the first study to investigate the association between fracture risk and clopidogrel use in stroke and TIA patients. It is particularly important to elucidate the effect of clopidogrel in stroke patients. First, they are at increased risk of osteoporosis and subsequent fractures due to immobilization and fall tendency and they are more vulnerable than other patient. Next, we have previously shown that clopidogrel treatment is associated with an increased risk of fracture in a nationwide cohort study including all patients prescribed clopidogrel Denmark (Jørgensen et al., 2012). Finally, we found that the patients with the highest risk where those receiving long-term treatment (more than 1 year) and as clopidogrel treatment in stroke patients is life-long, it is highly relevant to address the association of clopidogrel treatment on fracture risk in this particular patient category. In contrast to our previous study that included patients prescribed clopidogrel for any indication, we only find a marginally increased risk of osteoporotic fractures, and after adjusting for multiple confounders known to predispose to osteoporosis and fractures, we actually find a reduced risk of all fracture types. This is even more pronounced when we stratify for dose, where less adherent patients have even more reduced fracture risk as compared to both non-users and adherent patients receiving recommended doses. The obvious explanation for this would be that clopidogrel, at least in lower doses or shorter duration, affects bone metabolism and protects against fractures. This is supported by an *in vivo* study in which P2Y12 null mice had reduced osteoclastic activity and were partially protected against pathological bone loss (Su et al., 2012). However, another *in vivo* study from our own group found that clopidogrel treatment of mice induced bone loss and reduced bone strength (Syberg et al., 2012), so the effects of clopidogrel on bone cells and bone metabolism are not fully elucidated yet. Another explanation for the reduced fracture risk in less adherent patients could be that these patients stop the treatment due to side effects or they could be more severely affected by the stroke and are thus completely immobilized and thus in bed for prolonged periods of time, thus reducing the risk of falls and subsequent fractures.

As fracture risk differs between men and women we stratified the analyses according to gender. Interestingly, we found that clopidogrel treatment in men is associated with a lower fracture risk than in women. It has previously been shown that the effects of clopidogrel on platelet function are gender dependent (Hobson et al., 2009; Patti et al., 2014), and our data suggests that this might be a more universal gender-specific effect of clopidogrel in all target organs. However, differences in underlying comorbidities could also lead to over- or underadjustment for confounders in the analyses, falsely demonstrating an effect of gender on the response to clopidogrel.

Due to the centrally organized healthcare system in Denmark, a broad range of healthcare information is collected and can be collated based on the unique identification number for each citizen in Denmark. This enabled us to perform a large-scale population-based designed study. This also made it possible to collect data on confounders and exposure before the occurrence of fracture, thereby eliminating the risk of recall bias. Moreover, as all collected prescriptions are registered with the Danish Medicines Agency, it has been possible to include all patients prescribed clopidogrel in the study, thereby reducing the risk of selection bias. Finally, as almost all fractures are treated in public emergency departments and hospitals covered by the databases, collection of fracture data is considered almost complete, though there can be a minor risk of coding errors by the discharging physicians.

Though the strength of the study is the large-scale design, the optimal design would have been a prospective, randomized trial as optimal confounder-control could have been obtained. Such study should have included the determination of circulating markers of bone turnover to determine the effects of clopidogrel on bone formation and bone resorption in the patients. However, it would not have been feasible to conduct such a trial, as the cost of a sufficiently powered study with fracture as endpoint would have been immense. Moreover, it is not ethically justifiable to

TABLE 5 | The risk of any fractures and of the three major groups of osteoporotic fractures (hip, forearm, and spine) by dose of clopidogrel in all users.

Crude relative risk	Any fracture HR (95% CI)	Hip fracture HR (95% CI)	Forearm fracture HR (95% CI)	Spine fracture HR (95% CI)
Clopidogrel (never use as reference)				
<0.1 DDD/day	0.77 (0.74–0.81)*	0.54 (0.48–0.60)*	0.83 (0.74–0.92)*	0.77 (0.63–0.94)*
0.1–0.39 DDD/day	0.81 (0.760.85)*	0.62 (0.55–0.69)*	0.81 (0.72–0.91)*	0.64 (0.50–0.80)*
0.40–0.79 DDD/day	0.86 (0.80–0.92)*	0.60 (0.52–0.70)*	0.96 (0.83–1.12)	0.69 (0.51–0.94)*
≥0.8 DDD/day	1.04 (0.99–1.11)	0.90 (0.81–1.00)*	1.14 (1.00–1.29)*	1.00 (0.79–1.25)
TIA	1.04 (0.97–1.11)	1.10 (0.96–1.26)	1.05 (0.89–1.25)	1.07 (0.79–1.44)
Ischaemic stroke	1.11 (1.04–1.18)*	1.02 (0.82–1.27)	0.98 (0.74–1.30)	1.24 (0.80–1.92)
Haemorrhagic stroke	1.04 (0.92–1.17)	1.14 (1.02–1.28)*	0.94 (0.81–1.10)	1.04 (0.81–1.34)

*Risk of fracture is presented as crude relative risk, hazard ratio adjusted for multiple confounders. Each individual row represents the risk of fracture of one exposure variable (e.g., clopidogrel) when adjusted for the other exposures. Multiple confounders: Prior alcoholism, prior fractures, Charlson index, income, living alone or not, spironolactone use, use of bronchodilator drugs (proxy for smoking), use of drugs for smoking cessation (proxy for smoking), systemic corticosteroids, statin use, ACE use, ACE + diuretics use, combined alpha plus betablocker use, other diuretics use, betablocker use, betablocker plus other drug combined, calcium channel blocker, thiazide diuretics, loop diuretics, dipyridamole use, and acetylsalicylic use. HR, Hazard Ratio; CI, Confidence Interval; TIA, Transitory Ischemic Attack. *Two-tailed P < 0.05.*

TABLE 6 | The risk of any fractures and of the three major groups of osteoporotic fractures (hip, forearm, and spine) by dose of clopidogrel stratified by gender.

Crude relative risk	Any fracture HR (95% CI)		Hip fracture HR (95% CI)	
	Men	Women	Men	Women
Clopidogrel (never use as reference)				
<0.1 DDD/day	0.78 (0.72–0.83)*	0.80 (0.75–0.86)*	0.49 (0.42–0.58)*	0.61 (0.53–0.70)*
0.1–0.39 DDD/day	0.81 (0.75–0.87)*	0.86 (0.79–0.92)*	0.52 (0.44–0.62)*	0.76 (0.66–0.87)*
0.40–0.79 DDD/day	0.81 (0.73–0.90)*	0.93 (0.84–1.03)	0.52 (0.41–0.66)*	0.70 (0.58–0.85)*
≥0.8 DDD/day	0.97 (0.89–1.07)	1.01 (0.93–1.08)	0.79 (0.66–0.94)*	0.91 (0.80–1.04)
TIA	1.07 (0.97–1.19)	0.99 (0.91–1.09)	1.11 (0.90–1.36)	1.06 (0.89–1.27)
Ischaemic stroke	1.17 (1.07–1.29)*	1.05 (0.96–1.15)	1.11 (0.82–1.51)	0.94 (0.69–1.29)
Haemorrhagic stroke	1.03 (0.87–1.23)	1.06 (0.89–1.25)	1.31 (1.11–1.54)*	1.02 (0.88–1.19)

*Risk of fracture is presented as crude relative risk, hazard ratio adjusted for multiple confounders. Each individual row represents the risk of fracture of one exposure variable (e.g., clopidogrel) when adjusted for the other exposures. Multiple confounders: Prior alcoholism, prior fractures, Charlson index, income, living alone or not, spironolactone use, use of bronchodilator drugs (proxy for smoking), use of drugs for smoking cessation (proxy for smoking), systemic corticosteroids, statin use, ACE use, ACE + diuretics use, combined alpha plus betablocker use, other diuretics use, betablocker use, betablocker plus other drug combined, calcium channel blocker, thiazide diuretics, loop diuretics, dipyridamole use, and acetylsalicylic use. HR, Hazard Ratio; CI, Confidence Interval; TIA, Transitory Ischemic Attack. *Two-tailed P < 0.05.*

conduct a placebo-controlled trial, as clopidogrel is part of the standard, recommended treatment after an ischaemic stroke as well as after other cardiovascular diseases.

In our study, we have extensively controlled for multiple confounders in relation to fractures, but as in all observational studies there might still be residual confounding because of possible differences in comorbidities. Especially, the choice of prescribing clopidogrel to the stroke patient is dependent on the type of stroke (haemorrhagic, ischaemic) and possibly also the general condition of the patient. Thus, the severity of neurological deficit after the cerebrovascular event might be different between the treatment groups, which we are not able to control for with the current design. Also, differences in extent of exercise and mobilization and thus the risk of falls has not been possible to adjust for, as this information is not contained in any registers.

Future studies should address the effects of the newer P2Y12 receptor antagonists, prasugrel and ticagrelor, as they have other modes of function on the receptor. However, as they were marketed later than clopidogrel and have not been implemented as part of the standard of care in the treatment of stroke in Denmark, the number of patients treated would not be sufficient and the study therefore not sufficiently powered to determine the effects on osteoporotic fractures.

CONCLUSION

Patients with stroke have increased risk of osteoporotic fractures, but treatment with the widely used platelet inhibitor, clopidogrel, does not seem to increase the risk of fractures. In contrast, less adherent patients have lower risk of fractures than non-users. This might be due to a bone-protective effect of clopidogrel at lower doses or it might be due to differences in comorbidities between patients exposed to suboptimal doses of clopidogrel and patients treated with recommended doses. Thus, clopidogrel is not associated with deleterious effects on bone in stroke patients, but might even reduce the risk of fracture in these patients. However, further studies should investigate the exact effects of clopidogrel on bone metabolism.

Finally, in light of the high risk of fractures in stroke patient *per se* and the large number of underlying risk factors, careful attention should be given to the bone status of these patients. Clinicians should carefully consider additional evaluation

of the bone status of stroke survivors and treatment should be given to prevent development or progression of osteoporosis.

AUTHOR CONTRIBUTIONS

Conception and design of the study: NJ, PV, HI, and PS. Acquisition, analysis, and interpretation of data: NJ, PV, HI, and PS. Drafting of the work: NJ and PV. Revising it critically for intellectual content: NJ, PV, HI, and PS. Final approval of the version to be published: NJ, PV, HI, and PS. Agreement to be accountable for all aspects of the work in ensuring that questions related to the accuracy or integrity of any part of the work are appropriately investigated and resolved: NJ, PV, HI, and PS.

FUNDING

The work was kindly supported by the European Commission under the 7th Framework Programme (proposal #202231) performed as a collaborative project among the members of the ATPBone Consortium (Copenhagen University, University College London, University of Maastricht, University of Ferrara, University of Liverpool, University of Sheffield, and Université Libre de Bruxelles), and is a substudy under the main study "Fighting osteoporosis by blocking nucleotides: purinergic signaling in bone formation and homeostasis." Furthermore, the work was supported by a grant from Jacob and Olga Madsen's Foundation.

REFERENCES

Andersen, T. F., Madsen, M., Jorgensen, J., Mellemkjoer, L., and Olsen, J. H. (1999). The Danish National Hospital Register. A valuable source of data for modern health sciences. *Dan. Med. Bull.* 46, 263–268.

Brown, D. L., Morgenstern, L. B., Majersik, J. J., Kleerekoper, M., and Lisabeth, L. D. (2008). Risk of fractures after stroke. *Cerebrovasc. Dis.* 25, 95–99. doi: 10.1159/000111997

Grove, E. L., Wurtz, M., Schwarz, P., Jorgensen, N. R., and Vestergaard, P. (2013). Gastrointestinal events with clopidogrel: a nationwide population-based cohort study. *J. Gen. Intern. Med.* 28, 216–222. doi: 10.1007/s11606-012-2208-0

Hobson, A. R., Qureshi, Z., Banks, P., and Curzen, N. (2009). Gender and responses to aspirin and clopidogrel: insights using short thrombelastography. *Cardiovasc. Ther.* 27, 246–252. doi: 10.1111/j.1755-5922.2009.00106.x

Jørgensen, N. R., Grove, E. L., Schwarz, P., and Vestergaard, P. (2012). Clopidogrel and the risk of osteoporotic fractures: a nationwide cohort study. *J. Intern. Med.* 272, 385–393. doi: 10.1111/j.1365-2796.2012.02535.x

Kanis, J. A., Johansson, H., Johnell, O., Oden, A., De Laet, C., Eisman, J. A., et al. (2005). Alcohol intake as a risk factor for fracture. *Osteoporos. Int.* 16, 737–742. doi: 10.1007/s00198-004-1734-y

Kernan, W. N., Ovbiagele, B., Black, H. R., Bravata, D. M., Chimowitz, M. I., Ezekowitz, M. D., et al. (2014). Guidelines for the prevention of stroke in patients with stroke and transient ischemic attack: a guideline for healthcare professionals from the American Heart Association/American Stroke Association. *Stroke* 45, 2160–2236. doi: 10.1161/STR.0000000000000024

Klotzbuecher, C. M., Ross, P. D., Landsman, P. B., Abbott, T. A. III, and Berger, M. (2000). Patients with prior fractures have an increased risk of future fractures: a summary of the literature and statistical synthesis. *J. Bone Miner. Res.* 15, 721–739. doi: 10.1359/jbmr.2000.15.4.721

Mosbech, J., Jorgensen, J., Madsen, M., Rostgaard, K., Thornberg, K., and Poulsen, T. D. (1995). The national patient registry. Evaluation of data quality. *Ugeskr. Laeger* 157, 3741–3745.

Munk-Jørgensen, P., and Mortensen, P. B. (1997). The Danish Psychiatric Central Register. *Dan. Med. Bull.* 44, 82–84.

Patti, G., De Caterina, R., Abbate, R., Andreotti, F., Biasucci, L. M., Calabrò, P., et al. (2014). Platelet function and long-term antiplatelet therapy in women: Is there a gender-specificity? A 'state-of-the-art' paper. *Eur. Heart J.* 35, 2213–2223. doi: 10.1093/eurheartj/ehu279

Ramnemark, A., Nyberg, L., Borssen, B., Olsson, T., and Gustafson, Y. (1998). Fractures after stroke. *Osteoporos. Int.* 8, 92–95. doi: 10.1007/s001980050053

Ramnemark, A., Nyberg, L., Lorentzon, R., Englund, U., and Gustafson, Y. (1999). Progressive hemiosteoporosis on the paretic side and increased bone mineral density in the nonparetic arm the first year after severe stroke. *Osteoporos. Int.* 9, 269–275. doi: 10.1007/s001980050147

Rejnmark, L., Vestergaard, P., and Mosekilde, L. (2005). Reduced fracture risk in users of thiazide diuretics. *Calcif. Tissue Int.* 76, 167–175. doi: 10.1007/s00223-004-0084-2

Rejnmark, L., Vestergaard, P., and Mosekilde, L. (2006a). Treatment with beta-blockers, ACE inhibitors, and calcium-channel blockers is associated with a reduced fracture risk: a nationwide case-control study. *J. Hypertens.* 24, 581–589.

Rejnmark, L., Vestergaard, P., and Mosekilde, L. (2006b). Fracture risk in patients treated with loop diuretics. *J. Intern. Med.* 259, 117–124.

Sato, Y., Kuno, H., Kaji, M., Etoh, K., and Oizumi, K. (2000). Influence of immobilization upon calcium metabolism in the week following hemiplegic stroke. *J. Neurol. Sci.* 175, 135–139. doi: 10.1016/S0022-510X(00)00298-7

Su, X., Floyd, D. H., Hughes, A., Xiang, J., Schneider, J. G., Uluckan, O., et al. (2012). The ADP receptor P2RY12 regulates osteoclast function and pathologic bone remodeling. *J. Clin. Invest.* 122, 3579–3592. doi: 10.1172/JCI38576

Syberg, S., Brandao-Burch, A., Patel, J. J., Hajjawi, M., Arnett, T. R., Schwarz, P., et al. (2012). Clopidogrel (Plavix), a $P2Y_{12}$ receptor antagonist, inhibits bone cell function in vitro and decreases trabecular bone in vivo. *J. Bone Miner. Res.* 27, 2373–2386. doi: 10.1002/jbmr.1690

Truelsen, T., Piechowski-Jozwiak, B., Bonita, R., Mathers, C., Bogousslavsky, J., and Boysen, G. (2006). Stroke incidence and prevalence in Europe: a review of available data. *Eur. J. Neurol.* 13, 581–598. doi: 10.1111/j.1468-1331.2006.01138.x

Vestergaard, P., Emborg, C., Stoving, R. K., Hagen, C., Mosekilde, L., and Brixen, K. (2002). Fractures in patients with anorexia nervosa, bulimia nervosa, and other eating disorders–a nationwide register study. *Int. J. Eat. Disord.* 32, 301–308. doi: 10.1002/eat.10101

Vestergaard, P., and Mosekilde, L. (2002). Fracture risk in patients with celiac Disease, Crohn's disease, and ulcerative colitis: a nationwide follow-up study of 16,416 patients in Denmark. *Am. J. Epidemiol.* 156, 1–10. doi: 10.1093/aje/kwf007

Vestergaard, P., Steinberg, T. H., Schwarz, P., and Jorgensen, N. R. (2012). Use of the oral platelet inhibitors dipyridamole and acetylsalicylic acid is associated with increased risk of fracture. *Int. J. Cardiol.* 160, 36–40. doi: 10.1016/j.ijcard.2011.03.026

Yuan, Z. C., Mo, H., Guan, J., He, J. L., and Wu, Z. J. (2016). Risk of hip fracture following stroke, a meta-analysis of 13 cohort studies. *Osteoporos. Int.* 27, 2673–2679. doi: 10.1007/s00198-016-3603-x

Conflict of Interest Statement: The authors declare that the research was conducted in the absence of any commercial or financial relationships that could be construed as a potential conflict of interest.

frontiers in Pharmacology

ORIGINAL RESEARCH
published: 08 November 2017
doi: 10.3389/fphar.2017.00811

Post-inflammatory Ileitis Induces Non-neuronal Purinergic Signaling Adjustments of Cholinergic Neurotransmission in the Myenteric Plexus

*Cátia Vieira, Fátima Ferreirinha, Maria T. Magalhães-Cardoso, Isabel Silva, Patrícia Marques and Paulo Correia-de-Sá**

Laboratório de Farmacologia e Neurobiologia, Center for Drug Discovery and Innovative Medicines (MedInUP), Instituto de Ciências Biomédicas de Abel Salazar, Universidade do Porto, Porto, Portugal

OPEN ACCESS

Edited by:
Francisco Ciruela, University of Barcelona, Spain

Reviewed by:
Robson Coutinho-Silva, Universidade Federal do Rio de Janeiro, Brazil
Romain Lefebvre, Ghent University, Belgium

***Correspondence:**
Paulo Correia-de-Sá
farmacol@icbas.up.pt

Specialty section:
This article was submitted to Experimental Pharmacology and Drug Discovery, a section of the journal Frontiers in Pharmacology

Received: *15 August 2017*
Accepted: *26 October 2017*
Published: *08 November 2017*

Citation:
Vieira C, Ferreirinha F, Magalhães-Cardoso MT, Silva I, Marques P and Correia-de-Sá P (2017) Post-inflammatory Ileitis Induces Non-neuronal Purinergic Signaling Adjustments of Cholinergic Neurotransmission in the Myenteric Plexus. Front. Pharmacol. 8:811. doi: 10.3389/fphar.2017.00811

Uncoupling between ATP overflow and extracellular adenosine formation changes purinergic signaling in post-inflammatory ileitis. Adenosine neuromodulation deficits were ascribed to feed-forward inhibition of ecto-5′-nucleotidase/CD73 by high extracellular adenine nucleotides in the inflamed ileum. Here, we hypothesized that inflammation-induced changes in cellular density may also account to unbalance the release of purines and their influence on [^{3}H]acetylcholine release from longitudinal muscle-myenteric plexus preparations of the ileum of 2,4,6-trinitrobenzenesulfonic acid (TNBS)-treated rats. The population of S100β-positive glial cells increase, whereas Ano-1-positive interstitial cells of Cajal (ICCs) diminished, in the ileum 7-days after the inflammatory insult. In the absence of changes in the density of VAChT-positive cholinergic nerves detected by immunofluorescence confocal microscopy, the inflamed myenteric plexus released smaller amounts of [^{3}H]acetylcholine which also became less sensitive to neuronal blockade by tetrodotoxin (1 μM). Instead, [^{3}H]acetylcholine release was attenuated by sodium fluoroacetate (5 mM), carbenoxolone (10 μM) and A438079 (3 μM), which prevent activation of glial cells, pannexin-1 hemichannels and P2X7 receptors, respectively. Sodium fluoroacetate also decreased ATP overflow without significantly affecting the extracellular adenosine levels, thus indicating that surplus ATP release parallels reactive gliosis in post-inflammatory ileitis. Conversely, loss of ICCs may explain the lower amounts of adenosine detected in TNBS-treated preparations, since blockade of Ca_v3 (T-type) channels existing in ICCs with mibefradil (3 μM) or inhibition of the equilibrative nucleoside transporter 1 with dipyridamole (0.5 μM), both decreased extracellular adenosine. Data indicate that post-inflammatory ileitis operates a shift on purinergic neuromodulation reflecting the upregulation of ATP-releasing enteric glial cells and the depletion of ICCs accounting for decreased adenosine overflow via equilibrative nucleoside transporters.

Keywords: post-inflammatory ileitis, acetylcholine release, adenosine release, ATP release, myenteric plexus, enteric glia, interstitial cells of Cajal

INTRODUCTION

Inflammation of the gastrointestinal (GI) tract triggers a series of adaptive morphological, chemical and functional changes in the cellular components responsible for maintaining gut homeostasis (Sharkey and Kroese, 2001). These involve the number and chemical coding of enteric neurons, but also the relative abundance and activity of adjacent non-neuronal cells such as enteric glia, interstitial cells of Cajal, fibroblast-like cells and smooth muscle fibers, which are directly or indirectly influenced by inflammatory cells infiltrates. Adaptive cellular responses may impact on the coordination of motor function, local blood flow, GI secretions and also on the endocrine and immune reactions (Costa et al., 2000). As a matter of fact, the post-inflammatory status is frequently accompanied by significant changes in enteric motility (Pontell et al., 2009; Vieira et al., 2014).

Changes in the release of purines together with adaptive modifications of purinoceptors expression and/or function are hallmarks of inflammatory reactions in most tissues, with the GI tract being no exception (reviewed in Roberts et al., 2012). Although purinergic signaling modifications underlying inflammatory responses of the GI tract are not fully understood, the extreme plasticity of the purinergic system and its pathophysiological impact on immune reactions, enteric neuronal networking and cellular communication make drugs targeting the purinergic cascade ideal candidates for treating inflammatory GI diseases. Purines, such as ATP and adenosine, are released from activated infiltrating inflammatory cells (Marquardt et al., 1984), as well from resident neuronal and non-neuronal enteric cells (Stead et al., 1989; Bogers et al., 2000). ATP released in response to inflammatory mediators is crucial for neutrophil activation and immune defense (Lazarowski et al., 2011), but can also function as a danger signal preventing cells invasion of immune-privileged tissues, like myenteric ganglia (Bradley et al., 1997).

In healthy individuals, ATP is co-released by vesicular exocytosis from enteric neurons with other neurotransmitters, like acetylcholine (ACh; Burnstock, 1976), which is the main responsible for gut motility. Mounting evidences indicate that ATP release from non-neuronal cells is also critical to control organ functions, in both normal and stressful conditions (Bodin and Burnstock, 2001; Lazarowski et al., 2011; Mutafova-Yambolieva, 2012; Pinheiro et al., 2013; Silva et al., 2015). Non-neuronal release of ATP may be carried out by vesicular ATP transporters (VNUT) (Sawada et al., 2008; Lazarowski et al., 2011), as well as via other mechanisms involving activation of ABC proteins and hemichannels containing connexins and/or pannexins (Bodin and Burnstock, 2001; Lazarowski et al., 2011; Pinheiro et al., 2013; Carneiro et al., 2014; Timóteo et al., 2014; Silva et al., 2015).

Once released from either neuronal or non-neuronal cells, ATP modifies organ functions by activating directly ionotropic P2X and metabotropic P2Y purinoceptors or indirectly, via P1 receptors, after being metabolized into adenosine through ecto-nucleotidases. At the myenteric neuromuscular synapse, ATP transiently facilitates [^{3}H]ACh release from non-stimulated nerve terminals via the activation of P2X (most probably P2X2 or P2X2/3) receptors (Duarte-Araújo et al., 2009). Fast conversion of ATP directly into AMP catalyzed by NTPDases 2 and 3 (Vieira et al., 2014) and, subsequent, formation of adenosine by ecto-5′-nucleotidase/CD73, controls evoked [^{3}H]ACh release through stimulation of high-affinity excitatory A_{2A} and/or inhibitory A_1 receptors located on nerve terminals and ganglion cells bodies of myenteric neurons, respectively (Duarte-Araújo et al., 2004a, 2009; Vieira et al., 2011). However, inflammation may lead to overexpression of NTPDase2 at the myenteric synapse (Vieira et al., 2014), which is a preferential nucleoside triphosphatase hydrolysing ADP 10 to 15 times less efficiently than ATP (Kukulski et al., 2011). This favors ADP accumulation instead of adenosine and subsequent down-regulation of enteric neuromuscular transmission through the activation of inhibitory $P2Y_1$ receptors (Duarte-Araújo et al., 2009).

In contrast to ATP, adenosine is not stored nor released from synaptic vesicles. The nucleoside is involved in the fine-tuning modulation of enteric neuromuscular functions, influencing nerve-evoked neurotransmitters release, smooth muscle contractility, peristaltic reflexes and, ultimately, the GI transit (reviewed in Antonioli et al., 2011b). Membrane-bound adenosine receptor subtypes are heterogeneously distributed throughout the gut. Our group has contributed to elucidate the localization and function of all four adenosine receptor subtypes at the longitudinal muscle–myenteric plexus of the rat ileum (Vieira et al., 2011) and to uncover the complexities underlying differential activation of adenosine receptors, namely inhibitory A_1 and excitatory A_{2A}, which are major contributors to control ACh release from cholinergic enteric neurons (Duarte-Araújo et al., 2004a; Correia-de-Sá et al., 2006). Data suggest that adenosine inactivation systems, both adenosine deaminase and equilibrative nucleoside transporters, located in close proximity to the nucleoside release / production sites at the myenteric synapse are the key determinants for the predominant excitatory tone mediated by A_{2A} receptors. Under normal physiological conditions, this microenvironment restricts endogenous adenosine actions to the synaptic region where A_{2A} receptors are concentrated on cholinergic nerve terminals, thus preventing activation of other receptor subtypes located more abundantly in extrasynaptic regions (e.g., myenteric cell bodies and enteric glia). Yet, this scenario may change under pathological conditions (see e.g., De Man et al., 2003; Antonioli et al., 2011a; Zoppellaro et al., 2013).

Concerning adenosine production, our group demonstrated that the ecto-nucleotidase pathway contributes only partially to the total interstitial adenosine concentration in the rat myenteric plexus (Correia-de-Sá et al., 2006). Adenosine released as such from either neuronal or non-neuronal cells seems to be the main source of endogenous adenosine in the enteric nervous system (Duarte-Araújo et al., 2004a). This release is sought to be mediated by facilitated diffusion via equilibrative nucleoside transporters (Duarte-Araújo et al., 2004a; Correia-de-Sá et al., 2006) existing in interstitial cells of Cajal (ICCs) (Vieira et al., 2014), among other cells. Another potential source of endogenous adenosine could be adenosine 3′,5′-cyclic monophosphate (cAMP) extruded from activated cells, which

can be converted to AMP and then to adenosine by ecto-phosphodiesterase and ecto-5′-nucleotidase/CD73, respectively (Giron et al., 2008). Likewise, β-NAD^+ released from stimulated enteric nerve varicosities (Hwang et al., 2011; Durnin et al., 2013) could also serve as adenosine precursor. But again, the last two sources of adenosine depend on the activity of ecto-5′-nucleotidase/CD73, which apparently accounts only partially for endogenous adenosine accumulation in the myenteric plexus of the rat ileum (Vieira et al., 2014).

Uncoupling between ATP overflow and extracellular adenosine formation has been observed in post-inflammatory ileitis (Vieira et al., 2014). This situation disrupts the purinergic control of gut motility and has been ascribed to feed-forward inhibition of ecto-5′-nucleotidase/CD73 by high extracellular levels of adenine nucleotides together with augmentation of adenosine deaminase (ADA) activity in the inflamed ileum. While these findings explain, at least partially, the loss of adenosine neuromodulation in the inflamed ileum, they miss the point regarding enhancement of the ATP-mediated tone. In this study, we hypothesized that inflammation-induced changes in the density of specific enteric resident cells could also account to unbalance the release of purines and, thus, their influence on evoked [^{3}H]ACh release from longitudinal muscle-myenteric plexus preparations of rats with TNBS-induced post-inflammatory ileitis.

MATERIALS AND METHODS

TNBS-Induced Intestinal Inflammation Rat Model

The animals were provided free access to standard laboratory chow and water. Animal care and experimental procedures were carried out in accordance with the United Kingdom Animals (Scientific Procedures) Act 1986 and followed the European Communities Council Directive of 24 November 1986 (86/609/EEC) and the National Institutes of Health Guide for Care and Use of Laboratory animals (NIH Publications No. 80-23) revised 1996. All studies involving animals are reported in accordance with ARRIVE guidelines for reporting experiments involving animals (McGrath et al., 2010). This study and all its procedures were approved by the Ethics Committee and the Animal Welfare Responsible Organism of ICBAS-UP (Decision N° 224/2017).

Rats (Wistar, ∼200 g; CharlesRiver, Barcelona, Spain) of both gender were kept at a constant temperature (21°) and a regular light- (06.30–19.30 h) dark (19.30–06.30 h) cycle, with food and water) and a regular light- (06.30–19.30 h) dark (19.30–06.30 h) cycle, with food and water *ad libitum*. Intestinal inflammation was produced by the instillation of 2,4,6-trinitrobenzenesulfonic acid (TNBS) into the lumen of the rat ileum, according to the procedures described in a previous study from our group (Vieira et al., 2014) and confirmed in haematoxylin-eosin stained histological sections using the Pontell and Jergens criteria (Jergens, 1999; Wirtz and Neurath, 2007; Engel et al., 2008; Pontell et al., 2009). After a fasting period of 4–8 h with free access to drinking water, rats underwent median laparotomy under anesthesia with medetomidine (10 mg/Kg) plus ketamine (75 mg/Kg) subcutaneously. At the end of the procedure animals were retrieved with atipamezole (10 mg/Kg) subcutaneously. The terminal ileal loop was gently exteriorized, and TNBS (40 mM, 1 mL) was injected through the enteric wall into the lumen of the ileum with a 29G (0.3366 mm OD) beveled needle, 10 cm proximal to the ileocolonic junction. Controls received 1 mL of 0.9% saline. Sixty minutes after surgery, the rats were allowed to eat and drink *ad libitum*. After surgery, pain was controlled with tramadol hydrochloride (10 mg/Kg) subcutaneously. To have a control of the time course of body weight loss and recovery after injection of TNBS, rats were weighed prior to TNBS administration and daily following surgery. Animals with intestinal inflammation (TNBS) transiently lose weight for 3–4 days after surgery and regain weight thereafter. Seven days after surgery, animals were sacrificed following an overnight fasting period.

[^{3}H]Acetylcholine Release Experiments

Eight centimeters sections of the rat ileum not including the terminal one centimeter and the injected proximal portion were used. The longitudinal muscle strip with the myenteric plexus attached was separated from the underlying circular muscle according to the method of Paton and Vizi (1969). This preparation is abundant in cholinergic neurons, mainly excitatory neurons projecting to the longitudinal muscle (25%) that receive inputs from intrinsic primary afferents (26%) and from ascending and descending pathways (17%) (Costa et al., 1996).

The procedures used for labeling the preparations and measuring evoked [^{3}H] acetylcholine ([^{3}H]ACh) release were previously described (Vizi et al., 1984; Duarte-Araújo et al., 2004a; Correia-de-Sá et al., 2006; Vieira et al., 2011) and used with minor modifications. Isolated longitudinal muscle-myenteric plexus (LM-MP) strips were subdivided into 2-cm pieces, which were randomly mounted in 365 μL chambers of a semi-automated 12-sample superfusion system (SF-12 Suprafusion 1000, Brandel, Gaithersburg, MD, United States) heated at 37°C. The preparations were superfused with gassed (95% O_2 and 5% CO_2) Tyrode's solution containing (mM): NaCl 137, KCl 2.7, $CaCl_2$ 1.8, $MgCl_2$ 1, NaH_2PO_4 0.4, $NaHCO_3$ 11.9 and glucose 11.2. After a 30-min equilibration period, nerve terminals were labeled during 40 min with 1 μM of [^{3}H]choline (specific activity 5 μCi/nmol) under electrical field stimulation (1 Hz frequency, 1 ms pulse width, 75 mA) using two platinum-made grid electrodes placed above and below the muscle strip (transmural EFS stimulation). Following loading, the washout superfusion (1 ml/min) of the preparations was performed during 80 min with Tyrode's solution supplemented with the choline uptake inhibitor, hemicholinium-3 (10 μM). Tritium outflow was evaluated by liquid scintillation spectrometry (TriCarb2900TR, Perkin Elmer, and Boston, MA, United States; % counting efficiency: 56 ± 2%) in 0.6 ml bath samples automatically collected every 1 min using the SF-12 suprafusion system. [^{3}H]ACh release was evoked by two periods of EFS (S_1 and S_2), each consisting of 200 square wave pulses of 1 ms duration delivered at a 5-Hz frequency. The area of the peak corresponding

to evoked [^{3}H]ACh release was calculated as the sum of the differences between the total radioactivity present in the 4 samples collected after stimulus application and the basal tritium outflow (see **Figure 3A**). Baseline values were inferred by linear regression of the radioactivity decay immediately before stimulus and after its return to baseline (e.g., Duarte-Araújo et al., 2004a; Correia-de-Sá et al., 2006; Vieira et al., 2011, 2014). Test drugs were added 8 min before S_2 and were present up to the end of the experiments. The change in the ratio between the evoked [^{3}H]ACh release during the two stimulation periods (S_2/S_1) relative to that observed in control conditions (in the absence of test drugs) was taken as a measure of the effect of the tested drugs; in the absence of test drugs, the calculated S_2/S_1 ratios were 0.83 ± 0.07 ($n = 6$) and 0.80 ± 0.09 ($n = 6$) in control and TNBS-treated samples, respectively (see **Figure 5A**). Positive and negative values represent facilitation and inhibition of evoked [^{3}H]ACh release, respectively. None of the drugs significantly ($P > 0.05$) changed the basal tritium outflow.

Release of ATP and Adenine Nucleosides (Adenosine plus Inosine)

The procedures used to measure ATP and adenine nucleosides were previously described (Vieira et al., 2014). Experiments were performed using an automated perfusion system for sample collecting for given time periods, therefore improving the efficacy of HPLC (with diode array detection) and bioluminescence analysis. After a 30-min equilibration period, the preparations were incubated with 1.8 mL gassed Tyrode's solution, which was automatically changed every 15 min by emptying and refilling the organ bath with the solution in use. The preparations were electrically stimulated once, 15 min after starting sample collection (zero time), using 3000 square wave pulses of 1-ms duration delivered at a 5-Hz frequency. In these experiments, only the sample collected before stimulus application and the two samples collected after stimulation were retained for analysis. Bath aliquots (50–250 μL) were frozen in liquid nitrogen immediately after collection, stored at −20°C (the enzymes are stable for at least 4 weeks) and analyzed within 1 week of collection by HPLC with diode array detection (Finigan Thermo Fisher Scientific System LC/DAD, equipped with an Accela Pump coupled to an Accela Autosample, a diode array detector and an Accela PDA running the X-Calibur software chromatography manager). Chromatographic separation was carried out through a Hypersil GOLD C18 column (5 μM, 2.1 mm × 150 mm) equipped with a guard column (5 μm, 2.1 mm × 1 mm) using an elution gradient composed of ammonium acetate (5 mM, with a pH of 6 adjusted with acetic acid) and methanol. During the procedure the flow rate was set at 200 μL per min and the column temperature was maintained at 20°C. The autosampler was set at 4°C and 50 μL of standard or sample solution was injected, in duplicate, for each HPLC analysis. In order to obtain chromatograms and quantitative analysis with maximal sensibility, the diode array detection wavelength was set at 259 nm for adenosine and 248 nm for inosine (**Supplementary Figure S1**).

The ATP content of the same samples was evaluated in parallel with the luciferin-luciferase ATP bioluminescence assay kit HS II (Roche Applied Science, Indianapolis, IN, United States). Luminescence was determined using a multi detection microplate reader (SynergyHT, BioTek Instruments).

Stimulation-evoked release of adenine nucleotides and nucleosides was calculated by subtracting the basal release, measured in the sample collected before stimulation, from the total release of adenine nucleotides and nucleosides determined in the sample collected immediately after stimulus application.

Myographic Recordings of Ileal Contractile Activity

The contractile activity of the LM-MP was recorded as previously described (Vieira et al., 2009, 2011; Mendes et al., 2015). Ileum strips from control and TNBS-treated rats were mounted along the longitudinal axis in 14 ml capacity perfusion chambers connected to isometric force transducers. The changes in tension were recorded continuously with a PowerLab data acquisition system (Chart 5, v.4.2; AD Instruments, United States). Tissues were preloaded with 0.5 g of tension and allowed to equilibrate for 90 min under continuous superfusion with gassed (95% O_2 and 5% CO_2) Tyrode's solution at 37°C.

Immunofluorescence Staining and Confocal Microscopy Observation

LM-MP fragments were isolated from the rat ileum as previously described. The LM-MP fragments were stretched to all directions and pinned onto Petri dishes coated with Sylgard®. The tissues, then, were fixed in PLP solution (paraformaldehyde 2%, lysine 0.075 M, sodium phosphate 0.037 M, sodium periodate 0.01 M) for 16 h at 4°C, unless stated otherwise. Following fixation, the preparations were washed three times for 10 min each using 0.1 M phosphate buffer. At the end of the washout period, tissues were cryoprotected during 16 h with a solution containing anhydrous glycerol 20% and phosphate buffer 0.1 M at 4°C and, then, stored at −20°C for further processing. Once defrosted, tissue fragments were washed with phosphate saline buffer (PBS) and incubated with a blocking buffer, consisting in fetal bovine serum 10%, bovine serum albumin 1%, triton X-100 1% in PBS, for 2 h; washout was facilitated by constant stirring of the samples. After blocking and permeabilization, samples were incubated with selected primary antibodies (see **Table 1**) diluted in the incubation buffer (fetal bovine serum 5%, serum albumin 1%, Triton X-100 1% in PBS), at 4°C, for 48 h. For double immunostaining, antibodies were combined before application to tissue samples. Please note that ICCs immunofluorescence staining using antibodies against Ano-1 and c-Kit required the use of acetone as tissue fixative, which difficult double immunostaining with other primary antibodies. For the c-Kit/M_3 double immunostaining, tissues were fixed with acetone/formaldehyde solution (50% acetone, 2% PFA in PBS) for 10 min at 4°C, whereas the best results with Ano-1 antibody were obtained in tissues fixed with 100% acetone for 10 min at −20°C. Following the washout of primary antibodies with PBS supplemented with Triton X 1% (3 cycles of 10 min),

tissue samples were incubated with species-specific secondary antibodies in the dark for 2 h, at room temperature. In some experiments tetramethylrhodamine-conjugated α-bungarotoxin (BTX-rhod, 1.25 μM) was incubated together with secondary antibodies to label ionotropic nicotinic receptors containing α7 subunits. Finally, tissue samples were mounted on optical-quality glass slides using VectaShield as mounting media (VectorLabs) and stored at 4°C. Observations were performed and analyzed with a laser scanning confocal microscope (Olympus FV1000, Tokyo, Japan).

The images were stored in TIFF format with the same resolution and, subsequently, analyzed with the ImageJ® software version 1.46r (National Institutes of Health) in order to quantify the density of stained cell constituents of the LM-MP. Settings such as the area, the integrated density and the mean gray value were measured systematically in all analyzed images; background settings were obtained from an area of the section untreated with the primary-antibody. The values obtained were used to calculate the corrected total cryosection fluorescence (CTCF) using a formula published in the website[1].

Co-localization was assessed by calculating the Pearson's linear correlation coefficient (ρ) and the staining overlap for each confocal micrograph stained with two fluorescent dyes using the Olympus Fluoview 4.2 Software (Olympus FV1000, Tokyo, Japan) (see e.g., Barros-Barbosa et al., 2015, 2016a,b). The ρ value is a measure of pixel-by-pixel covariance in the signal levels of two images (stainings) and varies between +1 and −1, inclusive, where 1 is total positive correlation, 0 is no correlation, and −1 is total negative correlation; because it subtracts the mean intensity from each pixel's intensity value, the ρ coefficient is independent of signal levels and signal offset (background). Thus, the Pearson's linear correlation coefficient can be measured in two-color images without any form of preprocessing, making it both simple and relatively safe from user bias (Dunn et al., 2011). Because (1) ρ may be less sensitive to differences in signal intensity between the components of an image caused by different labeling with fluorocromes, photobleaching or different settings of amplifiers, and (2) the negative values of ρ are difficult to interpret when the degree of overlap is the quantity to be measured, the subtraction of the averages of the two colors can be omitted to create the overlap coefficient, which varies between +1 (total overlap) and 0 (no overlap); as with the Pearson's, this coefficient is not dependent on the magnitude of the signal (gain), but does depend on the background.

[1]http://sciencetechblog.com/2011/05/24/measuring-cell-fluorescence-using-imagej

Materials and Solutions

2,4,6-trinitrobenzenesulphonic acid (TNBS); carbenoxolone, choline chloride, paraformaldehyde (prills), lysine, sodium periodate, anhydrous glycerol, fetal bovine serum (Sigma, St Louis, MO, United States); serum albumin, triton X-100, methanol, potassium dihydrogen phosphate (KH_2PO_4) (Merck, Darmstadt, Germany); 3-[[5-(2,3-dichlorophenyl)-1H-tetrazol-1-yl]methyl]pyridine hydrochloride (A438079), mibefradil dihydrochloride, N^G-nitro-L-arginine methyl ester

TABLE 1 | Primary and secondary antibodies used in immunohistochemistry experiments.

Antigen	Code	Species	Dilution	Supplier
Primary antibodies				
NF200	ab8135	Rabbit (rb)	1:1000	ABCAM
nNOS	ab1376	Goat (gt)	1:300	ABCAM
S100β	Ab868	Rabbit (rb)	1:400	ABCAM
Ano-1	Ab53212	Rabbit (rb)	1:100	ABCAM
P2X7	APR-004	Rabbit (rb)	1:50	Alomone
M3	AMR-006	Rabbit (rb)	1:50	Alomone
ENT1	ANT-051	Rabbit (rb)	1:100	Alomone
VaChT	AB1588	Guinea-pig (gp)	1:500	Chemicon
ChAT	AB 144P	Goat (gt)	1:100	Chemicon
GFAP	MAB360	Mouse (ms)	1:600	Chemicon
Vimentin	M0725	Mouse (ms)	1:150	Dako
c-Kit	SC-1494	Goat (gt)	1:50	Santa Cruz
CD206	SC-34577	Goat (gt)	1:50	Santa Cruz
CD11B/αM	Sc-53086	Mouse (ms)	1:50	Santa Cruz
PGP 9.5	7863-1004	Mouse (ms)	1:750	Serotec
Secondary antibodies				
Alexa Fluor 488 anti-rb	A-21206	Donkey	1:1000	Molecular probes
Alexa Fluor 488 anti-ms	A21202	Donkey	1:1000	Molecular probes
Alexa Fluor 568 anti-gt	A11057	Donkey	1:1000	Molecular probes
Alexa Fluor 568 anti-ms	A-10037	Donkey	1:1000	Molecular probes
Alexa Fluor 633 anti-ms	A21052	Goat	1:1000	Molecular probes
TRITC 568 anti-gp	706-025-148	Donkey	1:150	Jackson Immuno Res.
Dylight 649 anti-gp	706-025-148	Donkey	1:100	Jackson Immuno Res.

hydrochloride (L-NAME), 2′,3′-O-(2,4,6-trinitrophenyl)adenosine-5′-triphosphate tetra(triethylammonium) salt (TNP-ATP); tetrodotoxin (TTX) (Tocris Cookson Inc., United Kingdom); Sodium Fluoroacetate (Supelco); Apamin was from Abcam Biochemicals (Cambridge, United Kingdom); tetramethylrhodamine-conjugated α-bungarotoxin (BTX-rhod) was from ThermoFisher Scientific (Waltham, MA, United States); [methyl-^{3}H]-choline chloride (ethanol solution, 80 Ci mmol^{-1}) (Amersham, United Kingdom); ATP bioluminescence assay kit HS II (Roche Applied Science, Indianapolis, IN, United States); medetomidine hydrochloride (Domitor, Pfizer Animal Health); atipamezole hydrochloride (Antisedan, Orion, Espoo, Finland); ketamine hydrochloride (Imalgene, Merial, Lyon, France); Sodium chloride 0.9%, tramadol hydrochloride (Labesfal, Santiago de Besteiros, Portugal).

All drugs were prepared in distilled water. All stock solutions were stored as frozen aliquots at −20°C. Dilutions of these stock solutions were made daily and appropriate solvent controls were done. No statistically significant differences between control experiments, made in the absence or in the presence of the solvents at the maximal concentrations used (0.5% v/v), were observed. The pH of the perfusion solution did not change by the addition of the drugs in the maximum concentrations applied to the preparations.

Presentation of Data and Statistical Analysis

The values are expressed as mean ± SEM, with n indicating the number of animals used for a particular set of experiments. Statistical analysis of data was carried out using unpaired Student's *t*-test with Welch correction. $P < 0.05$ represents significant differences.

RESULTS

Post-inflammatory Ileitis Causes an Increase in Enteric Glial Cells (Types III and IV) and a Partial Loss of Pacemaker Interstitial Cells of Cajal (ICCs)

Structural changes accompanied by neuronal cell death have been observed in chronic intestinal inflammation (Sanovic et al., 1999; Linden et al., 2005; Venkataramana et al., 2015). However, we found no obvious changes in the amount of neurons stained positively against (1) neurofilament NF200 expressed predominantly in Dogiel type I and II neurons (Hu et al., 2002), and (2) a pan-neuronal marker, protein gene product 9.5 (PGP 9.5), in the myenteric plexus 7 days after instillation of TNBS into the lumen of ileum compared to control rats treated with saline (**Figures 1c-f**). This is compatible with Moreels et al. (2001) findings showing that TNBS-induced ileitis in the rat lacks the chronic inflammatory phase and is characterized by an (sub)acute transmural inflammation that is accompanied by functional abnormalities of neuronal activity, which persists for at least 8 weeks without obvious neuronal loss (Stewart et al., 2003; Nurgali et al., 2007). Notwithstanding this, these authors found alterations in longitudinal muscle contractility which was attributed to structural thickness of the ileal wall.

Confocal micrographs show that neuronal cells are grouped in small clusters (enteric ganglia), which are interconnected by nerve fiber bundles from whom emerge small diameter nerve terminals (see e.g., Furness, 2006). Inflammatory infiltrates consisting of monocytes/macrophages exhibiting immunoreactivity against the integrin CD11B/OX42 were found surrounding the myenteric plexus of TNBS-treated rats (**Figure 1b**), but not in preparations from control animals (**Figure 1a**). The absence of inflammatory cells inside myenteric ganglia has been observed before (see also **Figures 3C**, **6**) and this is why myenteric ganglia are considered an immune-privileged tissue (Bradley et al., 1997).

Enteric glial cells express astrocytic cell markers, including the intermediate filament glial fibrillary acidic protein (GFAP) and the calcium-binding protein S100β (Gulbransen and Sharkey, 2012). Subtypes of enteric glia are classified in: type I, intraganglionic cells; type II, within interganglionic fibers; type III, form a matrix in the extraganglionic region remaining in close association with neuronal bundles; and type IV, elongated glia running with nerve fibers within the musculature (Boesmans et al., 2015). **Figures 1g–j** (and adjacent bar graphs) show that the myenteric plexus of rats treated with TNBS exhibits increased amounts of GFAP- and S100β-positive glial cells. Major differences in GFAP- and S100β-immunostaining were found at the neuromuscular region, meaning that TNBS treatment affects predominantly glial cells in the extraganglionic (glial type III) and intramuscular (glial type IV) regions. Thus, in contrast to the absence of significant structural changes in the neuronal cell population, TNBS-induced ileitis stimulates enteric glial cells proliferation (Bradley et al., 1997) or, at least, the increase in expression and/or synthesis of glial protein cell markers (Cabarrocas et al., 2003), in a similar manner to that observed in astrocytes of the CNS (Lhermitte et al., 1980; Rühl et al., 2004).

Interstitial cells of Cajal (ICCs) are known to act as pacemaker cells and integrators of nerve activity and smooth muscle contraction (Sanders, 1996). The number of these cells can significantly change in pathological conditions (Ekblad et al., 1998). Using vimentin, a characteristic intermediate filament of mesenchymal cells like ICC/FLC, we show here that the density of vimentin-positive cells decrease significantly in the myenteric plexus of TNBS-induced ileitis (**Figure 1l**) compared to control preparations (**Figure 1k**); the bar chart does not show data regarding the corrected total cryosection fluorescence (CTCF) staining of vimentin in control and TNBS-treated rats because only two animals per group were analyzed. Notwithstanding this, our data show that staining with anoctamine-1 (Ano-1), a calcium-activated chloride channel involved in the pacemaker activity of ICCs (Gomez-Pinilla et al., 2009), also decreased in density 7-days after instillation of TNBS into the lumen of the rat ileum (**Figure 2A**). Bar charts next to the confocal micrographs show that the partial loss of Ano-1 immunoreactivity was detected focusing both in the ganglion layer (myenteric stellate cells; **Figures 2Aa,b**) and in the neuromuscular region (intramuscular

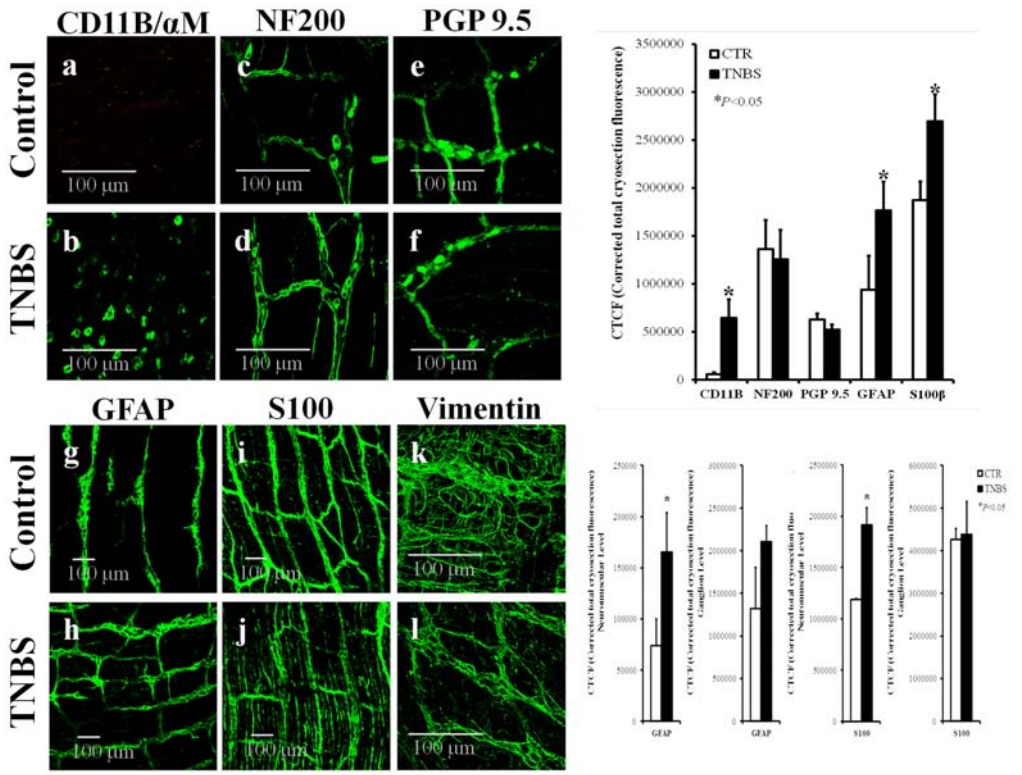

FIGURE 1 | Confocal micrographs of whole-mount preparations of the longitudinal muscle-myenteric plexus of the ileum of control (CTR) and TNBS-treated rats. Z-stacks illustrate the immunoreactivity against CD11B/αM (OX42) (marker of inflammatory cells) **(a,b)**, NF200 (neurofilament expressed in neurons) **(c,d)**, PGP9.5 (pan-neuronal cell marker) **(e,f)**, GFAP **(g,h)** and S100β **(i,j)** (enteric glial cells markers), and vimentin (intermediate filament of mesenchymal cells, like ICCs and FLCs) **(k,l)**. Images are representative of at least four different animals per group, except for vimentin where only two rats were analyzed in each group. Scale bars = 100 µm. Bar charts at the right hand-side panels represents mean ± SEM of corrected total cryosection fluorescence (CTCF) staining for each cell marker; CTCF staining discriminated by ganglion level and neuromuscular region are also shown for GFAP and S100β antibodies. $^*P < 0.05$ (unpaired Student's *t*-test with Welch correction) represent significant differences from control animals.

spindle-shape cells, **Figures 2Ac,d**) of inflamed LM-MP preparations.

The loss of ICC/FLC may affect the frequency of spontaneous enteric contractions (Kinoshita et al., 2007). In fact, myographic recordings demonstrate that spontaneous contractions of LM-MP preparations of the ileum of TNBS-treated animals were less frequent ($P < 0.05$) than those observed in control animals (**Figure 2Bi**). The amplitude of spontaneous contractions had a tendency to increase in TNBS-treated preparations, though without reaching statistical significance ($P > 0.05$) (**Figure 2Bii**).

Myenteric Neurons from the Ileum of TNBS-Treated Rats Release Smaller Amounts of [^{3}H]ACh, But No Relationship Exists between Cholinergic Hypoactivity and Nitrergic Inhibitory Signals

ACh is the prime regulator of intestinal motility and is the most important excitatory neurotransmitter in the myenteric plexus (Costa et al., 1996). **Figure 3A** shows that cholinergic neurons from the myenteric plexus of TNBS-treated rats release significantly less amounts of [^{3}H]ACh (see also Collins et al., 1992a; Davis et al., 1998) despite no obvious changes were detected by confocal microscopy in the density of cholinergic nerve fibers stained specifically against the vesicular acetylcholine transporter (VAChT) (Arvidsson et al., 1997) (**Figure 3B**).

Conversely, we found that TNBS-treated rats had higher immunoreactivity against choline acetyltransferase (ChAT), the enzyme that catalyzes the transfer of an acetyl group from the coenzyme, acetyl-CoA, to choline yielding ACh (**Figure 3C**). Bar charts next to the micrographs show that changes are detected both in the ganglion layer and in the neuromuscular region of TNBS-treated preparations. Increases in ChAT-immunoreactivity may be due to the presence of this enzyme inside CD11B-positive inflammatory cells surrounding myenteric ganglia and infiltrating the intramuscular layer of TNBS-treated rats (**Figure 3C**). In inflamed preparations, CD11B co-localizes with ChAT in a subset of ChAT-positive myenteric cells as indicated by the staining overlap (0.185 ± 0.091, $n = 8$, $P < 0.001$) and the Pearson's coefficient (0.226 ± 0.082, $n = 8$, $P < 0.001$)

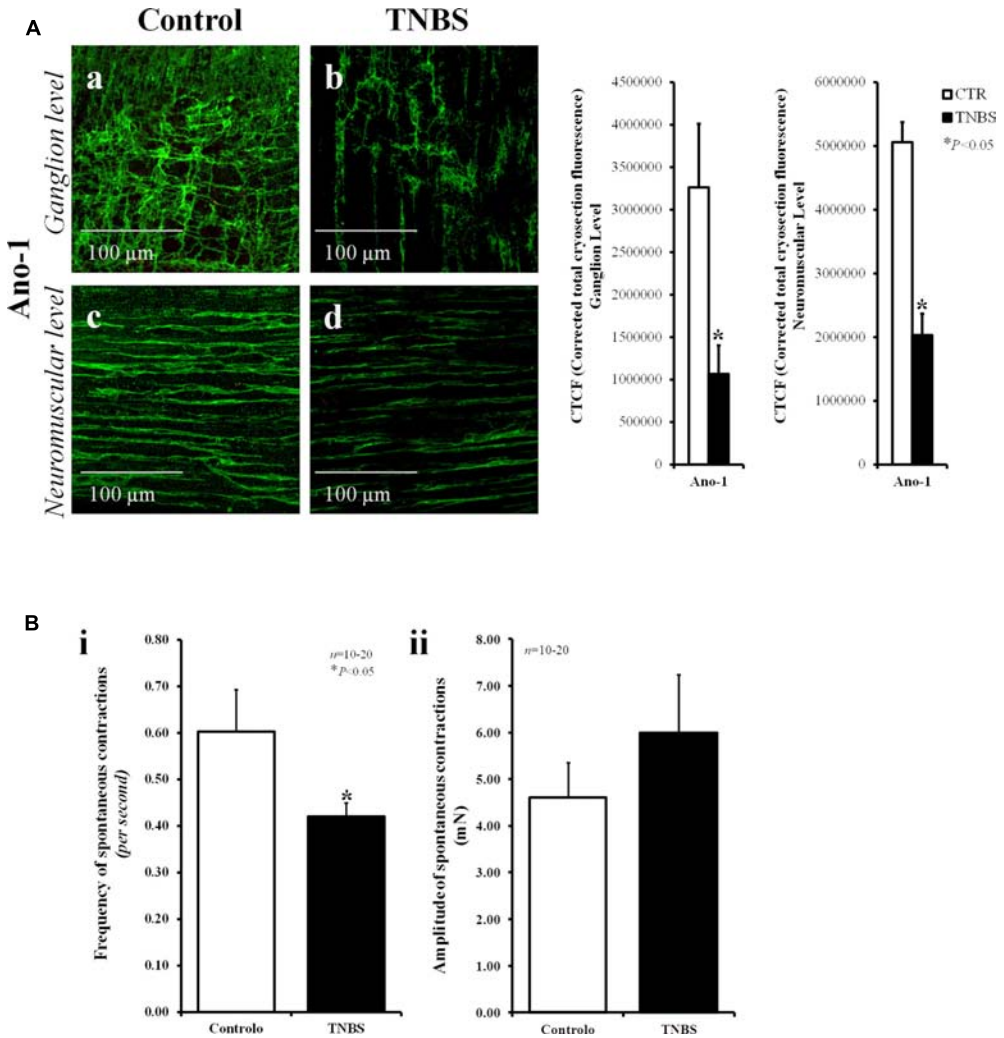

FIGURE 2 | The partial loss of anoctamine-1 (Ano-1)-positive ICCs in the myenteric plexus of TNBS-treated rats correlates with the reduction in the frequency of spontaneous contractions of the rat ileum. **(A)** Confocal micrographs of whole-mount preparations of the ileum of control and TNBS-injected rats taken at the myenteric ganglion level **(a,b)** and at the longitudinal smooth muscle layer **(c,d)**. Shown is the immunoreactivity against Ano-1, a calcium-activated chloride channel involved in the pacemaker activity of ICCs. Images are representative of at least five different animals per group. Scale bars = 100 µm. Bar charts at the right hand-side panel represents mean ± SEM of corrected total cryosection fluorescence (CTCF) of Ano-1 staining at the ganglion level and at the neuromuscular region. **(B)** Histograms representing the frequency **(i)** and the amplitude **(ii)** of spontaneous myographic contractions of the ileum from control rats and TNBS-treated animals. The data are mean ± SEM of an *n* number of animals. $^*P < 0.05$ (unpaired Student's *t*-test with Welch correction) represents significant differences from control animals.

scores. Co-localization of CD11b and ChAT indicate that inflammatory cells are able to synthesize ACh and might contribute to non-neuronal ACh release (volume cholinergic transmission) under certain conditions, like an inflammatory insult.

The lack of obvious changes in the density of VAChT-positive cholinergic nerve fibers, prompted us to investigate whether cholinergic nerve hypoactivity had any relationship with increased volume inhibitory neurotransmission operated by NO, which can be released from neighboring nitrergic nerves, enteric glia cells and/or infiltrating immunocytes (MacEachern et al., 2015; see also **Figure 4A**). This was hypothesized because up-regulation of nitric oxide synthase (NOS) activity and enhancement of NO-mediated inhibitory neurotransmission were demonstrated in chronic inflammatory bowel diseases (Miller et al., 1993). **Figure 4B** shows that inhibition of NOS activity with L-NAME (100 µM) had no effect on evoked [^{3}H]ACh release from the LM-MP of the ileum of control and TNBS-treated rats, indicating that NO does not mediate inhibition of [^{3}H]ACh release in TNBS-induced ileitis. Quantification of neuronal NOS-immunoreactivity in the myenteric plexus of the ileum of TNBS-treated animals was not significantly ($P < 0.05$) different from control rats, both at the ganglion level and at the neuromuscular region (**Figure 4A** and adjacent bar charts).

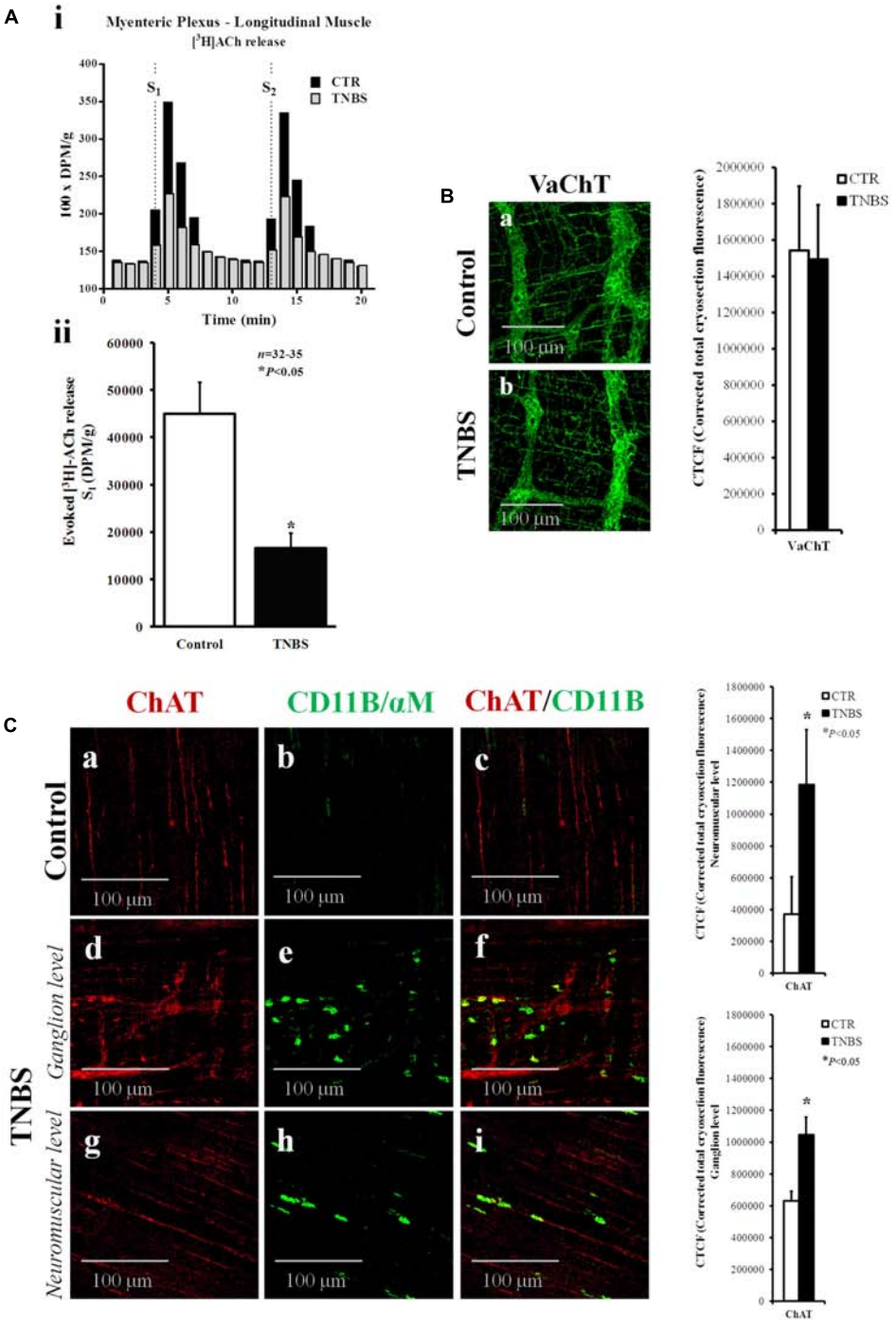

FIGURE 3 | Electrically stimulated myenteric neurons of TNBS-treated rats release smaller amounts of [^{3}H]ACh. **(Ai)** Ordinates represent tritium outflow from typical experiments using myenteric plexus-longitudinal muscle preparations from the ileum of control (CTR) and TNBS-treated rats expressed in disintegrations per min (DPM)/g of wet tissue. Abscissa indicates the times at which samples were collected. [^{3}H]ACh release was elicited by electrical field stimulation (5 Hz, 1 ms, 200 pulses) twice, starting at 4th (S_1) and 13th (S_2) minutes after the end of washout (zero time). **(Aii)** Shown is the amount of [^{3}H]ACh released from electrically stimulated myenteric neurons of the ileum of control and TNBS-treated rats during S_1 in DPM/g of wet tissue. $^*P < 0.05$ (unpaired Student's *t*-test with Welch correction) represents a significant difference from control animals. **(B,C)** Confocal micrographs of whole-mount preparations of the longitudinal muscle-myenteric plexus of the ileum from control and TNBS-treated rats stained against the vesicular ACh transporter (VAChT) and choline acetyltransferase (ChAT). Please note the presence of ChAT immunoreactivity inside CD11B-positive inflammatory cells surrounding myenteric ganglia and infiltrating the intramuscular layer of TNBS-treated rats. Images are representative of at least five animals per group. Scale bar = 100 µm. Bar charts at right hand-side panels represent mean ± SEM of corrected total cryosection fluorescence (CTCF) staining against VAChT and ChAT, respectively. $^*P < 0.05$ (unpaired Student's *t*-test with Welch correction) represents a significant difference from control animals.

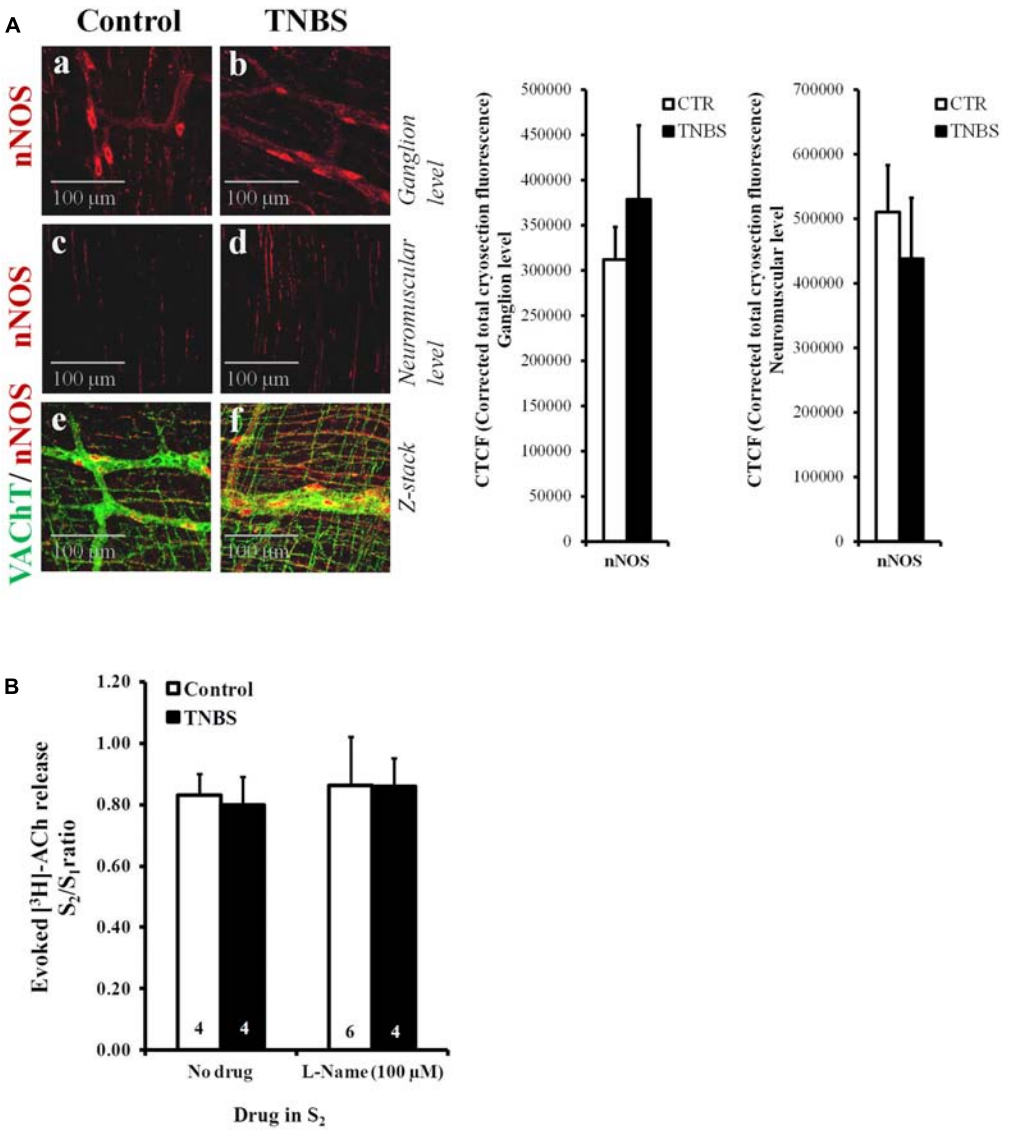

FIGURE 4 | (A) Confocal micrographs of whole-mount preparations of the longitudinal muscle-myenteric plexus of the ileum from control and TNBS-treated rats taken at the myenteric ganglion level **(a,b)** and at the longitudinal smooth muscle layer **(c,d)**. Shown is the immunoreactivity against neuronal NOS (nNOS). Z-stacks presented in panels **(e)** and **(f)** show that nNOS-positive nitrergic nerve fibers (red) are adjacent, but do not co-localize, with VAChT immunoreactivity (green). Images are representative of at least four individuals per group. Scale bar = 100 µM. Bar charts at the right hand-side panel represent mean ± SEM of corrected total cryosection fluorescence (CTCF) nNOS staining detected at the ganglion level and at the neuromuscular region. **(B)** Effect of the nitric oxide synthase (NOS) inhibitor, L-Name (100 µM), on [^{3}H]ACh released from stimulated myenteric neurons of the ileum of control and TNBS-treated rats. After loading and washout periods, [^{3}H]ACh release was elicited by two trains (S_1 and S_2) of electrical field stimulation, each consisting of 200 pulses delivered at a 5 Hz frequency. L-Name (100 µM) was applied 8 min before S_2. The ordinates are changes in S_2/S_1 ratios compared to the S_2/S_1 ratio obtained without addition of any drug. The data are means ± SEM of four to six individuals.

Post-inflammatory Shift from Neuronal to Non-neuronal Control of Evoked [^{3}H]ACh Release from Stimulated Myenteric Neurons

Figure 5A shows that [^{3}H]ACh release from electrical-stimulated ileal myenteric neurons of healthy rats was almost prevented ($P < 0.05$) by the blockage of nerve action potentials with tetrodotoxin (TTX, 1 µM). This confirms our previous observations, where we also demonstrated that [^{3}H]ACh excoytosis from depolarized myenteric nerve terminals depended on Ca^{2+} influx through voltage-sensitive channels (Duarte-Araújo et al., 2004a,b; Correia-de-Sá et al., 2006). Interestingly, inhibition of electrically driven [^{3}H]ACh outflow from TNBS-treated preparations was much less sensitive to TTX (1 µM) than control preparations (**Figure 5A**), but transmitter release was still fully prevented ($P < 0.05$) in Ca^{2+}-free conditions, i.e., the S_2/S_1 ratio decreased from 0.80 ± 0.09 ($n = 6$) to 0.13 ± 0.01

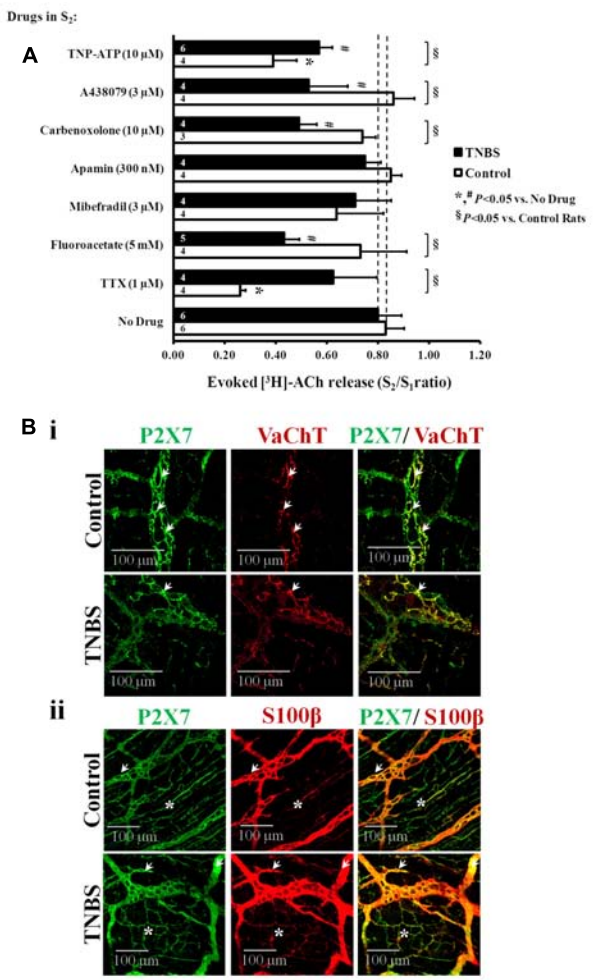

FIGURE 5 | (A) Effects of TTX (1 μM, a nerve action potential blocker), sodium fluoroacetate (5 mM, a glial cell metabolism uncoupler), mibefradil (3 μM, an inhibitor of Ca_v3 (T-type) channels existing in ICCs), apamin (0.3 μM, an inhibitor of small-conductance KCa2 (SK3) channels characteristic of FLCs), carbenoxolone (10 μM, a pannexin-1 inhibitor), A438079 (3 μM, a P2X7 receptor antagonist) and TNP-ATP (10 μM, a blocker of ionotropic P2X2 and P2X2/3 receptors) on electrically evoked [^{3}H]-ACh release from the LM-MP of the rat ileum of control and TNBS-treated rats. After loading and washout periods, [^{3}H]ACh release was elicited by two trains (S_1 and S_2) of electrical field stimulation, each consisting of 200 pulses delivered at a 5 Hz frequency. Drugs were applied 8 min before S_2. Abscissa is changes in S_2/S_1 ratios compared to the S_2/S_1 ratio obtained without addition of any drug. The data are means ± SEM of three to six individuals. $^{*,\#}P < 0.05$ (unpaired Student's *t*-test with Welch correction) represent significant differences from the situation where no drugs were added to control and TNBS-treated preparations, respectively (dashed vertical lines); § $P < 0.05$ (unpaired Student's *t*-test with Welch correction) represent significant differences from control animals. Confocal micrographs of whole-mount preparations of the longitudinal muscle-myenteric plexus of the ileum from control and TNBS-treated rats. Shown is the P2X7 receptor immunoreactivity in preparations also stained against the vesicular ACh transporter (VAChT, **Bi**) and the enteric glial cell marker (S100β, **Bii**). The P2X7 receptor co-localizes partially with VAChT at the ganglion level (**Bi**, white arrows); a more extensive co-localization exists between the P2X7 receptor and the glial cell marker, S100β **(Bii)**, both at myenteric ganglia (white arrows) and at the neuromuscular layer (asteriks) of control and TNBS-treated preparations. Z-stack images are representative of at least four animals per group. Scale bar = 100 μm.

($n = 4$) upon removing Ca^{2+} from the Tyrode's solution. Thus, the results suggest that [^{3}H]ACh outflow in TNBS-induced ileitis is likely due to exocytosis triggered via direct axonal activation by a non-neuronal released activator (see e.g., Broadhead et al., 2012; Gulbransen et al., 2012).

Under the present experimental conditions, the influence of smooth muscle contractions was ruled out since the Ca_v1 (L-type) channel blocker, nifedipine (1 μM), depressed ACh-induced contractions of the longitudinal muscle without affecting the release of [^{3}H]ACh from stimulated LM-MP of both control (Correia-de-Sá et al., 2006) and TNBS-treated rats (unpublished observations). Likewise, we discarded the participation of ICCs and fibroblasts-like cells (FLCs) in the regulation of evoked [^{3}H]ACh release in both animal groups, because the transmitter release was not ($P > 0.05$) affected when the experiments were performed in the presence of selective inhibitors of ICCs and FLCs activity (**Figure 5A**), namely mibefradil (3 μM) and apamin (0.3 μM) which block specifically voltage-sensitive Ca_v3 (T-type) and small-conductance $K_{Ca}2$ (SK3) channels that are characteristic of these cells, respectively (Fujita et al., 2003).

Next, we tested whether the gliotoxin, sodium fluoroacetate (5 mM) (MacEachern et al., 2015), could affect [^{3}H]ACh release from stimulated myenteric neurons. **Figure 5A**, shows that while sodium fluoroacetate (5 mM) was unable to change transmitter release in preparations from healthy rats, it significantly ($P < 0.05$) decreased evoked [^{3}H]ACh release from myenteric neurons of TNBS-treated animals. These results led us to the hypothesis that the cholinergic tone is kept to a minimum due to the release of an excitatory gliotransmitter from proliferating enteric glial cells in post-inflammatory ileitis.

ATP May Be the Putative Excitatory Gliotransmitter Responsible for Keeping the Cholinergic Tone in Post-inflammatory Ileitis

The nature of the putative excitatory gliotransmitter regulating ACh release from inflamed myenteric neurons is uncertain. Considering our previous observations that (1) ATP can be released from both neuronal and non-neuronal cells, and that (2) it can increase the release of [^{3}H]ACh from resting myenteric nerve terminals through the activation of ionotropic P2X receptors in the presence of TTX (Duarte-Araújo et al., 2009), we designed experiments to test if endogenous ATP could play any role in the regulation of ACh release in TNBS-induced ileitis.

Recently, our group demonstrated that ATP can be released from non-neuronal cells through hemichannels containing pannexin-1 and this mechanism can lead to a "vicious cycle" where ATP can induce the release of ATP via the activation of ionotropic P2X and metabotropic P2Y receptors under normal and pathological conditions (Pinheiro et al., 2013; Noronha-Matos et al., 2014; Timóteo et al., 2014; Certal et al., 2015; Silva et al., 2015). High extracellular ATP levels, such as those detected after an inflammatory insult, can stimulate low-affinity P2X7 receptors, which often but not exclusively couple to pannexin-1 to promote ATP outflow, via the pannexin-1 hemichannel or the P2X7 receptor pore (Gulbransen and Sharkey, 2012;

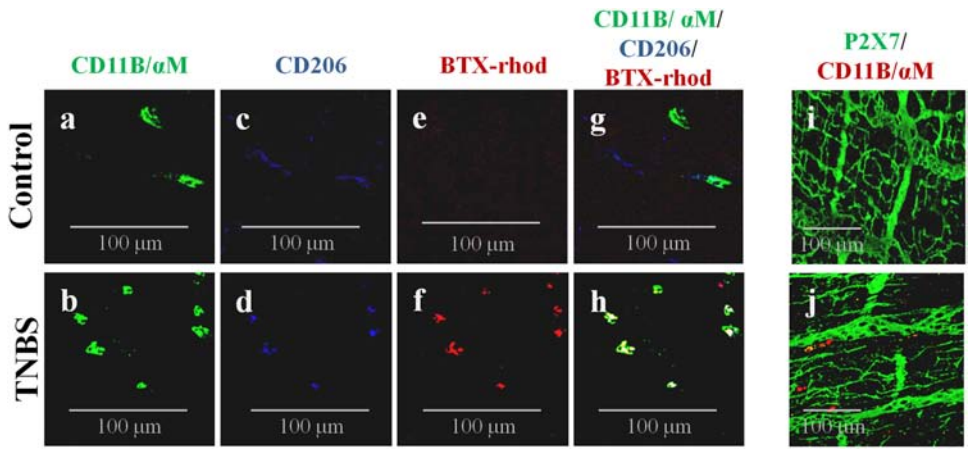

FIGURE 6 | CD11B-immunoreactive inflammatory cells surrounding myenteric ganglia and infiltrating the intramuscular layer of TNBS-treated rats also stain positively against CD206 (a cell marker of anti-inflammatory M2 macrophages) and tetramethylrhodamine-conjugated α-bungarotoxin (BTX-rhod) identifying α7 subunit-containing nicotinic receptors both in Control **(a,c,e,g)** and TNBS-treated **(b,d,f,h)** rats. Confocal micrographs of whole-mount preparations of the longitudinal muscle-myenteric plexus of the ileum of Control **(i)** and TNBS-treated **(j)** rats show that CD11B-positive cells do not express the P2X7 receptor. Images are representative of at least four animals per group. Scale bar = 100 μm.

Diezmos et al., 2013). This prompted us to investigate the role of pannexin-1 hemichannels and P2X7 receptors on [^{3}H]ACh release from stimulated LM-MP preparations of control and TNBS-treated rats using specific inhibitors.

Figure 5A, shows that selective blockage of pannexin-1 hemichannels and P2X7 receptors respectively with carbenoxolone (10 μM) and A438079 (3 μM) significantly ($P < 0.05$) decreased [^{3}H]ACh release from myenteric neurons of TNBS-treated rats, but not of their control littermates. The magnitude of the inhibitory effects on transmitter release produced by carbenoxolone (10 μM) and A438079 (3 μM) was about the same of that observed upon blocking glial cells activity with sodium fluoroacetate (5 mM) (**Figure 5A**). Notwithstanding the fact that P2X7 receptors are present in VAChT-positive cholinergic nerve terminals in myenteric ganglia (**Figure 5Bi**), the distribution of the P2X7 immunoreactivity in the myenteric plexus of both groups of animals accompanies that of the glial cell marker, S100β (**Figure 5Bii**). Co-localization of the P2X7 receptor and the S100β glial marker has been demonstrated before in the rat myenteric plexus (Vanderwinden et al., 2003; Gulbransen and Sharkey, 2012). This feature was confirmed and expanded to post-inflammatory ileitis in our experimental settings as demonstrated by the elevated scores of the staining overlap (0.706 ± 0.059 and 0.703 ± 0.001 in control and TNBS-treated rats, respectively; 4 animals per group, $P < 0.01$) and the Pearson's coefficient ($\rho = 0.674 \pm 0.074$ and $\rho = 0.665 \pm 0.006$ in control and TNBS-treated rats, respectively; 4 animals per group, $P < 0.01$) obtained by merging the two fluorescence channels (yellow staining; see **Figure 5Bii**).

We discarded the presence of P2X7 receptors in CD11B$^+$/ChAT$^+$ inflammatory cells surrounding myenteric ganglia and/or infiltrating the intramuscular layer of the ileum of TNBS-treated rats (**Figures 6i,j**), thus eliminating the contribution of P2X7 receptors to TTX-resistant ACh release from these cells. Notwithstanding this, our data show that a subset of CD11B-labeled cells present in the myenteric plexus of TNBS-treated rats are also positive to the scavenger mannose C-type receptor, CD206, and to tetramethylrhodamine-conjugated α-bungarotoxin (BTX-rhod) (**Figures 6a–h**). Co-localization of CD11B and CD206 is reflected by increases in the staining overlap from 0.170 ± 0.028 in control animals to 0.431 ± 0.169 in TNBS-treated rats, while the same occurred concerning the Pearson's coefficient, i.e., the ρ value increased from 0151 ± 0.027 in control animals to 0.411 ± 0.178 in TNBS-treated rats (4 animals per group, $P < 0.01$). A similar situation was verified when double immunolabelling CD11B or CD206 positive inflammatory cells with BTX-rhod. This labeling pattern suggests that CD11B-positive inflammatory cells next to myenteric neurons of TNBS-treated rats have an increasing proportion of anti-inflammatory macrophages of the M2 subtype (**Figures 6a–h**; Rõszer, 2015) carrying α7 nicotinic receptors, which cohabitate with a still significant amount of CD11B$^+$/CD206$^-$ cells (most probably monocytes-derived pro-inflammatory M1 macrophages). Activation of α7 subunit-containing nicotinic receptors by ACh in resident M2 macrophages modulates ATP-induced Ca^{2+} responses which play a key role in the gastrointestinal cholinergic anti-inflammatory pathway (Matteoli et al., 2014).

Murine enteric neurons express mainly P2X2 and P2X3 subunit-containing receptors (Galligan, 2002; Castelucci et al., 2002; Ren et al., 2003), which are responsible for ATP-induced Ca^{2+} transients (Ohta et al., 2005) and [^{3}H]ACh overflow from resting myenteric neurons in the presence of TTX (Duarte-Araújo et al., 2009). Fast desensitizing homomeric P2X2 and/or heteromeric P2X2/3 receptor channels can be blocked by micromolar concentrations of trinitrophenyl-substituted nucleotides, especially TNP-ATP (Virginio et al., 1998). In control rats, TNP-ATP (10 μM) reduced the release of [^{3}H]ACh by

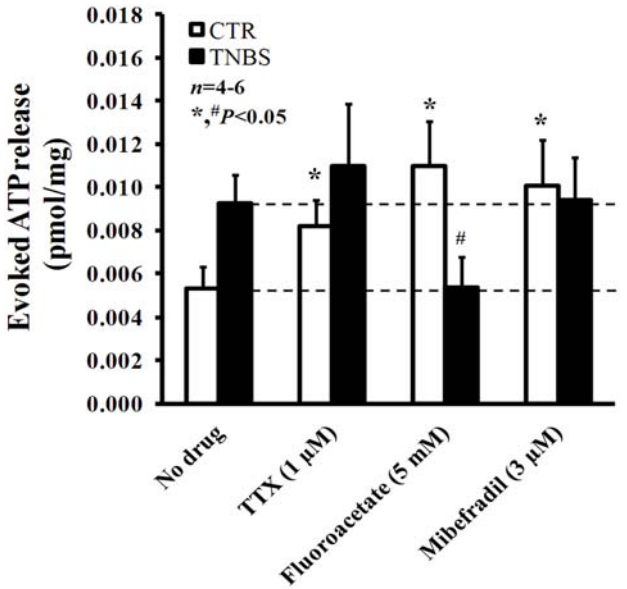

FIGURE 7 | Effects of TTX (1 μM), sodium fluoroacetate (5 mM) and mibefradil (3 μM) on ATP release from stimulated longitudinal muscle-myenteric plexus preparations of the ileum from control and TNBS-treated rats. Drugs were in contact with the preparations for at least 15 min before stimulus application (5 Hz frequency, 3000 pulses of 1 ms duration). Samples from the incubation media were collected and analyzed using the luciferin-luciferase bioluminescence assay for ATP quantification (this figure); aliquots of the same samples were used in parallel to measure their content in adenosine (plus inosine) by HPLC with diode array detection (results in **Figure 8**). Ordinates represent stimulation-induced increases in ATP above baseline levels determined immediately before the stimulus application; results are expressed in pmol/mg of tissue. The data are means ± SEM of four to six animals. $^{*,\#}P < 0.05$ (unpaired Student's *t*-test with Welch correction) represent significant differences from the amount of ATP released in the absence of any drug added to preparations from control and TNBS-treated animals (dashed horizontal lines), respectively.

53 ± 10% ($n = 4$), but its effect was significantly decreased to 17 ± 5% ($n = 5$, $P < 0.05$) in the ileum of TNBS-treated animals (**Figure 5A**). These findings raise the question about the purinoceptor subtype involved in ATP-induced transmitter release from myenteric neurons in post-inflammatory ileitis, a situation where the extracellular concentration of the nucleotide dramatically increases (Vieira et al., 2014). The low-affinity/slow-desensitizing P2X7 receptor is the most probable candidate, because (1) evoked [^{3}H]ACh release was significantly attenuated by A438079 (3 μM) (**Figure 5A**), and (2) VAChT-positive cholinergic myenteric nerve terminals exhibit P2X7 receptor immunoreactivity (**Figure 5Bi**).

Post-inflammatory Myenteric Glial Cells Release Higher Amounts of ATP

In a previous study from our group, we demonstrated that ATP is released in higher amounts from electrically stimulated TNBS-treated preparations than in control tissues (Vieira et al., 2014). High post-inflammatory ATP levels are comparable to those obtained in control LM-MP preparations submitted to blockage of action potentials generation, of glial cells metabolism and of ICCs activation respectively with TTX (1 μM), sodium fluoroacetate (5 mM) and mibefradil (3 μM) (**Figure 7**). These findings indicate that all these cells contribute to keep low extracellular ATP levels in normal physiological conditions. However, this scenario changes considerably in TNBS-induced ileitis. From the inhibitors used to target specifically the three resident cell types in the myenteric plexus, only sodium fluoroacetate (5 mM) was able to decrease significantly ($P < 0.05$) the release of ATP in post-inflammatory ileitis, while TTX (1 μM) and mibefradil (3 μM) were both ineffective (**Figure 7**).

This suggests that increased overflow of ATP after an inflammatory insult may possibly result from activation of proliferating glial cells. Interestingly, the pharmacology affecting ATP overflow from stimulated ileal preparations of TNBS-treated rats (**Figure 7**) looks like that verified by measuring the release of [^{3}H]ACh (**Figure 5A**), further strengthening our hypothesis that ATP may be the putative excitatory gliotransmitter responsible for keeping to a minimum the cholinergic tone in TNBS-induced ileitis.

Moreover, blockade of pannexin-1 hemichannels with carbenoxolone (10 μM) and P2X7 receptors with A438079 (3 μM) significantly ($P < 0.05$) decreased ATP overflow in TNBS-treated rats; while carbenoxolone (10 μM) was more active in decreasing the resting release of the nucleotide (from 5.1 ± 0.3 to 2.8 ± 0.4 fmol/mg, $n = 4$), A438079 (3 μM) depressed the release of ATP induced by electrical stimulation to the control level (from 9.2 ± 0.8 to 5.1 ± 0.6 fmol/mg, $n = 4$). These results suggest that pannexin-1 hemichannels may drive ATP release even during resting conditions, while ATP-induced ATP release via the activation of low affinity P2X7 receptors requires high extracellular levels of the nucleotide that might be favored by electrical stimulation of the tissue.

Deficient Extracellular Adenosine Accumulation in Post-inflammatory Ileitis Parallels the Loss of ICCs

Although adenosine may be released from activated inflammatory cells (Marquardt et al., 1984) in the vicinity of myenteric neurons (Bogers et al., 2000), the loss of adenosine neuromodulatory control of evoked [^{3}H]ACh release in TNBS-induced ileitis detected in a previous report results mainly from deficient accumulation of the nucleoside at the myenteric synapse (Vieira et al., 2014); this was verified despite the increase in ATP content of the same samples. Uncoupling between ATP overflow and adenosine levels in post-inflammatory ileitis was ascribed to feed-forward inhibition of ecto-5′-nucleotidase/CD73 and upregulation of adenosine deaminase. Here, we decided to evaluate the putative contribution of inflammation-induced cell density changes in the myenteric plexus to adenosine deficiency. To this end, we measured in parallel to the ATP levels the extracellular concentration of adenosine and of its deamination metabolite, inosine, by HPLC (with diode array detection) immediately before and after electrical stimulation of LM-MP preparations of both control and TNBS-treated rats in the presence of cell-specific activity inhibitors. **Figure 8A**

shows that the amounts of adenosine (plus inosine) released into the extracellular fluid following stimulation of the LM-MP are much higher in healthy controls than in TNBS-treated rats. It is worth to note that the amount of adenosine (plus inosine) accumulated in the LM-MP of healthy rats following electrical field stimulation was 7,000-fold higher than the ATP concentration in the same collected samples. It is also important to notice that we were unable to detect β-NAD^+ and/or cyclic AMP in our collected samples, neither before nor after electrical stimulation of the preparations; this was verified despite our chromatographic system is suitable to detect standards of these putative adenosine precursors in the same (picomolar) concentration range (data not shown). In view of this, stoichiometric conversion of ATP (or other released adenine nucleotide) into adenosine by ectonucleotidases can barely be considered a major source of the nucleoside in the myenteric plexus of the rat ileum (see e.g., Correia-de-Sá et al., 2006), thus confirming our previous suspicions that high amounts of adenosine may be released as such from neuronal and/or non-neuronal cells (Duarte-Araújo et al., 2004a).

Stimulus-evoked adenosine (plus inosine) release was partially dependent on neuronal activity in preparations from healthy rats, but not in the ileum of TNBS-treated animals. This was assumed because pre-treatment of the preparations with TTX (1 μM) reduced by about 50% the outflow of adenine nucleosides in control tissues with no effect on TNBS-treated preparations (**Figure 8A**). This means that the neuronal source of adenosine may be severely affected in TNBS-induced ileitis due to neuronal cells dysfunction (see above). Even though we considered unlikely that proliferating glial cells could contribute to adenosine deficits in the inflamed myenteric plexus of the rat ileum, we tested the effect of the glial cell metabolic uncoupler, sodium fluoroacetate (5 mM). Inhibition of glial cells metabolism caused a significant ($P < 0.05$), yet of smaller magnitude compared TTX, reduction of adenosine outflow from stimulated LM-MP preparations of control rats, whereas sodium fluoroacetate (5 mM) had only a minor effect ($P > 0.05$) in the myenteric plexus isolated from TNBS-treated rats (**Figure 8A**). The inhibitory action of sodium fluoroacetate (5 mM) was slightly more evident in healthy tissues than in TNBS-treated preparations, which is in agreement with the proposed uncoupling between ATP overflow and adenosine formation secondary to the inflammatory insult.

Prevention of smooth muscle contractions with the voltage-sensitive Ca_v1 (L-type) channel inhibitor, nifedipine (5 μM), did not affect the release of adenosine (plus inosine) in both animal groups (Correia-de-Sá et al., 2006; Vieira et al., 2009, 2014). However, blockade of Ca_v3 (T-type) channels expressed in ICCs with mibefradil (3 μM) significantly ($P < 0.05$) attenuated the release of adenosine (plus inosine) from both control and TNBS-treated animals. Taking into consideration previous findings from our laboratory demonstrating that the nucleoside transport inhibitor, dipyridamole (0.5 μM), decreased proportionally and by a similar amount the outflow of adenosine (plus inosine) to that obtained with mibefradil (3 μM) from both control and inflamed tissues (Vieira et al., 2014), it is very likely that adenosine accumulated in the ileum following an inflammatory insult originates predominantly from activated ICCs via a dipyridamole-sensitive equilibrative nucleoside transporter (ENT). The presence of ENT1-immunoreactivity in ICC-like cells located in the myenteric plexus of the ileum of control and TNBS-treated rats is shown in **Figure 8Bi**. The decrease in ENT1 immunoreactivity seems to parallel that of Ano-1 positive ICCs in the myenteric plexus of the ileum of TNBS-injected animals (see **Figures 2A**, **8Bi**).

In a previous study, we showed that adenosine outflow via dipyridamole-sensitive ENT-1 may be positively modulated by muscarinic M_3 receptors in the LM-MP of the rat ileum leading to activation of facilitatory A_{2A} receptors on cholinergic nerve terminals (Vieira et al., 2009). Signals from myenteric motor nerves onto ICCs involve M_3 receptors in mice intestine (Wang et al., 2003; So et al., 2009), indicating that a close relationship between enteric excitatory nerve terminals and intramuscular ICCs is fundamental to modulate cholinergic neurotransmission in the enteric nervous system (Wang et al., 2003). **Figure 8C** shows that muscarinic M_3 receptors are located in a small subset of c-Kit positive ICCs in myenteric ganglia, but this proportion significantly increases in c-Kit expressing intramuscular ICCs. Similar results were obtained in murine small intestine and gastric fundus (Epperson et al., 2000; Lecci et al., 2002), with muscarinic M_3 receptors staining outside c-Kit-labeled cells most probably located in enteric neurons. Interestingly, muscarinic M_3 receptors immunoreactivity substantially decreased in extraganglionic myenteric cells of TNBS-injected animals compared to their control littermates (**Figure 8Bii**). This pattern resembles that obtained in micrographs stained with ENT1 and Ano-1 antibodies (see **Figures 2A**, **8Bi**, respectively). Unfortunately, we were unable to double label LM-MP preparations with ENT1 plus M_3 and ENT-1 plus Ano-1 because the available antibodies were raised in the same host species (rabbit) (see **Table 1**); in addition, we felt technical difficulties when attempting to target ENT-1 in c-Kit-stained ICCs because the latter requires the use of a tissue fixative solution containing 50% acetone and 2% PFA in PBS, which revealed incompatible with the ENT-1 immunostaining.

DISCUSSION

TNBS-Induced Ileitis Affects Cholinergic Function without Neuronal Cell Loss: A Model to Study Neuronal to Non-neuronal Cell Communication after Inflammatory Insults

A number of key cellular players may be involved in the reaction to inflammatory insults by the gastrointestinal system. These include inflammatory cells, such as granulocytes, lymphocytes, mast cells, monocytes and macrophages, which release numerous cytokines, pro-inflammatory peptides, neuroactive and neurotrophic factors, noxious compounds,

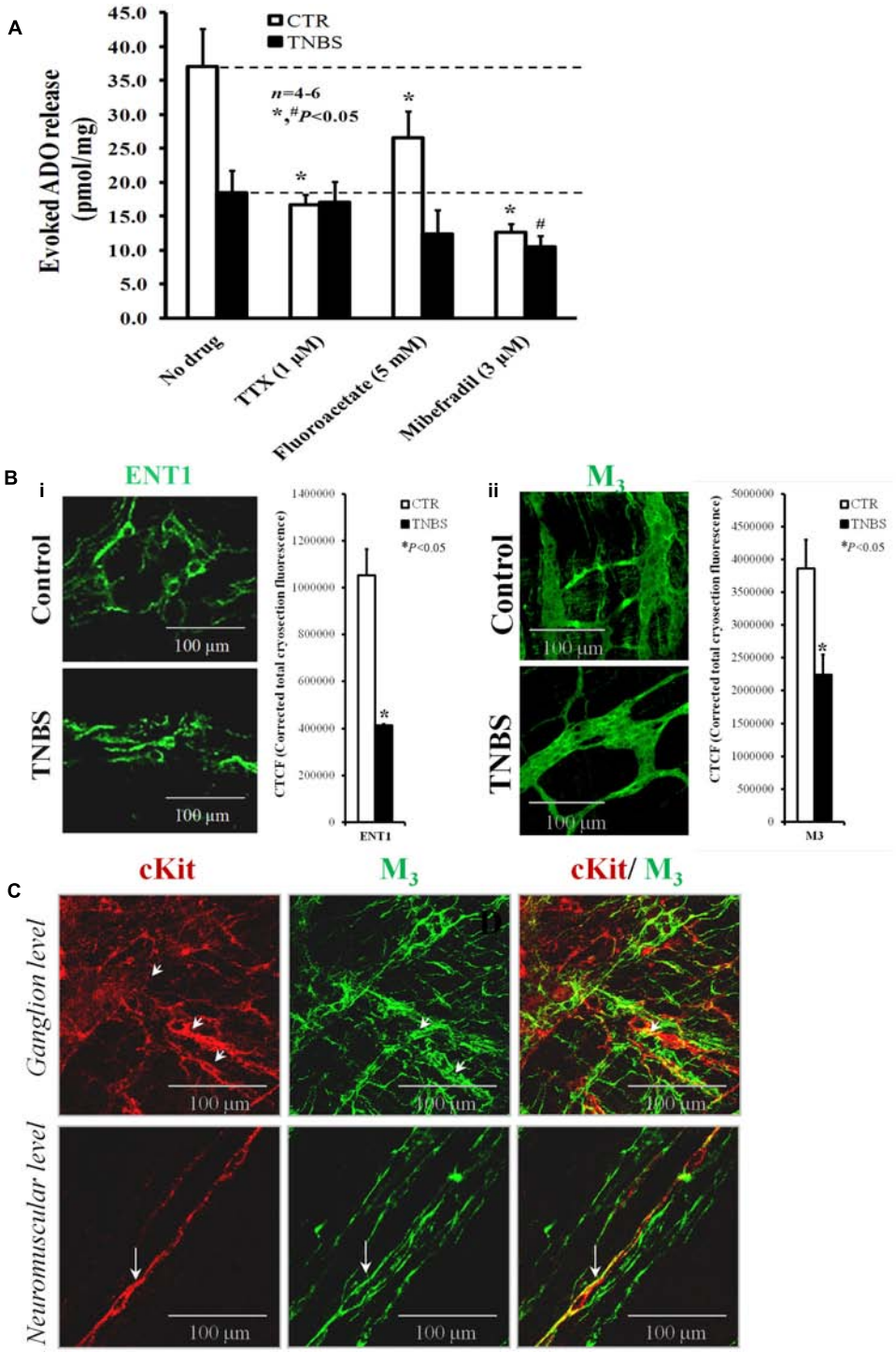

FIGURE 8 | (A) Shows the effects of TTX (1 μM), sodium fluoroacetate (5 mM) and mibefradil (3 μM) on evoked adenosine (plus inosine) release from stimulated LM-MP ileal preparations of control and TNBS-treated rats. Drugs were in contact with the preparations for at least 15 min before EFS. Samples from the incubation media were collected and analyzed by HPLC with diode array detection to evaluate their content in adenine nucleosides (see **Supplementary Figure S1**); aliquots of the same samples were tested in parallel using the luciferin-luciferase bioluminescence assay for ATP quantification (results in **Figure 7**). Ordinates represent stimulation-induced increases in adenosine (plus inosine) above baseline levels determined immediately before EFS; results are expressed in pmol/mg of tissue. The data are means ± SEM of four to six individuals. $^{*,\#}P < 0.05$ (unpaired Student's *t*-test with Welch correction) represent significant differences from the amount of adenosine (plus inosine) released in the absence of any drug added to preparations from control and TNBS-treated animals (dashed horizontal lines), respectively.

(Continued)

FIGURE 8 | Continued
(B) Shown are confocal micrographs of whole-mount preparations of the longitudinal muscle-myenteric plexus of the ileum from control and TNBS-treated rats stained against the equilibrative nucleoside transporter 1 (ENT1) (i) and the muscarinic M_3 receptor. The staining pattern of both antibodies resembles that obtained for anoctamine-1 (Ano-1)-positive interstitial cells at the ganglion level shown **Figure 2**. Images are representative of at least four individuals per group. Scale bar = 100 μM. Bar charts at the right hand-side panels represents mean ± SEM of corrected total cryosection fluorescence (CTCF) of ENT-1 and muscarinic M_3 antibodies staining, respectively. $^*P < 0.05$ (unpaired Student's *t*-test with Welch correction) represent significant differences from control animals. **(C)** Shown is confocal micrographs of whole-mount preparations of the longitudinal muscle-myenteric plexus (LM-MP) of the ileum of control rats. Please note that the majority of c-Kit positive interstitial cells of Cajal (ICCs, red) at the neuromuscular region are endowed with muscarinic M_3 receptors (green) (long arrows); although co-localization of c-kit (red) and muscarinic M_3 receptor (green) is still apparent at the myenteric ganglion level (small arrows), most of the cells express only one of these markers. Yellow staining denotes co-localization when overlaying the green and red confocal channels.

inflammatory enzymes and other danger signaling molecules. Enteric plasticity comprises a wide range of structural and/or functional changes in enteric neurons, glial cells and interstitial cells (ICC/FLC). As a result of adaptive responses to different types of pathophysiological conditions, enteric neurons are able to rapidly change their structure, function and chemical phenotype in order to maintain homeostasis of gut functions. In contrast to long-term functional abnormalities in the activity of neuronal cells described by several authors (Stewart et al., 2003; Nurgali et al., 2007) and confirmed in the present study by denoting hypoactivity of cholinergic neurotransmission, we found no obvious modifications in the cellular density and distribution of specific neuronal cell markers (e.g., NF200, PGP 9.5, VAChT, nNOS) in TNBS-induced ileitis. In this sense, ileitis caused by TNBS differs from other chronic inflammatory disease models because it lacks the chronic inflammatory phase (Moreels et al., 2001) that is usually accompanied by neuronal cell loss (Sanovic et al., 1999; Linden et al., 2005; Venkataramana et al., 2015). Notwithstanding, this constrain may be turned into an advantage characteristic of this animal model if one wants to investigate the adaptive changes of neuronal to non-neuronal cells communication after a transient inflammatory insult, as we aimed in this work.

Results show that stimulated myenteric neurons release smaller amounts of [^{3}H]ACh in the ileum of TNBS-treated rats compared to their control littermates, without evidence of any alteration in the density of VAChT-positive cholinergic nerve fibers in the myenteric plexus. Likewise, significant decreases in [^{3}H]choline uptake, acetylcholine release and contractile responses to stimulation of enteric nerves have been observed in rats with colitis induced by TNBS (Poli et al., 2001). These results imply a functional loss, not corresponding to cellular depletion, of cholinergic neurotransmission in inflamed tissues (Collins et al., 1992a). The mechanism underlying attenuation of ACh release in the inflamed rat intestine has been a matter of debate in the literature, but so far there is no unifying theory given the contradictory findings when looking at different immune cell players and inflammatory mediators (e.g., Davis et al., 1998). This is so, even though evidences have been produced showing that cytokines may directly change neurotransmitters content and release (Collins et al., 1992b). This contention strengthens our hypothesis that functional and structural adaptations of resident non-neuronal myenteric cell populations of the rat ileum may play a relevant role in the mechanisms underlying downregulation of cholinergic neurotransmission in TNBS-induced ileitis.

Post-inflammatory Depletion of ICCs Correlates with Adenosine Deficiency and Decreased Frequency of Spontaneous Contractions in the Ileum of TNBS-Treated Rats

Using immunofluorescence confocal microscopy, we show here that the LM-MP of the rat ileum becomes deficient in Ano-1 positive ICCs, both in the ganglion layer (myenteric stellate cells) and at the neuromuscular region (intramuscular spindle-shape cells). The same occurred regarding immunostaining against vimentin, which is an intermediate filament protein also present in FLCs. Porcher et al. (2002) demonstrated an almost complete abolition of interstitial cells in biopsy samples from patients with Crohn's disease. In the more severe colitis rat model, muscularis resident macrophages have been implicated in the loss of ICCs detected 7-days after instillation of TNBS (Kinoshita et al., 2007). TNF-α secreted from classically activated M1 macrophages reduces the number of cultured ICCs, whereas the conditioned medium from M2 macrophages had no effect (Eisenman et al., 2017). Co-localization studies show here that despite the increasing proportion of CD11B$^+$/CD206$^+$/BTX-rhod$^+$ anti-inflammatory M2 macrophages (see Rõszer, 2015) next to myenteric neurons of TNBS-treated rats, these cells cohabitate with a still important subset of CD11B$^+$/CD206$^-$ inflammatory cells, most probably composed of monocytes-derived pro-inflammatory M1 macrophages. This inflammatory cell pattern may be responsible for the loss of ICCs detected in post-inflammatory ileitis and may account to the decrease in the frequency of spontaneous contractions of LM-MP preparations of the ileum of TNBS-treated rats, as these cells have been implicated in the generation of electrical slow waves regulating the phasic contractile activity of the gastrointestinal smooth muscle (Kinoshita et al., 2007).

To our knowledge, this is the first report showing a relationship between the loss of ICCs in the myenteric plexus of the rat ileum following an inflammatory insult and depletion of extracellular adenosine compared to the normal physiological condition. This was concluded because the lowest extracellular adenosine levels in the ileum were detected upon blocking the activity of ICCs with the Ca_v3 (T-type) channel inhibitor, mibefradil, both in control conditions and after the inflammatory insult with TNBS. Therefore, it is highly

likely that this mechanism, together with the feed-forward inhibition of ecto-5′-nucleotidase/CD73 and upregulation of adenosine deaminase shown in our previous study (Vieira et al., 2014), may concur to prevent adenosine-mediated actions in post-inflammatory ileitis. Considering that, under normal physiological conditions, endogenous adenosine facilitates [^{3}H]ACh release from stimulated myenteric neurons through the preferential activation of pre-junctional A_{2A} receptors (Duarte-Araújo et al., 2004a), one may speculate that cholinergic hypoactivity in TNBS-induced ileitis is dependent on the loss of adenosine A_{2A} receptor-mediated neurofacilitation. Although not explored in this study cholinergic nerve hypoactivity in TNBS-induced ileitis may also be due to reinforcement of the muscarinic M_2-receptor-mediated pre-synaptic auto-inhibition (Takeuchi et al., 2005; Vieira et al., 2009). Yet, even if this mechanism is verified it may be cut-short by the resultant decline of [^{3}H]ACh release from inflamed myenteric nerves. One must also not forget that neurons are an important source of extracellular adenosine in the ileum of healthy animals (Correia-de-Sá et al., 2006) and this resource may turn to be deficient accompanying inflammation-induced functional abnormalities of myenteric neurons, which cannot be compensated by the concurrent loss of interstitial cells.

Depletion of ICCs Downregulates M_3 Receptor-Mediated Adenosine Overflow via ENT1, Decreasing Facilitation of Cholinergic Neurotransmission via Pre-synaptic A_{2A} Receptors

Purinergic re-enforcement to maintain cholinergic neurotransmission during high enteric nerve activity or whenever endogenous levels of adenosine become elevated has been observed in hypoxia, inflammation and postoperative ileum (Milusheva et al., 1990; De Man et al., 2003; Kadowaki et al., 2003). In a previous study, we provided evidence suggesting that muscarinic M_3 receptors activation by neuronally released ACh triggers a positive feedback loop leading to facilitation of transmitter release that is indirectly mediated by adenosine outflow and activation of pre-junctional A_{2A} receptors (Vieira et al., 2009). Yet, at that time we had no information regarding the cellular players of the tripartite myenteric neuromuscular synapse involved in this pathway. Nowadays, we learned that c-kit positive ICCs are endowed with muscarinic M_3 receptors coupled to $G_{q/11}$ (reviewed in Ward and Sanders, 2001; Goyal, 2013; see also **Figure 8**) and these receptors can be activated by inhibiting endogenous ACh breakdown with physostigmine resulting in adenosine overflow from the myenteric plexus of healthy rats (Vieira et al., 2009). Activation of phospholipase C (PLC) by muscarinic M_3 receptors causes the formation of IP_3 and DAG with subsequent recruitment of intracellular Ca^{2+} and protein kinase C activation, respectively (Koh and Rhee, 2013). Increases in intracellular Ca^{2+} can strengthen activation of protein kinase C, which subsequently stimulates adenosine outflow via the equilibrative transporter ENT1 (Coe et al., 2002). Increase in protein kinase C activity might also stimulate 5′-nucleotidase inside cells (Obata et al., 2001) and/or inhibit adenosine kinase (Sinclair et al., 2000), enhancing intracellular adenosine accumulation and the efflux of the nucleoside from the cells. These hypotheses were confirmed in the myenteric plexus of healthy rats incubated with the protein kinase C activator, phorbol 12-myristate 13-acetate, whereas extracellular adenosine accumulation was prevented by inhibiting ENT1 with dipyridamole (Vieira et al., 2009).

Using immunofluorescence confocal microscopy, we show here that the density of muscarinic M_3 receptors decreased significantly in the myenteric plexus of the ileum of TNBS-treated rats. Downmodulation of M_3 receptors-immunolabelling was more significant at the intramuscular level and paralleled the decrease in the immunostaining against ENT1 and Ano-1 in LM-MP preparations of rats injected with TNBS. In this context, our current vision is that the loss of ICCs expressing muscarinic M_3 receptors in TNBS-induced ileitis contributes to reduce extracellular adenosine accumulation, breaking down the amplification loop initiated by ACh release from myenteric neurons that is mediated by muscarinic M_3 receptors-induced adenosine overflow from ICCs, and concluded through the activation of facilitatory A_{2A} receptors on cholinergic nerve terminals. To our knowledge, this is the first time adenosine released from myenteric ICCs is implicated in functional cholinergic nerve abnormalities in post-inflammatory ileitis.

Surplus ATP Released from Proliferating Glial Cells Contributes to Sustain Cholinergic Tonus at Minimum in TNBS-Induced Post-inflammatory Ileitis

While the findings discussed so far may justify the downregulation of cholinergic neurotransmission in TNBS-induced ileitis, they fail to explain why ACh release from inflamed myenteric neurons becomes partially resistant to blockade of nerve action potentials by TTX and the mechanism(s) underlying the TTX-resistant transmitter release that is low, but still significant, in inflamed preparations. The appearance of TTX-resistant sodium currents has been observed before in TNBS-induced ileitis (Stewart et al., 2003). Interestingly, the pharmacology concerning the modulation of [^{3}H]ACh release from myenteric motor neurons of TNBS-treated rats is remarkably similar to that obtained when attempting to control ATP release in the same preparations. Notwithstanding the fact that inflammation-induced variations in the myenteric concentrations of ACh and ATP diverge (i.e., ACh decreases and ATP increases), the release of the two transmitters were significantly reduced in the presence of the gliotoxin, sodium fluoroacetate, but it was not affected by the neuronal activation blocker, TTX. These results led us to suggest that enteric glia cells are crucial to maintain ACh release from inflamed myenteric neurons and that ATP released from these cells may be the excitatory gliotransmitter responsible for keeping cholinergic tonus at minimum in TNBS-induced ileitis.

As a matter of fact, we observed increases in GFAP- and S100β-immunoreactivities in TNBS-induced ileitis suggesting that the inflammatory insult may stimulate enteric glial cells proliferation (Bradley et al., 1997) and/or activate the

expression/synthesis of glial protein cell markers (Cabarrocas et al., 2003). The release of cytokines and growth factors from inflammatory and immune cells may promote glial cells proliferation (Fields and Burnstock, 2006). On the other hand, enteric glial cells may secrete high amounts of neurotrophic factors, like NGF and GDNF, which may change the neurochemical code and content of neurotransmitters in myenteric neurons, even if they do not vary in terms of density (Von Boyen and Steinkamp, 2010). Enteric glia cells may also be a source of pro-inflammatory cytokines, such as IL-6 and IL-1β (Stoffels et al., 2014), with the latter being associated with the suppression of ACh release from the myenteric plexus (Van Assche and Collins, 1996). However, if this were the case in TNBS-induced ileitis, blockade of enteric glia cells metabolism would enhance, rather than decrease, evoked [^{3}H]ACh release from myenteric motor neurons. Moreover, enteric glia contain neurotransmitter precursors, uptake and degrade neuroactive substances, express neurotransmitter receptors and provide neurosupporting actions (Vasina et al., 2006). Regarding recovery from inflammatory adaptive cell changes, it appears that enteric glial dysfunction does not persist after the resolution of intestinal inflammation in TNBS-treated animals, indicating that attempts to correct glial cells dysfunction may be restricted to the course of inflammatory adaptations (MacEachern et al., 2015).

The function of enteric glial cells is intimately tied to the levels of purines and membrane-bound ectonucleotidases, which regulate the availability of P2 receptor ligands (Braun et al., 2004; Lavoie et al., 2011). Data from this study suggest that surplus ATP released by the myenteric plexus after an inflammatory insult may originate from proliferating glial cells, because ATP accumulation was reduced to control levels in the presence of the specific glial metabolic uncoupler, sodium fluoroacetate. ATP released from glial cells, acting most likely via pre-junctional homodimer P2X2 or heterodimer P2X2/3 receptors sensitive to TNP-ATP, may trigger the release of ACh directly from cholinergic nerve terminals (Galligan, 2002; Castelucci et al., 2002; Ren et al., 2003; Ohta et al., 2005; Duarte-Araújo et al., 2009; see also **Figure 5A**). Ionotropic P2X receptor subtypes are Ca^{2+} permeable non-selective cation channels (also permeable to Na^+), which can also inhibit membrane potassium conductance in enteric neurons (Barajas-López et al., 1996). Via these mechanisms, ATP can cause membrane depolarization leading to a secondary opening of voltage-gated Ca^{2+} channels and to transmitter exocytosis in the absence of action potential generation (Duarte-Araújo et al., 2009; see also Barthó et al., 2006), thus contributing to the maintenance of the cholinergic tone within a certain extent. Redistribution of NTPDase2, but not NTPDase3 from ganglia to the neuromuscular region leads to preferential ADP accumulation from released ATP, particularly when extracellular ATP levels reach the V_{max} for NTPDase3 (Duarte-Araújo et al., 2009) like that occurring in inflamed neuromuscular synapses (Vieira et al., 2014). Inflammation-induced increase in the expression of NTPDase2 in intramuscular glia may also contribute to restrain nerve-evoked ACh release in TNBS-induced ileitis due to the activation of ADP-sensitive inhibitory $P2Y_1$ receptors in myenteric nerve terminals (Duarte-Araújo et al., 2009), yet this hypothesis needs further experimental confirmation.

The Post-inflammatory Shift from Neuronal to Non-neuronal ACh Release Involves Ionotropic P2X7 Receptors and ATP Release via Pannexin-1 Hemichannels from Proliferating Glial Cells

Next we attempted to investigate the mechanism underlying the control shift from neuronal to non-neuronal of ACh release in TNBS-induced ileitis. Results show that evoked ACh release from inflamed myenteric neurons was attenuated by blocking the P2X7 receptor-pannexin-1 pathway respectively with A438079 and carbenoxolone in a similar manner to that verified with sodium fluoroacetate. Interestingly, the P2X7 receptor immunoreactivity in the myenteric plexus of the rat ileum is remarkably similar to that obtained for the glial cell marker, S100β, indicating that they may co-localize as shown previously (Vanderwinden et al., 2003; Gulbransen and Sharkey, 2012). Despite this, the P2X7 receptor is also expressed in neuronal soma and nerve terminals, but it is absent from smooth muscle fibers, interstitial cells and anti-inflammatory M2 macrophages ($CD11B^+/CD206^+$cells).

The ionotropic P2X7 receptor is a non-selective cation channel allowing Na^+ and Ca^{2+} influx and K^+ efflux in the presence of high-micromolar ATP concentrations (Morandini et al., 2014). This receptor has been largely associated with inflammatory diseases, including inflammatory bowel diseases (Diezmos et al., 2013), and it can signal through caspase-1 to cause the production of pro-inflammatory IL-1β and IL-18 (Kurashima et al., 2012), as well as TNF-α and nitric oxide (Alves et al., 2013), from inflammatory cells. Prophylactic systemic P2X7 receptor blockade attenuates the severity of mucosal damage, lowers macrophage and T-cells infiltration, and prevents the production of pro-inflammatory cytokines like TNF-α and IL-1β (with no changes detected in anti-inflammatory TGF-β and IL-10) secondary to experimental colitis in rats (Marques et al., 2014). This information is supported by our findings showing that resident anti-inflammatory M2 macrophages ($CD11B^+/CD206^+$cells) in the myenteric plexus of the rat ileum do not express P2X7 receptors 7 days after the inflammatory insult. The corollary of this finding may be that P2X7-mediated pro-inflammatory actions in inflammatory bowel diseases are undertaken by monocyte-derived macrophages polarized toward the M1 phenotype ($CD11B^+/CD206^-$ cells). Macrophages of the M1 subtype overexpressing the P2X7 receptor were found in the inflamed mucosa and have been implicated in the pathogenesis of Crohn's disease in human patients (Neves et al., 2014). These cells usually contribute to initiate and sustain inflammation through the release of large amounts of cytokines (e.g., IL-1β, TNF-α, IL-12, IL-18, and IL-23) and NO from L-arginine, whereas anti-inflammatory M2 macrophages are most often involved in phagocytic activity, immune confinement and tissue remodeling during the healing phase of inflammatory insults. It also became clear from our data that maintenance of the non-neuronal cholinergic tone attributed to activation of P2X7 receptors in

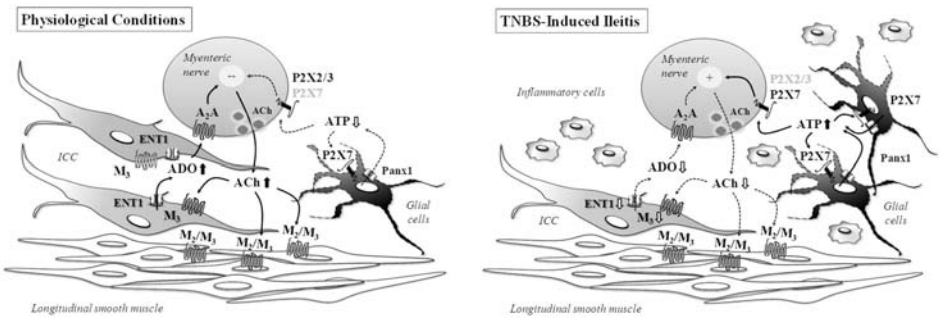

FIGURE 9 | Inflammation-induced cholinergic hypoactivity is deeply dependent on the purinergic shift from a preferential adenosinergic tone under physiological conditions to a more prevalent ATP-mediated control of ACh release in TNBS-induced ileitis. The post-inflammatory loss of ICCs correlates with adenosine deficiency in the ileum of TNBS-treated rats breaking down facilitation of cholinergic neurotransmission operated by muscarinic M_3 receptors-induced adenosine overflow from ICCs via ENT-1 and activation of pre-junctional facilitatory A_{2A} receptors. Adenosine depletion contrasts with the excess of ATP released from proliferating glial cells after the inflammatory insult and may also be explained by deficient formation from release adenine nucleotides by NTPDase cascade redistribution and excess of catabolism by adenosine deaminase (ADA) overproduction in inflammatory tissues (see Vieira et al., 2014). Extracellular ATP accumulation contributes to maintain the cholinergic tone at a minimum through the activation of high affinity / fast desensitizing pre-junctional P2X2 and/or P2X2/3 receptors. Inflammatory-induced neuronal to non-neuronal shift of ACh release is also intimately tight to a mechanism involving low affinity / slow desensitizing ionotropic P2X7 receptors and surplus ATP release via pannexin-1 hemichannels from proliferating glial cells. This scenario admits that post-inflammatory ileitis recapitulates an ancestral mechanism by which ATP released by glial cells directly (via ionotropic P2X receptors) stimulates ACh release from cholinergic nerve terminals even when these cells are disturbed and unable to generate normal action potentials. ACh: acetylcholine; ADO: adenosine; ENT1: equilibrative nucleoside transporter 1; ICC: interstitial cells of Cajal; Panx1: pannexin-1 hemichannels. Solid arrows indicate preferential mechanisms, while dotted arrows are assigned to deficient paths.

post-inflammatory ileitis cannot be due to ACh release from $CD11B^+/CD206^+/ChAT^+$ inflammatory cells infiltrating the myenteric plexus because these cells do not express this receptor.

Pannexin-1 is also expressed in a variety of immune cells and is required for caspase-1 cleavage in response to P2X7 receptor activation (Pelegrin and Surprenant, 2006). Downregulation of pannexin-1 is associated with pro-inflammatory responses, whereas the opposite promotes anti-inflammatory reactions (Sáez et al., 2014). Pannexin-1, along with pannexin-2, is expressed in all layers of the human colon, including the mucosa, muscularis mucosa, submucosa and muscularis externa, where it is found preferentially in enteric ganglia, but also in the endothelium of blood vessels, epithelial cells and goblet cells (Diezmos et al., 2013; Maes et al., 2015). The P2X7 receptor and pannexin-1 hemichannels form signaling complexes in several cell types and both structures may concur to release ATP from non-neuronal cells under physiological and pathological conditions. Interestingly, the selective P2X7 receptor antagonist, A438079, and the specific pannexin-1 inhibitor, carbenoxolone, did not modify evoked ACh release in the ileum of healthy rats where myenteric ATP levels are low, but they significantly decreased [^{3}H]ACh overflow from preparations of TNBS-treated rats in conditions where extracellular ATP release from proliferating glial cells is assumed to be high. It has also been shown that activation of the P2X7 receptor in enteric neurons may elicit ATP release through pannexin-1 hemichannels and this may act as a danger signal for neurons (Gulbransen et al., 2012). However, this mechanism is unlikely to modulate [^{3}H]ACh outflow in post-inflammatory ileitis because no substantial neuronal loss was observed in our experimental conditions and the transmitter release in TNBS-induced ileitis was TTX-resistant, yet fluoroacetate-sensitive, indicating a dominant participation of enteric glial cells.

Pivotal Role of Enteric Glia and ICCs to Maintain the Integrity of Gut Function as Part of a General Strategy to Respond to GI Tract Disorders Involving Purinergic Signaling

It has been proposed that enteric glial cells may play a critical role in maintaining the integrity of the bowel and that their loss or dysfunction might contribute to cellular mechanisms of inflammatory bowel diseases. A fulminating and fatal jejuno-ileitis is produced 7–14 days after ablation of enteric glia in adult transgenic mice, with almost none effects in other parts of the GI tract including the colon (Bush et al., 1998). It remains, however, to be explored whether deficits in ATP outflow from deficient glial cells play a role in triggering this disease process. This would be clinically relevant, since we predict here that the nucleotide may be an important gliotransmitter responsible for sustaining cholinergic tone after an inflammatory insult and this might contribute to avoid degeneration of myenteric neurons as already proved for glutamate in the CNS (Bush et al., 1999). In this context, the vasoactive properties of released adenine nucleotides and nucleosides may also contribute to microvascular disturbances and certain changes resembling ischemic bowel (see e.g., Mendes et al., 2015).

Thus, similarities in the appearance of end-stage pathology in various bowel conditions (e.g., inflammation, hypoxia/ischemia, diabetes) suggest that the gut may have limited ways of responding when it is defective (Bush et al., 1998). For this reason it is important to identify single events that are able to trigger complex pathological cascades. Our working hypothesis in this study was that inflammation-induced cell density changes in the myenteric plexus may unbalance the release of purines and, thus,

their influence on ACh release from stimulated enteric nerves. We clearly demonstrated that inflammation-induced cholinergic hypoactivity is deeply dependent on the purinergic shift from a preferential adenosinergic tone under physiological conditions to a more prevalent ATP-mediated control of ACh release in TNBS-induced ileitis (**Figure 9**). The adenosine neuromodulation deficit parallels the partial loss of ICCs population in the inflamed myenteric plexus and contributes to explain the brake of the cholinergic amplification loop operated by facilitatory muscarinic M_3 and adenosine A_{2A} receptors, which is responsible for keeping the safety margin of myenteric neuromuscular transmission under stressful conditions. On the other hand, proliferating and/or reactive enteric glial cells markedly influence the amount of ATP at the inflamed myenteric synapse by creating a vicious cycle that promote the release of the nucleotide through a mechanism involving the P2X7 receptor/pannexin-1 pathway. Data suggest that ATP may be the excitatory gliotransmitter responsible for keeping the cholinergic tone above a critical minimum in post-inflammatory ileitis. Inflammation may, thus, recapitulate an ancestral mechanism by which ATP released by glial cells directly (via ionotropic P2X receptors) stimulates ACh release from cholinergic nerve terminals even when these cells are disturbed and unable to generate normal action potentials.

CONCLUSION

This study provides a deeper understanding of the pathophysiological impact of purines in the communication between non-neuronal cells and neurons underlying the dysregulation of cholinergic neurotransmission in post-inflammatory ileitis. Data suggest that the purinergic cascade (e.g., ATP release mechanisms, ecto-nucleotidase enzymes and purinoceptors activation) may offer novel therapeutic targets to overcome long-term cholinergic neurotransmission deficits affecting motility in inflammatory bowel diseases.

AUTHOR CONTRIBUTIONS

CV, FF, MTMC, IS, PM, and PC-dS contributed significantly for the experimental design, data acquisition, and interpretation of the results obtained; CV carried out surgical procedures and monitored postoperative animal welfare; CV, IS, and PM performed *in vitro* myographic recordings and experiments to measure ACh, ATP and adenosine release; CV and MTMC quantified adenine nucleotides and nucleosides by HPLC; CV and FF performed immunofluorescence staining and confocal microscopy observations; CV and PC-dS drafted and revised the manuscript; PC-dS supervised the project in all its dimensions; all authors approved the submitted version of the manuscript and agreed that all aspects of the work are accurate.

FUNDING

This research was partially supported by FCT (FCT projects Pest-OE/SAU/UI215/2014 and UID/BIM/4308/2016) with the participation of FEDER funding. CV and IS were in receipt of Ph.D. studentships by FCT (SFRH/BD/79091/2011 and SFRH/BD/88855/2012, respectively).

ACKNOWLEDGMENTS

The authors acknowledge the valuable collaboration of Professor Margarida Duarte-Araújo in the implementation of TNBS-induced intestinal inflammation rat model in our lab. The authors also wish to thank Mrs. Maria Helena Costa e Silva and Belmira Silva for technical assistance.

SUPPLEMENTARY MATERIAL

The Supplementary Material for this article can be found online at: https://www.frontiersin.org/articles/10.3389/fphar.2017.00811/full#supplementary-material

FIGURE S1 | Images depict HPLC chromatograms obtained by injecting either adenosine (ADO) plus inosine (INO) standard solutions (upper panel) or experimental bath samples collected immediately before (Pre-EFS) and after (Post-EFS) stimulation of longitudinal muscle-myenteric plexus (LM-MP) preparations of the ileum from control and TNBS-treated rats. Please note that basal levels of ADO plus INO are inferior in TNBS-treated than in control preparations. Electrical field stimulation (EFS, 5 Hz frequency, 3000 pulses, 1 ms width) increases the ADO plus INO content of bathing samples obtained from both animal groups, but the maximal release of nucleosides was still lower in TNBS-treated rats than in control animals.

REFERENCES

Alves, L. A., Bezerra, R. J., Faria, R. X., Ferreira, L. G., and da, Silva Frutuoso V (2013). Physiological roles and potential therapeutic applications of the P2X7 receptor in inflammation and pain. *Molecules* 18, 10953–10972. doi: 10.3390/molecules180910953

Antonioli, L., Fornai, M., Colucci, R., Awwad, O., Ghisu, N., Tuccori, M., et al. (2011a). Differential recruitment of high affinity A1 and A2A adenosine receptors in the control of colonic neuromuscular function in experimental colitis. *Eur. J. Pharmacol.* 650, 639–649. doi: 10.1016/j.ejphar.2010.10.041

Antonioli, L., Fornai, M., Colucci, R., Tuccori, M., and Blandizzi, C. (2011b). A holistic view of adenosine in the control of intestinal neuromuscular functions: the enteric 'purinome' concept. *Br. J. Pharmacol.* 164, 1577–1579. doi: 10.1111/j.1476-5381.2011.01529.x

Arvidsson, U., Riedl, M., Elde, R., and Meister, B. (1997). Vesicular acetylcholine transporter (VAChT) protein: a novel and unique marker for cholinergic neurons in the central and peripheral nervous systems. *J. Comp. Neurol.* 378, 454–467. doi: 10.1002/(SICI)1096-9861(19970224)378:4<454::AID-CNE2>3.0.CO;2-1

Barajas-López, C., Huizinga, J. D., Collins, S. M., Gerzanich, V., Espinosa-Luna, R., and Peres, A. L. (1996). P2X-purinoceptors of myenteric neurones from the guinea-pig ileum and their unusual pharmacological properties. *Br. J. Pharmacol.* 119, 1541–1548. doi: 10.1111/j.1476-5381.1996.tb16070.x

Barros-Barbosa, A. R., Ferreirinha, F., Oliveira, Â., Mendes, M., Lobo, M. G., Santos, A., et al. (2016a). Adenosine A2A receptor and ecto-5′-nucleotidase/CD73 are upregulated in hippocampal astrocytes of human patients with mesial temporal lobe epilepsy (MTLE). *Purinergic Signal.* 12, 719–734.

Barros-Barbosa, A. R., Fonseca, A. L., Guerra-Gomes, S., Ferreirinha, F., Santos, A., Rangel, R., et al. (2016b). Up-regulation of P2X7 receptor-mediated inhibition of GABA uptake by nerve terminals of the human epileptic neocortex. *Epilepsia* 57, 99–110. doi: 10.1111/epi.13263

Barros-Barbosa, A. R., Lobo, M. G., Ferreirinha, F., Correia-de-Sá, P., and Cordeiro, J. M. (2015). P2X7 receptor activation downmodulates Na^+-dependent high-affinity GABA and glutamate transport into rat brain cortex synaptosomes. *Neuroscience* 306, 74–90. doi: 10.1016/j.neuroscience.2015.08.026

Barthó, L., Undi, S., Benkó, R., Wolf, M., Lázár, Z., Lénárd, L. Jr., et al. (2006). Multiple motor effects of ATP and their inhibition by P_2 purinoceptor antagonist, pyridoxalphosphate-6-azophenyl-2′,4′-disulphonic acid in the small intestine of the guine-pig. *Basic Clin. Pharmacol. Toxicol.* 98, 488–495. doi: 10.1111/j.1742-7843.2006.pto_369.x

Bodin, P., and Burnstock, G. (2001). Purinergic signalling: ATP release. *Neurochem. Res.* 26, 959–969. doi: 10.1023/A:1012388618693

Boesmans, W., Lasrado, R., Vanden, Berghe P, and Pachnis, V. (2015). Heterogeneity and phenotypic plasticity of glial cells in the mammalian enteric nervous system. *Glia* 63, 229–241. doi: 10.1002/glia.22746

Bogers, J., Moreels, T., De, Man J, Vrolix, G., Jacobs, W., Pelckmans, P., et al. (2000). Schistosoma mansoni infection causing diffuse enteric inflammation and damage of the enteric nervous system in the mouse small intestine. *Neurogastroenterol. Motil.* 12, 431–440. doi: 10.1046/j.1365-2982.2000.00219.x

Bradley, J. S. Jr., Parr, E. J., and Sharkey, K. A. (1997). Effects of inflammation on cell proliferation in the MP of the guinea-pig ileum. *Cell Tissue Res.* 289, 455–461. doi: 10.1007/s004410050891

Braun, N., Sévigny, J., Robson, S. C., Hammer, K., Hanani, M., and Zimmermann, H. (2004). Association of the ecto-ATPase NTPDase2 with glial cells of the peripheral nervous system. *Glia* 45, 124–132. doi: 10.1002/glia.10309

Broadhead, M. J., Bayguinov, P. O., Okamoto, T., Heredia, D. J., and Smith, T. K. (2012). Ca^{2+} transients in myenteric glial cells during the colonic migrating motor complex in the isolated murine large intestine. *J. Physiol.* 590, 335–350. doi: 10.1113/jphysiol.2011.219519

Burnstock, G. (1976). Do some nerve cells release more than one transmitter? *Neuroscience* 1, 239–248.

Bush, T. G., Puvanachandra, N., Horner, C. H., Polito, A., Ostenfeld, T., Svendsen, C. N., et al. (1999). Leukocyte infiltration, neuronal degeneration, and neurite outgrowth after ablation of scar-forming, reactive astrocytes in adult transgenic mice. *Neuron* 23, 297–308. doi: 10.1016/S0896-6273(00)80781-3

Bush, T. G., Savidge, T. C., Freeman, T. C., Cox, H. J., Campbell, E. A., Mucke, L., et al. (1998). Fulminant jejuno-ileitis following ablation of enteric glia in adult transgenic mice. *Cell* 93, 189–201. doi: 10.1016/S0092-8674(00)81571-8

Cabarrocas, J., Savidge, T. C., and Liblau, R. S. (2003). Role of enteric glial cells in inflammatory bowel disease. *Glia* 41, 81–93. doi: 10.1002/glia.10169

Carneiro, I., Timóteo, M. A., Silva, I., Vieira, C., Baldaia, C., Ferreirinha, F., et al. (2014). Activation of P2Y6 receptors increases the voiding frequency in anaesthetized rats by releasing ATP from the bladder urothelium. *Br. J. Pharmacol.* 171, 3404–3419. doi: 10.1111/bph.12711

Castelucci, P., Robbins, H. L., Poole, D. P., and Furness, J. B. (2002). The distribution of purine P2X(2) receptors in the guinea-pig enteric nervous system. *Histochem. Cell Biol.* 117, 415–422. doi: 10.1007/s00418-002-0404-4

Certal, M., Vinhas, A., Pinheiro, A. R., Ferreirinha, F., Barros-Barbosa, A. R., Silva, I., et al. (2015). Calcium signaling and the novel anti-proliferative effect of the UTP-sensitive P2Y11 receptor in rat cardiac myofibroblasts. *Cell Calcium* 58, 518–533. doi: 10.1016/j.ceca.2015.08.004

Coe, I., Zhang, Y., McKenzie, T., and Naydenova, Z. (2002). PKC regulation of the human equilibrative nucleoside transporter, hENT1. *FEBS Lett.* 517, 201–205. doi: 10.1016/S0014-5793(02)02622-4

Collins, S. M., Blennerhassett, P., Vermillion, D. L., Davis, K., Langer, J., and Ernst, P. B. (1992a). Impaired acetylcholine release in the inflamed rat intestine is T cell independent. *Am. J. Physiol.* 263(2 Pt 1), G198–G201.

Collins, S. M., Hurst, S. M., Main, C., Stanley, E., Khan, I., Blennerhassett, P., et al. (1992b). Effect of inflammation of enteric nerves. Cytokine-induced changes in neurotransmitter content and release. *Ann. N. Y. Acad. Sci.* 664, 415–424.

Correia-de-Sá, P., Adães, S., Timóteo, M. A., Vieira, C., Magalhães-Cardoso, T., Nascimento, C., et al. (2006). Fine-tuning modulation of myenteric motoneurons by endogenous adenosine: on the role of secreted adenosine deaminase. *Auton. Neurosci.* 12, 211–224. doi: 10.1016/j.autneu.2006.02.004

Costa, M., Brookes, S., and Hennig, G. (2000). Anatomy and physiology of the enteric nervous system. *Gut* 47(Suppl. 4), iv15–iv19. doi: 10.1136/gut.47.suppl_4.iv15

Costa, M., Brookes, S. J., Steele, P. A., Gibbins, I., Burcher, E., and Kandiah, C. J. (1996). Neurochemical classification of myenteric neurons in the guinea-pig ileum. *Neuroscience* 75, 949–967. doi: 10.1016/0306-4522(96)00275-8

Davis, K. A., Masella, J., and Blennerhassett, M. G. (1998). Acetylcholine metabolism in the inflamed rat intestine. *Exp. Neurol.* 152, 251–258. doi: 10.1006/exnr.1998.6839

De Man, J. G., Seerden, T. C., De Winter, B. Y., Van Marck, E. A., Herman, A. G., and Pelckmans, P. A. (2003). Alteration of the purinergic modulation of enteric neurotransmission in the mouse ileum during chronic intestinal inflammation. *Br. J. Pharmacol.* 139, 172–184. doi: 10.1038/sj.bjp.0705218

Diezmos, E. F., Sandow, S. L., Markus, I., Shevy, Perera D, Lubowski, D. Z., King, D. W., et al. (2013). Expression and localization of pannexin-1 hemichannels in human colon in health and disease. *Neurogastroenterol. Motil.* 25, e395–e405. doi: 10.1111/nmo.12130

Duarte-Araújo, M., Nascimento, C., Alexandrina, Timóteo M, Magalhães-Cardoso, T., and Correia-de-Sá, P. (2004a). Dual effects of adenosine on acetylcholine release from myenteric motoneurons are mediated by junctional facilitatory A2A and extrajunctional inhibitory A1 receptors. *Br. J. Pharmacol.* 141, 925–934.

Duarte-Araújo, M., Nascimento, C., Timóteo, M. A., Magalhães-Cardoso, M. T., and Correia-de-Sá, P. (2009). Relative contribution of ecto-ATPase and ecto-ATPDase pathways to the biphasic effect of ATP on acetylcholine release from myenteric motoneurons. *Br. J. Pharmacol.* 156, 519–533. doi: 10.1111/j.1476-5381.2008.00058.x

Duarte-Araújo, M., Timóteo, M. A., and Correia-de-Sá, P. (2004b). Adenosine activating A2A-receptors coupled to adenylate cyclase/cyclic AMP pathway downregulates nicotinic autoreceptor function at the rat myenteric nerve terminals. *Neurochem. Int.* 45, 641–651. doi: 10.1016/j.neuint.2004.03.027

Dunn, K. W., Kamocka, M. M., and McDonald, J. H. (2011). A practical guide to evaluating colocalization in biological microscopy. *Am. J. Physiol. Cell Physiol.* 300, C723–C742. doi: 10.1152/ajpcell.00462.2010

Durnin, L., Sanders, K. M., and Mutafova-Yambolieva, V. N. (2013). Differential release of β-NAD^+ and ATP upon activation of enteric motor neurons in primate and murine colons. *Neurogastroenterol. Motil.* 25, e194–e204. doi: 10.1111/nmo.12069

Eisenman, S. T., Gibbons, S. J., Verhulst, P. J., Cipriani, G., Saur, D., and Farrugia, G. (2017). Tumor necrosis factor alpha derived from classically activated "M1" macrophages reduces interstitial cell of Cajal numbers. *Neurogastroenterol. Motil.* 29:e12984. doi: 10.1111/nmo.12984

Ekblad, E., Sjuve, R., Arner, A., and Sundler, F. (1998). Enteric neuronal plasticity and a reduced number of interstitial cells of Cajal in hypertrophic rat ileum. *Gut* 42, 836–844. doi: 10.1136/gut.42.6.836

Engel, M. A., Kellermann, C. A., Rau, T., Burnat, G., Hahn, E. G., and Konturek, P. C. (2008). Ulcerative colitis in AKR mice is attenuated by intraperitoneally administered anandamide. *J. Physiol. Pharmacol.* 59, 673–689.

Epperson, A., Hatton, W. J., Callaghan, B., Doherty, P., Walker, R. L., Sanders, K. M., et al. (2000). Molecular markers expressed in cultured and freshly isolated interstitial cells of Cajal. *Am. J. Physiol. Cell Physiol.* 279, C529–C539.

Fields, R. D., and Burnstock, G. (2006). Purinergic signalling in neuron-glia interactions. *Nat. Rev. Neurosci.* 7, 423–436. doi: 10.1038/nrn1928

Fujita, A., Takeuchi, T., Jun, H., and Hata, F. (2003). Localization of Ca^{2+}-activated K^+ channel, SK3, in fibroblast-like cells forming gap junctions with smooth muscle cells in the mouse small intestine. *J. Pharmacol. Sci.* 92, 35–42. doi: 10.1254/jphs.92.35

Furness, J. B. (2006). *The Enteric Nervous System*. Oxford: Blackwell publishing.

Galligan, J. J. (2002). Pharmacology of synaptic transmission in the enteric nervous system. *Curr. Opin. Pharmacol.* 2, 623–629. doi: 10.1016/S1471-4892(02)00212-6

Giron, M. C., Bin, A., Brun, P., Etteri, S., Bolego, C., Florio, C., et al. (2008). Cyclic AMP in rat ileum: evidence for the presence of an extracellular cyclic AMP-adenosine pathway. *Gastroenterology* 134, 1116–1126. doi: 10.1053/j.gastro.2008.01.030

Gomez-Pinilla, P. J., Gibbons, S. J., Bardsley, M. R., Lorincz, A., Pozo, M. J., Pasricha, P. J., et al. (2009). Ano1 is a selective marker of interstitial cells

of Cajal in the human and mouse gastrointestinal tract. *Am. J. Physiol. Gastrointest. Liver Physiol.* 296, G1370–G1381. doi: 10.1152/ajpgi.00074.2009

Goyal, R. K. (2013). Revised role of interstitial cells of Cajal in cholinergic neurotransmission in the gut. *J. Physiol.* 591(Pt 21), 5413–5414. doi: 10.1113/jphysiol.2013.264135

Gulbransen, B. D., Bashashati, M., Hirota, S. A., Gui, X., Roberts, J. A., MacDonald, J. A., et al. (2012). Activation of neuronal P2X7 receptor-Pannexin-1 mediates death of enteric neurons during colitis. *Nat. Med.* 18, 600–604. doi: 10.1038/nm.2679

Gulbransen, B. D., and Sharkey, K. A. (2012). Novel functional roles for enteric glia in the gastrointestinal tract. *Nat. Rev. Gastroenterol. Hepatol.* 9, 625–632. doi: 10.1038/nrgastro.2012.138

Hu, H. Z., Gao, N., Lin, Z., Gao, C., Liu, S., Ren, J., et al. (2002). Chemical coding and electrophysiology of enteric neurons expressing neurofilament 145 in guinea pig gastrointestinal tract. *J. Comp. Neurol.* 442, 189–203. doi: 10.1002/cne.1424

Hwang, S. J., Durnin, L., Dwyer, L., Rhee, P. L., Ward, S. M., Koh, S. D., et al. (2011). β-nicotinamide adenine dinucleotide is an enteric inhibitory neurotransmitter in human and nonhuman primate colons. *Gastroenterology* 140, 608–617. doi: 10.1053/j.gastro.2010.09.039

Jergens, A. E. (1999). Inflammatory bowel disease. Current perspectives. *Vet. Clin. North Am. Small Anim. Pract.* 29, 501–521. doi: 10.1016/S0195-5616(99)50032-6

Kadowaki, M., Nagakura, Y., Tokita, K., Hanaoka, K., and Tomoi, M. (2003). Adenosine A1 receptor blockade reverses experimental postoperative ileus in rat colon. *Eur. J. Pharmacol.* 458, 197–200. doi: 10.1016/S0014-2999(02)02766-8

Kinoshita, K., Horiguchi, K., Fujisawa, M., Kobirumaki, F., Yamato, S., Hori, M., et al. (2007). Possible involvement of muscularis resident macrophages in impairment of interstitial cells of Cajal and myenteric nerve systems in rat models of TNBS-induced colitis. *Histochem. Cell Biol.* 127, 41–53. doi: 10.1007/s00418-006-0223-0

Koh, S. D., and Rhee, P. L. (2013). Ionic conductance(s) in response to post-junctional potentials. *J. Neurogastroenterol. Motil.* 19, 426–432. doi: 10.5056/jnm.2013.19.4.426

Kukulski, F., Lévesque, S. A., and Sévigny, J. (2011). Impact of ectoenzymes on P2 and P1 receptor signaling. *Adv. Pharmacol.* 61, 263–299. doi: 10.1016/B978-0-12-385526-8.00009-6

Kurashima, Y., Amiya, T., Nochi, T., Fujisawa, K., Haraguchi, T., Iba, H., et al. (2012). Extracellular ATP mediates mast cell-dependent intestinal inflammation through P2X7 purinoceptors. *Nat. Commun.* 3:1034. doi: 10.1038/ncomms2023

Lavoie, E. G., Gulbransen, B. D., Martín-Satué, M., Aliagas, E., Sharkey, K. A., and Sévigny, J. (2011). Ectonucleotidases in the digestive system: focus on NTPDase3 localization. *Am. J. Physiol. Gastrointest. Liver Physiol.* 300, G608–G620. doi: 10.1152/ajpgi.00207.2010

Lazarowski, E. R., Sesma, J. I., Seminario-Vidal, L., and Kreda, S. M. (2011). Molecular mechanisms of purine and pyrimidine nucleotide release. *Adv. Pharmacol.* 61, 221–261. doi: 10.1016/B978-0-12-385526-8.00008-4

Lecci, A., Santicioli, P., and Maggi, C. A. (2002). Pharmacology of transmission to gastrointestinal muscle. *Curr. Opin. Pharmacol.* 2, 630–641. doi: 10.1016/S1471-4892(02)00225-4

Lhermitte, F., Gray, F., Lyon-Caen, O., Pertuiset, B. F., and Bernard, P. (1980). Paralysis of digestive tract with lesions of myenteric plexuses. A new paraneoplastic syndrome. *Rev. Neurol.* 136, 825–836.

Linden, D. R., Couvrette, J. M., Ciolino, A., McQuoid, C., Blaszyk, H., Sharkey, K. A., et al. (2005). Indiscriminate loss of myenteric neurones in the TNBS-inflamed guinea-pig distal colon. *Neurogastroenterol. Motil.* 17, 751–760. doi: 10.1111/j.1365-2982.2005.00703.x

MacEachern, S. J., Patel, B. A., Keenan, C. M., Dicay, M., Chapman, K., McCafferty, D. M., et al. (2015). Inhibiting inducible nitric oxide synthase in enteric glia restores electrogenic ion transport in mice with colitis. *Gastroenterology* 149, 445.e3–455.e3. doi: 10.1053/j.gastro.2015.04.007

Maes, M., Cogliati, B., Crespo, Yanguas S, Willebrords, J., and Vinken, M. (2015). Roles of connexins and pannexins in digestive homeostasis. *Cell Mol. Life Sci.* 72, 2809–2821. doi: 10.1007/s00018-015-1961-8

Marquardt, D. L., Gruber, H. E., and Wasserman, S. I. (1984). Adenosine release from stimulated mast cells. *Proc. Natl. Acad. Sci. U.S.A.* 81, 6192–6196. doi: 10.1073/pnas.81.19.6192

Marques, C. C., Castelo-Branco, M. T., Pacheco, R. G., Buongusto, F., do Rosário, A. Jr., Schanaider, A., et al. (2014). Prophylactic systemic P2X7 receptor blockade prevents experimental colitis. *Biochim. Biophys. Acta* 1842, 65–78. doi: 10.1016/j.bbadis.2013.10.012

Matteoli, G., Gomez-Pinilla, P. J., Nemethova, A., Di Giovangiulio, M., Cailotto, C., van Bree, S. H., et al. (2014). A distinct vagal anti-inflammatory pathway modulates intestinal muscularis resident macrophages independent of the spleen. *Gut* 63, 938–948. doi: 10.1136/gutjnl-2013-304676

McGrath, J. C., Drummond, G. B., McLachlan, E. M., Kilkenny, C., and Wainwright, C. L. (2010). Guidelines for reporting experiments involving animals: the ARRIVE guidelines. *Br. J. Pharmacol.* 160, 1573–1576. doi: 10.1111/j.1476-5381.2010.00873.x

Mendes, C. E., Palombit, K., Vieira, C., Silva, I., Correia-de-Sá, P., and Castelucci, P. (2015). The effect of ischemia and reperfusion on enteric glial cells and contractile activity in the ileum. *Dig. Dis. Sci.* 60, 2677–2689. doi: 10.1007/s10620-015-3663-3

Miller, M. J., Sadowska-Krowicka, H., Chotinaruemol, S., Kakkis, J. L., and Clark, D. A. (1993). Amelioration of chronic ileitis by nitric oxide synthase inhibition. *J. Pharmacol. Exp. Ther.* 264, 11–16.

Milusheva, E., Sperlágh, B., Kiss, B., Szporny, L., Pásztor, E., Papasova, M., et al. (1990). Inhibitory effect of hypoxic condition on acetylcholine release is partly due to the effect of adenosine released from the tissue. *Brain Res. Bull.* 24, 369–373. doi: 10.1016/0361-9230(90)90091-D

Morandini, A. C., Savio, L. E., and Coutinho-Silva, R. (2014). The role of P2X7 receptor in infectious inflammatory diseases and the influence of ectonucleotidases. *Biomed. J.* 37, 169–177. doi: 10.4103/2319-4170.127803

Moreels, T. G., De Man, J. G., Dick, J. M., Nieuwendijk, R. J., De Winter, B. Y., Lefebvre, R. A., et al. (2001). Effect of TNBS-induced morphological changes on pharmacological contractility of the rat ileum. *Eur. J. Pharmacol.* 423, 211–222. doi: 10.1016/S0014-2999(01)01088-3

Mutafova-Yambolieva, V. N. (2012). Neuronal and extraneuronal release of ATP and NAD^+ in smooth muscle. *IUBMB Life* 64, 817–824. doi: 10.1002/iub.1076

Neves, A. R., Castelo-Branco, M. T., Figliuolo, V. R., Bernardazzi, C., Buongusto, F., Yoshimoto, A., et al. (2014). Overexpression of ATP-activated P2X7 receptors in the intestinal mucosa is implicated in the pathogenesis of Crohn's disease. *Inflamm. Bowel Dis.* 20, 444–457. doi: 10.1097/01.MIB.0000441201.10454.06

Noronha-Matos, J. B., Coimbra, J., Sá-e-Sousa, A., Rocha, R., Marinhas, J., Freitas, R., et al. (2014). P2X7-induced zeiosis promotes osteogenic differentiation and mineralization of postmenopausal bone marrow-derived mesenchymal stem cells. *FASEB J.* 28, 5208–5222. doi: 10.1096/fj.14-257923

Nurgali, K., Nguyen, T. V., Matsuyama, H., Thacker, M., Robbins, H. L., and Furness, J. B. (2007). Phenotypic changes of morphologically identified guinea-pig myenteric neurons following intestinal inflammation. *J. Physiol.* 583(Pt 2), 593–609. doi: 10.1113/jphysiol.2007.135947

Obata, T., Kubota, S., and Yamanaka, Y. (2001). Histamine increases interstitial adenosine concentration via activation of ecto-5′-nucleotidase in rat hearts in vivo. *J. Pharmacol. Exp. Ther.* 298, 71–76.

Ohta, T., Kubota, A., Murakami, M., Otsuguro, K., and Ito, S. (2005). P2X2 receptors are essential for $[Ca^{2+}]_i$ increases in response to ATP in cultured rat myenteric neurons. *Am. J. Physiol. Gastrointest. Liver Physiol.* 289, G935–G948. doi: 10.1152/ajpgi.00017.2005

Paton, W. D. M., and Vizi, E. S. (1969). The inhibitory action of noradrenaline and adrenaline on acetylcholine output by guinea pig-ileum longitudinal muscle strip. *Br. J. Pharmacol.* 35, 10–28. doi: 10.1111/j.1476-5381.1969.tb07964.x

Pelegrin, P., and Surprenant, A. (2006). Pannexin-1 mediates large pore formation and interleukin-1β release by the ATP-gated P2X7 receptor. *EMBO J.* 25, 5071–5082. doi: 10.1038/sj.emboj.7601378

Pinheiro, A. R., Paramos-de-Carvalho, D., Certal, M., Costa, M. A., Costa, C., Magalhães-Cardoso, M. T., et al. (2013). Histamine induces ATP release from human subcutaneous fibroblasts, via pannexin-1 hemichannels, leading to Ca^{2+} mobilization and cell proliferation. *J. Biol. Chem.* 288, 27571–27583. doi: 10.1074/jbc.M113.460865

Poli, E., Lazzaretti, M., Grandi, D., Pozzoli, C., and Coruzzi, G. (2001). Morphological and functional alterations of the myenteric plexus in rats

with TNBS-induced colitis. *Neurochem. Res.* 26, 1085–1093. doi: 10.1023/A:1012313424144

Pontell, L., Castelucci, P., Bagyánszki, M., Jovic, T., Thacker, M., Nurgali, K., et al. (2009). Structural changes in the epithelium of the small intestine and immune cell infiltration of enteric ganglia following acute mucosal damage and local inflammation. *Virchows Arch.* 455, 55–65. doi: 10.1007/s00428-009-0795-x

Porcher, C., Baldo, M., Henry, M., Orsoni, P., Julé, Y., and Ward, S. M. (2002). Deficiency of interstitial cells of Cajal in the small intestine of patients with Crohn's disease. *Am. J. Gastroenterol.* 97, 118–125. doi: 10.1111/j.1572-0241.2002.05430.x

Ren, J., Bian, X., DeVries, M., Schnegelsberg, B., Cockayne, D. A., Ford, A. P., et al. (2003). P2X2 subunits contribute to fast synaptic excitation in myenteric neurons of the mouse small intestine. *J. Physiol.* 552(Pt 3), 809–821.

Roberts, J. A., Lukewich, M. K., Sharkey, K. A., Furness, J. B., Mawe, G. M., and Lomax, A. E. (2012). The roles of purinergic signaling during gastrointestinal inflammation. *Curr. Opin. Pharmacol.* 12, 659–666. doi: 10.1016/j.coph.2012.09.011

Rõszer, T. (2015). Understanding the mysterious M2 macrophage through activation markers and effector mechanisms. *Mediators Inflamm.* 2015:816460. doi: 10.1155/2015/816460

Rühl, A., Nasser, Y., and Sharkey, K. A. (2004). Enteric glia. *Neurogastroenterol. Motil.* 16(Suppl. 1), 44–49. doi: 10.1111/j.1743-3150.2004.00474.x

Sáez, P. J., Shoji, K. F., Aguirre, A., and Sáez, J. C. (2014). Regulation of hemichannels and gap junction channels by cytokines in antigen-presenting cells. *Mediators Inflamm.* 2014:742734. doi: 10.1155/2014/742734

Sanders, K. M. (1996). A case for interstitial cells of Cajal as pacemakers and mediators of neurotransmission in the gastrointestinal tract. *Gastroenterology* 111, 492–515. doi: 10.1053/gast.1996.v111.pm8690216

Sanovic, S., Lamb, D. P., and Blennerhassett, M. G. (1999). Damage to the enteric nervous system in experimental colitis. *Am. J. Pathol.* 155, 1051–1057. doi: 10.1016/S0002-9440(10)65207-8

Sawada, K., Echigo, N., Juge, N., Miyaji, T., Otsuka, M., Omote, H., et al. (2008). Identification of a vesicular nucleotide transporter. *Proc. Natl. Acad. Sci. U.S.A.* 105, 5683–5686. doi: 10.1073/pnas.0800141105

Sharkey, K. A., and Kroese, A. B. (2001). Consequences of intestinal inflammation on the enteric nervous system: neuronal activation induced by inflammatory mediators. *Anat. Rec.* 262, 79–90. doi: 10.1002/1097-0185(20010101)262:1<79::AID-AR1013>3.0.CO;2-K

Silva, I., Ferreirinha, F., Magalhães-Cardoso, M. T., Silva-Ramos, M., and Correia-de-Sá, P. (2015). Activation of P2Y6 receptors facilitates nonneuronal adenosine triphosphate and acetylcholine release from urothelium with the lamina propria of men with bladder outlet obstruction. *J. Urol.* 194, 1146–1154. doi: 10.1016/j.juro.2015.05.080

Sinclair, C. J., Shepel, P. N., Geiger, J. D., and Parkinson, F. E. (2000). Stimulation of nucleoside efflux and inhibition of adenosine kinase by A1 adenosine receptor activation. *Biochem. Pharmacol.* 59, 477–483. doi: 10.1016/S0006-2952(99)00350-0

So, K. Y., Kim, S. H., Sohn, H. M., Choi, S. J., Parajuli, S. P., Choi, S., et al. (2009). Carbachol regulates pacemaker activities in cultured interstitial cells of Cajal from the mouse small intestine. *Mol. Cells* 27, 525–531. doi: 10.1007/s10059-009-0076-1

Stead, R. H., Dixon, M. F., Bramwell, N. H., Riddell, R. H., and Bienenstock, J. (1989). Mast cells are closely apposed to nerves in the human gastrointestinal mucosa. *Gastroenterology* 97, 575–585. doi: 10.1016/0016-5085(89)90627-6

Stewart, T., Beyak, M. J., and Vanner, S. (2003). Ileitis modulates potassium and sodium currents in guinea pig dorsal root ganglia sensory neurons. *J. Physiol.* 552(Pt 3), 797–807. doi: 10.1113/jphysiol.2003.046409

Stoffels, B., Hupa, K. J., Snoek, S. A., van, Bree S, Stein, K., Schwandt, T., et al. (2014). Postoperative ileus involves interleukin-1 receptor signaling in enteric glia. *Gastroenterology* 146, 176.e1–187.e1. doi: 10.1053/j.gastro.2013.09.030

Takeuchi, T., Fujinami, K., Goto, H., Fujita, A., Taketo, M. M., Manabe, T., et al. (2005). Roles of M2 and M4 muscarinic receptors in regulating acetylcholine release from myenteric neurons of mouse ileum. *J. Neurophysiol.* 93, 2841–2848. doi: 10.1152/jn.00986.2004

Timóteo, M. A., Carneiro, I., Silva, I., Noronha-Matos, J. B., Ferreirinha, F., Silva-Ramos, M., et al. (2014). ATP released via pannexin-1 hemichannels mediates bladder overactivity triggered by urothelial P2Y6 receptors. *Biochem. Pharmacol.* 87, 371–379. doi: 10.1016/j.bcp.2013.11.007

Van Assche, G., and Collins, S. M. (1996). Leukemia inhibitory factor mediates cytokine-induced suppression of myenteric neurotransmitter release from rat intestine. *Gastroenterology* 111, 674–681. doi: 10.1053/gast.1996.v111.pm8780572

Vanderwinden, J. M., Timmermans, J. P., and Schiffmann, S. N. (2003). Glial cells, but not interstitial cells, express P2X7, an ionotropic purinergic receptor, in rat gastrointestinal musculature. *Cell Tissue Res.* 312, 149–154.

Vasina, V., Barbara, G., Talamonti, L., Stanghellini, V., Corinaldesi, R., Tonini, M., et al. (2006). Enteric neuroplasticity evoked by inflammation. *Auton. Neurosci.* 126-127, 264–272. doi: 10.1016/j.autneu.2006.02.025

Venkataramana, S., Lourenssen, S., Miller, K. G., and Blennerhassett, M. G. (2015). Early inflammatory damage to intestinal neurons occurs via inducible nitric oxide synthase. *Neurobiol. Dis.* 75, 40–52. doi: 10.1016/j.nbd.2014.12.014

Vieira, C., Duarte-Araújo, M., Adães, S., Magalhães-Cardoso, T., and Correia-de-Sá, P. (2009). Muscarinic M3 facilitation of acetylcholine release from rat myenteric neurons depends on adenosine outflow leading to activation of excitatory A_{2A} receptors. *Neurogastroenterol. Motil.* 21, 1118–e95. doi: 10.1111/j.1365-2982.2009.01326.x

Vieira, C., Ferreirinha, F., Silva, I., Duarte-Araújo, M., and Correia-de-Sá, P. (2011). Localization and function of adenosine receptor subtypes at the longitudinal muscle-myenteric plexus of the rat ileum. *Neurochem. Int.* 59, 1043–1055. doi: 10.1016/j.neuint.2011.08.016

Vieira, C., Magalhães-Cardoso, M. T., Ferreirinha, F., Silva, I., Dias, A. S., Pelletier, J., et al. (2014). Feed-forward inhibition of CD73 and upregulation of adenosine deaminase contribute to the loss of adenosine neuromodulation in postinflammatory ileitis. *Mediators Inflamm.* 2014:254640. doi: 10.1155/2014/254640

Virginio, C., Robertson, G., Surprenant, A., and North, R. A. (1998). Trinitrophenyl-substituted nucleotides are potent antagonists selective for P2X1, P2X3, and heteromeric P2X2/3 receptors. *Mol. Pharmacol.* 53, 969–973.

Vizi, E. S., Ono, K., Adam-Vizi, V., Duncalf, D., and Földes, F. F. (1984). Presynaptic inhibitory effect of Met-enkephalin on [14C] acetylcholine release from the myenteric plexus and its interaction with muscarinic negative feedback inhibition. *J. Pharmacol. Exp. Ther.* 230, 493–499.

Von Boyen, G., and Steinkamp, M. (2010). The role of enteric glia in gut inflammation. *Neuron Glia Biol.* 6, 231–236. doi: 10.1017/S1740925X11000068

Wang, X. Y., Ward, S. M., Gerthoffer, W. T., and Sanders, K. M. (2003). PKC-ε translocation in enteric neurons and interstitial cells of Cajal in response to muscarinic stimulation. *Am. J. Physiol. Gastrointest. Liver Physiol.* 258, G593–G601.

Ward, S. M., and Sanders, K. M. (2001). Interstitial cells of Cajal: primary targets of enteric motor innervation. *Anat. Rec.* 262, 125–135. doi: 10.1002/1097-0185(20010101)262:1<125::AID-AR1017>3.0.CO;2-I

Wirtz, S., and Neurath, M. F. (2007). Mouse models of inflammatory bowel disease. *Adv. Drug Rev.* 59, 1073–1083. doi: 10.1016/j.addr.2007.07.003

Zoppellaro, C., Bin, A., Brun, P., Banzato, S., Macchi, V., Castagliuolo, I., et al. (2013). Adenosine-mediated enteric neuromuscular function is affected during herpes simplex virus type 1 infection of rat enteric nervous system. *PLOS ONE* 8:e72648. doi: 10.1371/journal.pone.0072648

Conflict of Interest Statement: The authors declare that the research was conducted in the absence of any commercial or financial relationships that could be construed as a potential conflict of interest.

frontiers in Pharmacology

ORIGINAL RESEARCH
published: 10 October 2017
doi: 10.3389/fphar.2017.00719

Changes in P2Y Purinergic Receptor Expression in the Ciliary Body in a Murine Model of Glaucoma

Begoña Fonseca[1], Alejandro Martínez-Águila[1], María J. Pérez de Lara[1], Maria Teresa Miras-Portugal[2], Rosa Gómez-Villafuertes[2†] and Jesús Pintor[1†]*

[1] Departamento de Bioquímica y Biología Molecular IV, Facultad de Óptica y Optometría, Universidad Complutense de Madrid, Madrid, Spain, [2] Departamento de Bioquímica y Biología Molecular IV, Facultad de Veterinaria, Universidad Complutense de Madrid, Madrid, Spain

Glaucoma is a neuropathology, often accompanied by an elevated intraocular pressure (IOP), which can lead to blindness. Since DBA/2J mice develop glaucoma, several studies of the physiopathology of glaucoma have been reported in this animal model. It is also known that purinergic receptors are involved in the pathology of glaucoma by controlling aqueous humor production and drainage and therefore controlling IOP. There are no studies on purinergic receptors in the DBA/2J model of glaucoma and their relation to the development of the pathology, so the aim of this study was to make an approach to the purinergic mechanisms involved in glaucoma. All the experiments were performed using DBA/2J and C57BL/6J mice and investigating $P2Y_1$, $P2Y_2$, and $P2Y_6$ receptors. IOP measurements were made with a non-invasive rebound tonometer, and animals were instilled with diadenosine tetraphosphate (Ap_4A) and the corresponding purinergic antagonists in order to see their effects on IOP. The expression of mRNA for $P2Y_1$, $P2Y_2$, and $P2Y_6$ purinergic receptors was carried out by quantitative real-time PCR. Additionally, P2Y-receptor expression was performed by immunohistochemical techniques carried out on the ciliary processes. The results showed that IOP decreases when Ap_4A was instilled and that the expressions of the analyzed purinergic receptors were stable throughout all the ages under study in the C57BL/6J mice (control mice). On the other hand, there were significant changes in the purinergic receptor expression in DBA/2J suggesting that elevated IOP in these animals could be related to an increase of $P2Y_2$ expression and a decrease in $P2Y_1$ receptors.

Keywords: Ap_4A, ciliary body, DBA/2J, eye, glaucoma, P2Y receptors

Edited by:
Francisco Ciruela, University of Barcelona, Spain

Reviewed by:
Claire H. Mitchell, University of Pennsylvania, United States
Lin-Hua Jiang, University of Leeds, United Kingdom

***Correspondence:**
Jesús Pintor
jpintor@vet.ucm.es

† These authors have contributed equally to this work.

Specialty section:
This article was submitted to Experimental Pharmacology and Drug Discovery, a section of the journal Frontiers in Pharmacology

Received: *12 June 2017*
Accepted: *25 September 2017*
Published: *10 October 2017*

Citation:
Fonseca B, Martínez-Águila A, Pérez de Lara MJ, Miras-Portugal MT, Gómez-Villafuertes R and Pintor J (2017) Changes in P2Y Purinergic Receptor Expression in the Ciliary Body in a Murine Model of Glaucoma. Front. Pharmacol. 8:719. doi: 10.3389/fphar.2017.00719

INTRODUCTION

DBA/2J mouse strain has become a popular model for studying glaucoma, because it develops the pathology spontaneously. DBA/2J mice contain mutations in two genes, *Tyrp1* and *Gpnmb*, encoding tyrosinase-related and glycosylated transmembrane proteins, respectively. These mutations lead to pigment dispersion, iris transillumination, iris atrophy, and anterior synechia (Anderson et al., 2002). Due to the blockade of aqueous outflow, DBA/2J mice suffer from ocular hypertension by the age of 9 months, which is accompanied by the canonical symptoms of a glaucoma-related death of retinal ganglion cells (RGCs), optic nerve atrophy and cupping, as well

as visual deficits (Libby et al., 2005). The pathophysiology of glaucoma remains in part unknown, although there are several studies demonstrating that elevated intraocular pressure (IOP) affects disease development, leading to a progressive optic neuropathy characterized by functional and structural impairment of ocular tissues that may result in the loss of vision (Davson, 1993). This elevated IOP mainly leads to glaucoma as a result of impeded aqueous humor outflow (Tomarev, 2001). Aqueous humor is produced by the ciliary epithelium in the posterior chamber of the eye and circulates through the pupil to the anterior chamber, where it drains through the trabecular meshwork into Schlemm's canal and episcleral veins (Morrison and Acott, 2003). Thus, the ciliary processes provide the pressure inside the eye, which is maintained as a balance between the production and the drainage of the aqueous humor throughout the trabecular meshwork.

It is well known that purinergic P2 receptors, which are activated by extracellular nucleotides, can be involved in aqueous humor production and drainage and are therefore involved in IOP control (Guzman-Aranguez et al., 2013). P2 receptors are classified into two subfamilies: G protein-coupled P2Y receptors and ligand-gated cation channels called P2X receptors. So far, seven P2X subunits (P2X1-7) and eight P2Y receptors ($P2Y_{1,2,4,6,11,12,13,14}$) have been cloned and characterized in humans, according to their agonist sensitivity, sequence identities, and signal transduction mechanisms (Burnstock, 2000; Abbracchio et al., 2006). P2Y receptors contain seven hydrophobic transmembrane domains connected by three extracellular loops and three intracellular loops. The extracellular amino-terminus presents sites for glycosylation and the intracellular domain contains potential sites for phosphorylation, which may participate in receptor desensitization and internalization. P2Y receptors can be characterized according to their responses to nucleotide agonists and subtype-preferring antagonists. Adenine nucleotides, such as ADP or its synthetic analogous 2-methylthio-ADP (2-MeSADP), can activate selectively $P2Y_1$ receptors (Waldo and Harden, 2004), whereas uracil nucleotides activate $P2Y_6$ receptors (Nicholas et al., 1996). Moreover, both adenine and uracil nucleotides (ATP and UTP) activate equipotently $P2Y_2$ receptors (Lazarowski et al., 1995).

$P2Y_1$ and $P2Y_2$ receptors are expressed in rabbit ciliary body epithelial cells, which may be responsible for the action of 2-MeSATP, ATPγS, as well as other P2Y agonists (Farahbakhsh and Cilluffo, 2002). The expression of $P2Y_1$, $P2Y_2$, and $P2Y_4$ receptors in bovine trabecular meshwork has also been reported (Soto et al., 2005) as well as the presence of $P2Y_6$ and $P2Y_{11}$ receptors in rat ocular structures (Pintor et al., 2004).

The dinucleotide diadenosine tetraphosphate (Ap_4A) (Guzman-Aranguez et al., 2011) shows a hypotensive effect when instilled topically in the eye (Fonseca et al., 2016), which is related to an increase in the outflow of the aqueous humor through activation of several purinergic receptors, mainly the $P2Y_1$ (Schachter et al., 1996; Soto et al., 2005).

Most of the experiments performed to analyze the modulation of aqueous humor production and drainage by purinergic receptors previously described in the scientific literature, have been carried out on normotensive mice models or on induced models of glaucoma. Here we characterize the presence of $P2Y_1$, $P2Y_2$, and $P2Y_6$ receptors in the ciliary processes of the eye of control versus glaucomatous mice and analyze the expression levels of these receptors during aging and the development of the pathology in these animals.

MATERIALS AND METHODS

Animals

Experiments were performed on adult female C57BL/6J ($n = 30$) (control animals) and DBA/2J ($n = 30$) (glaucomatous animals) mice obtained from the European distributor of Jackson Laboratories Mice (Charles River Laboratories). All animal maintenance and experimental procedures followed Spanish and European guidelines for animal care in the laboratory and animal research (Guide for the Care and Use of Laboratory Animals) and the ARVO Statement for the Use of Animals in Ophthalmic and Vision Research. Mice were housed (1–4 mice per cage) in temperature and light-controlled rooms maintained according to a 12-h/12-h light/dark cycle; all animals were fed *ad libitum*. DBA/2J and C57BL/6J mice were studied at 3, 6, 9, and 12 months of age.

All this study has been approved by the Animal Experimental Committee of the Universidad Complutense de Madrid and Comunidad de Madrid, reference 45/057949.9/16.

Intraocular Pressure (IOP) Measurements

Intraocular pressure (IOP) was measured using a non-invasive rebound tonometer (Tono-lab®; Tiolat, OY, Helsinki, Finland). The tonometer was fixed so that the probe tip was aligned with the optical axis of the eye, at a distance of 1–4 mm. In order to avoid the effect of the circadian rhythm, the IOP was always tested at the same time of day. Six consecutive measurements were taken for each reading, and three readings were obtained on each eye (Fonseca et al., 2016).

In order to study the effect of Ap_4A, two IOP measurements were taken before Ap_4A was instilled. A single application of 2 µl drops with a micropipette at 100 µM was instilled once every hour for 6 h. To study the effect of the antagonists of purinergic receptors, these blockers were instilled in 2 µl drops with a micropipette at 100 µM 30 min before Ap_4A at a concentration of 100 µM, measuring IOP in the same way as previously described (Fonseca et al., 2016). The antagonists assayed in the current study were pyridoxalphosphate-6-azophenyl-2',4'-disulfonic acid (PPADS), suramin and reactive blue 2 (RB-2, a non-selective P2 antagonists), 2'-deoxy-N6-methyladenosine 3',5'-bisphosphate tetrasodium salt (MRS2179, a $P2Y_1$ antagonist), and N,N″-1,4-butanediylbis(N′-(3-isothiocyanatophenyl))thiourea (MRS2578, a $P2Y_6$ antagonist). All the doses (concentrations), volumes, and times of measurement have been controlled according to Fonseca et al. (2016).

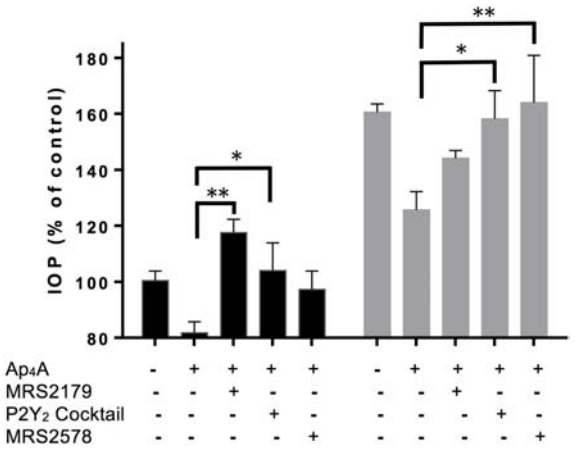

FIGURE 1 | Effect of P2 receptor antagonists on IOP reduction mediated by Ap_4A in C57BL/6J versus DBA/2J mice. Two IOP measurements were taken before a single dose of either vehicle or 100 μM Ap_4A was instilled, and 3 h later, IOP was measured again. When indicated, purinergic antagonists, all tested at 100 μM, were instilled 30 min before Ap_4A. MRS2179 and MRS2578 are antagonists of $P2Y_1$ and $P2Y_6$ receptors, respectively. "$P2Y_2$ cocktail" contains PPADS, suramin, and RB-2. Data are the mean ± SEM of 4 mice (*$p < 0.05$, **$p < 0.01$; one-way ANOVA with Dunnett's multiple comparisons test).

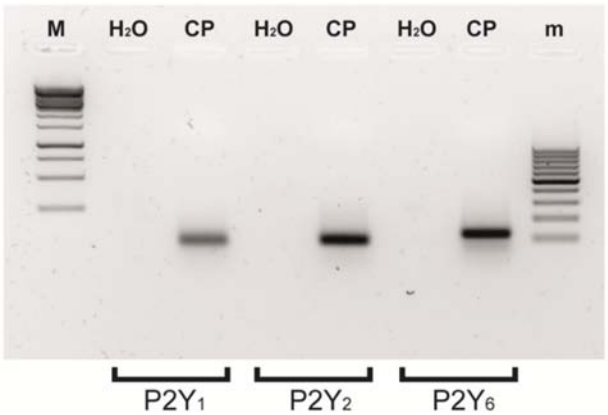

FIGURE 2 | Several metabotropic P2Y receptors are simultaneously expressed in the eye ciliary processes of C57BL/6J mice. RT-PCR expression of $P2Y_1$, $P2Y_2$, and $P2Y_6$ receptors. Molecular weights of the bands were around 100 bp and were amplified from adult C57BL/6J mouse ciliary processes (CP) mRNA extracts. No amplification products were observed in parallel assays carried out without template (H_2O). M: 1 Kb DNA ladder (10000-250 pb); m: 100 bp DNA ladder (1000–1100 bp).

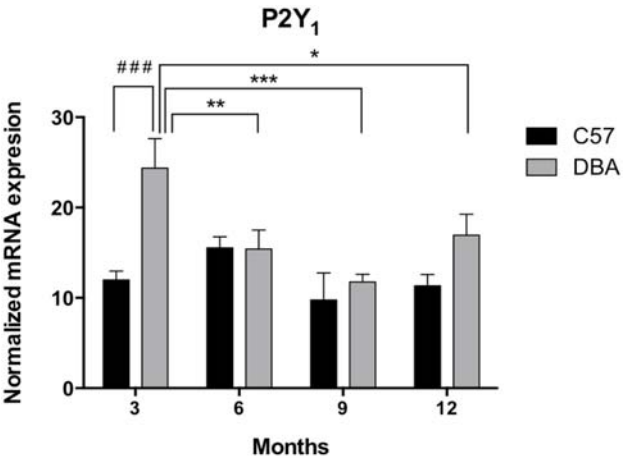

FIGURE 3 | Temporal pattern of $P2Y_1$ transcript expression in ciliary processes of C57BL/6J versus DBA/2J mice. Total RNA from ciliary processes of either control (C57BL/6J) or glaucomatous (DBA/2J) animals of 3, 6, 9, or 12 months of age was extracted and $P2Y_1$ mRNA was quantified by Q-PCR as described in the Section "Materials and Methods." Values were normalized to the content of GAPDH transcript. Results are the mean ± SEM of 24 animals of each strain (*$p < 0.05$, **$p < 0.01$, ***$p < 0.001$ versus same mice strain; $^{###}p < 0.001$ versus different mice strain; two-way ANOVA with Sidak's post-test).

RNA Isolation and RT-PCR

Total RNA from isolated ciliary bodies and iris of DBA/2J ($n = 24$) and C57BL/6 ($n = 24$) mice was extracted using Speedtools total RNA extraction kit (Biotools, Madrid, Spain), following the manufacturer's instructions. After digestion with TURBO DNase (Ambion, Austin, TX, United States), total RNA was quantified and reverse transcribed using M-MLV reverse transcriptase, 6 μg of random primers and 350 μM dNTPs (Invitrogen, San Francisco, CA, United States). Due to the small size of the tissues and in order to improve sensitivity of PCR analysis, pre-amplification reactions were carried out using DNA AmpliTools Master Mix (Biotools), 5 μL of the RT product and specific commercial oligonucleotide primers for mouse $P2Y_1$, $P2Y_2$, and $P2Y_6$ receptors (Applied Biosystems). Moreover, non-template control was amplified to check for contamination during the procedure. Pre-amplification reactions were performed on a 2720 Thermal Cycler (Applied Biosystems) with the following program: initial denaturation step at 94°C for 5 min followed by 14 cycles of amplification (94°C for 30 s, 60°C for 30 s, and 72°C for 30 s). Then, 5 μL of the pre-amplified product diluted 1/5 in water was used for the subsequent PCR assay. PCR reactions were identical to pre-amplification ones, with the exception of the number of cycles, which were 40 in the last case. Amplified PCR products were electrophoresed on a 2% agarose gel and visualized by SYBR® Safe DNA gel stain (Invitrogen). DNA ladders used were GeneRuler 1 Kb and 100 bp (Thermo Scientific).

Quantitative Real-Time PCR

Following pre-amplification, 5 μL of the each product diluted 1/5 in water were used for the subsequent quantitative real-time PCR (Q-PCR) assay. Q-PCR reactions were carried out using LuminoCt® Q-PCR Readymix (Sigma–Aldrich, St. Louis, MO, United States), 5 μL of the RT product, and specific commercial oligonucleotide primers and TaqMan MGB probes for mouse $P2Y_1$, $P2Y_2$, and $P2Y_6$ receptors, as well as for GAPDH (all from Applied Biosystems). Fast thermal cycling was performed using a StepOnePlus® Real-Time System (Applied Biosystems, Foster City, CA, United States) as follows: denaturation, one cycle of

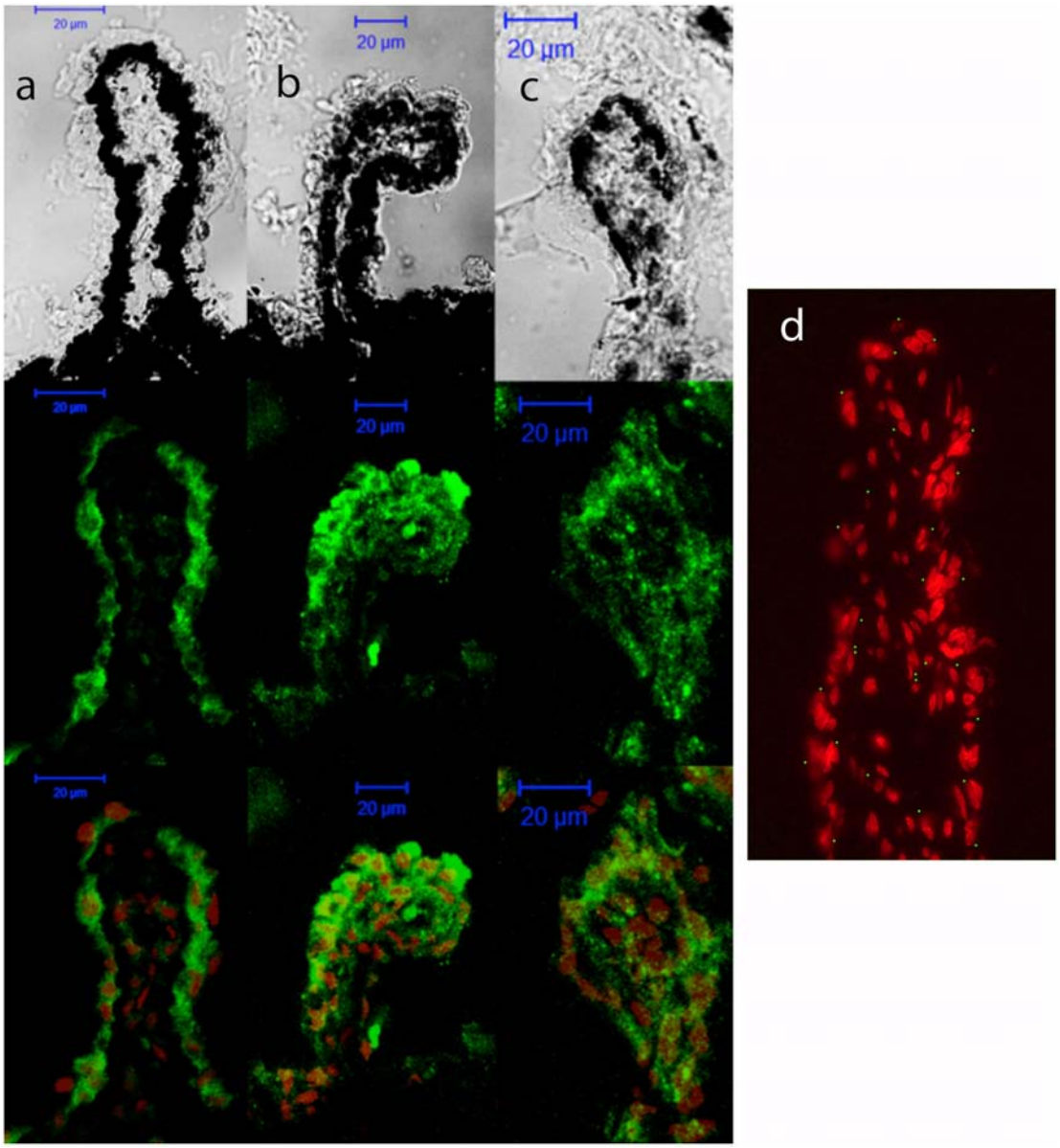

FIGURE 4 | Cellular distribution of $P2Y_1$ receptor in ciliary processes of C57BL/6J versus DBA/2J mice. Immunofluorescence images of ciliary processes from 3-month-old C57BL/6J **(a)**, 3-month-old DBA/2J **(b)**, and 12-month-old DBA/2J **(c)** mice labeled with antibodies against $P2Y_1$ receptor (green). Nuclei were counterstained with propidium iodide (red). **(d)** Negative control was carried out by substituting the $P2Y_1$ primary antibody by the same volume of PBS/TX-100 solution. Phase-contrast and confocal images show that $P2Y_1$ immunostaining is mainly located in non-pigmented epithelium of ciliary processes, being enhanced in DBA/2J versus C57BL/6J at the age of 3 months. Scale bar: 20 µm.

95°C for 20 s, followed by 40 cycles each of 95°C for 1 s and 60°C for 20 s. The results were normalized as indicated by the parallel amplification of the GAPDH housekeeping gene. Thus, Q-PCR graphs indicate the ratio between P2Y and GAPDH transcripts multiplied by the 10e4 factor in order to represent *Y*-axis values higher than 1.

Immunohistochemistry

C57BL/6J and DBA/2J mice at 3 and 12 months of age ($n = 6$ animals for each group) were euthanized with an intraperitoneal injection overdose of pentobarvital (Dolethal; Vetoquinol®; Especialidades Veterinarias, S.A., Alcobendas, Madrid, Spain) and perfused pericardially with phosphate buffer saline (PBS) followed by a solution of 4% paraformaldehyde in PBS 0.1 M, pH 7.4 at 4°C. The eyes were enucleated and dissected with curved forceps and sterile scissors. The anterior pole was immersed in paraformaldehyde (PFA) fixative solution for 1 h at 4°C and was washed in PBS, and rinsed in 11% sucrose solution for 1 h and 33% sucrose solution overnight at 4°C as cryoprotection procedure. Finally, the structures were embedded in tissue

medium freezing medium (Tissue-Tek© OCT) using liquid N_2 and vertical sections (10 μm thick) were cut on a cryostat (Microm, Walldorf, Germany) and collected on poly-L lysine-coated slides and stored at −20°C until use.

Frozen sections were rinsed in PBS 1× and permeabilized with PBS-containing 0.25% Triton X-100 (TX-100) for 30 min. To avoid non-specific staining, sections were incubated with the blocking solution containing 10% normal donkey serum (NDS; Jackson ImmunoResearch, West Grove, PA, United States) and 0.1% TX-100 in PBS for 1 h at room temperature. Then, the following primary antibodies diluted in PBS containing 0.1% TX-100 were incubated at 4°C overnight: goat anti-$P2Y_1$ (Santa Cruz Biotechnology, Inc., Santa Cruz, CA, United States; sc-15204, 1:100), rabbit anti-$P2Y_2$ (Alomone Labs Israel, APR-010, 1:100) goat anti-$P2Y_6$ (Santa Cruz Biotechnology, Inc., Santa Cruz, CA, United States; sc-15215, 1:75) diluted in PBS-0.1% TX-100 were incubated at 4°C overnight. Finally, tissue sections were washed in PBS containing 0.1% TX-100 and incubated. The secondary antibody donkey anti-rabbit Alexa Fluor 488 IgG (H+L) (Jackson ImmunoResearch, West Grove, PA, United States) was diluted 1:200 in PBS containing 0.1% TX-0.1% for 1 h in darkness at room temperature. Nuclei were stained with propidium iodide (red, Sigma–Aldrich, St. Louis, MO, United States) diluted 1:500 in PBS for 10 min. Finally, sections were rinsed and mounted in Vectashield (Vector Laboratories, Palex Medical, Barcelona, Spain) and coverslipped. Negative controls were carried out by following the same procedures but, in each case, the primary antibody was substituted by the same volume of PBS/TX-100 solution. For the analysis, the images were acquired using a laser-scanning microscope (Zeiss LSM 5, Jena, Germany) at 40× magnification and exported as tiff files for further analysis.

Statistical Analysis

All data are presented as the mean ± SEM. Statistical differences were calculated using one-way ANOVA test with Dunnett's post-test plotting and fitting were carried out by GraphPad Prism 6 computer program (GraphPad Software).

RESULTS

Activation of P2Y Receptors Decreases IOP in C57BL/6J and DBA/2J Mice Strains

Ap_4A has been reported as an agonist of $P2Y_1$, $P2Y_2$, and $P2Y_6$ receptors (Patel et al., 2001; Pintor et al., 2002). In a previous study, we have demonstrated that the instillation of Ap_4A was able to significantly decrease IOP in both control C57BL/6J and glaucomatous DBA/2J aged mice, with a maximal effect after 3 h of treatment (Fonseca et al., 2016). In the current study, we tested the effect of different P2Y receptor antagonists on the IOP reduction mediated by Ap_4A in 12-month-old C57BL/6J versus DBA/2J mice (**Figure 1**). It was noticed that the Ap_4A effect on control animals was completely blocked by either MRS2179, a $P2Y_1$ antagonist ($^{**}p < 0.005$), or a cocktail of suramin, PPADS and RB-2, which altogether inhibits $P2Y_2$ receptor ($^{*}p < 0.05$), whereas MRS2578, a $P2Y_6$ antagonist, did not show a significant effect on the Ap_4A hypotensive effect. On the contrary, in glaucomatous animals, the $P2Y_1$ antagonist did not modify the Ap_4A effect, whereas either the "$P2Y_2$ cocktail" or the $P2Y_6$ antagonist MRS2578 was able to prevent the IOP fall induced by Ap_4A. We have also performed RT-PCR experiments demonstrating that $P2Y_1$, $P2Y_2$, and $P2Y_6$ transcripts were expressed in the ciliary processes of C57BL/6J mice (**Figure 2**). These results suggested that the expression levels of P2Y receptors could differ between control and glaucomatous animals. In order to check this possibility, we analyzed, by Q-PCR and immunohistochemistry, the expression levels of $P2Y_1$, $P2Y_2$, and $P2Y_6$ receptors in the ciliary processes of both C57BL/6J and DBA/2J mice at different ages.

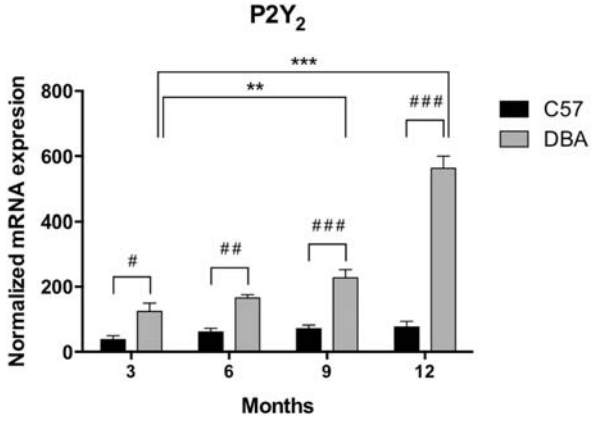

FIGURE 5 | Temporal pattern of $P2Y_2$ mRNA levels in ciliary processes of C57BL/6J versus DBA/2J mice. Total RNA from ciliary processes of either control (C57BL/6J) or glaucomatous (DBA/2J) animals of 3, 6, 9, or 12 months of age was extracted and $P2Y_2$ mRNA was quantified by Q-PCR as described in the Section "Materials and Methods." GAPDH was used as a control for differences in cDNA input. Results are the mean ± SEM of 24 animals of each strain ($^{**}p < 0.01$, $^{***}p < 0.001$ versus same mice strain; $^{\#}p < 0.05$, $^{\#\#}p < 0.01$ $^{\#\#\#}p < 0.001$ versus different mice strain; two-way ANOVA with Sidak's post-test).

Expression of $P2Y_1$ Receptors in Ciliary Processes of C57BL/6J and DBA/2J Mice

First, the expression levels of $P2Y_1$ transcript were compared between the control and glaucomatous mice of 3, 6, 9, and 12 months of age by Q-PCR. In C57BL/6J mice, $P2Y_1$ mRNA expression remained invariable during the adult life of the animals (**Figure 3**, black bars). Interestingly, $P2Y_1$ expression in DBA/2J mice was twofold higher than in C57BL/6J animals at 3-month-old ($p = 0.005$), but decreased to control values in older mice (**Figure 3**, gray bars). Immunohistochemical studies revealed that the $P2Y_1$ receptor was widely distributed over all in the non-pigmented epithelium of the ciliary process of the eye in both C57BL/6 and DBA/2J mice. However, as observed in transcript levels, $P2Y_1$ receptor expression

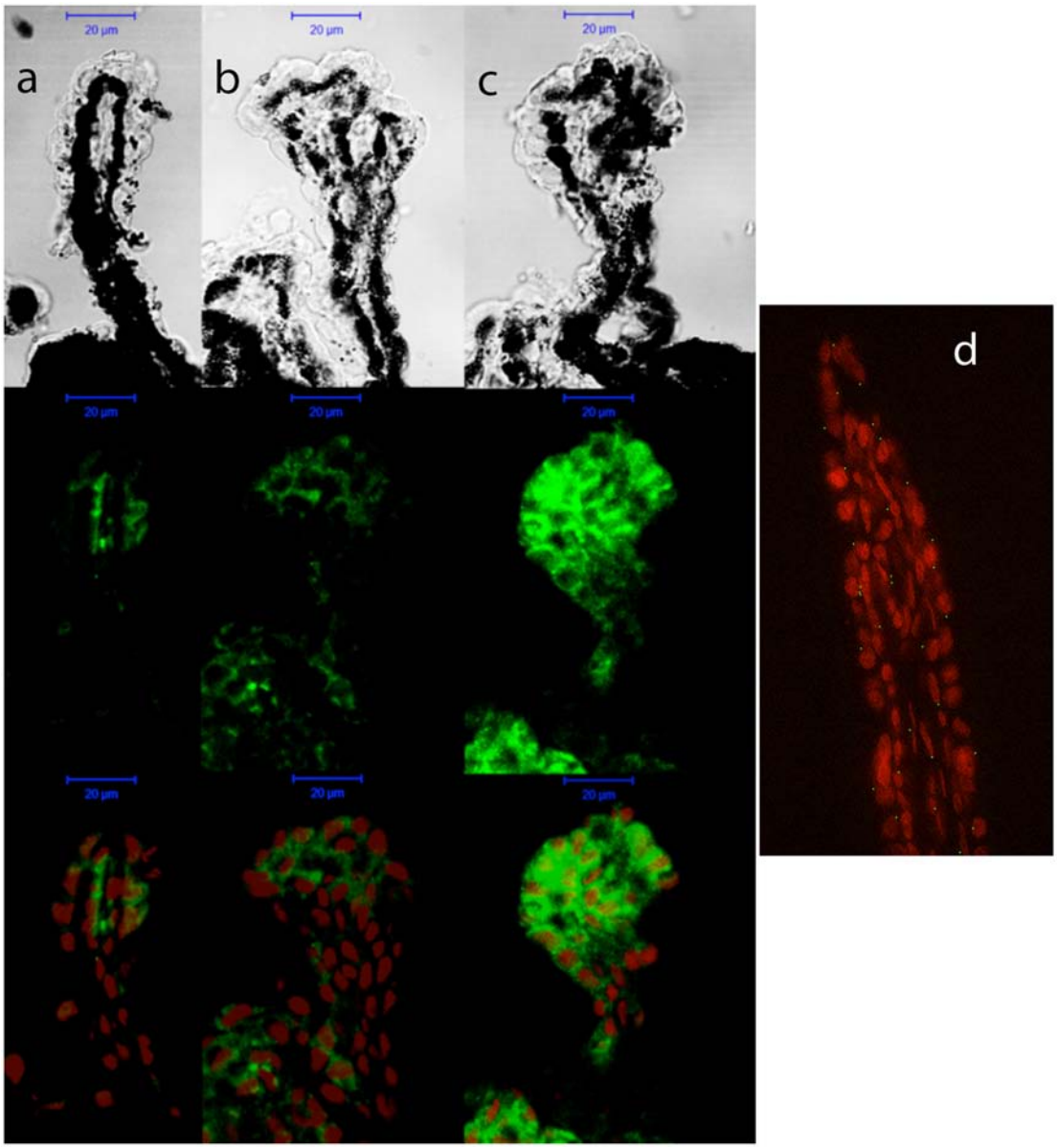

FIGURE 6 | Cellular distribution of $P2Y_2$ receptor in ciliary processes of C57BL/6J versus DBA/2J mice. Immunofluorescence images of ciliary processes from 3-month-old C57BL/6J **(a)**, 3-month-old DBA/2J **(b)**, and 12-month-old DBA/2J **(c)** mice labeled with antibodies against $P2Y_2$ receptor (green). Nuclei were counterstained with propidium iodide (red). **(d)** Negative control carried out by substituting the $P2Y_2$ primary antibody by the same volume of PBS/TX-100 solution. Phase-contrast and confocal images show that the $P2Y_2$ receptor is mainly located in the non-pigmented epithelium of ciliary processes, and its expression is strongly increased in old DBA/2J mice compared to young animals. Scale bar: 20 µm.

was enhanced in 3-month-old DBA/2J animals compared to 12-month-old ones and also compared to 3-month-old C57BL/6 mice (**Figure 4**).

Expression of $P2Y_2$ Receptors in Ciliary Processes of C57BL/6J and DBA/2J Mice

As shown for $P2Y_1$ transcript, $P2Y_2$ mRNA expression remained invariable during the adult life of C57BL/6J mice (**Figure 5**, black bars). However, a pathology-dependent rise in $P2Y_2$ transcript levels was found in glaucomatous mice, reaching a sixfold increase in 12-month-old DBA/2J mice compared to control ones ($p = 0.005$), although a significant increase was already observed in 6-month-old mice (**Figure 5**, gray bars). $P2Y_2$ protein was also found in the non-pigmented epithelium of the ciliary processes of both C57BL/6J and DBA/2J animals, although, as expected, a huge increment in the fluorescent signal coupled to $P2Y_2$ receptor was found in 12-month-old DBA/2J mice compared to young animals of both strains (**Figure 6**).

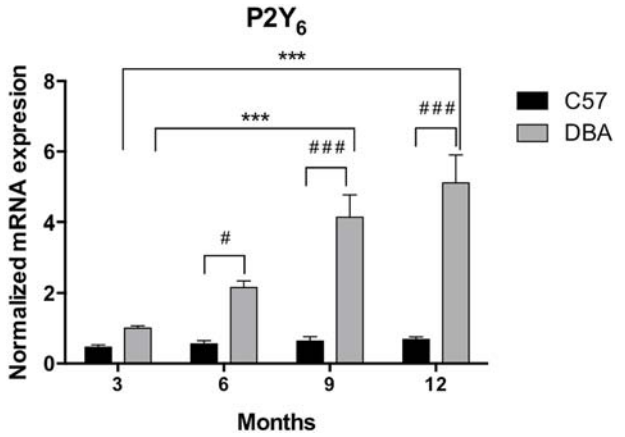

FIGURE 7 | Temporal pattern of $P2Y_6$ transcript expression in ciliary processes of C57BL/6J versus DBA/2J mice. Total RNA from ciliary processes of either control (C57BL/6J) or glaucomatous (DBA/2J) animals of 3, 6, 9, or 12 months of age was extracted and $P2Y_6$ mRNA was quantified by Q-PCR as described in the Section "Materials and Methods." Values were normalized to the content of GAPDH transcript. Results are the mean ± SEM of 24 animals of each strain ($^{***}p < 0.001$ versus same mice strain; $^{\#}p < 0.05$, $^{\#\#\#}p < 0.001$ versus different mice strain; two-way ANOVA with Sidak's post-test).

Expression of $P2Y_6$ Receptors in Ciliary Processes of C57BL/6J and DBA/2J Mice

The expression pattern of $P2Y_6$ receptors was very similar to that observed for $P2Y_2$ receptors. As shown in **Figure 7**, $P2Y_6$ transcript levels remained constant in C57BL/6J mice (black bars), but an age-dependent increase in $P2Y_6$ mRNA was observed in *DBA/2J* mice (gray bars). This increment was significant in 6-month-old animals and was progressively rising until reaching a sixfold increase in 12-month-old DBA/2J mice compared to control ones ($p = 0.005$). Immunohistochemical studies confirmed that the $P2Y_6$ receptor was also located in the non-pigmented epithelium of the ciliary body of the eye of both mice strains. Moreover, as observed in transcript levels, $P2Y_6$ receptor expression was significantly higher in 12-month-old DBA/2J animals compared to young ones and also compared to young C57BL/6 mice (**Figure 8**).

DISCUSSION

The existence of nucleotides in the aqueous humor (Mitchell et al., 1998; Pintor et al., 2003), as well as the participation of P2 purinergic receptors in the regulation of IOP, has already been described in the scientific literature (Crooke et al., 2008). Mono and dinucleotides, both in the μM range, are able to activate P2 receptors, which in turn modify both the synthesis and drainage of the aqueous humor. In normotensive animal models, $P2Y_1$ and $P2Y_2$ receptors are located in the trabecular meshwork and the ciliary body, respectively (Soto et al., 2005; Martin-Gil et al., 2012). When the activation of $P2Y_1$ receptors is carried out by Ap_4A in the trabecular meshwork, the observed effect is a reduction in IOP (Soto et al., 2005), whereas the activation of $P2Y_2$ receptors in the ciliary body produces a hypertensive effect (Martin-Gil et al., 2012). $P2Y_2$ receptors exert this effect by increasing the presence of Aquaporin-1 in the ciliary body epithelial cell membranes (Martin-Gil and Pintor, 2010; Pintor et al., 2011). Finally, the activation of $P2Y_6$ receptor by molecules such as uridine diphosphate (UDP), reduces IOP in the New Zealand normotensive model (Markovskaya et al., 2008).

Ap_4A is a molecule present in the aqueous humor of animal models such as rabbits or mice (Pintor et al., 2003), but is also present in normal and glaucomatous human patients (Castany et al., 2011). Therefore, this dinucleotide seems to be involved in the pathophysiology of glaucoma, mainly by acting on P2 purinergic receptors. In this sense, the release of Ap_4A is produced by the activation of a pressure sensor, a TRPV4 channel, which is activated by the abnormal IOP often associated to glaucoma (Pintor et al., 2011). The TRPV4-induced Ap_4A release will stimulate mainly the $P2Y_2$ receptor present in the ciliary body, which mobilizes Aquaporin-1 from intracellular reservoirs to the plasma membrane of the ciliary epithelium (Martin-Gil and Pintor, 2010). This increase in the aquaporins facilitates the production of aqueous humor contributing to the elevation of IOP and therefore priming the described process.

In this current study, using a glaucoma animal model, we have analyzed the expression levels of three P2Y metabotropic receptors ($P2Y_1$, $P2Y_2$, and $P2Y_6$), which are known to be activated by Ap_4A (Guzman-Aranguez et al., 2007), in the ciliary body and iris of control (C57BL/6) and glaucomatous (DBA/2J) mice. Our results demonstrate that control animals express constant levels of $P2Y_1$, $P2Y_2$, and $P2Y_6$ receptors throughout their lives, in clear contrast to the glaucomatous strain, where more remarkable changes are observed. In this sense, $P2Y_1$ receptor expression is significantly reduced at both mRNA and protein levels in aged DBA/2J mice. On the contrary, however, $P2Y_2$ and $P2Y_6$ receptor expressions are enhanced in aged DBA/2J mice, correlating in time with the pathology development. Similar differences between control and glaucomatous mice have also been found when analyzing the retinal electrophysiology in both strains, observing a gradual ganglion cell death in DBA/2J model (Perez de Lara et al., 2014). Moreover, the retinal ATP released increases in the glaucomatous mouse, but not in the control one when the pathology is fully established (12 months of age). In addition, the expression of the vesicular nucleotide transporter (VNUT) is significantly increased during the development of glaucoma in DBA/2J mice, reaching maximal levels at 12 months of age (Perez de Lara et al., 2015). Altogether, this evidence suggests that the alteration in the purinergic system observed in the DBA/2J is related to the pathology development and not to mice aging.

We have also established that micromolar concentrations of Ap_4A significantly reduce IOP in DBA/2J mice, once the pathology is fully developed. Moreover, a chronic treatment with the dinucleotide for 3 months is able to ameliorate the elevation in IOP in the glaucomatous mice in a very significant manner (Fonseca et al., 2016). These results indicate that the predominant physiological effect of Ap_4A is the reduction of IOP, although the expression of both $P2Y_2$ and $P2Y_6$ in DBA/2J mice is increased

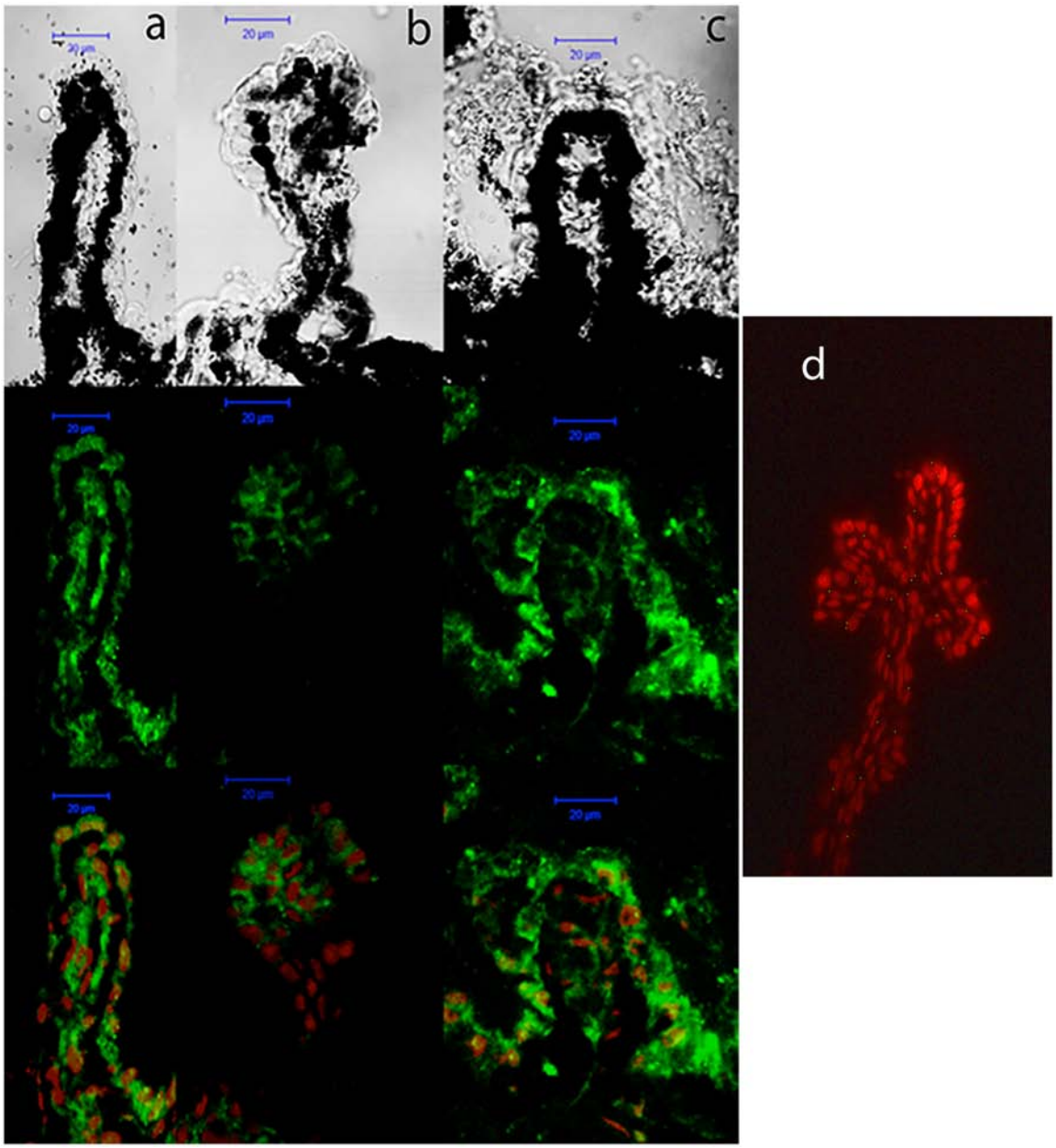

FIGURE 8 | Cellular distribution of $P2Y_6$ receptor in ciliary processes of C57BL/6J versus DBA/2J mice. Immunofluorescence images of ciliary processes from 3-month-old C57BL/6J **(a)**, 3-month-old DBA/2J **(b)**, and 12-month-old DBA/2J **(c)** mice labeled with antibodies against $P2Y_6$ receptor (green). Nuclei were counterstained with propidium iodide (red). **(d)** Negative control was carried out by substituting the $P2Y_6$ primary antibody by the same volume of PBS/TX-100 solution. Phase-contrast and confocal images show that the $P2Y_6$ receptor is mainly located in the non-pigmented epithelium of ciliary processes, and its expression is increased in 12-month-old DBA/2J mice compared to 3-month-old animals. Scale bar: 20 µm.

and both receptors mediate opposite effects on IOP (Fonseca et al., 2016).

Previous studies reported that $P2Y_2$ receptor activation in the ciliary body exerted a hypertensive effect on IOP, which could be inhibited by antagonism or silencing of that receptor (Martin-Gil et al., 2012). The hypertensive role of the $P2Y_2$ receptor in the ciliary body correlated well with the abnormally elevated concentration of Ap_4A found in glaucoma patients, as previously commented (Castany et al., 2011). However, the topical application of this dinucleotide reduces IOP, so its use in the treatment of glaucoma cannot be discarded (Fonseca et al., 2016).

In our experimental model, the reduction in the expression of the $P2Y_1$ receptor in glaucomatous mice could produce an elevation in IOP, since the treatment with the specific antagonist MRS2179 prevented the hypotensive effect of Ap_4A

(Fonseca et al., 2016). An increase $P2Y_2$ expression could have similar consequences, since its activation exerted a hypertensive effect (Fonseca et al., 2016). Thus, the pathology-related increased in $P2Y_2$ receptor expression and its activation by endogenous Ap_4A could justify high IOP values measured in the glaucomatous mice. Interestingly, exogenous applications of high doses of Ap_4A have hypotensive effects, probably by activating the $P2Y_6$ receptor, which is elevated in the glaucomatous mice. Noteworthy is that the high Ap_4A concentration (about 300 nM) found in the aqueous humor of glaucoma patients is unable to reduce IOP, probably because this concentration is enough to stimulate the hypertensive $P2Y_2$ receptor, but insufficient to activate the hypotensive $P2Y_6$, which requires micromolar concentrations (Guzman-Aranguez et al., 2007). Further studies will be necessary to clarify this refined equilibrium.

The pathogenesis of glaucoma is not fully understood, but most of the studies indicate that the level of IOP is linked to RGC's death (Hollands et al., 2013). The rise in IOP causes mechanical stress and strain affecting eye posterior structures such as the lamina cribrosa and adjacent tissues, thus causing the deformation by compression of the lamina cribrosa. Consequently, the optic nerve axonal damage reduces the retrograde axonal transport (Burgoyne et al., 2005). This process produces the RGC's death and the subsequent blindness. Slowing disease progression, by reducing IOP, can be suggested according to the changes in the expression of P2Y receptors sensitive to the dinucleotide Ap_4A presented in this manuscript. A previous study has already proved the hypotensive effect of this compound on the DBA/2J glaucoma model (Fonseca et al., 2016). Therefore, the application of Ap_4A may help to reduce IOP in humans if the changes in the P2Y receptors are similar to the ones described in the glaucomatous mice.

In summary, we have demonstrated that the expression of some P2Y receptors, $P2Y_1$, $P2Y_2$, and $P2Y_6$, changes during the development of the glaucomatous pathology in a mouse model. The prevalence of the $P2Y_2$ receptor between 9 and 12 months of age, together with the rise in Ap_4A concentration, may be a contributing factor that helps explain why the pressure is abnormally elevated when the pathology is fully established.

AUTHOR CONTRIBUTIONS

BF: Contributed in PCR, immunohistochemistry. AM-Á: Contributed in PCR, immunohistochemistry. MPdL: Contributed in IOP measurements. MTM-P: Contributed in paper organization and writing. RG-V: Contributed in PCR, statistical analysis, and writing. JP: Contributed in paper design, organization, and writing.

FUNDING

This work has been supported by the research grants SAF2013-44416-R, SAF2016-77084-R, RETICS RD12/0034/0003, and Universidad Complutense PR1/07-14890. BF is a fellowship holder of Universidad Complutense de Madrid.

ACKNOWLEDGMENT

We thank Penny Rollinson for her help in the preparation of this manuscript.

REFERENCES

Abbracchio, M. P., Burnstock, G., Boeynaems, J. M., Barnard, E. A., Boyer, J. L., Kennedy, C., et al. (2006). International Union of Pharmacology LVIII: update on the P2Y G protein-coupled nucleotide receptors: from molecular mechanisms and pathophysiology to therapy. *Pharmacol. Rev.* 58, 281–341. doi: 10.1124/pr.58.3.3

Anderson, M. G., Smith, R. S., Hawes, N. L., Zabaleta, A., Chang, B., Wiggs, J. L., et al. (2002). Mutations in genes encoding melanosomal proteins cause pigmentary glaucoma in DBA/2J mice. *Nat. Genet.* 30, 81–85. doi: 10.1038/ng794

Burgoyne, C. F., Downs, J. C., Bellezza, A. J., Suh, J. K., and Hart, R. T. (2005). The optic nerve head as a biomechanical structure: a new paradigm for understanding the role of IOP-related stress and strain in the pathophysiology of glaucomatous optic nerve head damage. *Prog. Retin. Eye Res.* 24, 39–73. doi: 10.1016/j.preteyeres.2004.06.001

Burnstock, G. (2000). P2X receptors in sensory neurones. *Br. J. Anaesth.* 84, 476–488. doi: 10.1093/oxfordjournals.bja.a013473

Castany, M., Jordi, I., Catala, J., Gual, A., Morales, M., Gasull, X., et al. (2011). Glaucoma patients present increased levels of diadenosine tetraphosphate, Ap(4)A, in the aqueous humour. *Exp. Eye Res.* 92, 221–226. doi: 10.1016/j.exer.2010.12.004

Crooke, A., Guzman-Aranguez, A., Peral, A., Abdurrahman, M. K., and Pintor, J. (2008). Nucleotides in ocular secretions: their role in ocular physiology. *Pharmacol. Ther.* 119, 55–73. doi: 10.1016/j.pharmthera.2008.04.002

Davson, H. (ed.). (1993). "The aqueous humour and the intraocular pressure," in *Physiology of the Eye* (New York: Pergamon Press), 34–95.

Farahbakhsh, N. A., and Cilluffo, M. C. (2002). P2 purinergic receptor-coupled signaling in the rabbit ciliary body epithelium. *Invest. Ophthalmol. Vis. Sci.* 43, 2317–2325.

Fonseca, B., Martinez-Aguila, A., De Lara, M. J., and Pintor, J. (2016). Diadenosine tetraphosphate as a potential therapeutic nucleotide to treat glaucoma. *Purinergic Signal.* 13, 171–177. doi: 10.1007/s11302-016-9547-y

Guzman-Aranguez, A., Crooke, A., Peral, A., Hoyle, C. H., and Pintor, J. (2007). Dinucleoside polyphosphates in the eye: from physiology to therapeutics. *Prog. Retin. Eye Res.* 26, 674–687. doi: 10.1016/j.preteyeres.2007.09.001

Guzman-Aranguez, A., Loma, P., and Pintor, J. (2011). Focus on molecules: diadenosine tetraphosphate. *Exp. Eye Res.* 92, 96–97. doi: 10.1016/j.exer.2010.12.007

Guzman-Aranguez, A., Santano, C., Martin-Gil, A., Fonseca, B., and Pintor, J. (2013). Nucleotides in the eye: focus on functional aspects and therapeutic perspectives. *J. Pharmacol. Exp. Ther.* 345, 331–341. doi: 10.1124/jpet.112.202473

Hollands, H., Johnson, D., Hollands, S., Simel, D. L., Jinapriya, D., and Sharma, S. (2013). Do findings on routine examination identify patients at risk for primary open-angle glaucoma? The rational clinical examination systematic review. *JAMA* 309, 2035–2042. doi: 10.1001/jama.2013.5099

Lazarowski, E. R., Watt, W. C., Stutts, M. J., Boucher, R. C., and Harden, T. K. (1995). Pharmacological selectivity of the cloned human P2U-purinoceptor: potent activation by diadenosine tetraphosphate. *Br. J. Pharmacol.* 116, 1619–1627. doi: 10.1111/j.1476-5381.1995.tb16382.x

Libby, R. T., Anderson, M. G., Pang, I. H., Robinson, Z. H., Savinova, O. V., Cosma, I. M., et al. (2005). Inherited glaucoma in DBA/2J mice: pertinent disease features for studying the neurodegeneration. *Vis. Neurosci.* 22, 637–648. doi: 10.1017/S0952523805225130

Markovskaya, A., Crooke, A., Guzman-Aranguez, A. I., Peral, A., Ziganshin, A. U., and Pintor, J. (2008). Hypotensive effect of UDP on intraocular pressure in rabbits. *Eur. J. Pharmacol.* 579, 93–97. doi: 10.1016/j.ejphar.2007.10.040

Martin-Gil, A., De Lara, M. J., Crooke, A., Santano, C., Peral, A., and Pintor, J. (2012). Silencing of P2Y(2) receptors reduces intraocular pressure in New Zealand rabbits. *Br. J. Pharmacol.* 165, 1163–1172. doi: 10.1111/j.1476-5381.2011.01586.x

Martin-Gil, A., and Pintor, J. (2010). P2Y2 nucleotide receptors increase the presence of aquaporin-1 in rabbit non-pigmented ciliary epithelial cells. *Purinergic Signal.* 6, S155.

Mitchell, C. H., Carre, D. A., Mcglinn, A. M., Stone, R. A., and Civan, M. M. (1998). A release mechanism for stored ATP in ocular ciliary epithelial cells. *Proc. Natl. Acad. Sci. U.S.A.* 95, 7174–7178. doi: 10.1073/pnas.95.12.7174

Morrison, J. C., and Acott, T. S. (2003). "Anatomy and physiology of aqueous humor outflow," in *Glaucoma: Science and Practice*, eds J. C. Morrison and I. P. Pollack (New York: Thieme), 34–41.

Nicholas, R. A., Watt, W. C., Lazarowski, E. R., Li, Q., and Harden, K. (1996). Uridine nucleotide selectivity of three phospholipase C-activating P2 receptors: identification of a UDP-selective, a UTP-selective, and an ATP- and UTP-specific receptor. *Mol. Pharmacol.* 50, 224–229.

Patel, K., Barnes, A., Camacho, J., Paterson, C., Boughtflower, R., Cousens, D., et al. (2001). Activity of diadenosine polyphosphates at P2Y receptors stably expressed in 1321N1 cells. *Eur. J. Pharmacol.* 430, 203–210. doi: 10.1016/S0014-2999(01)01401-7

Perez de Lara, M. J., Guzman-Aranguez, A., De La Villa, P., Diaz-Hernandez, J. I., Miras-Portugal, M. T., and Pintor, J. (2015). Increased levels of extracellular ATP in glaucomatous retinas: Possible role of the vesicular nucleotide transporter during the development of the pathology. *Mol. Vis.* 21, 1060–1070.

Perez de Lara, M. J., Santano, C., Guzman-Aranguez, A., Valiente-Soriano, F. J., Aviles-Trigueros, M., Vidal-Sanz, M., et al. (2014). Assessment of inner retina dysfunction and progressive ganglion cell loss in a mouse model of glaucoma. *Exp. Eye Res.* 122, 40–49. doi: 10.1016/j.exer.2014.02.022

Pintor, J., Martin-Gil, A., and Fonseca, B. (2011). Activation of TRPV4 induces the release of diadenosine tetraphosphate to the aqueous humour. *Invest. Ophthalmol. Vis. Sci.* 52, 2052.

Pintor, J., Peral, A., Hoyle, C. H., Redick, C., Douglass, J., Sims, I., et al. (2002). Effects of diadenosine polyphosphates on tear secretion in New Zealand white rabbits. *J. Pharmacol. Exp. Ther.* 300, 291–297. doi: 10.1124/jpet.300.1.291

Pintor, J., Peral, A., Pelaez, T., Martin, S., and Hoyle, C. H. (2003). Presence of diadenosine polyphosphates in the aqueous humor: their effect on intraocular pressure. *J. Pharmacol. Exp. Ther.* 304, 342–348. doi: 10.1124/jpet.102.041368

Pintor, J., Sanchez-Nogueiro, J., Irazu, M., Mediero, A., Pelaez, T., and Peral, A. (2004). Immunolocalisation of P2Y receptors in the rat eye. *Purinergic Signal.* 1, 83–90. doi: 10.1007/s11302-004-5072-5

Schachter, J. B., Li, Q., Boyer, J. L., Nicholas, R. A., and Harden, T. K. (1996). Second messenger cascade specificity and pharmacological selectivity of the human P2Y1-purinoceptor. *Br. J. Pharmacol.* 118, 167–173. doi: 10.1111/j.1476-5381.1996.tb15381.x

Soto, D., Pintor, J., Peral, A., Gual, A., and Gasull, X. (2005). Effects of dinucleoside polyphosphates on trabecular meshwork cells and aqueous humor outflow facility. *J. Pharmacol. Exp. Ther.* 314, 1042–1051. doi: 10.1124/jpet.105.085274

Tomarev, S. I. (2001). Eyeing a new route along an old pathway. *Nat. Med.* 7, 294–295. doi: 10.1038/85432

Waldo, G. L., and Harden, T. K. (2004). Agonist binding and Gq-stimulating activities of the purified human P2Y1 receptor. *Mol. Pharmacol.* 65, 426–436. doi: 10.1124/mol.65.2.426

Conflict of Interest Statement: The authors declare that the research was conducted in the absence of any commercial or financial relationships that could be construed as a potential conflict of interest.

frontiers in Pharmacology

ORIGINAL RESEARCH
published: 04 October 2017
doi: 10.3389/fphar.2017.00700

Antiparkinsonian Efficacy of Guanosine in Rodent Models of Movement Disorder

Caio M. Massari[1†], Marc López-Cano[2,3†], Fabiana Núñez[2,3†], Víctor Fernández-Dueñas[2,3], Carla I. Tasca[1,4‡] and Francisco Ciruela[2,3*‡]*

[1] Programa de Pós-graduação em Bioquímica, Centro de Ciências Biológicas, Universidade Federal de Santa Catarina, Florianópolis, Brazil, [2] Unitat de Farmacologia, Departament de Patologia i Terapèutica Experimental, Facultat de Medicina, Bellvitge Institute for Biomedical Research, Universitat de Barcelona, Barcelona, Spain, [3] Institut de Neurociències, Universitat de Barcelona, Barcelona, Spain, [4] Departamento de Bioquímica, Centro de Ciências Biológicas, Universidade Federal de Santa Catarina, Florianópolis, Brazil

OPEN ACCESS

Edited by:
Hugo Geerts,
In Silico Biosciences, Belgium

Reviewed by:
Roberto Coccurello,
Fondazione Santa Lucia (IRCCS), Italy
Diogo O. Souza,
Federal University of Rio Grande do Sul (UFRGS), Brazil

***Correspondence:**
Carla I. Tasca
carla.tasca@ufsc.br
Francisco Ciruela
fciruela@ub.edu

[†] These authors have contributed equally to this work.
[‡] These authors jointly directed this work.

Specialty section:
This article was submitted to Experimental Pharmacology and Drug Discovery, a section of the journal Frontiers in Pharmacology

Received: 30 June 2017
Accepted: 20 September 2017
Published: 04 October 2017

Citation:
Massari CM, López-Cano M, Núñez F, Fernández-Dueñas V, Tasca CI and Ciruela F (2017) Antiparkinsonian Efficacy of Guanosine in Rodent Models of Movement Disorder. Front. Pharmacol. 8:700. doi: 10.3389/fphar.2017.00700

Guanosine (GUO) is a guanine-based purine nucleoside with important trophic functions and promising neuroprotective properties. Although the neuroprotective effects of GUO have been corroborated in cellular models of Parkinson's disease (PD), its efficacy as an antiparkinsonian agent has not been fully explored in PD animal models. Accordingly, we evaluated the effectiveness of GUO in reversing motor impairments in several rodent movement disorder models, including catalepsy, tremor, and hemiparkinsonism. Our results showed that orally administered GUO antagonized reserpine-mediated catalepsy, reduced reserpine-induced tremulous jaw movements, and potentiated the number of contralateral rotations induced by L-3,4-dihydroxyphenylalanine in unilaterally 6-hydroxidopamine-lesioned rats. In addition, at 5 and 7.5 mg/kg, GUO inhibited L-DOPA-induced dyskinesia in rats chronically treated with a pro-dopaminergic agent. Overall, we describe the therapeutic potential of GUO, which may be effective not only for reversing parkinsonian motor impairments but also for reducing dyskinesia induced by treatment for PD.

Keywords: guanosine, Parkinson's disease, catalepsy, tremor, hemiparkinsonism, dyskinesia

INTRODUCTION

Parkinson's disease (PD) is a neurodegenerative condition of the central nervous system (CNS) characterized by bradykinesia, tremor, and rigidity (Poewe and Mahlknecht, 2009). The disorder, which is secondary to the loss of dopamine neurons in the substantia nigra, affects approximately 1% of the population over the age of 65 years (Meissner et al., 2011). Since the 1970s, the main therapeutic approach has consisted of administrating L-3,4-dihydroxyphenylalanine (L-DOPA) or other dopamine receptor agonists, aiming to reestablish normal function in the affected dopaminergic signaling circuitry (Poewe, 2009). However, adverse effects appear with the long consumption of dopaminergic drugs (Huot et al., 2013), among which dyskinesia -specifically L-DOPA-induced dyskinesia (LID)- is one of most often reported and most likely to impede normal life. Antiparkinsonian drugs are even classified clinically based on their probability of inducing dyskinesia, and it has been shown that rotating these drugs can diminish the appearance of these adverse motor effects. Nevertheless, novel agents are clearly needed to improve the management of PD (Schapira et al., 2006).

Over recent years, new drugs have been developed that not only improve the clinical response to classical drugs but that also alleviate undesired side effects. Among these, purine-based drugs, specifically adenosine A_{2A} receptor ($A_{2A}R$) antagonists, represent realistic and promising non-dopaminergic treatment options (Schapira et al., 2006). The nucleoside guanosine (GUO) is a guanine-based purine that crosses the blood–brain barrier (Jiang et al., 2008) and induces behavioral effects in rodents. GUO has been demonstrated to exert anticonvulsive (Lara et al., 2001), antinociceptive (Schmidt et al., 2010), anxiolytic-like (Almeida et al., 2017), and antidepressant-like effects (Bettio et al., 2014). In addition, it may have trophic and neuroprotective effects in neural cells (Rathbone et al., 1999; Lanznaster et al., 2016), possibly though adenosine receptors modulation (Dal-Cim et al., 2013). Furthermore, GUO can modulate glutamatergic transmission by stimulating its uptake through transporters and increasing glutamine synthetase activity and glutamate turnover, thereby reducing extracellular glutamate levels and protecting from excitotoxicity (Molz et al., 2011; Dal-Cim et al., 2016). Similarly, GUO-induced neuroprotection in ischemia-like models has been shown to promote the reduction of nitroxidative stress, prevent the alteration of mitochondrial membrane potentials (Thomaz et al., 2016), and control the inflammatory response. These effects occur through inhibition of the transcription factor NF-κB translocation to the nucleus (Dal-Cim et al., 2013), and through the reduction of inflammatory cytokines (Hansel et al., 2015).

The biochemical mechanisms responsible for neurodegeneration in PD are oxidative stress, mitochondrial damage, exacerbated inflammatory response, and glutamatergic excitotoxicity (Dexter and Jenner, 2013). Given the effects of GUO, its use offers a promising therapeutic approach. Interestingly, metabolomic analysis in a PD transgenic mouse model showed decreased GUO levels in the brains of adult transgenic mice with concurrent motor symptoms (Chen et al., 2015). Moreover, reduced striatal GUO levels have been observed after reserpine treatment (Loeffler et al., 1998). The administration of reserpine to rodents gives the classic acute pharmacological model of PD by creating a transient parkinsonian-like state (Duty and Jenner, 2011). Reserpine inhibits vesicular monoamine transport in the CNS, leading to monoamine depletion and motor impairments that resemble PD (e.g., hypokinesia, catalepsy, and oral tremor) (Leão et al., 2015).

In this study, we investigated the pharmacological use of GUO in animal models with motor impairments that resemble PD. Locomotor activity and the effects of GUO were investigated in mice with reserpine-mediated catalepsy and reserpine-induced tremulous jaw movements (TJMs). Contralateral rotations induced by L-DOPA in unilaterally 6-OHDA-lesioned rats were also assessed. Finally, we tested the effect of GUO in hemiparkinsonian rats on the development of LID. We aimed to provide evidence in support of GUO as a novel agent for improving the management of PD.

MATERIALS AND METHODS

Animals

Male Swiss albino mice (30–50 g; from the animal facility of the Federal University of Santa Catarina, Florianópolis, Brazil) and Sprague–Dawley rats (240–250 g; Charles River Laboratories, L'Arbresle, France) were used. Animals were housed in standard cages with free access to food and water, and were maintained under controlled standard conditions (12 h dark/light cycles starting at 7:30 a.m., 22°C temperature, and 66% humidity). All manipulations were carried out between 0900 and 1600 h. Procedures in this study were performed in accordance with relevant guidance from the National Institute of Health Guide for the Care and Use of Laboratory Animals (NIH Publications no. 80-23), the Guide for the Care and Use of Laboratory Animals (Clark et al., 1997), and European Union directives (2010/63/EU). The ethics committees of the relevant institutions (CEUA/UFSC and CEEA/UB) approved the protocol. Efforts were made to minimize suffering and reduce the number of animals used in the experiments.

Drugs

Reserpine (Sigma-Aldrich, St. Louis, MO, United States) was dissolved in 0.1% acetic acid for subcutaneous (s.c.) administration. GUO (Sigma-Aldrich) was dissolved in saline (NaCl 0.9%) containing 0.5% methylcellulose for oral (p.o.) administration. The 6-hydroxydopamine (6-OHDA; Sigma–Aldrich) was dissolved in a saline solution containing 0.05% ascorbic acid. DL-serine 2-(2,3,4-trihydroxybenzyl) hydrazide hydrochloride (benserazide; Sigma-Aldrich) and 3,4-Dihydroxy-L-phenylalanine (L-DOPA; Abcam Biochemicals, Cambridge, United Kingdom) were dissolved in saline for intraperitoneal (i.p.) administration.

Assessment of TJMs

Mice were administered reserpine (1 mg/kg, s.c.) or vehicle (0.1% acetic acid solution) twice at an interval of 48 h. GUO (3, 5, 7.5, or 10 mg/kg; p.o.) was administrated 20 min before behavioral testing and 24 h after the last injection of reserpine (**Figure 1A**). To quantify the occurrence of oral dyskinesia, mice were placed individually in a glass cylinder (13 cm diameter) and hand-operated counters were used to count TJM frequency. Mirrors were placed under the floor and behind the back wall of the cylinder to allow observation when the animal faced away from the observer. TJMs were defined as rapid vertical deflections of the lower jaw that resembled chewing, but were not directed at any particular stimulus (Salamone et al., 1998). If TJM occurred during a period of grooming, they were discounted. The incidence of these oral movements was measured continuously for 10 min.

Catalepsy Trial

After treatment with reserpine alone or reserpine plus GUO (**Figure 1A**), catalepsy behavior was assessed by placing the forepaws of mice on a horizontal bar (6 mm diameter) positioned at 4.5 cm above the bench surface. The duration of catalepsy,

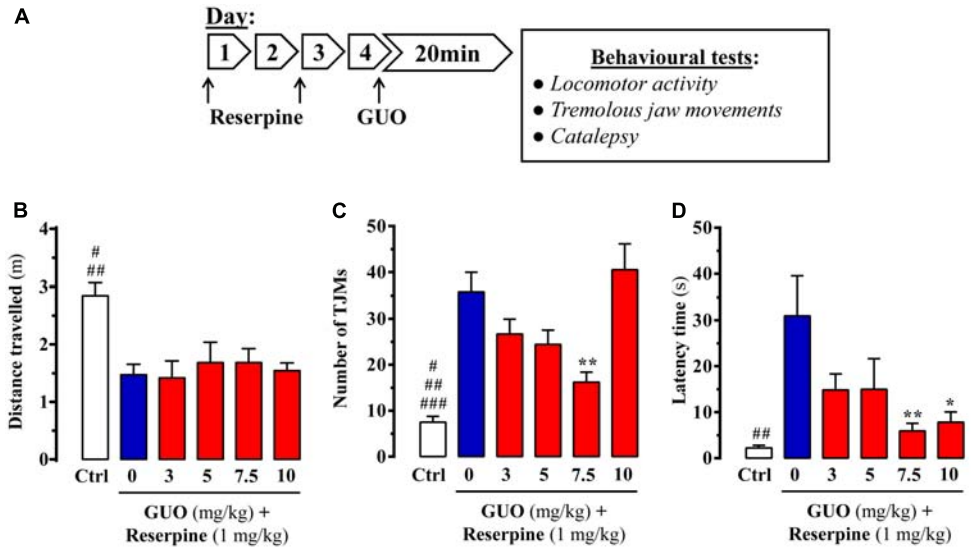

FIGURE 1 | Effect of guanosine (GUO) on reserpine-induced motor disturbances in mice. **(A)** Treatment schedule depicting the administration regimen of reserpine (1 mg/ml; s.c.), guanosine (GUO, 0, 3, 5, 7.5, 10 mg/kg, p.o.) and behavioral testing. **(B)** Spontaneous locomotor activity of mice treated with saline (control mice = Ctrl), or GUO (3, 5, 7.5, or 10 mg/kg, p.o.) after reserpine administration (see **A**) was evaluated in the open-field test. The distance traveled (m) was measured during 10 min. Results are presented as means ± SEM (n = 9–10 animals). $^{\#}P < 0.05$ and $^{\#\#}P < 0.01$ one-way ANOVA with Tukey's *post hoc* test when compared to 5 and 7.5 mg/kg GUO ($^{\#}$), and to 0, 3, and 10 mg/kg GUO ($^{\#\#}$). **(C)** Reserpine-induced orofacial dyskinesia evaluated by tremulous jaw movements (TJMs) frequency during 10 min. Results are presented as means ± SEM (n = 6 animals). $^{\#}P < 0.05$, $^{\#\#}P < 0.01$, and $^{\#\#\#}P = 0.001$ one-way ANOVA with Tukey's *post hoc* test when compared to 5 mg/kg GUO ($^{\#}$), to 3 mg/kg GUO ($^{\#\#}$) and to 0 and 10 mg/kg GUO ($^{\#\#\#}$). $^{**}P < 0.01$ one-way ANOVA with Dunnett's *post hoc* test when compared to vehicle-treated (0 mg/kg GUO) animals. **(D)** Reserpine-induced catalepsy in mice evaluated by the latency scape in the bar test. Results are presented as means ± SEM (n = 9 animals). $^{\#\#}P < 0.01$ one-way ANOVA with Tukey's *post hoc* test when compared 0 mg/kg GUO. $^{*}P < 0.05$ and $^{**}P < 0.01$ one-way ANOVA with Dunnett's *post hoc* test when compared to 0 mg/kg GUO.

which was defined as an immobile posture, was measured while the animal kept both forepaws on the bar, with a cut-off maximum of 180 s. Three trials were carried out and the results were analyzed using the mean value of the three trials, as adapted from Santos et al. (2013).

Spontaneous Locomotor Activity

The spontaneous locomotor activity of mice after reserpine or reserpine plus GUO treatment was tested in the open-field test. The apparatus consisted of an acrylic box measuring 45 cm × 45 cm × 45 cm, with each mouse placed in the center and recorded for 10 min with a video camera system. The distance traveled by each animal was analyzed using Bonther Activity Monitoring software (Bonther, Co., Brazil).

The spontaneous locomotor activity of rats was tested in an open-field Plexiglas® arena box measuring 1 m × 1 m × 1 m. Each rat was placed in the center and recorded for 5 min, as described above.

Hemiparkinsonian Animal Model

Experimental hemiparkinsonism was induced in rats by unilateral injection of 6-OHDA in the medial forebrain bundle, as previously described (Fernández-Dueñas et al., 2015). Rats were stereotaxically injected with 6-OHDA (8 μg of 6-OHDA in 4 μL of saline containing 0.05% ascorbic acid) at anterior–posterior (AP; −2.2 mm), medial–lateral (ML; −1.5 mm), and dorsal–ventral (DV; −7.8 mm) locations with respect to the bregma (Paxinos and Watson, 2007). To minimize damage to noradrenergic neurons, rats were pretreated with desipramine hydrochloride (10 mg/kg, i.p.) 20 min before surgery.

Three weeks later the extent of dopamine deafferentation was checked by assessing the rotating behavioral response to L-DOPA administration. In brief, rats were injected with L-DOPA (50 mg/kg, i.p.) in the presence of benserazide hydrochloride (25 mg/kg, i.p.), an inhibitor of DOPA decarboxylase that minimizes peripheral metabolization of L-DOPA, and the number of full contralateral turns were recorded during a 2 h period. Dopamine deafferentation was considered successful in animals made at least 200 net contralateral rotations.

Thereafter, animals were housed for 3 weeks before being used in the behavioral analyses. GUO was administered orally in a vehicle (0.5% methylcellulose and 2% DMSO) 40 min before benserazide (25 mg/kg; i.p.). Subsequently, L-DOPA (6 mg/kg; i.p.) was delivered after 20 min. The animals were then placed in the rotametry chambers, as previously described (Hodgson et al., 2009), and the number of contralateral rotations was recorded over a 2 h period.

LIDs and Abnormal Involuntary Movements Rating

L-DOPA-induced dyskinesia were triggered in hemiparkinsonian rats by twice daily administration of L-DOPA (6 mg/kg, i.p.) plus benserazide hydrochloride (15 mg/kg, i.p) for 22 consecutive days. L-DOPA-induced abnormal involuntary movements

(AIMs) were scored by a blinded experimenter following a previously described rat dyskinesia scale (Winkler et al., 2002). In brief, rats were injected with L-DOPA, placed in individual transparent plastic cages, and observed every 20 min for 220 min. Three AIM subtypes were monitored (i.e., axial, forelimb, and orolingual) and their respective severity scored from 0 to 4, as previously described (Winkler et al., 2002). Enhanced manifestations of otherwise normal behaviors, such as rearing, sniffing, grooming, and gnawing, were not included. AIM ratings were performed on treatment days 1, 7, 14, and 22 during the chronic L-DOPA administration phase. We calculated integrated AIM scores for each animal and behavioral session using the sum of all three AIM subtypes. AIM was also expressed as an area under the curve (AUC) analysis.

Data Analysis

Data are represented as means ± SEM. Comparisons among experimental and control groups were performed by one-way analysis of variance (ANOVA) followed by Dunnett's *post hoc* test when comparing GUO treatments or Tukey's *post hoc* test when comparing to internal control within the behavioral test, if any. Statistical significance was accepted when $P < 0.05$.

RESULTS

GUO Modulation of Reserpine-Induced Motor Disturbances

Reserpine administration to mice was performed to evaluate the ability of GUO to counteract reserpine-mediated changes (**Figure 1A**). We first determined the change in spontaneous locomotor activity. While it was significantly reduced by reserpine administration, acute GUO treatment (3, 5, 7.5, or 10 mg/kg, p.o.) was unable to reverse the change [$F_{(4,43)} = 0.2241$, $P = 0.9234$] (**Figure 1B**).

Next, we assessed the ability of GUO to reduce reserpine-induced TJMs, a parameter known to ameliorate by antiparkinsonian drugs (Collins-Praino et al., 2011). Reserpine-administered animals did, indeed, show a significant increase in TJMs that was partially blocked by GUO administration (**Figure 1C**). One-way ANOVA revealed significant differences between the GUO-treated reserpinized mice [$F_{(4,23)} = 5.603$, $P = 0.0027$], with a significant reduction in reserpine-mediated TJMs observed at 7.5 mg/kg GUO ($P < 0.01$) (**Figure 1C**). Interestingly, treatment with 10 mg/kg of GUO was unable to preclude reserpine-induced TJMs, thus resulting in a U-shaped dose-dependent GUO activity (**Figure 1C**).

Finally, reserpine-induced catalepsy was assessed as an experimental model of akinesia and bradykinesia (Duty and Jenner, 2011). Reserpine treatment induced a cataleptic state, as measured by the latency time of mice to move forepaws from the bar in the bar test, and acute GUO treatment significantly attenuated this increase in latency time [$F_{(4,40)} = 3.518$, $P = 0.0149$] (**Figure 1D**). GUO induced significant reductions in reserpine-mediated catalepsy at doses of 7.5 mg/kg ($P < 0.01$) and 10 mg/kg ($P < 0.05$) (**Figure 1D**).

Overall, although GUO did not reverse reserpine-induced locomotor activity depression, it did ameliorate TJM and catalepsy symptoms in reserpinized mice. Therefore, we considered that antiparkinsonian efficacy was shown in this classical pharmacological animal model of acute PD.

Antiparkinsonian Effect of GUO in 6-OHDA-Lesioned Rats

After assessing the effects of GUO on reserpinized mice, we evaluated its effectiveness in unilateral 6-OHDA-lesioned rats, a classic animal model of experimental parkinsonism based on toxin-mediated destruction of the dopaminergic nigrostriatal pathway (Schwarting and Huston, 1996). Accordingly, we evaluated the impact of acute GUO treatment on spontaneous locomotor activity and contralateral rotation in 6-OHDA-lesioned rats (**Figure 2A**). First, we assessed spontaneous locomotor activity of control and hemiparkinsonian animals. While in 6-OHDA-lesioned animals GUO did not have any effect, in saline-lesioned mice the one-way ANOVA analysis revealed a significant GUO-induced increase in spontaneous locomotor activity at 3 mg/kg ($P < 0.05$) (**Figure 2B**). Overall, GUO was unable to potentiate spontaneous locomotor activity in 6-OHDA-lesioned rats.

In the hemiparkinsonian animal model, asymmetric motor behavior is observed following dopaminergic treatment (i.e., L-DOPA) because of unilateral dopamine depletion in the nigrostriatal pathway (Duty and Jenner, 2011). Interestingly, when using submaximal doses of L-DOPA, it is possible to potentiate contralateral rotations with other pro-dopaminergic drugs (e.g., $A_{2A}R$ antagonists) (for review, see Vallano et al., 2011). Therefore, we determined whether GUO could promote contralateral rotations in 6-OHDA-lesioned animals with submaximal (6 mg/kg) L-DOPA dosing in hemiparkinsonian rats (**Figure. 2C**). GUO administration alone, up to 10 mg/kg, did not result in asymmetric turning behavior in 6-OHDA-lesioned rats (data not shown). However, GUO did dose-dependently induce contralateral turning behavior when administrated before the subthreshold dose of L-DOPA (**Figure 2C**). One-way ANOVA revealed significant differences between GUO treatments [$F_{(3,36)} = 11.65$, $P < 0.001$] (**Figure 2C**), with GUO inducing significant contralateral rotations at 3 mg/kg ($P < 0.05$) and 10 mg/kg ($P < 0.001$) (**Figure 2C**). Overall, GUO enhanced the effects of L-DOPA with a minimum efficacious oral dose of 3 mg/kg.

Antidyskinetic Effect of GUO in the LID Rat Model

Chronic L-DOPA use in PD is associated with the development of LIDs. Therefore, we assessed the potential antidyskinetic activity of GUO after inducing LIDs in 6-OHDA-lesioned rats through chronic L-DOPA administration and monitoring for the emergence of AIMs over time (**Figure 3A**). AIM severity significantly ($P < 0.01$) increased after 1 week of L-DOPA treatment (**Figure 3A**, inset, day 7), thus LID increased during the first 40 min L-DOPA post-injection and remaining elevated for an additional 40 min (**Figure 3A**, day 7). After

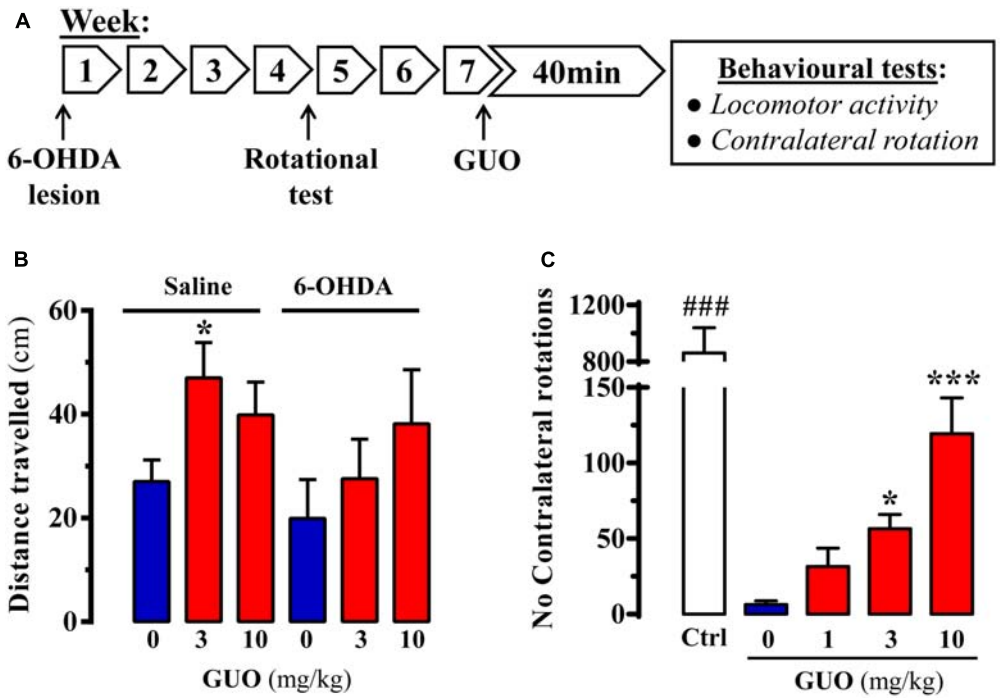

FIGURE 2 | Effect of guanosine (GUO) on hemiparkinsonian rats. **(A)** Treatment schedule depicting the 6-OHDA lesion, rotational test (see section "Materials and Methods") and the administration regimen of guanosine (GUO, 0, 1, 3, 10 mg/kg, p.o.) and behavioral testing. **(B)** Total distance traveled in the open-field test by either saline- or 6-OHDA-lesioned rats administered with L-DOPA after GUO treatment (3 or 10 mg/kg, p.o.). The distance traveled (cm) was measured during 5 min. Values correspond to the mean ± SEM (n = 12). $^{*}P < 0.05$ one-way ANOVA with Dunnett's *post hoc* test when compared to 0 mg/kg GUO. **(C)** GUO-mediated potentiation of L-DOPA-induced contralateral rotations in 6-OHDA-lesioned rats. The number of contralateral rotations in 6-OHDA-lesioned rats orally administered with vehicle or GUO (1, 3, or 10 mg/kg) was monitored during a 2 h period. The control group (Ctrl) was administered with L-DOPA (50 mg/kg, i.p.). Values correspond to the mean ± SEM (n = 10). $^{###}P < 0.001$ one-way ANOVA with Tukey's *post hoc* test when compared to 0, 1, 3, and 10 mg/kg GUO. $^{*}P < 0.05$ and $^{***}P < 0.001$ one-way ANOVA with Dunnett's *post hoc* test when compared to 0 mg/kg GUO.

2 weeks of L-DOPA treatment, the increase in LID was higher ($P < 0.001$) (**Figure 3A**, inset, day 14) and sustained in time (i.e., 150 min) (**Figure 3A**, day 14). Finally, after 3 weeks of L-DOPA administration a similar AIMs increase and sustained LID incidences were observed (**Figure 3A**, day 22), thus reaching a LID plateau. Interestingly, the observed time-course in our LID animal model resembled the so-called peak-dose dyskinesia in PD (Fahn, 2000). Thus, we showed that GUO treatment produced a U-shaped dose-dependent antidyskinetic activity in animals administered with L-DOPA for 3 weeks (**Figure 3B**). One-way ANOVA revealed significant differences between GUO treatments [$F_{(5,47)} = 11.65$, $P = 4.866$] (**Figure 3B**), with significantly maximal GUO-induced antidyskinetic activity observed at 5 mg/kg ($P < 0.001$) and 7.5 mg/kg ($P < 0.05$) (**Figure 3B**). Overall, GUO showed antidyskinetic activity in the LID animal model.

DISCUSSION

Given that dopamine replacement is the first line therapy in PD, treatment with L-DOPA or dopamine agonists (i.e., ropinirole, pramipexole, apomorphine) is the mainstay of clinical management (Poewe and Mahlknecht, 2009). Unfortunately, while dopamine-targeted therapies properly address PD-associated motor disturbances, they also have considerable acute and chronic side effect, including hallucinations, constipation, nausea, somnolence, on/off effects, and dyskinesia (Eggert et al., 2008). In addition, these therapies not only show a progressive decline in efficacy over time but they also do not address common mood, postural instability, or cognitive disturbances. Thus, approaches that indirectly modulate dopaminergic neurotransmission have emerged as potential alternatives to handle side effects associated with PD therapy (Fox et al., 2008).

In this study, we have shown the effectiveness of GUO, a naturally occurring guanine-based purine nucleoside, in three rodent models of impaired movement: (1) the reserpine-induced TJM and catalepsy model in mice, (2) the hemiparkinsonian model of PD in rats, and (3) the LID model in rats. Although GUO was unable to improve spontaneous locomotor activity in reserpine-treated mice, it did ameliorate TJMs and catalepsy in those mice. In addition, GUO potentiated L-DOPA-induced contralateral rotations in unilaterally 6-OHDA-lesioned rats and showed antidyskinetic efficacy in the LID model. Collectively, these results support the hypothesis that GUO has potential use in PD management, including for reducing dyskinesia when used in combination with L-DOPA.

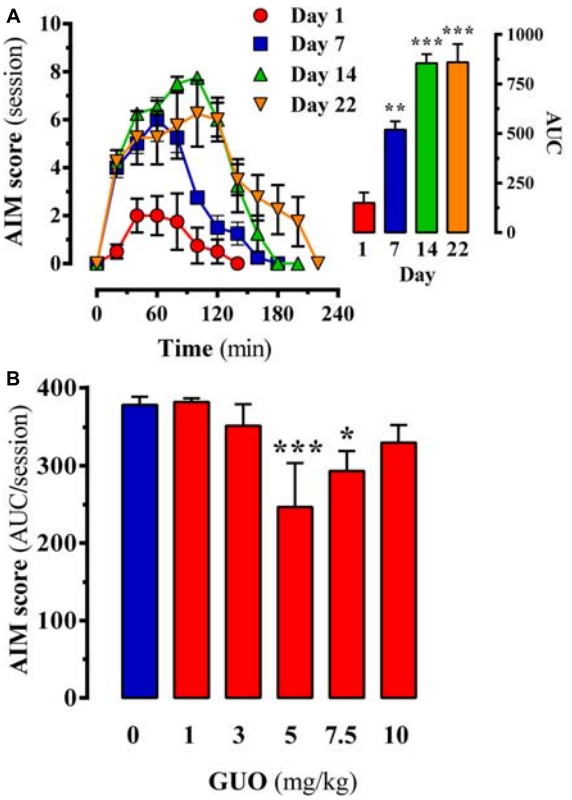

FIGURE 3 | Effect of guanosine (GUO) on dyskinetic rats. **(A)** Development of L-DOPA induced motor side effects (i.e., LIDs) following chronic (22 days) L-DOPA (6 mg/kg) administration. AIMs score was measured during a 220-min session on days 1, 7, 14, and 22 immediately after the corresponding daily L-DOPA injection. **(B)** LIDs attenuation in chronic (22 days) L-DOPA (6 mg/kg) administered rats following GUO administration. The total AIMs score AUC obtained over 220 min following co-administration of L-DOPA (6 mg/kg) plus vehicle or GUO (1, 3, 5, 7.5, or 10 mg/kg) are presented as mean score ± SEM ($n = 6$). $^{*}P < 0.05$ and $^{***}P < 0.001$ one-way ANOVA with Dunnett's *post hoc* test when compared to 0 mg/kg GUO.

Guanosine has been shown to exert neuroprotective effects in cellular models of PD. For instance, dopaminergic neurons differentiated from human SH-SY5Y neuroblastoma cells were shown to be protected from 6-OHDA-induced toxicity by GUO treatment (Giuliani et al., 2012). The protective effects of GUO were also observed in C6 glioma cells (as a model of astrocytes) when incubated with 6-OHDA (Giuliani et al., 2014). Similarly, GUO neuroprotection has been evidenced against other PD-related toxins, such as 1-methyl-4-phenylpyridinium (MPP^+). Of note, MPP^+ is taken up by dopaminergic neurons and accumulates in their mitochondria, where it inhibits complex I of the electron transport chain and ultimately causes neuronal cell death. In SH-SY5Y cells, GUO given after as long as 24 h after MPP^+ was able to reduce MPP^+-induced caspase-3 activity (Pettifer et al., 2007).

Despite *in vitro* evaluations, data from *in vivo* GUO treatment in PD models are scarce. Chronic treatment with GUO (8 mg/kg for 8 weeks) can significantly reduce bradykinesia in proteasome inhibitor (PSI)-treated rats (Su et al., 2009), which is an animal model for slow-onset PD (McNaught et al., 2004). In addition, chronic GUO treatment reduced apoptotic cell death, induced proliferation of neural progenitor/stem cells, and increased the number of tyrosine hydroxylase-positive cells in the substantia nigra in a PSI model of PD (Su et al., 2009). However, the acute effect and efficacy of GUO in reversing motor impairments in rodent models of movement disorders, including catalepsy, tremor, and hemiparkinsonism, have not previously been addressed.

Reserpine administration to rodents is a primary model for assessing potential PD treatments. L-DOPA efficacy was first reported in this model by observing that it improved the reserpine-induced akinetic state (Carlsson et al., 1957). Even though reserpine does not induce dopaminergic neurodegeneration, the model produces key motor disturbances consistent with those of PD; for example, mice show decreased spontaneous locomotor activity, which correlates to hypokinesia in PD. However, although reserpine-induced catalepsy and TJM were fully reversed, GUO treatment had no effect on spontaneous locomotor activity at the doses tested in this study.

Regarding the hemiparkinsonian rats, unilateral 6-OHDA lesions did not reduce, and subsequent GUO treatment did not increase, spontaneous locomotor activity. Conversely, GUO administration before the subthreshold dose of L-DOPA induced, in a dose-dependent manner, contralateral turning behavior that indicates a pro-dopaminergic action (i.e., GUO enhanced the effects of L-DOPA). Moreover, GUO exerted an antidyskinetic effect in rats chronically treated with L-DOPA. Besides L-DOPA beneficial effects, this long-term therapy leads to development of adverse motor responses, named LID. LIDs, in particular, are a great burden that affects 40–50% of PD patients who undergo L-DOPA treatment for 4–6 years (Ahlskog and Muenter, 2001). Taken together, results from reserpinized mice and hemiparkisonian rats demonstrated that GUO did not alter spontaneous locomotor activity. Interestingly, GUO presented antidyskinetic effect (reducing TJMs in mice and AIMs in the LID model in rats), although it was not observed in the higher dose tested (10 mg/kg). Thus, this surprising U-shaped dose-response of GUO efficacy alleviating TJMs and LID will deserve further investigation in the future. Yet, GUO effect on reserpine-induced catalepsy in mice and potentiation of L-DOPA-induced contralateral rotations in 6-OHDA-lesioned rats was observed in all doses tested. Overall, our data provide evidence that GUO treatment may not only improve the motor symptoms of PD but may also have a potential efficacy on L-DOPA side effects. Thus, the potential clinical importance of this finding is significant.

Importantly, we demonstrated the antiparkinsonian efficacy of GUO in a series of PD rodent models, consistent with other $A_{2A}R$ antagonists (Vallano et al., 2011). Indeed, istradefylline (Jenner, 2005) has recently been licensed for use in Japan as an adjuvant to L-DOPA treatment for reducing off-times produced by dopaminergic drugs (Mizuno et al., 2010; Kondo and Mizuno, 2015; Müller, 2015). The molecular target of GUO has not yet been fully characterized and no GUO receptor has been identified, though some studies have suggested its existence (Traversa et al., 2002; Volpini et al., 2011). Alternatively, it has been proposed that GUO might function by altering adenosine

receptor functioning (Dal-Cim et al., 2011, 2013; Ciruela, 2013; Lanznaster et al., 2016). Hence, the antiparkinsonian efficacy of GUO might in fact be related to $A_{2A}R$ function, thus its relationship with $A_{2A}R$ blockade should be further investigated as previously done while assessing similar non-dopaminergic approaches to PD therapy (Kase et al., 2003; Coccurello et al., 2004). Therefore, more experimental work is needed to elucidate the mechanism by which GUO exerts its antiparkinsonian action.

In summary, we have shown the remarkable potential of GUO to ameliorate parkinsonian symptoms in experimental animal models of movement disorders. Subject to further development, GUO is likely to become an excellent candidate for a clinical proof-of-concept study for purinergic-based treatment in PD.

AUTHOR CONTRIBUTIONS

CM performed *in vivo* experiments and analyzed data; ML-C performed *in vivo* experiments and analyzed data; FN performed experiments; VF-D designed experiments and wrote the paper; CT conceived and supervised the project, designed experiments, analyzed data and wrote the paper; FC conceived and supervised the project, designed experiments, analyzed data and wrote the paper.

ACKNOWLEDGMENTS

This work was supported by MINECO/ISCIII (SAF2014-55700-P and PIE14/00034), the Catalan government (2014 SGR 1054), Fundació la Marató de TV3 (Grant 20152031), FWO (SBO-140028) to FC; and by the Brazilian funding agencies, CAPES (PVE 052/2012), CNPq (INCT for Excitotoxicity and Neuroprotection) and FAPESC (NENASC/PRONEX) to CIT. CIT is recipient of CNPq productivity fellowship. We thank Esther Castaño and Benjamín Torrejón, from the CCiT-Bellvitge Campus of the University of Barcelona, for technical assistance.

REFERENCES

Ahlskog, J. E., and Muenter, M. D. (2001). Frequency of levodopa-related dyskinesias and motor fluctuations as estimated from the cumulative literature. *Mov. Disord.* 16, 448–458. doi: 10.1002/mds.1090

Almeida, R. F., Comasseto, D. D., Ramos, D. B., Hansel, G., Zimmer, E. R., Loureiro, S. O., et al. (2017). Guanosine anxiolytic-like effect involves adenosinergic and glutamatergic neurotransmitter systems. *Mol. Neurobiol.* 54, 423–436. doi: 10.1007/s12035-015-9660-x

Bettio, L. E. B., Freitas, A. E., Neis, V. B., Santos, D. B., Ribeiro, C. M., Rosa, P. B., et al. (2014). Guanosine prevents behavioral alterations in the forced swimming test and hippocampal oxidative damage induced by acute restraint stress. *Pharmacol. Biochem. Behav.* 127, 7–14. doi: 10.1016/j.pbb.2014.10.002

Carlsson, A., Lindqvist, M., and Magnusson, T. (1957). 3,4-Dihydroxy phenylalanine and 5-hydroxytryptophan as reserpine antagonists. *Nature* 180:1200. doi: 10.1038/1801200a0

Chen, X., Xie, C., Sun, L., Ding, J., and Cai, H. (2015). Longitudinal metabolomics profiling of Parkinson's disease-related α-synuclein a53t transgenic mice. *PLOS ONE* 10:e0136612. doi: 10.1371/journal.pone.0136612

Ciruela, F. (2013). Guanosine behind the scene. *J. Neurochem.* 126, 425–427. doi: 10.1111/jnc.12328

Clark, J. D., Gebhart, G. F., Gonder, J. C., Keeling, M. E., and Kohn, D. F. (1997). Special report: the 1996 guide for the care and use of laboratory animals. *ILAR J.* 38, 41–48. doi: 10.1093/ilar.38.1.41

Coccurello, R., Breysse, N., and Amalric, M. (2004). Simultaneous blockade of adenosine A2A and metabotropic glutamate mGlu5 receptors increase their efficacy in reversing Parkinsonian deficits in rats. *Neuropsychopharmacology* 29, 1451–1461. doi: 10.1038/sj.npp.1300444

Collins-Praino, L. E., Paul, N. E., Rychalsky, K. L., Hinman, J. R., Chrobak, J. J., Senatus, P. B., et al. (2011). Pharmacological and physiological characterization of the tremulous jaw movement model of parkinsonian tremor: potential insights into the pathophysiology of tremor. *Front. Syst. Neurosci.* 5:49. doi: 10.3389/fnsys.2011.00049

Dal-Cim, T., Ludka, F. K., Martins, W. C., Reginato, C., Parada, E., Egea, J., et al. (2013). Guanosine controls inflammatory pathways to afford neuroprotection of hippocampal slices under oxygen and glucose deprivation conditions. *J. Neurochem.* 126, 437–450. doi: 10.1111/jnc.12324

Dal-Cim, T., Martins, W. C., Santos, A. R., and Tasca, C. I. (2011). Guanosine is neuroprotective against oxygen/glucose deprivation in hippocampal slices via large conductance Ca^{2+}-activated K^+ channels, phosphatidilinositol-3 kinase/protein kinase B pathway activation and glutamate uptake. *Neuroscience* 183, 212–220. doi: 10.1016/j.neuroscience.2011.03.022

Dal-Cim, T., Martins, W. C., Thomaz, D. T., Coelho, V., Poluceno, G. G., Lanznaster, D., et al. (2016). Neuroprotection promoted by guanosine depends on glutamine synthetase and glutamate transporters activity in hippocampal slices subjected to oxygen/glucose deprivation. *Neurotox. Res.* 29, 460–468. doi: 10.1007/s12640-015-9595-z

Dexter, D. T., and Jenner, P. (2013). Parkinson disease: from pathology to molecular disease mechanisms. *Free Radic. Biol. Med.* 62, 132–144. doi: 10.1016/j.freeradbiomed.2013.01.018

Duty, S., and Jenner, P. (2011). Animal models of Parkinson's disease: a source of novel treatments and clues to the cause of the disease. *Br. J. Pharmacol.* 164, 1357–1391. doi: 10.1111/j.1476-5381.2011.01426.x

Eggert, K. M., Reese, J. P., Oertel, W. H., and Dodel, R. (2008). Cost effectiveness of pharmacotherapies in early Parkinson's disease. *CNS Drugs* 22, 841–860. doi: 10.2165/00023210-200822100-00005

Fahn, S. (2000). The spectrum of levodopa-induced dyskinesias. *Ann. Neurol.* 47, S2–S9.

Fernández-Dueñas, V., Taura, J. J., Cottet, M., Gómez-Soler, M., López-Cano, M., Ledent, C., et al. (2015). Untangling dopamine-adenosine receptor-receptor assembly in experimental parkinsonism in rats. *Dis. Models Mech.* 8, 57–63. doi: 10.1242/dmm.018143

Fox, S. H., Brotchie, J. M., and Lang, A. E. (2008). Non-dopaminergic treatments in development for Parkinson's disease. *Lancet Neurol.* 7, 927–938. doi: 10.1016/S1474-4422(08)70214-X

Giuliani, P., Ballerini, P., Buccella, S., Ciccarelli, R., Rathbone, M. P., Romano, S., et al. (2014). Guanosine protects glial cells against 6-hydroxydopamine toxicity. *Adv. Exp. Med. Biol.* 837, 23–33. doi: 10.1007/5584_2014_73

Giuliani, P., Romano, S., Ballerini, P., Ciccarelli, R., Petragnani, N., Cicchitti, S., et al. (2012). Protective activity of guanosine in an in vitro model of Parkinson's disease. *Panminerva Med.* 54, 43–51.

Hansel, G., Tonon, A. C., Guella, F. L., Pettenuzzo, L. F., Duarte, T., Duarte, M. M. M. F., et al. (2015). Guanosine protects against cortical focal ischemia. Involvement of Inflammatory Response. *Mol. Neurobiol.* 52, 1791–1803. doi: 10.1007/s12035-014-8978-0

Hodgson, R. A., Bertorelli, R., Varty, G. B., Lachowicz, J. E., Forlani, A., Fredduzzi, S., et al. (2009). Characterization of the potent and highly selective A2A receptor antagonists preladenant and SCH 412348 [7-[2-[4-2,4-difluorophenyl]-1-piperazinyl]ethyl]-2-(2-furanyl)-7H-pyrazolo[4,3-e][1,2,4]triazolo[1,5-c]pyrimidin-5-amine] in rodent models of movement disorders and depression. *J. Pharmacol. Exp. Ther.* 330, 294–303. doi: 10.1124/jpet.108.149617

Huot, P., Johnston, T. H., Koprich, J. B., Fox, S. H., and Brotchie, J. M. (2013). The pharmacology of L-DOPA-induced dyskinesia in Parkinson's disease. *Pharmacol. Rev.* 65, 171–222. doi: 10.1124/pr.111.005678

Jenner, P. (2005). Istradefylline, a novel adenosine A2A receptor antagonist, for the treatment of Parkinson's disease. *Expert Opin. Investig. Drugs* 14, 729–738. doi: 10.1517/13543784.14.6.729

Jiang, S., Ballerini, P., Buccella, S., Giuliani, P., Jiang, C., Huang, X., et al. (2008). Remyelination after chronic spinal cord injury is associated with proliferation of endogenous adult progenitor cells after systemic administration of guanosine. *Purinergic Signal.* 4, 61–71. doi: 10.1007/s11302-007-9093-8

Kase, H., Aoyama, S., Ichimura, M., Ikeda, K., Ishii, A., Kanda, T., et al. (2003). Progress in pursuit of therapeutic A2A antagonists: the adenosine A2A receptor selective antagonist KW6002: research and development toward a novel nondopaminergic therapy for Parkinson's disease. *Neurology* 61, S97–S100. doi: 10.1212/01.WNL.0000095219.22086.31

Kondo, T., and Mizuno, Y. (2015). A long-term study of istradefylline safety and efficacy in patients with Parkinson disease. *Clin. Neuropharmacol.* 38, 41–46. doi: 10.1097/WNF.0000000000000073

Lanznaster, D., Dal-Cim, T., Piermartiri, T. C. B., and Tasca, C. I. (2016). Guanosine: a neuromodulator with therapeutic potential in brain disorders. *Aging Dis.* 7, 657–679. doi: 10.14336/AD.2016.0208

Lara, D. R., Schmidt, A. P., Frizzo, M. E., Burgos, J. S., Ramírez, G., and Souza, D. O. (2001). Effect of orally administered guanosine on seizures and death induced by glutamatergic agents. *Brain Res.* 912, 176–180. doi: 10.1016/S0006-8993(01)02734-2

Leão, A. H. F. F., Sarmento-Silva, A. J., Santos, J. R., Ribeiro, A. M., and Silva, R. H. (2015). Molecular, neurochemical, and behavioral hallmarks of reserpine as a model for Parkinson's disease: new perspectives to a long-standing model. *Brain Pathol.* 25, 377–390. doi: 10.1111/bpa.12253

Loeffler, D. A., LeWitt, P. A., Juneau, P. L., Camp, D. M., DeMaggio, A. J., Milbury, P., et al. (1998). Altered guanosine and guanine concentrations in rabbit striatum following increased dopamine turnover. *Brain Res. Bull.* 45, 297–299. doi: 10.1016/S0361-9230(97)00367-5

McNaught, K. S. P., Perl, D. P., Brownell, A.-L., and Olanow, C. W. (2004). Systemic exposure to proteasome inhibitors causes a progressive model of Parkinson's disease. *Ann. Neurol.* 56, 149–162. doi: 10.1002/ana.20186

Meissner, W. G., Frasier, M., Gasser, T., Goetz, C. G., Lozano, A., Piccini, P., et al. (2011). Priorities in Parkinson's disease research. *Nat. Rev. Drug Discov.* 10, 377–393. doi: 10.1038/nrd3430

Mizuno, Y., Hasegawa, K., Kondo, T., Kuno, S., Yamamoto, M., and Group, J. I. S. (2010). Clinical efficacy of istradefylline (KW-6002) in Parkinson's disease: a randomized, controlled study. *Mov. Disord.* 25, 1437–1443. doi: 10.1002/mds.23107

Molz, S., Dal-Cim, T., Budni, J., Martín-de-Saavedra, M. D., Egea, J., Romero, A., et al. (2011). Neuroprotective effect of guanosine against glutamate-induced cell death in rat hippocampal slices is mediated by the phosphatidylinositol-3 kinase/Akt/ glycogen synthase kinase 3β pathway activation and inducible nitric oxide synthase inhibition. *J. Neurosci. Res.* 89, 1400–1408. doi: 10.1002/jnr.22681

Müller, T. (2015). The safety of istradefylline for the treatment of Parkinson's disease. *Expert Opin. Drug Saf.* 14, 769–775. doi: 10.1517/14740338.2015.1014798

Paxinos, G., and Watson, C. (2007). *The Rat Brain in Stereotaxic Coordinates,* 6th Edn. Amsterdam: Elsevier.

Pettifer, K. M., Jiang, S., Bau, C., Ballerini, P., D'Alimonte, I., Werstiuk, E. S., et al. (2007). MPP^+-induced cytotoxicity in neuroblastoma cells: antagonism and reversal by guanosine. *Purinergic Signal.* 3, 399–409. doi: 10.1007/s11302-007-9073-z

Poewe, W. (2009). Treatments for Parkinson disease–past achievements and current clinical needs. *Neurology* 72, S65–S73. doi: 10.1212/WNL.0b013e31819908ce

Poewe, W., and Mahlknecht, P. (2009). The clinical progression of Parkinson's disease. *Parkinsonism Relat. Disord.* 15(Suppl. 4), S28–S32. doi: 10.1016/S1353-8020(09)70831-4

Rathbone, M. P., Middlemiss, P. J., Gysbers, J. W., Andrew, C., Herman, M. A., Reed, J. K., et al. (1999). Trophic effects of purines in neurons and glial cells. *Prog. Neurobiol.* 59, 663–690. doi: 10.1016/S0301-0082(99)00017-9

Salamone, J. D., Mayorga, A. J., Trevitt, J. T., Cousins, M. S., Conlan, A., and Nawab, A. (1998). Tremulous jaw movements in rats: a model of parkinsonian tremor. *Prog. Neurobiol.* 56, 591–611. doi: 10.1016/S0301-0082(98)00053-7

Santos, J. R., Cunha, J. A. S., Dierschnabel, A. L., Campêlo, C. L. C., Leão, A. H. F. F., Silva, A. F., et al. (2013). Cognitive, motor and tyrosine hydroxylase temporal impairment in a model of parkinsonism induced by reserpine. *Behav. Brain Res.* 253, 68–77. doi: 10.1016/j.bbr.2013.06.031

Schapira, A. H., Bezard, E., Brotchie, J., Calon, F., Collingridge, G. L., Ferger, B., et al. (2006). Novel pharmacological targets for the treatment of Parkinson's disease. *Nat. Rev. Drug Discov.* 5, 845–854. doi: 10.1038/nrd2087

Schmidt, A., Bohmer, A., Schallenberger, C., Antunes, C., Tavares, R., Wofchuk, S., et al. (2010). Mechanisms involved in the antinociception induced by systemic administration of guanosine in mice. *Br. J. Pharmacol.* 159, 1247–1263. doi: 10.1111/j.1476-5381.2009.00597.x

Schwarting, R. K., and Huston, J. P. (1996). The unilateral 6-hydroxydopamine lesion model in behavioral brain research. Analysis of functional deficits, recovery and treatments. *Prog. Neurobiol.* 50, 275–331. doi: 10.1016/S0301-0082(96)00040-8

Su, C., Elfeki, N., Ballerini, P., D'Alimonte, I., Bau, C., Ciccarelli, R., et al. (2009). Guanosine improves motor behavior, reduces apoptosis, and stimulates neurogenesis in rats with parkinsonism. *J. Neurosci. Res.* 87, 617–625. doi: 10.1002/jnr.21883

Thomaz, D. T., Dal-Cim, T. A., Martins, W. C., Cunha, M. P., Lanznaster, D., de Bem, A. F., et al. (2016). Guanosine prevents nitroxidative stress and recovers mitochondrial membrane potential disruption in hippocampal slices subjected to oxygen/glucose deprivation. *Purinergic Signal.* 12, 707–718. doi: 10.1007/s11302-016-9534-3

Traversa, U., Bombi, G., Di Iorio, P., Ciccarelli, R., Werstiuk, E. S., and Rathbone, M. P. (2002). Specific [(3)H]-guanosine binding sites in rat brain membranes. *Br. J. Pharmacol.* 135, 969–976. doi: 10.1038/sj.bjp.0704542

Vallano, A., Fernandez-Duenas, V., Pedros, C., Arnau, J. M., and Ciruela, F. (2011). An update on adenosine A2A receptors as drug target in Parkinson's disease. *CNS Neurol. Disord. Drug Targets* 10, 659–669. doi: 10.2174/187152711797247803

Volpini, R., Marucci, G., Buccioni, M., Dal Ben, D., Lambertucci, C., Lammi, C., et al. (2011). Evidence for the existence of a specific g protein-coupled receptor activated by guanosine. *ChemMedChem* 6, 1074–1080. doi: 10.1002/cmdc.201100100

Winkler, C., Kirik, D., Björklund, A., and Cenci, M. A. (2002). L-DOPA-induced dyskinesia in the intrastriatal 6-hydroxydopamine model of Parkinson's disease: relation to motor and cellular parameters of nigrostriatal function. *Neurobiol. Dis.* 10, 165–186. doi: 10.1006/nbdi.2002.0499

Conflict of Interest Statement: The authors declare that the research was conducted in the absence of any commercial or financial relationships that could be construed as a potential conflict of interest.

frontiers in Pharmacology

REVIEW
published: 25 September 2017
doi: 10.3389/fphar.2017.00661

Purinergic Signalling: Therapeutic Developments

Geoffrey Burnstock[1,2]*

[1] Autonomic Neuroscience Centre, University College Medical School, London, United Kingdom, [2] Department of Pharmacology and Therapeutics, The University of Melbourne, Melbourne, VIC, Australia

Purinergic signalling, i.e., the role of nucleotides as extracellular signalling molecules, was proposed in 1972. However, this concept was not well accepted until the early 1990's when receptor subtypes for purines and pyrimidines were cloned and characterised, which includes four subtypes of the P1 (adenosine) receptor, seven subtypes of P2X ion channel receptors and 8 subtypes of the P2Y G protein-coupled receptor. Early studies were largely concerned with the physiology, pharmacology and biochemistry of purinergic signalling. More recently, the focus has been on the pathophysiology and therapeutic potential. There was early recognition of the use of P1 receptor agonists for the treatment of supraventricular tachycardia and A_{2A} receptor antagonists are promising for the treatment of Parkinson's disease. Clopidogrel, a $P2Y_{12}$ antagonist, is widely used for the treatment of thrombosis and stroke, blocking $P2Y_{12}$ receptor-mediated platelet aggregation. Diquafosol, a long acting $P2Y_2$ receptor agonist, is being used for the treatment of dry eye. P2X3 receptor antagonists have been developed that are orally bioavailable and stable *in vivo* and are currently in clinical trials for the treatment of chronic cough, bladder incontinence, visceral pain and hypertension. Antagonists to P2X7 receptors are being investigated for the treatment of inflammatory disorders, including neurodegenerative diseases. Other investigations are in progress for the use of purinergic agents for the treatment of osteoporosis, myocardial infarction, irritable bowel syndrome, epilepsy, atherosclerosis, depression, autism, diabetes, and cancer.

Keywords: ATP, adenosine, CNS diseases, peripheral diseases, infection, inflammation

OPEN ACCESS

Edited by:
Kenneth A. Jacobson, National Institutes of Health (NIH), United States

Reviewed by:
Stanko S. Stojilkovic, National Institutes of Health (NIH), United States
Rennolds S. Ostrom, Chapman University, United States

***Correspondence:**
Geoffrey Burnstock
g.burnstock@ucl.ac.uk

Specialty section:
This article was submitted to Experimental Pharmacology and Drug Discovery, a section of the journal Frontiers in Pharmacology

Received: *07 August 2017*
Accepted: *05 September 2017*
Published: *25 September 2017*

Citation:
Burnstock G (2017) Purinergic Signalling: Therapeutic Developments. Front. Pharmacol. 8:661. doi: 10.3389/fphar.2017.00661

INTRODUCTION

Purinergic signalling, i.e., nucleotides as extracellular signalling molecules, was proposed in 1972 (Burnstock, 1972). However, this concept was not well accepted until the 1990's when receptor subtypes for purines and pyrimidines were cloned and characterised, which includes four subtypes of the P1 (adenosine) receptor, seven subtypes of P2X ion channel receptors, and eight subtypes of the P2Y G protein-coupled receptor (Ralevic and Burnstock, 1998). Early studies were largely concerned with the physiology, pharmacology and biochemistry of purinergic signalling (Burnstock, 2007). Adenosine 5′-triphosphate (ATP) is a cotransmitter with classical transmitters in both the peripheral and central nervous systems. In addition, purines are powerful extracellular messengers to non-neuronal cells, including secretory, exocrine and endocrine, endothelial, immune, musculo-skeletal and inflammatory cells (Burnstock and Knight, 2004). Purinergic signalling is rapid in neurotransmission, neuromodulation and in secretion, but is also long-term in proliferation, differentiation, migration and death in development and regeneration (Burnstock, 2016f).

More recently, the focus has been on the pathophysiology and therapeutic potential of both P1 (Chen et al., 2013; de Lera Ruiz et al., 2014; Layland et al., 2014; Liu and Xia, 2015; Borea et al., 2016) and P2 (Burnstock and Kennedy, 2011; Bartlett et al., 2014; Ford et al., 2015; Burnstock, 2016e) receptors. Reviews focussed on different aspects of purinergic pathophysiology are also available, including inflammatory and immune disorders (Arulkumaran et al., 2011; Junger, 2011; Hansson et al., 2016); cancer (Burnstock and Di Virgilio, 2013; Di Virgilio and Adinolfi, 2017); gout and fibrosis (Gicquel et al., 2017); P2X7 receptors (R) as therapeutic targets (Romagnoli et al., 2008); medicinal chemistry of purinoceptors (Jacobson and Muller, 2016); pain (Burnstock and Sawynok, 2010; Alves et al., 2013; Kuan and Shyu, 2016; Sawynok, 2016) and adenosine kinase inhibitors (Kowaluk and Jarvis, 2000). A number of purine-related compounds have been patented. Therapeutic developments for disorders of different systems in the body will now follow. Reviews concerned with the early literature will be quoted, so the focus of this review will be concerned largely with the most recent findings.

DISORDERS OF THE CENTRAL NERVOUS SYSTEM (CNS)

Investigations into purinergic signalling and its roles in disorders of the CNS have been reported, for instance following surgery, stroke, accidents and ischemia, neurodegenerative diseases (such as Parkinson's, Alzheimer's and Huntington's diseases), multiple sclerosis (MS), amyotrophic lateral sclerosis (ALS), epilepsy and neuropsychiatric disorders (including schizophrenia, depression and anxiety). Reviews covering this topic are available (Burnstock, 2008b; Burnstock et al., 2011), including the recent attention to the development of centrally penetrant P2X7R antagonists for the treatment of CNS disorders (Burnstock and Verkhratsky, 2012; Puchalowicz et al., 2014; Sperlagh and Illes, 2014; Burnstock, 2015b; Cisneros-Mejorado et al., 2015b).

Neurodegenerative Diseases

Neurodegeneration in the CNS is associated with inflammation and damage to both neurons and glia (Rama Rao and Kielian, 2015). Reviews are available that include coverage of early papers concerned with neurodegenerative diseases (Puchalowicz et al., 2014; Santiago et al., 2014; Fasullo and Endres, 2015; Förster and Reiser, 2015; Burnstock, 2016a; Fumagalli et al., 2016). Recent attention has been directed toward the use of P2X7R antagonists for the treatment of neurodegenerative diseases (Metzger et al., 2017). However, adenosine acting via A_{2A}R has also been claimed as a promising therapeutic agent for the prevention and treatment of neurodegenerative diseases (Cunha, 2016; Harmse et al., 2016; Olatunji et al., 2016).

Alzheimer's Disease (AD)

There is progressive cognitive impairment in AD, with prominent deficits in short term memory. The potential of purinergic drugs for the treatment of AD has attracted much interest in recent years. Previous studies have led to the proposal that both P2X7R and $P2Y_4$R antagonists are potential therapeutic targets for the treatment of AD (Erb et al., 2015; Miras-Portugal et al., 2015; Woods et al., 2016). It has been suggested that the blockade of $P2Y_1$R may have therapeutic potential against cognitive disturbances in AD (Guzman and Gerevich, 2016). β-Amyloid increased release of ATP, which potentiated excitatory synaptic activity via P2XR, effects that were blocked by P2X antagonists (Sáez-Orellana et al., 2016). The glycosylphosphatidylinositol-anchored prion protein binds to and modulates the expression of P2X4R, which may be involved in AD (Carneiro et al., 2016). Recently, a potential role has been proposed for ATP-sensitive potassium channel (K_{ATP}) modulation as a therapeutic strategy against AD (Salgado-Puga et al., 2017).

Adenosine A_3R agonists suppress amyloid-β protein precursor internalisation and amyloid-β generation (Li S. et al., 2015). Hippocampal adenosine A_{2A}R up-regulation is necessary to trigger memory dysfunction in AD (Cunha, 2015).

Parkinson's Disease (PD)

The involvement of adenosine A_{2A}R in PD and their interactions with dopamine receptors has attracted most attention (see Jenner, 2014). A_{2A}R antagonists have been proposed for the treatment of PD (Jenner, 2014; Mori, 2014; Pinna, 2014; Navarro et al., 2016). K_{ATP} (Dragicevic et al., 2015) and P2X1R (Gan et al., 2015; Navarro et al., 2016; Yang Z. et al., 2016) in PD have also been reported, perhaps indicating new therapeutic targets. Clinical trials istradefylline, an A_{2A}R antagonist, have taken place and it may have a beneficial effect in conjunction with commonly used anti-Parkinson's therapies (Tao and Liang, 2015; Uchida et al., 2015; Vorovenci and Antonini, 2015), although in a later study, istradefylline was shown to enhance amyloid-β generation and γ-secretase activity (Lu et al., 2016). Oligomerisation kinetics of A_{2A} and dopamine D_2R have important implications for PD (Casadó-Anguera et al., 2016; Ferré et al., 2016; Guixà-González et al., 2016). Clinical trials for A_{2A} antagonists for PD are assessed in a review (Navarro et al., 2016). A_{2A}R inhibition stopped rotenone-induced motor impairment in a rat model of PD (Fathalla et al., 2016). A_1 as well as A_{2A}R antagonists were recommended as promising candidates for treatment of PD in a recent paper (Essawy et al., 2017).

P2X7R antagonists have also been implicated in this disease (Jörg et al., 2014; Wang et al., 2017). A P2X7R antagonist, brilliant blue G, was recently shown to be protective in a lipopolysaccharide (LPS) animal model of PD (Wang et al., 2017).

Huntington's Disease (HD)

Earlier studies reported that A_{2A}R agonists could be therapeutically useful for HD and that P2X7R antagonists inhibited neuronal apoptosis and attenuated body weight loss and motor co-ordination deficit in HD patients. Adenosine A_{2A}R inhibition reversed working memory deficits of HD at early stages models and it was proposed that A_{2A}R antagonists may therapeutically reverse the cognitive deficits in HD patients (Li W. et al., 2015). In earlier publications, A_1R agonists were suggested to be therapeutic targets (Ferrante et al., 2014; Lee and Chern, 2014). It has been claimed that K_{ATP} channels may be potential targets for treatment of HD (Gupta and Sharma, 2014).

Inhibition of equilibrative nucleoside transporter 1 enhances the adenosine level and may be a potential therapeutic approach for treating HD (Kao et al., 2017).

Amyotrophic Lateral Sclerosis

Involvement of $A_{2A}R$, P2X4R and P2X7R in ALS has been reported (Volonté et al., 2016). A_1R have also been implicated in ALS (Nascimento et al., 2015). Preconditioning with latrepirdine, an adenosine 5′-monophosphate (AMP)-activated protein kinase activator, was beneficial in the SOD1 mouse model of ALS (Coughlan et al., 2015). $A_{2A}R$ activation facilitated neuromuscular transmission in SOD1 mice during the pre-symptomatic but not symptomatic phase of the disease (Nascimento et al., 2014). Pharmacological inhibition of $A_{2A}R$ protects against degeneration of spinal motor neurons in the mouse SOD1G93A ALS model (Ng et al., 2015).

P2X7R expression was significantly reduced, leading to Ca^{2+} disturbances in peripheral blood mononuclear cells in ALS patients (Liu J. et al., 2016). Low concentrations of endogenous ATP acting on P2X7R induced motor neuron death (Gandelman et al., 2013). Spinal cord pathology was reduced by P2X7R inhibitors in the mouse SOD1 ALS model (Apolloni et al., 2014).

Multiple Sclerosis

P2X7R and the P2YR-like GPR17 are involved in MS (Plemel et al., 2014; Burnstock, 2015c; Ou et al., 2016). There is upregulation of ecto-5′-nucleotidase (CD73) in experimental autoimmune encephalomyelitis, which is an MS animal model (Lavrnja et al., 2015). Genetic variants in P2X7R affect susceptibility to MS (Gu et al., 2015; Sadovnick et al., 2017).

Brain Injury, Neuroprotection, and Neuroregeneration

Brain Injury

The importance of inflammation in the responses to brain injury has been reviewed and the involvement of P1R and P2R (Fiebich et al., 2014; Beamer et al., 2016) and of P2X7R in particular (Burnstock, 2016b; Giuliani A.L. et al., 2017). The roles of purinergic signalling in neurodegeneration as a consequence of brain injury, neuroprotection and neuroregeneration have been discussed in reviews (Hu et al., 2014; Burnstock, 2016a). Ectonucleotidase activities and nucleotide levels in serum are altered by brain stab injury (Parabucki et al., 2014; Laketa et al., 2015). P2X7R antagonists appear to be effective as a treatment for radiation injury (Xu et al., 2015). Astrocytic *p*-connexin 43 stimulates neuronic autophagy through P2X7R activation in the hippocampus, resulting in brain injury-induced cognitive deficit repair (Sun L. et al., 2015). P2X7R antagonists have been implicated as a novel target to prevent secondary neurological injury after traumatic brain injury (Kimbler et al., 2012) and after spinal cord injury (Peng et al., 2009). P2X7R antagonists could be therapeutically effective to treat stroke patients (Kuan et al., 2015). P2X7R stimulation in acute ischaemic stroke is beneficial by restricting early oedema formation and perhaps by modulating responses of glia (Kaiser et al., 2016). Hypoxic-ischaemic brain injury increases intracellular Ca^{2+} in oligodendrocytes, which is partly mediated by P2X7R (Fern et al., 2014). P2X7R antagonists may provide a new target for the treatment of cerebral ischaemia (Bai and Li, 2013; Yu Q. et al., 2013) and for the prevention of ischaemic damage to oligodendrocytes (Domercq et al., 2010). P2X7 antagonists or inhibition of pannexin-1 channels reduced brain damage following ischaemia (Cisneros-Mejorado et al., 2015a; Mahi et al., 2015).

Activation of upregulated $P2Y_1R$ results in neuroblast migration to sites of brain damage (Cao et al., 2015). Microglial $P2Y_{12}R$ activation follows neuronal injury (Swiatkowski et al., 2016). $A_{2A}R$ activation was suggested for the treatment of brain injury and subsequent neuroinflammation (Dai and Zhou, 2011). $A_{2A}R$ on cells derived from bone marrow modulate white matter lesions following chronic cerebral hypoperfusion (Ran et al., 2015). Diadenosine tetraphosphate (Ap_4A) may be a good candidate for traumatic spinal cord injury treatment (Reigada et al., 2017). Adenosine kinase facilitated astrogliosis after traumatic brain injury and its inhibition in reactive astrocytes ameliorated astrogliosis-induced cell death (Jin et al., 2016).

ATP and adenosine concentrations in the brain were significantly raised during brain ischaemia to stimulate P1R and P2R (Cisneros-Mejorado et al., 2015b; Pedata et al., 2016). P2X4R expressed by microglia are involved in post-ischaemic brain inflammation (Cheng et al., 2014). P2X4R are required for neuroprotection via ischemic preconditioning (Ozaki et al., 2016). Neuronal K_{ATP} channels play a role in hypoxic preconditioning where they decrease neonatal hypoxic-ischaemic brain injury; it has been proposed that openers of K_{ATP} channels may prove to be therapeutically beneficial (Sun H.S. et al., 2015). Intranasal administration of guanosine reduced ischaemic brain damage in rats (Ramos et al., 2016). Ambiguously, both $A_{2A}R$ agonists and antagonists may protect against ischaemic brain injury (Pedata et al., 2014). A_1R contribute to immune responses following neonatal hypoxic ischaemic brain injury (Winerdal et al., 2016). A valuable review of the involvement of P1R, P2XR and P2YR in brain ischemia is available (Pedata et al., 2016).

Neuroprotection and Neuroregeneration

This topic is explored in recent reviews (Rodrigues et al., 2015; Burnstock, 2016a; Illes et al., 2016). Inhibition of P2XR and P2YR as well as activation of P1R following ATP breakdown to adenosine released from CNS cells, have been shown to be neuroprotective. Activation of the pannexin 1/P2X7R complex contribute to the neuroprotection that occurs after ischaemic pre- and post-conditioning (Mahi et al., 2015). Docosahexaenoic acid in the diet is thought to be a purinergic modulator via P2XR where it protects against neurodegenerative diseases (Molz et al., 2015). Neuroprotection mediated by microglia is associated with P2X7R activation and release of tumour necrosis factor-α (Masuch et al., 2016). Blockade of P2X7R provides neuroprotection against stroke, traumatic brain injury and subarachnoid haemorrhage (Zhao H. et al., 2016). P2X7R antagonists improve recovery after spinal cord injury (Wang et al., 2004). From a recent study on $P2Y_2R$ knockout (KO) mice and murine cell lines, it was concluded that $P2Y_2R$ play a neuroprotective role in neurological disorders, especially AD (de Diego-Garcia et al., 2017). Neuroprotection is claimed to

be mediated by $P2Y_{13}$ nucleotide receptors in neurons (Pérez-Sen et al., 2015). Activation of $P2Y_2R$ evokes regeneration of glial cells and nerves and the P2YR-like GPR17 evokes oligodendrocyte regeneration. Neural stem cell activation leads to neuroregeneration, probably via P2X4R and P2X7R. Reviews focused on the roles played by P2X4R and P2X7R (Miras-Portugal et al., 2015) and $A_{2A}R$ (Ribeiro et al., 2016) in neurodegeneration and neuroprotection have been published.

Psychiatric Disorders

Several antipsychotic drugs (e.g., chlorpromazine, fluspirilene, and haloperidol) were found to antagonise responses mediated by P2XR. These antipsychotic drugs act therapeutically by inhibiting dopaminergic hyperactivity by suppressing P2X-mediated effects (see Burnstock, 2015b). Brain penetrant P2X7R antagonists are being developed as drug targets for psychiatric diseases (Bhattacharya and Biber, 2016). Reviews about purinergic signalling in psychiatric disorders, such as addiction, depression, schizophrenia, bipolar disorder and autism, have been previously published (Yamada et al., 2014; Lindberg et al., 2015; Krügel, 2016). The possibility has been raised that P1R agonists might be beneficial in the therapy of psychiatric disorders (Cieslak et al., 2016).

Schizophrenia

Adenosine neuromodulation in schizophrenia has received the most attention (see Rial et al., 2014; Ciruela et al., 2015; Turcin et al., 2016). Deletion of $A_{2A}R$ from astrocytes interferes with glutamate homeostasis resulting in cognitive and psychomotor impairment in schizophrenia (Matos et al., 2015). It has been suggested that P2X7R and pannexin 1 channels are involved (see Burnstock and Verkhratsky, 2012; Avendano et al., 2015).

Bipolar Disorder

P2X7R, mediating neuroinflammation via microglial activity, contribute to bipolar disorder (see Gubert et al., 2013, 2016; Barron et al., 2014). Serum concentrations of uric acid increase in different clinical phases of bipolar disorder (Albert et al., 2015) and in those patients treated with lithium (Muti et al., 2015). The purinergic system may become dysregulated during manic episodes and it has been proposed that raised uric acid levels could be a useful indicator of bipolar disorder manic phases (Bartoli et al., 2017a). Purinergic modulators that reduce levels of uric acid may be therapeutically beneficial (Bartoli et al., 2017b). However, a decrease in serum adenosine levels in bipolar disorder patients was reported (Gubert et al., 2016).

Depression and Anxiety

Reviews describing the roles of both P1 (A_1 and A_{2A}) and P2X7R in mood disorders are available (Yamada et al., 2014; Ortiz et al., 2015). Antidepressant effects of P2X7 antagonists have been reported (Pereira et al., 2013; Zhang K. et al., 2016). P2X2R in the medial prefrontal cortex mediate the antidepressant-like actions of ATP released from astrocytes (Cao et al., 2013). Brilliant blue G, a P2X7R antagonist, had antidepressant and anti-inflammatory actions in mice after LPS administration (Ma et al., 2014). The P2X7R antagonist, A-804598, affected neuroimmune and behavioural features of stress (Catanzaro et al., 2014). Stress-related mood disorders activate the inflammasome via release of ATP and stimulation of P2X7R (Iwata et al., 2016). Co-expression of wild-type P2X7R with the polymorphism variant Gln460Arg alters receptor function associated with mood disorders (Aprile-Garcia et al., 2016). Increased K_{ATP} channel activity due to a mutation led to reduced anxiety in mice (Lahmann et al., 2014). K_{ATP} channels are involved in the pathogenesis of depression and may be a therapeutic target for this disorder (Fan et al., 2016). Altered levels of several ATP-dependent chromatin remodelling factors may be linked to high trait anxiety (Wille et al., 2016).

$A_{2A}R$ antagonists were reported to have antidepressant activity (Yamada et al., 2014). Creatine and ketamine had antidepressant effects, probably mediated by activation of A_1R and $A_{2A}R$ (Cunha et al., 2015). Caffeine, acting as an $A_{2A}R$ antagonist, prevented depression triggered by chronic stress (Kaster et al., 2015; Dziubina et al., 2016). Striatal and extrastriatal $A_{2A}R$ in the forebrain regulate fear responses in mice (Wei et al., 2014). $A_{2A}R$ mediated increased interleukin (IL)-1β in the brain contributed to anxiety (Chiu et al., 2014). Fear and anxiety in a mouse model of post-traumatic stress disorder were alleviated by administration of a derivative of adenosine, WS0701 (Huang et al., 2014). A_1R agonists have been used to treat anxiety, but have troublesome side-effects so positive allosteric modulators have been developed as potent anxiolytic agents (Vincenzi et al., 2016). An antidepressant-like effect of inosine in mice has been reported (Gonçalves et al., 2017).

Autism

Adenosine in addition to suramin, a non-selective ATP antagonist, are reported to improve behaviour in autistic individuals (Masino et al., 2013; Naviaux et al., 2014, 2015; Hamidpour et al., 2016).

Addiction

Targeting $A_{2A}R$ may offer strategies for combating drug addiction. Striatopallidal $A_{2A}R$ signalling in the dorsomedial striatum has been suggested as a therapeutic target in drug addiction by reducing habit formation (Li et al., 2016). Caffeine potentiates the addictive effects of drugs of abuse, including cocaine and amphetamine derivatives (Ferrée, 2016).

Treatment of rodents with a P2X3R antagonist diminished opioid tolerance (Tai et al., 2010) and tolerance to morphine-induced antinociception (Ma et al., 2015). Lead-induced neuroinflammation via P2X7R may be responsible for the intensification of morphine tolerance (Baranowska-Bosiacka et al., 2016). Opiate-induced changes in brain adenosine levels may be associated with opiate addiction and withdrawal (Wu et al., 2013).

Adenosine, acting via $A_{2A}R$, regulates addiction induced by cocaine. Women are more sensitive to cocaine and are therefore more vulnerable to becoming addicted. Adenosine antagonists may be an effective treatment (Broderick and Malave, 2014). A_{2A}-D_2 receptor-receptor interactions in the dorsal striatum are differentially affected by cocaine, which contributes to compulsive drug seeking (Pintsuk et al., 2016).

Interactions between striatal A_{2A} and glutamate (mGlu5) receptors modulate the drug-seeking effects of methamphetamine (Wright S.R. et al., 2016). Methamphetamine produces alterations in adenosine receptor expression in the nucleus accumbens (Kavanagh et al., 2015). A_{2A}R antagonism in dorsomedial striatum reduces methamphetamine addiction (Furlong et al., 2015). Adenosine A_{2A}R integrate the rewarding and motivational behaviours of methamphetamine (Chesworth et al., 2016). Behavioural sensitisation provides a model in animals for drug craving that underlies human addiction and sensitisation to amphetamine was reduced by $P2Y_1$R antagonists in the mesocortico-limbic dopaminergic system (Krügel et al., 2013).

A_{2A}R agonist treatment can help counteract nicotine addiction (Jastrzebska et al., 2014). A_{2A}R are a potential target for the treatment of alcohol abuse (Micioni Di Bonaventura et al., 2012; Houchi et al., 2013). Regulation in adenosine signalling in striatal circuits in alcohol addiction was reviewed (Nam et al., 2013). A_1R signalling contributes to the regulation of basolateral amygdala excitability and to the pathophysiology of alcohol addiction (Rau et al., 2014). A review of alcohol addiction discusses the role of adenosine (Michalak and Biala, 2016). P2X4R modulate synaptic signalling associated with alcohol addiction (Franklin et al., 2014; Khoja et al., 2016).

Epilepsy

Early focus was on the role of P1R in epileptic seizures, but P2X4R and P2YR, but especially P2X7R antagonists have been recently explored as neuroleptic agents (see Burnstock, 2015b; Engel et al., 2016; Rassendren and Audinat, 2016; Beamer et al., 2017; Cieslak et al., 2017). Seizure-induced increases in microglial process numbers were reduced and kainate-induced seizure behaviours were exacerbated in $P2Y_{12}$ KO mice (Eyo et al., 2014). Antiepileptic consequences of deep brain stimulation may be mediated by P1R activation (Miranda et al., 2014). P2X3R expression was upregulated in epileptic rats and humans and it was postulated that P2X3R antagonists might be therapeutically effective (Zhou X. et al., 2016). The release of adenosine and ATP during on-going epileptiform activity was measured with microelectrode biosensors (Frenguelli and Wall, 2016). ATP levels were increased during epileptic seizures, which were not of neuronal origin (Lietsche et al., 2016). There is an insightful Editorial about purinergic signalling-induced neuroinflammation in epilepsy (Engel, 2016).

A role for post-transcriptional control of the P2X7R expression has been proposed and therapeutic targeting of microRNA-22 was suggested to prevent development of epilepsy and inflammation (Jimenez-Mateos et al., 2015). Purinergic signalling, via P2X7R, regulates neonatal seizures associated with hypophosphatasia, an inherited metabolic bone disease characterised by spontaneous seizures (Sebastián-Serrano et al., 2016). P2X7R antagonists were effective against hypoxia-induced neonatal seizures in mice (Rodriguez-Alvarez et al., 2017).

Migraine

The role of ATP in migraine was initially suggested to involve vascular events (see Burnstock and Verkhratsky, 2012; Haanes and Edvinsson, 2014). Later, P2X3R in nociceptive brain areas, including the thalamus and trigeminal nucleus, were investigated and their interaction with $P2Y_1$R in trigeminal neurons (Hullugundi et al., 2014; Marchenkova et al., 2016). The therapeutic potential of antagonists to P2X7R for migraine treatment has been proposed (Gölöncsér and Sperlágh, 2014), as well as P2X3R and P2X2/3R antagonists (Kilinc et al., 2015; Yegutkin et al., 2016). Reviews have been published about the roles and therapeutic potential of purinergic signalling in the aetiology of migraine (Cieslak et al., 2015; Yegutkin et al., 2016).

Neuropathic Pain

P1R and P2R involvement in neuropathic pain has been discussed in reviews (Burnstock and Sawynok, 2010; Burnstock et al., 2011; Burnstock, 2014a, 2016c). The discovery by Inoue and colleagues that antagonists to P2X4R on microglia are effective against neuropathic pain was particularly important (see Tsuda, 2016). Antagonists to P2X7R and $P2Y_{12}$R also act on microglia to reduce neuropathic pain (see Tsuda and Inoue, 2016; Tsuda, 2017). A_3R agonists delay the development of neuropathic pain (Janes et al., 2016). Glial $P2Y_2$R are potential targets for the management of trigeminal-related pain (Magni et al., 2015). Pannexin 1 and P2X7R interactions have been suggested to play a role in chronic pain (Bravo et al., 2015). P2X7R antagonists have been recommended for the treatment of central post-stroke pain (Kuan et al., 2015). A review discusses the use of P2XR subtype antagonists for the treatment of central neuropathic pain (Kuan and Shyu, 2016). Purinergic signalling in the spinal dorsal horn and anterior cingulate cortex appear to be involved in neuropathic pain (Tsuda et al., 2017). P2X3 and P2X2/3R blockade has also been claimed to reduce chronic pain (Cantin et al., 2012; Xu et al., 2012; Giniatullin and Nistri, 2013).

Brain Tumours

Neuroblastoma, a rare childhood tumour, expresses P2X7R, which mediate proliferation. The P2X7R appears to be a regulator of neuroblastoma metabolic activity, angiogenesis and growth and may be a target for neuroblastoma treatment (Amoroso et al., 2015; Gomez-Villafuertes et al., 2015). The action of the antitumor agent, temozolomide, was increased by the antiproliferative actions of P2X7R agonists and antagonists to A_3R and $P2Y_1$R on human glioblastoma (D'Alimonte et al., 2015). P2X4R may also be involved in human neuroblastoma (Gualix et al., 2015).

P2X7R were over-expressed in human malignant gliomas and P2X7R antagonists decreased tumour cell numbers (Fang et al., 2015; Morrone et al., 2016; McLarnon, 2017). Extracellular nucleotides control glioma growth via P2X7R and $P2Y_6$R activation (Braganhol et al., 2015). P2X7 and A_{2A}R activation leads to release of cytokines by macrophages, which was prevented by antagonists to these receptors (Bergamin et al., 2015). P2X7R antagonists blocked the cell cytotoxicity caused by irradiation for glioma (Gehring et al., 2015). Purine nucleoside phosphorylase is released from rat C6 glioma cells, contributing to the purinergic system homeostasis and exhibiting a pathophysiological role (Giuliani P. et al., 2017).

It was claimed that K_{ATP} channels are associated with tumorigenesis of human glioma (Ru et al., 2014). A_3R blockade enhances the actions of antitumour drugs used against human glioblastoma stem-like cells (Torres A. et al., 2016). A_1 and $A_{2B}R$ also sensitise glioblastoma stem cells to chemotherapy (Daniele et al., 2014). $P2Y_2R$ interactions with caveolin-1 represents a novel target for human astrocytoma cells (Martinez et al., 2016).

Sleep Disorders

$P2Y_{11}R$ appear to be associated with narcolepsy (Kornum et al., 2011). Reduced endothelial dilation to ATP in cerebral arteries occurred in a rat model of obstructive sleep apnoea (Crossland et al., 2013). Adenosine is a key player in the regulation and maintenance of sleep-wake dependent neural activity changes, where dysregulation can lead to sleep-wake disorders (Holst et al., 2016). The $A_{2A}R$ antagonist, SCH58261, overcame the blood–brain barrier dysfunction as a result of sleep restriction (Hurtado-Alvarado et al., 2016).

CARDIOVASCULAR DISEASES

Reviews about this topic are available (Erlinge and Burnstock, 2008; Headrick et al., 2013; Burnstock and Ralevic, 2014; Burnstock, 2015a; Burnstock and Pelleg, 2015; Ralevic, 2015; Sousa and Diniz, 2017).

Heart Diseases

Heart Failure

In chronic heart failure adenosine accumulates, probably as a result of lowered adenosine deaminase (ADA) gene expression and raised CD73 activity. Adenosine therapy mediated by A_1R and A_3R is cardioprotective for chronic heart failure (Greene et al., 2016; Voors et al., 2017). A_1R agonists attenuate cardiac hypertrophy and prevent heart failure in a mouse model (left-ventricular pressure-overload) and in a rat model (neonatal cardiac myocyte) (Chuo et al., 2016). $A_{2B}R$ agonists exert stronger cardioprotective effects against cardiac ischaemia/reperfusion injury compared to $A_{2A}R$ activation in rats (Ke et al., 2015). CD73 and $A_{2B}R$ agonists have been considered as therapeutic agents for myocardial ischaemia. Genetic deletion of CD39 results in increased myocardial ischaemia-reperfusion injury (Smith et al., 2016). Inflammatory responses initiated during ischemia-mediated immune injury may be regulated by adenosine (Boros et al., 2016).

Early studies were concerned with the role of adenosine in ischaemic and reperfusion injuries. However, there is also interest in the role of ATP. Application of ATP, prior to or just after cardiac ischaemia is cardioprotective (Ren et al., 2016). ATP released from the ischaemic myocardium causes reflex responses mediated by cardiac sympathetic afferent nerves (Dong et al., 2016). P2YR are important therapeutic targets in myocardial protection during ischemia/reperfusion (Djerada et al., 2017). $P2Y_6R$ could be a therapeutic target to regulate cardiac hypertrophy (Clouet et al., 2016). There is increased expression of $P2Y_2$ and P2X1R in the hearts of rats with congestive heart failure.

P2X4R are needed for neuroprotection via ischemic preconditioning (Ozaki et al., 2016). P2X3R expression increased in dorsal root ganglion (DRG) and superior cervical ganglia neurons, resulting in exaggerated sympathoexcitatory reflexes. NONRATT021972 siRNA decreases the upregulation of P2X7R and improves cardiac function after myocardial ischemia (Tu et al., 2016). Mitochondrial K_{ATP} channels provide protection against myocardial ischemia/reperfusion injury (Wang et al., 2015; Shimizu and Calvert, 2016). K_{ATP} channels maintain high energy phosphates and myocardial perfusion in heart failure (Jameel et al., 2016).

Myocardial Infarction

A clinical trial (Acute Myocardial Infarction Study of Adenosine) concluded that infusion for 3 h of adenosine resulted in a reduction of infarct size (Yetgin et al., 2015; Bulluck et al., 2016). Protection against myocardial infarction was mediated by A_1R in the rabbit heart. The A_3R agonist IB-MECA produced cardioprotection against myocardial infarction (Tian et al., 2015). Microglial P2X7R in the rat hypothalamic paraventricular nuclei regulate the sympathoexcitatory responses in acute myocardial infarction (Du D. et al., 2015). Loss of mouse $P2Y_4R$ protects against myocardial infarction (Horckmans et al., 2015). CD39 reduced infarct size following ischaemia-reperfusion injury (Smith et al., 2016). $P2Y_{12}R$ antagonists have been recommended for long-term protection of patients, post-myocardial infarction (Alexopoulos et al., 2016). The K_{ATP} channel opener, natakalim, improves ventricular remodelling of congestive heart failure after myocardial infarction (Jin, 2016).

Atrial Fibrillation

Adenosine reduces post-operative atrial fibrillation (AF). Up-regulation of $A_{2A}R$ involves abnormal calcium handling in AF. Prevention of $A_{2A}R$ activation in patients with AF may sustain uniform beat-to-beat responses at higher beating frequencies (Molina et al., 2016). Adenosine-guided pulmonary vein isolation following a randomised clinical trial was recommended to treat paroxysmal AF (Macle et al., 2015), although this has been queried in a more recent clinical trial (Ghanbari et al., 2016). ATP-induced AF has also been investigated (Hasebe et al., 2016). The efficacy of the $P2Y_{12}$ antagonists ticagrelor and prasugrel are not affected in AF (Ondrakova et al., 2016). The roles of adenosine and ATP in atrial arrhythmias and fibrillation have been discussed (Jared Bunch, 2015; Belhassen and Michowitz, 2016).

Supraventricular Tachycardia

Acute therapy by ATP for paroxysmal supraventricular tachycardia was used in the late 1940's. In patients with paroxysmal supraventricular tachycardia bolus injection of Adenocard (adenosine) is clinically prescribed to slow conduction time via the atrioventricular node, via A_1R (Sachdeva and Gupta, 2013). Treatment of paroxysmal supraventricular tachycardia by adenosine and ATP is discussed (Lerman, 2015). To provoke vasovagal reaction in syncope patients ATP and adenosine are administered together with the head-up tilt table test (Fragakis et al., 2015).

Cardiomyopathy

Cardiomyopathy can be an inherited disease, but can occur as a result of vitamin B deficiency, amyloidosis, alcoholism or viral infections. ATP synthase disruption contributes to diabetic cardiomyopathy (Ni et al., 2016). P2X7R involvement in dilated cardiomyopathy has been reported (Martinez et al., 2015).

Cardiac Fibrosis and myocarditis

$P2Y_{11}R$ agonists reduce cardiac fibrosis (Certal et al., 2015). Extracellular nucleotide regulation of signalling in cardiac fibrosis has been discussed (Novitskaya et al., 2016). The P2X7R antagonist, A740003, reduces experimental autoimmune myocarditis, suggesting a treatment for clinical myocarditis (Zempo et al., 2015).

Angina

ATP injections to treat angina pectoris associated with coronary disease were used during the 1940s, while AMP was used to treat angina. ATP treatment for patients with coronary insufficiency was also used early. Intracoronary administration of adenosine results in angina pain. Intracoronary administration of adenosine in patients with unstable angina produced decreased myonecrosis and improved coronary blood flow (Kizilirmak et al., 2015). In vascular pain, which encompasses pelvic and ischaemic pain, migraine and angina, it is thought that release of ATP from endothelial cells during reactive hyperaemia after vasospasm diffuses through the microvascular wall to activate P2X3R on perivascular sensory nerves to send impulses that travel to pain centres in the brain via the spinal cord (Joseph et al., 2015). P2X2/3R expressed on airway nociceptive sensory nerves mediate cardiovascular reflexes in conscious rats (Hooper et al., 2016).

Cardiac Transplants

Responses of the transplanted human heart to adenosine show supersensitivity. Protection of cardiac grafts from cold ischaemia/reperfusion injury is caused by donor pretreatment with AMP-activated protein kinase (Yang C. et al., 2016). Treatment with P2XR antagonists prolongs cardiac transplant survival.

Vascular Diseases

Hypertension

It has been proposed in a recent review (Burnstock, 2017) that there are five different ways that purinergic signalling can contribute to the development of hypertension:

(1) ATP released as a cotransmitter from sympathetic nerves together with noradrenaline (NA) contributes, via P2X1R, to the vasoconstriction that results from increased sympathetic vasomotor activity in hypertension. Therefore, P2X1R antagonists should be useful for the treatment of hypertension, especially since there is a substantial increase in ATP relative to NA released from sympathetic nerves in spontaneously hypertensive rats (Brock and Van Helden, 1995; Goonetilleke et al., 2013).

(2) Release of ATP from endothelial cells by shear stress as a result of changes in blood flow acts on P2YR and P2X4R on endothelial cells to release nitric oxide (NO) resulting in vasodilation. Introduction of $P2Y_1$, $P2Y_2$, and P2X4 agonists would cause increased vasodilation in hypertension.

(3) Brain stem and hypothalamic neurons mediate sympathetic nerve activity. Recent studies show that P2X3R antagonists are antihypertensive, due to reduced sympathetic nerve activity as a result of increased peripheral P2X3R-mediated carotid body chemoreceptor reflexes (Pijacka et al., 2016).

(4) P2X7R in the kidney contribute to the pathophysiology of hypertension and P2X7R antagonists may have promise as clinical antihypertensive agents.

(5) In hypertensive patients adenosine activates the vascular renin-angiotensin system. P1R agonists have been suggested for the treatment of hypertension (Ho M.F. et al., 2016).

Recently, $P2Y_6R$ were shown to age-dependently promote vascular remodelling in a mouse model, an effect inhibited by MRS2578, suggesting that $P2Y_6R$ are a therapeutic target for the prevention of age-related hypertension (Sunggip et al., 2017).

Atherosclerosis

ATP signalling influences the development of atherosclerosis (Burnstock, 2008a; Ferrari et al., 2015). Endothelial and smooth muscle cell proliferation are promoted by adenosine and ATP in atherosclerosis via $P2Y_1$, $P2Y_2$, and P1R. In a human model, adenosine, via $A_{2A}R$, modulates foam cell formation (Reiss and Cronstein, 2012). A_{2B} and A_3 antagonists reduce atherosclerotic plaque development. There are increased concentrations of circulating adenosine 5′-diphosphate (ADP) and ATP in atherosclerosis (Jalkanen et al., 2015). Uridine 5′-triphosphate (UTP), via $P2Y_2R$, induces expression of vascular cell adhesion molecule-1 in coronary artery endothelial cells, which leads to the monocyte recruitment associated with atherosclerosis development. Upregulated $P2Y_2R$ mediate intimal hyperplasia in collared rabbit carotid artery. $P2Y_1R$ antagonists are a therapeutic target for neointima formation (Liu R. et al., 2015). Endothelial P2X4R play a more important role in intense proliferation in atherosclerosis than $P2Y_2R$. ATP, by inducing leukocyte recruitment in mice, contributes to atherogenesis, via $P2Y_2$, $P2Y_6$, P2X4, and P2X7R. P2X7R are over-expressed in atherosclerosis and P2X7R deficiency leads to less plaque formation (Stachon et al., 2016). CD39 mRNA-coated stents may be a treatment for atherosclerosis (Abraham et al., 2015).

Atherosclerosis of coronary vessels is called coronary artery disease or coronary artery syndrome. $P2Y_{12}R$ antagonists combined with aspirin are beneficial for patients with acute coronary syndrome (De Luca et al., 2016; Rollini et al., 2016). $A_{2A}R$ on coronary arteries have also been claimed to be involved in coronary artery disease (Gariboldi et al., 2017).

Vascular Injury, Angiogenesis and Restenosis

An initiating event in the pathogenesis of vascular diseases is often vascular injury. Injured cells release ATP, which, together with adenosine, evoke endothelial and smooth muscle cell growth, proliferation, migration and death. Adenosine, following breakdown of ATP, is protective against ischaemic injury. $P2Y_{12}R$ antagonists are prescribed as prevention against ischaemic stroke (Liu F. et al., 2015). $P2Y_2R$ mediate regulation of endothelial inflammation and angiogenesis (Gidlöf et al., 2015).

Sustained control of proliferation of endothelial and smooth muscle cells as a result of P1 and P2YR activation during vascular remodelling in restenosis after angioplasty has been reported and therapeutic possibilities are being explored (Burnstock, 2002). Activation of $A_{2B}R$ stimulates angiogenesis in human microvascular endothelial cells (Du X. et al., 2015). Adenosine, via $A_{2A}R$, stimulates wound healing and angiogenesis following tissue injury in mice. CD39 administration decreases injury-induced platelet deposition and recruitment of leukocytes and inhibits neointimal hyperplasia. A review discusses the vascular actions of P2XR in renal injury (Howarth et al., 2015).

Thrombosis, Inflammation, and Stroke

Nucleotides are extracellular mediators of vascular inflammation and thrombosis. Clopidogrel, a $P2Y_{12}$ antagonist, inhibits aggregation in platelets and is widely prescribed for thrombosis and stroke (Sarafoff et al., 2012). Other $P2Y_{12}$ antagonists have been developed, including ticlopidine, cangrelor, ticagrelor, prasugrel, elinogrel, BX 667, and PSB 0739. $P2Y_1R$ antagonists also have antithrombotic actions and have been recommended as a complement to current $P2Y_{12}$ anti-platelet strategies. The $P2Y_6R$ may be a therapeutic target for systemic inflammatory responses. Review articles are available about purinergic signalling in thrombosis and inflammation, including the use of different oral or intravenous $P2Y_{12}R$ antagonists (Tang et al., 2015; Nylander and Schulz, 2016; Rollini et al., 2017). P2X7R are pro-thrombotic and genetic KO of the gene for the P2X7R was shown to be protective in a mouse carotid artery thrombosis model (Furlan-Freguia et al., 2011). Adenosine, via $A_{2A}R$ and A_3R, had antithrombotic effects (Cristalli et al., 1994; Hofer et al., 2013).

Migraine

Migraine pain involves two distinct cerebrovascular phases: an initial vasoconstriction (with no pain), followed by vasodilation (reactive hyperaemia) associated with pain. A purinergic hypothesis for migraine was proposed in 1981 (Burnstock, 1981). It was suggested that after the initial vasospasm ATP and adenosine (following breakdown of ATP) may mediate the vasodilation during reactive hyperaemia associated with pain. It was also hypothesised that stimulation of P2X3R on sensory nerve terminals located on the adventitia of the cerebral microvasculature by ATP contributed to the migraine pain. Data has also been presented recently that is consistent with the purinergic hypothesis of migraine pain (Yegutkin et al., 2016). P2X3R antagonists have been proposed as potential candidates for migraine treatment (Waeber and Moskowitz, 2003). The non-steroidal anti-inflammatory compound, naproxen, currently in use for migraine pain, blocks P2X3R-mediated responses in trigeminal neurons of the rat. Migraine could involve a chronic disorder of the sympathetic nervous system, where increased release of the sympathetic cotransmitter ATP contributes to the initial vasospasm.

Adenosine may also be involved in migraine. Adenosine infusion resulted in symptoms that were migraine-like and withdrawal of the P1R antagonists theophylline and caffeine also resulted in migraine-like symptoms. Clinical trials with the adenosine uptake inhibitor dipyridamole, that results in increased extracellular adenosine, were halted due to the increase of migraine attacks in all patients. Overactive P2YR on glial cells may contribute to pain transduction during migraine. Reviews have been published about the role of purinergic signalling in the aetiology of migraine and the potential of purinergic compounds (Cieslak et al., 2015; Jacobs and Dussor, 2016).

Diabetic Vascular Disease

There is pre-junctional A_1R-mediated sympathetic neurotransmission and ATP-mediated endothelial vasodilatation in mesenteric arteries of streptozotocin (STZ) diabetic rats (Burnstock and Novak, 2013). There is enhanced $A_{2A}R$-mediated increase in coronary flow in type 1 diabetic mice (Labazi et al., 2016). UTP, ATP and adenosine evoked vasodilation is reduced in the circulation of skeletal muscle of type 2 diabetic patients. Erythrocyte release of ATP is diminished in type 2 diabetics, supporting the view that a defect in the physiology of erythrocytes may contribute to diabetic vascular disease. Erythrocytes are less deformable in type 2 diabetes leading to lowered levels of deformation-induced ATP release. Low erythrocyte ATP release may contribute to the prevention and treatment of diabetic peripheral vascular disease (Richards et al., 2015). P2X7R expression by monocytes might play a role in the pathological changes of type 2 diabetes mellitus (Wu et al., 2015).

Aortic Valve Disease

ATP inhibits mineralisation of the aortic valve seen in calcific aortic valve disease (Côté et al., 2012). Increased levels of ectonucleotidase are found in calcific aortic valve disease and inhibition of ectonucleotidase with ARL67156 prevented disease development in rats.

Blood Cell Diseases

Adenosine is a potential therapeutic target for the prevention and treatment of sickle cell disease (Fu and Davies, 2015). The circulating levels of adenosine are elevated in pregnant women with sickle cell disease (Ashimi et al., 2015). Amyloid-β peptide inhibits ATP release from erythrocytes, suggesting that in AD, vascular amyloid peptide may play a role.

DISEASES OF THE AIRWAYS

Reviews covering the early literature are available (Burnstock et al., 2012a; McGovern and Mazzone, 2014).

Inflammation occurs in most diseases of the airways, including chronic obstructive pulmonary disease (COPD),

dyspnea, asthma, cystic fibrosis (CF), allergy, infection and injury. Purine nucleotide release from airway epithelial cells is raised in inflammatory processes and has an important role in the pathophysiology of chronic lung disease. P2X7R are a therapeutic target in lung hypersensitivity reactions seen in chronic inflammatory responses. P2X7R modulate lung inflammatory, fibrotic and functional changes in silicosis, an occupational lung disease (Monção-Ribeiro et al., 2014). P2X4R mediate acute airway inflammation by regulating dendritic cell function (Wiesler et al., 2016). Vagal parasympathetic reflex bronchoconstriction has a role in inflammatory airway disease. Mucin hypersecretion is stimulated in various respiratory diseases and silencing of MUC8 by siRNA increased $P2Y_2R$-induced airway inflammation (Cha et al., 2015). $P2Y_2R$ have also been claimed to downregulate MUC5AC gene expression (Jeong et al., 2016). Nucleotides released during airway inflammation activate $P2Y_6R$ leading to further release of inflammatory cytokines (Hao et al., 2014). Anti-inflammatory effects of adenosine in the lung have been described involving immune cells.

Asthma

A role of adenosine in asthma has been considered for many years, because it is a powerful bronchoconstrictor in asthmatic, but not healthy lungs and P1R antagonists have been used for the treatment of asthma (see Cicala and Ialenti, 2013). It was suggested earlier that the bronchoconstriction evoked by adenosine in asthma was as a result of indirect actions by release of leukotrienes, histamine or endothelin (see Burnstock et al., 2012a). In early reports, A_{2A}, A_{2B}, and A_3R were all claimed to mediate inhibition of allergic airway inflammation and mast cells were shown to be involved. Expression of adenosine receptors on monocytes from patients with asthma contributes to the progression of the disease (Yuryeva et al., 2015). $A_{2A}R$ are involved in the immunological pathogenesis of asthma (Wang et al., 2016).

The roles of nucleotides in asthma has gained attention. In human lung mast cells, ATP is an important modulator of histamine release. Attenuated P2X7R function gives protection from asthma and was suggested to be age related. ATP in sputum was significantly elevated in patients with asthma, which was correlated with the percentage of neutrophils in sputum (Soma et al., 2016). Impaired P2X1R-mediated adhesion in eosinophils from asthmatic patients has been reported (Wright A. et al., 2016). $P2Y_6R$ activation was effective for treatment of a mouse model of asthma (Chetty et al., 2016).

In allergic asthma, inhalation of allergens, such as pollen spores or house dust mite allergen, or triggers such as viral infection or air pollution, trigger inflammation. For an immune response to be triggered by allergens, activation of dendritic cells is required. In allergic asthmatics, bronchoconstriction following inhaled adenosine was mediated by A_1R. Selective antagonists to $A_{2B}R$ improve inflammatory conditions in allergic asthma (Basu et al., 2017). ATP plays a role in inflammation in allergic asthma by recruitment and activation of inflammatory cells. $P2Y_1R$ are involved in allergic airway inflammation, probably by regulating maturation of dendritic cells. It has also been proposed that $P2Y_2R$ in the respiratory epithelium are important sensors for airborne allergens. P2X7R have been implicated in the pathophysiology of allergy-induced lung inflammation. Activating P2X7R on hematopoietic cells, namely eosinophils or dendritic cells, may be a therapeutic approach to treat allergic asthma. Oxatomide, an anti-allergic antihistamine, is claimed to also act as a P2X7R antagonist (Yoshida et al., 2015). P2R act as modulators of rat eosinophil recruitment in allergic inflammation (Alberto et al., 2016). Asthmatic patients exhibit hypersensitivity to aerosolised ATP, but the effects of ATP are not mediated by adenosine (Basoglu et al., 2017).

Chronic Obstructive Pulmonary Disease (COPD)

COPD emphysema and chronic bronchitis. COPD is caused by gas or noxious particles, particularly in tobacco smoke, trigging a lung inflammatory response that when in the larger airways is called chronic bronchitis while in the alveoli is called emphysema.

The role of adenosine receptors in COPD has been the main emphasis to date. Combined stimulation of A_{2B} and glucocorticoid receptors in epithelial cells of human airways induces genes that have anti-inflammatory potential for COPD (Greer et al., 2013). $A_{2B}R$ on human mast cells were claimed to be a strategic target for COPD and inhaled $A_{2A}R$ agonists have been used for the treatment of COPD. A_1, A_{2B}, and A_3R antagonists have also been used to treat COPD (Basu et al., 2017).

ATP is implicated in COPD as well as adenosine. COPD is characterised by up-regulation of ATP in bronchoalveolar lavage fluid, which promotes inflammation and tissue degradation. ATP-induced pulmonary vasodilation occurs in patients with COPD. Activation of P2X7R signalling by cigarette smoke appears to play a role in the pathogenesis of emphysema. Cigarette smoke induces neutrophil ATP release via P2X7 and probably $P2Y_2R$ activation. Aerosolised ATP exacerbates the symptoms of COPD (Basoglu et al., 2015). A valuable review about purinergic signalling and COPD has been published recently (Pelleg et al., 2016).

Airway Infections

Antibiotics, including erythromycin, are used widely for the treatment of lower and upper respiratory tract infections. Erythromycin blocks the P2XR-mediated Ca^{2+} influx and could represent one mechanism by which it exerts its effects. The airway epithelium has a role in activating the innate immune response during lung bacterial infections to fight the infection. Over-expression of the ectonucleotidase, CD39, promotes bacteria-induced inflammation, mediated largely by P2X7R in mouse airways. It has been proposed that P2X7R agonists together with low molecular weight anti-tuberculosis medicines could be used to treat multi-drug-resistant tuberculosis (TB) (Soares-Bezerra et al., 2015), although caution was advised as a polymorphism of the P2X7R was reported to increase the risk of recurrence of TB (Fernando et al., 2007). In infectious inflammatory diseases the roles of P2X7R and ectonucleotidases have been reviewed (Morandini et al., 2014). Polymorphisms of the P2X7R gene are

associated with the prognosis and risk of human TB (Zheng X. et al., 2017). Data has been presented to support the view that P2X7R antagonists should be used to treat the aggressive forms of TB (Amaral et al., 2014). Selective, orally bioavailable and potent ATP synthase inhibitors show activity against both non-replicating and replicating TB (Singh et al., 2015). P2X7R contain the spread of *Toxoplasma gondii in vivo* (Corrêa et al., 2017). The role of purinergic signalling in a mouse model of pneumococcal meningitis has been explored (Zierhut et al., 2017). The authors showed that although P2X7R activated the NLRP3 inflammasome/IL-1β pathway that mediates inflammation in pneumococcal meningitis, neither suramin nor brilliant blue G affected the disease, possibly because of meningitis-associated down-regulation of brain P2X7R expression and/or a decrease in ATP levels in cerebrospinal fluid.

Adenosine protects against *Streptococcus pneumoniae* infection of the lungs by pulmonary neutrophil recruitment regulation (Bou Ghanem et al., 2015). Macrophages that engulf bacteria produce adenosine that suppresses sensitisation in response to early-life infections (Pei and Linden, 2016). Chemokine release and leukocyte recruitment are modulated by nucleotides in inflamed airways via an action on P2YR on immune and epithelial cells. Mucociliary clearance is the initial defence against infections of the airways. Airway epithelium releases ATP into the surface liquid layer that controls mucus clearance via P2R and, following breakdown to adenosine, also through P1R. Pulmonary TB patients had higher ADA activity in bronchoalveolar lavage fluid and in the sputum.

Infection with the malaria protozoan parasite, *Plasmodium falciparum*, induces ATP release from erythrocytes. Rupture of erythrocytes releases ATP during the blood-stage of *P. chabaudi* malaria that increases P2X7R expression on $CD4^+$ T cells. Platelet ADA, CD39, and CD73 expression was reduced in *Trypanosoma evansi* infected rats. A review about purinergic signalling and malaria-infected erythrocytes is available (Huber, 2012). Haemolysis produced by leukotoxin, a bacterial virulence factor, was increased by ATP release and P2XR activation of human erythrocytes.

P2X7R activation regulates inflammatory responses during acute viral infection (Lee et al., 2012) and is involved in the exacerbated immune response seen during influenza virus infection (Leyva-Grado et al., 2017). ATP, released by activated macrophages and damaged cells, modulates lung inflammation in pneumonia in cattle. Both pulmonary microvascular endothelial cells and epithelial cells expressed P2X7R mRNA.

The pneumovirus respiratory syncytial virus commonly causes childhood lower respiratory tract diseases. It reduces alveolar clearance, probably via UTP, released by the bronchoalveolar epithelium following infection, suggesting that $P2Y_2R$ antagonists may be therapeutically important for the treatment of severe respiratory syncytial virus bronchiolitis (Vanderstocken et al., 2012). Rhinoviral stimuli and ATP signalling contribute to human bronchial smooth muscle production of IL-33 by severe asthmatics (Calvén et al., 2015). ATP is involved in the expression and release of a major airway mucin, MUC5AC, mainly via $P2Y_2R$ and it was suggested that modulation of this pathway could be useful clinically for mucus hypersecretion following viral infections (Shishikura et al., 2016).

Lung Injury

Acute respiratory stress syndrome and lung injury can lead to respiratory failure. There is a protective effect of ATP-$MgCl_2$ in ischaemia-reperfusion lung injury. Alveolar macrophages contribute substantially to chronic lung inflammation development, including silicosis, idiopathic pulmonary fibrosis, hypersensitivity pneumonitis, sarcoidosis, and asbestosis.

Alveolar macrophages express P2X7R, which stimulate the IL-1 to IL-5 proinflammatory cytokine cascade and may be clinically relevant in lung hypersensitivity reactions occurring due to chronic inflammation. P2X7R are involved in the pathophysiology of LPS-induced lung injury and LPS-induced inflammation occurs independently of $P2Y_1R$ (Liverani, 2017). There is up-regulation of pulmonary P2X4 and P2X7R in both acute and chronic lung injury and P2X7R deletion, but not P2X4 deletion, was lung protective (Hafner et al., 2017). The initial inflammatory cells recruited during lung injury are pulmonary neutrophils and P2X7R antagonists reduced neutrophil infiltration and proinflammatory cytokine levels (Mishra et al., 2016).

Neuroendocrine body cells lining the lung epithelium at intervals, release ATP in response to distension, which then stimulates P2X3R to activate vagal sensory fibres that originate in the nodose ganglion (Brouns et al., 2003). This mechanism may control reflex responses to noxious gases and hyperventilation. Ventilator-induced lung injury may involve ATP release from neuroepithelial cell bodies in response to stretch and therefore may be therapeutically relevant.

Pulmonary fibrosis can be caused by injury. In patients with idiopathic pulmonary fibrosis $A_{2B}R$ signalling may promote the production of inflammatory and fibrotic mediators. Extracellular adenosine levels are closely associated with the progression of pulmonary fibrosis (Luo F. et al., 2016). Adenosine production by CD73 enhanced radiation-induced lung fibrosis (Wirsdörfer et al., 2016). LPS caused increased expression of A_1, A_{2A}, and A_{2B} and P2YR, and decreased expression of A_3R, while mechanical ventilation reduced $P2Y_4$ mRNA levels. Both A_{2A} and $A_{2B}R$ were claimed to attenuate acute lung injury. Upregulated $A_{2A}R$ activation is likely to improve the healing process after acute LPS-induced lung injury (Friebe et al., 2014). A protective role for $A_{2B}R$ signalling has been reported to counter ischaemic lung injury (Densmore et al., 2017). Protective effects of A_3R activation in attenuating reperfusion lung injury has also been reported. Inhibition of adenosine kinase attenuates acute lung injury (Köhler et al., 2016). Inhaled $A_{2B}R$ agonists have been recommended for the treatment of acute lung injury (Hoegl et al., 2015). Adenosine is detrimental in lung recovery following hyperoxic lung injury (Davies et al., 2016). Reviews have been written about adenosine receptors as potential therapeutic targets for acute respiratory stress syndrome and acute lung injury (Schepp and Reutershan, 2008; Eckle et al., 2009).

Cystic Fibrosis (CF)

Cystic fibrosis is hereditary as a result of a loss of function gene mutation in the cystic fibrosis transmembrane conductance regulator (CFTR) protein. Some outstanding reviews about purinergic signalling in CF have been published (Burnstock et al., 2012a; Della Latta et al., 2013). The regulation of ion transport by UTP and ATP in CF and normal human airway epithelium was proposed early, in retrospect probably via $P2Y_2$ and/or $P2Y_4R$. P2R compounds for the treatment of CF to restore Cl^- secretion and/or inhibit Na^+ absorption are being investigated. Lipoxin A_4, which stops inflammation, is inadequately produced in patients with CF, but it stimulates apical ATP release, which activates $P2Y_{11}R$ resulting in epithelial repair (Higgins et al., 2014). With the R117H mutation associated with mild forms of CF, there are faults with the gating conformational changes in the CFTR transmembrane domains, although the function of the nucleotide binding domains are unchanged (Yu et al., 2016). Gating of the R117H-CFTR was shown to be almost completely rectified by combined treatment with an ATP analogue [N^6-(2-phenylethyl)-2′-deoxy-ATP], VX-770 (Ivacaftor, currently used to treat CF) and nitrate ions (NO_3^-). The authors concluded that future therapeutic developments might include the complementary use of ATP analogues with VX-770.

Cl^- secretion across CF airway epithelia is restored by ATP by triggering calcium entry via P2XR. It was suggested that P2X4/6 heteromultimer receptors might be involved. CFTR activity is necessary for ATP release following erythrocyte deformation. CFTR is reduced or absent in CF and mechanical deformation of erythrocytes does not induce ATP release. Increasing nucleotide release via motion could have therapeutic implications for CF patients. Women with CF showed reduced survival compared with males. Oestrogen may lower breathing-induced release of ATP and ATP receptor-mediated $[Ca^{2+}]_i$ increase that induces Cl^- secretion. Anti-oestrogens may therefore be beneficial in the treatment of CF.

A_1R agonists release $[Ca^{2+}]_i$ and activate Cl^- and K^+ currents in CF epithelial cells of the airways. A_1 and $A_{2A}R$ participate in regulation of Cl^- secretion in CF airway epithelial cells. Bronchoalveolar lavage from CF patients contained high concentrations of adenosine, correlating with higher 5′-nucleotidase and lower ADA activity. Adenosine regulates CFTR via $A_{2B}R$. The exhaled breath condensate biomarker, adenosine, tracks changes in lung function in CF (Esther et al., 2013). There is increased airway adenosine metabolism in early CF (Esther et al., 2015).

Lung Cancer

Human lung A549 epithelial-like adenocarcinoma cells express P2UR (i.e., $P2Y_2$ and/or $P2Y_4$) that mediate increases in $[Ca^{2+}]_i$. In A549 cells there is calcium-dependent UTP and ATP release (with subsequent increase in adenosine levels). Erythromycin selectively inhibits influx of Ca^{2+} induced via P2X4R stimulation in A549 lung tumour cells. A549 cells express $P2Y_2$, $P2Y_4$, and $P2Y_6$, and P2X4R. ATP induces dose-dependent inhibition of growth of cell lines, including human mesothelioma (MER082), human papillary lung adenocarcinoma (H441), human squamous cell lung carcinoma (H520), human large cell lung carcinoma (H460), human small cell lung carcinoma (GLC4) and the PC14 lung adenocarcinoma cell line. ATP was released from Calu-3 cells derived from human lung adenocarcinoma, probably in response to $P2Y_2R$ activation. UTP, ATP and uridine diphosphate stimulate proliferation of lung tumour A549 cells through $P2Y_2$ and $P2Y_6R$.

Autocrine ATP release and P2X7R activation affects the migration of human lung cancer cells (Takai et al., 2014). A significant increase in survival of non-small cell lung cancer patients with high P2X7R expression was identified compared to patients with low P2X7R expression (Boldrini et al., 2015). Nucleotides released by radiochemotherapy induce chemotaxis, adhesion and proliferation of human lung cancer cells and metastasis was inhibited in immunodeficient mice by purinergic receptor antagonists (Schneider et al., 2015). An association of P2X7, P2X4, and $P2Y_1R$ with distant metastatic lung tumours was observed and increased degradation of ATP and ADP by CD39, which influence tumour growth and metastasisation (Hofman et al., 2015). ATP promotes cell survival by inducing a long lasting and sustained increase in $[Ca^{2+}]_i$ in lung cancer cells (Song et al., 2016). ATP binding cassette E1 promotes growth, invasion and metastasis of lung adenocarcinoma cells (Tian Y. et al., 2016). Ecto-5′-nucleotidase (CD73) inhibitors are currently under clinical trial to treat non-small cell lung cancer (Zhu et al., 2017).

$A_{2B}R$ on host immune cells may participate in promoting angiogenesis and suppressing immunity and $A_{2B}R$ KO mice showed reduced growth in a Lewis lung carcinoma isograft model. ATP increased the cytotoxicity of cisplatin, a common anti-cancer drug for the treatment of lung cancer, in the H460 carcinoma cell line. An A_3R agonist inhibited cell proliferation by stopping the cell cycle and by apoptosis in A549 cells. Antagonism of $A_{2A}R$ expressed by lung adenocarcinoma tumour cells inhibited their growth (Mediavilla-Varela et al., 2013). $A_{2A}R$ expression and CD73 have opposing prognostic effects in non-small cell lung cancer (Inoue et al., 2017).

Cachexia often occurs in lung cancer patients. In clinical trials, infusion of ATP in advanced non-small cell lung cancer patients contributed beneficially by increasing body weight, muscle strength and quality of life, as well as enhancing survival (Agteresch et al., 2003). ATP has been claimed to reduce radiation-induced damage in patients with non-small cell lung cancer (Swennen et al., 2008).

Chronic Cough

The therapeutic promise of P2X3R antagonists for the treatment of chronic cough was first recognised by Ford and Undem (2013). P2X3R are expressed by airway afferent nerves and mediate hypersensitivity of the cough reflex, which is dramatically reduced by the oral P2X3 antagonist, AF-219 (Abdulqawi et al., 2015). Central A_1R were shown to suppress cough (El-Hashim et al., 2016).

Pleurisy

Inosine contributed with adenosine to exert, via A_2R, anti-inflammatory effects in pleural inflammation (da Rocha Lapa et al., 2012).

Lung Allograft

Ecto-5′-nucleotidase (CD73) reduced rejection of airway allografts by stimulating $A_{2A}R$, which is a negative modulator of lymphocyte recruitment into the allograft. P2X7R antagonists prolong mouse lung allograft survival (Liu et al., 2014).

DISEASES OF THE SPECIAL SENSES

Purinergic signalling is involved in the physiology of the nasal organs, ear, eye and tongue. Purinergic drugs are being explored for corneal injury, retinal detachment, glaucoma, dry eye, retinitis, uveitis, rhinosinusitis, diabetic retinopathy, macular degeneration, noxious odour damage, Ménière's disease, sensorineural deafness, tinnitus and taste defects (Burnstock, 2006; Housley et al., 2009).

Eye

The early literature up to 2006 was reviewed (Burnstock, 2006) and there are more recent reviews covering the treatment of ocular diseases by purinergic drugs (Guzman-Aranguez et al., 2014; Sanderson et al., 2014; Beckel et al., 2016; Lee et al., 2016; Reichenbach and Bringmann, 2016).

Glaucoma is characterised by progressive degeneration of retinal ganglion cells and visual loss. Elevated intraocular pressure reduction is the treatable risk factor for glaucoma. P2X7R antagonists are being explored for the treatment of glaucoma (Krizaj et al., 2014; Pérez de Lara et al., 2015; Sakamoto et al., 2015). There is elevation of extracellular ATP and upregulation of NTPDase1 in animal models of chronic glaucoma (Lu et al., 2015). Cromakalim, a K_{ATP} channel opener, lowers intraocular pressure (Roy Chowdhury et al., 2015, 2016). Evidence for the use of adenosine receptor antagonists for the treatment of glaucoma has also been presented (Zhong et al., 2013; Agarwal and Agarwal, 2014). Ap_4A improves adrenergic anti-glaucomatous therapeutic effectiveness (Loma et al., 2015) and has recently been claimed to be an effective compound for the treatment of glaucoma (Fonseca et al., 2017).

Treatment for dry eye by a long lasting $P2Y_2R$ agonist, diquafosol, was developed by Inspire Pharmaceuticals, Inc. and is currently in use in Japan and Korea (see Lau et al., 2014).

A $P2Y_2R$ agonist, INS37217, enhances subretinal fluid reabsorption and is recommended for the treatment of retinal detachment (Maminishkis et al., 2002; Meyer et al., 2002).

P2X7R antagonist and A_3R agonists have been implicated for the treatment of diabetic neuropathy and retinopathy (Sugiyama, 2014; Reichenbach and Bringmann, 2016), photoreceptor neurodegeneration (Hu et al., 2015; Ho T. et al., 2016), retinitis (Corso et al., 2016) and uveitis (Zhao R. et al., 2016).

The roles of $P2Y_2$ and P2X7R in corneal wound healing have been reviewed (Minns and Trinkaus-Randall, 2016; Minns et al., 2016). P2X7R activation in oxysterol cytotoxicity may be a target for the treatment of age-related macular degeneration (Olivier et al., 2016).

Ear

In the auditory system ATP depressed sound-evoked action potentials in the auditory nerve by stimulating P2YR. Acoustic over-stimulation can cause permanent hearing loss due to damage and death of cochlea hair cells. Noise exposure promotes the release of ATP into endolymph. ATP regulates hearing sensitivity and could be useful to treat sensorineural deafness, Ménières disease and tinnitus. UTP infusion into the deafened guinea pig inner ear rescued auditory neurons (Fransson et al., 2009). P2XR-mediated control of cochlear gap junctions may be protective by reducing hearing sensitivity to noise stress (Zhu and Zhao, 2012), perhaps via P2X2R (Yan et al., 2013; Mittal et al., 2016). Susceptibility to hearing loss and noise-induced neural injury in the mouse cochlea is regulated by $A_{2A}R$ (Vlajkovic et al., 2017).

Olfactory Organs

Purinergic receptors are expressed in the nasal mucosa, including P2X3R on olfactory neurons. There is enhanced odour sensitivity in the presence of antagonists to P2R suggesting that endogenous ATP at a low level normally decreases odour responsiveness. Chemosensory trigeminal neurons express P2X2R, which contribute to control of odour recognition (Housley et al., 2009). Activation of P2X3R negatively modulates the odour response, indicating a protective strategy for olfactory sensory neurons (Yu, 2015). Olfactory nerves and secretory cells in the vomeronasal organ express purinoceptors. Heat-shock protein induction by noxious odour damage is inhibited by P2R antagonists *in vivo*. The inhibitory effect of ATP in odour responses may contribute to the reduction of odour sensitivity following exposure to noxious fumes and could be a new mechanism for neuroprotection (Yu and Zhang, 2014). ATP release following injury leads to post-injury neuroregeneration and may result in the development of therapies to restore loss of smell (Hayoz et al., 2012). $P2Y_1R$ increase neuronal network activity in the developing olfactory bulb (Fischer et al., 2012). Purinergic signalling serves as a paracrine signal in regulating the neurogenesis of mouse olfactory epithelium (Gao L. et al., 2010). It has been claimed that purinoceptors are a therapeutic target to alleviate or restore loss of olfactory sensory neurons by the mycotoxin, satratoxin (Jia et al., 2011). Activation of A_2R may be a novel therapeutic approach for enhancing nasal mucociliary clearance in chronic rhinosinusitis (Hua et al., 2013).

Tongue

ATP is a key neurotransmitter in the taste system, acting largely via P2X2/3 heteromultimer receptors (Kinnamon and Finger, 2013; Vandenbeuch et al., 2015). Consequently, disruption of taste function may be an unintentional consequence of therapeutic trials of pain, chronic cough and other conditions using purinergic P2X3R antagonists (Vandenbeuch et al., 2013).

IMMUNE SYSTEM AND INFLAMMATION

P2X7, $P2Y_1$, and $P2Y_2R$ on immune and inflammatory cells are important in immunomodulation and inflammation, and the purinergic contribution to neuroinflammation underlying neuropathology has been discussed in several recent reviews (Jacob et al., 2013; Takenouchi et al., 2014; Di Virgilio and Vuerich, 2015; Beamer et al., 2016). The role of P2X7R in particular in diseases related to neuroinflammation and the use of P2X7R centrally penetrant antagonists has been highlighted (Baudelet et al., 2015; Di Virgilio, 2015; Gentile et al., 2015; Burnstock, 2016b; Danquah et al., 2016; Karmakar et al., 2016; Rech et al., 2016; Corrêa et al., 2017; Giuliani A.L. et al., 2017; Jiang et al., 2017; Zheng B. et al., 2017). It has been claimed that activation of P2X1R on neutrophils and platelets is involved in regulation of thrombo-inflammation (Oury et al., 2015). $P2Y_{12}R$ activation modulates sepsis-induced inflammation (Liverani et al., 2016). Adenosine, acting mainly via $A_{2A}R$, is also involved in neoplastic and inflammatory and immune-mediated disease states (Antonioli et al., 2014a; da Rocha Lapa et al., 2014; Cekic and Linden, 2016; Ingwersen et al., 2016; Zhang X. et al., 2016; Faas et al., 2017).

INFECTION

Reviews have been published concerned with purinergic signalling in immune cell trafficking at sites of infection (Ferrari et al., 2016b) and P2X7R in infectious inflammatory diseases (Morandini et al., 2014). Apoptosis of macrophages via ATP-stimulated P2X7R leads to the killing of the mycobacteria they contain, which may lead to new strategies to combat bacterial infections. The cytotoxic effects of ATP on macrophages are through P2X7R, while the bactericidal actions of ATP (and UTP) may be though $P2Y_2R$. There is a valuable article about purinergic signalling in infection and autoimmune diseases (Savio and Coutinho-Silva, 2016). The P2X7R is a potential target for the treatment of *Clostridium perfringens* type C infection (Nagahama et al., 2015). P2X7R activation modulates cell death during *Porphyromonas gingivalis* infection (Almeida-da-Silva et al., 2016). P2X7 and P2X4R activation is protective during severe *Escherichia coli* infection (Greve et al., 2017). P2X7R develop the inflammatory response associated with sepsis (Santana et al., 2015) and might serve as a therapeutic target to ameliorate brain damage in sepsis (Savio et al., 2016). $A_{2A}R$ have also been recommended as a therapeutic target to treat sepsis (Sivak et al., 2016). The role of purinergic signalling in the immune response in sepsis has been reviewed (Ledderose et al., 2016). ATP protects against sepsis through P2X7R on macrophages by enhancing intracellular bacterial killing (Csóka et al., 2015). *Chlamydiae* are intracellular bacterial pathogens and these infections are influenced by inflammasomes and purinergic signalling (Pettengill et al., 2016). Purines modulate the inflammatory response in rats infected by *Cryptococcus neoformans* (de Azevedo et al., 2016). ADP facilitates monocyte recruitment in bacterial infection (Zhang X. et al., 2016). ATP synthase has been proposed as a target to kill *Mycobacterium tuberculosis* (Tantry et al., 2017). Purinergic enzymatic activities in lymphocytes and cardiomyocytes modulated the inflammatory responses of mice infected by *T. cruzi* (do Carmo et al., 2017). Adenosine restored LPS-inhibited chemotaxis via A_1R, making this a promising therapeutic strategy for infectious diseases (Xu et al., 2017).

Infection by *Schistosoma mansoni*, a parasitic blood fluke, results in thymic atrophy. The cloning and characterisation of a P2XR (schP2X) from *S. mansoni* was the first non-vertebrate ATP-gated ion channel, which could be an alternative drug target to treat schistosomiasis (see Burnstock and Kennedy, 2011). Purinergic signalling influences the immune response to infection by *Leishmania*, a protozoan parasite (Chaves et al., 2014; Figueiredo et al., 2016). Purinergic signalling is involved in *Trichomonas vaginalis* parasite infection (Menezes and Tasca, 2016). The dysfunction of P1, P2Y and P2X7R and NTPDases are likely to contribute to morbidity due to human schistosomiasis (Silva, 2016). P2X7R are important in parasite control as they regulate T effector cells and inflammation during *L. amazonensis* infection (Figliuolo et al., 2017a). A commentary about ATP as an initiator of immunity to parasitic infections has been published (Nelson et al., 2017).

P2X7R modulate the antiviral and inflammatory processes that occur during Dengue virus-2 infection (Corrêa et al., 2016) and exacerbate the immune response that occurs during influenza virus infection (Leyva-Grado et al., 2017). P2X4R antagonists reduce herpetic pain (Matsumura et al., 2016). Both P2X4 and P2X7R are involved in hepatitis C virus infection (Manzoor et al., 2016). Purinoceptors are putative targets for the treatment of HIV-1 infection (Pacheco et al., 2014). Ribavirin, an adenosine analogue, exhibited potent antiviral activities (Hao et al., 2017).

ENDOCRINE DISEASES

Purinoceptors are expressed widely by endocrine glands (Burnstock and Knight, 2004). Actions of purines have been described in the pituitary gland, with implications for pathological as well as physiological states. 5′-Nucleotidase activity in platelets is changed by hyper- and hypothyroidism and could be a further mechanism by which alterations in thyroid hormones are related to vascular diseases. The role of purinergic signalling in thyroid hormone activities in health and disease has been reviewed (Silveira et al., 2013). In the ovary, follicular atresia involves cellular degeneration that is due to apoptosis evoked by P2X7R activation in both somatic and germinal follicular cells. Adiponectin, secreted by adipocytes, is anti-inflammatory, protecting against fatty liver disorder, insulin-resistant type 2 diabetes and atherosclerosis. A review including the limited knowledge of purinergic signalling in the endocrine system has been published (Burnstock, 2014b).

Diabetes

Fibroblast P2YR are impaired in type 2 diabetes, which leads to lower glucose uptake, indicating that P2YR could be therapeutically useful as antidiabetic drugs. Analogues of the $P2Y_1R$ agonist, 2-methylthio ADP, have been developed for

the treatment of type 2 diabetes (Yelovitch et al., 2012). P2YR activation potentiates insulin secretion making it a promising therapeutic target for type 2 diabetes (Zhang et al., 2015b; DeOliveira et al., 2017). Adenosine, acting via $A_{2A}R$, increases pancreatic β-cell proliferation, and has been suggested as a therapeutic target for diabetes (Schulz et al., 2016). Uridine adenosine tetraphosphate may be a therapeutic target for diabetes (Matsumoto et al., 2015).

There is an enhancement of P2X7R-induced apoptosis on the retinal microvasculature in early diabetes. P2X7R located on glucagon-containing α cells in pancreatic islets in STZ-induced diabetic animals increase and they migrate centrally to replace missing insulin-containing β cells. P2X7R antagonists have been proposed as a therapeutic target to cause immunosuppression and tolerance induction in pancreatic islet transplantation (Aikin, 2013; Vergani et al., 2013). NONRATT021972 siRNA decreases the expression of P2X7 mRNA and protein in DRG, reducing mechanical and thermal hyperalgesia in type 2 diabetic rats (Liu et al., 2016c). Type 1 diabetes impairs P2X7R signalling in osteocytes that affects osteoblast function and maintenance of bone health (Seref-Ferlengez et al., 2016). STZ-induced type 1 diabetes was prevented in P2X7R KO mice (Vieira et al., 2016). Diabetic sympathetic neuropathy in type 2 diabetic rats was reduced by decreasing the expression of P2X7R in superior cervical ganglia (Wu et al., 2016). P2X7R are expressed in pancreatic cancer cells. P2X7R antagonists are likely to be effective therapeutic agents (Giannuzzo et al., 2016).

P2X3R antagonists have been proposed for the treatment of diabetic neuropathic pain (Guo et al., 2015; Zhang et al., 2015b; Peng et al., 2017; Rao et al., 2017). Recently P2X7R have also been claimed to be involved in painful diabetic neuropathy in rats (Liu et al., 2017). P2X7R polymorphisms are associated with severe diabetic neuropathic pain scores (Ursu et al., 2014). A_1R agonists improve mechanical allodynia in a painful diabetic neuropathy mouse model (Katz et al., 2015).

There is up-regulation of hippocampal $A_{2A}R$ in STZ-diabetes and $A_{2A}R$ antagonists gave neuroprotection. $A_{2A}R$ are a therapeutic target for diabetic retinopathy (Ibrahim et al., 2011). Reduced expression of A_1R in pancreatic α-cells could result in the development of type 1 diabetes (Yip et al., 2013). There is increased expression of $A_{2B}R$ in women with gestational diabetes mellitus (Wojcik et al., 2014). In diabetic rats, $A_{2B}R$ agonists improve erectile function (Wen et al., 2015). It was suggested that reduction in A_3R expression/function may slow the progression of diabetic neuropathy (Yan H. et al., 2016). Blockade of ATP synthase interaction with cyclophilin D has been proposed as a promising therapeutic target to treat diabetic encephalopathy (Yan S. et al., 2016).

K_{ATP} channels have neuroprotective effects in patients with type 2 diabetes (Liu R. et al., 2016; Rubaiy, 2016). $P2Y_1$ and $P2Y_2R$ mediate relaxation of the rat corpus cavernosum and may improve erectile function in men with diabetes (Gür et al., 2009).

An $A_{2A}R$ agonist was shown to enhance healing of chronic diabetic foot ulcers in a clinical trial (Squadrito et al., 2014; Montesinos et al., 2015). Adenosine kinase inhibitors attenuate inflammation in diabetic retinopathy (Elsherbiny et al., 2013a). Retinal inflammation in diabetic retinopathy is mediated by ADA2 and the anti-inflammatory activity of $A_{2A}R$ signalling is impaired with increased ADA2 activity (Elsherbiny et al., 2013b).

Several reviews about purinergic signalling in diabetes and its therapeutic potential are available (Burnstock and Novak, 2013; Cieslak and Roszek, 2014; Antonioli et al., 2015; Fotino et al., 2015; Kishore et al., 2015; Merighi et al., 2015; Vindeirinho et al., 2016). The involvement of purinergic signalling in diabetic nephropathy is discussed later in the Section on Kidney.

OBESITY

ATP released as a cotransmitter from sympathetic nerves, stimulates brown adipocytes. ATP stimulates lipogenesis in rat adipocytes, regulating fat stores not via established hormones. Adipocytes express two different P2YR subtypes and $P2Y_{11}R$ activation inhibited insulin-stimulated lepton production and lipolysis stimulation. $P2Y_4R$ mediate inhibition of cardiac fat formation (Lemaire et al., 2016). The anti-obesity effects of sesamol, a potent anti-inflammatory compound, is mediated by AMP-activated protein kinase (Go et al., 2017). Blocking $P2Y_6R$ activation in the CNS with the antagonist MRS2578 inhibits feeding in mice (Steculorum et al., 2017).

Some ATP effects are as a result of adenosine, after breakdown of ATP, which is also involved in the activities of adipocytes. Adenosine increased lipolysis and induced thermogenesis in brown adipocytes via $A_{2A}R$ (Gnad et al., 2014). They showed that $A_{2A}R$ antagonists counteract high fat-induced obesity in mice. Administration of $A_{2A}R$ agonists to obese mice caused improvements in glucose homeostasis and adipose tissue inflammation, suggesting that this may show promise for therapeutic treatment of obesity (DeOliveira et al., 2017).

There is disturbance of adiponectin secretion in obese patients and adiponectin release is controlled by ATP (Yamauchi and Kadowaki, 2013). A combination of Ca^{2+} and ATP augments vesicular release of adiponectin (Komai et al., 2014). Both ATP and adenosine have roles in the regulation of leptin secretion from adipocytes (Szkudelski, 2007). There is abnormal fat distribution in P2X7R KO mice (Beaucage et al., 2014). Manipulation of P2XR signalling may represent a novel therapeutic target in metabolically unhealthy obesity under inflammatory conditions (Pandolfi et al., 2016). There is protection of rats on high fat diet by adenosine (Lee, 2015). Perivascular adipose tissue of heavy smokers has increased expression of P2X7R and inflammasome components leading to increased release of inflammatory cytokines (Rossi et al., 2014).

GUT DISORDERS

Purinergic signalling plays an important role in a variety of gut activities (Liñán-Rico et al., 2015; Burnstock, 2016d; Chaudhury et al., 2016). ATP is a cotransmitter in non-adrenergic, non-cholinergic inhibitory nerves involved in peristalsis, a synaptic transmitter in submucosal and myenteric ganglia, it mediates mucosal secretion and vascular control of the

gastrointestinal tract. Both interstitial cells of Cajal and enteric glial cells express P2R.

Investigations of purinoceptors as therapeutic candidates for gut disorders are underway (Antonioli et al., 2013; Ochoa-Cortes et al., 2014; Burnstock, 2016d).

Inflammatory Bowel Disease (IBD)

Nucleotides and their receptors are involved in the pathogenesis of IBD, of which ulcerative colitis (UC) and Crohn's disease are the main types. $P2Y_6R$ are highly expressed on the T cells infiltrating IBD, suggesting that $P2Y_6R$ may play a role in the pathogenesis of IBD. P2X7R agonists are involved in colonic motor dysfunction associated with bowel inflammation in rats (Antonioli et al., 2014b) and are over-expressed in gut mucosa of patients with IBD. P2X7R KO mice are protected against gut inflammation (Figliuolo et al., 2017b). ATP activates mast cells, which further promote the inflammatory process (Kurashima and Kiyono, 2016). Oestrogen receptor β activation plays a therapeutic role in IBD by down-regulation of P2X3 and P2X7R (Ma B. et al., 2016). The roles of P2X7R in IBD are discussed in reviews (Kurashima et al., 2015; Diezmos et al., 2016).

P2X7R-expressing enteric neurons are differentially affected in UC based on their chemical codes (da Silva et al., 2015). In a later paper, it was shown that UC affected secretory and vasodilatory neurons, enteric sensory neurons and enteric glia of the submucosal plexus expressing P2X7R (da Silva et al., 2017). The P2X7R antagonist, A438079, down-regulated the production of proinflammatory cytokines and attenuated murine colitis, indicating that P2X7R mediate inflammatory responses during UC (Wan P. et al., 2016). Activation of P2X7R triggers the death of mucosal regulatory T cells (Figliuolo et al., 2017b). There was P2XR enhancement in an animal model of UC. MicroRNA-16 and microRNA-206 have pro-inflammatory roles in UC by down-regulating A_{2A} and A_3R expression (Tian T. et al., 2016; Wu et al., 2017).

There is increased expression of P2X7R in the inflamed mucosa in Crohn's disease, suggesting that P2X7R antagonists may be targets for treatment of Crohn's disease (Neves et al., 2014; Eser et al., 2015; Wan P. et al., 2016; Figliuolo et al., 2017b). P2X3R antagonists are being explored as therapeutic agents against colic and UC pain (Eser et al., 2015), as well as antibodies against P2X3R (Deiteren et al., 2015; Diezmos et al., 2016; Shcherbatko et al., 2016).

The potential of P2X3R to treat irritable bowel syndrome has been suggested. In diarrhoea-predominant irritable bowel syndrome there is increased expression of $P2Y_1$ and $P2Y_2R$, which was associated with abdominal pain (Luo Y. et al., 2016). P2X7R in DRG play a role in transmission of the nociceptive signal from the gut (Liu S. et al., 2015). A review about purinergic mediators in the control of intestinal inflammation and irritable bowel syndrome is available (Kurashima et al., 2015).

Motility Disorders

Purinergic signalling is involved in gastrointestinal motility disorders, including diarrhoea and constipation (Jiménez et al., 2014). Purinergic fast inhibitory junction potentials are impaired in Hirschsprung's disease (Jiménez et al., 2015). P2X4 and P2X7R activity was potentiated in enteric glia isolated from mice treated long-term with morphine (Bhave et al., 2017).

A review focuses on the pathophysiological roles of P2YR in inflammation (Wan H.X. et al., 2016). Aged mice have a lower ability to deal with inflammation evoked by *Candida albicans* infection, due to a lower gut density of $A_{2A}R$, which reduce inflammation (Rodrigues et al., 2016).

Colorectal Cancer

Apoptosis is induced by extracellular ATP and ATP also reduced growth of primary cultures of colorectal carcinomas, possibly via $P2Y_2R$ (see Burnstock and Di Virgilio, 2013; Wan H.X. et al., 2016). Purinergic responses of HT-29 cells, a colonic adenocarcinoma cell line, are mediated by $P2Y_2$ and/or $P2Y_4R$. Enhanced expression of $A_{2B}R$ on colorectal cancer cells that are proliferating suggests that antagonists to $A_{2B}R$ may be a promising therapeutic target for colorectal cancer (Ma et al., 2010; Molck et al., 2016). 8-Chloro adenosine inhibited growth of colorectal cancer cell lines 80514 and HCT116 *in vivo* and *in vitro*. A phase II, multi-centre study of CF101, an A_3R agonist, showed stabilisation of tumour in 35% of refractory metastatic colorectal cancer patients. P2X7R antagonists reduce tumour occurrence in a colitis-associated cancer mouse model (Hofman et al., 2015). There is high expression of the ectonucleotidase CD39 in human rectal adenocarcinoma (Zhang et al., 2015a).

DISEASES OF THE KIDNEY

Reviews are available (Burnstock et al., 2014a; Menzies et al., 2017; Oyarzun et al., 2017), including one that focuses on the roles played by ATP released as a cotransmitter from sympathetic nerves in renal diseases (Burnstock and Loesch, 2017).

Purinoceptors are richly expressed in the glomerulus, renal vascular system and nephron in the kidney, including subtypes involved in the regulation of glomerular filtration, renin secretion and transport of nutrients, ions, water and toxins. The distribution of NTPDases 1 and 2 parallels the distribution of P2R in the kidney, influencing physiological and pathophysiological renal events (see Burnstock et al., 2014a). Adenosine and ATP have protective effects against renal ischaemic-reperfusion injury, and have been investigated for transplantation-induced erythrocytosis and chronic renal failure treatment. It has been suggested that nephron luminal P2R are part of an epithelial 'secretory' defence mechanism against harmful particles or bacteria. Increased expression of P2X7R in glomerulonephritis, hypertension, polycystic kidney disease (PKD) and diabetes may be therapeutically relevant as a novel treatment of kidney failure.

Renal Injury and Failure

ATP contributes to kidney remodelling and progression toward chronic renal failure (with associated sympathetic overactivity). P2X7R are expressed weakly in healthy glomerulus, but after glomerular injury (e.g., in hypertension and diabetes) are upregulated, mostly in podocytes, but also in mesangial and

endothelial cells (Vonend et al., 2004). P2X7R play a role in altered intracellular calcium homeostasis in peripheral blood mononuclear cells of chronic kidney disease patients (Lajdova et al., 2012). P2X7R mediate deleterious renal epithelial-fibroblast cross-talk. P2X7R antagonists may be therapeutic targets to prevent and treat morbidity and mortality in kidney injury (Zarjou and Agarwal, 2011). P2X7R antagonists were protective against ischaemic acute kidney injury in mice (Yan et al., 2015). Arterial calcification is a feature in chronic kidney disease patients and ATP signalling is involved (see Fish et al., 2013). Cyclosporine is a potent immunosuppressive agent, but with limitations because of its side effect of nephrotoxicity. However, treatment with ATP following pre-treatment with verapamil greatly reduces nephrotoxicity. ATP is an important contributor to innate immunity regulation in primary idiopathic nephrotic syndrome. There is increased renal fibrosis in P2X4R-deficient mice following unilateral ureteric obstruction (Kim et al., 2014).

Adenosine mediates haemodynamic changes in adult renal failure. A_{2B}R-mediated IL-6 induction contributes to renal fibrogenesis and this receptor has therapeutic potential for treatment of chronic kidney disease (Grenz et al., 2012). Dendritic cells and macrophages activated by A_{2A}R agonists attenuate acute renal injury (Li et al., 2012; Truong et al., 2016). There is a review describing A_{2A}R in acute kidney injury (Vincent and Okusa, 2015).

Polycystic Kidney Disease (PKD)

The genetic disorder PKD results in abnormal proliferation of tubular cells of the adult nephron, leading to progressive dilation of tubules and formation of fluid-filled cysts that destroy by compression neighbouring tissue. In the cysts ATP is released at high concentrations. The *Caenorhabditis elegans* nematode is an animal model for investigating basic molecular mechanisms underlying human autosomal dominant PKD; the *C. elegans* PKD-2 and LOV-1 proteins are homologues of human polycystin (PC)-1 and PC-2 proteins. Nucleotide release is involved in both fluid flow and pressure responses and its role in altered mechanosensory transduction in PKD is considered in a review (Patel and Honoré, 2010).

Cysts in the collecting ducts of the *cpk*/*cpk* mouse model of congenital PKD express P2X7R, where they mediate cyst development. $P2Y_1$, $P2Y_2$, $P2Y_4$, $P2Y_6$, P2X5, and P2X7R were found on the lining epithelial cells of renal cysts in the rat Han:SPRD cy/+ model of autosomal dominant PKD. Expression of mRNA and protein for $P2Y_2$, $P2Y_6$, and P2X7R increased substantially as the disease developed. ATP inhibits renal cyst growth, via P2X7R. The P2X7R antagonists, oxidised ATP and A-438079, reduced cyst formation via extracellular signal-regulated kinase-dependent pathways in a zebrafish model of PKD (Chang et al., 2011). Nucleotides in the lumen fluid of cysts stimulate P2YR resulting in increased growth of Madin Darby canine kidney-derived cysts. Knocking out PKD-1 gene expression increased A_3R in human renal cells (Aguiari et al., 2009). There is a review about the functional and therapeutic importance of purinergic signalling in PKD (Ilatovskaya et al., 2016).

Ischaemia

Proximal tubular ATP declines rapidly in ischaemic acute renal failure. There was early recognition that there was restoration after ischaemia by perfusion of ATP-$MgCl_2$ and A_3R KO mice were shown to be protected against ischaemic renal failure. The ectonucleotidase CD73 protects the kidney from ischaemia-reperfusion injury via production of adenosine and free radical reduction (Jian et al., 2012). The role of adenosine in protection from renal ischaemia-reperfusion injury has been investigated and discussed in reviews (Yap and Lee, 2012; Roberts et al., 2013; Sashindranath et al., 2017).

Nephritis

Glomerulonephritis is one of the leading causes of end-stage renal disease. Increased expression of pro-apoptotic P2X7R has been demonstrated in both experimental and human glomerulonephritis, which suggests that P2X7R antagonists may have therapeutic potential (Deplano et al., 2013). It was shown later that P2X7R-deficiency attenuated renal injury in experimental glomerulonephritis (Taylor et al., 2009). P2X7R blockade attenuates lupus nephritis by inhibiting inflammasome activation (Zhao et al., 2013) and protects against cisplatin-induced nephrotoxicity (Zhang et al., 2014). The P2R antagonist, pyridoxal-phosphate-6-azophenyl-2′,4′-disulfonate (PPADS), effectively inhibits mesangial cell proliferation in a rat mesangial proliferative glomerulonephritis model. Tubuloglomerular feedback is greatly reduced in Thy-1 nephritic rats, but exogenous 5′-nucleotidase improved it. In $P2Y_1$R KO mice, there is protection against fibrosis and death by renal failure as a result of experimental crescentic glomerulonephritis. Adenosine uptake inhibitors attenuated glomerulonephritis in mice. A_{2A}R agonists may treat macrophage-mediated experimental glomerulonephritis. A_{2A}R agonists reduced inflammation in mouse kidneys, suggesting a therapeutic approach for human lupus nephritis.

Hypertension

Hypertension is a feature of chronic renal disease; this is due largely to sympathetic overactivity as a result of afferent signals from the kidney and triggering sympathetic tone resetting by activation of hypothalamic centres (Orth et al., 2001). ATP is a cotransmitter released from sympathetic nerves, whose activity is increased in hypertension.

There is an enhanced P2R-mediated vasoconstriction of both efferent and afferent arterioles in chronic angiotensin II-induced hypertensive rats, with predominant P2X1 and P2X7R control of glomerular haemodynamics (Franco et al., 2017). In connexin 30 KO mice, epithelial sodium channels that are unable to respond to changes in sodium levels as a result of reduced paracrine ATP feedback regulation may play a role in salt-sensitive hypertension. Mice lacking $P2Y_2$R have salt-resistant hypertension. The P2X7R is expressed weakly in healthy kidney glomerulus, but expression is significantly increased in hypertension (Vonend et al., 2004; Menzies et al., 2015). P2X7R antagonists inhibited the development

of renal injury and salt-sensitive hypertension in Dahl salt-sensitive rats (Ji et al., 2012). Activation of A_1R in mouse proximal tubules, modulated deoxycorticosterone acetate-salt hypertension.

Diabetic Nephropathy

Adenosine receptor agonists protect STZ-diabetic rats from nephropathy (Taskiran et al., 2016). A review discusses the role of $A_{2B}R$ antagonists as therapeutic treatment of diabetic nephropathy (Quezada et al., 2013). CD73 generation of adenosine attenuates diabetic nephropathy (Tak et al., 2014). A_3R antagonists reduced fibrosis in diabetic nephropathy (Kretschmar et al., 2016). AMP-activated protein kinase has been proposed as a potential treatment of diabetic nephropathy (Cameron et al., 2016). Chronic $A_{2A}R$ stimulation prevents proteinuria and glomerular damage in experimental diabetes (Persson et al., 2015).

P2X7R agonists evoke renal inflammation and injury induced by high-fat diet in type 2 diabetes, suggesting that P2X7R antagonists might be of therapeutic interest (Solini et al., 2013). P2X7R expression was increased in the STZ diabetic rat model (Vonend et al., 2004). It has been suggested that P2X7R antagonists may be a useful coadjuvant treatment to delay the progression of diabetic nephropathy (Rodrigues et al., 2014). Data has been presented to suggest that activation of P2X7R contributes to the high prevalence of kidney disease found in diabetics (Rodrigues et al., 2014; Menzies et al., 2017). Deletion of the $P2Y_2R$ reduced the development of nephrogenic diabetes insipidus polyuria induced by lithium. Blockade of $P2Y_{12}R$ in the renal collecting duct alleviates nephrogenic diabetes insipidus (Zhang et al., 2015c).

Nephrotoxicant Injury

Drug-induced nephrotoxicity was reduced by ATP-$MgCl_2$. A_1R antagonists are protective against cisplatin-induced acute kidney injury in rats (Gill et al., 2009). Adenosine antagonists are protective against acute renal failure. A_1R antagonists also reduce nephrotoxicity induced by the immunosuppressive agent cyclosporine. Cyclosporine increases plasma adenosine levels in kidney transplant patients. A_3R antagonism is effective against acute tacrolimus toxicity.

Cancer

P2X7R are strongly expressed on human embryonic kidney tumours, associated with increased proliferation (Adinolfi et al., 2012). The anthraquinone, emodin, inhibits human embryonic kidney cancer cell invasiveness by antagonising P2X7R (Jelassi et al., 2013). A prognostic indicator for post-operative cancer-specific survival of clear-cell renal cell carcinoma patients is P2X7R expression (Liu Z. et al., 2015).

DISEASES OF THE LOWER URINARY TRACT

The early literature has been thoroughly reviewed (Burnstock, 2014d; Keay et al., 2014).

Urinary Bladder

In contrast to laboratory animals, where the purinergic component of bladder parasympathetic cotransmission is about 50%, in healthy human bladder it is approximately 2% although ATP receptors are expressed by the smooth muscle. In pathological conditions, however, such as neurogenic bladder, outflow obstruction and interstitial cystitis (IC), the purinergic component can be as much as 40% and is consequently a therapeutic target. Botulinum neurotoxin type A (BTXA) is often used to treat bladder incontinence, where it inhibits ATP release as well as acetylcholine (ACh) release both from parasympathetic nerves and urothelial cells. Bladder epithelial cell release of ATP from patients with IC was substantially higher compared to healthy controls. Dysfunction in micturition involves P2X3R in rats with chronic spinal cord-injury, suggesting that P2X3R antagonists could be used to treat neurogenic bladder dysfunction.

Overactive Bladder (OAB) Syndrome

There are valuable reviews that discuss the roles of purinergic signalling in OAB (Meng et al., 2012; Sacco et al., 2015). OAB syndrome, which increases in old age, is characterised by frequency, nocturia and urgency, with or without urge incontinence. Women with an OAB exhibit higher ATP levels in their urine compared to controls, suggesting that this could be used as a prognostic marker for detrusor overactivity (Cheng et al., 2013; Silva-Ramos et al., 2013). The increased urine ATP concentration is due to increased release of ATP from proliferating urothelium and reduced metabolism of ATP (Silva-Ramos et al., 2013). P2X3R are present in the human bladder and, when upregulated, may play a role in the pathophysiology of OAB.

Patients with metabolic syndrome, where the risk of developing cardiovascular disease and diabetes is increased, exhibit a higher incidence of OAB. P2X3R expression is increased in subepithelial sensory nerves resulting in increased bladder activity. OAB is common among PD patients and inhibition of overactivity by $A_{2A}R$ antagonists occurs, probably by acting in the CNS to regulate the micturition reflex (Kitta et al., 2012). Uridine diphosphate via $P2Y_6R$ regulates abnormal smooth muscle activity in the OAB and increases contractions due to P2X1R activation (Yu W. et al., 2013). $P2Y_6$-deficiency increases micturition frequency and reduces contractility in the mouse urinary bladder (Kira et al., 2017).

Unstable Bladder

Unstable bladder (also referred to as detrusor instability or detrusor hyperreflexia) is either neurogenic or idiopathic in origin. Neurogenic detrusor instability can occur as a result of a stroke, or pelvic or spinal cord injury, as well as in PD and MS. Neurogenic bladders are hyper-responsive to ATP, via P2X3R.

Expression of P2X2R in both urothelium and detrusor muscle of suprasacral spinal cord injury patients are similar to P2X2R expression in bladder tissue from idiopathic overactive bladder patients. ATP levels increased in the rat spinal cord-injured bladder that activates P2X3 and P2X2/3R on afferent nerve fibres resulting in neurogenic bladder overactivity (Munoz et al., 2012).

P2YR agonists ADP, UTP and uridine diphosphate originating in the urothelium augment the contractile overactivity following spinal cord injury. Sympathetic nerve hyperactivity may play a role in reflex sympathetic dystrophy where increased ATP would be released as a cotransmitter to activate P2X1R on smooth muscle resulting in increased contractions of the bladder and P2X3R on sensory nerve fibre terminals resulting in bladder reflexes and nociception. Inhibition of P2X7R expressed at spinal cord injury sites improved the dysfunction of neurogenic bladder (Munoz et al., 2017).

Urothelial cell ATP release (both resting and evoked) was substantially more from rat bladders following chronic spinal cord injury, contributing to bladder hyperactivity development. In a mouse bladder overactivity model, bradykinin facilitated the release of ATP from nerve terminals via prejunctional receptors (Fabiyi and Brading, 2006).

In the absence of P2X3R in KO mice, there is bladder hyperactivity (Cockayne et al., 2000; Vlaskovska et al., 2001). AF-219, a P2X3 and P2X2/3R antagonist that is metabolically stable and orally bioavailable, is being investigated as a treatment for urinary tract dysfunction (Ford and Cockayne, 2011).

Idiopathic detrusor instability patients show abnormal bladder purinergic transmission, which may contribute to the symptoms of OAB (Andersson and Hedlund, 2002; O'Reilly et al., 2002). There is greater potency of ATP via P2X1R for generating detrusor contractions in unstable bladder patients. Urothelial release of ATP from human bladders from patients with detrusor overactivity occurs in both idiopathic and neurogenic conditions (Kumar et al., 2010). Oxybutynin, administered chronically, results in a shift from muscarinic to purinergic transmission in the rat bladder wall. Expression of P2X3R is increased on suburothelial sensory nerve fibres in idiopathic detrusor overactivity patients (Liu H. et al., 2013).

Interstitial Cystitis (IC)/Bladder Pain Syndrome

The possible roles of ATP and adenosine in IC/bladder pain syndrome are discussed in a review (Veselá et al., 2012a). Hypoosmotic mechanical stimulation of urothelial cells released ATP that was substantially increased in cyclophosphamide-induced inflamed bladder (Smith et al., 2005). In rats with cystitis induced by hydrochloric acid, purinergic receptors were lost, although release of ATP from mucosal cells was increased.

Contractions of the rat bladder mediated by parasympathetic nerve stimulation and release of ATP and ACh, were reduced in cyclophosphamide-induced cystitis (Veselá et al., 2012b), while P2XR function in sensory neurons was enhanced. The purinergic component was abolished in the neurogenic bladder following desensitisation with α,β-methylene ATP (α,β-meATP). ATP release due to stretch from bladder urothelium from IC patients was greater compared to healthy urothelium and P2X3R expression was upregulated. Urothelial cells from cats with feline IC responded to α,β-meATP, indicating increased expression of urothelial P2XR. There is mechanical hypersensitivity of the bladder in feline IC together with greater release of ATP from the urothelium; P2X1R expression is reduced and $P2Y_2R$ expression is lost.

A_1R blockade during the initial phase of IC/bladder pain syndrome was suggested as a treatment for this condition (*Aronsson et al., 2012*). The A_1R in rat urinary bladder is decreased in cyclophosphamide-induced cystitis (Veselá et al., 2011).

In neutrophils and macrophages in the submucosa of the bladder from mice with cyclophosphamide-induced haemorrhagic cystitis, expression of P2X7R is increased (Martins et al., 2012). Treatment with A-438079, a P2X7R antagonist, or genetic ablation of this receptor reduced nociceptive behaviour.

Outflow Obstruction

P2X1R expression in smooth muscle of the bladder was increased in the human obstructed bladder. In animal models of outlet obstruction, *in vivo* release of ATP from urothelial cells was increased compared to controls (Akino et al., 2011). Contractions to ATP were reduced in obstructed urinary bladder of rats (Sjuve Scott et al., 2004). There is P2X3R up-regulation in interstitial cells of Cajal in an experimental rat model of partial bladder outflow obstruction (Li et al., 2013). In the pig, partial bladder outlet obstruction resulted in reduced contractions in response to electrical field stimulation as well as to purinergic agonists (Milicic et al., 2006), but in the rat partial outlet obstruction model, contractions to ATP were increased after 2 weeks and 3 months (Murakami et al., 2008). Patients with bladder outflow obstruction release higher amounts of ATP into the urine (Silva-Ramos et al., 2016).

Botulinum Toxin A (BTXA) and ATP Release

BTXA is increasingly being used to treat detrusor overactivity. In an early paper, it was shown that BTXA inhibited ATP as well as ACh release from parasympathetic nerves. Recently, BTX has been shown to inhibit ATP release from the urothelium (Chancellor et al., 2008; Ikeda Y. et al., 2012; Cruz, 2013). Daytime frequency, urgency, nocturia and pain were decreased by injection of BTXA into the human bladder. BTX is used to treat OAB syndrome and bladder hypersensory states (Apostolidis et al., 2005; Atiemo et al., 2005).

Chronic Alcohol Consumption and Bladder Function

Chronic consumption of ethanol impairs purinoceptor-mediated relaxation of detrusor smooth muscle of the rat (Calvert et al., 2002). Ethanol also alters neuronal P2XR.

Diabetic Bladder

Damage to human urinary bladder autonomic nerves and disturbances in micturition in diabetes have been recognised for many years. Urothelial release of ATP has been reported to play a role in bladder dysfunction in type 2 diabetes (Wang Z. et al., 2013). There is a transient increase in sensitivity of the STZ rat whole bladder preparation to α,β-meATP. The cholinergic component of nerve-mediated contractions was reduced in diabetic rat and rabbit bladders, but the purinergic component was increased (Mumtaz et al., 2006).

In STZ mice, the urinary bladder had weaker nerve-mediated contractions in response to electrical field stimulation in contrast to normal mouse bladder. Ca^{2+} regulation of ATP release may be impaired in diabetes. Increased adenosine-

and ATP-mediated relaxant responses, together with increased ATP-mediated contractile responses were observed in bladders from 8-week STZ diabetic rats. The enhanced contractions of STZ-diabetic rat bladders to nerve stimulation and ATP peaked between 6 and 9 weeks, but dropped to control levels by 12–20 weeks (Daneshgari et al., 2006). There is also an increase in release of ATP in STZ female rat bladders (Munoz et al., 2008). There is upregulation of P2X1R in the bladder of STZ-induced diabetes in the early phase, but downregulation of the P2X2R (Liu et al., 2008). Bladder overactivity occurring 2 months after induction of diabetes with STZ was accompanied by enhanced expression of $P2Y_2$ and $P2Y_4R$ (Suadicani et al., 2009).

Bacterial Infection

Bacterial infection of the bladder causes urgency, urinary incontinence and overactivity. Urine ATP concentrations were reduced during episodes of bacteriuria (Walsh et al., 2013). An ATP assay method has been employed for many years to test for bacteriuria in urine.

Bladder Cancer

The growth of bladder cancer cells is reduced by ATP, both *in vivo* and *in vitro* (Shabbir et al., 2008; Shabbir and Burnstock, 2009). Doxorubicin, used to treat bladder cancer, has side effects, such as increased urgency and urinary frequency. Quercetin, a plant-derived flavonoid, prevents bladder cancer in cells lines, by suppressing cell proliferation and inducing arrest of the cell cycle or cell death by inhibiting the activity of ecto-nucleotidases (Rockenbach et al., 2013). In humans with bladder papillary carcinoma urothelial differentiation was correlated with the expression and localisation of P2X3 and P2X5R (Sterle et al., 2014). High CD73 immunoreactivity was associated with reduced bladder tumour progression (Wettstein et al., 2015). P2X7R protein favoured survival of patients with bladder urothelial cell carcinoma (Hu J. et al., 2016).

Bladder Pain

In 1995, P2X3 homomultimer and P2X2/3 heteromultimer receptors were cloned and were localised on sensory nerve endings. Purinergic mechanosensory transduction was proposed (Burnstock, 1999), suggesting that release of ATP from urothelial cells as a result of distension stimulates P2X3 and P2X2/3R on suburothelial sensory nerve endings to activate high threshold nociceptive nerve fibres that reach the cortex pain centres (Burnstock, 2009). Distension of the bladder stimulates discharge in the nociceptive sensory nerves, which can be mimicked by ATP and can be inhibited by P2X3R antagonists (Vlaskovska et al., 2001). Stimulation of bladder P2X3R sensitises bladder afferent nerves, mimicking the sensitising effect of cyclophosphamide-induced cystitis. P2X3R are a potential target for therapeutic treatment of bladder pain. $P2Y_2R$ are also expressed on bladder sensory nerves and are claimed to mediate increased stimulation of P2XR-mediated activity, playing a role in bladder pain syndrome (IC) (Chen et al., 2010).

Urethra

The principal non-adrenergic, non-cholinergic inhibitory transmitter to the urethra is NO, but a small component of purinergic neurotransmission is also involved (Andersson, 2001). ATP causes urethral relaxation, probably via $P2Y_1R$, in pigs, guinea-pigs, rabbits and hamsters. The responses to non-adrenergic, non-cholinergic nerve stimulation were blocked by α,β-meATP, indicating that the P2X1R subtype was involved.

Sensory nerve fibres supplying the urethra may release ATP during axon reflex activity. Prostaglandins, produced following stimulation of P2YR, contribute to contractions of the urethra in pathophysiological conditions. In the rat, SC19220 (a prostaglandin E1 antagonist), lowered detrusor tone leading to increased bladder capacity and decreased voiding efficiency. Some sensory functions in the urethra are mediated by afferent fibres that express P2X3R (Canda et al., 2006). A review that discusses the therapeutic opportunities offered by K_{ATP} channels in the urethra is available (Kyle, 2014).

Ureter

The ureter motor innervation is sparse, perhaps because peristaltic activity is not neurogenic, but myogenic. The dominant nerves in the ureter are sensory, confined mainly to the suburothelial plexus. These nerves contribute to vesicoureteral reflux that activates reflexes that modulate urine delivery to the bladder.

ATP constricts the pig ureter, while intravesical adenosine evoked relaxation via $A_{2B}R$. In the ureter, ATP, α,β-meATP and adenosine evoked transient decreases in the frequency of peristalsis. In the rat ureter expression of P2X1R was shown on smooth muscle, while P2X5 and perhaps P2X7R are expressed on urothelium and P2X6R in the layer beneath the urothelium. P2X3R are localised on subepithelial sensory nerves that mediate nociception produced by release of ATP following distension of urothelial cells (Knight et al., 2002; Rong and Burnstock, 2004). Some ureter purinoceptors are likely to participate in long-term (trophic) events during development and regeneration, such as cell proliferation, differentiation, migration and cell death. The human ureter releases ATP in response to distension and human ureteric suburothelial sensory nerves express P2X3R (Calvert et al., 2008b). In a review of the pharmacology and physiology of the human ureter, it was proposed that purinergic receptors may prove to be analgesic targets to treat ureteral colicky pain and to facilitate ureteral stone passage (Canda et al., 2007).

Seven days after unilateral ureteral obstruction of wild-type mice, it was shown that there was increased expression of P2X7R associated with fibrogenic responses and inflammation in the cortex. However, in P2X7R KO mice, the alterations seen in the wild-type mice were not present. It was suggested that P2X7R antagonists may play a role in preventing renal interstitial fibrosis. In $A_{2A}R$ KO mice with unilateral ureteral obstruction, there was a substantially increased progression of renal interstitial fibrosis (Xiao et al., 2013).

DISEASES OF THE LIVER

In the liver, the two epithelial cell types that secrete bile, i.e., hepatocytes and cholangiocytes, express purinoceptor in the plasma membrane. Modulation of the release of ATP

and purinergic signalling may be novel strategies to manage cholestasis and other bile flow disorders. Both quiescent and activated hepatic stellate cells (HSC) express purinergic receptors: $P2Y_2$ and $P2Y_4R$ on quiescent and $P2Y_6R$ on activated HSC. P2YR on satellite cells could be a therapeutic target to treat or prevent liver fibrosis. Reviews concerned with purinergic signalling in liver disease are available (Burnstock et al., 2014b; Vaughn et al., 2014).

Liver Injury, Inflammation, Immune Regulation and Repair

Purinergic signalling regulates the immune response in the liver. In A_1R KO mice α-naphthylisothiocyanate-induced cholestatic liver injury was decreased. CD39-deficient mice treated with adenosine, probably via $A_{2A}R$, were protected from reperfusion injury (Sun et al., 2011). A_1R antagonists abolished ischaemic preconditioning. After the resection of bile-duct-ligated cirrhotic livers, an $A_{2A}R$ agonist improved liver function (Iskandarov et al., 2016). Inhalation of high concentrations of hydrogen protects against ischaemia/reperfusion injury through $A_{2A}R$ activation (Li H. et al., 2017). Adenosine, via A_{2B} or A_3R, accelerates the cell cycle during partial hepatectomy-induced liver regeneration in rats (Mendieta-Condado et al., 2007). In mice, ATL-146e, a selective $A_{2A}R$ agonist, prevented concanavalin A-induced acute liver injury.

$P2Y_2R$ activation in mice makes a major contribution to endotoxin-induced acute liver injury (Samuel et al., 2010). In mice with acute liver injury, $P2Y_2R$ mediate neutrophil infiltration, regulating immune responses associated with death of hepatocytes. $P2Y_2R$ antagonists might be useful to treat inflammatory liver disease (Ayata et al., 2012). A review discusses the role of purinergic signalling in sterile liver injury (Oliveira et al., 2013).

Infusion of ATP-$MgCl_2$ was shown early to improve hepatic function and survival following hepatic ischaemia and after reperfusion. During ischaemia there is a substantial loss of ATP from hepatocytes. Resistance of hepatocytes to hypoxia is promoted by $P2Y_2R$. In mice, CD39 deletion from natural killer (NK) cells reduced hepatic ischaemia/reperfusion injury, indicating that during liver regeneration ATP modulates NK cell function. UTP acting via $P2Y_2$ and/or $P2Y_4R$ before induction of ischaemia attenuates post-ischaemic hepatocyte apoptosis resulting in a reduction of liver damage (Ben-Ari et al., 2009). Platelet aggregation triggered by ADP may have a role in ischaemia reperfusion injury (Schulte am Esch et al., 2010).

ATP released from sympathetic nerves and from hepatocytes, may participate in the regulation of liver repair. In $P2Y_2R$ KO mice, hepatocellular proliferation is impaired, indicating that ATP has a trophic role in liver regeneration and growth after injury (Thevananther et al., 2008). ATP release following partial hepatectomy in rats regulates liver regeneration. Apyrase (CD39/NTPDase1) reduces extracellular ATP allowing NK cells to play a role in the regulation of the immune response and to improve liver regeneration (Graubardt et al., 2013). After partial hepatectomy, liver regeneration is enhanced by the K_{ATP} opener, diazoxide (Nakagawa et al., 2012).

Hepatocyte lipoapoptosis contributes to hepatic inflammation in lipotoxic liver injury. Pannexin1 may contribute to hepatic inflammation by increasing ATP release in lipotoxic liver injury (Xiao et al., 2012). Acetaminophen (APAP), used to reduce pain and fever, may damage hepatocytes. In mouse APAP-induced inflammation models, full injury following an overdose involved P2X7R activation (Amaral et al., 2013). P2X7R activate hepatic caspase-1 as well as the migration of neutrophils into the liver, suggesting that ATP may play a major role in the development of inflammasomes following overdose of APAP (Hoque et al., 2012). A438079, a P2X7R antagonist, is protective against APAP-induced liver injury (Xie et al., 2013). P2X4R are involved in liver regeneration after partial hepatectomy in mice (Besnard et al., 2016). P2X1R-regulated IL-22 secretion is required for liver regeneration (Kudira et al., 2016).

Fibrosis and Hepatic Stellate Cells (HSC)

Liver fibrosis followed by cirrhosis is a common cause of liver failure. HSC are the main fibrogenic cells of the liver, which express nucleotide receptors that are functional (Kruglov et al., 2007) and mediate phospholipase D activity (Benitez-Rajal et al., 2006).

Adenosine $A_{2B}R$ play pro-fibrotic roles in human HSC (Zhong et al., 2007). During fibrosis, HSC proliferate and undergo senescence and $A_{2A}R$ mediate both these key processes, suggesting that $A_{2A}R$ antagonists are potential antifibrotics (Ahsan, 2011). $A_{2A}R$ contribute to the pathogenesis of hepatic fibrosis and $A_{2A}R$ antagonists may reduce ethanol-induced stellate cell activation and fibrosis (Szuster-Ciesielska et al., 2012; Chiang et al., 2013). MRS1754, an $A_{2B}R$ antagonist, reduced hepatic collagen deposition during fibrosis progression (Stoll et al., 2012).

Activation of $P2Y_2$ and $P2Y_6R$ regulates procollagen-1 transcription and may be targets to treat or prevent liver fibrosis, thereby avoiding cirrhosis and chronic liver failure. PPADS, a P2R antagonist, inhibited HSC proliferation and prevented the development of non-biliary liver fibrosis (Dranoff et al., 2007). NTPDase2 is a preferential ATPase that greatly influences inflammation and biliary type fibrogenesis. Ecto-5′-nucleotidase (CD73) gene expression in HSC and portal fibroblasts increased during myofibroblastic differentiation and is a therapeutic target for antifibrotic therapy (Fausther et al., 2012).

Human platelet ATP release contributes to reduced type I collagen production and HSC activation *in vitro* (Ikeda N. et al., 2012). In progressive fibrosis, eicosapentaenoic acid replenishes hepatic levels of ATP leading to a reduction of steatosis and inflammation (Jia et al., 2012). Blockade of the P2X7R-NLRP3 inflammasome axis is considered to be a potential therapeutic target for liver fibrosis (Jiang et al., 2017).

Cirrhosis

Liver injury induced by alcohol is associated with enhanced inflammatory responses and adenosine, acting via $A_{2A}R$, may prove to be an effective strategy for reducing liver injury (Pritchard et al., 2011). During fulminant hepatitis, $A_{2A}R$ contribute to the anti-inflammatory actions that limit liver damage (Choukèr et al., 2008). In cirrhosis, platelet dysfunction

is partly mediated by purinergic signalling. Cerebral A_1R are involved in liver cirrhosis (Boy et al., 2008). Ectonucleotidase NTPDase 2 is down-regulated in biliary cirrhosis. It has also been claimed that endogenous A_1R activation may protect mice against liver injury induced by acute ethanol by reducing oxidative stress and decreasing the accumulation of lipid (Yang et al., 2013). ATP-$MgCl_2$ was used early to improve survival following massive hepatectomy in cirrhotic rats and adenosine partially reversed cirrhosis induced by carbon tetrachloride. In alcoholic liver disease, ATP and uric acid mediate inflammatory cross-talk between immune cells and hepatocytes (Petrasek et al., 2015). $A_{2A}R$ are involved in the pathogenesis of hepatic cirrhosis (Chan et al., 2006).

Hepatitis

In vitro infection by duck hepatitis B virus, *Rous sarcoma* virus, and hepatitis delta virus was inhibited by suramin. Sympathetic nerves influence immune-mediated experimental hepatitis (Neuhuber and Tiegs, 2004) and ATP released as a cotransmitter with NA is probably involved. In autoimmune hepatitis P2X7R regulate NKT cells (Kawamura et al., 2006). P2X7R activation participates in hepatitis delta and hepatitis B virus infection of human hepatocytes (Taylor and Han, 2010). Leptin-induced GLUT4 function in stellate cells in non-alcoholic steatohepatitis is mediated by P2X7R (Chandrashekaran et al., 2016). Chronic hepatitis C virus infection evokes progressive liver disease, exhibiting cirrhosis, insulin resistance, fibrosis and finally liver cancer. P2X4 and P2X7R may be a major component of the purinergic signalling complex in hepatitis C virus-induced liver pathogenesis (Manzoor et al., 2016). In rats, $A_{2A}R$ stimulation inhibited hepatocyte lipotoxicity and non-alcoholic steatohepatitis (Imarisio et al., 2012). Adenosine, via $A_{2A}R$, controls NKT-cell-dependent hepatitis induction (Subramanian et al., 2014). Purinergic mechanisms involved in autoimmune hepatitis have been reviewed (Kapila et al., 2013).

Liver Transplantation

Human liver can be maintained successfully under hypothermic conditions for a maximum of 10 h using adenosine at high concentrations, although overcoming ischaemic damage is a major obstacle. However, infusion of ATP can preserve cells injured sublethally by enhancing their recovery following ischaemic injury and purinergic receptor antagonists prevent cold preservation-induced cell death. Upregulation of CD39 post-adenoviral infection prolongs transplant graft survival. After transplantation regeneration of the donor liver is important and ATP, via $P2Y_2R$, activates hepatocyte cell cycle progression and proliferation *in vitro* and modulates growth factor activities *in vivo* (Thevananther et al., 2004). $A_{2A}R$ stimulation down regulated adhesion molecules, proinflammatory cytokines and ultimately improved liver function following liver transplantation in rats (Tang et al., 2010). In post-transplant allografts, purinergic signalling is used to predict as well as monitor progression of fibrosis and rejection. Blood from acute rejection patients showed raised intracellular levels of ATP in $CD4^+$ lymphocytes (Qu et al., 2017).

Liver Cancer

Primary liver malignant tumours are subdivided in to hepatocarcinoma, bile duct carcinoma (cholangiocarcinoma) and hepatocholangiocarcinoma. ATP increases calcium uptake by rat hepatoma cells, probably via $P2Y_2$ or $P2Y_4R$ subtypes. There is upregulation of $P2Y_2R$ in human hepatocellular carcinoma cells (Tak et al., 2016), which mediates proliferation and migration of the cells (Xie et al., 2014). Carcinoma-specific expression of $P2Y_{11}R$ make a major contribution to ATP-induced signalling that controls cell migration in human hepatocellular carcinoma cells (Khalid et al., 2017). CD39 KO mice showed an increased incidence of spontaneous and induced hepatocellular carcinoma. Intra-arterial injection of an inhibitor of ATP production was suggested as a novel liver cancer therapy. The effects of ATP infusions *in vivo* on rat hepatocarcinomas have been investigated (Frontini et al., 2011). P2X3R over-expression is involved in poor recurrence-free survival in hepatocellular carcinoma patients and identifies the P2X3R as a potential therapeutic target (Maynard et al., 2015). Inhibition by adenosine of hepatoma cell growth was reported early.

The A_3R agonist, CF101, inhibited liver metastasis (following colon carcinoma) (Bar-Yehuda et al., 2008). CF102, another selective A_3R agonist, has anti-inflammatory and anti-tumour effects on the liver and was studied in a clinical trial for hepatocellular carcinoma patients (Stemmer et al., 2010). $A_{2B}R$ are strongly expressed in human hepatoma cellular carcinoma (Xiang et al., 2006). Mouse regulatory T cell CD39 expression mediated inhibition of NK cell activity and promoted hepatic metastatic tumour growth (Sun et al., 2013). Liver metastasis from colorectal cancer is one of the main causes of cancer-related morbidity and ATP-chemotherapy may effectively treat initially unresectable colorectal liver metastasis (Hur et al., 2012). In hepatocellular carcinoma, up-regulation of ATP-binding cassette transporter genes is mediated by cellular microRNAs (Borel et al., 2012).

DISEASES OF THE REPRODUCTIVE SYSTEM

Reviews are available about purinergic signalling in the reproductive system in both health and disease (Burnstock, 2014c; Gorodeski, 2015).

Disorders of the Male Reproductive Tract

Erectile Dysfunction

Abnormalities in purinergic signalling, including impaired ATP-mediated cavernosal relaxation, may contribute to erectile dysfunction associated with prostate enlargement and diabetes and may provide a target for therapy (Hupertan et al., 2012; Wen and Xia, 2012). Normal penile erectile function involves a fine balance between contraction and relaxation in the corpus cavernosum smooth muscle. The strong relaxation induced by ATP via P2YR on human corpus cavernosum is comparable to that produced by NO, thus ATP together with an NO donor may prove to be effective for erectile disorders (Hupertan et al., 2012). ATP released from sympathetic nerves leads to relaxation

of cavernosum smooth muscle via $P2Y_4R$, whereas ADP, after breakdown of ATP released from endothelial cells, acts via $P2Y_1R$ on endothelial cells to produce relaxation via NO (Calvert et al., 2008a). P2XR might also be involved (Gur et al., 2007; Phillips et al., 2014).

In anaesthetised dogs, ATP and adenosine induce penile tumescence, probably via A_2R; pelvic nerve stimulation also produced tumescence. Impaired adenosine signalling via A_1R contributes to erectile dysfunction (Ning et al., 2012a). Elevated adenosine signalling, via $A_{2B}R$, may contribute to priapism, where there is persistent penile erection lasting at least 4 h without sexual excitation (Dai et al., 2009; Ning et al., 2012b). A review highlights adenosine signalling in penile tissue as a potential therapeutic target to treat erectile disorders (Wen and Xia, 2012). Impaired erectile function occurs in CD73 KO mice resulting in decreased endogenous adenosine. Corpus cavernosum from men suffering from vasculogenic erectile dysfunction show lower ectonucleotidase CD39 activity resulting in ATP accumulation. Human corpus cavernosum relaxation by P2R agonists was substantially reduced in erectile dysfunction patients (Faria et al., 2010). ATP release from cavernosal tissue increased in patients following prostatectomy. Activating ATP-mediated pathways may restore erectile function in diabetics where there is impaired NO bioavailability. It has been suggested that P2X3 antagonists may improve recovery of erectile function (Li C.L. et al., 2015).

Male Fertility and Contraception

ATP increases the fertilising potential of sperm in humans and is used to treat spermatozoa during *in vitro* fertilisation. In P2X1R KO mice fertility was diminished with decreased number of spermatozoa in the ejaculate (Mulryan et al., 2000). This raises the possibility that P2X1R antagonists would provide a safe and effective contraceptive (White et al., 2013). In rat testes, during spermatogenesis there is differential, stage-dependent immunostaining for P2XR subtypes (Glass et al., 2001), suggesting purinergic targets for both fertility and contraception. ATP triggers the acrosome reaction via P2X7R in human spermatozoa (Torres-Fuentes et al., 2015). Purinergic signalling plays a role in the maturation of sperm cells in the testes. When the selective P2X1 and P2X3R desensitiser, α,β-meATP, was injected into the cauda epididymis, fertility in male rats was impaired. Adenosine stimulates human sperm motility via A_2R.

Prostatic Hyperplasia

Purinergic compounds have been suggested for the therapeutic treatment of benign prostatic hyperplasia (Andersson et al., 2002). Injection of BTX into the prostate, which reduces ATP and ACh release, treats bladder obstruction hyperactivity, by decreasing prostate size and as such improving urine flow rate (Chuang and Chancellor, 2006).

Disorders of the Female Reproductive Tract

Regulating the proliferation of ovarian granulosa cells as well as steroidogenesis contributes to ovarian pathophysiology, since in rats with polycystic ovarian syndrome, theca hyperplasia occurs (Salvetti et al., 2009). The hydrolysis of ADP and ATP was reduced by ovariectomy and oestradiol replacement therapy (Pochmann et al., 2004). Ovarian tumours arise largely from the surface of squamous-to-cuboid mesothelium covering the ovary. ATP stimulated mitogen-activated kinase in neoplastic and pre-neoplastic surface epithelium, suggesting that co-released ATP from sympathetic nerves may contribute to the regulation of cell proliferation in neoplastic epithelial cells from the surface of the ovary (Choi et al., 2003).

In the human fallopian tube, ATP-mediated contractions are increased during acute purulent inflammation, probably as a result of upregulation of P2X1 and P2X2R (Ziganshin et al., 2008). It has been claimed that targeting P2X7R may lead to new treatments to prevent uterine contractions in preterm deliveries. A naturally occurring P2X7 splice variant, the P2X7jR, blocks P2X7R-mediated actions (Feng et al., 2006). It is co-expressed with P2X7R in female reproductive tract epithelia. The P2X7j isoform hetero-oligomerises with the P2X7R and co-expression of P2X7R and P2X7jR blocks ATP-induced pore formation, and abolishes agonist-induced apoptosis. $P2Y_2R$ agonists may be a non-hormonal alternative therapy for treating vaginal dryness in post-menopausal women. ATP is considered as a therapeutic target to control uterine activity during difficult labours (Zafrah and Alotaibi, 2017).

The P2X7R contributes to the control of cervical infections. P2X7R-mediated activation of cervical epithelial cells inhibits *Chlamydia* and mycobacteria infection (Darville et al., 2007). ATP regresses endometriosis in a rat model (Zhang C. et al., 2016). Adenosine in the placenta mediates the placental disturbances induced by alcohol, perhaps contributing to the pathogenesis of foetal alcohol syndrome (Acevedo et al., 1997). Adenosine protects vaginal epithelial cells from *T. vaginalis* cytotoxicity (Menezes and Tasca, 2016). Plasma adenosine is raised in hyperemesis gravidarum (severe morning sickness) and serves as a prejunctional modulator of sympathetic neurotransmission, which limits further progression of this pregnancy-related disease (Yoneyama et al., 2004).

Preeclampsia

ATP infusion in pregnant rats involved an inflammatory response that occurs in preeclampsia (Spaans et al., 2014a). Elevated placental adenosine signalling contributes to the pathogenesis of preeclampsia (Iriyama et al., 2015). Hypoxia stimulates ATP release, which is rapidly broken down to adenosine by ectonucleotidases and women with preeclampsia and their foetuses have increased circulating adenosine concentrations. There is elevation of adenosine $A_{2A}R$ expression in placental biopsies, villous explants and placental microvillous membranes (von Versen-Höynck et al., 2009). In preeclampsia $A_{2B}R$ on microvascular endothelial cells have also been implicated (Escudero et al., 2008). Reduced adenosine-mediated angiogenesis in preeclamptic pregnancies may be associated with hypertension development in the offspring (Escudero et al., 2014). The interaction between $A_{2A}R$ and the angiotensin system may be involved in the early growth of the placenta. $A_{2A}R$ expression is raised in pre-eclampsia, perhaps

as a consequence of poor placental perfusion in preeclampsia (Kurlak et al., 2015). Elevation of ADA activity in women with preeclampsia may contribute to their increased levels of uric acid and pro-inflammatory immune activity (Giorgi et al., 2016). Release of ATP increases in preeclampsia following hypoxia and oxidative/nitrative stress, which acts on P2X4R to influence homeostasis of the placenta (Roberts et al., 2007). There is deficient spiral artery remodelling and trophoblast invasion in preeclampsia, both of which may be inhibited by ATP-induced activated macrophages (Spaans et al., 2014b). It was concluded from a study of the relationship between the foeto-placental adenosine release and utero-placental circulatory insufficiency in pregnancies featuring preeclampsia, that foetal plasma adenosine increases before utero-placental insufficiency induces generalised foetal hypoxia (Yoneyama et al., 1996).

Malignant Cancer of Reproductive Organs

Prostate Cancer

Prostate cancer is the second most common male cancer and the third leading cause of cancer death. Prostate cancer cells are sensitive to extracellular ATP. ATP and adenosine inhibit the growth of human prostate cancer cells (Lertsuwan et al., 2017), identified at that time to act via $P2Y_1$, $P2Y_2$ and/or $P2Y_4$, $P2Y_6$ and $P2Y_{11}$R subtypes. Activation of $P2Y_1$R inhibited growth and induced cell death of prostate cancer PC-3 cells and $P2Y_1$R agonists were claimed to be therapeutically promising for prostate cancer (Wei et al., 2011).

However, prostate tumour cells were shown later to also express P2X4, P2X5, and P2X7R in PC-3 cells and P2X4 and P2X5R in DU145 cells. ATP inhibited tumour cell growth, but not by UTP or adenosine, while 2′(3′)-*O*-(4-benzoylbenzoyl) ATP increased apoptotic cell death in PC-3 cells, probably via P2X7R. CD73 KO mice resist prostate carcinogenesis and CD73 promoted *de novo* prostate tumorigenesis. Anti-CD73 monoclonal antibodies decreased tumour growth and metastasis in the prostate (Stagg et al., 2012).

There are many polymorphisms of the P2X7R (Fuller et al., 2009), which, as well as resulting in loss of function, alter receptor activity. Cytolytic P2X7R expression was found in 116 prostate cancer pathology specimens (Slater et al., 2004). In normal tissues from patients with no evidence of cancer, P2X7R were not expressed, suggesting that the appearance of P2X7R is an early marker of prostate cancer.

Prostate tumour cell proliferation is inhibited by adenosine. A_3R activation by IB-MECA inhibited proliferation of prostate cancer cells and induced cell cycle arrest and apoptosis (Aghaei et al., 2012). Activation of A_3R suppressed prostate cancer metastasis (Jajoo et al., 2009). The ATP synthase β subunit also plays a role in prostate cancer metastasis (Li W. et al., 2017).

Breast Cancer

Inhibition of growth of human breast cancer cells by ATP was shown for the first time in 1993. Chemotherapeutic ATP release from breast tumour cells of mice increased tumour regression through apoptosis and it was suggested that $P2Y_2$ and/or $P2Y_4$R were involved. Oestrogen, acting via oestrogen receptor α, promoted proliferation of breast cancer cells by down-regulating expression of $P2Y_2$R and reducing $P2Y_2$R-induced increase in $[Ca^{2+}]_i$ (Li et al., 2011). $P2Y_2$R activation by ATP released from cancer cells induces the invasion of metastatic breast cancer cells (Eun et al., 2015). Up-regulation of $P2Y_6$R occurs in the mesenchymal phenotype of breast cancer cells and inhibition of $P2Y_6$R may be a useful therapeutic target for metastasis of breast cancer (Azimi et al., 2016; Ma X. et al., 2016).

Antibody therapy with anti-CD73 inhibited breast tumour growth and metastasis (Stagg et al., 2010). Bisphosphonates are also effective inhibitors of breast cancer (Fehm et al., 2012). Proteomic analysis of human breast carcinoma revealed upregulation of ATP synthase in tumours and the ATP synthase inhibitor, aurovertin B, inhibited proliferation of several breast cancer cell lines (Huang et al., 2008). Malignant breast carcinoma cells release ATP making the pre-metastatic environment suitable for micro-metastasis in lymph nodes and associated afferent lymph vessels (Kawai et al., 2008).

In breast tumour cells ATP increased $[Ca^{2+}]_i$ and high concentrations produced apoptosis via P2X7R. Activation of P2X7R in the human breast cancer cell line, T47D, increased cell migration and development of metastases, suggesting that P2X7R antagonists may have therapeutic roles (Xia et al., 2015). The role of hypoxia in the regulation of tumour progression has been debated. However, P2X7R expression is increased by hypoxia and hypoxia-driven increase in P2X7R enhances tumour cell invasion and migration. Silencing of P2X5R inhibited cell proliferation and may be a new mechanism to target cancer metastasis.

A_1 and A_3R mRNA are expressed on human breast tumours (Panjehpour et al., 2012). Adenosine induces tumour cell proliferation and migration of T-47D and MCF-7 breast carcinoma cell lines (Mujoomdar et al., 2004). MDA-MB-231, a human breast cancer cell line, expressed A_{2B}R, which mediated cell proliferation and A_{2B}R inhibition slowed growth of breast tumours (Cekic et al., 2012). A_3R agonists reduced bone metastasis of breast cancer, suggesting a therapeutic approach to bone-residing breast cancer (Varani et al., 2013).

Cervical Cancer

HeLa cells from human cervical cancer are used to study purinergic signalling involvement in cancer. Activation of $P2Y_2$ R with UTP and ATP caused proliferation of HeLa cells. $P2Y_4$ and $P2Y_6$ R expression increased during proliferation. Stimulation of $P2Y_1$R on HeLa cells triggered epidermal growth factor receptor mitogen signalling and $P2Y_1$ antagonists reduced proliferation. Permeabilisation of cervical cancer cells to a cytotoxin is activated by P2YR (Bukhari et al., 2015). $P2Y_6$R activation induces HeLa cell migration (Gendaszewska-Darmach and Szustak, 2016). Oestrogen reversed the apoptotic activity mediated by P2X7R in normal human cervix, but not in cervical epithelial cancer cells. A truncated P2X7R variant (P2X7-j), expressed in cervical cancer cells, antagonised the P2X7R through hetero-oligomerisation. Gentle mechanical stimulation released ATP from HeLa cells. The presence of ectonucleotidase in human cervical cancer cell regulates the levels of nucleotides, limiting their effects (Beckenkamp et al., 2014).

Ovarian Cancer

ATP raised $[Ca^{2+}]_i$ and stimulated growth of SKOV-3 and OVCAR-3 human ovarian carcinoma cells. ATP may act as a messenger to control the ovarian epithelial cell cycle through $P2Y_2R$ on human ovarian cancer cells. A_2R antagonists inhibited angiogenic activity of human ovarian cancer cells. The treatment of human ovarian carcinoma with cisplatin in the presence of ATP results in additive cytotoxicity (Rotte et al., 2010). P2X7R were highly expressed in both human ovarian tumours and ovarian cancer cell lines and paracrine release of ATP acts on P2X7R to cause proliferation of ovarian cancer cells (Vazquez-Cuevas et al., 2014).

Uterine Cancer

$P2Y_2R$ play a role in the control of the cell cycle and in the suppression of proliferation of human endometrial carcinoma cells. The P2X7R has been used as a biomarker for uterine epithelial cancers. There is decreased P2X7R expression on endometrial epithelium in pre-cancerous and cancer cells (Li et al., 2007, 2009). Activation of P2X7R-dependent apoptosis has a chemotherapeutic growth-preventive effect on pre-cancerous and early cancerous epithelial lesions (Fu et al., 2009; Gorodeski, 2009). Loss of CD73 in endometrial cancer allows for tumour progression (Bowser et al., 2016). A higher proportion of ADA2*1/*1 genotype was observed in women with uterine leiomyomas (Gloria-Bottini et al., 2016).

SKIN DISEASES

Reviews about purinergic signalling in the skin during health and disease have been published (Burnstock et al., 2012b; Geraghty et al., 2016). Changes in P2R subtype expression occurs in the epidermis during proliferative disorders, such as psoriasis and scleroderma, and $P2Y_2R$ may be a novel target to treat these disorders. ATP plays an important role in wound healing, the defence response, innate immunity and inflammation in the skin and might be an important therapeutically in psoriasis and scleroderma.

Psoriasis

Psoriasis is a chronic skin disease involving epidermal hyperproliferation. ATP and parathyroid hormone-related protein increased proliferation in HaCaT cells and may account for the hyperproliferation that occurs in psoriasis. $P2Y_2R$ contribute to epidermal homeostasis and indicate a possible therapy for psoriasis. $P2Y_{11}R$ mediate IL-6 production in human keratinocytes, which is important in psoriasis (Ishimaru et al., 2013). P2X7R signalling induces inflammation leading to differentiation of Th17 lymphocytes, which are involved in the pathogenesis and potential treatment of psoriasis (Killeen et al., 2013). P2X7R play a role in shaping the inflammatory microenvironment in psoriasis (Lioi et al., 2015). Strong P2X7R expression is confined to the basal layer cell membrane, while $P2Y_1R$ were expressed all through the psoriatic epidermis.

In the blood of psoriasis patients, there are high levels of adenosine. Adenosine raised cyclic AMP levels in lesions of epidermis from psoriasis patients. There is a defective purine nucleotide synthetic pathway in patients with psoriasis and nucleotide metabolism is altered in psoriatic keratinocytes. In psoriasis patients, ADA levels were significantly elevated in both serum and epidermis. It was concluded from a clinical trial that caffeine, a P1R antagonist, is an inexpensive, safe and effective treatment for psoriasis. The role of adenosine as an endogenous mediator of the pathogenesis of psoriasis has been reviewed (Festugato, 2015) and clinical trials for the use of A_3R agonists for the treatment of psoriasis described (Borea et al., 2015; Kofoed et al., 2015). $A_{2A}R$ are upregulated in psoriasis and $A_{2A}R$ agonists may counteract inflammation in this disease (Merighi et al., 2017). $A_{2B}R$ are also expressed by human epidermal keratinocytes and their expression is reduced in psoriasis (Andrés et al., 2017).

Scleroderma

Scleroderma encompasses a spectrum of disorders that cause dermal fibrosis and systemic sclerosis (SSc). SSc is a severe disease of the connective tissue of affected organs, including the skin. Adenosine $A_{2A}R$ contribute to the pathogenesis of dermal fibrosis and may be a therapeutic target to treat and prevent dermal fibrosis in scleroderma (Chan and Cronstein, 2010). Fibroblasts from SSc patients had a high rate of spontaneous IL-6 release, which was increased by ATP stimulation. SSc fibroblasts expressed mRNA for P2X3, P2X4, P2X7, $P2Y_1$, $P2Y_2$, $P2Y_4$, and $P2Y_6$, suggesting a possible therapeutic role for P2R antagonists in SSc patients via modulation of fibroblast function.

Skin Inflammation

The skin is an immune defence organ. Chemical, immune-specific or physical insults evoke increased expression of proinflammatory mediators, in particular keratinocytes release chemokines. Release of ATP is associated with inflammation of the skin, as well as increase in expression of, in particular, P2X7 and perhaps $P2Y_1R$, and subsequent release of proinflammatory cytokines. Skin inflammation is reduced by P2X7R antagonists.

In ectonucleotidase (CD39) KO mice, rapid ATP release from keratinocytes is triggered by irritant chemicals causing exacerbated skin inflammation. Ultraviolet (UV) radiation evokes ATP release from keratinocytes and $P2Y_6R$ mediate UV radiation-induced inflammatory responses (Takai et al., 2011). ATP, when released after trauma or infection, may enhance immunoresponses and P2R agonists may increase vaccine efficacy. A_1 and A_2R may function as cutaneous neurogenic pro-inflammatory mediators. Human skin keratinocytes infected by *Staphylococcus aureus*, which releases α-toxin, exhibited a transient reduction in cellular ATP levels (Suriyaphol et al., 2009). P2X3 and P2X2/3 nociceptive receptors on sensory nerve endings are increased in inflamed skin and antagonists to these receptors have been developed as analgesics.

Wound Healing

Topically applied A_{2B} and particularly $A_{2A}R$ agonists promote cutaneous wound healing in both healthy and diabetic conditions. $A_{2A}R$ agonists also promote collagen production by

dermal fibroblasts. Adenosine inhibits proliferation of vascular smooth muscle cells via A_2R activation. A review discusses the involvement of A_{2A} and $A_{2B}R$ signalling in wound healing and fibrosis (Shaikh and Cronstein, 2016).

ATP and ADP also play a role in wound healing. ATP, released by damaged cells and physiologically during gentle mechanical stimulation, contributes to wound healing, tissue repair and regeneration. Cutaneous wound healing is accelerated by Mg-ATP, probably by increasing synthesis of vascular endothelial growth factor. Release of ATP from platelets and other cells during wound healing results in an increase in $[Ca^{2+}]_i$ in keratinocytes, associated with epidermal growth and differentiation. ATP improves ischaemic skin flap survival after surgery, while P2R antagonists accelerate barrier repair.

There is acute inflammation in the initial phase of wound healing. ATP is involved in the development of inflammation through P2X7R-mediated production and release of cytokines from immune cells. The presence of P2X7R on immune cells mediates killing of intracellular pathogens by stimulating apoptosis of the host macrophage, chemo-attraction and cell adhesion. In contrast, adenosine has anti-inflammatory effects. ATP released following infection and trauma acts as an endogenous adjuvant to increase the immune response and P2R agonists may enhance the efficacy of vaccines.

Wound healing also involves new vessel growth (angiogenesis) and both ATP and adenosine contribute to cell proliferation and migration during angiogenesis. In cultured porcine artery smooth muscle cells, ADP and ATP stimulate DNA synthesis and cell proliferation. ATP and UTP are mitogenic in human vascular smooth muscle cells and $P2Y_2$ and $P2Y_4R$ might be involved.

Wound healing is delayed in denervated wounds. In a rat model of this, P2X5, P2X7, $P2Y_1$, and $P2Y_2R$ expression was altered in the epidermis. $P2Y_1R$ expression was increased in the basal proliferating layer of keratinocytes in the regenerating epidermis, while $P2Y_2R$ were significantly decreased. ATP and UTP, probably via $P2Y_2R$, increased proliferation of the MCS-P5 murine keratinocyte cell line, and enhanced wound healing in mice (Kehasse et al., 2013; Jin et al., 2014). ATP release and P2YR signalling mediate electric field-stimulated directional keratinocyte migration (Riding and Pullar, 2016). A review discussed the clinical applications of purinergic compounds to enhance wound healing (Gendaszewska-Darmach and Kucharska, 2011).

Warts

Warts are caused by human papillomavirus infection of epidermis basal keratinocytes. P2X5R staining was increased in warts. P2X7R immunoreactivity was found in hyperkeratotic areas of the stratum corneum and in nuclei of koilocytes in the wart suprabasal layers. The nuclei positive for P2X7R were shrunken, showing much more intense P2X7R staining. The expression of P2X7R in the nucleus of human papillomavirus-infected cells was associated with disruption of the cellular machinery. P2X7R agonists may be used to trigger apoptosis in these virally infected cells. P2X5 and P2X7R are being explored for the treatment of warts.

Allergy

Contact allergen sensitisation involves immune system activation by endogenous danger signals. P2X7R KO mice exhibit resistance to contact hypersensitivity. P2X7R KO dendritic cells do not induce sensitisation in response to contact allergens or release IL-1β in response to ATP. This suggests that P2X7R are crucial for release of ATP from skin in response to contact allergens. Interference with P2X7R signalling could be a therapeutic approach to prevent allergic contact dermatitis.

Hailey–Hailey and Darier Diseases

These are autosomal dominant skin disorders and are characterised by epidermal keratinocyte dissociation (acantholysis) at the epidermis suprabasal layer. In lesions $P2Y_2R$ are not localised on acantholytic cells, but P2X7R appear in the plasma membranes, potentially mediating apoptosis.

Barrier Function

The skin protects the water-rich internal organs from environmental dryness, with the stratum corneum being critical to the water-impermeable barrier. Topical application of ATP and α,β-meATP via P2XR delayed barrier recovery, damaged by surfactant, organic solvent or tape stripping. P2R antagonists, however, accelerated barrier repair. In mice skin wounds healed faster following treatment with ATP-encapsulated fusogenic lipid vesicles rather than with lipid vesicles. PPADS, a P2XR antagonist, accelerates skin barrier repair and prevented epidermal hyperplasia.

Burns

There is increased concentration of adenosine in burn blister fluid, and depletion of ATP in skin after thermal injury. ATP has a protective effect against skin burns. ATP-$MgCl_2$ administration following burn injury reversed the damage to the intravascular clearing of lipid emulsions within the reticuloendothelial immune system. Glucose metabolism was affected by ATP in thermally injured skin.

Burn injury produces severe pain and the relieving effects of tetramethylpyrazine, a Chinese medicine, are claimed to be due to it acting as a P2X3R antagonist (Gao Y. et al., 2010). Skin P2X3R expression was increased on sensory nerve terminals in first and second degree burns, but, following treatment with tetramethylpyrazine, P2X3R expression was reduced. P2X3R may play a role in the short-lasting thermal hyperalgesia induced by mild heat injury (Füredi et al., 2010). After a superficial skin burn, adenosine reduced the skin area showing hypersensitivity.

Pain

Skin pain is associated with changes in sympathetic nerve activity and ATP released from rat sympathetic nerves as a cotransmitter with NA may modulate cutaneous nociceptors. P2X3R are expressed on sensory neurons in DRG, nodose and trigeminal ganglia that innervate cutaneous tissues. ATP and ADP stimulate skin afferent nerve terminals and skin cell damage stimulates nociceptive sensory nerves via ATP release. In rat skin with carrageenan-induced inflammation, nociceptors can be

selectively activated with α,β-meATP, indicating the involvement of P2X3R. ATP contributes to the enhanced sensitivity of inflamed skin nociceptors, leading to heat hyperalgesia. P2X3R antagonists are anti-nociceptive. UV light evokes hypersensitivity of skin to ATP-induced pain. After subcutaneous bee venom injection, there is reduction of prolonged pain by PPADS, and it was suggested that stimulation of P2XR in the spinal cord contributes to cutaneous pain. The terminals of nociceptive neurons in the skin are targets for P2X3R antagonists. UTP sensitises a subpopulation of cutaneous C-fibre nociceptors to mechanical stimuli. There is increased P2X3R expression on calcitonin gene-related peptide-positive sensory fibres during the growth of tumours, mediating nociception. Increased expression of skin glial cell neurotrophic factor increases the mechanical sensitivity of nociceptive afferents expressing P2X3R.

Ecto-5′-nucleotidase (CD73) is located on nociceptive terminals and epidermal keratinocytes in the epidermis, which, by hydrolysing AMP to adenosine, is suggested to be anti-nociceptive. Blockade of peripheral $P2Y_1R$ prevents thermal hyperalgesia (Kwon et al., 2014). Mechanical allodynia is induced by α,β-meATP, which sensitises P2X3R on cutaneous nociceptive sensory fibres (Ren et al., 2015).

Reviews with coverage of purinergic signalling and cutaneous pain are available (Zhu and Lu, 2010; Burnstock, 2016c).

Dermatitis

In irritant dermatitis, there is a pathogenic role for keratinocyte-derived ATP. The necrosis produced by the chemical irritant croton oil was prevented by the pre-treatment with A438079, a selective P2X7R antagonist (Zanin et al., 2015). Topical application of A_{2A} antagonists prevents radiation dermatitis (Perez-Aso et al., 2016).

Skin Cancer

Different subtypes of P1R and P2R are involved in skin cancer, playing roles in differentiation, apoptosis and proliferation. The roles of purinoceptors are complicated because there are multiple receptor subtypes on the same cell, which can have opposing effects. For example, $P2Y_2R$ mediate an increase in tumour cell numbers, while $P2Y_1$, P2X5, and P2X7R mediate a decrease in cell numbers. In cancers of the skin, proliferation outweighs apoptotic cell death.

UV light is a stimulus for the genesis of cutaneous cancer, including basal and squamous cell carcinoma as well as melanoma, where the UV-B component has the most severe effects. UV-B irradiation decreases the amount of P2X1, $P2Y_2$, and P2X7R, which contributes to the malignant transformation of keratinocytes (Ruzsnavszky et al., 2011).

Basal and Squamous Cell Carcinomas

Basal cell and squamous cell carcinoma are tumours that generally occur after the age of 50, squamous cell carcinoma being the more common and aggressive of the two. Nucleoside analogues reduced basal cell carcinoma growth. A human cutaneous squamous cell (epidermal) carcinoma cell line, A431, express P2R that induce increases in $[Ca^{2+}]_i$. ATP-stimulated A431 cells induced production of inositol-trisphosphate, suggesting the involvement of P2YR. P2X5 and P2YR were strongly expressed on both squamous and basal cell carcinomas. P2X7R are expressed in apoptotic cells in superficial multifocal and infiltrative cells and in the necrotic centre of nodular basal cell carcinomas. Expression of $P2Y_1R$ was confined to the stroma surrounding tumours. $P2Y_4R$ were present only in basal cell carcinomas. ATP and UTP at low concentrations induced an increase in the number of A431 cells, while high concentrations substantially decreased cell numbers.

ATP via P2X7R caused apoptosis of A431 cells and UTP and adenosine (after ATP breakdown) also induced cell death (Völkl et al., 2008). 2′(3′)-*O*-(4-Benzoylbenzoyl) ATP, a potent P2X7R agonist, reduced skin carcinoma and papilloma and formation (Fu et al., 2009). ADA in saliva was shown to be a diagnostic marker of tongue squamous cell carcinoma (Rai et al., 2011).

Melanoma

Malignant melanoma, which is highly metastatic, is derived from melanocytes. ATP inhibited the growth of both human and animal melanoma cells *in vivo*. CD39 is over-expressed in differentiated human melanomas. Expression of P2X7R was increased in superficial spreading melanoma patients, which were later shown to be functional and may be a therapeutic target for melanoma therapy (White et al., 2005). A low pH environment as seen in solid tumours induced ATP release from B16 melanoma cells, which increases proliferation via P2X7R. Oxidised ATP, a P2X7R antagonist, inhibited tumour growth (Hattori et al., 2012). $P2Y_1$, $P2Y_2$, and $P2Y_6R$ mRNA and protein expression was observed in human melanomas. The presence of $P2Y_1$ and P2X7R, which had been suggested to be therapeutic targets for melanoma treatment using ATP, was demonstrated by immunohistochemistry (White et al., 2009). The release of ATP from murine B16 melanoma cells was shown to upregulate CD39 expression on regulatory T cells. Dying tumour cells release ATP, which accumulates at high concentrations and acts as an immune danger signal, although it can also kill adjacent tumour cells directly via P2X7R (Feng et al., 2011). Accelerated melanoma tumour progression in mice lacking P2X7R has been reported (Adinolfi et al., 2015). γ-Irradiation that induces arrest in tumour cell growth and death, induced P2X7R-dependent release of ATP from B16 cells (Ohshima et al., 2010).

In an animal model of melanoma, tumour growth was reduced in CD73 KO mice (Yegutkin et al., 2011). Implanting B16 cells into CD73 KO mice, thereby decreasing the production of adenosine, resulted in reduced tumour growth (Ring et al., 2011). Adenosine potentiated the *in vivo* actions of chemotherapeutic agents. Antimetastatic therapies based on inhibition of A_1R activation have been suggested. A_1, A_{2A}, A_{2B} and A_3R subtypes are expressed in the A375 human malignant melanoma cell line. A_3R activation resulted in growth inhibition of melanoma cells (Morello et al., 2011). However, another study claimed that adenosine, acting through A_3R, induced cell proliferation of human malignant melanoma C32 cells (Soares et al., 2012). $A_{2B}R$ antagonists impaired IL-8 production that is raised in malignant melanoma patients, while A_3R antagonists decreased vascular endothelial growth factor that promotes human carcinoma cell angiogenesis and metastasis (Merighi et al., 2009). Adenosine is

a potent immunoregulatory factor modulating cytotoxic activity and cytokine production of anti-melanoma specific T cells.

In conclusion, $P2Y_2R$ mediate proliferation, P2X5R mediate differentiation (i.e., are antiproliferative) and P2X7R mediate cell death. Therefore, $P2Y_2R$ antagonists and P2X5 and P2X7R agonists have therapeutic potential for the treatment of skin cancer.

MUSCULOSKELETAL DISEASES

Reviews that include discussion of the pathophysiology of musculoskeletal diseases have been published (Burnstock et al., 2013; Young et al., 2013; Agrawal and Gartland, 2015; Jørgensen et al., 2015; Orriss et al., 2016). There are multiple purinoceptor subtypes expressed by bone and cartilage, which are potential targets for original therapeutic strategies to inhibit bone resorption in osteoporosis, rheumatoid arthritis (RA), periodontitis and tumour-induced osteolysis.

Muscular Dystrophy

ATP was used early to treat myopathies, although the mechanism of action was not known. Allopurinol has been used for the treatment of Duchenne muscular dystrophy (DMD). It counteracts low purine nucleotide degradation levels that occur in Duchenne muscle, but chronic administration of allopurinol failed to improve DMD symptoms. Lymphoblastoid cells from DMD patients were found to be highly sensitive to ATP stimulation.

The *mdx* model of DMD, lacking the dystrophin protein, mimics muscle damage and subsequent regeneration. Sequential expression of P2X5, $P2Y_1$ and P2X2R was described during muscle regeneration in the *mdx* model (Ryten et al., 2004). It was claimed recently that a $P2Y_2R$ antagonist may ameliorate cardiomyopathy in DMD (De Oliveira Moreira et al., 2017). $P2Y_1R$ were expressed on infiltrating immune cells. A purinergic dystrophic phenotype was seen during the earliest stage of developing dystrophic muscle. Dystrophic myoblasts express P2X4 and P2X7R proteins and it was claimed that antagonists to these receptors may be of potential therapeutic benefit. ATP signalling is altered in muscular dystrophy, but was partly recovered after nifedipine treatment (Valladares et al., 2014). It was claimed that dihydropyridines may be used as a therapeutical tool to reduce muscle damage observed in dystrophic muscles. It was suggested that P2XR antagonists alter the adaptive immune component in the muscle infiltrates in DMD and are a promising therapeutic approach to treat DMD (Gazzerro et al., 2015).

Myofascial pain is a feature of DMD and ATP stimulates myofascial nociceptors. P2X7R upregulation occurs in dystrophic *mdx* mouse muscles and treatment with P2X7R antagonists slows the progression of DMD (Sinadinos et al., 2015). Sensitivity to ATP is higher, release of ATP is greater and expression of $P2Y_2R$ is increased, but $P2Y_1R$ expression is decreased in *mdx* mice. A review about purinergic receptors in DMD was published (Krasowska et al., 2014).

Myasthenia Gravis (MG)

Myasthenia gravis is an autoimmune disease, which affects the neuromuscular junction. Lack of neuronal $A_{2A}R$-mediated Ca_v 1 (L-type) influx causes tetanic failure in MG (Noronha-Matos et al., 2011). It was suggested that the adenosinergic pathway was dysfunctional in autoimmune MG and that stimulation of CD73 activity and $A_{2A}R$ may have therapeutic potential for MG (Oliveira et al., 2015).

Fibromyalgia

Fibromyalgia (a musculoskeletal disease) is characterised by allodynia, as well as mood disorders. In fibromyalgia patients, there are decreased levels of ATP in platelets perhaps contributing to the pathogenesis of the disease (Bazzichi et al., 2008).

Osteoporosis

Osteoporosis, characterised by bone mass loss (bone mineral density decrease), leads to a high risk of bone fracture. The P2X7R is considered to be important in relation to the treatment of osteoporosis (Kvist et al., 2014). P2X7R plays a critical role in both cortical and cancellous bone mass augmentation and were shown to stimulate cancellous and periosteal bone formation and inhibit cancellous bone resorption during growth. Single nucleotide polymorphisms of the P2X7R gene are associated with the risk of fractures, decrease in bone mineral density and osteoporosis. P2X7R are involved in the formation of human osteoclasts. P2X7R antagonists are being considered for the treatment of osteoporosis and with remodelling disorders, where bone mass is reduced (Jørgensen et al., 2011). Skeletal pain accompanies osteoporosis and P2X2/3R might have a role in osteoporosis patients under a high bone turnover state (Iba and Yamashita, 2016). P2X5R may be a therapeutic target for treatment for inflammatory bone loss (Kim et al., 2017). Polymorphisms in the P2X4 and P2X7R genes (Husted et al., 2013) and the Leu46Pro polymorphism of the human $P2Y_2R$ gene were linked to bone mineral density and the risk of osteoporosis in Dutch fracture patients (Wesselius et al., 2013). It was suggested that clopidogrel, a $P2Y_{12}R$ antagonist used for stroke and thrombosis, increases the risk of fractures in osteoporotic patients (Jørgensen et al., 2012). $P2Y_{13}R$ antagonists have also been proposed for the treatment of osteoporosis (Wang N. et al., 2013).

Adenosine receptors are involved in osteoporosis (McPhee and Whiting, 1989). *Trans*-differentiation of osteoblasts to adipocytes, which involves $A_{2B}R$, may contribute to the pathogenesis of osteoporosis (Rayalam et al., 2011). P1R might be targets for treating osteoporosis and other diseases characterised by excessive bone turnover.

Osteoarthritis (OA)

Osteoarthritis is a degenerative joint disease as a result of wear of the articular cartilage due to abnormal load to the joint or from infection, trauma or due to ageing. The pain from OA is due largely to inflammation. Increased ATP levels and 5′-nucleotidase activity are present in osteoarthritic joint synovial fluid, compared to the joints from RA patients, particularly from osteoarthritic patients where deposition of

calcium-containing crystals were also present. ATP contributes to pathologic mineralisation in articular cartilage and therefore P2R antagonists might provide therapeutic tools for crystal-associated arthritis (Costello et al., 2011). ATP levels in knee synovial fluid of patients with OA are related to pain intensity (Kumahashi et al., 2011). P2X3 and P2X2/3R play an important role in the development of articular hyperalgesia of arthritic joints (Teixeira et al., 2016). In the long-term complications following total hip arthroplasty, different polymorphic variants of the P2X7R are associated with high or reduced periprosthetic osteolysis (Mrazek et al., 2010). There are elevated concentrations of ATP in the synovial fluid of dogs with OA (Torres B.T. et al., 2016). Purinergic signalling, via P2R, produces calcium oscillations in migratory chondrogenic progenitor cells isolated from OA cartilage (Matta et al., 2015). Platelets promote cartilage repair and chondrocyte proliferation via release of ADP in a rodent model of OA, suggesting that $P2Y_1$ or $P2Y_{12}R$ agonists may be useful for treatment of OA (Zhou Q. et al., 2016). Treatment with the selective P2X7R antagonist, AZD9056, produced pain-relieving and anti-inflammatory effects in rats with OA (Hu H. et al., 2016).

Adenosine signalling is also involved in OA. Adenosine, produced following breakdown of ATP, is released from chondrocytes and contributes to tissue damage in arthritic conditions. The regulation of LPS-induced IL-6 release involves $A_{2A}R$, indicating that adenosine has a regulatory role in controlling osteoclastogenesis and inflammation. Electromagnetic field stimulation up-regulates $A_{2A}R$ in synovial fibroblasts and adenosine, acting through both A_1 and $A_{2A}R$, had anti-inflammatory activity to control joint inflammation (De Mattei et al., 2009). A_{2A} and A_3R agonists modulate prostaglandin E_2 and cytokine release in human osteoarthritic fibroblasts (Ongaro et al., 2012). Adenosine receptors also mediate regulation of inflammatory responses in human synoviocytes (Varani et al., 2010b). $A_{2A}R$ agonists are used to reduce joint destruction due to septic arthritis (Cohen et al., 2004). $A_{2A}R$ deletion resulted in the development of OA in mice, suggesting that $A_{2A}R$ agonists might be a target for the treatment of OA (Corciulo et al., 2017).

Rheumatoid Arthritis (RA)

The potential involvement in RA of purinergic signalling was recognised first in the 1990's when concentrations of adenosine, after released ATP was broken down, were reduced in synovial fluid in RA compared to OA. Increased levels of adenosine as a treatment for RA was suggested. UTP and ATP activate calcium-mobilising P2UR to synergistically act with IL-1 to stimulate release of prostaglandin E_2 from human rheumatoid synovial cells. Hypotonic stress promotes ATP release and cell proliferation via transient receptor potential vanilloid 4 activation in RA rat synovial fibroblasts (Hu et al., 2017).

IL-1β is a proinflammatory cytokine that substantially contributes to the progression of RA. ATP, through P2X7R, induced increased levels of IL-1β in RA patient blood samples compared to control samples. Mononuclear cells from these patients were more sensitive to stimulation by ATP, possibly because of P2X7R genetic polymorphism (Portales-Cervantes et al., 2012). P2X7R are involved in the pathogenesis of RA and systemic lupus erythematosus (Portales-Cervantes et al., 2010). P2X7R mRNA and protein are expressed in human rheumatoid synoviocytes. Studies of arthritis animal models suggest an *in vivo* role for the P2X7R in the progression of this inflammatory disease. There was a lower incidence and reduced severity of the symptoms of arthritis induced by anti-collagen treatment in P2X7R KO mice. Therefore targeting the P2X7R may be a potential treatment for RA. P2X7R antagonists in the collagen-induced animal model of RA reduced destruction of peripheral inflammatory tissue. In a later study, it was claimed that AZD9056, a P2X7R antagonist, was not effective against RA (Keystone et al., 2012). P2X7R antagonists are being investigated for clinical use against inflammatory joint pain (Beswick et al., 2010). A multicentre, double-blind, placebo-controlled clinical trial showed that ATP infusions reduced inflammation and disease symptoms in patients with RA (Bours et al., 2010).

Bovine chondrocytes express P2X1 and P2X3R and following stimulation there was release of inflammatory mediators. Therefore antagonists to these receptors may be therapeutically useful for articular cartilage resorption and diseases involving inflammation. There was an increased platelet response to ADP in RA patients (Mac Mullan et al., 2010).

Sympathetic nerves mediate proinflammatory responses during the initial phase of arthritis induced by type II collagen, probably via cytokines such as interferon-γ released in response to the sympathetic cotransmitters ATP and NA (Straub et al., 2008). α,β-MeATP-sensitive P2XR (probably P2X3) are expressed on rat knee joint peripheral nociceptive afferent fibres and the increased ATP levels in damaged and inflamed tissues, may contribute to nociception and pain. P2X3R were found on nociceptive sensory fibres in lumber facet joints, where low back pain originates (Ishikawa et al., 2005). Changes in P2X3R expression on DRG neurons that label isolectin B4 were seen following the induction of RA (Averill et al., 2008). P2X3R expressed on trigeminal ganglia also contribute to orofacial pressure pain in monoarthritis of the temporomandibular joint. Plasma extravasation in the rat knee joint induced by bradykinin was enhanced by ATP, released as a cotransmitter from sympathetic nerves. Intravenous guanethidine, which inhibits release of sympathetic cotransmitters, proved to be effective in RA patients. *Uncaria tomentosa* extract affects the metabolism of adenine nucleotides and has been suggested as an adjuvant to treat arthritis (Castilhos et al., 2015).

The evidence showing a role for adenosine in RA has been reviewed (Varani et al., 2010a). Increased activity of ADA was seen in synovial fluid from patients with RA as well as in rheumatoid synovial fibroblasts (Nakamachi et al., 2003). The ImmuKnow assay might effectively identify RA patients that are more at risk of developing infections (Akimoto et al., 2013). Signalling via the $A_{2A}R$ caused modification of the cytokine milieu in RA (Masahiro et al., 2003). Over-expression of A_3R was observed in peripheral blood mononuclear cells of RA patients. Patients with RA had greater expression A_3R in the synovium (Stamp et al., 2012). There are increased levels of A_{2A} and A_3R on the lymphocytes and neutrophils of RA patients. In the dorsal horn of rats with induced RA, A_1R agonists decreased

activation of *c-fos* and astrocytes. In a later study of the adjuvant-induced monoarthritis model an A_3 specific agonist prevented bone resorption. ATP, working via A_2R, also reduced joint injury. A phase II clinical trial provided evidence for A_3R agonists as a treatment for RA (Fishman et al., 2008; Silverman et al., 2008). CGS 21680, an agonist of the $A_{2A}R$, reduced progression of murine type II collagen-induced arthritis (Mazzon et al., 2011). $A_{2A}R$ agonists ameliorate adjuvant-induced arthritis in rats (Vincenzi et al., 2013). Methotrexate (MTX) is often used to treat RA. In human joints with inflammatory disease, MTX treatment involved $A_{2A}R$. Adenosine via $A_{2B}R$ prevented MTX-induced inhibition of osteoclast bone destruction in arthritis induced by adjuvant (Teramachi et al., 2011). In RA patients treated with MTX, studies of polymorphisms of the genes involved in adenosine release concluded that genotyping may help identify patients who would most benefit from MTX treatment (Wessels et al., 2006). Anti-tumour necrosis factor-α has also been used to treat RA, but it raises the risk of reactivating tuberculosis. ADA assay is a specific and sensitive test for the quick diagnosis of rheumatoid effusions (Zakeri et al., 2012).

Tooth Pain

There are many sensory nerves, originating in the trigeminal ganglia, expressing P2X3R in tooth pulp and ATP is released from odontoblasts in response to mechanical stimulation to act on these receptors, resulting in pain (Shibukawa et al., 2015). LPS-induced pulp inflammation increased the expression of P2XR in trigeminal sensory nerves (Chen et al., 2014). Mechanical or cold stimulation of odontoblast processes in dentin tubules, results in ATP release and dental pain (Liu X. et al., 2015). Therefore P2X3R antagonists may be therapeutically useful to reduce toothache.

Bone Cancer Pain

Bone metastases, common in prostate and breast cancer patients, may cause substantial bone loss and pain. Purinergic signalling involvement in bone cancer was initially reported in the 1990's when P2U (i.e., $P2Y_2/P2Y_4$) receptors were cloned from osteoclastoma. The expression of $P2Y_2R$ from human osteoclasts from bone giant cell tumour was later reported. Butyl benzyl phthalate, which interferes with mammalian ion channel receptors, inhibited ATP-induced cell proliferation via P2XR in human osteosarcoma HOS cells (Liu and Chen, 2010). ATP was used in autologous bone marrow transplantation for removing residual tumour cells. In mice, a type of human apyrase, APT102, in addition to aspirin disrupts bone metastasis (Uluçkan et al., 2008). Release of ATP from tumour cells further stimulates osteoclast formation and activity, contributing to bone destruction that often happens around tumour metastases. Bisphosphonates, used to treat osteoporosis, treat bone cancer and may involve apoptosis induced by ApppI, an ATP analogue produced by bisphosphonates (Sillero et al., 2009).

Purinergic signalling plays a role in bone cancer pain. Bone pain can be relieved by radiation therapy, which may be related to the Ca^{2+}-signalling cascade, mediated by P2X6R. In a mouse model of cancer pain, increased expression of P2X3R on calcitonin gene-related peptide immunoreactive DRG neurons during tumour growth, it was claimed that ATP had a role in cancer-related pain (Liu M. et al., 2013). In rats, systemic inhibition of P2X3 and P2X2/3R with AF-353 strongly attenuated bone cancer pain-related behaviour (Kaan et al., 2010). In mice, administration of A-317491, a selective P2X3 and P2X2/3R antagonist, attenuated the early stages of bone pain in cancer (Hansen et al., 2012). Functional up-regulation of P2X3R has been described in DRG of bone cancer pain in a rat model (Wu et al., 2012).

In P2X7R KO mice, bone cancer pain-related behaviours had an earlier onset (Hansen et al., 2011). Most human osteosarcomas expressed P2X7R isoforms A and B (Giuliani et al., 2014) and P2X7R are involved in cancer-induced bone pain and P2X7R antagonists were suggested as a useful analgesic target (Falk et al., 2015). $P2Y_1R$ signalling in the DRG and spinal cord may mediate pain from bone cancer (Chen et al., 2012). Activation of K_{ATP} channels at the spinal cord level reduces pain associated with bone cancer (Xia et al., 2014). Stimulation by AMP-activated protein kinase suppresses neuroinflammation and reduces bone cancer pain (Song et al., 2015).

Myeloma

Multiple myeloma (cancer of plasma cells) involves osteolytic bone lesions, due largely to enhanced osteoclast activity. A_2R may be therapeutically useful to treat and prevent multiple myeloma-induced bone disease as activation of $A_{2A}R$ reduces osteoclast function, while activation of $A_{2B}R$ stimulates osteoblast differentiation (He et al., 2012). 8-Amino-adenosine is another possible therapeutic compound for the treatment of multiple myeloma.

Severe Combined Immunodeficiency

A major cause of severe combined immunodeficiency are genetic defects in the ADA gene. Lack of ADA causes accumulation of adenosine. Bone defects as a result of reduced osteoclastogenesis together with a defect in osteoblast function leading to low bone formation were seen in about a half of early-onset ADA-deficient patients (Sauer et al., 2009). Further, the microenvironment of bone marrow in ADA KO mice had a lower ability to support haematopoiesis. In ADA KO mice, treatment with gene therapy, bone marrow transplantation or enzyme replacement, led to a full recovery. ADA-transduced hematopoietic stem cell gene therapy also enhanced the growth of children with this disease.

Dwarfism (Achondroplasia)

This is a congenital dysplasia of the skeleton as a result in a mutation in the gene encoding fibroblast growth factor receptor type 3 (FGR3). Ap_4A diminished the expression of the achondroplasic FGFR3 receptor and $P2Y_1$, $P2Y_2$, $P2Y_6$, and $P2Y_{11}R$ are expressed by achondroplasic chondrocytes mediating the action of Ap_4A (Guzmán-Aránguez et al., 2008). Ap_4A reversed the morphological changes supporting a therapeutic role for Ap_4A as a possible treatment of dwarfism (Huete et al., 2011).

Paget's Disease

There is an increase in osteoclast numbers in Paget's disease, leading to an increase in bone resorption and a high turnover of bone. Bisphosphonates have been employed as a treatment for Paget's disease and P2X7 antagonists have also been considered (Agrawal et al., 2010).

Ossification of the Posterior Longitudinal Ligament of the Spine

This disease causes neurological damage as a result of ectopic bone formation in spinal ligaments. In this disease, extracellular ATP in ossification of cell cultures of the posterior longitudinal ligament of the spine (OPLL) is increased. $P2Y_1R$ are highly expressed in OPLL cells. Mechanical stress and ATP increase the levels of osteopontin and alkaline phosphatase mRNA in OPLL cells, effects that can be inhibited by MRS2179, a selective $P2Y_1R$ antagonist. Over-expression of $P2Y_1R$ in OPLL-induced mineralisation resulted in ectopic bone formation in the spinal ligament cells of patients with OPLL (Tanaka et al., 2011).

CONCLUDING COMMENTS

Clinical interventions involving purinergic signalling are just beginning. However, the beginning and future of purinergic compounds for the treatment of a wide range of diseases is described in this review. $P2Y_{12}R$ antagonists, such as clopidogrel and ticagrelor, are currently in wide use for stroke and thrombosis, as are $P2Y_2R$ agonists for dry eye and A_1R agonists for supraventricular tachycardia. The use of P2X7R antagonists for the treatment of inflammatory diseases is promising, but the presence of polymorphic variations of this receptor is holding up the development of selective antagonists appropriate for each disease. P2X3R antagonists are in clinical trials for use against visceral pain, chronic cough and hypertension. $A_{2A}R$ agonists are in use for the treatment of PD, and perhaps soon in wider use. P2X1R antagonists are being investigated for treatment of bladder disorders and hypertension, while P2X4, P2X7 and A_3R antagonists are being explored for neuropathic pain. Treatments with inhalation of ectonucleotidases to alter the balance of ATP and adenosine and inhibitors of ATP release, are also a therapeutic approach being explored. The development of novel purinergic compounds by medicinal chemists that are orally available and stable *in vivo* would be a significant advantage in developing therapeutic approaches, including centrally penetrant P2X7R antagonists (Able et al., 2011).

The majority of the therapeutic approaches for many heart disorders based on purinergic signalling manipulation are not fully understood yet and strategies to overcome the side-effects of treatment need to be considered. The pathophysiological roles of purinergic signalling in blood vessels are clearer and it plays an important role in controlling vascular tone and remodelling. Immunologic factors related to purinergic signalling are attracting more attention and should be considered (Cekic and Linden, 2016). Human embryonic stem cells are able to self-renew and have the potential to differentiate into different cell types, including cardiovascular progenitor cells. This system of differentiation is being investigated for cardiac regenerative therapy (Huang et al., 2016). The single nucleotide polymorphisms in purinergic receptor genes and their association with diseases are being explored for potential use as diagnosis biomarkers (see Caseley et al., 2014). Purinoceptors modulate neural stem cell proliferation, differentiation, migration and cell death and could be therapeutic approaches for the treatment of neurological and psychiatric illnesses (Illes and Rubini, 2017). MicroRNAs modulating purinergic signalling are gaining interest as potential original therapeutic targets and disease biomarkers (Ferrari et al., 2016a).

Although still in its infancy, clinical use of purinergic compounds has started. Several relevant pharmacological interventions are currently in clinical use. The lack of more established purinergic therapies may be due to there being relatively few receptor subtype-specific agonists and antagonists that are both effective and stable *in vivo* (see Jacobson and Muller, 2016). In some situations, a degree of redundancy is present, with several different subtypes of receptor mediating similar functional effects. Purinergic signalling is implicated in multiple disorders and therefore offers many potential future therapeutic targets. It should be noted, however, that since most purinoceptors are ubiquitous, to selectively target specific cell types may prove to be a challenge. As well as the development of selective agonists and antagonists, therapeutic strategies will probably include compounds that control P2R expression, inhibitors of extracellular ATP breakdown and inhibitors or enhancers of ATP transport. Understanding the interactions of purinergic signalling with other established signalling systems will be necessary.

AUTHOR CONTRIBUTIONS

The author confirms being the sole contributor of this work and approved it for publication.

ACKNOWLEDGMENT

I am greatly indebted to Dr. Gillian E. Knight for the excellent editorial work in the preparation of this manuscript.

REFERENCES

Abdulqawi, R., Dockry, R., Holt, K., Layton, G., Mccarthy, B. G., Ford, A. P., et al. (2015). P2X3 receptor antagonist (AF-219) in refractory chronic cough: a randomised, double-blind, placebo-controlled phase 2 study. *Lancet* 385, 1198–1205. doi: 10.1016/S0140-6736(14)61255-1

Able, S. L., Fish, R. L., Bye, H., Booth, L., Logan, Y. R., Nathaniel, C., et al. (2011). Receptor localization, native tissue binding and ex vivo occupancy for centrally penetrant P2X7 antagonists in the rat. *Br. J. Pharmacol.* 162, 405–414. doi: 10.1111/j.1476-5381.2010.01025.x

Abraham, M. K., Nolte, A., Reus, R., Behring, A., Zengerle, D., Avci-Adali, M., et al. (2015). In vitro study of a novel stent coating using

modified CD39 messenger RNA to potentially reduce stent angioplasty-associated complications. *PLOS ONE* 10:e0138375. doi: 10.1371/journal.pone.0138375

Acevedo, C. G., Huambachano, A., Perez, E., Rojas, S., Bravo, I., and Contreras, E. (1997). Effect of ethanol on human placental transport and metabolism of adenosine. *Placenta* 18, 387–392. doi: 10.1016/S0143-4004(97)80038-0

Adinolfi, E., Capece, M., Franceschini, A., Falzoni, S., Giuliani, A. L., Rotondo, A., et al. (2015). Accelerated tumor progression in mice lacking the ATP receptor P2X7. *Cancer Res.* 75, 635–644. doi: 10.1158/0008-5472.CAN-14-1259

Adinolfi, E., Raffaghello, L., Giuliani, A. L., Cavazzini, L., Capece, M., Chiozzi, P., et al. (2012). Expression of P2X7 receptor increases in vivo tumor growth. *Cancer Res.* 72, 2957–2969. doi: 10.1158/0008-5472.CAN-11-1947

Agarwal, R., and Agarwal, P. (2014). Newer targets for modulation of intraocular pressure: focus on adenosine receptor signaling pathways. *Expert Opin. Ther. Targets* 18, 527–539. doi: 10.1517/14728222.2014.888416

Aghaei, M., Karami-Tehrani, F., Panjehpour, M., Salami, S., and Fallahian, F. (2012). Adenosine induces cell-cycle arrest and apoptosis in androgen-dependent and -independent prostate cancer cell lines, LNcap-FGC-10, DU-145, and PC3. *Prostate* 72, 361–375. doi: 10.1002/pros.21438

Agrawal, A., Buckley, K. A., Bowers, K., Furber, M., Gallagher, J. A., and Gartland, A. (2010). The effects of P2X7 receptor antagonists on the formation and function of human osteoclasts in vitro. *Purinergic Signal.* 6, 307–315. doi: 10.1007/s11302-010-9181-z

Agrawal, A., and Gartland, A. (2015). P2X7 receptors: role in bone cell formation and function. *J. Mol. Endocrinol.* 54, R75–R88. doi: 10.1530/JME-14-0226

Agteresch, H. J., Burgers, S. A., Van Der Gaast, A., Wilson, J. H., and Dagnelie, P. C. (2003). Randomized clinical trial of adenosine 5′-triphosphate on tumor growth and survival in advanced lung cancer patients. *Anticancer Drugs* 14, 639–644. doi: 10.1097/00001813-200309000-00009

Aguiari, G., Varani, K., Bogo, M., Mangolini, A., Vincenzi, F., Durante, C., et al. (2009). Deficiency of polycystic kidney disease-1 gene (PKD1) expression increases A3 adenosine receptors in human renal cells: implications for cAMP-dependent signalling and proliferation of PKD1-mutated cystic cells. *Biochim. Biophys. Acta* 1792, 531–540. doi: 10.1016/j.bbadis.2009.03.001

Ahsan, M. K. (2011). The adenosine A2 receptor enhances primary rat HSC proliferation and inhibits senescence by down-regulation of P53 and RB. *Hepatology* 54, 750A–751A. doi: 10.3389/fphar.2014.00069

Aikin, R. A. (2013). Targeting purinergic receptors in islet transplantation. *Diabetes Metab. Res. Rev.* 62, 1394–1395. doi: 10.2337/db13-0211

Akimoto, M., Yunoue, S., Otsubo, H., Yoshitama, T., Kodama, K., Matsushita, K., et al. (2013). Assessment of peripheral blood CD4+ adenosine triphosphate activity in patients with rheumatoid arthritis. *Mod. Rheumatol.* 23, 19–27. doi: 10.1007/s10165-012-0621-1

Akino, H., Nagase, K., Watanabe, N., Tanase, K., Oyama, N., Miwa, Y., et al. (2011). ATP release from blassers is increased in-vivo and suppressed by alpha-1 adrenoceptor blocker in a rat model of bladder outlet obstruction. *Eur. Urol. Suppl.* 10, 303–304. doi: 10.1016/S1569-9056(11)60955-X

Albert, U., De Cori, D., Aguglia, A., Barbaro, F., Bogetto, F., and Maina, G. (2015). Increased uric acid levels in bipolar disorder subjects during different phases of illness. *J. Affect. Disord* 173, 170–175. doi: 10.1016/j.jad.2014.11.005

Alberto, A. V., Faria, R. X., De Menezes, J. R., Surrage, A., Da Rocha, N. C., Ferreira, L. G., et al. (2016). Role of P2 receptors as modulators of rat eosinophil recruitment in allergic inflammation. *PLOS ONE* 11:e0145392. doi: 10.1371/journal.pone.0145392

Alexopoulos, D., Xanthopoulou, I., Moulias, A., and Lekakis, J. (2016). Long-term P2Y12-receptor antagonists in post-myocardial infarction patients: facing a new trilemma? *J. Am. Coll. Cardiol.* 68, 1223–1232. doi: 10.1016/j.jacc.2016.05.088

Almeida-da-Silva, C. L., Morandini, A. C., Ulrich, H., Ojcius, D. M., and Coutinho-Silva, R. (2016). Purinergic signaling during *Porphyromonas gingivalis* infection. *Biomed. J.* 39, 251–260. doi: 10.1016/j.bj.2016.08.003

Alves, L. A., Bezerra, R. J., Faria, R. X., Ferreira, L. G., and Da Silva Frutuoso, V. (2013). Physiological roles and potential therapeutic applications of the P2X7 receptor in inflammation and pain. *Molecules* 18, 10953–10972. doi: 10.3390/molecules180910953

Amaral, E. P., Ribeiro, S. C., Lanes, V. R., Almeida, F. M., De Andrade, M. R., Bomfim, C. C., et al. (2014). Pulmonary infection with hypervirulent Mycobacteria reveals a crucial role for the P2X7 receptor in aggressive forms of tuberculosis. *PLOS Pathog.* 10:e1004188. doi: 10.1371/journal.ppat.1004188

Amaral, S. S., Oliveira, A. G., Marques, P. E., Quintão, J. L., Pires, D. A., Resende, R. R., et al. (2013). Altered responsiveness to extracellular ATP enhances acetaminophen hepatotoxicity. *Cell Commun. Signal.* 11:10. doi: 10.1186/1478-811X-11-10

Amoroso, F., Capece, M., Rotondo, A., Cangelosi, D., Ferracin, M., Franceschini, A., et al. (2015). The P2X7 receptor is a key modulator of the PI3K/GSK3β/VEGF signaling network: evidence in experimental neuroblastoma. *Oncogene* 34, 5240–5251. doi: 10.1038/onc.2014.444

Andersson, K. E. (2001). Neurotransmission and drug effects in urethral smooth muscle. *Scand. J. Urol. Nephrol. Suppl.* 207, 26–34. doi: 10.1080/003655901750174854

Andersson, K. E., Chapple, C. R., and Höfner, K. (2002). Future drugs for the treatment of benign prostatic hyperplasia. *World J. Urol.* 19, 436–442. doi: 10.1007/s00345-002-0253-8

Andersson, K. E., and Hedlund, P. (2002). Pharmacologic perspective on the physiology of the lower urinary tract. *Urology* 60, 13–20. doi: 10.1016/S0090-4295(02)01786-7

Andrés, R. M., Terencio, M. C., Arasa, J., Payá, M., Valcuende-Cavero, F., Navalón, P., et al. (2017). Adenosine A2A and A2B receptors differentially modulate keratinocyte proliferation: possible deregulation in psoriatic epidermis. *J. Invest. Dermatol.* 137, 123–131. doi: 10.1016/j.jid.2016.07.028

Antonioli, L., Blandizzi, C., Csóka, B., Pacher, P., and Haskó, G. (2015). Adenosine signalling in diabetes mellitus - pathophysiology and therapeutic considerations. *Nat. Rev. Endocrinol.* 11, 228–241. doi: 10.1038/nrendo.2015.10

Antonioli, L., Colucci, R., Pellegrini, C., Giustarini, G., Tuccori, M., Blandizzi, C., et al. (2013). The role of purinergic pathways in the pathophysiology of gut diseases: pharmacological modulation and potential therapeutic applications. *Pharmacol. Ther.* 139, 157–188. doi: 10.1016/j.pharmthera.2013.04.002

Antonioli, L., Csóka, B., Fornai, M., Colucci, R., Kókai, E., Blandizzi, C., et al. (2014a). Adenosine and inflammation: what's new on the horizon? *Drug Discov. Today* 19, 1051–1068. doi: 10.1016/j.drudis.2014.02.010

Antonioli, L., Giron, M. C., Colucci, R., Pellegrini, C., Sacco, D., Caputi, V., et al. (2014b). Involvement of the P2X7 purinergic receptor in colonic motor dysfunction associated with bowel inflammation in rats. *PLOS ONE* 9:e116253. doi: 10.1371/journal.pone.0116253

Apolloni, S., Amadio, S., Parisi, C., Matteucci, A., Potenza, R. L., Armida, M., et al. (2014). Spinal cord pathology is ameliorated by P2X7 antagonism in a SOD1-mutant mouse model of amyotrophic lateral sclerosis. *Dis. Model Mech.* 7, 1101–1109. doi: 10.1242/dmm.017038

Apostolidis, A., Popat, R., Yiangou, Y., Cockayne, D., Ford, A. P., Davis, J. B., et al. (2005). Decreased sensory receptors P2X3 and TRPV1 in suburothelial nerve fibers following intradetrusor injections of botulinum toxin for human detrusor overactivity. *J. Urol.* 174, 977–982. doi: 10.1097/01.ju.0000169481.42259.54

Aprile-Garcia, F., Metzger, M. W., Paez-Pereda, M., Stadler, H., Acuña, M., Liberman, A. C., et al. (2016). Co-Expression of wild-type P2X7R with Gln460Arg variant alters receptor function. *PLOS ONE* 11:e0151862. doi: 10.1371/journal.pone.0151862

Aronsson, P., Johnsson, M., Vesela, R., Winder, M., and Tobin, G. (2012). Adenosine receptor antagonism suppresses functional and histological inflammatory changes in the rat urinary bladder. *Auton. Neurosci.* 171, 49–57. doi: 10.1016/j.autneu.2012.10.006

Arulkumaran, N., Unwin, R. J., and Tam, F. W. (2011). A potential therapeutic role for P2X7 receptor (P2X7R) antagonists in the treatment of inflammatory diseases. *Expert Opin. Investig. Drugs* 20, 897–915. doi: 10.1517/13543784.2011.578068

Ashimi, O., Parchim, N., Zhang, Y., Song, A., Iriyama, T., Sibai, B., et al. (2015). Circulating adenosine levels are elevated in pregnant women with sickle cell disease through 2,3-DPG induction. *Am. J. Obstet. Gynecol.* 212, S409–S410. doi: 10.1016/j.ajog.2014.10.1060

Atiemo, H., Wynes, J., Chuo, J., Nipkow, L., Sklar, G. N., and Chai, T. C. (2005). Effect of botulinum toxin on detrusor overactivity induced by intravesical adenosine triphosphate and capsaicin in a rat model. *Urology* 65, 622–626. doi: 10.1016/j.urology.2004.10.057

Avendano, B. C., Montero, T. D., Chávez, C. E., Von Bernhardi, R., and Orellana, J. A. (2015). Prenatal exposure to inflammatory conditions increases Cx43 and Panx1 unopposed channel opening and activation of astrocytes in the offspring effect on neuronal survival. *Glia* 63, 2058–2072. doi: 10.1002/glia.22877

Averill, S., Inglis, J. J., King, V. R., Thompson, S. W., Cafferty, W. B., Shortland, P. J., et al. (2008). Reg-2 expression in dorsal root ganglion neurons after adjuvant-induced monoarthritis. *Neuroscience* 155, 1227–1236. doi: 10.1016/j.neuroscience.2008.06.049

Ayata, C. K., Ganal, S. C., Hockenjos, B., Willim, K., Vieira, R. P., Grimm, M., et al. (2012). Purinergic P2Y2 receptors promote neutrophil infiltration and hepatocyte death in mice with acute liver injury. *Gastroenterology* 143, 1620–1629. doi: 10.1053/j.gastro.2012.08.049

Azimi, I., Beilby, H., Davis, F. M., Marcial, D. L., Kenny, P. A., Thompson, E. W., et al. (2016). Altered purinergic receptor-Ca2+ signaling associated with hypoxia-induced epithelial-mesenchymal transition in breast cancer cells. *Mol. Oncol.* 10, 166–178. doi: 10.1016/j.molonc.2015.09.006

Bai, H. Y., and Li, A. P. (2013). P2X7 receptors in cerebral ischemia. *Neurosci. Bull.* 29, 390–398. doi: 10.1007/s12264-013-1338-7

Baranowska-Bosiacka, I., Listos, J., Gutowska, I., Hoy-Mokrzynska, A., Kolasa-Wolosiuk, A., Tarnowski, M., et al. (2016). Effects of perinatal exposure to lead (Pb) on purine receptor expression in the brain and gliosis in rats tolerant to morphine analgesia. *Toxicology* 339, 19–33. doi: 10.1016/j.tox.2015.10.003

Barron, M. L., Werry, E. L., Mcgregor, I. S., and Kassiou, M. (2014). "P2X7 in bipolar and depressive disorders," in *Pathologies of Calcium Channels*, eds N. Weiss and A. Koschak (Berlin: Springer), 635–661.

Bartlett, R., Stokes, L., and Sluyter, R. (2014). The P2X7 receptor channel: recent developments and the use of P2X7 antagonists in models of disease. *Pharmacol. Rev.* 66, 638–675. doi: 10.1124/pr.113.008003

Bartoli, F., Carrà, G., and Clerici, M. (2017a). Update on bipolar disorder biomarker candidates: what about uric acid/adenosine hypothesis? *Expert Rev. Mol. Diagn.* 17, 105–106. doi: 10.1080/14737159.2017.1270757

Bartoli, F., Crocamo, C., Dakanalis, A., Brosio, E., Miotto, A., Capuzzi, E., et al. (2017b). Purinergic system dysfunctions in subjects with bipolar disorder: a comparative cross-sectional study. *Compr. Psychiatry* 73, 1–6. doi: 10.1016/j.comppsych.2016.09.011

Bar-Yehuda, S., Stemmer, S. M., Madi, L., Castel, D., Ochaion, A., Cohen, S., et al. (2008). The A3 adenosine receptor agonist CF102 induces apoptosis of hepatocellular carcinoma via de-regulation of the Wnt and NF-κB signal transduction pathways. *Int. J. Oncol.* 33, 287–295.

Basoglu, O. K., Barnes, P. J., Kharitonov, S. A., and Pelleg, A. (2015). Effects of aerosolized adenosine 5′-triphosphate in smokers and patients with COPD. *Chest* 148, 430–435. doi: 10.1378/chest.14-2285

Basoglu, O. K., Pelleg, A., Kharitonov, S. A., and Barnes, P. J. (2017). Contrasting effects of ATP and adenosine on capsaicin challenge in asthmatic patients. *Pulm. Pharmacol. Ther.* 45, 13–18. doi: 10.1016/j.pupt.2017.04.004

Basu, S., Barawkar, D. A., Ramdas, V., Patel, M., Waman, Y., Panmand, A., et al. (2017). Design and synthesis of novel xanthine derivatives as potent and selective A2B adenosine receptor antagonists for the treatment of chronic inflammatory airway diseases. *Eur. J. Med. Chem.* 134, 218–229. doi: 10.1016/j.ejmech.2017.04.014

Baudelet, D., Lipka, E., Millet, R., and Ghinet, A. (2015). Involvement of the P2X7 purinergic receptor in inflammation: an update of antagonists series since 2009 and their promising therapeutic potential. *Curr. Med. Chem.* 22, 713–729. doi: 10.2174/0929867322666141212120926

Bazzichi, L., Giannaccini, G., Betti, L., Fabbrini, L., Schmid, L., Palego, L., et al. (2008). ATP, calcium and magnesium levels in platelets of patients with primary fibromyalgia. *Clin. Biochem.* 41, 1084–1090. doi: 10.1016/j.clinbiochem.2008.06.012

Beamer, E., Fischer, W., and Engel, T. (2017). The ATP-gated P2X7 receptor as a target for the treatment of drug-resistant epilepsy. *Front. Neurosci.* 11:21. doi: 10.3389/fnins.2017.00021

Beamer, E., Gölöncsér, F., Horváth, G., Bekö, K., Otrokocsi, L., Koványi, B., et al. (2016). Purinergic mechanisms in neuroinflammation: an update from molecules to behavior. *Neuropharmacology* 104, 94–104. doi: 10.1016/j.neuropharm.2015.09.019

Beaucage, K. L., Xiao, A., Pollmann, S. I., Grol, M. W., Beach, R. J., Holdsworth, D. W., et al. (2014). Loss of P2X7 nucleotide receptor function leads to abnormal fat distribution in mice. *Purinergic Signal.* 10, 291–304. doi: 10.1007/s11302-013-9388-x

Beckel, J. M., Lu, W., Civan, M. M., and Mitchell, C. H. (2016). Treatment of retinal disorders with purinergic drugs: beyond receptors. *J. Ocul. Pharmacol. Ther.* 32, 488–489. doi: 10.1089/jop.2016.29020.jbe

Beckenkamp, A., Santana, D. B., Bruno, A. N., Calil, L. N., Casali, E. A., Paccez, J. D., et al. (2014). Ectonucleotidase expression profile and activity in human cervical cancer cell lines. *Biochem. Cell Biol.* 92, 95–104. doi: 10.1139/bcb-2013-0051

Belhassen, B., and Michowitz, Y. (2016). Unmasking right atrial fibrillation: a new indication of adenosine triphosphate test? *Heart Rhythm* 13, 364–365. doi: 10.1016/j.hrthm.2015.10.020

Ben-Ari, Z., Pappo, O., Yitzhaki, S., Cheporko, Y., Shainberg, A., Zinman, T., et al. (2009). Uridine-5′-triphosphate protects against hepatic-ischemic/reperfusion injury in mice. *Transplantation* 87, 1155–1162. doi: 10.1097/TP.0b013e31819e3cdc

Benitez-Rajal, J., Lorite, M. J., Burt, A. D., Day, C. P., and Thompson, M. G. (2006). Phospholipase D and extracellular signal-regulated kinase in hepatic stellate cells: effects of platelet-derived growth factor and extracellular nucleotides. *Am. J Physiol. Gastrointest. Liver Physiol.* 291, G977–G986. doi: 10.1152/ajpgi.00041.2006

Bergamin, L. S., Braganhol, E., Figueiró, F., Casali, E. A., Zanin, R. F., Sévigny, J., et al. (2015). Involvement of purinergic system in the release of cytokines by macrophages exposed to glioma-conditioned medium. *J. Cell Biochem.* 116, 721–729. doi: 10.1002/jcb.25018

Besnard, A., Gautherot, J., Julien, B., Tebbi, A., Garcin, I., Doignon, I., et al. (2016). The P2X4 purinergic receptor impacts liver regeneration after partial hepatectomy in mice through the regulation of biliary homeostasis. *Hepatology* 64, 941–953. doi: 10.1002/hep.28675

Beswick, P. J., Billinton, A., Chambers, L. J., Dean, D. K., Fonfria, E., Gleave, R. J., et al. (2010). Structure-activity relationships and in vivo activity of (1H-pyrazol-4-yl)acetamide antagonists of the P2X7 receptor. *Bioorg. Med. Chem. Lett.* 20, 4653–4656. doi: 10.1016/j.bmcl.2010.05.107

Bhattacharya, A., and Biber, K. (2016). The microglial ATP-gated ion channel P2X7 as a CNS drug target. *Glia* 64, 1772–1787. doi: 10.1002/glia.23001

Bhave, S., Gade, A., Kang, M., Hauser, K. F., Dewey, W. L., and Akbarali, H. I. (2017). Connexin-purinergic signaling in enteric glia mediates the prolonged effect of morphine on constipation. *FASEB J.* 31, 2649–2660. doi: 10.1096/fj.201601068R

Boldrini, L., Giordano, M., Alì, G., Melfi, F., Romano, G., Lucchi, M., et al. (2015). P2X7 mRNA expression in non-small cell lung cancer: MicroRNA regulation and prognostic value. *Oncol. Lett.* 9, 449–453.

Borea, P. A., Gessi, S., Merighi, S., and Varani, K. (2016). Adenosine as a multi-signalling guardian angel in human diseases: when, where and how does it exert its protective effects? *Trends Pharmacol. Sci.* 37, 419–434. doi: 10.1016/j.tips.2016.02.006

Borea, P. A., Varani, K., Vincenzi, F., Baraldi, P. G., Tabrizi, M. A., Merighi, S., et al. (2015). The A3 adenosine receptor: history and perspectives. *Pharmacol. Rev.* 67, 74–102. doi: 10.1124/pr.113.008540

Borel, F., Han, R., Visser, A., Petry, H., Van Deventer, S. J., Jansen, P. L., et al. (2012). Adenosine triphosphate-binding cassette transporter genes up-regulation in untreated hepatocellular carcinoma is mediated by cellular microRNAs. *Hepatology* 55, 821–832. doi: 10.1002/hep.24682

Boros, D., Thompson, J., and Larson, D. F. (2016). Adenosine regulation of the immune response initiated by ischemia reperfusion injury. *Perfusion* 31, 103–110. doi: 10.1177/0267659115586579

Bou Ghanem, E. N., Clark, S., Roggensack, S. E., Mciver, S. R., Alcaide, P., Haydon, P. G., et al. (2015). Extracellular adenosine protects against *Streptococcus pneumoniae* lung infection by regulating pulmonary neutrophil recruitment. *PLOS Pathog.* 11:e1005126. doi: 10.1371/journal.ppat.1005126

Bours, M. J., Peeters, R. H., Landewé, R. B., Beijer, S., Arts, I. C., and Dagnelie, P. C. (2010). Adenosine 5′-triphosphate infusions reduced disease activity and inflammation in a patient with active rheumatoid arthritis. *Rheumatology (Oxford)* 49, 2223–2225. doi: 10.1093/rheumatology/keq177

Bowser, J. L., Blackburn, M. R., Shipley, G. L., Molina, J. G., Dunner, K. Jr., and Broaddus, R. R. (2016). Loss of CD73-mediated actin polymerization promotes endometrial tumor progression. *J. Clin. Invest.* 126, 220–238. doi: 10.1172/JCI79380

Boy, C., Meyer, P. T., Kircheis, G., Holschbach, M. H., Herzog, H., Elmenhorst, D., et al. (2008). Cerebral A1 adenosine receptors (A1AR) in liver cirrhosis. *Eur. J. Nucl. Med. Mol. Imaging* 35, 589–597. doi: 10.1007/s00259-007-0586-z

Braganhol, E., Kukulski, F., Lévesque, S. A., Fausther, M., Lavoie, E. G., Zanotto-Filho, A., et al. (2015). Nucleotide receptors control IL-8/CXCL8 and MCP-1/CCL2 secretions as well as proliferation in human glioma cells. *Biochim. Biophys. Acta* 1852, 120–130. doi: 10.1016/j.bbadis.2014.10.014

Bravo, D., Maturana, C. J., Pelissier, T., Hernández, A., and Constandil, L. (2015). Interactions of pannexin 1 with NMDA and P2X7 receptors in central nervous system pathologies: possible role on chronic pain. *Pharmacol. Res.* 101, 86–93. doi: 10.1016/j.phrs.2015.07.016

Brock, J. A., and Van Helden, D. F. (1995). Enhanced excitatory junction potentials in mesenteric arteries from spontaneously hypertensive rats. *Pflügers Arch. Eur. J. Physiol.* 430, 901–908. doi: 10.1007/BF01837403

Broderick, P. A., and Malave, L. B. (2014). Cocaine shifts the estrus cycle out of phase and caffeine restores it. *J. Caffeine Res.* 4, 109–113. doi: 10.1089/jcr.2014.0015

Brouns, I., Van Genechten, J., Burnstock, G., Timmermans, J.-P., and Adriaensen, D. (2003). Ontogenesis of P2X3 receptor-expressing nerve fibres in the rat lung, with special reference to neuroepithelial bodies. *Biomed. Res.* 14, 80–86.

Bukhari, M., Deng, H., Jones, N., Towne, Z., Woodworth, C. D., and Samways, D. S. (2015). Selective permeabilization of cervical cancer cells to an ionic DNA-binding cytotoxin by activation of P2Y receptors. *FEBS Lett.* 589, 1498–1504. doi: 10.1016/j.febslet.2015.04.044

Bulluck, H., Sirker, A., Loke, Y. K., Garcia-Dorado, D., and Hausenloy, D. J. (2016). Clinical benefit of adenosine as an adjunct to reperfusion in ST-elevation myocardial infarction patients: an updated meta-analysis of randomized controlled trials. *Int. J. Cardiol.* 202, 228–237. doi: 10.1016/j.ijcard.2015.09.005

Burnstock, G. (1972). Purinergic nerves. *Pharmacol. Rev.* 24, 509–581.

Burnstock, G. (1981). Pathophysiology of migraine: a new hypothesis. *Lancet* 317, 1397–1399. doi: 10.1016/S0140-6736(81)92572-1

Burnstock, G. (1999). Release of vasoactive substances from endothelial cells by shear stress and purinergic mechanosensory transduction. *J. Anat.* 194, 335–342. doi: 10.1046/j.1469-7580.1999.19430335.x

Burnstock, G. (2002). Purinergic signalling and vascular cell proliferation and death. *Arterioscler. Thromb. Vasc. Biol.* 22, 364–373. doi: 10.1161/hq0302.105360

Burnstock, G. (2006). Pathophysiology and therapeutic potential of purinergic signaling. *Pharmacol. Rev.* 58, 58–86. doi: 10.1124/pr.58.1.5

Burnstock, G. (2007). Purine and pyrimidine receptors. *Cell. Mol. Life Sci.* 64, 1471–1483. doi: 10.1007/s00018-007-6497-0

Burnstock, G. (2008a). Dual control of vascular tone and remodelling by ATP released from nerves and endothelial cells. *Pharmacol. Rep.* 60, 12–20.

Burnstock, G. (2008b). Purinergic signalling and disorders of the central nervous system. *Nat. Rev. Drug Discov.* 7, 575–590. doi: 10.1038/nrd2605

Burnstock, G. (2009). Purinergic mechanosensory transduction and visceral pain. *Mol. Pain* 5:69. doi: 10.1186/1744-8069-5-69

Burnstock, G. (2014a). The erasmus lecture 2012, Academia Europaea. The concept of cotransmission: focus on ATP as a cotransmitter and its significance in health and disease. *Eur. Rev.* 22, 1–17. doi: 10.1017/S1062798713000586

Burnstock, G. (2014b). Purinergic signalling in endocrine organs. *Purinergic Signal.* 10, 189–231. doi: 10.1007/s11302-013-9396-x

Burnstock, G. (2014c). Purinergic signalling in the reproductive system in health and disease. *Purinergic Signal.* 10, 157–187. doi: 10.1007/s11302-013-9399-7

Burnstock, G. (2014d). Purinergic signalling in the urinary tract in health and disease. *Purinergic Signal.* 10, 103–155. doi: 10.1007/s11302-013-9395-y

Burnstock, G. (2015a). Blood cells: an historical account of the roles of purinergic signalling. *Purinergic Signal.* 11, 411–434. doi: 10.1007/s11302-015-9462-7

Burnstock, G. (2015b). Physiopathological roles of P2X receptors in the central nervous system. *Curr. Med. Chem.* 22, 819–844.

Burnstock, G. (2015c). Purinergic signalling in neuroregeneration. *Neural Regen. Res.* 10, 1919. doi: 10.4103/1673-5374.165300

Burnstock, G. (2016a). An introduction to the roles of purinergic signalling in neurodegeneration, neuroprotection and neuroregeneration. *Neuropharmacology* 104, 4–17. doi: 10.1016/j.neuropharm.2015.05.031

Burnstock, G. (2016b). P2X ion channel receptors and inflammation. *Purinergic Signal.* 12, 59–67. doi: 10.1007/s11302-015-9493-0

Burnstock, G. (2016c). Purinergic receptors and pain - an update. *Front. Med. Chem.* 9:3–55. doi: 10.2174/9781681082493116090003

Burnstock, G. (2016d). "Purinergic signalling in the gut," in *The Enteric Nervous System. 30 Years Later*, Vol. 891, eds S. Brierley and M. Costa (Berlin: Springer), 91–112.

Burnstock, G. (2016e). Purinergic signalling: pathophysiology and therapeutic potential. *J. Drug Res. Dev.* 2. doi: 10.16966/2470-1009.122

Burnstock, G. (2016f). Short- and long-term (trophic) purinergic signalling. *Philos. Trans. R. Soc. B Biol. Sci.* 371:20150422. doi: 10.1098/rstb.2015.0422

Burnstock, G. (2017). Purinergic signalling in the cardiovascular system. *Circ. Res.* 120, 207–228. doi: 10.1161/CIRCRESAHA.116.309726

Burnstock, G., Arnett, T. R., and Orriss, I. R. (2013). Purinergic signalling in the musculoskeletal system. *Purinergic Signal.* 9, 541–572. doi: 10.1007/s11302-013-9381-4

Burnstock, G., Brouns, I., Adriaensen, D., and Timmermans, J. P. (2012a). Purinergic signalling in the airways. *Pharmacol. Rev.* 64, 834–868. doi: 10.1124/pr.111.005389

Burnstock, G., and Di Virgilio, F. (2013). Purinergic signalling in cancer. *Purinergic Signal.* 9, 491–540. doi: 10.1007/s11302-013-9372-5

Burnstock, G., Evans, L., and Bailey, M. (2014a). Purinergic signalling in the kidney in health and disease. *Purinergic Signal.* 10, 71–101. doi: 10.1007/s11302-013-9400-5

Burnstock, G., and Kennedy, C. (2011). "P2X receptors in health and disease," in *Purine and Pyrimidine Receptor Pharmacology*, eds K. A. Jacobson and J. Linden (Burlington: Academic Press), 333–372.

Burnstock, G., and Knight, G. E. (2004). Cellular distribution and functions of P2 receptor subtypes in different systems. *Int. Rev. Cytol.* 240, 31–304. doi: 10.1016/S0074-7696(04)40002-3

Burnstock, G., Knight, G. E., and Greig, A. V. H. (2012b). Purinergic signalling in healthy and diseased skin. *J. Invest. Dermatol.* 132, 526–546. doi: 10.1038/jid.2011.344

Burnstock, G., Krügel, U., Abbracchio, M. P., and Illes, P. (2011). Purinergic signalling: from normal behaviour to pathological brain function. *Prog. Neurobiol.* 95, 229–274. doi: 10.1016/j.pneurobio.2011.08.006

Burnstock, G., and Loesch, A. (2017). Sympathetic innervation of the kidney in health and disease: emphasis on the role of purinergic cotransmission. *Auton. Neurosci.* 204, 4–16. doi: 10.1016/j.autneu.2016.05.007

Burnstock, G., and Novak, I. (2013). Purinergic signalling and diabetes. *Purinergic Signal.* 9, 307–324. doi: 10.1007/s11302-013-9359-2

Burnstock, G., and Pelleg, A. (2015). Cardiac purinergic signalling in health and disease. *Purinergic Signal.* 11, 1–46. doi: 10.1007/s11302-014-9436-1

Burnstock, G., and Ralevic, V. (2014). Purinergic signaling and blood vessels in health and disease. *Pharmacol. Rev.* 66, 102–192. doi: 10.1124/pr.113.008029

Burnstock, G., and Sawynok, J. (2010). "ATP and adenosine receptors and pain," in *Pharmacology of Pain*, eds P. Beaulieu, D. Lussier, F. Porreca, and A. H. Dickenson (Seattle: IASP Press), 303–326.

Burnstock, G., Vaughn, B., and Robson, S. (2014b). Purinergic signalling in the liver in health and disease. *Purinergic Signal.* 10, 51–70. doi: 10.1007/s11302-013-9398-8

Burnstock, G., and Verkhratsky, A. (2012). *Purinergic Signalling and the Nervous System*. Berlin: Springer.

Calvén, J., Akbarshahi, H., Menzel, M., Ayata, C. K., Idzko, M., Bjermer, L., et al. (2015). Rhinoviral stimuli, epithelial factors and ATP signalling contribute to bronchial smooth muscle production of IL-33. *J. Transl. Med.* 13, 281. doi: 10.1186/s12967-015-0645-3

Calvert, R. C., Banks, F. C., Thompson, C. S., Mikhailidis, D. P., and Morgan, R. J. (2002). Chronic ethanol consumption impairs adrenoceptor- and purinoceptor-mediated relaxations in isolated rat detrusor smooth muscle. *BJU. Int* 89, 793–794. doi: 10.1046/j.1464-410X.2002.t01-4-02801.x

Calvert, R. C., Khan, M. A., Thompson, C. S., Mikhailidis, D. P., and Burnstock, G. (2008a). A functional study of purinergic signalling in the normal and pathological rabbit corpus cavernosum. *BJU Int.* 101, 1043–1047. doi: 10.1111/j.1464-410X.2007.07385.x

Calvert, R. C., Thompson, C. S., and Burnstock, G. (2008b). ATP release from the human ureter on distension and P2X3 receptor expression on suburothelial sensory nerves. *Purinergic Signal.* 4, 377–381. doi: 10.1007/s11302-008-9123-1

Cameron, K. O., Kung, D. W., Kalgutkar, A. S., Kurumbail, R. G., Miller, R., Salatto, C. T., et al. (2016). Discovery and preclinical characterization of 6-chloro-5-[4-(1-hydroxycyclobutyl)phenyl]-1H-indole-3-carboxylic acid (PF-06409577),

a direct activator of adenosine monophosphate-activated protein kinase (AMPK), for the potential treatment of diabetic nephropathy. *J. Med. Chem.* 59, 8068–8081. doi: 10.1021/acs.jmedchem.6b00866

Canda, A. E., Cross, R. L., and Chapple, C. R. (2006). Pharmacology of the lower urinary tract and management of overactive bladder. *J. Turk. Ger. Gynecol. Assoc.* 7, 146–158.

Canda, A. E., Turna, B., Cinar, G. M., and Nazli, O. (2007). Physiology and pharmacology of the human ureter: basis for current and future treatments. *Urol. Int.* 78, 289–298. doi: 10.1159/000100830

Cantin, L. D., Bayrakdarian, M., Buon, C., Grazzini, E., Hu, Y. J., Labrecque, J., et al. (2012). Discovery of P2X3 selective antagonists for the treatment of chronic pain. *Bioorg. Med. Chem. Lett.* 22, 2565–2571. doi: 10.1016/j.bmcl.2012.01.124

Cao, L., Pu, J., Scott, R. H., Ching, J., and Mccaig, C. D. (2015). Physiological electrical signals promote chain migration of neuroblasts by up-regulating P2Y1 purinergic receptors and enhancing cell adhesion. *Stem Cell Rev.* 11, 75–86. doi: 10.1007/s12015-014-9524-1

Cao, X., Li, L. P., Wang, Q., Wu, Q., Hu, H. H., Zhang, M., et al. (2013). Astrocyte-derived ATP modulates depressive-like behaviors. *Nat. Med.* 19, 773–777. doi: 10.1038/nm.3162

Carneiro, M. V., Americo, T. A., Guimarães, M. Z., and Linden, R. (2016). The prion protein selectively binds to and modulates the content of purinergic receptor P2X4R. *Biochem. Biophys. Res. Commun.* 472, 293–298. doi: 10.1016/j.bbrc.2016.02.122

Casadó-Anguera, V., Bonaventura, J., Moreno, E., Navarro, G., Cortés, A., Ferré, S., et al. (2016). Evidence for the heterotetrameric structure of the adenosine A2A-dopamine D2 receptor complex. *Biochem. Soc. Trans.* 44, 595–600. doi: 10.1042/BST20150276

Caseley, E. A., Muench, S. P., Roger, S., Mao, H. J., Baldwin, S. A., and Jiang, L. H. (2014). Non-synonymous single nucleotide polymorphisms in the P2X receptor genes: association with diseases, impact on receptor functions and potential use as diagnosis biomarkers. *Int. J. Mol. Sci.* 15, 13344–13371. doi: 10.3390/ijms150813344

Castilhos, L. G., Rezer, J. F., Ruchel, J. B., Thorstenberg, M. L., Jaques, J. A., Schlemmer, J. B., et al. (2015). Effect of *Uncaria tomentosa* extract on purinergic enzyme activities in lymphocytes of rats submitted to experimental adjuvant arthritis model. *BMC Complement. Altern. Med.* 15:189. doi: 10.1186/s12906-015-0694-4

Catanzaro, J. M., Hueston, C. M., Deak, M. M., and Deak, T. (2014). The impact of the P2X7 receptor antagonist A-804598 on neuroimmune and behavioral consequences of stress. *Behav. Pharmacol.* 25, 582–598. doi: 10.1097/FBP.0000000000000072

Cekic, C., and Linden, J. (2016). Purinergic regulation of the immune system. *Nat. Rev. Immunol.* 16, 177–192. doi: 10.1038/nri.2016.4

Cekic, C., Sag, D., Li, Y., Theodorescu, D., Strieter, R. M., and Linden, J. (2012). Adenosine A2B receptor blockade slows growth of bladder and breast tumor. *J. Immunol.* 188, 198–205. doi: 10.4049/jimmunol.1101845

Certal, M., Vinhas, A., Pinheiro, A. R., Ferreirinha, F., Costa, M. A., and Correia-De-Sá, P. (2015). Novel anti-fibrotic effect of the UTP-sensitive P2Y11 receptor in rat cardiac myofibroblasts. *Auton. Neurosci.* 192, 72. doi: 10.1016/j.ceca.2015.08.004

Cha, H. J., Jung, M. S., Ahn, D. W., Choi, J. K., Ock, M. S., Kim, K. S., et al. (2015). Silencing of MUC8 by siRNA increases P2Y2-induced airway inflammation. *Am. J. Physiol. Lung. Cell Mol. Physiol.* 308, L495–L502. doi: 10.1152/ajplung.00332.2014

Chan, E. S., and Cronstein, B. N. (2010). Adenosine in fibrosis. *Mod. Rheumatol.* 20, 114–122. doi: 10.1007/s10165-009-0251-4

Chan, E. S., Montesinos, M. C., Fernandez, P., Desai, A., Delano, D. L., Yee, H., et al. (2006). Adenosine A2A receptors play a role in the pathogenesis of hepatic cirrhosis. *Br. J. Pharmacol.* 148, 1144–1155. doi: 10.1038/sj.bjp.0706812

Chancellor, M. B., Fowler, C. J., Apostolidis, A., De Groat, W. C., Smith, C. P., Somogyi, G. T., et al. (2008). Drug insight: biological effects of botulinum toxin A in the lower urinary tract. *Nat. Clin. Pract. Urol.* 5, 319–328. doi: 10.1038/ncpuro1124

Chandrashekaran, V., Das, S., Seth, R. K., Dattaroy, D., Alhasson, F., Michelotti, G., et al. (2016). Purinergic receptor X7 mediates leptin induced GLUT4 function in stellate cells in nonalcoholic steatohepatitis. *Biochim. Biophys. Acta* 1862, 32–45. doi: 10.1016/j.bbadis.2015.10.009

Chang, M. Y., Lu, J. K., Tian, Y. C., Chen, Y. C., Hung, C. C., Huang, Y. H., et al. (2011). Inhibition of the P2X7 receptor reduces cystogenesis in PKD. *J. Am. Soc. Nephrol.* 22, 1696–1706. doi: 10.1681/ASN.2010070728

Chaudhury, A., Dendi, V. S., and Mirza, W. (2016). Colligative property of ATP: implications for enteric purinergic neuromuscular neurotransmission. *Front. Physiol.* 7:500. doi: 10.3389/fphys.2016.00500

Chaves, M. M., Marques-Da-Silva, C., Monteiro, A. P., Canetti, C., and Coutinho-Silva, R. (2014). Leukotriene B4 modulates P2X7 receptor-mediated *Leishmania amazonensis* elimination in murine macrophages. *J. Immunol.* 192, 4765–4773. doi: 10.4049/jimmunol.1301058

Chen, J., Wang, L., Zhang, Y., and Yang, J. (2012). P2Y1 purinoceptor inhibition reduces extracellular signal-regulated protein kinase 1/2 phosphorylation in spinal cord and dorsal root ganglia: implications for cancer-induced bone pain. *Acta Biochim. Biophys. Sin. (Shanghai)* 44, 367–372. doi: 10.1093/abbs/gms007

Chen, J. F., Eltzschig, H. K., and Fredholm, B. B. (2013). Adenosine receptors as drug targets - what are the challenges? *Nat. Rev. Drug Discov.* 12, 265–286. doi: 10.1038/nrd3955

Chen, X., Molliver, D. C., and Gebhart, G. F. (2010). The P2Y2 receptor sensitizes mouse bladder sensory neurons and facilitates purinergic currents. *J. Neurosci.* 30, 2365–2372. doi: 10.1523/JNEUROSCI.5462-09.2010

Chen, Y., Zhang, L., Yang, J., Zhang, L., and Chen, Z. (2014). LPS-induced dental pulp inflammation increases expression of ionotropic purinergic receptors in rat trigeminal ganglion. *Neuroreport* 25, 991–997. doi: 10.1097/WNR.0000000000000193

Cheng, R. D., Ren, J. J., Zhang, Y. Y., and Ye, X. M. (2014). P2X4 receptors expressed on microglial cells in post-ischemic inflammation of brain ischemic injury. *Neurochem. Int.* 67, 9–13. doi: 10.1016/j.neuint.2014.01.011

Cheng, Y., Mansfield, K. J., Allen, W., Millard, R. J., Burcher, E., and Moore, K. H. (2013). Correlation between cystometric volumes, ATP release, and pH in women with overactive bladder versus controls. *Neurourol. Urodyn.* 32, 969–973. doi: 10.1002/nau.22344

Chesworth, R., Brown, R. M., Kim, J. H., Ledent, C., and Lawrence, A. J. (2016). Adenosine 2A receptors modulate reward behaviours for methamphetamine. *Addict. Biol.* 21, 407–421. doi: 10.1111/adb.12225

Chetty, A., Sharda, A., Warburton, R., Chen, T., Xue, C., Castellot, J., et al. (2016). Effect of a purinergic P2Y6 receptor agonist on airway remodeling and responsiveness in a mouse model of asthma. *Am. J. Respir. Crit. Care Med.* 193, A2173.

Chiang, D. J., Roychowdhury, S., Bush, K., Mcmullen, M. R., Pisano, S., Niese, K., et al. (2013). Adenosine 2A receptor antagonist prevented and reversed liver fibrosis in a mouse model of ethanol-exacerbated liver fibrosis. *PLOS ONE* 8:e69114. doi: 10.1371/journal.pone.0069114

Chiu, G. S., Darmody, P. T., Walsh, J. P., Moon, M. L., Kwakwa, K. A., Bray, J. K., et al. (2014). Adenosine through the A2A adenosine receptor increases IL-1β in the brain contributing to anxiety. *Brain Behav. Immun.* 41, 218–231. doi: 10.1016/j.bbi.2014.05.018

Choi, K. C., Tai, C. J., Tzeng, C. R., Auersperg, N., and Leung, P. C. (2003). Adenosine triphosphate activates mitogen-activated protein kinase in pre-neoplastic and neoplastic ovarian surface epithelial cells. *Biol. Reprod.* 68, 309–315. doi: 10.1095/biolreprod.102.006551

Choukèr, A., Thiel, M., Lukashev, D., Ward, J. M., Kaufmann, I., Apasov, S., et al. (2008). Critical role of hypoxia and A2A adenosine receptors in liver tissue-protecting physiological anti-inflammatory pathway. *Mol. Med.* 14, 116–123. doi: 10.2119/2007-00075.Chouker

Chuang, Y. C., and Chancellor, M. B. (2006). The application of botulinum toxin in the prostate. *J. Urol.* 176, 2375–2382. doi: 10.1016/j.juro.2006.07.127

Chuo, C. H., Devine, S. M., Scammells, P. J., Krum, H., Christopoulos, A., May, L. T., et al. (2016). VCP746, a novel A1 adenosine receptor biased agonist, reduces hypertrophy in a rat neonatal cardiac myocyte model. *Clin. Exp. Pharmacol. Physiol.* 43, 976–982. doi: 10.1111/1440-1681.12616

Cicala, C., and Ialenti, A. (2013). Adenosine signaling in airways: toward a promising antiasthmatic approach. *Eur. J. Pharmacol.* 714, 522–525. doi: 10.1016/j.ejphar.2013.06.033

Cieslak, M., Czarnecka, J., and Roszek, K. (2016). The roles of purinergic signaling in psychiatric disorders. *Acta Biochim. Pol.* 63, 1–9. doi: 10.18388/abp.2015_1004

Cieslak, M., Czarnecka, J., Roszek, K., and Komoszynski, M. (2015). The role of purinergic signaling in the etiology of migraine and novel antimigraine treatment. *Purinergic Signal.* 11, 307–316. doi: 10.1007/s11302-015-9453-8

Cieslak, M., and Roszek, K. (2014). Purinergic signaling in the pancreas and the therapeutic potential of ecto-nucleotidases in diabetes. *Acta Biochim. Pol.* 61, 655–662.

Cieslak, M., Wojtczak, A., and Komoszynski, M. (2017). Role of the purinergic signaling in epilepsy. *Pharmacol. Rep.* 69, 130–138. doi: 10.1016/j.pharep.2016.09.018

Ciruela, F., Fernández-Dueñas, V., Contreras, F., Arnau, J. M., Menchón, J. M., Vallano, A., et al. (2015). "Adenosine in the neurobiology of schizophrenia: potential adenosine receptor-based pharmacotherapy," in *Psychiatry and Neuroscience Update: Bridging the Divide*, eds P. Á Gargiulo and H. L. M. Arroyo (Cham: Springer International Publishing), 375–388.

Cisneros-Mejorado, A., Gottlieb, M., Cavaliere, F., Magnus, T., Koch-Nolte, F., Scemes, E., et al. (2015a). Blockade of P2X7 receptors or pannexin-1 channels similarly attenuates postischemic damage. *J. Cereb. Blood Flow Metab.* 35, 843–850. doi: 10.1038/jcbfm.2014.262

Cisneros-Mejorado, A., Perez-Samartin, A., Gottlieb, M., and Matute, C. (2015b). ATP signaling in brain: release, excitotoxicity and potential therapeutic targets. *Cell. Mol. Neurobiol.* 35, 1–6. doi: 10.1007/s10571-014-0092-3

Clouet, S., Di Pietrantonio, L., Daskalopoulos, E. P., Esfahani, H., Horckmans, M., Vanorlé, M., et al. (2016). Loss of mouse P2Y6 nucleotide receptor is associated with physiological macrocardia and amplified pathological cardiac hypertrophy. *J. Biol. Chem.* 291, 15841–15852. doi: 10.1074/jbc.M115.684118

Cockayne, D. A., Hamilton, S. G., Zhu, Q.-M., Dunn, P. M., Zhong, Y., Novakovic, S., et al. (2000). Urinary bladder hyporeflexia and reduced pain-related behaviour in P2X3-deficient mice. *Nature* 407, 1011–1015. doi: 10.1038/35039519

Cohen, S. B., Gill, S. S., Baer, G. S., Leo, B. M., Scheld, W. M., and Diduch, D. R. (2004). Reducing joint destruction due to septic arthrosis using an adenosine 2A receptor agonist. *J. Orthop. Res.* 22, 427–435. doi: 10.1016/j.orthres.2003.08.011

Corciulo, C., Lendhey, M., Wilder, T., Schoen, H., Cornelissen, A. S., Chang, G., et al. (2017). Endogenous adenosine maintains cartilage homeostasis and exogenous adenosine inhibits osteoarthritis progression. *Nat. Commun.* 8:15019. doi: 10.1038/ncomms15019

Corrêa, G., Almeida, L. C., Moreira-Souza, A. C., Savio, L. E., Takiya, C. M., Marques-Da-Silva, C., et al. (2017). Inflammatory early events associated to the role of P2X7 receptor in acute murine toxoplasmosis. *Immunobiology* 222, 676–683. doi: 10.1016/j.imbio.2016.12.007

Corrêa, G., Lindenberg, C. D. A., Fernandes-Santos, C., Gandini, M., Petitinga, P. F., Coutinho-Silva, R., et al. (2016). The purinergic receptor P2X7 role in control of Dengue virus-2 infection and cytokine/chemokine production in infected human monocytes. *Immunobiology* 221, 794–802. doi: 10.1016/j.imbio.2016.02.003

Corso, L., Cavallero, A., Baroni, D., Garbati, P., Prestipino, G., Bisti, S., et al. (2016). Saffron reduces ATP-induced retinal cytotoxicity by targeting P2X7 receptors. *Purinergic Signal.* 12, 161–174. doi: 10.1007/s11302-015-9490-3

Costello, J. C., Rosenthal, A. K., Kurup, I. V., Masuda, I., Medhora, M., and Ryan, L. M. (2011). Parallel regulation of extracellular ATP and inorganic pyrophosphate: roles of growth factors, transduction modulators, and ANK. *Connect. Tissue Res.* 52, 139–146. doi: 10.3109/03008207.2010.491928

Côté, N., El Husseini, D., Pepin, A., Guauque-Olarte, S., Ducharme, V., Bouchard-Cannon, P., et al. (2012). ATP acts as a survival signal and prevents the mineralization of aortic valve. *J. Mol. Cell Cardiol.* 52, 1191–1202. doi: 10.1016/j.yjmcc.2012.02.003

Coughlan, K. S., Mitchem, M. R., Hogg, M. C., and Prehn, J. H. (2015). "Preconditioning" with latrepirdine, an adenosine 5′-monophosphate-activated protein kinase activator, delays amyotrophic lateral sclerosis progression in SOD1(G93A) mice. *Neurobiol. Aging* 36, 1140–1150. doi: 10.1016/j.neurobiolaging.2014.09.022

Cristalli, G., Vittori, S., Thompson, R. D., Padgett, W. L., Shi, D., Daly, J. W., et al. (1994). Inhibition of platelet aggregation by adenosine receptor agonists. *Naunyn Schmiedebergs Arch. Pharmacol.* 349, 644–650.

Crossland, R. F., Durgan, D. J., Lloyd, E. E., Phillips, S. C., Reddy, A. K., Marrelli, S. P., et al. (2013). A new rodent model for obstructive sleep apnea: effects on ATP-mediated dilations in cerebral arteries. *Am. J. Physiol. Regul. Integr. Comp. Physiol.* 305, R334–R342. doi: 10.1152/ajpregu.00244.2013

Cruz, F. (2013). Targets for botulinum toxin in the lower urinary tract. *Neurourol. Urodyn.* 33, 31–38. doi: 10.1002/nau.22445

Csóka, B., Németh, Z. H., Törö, G., Idzko, M., Zech, A., Koscsó, B., et al. (2015). Extracellular ATP protects against sepsis through macrophage P2X7 purinergic receptors by enhancing intracellular bacterial killing. *FASEB J.* 29, 3626–3637. doi: 10.1096/fj.15-272450

Cunha, M. P., Pazini, F. L., Rosa, J. M., Ramos-Hryb, A. B., Oliveira, Á, Kaster, M. P., et al. (2015). Creatine, similarly to ketamine, affords antidepressant-like effects in the tail suspension test via adenosine A1 and A2A receptor activation. *Purinergic Signal.* 11, 215–227. doi: 10.1007/s11302-015-9446-7

Cunha, R. (2015). Hippocampal adenosine A2A receptor up-regulation isnecessary and sufficient to trigger memory dysfunction inAlzheimer's disease. *J. Neurochem.* 134, 322.

Cunha, R. A. (2016). How does adenosine control neuronal dysfunction and neurodegeneration? *J. Neurochem.* 139, 1019–1055. doi: 10.1111/jnc.13724

da Rocha Lapa, F., Da Silva, M. D., De Almeida Cabrini, D., and Santos, A. R. (2012). Anti-inflammatory effects of purine nucleosides, adenosine and inosine, in a mouse model of pleurisy: evidence for the role of adenosine A2 receptors. *Purinergic Signal.* 8, 693–704. doi: 10.1007/s11302-012-9299-2

da Rocha Lapa, F., Júnior, S. J. M., Cerutti, M. L., and Santos, A. R. S. (2014). "Pharmacology of adenosine receptors and their signaling role in immunity and inflammation," in *Pharmacology and Therapeutics*, ed. S. J. T. Gowder (Rijeka: InTech), 85–130.

da Silva, M. V., Marosti, A. R., Mendes, C. E., Palombit, K., and Castelucci, P. (2015). Differential effects of experimental ulcerative colitis on P2X7 receptor expression in enteric neurons. *Histochem. Cell Biol.* 143, 171–184. doi: 10.1007/s00418-014-1270-6

da Silva, M. V., Marosti, A. R., Mendes, C. E., Palombit, K., and Castelucci, P. (2017). Submucosal neurons and enteric glial cells expressing the P2X7 receptor in rat experimental colitis. *Acta Histochem.* 119, 481–494. doi: 10.1016/j.acthis.2017.05.001

Dai, S. S., and Zhou, Y. G. (2011). Adenosine 2A receptor: a crucial neuromodulator with bidirectional effect in neuroinflammation and brain injury. *Rev. Neurosci.* 22, 231–239. doi: 10.1515/RNS.2011.020

Dai, Y., Zhang, Y., Phatarpekar, P., Mi, T., Zhang, H., Blackburn, M. R., et al. (2009). Adenosine signaling, priapism and novel therapies. *J. Sex. Med.* 6(Suppl. 3), 292–301. doi: 10.1111/j.1743-6109.2008.01187.x

D'Alimonte, I., Nargi, E., Zuccarini, M., Lanuti, P., Di Iorio, P., Giuliani, P., et al. (2015). Potentiation of temozolomide antitumor effect by purine receptor ligands able to restrain the in vitro growth of human glioblastoma stem cells. *Purinergic Signal.* 11, 331–346. doi: 10.1007/s11302-015-9454-7

Daneshgari, F., Liu, G., and Imrey, P. B. (2006). Time dependent changes in diabetic cystopathy in rats include compensated and decompensated bladder function. *J. Urol.* 176, 380–386. doi: 10.1016/S0022-5347(06)00582-9

Daniele, S., Zappelli, E., Natali, L., Martini, C., and Trincavelli, M. L. (2014). Modulation of A1 and A2B adenosine receptor activity: a new strategy to sensitise glioblastoma stem cells to chemotherapy. *Cell. Death Dis.* 5, e1539. doi: 10.1038/cddis.2014.487

Danquah, W., Meyer-Schwesinger, C., Rissiek, B., Pinto, C., Serracant-Prat, A., Amadi, M., et al. (2016). Nanobodies that block gating of the P2X7 ion channel ameliorate inflammation. *Sci. Transl. Med.* 8, 366ra162. doi: 10.1126/scitranslmed.aaf8463

Darville, T., Welter-Stahl, L., Cruz, C., Sater, A. A., Andrews, C. W. Jr., and Ojcius, D. M. (2007). Effect of the purinergic receptor P2X7 on Chlamydia infection in cervical epithelial cells and vaginally infected mice. *J. Immunol.* 179, 3707–3714. doi: 10.4049/jimmunol.179.6.3707

Davies, J., Li, H., Karmouty-Quintana, H., Chen, N. Y., Weng, T., Molina, J., et al. (2016). Extracellular adenosine is detrimental in lung recovery following hyperoxic lung injury in a murine model of bronchopulmonary dysplasia. *Am. J. Respir. Crit. Care Med.* 193, A3850.

de Azevedo, M. I., Ferreiro, L., Da Silva, A. S., Tonin, A. A., Monteiro, D. U., Casali, E. A., et al. (2016). Participation of purines in the modulation of inflammatory response in rats experimentally infected by *Cryptococcus neoformans*. *Microb. Pathog.* 99, 36–40. doi: 10.1016/j.micpath.2016.07.015

de Diego-Garcia, L., Ramírez-Escudero, M., Sebastián-Serrano, A., Diaz-Hernández, J. I., Pintor, J., Lucas, J. J., et al. (2017). Regulation of proteasome activity by P2Y2 receptor underlies the neuroprotective effects of extracellular

nucleotides. *Biochim. Biophys. Acta* 1863, 43–51. doi: 10.1016/j.bbadis.2016.10.012

de Lera Ruiz, M., Lim, Y. H., and Zheng, J. (2014). Adenosine A2A receptor as a drug discovery target. *J. Med. Chem.* 57, 3623–3650. doi: 10.1021/jm4011669

De Luca, L., Capranzano, P., Patti, G., and Parodi, G. (2016). Switching of platelet P2Y12 receptor inhibitors in patients with acute coronary syndromes undergoing percutaneous coronary intervention: review of the literature and practical considerations. *Am. Heart J.* 176, 44–52. doi: 10.1016/j.ahj.2016.03.006

De Mattei, M., Varani, K., Masieri, F. F., Pellati, A., Ongaro, A., Fini, M., et al. (2009). Adenosine analogs and electromagnetic fields inhibit prostaglandin E2 release in bovine synovial fibroblasts. *Osteoarthritis Cartilage* 17, 252–262. doi: 10.1016/j.joca.2008.06.002

Deiteren, A., Van Der Linden, L., De Wit, A., Ceuleers, H., Buckinx, R., Timmermans, J. P., et al. (2015). P2X3 receptors mediate visceral hypersensitivity during acute chemically-induced colitis and in the post-inflammatory phase via different mechanisms of sensitization. *PLOS ONE* 10:e0123810. doi: 10.1371/journal.pone.0123810

Della Latta, V., Cabiati, M., Rocchiccioli, S., Del Ry, S., and Morales, M. A. (2013). The role of the adenosinergic system in lung fibrosis. *Pharmacol. Res.* 76, 182–189. doi: 10.1016/j.phrs.2013.08.004

Densmore, J. C., Schaid, T. R., Jeziorczak, P. M., Medhora, M., Audi, S., Nayak, S., et al. (2017). Lung injury pathways: adenosine receptor 2B signaling limits development of ischemic bronchiolitis obliterans organizing pneumonia. *Exp. Lung Res.* 43, 38–48. doi: 10.1080/01902148.2017.1286697

De Oliveira Moreira, D., Santo Neto, H., and Marques, M. J. (2017). P2Y2 purinergic receptors are highly expressed in cardiac and diaphragm muscles of mdx mice, and their expression is decreased by suramin. *Muscle Nerve* 55, 116–121. doi: 10.1002/mus.25199

DeOliveira, C. C., Paiva Caria, C. R., Ferreira Gotardo, E. M., Ribeiro, M. L., and Gambero, A. (2017). Role of A1 and A2A adenosine receptor agonists in adipose tissue inflammation induced by obesity in mice. *Eur. J. Pharmacol.* 799, 154–159. doi: 10.1016/j.ejphar.2017.02.017

Deplano, S., Cook, H. T., Russell, R., Franchi, L., Schneiter, S., Bhangal, G., et al. (2013). P2X7 receptor-mediated Nlrp3-inflammasome activation is a genetic determinant of macrophage-dependent crescentic glomerulonephritis. *J. Leukoc. Biol.* 93, 127–134. doi: 10.1189/jlb.0612284

Diezmos, E. F., Bertrand, P. P., and Liu, L. (2016). Purinergic signaling in gut inflammation: the role of connexins and pannexins. *Front. Neurosci.* 10:311. doi: 10.3389/fnins.2016.00311

Di Virgilio, F. (2015). P2X receptors and inflammation. *Curr. Med. Chem.* 22, 866–877. doi: 10.2174/0929867322666141210155311

Di Virgilio, F., and Adinolfi, E. (2017). Extracellular purines, purinergic receptors and tumor growth. *Oncogene* 36, 293–303. doi: 10.1038/onc.2016.206

Di Virgilio, F., and Vuerich, M. (2015). Purinergic signaling in the immune system. *Auton. Neurosci.* 191, 117–123. doi: 10.1016/j.autneu.2015.04.011

Djerada, Z., Feliu, C., Richard, V., and Millart, H. (2017). Current knowledge on the role of P2Y receptors in cardioprotection against ischemia-reperfusion. *Pharmacol. Res.* 118, 5–18. doi: 10.1016/j.phrs.2016.08.009

do Carmo, G. M., Doleski, P. H., De Sá, M. F., Grando, T. H., Bottari, N. B., Leal, D. B., et al. (2017). Purinergic enzymatic activities in lymphocytes and cardiomyocytes of mice acutely infected by *Trypanosoma cruzi* modulating the inflammatory responses. *Exp. Parasitol.* 175, 44–50. doi: 10.1016/j.exppara.2017.02.002

Domercq, M., Perez-Samartin, A., Aparicio, D., Alberdi, E., Pampliega, O., and Matute, C. (2010). P2X7 receptors mediate ischemic damage to oligodendrocytes. *Glia* 58, 730–740. doi: 10.1002/glia.20958

Dong, F., Yang, X. J., Jiang, T. B., and Chen, Y. (2016). Ischemia triggered ATP release through Pannexin-1 channel by myocardial cells activates sympathetic fibers. *Microvasc. Res.* 104, 32–37. doi: 10.1016/j.mvr.2015.11.005

Dragicevic, E., Schiemann, J., and Liss, B. (2015). Dopamine midbrain neurons in health and Parkinson's disease: emerging roles of voltage-gated calcium channels and ATP-sensitive potassium channels. *Neuroscience* 284, 798–814. doi: 10.1016/j.neuroscience.2014.10.037

Dranoff, J. A., Kruglov, E. A., Abreu-Lanfranco, O., Nguyen, T., Arora, G., and Jain, D. (2007). Prevention of liver fibrosis by the purinoceptor antagonist pyridoxal-phosphate-6-azophenyl-2′,4′-disulfonate (PPADS). *In Vivo* 21, 957–965.

Du, D., Jiang, M., Liu, M., Wang, J., Xia, C., Guan, R., et al. (2015). Microglial P2X7 receptor in the hypothalamic paraventricular nuclei contributes to sympathoexcitatory responses in acute myocardial infarction rat. *Neurosci. Lett.* 587, 22–28. doi: 10.1016/j.neulet.2014.12.026

Du, X., Ou, X., Song, T., Zhang, W., Cong, F., Zhang, S., et al. (2015). Adenosine A2B receptor stimulates angiogenesis by inducing VEGF and eNOS in human microvascular endothelial cells. *Exp. Biol. Med.* 240, 1472–1479. doi: 10.1177/1535370215584939

Dziubina, A., Szmyd, K., Zygmunt, M., Sapa, J., Dudek, M., Filipek, B., et al. (2016). Evaluation of antidepressant-like and anxiolytic-like activity of purinedione-derivatives with affinity for adenosine A2A receptors in mice. *Pharmacol. Rep.* 68, 1285–1292. doi: 10.1016/j.pharep.2016.07.008

Eckle, T., Koeppen, M., and Eltzschig, H. K. (2009). Role of extracellular adenosine in acute lung injury. *Physiology* 24, 298–306. doi: 10.1152/physiol.00022.2009

El-Hashim, A. Z., Mathew, S., and Spina, D. (2016). The A1 adenosine receptor is a novel inhibitory receptor that regulates the cough reflex via a central mechanism of action. *Am. J. Respir. Crit. Care Med.* 193, A6003–A6003.

Elsherbiny, N. M., Ahmad, S., Naime, M., Elsherbini, A. M., Fulzele, S., Al-Gayyar, M. M., et al. (2013a). ABT-702, an adenosine kinase inhibitor, attenuates inflammation in diabetic retinopathy. *Life Sci.* 93, 78–88. doi: 10.1016/j.lfs.2013.05.024

Elsherbiny, N. M., Naime, M., Ahmad, S., Elsherbini, A. M., Mohammad, S., Fulzele, S., et al. (2013b). Potential roles of adenosine deaminase-2 in diabetic retinopathy. *Biochem. Biophys. Res. Commun.* 436, 355–361. doi: 10.1016/j.bbrc.2013.05.023

Engel, T. (2016). Purinergic signaling-induced neuroinflammation and status epilepticus. *Expert. Rev. Neurother.* 16, 735–737. doi: 10.1586/14737175.2016.1164036

Engel, T., Alves, M., Sheedy, C., and Henshall, D. C. (2016). ATPergic signalling during seizures and epilepsy. *Neuropharmacology* 104, 140–153. doi: 10.1016/j.neuropharm.2015.11.001

Erb, L., Cao, C., Ajit, D., and Weisman, G. A. (2015). P2Y receptors in Alzheimer's disease. *Biol. Cell* 107, 1–21. doi: 10.1111/boc.201400043

Erlinge, D., and Burnstock, G. (2008). P2 receptors in cardiovascular regulation and disease. *Purinergic Signal.* 4, 1–20. doi: 10.1007/s11302-007-9078-7

Escudero, C., Casanello, P., and Sobrevia, L. (2008). Human equilibrative nucleoside transporters 1 and 2 may be differentially modulated by A2B adenosine receptors in placenta microvascular endothelial cells from pre-eclampsia. *Placenta* 29, 816–825. doi: 10.1016/j.placenta.2008.06.014

Escudero, C., Roberts, J. M., Myatt, L., and Feoktistov, I. (2014). Impaired adenosine-mediated angiogenesis in preeclampsia: potential implications for fetal programming. *Front. Pharmacol.* 5:134. doi: 10.3389/fphar.2014.00134

Eser, A., Colombel, J. F., Rutgeerts, P., Vermeire, S., Vogelsang, H., Braddock, M., et al. (2015). Safety and efficacy of an oral inhibitor of the purinergic receptor P2X7 in adult patients with moderately to severely active Crohn's disease: a randomized placebo-controlled, double-blind, phase IIa study. *Inflamm. Bowel Dis.* 21, 2247–2253. doi: 10.1097/MIB.0000000000000514

Essawy, S. S., Tawfik, M. K., and Korayem, H. E. (2017). Effects of adenosine receptor antagonists in MPTP mouse model of Parkinson's disease: mitochondrial DNA integrity. *Arch. Med. Sci.* 13, 659–669. doi: 10.5114/aoms.2017.67284

Esther, C. R. Jr., Olsen, B. M., Lin, F. C., Fine, J., and Boucher, R. C. (2013). Exhaled breath condensate adenosine tracks lung function changes in cystic fibrosis. *Am. J. Physiol. Lung. Cell Mol. Physiol.* 304, L504–L509. doi: 10.1152/ajplung.00344.2012

Esther, C. R., Muhlebach, M. M., Turkovic, L., Rosenow, T., Boucher, R. C., and Stick, S. M. (2015). Increased airway adenosine metabolism and oxidative stress in early cystic fibrosis lung disease. *Am. J. Respir. Crit. Care Med.* 191, A1032.

Eun, S. Y., Ko, Y. S., Park, S. W., Chang, K. C., and Kim, H. J. (2015). P2Y2 nucleotide receptor-mediated extracellular signal-regulated kinases and protein kinase C activation induces the invasion of highly metastatic breast cancer cells. *Oncol. Rep.* 34, 195–202. doi: 10.3892/or.2015.3972

Eyo, U. B., Peng, J., Swiatkowski, P., Mukherjee, A., Bispo, A., and Wu, L. J. (2014). Neuronal hyperactivity recruits microglial processes via neuronal NMDA receptors and microglial P2Y12 receptors after status epilepticus. *J. Neurosci.* 34, 10528–10540. doi: 10.1523/JNEUROSCI.0416-14.2014

Faas, M. M., Sáez, T., and De Vos, P. (2017). Extracellular ATP and adenosine: the Yin and Yang in immune responses? *Mol. Aspects Med.* 55, 9–19. doi: 10.1016/j.mam.2017.01.002

Fabiyi, A. C., and Brading, A. F. (2006). The use of the isolated mouse whole bladder for investigating bladder overactivity. *J. Pharmacol. Exp. Ther.* 319, 1386–1394. doi: 10.1124/jpet.106.108902

Falk, S., Schwab, S. D., Frosig-Jorgensen, M., Clausen, R. P., Dickenson, A. H., and Heegaard, A. M. (2015). P2X7 receptor-mediated analgesia in cancer-induced bone pain. *Neuroscience* 291, 93–105. doi: 10.1016/j.neuroscience.2015.02.011

Fan, Y., Kong, H., Ye, X., Ding, J., and Hu, G. (2016). ATP-sensitive potassium channels: uncovering novel targets for treating depression. *Brain Struct. Funct.* 221, 3111–3122. doi: 10.1007/s00429-015-1090-z

Fang, J., Chen, X., Wang, S., Xie, T., Du, X., Liu, H., et al. (2015). The expression of P2X7 receptors in EPCs and their potential role in the targeting of EPCs to brain gliomas. *Cancer Biol. Ther.* 16, 498–510. doi: 10.1080/15384047.2015.1016663

Faria, M., Timóteo, M. A., Lafuente-De-Carvalho, M., and Correia-De-Sá, P. (2010). P2 purinoceptor subtyope changes in patients with vasculogenic erectile dysfunction. *Purinergic Signal.* 6, S115.

Fasullo, M., and Endres, L. (2015). Nucleotide salvage deficiencies, DNA damage and neurodegeneration. *Int. J. Mol. Sci.* 16, 9431–9449. doi: 10.3390/ijms16059431

Fathalla, A. M., Soliman, A. M., Ali, M. H., and Moustafa, A. A. (2016). Adenosine A2A receptor blockade prevents rotenone-induced motor impairment in a rat model of Parkinsonism. *Front. Behav. Neurosci.* 10:35. doi: 10.3389/fnbeh.2016.00035

Fausther, M., Sheung, N., Saiman, Y., Bansal, M. B., and Dranoff, J. A. (2012). Activated hepatic stellate cells upregulate transcription of ecto-5′-nucleotidase/CD73 via specific SP1 and SMAD promoter elements. *Am. J. Physiol. Gastrointest. Liver Physiol.* 303, G904–G914. doi: 10.1152/ajpgi.00015.2012

Fehm, T., Zwirner, M., Wallwiener, D., Seeger, H., and Neubauer, H. (2012). Antitumor activity of zoledronic acid in primary breast cancer cells determined by the ATP tumor chemosensitivity assay. *BMC Cancer* 12:308. doi: 10.1186/1471-2407-12-308

Feng, L., Sun, X., Csizmadia, E., Han, L., Bian, S., Murakami, T., et al. (2011). Vascular CD39/ENTPD1 directly promotes tumor cell growth by scavenging extracellular adenosine triphosphate. *Neoplasia* 13, 206–216. doi: 10.1593/neo.101332

Feng, Y. H., Li, X., Wang, L., Zhou, L., and Gorodeski, G. I. (2006). A truncated P2X7 receptor variant (P2X7-j) endogenously expressed in cervical cancer cells antagonizes the full-length P2X7 receptor through hetero-oligomerization. *J. Biol. Chem.* 281, 17228–17237. doi: 10.1074/jbc.M602999200

Fern, R. F., Matute, C., and Stys, P. K. (2014). White matter injury: ischemic and nonischemic. *Glia* 62, 1780–1789. doi: 10.1002/glia.22722

Fernando, S. L., Saunders, B. M., Sluyter, R., Skarratt, K. K., Goldberg, H., Marks, G. B., et al. (2007). A polymorphism in the P2X7 gene increases susceptibility to extrapulmonary tuberculosis. *Am. J. Respir. Crit. Care Med.* 175, 360–366. doi: 10.1164/rccm.200607-970OC

Ferrante, A., Martire, A., Pepponi, R., Varani, K., Vincenzi, F., Ferraro, L., et al. (2014). Expression, pharmacology and functional activity of adenosine A1 receptors in genetic models of Huntington's disease. *Neurobiol. Dis.* 71, 193–204. doi: 10.1016/j.nbd.2014.08.013

Ferrari, D., Bianchi, N., Eltzschig, H. K., and Gambari, R. (2016a). MicroRNAs modulate the purinergic signaling network. *Trends Mol. Med.* 22, 905–918. doi: 10.1016/j.molmed.2016.08.006

Ferrari, D., Mcnamee, E. N., Idzko, M., Gambari, R., and Eltzschig, H. K. (2016b). Purinergic signaling during immune cell trafficking. *Trends Immunol.* 37, 399–411. doi: 10.1016/j.it.2016.04.004

Ferrari, D., Vitiello, L., Idzko, M., and La Sala, A. (2015). Purinergic signaling in atherosclerosis. *Trends Mol. Med.* 21, 184–192. doi: 10.1016/j.molmed.2014.12.008

Ferré, S., Bonaventura, J., Tomasi, D., Navarro, G., Moreno, E., Cortés, A., et al. (2016). Allosteric mechanisms within the adenosine A2A-dopamine D2 receptor heterotetramer. *Neuropharmacology* 104, 154–160. doi: 10.1016/j.neuropharm.2015.05.028

Ferrée, S. (2016). Mechanisms of the psychostimulant effects of caffeine: implications for substance use disorders. *Psychopharmacology* 233, 1963–1979. doi: 10.1007/s00213-016-4212-2

Festugato, M. (2015). Adenosine: an endogenous mediator in the pathogenesis of psoriasis. *An. Bras. Dermatol.* 90, 862–867. doi: 10.1590/abd1806-4841.20153689

Fiebich, B. L., Akter, S., and Akundi, R. S. (2014). The two-hit hypothesis for neuroinflammation: role of exogenous ATP in modulating inflammation in the brain. *Front. Cell Neurosci.* 8:260. doi: 10.3389/fncel.2014.00260

Figliuolo, V. R., Chaves, S. P., Savio, L. E. B., Thorstenberg, M. L. P., Machado Salles, E., Takiya, C. M., et al. (2017a). The role of the P2X7 receptor in murine cutaneous leishmaniasis: aspects of inflammation and parasite control. *Purinergic Signal.* 13, 143–152. doi: 10.1007/s11302-016-9544-1

Figliuolo, V. R., Savio, L. E. B., Safya, H., Nanini, H., Bernardazzi, C., Abalo, A., et al. (2017b). P2X7 receptor promotes intestinal inflammation in chemically induced colitis and triggers death of mucosal regulatory T cells. *Biochim. Biophys. Acta* 1863, 1183–1194. doi: 10.1016/j.bbadis.2017.03.004

Figueiredo, A. B., Souza-Testasicca, M. C., and Afonso, L. C. (2016). Purinergic signaling and infection by *Leishmania*: a new approach to evasion of the immune response. *Biomed. J.* 39, 244–250. doi: 10.1016/j.bj.2016.08.004

Fischer, T., Rotermund, N., Lohr, C., and Hirnet, D. (2012). P2Y1 receptor activation by photolysis of caged ATP enhances neuronal network activity in the developing olfactory bulb. *Purinergic Signal.* 8, 191–198. doi: 10.1007/s11302-011-9286-z

Fish, R. S., Klootwijk, E., Tam, F. W. K., Kleta, R., Wheeler, D. C., Unwin, R. J., et al. (2013). ATP and arterial calcification. *Eur. J. Clin. Invest.* 43, 405–412. doi: 10.1111/eci.12055

Fishman, P., Ochaion, A., Cohen, S., Patoka, R., Barer, F., and Bar-Yehuda, S. (2008). The anti-inflammatory effect of A3 adenosine receptor agonists: a novel targeted therapy for rheumatoid arthritis. *Expert Opin. Investig. Drugs* 16, 1601–1613. doi: 10.1517/13543784.16.10.1601

Fonseca, B., Martinez-Aguila, A., De Lara, M. J. P., and Pintor, J. (2017). Diadenosine tetraphosphate as a potential therapeutic nucleotide to treat glaucoma. *Purinergic Signal.* 13, 171–177. doi: 10.1007/s11302-016-9547-y

Ford, A. P., and Cockayne, D. A. (2011). ATP and P2X purinoceptors in urinary tract disorders. *Handb. Exp. Pharmacol.* 202, 485–526. doi: 10.1007/978-3-642-16499-6_22

Ford, A. P., and Undem, B. J. (2013). The therapeutic promise of ATP antagonism at P2X3 receptors in respiratory and urological disorders. *Front. Cell Neurosci.* 7:267. doi: 10.3389/fncel.2013.00267

Ford, A. P., Undem, B. J., Birder, L. A., Grundy, D., Pijacka, W., and Paton, J. F. (2015). P2X3 receptors and sensitization of autonomic reflexes. *Auton. Neurosci.* 191, 16–24. doi: 10.1016/j.autneu.2015.04.005

Förster, D., and Reiser, G. (2015). Supportive or detrimental roles of P2Y receptors in brain pathology?—The two faces of P2Y receptors in stroke and neurodegeneration detected in neural cell and in animal model studies. *Purinergic Signal.* 11, 441–454. doi: 10.1007/s11302-015-9471-6

Fotino, C., Vergani, A., Fiorina, P., and Pileggi, A. (2015). P2X receptors and diabetes. *Curr. Med. Chem.* 22, 891–901. doi: 10.2174/0929867321666141012173520

Fragakis, N., Antoniadis, A. P., Saviano, M., Vassilikos, V., and Pappone, C. (2015). The use of adenosine and adenosine triphosphate testing in the diagnosis, risk stratification and management of patients with syncope: current evidence and future perspectives. *Int. J. Cardiol.* 183, 267–273. doi: 10.1016/j.ijcard.2015.01.089

Franco, M., Bautista-Perez, R., Cano-Martinez, A., Pacheco, U., Santamaria, J., Del Valle-Mondragon, L., et al. (2017). Physiopathological implications of P2X1 and P2X7 receptors in regulation of glomerular hemodynamics in angiotensin II-induced hypertension. *Am. J. Physiol. Renal Physiol.* 313, F9–F19. doi: 10.1152/ajprenal.00663.2016

Franklin, K. M., Asatryan, L., Jakowec, M. W., Trudell, J. R., Bell, R. L., and Davies, D. L. (2014). P2X4 receptors (P2X4Rs) represent a novel target for the development of drugs to prevent and/or treat alcohol use disorders. *Front. Neurosci.* 8:176. doi: 10.3389/fnins.2014.00176

Fransson, A., Järlebark, L. E., and Ulfendahl, M. (2009). In vivo infusion of UTP and uridine to the deafened guinea pig inner ear: effects on response thresholds and neural survival. *J. Neurosci. Res.* 87, 1712–1717. doi: 10.1002/jnr.21969

Frenguelli, B. G., and Wall, M. J. (2016). Combined electrophysiological and biosensor approaches to study purinergic regulation of epileptiform activity in cortical tissue. *J. Neurosci. Methods* 260, 202–214. doi: 10.1016/j.jneumeth.2015.09.011

Friebe, D., Yang, T., Schmidt, T., Borg, N., Steckel, B., Ding, Z., et al. (2014). Purinergic signaling on leukocytes infiltrating the LPS-injured lung. *PLOS ONE* 9:e95382. doi: 10.1371/journal.pone.0095382

Frontini, A. V., Cd, D. L. V. E., Nicolorich, M. V., Naves, A., Schwarzbaum, P., and Venera, G. D. (2011). In vivo effects of adenosine 5′-triphosphate on rat preneoplastic liver. *Medicina* 71, 139–145.

Fu, S., and Davies, K. P. (2015). Opiorphin-dependent upregulation of CD73 (a key enzyme in the adenosine signaling pathway) in corporal smooth muscle cells exposed to hypoxic conditions and in corporal tissue in pre-priapic sickle cell mice. *Int. J. Impot. Res.* 27, 140–145. doi: 10.1038/ijir.2015.5

Fu, W., Mccormick, T., Qi, X., Luo, L., Zhou, L., Li, X., et al. (2009). Activation of P2X7-mediated apoptosis Inhibits DMBA/TPA-induced formation of skin papillomas and cancer in mice. *BMC Cancer* 9:114. doi: 10.1186/1471-2407-9-114

Fuller, S. J., Stokes, L., Skarratt, K. K., Gu, B. J., and Wiley, J. S. (2009). Genetics of the P2X7 receptor and human disease. *Purinergic Signal.* 5, 257–262. doi: 10.1007/s11302-009-9136-4

Fumagalli, M., Lecca, D., and Abbracchio, M. P. (2016). CNS remyelination as a novel reparative approach to neurodegenerative diseases: the roles of purinergic signaling and the P2Y-like receptor GPR17. *Neuropharmacology* 104, 82–93. doi: 10.1016/j.neuropharm.2015.10.005

Füredi, R., Bölcskei, K., Szolcsányi, J., and Pethö, G. (2010). Comparison of the peripheral mediator background of heat injury- and plantar incision-induced drop of the noxious heat threshold in the rat. *Life Sci.* 86, 244–250. doi: 10.1016/j.lfs.2009.12.010

Furlan-Freguia, C., Marchese, P., Gruber, A., Ruggeri, Z. M., and Ruf, W. (2011). P2X7 receptor signaling contributes to tissue factor-dependent thrombosis in mice. *J. Clin. Invest.* 121, 2932–2944. doi: 10.1172/JCI46129

Furlong, T. M., Supit, A. S., Corbit, L. H., Killcross, S., and Balleine, B. W. (2015). Pulling habits out of rats: adenosine 2A receptor antagonism in dorsomedial striatum rescues meth-amphetamine-induced deficits in goal-directed action. *Addict. Biol.* 22, 172–183. doi: 10.1111/adb.12316

Gan, M., Moussaud, S., Jiang, P., and Mclean, P. J. (2015). Extracellular ATP induces intracellular alpha-synuclein accumulation via P2X1 receptor-mediated lysosomal dysfunction. *Neurobiol. Aging* 36, 1209–1220. doi: 10.1016/j.neurobiolaging.2014.10.037

Gandelman, M., Levy, M., Cassina, P., Barbeito, L., and Beckman, J. S. (2013). P2X7 receptor-induced death of motor neurons by a peroxynitrite/FAS-dependent pathway. *J. Neurochem.* 126, 382–388. doi: 10.1111/jnc.12286

Gao, L., Cao, L., Qui, Y., Su, Z., Burnstock, G., Xiang, Z., et al. (2010). Blocking P2X receptors can inhibit the injury-induced proliferation of olfactory epithelium progenitor cells in adult mouse. *Int. J. Pediatr. Otorhinolaryngol.* 74, 747–751. doi: 10.1016/j.ijporl.2010.03.030

Gao, Y., Xu, C., Yu, K., Li, G., Wan, F., Liu, S., et al. (2010). Effect of tetramethylpyrazine on DRG neuron P2X3 receptor involved in transmitting pain after burn. *Burns* 36, 127–134. doi: 10.1016/j.burns.2009.04.032

Gariboldi, V., Vairo, D., Guieu, R., Marlingue, M., Ravis, E., Lagier, D., et al. (2017). Expressions of adenosine A2A receptors in coronary arteries and peripheral blood mononuclear cells are correlated in coronary artery disease patients. *Int. J. Cardiol.* 230, 427–431. doi: 10.1016/j.ijcard.2016.12.089

Gazzerro, E., Baldassari, S., Assereto, S., Fruscione, F., Pistorio, A., Panicucci, C., et al. (2015). Enhancement of muscle T regulatory cells and improvement of muscular dystrophic process in mdx mice by blockade of extracellular ATP/P2X axis. *Am. J. Pathol.* 185, 3349–3360. doi: 10.1016/j.ajpath.2015.08.010

Gehring, M. P., Kipper, F., Nicoletti, N. F., Sperotto, N. D., Zanin, R., Tamajusuku, A. S., et al. (2015). P2X7 receptor as predictor gene for glioma radiosensitivity and median survival. *Int. J. Biochem. Cell Biol.* 68, 92–100. doi: 10.1016/j.biocel.2015.09.001

Gendaszewska-Darmach, E., and Kucharska, M. (2011). Nucleotide receptors as targets in the pharmacological enhancement of dermal wound healing. *Purinergic Signal.* 7, 193–206. doi: 10.1007/s11302-011-9233-z

Gendaszewska-Darmach, E., and Szustak, M. (2016). Thymidine 5′-O-monophosphorothioate induces HeLa cell migration by activation of the P2Y6 receptor. *Purinergic Signal.* 12, 199–209. doi: 10.1007/s11302-015-9492-1

Gentile, D., Natale, M., Lazzerini, P. E., Capecchi, P. L., and Laghi-Pasini, F. (2015). The role of P2X7 receptors in tissue fibrosis: a brief review. *Purinergic Signal.* 11, 435–440. doi: 10.1007/s11302-015-9466-3

Geraghty, N. J., Watson, D., Adhikary, S. R., and Sluyter, R. (2016). P2X7 receptor in skin biology and diseases. *World J. Dermatol.* 5, 72–83. doi: 10.5314/wjd.v5.i2.72

Ghanbari, H., Jani, R., Hussain-Amin, A., Al-Assad, W., Huether, E., Ansari, S., et al. (2016). Role of adenosine after antral pulmonary vein isolation of paroxysmal atrial fibrillation: a randomized controlled trial. *Heart Rhythm* 13, 407–415. doi: 10.1016/j.hrthm.2015.10.016

Giannuzzo, A., Saccomano, M., Napp, J., Ellegaard, M., Alves, F., and Novak, I. (2016). Targeting of the P2X7 receptor in pancreatic cancer and stellate cells. *Int. J. Cancer* 139, 2540–2552. doi: 10.1002/ijc.30380

Gicquel, T., Le Dare, B., Boichot, E., and Lagente, V. (2017). Purinergic receptors: new targets for the treatment of gout and fibrosis. *Fundam. Clin. Pharmacol.* 31, 136–146. doi: 10.1111/fcp.12256

Gidlöf, O., Sathanoori, R., Magistri, M., Faghihi, M. A., Wahlestedt, C., Olde, B., et al. (2015). Extracellular uridine triphosphate and adenosine triphosphate attenuate endothelial inflammation through miR-22-mediated ICAM-1 inhibition. *J. Vasc. Res.* 52, 71–80. doi: 10.1159/000431367

Gill, A., Wortham, K., Costa, D., Davis, W., Ticho, B., and Whalley, E. (2009). Protective effect of tonapofylline (BG9928), an adenosine A1 receptor antagonist, against cisplatin-induced acute kidney injury in rats. *Am. J. Nephrol.* 30, 521–526. doi: 10.1159/000248762

Giniatullin, R., and Nistri, A. (2013). Desensitization properties of P2X3 receptors shaping pain signaling. *Front. Cell Neurosci.* 7:245. doi: 10.3389/fncel.2013.00245

Giorgi, V. S., Witkin, S. S., Bannwart-Castro, C. F., Sartori, M. S., Romao-Veiga, M., Borges, V. T., et al. (2016). Elevated circulatingadenosine deaminase activity in women with preeclampsia: association with pro-inflammatory cytokine production and uric acid levels. *Pregnancy Hypertens.* 6, 400–405. doi: 10.1016/j.preghy.2016.09.004

Giuliani, A. L., Colognesi, D., Ricco, T., Roncato, C., Capece, M., Amoroso, F., et al. (2014). Trophic activity of human P2X7 receptor isoforms A and B in osteosarcoma. *PLOS ONE* 9:e107224. doi: 10.1371/journal.pone.0107224

Giuliani, A. L., Sarti, A. C., Falzoni, S., and Di Virgilio, F. (2017). The P2X7 receptor-interleukin-1 liaison. *Front. Pharmacol.* 8:123. doi: 10.3389/fphar.2017.00123

Giuliani, P., Zuccarini, M., Buccella, S., Pena-Altamira, L. E., Polazzi, E., Virgili, M., et al. (2017). Evidence for purine nucleoside phosphorylase (PNP) release from rat C6 glioma cells. *J. Neurochem.* 141, 208–221. doi: 10.1111/jnc.14004

Glass, R., Bardini, M., Robson, T., and Burnstock, G. (2001). Expression of nucleotide P2X receptor subtypes during spermatogenesis in the adult rat testis. *Cells Tissues Org.* 169, 377–387. doi: 10.1159/000047905

Gloria-Bottini, F., Saccucci, P., Ammendola, M., Neri, A., Magrini, A., and Bottini, E. (2016). Genetic variability within Adenosine Deaminase gene and uterine leiomyomas. *Eur. J. Obstet. Gynecol. Reprod. Biol.* 199, 108–109. doi: 10.1016/j.ejogrb.2016.02.002

Gnad, T., Scheibler, S., Von Kügelgen, I., Scheele, C., Kilic, A., Glode, A., et al. (2014). Adenosine activates brown adipose tissue and recruits beige adipocytes via A2A receptors. *Nature* 516, 395–399. doi: 10.1038/nature13816

Go, G., Sung, J.-S., Jee, S.-C., Kim, M., Jang, W.-H., Kang, K.-Y., et al. (2017). In vitro anti-obesity effects of sesamol mediated by adenosine monophosphate-activated protein kinase and mitogen-activated protein kinase signaling in 3T3-L1 cells. *Food Sci. Biotechnol.* 26, 195–200. doi: 10.1007/s10068-017-0026-1

Gölöncsér, F., and Sperlágh, B. (2014). Effect of genetic deletion and pharmacological antagonism of P2X7 receptors in a mouse animal model of migraine. *J. Headache Pain* 15:24. doi: 10.1186/1129-2377-15-24

Gomez-Villafuertes, R., Garcia-Huerta, P., Diaz-Hernandez, J. I., and Miras-Portugal, M. T. (2015). PI3K/Akt signaling pathway triggers P2X7 receptor expression as a pro-survival factor of neuroblastoma cells under limiting growth conditions. *Sci. Rep.* 5:18417. doi: 10.1038/srep18417

Gonçalves, F. M., Neis, V. B., Rieger, D. K., Lopes, M. W., Heinrich, I. A., Costa, A. P., et al. (2017). Signaling pathways underlying the antidepressant-like effect of inosine in mice. *Purinergic Signal.* 13, 203–214. doi: 10.1007/s11302-016-9551-2

Goonetilleke, L., Ralevic, V., and Dunn, W. R. (2013). Influence of pressure on adenosine triphosphate function as a sympathetic neurotransmitter in small mesenteric arteries from the spontaneously hypertensive rat. *J. Hypertens.* 31, 312–320. doi: 10.1097/HJH.0b013e32835bd74d

Gorodeski, G. I. (2009). P2X7-mediated chemoprevention of epithelial cancers. *Expert. Opin. Ther. Targets* 13, 1313–1332. doi: 10.1517/14728220903277249

Gorodeski, G. I. (2015). Purinergic signalling in the reproductive system. *Auton. Neurosci.* 191, 82–101. doi: 10.1016/j.autneu.2015.04.008

Graubardt, N., Fahrner, R., Trochsler, M., Keogh, A., Breu, K., Furer, C., et al. (2013). Promotion of liver regeneration by natural killer cells in a murine model is dependent on extracellular adenosine triphosphate phosphohydrolysis. *Hepatology* 57, 1969–1979. doi: 10.1002/hep.26008

Greene, S. J., Sabbah, H. N., Butler, J., Voors, A. A., Abrecht-Küpper, B. E., Düngen, H. D., et al. (2016). Partial adenosine A1 receptor agonism: a potential new therapeutic strategy for heart failure. *Heart Fail. Rev.* 21, 95–102. doi: 10.1007/s10741-015-9522-7

Greer, S., Page, C. W., Joshi, T., Yan, D., Newton, R., and Giembycz, M. A. (2013). Concurrent agonism of adenosine A2B and glucocorticoid receptors in human airway epithelial cells cooperatively induces genes with anti-inflammatory potential: a novel approach to treat chronic obstructive pulmonary disease. *J. Pharmacol. Exp. Ther.* 346, 473–485. doi: 10.1124/jpet.113.206284

Grenz, A., Kim, J.-H., Bauerle, J. D., Tak, E., Eltzschig, H. K., and Clambey, E. T. (2012). Adora2b adenosine receptor signaling protects during acute kidney injury via inhibition of neutrophil-dependent TNF-α release. *J. Immunol.* 189, 4566–4573. doi: 10.4049/jimmunol.1201651

Greve, A. S., Skals, M., Fagerberg, S. K., Tonnus, W., Ellermann-Eriksen, S., Evans, R. J., et al. (2017). P2X1, P2X4, and P2X7 receptor knock out mice expose differential outcome of sepsis induced by α-haemolysin producing *Escherichia coli*. *Front. Cell Infect. Microbiol.* 7:113. doi: 10.3389/fcimb.2017.00113

Gu, B. J., Field, J., Dutertre, S., Ou, A., Kilpatrick, T. J., Lechner-Scott, J., et al. (2015). A rare P2X7 variant Arg307Gln with absent pore formation function protects against neuroinflammation in multiple sclerosis. *Hum. Mol. Genet.* 24, 5644–5654. doi: 10.1093/hmg/ddv278

Gualix, J., León-Otegui, M., Recuero, M., Bullido, M. J., Valdivieso, F., and Miras-Portugal, M. T. (2015). Functional characterization of P2Y1 and P2X4 receptors in human neuroblastoma SK-N-MC cells. *An. Real Acad. Farm.* 81, 247–257.

Gubert, C., Fries, G. R., Wollenhaupt De Aguiar, B., Ribeiro, A. R., Busnello, J. V., Ribeiro, L., et al. (2013). The P2X7 purinergic receptor as a molecular target in bipolar disorder. *Neuropsychiatry Neuropsychol.* 8, 1–7.

Gubert, C., Jacintho Moritz, C. E., Vasconcelos-Moreno, M. P., Quadros Dos Santos, B. T., Sartori, J., Fijtman, A., et al. (2016). Peripheral adenosine levels in euthymic patients with bipolar disorder. *Psychiatry Res.* 246, 421–426. doi: 10.1016/j.psychres.2016.10.007

Guixà-González, R., Javanainen, M., Gómez-Soler, M., Cordobilla, B., Domingo, J. C., Sanz, F., et al. (2016). Membrane omega-3 fatty acids modulate the oligomerisation kinetics of adenosine A2A and dopamine D2 receptors. *Sci. Rep.* 6:19839. doi: 10.1038/srep19839

Guo, J., Fu, X., Cui, X., and Fan, M. (2015). Contributions of purinergic P2X3 receptors within the midbrain periaqueductal gray to diabetes-induced neuropathic pain. *J. Physiol. Sci.* 65, 99–104. doi: 10.1007/s12576-014-0344-5

Gupta, S., and Sharma, B. (2014). Protective effects of phosphodiesterase-1 (PDE1) and ATP sensitive potassium (KATP) channel modulators against 3-nitropropionic acid induced behavioral and biochemical toxicities in experimental Huntington×s disease. *Eur. J. Pharmacol.* 732, 111–122. doi: 10.1016/j.ejphar.2014.03.032

Gür, S., Kadowitz, P. J., Abdel-Mageed, A. S., Kendirci, M., Sikka, S. C., Burnstock, G., et al. (2009). Management of erectile function by penile purinergic P2 receptors in the diabetic rat. *J. Urol.* 181, 2375–2382. doi: 10.1016/j.juro.2009.01.002

Gur, S., Kadowitz, P. J., and Hellstrom, W. J. (2007). Purinergic (P2) receptor control of lower genitourinary tract function and new avenues for drug action: an overview. *Curr. Pharm. Des.* 13, 3236–3244. doi: 10.2174/138161207782341277

Guzman, S. J., and Gerevich, Z. (2016). P2Y receptors in synaptic transmission and plasticity: therapeutic potential in cognitive dysfunction. *Neural Plast.* 2016:1207393. doi: 10.1155/2016/1207393

Guzman-Aranguez, A., Gasull, X., Diebold, Y., and Pintor, J. (2014). Purinergic receptors in ocular inflammation. *Mediators Inflamm.* 2014:320906. doi: 10.1155/2014/320906

Guzmán-Aránguez, A., Irazu, M., Yayon, A., and Pintor, J. (2008). P2Y receptors activated by diadenosine polyphosphates reestablish Ca^{2+} transients in achondroplasic chondrocytes. *Bone* 42, 516–523. doi: 10.1016/j.bone.2007.10.023

Haanes, K. A., and Edvinsson, L. (2014). Expression and characterization of purinergic receptors in rat middle meningeal artery-potential role in migraine. *PLOS ONE* 9:e108782. doi: 10.1371/journal.pone.0108782

Hafner, S., Wagner, K., Weber, S., Gröger, M., Wepler, M., Mccook, O., et al. (2017). Role of the purinergic receptor P2XR4 after blunt chest trauma in cigarette smoke-exposed mice. *Shock* 47, 193–199. doi: 10.1097/SHK.0000000000000726

Hamidpour, R., Hamidpour, S., Hamidpour, M., Zarabi, M., Sohraby, M., and Shalari, M. (2016). Antipurinergic therapy with suramin as a treatment for autism spectrum disorder. *J. Biomed. Sci.* 5, 14. doi: 10.4172/2254-609X.100028

Hansen, R. R., Nasser, A., Falk, S., Baldvinsson, S. B., Ohlsson, P. H., Bahl, J. M., et al. (2012). Chronic administration of the selective P2X3, P2X2/3 receptor antagonist, A-317491, transiently attenuates cancer-induced bone pain in mice. *Eur. J. Pharmacol.* 688, 27–34. doi: 10.1016/j.ejphar.2012.05.008

Hansen, R. R., Nielsen, C. K., Nasser, A., Thomsen, S. I., Eghorn, L. F., Pham, Y., et al. (2011). P2X7 receptor-deficient mice are susceptible to bone cancer pain. *Pain* 152, 1766–1776. doi: 10.1016/j.pain.2011.03.024

Hansson, E., Werner, T., Björklund, U., and Skiöldebrand, E. (2016). Therapeutic innovation: inflammatory-reactive astrocytes as targets of inflammation. *IBRO Rep.* 1, 1–9. doi: 10.1016/j.ibror.2016.06.001

Hao, Y., Liang, J. F., Chow, A. W., Cheung, W. T., and Ko, W. H. (2014). P2Y6 receptor-mediated proinflammatory signaling in human bronchial epithelia. *PLOS ONE* 9:e106235. doi: 10.1371/journal.pone.0106235

Hao, Y., Zhou, G., Wu, W., Zhang, Y., Tao, L., Yao, J., et al. (2017). Synthesis and antiviral evaluation of novel N-6 substituted adenosine analogues. *Tetrahedron Lett.* 58, 190–193. doi: 10.1016/j.tetlet.2016.11.059

Harmse, R., Van Der Walt, M. M., Petzer, J. P., and Terre'blanche, G. (2016). Discovery of 1,3-diethyl-7-methyl-8-(phenoxymethyl)-xanthine derivatives as novel adenosine A1 and A2A receptor antagonists. *Bioorg. Med. Chem. Lett.* 26, 5951–5955. doi: 10.1016/j.bmcl.2016.10.086

Hasebe, H., Yoshida, K., Iida, M., Hatano, N., Muramatsu, T., and Aonuma, K. (2016). Right-to-left frequency gradient during atrial fibrillation initiated by right atrial ectopies and its augmentation by adenosine triphosphate: implications of right atrial fibrillation. *Heart Rhythm* 13, 354–363. doi: 10.1016/j.hrthm.2015.09.030

Hattori, F., Ohshima, Y., Seki, S., Tsukimoto, M., Sato, M., Takenouchi, T., et al. (2012). Feasibility study of B16 melanoma therapy using oxidized ATP to target purinergic receptor P2X7. *Eur. J. Pharmacol.* 695, 20–26. doi: 10.1016/j.ejphar.2012.09.001

Hayoz, S., Jia, C., and Hegg, C. (2012). Mechanisms of constitutive and ATP-evoked ATP release in neonatal mouse olfactory epithelium. *BMC Neurosci.* 13:53. doi: 10.1186/1471-2202-13-53

He, W., Mazumder, A., Wilder, T., and Cronstein, B. N. (2012). Adenosine regulates bone metabolism via A_1, A_{2A} and A_{2B} receptors in bone marrow cells from normal humans and patients with multiple myeloma. *FASEB J.* 27, 3446–3454. doi: 10.1096/fj.13-231233

Headrick, J. P., Ashton, K. J., Rose'meyer, R. B., and Peart, J. N. (2013). Cardiovascular adenosine receptors: expression, actions and interactions. *Pharmacol. Ther.* 140, 92–111. doi: 10.1016/j.pharmthera.2013.06.002

Higgins, G., Buchanan, P., Perriere, M., Al-Alawi, M., Costello, R. W., Verriere, V., et al. (2014). Activation of P2RY11 and ATP release by lipoxin A4 restores the airway surface liquid layer and epithelial repair in cystic fibrosis. *Am. J. Respir. Cell Mol. Biol.* 51, 178–190. doi: 10.1165/rcmb.2012-0424OC

Ho, M. F., Low, L. M., and Rose'meyer, R. B. (2016). Pharmacology of the adenosine A3 receptor in the vasculature and essential hypertension. *PLOS ONE* 11:e0150021. doi: 10.1371/journal.pone.0150021

Ho, T., Aplin, F. P., Jobling, A. I., Phipps, J. A., De Iongh, R. U., Greferath, U., et al. (2016). Localization and possible function of P2X receptors in normal and diseased retinae. *J Ocul. Pharmacol. Ther.* 32, 509–517. doi: 10.1089/jop.2015.0158

Hoegl, S., Brodsky, K. S., Blackburn, M. R., Karmouty-Quintana, H., Zwissler, B., and Eltzschig, H. K. (2015). Alveolar epithelial A2B adenosine receptors in pulmonary protection during acute lung injury. *J. Immunol.* 195, 1815–1824. doi: 10.4049/jimmunol.1401957

Hofer, M., Pospisil, M., Dusek, L., Hoferova, Z., Weiterova, L., and Komurkova, D. (2013). Erythropoiesis- and thrombopoiesis-characterizing parameters in adenosine A3 receptor knock-out mice. *Physiol. Res.* 62, 305–311.

Hofman, P., Cherfils-Vicini, J., Bazin, M., Ilie, M., Juhel, T., Hébuterne, X., et al. (2015). Genetic and pharmacological inactivation of the purinergic P2RX7 receptor dampens inflammation but increases tumor incidence in a mouse model of colitis-associated cancer. *Cancer Res.* 75, 835–845. doi: 10.1158/0008-5472.CAN-14-1778

Holst, S. C., Valomon, A., and Landolt, H. P. (2016). Sleep pharmacogenetics: personalized sleep-wake therapy. *Annu. Rev. Pharmacol. Toxicol.* 56, 577–603. doi: 10.1146/annurev-pharmtox-010715-103801

Hooper, J. S., Hadley, S. H., Morris, K. F., Breslin, J. W., Dean, J. B., and Taylor-Clark, T. E. (2016). Characterization of cardiovascular reflexes evoked by airway stimulation with allylisothiocyanate, capsaicin, and ATP in Sprague-Dawley rats. *J. Appl. Physiol.* 120, 580–591. doi: 10.1152/japplphysiol.00944.2015

Hoque, R., Sohail, M. A., Salhanick, S., Malik, A. F., Ghani, A., Robson, S. C., et al. (2012). P2X7 receptor-mediated purinergic signaling promotes liver injury in acetaminophen hepatotoxicity in mice. *Am. J. Physiol. Gastrointest. Liver Physiol.* 302, G1171–G1179. doi: 10.1152/ajpgi.00352.2011

Horckmans, M., Esfahani, H., Beauloye, C., Clouet, S., Di Pietrantonio, L., Robaye, B., et al. (2015). Loss of mouse P2Y4 nucleotide receptor protects against myocardial infarction through endothelin-1 downregulation. *J. Immunol.* 194, 1874–1881. doi: 10.4049/jimmunol.1401364

Houchi, H., Persyn, W., Legastelois, R., and Naassila, M. (2013). The adenosine A2A receptor agonist CGS 21680 decreases ethanol self-administration in both non-dependent and dependent animals. *Addict. Biol.* 18, 812–825. doi: 10.1111/adb.12032

Housley, G. D., Bringmann, A., and Reichenbach, A. (2009). Purinergic signaling in special senses. *Trends Neurosci.* 32, 128–141. doi: 10.1016/j.tins.2009.01.001

Howarth, A. R., Conway, B. R., and Bailey, M. A. (2015). Vascular and inflammatory actions of P2X receptors in renal injury. *Auton. Neurosci.* 191, 135–140. doi: 10.1016/j.autneu.2015.05.001

Hu, F., Hui, Z., Wei, W., Yang, J., Chen, Z., Guo, B., et al. (2017). Hypotonic stress promotes ATP release, reactive oxygen species production and cell proliferation via TRPV4 activation in rheumatoid arthritis rat synovial fibroblasts. *Biochem. Biophys. Res. Commun.* 486, 108–115. doi: 10.1016/j.bbrc.2017.03.008

Hu, H., Yang, B., Li, Y., Zhang, S., and Li, Z. (2016). Blocking of the P2X7 receptor inhibits the activation of the MMP-13 and NF-κB pathways in the cartilage tissue of rats with osteoarthritis. *Int. J. Mol. Med.* 38, 1922–1932. doi: 10.3892/ijmm.2016.2770

Hu, J., Ye, F., Cui, M., Lee, P., Wei, C., Hao, Y., et al. (2016). Protein profiling of bladder urothelial cell carcinoma. *PLOS ONE* 11:e0161922. doi: 10.1371/journal.pone.0161922

Hu, S. J., Calippe, B., Lavalette, S., Roubeix, C., Montassar, F., Housset, M., et al. (2015). Upregulation of P2RX7 in Cx3cr1-deficient mononuclear phagocytes leads to increased interleukin-1β secretion and photoreceptor neurodegeneration. *J. Neurosci.* 35, 6987–6996. doi: 10.1523/JNEUROSCI.3955-14.2015

Hu, X., Liou, A. K., Leak, R. K., Xu, M., An, C., Suenaga, J., et al. (2014). Neurobiology of microglial action in CNS injuries: receptor-mediated signaling mechanisms and functional roles. *Prog. Neurobiol.* 11, 60–84. doi: 10.1016/j.pneurobio.2014.06.002

Hua, X., Naselsky, W. C., Bennett, W. D., Ledent, C., Senior, B. A., and Tilley, S. L. (2013). Adenosine increases nasal mucociliary clearance rate in mice through A2A and A2B adenosine receptors. *Laryngoscope* 123, 306–310. doi: 10.1002/lary.23586

Huang, J., Zhang, M., Zhang, P., Liang, H., Ouyang, K., and Yang, H. T. (2016). Coupling switch of P2Y-IP3 receptors mediates differential Ca^{2+} signaling in human embryonic stem cells and derived cardiovascular progenitor cells. *Purinergic Signal.* 12, 465–478. doi: 10.1007/s11302-016-9512-9

Huang, T. C., Chang, H. Y., Hsu, C. H., Kuo, W. H., Chang, K. J., and Juan, H. F. (2008). Targeting therapy for breast carcinoma by ATP synthase inhibitor aurovertin B. *J. Proteome Res.* 7, 1433–1444. doi: 10.1021/pr700742h

Huang, Z. L., Liu, R., Bai, X. Y., Zhao, G., Song, J. K., Wu, S., et al. (2014). Protective effects of the novel adenosine derivative WS0701 in a mouse model of posttraumatic stress disorder. *Acta Pharmacol. Sin.* 35, 24–32. doi: 10.1038/aps.2013.143

Huber, S. M. (2012). Purinoceptor signaling in malaria-infected erythrocytes. *Microbes Infect.* 14, 779–786. doi: 10.1016/j.micinf.2012.04.009

Huete, F., Guzmán-Aránguez, A., Ortin, J., Hoyle, C. H., and Pintor, J. (2011). Effects of diadenosine tetraphosphate on FGF9-induced chloride flux changes in achondroplastic chondrocytes. *Purinergic Signal.* 7, 243–249. doi: 10.1007/s11302-011-9234-y

Hullugundi, S. K., Ansuini, A., Ferrari, M. D., Van Den Maagdenberg, A. M., and Nistri, A. (2014). A hyperexcitability phenotype in mouse trigeminal sensory neurons expressing the R192Q Cacna1a missense mutation of familial hemiplegic migraine type-1. *Neuroscience* 266, 244–254. doi: 10.1016/j.neuroscience.2014.02.020

Hupertan, V., Neuzillet, Y., Stücker, O., Pons, C., Leammel, E., and Lebret, T. (2012). Effects of nucleotides adenosine monophosphate and adenosine triphosphate in combination with L-arginine on male rabbit corpus cavernosum tissue. *Int. J. Androl.* 35, 860–866. doi: 10.1111/j.1365-2605.2012.01290.x

Hur, H., Kim, N. K., Kim, H. G., Min, B. S., Lee, K. Y., Shin, S. J., et al. (2012). Adenosine triphosphate-based chemotherapy response assay-guided chemotherapy in unresectable colorectal liver metastasis. *Br. J. Cancer* 106, 53–60. doi: 10.1038/bjc.2011.469

Hurtado-Alvarado, G., Domínguez-Salazar, E., Velázquez-Moctezuma, J., and Gómez-González, B. (2016). A2A adenosine receptor antagonism reverts the blood-brain barrier dysfunction induced by sleep restriction. *PLOS ONE* 11:e0167236. doi: 10.1371/journal.pone.0167236

Husted, L. B., Harsløf, T., Stenkjær, L., Carstens, M., Jørgensen, N. R., and Langdahl, B. L. (2013). Functional polymorphisms in the P2X7 receptor gene are associated with osteoporosis. *Osteoporos. Int.* 24, 949–959. doi: 10.1007/s00198-012-2035-5

Iba, K., and Yamashita, T. (2016). "Osteoclast-mediated pain in osteoporosis," in *Osteoporosis in Orthopedics: Assessment and Therapeutic Options*, eds Y. Shimada and N. Miyakoshi (Tokyo: Springer), 23–34. doi: 10.1007/978-4-431-55778-4_2

Ibrahim, A. S., El-Shishtawy, M. M., Zhang, W., Caldwell, R. B., and Liou, G. I. (2011). A2A adenosine receptor (A2AAR) as a therapeutic target in diabetic retinopathy. *Am. J. Pathol.* 178, 2136–2145. doi: 10.1016/j.ajpath.2011.01.018

Ikeda, N., Murata, S., Maruyama, T., Tamura, T., Nozaki, R., Kawasaki, T., et al. (2012). Platelet-derived adenosine 5′-triphosphate suppresses activation of human hepatic stellate cell: in vitro study. *Hepatol. Res.* 42, 91–102. doi: 10.1111/j.1872-034X.2011.00893.x

Ikeda, Y., Zabbarova, I. V., Birder, L. A., De Groat, W. C., Mccarthy, C. J., Hanna-Mitchell, A. T., et al. (2012). Botulinum neurotoxin serotype A suppresses neurotransmitter release from afferent as well as efferent nerves in the urinary bladder. *Eur. Urol.* 62, 1157–1164. doi: 10.1016/j.eururo.2012.03.031

Ilatovskaya, D. V., Palygin, O., and Staruschenko, A. (2016). Functional and therapeutic importance of purinergic signaling in polycystic kidney disease. *Am. J. Physiol. Renal Physiol.* 311, F1135–F1139. doi: 10.1152/ajprenal.00406.2016

Illes, P., and Rubini, P. (2017). Regulation of neural stem/progenitor cell functions by P2X and P2Y receptors. *Neural Regen. Res.* 12, 395–396. doi: 10.4103/1673-5374.202937

Illes, P., Verkhratsky, A., Burnstock, G., and Sperlagh, B. (2016). Purines in neurodegeneration and neuroregeneration. *Neuropharmacology* 104, 1–3. doi: 10.1016/j.neuropharm.2016.01.020

Imarisio, C., Alchera, E., Sutti, S., Valente, G., Boccafoschi, F., Albano, E., et al. (2012). Adenosine A_{2A} receptor stimulation prevents hepatocyte lipotoxicity and non-alcoholic steatohepatitis (NASH) in rats. *Clin. Sci.* 123, 323–332. doi: 10.1042/CS20110504

Ingwersen, J., Wingerath, B., Graf, J., Lepka, K., Hofrichter, M., Schröter, F., et al. (2016). Dual roles of the adenosine A2a receptor in autoimmune neuroinflammation. *J. Neuroinflammation* 13, 48. doi: 10.1186/s12974-016-0512-z

Inoue, Y., Yoshimura, K., Kurabe, N., Kahyo, T., Kawase, A., Tanahashi, M., et al. (2017). Prognostic impact of CD73 and A2A adenosine receptor expression in non-small-cell lung cancer. *Oncotarget* 8, 8738–8751. doi: 10.18632/oncotarget.14434

Iriyama, T., Sun, K., Parchim, N. F., Li, J., Zhao, C., Song, A., et al. (2015). Elevated placental adenosine signaling contributes to the pathogenesis of preeclampsia. *Circulation* 131, 730–741. doi: 10.1161/CIRCULATIONAHA.114.013740

Ishikawa, T., Miyagi, M., Ohtori, S., Aoki, Y., Ozawa, T., Doya, H., et al. (2005). Characteristics of sensory DRG neurons innervating the lumbar facet joints in rats. *Eur. Spine J.* 14, 559–564. doi: 10.1007/s00586-004-0834-x

Ishimaru, M., Tsukimoto, M., Harada, H., and Kojima, S. (2013). Involvement of P2Y11 receptor in IFN-γ-induced IL-6 production in human keratinocytes. *Eur. J. Pharmacol.* 703, 67–73. doi: 10.1016/j.ejphar.2013.02.020

Iskandarov, E., Kadaba Srinivasan, P., Xin, W., Bleilevens, C., Afify, M., Hamza, A., et al. (2016). Protective effects of adenosine receptor agonist in a cirrhotic liver resection model. *Hepat. Mon.* 16:e36821. doi: 10.5812/hepatmon.36821

Iwata, M., Ota, K. T., Li, X. Y., Sakaue, F., Li, N., Dutheil, S., et al. (2016). Psychological stress activates the inflammasome via release of adenosine triphosphate and stimulation of the purinergic type 2X7 receptor. *Biol. Psychiatry* 80, 12–22. doi: 10.1016/j.biopsych.2015.11.026

Jacob, F., Novo, C. P., Bachert, C., and Crombruggen, K. (2013). Purinergic signaling in inflammatory cells: P2 receptor expression, functional effects, and modulation of inflammatory responses. *Purinergic Signal.* 9, 285–306. doi: 10.1007/s11302-013-9357-4

Jacobs, B., and Dussor, G. (2016). Neurovascular contributions to migraine: moving beyond vasodilation. *Neuroscience* 338, 130–144. doi: 10.1016/j.neuroscience.2016.06.012

Jacobson, K. A., and Muller, C. E. (2016). Medicinal chemistry of adenosine, P2Y and P2X receptors. *Neuropharmacology* 104, 31–49. doi: 10.1016/j.neuropharm.2015.12.001

Jajoo, S., Mukherjea, D., Watabe, K., and Ramkumar, V. (2009). Adenosine A3 receptor suppresses prostate cancer metastasis by inhibiting NADPH oxidase activity. *Neoplasia* 11, 1132–1145. doi: 10.1593/neo.09744

Jalkanen, J., Yegutkin, G. G., Hollmén, M., Aalto, K., Kiviniemi, T., Salomaa, V., et al. (2015). Aberrant circulating levels of purinergic signaling markers are associated with several key aspects of peripheral atherosclerosis and thrombosis. *Circ. Res.* 116, 1206–1215. doi: 10.1161/CIRCRESAHA.116.305715

Jameel, M. N., Xiong, Q., Mansoor, A., Bache, R. J., and Zhang, J. (2016). ATP sensitive K^+ channels are critical for maintaining myocardial perfusion and high energy phosphates in the failing heart. *J. Mol. Cell. Cardiol.* 92, 116–121. doi: 10.1016/j.yjmcc.2016.02.005

Janes, K., Symons-Liguori, A. M., Jacobson, K. A., and Salvemini, D. (2016). Identification of A3 adenosine receptor agonists as novel non-narcotic analgesics. *Br. J. Pharmacol.* 173, 1253–1267. doi: 10.1111/bph.13446

Jared Bunch, T. (2015). One drug, two outcomes after atrial fibrillation ablation: the situational irony of adenosine. *Eur. Heart J.* 36, 3288–3290. doi: 10.1093/eurheartj/ehv473

Jastrzebska, J., Nowak, E., Smaga, I., Bystrowska, B., Frankowska, M., Bader, M., et al. (2014). Adenosine A2A receptor modulation of nicotine-induced locomotor sensitization. A pharmacological and transgenic approach. *Neuropharmacology* 81, 318–326. doi: 10.1016/j.neuropharm.2014.03.002

Jelassi, B., Anchelin, M., Chamouton, J., Cayuela, M. L., Clarysse, L., Li, J., et al. (2013). Anthraquinone emodin inhibits human cancer cell invasiveness by antagonizing P2X7 receptors. *Carcinogenesis* 34, 1487–1496. doi: 10.1093/carcin/bgt099

Jenner, P. (2014). An overview of adenosine A2A receptor antagonists in Parkinson's disease. *Int. Rev. Neurobiol.* 119, 71–86. doi: 10.1016/B978-0-12-801022-8.00003-9

Jeong, J. Y., Kim, J., Kim, B., Kim, J., Shin, Y., Kim, J., et al. (2016). IL-1ra secreted by ATP-induced P2Y2 negatively regulates MUC5AC overproduction via PLCβ3 during airway inflammation. *Mediators Inflamm.* 2016:7984853. doi: 10.1155/2016/7984853

Ji, X., Naito, Y., Hirokawa, G., Weng, H., Hiura, Y., Takahashi, R., et al. (2012). P2X7 receptor antagonism attenuates the hypertension and renal injury in Dahl salt-sensitive rats. *Hypertens. Res.* 35, 173–179. doi: 10.1038/hr.2011.153

Jia, C., Sangsiri, S., Belock, B., Iqbal, T. R., Pestka, J. J., and Hegg, C. C. (2011). ATP mediates neuroprotective and neuroproliferative effects in mouse olfactory epithelium following exposure to satratoxin G in vitro and in vivo. *Toxicol. Sci.* 124, 169–178. doi: 10.1093/toxsci/kfr213

Jia, X., Naito, H., Yetti, H., Tamada, H., Kitamori, K., Hayashi, Y., et al. (2012). The modulation of hepatic adenosine triphosphate and inflammation by eicosapentaenoic acid during severe fibrotic progression in the SHRSP5/Dmcr rat model. *Life Sci.* 90, 934–943. doi: 10.1016/j.lfs.2012.04.029

Jian, R., Sun, Y., Wang, Y., Yu, J., Zhong, L., and Zhou, P. (2012). CD73 protects kidney from ischemia-reperfusion injury through reduction of free radicals. *APMIS* 120, 130–138. doi: 10.1111/j.1600-0463.2011.02827.x

Jiang, S., Zhang, Y., Zheng, J. H., Li, X., Yao, Y. L., Wu, Y. L., et al. (2017). Potentiation of hepatic stellate cell activation by extracellular ATP is dependent on P2X7R-mediated NLRP3 inflammasome activation. *Pharmacol. Res.* 117, 82–93. doi: 10.1016/j.phrs.2016.11.040

Jiménez, M., Clavé, P., Accarino, A., and Gallego, D. (2014). Purinergic neuromuscular transmission in the gastrointestinal tract; functional basis for future clinical and pharmacological studies. *Br. J. Pharmacol.* 171, 4360–4375. doi: 10.1111/bph.12802

Jiménez, M., De Diego, M., Martínez-Cutillas, M., Mañé Reed, N., Gallego, D., Ojanguren, M., et al. (2015). Purinergic and nitrergic inhibitory neuromuscular transmission in ganglionic, transitional and aganglionic segments from Hirschsprung's disease patients. *Neurogastroenterol. Motil.* 27, 71.

Jimenez-Mateos, E. M., Arribas-Blazquez, M., Sanz-Rodriguez, A., Concannon, C., Olivos-Ore, L. A., Reschke, C. R., et al. (2015). microRNA targeting of the P2X7 purinoceptor opposes a contralateral epileptogenic focus in the hippocampus. *Sci. Rep.* 5:17486. doi: 10.1038/srep17486

Jin, F. (2016). Analysis on mechanism of ATP-sensitive K^+ channel opener natakalim improving congestive heart failure after myocardial infarction. *Exp. Ther. Med.* 12, 3993–3997. doi: 10.3892/etm.2016.3853

Jin, H., Seo, J., Eun, S. Y., Joo, Y. N., Park, S. W., Lee, J. H., et al. (2014). P2Y2R activation by nucleotides promotes skin wound-healing process. *Exp. Dermatol.* 23, 480–485. doi: 10.1111/exd.12440

Jin, W., Xu, W., Chen, J., Zhang, X., Shi, L., and Ren, C. (2016). Adenosine kinase facilitated astrogliosis-induced cortical neuronal death in traumatic brain injury. *J. Mol. Histol.* 47, 259–271. doi: 10.1007/s10735-016-9670-7

Jörg, M., Scammells, P. J., and Capuano, B. (2014). The dopamine D2 and adenosine A2A receptors: past, present and future trends for the treatment of Parkinson's disease. *Curr. Med. Chem.* 21, 3188–3210. doi: 10.2174/13892002156661402171107l6

Jørgensen, N. R., Boeynaems, J. M., and Di Virgilio, F. (2011). European meeting "P2 receptors: new targets for the treatment of osteoporosis". *Purinergic Signal.* 7, 275–276. doi: 10.1007/s11302-011-9223-1

Jørgensen, N. R., Grove, E. L., Schwarz, P., and Vestergaard, P. (2012). Clopidogrel and the risk of osteoporotic fractures: a nationwide cohort study. *J. Intern. Med.* 272, 385–393. doi: 10.1111/j.1365-2796.2012.02535.x

Jørgensen, N. R., Syberg, S., and Ellegaard, M. (2015). The role of P2X receptors in bone biology. *Curr. Med. Chem.* 22, 902–914. doi: 10.2174/0929867321666141215094749

Joseph, E. K., Green, P. G., Ferrari, L. F., and Levine, J. D. (2015). Homocysteine-induced attenuation of vascular endothelium-dependent hyperalgesia in the rat. *Neuroscience* 284, 678–684. doi: 10.1016/j.neuroscience.2014.10.056

Junger, W. G. (2011). Immune cell regulation by autocrine purinergic signalling. *Nat. Rev. Immunol.* 11, 201–212. doi: 10.1038/nri2938

Kaan, T. K., Yip, P. K., Patel, S., Davies, M., Marchand, F., Cockayne, D. A., et al. (2010). Systemic blockade of P2X3 and P2X2/3 receptors attenuates bone cancer pain behaviour in rats. *Brain* 133, 2549–2564. doi: 10.1093/brain/awq194

Kaiser, M., Penk, A., Franke, H., Krügel, U., Norenberg, W., Huster, D., et al. (2016). Lack of functional P2X7 receptor aggravates brain edema development after middle cerebral artery occlusion. *Purinergic Signal.* 12, 453–463. doi: 10.1007/s11302-016-9511-x

Kao, Y. H., Lin, M. S., Chen, C. M., Wu, Y. R., Chen, H. M., Lai, H. L., et al. (2017). Targeting ENT1 and adenosine tone for the treatment of Huntington's disease. *Hum. Mol. Genet.* 26, 467–478. doi: 10.1093/hmg/ddw402

Kapila, N., Higa, J. T., Longhi, M. S., and Robson, S. C. (2013). Autoimmune hepatitis: clinical review with insights into the purinergic mechanism of disease. *J. Clin. Transl. Hepatol.* 1, 79–86. doi: 10.14218/JCTH.2013.00015

Karmakar, M., Katsnelson, M. A., Dubyak, G. R., and Pearlman, E. (2016). Neutrophil P2X7 receptors mediate NLRP3 inflammasome-dependent IL-1β secretion in response to ATP. *Nat. Commun.* 7:10555. doi: 10.1038/ncomms10555

Kaster, M. P., Machado, N. J., Silva, H. B., Nunes, A., Ardais, A. P., Santana, M., et al. (2015). Caffeine acts through neuronal adenosine A2A receptors to prevent mood and memory dysfunction triggered by chronic stress. *Proc. Natl. Acad. Sci. U.S.A* 112, 7833–7838. doi: 10.1073/pnas.1423088112

Katz, N. K., Ryals, J. M., and Wright, D. E. (2015). Central or peripheral delivery of an adenosine A1 receptor agonist improves mechanical allodynia in a mouse model of painful diabetic neuropathy. *Neuroscience* 285, 312–323. doi: 10.1016/j.neuroscience.2014.10.065

Kavanagh, K. A., Schreiner, D. C., Levis, S. C., O'neill, C. E., and Bachtell, R. K. (2015). Role of adenosine receptor subtypes in methamphetamine reward and

reinforcement. *Neuropharmacology* 89, 265–273. doi: 10.1016/j.neuropharm.2014.09.030

Kawai, Y., Kaidoh, M., and Ohhashi, T. (2008). MDA-MB-231 produces ATP-mediated ICAM-1-dependent facilitation of the attachment of carcinoma cells to human lymphatic endothelial cells. *Am. J. Physiol. Cell Physiol.* 295, C1123–C1132. doi: 10.1152/ajpcell.00247.2008

Kawamura, H., Aswad, F., Minagawa, M., Govindarajan, S., and Dennert, G. (2006). P2X7 receptors regulate NKT cells in autoimmune hepatitis. *J. Immunol.* 176, 2152–2160. doi: 10.4049/jimmunol.176.4.2152

Ke, J., Yao, B., Li, T., Cui, S., and Ding, H. (2015). A2 adenosine receptor-mediated cardioprotection against reperfusion injury in rat hearts is associated with autophagy downregulation. *J. Cardiovasc. Pharmacol.* 66, 25–34. doi: 10.1097/FJC.0000000000000239

Keay, S. K., Birder, L. A., and Chai, T. C. (2014). Evidence for bladder urothelial pathophysiology in functional bladder disorders. *Biomed Res. Int.* 2014:865463. doi: 10.1155/2014/865463

Kehasse, A., Rich, C. B., Lee, A., Mccomb, M. E., Costello, C. E., and Trinkaus-Randall, V. (2013). Epithelial wounds induce differential phosphorylation changes in response to purinergic and EGF receptor activation. *Am. J. Pathol.* 183, 1841–1852. doi: 10.1016/j.ajpath.2013.08.015

Keystone, E. C., Wang, M. M., Layton, M., Hollis, S., and Mcinnes, I. B. (2012). Clinical evaluation of the efficacy of the P2X7 purinergic receptor antagonist AZD9056 on the signs and symptoms of rheumatoid arthritis in patients with active disease despite treatment with methotrexate or sulphasalazine. *Ann. Rheum. Dis.* 71, 1630–1635. doi: 10.1136/annrheumdis-2011-143578

Khalid, M., Brisson, L., Tariq, M., Hao, Y., Guibon, R., Fromont, G., et al. (2017). Carcinoma-specific expression of P2Y11 receptor and its contribution in ATP-induced purinergic signalling and cell migration in human hepatocellular carcinoma cells. *Oncotarget* 8, 37278–37290. doi: 10.18632/oncotarget.16191

Khoja, S., Shah, V., Garcia, D., Asatryan, L., Jakowec, M. W., and Davies, D. L. (2016). Role of purinergic P2X4 receptors in regulating striatal dopamine homeostasis and dependent behaviors. *J. Neurochem.* 139, 134–148. doi: 10.1111/jnc.13734

Kilinc, E., Koroleva, K., Guerrero Toro, C., Töre, F., and Giniatullin, R. (2015). The role of adenosine triphosphate and its receptors in migraine pathophysiology. *Acta Physiol.* 215, 44.

Killeen, M. E., Ferris, L., Kupetsky, E. A., Falo, L. Jr., and Mathers, A. R. (2013). Signaling through purinergic receptors for ATP induces human cutaneous innate and adaptive Th17 responses: implications in the pathogenesis of psoriasis. *J. Immunol.* 190, 4324–4336. doi: 10.4049/jimmunol.1202045

Kim, H., Walsh, M. C., Takegahara, N., Middleton, S. A., Shin, H. I., Kim, J., et al. (2017). The purinergic receptor P2X5 regulates inflammasome activity and hyper-multinucleation of murine osteoclasts. *Sci. Rep.* 7, 196. doi: 10.1038/s41598-017-00139-2

Kim, M. J., Turner, C. M., Hewitt, R., Smith, J., Bhangal, G., Pusey, C. D., et al. (2014). Exaggerated renal fibrosis in P2X4 receptor-deficient mice following unilateral ureteric obstruction. *Nephrol. Dial. Transplant.* 29, 1350–1361. doi: 10.1093/ndt/gfu019

Kimbler, D. E., Shields, J., Yanasak, N., Vender, J. R., and Dhandapani, K. M. (2012). Activation of P2X7 promotes cerebral edema and neurological injury after traumatic brain injury in mice. *PLOS ONE* 7:e41229. doi: 10.1371/journal.pone.0041229

Kinnamon, S. C., and Finger, T. E. (2013). A taste for ATP: neurotransmission in taste buds. *Front. Cell Neurosci.* 7:264. doi: 10.3389/fncel.2013.00264

Kira, S., Yoshiyama, M., Tsuchiya, S., Shigetomi, E., Miyamoto, T., Nakagomi, H., et al. (2017). P2Y6-deficiency increases micturition frequency and attenuates sustained contractility of the urinary bladder in mice. *Sci. Rep.* 7, 771. doi: 10.1038/s41598-017-00824-2

Kishore, B. K., Carlson, N. G., Ecelbarger, C. M., Kohan, D. E., Müller, C. E., Nelson, R. D., et al. (2015). Targeting renal purinergic signalling for the treatment of lithium-induced nephrogenic diabetes insipidus. *Acta Physiol.* 214, 176–188. doi: 10.1111/apha.12507

Kitta, T., Chancellor, M. B., De Groat, W. C., Kuno, S., Nonomura, K., and Yoshimura, N. (2012). Suppression of bladder overactivity by adenosine A2A receptor antagonist in a rat model of Parkinson disease. *J. Urol.* 187, 1890–1897. doi: 10.1016/j.juro.2011.12.062

Kizilirmak, F., Gunes, H. M., Demir, G. G., Gokdeniz, T., Guler, E., Cakal, B., et al. (2015). Impact of intracoronary adenosine on myonecrosis in patients with unstable angina pectoris undergoing percutaneous coronary intervention. *Cardiovasc. Drugs Ther.* 29, 519–526. doi: 10.1007/s10557-015-6631-4

Knight, G. E., Bodin, P., De Groat, W. C., and Burnstock, G. (2002). ATP is released from guinea pig ureter epithelium on distension. *Am. J. Physiol. Renal Physiol.* 282, F281–F288. doi: 10.1152/ajprenal.00293.2000

Kofoed, K., Skov, L., and Zachariae, C. (2015). New drugs and treatment targets in psoriasis. *Acta Derm. Venereol.* 95, 133–139. doi: 10.2340/00015555-1931

Köhler, D., Streienberger, A., Morote-García, J. C., Granja, T. F., Schneider, M., Straub, A., et al. (2016). Inhibition of adenosine kinase attenuates acute lung injury. *Crit. Care Med.* 44, e181–e189. doi: 10.1097/CCM.0000000000001370

Komai, A. M., Brännmark, C., Musovic, S., and Olofsson, C. S. (2014). PKA-independent cAMP stimulation of white adipocyte exocytosis and adipokine secretion: modulations by Ca^{2+} and ATP. *J. Physiol.* 592, 5169–5186. doi: 10.1113/jphysiol.2014.280388

Kornum, B. R., Kawashima, M., Faraco, J., Lin, L., Rico, T. J., Hesselson, S., et al. (2011). Common variants in P2RY11 are associated with narcolepsy. *Nat. Genet.* 43, 66–71. doi: 10.1038/ng.734

Kowaluk, E. A., and Jarvis, M. F. (2000). Therapeutic potential of adenosine kinase inhibitors. *Expert Opin. Investig. Drugs* 9, 551–564. doi: 10.1517/13543784.9.3.551

Krasowska, E., Róg, J., Sinadinos, A., Young, C. N., Górecki, D. C., and Zablocki, K. (2014). Purinergic receptors in skeletal muscles in health and in muscular dystrophy. *Postepy Biochem.* 60, 483–489.

Kretschmar, C., Oyarzún, C., Villablanca, C., Jaramillo, C., Alarcón, S., Perez, G., et al. (2016). Reduced adenosine uptake and its contribution to signaling that mediates profibrotic activation in renal tubular epithelial cells: implication in diabetic nephropathy. *PLOS ONE* 11:e0147430. doi: 10.1371/journal.pone.0147430

Krizaj, D., Ryskamp, D. A., Tian, N., Tezel, G., Mitchell, C. H., Slepak, V. Z., et al. (2014). From mechanosensitivity to inflammatory responses: new players in the pathology of glaucoma. *Curr. Eye Res.* 39, 105–119. doi: 10.3109/02713683.2013.836541

Krügel, U. (2016). Purinergic receptors in psychiatric disorders. *Neuropharmacology* 104, 212–225. doi: 10.1016/j.neuropharm.2015.10.032

Krügel, U., Köles, L., and Illes, P. (2013). Integration of neuronal and glial signalling by pyramidal cells of the rat prefrontal cortex; control of cognitive functions and addictive behaviour by purinergic mechanisms. *Neuropsychopharmacol. Hung.* 15, 206–213.

Kruglov, E. A., Correa, P. R., Arora, G., Yu, J., Nathanson, M. H., and Dranoff, J. A. (2007). Molecular basis for calcium signaling in hepatic stellate cells. *Am. J. Physiol. Gastrointest. Liver Physiol.* 292, G975–G982.

Kuan, Y. H., Shih, H. C., Tang, S. C., Jeng, J. S., and Shyu, B. C. (2015). Targeting P2X7 receptor for the treatment of central post-stroke pain in a rodent model. *Neurobiol. Dis.* 78, 134–145. doi: 10.1016/j.nbd.2015.02.028

Kuan, Y. H., and Shyu, B. C. (2016). Nociceptive transmission and modulation via P2X receptors in central pain syndrome. *Mol. Brain* 9, 58. doi: 10.1186/s13041-016-0240-4

Kudira, R., Malinka, T., Kohler, A., Dosch, M., De Aguero, M. G., Melin, N., et al. (2016). P2X1-regulated IL-22 secretion by innate lymphoid cells is required for efficient liver regeneration. *Hepatology* 63, 2004–2017. doi: 10.1002/hep.28492

Kumahashi, N., Naitou, K., Nishi, H., Oae, K., Watanabe, Y., Kuwata, S., et al. (2011). Correlation of changes in pain intensity with synovial fluid adenosine triphosphate levels after treatment of patients with osteoarthritis of the knee with high-molecular-weight hyaluronic acid. *Knee* 18, 160–164. doi: 10.1016/j.knee.2010.04.013

Kumar, V., Chapple, C. R., Rosario, D., Tophill, P. R., and Chess-Williams, R. (2010). In vitro release of adenosine triphosphate from the urothelium of human bladders with detrusor overactivity, both neurogenic and idiopathic. *Eur. Urol.* 57, 1087–1092. doi: 10.1016/j.eururo.2009.11.042

Kurashima, Y., and Kiyono, H. (2016). "Physiological and pathological inflammation at the mucosal frontline," in *Chronic Inflammation: Mechanisms and Regulation*, eds M. Miyasaka and K. Takatsu (Tokyo: Springer), 567–590.

Kurashima, Y., Kiyono, H., and Kunisawa, J. (2015). Pathophysiological role of extracellular purinergic mediators in the control of intestinal inflammation. *Mediators Inflamm.* 2015:427125. doi: 10.1155/2015/427125

Kurlak, L. O., Williams, P. J., Bulmer, J. N., Broughton Pipkin, F., and Mistry, H. D. (2015). Placental expression of adenosine A2A receptor and hypoxia inducible factor-1 alpha in early pregnancy, term and pre-eclamptic pregnancies:

interactions with placental renin-angiotensin system. *Placenta* 36, 611–613. doi: 10.1016/j.placenta.2015.02.011

Kvist, T. M., Schwarz, P., and Jørgensen, N. R. (2014). The P2X7 receptor: a key player in immune-mediated bone loss? *Sci. World J.* 2014:954530. doi: 10.1155/2014/954530

Kwon, S. G., Roh, D. H., Yoon, S. Y., Moon, J. Y., Choi, S. R., Choi, H. S., et al. (2014). Blockade of peripheral P2Y1 receptors prevents the induction of thermal hyperalgesia via modulation of TRPV1 expression in carrageenan-induced inflammatory pain rats: involvement of p38 MAPK phosphorylation in DRGs. *Neuropharmacology* 79, 368–379. doi: 10.1016/j.neuropharm.2013.12.005

Kyle, B. D. (2014). Ion channels of the mammalian urethra. *Channels* 8, 393–401. doi: 10.4161/19336950.2014.954224

Labazi, H., Teng, B., Zhou, Z., and Mustafa, S. J. (2016). Enhanced A2A adenosine receptor-mediated increase in coronary flow in type I diabetic mice. *J. Mol. Cell. Cardiol.* 90, 30–37. doi: 10.1016/j.yjmcc.2015.11.033

Lahmann, C., Clark, R. H., Iberl, M., and Ashcroft, F. M. (2014). A mutation causing increased KATP channel activity leads to reduced anxiety in mice. *Physiol. Behav.* 129, 79–84. doi: 10.1016/j.physbeh.2014.02.031

Lajdova, I., Oksa, A., Chorvat, J. D., Topor, P., and Spustova, V. (2012). Purinergic P2X7 receptors participate in disturbed intracellular calcium homeostasis in peripheral blood mononuclear cells of patients with chronic kidney disease. *Kidney Blood Press. Res.* 35, 48–57. doi: 10.1159/000330349

Laketa, D., Savic, J., Bjelobaba, I., Lavrnja, I., Vasic, V., Stojiljkovic, M., et al. (2015). Brain injury alters ectonucleotidase activities and adenine nucleotide levels in rat serum. *J. Med. Biochem.* 34, 215–222. doi: 10.2478/jomb-2014-0025

Lau, O. C., Samarawickrama, C., and Skalicky, S. E. (2014). P2Y2 receptor agonists for the treatment of dry eye disease: a review. *Clin. Ophthalmol.* 8, 327–334. doi: 10.2147/OPTH.S39699

Lavrnja, I., Laketa, D., Savic, D., Bozic, I., Bjelobaba, I., Pekovic, S., et al. (2015). Expression of a second ecto-5′-nucleotidase variant besides the usual protein in symptomatic phase of experimental autoimmune encephalomyelitis. *J. Mol. Neurosci.* 55, 898–911. doi: 10.1007/s12031-014-0445-x

Layland, J., Carrick, D., Lee, M., Oldroyd, K., and Berry, C. (2014). Adenosine: physiology, pharmacology, and clinical applications. *JACC Cardiovasc. Interv.* 7, 581–591. doi: 10.1016/j.jcin.2014.02.009

Ledderose, C., Bao, Y., Kondo, Y., Fakhari, M., Slubowski, C., Zhang, J., et al. (2016). Purinergic signaling and the immune response in sepsis: a review. *Clin. Ther.* 38, 1054–1065. doi: 10.1016/j.clinthera.2016.04.002

Lee, B. H., Hwang, D. M., Palaniyar, N., Grinstein, S., Philpott, D. J., and Hu, J. (2012). Activation of P2X7 receptor by ATP plays an important role in regulating inflammatory responses during acute viral infection. *PLOS ONE* 7:e35812. doi: 10.1371/journal.pone.0035812

Lee, C. F., and Chern, Y. (2014). Adenosine receptors and Huntington's disease. *Int. Rev. Neurobiol.* 119, 195–232. doi: 10.1016/B978-0-12-801022-8.00010-6

Lee, C. Y. (2015). Adenosine protects Sprague Dawley rats from high-fat diet and repeated acute restraint stress-induced intestinal inflammation and altered expression of nutrient transporters. *J. Anim. Physiol. Anim. Nutr.* 99, 317–325. doi: 10.1111/jpn.12247

Lee, D., Myers, J. S., and Katz, L. J. (2016). The role of adenosine receptor agonists in ocular disorders. *Drugs Future* 41, 547–552. doi: 10.1358/dof.2016.041.09.2533858

Lemaire, A., Vanorlé, M., Horckmans, M., Di Pietrantonio, L., Clouet, S., Robaye, B., et al. (2016). Mouse P2Y4 nucleotide receptor is a negative regulator of cardiac adipose-derived stem cell differentiation and cardiac fat formation. *Stem Cells Dev.* 26, 363–373. doi: 10.1089/scd.2016.0166

Lerman, B. B. (2015). Ventricular tachycardia: mechanistic insights derived from adenosine. *Circ. Arrhythm. Electrophysiol.* 8, 483–491. doi: 10.1161/CIRCEP.115.001693

Lertsuwan, K., Peters, W., Johnson, L., Lertsuwan, J., Marwa, I., and Sikes, R. A. (2017). Purinergic receptor expression and cellular responses to purinergic agonists in human prostate cancer cells. *Anticancer Res.* 37, 529–537. doi: 10.21873/anticanres.11345

Leyva-Grado, V. H., Ermler, M. E., Schotsaert, M., Gonzalez, M. G., Gillespie, V., Lim, J. K., et al. (2017). Contribution of the purinergic receptor P2X7 to development of lung immunopathology during influenza virus infection. *mBio* 8:e00229-17. doi: 10.1128/mBio.00229-17

Li, C. L., Yang, X. L., Wang, J. J., Du, G. H., Yang, W. M., and Zhang, H. P. (2015). Effects of intracavernous injection of P2X3 and NK1 receptor antagonists on erectile dysfunction induced by spinal cord transection in rats. *Andrologia* 47, 25–29. doi: 10.1111/and.12217

Li, H., Chen, O., Ye, Z., Zhang, R., Hu, H., Zhang, N., et al. (2017). Inhalation of high concentrations of hydrogen ameliorates liver ischemia/reperfusion injury through A2A receptor mediated PI3K-Akt pathway. *Biochem. Pharmacol.* 130, 83–92. doi: 10.1016/j.bcp.2017.02.003

Li, H. J., Wang, L. Y., Qu, H. N., Yu, L. H., Burnstock, G., Ni, X., et al. (2011). P2Y2 receptor-mediated modulation of estrogen-induced proliferation of breast cancer cells. *Mol. Cell. Endocrinol.* 338, 28–37. doi: 10.1016/j.mce.2011.02.014

Li, L., Huang, L., Ye, H., Song, S. P., Bajwa, A., Lee, S. J., et al. (2012). Dendritic cells tolerized with adenosine A2AR agonist attenuate acute kidney injury. *J. Clin. Invest.* 122, 3931–3942. doi: 10.1172/JCI63170

Li, S., Geiger, N. H., Soliman, M. L., Hui, L., Geiger, J. D., and Chen, X. (2015). Caffeine, through adenosine A3 receptor-mediated actions, suppresses amyloid-β protein precursor internalization and amyloid-β generation. *J. Alzheimers Dis.* 47, 73–83. doi: 10.3233/JAD-142223

Li, W., Li, Y., Li, G., Zhou, Z., Chang, X., Xia, Y., et al. (2017). Ectopic expression of the ATP synthase beta subunit on the membrane of PC-3M cells supports its potential role in prostate cancer metastasis. *Int. J. Oncol.* 50, 1312–1320. doi: 10.3892/ijo.2017.3878

Li, W., Silva, H. B., Real, J., Wang, Y. M., Rial, D., Li, P., et al. (2015). Inactivation of adenosine A2A receptors reverses working memory deficits at early stages of Huntington's disease models. *Neurobiol. Dis.* 79, 70–80. doi: 10.1016/j.nbd.2015.03.030

Li, X., Qi, X., Zhou, L., Catera, D., Rote, N. S., Potashkin, J., et al. (2007). Decreased expression of P2X7 in endometrial epithelial pre-cancerous and cancer cells. *Gynecol. Oncol.* 106, 233–243. doi: 10.1016/j.ygyno.2007.03.032

Li, X., Qi, X., Zhou, L., Fu, W., Bdul-Karim, F. W., Maclennan, G., et al. (2009). P2X7 receptor expression is decreased in epithelial cancer cells of ectodermal, uro-genital sinus, and distal paramesonephric duct origin. *Purinergic Signal.* 5, 351–368. doi: 10.1007/s11302-009-9161-3

Li, Y., He, Y., Chen, M., Pu, Z., Chen, L., Li, P., et al. (2016). Optogenetic activation of adenosine A2A receptor signaling in the dorsomedial striatopallidal neurons suppresses goal-directed behavior. *Neuropsychopharmacology* 41, 1003–1013. doi: 10.1038/npp.2015.227

Li, Y., Xue, L., Miao, Q., Mao, F., Yao, L., Yuan, J., et al. (2013). Expression and electrophysiological characteristics of P2X3 receptors in interstitial cells of Cajal in rats with partial bladder outlet obstruction. *BJU Int.* 111, 843–851. doi: 10.1111/j.1464-410X.2012.11408.x

Lietsche, J., Imran, I., and Klein, J. (2016). Extracellular levels of ATP and acetylcholine during lithium-pilocarpine induced status epilepticus in rats. *Neurosci. Lett.* 611, 69–73. doi: 10.1016/j.neulet.2015.11.028

Liñán-Rico, A., Wunderlich, J. E., Enneking, J. T., Tso, D. R., Grants, I., Williams, K. C., et al. (2015). Neuropharmacology of purinergic receptors in human submucous plexus: involvement of P2X1, P2X2, P2X3 channels, P2Y and A3 metabotropic receptors in neurotransmission. *Neuropharmacology* 95, 83–99. doi: 10.1016/j.neuropharm.2015.02.014

Lindberg, D., Shan, D., Ayers-Ringler, J., Oliveros, A., Benitez, J., Prieto, M., et al. (2015). Purinergic signaling and energy homeostasis in psychiatric disorders. *Curr. Mol. Med.* 15, 275–295. doi: 10.2174/1566524015666150330163724

Lioi, A. B., Ferrari, B. M., Dubyak, G. R., Weinberg, A., and Sieg, S. F. (2015). Human β defensin-3 increases CD86 expression on monocytes by activating the ATP-gated channel P2X7. *J. Immunol.* 195, 4438–4445. doi: 10.4049/jimmunol.1401319

Liu, F., Tantry, U. S., and Gurbel, P. A. (2015). P2Y12 receptor inhibitors for secondary prevention of ischemic stroke. *Expert Opin. Pharmacother.* 16, 1149–1165. doi: 10.1517/14656566.2015.1035256

Liu, G., Li, M., and Daneshgari, F. (2008). Temporal expression of muscarinic and purinergic receptors in diabetic rat bladder. *Neurourol. Urodyn.* 27, 594–595.

Liu, H., Jiang, Y., and Kuo, H. (2013). Increased suburothelial nerve fiber and purinergic P2X3 receptor expressions in patients with idiopathic detrusor overactivity and their relationship with botulinum toxin A therapeutic outcome. *Neurourol. Urodyn.* 32, 733–735.

Liu, H., and Xia, Y. (2015). Beneficial and detrimental role of adenosine signaling in diseases and therapy. *J. Appl. Physiol.* 119, 1173–1182. doi: 10.1152/japplphysiol.00350.2015

Liu, J., Prell, T., Stubendorff, B., Keiner, S., Ringer, T., Gunkel, A., et al. (2016). Down-regulation of purinergic P2X7 receptor expression and intracellular calcium dysregulation in peripheral blood mononuclear cells of patients with amyotrophic lateral sclerosis. *Neurosci. Lett.* 630, 77–83. doi: 10.1016/j.neulet.2016.07.039

Liu, K., Vergani, A., Zhao, P., Ben, N. M., Wu, X., Iken, K., et al. (2014). Inhibition of the purinergic pathway prolongs mouse lung allograft survival. *Am. J. Respir. Cell Mol. Biol.* 51, 300–310. doi: 10.1165/rcmb.2013-0362OC

Liu, M., Yang, H., Fang, D., Yang, J. J., Cai, J., Wan, Y., et al. (2013). Upregulation of P2X3 receptors by neuronal calcium sensor protein VILIP-1 in dorsal root ganglions contributes to the bone cancer pain in rats. *Pain* 154, 1551–1568. doi: 10.1016/j.pain.2013.04.022

Liu, P. S., and Chen, C. Y. (2010). Butyl benzyl phthalate suppresses the ATP-induced cell proliferation in human osteosarcoma HOS cells. *Toxicol. Appl. Pharmacol.* 244, 308–314. doi: 10.1016/j.taap.2010.01.007

Liu, R., Ma, S., Lu, Z., Shen, H., Sun, L., and Wei, M. (2015). The ADP antagonist MRS2179 regulates the phenotype of smooth muscle cells to limit intimal hyperplasia. *Cardiovasc. Drugs Ther.* 29, 23–29. doi: 10.1007/s10557-014-6561-6

Liu, R., Wang, H., Xu, B., Chen, W., Turlova, E., Dong, N., et al. (2016). Cerebrovascular safety of sulfonylureas: the role of KATP channels in neuroprotection and the risk of stroke in patients with type 2 diabetes. *Diabetes Metab. Res. Rev.* 65, 2795–2809. doi: 10.2337/db15-1737

Liu, S., Shi, Q., Zhu, Q., Zou, T., Li, G., Huang, A., et al. (2015). P2X7 receptor of rat dorsal root ganglia is involved in the effect of moxibustion on visceral hyperalgesia. *Purinergic Signal.* 11, 161–169. doi: 10.1007/s11302-014-9439-y

Liu, S., Zou, L., Xie, J., Xie, W., Wen, S., Xie, Q., et al. (2016). LncRNA NONRATT021972 siRNA regulates neuropathic pain behaviors in type 2 diabetic rats through the $P2X_7$ receptor in dorsal root ganglia. *Mol. Brain* 9, 44. doi: 10.1186/s13041-016-0226-2

Liu, W., Ao, Q., Guo, Q., He, W., Peng, L., Jiang, J., et al. (2017). miR-9 mediates CALHM1-activated ATP-P2X7R signal in painful diabetic neuropathy rats. *Mol. Neurobiol.* 54, 922–929. doi: 10.1007/s12035-016-9700-1

Liu, X., Wang, C., Fujita, T., Malmstrom, H. S., Nedergaard, M., Ren, Y. F., et al. (2015). External dentin stimulation induces ATP release in human teeth. *J. Dent. Res.* 94, 1259–1266. doi: 10.1177/0022034515592858

Liu, Z., Liu, Y., Xu, L., An, H., Chang, Y., Yang, Y., et al. (2015). P2X7 receptor predicts postoperative cancer-specific survival of patients with clear-cell renal cell carcinoma. *Cancer Sci.* 106, 1224–1231. doi: 10.1111/cas.12736

Liverani, E. (2017). Lung injury during LPS-induced inflammation occurs independently of the receptor P2Y1. *Purinergic Signal.* 13, 119–125. doi: 10.1007/s11302-016-9543-2

Liverani, E., Rico, M. C., Tsygankov, A. Y., Kilpatrick, L. E., and Kunapuli, S. P. (2016). P2Y12 receptor modulates sepsis-induced inflammation. *Arterioscler. Thromb. Vasc. Biol.* 36, 961–971. doi: 10.1161/ATVBAHA.116.307401

Loma, P., Guzman-Aranguez, A., Perez De Lara, M. J., and Pintor, J. (2015). Diadenosine tetraphosphate improves adrenergic anti-glaucomatous drug delivery and efficiency. *Exp. Eye Res.* 134, 141–147. doi: 10.1016/j.exer.2015.02.014

Lu, J., Cui, J., Li, X., Wang, X., Zhou, Y., Yang, W., et al. (2016). An anti-Parkinson's disease drug via targeting adenosine A2A receptor enhances amyloid-β generation and γ-secretase activity. *PLOS ONE* 11:e0166415. doi: 10.1371/journal.pone.0166415

Lu, W., Hu, H., Sévigny, J., Gabelt, B. T., Kaufman, P. L., Johnson, E. C., et al. (2015). Rat, mouse, and primate models of chronic glaucoma show sustained elevation of extracellular ATP and altered purinergic signaling in the posterior eye. *Invest. Ophthalmol. Vis. Sci.* 56, 3075–3083. doi: 10.1167/iovs.14-15891

Luo, F., Le, N. B., Mills, T., Chen, N. Y., Karmouty-Quintana, H., Molina, J. G., et al. (2016). Extracellular adenosine levels are associated with the progression and exacerbation of pulmonary fibrosis. *FASEB J.* 30, 874–883. doi: 10.1096/fj.15-274845

Luo, Y., Feng, C., Wu, J., Wu, Y., Liu, D., Wu, J., et al. (2016). P2Y1, P2Y2, and TRPV1 receptors are increased in diarrhea-predominant irritable bowel syndrome and P2Y2 correlates with abdominal pain. *Dig. Dis. Sci.* 61, 2878–2886. doi: 10.1007/s10620-016-4211-5

Ma, B., Jiang, Q., Li, W., and Li, Z. (2016). Estrogen receptor beta (ERβ) activation plays a therapeutic role in murine models of inflammatory bowel disease (IBD) via inhibiting P2X3 and P2X7 receptors. *FASEB J.* 30, 1023–1023.

Ma, D. F., Kondo, T., Nakazawa, T., Niu, D. F., Mochizuki, K., Kawasaki, T., et al. (2010). Hypoxia-inducible adenosine A2B receptor modulates proliferation of colon carcinoma cells. *Hum. Pathol.* 41, 1550–1557. doi: 10.1016/j.humpath.2010.04.008

Ma, M., Ren, Q., Zhang, J. C., and Hashimoto, K. (2014). Effects of brilliant blue G on serum tumor necrosis factor-α levels and depression-like behavior in mice after lipopolysaccharide administration. *Clin. Psychopharmacol. Neurosci.* 12, 31–36. doi: 10.9758/cpn.2014.12.1.31

Ma, X., Pan, X., Wei, Y., Tan, B., Yang, L., Ren, H., et al. (2016). Chemotherapy-induced uridine diphosphate release promotes breast cancer metastasis through P2Y6 activation. *Oncotarget* 7, 29036–29050. doi: 10.18632/oncotarget.8664

Ma, X., Xu, T., Xu, H., and Jiang, W. (2015). Blockade and reversal of spinal morphine tolerance by P2X3 receptor antagonist. *Behav. Pharmacol.* 26, 260–267. doi: 10.1097/FBP.0000000000000105

Mac Mullan, P. A., Peace, A. J., Madigan, A. M., Tedesco, A. F., Kenny, D., and Mccarthy, G. M. (2010). Platelet hyper-reactivity in active inflammatory arthritis is unique to the adenosine diphosphate pathway: a novel finding and potential therapeutic target. *Rheumatology* 49, 240–245. doi: 10.1093/rheumatology/kep377

Macle, L., Khairy, P., Weerasooriya, R., Novak, P., Verma, A., Willems, S., et al. (2015). Adenosine-guided pulmonary vein isolation for the treatment of paroxysmal atrial fibrillation: an international, multicentre, randomised superiority trial. *Lancet* 386, 672–679. doi: 10.1016/S0140-6736(15)60026-5

Magni, G., Merli, D., Verderio, C., Abbracchio, M. P., and Ceruti, S. (2015). P2Y2 receptor antagonists as anti-allodynic agents in acute and sub-chronic trigeminal sensitization: role of satellite glial cells. *Glia* 63, 1256–1269. doi: 10.1002/glia.22819

Mahi, N., Kumar, A., Jaggi, A. S., Singh, N., and Dhawan, R. (2015). Possible role of pannexin 1/P2x7 purinoceptor in neuroprotective mechanism of ischemic postconditioning in mice. *J. Surg. Res.* 196, 190–199. doi: 10.1016/j.jss.2015.02.050

Maminishkis, A., Jalickee, S., Blaug, S. A., Rymer, J., Yerxa, B. R., Peterson, W. M., et al. (2002). The P2Y2 receptor agonist INS37217 stimulates RPE fluid transport in vitro and retinal reattachment in rat. *Invest. Ophthalmol. Vis. Sci.* 43, 3555–3566.

Manzoor, S., Akhtar, U., Naseem, S., Khalid, M., Mazhar, M., Parvaiz, F., et al. (2016). Ionotropic purinergic receptors P2X4 and P2X7: proviral or antiviral? An insight into P2X receptor signaling and hepatitis C virus infection. *Viral Immunol.* 29, 401–408. doi: 10.1089/vim.2016.0008

Marchenkova, A., Van Den Maagdenberg, A. M., and Nistri, A. (2016). Loss of inhibition by brain natriuretic peptide over P2X3 receptors contributes to enhanced spike firing of trigeminal ganglion neurons in a mouse model of familial hemiplegic migraine type-1. *Neuroscience* 331, 197–205. doi: 10.1016/j.neuroscience.2016.06.034

Martinez, C. G., Zamith-Miranda, D., Da Silva, M. G., Ribeiro, K. C., Brandão, I. T., Silva, C. L., et al. (2015). P2x7 purinergic signaling in dilated cardiomyopathy induced by auto-immunity against muscarinic M2 receptors: autoantibody levels, heart functionality and cytokine expression. *Sci. Rep.* 5:16940. doi: 10.1038/srep16940

Martinez, N. A., Ayala, A. M., Martinez, M., Martinez-Rivera, F. J., Miranda, J. D., and Silva, W. I. (2016). Caveolin-1 regulates the P2Y2 receptor signaling in human 1321N1 astrocytoma cells. *J. Biol. Chem.* 291, 12208–12222. doi: 10.1074/jbc.M116.730226

Martins, J. P., Silva, R. B., Coutinho-Silva, R., Takiya, C. M., Battastini, A. M., Morrone, F. B., et al. (2012). The role of P2X7 purinergic receptors in inflammatory and nociceptive changes accompanying cyclophosphamide-induced haemorrhagic cystitis in mice. *Br. J. Pharmacol.* 165, 183–196. doi: 10.1111/j.1476-5381.2011.01535.x

Masahiro, K., Nakamachi, Y., Kosaka, H., Nakazawa, T., Tsuji, G., and Kumagai, S. (2003). Modification of cytokine milieu in rheumatoid arthritis by signalling through A2A adenosine receptors. *FASEB J.* 17, C69.

Masino, S. A., Kawamura, M. Jr., Cote, J. L., Williams, R. B., and Ruskin, D. N. (2013). Adenosine and autism: a spectrum of opportunities. *Neuropharmacology* 68, 116–121. doi: 10.1016/j.neuropharm.2012.08.013

Masuch, A., Shieh, C. H., Van Rooijen, N., Van Calker, D., and Biber, K. (2016). Mechanism of microglia neuroprotection: involvement of P2X7, TNFα, and valproic acid. *Glia* 64, 76–89. doi: 10.1002/glia.22904

Matos, M., Shen, H. Y., Augusto, E., Wang, Y., Wei, C. J., Wang, Y. T., et al. (2015). Deletion of adenosine A2A receptors from astrocytes disrupts glutamate homeostasis leading to psychomotor and cognitive impairment: relevance to schizophrenia. *Biol. Psychiatry* 78, 763–774. doi: 10.1016/j.biopsych.2015.02.026

Matsumoto, T., Goulopoulou, S., Taguchi, K., Tostes, R. C., and Kobayashi, T. (2015). Constrictor prostanoids and uridine adenosine tetraphosphate: vascular mediators and therapeutic targets in hypertension and diabetes. *Br. J. Pharmacol.* 172, 3980–4001. doi: 10.1111/bph.13205

Matsumura, Y., Yamashita, T., Sasaki, A., Nakata, E., Kohno, K., Masuda, T., et al. (2016). A novel P2X4 receptor-selective antagonist produces anti-allodynic effect in a mouse model of herpetic pain. *Sci. Rep.* 6:32461. doi: 10.1038/srep32461

Matta, C., Fodor, J., Miosge, N., Takács, R., Juhász, T., Rybaltovszki, H., et al. (2015). Purinergic signalling is required for calcium oscillations in migratory chondrogenic progenitor cells. *Pflugers Arch.* 467, 429–442. doi: 10.1007/s00424-014-1529-8

Maynard, J. P., Lee, J. S., Sohn, B. H., Yu, X., Lopez-Terrada, D., Finegold, M. J., et al. (2015). P2X3 purinergic receptor overexpression is associated with poor recurrence-free survival in hepatocellular carcinoma patients. *Oncotarget* 6, 41162–41179. doi: 10.18632/oncotarget.6240

Mazzon, E., Esposito, E., Impellizzeri, D., Di Paola, R., Melani, A., Bramanti, P., et al. (2011). CGS 21680, an agonist of the adenosine (A2A) receptor, reduces progression of murine type II collagen-induced arthritis. *J. Rheumatol.* 38, 2119–2129. doi: 10.3899/jrheum.110111

McGovern, A. E., and Mazzone, S. B. (2014). Neural regulation of inflammation in the airways and lungs. *Auton. Neurosci.* 182, 95–101. doi: 10.1016/j.autneu.2013.12.008

McLarnon, J. G. (2017). Roles of purinergic P2X7 receptor in glioma and microglia in brain tumors. *Cancer Lett.* 402, 93–99. doi: 10.1016/j.canlet.2017.05.004

McPhee, M. D., and Whiting, S. J. (1989). The effect of adenosine and adenosine analogues on methylxanthine-induced hypercalciuria in the rat. *Can. J. Physiol. Pharmacol.* 67, 1278–1282. doi: 10.1139/y89-203

Mediavilla-Varela, M., Luddy, K., Noyes, D., Khalil, F. K., Neuger, A. M., Soliman, H., et al. (2013). Antagonism of adenosine A2A receptor expressed by lung adenocarcinoma tumor cells and cancer associated fibroblasts inhibits their growth. *Cancer Biol. Ther.* 14, 860–868. doi: 10.4161/cbt.25643

Mendieta-Condado, E., Chagoya de Sanchez, V., and Hernandez-Munoz, R. (2007). Adenosine can accelerate the cell cycle during rat liver regeneration induced by partial hepatectomy. *J. Hepatol.* 46, S142–S143. doi: 10.1124/jpet.109.156620

Menezes, C. B., and Tasca, T. (2016). Trichomoniasis immunity and the involvement of the purinergic signaling. *Biomed. J.* 39, 234–243. doi: 10.1016/j.bj.2016.06.007

Meng, E., Lin, W. Y., Lee, W. C., and Chuang, Y. C. (2012). Pathophysiology of overactive bladder. *LUTS* 4, 48–55. doi: 10.1111/j.1757-5672.2011.00122.x

Menzies, R. I., Tam, F. W., Unwin, R. J., and Bailey, M. A. (2017). Purinergic signaling in kidney disease. *Kidney Int.* 91, 315–323. doi: 10.1016/j.kint.2016.08.029

Menzies, R. I., Unwin, R. J., and Bailey, M. A. (2015). Renal P2 receptors and hypertension. *Acta Physiol.* 213, 232–241. doi: 10.1111/apha.12412

Merighi, S., Borea, P. A., and Gessi, S. (2015). Adenosine receptors and diabetes: focus on the A2B adenosine receptor subtype. *Pharmacol. Res.* 99, 229–236. doi: 10.1016/j.phrs.2015.06.015

Merighi, S., Borea, P. A., Varani, K., and Gessi, S. (2017). Deregulation of adenosine receptors in psoriatic epidermis: an option for therapeutic treatment. *J. Invest. Dermatol.* 137, 11–13. doi: 10.1016/j.jid.2016.08.001

Merighi, S., Simioni, C., Gessi, S., Varani, K., Mirandola, P., Tabrizi, M. A., et al. (2009). A2B and A3 adenosine receptors modulate vascular endothelial growth factor and interleukin-8 expression in human melanoma cells treated with etoposide and doxorubicin. *Neoplasia* 11, 1064–1073. doi: 10.1593/neo.09768

Metzger, M. W., Walser, S. M., Aprile-Garcia, F., Dedic, N., Chen, A., Holsboer, F., et al. (2017). Genetically dissecting P2rx7 expression within the central nervous system using conditional humanized mice. *Purinergic Signal.* 13, 153–170. doi: 10.1007/s11302-016-9546-z

Meyer, C. H., Hotta, K., Peterson, W. M., Toth, C. A., and Jaffe, G. J. (2002). Effect of INS37217, a P2Y2 receptor agonist, on experimental retinal detachment and electroretinogram in adult rabbits. *Invest. Ophthalmol. Vis. Sci.* 43, 3567–3574.

Michalak, A., and Biala, G. (2016). Alcohol dependence - neurobiology and treatment. *Acta Pol. Pharm.* 73, 3–12.

Micioni Di Bonaventura, M. V., Cifani, C., Lambertucci, C., Volpini, R., Cristalli, G., Froldi, R., et al. (2012). Effects of A2A adenosine receptor blockade or stimulation on alcohol intake in alcohol-preferring rats. *Psychopharmacology* 219, 945–957. doi: 10.1007/s00213-011-2430-1

Milicic, I., Buckner, S. A., Daza, A., Coghlan, M., Fey, T. A., Brune, M. E., et al. (2006). Pharmacological characterization of urinary bladder smooth muscle contractility following partial bladder outlet obstruction in pigs. *Eur. J. Pharmacol.* 532, 107–114. doi: 10.1016/j.ejphar.2005.12.076

Minns, M. S., Teicher, G., Rich, C. B., and Trinkaus-Randall, V. (2016). Purinoreceptor P2X7 regulation of Ca^{2+} mobilization and cytoskeletal rearrangement is required for corneal reepithelialization after injury. *Am. J. Pathol.* 186, 285–296. doi: 10.1016/j.ajpath.2015.10.006

Minns, M. S., and Trinkaus-Randall, V. (2016). Purinergic signaling in corneal wound healing: a tale of 2 receptors. *J. Ocul. Pharmacol. Ther.* 32, 498–503. doi: 10.1089/jop.2016.0009

Miranda, M. F., Hamani, C., De Almeida, A. C., Amorim, B. O., Macedo, C. E., Fernandes, M. J., et al. (2014). Role of adenosine in the antiepileptic effects of deep brain stimulation. *Front. Cell. Neurosci.* 8:312. doi: 10.3389/fncel.2014.00312

Miras-Portugal, M. T., Diaz-Hernandez, J. I., Gomez-Villafuertes, R., Diaz-Hernandez, M., Artalejo, A. R., and Gualix, J. (2015). Role of P2X7 and P2Y2 receptors on α-secretase-dependent APP processing: control of amyloid plaques formation "in vivo" by P2X7 receptor. *Comput. Struct. Biotechnol. J.* 13, 176–181. doi: 10.1016/j.csbj.2015.02.005

Mishra, A., Guo, Y., Zhang, L., More, S., Weng, T., Chintagari, N. R., et al. (2016). A critical role for P2X7 receptor-induced VCAM-1 shedding and neutrophil infiltration during acute lung injury. *J. Immunol.* 197, 2828–2837. doi: 10.4049/jimmunol.1501041

Mittal, R., Chan, B., Grati, M., Mittal, J., Patel, K., Debs, L. H., et al. (2016). Molecular structure and regulation of P2X receptors with a special emphasis on the role of P2X2 in the auditory system. *J. Cell. Physiol.* 231, 1656–1670. doi: 10.1002/jcp.25274

Molck, C., Ryall, J., Failla, L. M., Coates, J. L., Pascussi, J. M., Heath, J. K., et al. (2016). The A2b adenosine receptor antagonist PSB-603 promotes oxidative phosphorylation and ROS production in colorectal cancer cells via adenosine receptor-independent mechanism. *Cancer Lett.* 383, 135–143. doi: 10.1016/j.canlet.2016.09.018

Molina, C. E., Llach, A., Herraiz-Martínez, A., Tarifa, C., Barriga, M., Wiegerinck, R. F., et al. (2016). Prevention of adenosine A2A receptor activation diminishes beat-to-beat alternation in human atrial myocytes. *Basic Res. Cardiol.* 111, 5. doi: 10.1007/s00395-015-0525-2

Molz, S., Olescowicz, G., Kraus, J. R., Ludka, F. K., and Tasca, C. I. (2015). Purine receptors are required for DHA-mediated neuroprotection against oxygen and glucose deprivation in hippocampal slices. *Purinergic Signal.* 11, 117–126. doi: 10.1007/s11302-014-9438-z

Monção-Ribeiro, L. C., Faffe, D. S., Santana, P. T., Vieira, F. S., Da Graca, C. L., Marques-Da-Silva, C., et al. (2014). P2X7 receptor modulates inflammatory and functional pulmonary changes induced by silica. *PLOS ONE* 9:e110185. doi: 10.1371/journal.pone.0110185

Montesinos, M. C., Desai-Merchant, A., and Cronstein, B. N. (2015). Promotion of wound healing by an agonist of adenosine A2A receptor is dependent on tissue plasminogen activator. *Inflammation* 38, 2036–2041. doi: 10.1007/s10753-015-0184-3

Morandini, A. C., Savio, L. E., and Coutinho-Silva, R. (2014). The role of P2X7 receptor in infectious inflammatory diseases and the influence of ectonucleotidases. *Biomed. J.* 37, 169–177. doi: 10.4103/2319-4170.127803

Morello, S., Sorrentino, R., Montinaro, A., Luciano, A., Maiolino, P., Ngkelo, A., et al. (2011). $NK1.1^+$ cells and $CD8^+$ T cells mediate the antitumor activity of Cl-IB-MECA in a mouse melanoma model. *Neoplasia* 13, 365–373. doi: 10.1593/neo.101628

Mori, A. (2014). Mode of action of adenosine A2A receptor antagonists as symptomatic treatment for Parkinson's disease. *Int. Rev. Neurobiol.* 119, 87–116. doi: 10.1016/B978-0-12-801022-8.00004-0

Morrone, F. B., Gehring, M. P., and Nicoletti, N. F. (2016). Calcium channels and associated receptors in malignant brain tumor therapy. *Mol. Pharmacol.* 90, 403–409. doi: 10.1124/mol.116.103770

Mrazek, F., Gallo, J., Stahelova, A., and Petrek, M. (2010). Functional variants of the P2RX7 gene, aseptic osteolysis, and revision of the total hip arthroplasty: a preliminary study. *Hum. Immunol.* 71, 201–205. doi: 10.1016/j.humimm.2009.10.013

Mujoomdar, M., Bennett, A., Hoskin, D., and Blay, J. (2004). Adenosine stimulation of proliferation of breast carcinoma cell lines: evaluation of the [3H]thymidine assay system and modulatory effects of the cellular microenvironment in vitro. *J. Cell. Physiol.* 201, 429–438. doi: 10.1002/jcp.20089

Mulryan, K., Gitterman, D. P., Lewis, C. J., Vial, C., Leckie, B. J., Cobb, A. L., et al. (2000). Reduced vas deferens contraction and male infertility in mice lacking P2X1 receptors. *Nature* 403, 86–89. doi: 10.1038/47495

Mumtaz, F. H., Lau, D. H., Siddiqui, E. J., Morgan, R. J., Thompson, C. S., and Mikhailidis, D. P. (2006). Changes in cholinergic and purinergic neurotransmission in the diabetic rabbit bladder. *In Vivo* 20, 1–4.

Munoz, A., Romain, Z., Munch, E., Gangitano, D., Boone, T., Smith, C., et al. (2008). Changes in purinergic and nitrergic sensory signals in female rats during early diabetes. *Neurourol. Urodyn.* 28, 110–111.

Munoz, A., Somogyi, G. T., Boone, T. B., Ford, A. P., and Smith, C. P. (2012). Modulation of bladder afferent signals in normal and spinal cord-injured rats by purinergic P2X3 and P2X2/3 receptors. *BJU Int.* 110, E409–E414. doi: 10.1111/j.1464-410X.2012.11189.x

Munoz, A., Yazdi, I. K., Tang, X., Rivera, C., Taghipour, N., Grossman, R. G., et al. (2017). Localized inhibition of P2X7R at the spinal cord injury site improves neurogenic bladder dysfunction by decreasing urothelial P2X3R expression in rats. *Life Sci.* 171, 60–67. doi: 10.1016/j.lfs.2016.12.017

Murakami, S., Yoshida, M., Masunaga, K., Maeda, Y., and Ueda, S. (2008). Change in acetylcholine release from rat bladder with partial outlet obstruction. *BJU Int.* 101, 633–639. doi: 10.1111/j.1464-410X.2007.07325.x

Muti, M., Del Grande, C., Musetti, L., Marazziti, D., Turri, M., Cirronis, M., et al. (2015). Serum uric acid levels and different phases of illness in bipolar I patients treated with lithium. *Psychiatry Res.* 225, 604–608. doi: 10.1016/j.psychres.2014.11.038

Nagahama, M., Seike, S., Shirai, H., Takagishi, T., Kobayashi, K., Takehara, M., et al. (2015). Role of P2X7 receptor in *Clostridium perfringens* beta-toxin-mediated cellular injury. *Biochim. Biophys. Acta* 1850, 2159–2167. doi: 10.1016/j.bbagen.2015.08.011

Nakagawa, Y., Yoshioka, M., Abe, Y., Uchinami, H., Ohba, T., Ono, K., et al. (2012). Enhancement of liver regeneration by adenosine triphosphate-sensitive K+ channel opener (diazoxide) after partial hepatectomy. *Transplantation* 93, 1094–1100. doi: 10.1097/TP.0b013e31824ef1d1

Nakamachi, Y., Koshiba, M., Nakazawa, T., Hatachi, S., Saura, R., Kurosaka, M., et al. (2003). Specific increase in enzymatic activity of adenosine deaminase 1 in rheumatoid synovial fibroblasts. *Arthritis Rheum.* 48, 668–674. doi: 10.1002/art.10956

Nam, H. W., Bruner, R. C., and Choi, D. S. (2013). Adenosine signaling in striatal circuits and alcohol use disorders. *Mol. Cells* 36, 195–202. doi: 10.1007/s10059-013-0192-9

Nascimento, F., Pousinha, P. A., Correia, A. M., Gomes, R., Sebastião, A. M., and Ribeiro, J. A. (2014). Adenosine A2A receptors activation facilitates neuromuscular transmission in the pre-symptomatic phase of the SOD1(G93A) ALS mice, but not in the symptomatic phase. *PLOS ONE* 9:e104081. doi: 10.1371/journal.pone.0104081

Nascimento, F., Sebastião, A. M., and Ribeiro, J. A. (2015). Presymptomatic and symptomatic ALS SOD1(G93A) mice differ in adenosine A1 and A2A receptor-mediated tonic modulation of neuromuscular transmission. *Purinergic Signal.* 11, 471–480. doi: 10.1007/s11302-015-9465-4

Navarro, G., Borroto-Escuela, D. O., Fuxe, K., and Franco, R. (2016). Purinergic signaling in Parkinson's disease. Relevance for treatment. *Neuropharmacology* 104, 161–168. doi: 10.1016/j.neuropharm.2015.07.024

Naviaux, J. C., Schuchbauer, M. A., Li, K., Wang, L., Risbrough, V. B., Powell, S. B., et al. (2014). Reversal of autism-like behaviors and metabolism in adult mice with single-dose antipurinergic therapy. *Transl. Psychiatry* 4, e400. doi: 10.1038/tp.2014.33

Naviaux, J. C., Wang, L., Li, K., Bright, A. T., Alaynick, W. A., Williams, K. R., et al. (2015). Antipurinergic therapy corrects the autism-like features in the Fragile X (*Fmr1* knockout) mouse model. *Mol. Autism* 6:1. doi: 10.1186/2040-2392-6-1

Nelson, S., Kiyono, H., and Kurashima, Y. (2017). Epithelial extracellular ATP: an initiator of immunity to parasitic infections. *Immunol. Cell Biol.* 95, 117–118. doi: 10.1038/icb.2016.106

Neuhuber, W. L., and Tiegs, G. (2004). Innervation of immune cells: evidence for neuroimmunomodulation in the liver. *Anat. Rec. A Discov. Mol. Cell. Evol. Biol.* 280, 884–892. doi: 10.1002/ar.a.20093

Neves, A. R., Castelo-Branco, M. T., Figliuolo, V. R., Bernardazzi, C., Buongusto, F., Yoshimoto, A., et al. (2014). Overexpression of ATP-activated P2X7 receptors in the intestinal mucosa is implicated in the pathogenesis of Crohn's disease. *Inflamm. Bowel Dis.* 20, 444–457. doi: 10.1097/01.MIB.0000441201.10454.06

Ng, S. K., Higashimori, H., Tolman, M., and Yang, Y. (2015). Suppression of adenosine 2a receptor (A2aR)-mediated adenosine signaling improves disease phenotypes in a mouse model of amyotrophic lateral sclerosis. *Exp. Neurol.* 267, 115–122. doi: 10.1016/j.expneurol.2015.03.004

Ni, R., Zheng, D., Xiong, S., Hill, D. J., Sun, T., Gardiner, R. B., et al. (2016). Mitochondrial calpain-1 disrupts ATP synthase and induces superoxide generation in type 1 diabetic hearts: a novel mechanism contributing to diabetic cardiomyopathy. *Diabetes Metab. Res. Rev.* 65, 255–268. doi: 10.2337/db15-0963

Ning, C., Wen, J., Zhang, Y., Blackburn, M., Kellems, R., and Xia, Y. (2012a). Impaired adenosine signaling contributes to erectile dysfunction. *J. Sex. Med.* 9, 183–298. doi: 10.1161/ATVBAHA.111.226803

Ning, C., Zhang, Y., Wen, J., Blackburn, M., Kellems, R., and Xia, Y. (2012b). Adenosine signaling in priapism and novel therapies. *J. Sex. Med.* 9, 223.

Noronha-Matos, J. B., Morais, T., Trigo, D., Timóteo, M. A., Magalhães-Cardoso, M. T., Oliveira, L., et al. (2011). Tetanic failure due to decreased endogenous adenosine A2A tonus operating neuronal Cav 1 (L-type) influx in Myasthenia gravis. *J. Neurochem.* 117, 797–811. doi: 10.1111/j.1471-4159.2011.07216.x

Novitskaya, T., Chepurko, E., Covarrubias, R., Novitskiy, S., Ryzhov, S. V., Feoktistov, I., et al. (2016). Extracellular nucleotide regulation and signaling in cardiac fibrosis. *J. Mol. Cell. Cardiol.* 93, 47–56. doi: 10.1016/j.yjmcc.2016.02.010

Nylander, S., and Schulz, R. (2016). Effects of P2Y12 receptor antagonists beyond platelet inhibition - comparison of ticagrelor with thienopyridines. *Br. J. Pharmacol.* 173, 1163–1178. doi: 10.1111/bph.13429

Ochoa-Cortes, F., Liñán-Rico, A., Jacobson, K. A., and Christofi, F. L. (2014). Potential for developing purinergic drugs for gastrointestinal diseases. *Inflamm. Bowel Dis.* 20, 1259–1287. doi: 10.1097/MIB.0000000000000047

Ohshima, Y., Tsukimoto, M., Takenouchi, T., Harada, H., Suzuki, A., Sato, M., et al. (2010). γ-Irradiation induces P2X7 receptor-dependent ATP release from B16 melanoma cells. *Biochim. Biophys. Acta* 1800, 40–46. doi: 10.1016/j.bbagen.2009.10.008

Olatunji, O. J., Feng, Y., Olatunji, O. O., Tang, J., Ouyang, Z., Su, Z., et al. (2016). Neuroprotective effects of adenosine isolated from *Cordyceps cicadae* against oxidative and ER stress damages induced by glutamate in PC12 cells. *Environ. Toxicol. Pharmacol.* 44, 53–61. doi: 10.1016/j.etap.2016.02.009

Oliveira, A. G., Marques, P. E., Amaral, S. S., Quintão, J. L., Cogliati, B., Dagli, M. L., et al. (2013). Purinergic signalling during sterile liver injury. *Liver Int.* 33, 353–361. doi: 10.1111/liv.12109

Oliveira, L., Correia, A., Costa, A. C., Guerra-Gomes, S., Ferreirinha, F., Magalhães-Cardoso, M. T., et al. (2015). Deficits in endogenous adenosine formation by ecto-5′-nucleotidase/CD73 impair neuromuscular transmission and immune competence in experimental autoimmune myasthenia gravis. *Mediators Inflamm.* 2015:460610. doi: 10.1155/2015/460610

Olivier, E., Dutot, M., Regazzetti, A., Leguillier, T., Dargere, D., Auzeil, N., et al. (2016). P2X7-pannexin-1 and amyloid β-induced oxysterol input in human retinal cell: role in age-related macular degeneration? *Biochimie* 127, 70–78. doi: 10.1016/j.biochi.2016.04.014

Ondrakova, M., Knot, J., Ulman, J., Maly, M., and Motovska, Z. (2016). Efficacy of P2Y12 receptor antagonists in patients with atrial fibrillation according to the CHA2DS2VASc score. *Int. J. Cardiol.* 207, 84–86. doi: 10.1016/j.ijcard.2016.01.039

Ongaro, A., Varani, K., Masieri, F. F., Pellati, A., Massari, L., Cadossi, R., et al. (2012). Electromagnetic fields (EMFs) and adenosine receptors modulate

prostaglandin E(2) and cytokine release in human osteoarthritic synovial fibroblasts. *J. Cell. Physiol.* 227, 2461–2469. doi: 10.1002/jcp.22981

O'Reilly, B. A., Kosaka, A. H., Knight, G. E., Chang, T. K., Ford, A. P. D. W., Rymer, J. M., et al. (2002). P2X receptors and their role in female idiopathic detrusor instability. *J. Urol.* 167, 157–164. doi: 10.1016/S0022-5347(05)65403-1

Orriss, I. R., Arnett, T. R., and Russell, R. G. (2016). Pyrophosphate: a key inhibitor of mineralisation. *Curr. Opin. Pharmacol.* 28, 57–68. doi: 10.1016/j.coph.2016.03.003

Orth, S. R., Amann, K., Strojek, K., and Ritz, E. (2001). Sympathetic overactivity and arterial hypertension in renal failure. *Nephrol. Dial. Transplant.* 16(Suppl. 1), 67–69. doi: 10.1093/ndt/16.suppl_1.67

Ortiz, R., Ulrich, H., Zarate, C. A. Jr., and Machado-Vieira, R. (2015). Purinergic system dysfunction in mood disorders: a key target for developing improved therapeutics. *Prog. Neuropsychopharmacol. Biol. Psychiatry* 57, 117–131. doi: 10.1016/j.pnpbp.2014.10.016

Ou, Z., Sun, Y., Lin, L., You, N., Liu, X., Li, H., et al. (2016). Olig2-targeted G-protein-coupled receptor Gpr17 regulates oligodendrocyte survival in response to lysolecithin-induced demyelination. *J. Neurosci.* 36, 10560–10573. doi: 10.1523/JNEUROSCI.0898-16.2016

Oury, C., Lecut, C., Hego, A., Wéra, O., and Delierneux, C. (2015). Purinergic control of inflammation and thrombosis: role of P2X1 receptors. *Comput. Struct. Biotechnol. J.* 13, 106–110. doi: 10.1016/j.csbj.2014.11.008

Oyarzun, C., Garrido, W., Alarcon, S., Yanez, A., Sobrevia, L., Quezada, C., et al. (2017). Adenosine contribution to normal renal physiology and chronic kidney disease. *Mol. Aspects Med.* 55, 75–89. doi: 10.1016/j.mam.2017.01.004

Ozaki, T., Muramatsu, R., Sasai, M., Yamamoto, M., Kubota, Y., Fujinaka, T., et al. (2016). The P2X4 receptor is required for neuroprotection via ischemic preconditioning. *Sci. Rep.* 6:25893. doi: 10.1038/srep25893

Pacheco, P. A., Faria, R. X., Ferreira, L. G., and Paixão, I. C. (2014). Putative roles of purinergic signaling in human immunodeficiency virus-1 infection. *Biol. Direct* 9:21. doi: 10.1186/1745-6150-9-21

Pandolfi, J. B., Ferraro, A. A., Sananez, I., Gancedo, M. C., Baz, P., Billordo, L. A., et al. (2016). ATP-induced inflammation drives tissue-resident Th17 cells in metabolically unhealthy obesity. *J. Immunol.* 196, 3287–3296. doi: 10.4049/jimmunol.1502506

Panjehpour, M., Hemati, S., and Forghani, M. A. (2012). Expression of A1 and A3 adenosine receptors in human breast tumors. *Tumori* 98, 137–141. doi: 10.1700/1053.11512

Parabucki, A., Savic, D., Laketa, D., Pekovic, S., Stojiljkovic, M., Nedeljkovic, N., et al. (2014). Expression of major ectonucleotidases after cortical stab brain injury in rats: a real-time PCR study. *Arch. Biol. Sci. Belgrade* 66, 149–155. doi: 10.2298/ABS1401148P

Patel, A., and Honoré, E. (2010). Polycystins and renovascular mechanosensory transduction. *Nat. Rev. Nephrol.* 6, 530–538. doi: 10.1038/nrneph.2010.97

Pedata, F., Dettori, I., Coppi, E., Melani, A., Fusco, I., Corradetti, R., et al. (2016). Purinergic signalling in brain ischemia. *Neuropharmacology* 104, 105–130. doi: 10.1016/j.neuropharm.2015.11.007

Pedata, F., Pugliese, A. M., Coppi, E., Dettori, I., Maraula, G., Cellai, L., et al. (2014). Adenosine A2A receptors modulate acute injury and neuroinflammation in brain ischemia. *Mediators Inflamm.* 2014:805198. doi: 10.1155/2014/805198

Pei, H., and Linden, J. (2016). Adenosine influences myeloid cells to inhibit aeroallergen sensitization. *Am. J. Physiol. Lung Cell. Mol. Physiol.* 310, L985–L992. doi: 10.1152/ajplung.00330.2015

Pelleg, A., Schulman, E. S., and Barnes, P. J. (2016). Extracellular adenosine 5′-triphosphate in obstructive airway diseases. *Chest* 150, 908–915. doi: 10.1016/j.chest.2016.06.045

Peng, H., Zou, L., Xie, J., Wu, H., Wu, B., Zhu, G., et al. (2017). lncRNA NONRATT021972 siRNA decreases diabetic neuropathic pain mediated by the P2X3 receptor in dorsal root ganglia. *Mol. Neurobiol.* 54, 511–523. doi: 10.1007/s12035-015-9632-1

Peng, W., Cotrina, M. L., Han, X., Yu, H., Bekar, L., Blum, L., et al. (2009). Systemic administration of an antagonist of the ATP-sensitive receptor P2X7 improves recovery after spinal cord injury. *Proc. Natl. Acad. Sci. U.S.A.* 106, 12489–12493. doi: 10.1073/pnas.0902531106

Pereira, V. S., Casarotto, P. C., Hiroaki-Sato, V. A., Sartim, A. G., Guimarães, F. S., and Joca, S. R. (2013). Antidepressant- and anticompulsive-like effects of purinergic receptor blockade: involvement of nitric oxide. *Eur. Neuropsychopharmacol.* 23, 1769–1778. doi: 10.1016/j.euroneuro.2013.01.008

Pérez de Lara, M. J., Guzmán-Aránguez, A., De La Villa, P., Díaz-Hernández, J. I., Miras-Portugal, M. T., and Pintor, J. (2015). Increased levels of extracellular ATP in glaucomatous retinas: possible role of the vesicular nucleotide transporter during the development of the pathology. *Mol. Vis.* 21, 1060–1070.

Perez-Aso, M., Mediero, A., Low, Y. C., Levine, J., and Cronstein, B. N. (2016). Adenosine A2A receptor plays an important role in radiation-induced dermal injury. *FASEB J.* 30, 457–465. doi: 10.1096/fj.15-280388

Pérez-Sen, R., Queipo, M. J., Morente, V., Ortega, F., Delicado, E. G., and Miras-Portugal, M. T. (2015). Neuroprotection mediated by P2Y13 nucleotide receptors in neurons. *Comput. Struct. Biotechnol. J.* 13, 160–168. doi: 10.1016/j.csbj.2015.02.002

Persson, P., Friederich-Persson, M., Fasching, A., Hansell, P., Inagi, R., and Palm, F. (2015). Adenosine A2 a receptor stimulation prevents proteinuria in diabetic rats by promoting an anti-inflammatory phenotype without affecting oxidative stress. *Acta Physiol.* 214, 311–318. doi: 10.1111/apha.12511

Petrasek, J., Iracheta-Vellve, A., Saha, B., Satishchandran, A., Kodys, K., Fitzgerald, K. A., et al. (2015). Metabolic danger signals, uric acid and ATP, mediate inflammatory cross-talk between hepatocytes and immune cells in alcoholic liver disease. *J. Leukoc. Biol.* 98, 249–256. doi: 10.1189/jlb.3AB1214-590R

Pettengill, M. A., Abdul-Sater, A., Coutinho-Silva, R., and Ojcius, D. M. (2016). Danger signals, inflammasomes, and the intricate intracellular lives of chlamydiae. *Biomed. J.* 39, 306–315. doi: 10.1016/j.bj.2016.07.001

Phillips, E., Carpenter, C., and Oates, R. D. (2014). Ejaculatory dysfunction. *Urol. Clin. North Am.* 41, 115–128. doi: 10.1016/j.ucl.2013.08.018

Pijacka, W., Moraes, D. J. A., Ratcliffe, L. E. K., Nightingale, A. K., Hart, E. C., Da Silva, M. P., et al. (2016). Purinergic receptors in the carotid body as a new drug target for controlling hypertension. *Nat. Med.* 22, 1151–1159. doi: 10.1038/nm.4173

Pinna, A. (2014). Adenosine A2A receptor antagonists in Parkinson's disease: progress in clinical trials from the newly approved istradefylline to drugs in early development and those already discontinued. *CNS Drugs* 28, 455–474. doi: 10.1007/s40263-014-0161-7

Pintsuk, J., Borroto-Escuela, D. O., Pomierny, B., Wydra, K., Zaniewska, M., Filip, M., et al. (2016). Cocaine self-administration differentially affects allosteric A2A-D2 receptor-receptor interactions in the striatum. Relevance for cocaine use disorder. *Pharmacol. Biochem. Behav.* 144, 85–91. doi: 10.1016/j.pbb.2016.03.004

Plemel, J. R., Keough, M. B., Duncan, G. J., Sparling, J. S., Yong, V. W., Stys, P. K., et al. (2014). Remyelination after spinal cord injury: is it a target for repair? *Prog. Neurobiol.* 117, 54–72. doi: 10.1016/j.pneurobio.2014.02.006

Pochmann, D., Rucker, B., Battastini, A. M., and Sarkis, J. J. (2004). Ovariectomy and estradiol replacement therapy alters the adenine nucleotide hydrolysis in rat blood serum. *Thromb. Res.* 114, 275–281. doi: 10.1016/j.thromres.2004.06.021

Portales-Cervantes, L., Niño-Moreno, P., Doníz-Padilla, L., Baranda-Candido, L., García-Hernández, M., Salgado-Bustamante, M., et al. (2010). Expression and function of the P2X7 purinergic receptor in patients with systemic lupus erythematosus and rheumatoid arthritis. *Hum. Immunol.* 71, 818–825. doi: 10.1016/j.humimm.2010.05.008

Portales-Cervantes, L., Niño-Moreno, P., Salgado-Bustamante, M., García-Hernández, M. H., Baranda-Candido, L., Reynaga-Hernández, E., et al. (2012). The His155Tyr (489C>T) single nucleotide polymorphism of P2RX7 gene confers an enhanced function of P2X7 receptor in immune cells from patients with rheumatoid arthritis. *Cell. Immunol.* 276, 168–175. doi: 10.1016/j.cellimm.2012.05.005

Pritchard, M., Mandal, P., Chiang, D. J., Ndum, O., and Nagy, L. E. (2011). Adenosine and adenosine signaling contribute to the anti-inflammatory effect of globular adiponectin in macrophages. *Hepatology* 54, 1099A–1100A.

Puchalowicz, K., Tarnowski, M., Baranowska-Bosiacka, I., Chlubek, D., and Dziedziejko, V. (2014). P2X and P2Y receptors-role in the pathophysiology of the nervous system. *Int. J. Mol. Sci.* 15, 23672–23704. doi: 10.3390/ijms151223672

Qu, W., Zhu, Z. J., Sun, L. Y., Wei, L., Liu, Y., and Zeng, Z. G. (2017). Correlation between survival interval and CD4+ T-cell intracellular ATP levels in liver transplant recipients. *Transplant. Proc.* 49, 316–321. doi: 10.1016/j.transproceed.2016.11.044

Quezada, C., Alarcón, S., Jaramillo, C., Muñoz, D., Oyarzún, C., and San Martín, R. (2013). Targeting adenosine signaling to treatment of diabetic nephropathy. *Curr. Drug Targets* 14, 490–496. doi: 10.2174/1389450111314040010

Rai, B., Kaur, J., Jacobs, R., and Anand, S. C. (2011). Adenosine deaminase in saliva as a diagnostic marker of squamous cell carcinoma of tongue. *Clin. Oral Investig.* 15, 347–349. doi: 10.1007/s00784-010-0404-z

Ralevic, V. (2015). P2X receptors in the cardiovascular system and their potential as therapeutic targets in disease. *Curr. Med. Chem.* 22, 851–865. doi: 10.2174/0929867321666141215094050

Ralevic, V., and Burnstock, G. (1998). Receptors for purines and pyrimidines. *Pharmacol. Rev.* 50, 413–492.

Rama Rao, K. V., and Kielian, T. (2015). Neuron-astrocyte interactions in neurodegenerative diseases: role of neuroinflammation. *Clin. Exp. Neuroimmunol.* 6, 245–263. doi: 10.1111/cen3.12237

Ramos, D. B., Muller, G. C., Rocha, G. B., Dellavia, G. H., Almeida, R. F., Pettenuzzo, L. F., et al. (2016). Intranasal guanosine administration presents a wide therapeutic time window to reduce brain damage induced by permanent ischemia in rats. *Purinergic Signal.* 12, 149–159. doi: 10.1007/s11302-015-9489-9

Ran, H., Duan, W., Gong, Z., Xu, S., Zhu, H., Hou, X., et al. (2015). Critical contribution of adenosine A2A receptors in bone marrow-derived cells to white matter lesions induced by chronic cerebral hypoperfusion. *J. Neuropathol. Exp. Neurol.* 74, 305–318. doi: 10.1097/NEN.0000000000000174

Rao, S., Liu, S., Zou, L., Jia, T., Zhao, S., Wu, B., et al. (2017). The effect of sinomenine in diabetic neuropathic pain mediated by the P2X3 receptor in dorsal root ganglia. *Purinergic Signal.* 13, 227–235. doi: 10.1007/s11302-016-9554-z

Rassendren, F., and Audinat, E. (2016). Purinergic signaling in epilepsy. *J. Neurosci. Res.* 94, 781–793. doi: 10.1002/jnr.23770

Rau, A. R., Ariwodola, O. J., and Weiner, J. L. (2014). Presynaptic adenosine A1 receptors modulate excitatory transmission in the rat basolateral amygdala. *Neuropharmacology* 77, 465–474. doi: 10.1016/j.neuropharm.2013.10.029

Rayalam, S., Yang, J. Y., La-Fera, M. A., and Baile, C. A. (2011). Novel molecular targets for prevention of obesity and osteoporosis. *J. Nutr. Biochem.* 22, 1099–1104. doi: 10.1016/j.jnutbio.2010.11.009

Rech, J. C., Bhattacharya, A., Letavic, M. A., and Savall, B. M. (2016). The evolution of P2X7 antagonists with a focus on CNS indications. *Bioorg. Med. Chem. Lett.* 26, 3838–3845. doi: 10.1016/j.bmcl.2016.06.048

Reichenbach, A., and Bringmann, A. (2016). Purinergic signaling in retinal degeneration and regeneration. *Neuropharmacology* 104, 194–211. doi: 10.1016/j.neuropharm.2015.05.005

Reigada, D., Navarro-Ruiz, R. M., Caballero-López, M. J., Del Águila, Á, Muñoz-Galdeano, T., Maza, R. M., et al. (2017). Diadenosine tetraphosphate (Ap4A) inhibits ATP-induced excitotoxicity: a neuroprotective strategy for traumatic spinal cord injury treatment. *Purinergic Signal.* 13, 75–87. doi: 10.1007/s11302-016-9541-4

Reiss, A. B., and Cronstein, B. N. (2012). Regulation of foam cells by adenosine. *Arterioscler. Thromb. Vasc. Biol.* 32, 879–886. doi: 10.1161/ATVBAHA.111.226878

Ren, C., Qiu, C. Y., Gan, X., Liu, T. T., Qu, Z. W., Rao, Z., et al. (2015). Prokineticin 2 facilitates mechanical allodynia induced by α,β-methylene ATP in rats. *Eur. J. Pharmacol.* 767, 24–29. doi: 10.1016/j.ejphar.2015.09.047

Ren, M., Liu, Y., Zhao, H., Dong, S., Jiang, Z., Li, K., et al. (2016). Adenosine triphosphate postconditioning is associated with better preserved global and regional cardiac function during myocardial ischemia and reperfusion: a speckle tracking imaging-based echocardiologic study. *Cardiovasc. Ther.* 34, 343–351. doi: 10.1111/1755-5922.12205

Rial, D., Lara, D. R., and Cunha, R. A. (2014). The adenosine neuromodulation system in schizophrenia. *Int. Rev. Neurobiol.* 119, 395–449. doi: 10.1016/B978-0-12-801022-8.00016-7

Ribeiro, F. F., Xapelli, S., Miranda-Lourenco, C., Tanqueiro, S. R., Fonseca-Gomes, J., Diogenes, M. J., et al. (2016). Purine nucleosides in neuroregeneration and neuroprotection. *Neuropharmacology* 104, 226–242. doi: 10.1016/j.neuropharm.2015.11.006

Richards, J. P., Bowles, E. A., Gordon, W. R., Ellsworth, M. L., Stephenson, A. H., and Sprague, R. S. (2015). Mechanisms of C-peptide-mediated rescue of low O2-induced ATP release from erythrocytes of humans with Type 2 diabetes. *Am. J. Physiol. Regul. Integr. Comp. Physiol.* 308, R411–R418. doi: 10.1152/ajpregu.00420.2014

Riding, A., and Pullar, C. E. (2016). ATP release and P2Y receptor signaling are essential for keratinocyte galvanotaxis. *J. Cell. Physiol.* 231, 181–191. doi: 10.1002/jcp.25070

Ring, S., Enk, A., and Mahnke, K. (2011). A role for adenosine triphosphate in regulating immune responses during melanoma growth. *J. Invest. Dermatol.* 131, S91.

Roberts, V., Lu, B., Rajakumar, S., Cowan, P. J., and Dwyer, K. M. (2013). The CD39-adenosinergic axis in the pathogenesis of renal ischemia-reperfusion injury. *Purinergic Signal.* 9, 135–143. doi: 10.1007/s11302-012-9342-3

Roberts, V. H., Webster, R. P., Brockman, D. E., Pitzer, B. A., and Myatt, L. (2007). Post-translational modifications of the P2X4 purinergic receptor subtype in the human placenta are altered in preeclampsia. *Placenta* 28, 270–277. doi: 10.1016/j.placenta.2006.04.008

Rockenbach, L., Bavaresco, L., Fernandes, F. P., Cappellari, A. R., Barrios, C. H., Bueno, M. F., et al. (2013). Alterations in the extracellular catabolism of nucleotides are involved in the antiproliferative effect of quercetin in human bladder cancer T24 cells. *Urol. Oncol.* 31, 1204–1211. doi: 10.1016/j.urolonc.2011.10.009

Rodrigues, A. M., Bergamaschi, C. T., Fernandes, M. J., Paredes-Gamero, E. J., Buri, M. V., Ferreira, A. T., et al. (2014). P2X7 receptor in the kidneys of diabetic rats submitted to aerobic training or to N-acetylcysteine supplementation [corrected]. *PLOS ONE* 9:e97452. doi: 10.1371/journal.pone.0097452

Rodrigues, L., Miranda, I. M., Andrade, G. M., Mota, M., Cortes, L., Rodrigues, A. G., et al. (2016). Blunted dynamics of adenosine A2A receptors is associated with increased susceptibility to *Candida albicans* infection in the elderly. *Oncotarget* 7, 62862–62872. doi: 10.18632/oncotarget.11760

Rodrigues, R. J., Tomé, A. R., and Cunha, R. A. (2015). ATP as a multi-target danger signal in the brain. *Front. Neurosci.* 9:148. doi: 10.3389/fnins.2015.00148

Rodriguez-Alvarez, N., Jimenez-Mateos, E. M., Engel, T., Quinlan, S., Reschke, C. R., Conroy, R. M., et al. (2017). Effects of P2X7 receptor antagonists on hypoxia-induced neonatal seizures in mice. *Neuropharmacology* 116, 351–363. doi: 10.1016/j.neuropharm.2017.01.005

Rollini, F., Franchi, F., and Angiolillo, D. J. (2016). Switching P2Y12-receptor inhibitors in patients with coronary artery disease. *Nat. Rev. Cardiol.* 13, 11–27. doi: 10.1038/nrcardio.2015.113

Rollini, F., Franchi, F., and Angiolillo, D. J. (2017). Drug-drug interactions when switching between intravenous and oral P2Y12 receptor inhibitors: how real is it? *JACC Cardiovasc. Interv.* 10, 130–132. doi: 10.1016/j.jcin.2016.11.021

Romagnoli, R., Baraldi, P. G., Cruz-Lopez, O., Lopez-Cara, C., Preti, D., Borea, P. A., et al. (2008). The P2X7 receptor as a therapeutic target. *Expert Opin. Ther. Targets* 12, 647–661. doi: 10.1517/14728222.12.5.647

Rong, W., and Burnstock, G. (2004). Activation of ureter nociceptors by exogenous and endogenous ATP in guinea pig. *Neuropharmacology* 47, 1093–1101. doi: 10.1016/j.neuropharm.2004.08.003

Rossi, C., Santini, E., Chiarugi, M., Salvati, A., Comassi, M., Vitolo, E., et al. (2014). The complex P2X7 receptor/inflammasome in perivascular fat tissue of heavy smokers. *Eur. J. Clin. Invest.* 44, 295–302. doi: 10.1111/eci.12232

Rotte, A., Garmann, D., Buss, I., and Jaehde, U. (2010). Effect of extracellular ATP on cisplatin-induced cytotoxicity in human ovarian carcinoma cells. *Chemotherapy* 56, 1–8. doi: 10.1159/000287351

Roy Chowdhury, U., Bahler, C. K., Holman, B. H., Dosa, P. I., and Fautsch, M. P. (2015). Ocular hypotensive effects of the ATP-sensitive potassium channel opener cromakalim in human and murine experimental model systems. *PLOS ONE* 10:e0141783. doi: 10.1371/journal.pone.0141783

Roy Chowdhury, U., Viker, K. B., Stoltz, K. L., Holman, B. H., Fautsch, M. P., and Dosa, P. I. (2016). Analogs of the ATP-sensitive potassium (KATP) channel opener cromakalim with in vivo ocular hypotensive activity. *J. Med. Chem.* 59, 6221–6231. doi: 10.1021/acs.jmedchem.6b00406

Ru, Q., Tian, X., Wu, Y. X., Wu, R. H., Pi, M. S., and Li, C. Y. (2014). Voltage-gated and ATP-sensitive K+ channels are associated with cell proliferation and tumorigenesis of human glioma. *Oncol. Rep.* 31, 842–848. doi: 10.3892/or.2013.2875

Rubaiy, H. N. (2016). The therapeutic agents that target ATP-sensitive potassium channels. *Acta Pharm.* 66, 23–34. doi: 10.1515/acph-2016-0006

Ruzsnavszky, O., Telek, A., Gönczi, M., Balogh, A., Remenyik, E., and Csernoch, L. (2011). UV-B induced alteration in purinergic receptors and signaling on HaCaT keratinocytes. *J. Photochem. Photobiol. B* 105, 113–118. doi: 10.1016/j.jphotobiol.2011.07.009

Ryten, M., Yang, S. Y., Dunn, P. M., Goldspink, G., and Burnstock, G. (2004). Purinoceptor expression in regenerating skeletal muscle in the mdx mouse model of muscular dystrophy and in satellite cell cultures. *FASEB J.* 18, 1404–1406. doi: 10.1096/fj.03-1175fje

Sacco, E., Recupero, S. M., Bientinesi, R., Palermo, G., D'agostino, D., Currò, D., et al. (2015). Pioneering drugs for overactive bladder and detrusor overactivity: ongoing research and future directions. *World J. Obstet. Gynecol.* 4, 24–39.

Sachdeva, S., and Gupta, M. (2013). Adenosine and its receptors as therapeutic targets: an overview. *Saudi. Pharm. J.* 21, 245–253. doi: 10.1016/j.jsps.2012.05.011

Sadovnick, A. D., Gu, B. J., Traboulsee, A. L., Bernales, C. Q., Encarnacion, M., Yee, I. M., et al. (2017). Purinergic receptors P2RX4 and P2RX7 in familial multiple sclerosis. *Hum. Mutat.* 38, 736–744. doi: 10.1002/humu.23218

Sáez-Orellana, F., Godoy, P. A., Bastidas, C. Y., Silva-Grecchi, T., Guzmán, L., Aguayo, L. G., et al. (2016). ATP leakage induces P2XR activation and contributes to acute synaptic excitotoxicity induced by soluble oligomers of β-amyloid peptide in hippocampal neurons. *Neuropharmacology* 100, 116–123. doi: 10.1016/j.neuropharm.2015.04.005

Sakamoto, K., Endo, K., Suzuki, T., Fujimura, K., Kurauchi, Y., Mori, A., et al. (2015). P2X7 receptor antagonists protect against N-methyl-D-aspartic acid-induced neuronal injury in the rat retina. *Eur. J Pharmacol.* 756, 52–58. doi: 10.1016/j.ejphar.2015.03.008

Salgado-Puga, K., Rodriguez-Colorado, J., Prado-Alcala, R. A., and Pena-Ortega, F. (2017). Subclinical doses of ATP-sensitive potassium channel modulators prevent alterations in memory and synaptic plasticity induced by amyloid-β. *J. Alzheimers Dis.* 57, 205–226. doi: 10.3233/JAD-160543

Salvetti, N. R., Panzani, C. G., Gimeno, E. J., Neme, L. G., Alfaro, N. S., and Ortega, H. H. (2009). An imbalance between apoptosis and proliferation contributes to follicular persistence in polycystic ovaries in rats. *Reprod. Biol. Endocrinol.* 7:68. doi: 10.1186/1477-7827-7-68

Samuel, S. S., Mani, A., Tachett, B., Desai, M., and Thevananther, S. (2010). P2Y2 purinergic receptor activation is essential for endotoxin-induced acute liver injury in mice. *Hepatology* 52:608A.

Sanderson, J., Dartt, D. A., Trinkaus-Randall, V., Pintor, J., Civan, M. M., Delamere, N. A., et al. (2014). Purines in the eye: recent evidence for the physiological and pathological role of purines in the RPE, retinal neurons, astrocytes, Muller cells, lens, trabecular meshwork, cornea and lacrimal gland. *Exp. Eye Res.* 127, 270–279. doi: 10.1016/j.exer.2014.08.009

Santana, P. T., Benjamim, C. F., Martinez, C. G., Kurtenbach, E., Takiya, C. M., and Coutinho-Silva, R. (2015). The P2X7 receptor contributes to the development of the exacerbated inflammatory response associated with sepsis. *J. Innate Immun.* 7, 417–427. doi: 10.1159/000371388

Santiago, A. R., Baptista, F. I., Santos, P. F., Cristóvão, G., Ambrósio, A. F., Cunha, R. A., et al. (2014). Role of microglia adenosine A2A receptors in retinal and brain neurodegenerative diseases. *Mediators Inflamm.* 2014:465694. doi: 10.1155/2014/465694

Sarafoff, N., Byrne, R. A., and Sibbing, D. (2012). Clinical use of clopidogrel. *Curr. Pharm. Des.* 18, 5224–5239. doi: 10.2174/138161212803251853

Sashindranath, M., Dwyer, K. M., Dezfouli, S., Selan, C., Crikis, S., Lu, B., et al. (2017). Development of a novel strategy to target CD39 antithrombotic activity to the endothelial-platelet microenvironment in kidney ischemia-reperfusion injury. *Purinergic Signal.* 13, 259–265. doi: 10.1007/s11302-017-9558-3

Sauer, A. V., Mrak, E., Hernandez, R. J., Zacchi, E., Cavani, F., Casiraghi, M., et al. (2009). ADA-deficient SCID is associated with a specific microenvironment and bone phenotype characterized by RANKL/OPG imbalance and osteoblast insufficiency. *Blood* 114, 3216–3226. doi: 10.1182/blood-2009-03-209221

Savio, L. E., Andrade, M. G., De Andrade Mello, P., Santana, P. T., Moreira-Souza, A. C., Kolling, J., et al. (2016). P2X7 receptor signaling contributes to sepsis-associated brain dysfunction. *Mol. Neurobiol.* 54, 6459–6470. doi: 10.1007/s12035-016-0168-9

Savio, L. E., and Coutinho-Silva, R. (2016). Purinergic signaling in infection and autoimmune disease. *Biomed. J.* 39, 304–305. doi: 10.1016/j.bj.2016.09.002

Sawynok, J. (2016). Adenosine receptor targets for pain. *Neuroscience* 338, 1–18. doi: 10.1016/j.neuroscience.2015.10.031

Schepp, C. P., and Reutershan, J. (2008). Bench-to-bedside review: adenosine receptors–promising targets in acute lung injury? *Crit. Care* 12:226. doi: 10.1186/cc6990

Schneider, G., Glaser, T., Lameu, C., Bdelbaset-Ismail, A., Sellers, Z. P., Moniuszko, M., et al. (2015). Extracellular nucleotides as novel, underappreciated pro-metastatic factors that stimulate purinergic signaling in human lung cancer cells. *Mol. Cancer* 14:201. doi: 10.1186/s12943-015-0469-z

Schulte am Esch, J., Akyildiz, A., Tustas, R. Y., Ganschow, R., Schmelzle, M., Krieg, A., et al. (2010). ADP-dependent platelet function prior to and in the early course of pediatric liver transplantation and persisting thrombocytopenia are positively correlated with ischemia/reperfusion injury. *Transpl. Int.* 23, 745–752. doi: 10.1111/j.1432-2277.2010.01054.x

Schulz, N., Liu, K. C., Charbord, J., Mattsson, C. L., Tao, L., Tworus, D., et al. (2016). Critical role for adenosine receptor A2a in β-cell proliferation. *Mol. Metab.* 5, 1138–1146. doi: 10.1016/j.molmet.2016.09.006

Sebastián-Serrano, A., Engel, T., De Diego-García, L., Olivos-Oré, L. A., Arribas-Blázquez, M., Martínez-Frailes, C., et al. (2016). Neurodevelopmental alterations and seizures developed by mouse model of infantile hypophosphatasia are associated with purinergic signalling deregulation. *Hum. Mol. Genet.* 25, 4143–4156. doi: 10.1093/hmg/ddw248

Seref-Ferlengez, Z., Maung, S., Schaffler, M. B., Spray, D. C., Suadicani, S. O., and Thi, M. M. (2016). P2X7R-Panx1 complex impairs bone mechanosignaling under high glucose levels associated with Type-1 diabetes. *PLOS ONE* 11:e0155107. doi: 10.1371/journal.pone.0155107

Shabbir, M., and Burnstock, G. (2009). Purinergic receptor-mediated effects of ATP in urogenital malignant diseases. *Int. J. Urol.* 16, 143–150. doi: 10.1111/j.1442-2042.2008.02207.x

Shabbir, M., Ryten, M., Thompson, C. S., Mikhailidis, D. P., and Burnstock, G. (2008). Purinergic receptor-mediated effects of ATP in high-grade bladder cancer. *BJU Int.* 101, 106–112.

Shaikh, G., and Cronstein, B. (2016). Signaling pathways involving adenosine A2A and A2B receptors in wound healing and fibrosis. *Purinergic Signal.* 12, 191–197. doi: 10.1007/s11302-016-9498-3

Shcherbatko, A., Foletti, D., Poulsen, K., Strop, P., Zhu, G., Hasa-Moreno, A., et al. (2016). Modulation of P2X3 and P2X2/3 receptors by monoclonal antibodies. *J. Biol. Chem.* 291, 12254–12270. doi: 10.1074/jbc.M116.722330

Shibukawa, Y., Sato, M., Kimura, M., Sobhan, U., Shimada, M., Nishiyama, A., et al. (2015). Odontoblasts as sensory receptors: transient receptor potential channels, pannexin-1, and ionotropic ATP receptors mediate intercellular odontoblast-neuron signal transduction. *Pflugers. Arch.* 467, 843–863. doi: 10.1007/s00424-014-1551-x

Shimizu, Y., and Calvert, J. W. (2016). Recycling KATP channels for cardioprotection. *Am. J. Physiol. Heart Circ. Physiol.* 310, H1381–H1382. doi: 10.1152/ajpheart.00309.2016

Shishikura, Y., Koarai, A., Sugiura, H., Aizawa, H., Hashimoto, Y., Numakura, T., et al. (2016). Extracellular ATP involves in dsRNA-induced MUC5AC production via P2Y2R in human airway epithelium. *Am. J. Respir. Crit. Care Med.* 193, A5851.

Sillero, M. A., De Diego, A., Tavares, J. E., Silva, J. A., Pérez-Zúñiga, F. J., and Sillero, A. (2009). Synthesis of ATP derivatives of compounds of the mevalonate pathway (isopentenyl di- and triphosphate; geranyl di- and triphosphate, farnesyl di- and triphosphate, and dimethylallyl diphosphate) catalyzed by T4 RNA ligase, T4 DNA ligase and other ligases Potential relationship with the effect of bisphosphonates on osteoclasts. *Biochem. Pharmacol.* 78, 335–343. doi: 10.1016/j.bcp.2009.04.028

Silva, C. L. (2016). Purinergic signaling in schistosomal infection. *Biomed. J.* 39, 316–325. doi: 10.1016/j.bj.2016.06.006

Silva-Ramos, M., Silva, I., Oliveira, J. C., and Correia-De-Sa, P. (2016). Increased urinary adenosine triphosphate in patients with bladder outlet obstruction due to benign prostate hyperplasia. *Prostate* 76, 1353–1363. doi: 10.1002/pros.23207

Silva-Ramos, M., Silva, I., Oliveira, O., Ferreira, S., Reis, M. J., Oliveira, J. C., et al. (2013). Urinary ATP may be a dynamic biomarker of detrusor overactivity in women with overactive bladder syndrome. *PLOS ONE* 8:e64696. doi: 10.1371/journal.pone.0064696

Silveira, G. F., Buffon, A., and Bruno, A. N. (2013). New approaches to thyroid hormones and purinergic signaling. *J. Thyroid Res.* 2013:434727. doi: 10.1155/2013/434727

Silverman, M. H., Strand, V., Markovits, D., Nahir, M., Reitblat, T., Molad, Y., et al. (2008). Clinical evidence for utilization of the A3 adenosine receptor as a target to treat rheumatoid arthritis: data from a phase II clinical trial. *J. Rheumatol.* 35, 41–48.

Sinadinos, A., Young, C. N., Al-Khalidi, R., Teti, A., Kalinski, P., Mohamad, S., et al. (2015). P2RX7 purinoceptor: a therapeutic target for ameliorating the symptoms of duchenne muscular dystrophy. *PLOS Med.* 12:e1001888. doi: 10.1371/journal.pmed.1001888

Singh, S., Roy, K. K., Khan, S. R., Kashyap, V. K., Sharma, A., Jaiswal, S., et al. (2015). Novel, potent, orally bioavailable and selective mycobacterial ATP synthase inhibitors that demonstrated activity against both replicating and non-replicating *M. tuberculosis*. *Bioorg. Med. Chem.* 23, 742–752. doi: 10.1016/j.bmc.2014.12.060

Sivak, K. V., Vasin, A. V., Egorov, V. V., Tsevtkov, V. B., Kuzmich, N. N., Savina, V. A., et al. (2016). Adenosine A2A receptor as a drug target for treatment of sepsis. *Mol. Biol.* 50, 231–245. doi: 10.7868/S0026898416020233

Sjuve Scott, R., Uvelius, B., and Arner, A. (2004). Changes in intracellular calcium concentration and P2X1 receptor expression in hypertrophic rat urinary bladder smooth muscle. *Neurourol. Urodyn.* 23, 361–366. doi: 10.1002/nau.20047

Slater, M., Danieletto, S., Gidley-Baird, A., Teh, L. C., and Barden, J. A. (2004). Early prostate cancer detected using expression of non-functional cytolytic P2X7 receptors. *Histopathology* 44, 206–215. doi: 10.1111/j.0309-0167.2004.01798.x

Smith, C. P., Vemulakonda, V. M., Kiss, S., Boone, T. B., and Somogyi, G. T. (2005). Enhanced ATP release from rat bladder urothelium during chronic bladder inflammation: effect of botulinum toxin A. *Neurochem. Int.* 47, 291–297. doi: 10.1016/j.neuint.2005.04.021

Smith, S. B., Xu, Z., Novitskaya, T., Zhang, B., Chepurko, E., Pu, X. A., et al. (2016). Impact of cardiac-specific expression of CD39 on myocardial infarct size in mice. *Life Sci.* 179, 54–59. doi: 10.1016/j.lfs.2016.10.016

Soares, A. F., Diniz, C., and Fresco, P. (2012). A3-adenosine receptor effects on malignant melanoma cells. *FEBS J.* 279:547.

Soares-Bezerra, R. J., Pinho, R. T., Bisaggio Rda, C., Benevolo-De-Andrade, T. C., and Alves, L. A. (2015). The search for new agonists to P2X7R for clinical use: tuberculosis as a possible target. *Cell Physiol. Biochem.* 37, 409–418. doi: 10.1159/000430364

Solini, A., Menini, S., Rossi, C., Ricci, C., Santini, E., Blasetti Fantauzzi, C., et al. (2013). The purinergic 2X7 receptor participates in renal inflammation and injury induced by high-fat diet: possible role of NLRP3 inflammasome activation. *J. Pathol.* 231, 342–353. doi: 10.1002/path.4237

Soma, T., Kobayashi, T., Nakagome, K., and Nagata, M. (2016). Clinical implication of adenosine triphosphate in sputum in asthma. *Am. J. Respir. Crit. Care Med.* 193, A1394.

Song, H., Han, Y., Pan, C., Deng, X., Dai, W., Hu, L., et al. (2015). Activation of adenosine monophosphate-activated protein kinase suppresses neuroinflammation and ameliorates bone cancer pain: involvement of inhibition on mitogen-activated protein kinase. *Anesthesiology* 123, 1170–1185. doi: 10.1097/ALN.0000000000000856

Song, S., Jacobson, K. N., Mcdermott, K. M., Reddy, S. P., Cress, A. E., Tang, H., et al. (2016). ATP promotes cell survival via regulation of cytosolic [Ca2+] and Bcl-2/Bax ratio in lung cancer cells. *Am. J. Physiol. Cell Physiol.* 310, C99–C114. doi: 10.1152/ajpcell.00092.2015

Sousa, J. B., and Diniz, C. (2017). The adenosinergic system as a therapeutic target in the vasculature: new ligands and challenges. *Molecules* 22:E752. doi: 10.3390/molecules22050752

Spaans, F., Melgert, B. N., Borghuis, T., Klok, P. A., De Vos, P., Bakker, W. W., et al. (2014a). Extracellular adenosine triphosphate affects systemic and kidney immune cell populations in pregnant rats. *Am. J. Reprod. Immunol.* 72, 305–316. doi: 10.1111/aji.12267

Spaans, F., Melgert, B. N., Chiang, C., Borghuis, T., Klok, P. A., De Vos, P., et al. (2014b). Extracellular ATP decreases trophoblast invasion, spiral artery remodeling and immune cells in the mesometrial triangle in pregnant rats. *Placenta* 35, 587–595. doi: 10.1016/j.placenta.2014.05.013

Sperlagh, B., and Illes, P. (2014). P2X7 receptor: an emerging target in central nervous system diseases. *Trends Pharmacol. Sci.* 35, 537–547. doi: 10.1016/j.tips.2014.08.002

Squadrito, F., Bitto, A., Altavilla, D., Arcoraci, V., De Caridi, G., De Feo, M. E., et al. (2014). The effect of PDRN, an adenosine receptor A2A agonist, on the healing of chronic diabetic foot ulcers: results of a clinical trial. *J. Clin. Endocrinol. Metab.* 99, E746–E753. doi: 10.1210/jc.2013-3569

Stachon, P., Heidenreich, A., Merz, J., Hoppe, N., Bode, C., Idzko, M., et al. (2016). Deficiency of purinergic receptor P2X7 reduces atherosclerosis in mice. *Circulation* 134(Suppl._1), A16502.

Stagg, J., Beavis, P. A., Divisekera, U., Liu, M. C., Moller, A., Darcy, P. K., et al. (2012). CD73-deficient mice are resistant to carcinogenesis. *Cancer Res.* 72, 2190–2196. doi: 10.1158/0008-5472.CAN-12-0420

Stagg, J., Divisekera, U., Mclaughlin, N., Sharkey, J., Pommey, S., Denoyer, D., et al. (2010). Anti-CD73 antibody therapy inhibits breast tumor growth and metastasis. *Proc. Natl. Acad. Sci. U.S.A.* 107, 1547–1552. doi: 10.1073/pnas.0908801107

Stamp, L. K., Hazlett, J., Roberts, R. L., Frampton, C., Highton, J., and Hessian, P. A. (2012). Adenosine receptor expression in rheumatoid synovium: a basis for methotrexate action. *Arthritis Res. Ther.* 14:R138. doi: 10.1186/ar3871

Steculorum, S. M., Timper, K., Engström Ruud, L., Evers, N., Paeger, L., Bremser, S., et al. (2017). Inhibition of P2Y6 signaling in AgRP neurons reduces food intake and improves systemic insulin sensitivity in obesity. *Cell Rep.* 18, 1587–1597. doi: 10.1016/j.celrep.2017.01.047

Stemmer, S., Silverman, M. H., Kerns, W. D., Bar-Yehuda, S., Fishman, S., Harpaz, Z., et al. (2010). Phase 1/2 trial of CF102, a selective A3 adenosine receptor (A3AR) agonist, in patients with hepatocellular carcinoma (HCC). *Eur. J. Cancer* 8:122. doi: 10.1634/theoncologist.2012-0211

Sterle, I., Zupancic, D., and Romih, R. (2014). Correlation between urothelial differentiation and sensory proteins P2X3, P2X5, TRPV1, and TRPV4 in normal urothelium and papillary carcinoma of human bladder. *Biomed. Res. Int.* 2014:805236. doi: 10.1155/2014/805236

Stoll, M., Kim, Y. O., Bebich, B., Robson, S. C., and Schuppan, D. (2012). The selective adenosine 2B receptor antagonist MRS1754 mitigates hepatic collagen deposition during fibrosis progression and induces mild fibrosis regression. *Gastroenterology* 142, S974–S975. doi: 10.1016/S0016-5085(12)63778-0

Straub, R. H., Rauch, L., Fassold, A., Lowin, T., and Pongratz, G. (2008). Neuronally released sympathetic neurotransmitters stimulate splenic interferon-γ secretion from T cells in early type II collagen-induced arthritis. *Arthritis Rheum.* 58, 3450–3460. doi: 10.1002/art.24030

Suadicani, S. O., Urban-Maldonado, M., Tar, M. T., Melman, A., and Spray, D. C. (2009). Effects of ageing and streptozotocin-induced diabetes on connexin43 and P2 purinoceptor expression in the rat corpora cavernosa and urinary bladder. *BJU Int.* 103, 1686–1693. doi: 10.1111/j.1464-410X.2008.08337.x

Subramanian, M., Kini, R., Madasu, M., Ohta, A., Nowak, M., Exley, M., et al. (2014). Extracellular adenosine controls NKT-cell-dependent hepatitis induction. *Eur. J. Immunol.* 44, 1119–1129. doi: 10.1002/eji.201343866

Sugiyama, T. (2014). Role of P2X7 receptors in the development of diabetic retinopathy. *World J. Diabetes* 5, 141–145. doi: 10.4239/wjd.v5.i2.141

Sun, H. S., Xu, B., Chen, W., Xiao, A., Turlova, E., Alibraham, A., et al. (2015). Neuronal KATP channels mediate hypoxic preconditioning and reduce subsequent neonatal hypoxic-ischemic brain injury. *Exp. Neurol.* 263, 161–171. doi: 10.1016/j.expneurol.2014.10.003

Sun, L., Gao, J., Zhao, M., Cui, J., Li, Y., Yang, X., et al. (2015). A novel cognitive impairment mechanism that astrocytic p-connexin 43 promotes neuronic autophagy via activation of P2X7R and down-regulation of GLT-1 expression in the hippocampus following traumatic brain injury in rats. *Behav. Brain Res.* 291, 315–324. doi: 10.1016/j.bbr.2015.05.049

Sun, X., Han, L., Seth, P., Bian, S., Li, L., Csizmadia, E., et al. (2013). Disordered purinergic signaling and abnormal cellular metabolism are associated with development of liver cancer in Cd39/ENTPD1 null mice. *Hepatology* 57, 205–216. doi: 10.1002/hep.25989

Sun, X., Imai, M., Nowak-Machen, M., Guckelberger, O., Enjyoji, K., Wu, Y., et al. (2011). Liver damage and systemic inflammatory responses are exacerbated by the genetic deletion of CD39 in total hepatic ischemia. *Purinergic Signal.* 7, 427–434. doi: 10.1007/s11302-011-9239-6

Sunggip, C., Nishimura, A., Shimoda, K., Numaga-Tomita, T., Tsuda, M., and Nishida, M. (2017). Purinergic P2Y6 receptors: A new therapeutic target of age-dependent hypertension. *Pharmacol. Res.* 120, 51–59. doi: 10.1016/j.phrs.2017.03.013

Suriyaphol, G., Sarikaputi, M., and Suriyaphol, P. (2009). Differential responses of cells from human skin keratinocyte and bovine mammary epithelium to attack by pore-forming *Staphylococcus aureus* α-toxin. *Comp. Immunol. Microbiol. Infect. Dis.* 32, 491–502. doi: 10.1016/j.cimid.2008.07.002

Swennen, E. L., Dagnelie, P. C., Van Den Beucken, T., and Bast, A. (2008). Radioprotective effects of ATP in human blood ex vivo. *Biochem. Biophys. Res. Commun.* 367, 383–387. doi: 10.1016/j.bbrc.2007.12.125

Swiatkowski, P., Murugan, M., Eyo, U. B., Wang, Y., Rangaraju, S., Oh, S. B., et al. (2016). Activation of microglial P2Y12 receptor is required for outward potassium currents in response to neuronal injury. *Neuroscience* 318, 22–33. doi: 10.1016/j.neuroscience.2016.01.008

Szkudelski, T. (2007). Intracellular mediators in regulation of leptin secretion from adipocytes. *Physiol. Res.* 56, 503–512.

Szuster-Ciesielska, A., Sztanke, K., and Kandefer-Szerszen, M. (2012). A novel fused 1,2,4-triazine aryl derivative as antioxidant and nonselective antagonist of adenosine A2A receptors in ethanol-activated liver stellate cells. *Chem. Biol. Interact.* 195, 18–24. doi: 10.1016/j.cbi.2011.10.004

Tai, Y. H., Cheng, P. Y., Tsai, R. Y., Chen, Y. F., and Wong, C. S. (2010). Purinergic P2X receptor regulates N-methyl-D-aspartate receptor expression and synaptic excitatory amino acid concentration in morphine-tolerant rats. *Anesthesiology* 113, 1163–1175. doi: 10.1097/ALN.0b013e3181f11aa2

Tak, E., Jun, D. Y., Kim, S. H., Park, G. C., Lee, J., Hwang, S., et al. (2016). Upregulation of P2Y2 nucleotide receptor in human hepatocellular carcinoma cells. *J. Int. Med. Res.* 44, 1234–1247. doi: 10.1177/0300060516662135

Tak, E., Ridyard, D., Kim, J. H., Zimmerman, M., Werner, T., Wang, X. X., et al. (2014). CD73-dependent generation of adenosine and endothelial Adora2b signaling attenuate diabetic nephropathy. *J. Am. Soc. Nephrol.* 25, 547–563. doi: 10.1681/ASN.2012101014

Takai, E., Tsukimoto, M., Harada, H., and Kojima, S. (2011). Involvement of P2Y6 receptor in p38 MAPK-mediated COX-2 expression in response to UVB irradiation of human keratinocytes. *Radiat. Res.* 175, 358–366. doi: 10.1667/RR2375.1

Takai, E., Tsukimoto, M., Harada, H., and Kojima, S. (2014). Autocrine signaling via release of ATP and activation of P2X7 receptor influences motile activity of human lung cancer cells. *Purinergic Signal.* 10, 487–497. doi: 10.1007/s11302-014-9411-x

Takenouchi, T., Tsukimoto, M., Hashimoto, M., and Kitani, H. (2014). Inflammasome activation by danger signals: extracellular ATP and pH. *Inflammasome* 1, 76–80. doi: 10.2478/infl-2014-0008

Tanaka, S., Kudo, H., Asari, T., Ono, A., Motomura, S., Toh, S., et al. (2011). P2Y1 transient overexpression induced mineralization in spinal ligament cells derived from patients with ossification of the posterior longitudinal ligament of the cervical spine. *Calcif. Tissue Int.* 88, 263–271. doi: 10.1007/s00223-010-9456-y

Tang, J., Li, M. P., Zhou, H. H., and Chen, X. P. (2015). Platelet inhibition agents: current and future P2Y12 receptor antagonists. *Curr. Vasc. Pharmacol.* 13, 566–577. doi: 10.2174/15701611126661411271622O9

Tang, L. M., Zhu, J. F., Wang, F., Qian, J., Zhu, J., Mo, Q., et al. (2010). Activation of adenosine A2A receptor attenuates inflammatory response in a rat model of small-for-size liver transplantation. *Transplant. Proc.* 42, 1915–1920. doi: 10.1016/j.transproceed.2010.02.084

Tantry, S. J., Markad, S. D., Shinde, V., Bhat, J., Balakrishnan, G., Gupta, A. K., et al. (2017). Discovery of imidazo[1,2-a]pyridine ethers and squaramides as selective and potent inhibitors of mycobacterial adenosine triphosphate (ATP) synthesis. *J. Med. Chem.* 60, 1379–1399. doi: 10.1021/acs.jmedchem.6b01358

Tao, Y., and Liang, G. (2015). Efficacy of adenosine A2A receptor antagonist istradefylline as augmentation for Parkinson's disease: a meta-analysis of randomized controlled trials. *Cell Biochem. Biophys.* 71, 57–62. doi: 10.1007/s12013-014-0162-7

Taskiran, E., Erbas, O., Yigittürk, G., Meral, A., Akar, H., and Taskiran, D. (2016). Exogenously administered adenosine attenuates renal damage in streptozotocin-induced diabetic rats. *Ren. Fail.* 38, 1276–1282. doi: 10.1080/0886022X.2016.1207054

Taylor, J. M., and Han, Z. (2010). Purinergic receptor functionality is necessary for infection of human hepatocytes by hepatitis delta virus and hepatitis B virus. *PLOS ONE* 5:e15784. doi: 10.1371/journal.pone.0015784

Taylor, S. R. J., Turner, C. M., Elliott, J. I., Hewitt, R., Pickering, M., Cook, H. T., et al. (2009). P2X7-deficiency ameliorates accelerated nephrotoxic nephritis in mice. *J. Am. Soc. Nephrol.* 20, 1275–1281. doi: 10.1681/ASN.2008060559

Teixeira, J. M., Bobinski, F., Parada, C. A., Sluka, K. A., and Tambeli, C. H. (2016). P2X3 and P2X2/3 receptors play a crucial role in articular hyperalgesia development through inflammatory mechanisms in the knee joint experimental synovitis. *Mol. Neurobiol.* doi: 10.1007/s12035-016-0146-2 [Epub ahead of print].

Teramachi, J., Kukita, A., Li, Y. J., Ushijima, Y., Ohkuma, H., Wada, N., et al. (2011). Adenosine abolishes MTX-induced suppression of osteoclastogenesis and inflammatory bone destruction in adjuvant-induced arthritis. *Lab. Invest.* 91, 719–731. doi: 10.1038/labinvest.2011.9

Thevananther, S., Sun, H., Hernandez, A., Awad, S. S., and Karpen, S. J. (2008). Impaired hepatocellular proliferation in P2Y2 purinergic receptor knockout mice: mitogenic role of extracellular ATP. *Hepatology* 44:206A.

Thevananther, S., Sun, H., Li, D., Arjunan, V., Awad, S. S., Wyllie, S., et al. (2004). Extracellular ATP activates c-jun N-terminal kinase signaling and cell cycle progression in hepatocytes. *Hepatology* 39, 393–402. doi: 10.1002/hep.20075

Tian, T., Zhou, Y., Feng, X., Ye, S., Wang, H., Wu, W., et al. (2016). MicroRNA-16 is putatively involved in the NF-κB pathway regulation in ulcerative colitis through adenosine A2a receptor (A2aAR) mRNA targeting. *Sci. Rep.* 6:30824. doi: 10.1038/srep30824

Tian, Y., Marshall, M., French, B. A., Linden, J., and Yang, Z. (2015). The infarct-sparing effect of IB-MECA against myocardial ischemia/reperfusion injury in mice is mediated by sequential activation of adenosine A3 and A2A receptors. *Basic Res. Cardiol.* 110:16. doi: 10.1007/s00395-015-0473-x

Tian, Y., Tian, X., Han, X., Chen, Y., Song, C. Y., Zhang, Y. B., et al. (2016). Expression of ATP binding cassette E1 enhances viability and invasiveness of lung adenocarcinoma cells in vitro. *Mol. Med. Rep.* 14, 1345–1350. doi: 10.3892/mmr.2016.5388

Torres, A., Vargas, Y., Uribe, D., Jaramillo, C., Gleisner, A., Salazar-Onfray, F., et al. (2016). Adenosine A3 receptor elicits chemoresistance mediated by multiple resistance-associated protein-1 in human glioblastoma stem-like cells. *Oncotarget* 7, 67373–67386. doi: 10.18632/oncotarget.12033

Torres, B. T., Jimenez, D. A., and Budsberg, S. C. (2016). Elevated synovial fluid concentration of adenosine triphosphate in dogs with osteoarthritis or sodium urate-induced synovitis of the stifle. *Vet. Comp. Orthop. Traumatol.* 29, 344–346. doi: 10.3415/VCOT-15-06-0111

Torres-Fuentes, J. L., Rios, M., and Moreno, R. D. (2015). Involvement of a P2X7 receptor in the acrosome reaction induced by ATP in rat spermatozoa. *J. Cell. Physiol.* 230, 3068–3075. doi: 10.1002/jcp.25044

Truong, L. D., Trostel, J., Mcmahan, R., Chen, J. F., and Garcia, G. E. (2016). Macrophage A2A adenosine receptors are essential to protect from progressive kidney injury. *Am. J. Pathol.* 186, 2601–2613. doi: 10.1016/j.ajpath.2016.06.017

Tsuda, M. (2016). Microglia in the spinal cord and neuropathic pain. *J. Diabetes Investig.* 7, 17–26. doi: 10.1111/jdi.12379

Tsuda, M. (2017). P2 receptors, microglial cytokines and chemokines, and neuropathic pain. *J. Neurosci. Res.* 95, 1319–1329. doi: 10.1002/jnr.23816

Tsuda, M., and Inoue, K. (2016). Neuron-microglia interaction by purinergic signaling in neuropathic pain following neurodegeneration. *Neuropharmacology* 104, 76–81. doi: 10.1016/j.neuropharm.2015.08.042

Tsuda, M., Koga, K., Chen, T., and Zhuo, M. (2017). Neuronal and microglial mechanisms for neuropathic pain in the spinal dorsal horn and anterior cingulate cortex. *J. Neurochem.* 141, 486–498. doi: 10.1111/jnc.14001

Tu, G., Zou, L., Liu, S., Wu, B., Lv, Q., Wang, S., et al. (2016). Long noncoding NONRATT021972 siRNA normalized abnormal sympathetic activity mediated by the upregulation of P2X7 receptor in superior cervical ganglia after myocardial ischemia. *Purinergic Signal.* 12, 521–535. doi: 10.1007/s11302-016-9518-3

Turcin, A., Dolzan, V., Porcelli, S., Serretti, A., and Plesnicar, B. K. (2016). Adenosine hypothesis of antipsychotic drugs revisited: pharmacogenomics variation in nonacute schizophrenia. *OMICS* 20, 283–289. doi: 10.1089/omi.2016.0003

Uchida, S., Soshiroda, K., Okita, E., Kawai-Uchida, M., Mori, A., Jenner, P., et al. (2015). The adenosine A2A receptor antagonist, istradefylline enhances the anti-parkinsonian activity of low doses of dopamine agonists in MPTP-treated common marmosets. *Eur. J. Pharmacol.* 747, 160–165. doi: 10.1016/j.ejphar.2014.11.038

Uluçkan, Ö., Eagleton, M. C., Floyd, D. H., Morgan, E. A., Hirbe, A. C., Kramer, M., et al. (2008). APT102, a novel adpase, cooperates with aspirin to disrupt bone metastasis in mice. *J. Cell. Biochem* 104, 1311–1323. doi: 10.1002/jcb.21709

Ursu, D., Ebert, P., Langron, E., Ruble, C., Munsie, L., Zou, W., et al. (2014). Gain and loss of function of P2X7 receptors: mechanisms, pharmacology and

relevance to diabetic neuropathic pain. *Mol. Pain* 10:37. doi: 10.1186/1744-8069-10-37

Valladares, D., Altamirano, F., Henríquez-Olguín, C., Díaz-Vegas, A., Intriago, G., Contreras-Ferrat, A., et al. (2014). ATP signaling complex is altered in muscular dystrophy and was partly recovered after nifedipine treatment. *FASEB J.* 28, 762.3.

Vandenbeuch, A., Anderson, C. B., Parnes, J., Enjyoji, K., Robson, S. C., Finger, T. E., et al. (2013). Role of the ectonucleotidase NTPDase2 in taste bud function. *Proc. Natl. Acad. Sci. U.S.A.* 110, 14789–14794. doi: 10.1073/pnas.1309468110

Vandenbeuch, A., Larson, E. D., Anderson, C. B., Smith, S. A., Ford, A. P., Finger, T. E., et al. (2015). Postsynaptic P2X3-containing receptors in gustatory nerve fibres mediate responses to all taste qualities in mice. *J. Physiol.* 593, 1113–1125. doi: 10.1113/jphysiol.2014.281014

Vanderstocken, G., Van De Paar, E., Robaye, B., Di Pietrantonio, L., Bondue, B., Boeynaems, J. M., et al. (2012). Protective role of P2Y2 receptor against lung infection induced by pneumonia virus of mice. *PLOS ONE* 7:e50385. doi: 10.1371/journal.pone.0050385

Varani, K., Padovan, M., Govoni, M., Vincenzi, F., Trotta, F., and Borea, P. A. (2010a). The role of adenosine receptors in rheumatoid arthritis. *Autoimmun. Rev.* 10, 61–64. doi: 10.1016/j.autrev.2010.07.019

Varani, K., Vincenzi, F., Targa, M., Paradiso, B., Parrilli, A., Fini, M., et al. (2013). The stimulation of A3 adenosine receptors reduces bone-residing breast cancer in a rat preclinical model. *Eur. J. Cancer* 49, 482–491. doi: 10.1016/j.ejca.2012.06.005

Varani, K., Vincenzi, F., Tosi, A., Targa, M., Masieri, F. F., Ongaro, A., et al. (2010b). Expression and functional role of adenosine receptors in regulating inflammatory responses in human synoviocytes. *Br. J. Pharmacol.* 160, 101–115. doi: 10.1111/j.1476-5381.2010.00667.x

Vaughn, B. P., Robson, S. C., and Longhi, M. S. (2014). Purinergic signaling in liver disease. *Dig. Dis.* 32, 516–524. doi: 10.1159/000360498

Vazquez-Cuevas, F. G., Martinez-Ramirez, A. S., Robles-Martinez, L., Garay, E., Garcia-Carranca, A., Perez-Montiel, D., et al. (2014). Paracrine stimulation of P2X7 receptor by ATP activates a proliferative pathway in ovarian carcinoma cells. *J. Cell. Biochem.* 115, 1955–1966. doi: 10.1002/jcb.24867

Vergani, A., Fotino, C., D'addio, F., Tezza, S., Podetta, M., Gatti, F., et al. (2013). Effect of the purinergic inhibitor oxidized ATP in a model of islet allograft rejection. *Diabetes Metab. Res. Rev.* 62, 1665–1675. doi: 10.2337/db12-0242

Veselá, R., Aronsson, P., Andersson, M., Wsol, V., and Tobin, G. (2012a). The potential of non-adrenergic, non-cholinergic targets in the treatment of interstitial cystitis/painful bladder syndrome. *J. Physiol. Pharmacol.* 63, 209–216.

Veselá, R., Aronsson, P., and Tobin, G. (2011). Functional and morphological examinations of P1A1 purinoceptors in the normal and inflamed urinary bladder of the rat. *Auton. Neurosci.* 159, 26–31. doi: 10.1016/j.autneu.2010.07.008

Veselá, R., Asklund, H., Aronsson, P., Johnsson, M., Wsol, V., Andersson, M., et al. (2012b). Coupled nitric oxide and autonomic receptor functional responses in the normal and inflamed urinary bladder of the rat. *Physiol. Res.* 61, 371–380.

Vieira, F. S., Nanini, H. F., Takiya, C. M., and Coutinho-Silva, R. (2016). P2X7 receptor knockout prevents streptozotocin-induced type 1 diabetes in mice. *Mol. Cell. Endocrinol.* 419, 148–157. doi: 10.1016/j.mce.2015.10.008

Vincent, I. S., and Okusa, M. D. (2015). Adenosine 2A receptors in acute kidney injury. *Acta Physiol.* 214, 303–310. doi: 10.1111/apha.12508

Vincenzi, F., Padovan, M., Targa, M., Corciulo, C., Giacuzzo, S., Merighi, S., et al. (2013). A2A adenosine receptors are differentially modulated by pharmacological treatments in rheumatoid arthritis patients and their stimulation ameliorates adjuvant-induced arthritis in rats. *PLOS ONE* 8:e54195. doi: 10.1371/journal.pone.0054195

Vincenzi, F., Ravani, A., Pasquini, S., Merighi, S., Gessi, S., Romagnoli, R., et al. (2016). Positive allosteric modulation of A1 adenosine receptors as a novel and promising therapeutic strategy for anxiety. *Neuropharmacology* 111, 283–292. doi: 10.1016/j.neuropharm.2016.09.015

Vindeirinho, J., Santiago, A. R., Cavadas, C., Ambrósio, A. F., and Santos, P. F. (2016). The adenosinergic system in diabetic retinopathy. *J. Diabetes Res.* 2016:4270301. doi: 10.1155/2016/4270301

Vlajkovic, S. M., Ambepitiya, K., Barclay, M., Boison, D., Housley, G. D., and Thorne, P. R. (2017). Adenosine receptors regulate susceptibility to noise-induced neural injury in the mouse cochlea and hearing loss. *Hear. Res.* 345, 43–51. doi: 10.1016/j.heares.2016.12.015

Vlaskovska, M., Kasakov, L., Rong, W., Bodin, P., Bardini, M., Cockayne, D. A., et al. (2001). P2X3 knockout mice reveal a major sensory role for urothelially released ATP. *J. Neurosci.* 21, 5670–5677.

Völkl, T., Ogilvie, A., Neuhuber, W., and Ogilvie, A. (2008). Cell death induced by uridine 5′-triphosphate (UTP) in contrast to adenosine 5′-triphosphate (ATP) in human epidermoid carcinoma cells (A-431). *Cell Physiol. Biochem.* 22, 441–454. doi: 10.1159/000185491

Volonté, C., Apolloni, S., Parisi, C., and Amadio, S. (2016). Purinergic contribution to amyotrophic lateral sclerosis. *Neuropharmacology* 104, 180–193. doi: 10.1016/j.neuropharm.2015.10.026

von Versen-Höynck, F., Rajakumar, A., Bainbridge, S. A., Gallaher, M. J., Roberts, J. M., and Powers, R. W. (2009). Human placental adenosine receptor expression is elevated in preeclampsia and hypoxia increases expression of the A2A receptor. *Placenta* 30, 434–442. doi: 10.1016/j.placenta.2009.02.004

Vonend, O., Turner, C., Chan, C. M., Loesch, A., Dell'anna, G. C., Srai, S. K., et al. (2004). Glomerular expression of the ATP-sensitive P2X7 receptor in diabetic and hypertensive rat models. *Kidney Int.* 66, 157–166. doi: 10.1111/j.1523-1755.2004.00717.x

Voors, A. A., Dungen, H. D., Senni, M., Nodari, S., Agostoni, P., Ponikowski, P., et al. (2017). Safety and tolerability of neladenoson bialanate, a novel oral partial adenosine A1 receptor agonist, in patients with chronic heart failure. *J. Clin. Pharmacol.* 57, 440–451. doi: 10.1002/jcph.828

Vorovenci, R. J., and Antonini, A. (2015). The efficacy of oral adenosine A2A antagonist istradefylline for the treatment of moderate to severe Parkinson's disease. *Expert Rev. Neurother.* 15, 1383–1390. doi: 10.1586/14737175.2015.1113131

Waeber, C., and Moskowitz, M. A. (2003). Therapeutic implications of central and peripheral neurologic mechanisms in migraine. *Neurology* 61, S9–S20. doi: 10.1212/WNL.61.8_suppl_4.S9

Walsh, C. A., Cheng, Y., Mansfield, K. J., Parkin, K., Mukerjee, C., and Moore, K. H. (2013). Decreased intravesical adenosine triphosphate in patients with refractory detrusor overactivity and bacteriuria. *J. Urol.* 189, 1383–1387. doi: 10.1016/j.juro.2012.10.003

Wan, H. X., Hu, J. H., Xie, R., Yang, S. M., and Dong, H. (2016). Important roles of P2Y receptors in the inflammation and cancer of digestive system. *Oncotarget* 7, 28736–28747. doi: 10.18632/oncotarget.7518

Wan, P., Liu, X., Xiong, Y., Ren, Y., Chen, J., Lu, N., et al. (2016). Extracellular ATP mediates inflammatory responses in colitis via P2 x 7 receptor signaling. *Sci. Rep.* 6:19108. doi: 10.1038/srep19108

Wang, C., Hu, S. M., Xie, H., Qiao, S. G., Liu, H., and Liu, C. F. (2015). Role of mitochondrial ATP-sensitive potassium channel-mediated PKC-ε in delayed protection against myocardial ischemia/reperfusion injury in isolated hearts of sevoflurane-preconditioned rats. *Braz. J. Med. Biol. Res.* 48, 528–536. doi: 10.1590/1414-431X20143876

Wang, L., Wan, H., Tang, W., Ni, Y., Hou, X., Pan, L., et al. (2016). Critical roles of adenosine A2A receptor in regulating the balance of Treg/Th17cells in allergic asthma. *Clin. Respir. J.* doi: 10.1111/crj.12503 [Epub ahead of print].

Wang, N., Rumney, R. M., Yang, L., Robaye, B., Boeynaems, J. M., Skerry, T. M., et al. (2013). The P2Y13 receptor regulates extracellular ATP metabolism and the osteogenic response to mechanical loading. *J. Bone Miner. Res.* 28, 1446–1456. doi: 10.1002/jbmr.1877

Wang, X., Arcuino, G., Takano, T., Lin, J., Peng, W. G., Wan, P., et al. (2004). P2X7 receptor inhibition improves recovery after spinal cord injury. *Nat. Med.* 10, 821–827. doi: 10.1038/nm1082

Wang, X. H., Xie, X., Luo, X. G., Shang, H., and He, Z. Y. (2017). Inhibiting purinergic P2X7 receptors with the antagonist brilliant blue G is neuroprotective in an intranigral lipopolysaccharide animal model of Parkinson's disease. *Mol. Med. Rep.* 15, 768–776. doi: 10.3892/mmr.2016.6070

Wang, Z., Cristofaro, V., Cheng, Z., Xiao, X., Ge, R., Sullivan, M., et al. (2013). Urothelium-released ATP contributes to bladder dysfunction in type 2 diabetes. *J. Urol.* 189, e116. doi: 10.1016/j.juro.2013.02.1668

Wei, C. J., Augusto, E., Gomes, C. A., Singer, P., Wang, Y., Boison, D., et al. (2014). Regulation of fear responses by striatal and extrastriatal adenosine A2A

receptors in forebrain. *Biol. Psychiatry* 75, 855–863. doi: 10.1016/j.biopsych.2013.05.003

Wei, Q., Costanzi, S., Liu, Q. Z., Gao, Z. G., and Jacobson, K. A. (2011). Activation of the P2Y1 receptor induces apoptosis and inhibits proliferation of prostate cancer cells. *Biochem. Pharmacol.* 82, 418–425. doi: 10.1016/j.bcp.2011.05.013

Wen, J., Wang, B., Du, C., Xu, G., Zhang, Z., Li, Y., et al. (2015). A2B adenosine receptor agonist improves erectile function in diabetic rats. *Tohoku J. Exp. Med.* 237, 141–148. doi: 10.1620/tjem.237.141

Wen, J., and Xia, Y. (2012). Adenosine signaling: good or bad in erectile function? *Arterioscler. Thromb. Vasc. Biol.* 32, 845–850. doi: 10.1161/ATVBAHA.111.226803

Wesselius, A., Bours, M. J., Jørgensen, N. R., Wiley, J., Gu, B., Van Helden, S., et al. (2013). Non-synonymous polymorphisms in the P2RX4 are related to bone mineral density and osteoporosis risk in a cohort of Dutch fracture patients. *Purinergic Signal.* 9, 123–130. doi: 10.1007/s11302-012-9337-0

Wessels, J. A., Kooloos, W. M., De Jonge, R., De Vries-Bouwstra, J. K., Allaart, C. F., Linssen, A., et al. (2006). Relationship between genetic variants in the adenosine pathway and outcome of methotrexate treatment in patients with recent-onset rheumatoid arthritis. *Arthritis Rheum.* 54, 2830–2839. doi: 10.1002/art.22032

Wettstein, M. S., Buser, L., Hermanns, T., Roudnicky, F., Eberli, D., Baumeister, P., et al. (2015). CD73 predicts favorable prognosis in patients with nonmuscle-invasive urothelial bladder cancer. *Dis. Markers* 2015:785461. doi: 10.1155/2015/785461

White, C. W., Choong, Y. T., Short, J. L., Exintaris, B., Malone, D. T., Allen, A. M., et al. (2013). Male contraception via simultaneous knockout of α1A-adrenoceptors and P2X1-purinoceptors in mice. *Proc. Natl. Acad. Sci U.S.A.* 110, 20825–20830. doi: 10.1073/pnas.1318624110

White, N., Butler, P. E. M., and Burnstock, G. (2005). Human melanomas express functional P2X7 receptors. *Cell Tissue Res.* 321, 411–418. doi: 10.1007/s00441-005-1149-x

White, N., Knight, G. E., Butler, P. E. M., and Burnstock, G. (2009). An in vivo model of melanoma: treatment with ATP. *Purinergic Signal.* 5, 327–333. doi: 10.1007/s11302-009-9156-0

Wiesler, B., Zech, A., and Idzko, M. (2016). The purinergic receptor P2X4 mediates acute airway inflammation by regulating dendritic cell function. *Am. J. Respir. Crit. Care Med.* 193, A7543.

Wille, A., Amort, T., Singewald, N., Sartori, S. B., and Lusser, A. (2016). Dysregulation of select ATP-dependent chromatin remodeling factors in high trait anxiety. *Behav. Brain Res.* 311, 141–146. doi: 10.1016/j.bbr.2016.05.036

Winerdal, M., Winerdal, M. E., Wang, Y. Q., Fredholm, B. B., Winqvist, O., and Ådén, U. (2016). Adenosine A1 receptors contribute to immune regulation after neonatal hypoxic ischemic brain injury. *Purinergic Signal.* 12, 89–101. doi: 10.1007/s11302-015-9482-3

Wirsdörfer, F., De Leve, S., Cappuccini, F., Eldh, T., Meyer, A. V., Gau, E., et al. (2016). Extracellular adenosine production by ecto-5′-nucleotidase (CD73) enhances radiation-induced lung fibrosis. *Cancer Res.* 76, 3045–3056. doi: 10.1158/0008-5472.CAN-15-2310

Wojcik, M., Zieleniak, A., Mac-Marcjanek, K., Wozniak, L. A., and Cypryk, K. (2014). The elevated gene expression level of the A2B adenosine receptor is associated with hyperglycemia in women with gestational diabetes mellitus. *Diabetes Metab. Res. Rev.* 30, 42–53. doi: 10.1002/dmrr.2446

Woods, L. T., Ajit, D., Camden, J. M., Erb, L., and Weisman, G. A. (2016). Purinergic receptors as potential therapeutic targets in Alzheimer's disease. *Neuropharmacology* 104, 169–179. doi: 10.1016/j.neuropharm.2015.10.031

Wright, A., Mahaut-Smith, M., Symon, F., Sylvius, N., Ran, S., Bafadhel, M., et al. (2016). Impaired P2X1 receptor-mediated adhesion in eosinophils from asthmatic patients. *J. Immunol.* 196, 4877–4884. doi: 10.4049/jimmunol.1501585

Wright, S. R., Zanos, P., Georgiou, P., Yoo, J. H., Ledent, C., Hourani, S. M., et al. (2016). A critical role of striatal A2A R-mGlu R interactions in modulating the psychomotor and drug-seeking effects of methamphetamine. *Addict. Biol.* 21, 811–825. doi: 10.1111/adb.12259

Wu, B., Zhang, C., Zou, L., Ma, Y., Huang, K., Lv, Q., et al. (2016). LncRNA uc.*48*+ siRNA improved diabetic sympathetic neuropathy in type 2 diabetic rats mediated by P2X7 receptor in SCG. *Auton. Neurosci.* 197, 14–18. doi: 10.1016/j.autneu.2016.04.001

Wu, H., Nie, Y., Xiong, H., Liu, S., Li, G., Huang, A., et al. (2015). P2X7 receptor expression in peripheral blood monocytes is correlated with plasma C-reactive protein and cytokine levels in patients with type 2 diabetes mellitus: a preliminary report. *Inflammation* 38, 2076–2081. doi: 10.1007/s10753-015-0189-y

Wu, J. X., Xu, M. Y., Miao, X. R., Lu, Z. J., Yuan, X. M., Li, X. Q., et al. (2012). Functional up-regulation of P2X3 receptors in dorsal root ganglion in a rat model of bone cancer pain. *Eur. J. Pain* 16, 1378–1388. doi: 10.1002/j.1532-2149.2012.00149.x

Wu, M., Sahbaie, P., Zheng, M., Lobato, R., Boison, D., Clark, J. D., et al. (2013). Opiate-induced changes in brain adenosine levels and narcotic drug responses. *Neuroscience* 228, 235–242. doi: 10.1016/j.neuroscience.2012.10.031

Wu, W., He, Y., Feng, X., Ye, S., Wang, H., Tan, W., et al. (2017). MicroRNA-206 is involved in the pathogenesis of ulcerative colitis via regulation of adenosine A3 receptor. *Oncotarget* 8, 705–721. doi: 10.18632/oncotarget.13525

Xia, H., Zhang, D., Yang, S., Wang, Y., Xu, L., Wu, J., et al. (2014). Role of ATP-sensitive potassium channels in modulating nociception in rat model of bone cancer pain. *Brain Res.* 1554, 29–35. doi: 10.1016/j.brainres.2014.01.032

Xia, J., Yu, X., Tang, L., Li, G., and He, T. (2015). P2X7 receptor stimulates breast cancer cell invasion and migration via the AKT pathway. *Oncol. Rep.* 34, 103–110. doi: 10.3892/or.2015.3979

Xiang, H. J., Liu, Z. C., Wang, D. S., Chen, Y., Yang, Y. L., and Dou, K. F. (2006). Adenosine A2b receptor is highly expressed in human hepatocellular carcinoma. *Hepatol. Res.* 36, 56–60. doi: 10.1016/j.hepres.2006.06.008

Xiao, F., Waldrop, S. L., Khimji, A. K., and Kilic, G. (2012). Pannexin1 contributes to pathophysiological ATP release in lipoapoptosis induced by saturated free fatty acids in liver cells. *Am. J. Physiol. Cell Physiol.* 303, C1034–C1044. doi: 10.1152/ajpcell.00175.2012

Xiao, H., Si, L. Y., Liu, W., Li, N., Meng, G., Yang, N., et al. (2013). The effects of adenosine A2A receptor knockout on renal interstitial fibrosis in a mouse model of unilateral ureteral obstruction. *Acta Histochem.* 115, 315–319. doi: 10.1016/j.acthis.2012.09.002

Xie, R., Xu, J., Wen, G., Jin, H., Liu, X., Yang, Y., et al. (2014). The P2Y2 nucleotide receptor mediates the proliferation and migration of human hepatocellular carcinoma cells induced by ATP. *J. Biol. Chem.* 289, 19137–19149. doi: 10.1074/jbc.M113.540047

Xie, Y., Williams, C. D., Mcgill, M. R., Lebofsky, M., Ramachandran, A., and Jaeschke, H. (2013). Purinergic receptor antagonist A438079 protects against acetaminophen-induced liver injury by inhibiting P450 isoenzymes, not by inflammasome activation. *Toxicol. Sci.* 131, 325–335. doi: 10.1093/toxsci/kfs283

Xu, J., Chu, K. L., Brederson, J. D., Jarvis, M. F., and Mcgaraughty, S. (2012). Spontaneous firing and evoked responses of spinal nociceptive neurons are attenuated by blockade of P2X3 and P2X2/3 receptors in inflamed rats. *J. Neurosci. Res.* 90, 1597–1606. doi: 10.1002/jnr.23042

Xu, P., Xu, Y., Hu, B., Wang, J., Pan, R., Murugan, M., et al. (2015). Extracellular ATP enhances radiation-induced brain injury through microglial activation and paracrine signaling via P2X7 receptor. *Brain Behav. Immun.* 50, 87–100. doi: 10.1016/j.bbi.2015.06.020

Xu, X., Zheng, S., Xiong, Y., Wang, X., Qin, W., Zhang, H., et al. (2017). Adenosine effectively restores endotoxin-induced inhibition of human neutrophil chemotaxis via A1 receptor-p38 pathway. *Inflamm. Res.* 66, 353–364. doi: 10.1007/s00011-016-1021-3

Yamada, K., Kobayashi, M., and Kanda, T. (2014). Involvement of adenosine A2A receptors in depression and anxiety. *Int. Rev. Neurobiol.* 119, 373–393. doi: 10.1016/B978-0-12-801022-8.00015-5

Yamauchi, T., and Kadowaki, T. (2013). Adiponectin receptor as a key player in healthy longevity and obesity-related diseases. *Cell Metab.* 17, 185–196. doi: 10.1016/j.cmet.2013.01.001

Yan, D., Zhu, Y., Walsh, T., Xie, D., Yuan, H., Sirmaci, A., et al. (2013). Mutation of the ATP-gated P2X2 receptor leads to progressive hearing loss and increased susceptibility to noise. *Proc. Natl. Acad. Sci. U.S.A.* 110, 2228–2233. doi: 10.1073/pnas.1222285110

Yan, H., Zhang, E., Feng, C., and Zhao, X. (2016). Role of A3 adenosine receptor in diabetic neuropathy. *J. Neurosci. Res.* 94, 936–946. doi: 10.1002/jnr.23774

Yan, S., Du, F., Wu, L., Zhang, Z., Zhong, C., Yu, Q., et al. (2016). F1F0 ATP synthase-cyclophilin D interaction contributes to diabetes-induced synaptic dysfunction and cognitive decline. *Diabetes Metab. Res. Rev.* 65, 3482–3494.

Yan, Y., Bai, J., Zhou, X., Tang, J., Jiang, C., Tolbert, E., et al. (2015). P2X7 receptor inhibition protects against ischemic acute kidney injury in mice. *Am. J. Physiol. Cell Physiol.* 308, C463–C472. doi: 10.1152/ajpcell.00245.2014

Yang, C., Xu, H., Cai, L., Du, X., Jiang, Y., Zhang, Y., et al. (2016). Donor pretreatment with adenosine monophosphate-activated protein kinase activator protects cardiac grafts from cold ischaemia/reperfusion injury. *Eur. J Cardiothorac. Surg.* 49, 1354–1360. doi: 10.1093/ejcts/ezv413

Yang, Z., Li, L., Zheng, J., Ma, H., Tian, S., Li, J., et al. (2016). Identification of a new series of potent adenosine A2A receptor antagonists based on 4-amino-5-carbonitrile pyrimidine template for the treatment of Parkinson's disease. *ACS Chem. Neurosci.* 7, 1575–1584. doi: 10.1021/acschemneuro.6b00218

Yang, P., Wang, Z., Zhan, Y., Wang, T., Zhou, M., Xia, L., et al. (2013). Endogenous A1 adenosine receptor protects mice from acute ethanol-induced hepatotoxicity. *Toxicology* 309, 100–106. doi: 10.1016/j.tox.2013.05.003

Yap, S. C., and Lee, H. T. (2012). Adenosine and protection from acute kidney injury. *Curr Opin. Nephrol. Hypertens* 21, 24–32. doi: 10.1097/MNH.0b013e32834d2ec9

Yegutkin, G. G., Guerrero-Toro, C., Kilinc, E., Koroleva, K., Ishchenko, Y., Abushik, P., et al. (2016). Nucleotide homeostasis and purinergic nociceptive signaling in rat meninges in migraine-like conditions. *Purinergic Signal.* 12, 561–574. doi: 10.1007/s11302-016-9521-8

Yegutkin, G. G., Marttila-Ichihara, F., Karikoski, M., Niemela, J., Laurila, J. P., Elima, K., et al. (2011). Altered purinergic signaling in CD73-deficient mice inhibits tumor progression. *Eur. J. Immunol.* 41, 1231–1241. doi: 10.1002/eji.201041292

Yelovitch, S., Barr, H. M., Camden, J., Weisman, G. A., Shai, E., Varon, D., et al. (2012). Identification of a promising drug candidate for the treatment of type 2 diabetes based on a P2Y1 receptor agonist. *J. Med. Chem.* 55, 7623–7635. doi: 10.1021/jm3006355

Yetgin, T., Uitterdijk, A., Te Lintel Hekkert, M., Merkus, D., Krabbendam-Peters, I., Van Beusekom, H. M., et al. (2015). Limitation of infarct size and no-reflow by intracoronary adenosine depends critically on dose and duration. *JACC Cardiovasc. Interv.* 8, 1990–1999. doi: 10.1016/j.jcin.2015.08.033

Yip, L., Taylor, C., Whiting, C. C., and Fathman, C. G. (2013). Diminished adenosine A1 receptor expression in pancreatic α-cells may contribute to the pathology of type 1 diabetes. *Diabetes Metab. Res. Rev.* 62, 4208–4219. doi: 10.2337/db13-0614

Yoneyama, Y., Sawa, R., Suzuki, S., Shin, S., Power, G. G., and Araki, T. (1996). The relationship between uterine artery Doppler velocimetry and umbilical venous adenosine levels in pregnancies complicated by preeclampsia. *Am. J. Obstet. Gynecol.* 174, 267–271. doi: 10.1016/S0002-9378(96)70406-4

Yoneyama, Y., Suzuki, S., Sawa, R., and Araki, T. (2004). Plasma adenosine concentrations increase in women with hyperemesis gravidarum. *Clin. Chim. Acta* 342, 99–103. doi: 10.1016/j.cccn.2003.12.004

Yoshida, K., Ito, M., and Matsuoka, I. (2015). P2X7 receptor antagonist activity of the anti-allergic agent oxatomide. *Eur. J. Pharmacol.* 767, 41–51. doi: 10.1016/j.ejphar.2015.10.002

Young, C. N. J., Sinadinos, A., and Gorecki, D. C. (2013). P2X receptor signaling in skeletal muscle health and disease. *Wiley Interdiscip. Rev. Membr. Transp. Signal.* 2, 265–274. doi: 10.1042/BJ20141551

Yu, Q., Guo, Z., Liu, X., Ouyang, Q., He, C., Burnstock, G., et al. (2013). Block of P2X7 receptors could partly reverse the delayed neuronal death in area CA1 of the hippocampus after transient global cerebral ischemia. *Purinergic Signal.* 9, 663–675. doi: 10.1007/s11302-013-9379-y

Yu, W., Sun, X., Robson, S. C., and Hill, W. G. (2013). Extracellular UDP enhances P2X-mediated bladder smooth muscle contractility via P2Y6 activation of the phospholipase C/inositol trisphosphate pathway. *FASEB J.* 27, 1895–1903. doi: 10.1096/fj.12-219006

Yu, Y. (2015). Nucleotide modulates odor response through activation of purinergic receptor in olfactory sensory neuron. *Biochem. Biophys. Res. Commun.* 463, 1006–1011. doi: 10.1016/j.bbrc.2015.06.050

Yu, Y., and Zhang, C. (2014). Purinergic signaling negatively regulates activity of an olfactory receptor in an odorant-dependent manner. *Neuroscience* 275, 89–101. doi: 10.1016/j.neuroscience.2014.05.055

Yu, Y. C., Sohma, Y., and Hwang, T. C. (2016). On the mechanism of gating defects caused by the R117H mutation in cystic fibrosis transmembrane conductance regulator. *J. Physiol.* 594, 3227–3244. doi: 10.1113/JP271723

Yuryeva, K., Saltykova, I., Ogorodova, L., Kirillova, N., Kulikov, E., Korotkaya, E., et al. (2015). Expression of adenosine receptors in monocytes from patients with bronchial asthma. *Biochem. Biophys. Res. Commun.* 464, 1314–1320. doi: 10.1016/j.bbrc.2015.07.141

Zafrah, H. A., and Alotaibi, M. F. (2017). The effect of extracellular ATP on rat uterine contraction from different gestational stages and its possible mechanisms of action. *J. Basic Clin. Physiol. Pharmacol.* 28, 209–217. doi: 10.1515/jbcpp-2016-0118

Zakeri, Z., Izadi, S., Niazi, A., Bari, Z., Zendeboodi, S., Shakiba, M., et al. (2012). Comparison of adenosine deaminase levels in serum and synovial fluid between patients with rheumatoid arthritis and osteoarthritis. *Int. J. Clin. Exp. Med.* 5, 195–200.

Zanin, R. F., Da Silva, G. L., Erig, T., Sperotto, N. D., Leite, C. E., Coutinho-Silva, R., et al. (2015). Decrease of serum adenine nucleotide hydrolysis in an irritant contact dermatitis mice model: potential P2X7R involvement. *Mol. Cell. Biochem.* 404, 221–228. doi: 10.1007/s11010-015-2381-7

Zarjou, A., and Agarwal, A. (2011). ATP as a death factor: purinergic signaling in renal epithelial-fibroblast cross talk. *Am. J. Physiol. Renal Physiol.* 300, F60–F61. doi: 10.1152/ajprenal.00593.2010

Zempo, H., Sugita, Y., Ogawa, M., Watanabe, R., Suzuki, J., and Isobe, M. (2015). A P2X7 receptor antagonist attenuates experimental autoimmune myocarditis via suppressed myocardial CD4+ T and macrophage infiltration and NADPH oxidase 2/4 expression in mice. *Heart Vessels* 30, 527–533. doi: 10.1007/s00380-014-0527-2

Zhang, B., Cheng, B., Li, F. S., Ding, J. H., Feng, Y. Y., Zhuo, G. Z., et al. (2015a). High expression of CD39/ENTPD1 in malignant epithelial cells of human rectal adenocarcinoma. *Tumour. Biol.* 36, 9411–9419. doi: 10.1007/s13277-015-3683-9

Zhang, C., Gao, L., Yi, Y., Han, H., Cheng, H., Ye, X., et al. (2016). Adenosine triphosphate regresses endometrial explants in a rat model of endometriosis. *Reprod. Sci.* 23, 924–930. doi: 10.1177/1933719115625847

Zhang, K., Liu, J., You, X., Kong, P., Song, Y., Cao, L., et al. (2016). P2X7 as a new target for chrysophanol to treat lipopolysaccharide-induced depression in mice. *Neurosci. Lett.* 613, 60–65. doi: 10.1016/j.neulet.2015.12.043

Zhang, X., Qin, J., Zou, J., Lv, Z., Tan, B., Shi, J., et al. (2016). Extracellular ADP facilitates monocyte recruitment in bacterial infection via ERK signaling. *Cell Mol. Immunol.* doi: 10.1038/cmi.2016.56 [Epub ahead of print].

Zhang, Y., Guo, Q., Li, X., Gao, J., Liu, Y., Yang, J., et al. (2015b). P2Y purinergic receptor-regulated insulin secretion is mediated by a cAMP/Epac/Kv channel pathway. *Biochem. Biophys. Res. Commun.* 460, 850–856. doi: 10.1016/j.bbrc.2015.03.121

Zhang, Y., Peti-Peterdi, J., Müller, C. E., Carlson, N. G., Baqi, Y., Strasburg, D. L., et al. (2015c). P2Y12 receptor localizes in the renal collecting duct and its blockade augments arginine vasopressin action and alleviates nephrogenic diabetes insipidus. *J. Am. Soc. Nephrol.* 26, 2978–2987. doi: 10.1681/ASN.2014010118

Zhang, Y., Yuan, F., Cao, X., Zhai, Z., Ganghuang, Du, X., et al. (2014). P2X7 receptor blockade protects against cisplatin-induced nephrotoxicity in mice by decreasing the activities of inflammasome components, oxidative stress and caspase-3. *Toxicol. Appl. Pharmacol.* 281, 1–10. doi: 10.1016/j.taap.2014.09.016

Zhao, H., Zhang, X., Dai, Z., Feng, Y., Li, Q., Zhang, J. H., et al. (2016). P2X7 receptor suppression preserves blood-brain barrier through inhibiting RhoA activation after experimental intracerebral hemorrhage in rats. *Sci. Rep.* 6:23286. doi: 10.1038/srep23286

Zhao, J., Wang, H., Dai, C., Wang, H., Zhang, H., Huang, Y., et al. (2013). P2X7 blockade attenuates lupus nephritis by inhibiting NLRP3/ASC/caspase-1 activation. *Arthritis Rheum.* 65, 3176–3185. doi: 10.1002/art.38174

Zhao, R., Liang, D., and Sun, D. (2016). Blockade of extracellular ATP effect by oxidized ATP effectively mitigated induced mouse experimental autoimmune uveitis (EAU). *PLOS ONE* 11:e0155953. doi: 10.1371/journal.pone.0155953

Zheng, B., Lai, R., Li, J., and Zuo, Z. (2017). Critical role of P2X7 receptors in the neuroinflammation and cognitive dysfunction after surgery. *Brain Behav. Immun.* 61, 365–374. doi: 10.1016/j.bbi.2017.01.005

Zheng, X., Li, T., Chen, Y., Pan, H., Zhang, Z., Dai, Y., et al. (2017). Genetic polymorphisms of the P2X7 gene associated with susceptibility to and prognosis of pulmonary tuberculosis. *Infect. Genet. Evol.* 53, 24–29. doi: 10.1016/j.meegid.2017.05.003

Zhong, H., Yang, L., Belardinelli, L., and Zeng, D. (2007). Pro-fibrotic roles of the A2B adenosine receptor in human primary hepatic stellate cells. *J. Hepatol.* 46, S135–S135. doi: 10.1016/S0168-8278(07)61943-6

Zhong, Y., Yang, Z., Huang, W. C., and Luo, X. (2013). Adenosine, adenosine receptors and glaucoma: an updated overview. *Biochim. Biophys. Acta* 1830, 2882–2890. doi: 10.1016/j.bbagen.2013.01.005

Zhou, Q., Xu, C., Cheng, X., Liu, Y., Yue, M., Hu, M., et al. (2016). Platelets promote cartilage repair and chondrocyte proliferation via ADP in a rodent model of osteoarthritis. *Platelets* 27, 212–222. doi: 10.3109/09537104.2015.1075493

Zhou, X., Ma, L. M., Xiong, Y., Huang, H., Yuan, J. X., Li, R. H., et al. (2016). Upregulated P2X3 receptor expression in patients with intractable temporal lobe epilepsy and in a rat model of epilepsy. *Neurochem. Res.* 41, 1263–1273. doi: 10.1007/s11064-015-1820-x

Zhu, J., Zeng, Y., Li, W., Qin, H., Lei, Z., Shen, D., et al. (2017). CD73/NT5E is a target of miR-30a-5p and plays an important role in the pathogenesis of non-small cell lung cancer. *Mol. Cancer* 16:34. doi: 10.1186/s12943-017-0591-1

Zhu, Y., and Zhao, H. B. (2012). ATP activates P2X receptors to mediate gap junctional coupling in the cochlea. *Biochem. Biophys. Res. Commun.* 426, 528–532. doi: 10.1016/j.bbrc.2012.08.119

Zhu, Y. J., and Lu, T. J. (2010). A multi-scale view of skin thermal pain: from nociception to pain sensation. *Philos. Trans. A Math. Phys. Eng. Sci.* 368, 521–559. doi: 10.1098/rsta.2009.0234

Zierhut, M., Dyckhoff, S., Masouris, I., Klein, M., Hammerschmidt, S., Pfister, H. W., et al. (2017). Role of purinergic signaling in experimental pneumococcal meningitis. *Sci. Rep.* 7:44625. doi: 10.1038/srep44625

Ziganshin, A. U., Vafina, Z. R., and Fatkullin, I. F. (2008). Contrasting effects of P2 receptor agonists on spontaneous contractility of human fallopian tubes with and without acute inflammation. *Pharmacol. Res.* 57, 56–59. doi: 10.1016/j.phrs.2007.11.004

Conflict of Interest Statement: The author declares that the research was conducted in the absence of any commercial or financial relationships that could be construed as a potential conflict of interest.

The reviewer SS and handling Editor declared their shared affiliation.

frontiers in Pharmacology

ORIGINAL RESEARCH
published: 13 September 2017
doi: 10.3389/fphar.2017.00638

Searching Novel Therapeutic Targets for Scleroderma: P2X7-Receptor Is Up-regulated and Promotes a Fibrogenic Phenotype in Systemic Sclerosis Fibroblasts

Daniela Gentile[1†], Pietro E. Lazzerini[1†], Alessandra Gamberucci[2†], Mariarita Natale[1], Enrico Selvi[1], Francesca Vanni[1], Alessandra Alì[2], Paolo Taddeucci[1], Silvia Del-Ry[3], Manuela Cabiati[3], Veronica Della-Latta[3], David J. Abraham[4], Maria A. Morales[3], Rosella Fulceri[2], Franco Laghi-Pasini[1‡] and Pier L. Capecchi[1‡]*

[1] Department of Medical Sciences, Surgery and Neurosciences, University of Siena, Siena, Italy, [2] Department of Molecular and Developmental Medicine, University of Siena, Siena, Italy, [3] Institute of Clinical Physiology, CNR, Pisa, Italy, [4] Division of Medicine, Department of Inflammation, Centre for Rheumatology and Connective Tissue Diseases, University College London, London, United Kingdom

OPEN ACCESS

Edited by:
Kenneth A. Jacobson,
National Institutes of Health (NIH),
United States

Reviewed by:
Anindya Bhattacharya,
Janssen, United States
Bruce Neil Cronstein,
NYU School of Medicine,
United States

***Correspondence:**
Pietro E. Lazzerini
lazzerini7@unisi.it

[†]Co-first authors.
[‡]Co-senior authors.

Specialty section:
This article was submitted to Experimental Pharmacology and Drug Discovery, a section of the journal Frontiers in Pharmacology

Received: 02 March 2017
Accepted: 29 August 2017
Published: 13 September 2017

Citation:
Gentile D, Lazzerini PE, Gamberucci A, Natale M, Selvi E, Vanni F, Alì A, Taddeucci P, Del-Ry S, Cabiati M, Della-Latta V, Abraham DJ, Morales MA, Fulceri R, Laghi-Pasini F and Capecchi PL (2017) Searching Novel Therapeutic Targets for Scleroderma: P2X7-Receptor Is Up-regulated and Promotes a Fibrogenic Phenotype in Systemic Sclerosis Fibroblasts. Front. Pharmacol. 8:638. doi: 10.3389/fphar.2017.00638

Objectives: Systemic sclerosis (SSc) is a connective tissue disorder presenting fibrosis of the skin and internal organs, for which no effective treatments are currently available. Increasing evidence indicates that the P2X7 receptor (P2X7R), a nucleotide-gated ionotropic channel primarily involved in the inflammatory response, may also have a key role in the development of tissue fibrosis in different body districts. This study was aimed at investigating P2X7R expression and function in promoting a fibrogenic phenotype in dermal fibroblasts from SSc patients, also analyzing putative underlying mechanistic pathways.

Methods: Fibroblasts were isolated by skin biopsy from 9 SSc patients and 8 healthy controls. P2X7R expression, and function (cytosolic free Ca^{2+} fluxes, α-smooth muscle actin [α-SMA] expression, cell migration, and collagen release) were studied. Moreover, the role of cytokine (interleukin-1β, interleukin-6) and connective tissue growth factor (CTGF) production, and extracellular signal-regulated kinases (ERK) activation in mediating P2X7R-dependent pro-fibrotic effects in SSc fibroblasts was evaluated.

Results: P2X7R expression and Ca^{2+} permeability induced by the selective P2X7R agonist 2′-3′-O-(4-benzoylbenzoyl)ATP (BzATP) were markedly higher in SSc than control fibroblasts. Moreover, increased αSMA expression, cell migration, CTGF, and collagen release were observed in lipopolysaccharides-primed SSc fibroblasts after BzATP stimulation. While P2X7-induced cytokine changes did not affect collagen production, it was completely abrogated by inhibition of the ERK pathway.

Conclusion: In SSc fibroblasts, P2X7R is overexpressed and its stimulation induces Ca^{2+}-signaling activation and a fibrogenic phenotype characterized by increased migration and collagen production. These data point to the P2X7R as a potential, novel therapeutic target for controlling exaggerated collagen deposition and tissue fibrosis in patients with SSc.

Keywords: systemic sclerosis, P2X7 receptor, dermal fibroblasts, collagen, fibrosis, ERK

INTRODUCTION

Systemic sclerosis (SSc; scleroderma) is a connective tissue disease (CTD) presenting with three major aspects: small vessel disease, autoantibody production, and fibroblasts dysfunction leading to exaggerated deposition of collagen and extracellular matrix (ECM), tissue fibrosis and organ dysfunction (Allanore et al., 2015). Clinical aspects and prognosis of SSc may diverge, most patients presenting skin thickening and changeable involvement of internal organs including lungs, heart, gastrointestinal tract, and kidneys (Allanore et al., 2015). Although, relatively rare (50–300 case per million), the disease has a relevant social impact since it typically affects young women leading to significant disability and mortality (Allanore et al., 2015). At the moment, no effective anti-fibrogenetic therapy is available for the disease (Allanore et al., 2015; Pattanaik et al., 2015).

Increasing evidence indicates that the purinergic system may play a key role in the fibrotic process, by regulating collagen and ECM production from the fibroblast. Although most studies focused on P1 adenosine receptors (Chan et al., 2006; Lazzerini et al., 2012; Perez-Aso et al., 2012, 2014), recent data suggest that also P2 purinergic receptors, particularly P2X7, may be actively involved in tissue fibrosis. The P2X7 receptor (P2X7R) is a nucleotide-gated ion channel chiefly involved in the inflammatory response triggered by the release of ATP from damaged cells. It is largely expressed in monocytes where it enhances the synthesis and/or promotes the release of lipopolysaccharide (LPS)-induced pro-inflammatory cytokines, particularly interleukin-1β (IL-1β) and interleukin-18, by activating the K+-dependent NALP3 inflammasome/caspase-1 pathway (Di Virgilio, 2007; Castrichini et al., 2014; Gicquel et al., 2015), but also possibly interleukin-6 (IL-6), via the Ca^{2+}-dependent MAP-Kinase/early growth response-1 gene systems, egr-1 (Solini et al., 1999; Caporali et al., 2008; Friedle et al., 2011). Accumulating data demonstrated that the P2X7R is also expressed in fibroblastic cells (Solini et al., 1999; Caporali et al., 2008; Friedle et al., 2011), promoting lung, kidney, pancreas, and cardiac fibrosis in animal models (Gentile et al., 2015).

Starting from such premises, and taking into consideration that no information exists on a possible role of P2X7R in modulating fibrosis in scleroderma, we here hypothesized that P2X7R activation may stimulate the collagen biosynthetic process in SSc fibroblasts, thus representing a potential pharmacological target for the treatment of the disease. This study is aimed at determining expression and function of the P2X7R by evaluating calcium flux, α-SMA expression, cell migration, and collagen production in human skin fibroblast from SSc patients as compared to healthy controls.

MATERIALS AND METHODS

Skin Biopsies

Dermal fibroblasts were prepared from 5-mm skin biopsies from the forearm of 9 SSc patients and 8 healthy volunteers matched for age and sex. The research received the approval by the Local Ethical Committee, and patients gave their informed consent in accordance with the Declaration of Helsinki. Demography of the subjects involved in the study is depicted in the Supplementary Table.

Dermal Fibroblasts Isolation and Culture

Skin specimens were digested using 1 mg/ml clostridial collagenase (Sigma-Aldrich, Milan, Italy) in phosphate buffered saline (PBS). Cell suspensions were plated out in 10 ml of Dulbecco's Modified Eagle Medium (DMEM) supplemented with L-glutamine (2 mM), fetal bovine serum (FBS; 10%), penicillin (200 U/ml) and streptomycin (200 μg/ml) in 100-mm culture dishes and incubated in a humidified atmosphere containing 5% CO_2. The experiments were conducted at the third passage in order to avoid changes in the original phenotype. Except where indicated otherwise, all the reagents cited above were from Euroclone (Pero, Italy).

Flow Cytometry Analysis of P2X7R Expression

Fibroblasts (1×10^5) were incubated with a specific polyclonal anti-P2X7R (extracellular) antibody fluorescein isothiocyanate (FITC) (Sigma-Aldrich, Milan, Italy) (Xie et al., 2014) for 30 min at 4°C. A rabbit IgG-FITC isotype control antibody was chosen to differentiate non-specific background fluorescence from specific antibody signal. Cells were analyzed with the Dako Galaxy Flow Cytometry System and the FlowMax software. The analysis was done on well-shaped living cells by setting FSC X SSC live gates that exclude cellular debris. After setting of appropriate gates 20,000 events were acquired for each sample. The expression of surface-labeled P2X7Rs was evaluated measuring both the percentage and the mean fluorescence intensity (MFI) of cells that were P2X7R positive using the FlowJo software, version 7.6.5. This analysis allows us to know the percentage of fibroblasts expressing P2X7R with respect to the total number of fibroblasts analyzed (% P2X7R+ cells) as well as the level of P2X7Rs expression per single cell, evaluated by its MFI.

Analysis of P2X7R mRNA by qRT-PCR

Total RNA was extracted from fibroblasts (1×10^6) using the RNeasy Mini kit (Qiagen S.p.A, Milano, Italy) following a standardized method (Del Ry et al., 2011). For cDNA synthesis, iScript cDNA Synthesis kit (Bio-Rad, Hercules, CA, USA) was used according to the manufacturer's instructions. Specific primers for P2X7R were synthesized by Qiagen (Hs_P2RX7_1_SG QuantiTect Primer Assay). Following recent guidelines (Vandesompele et al., 2002), three candidate reference genes [Eukaryotic translation elongation factor-1 alpha 1 (NM_001402), human ribosomal protein L13a (NM_012423) and ribosomal protein S4, X-Linked (NM_002046)], from among the most commonly cited in the literature, were selected and used to normalize mRNA expression data obtained by Real-Time PCR experiments. More details are provided in the Supplementary Material.

P2X7R-Induced Calcium Influx Measurement

P2X7R is an ATP-gated cation channel. It acts as a bifunctional molecule whose brief activation causes the rapid (within milliseconds) and reversible opening of a channel selective for small cations, that induces the entry of Ca^{2+} and Na^{+} and the efflux of K^{+} while a sustained stimulation causes the opening of a larger pore. From a physiological point of view, it has been demonstrated that the channel opening mediates the effects of the P2X7R on cytokine production, in particular IL-1β maturation and release (triggered by the K^{+} efflux), and IL-6 expression (activated by the Ca^{2+} influx; North, 2002; Di Virgilio, 2007; Friedle et al., 2011). In the present study we studied the P2X7R functional activation in terms of Ca^{2+} influx, evaluated by the analysis of the cytosolic Ca^{2+} ($[Ca^{2+}]_i$) elevation. Indeed, since both Ca^{2+} influx and K^{+} efflux results from the opening of the same cationic channel, Ca^{2+} measurement was here employed as a marker more in general reflecting the extent of P2X7R (and related intracellular pathways) activation.

P2X7R activation was induced by using 2′-3′-O-(4-benzoylbenzoyl)ATP (BzATP) a selective P2X7R synthetic agonist that exhibits 10 fold greater potency respect to the physiological activator ATP (Jacobson, 2010). Technical details are provided as Supplementary Material.

In order to describe the features of Ca^{2+} influx, the following parameters were measured: (i) the Area Under the Curve (AUC) as an expression of the area included under the curve of the $[Ca^{2+}]$i over the time for 5 min following the agonist addition [AUC (5′)] and (ii) the percentage (%) of responsive cells.

Culture Stimulation

Dermal fibroblasts were plated out in 500 μl of starvation medium (DMEM plus 0.5 % FBS). After 24 h in starvation, cells were primed with lipopolysaccharide (LPS, 1 μg/ml) from *E. coli* 026:B6 or vehicle for 24 h, and then stimulated with the P2X7R agonist BzATP (0.1 mM) for 30 min. Cells were also stimulated with LPS alone.

In order to confirm the specific involvement of the P2X7R in the observed effects, experiments with two different synthetic P2X7R antagonists were performed, by incubating for 2 h the LPS-primed cells with oxidized ATP (oATP, 200 μM) or A438079 (10–50 μM) before BzATP treatment.

The putative effects of IL-6 released by SSc fibroblasts upon P2X7R activation was investigated adding the recombinant human soluble IL6 receptor (IL6α, 10 ng/ml) to the BzATP+LPS-stimulated cells for 24 h.

Finally, the involvement of ERK-1/2 pathway in P2X7R activation-induced collagen production was evaluated by pre-treatement of the fibroblasts with the selective ERK-1/2 inhibitor FR-180204 (50 μM) for 30 min before BzATP+LPS stimulation.

LPS, BzATP, and oATP were purchased from Sigma-Aldrich (Milan, Italy). FR-180204, A438079 and soluble IL-6Rα from Tocris (Bristol, UK). Reagents were dissolved in dimethyl sulfoxide (DMSO, Sigma-Aldrich, Milan, Italy) or in distilled water. Accordingly, fibroblast cultures treated with the appropriate vehicle were used as basal samples.

Collagen Analysis

Collagen concentration was determined in the supernatant of the cells collected at the end of each treatment and stored at −20°C until used. By means of the EIA kit (Takara Bio Inc., Otsu, Japan) we evaluated the procollagen type I carboxy-terminal peptide (PIP) released in the culture supernatants as an expression of the collagen synthesis. PIP levels were measured as ng/ml. Technical details are reported as Supplementary Material.

Immunofluorescence Experiments

Fibroblasts were seeded on 13 mm glass coverslip and stimulated or not with LPS and BzATP in the presence or in the absence of A438079 (50 μM), as described in culture stimulation section. The cells were then fixed with paraformaldehyde 4% for 15′ at RT and permeabilized with Triton X-100 0.1% for 10′ at RT. After blocking with 1%BSA, 10% goat serum, 0.1% Tween-20 and 2 mM EDTA for 1 h at RT, the cells were incubated with a mouse anti-α smooth muscle actin (αSMA) antibody (Sigma-Aldrich, Saint Louis, MO, USA) 1:200, overnight at 4°C and then reacted with a goat anti-mouse cy3 1:5000 (Jackson Laboratories, Bar Harbor, ME). Nuclei were visualized by 4′,6-diamidino-2-phenylindole (DAPI, Sigma-Aldrich). After mounting the cells were examined in a fluorescence microscope Nikon Eclipse Ti coupled to a DS-Q1Mc camera and a NIS element software (Nikon, Tokio, Japan).

Scratch Wound Healing Assay

Fibroblasts were plated onto 24-well plates allowed to grow to confluency in the same medium as for cell culture. Once confluent, the medium was switched to starvation medium (DMEM plus 0.2% FBS) for 24 h to minimize the influence of hormones and growth factors. After the starvation period, the cells were scratched with a 200 μl pipette tip, washed two times with PBS to remove cellular debris after that treatments were applied. Wells were imaged at 0 and 48 h at 4x magnification with phase contrast Zeiss Axiocam. Image J was used to measure the area of the scratch remaining at the different time points. The free hand tool on Image J was used to draw around the scratch and area in mm^2 was measured after setting the field of view to 3,400 × 2,700 μm.

Cytokine Supernatant Assay

IL-1β and IL-6 cytokines release was analyzed in the culture supernatants using commercially available Bio-Plex-Pro Human Cytokine assay (BioRad Laboratories, Hercules, CA) according to the manufacturer's protocol. Sample were acquired by a Bio-Plex 200 system and after setting up the calibration the cytokines concentration were performed using the Bio-Plex Manager software v5.0 (BioRad).

Connective Tissue Growth Factor (CTGF) Supernatant Assay

CTGF concentration was measured in duplicate in culture supernatants of dermal fibroblasts from healthy controls and SSc patients after different treatments, by using the Human CTGF ELISA Kit (Cloude-Clone Corp., TX, USA) according to the manufacturer's instructions.

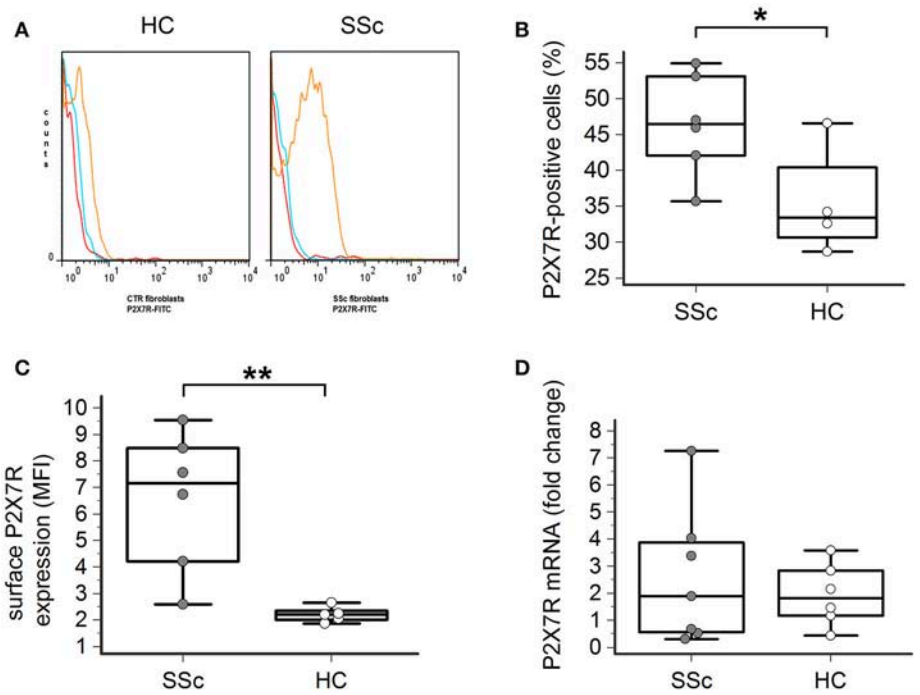

FIGURE 1 | P2X7R surface expression is increased in SSc dermal fibroblasts. **(A–C)** P2X7R surface expression in dermal fibroblasts from SSc patients and HC, as determined by flow cytometry: **(A)** original flow cytometry data representative of an experiment; **(B)** percentage of P2X7R positive cells, and **(C)** MFI values. SSc patients, $n = 6$; HC, $n = 5$. $^*p < 0.05$, two-tailed unpaired t-test; $^{**}p < 0.01$, two-tailed Mann–Whitney test. **(D)** P2X7R mRNA expression in dermal fibroblasts from SSc patients and HC, as determined by quantitative RT-PCR analysis. SSc patients, $n = 7$; HC, $n = 6$. p = not significant, two-tailed unpaired t-test. SSc, Systemic sclerosis; HC, healthy controls; P2X7R, P2X7 receptor; MFI, mean fluorescence intensity; RT-PCR, reverse transcription-polymerase chain reaction.

Statistical Analysis

All experiments were performed in duplicate or triplicate. Normal distribution of quantitative variables was preliminarily tested using the Kolmogorov–Smirnov test to select parametric (normal distribution) or non-parametric (non-normal distribution) inferential statistical methods. Accordingly, the following parametric or non-parametric statistical analyses were performed, respectively: the two-tailed unpaired t-test or the two-tailed Mann–Whitney test to evaluate differences in continuous variables between two groups. The repeated measures analysis of variance (RM-ANOVA) and the two-tailed Tukey–Kramer *post-hoc* multiple comparisons test, or the Friedman test (non-parametric RM-ANOVA), or Kruskal–Wallis test (one-way non-parametric ANOVA) and the two-tailed Dunn's *post-hoc* multiple comparison test to evaluate differences in continuous variables among more than two groups. Values of $p < 0.05$ were considered significant. All statistical analyses were done using GraphPad-InStat package (GraphPad, La Jolla, CA, USA).

RESULTS

P2X7R Surface Expression Is Increased in SSc Dermal Fibroblasts

Flow cytometry analysis showed that the P2X7R was expressed on the surface of both healthy and SSc dermal fibroblasts (**Figures 1A–C**). However, both the percentage of P2X7-positive cells (46 ± 7 vs. $35 \pm 6\%$, $p = 0.023$; **Figure 1B**) and, particularly, the total amount of the P2X7R expression was significantly higher in SSc than healthy fibroblasts, as demonstrated by the ∼3-times higher values of mean fluorescence intensity (MFI; 6.5 ± 2.6 vs. 2.2 ± 0.3, $p = 0.0087$; **Figure 1C**).

Such a phenomenon was not associated with an increased P2X7R gene expression by the cells, as real time-PCR analysis indicated that the levels of P2X7R mRNA were not significantly different in SSc patients when compared to healthy controls (2.6 ± 2.5 vs. 1.9 ± 1.1 fold-increase, $p = 0.58$; **Figure 1D**).

P2X7R-Mediated Calcium Influx Is Enhanced in Dermal Fibroblasts from SSc Patients

P2X7R stimulation with the receptor agonist BzATP resulted in calcium influx in normal and SSc dermal fibroblasts in the presence of extracellular Ca^{2+} (**Figure 2A**). However, significant differences between the two cell populations were found, indicative of an increased P2X7-dependent Ca^{2+} permeability in SSc fibroblasts. In fact, both the number of responding cells (54 ± 22 vs. $16 \pm 7\%$, $p = 0.0095$; **Figure 2C**), and the extent of Ca^{2+} uptake as assessed by the AUC ($9{,}527 \pm 3{,}396$ vs. $1{,}293 \pm 477$ nM, $p = 0.0093$; **Figure 2B**) were significantly higher when SSc cells were compared to healthy subject fibroblasts. Notably, pre-incubation of SSc fibroblasts with the P2X7R antagonist oATP significantly reduced BzATP-induced calcium influx, to values

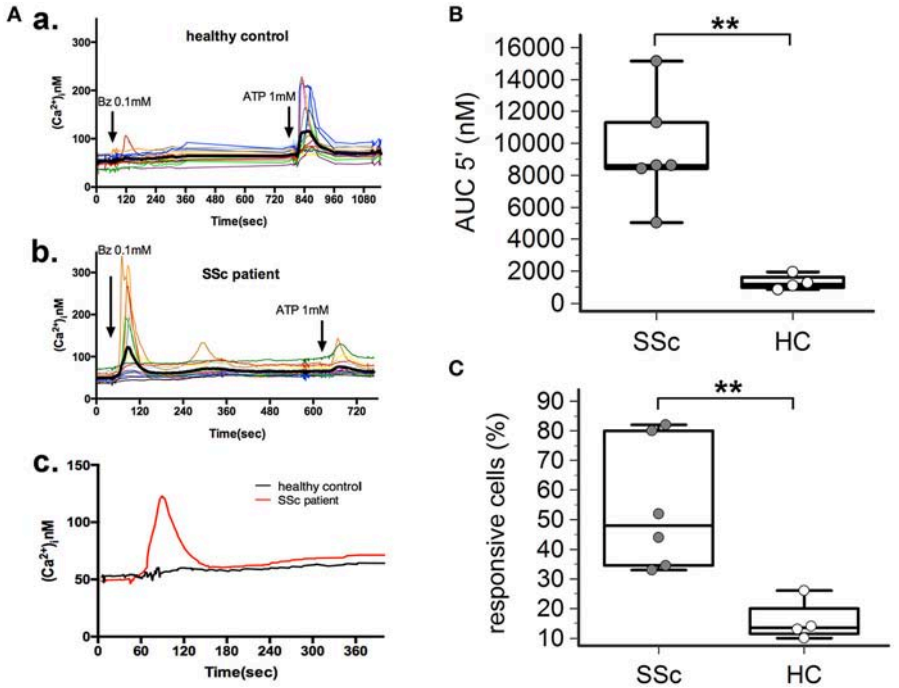

FIGURE 2 | P2X7R-mediated calcium influx is enhanced in dermal fibroblasts from SSc patients. BzATP-induced calcium entry in dermal fibroblasts from SSc patients and HC, as determined by single-cell fluorescence microscopy. **(A)** Representative plot of an experiment in one SSc patient **(a,c)** and one HC **(b,c)**. Each colored trace in **(a,b)** represents the response of individual cells while the thick black line in **(a,b)**, and the red and black lines in **(c)** represent the mean response of all the cells from the same culture dish. The arrow indicates the time when the agonist was added. **(B)** P2X7-induced Ca2+ uptake as assessed by the AUC 5′, in dermal fibroblasts from SSc patients and HC. SSc patients, $n = 6$; HC, $n = 4$. $^{**}p < 0.01$, two-tailed Mann–Whitney test. **(C)** Percentage of BzATP-responsive cells in SSc patients and HC. SSc patients, $n = 6$; HC, $n = 4$. $^{**}p < 0.01$, two-tailed Mann–Whitney test. SSc, Systemic sclerosis; HC, healthy controls; P2X7R, P2X7 receptor; Bz, 2′-3′-O-(4-benzoylbenzoyl)ATP; Ca2+, calcium; AUC 5′, area under the curve represents the area enclosed between the curve of the $[Ca^{2+}]$vs. the time for 5 min after the addition of the stimulus.

substantially comparable to controls (number of responding cells: 13±21%, $p = 0.015$; AUC: 2,342 ± 1,280 nM, $p = 0.0003$; **Figure 3**).

P2X7R Activation Stimulates Collagen Production in SSc Dermal Fibroblasts

In LPS-primed fibroblasts from SSc patients, BzATP-dependent P2X7R activation resulted in a clear-cut stimulation of collagen synthesis. As shown in the **Figure 4**, while cell stimulation with LPS or BzATP alone produced no changes in PIP release, LPS plus BzATP significantly increased supernatant PIP levels in SSc dermal fibroblasts (466.0 ± 313.9 vs. 277.0 ± 183.1 ng/ml in untreated cells, +76.7%; $p < 0.05$). This effect was not due to an increase in cells number after stimulation (62 ± 17.6 vs. 62.89 ± 22.8 cells/microscopic field analyzed in parallel experiments). Such a stimulating effect was completely removed when cultures were co-incubated with the P2X7R antagonist, oATP (**Figure 5**). On the contrary, none of the treatments induced appreciable effects on collagen synthesis in healthy subject cells.

P2X7R Stimulation Increases αSMA Bundles Expression in SSc Dermal Fibroblasts

Differentiation of fibroblast into myofibroblast can be marked by several morphological and functional changes, including cell dimension increase, collagen production and expression of contractile proteins such as αSMA. In particular, a well-recognized characteristic of the fully differentiated myofibroblast is the accumulation of cytoplasmatic microfilaments constituted by αSMA bundles (stress fibers) with high contractile activity (Talele et al., 2015; Garrett et al., 2017).

In basal conditions, healthy fibroblasts had a very weak reaction for αSMA when compared to SSc dermal fibroblasts (**Figure 6**). However, despite showing a high fluorescence intensity, SSc cells displayed a heterogeneous αSMA staining represented by a punctate and bundled pattern, with a prevalence of cells with punctate distribution (63 ± 24% of cells counted in at least five random fields of 3 separate coverslips for each of 4 different patients). P2X7R stimulation with LPS + BzATP markedly increased the percentage of large-size fibroblasts expressing well-developed αSMA microfilament bundles (from 37 ± 24 to 84 ± 14%; $p < 0.05$). Conversely, in the presence of the P2X7R inhibitor A438079, the percentage of αSMA stress fiber-positive cells significantly fell below the basal levels (19 ± 14%; **Figure 6**), thus suggesting a constitutive activity of the receptor in the SSc fibroblast. Culture stimulation with LPS + BzATP induced a slight increase of αSMA stress fiber-positive cells also in healthy fibroblasts (from 16 ± 4 to 30 ± 14%), an effect which was completely prevented by A438079 pre-incubation (15 ± 8%; **Figure 6**).

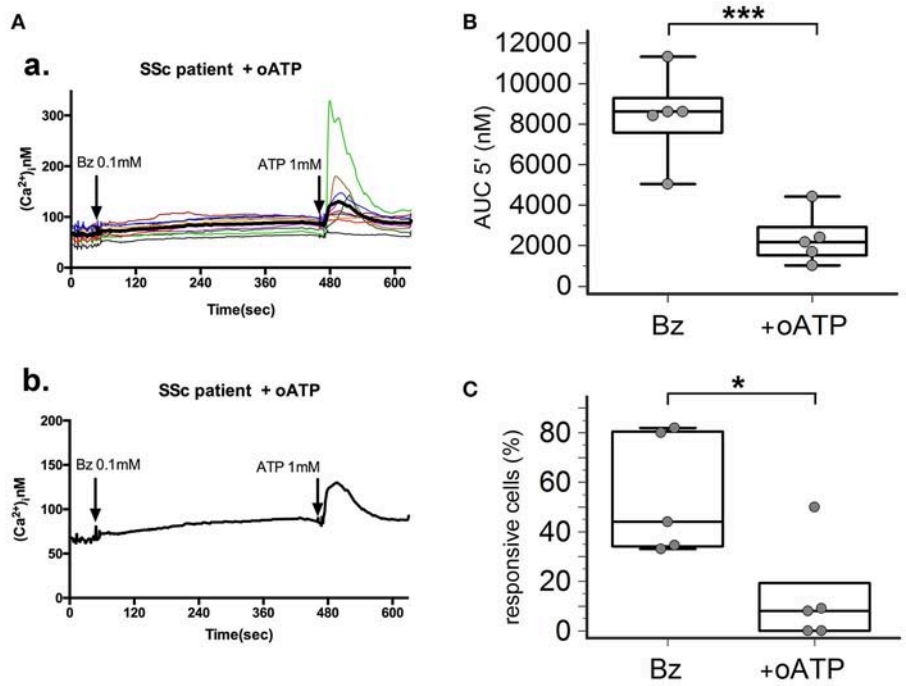

FIGURE 3 | P2X7R antagonism inhibits calcium influx in SSc dermal fibroblasts. Effect of the P2X7R antagonist oxATP (200 μM) on BzATP-induced calcium entry in dermal fibroblasts from SSc patients, as determined by single-cell fluorescence microscopy. **(A)** Representative plot of an experiment in one SSc patient **(a,b)**. Each colored trace in **(a)** represents the response of individual cells while the thick black line in **(a,b)** represent the mean response of all the cells from the same culture dish. The arrow indicates the time when the agonist was added. **(B)** P2X7-induced Ca2+ influx in dermal fibroblasts from SSc patients ($n = 5$) pre-incubated with oATP, as assessed by the AUC 5′. ***$p < 0.01$, two-tailed paired *t*-test. **(C)** Percentage of BzATP-responsive cells in SSc patients ($n = 5$) pre-incubated with oATP. *$p < 0.05$, two-tailed paired *t*-test. SSc, Systemic sclerosis; P2X7R, P2X7 receptor; Bz, 2′-3′-O-(4-benzoylbenzoyl)ATP; oATP, oxidized ATP; Ca2+, calcium; AUC 5′, area under the curve represents the area enclosed between the curve of the [Ca^{2+}]vs. the time for 5 min after the addition of the stimulus.

P2X7R Stimulation Increases SSc Dermal Fibroblasts Migration

As predicted by the enhanced expression of contractile proteins, wound healing experiments performed *in vitro* by using a scratch assay demonstrated that P2X7R also increased SSc fibroblast migration. After LPS priming, P2X7R stimulation with BzATP promoted wound healing as demonstrated by the increased SSc cell migration to closing the wound scratch (**Figures 7A,B**). This view was further confirmed by the evidence that culture co-incubation with the P2X7R-inhibitor A438079 completely abrogated the effect (**Figures 6A,B**).

P2X7R Activation Induces IL-6, But Not IL-1β, Release from SSc Dermal Fibroblasts

In order to provide information about the possible intracellular mechanisms involved in P2X7R-dependent collagen production in LPS-primed SSc dermal fibroblasts, we evaluated whether the LPS plus BzATP co-incubation was associated with the production of specific cytokines, particularly IL-1β and IL-6, as a possible result of the P2X7R-induced activation of the K^+-dependent NALP3 inflammasome/caspase-1 or the Ca^{2+}-dependent MAP-Kinase/egr-1 systems, respectively. As shown in **Figures 8A,B**, while no changes in IL-1β were observed (0.07 ± 0.02 vs. 0.09 ± 0.02 pg/ml; $p = 0.41$), co-treatment of SSc cells with LPS + BzATP induced a significant 2.4-fold increase in IL-6 supernatant levels (2.5 ± 2.6 vs. 6.0 ± 3.0 pg/ml; $p = 0.0032$).

IL-6 Does Not Contribute to P2X7R-Dependent Collagen Production from SSc Dermal Fibroblasts

Since human dermal fibroblasts (thus SSc fibroblasts) do not express on their surface the IL-6 receptor (transmembrane IL-6R, mIL-6R) required for activating classic signaling (Lazzerini et al., 2016), the possibility can be ruled out that the P2X7-dependent stimulating effect on collagen production observed *in-vitro* is the result of the above reported IL-6 increase, via an autocrine mechanism. Nevertheless, we evaluated the potential additive role of the P2X7R-dependent IL-6 increase in enhancing collagen production from SSc fibroblast via the soluble IL-6R (sIL-6R)-dependent transsignaling pathway, potentially relevant in SSc patients *in-vivo*. In fact, differently from *in vitro* conditions, the sIL-6R is freely available *in vivo* in human plasma where it is released by hepatocytes, leukocytes and megakaryocytes (Lazzerini et al., 2016). On these premises, LPS-primed SSc fibroblasts were stimulated with BzATP in the presence of sIL-6R, but no any further increase in collagen supernatant levels was observed (**Figure 8C**).

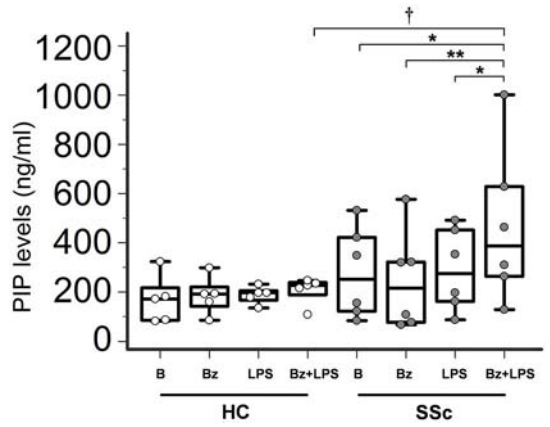

FIGURE 4 | P2X7R activation stimulates collagen production in SSc dermal fibroblasts. Spontaneous, Bz-, LPS-, and Bz+LPS-induced PIP release in the culture medium of dermal fibroblasts from SSc patients and HC. Cells starved for 24 h were primed with LPS (1 μg/ml) or vehicle for further 24 h, and then stimulated with Bz (0.1 mM) for 30 min; cells were also stimulated with LPS alone (24 h). SSc patients, $n = 6$; HC, $n = 5$. Comparisons within SSc patients: RM-ANOVA, $p = 0.0064$; *post-hoc* two-tailed Tukey–Kramer test, $^{*}p < 0.05$, $^{**}p < 0.01$. Comparisons within HC: Friedman test (non-parametric RM-ANOVA), $p =$ not significant. Comparison between SSc patients and HC: $^{\dagger}p < 0.05$, two-tailed Mann–Whitney test. SSc, Systemic sclerosis; HC, healthy controls; P2X7R, P2X7 receptor; B, baseline; Bz, 2′-3′-O-(4-benzoylbenzoyl)ATP; LPS, lipopolysaccharide; PIP, procollagen type I carboxy-terminal peptide; RM-ANOVA, repeated measures analysis of variance.

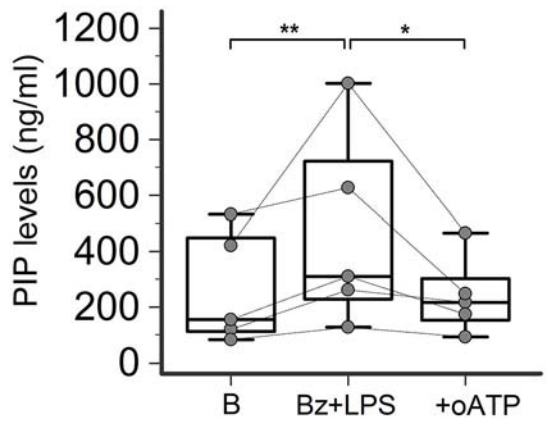

FIGURE 5 | P2X7R antagonism inhibits collagen production in SSc dermal fibroblasts. Effect of the P2X7R antagonist oATP (200 μM) on Bz+LPS-induced PIP release in the culture medium of dermal fibroblasts from SSc patients, as determined by EIA assay. SSc patients, $n = 5$. RM-ANOVA, $p = 0.0052$; *post-hoc* two-tailed Tukey–Kramer test, $^{*}p < 0.05$, $^{**}p < 0.01$. SSc, Systemic sclerosis; HC, healthy controls; P2X7R, P2X7 receptor; B, baseline; Bz, 2′-3′-O-(4-benzoylbenzoyl)ATP; LPS, lipopolysaccharide; oATP, oxidized ATP; PIP, procollagen type I carboxy-terminal peptide; RM-ANOVA, repeated measures analysis of variance.

P2X7R Activation Induces CTGF Release from Dermal Fibroblasts

The possible pathway involved in mediating P2X7R-induced SSc fibroblast activation was then further investigated by evaluating

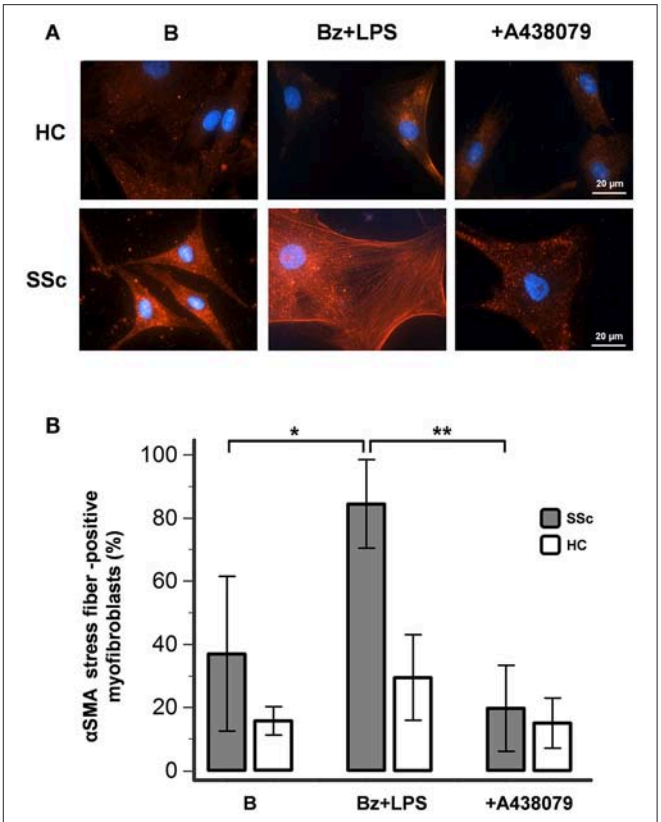

FIGURE 6 | P2X7R activation promotes myofibroblast differentiation of SSc dermal fibroblasts. Effect of Bz+LPS stimulation on the differentiation of dermal fibroblasts to myofibroblasts, identified as large size and αSMA bundle (stress fiber)-positive cells by immunofluorescence. Fibroblasts from SSc patients and HC were starved for 24 h and then primed with LPS (1 μg/ml) or vehicle for further 24 h, followed by stimulation with Bz (0.1 mM) for 30 min, alone or after 2 h pre-incubation with the P2X7R antagonist A438079 (50 μM). **(A)** Representative figure of an experiment performed in SSc and HC fibroblasts, respectively: in red the immunofluorescence for α-SMA, while nuclei were stained in blue with DAPI. Images were acquired with a 60X/1.49 Apo objective. **(B)** Effect of Bz+LPS and Bz+LPS+AR438079 on myofibroblast differentiation, as determined by the percentage of αSMA stress fiber-positive cells. Histograms represent results (mean ± standard deviation) of experiments performed by using fibroblasts from SSc patients ($n = 4$) and HC ($n = 3$). RM-ANOVA, $p = 0.012$; *post-hoc* two-tailed Tukey–Kramer test, $^{*}p < 0.05$, $^{**}p < 0.01$. P2X7R, P2X7 receptor; SSc, Systemic sclerosis; B, baseline; Bz, 2′-3′-O-(4-benzoylbenzoyl)ATP; LPS, lipopolysaccharide; HC, healthy controls; DAPI, 4′,6-diamidino-2-phenylindole; ANOVA, analysis of variance.

the effect of LPS + BzATP stimulation on the release of CTGF in the culture supernatant. Under these conditions, CTGF levels showed a clear-cut increase (∼6-fold, from 13.9 ± 6.3 to 91.6 ± 36.7 pg/ml) which was completely abrogated by culture pre-incubation with the P2X7 antagonists oATP (15.4 ± 0.4 pg/ml) or A438079 (50 μM: 13.9 ± 5.4 pg/ml; 10 μM:13.6 ± 1.8 pg/ml; **Figure 9**). CTGF release was also affected in healthy fibroblasts, although to a lesser extent: culture stimulation with LPS + BzATP induced a ∼2-fold CTGF increase (from 16.0 ± 0.4 to 27.4 ± 6.9 pg/ml), an effect which was completely prevented by oATP (13.4 ± 3.1 pg/ml) or A438079 (50 μM: 13.5 ± 2.5 pg/ml; 10 μM: 18.9 ± 4.8 pg/ml) pre-incubation (**Figure 9**).

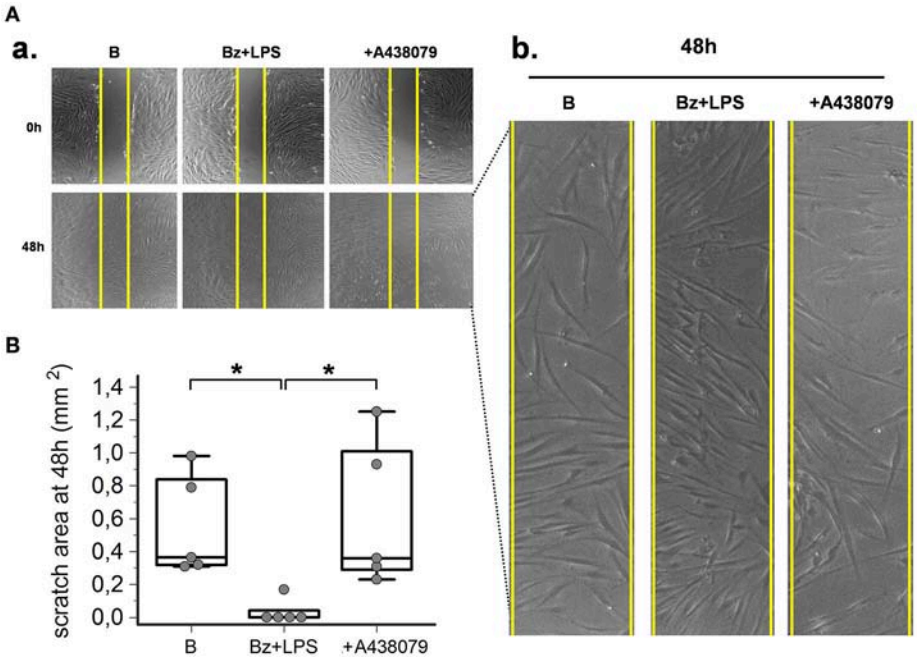

FIGURE 7 | P2X7R stimulation increases SSc fibroblasts migration. P2X7R-dependent migration of SSc dermal fibroblasts, as determined by *in vitro* scratch-wound healing assays. **(A) (a)** Representative figure of an experiment. Cells are stimulated with Bz+LPS alone or in association with the P2X7R antagonist A438079 (50 μM). Photos were taken immediately after wounding (0 h) and 48 h later. Yellow vertical lines show the scratch area, as initially measured at 0 h. **(b)** Magnification of the scratch area at 48 h. **(B)** Effect of Bz+LPS and Bz+LPS+AR438079 on SSc dermal fibroblast migration, as determined by the scratch area at 48 h. Plots represent 5 different experiments performed by using fibroblasts from 3 different SSc patients. Kruskal–Wallis test (non-parametric ANOVA), $p = 0.0083$; *post-hoc* two-tailed Dunn multiple comparison test, $^*p < 0.05$. SSc, Systemic sclerosis; P2X7R, P2X7 receptor; B, baseline; Bz, 2′-3′-O-(4-benzoylbenzoyl)ATP; LPS, lipopolysaccharide; ANOVA, analysis of variance.

ERK-1/2 Inhibition Completely Prevents P2X7R-Induced Collagen Production in SSc Dermal Fibroblasts

Increasing evidence indicates that LPS-besides constituting an essential stimulus for the activation of the NALP3 inflammasome via a Toll-like receptor-mediated mechanism- can also directly interact with the P2X7R by recognizing a sequence of the carboxy-end which contains a conserved LPS-binding domain (Denlinger et al., 2001). This interaction is required to induce LPS-dependent activation of the extracellular signal-regulated kinases (ERK1, ERK2; Denlinger et al., 2001), which in turn are involved in SSc fibroblast activation leading to collagen production (Bogatkevich et al., 2007; Chen et al., 2008). Thus, we evaluate the possible involvement of this pathway as the intracellular mechanism linking P2X7R and collagen production in LPS-primed SSc fibroblasts by pre-treating the cells with the ERK-1/2 inhibitor, FR-180204. **Figure 10** shows that the addition of this molecule to the cultures completely abrogated the P2X7R-dependent stimulating effect on collagen production, as assessed by supernatant PIP levels.

Notably, also P2X7R-induced CTGF release was fully reversed when fibroblast cultures were pre-incubated with FR-180204 (**Figure 9**).

DISCUSSION

The main findings of the present study are the following: (i) when compared to healthy controls, dermal fibroblasts from SSc patients display a higher P2X7R surface expression with an enhanced function in terms of Ca^{2+} influx; (ii) in LPS-primed SSc fibroblasts, P2X7R stimulation results in profibrotic effects by promoting enhanced αSMA expression, cell migration, CTGF, and collagen production; (iii) intracellular mechanisms underlying P2X7R-induced fibrogenic effects seem to involve a cytokine-independent pathway likely due to ERK-1/2 signaling activation. Altogether, these data point to the P2X7R as a potential, novel therapeutic target for controlling exaggerated collagen deposition and tissue fibrosis in patients with SSc.

The P2X7 protein is a 595 amino acids sequence consisting of an intracellular N-terminus, two hydrophobic transmembrane domains, an extracellular loop, and an intracellular C-terminus (North, 2002). The main structurally distinctive feature of the P2X7R is a long C-terminal tail (244 amino acids) that is essential for pore formation, receptor trafficking and stabilization of the P2X7R in the membrane. Moreover, it harbors multiple potential protein and lipid interaction motifs (Vandesompele et al., 2002; Smart et al., 2003). Although the most recognized role of P2X7R is the promotion of effector functions in monocytes/macrophages (cell proliferation, killing, nuclear factor-kB activation, cytokine

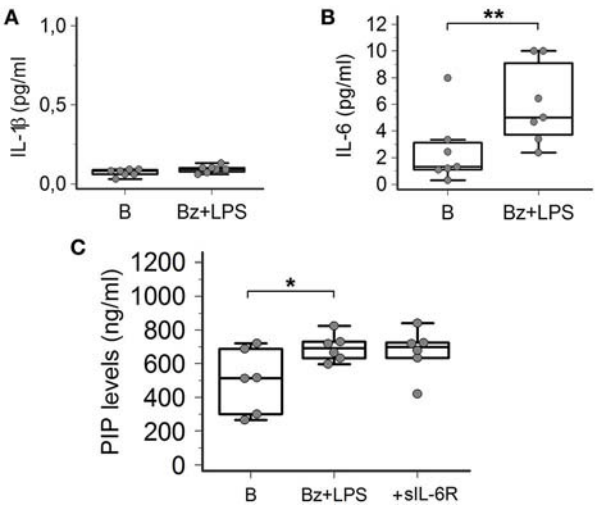

FIGURE 8 | P2X7R activation induces IL-6 release from SSc dermal fibroblasts, but the cytokine does not contribute to collagen production. **(A)** Effect of Bz+LPS stimulation on the IL-1β release in the culture medium of dermal fibroblasts from SSc patients; $n = 7$. p = not significant, two-tailed paired *t*-test. **(B)** Effect of Bz+LPS stimulation on the IL-6 release in the culture medium of dermal fibroblasts from SSc patients; $n = 7$. $^{**}p < 0.01$, two-tailed paired *t*-test. **(C)** Effect of the addition of the sIL-6R on Bz+LPS-induced PIP release in the culture medium of dermal fibroblasts from SSc patients, as determined by EIA assay; $n = 6$. RM-ANOVA, $p = 0.023$; *post-hoc* two-tailed Tukey–Kramer test, $^{*}p < 0.05$. SSc, Systemic sclerosis; P2X7R, P2X7 receptor; B, baseline; Bz, 2′-3′-O-(4-benzoylbenzoyl)ATP; LPS, lipopolysaccharide; IL-1β, interleukin-1β; IL-6, interleukin-6; sIL-6R, soluble interleukin-6 receptor; PIP, procollagen type I carboxy-terminal peptide; RM-ANOVA, repeated measures analysis of variance.

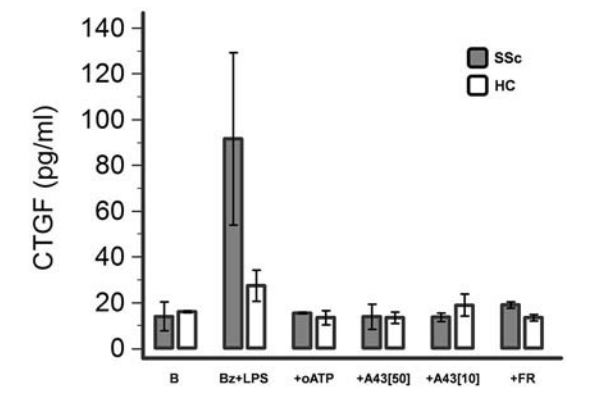

FIGURE 9 | P2X7R stimulation induces CTGF release from dermal fibroblasts, which is completely abrogated by P2X7R antagonism or ERK-1/2 inhibition. Effect of Bz+LPS stimulation on CTGF release in the culture medium of dermal fibroblasts from SSc patients ($n = 2$) and healthy controls ($n = 2$), as determined by ELISA assay, and its modulation by P2X7R antagonists (oATP 200 μM; A438079 10–50 μM) or an ERK-1/2 inhibitor (FR-180204 50 μM). CTGF, connective tissue growth factor; SSc, Systemic sclerosis; P2X7R, P2X7 receptor; B, baseline; Bz, 2′-3′-O-(4-benzoylbenzoyl)ATP; LPS, lipopolysaccharide; oATP, oxidized ATP; A43[50], A438079 50 μM; A43[10], A438079 10 μM; FR, FR-180204.

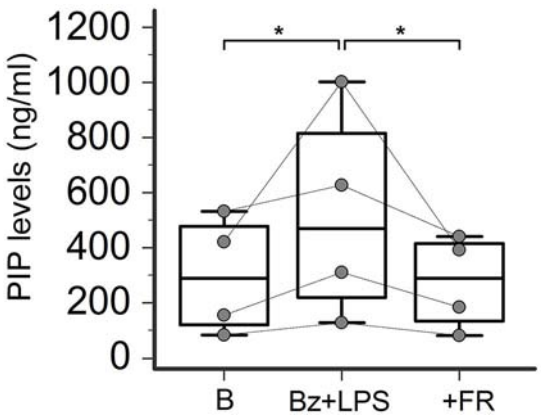

FIGURE 10 | ERK-1/2 inhibition completely prevents P2X7R-induced collagen production in SSc dermal fibroblasts. Effect of the ERK-1/2 inhibitor FR-180204 (50 μM) on Bz+LPS-induced PIP release in the culture medium of dermal fibroblasts from SSc patients, as determined by EIA assay. SSc patients, $n = 4$. RM-ANOVA, $p = 0.013$; *post-hoc* two-tailed Tukey–Kramer test, $^{*}p < 0.05$. SSc, Systemic sclerosis; P2X7R, P2X7 receptor; ERK-1/2, extracellular signal-regulated kinases-1/2; B, baseline; Bz, 2′-3′-O-(4-benzoylbenzoyl)ATP; LPS, lipopolysaccharide; FR, FR-180204; PIP, procollagen type I carboxy-terminal peptide; RM-ANOVA, repeated measures analysis of variance.

production, and release; Rossi et al., 2012) resulting in an amplification of the innate immune response, increasing recent evidence suggests that this receptor may also be actively involved in wound healing by stimulating reparation and fibrosis. Indeed, several studies have demonstrated that the P2X7R is expressed by a wide range of fibroblastic cells throughout the body, both in animals [heart (Kumagai et al., 2013), kidney (Ponnusamy et al., 2011), pancreas (Haanes et al., 2012), endometrium (Koshi et al., 2005)] and in humans [skin (Solini et al., 1999), synovium (Caporali et al., 2008), gingival, and dental pulp tissue (Jiang et al., 2015)]. In addition, increasing data from animal models indicate that P2X7R activation plays a key role in different forms of experimental fibrotic diseases. Gonçalves et al. (2006) demonstrated that kidneys from P2X7R-knockout (KO) mice with unilateral ureteral obstruction showed a lower immunostaining for transforming growth factor-β (TGF-β), and myofibroblasts when compared with wild-type mice. Moreover, P2X7R-KO mice airway-administered with bleomycin to induce lung fibrosis, presented dramatically reduced fibrosis markers, such as lung collagen content and matrix-remodeling proteins, than in control animals normally expressing the receptor (Riteau et al., 2010). More recently, beneficial effects of P2X7R antagonism on liver fibrosis were reported both in rats with bile duct ligation-induced cirrhosis, (Tung et al., 2015) and in mice with carbon tetrachloride-induced liver fibrosis (Huang et al., 2014). Keeping this in mind, we characterized the expression and function profile of the P2X7R in dermal fibroblasts from patients with SSc, a systemic fibrotic disorder of unknown origin, to test the hypothesis that a dysregulation of this receptor may play a role in this disease.

A first relevant finding from our study is the demonstration that in SSc dermal fibroblasts the surface expression of the P2X7R is substantially increased. In fact, both the percentage of

P2X7-positive cells and the mean number of receptors expressed on the cell membrane, as indicated by the MFI values, was significantly higher in fibroblasts from SSc patients than healthy controls. These data confirm and expand preliminary data from a seminal work from the group of Di Virgilio (Lo Monaco et al., 2007), in which for the first time evidence was provided that SSc dermal fibroblasts expressed mRNA for several P2 receptors, including the P2X7R; however, these authors did not perform any quantitative comparison with control cells. Indeed, in our study we found no significant difference in fibroblast P2X7R-mRNA content between SSc patients and healthy subjects, a datum suggesting that P2X7R up-regulation does not involve gene transcription but only cell surface expression of the molecule, possibly via an increased trafficking of the P2X7R protein to the plasma membrane. Indirect support to this view is provided by previous data on monocytes/macrophages. Gudipaty et al. (2001) demonstrated that during cytokine-driven differentiation in macrophages healthy human monocytes markedly increase the P2X7R number per cell (MFI > 10-fold) without any significant change in the mRNA content. Moreover, we found that monocytes from patients with a chronic inflammatory disorder such as Behçet's disease expressed significantly higher P2X7R membrane levels than healthy controls, with no difference in intracellular mRNA concentration (Castrichini et al., 2014). Notably, Gu et al. (2000) demonstrated that in monocytes from healthy humans most of P2X7R protein is localized inside the cell roughly an order of magnitude greater than that expressed on the membrane. On this basis, the authors hypothesized that this intracellular pool represents a reserve able to be recruited to the surface when the cell activates. Probably such a mechanism is operative also in SSc fibroblasts, thus explaining the high cell membrane P2X7R expression found in these patients.

Not only the expression, but also the function of the P2X7R as evaluated by agonist-induced Ca^{2+} influx, αSMA expression, cell migration, CTGF, and collagen release, was enhanced in SSc dermal fibroblasts.

As regards the P2X7R-dependent Ca^{2+} influx, a significantly higher ion permeability was observed in SSc patients when compared to healthy controls. In particular, SSc fibroblasts showed an enhanced reactivity to BzATP, a potent and selective synthetic P2X7R agonist, as demonstrated by the higher percentage of responsive cells, and the increased total amount of Ca^{2+} entry into the single cell in the time unit, as reflected by AUC 5′-values. Such results, together with the evidence that SSc fibroblast hyper-responsiveness significantly reduced after oATP pre-incubation, strongly support the active role of the P2X7R in the function of these cells.

Notably, these findings paralleled the differences in the expression pattern observed between the two groups, i.e., SSc fibroblasts expressed higher levels of P2X7R on a higher number of cells when compared to controls, thus suggesting that P2X7R overexpression is the main driver of receptor overactivity. In agreement with our data, a preliminary observation by Lo Monaco et al. (2007) found that SSc dermal fibroblasts showed an increased sensitivity to extracellular ATP than healthy controls in terms of intracellular Ca^{2+} changes. Moreover, some recent studies reported that P2X7R function was increased in peripheral blood mononuclear cells (PBMC) from patients with other autoimmune diseases, specifically rheumatoid arthritis (Al-Shukaili et al., 2008, 2011), and Behçet's disease (Castrichini et al., 2014). In particular, Al-Shukaili et al. (Al-Shukaili et al., 2008, 2011) demonstrated that in rheumatoid arthritis patients the increase in the P2X7R function, without any concomitant membrane expression enhancement, was associated to a higher prevalence of a gain-of-function receptor gene polymorphism in these subjects. Conversely, our data are poorly consistent with the hypothesis that SSc-associated changes in the receptor function are the result of a specific genetic substrate. In fact, currently known gain of function polymorphisms influence receptor properties without any appreciable significant effect on the membrane expression (Sun et al., 2010). Nevertheless, a novel single-nucleotide polymorphism (H155Y) enhancing P2X7R function via increased protein trafficking and surface expression has been recently identified (Bradley et al., 2011). Thus, this theoretical possibility cannot be completely ruled out.

Exaggerated fibroblast activation, as reflected by increased cell proliferation, migration, production of ECM proteins and collagen, represents a key feature in the pathogenesis of SSc (Allanore et al., 2015). Our data provide for the first time evidence that P2X7R may be actively involved in promoting this process. In fact, SSc fibroblast stimulation with selective receptor agonists resulted in a clear-cut increase in the myofibroblast phenotype, with higher propensity of these cells in releasing collagen and migrating to close wound scratch, and these effects were completely reversed by P2X7R antagonists pre-incubation. Notably, such changes took place only when receptor activation occurred in the setting of a cell priming with LPS. This datum first suggested that inflammatory molecules could represent crucial mediators in the genesis of the phenomenon. Indeed, it is well-recognized that in monocytes LPS-induced release of inflammatory cytokines, particularly IL-1β and IL-6, is markedly boosted by P2X7R activation (Di Virgilio, 2007; Castrichini et al., 2014; Gicquel et al., 2015). Moreover, both these molecules are produced by dermal fibroblasts upon LPS stimulation, (Tardif et al., 2004; Wang et al., 2011) and are able to induce a fibrogenic phenotype in these cells (Goldring and Krane, 1987; O'Reilly et al., 2014). Despite such premises, our data conflict with this interpretative hypothesis: LPS+BzATP incubation of SSc fibroblasts did not produce any change in IL-1β release, while IL-6, although reaching significantly higher levels with respect to basal conditions (but still quite low in absolute), did not show any appreciable impact on collagen production. In fact, reproducing the *in vivo* conditions by adding the sIL-6R to cell cultures in order to make possible IL-6-dependent transsignaling pathway activation, no any further increase in PIP levels was detected. As regards the apparently unexpected IL-1β findings, it should be noted that previous studies demonstrated that IL-1α, rather than IL-1β, peculiarly plays an important role in promoting the activation of SSc dermal fibroblasts (Kawaguchi, 1994; Higgins et al., 1999; Hutyrová et al., 2004; Kawaguchi et al., 2004). In fact, while it has been reported that IL-1α is expressed in these cells where induced a fibrogenic phenotype via an autocrine mechanism (Kawaguchi et al., 2004), IL-1β was not detectable in

both SSc fibroblast cell extracts and the supernatants (Kawaguchi, 1994).

An alternative intriguing mechanism by which the P2X7R could promote the development of a fibrogenic phenotype in fibroblasts may be the direct activation of intracellular pathways controlling collagen biosynthetic machinery, particularly the mitogen-activated protein kinase (MAPK) cascade. In fact, increasing evidence indicates that a key role in fibroblast activation is also played by ERK1/2, a member of the MAPK family (Mu et al., 2012). Specifically, it has been demonstrated that in SSc fibroblasts ERK1/2 activation contributes to increase the expression of fibrotic proteins, including collagen, as well as to the contraction of these cells (Bogatkevich et al., 2007; Chen et al., 2008; Lazzerini et al., 2012).

Several data suggest that the P2X7R can activate the ERK1/2 pathway in different cell types, although the mechanism of this coupling is still unclear (Amstrup and Novak, 2003; Gendron et al., 2003). Intriguingly, in addition of being activated by an increase in $[Ca^{2+}]_i$ (Gendron et al., 2003), it has been demonstrated that a sequence of the carboxy-end of the P2X7R contains a conserved LPS-binding domain (Coddou et al., 2011), and peptides derived from this sequence bind LPS *in vitro* and neutralize the ability of LPS to activate ERK1/2 in tissue cultured macrophages (Denlinger et al., 2001). Keeping this in mind, the carboxy-terminal domain of P2X7R may directly coordinate key signal transduction events related to LPS action also in SSc fibroblasts, specifically the ERK1/2 activation, eventually leading to the development of a pro-fibrotic phenotype. Our data support this point of view. Indeed, we demonstrated that LPS priming is required for P2X7R-induced collagen production from SSc cells, and that such an effect was completely abrogated when cultures were pre-incubated with a ERK1/2 inhibitor. The concomitant finding here provided that also CTGF release was induced by LPS+BzATP, and then fully reversed by both P2X7R antagonists and ERK1/2 inhibitors, points to MAPK-dependent CTGF production as a key event in promoting the P2X7R-induced fibrogenic phenotype in dermal fibroblasts. This hypothesis is supported by the evidence provided by Leask et al. (2003) that MAPK pathway activation can induce the CTGF promoter in human dermal fibroblasts.

Finally, we cannot ruled out that also indirect effects can contribute to the observed P2X7R-induced ERK1/2 signaling activation and profibrotic response. In fact, it has been demonstrated that P2X7R activation causes ATP release (Pellegatti et al., 2005; Brandao-Burch et al., 2012), which in turn can activate profibrotic P2Y2 and/or A2A receptors (in this case indirectly, by increasing extracellular adenosine concentrations), both exerting their effects through a MAPK signaling pathway (Pellegatti et al., 2011; Lazzerini et al., 2012; Lu et al., 2012).

In conclusion, our data provide for the first time evidence that in dermal fibroblasts from SSc patients both the expression and function of the P2X7R are increased with respect to healthy controls. In these cells, P2X7R stimulation induces a fibrogenic phenotype characterized by increased migration and collagen production, via activation of the ERK1/2 pathway. These findings, besides giving new insights on the pathophysiology of SSc-associated dermal fibrosis, rise the distinct possibility that drugs specifically blocking the P2X7R could represent a novel and attractive pharmacological target for anti-fibrogenetic therapy of the disease. Indeed, novel P2X7R inhibitors are available for clinical use [e.g., periodate-oxidized ATP, (Ferrero, 2009) CE-224,535, (Stock et al., 2012) and AZD9056 (Eser et al., 2015)]. Thus, P2X7R targeting may have translational potential with a possible relevant impact in morbidity and mortality in SSc patients.

ETHICS STATEMENT

Local Ethical Committee (Comitato Etico Regione Toscana—Area Vasta Sud Est) approved the study, and patients gave their oral and written informed consent in accordance with the Principles of the Declaration of Helsinki.

AUTHOR CONTRIBUTIONS

Conception and design of the work: PL, FL, PC. Substantial contributions to the acquisition of data for the work: DG, AG, ES, FV, AA, PT, MC, VD. Substantial contributions to the analysis of data for the work: DG, PL, AG, MN, ES, FL, PC. Substantial contributions to the interpretation of data for the work: PL, AG, MN, ES, RF, FL, PC. Drafting the work: DG, PL, AG, PC. Revising the draft of the work critically for important intellectual content: DG, PL, AG, SD, DA, MM, RF, FL, PC. Final approval of the version to be published: DG, PL, AG, MN, ES, FV, AA, PT, SD, MC, VD, DA, MM, RF, FL, PC. Agreement to be accountable for all aspects of the work in ensuring that questions related to the accuracy or integrity of any part of the work are appropriately investigated and resolved: DG, PL, AG, MN, ES, FV, AA, PT, SD, MC, VD, DA, MM, RF, FL, PL.

FUNDING

The work was supported by Grant Number #19427 from Arthritis Research UK.

SUPPLEMENTARY MATERIAL

The Supplementary Material for this article can be found online at: http://journal.frontiersin.org/article/10.3389/fphar.2017.00638/full#supplementary-material

REFERENCES

Allanore, Y., Simms, R., Distler, O., Trojanowska, M., Pope, J., Denton, C. P., et al. (2015). Systemic sclerosis. *Nat. Rev. Dis. Primers* 1:15002. doi: 10.1038/nrdp.2015.2

Al-Shukaili, A., Al-Kaabi, J., and Hassan, B. (2008). A comparative study of interleukin-1beta production and p2x7 expression after ATP stimulation by peripheral blood mononuclear cells isolated from rheumatoid arthritis patients and normal healthy controls. *Inflammation* 31, 84–90. doi: 10.1007/s10753-007-9052-0

Al-Shukaili, A., Al-Kaabi, J., Hassan, B., Al-Araimi, T., Al-Tobi, M., Al-Kindi, M., et al. (2011). P2X7 receptor gene polymorphism analysis in rheumatoid arthritis. *Int. J. Immunogenet.* 38, 389–396. doi: 10.1111/j.1744-313X.2011.01019.x

Amstrup, J., and Novak, I. (2003). P2X7 receptor activates extracellular signal-regulated kinases ERK1 and ERK2 independently of Ca2+ influx. *Biochem. J.* 374, 51–61. doi: 10.1042/bj20030585

Bogatkevich, G. S., Ludwicka-Bradley, A., Highland, K. B., Hant, F., Nietert, P. J., Singleton, C. B., et al. (2007). Down-regulation of collagen and connective tissue growth factor expression with hepatocyte growth factor in lung fibroblasts from white scleroderma patients via two signaling pathways. *Arthritis Rheum* 56, 3468–3477. doi: 10.1002/art.22874

Bradley, H. J., Baldwin, J. M., Goli, G. R., Johnson, B., Zou, J., Sivaprasadarao, A., et al. (2011). Residues 155 and 348 contribute to the determination of P2X7 receptor function via distinct mechanisms revealed by single-nucleotide polymorphisms. *J. Biol. Chem.* 286, 8176–8187. doi: 10.1074/jbc.M110.211284

Brandao-Burch, A., Key, M. L., Patel, J. J., Arnett, T. R., and Orriss, I. R. (2012). The P2X7 Receptor is an Important Regulator of Extracellular ATP Levels. *Front Endocrinol* 3:41. doi: 10.3389/fendo.2012.00041

Caporali, F., Capecchi, P. L., Gamberucci, A., Lazzerini, P. E., Pompella, G., Natale, M., et al. (2008). Human rheumatoid synoviocytes express functional P2X7 receptors. *J. Mol. Med.* 86, 937–949. doi: 10.1007/s00109-008-0365-8

Castrichini, M., Lazzerini, P. E., Gamberucci, A., Capecchi, P. L., Franceschini, R., Natale, M., et al. (2014). The purinergic P2×7 receptor is expressed on monocytes in Behçet's disease and is modulated by TNF-α. *Eur. J. Immunol.* 44, 227–238 doi: 10.1002/eji.201343353

Chan, E. S., Fernandez, P., Merchant, A. A., Montesinos, M. C., Trzaska, S., Desai, A., et al. (2006). Adenosine A2A receptors in diffuse dermal fibrosis: pathogenic role in human dermal fibroblasts and in a murine model of scleroderma. *Arthritis Rheum* 54, 2632–2642. doi: 10.1002/art.21974

Chen, Y., Leask, A., Abraham, D. J., Pala, D., Shiwen, X., Khan, K., et al. (2008). Heparan sulfate-dependent ERK activation contributes to the overexpression of fibrotic proteins and enhanced contraction by scleroderma fibroblasts. *Arthritis Rheum* 58, 577–585. doi: 10.1002/art.23146

Coddou, C., Stojilkovic, S. S., and Huidobro-Toro, J. P. (2011). Allosteric modulation of ATP-gated P2X receptor channels. *Rev. Neurosci.* 22, 335–354. doi: 10.1515/rns.2011.014

Del Ry, S., Cabiati, M., Vozzi, F., Battolla, B., Caselli, C., Forini, F., et al. (2011). Expression of C-type natriuretic peptide and its receptor NPR-B in cardiomyocytes. *Peptides* 32, 1713–1718. doi: 10.1016/j.peptides.2011.06.014

Denlinger, L. C., Fisette, P. L., Sommer, J. A., Watters, J. J., Prabhu, U., Dubyak, G. R., et al. (2001). Cutting edge: the nucleotide receptor P2X7 contains multiple protein- and lipid-interaction motifs including a potential binding site for bacterial lipopolysaccharide. *J. Immunol.* 167, 1871–1876. doi: 10.4049/jimmunol.167.4.1871

Di Virgilio, F. (2007). Liaisons dangereuses:P2X(7) and the inflammasome. *Trends Pharmacol. Sci.* 28, 465–472. doi: 10.1016/j.tips.2007.07.002

Eser, A., Colombel, J. F., Rutgeerts, P., Vermeire, S., Vogelsang, H., Braddock, M., et al. (2015). Safety and efficacy of an oral inhibitor of the purinergic receptor P2X7 in adult patients with moderately to severely active crohn's disease: a randomized placebo-controlled, double-blind, phase IIa study. *Inflamm. Bowel Dis.* 21, 2247–2253. doi: 10.1097/MIB.0000000000000514

Ferrero, M. E. (2009). A new approach to the inflammatory/autoimmune diseases. *Recent Pat. Antiinfect. Drug Discov.* 4, 108–113. doi: 10.2174/157489109788490343

Friedle, S. A., Brautigam, V. M., Nikodemova, M., Wright, M. L., and Watters, J. J. (2011). The P2X7-Egr pathway regulates nucleotide-dependent inflammatory gene expression in microglia. *Glia* 59, 1–13. doi: 10.1002/glia.21071

Garrett, S. M., Backer Frost, D., and Feghali-Bostwick, C. (2017). The mighty fibroblast and its utility in scleroderma research. *J. Scleroderma Relat. Disord.* 2, 100–107. doi: 10.5301/jsrd.5000240

Gendron, F. P., Neary, J. T., Theiss, P. M., Sun, G. Y., Gonzalez, F. A., and Weisman, G. A. (2003). Mechanisms of P2X7 receptor-mediated ERK1/2 phosphorylation in human astrocytoma cells. *Am. J. Physiol. Cell Physiol.* 284, C571–C581. doi: 10.1152/ajpcell.00286.2002

Gentile, D., Natale, M., Lazzerini, P. E., Capecchi, P. L., and Laghi-Pasini, F. (2015). The role of P2X7 receptors in tissue fibrosis: a brief review. *Purinergic Signal* 11, 435–440. doi: 10.1007/s11302-015-9466-3

Gicquel, T., Robert, S., Loyer, P., Victoni, T., Bodin, A., Ribault, C., et al. (2015). IL-1β production is dependent on the activation of purinergic receptors and NLRP3 pathway in human macrophages. *FASEB J.* 29, 4162–4173. doi: 10.1096/fj.14-267393

Goldring, M. B., and Krane, S. (1987). M. Modulation by recombinant interleukin 1 of synthesis of types I and III collagens and associated procollagen mRNA levels in cultured human cells. *J. Biol. Chem.* 262, 16724–16729.

Gonçalves, R. G., Gabrich, L., Rosário, A. Jr. (2006). The role of purinergic P2X7 receptors in the inflammation and fibrosis of unilateral ureteral obstruction in mice. *Kidney Int.* 70, 1599–1606. doi: 10.1038/sj.ki.5001804

Gu, B. J., Zhang, W. Y., Bendall, L. J., Chessell, I. P., Buell, G. N., and Wiley, J. S. (2000). Expression of P2X(7) purinoceptors on human lymphocytes and monocytes: evidence for nonfunctional P2X(7) receptors. *Am. J. Physiol. Cell Physiol.* 279, C1189–C1197.

Gudipaty, L., Humphreys, B. D., Buell, G., and Dubyak, G. R. (2001). Regulation of P2X7 nucleotide receptor function in human monocytes by extracellular ions and receptor density. *Am. J. Physiol. Cell Physiol.* 280, C943–C953.

Haanes, K. A., Schwab, A., and Novak, I. (2012). The P2X7 receptor supports both life and death in fibrogenic pancreatic stellate cells. *PLoS ONE* 7:e51164. doi: 10.1371/journal.pone.0051164

Higgins, G. C., Wu, Y., and Postlethwaite, A. E. (1999). Intracellular IL-1 receptor antagonist is elevated in human dermal fibroblasts that overexpress intracellular precursor IL-1 alpha. *J. Immunol.* 163, 3969–3975.

Huang, C., Yu, W., Cui, H., Wang, Y., Zhang, L., Han, F., et al. (2014). P2X7 blockade attenuates mouse liver fibrosis. *Mol. Med. Rep.* 9, 57–62. doi: 10.3892/mmr.2013.1807

Hutyrová, B., Lukác, J., Bosák, V., Buc, M., du Bois, R., and Petrek, M. (2004). Interleukin 1alpha single-nucleotide polymorphism associated with systemic sclerosis. *J. Rheumatol.* 31, 81–84.

Jacobson, K. A. (2010). P2X and P2Y Receptors. *Tocris Bioscience Scientific Review No.* 33.

Jiang, W., Lv, H., Wang, H., Wang, D., Sun, S., Jia, Q., et al. (2015). Activation of the NLRP3/caspase-1 inflammasome in human dental pulp tissue and human dental pulp fibroblasts. *Cell Tissue Res.* 361, 541–555. doi: 10.1007/s00441-015-2118-7

Kawaguchi, Y. (1994). IL-1 alpha gene expression and protein production by fibroblasts from patients with systemic sclerosis. *Clin. Exp. Immunol.* 97, 445–450. doi: 10.1111/j.1365-2249.1994.tb06108.x

Kawaguchi, Y., McCarthy, S. A., Watkins, S. C., and Wright, T. M. (2004). Autocrine activation by interleukin 1alpha induces the fibrogenic phenotype of systemic sclerosis fibroblasts. *J. Rheumatol.* 31, 1946–1954.

Koshi, R., Coutinho-Silva, R., Cascabulho, C. M., Henrique-Pons, A., Knight, G. E., Loesch, A., et al. (2005). Presence of the P2X(7) purinergic receptor on immune cells that invade the rat endometrium during oestrus. *J. Reprod. Immunol.* 66, 127–140. doi: 10.1016/j.jri.2005.04.006

Kumagai, S., Matsui, K., Kawaguchi, H., Yamashita, T., Mohri, T., Fujio, Y., et al. (2013). Cathelicidin antimicrobial peptide inhibits fibroblast migration via P2X7 receptor signaling. *Biochem. Biophys. Res. Commun.* 437, 609–614. doi: 10.1016/j.bbrc.2013.07.010

Lazzerini, P. E., Natale, M., Gianchecchi, E., Capecchi, P. L., Montilli, C., Zimbone, S., et al. (2012). Adenosine A2A receptor activation stimulates collagen production in sclerodermic dermal fibroblasts either directly and through a cross-talk with the cannabinoid system. *J. Mol. Med.* 90, 331–342. doi: 10.1007/s00109-011-0824-5

Lazzerini, P. E., Capecchi, P. L., Guidelli, G. M., Selvi, E., Acampa, M., and Laghi-Pasini, F. (2016). Spotlight on sirukumab for the treatment of rheumatoid arthritis: the evidence to date. *Drug Des. Dev. Ther.* 10, 3083–3098. doi: 10.2147/DDDT.S99898

Leask, A., Holmes, A., Black, C. M., and Abraham, D. J. (2003). Connective tissue growth factor gene regulation. Requirements for its induction by transforming growth factor-beta 2 in fibroblasts. *J. Biol. Chem.* 278, 13008–13015. doi: 10.1074/jbc.M210366200

Lo Monaco, A., Gulinelli, S., Castellino, G., Solini, A., Ferrari, D., La Corte, R., et al. (2007). Increased sensitivity to extracellular ATP of fibroblasts from patients affected by systemic sclerosis. *Ann. Rheum Dis.* 66, 1124–1125. doi: 10.1136/ard.2006.065078

Lu, D., Soleymani, S., Madakshire, R., and Insel, P. A. (2012). ATP released from cardiac fibroblasts via connexin hemichannels activates profibrotic P2Y2 receptors. *FASEB J.* 26, 2580–2591. doi: 10.1096/fj.12-204677

Mu, Y., Gudey, S. K., and Landström, M. (2012). Non-Smad signaling pathways. *Cell Tissue Res.* 347, 11–20. doi: 10.1007/s00441-011-1201-y

North, R. A. (2002). Molecular physiology of P2X receptors. *Physiol. Rev.* 82, 1013–1067. doi: 10.1152/physrev.00015.2002

O'Reilly, S., Ciechomska, M., Cant, R., and van Laar, J. M. (2014). Interleukin-6 (IL-6) trans signaling drives a STAT3-dependent pathway that leads to hyperactive transforming growth factor-β (TGF-β) signaling promoting SMAD3 activation and fibrosis via Gremlin protein. *J. Biol. Chem.* 289, 9952–9960. doi: 10.1074/jbc.M113.545822

Pattanaik, D., Brown, M., Postlethwaite, B. C., and Postlethwaite, A. E. (2015). Pathogenesis of systemic sclerosis. *Front. Immunol.* 6:272. doi: 10.3389/fimmu.2015.00272

Pellegatti, P., Falzoni, S., Donvito, G., Lemaire, I., and Di Virgilio, F. (2011). P2X7 receptor drives osteoclast fusion by increasing the extracellular adenosine concentration. *FASEB J.* 25, 1264–1274. doi: 10.1096/fj.10-169854

Pellegatti, P., Falzoni, S., Pinton, P., Rizzuto, R., and Di Virgilio, F. (2005). A novel recombinant plasma membrane-targeted luciferase reveals a new pathway for ATP secretion. *Mol. Biol. Cell* 16, 3659–3665. doi: 10.1091/mbc.E05-03-0222

Perez-Aso, M., Chiriboga, L., and Cronstein, B. N. (2012). Pharmacological blockade of adenosine A2A receptors diminishes scarring. *FASEB J* 26, 4254–4263. doi: 10.1096/fj.12-209627

Perez-Aso, M., Fernandez, P., Mediero, A., Chan, E. S., and Cronstein, B. N. (2014). Adenosine 2A receptor promotes collagen production by human fibroblasts via pathways involving cyclic AMP and AKT but independent of Smad2/3. *FASEB J.* 28, 802–812 doi: 10.1096/fj.13-241646

Ponnusamy, M., Ma, L., Gong, R., Pang, M., Chin, Y. E., and Zhuang, S. (2011). P2X7 receptors mediate deleterious renal epithelial-fibroblast cross talk. *Am. J. Physiol. Renal Physiol.* 300, F62–F70. doi: 10.1152/ajprenal.00473.2010

Riteau, N., Gasse, P., Fauconnier, L., Gombault, A., Couegnat, M., Fick, L., et al. (2010). Extracellular ATP is a danger signal activating P2X7 receptor in lung inflammation and fibrosis. *Am. J. Respir. Crit. Car. Med.* 182, 774–783. doi: 10.1164/rccm.201003-0359OC

Rossi, L., Salvestrini, V., Ferrari, D., Di Virgilio, F., and Lemoli, R. M. (2012). The sixth sense: hematopoietic stem cells detect danger through purinergic signaling. *Blood* 120, 2365–2375. doi: 10.1182/blood-2012-04-422378

Smart, M. L., Gu, B., Panchal, R. G., Wiley, J., Cromer, B., Williams, D. A., et al. (2003). P2X7 receptor cell surface expression and cytolytic pore formation are regulated by a distal C-terminal region. *J. Biol. Chem.* 278, 8853–8860. doi: 10.1074/jbc.M211094200

Solini, A., Chiozzi, P., Morelli, A., Fellin, R., and Di Virgilio, F. (1999). Human primary fibroblasts *in vitro* express a purinergic P2X7 receptor coupled to ion fluxes, microvesicle formation and IL-6 release. *J. Cell Sci.* 112, 297–305.

Stock, T. C., Bloom, B. J., Wei, N., Ishaq, S., Park, W., Wang, X., et al. (2012). Efficacy and safety of CE-224,535, an antagonist of P2X7 receptor, in treatment of patients with rheumatoid arthritis inadequately controlled by methotrexate. *J. Rheumatol.* 39, 720–727. doi: 10.3899/jrheum.110874

Sun, C., Chu, J., Singh, S., and Salter, R. D. (2010). Identification and characterization of a novel variant of the human P2X(7) receptor resulting in gain of function. *Purinergic Signal.* 6, 31–45. doi: 10.1007/s11302-009-9168-9

Talele, N. P., Fradette, J., Davies, J. E., Kapus, A., and Hinz, B. (2015). Expression of α-smooth muscle actin determines the fate of mesenchymal stromal cells. *Stem Cell Rep.* 4, 1016–1030. doi: 10.1016/j.stemcr.2015.05.004

Tardif, F., Ross, G., and Rouabhia, M. (2004). Gingival and dermal fibroblasts produce interleukin-1 beta converting enzyme and interleukin-1 beta but not interleukin-18 even after stimulation with lipopolysaccharide. *J. Cell. Physiol.* 198, 125–132. doi: 10.1002/jcp.10400

Tung, H. C., Lee, F. Y., Wang, S. S., Tsai, M. H., Lee, J. Y., Huo, T. I., et al. (2015). The beneficial effects of P2X7 antagonism in rats with bile duct ligation-induced cirrhosis. *PLoS ONE* 10:e0124654. doi: 10.1371/journal.pone.0124654

Vandesompele, J., De Preter, K., Pattyn, F., Poppe, B., Van Roy, N., De Paepe, A., et al. (2002). Accurate normalization of real-time quantitative RT-PCR data by geometric averaging of multiple internal control genes. *Genome Biol.* 3:research0034.1–research0034.11.

Wang, J., Hori, K., Ding, J., Huang, Y., Kwan, P., Ladak, A., et al. (2011). Toll-like receptors expressed by dermal fibroblasts contribute to hypertrophic scarring. *J. Cell. Physiol.* 226, 1265–1273. doi: 10.1002/jcp.22454

Xie, B., Chen, Y., Zhang, S., Wu, X., Zhang, Z., Peng, Y., et al. (2014). The expression of P2X7 receptors on peripheral blood mononuclear cells in patients with primary Sjögren's syndrome and its correlation with anxiety and depression. *Clin. Exp. Rheumatol.* 32, 354–360.

Conflict of Interest Statement: The authors declare that the research was conducted in the absence of any commercial or financial relationships that could be construed as a potential conflict of interest.

frontiers in Pharmacology

ORIGINAL RESEARCH
published: 08 March 2017
doi: 10.3389/fphar.2017.00115

Generation and Characterization of Specific Antibodies to the Murine and Human Ectonucleotidase NTPDase8

*Julie Pelletier[1], Mabrouka Salem[1,2], Joanna Lecka[1,2], Michel Fausther[1,2,3], François Bigonnesse[1] and Jean Sévigny[1,2]**

[1] Centre de recherche du CHU de Québec – Université Laval, Québec City, QC, Canada, [2] Département de Microbiologie-Infectiologie et d'Immunologie, Faculté de Médecine, Université Laval, Québec City, QC, Canada, [3] Division of Gastroenterology and Hepatology, Department of Internal Medicine, University of Arkansas for Medical Sciences, Little Rock, AR, USA

The ectonucleotidase nucleoside triphosphate diphosphohydrolase-8 (NTPDase8) is the last member of the Ecto-NTPDase family to be discovered and characterized. It is a transmembrane protein which regulates the concentration of the agonists of P1 and P2 receptors at the cell surface. The functions of the enzyme are still not known partly due to the lack of specific tools such as antibodies. In this work, guinea pig polyclonal antibodies against mouse NTPDase8 and mouse monoclonal antibodies against human NTPDase8 have been generated and characterized. For the production of antibodies against mouse NTPDase8 several techniques have been tried. Several peptide antigens in several hosts (rabbit, rat, hamster, and guinea pig) failed to give a positive reaction suggesting that NTPDase8 is poorly immunogenic. In this study, we describe the successful process that led to anti-mouse NTPDase8, namely the cDNA immunization technique. Monoclonal antibodies to human NTPDase8 were also obtained by cDNA immunization followed by a final injection with transfected human embryonic kidney (HEK 293T) cells expressing human NTPDase8. The specificity of these antibodies was evaluated by Western blot, immunocytochemistry, immunohistochemistry and flow cytometry. In contrast, all commercial antibodies to NTPDase8 peptides that we have tested failed to give a specific positive signal against the expressed NTPDase8 protein when used to probe Western blots. In addition, immunohistochemistry experiments confirmed the presence of NTPDase8 in mouse liver canaliculi. The tools generated in this work will help characterize NTPDase8 localization and function in future studies and its contribution to the modulation of P1 and P2 receptor activation.

Keywords: monoclonal antibodies, polyclonal antibodies, mouse NTPDase8, human NTPDase8, cDNA immunization

OPEN ACCESS

Edited by:
Kenneth A. Jacobson, National Institutes of Health, USA

Reviewed by:
Gennady G. Yegutkin, University of Turku, Finland
Terence L. Kirley, University of Cincinnati, USA

****Correspondence:***
Jean Sévigny
jean.sevigny@crchul.ulaval.ca

Specialty section:
This article was submitted to Experimental Pharmacology and Drug Discovery, a section of the journal Frontiers in Pharmacology

Received: *17 January 2017*
Accepted: *24 February 2017*
Published: *08 March 2017*

Citation:
Pelletier J, Salem M, Lecka J, Fausther M, Bigonnesse F and Sévigny J (2017) Generation and Characterization of Specific Antibodies to the Murine and Human Ectonucleotidase NTPDase8. Front. Pharmacol. 8:115. doi: 10.3389/fphar.2017.00115

INTRODUCTION

The activation of nucleotide (P2) and adenosine (P1) receptors is regulated in part by enzymes that regulate the concentration of their agonists at the cell surface. The most important enzymes that dephosphorylate nucleotides in the extracellular environment in physiological conditions are members of the Ecto-nucleoside triphosphate diphosphohydrolase (E-NTPDase) family (Beaudoin et al., 1996; Robson et al., 2006; Zimmermann et al., 2012). This family

of ectonucleotidases is composed of 8 members (NTPDase1 to -8; Robson et al., 2006; Zimmermann et al., 2012). NTPDase1, -2, -3, and -8 are expressed at the plasma membrane and they hydrolyse nucleotides at the cell surface with different abilities (Kukulski et al., 2005). These enzymes have been located in different systems and they have been reported to play distinct roles. To give a few examples, NTPDase1, which is expressed by several cell types which includes vascular endothelial cells and Tregs, has been shown to regulate vascular hemostasis and immune functions (Kukulski et al., 2011; Zimmermann et al., 2012; Yegutkin, 2014). NTPDase2, which is also expressed by several cell types, is found in type I cells of taste buds where it has been associated to taste functions (Bartel et al., 2006; Vandenbeuch et al., 2013). NTPDase3 has been detected in neurons in different organs. It was proposed that in the rat brain, NTPDase3 may modulate feeding and sleep–wake behavior (Belcher et al., 2005). In contrast to NTPDase1, -2, and -3, no function has yet been associated to NTPDase8. Finally, as NTPDase4, -5, -6, and -7 are mainly anchored to the membranes of intracellular organelles and as they hydrolyse nucleotides with lower affinities their functions are expected to differ from the one of the above plasma membrane bound NTPDases.

So far NTPDase8 was reported to be expressed only in a few tissues which includes rat (Fausther et al., 2007) and porcine (Sévigny et al., 2000) liver, and pig kidneys (Sévigny et al., 2000). The lack of tools such as antibodies limits the study of NTPDase8 structure and function. To date, some commercial antibodies against NTPDase8 are available, but their specificity has not been demonstrated. The goal of this work was to obtain specific antibodies against NTPDase8 and to demonstrate their specificity. As the commercial antibodies revealed to be unspecific, to achieve this goal we used several techniques of immunization. Following several unsuccessful attempts we finally ended with a convenient technique that we also describe here.

MATERIALS AND METHODS

Materials

Aprotinin, phenylmethanesulfonyl fluoride, ethylenediaminetetraacetic acid, sodium citrate, paraformaldehyde (PFA), 3,3′-diaminobenzidine (DAB), and hydrogen peroxide (H_2O_2) were purchased from Sigma-Aldrich (Oakville, ON, Canada). Tris(hydroxymethyl)aminomethane (Tris) was from VWR International (Montreal, QC, Canada). Dulbecco's modified Eagle's medium and antibiotic–antimycotic solution, NuPAGE lithium dodecyl sulfate sample, NuPAGE 4–12% Bis-Tris gels were obtained from Life Technologies (Burlington, ON, Canada). Fetal bovine serum (FBS) and goat serum were from Wisent (St-Bruno, QC, Canada). For Western blot and/or immunohistochemistry experiments the secondary antibodies used were either conjugated to horseradish peroxidase (HRP), namely goat anti-guinea pig, donkey anti-goat (Santa Cruz Biotechnology, Dallas, TX, USA), goat anti-mouse (Jackson ImmunoResearch Laboratories Inc. West Grove, PA, USA), donkey anti-rabbit (GE Healthcare Life Sciences, Baie d'Urfe, QC, Canada), rabbit anti-rat (Thermo Fisher Scientific, Rockford, IL, USA), or to biotin, namely goat anti-guinea pig, goat anti-rabbit (Jackson ImmunoResearch Laboratories Inc. West Grove, PA, USA), goat anti-mouse and goat anti-rat (Vector Laboratories, Burlington, ON, Canada). For flow cytometry experiments Alexa Fluor 594-goat anti-guinea pig and Alexa Fluor 633-goat anti-mouse were obtained from Life Technologies (Burlington, ON, Canada).

Animals and Plasmids

Female Sprague-Dawley rats, Hartley guinea pigs, LVG Golden Syrian hamsters, BALB/c mice, and New Zealand rabbits were obtained from Charles River Laboratories (Saint-Constant, QC, Canada). All procedures were approved by the Canadian Council on Animal Care and the Université Laval Animal Welfare Committee. The plasmids encoding mouse NTPDase1 (GenBank accession no. NM_009848; Enjyoji et al., 1999), mouse NTPDase2 (AY376711; Kukulski et al., 2005), mouse NTPDase3 (AY376710; Lavoie et al., 2004), mouse NTPDase8 (AY364442; Bigonnesse et al., 2004), human NTPDase1 (U87967; Kaczmarek et al., 1996), human NTPDase2 (NM_001246; Knowles and Chiang, 2003), a kind gift of Dr. A. F. Knowles (San Diego, CA, USA), human NTPDase3 (AF034840; Smith and Kirley, 1998), a kind gift of Dr. T. L. Kirley (Cincinnati, OH, USA), human NTPDase8 (AY430414; Fausther et al., 2007), or rat NTPDase8 (AY536920; Fausther et al., 2007) all in pcDNA 3.1 vector were used for antiserum generation and for/or cell transfection, as described below.

Polyclonal Antibody Production to Mouse NTPDase8 with Peptides and Recombinant Proteins Produced in Bacteria

High density multiple antigen peptides (MAPs) system generated using four lysine residues bearing four branching peptides were synthesized separately with two polypeptides: peptide 829 (MGLSWKERVFMALL) and peptide 830 (QWPANKEKDTGVVSQ) that correspond to amino acid 1–14 and 60–74, respectively. These two antigens were generated by the Proteomics Platform of the Centre de Recherche of the CHU de Québec. These peptides were injected at day 1, 43, 85, 127, 169, 211 in rabbits, at day 1, 29, 57, 92 in hamsters, and at day 1, 29, 57, 92, 146 in guinea pigs and rats. The amount of peptides injected was as follows: 400–650 μg for rabbits, 100–200 μg for rats and guinea pigs, and 100 μg for hamsters. The blood was collected prior to the first injection and 7 days post-injection. The peptides were diluted in phosphate-buffered solution (PBS) (in mM: 10.1 Na_2HPO_4, 1.8 KH_2PO_4, 136.9 NaCl, and 2.7 KCl, pH 7.4) and complete Freund's adjuvant was mixed at a ratio 1:1 with peptides for the first injection. Two other peptides conjugated to keyhole limpet hemocyanin (KLH) that correspond to amino acid 87-101 (SYTSDPTQAGESLKS) and 390-404 (VEVSYPGQERWLRDY) were also injected six times (125–250 μg) in rabbit. The blood was collected 7 days post-injection. Recombinant purified protein produced in bacteria corresponding to amino acid 361–441 of mouse NTPDase8, named as peptide 76, was

synthetized by the Molecular Biology and Production of Antibody Service of the Centre de Recherche du CHU de Québec. Rabbits were injected three times at day 1, 28, 56 and blood was collected 14 days after the second and the third injection.

Polyclonal Antibodies by cDNA Immunization

Genetic immunization was carried out with plasmids encoding mouse NTPDase8 diluted in PBS 0.8×. Rabbits were injected with 1 mL of mouse NTPDase8 cDNA (0.65–0.8 mg/mL) consisting of 10 intradermic (ID) sites of 50 μL each and two intramuscular (IM) sites of 250 μL each. Hamsters were injected with 0.1 mL of mouse NTPDase8 cDNA (1 mg/mL) consisting of two ID sites of 25 μL each and one IM site of 50 μL. Guinea pigs and rats were injected with 0.2 mL of mouse NTPDase8 cDNA (1 mg/mL) consisting of two ID sites of 50 μL each and one IM site of 100 μL. Rabbits and hamsters were injected at day 1, 15, 29, 99, 183, 253, 286, 316, 384, and at day 1, 15, 29, 99, 170, respectively, rats and guinea pigs were injected at day 1, 15, 29, 99, 170, 283. The intradermal injections were done in the dorsal skin and the IM injections were done in the hind leg. The blood was collected prior to the first injection and between 12 and 14 days after the third and the subsequent injection.

Monoclonal Antibody Production by cDNA Immunization

Hybridomas were generated in BALB/c mice by ID and IM injection with 100 μg of human NTPDase8 cDNA diluted in PBS 0.8× at day 1, 15, 29, 99, and 184. A final injection was made at day 297 using intact human embryonic kidney (HEK 293T) cells transfected with human NTPDase8 expression vector (see Cell Transfection and Western Blot). Spleen cells were collected 3 days after the prime boost cells injection and fusion with SP2/0 cells were done as previously described (Munkonda et al., 2009) with minor modifications. For this assay, the SP2/0 cells were combined with splenocytes at a ratio 1:5. The positive hybridomas were screened by enzyme-linked immunosorbent assay (ELISA). The hybridomas were cloned by limiting dilution and the produced immunoglobulins were purified on Protein A Sepharose CL-4B column as described (Munkonda et al., 2009).

ELISA and Isotyping for Monoclonal Antibodies

ELISA plates (96 wells) were coated overnight (O/N) with 500 ng per well of lysates from African green monkey kidney (COS-7) cells transiently transfected with human NTPDase8 or untransfected diluted in PBS. After washing with PBS-Tween 0.05% (PBS-T), the wells were incubated for 1 h at 37°C in a blocking solution (0.5% bovine serum albumin diluted in PBS-T). After washing, the supernatant from each hybridoma was added to the well and incubated for 2 h at room temperature (RT), followed by four washing steps. Then a goat anti-mouse IgG (H + L)-HRP (1:2500) diluted in the blocking solution was incubated for 2 h at RT followed by four washing steps. The Enhanced K-Blue® Substrate (Neogen Corporation, Lansing, MI, USA) was then added for 15 min and the reaction was stopped by the addition of an equal volume of 2 N sulphuric acid and absorbance at 450 nm was recorded. The isotype of the antibodies produced by each hybridoma was determined by a Mouse Immunoglobulin Isotyping ELISA Kit (BD Bioscience, Mississauga, ON, Canada) according to the manufacturer's instruction. In brief, monoclonal rat anti-mouse IgG1, IgG2a, IgG2b, IgG3, IgA, and IgM were coated O/N in 96-well plates. After a washing step and a blocking treatment, each monoclonal anti-human NTPDase8 antibody was transferred to the wells. After washing steps, a rat anti-mouse Ig conjugated to HRP was added to each well, and revealed with a substrate provided in the kit. The plate was then read at 450 nm.

Cell Transfection and Western Blot

COS-7 cells and HEK 293T cells were cultured and transiently transfected as indicated with mouse NTPDase8 or human NTPDase8 cDNA constructs as described previously (Kukulski et al., 2005). For Western blot assays, lysates from transfected or non-transfected COS-7 cells (6 μg, unless otherwise indicated) were resuspended in NuPAGE sample buffer, separated on NuPAGE 4–12% Bis-Tris gels under reduced or non-reduced conditions, as indicated, and transferred to an Immobilon-P membrane (Millipore, Bedford, MA, USA) by electroblotting according to the manufacturer's recommendation. Membranes were then blocked with 2.5% non-fat milk in PBS containing 0.15% Tween20®(pH 7.4) O/N at 4°C and subsequently probed with the primary antibodies. Appropriate secondary HRP-conjugated antibodies were used, and the membranes developed with the Western Lightning™ Plus-ECL system (PerkinElmer Life and Analytical Sciences, Waltham, MA, USA). In some experiments, a gel with a large sample well 6 cm long containing 120 μg of lysates, transferred and blocked as described above and then probed with antibodies using the Mini-Protean II multiscreen apparatus (Bio-Rad Laboratories Ltd., Mississauga, ON, Canada) in which 20 antibodies can be tested on one gel.

Immunocytochemistry and Immunohistochemistry

Mouse liver was collected after animal perfusion with 4% PFA, tissues were then fixed in 4% PFA for 2 h and incubated O/N in 4% sucrose at 4°C and frozen in Tissue-Tek® O.C.T.™ Compound (Sakura Finetek, Torrance, CA, USA). COS-7 cells or tissues sections (6 μm thick) of mouse liver were fixed in 10% phosphate-buffered formalin (Fisher Scientific, Ottawa, ON, Canada) mixed with cold acetone (Fisher Scientific, Ottawa, ON, Canada) and blocked in a PBS solution containing 7% normal goat serum for 30 min. COS-7 cells and tissue sections were incubated with the indicated primary antibody at 4°C. COS-7 cells and tissue sections were then treated with 0.15% H_2O_2 in PBS for 10 min to inactivate endogenous peroxidase, and with an avidin/biotin solution (Avidin/Biotin Blocking kit; Vector Laboratories, Burlington, ON, Canada) to prevent non-specific staining due to endogenous biotin.

This step was followed by incubation with an appropriate biotin-conjugated secondary antibody at a dilution of 1:1000. The avidin–biotinylated HRP complex (VectaStain Elite ABC kit; Vector Laboratories) was added to optimize the reaction. Peroxidase activity was revealed with DAB as the substrate. Nuclei were counterstained with aqueous hematoxylin (Biomeda, Foster City, CA, USA) in accordance with the manufacturer's instructions.

Flow Cytometry (FACS)

HEK 293T cells transfected with mouse or human NTPDase8, were detached from the plates with a citric saline solution (135 mM potassium chloride, 15 mM sodium citrate). Samples of 2.5×10^5 cells per tube were washed with an ice-cold PBS solution containing 1% FBS and 0.1% NaN_3 [fluorescence-activated cell sorting (FACS) buffer] followed by incubation with the primary antibodies (serum from polyclonal anti-mouse NTPDase8 or purified monoclonal antibodies to human NTPDase8) or negative control (guinea pig preimmune sera or control mouse IgG2a (Sigma-Aldrich, Oakville, ON, Canada)) in FACS buffer for 1 h. After washes with FACS buffer solution, the cells were incubated with an appropriate Alexa-conjugated secondary antibody for 30 min on ice, washed with FACS buffer, and analyzed by flow cytometry (BD LSR II, BD Biosciences, San Jose, CA USA).

Inhibition Assays

Inhibition assay were done as previously described (Munkonda et al., 2009) on cell lysates from human NTPDase8 transfected COS-7 cells at 37°C in two different buffers: modified Ringer buffer (120 mM NaCl, 5 mM KCl, 2.5 mM $CaCl_2$, 1.2 mM $MgSO_4$, 25 mM $NaHCO_3$, 5 mM dextrose, 80 mM Tris–HCl, pH 7.4) and Tris/calcium buffer (5 mM $CaCl_2$, 80 mM Tris–HCl, pH 7.4). After pre-incubation of the enzyme with the purified monoclonal antibodies to human NTPDase8 (5 μg/mL), substrate (ATP, 100 μM) was then added and incubated for 8–10 min, the reaction was then stopped with malachite green reagent. The inorganic phosphate released during the enzymatic reaction was measured as previously described with the malachite green assay (Baykov et al., 1988).

TABLE 1 | Antigen used and specificity of the antibodies to mouse and human NTPDase8.

Antigen	Conjugation	Host	Animals per group	Application				
				WB		IHC	ICC	FACS
				NR	Red.			
Antibodies to mouse NTPDase8 (accession number: AY364442)								
Expression vector encoding mouse NTPDase8	None	Rabbit	3	–	–	–	NT	NT
		Rat	6	–	NT	–	+ (2/6)	NT
		Hamster	6	–	NT	–	–	NT
		Guinea pig	6	+ (5/6)	NT	–	+ (5/6)	NT
		Guinea pig	5	++	–	++	++	++
Peptide 829 (aa 1–14): MGLSWKERVFMALL	MAPs	Rabbit	2	–	–	–	NT	NT
		Rat	3	NT	–	NT	NT	NT
		Hamster	3	NT	–	NT	NT	NT
		Guinea pig	3	NT	–	NT	NT	NT
Peptide 830 (aa 60–74): QWPANKEKDTGVVSQ	MAPs	Rabbit	2	–	–	–	NT	NT
		Rat	3	NT	–	NT	NT	NT
		Hamster	3	NT	–	NT	NT	NT
		Guinea pig	3	NT	–	NT	NT	NT
Peptide 6768 (aa 87–101): SYTSDPTQAGESLKS	KLH	Rabbit	2	NT	+	NT	NT	NT
Peptide 6970 (aa 390–404): VEVSYPGQERWLRDY	KLH	Rabbit	2	NT	–	NT	NT	NT
Peptide 76 (aa 361–441)	None	Rabbit	3	NT	–	NT	NT	NT
Santa Cruz Biotechnologies (sc-160611)[1]	Unknown	Goat	N/A	NT	–	NT	NT	NT
Antibodies to human NTPDase8 (accession number: AY430414)								
Expression vector encoding human NTPDase8	None	Mouse	9[2] (4 mAbs)	++	++	++	NT	+
Aviva Systems Biology (ARP44815_P050) Peptide aa 110–159	Unknown	Rabbit	N/A	NT	–	NT	NT	NT

Unless indicated otherwise with the number of reacting antisera over the total number of animals used for immunization, each animal in the same group reacted similarly in the experiments presented.

WB, Western blot; NR, non-reduced condition; Red., reduced condition; IHC, immunohistochemistry; ICC, immunocytochemistry; FACS, Fluorescence-activated cell sorting; NT, not tested; N/A, not applicable; aa, amino acid; mAbs, monoclonal antibodies. Results "–", absence of reaction or same signal as in the negative control; "+", weak positive reaction; "++", strong and specific reaction and therefore antibody appropriate for research purposes. [1]This antibody has been discontinued. [2]For the production of monoclonal antibodies to human NTPDase8, nine BALB/c mice were immunized. Seven out of the nine mice gave a positive reaction on Western blot in non-reduced conditions. The mouse with the sera with the highest titer was used for the generation of monoclonal antibodies, as described in Section "Materials and Methods." The four monoclonal antibodies obtained gave similar results for all experiments as indicated in the table.

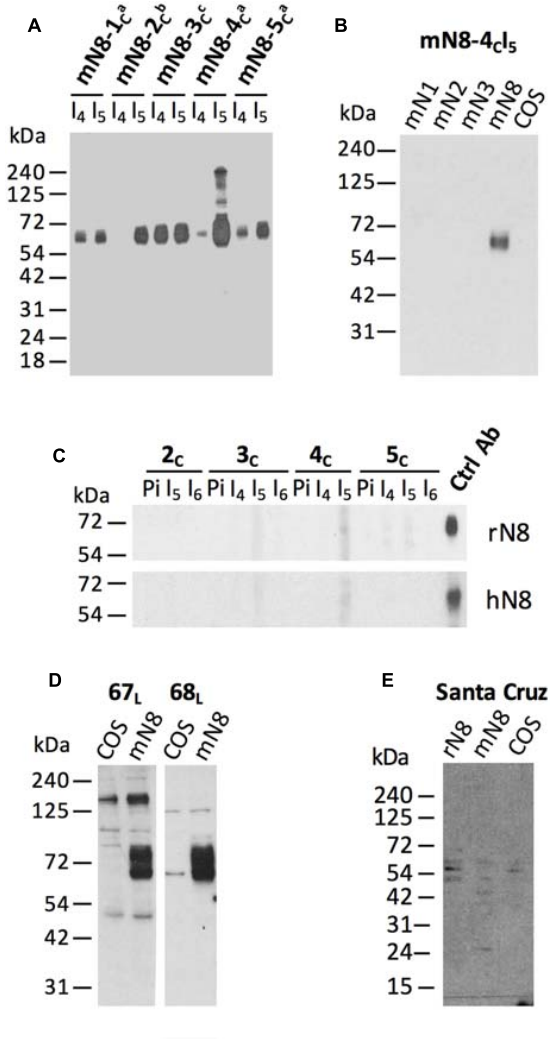

FIGURE 1 | Specificity of the polyclonal antibodies to mouse NTPDase8 by Western blot. (A) Lysates (120 μg) for one large well from COS-7 cells transfected with mouse NTPDase8, were subjected to electrophoresis and probed with the five guinea pig (mN8-1_c;-2_c;-3_c;-4_c; -5_c) antisera [bleeding after the fourth (I_4) and fifth (I_5) injection] against mouse NTPDase8 at different dilution (a: 1:1000; b: 1:500; c: 1:2000). **(B)** NTPDases specificity tested on lysates from COS-7 cells transfected with mouse NTPDase1 (mN1), -2 (mN2), -3 (mN3), -8 (mN8) or from non-transfected COS-7 cells (COS) and probed with the guinea pig anti-mouse NTPDase8 mN8-4_cI_5 at a dilution of 1:1000. **(C)** Species specificity tested on lysates (120 μg; large well) of COS-7 cells transfected with either rat (rN8) or human (hN8) NTPDase8 and incubated with four guinea pig antisera corresponding to the bleedings after the fourth (I_4), the fifth (I_5) and the sixth (I_6) injection or with the preimmune serum at a dilution of 1:500. Control antibodies to rat NTPDase8, rN8-8_cI_5 (1:1000) (previously described by Fausther et al., 2007) and to human NTPDase8, hN8-$C5_s$ (0.2 μg/mL) were used to confirm the presence of rat or human NTPDase8 protein in COS-7 lysates. **(D)** Lysates from COS-7 cells transfected with mouse NTPDase8 expression vector (mN8) or non-transfected (COS) and incubated with either mN8-67_LI_5 or mN8-68_LI_6 antiserum diluted 1:500 from rabbits immunized with peptide 6768 conjugated to KLH. **(E)** Lysate from COS-7 cells transfected with mouse (mN8) or rat (rN8) NTPDase8 or non-transfected (COS) and incubated with a commercial anti-mouse NTPDase8 (1:200) from Santa Cruz Biotechnology Inc. (Dallas, TX, USA). All gels were run under non-reduced conditions except in panel **(D)** and **(E)** where the protein samples were treated with β-mercaptoethanol.

RESULTS

For many years we struggled to produce antibodies to mouse NTPDase8. We will present below our unsuccessful attempts that may help other groups to avoid these problems and improve their chances of success. We also present an efficient and convenient technique that we used to obtain excellent antibodies to several ectonucleotidases that are now available at ectonucleotidases-ab.com. In addition, we have tested the antibodies produced by different companies against mouse and human NTPDase8.

Antibodies to Mouse NTPDase8

For the generation of mouse NTPDase8 antibodies, we first produced short peptides conjugated to KLH or in the form of MAPs. The number of animals tested for each antigen and conjugation type is indicated in **Table 1**. The MAPs was synthesized with peptide 829 and 830 corresponding to amino acid 1–14 and 60–74, respectively. These conjugated peptides and MAPs were injected in rabbits, hamsters, guinea pigs, and rats. The antiserum obtained for each animal was tested by Western blot under reduced condition. Note that all antisera generated from the immunization of peptides as an antigen were tested only by Western blot under denaturing conditions as this is the most likely technique that should work with such antigens. Generally, when no specific signal was obtained by Western blot with the sera from an animal immunized with peptides, no further experiments were done. The situation with intact and native proteins is different and will be described below. From all the sera with animals immunized with these MAPs, none of them gave a specific signal for mouse NTPDase8 (**Table 1** and data not shown).

Two other peptides conjugated to KLH, were injected in rabbits. The antisera from the rabbits injected with the peptide corresponding to amino acid 87–101 of mouse NTPDase8 showed a signal on lysate of mouse NTPDase8 transfected cells in Western blot (**Figure 1D**). Due to high level background, these antibodies were not further used in other techniques. No specific signal was obtained with the sera of rabbits injected with the KLH conjugated peptide corresponding to amino acid 390–404 (data not shown).

The service of Molecular Biology and Production of Antibody Service of the Centre de Recherche du CHU de Québec produced in bacteria a mouse NTPDase8 recombinant section from amino acid 361 to 441 (peptide 76). The peptide was purified by affinity chromatography on nickel-nitrilotriacetic acid resin, dialyzed and injected in rabbits. Again, none of the antisera obtained detected mouse NTPDase8 by Western blot in reduced condition (data not shown). Note that the peptides tested above were selected following *in silico* analysis using different programs to determine the hydrophobicity, antigenicity and sequence homology such as Peptool (BioTools Incorporated, Edmonton, AB, Canada) and Kyte and Doolittle hydrophobicity scale. The N-terminal region generally known to represent a good choice for immunization was also synthetized. Unfortunately, little success was obtained with these peptides as detailed above.

Injections of mouse NTPDase8 cDNA were then used in rabbits, hamsters, rats, and guinea pigs. The serum obtained for

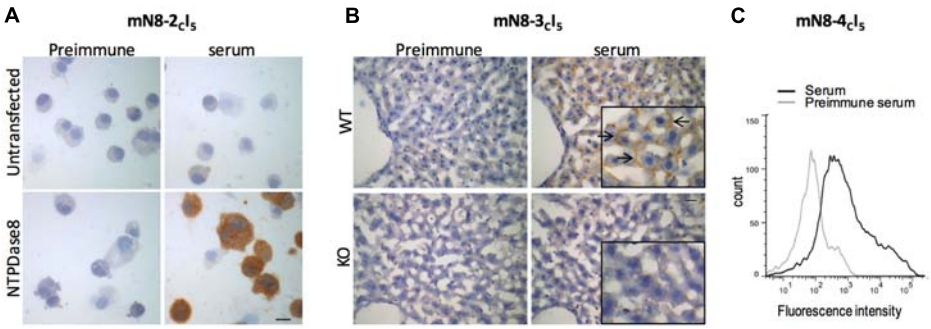

FIGURE 2 | Specificity of the best antisera for immunocytochemistry, immunohistochemistry, and flow cytometry. (A) Immunocytochemistry of COS-7 cells transfected with mouse NTPDase8 (lower panels) or non-transfected COS-7 cells (upper panels) were probed with the guinea pig anti-mouse NTPDase8 mN8-2_cI$_5$ (right panels), or with its preimmune serum (left panels), both at a 1:250 dilution. **(B)** Immunohistochemistry on a liver deficient in NTPDase8 expression (lower panels) or on a wild type (WT) mouse liver (upper panels) incubated with the preimmune serum (left panels) or the antiserum mN8-3_cI$_5$ (right panels) at a dilution of 1:500. Insets are 2× magnifications. Arrows show stained canaliculi. **(C)** Flow cytometry on mouse NTPDase8 transfected HEK 293T cells incubated with the mN8-4_cI$_5$ antiserum or its preimmune serum both at 1:80 dilution. In panels **(A)** and **(B)**, counterstaining of nuclei (blue) was performed with aqueous hematoxylin. Scale bar 25 μm.

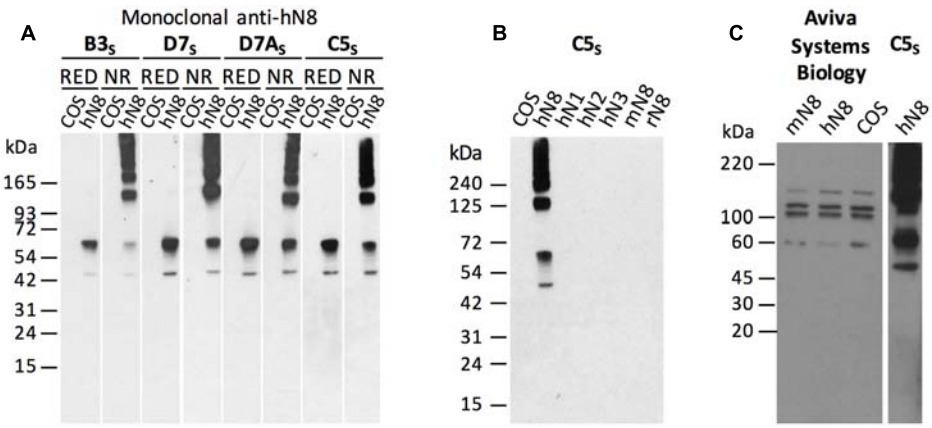

FIGURE 3 | Specificity of the mouse monoclonal antibodies to human NTPDase8 by Western blot. (A) Western blotting using lysates from COS-7 cells transfected with human NTPDase8 (hN8) or non-transfected cells (COS) in reduced (RED) or in non-reducing conditions (NR) were incubated separately with each anti-human NTPDase8 hybridoma, hN8-$B3_s$, -$D7_s$, -$D7A_s$, and -$C5_s$, as indicated. **(B)** Specificity of hN8-$C5_s$ (0.5 μg/mL) antibody on lysates from COS-7 transfected with human NTPDase1 (hN1), -2 (hN2), -3 (hN3), -8 (hN8), mouse NTPDase8 (mN8), rat NTPDase8 (rN8) or non-transfected cells (COS) in non-reduced condition. **(C)** A commercial anti-human NTPDase8 antibody from Aviva Systems Biology tested on lysates from COS-7 transfected with mouse (mN8) or human (hN8) NTPDase8 as well as non-transfected cells (COS) in reduced condition (left panel). A positive control in non-reduced conditions on a human NTPDase8 COS-7 cell lysate probed with hN8-$C5_s$ antibody was performed on the same gel. Additional note. Panels **(A)** and **(B)** represent two gels performed in the same time. The first 12 lanes of panel **(A)** constitute the first gel and the last four lanes were part of the gel presented in panel **(B)**. The last two lanes of panel **(A)** (COS and hN8) are reproduced in the first two lanes of panel **(B)**. Each demarcation shown in panels **(A)** and **(C)** represents a lane with non-reduced COS lysates used to stop diffusion of β-mercaptoethanol. These lanes were cut out of the data presented.

each animal was tested by Western blot. As the antigen here is the complete native form of mouse NTPDase8 produced by the host cells, the Western blots were first carried out in non-reducing conditions. No specific staining was obtained either with the rabbits, the hamsters or the rats (data not shown). On the other hand, the antisera developed by guinea pigs gave a weak signal on lysate from mouse NTPDase8 transfected COS-7 cells (data not shown). Of all the techniques used and from all species tested, the guinea pigs injected with cDNA was the technique and the species from which the best results were obtained. As the antisera of the first group of guinea pigs were positive but not sufficiently strong to work with, we repeated with a second series of five guinea pigs with the cDNA immunization technique. The sera of those last 5 guinea pigs gave a strong positive signal in Western blot with different intensity levels at the right molecular weight (**Figure 1A**). The detected band in Western blot for mouse NTPDase8 appears higher than the calculated molecular weight (54,650 Da) due to eight potential N-linked glycosylation sites. We do not have an explanation for the difference in immunoreactivity between the first groups of guinea pigs and the second group.

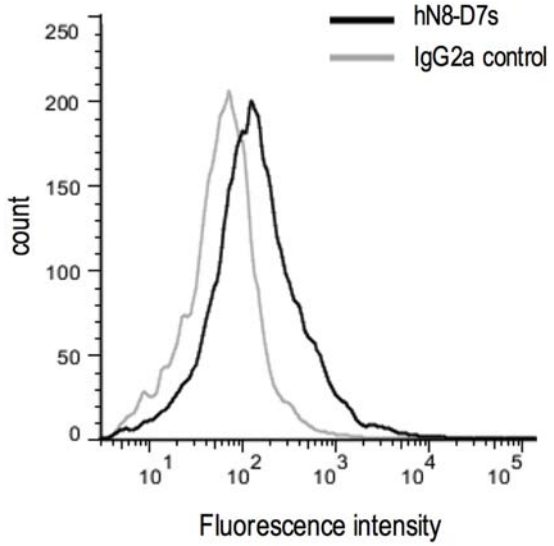

FIGURE 4 | Specificity of hN8-D7$_s$ by flow cytometry. Flow cytometry on human NTPDase8 transfected HEK 293T cells and incubated with an anti-human NTPDase8 (hN8-D7$_s$) or its isotype control both used at 10 μg/mL.

The cross-reactivity of the two best antibodies (mN8-3$_c$I$_5$ and mN8-4$_c$I$_5$) was tested on lysates of COS-7 cells transfected with other closely related members of the mouse E-NTPDase family as well as with non-transfected cells. **Figure 1B** shows that the antiserum mN8-4$_c$I$_5$ does not recognize mouse NTPDase1, -2, -3 or any other proteins from non-transfected COS-7 cells. Similar results were obtained for the other antibody tested: mN8-3$_c$I$_5$ (data not shown). The specificity was also confirmed on recombinant NTPDase8 from rat and human species, as shown on **Figure 1C**, no antiserum after the fourth (I$_4$), the fifth (I$_5$) and the sixth injection (I$_6$) of those guinea pigs (mN8-2$_c$; -3$_c$; -4$_c$; -5$_c$) cross-reacted with these two species. Similar results were obtained with mN8-1$_c$ on rat NTPDase8 (data not shown). These four guinea pig antisera (mN8-2$_c$; -3$_c$; -4$_c$; -5$_c$) were also tested in reduced conditions against mouse NTPDase8 but none of them recognized the protein reduced with β-mercaptoethanol (data not shown).

We next tested whether the best antisera on Western blot could immunolocalize NTPDase8 by immunocytochemistry and immunohistochemistry. The antisera mN8-2$_c$I$_5$ gave a strong positive signal on cells transfected with an expression vector encoding mouse NTPDase8 (**Figure 2A**, lower right panel). The absence of staining in non-transfected COS-7 cells confirmed the specificity of the reaction (**Figure 2A**, upper right panel). In addition, no signal could be detected with the preimmune serum either on non-transfected or NTPDase8 transfected COS-7 cells (**Figure 2A**, left panels). Similar results were obtained with the mN8-3$_c$I$_6$ and mN8-4$_c$I$_5$ antiserum (data not shown).

These antisera were also efficient and specific to detect the native NTPDase8 by immunohistochemistry, as evaluated by use of wild type and knockout mouse for *Entpd8* gene. We previously demonstrated the presence of NTPDase8 in rat (Fausther et al., 2007) and porcine liver canaliculi (Sévigny et al., 2000). We have also detected the presence of mRNA in mouse liver (Bigonnesse et al., 2004) suggesting that this protein may also be found in the same structure in mouse. As expected, mN8-3$_c$I$_5$ antiserum stained the canaliculi in the wild type mouse liver but not in the NTPDase8 knockout mouse (**Figure 2B**). Similar results were obtained with mN8-1$_c$I$_5$; -2$_c$I$_5$; -4$_c$I$_5$; -5$_c$I$_5$ antiserum (data not shown).

Each of the last five guinea pig anti-mouse NTPDase8 antisera was also efficient in flow cytometry. Indeed, they showed a shift in fluorescence intensity on cells transfected with a mouse NTPDase8 expression vector when compared with the preimmune serum (**Figure 2C** for mN8-4$_c$I$_5$ and data not shown for the other guinea pig antisera). Overall, these data indicate that the guinea pig antibodies detect the native mouse NTPDase8 protein.

In contrast to the immunization techniques that use native proteins as a source of antigen, as in the cDNA immunization technique with the full gene encoded as we did here, the commercial anti-mouse NTPDase8 from Santa Cruz Biotechnology Inc. was generated against a synthetic polypeptide. Therefore, if it can detect mouse NTPDase8 it must do in Western blot in denaturing and reduced conditions. In these conditions, the same non-specific bands were detected in both, lysates from transfected cells with mouse NTPDase8 and from non-transfected cells (**Figure 1E**).

Antibodies to Human NTPDase8

Hybridomas were generated from B-cells of BALB/c mice injected with human NTPDase8 cDNA. As our previous assays using only cDNA immunization were ineffective for some proteins (data not shown), we have made the final boost with intact HEK 293T cells transfected with the same human NTPDase8 expression vector to increase the titer and our chances of success in obtaining hybridomas. Even if the background would be expected to increase in the sera, this is not an issue with monoclonal antibodies. With this technique, we obtained four hybridomas by limiting dilution named hN8-B3$_s$, hN8-C5$_s$, hN8-D7$_s$, and hN8-D7A$_s$, which produced a positive response in ELISA on lysates of human NTPDase8 transfected cells, and a negative signal with lysates from non-transfected cells. The specificity of these monoclonal antibodies was tested by Western blot, ELISA, and flow cytometry.

The four hybridomas were tested in Western blot on lysates from COS-7 cells transfected with human NTPDase8 or non-transfected cells in reduced and non-reduced condition. As demonstrated in **Figure 3A**, human NTPDase8 antibodies recognize human NTPDase8 proteins in both reduced and non-reduced forms, suggesting that the higher bands observed over 65 kDa in the non-reduced samples are due to multimer formation. Indeed, none of these higher molecular weight bands are detected in the control sample proteins. Human NTPDase8 have a calculated molecular weight of 53,773 Da plus seven potential glycosylation sites for about 2–4 kDa each. In addition, the specificity of these four hybridomas was also tested in Western blot on other human NTPDases (NTPDase1, -2, -3) and

on other NTPDase8 species (mouse and rat) using lysates from transfected COS-7 transfected as well as from non-transfected cells. As illustrated in **Figure 3B**, the antibody named hN8-$C5_s$ detected only human NTPDase8. No cross-reaction was observed with human NTPDase1, -2, -3 nor with the mouse or rat NTPDase8 showing that these antibodies are highly specific. Similar results were obtained for the three other antibodies.

The isotype of the antibodies produced by these hybridomas were determined by ELISA using rat monoclonal antibodies specific for different mouse immunoglobulin which revealed that all four hybridomas are IgG2a (data not shown).

The four purified hybridomas anti-human NTPDase8 were tested by flow cytometry on human NTPDase8 transfected HEK 293T cells. All hybridomas produced a shift in the fluorescence at different intensity; the best antibody for this technique was hN8-D7s (diluted at 10 μg/mL; **Figure 4**), data not shown for the three other monoclonal antibodies.

These four monoclonal antibodies were also tested in enzyme activity inhibition assays but none of them were able to inhibit human NTPDase8 (data not shown).

The commercial anti-human NTPDase8 (Aviva Systems Biology, San Diego, CA, USA) was tested by Western blot. No specific staining at the expected molecular weight could be detected in reduced conditions. As seen in **Figure 3C**, the bands obtained were the same in the positive samples [COS-7 cells transfected with human NTPDase8 (hN8)] and in the negative control [non-transfected COS-7 cells (COS)].

DISCUSSION

In the present work, we have generated polyclonal antibodies against mouse NTPDase8 and four hybridomas that produce IgG2a against human NTPDase8. Many experimental approaches were necessary to generate antibodies against mouse NTPDase8, indeed, even if five different peptides were used to produce antibodies against mouse NTPDase8 injected in different hosts, and conjugated differently, only the peptides corresponding to amino acid 87–101 conjugated to KLH injected in rabbits gave a positive band on Western blot. The immunization with an expression vector encoding for the full coding sequence of mouse NTPDase8 in rabbit, guinea pig, rat, and hamster gave successful result only in guinea pigs (**Table 1**). This technique was also useful for the production of antibodies against several other ectonucleotidases (Sévigny et al., 2002; Bartel et al., 2006; Vekaria et al., 2006; Fausther et al., 2007, 2012; Martín-Satué et al., 2009). The guinea pig anti-mouse NTPDase8 antibodies were validated in different techniques. They are specific and efficient for immunohistochemistry, for immunocytochemistry, for flow cytometry as well as for Western blot but only in non-reduced conditions, suggesting that the epitope is discontinuous and part of a tertiary structure of the protein involving disulphide bridges. These antibodies were very specific to mouse NTPDase8 and they did not cross-react with cells transfected with the other NTPDases that show the highest homology to NTPDase8, between 39 and 44% identity, namely NTPDase1, -2, and -3 (Bigonnesse et al., 2004; Lavoie et al., 2004), or with NTPDase8 from rat and human species. The other NTPDases which are more different in structures and in amino acid sequence identity (lower than 25% identity to mouse NTPDase8) were not tested. All the difficulties that we encountered to produce antibodies to mouse NTPDase8, especially those using synthetized peptides, suggests that this protein is poorly immunogenic.

In addition, the antibody against mouse NTPDase8 allowed the localization of NTPDase8 in mouse liver canaliculi as we previously observed for rat NTPDase8 (Fausther et al., 2007).

To generate monoclonal antibodies against human NTPDase8, an injection of human NTPDase8 transfected HEK 293T cells at the last boost after several cDNA immunizations was determined to be an efficient technique. The monoclonal antibodies against human NTPDase8 were also validated with different techniques. Our results show that these monoclonal antibodies are efficient in all techniques tested: Western blot (reduced and non-reduced conditions), indirect ELISA, immunohistochemistry (data not shown) and flow cytometry (**Table 1**). The four hybridomas may originate from the same original B cell clone since all experiments performed yielded similar results with each of the four monoclonal antibodies and that all are IgG2a.

In addition, we also tested commercial antibodies to mouse and human NTPDase8. Neither of them detected a specific band on Western blot under the conditions used in our experiments. Indeed, the same background bands could be seen in both COS-7 extracts from cells overexpressing NTPDase8 and in COS-7 extract controls (**Figures 1E**, **3C**). The commercial antibodies were used at the concentration recommended by the companies. It is noteworthy that we allowed an overreaction to detect any minor bands. As a comparative control which is illustrated in **Figure 3C**, the amount of cell lysates loaded, containing human NTPDase8, and time of reaction resulted in an intense band with the hN8-$C5_s$ antibody. Similar results were obtained when comparing the reaction obtained with mN8-4_cI_5 antisera with the antibody from Santa Cruz (**Figure 1E** and data not shown).

CONCLUSION

In this work, we generated specific antibodies to mouse and human NTPDase8 with very convenient cDNA immunization techniques. These antibodies are useful for Western blot, ELISA, immunohistochemistry, immunocytochemistry, and flow cytometry. These antibodies allowed the immunolocalization of NTPDase8 in mouse liver canaliculi. It is noteworthy that the commercial antibodies tested here against mouse or human NTPDase8 failed to give a specific reaction. This reiterates previously published results evaluating other commercially available antibodies, which indicate that commercial antibodies need to be carefully validated before they can be correctly and

effectively used, e.g., for antibodies against angiotensin II AT_2 (Hafko et al., 2013), $P2Y_6$ (Yu and Hill, 2013), and alpha1-adrenergic receptor subtypes (Jensen et al., 2009).

AUTHOR CONTRIBUTIONS

JP performed Western blot, immunocytochemistry, activity tests, flow cytometry, and wrote the first draft of the manuscript; MS did immunohistochemistry assays; JL prepared the protein extracts; MF performed immunohistochemistry, immunocytochemistry, and Western blot; FB performed immunohistochemistry and immunocytochemistry; JS supervised the study.

FUNDING

This work was supported by a grant to J. Sévigny from the Canadian Institutes of Health Research (CIHR; MOP-102472). MS was a recipient of a scholarship from the Fonds de recherche du Québec-Santé (FRQS), MF of a doctoral Scholarship from the Government of Gabon and JS of a "Chercheur National" Scholarship award from the FRQS.

DISCLAIMER

The monies received to obtain the antibodies were reinvested into antibody generation and research.

REFERENCES

Bartel, D. L., Sullivan, S. L., Lavoie, E. G., Sévigny, J., and Finger, T. E. (2006). Nucleoside triphosphate diphosphohydrolase-2 is the ecto-ATPase of type I cells in taste buds. *J. Comp. Neurol.* 497, 1–12. doi: 10.1002/cne.20954

Baykov, A. A., Evtushenko, O. A., and Avaeva, S. M. (1988). A malachite green procedure for orthophosphate determination and its use in alkaline phosphatase-based enzyme immunoassay. *Anal. Biochem.* 171, 266–270. doi: 10.1016/0003-2697(88)90484-8

Beaudoin, A. R., Sévigny, J., and Picher, M. (1996). "ATP-diphosphohydrolases, apyrases, and nucleotide phosphohydrolases: biochemical properties and functions," in *ATPases*, ed. A. G. Lee (Greenwich: JAI Press Inc), 369–401. doi: 10.1016/s1874-5342(06)80015-2

Belcher, S. M., Zsarnovszky, A., Crawford, A. R., Hemani, H., Spurling, L., and Kirley, T. L. (2005). Immunolocalization of ectonucleoside triphosphate diphosphohydrolase 3 in rat brain: implication for modulation of multiple homeostatic systems including feeding and sleep-wake behaviors. *Neuroscience* 137, 1331–1346. doi: 10.1016/j.neuroscience.2005.08.086

Bigonnesse, F., Lévesque, S. A., Kukulski, F., Lecka, J., Robson, S. C., Fernandes, M. J. G., et al. (2004). Cloning and characterization of mouse nucleoside triphosphate diphosphohydrolase-8. *Biochemistry* 43, 5511–5519. doi: 10.1021/bi0362222

Enjyoji, K., Sévigny, J., Lin, Y., Frenette, P. S., Christie, P. D., Schulte Am Esch Ii, J., et al. (1999). Targeted disruption of CD39/ATP diphosphohydrolase results in disordered hemostasis and thromboregulation. *Nat. Med.* 5, 1010–1017. doi: 10.1038/12447

Fausther, M., Lecka, J., Kukulski, F., Lévesque, S. A., Pelletier, J., Zimmermann, H., et al. (2007). Cloning, purification and identification of the liver canalicular ecto-ATPase as NTPDase8. *Am. J. Physiol. Gastrointest. Liver Physiol.* 292, G785–G795.

Fausther, M., Lecka, J., Soliman, E., Kauffenstein, G., Pelletier, J., Sheung, N., et al. (2012). Coexpression of ecto-5′-nucleotidase/CD73 with specific NTPDases differentially regulates adenosine formation in the rat liver. *Am. J. Physiol. Gastrointest. Liver Physiol.* 302, G447–G459. doi: 10.1152/ajpgi.00165.2011

Hafko, R., Villapol, S., Nostramo, R., Symes, A., Sabban, E. L., Inagami, T., et al. (2013). Commercially available angiotensin II At(2) receptor antibodies are nonspecific. *PLoS ONE* 8:e69234. doi: 10.1371/journal.pone.0069234

Jensen, B. C., Swigart, P. M., and Simpson, P. C. (2009). Ten commercial antibodies for alpha-1-adrenergic receptor subtypes are nonspecific. *Naunyn Schmiedebergs Arch. Pharmacol.* 379, 409–412. doi: 10.1007/s00210-008-0368-6

Kaczmarek, E., Koziak, K., Sévigny, J., Siegel, J. B., Anrather, J., Beaudoin, A. R., et al. (1996). Identification and characterization of CD39 vascular ATP diphosphohydrolase. *J. Biol. Chem.* 271, 33116–33122. doi: 10.1074/jbc.271.51.33116

Knowles, A. F., and Chiang, W. C. (2003). Enzymatic and transcriptional regulation of human ecto-ATPase/E-NTPDase 2. *Arch. Biochem. Biophys.* 418, 217–227. doi: 10.1016/j.abb.2003.08.007

Kukulski, F., Lévesque, S. A., Lavoie, E. G., Lecka, J., Bigonnesse, F., Knowles, A. F., et al. (2005). Comparative hydrolysis of P2 receptor agonists by NTPDases 1, 2, 3 and 8. *Purinergic Signal.* 1, 193–204. doi: 10.1007/s11302-005-6217-x

Kukulski, F., Lévesque, S. A., and Sévigny, J. (2011). Impact of ectoenzymes on P2 and P1 receptor signaling. *Adv. Pharmacol.* 61, 263–299. doi: 10.1016/B978-0-12-385526-8.00009-6

Lavoie, É. G., Kukulski, F., Lévesque, S. A., Lecka, J., and Sévigny, J. (2004). Cloning and characterization of mouse nucleoside triphosphate diphosphohydrolase-3. *Biochem. Pharmacol.* 67, 1917–1926. doi: 10.1016/j.bcp.2004.02.012

Martín-Satué, M., Lavoie, E. G., Pelletier, J., Fausther, M., Csizmadia, E., Guckelberger, O., et al. (2009). Localization of plasma membrane bound NTPDases in the murine reproductive tract. *Histochem. Cell Biol.* 131, 615–628. doi: 10.1007/s00418-008-0551-3

Munkonda, M. N., Pelletier, J., Ivanenkov, V. V., Fausther, M., Tremblay, A., Kunzli, B., et al. (2009). Characterization of a monoclonal antibody as the first specific inhibitor of human NTP diphosphohydrolase-3: partial characterization of the inhibitory epitope and potential applications. *FEBS J.* 276, 479–496. doi: 10.1111/j.1742-4658.2008.06797.x

Robson, S. C., Sévigny, J., and Zimmermann, H. (2006). The E-NTPDase family of ectonucleotidases: structure function relationships and pathophysiological significance. *Purinergic Signal.* 2, 409–430. doi: 10.1007/s11302-006-9003-5

Sévigny, J., Robson, S. C., Waelkens, E., Csizmadia, E., Smith, R. N., and Lemmens, R. (2000). Identification and characterization of a novel hepatic canalicular ATP diphosphohydrolase. *J. Biol. Chem.* 275, 5640–5647. doi: 10.1074/jbc.275.8.5640

Sévigny, J., Sundberg, C., Braun, N., Guckelberger, O., Csizmadia, E., Qawi, I., et al. (2002). Differential catalytic properties and vascular topography of murine nucleoside triphosphate diphosphohydrolase 1 (NTPDase1) and NTPDase2 have implications for thromboregulation. *Blood* 99, 2801–2809. doi: 10.1182/blood.V99.8.2801

Smith, T. M., and Kirley, T. L. (1998). Cloning, sequencing, and expression of a human brain ecto-apyrase related to both the ecto-ATPases and CD39 ecto-apyrases. *Biochim. Biophys. Acta* 1386, 65–78. doi: 10.1016/S0167-4838(98)00063-6

Vandenbeuch, A., Anderson, C. B., Parnes, J., Enjyoji, K., Robson, S. C., Finger, T. E., et al. (2013). Role of the ectonucleotidase NTPDase2 in taste bud function. *Proc. Natl. Acad. Sci. U.S.A.* 110, 14789–14794. doi: 10.1073/pnas.1309468110

Vekaria, R. M., Shirley, D. G., Sévigny, J., and Unwin, R. J. (2006). Immunolocalization of ectonucleotidases along the rat nephron. *Am. J. Physiol. Renal Physiol.* 290, F550–F560. doi: 10.1152/ajprenal.00151.2005

Yegutkin, G. G. (2014). Enzymes involved in metabolism of extracellular nucleotides and nucleosides: functional implications and measurement of activities. *Crit. Rev. Biochem. Mol. Biol.* 49, 473–497. doi: 10.3109/10409238.2014.953627

Yu, W., and Hill, W. G. (2013). Lack of specificity shown by P2Y6 receptor antibodies. *Naunyn Schmiedebergs Arch. Pharmacol.* 386, 885–891. doi: 10.1007/s00210-013-0894-8

Zimmermann, H., Zebisch, M., and Strater, N. (2012). Cellular function and molecular structure of ecto-nucleotidases. *Purinergic Signal.* 8, 437–502. doi: 10.1007/s11302-012-9309-4

Conflict of Interest Statement: The authors declare that the research was conducted in the absence of any commercial or financial relationships that could be construed as a potential conflict of interest.

Advantages of publishing in Frontiers

OPEN ACCESS
Articles are free to read for greatest visibility and readership

FAST PUBLICATION
Around 90 days from submission to decision

HIGH QUALITY PEER-REVIEW
Rigorous, collaborative, and constructive peer-review

TRANSPARENT PEER-REVIEW
Editors and reviewers acknowledged by name on published articles

Frontiers
Avenue du Tribunal-Fédéral 34
1005 Lausanne | Switzerland

Visit us: www.frontiersin.org
Contact us: info@frontiersin.org | +41 21 510 17 00

REPRODUCIBILITY OF RESEARCH
Support open data and methods to enhance research reproducibility

DIGITAL PUBLISHING
Articles designed for optimal readership across devices

FOLLOW US
@frontiersin

IMPACT METRICS
Advanced article metrics track visibility across digital media

EXTENSIVE PROMOTION
Marketing and promotion of impactful research

LOOP RESEARCH NETWORK
Our network increases your article's readership